PDF Output of CLIC (clustering by inferred co-expression)

Dataset:

Num of genes in input gene set: 41

Total number of genes: 16978

CLIC PDF output has three sections:

1) Overview of Co-Expression Modules (CEMs)

- Heatmap shows pairwise correlations between all genes in the input query gene set.
- Red lines shows the partition of input genes into CEMs, ordered by CEM strength.
- Each row shows one gene, and the brightness of squares indicates its correlations with other genes.
- Gene symbols are shown at left side and on the top of the heatmap.

2) Details of each CEM and its expansion CEM+

- Top panel shows the posterior selection probability (dataset weights) for top GEO series datasets.
- Bottom panel shows the CEM genes (blue rows) as well as expanded CEM+ genes (green rows).
- Each column is one GEO series dataset, sorted by their posterior probability of being selected.
- The brightness of squares indicates the gene's correlations with CEM genes in the corresponding dataset.
- CEM+ includes genes that co-express with CEM genes in high-weight datasets, measured by LLR score.

3) Details of each GEO series dataset and its expression profile:

- Top panel shows the detailed information (e.g. title, summary) for the GEO series dataset.
- Bottom panel shows the background distribution and the expression profile for CEM genes in this dataset.

Overview of Co-Expression Modules (CEMs) with Dataset Weighting

Num of Genes in Query Geneset: 41. Num of CEMs: 1.

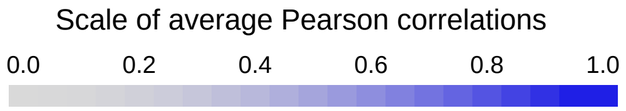

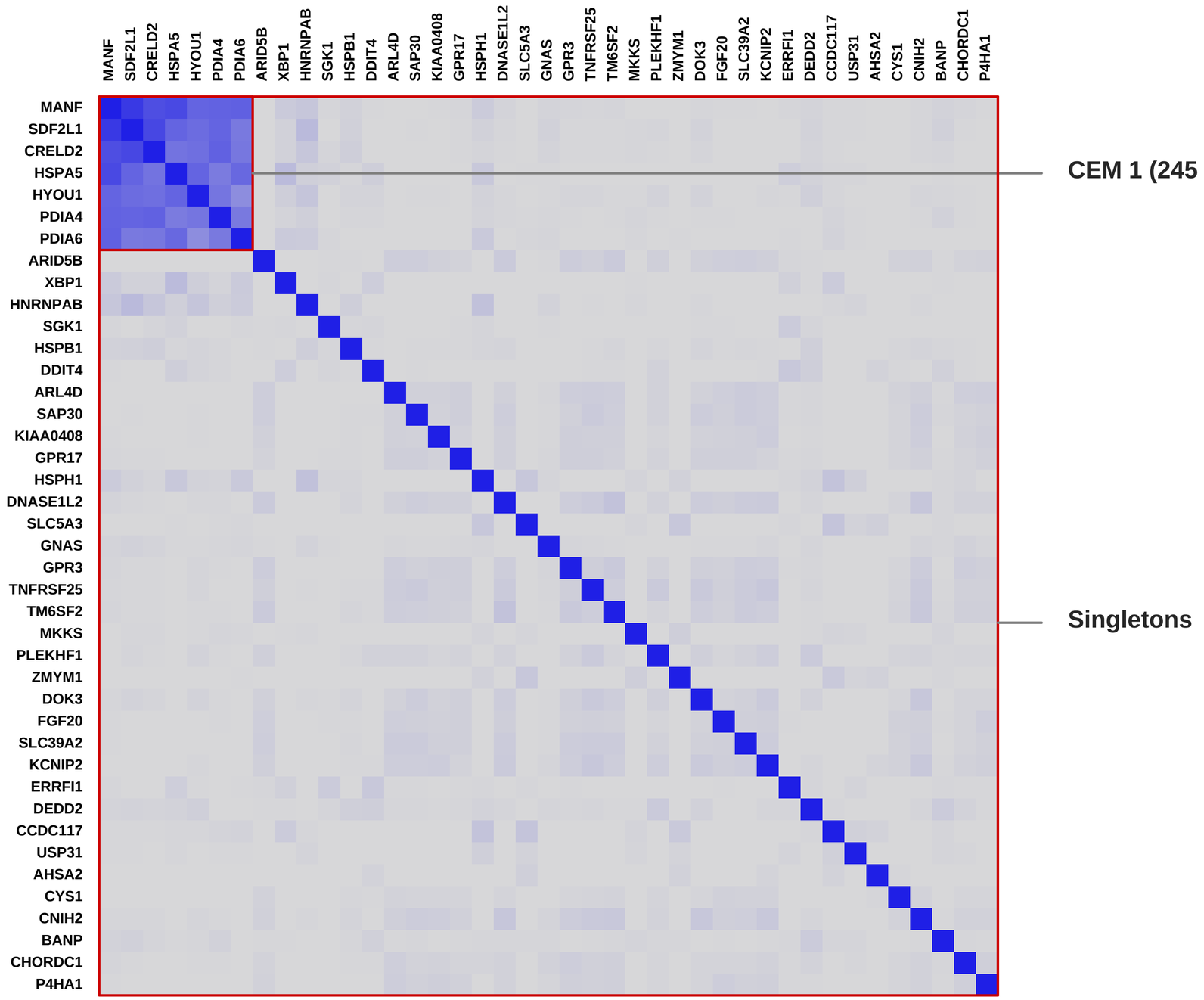

CEM 1, Gene set "", Page 1

Num of CEM Genes: 7. Num of Predicted Genes: 32. Num of Selected Datasets: 245. CEM Strength: 14.7

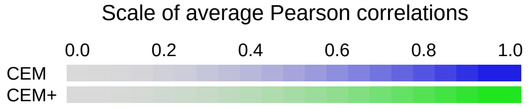

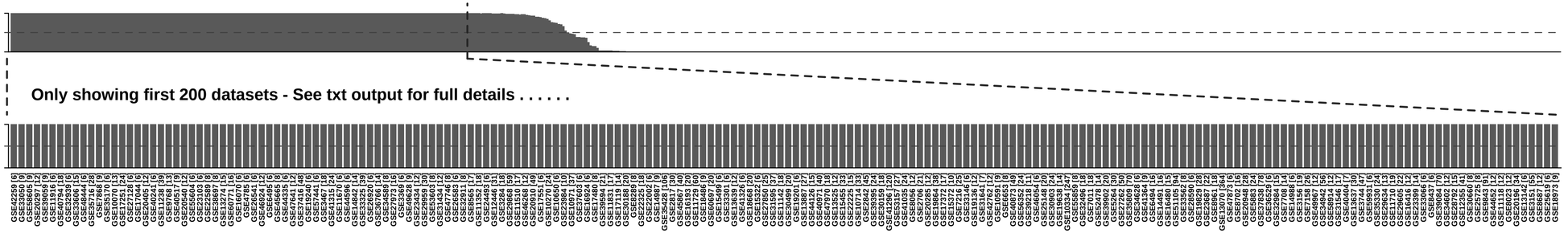

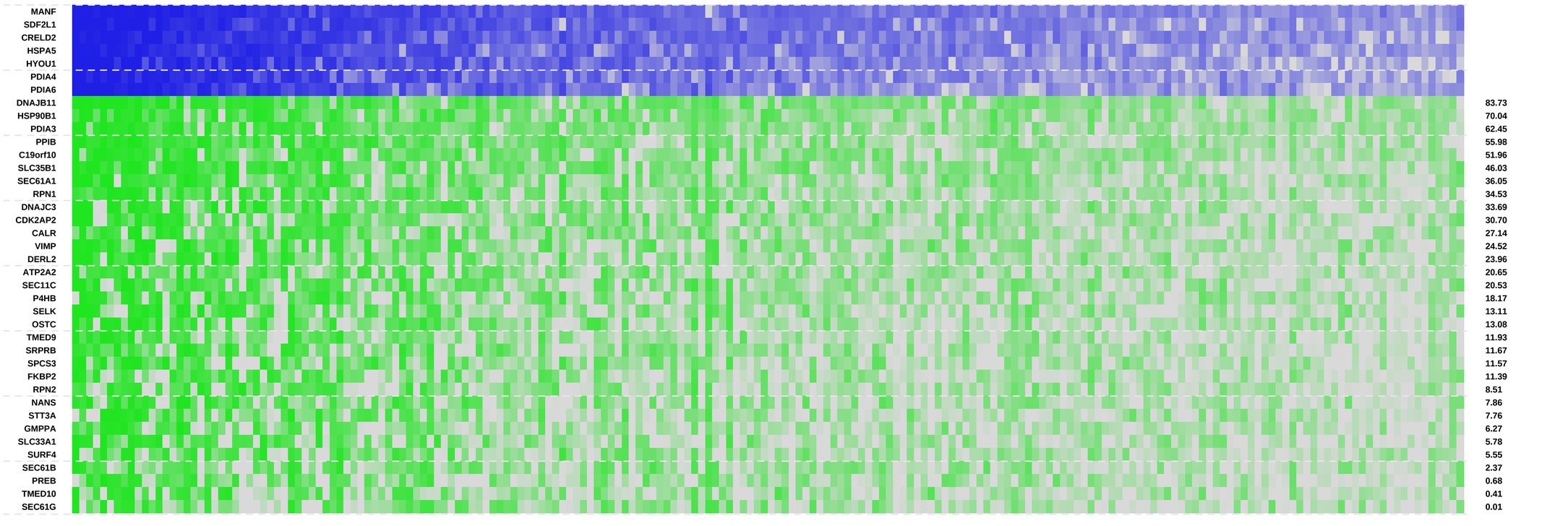

GEO Series "GSE42259" Expression Profiles

Num of samples in this series: 6

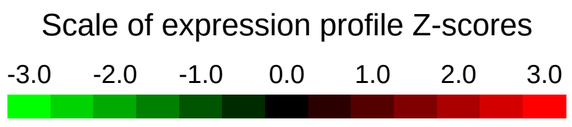

GEO Link:	http://www.ncbi.nlm.nih.gov/geo/query/acc.cgi?acc=GSE42259
Status:	Public on Jan 18 2013
Title:	Notch Pathway Activation Targets AML Cell Homeostasis and Differentiation: THP1 cell line
Organism:	Homo sapiens
Experiment type:	Expression profiling by array
Platform:	GPL570
Pubmed ID:	23359070
Summary & Design:	**Summary:** Expression data from untreated or Dll4-Fc treated THP1 cell line. We used Dll4-Fc stimulation of AML cells to study whether Notch activation has an impact on AML. We analyzed THP1 cell line in vitro treated with Dll4-Fc or vehicle control to determine genes affected by Notch activation. **Overall design:** THP1 cell line was cultured on plate coated with 30 nM Dll4-Fc or vehicle for 48 hours prior to RNA extraction and hybridization to Human Genome U133 Plus 2.0 Affymetrix arrays.

Background corr dist: KL-Divergence = 0.0294, L1-Distance = 0.0472, L2-Distance = 0.0026, Normal std = 0.7500

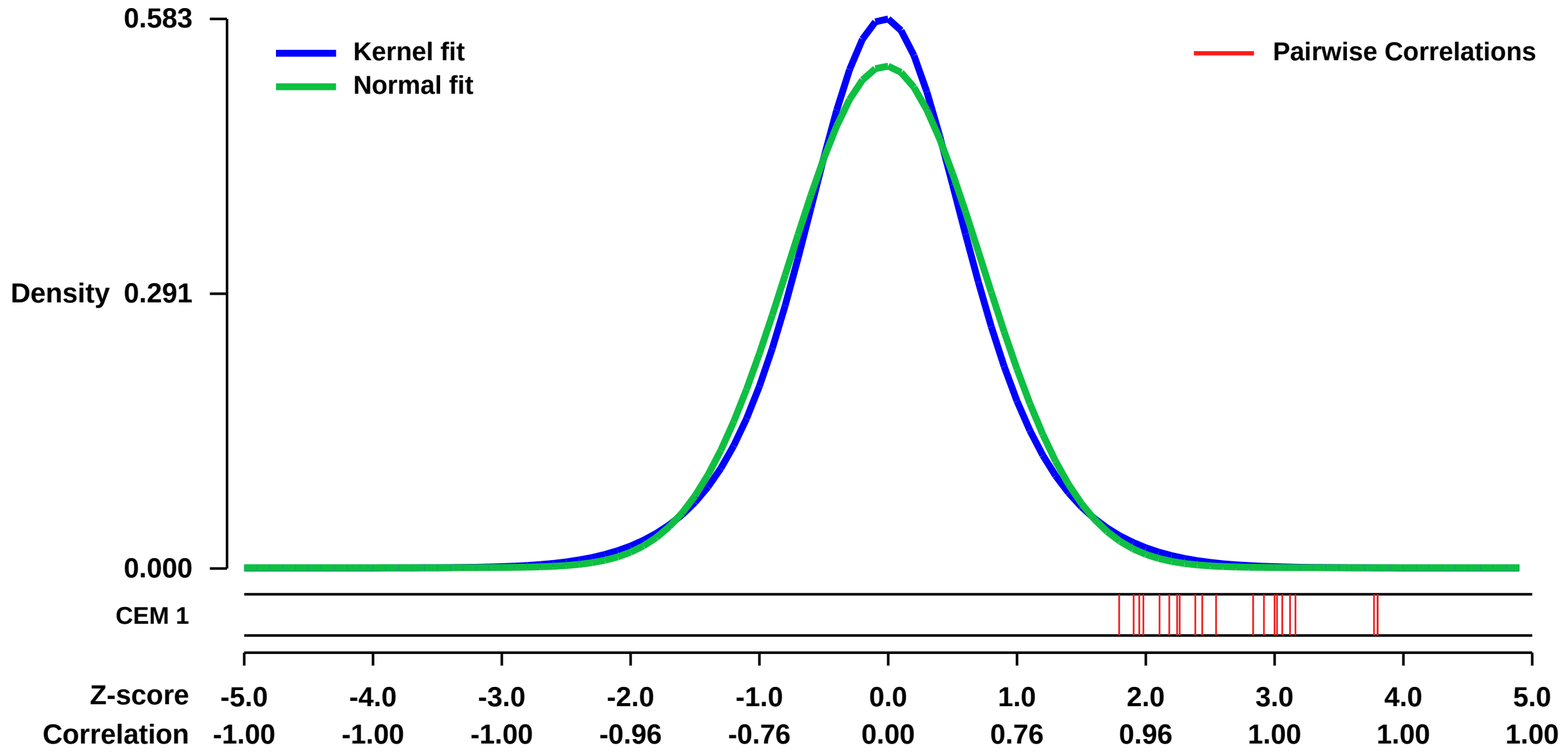

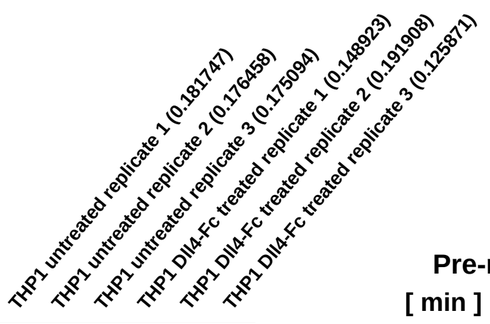

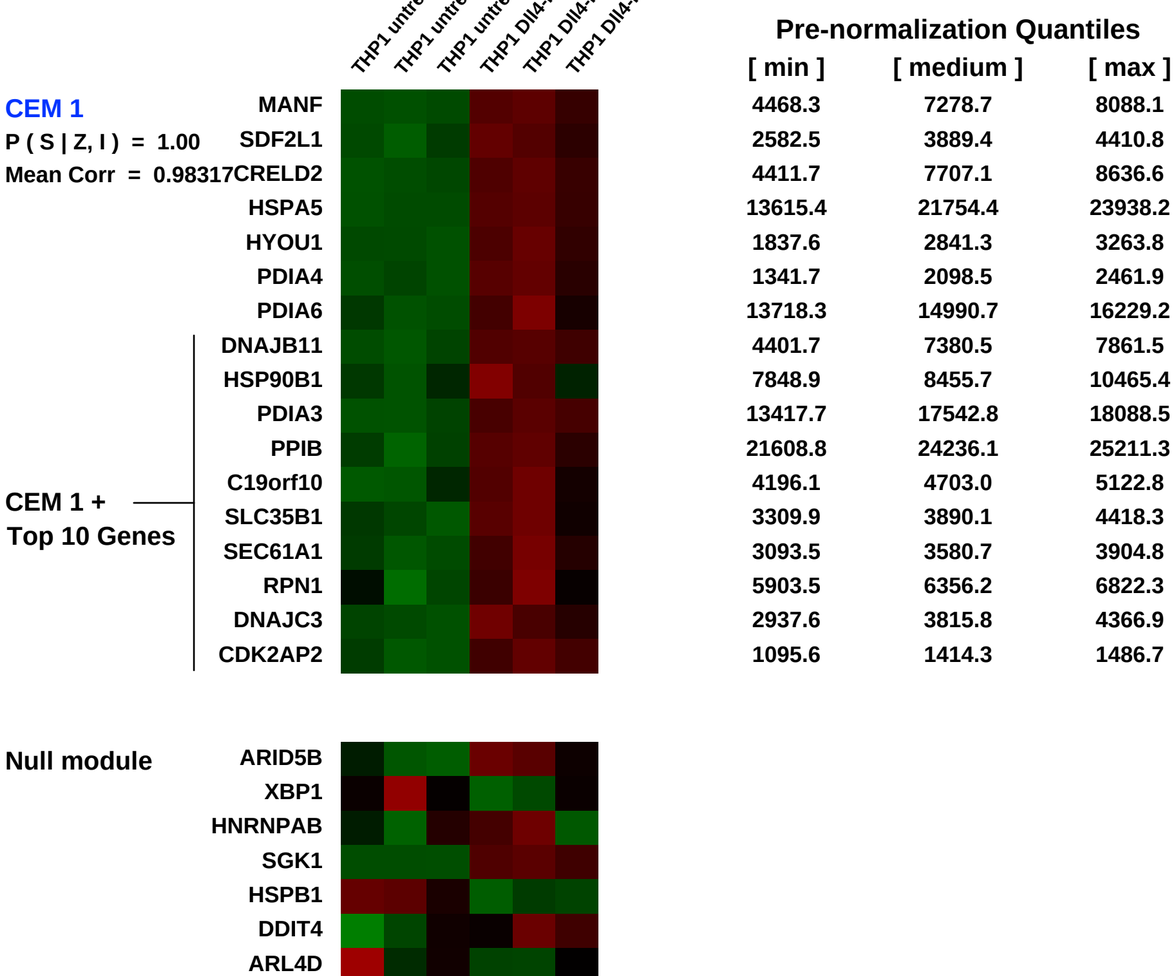

GEO Series "GSE33050" Expression Profiles

Num of samples in this series: 9

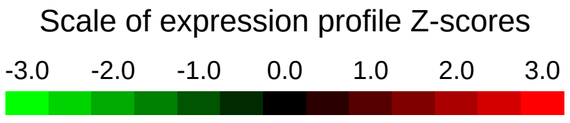

GEO Link:	http://www.ncbi.nlm.nih.gov/geo/query/acc.cgi?acc=GSE33050
Status:	Public on Oct 27 2011
Title:	GlcNAcylation of histone H2B facilitates its monoubiquitination [Affymetrix data]
Organism:	Homo sapiens
Experiment type:	Expression profiling by array
Platform:	GPL570
Pubmed ID:	22121020
Summary & Design:	**Summary:** We have found that histone H2B is GlcNAcylated at residue S112 by O-GlcNAc transferase and that H2B S112 GlcNAcylation fluctuates in response to extracellular glucose level. We have also found that H2B S112 GlcAcylation promotes H2B K120 ubiquitination. To investigate whether these histone modification correlate to transcriptional activation, we performed comprehensive gene expression analysis using Affymetrix GeneChip in HeLa cell cultured with different conditions, i.e. without glucose, with glucose and with FBS. **Overall design:** HeLa cells were cultured in DMEM with the following three conditions, 1) DMEM without glucose for 24 hours, 2) DMEM without glucose for 24 hours and followed by treatment with 4.5 g/L glucose for another 24 hours, 3) normal culture condition (DMEM with FBS). Total RNA was purified from these cells and each RNA was linearly amplified and hybridized to Affymetrix GeneChip.

Background corr dist: KL-Divergence = 0.0716, L1-Distance = 0.0382, L2-Distance = 0.0020, Normal std = 0.5247

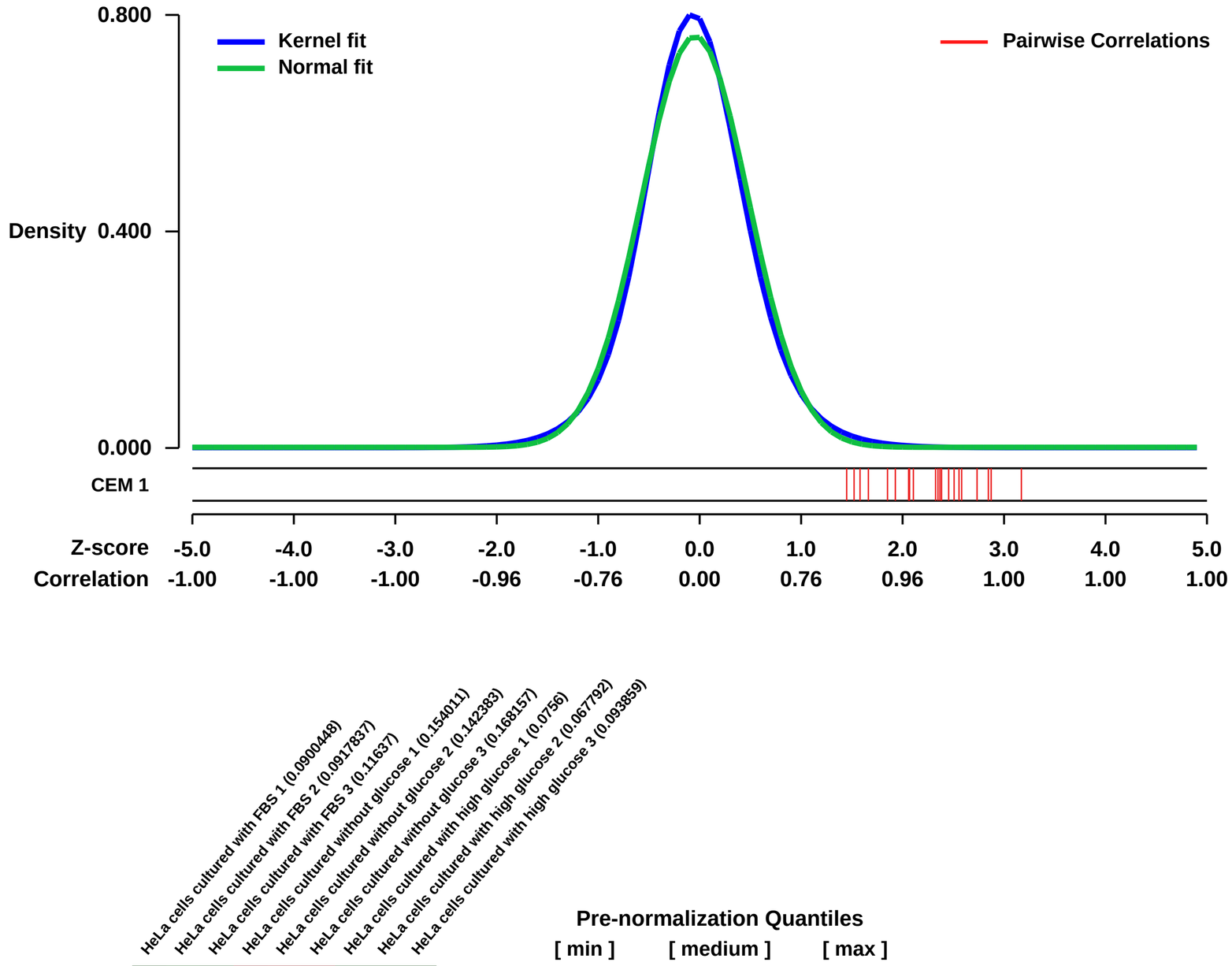

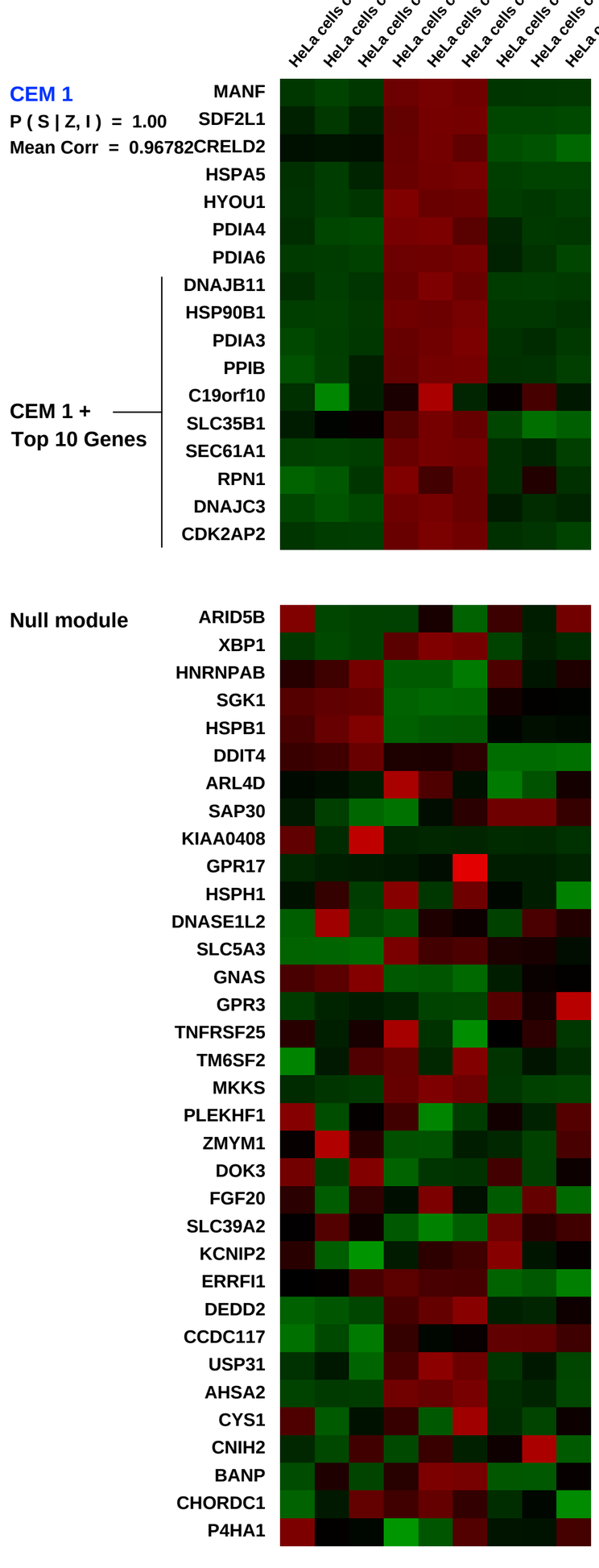

Pre-normalization Quantiles

	[min]	[medium]	[max]
MANF	2993.2	3411.4	9310.0
SDF2L1	1278.0	1771.5	3692.2
CRELD2	1639.3	3305.7	5812.7
HSPA5	15551.3	18348.4	42143.6
HYOU1	4295.6	4858.1	16317.3
PDIA4	1083.7	1440.3	3592.9
PDIA6	6511.7	6943.2	11109.5
DNAJB11	7496.1	7979.5	17376.0
HSP90B1	3330.2	3888.4	13891.5
PDIA3	10330.3	12265.2	28298.8
PPIB	14475.5	16601.8	26915.6
C19orf10	3894.0	4711.3	6168.7
SLC35B1	2647.0	3933.7	5403.2
SEC61A1	3766.7	4315.9	8638.1
RPN1	4038.8	4375.0	5481.4
DNAJC3	1333.3	2075.6	4461.6
CDK2AP2	1347.1	1532.8	3812.7

GEO Series "GSE58605" Expression Profiles

Num of samples in this series: 9

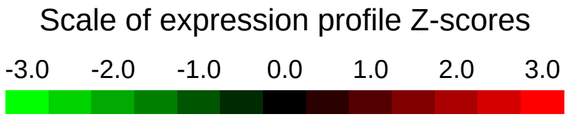

GEO Link:	http://www.ncbi.nlm.nih.gov/geo/query/acc.cgi?acc=GSE58605
Status:	Public on Sep 01 2014
Title:	Expression data from A549 cells infected by adenovirus not carrying virus associated sequences in the genome.
Organism:	Homo sapiens
Experiment type:	Expression profiling by array
Platform:	GPL570
Pubmed ID:	
Summary & Design:	**Summary:** Non-coding small RNAs are involved in viral life cycles. Adenovirus-encoding small RNAs, virus-associated RNAs (VA RNAs), are transcribed throughout the replication process, and the transcript levels depend on the copy numbers of the viral genome. Although the VA RNA transcription starts immediate early phase, little is known about the function in the early phase. Here we applied replication-deficient adenovirus vectors (AdVs) and novel VA-RNA deleted AdVs to analyze expression change of cellular gene mediated by VA RNAs. **Overall design:** Human lung cell, A549, were infected by VA(+) or VA(-) adenoviral vectors. After the designed preiod of infection, cells were harvested and RNA was extacted, followed by DNA microarray analysis.
Background corr dist:	KL-Divergence = 0.0944, L1-Distance = 0.0207, L2-Distance = 0.0006, Normal std = 0.4497

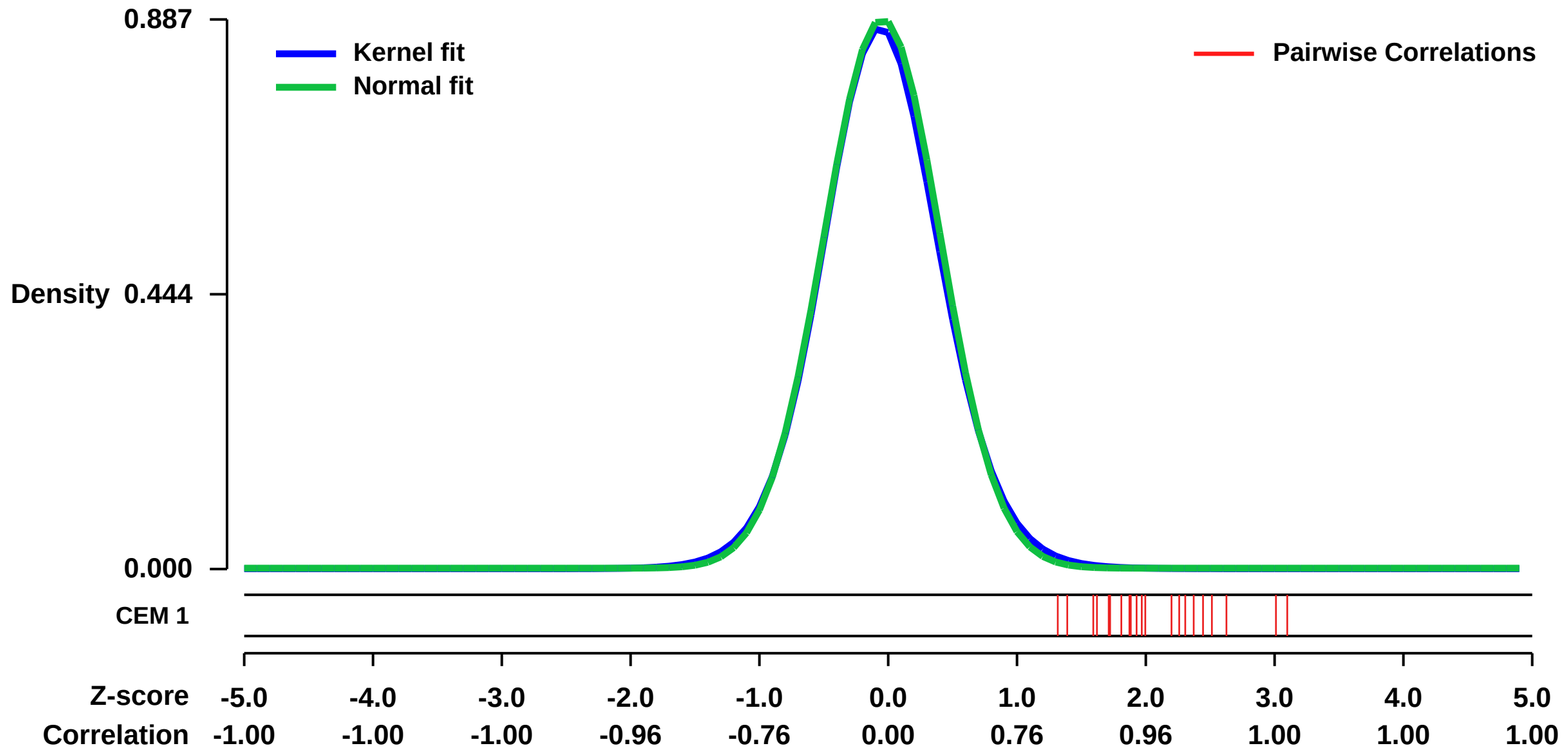

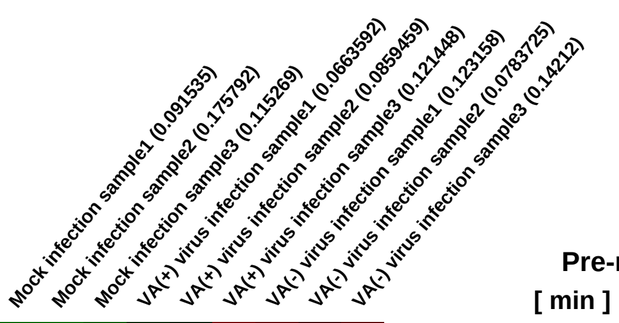

Pre-normalization Quantiles

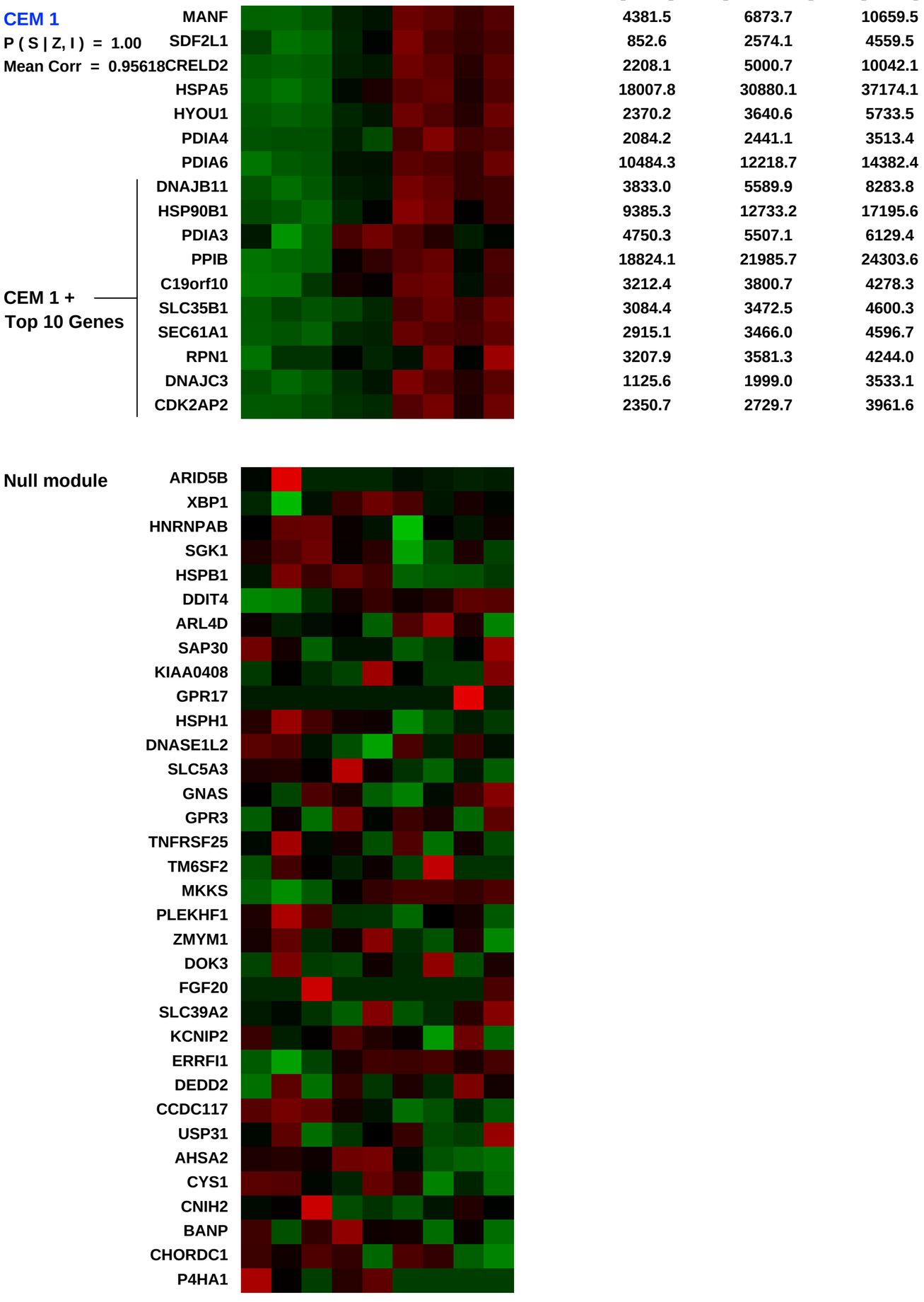

	[min]	[medium]	[max]
MANF	4381.5	6873.7	10659.5
SDF2L1	852.6	2574.1	4559.5
CRELD2	2208.1	5000.7	10042.1
HSPA5	18007.8	30880.1	37174.1
HYOU1	2370.2	3640.6	5733.5
PDIA4	2084.2	2441.1	3513.4
PDIA6	10484.3	12218.7	14382.4
DNAJB11	3833.0	5589.9	8283.8
HSP90B1	9385.3	12733.2	17195.6
PDIA3	4750.3	5507.1	6129.4
PPIB	18824.1	21985.7	24303.6
C19orf10	3212.4	3800.7	4278.3
SLC35B1	3084.4	3472.5	4600.3
SEC61A1	2915.1	3466.0	4596.7
RPN1	3207.9	3581.3	4244.0
DNAJC3	1125.6	1999.0	3533.1
CDK2AP2	2350.7	2729.7	3961.6
ARID5B			
XBP1			
HNRNPAB			
SGK1			
HSPB1			
DDIT4			
ARL4D			
SAP30			
KIAA0408			
GPR17			
HSPH1			
DNASE1L2			
SLC5A3			
GNAS			
GPR3			
TNFRSF25			
TM6SF2			
MKKS			
PLEKHF1			
ZMYM1			
DOK3			
FGF20			
SLC39A2			
KCNIP2			
ERRFI1			
DEDD2			
CCDC117			
USP31			
AHSA2			
CYS1			
CNIH2			
BANP			
CHORDC1			
P4HA1			

GEO Series "GSE20297" Expression Profiles

Num of samples in this series: 12

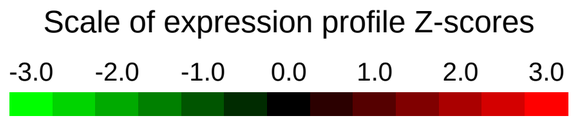

GEO Link:	http://www.ncbi.nlm.nih.gov/geo/query/acc.cgi?acc=GSE20297
Status:	Public on Dec 01 2010
Title:	The effects of terbutaline or GW9508 on TNF-alpha and IFN gamma (TNF-alpha + IFN gamma) stimulation by HaCaT
Organism:	Homo sapiens
Experiment type:	Expression profiling by array
Platform:	GPL570
Pubmed ID:	
Summary & Design:	**Summary:** G-protein coupled receptors (GPCRs) have diverse roles in physiological processes, including immunity. Gs-coupled GPCRs increase while Gi-coupled ones decrease intracellular cAMP. Previous studies suggest that, in epithelial cells, Gs-coupled GPCRs enhance whereas Gi-coupled GPCRs suppress pro-inflammatory immune responses. In order to examine the issue, we chose beta2 adrenergic receptor and GPR40 as representatives of Gs- and Gi- coupled GPCRs, respectively, and examined their effects on TNF-alpha and IFN-gamma-(TNF-alpha + IFN-gamma) induced gene expression by HaCaT. We used microarrays to detail the global changes of gene expression induced by a beta2 adrenergic receptor agonist terbutaline or GPR40 agonist GW9508 pre-treatment in TNF-alpha + IFN-gamma - stimulated HaCaT cells. **Overall design:** HaCaT cells were pre-treated with terbutaline or GW9508, TNF-alpha + IFN-gamma were then added, and cultured for another 24 h. Cells were then used for RNA extraction and hybridization on Affymetrix microarrays. We sought to clarify changes in gene expression after 1) TNF-alpha + IFN-gamma, 2) TNF-alpha + IFN-gamma + terbutaline, and 3) TNF-alpha + IFN-gamma + GW9508 treatment. To this end, we set 4 groups of samples; 1) unstimulated group, 2) TNF-alpha + IFN-gamma-stimulated group, 3) TNF-alpha + IFN-gamma + terbutaline-stimulated group, and 4) TNF-alpha + IFN-gamma + GW9508-stimulated group. In each group, HaCaT cells were stimulated in triplicate wells (n=3).

Background corr dist: KL-Divergence = 0.0778, L1-Distance = 0.0884, L2-Distance = 0.0124, Normal std = 0.5792

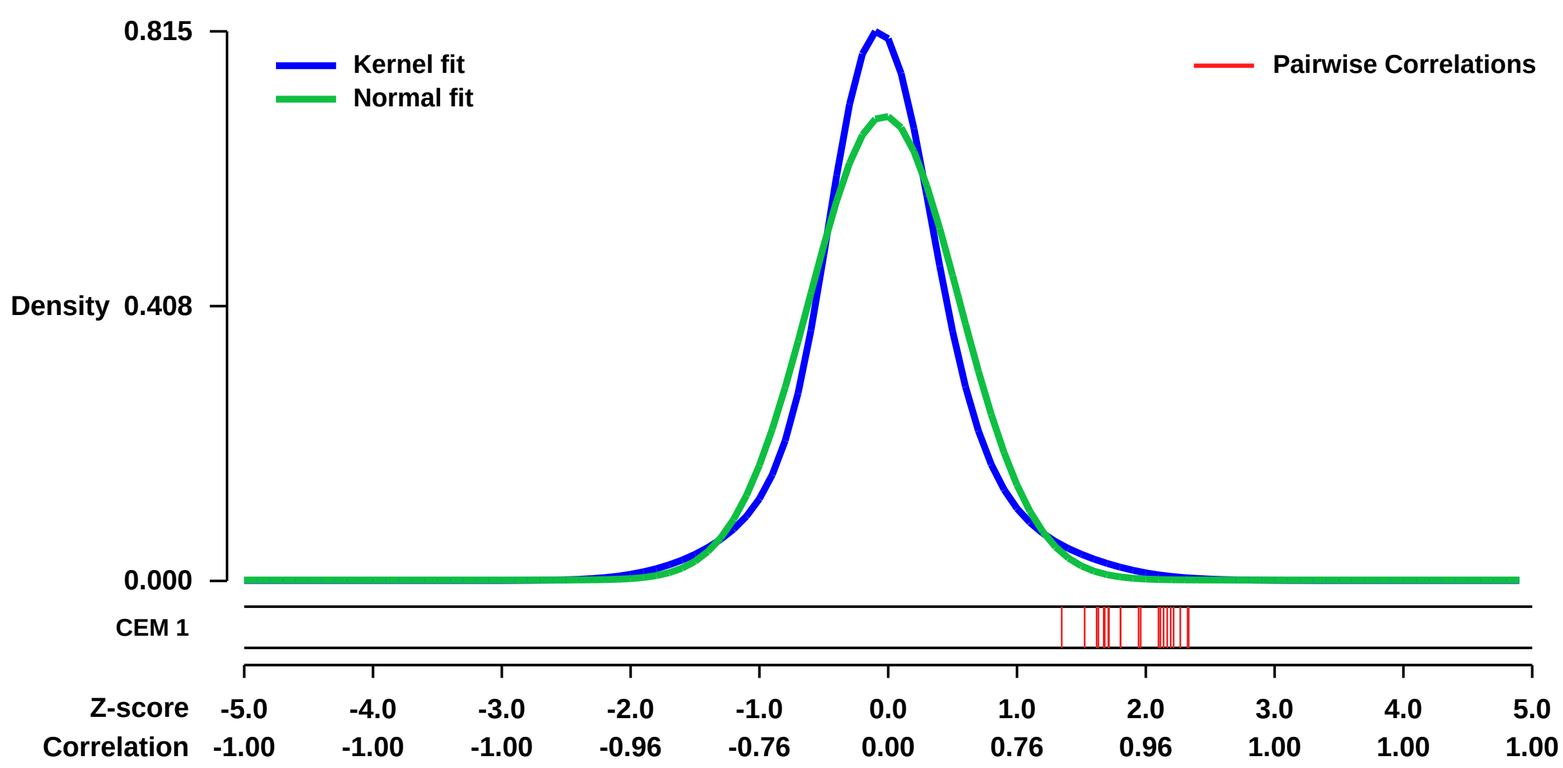

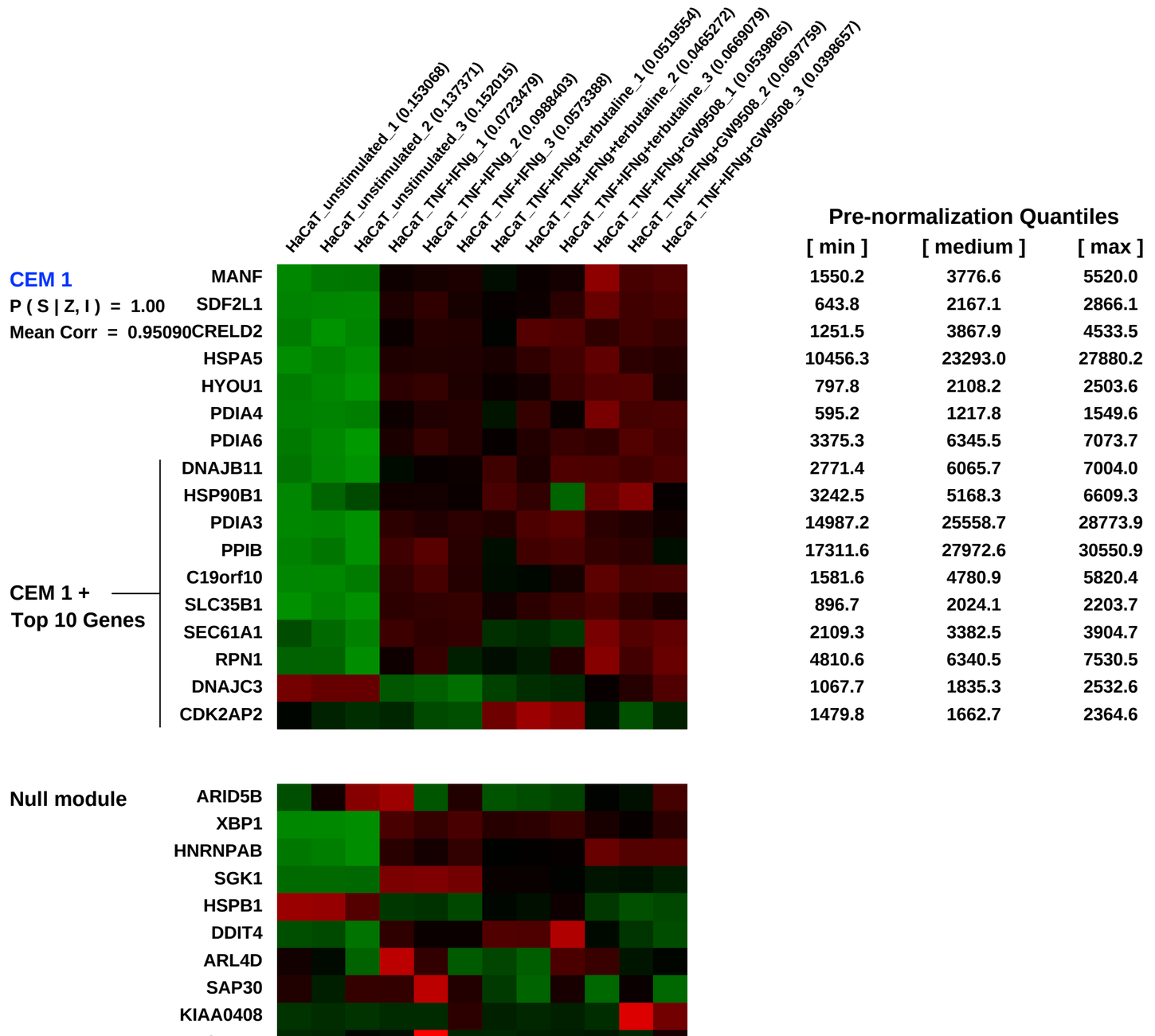

	Pre-normalization Quantiles		
	[min]	[medium]	[max]
MANF	1550.2	3776.6	5520.0
SDF2L1	643.8	2167.1	2866.1
CRELD2	1251.5	3867.9	4533.5
HSPA5	10456.3	23293.0	27880.2
HYOU1	797.8	2108.2	2503.6
PDIA4	595.2	1217.8	1549.6
PDIA6	3375.3	6345.5	7073.7
DNAJB11	2771.4	6065.7	7004.0
HSP90B1	3242.5	5168.3	6609.3
PDIA3	14987.2	25558.7	28773.9
PPIB	17311.6	27972.6	30550.9
C19orf10	1581.6	4780.9	5820.4
SLC35B1	896.7	2024.1	2203.7
SEC61A1	2109.3	3382.5	3904.7
RPN1	4810.6	6340.5	7530.5
DNAJC3	1067.7	1835.3	2532.6
CDK2AP2	1479.8	1662.7	2364.6
ARID5B			
XBP1			
HNRNPAB			
SGK1			
HSPB1			
DDIT4			
ARL4D			
SAP30			
KIAA0408			
GPR17			
HSPH1			
DNASE1L2			
SLC5A3			
GNAS			
GPR3			
TNFRSF25			
TM6SF2			
MKKS			
PLEKHF1			
ZMYM1			
DOK3			
FGF20			
SLC39A2			
KCNIP2			
ERRFI1			
DEDD2			
CCDC117			
USP31			
AHSA2			
CYS1			
CNIH2			
BANP			
CHORDC1			
P4HA1			

GEO Series "GSE39059" Expression Profiles

Num of samples in this series: 9

Scale of expression profile Z-scores

-3.0 -2.0 -1.0 0.0 1.0 2.0 3.0

GEO Link:	http://www.ncbi.nlm.nih.gov/geo/query/acc.cgi?acc=GSE39059
Status:	Public on Oct 01 2012
Title:	Changes in microRNA and mRNA expression with differentiation of human bronchial epithelial cells [mRNA]
Organism:	Homo sapiens
Experiment type:	Expression profiling by array
Platform:	GPL570
Pubmed ID:	23590309
Summary & Design:	**Summary:** Normal human bronchial epithelial (NHBE) cells cultured in an air-liquid interface (ALI) system form a polarized, pseudostratified epithelium composed of basal, ciliated and goblet cells that closely resemble the in vivo airway epithelium structure. ALI cultures of NHBE cells provide a unique in vitro system to investigate airway epithelial biology, including developmental, structural and physiologic aspects. In this study, we wanted to investigate mRNA expression patterns during airway epithelium differentiation. By using microarrays, we studied the changes in expression of mRNAs in normal human bronchial epithelial cells as they differentiate from an undifferentiated monolayer to a differentiated pseudostratified epithelium after 28 days of air-liquid interface (ALI) culture, when epithelial cells differentially express basal, ciliated and goblet cell markers. **Overall design:** Normal human bronchial epithelial cells were cultured in an air-liquid interface (ALI) system and harvested at three different time-points: subconfluent, confluent and day 28 of ALI. Samples were processed for total RNA extraction and hybridization on Affymetrix microarrays. All the experiments were performed by triplicate.

Background corr dist: KL-Divergence = 0.0352, L1-Distance = 0.0888, L2-Distance = 0.0097, Normal std = 0.8436

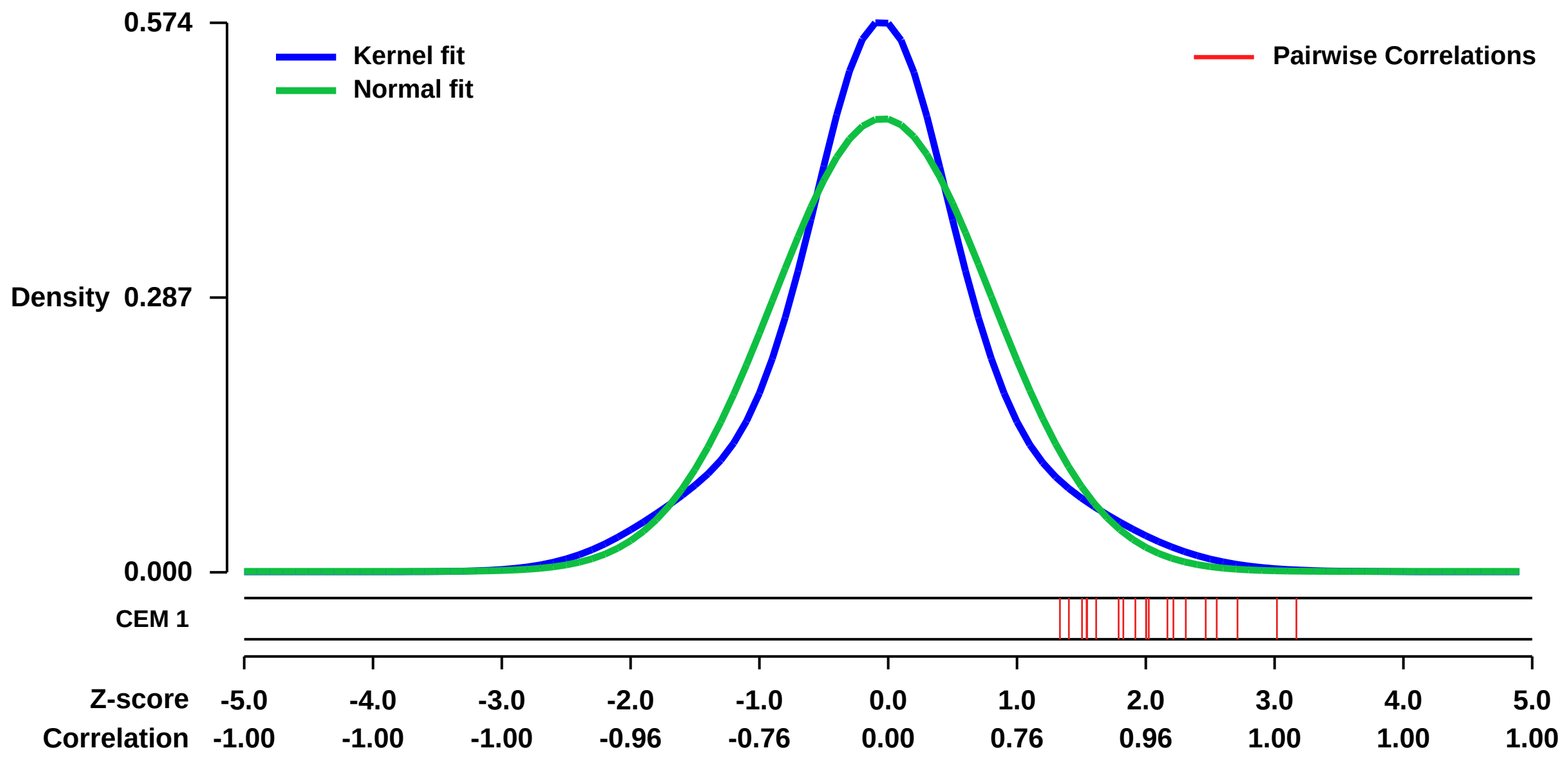

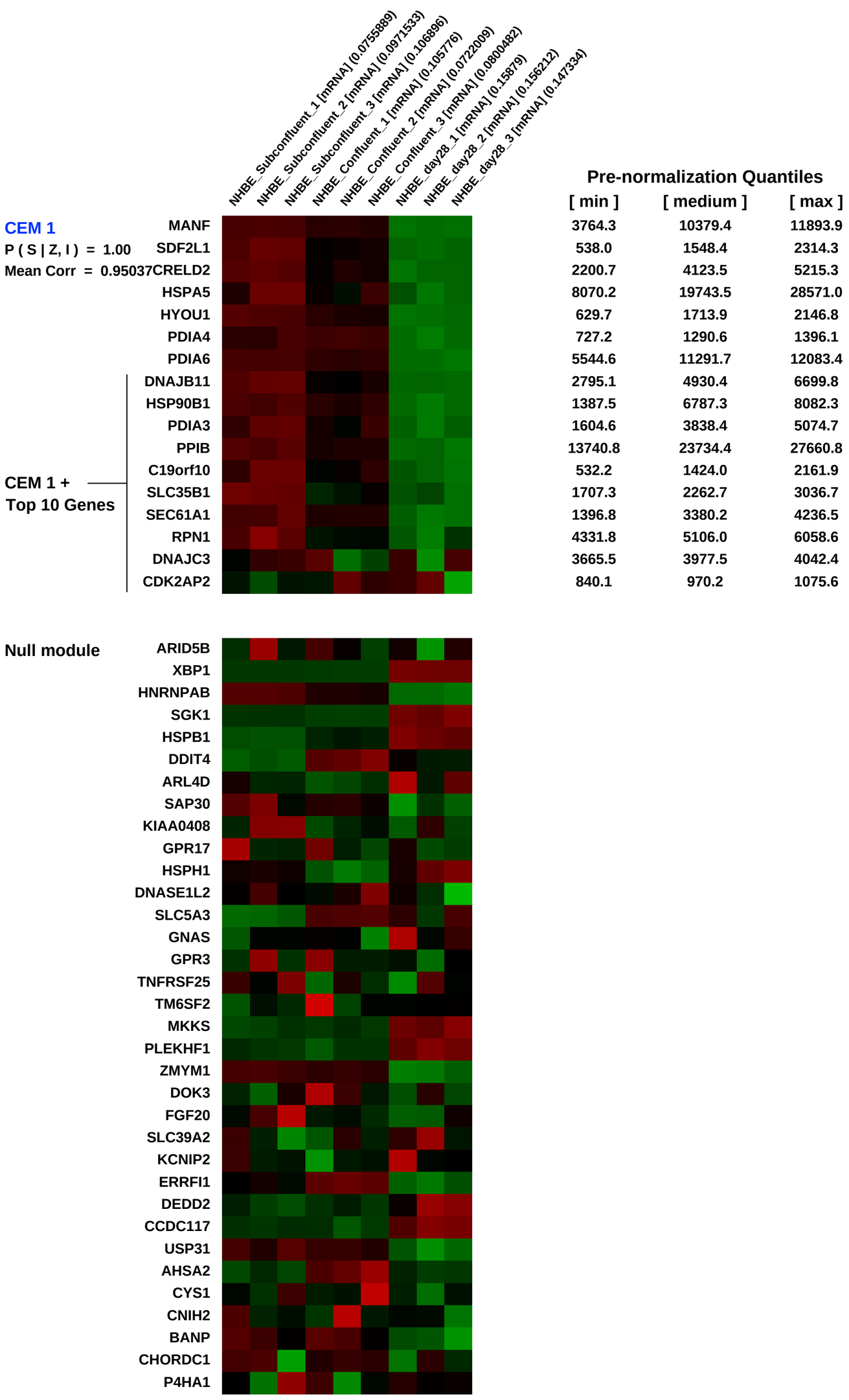

Pre-normalization Quantiles

	[min]	[medium]	[max]
MANF	3764.3	10379.4	11893.9
SDF2L1	538.0	1548.4	2314.3
CRELD2	2200.7	4123.5	5215.3
HSPA5	8070.2	19743.5	28571.0
HYOU1	629.7	1713.9	2146.8
PDIA4	727.2	1290.6	1396.1
PDIA6	5544.6	11291.7	12083.4
DNAJB11	2795.1	4930.4	6699.8
HSP90B1	1387.5	6787.3	8082.3
PDIA3	1604.6	3838.4	5074.7
PPIB	13740.8	23734.4	27660.8
C19orf10	532.2	1424.0	2161.9
SLC35B1	1707.3	2262.7	3036.7
SEC61A1	1396.8	3380.2	4236.5
RPN1	4331.8	5106.0	6058.6
DNAJC3	3665.5	3977.5	4042.4
CDK2AP2	840.1	970.2	1075.6

GEO Series "GSE11916" Expression Profiles

Num of samples in this series: 6

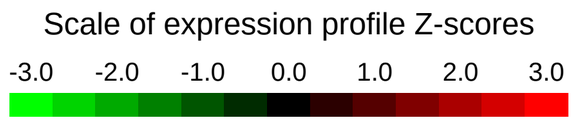

GEO Link:	**http://www.ncbi.nlm.nih.gov/geo/query/acc.cgi?acc=GSE11916**
Status:	**Public on Sep 30 2009**
Title:	**Comparison of TCF hyper-activated and control Huh7 cells - microarray data**
Organism:	**Homo sapiens**
Experiment type:	**Expression profiling by array**
Platform:	**GPL570**
Pubmed ID:	
Summary & Design:	**Summary:** **The Wnt signaling pathway is involved in many differentiation events during embryonic development and can lead to tumor formation after aberrant activation of its components. ¸ -catenin, a cytoplasmic component, plays a major role in the transduction of the canonical wnt/ ¸†-catenin signaling. The aim of this study was to identify novel genes that are regulated by active ¸†-catenin/TCF signaling in hepatocellular carcinoma. We selected and expanded isogenic clones from hepatocellular carcinoma-derived Huh7 cells with high and low ¸†-catenin/TCF activities. We showed that, high TCF activity Huh7 cells lead to bigger and more aggressive tumors when xenografted into nude mice. We used SAGE (Serial Analysis of Gene Expression), genome-wide microarray and in silico promoter analysis in parallel, to compare gene expression between low (basal) and high (transfected) ¸†-catenin/TCF activity clones, those had been xenografted into nude mice. We compared and contrasted SAGE and genome-wide microarray data, in parallel. Finally; after combined analysis, we identified BRI3 and HSF2 as novel targets of Wnt/¸†-catenin signaling in hepatocellular carcinoma.** **Overall design:** **High TCF activity Huh7 cell line (Huh7-S33Y) was compared to control Huh7 cell line (Huh7-Vec) by using 10 ug of total RNA isolated from each sample (15 ug of labeled cRNA was hybridized to the arrays). Triplicates are coming from same total RNA extraction.**

Background corr dist: KL-Divergence = 0.0553, L1-Distance = 0.0353, L2-Distance = 0.0014, Normal std = 0.6821

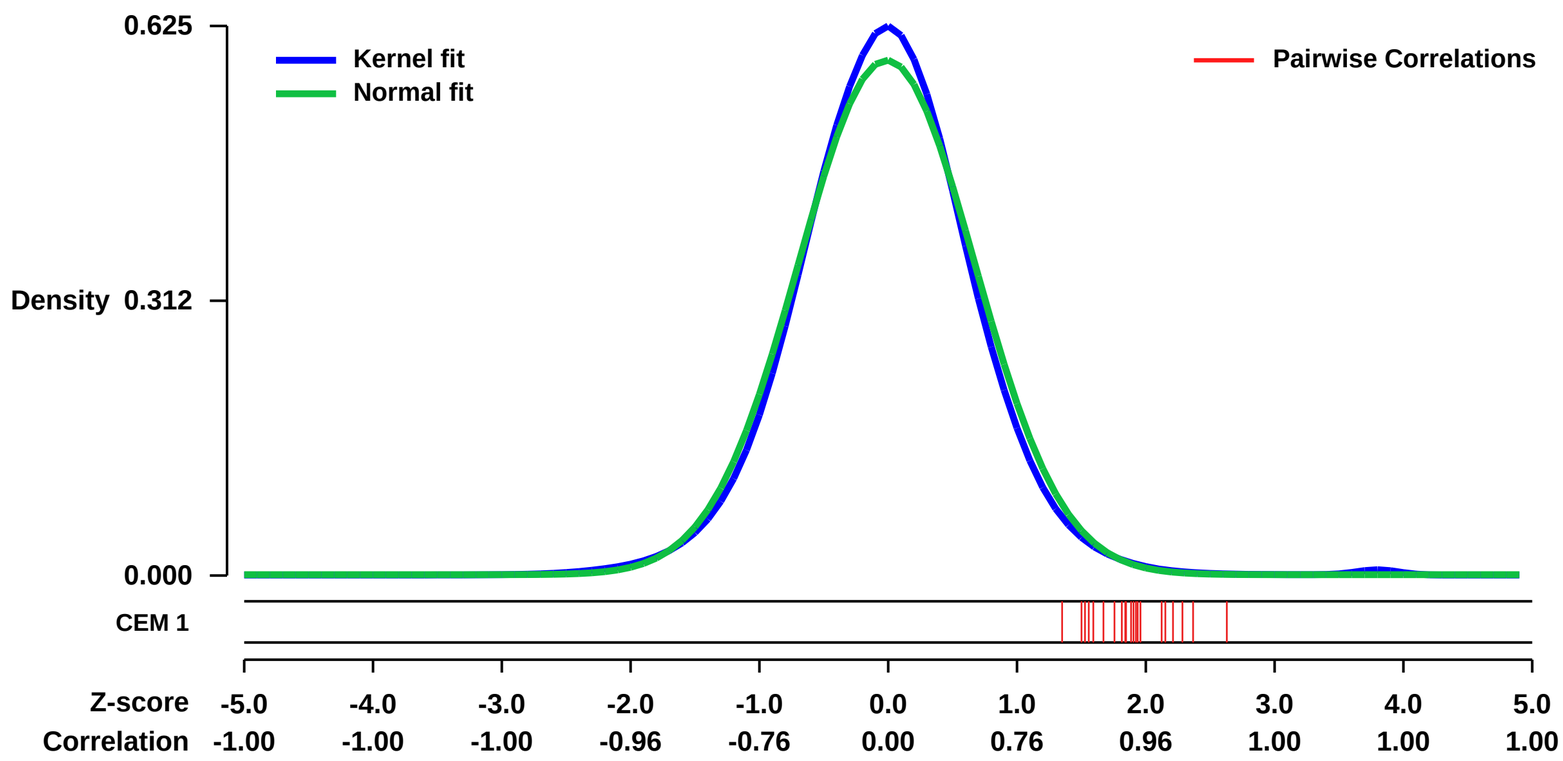

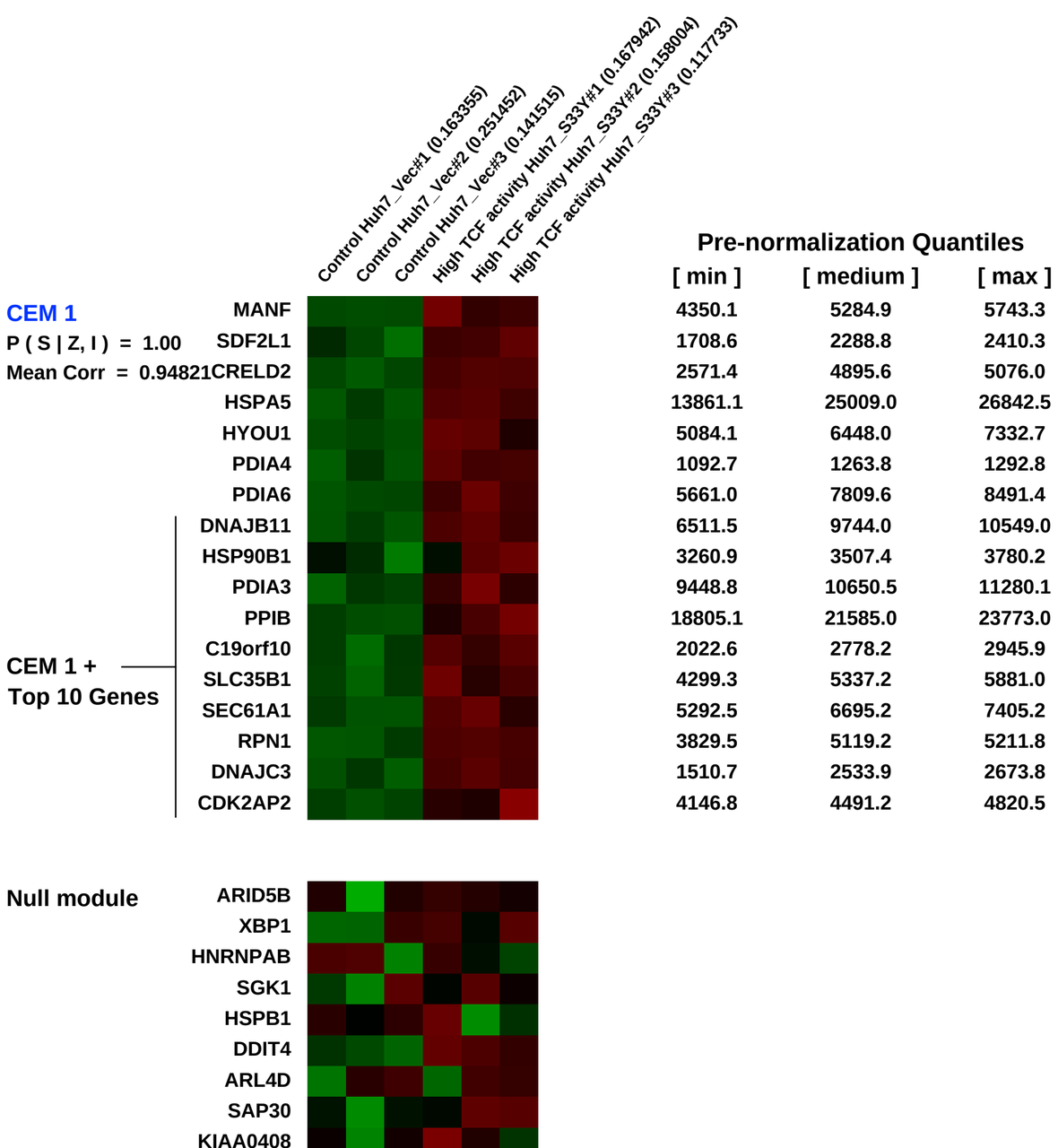

	Pre-normalization Quantiles		
	[min]	[medium]	[max]
MANF	4350.1	5284.9	5743.3
SDF2L1	1708.6	2288.8	2410.3
CRELD2	2571.4	4895.6	5076.0
HSPA5	13861.1	25009.0	26842.5
HYOU1	5084.1	6448.0	7332.7
PDIA4	1092.7	1263.8	1292.8
PDIA6	5661.0	7809.6	8491.4
DNAJB11	6511.5	9744.0	10549.0
HSP90B1	3260.9	3507.4	3780.2
PDIA3	9448.8	10650.5	11280.1
PPIB	18805.1	21585.0	23773.0
C19orf10	2022.6	2778.2	2945.9
SLC35B1	4299.3	5337.2	5881.0
SEC61A1	5292.5	6695.2	7405.2
RPN1	3829.5	5119.2	5211.8
DNAJC3	1510.7	2533.9	2673.8
CDK2AP2	4146.8	4491.2	4820.5
ARID5B			
XBP1			
HNRNPAB			
SGK1			
HSPB1			
DDIT4			
ARL4D			
SAP30			
KIAA0408			
GPR17			
HSPH1			
DNASE1L2			
SLC5A3			
GNAS			
GPR3			
TNFRSF25			
TM6SF2			
MKKS			
PLEKHF1			
ZMYM1			
DOK3			
FGF20			
SLC39A2			
KCNIP2			
ERRFI1			
DEDD2			
CCDC117			
USP31			
AHSA2			
CYS1			
CNIH2			
BANP			
CHORDC1			
P4HA1			

GEO Series "GSE40794" Expression Profiles

Num of samples in this series: 18

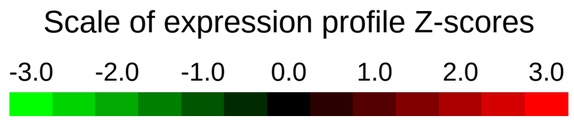

GEO Link:	http://www.ncbi.nlm.nih.gov/geo/query/acc.cgi?acc=GSE40794
Status:	Public on Mar 31 2013
Title:	Convergence of oncogenic and hormone receptor pathways promotes pro-metastatic phenotypes.
Organism:	Homo sapiens
Experiment type:	Expression profiling by array
Platform:	GPL570
Pubmed ID:	23257359
Summary & Design:	**Summary:** Cyclin D1b is a splice variant of the cell cycle regulator Cyclin D1 and is known to harbor divergent and highly oncogenic functions in human disease. While Cyclin D1b is induced during disease progression in many cancer types, the mechanisms underlying Cyclin D1b function remain poorly understood. Herein, models of human disease were utilized to resolve the downstream pathways requisite for the pro-tumorigenic functions of Cyclin D1b. Specifically, it was shown that Cyclin D1b modulates the expression of a large transcriptional network that cooperates with AR signaling to enhance tumor cell growth and invasive potential. Notably, Cyclin D1b promoted AR-dependent activation of genes associated with metastatic phenotypes. Further exploration determined that transcriptional induction of SNAI2 (Slug) was essential for Cyclin D1b- mediated proliferative and invasive properties, implicating Slug as a critical driver of disease progression. Importantly, Cyclin D1b expression highly correlated with that of Slug in clinical samples of advanced disease. Further, in vivo analyses provided strong evidence that Slug enhances both tumor growth and homing to distal soft tissues. Collectively, these findings reveal the underpinning mechanisms behind the pro-tumorigenic functions of Cyclin D1b, and demonstrate that the convergence of the Cyclin D1b-AR and Slug pathways results in the activation of processes critical for the promotion of lethal tumor phenotypes. Analysis of transcriptomes under the control of individual D-type cyclin isoforms in the hormone dependent prostate cancer cell line LNCaP in the presence and absence of androgen. **Overall design:** LNCaP cells cultured in charcoal dextran treated media were transduced with virus encoding Cyclin D1a, Cyclin D1b, or control GFP for 24 hours in biological triplicate. Cells were then stimulated with either 1nM DHT or 0.01% EtOH (vehicle control) for 16 hours and harvested for RNA

Background corr dist: KL-Divergence = 0.0785, L1-Distance = 0.0242, L2-Distance = 0.0007, Normal std = 0.4862

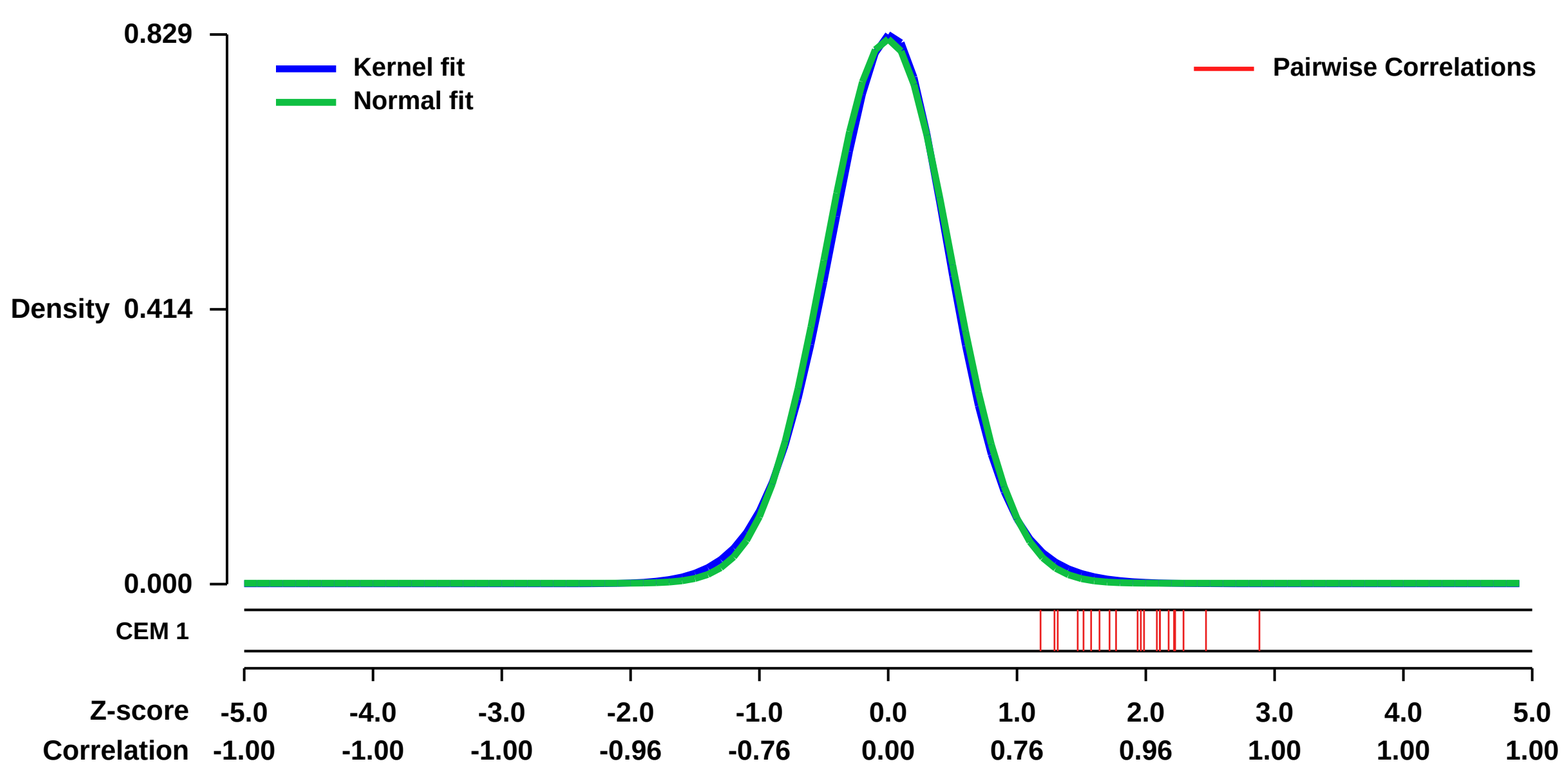

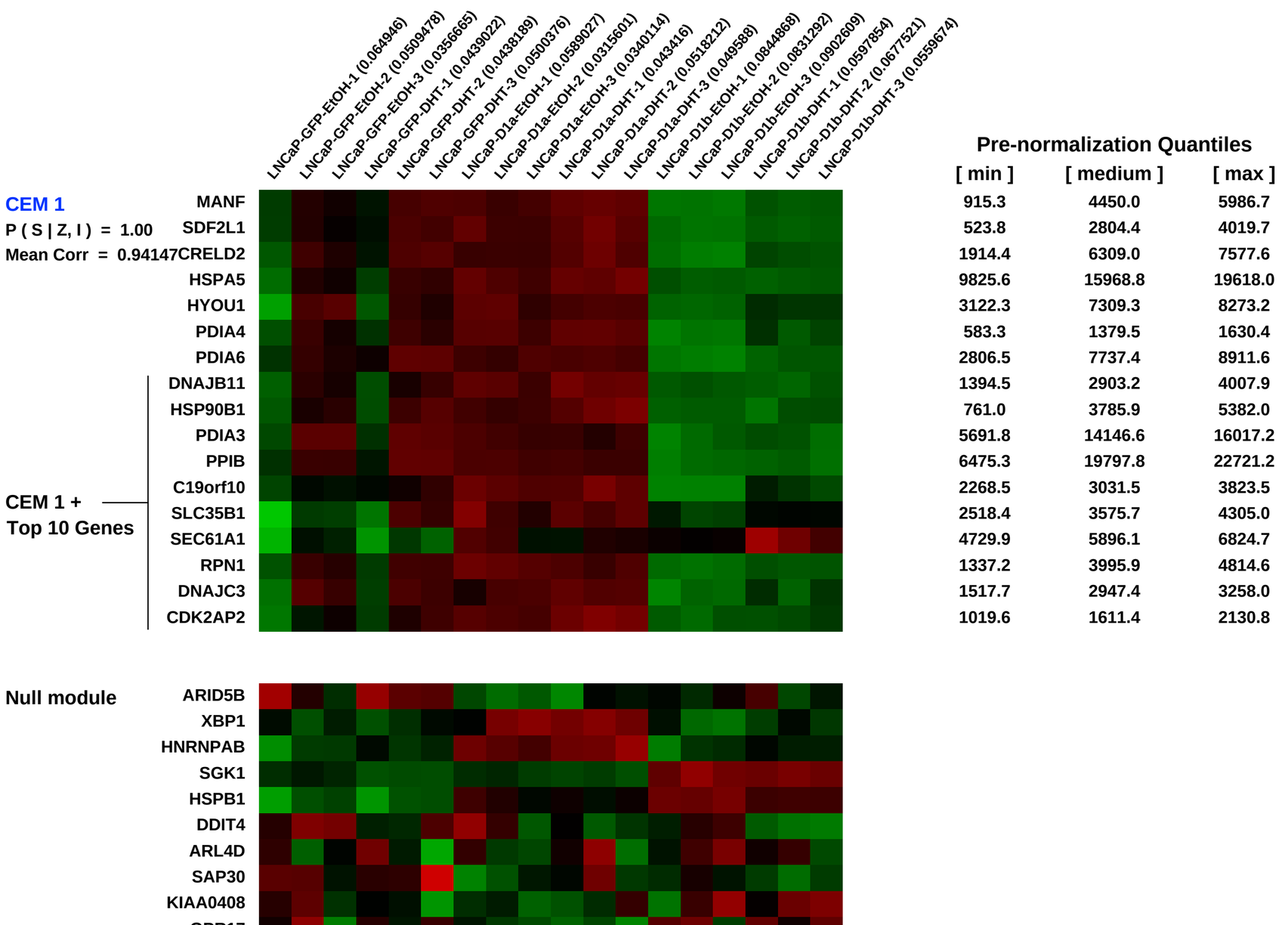

Pre-normalization Quantiles

	[min]	[medium]	[max]
MANF	915.3	4450.0	5986.7
SDF2L1	523.8	2804.4	4019.7
CRELD2	1914.4	6309.0	7577.6
HSPA5	9825.6	15968.8	19618.0
HYOU1	3122.3	7309.3	8273.2
PDIA4	583.3	1379.5	1630.4
PDIA6	2806.5	7737.4	8911.6
DNAJB11	1394.5	2903.2	4007.9
HSP90B1	761.0	3785.9	5382.0
PDIA3	5691.8	14146.6	16017.2
PPIB	6475.3	19797.8	22721.2
C19orf10	2268.5	3031.5	3823.5
SLC35B1	2518.4	3575.7	4305.0
SEC61A1	4729.9	5896.1	6824.7
RPN1	1337.2	3995.9	4814.6
DNAJC3	1517.7	2947.4	3258.0
CDK2AP2	1019.6	1611.4	2130.8

GEO Series "GSE32939" Expression Profiles

Num of samples in this series: 6

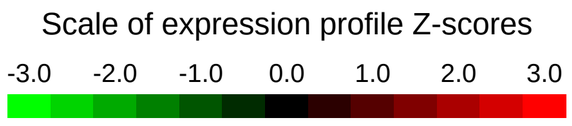

GEO Link:	http://www.ncbi.nlm.nih.gov/geo/query/acc.cgi?acc=GSE32939
Status:	Public on Oct 13 2011
Title:	CD4 on human monocytes
Organism:	Homo sapiens
Experiment type:	Expression profiling by array
Platform:	GPL570
Pubmed ID:	
Summary & Design:	**Summary:** We examined the efffects of ligating CD4 expressed by primary human peripheral blood monocytes with soluble MHC Class II. **Overall design:** 3 replicates are included. Fresh blood monocytes, obtained through negative selection via magnetic activted cell sorting (Miltenyi, Auburn, CA), from three separate individual donors were treated with RPMI-1640 medium alone or with medium containing sMHC II (1 ¸…g/ml) for three hours. Cells were harvested and RNA purified using the RNeasy procedure (Qiagen). RNA was then analyzed by the UCLA Clinical Microarray Core Laboratory using the Human U133 Plus 2.0 Array (Affimetrix). Data was analyzed using Dchip software. Visual inspection did not find any potential outliers or suspect areas. Data across all groups were normalized using the PM/MM difference.

Background corr dist: KL-Divergence = 0.0327, L1-Distance = 0.0223, L2-Distance = 0.0005, Normal std = 0.6596

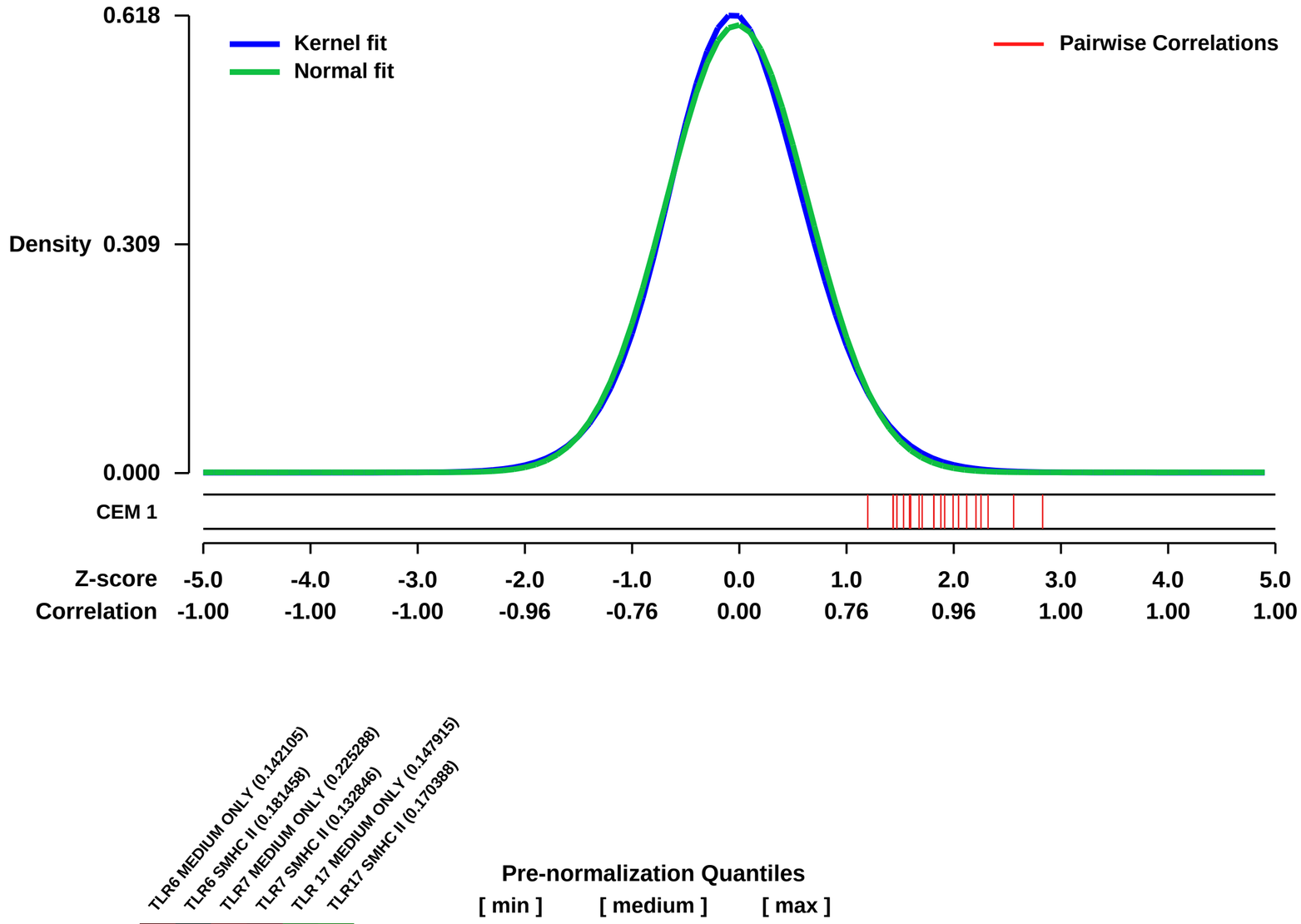

CEM 1
P (S | Z, I) = 1.00
Mean Corr = 0.94123

CEM 1 + Top 10 Genes

Null module

MANF	2195.7	5356.0	5705.8
SDF2L1	852.5	2436.6	2895.2
CRELD2	1210.5	2870.0	3654.9
HSPA5	7969.0	14205.5	16396.0
HYOU1	837.8	3217.6	3468.9
PDIA4	723.2	1500.8	1611.9
PDIA6	2908.2	7032.3	8929.2
DNAJB11	2174.2	4246.2	4428.9
HSP90B1	1112.1	4912.8	6109.7
PDIA3	7567.2	15068.1	15510.9
PPIB	10413.5	14560.1	15826.2
C19orf10	2430.1	4820.8	5154.6
SLC35B1	1075.1	1923.9	2334.3
SEC61A1	1802.5	2703.0	3315.7
RPN1	4091.4	6350.5	7463.0
DNAJC3	4222.5	5781.4	6038.1
CDK2AP2	788.9	1468.0	1903.4
ARID5B			
XBP1			
HNRNPAB			
SGK1			
HSPB1			
DDIT4			
ARL4D			
SAP30			
KIAA0408			
GPR17			
HSPH1			
DNASE1L2			
SLC5A3			
GNAS			
GPR3			
TNFRSF25			
TM6SF2			
MKKS			
PLEKHF1			
ZMYM1			
DOK3			
FGF20			
SLC39A2			
KCNIP2			
ERRFI1			
DEDD2			
CCDC117			
USP31			
AHSA2			
CYS1			
CNIH2			
BANP			
CHORDC1			
P4HA1			

GEO Series "GSE33606" Expression Profiles

Num of samples in this series: 15

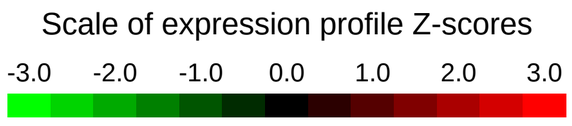

GEO Link:	http://www.ncbi.nlm.nih.gov/geo/query/acc.cgi?acc=GSE33606
Status:	Public on Nov 11 2011
Title:	Gene expression changes in human hepatocytes exposed to VX (O-ethyl S-[2-(diisopropylamino)ethyl] methylphosphonothiolate)
Organism:	Homo sapiens
Experiment type:	Expression profiling by array
Platform:	GPL570
Pubmed ID:	
Summary & Design:	**Summary:** Organophosphorus compounds induce hepatotoxicity through currently unknown mechanisms, which need to be unraveled by a comprehensive and systematic approach such as genome-wide gene expression analysis. We used microarrays to study gene expression changes in human hepatocytes after exposure to VX, and identified pathways underlying these changes. **Overall design:** Human hepatocytes were exposed to sublethal concentrations (0, 0.1, 10 ¿…M) of VX. RNA were extracted at different timepoints (0, 6 h) after VX exposure and hybridized to Affymetrix microarrays. Four biological repeats were used for each condition.

Background corr dist: KL-Divergence = 0.1080, L1-Distance = 0.0615, L2-Distance = 0.0062, Normal std = 0.4667

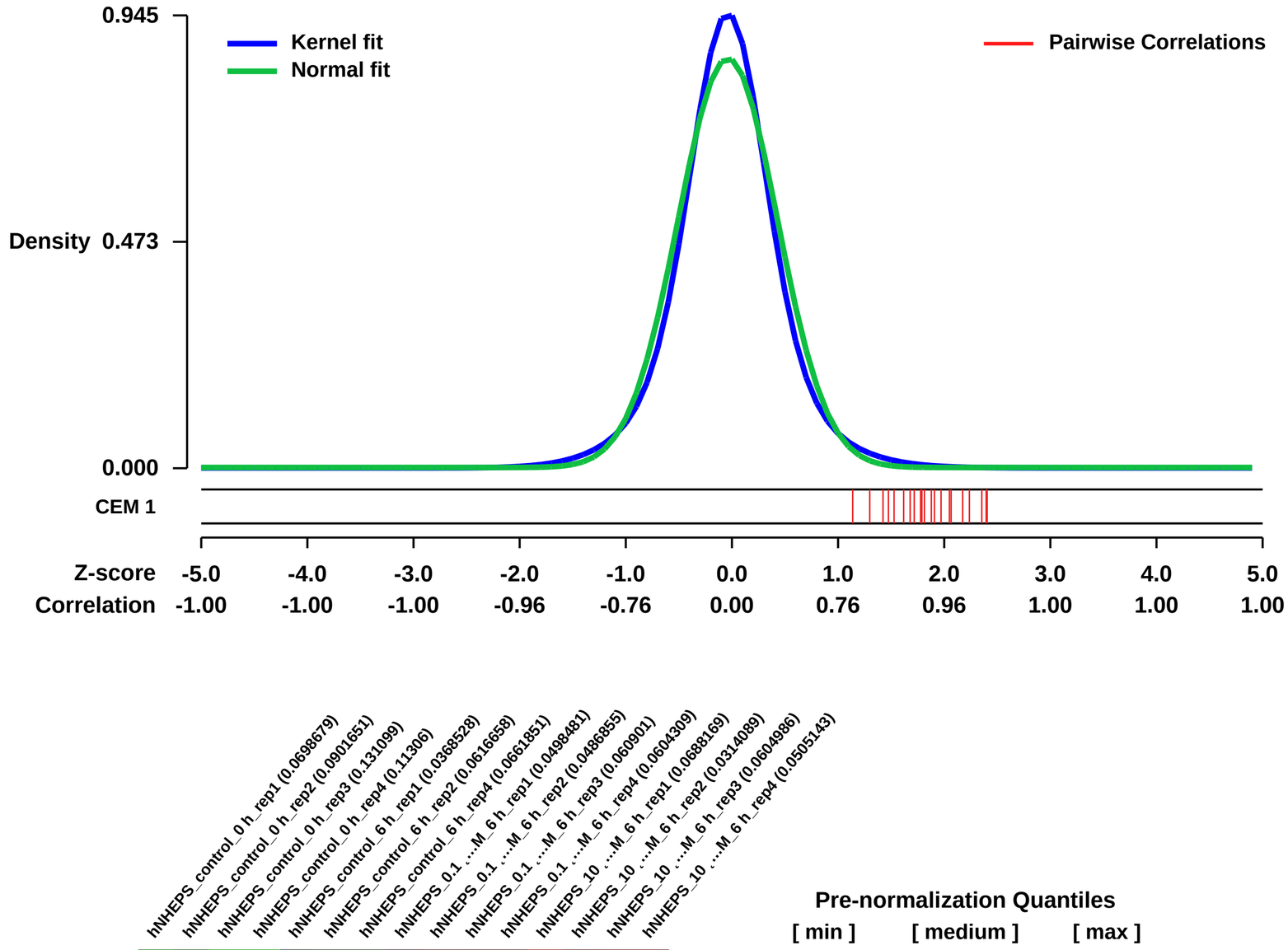

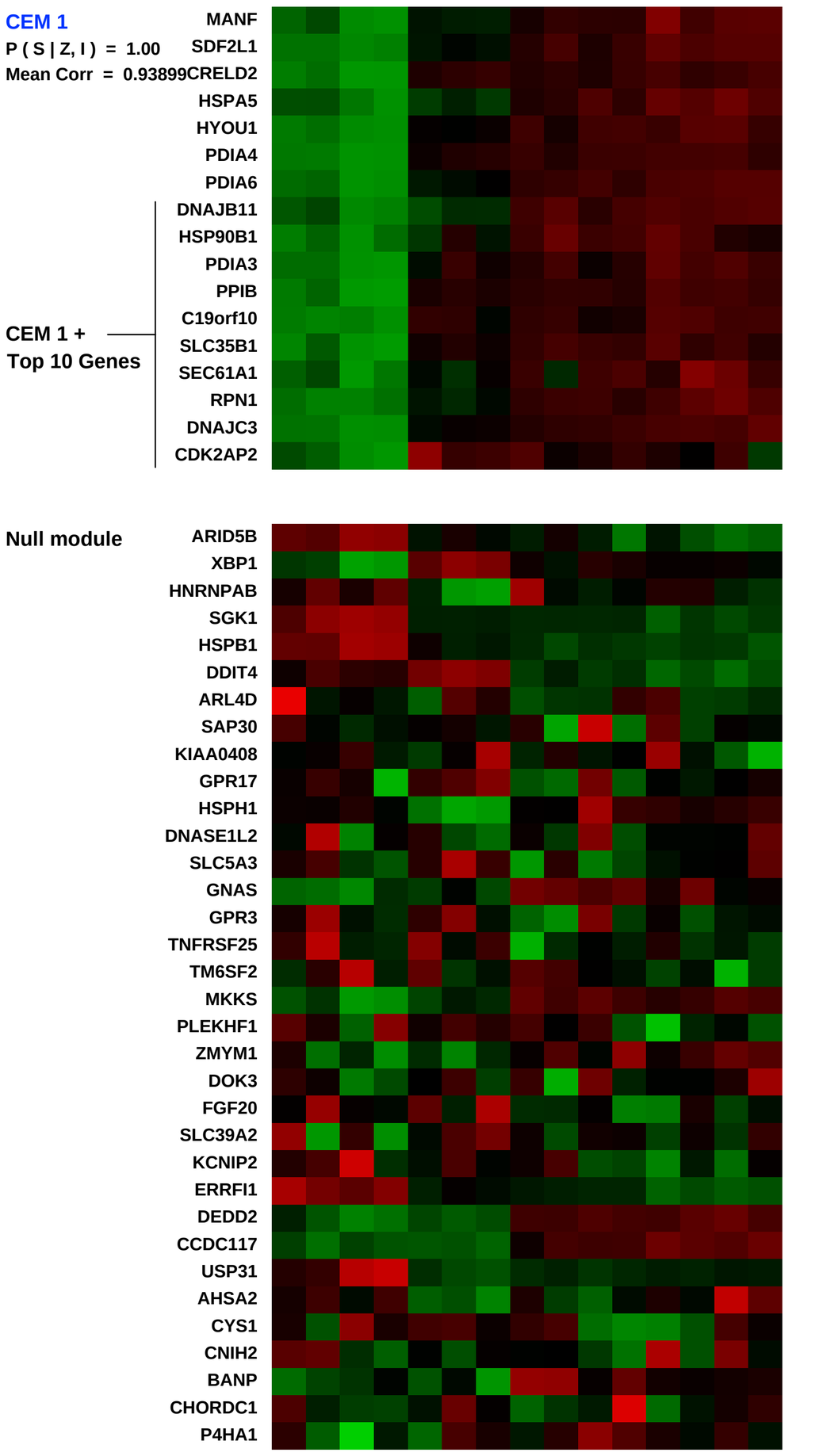

Pre-normalization Quantiles

[min]	[medium]	[max]
3823.0	7441.6	9722.3
1290.2	2983.4	3673.4
1741.0	4864.2	5291.3
25152.0	34648.5	38885.0
1332.9	2600.6	3126.5
812.5	2519.1	2817.7
7285.8	12736.7	13853.1
4570.0	6690.7	7250.8
7231.4	13706.0	16295.9
10016.5	17976.3	20571.9
19713.4	29236.8	31265.6
3199.6	4195.7	4395.4
2086.3	3878.8	4389.6
4027.2	5390.6	6443.5
5251.9	6979.2	7688.2
4449.0	8253.0	9581.3
637.1	925.5	1111.1

GEO Series "GSE48444" Expression Profiles

Num of samples in this series: 6

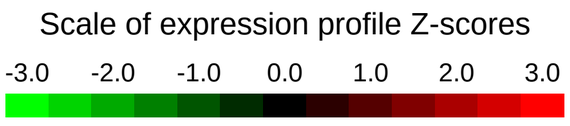

GEO Link:	http://www.ncbi.nlm.nih.gov/geo/query/acc.cgi?acc=GSE48444
Status:	Public on Jul 02 2013
Title:	Microarray-based gene expression data from BPLER tumor explants.
Organism:	Homo sapiens
Experiment type:	Expression profiling by array
Platform:	GPL570
Pubmed ID:	23948298
Summary & Design:	**Summary:** The gene expression of 6 different mouse xenografts initiated by BPLER cells analyzed by microarray. Basal-like triple negative breast cancers (TNBC) have poor prognosis. To study the basal-like transcriptional profile of tumors transformed by defined genetic elements, the human breast epithelial cell line BPLER was injected into NOD/SCID mice. The resulting tumors were excised for expression analysis. Keywords: breast cancer, BPLER, metastasis, tumor stem cells, tumor initiating cells, breast adenocarcinoma **Overall design:** BPLER cells were derived from human primary breast epithelial cells propagated in WIT medium (Ince et al, Cancer Cell, 2007). These cells were transformed with hTERT, SV40 early region and hRASV12 by retroviral transduction. BPLER have a TNBC-like phenotype in vitro and are highly enriched for tumor-initiating cells. To define the phenotype of BPLER-derived tumors in vivo, BPLER cells were injected in the mammary fat-pad of 6 NOD/SCID mice. Once tumors were palpable, mice were sacrificed and tumors excised. Total RNA was extracted using Trizol. The gene expression profile of each tumor was assessed by mRNA microarray analysis. Based on histology and principal component analysis of microarray data, BPLER tumors were remarkably similar to human primary TNBC encountered in the clinic (Petrocca et al, Cancer Cell, 2013).

Background corr dist: KL-Divergence = 0.0459, L1-Distance = 0.0296, L2-Distance = 0.0012, Normal std = 0.5966

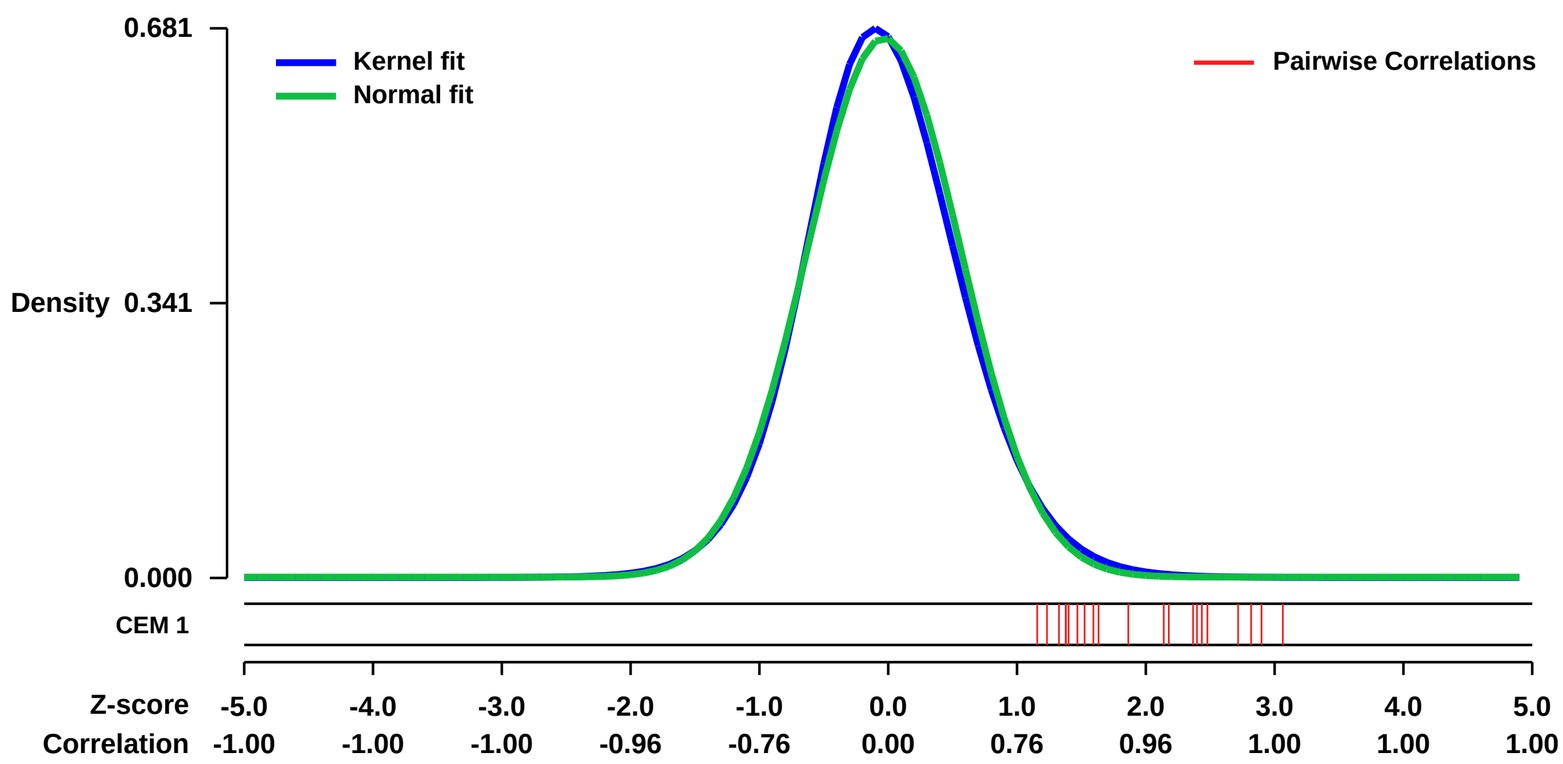

CEM 1
P (S | Z, I) = 1.00
Mean Corr = 0.93551

CEM 1 + Top 10 Genes

Null module

	Pre-normalization Quantiles		
	[min]	[medium]	[max]
MANF	2623.4	3666.4	13253.4
SDF2L1	701.3	1185.0	5529.3
CRELD2	1462.7	2404.7	5507.3
HSPA5	8428.3	10259.7	46177.5
HYOU1	2747.8	3669.6	14633.7
PDIA4	1373.2	1743.1	2831.4
PDIA6	3942.3	4802.3	10777.0
DNAJB11	2556.6	3364.9	10024.6
HSP90B1	913.4	1783.6	15816.2
PDIA3	6262.1	9165.1	14748.2
PPIB	9478.0	11128.0	20129.4
C19orf10	2602.5	3383.1	5482.4
SLC35B1	1543.6	1968.0	3994.0
SEC61A1	2893.9	3771.0	5484.6
RPN1	4428.2	4762.1	6038.1
DNAJC3	1222.4	2259.8	5686.3
CDK2AP2	849.1	944.2	2656.9
ARID5B			
XBP1			
HNRNPAB			
SGK1			
HSPB1			
DDIT4			
ARL4D			
SAP30			
KIAA0408			
GPR17			
HSPH1			
DNASE1L2			
SLC5A3			
GNAS			
GPR3			
TNFRSF25			
TM6SF2			
MKKS			
PLEKHF1			
ZMYM1			
DOK3			
FGF20			
SLC39A2			
KCNIP2			
ERRFI1			
DEDD2			
CCDC117			
USP31			
AHSA2			
CYS1			
CNIH2			
BANP			
CHORDC1			
P4HA1			

GEO Series "GSE35716" Expression Profiles

Num of samples in this series: 28

Scale of expression profile Z-scores

-3.0 -2.0 -1.0 0.0 1.0 2.0 3.0

GEO Link:	http://www.ncbi.nlm.nih.gov/geo/query/acc.cgi?acc=GSE35716
Status:	Public on Sep 01 2012
Title:	Transcriptional Signatures as a Disease-Specific and Predictive Inflammatory Biomarker for Type 1 Diabetes [Pneu_S3S24_10Pneu_4HC]
Organism:	Homo sapiens
Experiment type:	Expression profiling by array
Platform:	GPL570
Pubmed ID:	22972474
Summary & Design:	**Summary:** The complex milieu of inflammatory mediators associated with many diseases is often too dilute to directly measure in the periphery, necessitating development of more sensitive measurements suitable for mechanistic studies, earlier diagnosis, guiding selection of therapy, and monitoring interventions. Previously, we determined that plasma of recent-onset (RO) Type 1 diabetes (T1D) patients induce a proinflammatory transcriptional signature in fresh peripheral blood mononuclear cells (PBMC) relative to that of unrelated healthy controls (HC). Here, using an optimized cryopreserved PBMC-based protocol, we compared the signature found between unrelated healthy controls and patients with bacterial pneumonia. **Overall design:** UPN727 cells were stimulated with either plasma from unrelated healthy controls (n=18) or plasma from patients with bacterial pneumonia (n=10). Gene expression analysis was perfromed in order to evaluate the transcriptional signature associated with bacterial pneumonia.

Background corr dist: KL-Divergence = 0.1160, L1-Distance = 0.0256, L2-Distance = 0.0010, Normal std = 0.4152

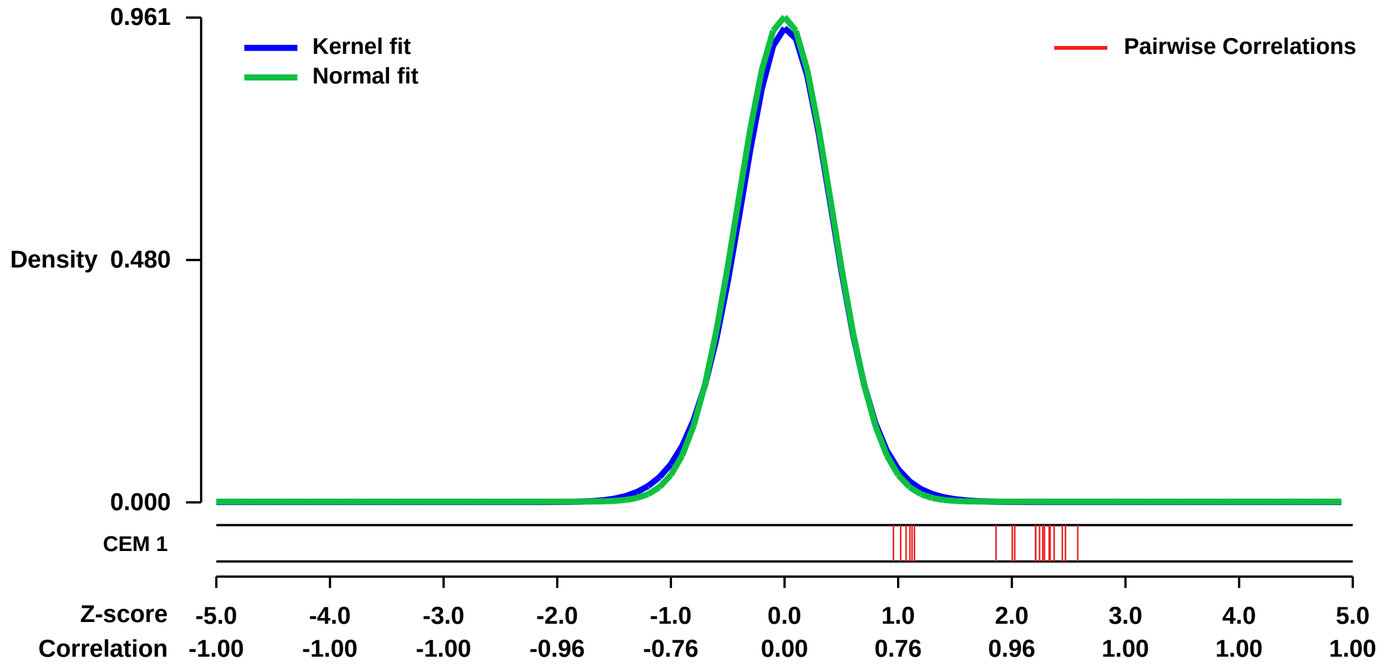

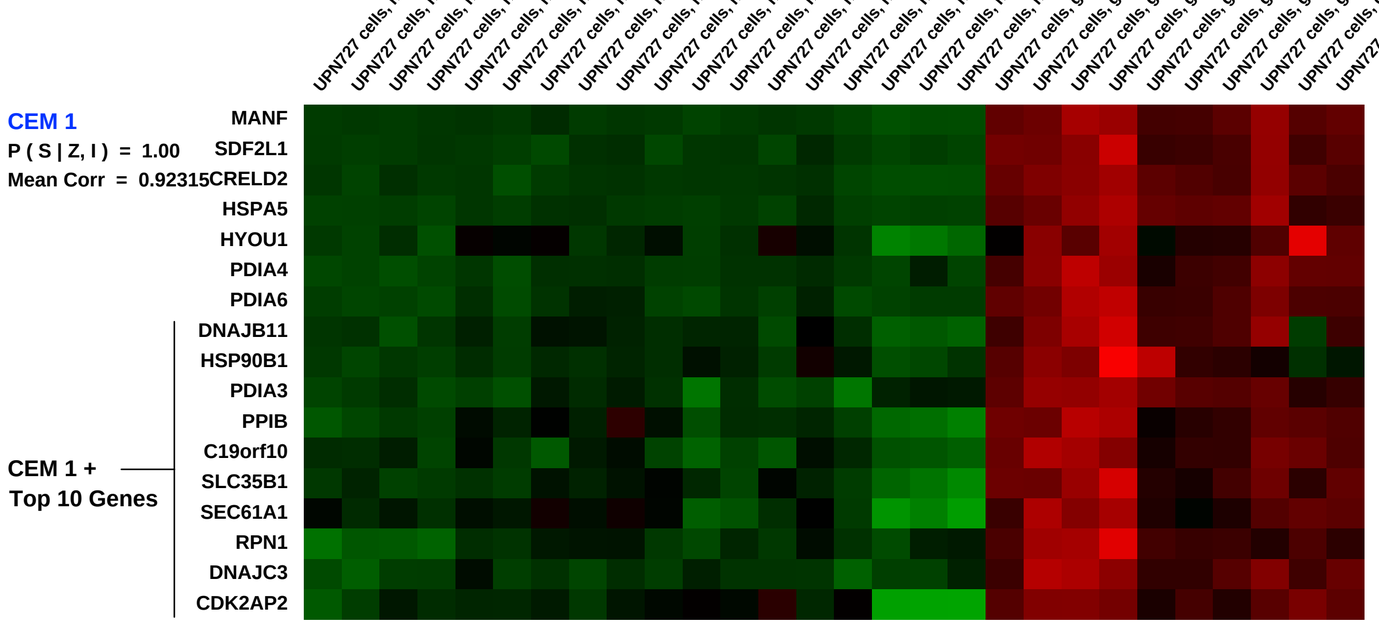

Pre-normalization Quantiles

[min]	[medium]	[max]
1747.2	2481.4	8417.2
665.1	1023.2	5479.7
1453.4	1905.2	5540.4
8450.2	11211.4	55250.1
940.3	1947.5	3914.5
426.0	590.0	1848.7
2903.5	3622.6	9615.1
2968.5	4174.8	8787.8
1771.3	2470.2	7060.0
2718.9	6446.8	14182.2
7437.2	10033.0	14603.7
1486.4	1873.1	2911.6
1126.0	1809.3	3132.1
1426.2	2194.4	3102.1
2516.3	3140.6	4875.5
1948.5	2506.3	4956.9
538.7	1211.4	1802.9

GEO Series "GSE7868" Expression Profiles

Num of samples in this series: 9

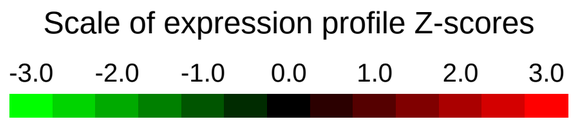

GEO Link:	http://www.ncbi.nlm.nih.gov/geo/query/acc.cgi?acc=GSE7868
Status:	Public on Sep 01 2007
Title:	Expression data from LNCaP cell line
Organism:	Homo sapiens
Experiment type:	Expression profiling by array
Platform:	GPL570
Pubmed ID:	17679089
Summary & Design:	**Summary:** Androgen receptor (AR) is a ligand-dependent transcription factor that plays a key role in the onset and progression of prostate cancer. Surprisingly little is known of AR binding sites and collaborating transcription factors in the human genome. Here we have identified the DNA sequence motifs that are significantly enriched within the authentic 90 AR target regions found on chromosomes 21 and 22 in human prostate cancer cells by combining chromatin immunoprecipitation for AR with chromosome-scale tiled oligonucleotide microarrays. By integrating the DNA sequence motif data with the gene expression profiles from human prostate cancers we identified the transcription factors that recognize each of these motifs. These factors form complexes with AR, bind to specific AR target regions and govern androgen-dependent transcription. Together with AR these collaborating transcription factors form a regulatory network that directs prostate cancer growth and survival and identify potential new opportunities for therapeutic intervention. **Keywords:** time course **Overall design:** The RNA samples are extracted from DHT 0, 4h and 16h treated LNCaP cells by using a RNeasy kit (Qiagen). The final RNAs submitted to Dana-Farber Cancer Institute (DFCI) Microarray Core Facility are all at 1.5ug/ul, A260/A280=2.1.

Background corr dist: KL-Divergence = 0.1110, L1-Distance = 0.0278, L2-Distance = 0.0013, Normal std = 0.4197

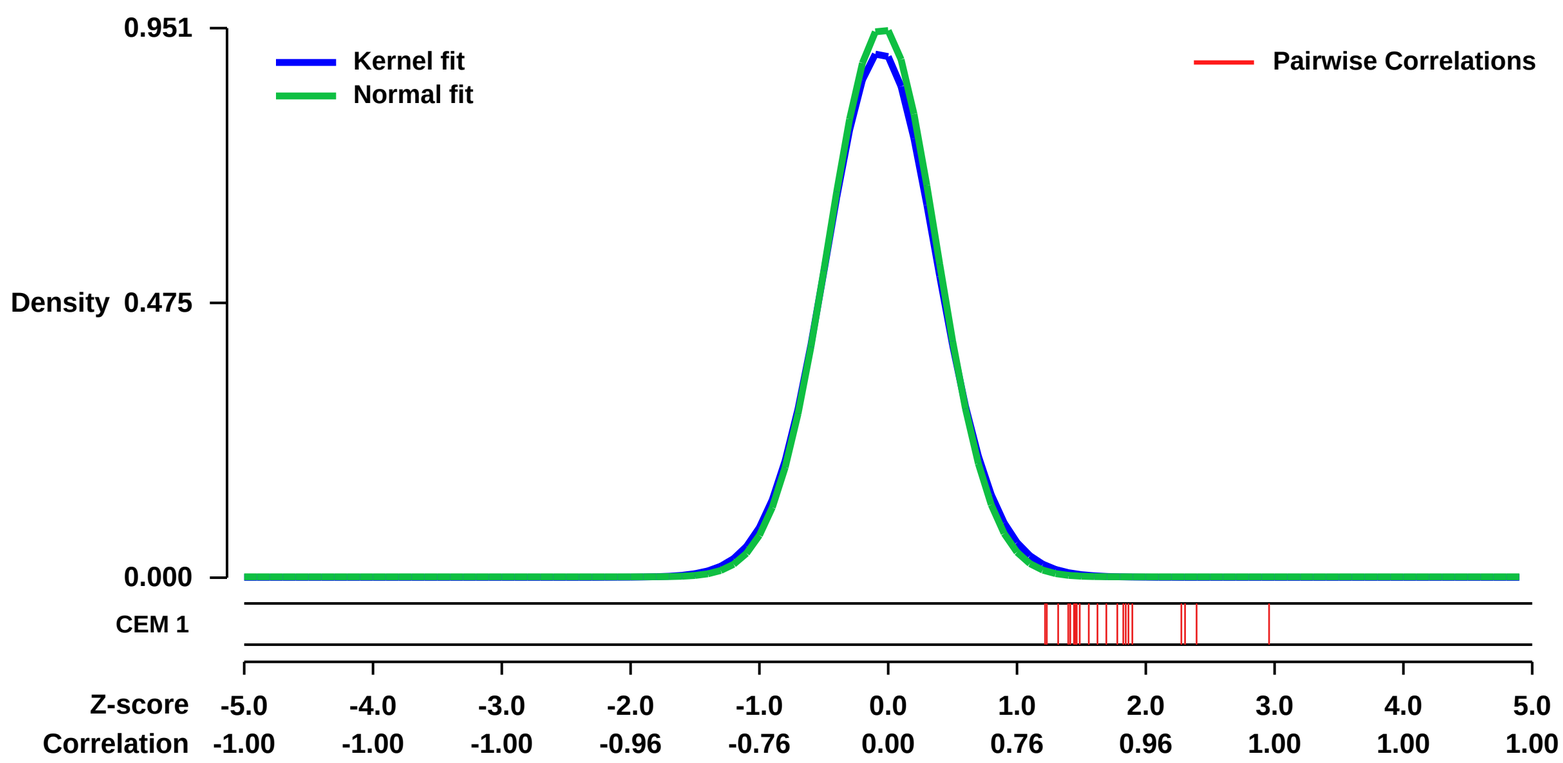

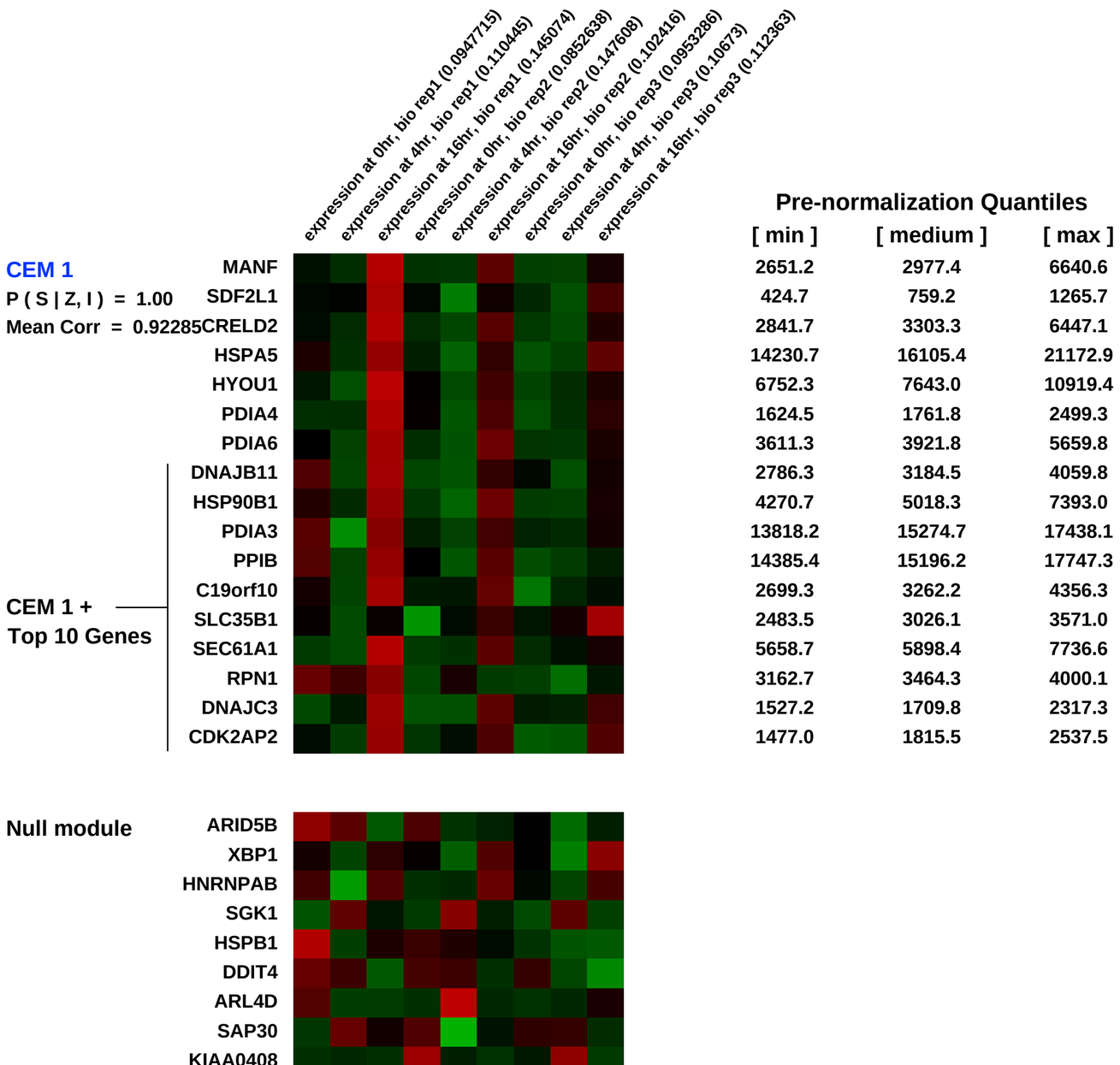

	Pre-normalization Quantiles		
	[min]	[medium]	[max]
MANF	2651.2	2977.4	6640.6
SDF2L1	424.7	759.2	1265.7
CRELD2	2841.7	3303.3	6447.1
HSPA5	14230.7	16105.4	21172.9
HYOU1	6752.3	7643.0	10919.4
PDIA4	1624.5	1761.8	2499.3
PDIA6	3611.3	3921.8	5659.8
DNAJB11	2786.3	3184.5	4059.8
HSP90B1	4270.7	5018.3	7393.0
PDIA3	13818.2	15274.7	17438.1
PPIB	14385.4	15196.2	17747.3
C19orf10	2699.3	3262.2	4356.3
SLC35B1	2483.5	3026.1	3571.0
SEC61A1	5658.7	5898.4	7736.6
RPN1	3162.7	3464.3	4000.1
DNAJC3	1527.2	1709.8	2317.3
CDK2AP2	1477.0	1815.5	2537.5
ARID5B			
XBP1			
HNRNPAB			
SGK1			
HSPB1			
DDIT4			
ARL4D			
SAP30			
KIAA0408			
GPR17			
HSPH1			
DNASE1L2			
SLC5A3			
GNAS			
GPR3			
TNFRSF25			
TM6SF2			
MKKS			
PLEKHF1			
ZMYM1			
DOK3			
FGF20			
SLC39A2			
KCNIP2			
ERRFI1			
DEDD2			
CCDC117			
USP31			
AHSA2			
CYS1			
CNIH2			
BANP			
CHORDC1			
P4HA1			

GEO Series "GSE35170" Expression Profiles

Num of samples in this series: 6

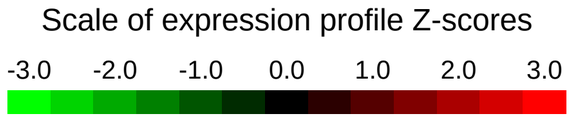

GEO Link:	http://www.ncbi.nlm.nih.gov/geo/query/acc.cgi?acc=GSE35170
Status:	Public on Dec 31 2012
Title:	Expression data from U87-2M1 glioma cells transduced with baculoviral control decoy vector or baculoviral miR-10b decoy vector
Organism:	Homo sapiens
Experiment type:	Expression profiling by array
Platform:	GPL570
Pubmed ID:	23034333
Summary & Design:	**Summary:** MicroRNA-10b may target numerous genes in gliomagenesis. The target genes of miR-10b may differ according to the cellular context. We used microarray analyses to determine the phenotypic effects and gene targets of miR-10b by silencing miR-10b in invasive U87-2M1 glioma cells. **Overall design:** Early passage U87-2M1 cells treated with the baculoviral control decoy vector or miR-10b decoy vector were selected for RNA extraction and hybridization on microarray

Background corr dist: KL-Divergence = 0.0337, L1-Distance = 0.0278, L2-Distance = 0.0008, Normal std = 0.6639

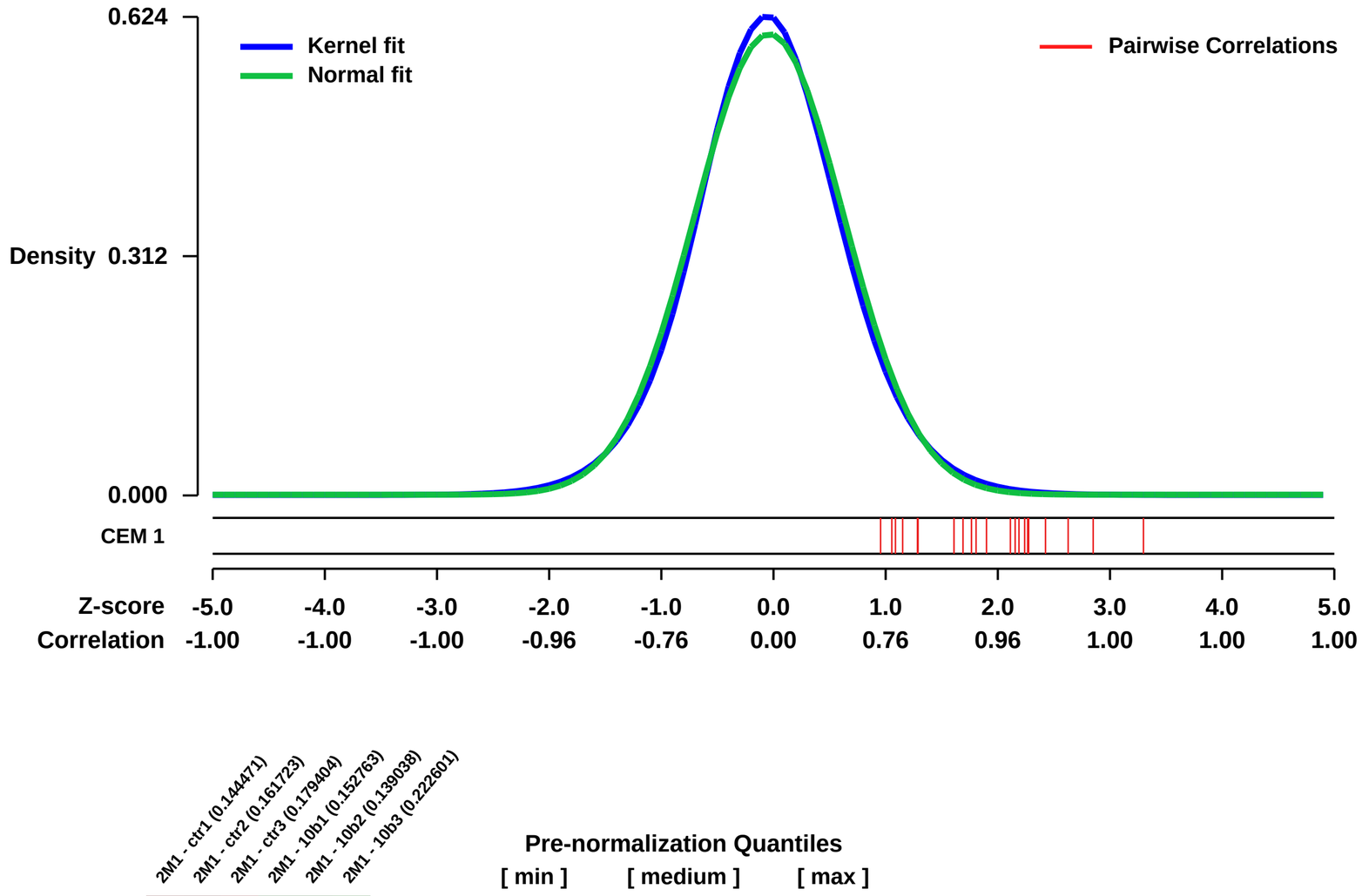

CEM 1
P (S | Z, I) = 1.00
Mean Corr = 0.92285

CEM 1 + Top 10 Genes

Null module

MANF	8686.1	12358.0	13335.2
SDF2L1	3260.8	5648.3	6221.4
CRELD2	5733.4	8732.6	9635.0
HSPA5	27826.5	33849.2	34683.2
HYOU1	1770.1	2877.1	3600.5
PDIA4	1156.9	1550.5	1712.3
PDIA6	6865.5	9130.3	9780.5
DNAJB11	6770.2	9927.3	10964.0
HSP90B1	5564.6	7414.5	12265.7
PDIA3	4827.8	6064.7	6753.8
PPIB	18226.5	20292.5	21147.3
C19orf10	4716.2	5395.0	5431.8
SLC35B1	2851.8	3056.3	3446.2
SEC61A1	6806.1	7401.4	7545.8
RPN1	4783.0	6015.0	6508.0
DNAJC3	4753.5	6972.7	7124.8
CDK2AP2	1655.7	2046.2	2160.3
ARID5B			
XBP1			
HNRNPAB			
SGK1			
HSPB1			
DDIT4			
ARL4D			
SAP30			
KIAA0408			
GPR17			
HSPH1			
DNASE1L2			
SLC5A3			
GNAS			
GPR3			
TNFRSF25			
TM6SF2			
MKKS			
PLEKHF1			
ZMYM1			
DOK3			
FGF20			
SLC39A2			
KCNIP2			
ERRFI1			
DEDD2			
CCDC117			
USP31			
AHSA2			
CYS1			
CNIH2			
BANP			
CHORDC1			
P4HA1			

GEO Series "GSE10070" Expression Profiles

Num of samples in this series: 13

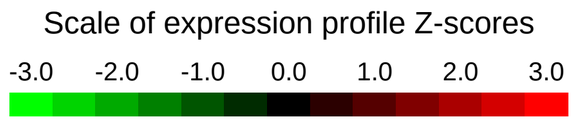

GEO Link:	http://www.ncbi.nlm.nih.gov/geo/query/acc.cgi?acc=GSE10070
Status:	Public on Jan 31 2008
Title:	Gene Expression in MCF10A cells through Differentiation on Transwells
Organism:	Homo sapiens
Experiment type:	Expression profiling by array
Platform:	GPL570
Pubmed ID:	19005683
Summary & Design:	**Summary:** To further understand the differences occurring in MCF10A cells as they polarize and differentiate in the Transwell´fi model, we performed gene expression profiling with Affymetrix Human Genome U133 Plus 2.0 Arrays. Four experimental time points, were sampled: conventional cultures of MCF10A cells grown on plastic (Monolayer) and MCF10A cells plated on Transwells´fi sampled at three TEER values, 200-300 ¸' cm2 (Base), 1400-1600 ¸' cm2 (Midpoint), and 3000-3200 ¸' cm2 (Plateau). **Keywords:** Mammary Epithelial Cell Differentiation **Overall design:** Cells are grown in monolayer to 90-95% confluency, trypsinized and counted for seeding onto permeable supports (Transwell´fi, 0.4 ´µm pores, polyester) in normal growth medium. MCF10A cells are seeded on 12-well Transwells´fi (Corning) at 105 cells/cm2. Both chambers of media were changed strictly on a 24-hour schedule. Transepithelial electrical resistance (TEER) is measured daily with Epithelial Volt-Ohm Meter (EVOM; World Precision Instruments), prior to media change. Total RNA was isolated at the indicated TEER listed above. Canonical monolayer MCF10A cells served as a control comparison. Each time point was performed on triplicate arrays except for Plateau (n=4).

Background corr dist: KL-Divergence = 0.0724, L1-Distance = 0.0849, L2-Distance = 0.0111, Normal std = 0.5904

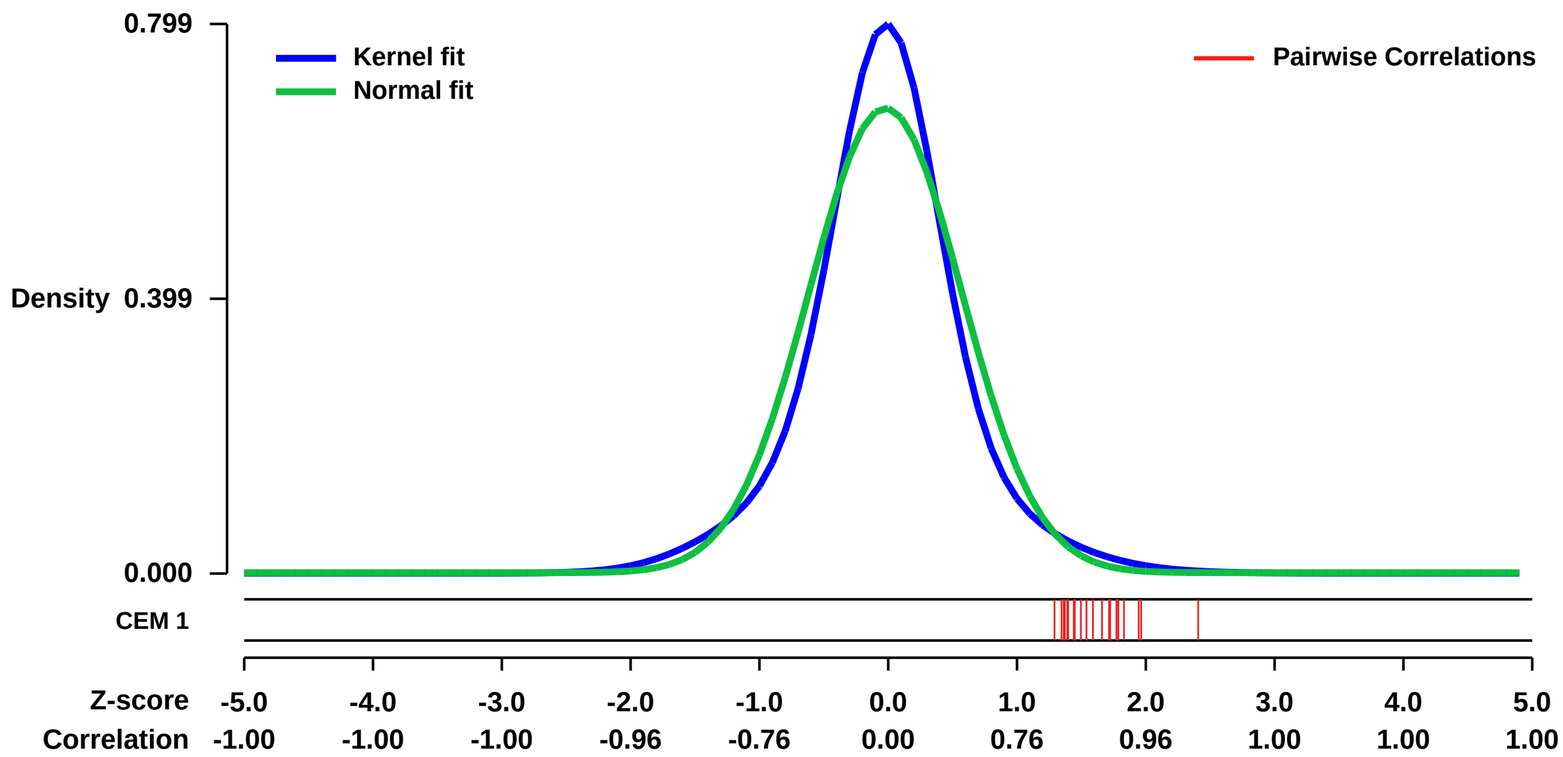

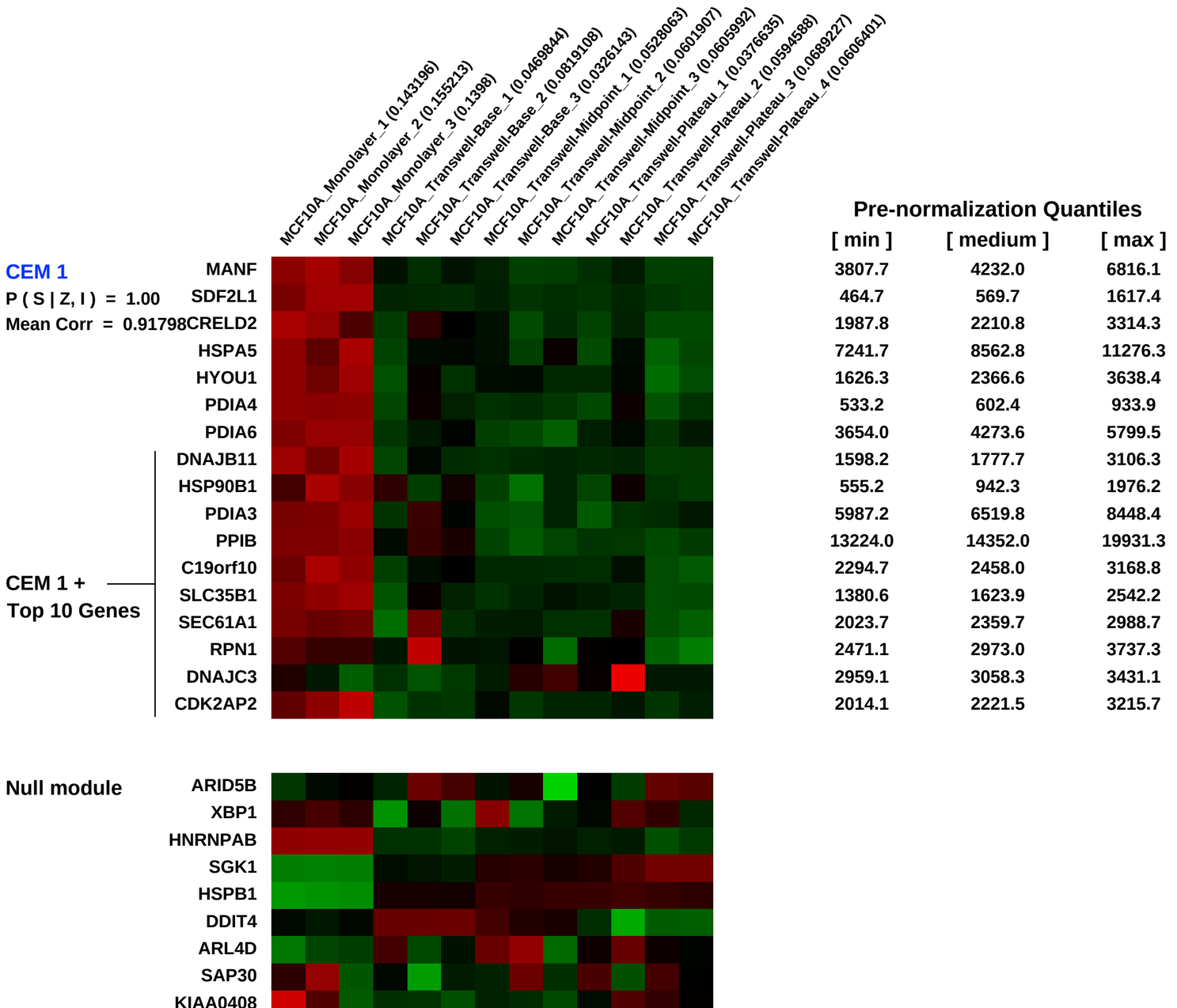

Pre-normalization Quantiles

	[min]	[medium]	[max]
MANF	3807.7	4232.0	6816.1
SDF2L1	464.7	569.7	1617.4
CRELD2	1987.8	2210.8	3314.3
HSPA5	7241.7	8562.8	11276.3
HYOU1	1626.3	2366.6	3638.4
PDIA4	533.2	602.4	933.9
PDIA6	3654.0	4273.6	5799.5
DNAJB11	1598.2	1777.7	3106.3
HSP90B1	555.2	942.3	1976.2
PDIA3	5987.2	6519.8	8448.4
PPIB	13224.0	14352.0	19931.3
C19orf10	2294.7	2458.0	3168.8
SLC35B1	1380.6	1623.9	2542.2
SEC61A1	2023.7	2359.7	2988.7
RPN1	2471.1	2973.0	3737.3
DNAJC3	2959.1	3058.3	3431.1
CDK2AP2	2014.1	2221.5	3215.7

GEO Series "GSE17251" Expression Profiles

Num of samples in this series: 24

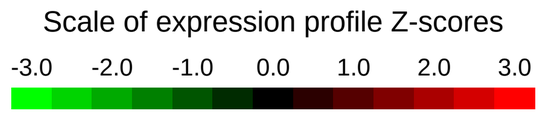

GEO Link:	http://www.ncbi.nlm.nih.gov/geo/query/acc.cgi?acc=GSE17251
Status:	Public on Sep 21 2009
Title:	Comparative analysis of gene regulation by the transcription factor PPAR‹– human
Organism:	Homo sapiens
Experiment type:	Expression profiling by array
Platform:	GPL570
Pubmed ID:	22215653

Summary & Design:

Summary:
Studies in mice have shown that PPAR‹– is an important regulator of hepatic lipid metabolism and the acute phase response. However, little information is available on the role of PPAR‹– in human liver. Here we set out to compare the function of PPAR‹– in mouse and human hepatocytes via analysis of target gene regulation. Primary hepatocytes from 6 human and 6 mouse donors were treated with PPAR‹– agonist Wy14643 and gene expression profiling was performed using Affymetrix GeneChips followed by a systems biology analysis. Baseline PPAR‹– expression was similar in human and mouse hepatocytes. Depending on species and time of exposure, Wy14643 significantly induced the expression of 362-672 genes. Surprisingly minor overlap was observed between the Wy14643-regulated genes from mouse and human, although more substantial overlap was observed at the pathway level. Xenobiotics metabolism and apolipoprotein synthesis were specifically regulated by PPAR‹– in human hepatocytes, whereas glycolysis-gluconeogenesis was regulated specifically in mouse hepatocytes. Most of the genes commonly regulated in mouse and human were involved in lipid metabolism and many represented known PPAR‹– targets, including CPT1A, HMGCS2, FABP, ACSL, and ADFP. Several genes were identified that were specifically induced by PPAR‹– in human (MBL2, ALAS1, CYP1A1, TSKU) or mouse (Fbp2, lgals4, Cd36, Ucp2, Pxmp4). Furthermore, several putative novel PPAR‹– targets were identified that were commonly regulated in both species, including CREB3L3, KLF10, KLF11 and MAP3K8. Our results suggest that PPAR‹– activation has a major impact on gene regulation in human hepatocytes. Importantly, the role of PPAR‹– as master regulator of hepatic lipid metabolism is generally well-conserved between mouse and human. Overall, however, PPAR‹– regulates a mostly divergent set of genes in mouse and human hepatocytes.

Keywords: Analysis of target gene regulation by using microarrays

Overall design:
Primary hepatocytes from 6 human subjects were treated with the PPAR‹– agonist Wy14643 for 6 and 24 hours, and gene expression profiling was performed using Affymetrix GeneChips. Human hepatocytes and Hepatocyte Culture Medium Bulletkit were purchased from Lonza Bioscience (Verviers, Belgium). Primary hepatocytes were isolated from surgical liver biopsies obtained from six individual donors who underwent surgery after informed consent was obtained for surgery with subsequent use of samples in experiments. Hepatocytes were isolated with two-step collagenase perfusion method and the viability of the cells was over 80%. Cells were plated on collagen-coated six-well plates and filled with maintenance medium. Upon arrival of the cells, the medium was discarded and was replaced by Hepatocyte Culture Medium (HCM) with additives. The additives included Gentamicin sulphate/Amphotercin-B, Bovine serum albumin (Fatty acid free), Transferrin, Ascorbic acid, Insulin, Epidermal growth factor, Hydrocortisone hemisuccinate. The next day, cells were incubated in fresh medium in the presence or absence of Wy14643 (50 microM) dissolved in DMSO for 6 and 24 hours, followed by RNA isolation.

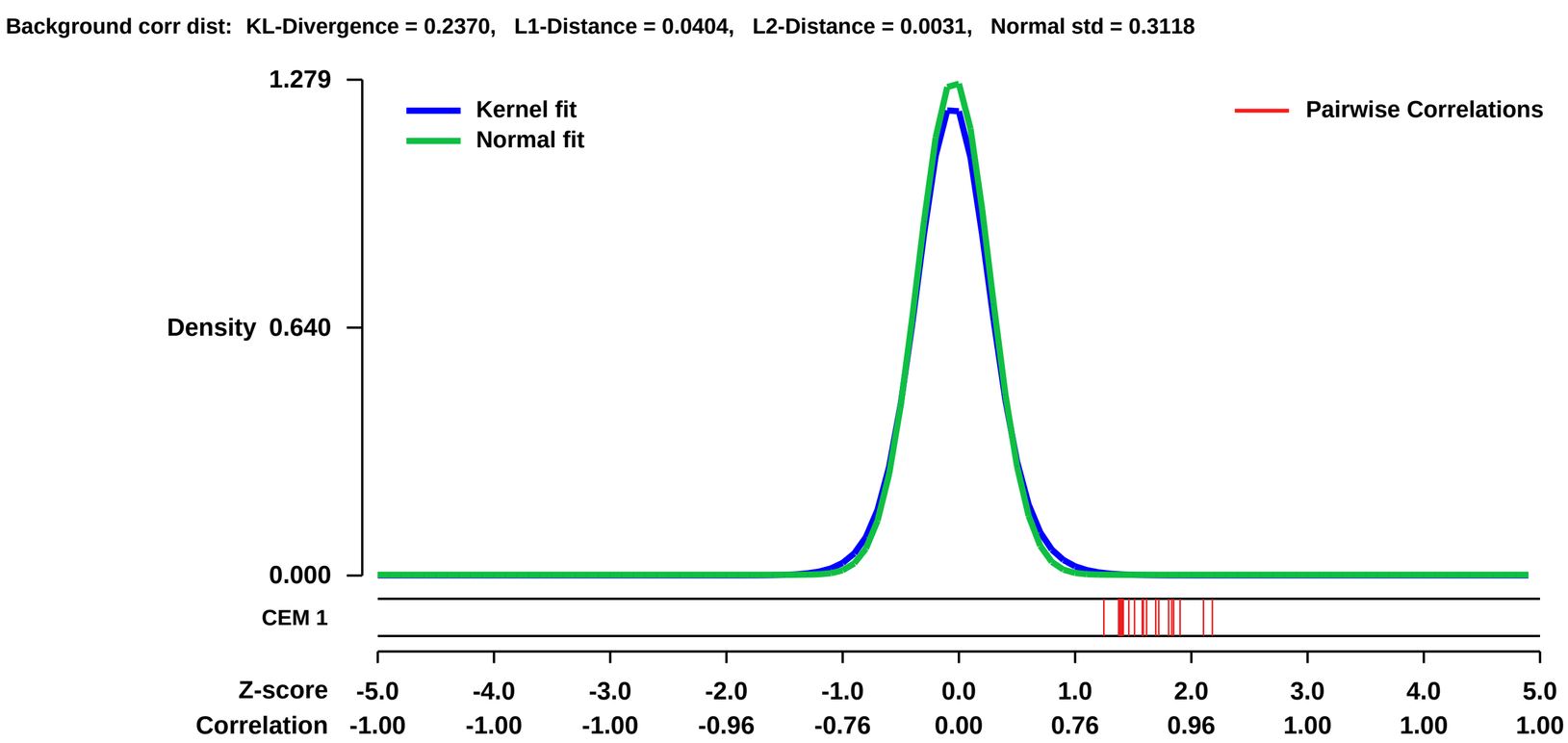

GEO Series "GSE27128" Expression Profiles

Num of samples in this series: 6

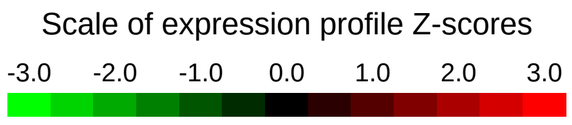

GEO Link:	http://www.ncbi.nlm.nih.gov/geo/query/acc.cgi?acc=GSE27128
Status:	Public on Feb 12 2011
Title:	Expression levels in strained vs. non-strained Calu-3 lung epithelial cells
Organism:	Homo sapiens
Experiment type:	Expression profiling by array
Platform:	GPL570
Pubmed ID:	24391213
Summary & Design:	**Summary:** Ventilator induced lung injury can lead to serious conditions like ARDS which are associated with a high mortality (around 30%, Stapleton et al., Chest, 2005). We hypothesized that changes of expression levels of different genes would lead us to the identification of critical target genes, which might influence the inflammation and outcome associated with this condition. We used human whole genome U133 Plus 2.0 microarrays to detail the changes of gene expression and identified distinct classes of up-regulated genes during this process. **Overall design:** Confluent non strained and strained human Calu-3 cells were selected for RNA extraction and hybridization on Affymetrix microarrays. The experiment was performed with 3 replicates.

Background corr dist: KL-Divergence = 0.0390, L1-Distance = 0.0282, L2-Distance = 0.0010, Normal std = 0.6280

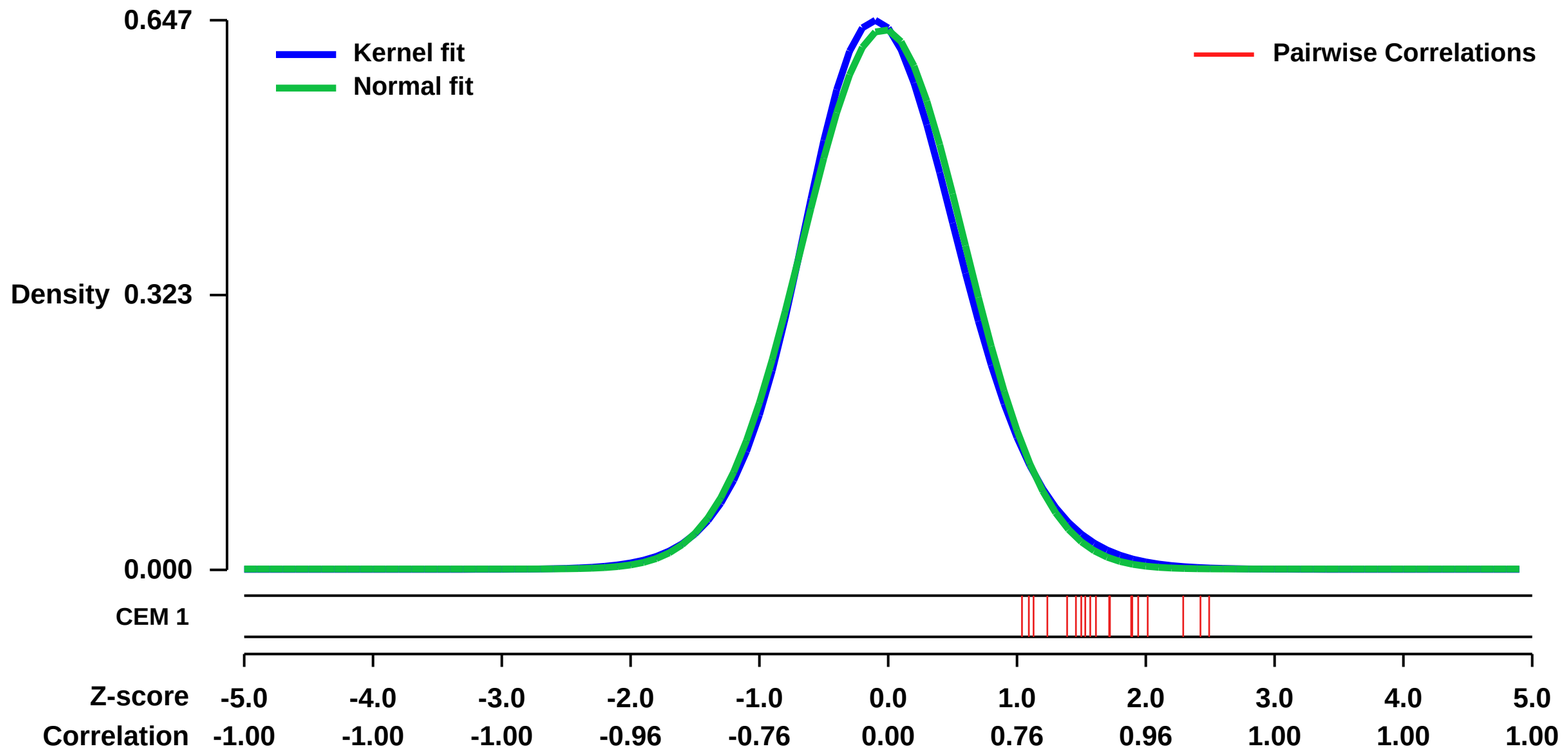

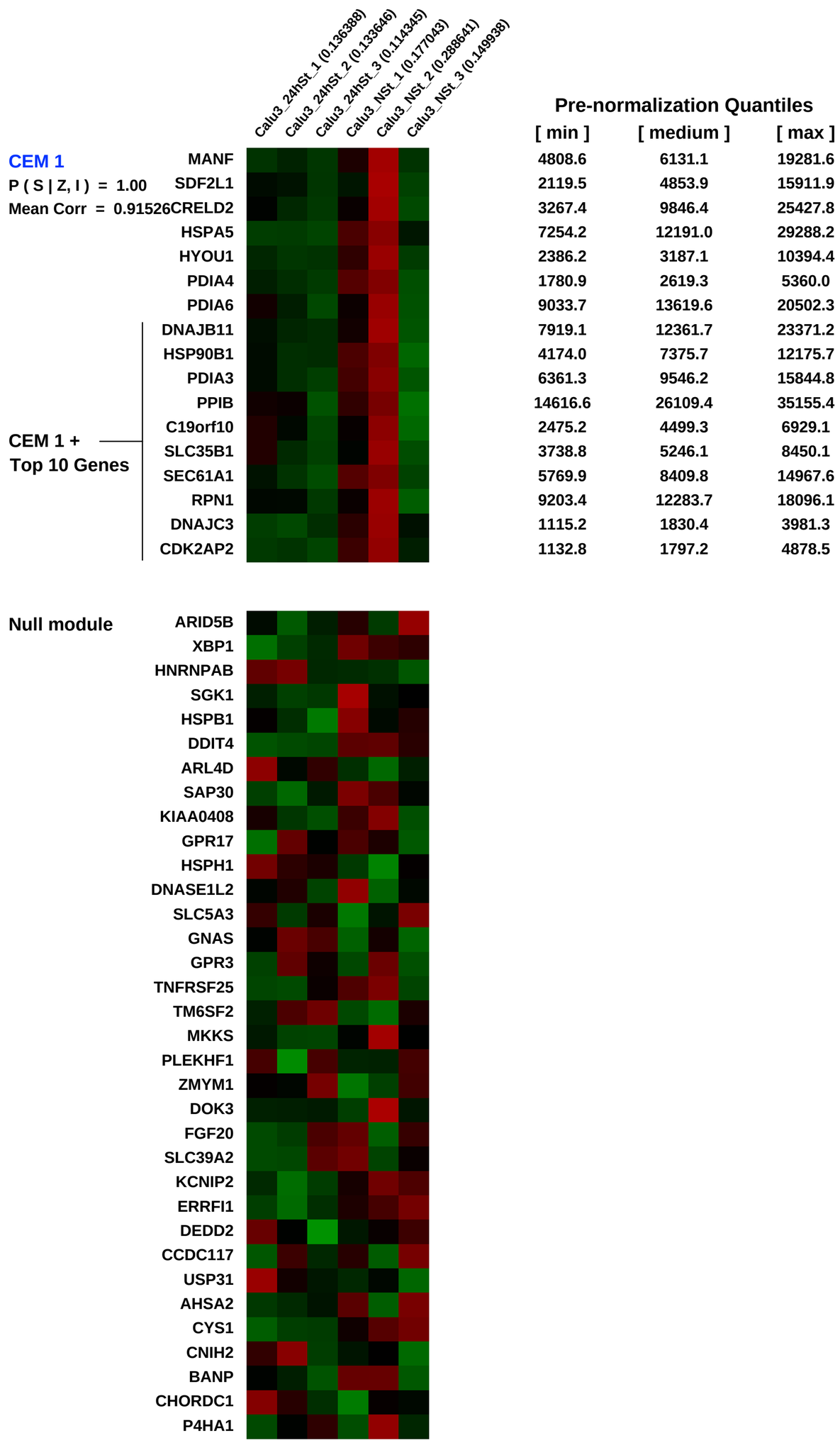

GEO Series "GSE17044" Expression Profiles

Num of samples in this series: 6

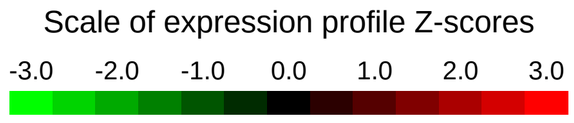

GEO Link:	http://www.ncbi.nlm.nih.gov/geo/query/acc.cgi?acc=GSE17044
Status:	Public on Dec 30 2009
Title:	Expression data from androgen treated LNCaP cells
Organism:	Homo sapiens
Experiment type:	Expression profiling by array
Platform:	GPL570
Pubmed ID:	19763266
Summary & Design:	**Summary:** Androgens are required for the development of normal prostate, and they are also linked to the development of prostate cancer. We used microarrays to understand the role of androgen in an androgen dependent, androgen receptor (AR) positive human metastatic cell line, LNCaP. **Overall design:** LNCaP cells were grown in RPMI medium and they were subjected to stay in phenol-red free, RPMI with charcoal stripped serum for 48h. Synthetic androgen R1881 was added and the cells were allowed to grow for 48h. Control cells were given with corresponding amount of ethanol as vehicle which is used for the solubilization of R1881. Cells were harvested and RNA was isolated for microarray analysis.

Background corr dist: KL-Divergence = 0.0179, L1-Distance = 0.0326, L2-Distance = 0.0017, Normal std = 0.7710

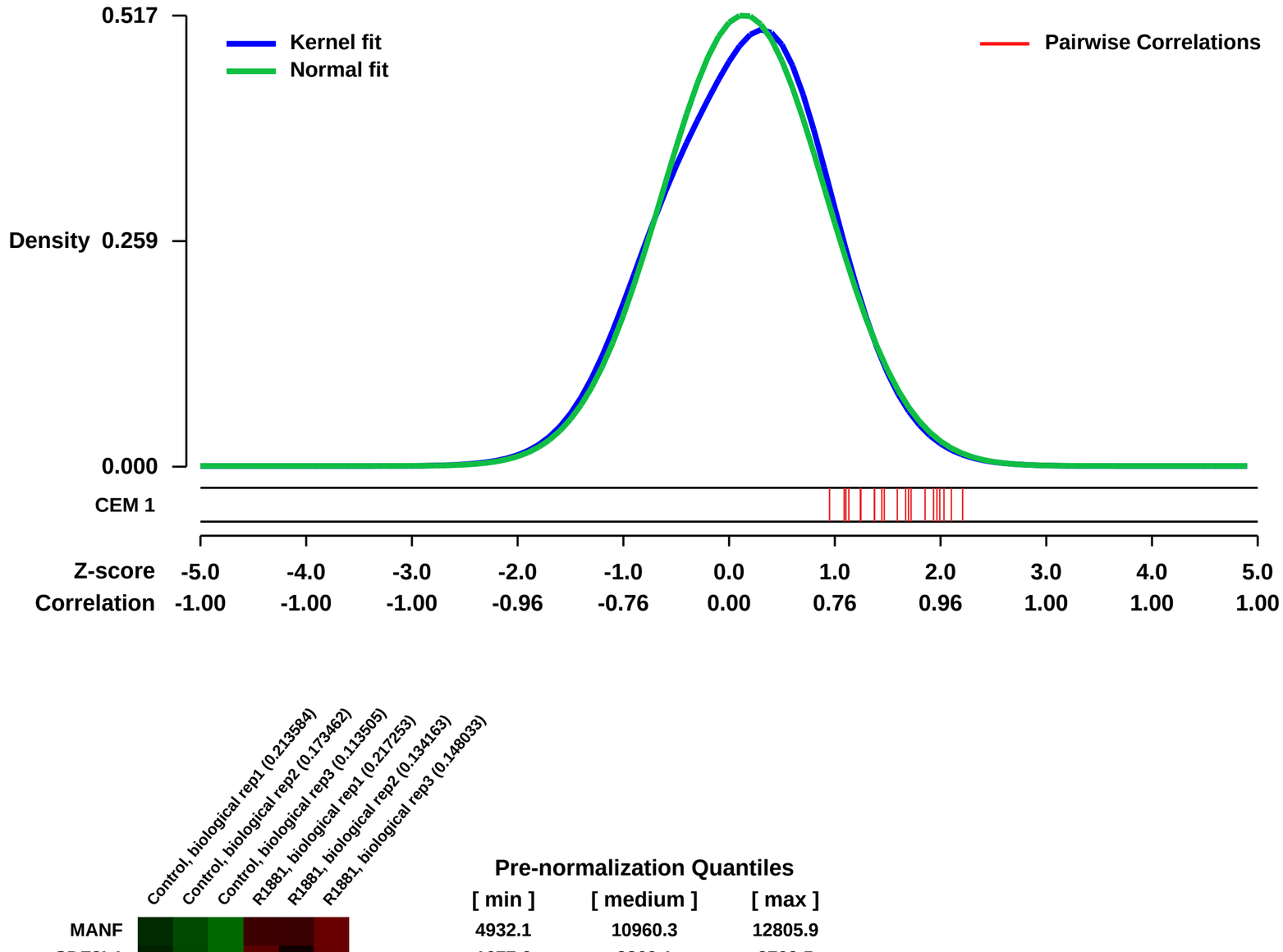

CEM 1
P (S | Z, I) = 1.00
Mean Corr = 0.89863

CEM 1 + Top 10 Genes

Null module

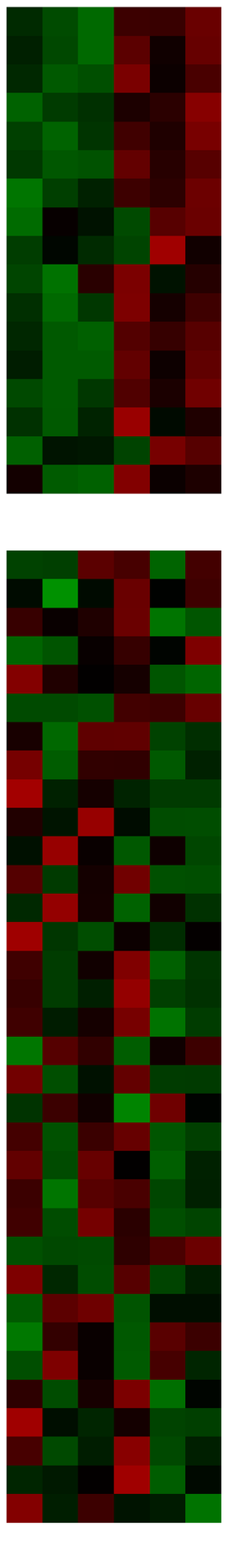

MANF	4932.1	10960.3	12805.9
SDF2L1	1677.6	2869.1	3709.5
CRELD2	3813.3	5939.8	8269.6
HSPA5	10302.8	18144.1	24797.7
HYOU1	3520.4	6561.9	8667.0
PDIA4	784.9	1201.8	1398.8
PDIA6	5290.4	7802.9	8805.1
DNAJB11	2134.2	3192.0	4104.3
HSP90B1	3289.2	4185.1	6553.7
PDIA3	7327.6	11148.2	13314.5
PPIB	17243.1	24461.0	30404.8
C19orf10	3110.6	7174.7	8065.9
SLC35B1	4051.2	5164.4	6081.5
SEC61A1	3393.0	5823.2	7593.9
RPN1	3668.1	5801.8	10200.9
DNAJC3	312.9	1025.1	2320.3
CDK2AP2	1436.6	3103.0	4707.7
ARID5B			
XBP1			
HNRNPAB			
SGK1			
HSPB1			
DDIT4			
ARL4D			
SAP30			
KIAA0408			
GPR17			
HSPH1			
DNASE1L2			
SLC5A3			
GNAS			
GPR3			
TNFRSF25			
TM6SF2			
MKKS			
PLEKHF1			
ZMYM1			
DOK3			
FGF20			
SLC39A2			
KCNIP2			
ERRFI1			
DEDD2			
CCDC117			
USP31			
AHSA2			
CYS1			
CNIH2			
BANP			
CHORDC1			
P4HA1			

GEO Series "GSE20405" Expression Profiles

Num of samples in this series: 12

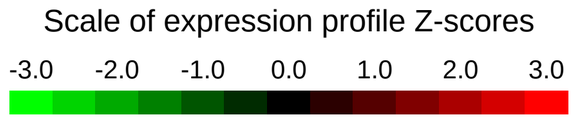

GEO Link:	http://www.ncbi.nlm.nih.gov/geo/query/acc.cgi?acc=GSE20405
Status:	Public on Jan 24 2014
Title:	HDAC and aminopeptidase inhibitor treatment of myeloma cells
Organism:	Homo sapiens
Experiment type:	Expression profiling by array
Platform:	GPL570
Pubmed ID:	
Summary & Design:	**Summary:** H929 human myeloma cells were exposed to aminopeptidase inhibitor (CHR-2797), HDAC inhibitor (CHR-3996), or a combinaion of the two agents, for 24 hours. Following this treatment RNA was extracted and microarrays used to determine gene expression changes. **Overall design:** Myeloma cells were exposed to chemotherapeutic agent for 24 hours.

Background corr dist: KL-Divergence = 0.0692, L1-Distance = 0.0839, L2-Distance = 0.0107, Normal std = 0.5943

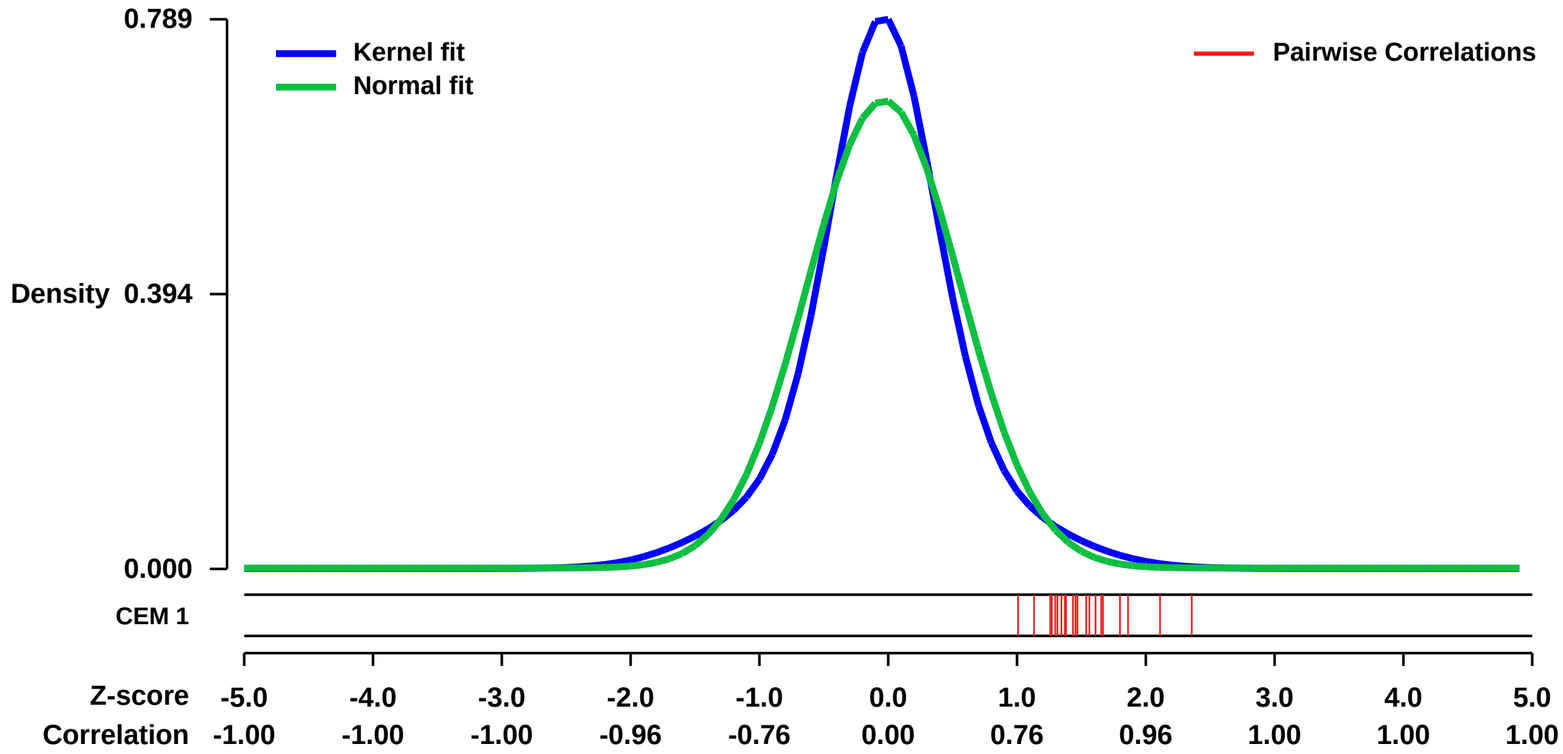

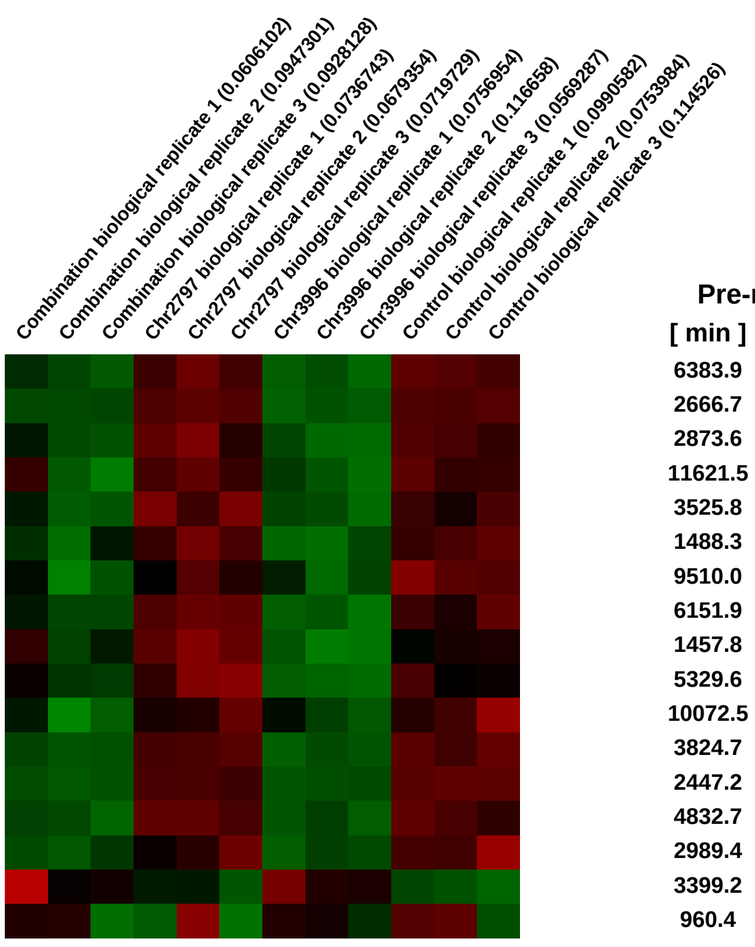

	Pre-normalization Quantiles [min]	[medium]	[max]
MANF	6383.9	10373.3	11586.0
SDF2L1	2666.7	6138.1	6482.3
CRELD2	2873.6	4998.2	6271.9
HSPA5	11621.5	15199.9	16088.0
HYOU1	3525.8	6027.2	7932.1
PDIA4	1488.3	1992.4	2185.1
PDIA6	9510.0	11731.4	13925.2
DNAJB11	6151.9	8810.3	10240.5
HSP90B1	1457.8	2119.2	2599.1
PDIA3	5329.6	6473.7	7720.0
PPIB	10072.5	12292.5	14070.4
C19orf10	3824.7	6973.1	7696.9
SLC35B1	2447.2	5251.7	5917.9
SEC61A1	4832.7	8704.0	10020.7
RPN1	2989.4	4897.4	7446.1
DNAJC3	3399.2	4190.0	5506.5
CDK2AP2	960.4	1174.0	1323.6
ARID5B			
XBP1			
HNRNPAB			
SGK1			
HSPB1			
DDIT4			
ARL4D			
SAP30			
KIAA0408			
GPR17			
HSPH1			
DNASE1L2			
SLC5A3			
GNAS			
GPR3			
TNFRSF25			
TM6SF2			
MKKS			
PLEKHF1			
ZMYM1			
DOK3			
FGF20			
SLC39A2			
KCNIP2			
ERRFI1			
DEDD2			
CCDC117			
USP31			
AHSA2			
CYS1			
CNIH2			
BANP			
CHORDC1			
P4HA1			

GEO Series "GSE40241" Expression Profiles

Num of samples in this series: 6

Scale of expression profile Z-scores

-3.0 -2.0 -1.0 0.0 1.0 2.0 3.0

GEO Link:	http://www.ncbi.nlm.nih.gov/geo/query/acc.cgi?acc=GSE40241
Status:	Public on Dec 31 2013
Title:	Expression data from Versican (VCAN) protein treated ovarian cancer cell line OVCA433
Organism:	Homo sapiens
Experiment type:	Expression profiling by array
Platform:	GPL570
Pubmed ID:	23824740
Summary & Design:	**Summary:** Advanced ovarian cancer is the most lethal gynecologic malignancy in the United States. Currently patients are treated by surgical cytoreductive surgery with the aim of reducing tumor burden to microscopic disease followed by adjuvant combined treatment with a platinum and taxane containing chemotherapy, which affords 80% of patients an initial complete response. However, Abdominal and pelvic recurrence rates are high and response to further chemotherapy is limited. Attempts at introducing biologic therapeutic agents to improve outcome in this disease are ongoing, while prognostic or predictive biomarkers that can stratify patients for treatment are still lacking. Using transcriptome profiling of microdissected tissue samples from high-grade serous ovarian cancer patients, we identified a cancer associated fibroblast (CAF) specific gene signature. Versican, which encodes a extracellular matrix protein, was one of the identified genes which demonstrated up-regulation in cancer stroma. To investigate the function roles, signaling machanism and the effect of versican treatment on ovarian cancer cells, transcriptome profiling of versican treated OVCA433 high-grade serous ovarian cancer cells was performed. **Overall design:** High grade serous ovarian cancer cell line OVCA433 was used. Total RNA was isolated from control samples and versican treated cancer cell samples at 48 hours post-treatment followed by cDNA synthesis, IVT and biotin labeling. Samples were then hybridized onto Affymetrix Human genome U133 plus 2.0 microarrays. For each treatment group, three independent samples were prepared for the microarray experiment.

Background corr dist: KL-Divergence = 0.0371, L1-Distance = 0.0308, L2-Distance = 0.0010, Normal std = 0.6558

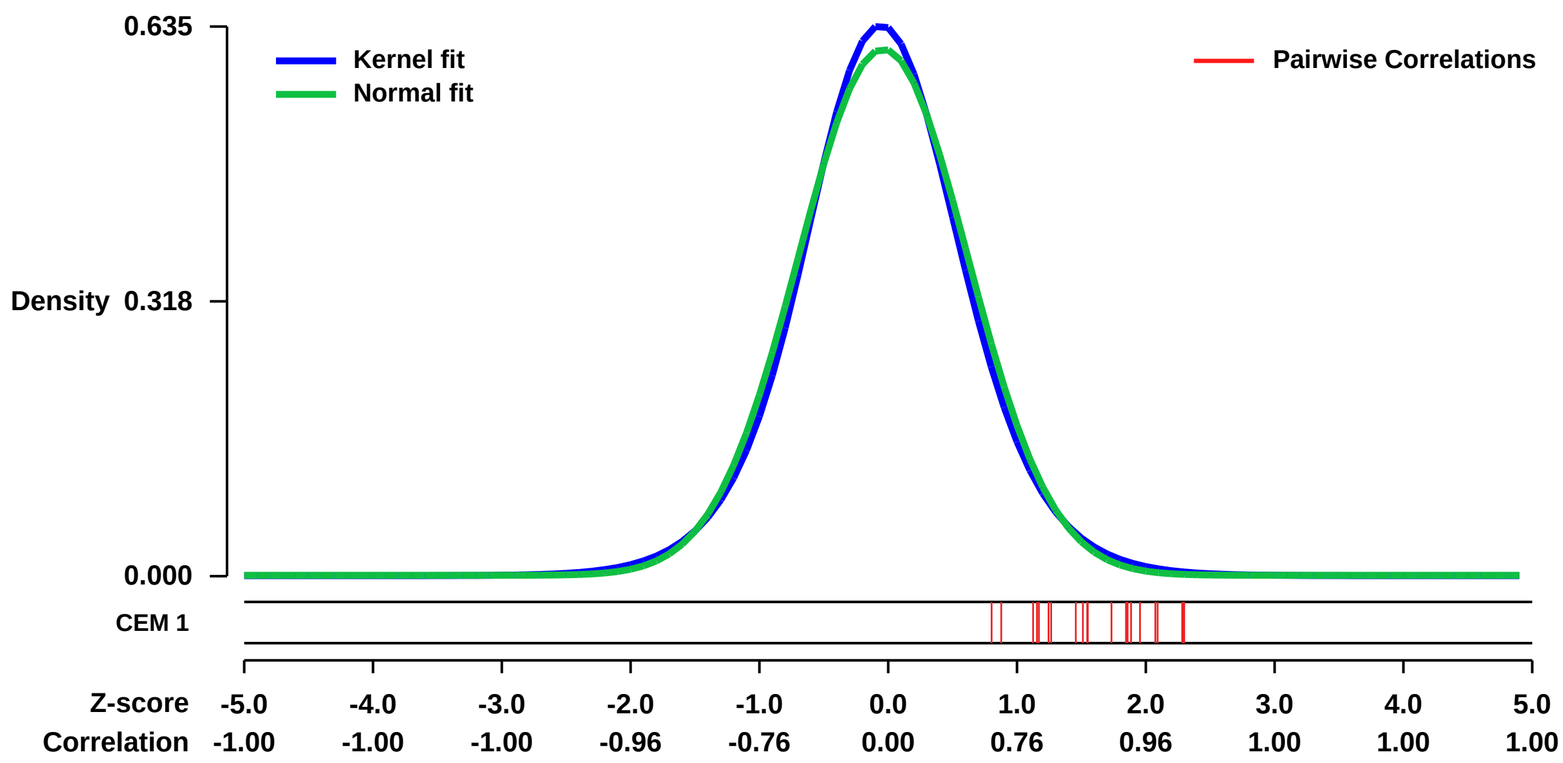

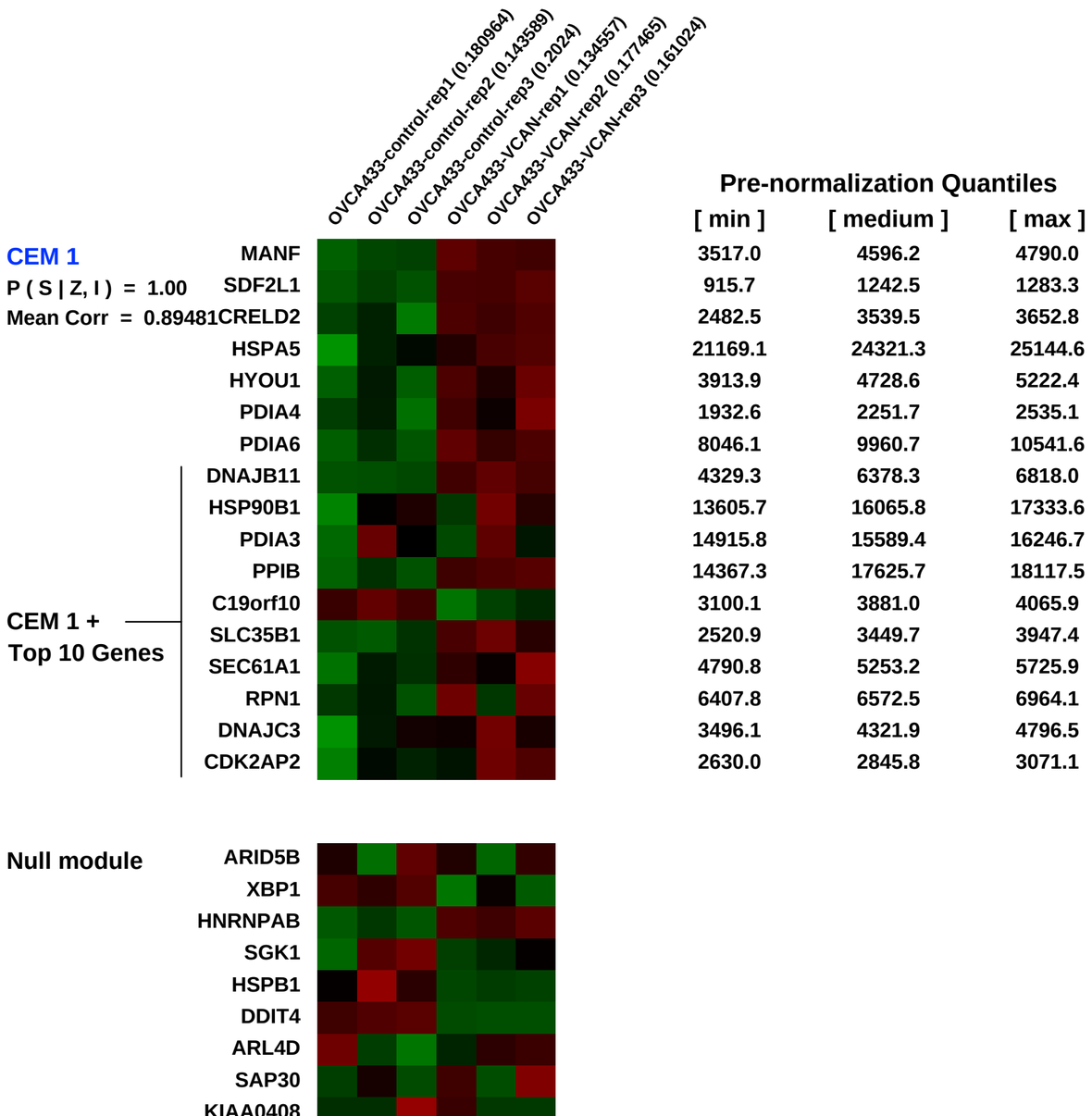

	Pre-normalization Quantiles		
	[min]	[medium]	[max]
MANF	3517.0	4596.2	4790.0
SDF2L1	915.7	1242.5	1283.3
CRELD2	2482.5	3539.5	3652.8
HSPA5	21169.1	24321.3	25144.6
HYOU1	3913.9	4728.6	5222.4
PDIA4	1932.6	2251.7	2535.1
PDIA6	8046.1	9960.7	10541.6
DNAJB11	4329.3	6378.3	6818.0
HSP90B1	13605.7	16065.8	17333.6
PDIA3	14915.8	15589.4	16246.7
PPIB	14367.3	17625.7	18117.5
C19orf10	3100.1	3881.0	4065.9
SLC35B1	2520.9	3449.7	3947.4
SEC61A1	4790.8	5253.2	5725.9
RPN1	6407.8	6572.5	6964.1
DNAJC3	3496.1	4321.9	4796.5
CDK2AP2	2630.0	2845.8	3071.1
ARID5B			
XBP1			
HNRNPAB			
SGK1			
HSPB1			
DDIT4			
ARL4D			
SAP30			
KIAA0408			
GPR17			
HSPH1			
DNASE1L2			
SLC5A3			
GNAS			
GPR3			
TNFRSF25			
TM6SF2			
MKKS			
PLEKHF1			
ZMYM1			
DOK3			
FGF20			
SLC39A2			
KCNIP2			
ERRFI1			
DEDD2			
CCDC117			
USP31			
AHSA2			
CYS1			
CNIH2			
BANP			
CHORDC1			
P4HA1			

GEO Series "GSE11238" Expression Profiles

Num of samples in this series: 39

Scale of expression profile Z-scores

-3.0 -2.0 -1.0 0.0 1.0 2.0 3.0

GEO Link: http://www.ncbi.nlm.nih.gov/geo/query/acc.cgi?acc=GSE11238
Status: Public on Apr 23 2008
Title: Vaccinia E3L mutant virus infected HeLa cell lines (langl-affy-human-215499)
Organism: Homo sapiens
Experiment type: Expression profiling by array
Platform: GPL570
Pubmed ID:

Summary & Design:

Summary:
Smallpox is a highly communicable, often fatal diseae. There is currently no licensed treatment for smallpox and vaccinia virus (VV) is currently used for immunization. While immunization with VV can provide good protection against exposure to the smallpox virus, the current vaccine is far from optimal. Complications occur in 1/1,000-1/10,000 vaccinees, with at least one death per million vaccinees. We have constructed recombinant VV strains which are less pathogenic, yet provide a protective immune response. These viruses contain various mutations in the E3L which is known to block the host antiviral response. Identifying the host genes involved in producing a strong protective immunological response to these attenuated viruses would not only increase our understanding of the proteins and pathways involved in effective smallpox vaccination, but aid in the development of alternative vaccine strains which enhance these specific immune responses.

We will determine gene expression patterns in HeLa cells at various times following infection with wtVV and several VV constructs containing mutations in the E3L gene.

The VV E3L gene product blocks the host antiviral response by sequestering viral danger signals, including double-stranded RNA and Z-DNA. VV constructs containing mutations in E3L which allow host cell recognition of either of these danger signals leads to a decrease in viral pathogensis. In this project we will dissect the cellular inflammatory response to infection with wtVV in comparison to VV containing mutations in the E3L gene. By understanding why certain strains of VV are non-pathogenic, yet highly immunogenic, it is possible to gain a better understanding on the mechanisms of poxvirus pathogenesis and the host response.

We will examine three times points following infection with VV: 2 HPI, 6 HPI and 9 HPI. These times points represent keys points in the virus replication cycle. Several VV constructs will be used which contain mutations in the E3L gene. These constructs alter the ability of E3L to sequester double-stranded RNA and/or Z-DNA and therefore have a direct effect on viral pathogenesis. Fourteen constructs will be used including: mock, wtVV, VVdelE3L, VVE3Ldel83N, VVE3Ldel37N, VVE3Ldel26C, VVE3Ldel7C, VVE3L Y48A, VVE3L P63A, VVE3L K167T, VV-ATV, VV-ADAR/E3L, VVdelK3L, VVdelK3L-E3Ldel37N. Cells will be infected at an MOI of 5 to allow infection of all cells. At each time point, cells will be harvested by scraping. RNA will be isolated using a Trizol RNA extraction protocol (Invitrogen) followed by RNA purification using the RNeasy cleanup kit available from Qiagen.

Keywords: time-course

Overall design:

Background corr dist: KL-Divergence = 0.1943, L1-Distance = 0.0309, L2-Distance = 0.0019, Normal std = 0.3459

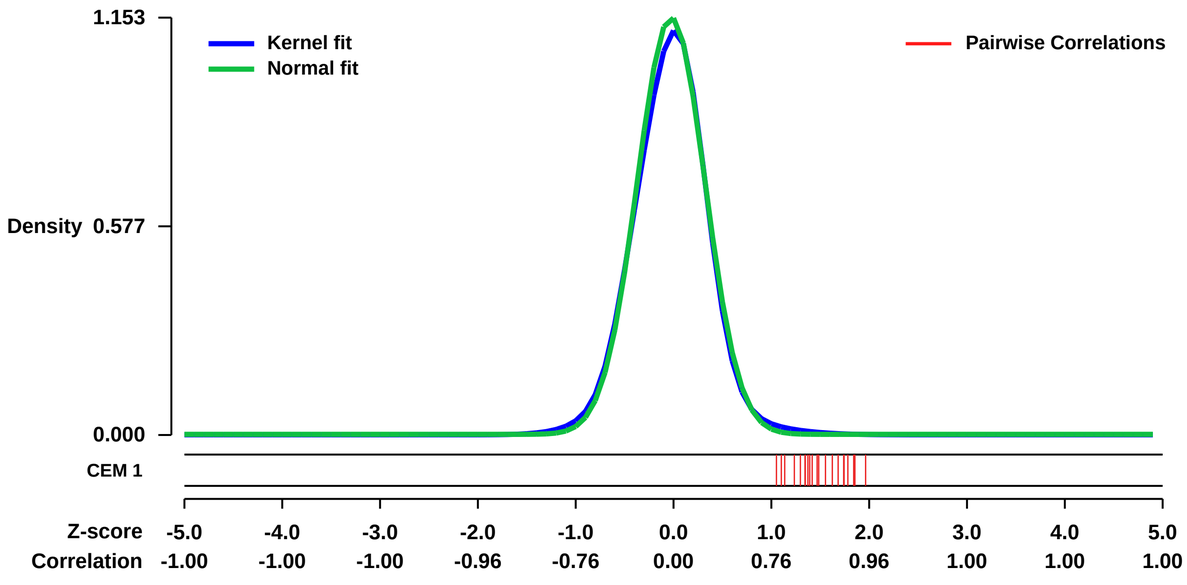

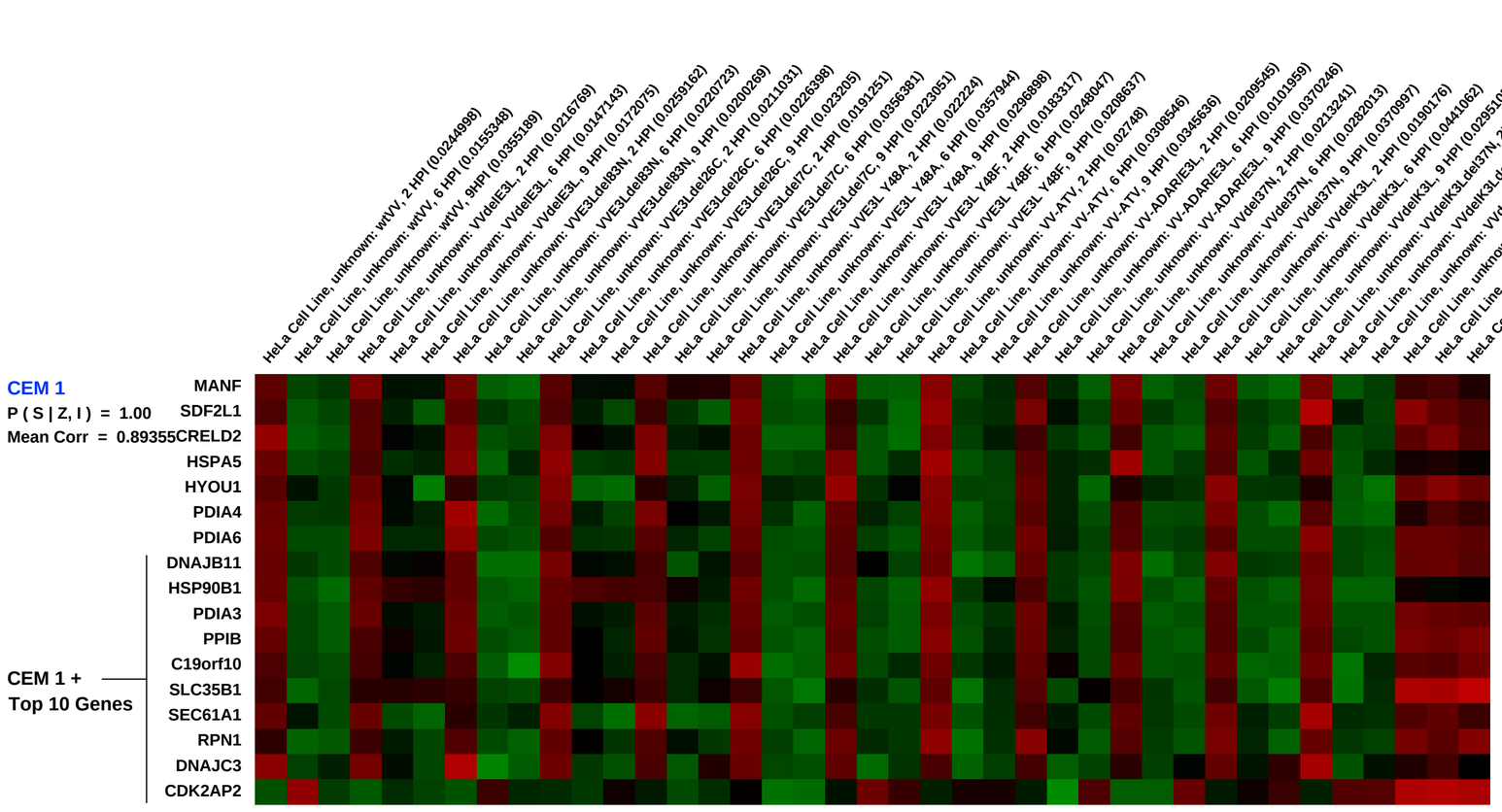

Pre-normalization Quantiles

[min]	[medium]	[max]
624.8	1972.3	4306.2
238.3	824.5	2991.4
563.8	2103.1	4903.8
7805.7	16195.4	46064.3
250.5	887.5	2127.4
162.2	716.5	2177.9
975.1	2328.7	8627.4
2483.4	4602.7	7555.6
1505.4	8811.9	19791.6
2398.0	5919.3	14066.5
3200.7	10166.6	27499.1
548.4	1981.9	4179.3
674.7	1742.9	3303.6
1111.4	2308.8	5846.3
748.5	2180.1	5432.7
589.5	1164.1	2140.2
61.4	351.6	884.8

GEO Series "GSE9768" Expression Profiles

Num of samples in this series: 13

Scale of expression profile Z-scores

-3.0 -2.0 -1.0 0.0 1.0 2.0 3.0

GEO Link: http://www.ncbi.nlm.nih.gov/geo/query/acc.cgi?acc=GSE9768
Status: Public on Dec 05 2007
Title: Identification of genes modulated by acid and bile in a Barrett's oesophagus cell line
Organism: Homo sapiens
Experiment type: Expression profiling by array
Platform: GPL570
Pubmed ID:

Summary & Design:

Summary:
The major aetiological risk factor for Barrett's oesophagus and oesophageal adenocarcinoma is gastroesophageal reflux. This study's aim was to identify genes involved in the celular response to reflux in vitro. The Barrettâ s oesophagus cell line, CP-A hTERT, was exposed to media with acid, deoxycholic acid or a primary bile salt mixture. RNA expression was compared with controls on Affymetrix U133 Plus 2.0 arrays. In CP-A hTERT, the greatest number of changes in gene expression was observed after treatment with deoxycholic acid, pH 4.5; 152 genes were up-regulated at 2 hours (91 at 6 hours) and 10 down-regulated at 2 hours (34 at 6 hours). 12 genes were identified and were subsequently assessed in patients with non-erosive reflux disease, oesophagitis, Barrett's oesophagus and oesophageal adenocarcinoma

Background and Aims: The major etiological risk factor for Barrettâ s esophagus and esophageal adenocarcinoma is gastro-esophageal reflux. This studyâ s aim was to identify genes involved in the cellular response to components of reflux both in vitro and in patients with reflux-related disease.

Methods: The Barrettâ s cell line, CP-A hTERT, was exposed to media with acid, deoxycholic acid or a primary bile salt mixture. RNA expression was compared with controls on Affymetrix U133 Plus 2.0 arrays. 12 genes of interest were analysed by Real Time PCR both in cell line and biopsies from 110 patients with non-erosive reflux disease, esophagitis, Barrettâ s esophagus and esophageal adenocarcinoma.

Results: In CP-A hTERT, the greatest number of changes in gene expression was observed after treatment with deoxycholic acid, pH 4.5. Of 12 genes analysed in biopsies, 10 were significantly different between the 4 groups with the largest change for anterior gradient homolog 2, which may modulate p53 function. This had highest expression in biopsies from Barrettâ s esophagus (median gene fold change for Barrettâ s esophagus versus non-erosive reflux disease, 411.2 (95% CI 290.5-682.7; p<0.01); esophageal adenocarcinoma versus non-erosive reflux disease 68.1 (20.5-161.4; p<0.01)). In addition 4 genes associated with development/differentiation were upregulated in Barrettâ s biopsies compared to those from non-erosive reflux disease (SEL1L, MFNG, CRIP1 and EFNA1).

Conclusions: Novel genes have been identified, whose expression is altered after acid and bile exposure in vitro and in biopsies from patients with reflux related diseases. These genes may have utility as biomarkers of response to reflux and should be assessed in prospective studies.

Keywords: Acid (pH 4.5) and bile (mixture of primary bile salts or the secondary bile salt deoxycholic acid, both at pH 4.5) challenge to a Barrett's oesophagus cell line. RNA extraction at 2 and 6 hours. Comparison of treatment RNA to control (non-treatment) RNA,

Overall design:
The Barrett's oesophagus cell line CP-A hTERT was treated with a 15 minute exposure of acid (pH 4.5), a mixture of primary bile acids (pH 4.5) or deoxycholic acid (pH 4.5). RNA extraction occurred in treatment and non-treated cells at 2 hours and 6 hours. The treatments were performed in duplicate on 2 different days. RNA was compared in each treatment to each control at the relevant time points, in a 2 x 2 manner by using Affymetrex U133 Plus 2.0 arrays. Results of 12 genes were confirmed by Real Time PCR and were subsequently assessed in patients with non-erosive reflux disease, oesophagitis, Barrett's oesophagus and oesophageal adenocarcinoma.

Background corr dist: KL-Divergence = 0.1329, L1-Distance = 0.0335, L2-Distance = 0.0024, Normal std = 0.3951

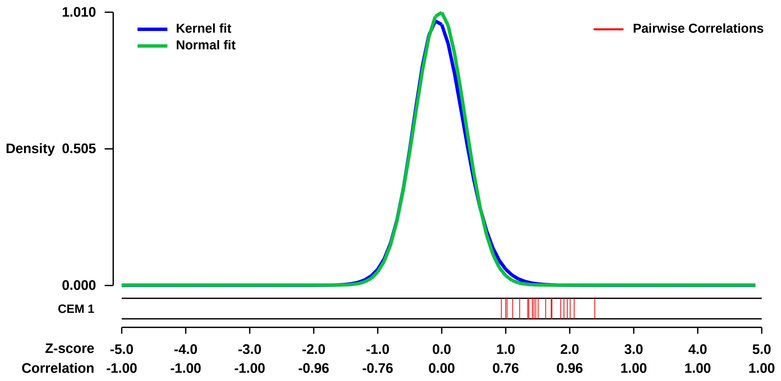

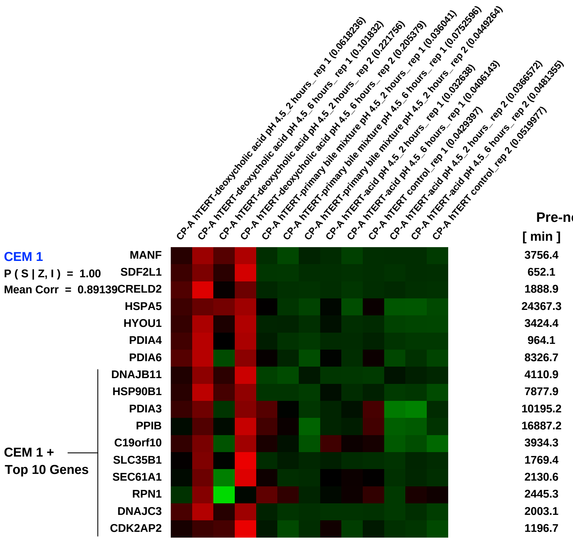

Pre-normalization Quantiles

	[min]	[medium]	[max]
CEM 1			
P (S | Z, I) = 1.00			
Mean Corr = 0.89139			
MANF	3756.4	5527.7	20421.3
SDF2L1	652.1	1053.2	12016.3
CRELD2	1888.9	2593.0	21973.2
HSPA5	24367.3	40984.1	75877.8
HYOU1	3424.4	5256.7	16641.5
PDIA4	964.1	1252.2	5759.2
PDIA6	8326.7	9928.7	18497.9
CEM 1 + Top 10 Genes			
DNAJB11	4110.9	6689.9	20619.0
HSP90B1	7877.9	10131.6	27399.3
PDIA3	10195.2	16424.7	24759.8
PPIB	16887.2	22446.9	35704.8
C19orf10	3934.3	6752.7	10348.9
SLC35B1	1769.4	2023.0	7145.1
SEC61A1	2130.6	5540.7	12253.1
RPN1	2445.3	5761.4	7474.5
DNAJC3	2003.1	2322.8	7430.1
CDK2AP2	1196.7	2154.1	7305.1

Null module

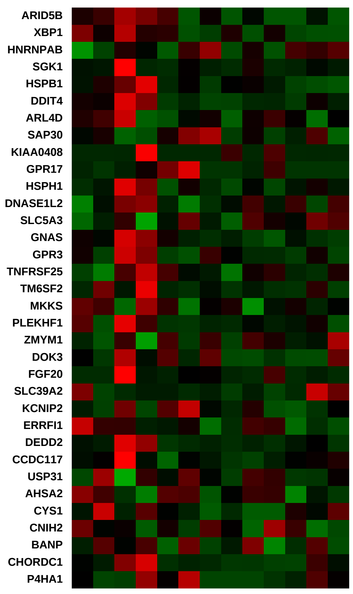

GEO Series "GSE40517" Expression Profiles

Num of samples in this series: 9

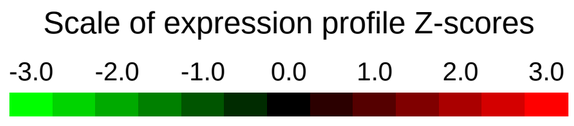

GEO Link:	**http://www.ncbi.nlm.nih.gov/geo/query/acc.cgi?acc=GSE40517**
Status:	**Public on Aug 31 2013**
Title:	**Selective Requirement for Mediator MED23 in Ras-active Lung Cancer**
Organism:	**Homo sapiens**
Experiment type:	**Expression profiling by array**
Platform:	**GPL570**
Pubmed ID:	

Summary & Design:

Summary:
K-RAS activating mutations occur frequently in non-small cell lung cancer (NSCLC), leading to aberrant activation of Ras-MAPK signaling pathway that contributes to the malignant phenotype. However, the development of Ras-targeted therapeutics remains challenging. Here, we show that MED23, a component of the multisubunit Mediator complex that is known to integrate signaling and gene activities, is selectively important for Ras-active lung cancer. By screening a large panel of human lung cancer cell lines with or without a Ras mutation, we found that Med23 RNAi specifically inhibits the proliferation and tumorigenicity of lung cancer cells with hyperactive Ras activity. Med23-deficiency in fibroblasts selectively inhibited the oncogenic transformation induced by Ras but not by c-Myc. Transcription factor ELK1, which is phosphorylated by MAPK for relaying the Ras signaling to MED23, was also required for the Ras-driven oncogenesis. Transcriptiome analysis revealed that MED23 and ELK1 co-regulate a common set of target genes enriched in regulating cell cycle and proliferation to support the Ras-dependency. Furthermore, correlated with the strength of Ras signaling as indicated by the ELK1 phosphorylation level, MED23 was up-regulated by Ras-transformation, and was found to be overexpressed in both Ras-mutated lung cancer cell lines and primary tumor samples. Remarkably, lower Med23 expression predicts better survival in Ras-active lung cancer patients and xenograft mice. Collectively, our findings demonstrate a critical role for MED23 in enabling the â Ras-addictionâ of lung carcinogenesis, thus providing a vulnerable target for the treatment of Ras-active lung cancer.

To gain a genome-wide understanding of how MED23 and ELK1 control gene expression in Ras-active lung cancer cells, we performed gene profiling experiments to analyze the transcriptomes from control, si-Med23, or si-Elk1 A549 cells.

Overall design:
The si-Ctrl, si-Med23 and si-Elk1 A549 cells were cultured in the normal condition. Then the cells were harvested for RNA extraction and hybridization on Affymetrix microarrays. The analysis contain 9 samples. si-Ctrl cells have three replicates (si-Ctrl#1, si-Ctrl#2 and si-Ctrl#3), and the si-Med23 or si-Elk1 group contains three different cell lines that harbor three different RNAi oligos against Med23 or Elk1 (si-Med23A, B, C and si-Elk1A, B, C).

Background corr dist: **KL-Divergence = 0.0666, L1-Distance = 0.0297, L2-Distance = 0.0011, Normal std = 0.5225**

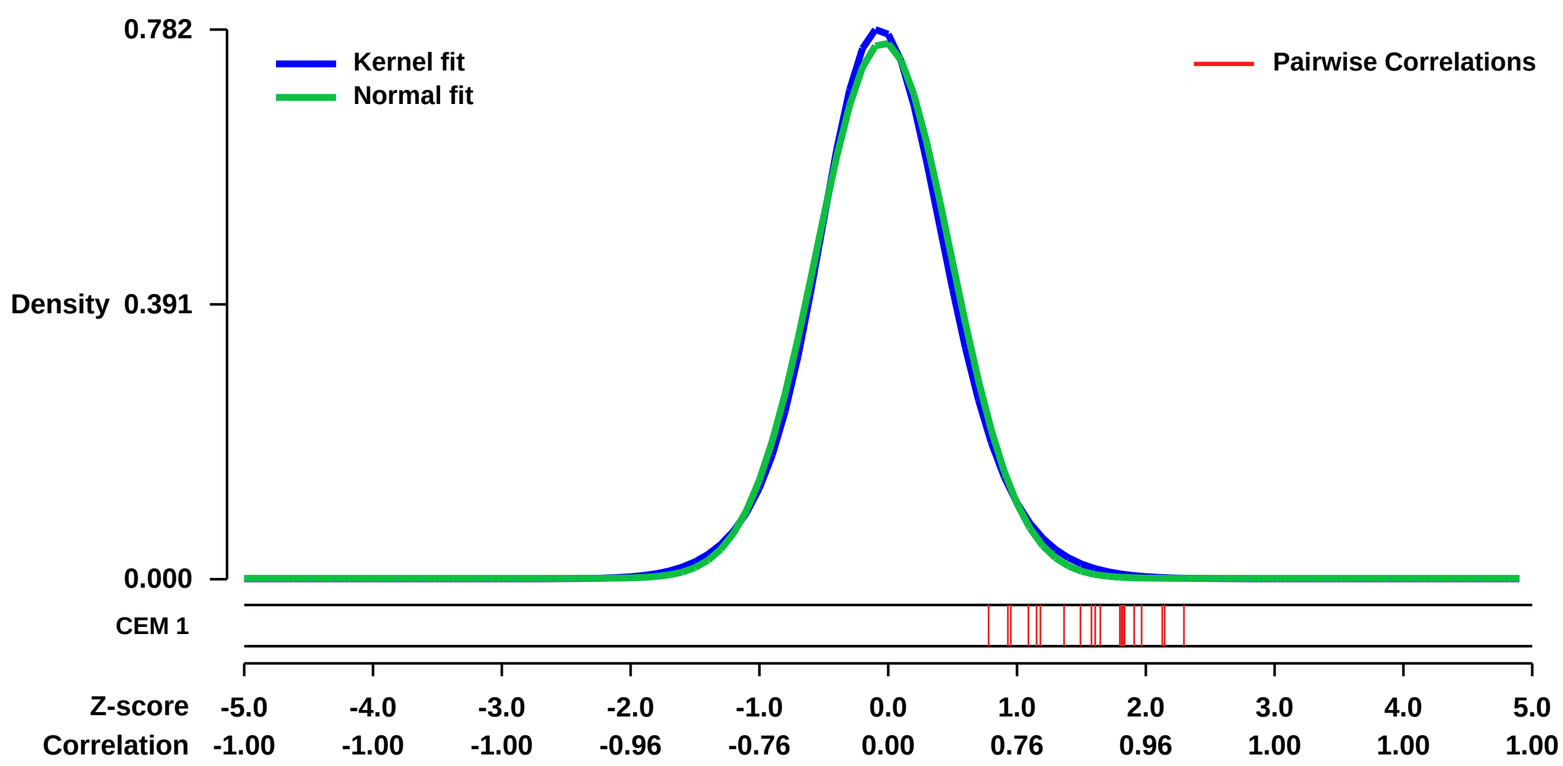

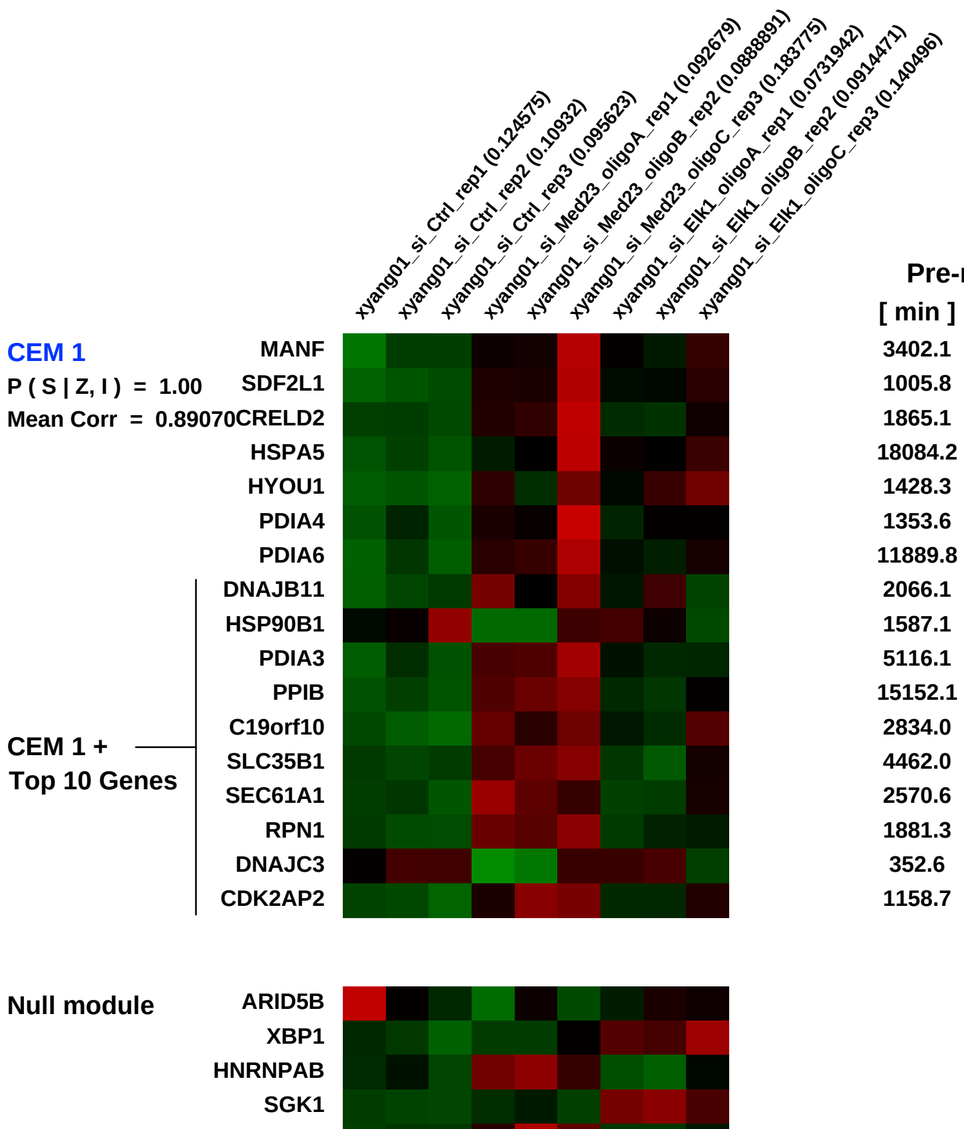

GEO Series "GSE20540" Expression Profiles

Num of samples in this series: 12

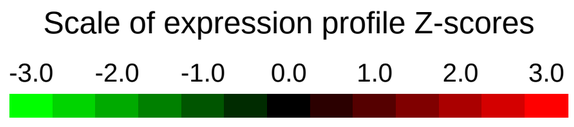

GEO Link:	http://www.ncbi.nlm.nih.gov/geo/query/acc.cgi?acc=GSE20540
Status:	Public on Mar 14 2010
Title:	Gene expression profiles of myeloma cells interacting with bone marrow stromal cells in vitro
Organism:	Homo sapiens
Experiment type:	Expression profiling by array
Platform:	GPL570
Pubmed ID:	20228816

Summary & Design:

Summary:
Conventional anti-cancer drug screening is typically performed in the absence of accessory cells (e.g. stromal cells) of the tumor microenvironment, which can profoundly alter anti-tumor drug activity. To address this major limitation, we have developed assays (e.g. the tumor cell-specific in vitro bioluminescence imaging (CS-BLI) assay) to selectively quantify tumor cell viability, in presence vs. absence of non-malignant stromal cells or drug treatment. These assays have allowed us to identify that neoplastic cells from diverse malignancies exhibit stroma-induced resistance to different anti-tumor agents. In this analysis, we evaluated the molecular changes triggered in myeloma cells by their in vitro interaction with stromal cells. The transcriptional profile of 3 human multiple myeloma (MM) cell lines (MM.1S, MM.1R, INA-6) co-cultured with stromal cells vs. when cultured alone was characterized by oligonucleotide microarray analysis, using the human U133 plus 2.0 Affymetrix GeneChip.

Overall design:
Three human multiple myeloma (MM) cell lines (MM.1S, MM.1R, INA-6) stably expressing green fluorescent protein (GFP) were cultured in vitro for 24hrs either alone or in the presence of the human bone marrow stromal cell line HS-5. Fluorescence activated cell sorting was used to separate the GFP+ MM cells from GFP- stromal cells. The gene expression profiles of MM cells after their co-culture with stromal cells were compared with the profiles of MM cells cultured alone, according to previously described protocols for total RNA extraction and purification; cDNA synthesis; production of biotin-labeled cRNA; hybridization of cRNA with U133plus2.0 Affymetrix gene chips; and scanning of image output files. Scanned image output files were analyzed using DNA-Chip Analyzer (dChip) (www.dchip.org), including conversion to DCP files, normalization and modeling, and averaging of duplicate chips according to standard parameters recommended by the software. For each cell line, the gene expression profile in the presence of stomal cells was compared to the profile of the same cell line cultured in the absence of stromal cells. Technical replicates for each condition were analyzed (total of 12 gene expression profiles).

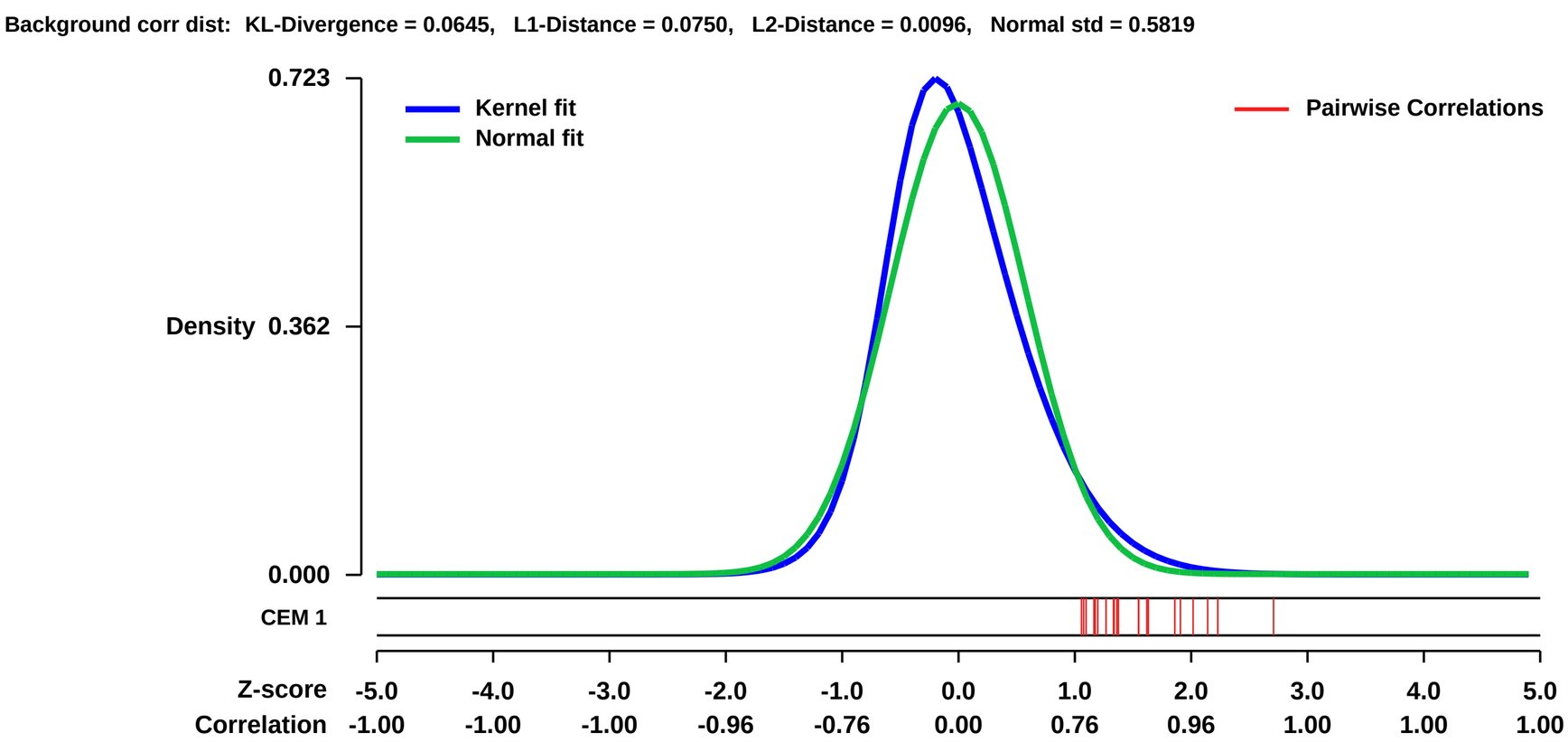

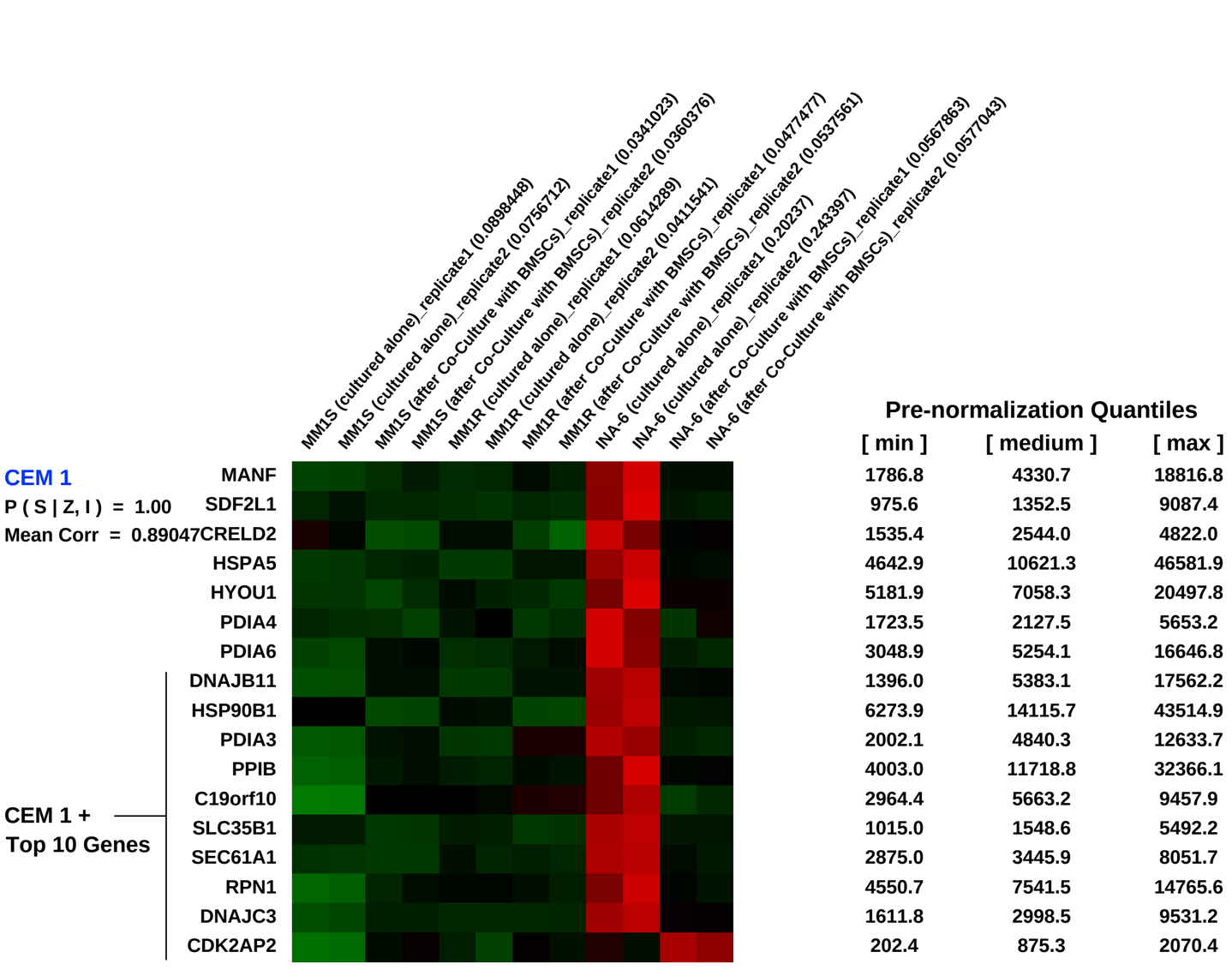

GEO Series "GSE55604" Expression Profiles

Num of samples in this series: 6

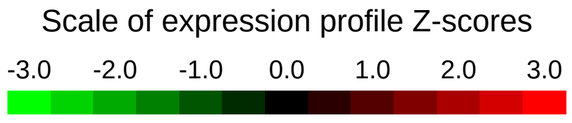

GEO Link:	http://www.ncbi.nlm.nih.gov/geo/query/acc.cgi?acc=GSE55604
Status:	Public on Apr 09 2014
Title:	A novel EMT-selective small molecule induces ER stress
Organism:	Homo sapiens
Experiment type:	Expression profiling by array
Platform:	GPL570
Pubmed ID:	24705811
Summary & Design:	**Summary:** Carcinoma cells can acquire key malignant traits by reprogramming their differentiation state via an epithelial-to-mesenchymal transition (EMT). Cancer cells that undergo EMT become invasive and resist a wide range of therapies including most chemotherapy drugs and radiation. Such cells are also able to efficiently seed primary and metastatic tumors, making them functionally indistinguishable from tumor-initiating or cancer stem-like cells (TICs or CSCs). Therefore, there is significant interest in finding vulnerabilities of cancer cells that have undergone EMT. A potent EMT-selective small molecule was discovered through a large-scale chemical screen. We used microarray analysis to understand the biological effects of this compound. **Overall design:** HMLE_ctrl (human MECs, infected with a pBabe-shGFP retrovirus) and HMLE_Twist (human MECs, infected with a pBabe-Twist retrovirus) cells were treated with solvent control (DMSO), 5 ´µM or 10 ´µM of Cmp302 for 6 hours. Microarray analysis was performed to profile global gene expression.

Background corr dist: KL-Divergence = 0.0178, L1-Distance = 0.0199, L2-Distance = 0.0004, Normal std = 0.7888

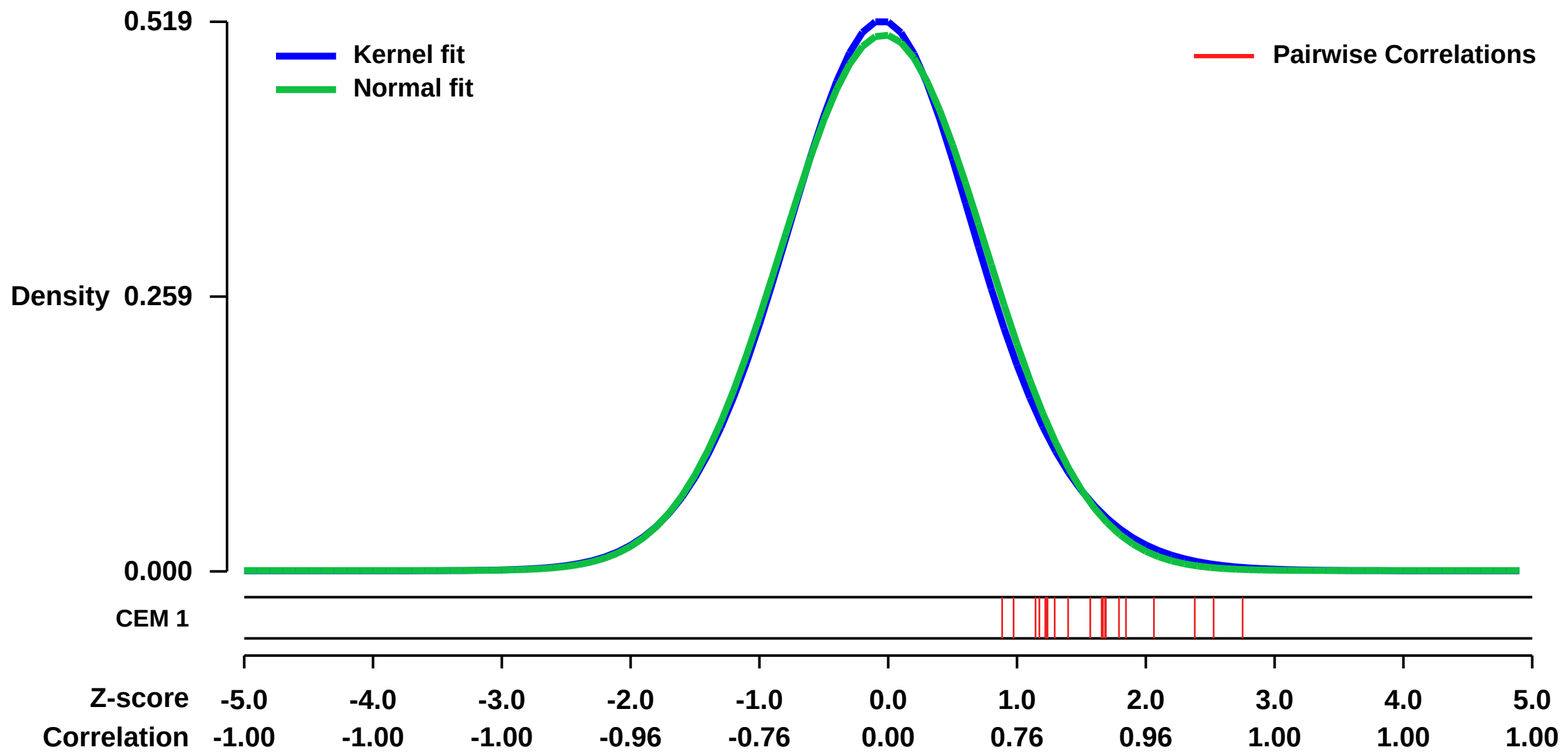

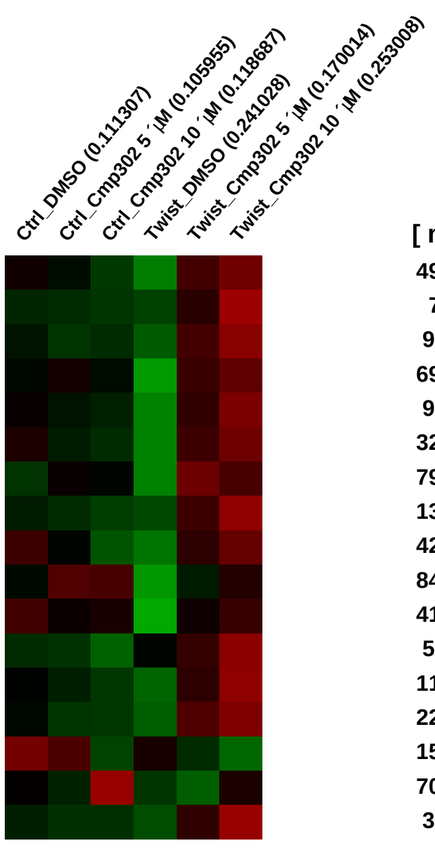

Pre-normalization Quantiles

		[min]	[medium]	[max]
CEM 1	MANF	4977.4	10152.2	13595.8
P (S | Z, I) = 1.00	SDF2L1	75.1	261.3	1542.3
Mean Corr = 0.88983	CRELD2	930.1	1858.0	3850.6
	HSPA5	6990.5	12588.3	15085.5
	HYOU1	930.1	2796.7	4362.3
	PDIA4	3261.2	6886.3	8785.3
	PDIA6	7919.5	8901.2	9618.8
CEM 1 + Top 10 Genes	DNAJB11	1352.3	2485.8	6892.8
	HSP90B1	4214.6	5601.7	6084.3
	PDIA3	8429.2	11432.7	12159.5
	PPIB	4185.5	7354.3	8020.7
	C19orf10	528.0	832.4	1305.9
	SLC35B1	1113.7	2119.5	3617.8
	SEC61A1	2227.5	3491.2	5408.0
	RPN1	1521.1	1912.4	2209.5
	DNAJC3	7041.3	7747.5	8806.7
	CDK2AP2	326.6	604.5	1699.5
Null module	ARID5B			
	XBP1			
	HNRNPAB			
	SGK1			
	HSPB1			
	DDIT4			
	ARL4D			
	SAP30			
	KIAA0408			
	GPR17			
	HSPH1			
	DNASE1L2			
	SLC5A3			
	GNAS			
	GPR3			
	TNFRSF25			
	TM6SF2			
	MKKS			
	PLEKHF1			
	ZMYM1			
	DOK3			
	FGF20			
	SLC39A2			
	KCNIP2			
	ERRFI1			
	DEDD2			
	CCDC117			
	USP31			
	AHSA2			
	CYS1			
	CNIH2			
	BANP			
	CHORDC1			
	P4HA1			

GEO Series "GSE23103" Expression Profiles

Num of samples in this series: 6

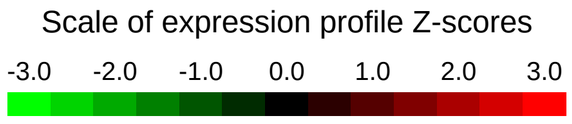

GEO Link:	http://www.ncbi.nlm.nih.gov/geo/query/acc.cgi?acc=GSE23103
Status:	Public on Jul 28 2010
Title:	HeLa SCY1-like 1 esiRNA knockdown
Organism:	Homo sapiens
Experiment type:	Expression profiling by array
Platform:	GPL570
Pubmed ID:	
Summary & Design:	**Summary:** Array-based characterisation of SCY1-like 1 (NM_020680.3) esiRNA knockdown **Overall design:** 3 controls vs. 3 target knock downs

Background corr dist: KL-Divergence = 0.0117, L1-Distance = 0.0111, L2-Distance = 0.0001, Normal std = 0.8309

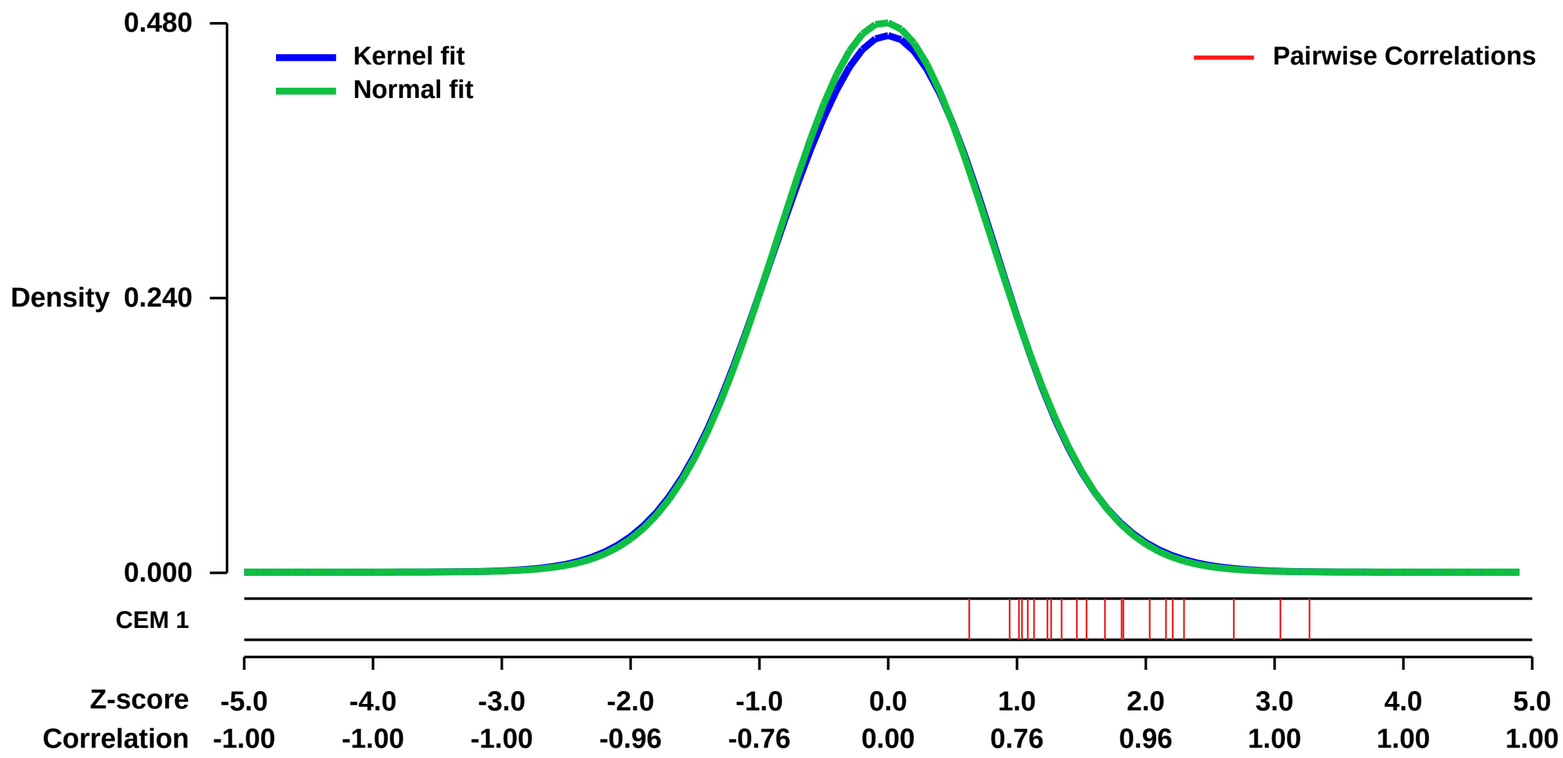

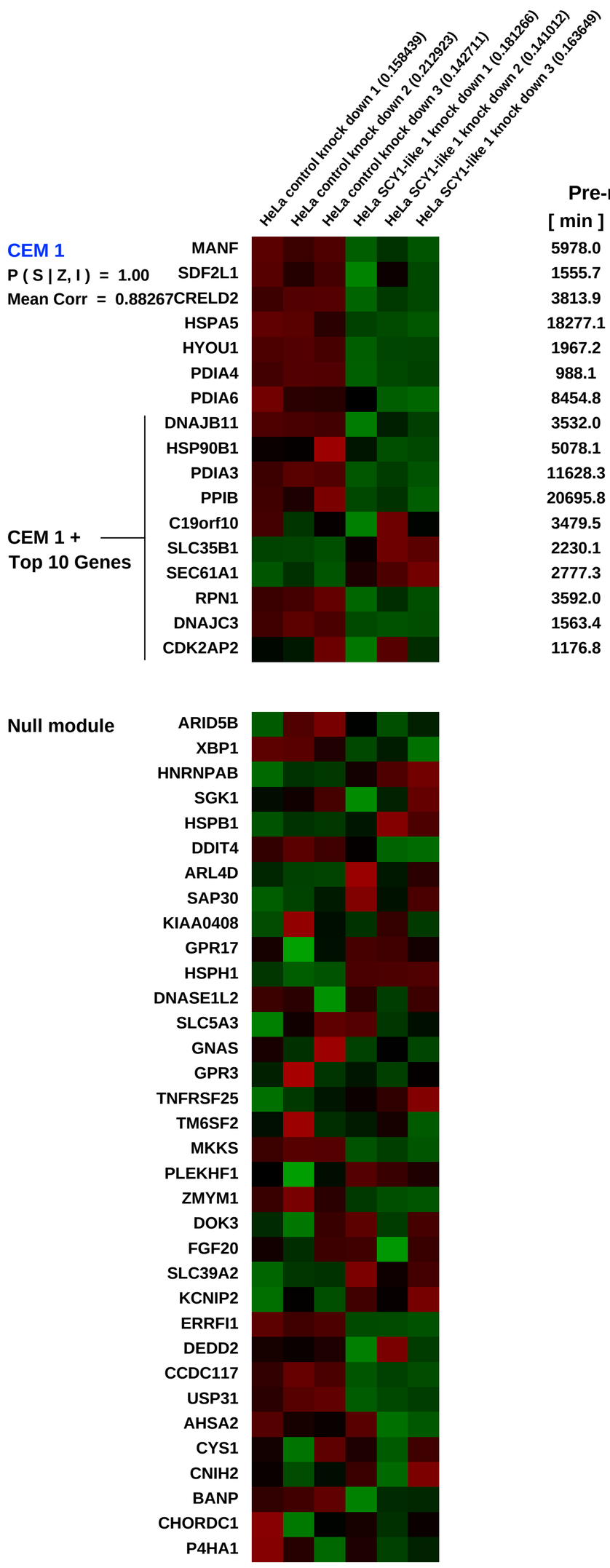

GEO Series "GSE22589" Expression Profiles

Num of samples in this series: 8

Scale of expression profile Z-scores

-3.0 -2.0 -1.0 0.0 1.0 2.0 3.0

GEO Link:	http://www.ncbi.nlm.nih.gov/geo/query/acc.cgi?acc=GSE22589
Status:	Public on Sep 09 2010
Title:	A cryptic sensor for HIV-1 activates antiviral innate immunity in dendritic cells
Organism:	Homo sapiens
Experiment type:	Expression profiling by array
Platform:	GPL570
Pubmed ID:	20829794
Summary & Design:	**Summary:** Dendritic cells (DC) serve a key function in host defense, linking innate detection of microbes to the activation of pathogen-specific adaptive immune responses. Whether there is cell-intrinsic recognition of HIV-1 by host innate pattern-recognition receptors and subsequent coupling to antiviral T cell responses is not yet known. DC are largely resistant to infection with HIV-1, but facilitate infection of co-cultured T-helper cells through a process of trans-enhancement. We show here that, when DC resistance to infection is circumvented, HIV-1 induces DC maturation, an antiviral type I interferon response and activation of T cells. This innate response is dependent on the interaction of newly-synthesized HIV-1 capsid (CA) with cellular cyclophilin A (CypA) and the subsequent activation of the transcription factor IRF3. Because the peptidyl-prolyl isomerase CypA also interacts with CA to promote HIV-1 infectivity, our results suggest that CA conformation has evolved under opposing selective pressures for infectivity versus furtiveness. Thus, a cell intrinsic sensor for HIV-1 exists in DC and mediates an antiviral immune response, but it is not typically engaged due to absence of DC infection. The virulence of HIV-1 may be related to evasion of this response, whose manipulation may be necessary to generate an effective HIV-1 vaccine. **Overall design:** We analyzed the gene expression profiles of uninfected human monocyte-derived dendritic cells (MDDCs) and MDDCs infected with an envelope-defective GFP-encoding VSV-G-pseudotyped HIV-1 vector (HIVGFP(G)) and with VSV-G pseudotyped virus-like particles derived from SIVmac to deliver Vpx (SIVVLP(G)), alone or in combination. Cells were infected at day 4 of differentiation and cells were harvested 48 hours later. RNA was extracted with TRIzol. RNA was labeled and hybridized to Human Genome U133A 2.0 arrays arrays following the Affymetrix protocols. Data were analyzed in R and Bioconductor.

Background corr dist: KL-Divergence = 0.0627, L1-Distance = 0.0287, L2-Distance = 0.0011, Normal std = 0.5332

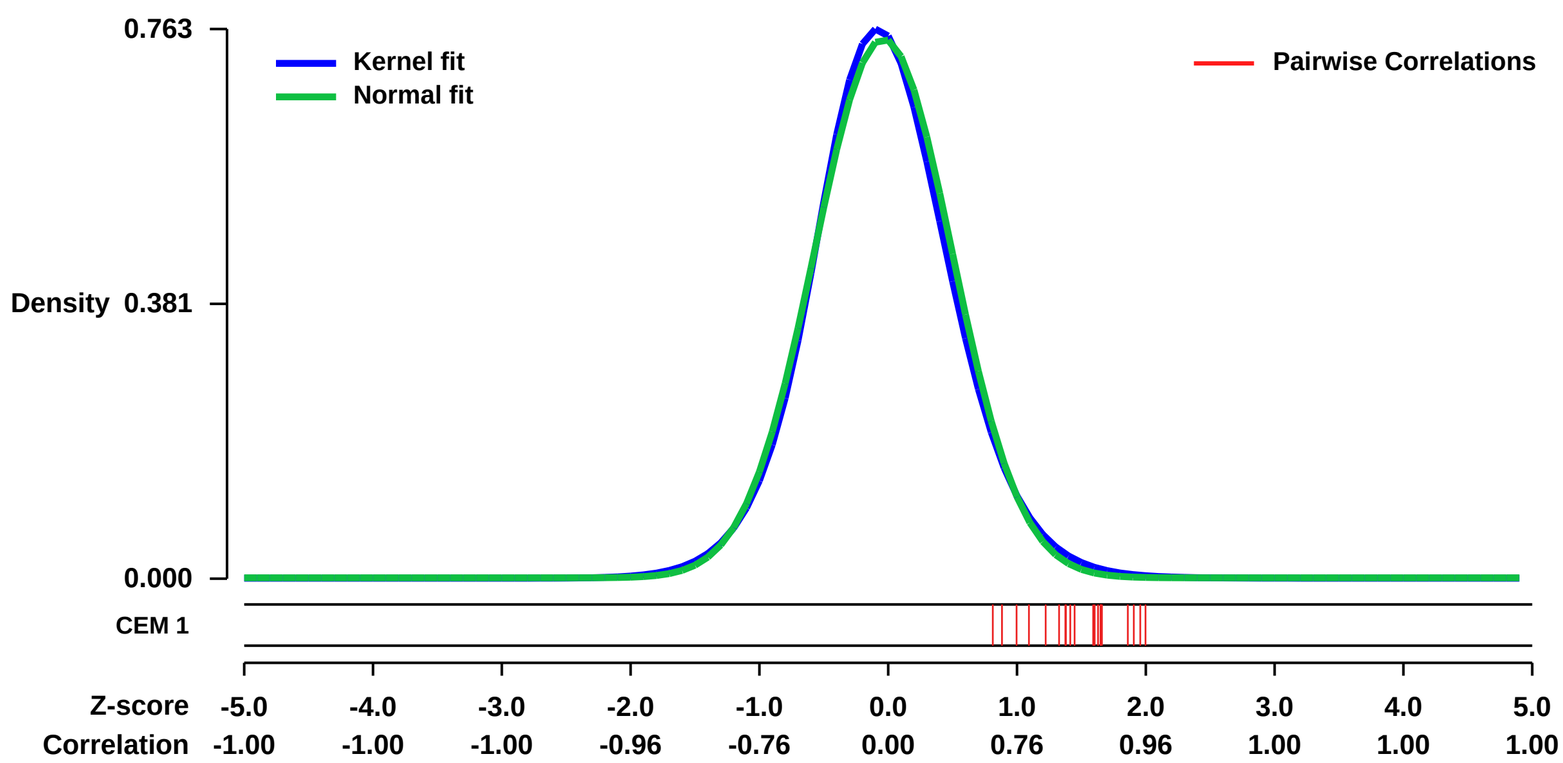

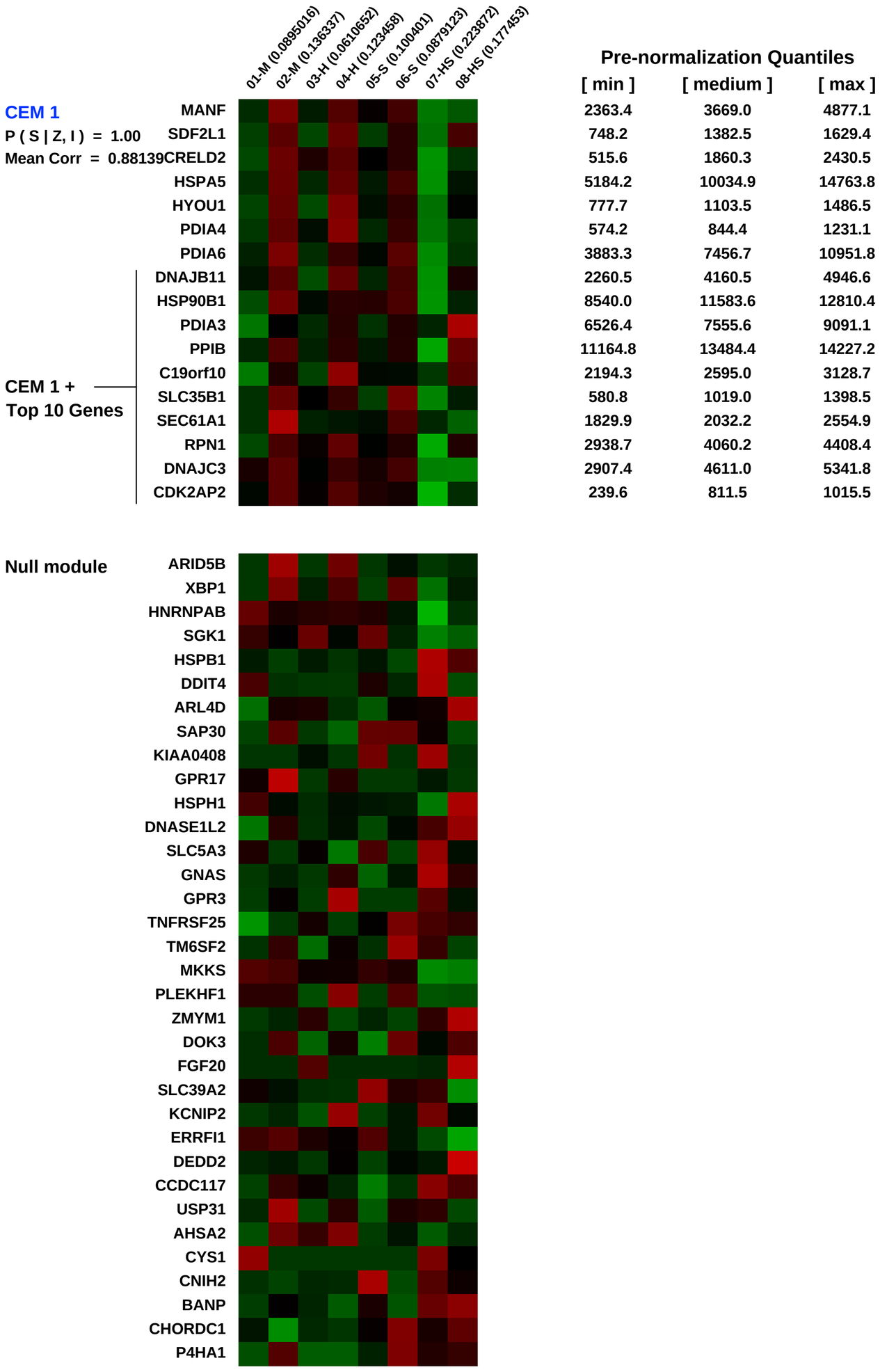

Pre-normalization Quantiles

	[min]	[medium]	[max]
MANF	2363.4	3669.0	4877.1
SDF2L1	748.2	1382.5	1629.4
CRELD2	515.6	1860.3	2430.5
HSPA5	5184.2	10034.9	14763.8
HYOU1	777.7	1103.5	1486.5
PDIA4	574.2	844.4	1231.1
PDIA6	3883.3	7456.7	10951.8
DNAJB11	2260.5	4160.5	4946.6
HSP90B1	8540.0	11583.6	12810.4
PDIA3	6526.4	7555.6	9091.1
PPIB	11164.8	13484.4	14227.2
C19orf10	2194.3	2595.0	3128.7
SLC35B1	580.8	1019.0	1398.5
SEC61A1	1829.9	2032.2	2554.9
RPN1	2938.7	4060.2	4408.4
DNAJC3	2907.4	4611.0	5341.8
CDK2AP2	239.6	811.5	1015.5

GEO Series "GSE38697" Expression Profiles

Num of samples in this series: 8

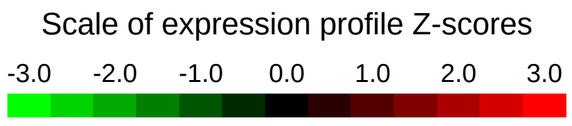

GEO Link:	http://www.ncbi.nlm.nih.gov/geo/query/acc.cgi?acc=GSE38697
Status:	Public on Jun 14 2012
Title:	Gene expression in human germinal center light zone and dark zone B cells
Organism:	Homo sapiens
Experiment type:	Expression profiling by array
Platform:	GPL570
Pubmed ID:	22740445
Summary & Design:	**Summary:** Microarrays of gene expression in human germinal center light zone and dark zone B cells sorted according to the expression of cell surface molecules CD83 and CXCR4 We used microarray data to identify genes differentially expressed by B cells in the light and dark zones of germinal centers from human tonsil specimens. **Overall design:** Germinal center B cells (CD19+CD38+IgD-) were sorted from pediatric tonsil discard specimens into light zone (CXCR4hi/CD83lo) and dark zone (CXCR4lo/CD83hi) populations, from which RNA was extracted

Background corr dist: KL-Divergence = 0.0652, L1-Distance = 0.0209, L2-Distance = 0.0005, Normal std = 0.5218

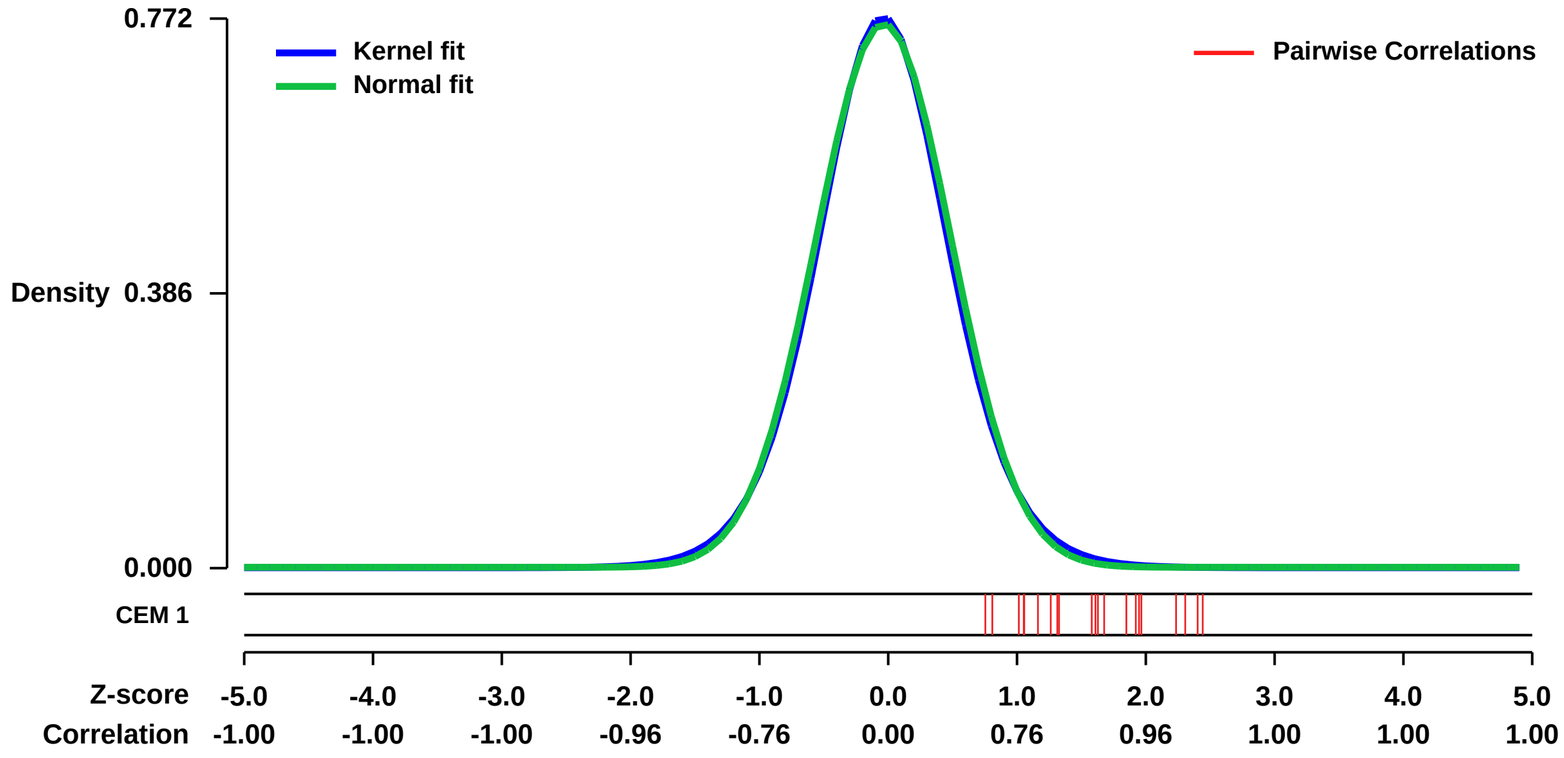

CEM 1
P (S | Z, I) = 1.00
Mean Corr = 0.88120

CEM 1 + Top 10 Genes

Null module

	Pre-normalization Quantiles [min]	[medium]	[max]
MANF	1626.0	2596.5	3239.4
SDF2L1	723.3	1107.1	1552.6
CRELD2	1528.7	2321.2	2794.3
HSPA5	5769.4	10836.5	13028.1
HYOU1	759.2	1488.3	2055.1
PDIA4	822.9	1229.8	2426.1
PDIA6	6451.0	10926.4	13270.5
DNAJB11	2648.2	3912.6	4491.4
HSP90B1	430.6	933.6	1413.0
PDIA3	4397.7	7244.6	8351.5
PPIB	7079.5	10469.6	11887.2
C19orf10	664.3	846.1	1005.1
SLC35B1	855.8	1034.9	1301.3
SEC61A1	1171.1	1466.9	1740.4
RPN1	1586.6	1820.3	1993.0
DNAJC3	904.8	1234.0	1440.2
CDK2AP2	1820.3	2615.1	2902.3
ARID5B			
XBP1			
HNRNPAB			
SGK1			
HSPB1			
DDIT4			
ARL4D			
SAP30			
KIAA0408			
GPR17			
HSPH1			
DNASE1L2			
SLC5A3			
GNAS			
GPR3			
TNFRSF25			
TM6SF2			
MKKS			
PLEKHF1			
ZMYM1			
DOK3			
FGF20			
SLC39A2			
KCNIP2			
ERRFI1			
DEDD2			
CCDC117			
USP31			
AHSA2			
CYS1			
CNIH2			
BANP			
CHORDC1			
P4HA1			

GEO Series "GSE13274" Expression Profiles

Num of samples in this series: 15

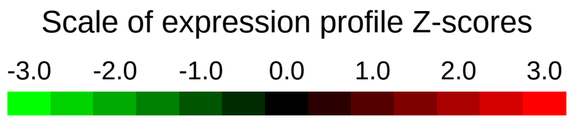

GEO Link:	http://www.ncbi.nlm.nih.gov/geo/query/acc.cgi?acc=GSE13274
Status:	Public on Nov 15 2008
Title:	Ad-HER-wt and Ad-HER2-ki infected HMECs
Organism:	Homo sapiens
Experiment type:	Expression profiling by array
Platform:	GPL570
Pubmed ID:	20179231
Summary & Design:	**Summary:** As an oncogene, use of HER2 vaccines in humans requires the development of HER2 immunotherapies with maximal immunologic potential, but minimal oncologic potential. To address these issues, we developed a recombinant adenoviral vector expressing a mutated HER2 inactivated for kinase function (Ad-HER2-ki). Ad-HER2-ki was highly expressed, but non-phosphorylated and elicited minimal transcription dysregulation in primary cells. In contrast, Ad-HER2-wt elicited a strong oncogenic signature associated with tumorigenesis. **Overall design:** Early Passage Human Mammary Epithelial cells (HMECs) were serum starved for 36hrs. and infected at a MOI of 150 with either Ad-GFP, Ad-HER2-wt, or Ad-HER2-ki vectors. At 18 hpi, RNA was extracted and transcriptomes evaluated by microarray. Five samples were infected per virus treatment, each a completely separate biologic replicate.

Background corr dist: KL-Divergence = 0.1464, L1-Distance = 0.0275, L2-Distance = 0.0012, Normal std = 0.3851

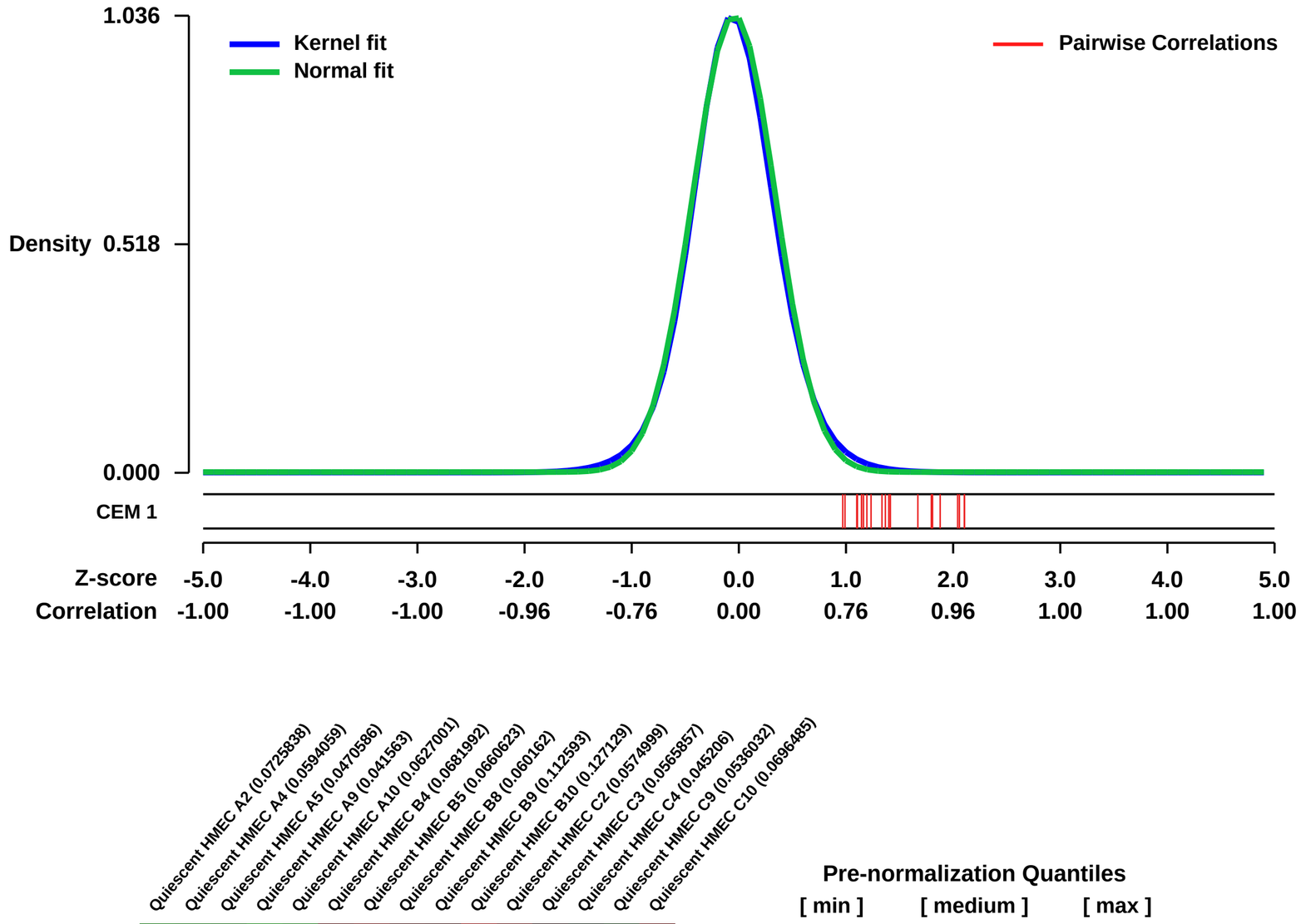

CEM 1
P (S | Z, I) = 1.00
Mean Corr = 0.87713

CEM 1 + Top 10 Genes

Null module

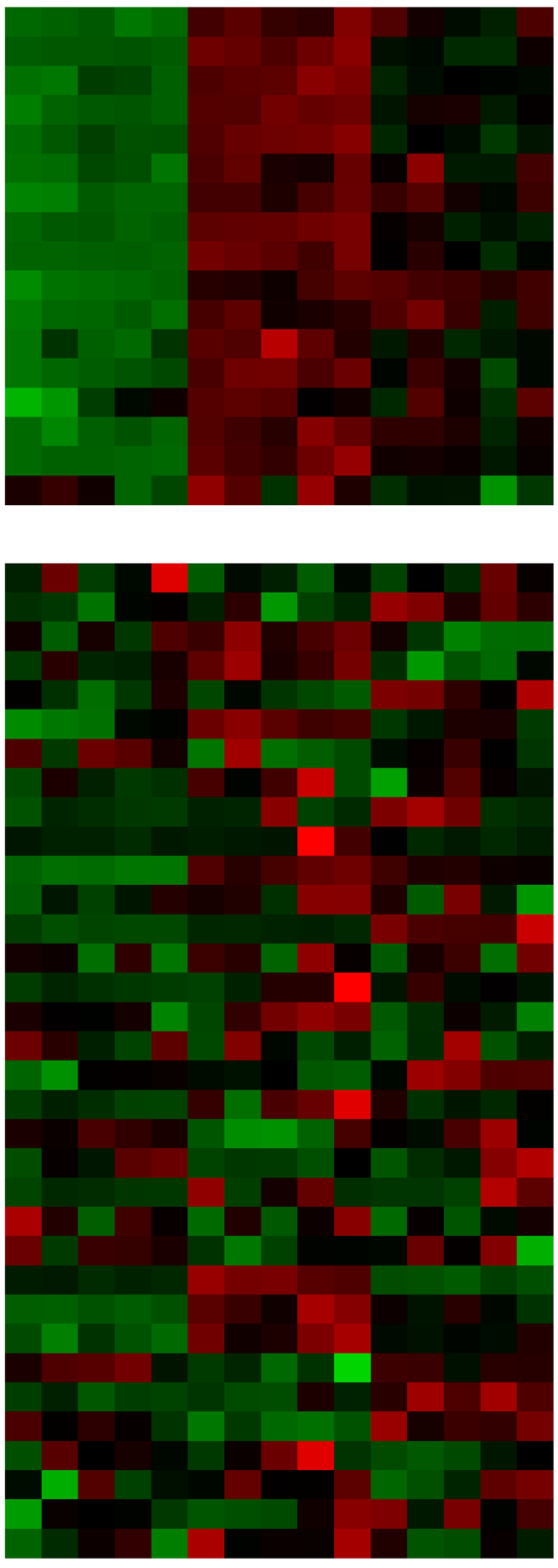

Pre-normalization Quantiles	[min]	[medium]	[max]
MANF	2251.8	5292.2	7640.4
SDF2L1	750.0	1587.8	3254.8
CRELD2	4980.8	8922.1	14030.0
HSPA5	34414.1	77027.9	112970.2
HYOU1	9703.7	16640.6	28986.5
PDIA4	868.1	1684.0	2573.4
PDIA6	5357.6	12389.5	15542.2
DNAJB11	5131.4	10868.3	20082.9
HSP90B1	5313.4	12014.1	20035.3
PDIA3	9402.6	19404.1	22453.1
PPIB	16007.5	28147.8	35488.6
C19orf10	4011.2	5363.7	8245.9
SLC35B1	1875.9	2942.2	4061.8
SEC61A1	14395.5	19655.7	21738.1
RPN1	1488.6	3331.4	4527.6
DNAJC3	2549.6	6310.8	10780.1
CDK2AP2	303.8	471.7	694.2

GEO Series "GSE60771" Expression Profiles

Num of samples in this series: 16

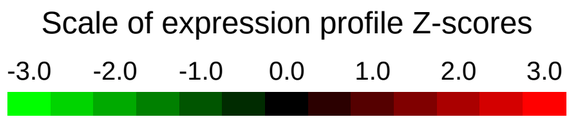

GEO Link:	**http://www.ncbi.nlm.nih.gov/geo/query/acc.cgi?acc=GSE60771**
Status:	**Public on Aug 27 2014**
Title:	**Testing gene expression changes in VCaP upon depletion of the mutated ETS transcription factor ERG**
Organism:	**Homo sapiens**
Experiment type:	**Expression profiling by array**
Platform:	**GPL570**
Pubmed ID:	
Summary & Design:	**Summary:** **VCaP cells expressing inducible shRNAs for either ERG or a non-targeting control were treated with Doxycycline for 1, 3, 7 and 10 days prior to collection** **This experiment is designed to see which genes and pathways are modulated by ERG knockdown** **Overall design:** **VCaP cells stably expressing a Doxycycline (dox)-inducible control nontargeting shRNA (Pak4) or an ERG shRNA (2217) were exposed to 100ng/ml Dox for the noted days.**

Background corr dist: **KL-Divergence = 0.2012, L1-Distance = 0.0385, L2-Distance = 0.0030, Normal std = 0.3327**

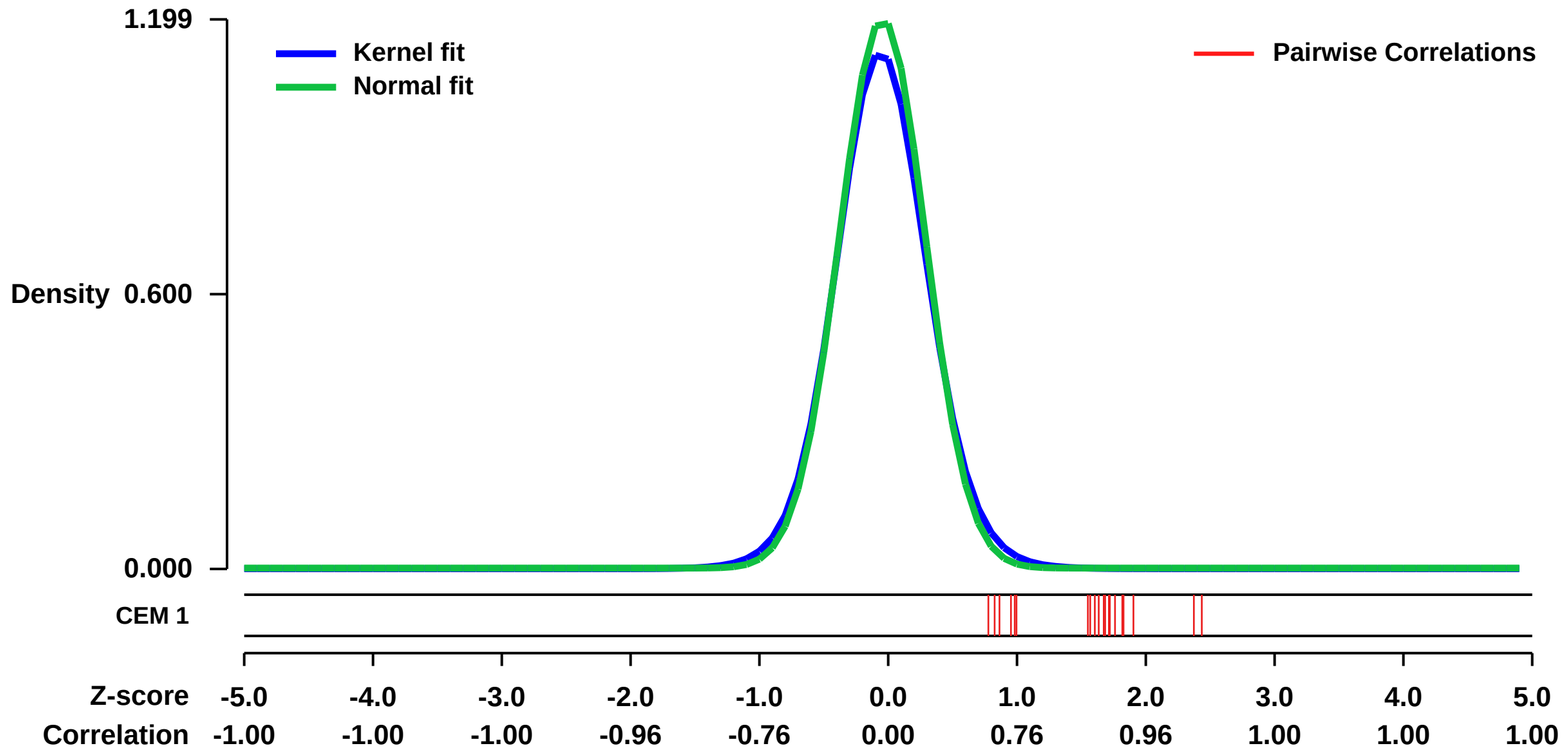

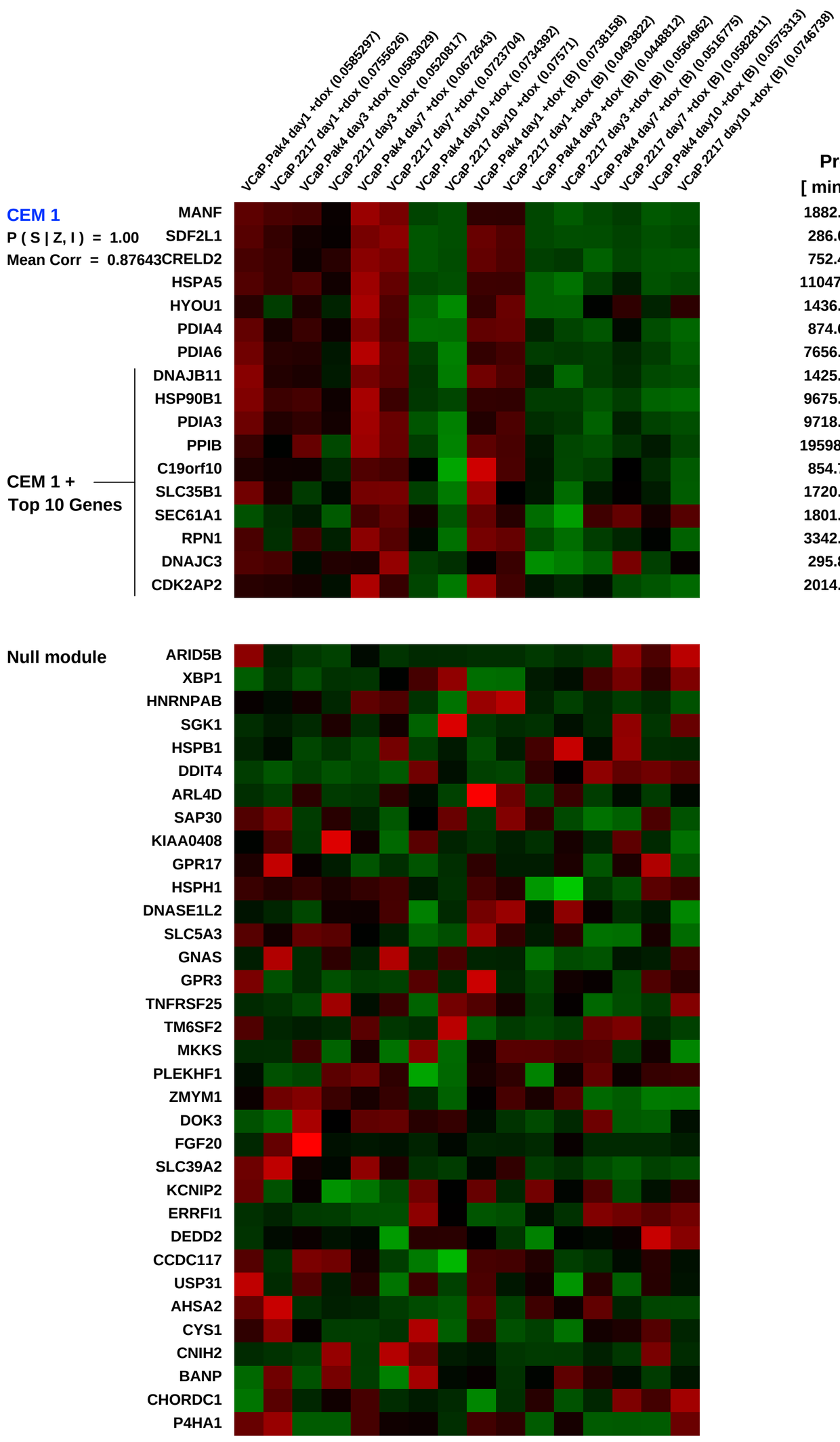

Pre-normalization Quantiles

	[min]	[medium]	[max]
MANF	1882.6	4440.6	8116.2
SDF2L1	286.0	1028.7	2096.2
CRELD2	752.4	1817.7	2983.0
HSPA5	11047.5	20990.5	31705.3
HYOU1	1436.9	2520.8	3412.9
PDIA4	874.6	1809.5	2704.4
PDIA6	7656.6	10799.8	16905.0
DNAJB11	1425.9	2452.7	4160.1
HSP90B1	9675.6	18674.7	30081.7
PDIA3	9718.6	14894.7	19936.8
PPIB	19598.2	24155.2	31850.3
C19orf10	854.7	1747.6	2859.3
SLC35B1	1720.8	2300.1	3140.1
SEC61A1	1801.0	2402.2	2675.6
RPN1	3342.9	4110.7	5229.3
DNAJC3	295.8	508.4	712.9
CDK2AP2	2014.8	2838.4	4329.0

GEO Series "GSE16070" Expression Profiles

Num of samples in this series: 6

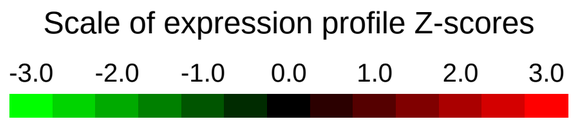

GEO Link:	http://www.ncbi.nlm.nih.gov/geo/query/acc.cgi?acc=GSE16070
Status:	Public on Sep 08 2009
Title:	Networking of differentially expressed genes in human MCF7 breast cancer cells resistant to methotrexate
Organism:	Homo sapiens
Experiment type:	Expression profiling by array
Platform:	GPL570
Pubmed ID:	19732436
Summary & Design:	**Summary:** **A summary of the work associated to these microarrays is the following:** **The need for an integrated view of all data obtained from high-throughput technologies gave rise to network analyses. These are especially useful to rationalize phenomena in terms of how external perturbations propagate through the expression of genes. To address this issue in the case of drug resistance, we constructed Biological Association Networks of genes differentially expressed in cell lines resistant to methotrexate (MTX). Seven cell lines representative of different types of cancer including colon cancer (HT29 and Caco2), breast cancer (MCF7 and MDA-MB-468), pancreatic cancer (MIA PaCa-2), erythroblastic leukemia (K562) and osteosarcoma (Saos-2), were used. The differential expression pattern between sensitive and MTX-resistant cells was determined by microarrays covering the whole human genome and analyzed with the GeneSpring GX software package, v.7.3.1. Genes deregulated in common in the two colon cancer cell lines studied, were subject of Biological Association Networks construction. Dikkopf homolog-1 (DKK1) was a clear node of this network, and functional validations of this target using a siRNA showed a chemosensitization toward MTX. Members of the UDP-glucuronosyltransferase 1A (UGT1A) family formed a network of differentially expressed genes in the two breast cancer cell lines studied. siRNA treatment against UGT1A showed also an increase in MTX sensitivity. Eukaryotic translation elongation factor 1 alpha 1 (EEF1A1) was a gene overexpressed in common among the pancreatic cancer, leukemia and osteosarcoma cell lines, and siRNA treatment against EEF1A1 produced a chemosensitization toward MTX. Biological Association Networks identified DKK1, UGT1As and EEF1A1 as important gene nodes in MTX-resistance. Treatments using iRNA technology against these three genes show chemosensitization toward MTX.** **Overall design:** **Two cell lines are compared, which are MCF7 breast cancer cells sensitive to methotrexate and MCF7 cells resistant to 10e-6M methotrexate. Six samples are provided which correspond to tripicates of each cell line. The samples provided were analyzed using the specific software GeneSpring GX.**

Background corr dist: KL-Divergence = 0.0387, L1-Distance = 0.0288, L2-Distance = 0.0010, Normal std = 0.6343

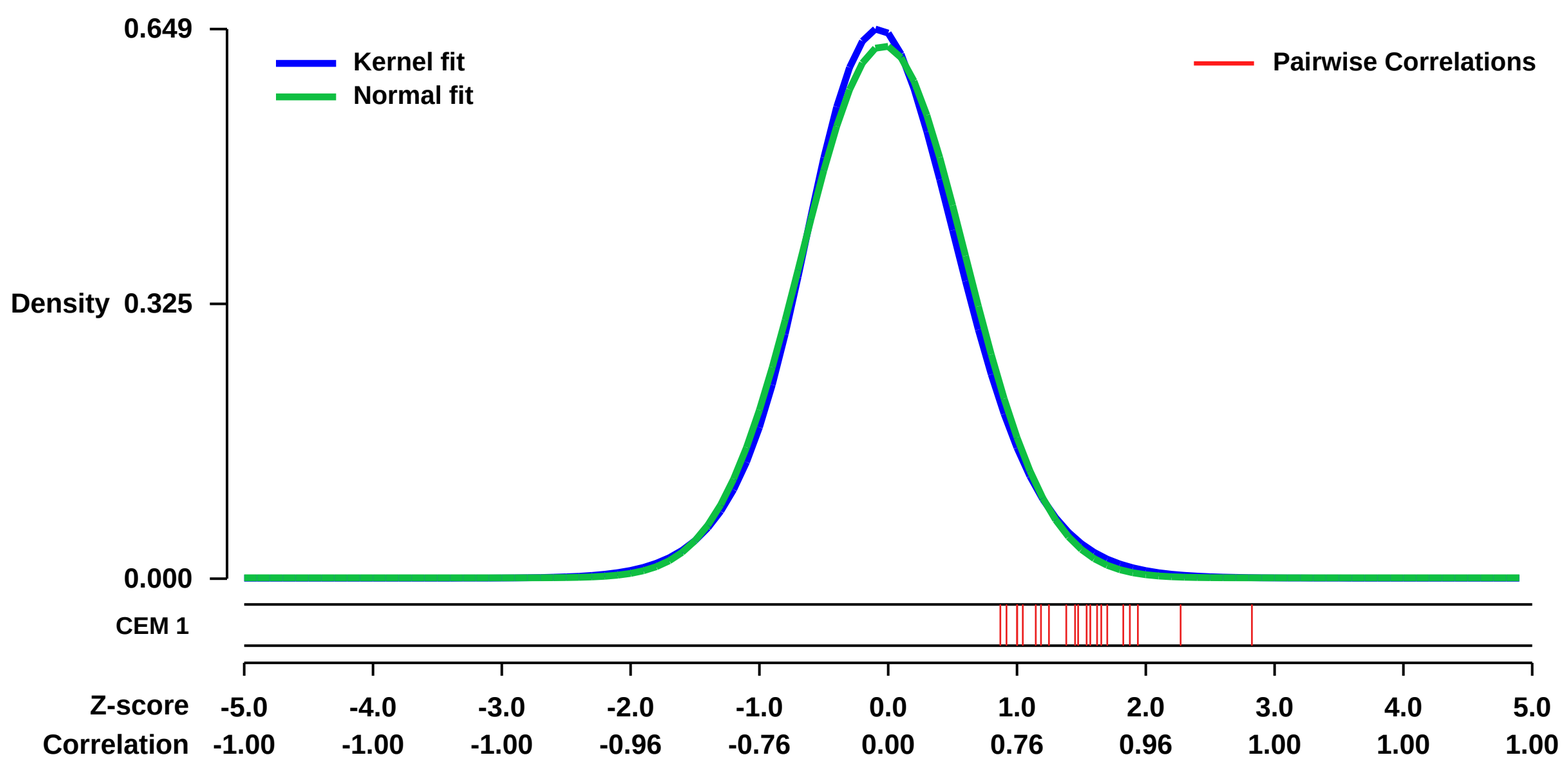

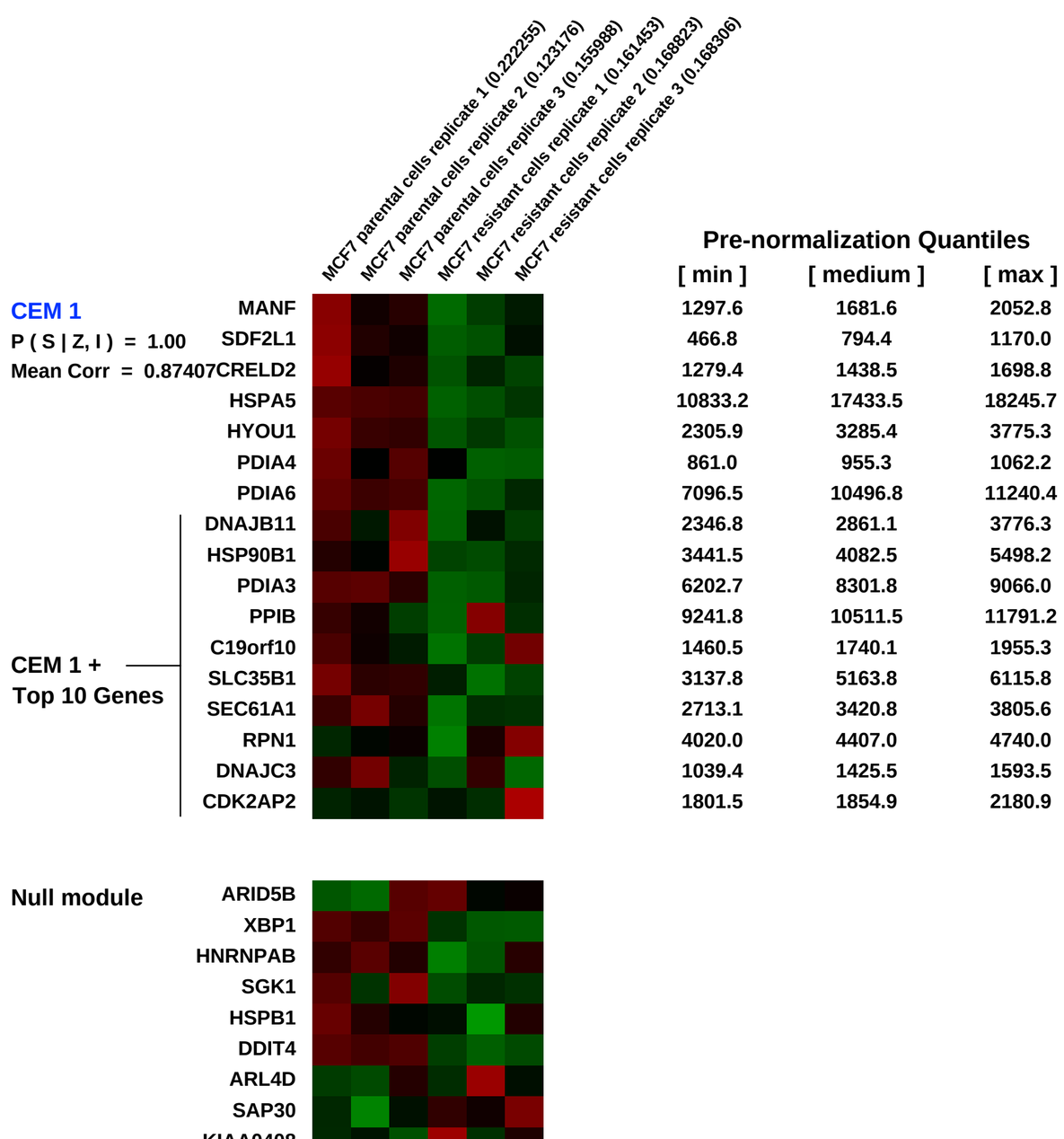

GEO Series "GSE4785" Expression Profiles

Num of samples in this series: 6

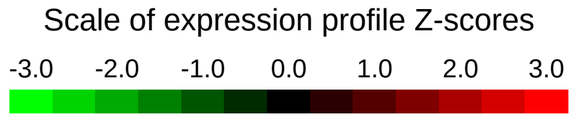

GEO Link:	http://www.ncbi.nlm.nih.gov/geo/query/acc.cgi?acc=GSE4785
Status:	Public on Jul 25 2006
Title:	Nef transfection of Jurkat T cells
Organism:	Homo sapiens
Experiment type:	Expression profiling by array
Platform:	GPL570
Pubmed ID:	16857233
Summary & Design:	**Summary:** Jurkat T cell line was transfected with SIV Nef controlled by an unducible promoter system. Nef was induced by addition of 10 micromolar pronasterone A and gene expression values were determined after 24 hrs. Control Jurkat cells were untransfected and treated with 10 micromolar pronasterone A and gene expressio values were determined after 24 hrs. **Keywords: SIV Nef, Jurkat, pronasterone A** **Overall design:** Controls: Non-transfected. 24 hr.

Background corr dist: KL-Divergence = 0.0357, L1-Distance = 0.0304, L2-Distance = 0.0011, Normal std = 0.6562

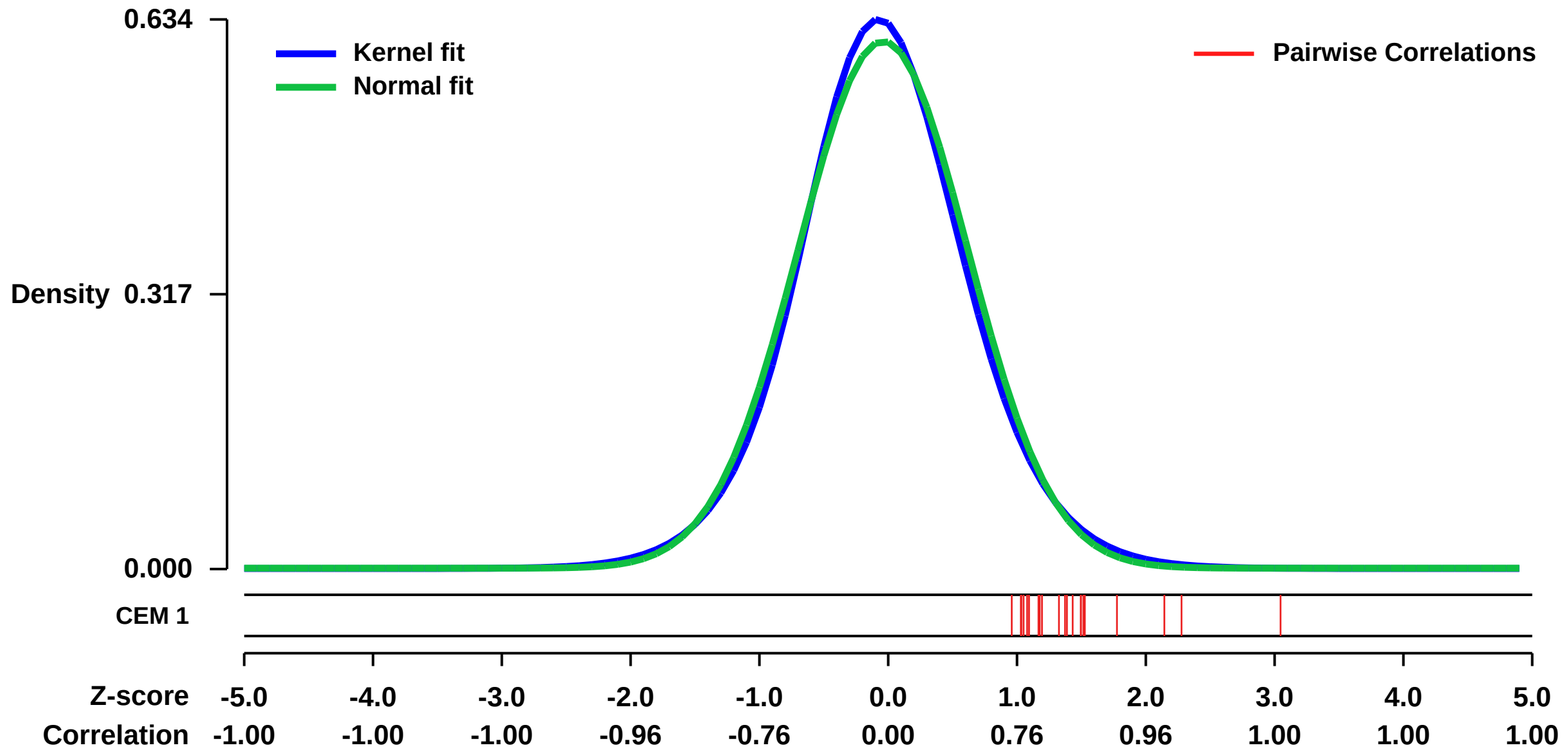

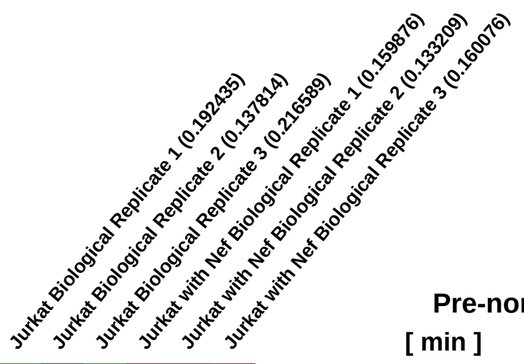

Pre-normalization Quantiles

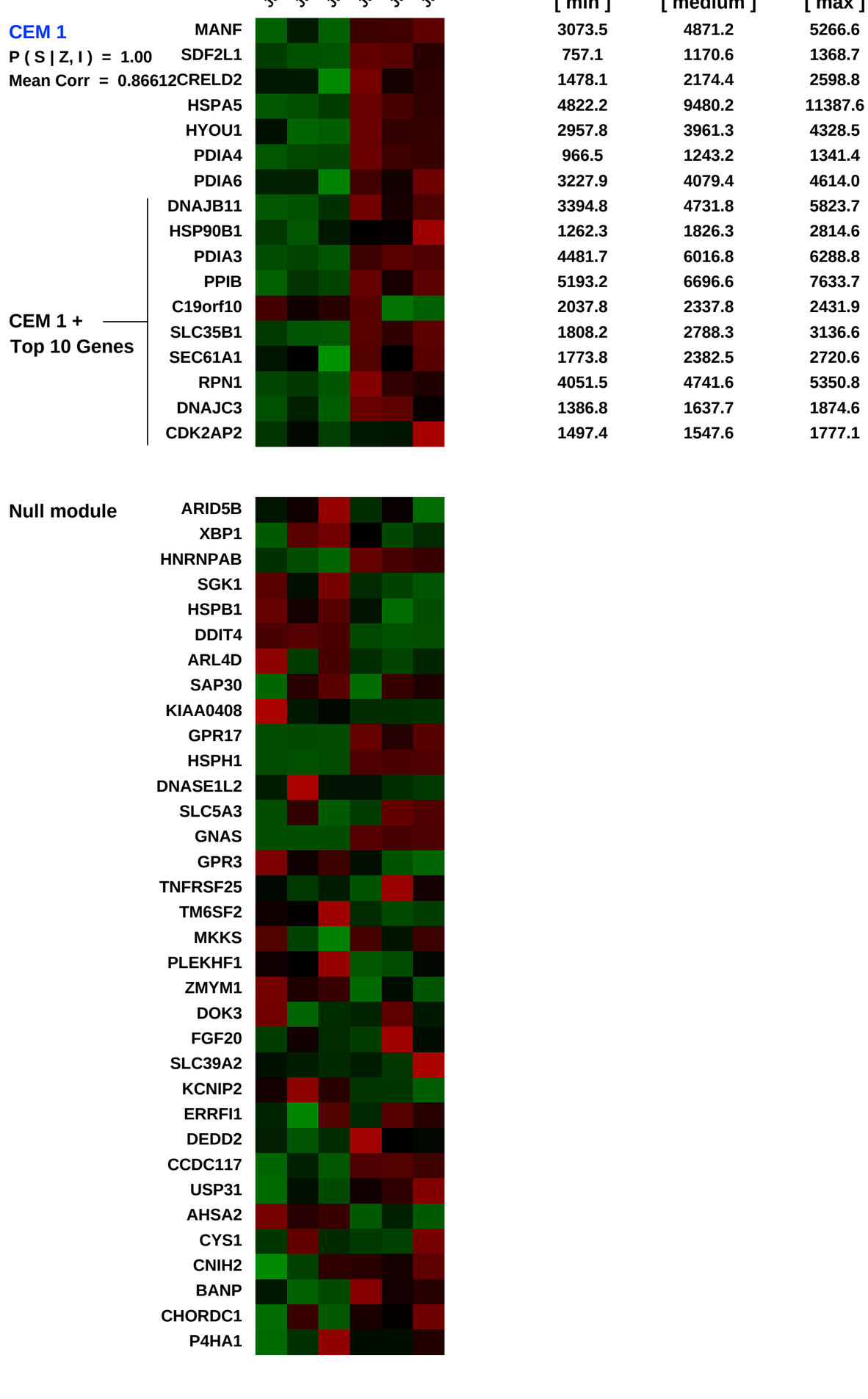

GEO Series "GSE26541" Expression Profiles

Num of samples in this series: 6

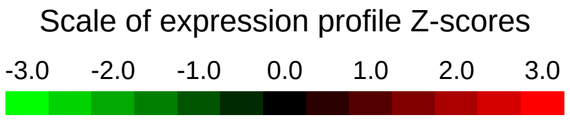

GEO Link:	http://www.ncbi.nlm.nih.gov/geo/query/acc.cgi?acc=GSE26541
Status:	Public on Jan 31 2012
Title:	Gene expression profiles of p53 depleted human mammary epithelial cells with their Ras-infected epithelial and mesenchymal derivatives
Organism:	Homo sapiens
Experiment type:	Expression profiling by array
Platform:	GPL570
Pubmed ID:	
Summary & Design:	**Summary:** The epithelial-mesenchymal transition (EMT) is an embryonic transdiffrentiation program which consists of the conversion of polarized epithelial cells into a motile mesenchymal phenotype. EMT is aberrantly reactivated during tumor progression, promoting metastatic dissemination. Herein, we demonstrate that EMT permissive conditions also favor tumor initiation by minimizing the number of events required for neoplastic transformation. We further demonstrated that even partial commitment of human mammary epithelial cells into an EMT program is sufficient to confer malignant properties, suggesting that the reactivation of embryonic EMT inducers participate to the primary tumor growth long before the initiation of the invasion-metastasis cascade. **Overall design:** Human mammary epithelial cells (HMEC) were sequentially depleted in p53 through RNA interference (shp53), transduced with H-RasG12V and immortalized by hTert. Two different Tert/shp53/Ras cell population emerge that display either an epithelial (Epi) or a mesenchymal (Mes) phenotype. Gene expression profiles of the Tert/shp53 control cells and of tert/shp53/Ras/Epi and Tert/shp53/Ras/Mes were analyzed.

Background corr dist: KL-Divergence = 0.0314, L1-Distance = 0.0513, L2-Distance = 0.0030, Normal std = 0.7621

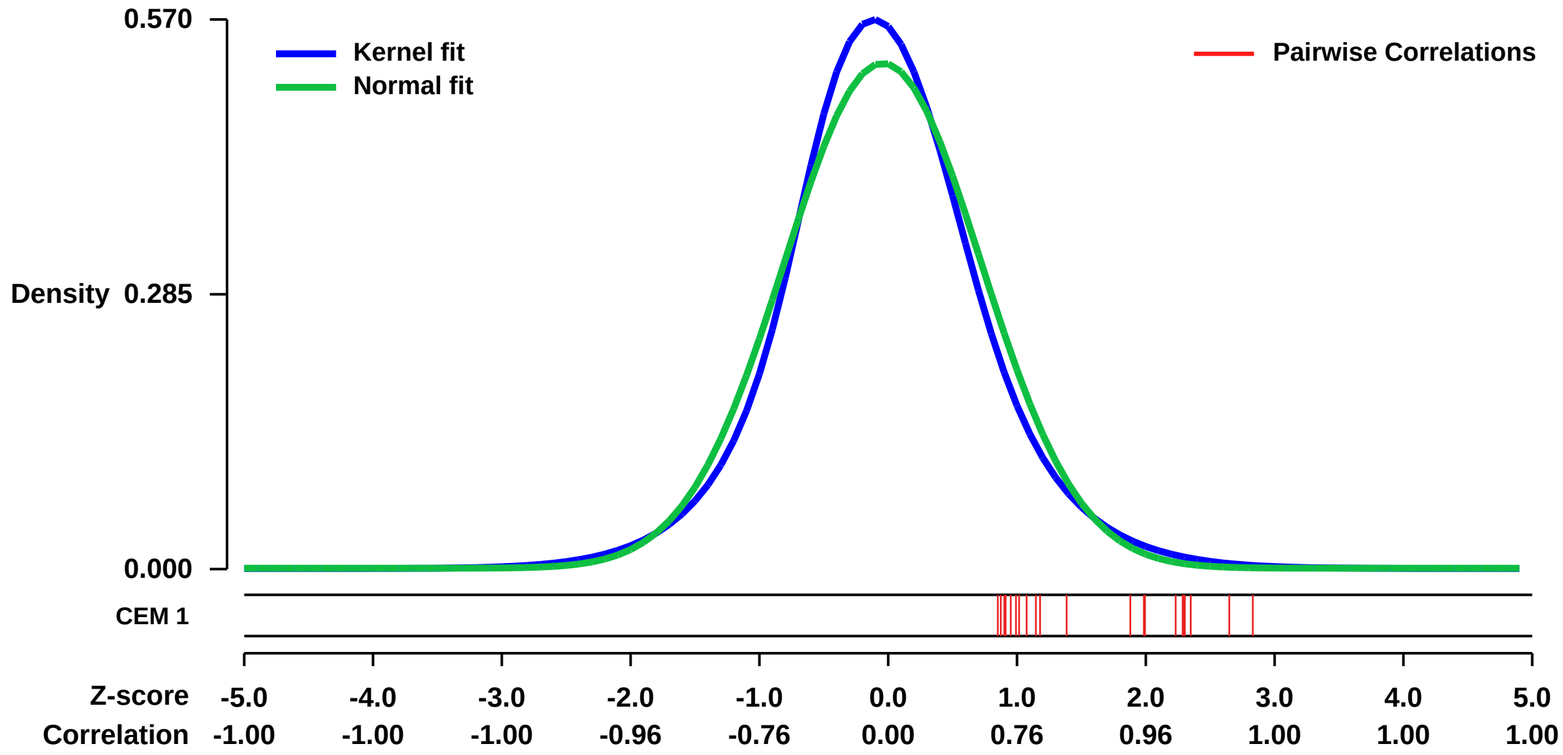

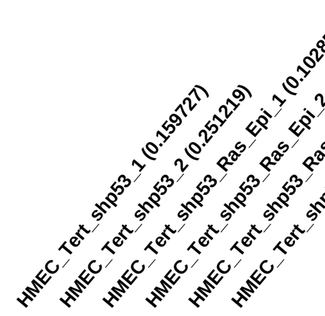

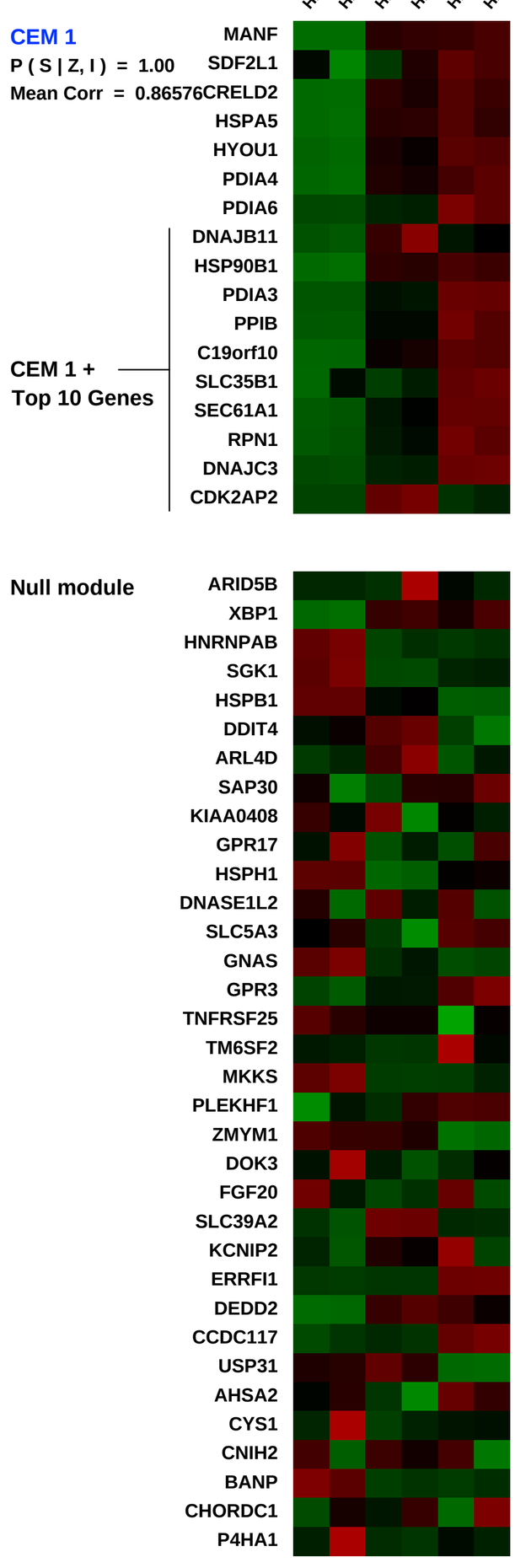

Pre-normalization Quantiles

	[min]	[medium]	[max]
MANF	4413.0	10168.8	11010.9
SDF2L1	788.7	1113.7	1235.9
CRELD2	1423.0	2912.6	3267.8
HSPA5	11949.8	21413.0	23674.0
HYOU1	1010.5	1586.6	1857.1
PDIA4	730.8	1805.1	2238.3
PDIA6	5416.8	6319.1	9560.4
DNAJB11	4279.7	4947.1	5957.2
HSP90B1	2097.3	6440.4	7152.4
PDIA3	11672.2	14341.6	18952.4
PPIB	12306.6	16364.3	22265.5
C19orf10	2756.3	7169.7	9574.3
SLC35B1	1437.7	1602.2	1809.0
SEC61A1	2187.8	3649.2	5322.6
RPN1	4337.1	5869.7	8298.3
DNAJC3	2028.8	2890.1	5347.1
CDK2AP2	835.4	979.7	1653.1
ARID5B			
XBP1			
HNRNPAB			
SGK1			
HSPB1			
DDIT4			
ARL4D			
SAP30			
KIAA0408			
GPR17			
HSPH1			
DNASE1L2			
SLC5A3			
GNAS			
GPR3			
TNFRSF25			
TM6SF2			
MKKS			
PLEKHF1			
ZMYM1			
DOK3			
FGF20			
SLC39A2			
KCNIP2			
ERRFI1			
DEDD2			
CCDC117			
USP31			
AHSA2			
CYS1			
CNIH2			
BANP			
CHORDC1			
P4HA1			

GEO Series "GSE46924" Expression Profiles

Num of samples in this series: 12

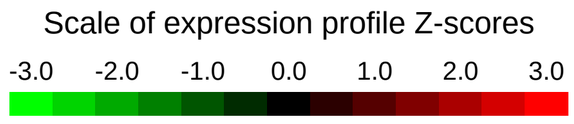

GEO Link:	http://www.ncbi.nlm.nih.gov/geo/query/acc.cgi?acc=GSE46924
Status:	Public on Aug 01 2013
Title:	27-Hydroxycholesterol links cholesterol and breast cancer pathophysiology.
Organism:	Homo sapiens
Experiment type:	Expression profiling by array
Platform:	GPL570
Pubmed ID:	24288332
Summary & Design:	**Summary:** **The cholesterol metabolite and SERM, 27HC, is the signaling molecule that links cholesterol to breast cancer pathophysiology** **Hypercholesterolemia is a risk factor for breast cancer, and patients taking statins demonstrate lower breast cancer incidence and decreased breast cancer recurrence, data that highlights the potential importance of the recent finding that 27-Hydroxycholesterol (27HC), a primary metabolite of cholesterol, acts as a selective estrogen receptor modulator (SERM). The goal of this study was to evaluate the impact of 27HC on breast cancer pathophysiology. Elevation of 27HC in murine models increased tumor growth in an estrogen receptor dependent manner. Importantly, a high cholesterol diet decreased the time to tumor onset and increased tumor growth, and this response required presence of CYP27A1. Within human breast cancer samples, CYP27A1 expression increasesd with grade, in addition to being highly expressed in tumor associated macrophages. Finally 27HC increases metastasis to the lung. The findings herein strongly support a role for 27HC in breast cancer pathophysiology, providing support for the exploration of potential chemopreventative benefits of lower cholesterol diets, and pharmacological inhibitors of HMG-CoA reductase or CYP27A1.** **Overall design:** **MCF-7 cells were treated as indicated in the presence of E2 or vehicle; RNA was isolated and used for preparation of label for 3' expression analysis.**

Background corr dist: **KL-Divergence = 0.0767, L1-Distance = 0.0256, L2-Distance = 0.0008, Normal std = 0.4939**

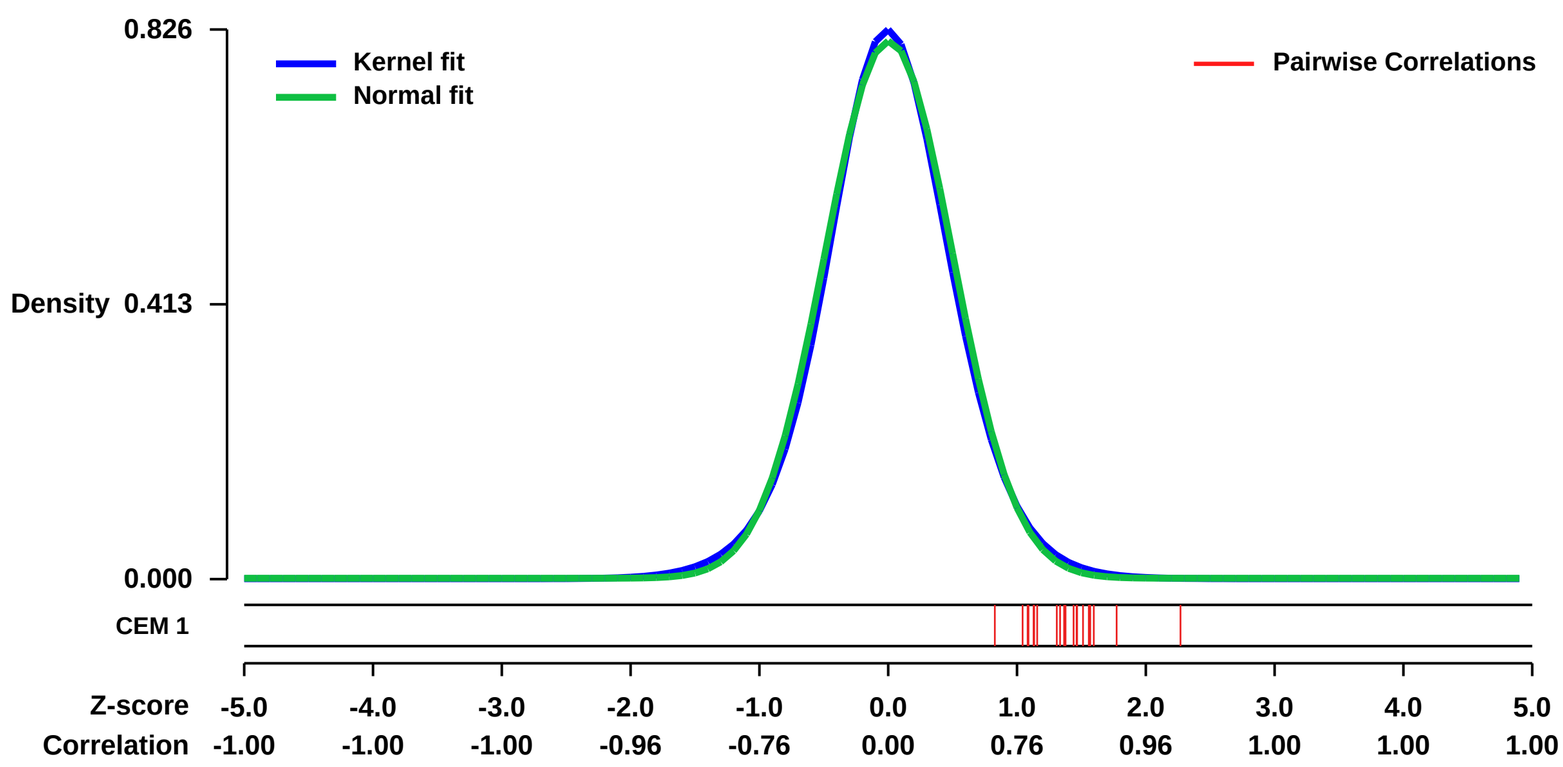

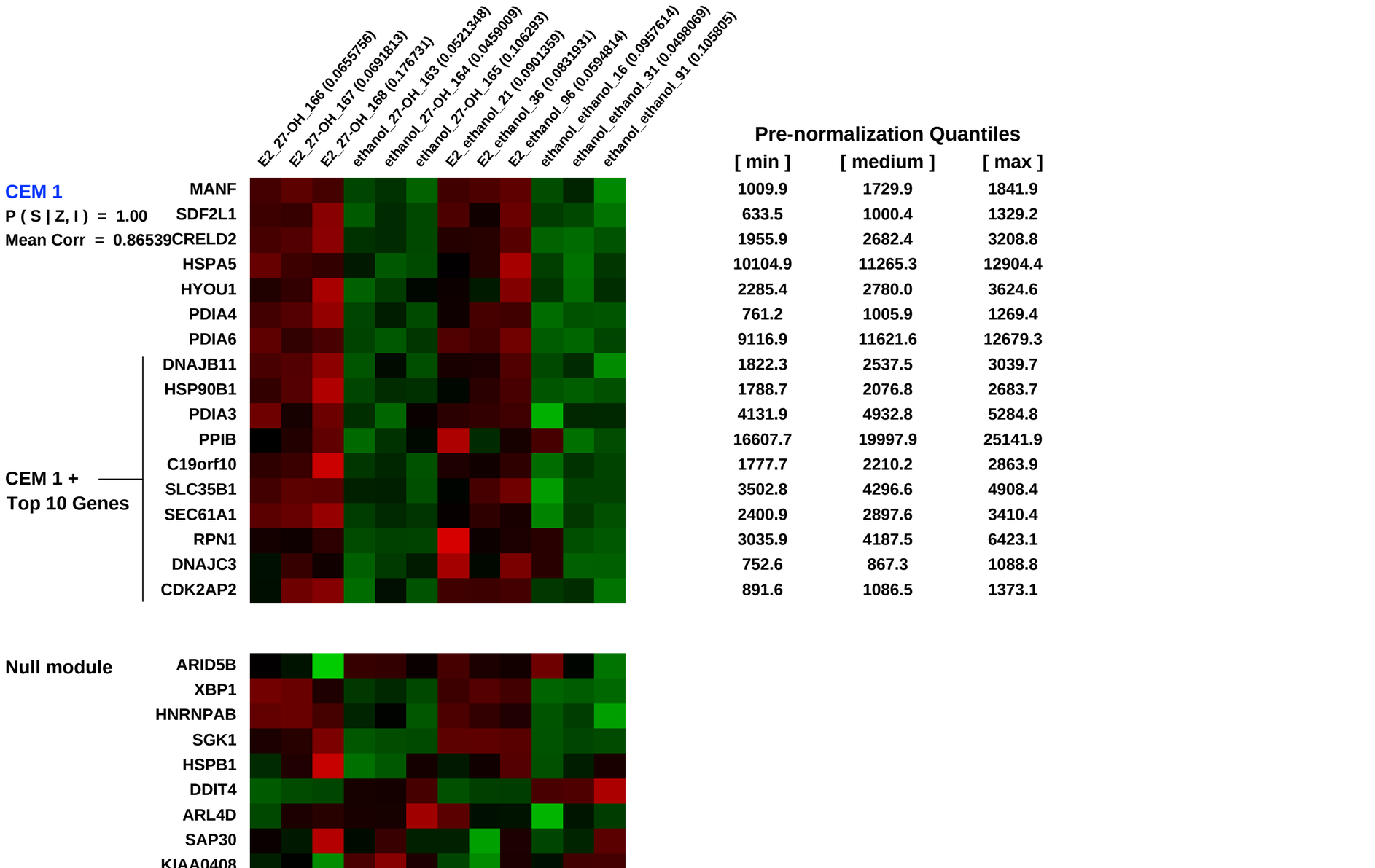

Pre-normalization Quantiles

	[min]	[medium]	[max]
MANF	1009.9	1729.9	1841.9
SDF2L1	633.5	1000.4	1329.2
CRELD2	1955.9	2682.4	3208.8
HSPA5	10104.9	11265.3	12904.4
HYOU1	2285.4	2780.0	3624.6
PDIA4	761.2	1005.9	1269.4
PDIA6	9116.9	11621.6	12679.3
DNAJB11	1822.3	2537.5	3039.7
HSP90B1	1788.7	2076.8	2683.7
PDIA3	4131.9	4932.8	5284.8
PPIB	16607.7	19997.9	25141.9
C19orf10	1777.7	2210.2	2863.9
SLC35B1	3502.8	4296.6	4908.4
SEC61A1	2400.9	2897.6	3410.4
RPN1	3035.9	4187.5	6423.1
DNAJC3	752.6	867.3	1088.8
CDK2AP2	891.6	1086.5	1373.1

GEO Series "GSE6495" Expression Profiles

Num of samples in this series: 6

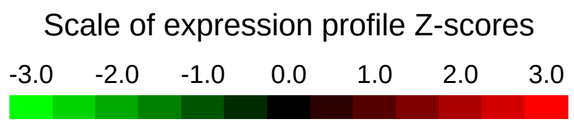

GEO Link:	http://www.ncbi.nlm.nih.gov/geo/query/acc.cgi?acc=GSE6495
Status:	Public on Dec 15 2006
Title:	NOTCH signaling in T-cell acute lymphoblastic leukemia cell lines
Organism:	Homo sapiens
Experiment type:	Expression profiling by array
Platform:	GPL570
Pubmed ID:	17560996
Summary & Design:	**Summary:** In T-cell acute lymphoblastic leukemia (T-ALL) NOTCH 1 receptors are frequently mutated. This leads to aberrantly high Notch signaling, but how this translates into deregulated cell cycle control and the transformed cell type is poorly understood. In this report, we analyze downstream responses resulting from the high level of NOTCH 1 signaling in T-ALL. Notch activity, measured immediately downstream of the NOTCH 1 receptor, is high, but expression of the canonical downstream Notch response genes HES 1 and HEY 2 is low both in primary cells from T-ALL patients and in T-ALL cell lines. This suggests that other immediate Notch downstream genes are activated, and we found that Notch signaling controls the levels of expression of the E3 ubiquitin ligase SKP2 and its target protein p27Kip1. We show that in T-ALL cell lines, recruitment of NOTCH 1 ICD to the SKP2 promoter was accompanied by high SKP2 and low p27Kip1 protein levels were low. In contrast, pharmacologically blocking Notch signaling reversed this picture and led to loss of NOTCH 1 ICD occupancy of the SKP2 promoter, decreased SKP2 and increased p27Kip1 expression. T-ALL cells show a rapid G1-S cell cycle transition, while blocked Notch signaling resulted in G0/G1 cell cycle arrest, also observed by transfection of p27Kip1 or, to a smaller extent, a dominant negative SKP2 allele. Collectively, our data suggest that the aberrantly high Notch signaling in T-ALL maintains SKP2 at a high level and reduces p27Kip1, which leads to more rapid cell cycle progression. **Keywords:** comparative genomic hybridization **Overall design:** Three independent cultures of the MOLT4 cell line before and 48 hours after addition of the gamma-secretase inhibitor DAPT (5 uM).

Background corr dist: KL-Divergence = 0.0495, L1-Distance = 0.0226, L2-Distance = 0.0006, Normal std = 0.5769

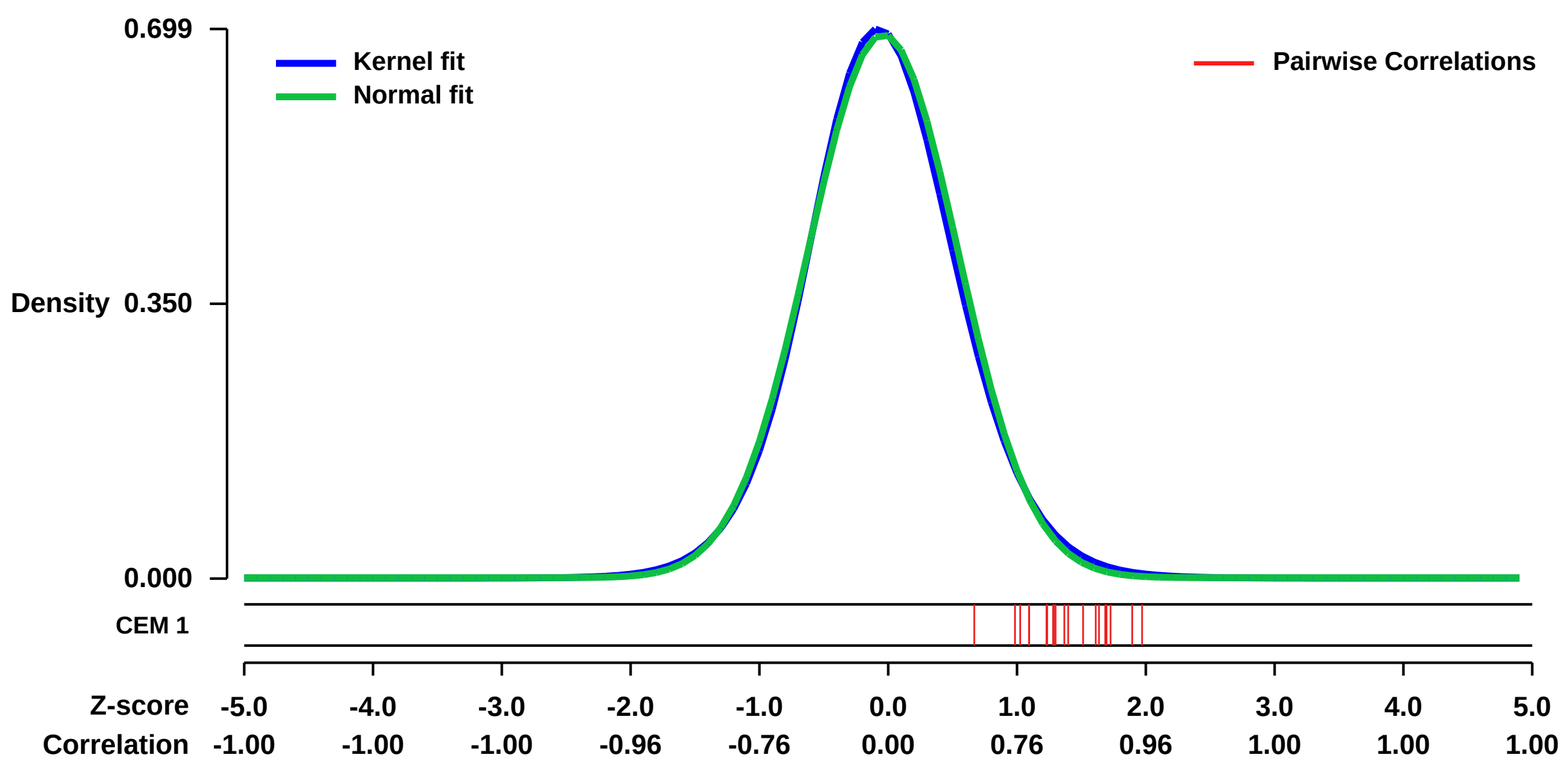

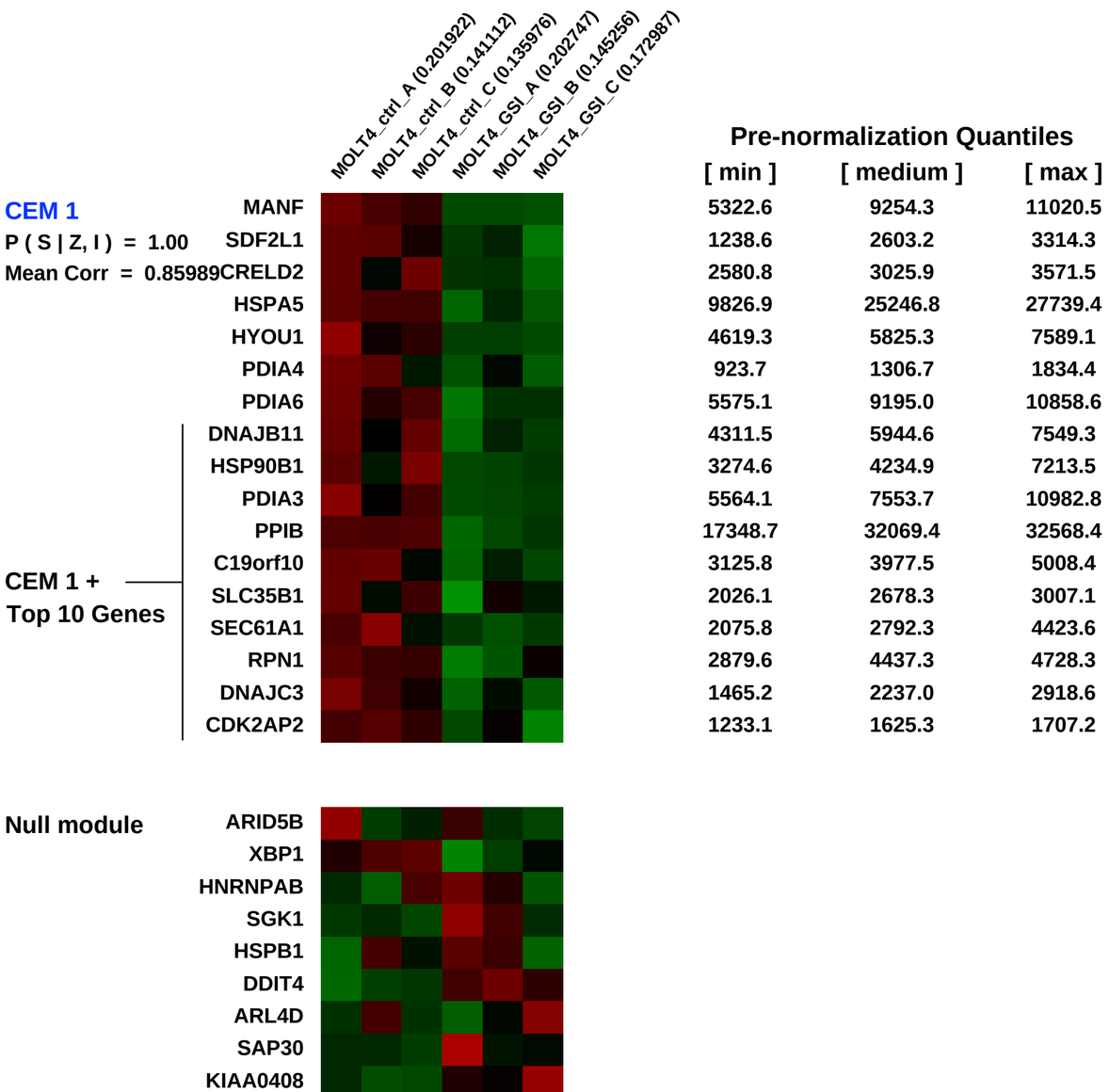

Pre-normalization Quantiles

	[min]	[medium]	[max]
MANF	5322.6	9254.3	11020.5
SDF2L1	1238.6	2603.2	3314.3
CRELD2	2580.8	3025.9	3571.5
HSPA5	9826.9	25246.8	27739.4
HYOU1	4619.3	5825.3	7589.1
PDIA4	923.7	1306.7	1834.4
PDIA6	5575.1	9195.0	10858.6
DNAJB11	4311.5	5944.6	7549.3
HSP90B1	3274.6	4234.9	7213.5
PDIA3	5564.1	7553.7	10982.8
PPIB	17348.7	32069.4	32568.4
C19orf10	3125.8	3977.5	5008.4
SLC35B1	2026.1	2678.3	3007.1
SEC61A1	2075.8	2792.3	4423.6
RPN1	2879.6	4437.3	4728.3
DNAJC3	1465.2	2237.0	2918.6
CDK2AP2	1233.1	1625.3	1707.2

GEO Series "GSE45665" Expression Profiles

Num of samples in this series: 8

Scale of expression profile Z-scores

-3.0 -2.0 -1.0 0.0 1.0 2.0 3.0

GEO Link:	http://www.ncbi.nlm.nih.gov/geo/query/acc.cgi?acc=GSE45665
Status:	Public on Apr 02 2013
Title:	Expression data (U133 Plus 2.0) from fibroblast like synoviocytes from patients with rheumatoid arthritis (RA-FLS) stimulated by DcR3
Organism:	Homo sapiens
Experiment type:	Expression profiling by array
Platform:	GPL570
Pubmed ID:	23912906
Summary & Design:	**Summary:** Decoy receptor 3 (DcR3), a member of the tumor necrosis factor receptor (TNFR) superfamily, competitively binds and inhibits members of the TNF family, including Fas ligand (FasL), LIGHT, and TL1A. DcR3 was recently reported not only to act as a decoy receptor for these TNFRs but also to play a role as a ligand for the pathogenesis of RA. We hypothesized that DcR3 regulates the gene expression in RA-FLS. We used to search for genes in which expression in RA-FLS is regulated by the ligation of DcR3. **Overall design:** RA-FLS were obtained from 4 RA patients (sample1-4). Each sample was incubated with control IgG1 or human DcR3-Fc. Gene expression in RA-FLS stimulated by DcR3-Fc was compared with that of their respective unstimulated controls.

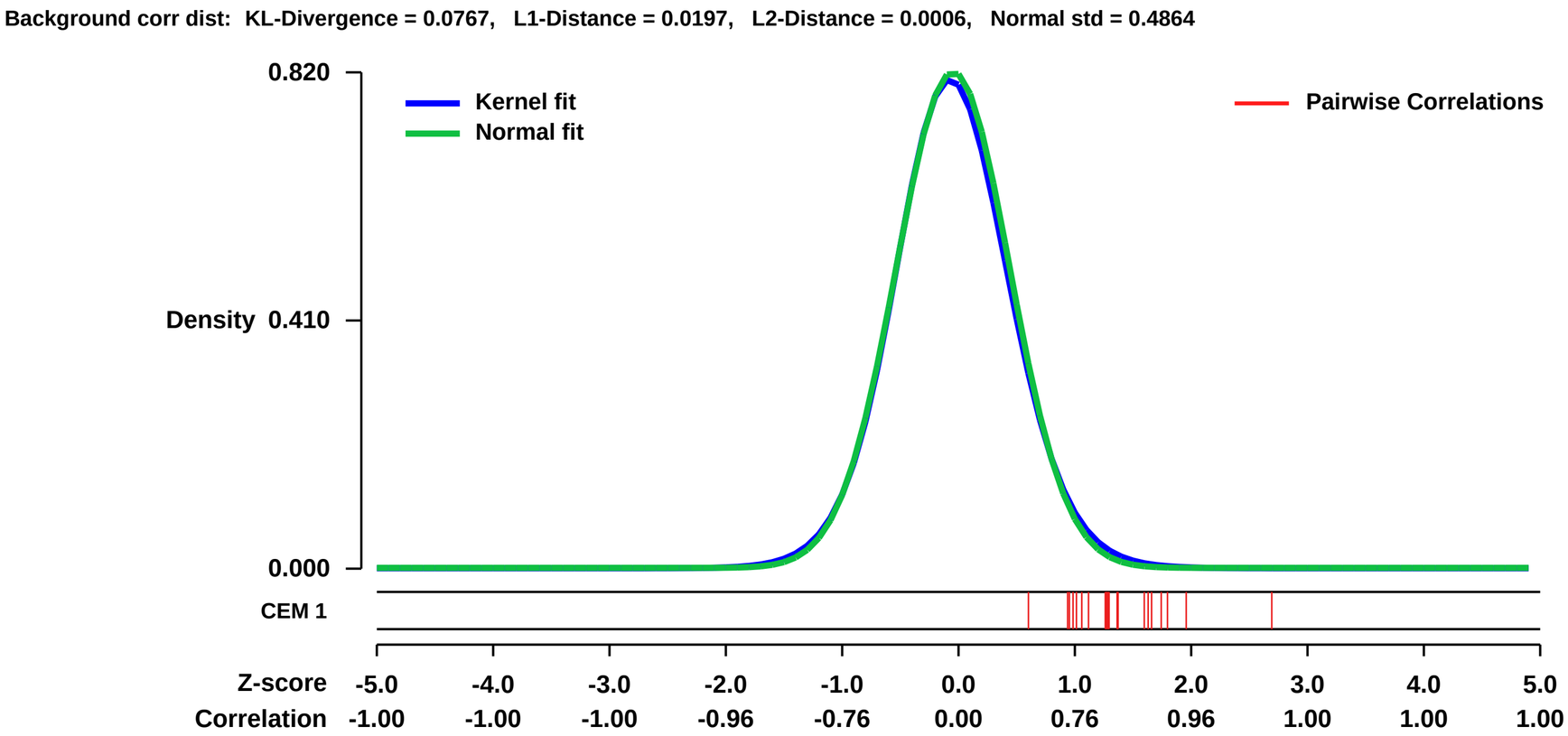

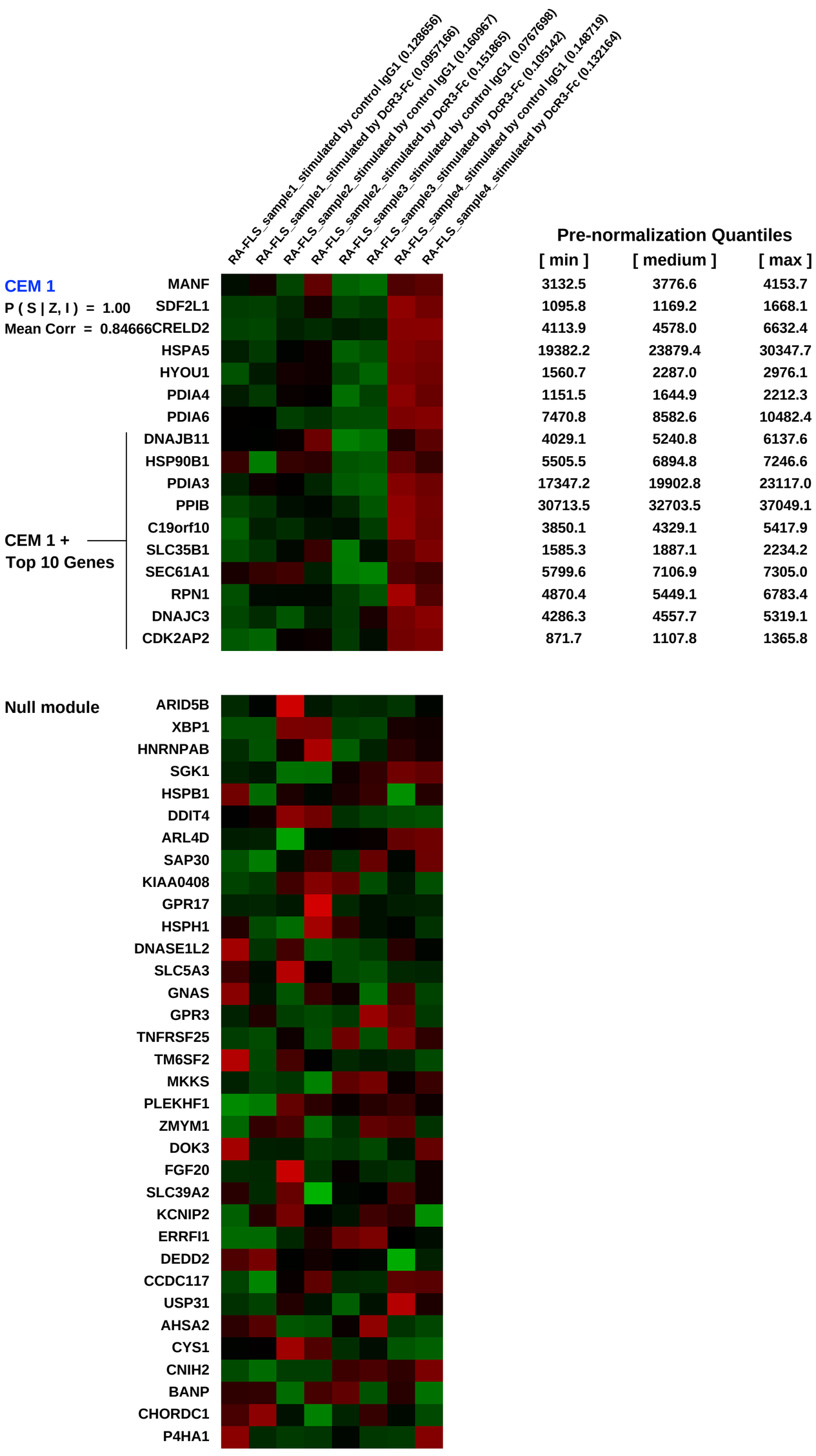

Pre-normalization Quantiles

	[min]	[medium]	[max]
MANF	3132.5	3776.6	4153.7
SDF2L1	1095.8	1169.2	1668.1
CRELD2	4113.9	4578.0	6632.4
HSPA5	19382.2	23879.4	30347.7
HYOU1	1560.7	2287.0	2976.1
PDIA4	1151.5	1644.9	2212.3
PDIA6	7470.8	8582.6	10482.4
DNAJB11	4029.1	5240.8	6137.6
HSP90B1	5505.5	6894.8	7246.6
PDIA3	17347.2	19902.8	23117.0
PPIB	30713.5	32703.5	37049.1
C19orf10	3850.1	4329.1	5417.9
SLC35B1	1585.3	1887.1	2234.2
SEC61A1	5799.6	7106.9	7305.0
RPN1	4870.4	5449.1	6783.4
DNAJC3	4286.3	4557.7	5319.1
CDK2AP2	871.7	1107.8	1365.8

GEO Series "GSE44335" Expression Profiles

Num of samples in this series: 6

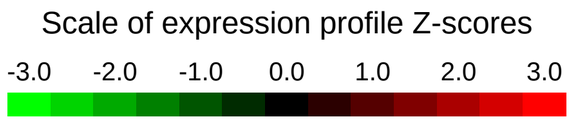

GEO Link:	http://www.ncbi.nlm.nih.gov/geo/query/acc.cgi?acc=GSE44335
Status:	Public on Feb 15 2013
Title:	HMLER cells expressing either FOXC2 or a vector control
Organism:	Homo sapiens
Experiment type:	Expression profiling by array
Platform:	GPL570
Pubmed ID:	23378344
Summary & Design:	**Summary:** We used microarrays to investigate the transcription profile of FOXC2 expression in a human mammary epithelial cell line. **Overall design:** HMLER cells were infected with either a control vector or a retroviral vector expressing FOXC2.

Background corr dist: KL-Divergence = 0.0257, L1-Distance = 0.0639, L2-Distance = 0.0045, Normal std = 0.8701

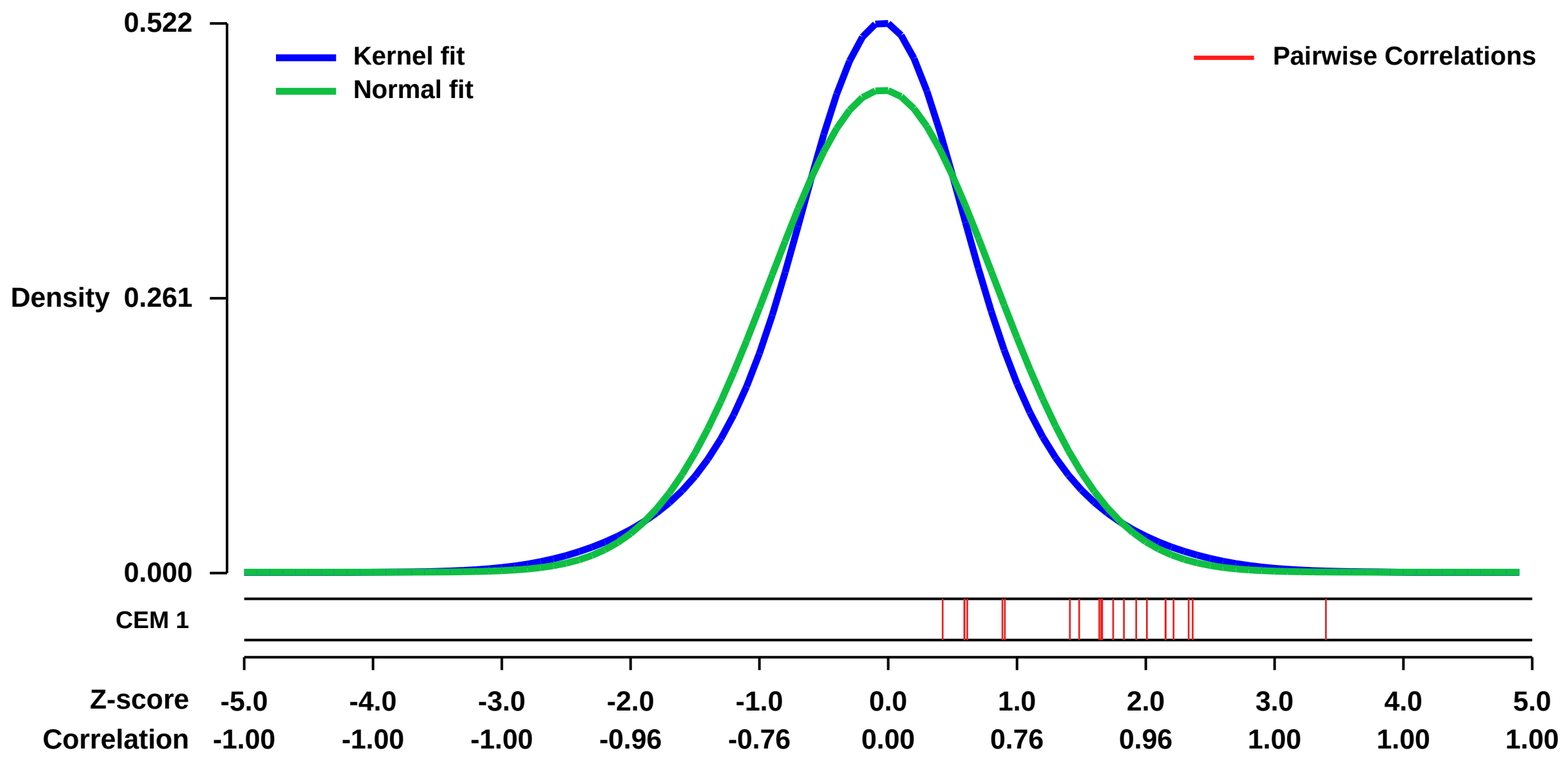

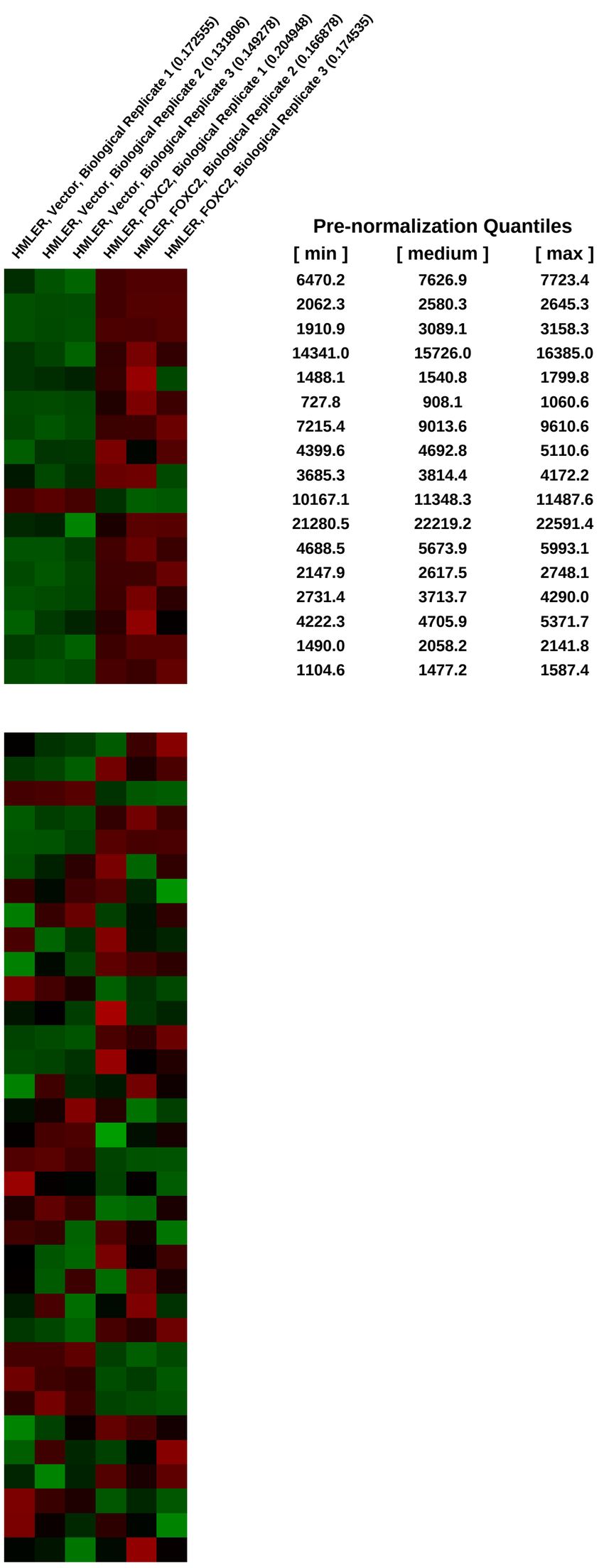

GEO Series "GSE47641" Expression Profiles

Num of samples in this series: 12

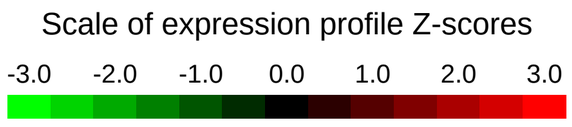

GEO Link:	http://www.ncbi.nlm.nih.gov/geo/query/acc.cgi?acc=GSE47641
Status:	Public on Jul 16 2013
Title:	Expression analysis of mock- or RAD21-transduced Kasumi1 cells
Organism:	Homo sapiens
Experiment type:	Expression profiling by array
Platform:	GPL570
Pubmed ID:	23955599
Summary & Design:	**Summary:** We recently identified recurrent mutations of cohesin complex in myeloid neoplasms through whole-exome sequencing analysis. RAD21 is one of the main components of the cohesin complex. In this study, to investigate the biological impact of wild-type RAD21 on Kasumi1 cells harboring RAD21 mutation, Kasumi1 cells were retrovirally transduced with either mock or wild-type RAD21, and expression array was performed. **Overall design:** Expression analysis was performed for mock- or wild-type RAD21-transduced Kasumi-1 cells in triplicate. The experiment was performed twice independently.

Background corr dist: KL-Divergence = 0.0619, L1-Distance = 0.0620, L2-Distance = 0.0059, Normal std = 0.5761

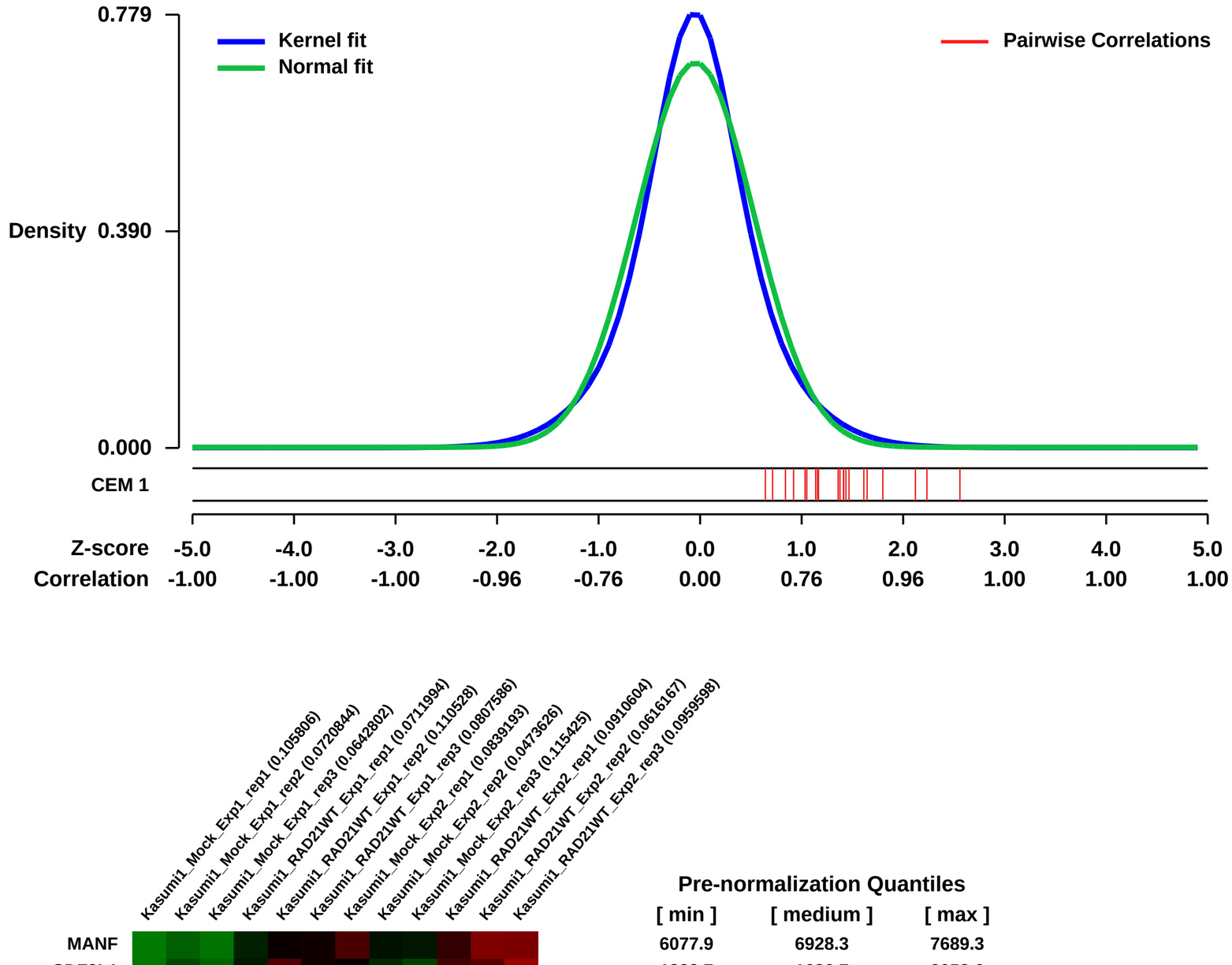

CEM 1
P (S | Z, I) = 1.00
Mean Corr = 0.84130

CEM 1 + Top 10 Genes

Null module

Pre-normalization Quantiles

	[min]	[medium]	[max]
MANF	6077.9	6928.3	7689.3
SDF2L1	1383.7	1686.7	2058.6
CRELD2	1423.6	1846.3	2169.3
HSPA5	12810.2	15264.0	17743.3
HYOU1	4474.1	5115.3	5850.2
PDIA4	1189.0	1325.5	1445.5
PDIA6	8675.2	10188.9	11863.8
DNAJB11	5356.4	5797.3	6419.1
HSP90B1	2518.7	7880.0	9253.9
PDIA3	6263.1	7377.0	9357.8
PPIB	12988.3	15225.9	17588.9
C19orf10	3468.9	4233.7	4638.9
SLC35B1	2955.8	3286.5	3651.5
SEC61A1	2385.4	2830.8	3040.0
RPN1	6024.8	6632.3	7251.9
DNAJC3	2866.9	3092.2	3229.1
CDK2AP2	526.3	599.0	714.5
ARID5B			
XBP1			
HNRNPAB			
SGK1			
HSPB1			
DDIT4			
ARL4D			
SAP30			
KIAA0408			
GPR17			
HSPH1			
DNASE1L2			
SLC5A3			
GNAS			
GPR3			
TNFRSF25			
TM6SF2			
MKKS			
PLEKHF1			
ZMYM1			
DOK3			
FGF20			
SLC39A2			
KCNIP2			
ERRFI1			
DEDD2			
CCDC117			
USP31			
AHSA2			
CYS1			
CNIH2			
BANP			
CHORDC1			
P4HA1			

GEO Series "GSE37416" Expression Profiles

Num of samples in this series: 48

Scale of expression profile Z-scores

-3.0 -2.0 -1.0 0.0 1.0 2.0 3.0

GEO Link:	http://www.ncbi.nlm.nih.gov/geo/query/acc.cgi?acc=GSE37416
Status:	Public on Oct 22 2012
Title:	Gene expression data from F. tularensis-exposed neutrophils
Organism:	Homo sapiens
Experiment type:	Expression profiling by array
Platform:	GPL570
Pubmed ID:	22986450
Summary & Design:	**Summary:** We demonstrated recently that both constitutive and FAS-triggered apoptosis of human neutrophils are profoundly impaired by Francisella tularensis, but how this is achieved is largely unknown. To test the hypothesis that changes in neutrophil gene expression contribute to this phenotype, we used human oligonucleotide microarrays to identify differentially regulated genes in cells infected with F. tularensis strain LVS compared with uninfected controls. In order to examine the effect of F. tularensis on the neutrophil transcriptome, we performed microarray expression analysis on human neutrophils treated with F. tularensis subsp. holarctica live vaccine strain (LVS). **Overall design:** Polymorphonuclear leukocytes (PMNs) were isolated from the blood of healthy donors. Control and F. tularensis-exposed PMNs were incubated at 37C for 0, 3, 6, 12, 24, and 48 hours.

Background corr dist: KL-Divergence = 0.0878, L1-Distance = 0.0617, L2-Distance = 0.0085, Normal std = 0.4688

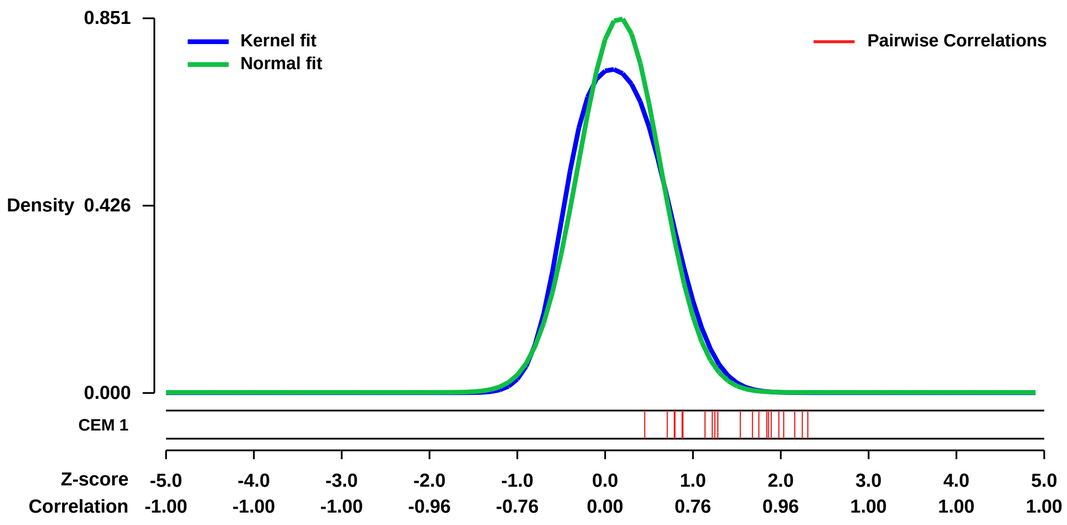

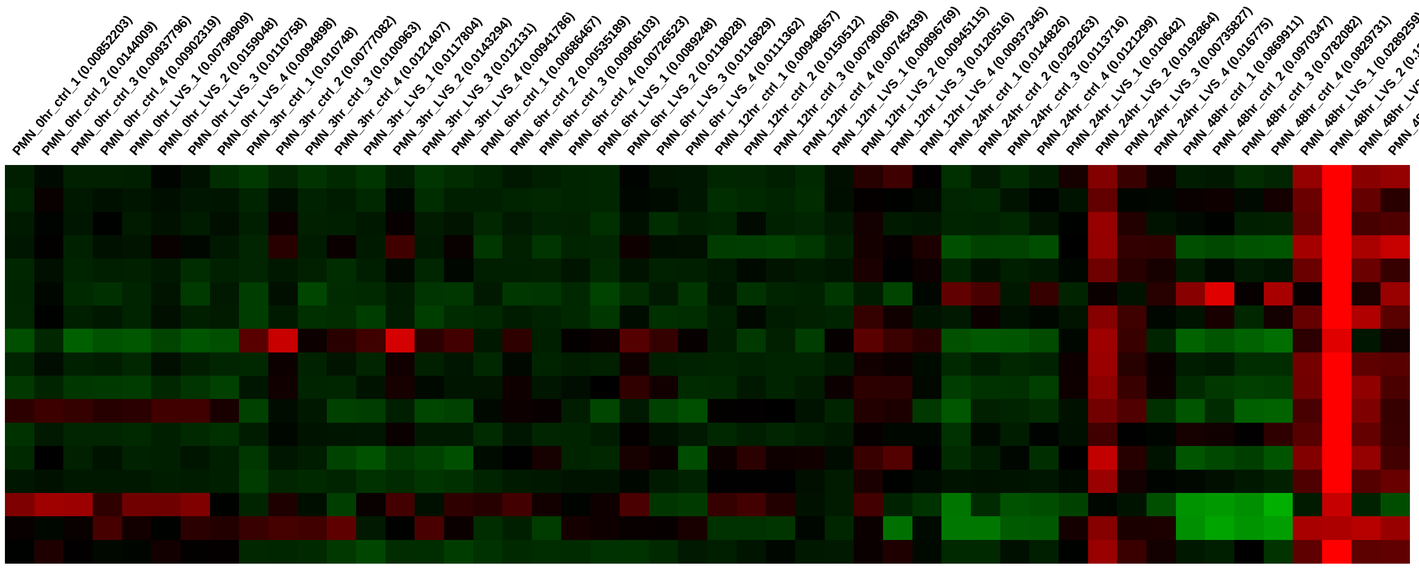

Pre-normalization Quantiles

	[min]	[medium]	[max]
MANF	504.4	1151.0	12150.4
SDF2L1	68.4	244.4	3599.5
CRELD2	313.6	648.3	8745.2
HSPA5	3085.3	8474.0	41519.4
HYOU1	228.0	558.7	8587.2
PDIA4	114.3	201.6	996.5
PDIA6	396.4	958.8	8824.0
DNAJB11	672.0	1842.0	4447.3
HSP90B1	126.2	713.5	19162.9
PDIA3	1888.7	3930.8	27024.8
PPIB	1845.0	4879.4	21452.9
C19orf10	144.4	423.6	5984.4
SLC35B1	481.2	786.7	2717.1
SEC61A1	249.7	946.0	10162.7
RPN1	628.6	3189.1	6279.4
DNAJC3	1384.0	5928.6	10526.6
CDK2AP2	171.5	532.6	4378.3

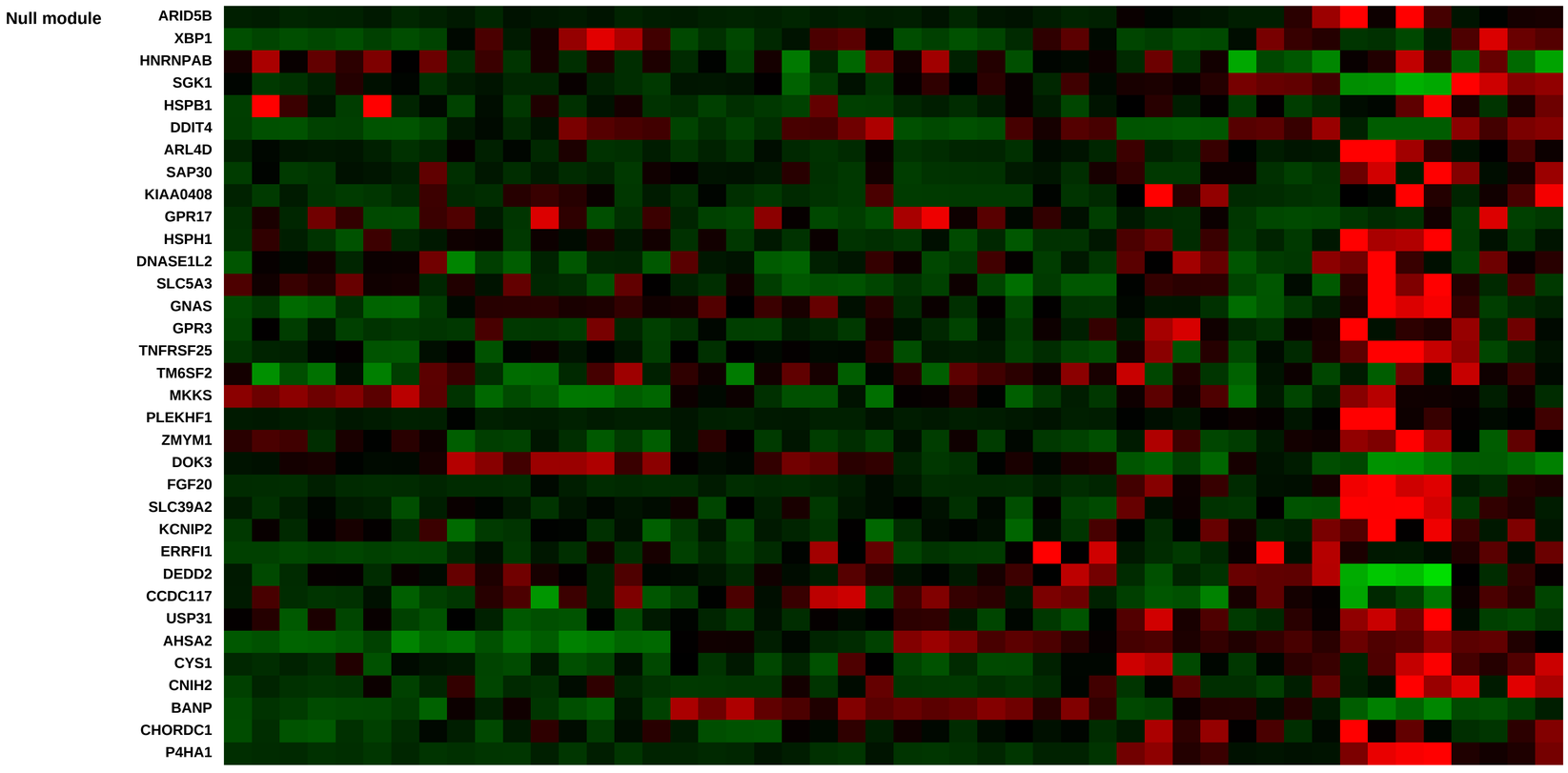

GEO Series "GSE19240" Expression Profiles

Num of samples in this series: 6

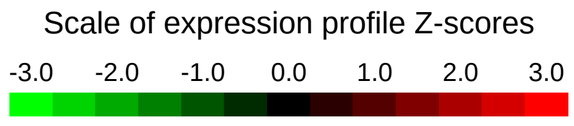

GEO Link:	http://www.ncbi.nlm.nih.gov/geo/query/acc.cgi?acc=GSE19240
Status:	Public on Jul 01 2010
Title:	Expression profile of IL-1beta stimulated and non-stimulated endothelial cells
Organism:	Homo sapiens
Experiment type:	Expression profiling by array
Platform:	GPL570
Pubmed ID:	21469100
Summary & Design:	**Summary:** Complete identification of the bone marrow niche remains one of the most progressing fields. Attempts to identify soluble factors involved in stem cell renewal have been less successful. We have previously shown that endothelial cells (EC) can induce the long-term proliferation of hematopoietic progenitor cells (HPC), especially when they had been subjected to an inflammatory stimulus like interleukins (IL) 1. To identify yet unknown growth factors, we compared the expression profile of IL-1 stimulated and non-stimulated endothelial cells. **Overall design:** Human endothelial cells were subjected to IL-1 for 4, 8, and 16 hours. Isolated mRNA was analyzed by oligonucleotide microarray chips covering over 46,000 human genes.

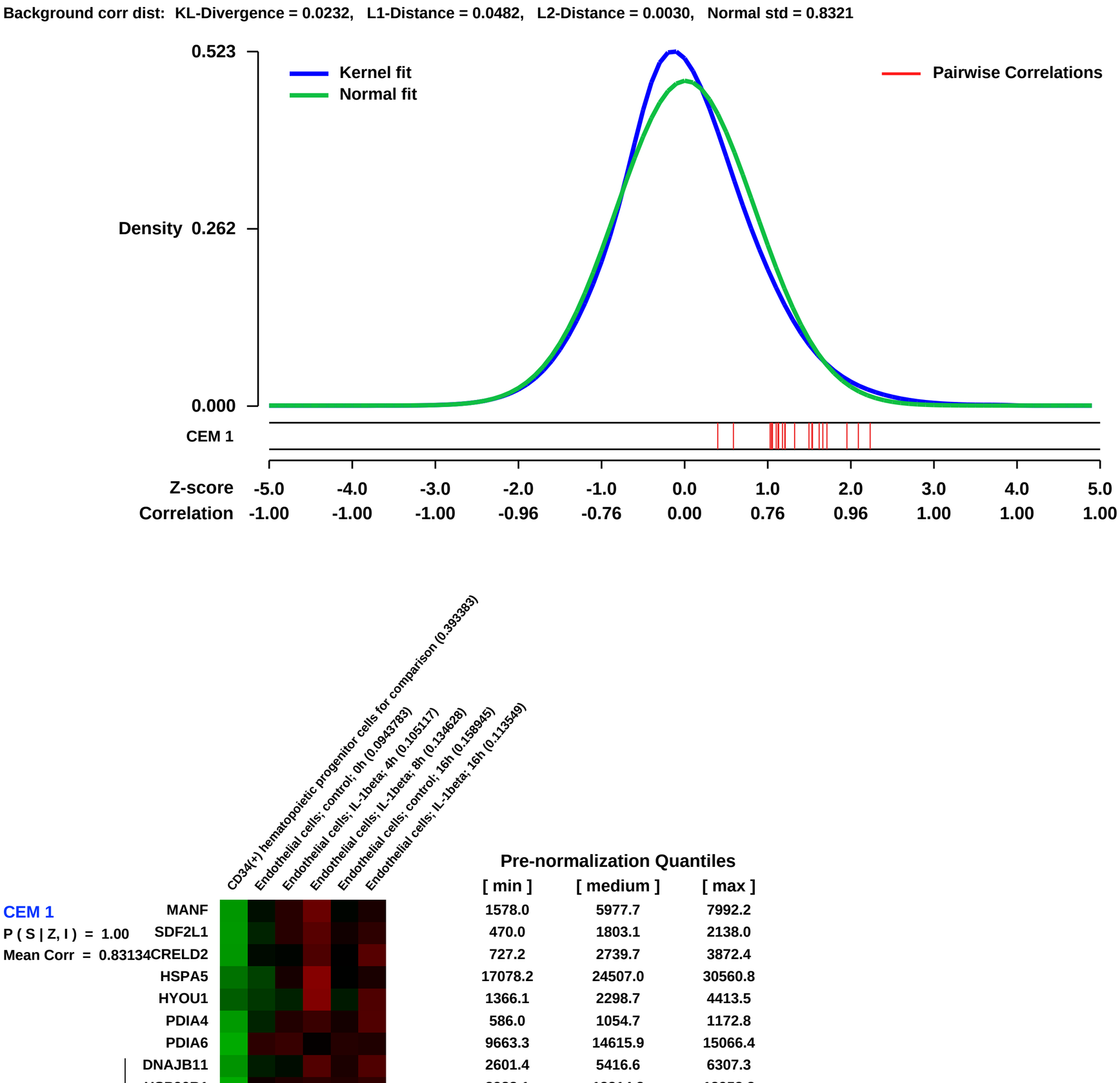

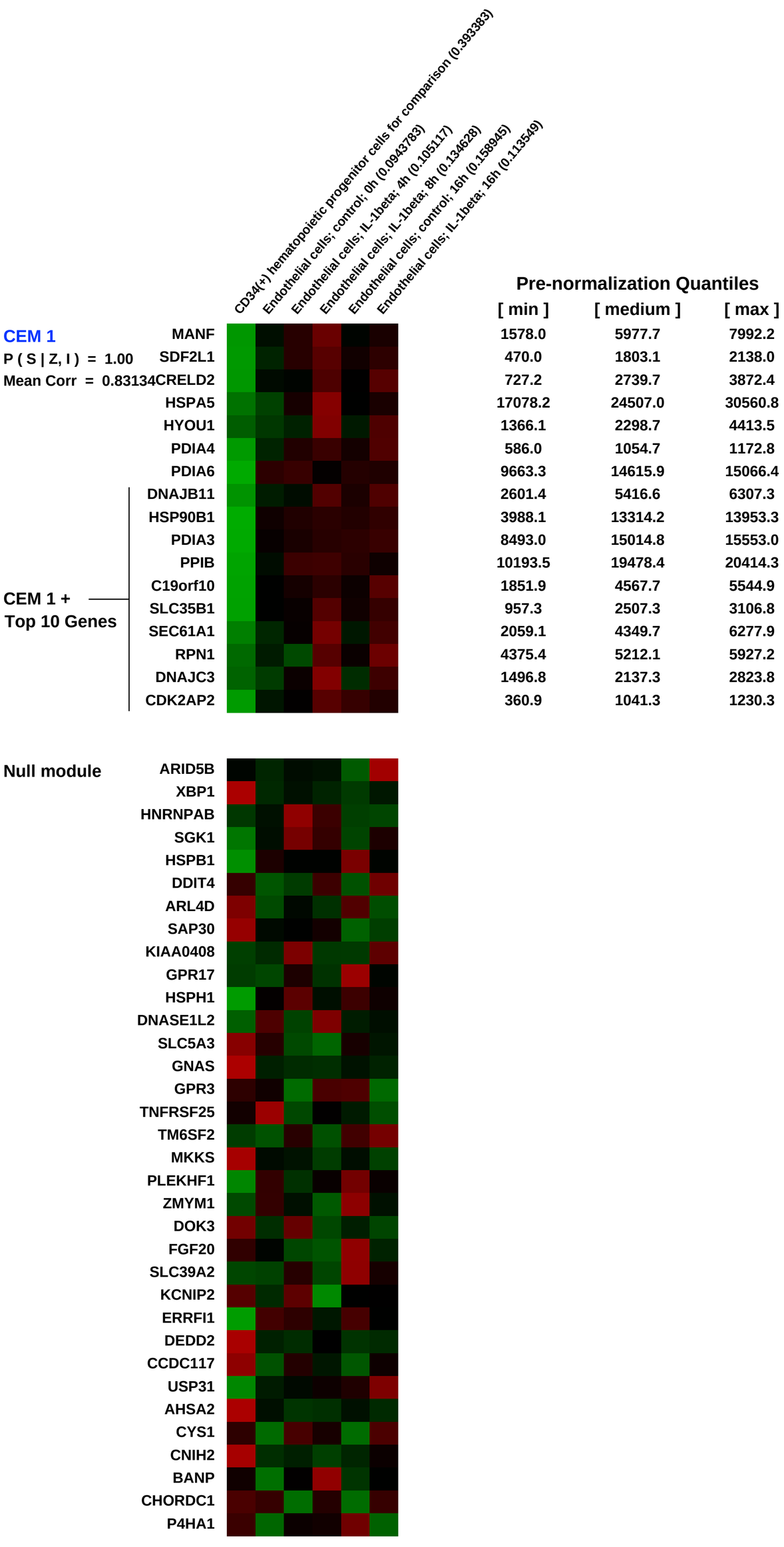

Pre-normalization Quantiles

	[min]	[medium]	[max]
MANF	1578.0	5977.7	7992.2
SDF2L1	470.0	1803.1	2138.0
CRELD2	727.2	2739.7	3872.4
HSPA5	17078.2	24507.0	30560.8
HYOU1	1366.1	2298.7	4413.5
PDIA4	586.0	1054.7	1172.8
PDIA6	9663.3	14615.9	15066.4
DNAJB11	2601.4	5416.6	6307.3
HSP90B1	3988.1	13314.2	13953.3
PDIA3	8493.0	15014.8	15553.0
PPIB	10193.5	19478.4	20414.3
C19orf10	1851.9	4567.7	5544.9
SLC35B1	957.3	2507.3	3106.8
SEC61A1	2059.1	4349.7	6277.9
RPN1	4375.4	5212.1	5927.2
DNAJC3	1496.8	2137.3	2823.8
CDK2AP2	360.9	1041.3	1230.3

GEO Series "GSE57441" Expression Profiles

Num of samples in this series: 6

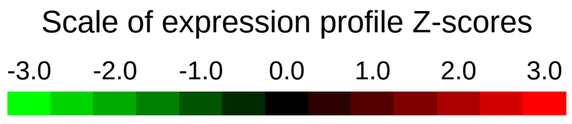

GEO Link:	http://www.ncbi.nlm.nih.gov/geo/query/acc.cgi?acc=GSE57441
Status:	Public on May 09 2014
Title:	Genes expression of cervical squamous cell carcinoma, CaSki cells, treated with or without recombinant TGF-b1 (2 ng/mL)
Organism:	Homo sapiens
Experiment type:	Expression profiling by array
Platform:	GPL570
Pubmed ID:	
Summary & Design:	**Summary:** Aggressive local invasion is the major way of spread in uterine cervical squamous cell carcinoma (CSCC). Although TGF-b facilitates invasion of various types of cancer cells, the role of TGF-b pathway in CSCC is unclear. Through array-based analysis, immunohistochemical staining of human endometrial cancer tissue, it is shown that interaction between CSCC cells and surrounding cancer asscocited fibroblasts (CAFs) activates TGF-b via TSP-1 secretion to facilitate CSCC invade, resulting in up-regulation of pSMAD3 in CSCC cells to promote invasion. These results suggest that activation of TGF-b induced by the interaction between CSCC cells and CAFs could play a key role in the initiation of tumor spreads. **Overall design:** We used microarrays to clarify the changes of gene expression along with recombinant TGF-b1 treatment and to confirm whether there are any changes on genes expression related to TGF-b pathway.

Background corr dist: KL-Divergence = 0.0381, L1-Distance = 0.0206, L2-Distance = 0.0004, Normal std = 0.6293

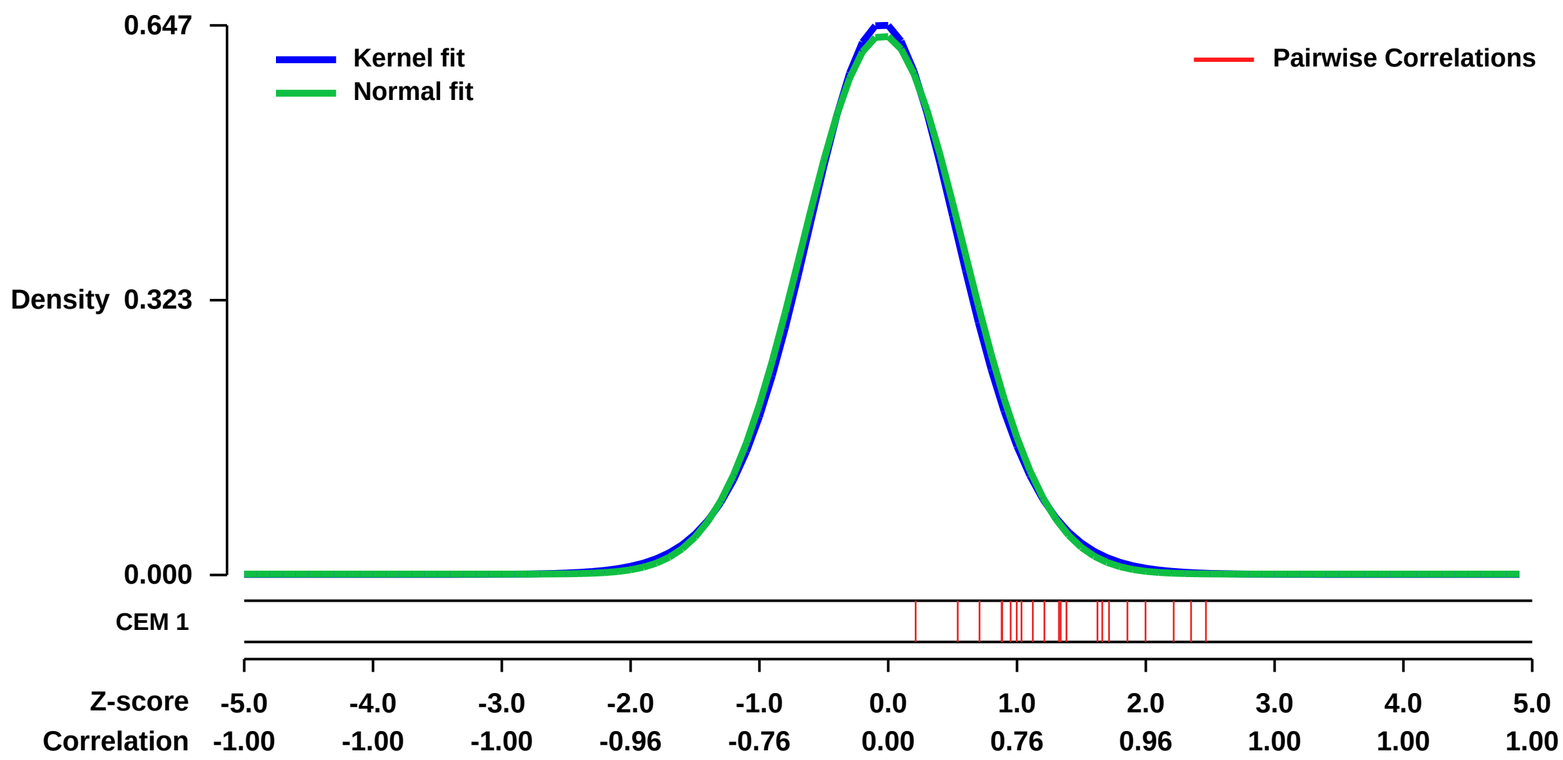

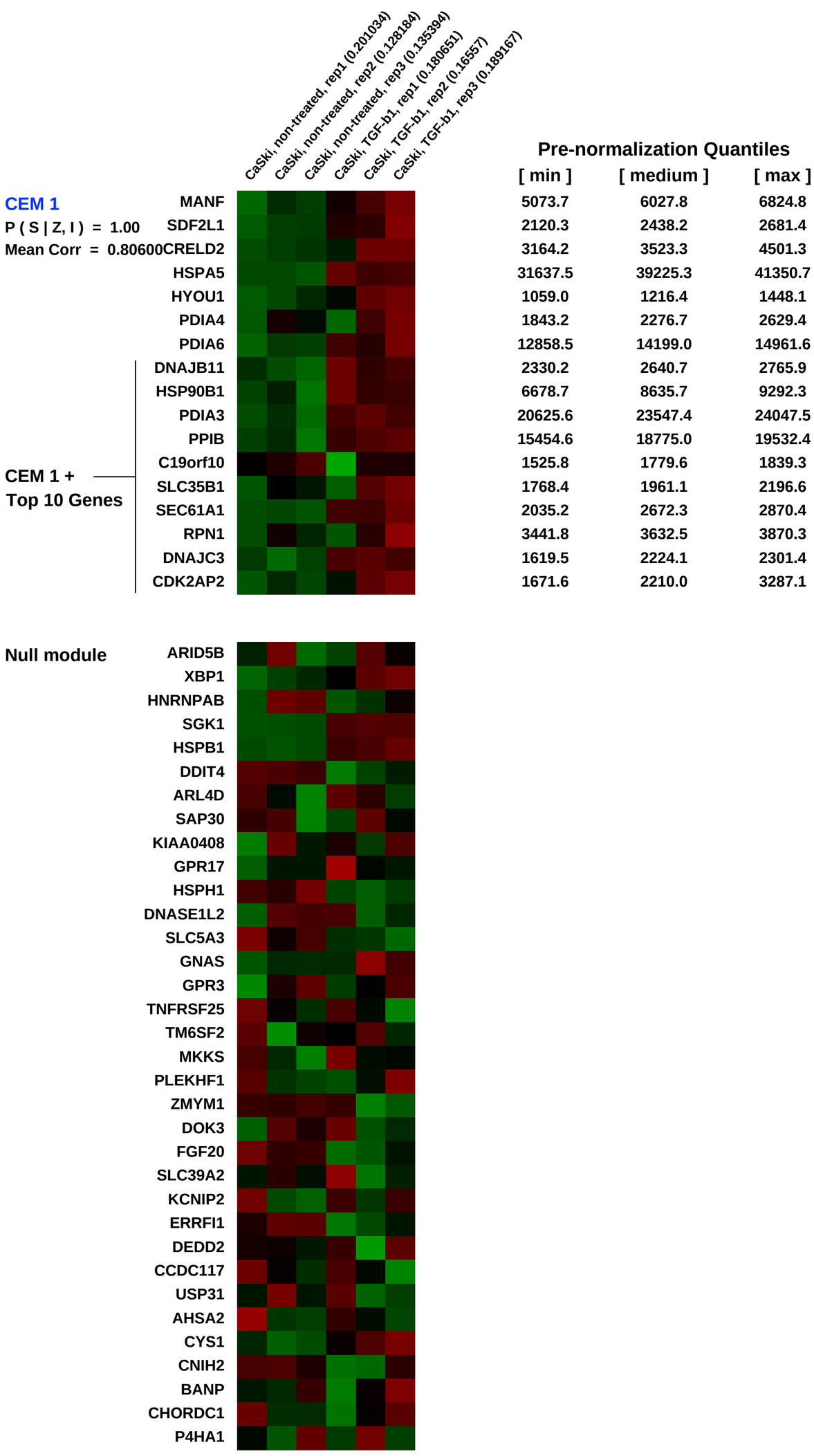

GEO Series "GSE3467" Expression Profiles

Num of samples in this series: 18

Scale of expression profile Z-scores

-3.0 -2.0 -1.0 0.0 1.0 2.0 3.0

GEO Link:	http://www.ncbi.nlm.nih.gov/geo/query/acc.cgi?acc=GSE3467
Status:	Public on Dec 19 2005
Title:	The role of micro-RNA genes in papillary thyroid carcinoma
Organism:	Homo sapiens
Experiment type:	Expression profiling by array
Platform:	GPL570
Pubmed ID:	16365291
Summary & Design:	**Summary:** We show that numerous miRNAs are transcriptionally up-regulated in papillary thyroid carcinoma (PTC) tumors compared with unaffected thyroid tissue. Among the predicted target genes of the three most upregulated miRNAs (miRs 221, 222 and 146b), only less than 15% showed significant downexpression in transcript level between tumor and unaffected tissue. The KIT gene which is known to be downregulated by miRNAs 221 and 222 displayed dramatic loss of transcript and protein in those tumors that had abundant mir-221, mir-222, and mir-146b transcript. Keywords: Disease state analysis **Overall design:** Total RNA was extracted from paired tumor and normal thyroid tissues from 9 PTC patients. The same set samples were applied to Custom miRNA microarray chips (OSU_CCC version 2.0) and Affymetrix HG-U133 plus 2 chips.

Background corr dist: KL-Divergence = 0.1161, L1-Distance = 0.0419, L2-Distance = 0.0037, Normal std = 0.4103

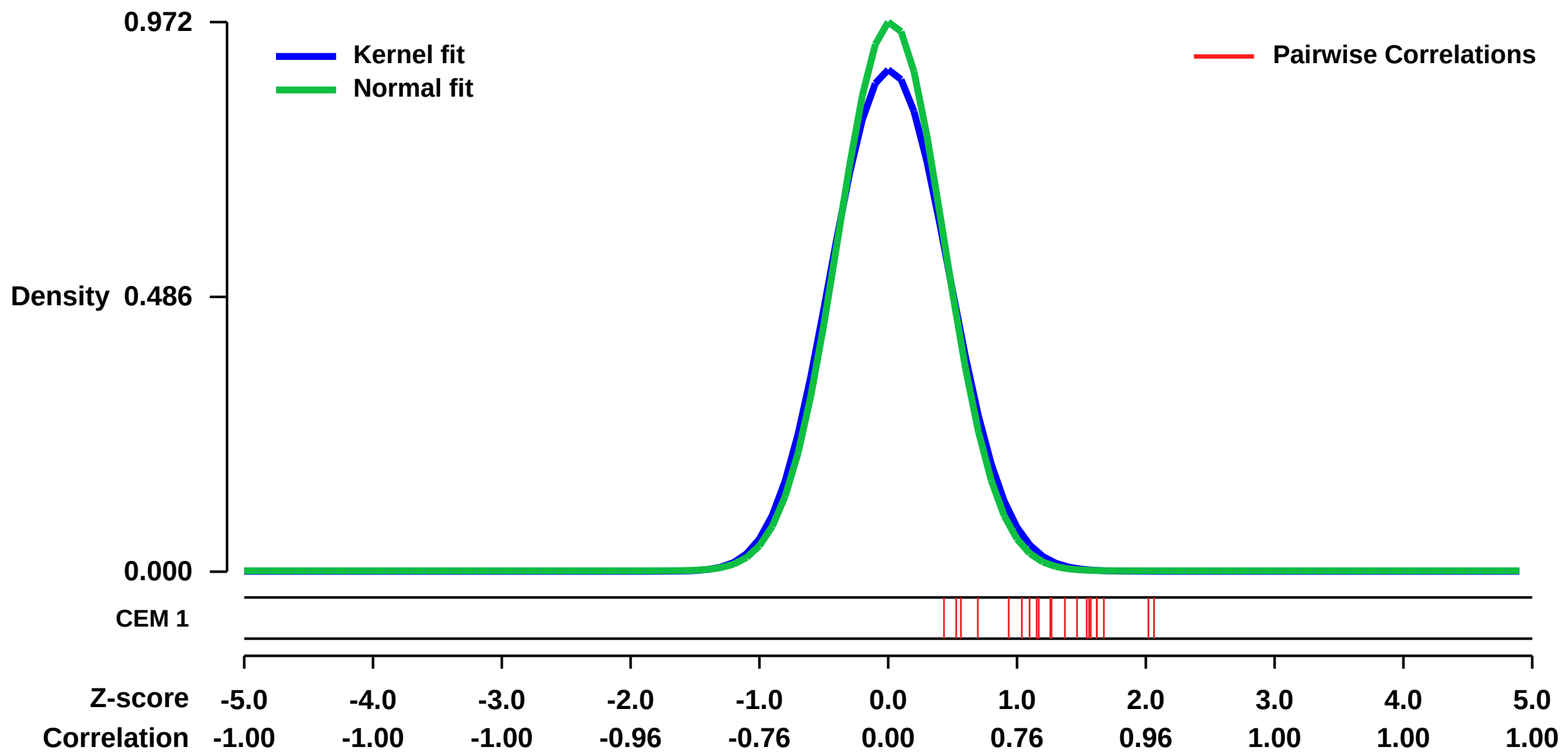

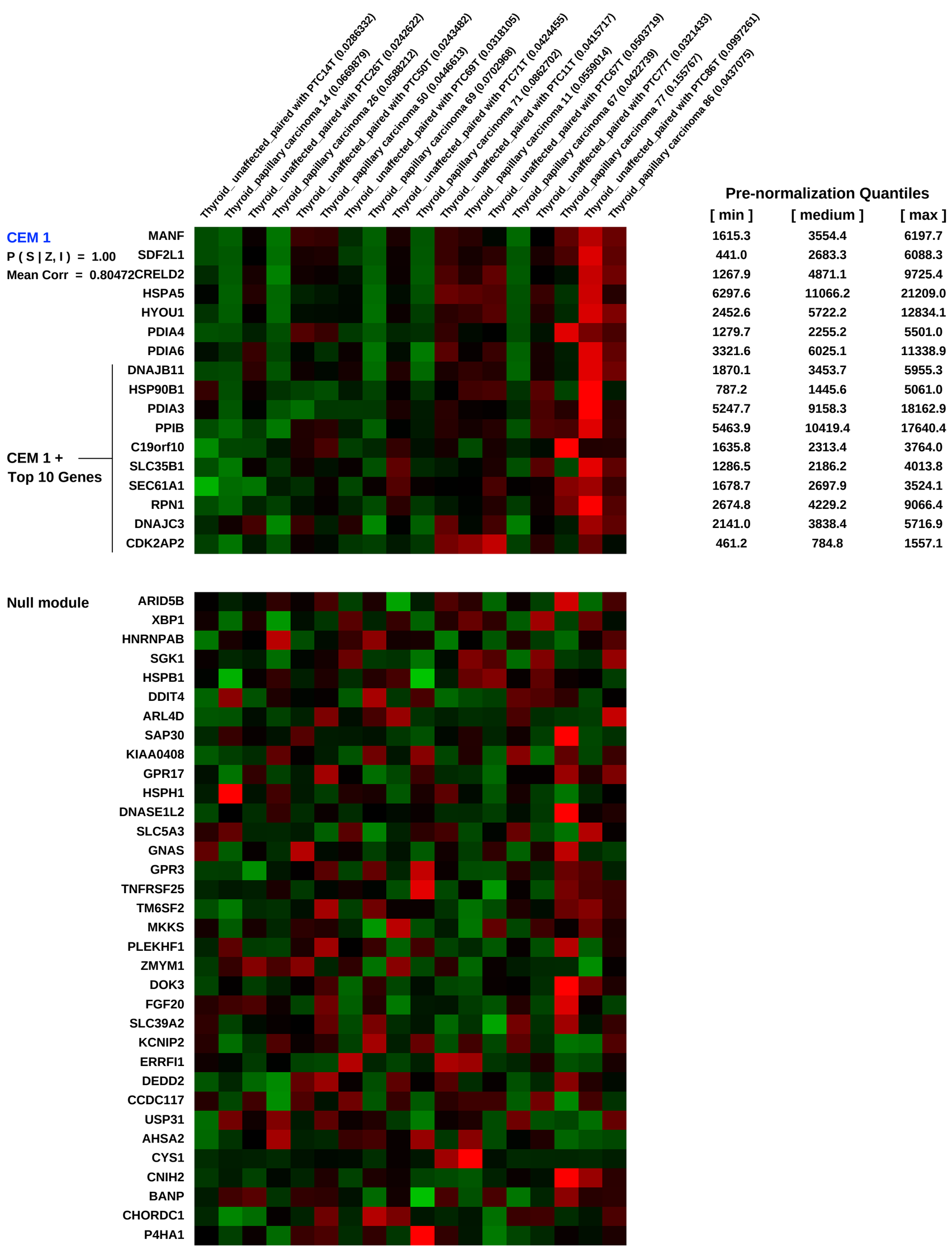

Pre-normalization Quantiles

	[min]	[medium]	[max]
MANF	1615.3	3554.4	6197.7
SDF2L1	441.0	2683.3	6088.3
CRELD2	1267.9	4871.1	9725.4
HSPA5	6297.6	11066.2	21209.0
HYOU1	2452.6	5722.2	12834.1
PDIA4	1279.7	2255.2	5501.0
PDIA6	3321.6	6025.1	11338.9
DNAJB11	1870.1	3453.7	5955.3
HSP90B1	787.2	1445.6	5061.0
PDIA3	5247.7	9158.3	18162.9
PPIB	5463.9	10419.4	17640.4
C19orf10	1635.8	2313.4	3764.0
SLC35B1	1286.5	2186.2	4013.8
SEC61A1	1678.7	2697.9	3524.1
RPN1	2674.8	4229.2	9066.4
DNAJC3	2141.0	3838.4	5716.9
CDK2AP2	461.2	784.8	1557.1

GEO Series "GSE41315" Expression Profiles

Num of samples in this series: 24

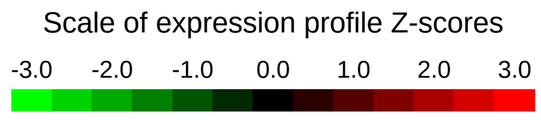

GEO Link:	http://www.ncbi.nlm.nih.gov/geo/query/acc.cgi?acc=GSE41315
Status:	Public on Oct 04 2012
Title:	Timecourse gene expression profiling of DLBCL cell line Karpas422 after EZH2 inhibitor treatment
Organism:	Homo sapiens
Experiment type:	Expression profiling by array
Platform:	GPL570
Pubmed ID:	23236167
Summary & Design:	**Summary:** Ezh2 protein is the enzymatic component of the Polycomb Repressive Complex (PRC)-2, which represses its target genes by methylating lysine 27 of histone H3 (H3K27) and regulates cell proliferation and differentiation during embryonic development. Recently, hot-spot mutations of Ezh2 have been identified in diffused large B cell lymphomas (DLBCLs) and follicular lymphomas (FLs). To investigate if tumor growth is dependent on the enzymatic activity of Ezh2, we have developed a potent and selective small molecule inhibitor, EI1, which inhibits the enzymatic activity of Ezh2 through direct binding and competing with the methyl group donor S-Adenosyl methionine (SAM). EI1-treated cells exhibit genome-wide loss of H3K27 methylation. Furthermore, inhibition of Ezh2 by EI1 in DLBCL cells carrying the Y641 mutations results in decreased proliferation, cell cycle arrest and apoptosis. These results provide strong validation of Ezh2 as a potential therapeutic target for the treatment of cancer with the Ezh2 mutation. In this microarray experiment we examined the global gene expression changes in DLBCL cell line Karpas422 (Ezh2Y641N) after EI1 treatment for up to 6 days. **Overall design:** Total RNA was prepared from KARPAS422 at 1 day, 2 days, 3 days, and 6 days after DMSO or EZH2 inhibitor (5 uM) treatment with biological triplicates and hybridized to Affimetrix U133 Plus 2 microarray chips according to the manufacturers protocol (Affymetrix, CA).

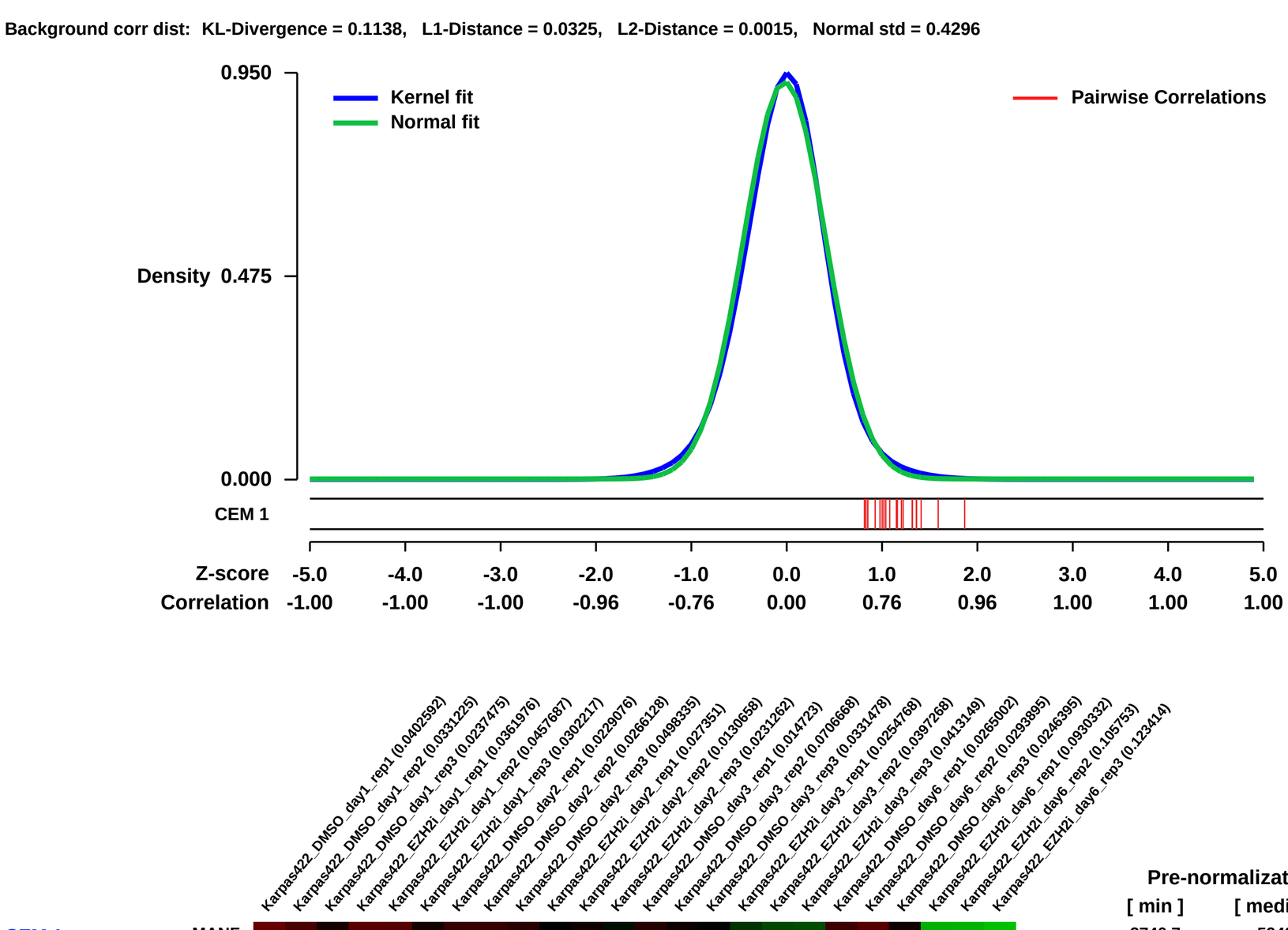

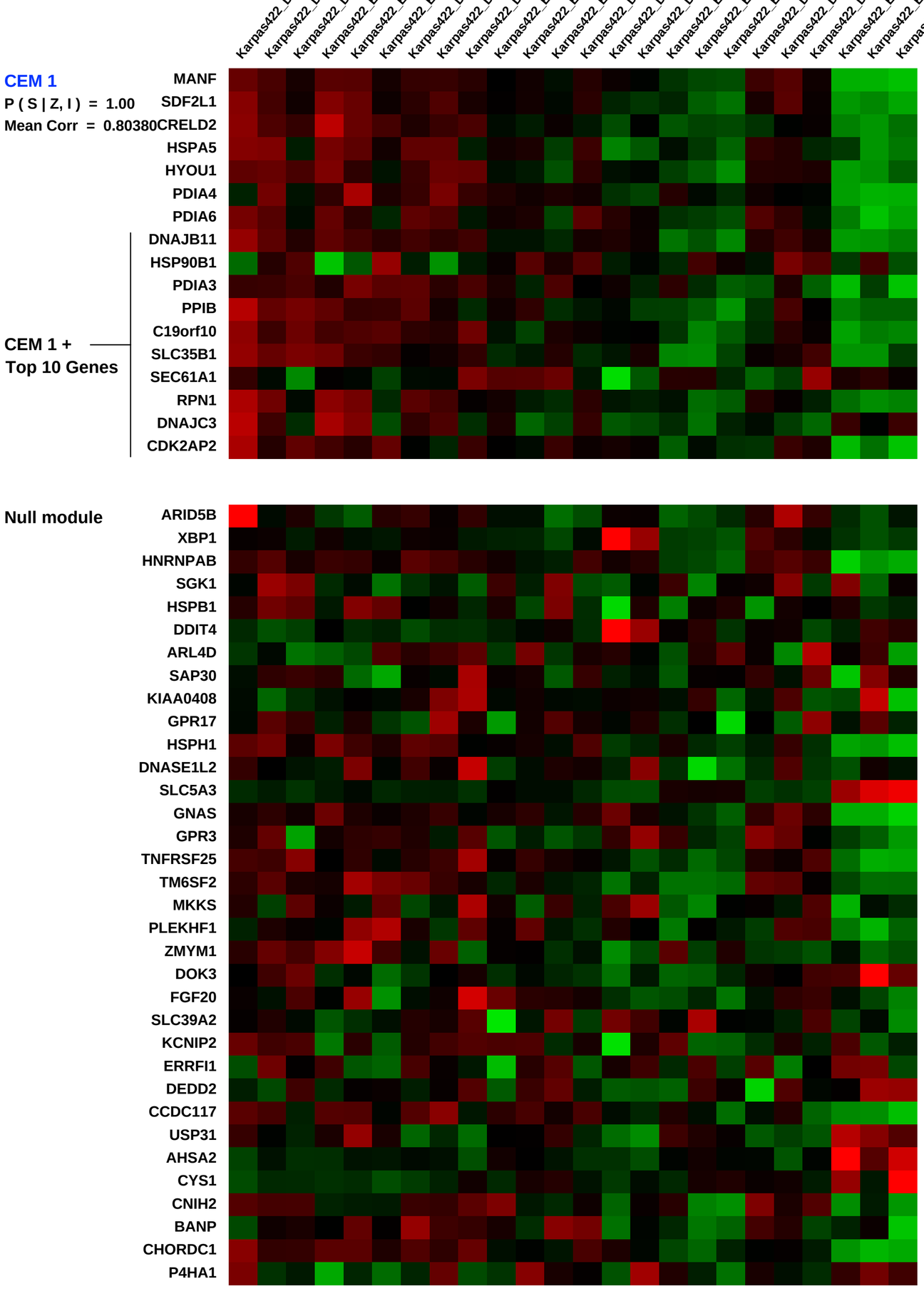

Pre-normalization Quantiles

[min]	[medium]	[max]
2740.7	5948.7	7169.1
1154.5	2108.9	2724.1
1909.1	2661.2	3626.6
9764.3	13055.6	15277.7
469.9	638.0	725.3
808.5	1173.1	1454.1
2996.8	4888.8	5767.5
6535.5	8833.0	10312.5
2368.3	3510.4	4275.5
5854.3	9442.5	10829.1
12878.4	14341.6	16101.1
891.5	1361.9	1707.2
1432.3	1885.8	2243.9
1621.3	1880.5	2051.2
2519.5	3272.5	4305.6
1052.4	1221.7	1550.5
1406.8	2126.8	2666.7

GEO Series "GSE11670" Expression Profiles

Num of samples in this series: 6

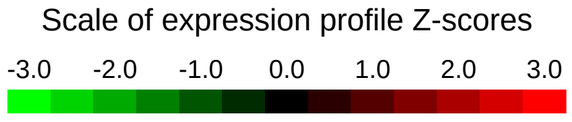

GEO Link:	http://www.ncbi.nlm.nih.gov/geo/query/acc.cgi?acc=GSE11670
Status:	Public on May 20 2009
Title:	Transcriptional profiling of ICL670 treated K562 cells
Organism:	Homo sapiens
Experiment type:	Expression profiling by array
Platform:	GPL570
Pubmed ID:	19298223
Summary & Design:	**Summary:** Iron plays a central role in the regulation of many cellular functions. Dysregulation of its metabolism leads an iron overload situation and iron depletion leads to an inhibition of cell proliferation. Recent reports demonstrated that ICL670 (Novartis) acts as a potent NF-kappa-B inhibitor and improves hematological data in a subset of MDS patients (Cilloni et al, Haematologica, s1: 238, 2007). However, the precise mechanism of anti-cancer effect of ICL670 is still uncertain. To evaluate the effect of ICL670, and to identify the moleclular pathways responsible for the observed reduced transfusion requirement during chelation therapy, we performed gene expression profiling to focus on the pathway involved in the anti-cancer effect of ICL670. **Overall design:** A human myeloid leukemia cell line, K562, was incubated with or without ICL670 for 16hrs.Gene expression profiling was done using an Affymerix GeneChip (U133 Plus 2.0). Statistical analysis was done by GeneSifter vizXlab, Seattle, WA).

Background corr dist: KL-Divergence = 0.0377, L1-Distance = 0.0334, L2-Distance = 0.0013, Normal std = 0.6549

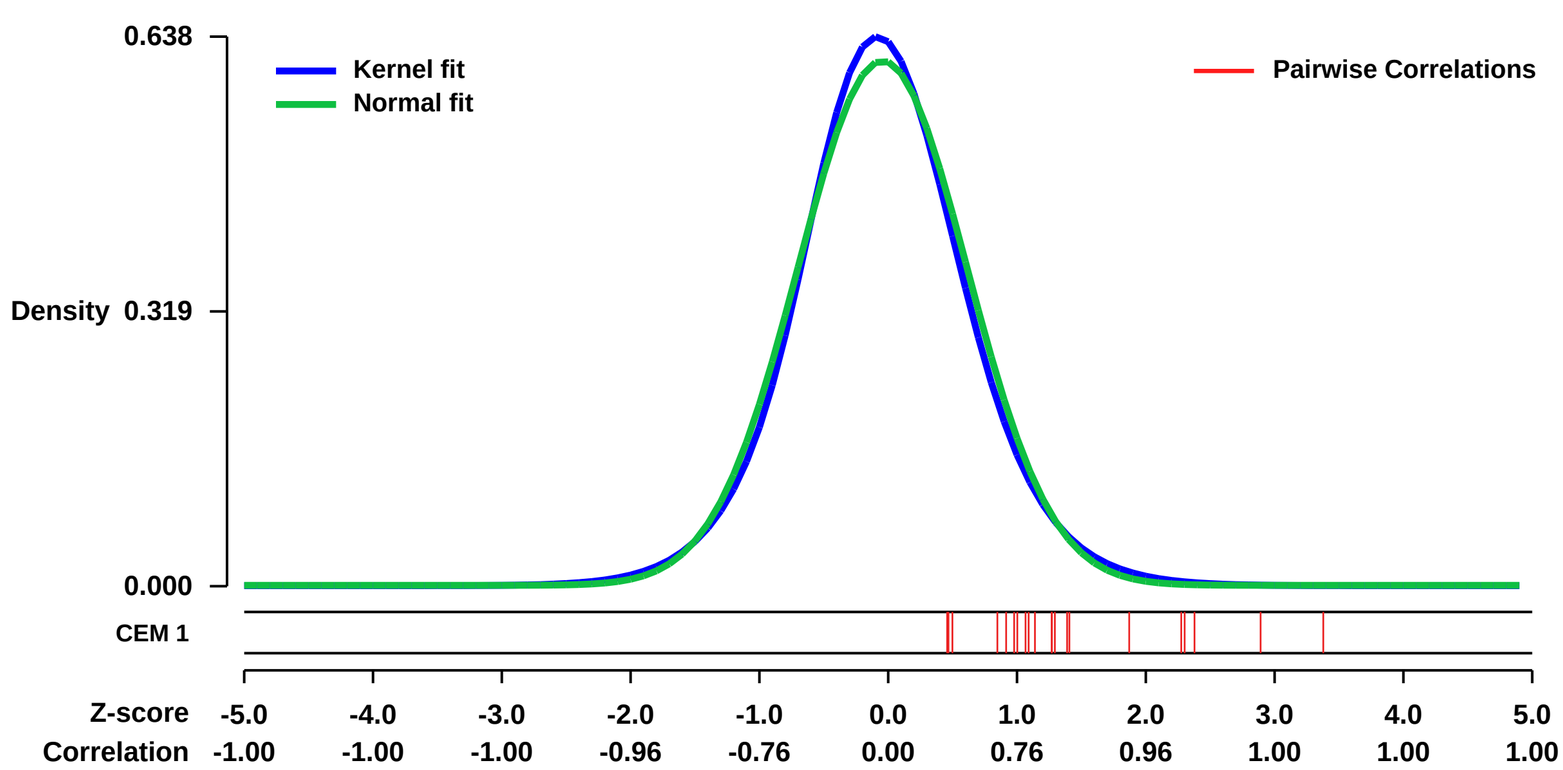

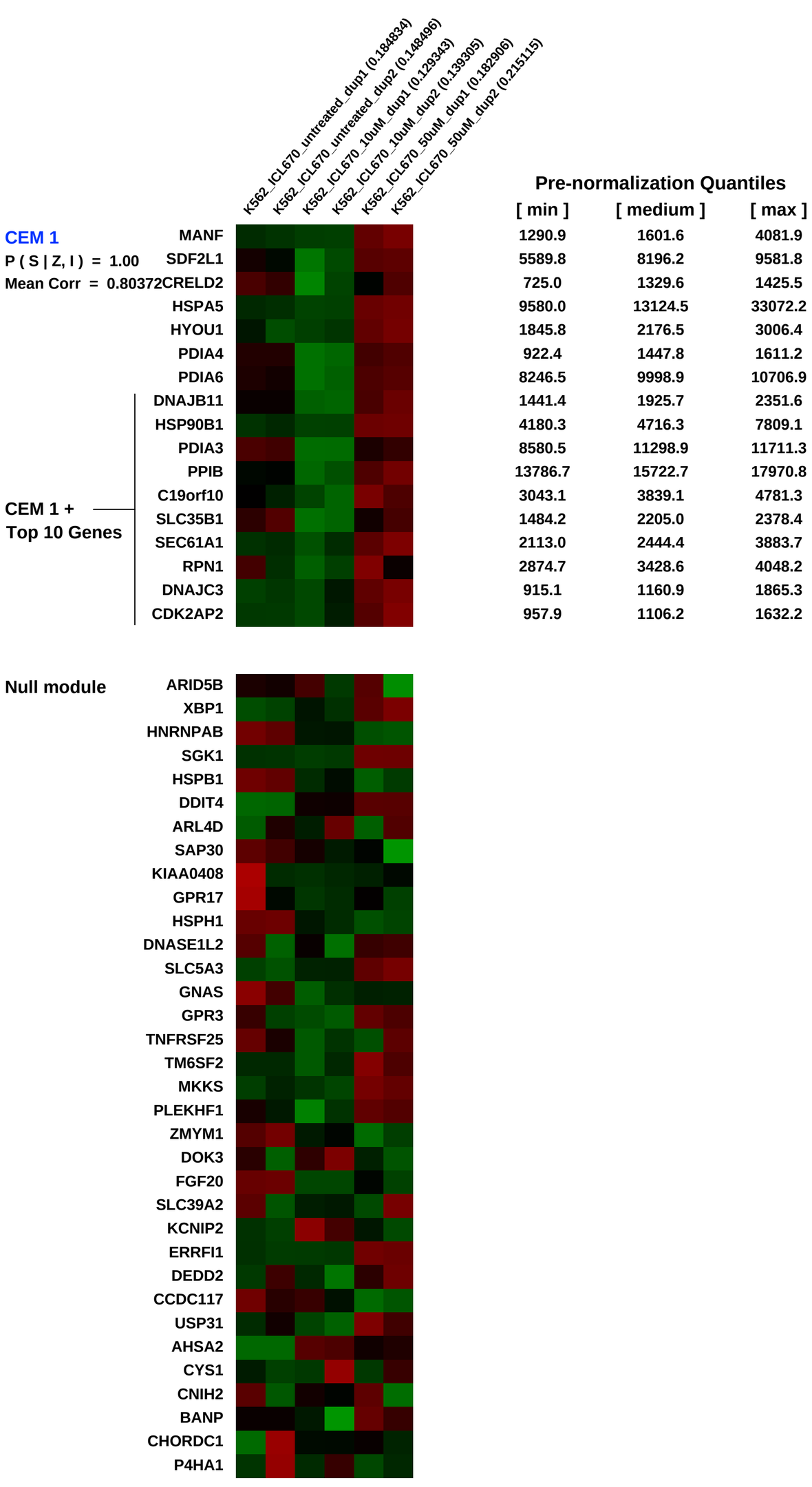

Pre-normalization Quantiles

	[min]	[medium]	[max]
MANF	1290.9	1601.6	4081.9
SDF2L1	5589.8	8196.2	9581.8
CRELD2	725.0	1329.6	1425.5
HSPA5	9580.0	13124.5	33072.2
HYOU1	1845.8	2176.5	3006.4
PDIA4	922.4	1447.8	1611.2
PDIA6	8246.5	9998.9	10706.9
DNAJB11	1441.4	1925.7	2351.6
HSP90B1	4180.3	4716.3	7809.1
PDIA3	8580.5	11298.9	11711.3
PPIB	13786.7	15722.7	17970.8
C19orf10	3043.1	3839.1	4781.3
SLC35B1	1484.2	2205.0	2378.4
SEC61A1	2113.0	2444.4	3883.7
RPN1	2874.7	3428.6	4048.2
DNAJC3	915.1	1160.9	1865.3
CDK2AP2	957.9	1106.2	1632.2

GEO Series "GSE44596" Expression Profiles

Num of samples in this series: 6

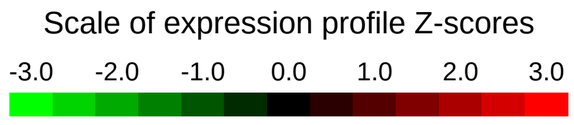

GEO Link:	http://www.ncbi.nlm.nih.gov/geo/query/acc.cgi?acc=GSE44596
Status:	Public on Feb 20 2014
Title:	The effect of Sparstolonin B (SsnB) on gene expression in HCAECs
Organism:	Homo sapiens
Experiment type:	Expression profiling by array
Platform:	GPL570
Pubmed ID:	23940584
Summary & Design:	**Summary:** Sparstolonin B is a novel bioactive compound isolated from Sparganium stoloniferum, an herb historically used in Traditional Chinese Medicine as an anti-tumor agent. SsnB has previously demonstrated anti-angiogenic properties. In functional assays, SsnB inhibited endothelial cell tube formation (Matrigel method) and cell migration (Transwell method) in a dose-dependent manner. We used microarrays to examine how SsnB affected the gene expression of human coronary artery endothelial cells (HCAECs), focusing in particular on pathways related to angiogenesis. **Overall design:** Three plates of HCAECs were exposed to 100 micromolar SsnB and three plates of HCAECs were exposed to Vehicle Control (1:1000 dilution of DMSO). After 24 hours, RNA was extracted for microarrays and gene expression was analyzed.

Background corr dist: KL-Divergence = 0.0344, L1-Distance = 0.0260, L2-Distance = 0.0007, Normal std = 0.6619

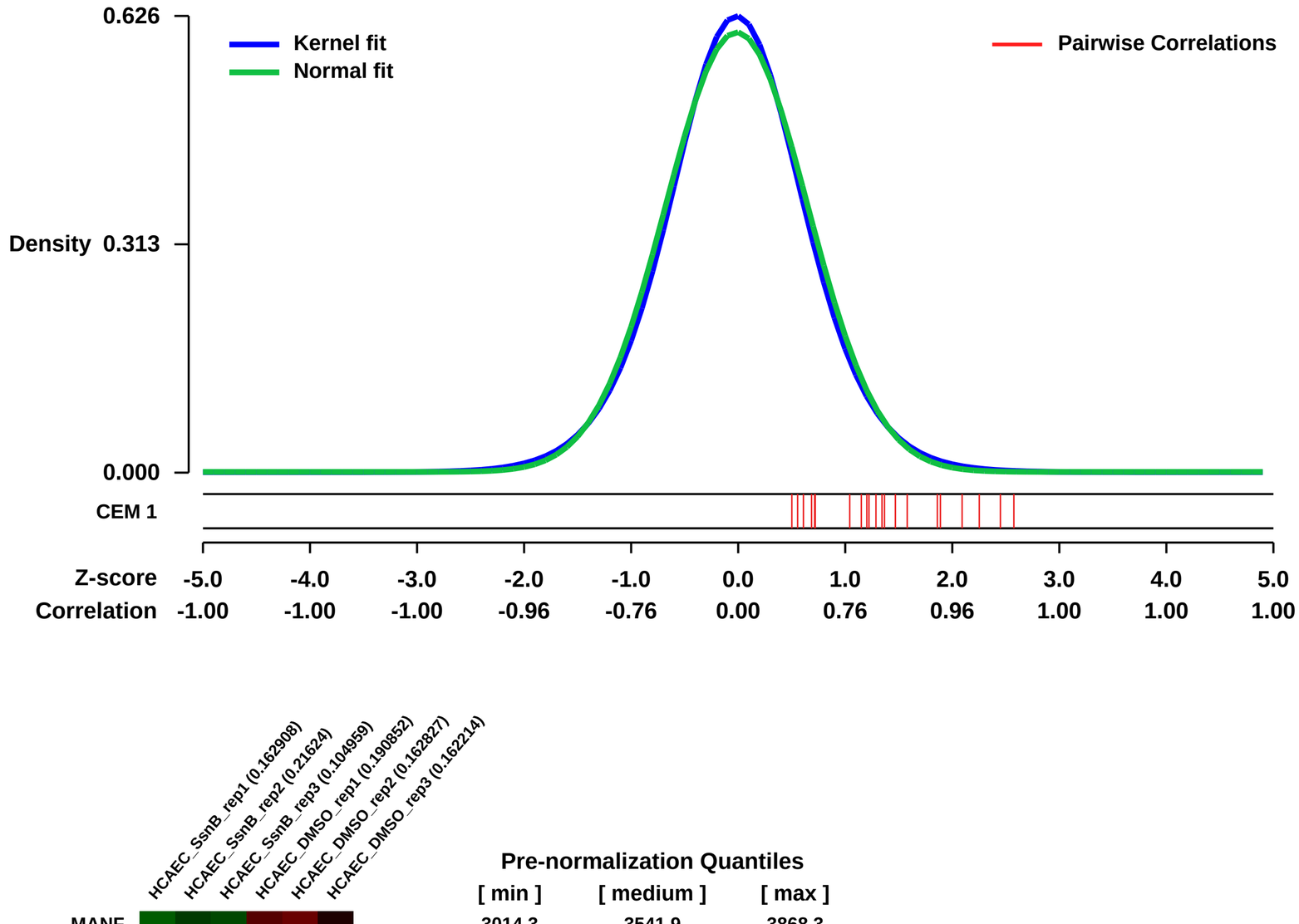

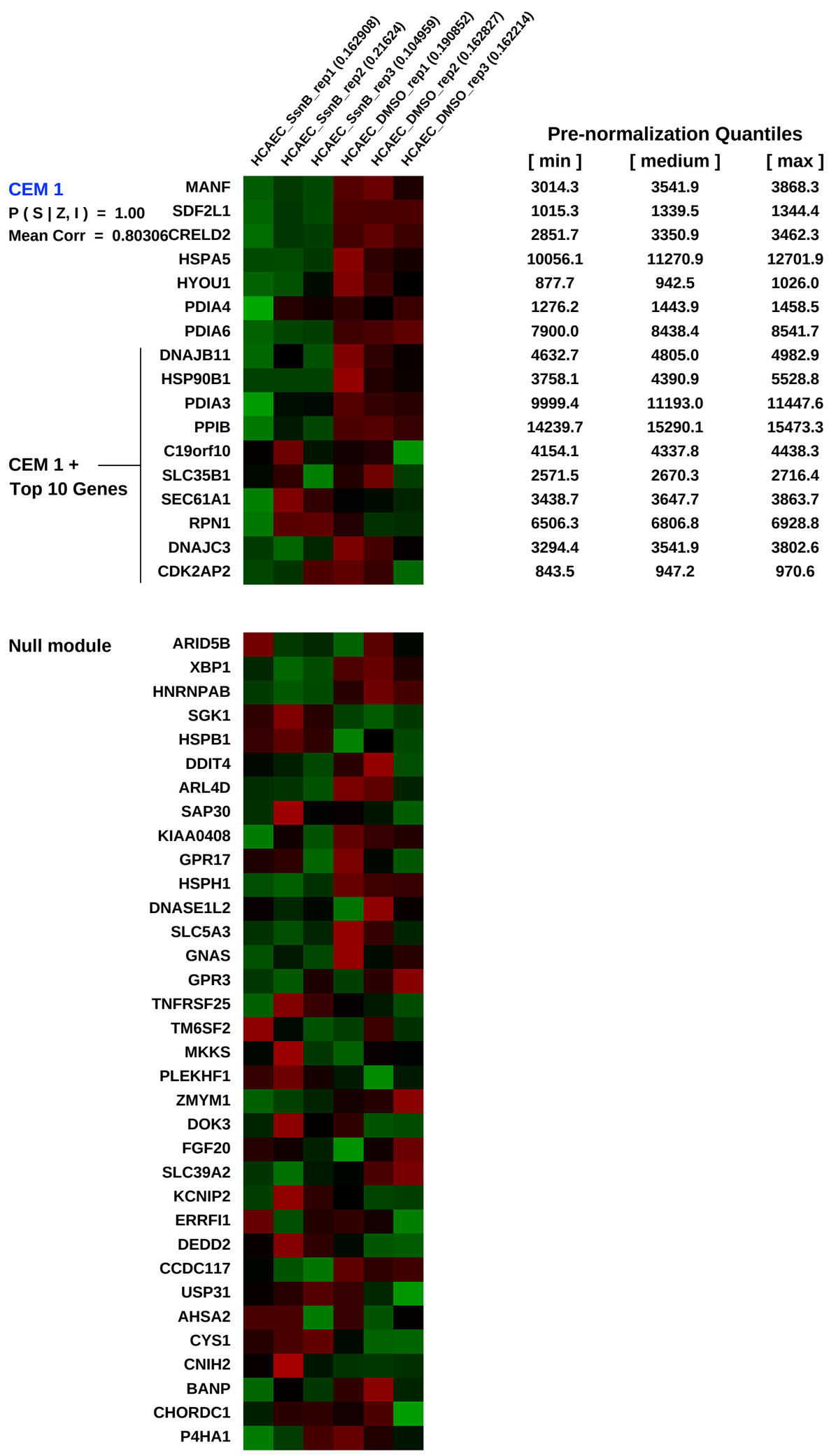

Pre-normalization Quantiles

	[min]	[medium]	[max]
MANF	3014.3	3541.9	3868.3
SDF2L1	1015.3	1339.5	1344.4
CRELD2	2851.7	3350.9	3462.3
HSPA5	10056.1	11270.9	12701.9
HYOU1	877.7	942.5	1026.0
PDIA4	1276.2	1443.9	1458.5
PDIA6	7900.0	8438.4	8541.7
DNAJB11	4632.7	4805.0	4982.9
HSP90B1	3758.1	4390.9	5528.8
PDIA3	9999.4	11193.0	11447.6
PPIB	14239.7	15290.1	15473.3
C19orf10	4154.1	4337.8	4438.3
SLC35B1	2571.5	2670.3	2716.4
SEC61A1	3438.7	3647.7	3863.7
RPN1	6506.3	6806.8	6928.8
DNAJC3	3294.4	3541.9	3802.6
CDK2AP2	843.5	947.2	970.6

GEO Series "GSE14842" Expression Profiles

Num of samples in this series: 14

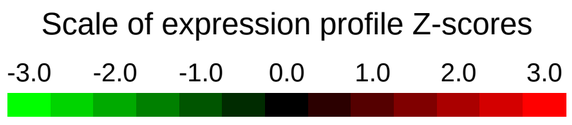

GEO Link: http://www.ncbi.nlm.nih.gov/geo/query/acc.cgi?acc=GSE14842

Status: Public on Feb 14 2009

Title: Expression data from IBS patients before and after treatment

Organism: Homo sapiens

Experiment type: Expression profiling by array

Platform: GPL570

Pubmed ID:

Summary & Design:

Summary:
Increased numbers of mast cells and their products have been linked to symptom onset and severity in patients with chronic diarrhea and abdominal pain. Although mast-cell inhibition ameliorates clinical manifestations and reduces mucosal inflammation, underlying molecular mechanisms remain unknown.

Keywords: Comparison of gene expression

Overall design:
Diarrhea-irritable bowel syndrome (d-IBS) patients were studied at baseline, or 6 months after natural evolution (control) or oral cromoglycate treatment. Jejunal biopsies were subjected to chip analysis (Affymetrix Human Genome U133 Plus 2.0 GeneChips).

Background corr dist: KL-Divergence = 0.1991, L1-Distance = 0.0493, L2-Distance = 0.0056, Normal std = 0.3313

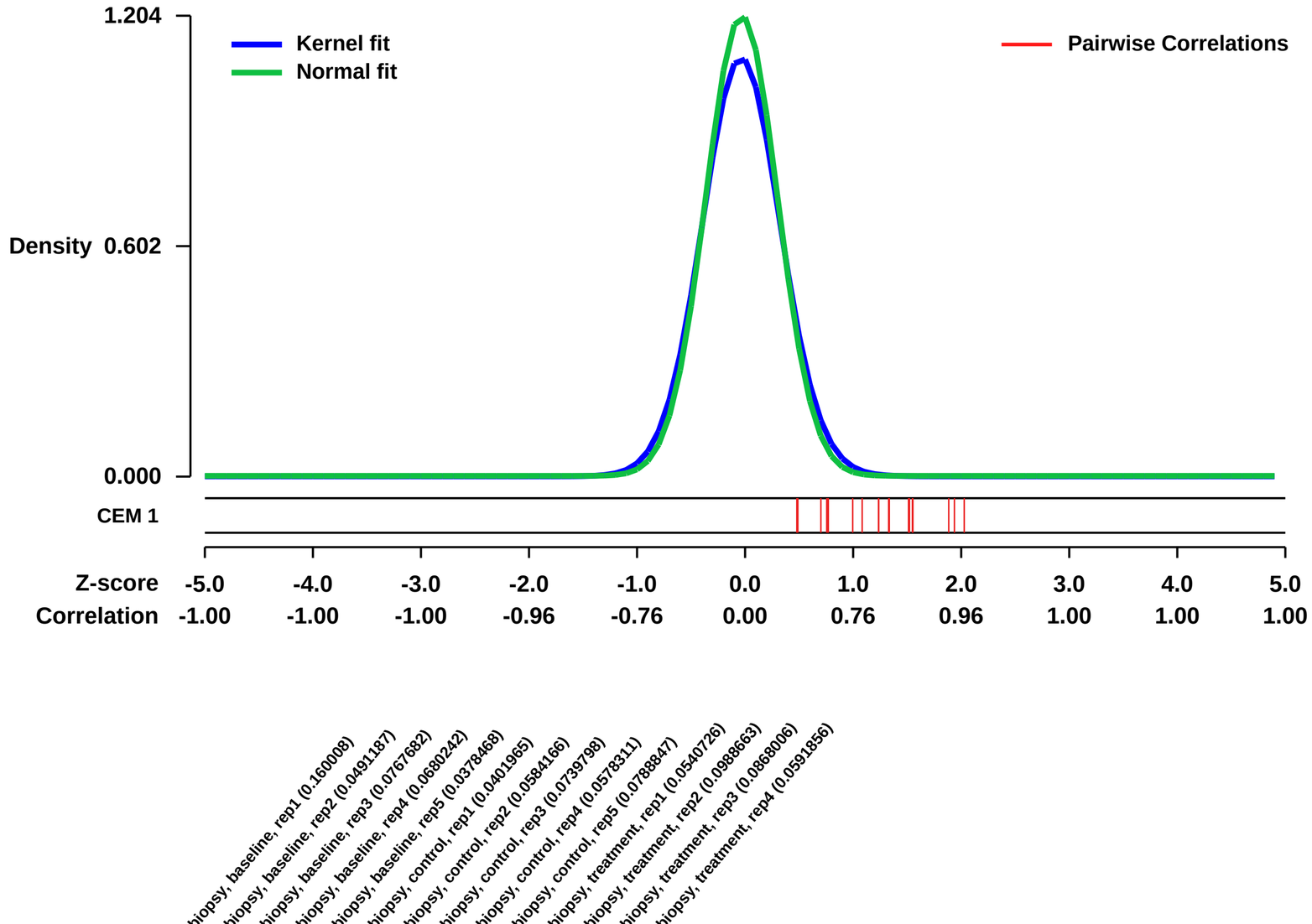

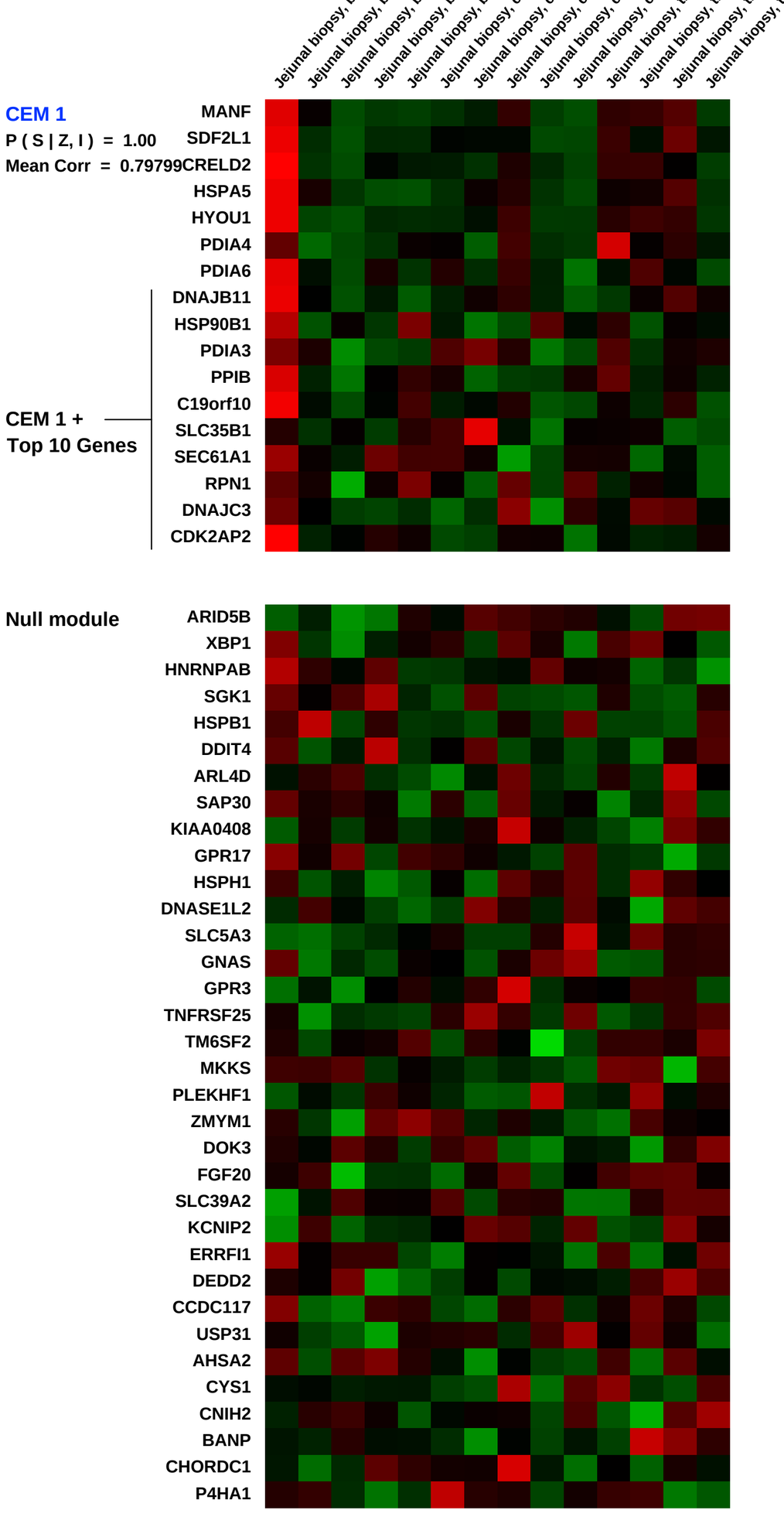

Pre-normalization Quantiles

	[min]	[medium]	[max]
MANF	1516.3	1733.7	2849.4
SDF2L1	713.2	902.9	1612.7
CRELD2	1481.2	1739.7	3136.1
HSPA5	10639.0	14226.3	22866.3
HYOU1	2207.8	2410.1	3737.3
PDIA4	774.3	904.9	1154.5
PDIA6	3375.6	4315.8	6584.5
DNAJB11	2784.1	3336.7	4780.2
HSP90B1	1914.4	2385.3	3236.3
PDIA3	6938.6	10428.5	12388.8
PPIB	10441.7	11840.0	14368.3
C19orf10	1743.1	1945.6	2604.5
SLC35B1	2888.6	3889.2	5730.7
SEC61A1	1816.4	2271.7	2639.9
RPN1	2378.9	2998.1	3361.8
DNAJC3	3103.3	3694.5	4336.6
CDK2AP2	674.9	860.8	1291.5

GEO Series "GSE33325" Expression Profiles

Num of samples in this series: 39

Scale of expression profile Z-scores

-3.0 -2.0 -1.0 0.0 1.0 2.0 3.0

GEO Link: http://www.ncbi.nlm.nih.gov/geo/query/acc.cgi?acc=GSE33325
Status: Public on Oct 29 2011
Title: Gene expression changes in human cardiomyocytes exposed to VX (O-ethyl S-[2-(diisopropylamino)ethyl] methylphosphonothiolate)
Organism: Homo sapiens
Experiment type: Expression profiling by array
Platform: GPL570
Pubmed ID:
Summary & Design:

Summary:
Organophosphorus compounds induce cardiotoxicity through currently unknown mechanisms, which need to be unraveled by a comprehensive and systematic approach such as genome-wide gene expression analysis.

We used microarrays to study gene expression changes in human cardiomyocytes after exposure to VX, and identified pathways underlying these changes.

Overall design:
Human cardiomyocytes were exposed to sublethal concentrations (0, 0.1, 10 ¸…M) of VX. RNA were extracted at different timepoints (0, 6, 24, 72 h) after VX exposure and hybridized to Affymetrix microarrays. Four biological repeats were used for each condition.

Background corr dist: KL-Divergence = 0.1642, L1-Distance = 0.0295, L2-Distance = 0.0012, Normal std = 0.3648

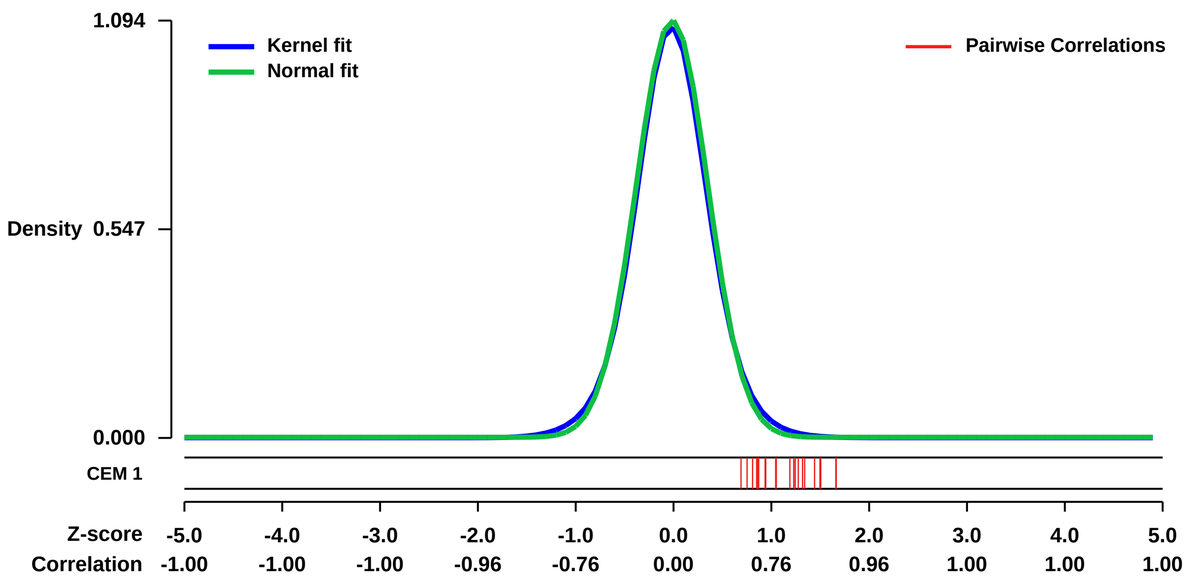

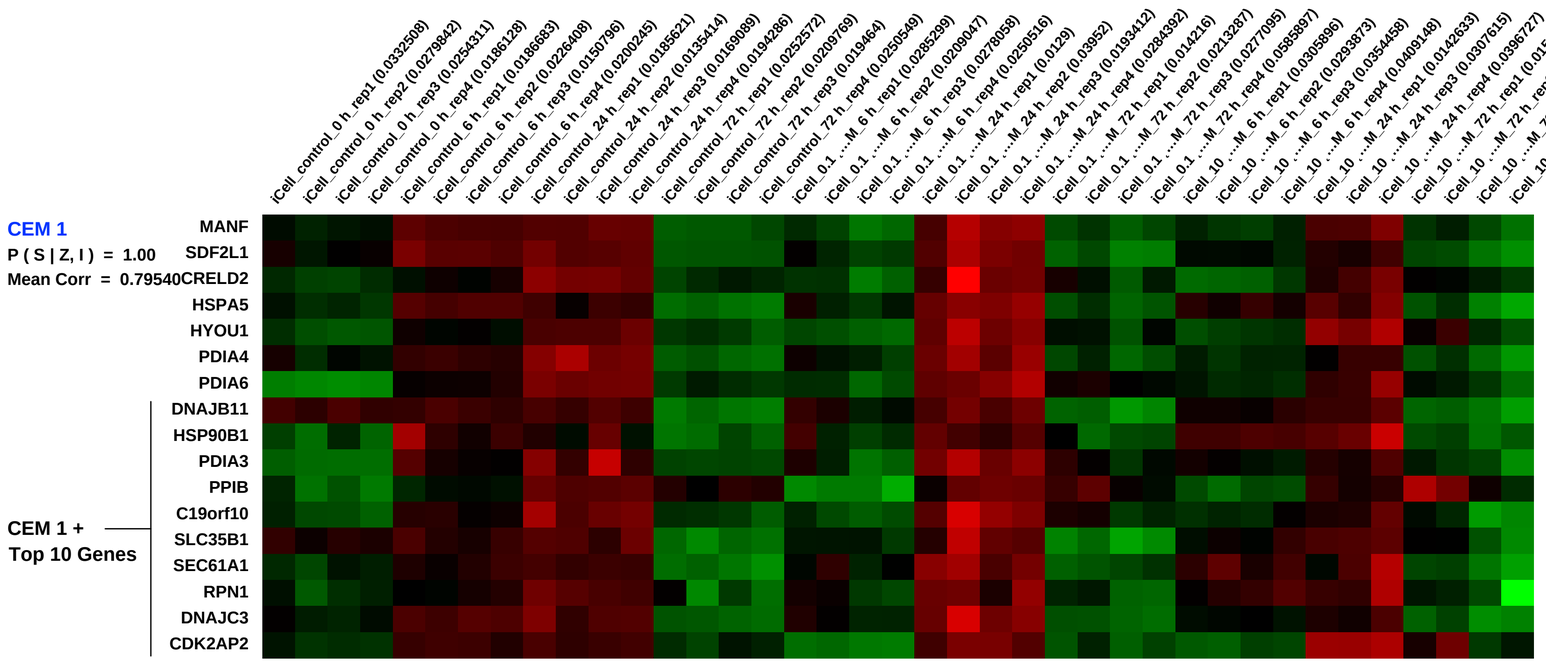

Pre-normalization Quantiles

[min]	[medium]	[max]
4042.4	5199.9	8075.8
891.3	1498.4	2281.4
1637.1	2104.8	3488.5
15944.6	23681.7	30050.4
1294.9	1643.2	2457.7
355.1	537.3	795.3
6737.0	8693.3	11519.5
4353.9	7052.4	8001.7
5903.3	8107.2	12522.7
8410.5	10629.7	13680.4
14969.7	18711.1	22149.5
1875.7	2424.4	3526.4
2154.9	2919.9	3705.8
2144.0	2867.1	3690.1
3303.5	4168.1	4726.5
2216.1	3561.3	5771.7
823.6	1383.0	2455.8

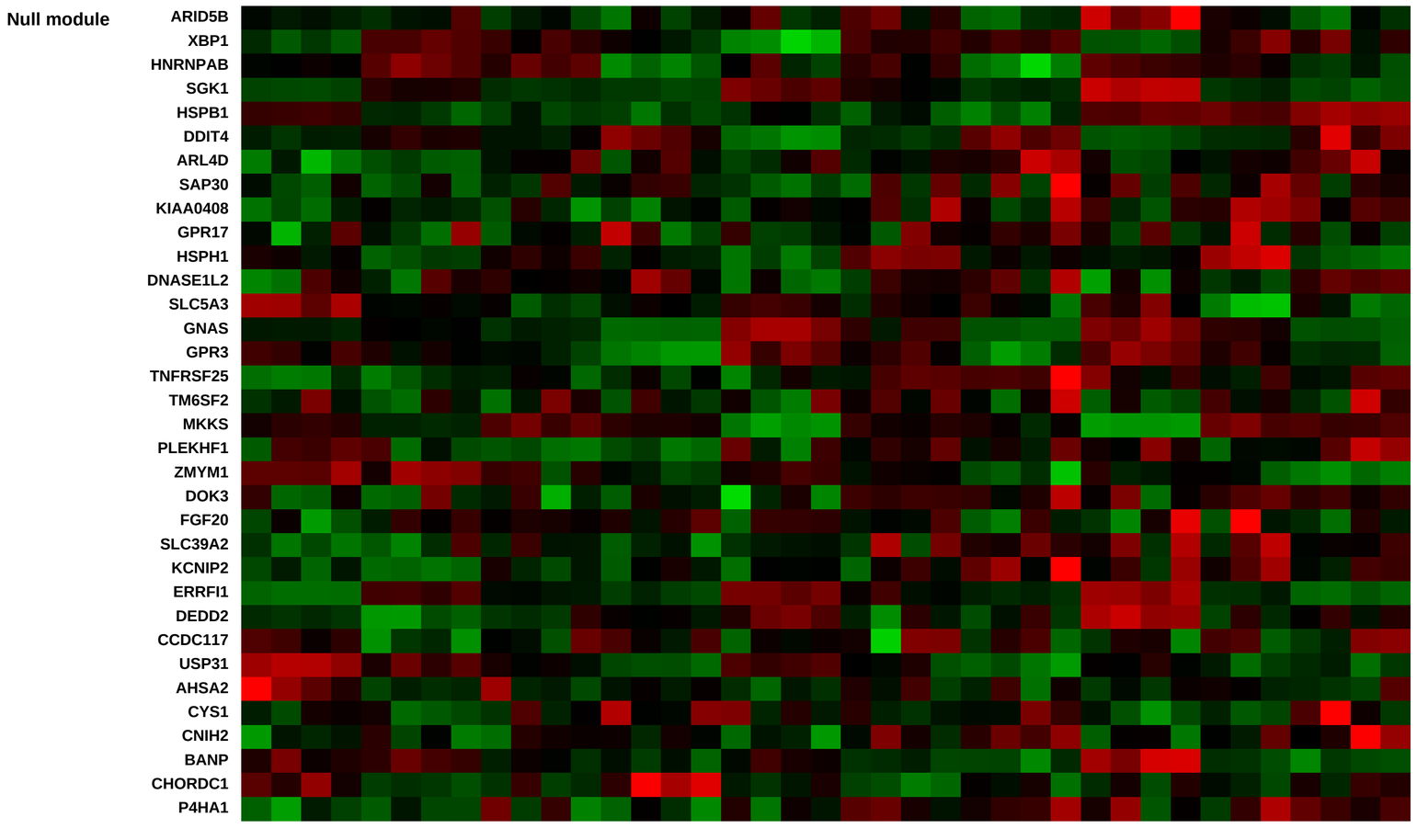

GEO Series "GSE26920" Expression Profiles

Num of samples in this series: 6

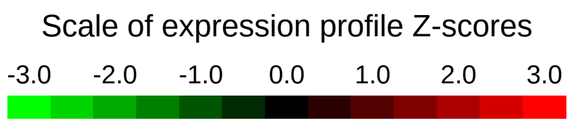

GEO Link:	**http://www.ncbi.nlm.nih.gov/geo/query/acc.cgi?acc=GSE26920**
Status:	**Public on Dec 31 2011**
Title:	**Iron Chelators Treatment on DMS-53 Human Lung Cancer Cell**
Organism:	**Homo sapiens**
Experiment type:	**Expression profiling by array**
Platform:	**GPL570**
Pubmed ID:	
Summary & Design:	**Summary:** **The molecular role of iron in gene expression remains poorly characterized. Moreover, the alterations in global gene expression after iron chelation remains unclear and are important to assess for understanding the molecular pathology of iron-depletion and the biological effects of iron chelators. We assessed the effect on whole genome gene expression of two iron chelators (desferrioxamine and Dp44mT). These studies are important for understanding the molecular and cellular effects of iron-depletion.** **Overall design:** **Total RNA was isolated from cells in 1 mL of TRIzol´fi reagent (Invitrogen). Samples were then prepared and hybridized to the Human Genome U133 Plus 2.0 430 2.0. The human GeneChip´fi U133 Plus 2.0 consists of greater than 47,000 transcripts and variants from over 38,500 well characterized human genes. On completion of hybridization and washing, microarray chips were scanned with the Affymetrix GeneChip´fi Scanner 3000 (Affymetrix).**

Background corr dist: KL-Divergence = 0.0165, L1-Distance = 0.0439, L2-Distance = 0.0023, Normal std = 0.8476

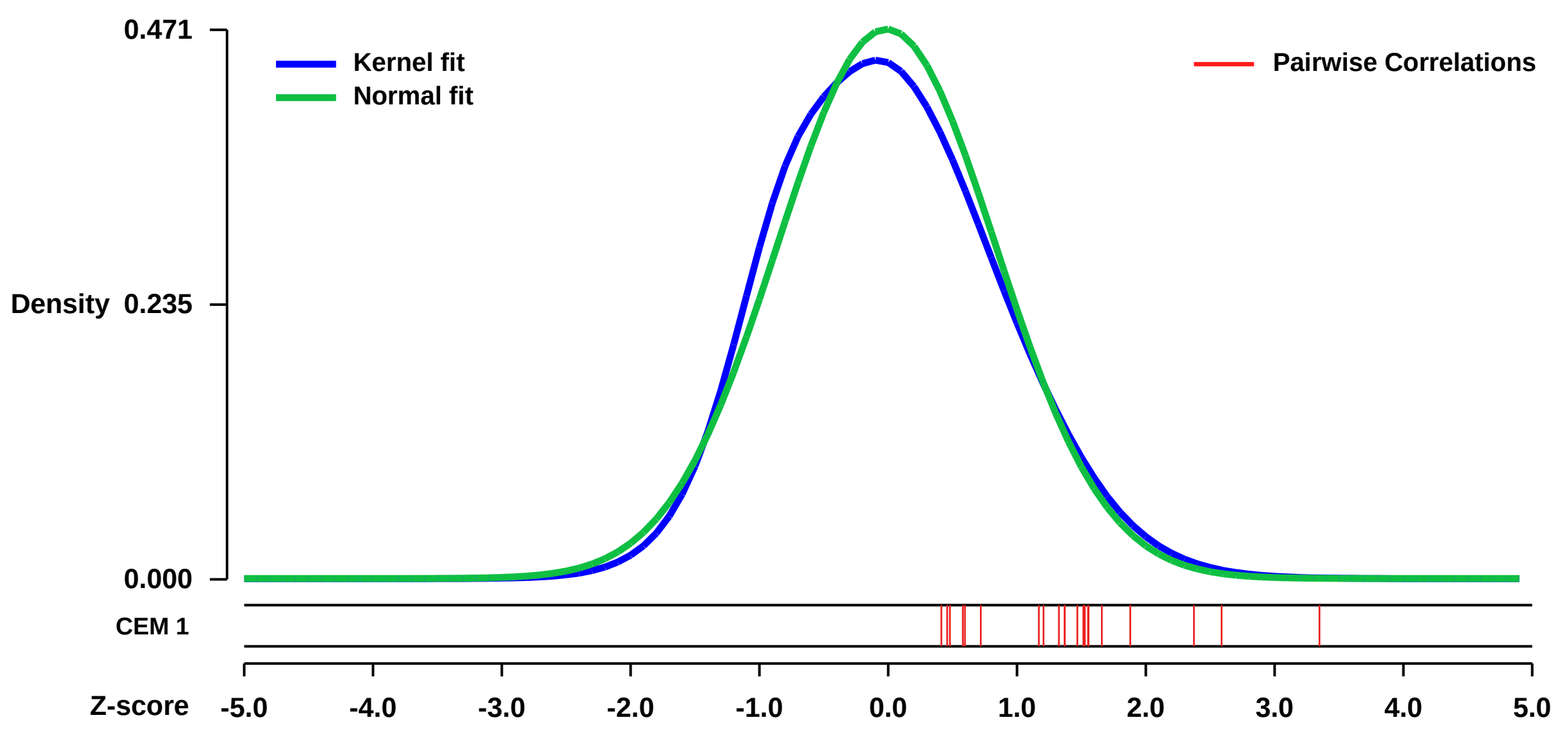

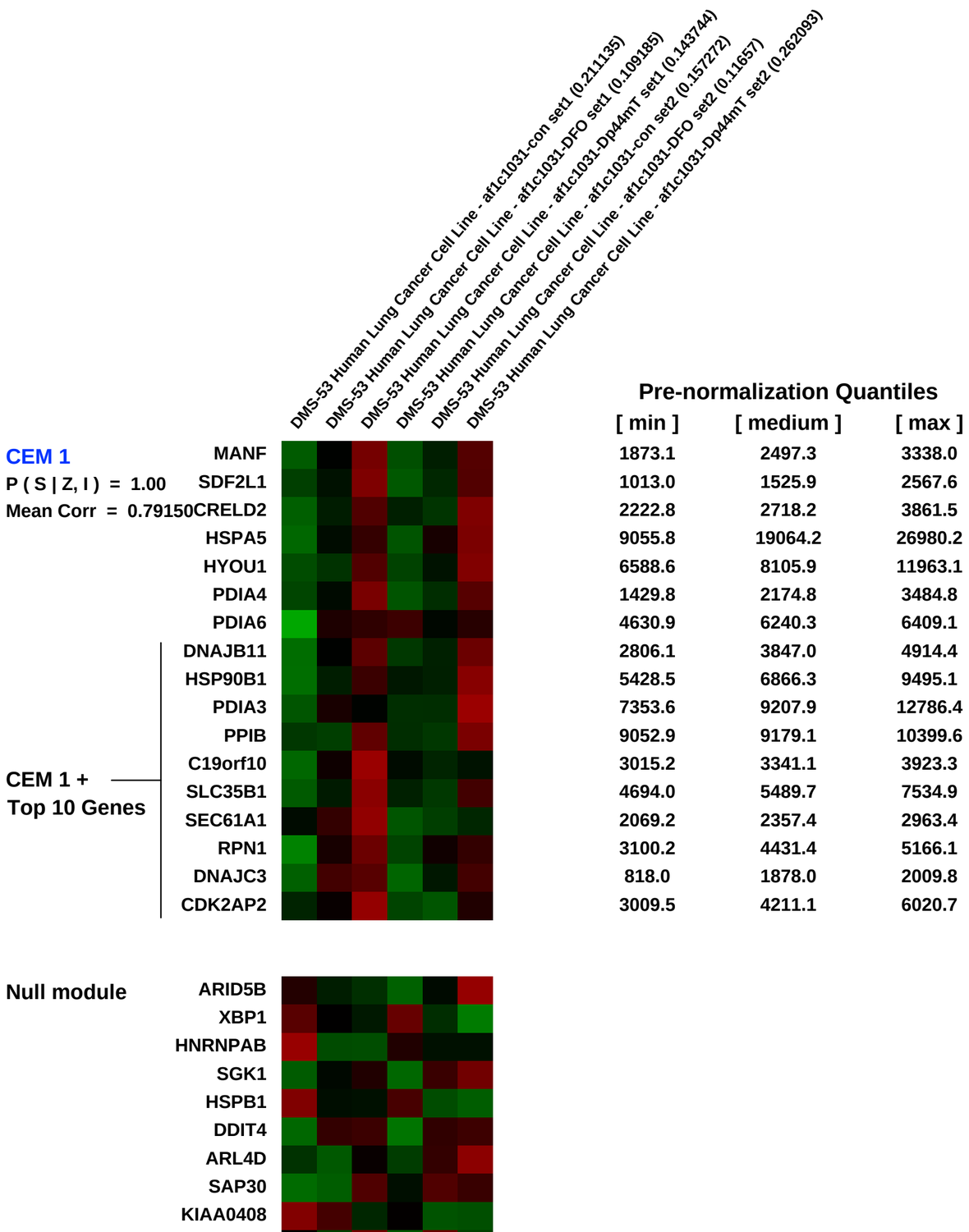

GEO Series "GSE36766" Expression Profiles

Num of samples in this series: 14

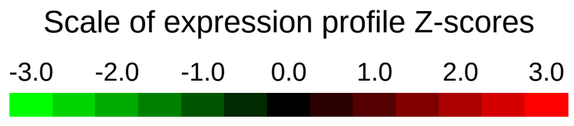

GEO Link:	http://www.ncbi.nlm.nih.gov/geo/query/acc.cgi?acc=GSE36766
Status:	Public on Jun 17 2013
Title:	Effect of human breast tumor supernatant on normal CD4+ T cells (Confirmation Set SN)
Organism:	Homo sapiens
Experiment type:	Expression profiling by array
Platform:	GPL570
Pubmed ID:	23778140
Summary & Design:	**Summary:** CD4+ helper T (Th) cells are critical regulators of immune responses but their role in breast cancer is currently unknown. This work aims to characterize Th cells infiltrating invasive primary human breast tumors, analyze the influence by the tumor microenvironment and identify Th cell specific prognostic gene signatures. CD4+ T cells isolated from the tumor (TIL), axillary lymph node (LN) and blood (PB) of 10 patients were analyzed on Affymetrix U133 Plus 2.0 arrays. A confirmation set of 60 patients were studied by flow cytometry, qRT-PCR or immunohistochemistry and analyzed according to the extent of the tumor immune infiltrate. Gene expression profiles of freshly isolated TIL were also compared with TIL that had been rested overnight or with CD4+ T cells [non-stimulated (NS) or stimulated (S)] from healthy donor PB treated with tumor supernatant (SN). Comparing gene expression profiles of donor blood derived memory CD4+ T cells [non-stimulated (NS) or stimulated (S)] with and without tumor supernatant (SN) treatment **Overall design:** Memory CD4+ T cells isolated from a healthy donor blood (NS or S) were treated (and as control: untreated samples in biological triplicate) with SN obtained from fresh breast tumor homogenates of 4 patients and analyzed on Affymetrix U133 Plus 2.0 arrays

Background corr dist: KL-Divergence = 0.0422, L1-Distance = 0.0159, L2-Distance = 0.0002, Normal std = 0.6047

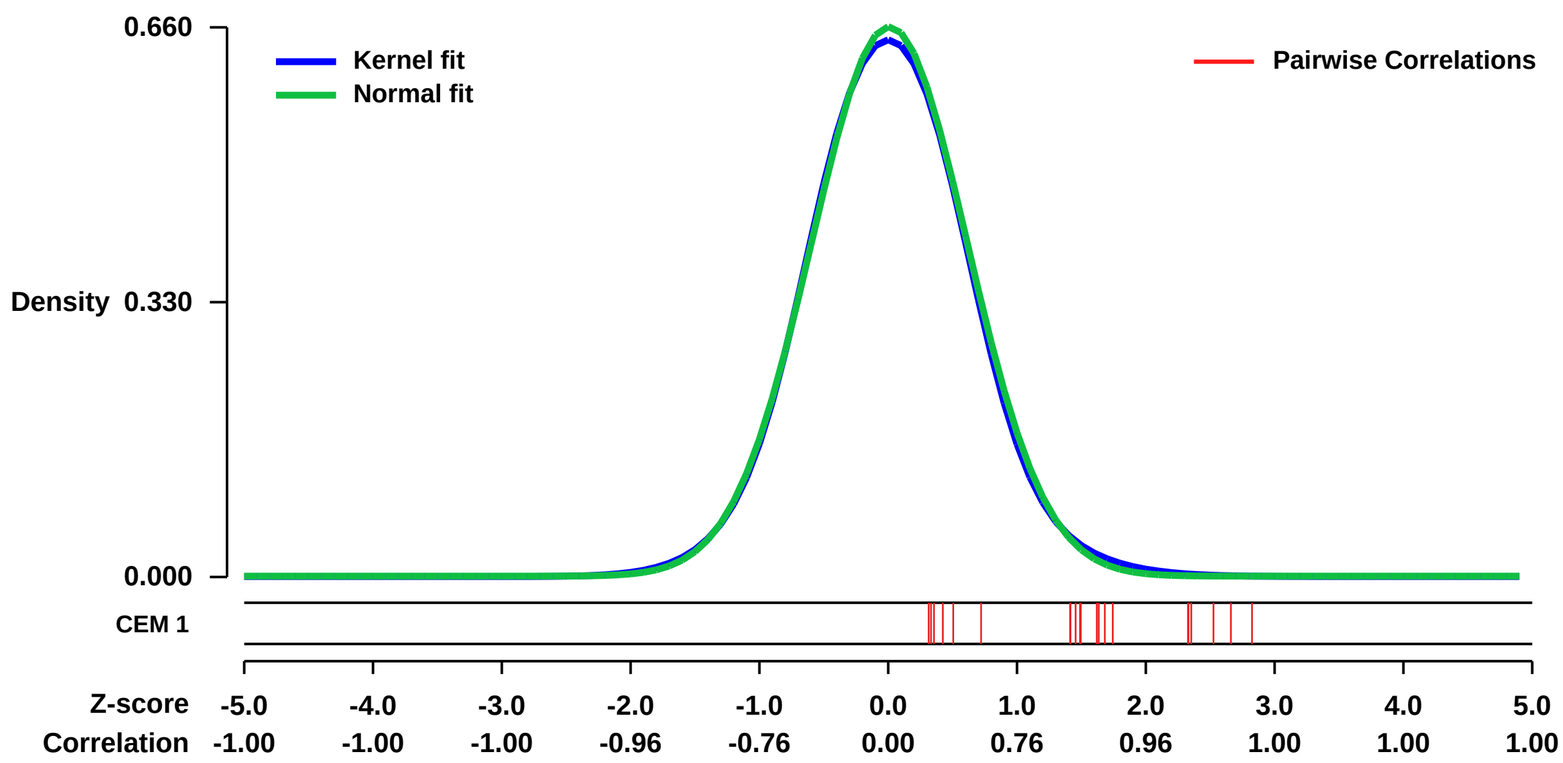

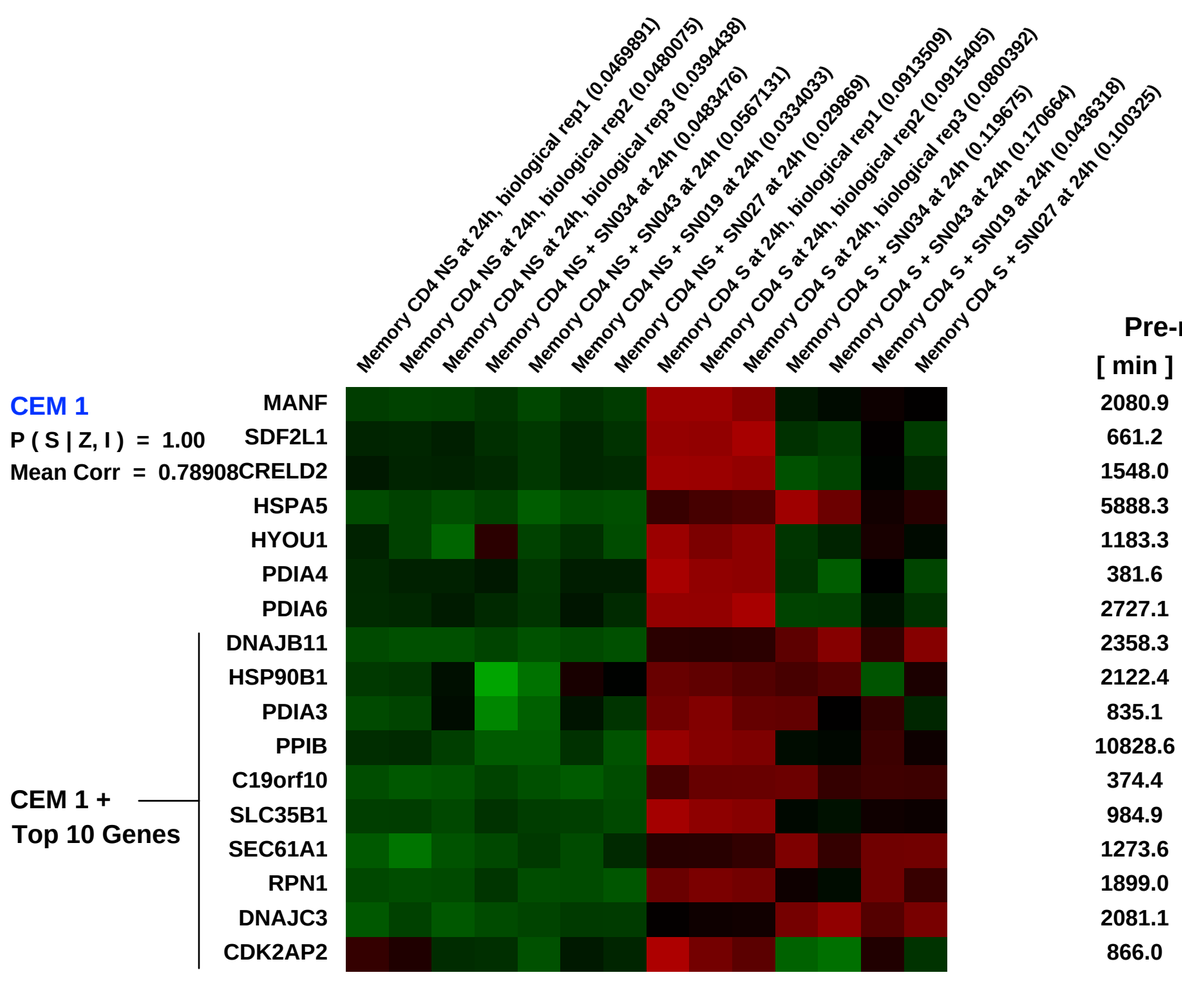

Pre-normalization Quantiles

	[min]	[medium]	[max]
MANF	2080.9	3084.5	6969.3
SDF2L1	661.2	823.9	2298.3
CRELD2	1548.0	2330.1	5687.5
HSPA5	5888.3	10028.9	15326.0
HYOU1	1183.3	1606.5	2819.8
PDIA4	381.6	552.1	1080.1
PDIA6	2727.1	3498.6	9287.2
DNAJB11	2358.3	6323.4	9412.6
HSP90B1	2122.4	4081.8	4918.3
PDIA3	835.1	1489.4	2244.8
PPIB	10828.6	12915.4	17241.2
C19orf10	374.4	720.3	856.1
SLC35B1	984.9	1470.8	3042.0
SEC61A1	1273.6	2033.9	2454.6
RPN1	1899.0	2811.1	4475.3
DNAJC3	2081.1	2995.4	4382.8
CDK2AP2	866.0	1258.4	2156.3

GEO Series "GSE34589" Expression Profiles

Num of samples in this series: 8

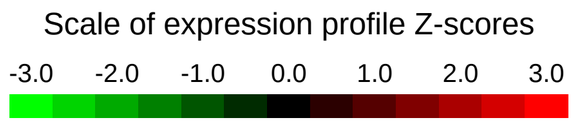

GEO Link:	http://www.ncbi.nlm.nih.gov/geo/query/acc.cgi?acc=GSE34589
Status:	Public on May 02 2013
Title:	Elk1 Directs a Critical Component of Growth Signaling by the Androgen Receptor in Prostate Cancer
Organism:	Homo sapiens
Experiment type:	Expression profiling by array
Platform:	GPL570
Pubmed ID:	23426362
Summary & Design:	**Summary:** Elk1 directs selective gene induction that is a substantial and critical component of growth signaling by AR in PC cells. **Overall design:** Gene expression in LNCaP cells was determined in androgen-depleted medium in response to R1881 in ELK1 knock down (via AR shRNA) or in cells treated with control shRNA.

Background corr dist: KL-Divergence = 0.0663, L1-Distance = 0.0248, L2-Distance = 0.0007, Normal std = 0.5220

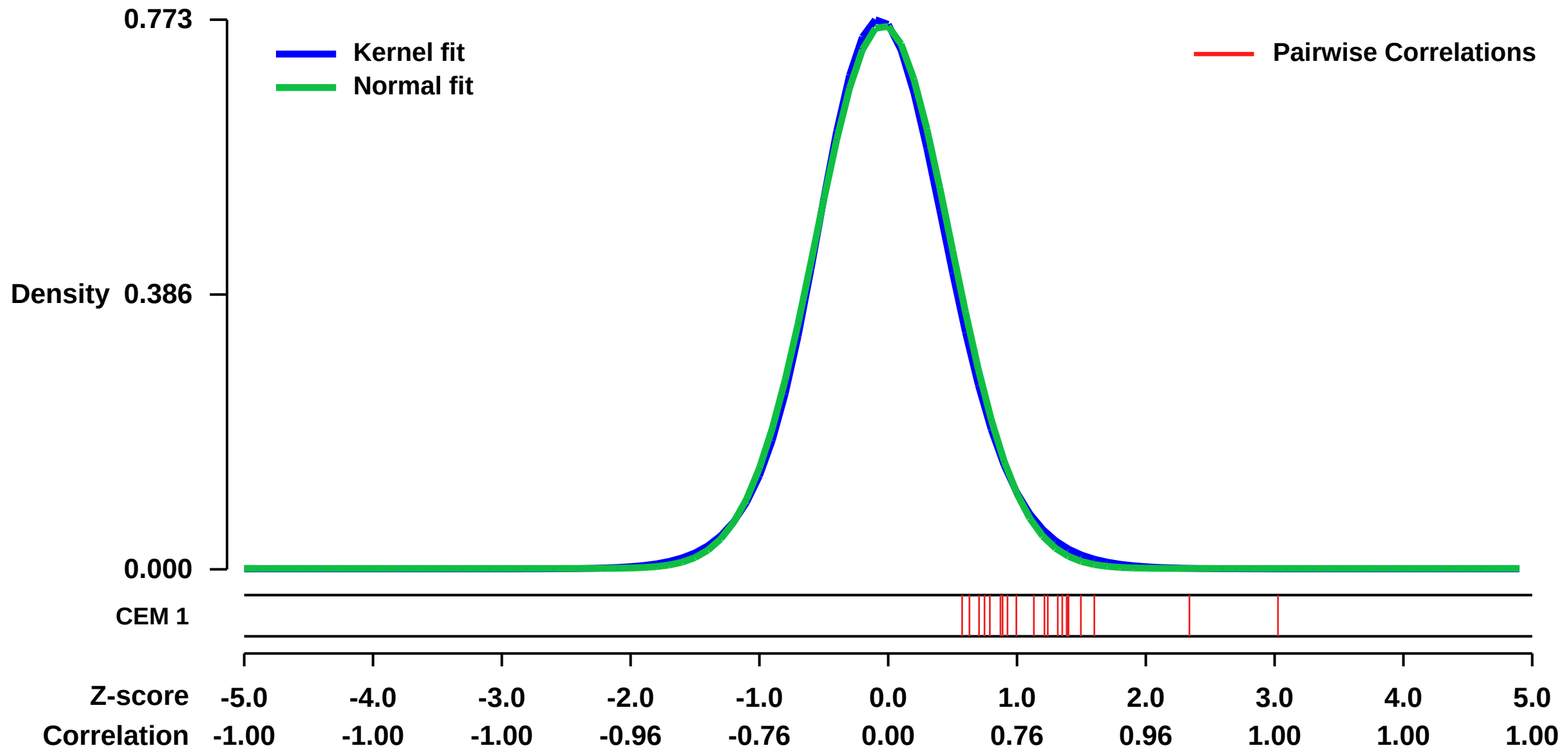

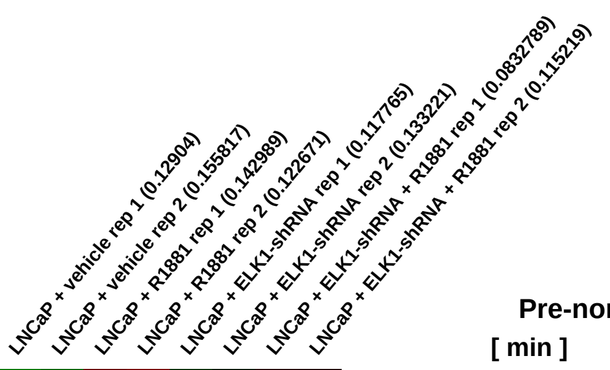

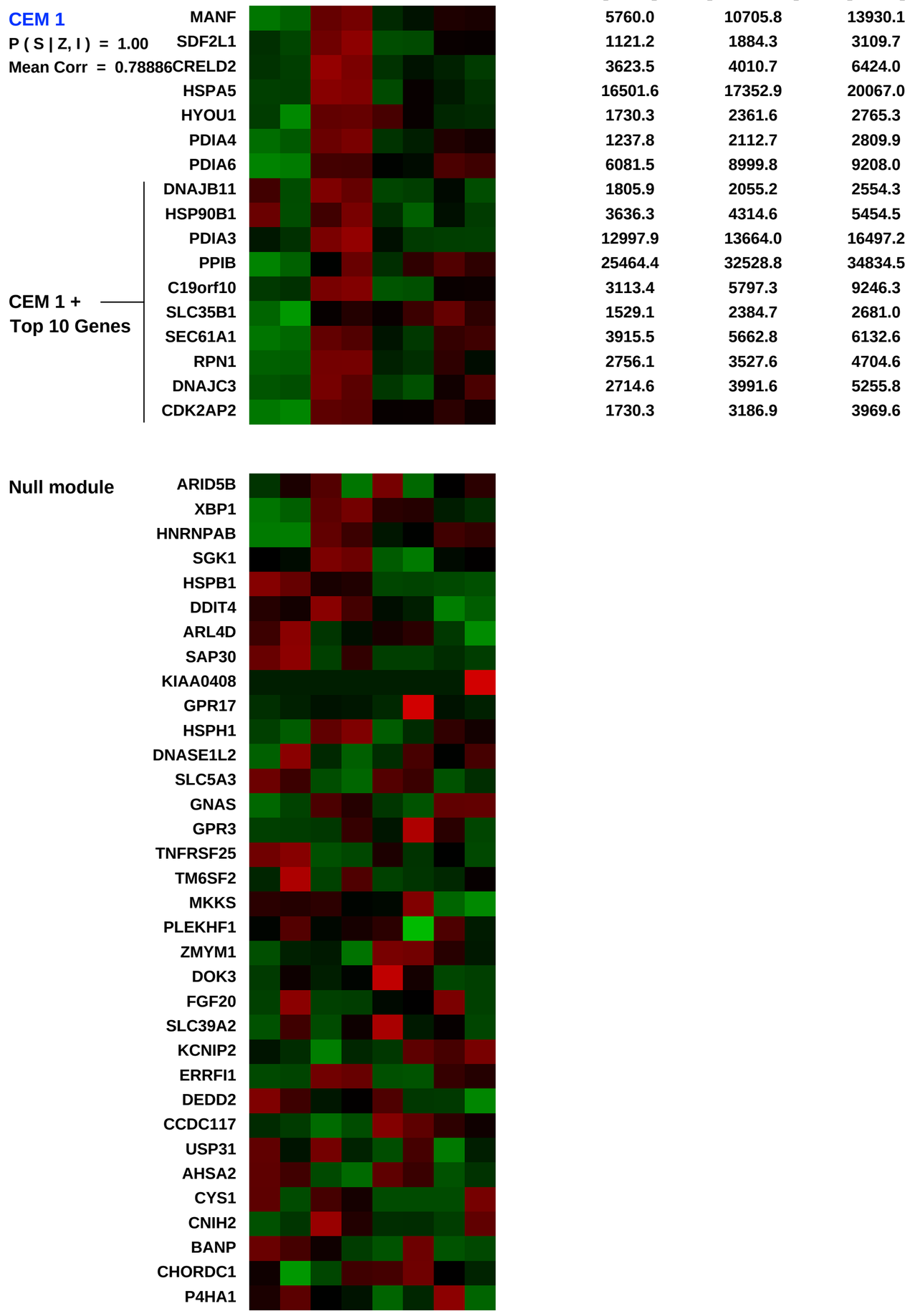

GEO Series "GSE27973" Expression Profiles

Num of samples in this series: 16

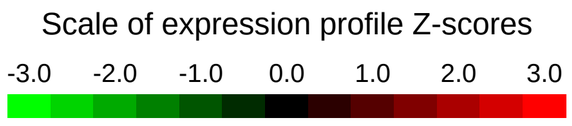

GEO Link:	http://www.ncbi.nlm.nih.gov/geo/query/acc.cgi?acc=GSE27973
Status:	Public on Mar 15 2011
Title:	Human airway epithelial responses to rhinovirus infection and cigarette smoke extract alone and in combination
Organism:	Homo sapiens
Experiment type:	Expression profiling by array
Platform:	GPL570
Pubmed ID:	22808255
Summary & Design:	**Summary:** This study was performed to test the hypothesis that cigarette smoke extract would alter the responses of primary cultures of human bronchial epithelial cells to infection with purified human rhinovirus 16. The data show marked alterations in rhinovirus-induced expression profiles of a number of genes in the presence of cigarette smoke extract (CSE). **Overall design:** Cultured epithelial cells from each of 4 donors were exposed to medium alone, rhinovirus 16 (RV16) alone, CSE alone, or RV16 in the presence of CSE. After a 24 h incubation gene expression was assessed.

Background corr dist: KL-Divergence = 0.2120, L1-Distance = 0.0476, L2-Distance = 0.0054, Normal std = 0.3244

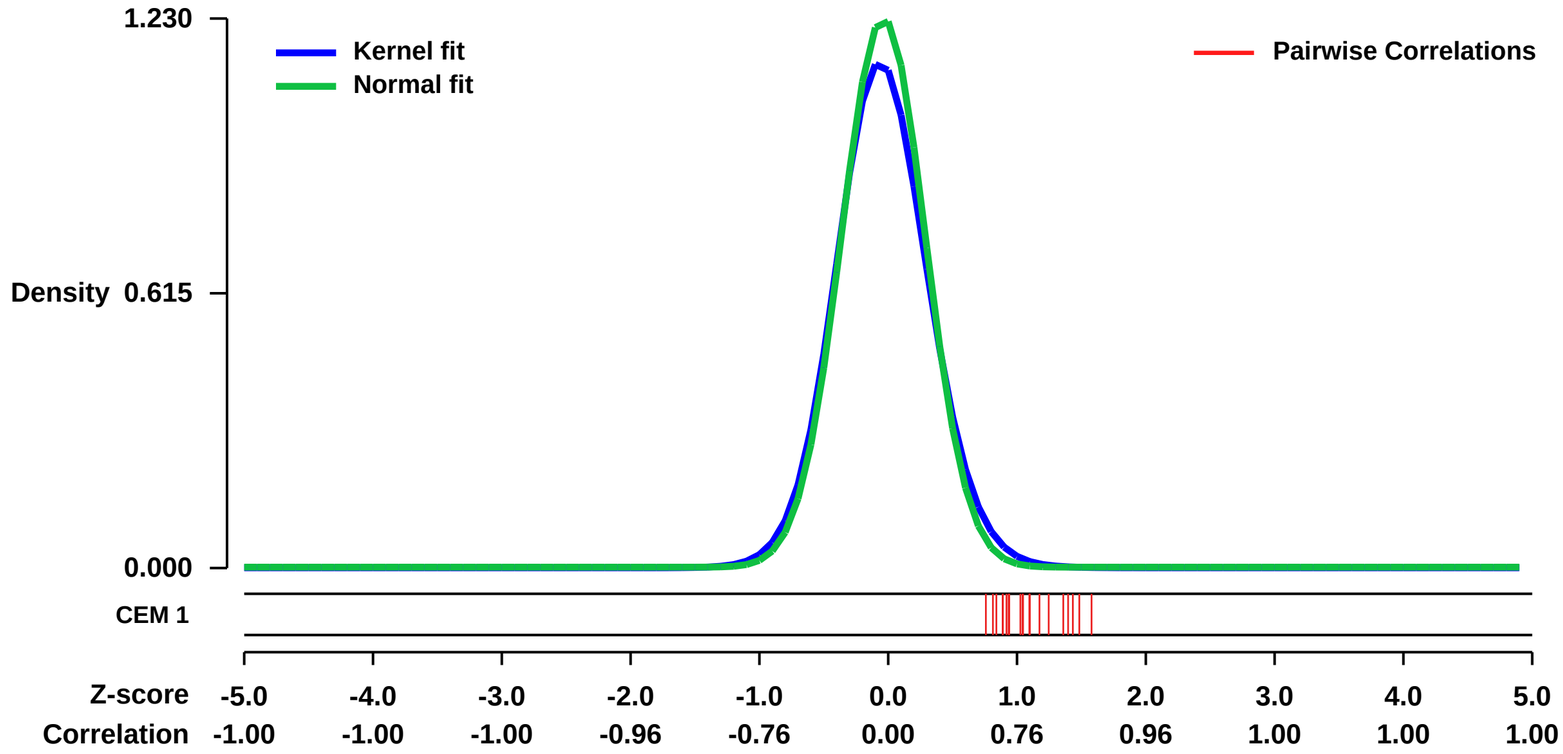

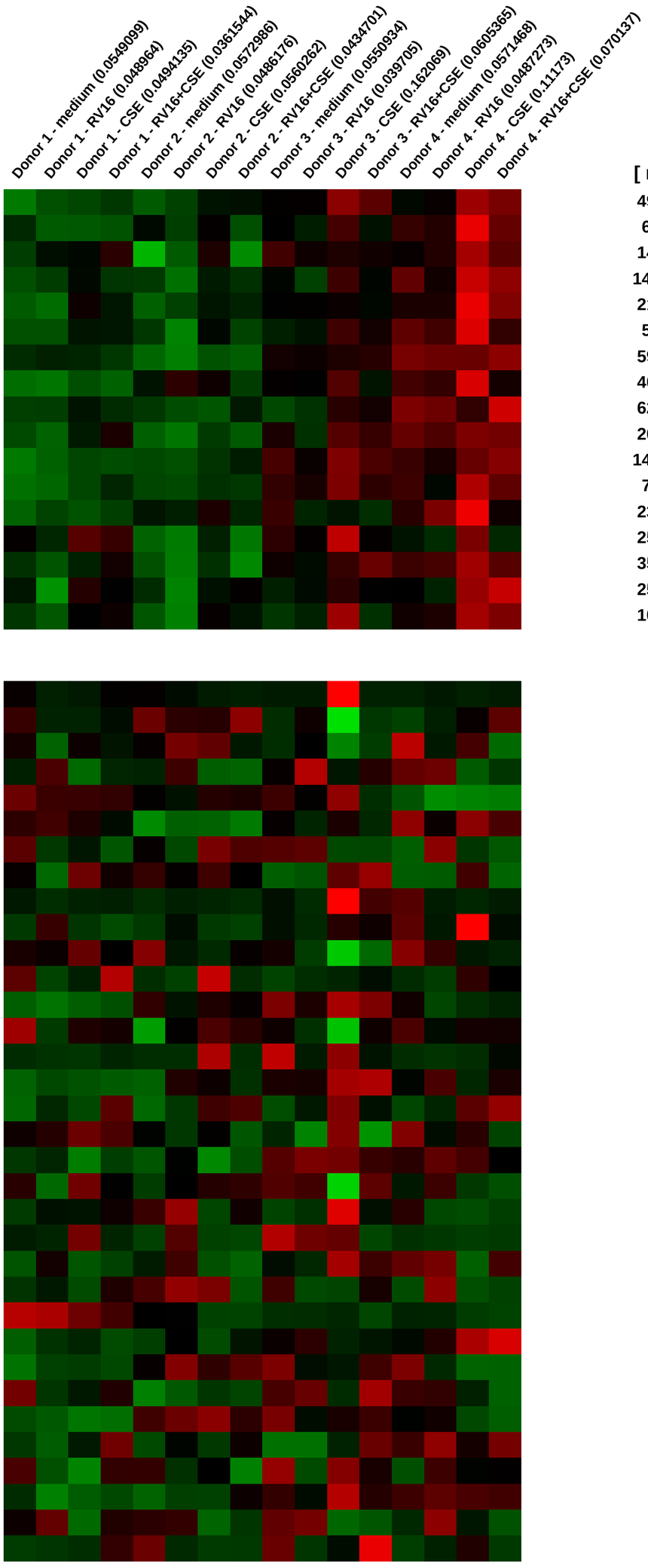

	Pre-normalization Quantiles		
	[min]	[medium]	[max]
MANF	4989.0	9146.2	15164.7
SDF2L1	695.8	1022.7	2012.5
CRELD2	1465.6	2912.4	4018.7
HSPA5	14811.2	25960.5	48046.7
HYOU1	2143.9	3011.7	4914.7
PDIA4	531.4	938.3	1789.7
PDIA6	5972.0	9562.7	12904.4
DNAJB11	4090.8	5001.7	6616.6
HSP90B1	6282.8	8824.1	18675.8
PDIA3	2012.1	3274.2	4130.6
PPIB	14721.6	22983.0	30782.0
C19orf10	707.6	1448.8	2700.3
SLC35B1	2317.7	2640.3	3713.1
SEC61A1	2542.0	3762.1	5557.0
RPN1	3511.8	4748.5	5939.1
DNAJC3	2500.5	3468.4	4800.8
CDK2AP2	1026.6	1524.8	2166.7

GEO Series "GSE3369" Expression Profiles

Num of samples in this series: 6

Scale of expression profile Z-scores

-3.0 -2.0 -1.0 0.0 1.0 2.0 3.0

GEO Link: http://www.ncbi.nlm.nih.gov/geo/query/acc.cgi?acc=GSE3369

Status: Public on Mar 31 2006

Title: Affymetrix U133Plus2.0 data sets of Human Myeloma Cellline JJN3 with non-specific, scrambled shRNA or CKS1B shRNA

Organism: Homo sapiens

Experiment type: Expression profiling by array

Platform: GPL570

Pubmed ID:

Summary & Design:

Summary:
This series represents Affymetrix U133Plus2.0 data sets of JJN3 transduced with levivirus expressing non-specific scrambled shRNA or CKS1B shRNA

Keywords: JJN3 CKS1B shRNA

Overall design:
This series represents Affymetrix U133Plus2.0 data sets of JJN3 transduced with levivirus expressing non-specific scrambled shRNA or CKS1B shRNA

Background corr dist: KL-Divergence = 0.0116, L1-Distance = 0.0384, L2-Distance = 0.0016, Normal std = 0.9474

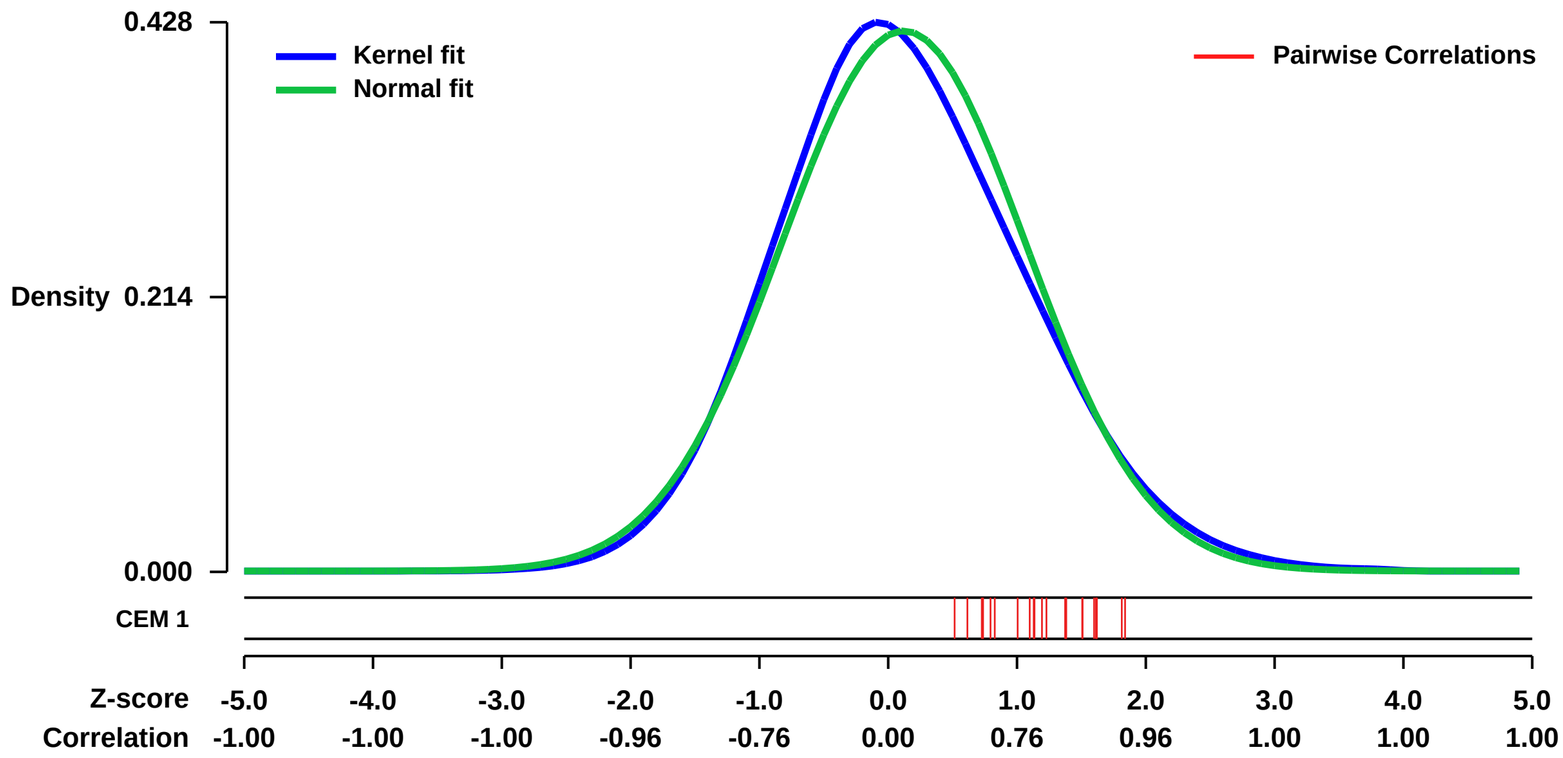

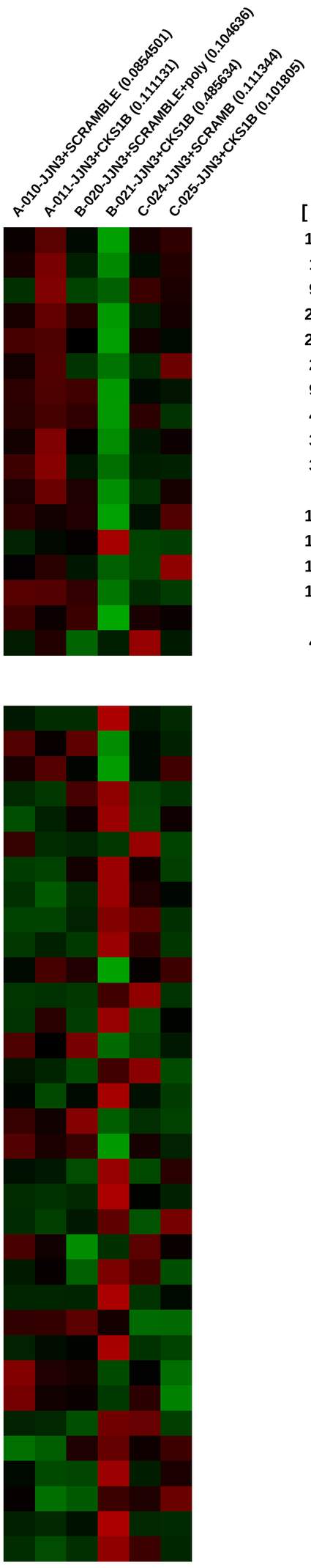

		Pre-normalization Quantiles [min]	[medium]	[max]
CEM 1	MANF	1018.1	3818.0	4829.3
P (S | Z, I) = 1.00	SDF2L1	145.0	1689.6	2615.9
Mean Corr = 0.79589	CRELD2	941.4	2058.1	2953.6
	HSPA5	2505.2	10783.6	14173.3
	HYOU1	2858.8	6429.2	7539.7
	PDIA4	212.5	1197.6	1855.7
	PDIA6	931.0	5165.0	5868.6
CEM 1 + Top 10 Genes	DNAJB11	442.3	4193.8	4660.3
	HSP90B1	300.4	4055.7	6860.4
	PDIA3	344.5	1918.2	4628.4
	PPIB	49.6	7593.1	10955.8
	C19orf10	1488.3	5242.1	6209.2
	SLC35B1	1416.4	2802.0	6885.8
	SEC61A1	1316.3	2948.6	5329.3
	RPN1	1465.5	3298.0	3678.3
	DNAJC3	12.8	1546.1	1826.2
	CDK2AP2	495.8	758.7	1374.6
Null module	ARID5B			
	XBP1			
	HNRNPAB			
	SGK1			
	HSPB1			
	DDIT4			
	ARL4D			
	SAP30			
	KIAA0408			
	GPR17			
	HSPH1			
	DNASE1L2			
	SLC5A3			
	GNAS			
	GPR3			
	TNFRSF25			
	TM6SF2			
	MKKS			
	PLEKHF1			
	ZMYM1			
	DOK3			
	FGF20			
	SLC39A2			
	KCNIP2			
	ERRFI1			
	DEDD2			
	CCDC117			
	USP31			
	AHSA2			
	CYS1			
	CNIH2			
	BANP			
	CHORDC1			
	P4HA1			

GEO Series "GSE49628" Expression Profiles

Num of samples in this series: 9

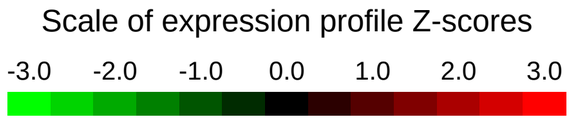

GEO Link:	http://www.ncbi.nlm.nih.gov/geo/query/acc.cgi?acc=GSE49628
Status:	Public on Sep 17 2013
Title:	Large-scale hypomethylated blocks associated with Epstein-Barr virus-induced B-cell immortalization [Expression Array]
Organism:	Homo sapiens
Experiment type:	Expression profiling by array
Platform:	GPL570
Pubmed ID:	24068705
Summary & Design:	**Summary:** To determine what DNA methylation and gene expression changes occur following EBV transformation. B-cells were isolated from 3 donors. Resting, CD40 activated and EBV transfromed cells from each donor was analyzed. Each sample was assayed using Affymetrix expression arrays and whole genome bisulfite sequenicng. Additional time points during transformation and activation were sequenced as well, but not assayed for expression. **Overall design:** B-cells were isolated from 3 donors. Resting, CD40 activated and EBV transfromed cells from each donor was analyzed.

Background corr dist: KL-Divergence = 0.0455, L1-Distance = 0.0192, L2-Distance = 0.0004, Normal std = 0.5853

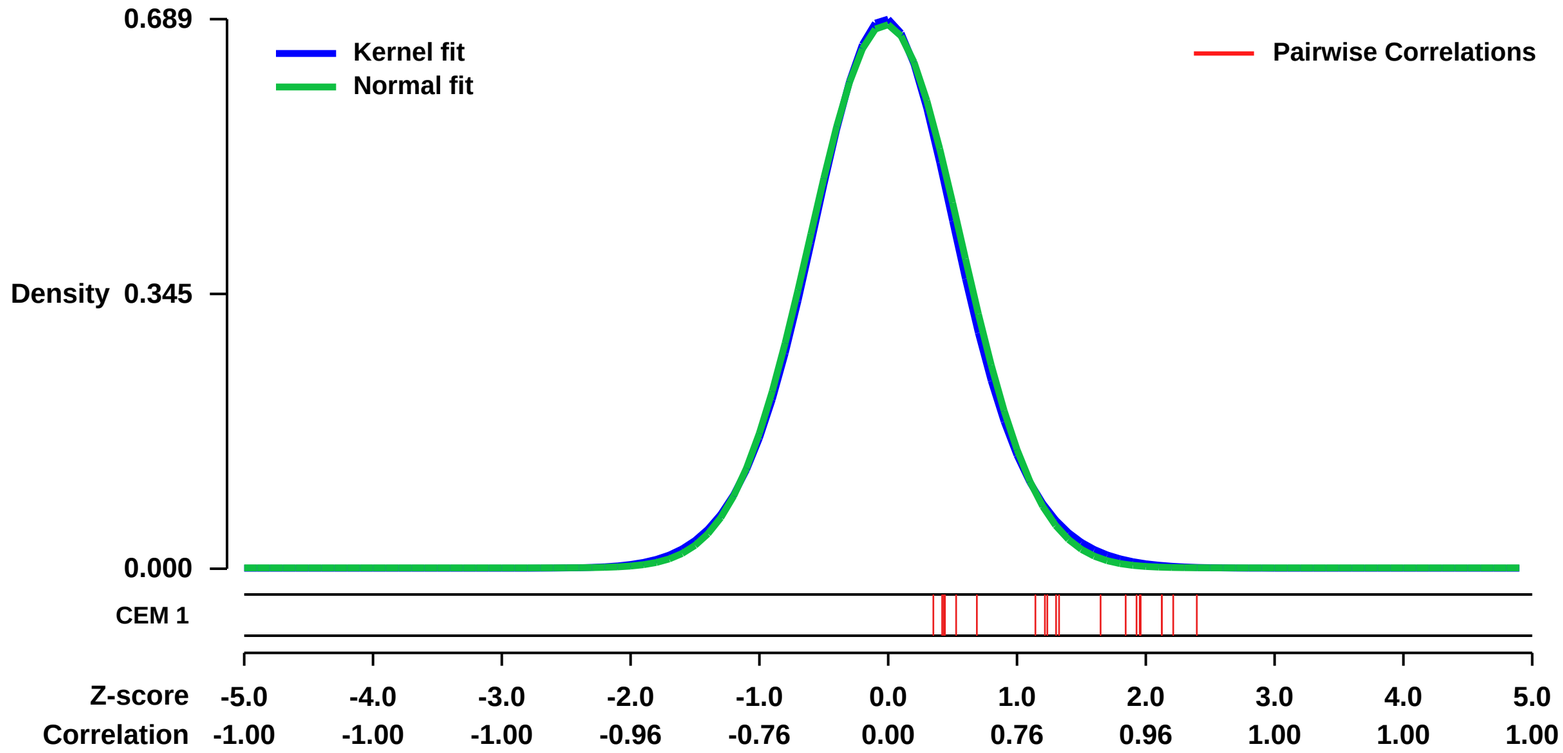

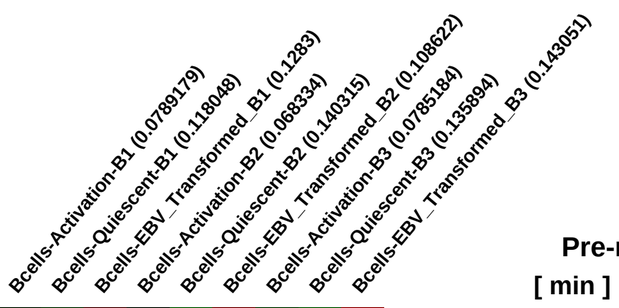

Pre-normalization Quantiles

		[min]	[medium]	[max]
CEM 1	MANF	1536.3	3412.5	7965.0
P (S | Z, I) = 1.00	SDF2L1	522.0	1249.6	3767.7
Mean Corr = 0.78508	CRELD2	1334.5	1977.8	4035.5
	HSPA5	5332.8	10006.0	18191.6
	HYOU1	736.5	1827.3	3253.1
	PDIA4	366.5	813.8	1456.4
	PDIA6	2819.5	7327.1	10363.9
CEM 1 + Top 10 Genes	DNAJB11	1726.9	2854.9	5038.1
	HSP90B1	736.8	1195.5	3356.4
	PDIA3	4016.7	6529.4	9514.8
	PPIB	5777.2	9229.4	15577.5
	C19orf10	1192.1	2296.2	3353.9
	SLC35B1	1107.3	1373.5	2244.6
	SEC61A1	1170.0	1580.7	2643.2
	RPN1	2388.7	2881.0	4144.9
	DNAJC3	1812.6	2415.6	4420.2
	CDK2AP2	500.6	1433.6	1966.1
Null module	ARID5B			
	XBP1			
	HNRNPAB			
	SGK1			
	HSPB1			
	DDIT4			
	ARL4D			
	SAP30			
	KIAA0408			
	GPR17			
	HSPH1			
	DNASE1L2			
	SLC5A3			
	GNAS			
	GPR3			
	TNFRSF25			
	TM6SF2			
	MKKS			
	PLEKHF1			
	ZMYM1			
	DOK3			
	FGF20			
	SLC39A2			
	KCNIP2			
	ERRFI1			
	DEDD2			
	CCDC117			
	USP31			
	AHSA2			
	CYS1			
	CNIH2			
	BANP			
	CHORDC1			
	P4HA1			

GEO Series "GSE23434" Expression Profiles

Num of samples in this series: 12

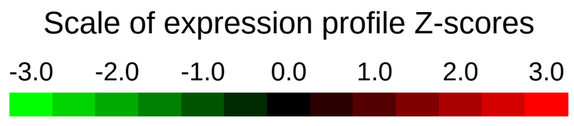

GEO Link:	http://www.ncbi.nlm.nih.gov/geo/query/acc.cgi?acc=GSE23434
Status:	Public on Aug 03 2012
Title:	Expression data from human Kidney cell line induced by PCB153
Organism:	Homo sapiens
Experiment type:	Expression profiling by array
Platform:	GPL570
Pubmed ID:	
Summary & Design:	**Summary:** Exposure to Polychlorobiphenyls (PCBs) is known to cause serious health effects in human but the gene expression profiles leading to development of differnet diseases is not fully understood. The knowledge of global gene expression will help us to devlop early diagnostic biomarkers for PCB induced health effects. We used microarrays to detail the global gene expression profile underlying the effects of PCB153 on human Kidney cells leading to identification of distinct classes of up-regulated and down-regulated genes and cellular processes. Keywords: time course **Overall design:** The HK2 cells are grown in Keratinocyte-Serum Free Medium supplemented 5ng/ml recombinant epidermal growth factor and 0.05mg/ml bovinepituitary extract and 1X Pennicilllin-Streptromycin and were treated with PCB153 for different times. Trizol extraction of total RNA was performed according to the manufacturer's instructions. Biotinylated cRNA were prepared according to the standard Affymetrix protocol from 6 microgram of total RNA (Expression Analysis Technical Manual, 2001, Affymetrix). Following fragmentation, 10 microgram of cRNA were hybridized for 16 hr at 45C on GeneChip Human Genome Array (HGU133 plus 2.0). GeneChips were washed and stained in the Affymetrix Fluidics Station 450 and scanned using the Affymetrix GeneArray Scanner 3000. The data were analyzed with Microarray Suite version 5.0 (MAS 5.0) using Affymetrix default analysis settings and global scaling as normalization method. The trimmed mean target intensity of each array was arbitrarily set to 150.

Background corr dist: KL-Divergence = 0.0882, L1-Distance = 0.0259, L2-Distance = 0.0011, Normal std = 0.4623

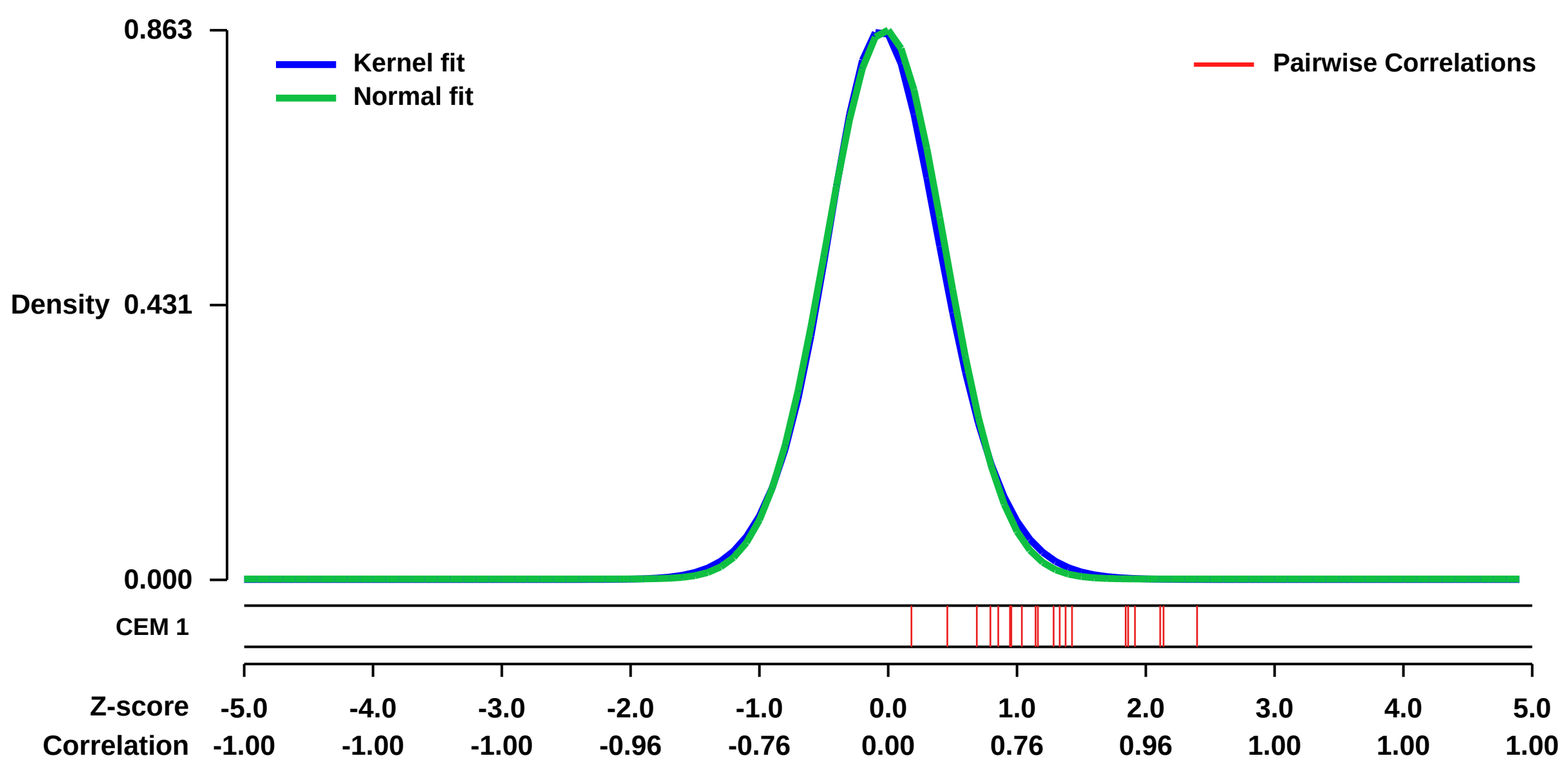

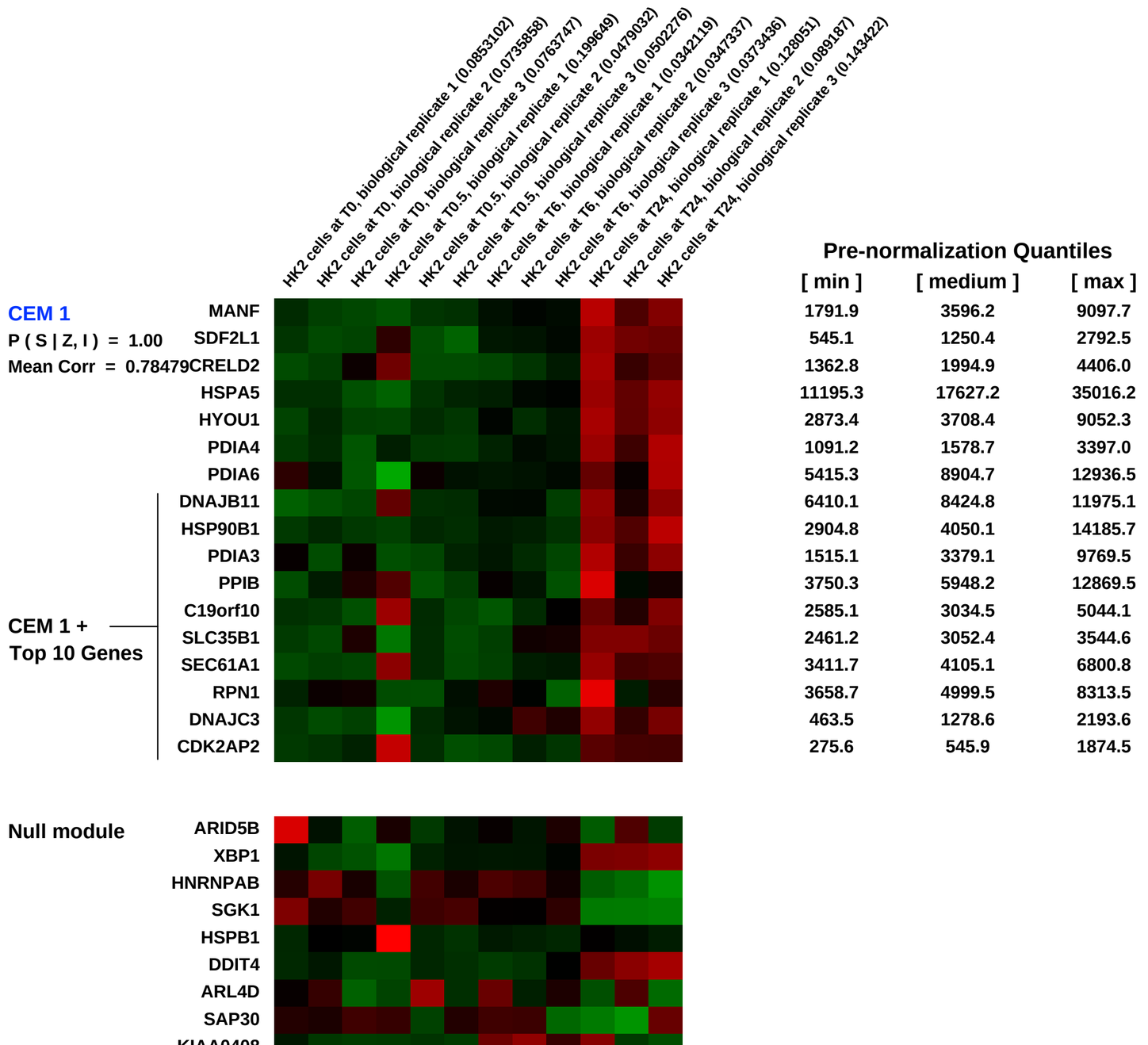

GEO Series "GSE29959" Expression Profiles

Num of samples in this series: 30

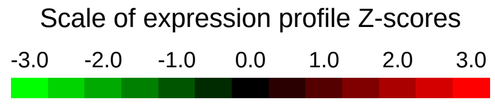

GEO Link:	http://www.ncbi.nlm.nih.gov/geo/query/acc.cgi?acc=GSE29959
Status:	Public on Aug 01 2011
Title:	Human T-ALL cell line response to inhibition of Notch signaling
Organism:	Homo sapiens
Experiment type:	Expression profiling by array
Platform:	GPL570
Pubmed ID:	21807868
Summary & Design:	**Summary:** Analysis of five Notch signaling-dependent human T-ALL cell lines (ALLSIL, DND41, HPBALL, KOPTK1, TALL-1) treated with gamma-secretase inhibitor (GSI) to block Notch signaling. Samples include parental cells, cells rescued by retroviral transduction with ICN (a GSI-independent form of activated Notch1), and cells retrovirally transduced with c-Myc (an important downstream target of Notch1). Results allow segregation of bona fide Notch targets from other genes affected by gamma-secretase inhibition as well as from targets downstream of c-Myc. **Overall design:** Thirty samples were analyzed. Five human T-ALL cell lines (ALLSIL, DND41, HPBALL, KOPTK1, TALL-1) were treated with gamma-secretase inhibitor (1.0 micromolar compound E) vs. DMSO vehicle control for 12 hours. Each cell line was also retrovirally transduced with ICN or c-Myc, FACS sorted, and then treated with GSI vs. DMSO.

Background corr dist: KL-Divergence = 0.2044, L1-Distance = 0.0369, L2-Distance = 0.0024, Normal std = 0.3398

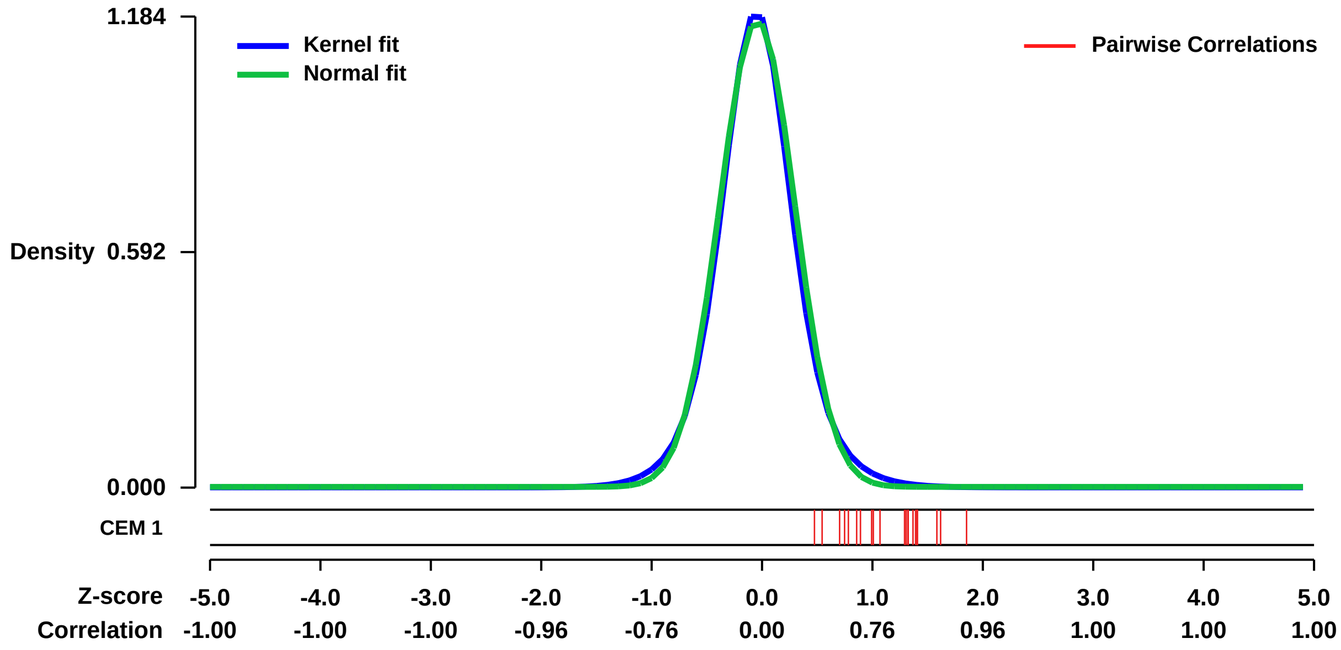

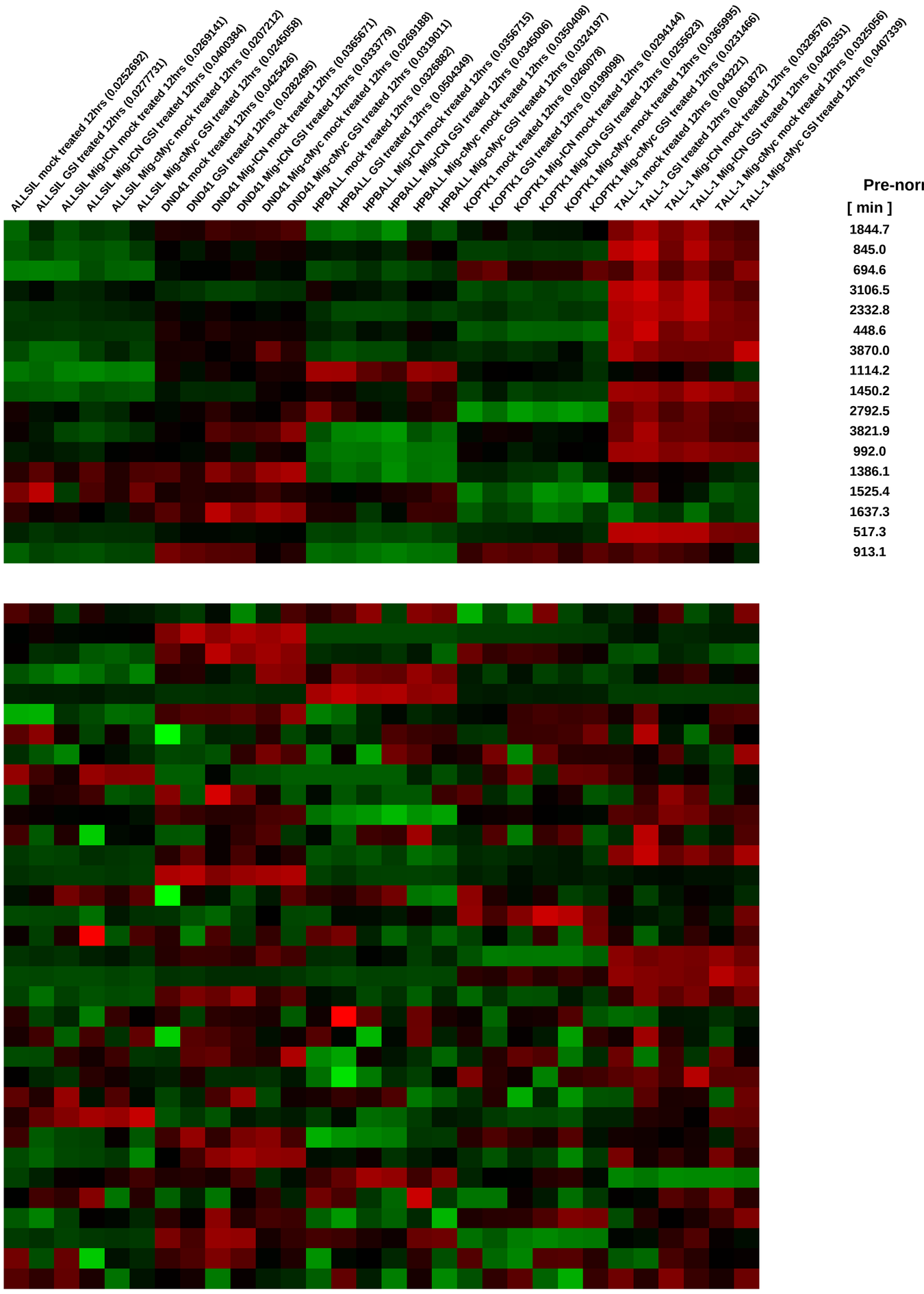

Pre-normalization Quantiles

	[min]	[medium]	[max]
ALLSIL_mock treated 12hrs (0.0252692)	1844.7	3077.1	4970.0
ALLSIL_GSI treated 12hrs (0.0277731)	845.0	1232.6	2447.8
ALLSIL Mig-ICN mock treated 12hrs (0.0269141)	694.6	1273.8	2026.1
ALLSIL Mig-ICN GSI treated 12hrs (0.0400384)	3106.5	5085.2	13571.3
ALLSIL Mig-cMyc mock treated 12hrs (0.0207212)	2332.8	2859.2	6277.6
ALLSIL Mig-cMyc GSI treated 12hrs (0.0245058)	448.6	975.4	2184.7
DND41 mock treated 12hrs (0.0425426)	3870.0	4845.6	7757.2
DND41 GSI treated 12hrs (0.0282495)	1114.2	1820.4	2640.6
DND41 Mig-ICN mock treated 12hrs (0.0365671)	1450.2	1895.6	3058.4
DND41 Mig-ICN GSI treated 12hrs (0.0333779)	2792.5	4040.6	4933.8
DND41 Mig-cMyc mock treated 12hrs (0.0269188)	3821.9	5812.5	7939.8
DND41 Mig-cMyc GSI treated 12hrs (0.0319011)	992.0	2033.1	3311.5
HPBALL mock treated 12hrs (0.0326882)	1386.1	2053.4	2770.8
HPBALL GSI treated 12hrs (0.0504349)	1525.4	1914.3	2267.7
HPBALL Mig-ICN mock treated 12hrs (0.0356715)	1637.3	2253.3	3220.5
HPBALL Mig-ICN GSI treated 12hrs (0.0345006)	517.3	875.4	2554.8
HPBALL Mig-cMyc mock treated 12hrs (0.0350408)	913.1	2271.9	2961.6
HPBALL Mig-cMyc GSI treated 12hrs (0.0324197)			
KOPTK1 mock treated 12hrs (0.0260078)			
KOPTK1 GSI treated 12hrs (0.0199098)			
KOPTK1 Mig-ICN mock treated 12hrs (0.0294144)			
KOPTK1 Mig-ICN GSI treated 12hrs (0.0255623)			
KOPTK1 Mig-cMyc mock treated 12hrs (0.0365995)			
KOPTK1 Mig-cMyc GSI treated 12hrs (0.0231466)			
TALL-1 mock treated 12hrs (0.043221)			
TALL-1 GSI treated 12hrs (0.061872)			
TALL-1 Mig-ICN mock treated 12hrs (0.0329576)			
TALL-1 Mig-ICN GSI treated 12hrs (0.0425351)			
TALL-1 Mig-cMyc mock treated 12hrs (0.0325056)			
TALL-1 Mig-cMyc GSI treated 12hrs (0.0407339)			

GEO Series "GSE53603" Expression Profiles

Num of samples in this series: 8

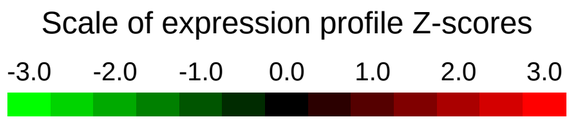

GEO Link:	http://www.ncbi.nlm.nih.gov/geo/query/acc.cgi?acc=GSE53603
Status:	Public on Mar 19 2014
Title:	Expression data from SKOV3 cells treated with SAHA or vehicle control
Organism:	Homo sapiens
Experiment type:	Expression profiling by array
Platform:	GPL570
Pubmed ID:	24631446
Summary & Design:	**Summary:** We performed a microarray experiment to assess SAHA-induced changes in expression of genes of the homologous recombination DNA repair pathway **Overall design:** SKOV-3 ovarian cancer cells were treated with 1´µM SAHA or vehicle-control (0.01% DMSO) for 6 or 24 hours, harvested and processed for RNA isolation. Data for both time-points for SAHA and vehicle-control treated cells were obtained in duplicate. Total RNA was isolated using the Qiagen RNeasy Kit (Qiagen, Valencia, CA) according to manufacturer's instructions. cDNA synthesis and hybridization on oligonucleotide microarrays (U133 Plus 2.0 Array GeneChip, Affymetrix, Inc., Santa Clara, CA) were carried out using standard protocols.

Background corr dist: KL-Divergence = 0.0579, L1-Distance = 0.0171, L2-Distance = 0.0003, Normal std = 0.5347

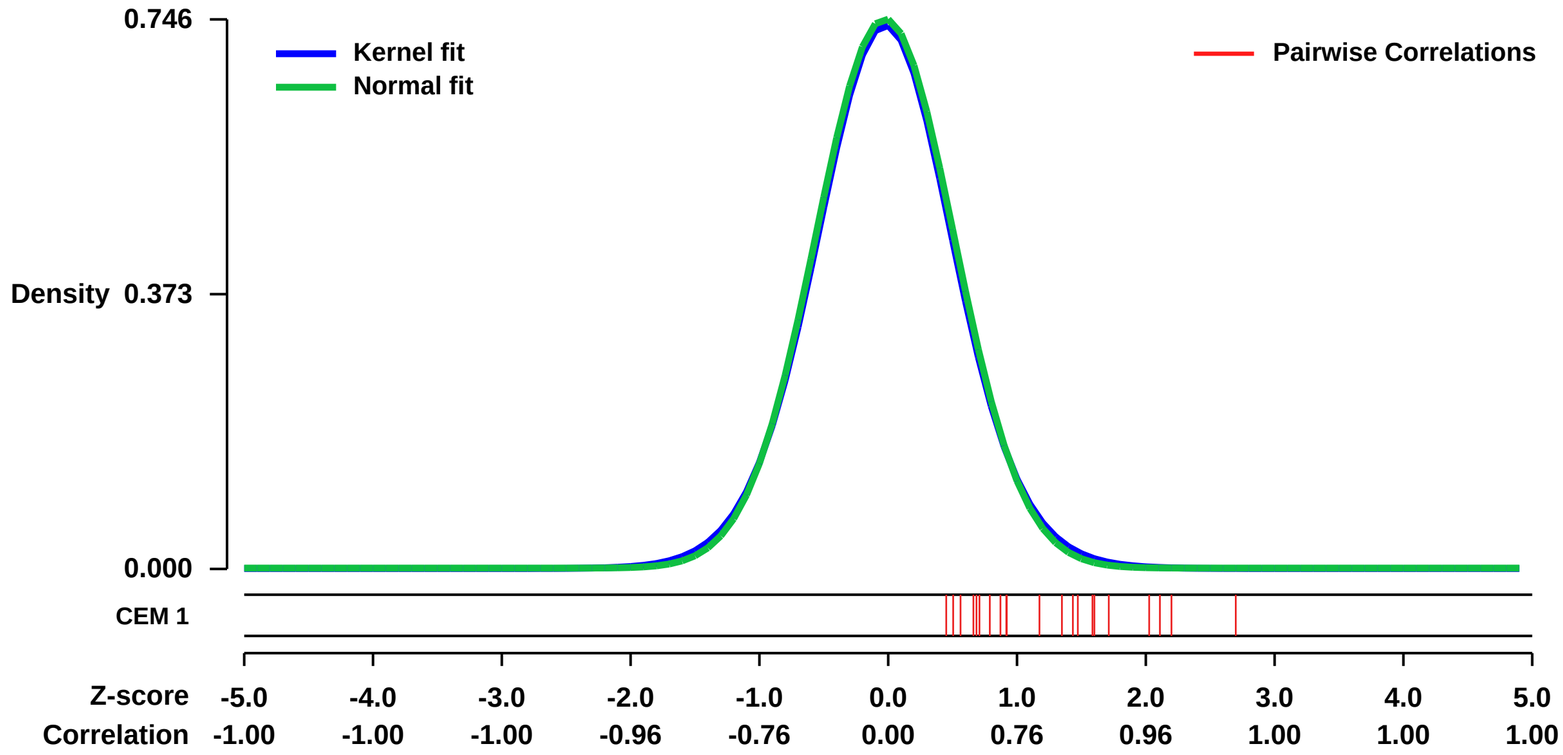

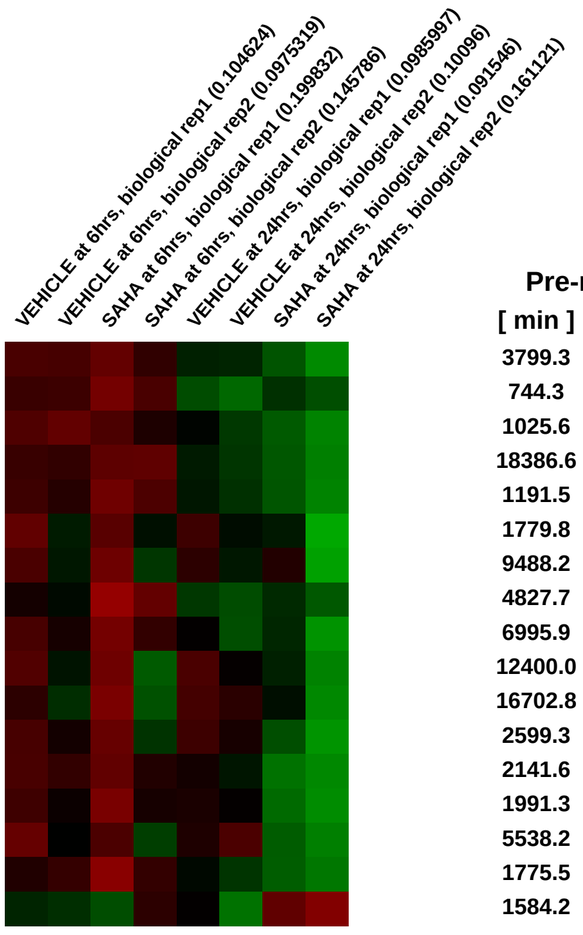

GEO Series "GSE31434" Expression Profiles

Num of samples in this series: 12

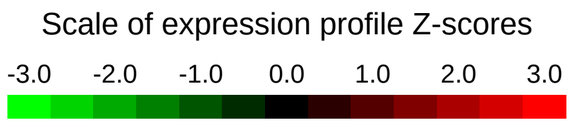

GEO Link:	http://www.ncbi.nlm.nih.gov/geo/query/acc.cgi?acc=GSE31434
Status:	Public on Sep 17 2012
Title:	Expression data from HeLa cells transfected with SLC44A5
Organism:	Homo sapiens
Experiment type:	Expression profiling by array
Platform:	GPL570
Pubmed ID:	22815983
Summary & Design:	**Summary:** We identified SLC44A5 as a gene associated with birth weight in cattle based on genome wide association studies. To identify the mechanisms involved in growth and choline transporter, we performed genome-wide mRNA expression analysis in HeLa cells transfected with SLC44A5. **Overall design:** HeLa cells were transfected with negative control, siRNA against SLC44A5, bovine SLC44A5 expression plasmid, and an empty vector control for RNA extraction and hybridization on Affymetrix microarrays.

Background corr dist: KL-Divergence = 0.0795, L1-Distance = 0.0371, L2-Distance = 0.0019, Normal std = 0.4972

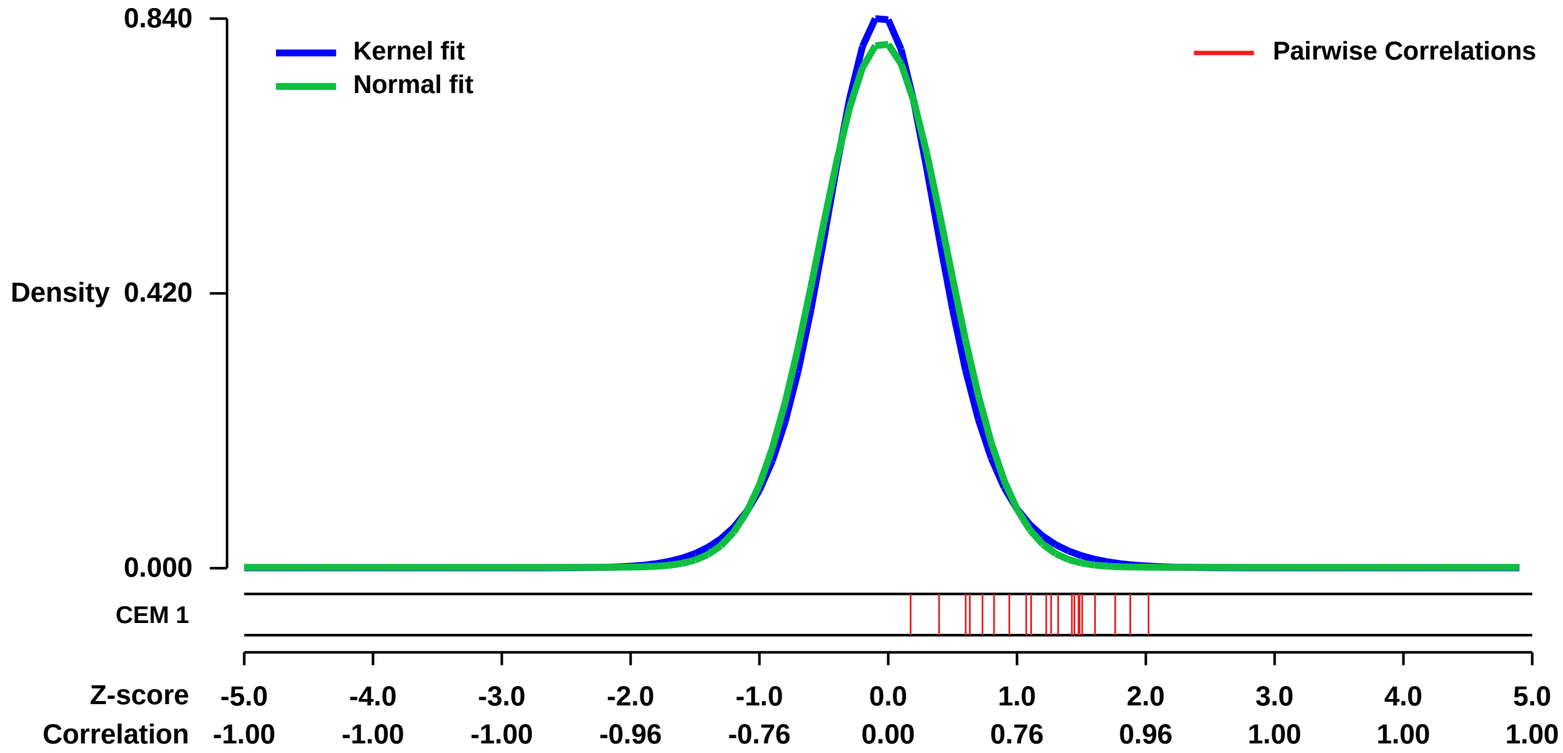

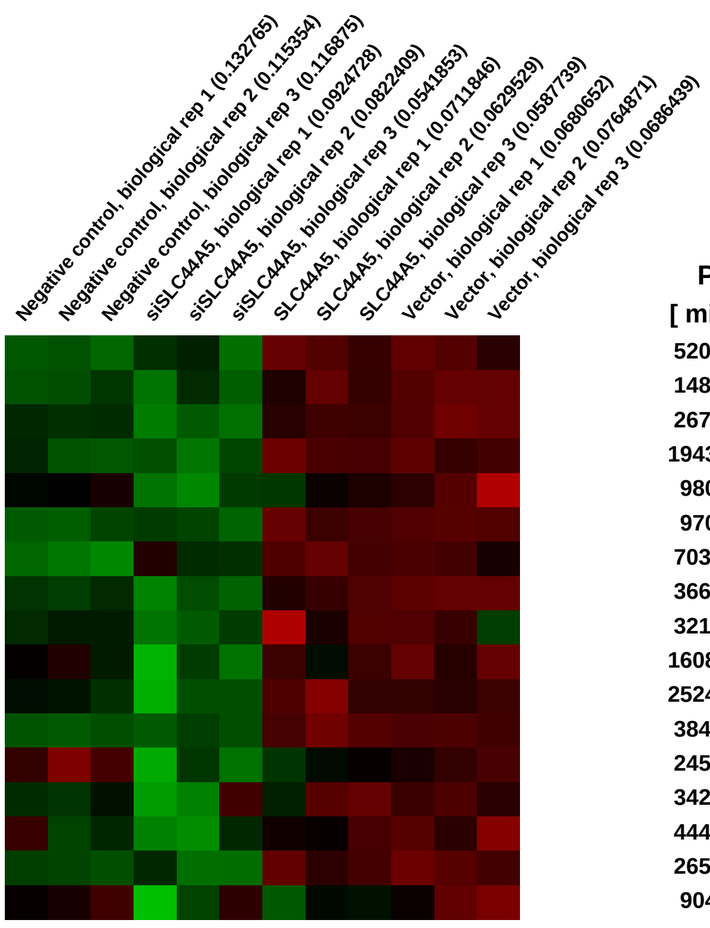

GEO Series "GSE47746" Expression Profiles

Num of samples in this series: 8

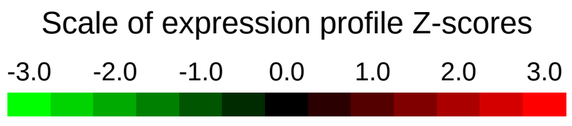

GEO Link:	http://www.ncbi.nlm.nih.gov/geo/query/acc.cgi?acc=GSE47746
Status:	Public on Nov 03 2013
Title:	Gene expression data of fibroblasts transduced with LacZ or p63+KLF4.
Organism:	Homo sapiens
Experiment type:	Expression profiling by array
Platform:	GPL570
Pubmed ID:	23921950
Summary & Design:	**Summary:** To determine if fibroblasts could be reprogrammed to a keratinocyte phenotype p63+KLF4 or LacZ expressing retroviruses were transduced into primary human neonatal fibroblasts. Global gene expression profiling using U133 plus 2.0 arrays were used to deteremine the extent of reprogramming to a keratinocyte phenoypte upon transduction with p63+KLF4. Fibroblasts transduced with p63+KLF4 were also treated +/- high calcium to determine if treatment with calcium could induce differentiation of these cells. Microarray analysis was also performed on cells treated +/- calcium. **Overall design:** For gene expression profiling, cultured human fibroblasts were infected with LacZ or p63+KLF4 expressing retroviruses. p63+KLF4 cells were also treated +/- calcium. Microarray analysis using Affymetrix HG-U133 2.0 plus arrays was performed on duplicate samples.

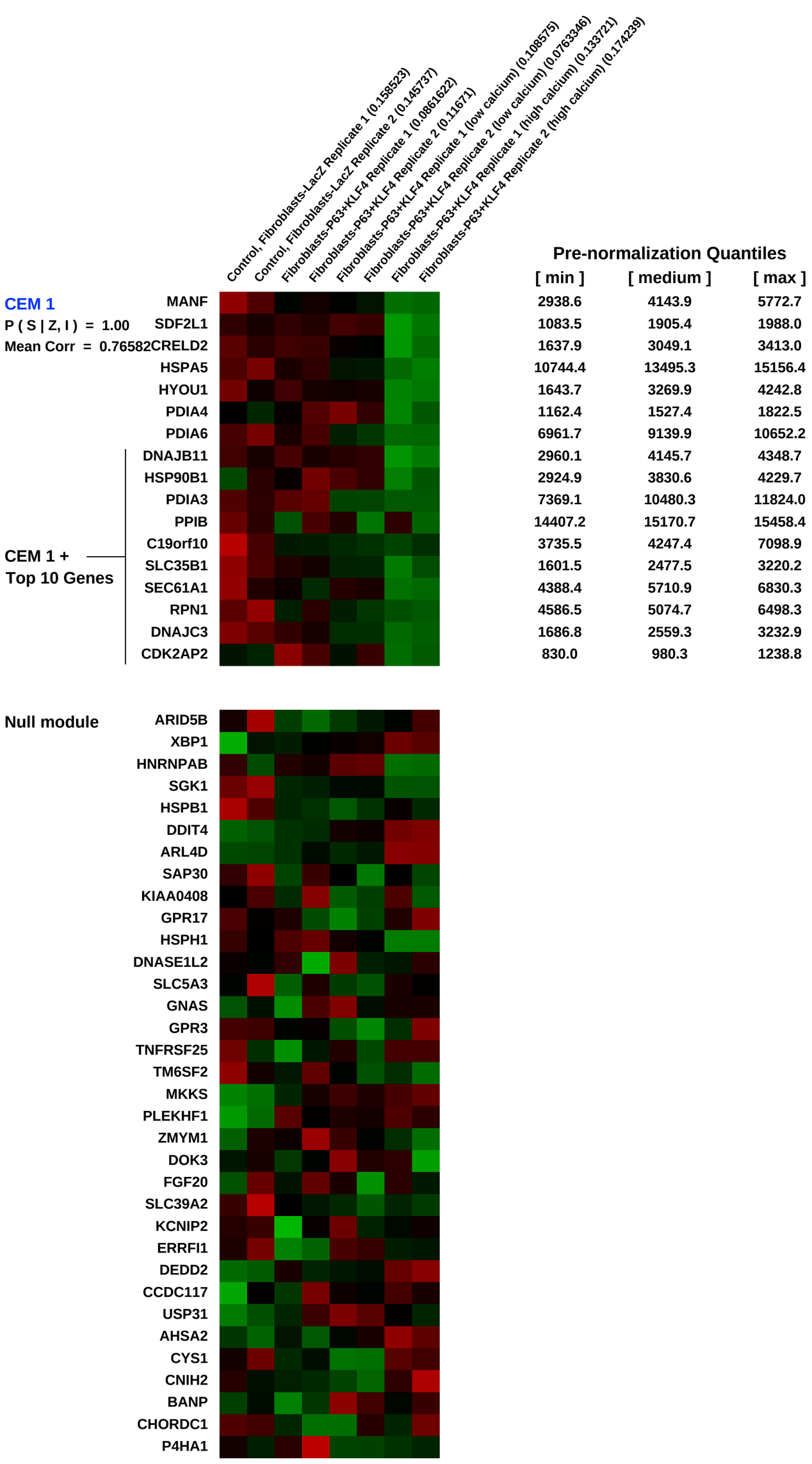

GEO Series "GSE26583" Expression Profiles

Num of samples in this series: 6

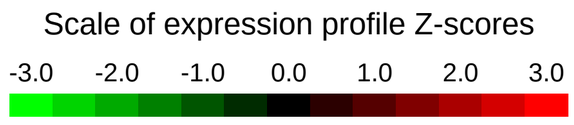

GEO Link:	http://www.ncbi.nlm.nih.gov/geo/query/acc.cgi?acc=GSE26583
Status:	Public on Jan 15 2014
Title:	Expression data of overexpression of ABF-1 in SKW cells
Organism:	Homo sapiens
Experiment type:	Expression profiling by array
Platform:	GPL570
Pubmed ID:	25070843
Summary & Design:	**Summary:** ABF-1, a bHLH trancriptional repressor expresses in human activated B cells. Overexpression of ABF-1 in a SKW lymphoblastoid cells suppressed IgM production. We used cDNA microarray to identify genes under ABF-1 regulation. **Overall design:** SKW cells ectopically expressed ABF-1-GFP or GFP were harvested for RNA extraction and array hybridization.

Background corr dist: KL-Divergence = 0.0226, L1-Distance = 0.0121, L2-Distance = 0.0002, Normal std = 0.7128

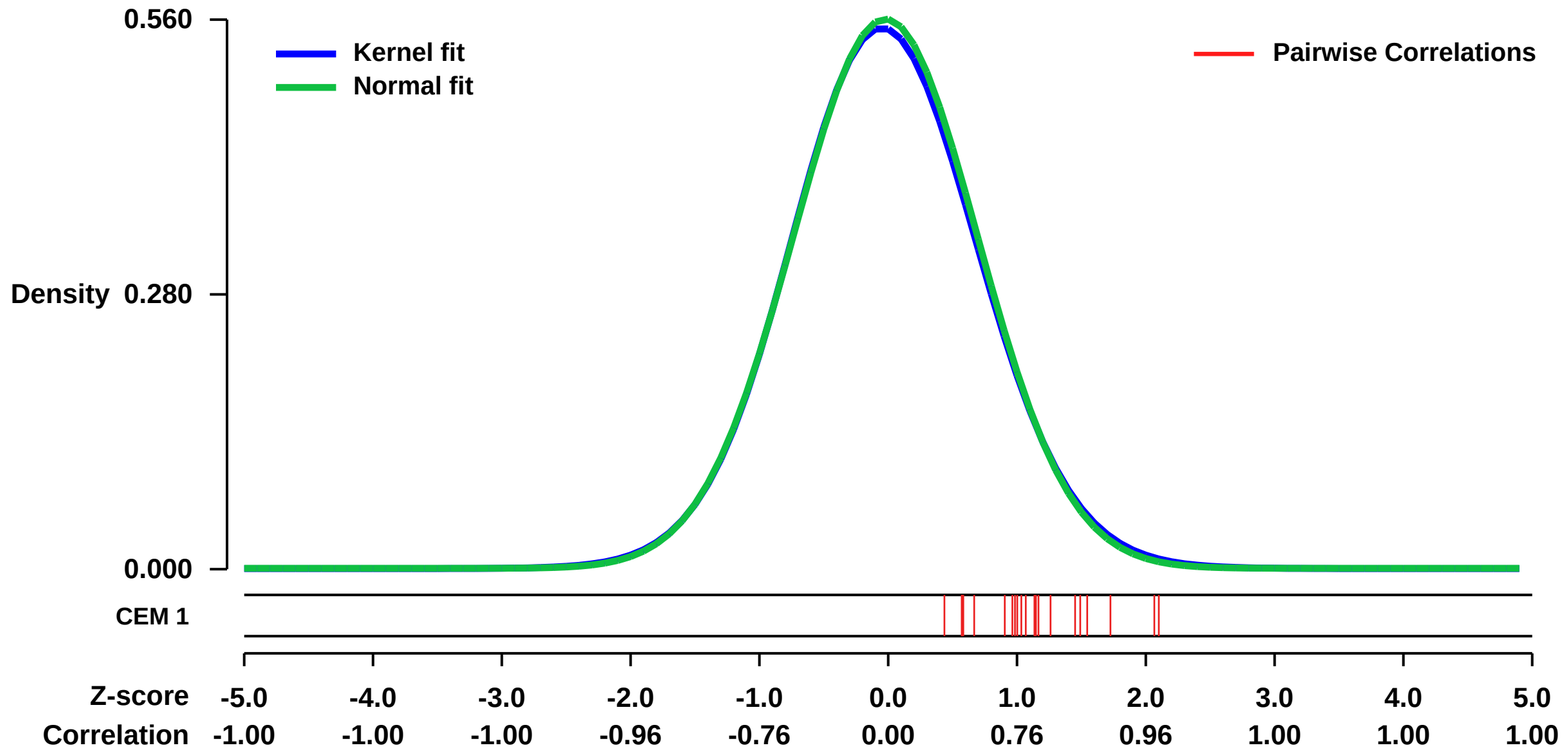

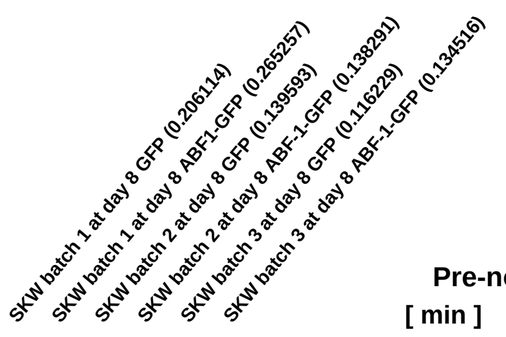

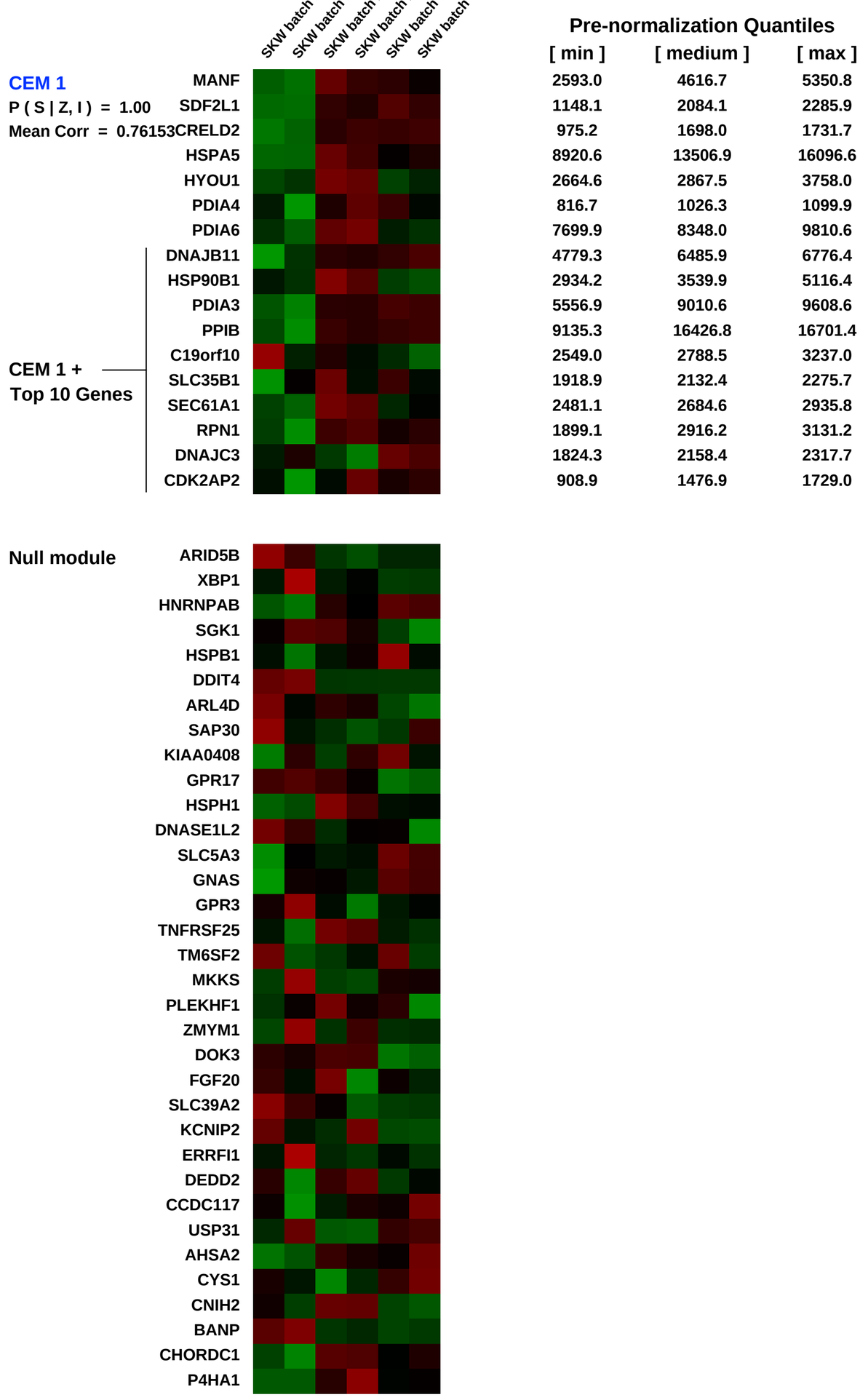

GEO Series "GSE32911" Expression Profiles

Num of samples in this series: 8

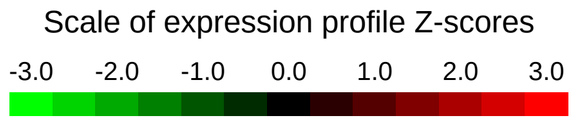

GEO Link:	http://www.ncbi.nlm.nih.gov/geo/query/acc.cgi?acc=GSE32911
Status:	Public on Oct 11 2012
Title:	Compound C prevents the unfolded protein response during glucose deprivation through a mechanism independent of AMPK and BMP signaling.
Organism:	Homo sapiens
Experiment type:	Expression profiling by array
Platform:	GPL570
Pubmed ID:	23029271
Summary & Design:	**Summary:** Inhibiting the unfolded protein response (UPR) can be a therapeutic approach, especially for targeting the tumor microenvironment. We found that compound C (also known as dorsomorphin) prevented the UPR and exerted enhanced cytotoxicity during glucose deprivation. The UPR-inhibiting activity of compound C was not associated with either AMPK or BMP signaling inhibition. **Overall design:** To induce the UPR, we treated HT1080 cells for 18 hours under ER stress conditions by adding 10 mM 2-Deoxy-D-glucose (2DG) to culture medium. UPR inhibitors (compound C, versipelostatin and phenformin) were added just before 2DG was added in medium. Total 8 samples were prepared for RNA extraction and hybridization on Affymetrix microarrays.

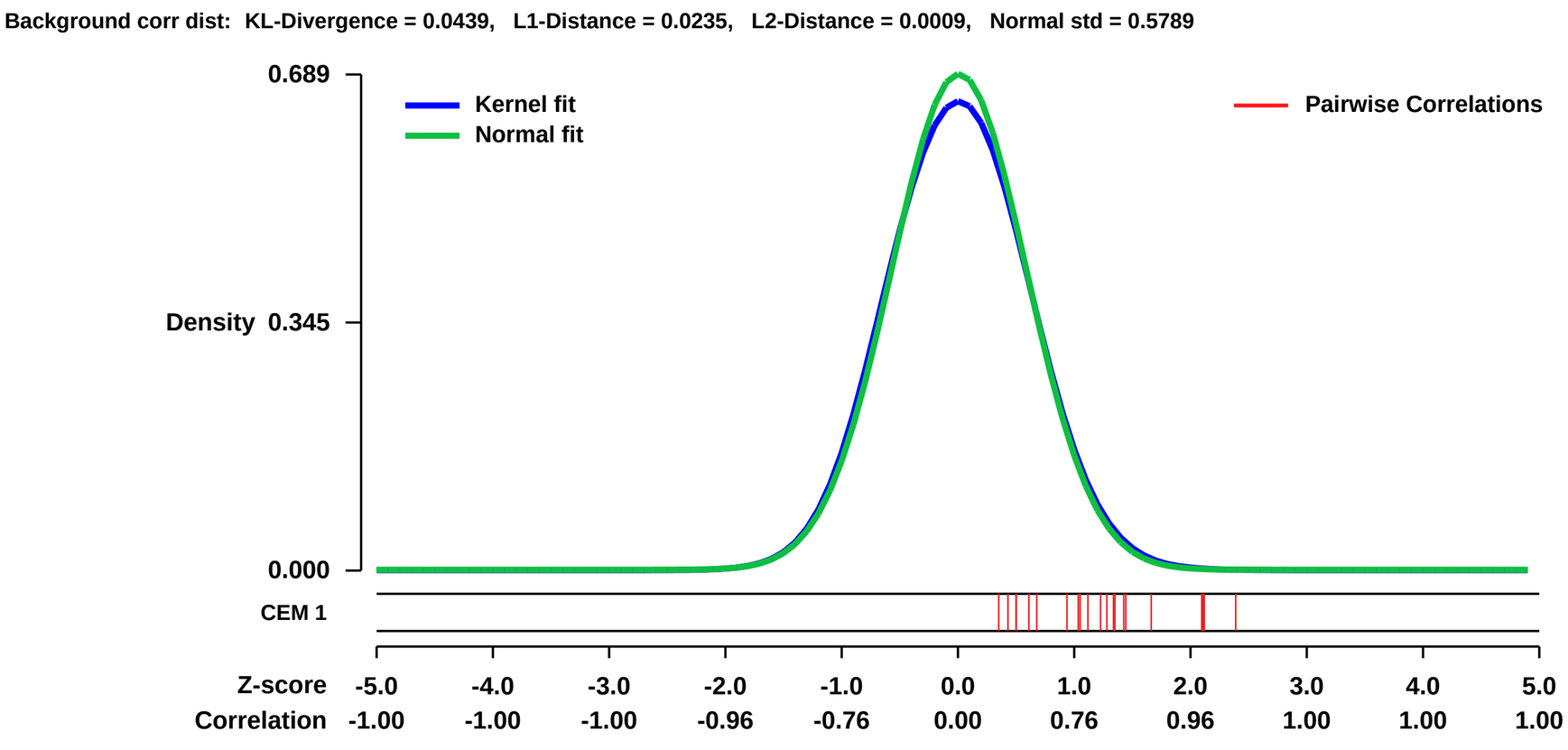

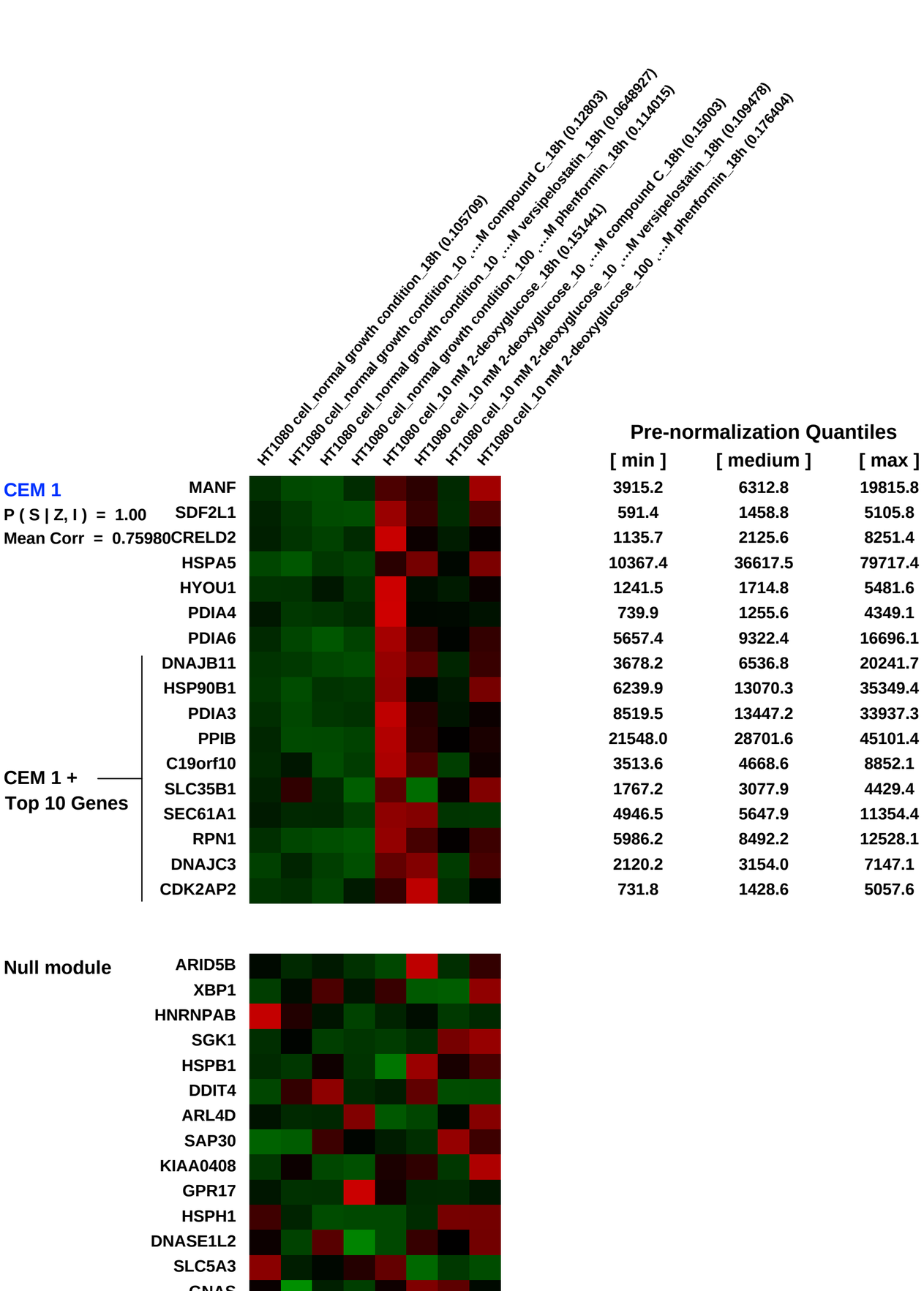

GEO Series "GSE8565" Expression Profiles

Num of samples in this series: 17

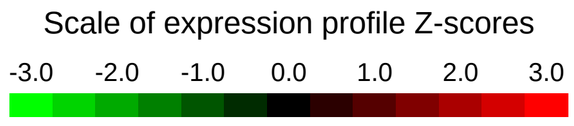

GEO Link:	http://www.ncbi.nlm.nih.gov/geo/query/acc.cgi?acc=GSE8565
Status:	Public on Apr 29 2008
Title:	Argyrin A is a p27 stabilizing drug with potent antiproliferative activity in vivo
Organism:	Homo sapiens
Experiment type:	Expression profiling by array
Platform:	GPL570
Pubmed ID:	18598941

Summary & Design:

Summary:
Reduction in the cellular levels of the cyclin kinase inhibitor p27kip1 are frequently found in many human cancers and correlate directly with patient prognosis. Specifically ubiquitin dependent proteasomal turnover has been shown to cause reduced p27 expression in many human cancers. We recently demonstated that expression of a stabilized version of p27kip1 (p27kip1T187A) in a genetically modified mouse significantly reduced the number of intestinal adenomatous polyps which progressed to invasive carcinomas. Based on this work we set out to identify compounds which lead to a re-expression of p27 in cancer tissues. In this work we identify Argyrin A a compound derived from myxobacterium archangium gephyra as a potent inducer of p27kip1 expression. Argyrin A induces apoptosis in human colon cancer xenografts and tumor vasculature in vivo leading to a profound reduction in tumor size at well tolerated levels. Argyrin A functions are strictly dependent on the expression of p27kip1 as neither tumor cells nor endothelial cells which do not express p27kip1 respond to this compound. Surprisingly the molecular mechanism by which Argyrin A exerts its p27 dependent biological function is through a potent inhibition of the 20S proteasome.

Keywords: protasome inhibitor, time course, MCF7 cells, genome wide gene expression response, siRNA

Overall design:
MCF7 cells were incubated with proteasome inhibitors bortezomib or Argyrin A or proteasome activity was reduced by treatment with siRNA against proteasomal subunits and gene expression profiles were determined at different timepoints thereafter.

Background corr dist: KL-Divergence = 0.1620, L1-Distance = 0.0337, L2-Distance = 0.0024, Normal std = 0.3701

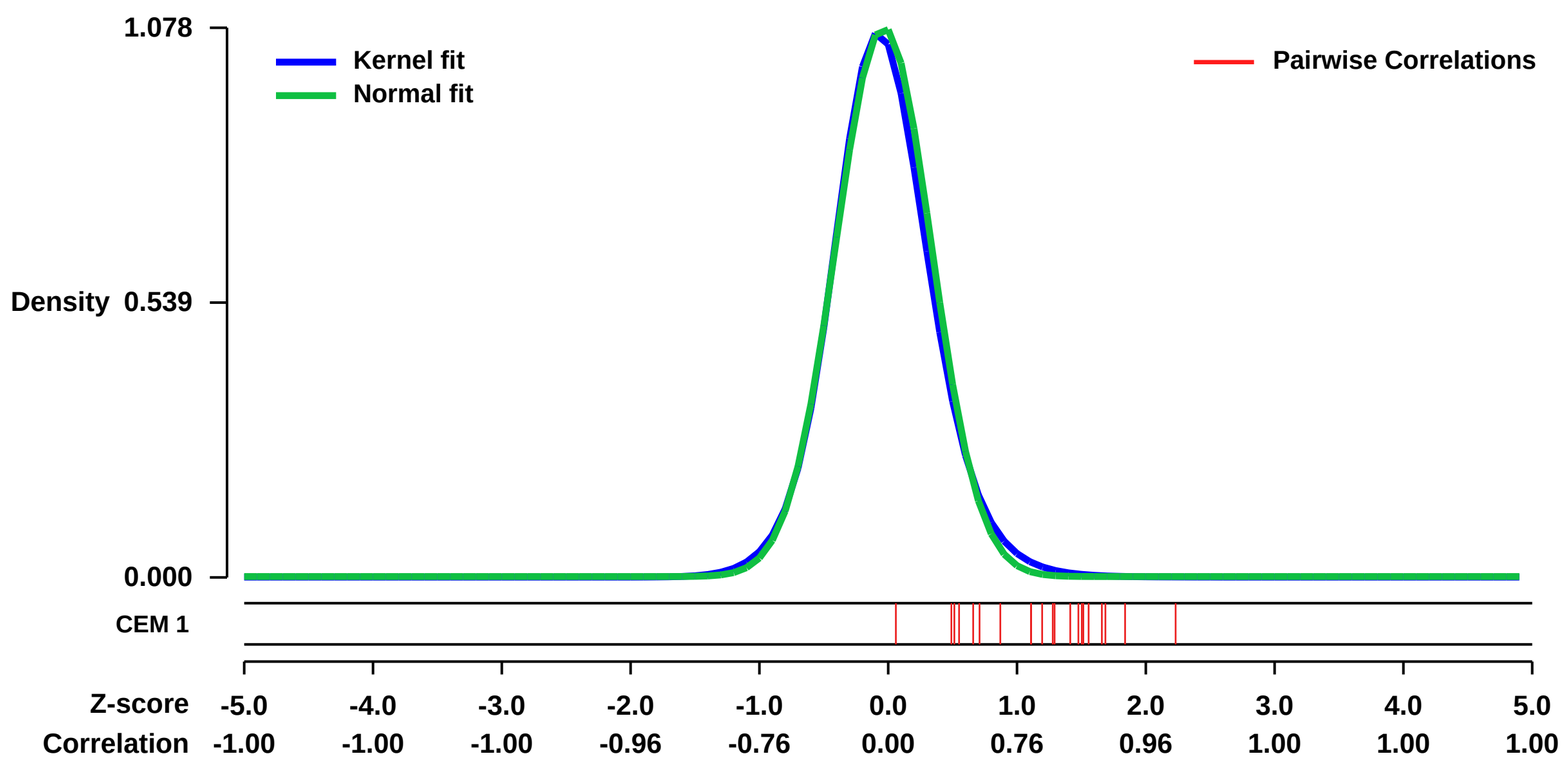

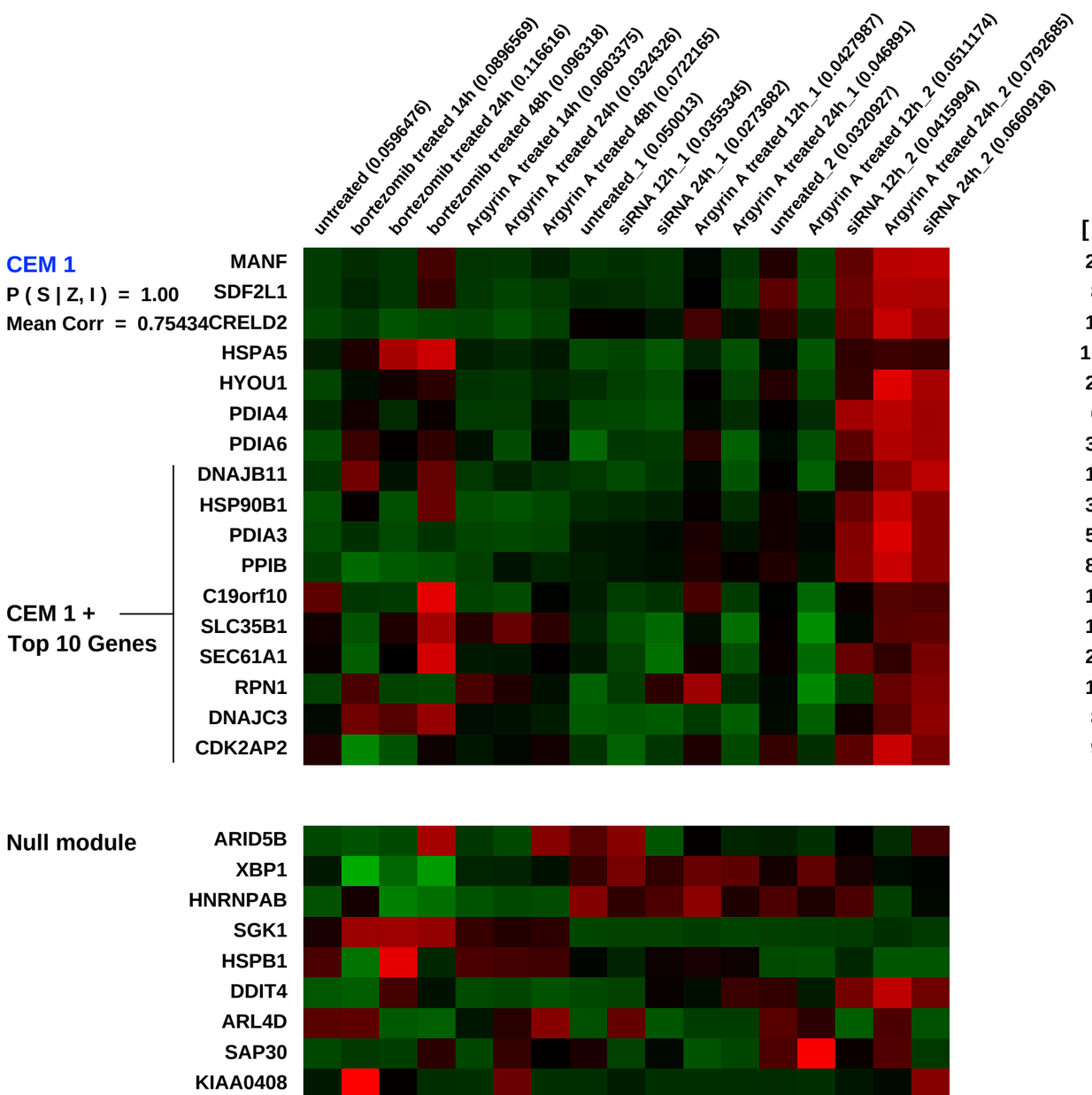

Pre-normalization Quantiles

[min]	[medium]	[max]
2098.7	2609.9	8621.6
884.1	1714.5	6912.9
1464.3	6367.7	23270.2
11293.5	21830.6	64151.4
2652.9	3988.0	13359.2
642.2	932.4	2551.3
3972.5	5680.8	9089.4
1543.0	2889.3	7513.7
3403.2	6108.2	17634.8
5673.8	10294.1	31473.7
8878.8	16380.8	35167.4
1366.2	1883.5	3669.2
1852.6	3920.7	6104.4
2175.5	3516.6	6013.7
1914.2	2879.6	4224.0
877.1	1527.3	2854.9
986.2	2067.5	3821.7

GEO Series "GSE11352" Expression Profiles

Num of samples in this series: 18

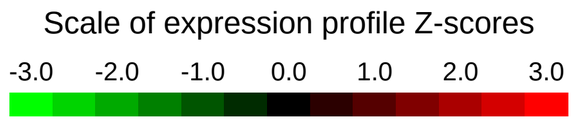

GEO Link:	http://www.ncbi.nlm.nih.gov/geo/query/acc.cgi?acc=GSE11352
Status:	Public on May 07 2008
Title:	Timecourse of estradiol (10nM) exposure in MCF7 breast cancer cells.
Organism:	Homo sapiens
Experiment type:	Expression profiling by array
Platform:	GPL570
Pubmed ID:	17542648

Summary & Design:

Summary:
Using a chromatin immunoprecipitation-paired end diTag cloning and sequencing strategy, we mapped estrogen receptor alpha (ERalpha) binding sites in MCF-7 breast cancer cells. We identified 1,234 high confidence binding clusters of which 94% are projected to be bona fide ERalpha binding regions. Only 5% of the mapped estrogen receptor binding sites are located within 5 kb upstream of the transcriptional start sites of adjacent genes, regions containing the proximal promoters, whereas vast majority of the sites are mapped to intronic or distal locations (>5 kb from 5' and 3' ends of adjacent transcript), suggesting transcriptional regulatory mechanisms over significant physical distances. Of all the identified sites, 71% harbored putative full estrogen response elements (EREs), 25% bore ERE half sites, and only 4% had no recognizable ERE sequences. Genes in the vicinity of ERalpha binding sites were enriched for regulation by estradiol in MCF-7 cells, and their expression profiles in patient samples segregate ERalpha-positive from ERalpha-negative breast tumors. The expression dynamics of the genes adjacent to ERalpha binding sites suggest a direct induction of gene expression through binding to ERE-like sequences, whereas transcriptional repression by ERalpha appears to be through indirect mechanisms. Our analysis also indicates a number of candidate transcription factor binding sites adjacent to occupied EREs at frequencies much greater than by chance, including the previously reported FOXA1 sites, and demonstrate the potential involvement of one such putative adjacent factor, Sp1, in the global regulation of ERalpha target genes. Unexpectedly, we found that only 22%-24% of the bona fide human ERalpha binding sites were overlapping conserved regions in whole genome vertebrate alignments, which suggest limited conservation of functional binding sites. Taken together, this genome-scale analysis suggests complex but definable rules governing ERalpha binding and gene regulation.

Keywords: time course

Overall design:
We used oligonucleotide expression microarrays (Affymetrix GeneChip U133 Plus 2.0) to identify estradiol (E2)-responsive genes in the estrogen-receptor positive breast cancer cell line, MCF7. MCF7 cells were grown to 30-50% confluency and exposed to 10 nM E2 (or vehicle only) at 12, 24, and 48 hours. Each timepoint was performed in triplicate (ie, biological replicates). Total RNA was isolated from cells using the Qiagen RNeasy kit, and 5 micrograms of total RNA was amplified, labeled and hybridized to the array according to the manufacturerâ s protocols.

Background corr dist: KL-Divergence = 0.2257, L1-Distance = 0.0390, L2-Distance = 0.0031, Normal std = 0.3181

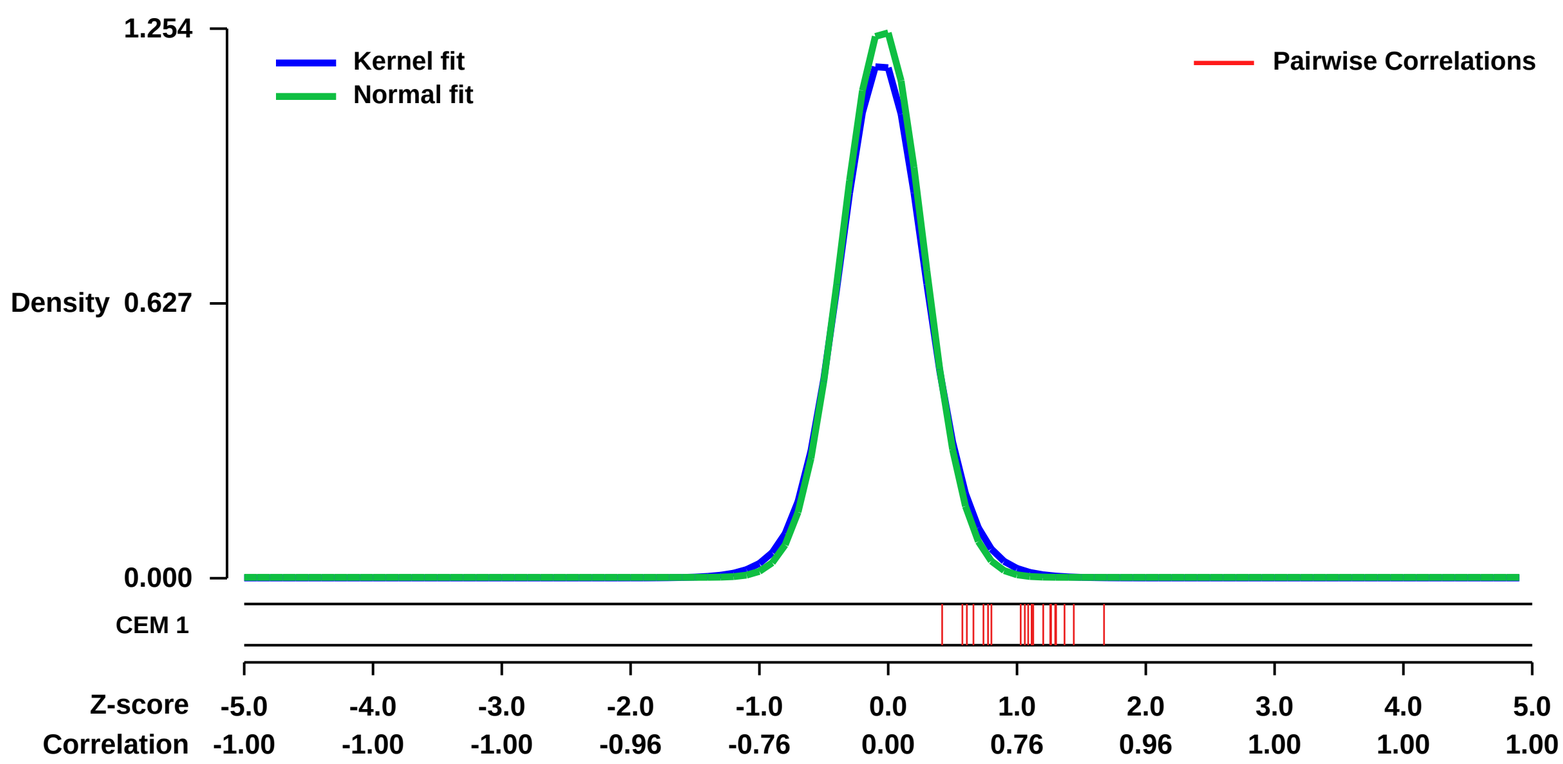

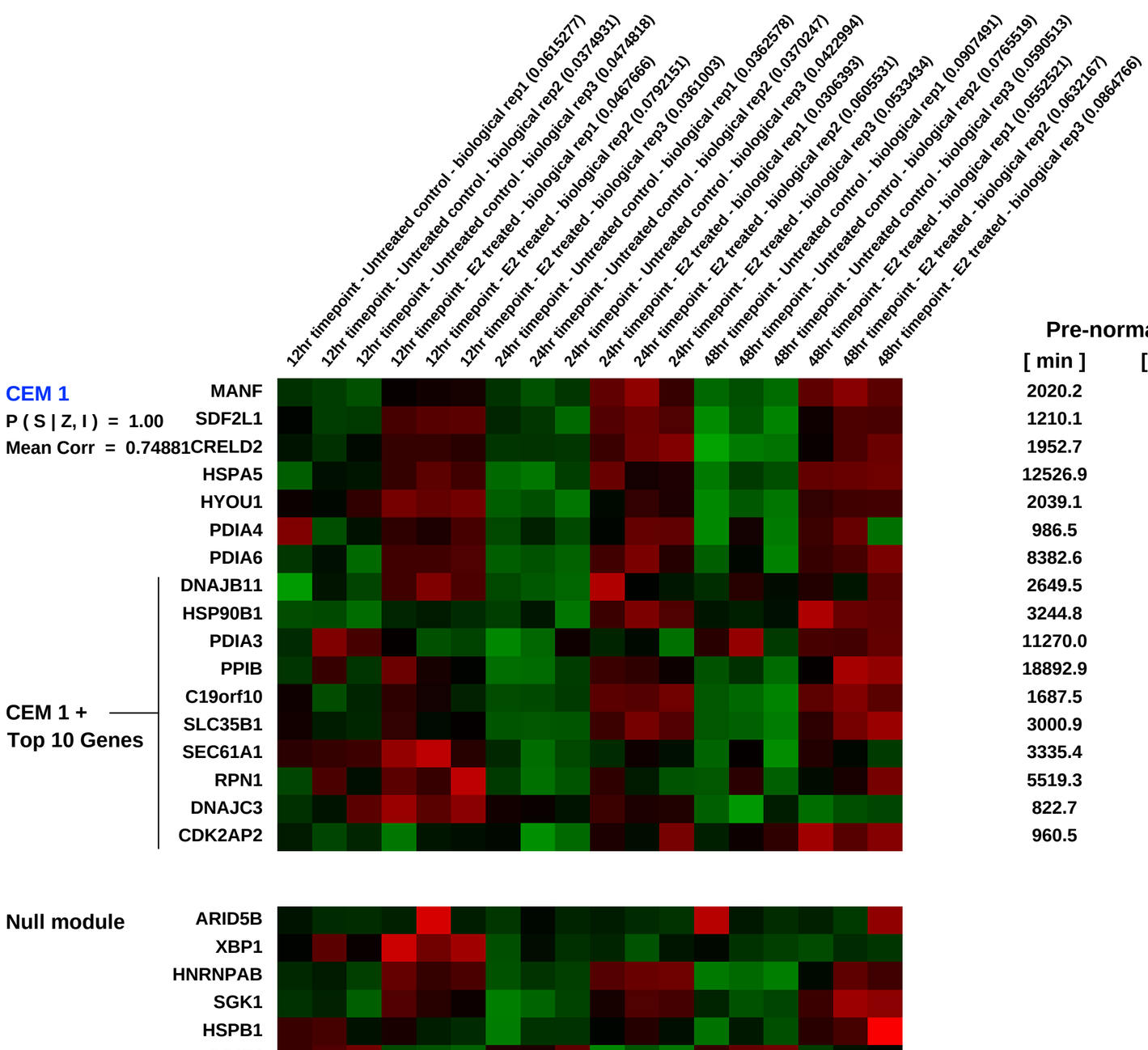

GEO Series "GSE24493" Expression Profiles

Num of samples in this series: 6

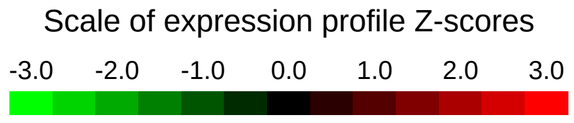

GEO Link:	http://www.ncbi.nlm.nih.gov/geo/query/acc.cgi?acc=GSE24493
Status:	Public on Oct 10 2010
Title:	Effect of Imatinib on chronic myelogenous leukemia
Organism:	Homo sapiens
Experiment type:	Expression profiling by array
Platform:	GPL570
Pubmed ID:	21911423
Summary & Design:	**Summary:** The Philadelphia chromosome (Ph) encodes the oncogenic BCR-ABL1 tyrosine kinase, which is present in almost every patient with chronic myeloid leukemia. In this study, the tyrosine kinase inhibitor Imatinib was used for pharmacological inhibition of BCR-ABL1. Gene expression profiles of CML cell lines were analyzed in response to Imatinib treatment. **Overall design:** Three CML cell lines (KU-812, KCL-22, JURL-MK1) were either treated with 10 ´µM STI571 (Imatinib) for 16 hours or cultured in absence of STI571.

Background corr dist: KL-Divergence = 0.0340, L1-Distance = 0.0221, L2-Distance = 0.0006, Normal std = 0.6526

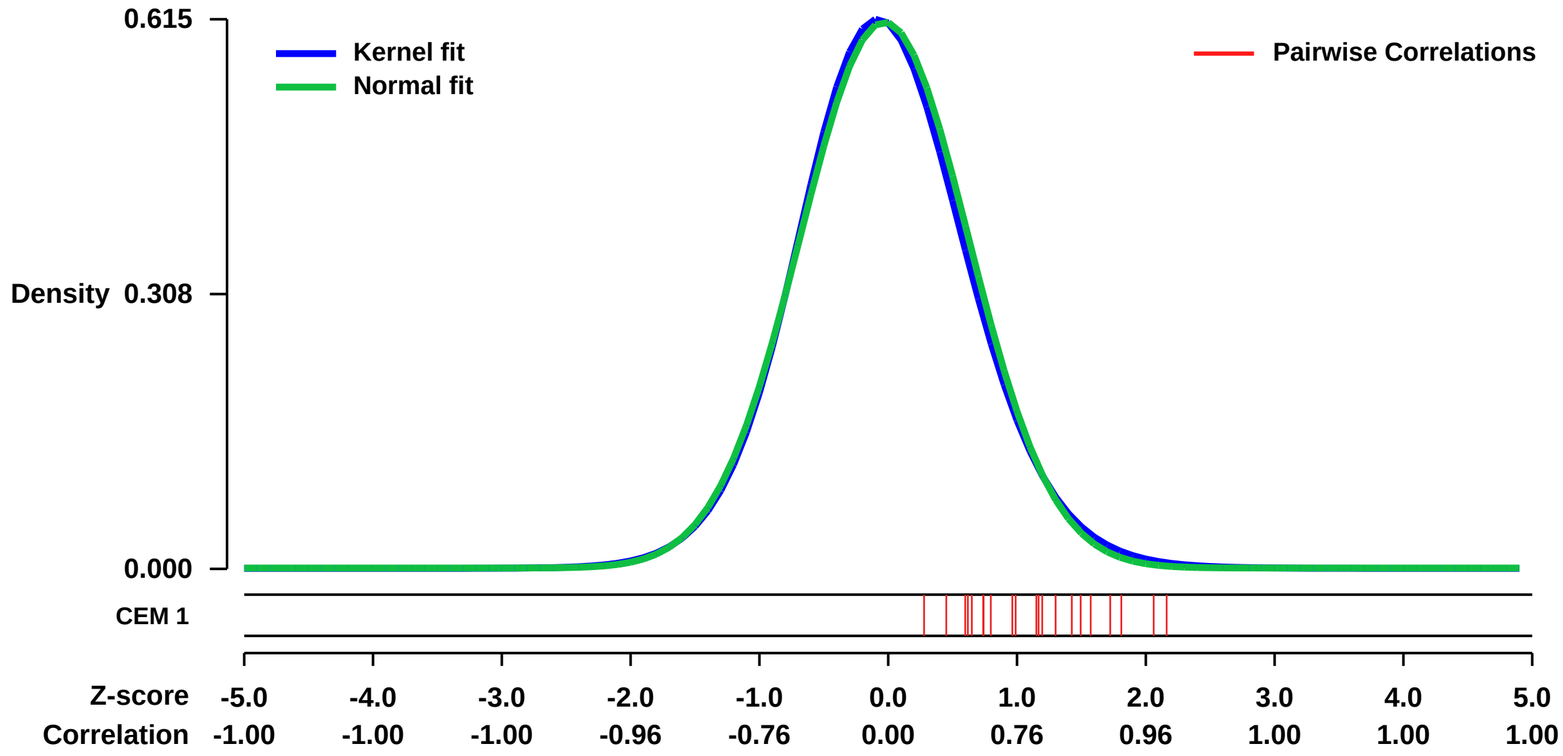

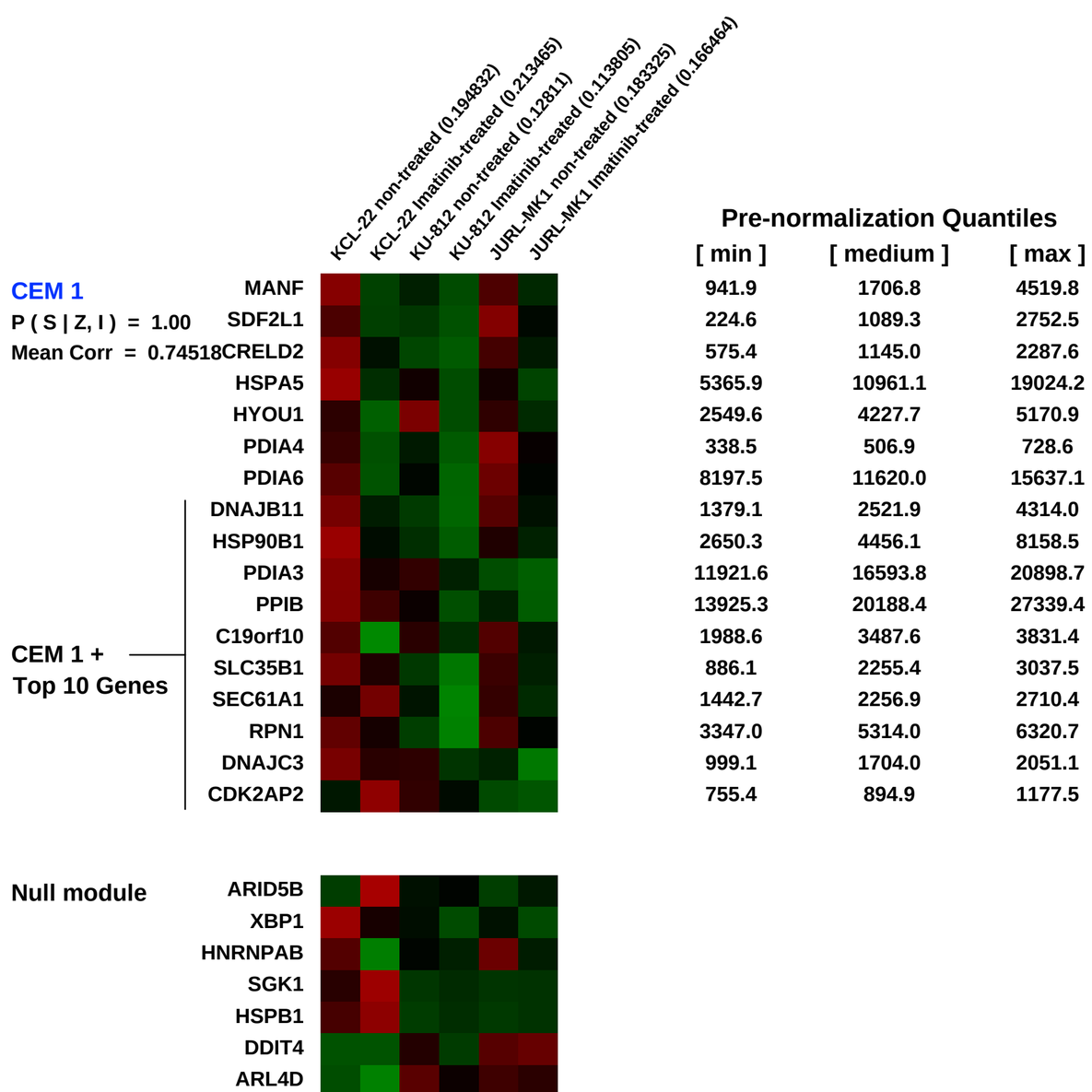

GEO Series "GSE12446" Expression Profiles

Num of samples in this series: 31

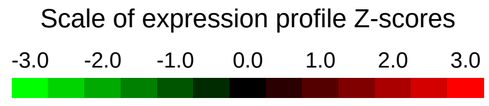

GEO Link:	http://www.ncbi.nlm.nih.gov/geo/query/acc.cgi?acc=GSE12446
Status:	Public on Aug 21 2008
Title:	Endometrium of hormone-treated postmenopausal women
Organism:	Homo sapiens
Experiment type:	Expression profiling by array
Platform:	GPL570
Pubmed ID:	17226044
Summary & Design:	**Summary:** **Title: Transcriptome analysis of human endometrial tissues from healthy post-menoupausal women reflecting the endometrial response to 3-weeks treatment with tibolone, E2 and E2+MPA.** **In an observational, open, non-randomized, controlled study uterine tissues were collected in order to generate endometrial gene expression profiles. healthy postmenopausal women were enrolled into the following treatment groups: Control-group; Tibolone-group, 2,5 mg of tibolone (administered orally) every day, starting 21 days prior to surgery; Estradiol-group, 2 mg of estradiol (administered orally) every day, starting 21 days prior to surgery; Estradiol+progestagen-group, 2 mg of estradiol (administered orally) and 5 mg of MPA (Medroxy Progesteroneacetate, administered orally) every day, starting 21 days prior to surgery. Pure (100%) endometrium was isolated from the snap-frozen uterine tissues and used for RNA isolation. RNA was labeled and hybridized to whole genome Affymetrix U133plus2 GeneChips containing 54,614 probe sets, representing approximately 47,000 transcripts.** **Relative to the control group, 940 genes are regulated in the endometrium of E2 treated patients, whereas only 198 genes are significantly regulated in endometria from tibolone or E2+MPA treated patients. Furthermore, only 9% of E2 regulated genes are also regulated by tibolone (85 out of 940), only 5% are also regulated by E2+MPA treatment and the overlap between tibolone and E2+MPA treatment is about 10%. This indicated that tibolone-treatment results in a weak endometrial profile similarity to E2 treatment and no profile similarity to E2+MPA treatment. A more detailed analysis showed that down stream processes, such as regulation of the cell cycle, angiogenesis and cell proliferation are almost not affected by tibolone treatment but, in contrast, are significantly affected by E2. For example, upon staining with Ki67, a marker for mitotic activity, significantly increased stromal as well as glandular cell proliferation was observed in the endometria from the E2-only treated group, while tibolone treatment resulted only in a slight increase in stromal cell proliferation (and no increase in glandular cell proliferation). These results indicate that in contrast to long-term tibolone use, short-term (21-days) use results in some estrogenic stimulation of the endometrium, which is clearly far less and rather different from what is observed during E2 treatment.** **References:** **Klaassens et al., 2006** **Hanifi-Moghaddam et al., 2007** **Verheul et al., 2007** **Overall design:** **Pure endometrium was isolated and used for profiling. 31 samples, 3 of which were duplicates, were analyzed.**

Background corr dist: **KL-Divergence = 0.2263, L1-Distance = 0.0628, L2-Distance = 0.0105, Normal std = 0.3156**

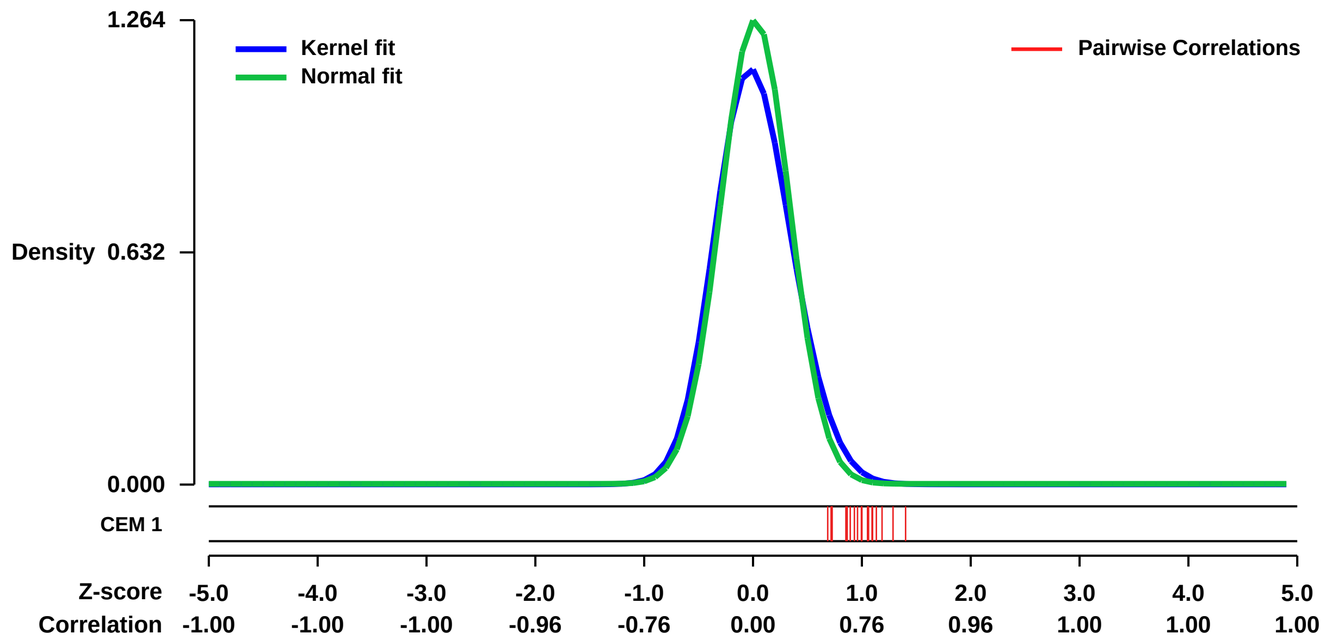

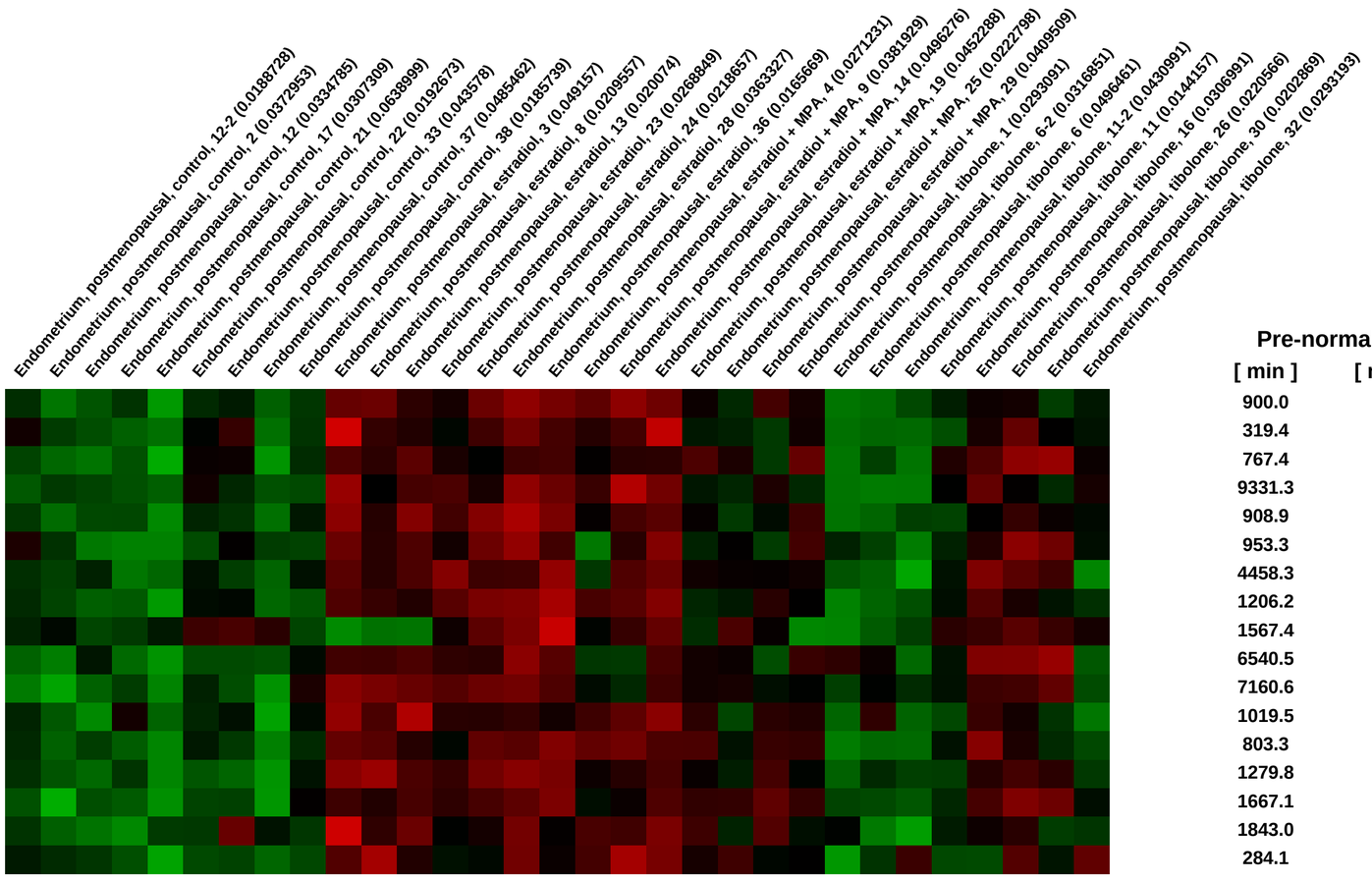

Pre-normalization Quantiles

	[min]	[medium]	[max]
CEM 1			
P (S | Z, I) = 1.00			
Mean Corr = 0.74513			
MANF	900.0	1571.6	2432.7
SDF2L1	319.4	508.1	873.7
CRELD2	767.4	1662.1	2349.3
HSPA5	9331.3	12374.1	16818.8
HYOU1	908.9	1767.4	2948.7
PDIA4	953.3	1367.6	1823.1
PDIA6	4458.3	7108.5	9267.1
CEM 1 + Top 10 Genes			
DNAJB11	1206.2	2070.3	3143.8
HSP90B1	1567.4	2406.8	3541.9
PDIA3	6540.5	10687.3	14380.6
PPIB	7160.6	13425.3	18806.0
C19orf10	1019.5	1572.2	2048.1
SLC35B1	803.3	1220.7	1763.0
SEC61A1	1279.8	2500.7	3838.1
RPN1	1667.1	3113.9	4036.6
DNAJC3	1843.0	2596.4	3618.4
CDK2AP2	284.1	626.9	1005.6
Null module			
ARID5B			
XBP1			
HNRNPAB			
SGK1			
HSPB1			
DDIT4			
ARL4D			
SAP30			
KIAA0408			
GPR17			
HSPH1			
DNASE1L2			
SLC5A3			
GNAS			
GPR3			
TNFRSF25			
TM6SF2			
MKKS			
PLEKHF1			
ZMYM1			
DOK3			
FGF20			
SLC39A2			
KCNIP2			
ERRFI1			
DEDD2			
CCDC117			
USP31			
AHSA2			
CYS1			
CNIH2			
BANP			
CHORDC1			
P4HA1			

GEO Series "GSE3284" Expression Profiles

Num of samples in this series: 18

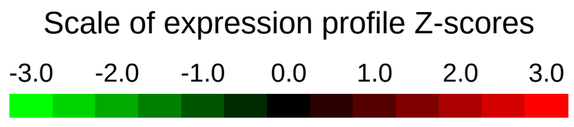

GEO Link:	http://www.ncbi.nlm.nih.gov/geo/query/acc.cgi?acc=GSE3284
Status:	Public on Sep 14 2005
Title:	A network-based analysis of systemic inflammation in humans
Organism:	Homo sapiens
Experiment type:	Expression profiling by array
Platform:	GPL570
Pubmed ID:	20233835
Summary & Design:	**Summary:** Oligonucleotide and complementary DNA microarrays are being used to subclassify histologically similar tumours, monitor disease progress, and individualize treatment regimens. However, extracting new biological insight from high-throughput genomic studies of human diseases is a challenge, limited by difficulties in recognizing and evaluating relevant biological processes from huge quantities of experimental data. Here we present a structured network knowledge-base approach to analyse genome-wide transcriptional responses in the context of known functional interrelationships among proteins, small molecules and phenotypes. This approach was used to analyse changes in blood leukocyte gene expression patterns in human subjects receiving an inflammatory stimulus (bacterial endotoxin). We explore the known genome-wide interaction network to identify significant functional modules perturbed in response to this stimulus. Our analysis reveals that the human blood leukocyte response to acute systemic inflammation includes the transient dysregulation of leukocyte bioenergetics and modulation of translational machinery. These findings provide insight into the regulation of global leukocyte activities as they relate to innate immune system tolerance and increased susceptibility to infection in humans. **Keywords:** Gene expression profiling of human blood leukocytes in response to in vivo endotoxin administration. **Overall design:** Healthy male and female subjects were intravenously administered either endotoxin or only vehicle (control). Arterial blood samples were collected before infusion (0 hours) and at post infusion times of 2, 4, 6, 9, and 24 hours. Blood leukocytes were isolated and analyzed using Affymetrix GeneChip arrays.

Background corr dist: KL-Divergence = 0.1629, L1-Distance = 0.0493, L2-Distance = 0.0053, Normal std = 0.3759

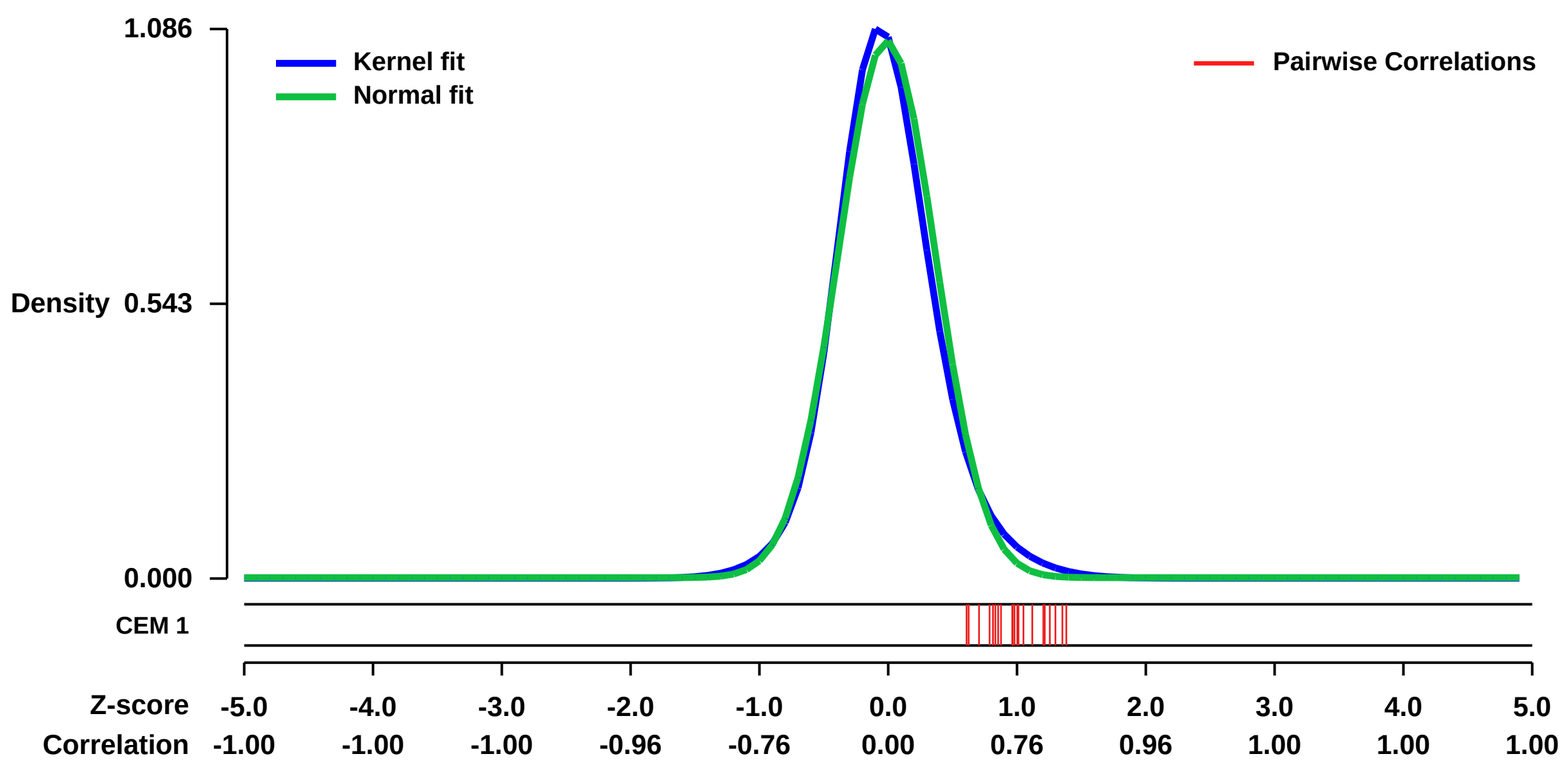

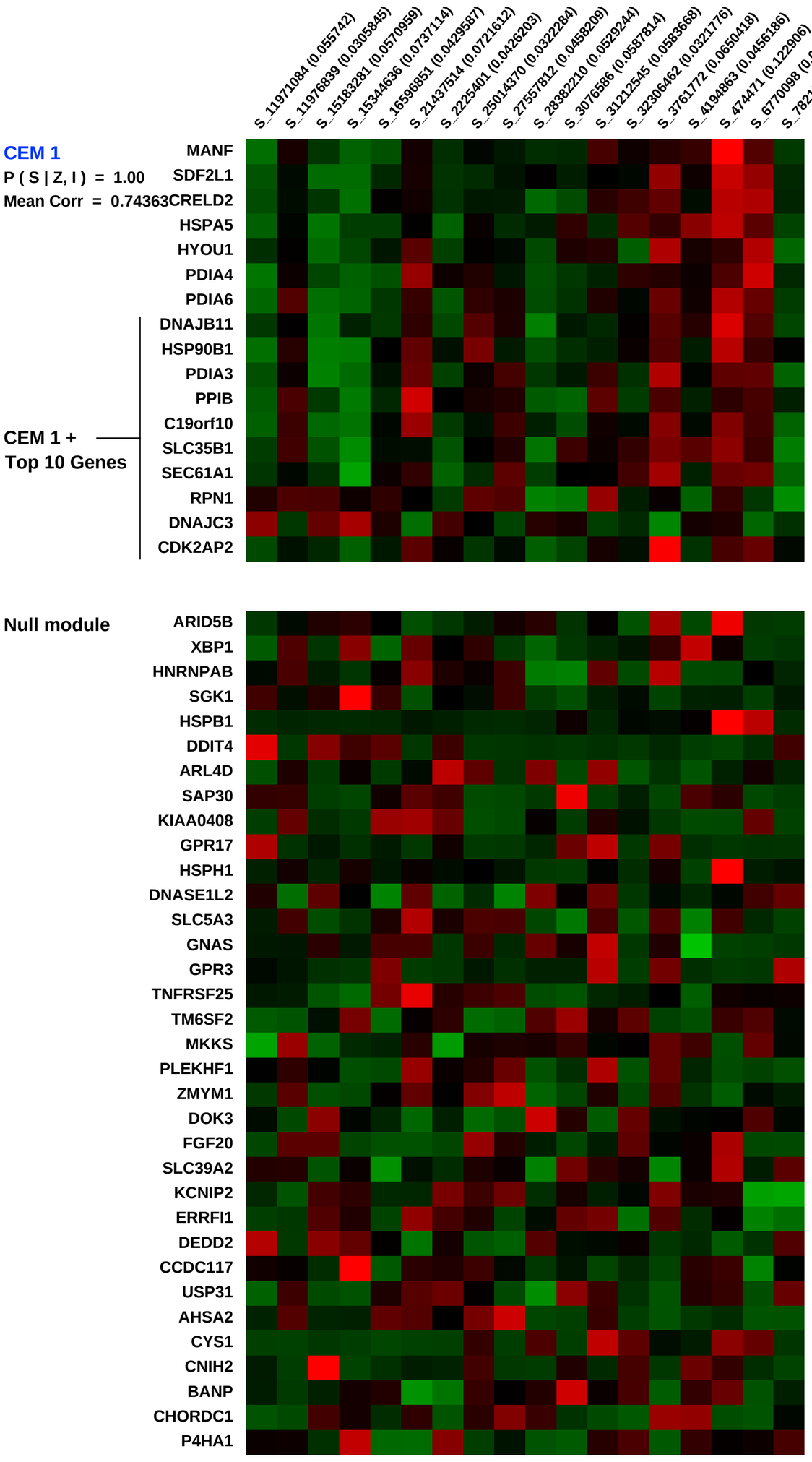

Pre-normalization Quantiles

[min]	[medium]	[max]
854.7	1384.6	2734.7
145.8	496.7	1240.2
411.5	1077.8	2390.9
2905.0	5958.6	11290.7
598.8	1130.0	1985.4
225.9	698.6	1406.4
1158.4	3762.2	7070.2
678.7	1325.2	2403.2
266.8	688.7	1327.9
1770.3	4508.2	8525.6
8754.2	12511.3	18864.9
492.1	946.3	1637.8
360.8	591.4	785.9
610.0	1308.2	1996.3
2350.5	3935.1	5293.4
2788.5	6908.0	10801.4
592.4	922.9	1998.5

GEO Series "GSE29868" Expression Profiles

Num of samples in this series: 59

Scale of expression profile Z-scores

-3.0 -2.0 -1.0 0.0 1.0 2.0 3.0

GEO Link: http://www.ncbi.nlm.nih.gov/geo/query/acc.cgi?acc=GSE29868
Status: Public on Sep 01 2011
Title: Inferring drug-induced gene regulatory relationships in primary human hepatocytes
Organism: Homo sapiens
Experiment type: Expression profiling by array
Platform: GPL570
Pubmed ID: 21757465

Summary & Design:

Summary:
Statins are widely used cholesterol-lowering drugs that inhibit HMG-CoA reductase, a key enzyme in cholesterol synthesis. In some cases, however, these drugs may cause a number of toxic side effects in hepatocytes and skeletal muscle tissue. Currently, the specific molecular mechanisms that cause these adverse effects are not sufficiently understood. In this work, genome-wide RNA expression changes in primary human hepatocytes of six individuals were measured at five time points upon atorvastatin treatment. A novel systems-level analysis workflow was applied to reconstruct regulatory mechanisms based on these drug-response data and available knowledge about transcription factor binding specificities, protein-protein interactions and protein-drug interactions. Several previously unknown transcription factors, regulatory cofactors and signaling molecules were found to be involved in atorvastatin-responsive gene expression. Some novel relationships, e.g., the regulatory influence of nuclear receptor NR2C2 on CYP3A4, were successfully validated in wet-lab experiments.

Overall design:
Whole-genome Affymetrix U133 Plus 2.0 (Affymetrix, Santa Clara, CA) microarray measurements were conducted using samples of primary human hepatocytes cultured from six individuals (i.e., hh62, hh65, hh67, hh79, hh80 and hh81). Each sample was treated with atorvastatin and dimethylsulfoxide (DMSO), which was used as a control substance. Microarray measurements were performed at five time points (6 h, 12 h, 24 h, 48 h and 72 h) after the drug stimulus.

Background corr dist: KL-Divergence = 0.1833, L1-Distance = 0.0481, L2-Distance = 0.0051, Normal std = 0.3425

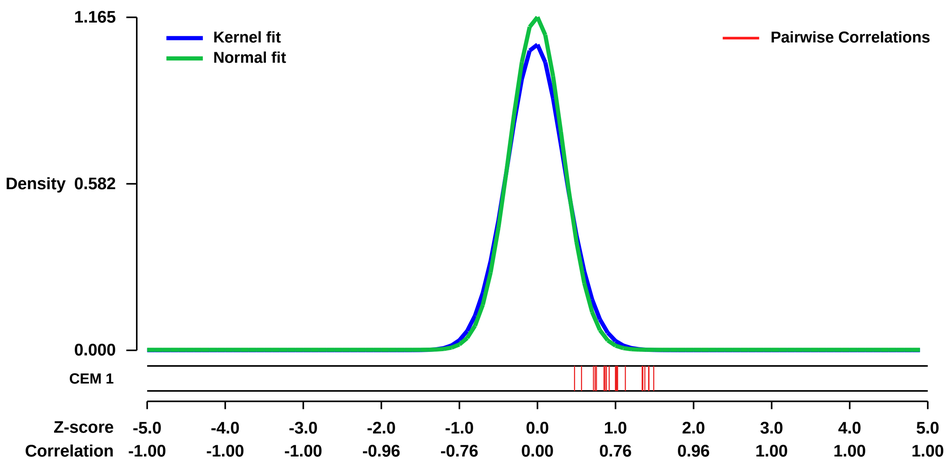

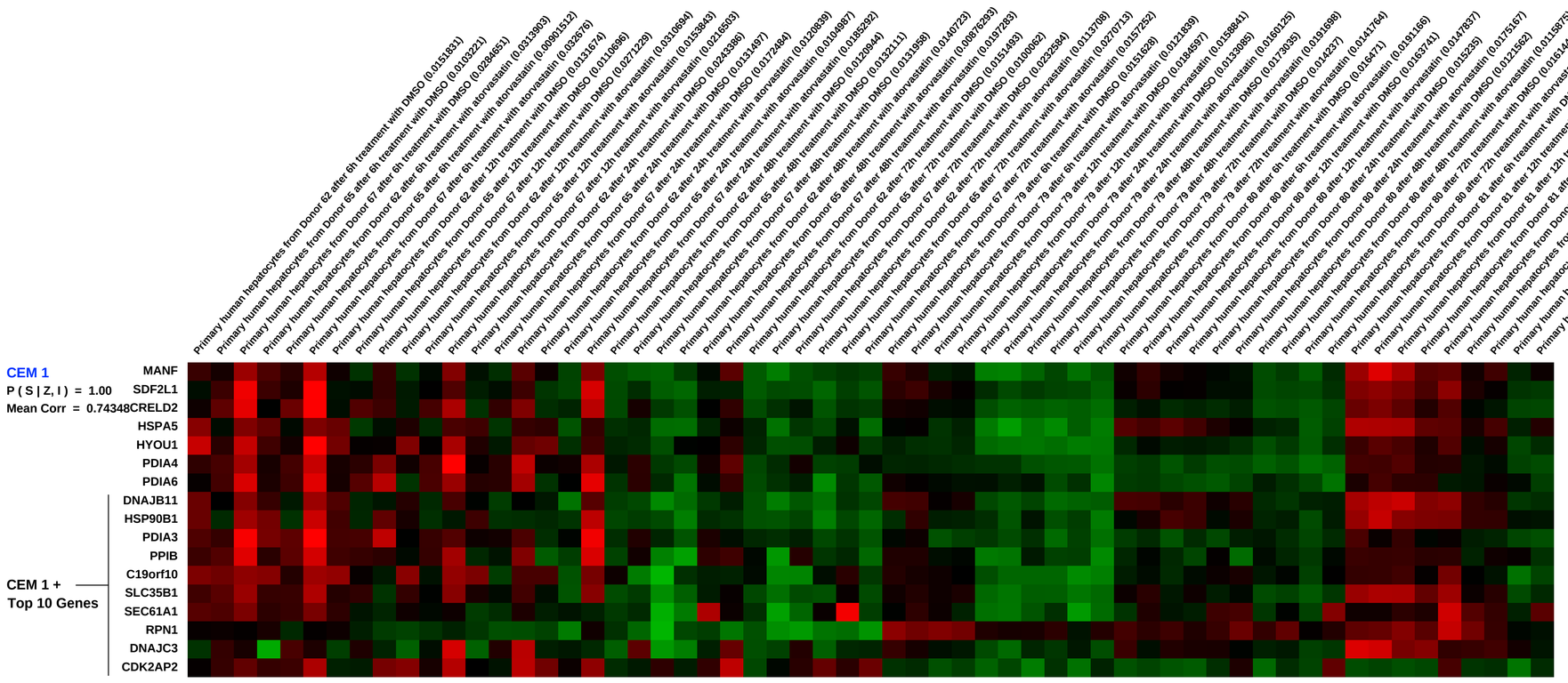

Pre-normalization Quantiles

[min]	[medium]	[max]
4867.1	8769.6	16286.8
1005.7	2916.3	9105.3
2232.4	6250.1	18725.9
12456.9	29837.8	51939.3
2127.8	5701.5	16453.9
1041.7	2455.7	6982.5
7688.1	12959.8	23508.2
2626.0	6219.0	13334.8
3500.0	9476.9	23584.5
6007.4	11012.2	29021.0
16582.5	23594.9	34142.1
2491.2	5311.7	7904.4
2037.4	4117.4	6774.0
3508.8	5714.6	8892.5
2678.1	5626.4	8592.1
3236.2	5911.6	10180.7
868.6	1619.5	3343.9

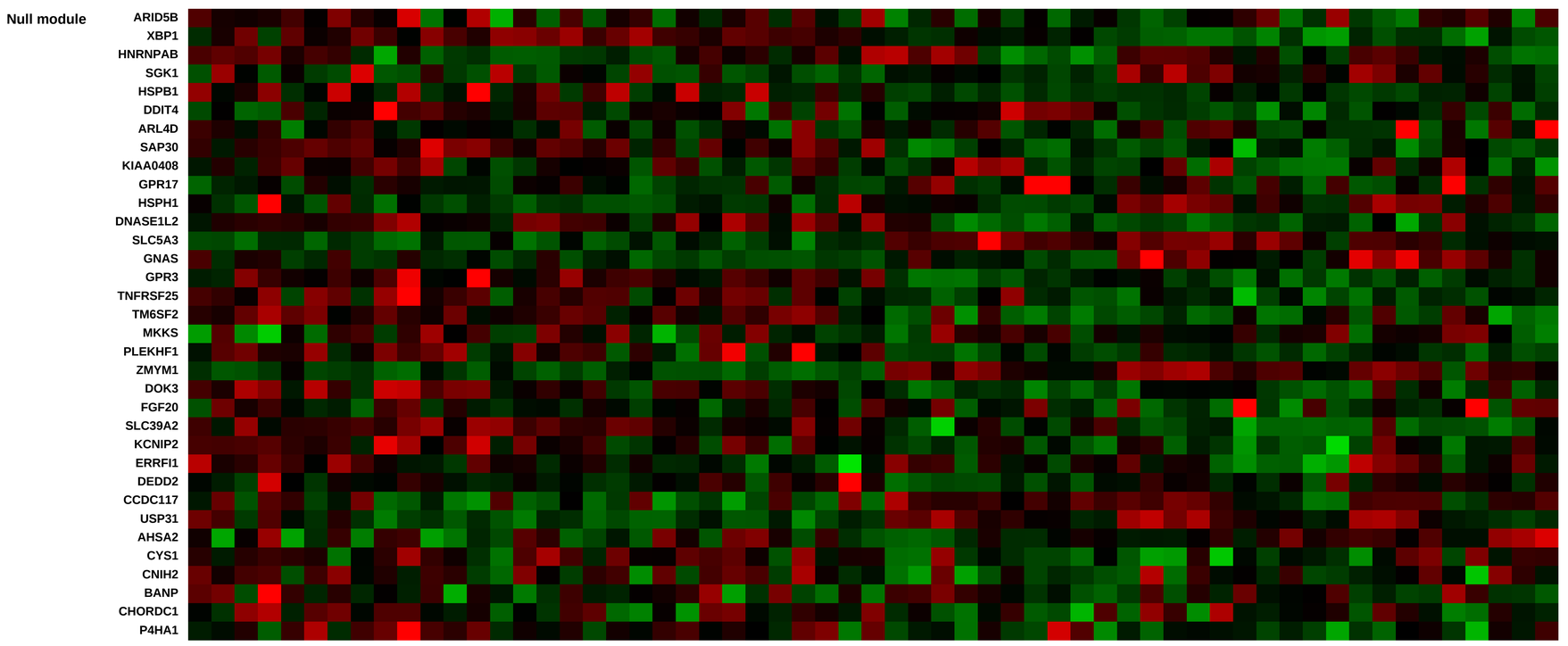

GEO Series "GSE11510" Expression Profiles

Num of samples in this series: 17

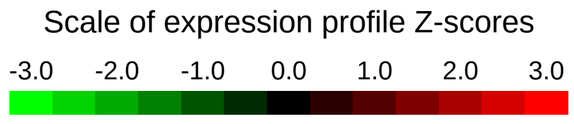

GEO Link: http://www.ncbi.nlm.nih.gov/geo/query/acc.cgi?acc=GSE11510

Status: Public on May 20 2008

Title: Taxonomy of placenta cells

Organism: Homo sapiens

Experiment type: Expression profiling by array

Platform: GPL570

Pubmed ID:

Summary & Design:

Summary:
The placenta is considered one of the candidate cell sources in cellular therapeutics because of a large number of cells and heterogenous cell population with myogenic potentials. We first analyzed myogenic potential of cells obtained from six parts of the placenta, i.e., umbilical cord, amniotic epithelium, amniotic mesoderm, chorionic plate, villous chorion (chorion frondosum), , and decidua basalis. Implantation of placenta-derived cells into dystrophic muscles of immunodeficient mdx mice restored sarcolemmal expression of human dystrophin. Co-existence of human and murine nuclei in one myotube and presence of human dystrophin in murine myotube suggests that human dystrophin expression is due to cell fusion between host murine myocytes and implanted human cells. In vitro analysis revealed that cells derived from amniotic mesoderm, chorionic plate, ,and villous chorion efficiently transdifferentiate into myotubes. These cells fused to C2C12 murine myoblasts by in vitro co-culturing, and murine myoblasts start to express human dystrophin after fusion. These results demonstrate that placenta-derived cells, especially extraembryonic mesodermal cells, have a myogenic potential and regenerative capacity of skeletal muscle. Determination of cell specification with the gene chip analysis revealed that each placental cell has a distinct expression pattern.

Keywords: Determination of cell specification

Overall design:
To isolate chorionic villi cells, we used the explant culture method, in which the cells were outgrown from pieces of chorionic villi attached to dishes. Chorionic villi cells were harvested with 0.25% trypsin and 1 mM EDTA, and overlaid onto the cultured fetal cardiomyocytes at 7 x 103/cm2. Every 2 days, the culture medium was replaced with fresh culture medium that was supplemented with 10% FBS and 1 ug/ml Amphotericin B (GIBCO). The morphology of the beating chorionic villi cells was evaluated under a fluorescent microscope.

Background corr dist: KL-Divergence = 0.1901, L1-Distance = 0.0477, L2-Distance = 0.0054, Normal std = 0.3401

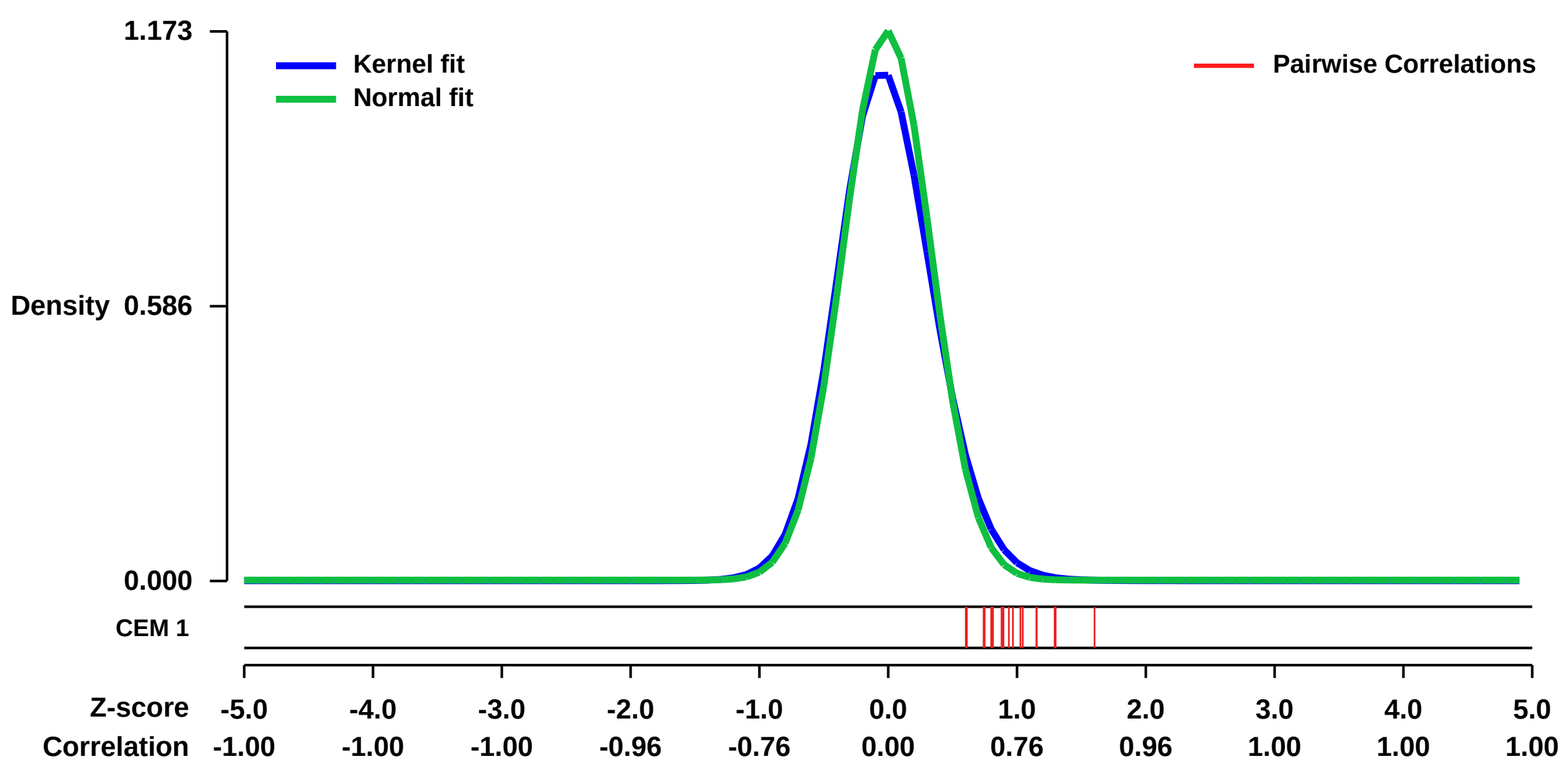

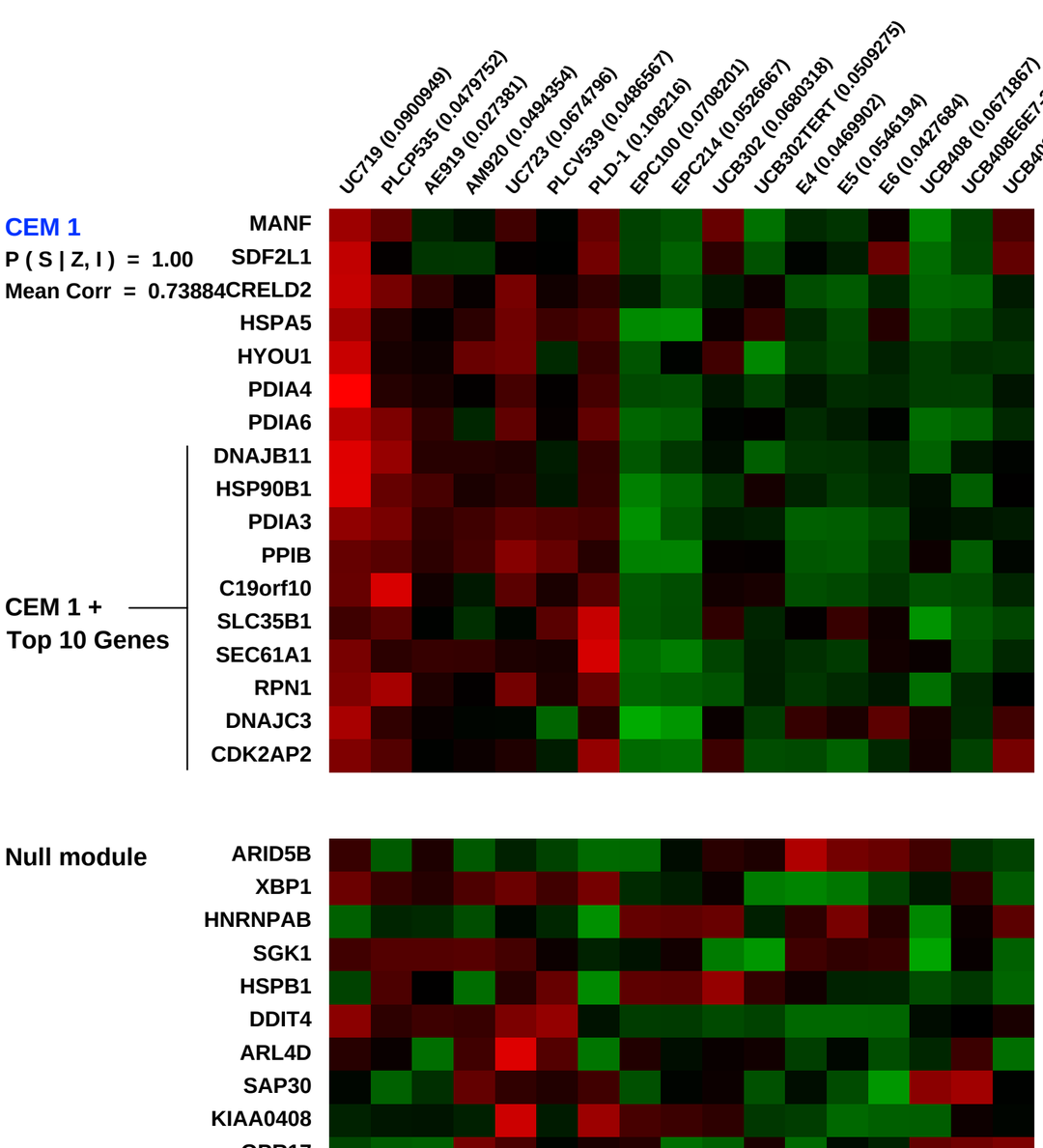

Pre-normalization Quantiles

	[min]	[medium]	[max]
MANF	1712.1	3496.1	6142.3
SDF2L1	461.3	879.7	1673.4
CRELD2	1500.9	2859.4	6827.1
HSPA5	8801.4	15041.6	21084.0
HYOU1	3025.0	5400.8	10805.6
PDIA4	944.5	1451.3	4247.4
PDIA6	4972.5	7345.4	11508.8
DNAJB11	3613.0	5076.1	9698.0
HSP90B1	2109.5	5334.1	12015.1
PDIA3	6234.9	10700.6	16572.3
PPIB	9099.5	13266.0	17169.6
C19orf10	3909.2	4938.5	8822.0
SLC35B1	1930.8	3001.5	4467.1
SEC61A1	4561.1	7815.5	12774.9
RPN1	3178.3	4261.7	6583.2
DNAJC3	855.0	2433.4	3820.1
CDK2AP2	493.7	862.5	1368.4

GEO Series "GSE46268" Expression Profiles

Num of samples in this series: 12

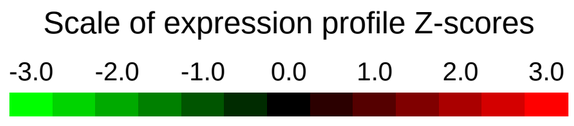

GEO Link:	http://www.ncbi.nlm.nih.gov/geo/query/acc.cgi?acc=GSE46268
Status:	Public on Dec 31 2013
Title:	Gene expression profile of human monocytes stimulated with all-trans retinoic acid (ATRA) or 1,25a-dihydroxyvitamin D3 (1,25D3)
Organism:	Homo sapiens
Experiment type:	Expression profiling by array
Platform:	GPL570
Pubmed ID:	24501203
Summary & Design:	**Summary:** A role for vitamin A in host defense against Mycobacterium tuberculosis has been suggested through epidemiological and in vitro studies; however, the antimicrobial mechanism is unclear. Here, we demonstrate that vitamin A mediates host defense through regulation of cellular cholesterol content. Comparison of monocytes stimulated with all-trans retinoic acid (ATRA) or 1,25-dihydroxyvitamin D3, the biologically active forms of vitamin A and vitamin D respectively, indicates that ATRA and 1,25D3 induce mechanistically distinct antimicrobial activities. Gene expression profiling reveals that ATRA but not 1,25D3 triggers a lipid metabolism and efflux pathway, including expression of lysosomal lipid transport gene NPC2. ATRA-induced decrease in total cellular cholesterol content, subcellular lipid reorganization, lysosomal acidification and antimicrobial activity are all dependent upon expression of NPC2. Finally, the addition of HIV-protease inhibitors known to inhibit cholesterol efflux, Ritonavir and Nelfinavir, blocked both ATRA-induced cholesterol decrease as well as antimicrobial activity. Taken together, these results suggest that the vitamin A-mediated host defense mechanism against M. tuberculosis requires regulation of cellular cholesterol. **Overall design:** Monocytes derived from four independent healthy blood donors that were stimulated with control (CTRL), ATRA or 1,25D3 at 10-8M for 18 hours.

Background corr dist: KL-Divergence = 0.1501, L1-Distance = 0.0355, L2-Distance = 0.0025, Normal std = 0.3736

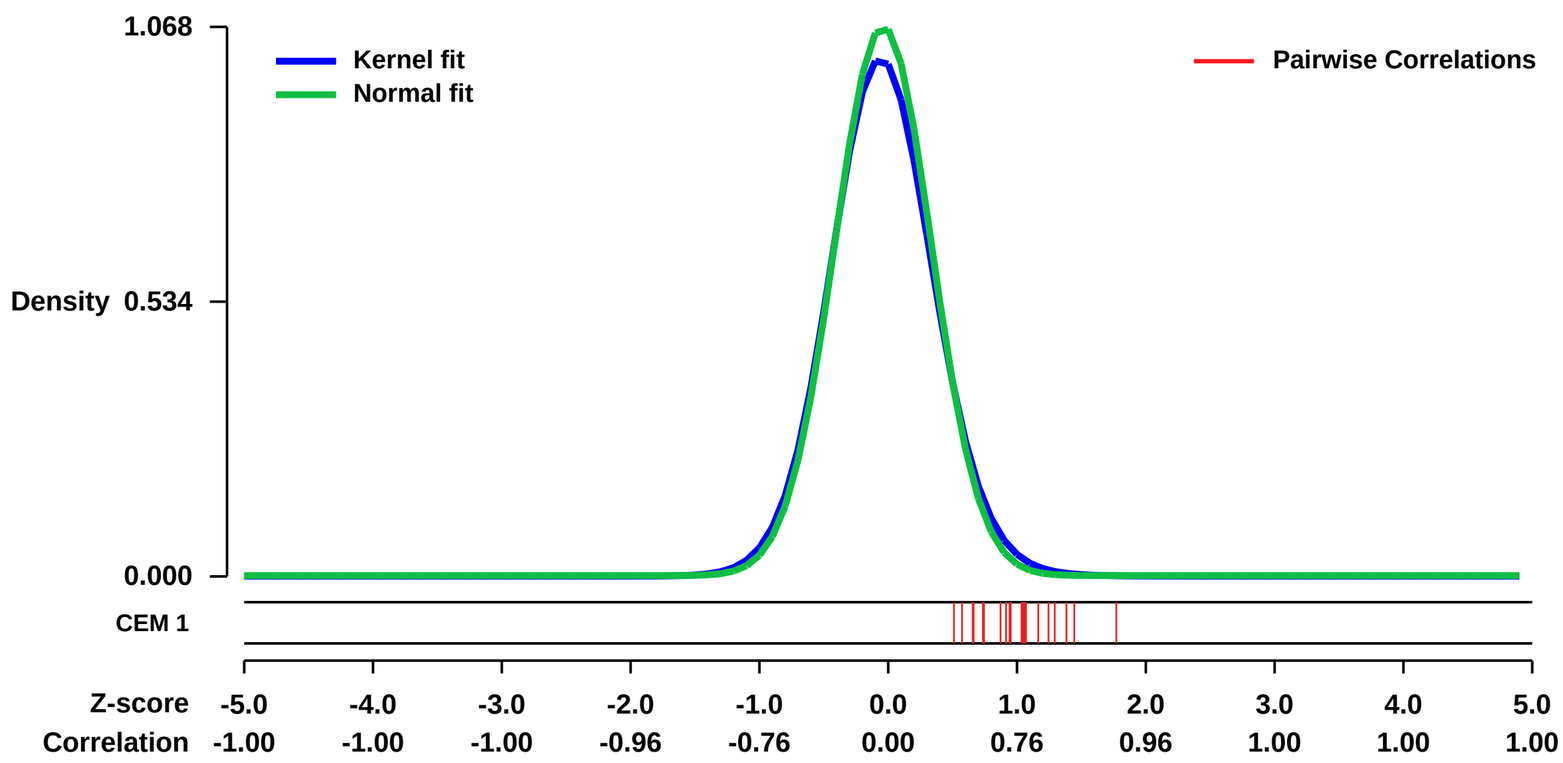

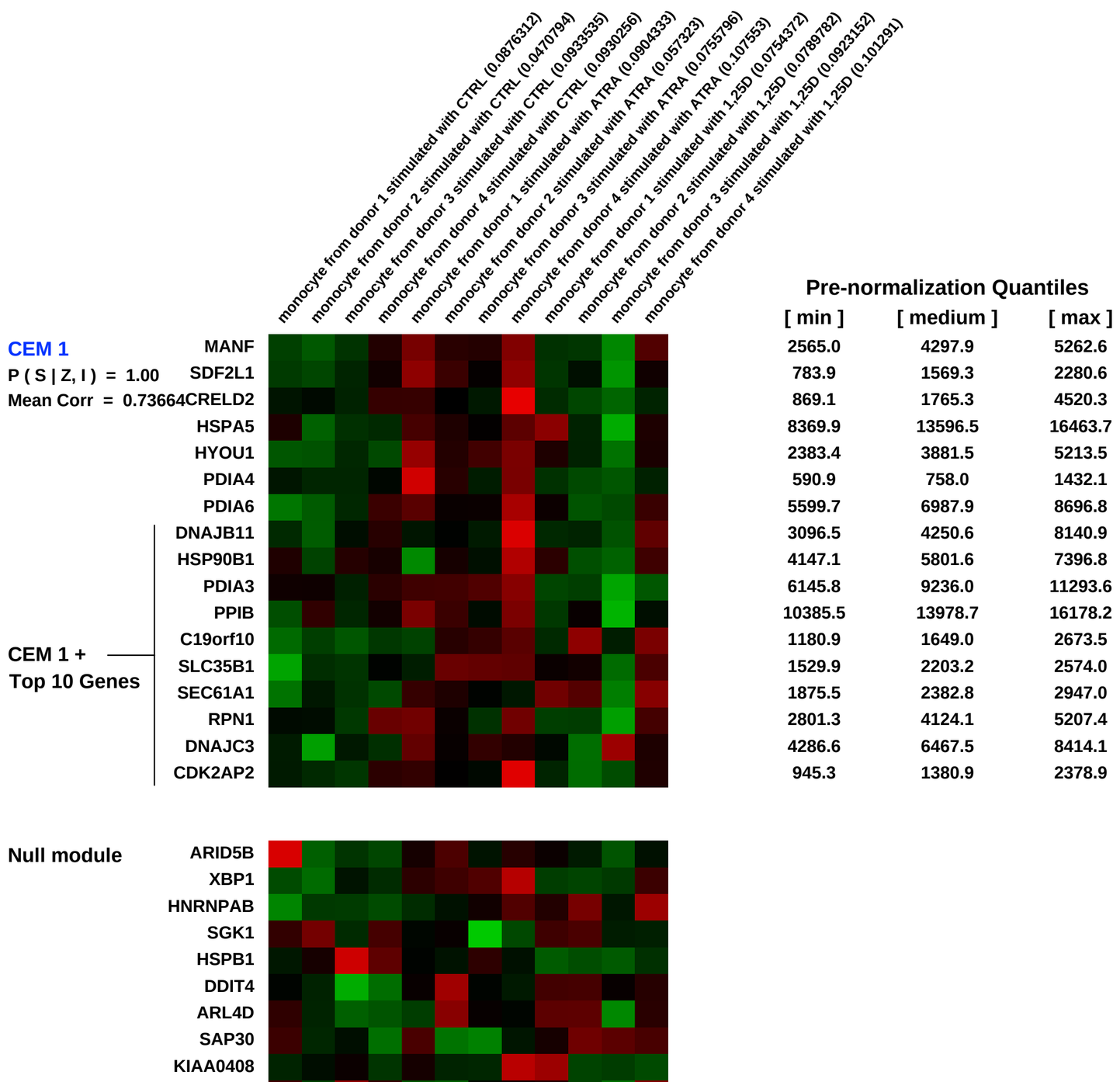

Pre-normalization Quantiles

	[min]	[medium]	[max]
MANF	2565.0	4297.9	5262.6
SDF2L1	783.9	1569.3	2280.6
CRELD2	869.1	1765.3	4520.3
HSPA5	8369.9	13596.5	16463.7
HYOU1	2383.4	3881.5	5213.5
PDIA4	590.9	758.0	1432.1
PDIA6	5599.7	6987.9	8696.8
DNAJB11	3096.5	4250.6	8140.9
HSP90B1	4147.1	5801.6	7396.8
PDIA3	6145.8	9236.0	11293.6
PPIB	10385.5	13978.7	16178.2
C19orf10	1180.9	1649.0	2673.5
SLC35B1	1529.9	2203.2	2574.0
SEC61A1	1875.5	2382.8	2947.0
RPN1	2801.3	4124.1	5207.4
DNAJC3	4286.6	6467.5	8414.1
CDK2AP2	945.3	1380.9	2378.9

GEO Series "GSE20910" Expression Profiles

Num of samples in this series: 49

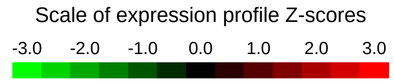

GEO Link:	http://www.ncbi.nlm.nih.gov/geo/query/acc.cgi?acc=GSE20910
Status:	Public on Jul 12 2011
Title:	Expression data from Down syndrome and non-Down syndrome pediatric acute lymphoblastic leukemia cases
Organism:	Homo sapiens
Experiment type:	Expression profiling by array
Platform:	GPL570
Pubmed ID:	21647151
Summary & Design:	**Summary:** Gene expression profiling (GEP) can reveal characteristic signatures associated with distinct biologic subtypes of acute lymphoblastic leukemia (ALL). We performed GEP on Down syndrome (DS) and comparison non-Down syndrome (NDS) ALL cases to identify biologic differences between these groups. **Overall design:** Ficoll-enriched, cryopreserved diagnostic bone marrow samples were obtained from patients with newly diagnosed B-precursor acute lymphoblastic leukemia.

Background corr dist: KL-Divergence = 0.3707, L1-Distance = 0.0942, L2-Distance = 0.0289, Normal std = 0.2571

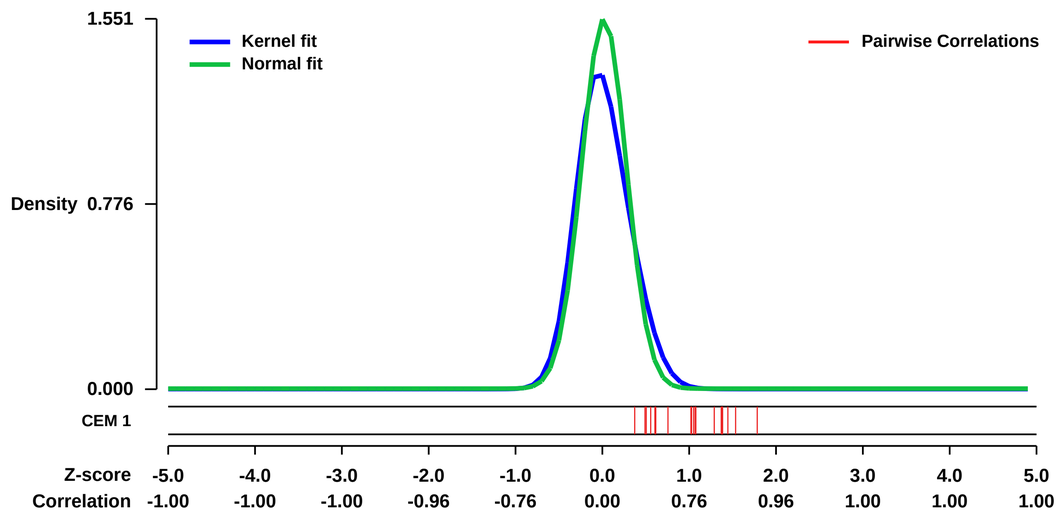

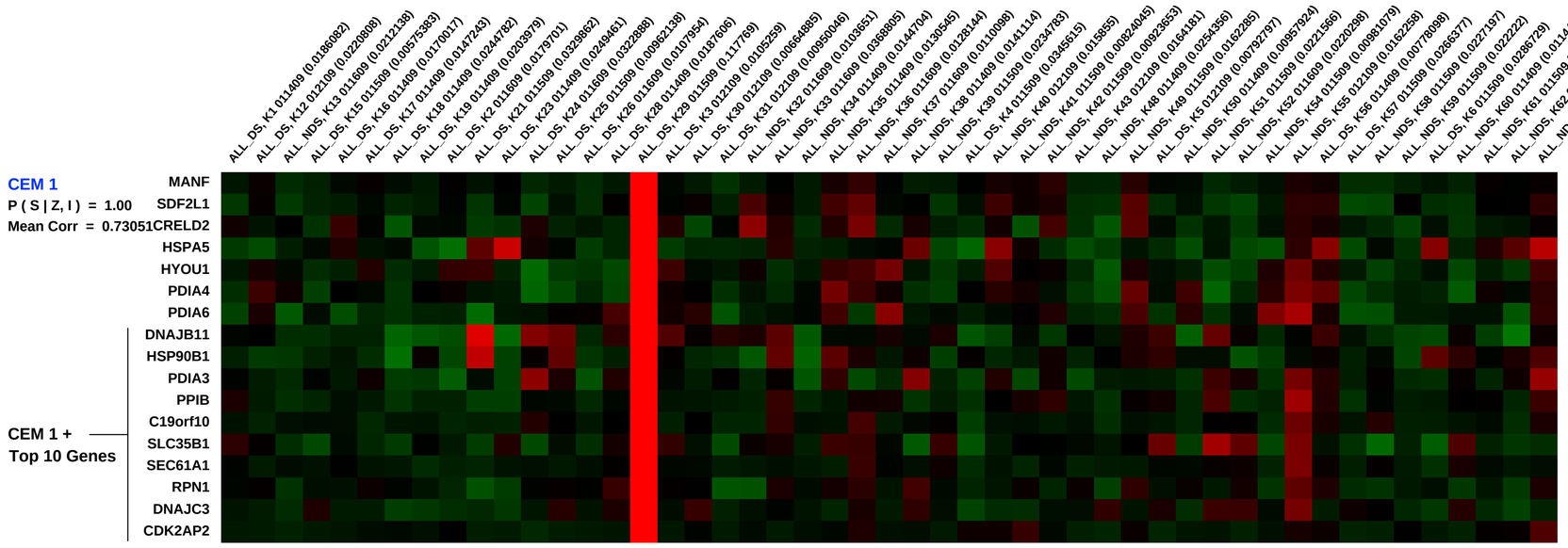

Pre-normalization Quantiles

[min]	[medium]	[max]
764.3	1747.8	17640.7
387.3	921.2	5723.2
1429.1	2773.8	12780.2
7168.6	21524.9	77011.9
382.0	834.1	3493.5
230.7	675.0	2993.2
5533.8	9777.4	30477.2
1754.9	3025.3	7202.3
2465.3	5277.4	17758.5
8133.0	12452.7	40612.9
12593.4	16907.9	74047.8
1214.8	2119.4	13192.5
927.2	1512.1	4454.1
1666.9	2288.7	13449.1
2013.9	3431.8	13728.9
851.1	1733.2	11769.8
248.3	625.9	11130.9

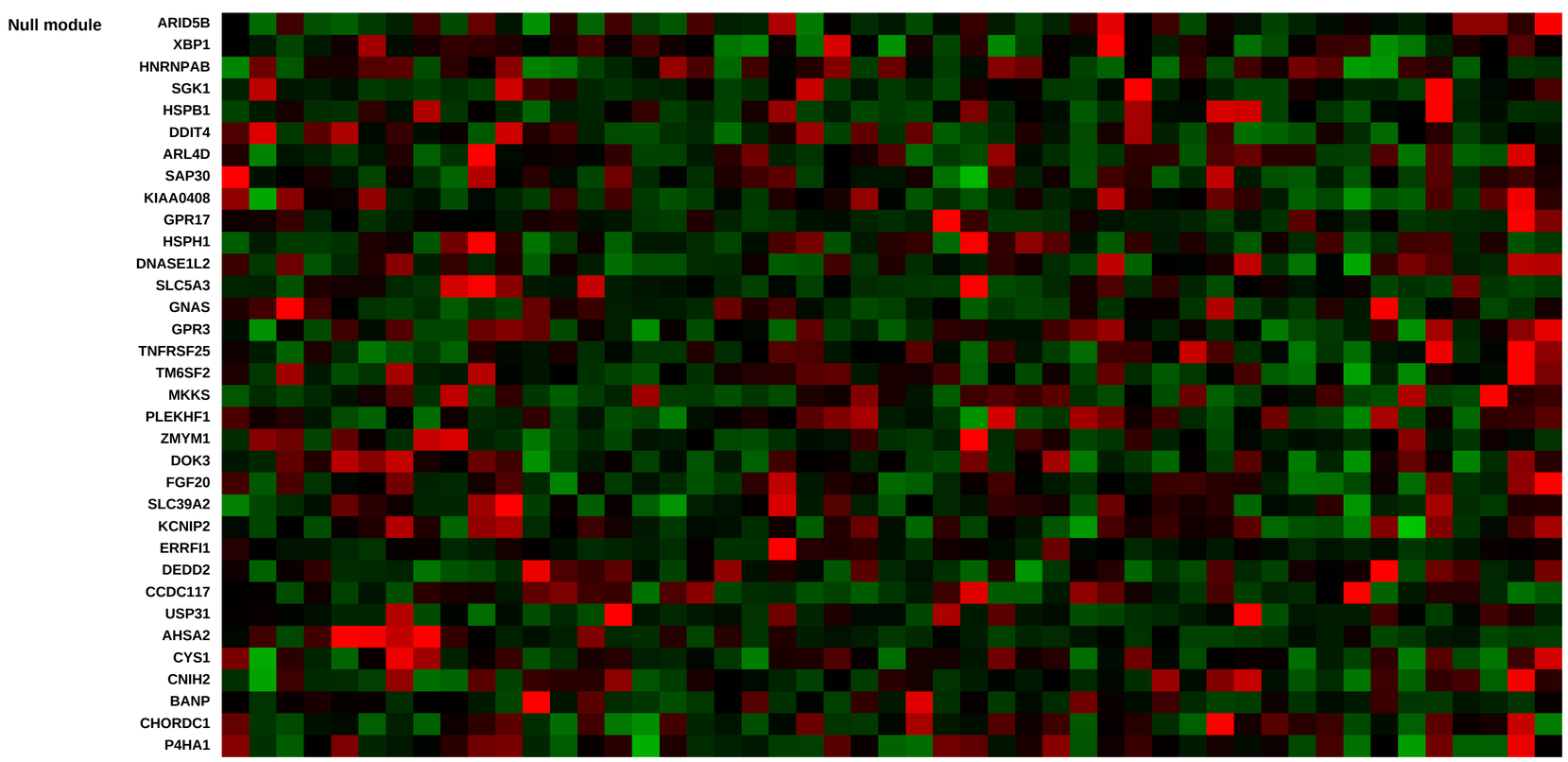

GEO Series "GSE17551" Expression Profiles

Num of samples in this series: 6

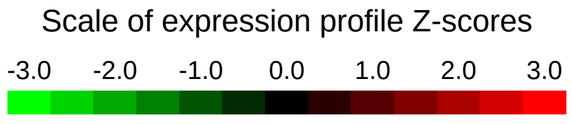

GEO Link:	http://www.ncbi.nlm.nih.gov/geo/query/acc.cgi?acc=GSE17551
Status:	Public on Aug 04 2010
Title:	Genes regulated after transient knock-down of Pirin in WM-266 cells
Organism:	Homo sapiens
Experiment type:	Expression profiling by array
Platform:	GPL570
Pubmed ID:	
Summary & Design:	**Summary:** Pirin (PIR) is a putative transcriptional regulator abundantly expressed in melanocytes and in a subset of primary and metastatic melanomas. Ablation of PIR in the melanoma cell lines results in induction of a senescence-like phenotype. **Keywords: Transcriptional regulation, knock-down using siRNA** **Overall design:** We analyzed gene expression profiles of WM-266.4 metastatic melanoma cells after knock-down of PIR, which was achieved using a pool of four PIR-siRNA duplexes (siPIR). A pool of four non-targeting siRNA duplexes was used as control of off-target transcriptional effects (siCTR). Cells that underwent transfection with no oligonucleotides (oligofectamine only) were also included to measure all non-specific effects (NO cells). For each sample, an RNA pool was obtained by mixing equal quantities of total RNA from each of three independent RNA extractions. Each biotin-labeled target was hybridized to two GeneChip HG-U133 Plus v.2 arrays.

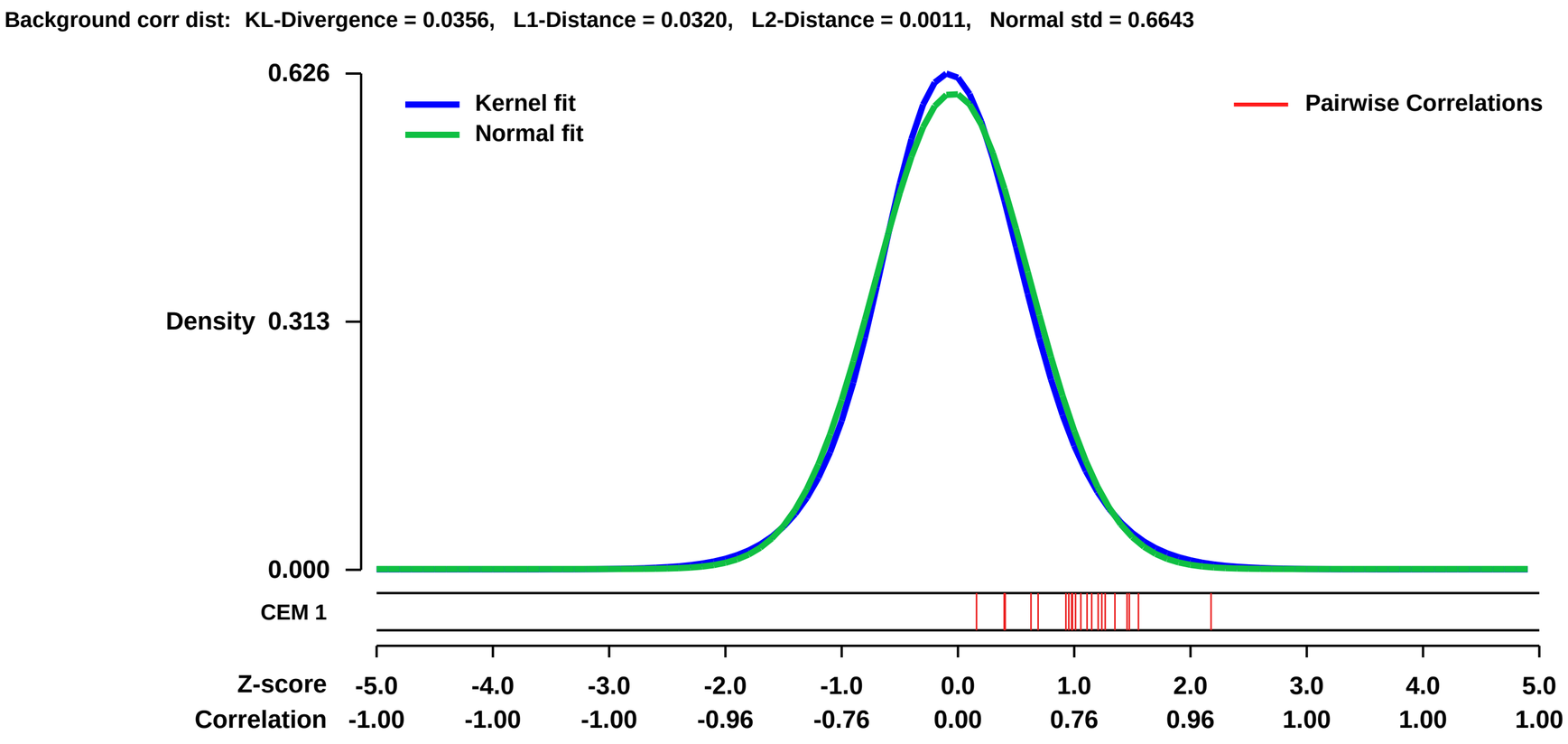

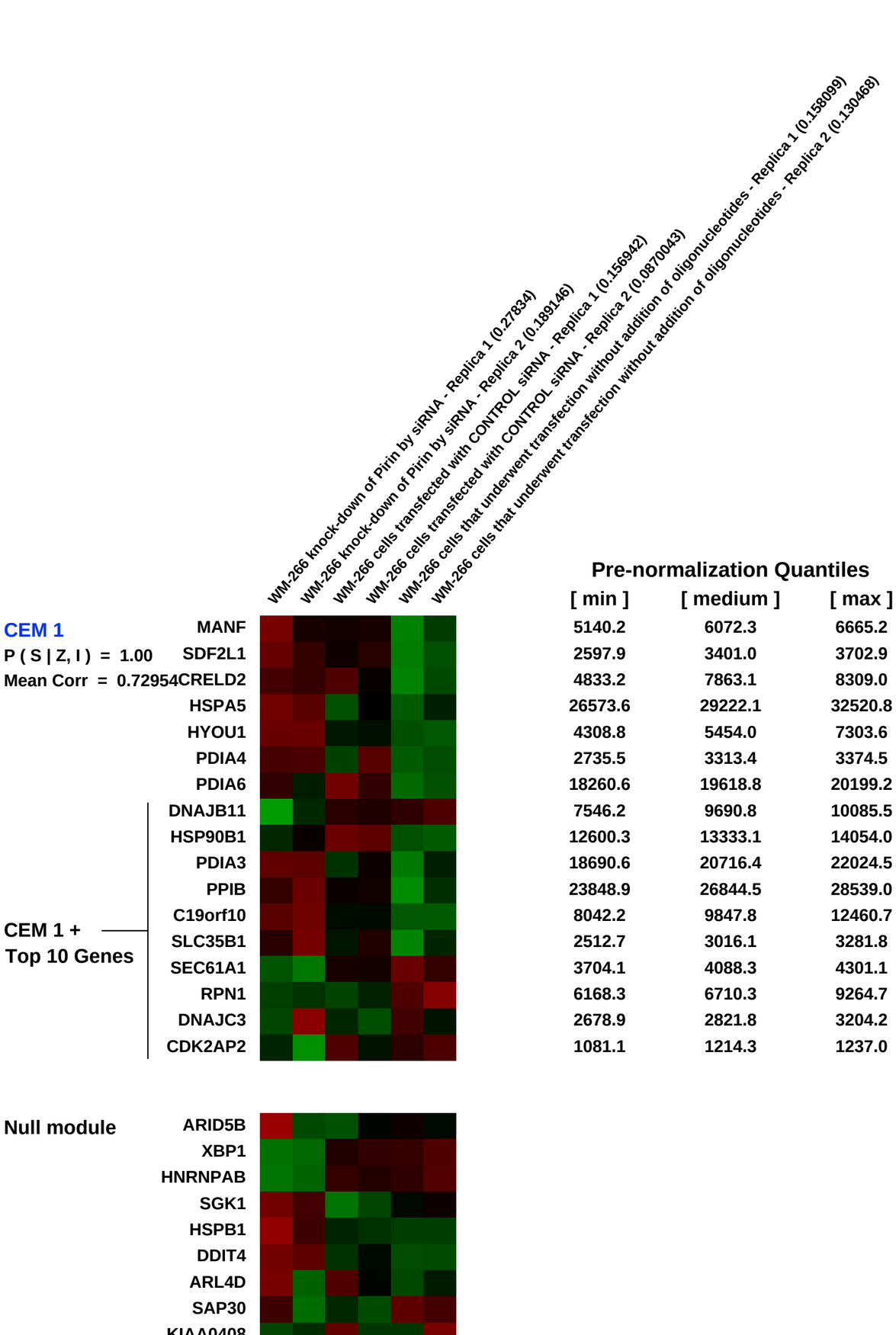

GEO Series "GSE10270" Expression Profiles

Num of samples in this series: 24

Scale of expression profile Z-scores

-3.0 -2.0 -1.0 0.0 1.0 2.0 3.0

GEO Link: http://www.ncbi.nlm.nih.gov/geo/query/acc.cgi?acc=GSE10270

Status: Public on Jan 26 2008

Title: Bisphenol A induces a profile of tumor aggressiveness in high-risk cells of breast cancer patients

Organism: Homo sapiens

Experiment type: Expression profiling by array

Platform: GPL570

Pubmed ID: 18381411

Summary & Design:

Summary:
Breast cancer outcome is highly variable. Whether inadvertent exposure to environmental xenobiotics evokes a biological response promoting cancer aggressiveness and a higher probability of tumor recurrence remains unknown. To determine specific molecular alterations, which arise in high-risk breast tissue in the presence of the ubiquitous xenoestrogen, bisphenol A (BPA), we employed non-malignant random periareolar fine needle aspirates (RPFNA) in a novel functional assay. Early events induced by BPA in epithelial-stromal cocultures derived from the contralateral tissue of breast cancer patients included gene expression patterns, which facilitate apoptosis evasion, endurance of microenvironmental stress, and cell cycle deregulation without a detectable increase in cell number. This BPA response profile was significantly associated with breast tumors characterized by high histologic grade (p<0.001), and large tumor size (p=0.002), resulting in decreased recurrence-free patient survival (p<0.001). Our assays demonstrate a biological â fingerprintâ of probable prior exposure to endocrine disrupting agents, and suggest a scenario in which their presence in the microenvironmental milieu of high-risk breast tissue could play a deterministic role in establishing and maintaining tumor aggressiveness and poor patient outcome.

Keywords: Gene expression, Epithelial, Breast cancer

Overall design:
The study included twelve patients undergoing breast biopsy or surgery for breast cancer. Random periareolar fine needle aspirates (RPFNA) were collected from the unaffected contralateral breast of these patients. Control and hormone treated RPFNA cell cultures were analyzed using Affymetrix GeneChip(TM) arrays

Background corr dist: KL-Divergence = 0.2511, L1-Distance = 0.0583, L2-Distance = 0.0085, Normal std = 0.3013

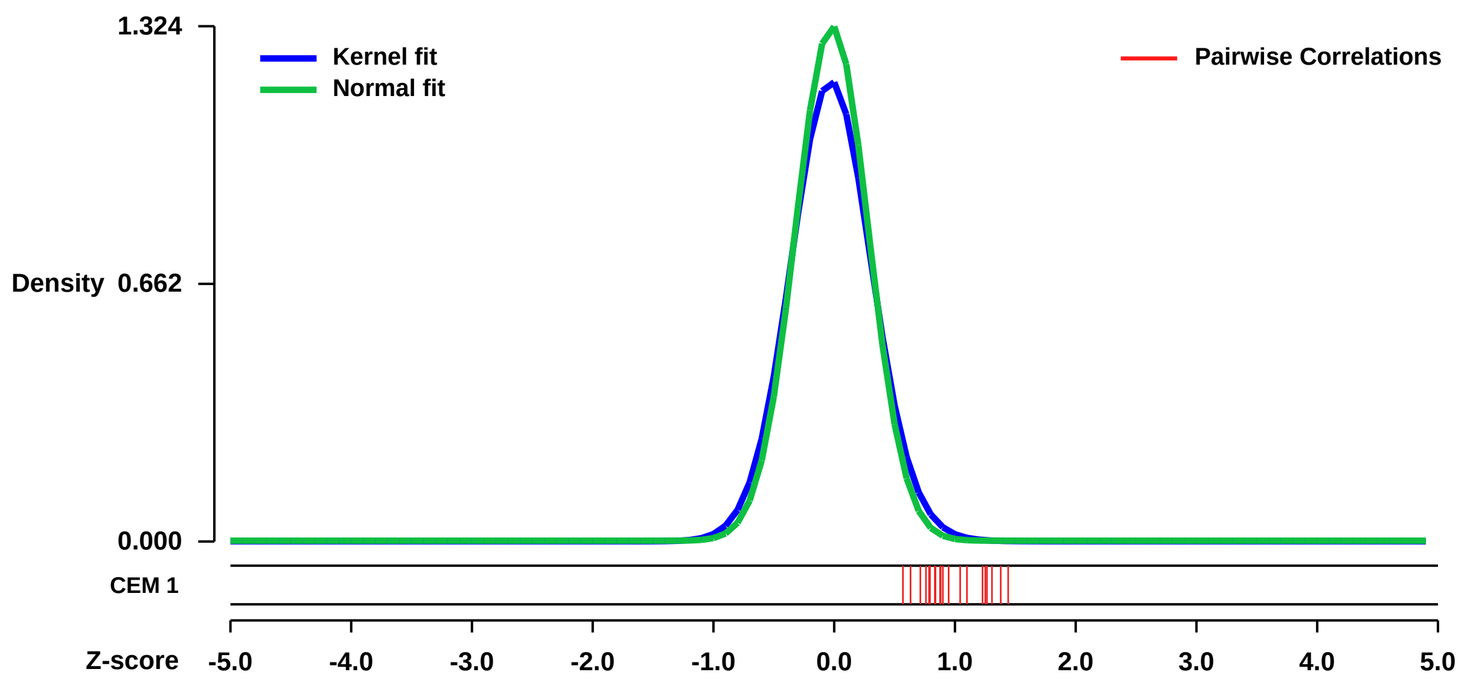

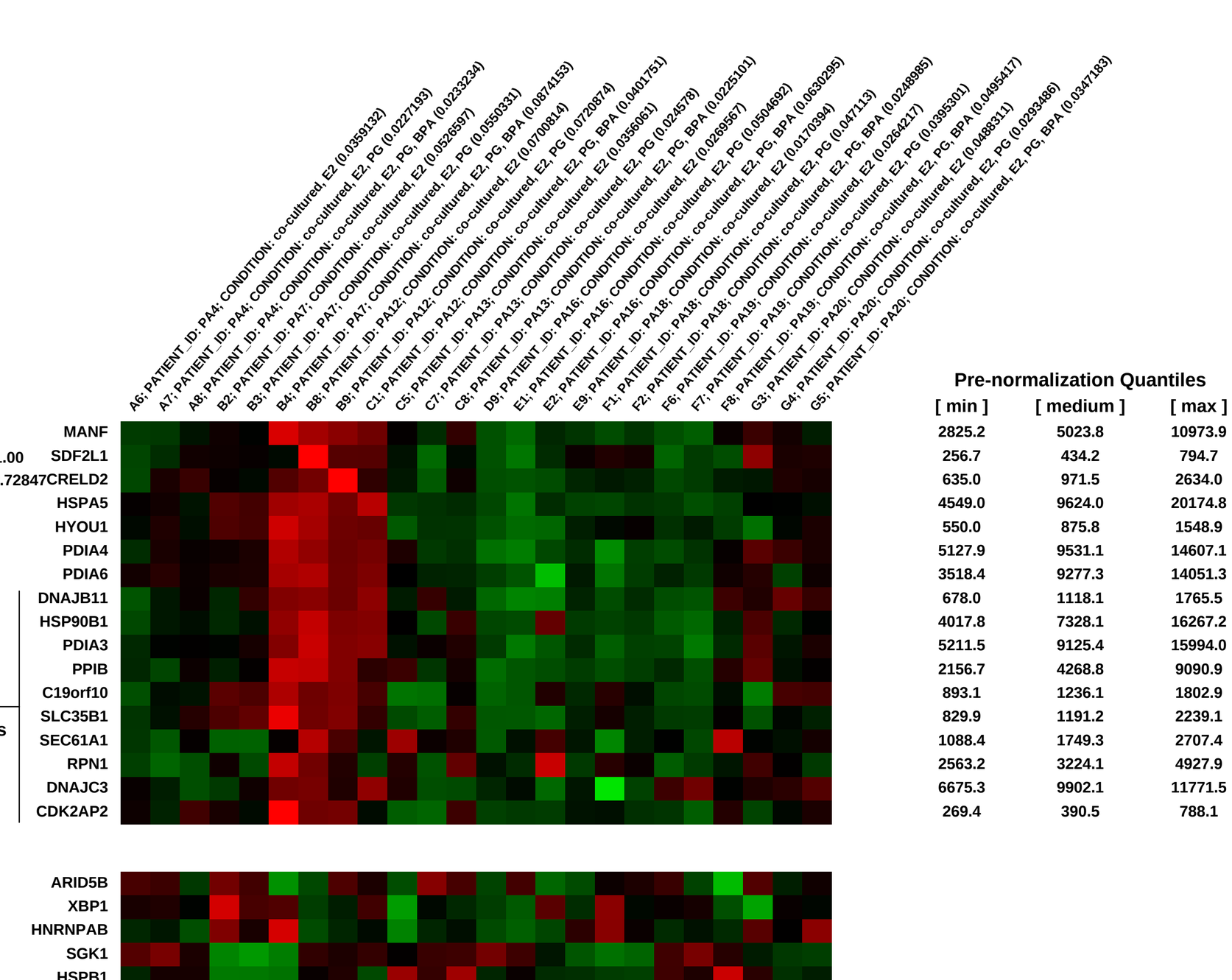

GEO Series "GSE10650" Expression Profiles

Num of samples in this series: 6

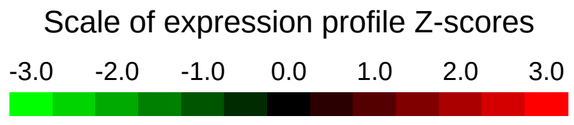

GEO Link:	http://www.ncbi.nlm.nih.gov/geo/query/acc.cgi?acc=GSE10650
Status:	Public on Feb 26 2009
Title:	HCT116 PCLKC
Organism:	Homo sapiens
Experiment type:	Expression profiling by array
Platform:	GPL570
Pubmed ID:	

Summary & Design:

Summary:
The gain of Protocadherin LKC (PCDH24) expression in colon carcinoma cell line HCT116 has been shown to induce contact inhibition, thereby completely abolishing tumor formation in vivo. To clarify the molecular mechanism, we performed DNA microarray analysis and compared gene-expression pattern between control and PCDH24-expressing HCT116 cells. Approximately 2000 genes were apparently changed their expression. Further proteomics analysis using 2-DE/MS confirmed the dramatic changes and provided additional information. We were aware that these changes are quite similar to the changes observed in epithelial-mesenchymal transition (EMT), most drastic changes in development and cancer metastasis. We thus further analyzed these changes using specific antibodies, and found distinct difference between these two phenomena. Among the differences, nuclear translocation of catenin beta 1 (CTNNB1) was inhibited by PCDH24-expression, subsequently some of the downstream nodes were suppressed. Although contact inhibition and cancer metastasis are completely opposite aspect of the cells, we expect that the identified differences will be key nodes to understand the relationship. We also expect that the nodes will be a target to modulate tumors arising stem cell transplantation (SCT), as well as a therapeutic target for cancer metastasis.

Keywords: dose response

Overall design:
Three HCT116 PCLKC cell lines (parental cells and two stable expression clones with random integration of the targeting vector, PCLKC-GFP, GFP) were studied.

Background corr dist: KL-Divergence = 0.0146, L1-Distance = 0.0501, L2-Distance = 0.0044, Normal std = 0.9244

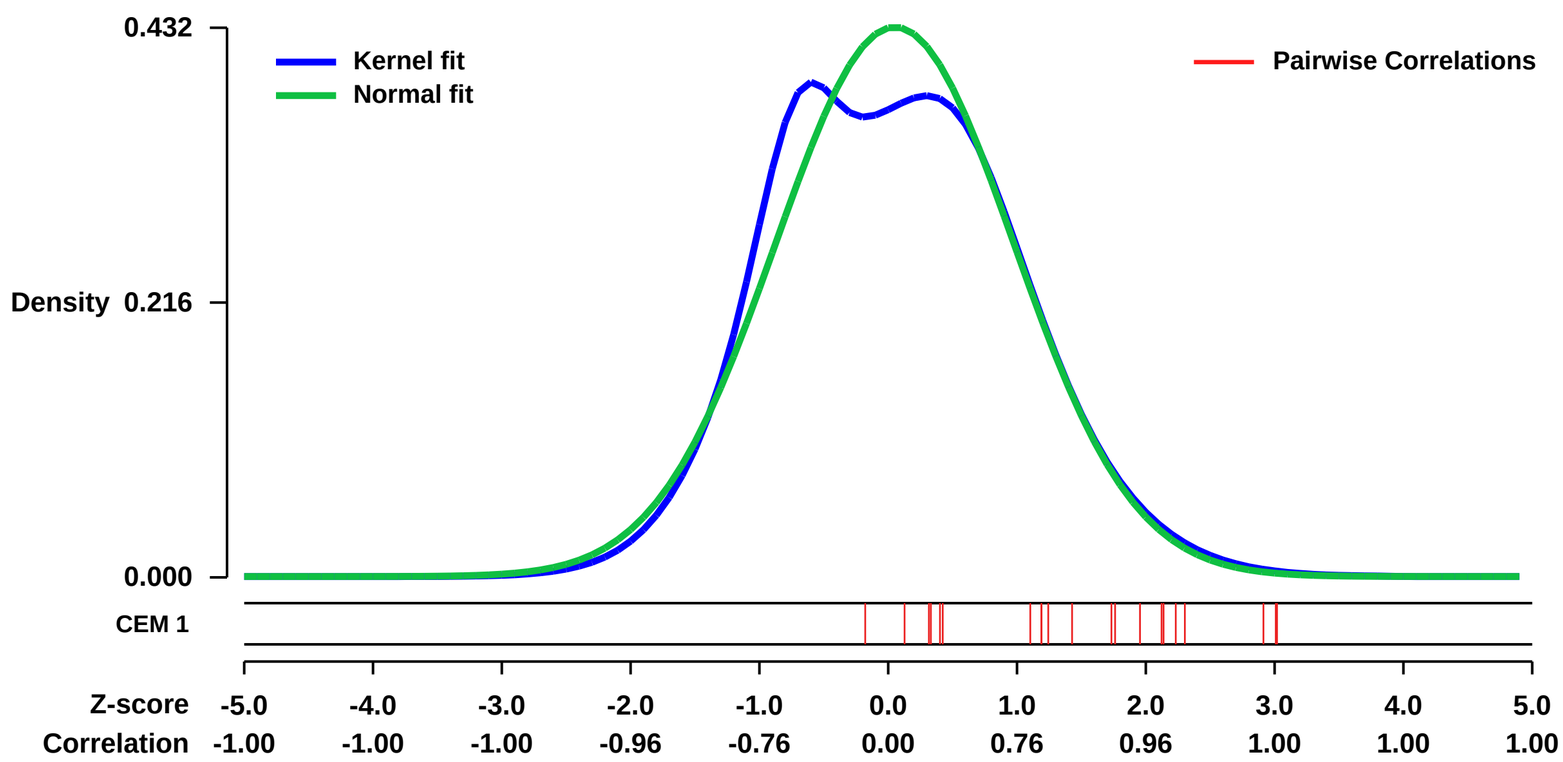

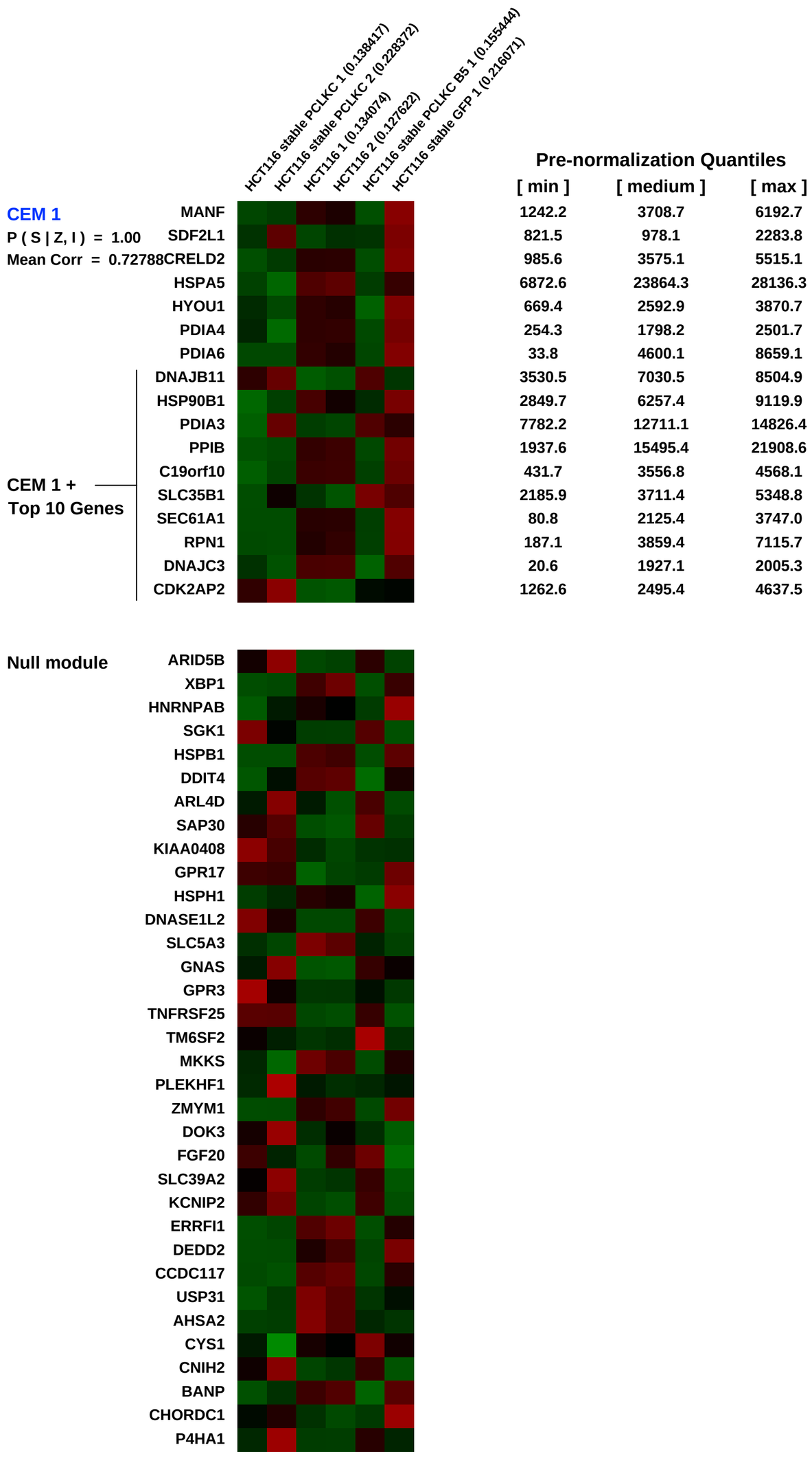

	Pre-normalization Quantiles		
	[min]	[medium]	[max]
MANF	1242.2	3708.7	6192.7
SDF2L1	821.5	978.1	2283.8
CRELD2	985.6	3575.1	5515.1
HSPA5	6872.6	23864.3	28136.3
HYOU1	669.4	2592.9	3870.7
PDIA4	254.3	1798.2	2501.7
PDIA6	33.8	4600.1	8659.1
DNAJB11	3530.5	7030.5	8504.9
HSP90B1	2849.7	6257.4	9119.9
PDIA3	7782.2	12711.1	14826.4
PPIB	1937.6	15495.4	21908.6
C19orf10	431.7	3556.8	4568.1
SLC35B1	2185.9	3711.4	5348.8
SEC61A1	80.8	2125.4	3747.0
RPN1	187.1	3859.4	7115.7
DNAJC3	20.6	1927.1	2005.3
CDK2AP2	1262.6	2495.4	4637.5
ARID5B			
XBP1			
HNRNPAB			
SGK1			
HSPB1			
DDIT4			
ARL4D			
SAP30			
KIAA0408			
GPR17			
HSPH1			
DNASE1L2			
SLC5A3			
GNAS			
GPR3			
TNFRSF25			
TM6SF2			
MKKS			
PLEKHF1			
ZMYM1			
DOK3			
FGF20			
SLC39A2			
KCNIP2			
ERRFI1			
DEDD2			
CCDC117			
USP31			
AHSA2			
CYS1			
CNIH2			
BANP			
CHORDC1			
P4HA1			

GEO Series "GSE23984" Expression Profiles

Num of samples in this series: 10

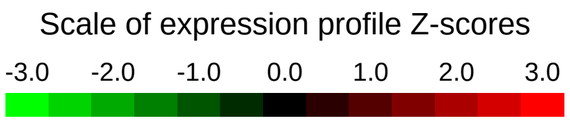

GEO Link:	http://www.ncbi.nlm.nih.gov/geo/query/acc.cgi?acc=GSE23984
Status:	Public on Nov 15 2010
Title:	Effects of TX527, a hypocalcemic vitamin D analog on human activated T lymphocytes
Organism:	Homo sapiens
Experiment type:	Expression profiling by array
Platform:	GPL570
Pubmed ID:	21131424
Summary & Design:	**Summary:** Hypocalcemic vitamin D analogs are appealing molecules to exploit the immunomodulatory actions of active vitamin D in vivo. The functional modulation of dendritic cells is regarded as the key mechanism underlying their ability to regulate T cell responses. In contrast, the direct actions of vitamin D and structural analogs on T lymphocytes remain less well characterized. Microarray analysis was performed to gain insight into the direct immunomodulatory actions of TX527, a hypocalcemic vitamin D analog, on human T lymphocytes. Gene expression analysis revealed that TX527 regulated a wide variety of genes involved in different aspects of T cell function, including cellular growth and proliferation, cell death, cellular development, cellular movement and cell-to-cell signalling and interaction. **Overall design:** Human CD3+ T cells, isolated from peripheral blood from healthy donors, were activated by anti-CD3/anti-CD28 and cultured in the presence of TX527 (10-8M) or vehicle (ethanol) for 10 days. Expression profiles of TX527-treated and vehicle-treated T cells were compared using Affymetrix Human Genome U133 Plus 2.0 Arrays.

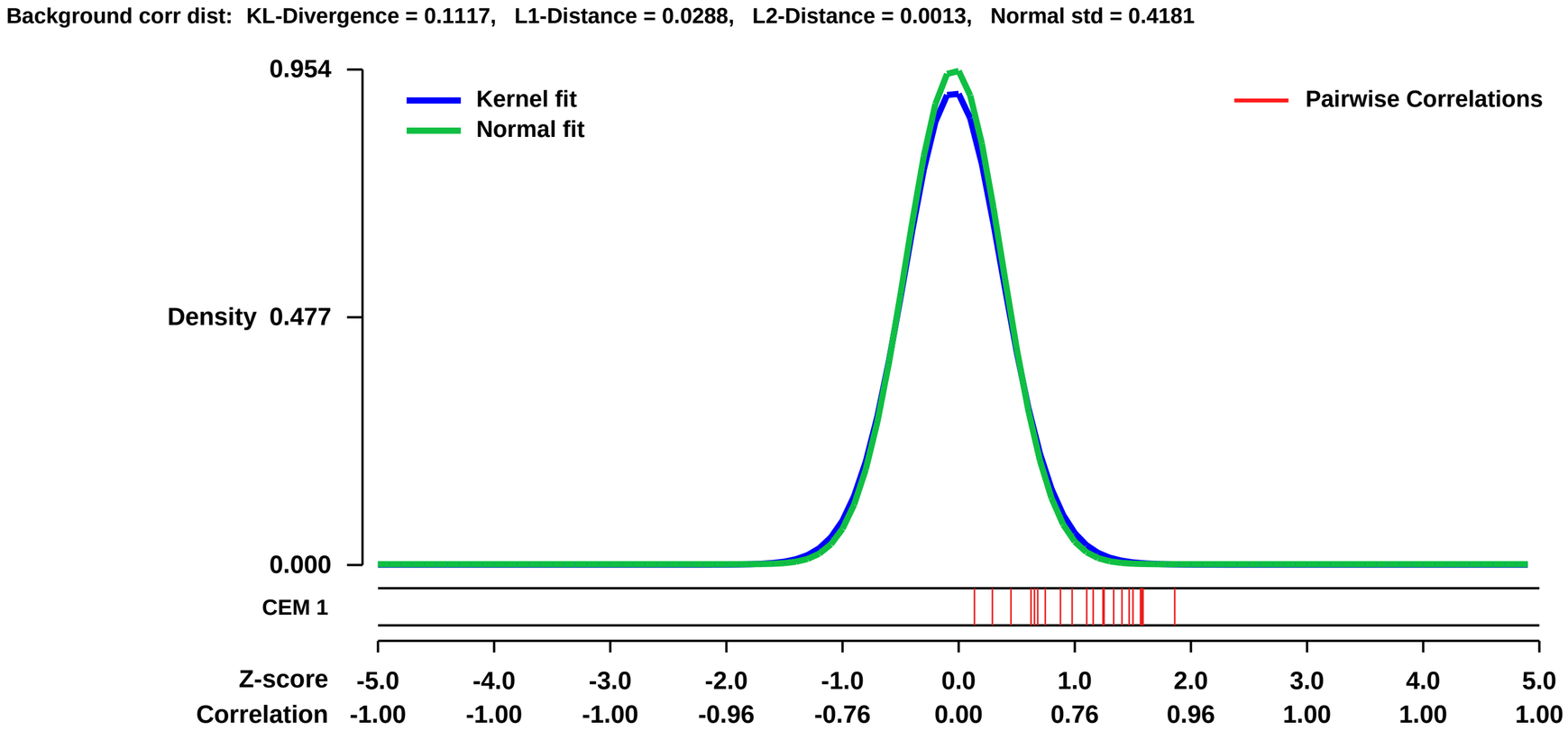

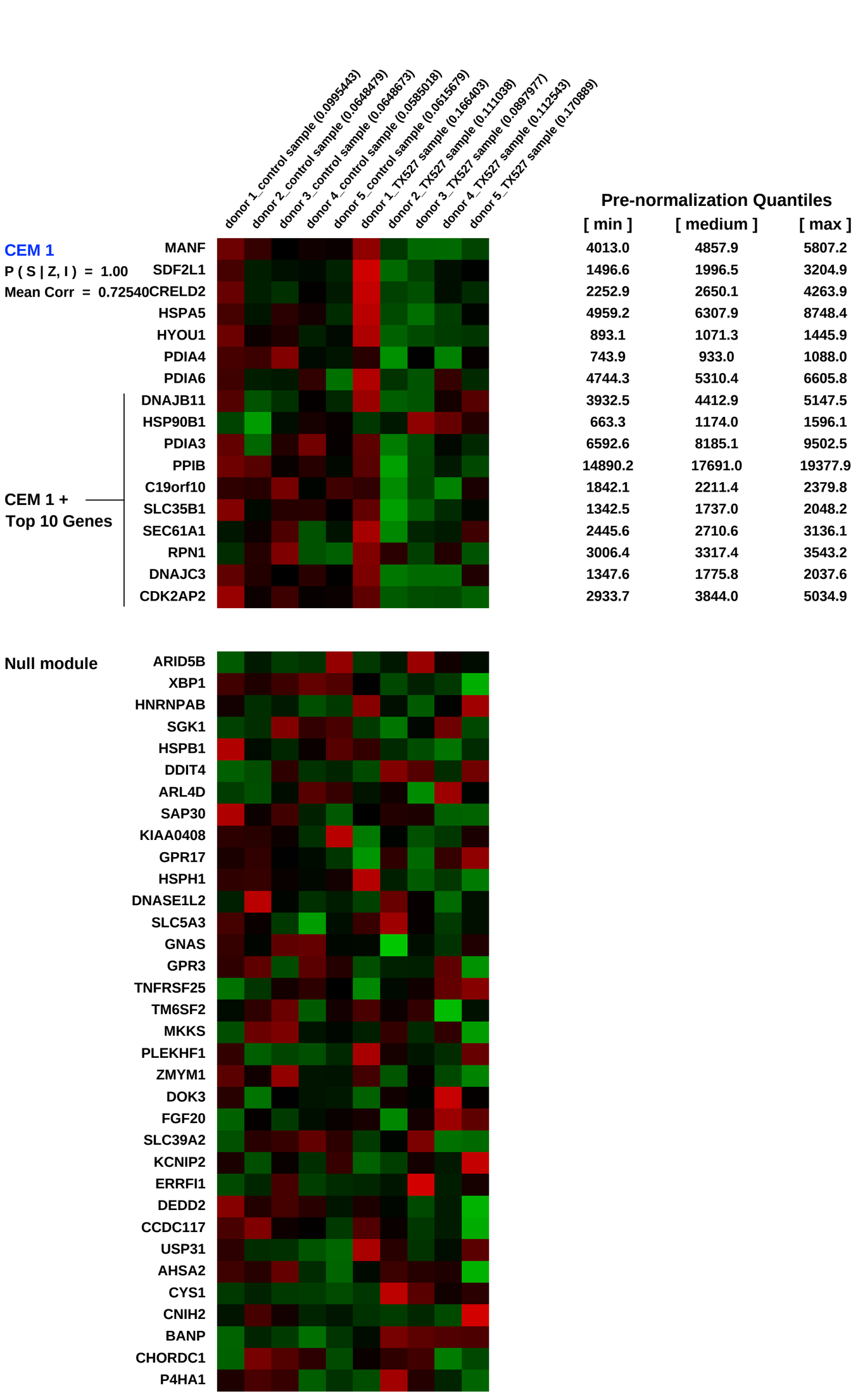

Pre-normalization Quantiles

[min]	[medium]	[max]
4013.0	4857.9	5807.2
1496.6	1996.5	3204.9
2252.9	2650.1	4263.9
4959.2	6307.9	8748.4
893.1	1071.3	1445.9
743.9	933.0	1088.0
4744.3	5310.4	6605.8
3932.5	4412.9	5147.5
663.3	1174.0	1596.1
6592.6	8185.1	9502.5
14890.2	17691.0	19377.9
1842.1	2211.4	2379.8
1342.5	1737.0	2048.2
2445.6	2710.6	3136.1
3006.4	3317.4	3543.2
1347.6	1775.8	2037.6
2933.7	3844.0	5034.9

GEO Series "GSE10971" Expression Profiles

Num of samples in this series: 37

Scale of expression profile Z-scores

-3.0 -2.0 -1.0 0.0 1.0 2.0 3.0

GEO Link:	http://www.ncbi.nlm.nih.gov/geo/query/acc.cgi?acc=GSE10971
Status:	Public on May 31 2008
Title:	Gene expression data from non-malignant fallopian tube epithelium and high grade serous carcinoma.
Organism:	Homo sapiens
Experiment type:	Expression profiling by array
Platform:	GPL570
Pubmed ID:	21263043
Summary & Design:	**Summary:** The purpose of this study was to identify molecular alterations potentially involved in predisposition to adnexal serous carcinoma (SerCa) in the non-malignant fallopian tube epithelium (FTE) of BRCA1/2-mutation carriers, given recent evidence implicating the distal FTE as a common source for SerCa. **Keywords: disease state analysis** **Overall design:** We obtained and compared gene expression profiles of laser capture microdissected non-malignant distal FTE from 12 known BRCA1/2-mutation carriers (FTEb) and 12 control women (FTEn) during the luteal and follicular phase, as well as 13 high grade tubal and ovarian SerCa.

Background corr dist: KL-Divergence = 0.4401, L1-Distance = 0.0827, L2-Distance = 0.0221, Normal std = 0.2395

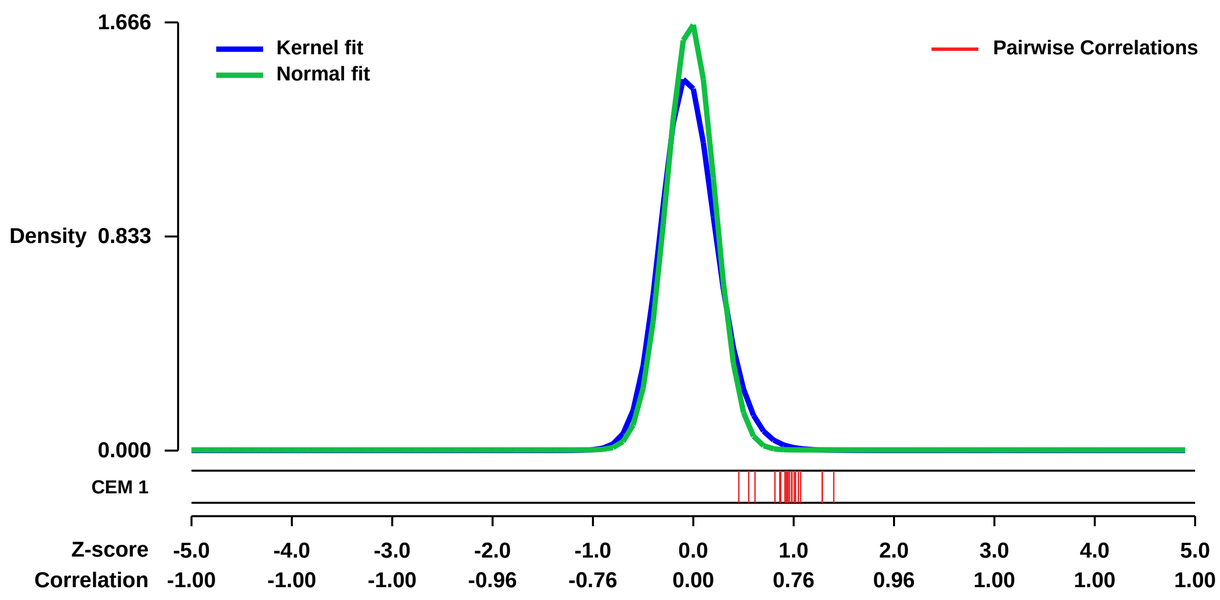

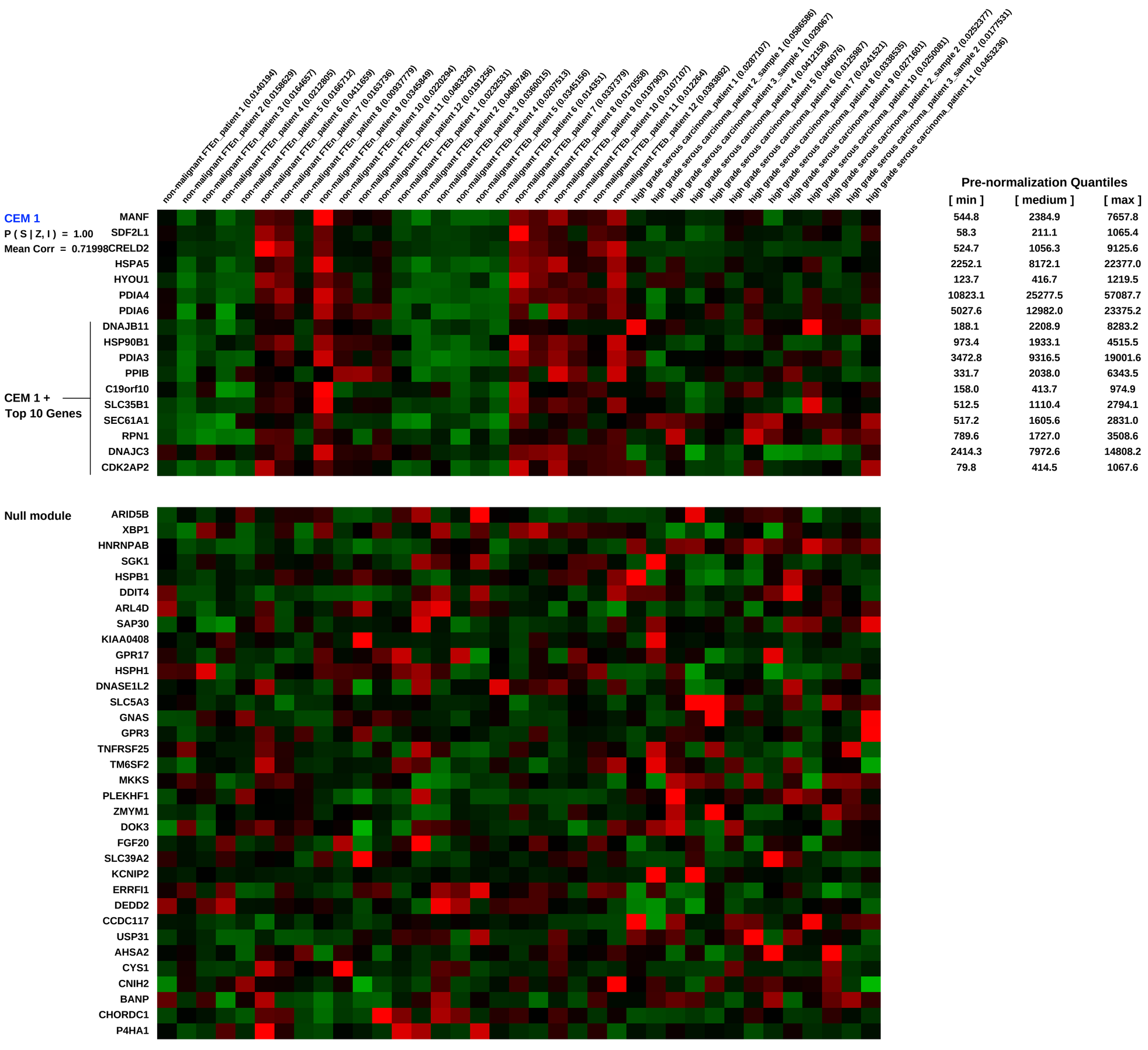

GEO Series "GSE37603" Expression Profiles

Num of samples in this series: 6

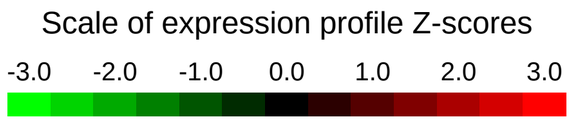

GEO Link:	http://www.ncbi.nlm.nih.gov/geo/query/acc.cgi?acc=GSE37603
Status:	Public on Apr 30 2014
Title:	Identification of WISP1 as an important survival factor in human mesenchymal stem cells
Organism:	Homo sapiens
Experiment type:	Expression profiling by array
Platform:	GPL570
Pubmed ID:	
Summary & Design:	**Summary:** WNT-induced secreted protein 1 (WISP1/CCN4), a member of the CCN protein family, acts as a downstream factor of the canonical WNT-signaling pathway. A dysregulated expression of WISP1 often reflects its oncogenic potential by inhibition of apoptosis, a necessary form of cell death that protect cell populations for transformation into malignant phenotypes. WISP1-signaling is also known to affect proliferation and differentiation of human mesenchymal stem cells (hMSCs), which are fundamental for the constitution and maintenance of the musculoskeletal system. Our study emphasizes the importance of WISP1-signaling for cell survival of primary human cells. Therefore, we established a successful down-regulation of endogenous WISP1 transcripts through gene silencing in hMSCs. We were able to demonstrate the consequence of cell death immediately after WISP1 down-regulation took place. Bioinformatical analyses of subsequent performed microarrays from WISP1 down-regulated vs. control samples confirmed this observation. We uncovered several clusters of differential expressed genes important for cellular apoptosis induction and immuno-regulatory processes, thereby indicating TRAIL-induced and p53-mediated apoptosis as well as IFNbeta-signaling. Since all of them act as potent inhibitors for malignant cell growth, in vitro knowledge about the connection with WISP1-signaling could help to find new therapeutic approaches concerning cancerogenesis and tumor growth in musculoskeletal tissues. **Overall design:** Knock-down versus controls.

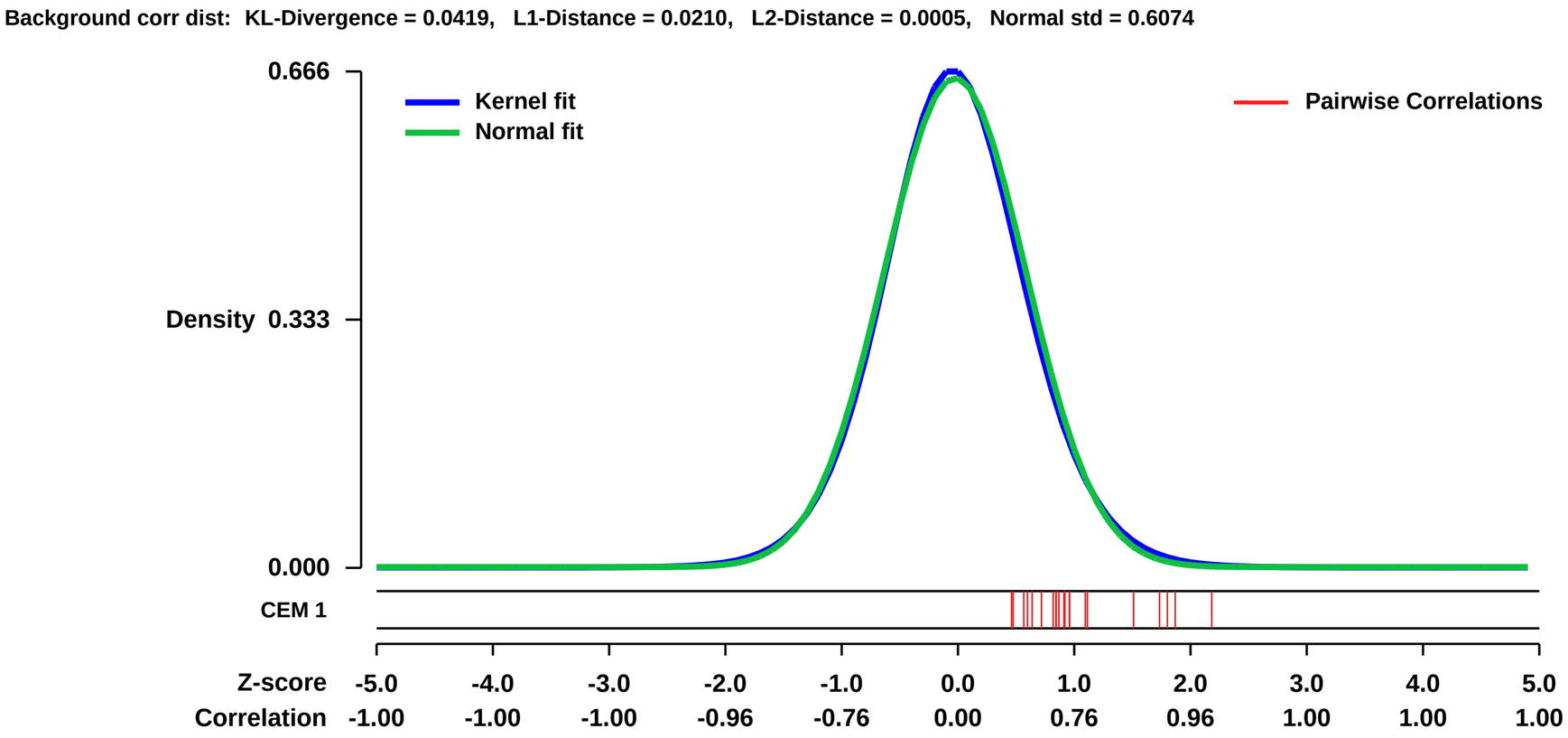

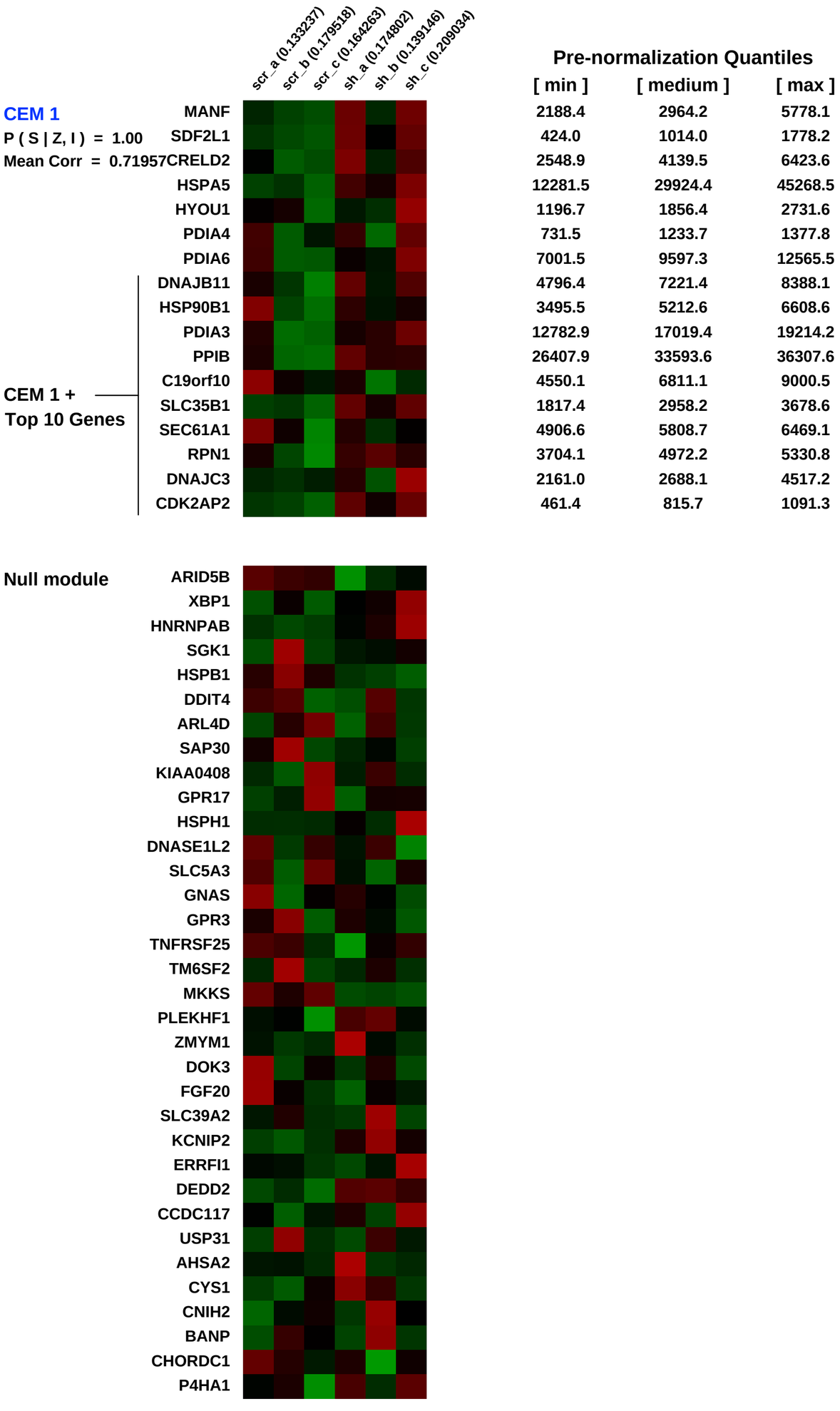

Pre-normalization Quantiles

	[min]	[medium]	[max]
MANF	2188.4	2964.2	5778.1
SDF2L1	424.0	1014.0	1778.2
CRELD2	2548.9	4139.5	6423.6
HSPA5	12281.5	29924.4	45268.5
HYOU1	1196.7	1856.4	2731.6
PDIA4	731.5	1233.7	1377.8
PDIA6	7001.5	9597.3	12565.5
DNAJB11	4796.4	7221.4	8388.1
HSP90B1	3495.5	5212.6	6608.6
PDIA3	12782.9	17019.4	19214.2
PPIB	26407.9	33593.6	36307.6
C19orf10	4550.1	6811.1	9000.5
SLC35B1	1817.4	2958.2	3678.6
SEC61A1	4906.6	5808.7	6469.1
RPN1	3704.1	4972.2	5330.8
DNAJC3	2161.0	2688.1	4517.2
CDK2AP2	461.4	815.7	1091.3

GEO Series "GSE16924" Expression Profiles

Num of samples in this series: 6

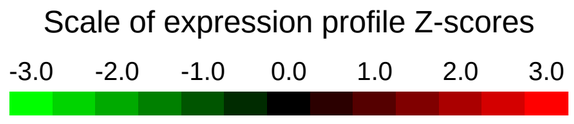

GEO Link:	http://www.ncbi.nlm.nih.gov/geo/query/acc.cgi?acc=GSE16924
Status:	Public on Dec 17 2009
Title:	Determining direct targets of the bHLH MIST1
Organism:	Homo sapiens
Experiment type:	Expression profiling by array
Platform:	GPL570
Pubmed ID:	20038531
Summary & Design:	**Summary:** The transcription factor MIST1 is required for final maturation of secretory cells of diverse tissues, including gastric digestive-enzyme secreting zymogenic (chief) cells (ZCs). Here, we show that MIST1 directly activates RAB26, RAB3D and several other genes. **Overall design:** We used microarrays to determine genes upregulated following transient MIST1 transfection. Two gastric cell lines were used: HGC-27 and AGS. Three chips were generated from each cell line: parental (untransfected), GFP+empty vector (a control for effects of transfection), and GFP+MIST1. The latter two chips were generated from cells flow sorted based on GFP fluorescence to isolate cells with high levels of transfection. Chips were analyzed by dChip to identify genes expressed in both MIST1-transfected cell populations relative to their respective controls in multiple Boolean 'AND' comparisons.

Background corr dist: KL-Divergence = 0.0184, L1-Distance = 0.0485, L2-Distance = 0.0027, Normal std = 0.8639

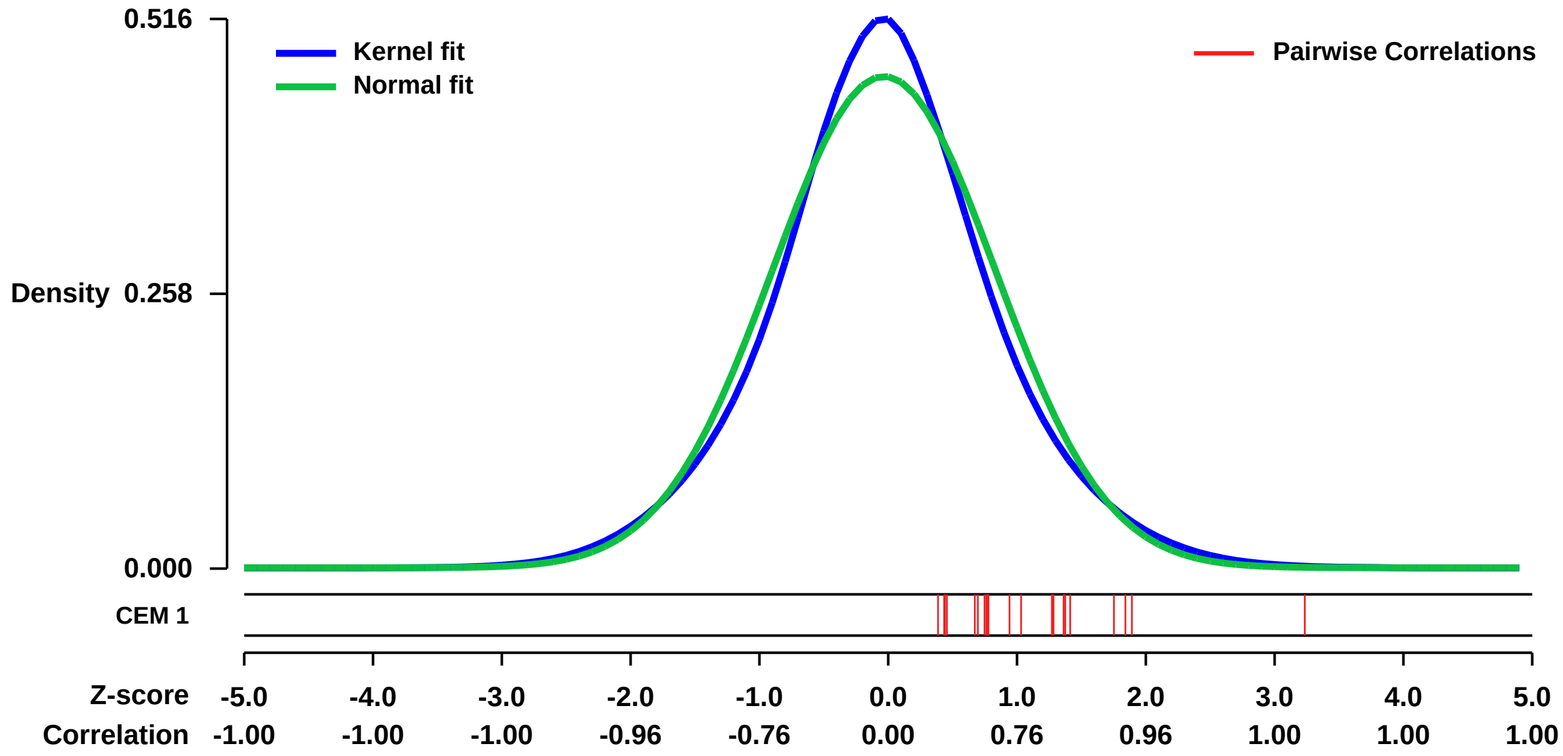

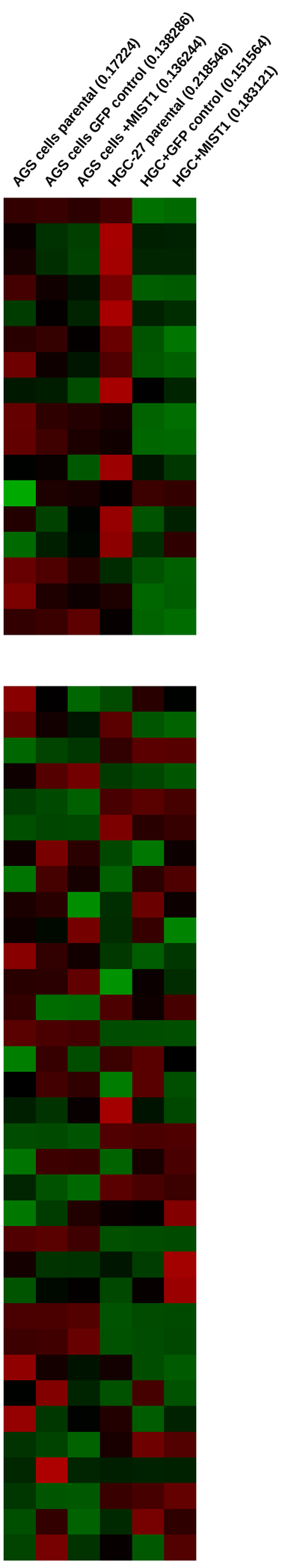

GEO Series "GSE17480" Expression Profiles

Num of samples in this series: 8

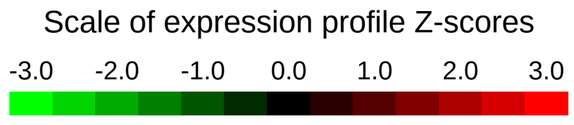

GEO Link:	http://www.ncbi.nlm.nih.gov/geo/query/acc.cgi?acc=GSE17480
Status:	Public on Dec 01 2009
Title:	Transcriptome profiling of fenretinide-treated and untreated CD34+ cells from 4 CML patients
Organism:	Homo sapiens
Experiment type:	Expression profiling by array
Platform:	GPL570
Pubmed ID:	24021153
Summary & Design:	**Summary:** Imatinib, as the first-line agent of chronic myeloid leukemia (CML), is ineffective in eradicating CML stem/progenitor cells, thus unable to prevent late relapse. Here we present data indicating that fenretinide preferentially targets CD34+ CML cells and enhances the efficacy of imatinib in CML. As tested by colony forming cell assays, both number and size of total colonies derived from CD34+ CML cells were significantly reduced by fenretinide, and by combining fenretinide with imatinib. In particular, colonies derived from erythroid progenitors and those derived from more primitive pluripotent progenitor cells were highly sensitive to fenretinide/fenretinide plus immtinib. Further data showed that fenretinide was able to induce apoptosis in CD34+ CML cells which were refractory to imatinib. Through transcriptome analysis and followed by molecular validation, we further showed that apoptosis induced by fenretinide in CD34+ CML cells was mediated by complex mechanisms of stress responses, probably triggered by elevated levels of intracellular reactive oxygen species. Thus, fenretinide combines with imatinib may represent a new strategy for the treatment of CML, in which fenretinide targets primitive CD34+ CML cells whereas imatinib targets leukemic blasts. This strategy may eventually reduce the risk of relapse and probably resistant as well in CML patients. **Overall design:** Transcriptome profiles of CML CD34+ cells with and without fenretinide treatment were analyzed using whole genome expression arrays (Affymetrix HG-U133 Plus 2.0) in four CML patients (CML32, CML33, CML34 and CML35, see Table 1). To minimize potential data biases, both treated and untreated cell samples were maintained in culture for 48 hours before hybridization.

Background corr dist: KL-Divergence = 0.0627, L1-Distance = 0.0192, L2-Distance = 0.0005, Normal std = 0.5187

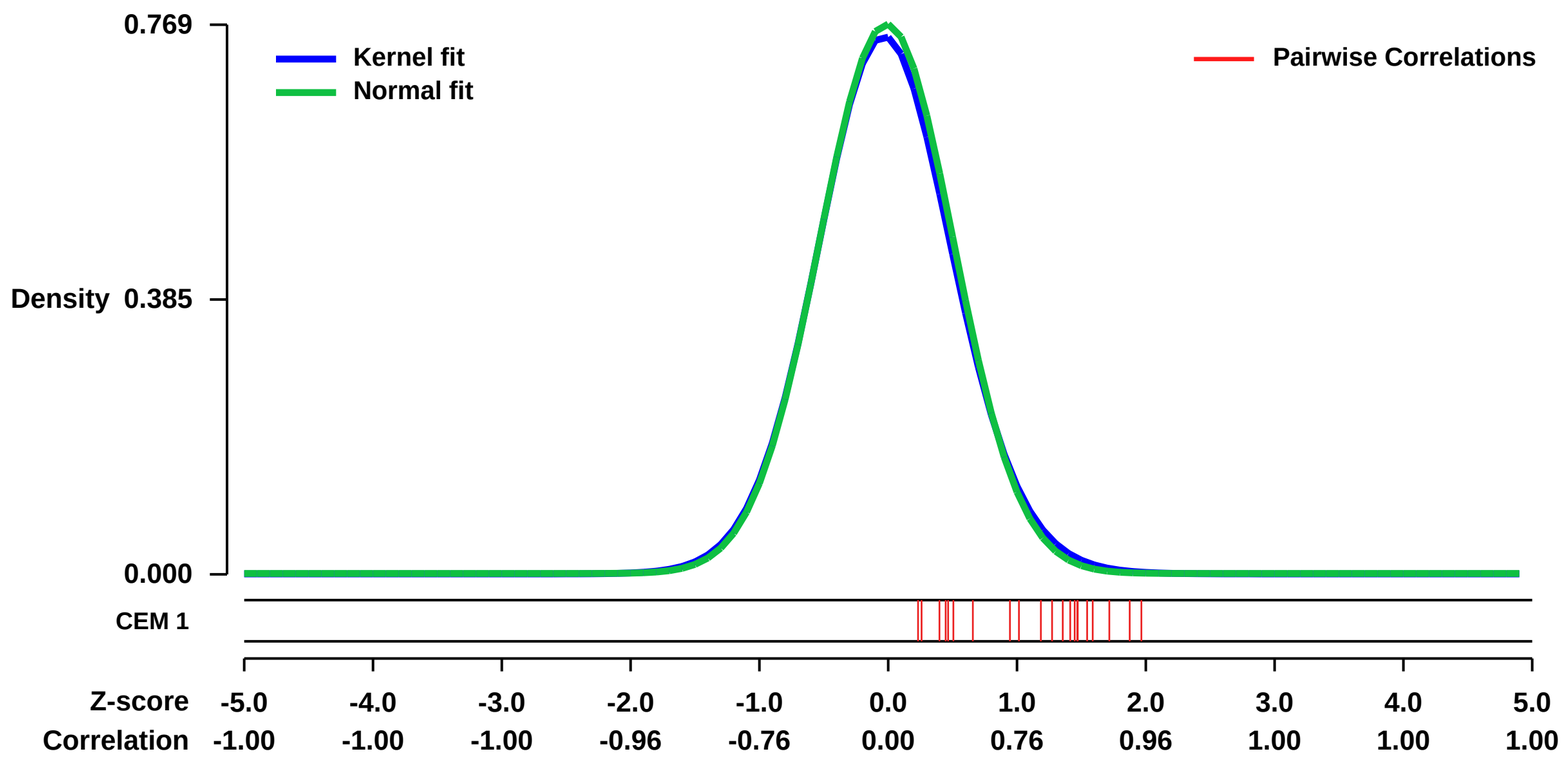

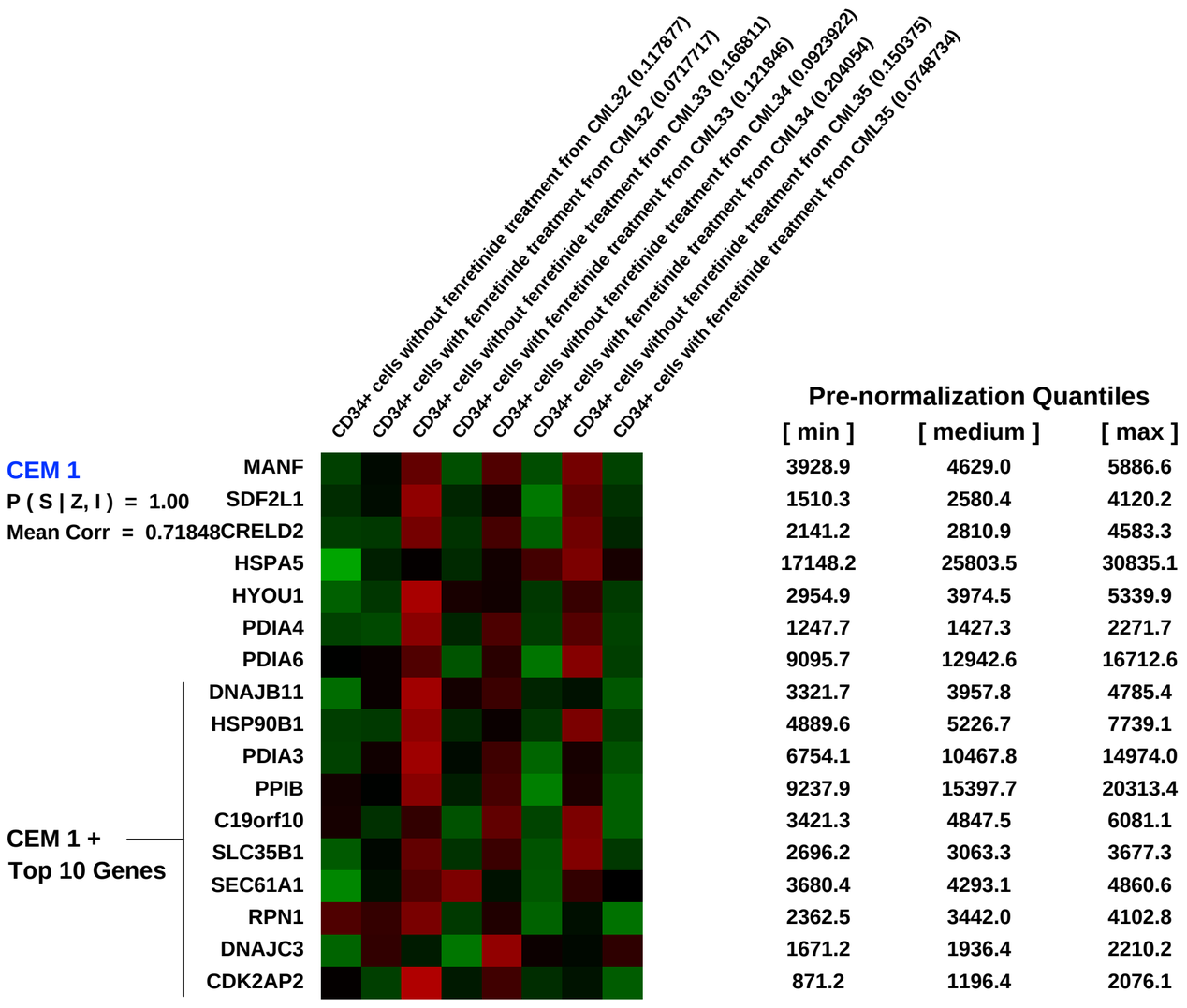

GEO Series "GSE39594" Expression Profiles

Num of samples in this series: 21

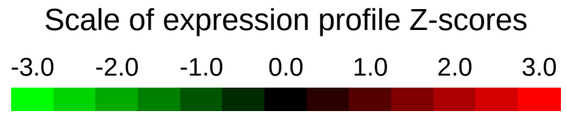

GEO Link:	http://www.ncbi.nlm.nih.gov/geo/query/acc.cgi?acc=GSE39594
Status:	Public on Jul 03 2013
Title:	Human naive CD4+ T cell activation transcriptome
Organism:	Homo sapiens
Experiment type:	Expression profiling by array
Platform:	GPL570
Pubmed ID:	23878307
Summary & Design:	**Summary:** We used microarrays to detail the global gene transcription underlying T cells activation during the first 24 hours after stimulation. **Overall design:** CD4+CD45RA+ T cells were sorted and cultured with different stimulatory conditions (Non-stimulated, anti-CD3 and anti-CD3 plus anti-CD28) for different times (0 hours, 4 hours and 24 hours). 3 replicates for each condition were analyzed.

Background corr dist: KL-Divergence = 0.1383, L1-Distance = 0.0304, L2-Distance = 0.0016, Normal std = 0.3879

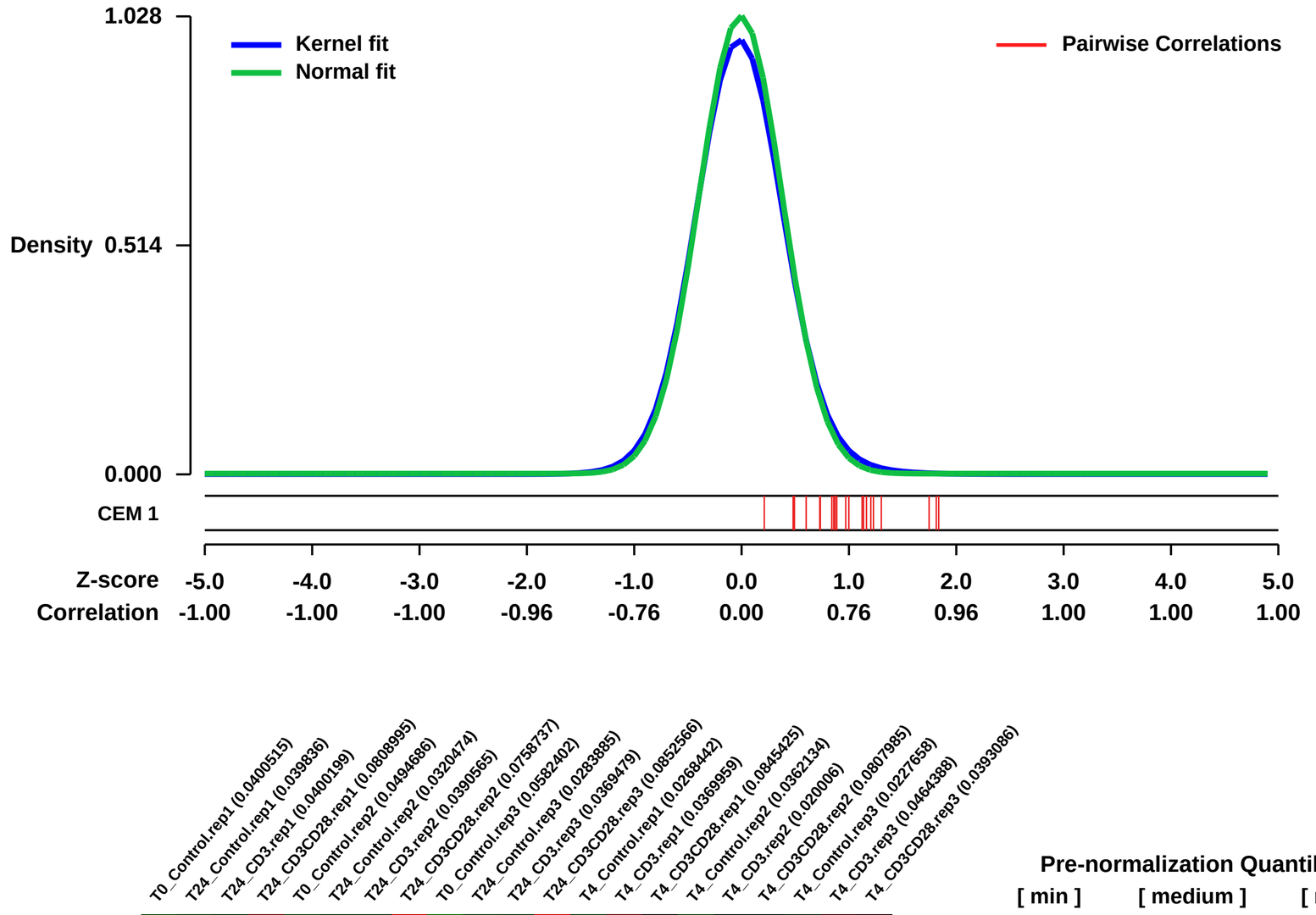

CEM 1
P (S | Z, I) = 1.00
Mean Corr = 0.71534

CEM 1 + Top 10 Genes

Null module

	Pre-normalization Quantiles [min]	[medium]	[max]
MANF	891.7	1910.5	5900.1
SDF2L1	418.2	523.5	1724.3
CRELD2	1500.8	1912.8	3444.5
HSPA5	2553.9	4408.8	8935.4
HYOU1	820.5	1266.4	2378.0
PDIA4	311.3	476.9	769.9
PDIA6	763.4	1367.0	5221.5
DNAJB11	903.6	1268.3	3455.3
HSP90B1	670.9	1023.4	2294.0
PDIA3	3126.1	4605.7	8474.5
PPIB	2273.6	5037.1	9287.4
C19orf10	839.9	1176.5	2744.0
SLC35B1	515.5	778.7	1798.4
SEC61A1	884.0	1018.5	1632.4
RPN1	1298.0	1732.5	2810.2
DNAJC3	1065.3	1302.5	1940.2
CDK2AP2	205.3	909.5	2454.2
ARID5B			
XBP1			
HNRNPAB			
SGK1			
HSPB1			
DDIT4			
ARL4D			
SAP30			
KIAA0408			
GPR17			
HSPH1			
DNASE1L2			
SLC5A3			
GNAS			
GPR3			
TNFRSF25			
TM6SF2			
MKKS			
PLEKHF1			
ZMYM1			
DOK3			
FGF20			
SLC39A2			
KCNIP2			
ERRFI1			
DEDD2			
CCDC117			
USP31			
AHSA2			
CYS1			
CNIH2			
BANP			
CHORDC1			
P4HA1			

GEO Series "GSE11831" Expression Profiles

Num of samples in this series: 17

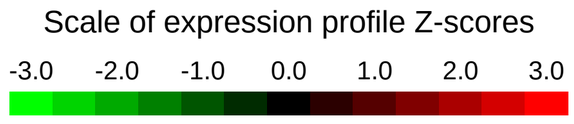

GEO Link:	http://www.ncbi.nlm.nih.gov/geo/query/acc.cgi?acc=GSE11831
Status:	Public on Jun 20 2008
Title:	Transcription profiling of biopsies from the descending colon of control subjects
Organism:	Homo sapiens
Experiment type:	Expression profiling by array
Platform:	GPL570
Pubmed ID:	19177426
Summary & Design:	**Summary:** These samples were all taken from patients who underwent investigations including colonoscopy but where all tests were normal and the diagnosis of irritable bowel syndrome was reached. These observations have been used as references in studies of colonic gene expression in inflammatory bowel diseases **Overall design:** 17 samples were analyzed each originating from an individual subject. No replicas.

Background corr dist: KL-Divergence = 0.1403, L1-Distance = 0.0480, L2-Distance = 0.0053, Normal std = 0.3824

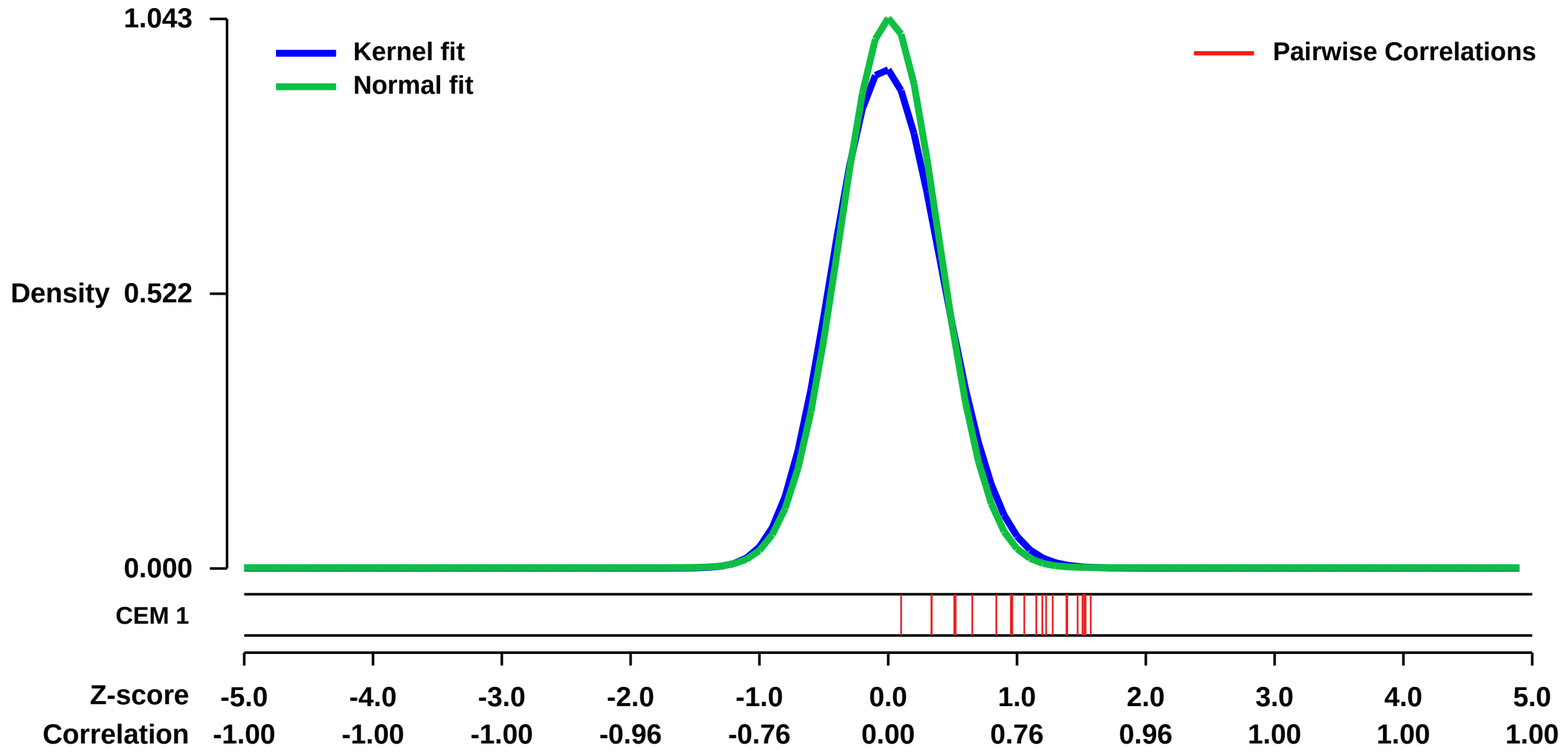

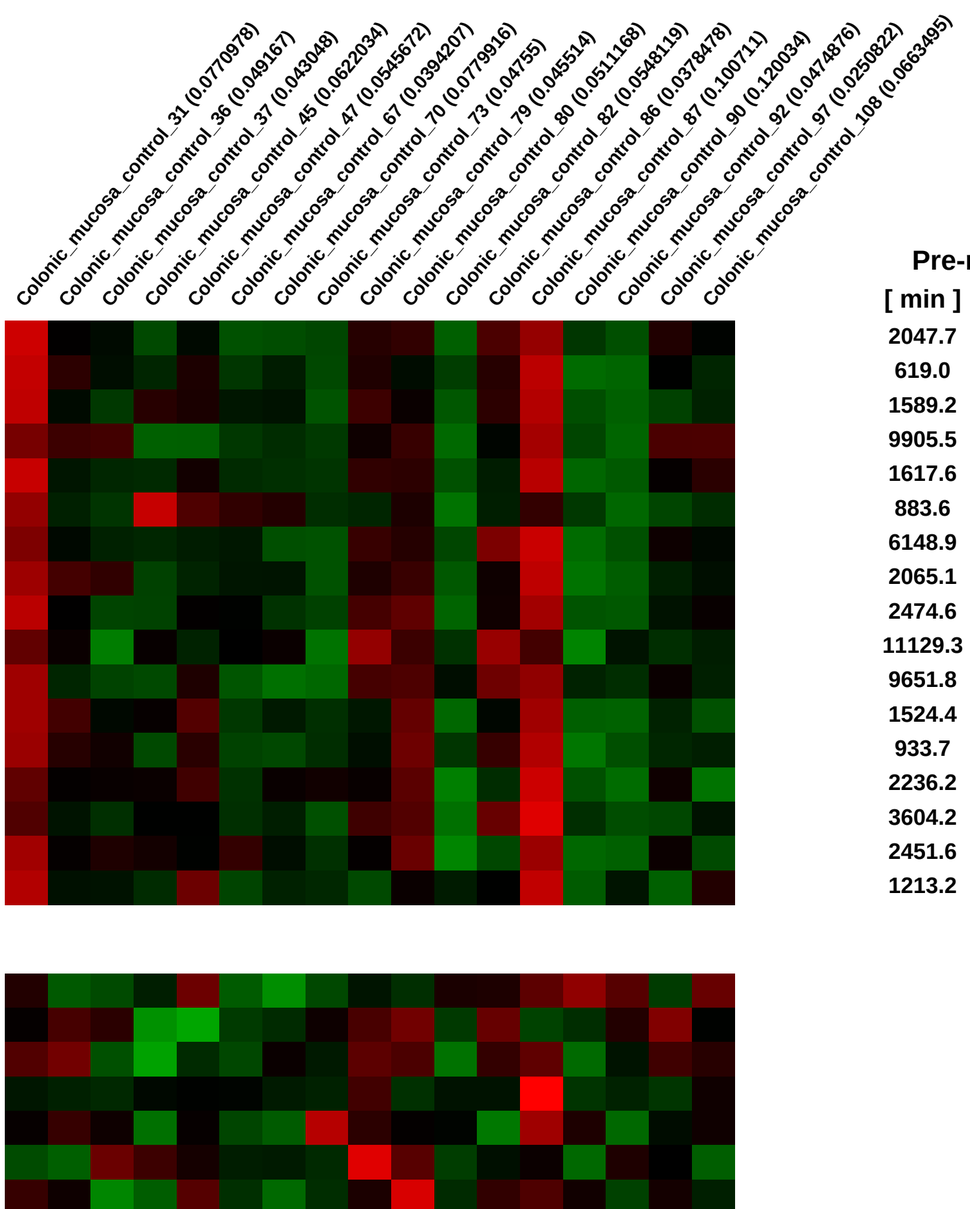

CEM 1
P (S | Z, I) = 1.00
Mean Corr = 0.70896

CEM 1 + Top 10 Genes

Null module

	Pre-normalization Quantiles [min]	[medium]	[max]
MANF	2047.7	3178.4	5984.6
SDF2L1	619.0	1257.6	2669.5
CRELD2	1589.2	2537.5	5084.6
HSPA5	9905.5	15412.4	24592.1
HYOU1	1617.6	2501.8	5239.8
PDIA4	883.6	1347.9	2650.8
PDIA6	6148.9	8255.7	13885.4
DNAJB11	2065.1	2969.9	4961.1
HSP90B1	2474.6	3214.7	4648.3
PDIA3	11129.3	15421.0	20383.7
PPIB	9651.8	13687.3	23117.4
C19orf10	1524.4	1963.3	2958.3
SLC35B1	933.7	1402.6	2505.5
SEC61A1	2236.2	2987.9	4080.6
RPN1	3604.2	4818.9	7967.3
DNAJC3	2451.6	3564.2	4837.0
CDK2AP2	1213.2	1468.4	2192.5
ARID5B			
XBP1			
HNRNPAB			
SGK1			
HSPB1			
DDIT4			
ARL4D			
SAP30			
KIAA0408			
GPR17			
HSPH1			
DNASE1L2			
SLC5A3			
GNAS			
GPR3			
TNFRSF25			
TM6SF2			
MKKS			
PLEKHF1			
ZMYM1			
DOK3			
FGF20			
SLC39A2			
KCNIP2			
ERRFI1			
DEDD2			
CCDC117			
USP31			
AHSA2			
CYS1			
CNIH2			
BANP			
CHORDC1			
P4HA1			

GEO Series "GSE17119" Expression Profiles

Num of samples in this series: 14

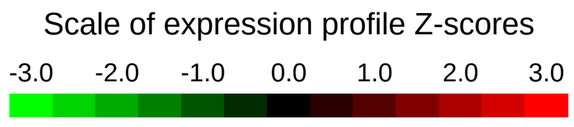

GEO Link:	http://www.ncbi.nlm.nih.gov/geo/query/acc.cgi?acc=GSE17119
Status:	Public on Jul 17 2009
Title:	Transcriptional profiling of a novel pro-angiogenic small molecule phthalimide neovascular factor 1 (PNF1)
Organism:	Homo sapiens
Experiment type:	Expression profiling by array
Platform:	GPL570
Pubmed ID:	19326468
Summary & Design:	**Summary:** We generated the transcriptional regulatory footprint of phthalimide neovascular factor 1 (PNF1)â a novel synthetic small molecule that exhibits significant in vitro endothelial potency and significant in vivo microvascular network expansionâ by performing comparative microarray analysis on PNF1-stimulated (versus control) human microvascular endothelial cells (HMVEC) spanning 1-48 h post-supplementation. We subsequently applied network analysis tools (including substantial libraries of information regarding known associations among network components) to elucidate key signaling components and pathways involved in the PNF1 mechanism-of-action. We identified that PNF1 first induces function of the tumor necrosis factor-alpha (TNF-¸–) signaling pathway, which in turn affects transforming growth factor-beta (TGF-¸†) signaling. **Overall design:** HMVEC (Cambrex, Walkersville, MD, USA) were cultured in endothelial growth medium 2-microvascular (bulletkit, BioWhittaker, Walkersville, MD, USA) supplemented as directed with 5% fetal bovine serum. The cells (passage 9) were plated at 2.5 x 104 cells/cm2 at 37 degrees Celsius in a humidified chamber with 5% carbon dioxide. They were grown to confluence. After confluence, medium was refreshed, and 30 ´µM PNF1 or 0.6% dimethyl sulfoxide (DMSO) vehicle control was added to the sample. Total RNA from the PNF1 (n=1 at each timepoint) and control (n=1 at each timepoint) samples was isolated 1, 2, 4, 8, 16, 24 and 48 h post-supplementation using an RNeasy kit (Qiagen, Inc., Valencia, CA, USA) according to the manufacturer's protocol.

Background corr dist: KL-Divergence = 0.1769, L1-Distance = 0.0375, L2-Distance = 0.0029, Normal std = 0.3502

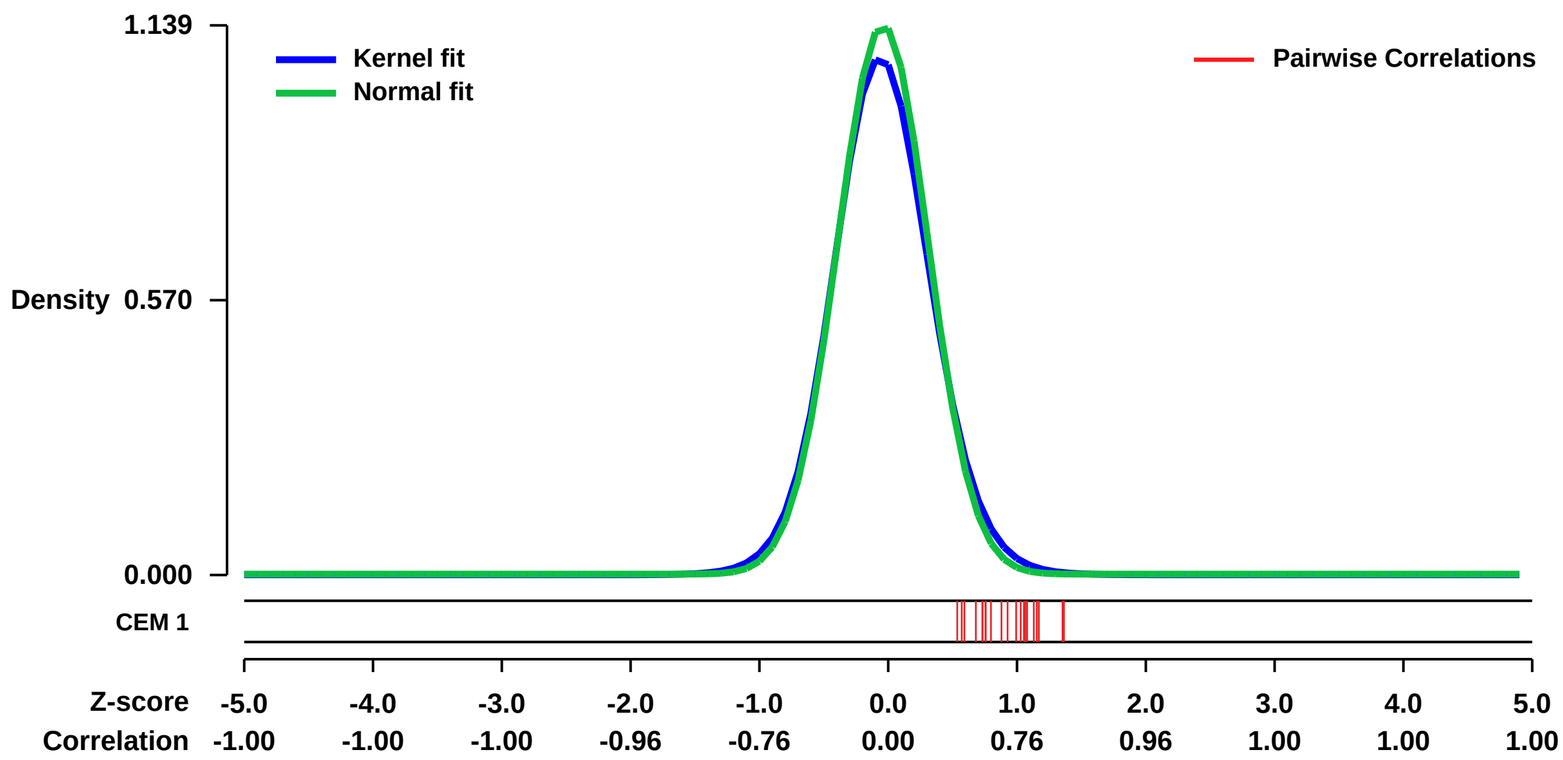

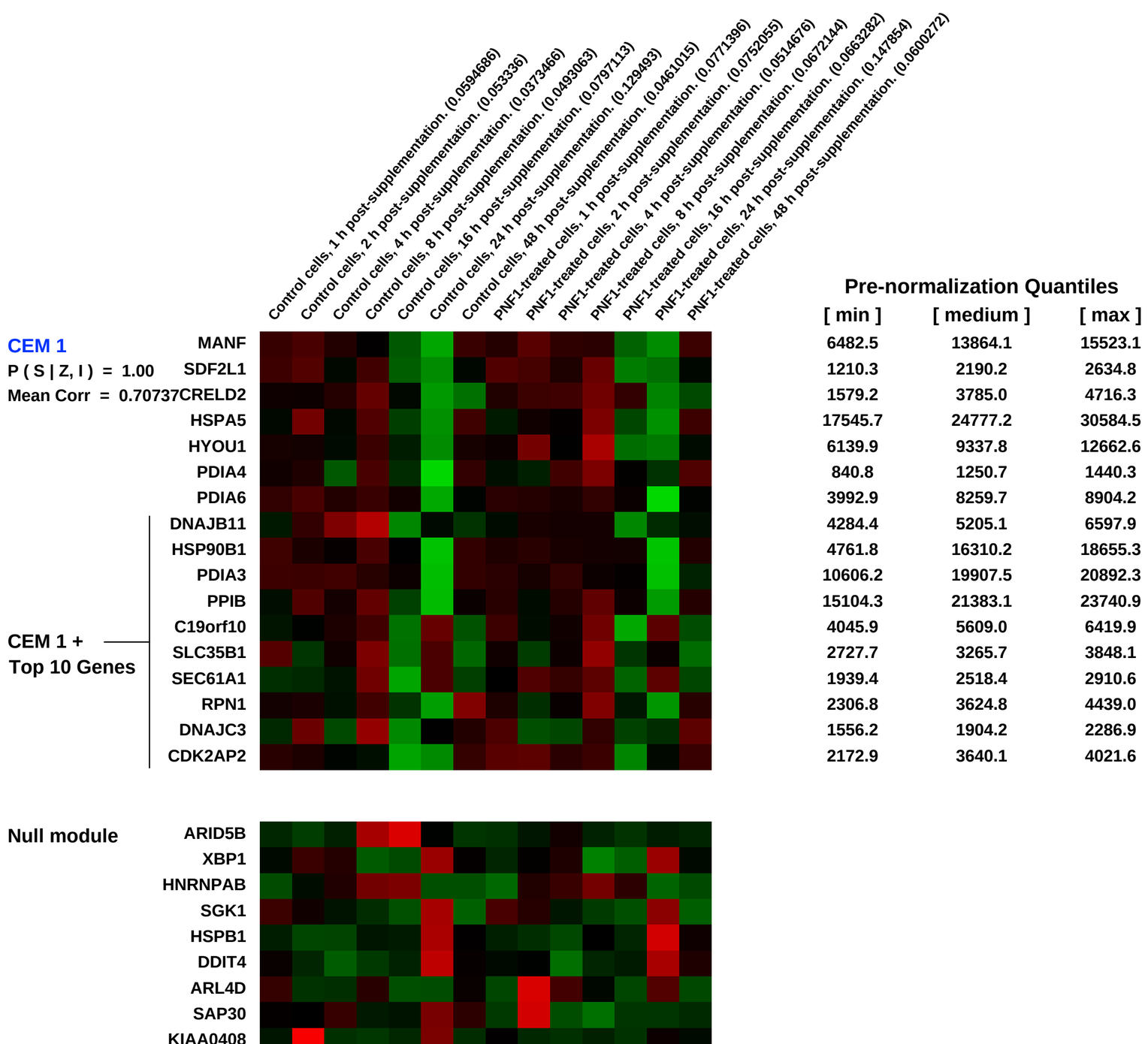

Pre-normalization Quantiles

	[min]	[medium]	[max]
MANF	6482.5	13864.1	15523.1
SDF2L1	1210.3	2190.2	2634.8
CRELD2	1579.2	3785.0	4716.3
HSPA5	17545.7	24777.2	30584.5
HYOU1	6139.9	9337.8	12662.6
PDIA4	840.8	1250.7	1440.3
PDIA6	3992.9	8259.7	8904.2
DNAJB11	4284.4	5205.1	6597.9
HSP90B1	4761.8	16310.2	18655.3
PDIA3	10606.2	19907.5	20892.3
PPIB	15104.3	21383.1	23740.9
C19orf10	4045.9	5609.0	6419.9
SLC35B1	2727.7	3265.7	3848.1
SEC61A1	1939.4	2518.4	2910.6
RPN1	2306.8	3624.8	4439.0
DNAJC3	1556.2	1904.2	2286.9
CDK2AP2	2172.9	3640.1	4021.6

GEO Series "GSE30188" Expression Profiles

Num of samples in this series: 20

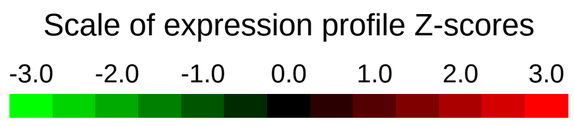

GEO Link:	http://www.ncbi.nlm.nih.gov/geo/query/acc.cgi?acc=GSE30188
Status:	Public on May 01 2013
Title:	Rho transcription inhibitor CCG-1423 effect on PC-3 cells
Organism:	Homo sapiens
Experiment type:	Expression profiling by array
Platform:	GPL570
Pubmed ID:	
Summary & Design:	**Summary:** Analysis of serum starved PC-3 cells treated with CCG-1423, Latrunculin B, or the transcription elongation inhibitor DRB for 2 or 24 hours. Results provide insights to potential therapeutic approaches to cancer metastasis. **Overall design:** As a control for non-specific transcription inhibition, DRB was used. All samples, 2-hr and 24-hr treated samples were compared to the 24-hr DMSO sample.

Background corr dist: KL-Divergence = 0.0850, L1-Distance = 0.0210, L2-Distance = 0.0006, Normal std = 0.4661

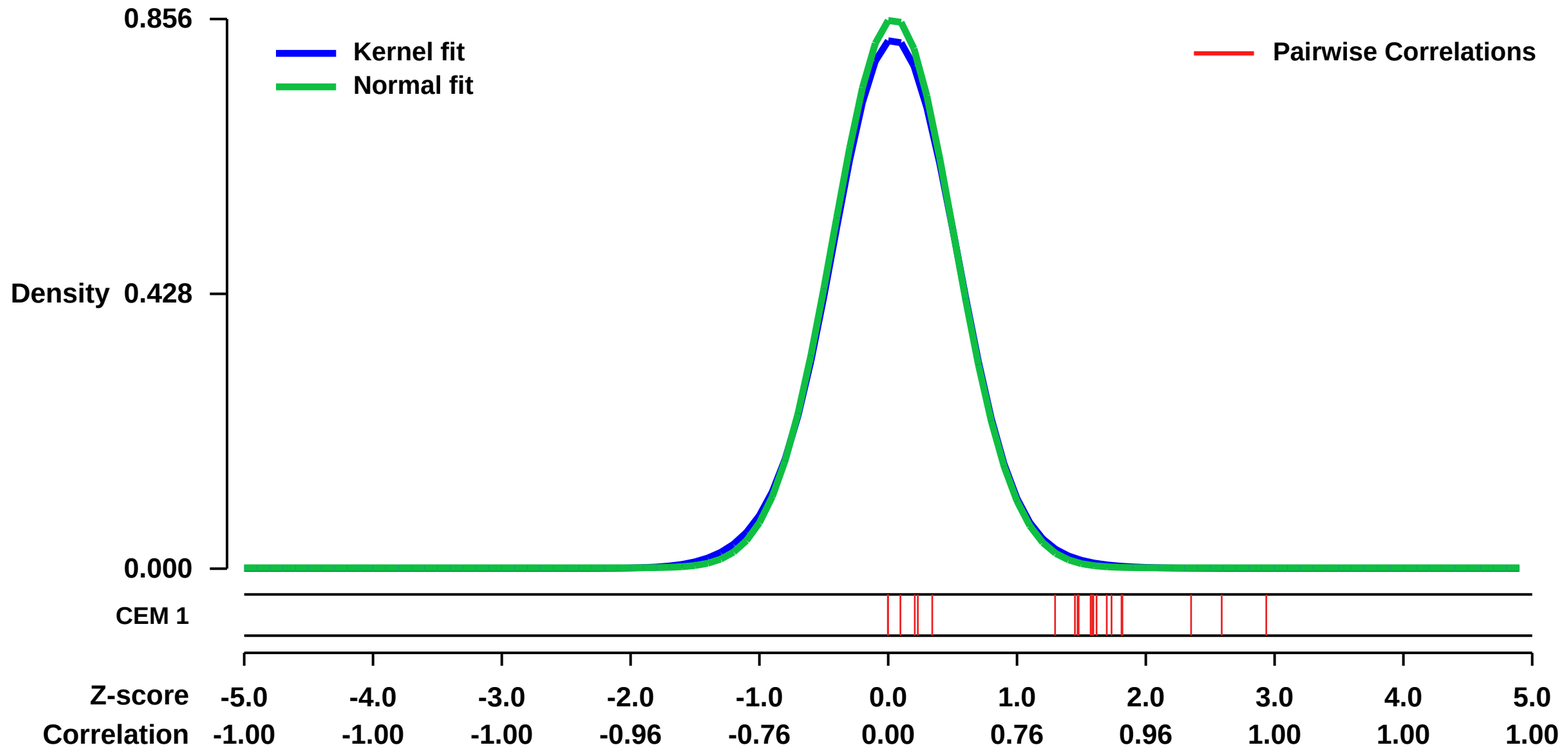

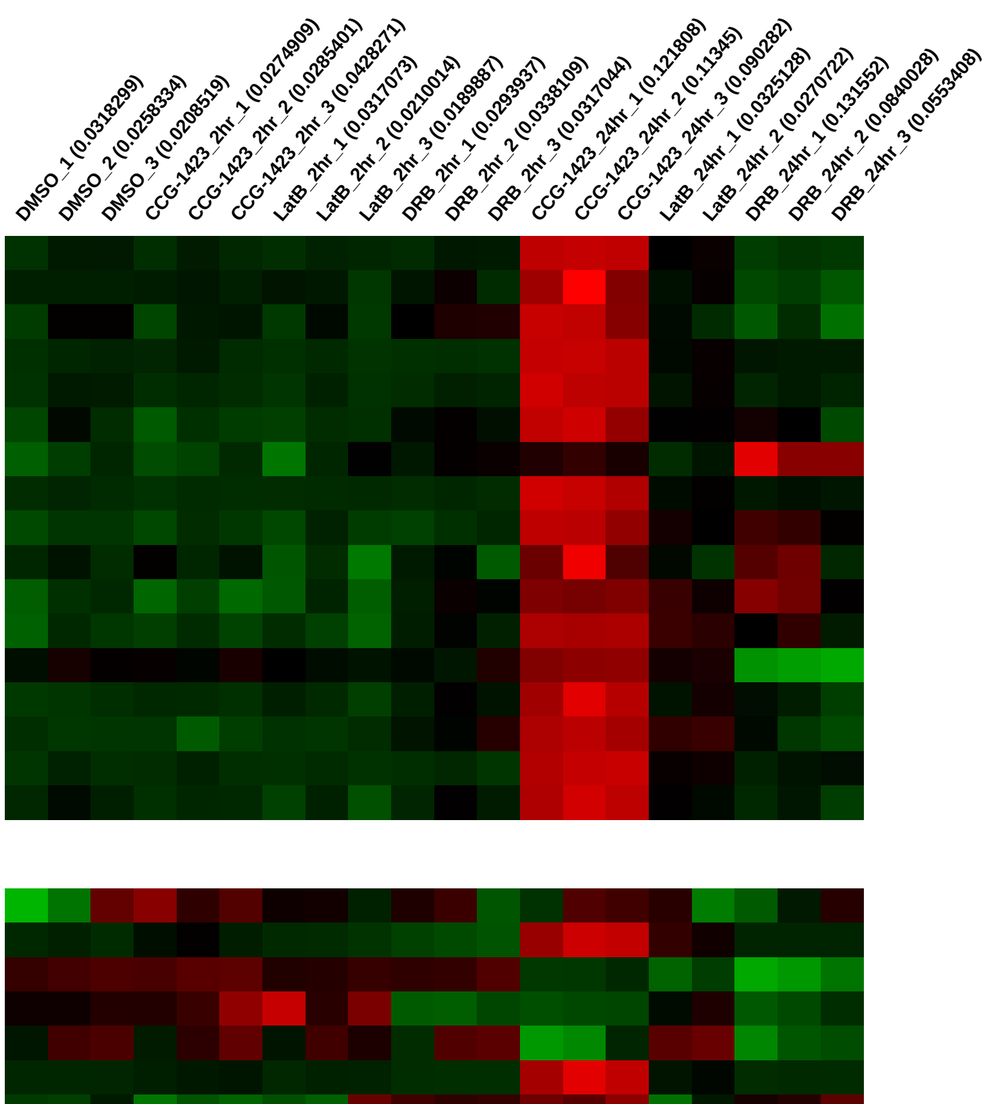

CEM 1
P (S | Z, I) = 1.00
Mean Corr = 0.70589

CEM 1 + Top 10 Genes

Null module

	Pre-normalization Quantiles [min]	[medium]	[max]
MANF	4336.7	5986.4	16669.4
SDF2L1	578.2	1031.6	3092.6
CRELD2	2537.0	3208.6	4563.0
HSPA5	10631.5	13225.6	48688.6
HYOU1	4283.1	5183.4	16677.8
PDIA4	1323.9	1723.6	2809.0
PDIA6	7910.6	9482.8	13507.1
DNAJB11	4391.0	4660.2	10598.1
HSP90B1	6375.7	7476.6	14505.0
PDIA3	8909.5	11376.6	17611.4
PPIB	13988.8	16960.2	21037.6
C19orf10	5157.7	6109.1	8878.4
SLC35B1	3265.7	5203.9	6759.4
SEC61A1	4851.8	5367.1	9472.1
RPN1	3111.8	3530.3	5542.6
DNAJC3	1085.6	1263.2	3440.0
CDK2AP2	2125.2	2606.2	4946.3
ARID5B			
XBP1			
HNRNPAB			
SGK1			
HSPB1			
DDIT4			
ARL4D			
SAP30			
KIAA0408			
GPR17			
HSPH1			
DNASE1L2			
SLC5A3			
GNAS			
GPR3			
TNFRSF25			
TM6SF2			
MKKS			
PLEKHF1			
ZMYM1			
DOK3			
FGF20			
SLC39A2			
KCNIP2			
ERRFI1			
DEDD2			
CCDC117			
USP31			
AHSA2			
CYS1			
CNIH2			
BANP			
CHORDC1			
P4HA1			

GEO Series "GSE8289" Expression Profiles

Num of samples in this series: 8

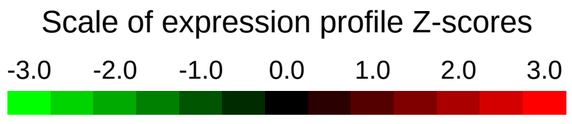

GEO Link:	http://www.ncbi.nlm.nih.gov/geo/query/acc.cgi?acc=GSE8289
Status:	Public on Jun 20 2008
Title:	HEK293 cells overexpressing HNF4a2 wild type or mutant forms C106R or R154X
Organism:	Homo sapiens
Experiment type:	Expression profiling by array
Platform:	GPL570
Pubmed ID:	18163890
Summary & Design:	**Summary:** Identification of genes regulated by the transcription factor HNF4a2 **Keywords: ordered** **Overall design:** We used microarrays to identify genes regulated by the transcription factor HNF4a2. HEK293 cell lines containing doxycyclin-inducible wilt type or mutant forms of HNF4a2m which were introduced by FRT/FLP mediated recombination into FLP-In T-REx 293 cells (Invitrogen) were treated for 24 hours with 1 ´µg/ml doxycyclin. Gene expression profiles of induced and noninduced cells were compared to identify HNF4 regulated targets.

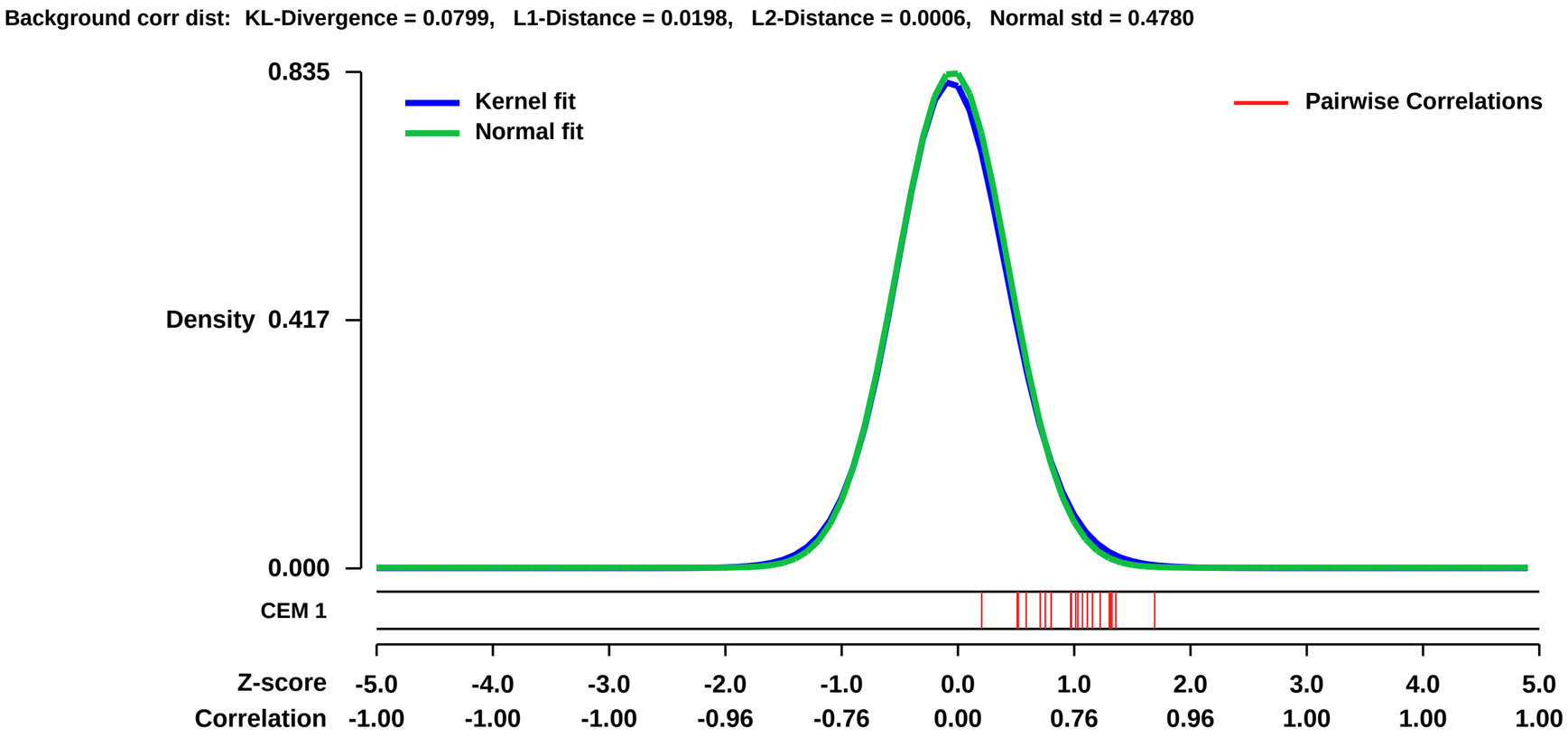

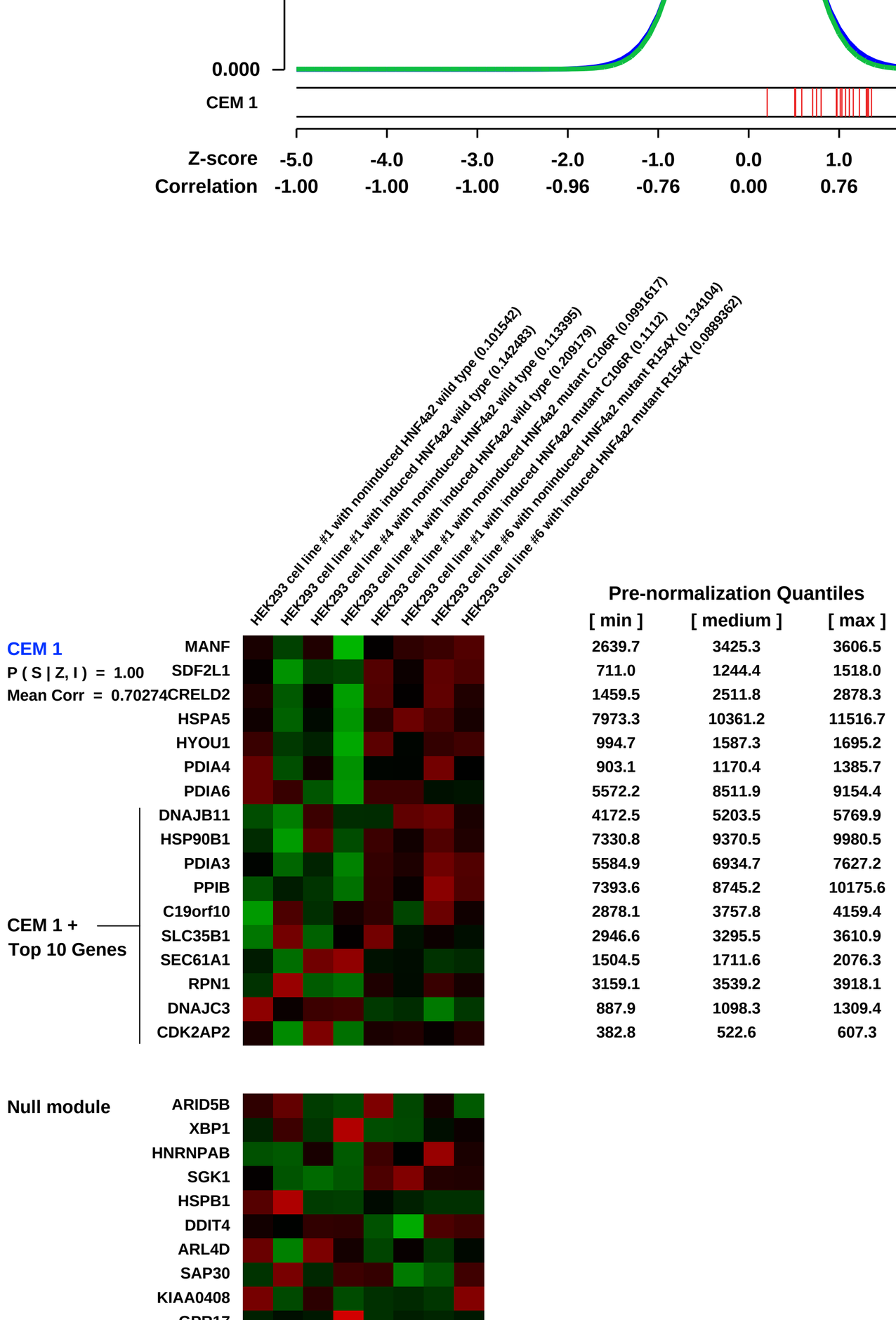

GEO Series "GSE22325" Expression Profiles

Num of samples in this series: 18

Scale of expression profile Z-scores

-3.0 -2.0 -1.0 0.0 1.0 2.0 3.0

GEO Link:	http://www.ncbi.nlm.nih.gov/geo/query/acc.cgi?acc=GSE22325
Status:	Public on Jul 01 2011
Title:	Expression data from interleukin-stimulated HUVEC
Organism:	Homo sapiens
Experiment type:	Expression profiling by array
Platform:	GPL570
Pubmed ID:	21669038
Summary & Design:	**Summary:** **In the hematopoietic microenvironment, endothelial cells (ECs) play an important role in the regulation of hematopoietic cell proliferation and trafficking. We previously demonstrated that EC stimulated with tumor necrosis factor alpha (TNF-¸–) induce the generation of dendritic cells from CD34(+) stem cells, whereas in contrast, interleukins were capable of inducing the proliferation of hematopoietic and myeloid progenitors.** **In order to identify potentially new soluble factors which greatly impact the self-renewal, proliferation and differentiation of CD34+ hematopoietic stem cells (HSC), we examined the expression profiles of IL-1^ , IL-3 and IL-6 stimulated human umbilical vein endothelial cells (HUVEC).** **Overall design:** **we processed seven different umbilical cords and isolated 129 samples for total RNA, and pooled them into 18 groups corresponding to each stimulant, control and time point.**

Background corr dist: KL-Divergence = 0.1954, L1-Distance = 0.0365, L2-Distance = 0.0025, Normal std = 0.3370

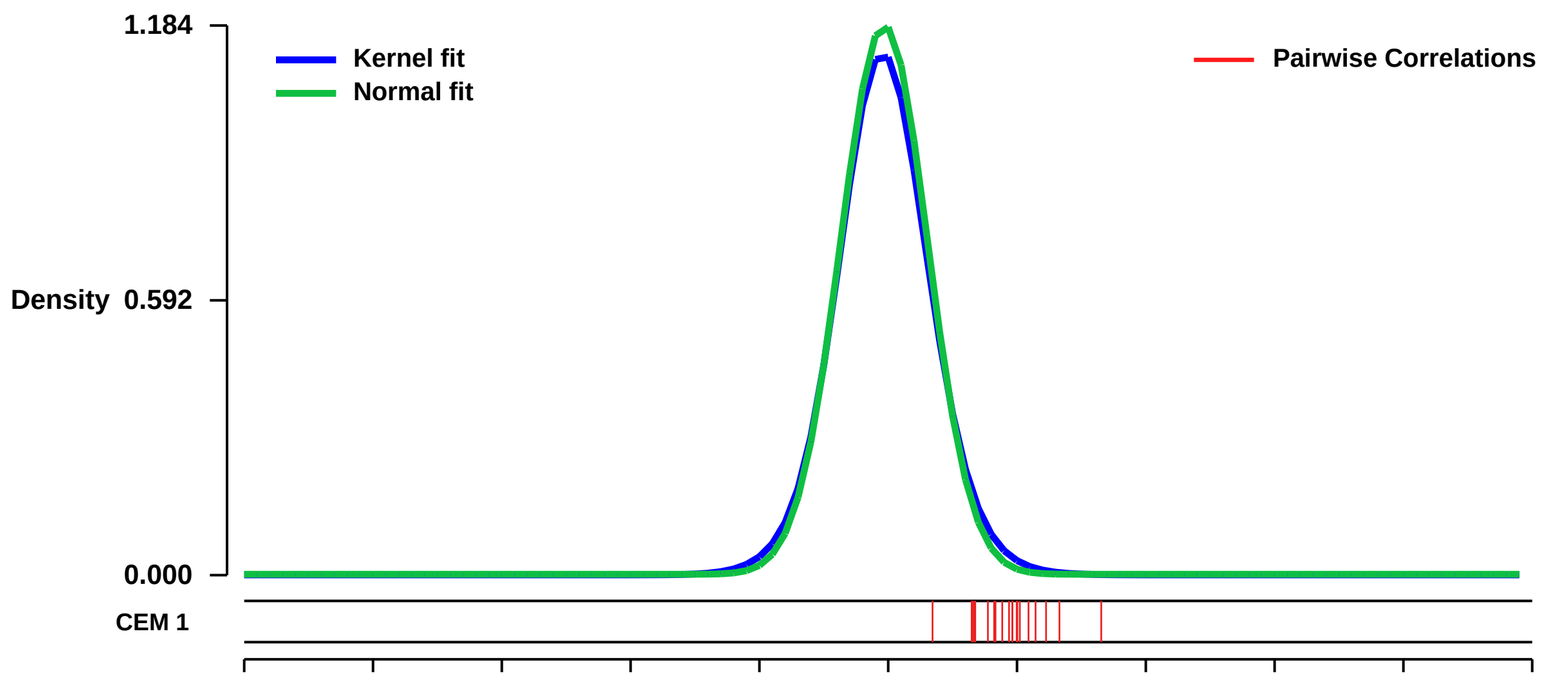

Z-score	-5.0	-4.0	-3.0	-2.0	-1.0	0.0	1.0	2.0	3.0	4.0	5.0
Correlation	-1.00	-1.00	-1.00	-0.96	-0.76	0.00	0.76	0.96	1.00	1.00	1.00

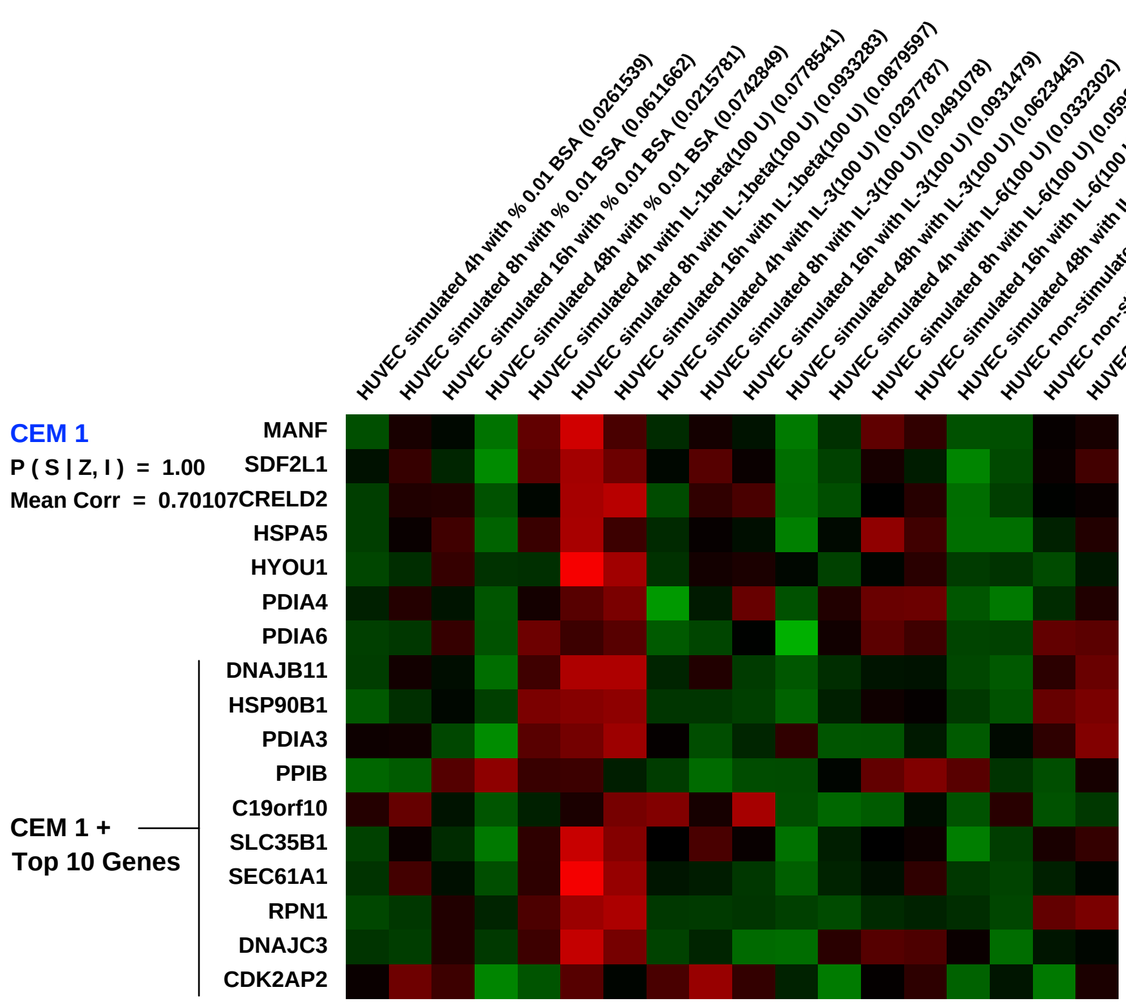

Pre-normalization Quantiles

	[min]	[medium]	[max]
MANF	3159.0	5022.2	7982.2
SDF2L1	550.6	1337.5	2145.7
CRELD2	1859.2	2610.0	3899.7
HSPA5	14757.9	21929.1	30574.5
HYOU1	1904.4	2312.1	4428.2
PDIA4	690.6	992.4	1171.6
PDIA6	8171.7	12888.4	15123.1
DNAJB11	2540.0	3749.6	6293.7
HSP90B1	4955.1	7539.6	14012.9
PDIA3	11411.1	13486.2	15647.3
PPIB	16412.3	18901.5	22484.6
C19orf10	4144.6	4733.2	5891.6
SLC35B1	1712.1	2291.9	3118.7
SEC61A1	2985.4	3702.2	6270.5
RPN1	2522.6	2980.8	5941.0
DNAJC3	1284.3	1808.9	2832.7
CDK2AP2	823.1	1092.5	1358.6

GEO Series "GSE22002" Expression Profiles

Num of samples in this series: 6

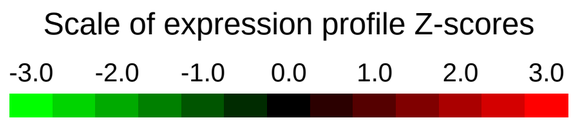

GEO Link:	http://www.ncbi.nlm.nih.gov/geo/query/acc.cgi?acc=GSE22002
Status:	Public on Aug 03 2010
Title:	Analysis of HeLa cells after transfection with miR-1 or miR-155, by microarray profiling
Organism:	Homo sapiens
Experiment type:	Expression profiling by array
Platform:	GPL570
Pubmed ID:	20703300
Summary & Design:	**Summary:** MicroRNAs (miRNAs) are endogenous ~22-nucleotide RNAs that mediate important gene-regulatory events by pairing to the mRNAs of protein-coding genes to direct their repression. Repression of these regulatory targets leads to decreased translational efficiency and/or decreased mRNA levels, but the relative contributions of these two outcomes have been largely unknown, particularly for endogenous targets expressed at low-to-moderate levels. Here, we use ribosome profiling to measure the overall effects on protein production and compare these to simultaneously measured effects on mRNA levels. For both ectopic and endogenous miRNA regulatory interactions, lowered mRNA levels account for most (â¥84%) of the decreased protein production. These results show that changes in mRNA levels closely reflect the impact of miRNAs on gene expression and indicate that destabilization of target mRNAs is the predominant reason for reduced protein output. **Overall design:** Examine mRNA expression levels in HeLa cells transfected with miR-1 or miR-155, versus mock-transfected cells, at two different time points post-transfection.

Background corr dist: KL-Divergence = 0.0398, L1-Distance = 0.0173, L2-Distance = 0.0003, Normal std = 0.6131

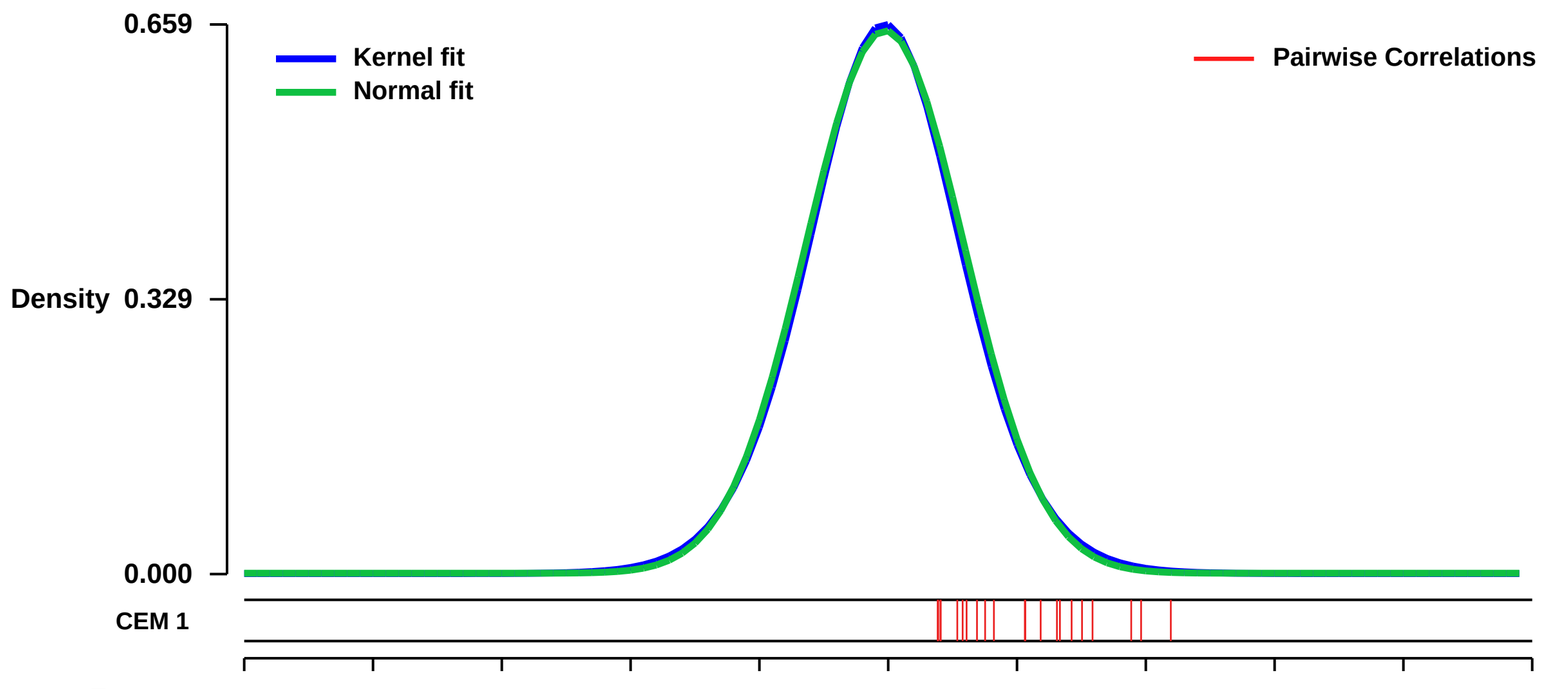

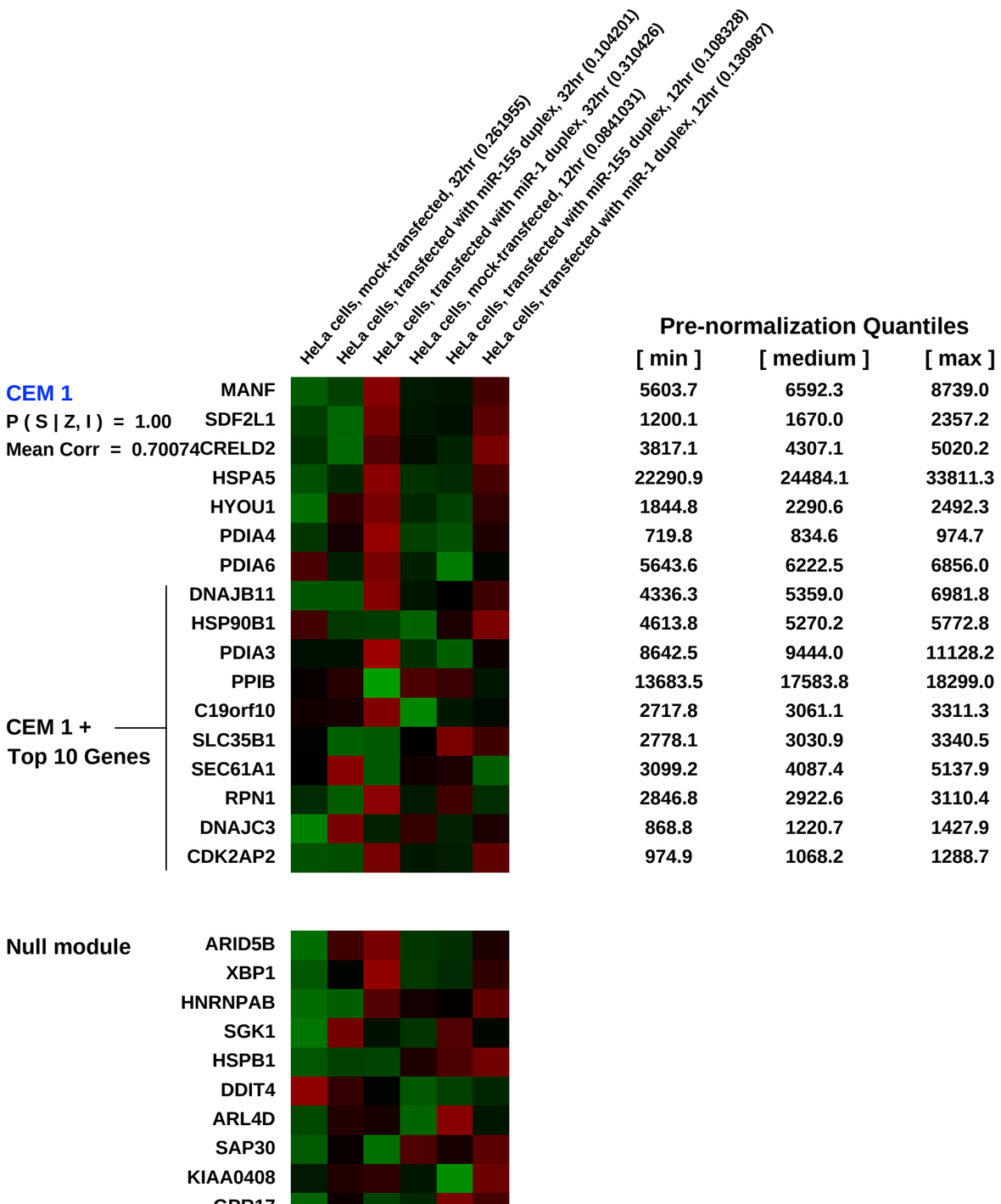

Pre-normalization Quantiles

	[min]	[medium]	[max]
MANF	5603.7	6592.3	8739.0
SDF2L1	1200.1	1670.0	2357.2
CRELD2	3817.1	4307.1	5020.2
HSPA5	22290.9	24484.1	33811.3
HYOU1	1844.8	2290.6	2492.3
PDIA4	719.8	834.6	974.7
PDIA6	5643.6	6222.5	6856.0
DNAJB11	4336.3	5359.0	6981.8
HSP90B1	4613.8	5270.2	5772.8
PDIA3	8642.5	9444.0	11128.2
PPIB	13683.5	17583.8	18299.0
C19orf10	2717.8	3061.1	3311.3
SLC35B1	2778.1	3030.9	3340.5
SEC61A1	3099.2	4087.4	5137.9
RPN1	2846.8	2922.6	3110.4
DNAJC3	868.8	1220.7	1427.9
CDK2AP2	974.9	1068.2	1288.7

GEO Series "GSE14987" Expression Profiles

Num of samples in this series: 9

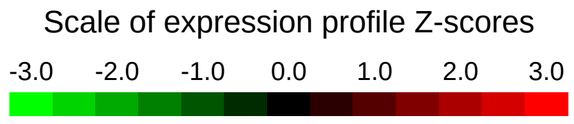

GEO Link:	http://www.ncbi.nlm.nih.gov/geo/query/acc.cgi?acc=GSE14987
Status:	Public on Feb 01 2010
Title:	Expression data from ERBB2 over-expression and EGF stimulation in MCF10A cells
Organism:	Homo sapiens
Experiment type:	Expression profiling by array
Platform:	GPL570
Pubmed ID:	20133671
Summary & Design:	**Summary:** Expression data from ERBB2 over-expression and EGF stimulation in MCF10A cells **Overall design:** The cells were transduced with retroviruses encoding vector control (pBabe) or pBabe-ErbB2. After infection cells were switched to assay medium supplemented with only 2% horse serum and no EGF. For EGF stimulation, cells transduced with empty vector were treated with EGF at 50 ng/ml for 2 hours before harvesting.

Background corr dist: KL-Divergence = 0.0740, L1-Distance = 0.0325, L2-Distance = 0.0014, Normal std = 0.5080

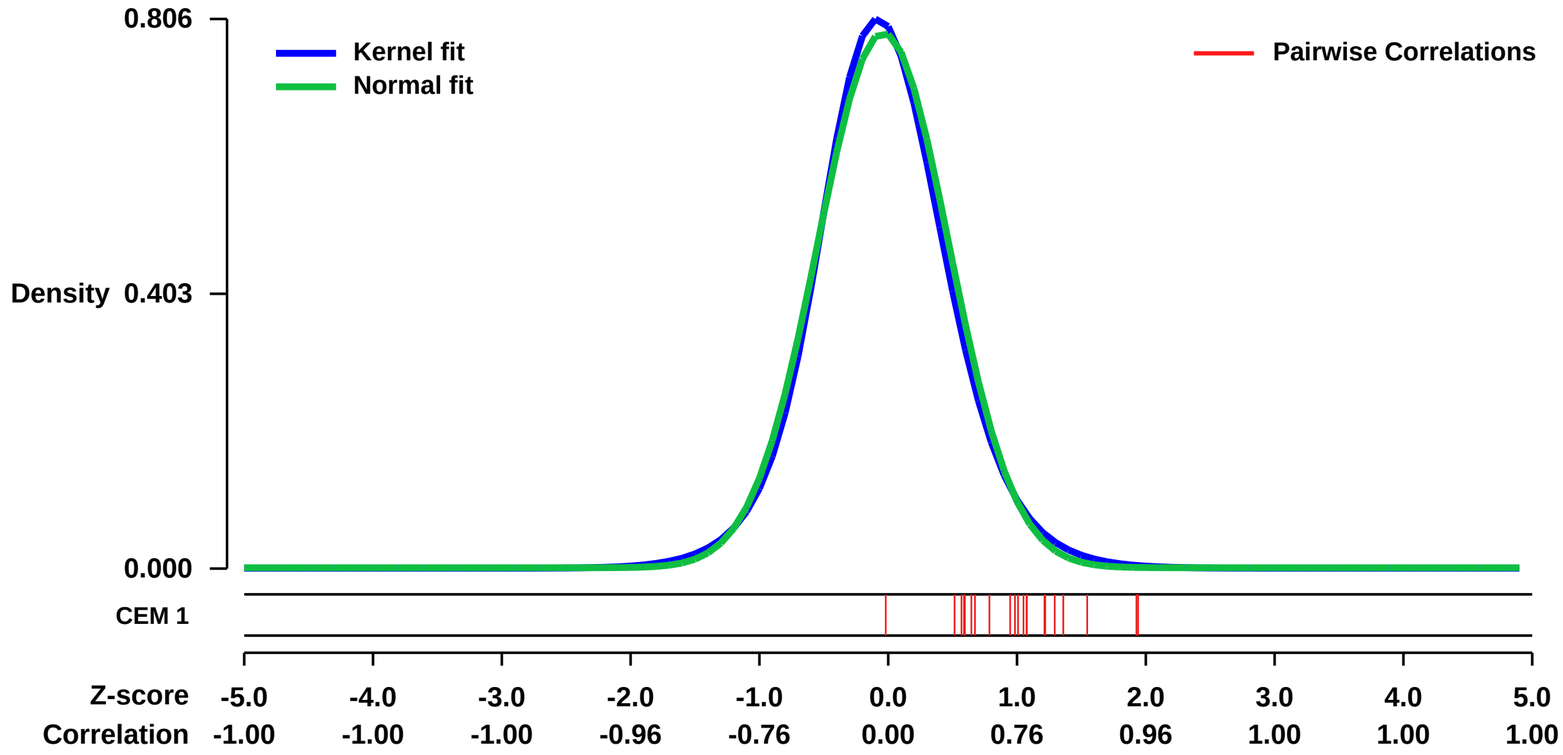

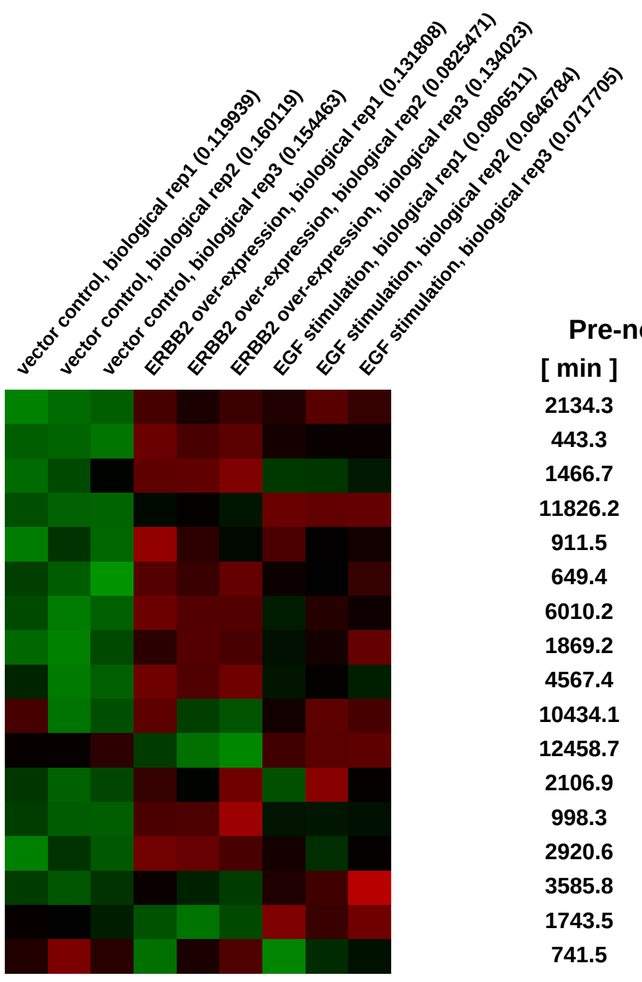

GEO Series "GSE35428" Expression Profiles

Num of samples in this series: 106

Details of this dataset are not shown due to large number of samples and the page size limit.

Find details in http://www.ncbi.nlm.nih.gov/geo/query/acc.cgi?acc=GSE35428

Background corr dist: KL-Divergence = 0.3718, L1-Distance = 0.0930, L2-Distance = 0.0234, Normal std = 0.2821

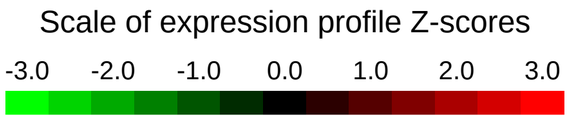

GEO Series "GSE2817" Expression Profiles

Num of samples in this series: 30

Scale of expression profile Z-scores

-3.0 -2.0 -1.0 0.0 1.0 2.0 3.0

GEO Link:	http://www.ncbi.nlm.nih.gov/geo/query/acc.cgi?acc=GSE2817
Status:	Public on Dec 15 2005
Title:	Wavelet modelling of microarray data provides chromosomal pattern of expression which predicts survival in gliomas
Organism:	Homo sapiens
Experiment type:	Expression profiling by array
Platform:	GPL570
Pubmed ID:	17140431
Summary & Design:	**Summary:** Genetic and epigenetic processes result in gene expression changes through alteration of the chromatin structure. The relative position of genes on chromosomes has therefore important functional implications and can be exploited to model microarray datasets. Gliomas are the most frequent primary brain tumours in adults and their prognosis is related to histology and grade. In oligodendrogliomas, allelic loss of 1p/19q and hypermethylation of MGMT promoter is associated with longer survival and chemosensitivity. In this work we used oligonucleotide microarray to study a group of 30 gliomas with various oligodendroglial and astrocytic components. We used an original approach combining a wavelet model of inter-probe genomic distance (CHROMOWAVE) and unsupervised method of analysis (Singular Value Decomposition) in order to discover new prognostic chromosomal patterns of gene expression. We identified a major pattern of variation that strongly correlated with survival (p= 0.007) and could be visualized as a genome-wide chromosomal pattern including widespread gene expression changes on 1p, 19q, 4, 18, 13 and 9q and multiple smaller clusters scattered along chromosomes. Gene expression changes on chromosomes 1p, 19q and 9q were significantly correlated with the allelic loss of these regions as measured by FISH. Differential expression of genes implicated in drug resistance was also a feature of this chromosomal pattern and in particular low expression of MGMT was correlated with favourable prognosis (p<0.0001). Remarkably, unsupervised analysis of the expression of individual genes and not of their chromosomal ensemble produced a pattern that could not be associated with prognosis, emphasizing the determinant role of the wavelet mathematical modelling. **Keywords: wavelet, glioma, unsupervised** **Overall design:** Unsupervised analysis using wavelet models of 30 diffuse gliomas

Background corr dist: KL-Divergence = 0.3754, L1-Distance = 0.0702, L2-Distance = 0.0143, Normal std = 0.2567

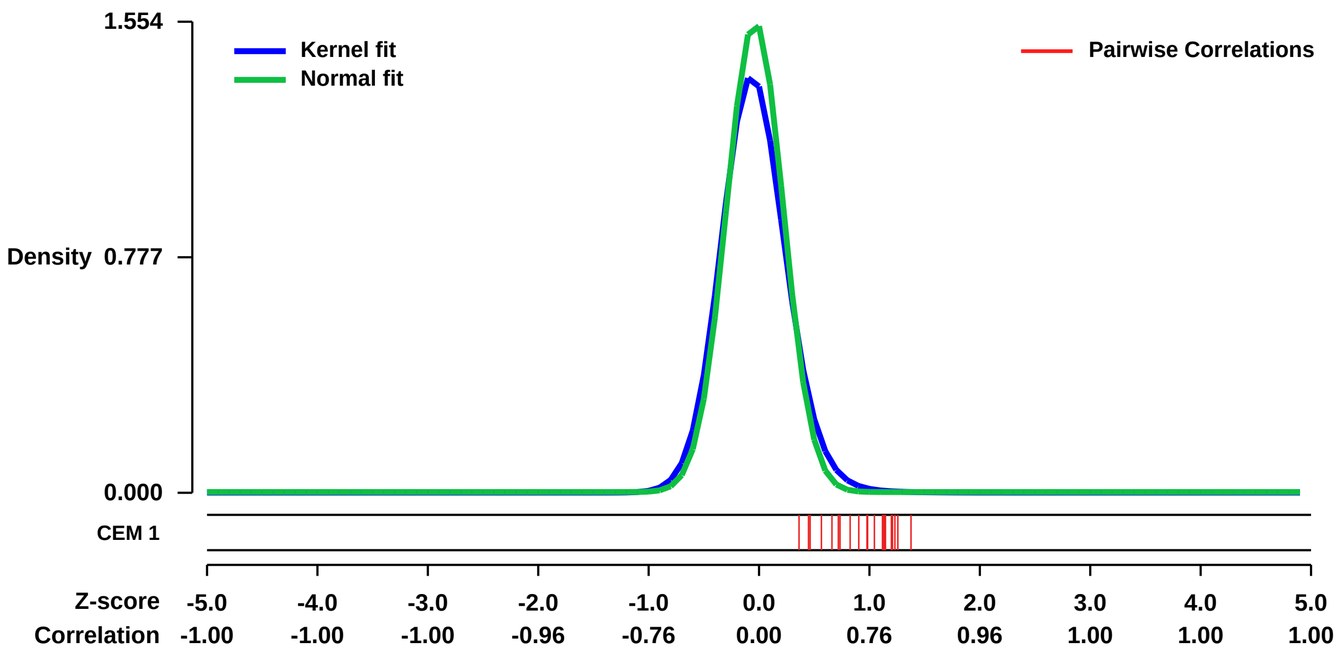

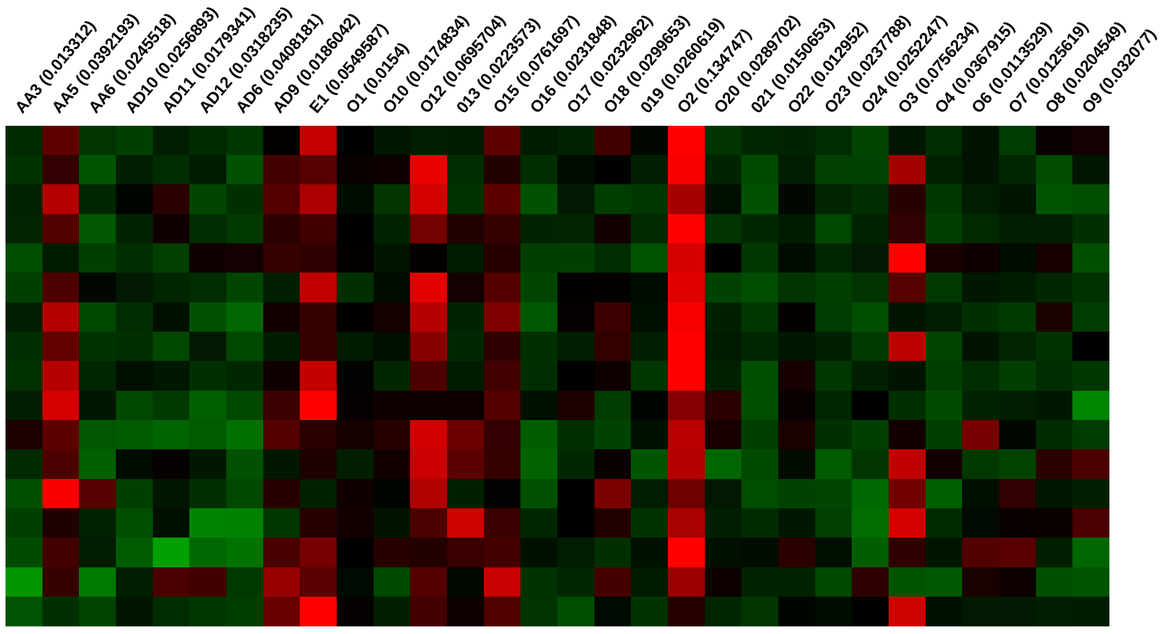

Pre-normalization Quantiles

[min]	[medium]	[max]
909.9	1342.3	5165.2
152.0	409.8	1698.3
922.4	1450.1	3768.0
4134.7	6795.1	26895.2
1611.7	2399.0	6162.7
317.7	524.2	1617.6
3305.6	5079.8	10899.4
1190.3	2039.6	8841.5
1531.7	2598.6	9769.0
2055.1	4427.2	10112.5
4969.7	8813.4	16668.1
1001.2	1391.7	2304.6
1036.4	1378.3	2510.1
966.8	2287.6	4855.0
909.0	2315.3	4971.9
703.9	1396.8	2439.6
493.5	791.5	2528.5

GEO Series "GSE45867" Expression Profiles

Num of samples in this series: 40

Scale of expression profile Z-scores

-3.0 -2.0 -1.0 0.0 1.0 2.0 3.0

GEO Link:	http://www.ncbi.nlm.nih.gov/geo/query/acc.cgi?acc=GSE45867
Status:	Public on Dec 30 2013
Title:	Effects of tocilizumab versus methotrexate therapy on gene expression profiles in the early rheumatoid arthrtis synovium
Organism:	Homo sapiens
Experiment type:	Expression profiling by array
Platform:	GPL570
Pubmed ID:	24449571
Summary & Design:	**Summary:** Rheumatoid arthritis (RA) is a chronic, systemic autoimmune inflammatory disease that is characterized by the presence of inflammatory cytokines, including interleukin-6 (IL-6). Here, we investigated the global molecular effects of Tocilizumab, an approved humanized anti-IL6 Receptor antibody, versus Methotrexate therapy, in synovial biopsy samples collected prospectively in early RA before and 12 weeks after administration of the drug. The results were compared with our previous data, generated in prospective cohorts of Adalimumab- and Rituximab-treated (Methotrexate- and anti-TNF-resistant, respectively) RA patients. We found that Tocilizumab induces a significant down-regulation of genes included in specific pathways: cytokines & chemokines (e.g. IL-6, IL-7, IL-22, CCL8, CCL11, CCL13, CCL19, CCL20), and T cell activation. By contrast, Tocilizumab induces a significant up-regulation of genes associated with healing processes. These effects are significantly more pronounced as compared to Methotrexate, Rituximab, or Adalimumab therapies. By opposition to the effects of Adalimumab, Tocilizumab therapy does not induce a decreased expression of genes involved in cell proliferation. **Overall design:** Paired synovial biopsy samples were obtained from the affected knee of early RA patients before and 12 weeks after initiation of Tocilizumab (n=12) or Methotrexate (n=8) therapy. SDAI remission criteria were computed prospectively before, 3 months and 6 months after administration of the drugs and patientsâ responses were defined according to their SDAI remission status at 6 months. Gene expression studies were performed using GeneChip Human Genome U133 Plus 2.0 arrays.

Background corr dist: KL-Divergence = 0.4424, L1-Distance = 0.0882, L2-Distance = 0.0262, Normal std = 0.2435

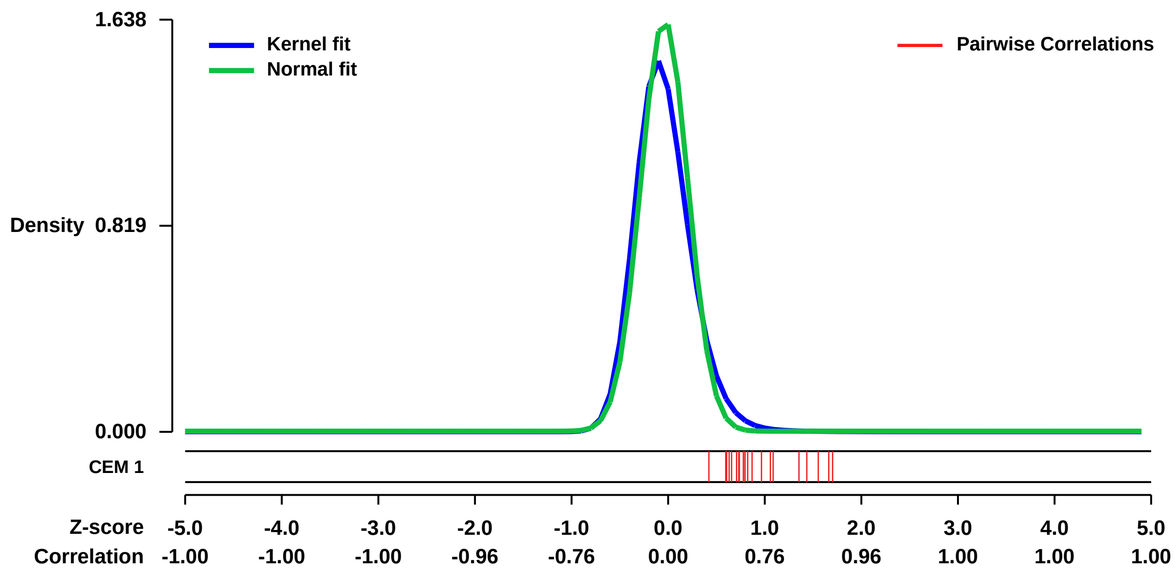

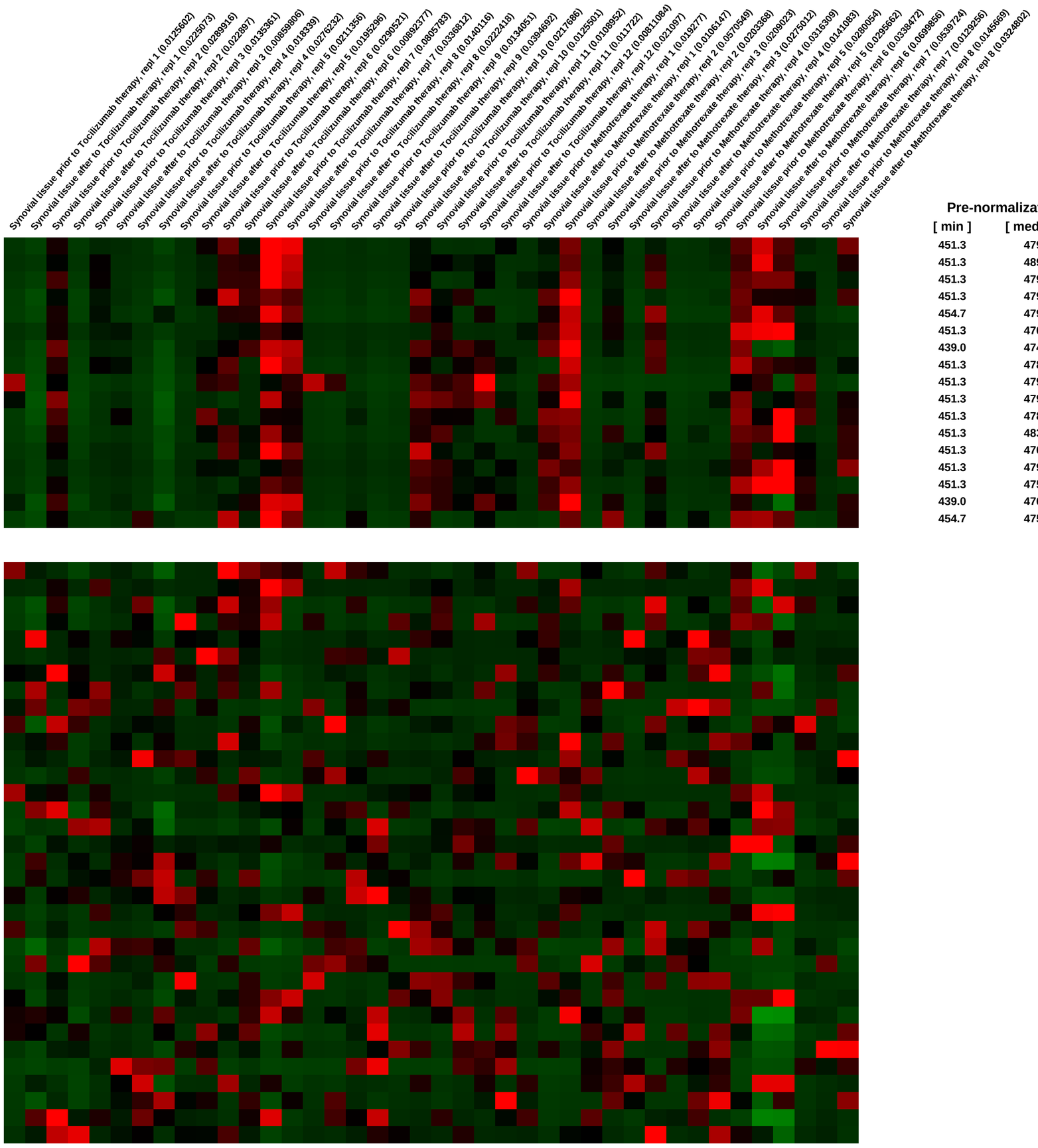

CEM 1
P (S | Z, I) = 1.00
Mean Corr = 0.69950

CEM 1 + Top 10 Genes

Null module

	MANF	SDF2L1	CRELD2	HSPA5	HYOU1	PDIA4	PDIA6	DNAJB11	HSP90B1	PDIA3	PPIB	C19orf10	SLC35B1	SEC61A1	RPN1	DNAJC3	CDK2AP2
Pre-normalization Quantiles [min]	451.3	451.3	451.3	451.3	454.7	451.3	439.0	451.3	451.3	451.3	451.3	451.3	451.3	451.3	451.3	439.0	454.7
[medium]	479.1	489.9	479.1	479.1	479.1	476.2	474.8	478.1	479.1	479.1	478.1	483.4	476.9	479.1	475.8	476.7	475.1
[max]	838.8	1453.8	1032.5	760.3	816.9	973.6	708.4	762.8	763.4	667.5	717.9	868.9	753.9	902.9	823.9	645.5	800.7

	ARID5B	XBP1	HNRNPAB	SGK1	HSPB1	DDIT4	ARL4D	SAP30	KIAA0408	GPR17	HSPH1	DNASE1L2	SLC5A3	GNAS	GPR3	TNFRSF25	TM6SF2	MKKS	PLEKHF1	ZMYM1	DOK3	FGF20	SLC39A2	KCNIP2	ERRFI1	DEDD2	CCDC117	USP31	AHSA2	CYS1	CNIH2	BANP	CHORDC1	P4HA1
Pre-normalization Quantiles [min]	451.3	451.3	451.3	451.3	451.3	451.3	451.3	451.3	451.3	451.3	451.3	451.3	451.3	451.3	451.3	451.3	451.3	451.3	451.3	451.3	451.3	451.3	451.3	451.3	451.3	451.3	451.3	451.3	451.3	451.3	451.3	451.3	451.3	451.3
[medium]	479.1	479.1	479.1	479.1	479.1	479.1	479.1	479.1	479.1	479.1	479.1	479.1	479.1	479.1	479.1	479.1	479.1	479.1	479.1	479.1	479.1	479.1	479.1	479.1	479.1	479.1	479.1	479.1	479.1	479.1	479.1	479.1	479.1	479.1
[max]	838.8	838.8	838.8	838.8	838.8	838.8	838.8	838.8	838.8	838.8	838.8	838.8	838.8	838.8	838.8	838.8	838.8	838.8	838.8	838.8	838.8	838.8	838.8	838.8	838.8	838.8	838.8	838.8	838.8	838.8	838.8	838.8	838.8	838.8

GEO Series "GSE16193" Expression Profiles

Num of samples in this series: 20

Scale of expression profile Z-scores

-3.0 -2.0 -1.0 0.0 1.0 2.0 3.0

GEO Link:	http://www.ncbi.nlm.nih.gov/geo/query/acc.cgi?acc=GSE16193
Status:	Public on May 21 2010
Title:	Interfering with Proximal TLR4 to NF-kappaB Signal Transduction in Human Monocytes
Organism:	Homo sapiens
Experiment type:	Expression profiling by array
Platform:	GPL570
Pubmed ID:	19956541
Summary & Design:	**Summary:** Carbon monoxide (CO) is an endogenous messenger that suppresses inflammation, modulates apoptosis and promotes vascular remodeling. Here, microarrays were employed to globally characterize the CO (250 ppm) suppression of early (1 h) LPS-induced inflammation in human monocytic THP-1 cells. CO suppressed 79 of 101 immediate-early genes induced by LPS; 19% (15/79) were transcription factors and most others were cytokines, chemokines and immune response genes. The prototypic effects of CO on transcription and protein production occurred early but decreased rapidly. CO activated p38 MAPK, ERK1/2 and Akt and caused an early and transitory delay in LPS-induced JNK activation. However, selective inhibitors of these kinases failed to block CO suppression of LPS-induced IL-1beta, an inflammation marker. Of CO-suppressed genes, 81% (64/79) were found to have promoters with putative NF-kappaB binding sites. CO was subsequently shown to block LPS-induced phosphorylation and degradation of IkappaBalpha in human monocytes, thereby inhibiting NF-kappaB signal transduction. CO broadly suppresses the initial inflammatory response of human monocytes to LPS by reshaping proximal events in TLR4 signal transduction such as stress kinase responses and early NF-kappaB activation. These rapid, but transient effects of CO may have therapeutic applications in acute pulmonary and vascular injury. **Overall design:** The microarrays were performed on THP-1 cells, a human monocytic cell line. Cells were treated with or without LPS (1 ´µg/ml) in presence or absence of carbon monoxide (250 ppm) for 1 h. Total RNA was isolated, reverse transcribed, labeled and hybridized to oligonucleotide microarrays.

Background corr dist: KL-Divergence = 0.3340, L1-Distance = 0.0685, L2-Distance = 0.0132, Normal std = 0.2675

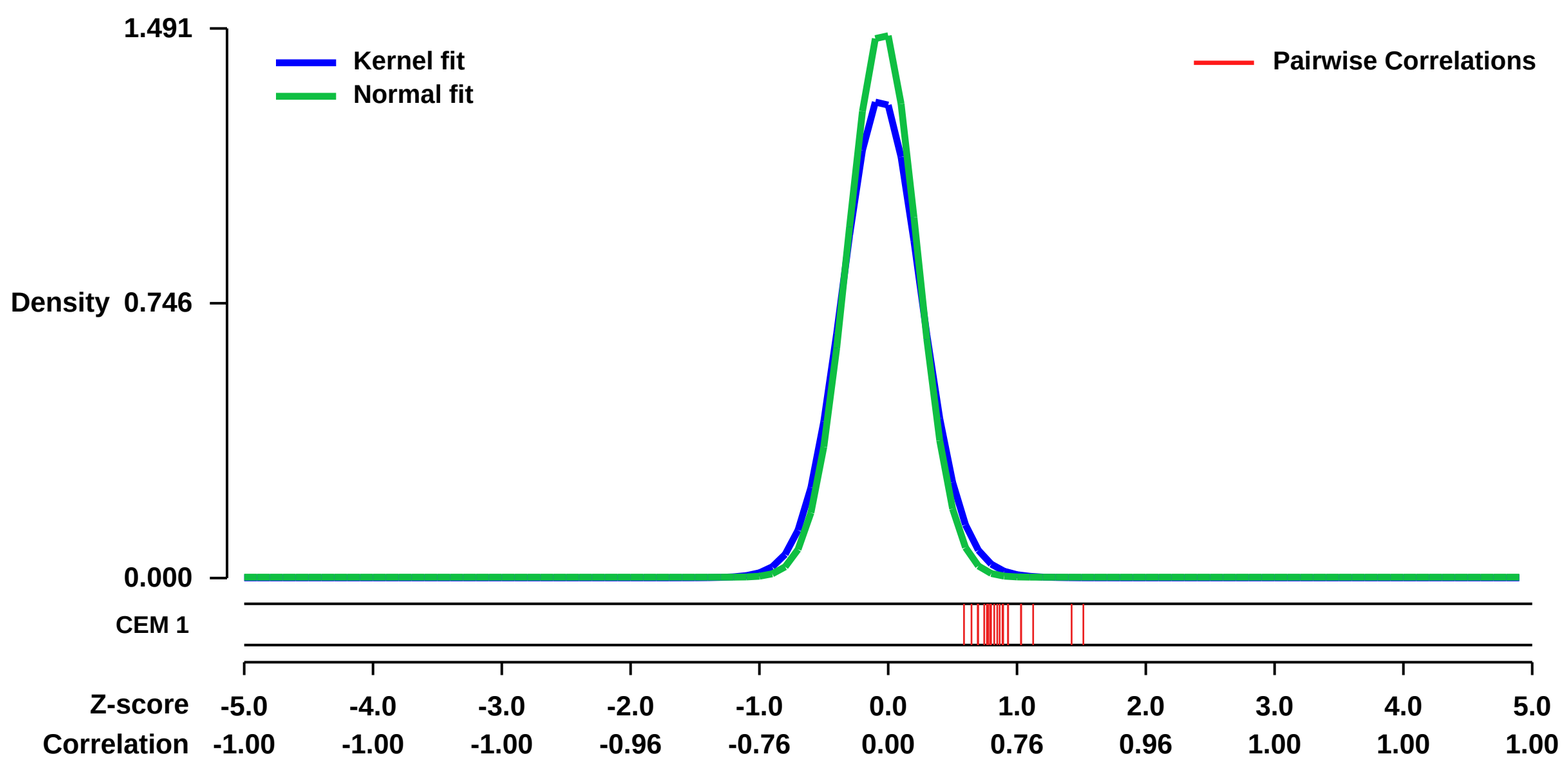

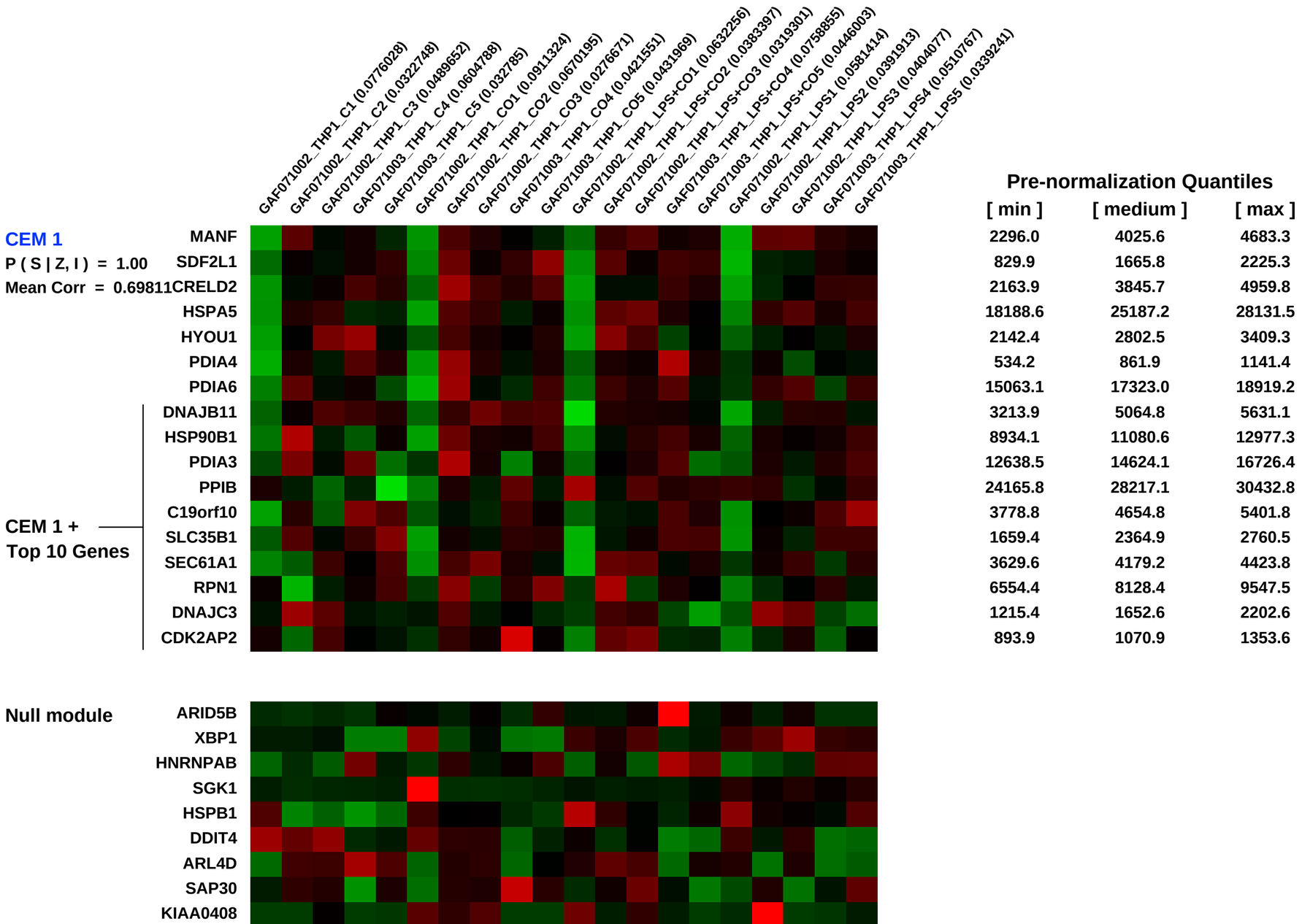

Pre-normalization Quantiles

	[min]	[medium]	[max]
MANF	2296.0	4025.6	4683.3
SDF2L1	829.9	1665.8	2225.3
CRELD2	2163.9	3845.7	4959.8
HSPA5	18188.6	25187.2	28131.5
HYOU1	2142.4	2802.5	3409.3
PDIA4	534.2	861.9	1141.4
PDIA6	15063.1	17323.0	18919.2
DNAJB11	3213.9	5064.8	5631.1
HSP90B1	8934.1	11080.6	12977.3
PDIA3	12638.5	14624.1	16726.4
PPIB	24165.8	28217.1	30432.8
C19orf10	3778.8	4654.8	5401.8
SLC35B1	1659.4	2364.9	2760.5
SEC61A1	3629.6	4179.2	4423.8
RPN1	6554.4	8128.4	9547.5
DNAJC3	1215.4	1652.6	2202.6
CDK2AP2	893.9	1070.9	1353.6

GEO Series "GSE11729" Expression Profiles

Num of samples in this series: 60

Scale of expression profile Z-scores

-3.0 -2.0 -1.0 0.0 1.0 2.0 3.0

GEO Link: http://www.ncbi.nlm.nih.gov/geo/query/acc.cgi?acc=GSE11729
Status: Public on Jul 30 2009
Title: H1299 EGF and Iressa stimulation
Organism: Homo sapiens
Experiment type: Expression profiling by array
Platform: GPL570
Pubmed ID: 19674104

Summary & Design:

Summary:
Controlled activation of epidermal growth factor receptor (EGFR) is systematically guaranteed at the molecular level, however aberrant activation of EGFR is frequently found in cancer. Transcription induced by EGFR activation often involves coordinated expression of genes that positively and negatively regulate the original signaling pathway, therefore alterations in EGFR kinase activity may reflect changes in gene expression associated with the pathway. In this study, we investigated transcriptional changes following EGF stimulation with or without the EGFR kinase inhibitor Iressa in H1299 human non-small-cell lung cancer cells (parental H1299, H1299 cells which overexpress wild-type: EGFR-WT and mutant EGFR: L858R). Our results clearly showed differences in transcriptional activity in the absence or presence of EGFR kinase activity, and genes sharing the same molecular functions showed distinct expression dynamics. The results showed particular enrichment of EGFR/ErbB signaling-related genes in a differentially expressed gene set, and significant protein expression of MIG6/RALT(ERRFI1), an EGFR negative regulator, was confirmed in L858R. High MIG6 protein expression was correlated with basal EGFR phosphorylation and inversely correlated with EGF-induced ERK phosphorylation levels. Investigation of NCI-60 cell lines showed that ERRFI1 expression was correlated with EGFR expression regardless of tissue type. These results suggest that cells accumulate MIG6 as an inherent negative regulator to suppress excess EGFR activity when basal EGFR kinase activity is considerably high. Taken together, an EGFR mutation can cause transcriptional changes to accommodate the activation potency of the original signaling pathway at the cellular level.

Overall design:
H1299 human non-small cell lung cancer cells were stimulated by the growth hormone (epidermal growth factor (EGF)) or EGFR kinase inhibitor (Iressa). Control was set as non-treated cells.

Background corr dist: KL-Divergence = 0.1652, L1-Distance = 0.0514, L2-Distance = 0.0069, Normal std = 0.3603

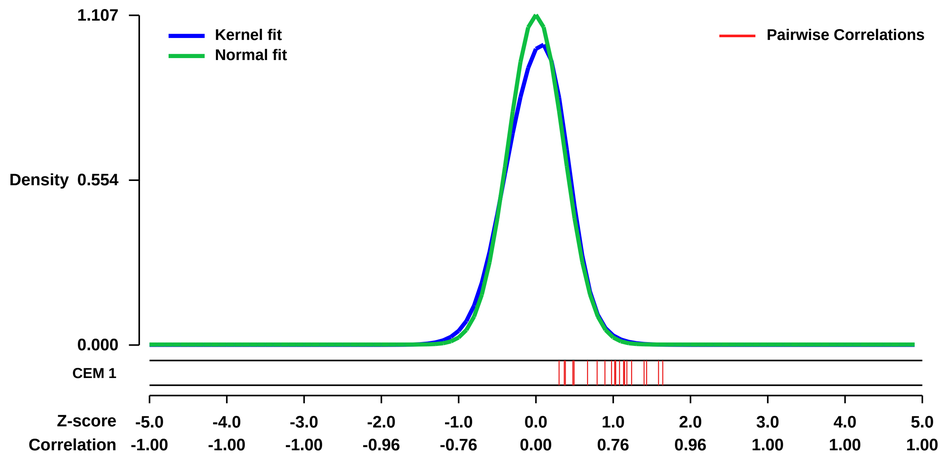

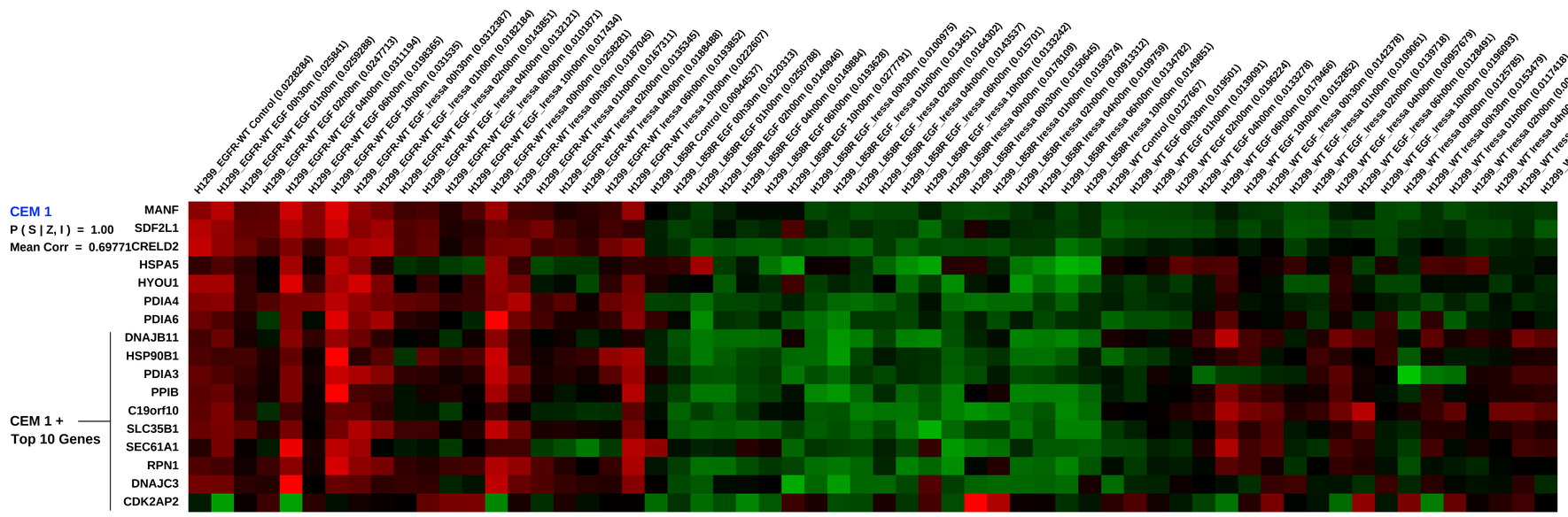

Pre-normalization Quantiles

[min]	[medium]	[max]
1786.8	2285.1	4709.3
622.5	826.1	1574.4
818.0	1128.6	1903.9
6220.3	9419.6	12183.9
1765.5	2497.3	3726.9
302.6	417.0	705.2
6286.1	8099.8	12730.9
1779.4	2895.9	4076.1
1756.0	2483.4	3816.1
3895.8	7329.0	10755.4
9526.9	13988.9	21318.5
2206.2	3075.6	4161.5
2307.4	3553.7	4829.5
2826.2	3584.6	4970.1
3905.9	5734.9	8699.4
507.3	704.3	1073.6
554.7	666.0	837.7

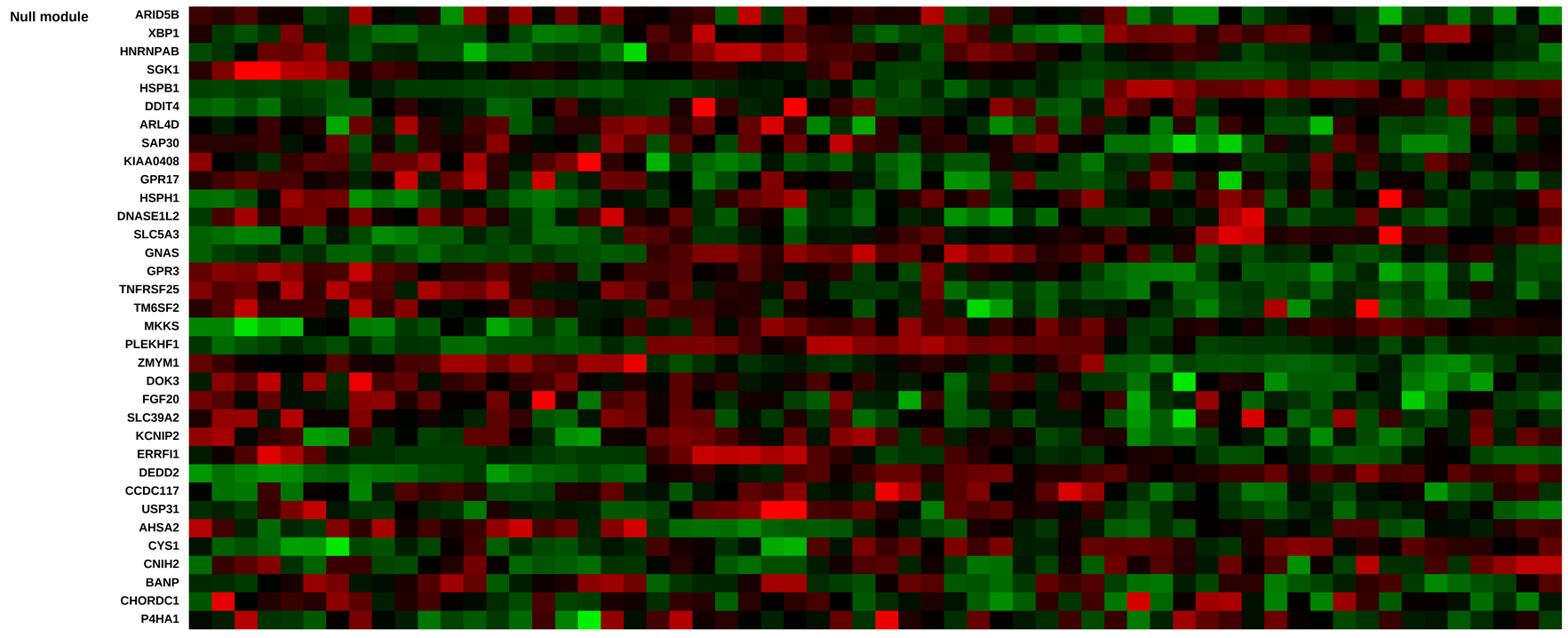

GEO Series "GSE18486" Expression Profiles

Num of samples in this series: 9

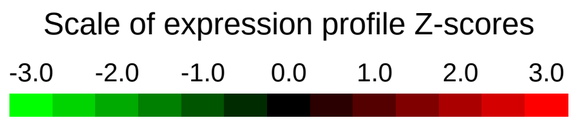

GEO Link:	http://www.ncbi.nlm.nih.gov/geo/query/acc.cgi?acc=GSE18486
Status:	Public on Jul 14 2010
Title:	CDK inhibitors PHA-848125 and PHA-690509 profiling on A2780
Organism:	Homo sapiens
Experiment type:	Expression profiling by array
Platform:	GPL570
Pubmed ID:	20679242
Summary & Design:	**Summary:** The effects of the CDK inhibitors PHA-848125 and PHA-690509 on the A2780 cell line were analysed by gene expression profiling. **Overall design:** The A2780 cell line was treated with PHA-848125 (CDk-125) or PHA-690509 (CDk-509) for 6 hours at a dose equal to 5 times the IC50. Untreated A2780 cells were used as a control. Three replicates per treatment.

Background corr dist: KL-Divergence = 0.0703, L1-Distance = 0.0343, L2-Distance = 0.0015, Normal std = 0.5225

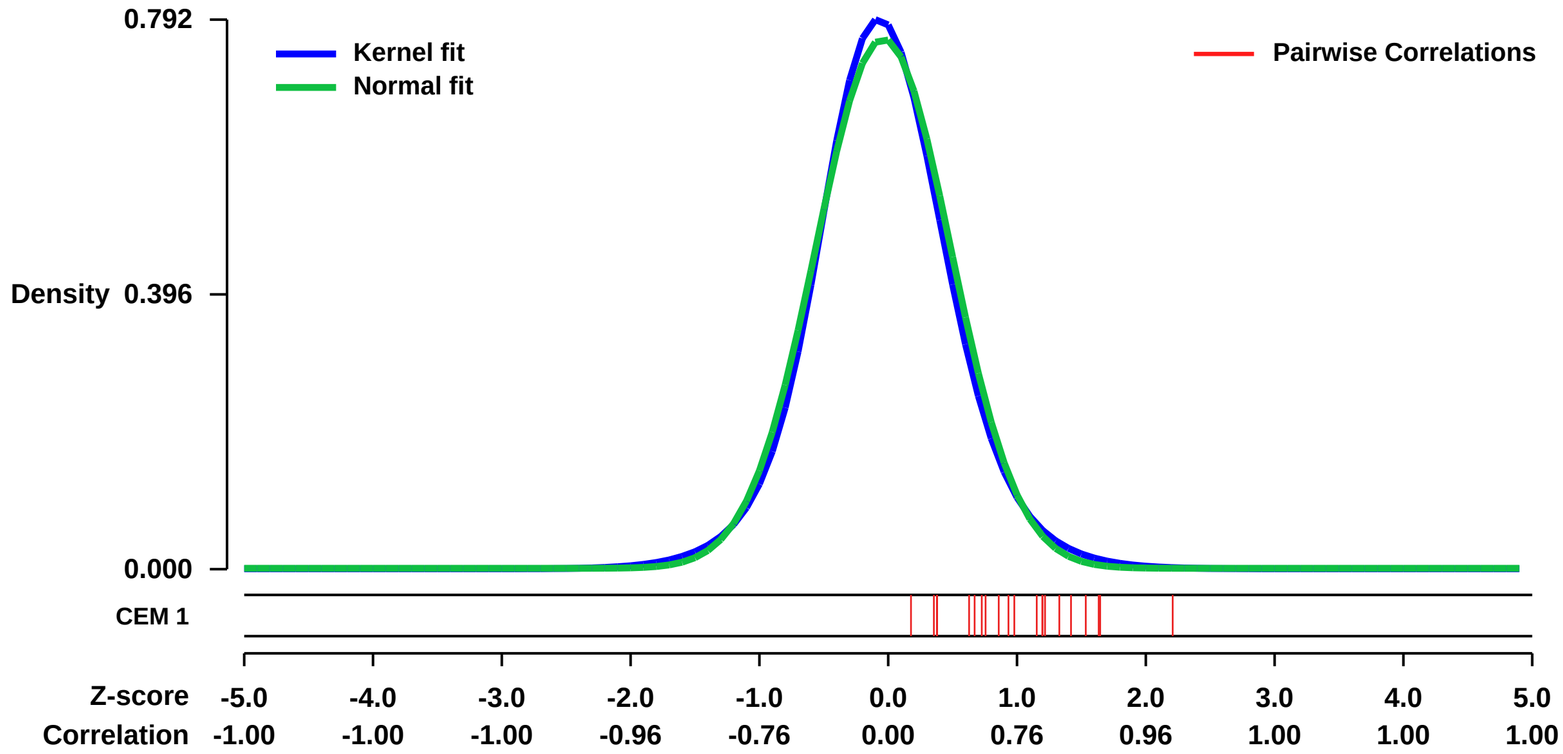

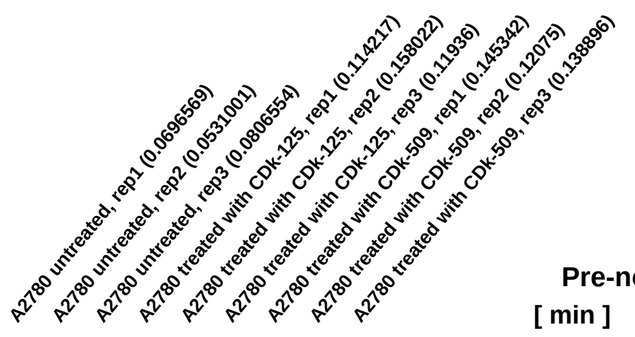

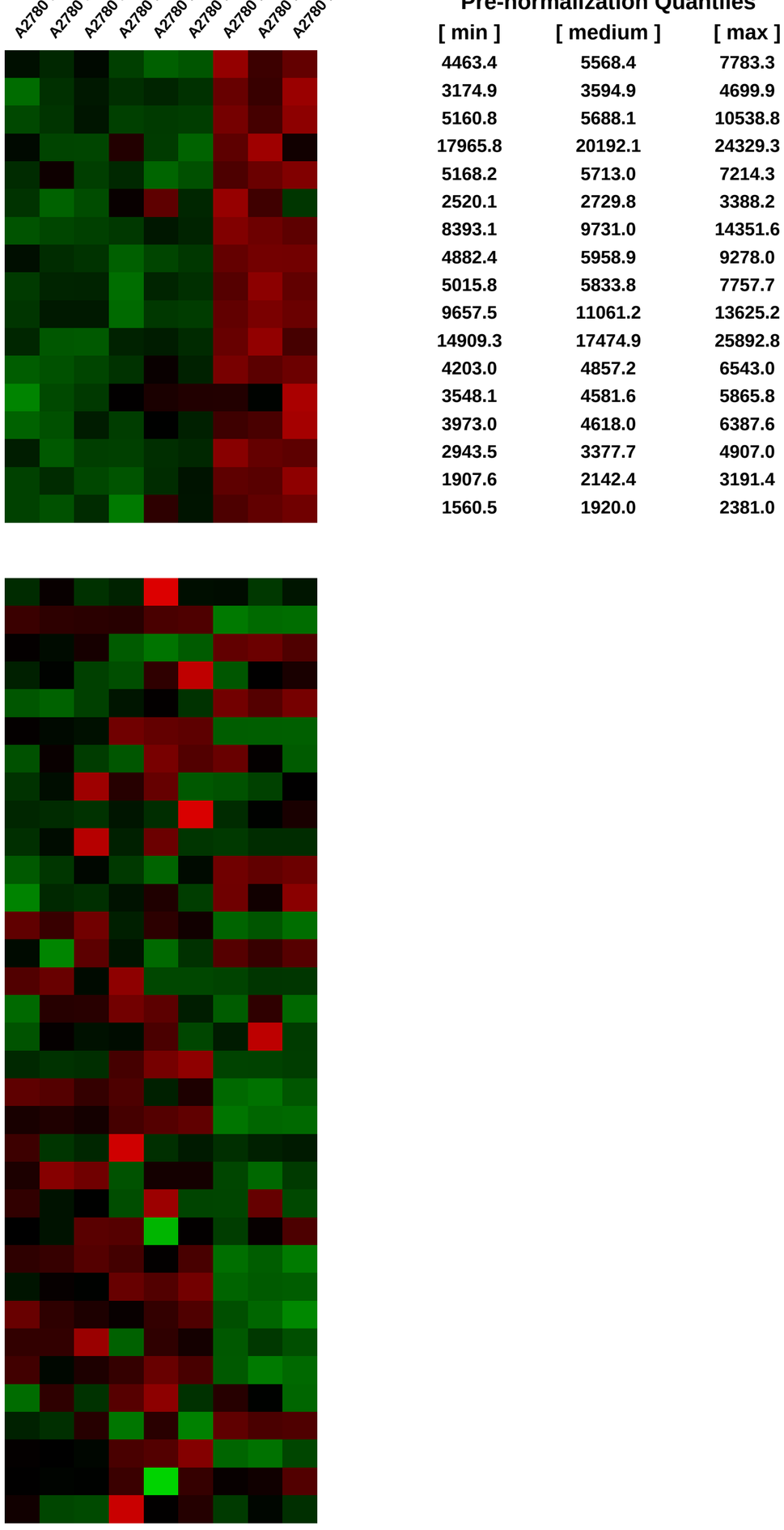

GEO Series "GSE60697" Expression Profiles

Num of samples in this series: 20

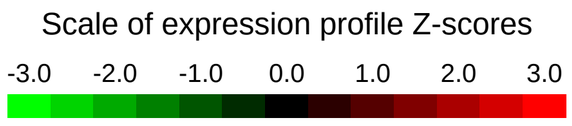

GEO Link:	**http://www.ncbi.nlm.nih.gov/geo/query/acc.cgi?acc=GSE60697**
Status:	**Public on Aug 26 2014**
Title:	**Expression data from 20 human colon cancer**
Organism:	**Homo sapiens**
Experiment type:	**Expression profiling by array**
Platform:	**GPL570**
Pubmed ID:	
Summary & Design:	**Summary:** **We obtained snap-frozen tissue samples from 20 colorectal cancer (CRC) patients with stage III disease who had undergone curative resection. The expression profiles were determined using Affymetrix Human Genome U133Plus 2.0 arrays.** **We used microarrays to identify potential gene deregulation correlated with the outcomes of colon cancer patients.** **Overall design:** **mRNA from 20 primary colorectal tumour samples were extracted and hybridized to HG-U133Plus 2.0 expression arrays. The NexusExp3 procedure was used to make calls of expression. Of the 20 patients, 7 had disease relapse within 3 years after surgery.**

Background corr dist: KL-Divergence = 0.3064, L1-Distance = 0.0665, L2-Distance = 0.0122, Normal std = 0.2791

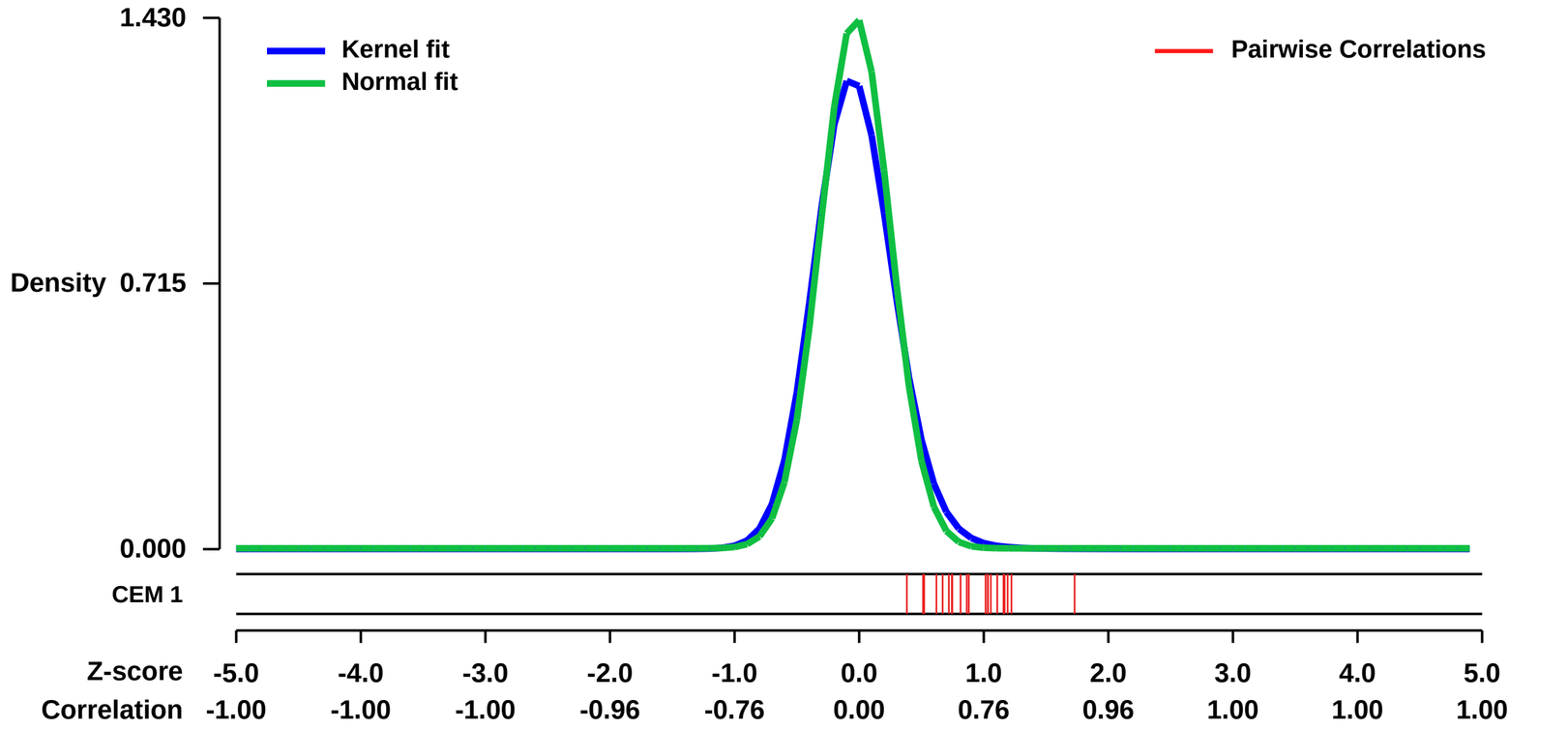

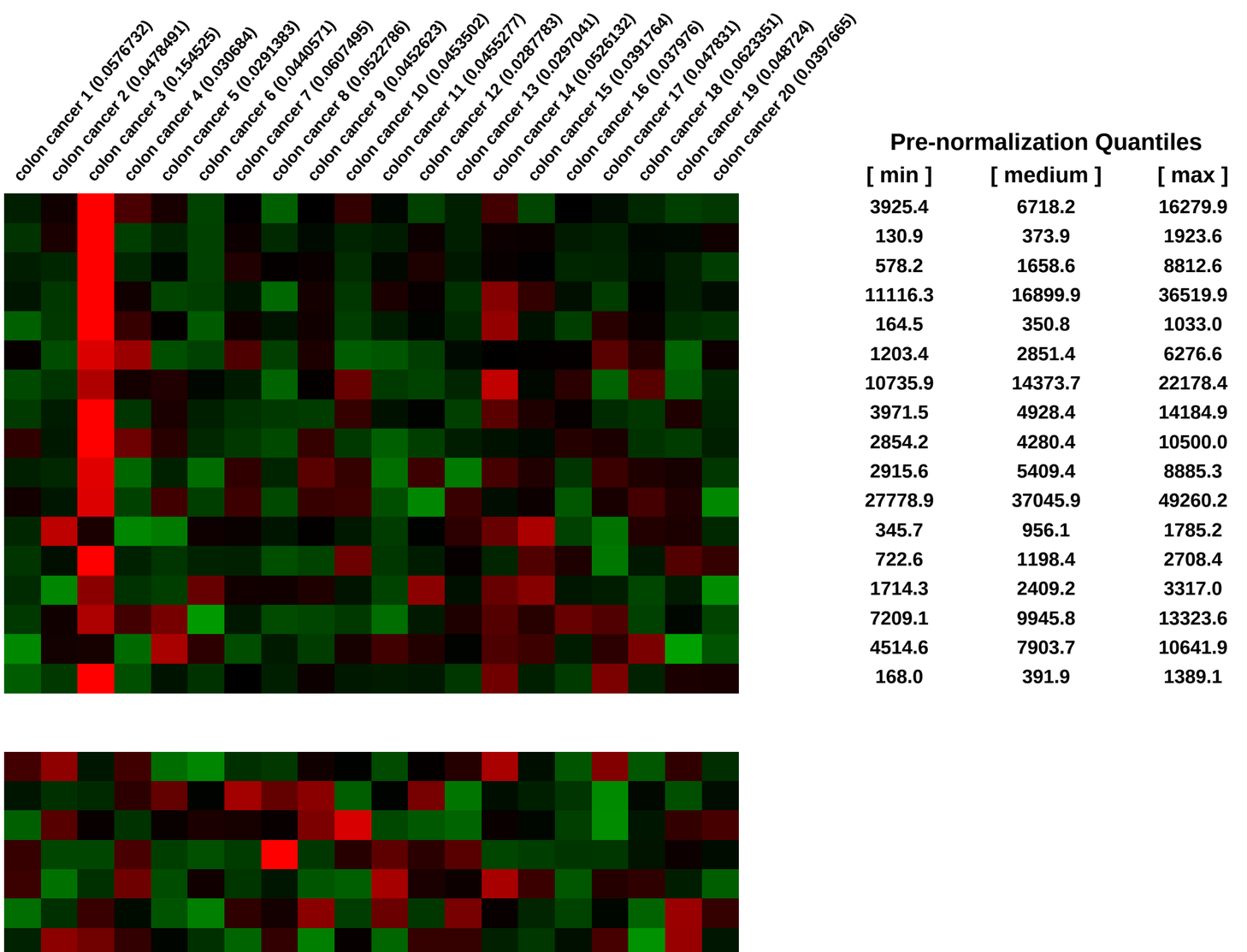

Pre-normalization Quantiles

	[min]	[medium]	[max]
CEM 1			
P (S | Z, I) = 1.00			
Mean Corr = 0.69385			
MANF	**3925.4**	**6718.2**	**16279.9**
SDF2L1	**130.9**	**373.9**	**1923.6**
CRELD2	**578.2**	**1658.6**	**8812.6**
HSPA5	**11116.3**	**16899.9**	**36519.9**
HYOU1	**164.5**	**350.8**	**1033.0**
PDIA4	**1203.4**	**2851.4**	**6276.6**
PDIA6	**10735.9**	**14373.7**	**22178.4**
CEM 1 + Top 10 Genes			
DNAJB11	**3971.5**	**4928.4**	**14184.9**
HSP90B1	**2854.2**	**4280.4**	**10500.0**
PDIA3	**2915.6**	**5409.4**	**8885.3**
PPIB	**27778.9**	**37045.9**	**49260.2**
C19orf10	**345.7**	**956.1**	**1785.2**
SLC35B1	**722.6**	**1198.4**	**2708.4**
SEC61A1	**1714.3**	**2409.2**	**3317.0**
RPN1	**7209.1**	**9945.8**	**13323.6**
DNAJC3	**4514.6**	**7903.7**	**10641.9**
CDK2AP2	**168.0**	**391.9**	**1389.1**
Null module			
ARID5B			
XBP1			
HNRNPAB			
SGK1			
HSPB1			
DDIT4			
ARL4D			
SAP30			
KIAA0408			
GPR17			
HSPH1			
DNASE1L2			
SLC5A3			
GNAS			
GPR3			
TNFRSF25			
TM6SF2			
MKKS			
PLEKHF1			
ZMYM1			
DOK3			
FGF20			
SLC39A2			
KCNIP2			
ERRFI1			
DEDD2			
CCDC117			
USP31			
AHSA2			
CYS1			
CNIH2			
BANP			
CHORDC1			
P4HA1			

GEO Series "GSE15499" Expression Profiles

Num of samples in this series: 6

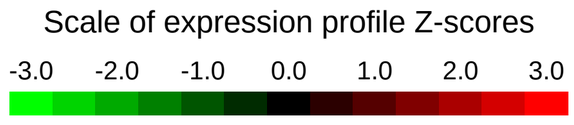

GEO Link:	http://www.ncbi.nlm.nih.gov/geo/query/acc.cgi?acc=GSE15499
Status:	Public on Apr 02 2009
Title:	HDAC5 is a repressor of angiogenesis and determines the angiogenic gene expression pattern of endothelial cells
Organism:	Homo sapiens
Experiment type:	Expression profiling by array
Platform:	GPL570
Pubmed ID:	19351956
Summary & Design:	**Summary:** Class IIa histone deacetylases (HDACs) are signal-responsive regulators of gene expression involved in vascular homeostasis. To investigate the differential role of class IIa HDACs for the regulation of angiogenesis, we used siRNA to specifically suppress the individual HDAC isoenzymes. Among the HDAC isoforms tested, silencing of HDAC5 exhibited a unique pro-angiogenic effect evidenced by increased endothelial cell migration, sprouting and tube formation. Consistently, overexpression of HDAC5 decreased sprout formation, indicating that HDAC5 is a negative regulator of angiogenesis. The anti-angiogenic activity of HDAC5 was independent of MEF2 binding and its deacetylase activity, but required a nuclear localization indicating that HDAC5 might affect the transcriptional regulation of gene expression. To identify putative HDAC5 targets, we performed microarray expression analysis. Silencing of HDAC5 increased the expression of fibroblast growth factor 2 (FGF2) and angiogenic guidance factors including Slit2. Antagonization of FGF2 or Slit2 reduced sprout induction in response to HDAC5 siRNA. ChIP assays demonstrate that HDAC5 binds to the promoter of FGF2 and Slit2. In summary, HDAC5 represses angiogenic genes, like FGF2 and Slit2, which causally contribute to capillary-like sprouting of endothelial cells. The de-repression of angiogenic genes by HDAC5 inactivation may provide a useful therapeutic target for induction of angiogenesis. **Overall design:** 6 samples: 3x siSCRAMBLED transfected HUVEC (control) + 3x siHDAC5 transfected HUVEC 24h after transfection

Background corr dist: KL-Divergence = 0.0300, L1-Distance = 0.0466, L2-Distance = 0.0030, Normal std = 0.7247

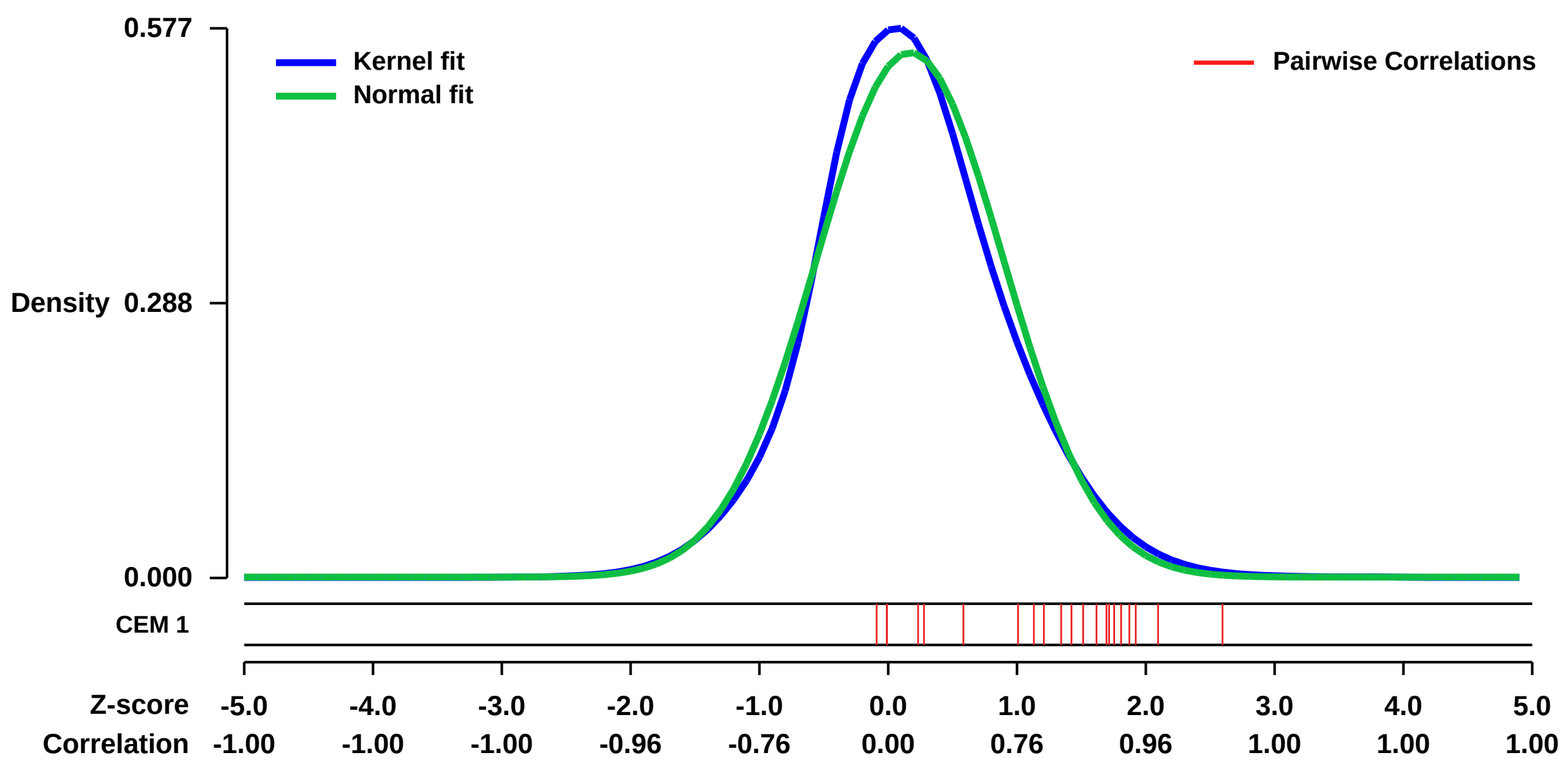

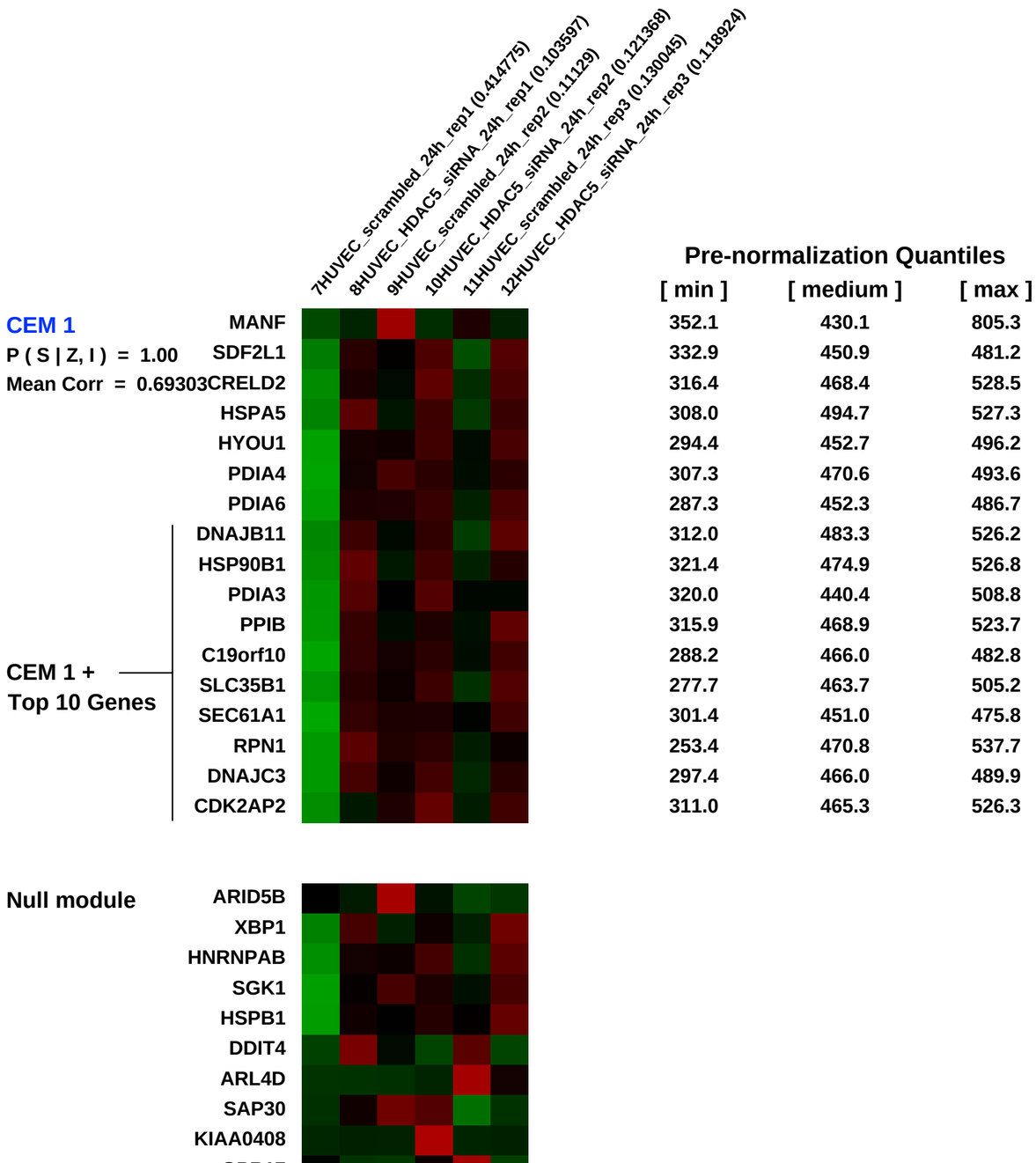

	Pre-normalization Quantiles		
	[min]	[medium]	[max]
MANF	352.1	430.1	805.3
SDF2L1	332.9	450.9	481.2
CRELD2	316.4	468.4	528.5
HSPA5	308.0	494.7	527.3
HYOU1	294.4	452.7	496.2
PDIA4	307.3	470.6	493.6
PDIA6	287.3	452.3	486.7
DNAJB11	312.0	483.3	526.2
HSP90B1	321.4	474.9	526.8
PDIA3	320.0	440.4	508.8
PPIB	315.9	468.9	523.7
C19orf10	288.2	466.0	482.8
SLC35B1	277.7	463.7	505.2
SEC61A1	301.4	451.0	475.8
RPN1	253.4	470.8	537.7
DNAJC3	297.4	466.0	489.9
CDK2AP2	311.0	465.3	526.3
ARID5B			
XBP1			
HNRNPAB			
SGK1			
HSPB1			
DDIT4			
ARL4D			
SAP30			
KIAA0408			
GPR17			
HSPH1			
DNASE1L2			
SLC5A3			
GNAS			
GPR3			
TNFRSF25			
TM6SF2			
MKKS			
PLEKHF1			
ZMYM1			
DOK3			
FGF20			
SLC39A2			
KCNIP2			
ERRFI1			
DEDD2			
CCDC117			
USP31			
AHSA2			
CYS1			
CNIH2			
BANP			
CHORDC1			
P4HA1			

GEO Series "GSE33301" Expression Profiles

Num of samples in this series: 6

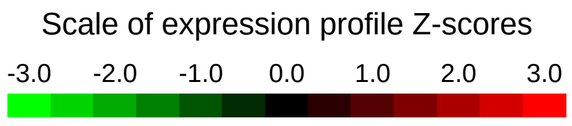

GEO Link:	http://www.ncbi.nlm.nih.gov/geo/query/acc.cgi?acc=GSE33301
Status:	Public on Oct 28 2011
Title:	Expression data from control and COUP-TFII siRNA treated HUVEC cells
Organism:	Homo sapiens
Experiment type:	Expression profiling by array
Platform:	GPL570
Pubmed ID:	22734039
Summary & Design:	**Summary:** COUP-TFII plays a critical role in angiogenesis during development. It has also been shown to suppress Notch signaling pathway to confer vein identity. However, the downstream targets and the mechanism mediate COUP-TFII function to regulate these processes remain elusive. To identify the downstream targets and the mechanism by which COUP-TFII regulates agiogenesis and vein specification, we knocked down COUP-TFII in HUVEC cells using COUP-TFII specific siRNA and used microarray analysis to identify downstream targets. Interestingly, we found the expression of many genes in the cell cycle pathway and Notch signaling pathway are significantly altered in the COUP-TFII depleted cells. **Overall design:** HUVEC Cells were transfected with siRNA (Control or COUP-TFII siRNA) duplexes (50 nM) and total RNA was isolated 48 hours later.

Background corr dist: KL-Divergence = 0.0358, L1-Distance = 0.0272, L2-Distance = 0.0008, Normal std = 0.6480

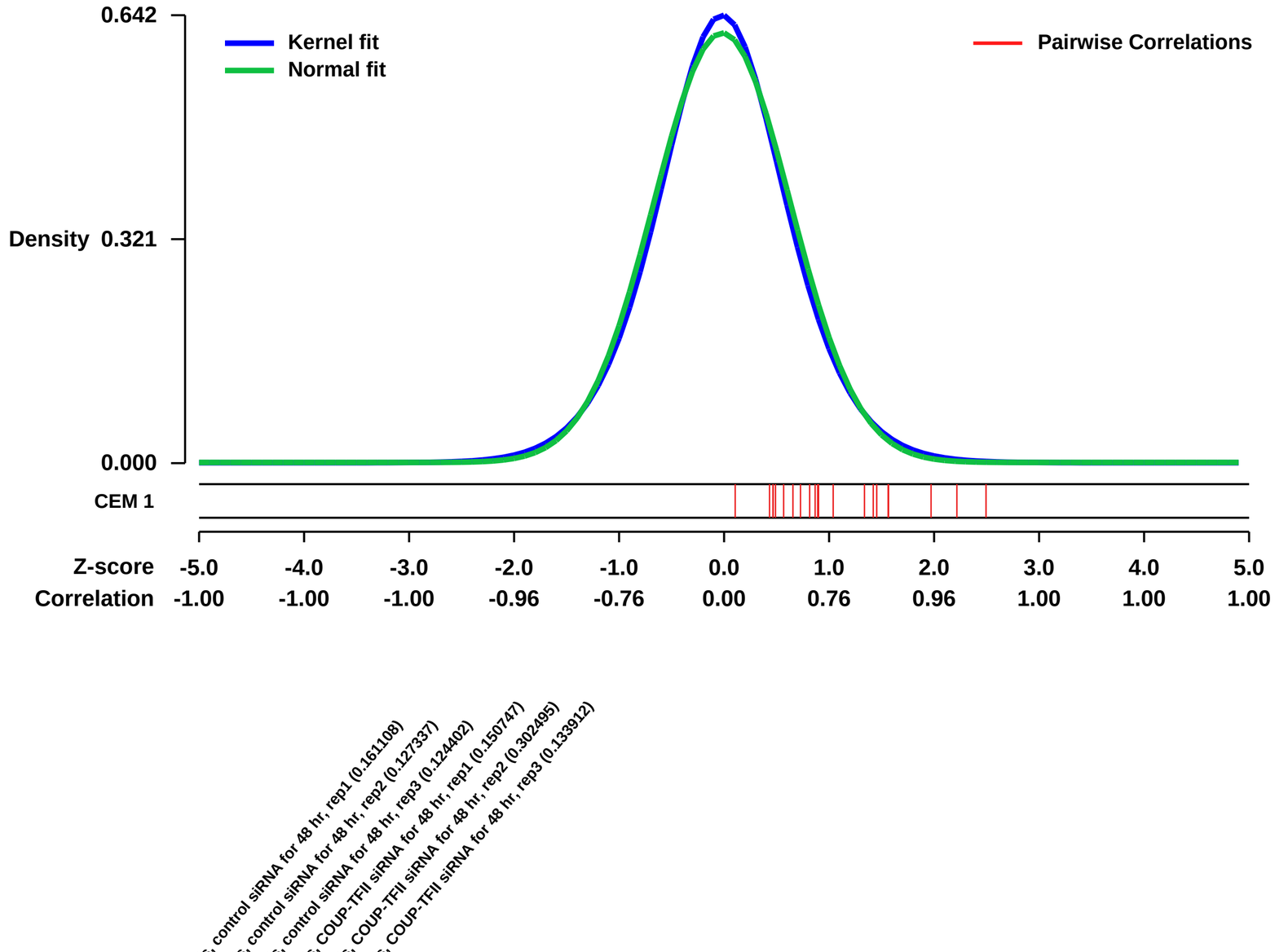

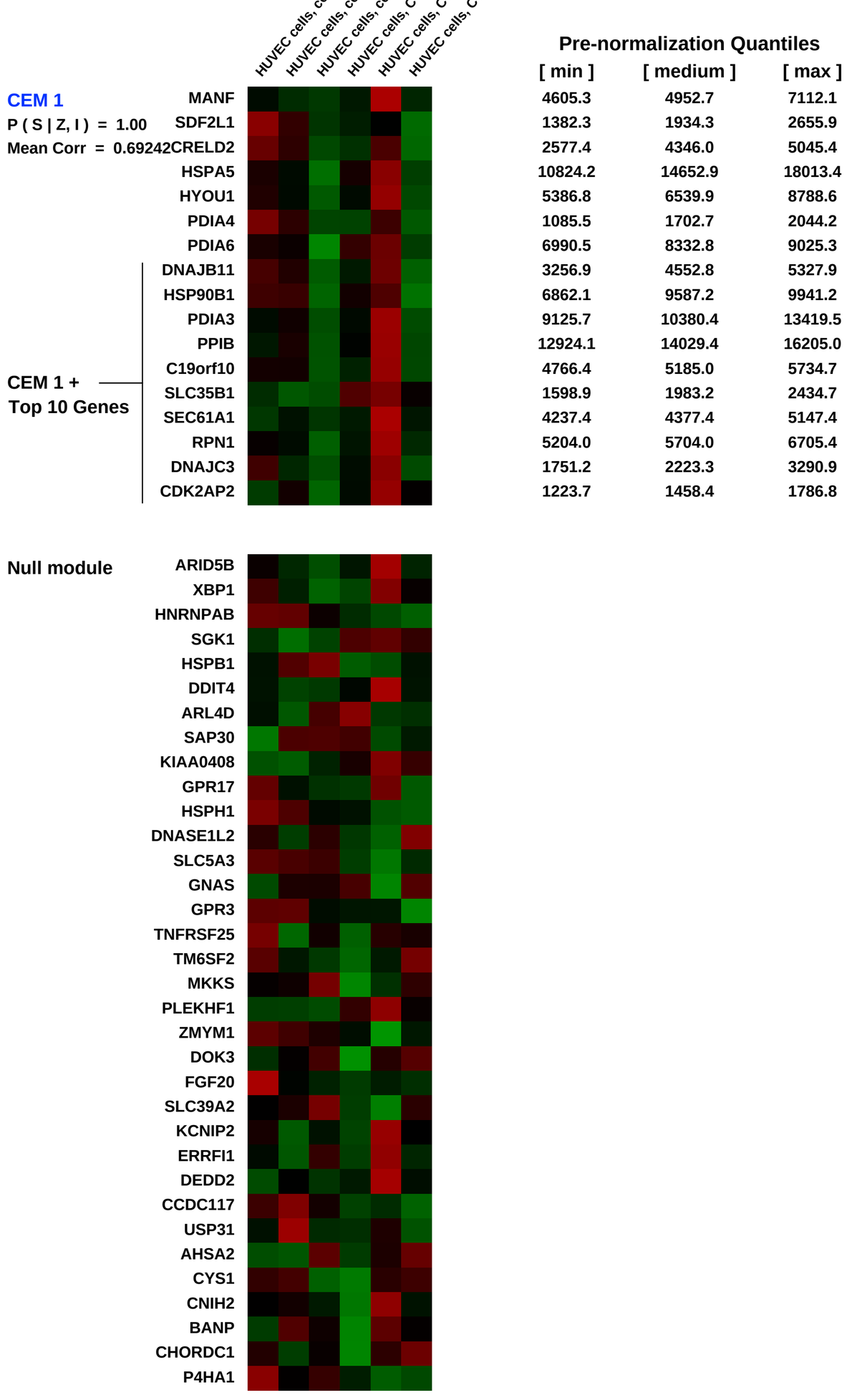

	Pre-normalization Quantiles		
	[min]	[medium]	[max]
MANF	4605.3	4952.7	7112.1
SDF2L1	1382.3	1934.3	2655.9
CRELD2	2577.4	4346.0	5045.4
HSPA5	10824.2	14652.9	18013.4
HYOU1	5386.8	6539.9	8788.6
PDIA4	1085.5	1702.7	2044.2
PDIA6	6990.5	8332.8	9025.3
DNAJB11	3256.9	4552.8	5327.9
HSP90B1	6862.1	9587.2	9941.2
PDIA3	9125.7	10380.4	13419.5
PPIB	12924.1	14029.4	16205.0
C19orf10	4766.4	5185.0	5734.7
SLC35B1	1598.9	1983.2	2434.7
SEC61A1	4237.4	4377.4	5147.4
RPN1	5204.0	5704.0	6705.4
DNAJC3	1751.2	2223.3	3290.9
CDK2AP2	1223.7	1458.4	1786.8

GEO Series "GSE13639" Expression Profiles

Num of samples in this series: 12

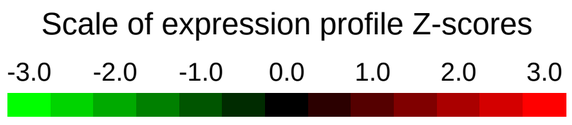

GEO Link:	http://www.ncbi.nlm.nih.gov/geo/query/acc.cgi?acc=GSE13639
Status:	Public on Feb 05 2009
Title:	Drosha or DGCR8 knockdown effects on mRNA levels in HeLa
Organism:	Homo sapiens
Experiment type:	Expression profiling by array
Platform:	GPL570
Pubmed ID:	19135890
Summary & Design:	**Summary:** Anaysis of mRNA changes in HeLa cells following knockdown of Drosha or DGCR8. Drosha is a nuclear RNase III that carries out microRNA (miRNA) processing by cleaving primary microRNA transcript (pri-miRNA). DGCR8 is an essential co-factor of Drosha. Keywords: gene expression array-based (RNA / in situ oligonucleotide) **Overall design:** siRNA against Drosha or DGCR8 were trasnfected into HeLa cells. siRNA against GFP was used as a control. Biologically duplicated total RNAs were prepared from HeLa cells, 24 hrs and 48 hrs after siRNA transfection.

Background corr dist: KL-Divergence = 0.1654, L1-Distance = 0.0404, L2-Distance = 0.0034, Normal std = 0.3587

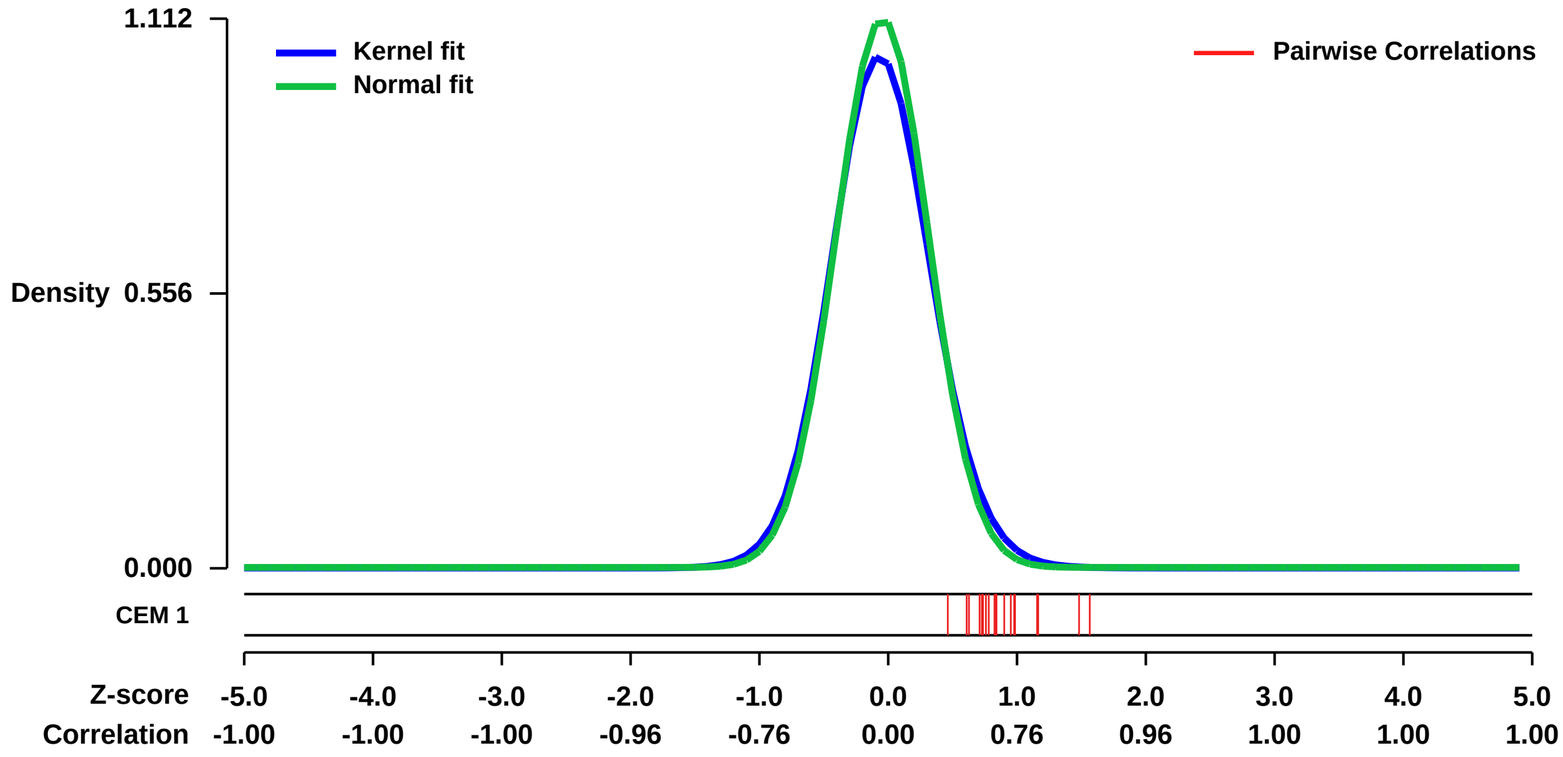

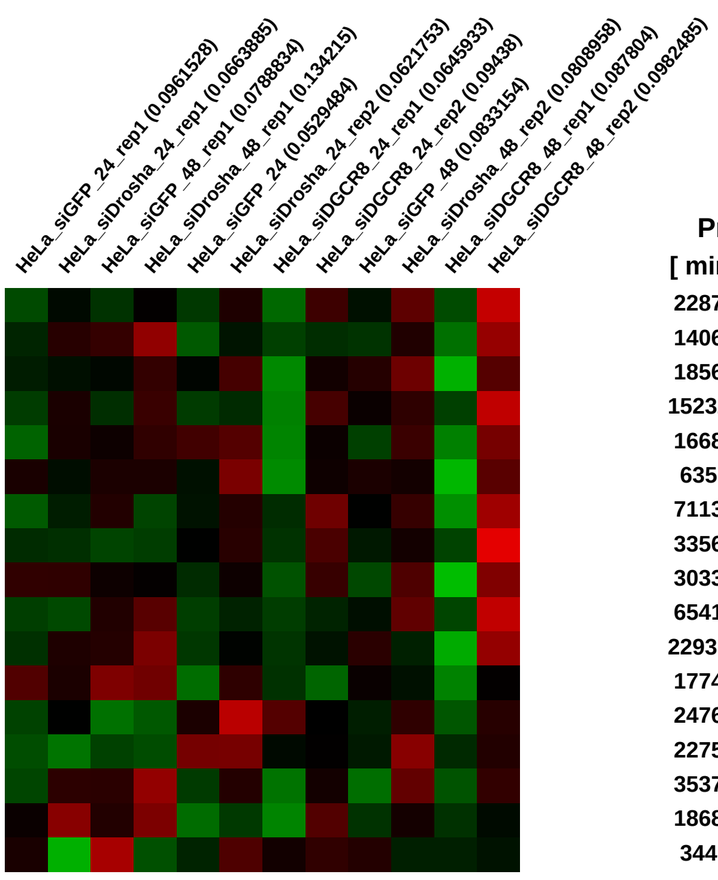

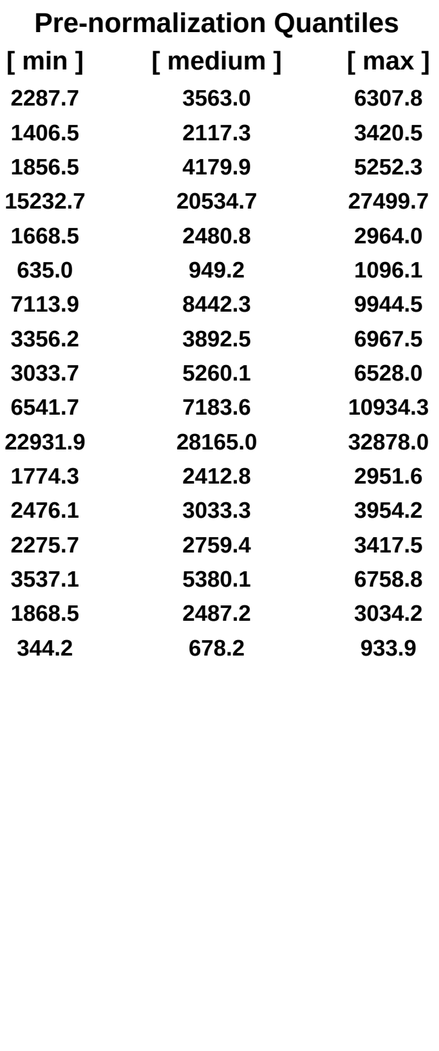

GEO Series "GSE41326" Expression Profiles

Num of samples in this series: 6

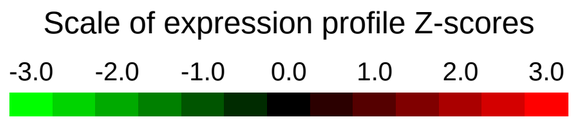

GEO Link:	http://www.ncbi.nlm.nih.gov/geo/query/acc.cgi?acc=GSE41326
Status:	Public on Oct 04 2012
Title:	Expression data from HepG2 cells before and after RNF43 knockdown
Organism:	Homo sapiens
Experiment type:	Expression profiling by array
Platform:	GPL570
Pubmed ID:	23136185
Summary & Design:	**Summary:** It has been demonstrated that Ring finger protein 43 (RNF43) is overexpressed in colorectal cancer and mediates cancer cell proliferation. We found that RNF43 was frequently overexpressed in HCC, and knockdown of RNF43 could induce apoptosis and inhibit proliferation, invasion, colony formation and xenograft growth of HCC cells. Suggesting that RNF43 is involved in tumorigenesis and progression of HCC. We used microarrays to profile gene expression patterns before and after RNF43 knockdown, and identified differentially expressed genes during this process. **Overall design:** HepG2 cells were transfected with RNF43 siRNA or negative control siRNA in triplicate. Forty-eight hours after transfection, total RNA was extracted,labeled and hybridized to HG-U133 Plus 2.0 arrays.

Background corr dist: KL-Divergence = 0.0397, L1-Distance = 0.0240, L2-Distance = 0.0006, Normal std = 0.6245

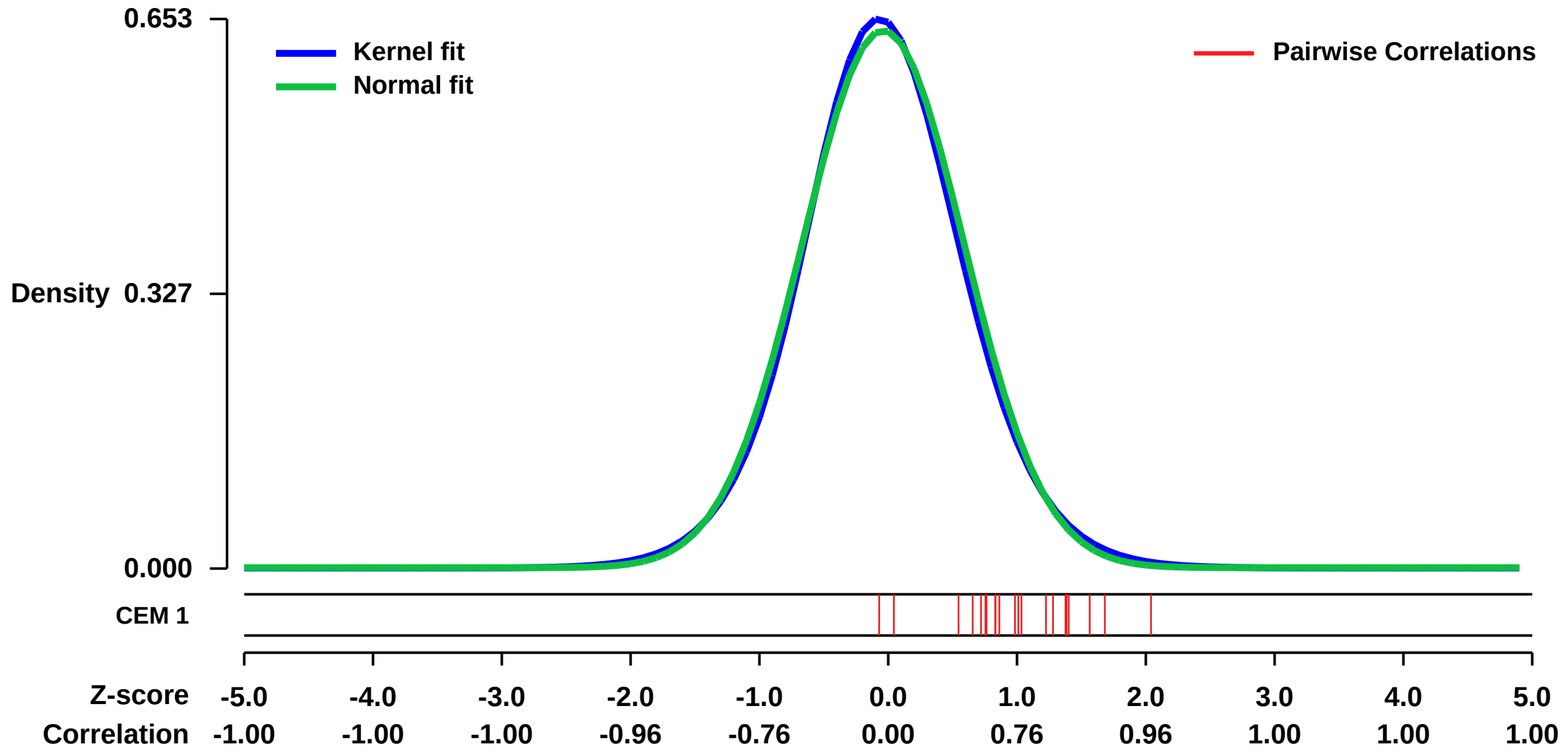

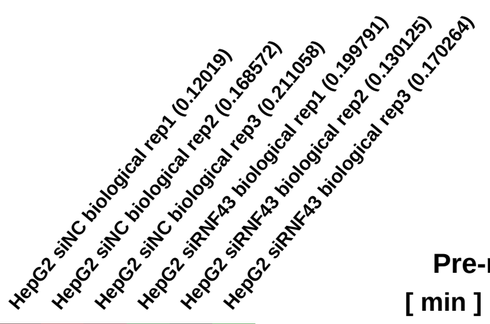

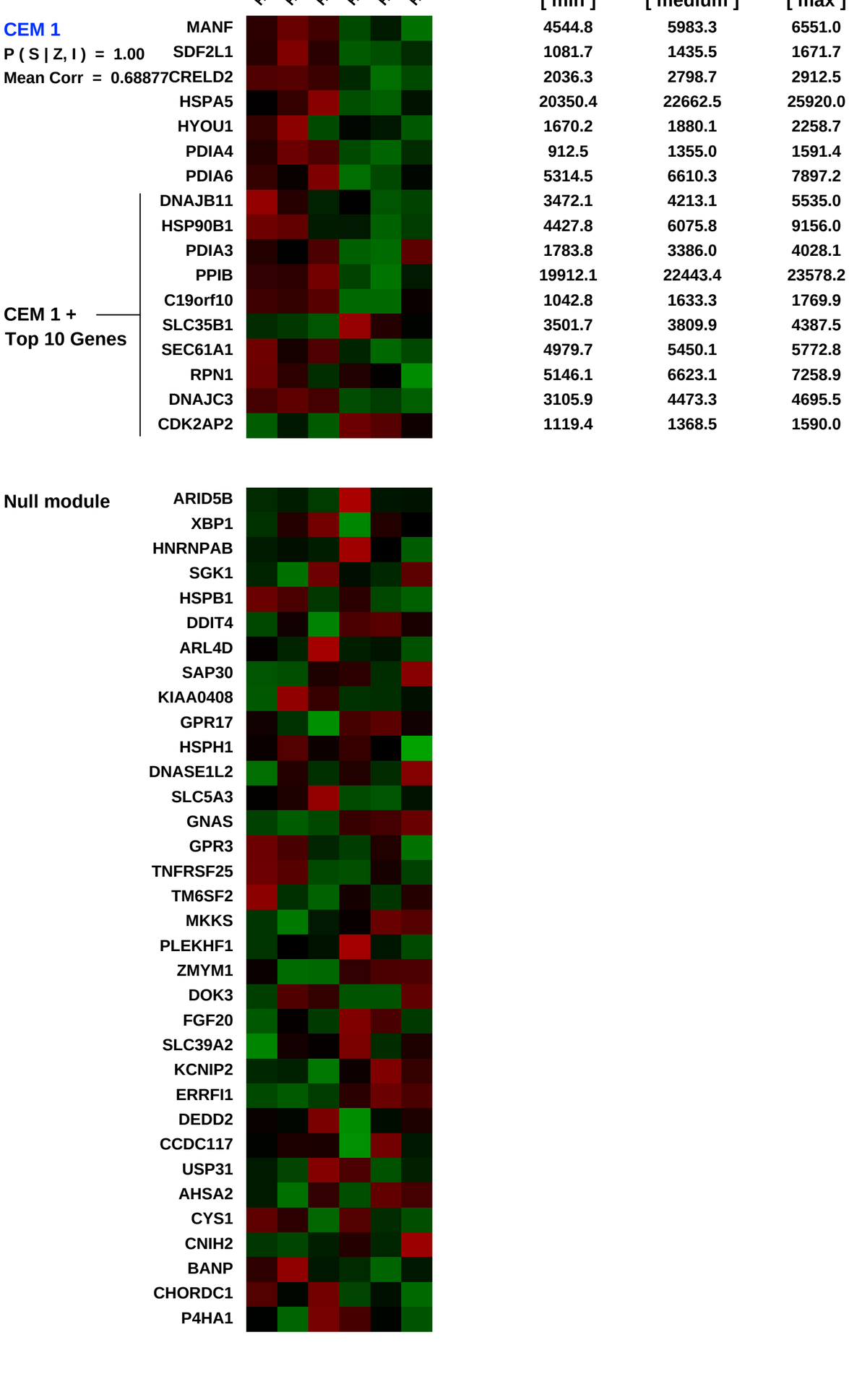

GEO Series "GSE18668" Expression Profiles

Num of samples in this series: 20

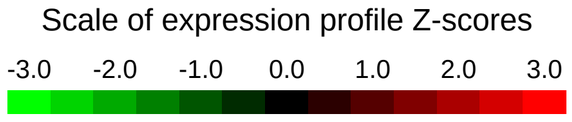

GEO Link:	http://www.ncbi.nlm.nih.gov/geo/query/acc.cgi?acc=GSE18668
Status:	Public on Jul 01 2011
Title:	Differentiation of NUT midline carcinoma by epigenomic reprogramming
Organism:	Homo sapiens
Experiment type:	Expression profiling by array
Platform:	GPL570
Pubmed ID:	21447744
Summary & Design:	**Summary:** Knockdown of the oncogene, BRD4-NUT, in a rare cancer, termed NUTmidline carcinoma (NMC), results in morphologic features consistent with squamous differentiation. Treatment with the HDAC-inhibitor, TSA, appears to cause the same phenotype. Here, we use gene expression profiling to compare the changes in gene expression following BRD4-NUT knockdown and TSA treatment. **Overall design:** RNA was extracted from two BRD4-NUT-expressing NMC cell lines, PER-403 and TC-797, 24h following siRNA knockdown versus control in duplicate. RNA was extracted from two BRD4-NUT-expressing NMC cell lines, PER-403 and TC-797, 24h following treatment with TSA versus etoh control in triplicate

Background corr dist: KL-Divergence = 0.1225, L1-Distance = 0.0288, L2-Distance = 0.0017, Normal std = 0.4092

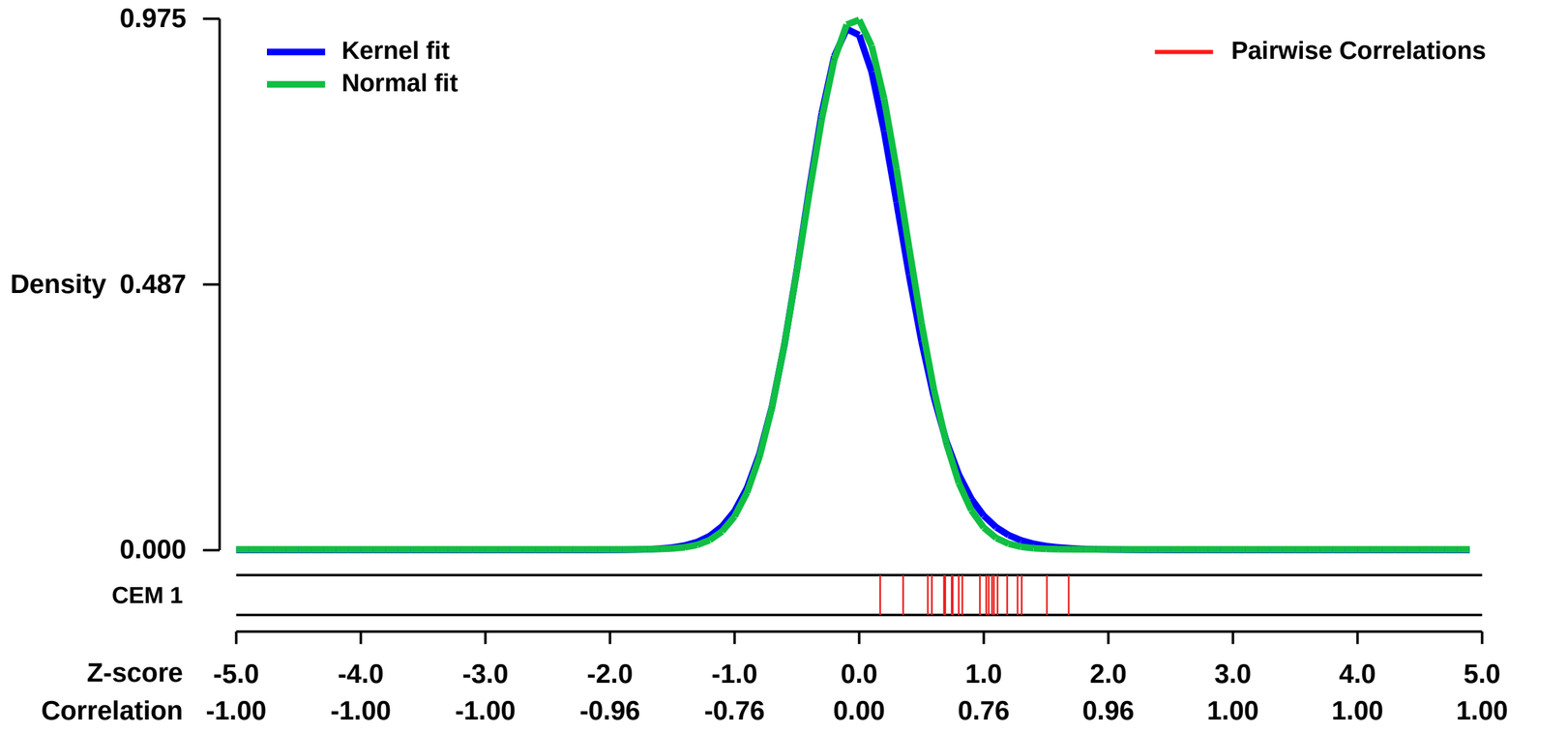

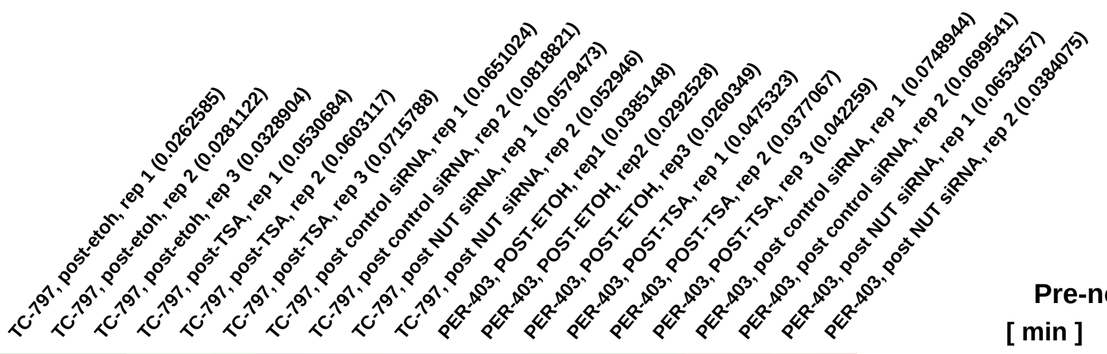

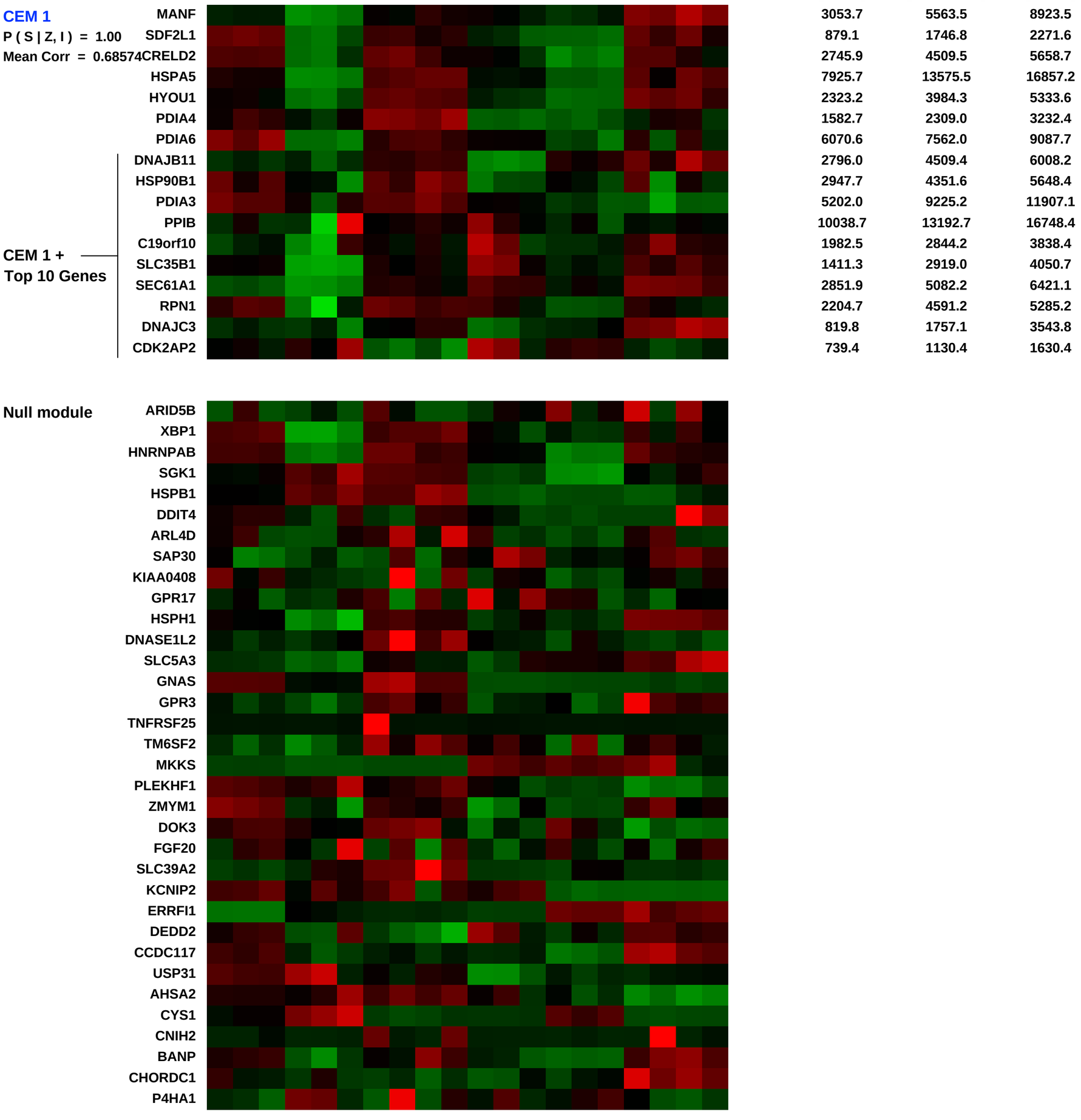

GEO Series "GSE15322" Expression Profiles

Num of samples in this series: 6

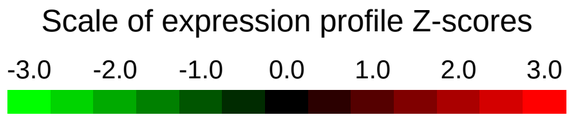

GEO Link:	http://www.ncbi.nlm.nih.gov/geo/query/acc.cgi?acc=GSE15322
Status:	Public on Mar 21 2009
Title:	Comparative transcriptomic profiling of human colon cells (CCD-18Co) exposed to an orange extract rich in flavanones
Organism:	Homo sapiens
Experiment type:	Expression profiling by array
Platform:	GPL570
Pubmed ID:	19728713
Summary & Design:	**Summary:** We used microarrays to investigate gene expression changes in human colon normal fibroblasts exposed to a bitter orange extract enriched in flavanones (and previously subjected to in vitro gastro-duodenal digestion) to determine possible modulatory beneficial effects induced by these plant-derived compounds on the colon cells. **Keywords: Comparative gene expression, Control vs Treated cells (response to exposure with xenobiotics plant polyphenols)** **Overall design:** We used ~90% confluent monolayers of colon CCD-18Co cells exposed to either small doses of pre-digested extract from bitter orange containing a mixture of flavanones (Treated) or equivalent quantities of digestive enzymes and salts (Control). Treatments were done in triplicate.

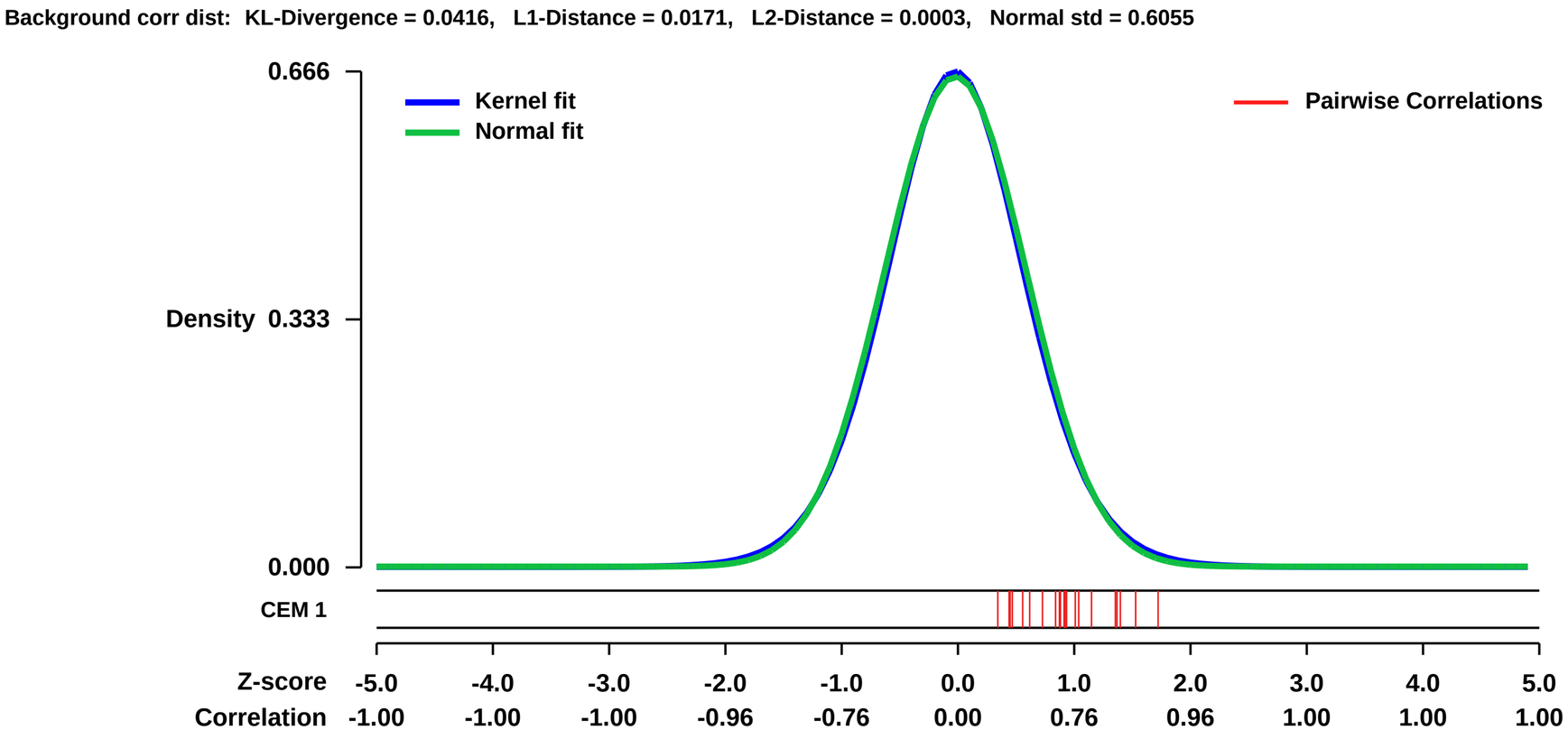

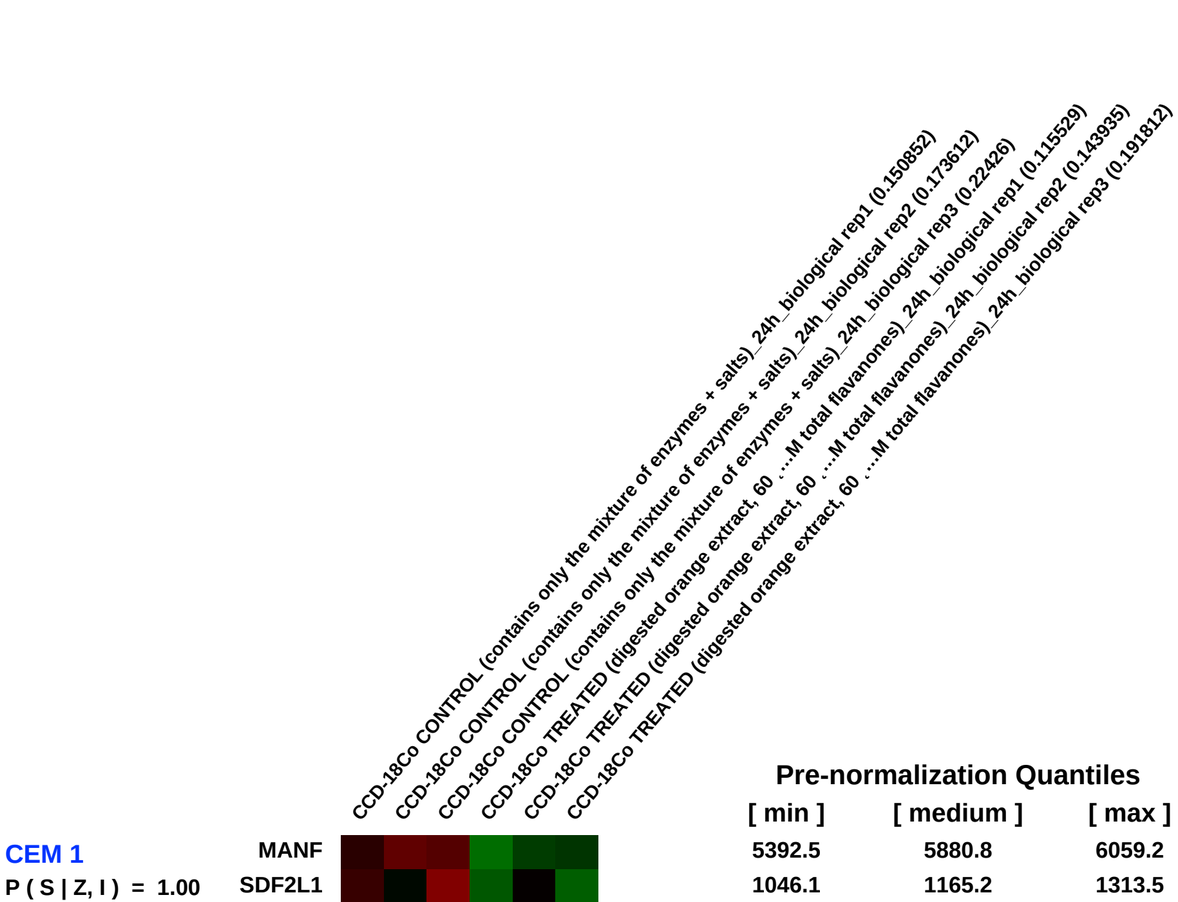

GEO Series "GSE27850" Expression Profiles

Num of samples in this series: 25

Scale of expression profile Z-scores

-3.0 -2.0 -1.0 0.0 1.0 2.0 3.0

GEO Link: http://www.ncbi.nlm.nih.gov/geo/query/acc.cgi?acc=GSE27850

Status: Public on Mar 09 2011

Title: HAV acute infection in chimpanzees

Organism: Pan troglodytes

Experiment type: Expression profiling by array

Platform: GPL570

Pubmed ID: 21690403

Summary & Design:

Summary:
Hepatitis A virus (HAV) is a hepatotropic human picornavirus that has been associated only with acute infection. Its pathogenesis is not well understood since there have been few recent studies in animal models using modern methodologies. We characterized HAV infections in three chimpanzees, quantifying viral RNA by qRT-PCR and examining critical aspects of the innate immune response including intrahepatic interferon-stimulated gene expression. We compared these infection profiles with similar studies of chimpanzees infected with hepatitis C virus (HCV), a hepatotropic flavivirus that frequently causes persistent infection. Surprisingly, HAV-infected animals exhibited very limited induction of type I interferon-stimulated genes in the liver compared to chimpanzees with acute resolving HCV infection, despite similar levels of viremia and 100-fold greater quantities of viral RNA in the liver. Minimal ISG15 and IFIT1 responses peaked 1-2 weeks after HAV challenge, then subsided despite continuing high hepatic viral loads. An acute inflammatory response at 3-4 weeks correlated with the appearance of virus-specific antibodies, and both apoptosis and proliferation of hepatocytes. Despite this, HAV RNA persisted in the liver for months, remaining present long after its clearance from serum and feces and revealing dramatic differences in the kinetics of clearance in the three compartments. Viral RNA was detected in the liver for significantly longer (35 to >48 weeks) than HCV RNA in animals with acute resolving HCV infection (10-20 weeks). Collectively, these findings suggest that early HAV infection is far stealthier than HCV infection and represents a distinctly different paradigm in viral-host interactions within the liver.

Overall design:
Chimpanzee liver was biopsied during an acute HAV infection. Chimp 1 and 2 had two baseline samples. Chimp 3 used the baselines from chimps 1 and 2. Chimp 1 had 8 samples during the HAV acute infection. Chimp 2 had 9 samples during the HAV acute infection. Chimp 3 had 4 samples during the HAV acute infection.

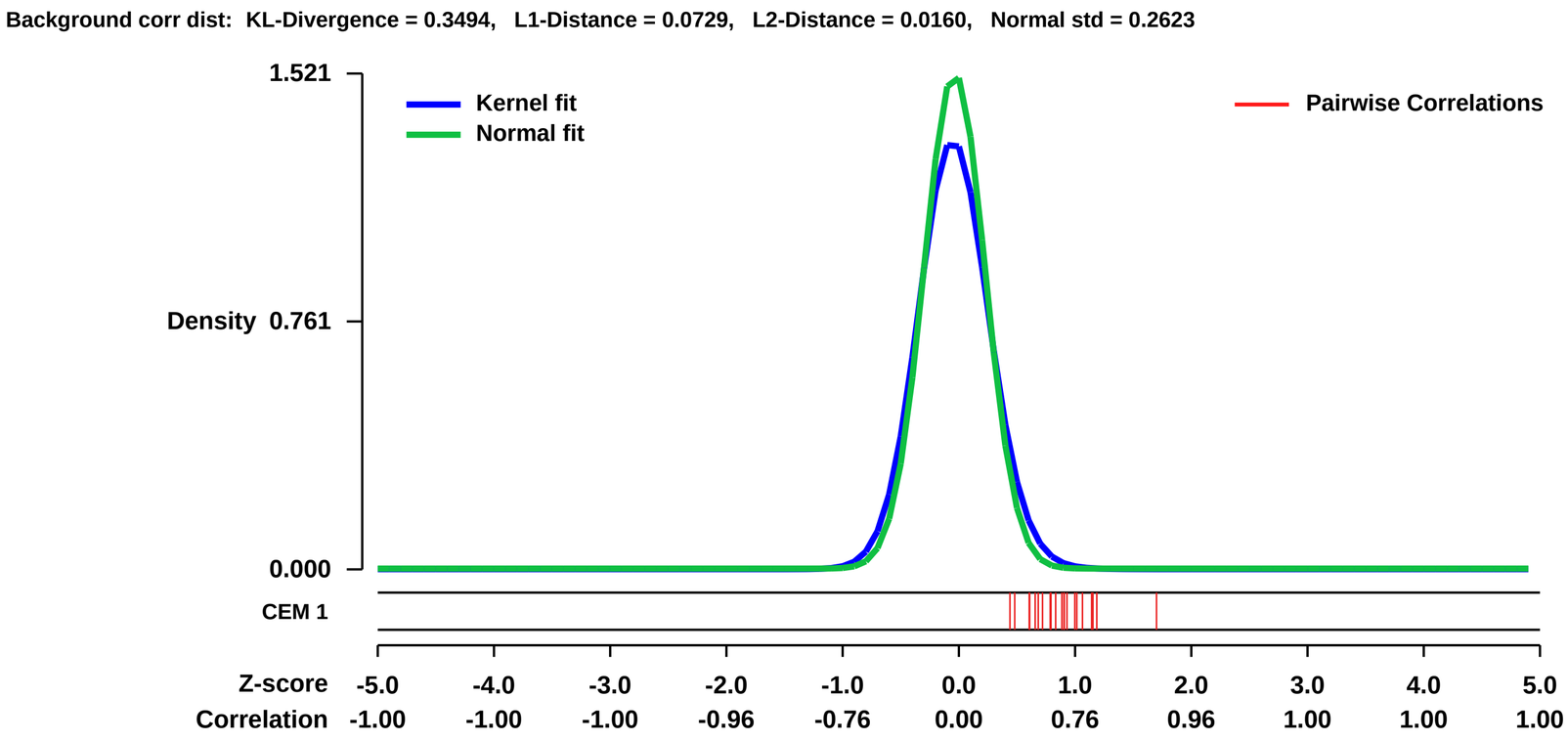

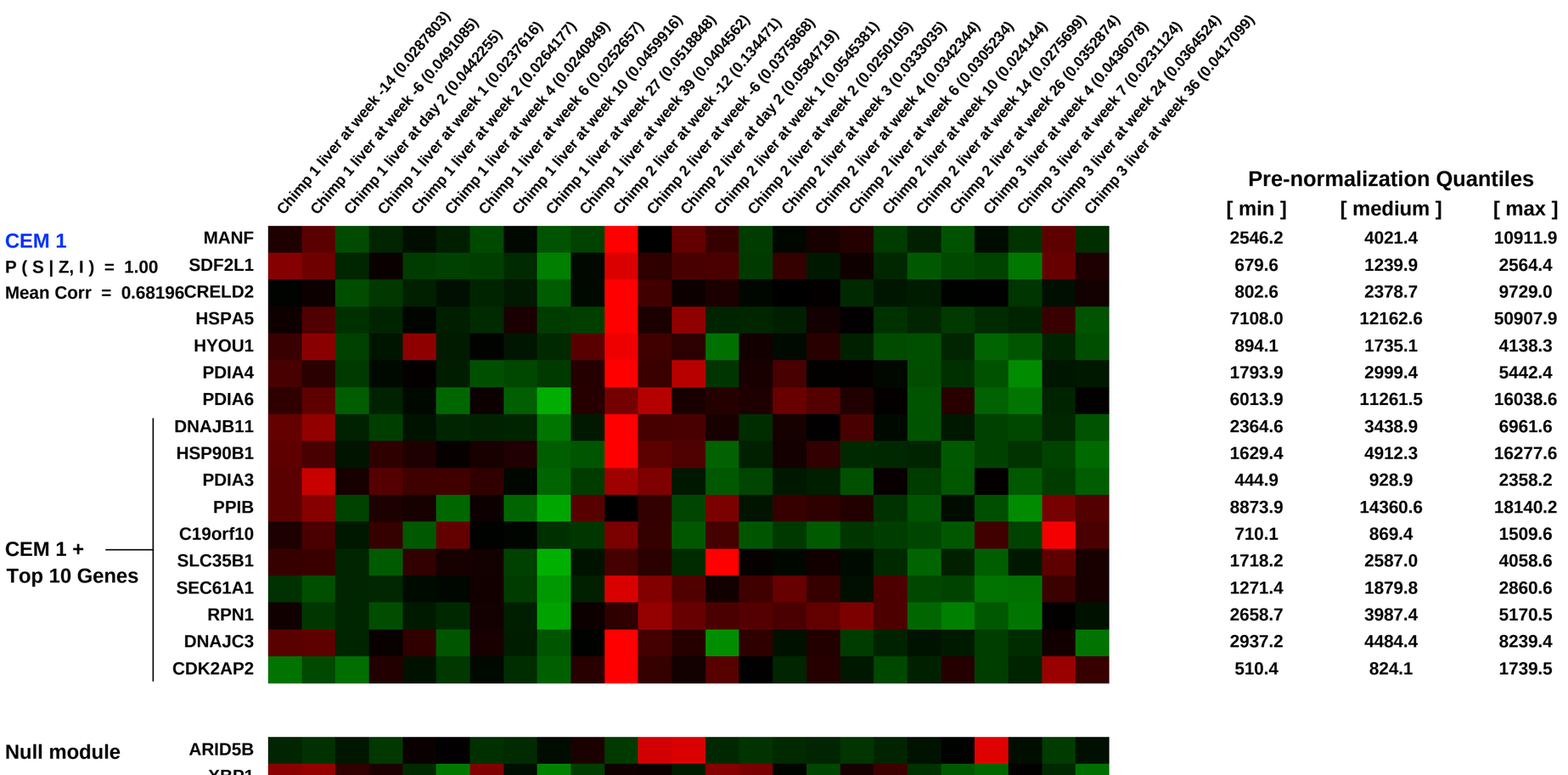

Pre-normalization Quantiles

	[min]	[medium]	[max]
MANF	2546.2	4021.4	10911.9
SDF2L1	679.6	1239.9	2564.4
CRELD2	802.6	2378.7	9729.0
HSPA5	7108.0	12162.6	50907.9
HYOU1	894.1	1735.1	4138.3
PDIA4	1793.9	2999.4	5442.4
PDIA6	6013.9	11261.5	16038.6
DNAJB11	2364.6	3438.9	6961.6
HSP90B1	1629.4	4912.3	16277.6
PDIA3	444.9	928.9	2358.2
PPIB	8873.9	14360.6	18140.2
C19orf10	710.1	869.4	1509.6
SLC35B1	1718.2	2587.0	4058.6
SEC61A1	1271.4	1879.8	2860.6
RPN1	2658.7	3987.4	5170.5
DNAJC3	2937.2	4484.4	8239.4
CDK2AP2	510.4	824.1	1739.5

GEO Series "GSE31595" Expression Profiles

Num of samples in this series: 37

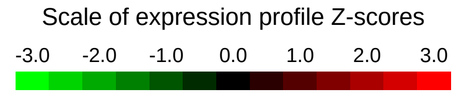

GEO Link:	http://www.ncbi.nlm.nih.gov/geo/query/acc.cgi?acc=GSE31595
Status:	Public on Sep 01 2011
Title:	Gene Expression Profiles in Stage II and III Colon Cancer. Application of a 128-gene signature
Organism:	Homo sapiens
Experiment type:	Third-party reanalysis
Platform:	GPL570
Pubmed ID:	
Summary & Design:	**Summary:** Purpose: A 128-gene signature has been proposed to predict poor outcomes in patients with stage II and III colorectal cancer. In the present study we aimed to validate this previously published 128-gene signature on external and independent data from patients with stage II and III colon cancer. **Overall design:** Tumor samples were obtained from 37 patients with stage II and III colon cancer, who underwent colon resection at the Department of Surgery, Roskilde Hospital, Denmark and the Department of Surgery, Bispebjerg Hospital, Denmark between 2001 and 2008. Purified tumor RNA was reverse-transcribed, labelled and hybridized to Affymetrix Human Genome U133 Plus 2.0 GeneChip Array (Affymetrix, Santa Clara, USA) according to the manufacturers instructions and scanned at the RH Microarray Center, Rigshospitalet, University of Copenhagen.

Background corr dist: KL-Divergence = 0.4153, L1-Distance = 0.0859, L2-Distance = 0.0236, Normal std = 0.2442

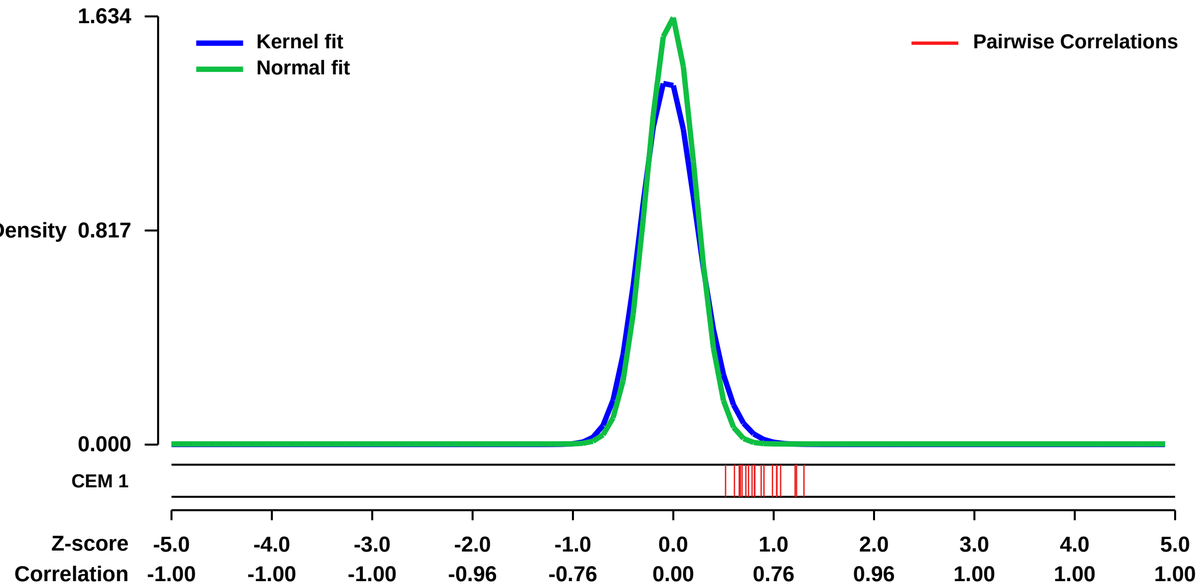

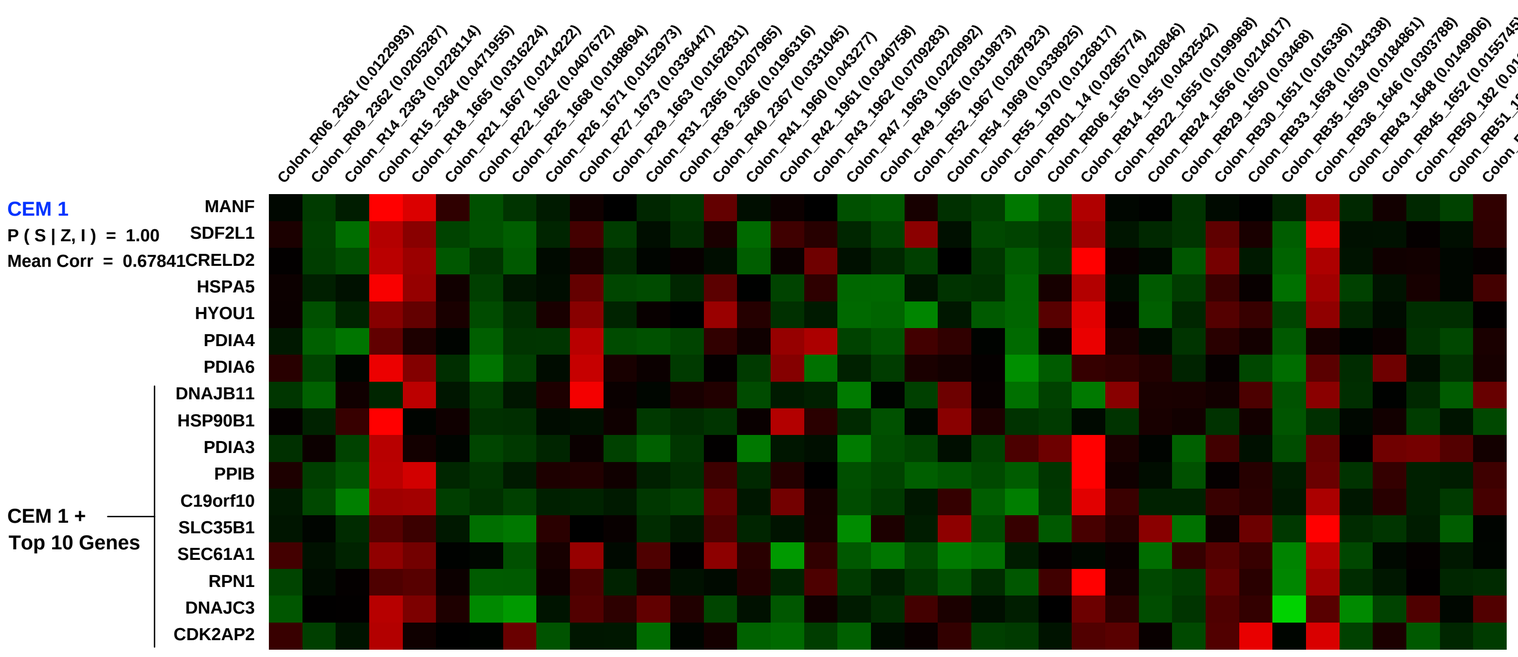

Pre-normalization Quantiles

	[min]	[medium]	[max]
MANF	1528.8	2874.7	6403.1
SDF2L1	817.3	1467.7	3231.0
CRELD2	1268.2	2229.4	5125.9
HSPA5	6496.6	8959.2	15843.4
HYOU1	1559.2	2979.9	6174.3
PDIA4	981.2	1947.1	3948.8
PDIA6	3494.4	5715.3	9591.5
DNAJB11	2753.8	3704.4	5752.2
HSP90B1	2346.2	3080.5	7071.2
PDIA3	3783.8	6447.2	13110.8
PPIB	7593.8	9846.2	20304.5
C19orf10	1559.6	2494.8	4837.5
SLC35B1	915.8	1604.6	3351.6
SEC61A1	2222.4	3243.5	4530.5
RPN1	2161.8	3169.9	6182.3
DNAJC3	1749.8	3514.8	5035.9
CDK2AP2	895.4	1271.9	2218.4

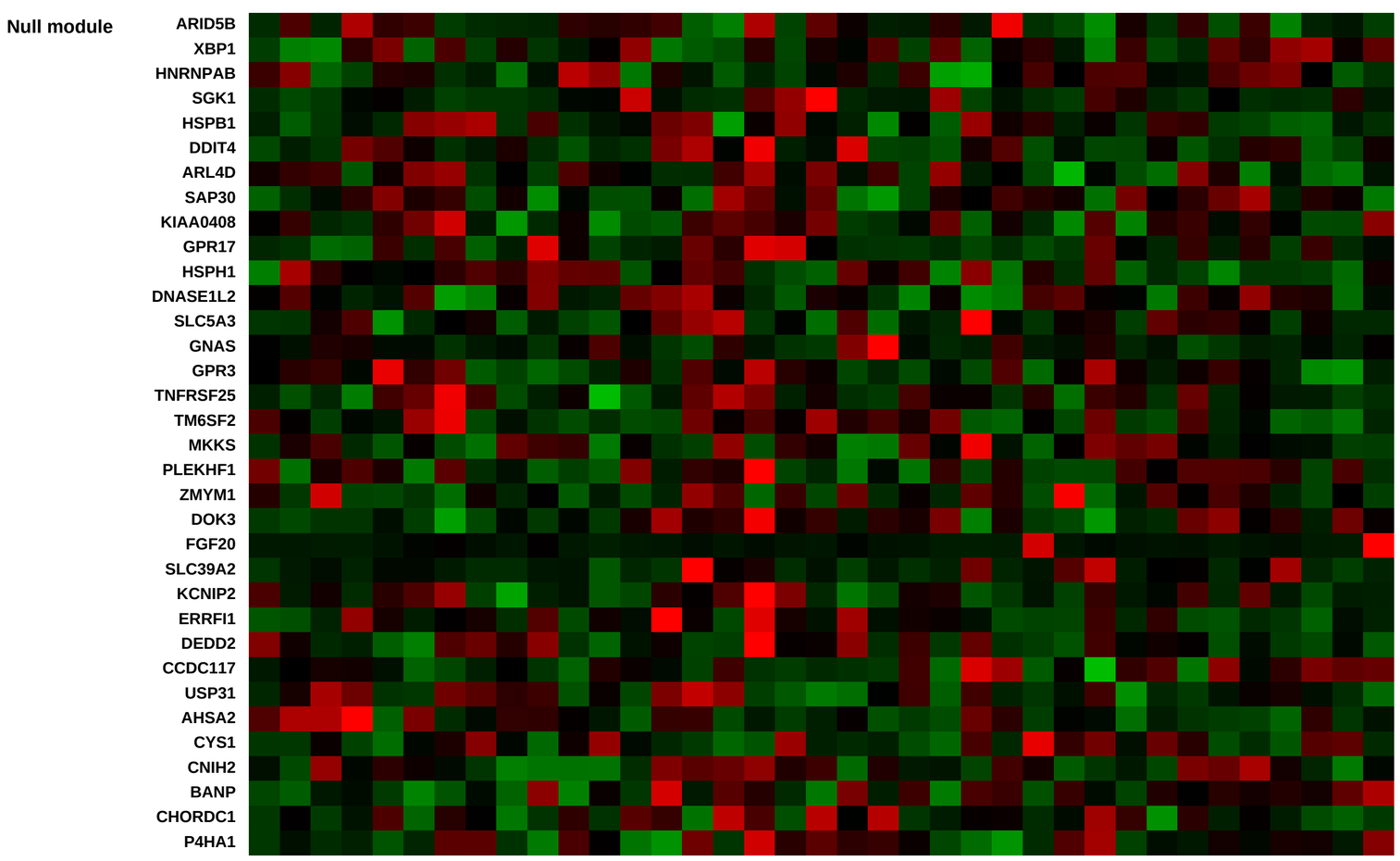

GEO Series "GSE11142" Expression Profiles

Num of samples in this series: 18

Scale of expression profile Z-scores

-3.0 -2.0 -1.0 0.0 1.0 2.0 3.0

GEO Link: http://www.ncbi.nlm.nih.gov/geo/query/acc.cgi?acc=GSE11142

Status: Public on Apr 12 2008

Title: Nicotine effect on CEM model T cell line (kuo-affy-human-232861)

Organism: Homo sapiens

Experiment type: Expression profiling by array

Platform: GPL570

Pubmed ID:

Summary & Design:

Summary:
The long-term objective of this project is to establish roles played in development and function of the immune system by nicotinic acetylcholine receptors (nAChR) and exposure to the tobacco alkaloid, nicotine. The planned gene chip studies will allow us to assess effects of nicotine exposure on gene expression in a model T cell line, and the findings are expected to help direct further efforts. One of the biomedically-relevant hypotheses of this project is that tobacco use and nicotine exposure affect immune system development.

To establish effects of nicotine exposure on gene expression in the CEM model T cell line.

Immune system nAChR acting as ion channels or via novel signaling cascades mediate their effects on T cell development by altering expression of genes involved in T cell receptor rearrangements, cytokine expression, and cell death/survival decisions.

CEM cells will be treated for one hour or one day with an effective dose of nicotine or with the same medium change but in the absence of nicotine.

Keywords: nicotine, T cell line

Overall design:

Background corr dist: KL-Divergence = 0.2044, L1-Distance = 0.0345, L2-Distance = 0.0022, Normal std = 0.3323

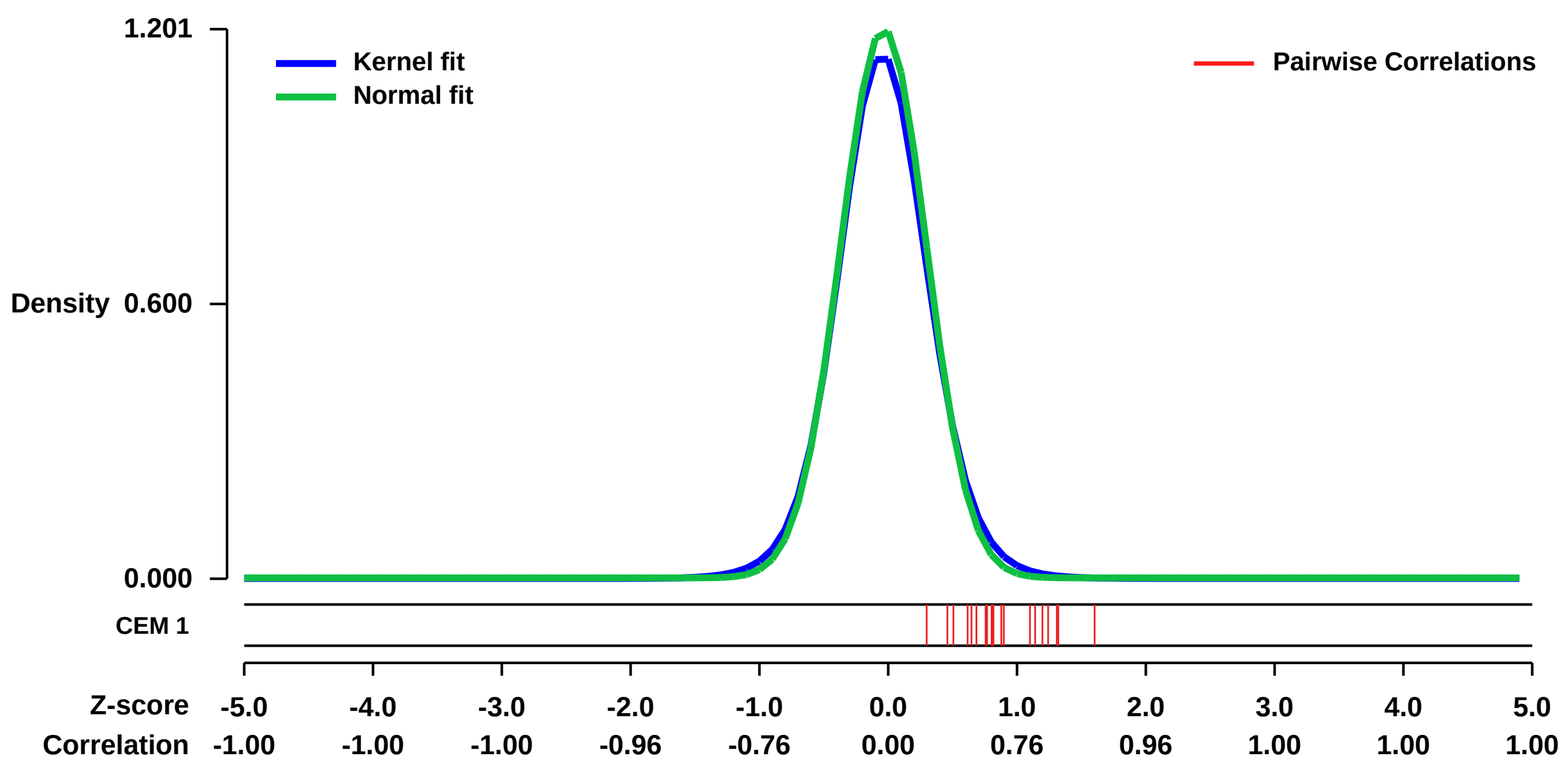

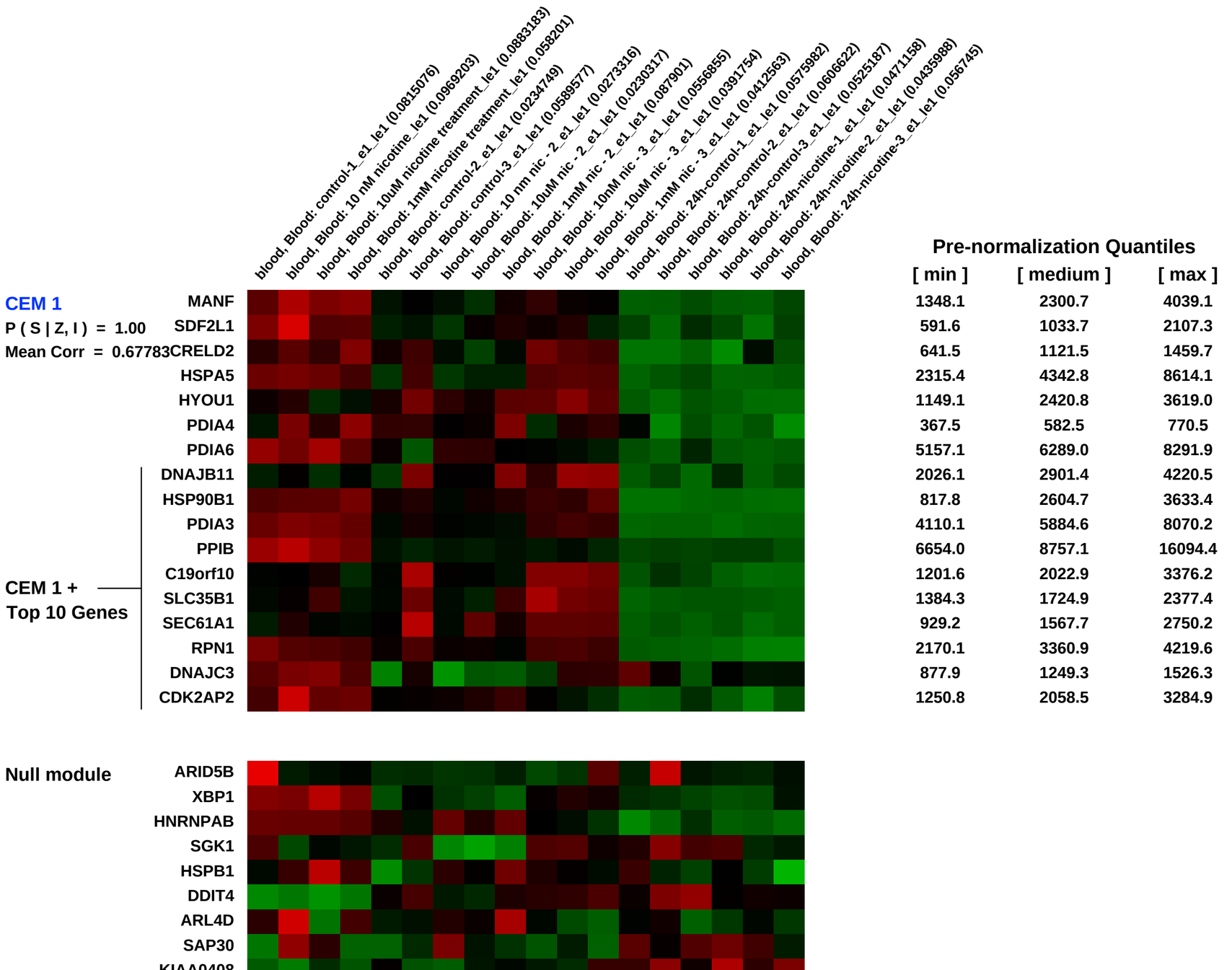

Pre-normalization Quantiles

	[min]	[medium]	[max]
MANF	1348.1	2300.7	4039.1
SDF2L1	591.6	1033.7	2107.3
CRELD2	641.5	1121.5	1459.7
HSPA5	2315.4	4342.8	8614.1
HYOU1	1149.1	2420.8	3619.0
PDIA4	367.5	582.5	770.5
PDIA6	5157.1	6289.0	8291.9
DNAJB11	2026.1	2901.4	4220.5
HSP90B1	817.8	2604.7	3633.4
PDIA3	4110.1	5884.6	8070.2
PPIB	6654.0	8757.1	16094.4
C19orf10	1201.6	2022.9	3376.2
SLC35B1	1384.3	1724.9	2377.4
SEC61A1	929.2	1567.7	2750.2
RPN1	2170.1	3360.9	4219.6
DNAJC3	877.9	1249.3	1526.3
CDK2AP2	1250.8	2058.5	3284.9

GEO Series "GSE30499" Expression Profiles

Num of samples in this series: 20

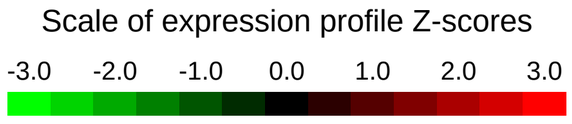

GEO Link:	http://www.ncbi.nlm.nih.gov/geo/query/acc.cgi?acc=GSE30499
Status:	Public on Jul 08 2011
Title:	Inhibition of nonsense-mediated RNA decay by the tumor microenvironment promotes tumorigenesis
Organism:	Homo sapiens
Experiment type:	Expression profiling by array
Platform:	GPL570
Pubmed ID:	21730287
Summary & Design:	**Summary:** Nonsense-mediated RNA decay (NMD) is regulated by a variety of cellular stresses. We expose U2OS cells to several stresses and assess RNA expression in the absence of transcription (i.e. stability). These studies identify transcripts that are stabilized by the physiological inhibition of NMD. **Overall design:** U2OS cells rendered hypoxia for three hours, treated with tunicamycin for three hours, treated with emetine for three hours, or depleted of Upf1/Rent1 were treated with DRB, and RNA was collected at 0, 1.5, 3 and 4.5 hrs.

Background corr dist: KL-Divergence = 0.0805, L1-Distance = 0.0456, L2-Distance = 0.0049, Normal std = 0.4749

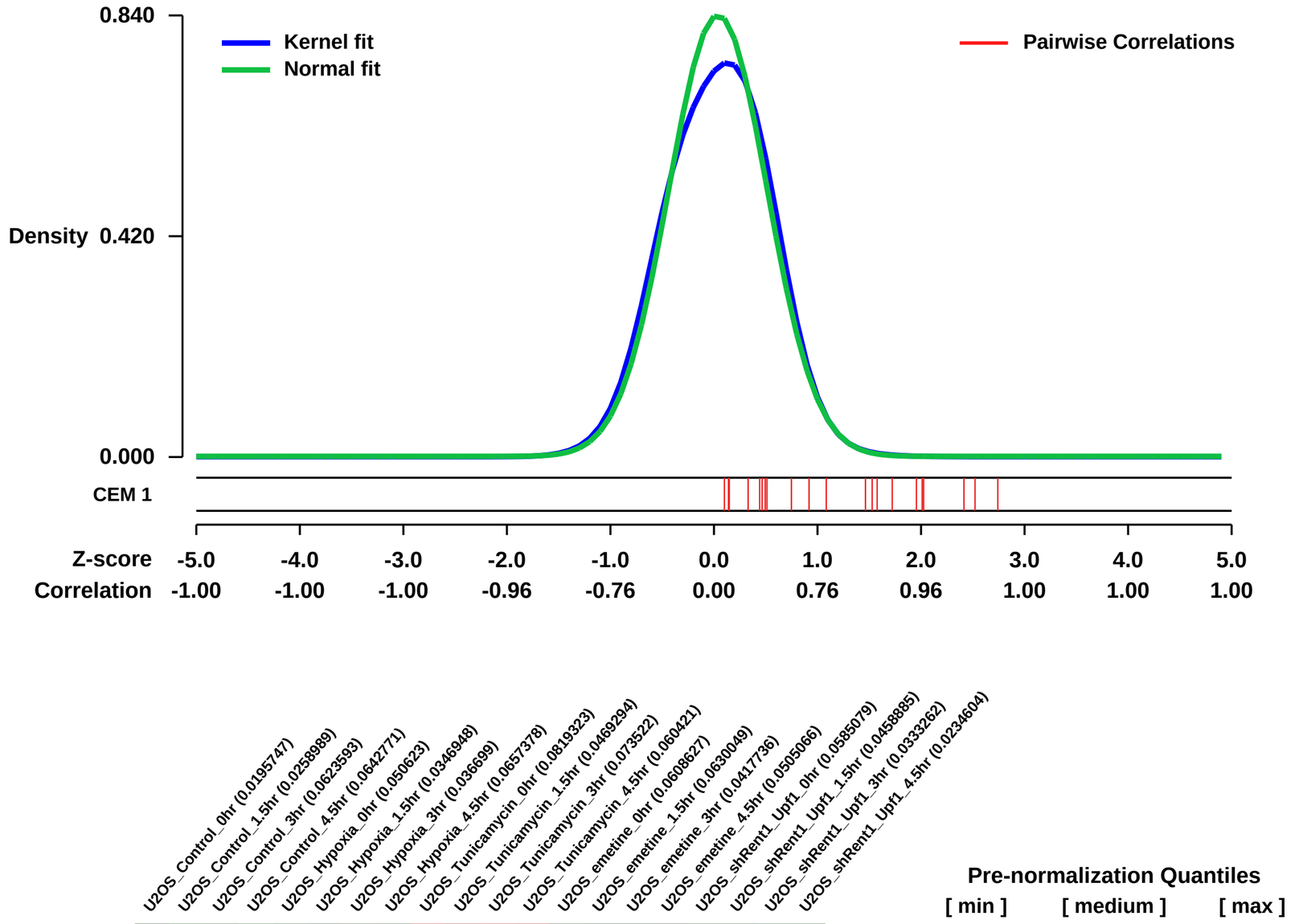

Pre-normalization Quantiles

	[min]	[medium]	[max]
CEM 1			
P (S | Z, I) = 1.00			
Mean Corr = 0.67410			
MANF	3491.1	4582.8	11314.1
SDF2L1	2502.6	3063.5	9027.4
CRELD2	4035.2	5133.9	10541.9
HSPA5	8684.5	9605.0	36797.7
HYOU1	1458.6	2272.6	4533.4
PDIA4	610.1	794.0	1131.4
PDIA6	9773.3	13656.0	18118.3
CEM 1 + Top 10 Genes			
DNAJB11	8219.6	9801.5	18800.0
HSP90B1	3189.2	4058.1	6861.5
PDIA3	2881.1	5835.9	9845.5
PPIB	28338.6	32877.1	38905.4
C19orf10	2132.8	3540.7	5261.5
SLC35B1	4305.9	6052.0	7164.3
SEC61A1	4396.3	6226.1	7679.1
RPN1	4023.9	5131.4	6924.8
DNAJC3	985.7	1358.5	4194.2
CDK2AP2	559.4	724.6	1967.5
Null module			
ARID5B			
XBP1			
HNRNPAB			
SGK1			
HSPB1			
DDIT4			
ARL4D			
SAP30			
KIAA0408			
GPR17			
HSPH1			
DNASE1L2			
SLC5A3			
GNAS			
GPR3			
TNFRSF25			
TM6SF2			
MKKS			
PLEKHF1			
ZMYM1			
DOK3			
FGF20			
SLC39A2			
KCNIP2			
ERRFI1			
DEDD2			
CCDC117			
USP31			
AHSA2			
CYS1			
CNIH2			
BANP			
CHORDC1			
P4HA1			

GEO Series "GSE19201" Expression Profiles

Num of samples in this series: 6

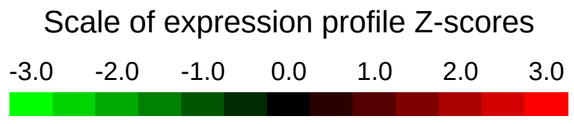

GEO Link:	http://www.ncbi.nlm.nih.gov/geo/query/acc.cgi?acc=GSE19201
Status:	Public on Nov 26 2009
Title:	Expression profiling of ATRA treated NB4 cells
Organism:	Homo sapiens
Experiment type:	Expression profiling by array
Platform:	GPL570
Pubmed ID:	20159610
Summary & Design:	**Summary:** NB4 is an APL derived cell line, carrying the t(15;17) translocation and expressing the PML/RARa fusion protein. Still, an important question that remains to be addressed is whether PML/RARa target genes are transcriptionally suppressed in primary APL cells and re-activated in all-trans retinoic acid (ATRA) treated NB4 cells. Gene expression of NB4 cells treated with ATRA at different time points were analyzed. **Overall design:** 6 samples at various times. No replicats.

Background corr dist: KL-Divergence = 0.0381, L1-Distance = 0.0285, L2-Distance = 0.0009, Normal std = 0.6415

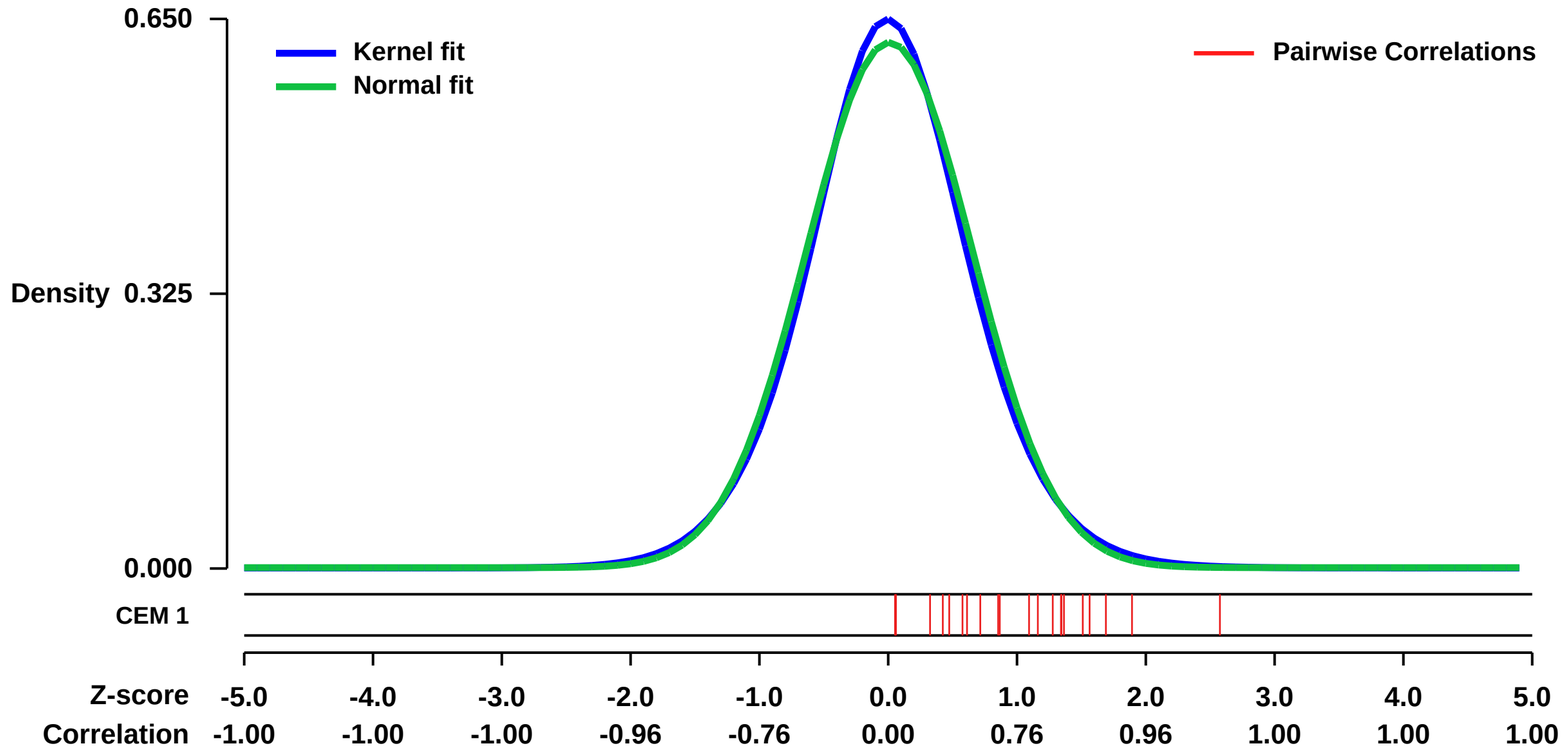

Pre-normalization Quantiles

		[min]	[medium]	[max]
CEM 1	MANF	3583.9	4022.9	6325.1
P (S | Z, I) = 1.00	SDF2L1	871.0	1173.6	1915.0
Mean Corr = 0.67331	CRELD2	979.4	1515.0	2252.4
	HSPA5	12944.5	21687.9	24783.0
	HYOU1	3478.9	4713.1	7159.9
	PDIA4	1008.1	1140.9	1443.8
	PDIA6	6707.2	9018.9	11261.0
CEM 1 + Top 10 Genes	DNAJB11	5717.4	7227.8	8487.7
	HSP90B1	4312.3	4896.1	8256.7
	PDIA3	10621.1	13176.4	15626.6
	PPIB	20501.4	23000.0	27817.1
	C19orf10	4506.2	4719.5	5382.7
	SLC35B1	2646.4	3296.7	4200.9
	SEC61A1	3386.6	3733.4	3914.2
	RPN1	3305.3	5087.9	5348.2
	DNAJC3	2821.6	3880.8	4918.2
	CDK2AP2	1038.4	1331.6	1920.8
Null module	ARID5B			
	XBP1			
	HNRNPAB			
	SGK1			
	HSPB1			
	DDIT4			
	ARL4D			
	SAP30			
	KIAA0408			
	GPR17			
	HSPH1			
	DNASE1L2			
	SLC5A3			
	GNAS			
	GPR3			
	TNFRSF25			
	TM6SF2			
	MKKS			
	PLEKHF1			
	ZMYM1			
	DOK3			
	FGF20			
	SLC39A2			
	KCNIP2			
	ERRFI1			
	DEDD2			
	CCDC117			
	USP31			
	AHSA2			
	CYS1			
	CNIH2			
	BANP			
	CHORDC1			
	P4HA1			

GEO Series "GSE13887" Expression Profiles

Num of samples in this series: 27

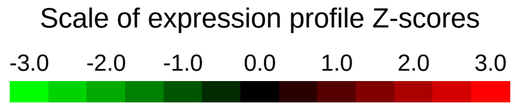

GEO Link:	http://www.ncbi.nlm.nih.gov/geo/query/acc.cgi?acc=GSE13887
Status:	Public on Feb 20 2009
Title:	Activation of mTOR controls the loss of TCR¸¶ in lupus T cells through HRES-1/Rab4-regulated lysosomal degradation
Organism:	Homo sapiens
Experiment type:	Expression profiling by array
Platform:	GPL570
Pubmed ID:	19201859
Summary & Design:	**Summary:** CD3-positive T cells were negatively isolated from 10 SLE patients and 9 healthy controls without SLE. All of the SLE samples and control samples were compared with one another to identify baseline differences in expression due to the disease. Next, T cell preparations from 4 of the control subjects were stimulated with either Nitric Oxide (NOC-18) 600 uM for 24hr or stimulated through CD3/CD28 for 24hr to determine which genes were responsive to these signaling mechanisms. Here, we show that activity of the mammalian target of rapamycin (mTOR), which is a sensor of the mitochondrial transmembrane potential, is increased in SLE T cells. Activation of mTOR was inducible by NO, a key trigger of MHP which in turn enhanced the expression of HRES-1/Rab4, a small GTPase that regulates recycling of surface receptors through early endosomes. Expression of HRES-1/Rab4 was increased in SLE T cells and, in accordance with its dominant impact on the endocytic recycling of CD4, it was inversely correlated with diminished CD4 expression. HRES-1/Rab4 over-expression was also inversely correlated with diminished TCR¸¶ protein levels. Combined with follow up studies, these results suggest that activation of mTOR causes the loss of TCR¸¶ in lupus T cells through HRES-1/Rab4-dependent lysosomal degradation. **Overall design:** 4 replicate CD3/CD28 stimulated T cell samples from 4 of the control subjects

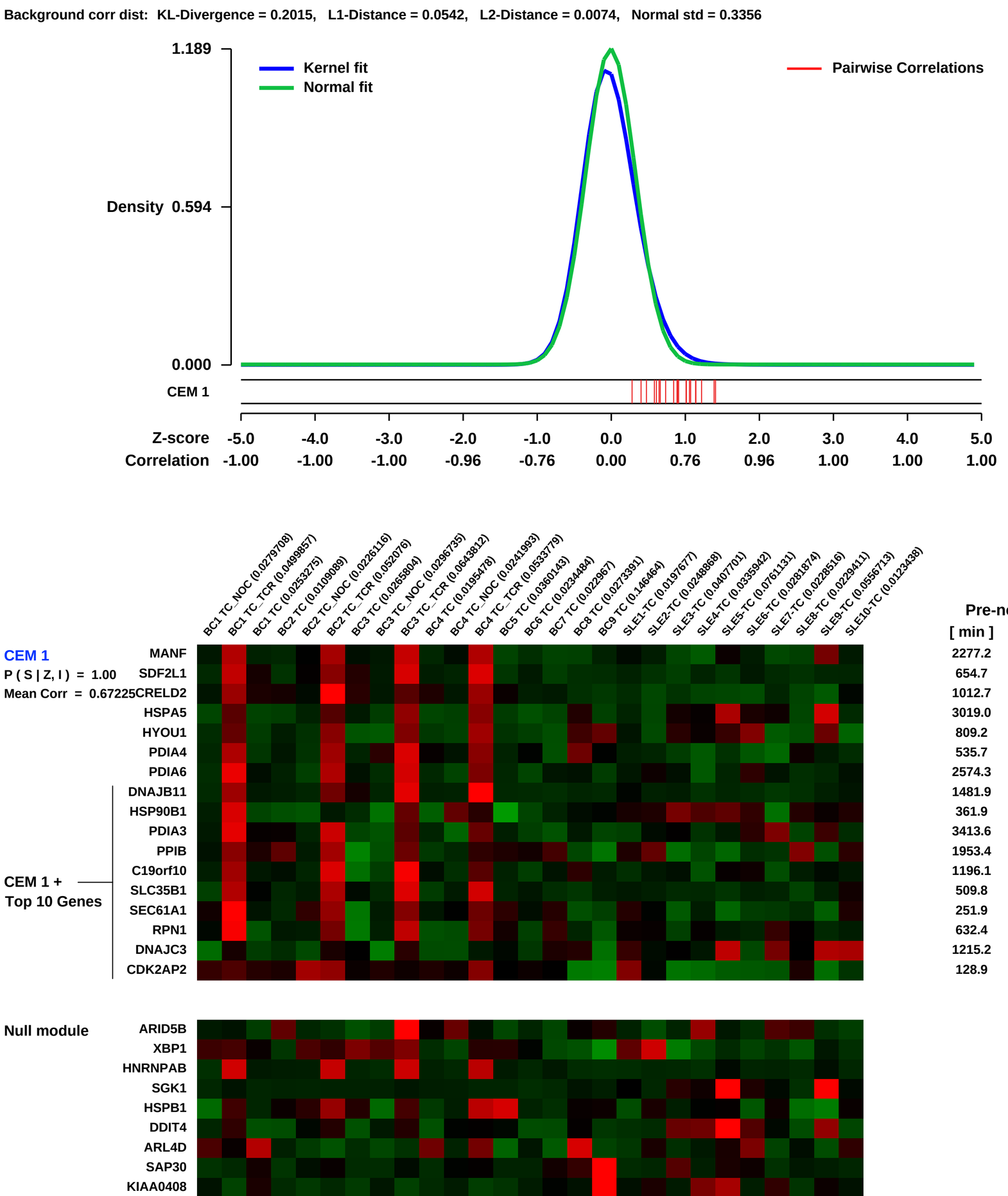

GEO Series "GSE44126" Expression Profiles

Num of samples in this series: 15

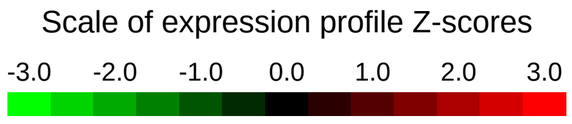

GEO Link:	http://www.ncbi.nlm.nih.gov/geo/query/acc.cgi?acc=GSE44126
Status:	Public on Aug 05 2013
Title:	Expression data from Human CD40L+ Tcells
Organism:	Homo sapiens
Experiment type:	Expression profiling by array
Platform:	GPL570
Pubmed ID:	23719298
Summary & Design:	**Summary:** To assess the nature of CD8+CD40L+ memory Tcells, we compared the gene expression to CD8+CD40L- and CD4+ counterparts, and found similarities in expression of genes encoding cytokines **Overall design:** PBMCs were isolated from five healthy donors. The cells were stimulated with PMA/Ionomycin for 6 h, and subsequently sorted into the CD4+CD45RA-CD40L+, CD8+CD45RA-CD40L-, CD8+CD45RA-CD40L+ populations by FACS-sort

Background corr dist: KL-Divergence = 0.1737, L1-Distance = 0.0427, L2-Distance = 0.0039, Normal std = 0.3506

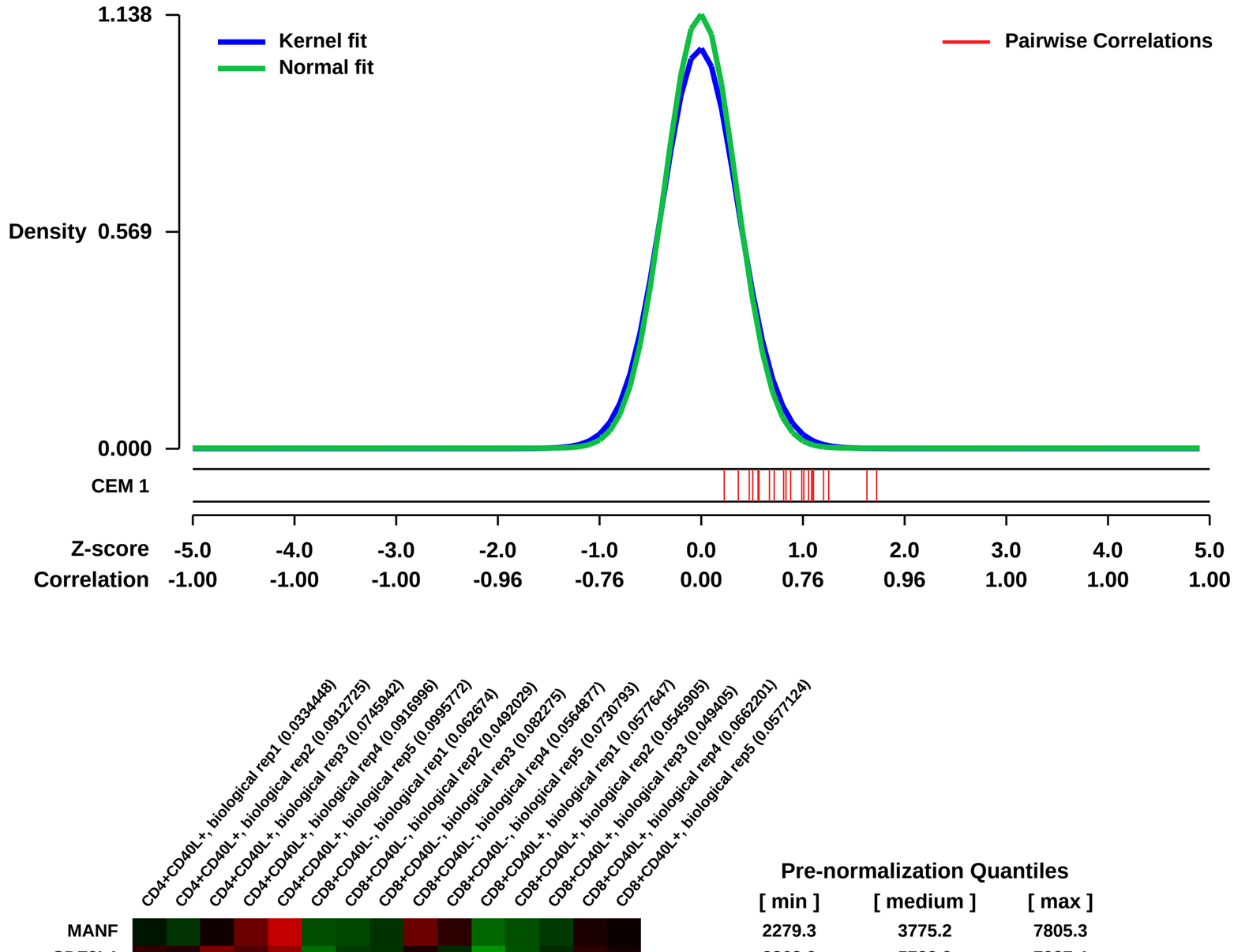

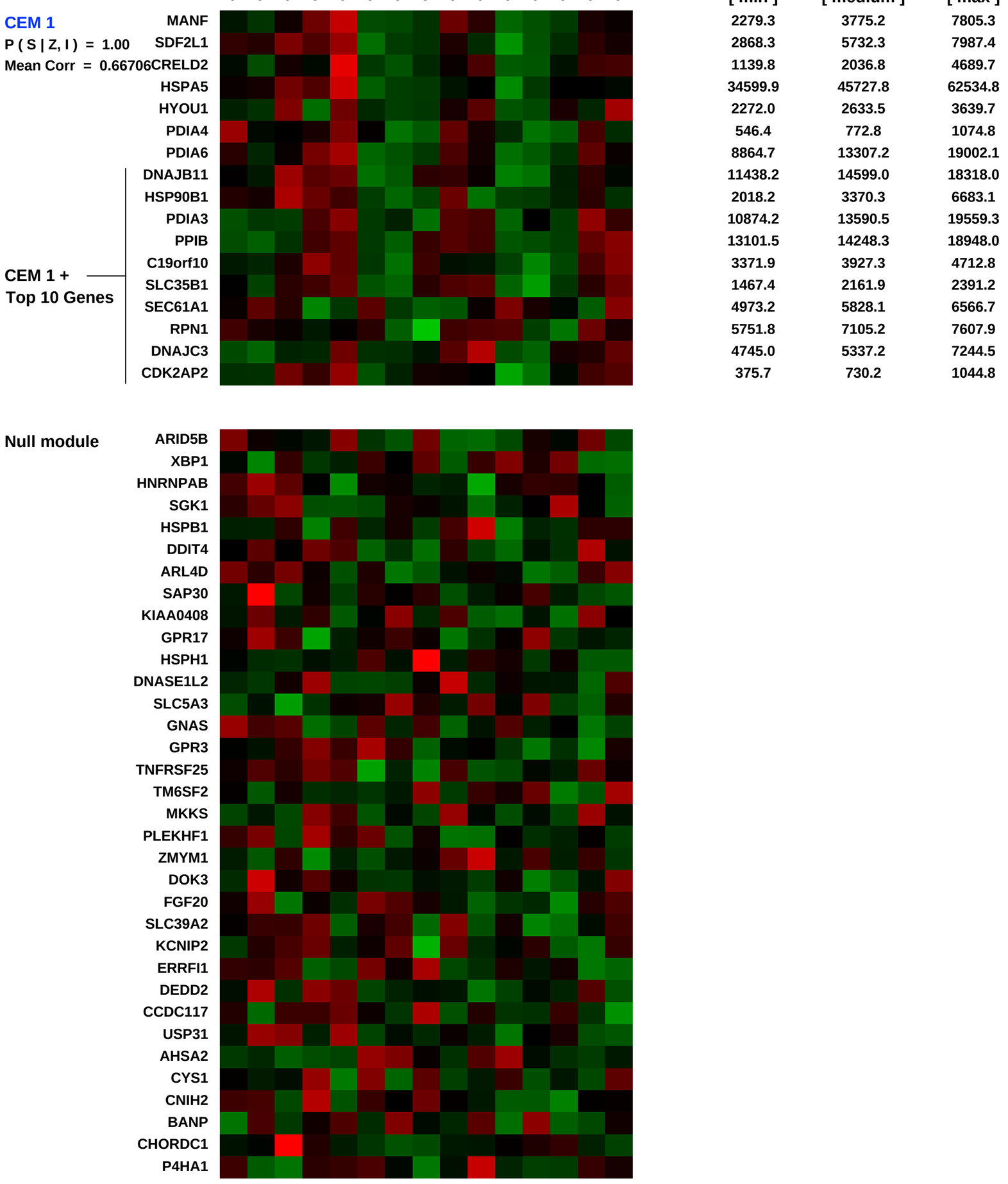

Pre-normalization Quantiles	[min]	[medium]	[max]
MANF	2279.3	3775.2	7805.3
SDF2L1	2868.3	5732.3	7987.4
CRELD2	1139.8	2036.8	4689.7
HSPA5	34599.9	45727.8	62534.8
HYOU1	2272.0	2633.5	3639.7
PDIA4	546.4	772.8	1074.8
PDIA6	8864.7	13307.2	19002.1
DNAJB11	11438.2	14599.0	18318.0
HSP90B1	2018.2	3370.3	6683.1
PDIA3	10874.2	13590.5	19559.3
PPIB	13101.5	14248.3	18948.0
C19orf10	3371.9	3927.3	4712.8
SLC35B1	1467.4	2161.9	2391.2
SEC61A1	4973.2	5828.1	6566.7
RPN1	5751.8	7105.2	7607.9
DNAJC3	4745.0	5337.2	7244.5
CDK2AP2	375.7	730.2	1044.8

GEO Series "GSE40971" Expression Profiles

Num of samples in this series: 40

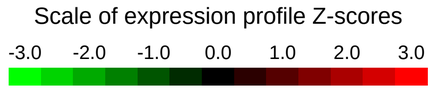

GEO Link:	http://www.ncbi.nlm.nih.gov/geo/query/acc.cgi?acc=GSE40971
Status:	Public on Oct 12 2012
Title:	Gene expression profiling of EZH2 mutant and wild type DLBCL cell lines treated with EZH2 inhibitor
Organism:	Homo sapiens
Experiment type:	Expression profiling by array
Platform:	GPL570
Pubmed ID:	23051747
Summary & Design:	**Summary:** We studied transcriptional changes by Affymetrix human microarrays in DLBCL cell lines as a result of treatment with GSK126, a potent, highly-selective, SAM-competitive, small molecule inhibitor of EZH2 In eukaryotes, epigenetic post-translational modification of histones is critical for regulation of chromatin structure and gene expression. EZH2 is the catalytic subunit of the Polycomb Repressive Complex 2 (PRC2) and is responsible for repressing target gene expression through methylation of histone H3 on lysine 27 (H3K27). Over-expression of EZH2 is implicated in tumorigenesis and correlates with poor prognosis in multiple tumor types. Recent reports have identified somatic heterozygous mutations of Y641 and A677 residues within the catalytic SET domain of EZH2 in diffuse large B-cell lymphoma (DLBCL) and follicular lymphoma (FL). The Y641 residue is the most frequently mutated residue, with 22% of GCB (Germinal Cell B-cell) DLBCL and FL harboring mutations at this site. These lymphomas exhibit increased H3K27 tri-methylation (H3K27me3) due to altered substrate preferences of the mutant enzymes. However, it is unknown whether direct inhibition of EZH2 methyltransferase activity alone will be effective in treating lymphomas carrying activating EZH2 mutations. Herein, we demonstrate that GSK126, a potent, highly-selective, SAM-competitive, small molecule inhibitor of EZH2 methyltransferase activity, decreases global H3K27me3 levels and reactivates silenced PRC2 target genes. GSK126 effectively inhibits the proliferation of EZH2 mutant DLBCL cell lines and dramatically inhibits the growth of EZH2 mutant DLBCL xenografts in mice. Together, these data demonstrate that pharmacological inhibition of EZH2 activity may provide a promising treatment for EZH2 mutant lymphoma. **Overall design:** 10 DLBCL cell lines (7 mutant and 3 wild type EZH2), that were differentially sensitive to GSK126 in proliferation assays, were treated for 72 hours, in duplicate (n=2), with either DMSO (vehicle) or 500nM of GSK126, a potent selective EZH2 inhibitor. EZH2 mutant cell lines are Pfeiffer, KARPAS-422, WSU-DLCL2, SU-DHL-10, SU-DHL-6, DB and SU-DHL-4. EZH2 wildtype cell lines are HT, OCI-LY-19 and Toledo.

Background corr dist: KL-Divergence = 0.3349, L1-Distance = 0.0543, L2-Distance = 0.0076, Normal std = 0.2709

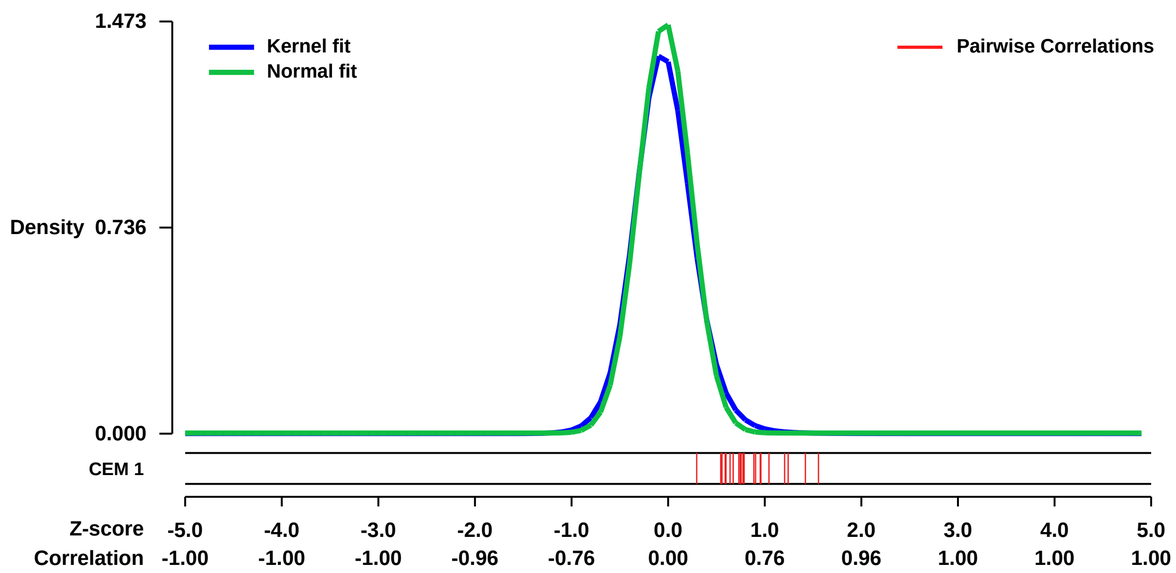

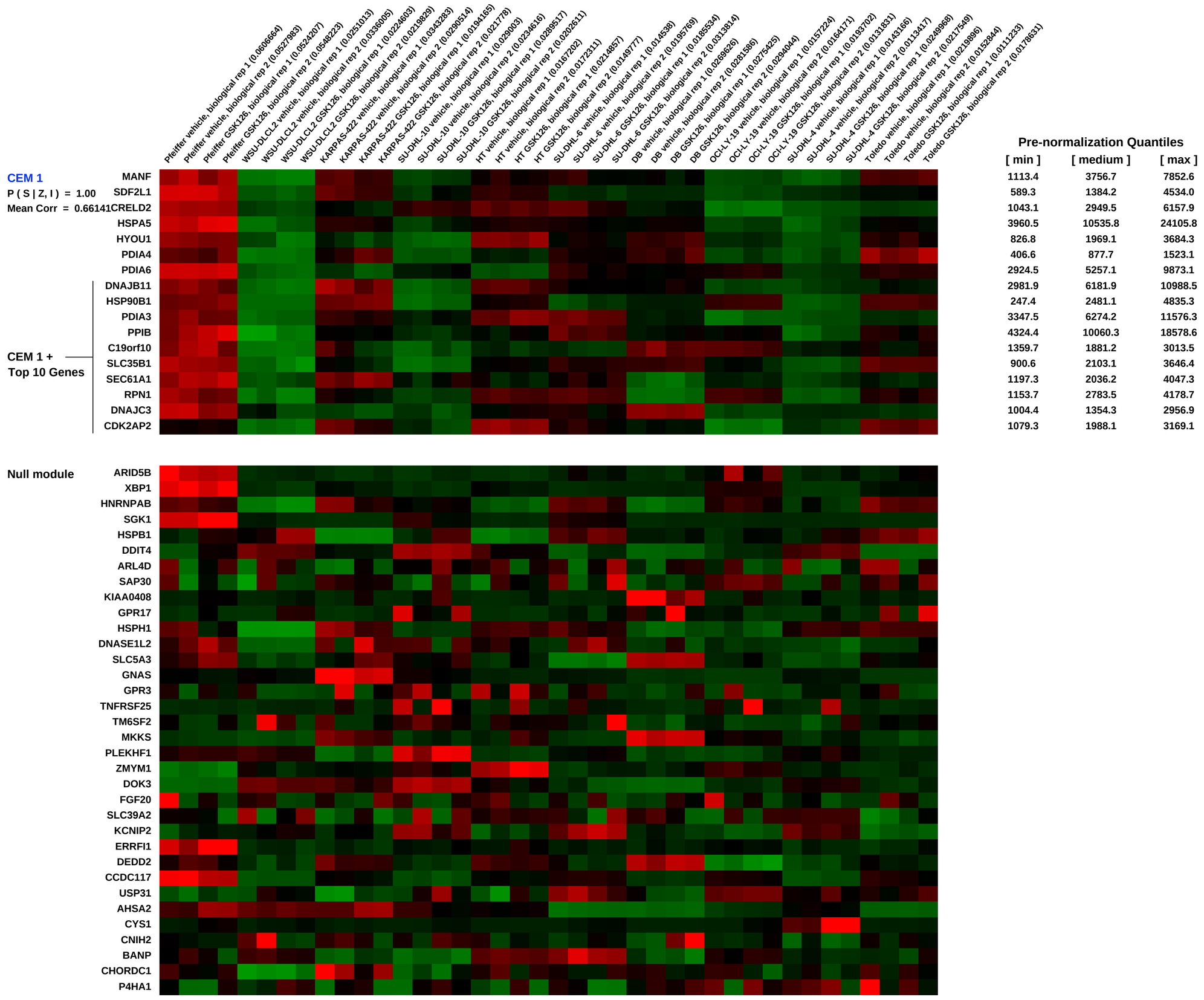

GEO Series "GSE47970" Expression Profiles

Num of samples in this series: 18

Scale of expression profile Z-scores

-3.0 -2.0 -1.0 0.0 1.0 2.0 3.0

GEO Link:	http://www.ncbi.nlm.nih.gov/geo/query/acc.cgi?acc=GSE47970
Status:	Public on Apr 30 2014
Title:	Cross-species gene expression analysis of species-specific differences in preclinical assessment of pharmaceutical compounds (human)
Organism:	Homo sapiens
Experiment type:	Expression profiling by array
Platform:	GPL570
Pubmed ID:	24823806
Summary & Design:	**Summary:** Significant qualitative and quantitative differences exist between humans and the animal models used in research. However, significant quantitative and qualitative differences exist between humans and the animal models used in research. This is as a result of genetic variation between human and the laboratory animal. Therefore the development of a system that would allow the assessment of all molecular differences between species after drug exposure would have a significant impact on drug evaluation for toxicity and efficacy. Here we describe a cross-species microarray methodology that identifies and selects orthologous probes after cross-species sequence comparison to develop an orthologous cross-species gene expression analysis tool. The assumptions made by the use of this orthologous gene expression strategy for cross-species extrapolation is that; conserved changes in gene expression equate to conserved pharmacodynamic endpoints. This assumption is supported by the fact that evolution and selection have maintained the structure and function of many biochemical pathways over time, resulting in the conservation of many important processes. We demonstrate this difference using a cross-species methodology by investigating species specific differences of the peroxisome proliferator activator receptor (PPAR) alpha in rat and human. **Overall design:** Human primary hepatocytes were treated with 30´µ 100´µEMD and 0.1% DMSO as vehicle control. All samples were incubated at 24hr and 72hr intervals before RNA extractions and hybridization onto Affymetrix human microarrays.

Background corr dist: KL-Divergence = 0.1316, L1-Distance = 0.0399, L2-Distance = 0.0033, Normal std = 0.3916

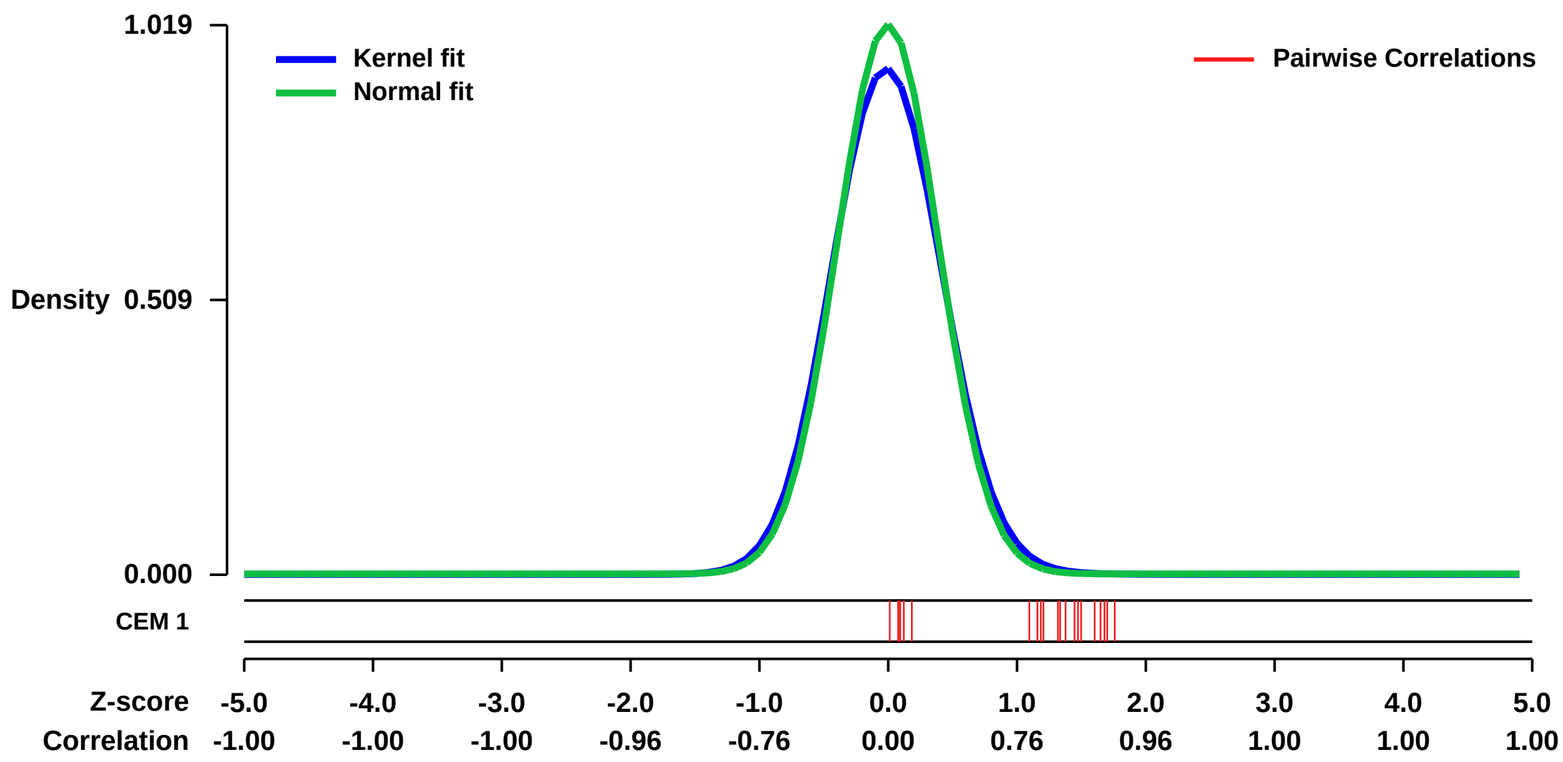

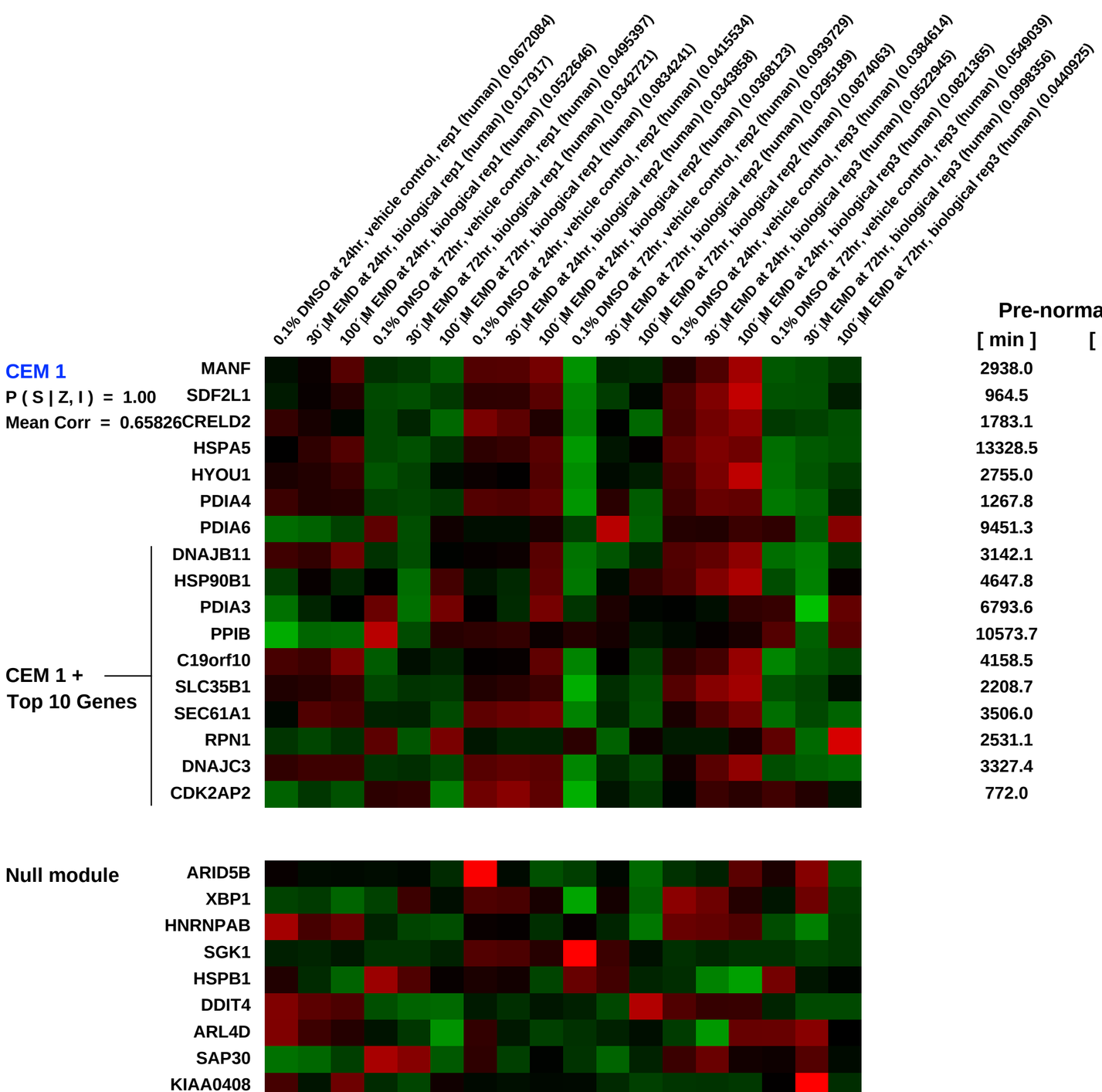

Pre-normalization Quantiles

	[min]	[medium]	[max]
MANF	2938.0	7677.4	13936.7
SDF2L1	964.5	3618.4	7984.0
CRELD2	1783.1	5253.4	9343.9
HSPA5	13328.5	35293.7	52731.5
HYOU1	2755.0	8935.5	17038.4
PDIA4	1267.8	3303.7	4023.8
PDIA6	9451.3	11312.3	13851.7
DNAJB11	3142.1	7247.0	11311.5
HSP90B1	4647.8	8655.0	13846.2
PDIA3	6793.6	11510.4	14440.2
PPIB	10573.7	19016.7	26119.2
C19orf10	4158.5	6814.2	9609.9
SLC35B1	2208.7	5204.4	7096.5
SEC61A1	3506.0	5764.6	8013.4
RPN1	2531.1	3358.0	5926.7
DNAJC3	3327.4	5732.4	7743.7
CDK2AP2	772.0	1764.2	2242.2

GEO Series "GSE13525" Expression Profiles

Num of samples in this series: 12

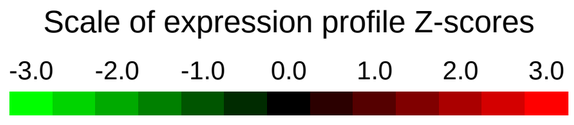

GEO Link:	http://www.ncbi.nlm.nih.gov/geo/query/acc.cgi?acc=GSE13525
Status:	Public on Jan 05 2009
Title:	Carboplatin-induced gene expression changes in vitro are prognostic of survival in epithelial ovarian cancer
Organism:	Homo sapiens
Experiment type:	Expression profiling by array
Platform:	GPL570
Pubmed ID:	19038057
Summary & Design:	**Summary:** We performed a time-course microarray experiment to define the transcriptional response to carboplatin in vitro, and to correlate this with clinical outcome in epithelial ovarian cancer (EOC). RNA was isolated from carboplatin and control-treated 36M2 ovarian cancer cells at several time points, followed by oligonucleotide microarray hybridization. Carboplatin induced changes in gene expression were assessed at the single gene as well as at the pathway level. Clinical validation was performed in publicly available microarray datasets using disease free and overall survival endpoints. Time-course and pathway analyses identified 317 genes and 40 pathways (designated time-course and pathway signatures) deregulated following carboplatin exposure. Both types of signatures were validated in two separate platinum-treated ovarian and NSCLC cell lines using published microarray data. Expression of time-course and pathway signature genes distinguished between patients with unfavorable and favorable survival in two independent ovarian cancer datasets. Among the pathways most highly induced by carboplatin in vitro, the NRF2, NF-kB, and cytokine and inflammatory response pathways were also found to be upregulated prior to chemotherapy exposure in poor prognosis tumors. **Overall design:** we treated the 36M2 cell line with carboplatin 100¸…M or vehicle-control for 24hrs and cells were harvested and processed for RNA isolation at 24, 30 and 36hrs after treatment.

Background corr dist: KL-Divergence = 0.1165, L1-Distance = 0.0246, L2-Distance = 0.0008, Normal std = 0.4149

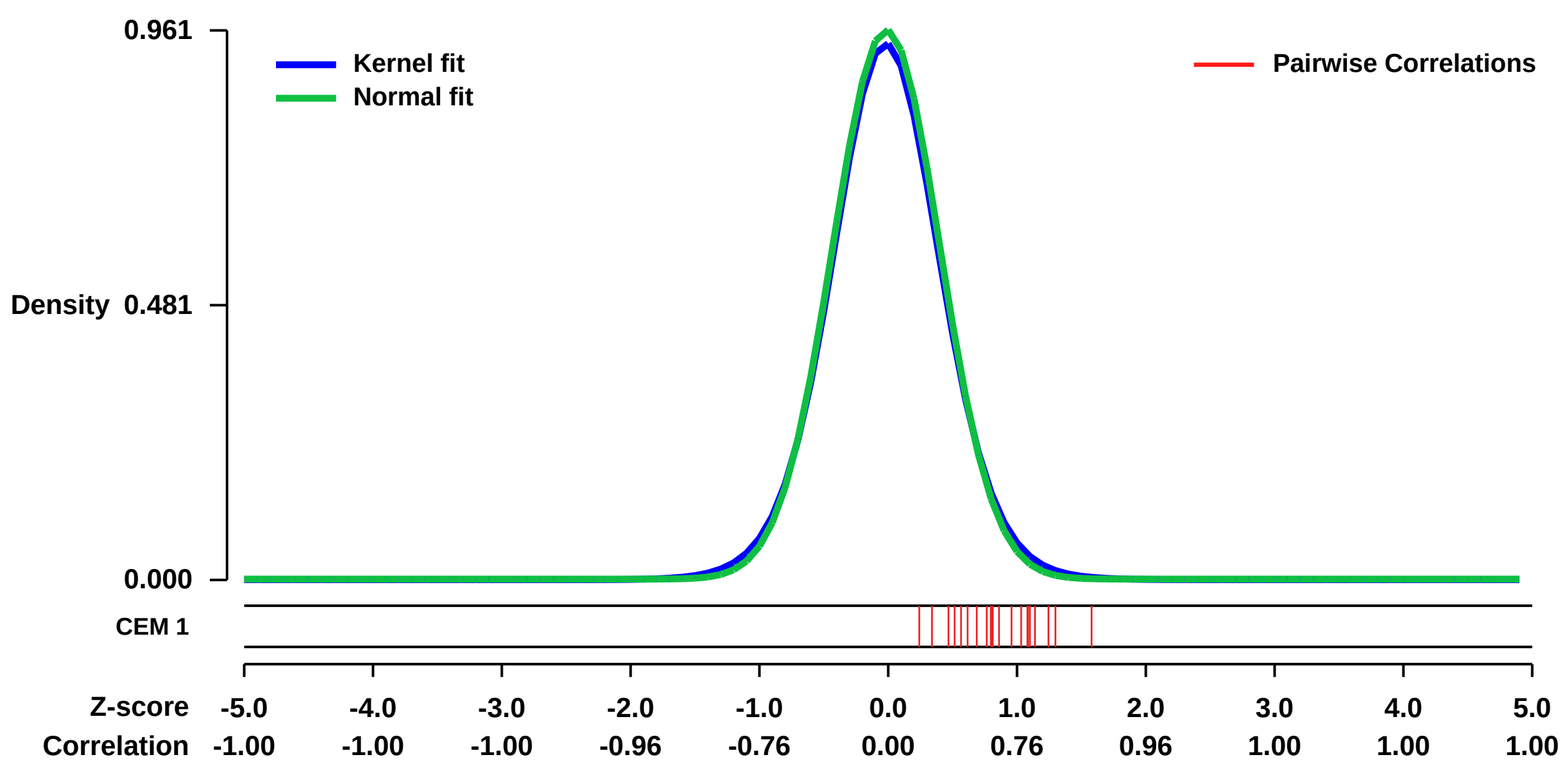

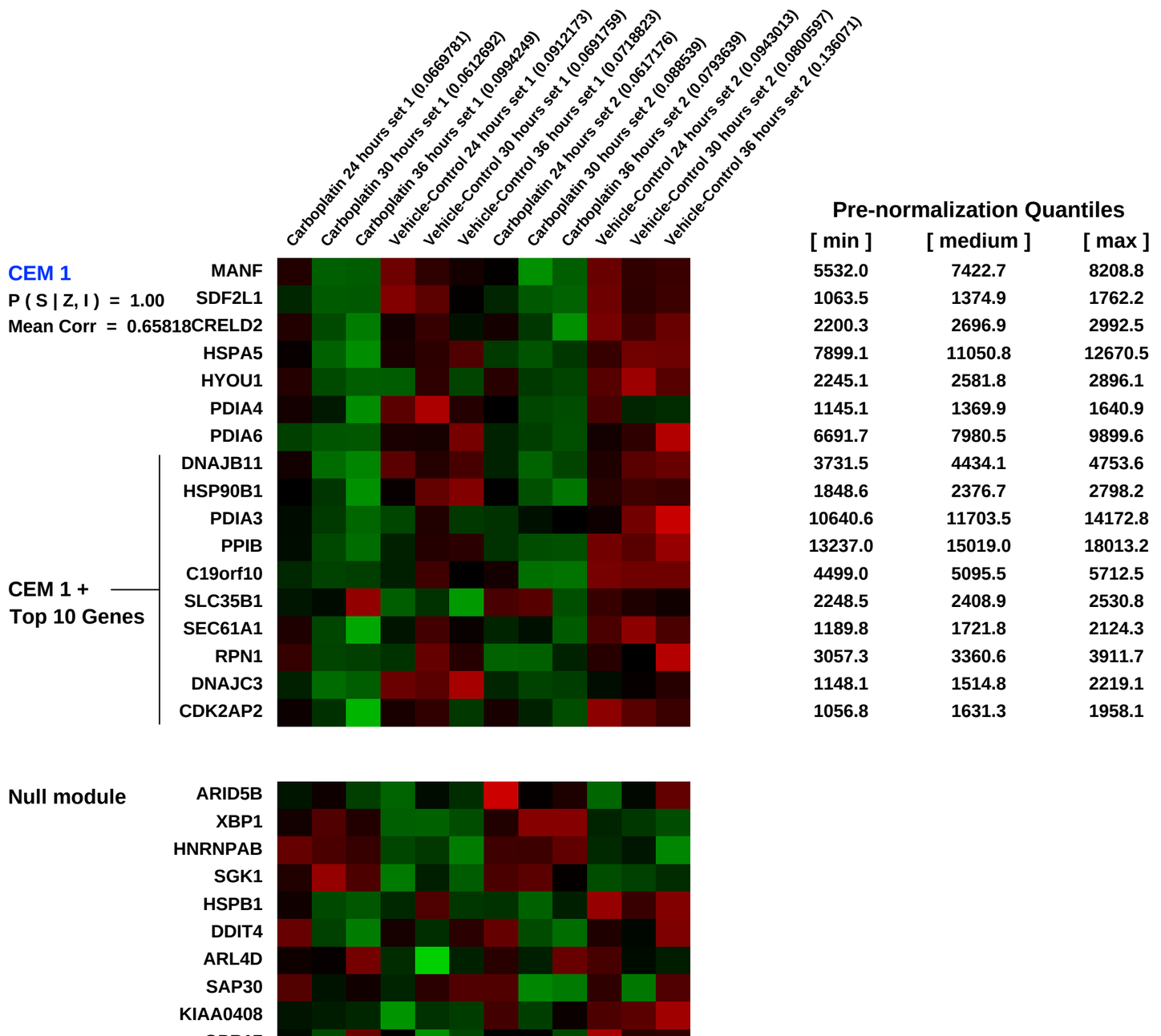

Pre-normalization Quantiles

	[min]	[medium]	[max]
MANF	5532.0	7422.7	8208.8
SDF2L1	1063.5	1374.9	1762.2
CRELD2	2200.3	2696.9	2992.5
HSPA5	7899.1	11050.8	12670.5
HYOU1	2245.1	2581.8	2896.1
PDIA4	1145.1	1369.9	1640.9
PDIA6	6691.7	7980.5	9899.6
DNAJB11	3731.5	4434.1	4753.6
HSP90B1	1848.6	2376.7	2798.2
PDIA3	10640.6	11703.5	14172.8
PPIB	13237.0	15019.0	18013.2
C19orf10	4499.0	5095.5	5712.5
SLC35B1	2248.5	2408.9	2530.8
SEC61A1	1189.8	1721.8	2124.3
RPN1	3057.3	3360.6	3911.7
DNAJC3	1148.1	1514.8	2219.1
CDK2AP2	1056.8	1631.3	1958.1

GEO Series "GSE15455" Expression Profiles

Num of samples in this series: 33

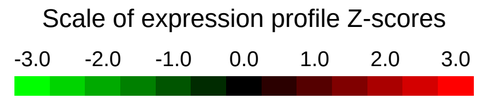

GEO Link:	http://www.ncbi.nlm.nih.gov/geo/query/acc.cgi?acc=GSE15455
Status:	Public on Oct 06 2009
Title:	GEMINI (Gastric Encyclopedia of Molecular Interactions and Nodes for Intervention) Phases A-C
Organism:	Homo sapiens
Experiment type:	Expression profiling by array
Platform:	GPL570
Pubmed ID:	19798449
Summary & Design:	**Summary:** Genome-wide mRNA expression profiles of 25 unique gastric cancer cell lines (GCCLs). Gastric cancer (GC) is the second leading cause of global cancer mortality, with individual gastric tumors displaying significant heterogeneity in their deregulation of various oncogenic pathways. We aim to identify major oncogenic pathways in GC that robustly impact patient survival and treatment response. We used an in silico strategy based on gene expression signatures and connectivity analytics to map patterns of oncogenic pathway activation in 25 unique GCCLs, and in 301 primary gastric cancers from three independent patient cohorts. Of 11 oncogenic pathways previously implicated in GC, we identified three predominant pathways (proliferation/stem cell, NF-kB, and Wnt/b-catenin) deregulated in the majority (>70%) of gastric tumors. Using a variety of proliferative, Wnt, and NF-kB-related assays, we experimentally validated the pathway predictions in multiple GC cell lines showing similar pathway activation patterns in vitro. Patients stratified at the level of individual pathways did not exhibit consistent differences in clinical outcome. However, patients grouped by oncogenic pathway combinations demonstrated robust and significant survival differences (e.g., high proliferation/high NF-kB vs. low proliferation/low NF-kB), suggesting that tumor behavior in GC is likely influenced by the combined effects of multiple oncogenic pathways. Our results demonstrate that GCs can be successfully taxonomized by oncogenic pathway activity into biologically and clinically relevant subgroups. **Keywords:** gastric cancer, cell culture **Overall design:** Profiling of 25 unique Gastric Cancer Cell Lines on Affymetrix GeneChip Human Genome U133 Plus 2.0 Array. Replicates are included for a total of 33 arrays.

Background corr dist: KL-Divergence = 0.5322, L1-Distance = 0.0996, L2-Distance = 0.0344, Normal std = 0.2198

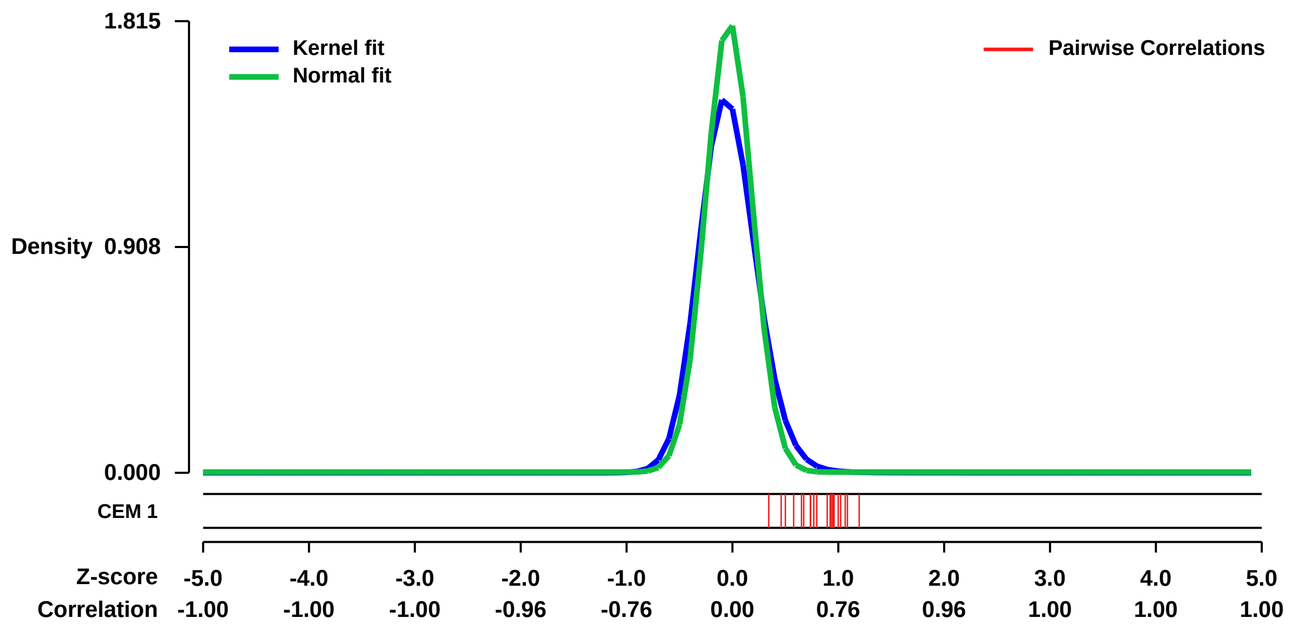

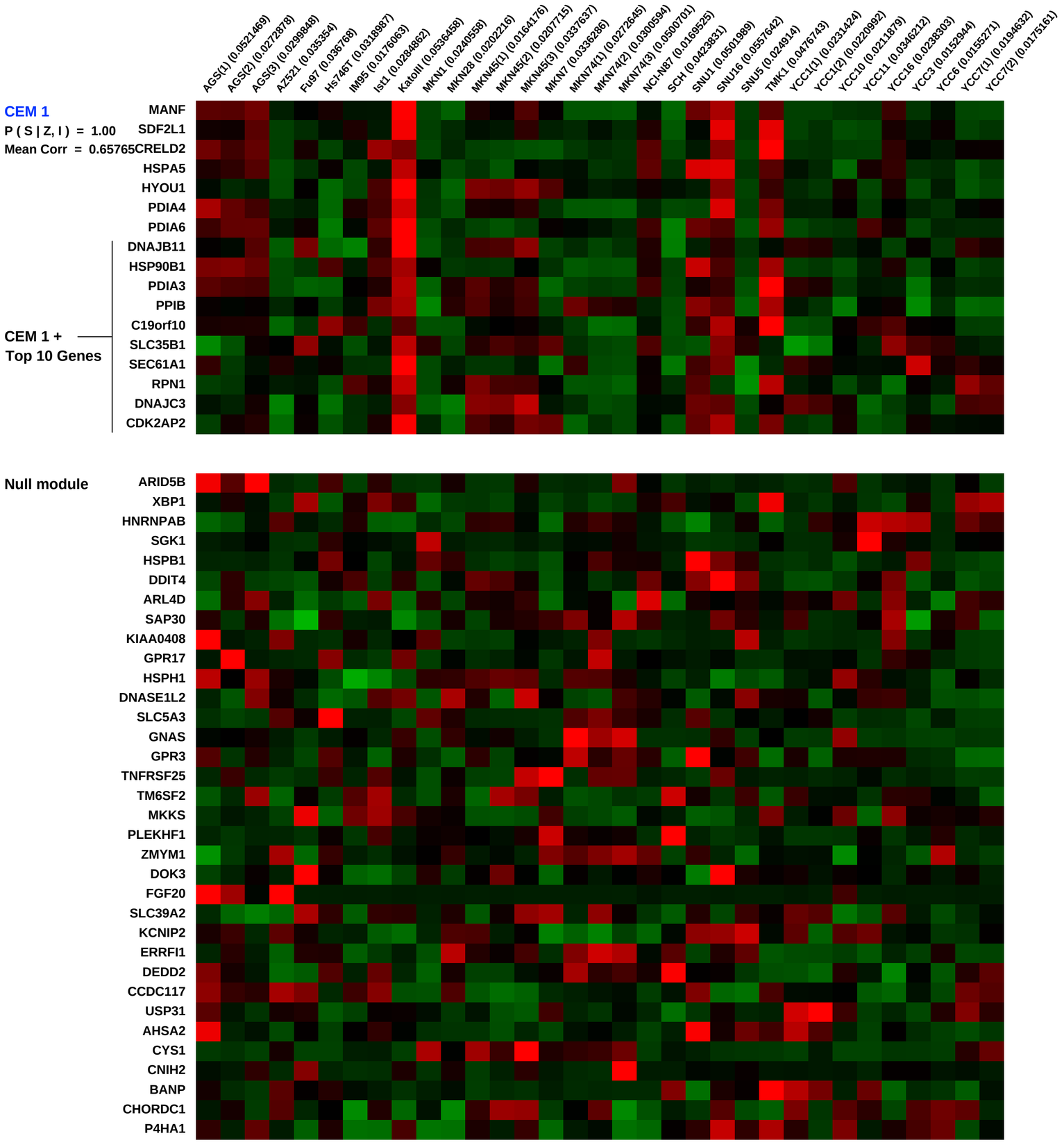

Pre-normalization Quantiles

[min]	[medium]	[max]
1314.1	3785.1	12364.3
324.9	1396.8	5782.8
1129.7	2275.9	9378.7
13994.6	24217.6	55084.4
1400.6	4440.5	16243.1
832.9	2206.1	6904.4
5385.3	10457.9	23637.2
1957.6	5048.9	12559.7
3741.7	6659.6	24479.5
8558.7	16295.1	38899.0
10963.5	20302.0	32502.4
1300.0	3427.7	8650.4
1140.7	2470.0	4408.6
1850.5	3210.4	6542.4
1782.7	4527.3	9384.2
701.0	2134.2	4842.6
645.9	1579.0	4204.3

GEO Series "GSE22225" Expression Profiles

Num of samples in this series: 15

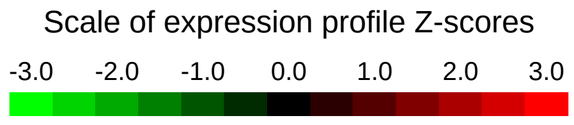

GEO Link:	http://www.ncbi.nlm.nih.gov/geo/query/acc.cgi?acc=GSE22225
Status:	Public on Jun 08 2011
Title:	CLN3 patients with differing progression of the disease
Organism:	Homo sapiens
Experiment type:	Expression profiling by array
Platform:	GPL570
Pubmed ID:	21863212
Summary & Design:	**Summary:** Mutations in the CLN3 gene lead to juvenile neuronal ceroid lipofuscinosis, a pediatric neurodegenerative disorder characterized by visual loss, epilepsy and psychomotor deterioration. Although most CLN3 patients carry the same 1 kb deletion in the CLN3 gene, their disease phenotype can be variable. The aims of this study were (1) to identify genes that are dysregulated in CLN3 disease regardless of the clinical course that could be useful as biomarkers, and (2) to find modifier genes that affect the progression rate of the disease. Genome-wide expression profiling was performed in 8 CLN3 patients, homozygous for the 1 kb deletion, with different disease progression and compared to seven age and gender matched controls. **Overall design:** Lymphocytes from eight patients diagnosed with CLN3 disease,all homozygous for the 1 kb deletion in the CLN3 gene and classified as having rapid (n = 2), average (n=4), and slow disease progression (n = 2), were used. These eight patients did not receive anticonvulsive medication. In addition, lymphocytes of seven age and gender matched controls were included in the study. Lymphocytes were prepared from fresh patient blood samples by Ficoll-gradient centrifugation (Biocoll´fi, Biochrom AG, Berlin, Germany) according to the manufacturerâ s protocol and used for RNA isolation (RNeasy´fi Micro Kit, Qiagen, Hilden, Germany).

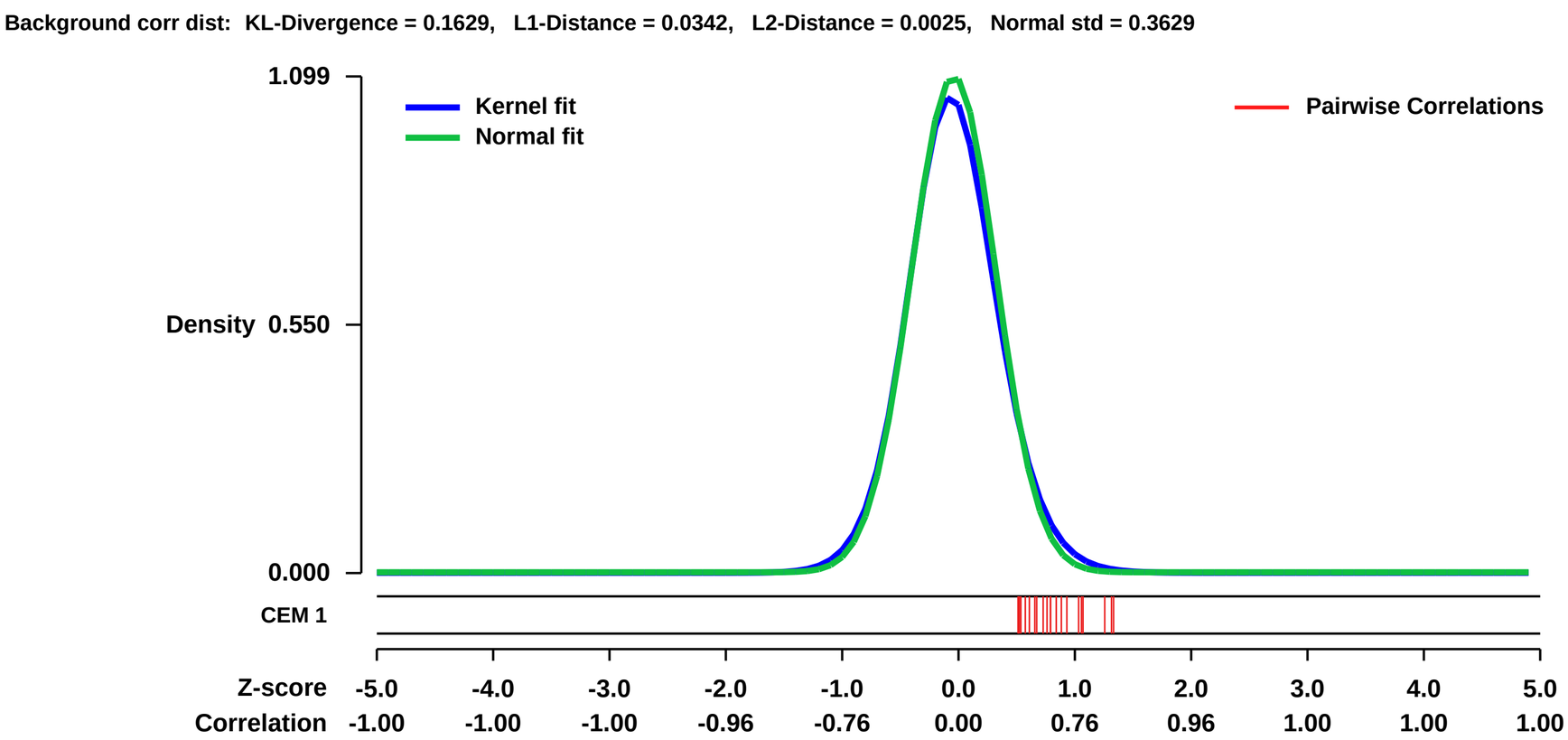

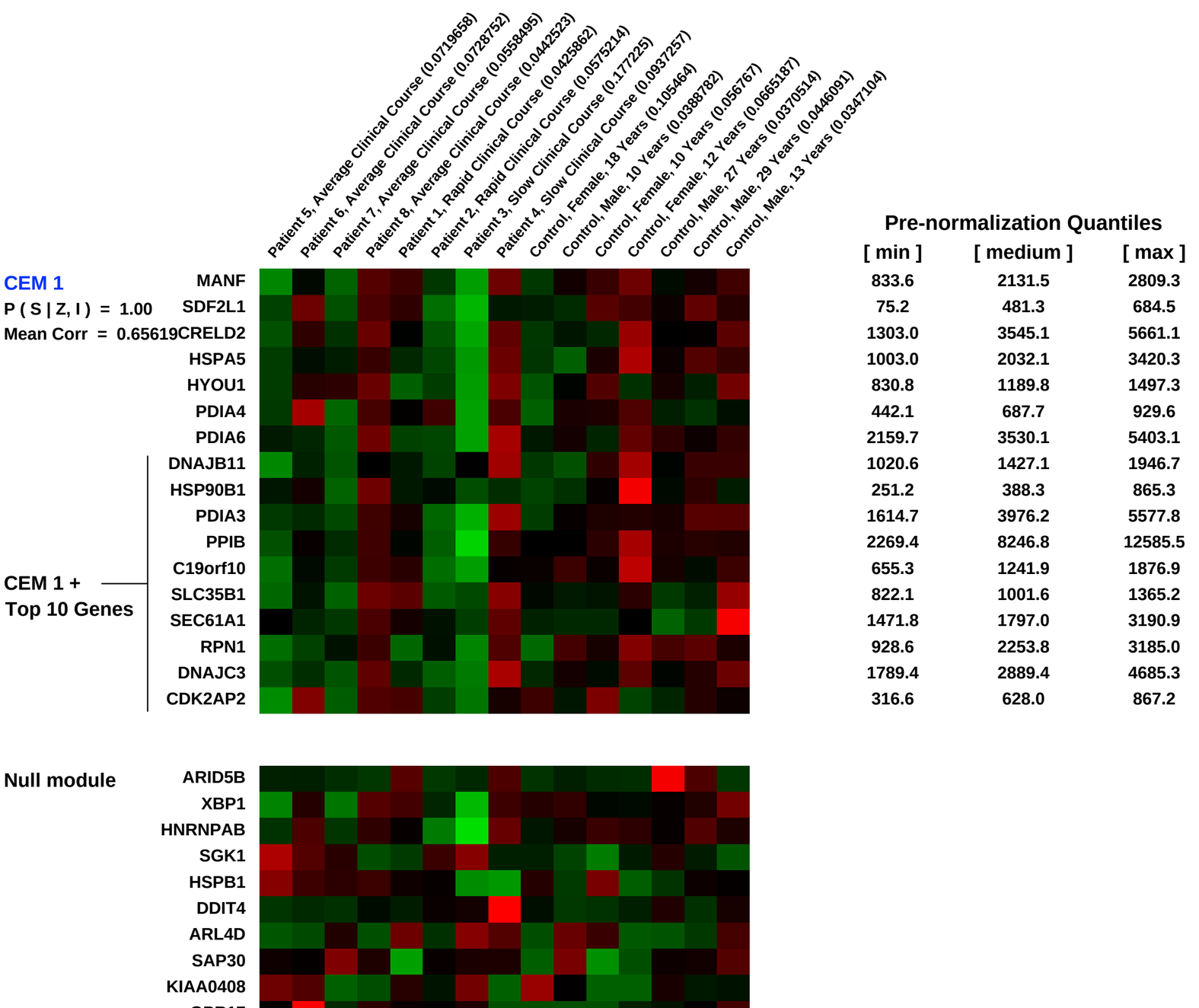

Pre-normalization Quantiles

	[min]	[medium]	[max]
MANF	833.6	2131.5	2809.3
SDF2L1	75.2	481.3	684.5
CRELD2	1303.0	3545.1	5661.1
HSPA5	1003.0	2032.1	3420.3
HYOU1	830.8	1189.8	1497.3
PDIA4	442.1	687.7	929.6
PDIA6	2159.7	3530.1	5403.1
DNAJB11	1020.6	1427.1	1946.7
HSP90B1	251.2	388.3	865.3
PDIA3	1614.7	3976.2	5577.8
PPIB	2269.4	8246.8	12585.5
C19orf10	655.3	1241.9	1876.9
SLC35B1	822.1	1001.6	1365.2
SEC61A1	1471.8	1797.0	3190.9
RPN1	928.6	2253.8	3185.0
DNAJC3	1789.4	2889.4	4685.3
CDK2AP2	316.6	628.0	867.2

GEO Series "GSE10714" Expression Profiles

Num of samples in this series: 33

Scale of expression profile Z-scores

-3.0 -2.0 -1.0 0.0 1.0 2.0 3.0

GEO Link:	http://www.ncbi.nlm.nih.gov/geo/query/acc.cgi?acc=GSE10714
Status:	Public on Jan 29 2009
Title:	Expression data from human colonic biopsy sample
Organism:	Homo sapiens
Experiment type:	Expression profiling by array
Platform:	GPL570
Pubmed ID:	20087348
Summary & Design:	**Summary:** Gene expression profile based classification of colonic diseases are suitable for identification of diagnostic mRNA expression patterns which can establish the basis of a new molecular biological diagnostic method **Keywords:** whole genomic expression **Overall design:** Total RNA was extracted from colonic biosy samples CRC and hybridized on Affymetrix HGU133 Plus 2.0 microarrays

Background corr dist: KL-Divergence = 0.4308, L1-Distance = 0.0811, L2-Distance = 0.0205, Normal std = 0.2405

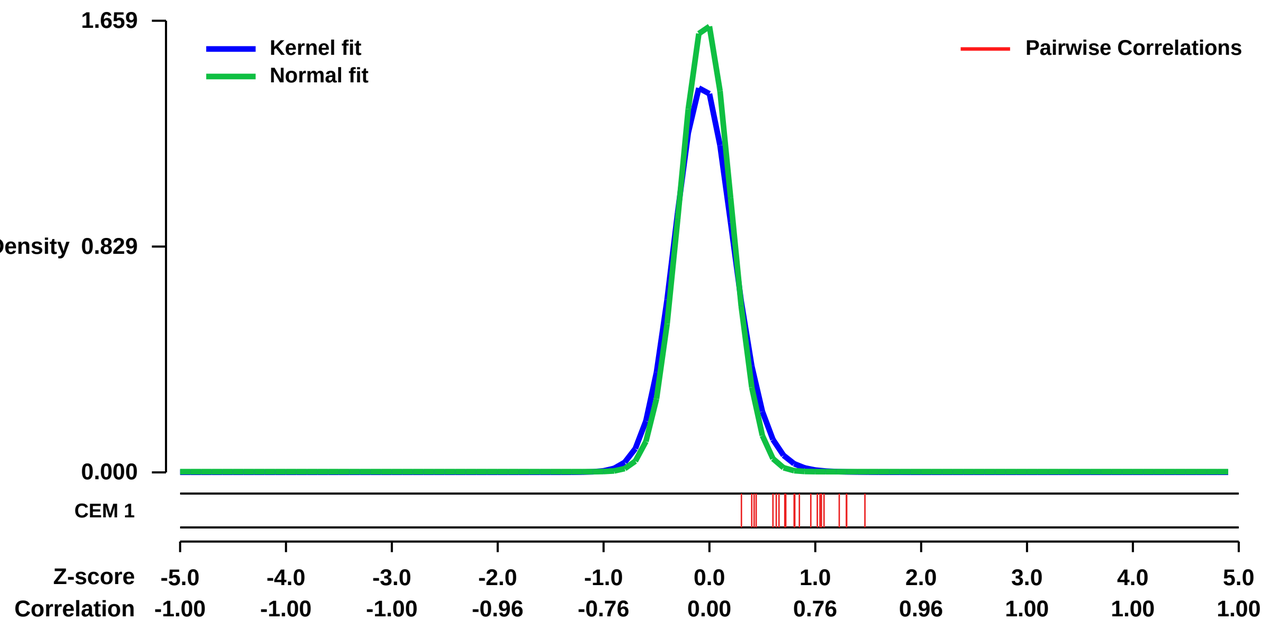

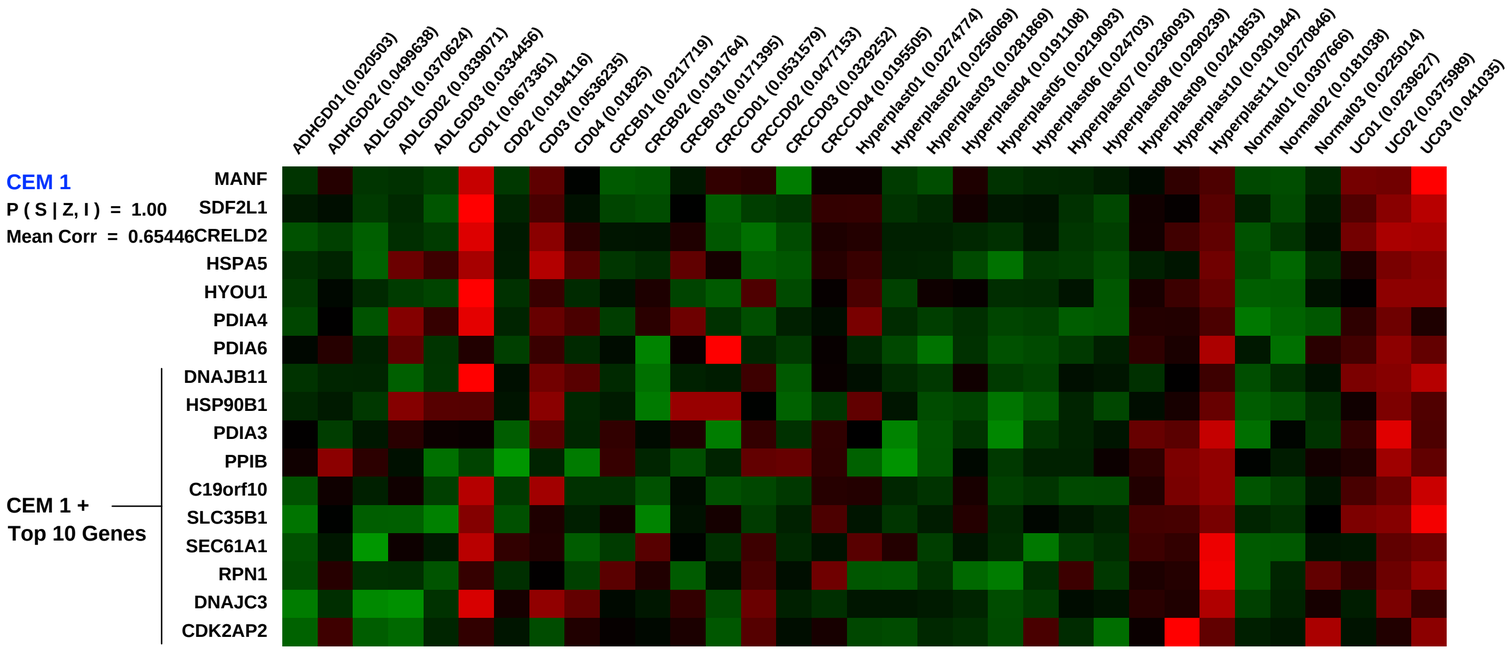

Pre-normalization Quantiles

[min]	[medium]	[max]
2689.6	4345.1	9294.0
1004.8	1738.9	5265.0
1559.7	3791.0	10236.0
10678.4	14795.7	25829.8
2630.7	3621.9	7799.7
896.9	1860.5	4698.0
5531.5	7417.8	12319.8
3045.7	4983.3	11693.9
2054.9	3834.7	7139.6
9988.9	15243.5	24459.6
14011.8	19948.7	26959.9
3646.0	4294.2	7645.0
980.3	1659.8	3296.8
2658.5	4006.7	6678.8
2673.7	4120.5	7566.2
2498.8	3981.5	6874.7
1201.8	1716.6	3332.0

GEO Series "GSE2842" Expression Profiles

Num of samples in this series: 45

Scale of expression profile Z-scores

-3.0 -2.0 -1.0 0.0 1.0 2.0 3.0

GEO Link:	http://www.ncbi.nlm.nih.gov/geo/query/acc.cgi?acc=GSE2842
Status:	Public on Nov 14 2005
Title:	Additional systems to Prednisolone treated childhood ALL samples
Organism:	Homo sapiens
Experiment type:	Expression profiling by array
Platform:	GPL570
Pubmed ID:	16293608
Summary & Design:	**Summary:** Glucocorticoids (GC) are in most chemotherapy protocols for lymphoid malignancies, particularly childhood acute lymphoblastic leukaemia (ALL) for their ability to induce apoptosis in malignant blast. The underlying mechanism, however, has so far only been investigated in model systems. This study comprises Affymetrix hgu133 plus 2.0 analyses of Peripheral blood lymphoblasts purified at three time points (0h, 6-8h, 24h after treatment initiation) from 13 children under therapy for ALL . Treated samples were compared to untreated (0h). For comparison, expression profiles were generated from an adult ALL patient, peripheral blood lymphocytes from GC-exposed healthy donors, GC-sensitive and -resistant ALL cell lines and mouse thymocytes treated with GC in vivo and in vitro. This second series comprises the additional samples mentioned above. Findings. An essentially complete list of GC-regulated candidate genes in clinical settings experimental and was generated, enabling immediate analysis of any gene with respect to its potential significance for GC-induced apoptosis in these systems. Gene regulations previously thought responsible for cell death in experimental systems were reconfirmed in few children only. In contrast, a small number of genes, most not implicated in GC-induced apoptosis previously, were co-ordinately regulated in the majority of children. Keywords: treatment response **Overall design:** Glucocorticoid treated samples of patients or cell lines or healthy donors were compared to their untreated or ethanol treated counterparts.

Background corr dist: KL-Divergence = 0.1239, L1-Distance = 0.0371, L2-Distance = 0.0027, Normal std = 0.4005

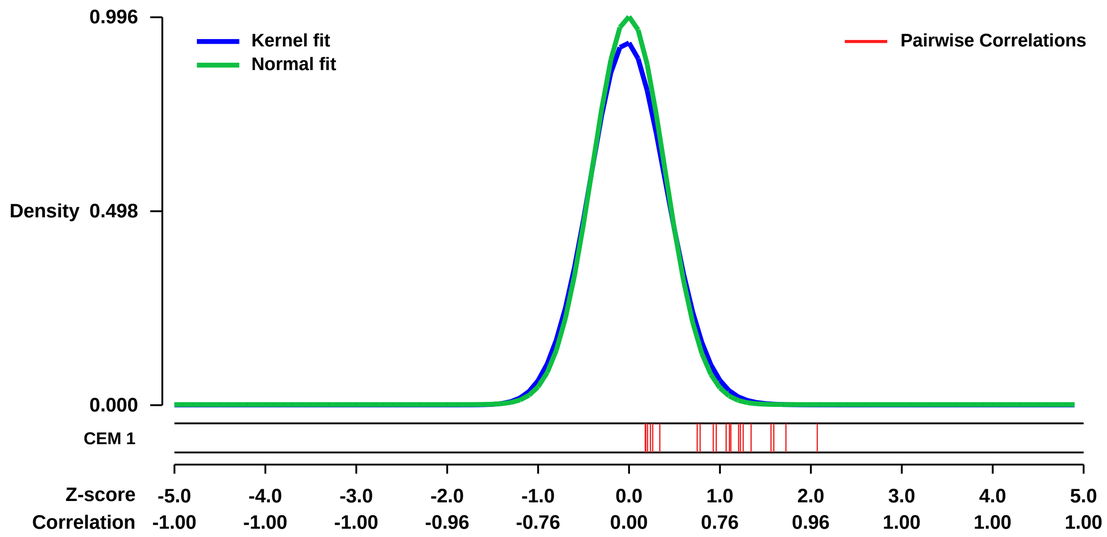

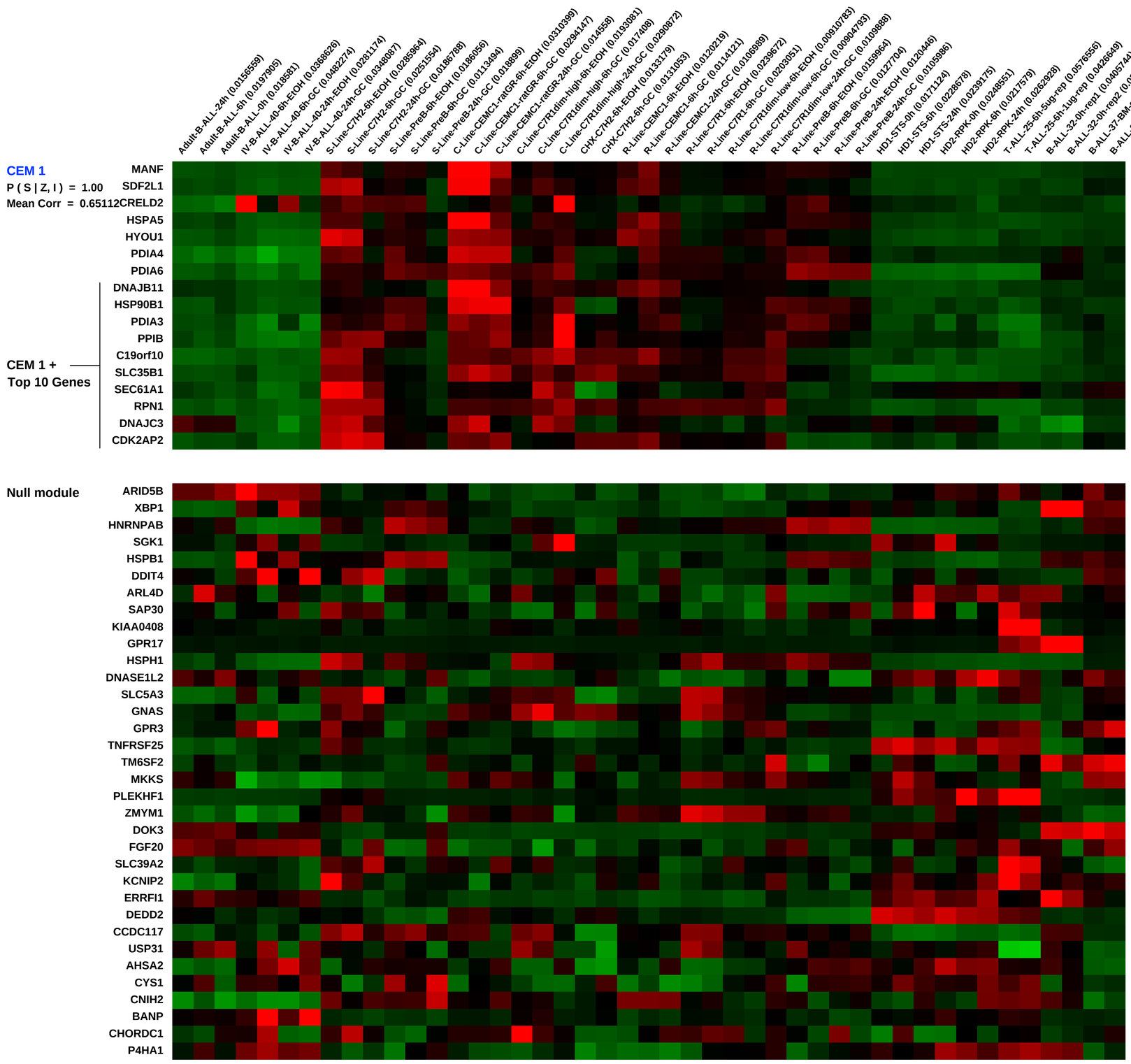

Pre-normalization Quantiles

[min]	[medium]	[max]
951.7	3441.5	13875.9
152.7	1543.8	6272.8
893.7	2003.6	6067.3
2186.8	9775.0	41422.6
748.5	2706.0	7914.1
244.1	804.2	1642.7
1575.4	8105.9	14951.3
1711.8	4023.4	14744.9
1111.1	2648.7	8050.0
3360.2	8656.0	20529.3
6770.9	18195.7	45120.6
773.7	1557.3	4245.0
894.4	2105.6	4587.3
1007.0	1900.6	4092.9
2184.2	3850.8	8855.8
774.2	1702.4	3175.8
591.7	1542.9	4584.1

GEO Series "GSE39395" Expression Profiles

Num of samples in this series: 24

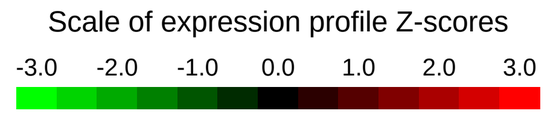

GEO Link:	http://www.ncbi.nlm.nih.gov/geo/query/acc.cgi?acc=GSE39395
Status:	Public on Jan 17 2013
Title:	Expression profiles of cell populations purified from human CRC (3 ways)
Organism:	Homo sapiens
Experiment type:	Expression profiling by array
Platform:	GPL570
Pubmed ID:	23153532
Summary & Design:	**Summary:** The survival of isolated metastatic cells and expansion into macroscopic tumour has been recognized as a limiting step for metastasis formation in several cancer types yet the determinants of this process remain largely uncharacterized. In colorectal cancer (CRC), we identify a transcriptional programme in tumour-associated stromal cells, which is intimately linked to a high risk of developing recurrent disease after therapy. A large proportion of CRCs display mutational inactivation of the TGF-beta pathway but paradoxically they are characterized by high TGF-beta production. In these tumours, TGF-beta instructs a transcriptional programme in stromal cells, which confers a high risk of developing metastatic disease. We purified by FACS [CD45(+),Epcam(-)], [CD45(-) Epcam(+)] and [CD45(-) Epcam(-)] cell populations from fresh CRC samples and assessed their gene expression profiles **Overall design:** Freshly obtained tumors from CRC patients (n=8) treated at Hospital del Mar (Barcelona, Spain) were minced and incubated with 0.1% Hyaluronidase and 0.1% Collagenase 1A. Pieces were then homogenized. Enzymatic reaction was stopped by adding 10% FBS and single cells were collected by sequential filtering. Cells were resuspended in Ammonium Chloride (0.15M) to lyse erythrocytes. Cells were stained with anti-hEpcam/TROP1-APC and anti-CD45-PE conjugated antibody. Dead cells were labeled with Propidium Iodide. Fluorescence Activated Cell Sorting (FACS) was used to separate cells.

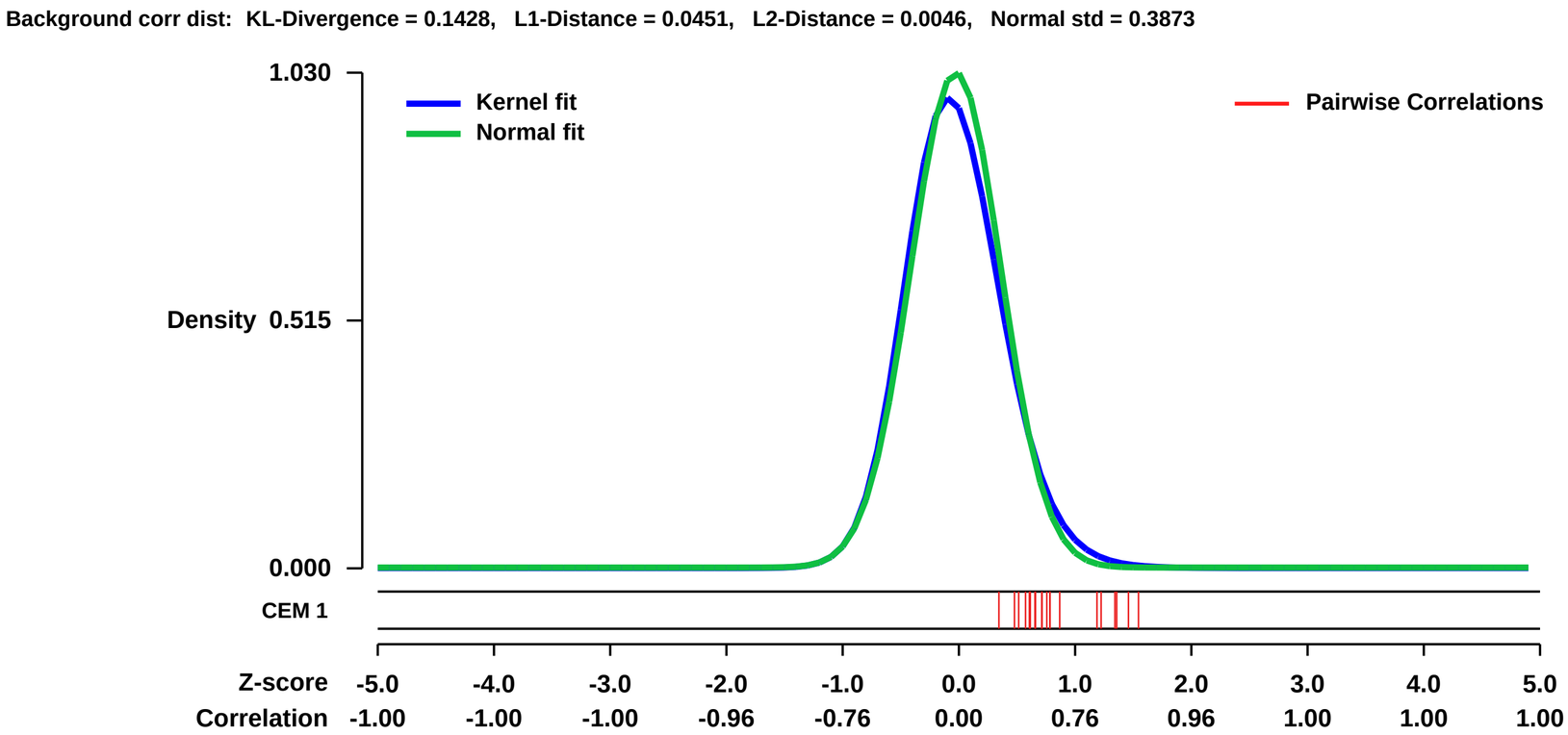

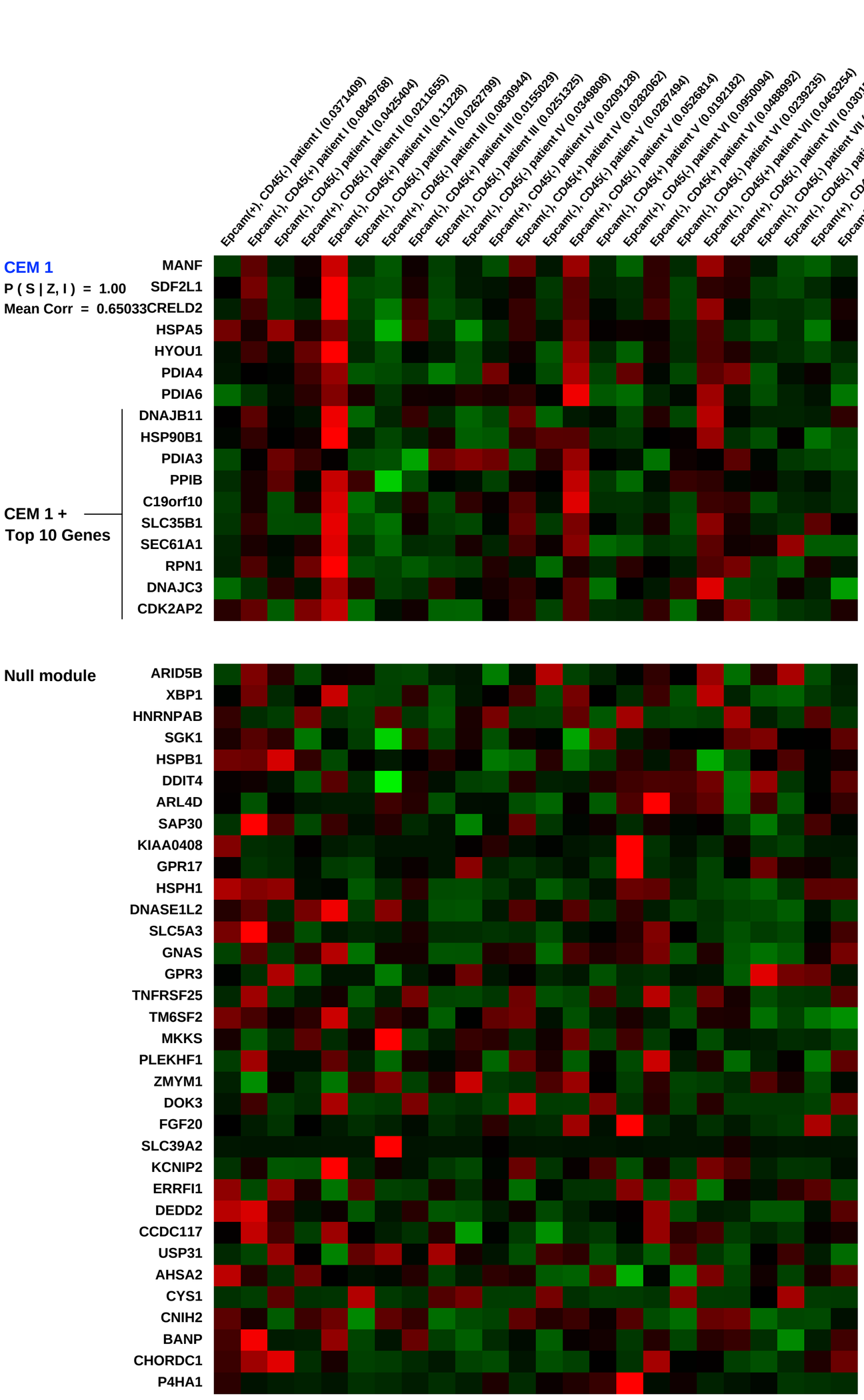

Pre-normalization Quantiles

[min]	[medium]	[max]
4963.3	6761.1	12585.9
210.7	528.1	2260.7
807.4	2194.3	6684.8
8214.9	11856.9	14488.4
735.0	1320.1	3713.1
5564.7	8262.3	12509.3
4611.9	5576.7	7807.3
2278.0	3218.8	6114.1
2116.0	2588.1	3694.1
4516.1	6257.6	7806.3
4649.3	9140.8	13862.3
1382.4	2014.0	4106.6
2446.1	3407.3	5600.3
2273.2	3243.2	5589.7
1013.4	1646.3	3780.7
3996.5	5217.6	6992.4
898.0	2112.1	4075.1

GEO Series "GSE30159" Expression Profiles

Num of samples in this series: 18

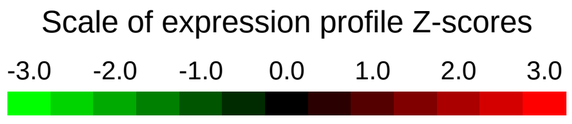

GEO Link:	http://www.ncbi.nlm.nih.gov/geo/query/acc.cgi?acc=GSE30159
Status:	Public on Apr 08 2012
Title:	Gene expression analysis of bone biospies from nine patients with endogenous Cushings syndrome before and after treatment
Organism:	Homo sapiens
Experiment type:	Expression profiling by array
Platform:	GPL570
Pubmed ID:	22450549
Summary & Design:	**Summary:** Glucose intolerance and diabetes mellitus are classical parts of endogenous Cushingâ s syndrome (CS), and insulin resistance is a feature of cortisol excess. CS patients display characteristics including hyperglycemia, abdominal obesity, reduced high-density lipoprotein cholesterol levels and elevated triglycerides, and arterial hypertension. Hypercortisolism is a well known cause of bone loss, and patients with CS frequently display low bone mass and fragility fractures. Cortisol excess inhibits bone formation, increases bone resorption, impairs calcium absorption from the gut, and affects the secretion of several hormones, cytokines, and growth factors with potential influence on bone metabolism. Bone biopsies from nine CS patients, before and mean 3 months after surgery, were screened for expressional candidate genes using Affymetrix human Gene Plus 2.0 Arrays. Analyses were performed to identify genes in glucocorticoid-induced osteoporosis and genes in glucose metabolism and energy homeostasis. **Overall design:** Expression levels were examined in bone biopsy samples from 9 patients with endogenous cushing syndrome, before and mean three months after surgery.

Background corr dist: KL-Divergence = 0.0822, L1-Distance = 0.0258, L2-Distance = 0.0011, Normal std = 0.4680

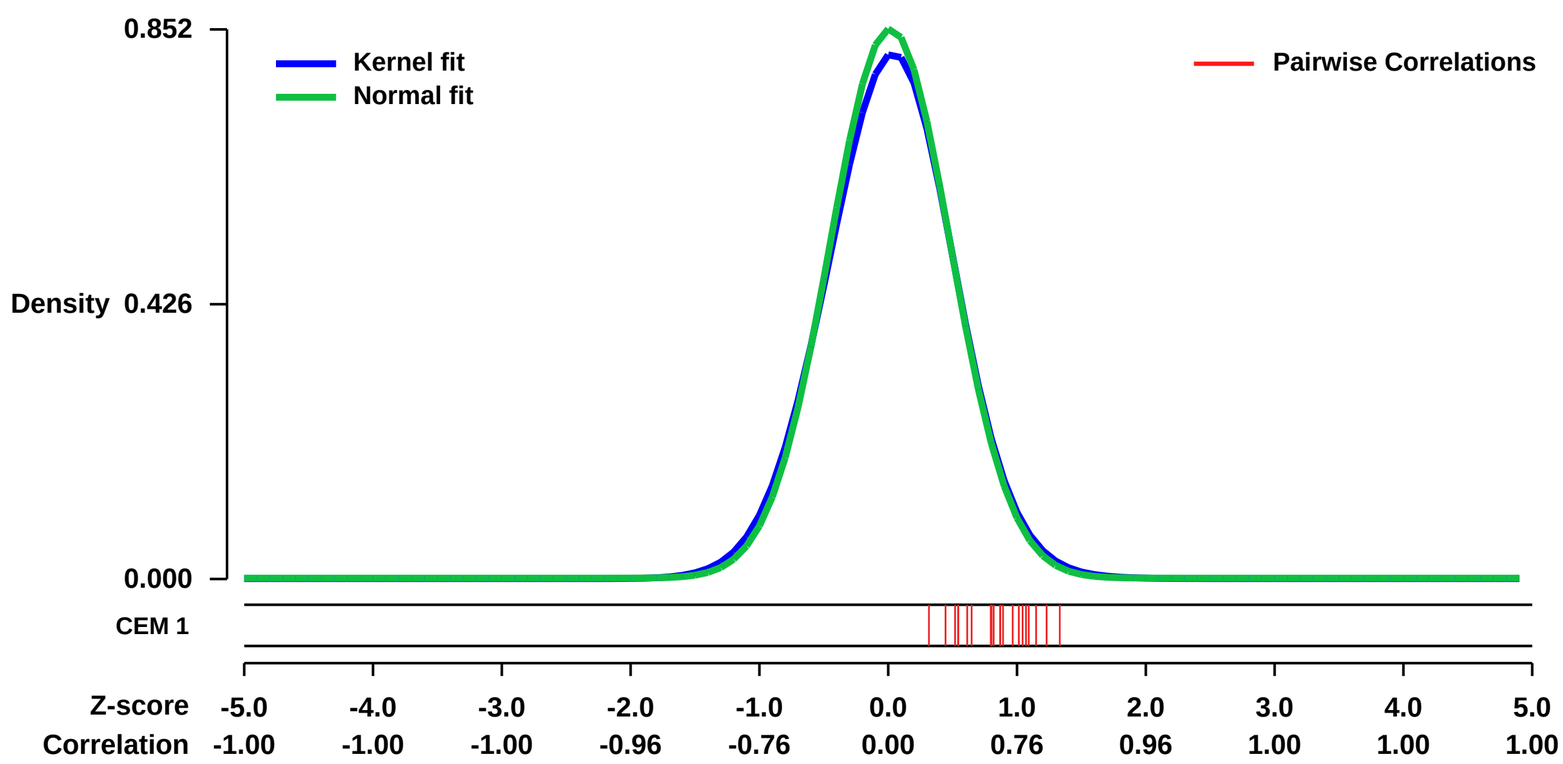

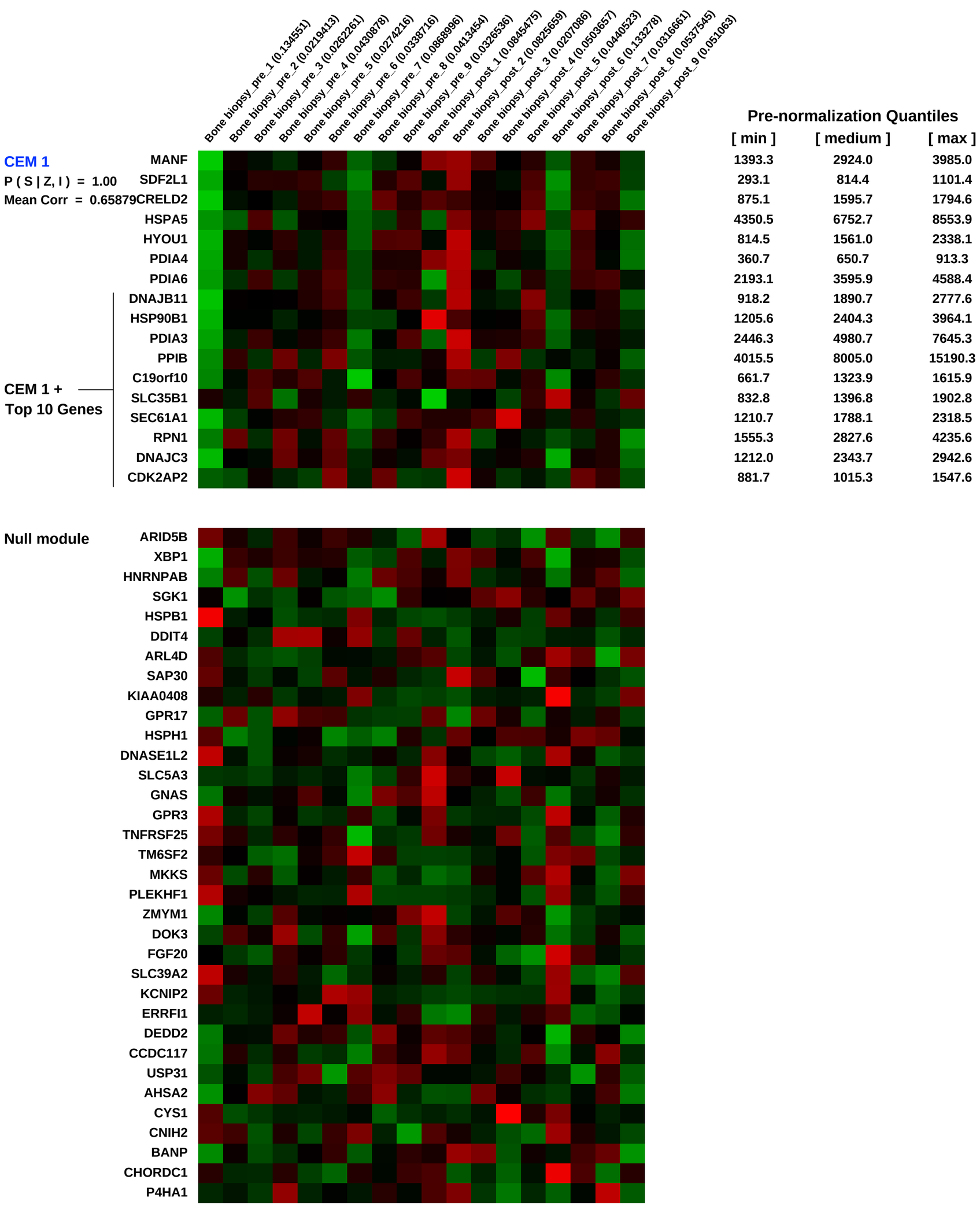

GEO Series "GSE41296" Expression Profiles

Num of samples in this series: 120

Details of this dataset are not shown due to large number of samples and the page size limit.

Find details in http://www.ncbi.nlm.nih.gov/geo/query/acc.cgi?acc=GSE41296

Background corr dist: KL-Divergence = 0.2722, L1-Distance = 0.0580, L2-Distance = 0.0089, Normal std = 0.2920

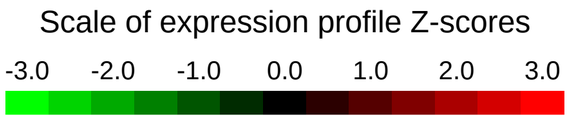

GEO Series "GSE53157" Expression Profiles

Num of samples in this series: 27

Scale of expression profile Z-scores

-3.0 -2.0 -1.0 0.0 1.0 2.0 3.0

GEO Link:	http://www.ncbi.nlm.nih.gov/geo/query/acc.cgi?acc=GSE53157
Status:	Public on Dec 10 2013
Title:	Gene expression profiling associated with the progression to poorly differentiated thyroid carcinomas
Organism:	Homo sapiens
Experiment type:	Expression profiling by array
Platform:	GPL570
Pubmed ID:	19809427
Summary & Design:	**Summary:** Poorly differentiated thyroid carcinomas (PDTC) represent a heterogeneous, aggressive entity, presenting features that suggest a progression from well-differentiated carcinomas. To elucidate the mechanisms underlying such progression and identify novel therapeutical targets, we assessed the genome-wide expression in normal thyroid tissues, well-differentiated thyroid carcinomas and PDTC. **Overall design:** PTC were screened for BRAF mutations and rearrangements of RET/PTC and, in addition, follicular variants were also analyzed for RAS mutations and PAX8-PPARG rearrangements. FTC were screened for RAS and PAX8-PPARG rearrangements. PDTC were analyzed for BRAF, RAS and PAX8-PPARG genes.

Background corr dist: KL-Divergence = 0.2909, L1-Distance = 0.0628, L2-Distance = 0.0108, Normal std = 0.2898

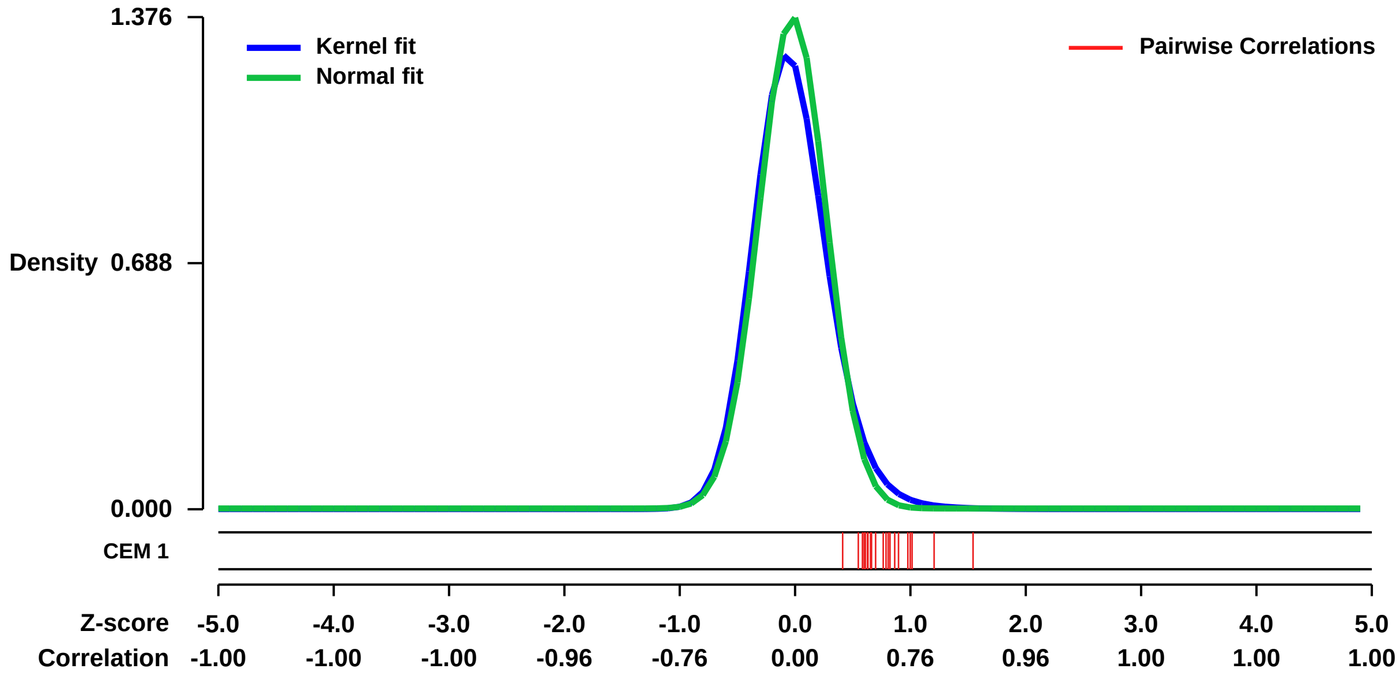

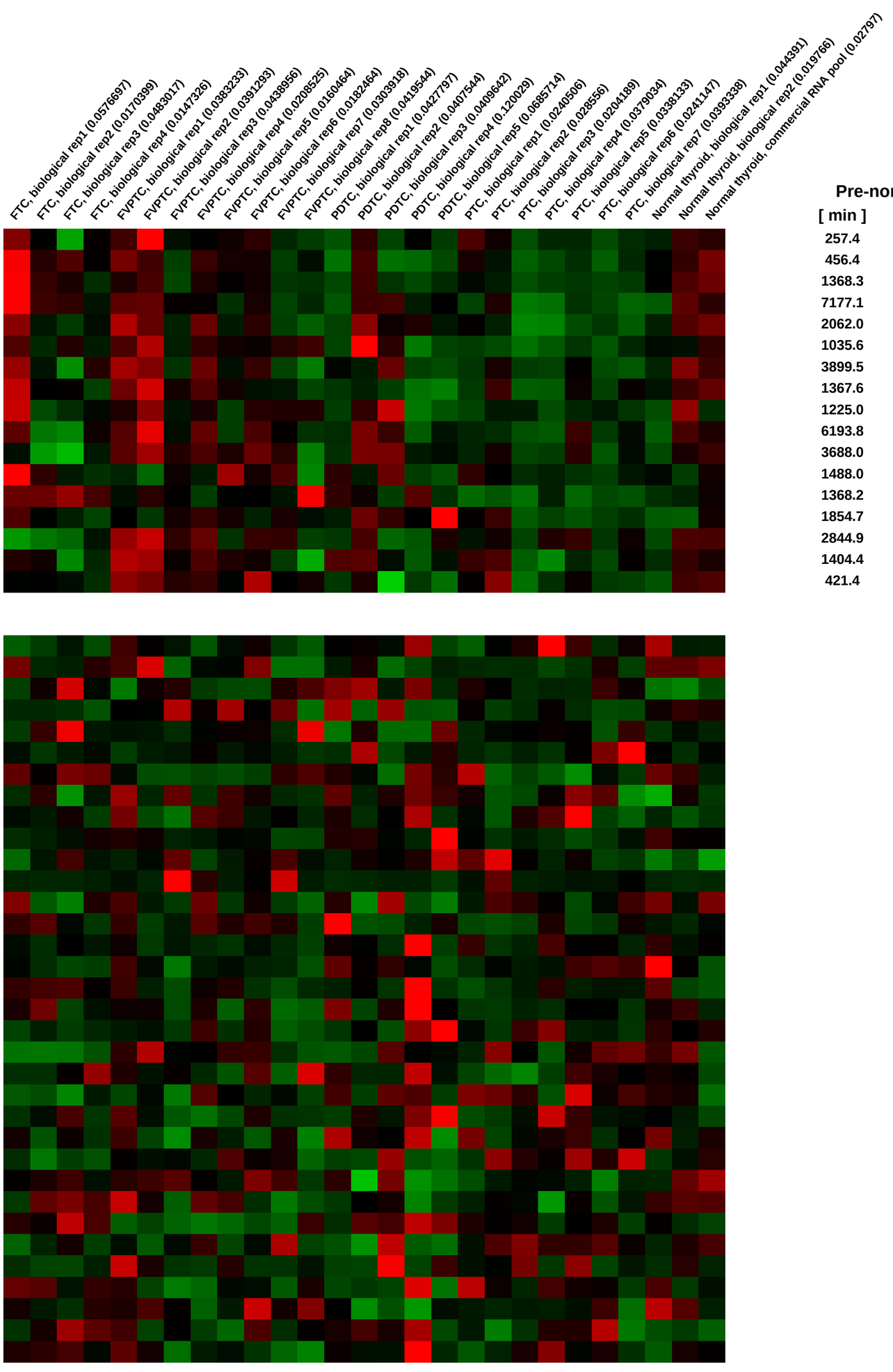

	Pre-normalization Quantiles		
	[min]	[medium]	[max]
MANF	257.4	3766.7	10296.0
SDF2L1	456.4	1655.2	4327.3
CRELD2	1368.3	2325.4	9061.0
HSPA5	7177.1	11868.5	22017.4
HYOU1	2062.0	4044.3	7503.8
PDIA4	1035.6	2318.2	5577.8
PDIA6	3899.5	6457.7	10263.9
DNAJB11	1367.6	2206.2	3884.6
HSP90B1	1225.0	3664.7	9326.6
PDIA3	6193.8	10711.6	19821.4
PPIB	3688.0	10924.4	17946.4
C19orf10	1488.0	2188.7	4211.3
SLC35B1	1368.2	2045.4	3841.2
SEC61A1	1854.7	2428.9	4603.5
RPN1	2844.9	5740.0	9025.9
DNAJC3	1404.4	3066.5	4591.6
CDK2AP2	421.4	1424.2	2280.8

GEO Series "GSE41035" Expression Profiles

Num of samples in this series: 24

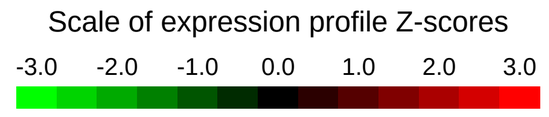

GEO Link:	http://www.ncbi.nlm.nih.gov/geo/query/acc.cgi?acc=GSE41035
Status:	Public on Nov 07 2012
Title:	FGFR3-shRNA induced transcriptional changes in RT112 bladder cancer cells
Organism:	Homo sapiens
Experiment type:	Expression profiling by array
Platform:	GPL570
Pubmed ID:	23019225
Summary & Design:	**Summary:** Aberrant activation of FGFR3 via overexpression or mutation is a frequent feature of bladder cancer; however, its molecular and cellular consequences and functional relevance to carcinogenesis are not well understood. In this study with a bladder carcinoma cell line expressing inducible FGFR3 shRNAs, we sought to identiy transcriptional targets of FGFR3 and investigate their contribution to bladder cancer development. **Overall design:** Bladder cancer cell line RT112 was transduced with a doxycycline-inducible control EGFP shRNA or three independent FGFR3 shRNAs, designated FGFR3 shRNA 2-4, FGFR3 shRNA 4-1 and FGFR3 shRNA 6-16. These four cell lines were treated with or without doxycycline for 48 hr to deplete FGFR3 protein prior to the isolation of mRNA for microarray analysis. Genes that were differentially expressed after doxycycline induction in all three FGFR3-depleted cell lines but not in the control cell line were considered potential FGFR3-regulated genes. Each treatment group was run in triplcates, and there are 24 samples.

Background corr dist: KL-Divergence = 0.1424, L1-Distance = 0.0265, L2-Distance = 0.0010, Normal std = 0.3853

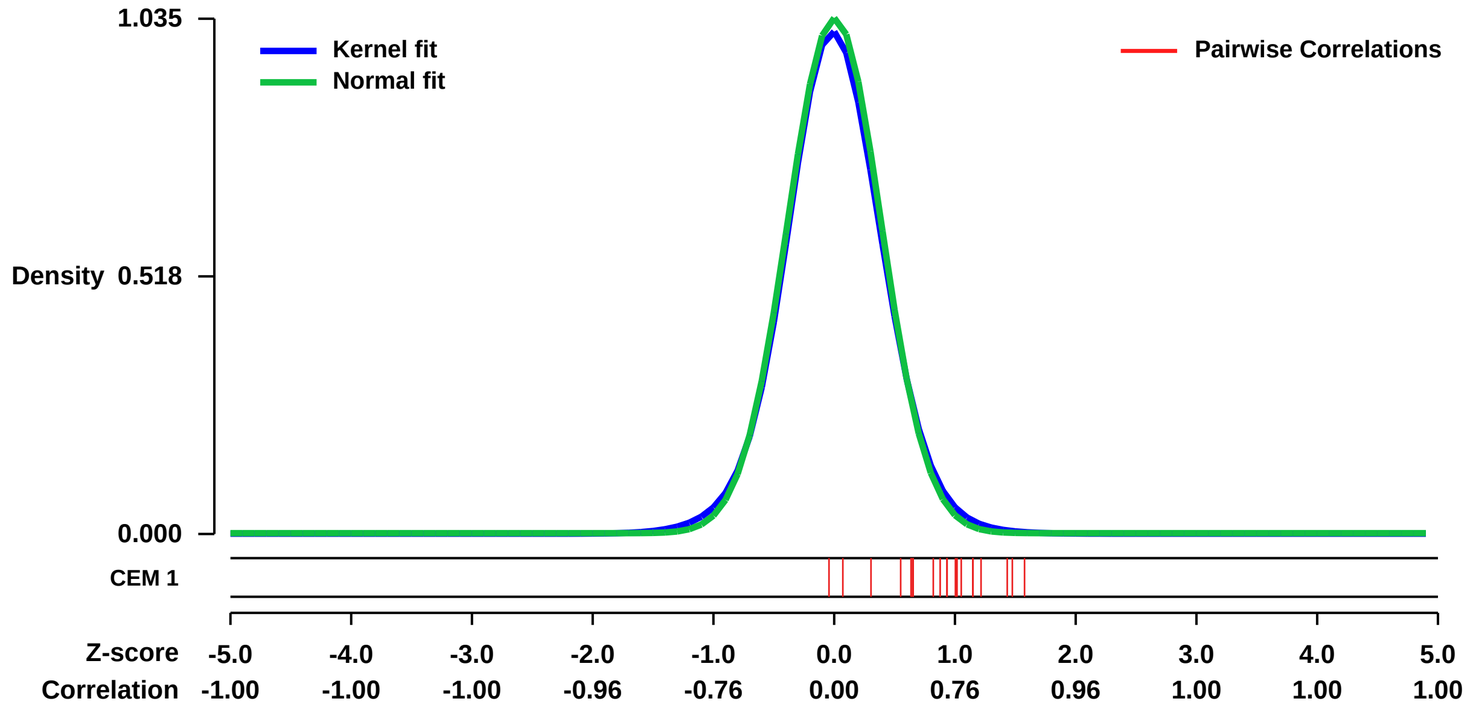

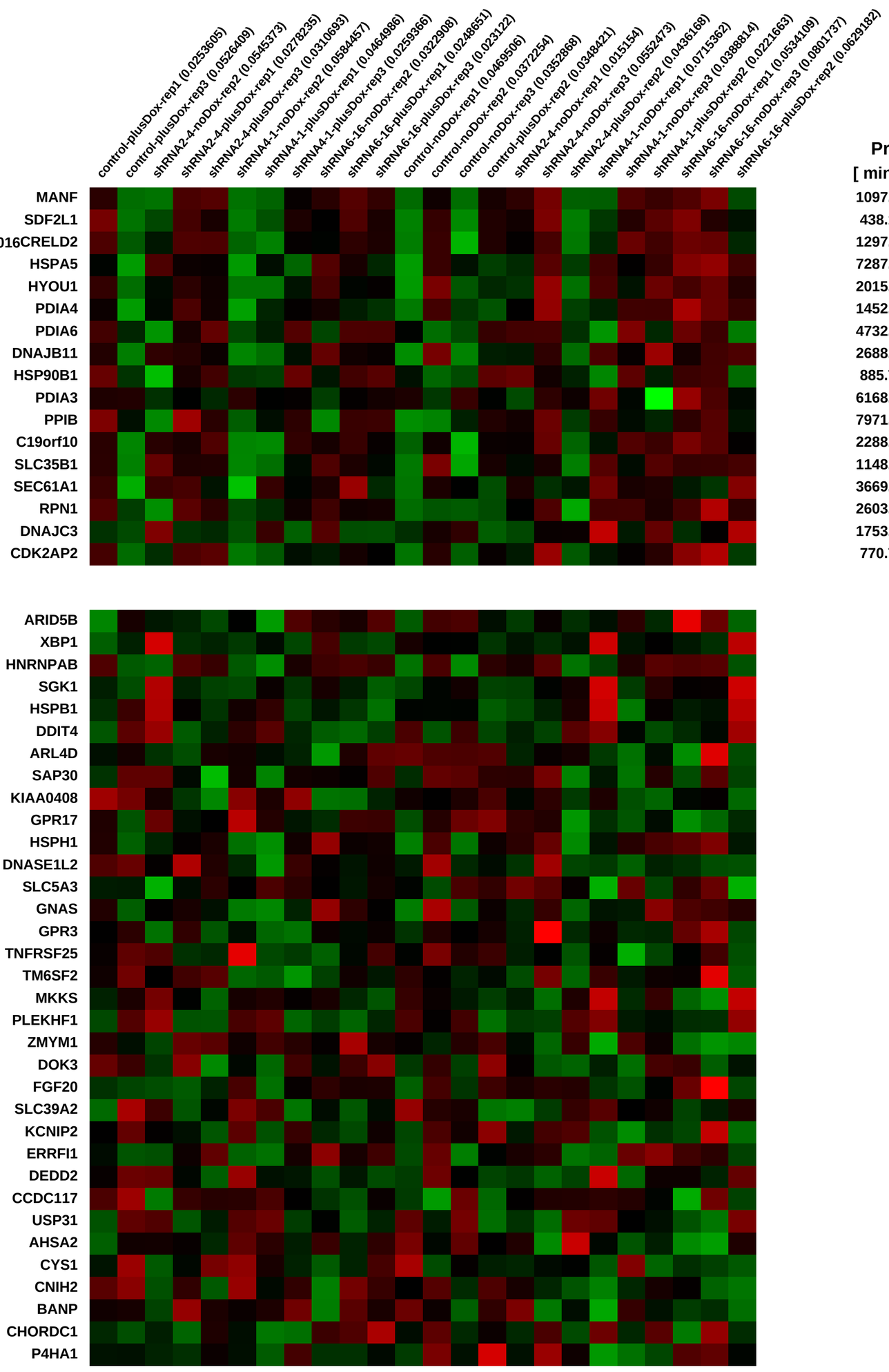

GEO Series "GSE8056" Expression Profiles

Num of samples in this series: 12

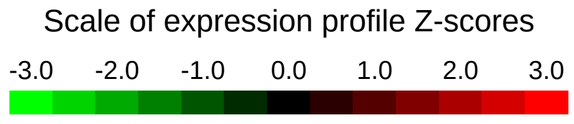

GEO Link:	http://www.ncbi.nlm.nih.gov/geo/query/acc.cgi?acc=GSE8056
Status:	Public on May 23 2010
Title:	Gene Expression Profiles in Thermally Injured Human Skin: A Temporal Microarray Analysis
Organism:	Homo sapiens
Experiment type:	Expression profiling by array
Platform:	GPL570
Pubmed ID:	19781859
Summary & Design:	**Summary:** Thermal injury incites inflammatory responses that often transcend the local environment and lead to structural deficiencies in skin that give way to scar formation. We hypothesized that extensive perturbations within burned skin following thermal insult and during subsequent events of wound repair induce vast alterations in gene expression that likely serve as a wound and systemic healing deterrent. A high-throughput microarray experiment was designed to analyze genetic expression patterns and identify potential genes to target for therapeutic augmentation or silencing. The study compares gene expression from burn wound margins at various times following thermal injury to expression observed in normal skin. Utilizing this design, we report that the totality of gene expression alterations is indeed enormous. Further, we observed that the differential expression of many inflammatory and immune response genes appear to be continually up-regulated in burn wound margins seven days or more after initial thermal insult. As it is well established that the inflammatory process must abate for wound healing to proceed, the finding of ongoing local inflammation is cause for further investigation. To our knowledge, this is the first report of the gene expression alterations induced by thermal injury of human skin. As such, it provides a wealth of data to mine with the ultimate goal of better understanding the local pathophysiologic changes at the site of thermal injury that not only affect wound healing capacity, but may also contribute to systemic derangements within the burn patient. **Keywords: time course, disease state analysis** **Overall design:** The study compares gene expression from burn wound margins at various times following thermal injury to expression observed in normal skin. All skin specimens were obtained in the operating room within minutes of being removed from the patient. Burn specimens were taken from wound margins. Harvested tissue at the burn wound margin maximized the capture of viable cells from the multiple lineages important to the healing process and minimized the inclusion of non-viable cells destroyed by full-thickness injury. After isolation, RNA samples were pooled equally by mass as to contain RNA from 5 tissue specimens for each array replicate.

Background corr dist: KL-Divergence = 0.0873, L1-Distance = 0.0311, L2-Distance = 0.0017, Normal std = 0.4592

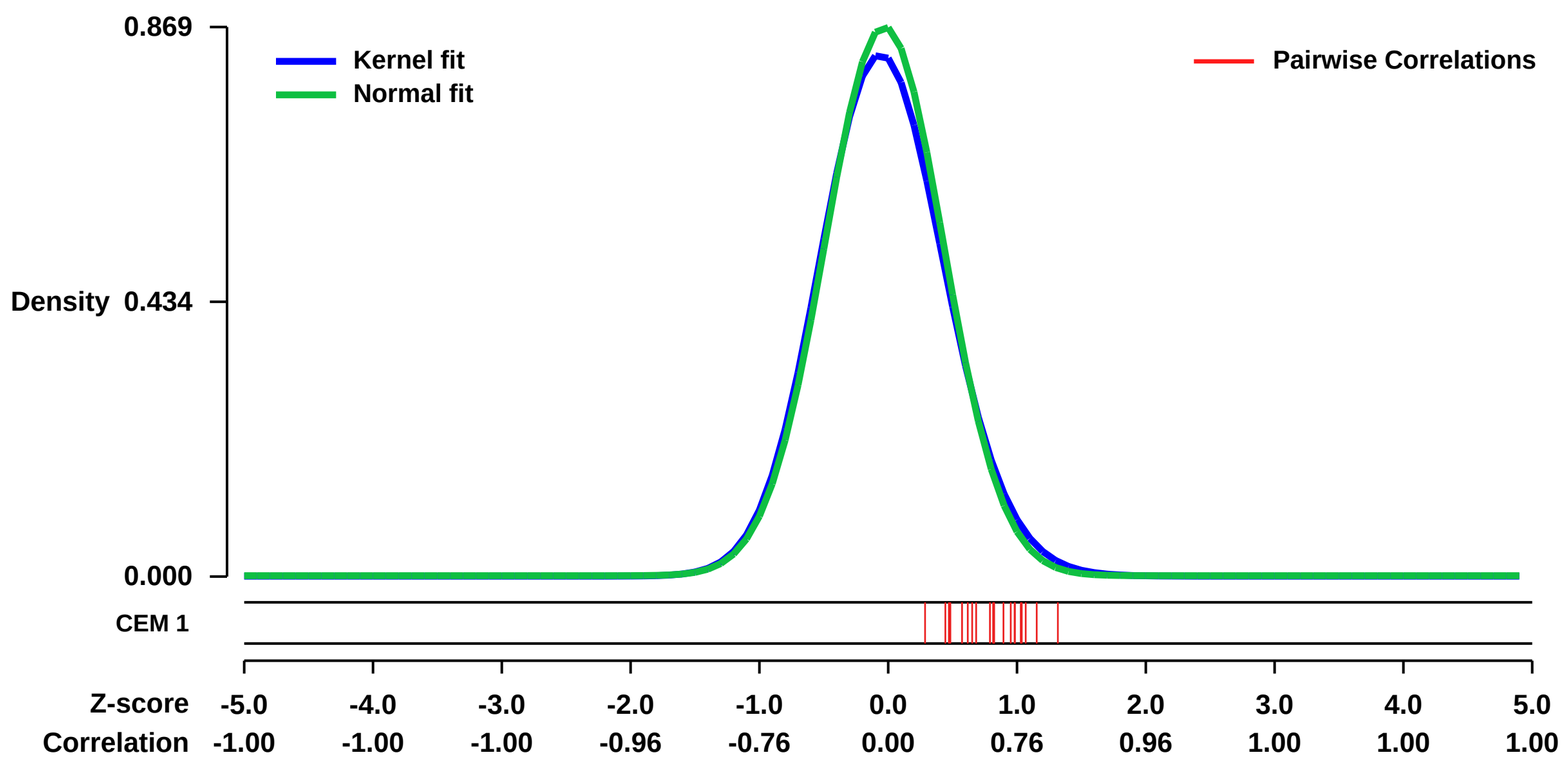

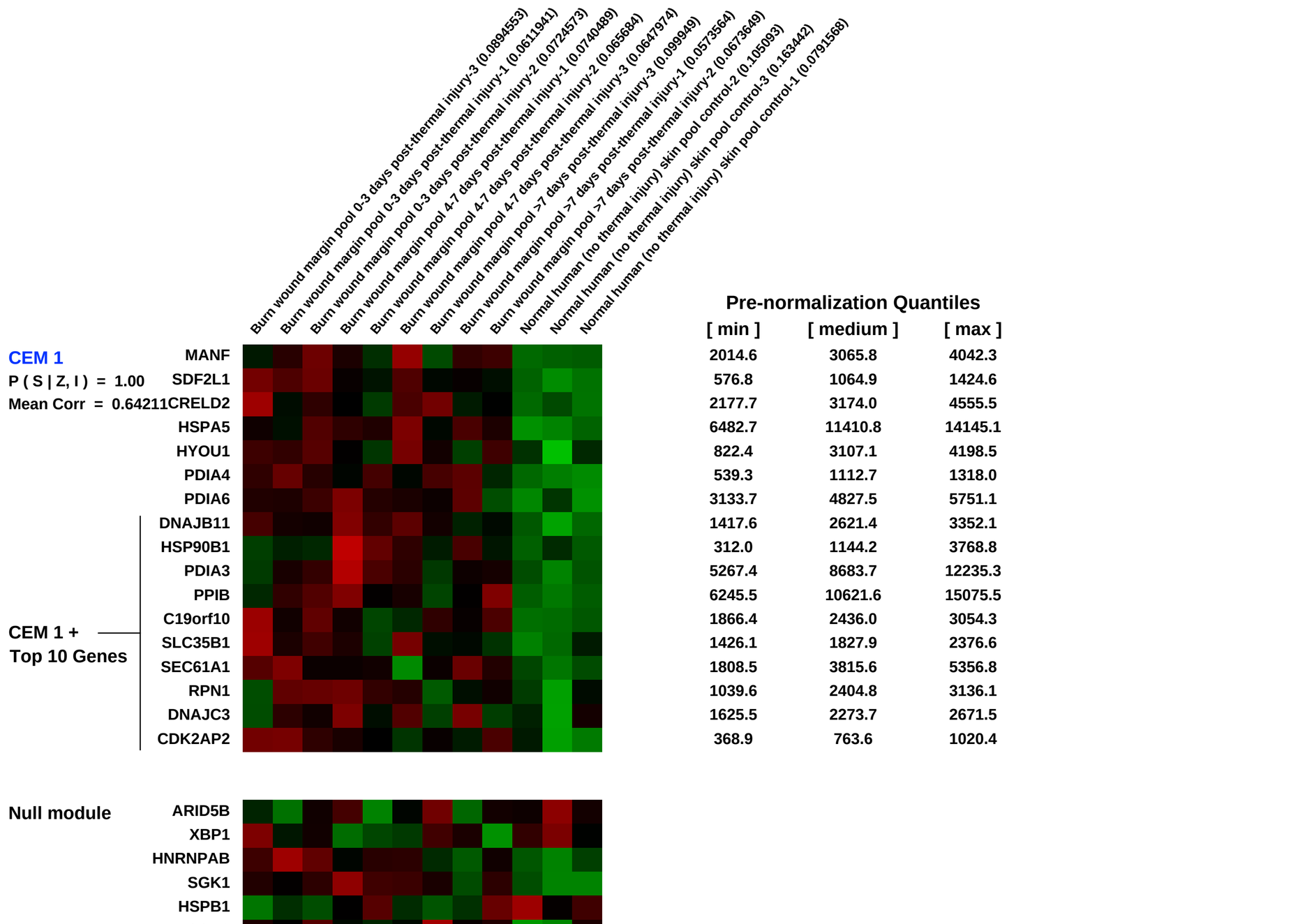

GEO Series "GSE2706" Expression Profiles

Num of samples in this series: 21

Scale of expression profile Z-scores

-3.0 -2.0 -1.0 0.0 1.0 2.0 3.0

GEO Link:	http://www.ncbi.nlm.nih.gov/geo/query/acc.cgi?acc=GSE2706
Status:	Public on Sep 01 2005
Title:	TLR agonists on human dendritic cells
Organism:	Homo sapiens
Experiment type:	Expression profiling by array
Platform:	GPL570
Pubmed ID:	15995707
Summary & Design:	**Summary:** Toll like receptors (TLRs) sense microbial products and initiate adaptive immune responses by activating dendritic cells (DCs). Since pathogens may contain several agonists we asked whether different TLRs may synergize in DC activation. We report that in human and mouse DC TLR3 or TLR4 potently synergize with TLR7, TLR8 or TLR9 in the induction of selected cytokine genes. Upon synergistic stimulation, IL-12, IL-23 and Delta-4 are induced at levels 50-100 fold higher than those induced by optimal concentrations of single agonists, leading to enhanced and sustained TH1 polarizing capacity. Using microarray analysis we show that only 1.5% of the transcripts induced by single TLR agonists are synergistically regulated by combinations of TLR4 and TLR8 agonists.. These results identify a combinatorial code by which DCs discriminate pathogens and provide (suggest) a rationale to design adjuvants for TH1 responses. Series_overall_design: 3 untreated, 3 treated with LPS at 2h, 3 treated with LPS at 8h, 3 treated with R848 at 2h, 3 treated with R848 at 8h, 3 treated with LPS + R848 at 2h, 3 treated with LPS + R848 at 8h Keywords: other Overall design:

Background corr dist: KL-Divergence = 0.2329, L1-Distance = 0.0428, L2-Distance = 0.0045, Normal std = 0.3167

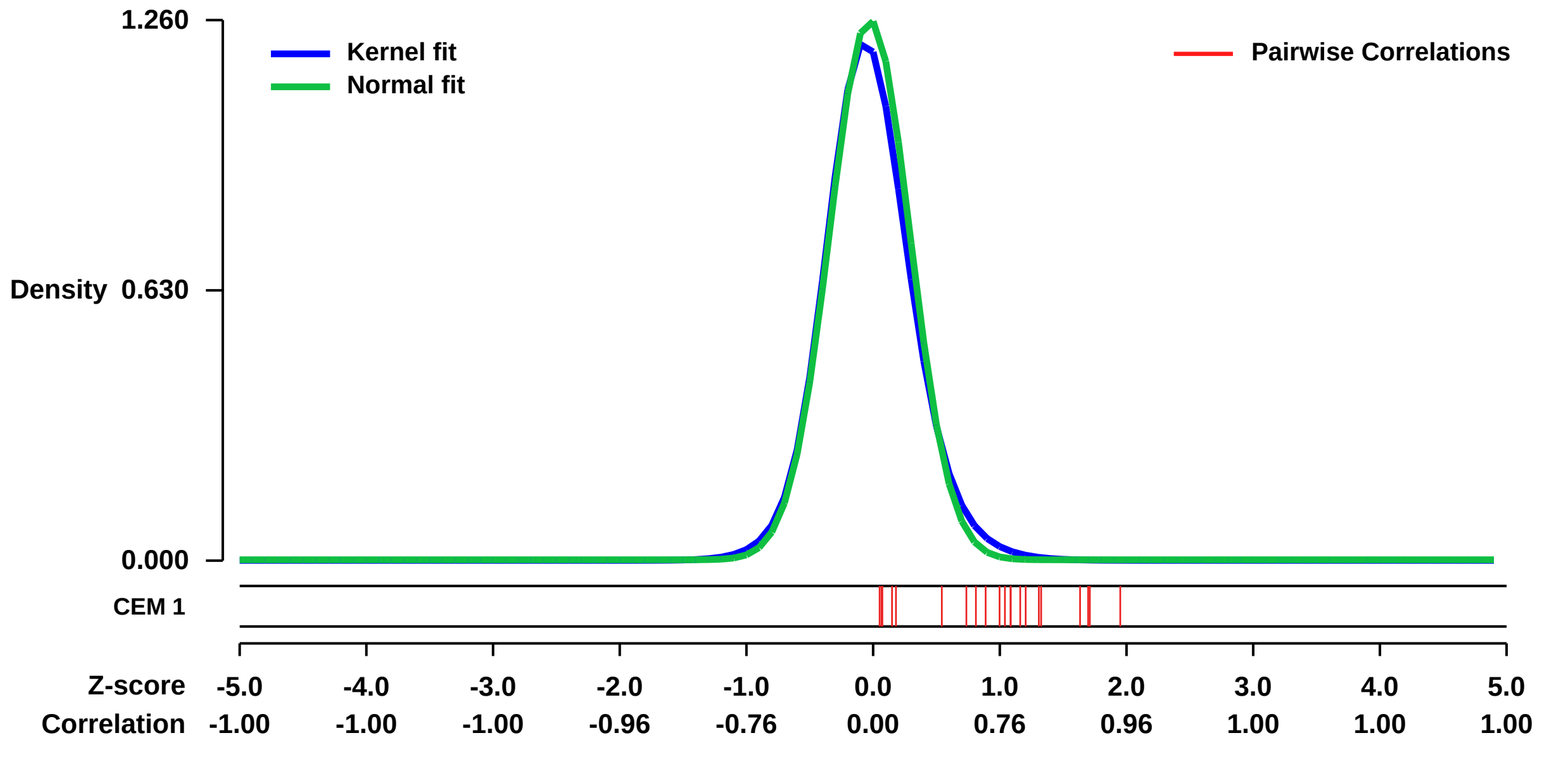

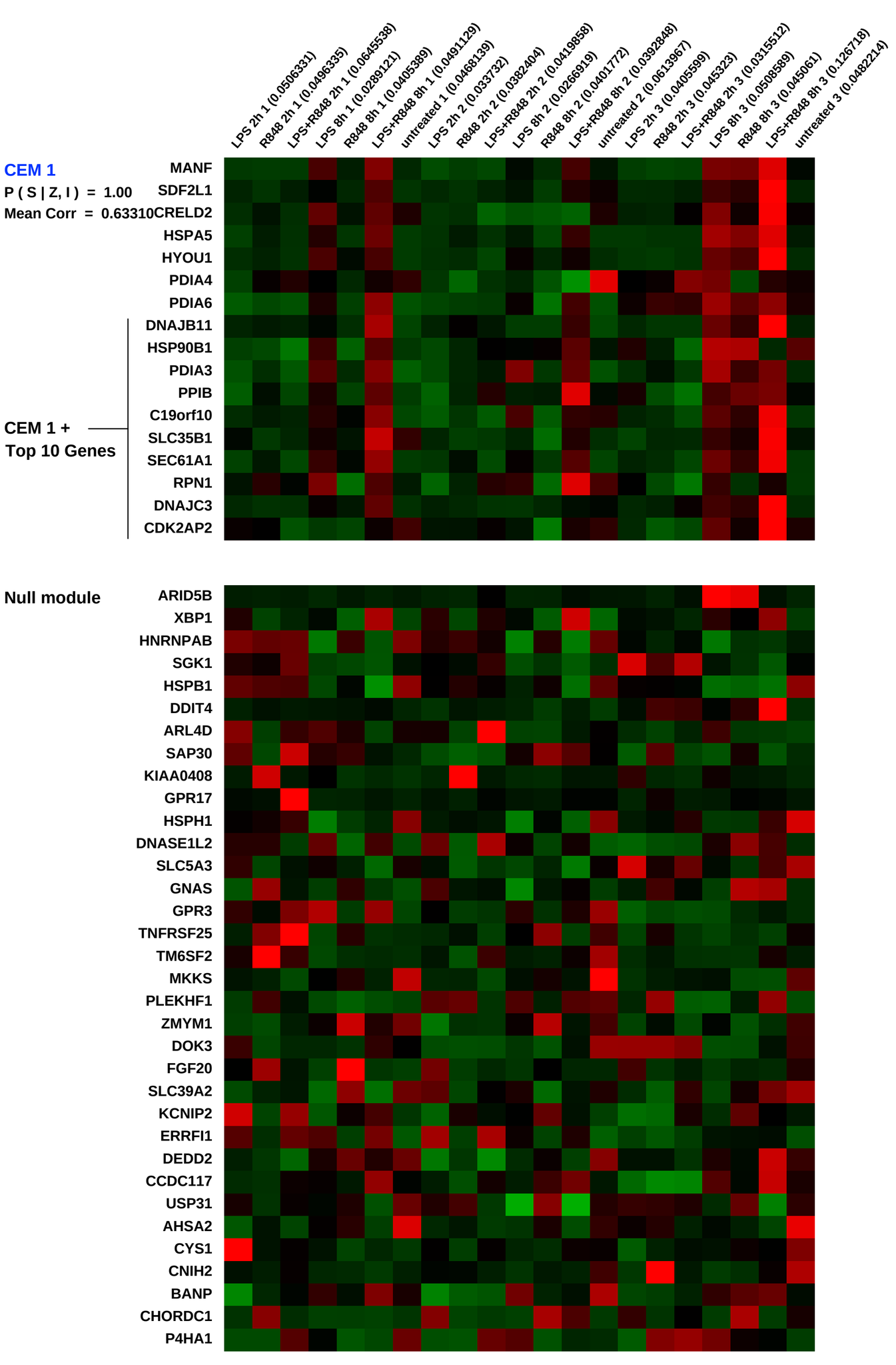

Pre-normalization Quantiles

	[min]	[medium]	[max]
MANF	1226.3	2076.6	7986.6
SDF2L1	660.7	1079.0	6794.2
CRELD2	536.4	981.7	2449.9
HSPA5	7049.8	9746.1	44905.5
HYOU1	745.8	1284.9	8057.6
PDIA4	297.4	880.0	1796.6
PDIA6	3659.3	7617.6	12333.2
DNAJB11	2553.8	3910.5	14427.7
HSP90B1	2632.6	4708.8	8950.8
PDIA3	8062.4	10848.2	21270.6
PPIB	5167.2	9223.1	18855.6
C19orf10	2641.6	3534.6	7824.1
SLC35B1	751.1	1200.4	2912.4
SEC61A1	2156.4	3169.2	10074.6
RPN1	1722.8	2984.2	5532.8
DNAJC3	2665.6	3383.6	15759.0
CDK2AP2	364.8	606.4	1168.8

GEO Series "GSE20285" Expression Profiles

Num of samples in this series: 12

Scale of expression profile Z-scores

-3.0 -2.0 -1.0 0.0 1.0 2.0 3.0

GEO Link:	http://www.ncbi.nlm.nih.gov/geo/query/acc.cgi?acc=GSE20285
Status:	Public on Mar 12 2010
Title:	Gene profiles induced by overexpression of wild-type and mutant Notch1 variants in MCF10A mammary epithelial cell line
Organism:	Homo sapiens
Experiment type:	Expression profiling by array
Platform:	GPL570
Pubmed ID:	20194747
Summary & Design:	**Summary:** Expression of a constitutively active Notch-1 intracellular domain (NICD) in MCF-10A cells was found to induce two distinct types of 3D structures: large, hyperproliferative structures and small, growth-arrested structures with reduced cell-to-matrix adhesion. These heterogeneous phenotypes reflect differences in Notch pathway activation levels. High Notch activity caused loss of cell adhesion and inhibition of proliferation, whereas low Notch activity maintained matrix adhesion and provoked a strong hyperproliferative response. In order to gain insight into the dosage-dependent transcriptional events triggered by Notch1 activation, gene expression profiles induced 48 hours after infection of MCF-10A cells with retroviral vectors expressing full-length Notch-1, L1601P+â P, or NICD were compared. Full-length Notch-1 induced the weakest effect, L1601P+â P induced an intermediate effect and NICD induced the strongest effect. Results provide insight into the dichotomous activites of Notch during development and tumorigenesis. **Overall design:** Twelve samples were harvested 48 h after retroviral infection with either vector control, full-length Notch1, Notch1 L1601P+â P, or NICD. Each condition was performed in triplicate.

Background corr dist: KL-Divergence = 0.0909, L1-Distance = 0.0307, L2-Distance = 0.0012, Normal std = 0.4749

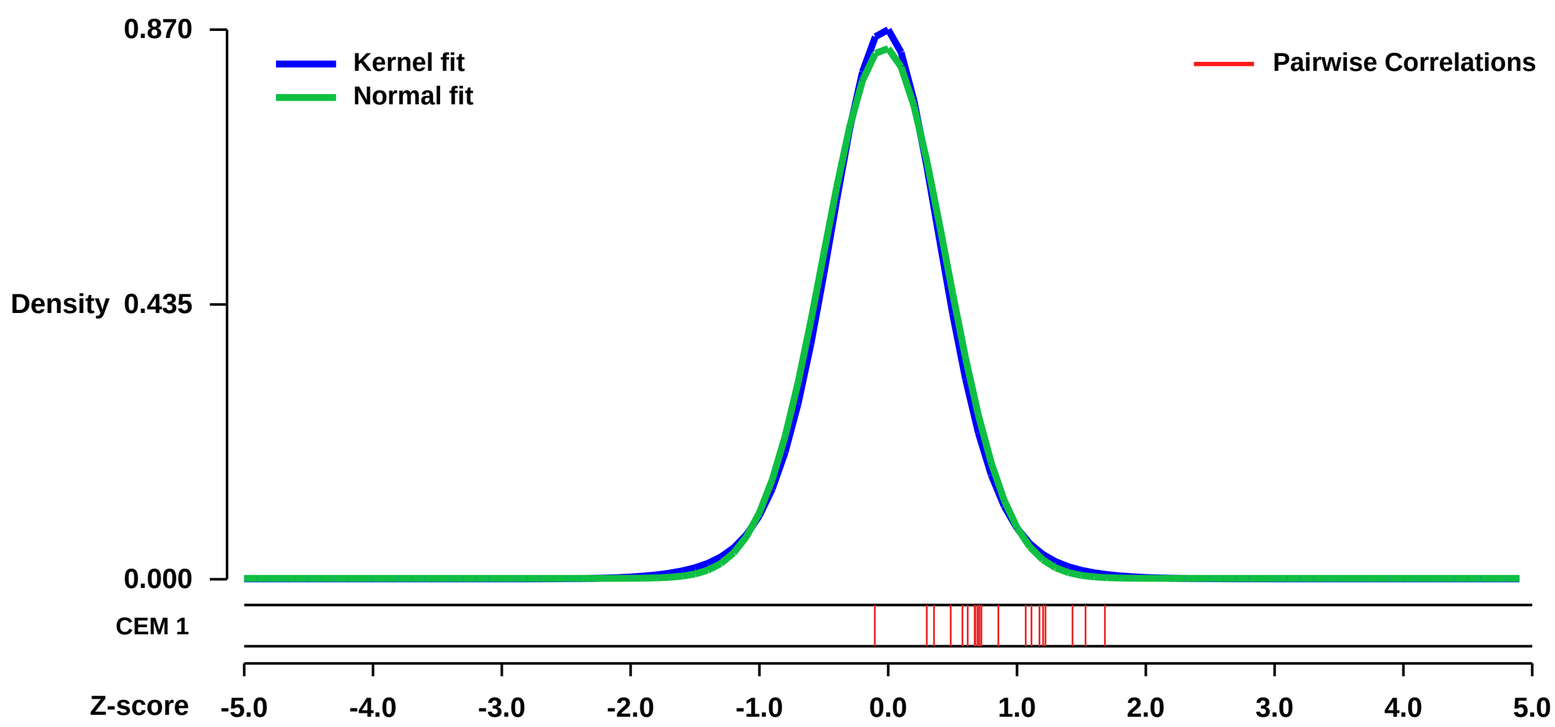

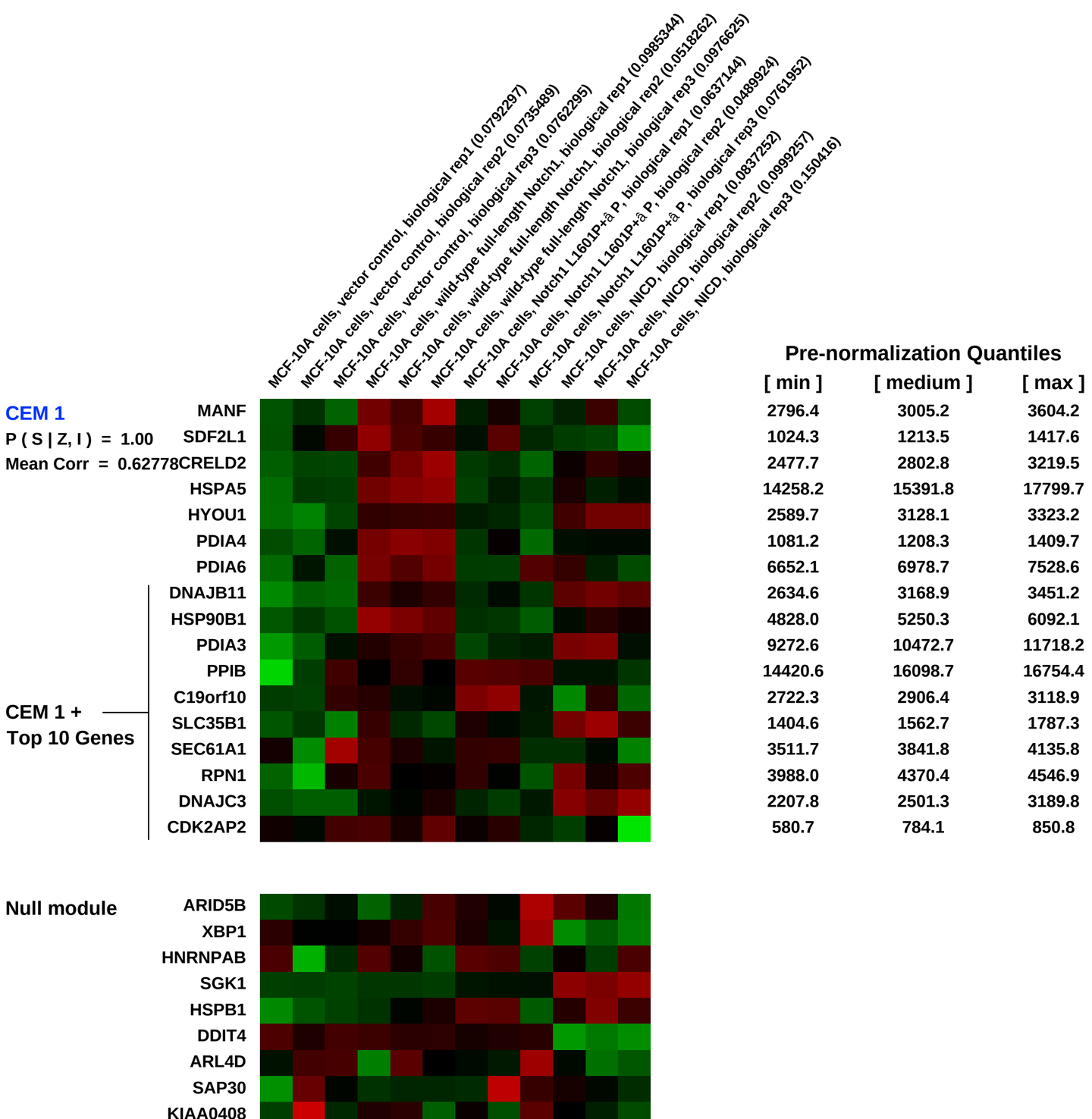

Pre-normalization Quantiles

	[min]	[medium]	[max]
MANF	2796.4	3005.2	3604.2
SDF2L1	1024.3	1213.5	1417.6
CRELD2	2477.7	2802.8	3219.5
HSPA5	14258.2	15391.8	17799.7
HYOU1	2589.7	3128.1	3323.2
PDIA4	1081.2	1208.3	1409.7
PDIA6	6652.1	6978.7	7528.6
DNAJB11	2634.6	3168.9	3451.2
HSP90B1	4828.0	5250.3	6092.1
PDIA3	9272.6	10472.7	11718.2
PPIB	14420.6	16098.7	16754.4
C19orf10	2722.3	2906.4	3118.9
SLC35B1	1404.6	1562.7	1787.3
SEC61A1	3511.7	3841.8	4135.8
RPN1	3988.0	4370.4	4546.9
DNAJC3	2207.8	2501.3	3189.8
CDK2AP2	580.7	784.1	850.8

GEO Series "GSE19864" Expression Profiles

Num of samples in this series: 38

Scale of expression profile Z-scores

-3.0 -2.0 -1.0 0.0 1.0 2.0 3.0

GEO Link:	http://www.ncbi.nlm.nih.gov/geo/query/acc.cgi?acc=GSE19864
Status:	Public on Jan 15 2010
Title:	Gene expression profiles after RNAi-mediated suppression of RB, p107 or p130 in growing, quiescent or ras-induced senescent IMR90 cells
Organism:	Homo sapiens
Experiment type:	Expression profiling by array
Platform:	GPL570
Pubmed ID:	20385362
Summary & Design:	**Summary:** The action of RB as a tumor suppressor has been difficult to define, in part, due to the redundancy of the related proteins p107 and p130. By coupling advanced RNAi technology to suppress RB, p107 or p130 with a genome wide analysis of gene expression in growing, quiescent or ras-senescent cells, we identified a unique and specific activity of RB in repressing DNA replication as cells exit the cell cycle into senescence, a tumor suppressive program. **Overall design:** Expression profiles of IMR90 cells before and after RNAi-mediated supppression of RB, p107 or p130 in growing, quiescent or ras-induced senescent conditions. RNA was extracted from growing, low serum (0.1% FBS), confluent, or ras-senescent cells.

Background corr dist: KL-Divergence = 0.2732, L1-Distance = 0.0626, L2-Distance = 0.0106, Normal std = 0.2909

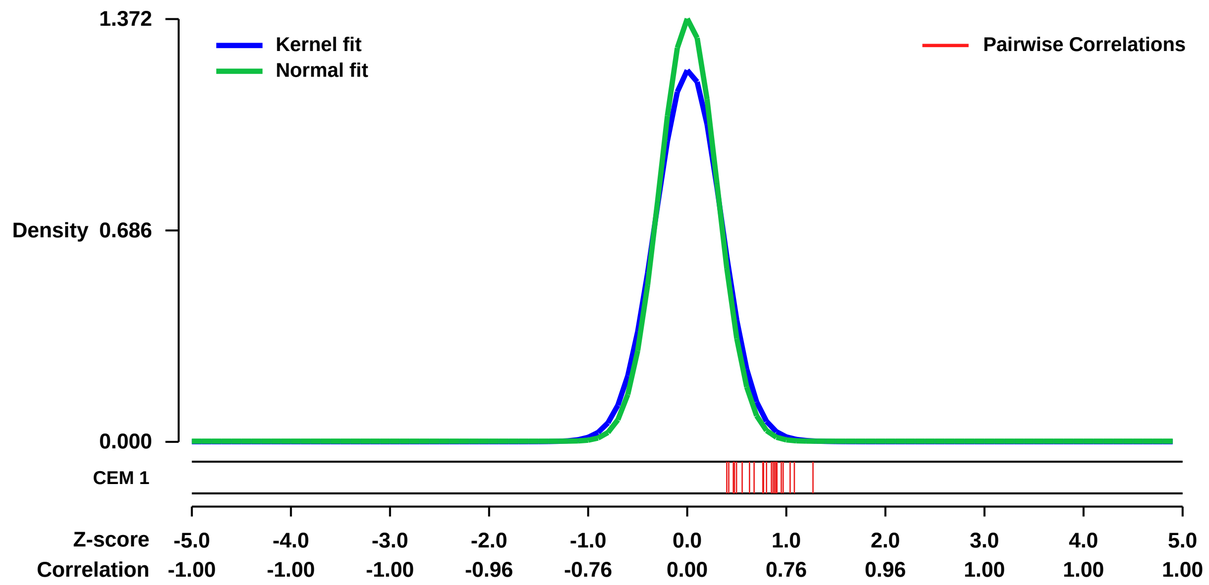

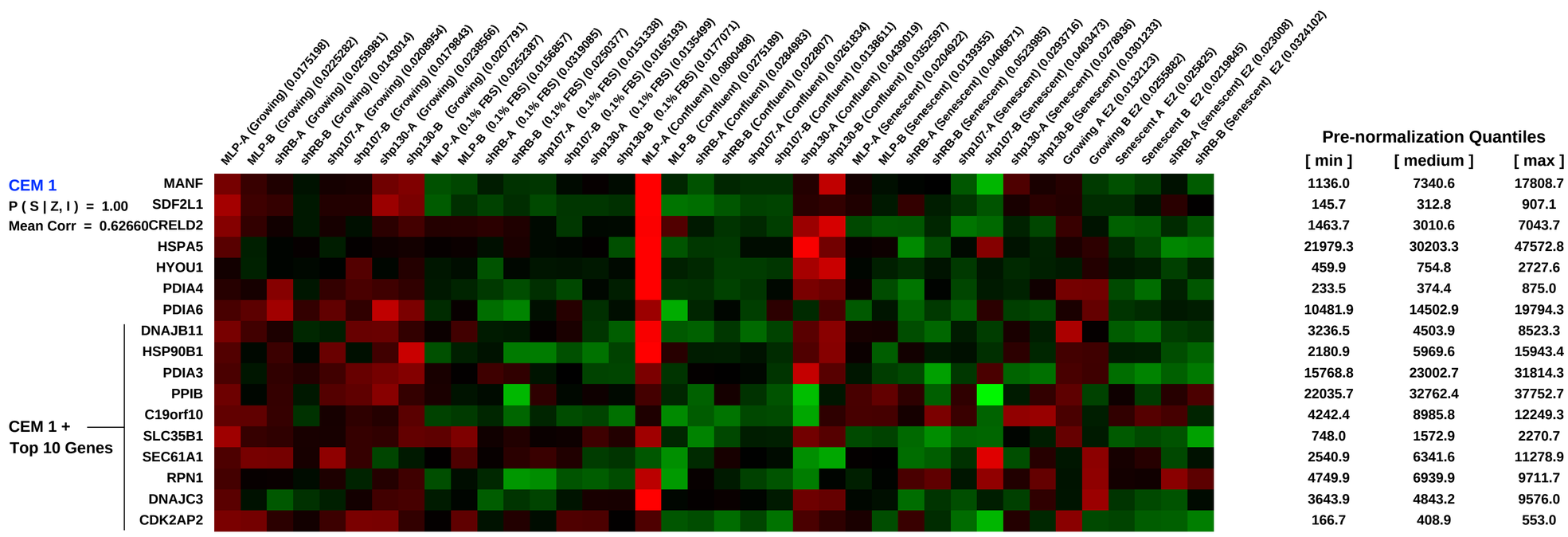

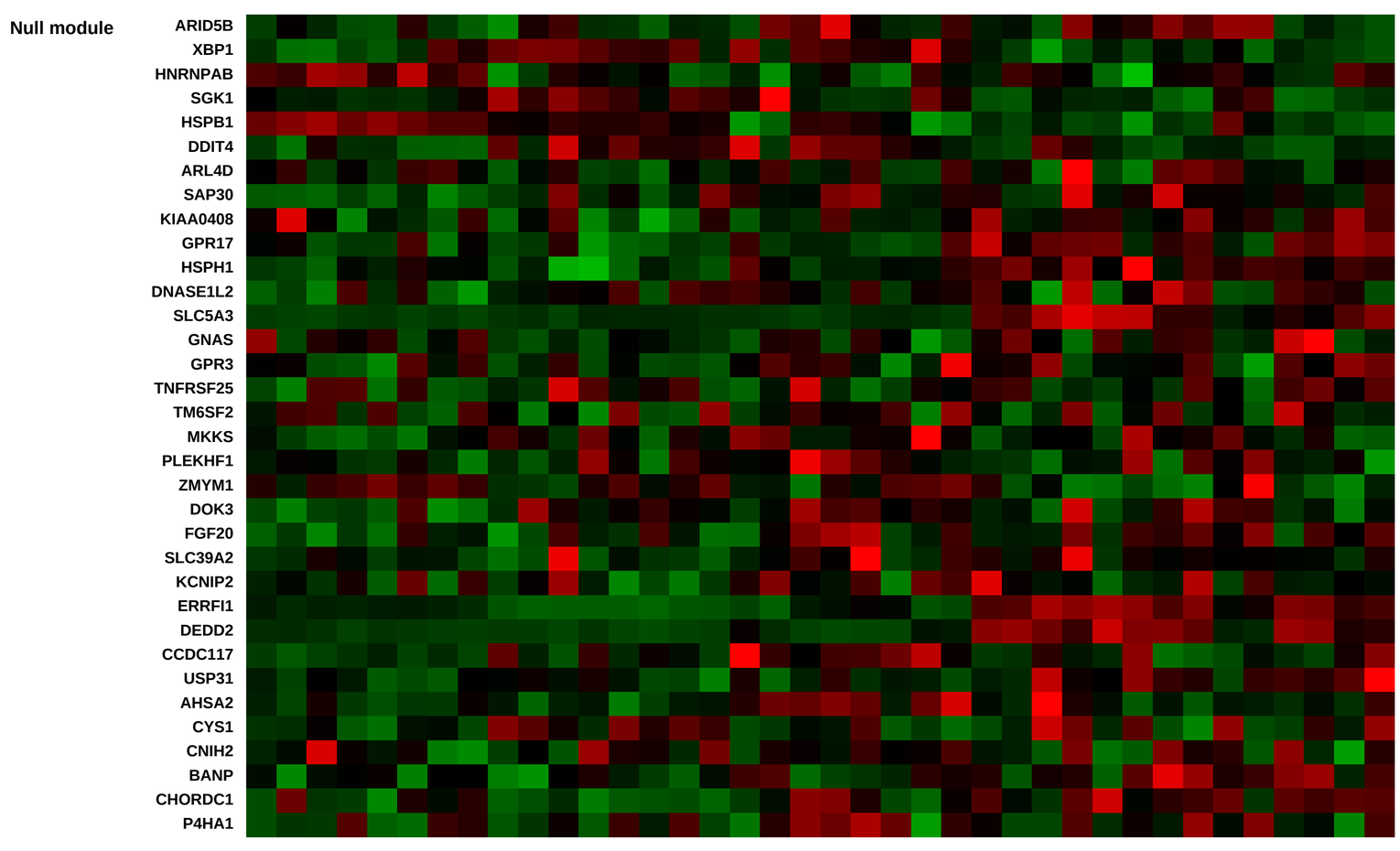

GEO Series "GSE17372" Expression Profiles

Num of samples in this series: 17

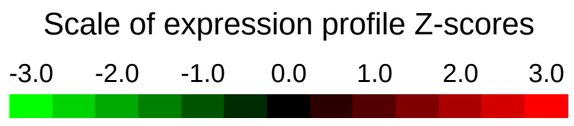

GEO Link:	http://www.ncbi.nlm.nih.gov/geo/query/acc.cgi?acc=GSE17372
Status:	Public on Jul 18 2012
Title:	Molecular Classification of AIDS-Related Lymphomas [including third-party data]
Organism:	Homo sapiens
Experiment type:	Expression profiling by array
Platform:	GPL570
Pubmed ID:	20216076
Summary & Design:	**Summary:** Gene expression profiling (GEP) of ARL patient samples was done to determine whether gene expression signatures derived from HIV- lymphomas retained their ability to molecularly classify HIV+ lymphomas. The GEP-based predictors robustly classified ARL tumors, distinguishing molecular Burkitt lymphoma (BL) and diffuse large B-cell lymphoma (DLBCL), as well as activated B-cell-like (ABC) and germinal center B-cell-like (GCB) molecular subtypes of DLBCL. Gene expression profiles were used to identify coordinately regulated gene sets and pathways that differ between HIV+ and HIV- lymphomas of corresponding molecular subtype. **Overall design:** [2] HIV- lymphoma, DLBCL cases: 200 of the 414 cases in Series GSE10846 (listed in the supplementary file below). These included all R-CHOP treated cases of either ABC or GCB subtype. These data were also used as is. These data were published in Lenz et al. NEJM 2008; Volume 359: 2313-2323.

Background corr dist: KL-Divergence = 0.1896, L1-Distance = 0.0609, L2-Distance = 0.0098, Normal std = 0.3460

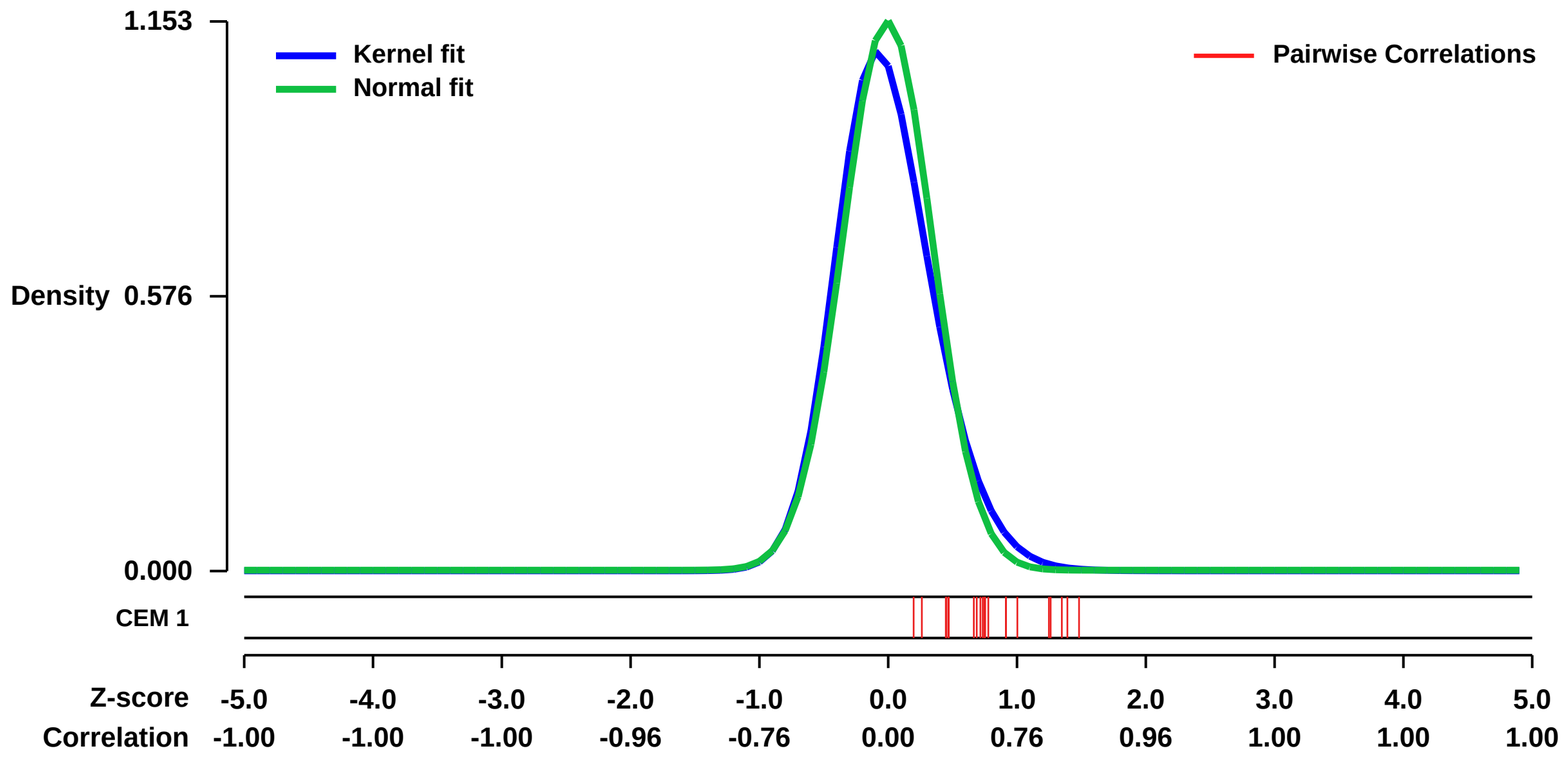

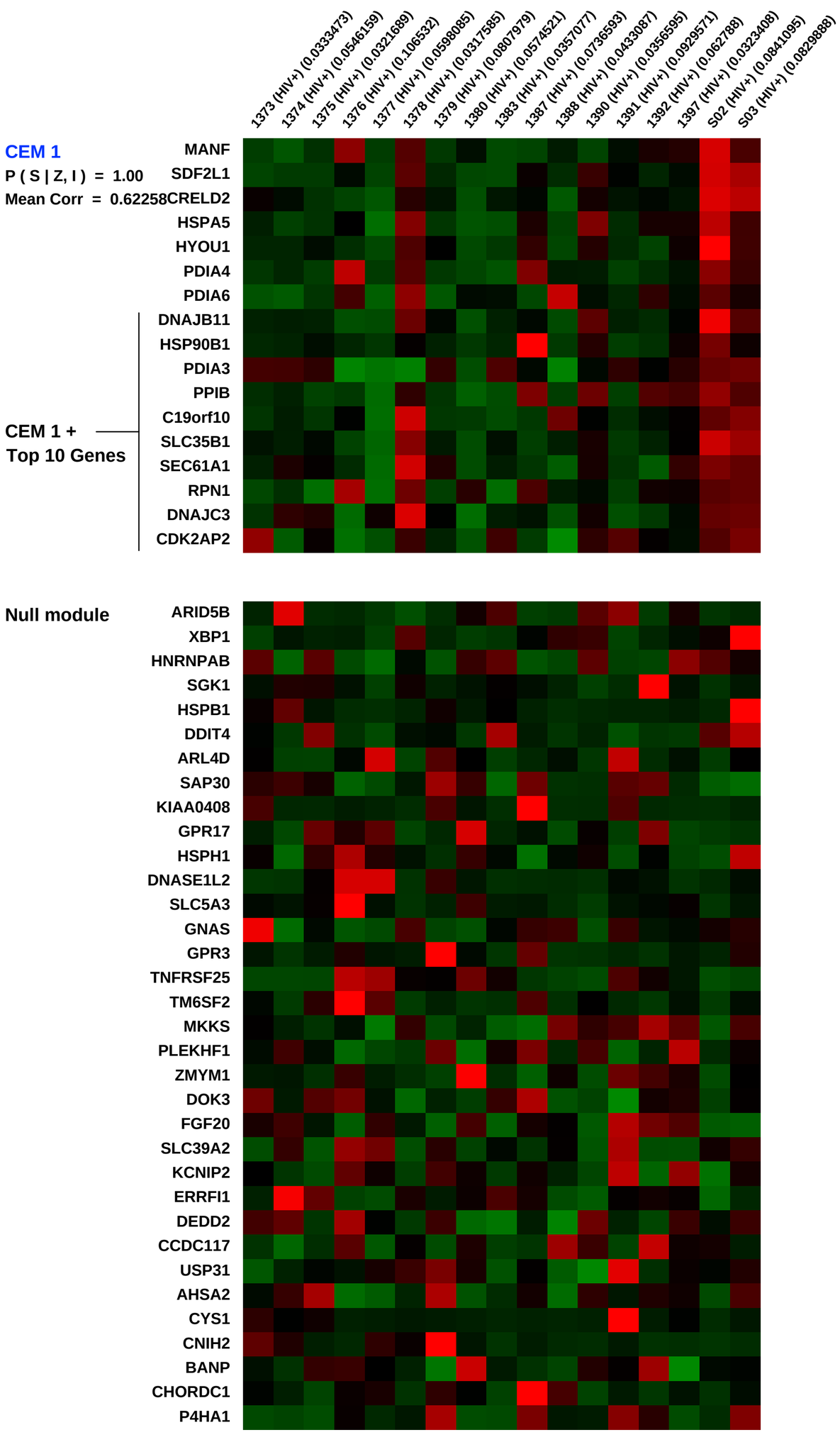

	Pre-normalization Quantiles		
	[min]	[medium]	[max]
MANF	1876.5	4082.0	13114.2
SDF2L1	739.2	1300.9	4985.7
CRELD2	667.8	2441.2	8588.3
HSPA5	7530.0	19098.1	50666.7
HYOU1	596.8	1330.9	7298.3
PDIA4	926.3	1554.4	4636.4
PDIA6	3439.5	10050.5	27153.5
DNAJB11	907.2	1868.3	7144.9
HSP90B1	565.0	6410.1	74064.0
PDIA3	1026.8	8936.1	12222.7
PPIB	2004.5	7049.6	22438.6
C19orf10	708.2	3175.7	10341.5
SLC35B1	69.6	986.1	3732.3
SEC61A1	673.8	2169.0	6727.8
RPN1	1389.2	2967.7	5803.2
DNAJC3	349.2	1801.6	5226.2
CDK2AP2	387.2	1330.6	2266.9

GEO Series "GSE15372" Expression Profiles

Num of samples in this series: 10

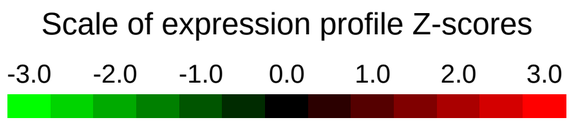

GEO Link:	http://www.ncbi.nlm.nih.gov/geo/query/acc.cgi?acc=GSE15372
Status:	Public on Apr 17 2009
Title:	Expression data from A2780 (cisplatin-sensitive) and Round5 A2780 (cisplatin-resistant) cell lines.
Organism:	Homo sapiens
Experiment type:	Expression profiling by array
Platform:	GPL570
Pubmed ID:	19505326
Summary & Design:	**Summary:** Cisplatin and carboplatin are the primary first-line therapies for the treatment of ovarian cancer. However, resistance to these platinum-based drugs occurs in the large majority of initially responsive tumors, subsequently resulting in a poor long-term prognosis. To model the onset of drug resistance, we measured gene expression alterations associated with cisplatin resistance. **Overall design:** We treated clonally derived, drug-sensitive A2780 epithelial ovarian cancer cells with increasing concentrations of cisplatin. After 5 cycles of drug selection, the isogenic drug-sensitive (parental A2780) and -resistant (Round5 A2780) cell lines were subjected to mRNA expression microarray analyses.

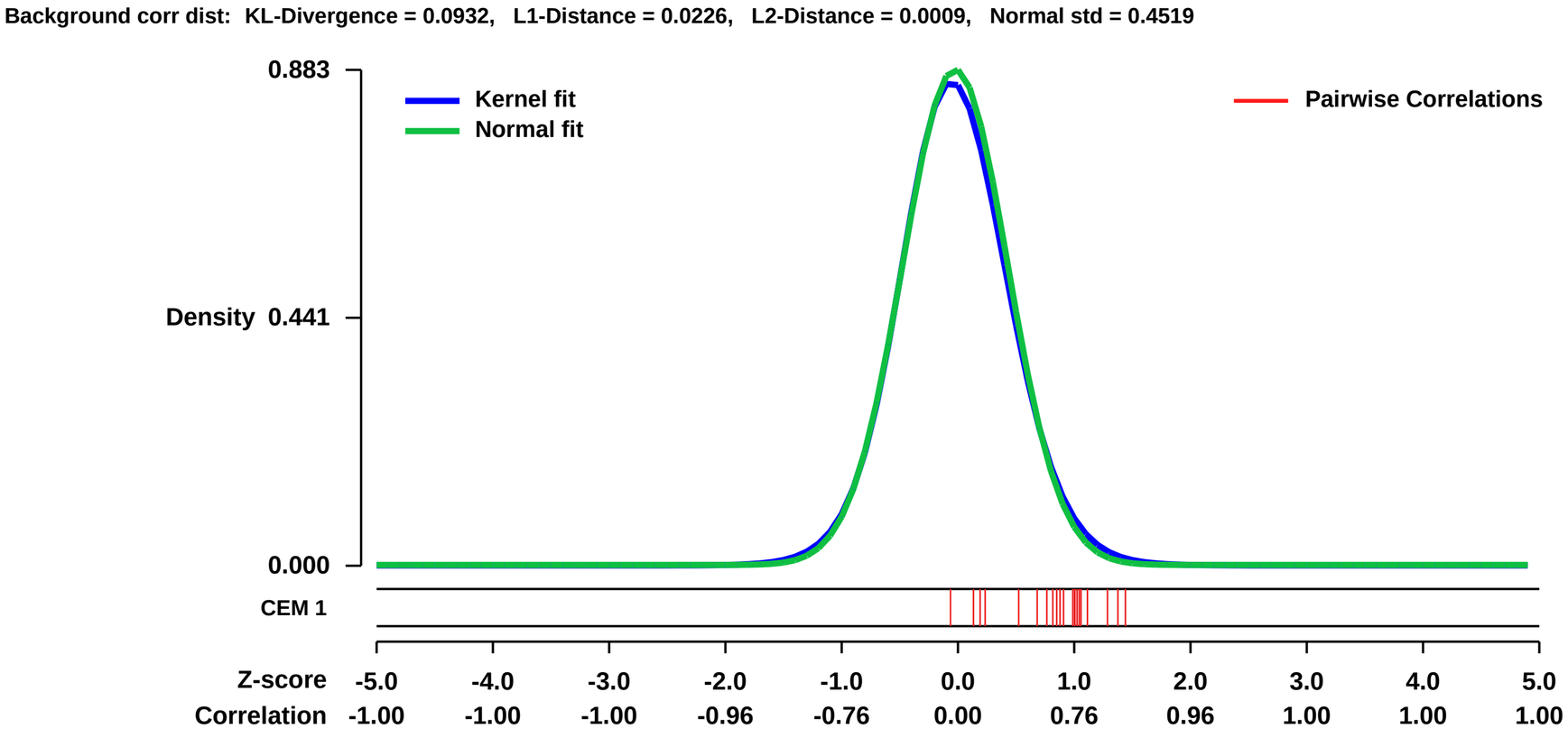

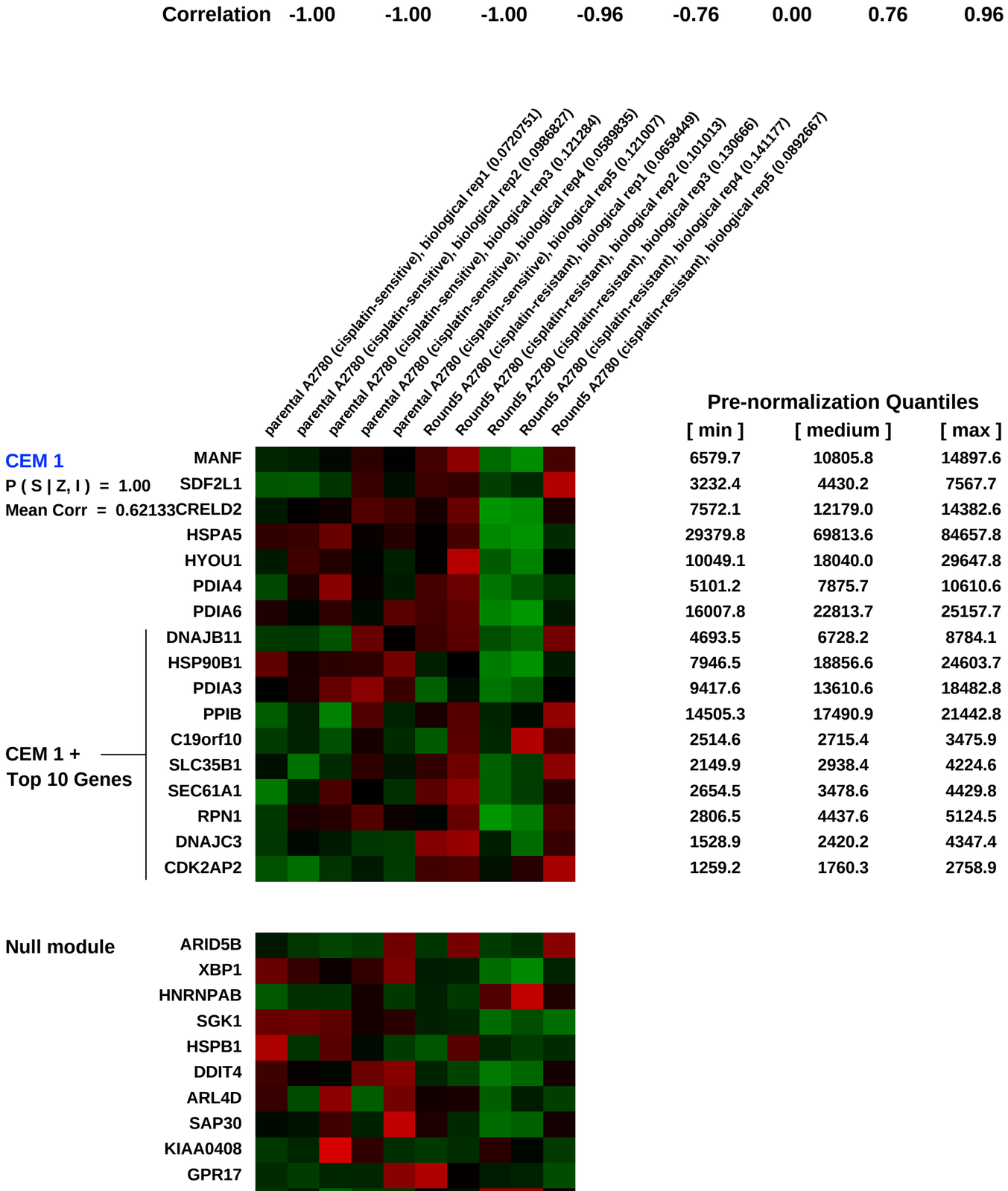

GEO Series "GSE7216" Expression Profiles

Num of samples in this series: 25

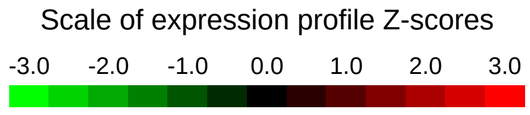

GEO Link:	http://www.ncbi.nlm.nih.gov/geo/query/acc.cgi?acc=GSE7216
Status:	Public on Mar 09 2007
Title:	Cytokine treated normal human epidermal keratinocytes
Organism:	Homo sapiens
Experiment type:	Expression profiling by array
Platform:	GPL570
Pubmed ID:	17277128
Summary & Design:	**Summary:** Normal human epidermal keratinocytes (NHEK) from neonatal foreskin were cultured in serum-free EpiLife medium with human KC growth supplement (0.2% bovine pituitary extract (v/v), 5ug bovine insulin, 5ug/ml bovine transferrin, 0.5ng/ml human EGF, and 0.18 ug/ml hydrocortisone) from Cascade Biologics. Cultures were treated with recombinant cytokines from R&D Systems. J Immunol. 2007 Feb 15;178(4):2229-40. **Keywords: cytokine response** **Overall design:** NHEK were treated with IL-19, IL20, IL-22, and IL24, with controls untreated, along with IL1b, IFN gamma, and KGF.

Background corr dist: KL-Divergence = 0.3434, L1-Distance = 0.0652, L2-Distance = 0.0117, Normal std = 0.2647

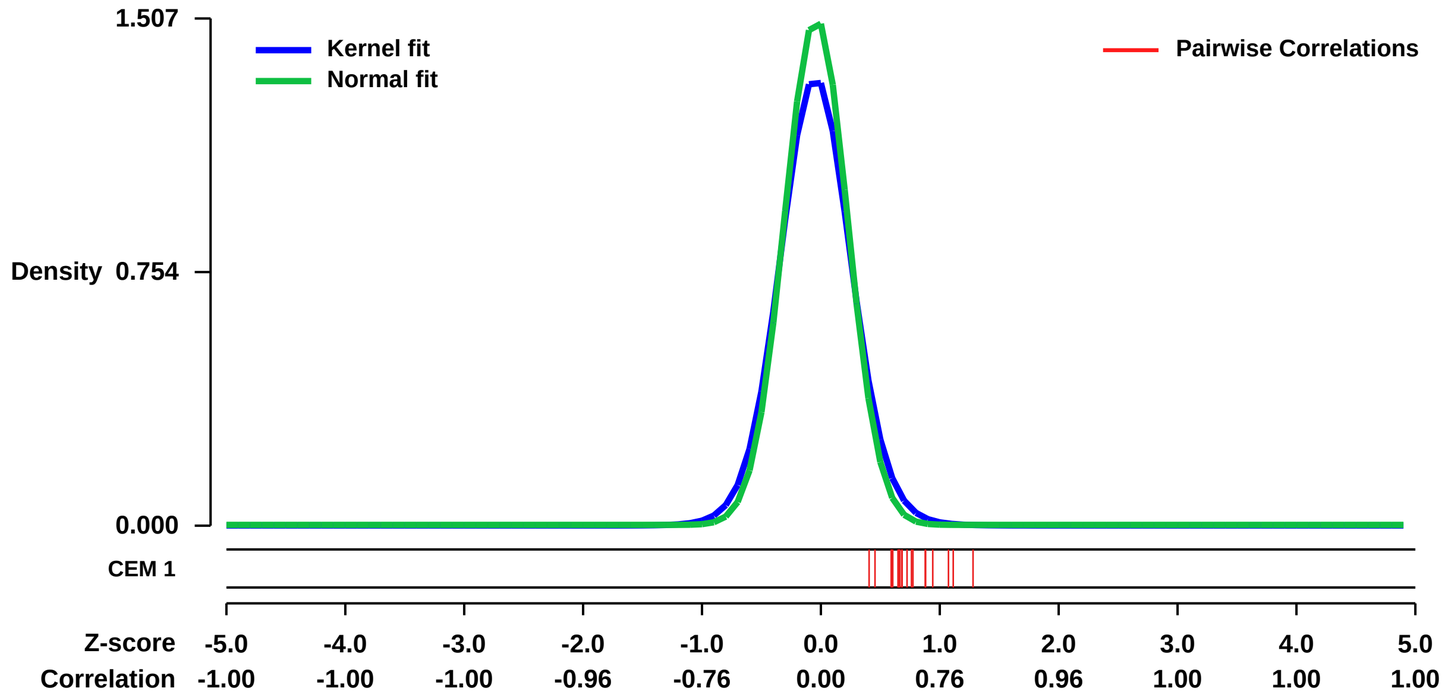

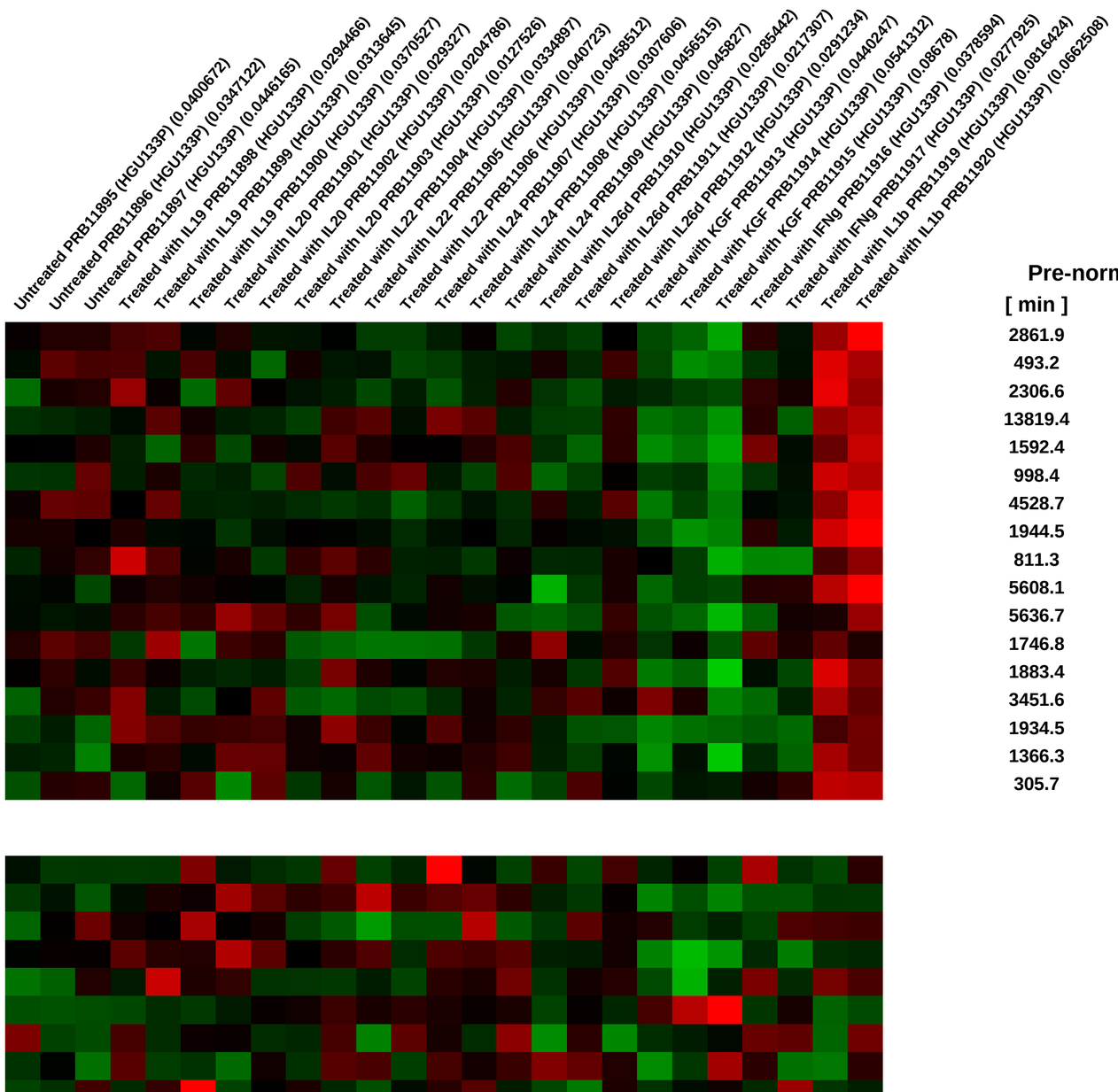

GEO Series "GSE33146" Expression Profiles

Num of samples in this series: 6

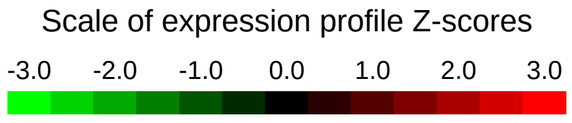

GEO Link:	http://www.ncbi.nlm.nih.gov/geo/query/acc.cgi?acc=GSE33146
Status:	Public on Jun 01 2012
Title:	Expression data from DKAT breast cancer cell line pre- and post-EMT
Organism:	Homo sapiens
Experiment type:	Expression profiling by array
Platform:	GPL570
Pubmed ID:	
Summary & Design:	**Summary:** The DKAT cell line is a novel model of triple-negative breast cancer that was isolated from the pleural effusion of a 35 year-old caucasian woman with triple-negative breast cancer. When cultured in serum-free media (MEGM, Lonza) this cell line exhibits an epithelial morphology and gene expression pattern. However, when cultured in the presence of serum (SCGM, Lonza) it undergoes a reversible EMT. We used microarrays to look at gene expression changes in the DKAT cell line when cultured in Mammary Epithelial Growth Media (MEGM, where DKAT cells have an epithelial morphology) vs Stromal Cell Growth Media (SCGM, where DKAT cells have a mesenchymal morphology). **Overall design:** DKAT breast cancer cells (passage 10) grown in MEGM (Lonza) were split and cultured in T75 flasks in either in MEGM or SCGM for 14 days. RNA was isolated using Qiagen RNeasy kit and hybridization on Affymetrix microarrays was performed. Three separate cDNA reactions were performed and these were run as technical replicates.

Background corr dist: KL-Divergence = 0.0326, L1-Distance = 0.0390, L2-Distance = 0.0017, Normal std = 0.7070

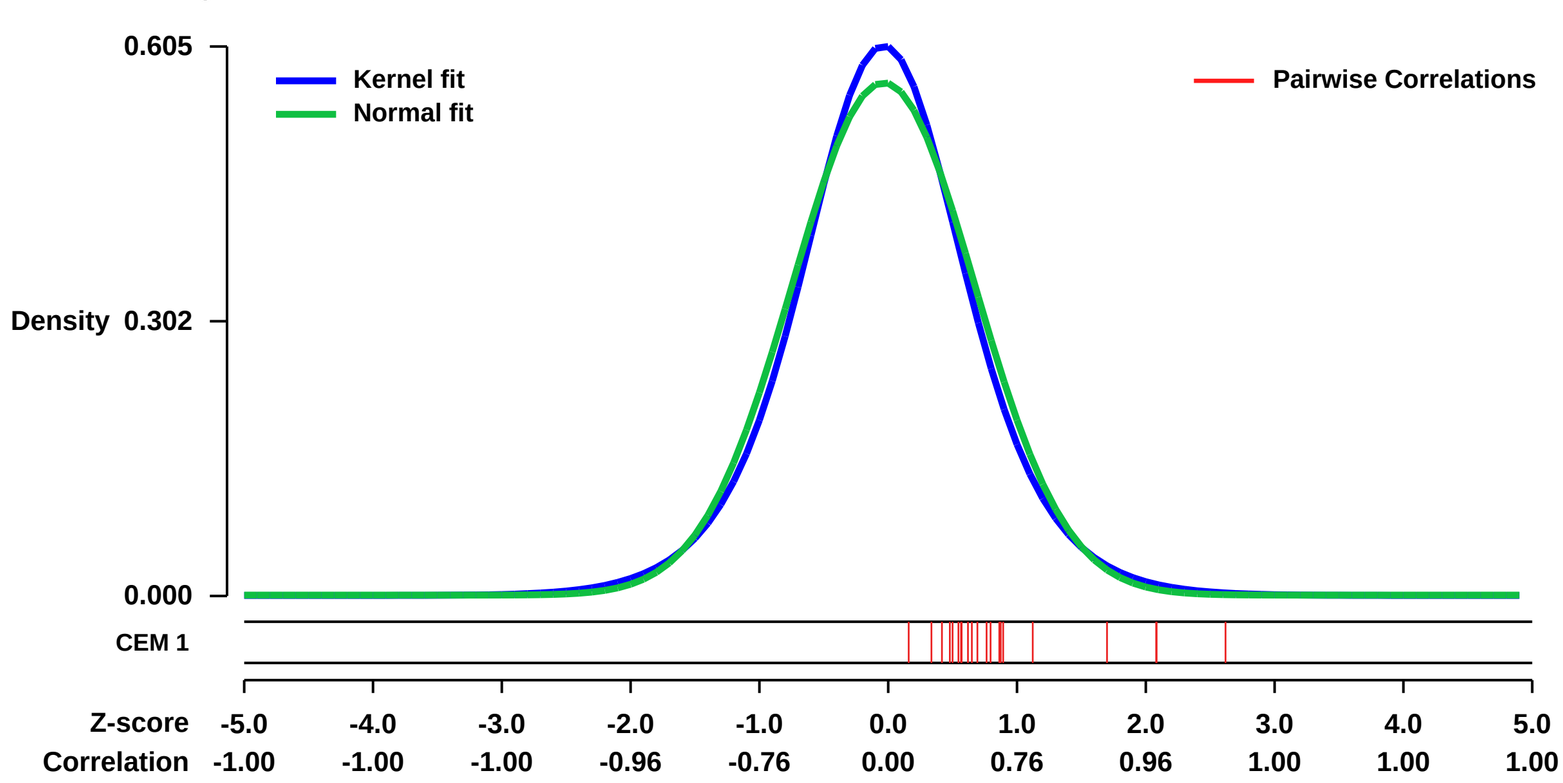

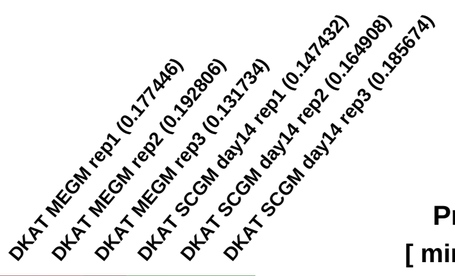

Pre-normalization Quantiles

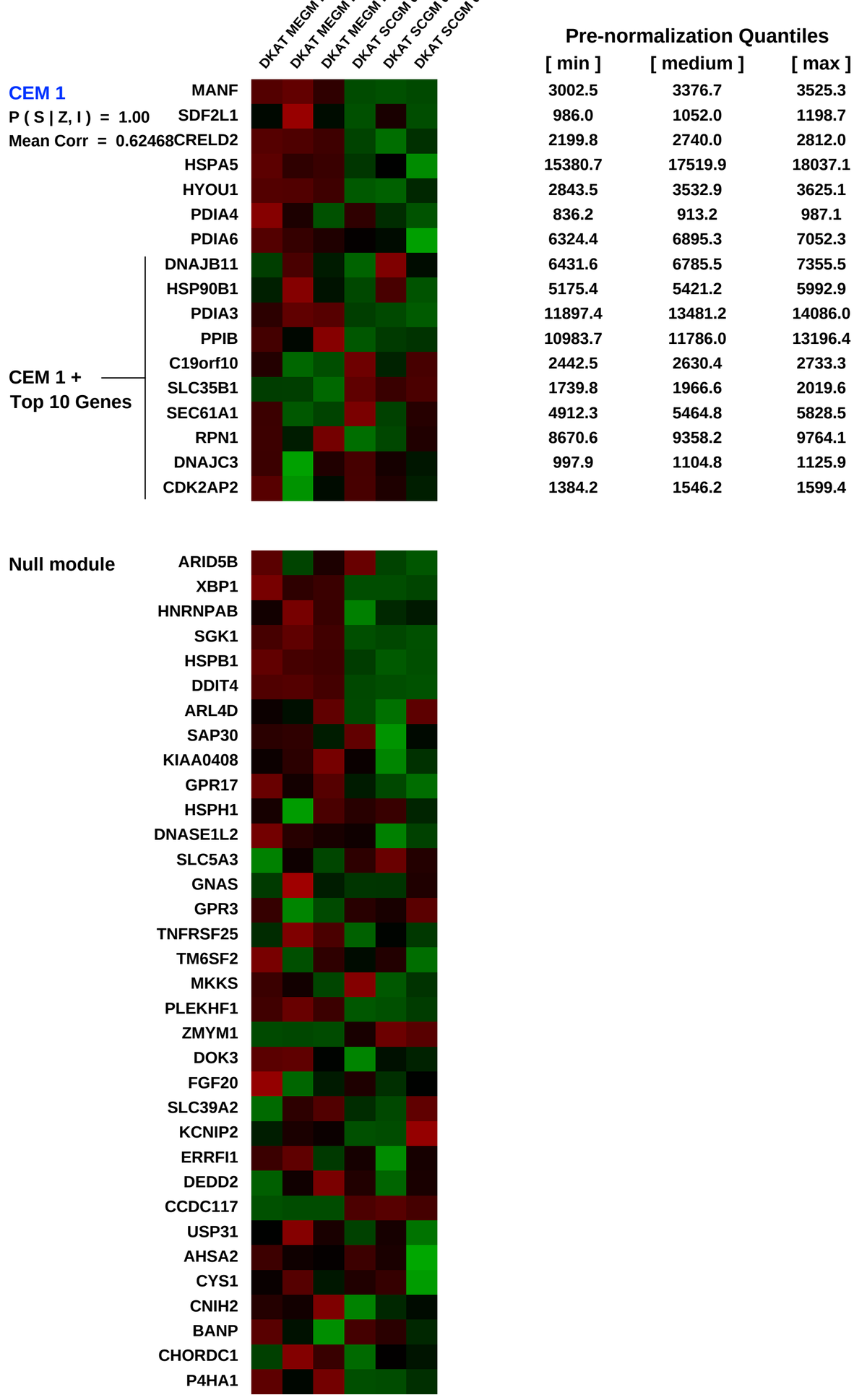

	[min]	[medium]	[max]
MANF	3002.5	3376.7	3525.3
SDF2L1	986.0	1052.0	1198.7
CRELD2	2199.8	2740.0	2812.0
HSPA5	15380.7	17519.9	18037.1
HYOU1	2843.5	3532.9	3625.1
PDIA4	836.2	913.2	987.1
PDIA6	6324.4	6895.3	7052.3
DNAJB11	6431.6	6785.5	7355.5
HSP90B1	5175.4	5421.2	5992.9
PDIA3	11897.4	13481.2	14086.0
PPIB	10983.7	11786.0	13196.4
C19orf10	2442.5	2630.4	2733.3
SLC35B1	1739.8	1966.6	2019.6
SEC61A1	4912.3	5464.8	5828.5
RPN1	8670.6	9358.2	9764.1
DNAJC3	997.9	1104.8	1125.9
CDK2AP2	1384.2	1546.2	1599.4
ARID5B			
XBP1			
HNRNPAB			
SGK1			
HSPB1			
DDIT4			
ARL4D			
SAP30			
KIAA0408			
GPR17			
HSPH1			
DNASE1L2			
SLC5A3			
GNAS			
GPR3			
TNFRSF25			
TM6SF2			
MKKS			
PLEKHF1			
ZMYM1			
DOK3			
FGF20			
SLC39A2			
KCNIP2			
ERRFI1			
DEDD2			
CCDC117			
USP31			
AHSA2			
CYS1			
CNIH2			
BANP			
CHORDC1			
P4HA1			

GEO Series "GSE19136" Expression Profiles

Num of samples in this series: 12

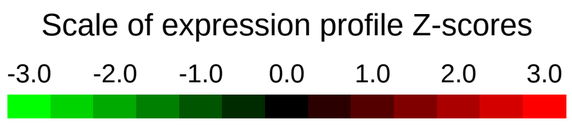

GEO Link:	**http://www.ncbi.nlm.nih.gov/geo/query/acc.cgi?acc=GSE19136**
Status:	**Public on Mar 01 2010**
Title:	**Gene expression response to implanted drug (paclitaxel)-eluting or bare metal stents in denuded human LIMA arteries**
Organism:	**Homo sapiens**
Experiment type:	**Expression profiling by array**
Platform:	**GPL570**
Pubmed ID:	
Summary & Design:	**Summary:** **[original title] Gene expression response to the implantation of drug (paclitaxel)-eluting or bare metal stents in denuded human LIMA arteries.** **Different clinical outcomes have been observed for paclitaxel-eluting and bare metal cardiovascular stents. The aim of this project was to identify genes that might be associated with the observed clinical outcomes.** **Overall design:** **Human left internal mammary artery (LIMA) was divided into three segments and and two of the segments were fitted with either a paclitaxel-eluting stent or a bare metal stent. The experiment includes three groups: control, paclitaxel-eluting stent, and bare metal stent, respectively. Each group includes four biological replicates (patients 1, 2, 4 and 5).**

Background corr dist: KL-Divergence = 0.1566, L1-Distance = 0.0371, L2-Distance = 0.0028, Normal std = 0.3669

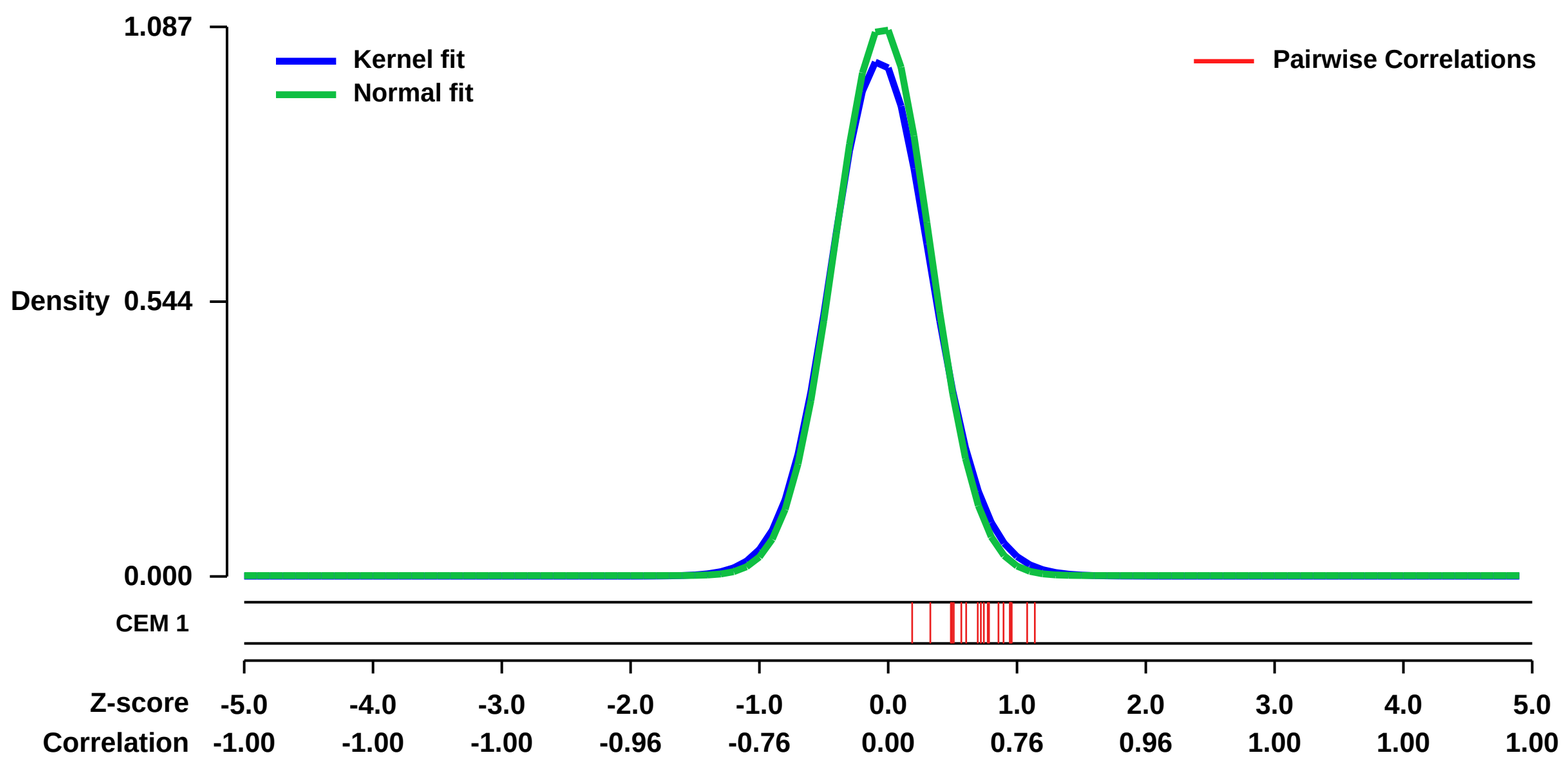

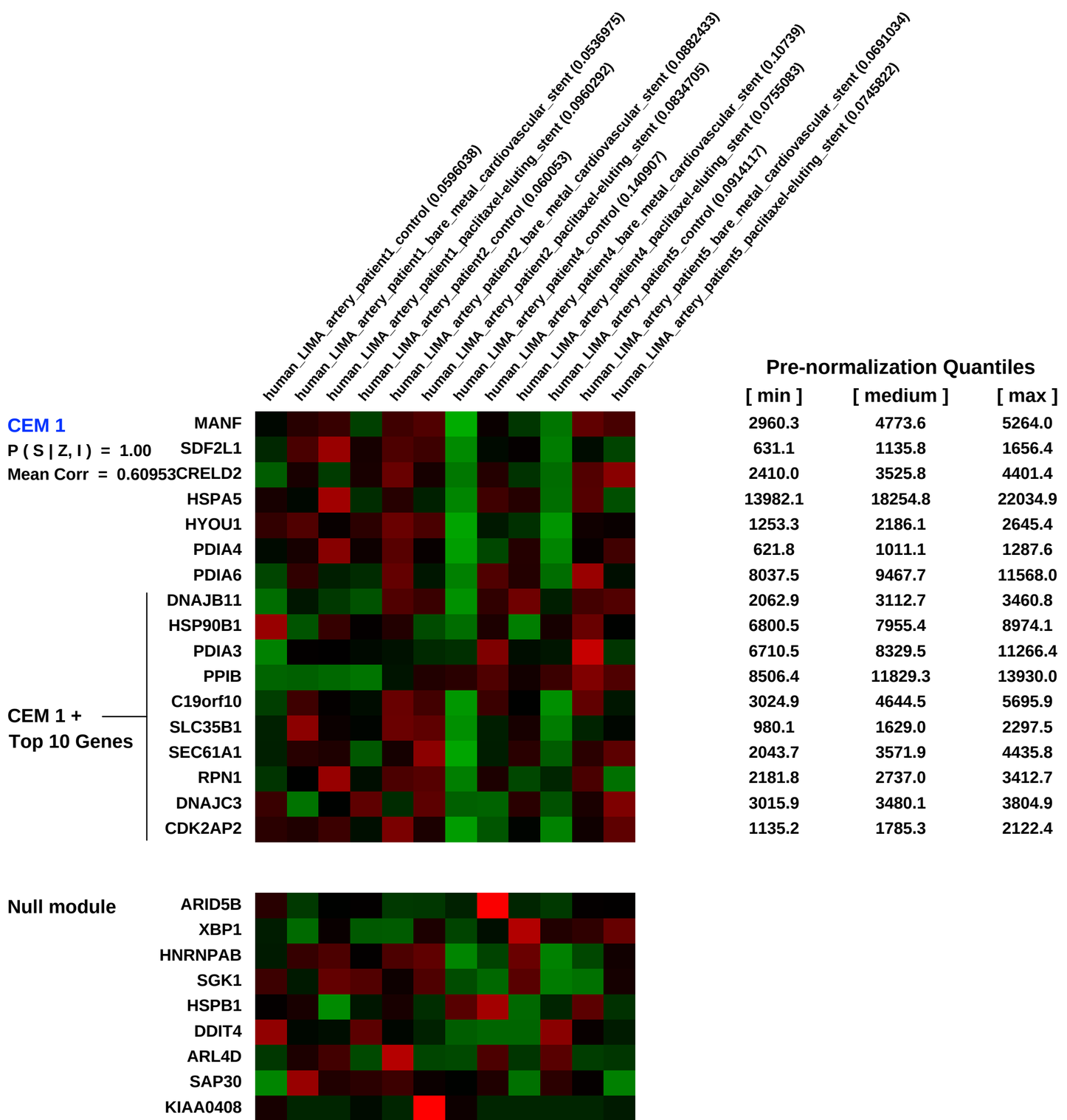

Pre-normalization Quantiles

	[min]	[medium]	[max]
MANF	2960.3	4773.6	5264.0
SDF2L1	631.1	1135.8	1656.4
CRELD2	2410.0	3525.8	4401.4
HSPA5	13982.1	18254.8	22034.9
HYOU1	1253.3	2186.1	2645.4
PDIA4	621.8	1011.1	1287.6
PDIA6	8037.5	9467.7	11568.0
DNAJB11	2062.9	3112.7	3460.8
HSP90B1	6800.5	7955.4	8974.1
PDIA3	6710.5	8329.5	11266.4
PPIB	8506.4	11829.3	13930.0
C19orf10	3024.9	4644.5	5695.9
SLC35B1	980.1	1629.0	2297.5
SEC61A1	2043.7	3571.9	4435.8
RPN1	2181.8	2737.0	3412.7
DNAJC3	3015.9	3480.1	3804.9
CDK2AP2	1135.2	1785.3	2122.4

GEO Series "GSE31641" Expression Profiles

Num of samples in this series: 7

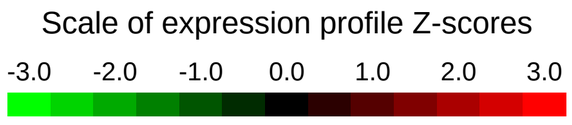

GEO Link:	http://www.ncbi.nlm.nih.gov/geo/query/acc.cgi?acc=GSE31641
Status:	Public on Dec 01 2012
Title:	Expression data from treatment of human melanocytes with phenolic compounds
Organism:	Homo sapiens
Experiment type:	Expression profiling by array
Platform:	GPL570
Pubmed ID:	
Summary & Design:	**Summary:** Vitiligo, an acquired disorder characterized by depigmented skin patches, results from loss of epidermal melanocytes. Etiology of vitiligo is not clearly understood but environmental, biochemical, genetic, and immune factors play a role in its pathogenesis. There is evidence that melanocyte death is perpetuated by an autoimmune response that causes lesions to spread. 4-tertiary butyl phenol (4TBP) and monobenzyl ether of hydroquinone (MBEH) are phenolic compounds that are known as environmental causes of vitiligo. We used microarray to detail the global gene expression that occurs following exposure of melanocytes to 4-TBP or MBEH to identified distinct classes of up-regulated genes that may contribute to melanocyte loss in vitiligo. We show that human melanocytes exposed to 4-TBP and MBEH show increased production of some inflammatory cytokines. Interleukin-6 (IL6) and IL8, in particular, are expressed at the periphery of vitiligo lesions and may contribute to recruitment of immune components to the areas, perpetuating melanocyte loss. **Overall design:** Cultured human epidermal melanocytes were treated with 4TBP or MBEH for 3, 6, or 24 hours and gene expression were compared with untreated cells.

Background corr dist: KL-Divergence = 0.0389, L1-Distance = 0.0319, L2-Distance = 0.0012, Normal std = 0.6320

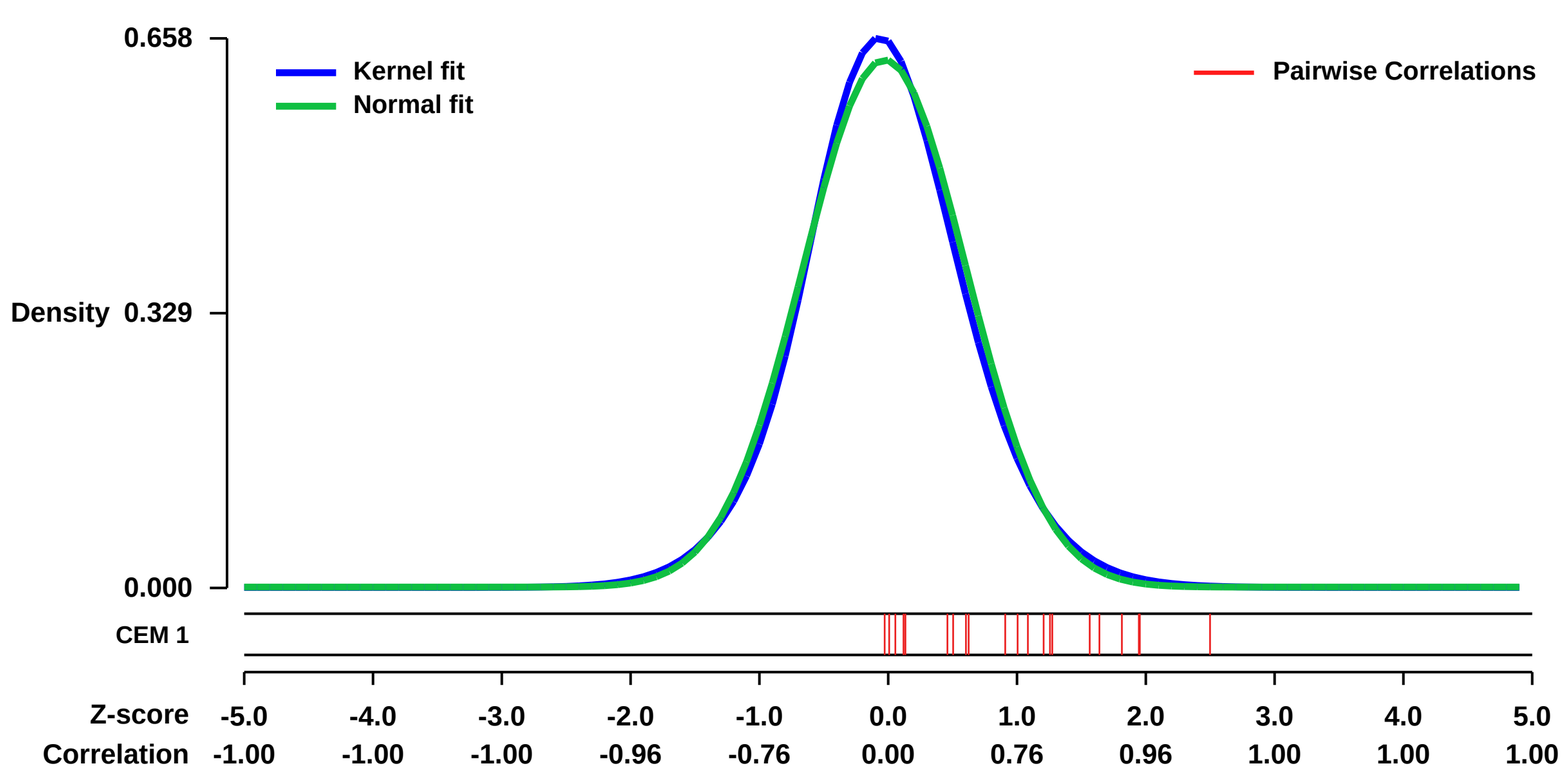

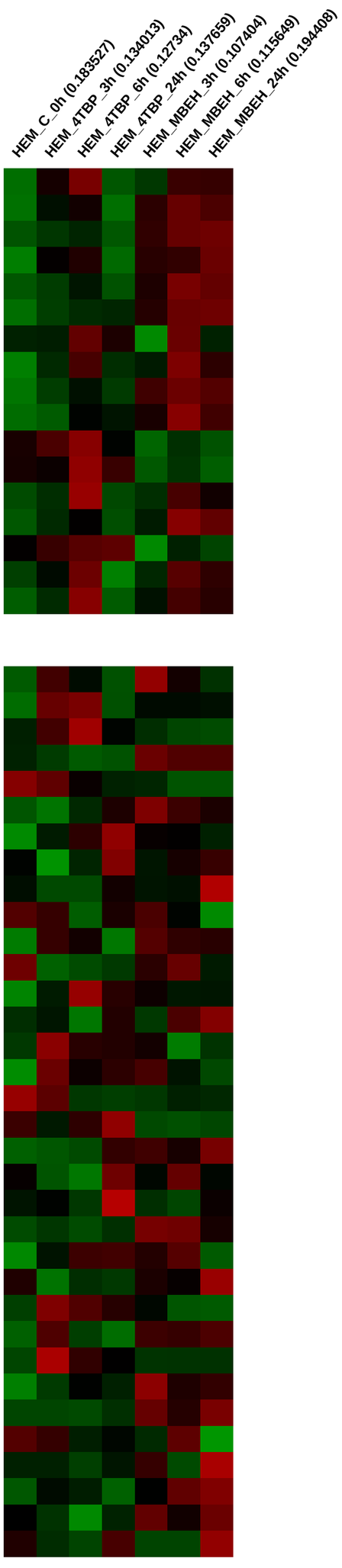

GEO Series "GSE42762" Expression Profiles

Num of samples in this series: 12

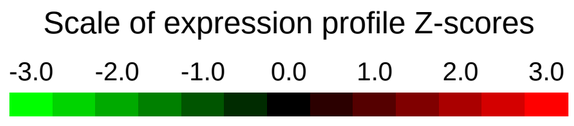

GEO Link:	http://www.ncbi.nlm.nih.gov/geo/query/acc.cgi?acc=GSE42762
Status:	Public on May 01 2013
Title:	FOXO3a Is A Major Target Of Inactivation By PI3K/AKT Signaling In Aggressive Neuroblastoma
Organism:	Homo sapiens
Experiment type:	Expression profiling by array
Platform:	GPL570
Pubmed ID:	23378341
Summary & Design:	**Summary:** Neuroblastoma is a pediatric tumor of the peripheral sympathetic nervous system with a highly variable prognosis. Activation of the PI3K/AKT pathway in neuroblastoma is correlated with poor patient prognosis, but the precise downstream effectors mediating this effect have not been determined. Here, we identify the forkhead transcription factor FOXO3a as a key target of the PI3K/AKT pathway in neuroblastoma. FOXO3a expression was elevated in low stage neuroblastoma tumors and normal embryonal neuroblasts, but reduced in late stage neuroblastoma. Inactivation of FOXO3a by AKT was essential for neuroblastoma cell survival. Treatment of neuroblastoma cells with the dual PI3K/mTOR inhibitor PI-103 activated FOXO3a and triggered apoptosis. This effect was rescued by FOXO3a silencing. Conversely, apoptosis induced by PI-103 or the AKT inhibitor MK-2206 was potentiated by FOXO3a overexpression. Further, levels of total or phosphorylated FOXO3a correlated closely with apoptotic sensitivity to MK-2206. In clinical specimens, there was an inverse relationship between gene expression signatures regulated by PI3K signaling and FOXO3a transcriptional activity. Moreover, high PI3K activity and low FOXO3a activity were each associated with an extremely poor prognosis. Our work indicates that expression of FOXO3a and its targets offer useful prognostic markers as well as biomarkers for PI3K/AKT inhibitor efficacy in neuroblastoma. **Overall design:** Affymetrix U133 Plus 2.0 profiling of SY5Y-TetR-FOXO3A cells treated with doxycycline and/or the PI3K/mTOR inhibitor PI-103. Each condition profiled in triplicate.

Background corr dist: KL-Divergence = 0.1022, L1-Distance = 0.0270, L2-Distance = 0.0011, Normal std = 0.4391

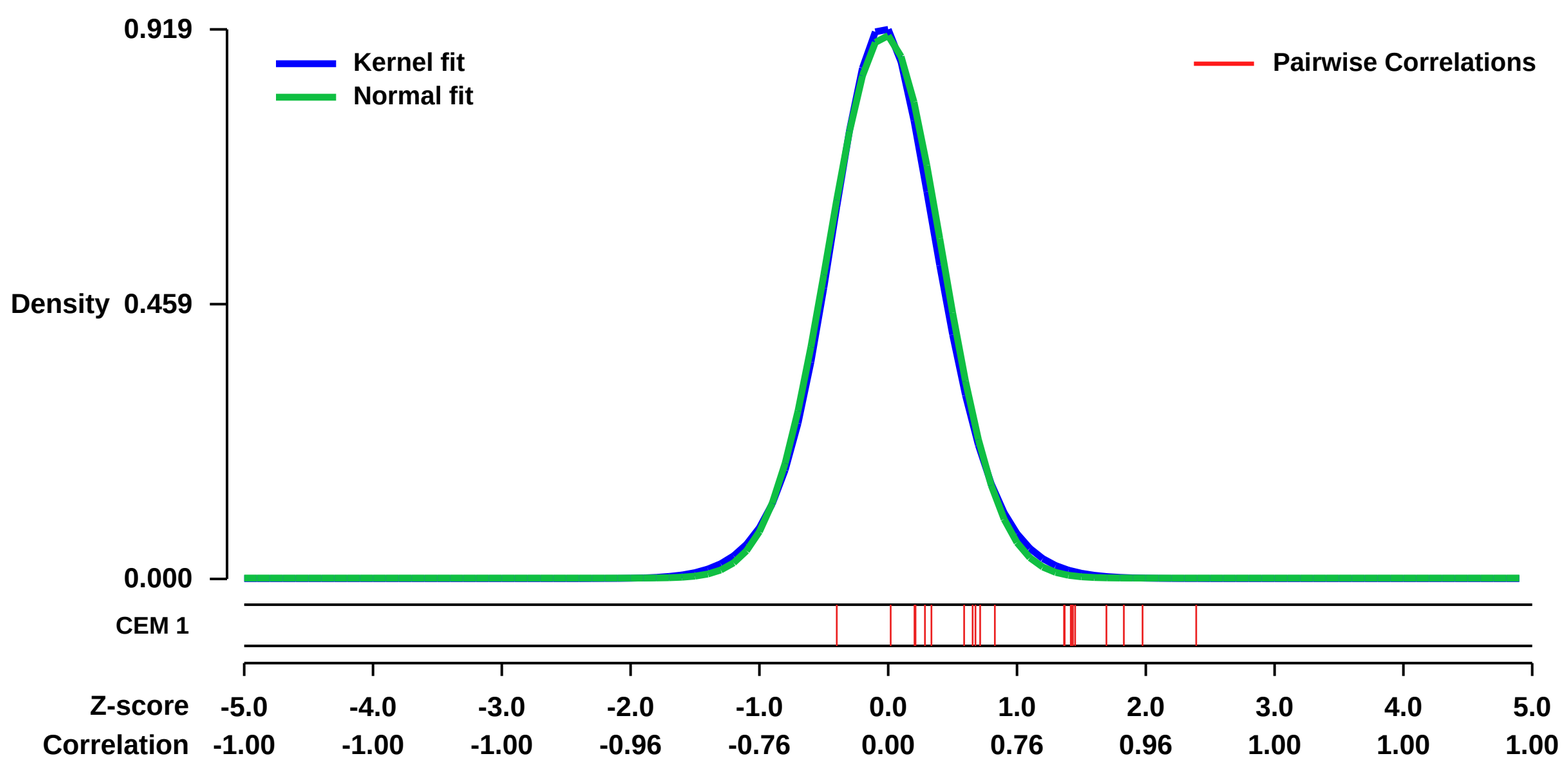

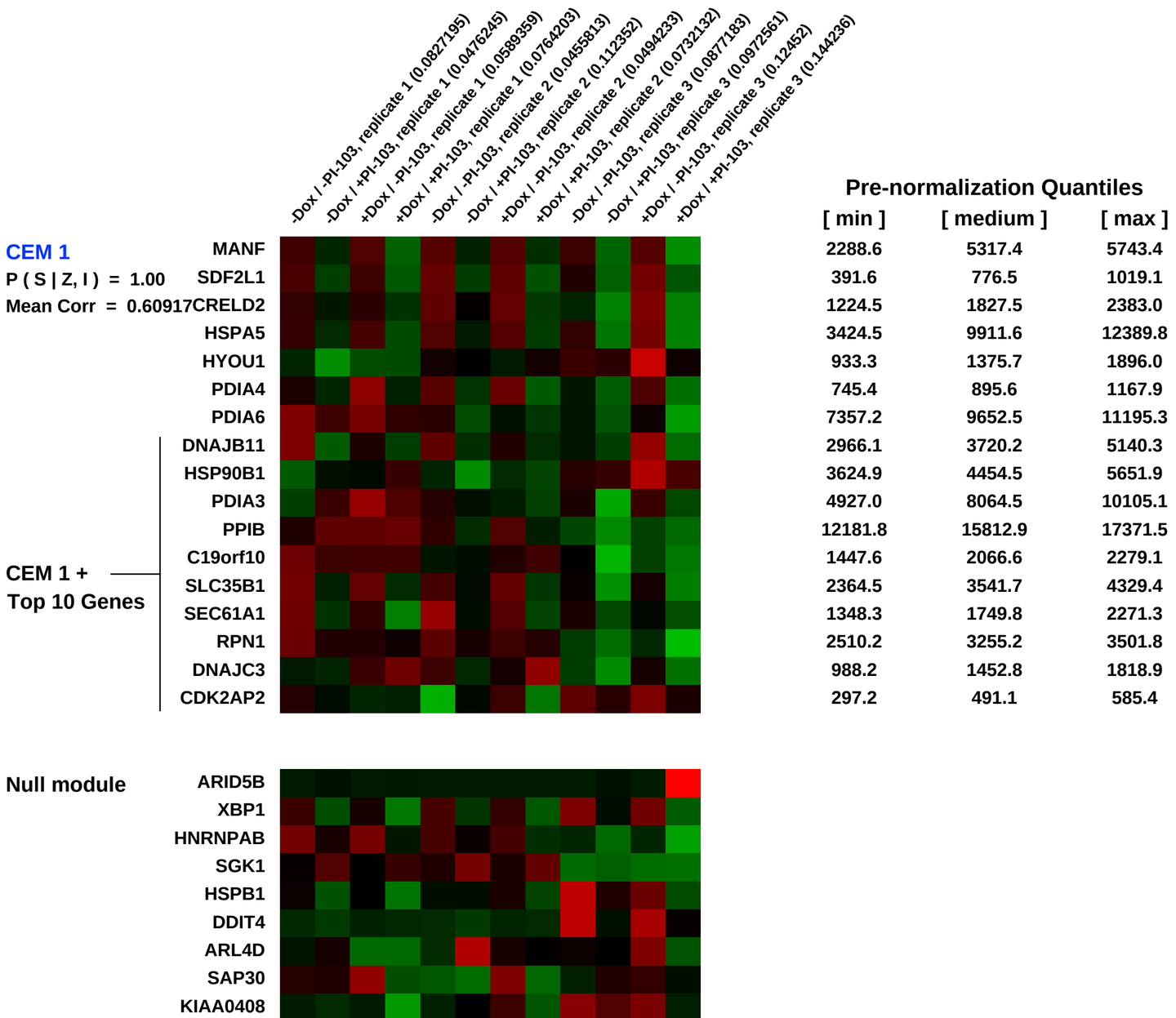

	Pre-normalization Quantiles		
	[min]	[medium]	[max]
MANF	2288.6	5317.4	5743.4
SDF2L1	391.6	776.5	1019.1
CRELD2	1224.5	1827.5	2383.0
HSPA5	3424.5	9911.6	12389.8
HYOU1	933.3	1375.7	1896.0
PDIA4	745.4	895.6	1167.9
PDIA6	7357.2	9652.5	11195.3
DNAJB11	2966.1	3720.2	5140.3
HSP90B1	3624.9	4454.5	5651.9
PDIA3	4927.0	8064.5	10105.1
PPIB	12181.8	15812.9	17371.5
C19orf10	1447.6	2066.6	2279.1
SLC35B1	2364.5	3541.7	4329.4
SEC61A1	1348.3	1749.8	2271.3
RPN1	2510.2	3255.2	3501.8
DNAJC3	988.2	1452.8	1818.9
CDK2AP2	297.2	491.1	585.4
ARID5B			
XBP1			
HNRNPAB			
SGK1			
HSPB1			
DDIT4			
ARL4D			
SAP30			
KIAA0408			
GPR17			
HSPH1			
DNASE1L2			
SLC5A3			
GNAS			
GPR3			
TNFRSF25			
TM6SF2			
MKKS			
PLEKHF1			
ZMYM1			
DOK3			
FGF20			
SLC39A2			
KCNIP2			
ERRFI1			
DEDD2			
CCDC117			
USP31			
AHSA2			
CYS1			
CNIH2			
BANP			
CHORDC1			
P4HA1			

GEO Series "GSE10591" Expression Profiles

Num of samples in this series: 9

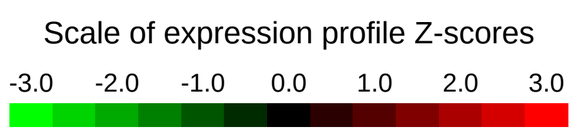

GEO Link:	http://www.ncbi.nlm.nih.gov/geo/query/acc.cgi?acc=GSE10591
Status:	Public on Aug 01 2008
Title:	Expression in HepG2 cells with overexpression of TMPRSS6 or its mutant version.
Organism:	Homo sapiens
Experiment type:	Expression profiling by array
Platform:	GPL570
Pubmed ID:	18451267
Summary & Design:	**Summary:** TMPRSS6 is a type II transmembrane serine protease and is revealed by our work to be part of a low-iron sensing pathway. When animal gets iron deficient, TMPRSS6 is required to shut off hepcidin gene, so as to allow iron to be uptaken from GI tract. The mutant mouse, which was generated by ENU mutagenesis, has developed microcytic anemia. The phenotype is caused by a splicing error in Tmprss6 gene. However, the mechanism of TMPRSS6 effect remains elusive. To gain further insight into the molecular components of the TMPRSS6 signaling pathway, we overexpressed either TMPRSS6 or its mutant version of protein in human liver carcinoma cell line HepG2 cells, and compared the transcription status betweem these two treatments. **Keywords:** genetic modification **Overall design:** Triplicate per transfection with wildtype Tmprss6 cDNA, mutant version of Tmprss6 cDNA and empty vector as control, respectively. 36 hours post transfection, cells were harvested and subjected to RNA extraction.

Background corr dist: KL-Divergence = 0.0789, L1-Distance = 0.0205, L2-Distance = 0.0005, Normal std = 0.4811

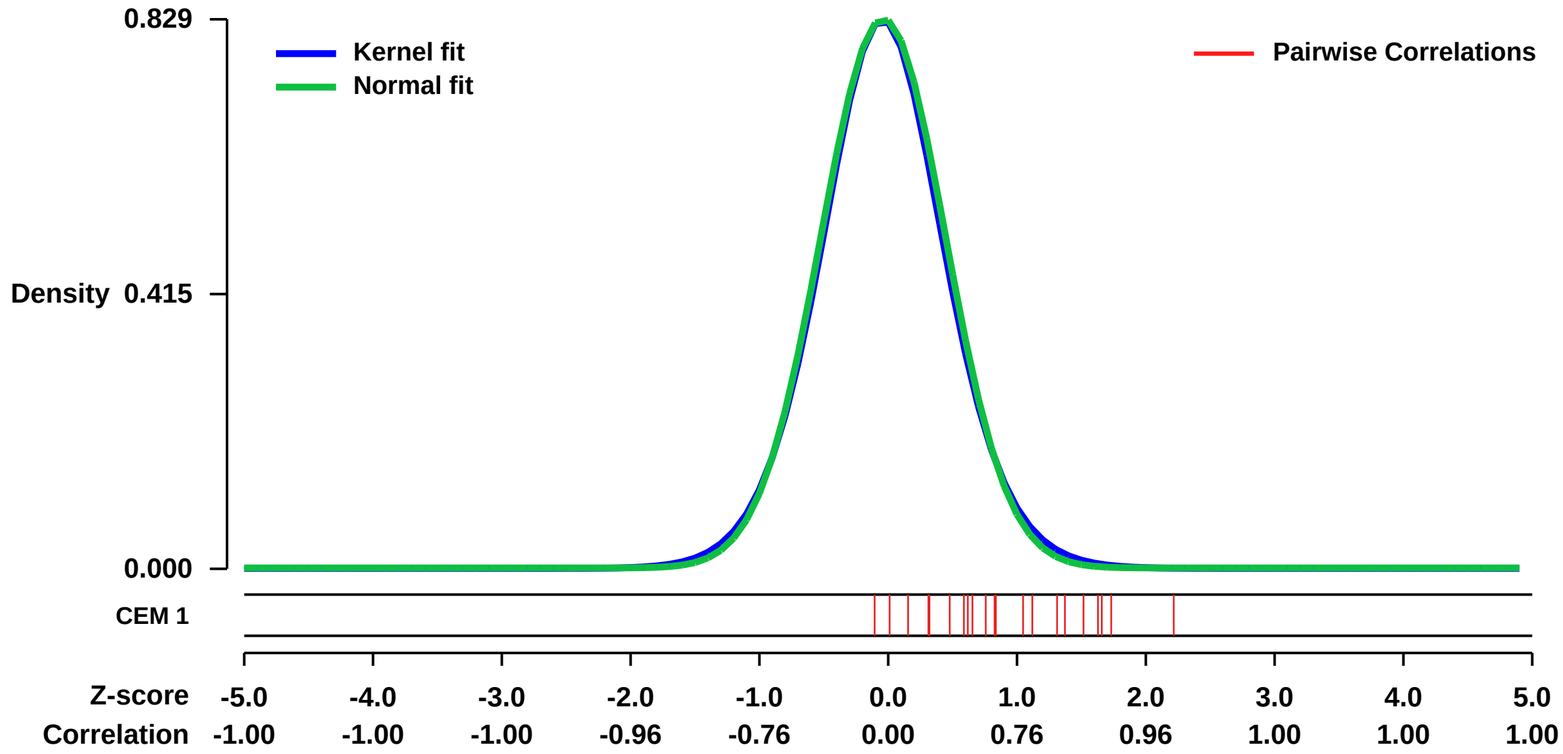

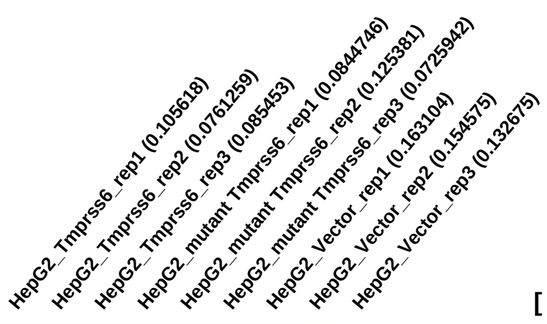

Pre-normalization Quantiles

		[min]	[medium]	[max]
CEM 1	MANF	5438.4	6801.5	7720.2
P (S | Z, I) = 1.00	SDF2L1	1173.3	1518.3	1932.6
Mean Corr = 0.60856	CRELD2	2647.6	3142.2	3683.8
	HSPA5	16569.1	20767.7	22419.6
	HYOU1	5738.5	7298.6	8000.3
	PDIA4	1947.4	2364.9	2823.6
	PDIA6	8573.6	9344.9	9801.0
CEM 1 + Top 10 Genes	DNAJB11	7244.4	8075.8	8722.7
	HSP90B1	3836.0	4863.8	5410.4
	PDIA3	10140.9	10574.1	11268.0
	PPIB	15936.1	17366.8	18888.3
	C19orf10	7557.6	7728.3	8775.7
	SLC35B1	2795.3	3715.3	4170.3
	SEC61A1	4902.5	5300.3	6056.5
	RPN1	5741.1	6072.2	6572.6
	DNAJC3	2195.1	2815.4	3156.6
	CDK2AP2	806.7	1024.8	1154.3
Null module	ARID5B			
	XBP1			
	HNRNPAB			
	SGK1			
	HSPB1			
	DDIT4			
	ARL4D			
	SAP30			
	KIAA0408			
	GPR17			
	HSPH1			
	DNASE1L2			
	SLC5A3			
	GNAS			
	GPR3			
	TNFRSF25			
	TM6SF2			
	MKKS			
	PLEKHF1			
	ZMYM1			
	DOK3			
	FGF20			
	SLC39A2			
	KCNIP2			
	ERRFI1			
	DEDD2			
	CCDC117			
	USP31			
	AHSA2			
	CYS1			
	CNIH2			
	BANP			
	CHORDC1			
	P4HA1			

GEO Series "GSE6653" Expression Profiles

Num of samples in this series: 8

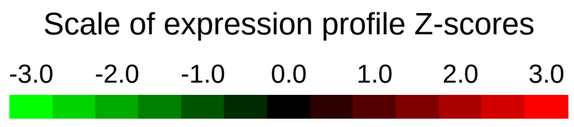

GEO Link:	http://www.ncbi.nlm.nih.gov/geo/query/acc.cgi?acc=GSE6653
Status:	Public on Jan 09 2007
Title:	Gene expression analysis of IOSE cells treated with TGFb1, a time course study
Organism:	Homo sapiens
Experiment type:	Expression profiling by array
Platform:	GPL570
Pubmed ID:	19615063
Summary & Design:	**Summary:** Unlike ovarian cancer, normal ovarian epithelium response to TGFb1 induced growth inhibition. This time course study tried to idenify genes that showed changes after additionof TGFb1 in immortalized ovarian surface epithelial cells (IOSE) which is derived from normal ovarian epithelial cells **Keywords: Time-course** **Overall design:** IOSE cells were treated with TGFb1 for 0, 3, 6, and 12hrs. Cells were harvested for total RNA extraction. Affymetrix expression microarray was performed to analyse gene expression changes.

Background corr dist: KL-Divergence = 0.0609, L1-Distance = 0.0190, L2-Distance = 0.0004, Normal std = 0.5219

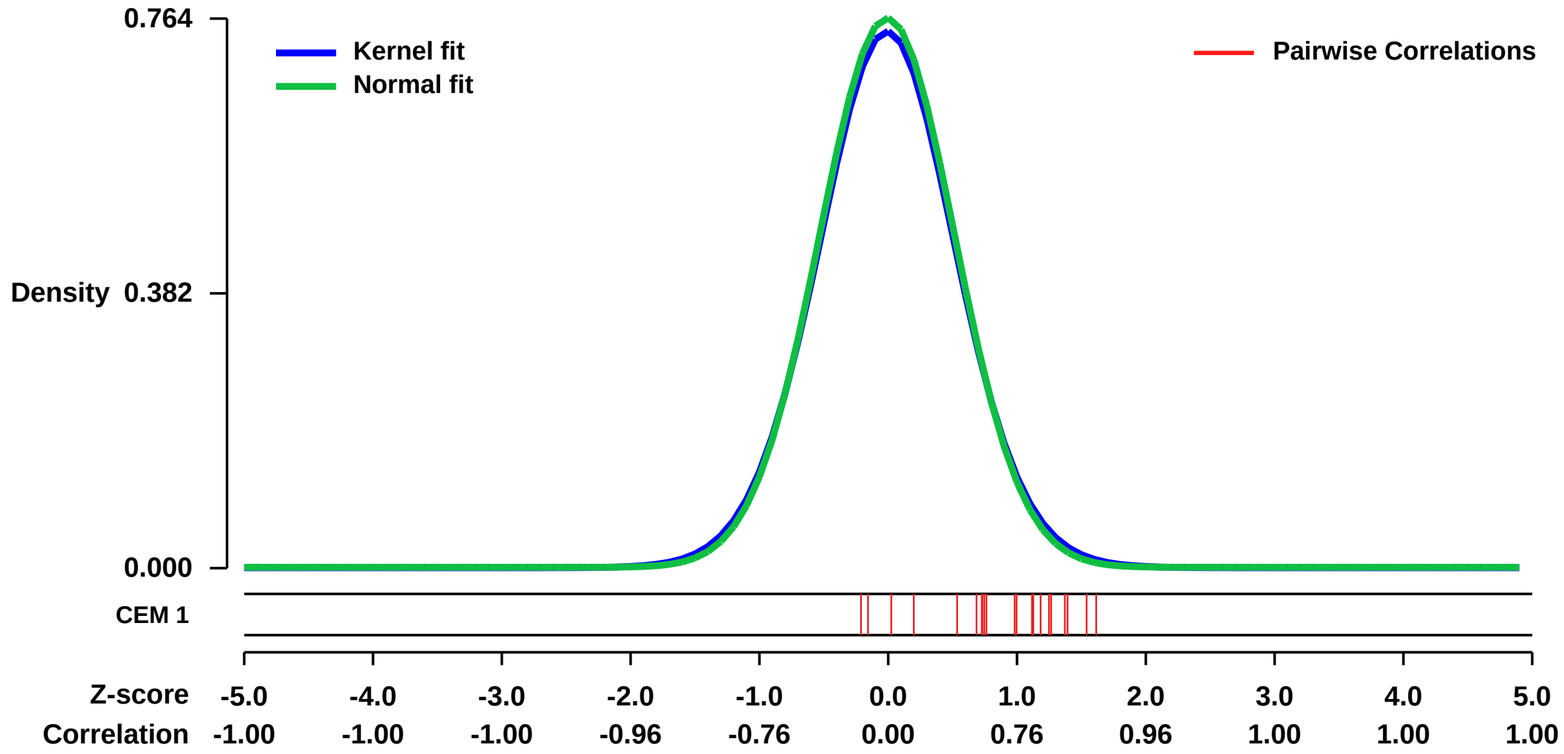

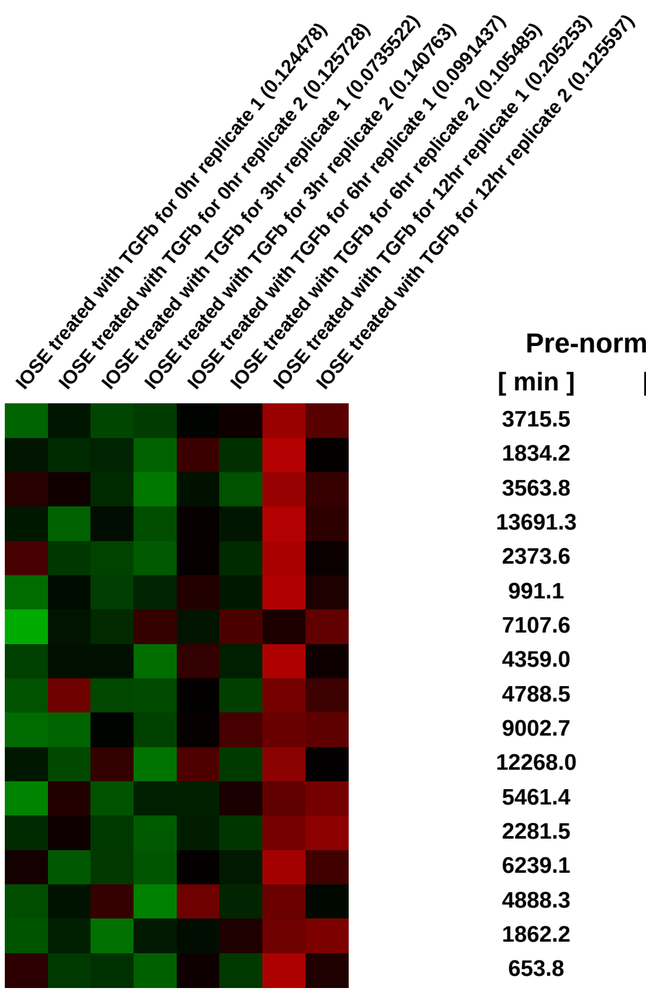

Pre-normalization Quantiles

	[min]	[medium]	[max]
MANF	3715.5	4710.9	6297.0
SDF2L1	1834.2	2354.1	3685.0
CRELD2	3563.8	4064.4	4565.4
HSPA5	13691.3	15473.7	19508.3
HYOU1	2373.6	3242.9	4698.1
PDIA4	991.1	1081.7	1257.6
PDIA6	7107.6	9352.6	10131.7
DNAJB11	4359.0	4824.8	5753.9
HSP90B1	4788.5	4988.3	5255.1
PDIA3	9002.7	10184.3	11215.3
PPIB	12268.0	14452.0	16961.0
C19orf10	5461.4	5991.7	6297.5
SLC35B1	2281.5	2438.8	2870.2
SEC61A1	6239.1	7018.3	8335.0
RPN1	4888.3	5175.1	5458.8
DNAJC3	1862.2	2230.4	2737.2
CDK2AP2	653.8	896.4	1245.4

GEO Series "GSE40873" Expression Profiles

Num of samples in this series: 49

Scale of expression profile Z-scores

-3.0 -2.0 -1.0 0.0 1.0 2.0 3.0

GEO Link:	http://www.ncbi.nlm.nih.gov/geo/query/acc.cgi?acc=GSE40873
Status:	Public on Apr 01 2013
Title:	Low SLC22A7 expression in noncancerous liver promotes hepatocellular carcinoma occurrence - a prospective study
Organism:	Homo sapiens
Experiment type:	Expression profiling by array
Platform:	GPL570
Pubmed ID:	23543312

Summary & Design:

Summary:
Background & Aims: The recurrence determines the postoperative prognosis of patients with hepatocellular carcinoma (HCC). It is unknown whether de novo HCCs derive from the liver with disability of an organic anion transport. This study was designed to elucidate the link between such transporters and the multicentric occurrence (MO) after radical hepatectomy.

Results: SLC22A7 expression was the best predictor of metastasis-free survival (MFS) as judged by the GA (Fold, 0.726; P=0.001). High SLC22A7 gene expression in noncancerous tissue prevent HCC occurrence after hepatectomy (Odds Ratio (OR), 0.2; 95%CI, 0.1-0.6; P=0.004). Multivariate analyses of MFS revealed the independent risk factor to be SLC22A7 expression (OR, 0.3; 95%CI, 0.1-1.0, P=0.043). Low SLC22A7 expression caused MO of HCC significantly (log-rank, P=0.001). In the validation study, multivariate analyses of MFS revealed the independent risk factor to be SLC22A7 expression (OR, 0.5; 95%CI, 0.3-0.8; P=0.012). As judged by Gene set-enrichment analysis, SLC22A7 down-regulation associated with mitochondrion (P=0.008; false discovery rate (FDR)=0.199; normalized enrichment score (NES) =1.804), oxidoreductase activity (P=0.006; FDR=0.157; NES=1.854) and fatty acid metabolic process (P=0.021; FDR=0.177; NES=1.723). Sirtuin3 also determined MFS (P= 0.018).

Conclusions: These pathways involving SLC22A7 dysfunction may promote the occurrence of HCC.

Overall design:
The 49 noncancerous liver tissues of HCC patients within Milan criteria, treated at our institution between January 2004 and August 2008, were examined as a training set by genome-wide gene expression analysis (GA). Cox proportional hazards regression analyses for MO-free survival (MFS) were performed to estimate the risk factors. Using the independent two institutional cohorts of 134 patients between September 2008 and December 2009, a validation study was employed using tissue microarrays.

Background corr dist: KL-Divergence = 0.2659, L1-Distance = 0.0815, L2-Distance = 0.0207, Normal std = 0.2987

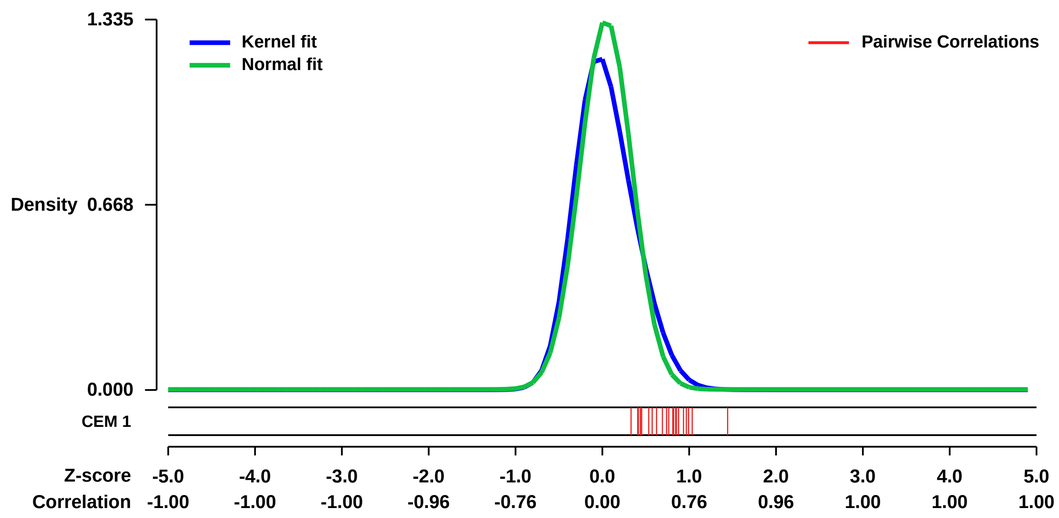

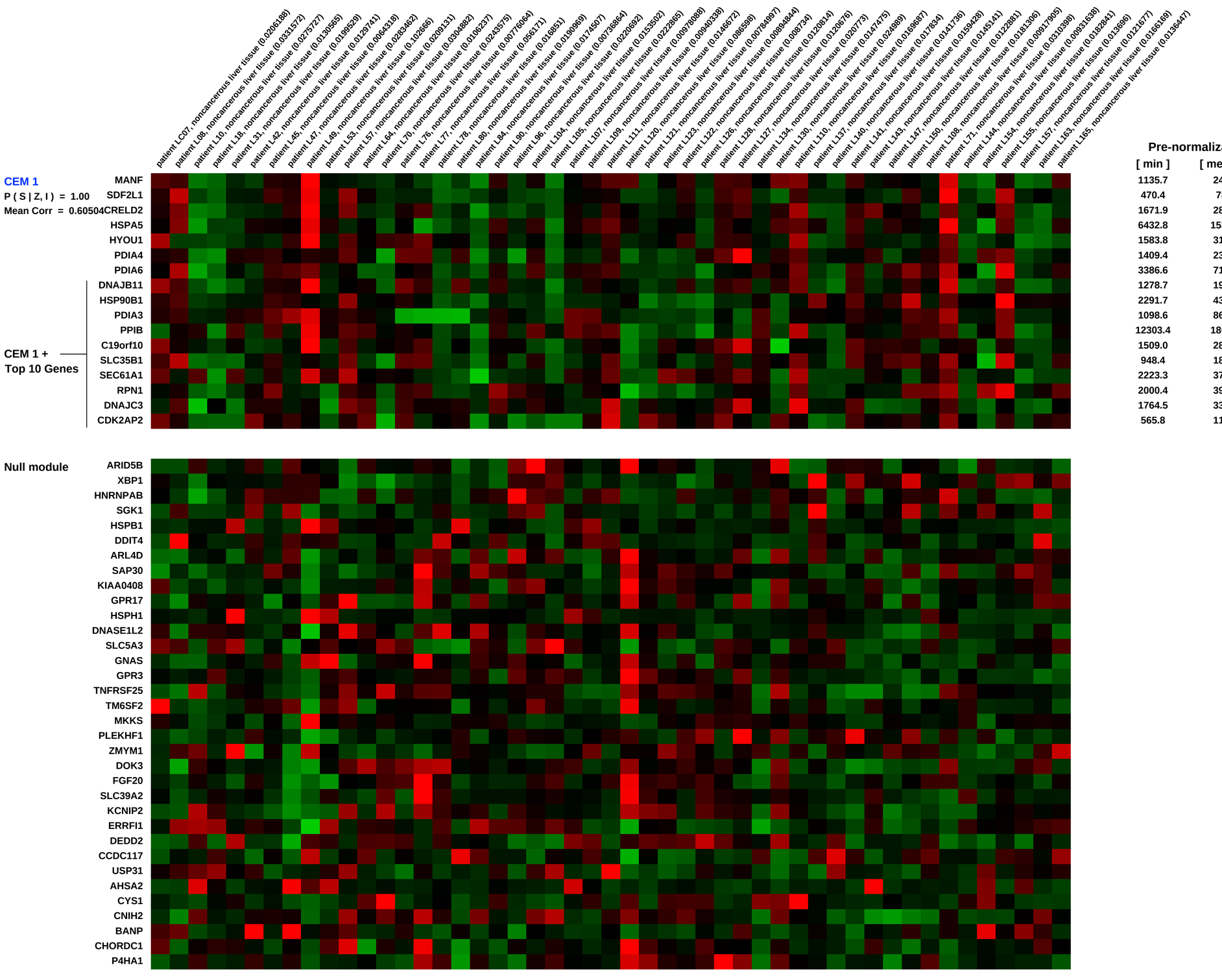

Pre-normalization Quantiles

	[min]	[medium]	[max]
MANF	1135.7	2444.1	5681.3
SDF2L1	470.4	782.8	2138.9
CRELD2	1671.9	2883.9	6321.3
HSPA5	6432.8	15380.9	29591.8
HYOU1	1583.8	3105.8	8986.4
PDIA4	1409.4	2310.7	4061.7
PDIA6	3386.6	7193.9	12936.2
DNAJB11	1278.7	1981.3	3886.8
HSP90B1	2291.7	4329.7	11379.7
PDIA3	1098.6	8679.4	18622.6
PPIB	12303.4	18075.5	28418.4
C19orf10	1509.0	2897.4	5120.7
SLC35B1	948.4	1826.7	2980.5
SEC61A1	2223.3	3775.0	5613.0
RPN1	2000.4	3997.9	6751.8
DNAJC3	1764.5	3384.3	5404.3
CDK2AP2	565.8	1173.6	1873.6

GEO Series "GSE56352" Expression Profiles

Num of samples in this series: 24

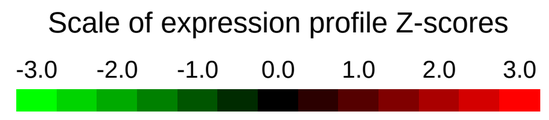

GEO Link:	http://www.ncbi.nlm.nih.gov/geo/query/acc.cgi?acc=GSE56352
Status:	Public on Mar 31 2014
Title:	Inhibition of BET bromodomain proteins as a therapeutic approach in prostate cancer
Organism:	Homo sapiens
Experiment type:	Expression profiling by array
Platform:	GPL570
Pubmed ID:	24293458
Summary & Design:	**Summary:** We analyzed transcriptional changes in 4 prostate cancer cell lines following treatment with the BET inhibitor I-BET762 using Affymetrix Human Genome U133 Plus 2.0 Arrays. **Overall design:** Four prostate cancer cell lines (NCI-H660, VCaP, LNCaP, PC-3) were treated with DMSO (control) or I-BET762 at 0.5uM or 10uM concentrations for 24 hours. Two biological replicates are included for each treatment group.

Background corr dist: KL-Divergence = 0.1318, L1-Distance = 0.0506, L2-Distance = 0.0050, Normal std = 0.4163

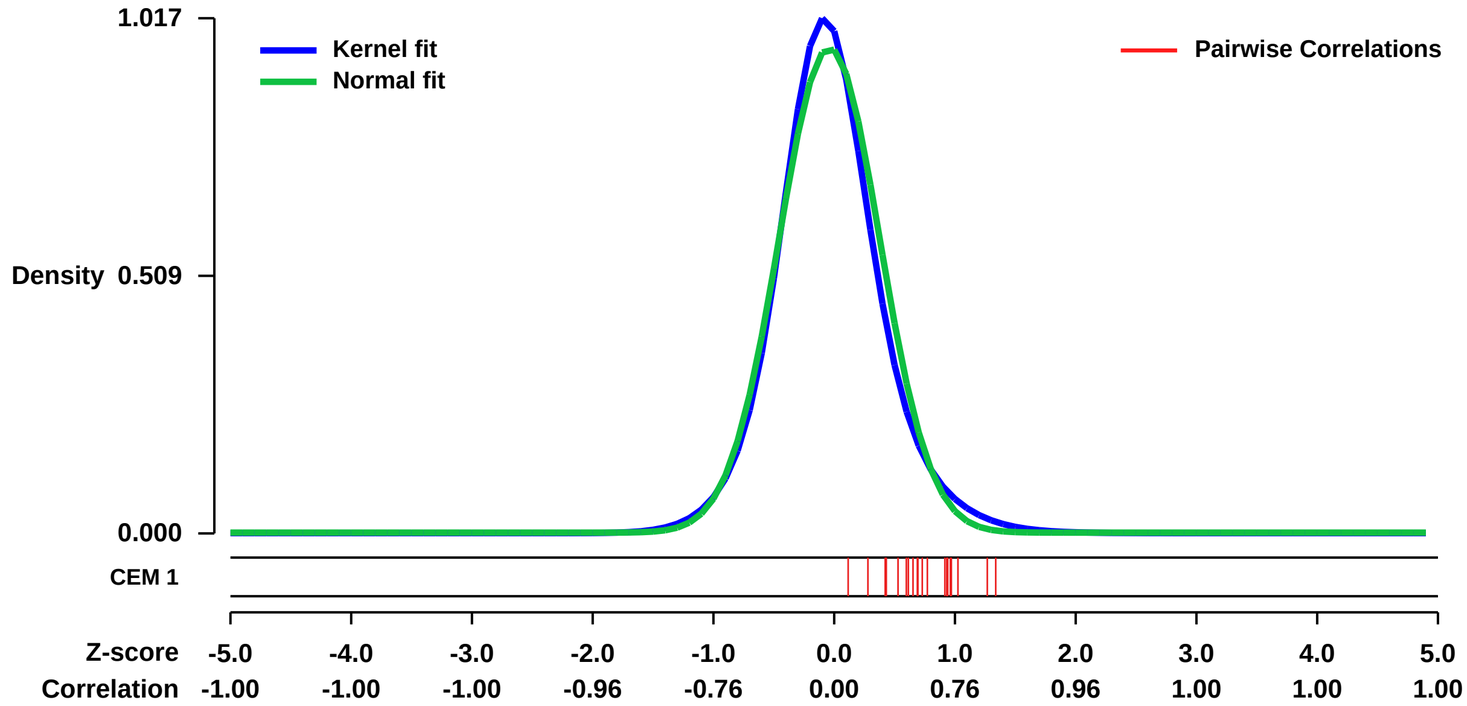

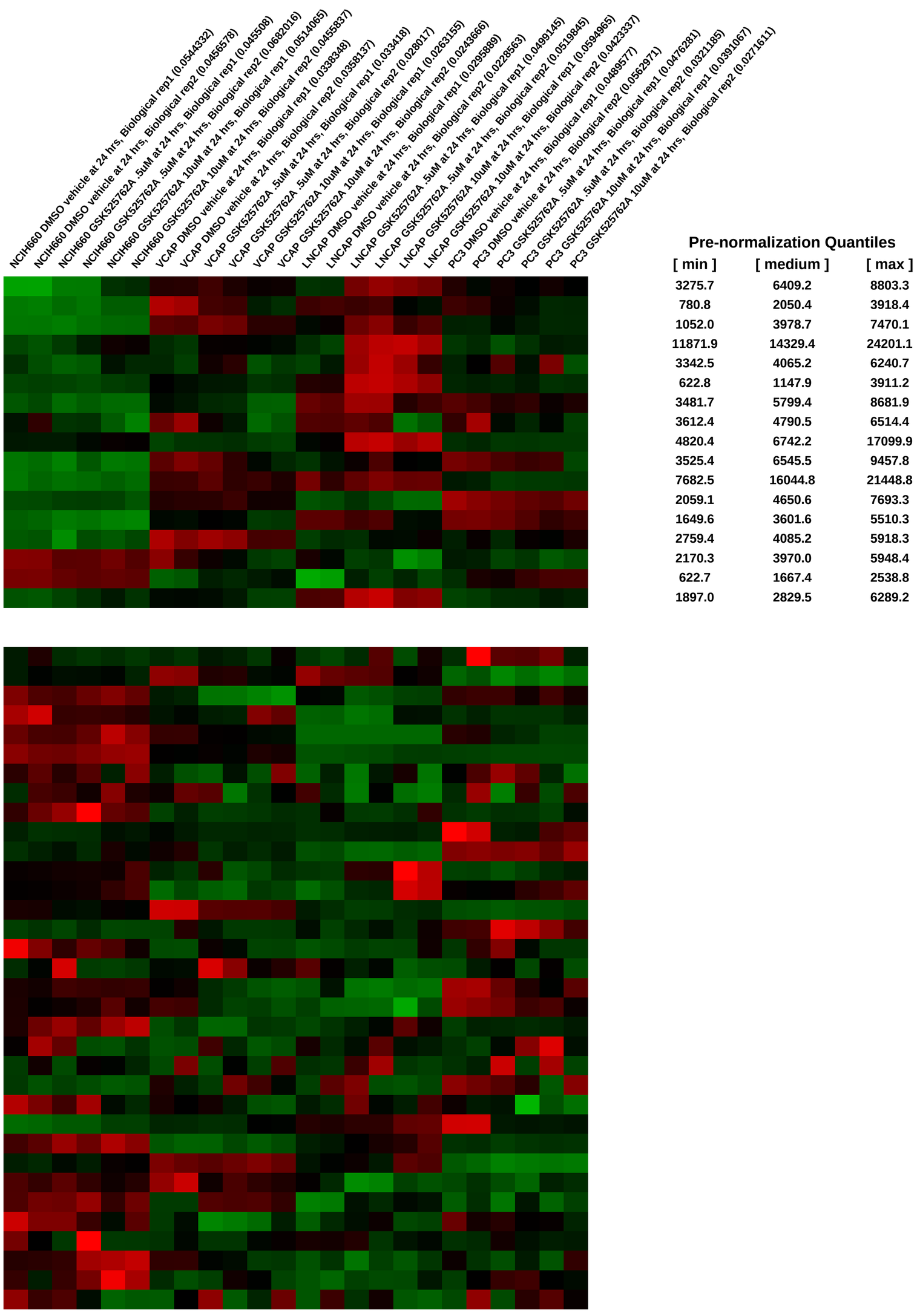

GEO Series "GSE39218" Expression Profiles

Num of samples in this series: 11

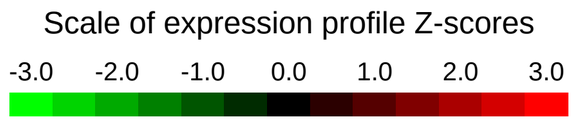

GEO Link:	http://www.ncbi.nlm.nih.gov/geo/query/acc.cgi?acc=GSE39218
Status:	Public on Nov 05 2012
Title:	Functional MYCN signature predicts outcome of neuroblastoma irrespective of MYCN amplification.
Organism:	Homo sapiens
Experiment type:	Expression profiling by array
Platform:	GPL570
Pubmed ID:	23091029
Summary & Design:	**Summary:** Neuroblastoma is a pediatric tumor of the sympathetic nervous system. MYCN (V-myc myelocytomatosis viral-related oncogene, neuroblastoma derived [avian]) is amplified in 20% of neuroblastomas, and these tumors carry a poor prognosis. However, tumors without MYCN amplification also may have a poor outcome. Here, we identified downstream targets of MYCN by shRNA-mediated silencing MYCN in neuroblastoma cells. From these targets, 157 genes showed an expression profile correlating with MYCN mRNA levels in NB88, a series of 88 neuroblastoma tumors, and therefore represent in vivo relevant MYCN pathway genes. This 157-gene signature identified very poor prognosis tumors in NB88 and independent neuroblastoma cohorts and was more powerful than MYCN amplification or MYCN expression alone. Remarkably, this signature also identified poor outcome of a group of tumors without MYCN amplification. Most of these tumors have low MYCN mRNA levels but high nuclear MYCN protein levels, suggesting stabilization of MYCN at the protein level. One tumor has an MYC amplification and high MYC expression. Chip-on-chip analyses showed that most genes in this signature are directly regulated by MYCN. MYCN induces genes functioning in cell cycle and DNA repair while repressing neuronal differentiation genes. The functional MYCN-157 signature recognizes classical neuroblastoma with MYCN amplification, as well as a newly identified group marked by MYCN protein stabilization. **Overall design:** IMR32 was transduced with control or shMYCN virus (duplo). For each experiment 3 time points were analyzed and 2 no virus controls.

Background corr dist: KL-Divergence = 0.0928, L1-Distance = 0.0405, L2-Distance = 0.0024, Normal std = 0.4704

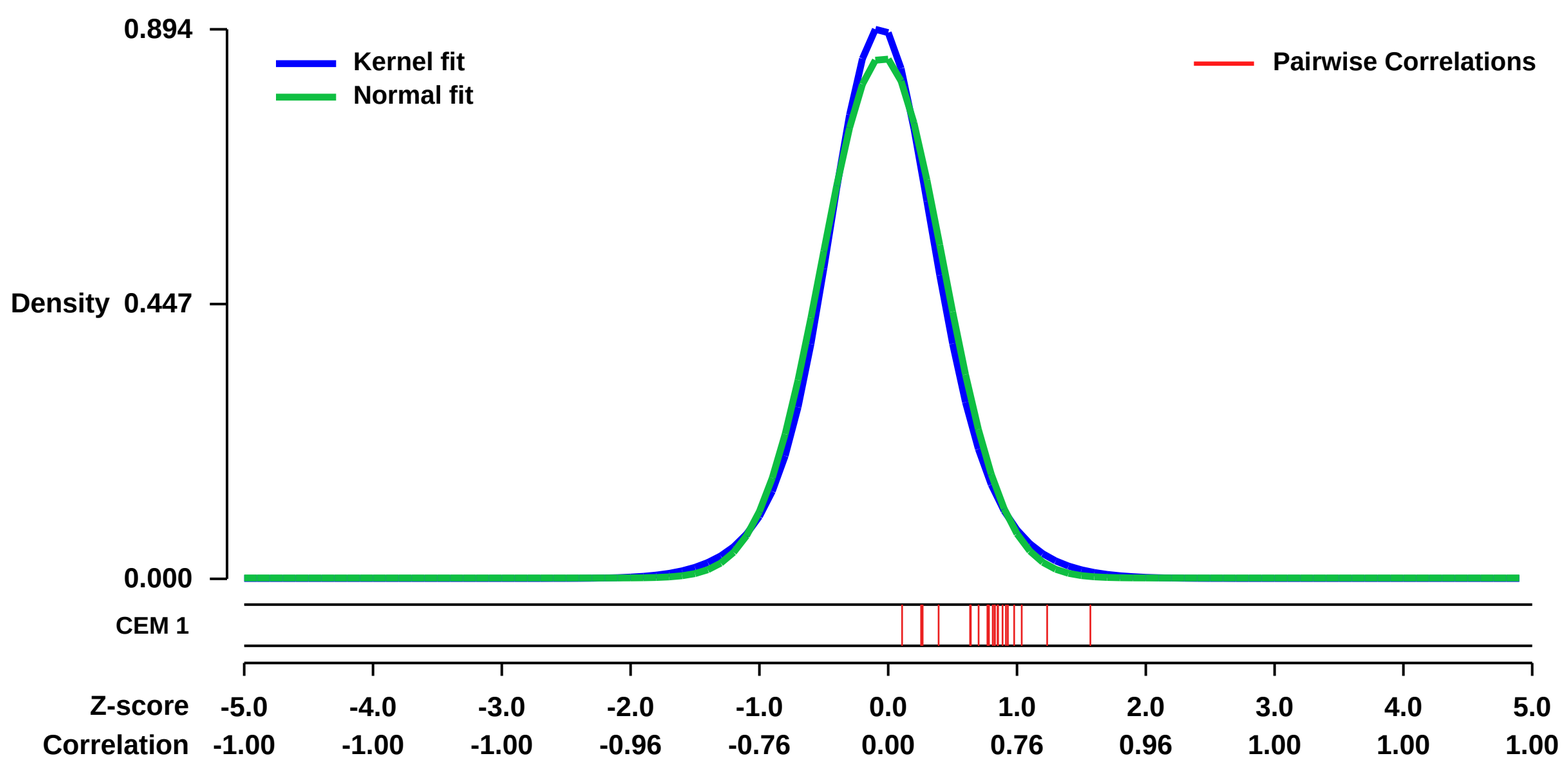

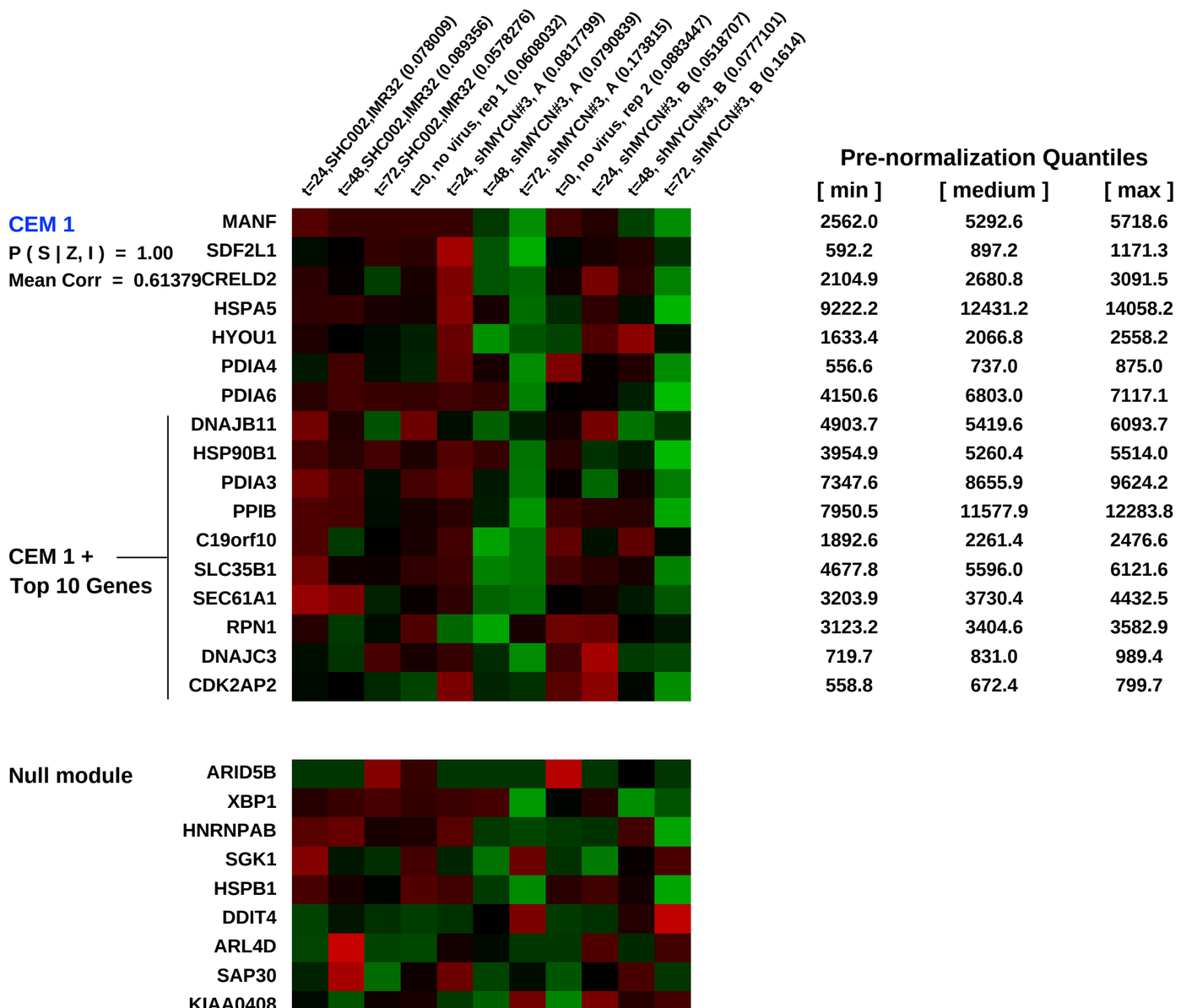

Pre-normalization Quantiles

	[min]	[medium]	[max]
MANF	2562.0	5292.6	5718.6
SDF2L1	592.2	897.2	1171.3
CRELD2	2104.9	2680.8	3091.5
HSPA5	9222.2	12431.2	14058.2
HYOU1	1633.4	2066.8	2558.2
PDIA4	556.6	737.0	875.0
PDIA6	4150.6	6803.0	7117.1
DNAJB11	4903.7	5419.6	6093.7
HSP90B1	3954.9	5260.4	5514.0
PDIA3	7347.6	8655.9	9624.2
PPIB	7950.5	11577.9	12283.8
C19orf10	1892.6	2261.4	2476.6
SLC35B1	4677.8	5596.0	6121.6
SEC61A1	3203.9	3730.4	4432.5
RPN1	3123.2	3404.6	3582.9
DNAJC3	719.7	831.0	989.4
CDK2AP2	558.8	672.4	799.7

GEO Series "GSE46054" Expression Profiles

Num of samples in this series: 6

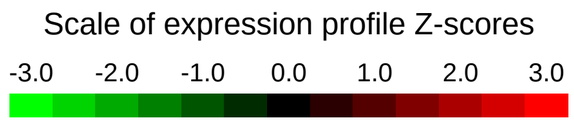

GEO Link:	http://www.ncbi.nlm.nih.gov/geo/query/acc.cgi?acc=GSE46054
Status:	Public on Apr 16 2013
Title:	Hela SPAG4 siRNA
Organism:	Homo sapiens
Experiment type:	Expression profiling by array
Platform:	GPL570
Pubmed ID:	23602831
Summary & Design:	**Summary:** In order to clarify the downstream target genes of SPAG4, we performed knockdown of SPAG4 using siRNA both under normoxia and hypoxia. **Overall design:** Hela cells are cultured for 24 hours under normoxia and hypoxia after knocking down of SPAG4 using different sequences of siRNA.

Background corr dist: KL-Divergence = 0.0459, L1-Distance = 0.0320, L2-Distance = 0.0013, Normal std = 0.6054

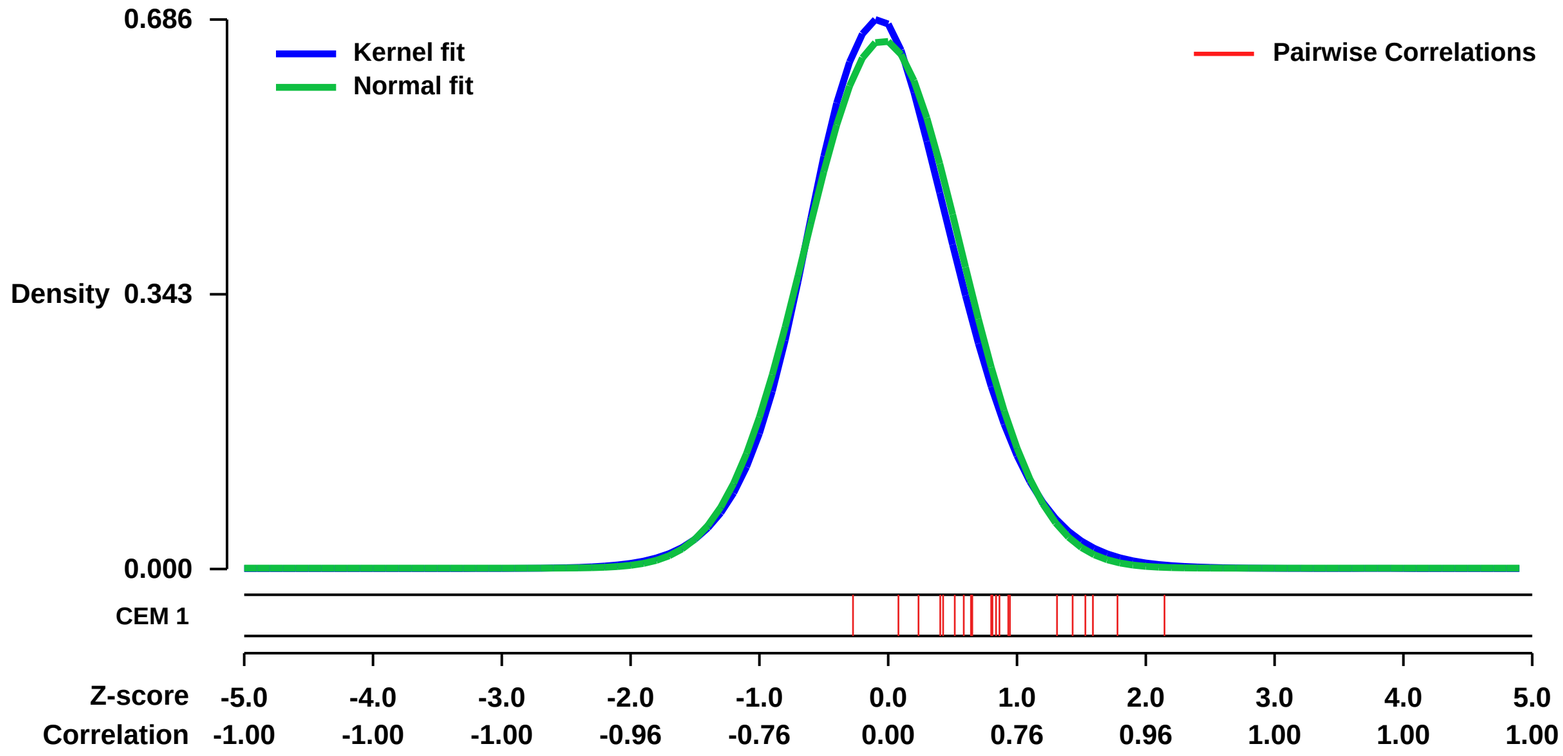

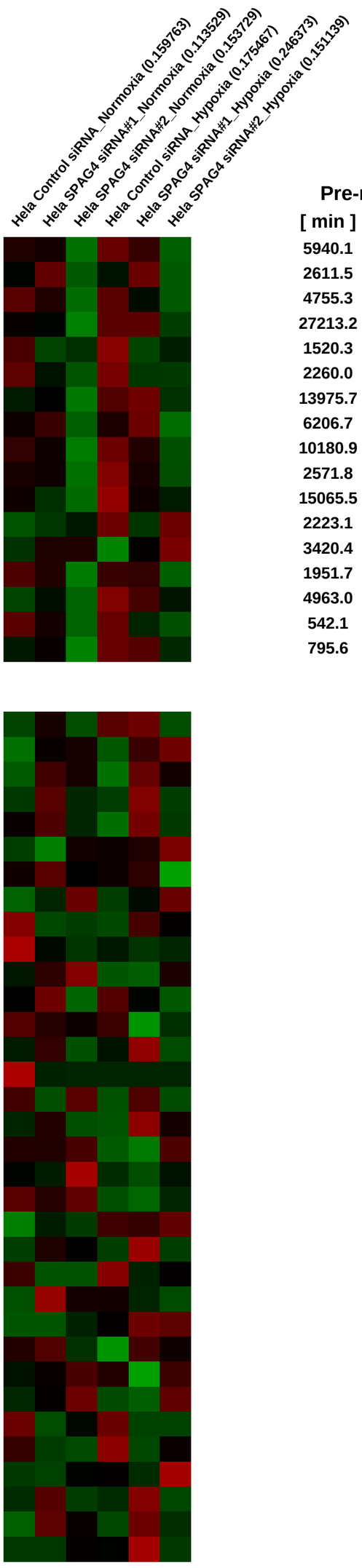

GEO Series "GSE25148" Expression Profiles

Num of samples in this series: 20

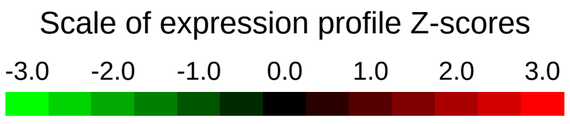

GEO Link:	http://www.ncbi.nlm.nih.gov/geo/query/acc.cgi?acc=GSE25148
Status:	Public on Jan 12 2011
Title:	Changes in gene expression in HEK-TLR2 cells in response to Helicobacter pylori lipopolysaccharide
Organism:	Homo sapiens
Experiment type:	Expression profiling by array
Platform:	GPL570
Pubmed ID:	21220698
Summary & Design:	**Summary:** This study set out to identify global changes in gene expression in human embryonic kidney (HEK) cells stably transfected with Toll-like receptor 2 (TLR2) over a 48 hour time-course, following stimulation with 10 ¸…g/ml lipopolysaccharide (LPS) from the gastric pathogen H. pylori. Microarray analysis was used to compare changes in gene expression between cells treated with 10 ¸…g/ml H. pylori LPS and untreated cells at the same time point. **Overall design:** Total RNA was harvested from HEK-TLR2 cells following treatment with LPS for 2, 4, 8, 24 and 48h or untreated cells at the same time-point. 2 independent experiments were carried out. RNA was labeled and hybridized to GeneChips to analyse changes in gene expression.

Background corr dist: KL-Divergence = 0.1321, L1-Distance = 0.0436, L2-Distance = 0.0041, Normal std = 0.3898

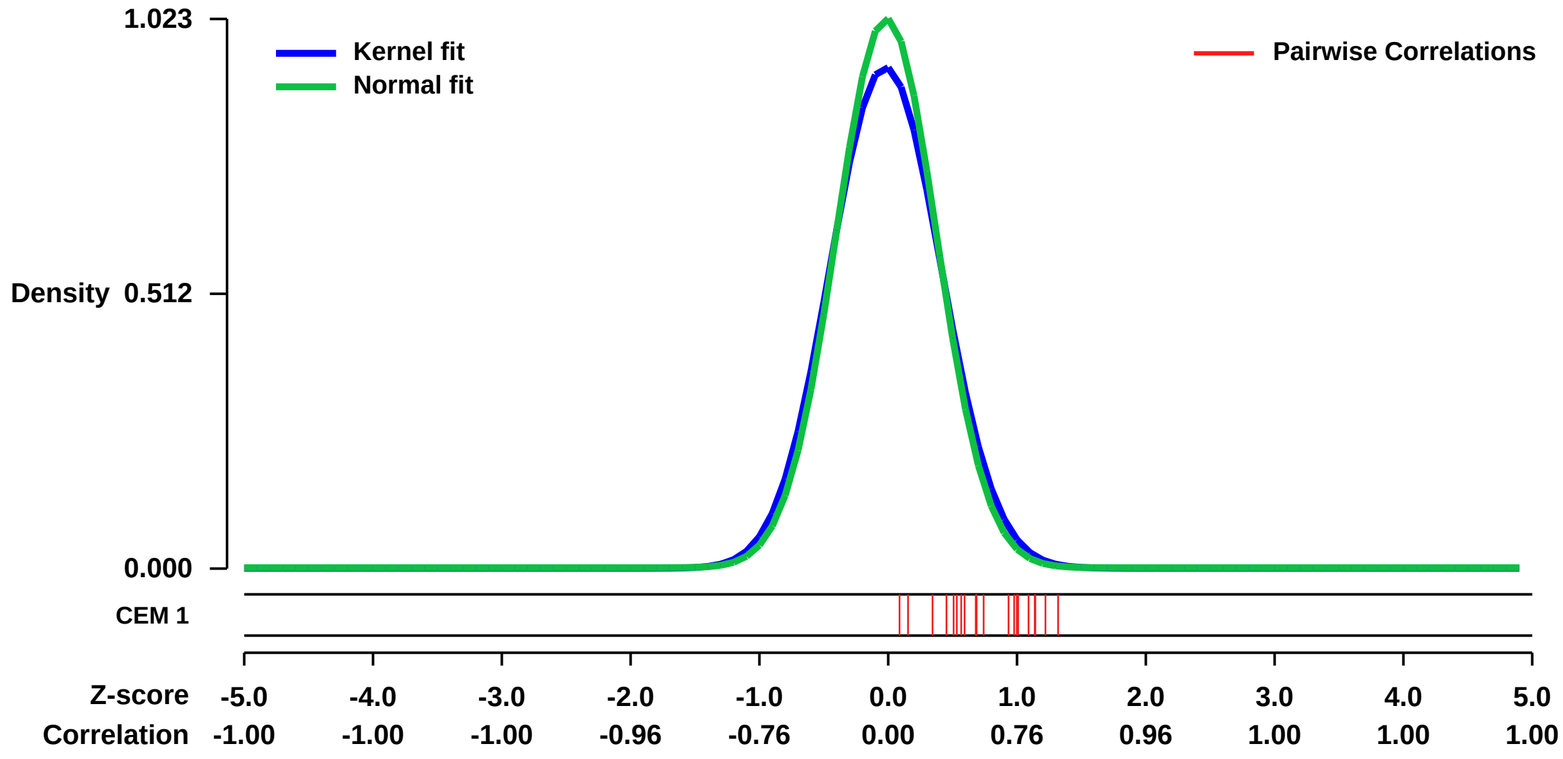

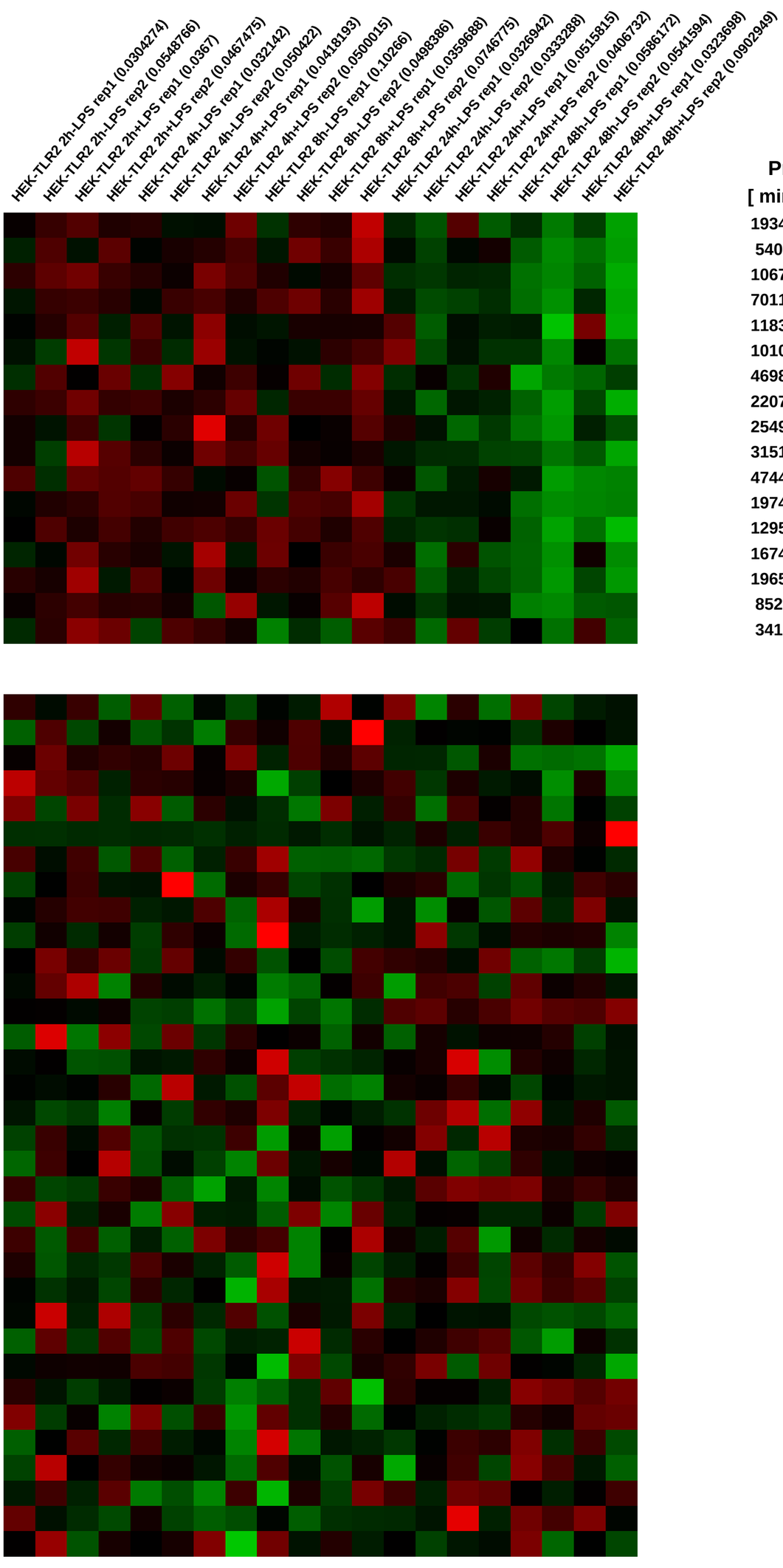

GEO Series "GSE30903" Expression Profiles

Num of samples in this series: 24

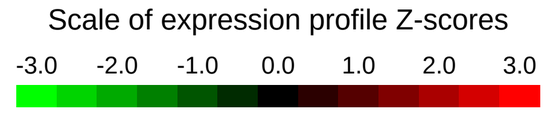

GEO Link:	http://www.ncbi.nlm.nih.gov/geo/query/acc.cgi?acc=GSE30903
Status:	Public on Feb 25 2012
Title:	Expression data from untreated and ATP treated AML blasts
Organism:	Homo sapiens
Experiment type:	Expression profiling by array
Platform:	GPL570
Pubmed ID:	22053107
Summary & Design:	**Summary:** In the present study, we investigated whether, and to what extent, P2Rs and their ligands are involved in the regulation of AML cells. Our findings show that AML blasts express several receptors belonging to the P2X and P2Y family. Although different samples respond differently to ATP and UTP stimulation (reflecting the variability intrinsic to the group of acute myeloid leukemias), all the tested samples appear to be responsive to purinergic signalling, as demonstrated by intracellular calcium mobilization. GEP analysis demonstrated that ATP induced the expression of cell cycle inhibitors and negative modulators of cell motility, such as inhibitors of GTPase activity. On the contrary, ATP inhibits the expression cell-cycle related genes (cyclins and CDKs), activators of cell motility (Rho GTPases regulators, matrix degradation enzyme and cytoskeleton proteins) and adhesion molecules involved in homing and engraftment. **Overall design:** Blast cells obtained from 12 AML patients (3 M0/M1; 3 M2; 3 M4; and 3 M5) were cultured for 24 h with or without 1 mM ATP. Total RNA from 106 ATP-treated and untreated cells was extracted to study variation of gene expression profile induced by ATP treatment in leukemic cells.

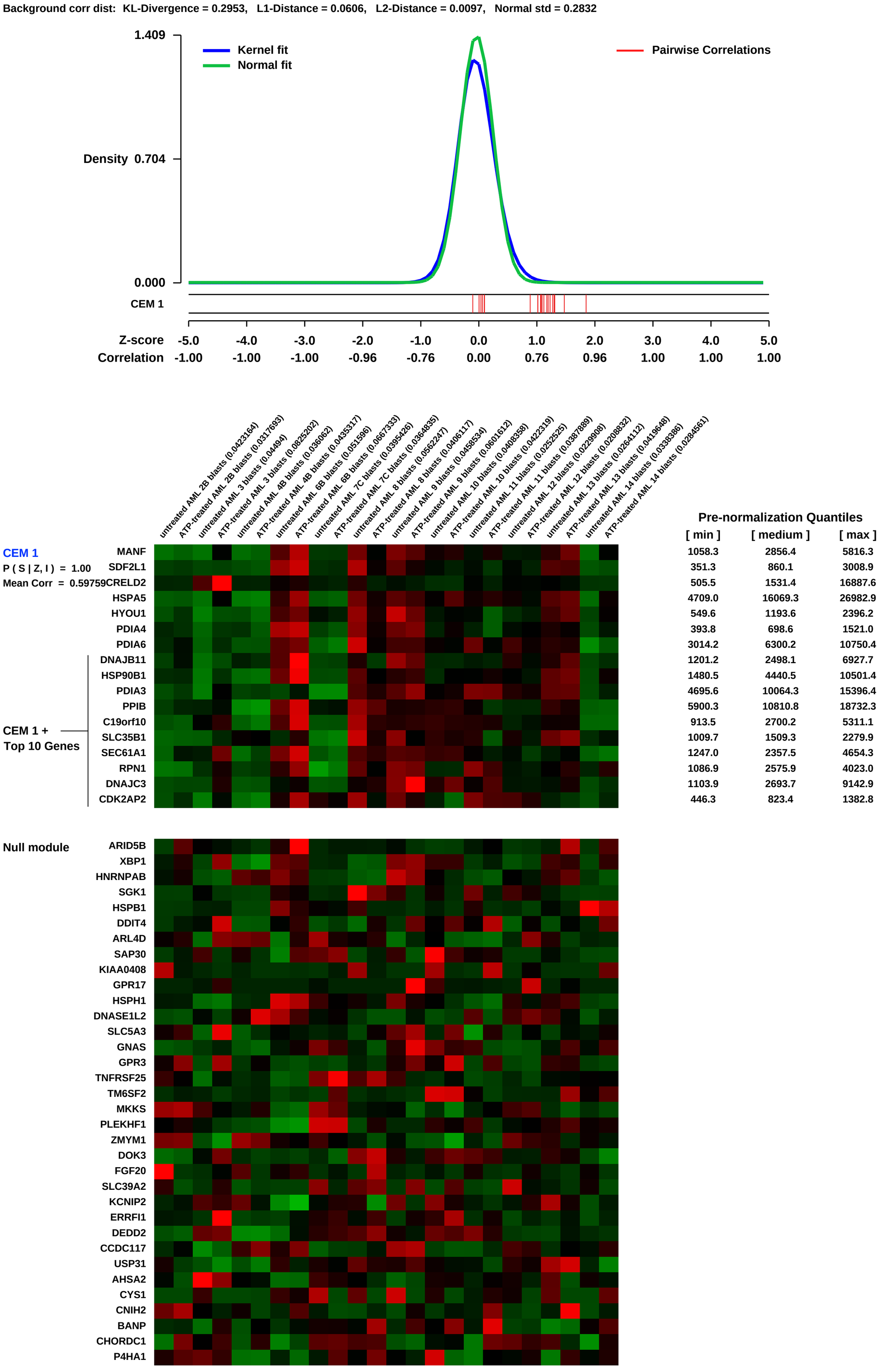

GEO Series "GSE19638" Expression Profiles

Num of samples in this series: 14

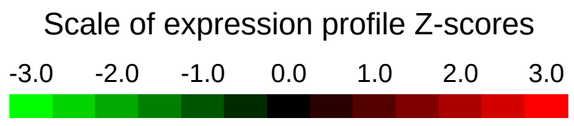

GEO Link:	http://www.ncbi.nlm.nih.gov/geo/query/acc.cgi?acc=GSE19638
Status:	Public on Jul 14 2010
Title:	Compounds profiling on MCF7
Organism:	Homo sapiens
Experiment type:	Expression profiling by array
Platform:	GPL570
Pubmed ID:	20679242
Summary & Design:	**Summary:** The effects of several compounds on the MCF7 human adenocarcinoma mammary cell line were analysed by gene expression profiling. **Overall design:** The MCF7 cell line was treated with the different compounds for 6 hours at a dose equal to 5 times the IC50. Untreated MCF7 cells were used as a control. Two replicates per treatment.

Background corr dist: KL-Divergence = 0.1132, L1-Distance = 0.0400, L2-Distance = 0.0024, Normal std = 0.4362

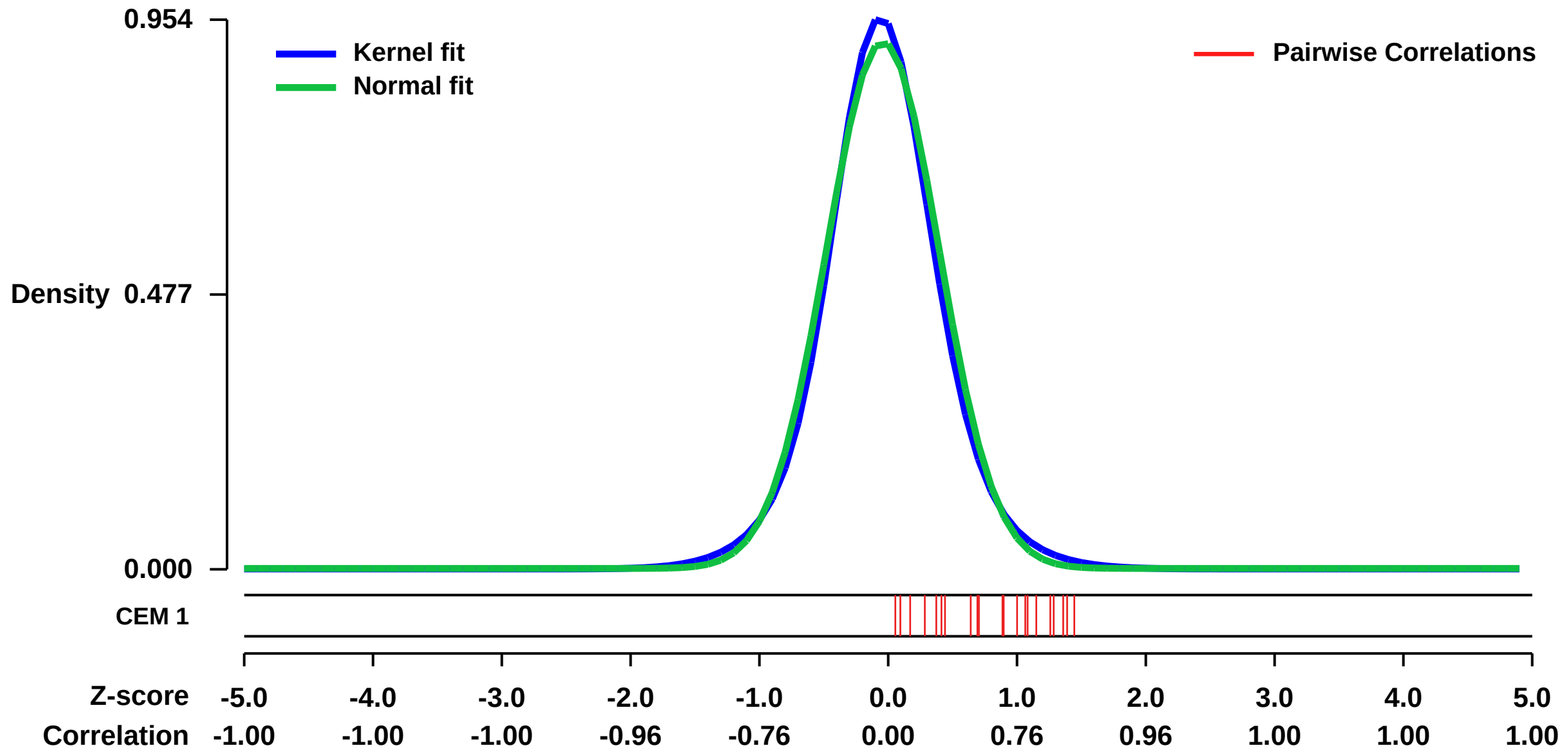

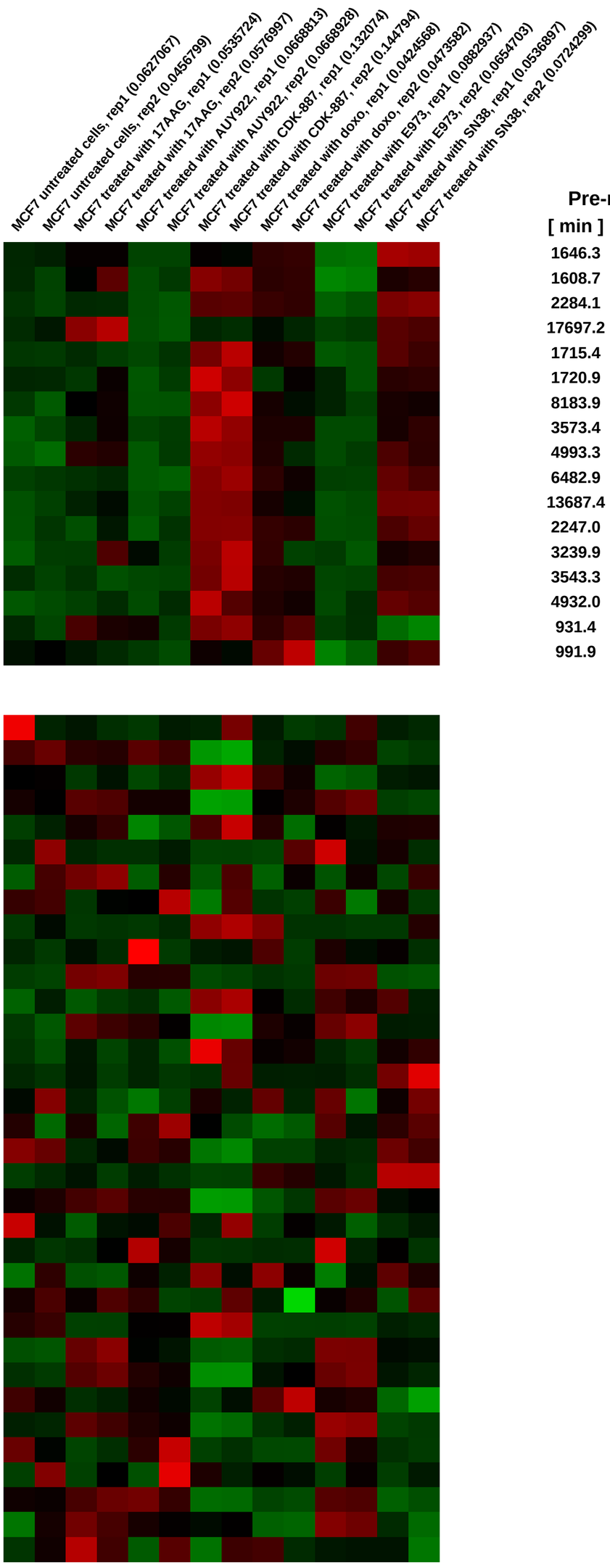

GEO Series "GSE10334" Expression Profiles

Num of samples in this series: 247

Details of this dataset are not shown due to large number of samples and the page size limit.

Find details in http://www.ncbi.nlm.nih.gov/geo/query/acc.cgi?acc=GSE10334

Background corr dist: KL-Divergence = 0.2353, L1-Distance = 0.0777, L2-Distance = 0.0181, Normal std = 0.3167

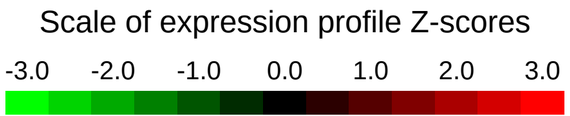

GEO Series "GSE55859" Expression Profiles

Num of samples in this series: 8

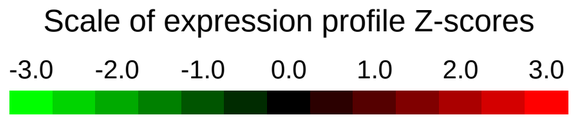

GEO Link:	http://www.ncbi.nlm.nih.gov/geo/query/acc.cgi?acc=GSE55859
Status:	Public on Sep 01 2014
Title:	Gene expression profile of TRAIL-sensitive and -resistant H460 cells
Organism:	Homo sapiens
Experiment type:	Expression profiling by array
Platform:	GPL570
Pubmed ID:	
Summary & Design:	**Summary:** We generated H460 cells with acquired TRAIL resistance by exposing the parental sentisitve cells to subtoxic concentrations of TRAIL for 6 months. Then we compared the gene expression profile of the sensitive versus the resistant cells. We generated acquired TRAIL-resistant H460 cells from the sentisitve cells by treating subtoxic range of TRAIL for 6 month. And we tried to compare the expressional profile of the genes between two cell types to isolate genes regulating acquired TRAIL-resistance **Overall design:** H460 cells were treated with subtoxic concentrations of TRAIL for 6 month. After confirmation of the resistance, the RNA was extracted and the gene expression profile was analyzed.

Background corr dist: KL-Divergence = 0.0490, L1-Distance = 0.0503, L2-Distance = 0.0033, Normal std = 0.6274

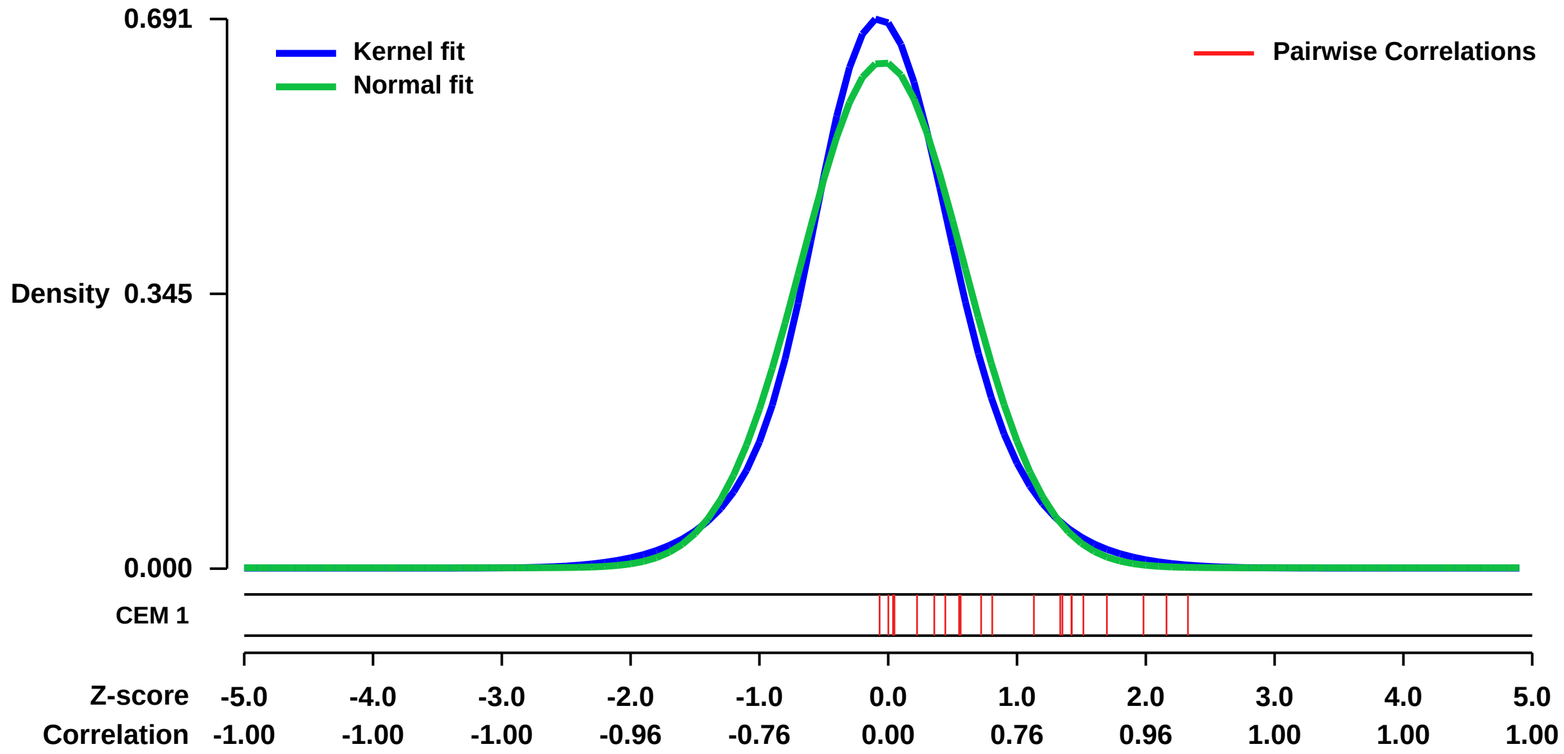

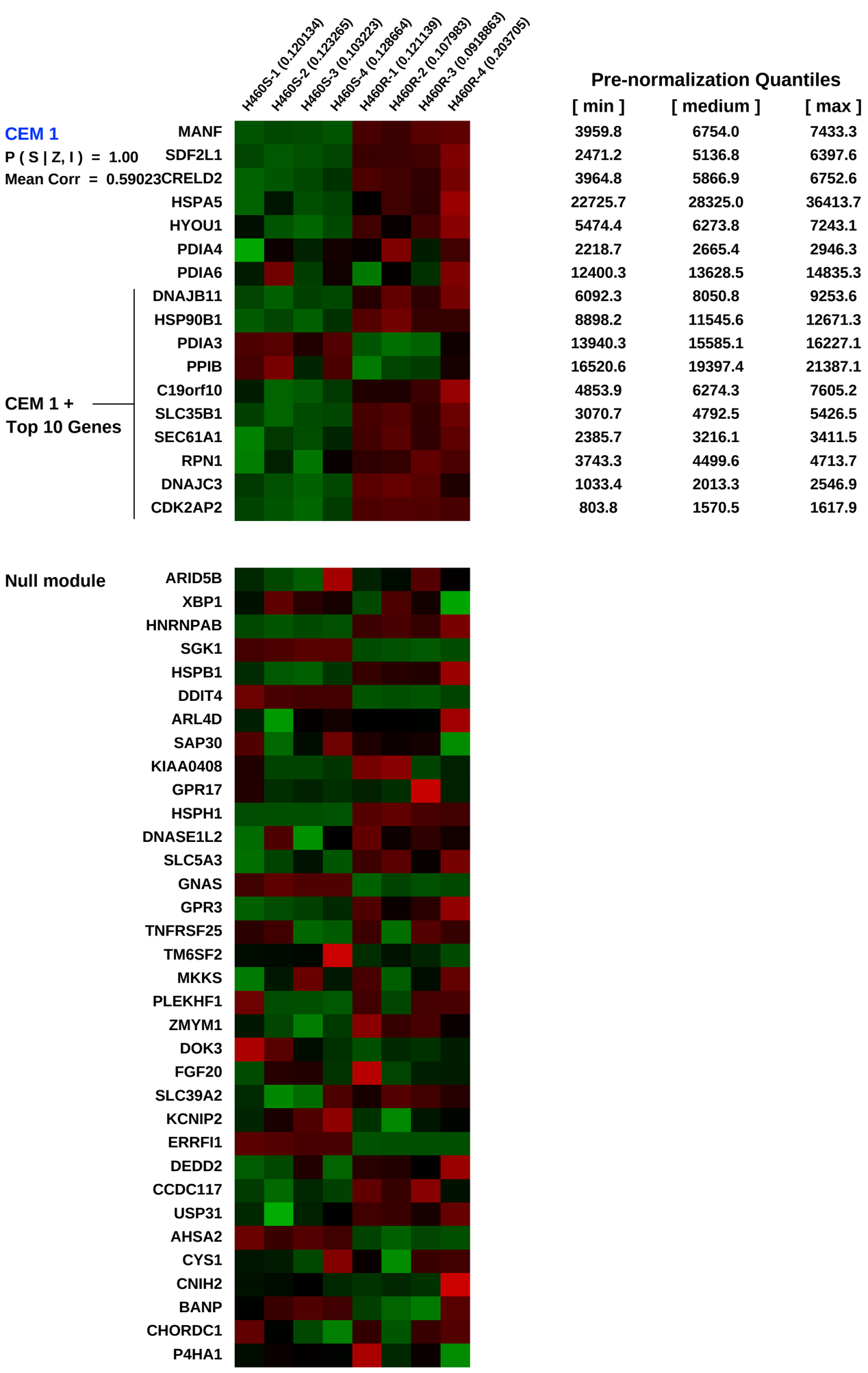

GEO Series "GSE32496" Expression Profiles

Num of samples in this series: 18

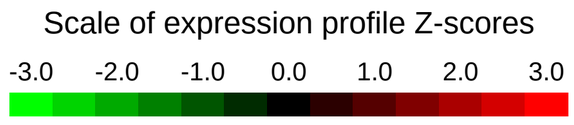

GEO Link:	http://www.ncbi.nlm.nih.gov/geo/query/acc.cgi?acc=GSE32496
Status:	Public on Nov 26 2012
Title:	GENOME-WIDE CpG ISLAND METHYLATION ANALYSIS IN NON-SMALL CELL LUNG CANCER PATIENTS [Affymetrix expression data]
Organism:	Homo sapiens
Experiment type:	Expression profiling by array
Platform:	GPL570
Pubmed ID:	23172663
Summary & Design:	**Summary:** Epigenetic changes largely contribute to the regulation of gene expression in cancer cells. DNA methylation is part of the epigenetic gene regulation complex which is relevant for the pathogenesis of cancer. We performed a genome-wide search for methylated CpG islands in tumors and corresponding non-malignant lung tissue samples of 101 stage I-III non-small cell lung cancer (NSCLC) patients by combining methylated DNA immunoprecipitation and microarray analysis using NimbleGen´·s 385K Human CpG Island plus Promoter arrays. By testing for differences in methylation between tumors and corresponding non-malignant lung tissues, we identified 298 tumor-specifically methylated genes. From many of these genes epigenetic regulation was unknown so far. Gene Ontology analysis revealed an over-representation of genes involved in regulation of gene expression and cell adhesion. Expression of 182 of 298 genes was found to be upregulated after 5-aza-2´·-deoxycytidine (Aza-dC) and/or trichostatin A (TSA) treatment of 3 NSCLC cell lines by Affymetrix microarray analysis. In addition, methylation of selected genes in primary NSCLCs and corresponding non-malignant lung tissue samples were analyzed by methylation-sensitive high resolution melting analysis (MS-HRM). Our results obtained by MS-HRM analysis confirmed our data obtained by MeDIP-chip analysis. Moreover, by comparing methylation results from MeDIP-chip analysis with clinico-pathological parameters of the patients we observed methylation of HOXA2 as potential parameter for shorter disease-free survival of NSCLC patients. In conclusion, using a genome-wide approach we identified a large number of tumor-specifically methylated genes in NSCLC patients. Our results stress the importance of DNA methylation for the pathogenesis of NSCLCs. **Overall design:** Overall, samples of 3 untreated, with Aza-dC treated and with Aza-dC/TSA treated NSCLC cell lines were hybridized to Affymetrix HG-U133_plus_2.0 microarrays (18 in total).

Background corr dist: KL-Divergence = 0.1045, L1-Distance = 0.0408, L2-Distance = 0.0027, Normal std = 0.4478

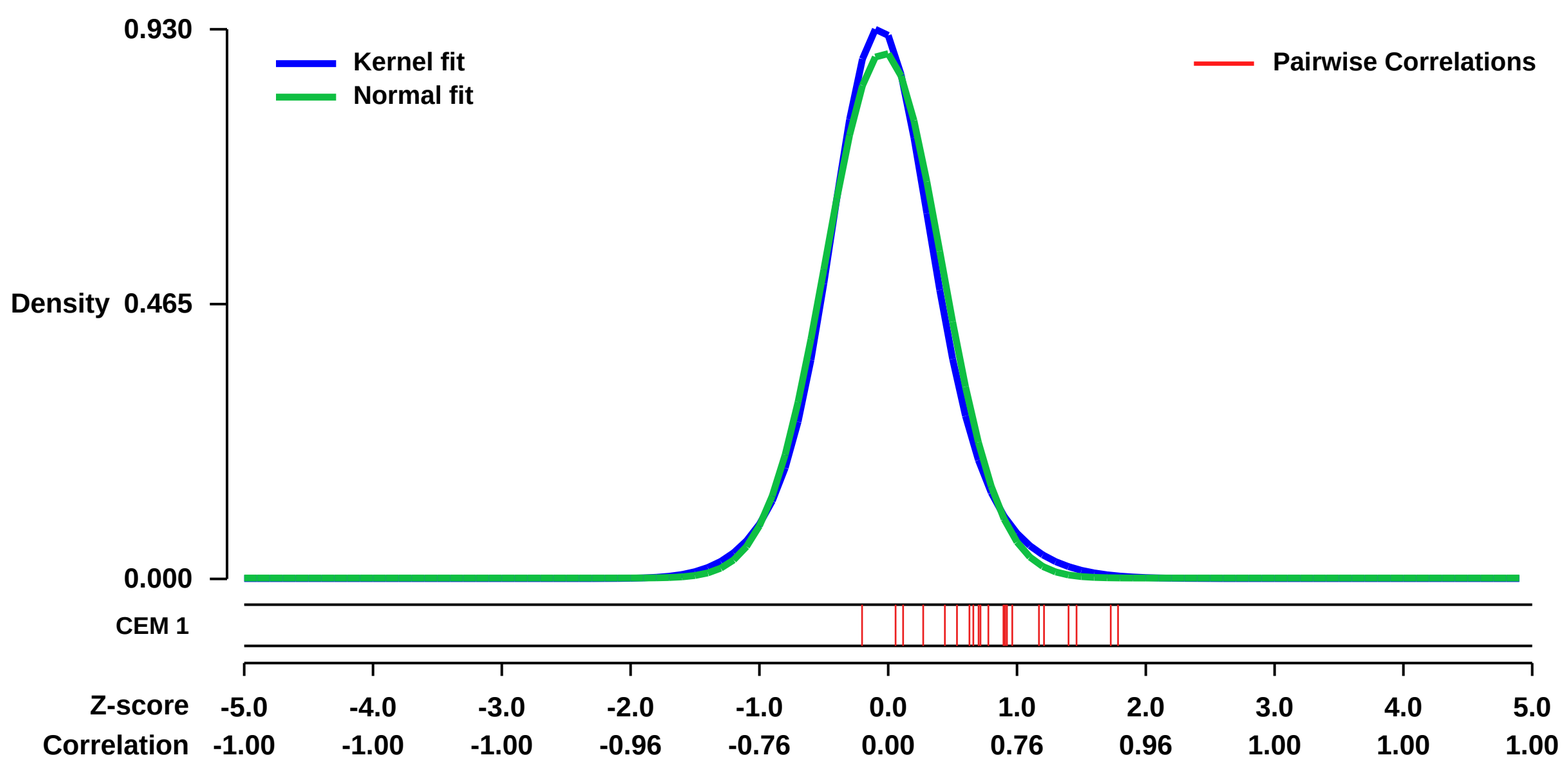

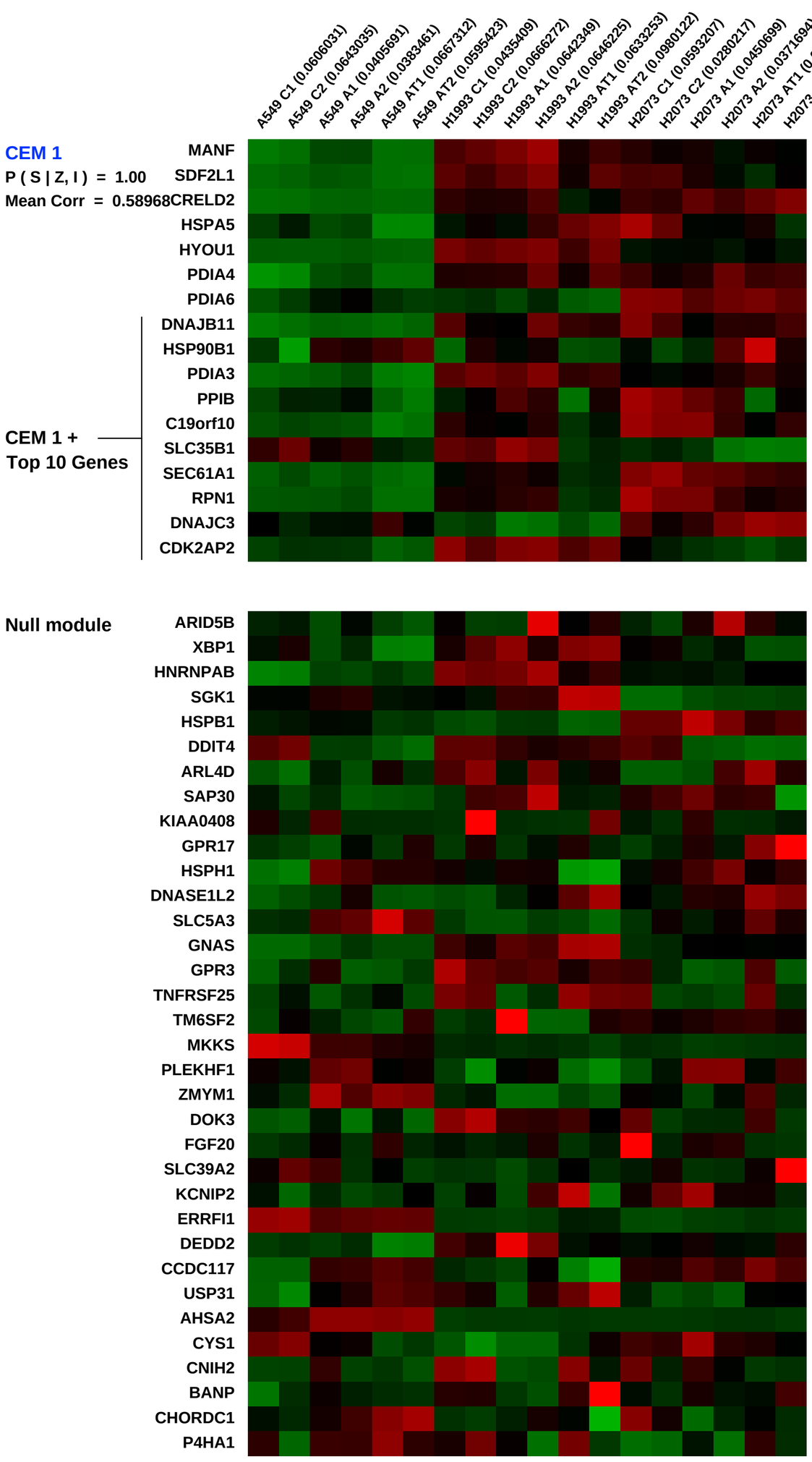

Pre-normalization Quantiles

	[min]	[medium]	[max]
MANF	2529.4	6300.7	10287.5
SDF2L1	879.3	3321.7	5376.6
CRELD2	1269.8	10210.1	16130.4
HSPA5	15040.3	22920.0	33351.3
HYOU1	872.4	4605.2	10467.3
PDIA4	951.8	2303.3	2814.6
PDIA6	9239.6	12157.3	19775.7
DNAJB11	2487.2	4696.6	5945.6
HSP90B1	3277.8	6208.5	9248.3
PDIA3	5490.7	10204.9	13531.4
PPIB	11467.1	15703.4	20937.8
C19orf10	2656.5	5500.1	9145.5
SLC35B1	2341.4	3561.8	5770.1
SEC61A1	1986.1	4061.7	6272.8
RPN1	1556.0	4076.5	7021.8
DNAJC3	553.2	1209.2	2085.5
CDK2AP2	923.2	1735.3	4741.8

GEO Series "GSE7011" Expression Profiles

Num of samples in this series: 18

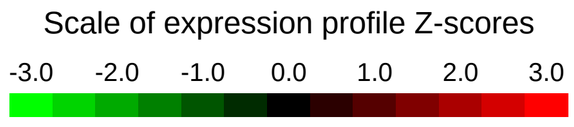

GEO Link:	http://www.ncbi.nlm.nih.gov/geo/query/acc.cgi?acc=GSE7011
Status:	Public on May 01 2008
Title:	Leukemia fusion-gene transduced human cord blood cells
Organism:	Homo sapiens
Experiment type:	Expression profiling by array
Platform:	GPL570
Pubmed ID:	18538732

Summary & Design:

Summary:
MLL-AF9 expression in normal human umbilical cord blood CD34+ cells leads to long-term proliferation of a myeloid progenitor cell with leukemogenic potential. Expression of a Core Binding Factor leukemia fusion (AML1-ETO or CBFbeta-SMMHC) in human CD34+ cells results in self-renewal of primitive progenitor cells with multilineage potential and stem cell ability, but these cells do not induce leukemia in immunodeficient mice. This comparative microarray study was initiated to determine how faithful these cell cultures are to the transcriptome of patient samples expressing each of these different fusion proteins, and to analyze the signaling pathways that are unique to CBF cultures and MLL-fusion cultures, with the hope of determining why the MLL-fusion cells are leukemogenic while the CBF cells are not.

Keywords: Disease state analysis; comparison of leukemia fusion gene expression in normal human hematopoietic progenitor cells

Overall design:
We have established a culture system whereby we retrovirally transduce human CD34+ cells, obtained from cord blood, with the leukemia fusion genes MLL-AF9 (MA9), AML1-ETO (AE) or CBFbetaMYH11 (CM). Cells expressing each of these fusion proteins are able to proliferate long-term in vitro in a cytokine dependent manner. These cultures resemble somewhat the blast samples from patients that contain these different fusion proteins, in that MA9 cells are predominantly monocytic (M5-like), AE cells have a large population of primitive CD34+ cells with continued abnormal differentiation (M2-like) and CM cells also contain a population of primitive CD34+ cells with continued abnormal differentiation but also have a significant population of abnormal eosinophils (M4Eo). We grow these cells in the presence of fetal bovine serum (FBS), and also grow them in serum-free conditions using the BIT supplement from Stem Cell Technologies. For the current experiments we used cell cultures that had been proliferating in vitro for 8-12 weeks, in either serum-free conditions or with FBS. Replicate samples were included in some instances, and the same clonal cultures that were grown under either BIT or FBS were also included.

Background corr dist: KL-Divergence = 0.1276, L1-Distance = 0.0308, L2-Distance = 0.0020, Normal std = 0.3998

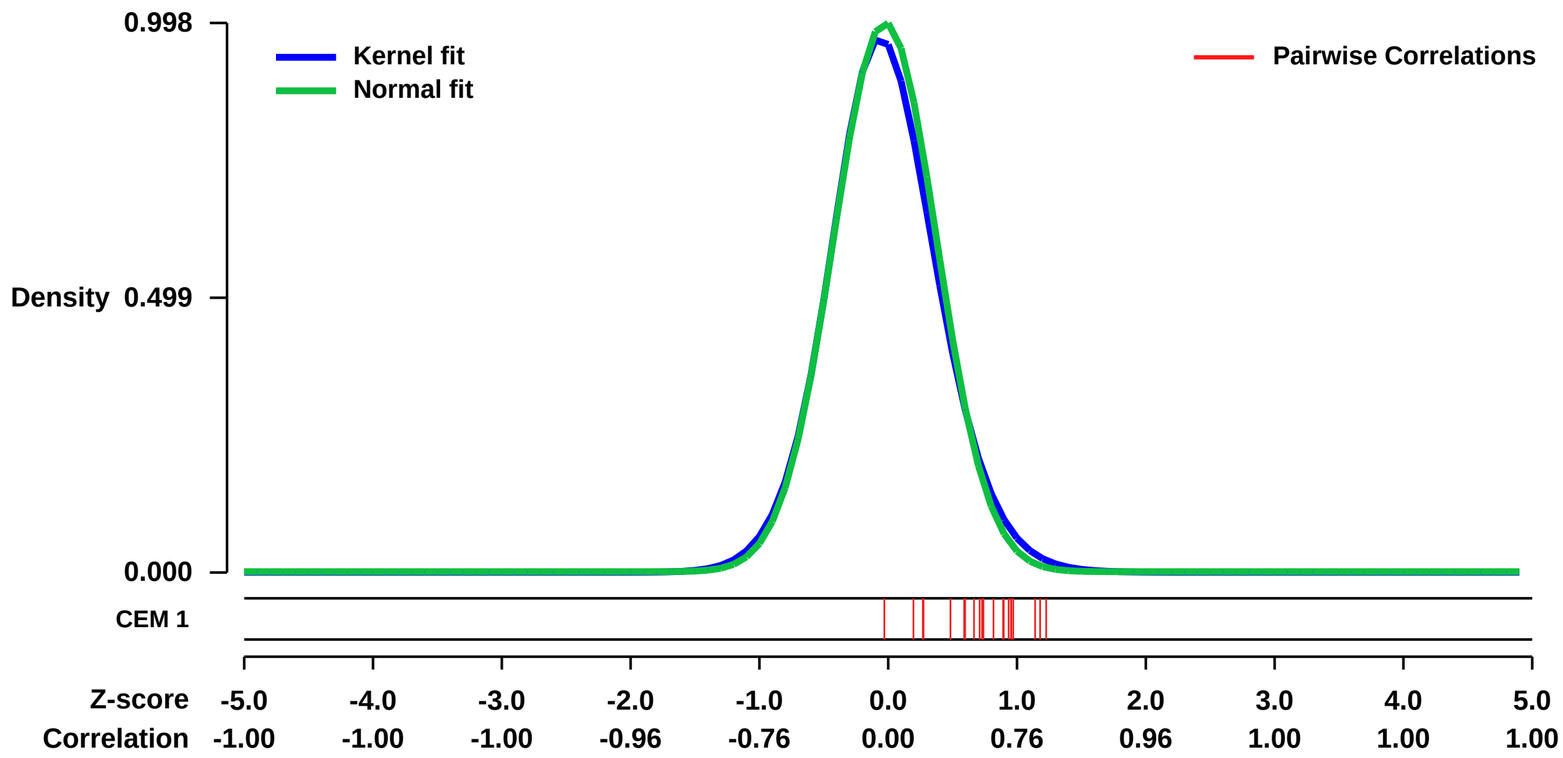

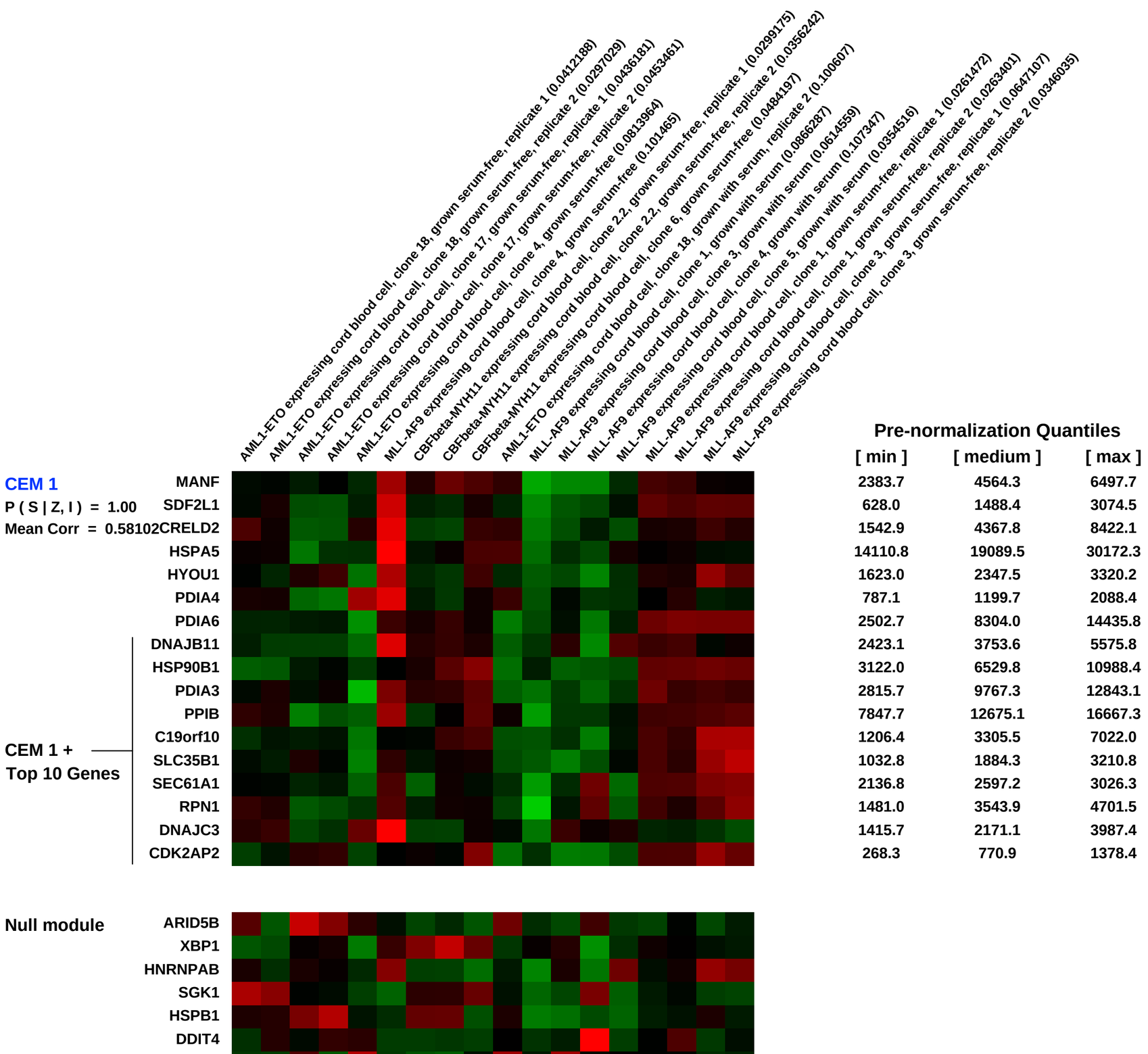

GEO Series "GSE52478" Expression Profiles

Num of samples in this series: 14

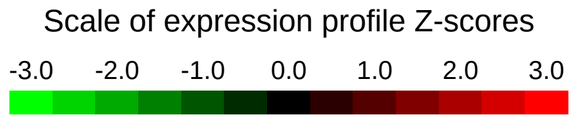

GEO Link:	http://www.ncbi.nlm.nih.gov/geo/query/acc.cgi?acc=GSE52478
Status:	Public on Nov 19 2013
Title:	The DNA Double-Strand Break Response Is Abnormal in Myeloblasts From Patients With Therapy-Related Acute Myeloid Leukemia [Affymetrix]
Organism:	Homo sapiens
Experiment type:	Expression profiling by array
Platform:	GPL570
Pubmed ID:	24304937
Summary & Design:	**Summary:** In order to examine if the upregulation of DNA repair genes on chromosome 8 was associated with the abnormal DSB phenotype observed in trisomy 8 (defined by array CGH or cytogenetics), we compared the mRNA levels of DNA repair genes on chromosome 8 in trisomy 8 t-AML patients versus normal t-AML gammaH2AX responders using gene expression array data. **Overall design:** Bone marrow cells taken directly from patients after written informed consent were cryopreserved, RNA extracted, and microarray analysis was performed using Affymetrix U133plus2 chips.

Background corr dist: KL-Divergence = 0.1716, L1-Distance = 0.0480, L2-Distance = 0.0054, Normal std = 0.3537

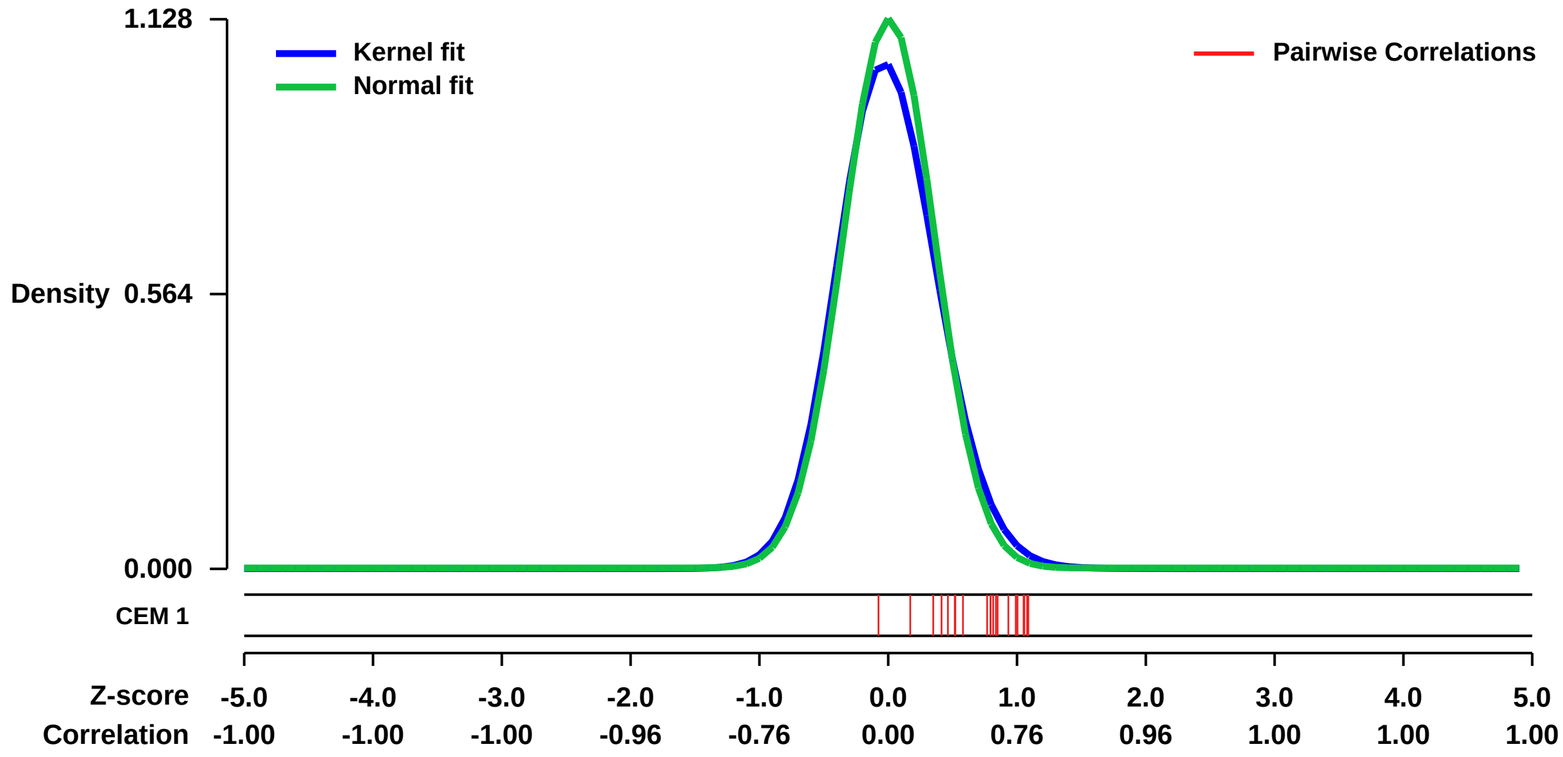

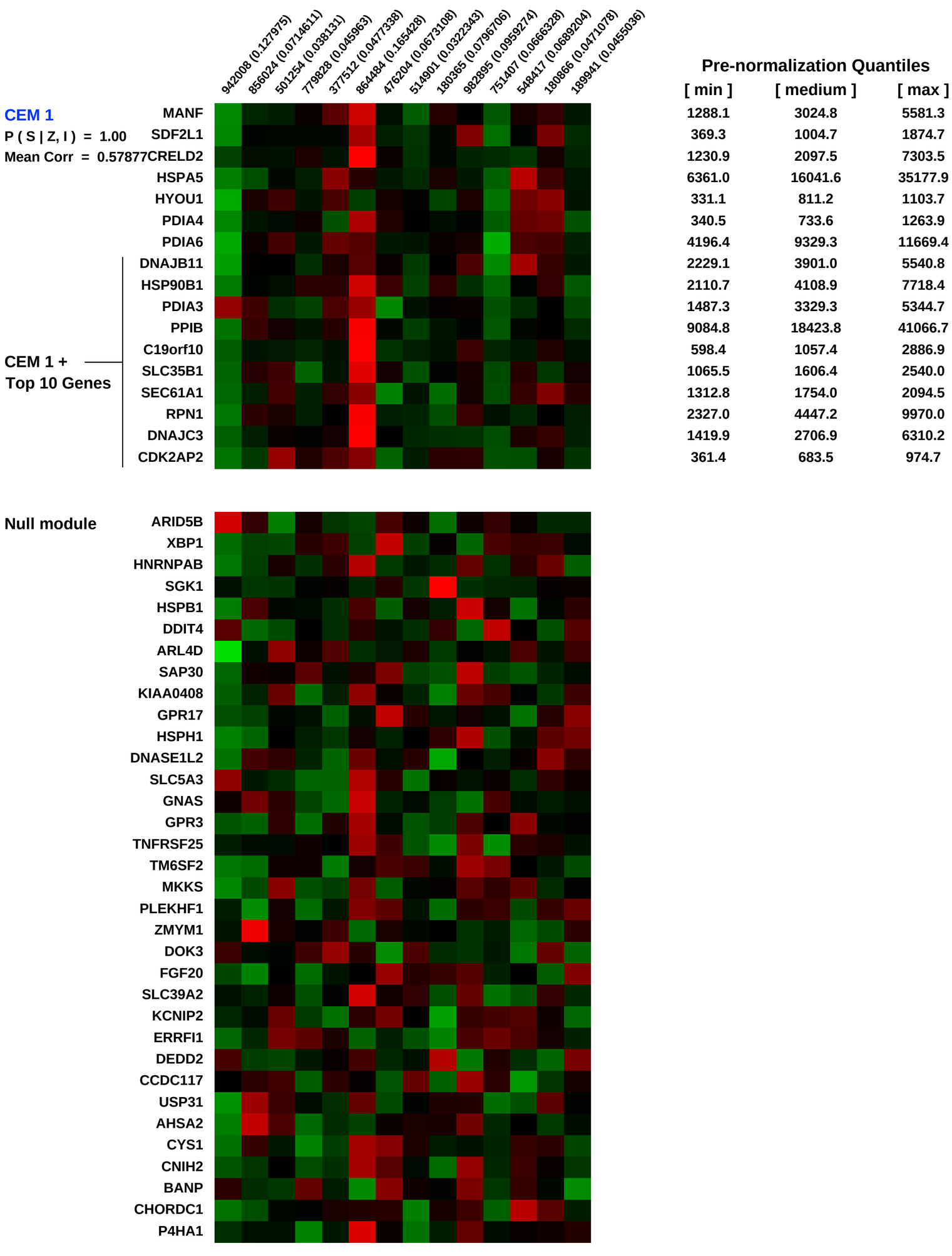

GEO Series "GSE39902" Expression Profiles

Num of samples in this series: 20

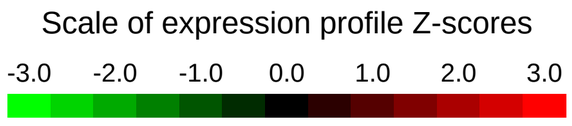

GEO Link:	http://www.ncbi.nlm.nih.gov/geo/query/acc.cgi?acc=GSE39902
Status:	Public on Dec 21 2012
Title:	Role of TAZ as mediator of Wnt signaling (MII)
Organism:	Homo sapiens
Experiment type:	Expression profiling by array
Platform:	GPL570
Pubmed ID:	23245942
Summary & Design:	**Summary:** To investigate the role of TAZ downstream of APC and beta-catenin in mammary epithelial cells cells, we compared the expression profiles of MCF10-T1k (MII) cells transfected with siControl, siAPC, siAPC+siTAZ, sibeta-catenin, or sibeta-catenin+siTAZ. **Keywords:** expression profiling by array **Overall design:** We collected RNA from MII cells transfected with siControl, siAPC, siAPC+siTAZ, sibeta-catenin, or sibeta-catenin+siTAZ. Cells were left untreated in normal culturing conditions before harvesting. Samples were then processed for total RNA extraction and hybridization on Affymetrix microarrays. Four biological replicas (A, B, C, D) were used for each of the 5 conditions (1: siControl, control cells; 2: siAPC cells; 3: siAPC+siTAZ cells; 4: sibeta-catenin (sibcat) cells; 5: sibeta-catenin+siTAZ) for a total of 20 samples.

Background corr dist: KL-Divergence = 0.1360, L1-Distance = 0.0498, L2-Distance = 0.0042, Normal std = 0.4143

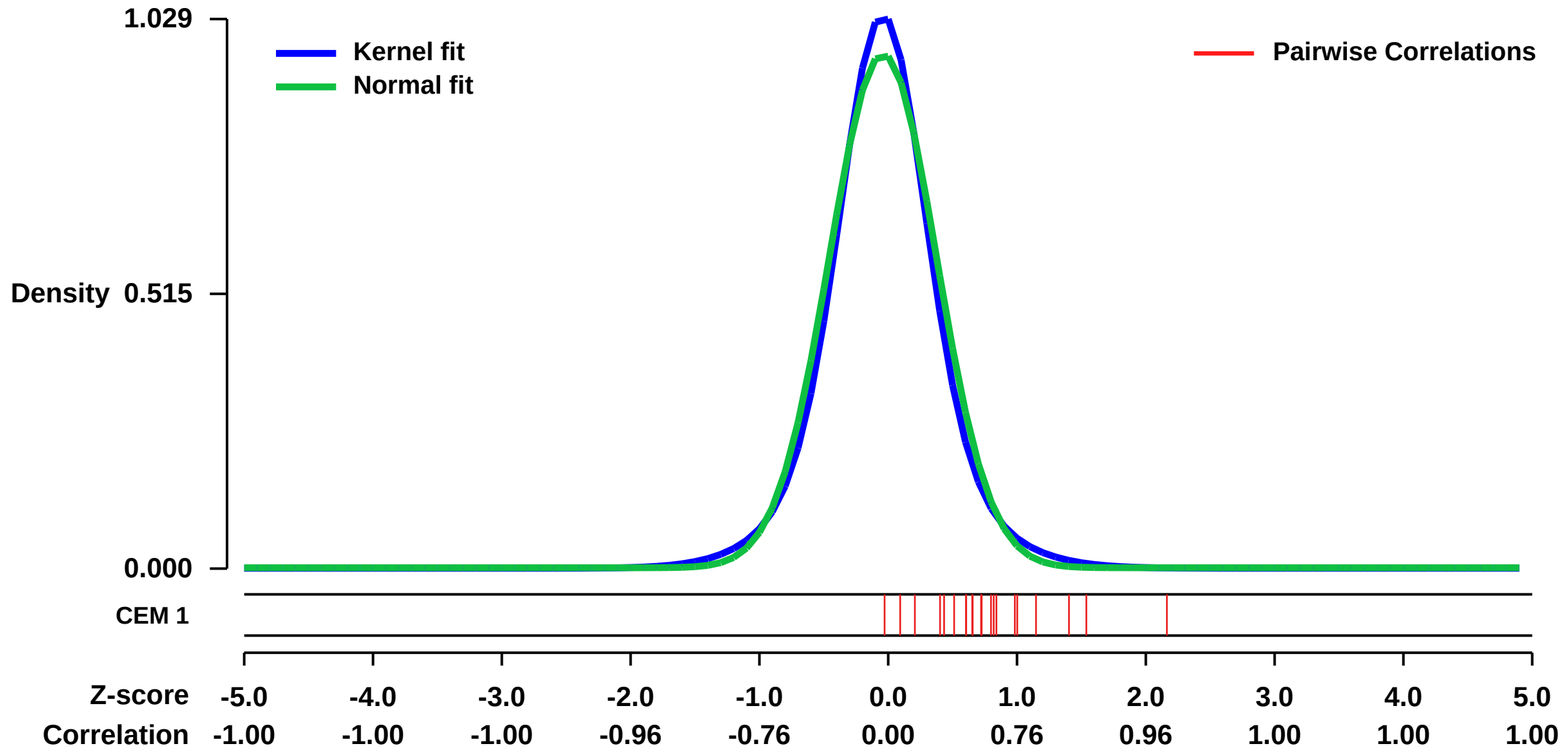

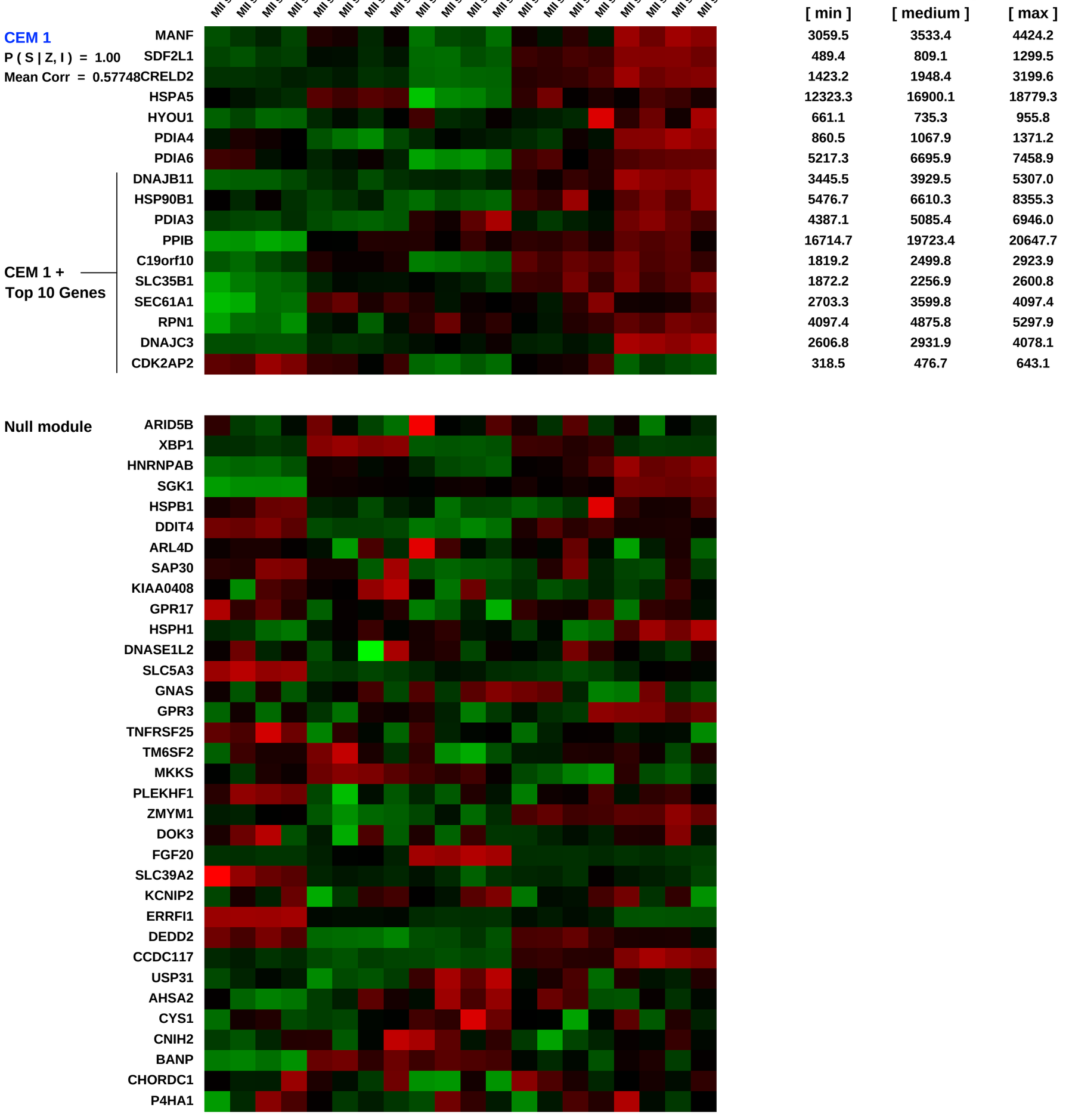

	Pre-normalization Quantiles [min]	[medium]	[max]
MANF	3059.5	3533.4	4424.2
SDF2L1	489.4	809.1	1299.5
CRELD2	1423.2	1948.4	3199.6
HSPA5	12323.3	16900.1	18779.3
HYOU1	661.1	735.3	955.8
PDIA4	860.5	1067.9	1371.2
PDIA6	5217.3	6695.9	7458.9
DNAJB11	3445.5	3929.5	5307.0
HSP90B1	5476.7	6610.3	8355.3
PDIA3	4387.1	5085.4	6946.0
PPIB	16714.7	19723.4	20647.7
C19orf10	1819.2	2499.8	2923.9
SLC35B1	1872.2	2256.9	2600.8
SEC61A1	2703.3	3599.8	4097.4
RPN1	4097.4	4875.8	5297.9
DNAJC3	2606.8	2931.9	4078.1
CDK2AP2	318.5	476.7	643.1

GEO Series "GSE5264" Expression Profiles

Num of samples in this series: 30

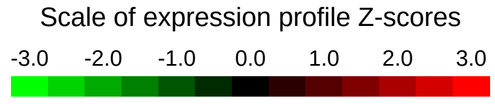

GEO Link:	http://www.ncbi.nlm.nih.gov/geo/query/acc.cgi?acc=GSE5264
Status:	Public on Jul 08 2006
Title:	Human bronchial epithelial cell differentiation time course
Organism:	Homo sapiens
Experiment type:	Expression profiling by array
Platform:	GPL570
Pubmed ID:	17413031
Summary & Design:	**Summary:** Microarray analysis was performed to identify transcriptional changes that occur during mucociliary differentiation of human primary bronchial epithelial cells cultured at an air-liquid interface (ALI). **Keywords: time course** **Overall design:** Cells from three different donors were cultured and collected at 11 different time points from day 0 to day 28 of ALI culture.

Background corr dist: KL-Divergence = 0.1998, L1-Distance = 0.0352, L2-Distance = 0.0021, Normal std = 0.3348

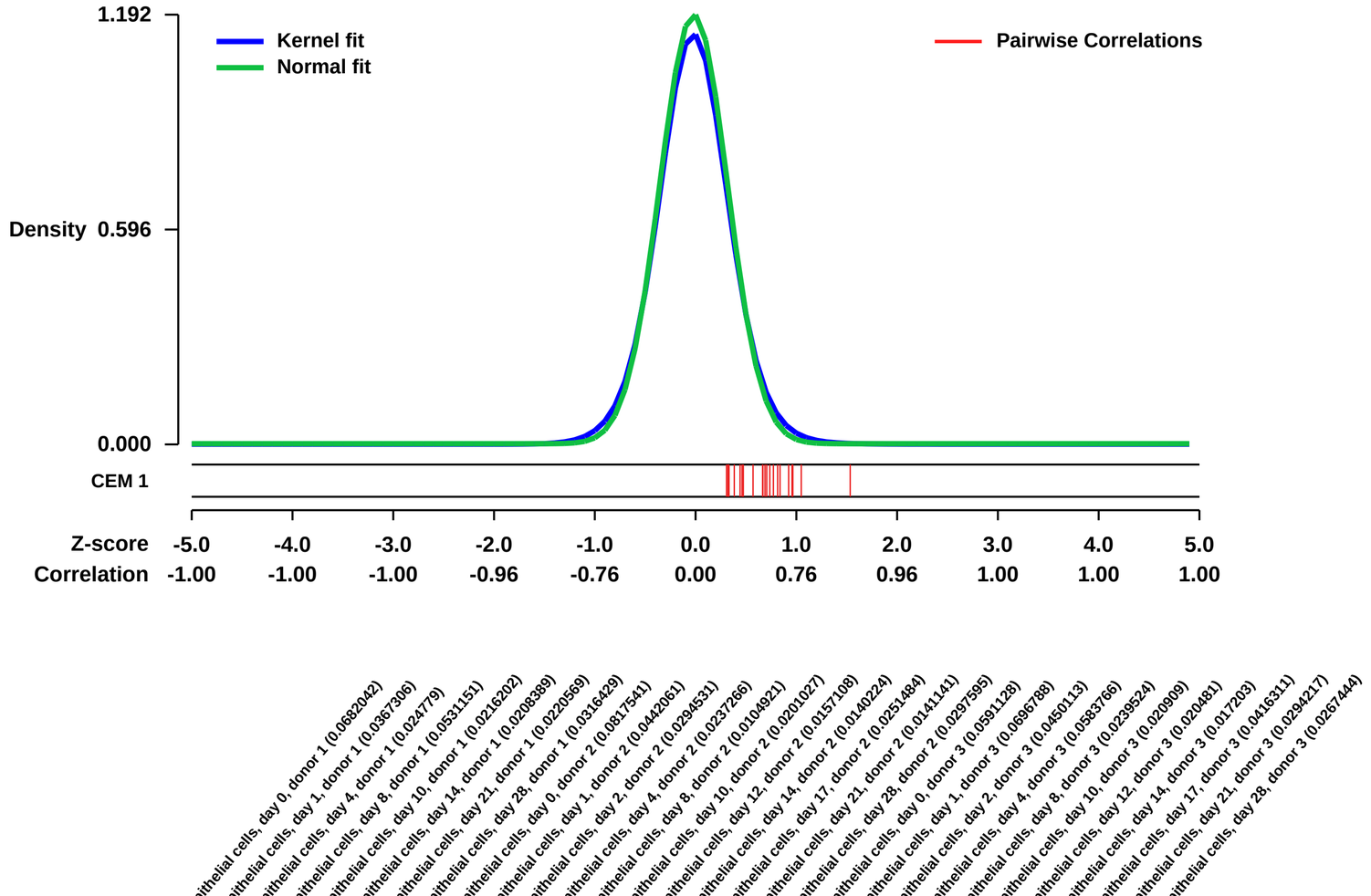

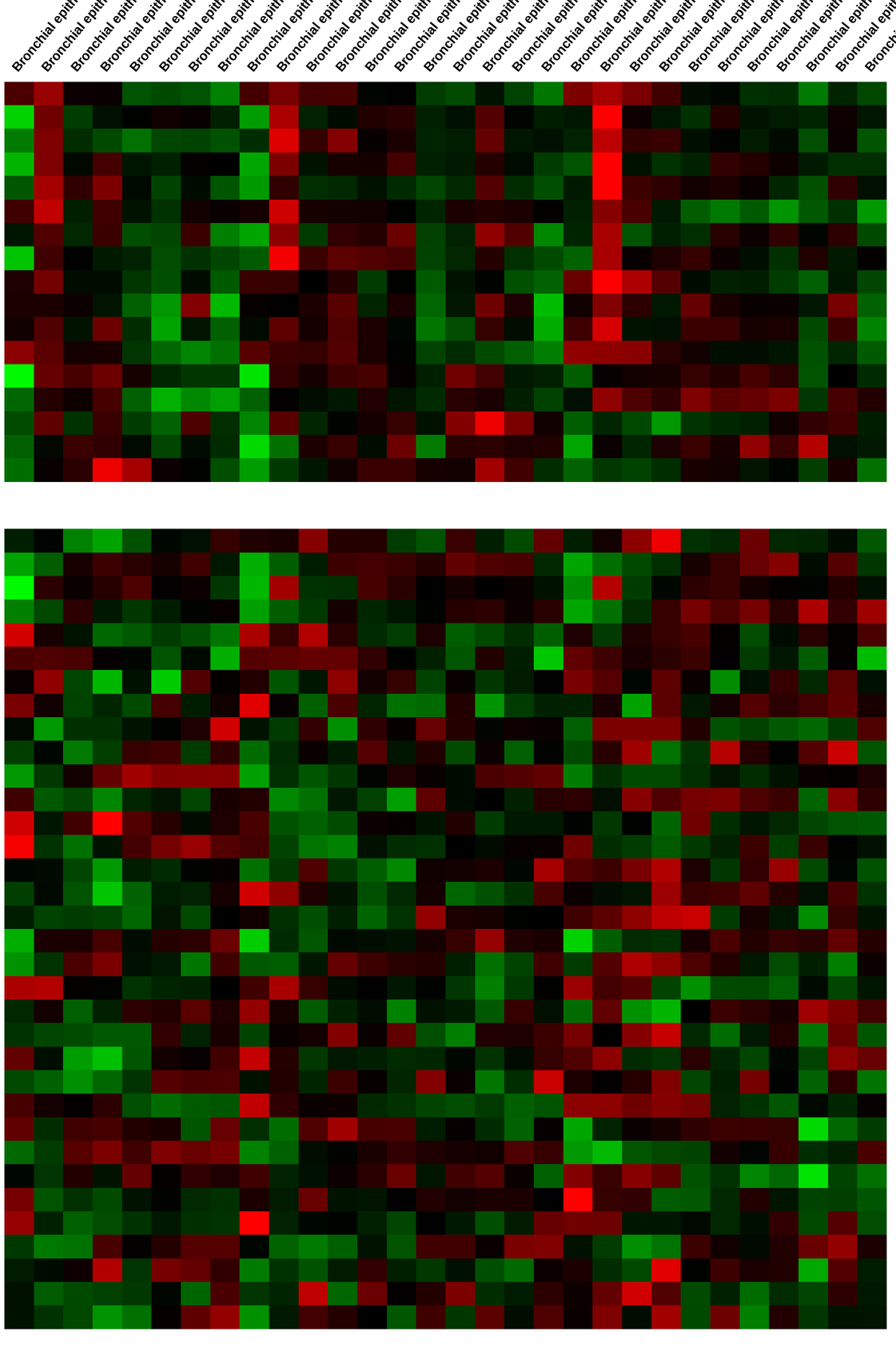

Pre-normalization Quantiles		
[min]	[medium]	[max]
1622.0	2448.6	3626.5
544.9	990.3	1637.7
2268.4	2849.3	4140.8
6502.5	8546.0	12077.3
2591.0	3586.9	5640.8
1149.3	1591.2	2129.3
3551.8	4505.7	5550.2
1726.8	2601.3	3695.6
1143.3	1505.8	2707.5
6356.7	7592.3	8302.6
6050.3	7602.1	9235.6
2190.7	2971.7	3861.3
1603.5	2612.7	2947.0
1927.6	2531.7	2933.2
2440.1	2837.5	3586.8
2058.6	2674.3	3070.1
954.3	1611.5	2517.6

GEO Series "GSE27262" Expression Profiles

Num of samples in this series: 50

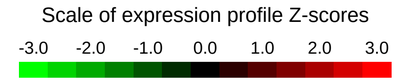

GEO Link:	http://www.ncbi.nlm.nih.gov/geo/query/acc.cgi?acc=GSE27262
Status:	Public on Apr 10 2013
Title:	Gene expression profiling of Non-small cell lung cancer in Taiwan
Organism:	Homo sapiens
Experiment type:	Expression profiling by array
Platform:	GPL570
Pubmed ID:	22726390
Summary & Design:	**Summary:** This study focus on the expression signature between tumor and adjacent normal tissues. **Overall design:** Tumor(T) and adjacent normal(N) tissue pairs from 25 stage I lung adenocarcinoma patients were selected for RNA extraction and hybridization on microarrays.

Background corr dist: KL-Divergence = 0.4460, L1-Distance = 0.0832, L2-Distance = 0.0230, Normal std = 0.2384

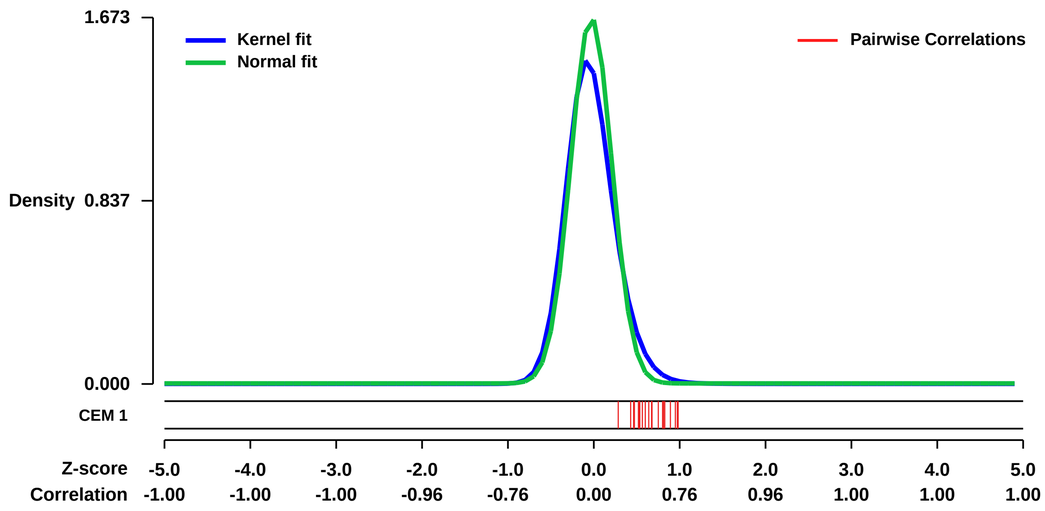

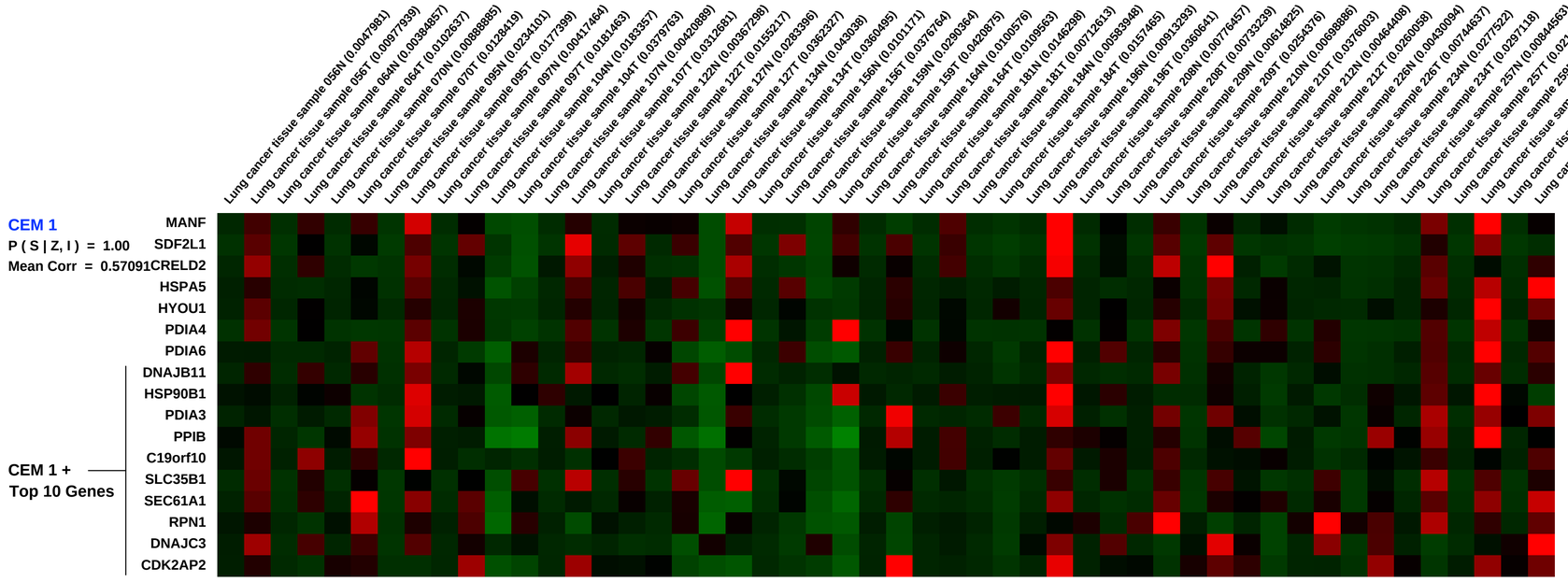

Pre-normalization Quantiles

[min]	[medium]	[max]
405.7	469.5	1067.4
397.2	471.8	1386.2
397.2	469.5	1036.6
405.8	469.5	1105.7
397.2	471.2	2289.1
399.7	469.7	2258.9
405.8	468.3	855.3
405.8	471.8	1423.0
405.8	469.4	810.5
395.2	472.7	830.9
395.2	468.2	680.9
395.2	468.2	1135.0
395.2	471.8	1341.6
395.2	472.7	932.9
405.8	468.3	777.1
425.6	469.5	891.0
395.2	470.6	977.8

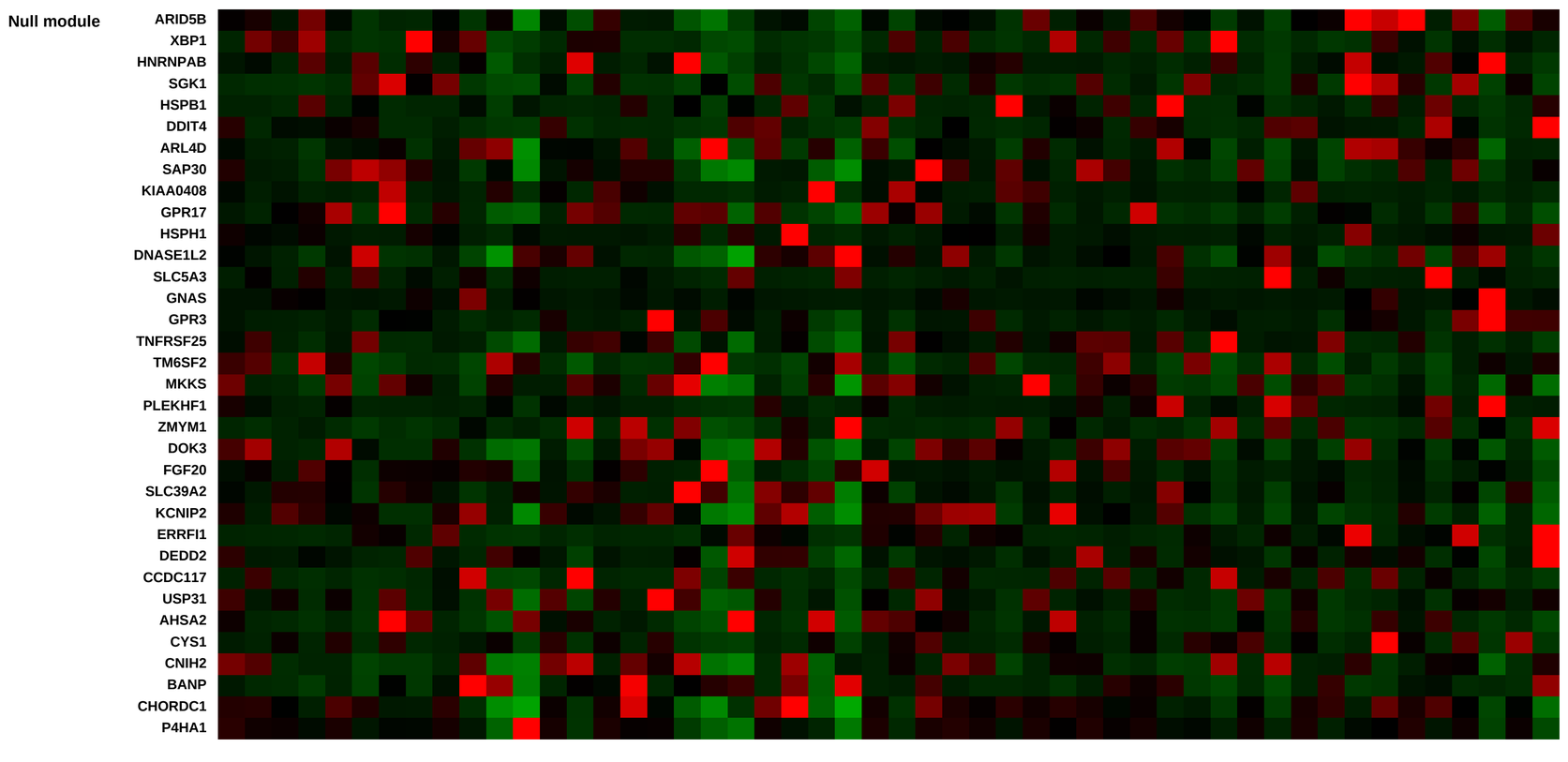

GEO Series "GSE35809" Expression Profiles

Num of samples in this series: 70

Scale of expression profile Z-scores

-3.0 -2.0 -1.0 0.0 1.0 2.0 3.0

GEO Link:	http://www.ncbi.nlm.nih.gov/geo/query/acc.cgi?acc=GSE35809
Status:	Public on Jul 05 2012
Title:	Gastric Cancer Subtyping (Australian Patient Cohort)
Organism:	Homo sapiens
Experiment type:	Expression profiling by array
Platform:	GPL570
Pubmed ID:	22735568
Summary & Design:	**Summary:** Genome-wide mRNA expression profiles of 70 primary gastric tumors from the Australian patient cohort. Like many cancers, gastric adenocarcinomas (gastric cancers) show considerable heterogeneity between patients. Thus, there is intense interest in using gene expression profiles to discover subtypes of gastric cancers with particular biological properties or therapeutic vulnerabilities. Identification of such subtypes could generate insights into the mechanisms of cancer progression or lay the foundation for personalized treatments. Here we report a robust gene-xpression-based clustering of a large collection of gastric adenocarcinomas from Singaporean patients [GSE34942 and GSE15459]. We developed and validated a classifier for the three subtypes in Australian patient cohort. **Overall design:** Profiling of 70 primary gastric tumors on Affymetrix GeneChip Human Genome U133 Plus 2.0 Array. All tumors were collected with approvals from Peter MacCallum Cancer Center, Australia; the Research Ethics Review Committee; and signed patient informed consent.

Background corr dist: KL-Divergence = 0.3989, L1-Distance = 0.0932, L2-Distance = 0.0293, Normal std = 0.2635

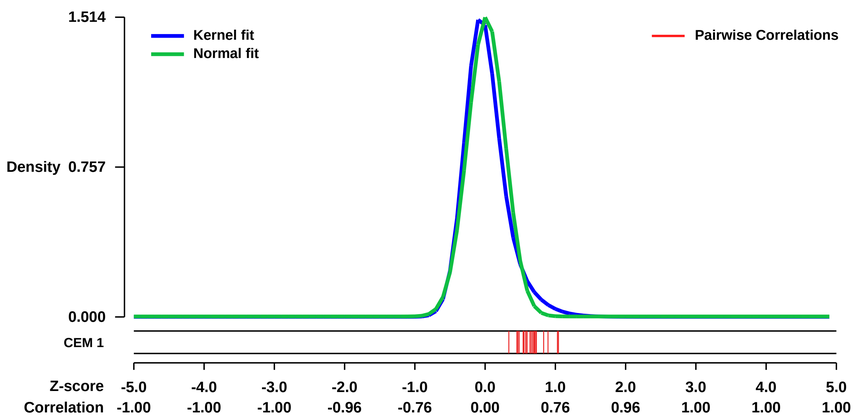

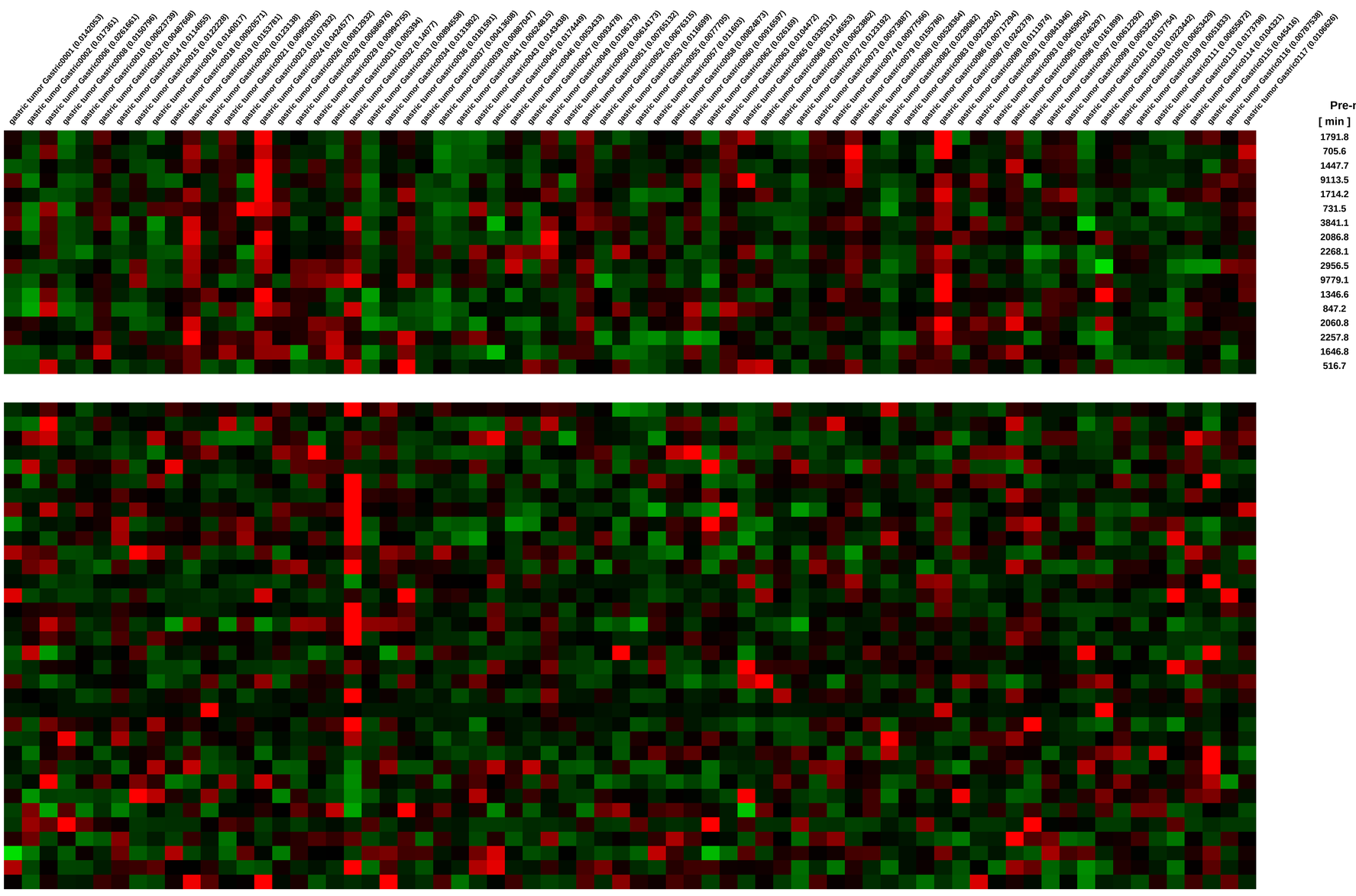

Pre-normalization Quantiles

[min]	[medium]	[max]
1791.8	2917.0	6127.0
705.6	1369.8	3385.4
1447.7	2852.8	10200.4
9113.5	13845.3	25082.2
1714.2	2898.7	7696.8
731.5	1703.6	3791.6
3841.1	7864.1	12647.2
2086.8	3524.9	10607.8
2268.1	3918.8	6619.3
2956.5	12019.5	21100.7
9779.1	15483.1	29481.5
1346.6	2784.1	5696.5
847.2	1739.3	3023.1
2060.8	3067.7	5113.1
2257.8	4212.6	7552.9
1646.8	3608.2	5937.1
516.7	953.6	2307.9

GEO Series "GSE34628" Expression Profiles

Num of samples in this series: 6

Scale of expression profile Z-scores

-3.0 -2.0 -1.0 0.0 1.0 2.0 3.0

GEO Link:	http://www.ncbi.nlm.nih.gov/geo/query/acc.cgi?acc=GSE34628
Status:	Public on Apr 11 2012
Title:	Gene expression timecourse from Dengue virus infected human endothelial cells
Organism:	Homo sapiens
Experiment type:	Expression profiling by array
Platform:	GPL570
Pubmed ID:	22496214
Summary & Design:	**Summary:** Dengue viruses cause two severe diseases that alter vascular fluid barrier functions, dengue hemorrhagic fever (DHF) and dengue shock syndrome (DSS). While the mechanisms that lead to vascular permeability are unknown, the endothelium plays a central role in regulating fluid and cellular efflux from capillaries. Thus, dysregulation of endothelial cells functions by dengue virus infection may contribute to pathogenesis and severe disease. We used microarrays to investigate the effect of dengue virus infection on gene expression within primary human endothelial cells at various times post infection and identified numerous upregulated antiviral and immune response genes. **Overall design:** Early passage primary endothelial cells (HUVECs) were mock infected (no virus) or infected with dengue virus and total RNA collected at 3 timepoints: 12, 24, and 48 hours post infection. Multiple timepoints were analyzed to identify changes in gene expression levels over time. Gene expression from both mock infected and dengue virus infected endothelial cells was evaluated to determine fold induction at each timepoint.

Background corr dist: KL-Divergence = 0.0443, L1-Distance = 0.0225, L2-Distance = 0.0006, Normal std = 0.6013

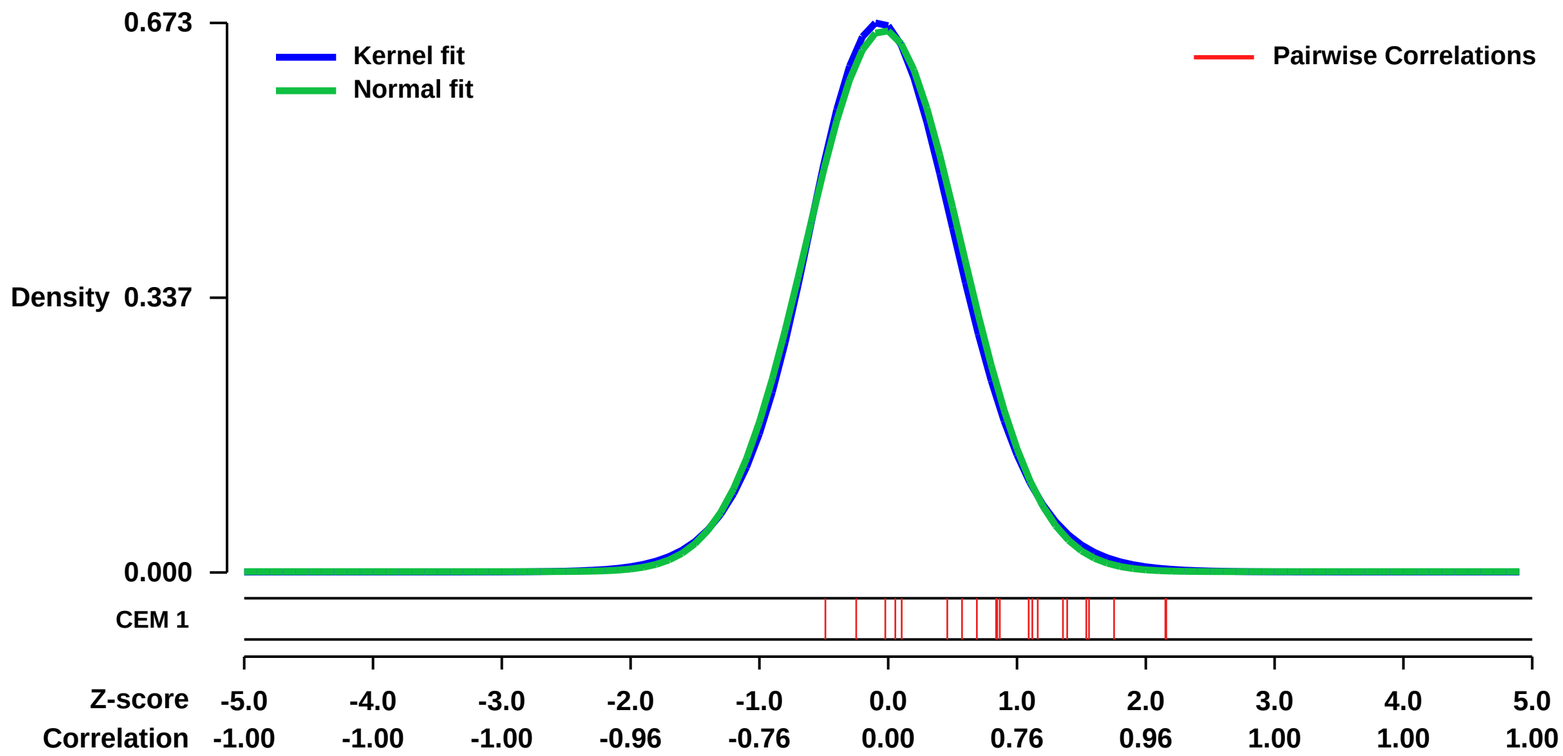

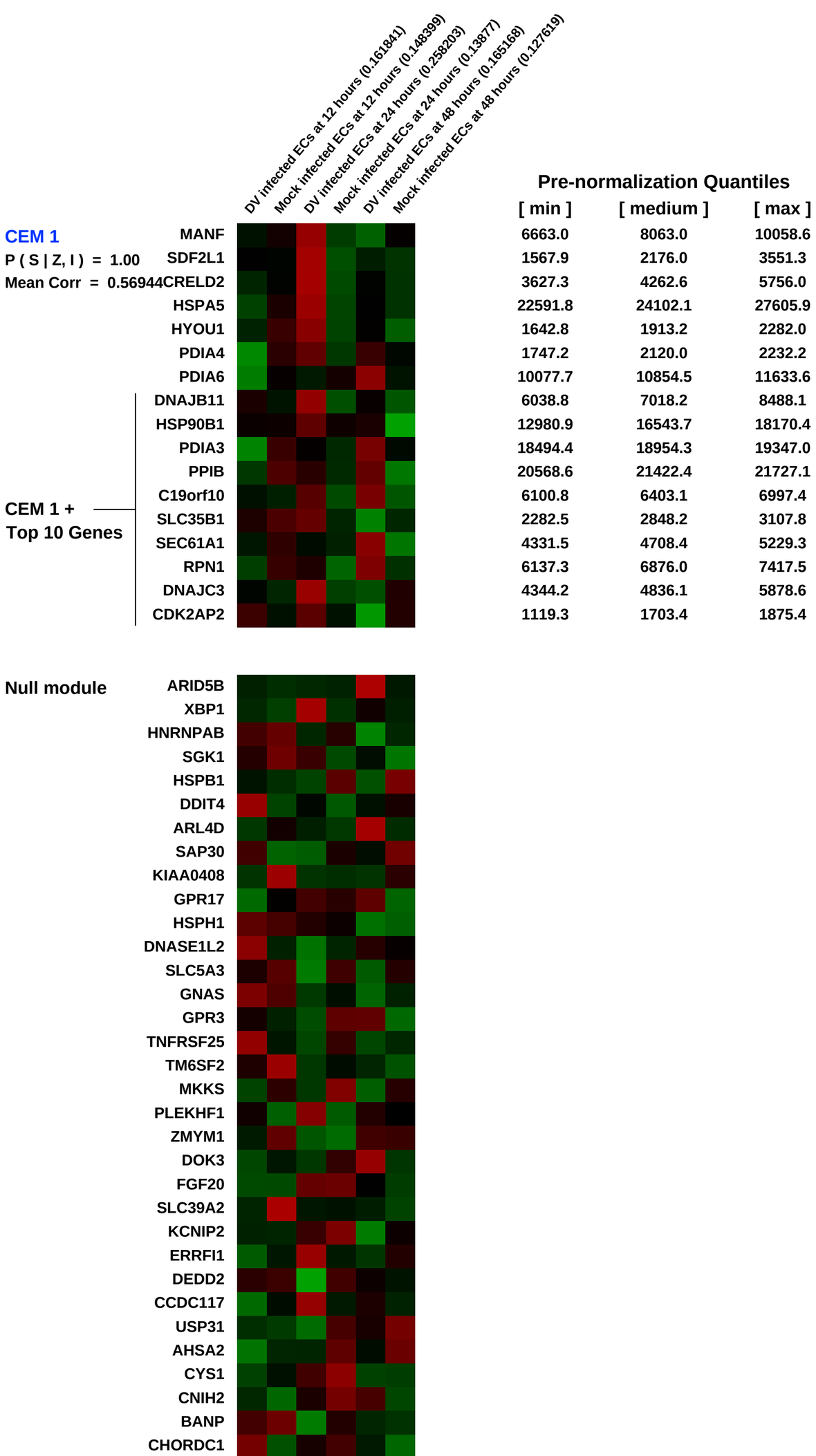

Pre-normalization Quantiles

	[min]	[medium]	[max]
MANF	6663.0	8063.0	10058.6
SDF2L1	1567.9	2176.0	3551.3
CRELD2	3627.3	4262.6	5756.0
HSPA5	22591.8	24102.1	27605.9
HYOU1	1642.8	1913.2	2282.0
PDIA4	1747.2	2120.0	2232.2
PDIA6	10077.7	10854.5	11633.6
DNAJB11	6038.8	7018.2	8488.1
HSP90B1	12980.9	16543.7	18170.4
PDIA3	18494.4	18954.3	19347.0
PPIB	20568.6	21422.4	21727.1
C19orf10	6100.8	6403.1	6997.4
SLC35B1	2282.5	2848.2	3107.8
SEC61A1	4331.5	4708.4	5229.3
RPN1	6137.3	6876.0	7417.5
DNAJC3	4344.2	4836.1	5878.6
CDK2AP2	1119.3	1703.4	1875.4

GEO Series "GSE41364" Expression Profiles

Num of samples in this series: 9

Scale of expression profile Z-scores

-3.0 -2.0 -1.0 0.0 1.0 2.0 3.0

GEO Link:	http://www.ncbi.nlm.nih.gov/geo/query/acc.cgi?acc=GSE41364
Status:	Public on Sep 17 2013
Title:	Expression data for HT29 cells treated with 5-aza-deoxy-cytidine [Affymetrix]
Organism:	Homo sapiens
Experiment type:	Expression profiling by array
Platform:	GPL570
Pubmed ID:	23902433
Summary & Design:	**Summary:** The RNA samples from HT-29 (ATCC) colon cancer cell line were reverse transcribed into cDNAs and categorized in 3 groups with different concentrations of 5-aza-deoxy-cytidine (5-Aza); in each group three replicative 150 mm cultures were treated with: 1) dimethyl sulfoxide (vehicle alone, 0 ¸…M 5-Aza); 2) 5¸…M 5-Aza and 3) 10 ¸…M 5-Aza; for five days We then used Affymetrix microarray platform to profile the gene expression of the 3 HT29 cell groups (3 replicates in each group) in order to search for differentially expressed genes **Overall design:** The transcriptional response of HT-29 (ATCC) colon cancer cell line under 3 concentrations of 5-aza-deoxy-cytidine was investigated based on their RNA expression profiles

Background corr dist: KL-Divergence = 0.0747, L1-Distance = 0.0228, L2-Distance = 0.0007, Normal std = 0.4934

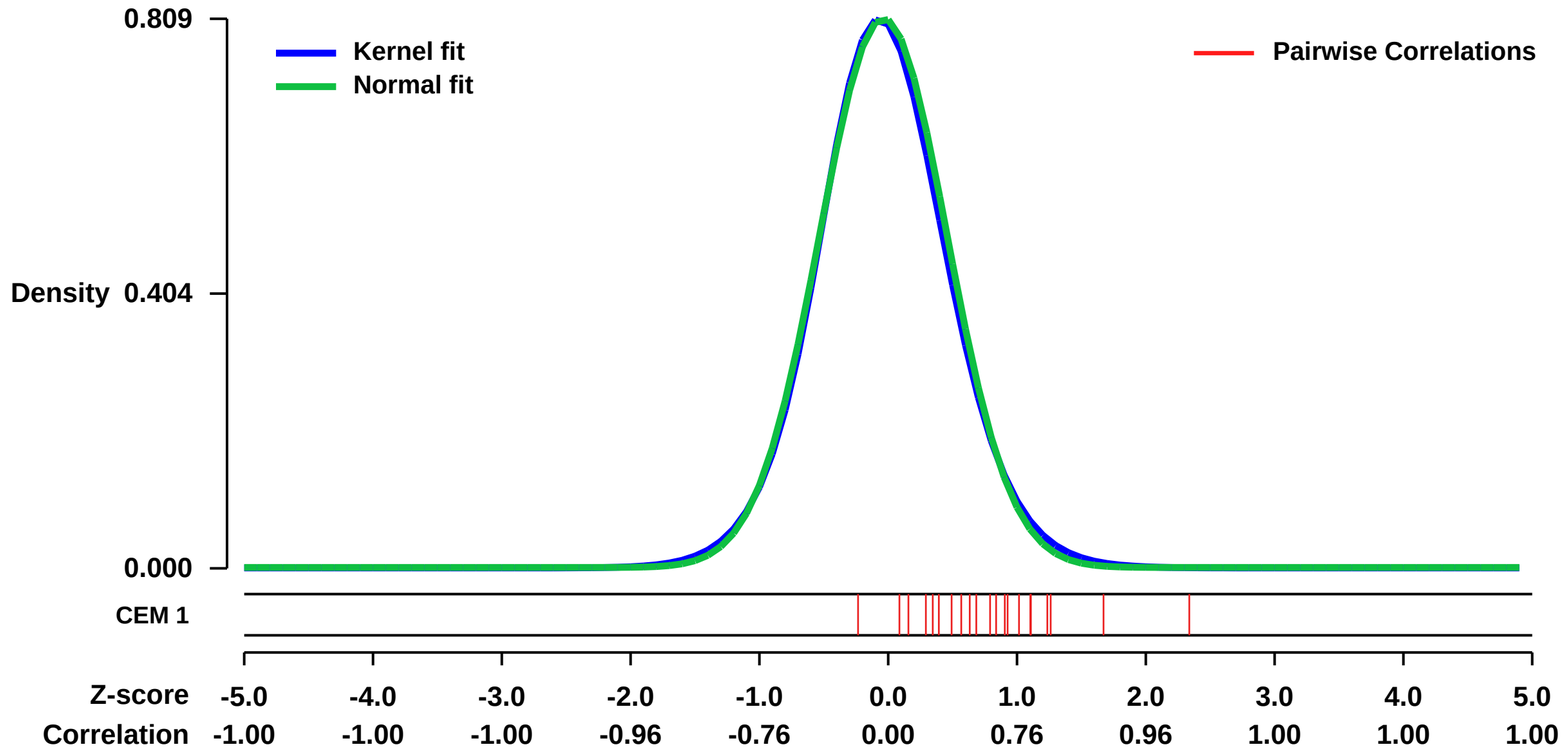

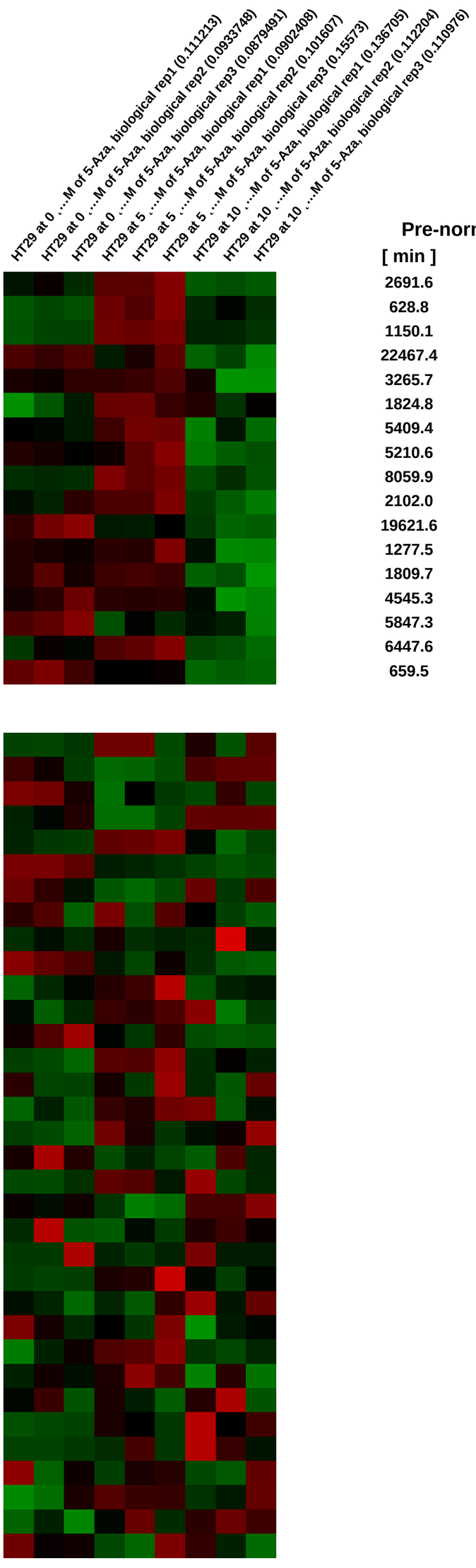

GEO Series "GSE6494" Expression Profiles

Num of samples in this series: 16

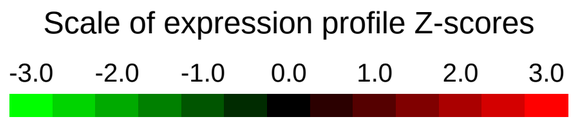

GEO Link:	http://www.ncbi.nlm.nih.gov/geo/query/acc.cgi?acc=GSE6494
Status:	Public on Jul 22 2010
Title:	Expression data from human liver cell line induced by PCB153
Organism:	Homo sapiens
Experiment type:	Expression profiling by array
Platform:	GPL570
Pubmed ID:	20638727
Summary & Design:	**Summary:** Exposure to Polychlorobiphenyls (PCBs) is known to cause serious health effects in human but the gene expression profiles leading to development of differnet diseases is not fully understood. The knowledge of global gene expression will help us to devlop early diagnostic biomarkers for PCB induced health effects. We used microarrays to detail the global gene expression profile underlying the effects of PCB153 on human liver cells leading to identification of distinct classes of up-regulated and down-regulated genes and cellular processes. Keywords: time course **Overall design:** The HepG2 cells were grown for 48 hours in DMEM supplemented with 10% FBS and 1X Pennicillin-Streptromycin and treated with PCB153 for different times. Trizol extraction of total RNA was performed according to the manufacturer's instructions. Biotinylated cRNA were prepared according to the standard Affymetrix protocol from 6 microgram of total RNA (Expression Analysis Technical Manual, 2001, Affymetrix). Following fragmentation, 10 microgram of cRNA were hybridized for 16 hr at 45C on GeneChip Human Genome Array (HGU133 plus 2.0). GeneChips were washed and stained in the Affymetrix Fluidics Station 450 and scanned using the Affymetrix GeneArray Scanner 3000. The data were analyzed with Microarray Suite version 5.0 (MAS 5.0) using Affymetrix default analysis settings and global scaling as normalization method. The trimmed mean target intensity of each array was arbitrarily set to 150.

Background corr dist: KL-Divergence = 0.1882, L1-Distance = 0.0387, L2-Distance = 0.0030, Normal std = 0.3410

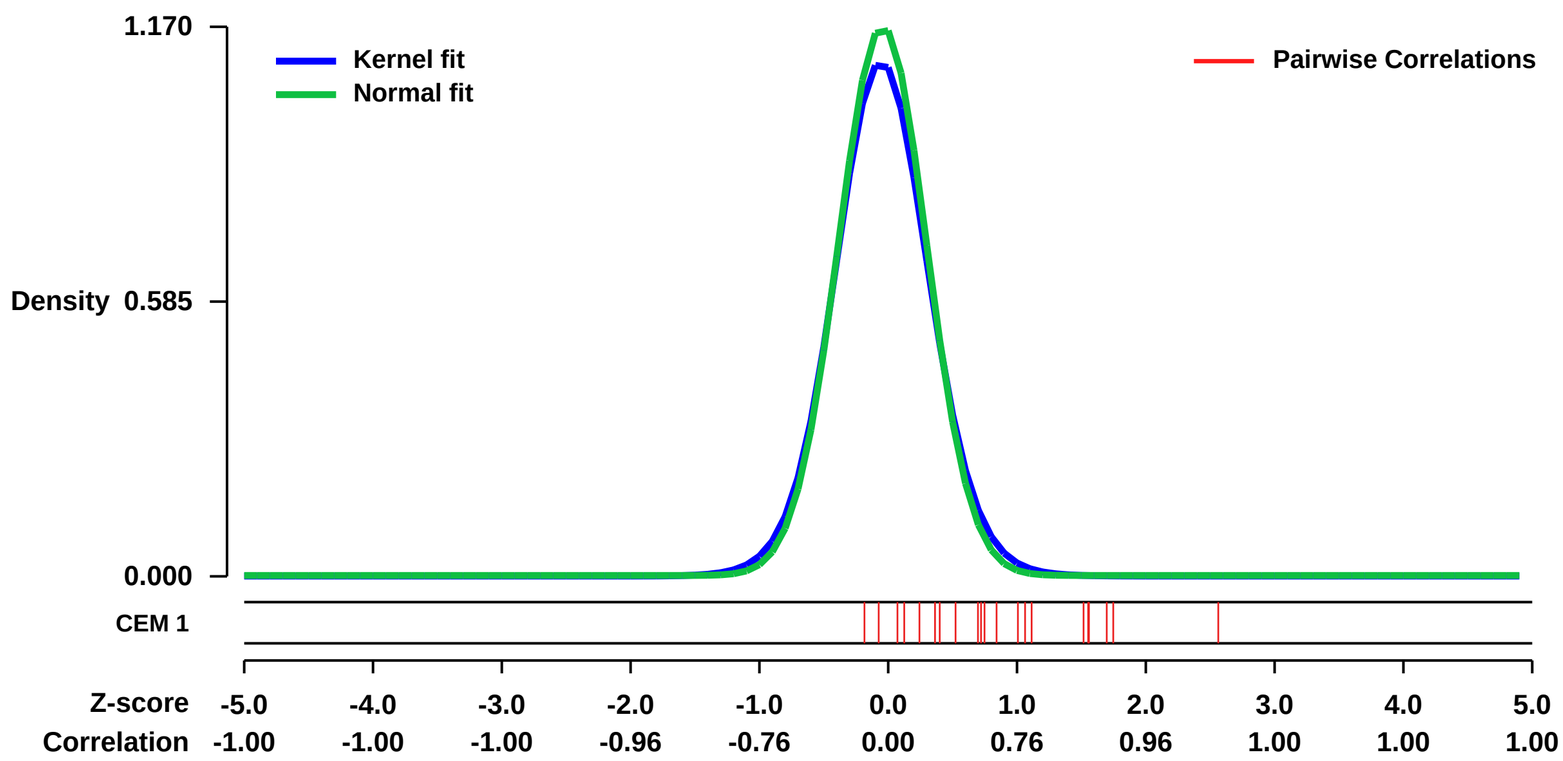

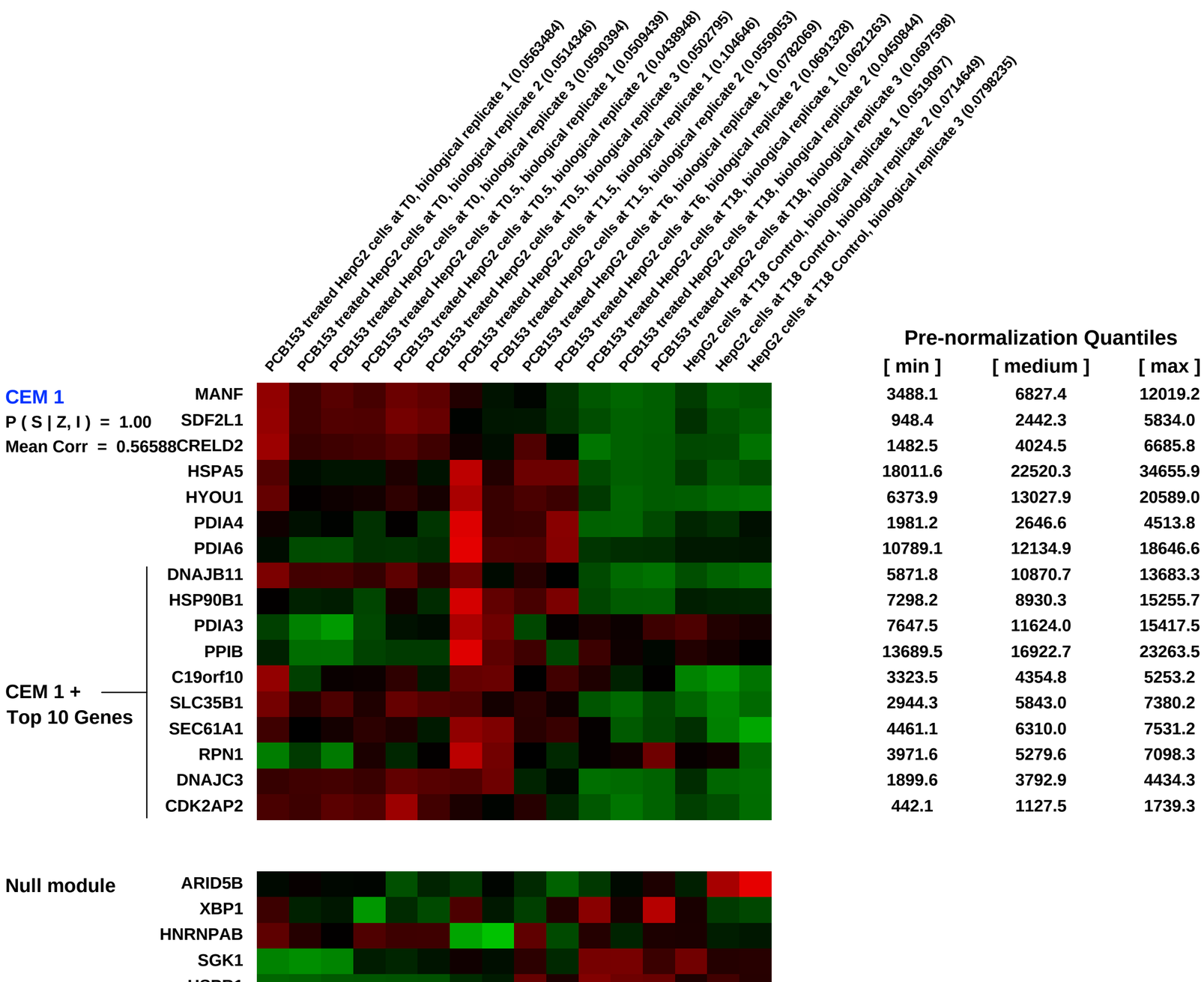

GEO Series "GSE14491" Expression Profiles

Num of samples in this series: 16

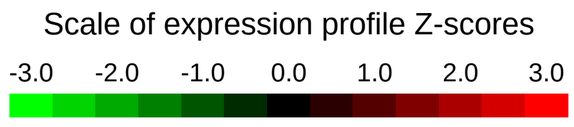

GEO Link:	http://www.ncbi.nlm.nih.gov/geo/query/acc.cgi?acc=GSE14491
Status:	Public on Apr 03 2009
Title:	TGF¸†/mutant-p53 jointly controlled genes
Organism:	Homo sapiens
Experiment type:	Expression profiling by array
Platform:	GPL570
Pubmed ID:	19345189
Summary & Design:	**Summary:** TGF¸† ligands act as tumor suppressors in early stage tumors but are paradoxically diverted into potent prometastatic factors in advanced cancers. The molecular nature of this switch remains enigmatic. We now show that TGF¸†-dependent cell migration, invasion and metastasis are empowered by mutant-p53. To investigate the specific gene expression program by which mutant-p53 and TGF¸† control invasion and metastasis in breast cancer cells, we compared the TGF¸† transcriptomic profile of control and mutant-p53 depleted MDA-MB-231 cells. Keywords: expression profiling by array **Overall design:** MDA-MB-231 cells, stably expressing either control (shGFP) or anti-p53 (shp53) short-hairpin RNAs, were left untreated or treated with TGFbeta. Samples were then processed for total RNA extraction and hybridization on Affymetrix microarrays. Four biological replicas (A, B, C, D) were used for each of the 4 conditions (1: untreated control; 2: TGFbeta treated control; 3: untreated p53-depleted cells; 4: TGFbeta treated mutant-p53-depleted cells), for a total of 16 samples.

Background corr dist: KL-Divergence = 0.1626, L1-Distance = 0.0343, L2-Distance = 0.0022, Normal std = 0.3628

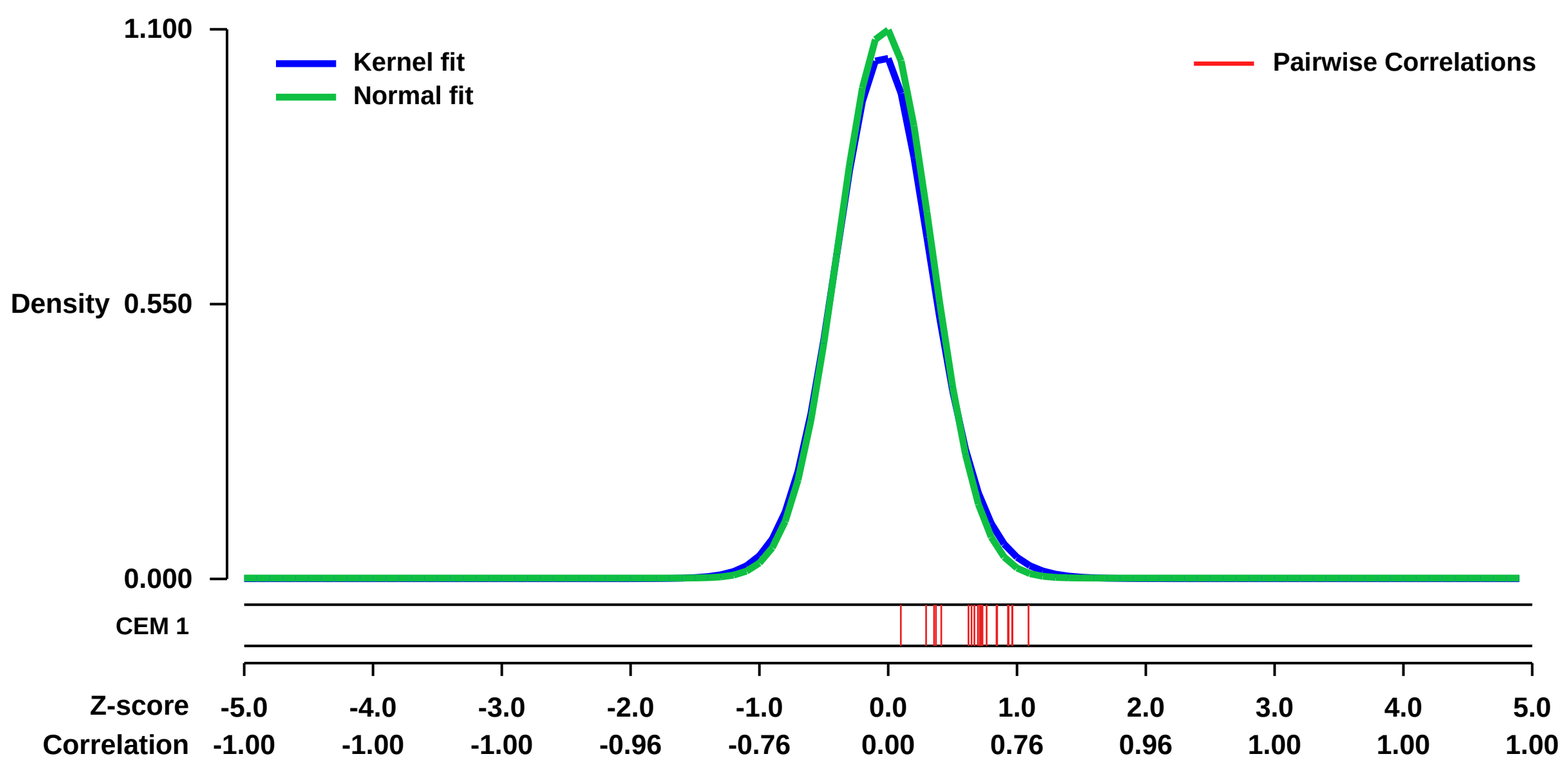

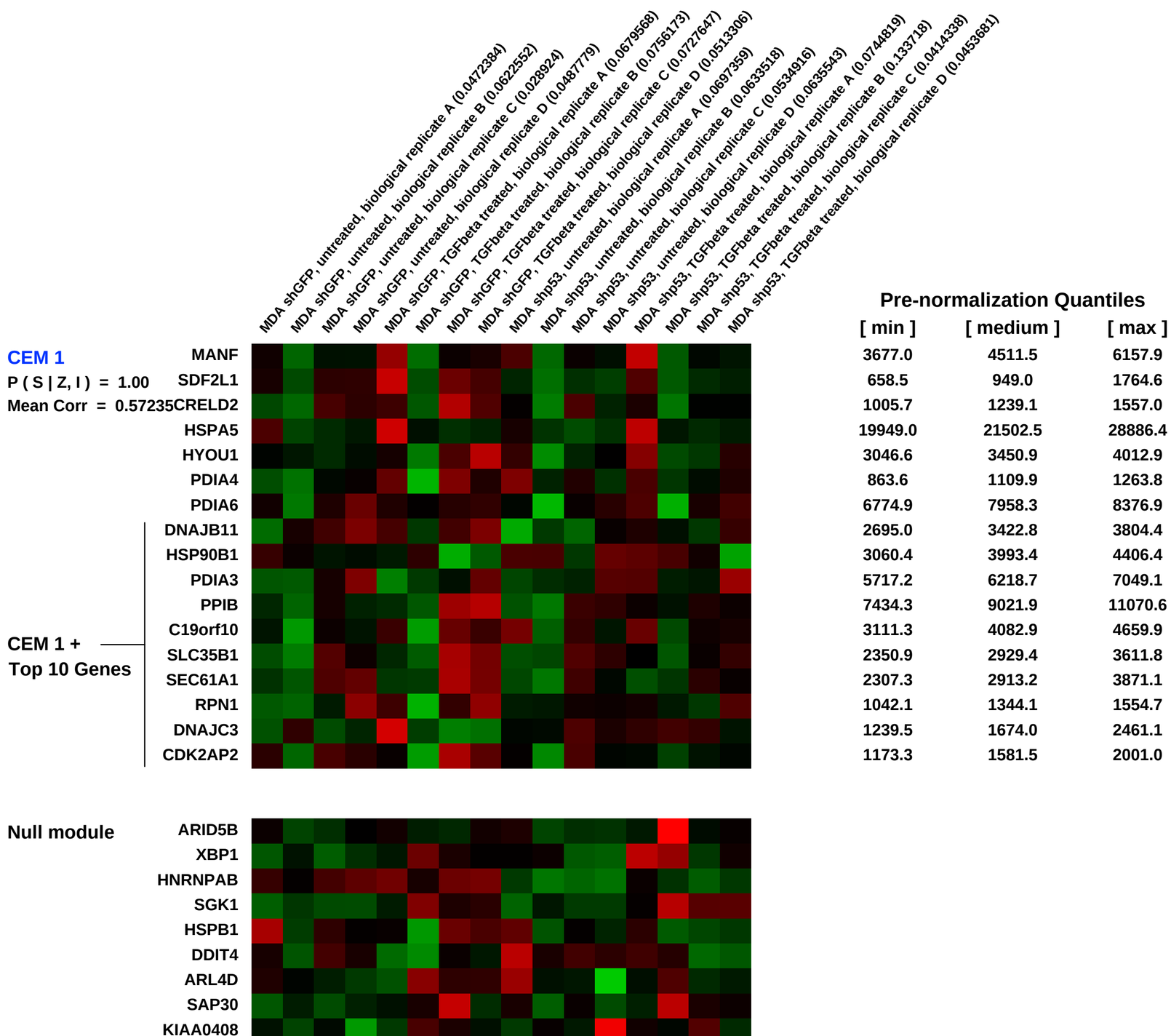

Pre-normalization Quantiles

	[min]	[medium]	[max]
MANF	3677.0	4511.5	6157.9
SDF2L1	658.5	949.0	1764.6
CRELD2	1005.7	1239.1	1557.0
HSPA5	19949.0	21502.5	28886.4
HYOU1	3046.6	3450.9	4012.9
PDIA4	863.6	1109.9	1263.8
PDIA6	6774.9	7958.3	8376.9
DNAJB11	2695.0	3422.8	3804.4
HSP90B1	3060.4	3993.4	4406.4
PDIA3	5717.2	6218.7	7049.1
PPIB	7434.3	9021.9	11070.6
C19orf10	3111.3	4082.9	4659.9
SLC35B1	2350.9	2929.4	3611.8
SEC61A1	2307.3	2913.2	3871.1
RPN1	1042.1	1344.1	1554.7
DNAJC3	1239.5	1674.0	2461.1
CDK2AP2	1173.3	1581.5	2001.0

GEO Series "GSE16480" Expression Profiles

Num of samples in this series: 15

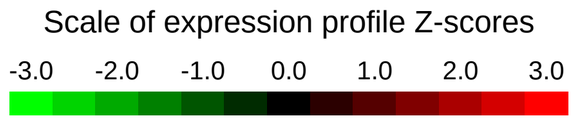

GEO Link:	http://www.ncbi.nlm.nih.gov/geo/query/acc.cgi?acc=GSE16480
Status:	Public on May 19 2014
Title:	Inactivation of CDK2 is synthetic lethal to MYCN-overexpressing cancer cells
Organism:	Homo sapiens
Experiment type:	Expression profiling by array
Platform:	GPL570
Pubmed ID:	19525400
Summary & Design:	**Summary:** Two genes have a synthetic lethal relationship when silencing or inhibition of one gene is only lethal in the context of a mutation or activation of the second gene. This situation offers an attractive therapeutic strategy, as inhibition of such a gene will only trigger cell death in tumor cells with an activated second oncogene but spare normal cells without activation of the second oncogene. Here we present evidence that CDK2 is synthetic lethal to neuroblastoma cells with MYCN amplification and overexpression. Neuroblastomas are childhood tumors with an often lethal outcome. Twenty percent of the tumors have MYCN amplification and these tumors are ultimately refractory to any therapy. Targeted silencing of CDK2 by three RNA interference techniques induced apoptosis in MYCN-amplified neuroblastoma cell lines, but not in MYCN single copy cells. Silencing of MYCN abrogated this apoptotic response in MYCN-amplified cells. Inversely, silencing of CDK2 in MYCN single copy cells did not trigger apoptosis, unless a MYCN transgene was activated. The MYCN induced apoptosis after CDK2 silencing was accompanied by nuclear stabilization of P53 and mRNA profiling showed up-regulation of P53 target genes. Silencing of P53 rescued the cells from MYCN-driven apoptosis. The synthetic lethality of CDK2 silencing in MYCN activated neuroblastoma cells can also be triggered by inhibition of CDK2 with a small molecule drug. Treatment of neuroblastoma cells with Roscovitine, a CDK inhibitor, at clinically achievable concentrations induced MYCN-dependent apoptosis. The synthetic lethal relation between CDK2 and MYCN indicates CDK2 inhibitors as potential MYCN-selective cancer therapeutics. **Overall design:** CDK2 shRNA in a tet repressor system was stably transfected in the IMR32 cell line. Time course analysis was performed in triplicate after induction of CDK2 shRNA at 5 time points.

Background corr dist: KL-Divergence = 0.1315, L1-Distance = 0.0403, L2-Distance = 0.0025, Normal std = 0.4116

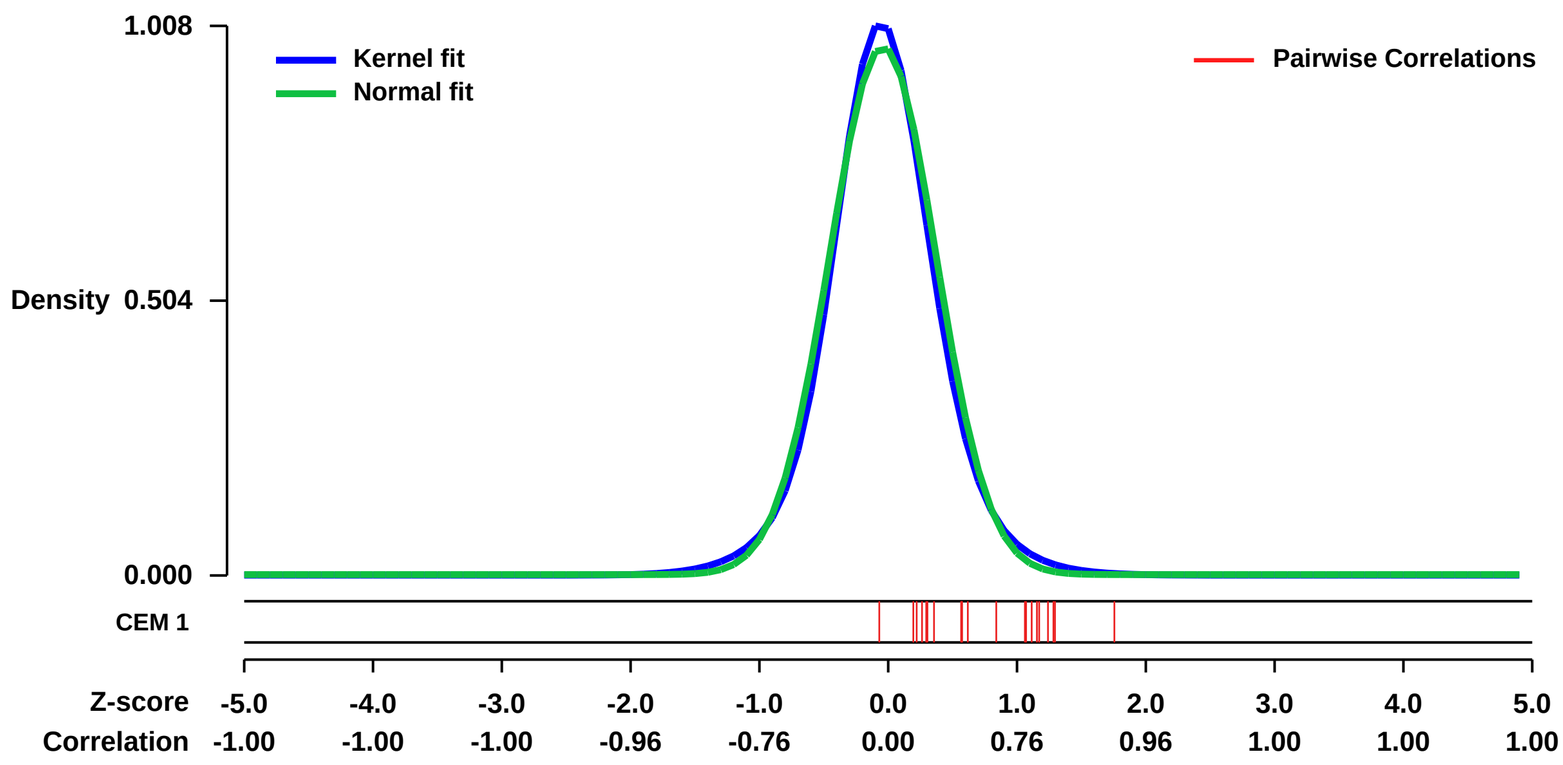

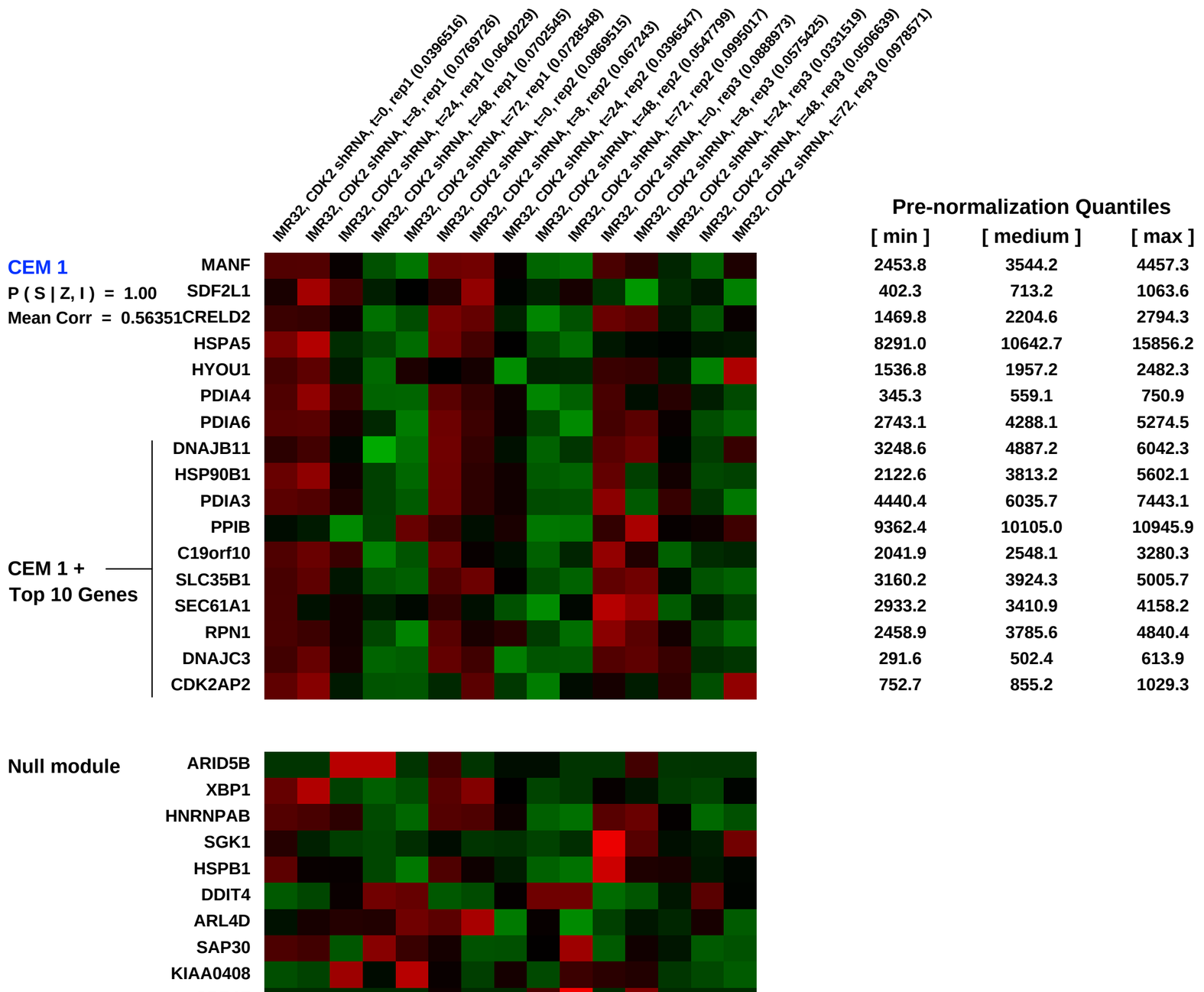

	Pre-normalization Quantiles [min]	[medium]	[max]
MANF	2453.8	3544.2	4457.3
SDF2L1	402.3	713.2	1063.6
CRELD2	1469.8	2204.6	2794.3
HSPA5	8291.0	10642.7	15856.2
HYOU1	1536.8	1957.2	2482.3
PDIA4	345.3	559.1	750.9
PDIA6	2743.1	4288.1	5274.5
DNAJB11	3248.6	4887.2	6042.3
HSP90B1	2122.6	3813.2	5602.1
PDIA3	4440.4	6035.7	7443.1
PPIB	9362.4	10105.0	10945.9
C19orf10	2041.9	2548.1	3280.3
SLC35B1	3160.2	3924.3	5005.7
SEC61A1	2933.2	3410.9	4158.2
RPN1	2458.9	3785.6	4840.4
DNAJC3	291.6	502.4	613.9
CDK2AP2	752.7	855.2	1029.3
ARID5B			
XBP1			
HNRNPAB			
SGK1			
HSPB1			
DDIT4			
ARL4D			
SAP30			
KIAA0408			
GPR17			
HSPH1			
DNASE1L2			
SLC5A3			
GNAS			
GPR3			
TNFRSF25			
TM6SF2			
MKKS			
PLEKHF1			
ZMYM1			
DOK3			
FGF20			
SLC39A2			
KCNIP2			
ERRFI1			
DEDD2			
CCDC117			
USP31			
AHSA2			
CYS1			
CNIH2			
BANP			
CHORDC1			
P4HA1			

GEO Series "GSE51105" Expression Profiles

Num of samples in this series: 94

Scale of expression profile Z-scores

-3.0 -2.0 -1.0 0.0 1.0 2.0 3.0

GEO Link: http://www.ncbi.nlm.nih.gov/geo/query/acc.cgi?acc=GSE51105

Status: Public on Apr 01 2014

Title: A signature predicting poor prognosis in gastric and ovarian cancer represents a coordinated macrophage and stromal-response.

Organism: Homo sapiens

Experiment type: Expression profiling by array

Platform: GPL570

Pubmed ID: 24658156

Summary & Design:

Summary:
Genome wide mRNA expression profiling of 94 gastric tumours derived from Australian based cohort was performed. . From this data we identified a cluster of co-expressed genes termed the stromal response cluster which almost perfectly differentiates tumor from its non-malignant gastric tissue and hence can be regarded as a highly tumor-specific gene expression signature. We show that these genes are consistently co-expressed across a range of independent gastric datasets as well as other cancer types suggesting a conserved functional role in cancer.

Overall design:
Profiling of 94 primary gastric tumors on Affymetrix GeneChip Human Genome U133 Plus 2.0 Arrays. All tumors were collected with approvals from Peter MacCallum Cancer Center, Australia; the Research Ethics Review Committee; and signed informed patient consent.

Background corr dist: KL-Divergence = 0.4661, L1-Distance = 0.0917, L2-Distance = 0.0291, Normal std = 0.2385

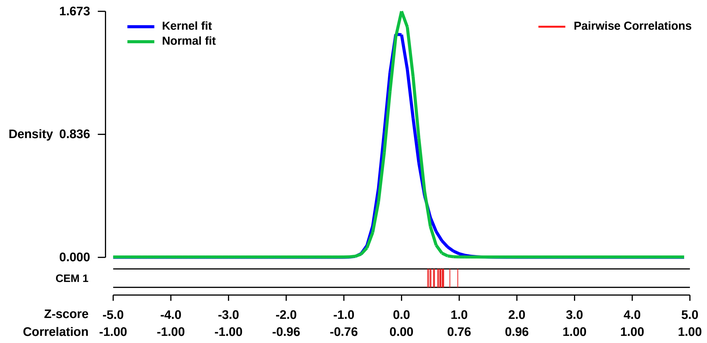

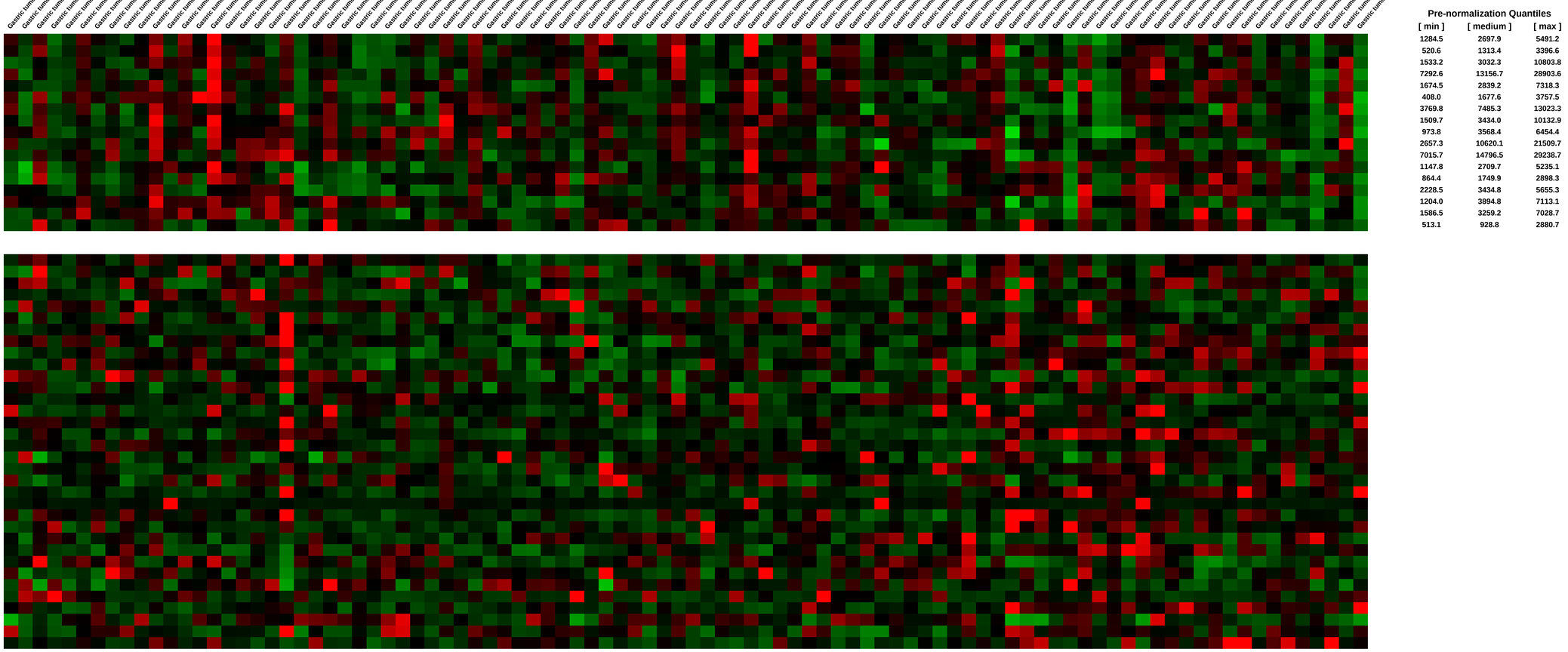

Pre-normalization Quantiles

	[min]	[medium]	[max]
CEM 1	1284.5	2697.9	5491.2
P (S | Z, I) = 1.00	520.6	1313.4	3396.6
Mean Corr = 0.56215	1533.2	3032.3	10803.8
HSPA5	7292.6	13156.7	28903.6
HYOU1	1674.5	2839.2	7318.3
PDIA4	408.0	1677.6	3757.5
PDIA6	3769.8	7485.3	13023.3
CEM 1 + Top 10 Genes	1509.7	3434.0	10132.9
	973.8	3568.4	6454.4
	2657.3	10620.1	21509.7
	7015.7	14796.5	29238.7
	1147.8	2709.7	5235.1
	864.4	1749.9	2898.3
	2228.5	3434.8	5655.3
	1204.0	3894.8	7113.1
	1586.5	3259.2	7028.7
	513.1	928.8	2880.7

GEO Series "GSE33562" Expression Profiles

Num of samples in this series: 8

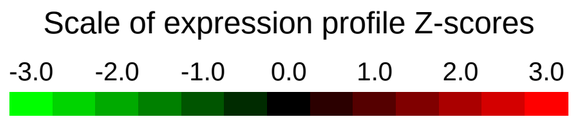

GEO Link:	http://www.ncbi.nlm.nih.gov/geo/query/acc.cgi?acc=GSE33562
Status:	Public on Nov 09 2011
Title:	Preclinical analysis of the gamma secretase inhibitor PF-030840214 in combination with glucocorticoids in T-cell acute lymphoblastic leukemia
Organism:	Homo sapiens
Experiment type:	Expression profiling by array
Platform:	GPL570
Pubmed ID:	22504949
Summary & Design:	**Summary:** T-cell acute lymphoblastic leukemia (T-ALL) is an aggressive hematologic cancer frequently associated with activating mutations in NOTCH1. Early studies identified NOTCH1 as an attractive therapeutic target for the treatment of T-ALL through the use of gamma-secretase inhibitors (GSIs). Here, we characterized the interaction between PF-03084014, a clinically-relevant GSI, and dexamethasone in preclinical models of glucocorticoid-resistant T-ALL. Combination treatment of the GSI PF-03084014 with glucocorticoids induced a synergistic antileukemic effect in human T-ALL cell lines and primary human T-ALL patient samples. Molecular characterization of the response to PF-03084014 plus glucocorticoids through gene expression profiling revealed transcriptional upregulation of the glucocorticoid receptor as the mechanism mediating the enhanced glucocorticoid response. Moreover, treatment with PF-03084014 and glucocorticoids in combination was highly efficacious in vivo, with enhanced reduction of tumor burden in a xenograft model of T-ALL. Finally, glucocorticoid treatment was highly effective at reversing PF-03084014-induced gastrointestinal toxicity via inhibition of goblet cell metaplasia. These results suggest that combination of PF-03084014 treatment with glucocorticoids may be well-tolerated and highly active for the treatment of glucorticoid-resistant T-ALL. **Overall design:** Duplicate samples of the CUTLL1 T-ALL cell line were treated with vehicle only (DMSO), the gamma-secretase inhibitor PF-03084014 (1 microM), dexamethasone (1 microM), or PF-03084014 (1 microM). plus dexamethasone (1 microM) for 48 hours. Gene expression profiling was analyzed to identify gene expression signatures assocuated with glucocorticoid treatment (dexamethasone), inhibition of NOTCH1 by gamma secretase inhibitor (PF-03084014) or the combination of both treatments.

Background corr dist: KL-Divergence = 0.0459, L1-Distance = 0.0176, L2-Distance = 0.0004, Normal std = 0.5777

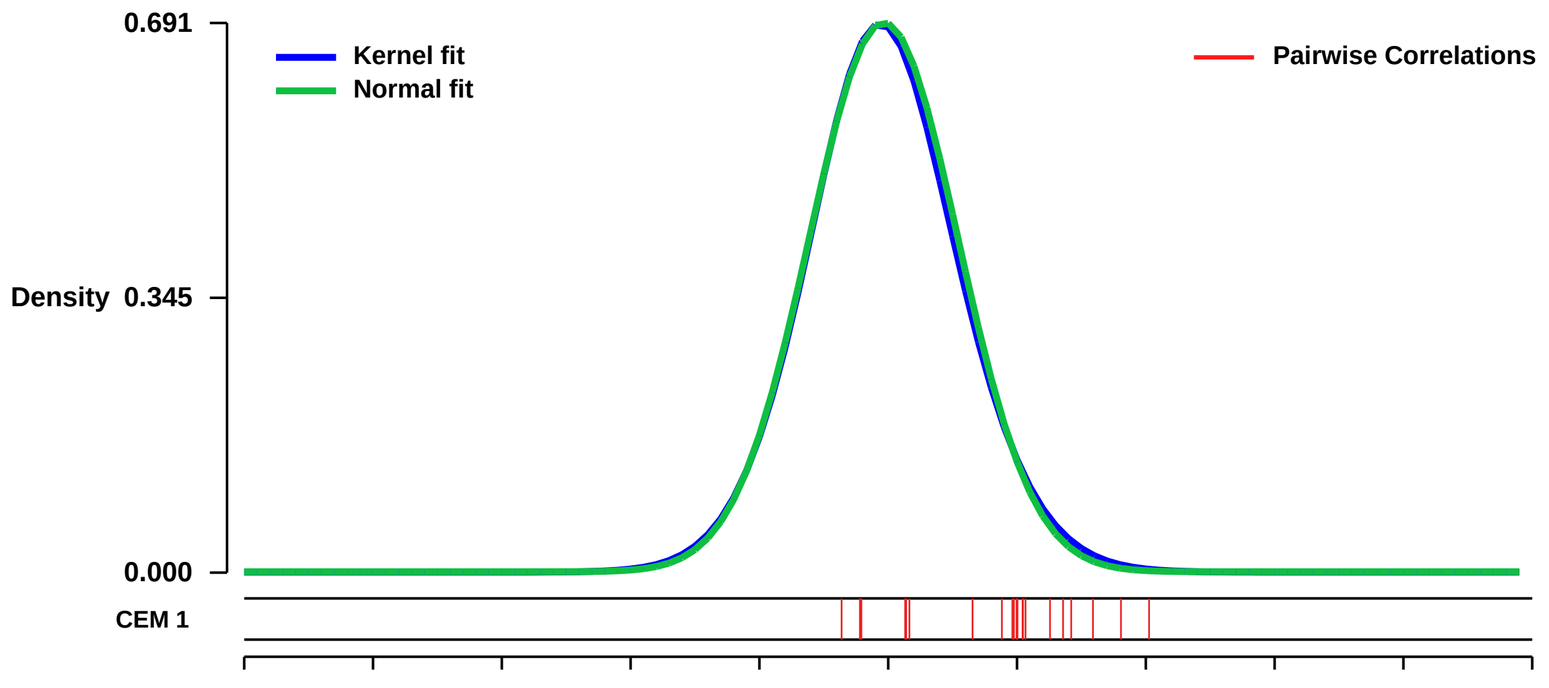

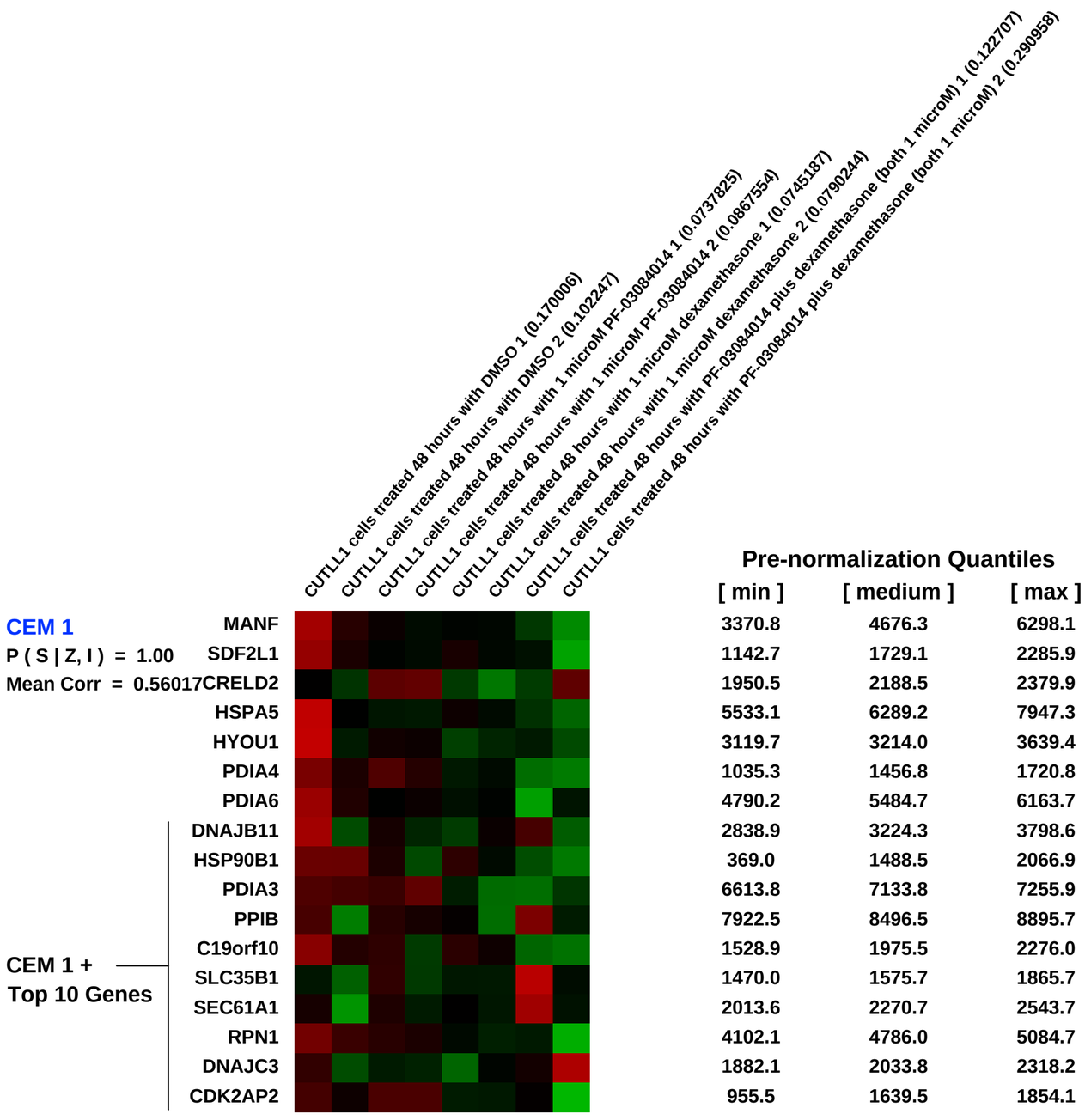

GEO Series "GSE28590" Expression Profiles

Num of samples in this series: 6

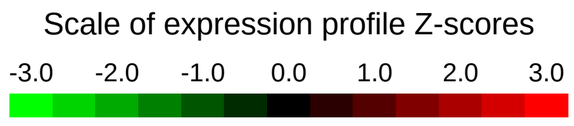

GEO Link:	http://www.ncbi.nlm.nih.gov/geo/query/acc.cgi?acc=GSE28590
Status:	Public on Jun 08 2011
Title:	Expression data of the human hepatoblastoma cell line HepG2 treated with TGF-beta
Organism:	Homo sapiens
Experiment type:	Expression profiling by array
Platform:	GPL570
Pubmed ID:	21646355
Summary & Design:	**Summary:** Smad2/3 are transcription factors that engage in TGF-beta-induced transcription. We determined and analyzed HepG2 and Hep3B-specific Smad2/3 binding sites by ChIP-chip. We used expression microarrays to compare the Smad2/3 and HNF4alpha binding sites identified by ChIP-chip or ChIP-seq, respectively, to TGF-beta-induced gene expressions. **Overall design:** HepG2 cells were transfected with control or HNF4A siRNAs and treated with 3 ng/ml TGF-beta for 0, 1.5 and 24 h (6 samples in total, no replicates). Total RNA was extracted and expression microarray analysis was performed as described in the protocols.

Background corr dist: KL-Divergence = 0.0434, L1-Distance = 0.0265, L2-Distance = 0.0008, Normal std = 0.6091

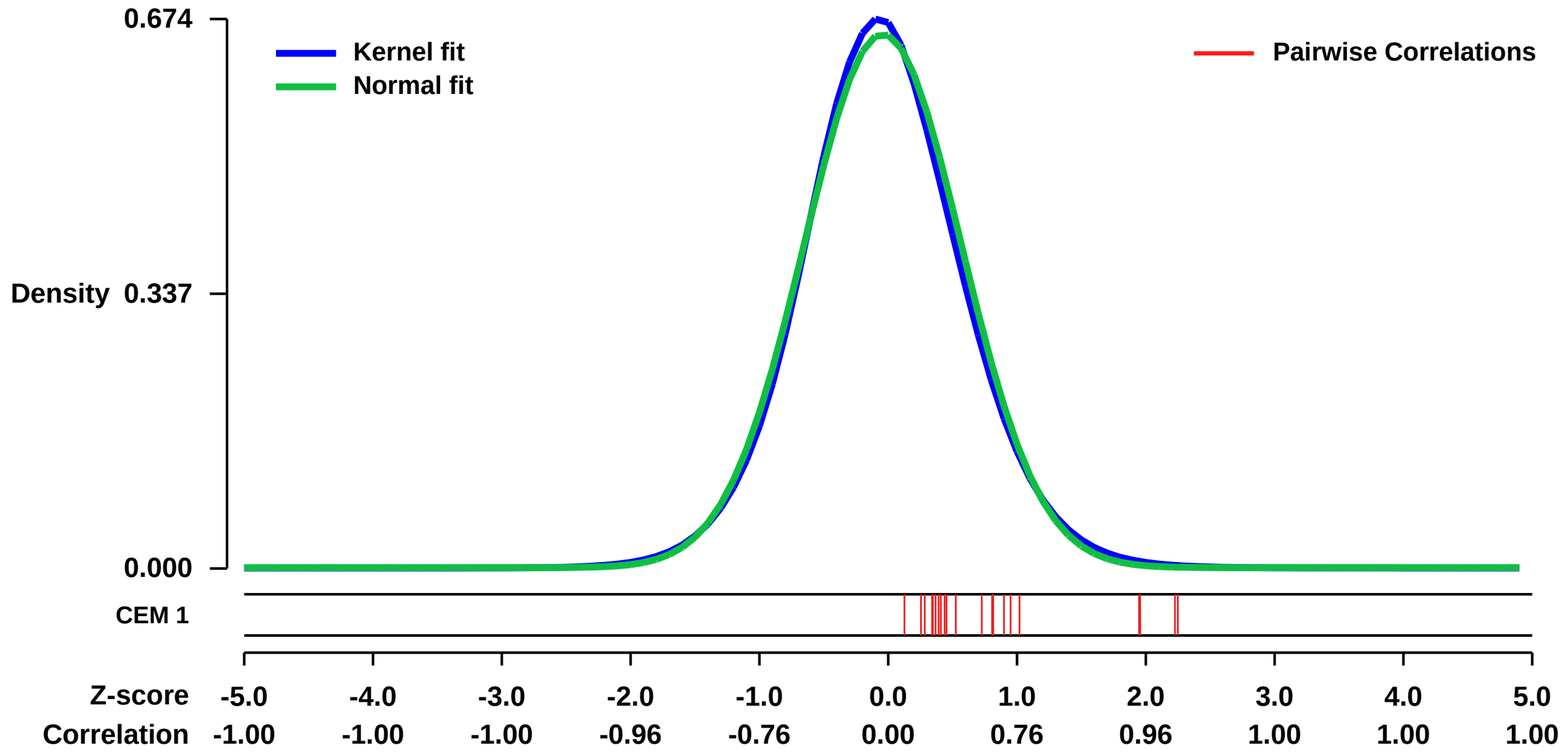

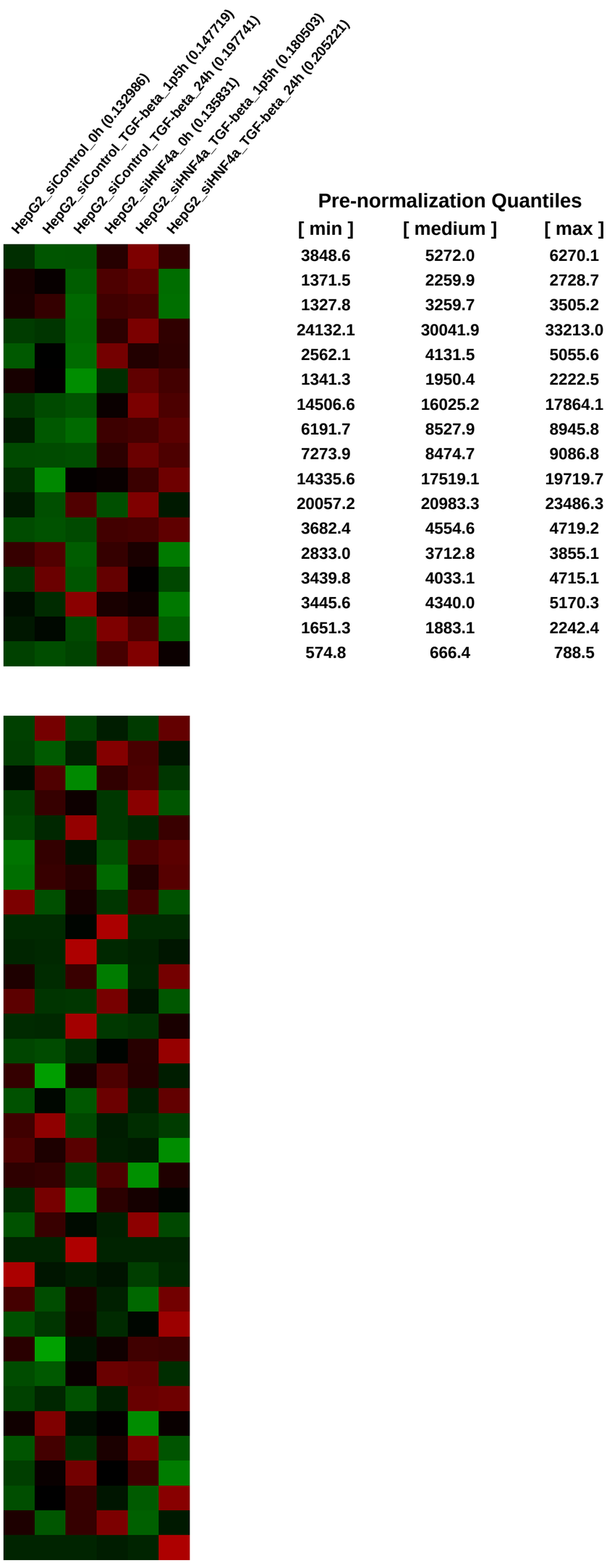

GEO Series "GSE19829" Expression Profiles

Num of samples in this series: 28

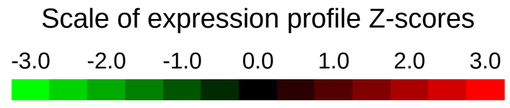

GEO Link:	http://www.ncbi.nlm.nih.gov/geo/query/acc.cgi?acc=GSE19829
Status:	Public on Jul 11 2010
Title:	A gene expression profile of BRCAness that is associated with outcome in ovarian cancer
Organism:	Homo sapiens
Experiment type:	Expression profiling by array
Platform:	GPL570
Pubmed ID:	20547991
Summary & Design:	**Summary:** A gene expression profile of BRCAness was defined in publicly available expression data of 61 patients with epithelial ovarian cancer (34 patients with BRCA-1 or BRCA-2 mutations and 27 patients with sporadic disease). This dataset is publicly available at http://jnci.oxfordjournals.org/cgi/content/full/94/13/990/DC1 The BRCAness profile was correlated with outcome in 70 patients with epithelial ovarian cancer and known outcome data. **Overall design:** Correlation with outcome

Background corr dist: KL-Divergence = 0.2896, L1-Distance = 0.0700, L2-Distance = 0.0144, Normal std = 0.2856

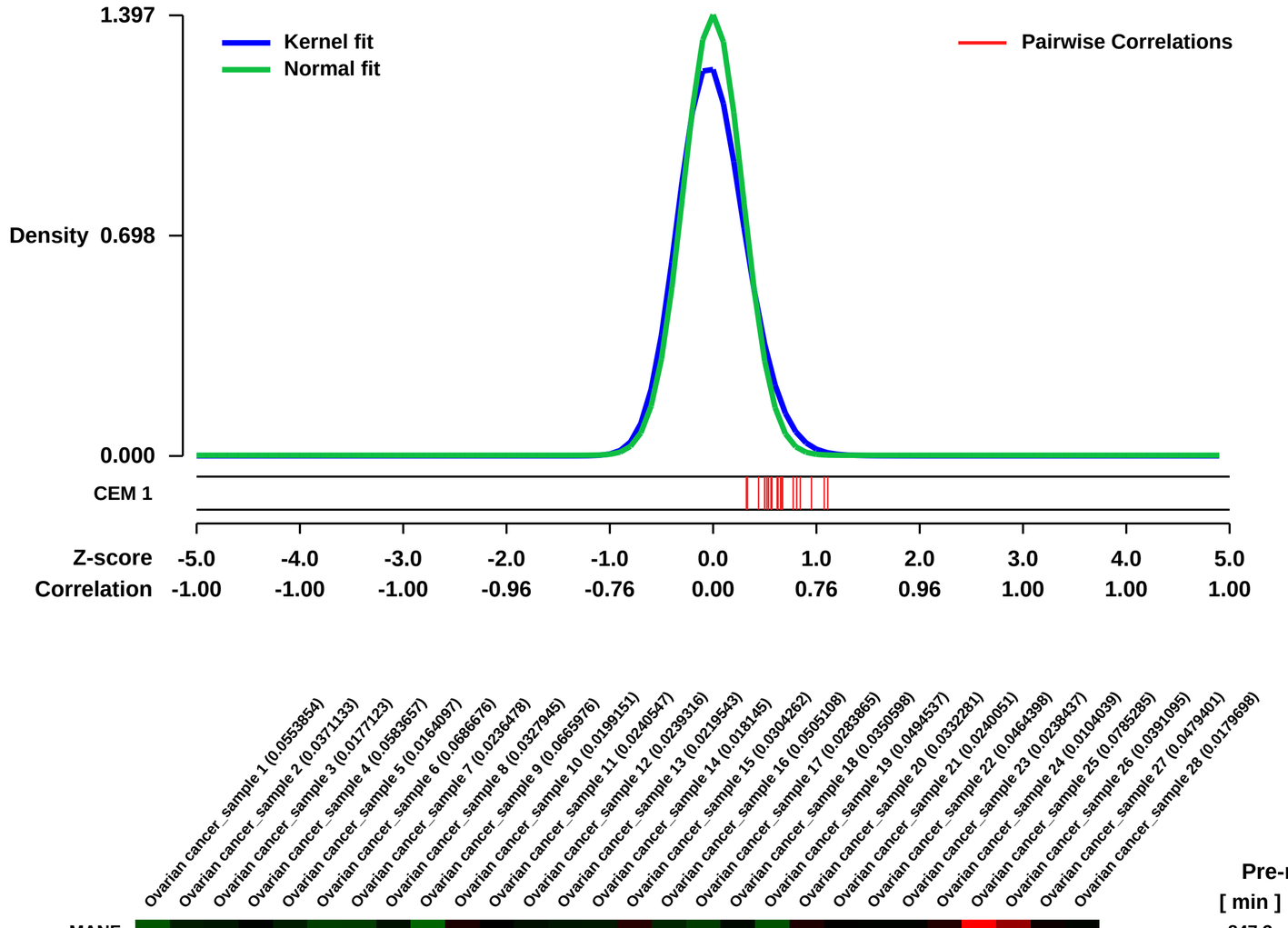

Pre-normalization Quantiles

[min]	[medium]	[max]
847.3	2084.3	7041.9
265.1	620.8	2478.1
903.0	1562.7	3581.7
3570.3	9039.6	14344.2
1883.1	4515.4	11609.9
379.1	1447.6	5829.4
2152.4	4197.0	6548.9
1243.1	2993.3	10303.3
1015.9	1606.3	4599.6
2108.5	5767.9	21040.1
5439.8	10282.9	20350.8
1150.7	2076.8	2703.6
732.7	1758.1	4368.9
1628.9	2769.9	4625.2
1773.8	3406.5	6291.5
731.7	1821.2	2729.2
197.5	877.8	2780.2

GEO Series "GSE23687" Expression Profiles

Num of samples in this series: 22

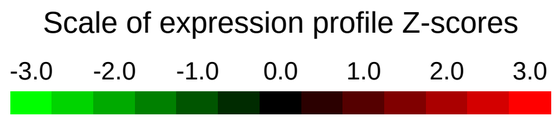

GEO Link:	http://www.ncbi.nlm.nih.gov/geo/query/acc.cgi?acc=GSE23687
Status:	Public on Sep 27 2010
Title:	Expression data from SPARKS CHARMS JIA cohort
Organism:	Homo sapiens
Experiment type:	Expression profiling by array
Platform:	GPL570
Pubmed ID:	20827233
Summary & Design:	**Summary:** Gene expression on peripheral blood mononuclear cells (PBMC) from SPARKS CHARMS juvenile idiopathic arthritis (JIA) cohort pre and post methotrexate therapy. This is the first study to our knowledge, to evaluate gene expression profiles in children with JIA before and after MTX, and to analyze genetic variation in differentially expressed genes. We have identified a gene, which may contribute to genetic variability in MTX response in JIA. **Overall design:** PBMC were isolated from blood samples taken from 11 patients with JIA pre methotrexate therapy and at 6 months into therapy

Background corr dist: KL-Divergence = 0.2068, L1-Distance = 0.0462, L2-Distance = 0.0047, Normal std = 0.3272

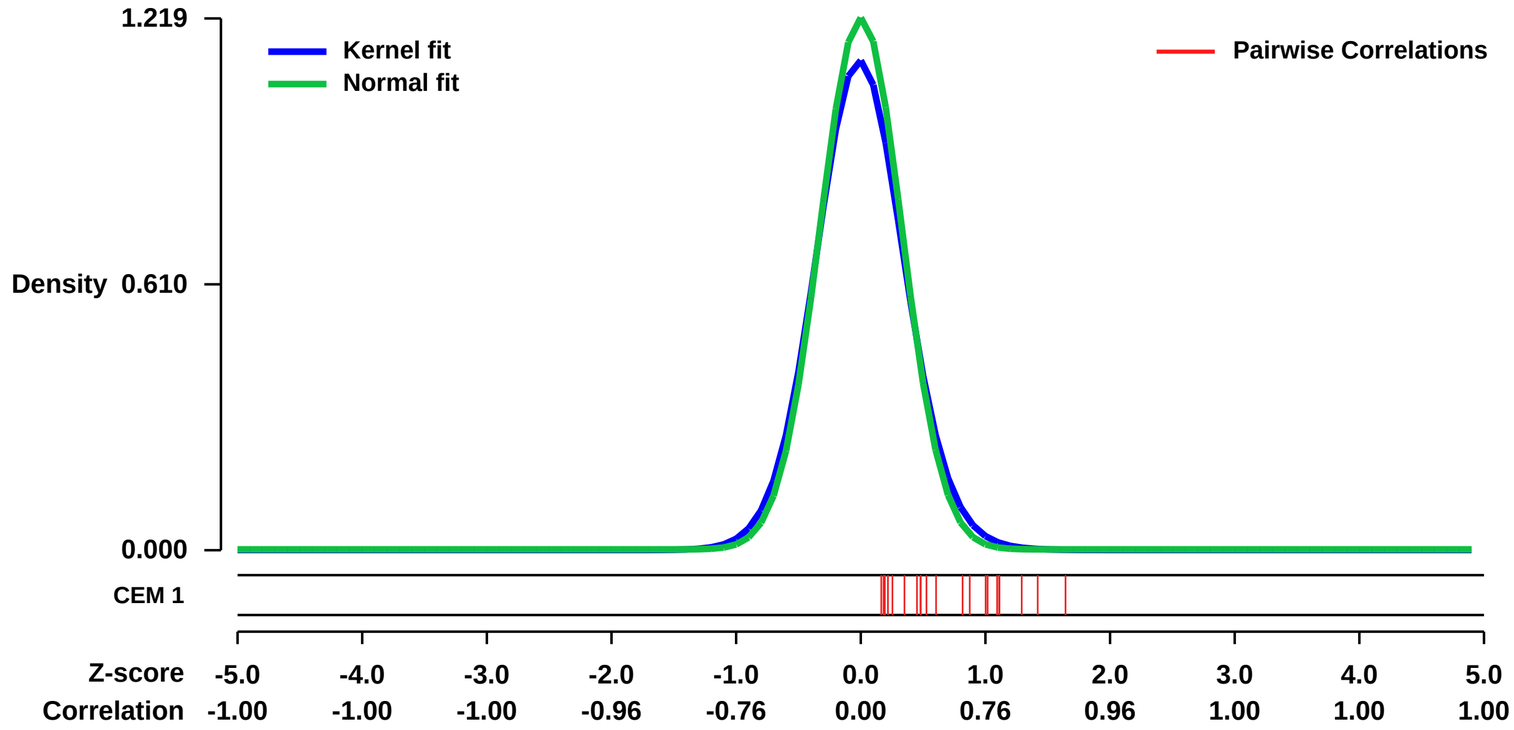

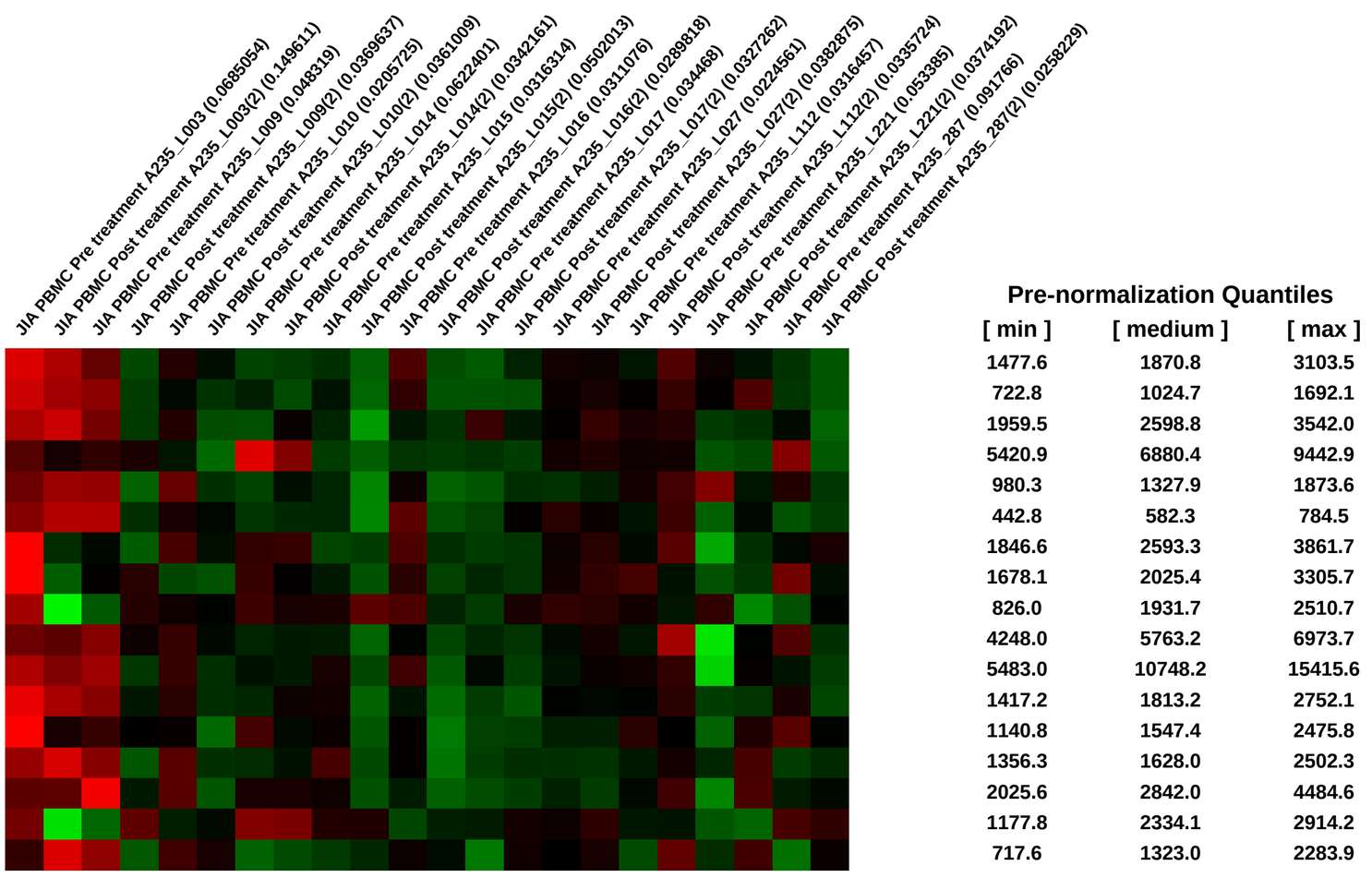

GEO Series "GSE8961" Expression Profiles

Num of samples in this series: 18

Scale of expression profile Z-scores

-3.0 -2.0 -1.0 0.0 1.0 2.0 3.0

GEO Link:	http://www.ncbi.nlm.nih.gov/geo/query/acc.cgi?acc=GSE8961
Status:	Public on Nov 10 2007
Title:	Identification of human metapneumovirus-induced gene networks in airway epithelial cells by microarray analysis
Organism:	Homo sapiens
Experiment type:	Expression profiling by array
Platform:	GPL570
Pubmed ID:	18234263
Summary & Design:	**Summary:** This experiment is designed to study the effects to HMPV on A549 over time **Keywords: time course** **Overall design:** Confluent monolayers of A549 cells were infected with hMPV at MOI of 1 in serum-free media and harvested at 6, 12, 24, 48, or 72 hours post-infection to extract total RNA using RNAqueous´fi-Midi Kit (Ambion, Austin, TX), according to manufacturerâ s instruction;3 Affymetrix HG-U133 plus 2.0 were used for hybridization.

Background corr dist: KL-Divergence = 0.1345, L1-Distance = 0.0292, L2-Distance = 0.0014, Normal std = 0.3992

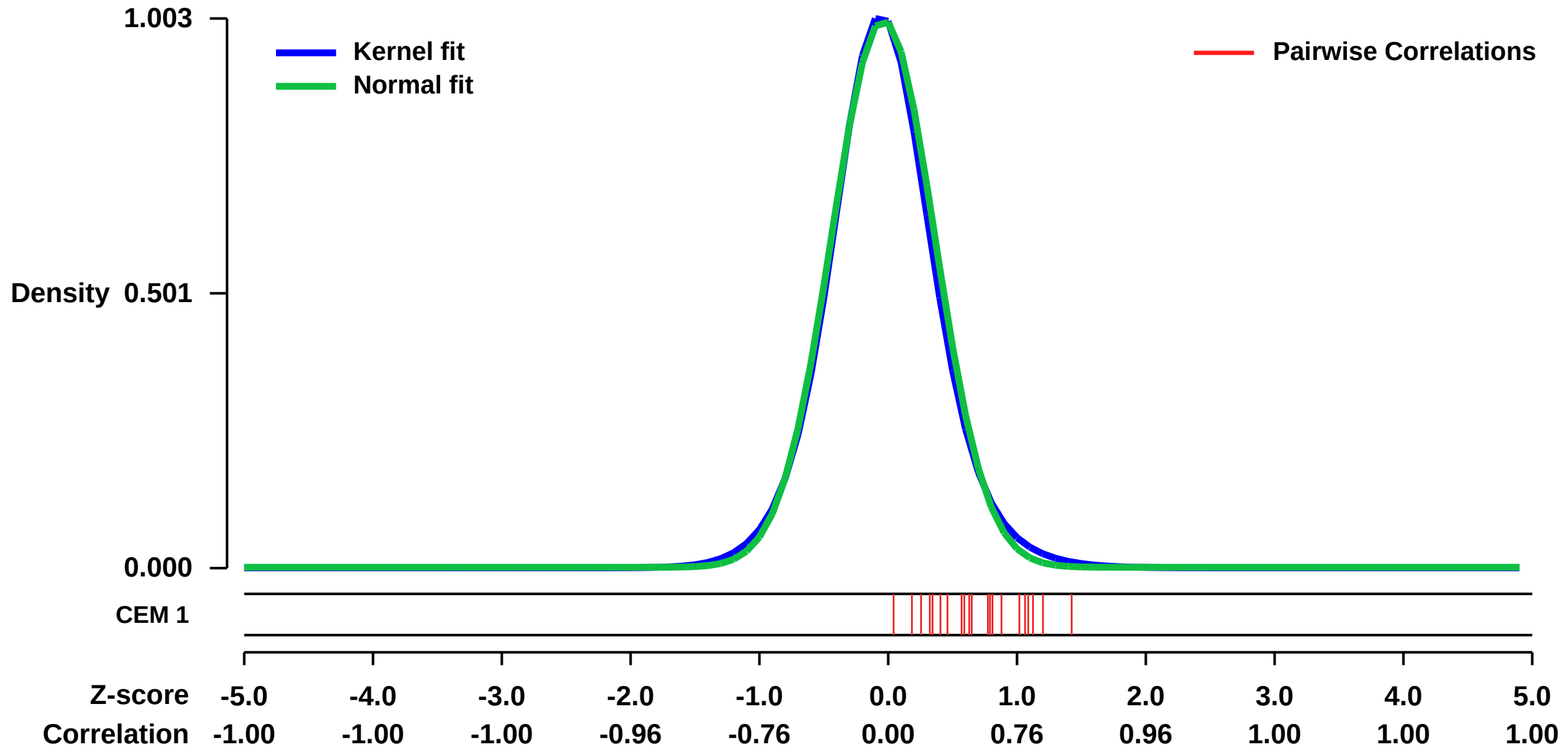

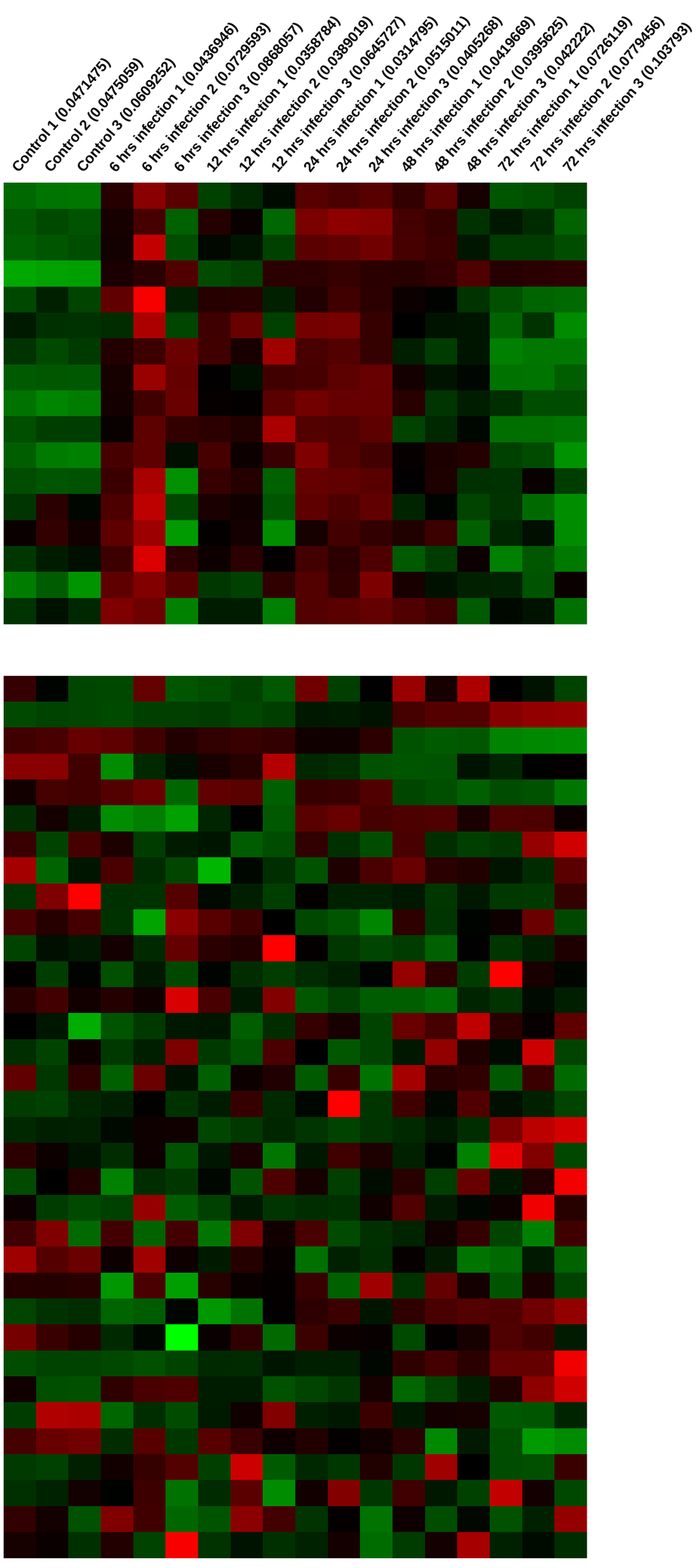

	Pre-normalization Quantiles		
	[min]	[medium]	[max]
MANF	1391.8	3496.7	5202.4
SDF2L1	272.1	1326.7	2570.8
CRELD2	682.4	1862.5	5312.9
HSPA5	6239.0	21153.3	23929.7
HYOU1	555.4	2077.4	5797.8
PDIA4	471.6	1168.0	2288.4
PDIA6	3424.3	9336.8	14673.3
DNAJB11	1708.4	3227.6	5167.2
HSP90B1	795.7	2202.4	3286.4
PDIA3	2495.4	6749.3	12275.1
PPIB	7754.5	15040.7	19166.1
C19orf10	1363.1	2935.1	4587.8
SLC35B1	1529.3	2918.5	4871.9
SEC61A1	143.7	2702.7	4694.2
RPN1	1454.3	2599.9	4298.6
DNAJC3	1035.7	1874.9	2505.8
CDK2AP2	121.4	835.6	1736.5
ARID5B			
XBP1			
HNRNPAB			
SGK1			
HSPB1			
DDIT4			
ARL4D			
SAP30			
KIAA0408			
GPR17			
HSPH1			
DNASE1L2			
SLC5A3			
GNAS			
GPR3			
TNFRSF25			
TM6SF2			
MKKS			
PLEKHF1			
ZMYM1			
DOK3			
FGF20			
SLC39A2			
KCNIP2			
ERRFI1			
DEDD2			
CCDC117			
USP31			
AHSA2			
CYS1			
CNIH2			
BANP			
CHORDC1			
P4HA1			

GEO Series "GSE13070" Expression Profiles

Num of samples in this series: 364

Details of this dataset are not shown due to large number of samples and the page size limit.

Find details in http://www.ncbi.nlm.nih.gov/geo/query/acc.cgi?acc=GSE13070

Background corr dist: KL-Divergence = 0.2712, L1-Distance = 0.0365, L2-Distance = 0.0023, Normal std = 0.2997

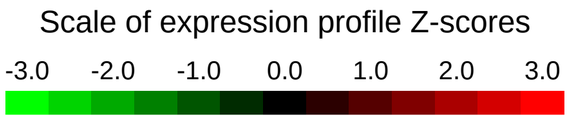

GEO Series "GSE47873" Expression Profiles

Num of samples in this series: 6

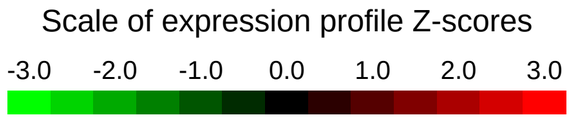

GEO Link:	http://www.ncbi.nlm.nih.gov/geo/query/acc.cgi?acc=GSE47873
Status:	Public on Jun 17 2013
Title:	Gene expression profiles MCF-10A cells overexpressing MBD2
Organism:	Homo sapiens
Experiment type:	Expression profiling by array
Platform:	GPL570
Pubmed ID:	
Summary & Design:	**Summary:** Methylated DNA binding protein 2 (MBD2) has been shown to bind specific methylated promoters and suppress transcription. Here we systematically investigate MBD2 suppression by overexpressing MBD2 in MCF-10A cells and generating gene expression profiles of overexpressing cells and normal MCF-10A cells. **Overall design:** MCF-10A cells were infected with MBD2 lentivirus in order to increase MBD2 expression. Total RNA was extracted from both infected and non-infected cells and hybridized to Affymetrix gene expression microarrays. Three technical replicates were hybridized for infected and non-infected cells.

Background corr dist: KL-Divergence = 0.0283, L1-Distance = 0.0229, L2-Distance = 0.0006, Normal std = 0.6907

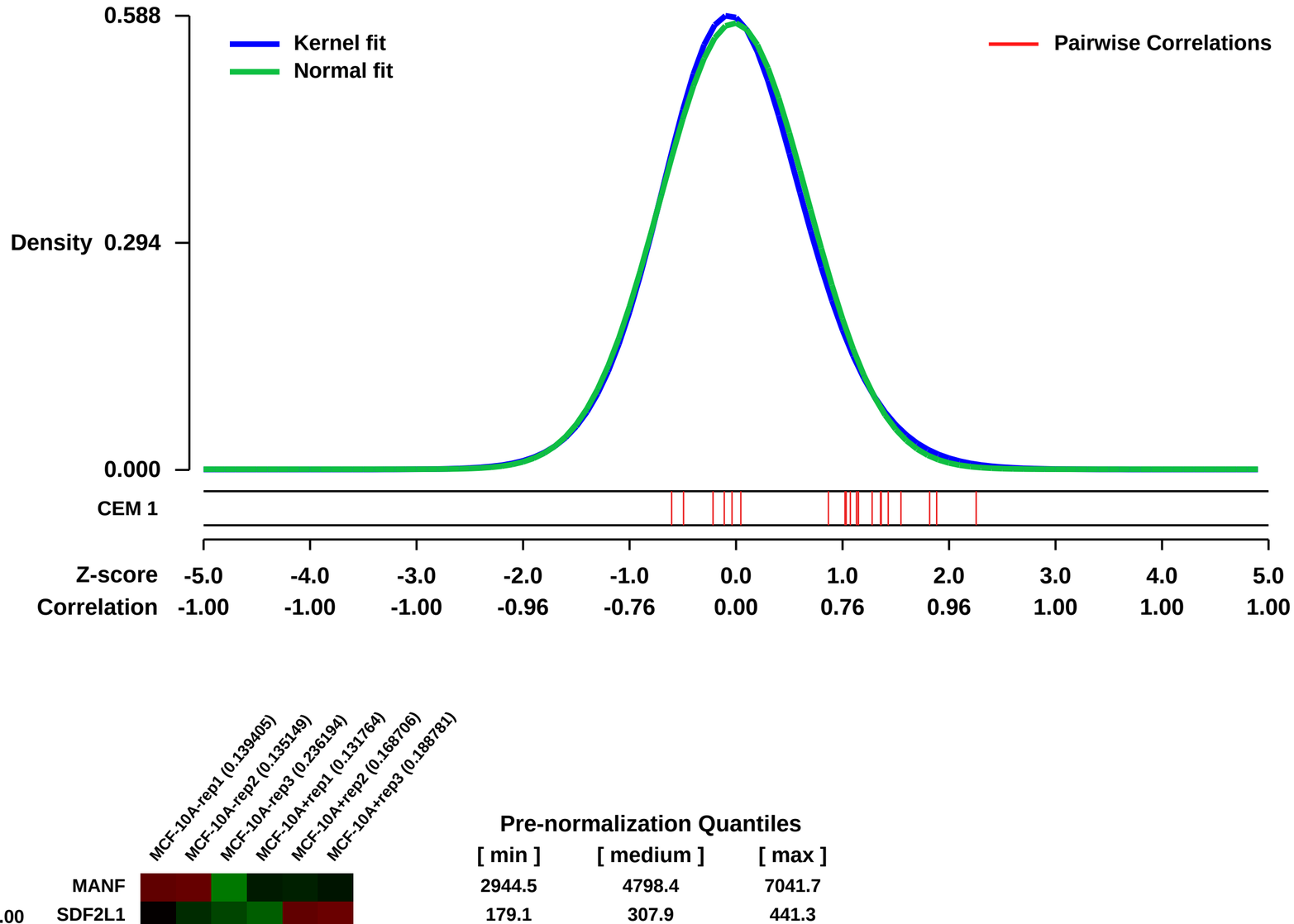

CEM 1
P (S | Z, I) = 1.00
Mean Corr = 0.54590

CEM 1 + Top 10 Genes

Null module

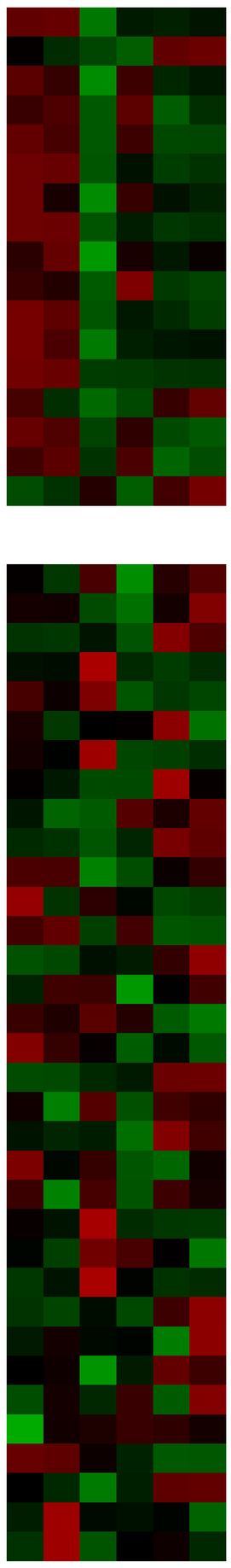

MANF	2944.5	4798.4	7041.7
SDF2L1	179.1	307.9	441.3
CRELD2	3596.7	6950.9	7634.4
HSPA5	12332.9	19631.6	21380.7
HYOU1	2390.2	4812.2	5414.4
PDIA4	1340.9	2264.0	3998.2
PDIA6	14792.5	21818.6	25411.5
DNAJB11	2055.1	2825.1	4739.2
HSP90B1	556.6	1521.2	1928.7
PDIA3	7102.5	14465.6	19861.7
PPIB	13107.5	16652.2	24662.1
C19orf10	1677.7	3360.9	5507.8
SLC35B1	1746.5	1882.7	4454.5
SEC61A1	3789.8	8730.4	10086.8
RPN1	3189.7	5280.3	6159.3
DNAJC3	8149.2	15341.8	16535.0
CDK2AP2	271.8	444.7	552.4
ARID5B			
XBP1			
HNRNPAB			
SGK1			
HSPB1			
DDIT4			
ARL4D			
SAP30			
KIAA0408			
GPR17			
HSPH1			
DNASE1L2			
SLC5A3			
GNAS			
GPR3			
TNFRSF25			
TM6SF2			
MKKS			
PLEKHF1			
ZMYM1			
DOK3			
FGF20			
SLC39A2			
KCNIP2			
ERRFI1			
DEDD2			
CCDC117			
USP31			
AHSA2			
CYS1			
CNIH2			
BANP			
CHORDC1			
P4HA1			

GEO Series "GSE8702" Expression Profiles

Num of samples in this series: 16

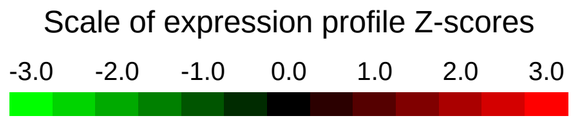

GEO Link:	http://www.ncbi.nlm.nih.gov/geo/query/acc.cgi?acc=GSE8702
Status:	Public on Feb 29 2008
Title:	Longitudinal Analysis of Progression to Androgen Independence
Organism:	Homo sapiens
Experiment type:	Expression profiling by array
Platform:	GPL570
Pubmed ID:	18302219
Summary & Design:	**Summary:** Following androgen ablation therapy (AAT), the vast majority of prostate cancer patients develop treatment resistance with a median time of 18-24 months to disease progression. To identify molecular targets that aid in prostate cancer cell survival and contribute to the androgen independent phenotype, we evaluated changes in LNCaP cell gene expression during 12 months of androgen deprivation. At time points reflecting critical growth and phenotypic changes, we performed Affymetrix expression array analysis to examine the effects of androgen deprivation during the acute response, during the period of apparent quiescence, and during the emergence of highly proliferative, androgen-independent prostate cancer cells (LNCaP-AI). We discovered alterations in gene expression for a host of molecules associated with promoting prostate cancer cell growth and survival, regulating cell cycle progression, apoptosis and adrenal androgen metabolism, in addition to AR co-regulators and markers of neuroendocrine disease. These findings illustrate the complexity and unpredictable nature of cancer cell biology and contribute greatly to our understanding of how prostate cancer cells likely survive AAT. The value of this longitudinal approach lies in the ability to examine gene expression changes throughout the cellular response to androgen deprivation; it provides a more dynamic illustration of those genes which contribute to disease progression in addition to specific genes which constitute a malignant androgen-independent phenotype. In conclusion, it is of great importance that we employ new approaches, such as the one proposed here, to continue exploring the cellular mechanisms of therapy resistance and identify promising targets to improve cancer therapeutics. **Keywords:** Time Course **Overall design:** To identify molecular targets that aid in prostate cancer cell survival and contribute to the androgen independent phenotype, we evaluated changes in LNCaP cell gene expression during 12 months of androgen deprivation. At time points reflecting critical growth and phenotypic changes, we performed Affymetrix expression array analysis to examine the effects of androgen deprivation during the acute response, during the period of apparent quiescence, and during the emergence of highly proliferative, androgen-independent prostate cancer cells (LNCaP-AI).

Background corr dist: KL-Divergence = 0.1700, L1-Distance = 0.0301, L2-Distance = 0.0019, Normal std = 0.3592

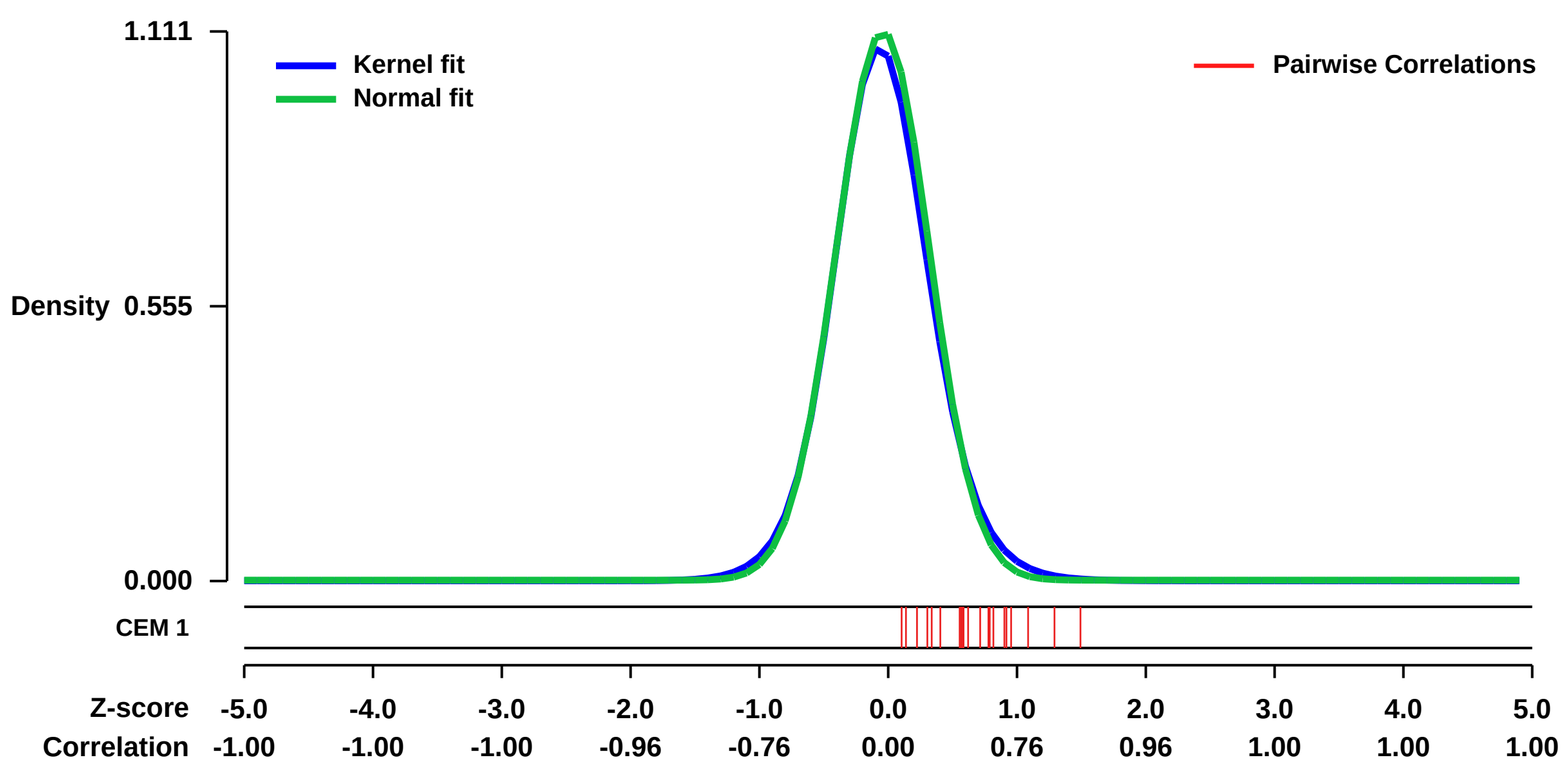

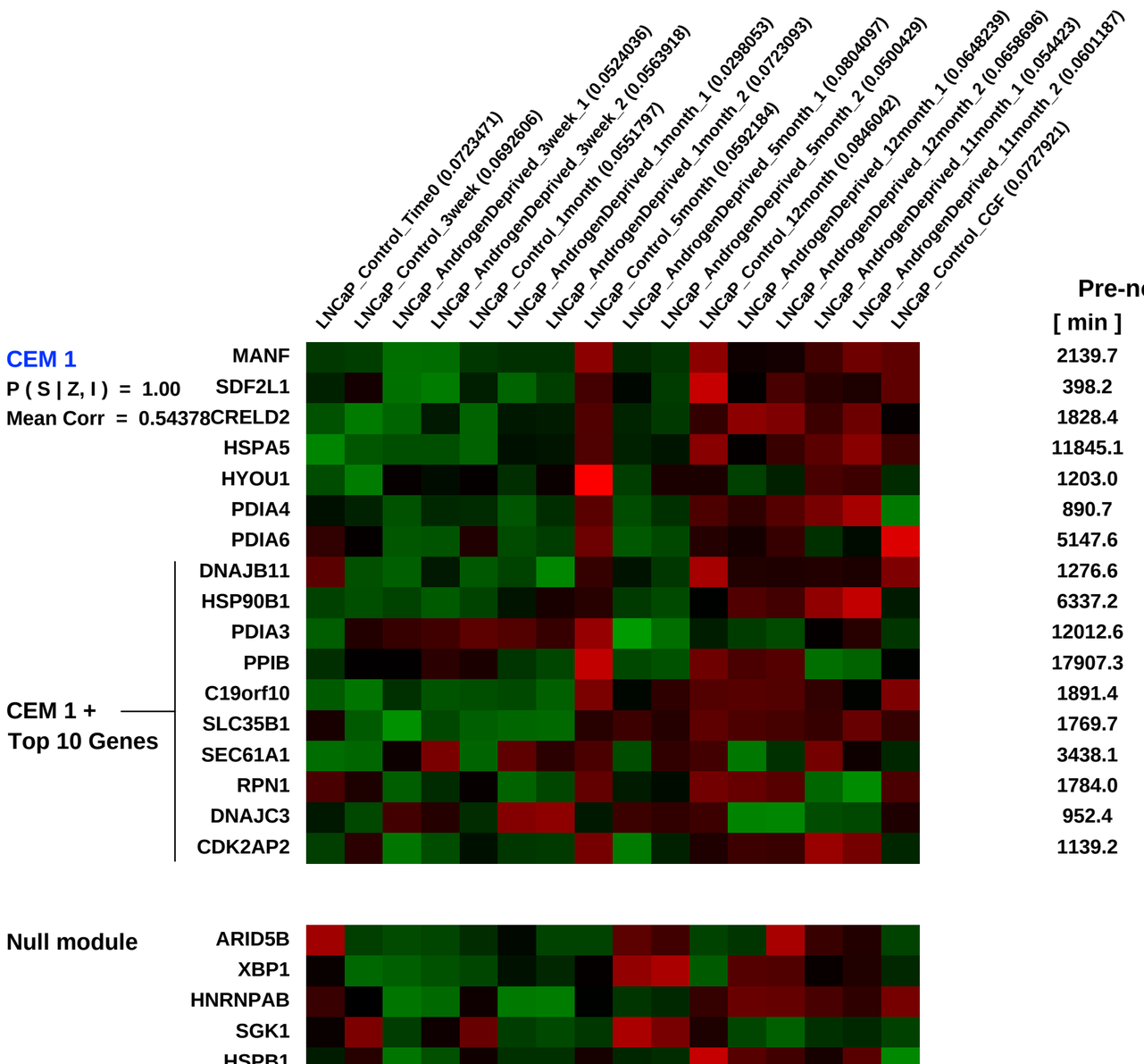

GEO Series "GSE20948" Expression Profiles

Num of samples in this series: 28

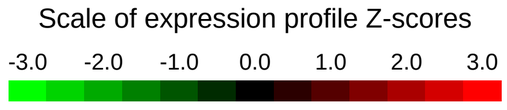

GEO Link:	http://www.ncbi.nlm.nih.gov/geo/query/acc.cgi?acc=GSE20948
Status:	Public on May 01 2010
Title:	The Effect of Hepatitis C Virus Infection on Host Gene Expression
Organism:	Homo sapiens
Experiment type:	Expression profiling by array
Platform:	GPL570
Pubmed ID:	20200238
Summary & Design:	**Summary:** Hepatitis C Virus is a leading cause of chronic liver disease. The identification and characterisation of key host cellular factors that play a role in the HCV replication cycle is important for the understanding of disease pathogenesis and the identification of novel anti-viral therapeutic targets. Gene expression profiling of HCV infected Huh7 cells by microarray analysis was performed to identify host cellular genes that are transcriptionally regulated by infection. The expression of host genes involved in cellular defence mechanisms (apoptosis, proliferation and anti-oxidant responses), cellular metabolism (lipid and protein metabolism) and intracellular transport (vesicle trafficking and cytoskeleton regulation) was significantly altered by HCV infection. The gene expression patterns identified provide insight into the potential mechanisms that contribute to HCV associated pathogenesis. These include an increase in pro-inflammatory and pro-apoptotic signalling and a decrease in the anti-oxidant response pathways of the infected cell. **Overall design:** 5x105 Huh7 cells were seeded in 25cm2 culture flasks and infected in triplicate either with the genotype 2a HCV clone, JFH-1 at a multiplicity of infection (MOI) of 3 or mock infected with an equal volume of concentrated conditioned growth medium. At 6, 12, 18, 24 and 48 hours post-infection, cellular RNA was extracted using TRIzol reagent (Invitrogen). Trizol lysates were shipped to Expression Analysis (NC, USA) where RNA was purified, quality tested using the Agilent Bioanalyser and hybridised onto Human U133 Plus 2.0 Affymetrix microarray chips for fluorescence data acquisition. In summary, a total of 30 RNA samples were analysed including 3x mock infected samples taken at 6, 12, 18, 24 and 48 hours post-treatment and 3x JFH-1 infected samples taken at 6, 12, 18, 24 and 48 hours post-infection. Two samples (Mock_6hrs_1 and JFH-1_6hrs_1) did not pass our data quality control measures and were therefore excluded from the statistical analysis.

Background corr dist: KL-Divergence = 0.2119, L1-Distance = 0.0328, L2-Distance = 0.0016, Normal std = 0.3302

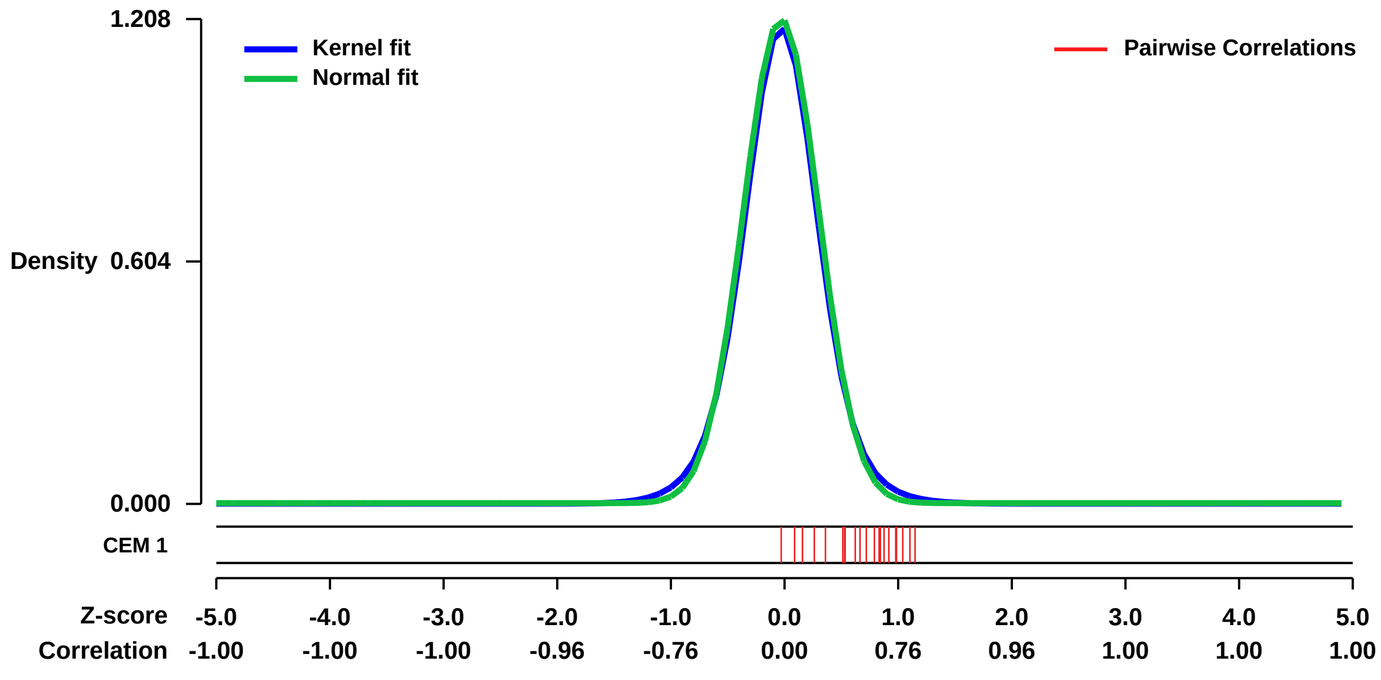

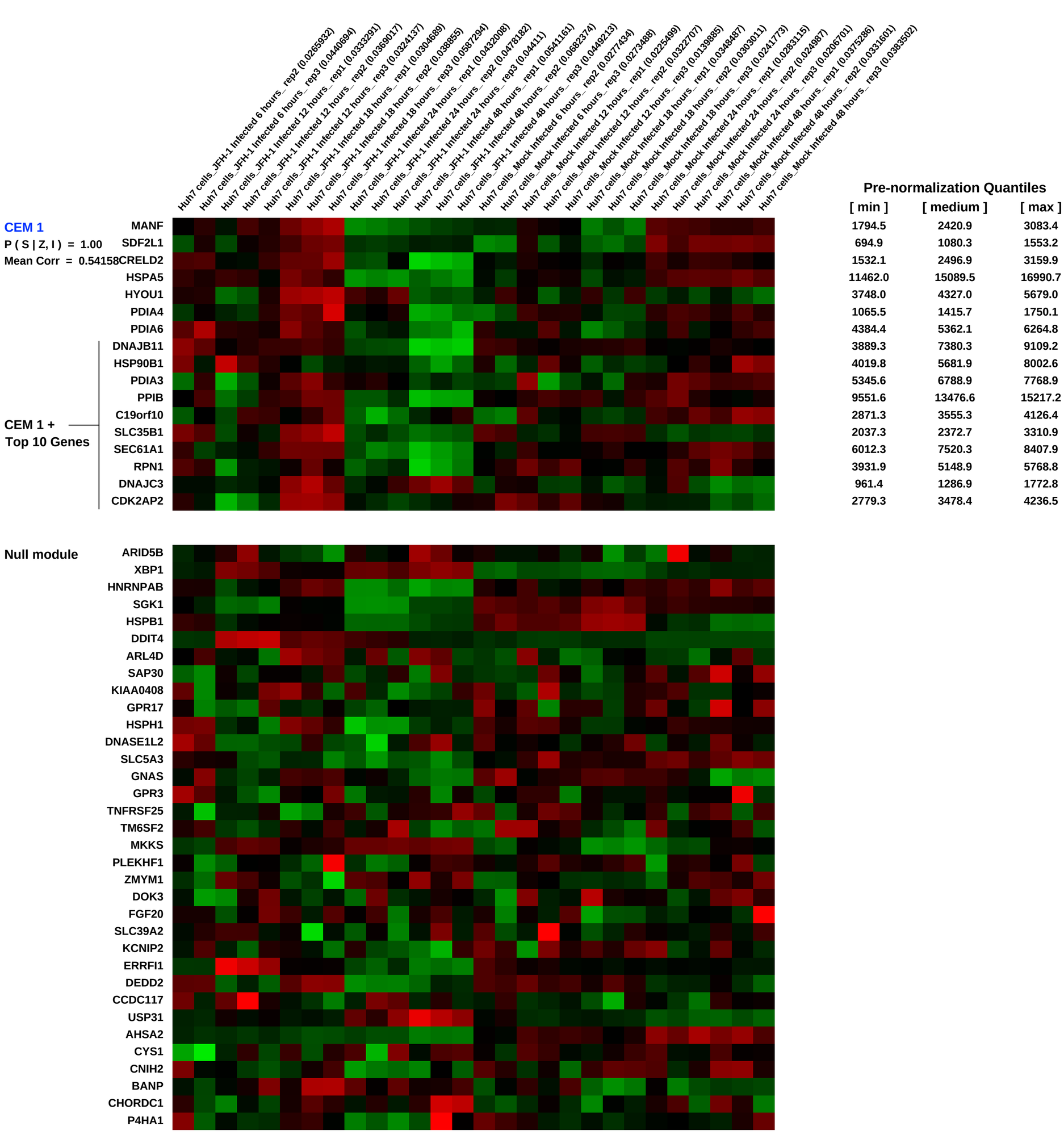

GEO Series "GSE5883" Expression Profiles

Num of samples in this series: 24

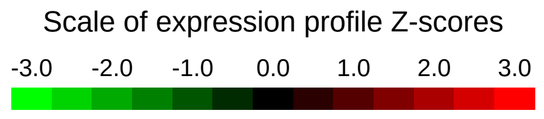

GEO Link: http://www.ncbi.nlm.nih.gov/geo/query/acc.cgi?acc=GSE5883

Status: Public on May 29 2009

Title: Lipopolysaccharide-induced Changes in Gene Expression in Human Lung Microvascular Endothelial Cells over Time

Organism: Homo sapiens

Experiment type: Expression profiling by array

Platform: GPL570

Pubmed ID:

Summary & Design:

Summary:
The vascular endothelium may play a role in the response to infectious agents and in the pathophysiology of disease processes resulting in capillary leak such as septic shock and acute respiratory distress syndrome. In order to study the effect of endotoxin on endothelial cell function, human lung microvascular endothelial cells in culture were exposed to lipopolysaccharide (LPS), 10 ng, for 4, 8, or 24 hours and changes in mRNA expression were studied using Affymetrix HG U133plus2 gene arrays. A principal components analysis revealed that LPS treatment was the primary source of variability in the data. LPS treatment of endothelial cells for 4, 8, or 24 hours resulted in the upregulation by two-fold or greater of 275, 260 and 141 genes respectively. LPS treatment resulted in the down regulation by 50% or greater of 176, 263 and 79 genes at 4, 8, or 24 hours respectively. Up regulated genes at 4 or 8 hours were enriched in those encoding for cytokines, secreted proteins, cell membrane proteins and proteins controlling signal transduction and transcriptional regulation. Down regulated genes at each of the time points included those coding for cell membrane proteins, transcriptional regulation and metabolism. At each time point, a significant proportion of the genes identified as changed were unique to that time point.

Keywords: Time course

Overall design:
In order to study the effect of endotoxin on endothelial cell function, human lung microvascular endothelial cells in culture were exposed to lipopolysaccharide (LPS), 10 ng, for 4, 8, or 24 hours and changes in mRNA expression were studied using Affymetrix HG U133plus2 gene arrays. Controls for each time point with no LPS exposure were also run. An N of 4 for each time point and treatment was used.

Background corr dist: KL-Divergence = 0.3703, L1-Distance = 0.0727, L2-Distance = 0.0157, Normal std = 0.2561

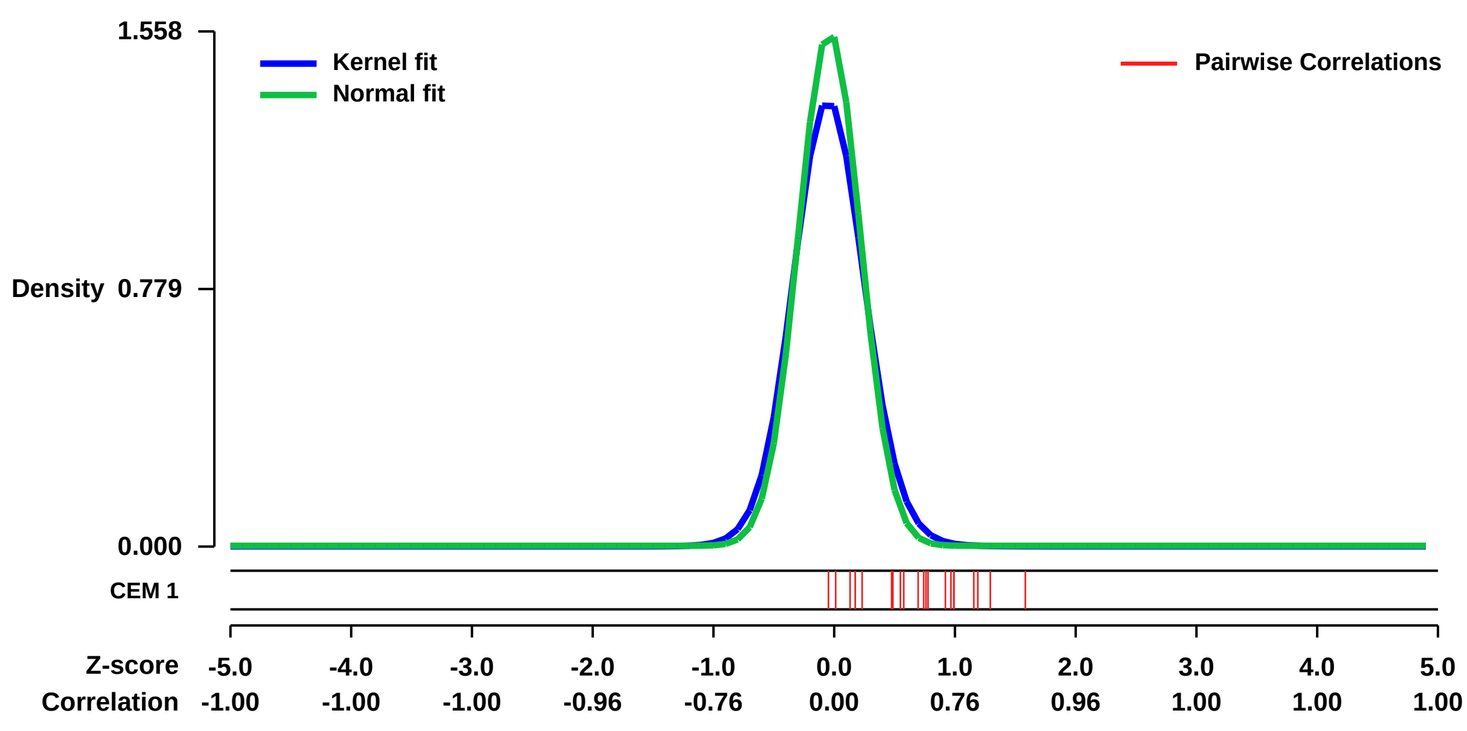

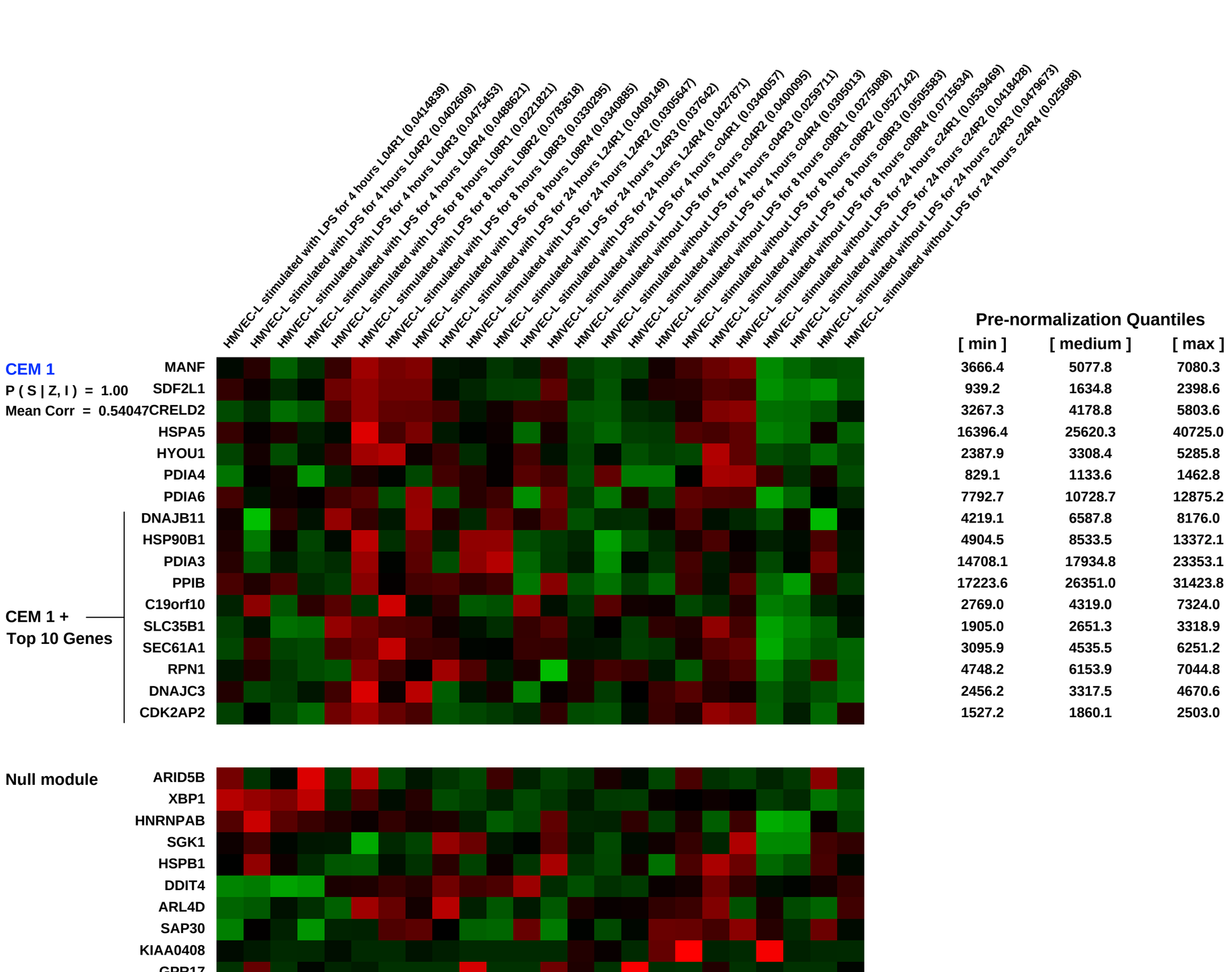

GEO Series "GSE37838" Expression Profiles

Num of samples in this series: 78

Scale of expression profile Z-scores

-3.0 -2.0 -1.0 0.0 1.0 2.0 3.0

GEO Link: http://www.ncbi.nlm.nih.gov/geo/query/acc.cgi?acc=GSE37838
Status: Public on Feb 13 2013
Title: Comparing molecular assessment of implantation biopsies with histologic and demographic risk assessment.
Organism: Homo sapiens
Experiment type: Expression profiling by array
Platform: GPL570
Pubmed ID: 23282320

Summary & Design:

Summary:
In deceased donor kidney transplantation, acute kidney injury (AKI) prioir to surgery is a major determinant of delayed graft function (DGF), but AKI is histologically silent and difficult to assess. We hypothesized that a molecular measurement of AKI would add power to conventional risk assessments to predict the early poor allograft function at first week post transplantation.

Overall design:
We performed microarrays on implantation biopsies taken during reperfusion in 70 deceased donor kidneys from 53 donors. Early poor function was classified by two definitions on day 7 post-transplantation: serum creatinine greater than 265 umol/L (3 mg/dL) or the requirement for dialysis. Donor age and related risk scores (Irish, Schold, KDRI) associated with worse early function, as expected, but histologic features (glomerulosclerosis; pathology risk scores (Remuzzi, MAPI)) correlated with donor age but not with poor function. However, molecular AKI signal, previously defined in kidneys with early injury, was the best single predictor of poor allograft function. The combination of donor age and the AKI signal improved the prediction of poor function. In addition, asssessments of tissue quality particularly donor age, Banff ct, Irish and KDRI scores, showed negative correlative trend with late graft function, whereas the AKI signal did not. Thus donor age and the molecular AKI signal are the main predictors of early impaired function, but have little impact on survival.

Background corr dist: KL-Divergence = 0.3519, L1-Distance = 0.0806, L2-Distance = 0.0201, Normal std = 0.2634

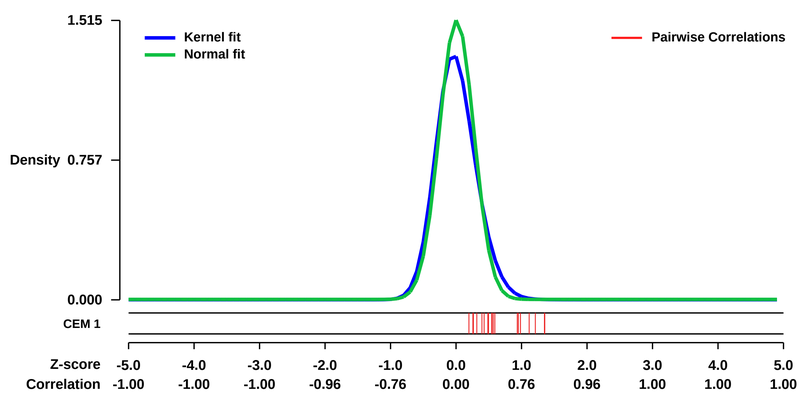

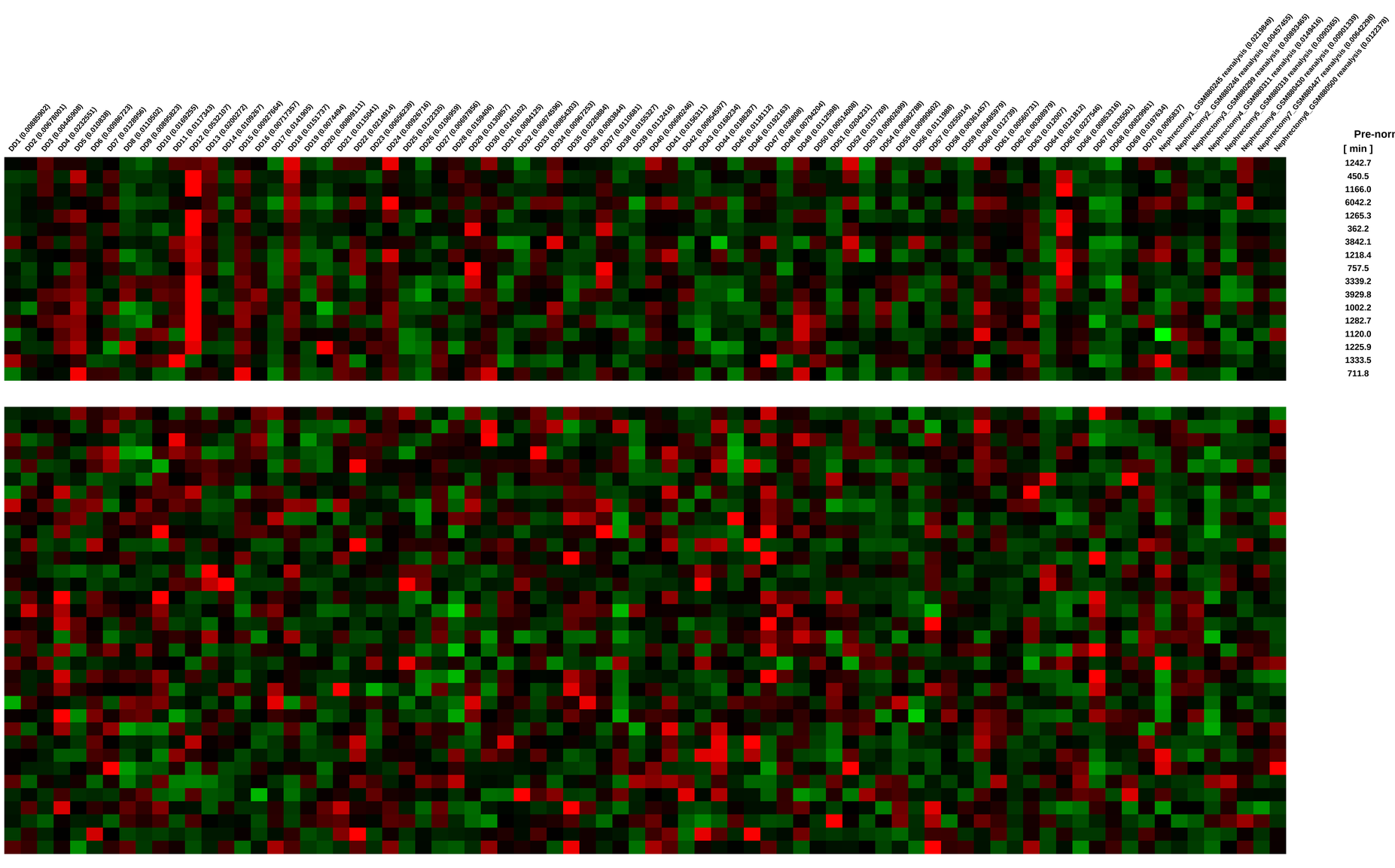

GEO Series "GSE36529" Expression Profiles

Num of samples in this series: 6

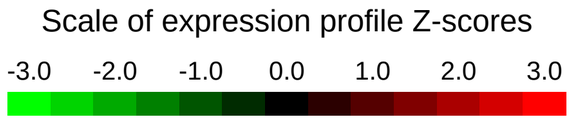

GEO Link:	http://www.ncbi.nlm.nih.gov/geo/query/acc.cgi?acc=GSE36529
Status:	Public on Mar 20 2013
Title:	Expression data from CtBP knockdown MCF-7 cells
Organism:	Homo sapiens
Experiment type:	Expression profiling by array
Platform:	GPL570
Pubmed ID:	23385593
Summary & Design:	**Summary:** CtBP is a global co-repressor by serving as transcriptional factor in multiple pathways. CtBP functioned as transcriptional factor by recruiting other cofactors such as G9a, HDAC1 and PcG proteins. CtBP is found to be over enriched in several type of tumor samples. To dipict the role of CtBP in globally regulating gene expression, we applied gene microarray technology to find out what subgroups of genes are mainly affected. **Overall design:** 6 MCF-7 cell samples, 3 with CtBP knockdown and 3 with control knock down.

Background corr dist: KL-Divergence = 0.0343, L1-Distance = 0.0196, L2-Distance = 0.0004, Normal std = 0.6463

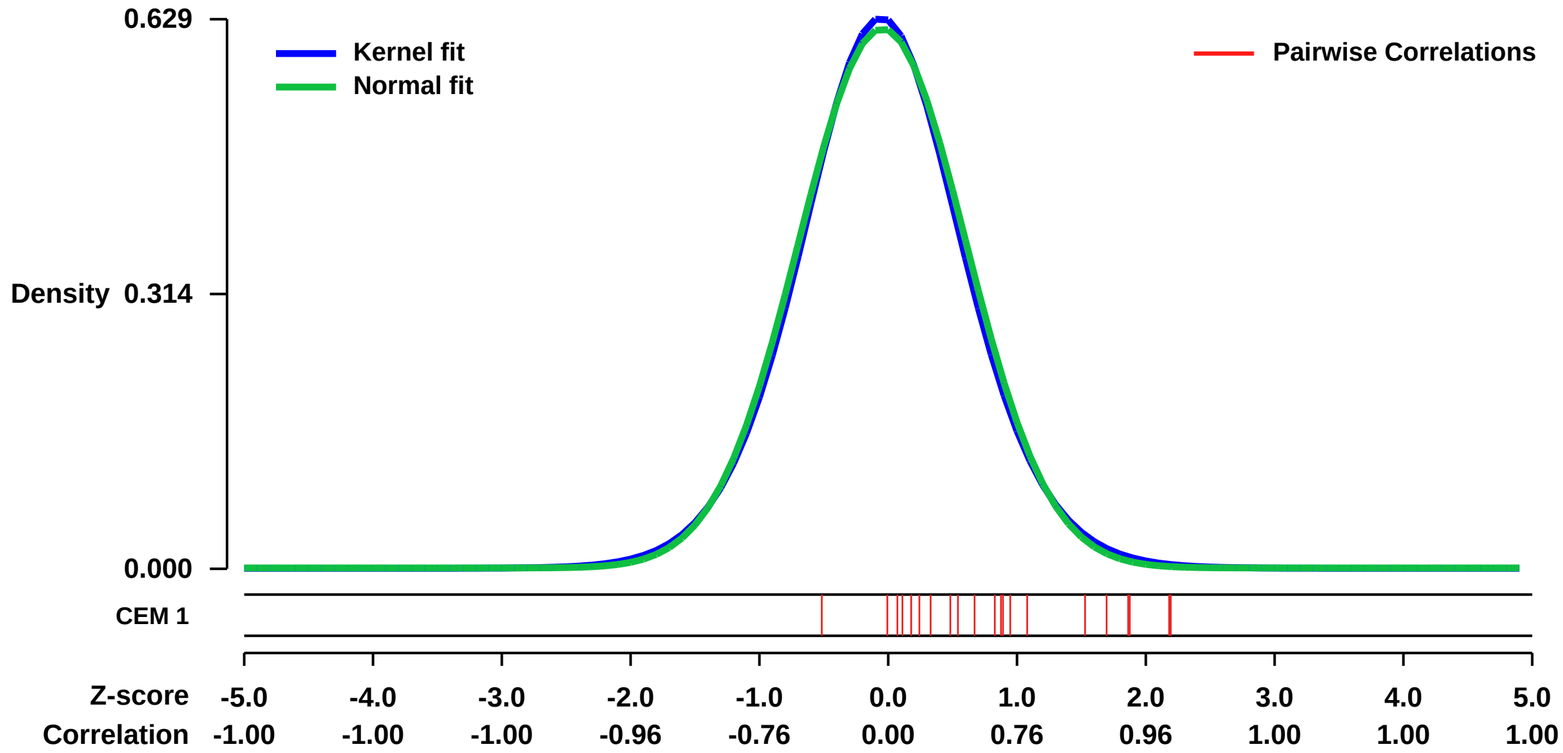

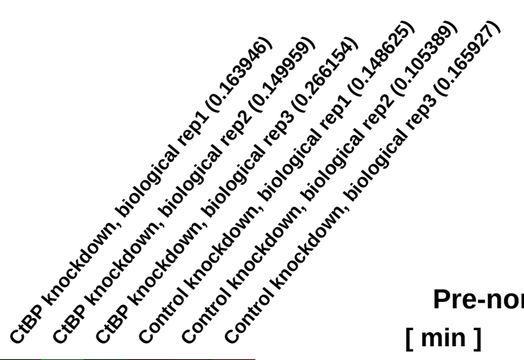

Pre-normalization Quantiles

		[min]	[medium]	[max]
CEM 1 P (S | Z, I) = 1.00 Mean Corr = 0.53753	MANF	3407.6	4593.7	5109.3
	SDF2L1	1515.6	1739.4	2020.4
	CRELD2	2794.2	3546.1	3900.1
	HSPA5	13237.2	21269.2	23541.4
	HYOU1	4663.2	7822.8	9950.2
	PDIA4	1668.0	1977.4	2161.3
	PDIA6	9427.5	10058.4	10824.9
CEM 1 + Top 10 Genes	DNAJB11	2814.2	4065.4	4431.3
	HSP90B1	7975.2	9430.5	12561.0
	PDIA3	8430.5	12029.7	13662.0
	PPIB	22816.1	26422.2	27457.5
	C19orf10	3754.2	4523.8	4788.3
	SLC35B1	4569.5	4655.7	4941.1
	SEC61A1	3178.2	4045.4	4365.1
	RPN1	6602.2	7478.7	8608.1
	DNAJC3	1553.0	2367.9	2399.1
	CDK2AP2	2273.0	2862.4	3774.5
Null module	ARID5B			
	XBP1			
	HNRNPAB			
	SGK1			
	HSPB1			
	DDIT4			
	ARL4D			
	SAP30			
	KIAA0408			
	GPR17			
	HSPH1			
	DNASE1L2			
	SLC5A3			
	GNAS			
	GPR3			
	TNFRSF25			
	TM6SF2			
	MKKS			
	PLEKHF1			
	ZMYM1			
	DOK3			
	FGF20			
	SLC39A2			
	KCNIP2			
	ERRFI1			
	DEDD2			
	CCDC117			
	USP31			
	AHSA2			
	CYS1			
	CNIH2			
	BANP			
	CHORDC1			
	P4HA1			

GEO Series "GSE32984" Expression Profiles

Num of samples in this series: 15

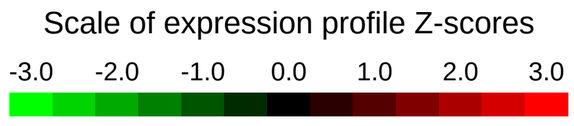

GEO Link:	http://www.ncbi.nlm.nih.gov/geo/query/acc.cgi?acc=GSE32984
Status:	Public on Feb 27 2012
Title:	Gene expression profiling of Human Umbilical Vein Endothelial Cells (HUVEC) after treatment with Erg or control antisense (GeneBloc)
Organism:	Homo sapiens
Experiment type:	Expression profiling by array
Platform:	GPL570
Pubmed ID:	22117042
Summary & Design:	**Summary:** The endothelial transcription factor Erg (Ets Related Gene) plays an important role in homeostasis and angiogenesis by regulating many endothelial functions including survival and junction stability. Here we show that Erg regulates endothelial cell migration. Transcriptome profiling of Erg-deficient endothelial cells (EC) identified 80 genes involved in cell migration as candidate Erg targets, including regulators of the Rho GTPases. Inhibition of Erg expression in human umbilical vein endothelial cells (HUVEC) resulted in decreased migration in vitro, whilst Erg over-expression using adenovirus caused increased migration. Live-cell imaging of Erg-deficient HUVEC showed a reduction in lamellipodia, in line with decreased motility. Both actin and tubulin cytoskeletons were disrupted in Erg-deficient EC, with a dramatic increase in tubulin acetylation. Amongst the most significant microarray hit was the cytosolic histone deacetylase (HDAC)-6, a regulator of cell migration. Rescue experiments confirmed that HDAC6 mediates the Erg-dependent regulation of tubulin acetylation and actin localization. **Overall design:** The functional role of Erg in EC was studied by gene expressing profiling using three separate HUVEC isolates treated with either control antisense or Erg-specific antisense for 24 or 48 hours.

Background corr dist: KL-Divergence = 0.1849, L1-Distance = 0.0373, L2-Distance = 0.0029, Normal std = 0.3440

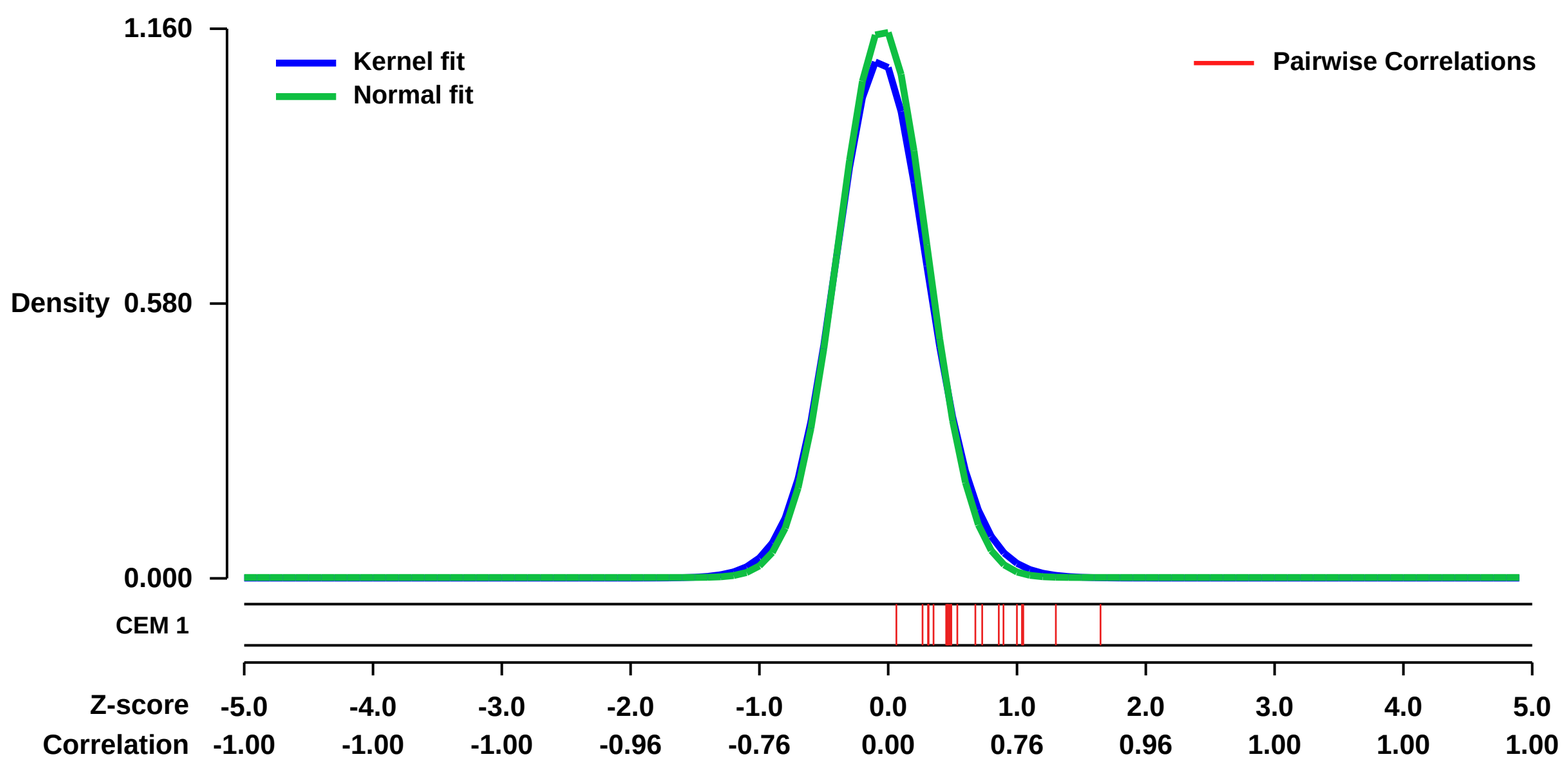

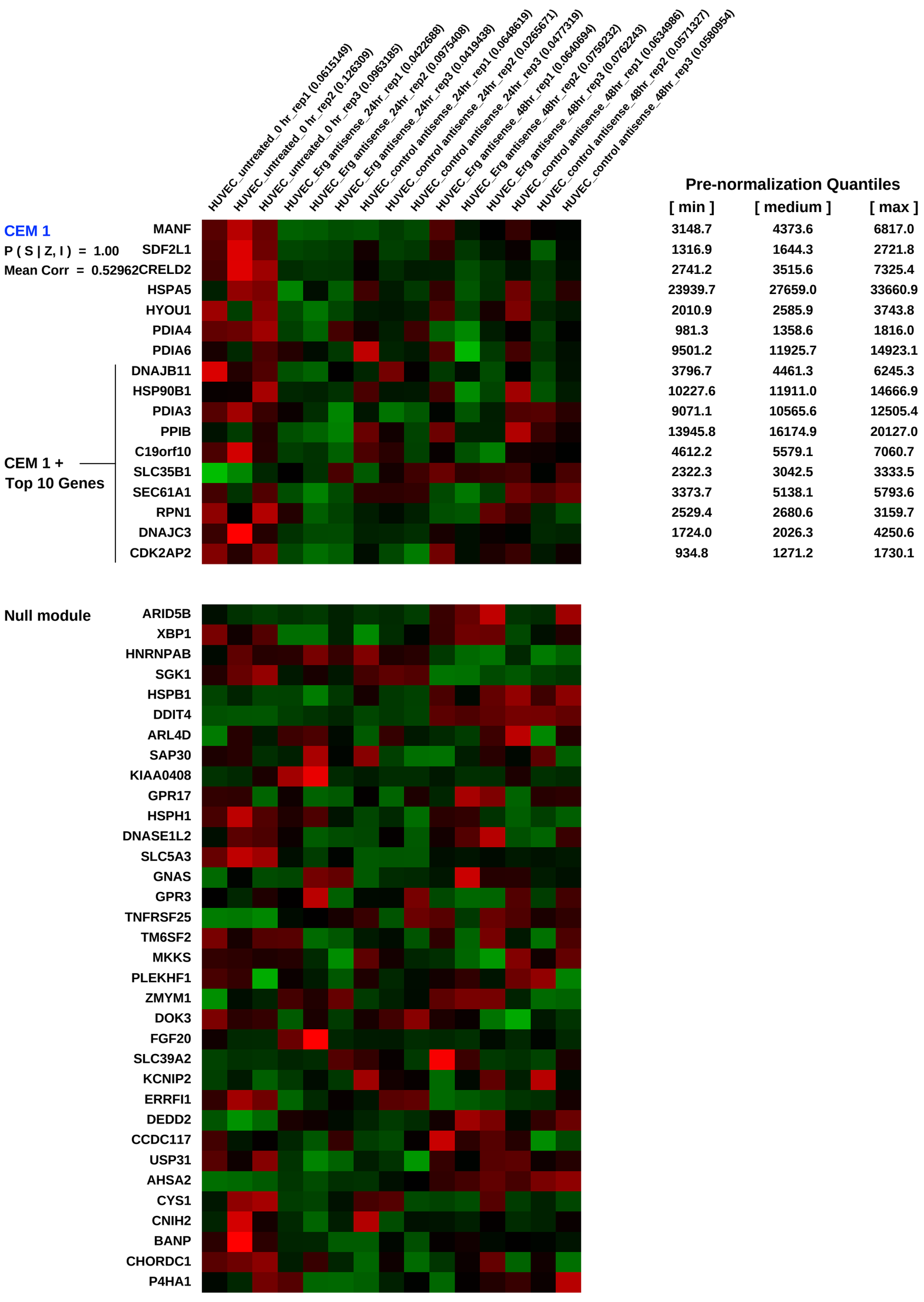

Pre-normalization Quantiles

	[min]	[medium]	[max]
MANF	3148.7	4373.6	6817.0
SDF2L1	1316.9	1644.3	2721.8
CRELD2	2741.2	3515.6	7325.4
HSPA5	23939.7	27659.0	33660.9
HYOU1	2010.9	2585.9	3743.8
PDIA4	981.3	1358.6	1816.0
PDIA6	9501.2	11925.7	14923.1
DNAJB11	3796.7	4461.3	6245.3
HSP90B1	10227.6	11911.0	14666.9
PDIA3	9071.1	10565.6	12505.4
PPIB	13945.8	16174.9	20127.0
C19orf10	4612.2	5579.1	7060.7
SLC35B1	2322.3	3042.5	3333.5
SEC61A1	3373.7	5138.1	5793.6
RPN1	2529.4	2680.6	3159.7
DNAJC3	1724.0	2026.3	4250.6
CDK2AP2	934.8	1271.2	1730.1

GEO Series "GSE7708" Expression Profiles

Num of samples in this series: 14

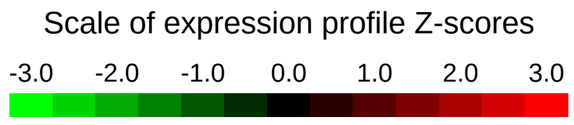

GEO Link:	http://www.ncbi.nlm.nih.gov/geo/query/acc.cgi?acc=GSE7708
Status:	Public on May 05 2007
Title:	Suppression of androgen receptor mediated gene expression by a sequence-specific DNA binding polyamide
Organism:	Homo sapiens
Experiment type:	Expression profiling by array
Platform:	GPL570
Pubmed ID:	17566103

Summary & Design:

Summary:
Androgen Receptor (AR) is essential for the growth and progression of prostate cancer in both hormone-sensitive and hormone-refractory disease. We have designed a sequence-specific DNA binding polyamide (1) that targets the consensus androgen response element (ARE). This polyamide binds the PSA promoter ARE, inhibits androgen-induced expression of PSA and several other AR-regulated genes in cultured prostate cancer cells, and reduces AR occupancy at the PSA promoter and enhancer. Down-regulation of PSA by this polyamide was comparable to that produced by the synthetic anti-androgen bicalutamide (Casodex) at the same concentration. Genome-wide expression analysis reveals that a similar number of transcripts are affected by treatment with the polyamide and with bicalutamide. Direct inhibition of AR-DNA binding by sequence-specific DNA binding small molecules could offer an alternative approach to antagonizing AR activity. A polyamide (2) that targets a different DNA sequence is included as a control.

Keywords: Gene expression changes in cultured LNCaP cells after DHT-stimulation and various treatment conditions

Overall design:
DHT (dihydrotestosterone)-stimulated LNCaP cells that were treatment with polyamide 1, polyamide 2, bicalutamide were compared to control cells that were also DHT-stimulated. Cells not stimulated with DHT were also compared to the DHT-stimulated controls. Three biological replicates were included for each treatment/condition except the no-DHT induced controls, which were in biological duplicate.

Background corr dist: KL-Divergence = 0.1758, L1-Distance = 0.0325, L2-Distance = 0.0019, Normal std = 0.3526

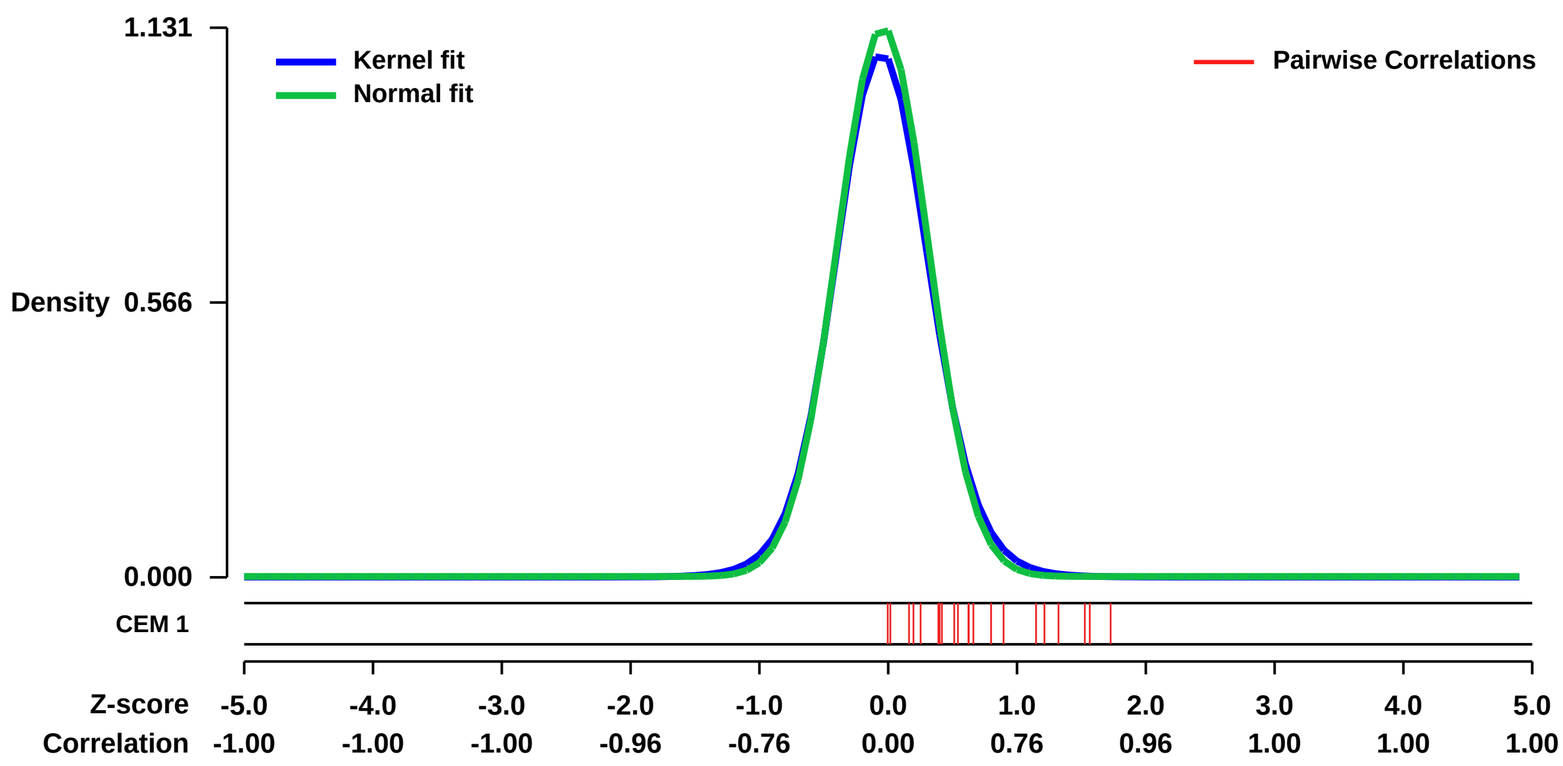

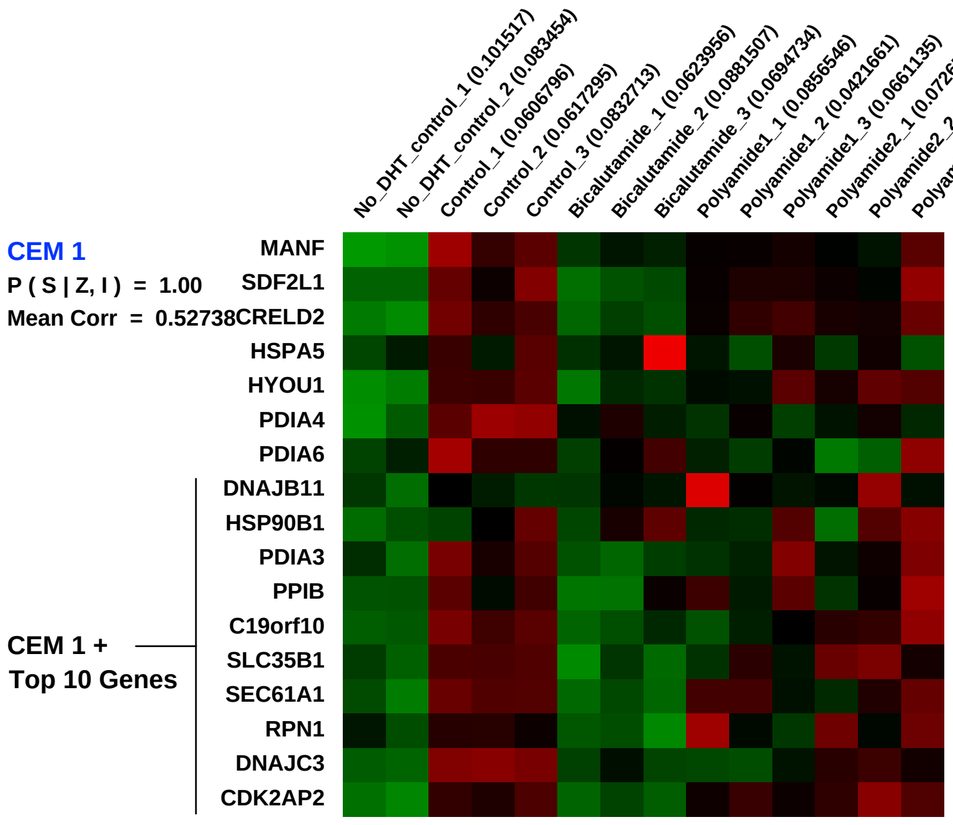

Pre-normalization Quantiles

	[min]	[medium]	[max]
No_DHT_control_1 (0.101517)	5322.2	7136.4	8875.5
No_DHT_control_2 (0.083454)	1176.8	1668.0	2206.4
Control_1 (0.0606796)	2945.2	4972.9	6090.0
Control_2 (0.0617295)	26601.3	28675.7	37630.9
Control_3 (0.0832713)	3159.0	4929.7	5717.8
Bicalutamide_1 (0.0623956)	1139.2	1478.4	1929.6
Bicalutamide_2 (0.0881507)	6828.9	8191.5	10189.7
Bicalutamide_3 (0.0694734)	2713.4	3277.6	4696.4
Polyamide1_1 (0.0856546)	9452.2	10854.6	12563.7
Polyamide1_2 (0.0421661)	17196.5	18883.4	21703.7
Polyamide1_3 (0.0661135)	20736.6	25222.7	30589.0
Polyamide2_1 (0.0726587)	3439.3	4614.2	6280.6
Polyamide2_2 (0.0464305)	2172.7	2796.2	3205.2
Polyamide2_3 (0.076306)	4705.4	6807.1	7786.0
	2672.3	3617.1	4812.3
	2192.0	3112.8	4724.9
	1692.0	2643.8	3248.6

GEO Series "GSE14988" Expression Profiles

Num of samples in this series: 6

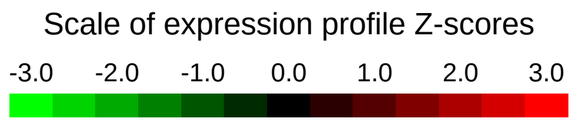

GEO Link:	http://www.ncbi.nlm.nih.gov/geo/query/acc.cgi?acc=GSE14988
Status:	Public on Feb 01 2010
Title:	Expression data from DHT stimulation vs. control in LNCaP cells
Organism:	Homo sapiens
Experiment type:	Expression profiling by array
Platform:	GPL570
Pubmed ID:	20133671
Summary & Design:	**Summary:** Expression data from DHT stimulation vs. control in LNCaP cells **Overall design:** LNCaP cells were maintained in phenol red-free RPMI supplemented with 10% charcoal/dextran stripped FCS for three days before stimulation with 100 nM dihydrotestosterone (DHT) for 48 hours

Background corr dist: KL-Divergence = 0.0432, L1-Distance = 0.0209, L2-Distance = 0.0005, Normal std = 0.6028

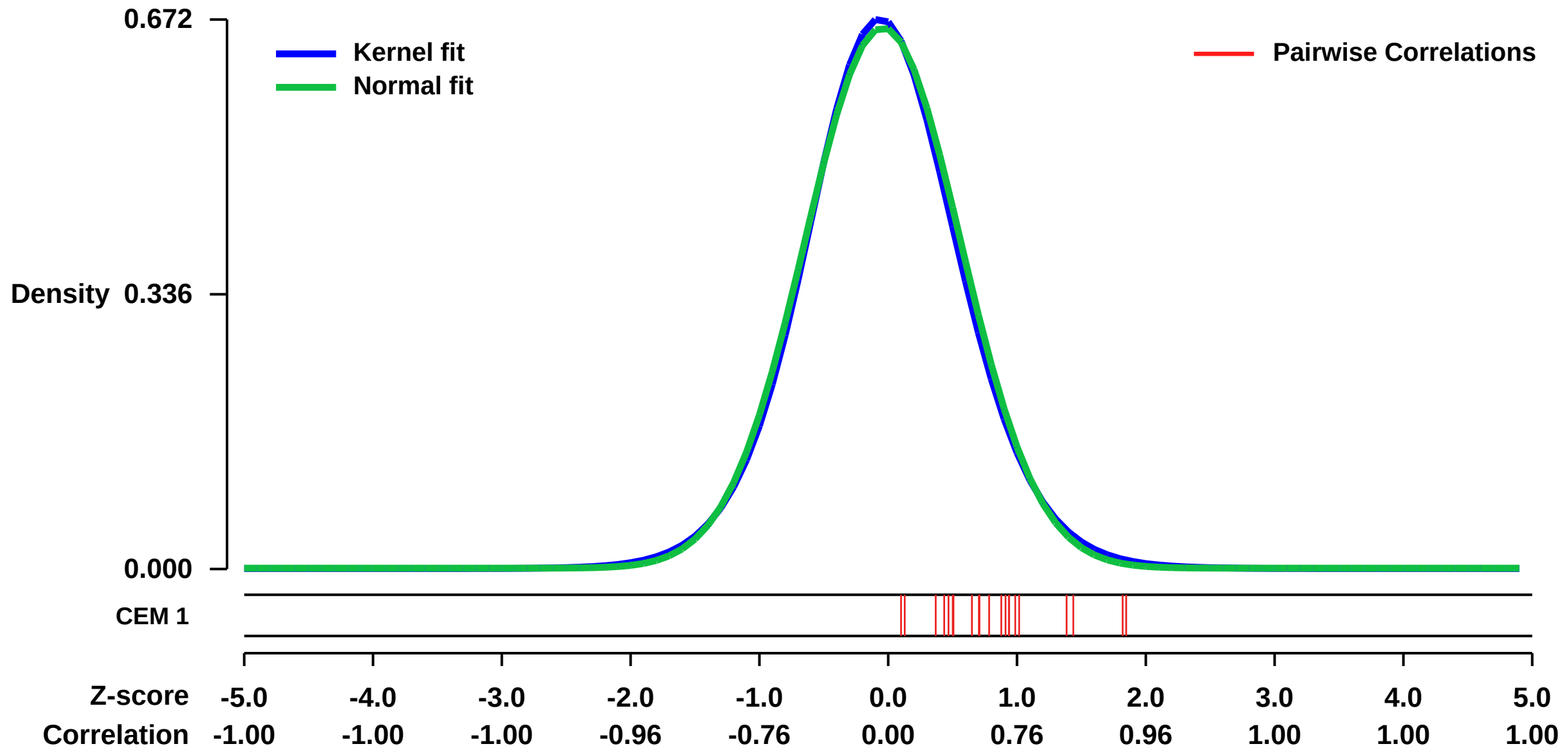

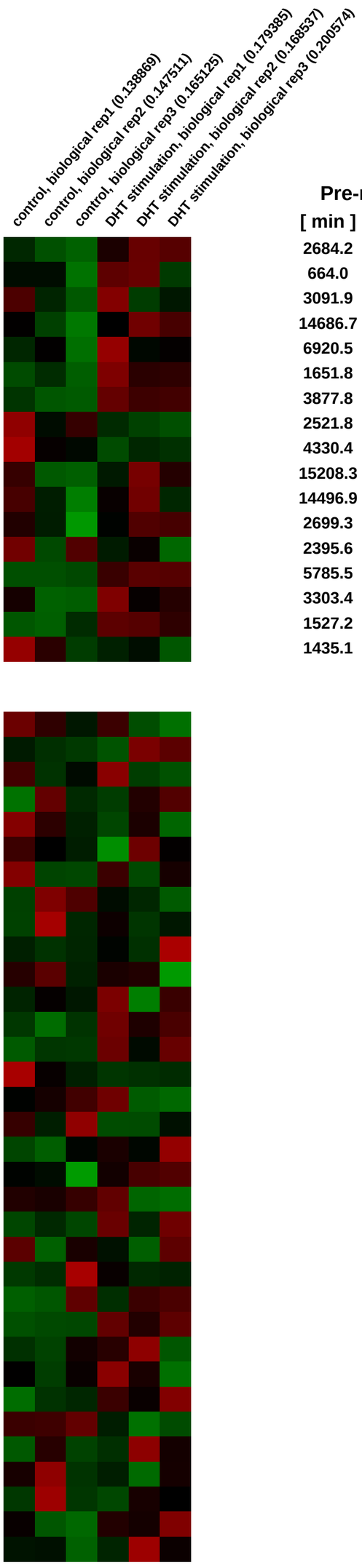

GEO Series "GSE3156" Expression Profiles

Num of samples in this series: 19

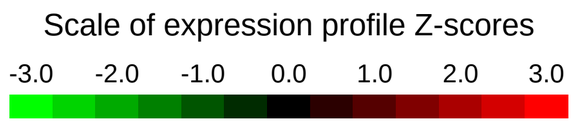

GEO Link:	http://www.ncbi.nlm.nih.gov/geo/query/acc.cgi?acc=GSE3156
Status:	Public on Nov 07 2005
Title:	Breast Cancer Cell Lines
Organism:	Homo sapiens
Experiment type:	Expression profiling by array
Platform:	GPL570
Pubmed ID:	16273092
Summary & Design:	**Summary:** Gene expression analysis on growing breast cancer cell lines. **Keywords: cancer cell line profiles** **Overall design:** see Bild, A. et.al.

Background corr dist: KL-Divergence = 0.3211, L1-Distance = 0.0717, L2-Distance = 0.0149, Normal std = 0.2738

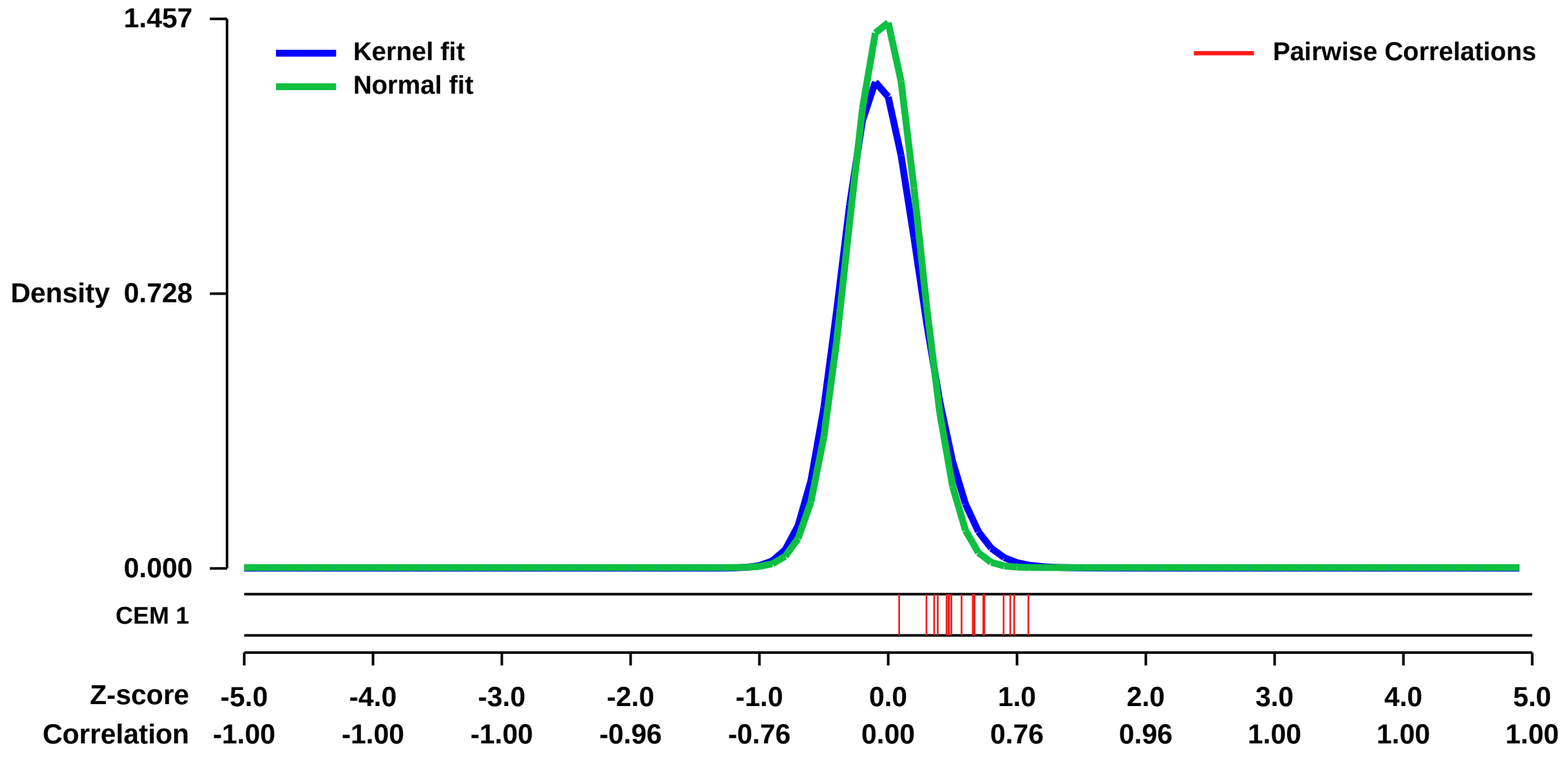

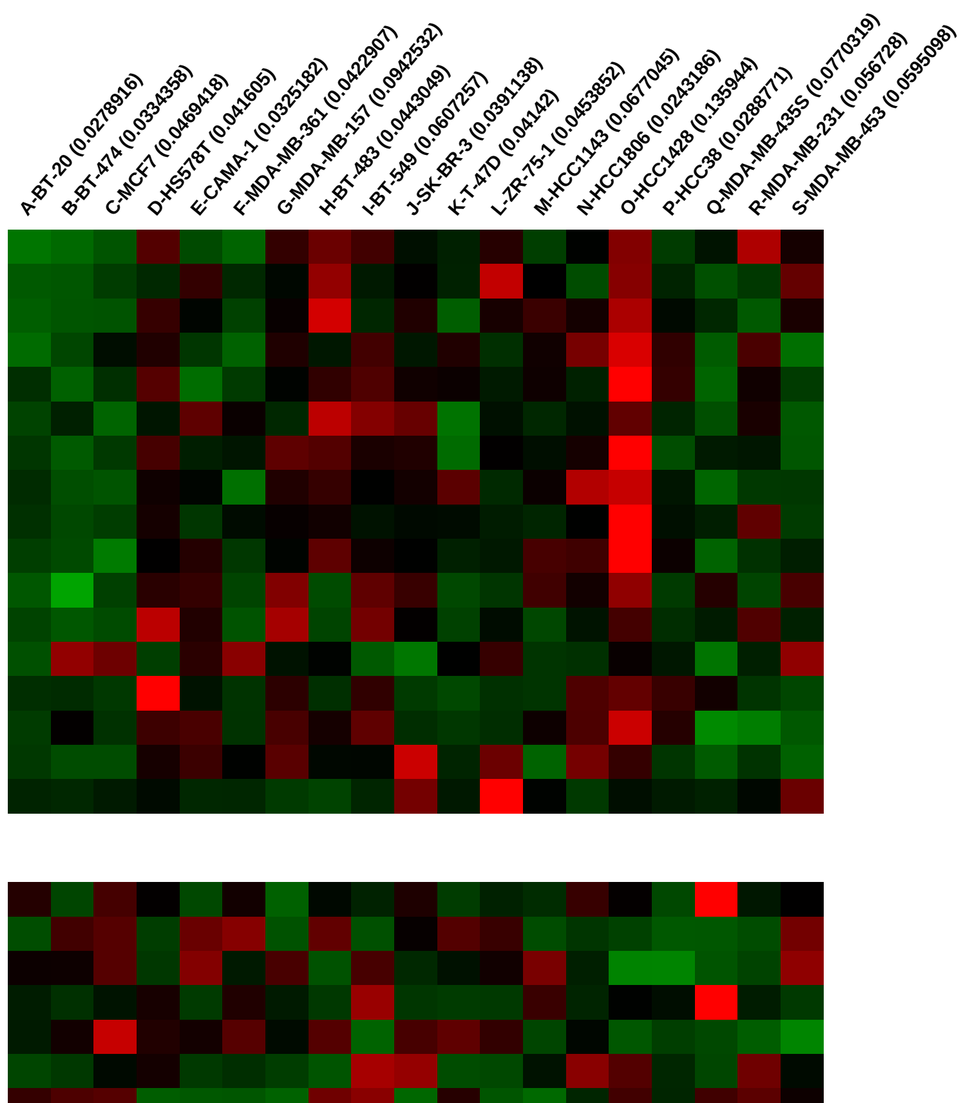

Pre-normalization Quantiles

	[min]	[medium]	[max]
CEM 1			
P (S | Z, I) = 1.00			
Mean Corr = 0.52428			
MANF	1342.0	2822.1	5541.8
SDF2L1	609.0	1349.6	4326.9
CRELD2	1761.2	4597.9	11474.0
HSPA5	7758.6	14097.2	29009.6
HYOU1	4908.8	8919.3	18733.6
PDIA4	1014.4	1733.1	3336.5
PDIA6	2946.1	5648.8	14385.1
CEM 1 + Top 10 Genes			
DNAJB11	4278.7	8111.1	15355.1
HSP90B1	1151.3	3636.4	17869.5
PDIA3	4555.2	11612.4	27343.5
PPIB	4576.7	13117.1	18980.6
C19orf10	1632.6	2819.8	6981.1
SLC35B1	1159.3	3286.6	6761.8
SEC61A1	3163.8	3871.5	12586.0
RPN1	2513.0	5733.4	10329.8
DNAJC3	1180.8	2685.7	6102.8
CDK2AP2	555.1	968.2	4112.4
Null module			
ARID5B			
XBP1			
HNRNPAB			
SGK1			
HSPB1			
DDIT4			
ARL4D			
SAP30			
KIAA0408			
GPR17			
HSPH1			
DNASE1L2			
SLC5A3			
GNAS			
GPR3			
TNFRSF25			
TM6SF2			
MKKS			
PLEKHF1			
ZMYM1			
DOK3			
FGF20			
SLC39A2			
KCNIP2			
ERRFI1			
DEDD2			
CCDC117			
USP31			
AHSA2			
CYS1			
CNIH2			
BANP			
CHORDC1			
P4HA1			

GEO Series "GSE7158" Expression Profiles

Num of samples in this series: 26

Scale of expression profile Z-scores

-3.0 -2.0 -1.0 0.0 1.0 2.0 3.0

GEO Link:	http://www.ncbi.nlm.nih.gov/geo/query/acc.cgi?acc=GSE7158
Status:	Public on Mar 01 2008
Title:	Genome Wide Gene Expression Study of Circulating Monocytes in human with extremely high vs. low bone mass
Organism:	Homo sapiens
Experiment type:	Expression profiling by array
Platform:	GPL570
Pubmed ID:	
Summary & Design:	**Summary:** Peak bone mass (PBM) is an important determinant of osteoporosis. Circulating monocytes may serve as early progenitors of osteoclasts and produce important molecules for bone metabolism. To search for genes functionally important for osteoclastogenesis, we performed a whole genome gene differential expression study of circulating monocytes in human subjects with extremely low vs. high peak bone mass. **Keywords: Circulating monocyte, Gene expression, Peak bone mass, DNA microarray** **Overall design:** We first recruited 878 healthy Chinese females aged 20-45 y with an average of 27.3 y when PBM is attainted and maintained. Then, we distributed the total sample according to the hip Z-score of PBM. From the bottom 100 and top 100 subjects of the PBM phenotypic distribution, we selected 12 subjects (Low-PBM 1-12) and 14 (High-PBM 1-14) with extremely low and high PBM for further DNA microarray experiments.Total RNA was extracted from monocytes

Background corr dist: KL-Divergence = 0.3919, L1-Distance = 0.0774, L2-Distance = 0.0184, Normal std = 0.2500

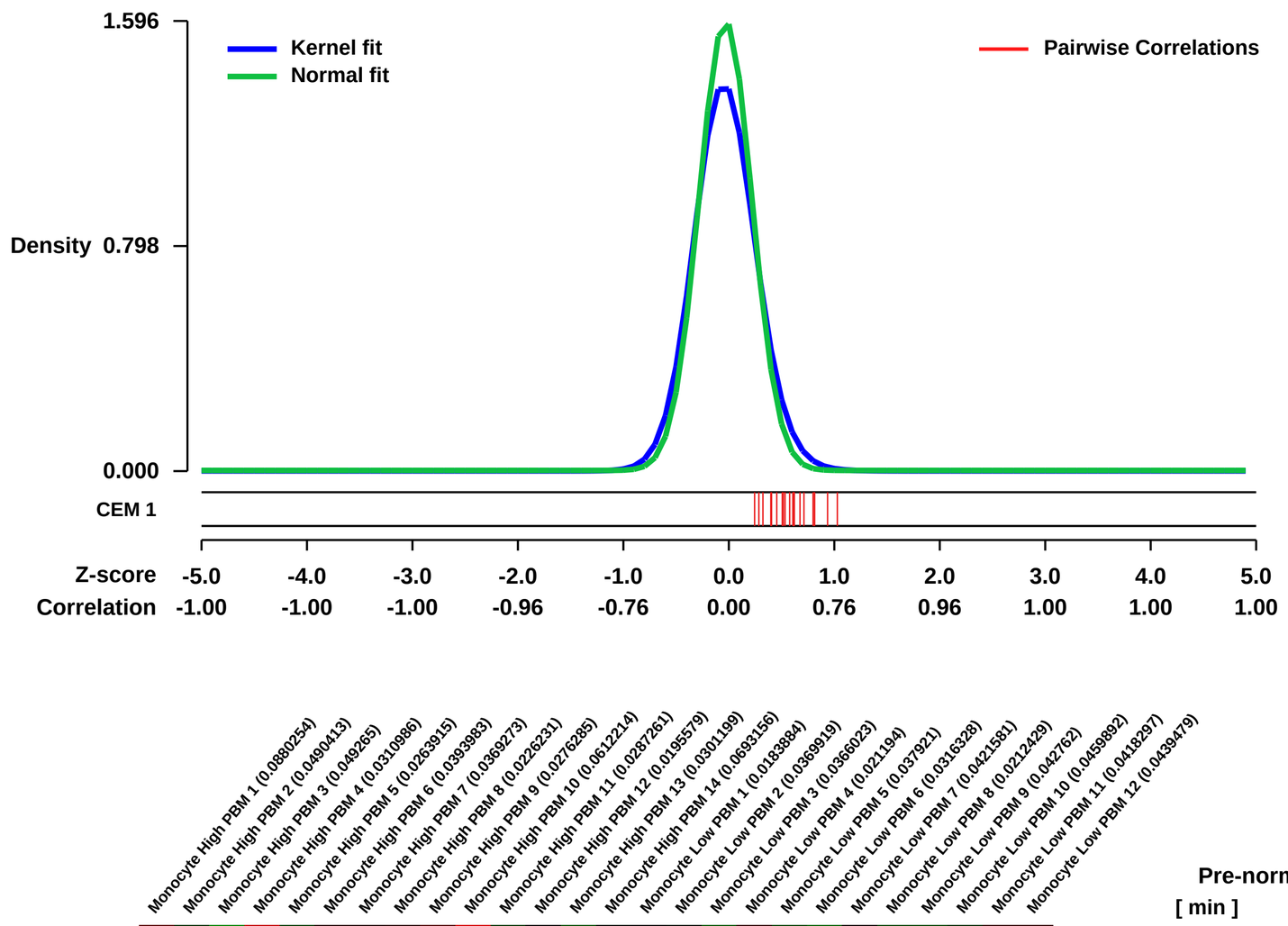

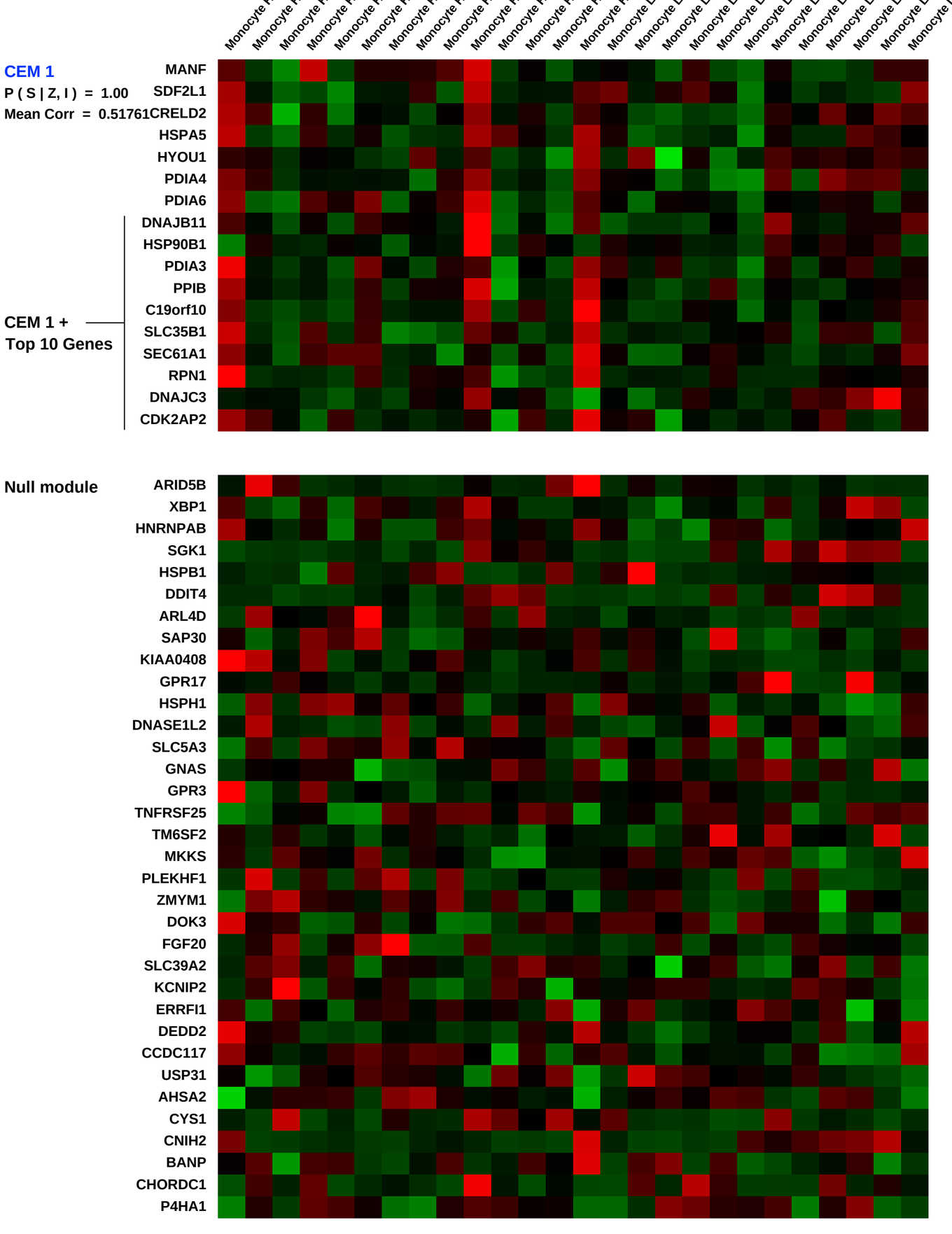

Pre-normalization Quantiles

[min]	[medium]	[max]
889.1	1436.7	2240.9
296.2	505.2	882.5
451.7	1111.7	1724.5
5095.5	7401.0	11819.7
478.2	1512.0	2103.1
407.8	555.7	747.3
2229.8	3035.3	4394.6
1313.9	1748.1	2871.6
738.0	1667.5	4408.8
4171.2	5848.3	8763.7
3877.3	7230.1	12377.8
1294.9	1767.5	3357.9
638.6	861.8	1315.7
928.5	1475.6	2466.6
1113.4	2122.5	4489.4
1378.0	1822.2	2590.9
362.2	729.8	1295.9

GEO Series "GSE49967" Expression Profiles

Num of samples in this series: 12

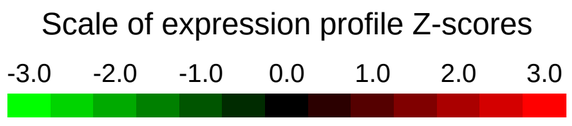

GEO Link:	http://www.ncbi.nlm.nih.gov/geo/query/acc.cgi?acc=GSE49967
Status:	Public on Nov 12 2013
Title:	Variability in functional p53 reactivation by Prima-1Met/APR-246 in Ewing sarcoma
Organism:	Homo sapiens
Experiment type:	Expression profiling by array
Platform:	GPL570
Pubmed ID:	24129240
Summary & Design:	**Summary:** Though p53 mutations are rare in Ewing sarcoma, there is a strong indication that p53-mutant tumors form a particularly bad prognosis group. As such, novel treatment strategies are warranted that would specifically target and eradicate tumor cells containing mutant-p53 in this subset of ES patients. PRIMA-1Met/APR-246 is a small organic molecule which has been shown to restore tumor suppressor function primarily to mutant p53 and to also induce cell death in various cancer cell types. **Overall design:** We analyzed the apoptosis inducibility on Ewing sarcoma cells harbouring different p53 mutations upon exposure to APR-246. Gene expression profiles of three STA-ET-7 cell lines established from the same patient at different stages of the disease was assessed by microarray analysis as these cell lines responded variably to APR-246.

Background corr dist: KL-Divergence = 0.1000, L1-Distance = 0.0225, L2-Distance = 0.0007, Normal std = 0.4431

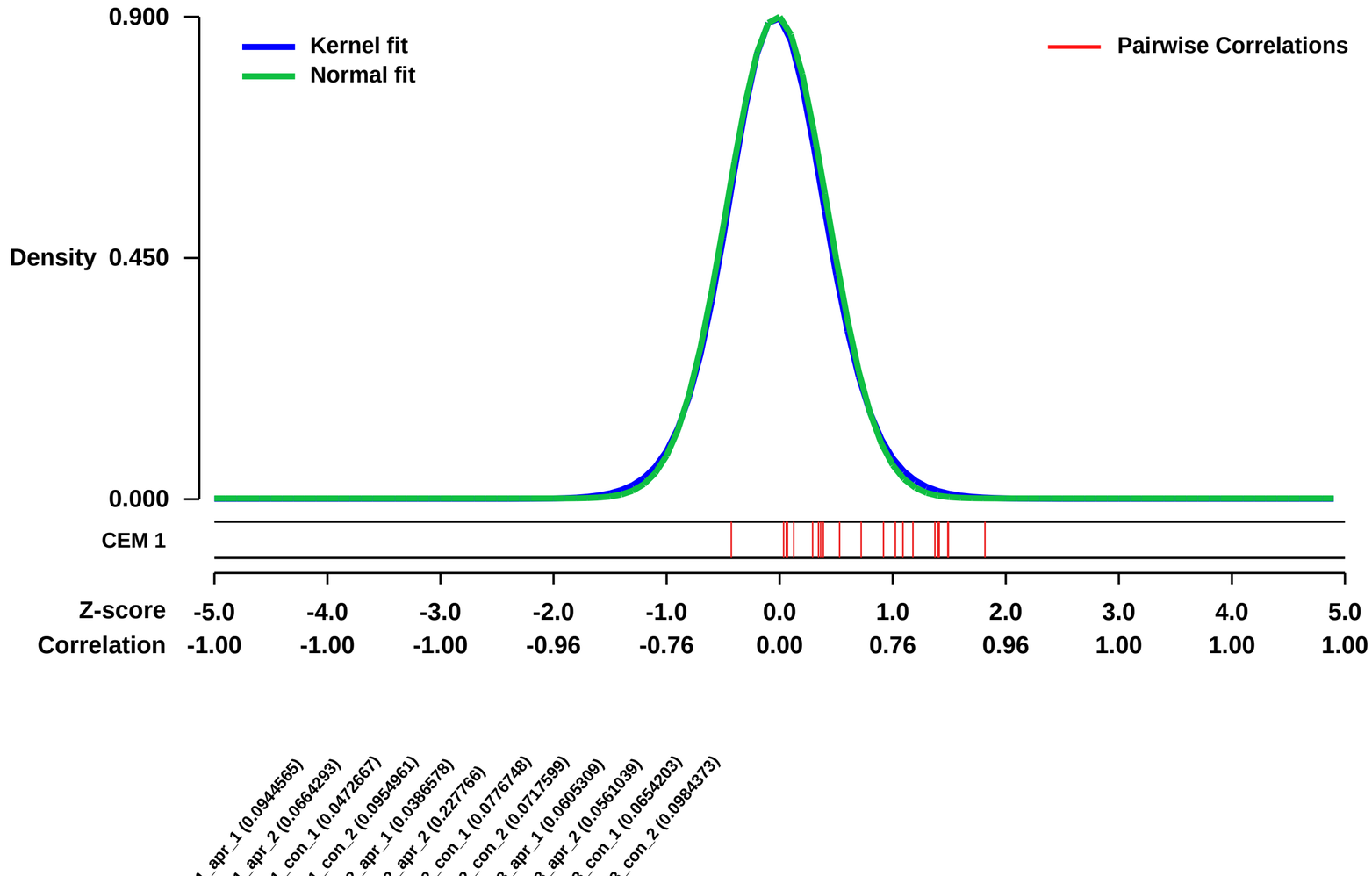

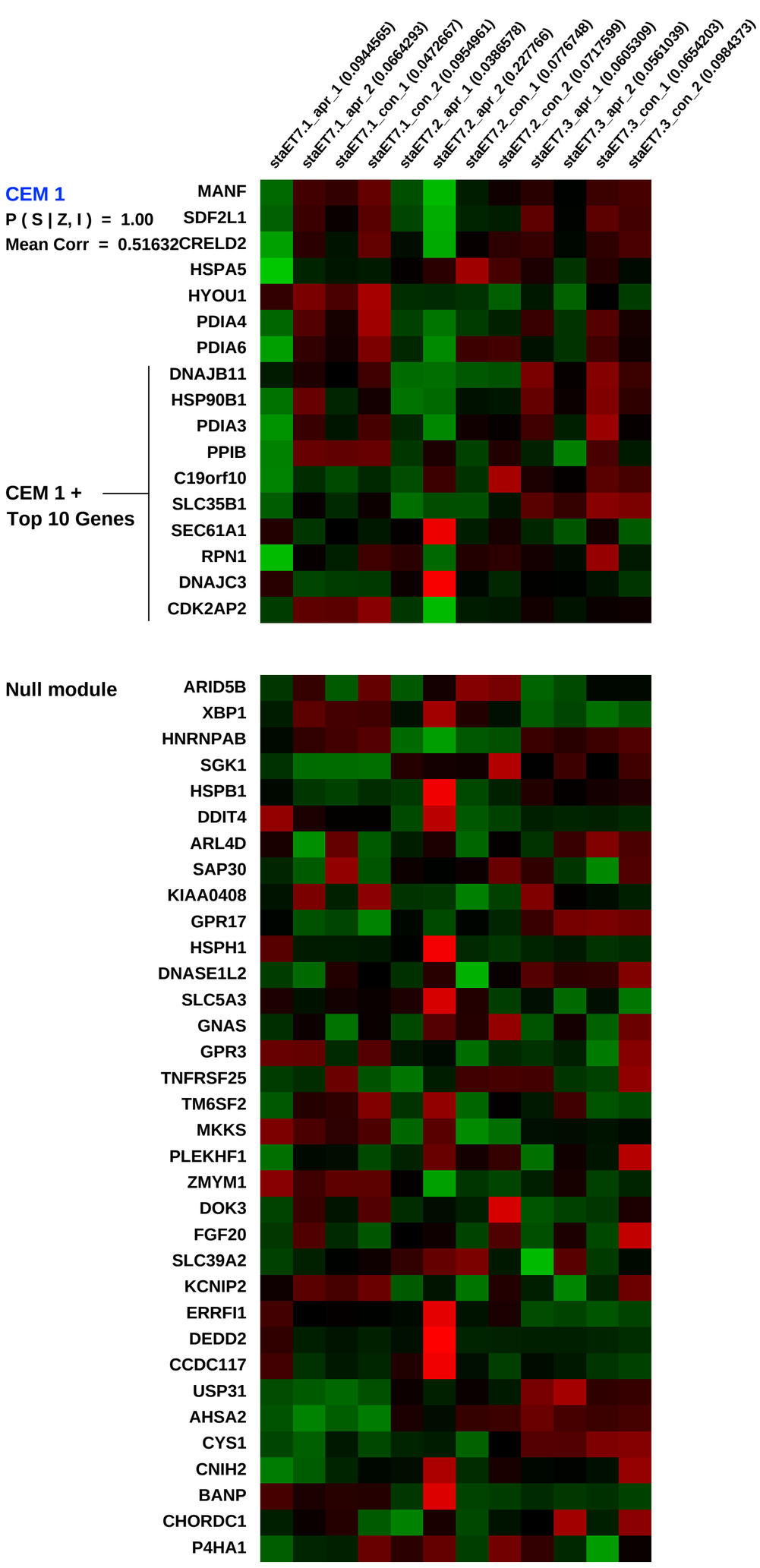

Pre-normalization Quantiles

	[min]	[medium]	[max]
MANF	2026.9	5634.9	6594.7
SDF2L1	303.1	1008.8	1339.8
CRELD2	1281.0	1962.5	2139.1
HSPA5	6969.7	11088.6	14256.4
HYOU1	1115.3	1368.1	1998.5
PDIA4	1958.1	2708.8	3454.4
PDIA6	2650.2	4267.2	5223.9
DNAJB11	3192.4	4712.8	6379.6
HSP90B1	4338.8	6383.8	8253.8
PDIA3	5575.9	7426.7	9206.6
PPIB	6353.8	7678.7	8314.9
C19orf10	2516.8	3127.9	3856.9
SLC35B1	1924.7	2790.0	3737.0
SEC61A1	1736.5	2018.3	2751.6
RPN1	2832.9	3729.1	4293.8
DNAJC3	1557.6	1740.3	2495.6
CDK2AP2	326.2	765.3	1046.5

GEO Series "GSE34942" Expression Profiles

Num of samples in this series: 56

Scale of expression profile Z-scores

-3.0 -2.0 -1.0 0.0 1.0 2.0 3.0

GEO Link: http://www.ncbi.nlm.nih.gov/geo/query/acc.cgi?acc=GSE34942
Status: Public on Sep 05 2014
Title: Gastric cancer subtyping (Singapore Patient Cohort, batch B)
Organism: Homo sapiens
Experiment type: Expression profiling by array
Platform: GPL570
Pubmed ID: 25053715

Summary & Design:

Summary:
Genome-wide mRNA expression profiles of 56 primary gastric tumors from the Singapore patient cohort, batch B. Like many cancers, gastric adenocarcinomas (gastric cancers) show considerable heterogeneity between patients. Thus, there is intense interest in using gene expression profiles to discover subtypes of gastric cancers with particular biological properties or therapeutic vulnerabilities.

Identification of such subtypes could generate insights into the mechanisms of cancer progression or lay the foundation for personalized treatments. Here we report a robust gene-expression-based clustering of a large collection of gastric adenocarcinomas (with GSE15459) from Singaporean patients.

Overall design:
Profiling of 56 primary gastric tumors on Affymetrix GeneChip Human Genome U133 Plus 2.0 Array. All tumors were collected with approvals from the National Cancer Centre, Singapore; the Research Ethics Review Committee; and signed patient informed consent.

Background corr dist: KL-Divergence = 0.4895, L1-Distance = 0.0879, L2-Distance = 0.0263, Normal std = 0.2281

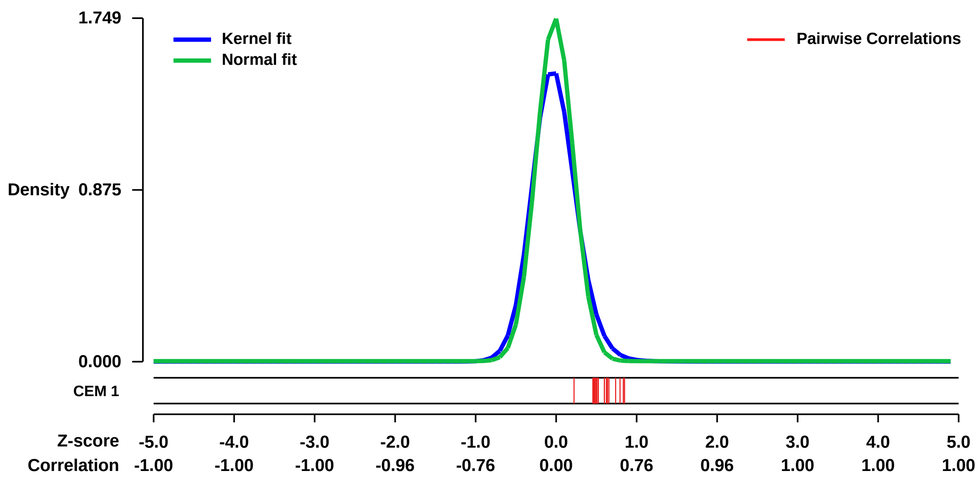

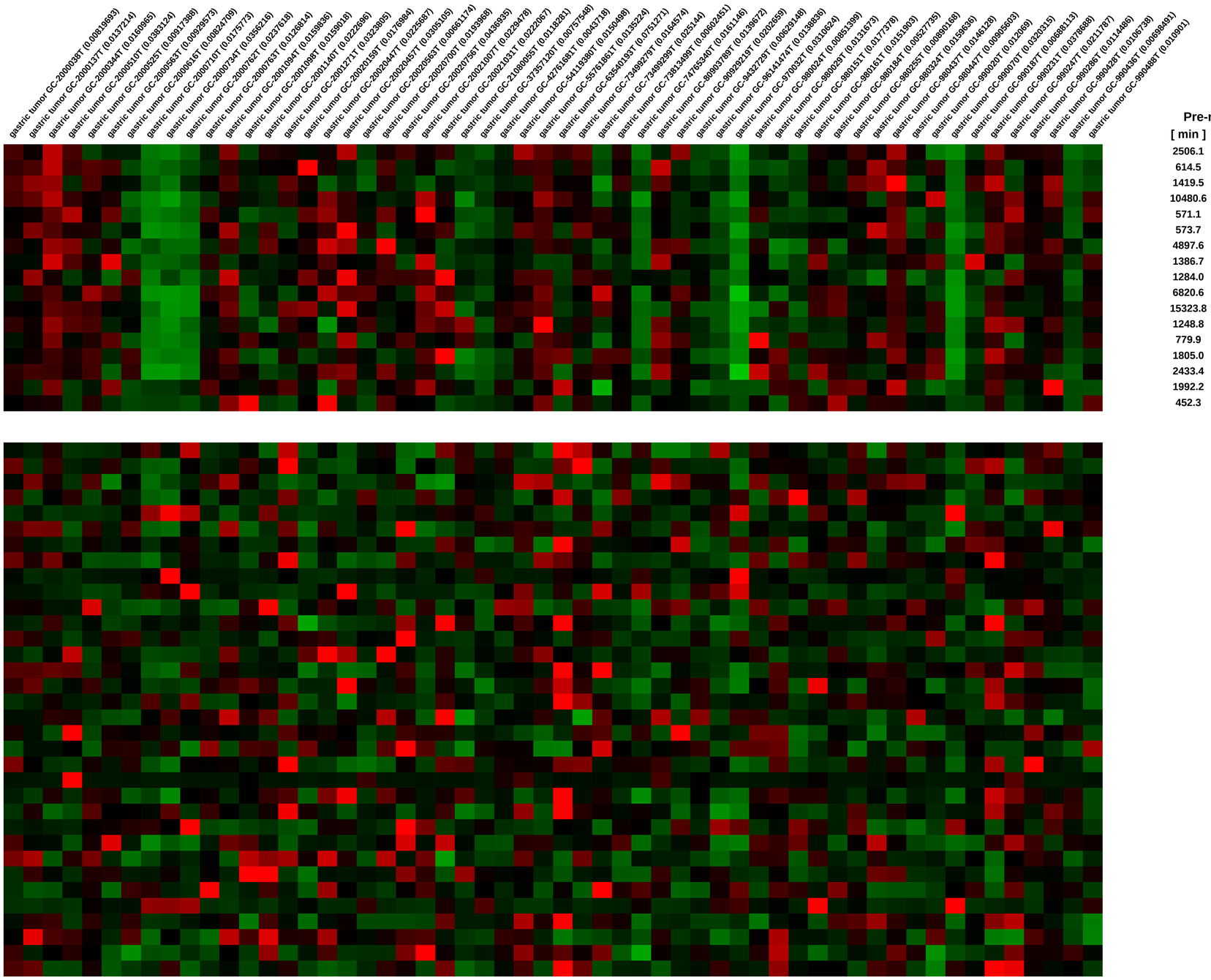

Pre-normalization Quantiles

[min]	[medium]	[max]
2506.1	6029.2	9966.3
614.5	1781.2	5261.0
1419.5	3217.9	7567.4
10480.6	18338.6	28163.7
571.1	1432.1	3441.1
573.7	3112.3	7347.6
4897.6	7943.3	14562.9
1386.7	4454.4	10356.9
1284.0	3020.1	6285.1
6820.6	16925.6	26946.8
15323.8	24491.2	38137.4
1248.8	3259.5	7128.8
779.9	1914.3	4904.1
1805.0	3366.9	6248.8
2433.4	5799.1	8629.7
1992.2	3921.3	7194.6
452.3	940.8	3688.2

GEO Series "GSE58914" Expression Profiles

Num of samples in this series: 12

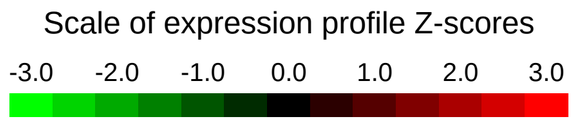

GEO Link:	http://www.ncbi.nlm.nih.gov/geo/query/acc.cgi?acc=GSE58914
Status:	Public on Aug 01 2014
Title:	Expression data from Epstein-Barr virus infection of immortalized normal oral keratinocytes
Organism:	Homo sapiens
Experiment type:	Expression profiling by array
Platform:	GPL570
Pubmed ID:	

Summary & Design:

Summary:
The oral cavity is the persistent reservoir for EBV with lifelong infection of resident epithelial and B cells. Infection of these cell types results in distinct EBV gene expression patterns that are regulated by epigenetic modifications involving DNA methylation and chromatin structure. Such regulation of EBV gene expression relies on viral manipulation of the host epigenetic machinery that may inadvertently result in long-lasting, oncogenic host epigenetic reprogramming. To test this hypothesis in the context of EBV infection of epithelial cells, we established a transient infection model to identify the epigenetic consequences after EBV infection of immortalized normal oral keratinocytes and subsequent viral loss.

With mounting evidence that EBV can induce epigenetic alterations, we developed a transient infection model where a clonal derivative (designated cl1) from a human telomerase immortalized normal oral keratinocyte (NOK) cell line was infected with a recombinant Akata EBV carrying neomycin resistance and GfP cassette in place of the BXLF1 open reading frame. Infected cells were passaged ten times, and then selection pressure was removed for an additional ten passages to allow for viral loss. Three transiently-infected EBV-negative clones were identified by single cell cloning (designated cl1, cl3, cl4). Uninfected parental clone and cells transfected with PTRUF5 plasmid were passaged alongside the transiently-infected clones. The transcription profiles were analyzed using Affymetrix microarray U133Plus2.0 arrays in duplicate.

Overall design:
NOK cells were single cell cloned (designated as cl1) and EBV infected by co-culture with a recombinant Akata EBV strain carrying neomcycin resistance and GFP expression cassette in place of EBV BXLF1. Cells were selected with 350 ug/ml G418. As a selection control, cells were transfected a plasmid carrying a neomycin resistance cassette. Cells were passaged 10 times with G418, followed by removal of selection pressure. After an additional 10 passages, cells were single cell cloned and the presence of EBV was determined by various methods. Three clones were identified as being EBV negative and said to be transiently infected. Uninfected parental and vector transfected cells were passaged in the same manner and also single cell cloned.

Background corr dist: KL-Divergence = 0.1799, L1-Distance = 0.0445, L2-Distance = 0.0044, Normal std = 0.3461

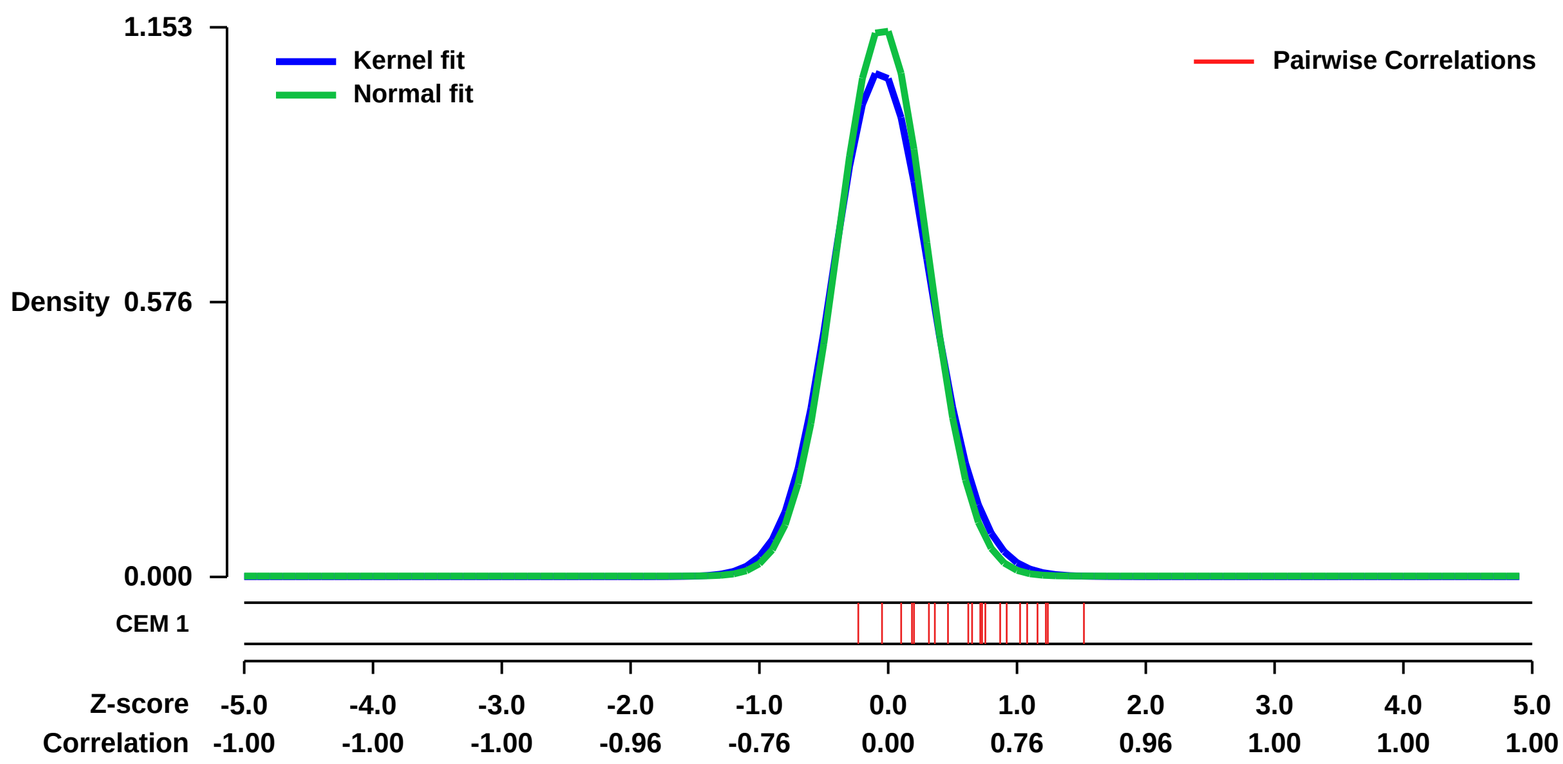

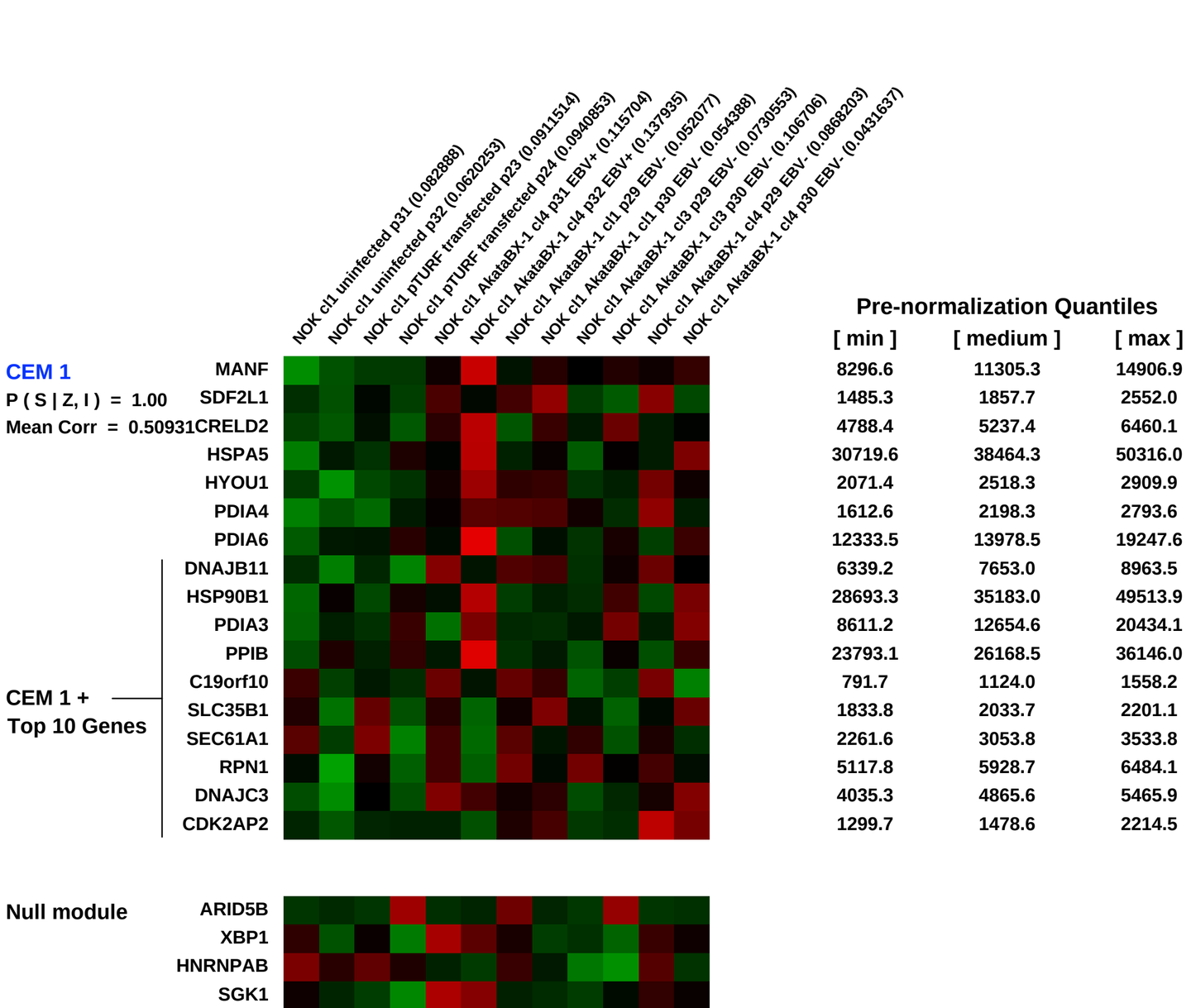

GEO Series "GSE31546" Expression Profiles

Num of samples in this series: 17

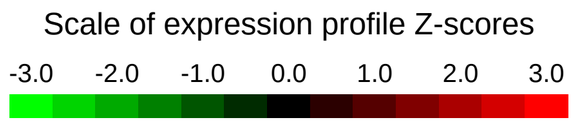

GEO Link:	**http://www.ncbi.nlm.nih.gov/geo/query/acc.cgi?acc=GSE31546**
Status:	**Public on Sep 06 2011**
Title:	**UMCCC Primary Lung Cancer Specimens**
Organism:	**Homo sapiens**
Experiment type:	**Expression profiling by array**
Platform:	**GPL570**
Pubmed ID:	
Summary & Design:	**Summary:** **Develop an EGFR mutation gene expression signature to aid in predicting response and clinical outcome and to identify genes associated with the EGFR-dependent phenotype** **Overall design:** **17 primary lung adenocarcinomas were analyzed with Affymetrix U133-plus2**

Background corr dist: **KL-Divergence = 0.2543, L1-Distance = 0.0590, L2-Distance = 0.0091, Normal std = 0.3012**

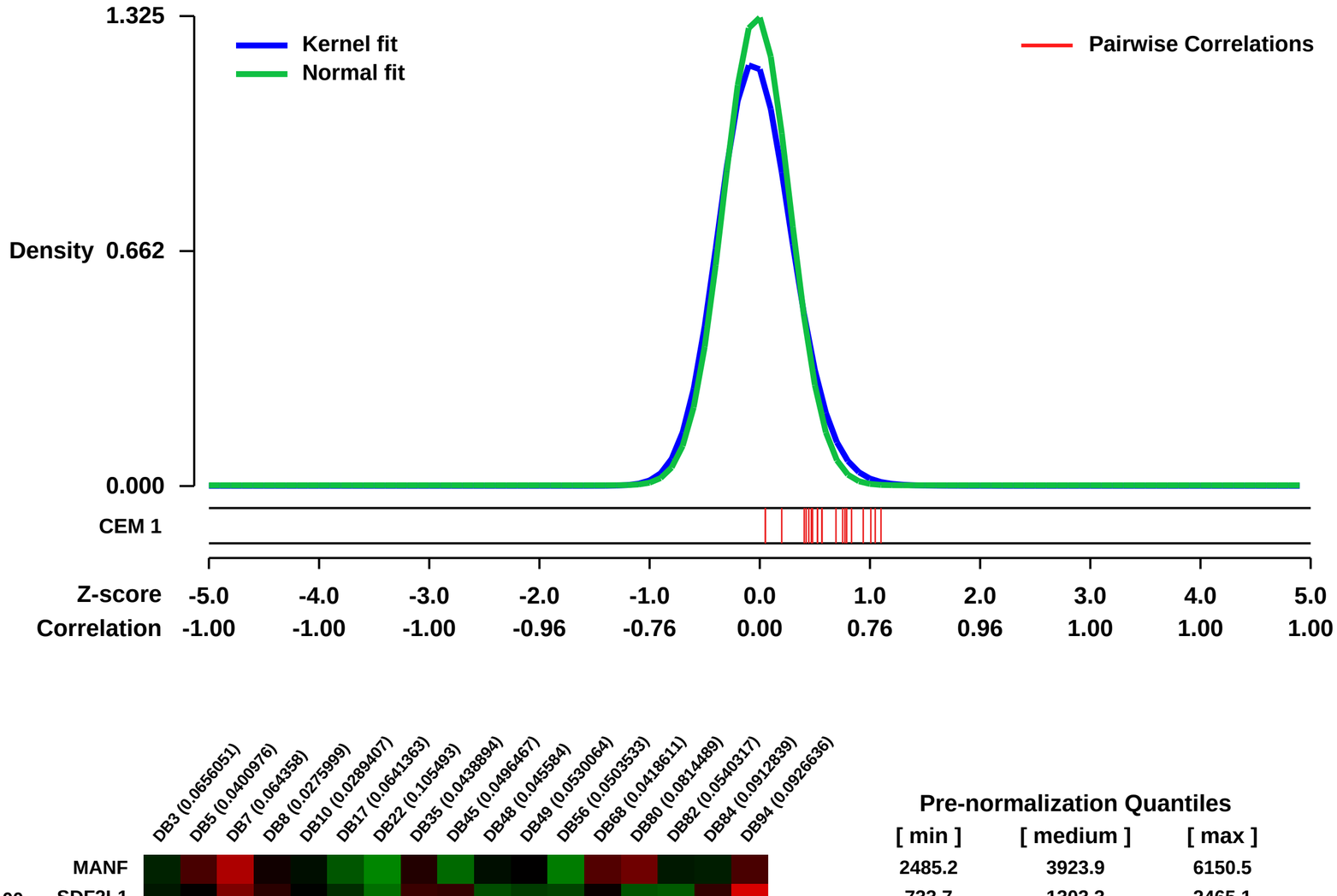

Pre-normalization Quantiles

		[min]	[medium]	[max]
CEM 1	**MANF**	**2485.2**	**3923.9**	**6150.5**
P (S | Z, I) = 1.00	**SDF2L1**	**733.7**	**1303.3**	**2465.1**
Mean Corr = 0.50798	**CRELD2**	**2010.9**	**4389.5**	**8120.8**
	HSPA5	**11373.7**	**12836.9**	**20274.9**
	HYOU1	**1551.1**	**2457.2**	**4559.6**
	PDIA4	**912.5**	**1381.0**	**3067.4**
	PDIA6	**3613.4**	**5601.0**	**8208.0**
CEM 1 + Top 10 Genes	**DNAJB11**	**2424.7**	**3475.0**	**6021.0**
	HSP90B1	**629.9**	**1052.1**	**3207.9**
	PDIA3	**4264.1**	**7342.8**	**13275.5**
	PPIB	**4479.5**	**8087.5**	**13563.2**
	C19orf10	**2208.9**	**3065.9**	**8234.2**
	SLC35B1	**2148.3**	**2761.5**	**4789.9**
	SEC61A1	**2061.0**	**2800.1**	**4890.5**
	RPN1	**1980.3**	**3098.6**	**5306.0**
	DNAJC3	**2334.9**	**4720.4**	**6991.9**
	CDK2AP2	**723.6**	**1190.5**	**2752.4**
Null module	**ARID5B**			
	XBP1			
	HNRNPAB			
	SGK1			
	HSPB1			
	DDIT4			
	ARL4D			
	SAP30			
	KIAA0408			
	GPR17			
	HSPH1			
	DNASE1L2			
	SLC5A3			
	GNAS			
	GPR3			
	TNFRSF25			
	TM6SF2			
	MKKS			
	PLEKHF1			
	ZMYM1			
	DOK3			
	FGF20			
	SLC39A2			
	KCNIP2			
	ERRFI1			
	DEDD2			
	CCDC117			
	USP31			
	AHSA2			
	CYS1			
	CNIH2			
	BANP			
	CHORDC1			
	P4HA1			

GEO Series "GSE40404" Expression Profiles

Num of samples in this series: 7

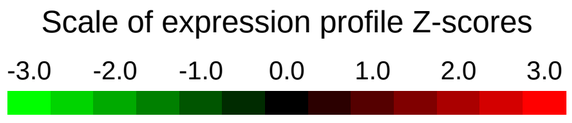

GEO Link:	http://www.ncbi.nlm.nih.gov/geo/query/acc.cgi?acc=GSE40404
Status:	Public on Aug 31 2012
Title:	Expression data from normal human fibroblasts expressing prelamin A or progerin, untreated or treated with farnesyltransferase inhibitor (FTI)
Organism:	Homo sapiens
Experiment type:	Expression profiling by array
Platform:	GPL570
Pubmed ID:	22948034
Summary & Design:	**Summary:** We compared the transcriptomes of isogenic diploid fibroblasts expressing progerin or elevated levels of wild-type prelamin A with that of wild-type fibroblasts. We subsequently used the reversion towards normal of two phenotypes, reduced cell growth and dismorphic nuclei, by treatment with farnesyltransferase inhibitor (FTI) or overexpression of ZMPSTE24, as a filtering strategy to identify genes linked to the onset of these two phenotypes. **Overall design:** We carried out microarray analyses of gene expression profiling in isogenic fibroblasts lines to identify the subset of genes whose expression patterns are strongly altered upon expression of progerin or elevated levels of wild-type lamin A. A filtering strategy was then used to identify potential key effectors. We searched for genes whose expression was reverted towards normal by treatment with farnesyl transferase inibitors (FTI) in both cell lines for 48 hours, or by overexpression of ZMPSTE24 in cells with elevated levels of prelamin A, conditions that improve cell proliferation and leads to a significant decrease in nuclear membrane abnormalities.

Background corr dist: KL-Divergence = 0.0576, L1-Distance = 0.0220, L2-Distance = 0.0007, Normal std = 0.5398

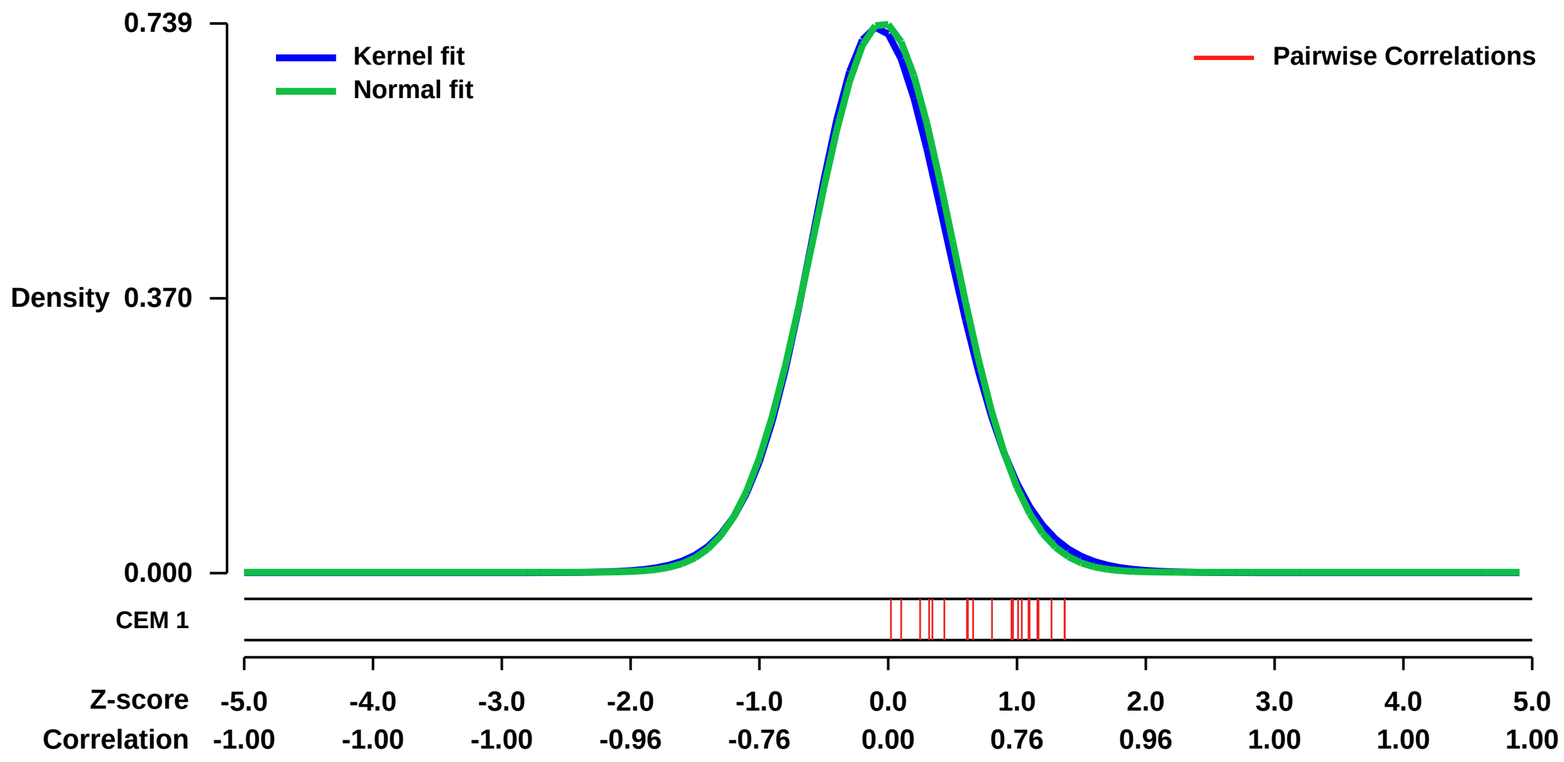

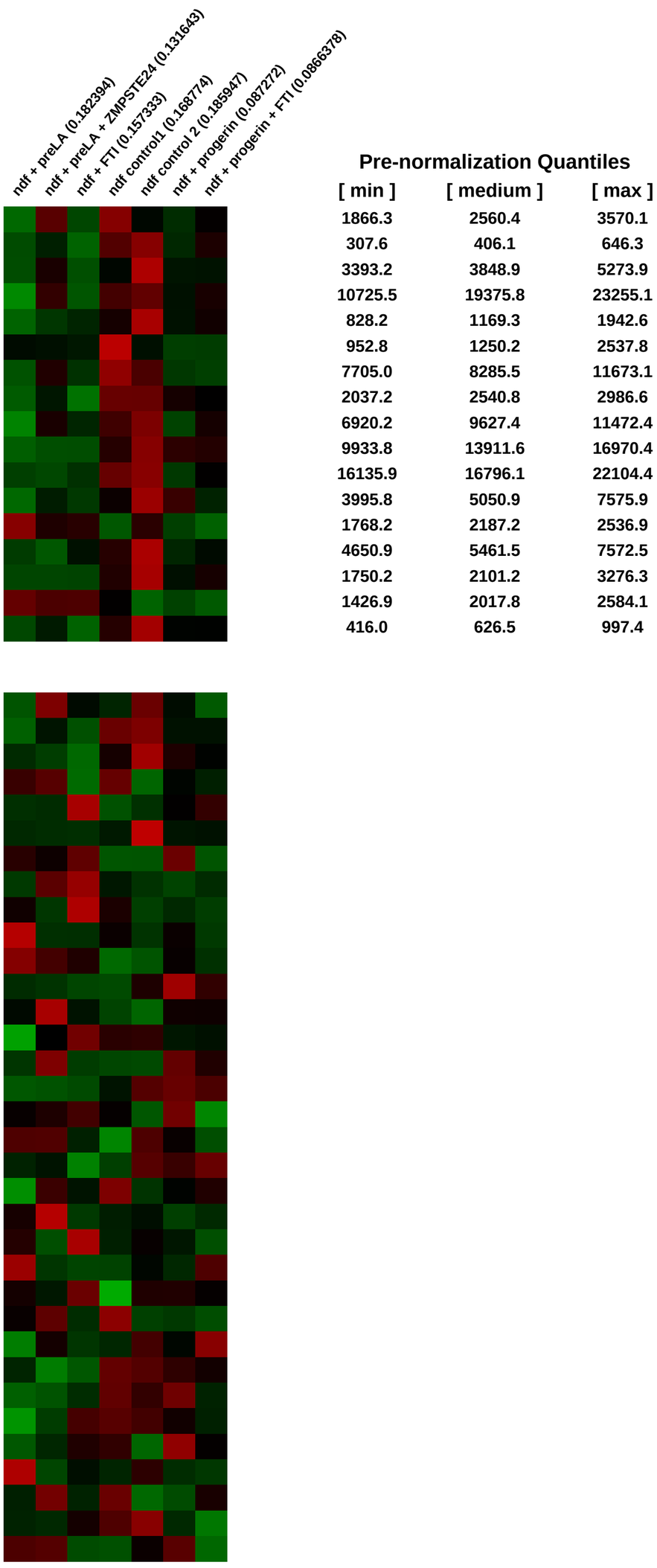

GEO Series "GSE13637" Expression Profiles

Num of samples in this series: 30

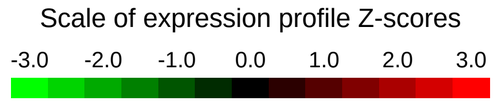

GEO Link:	http://www.ncbi.nlm.nih.gov/geo/query/acc.cgi?acc=GSE13637
Status:	Public on Dec 31 2009
Title:	Influenza virus infected HUVEC
Organism:	Homo sapiens
Experiment type:	Expression profiling by array
Platform:	GPL570
Pubmed ID:	21106851
Summary & Design:	**Summary:** To delineate specific patterns of signaling networks activated by H5N1 we used a comparative systems biology approach analyzing gene expression in endothelial cells infected with three different human and avian influenza strains of high and low pathogenicity. **Overall design:** HUVECs were infected with either PR8, FPV or H5N1 virus. We used wildtype HUVEC or HUVEC transfected with a dominant negative mutant of IKK2 (block of the NF-kB signaling pathway). In case of FPV infections we also blocked p38 MAP kinase with an SB-inhibitor.

Background corr dist: KL-Divergence = 0.3128, L1-Distance = 0.0593, L2-Distance = 0.0093, Normal std = 0.2762

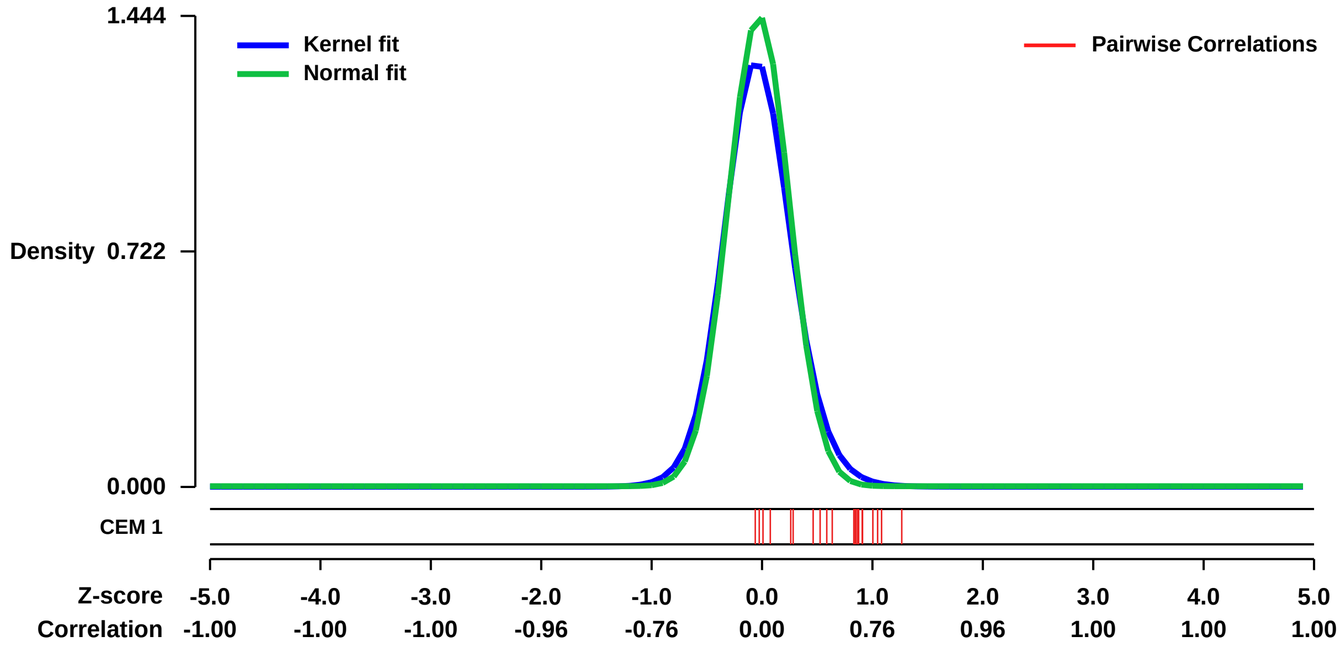

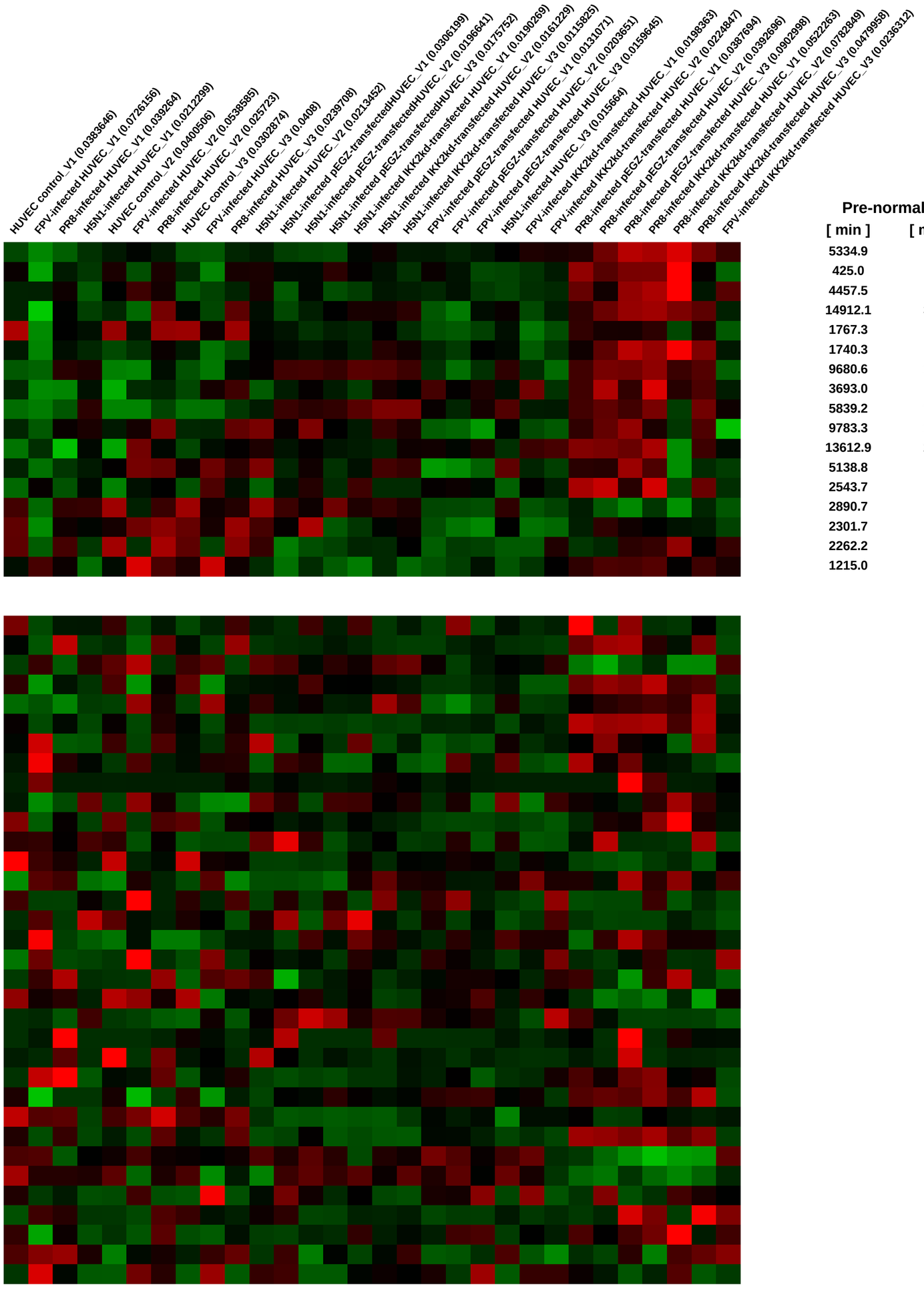

	Pre-normalization Quantiles		
	[min]	[medium]	[max]
MANF	5334.9	7459.2	12032.3
SDF2L1	425.0	1444.0	3204.5
CRELD2	4457.5	5516.7	10102.6
HSPA5	14912.1	30788.7	44074.9
HYOU1	1767.3	3559.8	6283.2
PDIA4	1740.3	2949.0	5602.0
PDIA6	9680.6	14976.6	18641.9
DNAJB11	3693.0	5453.3	7756.9
HSP90B1	5839.2	18932.1	28744.4
PDIA3	9783.3	17789.2	23371.7
PPIB	13612.9	23554.6	32861.7
C19orf10	5138.8	6886.7	8586.1
SLC35B1	2543.7	3427.1	5038.4
SEC61A1	2890.7	4900.5	6676.8
RPN1	2301.7	3860.4	5795.3
DNAJC3	2262.2	2855.3	4205.8
CDK2AP2	1215.0	2313.7	4220.1

GEO Series "GSE3744" Expression Profiles

Num of samples in this series: 47

Scale of expression profile Z-scores

-3.0 -2.0 -1.0 0.0 1.0 2.0 3.0

GEO Link:	http://www.ncbi.nlm.nih.gov/geo/query/acc.cgi?acc=GSE3744
Status:	Public on Feb 09 2006
Title:	Human breast tumor expression
Organism:	Homo sapiens
Experiment type:	Expression profiling by array
Platform:	GPL570
Pubmed ID:	20400965
Summary & Design:	**Summary:** Gene expression for 47 human breast tumor cases; (* normalized by GCRMA for global expression analysis) Keywords: Type **Overall design:** Gene expression of human breast tumor by Affymetrix Human Genome U133 Plus 2.0 Array

Background corr dist: KL-Divergence = 0.5069, L1-Distance = 0.0820, L2-Distance = 0.0244, Normal std = 0.2320

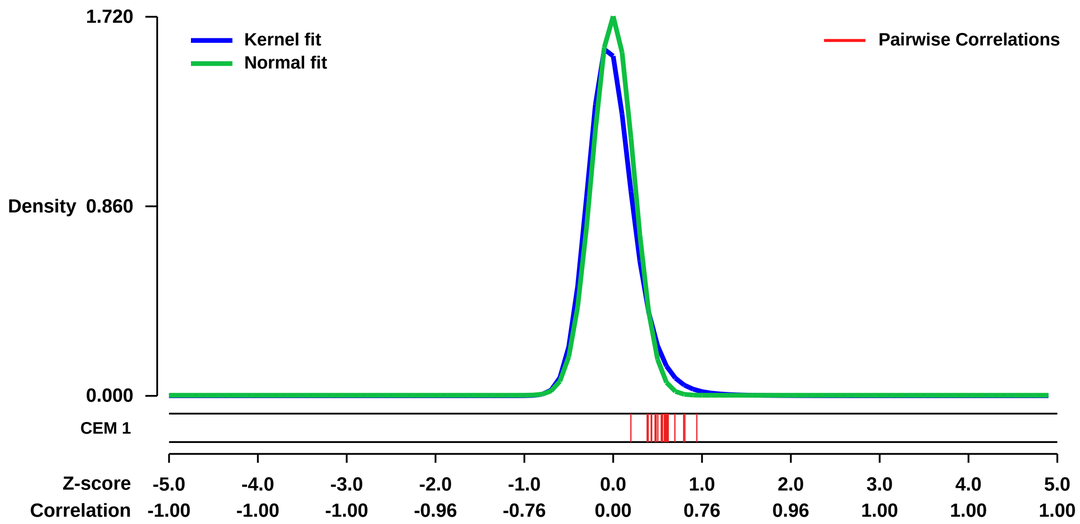

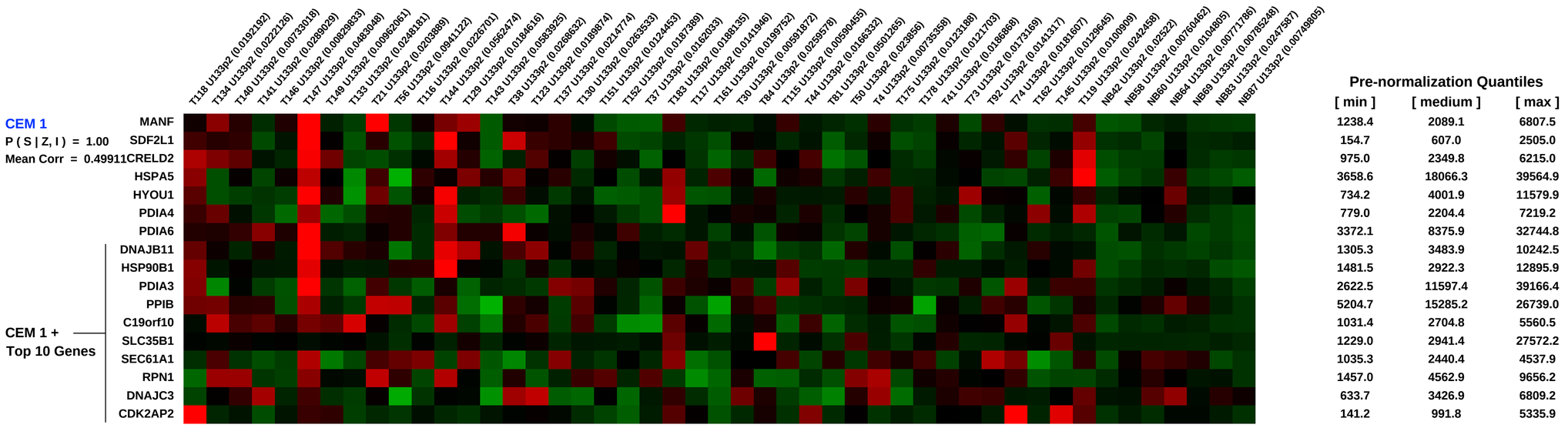

Pre-normalization Quantiles

[min]	[medium]	[max]
1238.4	2089.1	6807.5
154.7	607.0	2505.0
975.0	2349.8	6215.0
3658.6	18066.3	39564.9
734.2	4001.9	11579.9
779.0	2204.4	7219.2
3372.1	8375.9	32744.8
1305.3	3483.9	10242.5
1481.5	2922.3	12895.9
2622.5	11597.4	39166.4
5204.7	15285.2	26739.0
1031.4	2704.8	5560.5
1229.0	2941.4	27572.2
1035.3	2440.4	4537.9
1457.0	4562.9	9656.2
633.7	3426.9	6809.2
141.2	991.8	5335.9

GEO Series "GSE59931" Expression Profiles

Num of samples in this series: 6

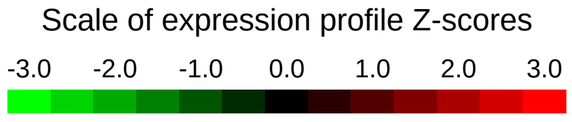

GEO Link:	http://www.ncbi.nlm.nih.gov/geo/query/acc.cgi?acc=GSE59931
Status:	Public on Jul 31 2014
Title:	Glutamine deprivation in U2OS cells
Organism:	Homo sapiens
Experiment type:	Expression profiling by array
Platform:	GPL570
Pubmed ID:	
Summary & Design:	**Summary:** **To understand the effects of glutamine deprivation on cell physiology we performed global analysis of gene expression in response to glutamine deprivation.** **U2OS cells were subjected to glutamine deprivation for 24h followed by RNA extraction and microarray analysis.** **Overall design:** **U2OS cells were plated overnight followed by treatment for 24h with glutamine-containing and glutamine-depleted media. Three biological replicates were assayed for each condition.**

Background corr dist: **KL-Divergence = 0.0303, L1-Distance = 0.0569, L2-Distance = 0.0041, Normal std = 0.7617**

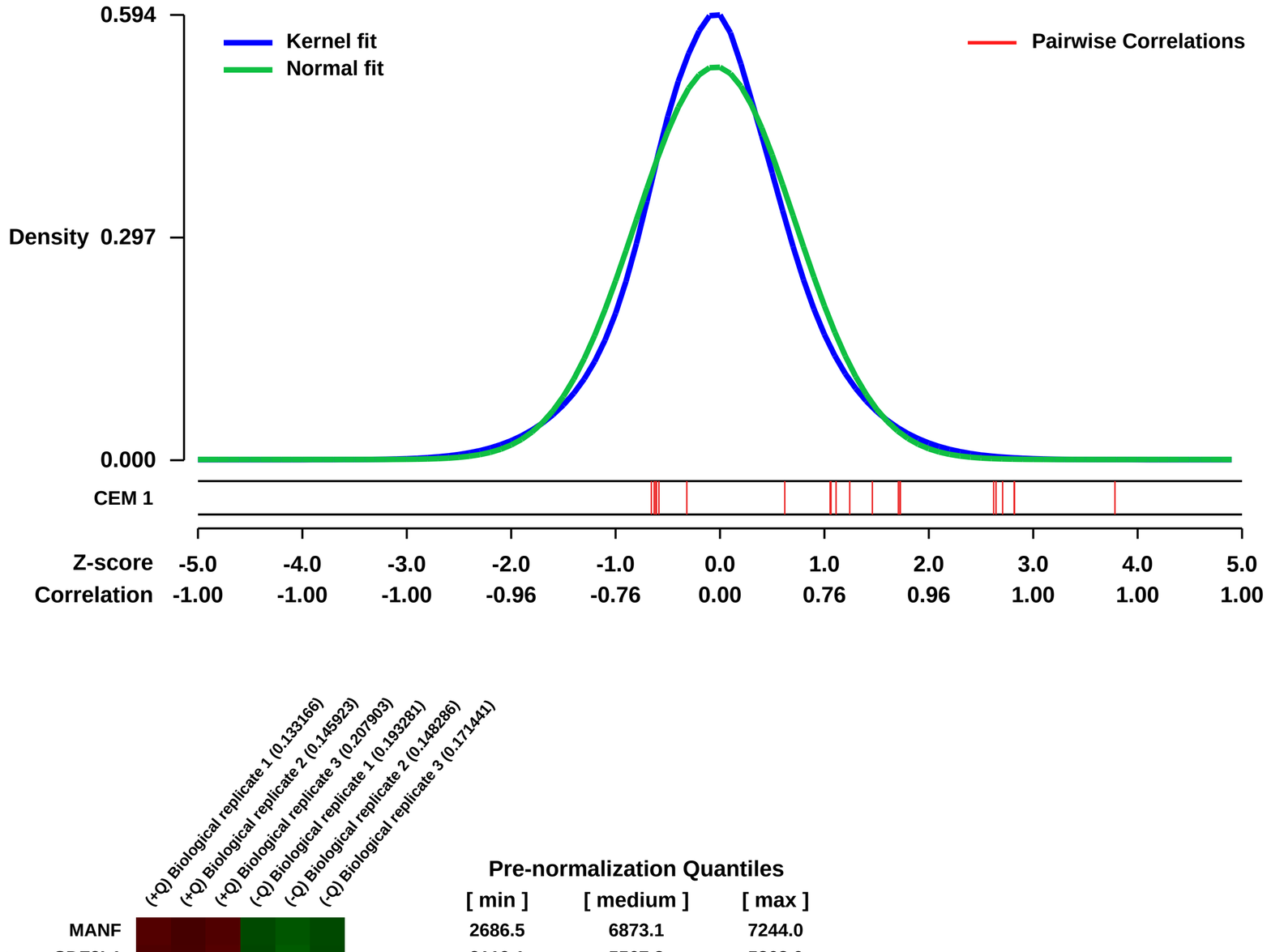

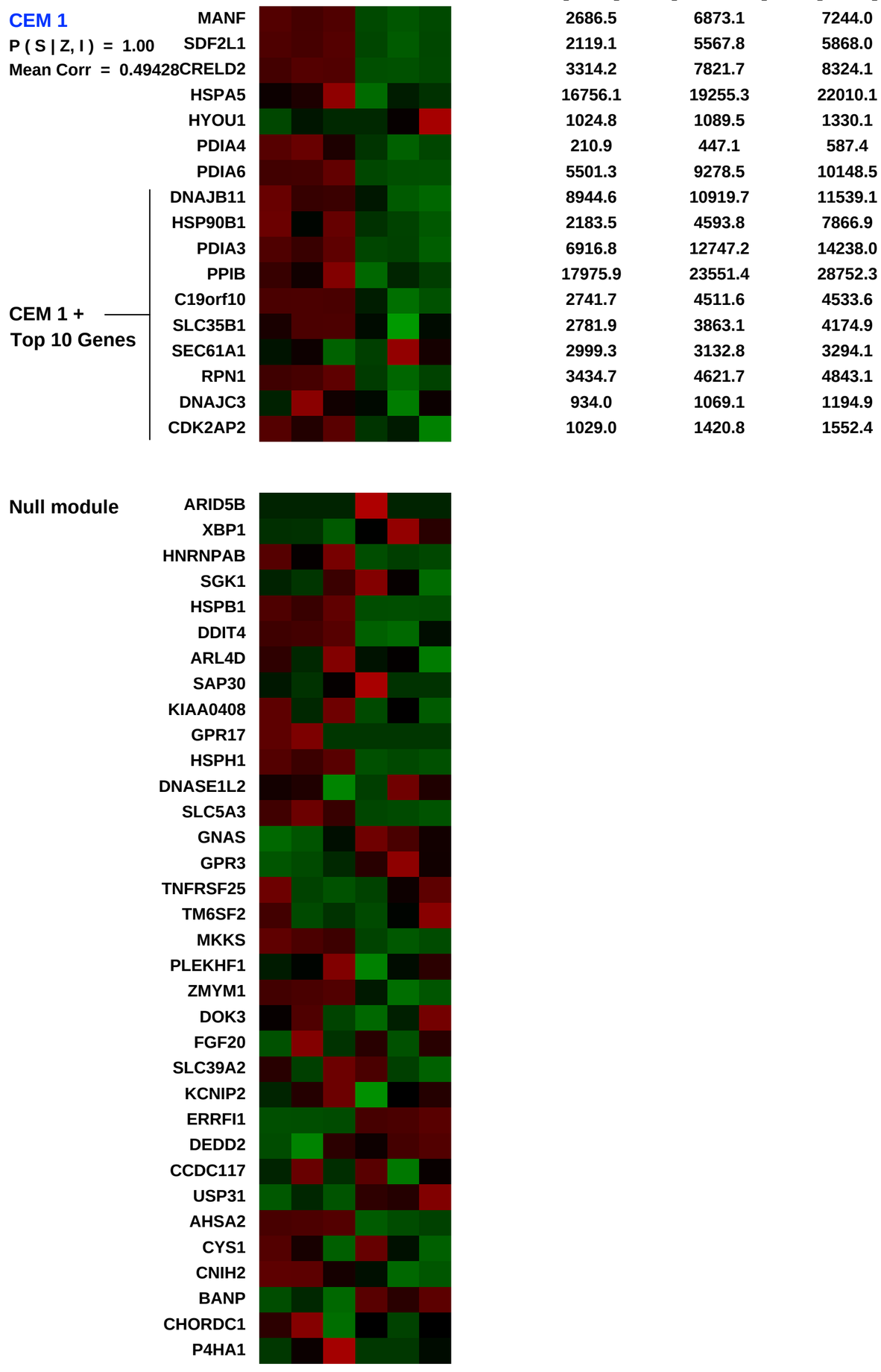

GEO Series "GSE35330" Expression Profiles

Num of samples in this series: 24

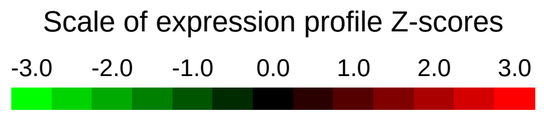

GEO Link:	http://www.ncbi.nlm.nih.gov/geo/query/acc.cgi?acc=GSE35330
Status:	Public on Dec 03 2012
Title:	Cellular senescence reprograms human NK cells to promote vascular remodeling
Organism:	Homo sapiens
Experiment type:	Expression profiling by array
Platform:	GPL570
Pubmed ID:	23184984
Summary & Design:	**Summary:** Natural killer (NK) cells are lymphocytes that participate in immune responses through their cytotoxic activity and secretion of cytokines and chemokines. They can be activated by interaction with ligands on target cells or by soluble mediators such as cytokines. In addition, soluble HLA-G, a major histocompatibility complex molecule secreted by fetal trophoblast cells during early pregnancy, stimulates resting NK cells to secrete proinflammatory and proangiogenic factors. Human NK cells are abundant in uterus, where they remain after implantation. Soluble HLA-G is endocytosed into early endosomes of NK cells where its receptor, CD158d, initiates a signaling cascade through DNA-PKcs, Akt and NF-kB3. The physiological relevance of this endosomal signaling pathway, and how the fate and function of NK cells during early pregnancy is regulated, is unknown. Here we show that soluble agonists of CD158d trigger DNA damage response signaling and p21 (CIP1/WAF1) expression to promote senescence in primary NK cells. CD158d engagement resulted in morphological alterations in cell size and shape, chromatin remodeling, and survival in the absence of proliferation, all hallmarks of senescence. Microarray analysis revealed a senescence signature of upregulated genes upon sustained activation through CD158d. The proinflammatory and proangiogenic factors secreted by these metabolically active NK cells are part of a senescence associated secretory phenotype (SASP) that promoted tissue remodeling and angiogenesis as assessed by functional readouts of vascular permeability and endothelial cell tube formation. We propose that ligand-induced senescence is a molecular switch for the sustained activation of NK cells in response to soluble HLA-G for the purpose of remodeling the maternal vasculature in early pregnancy. **Overall design:** Time series (4 hr, 16 hr, 64 hr) of NK cells treated with agonist (anti-CD158d mAb) or control. NK cells were from 4 donors.

Background corr dist: KL-Divergence = 0.3535, L1-Distance = 0.0737, L2-Distance = 0.0164, Normal std = 0.2608

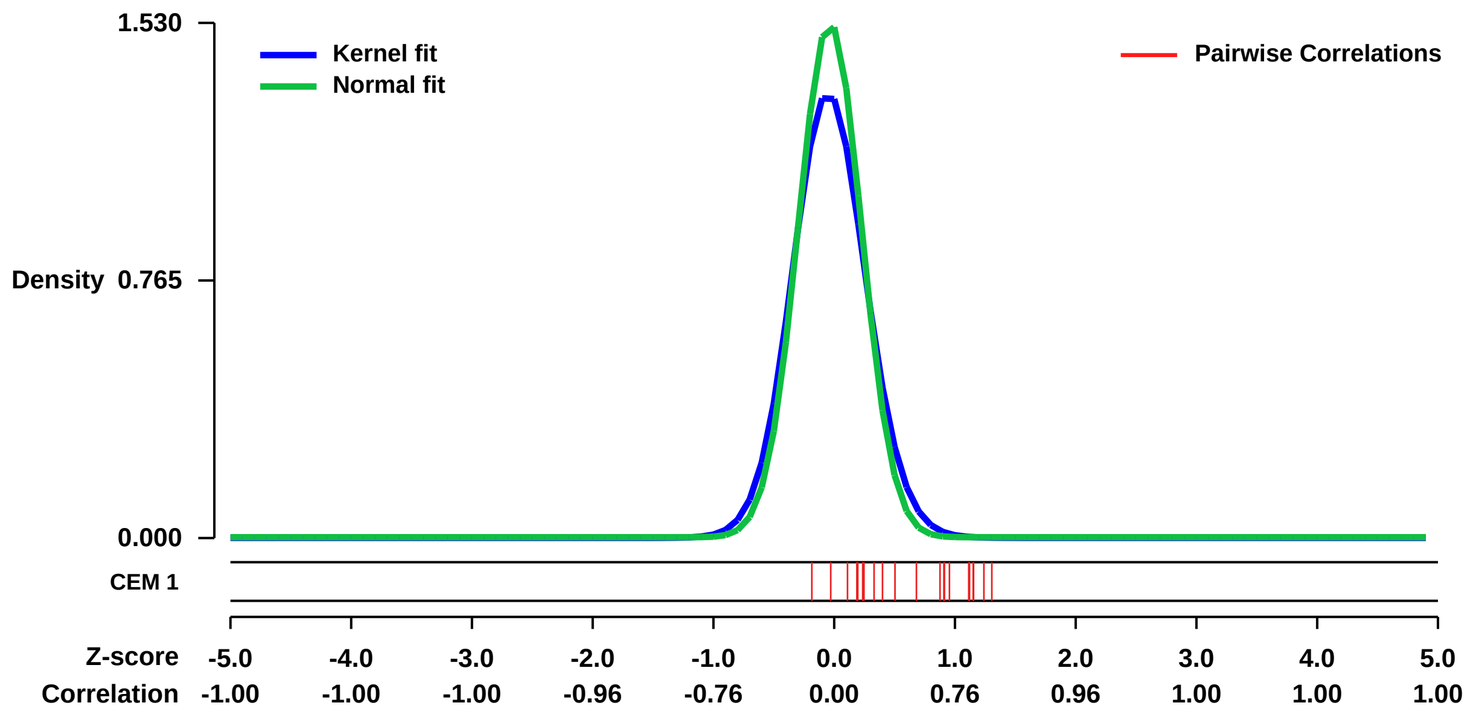

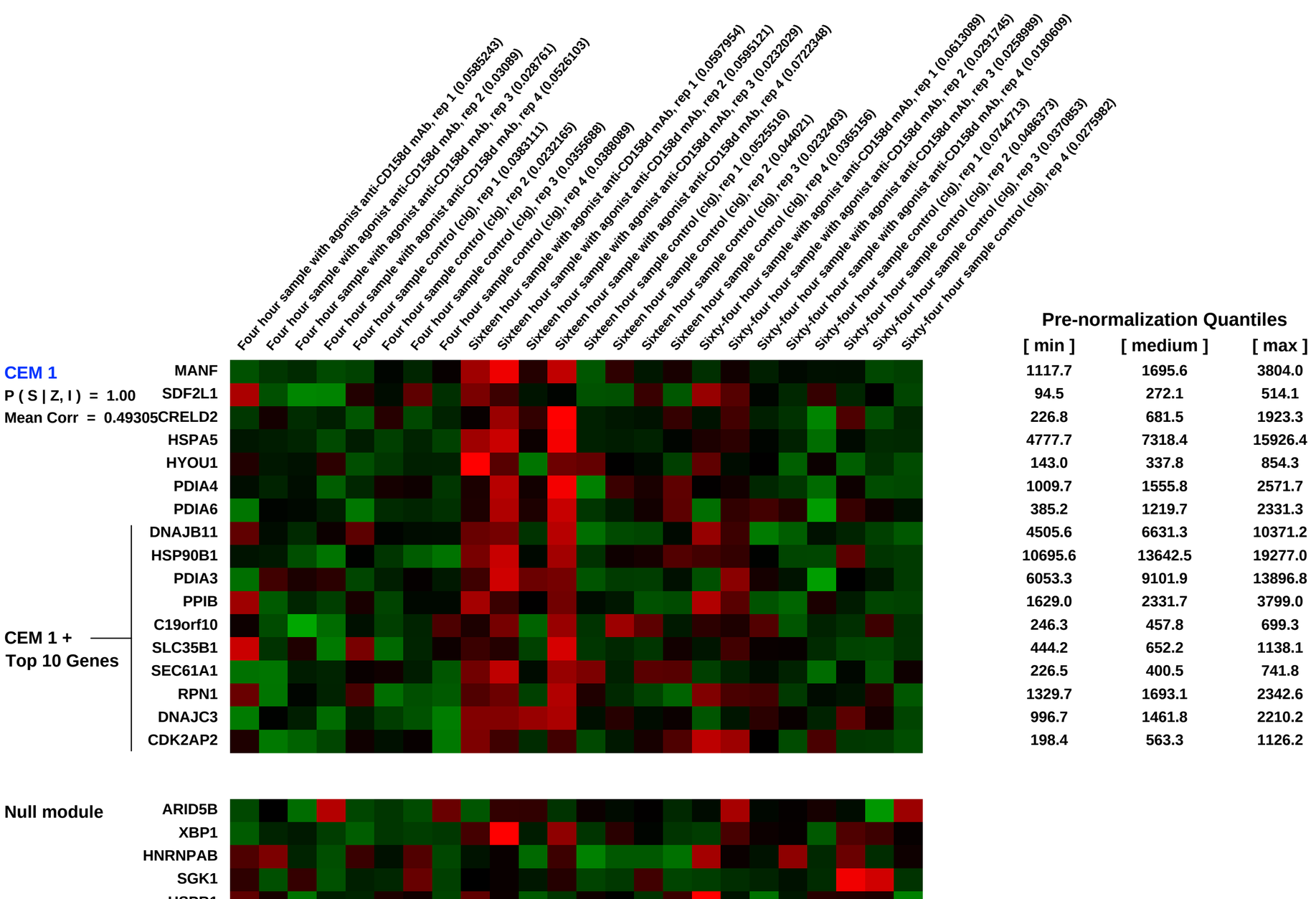

GEO Series "GSE29634" Expression Profiles

Num of samples in this series: 13

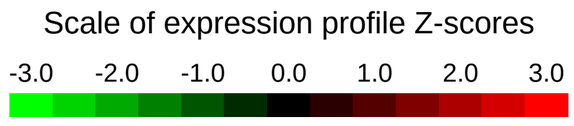

GEO Link:	**http://www.ncbi.nlm.nih.gov/geo/query/acc.cgi?acc=GSE29634**
Status:	**Public on Jun 01 2012**
Title:	**Oncogenic Activation Of FOXR1 by 11q23 Intrachromosomal Deletion-Fusions In Neuroblastoma**
Organism:	**Homo sapiens**
Experiment type:	**Expression profiling by array**
Platform:	**GPL570**
Pubmed ID:	
Summary & Design:	**Summary:** **Neuroblastoma tumors frequently show loss of heterozygosity of chromosome 11q with a shortest region of overlap in the 11q23 region. These deletions are thought to cause inactivation of tumor suppressor genes leading to haploinsufficiency. Alternatively, micro-deletions could lead to gene fusion products that are tumor-driving. To identify such events we analyzed a series of neuroblastomas by comparative genomic hybridization (CGH) and single nucleotide polymorphism (SNP) arrays and integrated these data with Affymetrix mRNA profiling data with the bioinformatic tool R2 (http://r2.amc.nl). We identified three neuroblastoma samples with small interstitial deletions at 11q23, upstream of the forkhead-box transcription factor FOXR1. Genes at the proximal side of the deletion were fused to FOXR1, resulting in fusion transcripts of MLL-FOXR1 and PAFAH1B2-FOXR1. FOXR1 expression has only been detected in early embryogenesis. Affymetrix microarray analysis showed high FOXR1 mRNA expression exclusively in the neuroblastomas with micro-deletions and rare cases of other tumor types, including osteosarcoma cell line HOS. RNAi silencing of FOXR1 strongly inhibited proliferation of HOS cells and triggered apoptosis. Expression profiling of these cells and reporter assays suggested that FOXR1 is a negative regulator of forkhead-box factor mediated transcription. The neural crest stem cell line JoMa1 proliferates in culture conditional to activity of a MYC-ER transgene. Over-expression of the wild-type FOXR1 could functionally replace MYC and drive proliferation of JoMa1. We conclude that FOXR1 is recurrently activated in neuroblastoma by intrachromosomal deletion/fusion events, resulting in over-expression of fusion transcripts. Forkhead-box transcription factors have not been previously implicated in neuroblastoma pathogenesis. Furthermore, this is the first identification of intrachromosomal fusion genes in neuroblastoma.** **Overall design:** **Time series Affymetrix U133p2 profiling of Osteosarcoma HOS cells transduced with FOXR1 targeted shRNAs or control shRNA**

Background corr dist: KL-Divergence = 0.1424, L1-Distance = 0.0269, L2-Distance = 0.0012, Normal std = 0.3847

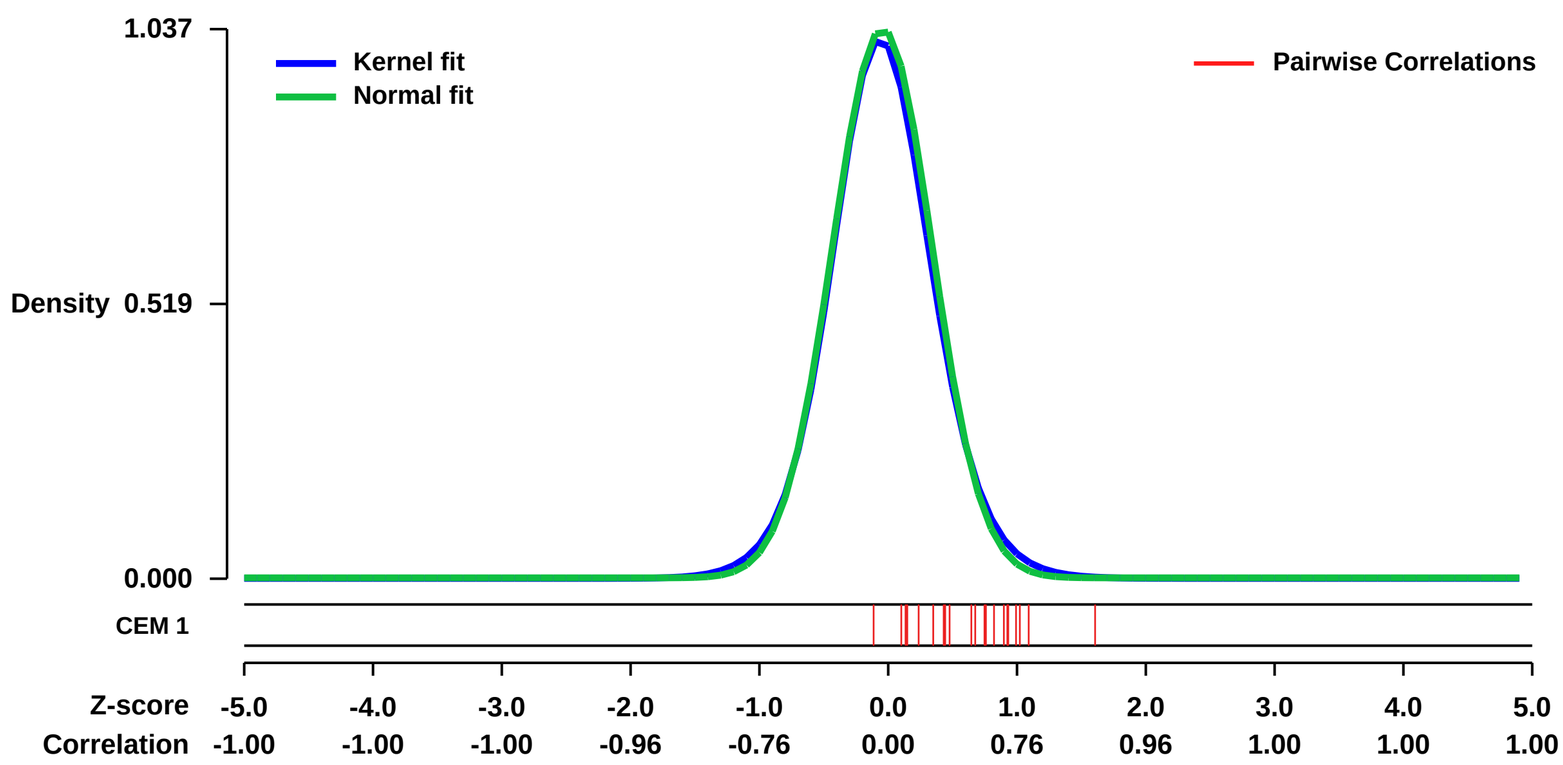

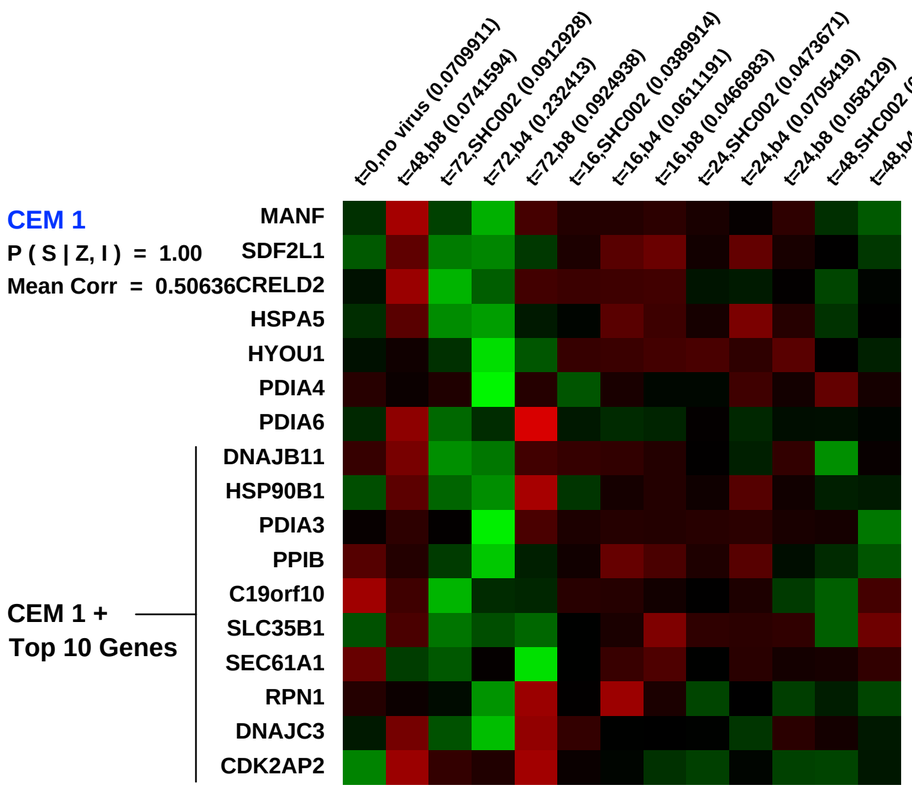

Pre-normalization Quantiles

	[min]	[medium]	[max]
MANF	2267.5	4193.3	5522.2
SDF2L1	776.9	1202.5	1449.0
CRELD2	1825.4	2451.3	3014.6
HSPA5	15438.2	19264.5	22198.4
HYOU1	3405.7	5437.3	6065.5
PDIA4	180.7	366.3	421.0
PDIA6	5861.7	6279.7	7542.2
DNAJB11	5035.5	6893.4	7779.8
HSP90B1	5871.4	7763.7	9604.7
PDIA3	2488.3	12444.0	14172.2
PPIB	12684.4	17301.4	19127.0
C19orf10	2931.6	3818.1	4449.1
SLC35B1	3752.2	4151.3	4430.9
SEC61A1	1949.0	3235.0	3673.0
RPN1	3167.3	3858.9	4583.5
DNAJC3	966.6	1378.7	1701.1
CDK2AP2	1482.9	1821.3	2271.7

GEO Series "GSE11710" Expression Profiles

Num of samples in this series: 19

Scale of expression profile Z-scores

-3.0 -2.0 -1.0 0.0 1.0 2.0 3.0

GEO Link:	http://www.ncbi.nlm.nih.gov/geo/query/acc.cgi?acc=GSE11710
Status:	Public on Oct 29 2008
Title:	TGF-beta-induced gene expression data and Smad2/3 binding sites of HaCaT keratinocytes
Organism:	Homo sapiens
Experiment type:	Genome binding/occupancy profiling by genome tiling array
Platform:	GPL570
Pubmed ID:	18955504
Summary & Design:	**Summary:** Smad2/3 are transcription factors that engage in TGF-beta-induced transcription. Here we analyzed the effect of identified Smad2/3 binding sites to transcription. We used expression microarrays to compare the Smad2/3 binding sites identified by ChIP-chip to TGF-beta-induced gene expressions. Keywords: time course We also examined the effect of either ETS1/TFAP2A/SMAD2/SMAD3 siRNAs on TGF-beta-induced gene expression change. **Overall design:** HaCaT cells were treated with TGF-beta3 for Smad2/3 ChIP-chip or RNA extraction and hybridization on Affymetrix microarrays.

Background corr dist: KL-Divergence = 0.2206, L1-Distance = 0.0432, L2-Distance = 0.0041, Normal std = 0.3199

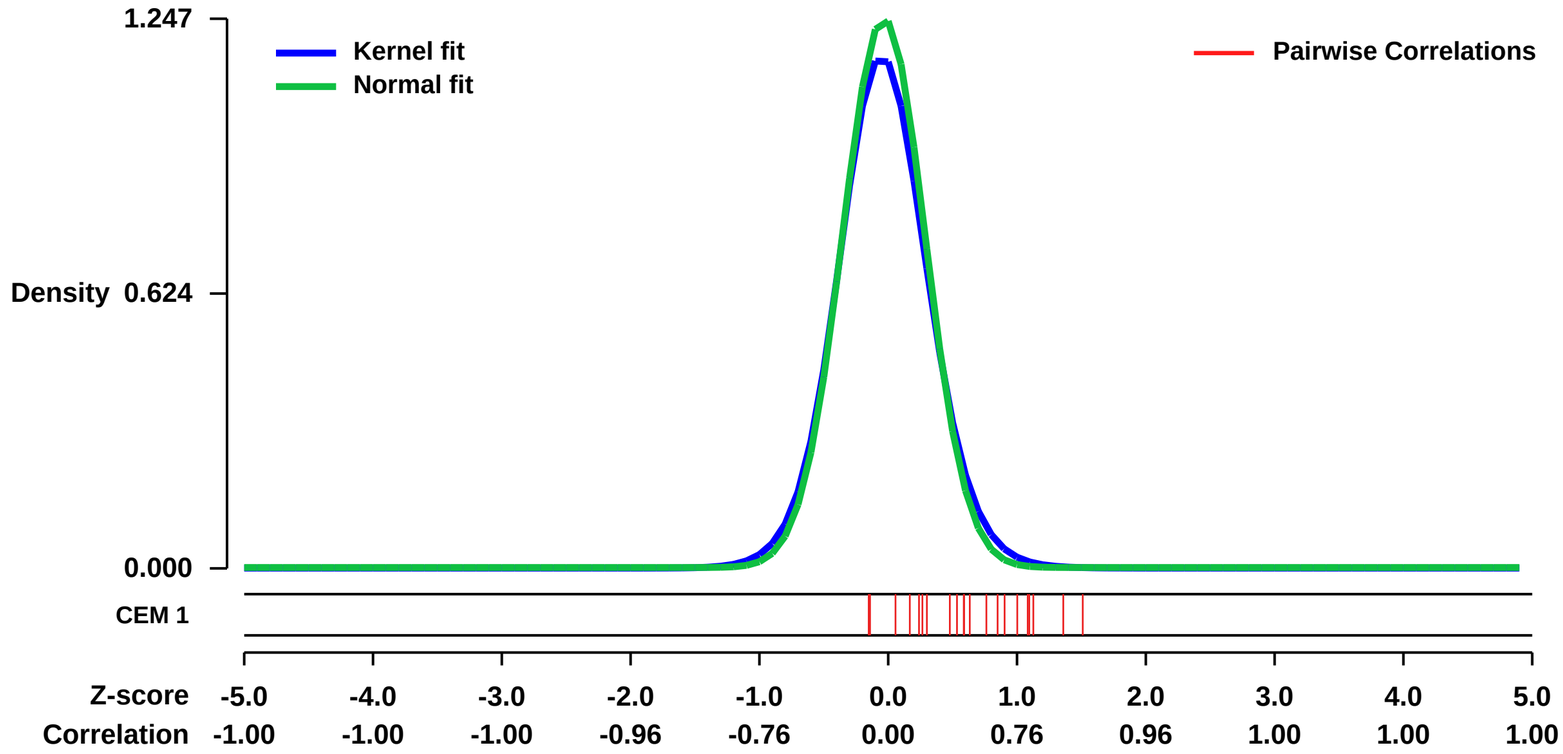

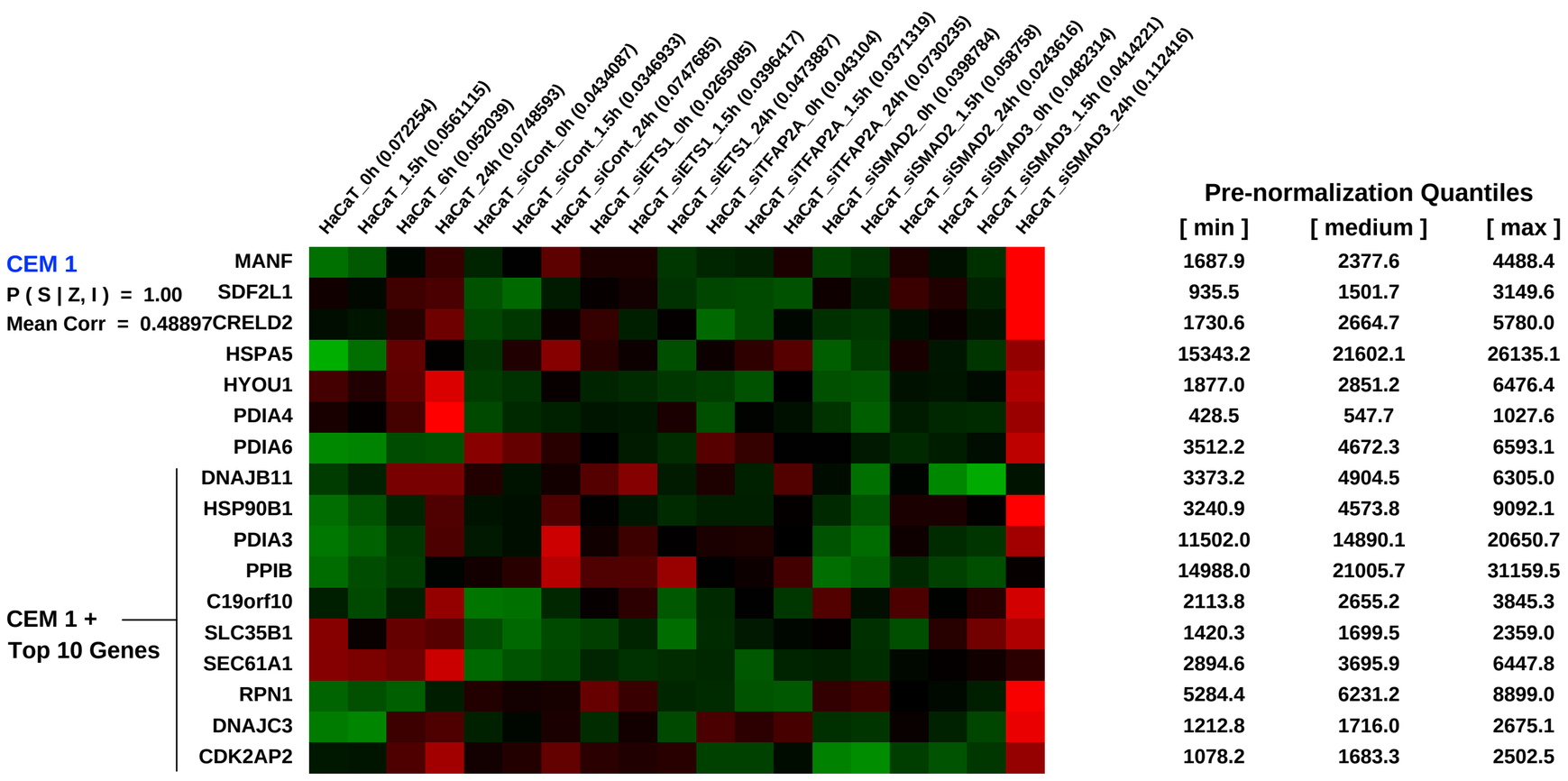

	Pre-normalization Quantiles [min]	[medium]	[max]
MANF	1687.9	2377.6	4488.4
SDF2L1	935.5	1501.7	3149.6
CRELD2	1730.6	2664.7	5780.0
HSPA5	15343.2	21602.1	26135.1
HYOU1	1877.0	2851.2	6476.4
PDIA4	428.5	547.7	1027.6
PDIA6	3512.2	4672.3	6593.1
DNAJB11	3373.2	4904.5	6305.0
HSP90B1	3240.9	4573.8	9092.1
PDIA3	11502.0	14890.1	20650.7
PPIB	14988.0	21005.7	31159.5
C19orf10	2113.8	2655.2	3845.3
SLC35B1	1420.3	1699.5	2359.0
SEC61A1	2894.6	3695.9	6447.8
RPN1	5284.4	6231.2	8899.0
DNAJC3	1212.8	1716.0	2675.1
CDK2AP2	1078.2	1683.3	2502.5

GEO Series "GSE29605" Expression Profiles

Num of samples in this series: 22

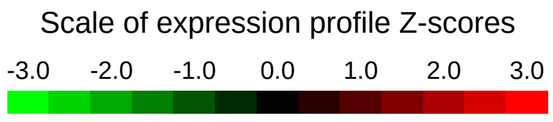

GEO Link:	**http://www.ncbi.nlm.nih.gov/geo/query/acc.cgi?acc=GSE29605**
Status:	**Public on Jun 01 2011**
Title:	**Gene expression data from chronic lymphocytic leukemia samples**
Organism:	**Homo sapiens**
Experiment type:	**Expression profiling by array**
Platform:	**GPL570**
Pubmed ID:	
Summary & Design:	**Summary:** **MicroRNA-155 is frequently over-expressed in CLL and is associated with worse clinical prognosis. To understand the role of miR-155 in CLL pathogenesis, we used microarrays to identify genes that are expressed at significantly lower levels in CLLs that harbor** **higher levels of miR-155 expression in an attempt to determine the relevant gene targets of miR-155 in CLL.** **Overall design:** **MiR-155 levels of 38 CLL samples were determined and ranked. 6 CLLs with the highest and 6 CLLs with the lowest miR-155 within the IgVH unmutated group, and 5 CLLs with the highest and 5 CLLs with the lowest miR-155 within the IgVH mutated group were selected for Affymetrix array analyses.**

Background corr dist: **KL-Divergence = 0.3507, L1-Distance = 0.0733, L2-Distance = 0.0159, Normal std = 0.2624**

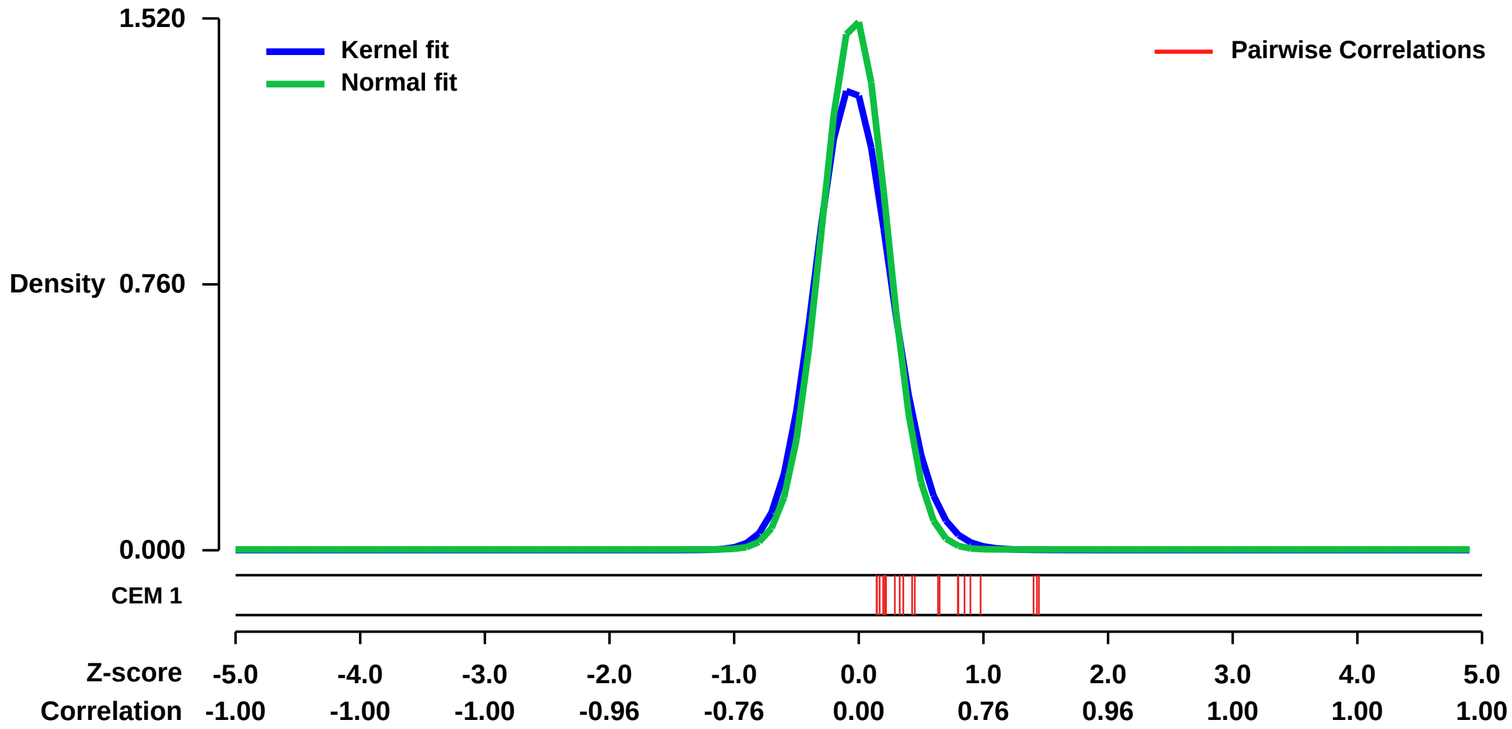

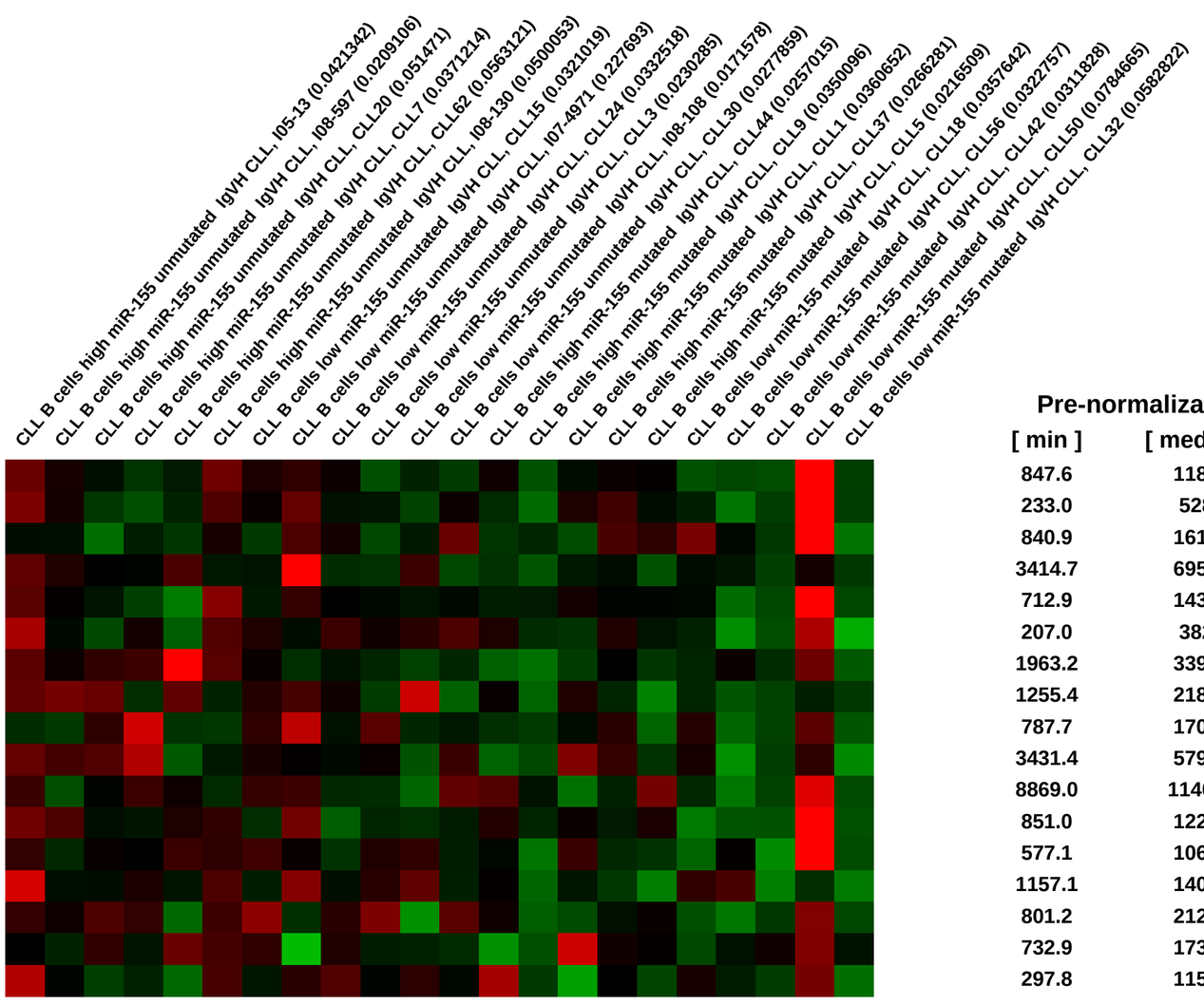

Pre-normalization Quantiles

[min]	[medium]	[max]
847.6	1184.6	2643.3
233.0	528.6	1326.9
840.9	1611.5	3599.0
3414.7	6953.5	24761.4
712.9	1432.3	3249.0
207.0	382.0	525.5
1963.2	3393.4	7589.4
1255.4	2189.2	4417.7
787.7	1700.4	4359.3
3431.4	5798.7	8329.8
8869.0	11404.1	17409.4
851.0	1223.5	2233.2
577.1	1068.0	2011.1
1157.1	1409.5	1912.2
801.2	2127.5	3180.3
732.9	1732.1	2813.4
297.8	1150.4	2139.7

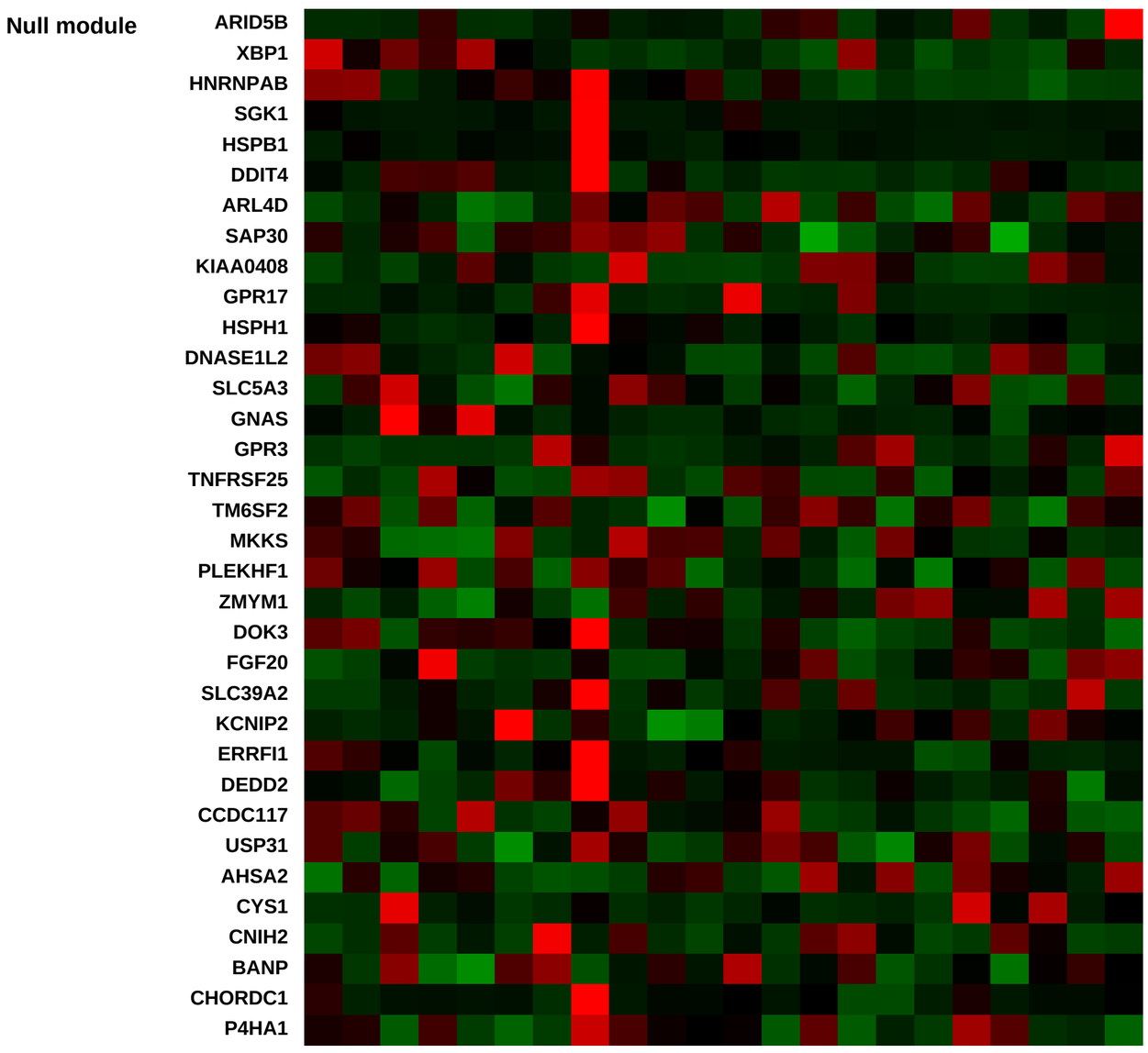

GEO Series "GSE16416" Expression Profiles

Num of samples in this series: 12

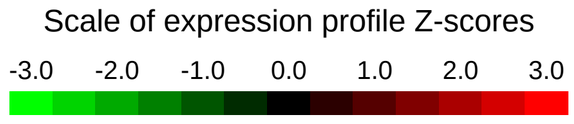

GEO Link:	http://www.ncbi.nlm.nih.gov/geo/query/acc.cgi?acc=GSE16416
Status:	Public on Sep 09 2011
Title:	Expression data from human primary fibroblasts treated with Trypanosoma cruzi-conditioned medium
Organism:	Homo sapiens
Experiment type:	Expression profiling by array
Platform:	GPL570
Pubmed ID:	21931601
Summary & Design:	**Summary:** The intracellular pathogen Trypanosoma cruzi secretes an activity that blocks TGF-¸†-dependent induction of connective tissue growth factor (CTGF/CCN2). Here, we address the mechanistic basis for T. cruzi-mediated interference of CTGF/CCN2 expression by examining host cell signaling pathways and the global inhibitory effect on TGF-¸†-dependent gene expression. We show that the expression of a discrete subset of TGF-¸†-inducible genes involved in cell proliferation, wound repair, and immune regulation are blocked by the soluble T. cruzi activity, demonstrating that this parasite-derived activity has broad, but specific effects on fibroblast gene regulation. **Overall design:** Primary human fibroblasts were treated with TGF-¸†, T. cruzi conditioned medium (PCM) and TGF-¸†/ PCM simultaneously. Untreated cells were also included as controls. Total RNA was extracted and gene expression levels analyzed with Affymetrix microarrays. Three independent biological replicates were included for each type of treatment.

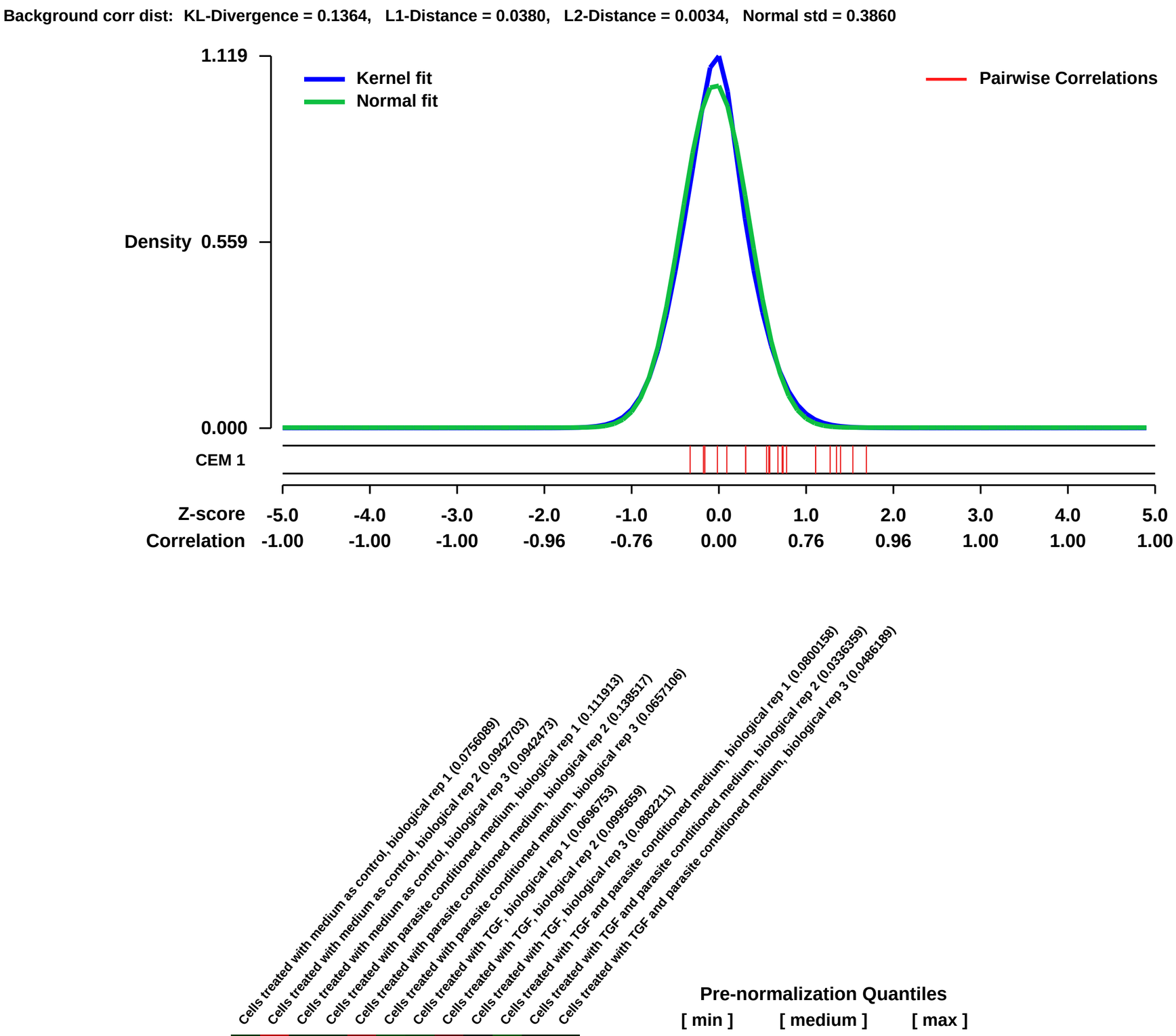

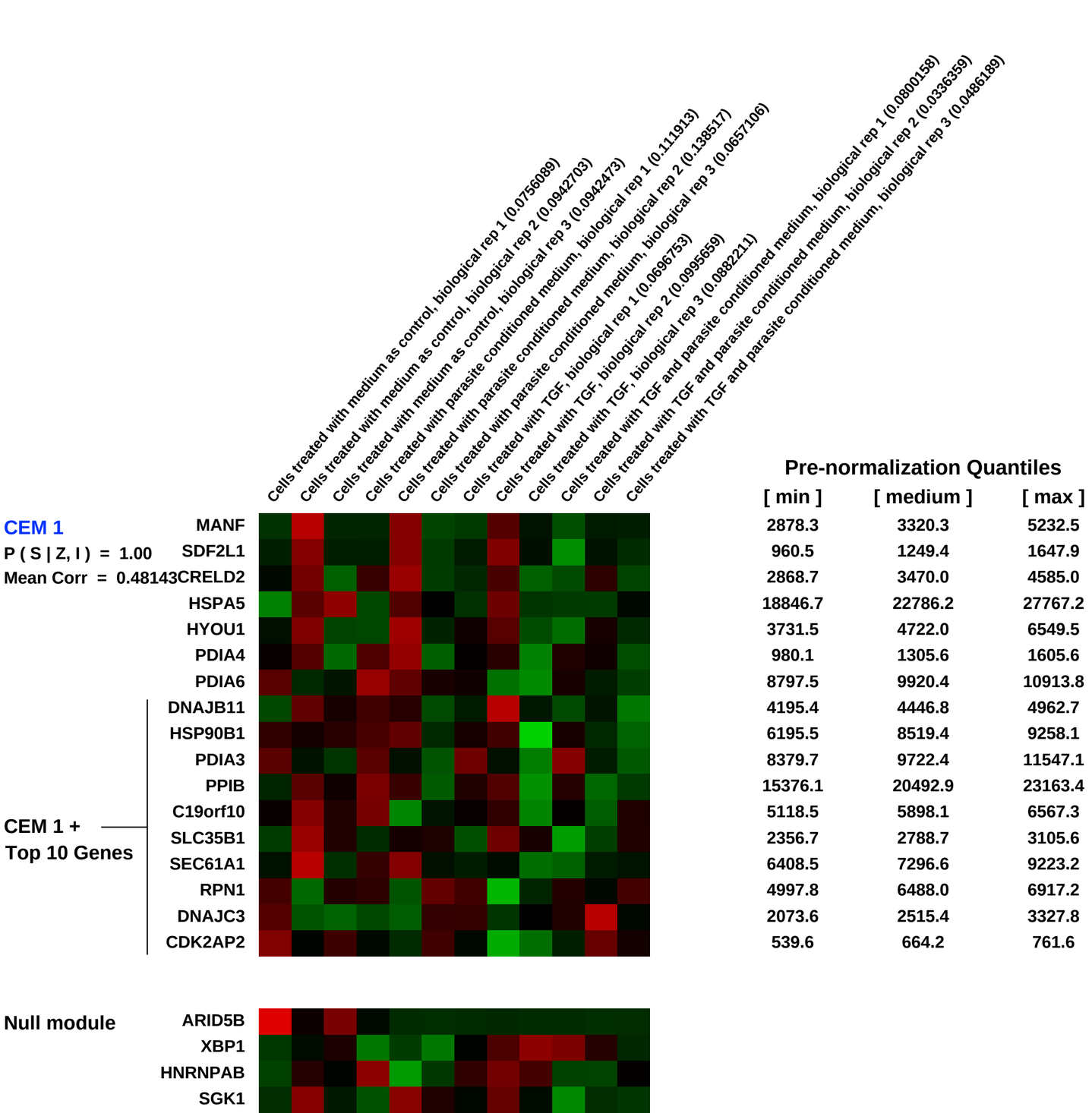

GEO Series "GSE23399" Expression Profiles

Num of samples in this series: 14

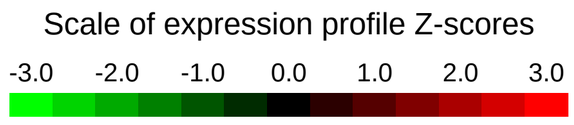

GEO Link:	http://www.ncbi.nlm.nih.gov/geo/query/acc.cgi?acc=GSE23399
Status:	Public on Aug 03 2010
Title:	Gene expression profling of human breast carcinoma-associated fibroblasts treated with paclitaxol or doxorubicin at therapeutically relevant doses
Organism:	Homo sapiens
Experiment type:	Expression profiling by array
Platform:	GPL570
Pubmed ID:	
Summary & Design:	**Summary:** **Systemic chemotherapy inflicts cytotoxic injuries on breast carcinoma-associated fibroblasts.** **We profiled the transcriptomes of human breast carcinoma-associated fibroblasts before and after clinically relevant cytotoxic stimuli induced by chemotheraputic agents.** **Overall design:** **Breast cancer associated fibroblasts (BCAFs) were isolated from the tumor specimen by mechanical dissociation and differential centrifugation. The cells at early passages were treated with paclitaxol or doxorubicin at clinically revealent concentration. Total RNA was extracted from the cells at different time points post-treatment for gene expression profiling.**

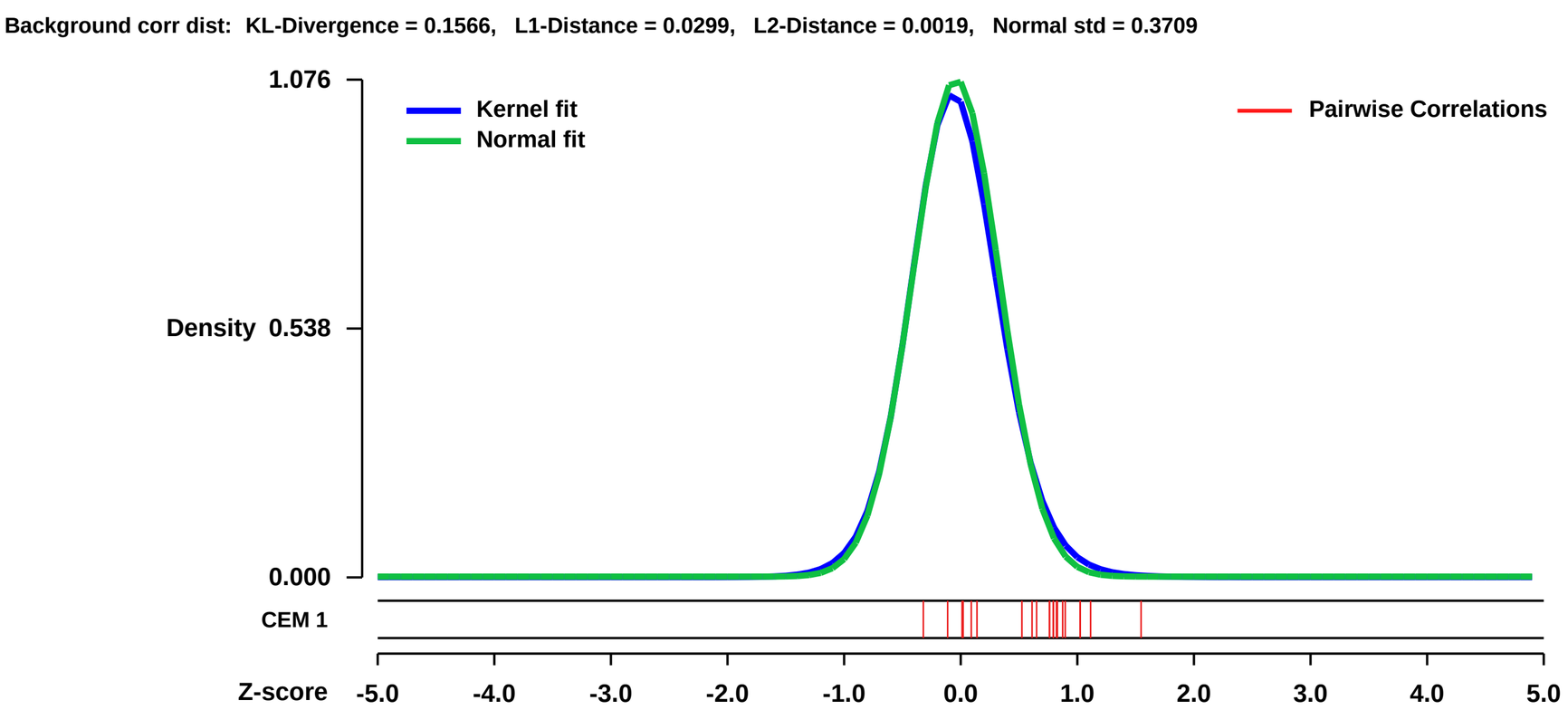

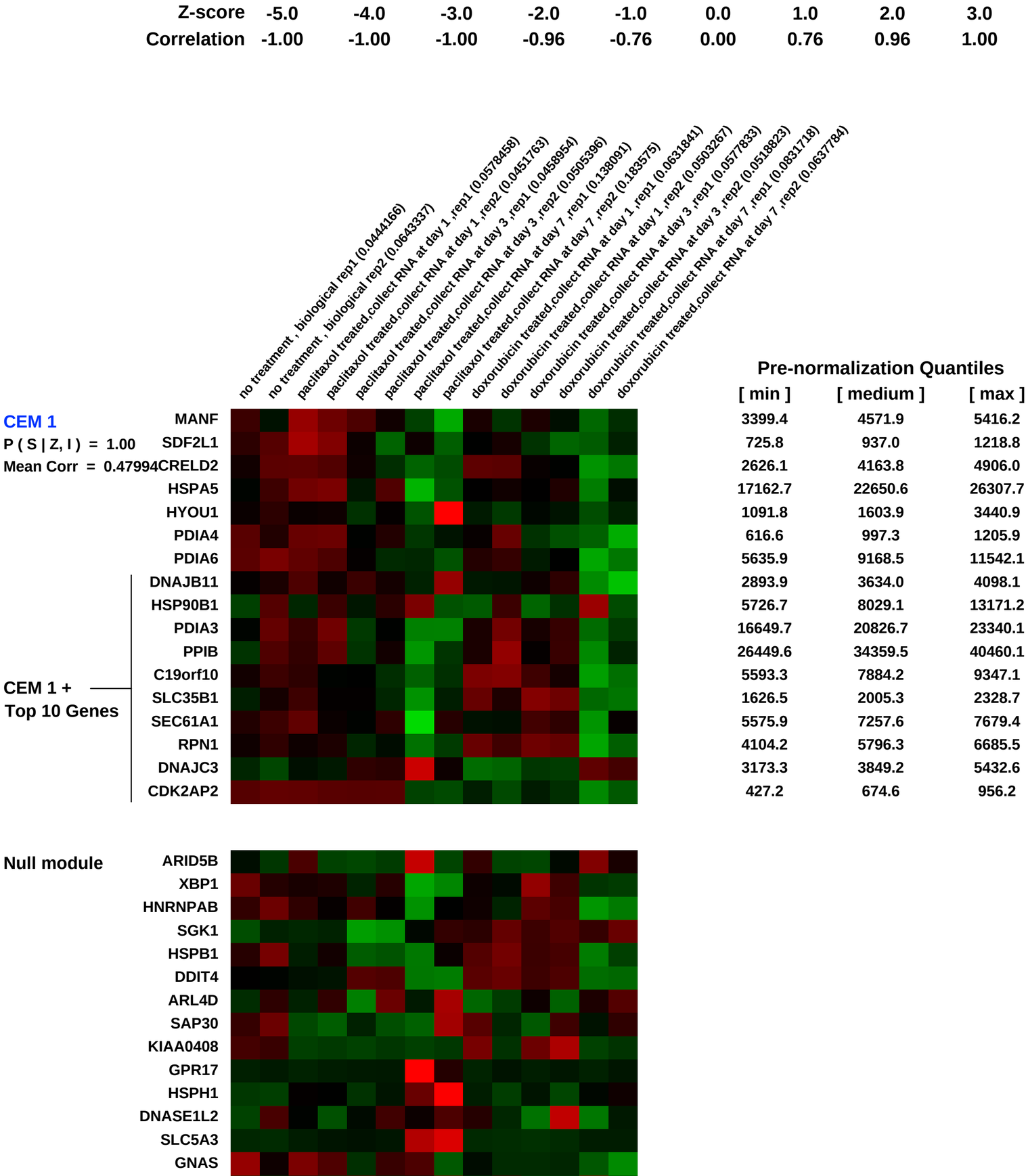

GEO Series "GSE33066" Expression Profiles

Num of samples in this series: 6

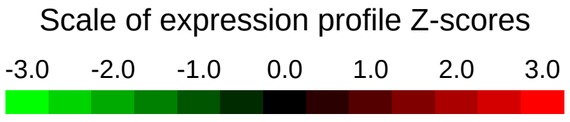

GEO Link:	http://www.ncbi.nlm.nih.gov/geo/query/acc.cgi?acc=GSE33066
Status:	Public on Mar 01 2012
Title:	Transcriptional analysis of primary adult human skin cells that express stage-specific embryonic antigen 3 (SSEA-3)
Organism:	Homo sapiens
Experiment type:	Expression profiling by array
Platform:	GPL570
Pubmed ID:	
Summary & Design:	**Summary:** Primary human skin cells were gated based on expression of stage-specific embryonic antigen 3 (SSEA3) with the high SSEA3 expressing cells (top 10%, categorized as SSEA3-positive or SSEA3-high) and negative SSEA3 expressing cells (bottom 10%, categorized as SSEA3-negative) purified into two different subpopulations. Sorted cells were allowed to adhere overnight under DMEM/F12 + 10% FBS culture conditions before total RNA was collected and global transcriptional analysis was performed. **Overall design:** We isolated primary adult human skin cells with either high SSEA3 expression or negative SSEA3 expression via FACS and analyzed via Affymetrix microarray analysis.

Background corr dist: KL-Divergence = 0.0476, L1-Distance = 0.0210, L2-Distance = 0.0005, Normal std = 0.5839

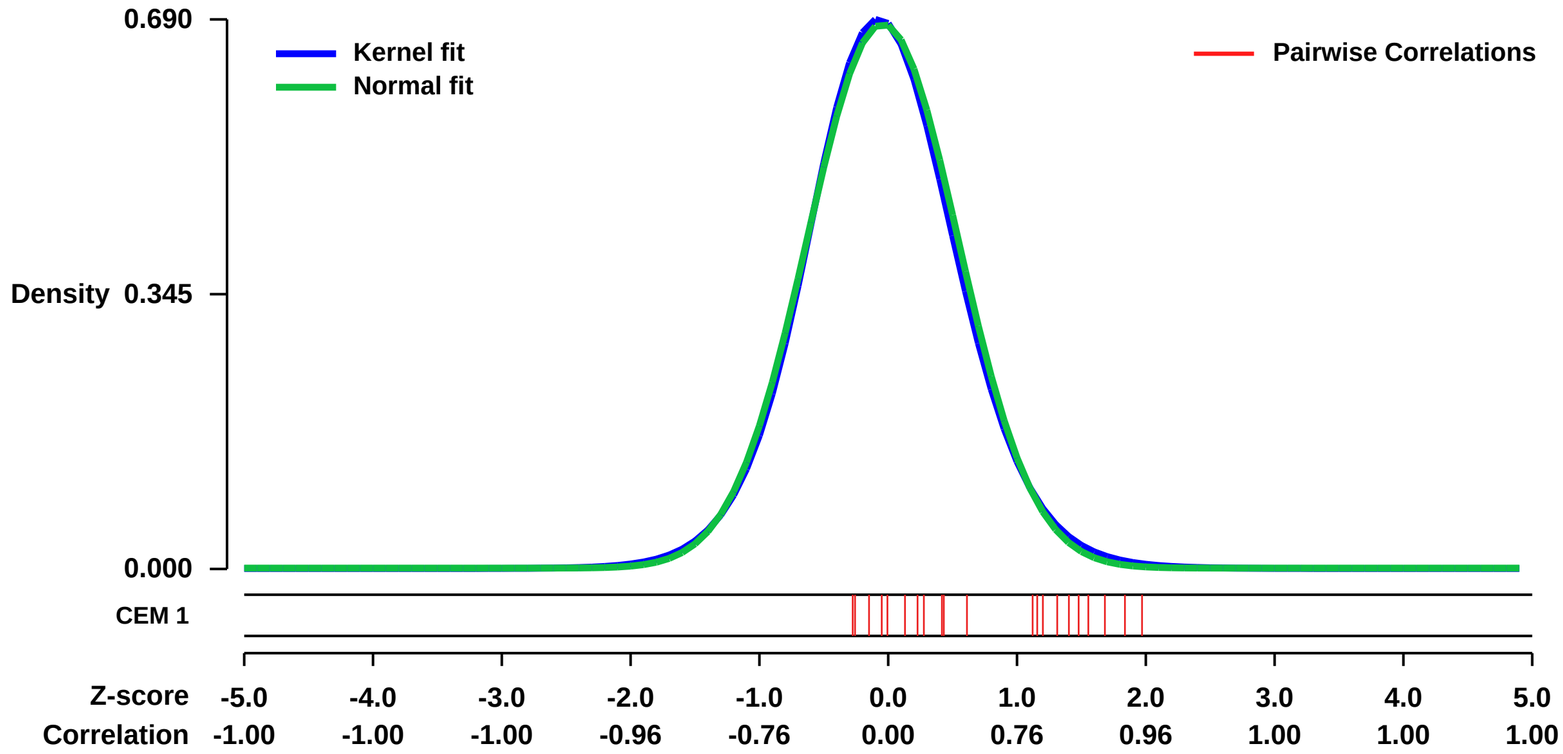

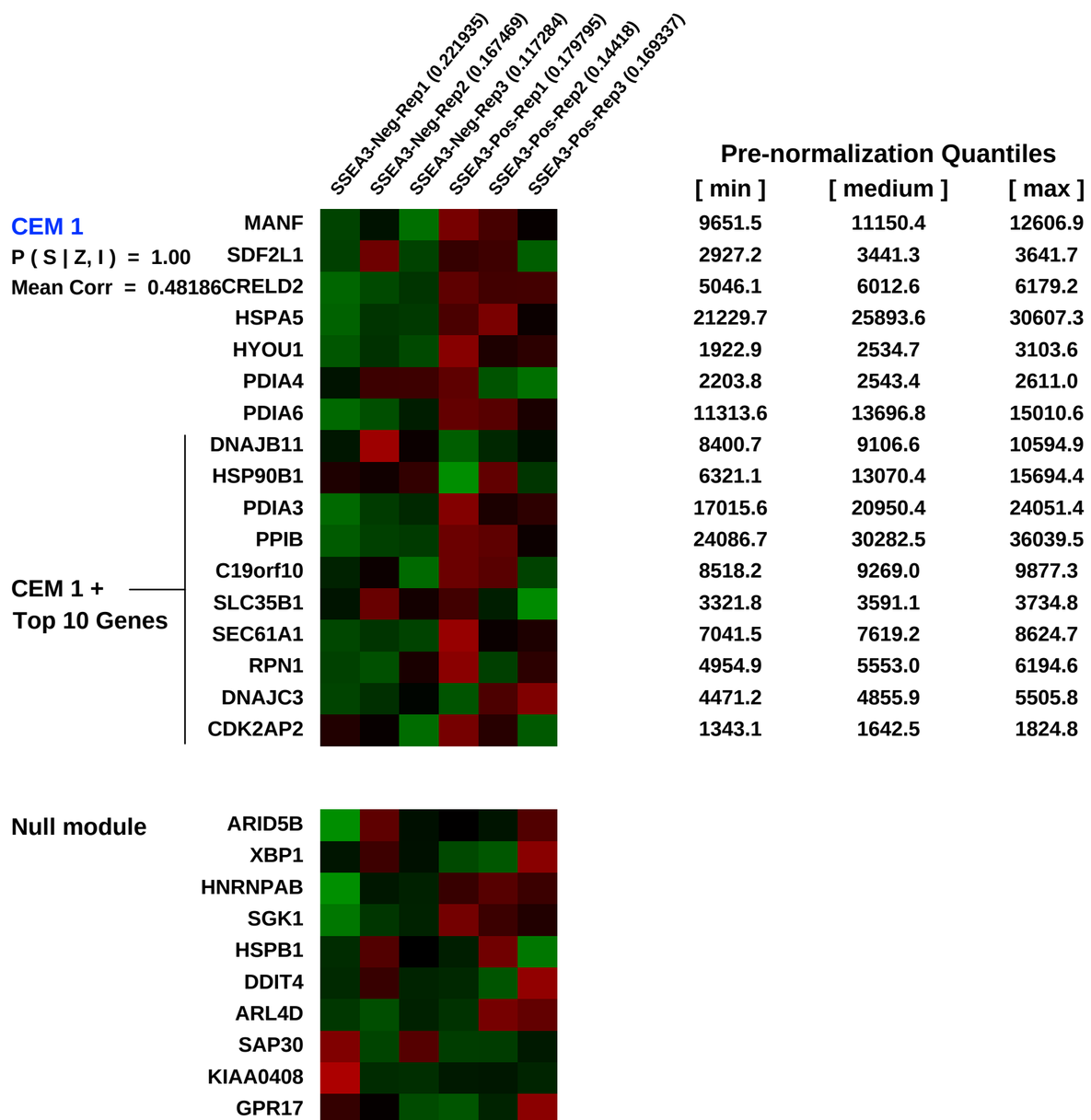

GEO Series "GSE8437" Expression Profiles

Num of samples in this series: 6

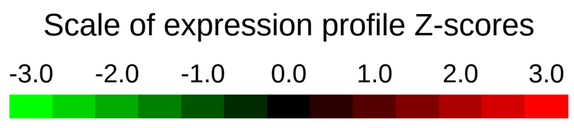

GEO Link:	http://www.ncbi.nlm.nih.gov/geo/query/acc.cgi?acc=GSE8437
Status:	Public on Jan 18 2008
Title:	IP Staufen2
Organism:	Homo sapiens
Experiment type:	Other
Platform:	GPL570
Pubmed ID:	18094122

Summary & Design:

Summary:
In human cells, Staufen2 is a double-stranded RNA-binding protein involved in several cellular functions. Although 51% identical to Staufen1, these proteins are nevertheless found in different RNA particles. In addition, differential splicing events generate Staufen2 isoforms that only differ at their N-terminal extremities. We used a genome wide approach to identify and compare the mRNA targets of mammalian Staufen2 isoforms. The mRNA content of Staufen mRNPs was identified by probing DNA microarrays with probes derived from mRNAs isolated from immunopurified Staufen2-containing complexes following transfection of HEK293T cells with Stau2-HA (59kDa) or Stau2-HA (62kDa) expressors. Our results indicate that 11% of the cellular RNAs expressed in HEK293T cells are found in Stau2-containing mRNPs. There is a predominance of mRNAs involved in cell metabolism, transport, transcription, regulation of cell processes and catalytic activity.

Keywords: Immunoprecipitation, Staufen, microarray

Overall design:
HEK293 cells were transiantly transfected with plasmids coding for Staufen2-HA isoforms. Cell extracts were immunoprecipitated using anti-HA antibodies and co-immunoprecipitated mRNAs were purified and used to hybridize microarrays. As control, cell extract from mock transfected cells were used.

Background corr dist: KL-Divergence = 0.0367, L1-Distance = 0.0431, L2-Distance = 0.0026, Normal std = 0.6730

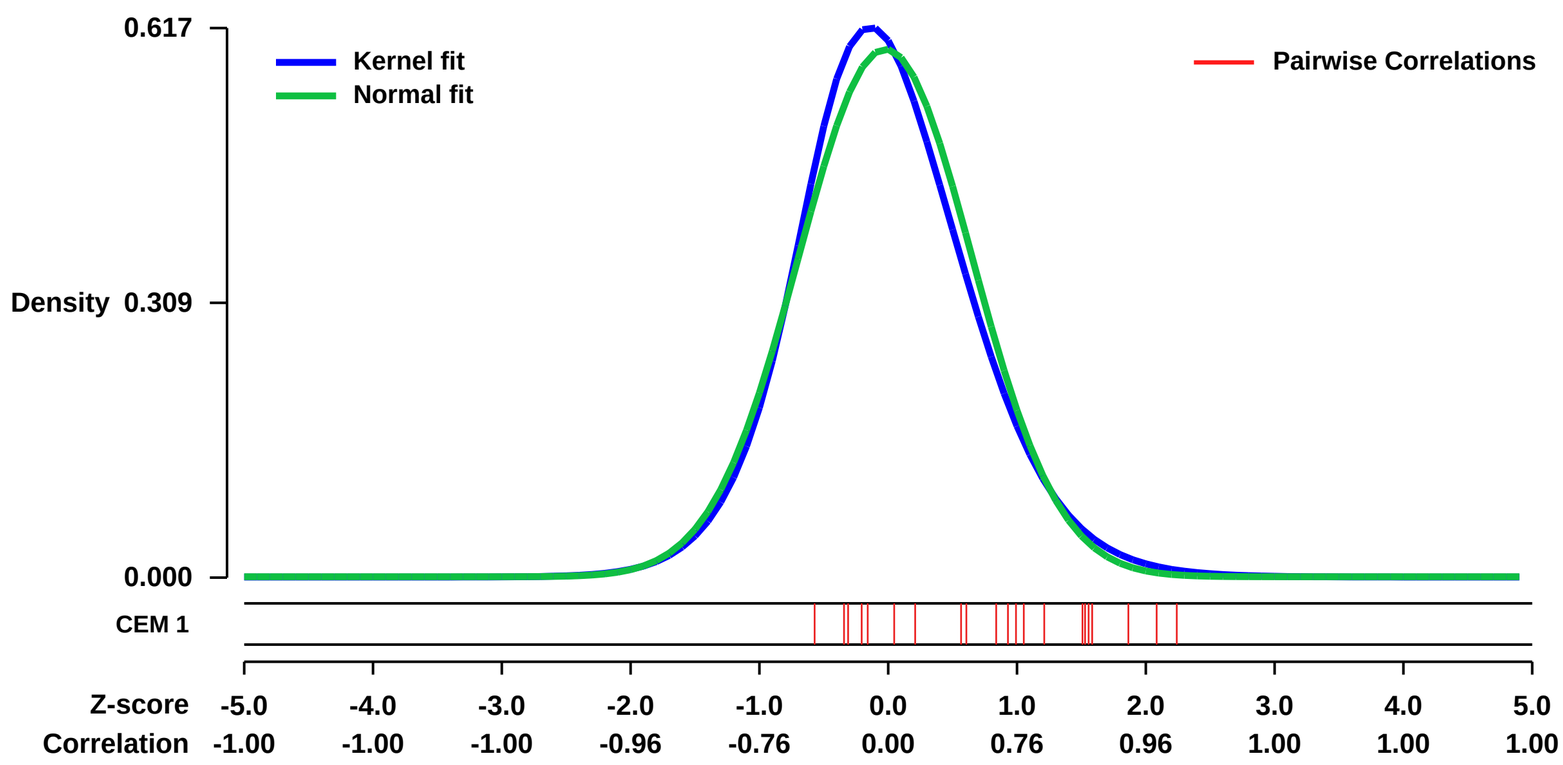

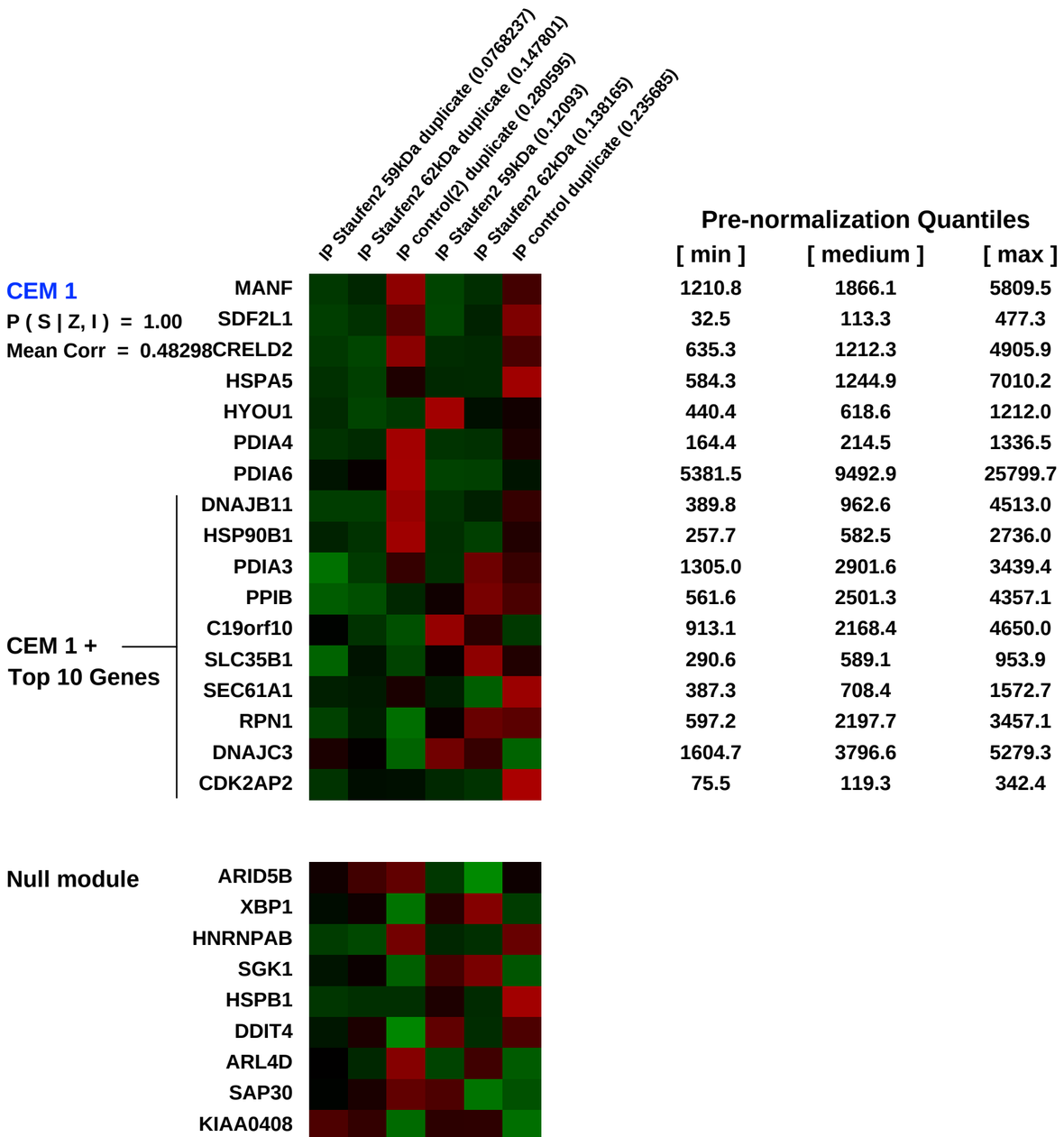

	Pre-normalization Quantiles		
	[min]	[medium]	[max]
MANF	1210.8	1866.1	5809.5
SDF2L1	32.5	113.3	477.3
CRELD2	635.3	1212.3	4905.9
HSPA5	584.3	1244.9	7010.2
HYOU1	440.4	618.6	1212.0
PDIA4	164.4	214.5	1336.5
PDIA6	5381.5	9492.9	25799.7
DNAJB11	389.8	962.6	4513.0
HSP90B1	257.7	582.5	2736.0
PDIA3	1305.0	2901.6	3439.4
PPIB	561.6	2501.3	4357.1
C19orf10	913.1	2168.4	4650.0
SLC35B1	290.6	589.1	953.9
SEC61A1	387.3	708.4	1572.7
RPN1	597.2	2197.7	3457.1
DNAJC3	1604.7	3796.6	5279.3
CDK2AP2	75.5	119.3	342.4
ARID5B			
XBP1			
HNRNPAB			
SGK1			
HSPB1			
DDIT4			
ARL4D			
SAP30			
KIAA0408			
GPR17			
HSPH1			
DNASE1L2			
SLC5A3			
GNAS			
GPR3			
TNFRSF25			
TM6SF2			
MKKS			
PLEKHF1			
ZMYM1			
DOK3			
FGF20			
SLC39A2			
KCNIP2			
ERRFI1			
DEDD2			
CCDC117			
USP31			
AHSA2			
CYS1			
CNIH2			
BANP			
CHORDC1			
P4HA1			

GEO Series "GSE39084" Expression Profiles

Num of samples in this series: 70

Scale of expression profile Z-scores

-3.0 -2.0 -1.0 0.0 1.0 2.0 3.0

GEO Link: http://www.ncbi.nlm.nih.gov/geo/query/acc.cgi?acc=GSE39084
Status: Public on Aug 04 2014
Title: Sporadic early-onset colorectal carcinoma is a distinct clinicopathological and molecular entity
Organism: Homo sapiens
Experiment type: Expression profiling by array
Platform: GPL570
Pubmed ID: 25083765

Summary & Design:

Summary:
Sporadic early onset colorectal carcinoma (EOCRC) is a growing problem that remains poorly understood. Clinical specificities and mechanisms of tumorigenesis might be relevant to both diagnosis and treatment. In this prospective study, clinicopathological features, genomic and gene expression profiles of sporadic EOCRC were compared to other well defined groups of CRC.

Overall design:
Seventy selected patients were divided into 4 groups according to age (< 45 or > 60 years) and mismatch repair status. Mutations of key genes involved in colorectal carcinogenesis (P53, KRAS, BRAF, PIK3CA) were detected and the methylator phenotype (CIMP) established. Gene expression profiles (GEP) were obtained using pangenomic Affymetrix GeneChip.

Background corr dist: KL-Divergence = 0.5686, L1-Distance = 0.0966, L2-Distance = 0.0330, Normal std = 0.2153

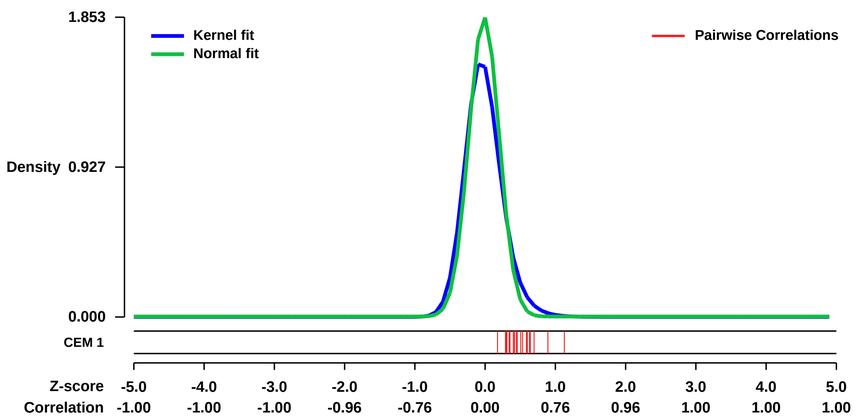

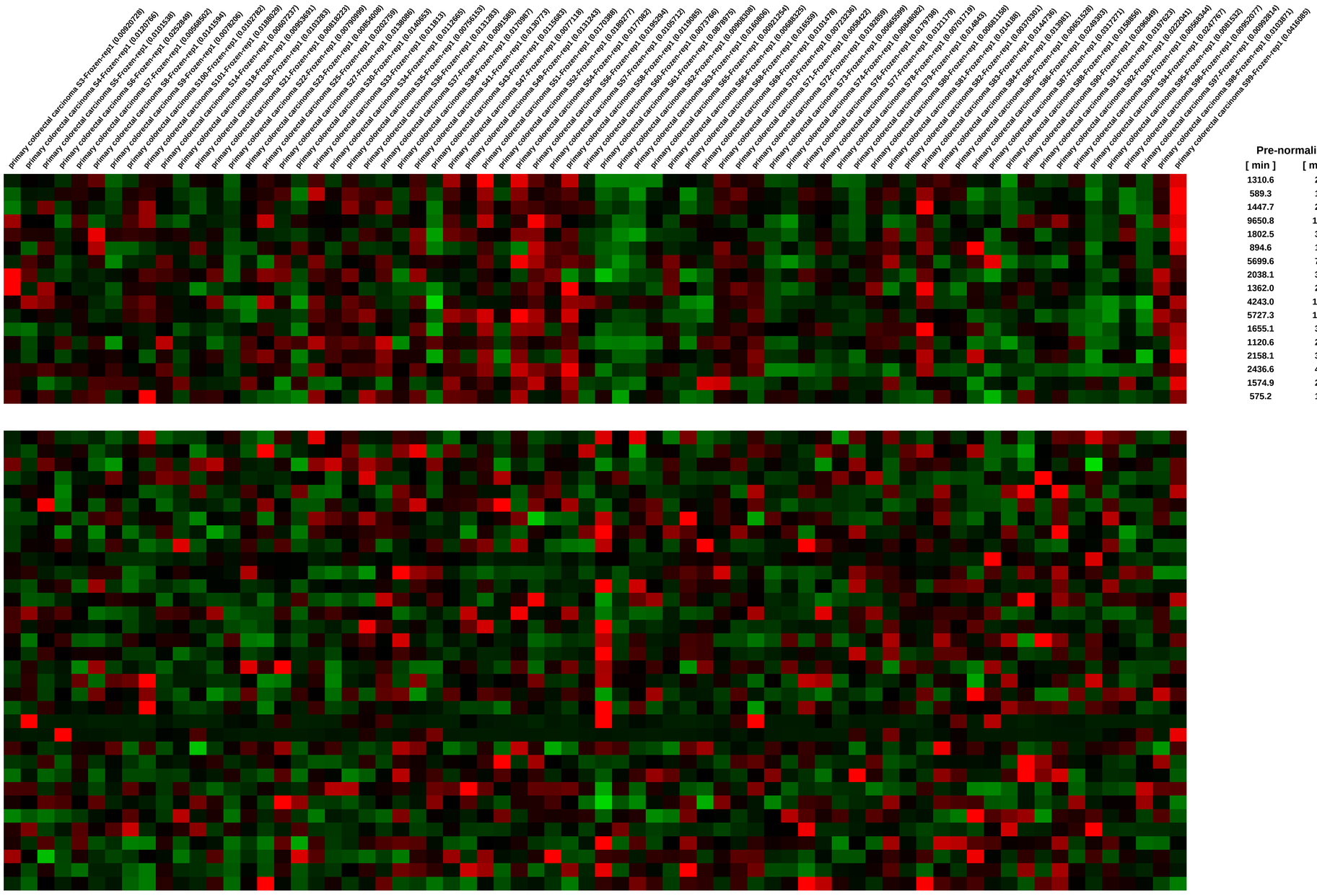

Pre-normalization Quantiles

[min]	[medium]	[max]
1310.6	2589.7	5283.5
589.3	1375.5	3345.2
1447.7	2862.7	7827.4
9650.8	14883.2	24176.1
1802.5	3541.5	7858.5
894.6	1590.3	3649.9
5699.6	7926.6	12412.8
2038.1	3441.8	5591.7
1362.0	2971.6	7221.6
4243.0	10162.0	15457.3
5727.3	13382.6	30871.0
1655.1	3731.5	8993.4
1120.6	2050.4	3278.0
2158.1	3440.5	5591.3
2436.6	4207.5	7362.2
1574.9	2868.6	5499.9
575.2	1390.6	2828.6

GEO Series "GSE34602" Expression Profiles

Num of samples in this series: 12

Scale of expression profile Z-scores

-3.0 -2.0 -1.0 0.0 1.0 2.0 3.0

GEO Link:	http://www.ncbi.nlm.nih.gov/geo/query/acc.cgi?acc=GSE34602
Status:	Public on Dec 22 2011
Title:	Expression data from 3 gamma-secretase or mock-treated mantle cell lymphoma (MCL) cell lines
Organism:	Homo sapiens
Experiment type:	Expression profiling by array
Platform:	GPL570
Pubmed ID:	22210878
Summary & Design:	**Summary:** We identified recurrent NOTCH1 mutations in 12% of MCLs. 2 out of 10 tested MCL cell lines (Rec-1 and SP-49) were sensitive to inhibition of the NOTCH pathway by gamma-secretase inhibition. The aim of this study was to identify transcriptional targets of NOTCH signaling in MCL. **Overall design:** 3 MCL cell lines (Mino, Rec-1, SP-49 treated with Mock or 1 micromolar compound E for 24 hours, in duplicate.

Background corr dist: KL-Divergence = 0.0852, L1-Distance = 0.0214, L2-Distance = 0.0006, Normal std = 0.4746

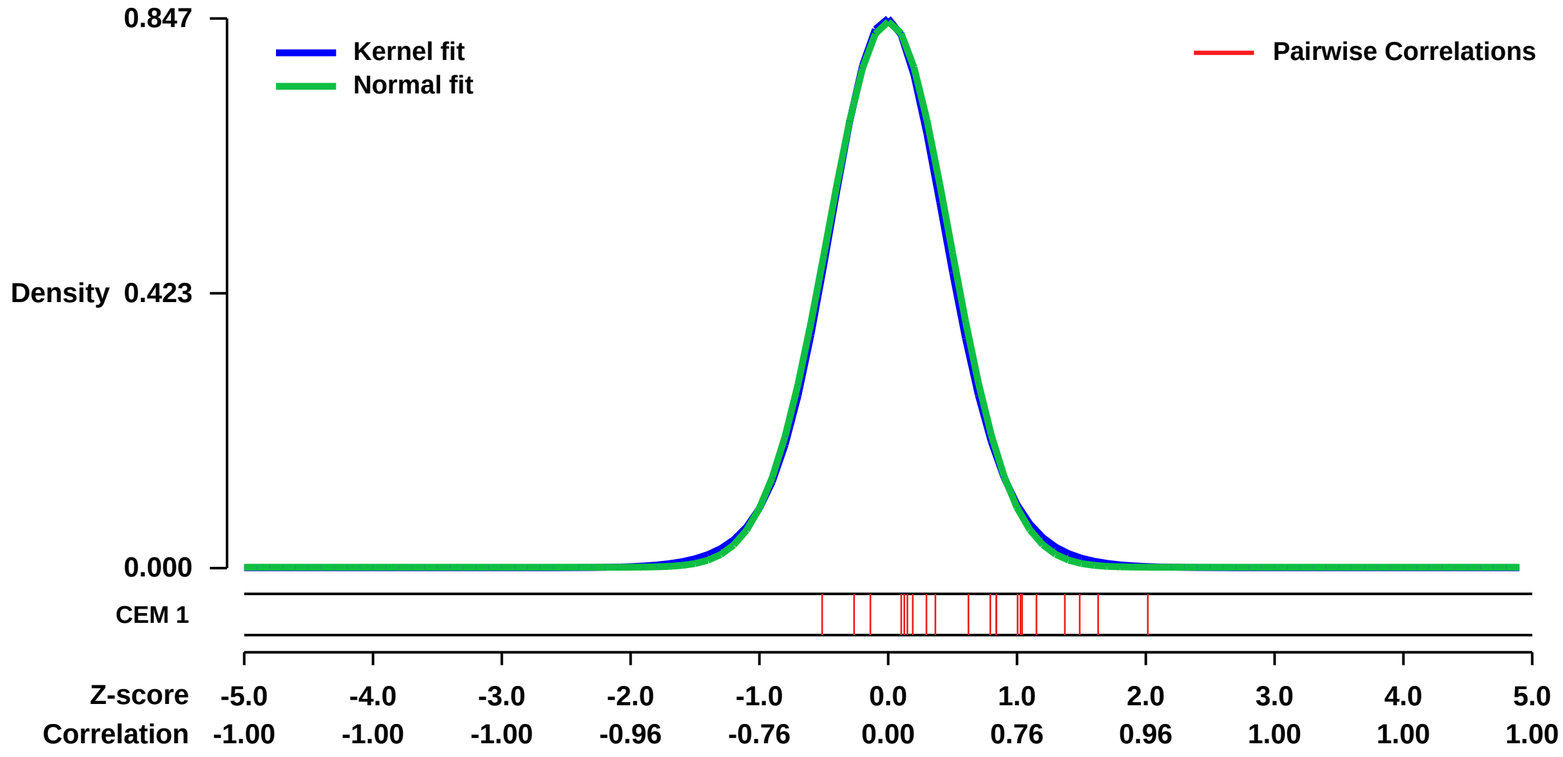

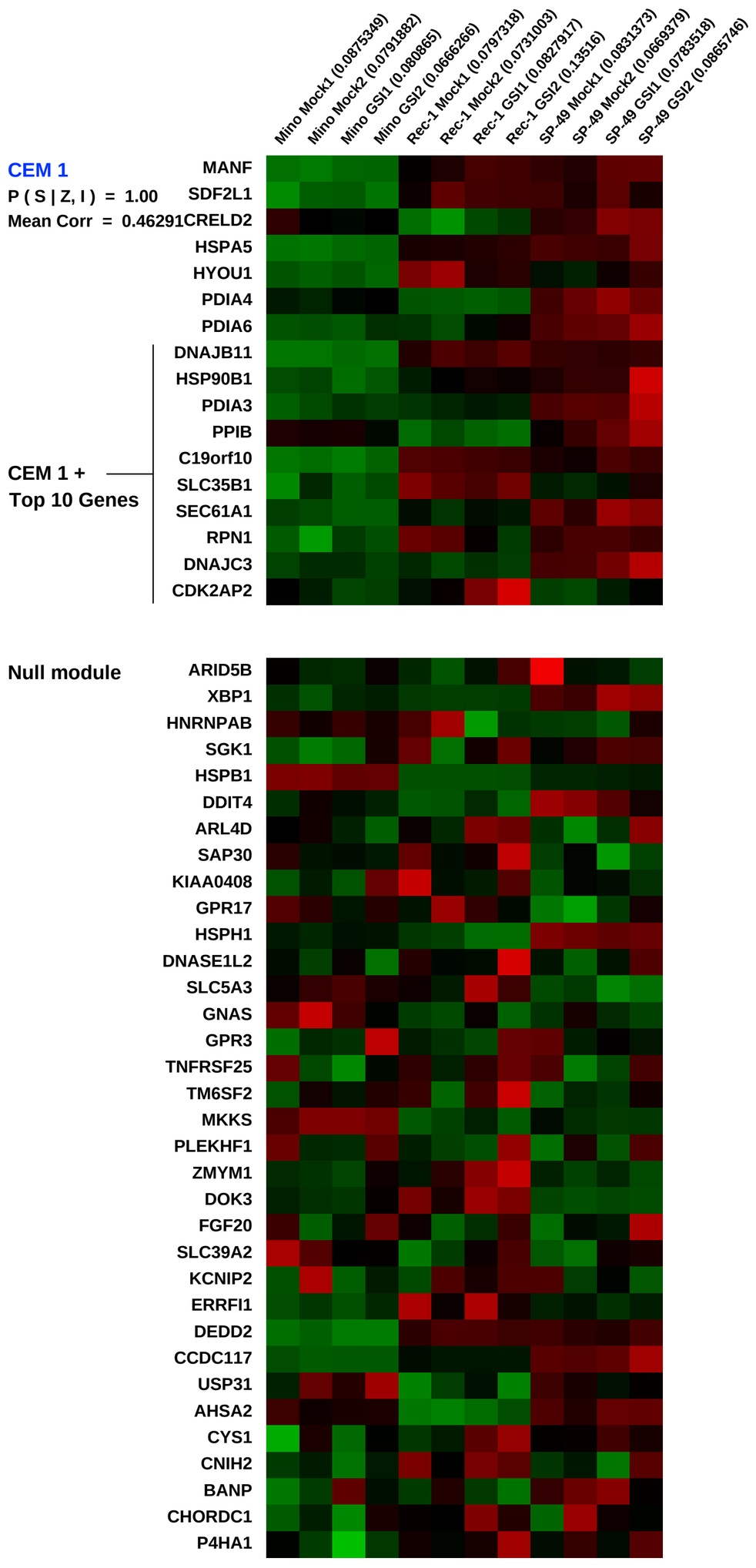

GEO Series "GSE28792" Expression Profiles

Num of samples in this series: 15

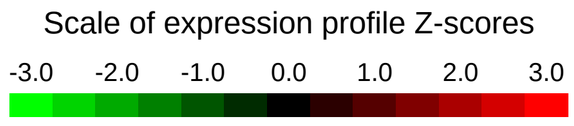

GEO Link:	http://www.ncbi.nlm.nih.gov/geo/query/acc.cgi?acc=GSE28792
Status:	Public on Apr 22 2011
Title:	Polydextrose fermentation metabolite effect on Caco-2 colon cancer cells
Organism:	Homo sapiens
Experiment type:	Expression profiling by array
Platform:	GPL570
Pubmed ID:	

Summary & Design:

Summary:
Analysis of non-differentiated Caco-2 intestinal epithelial cell line treated with polydextrose fermentation metabolites fermented for 48 hours in 4-stage in vitro colon simulator, in which the conditions mimic the human proximal, ascending, transverse and distal colon in sequence , as well as with medium, 100 mM NaCl and 5 mM butyrate. Polydextrose, a soluble fiber fermented in colon, was fermented with the in vitro colon simulator in three amounts of 0%, 1% and 2%. Results provide insight into the mechanisms underlying colon cancer cells and a comparison of a complex fiber metabolome to 5 mM butyrate and 100 mM NaCl. Furthermore, the results give insight of dosage effect of increasing the concentration of fiber.

High level of dietary fiber has been epidemiologically linked to protection against the risk for developing colon cancer. The mechanisms of this protection are not clear. Fermentation of dietary fiber in the colon results in production of for example butyrate that has drawn attention as a chemopreventive agent. Polydextrose, a soluble fiber that is only partially fermented in colon, was fermented in an in vitro colon simulator, in which the conditions mimic the human proximal, ascending, transverse and distal colon in sequence. The subsequent fermentation metabolome were applied on colon cancer cells, and the gene expression changes studied. Polydextrose fermentation down-regulated classes linked with cell cycle, and affected number of metabolically active cells. Further, up-regulated effects on classes linked with apoptosis implicate that polydextrose fermentation plays a role in induction of apoptosis in colon cancer cells. The up-regulated genes involved also key regulators of lipid metabolism, such as PPARg and PGC-1α–. These results offer hypotheses for the mechanisms of two health benefits linked with consumption of dietary fiber, reducing risk of development of colon cancer, and dyslipidemia.

Overall design:
Non-differentiated Caco-2 cells were treated with polydextrose fermentation metabolites from the vessels representing different parts of the colon, or with 100 mM NaCl or with 5 mM butyrate for 24 hours. For polydextrose fermentation three concentrations of polydextrose were used: 0%, 1% and 2% for a simulation that lasted for 48 hours. Polydextrose fermentation samples from total of 12 vessels, as well as from medium sample, 5 mM butyrate and 100 mM NaCl were analysed as single replica.

Background corr dist: KL-Divergence = 0.1278, L1-Distance = 0.0338, L2-Distance = 0.0019, Normal std = 0.4109

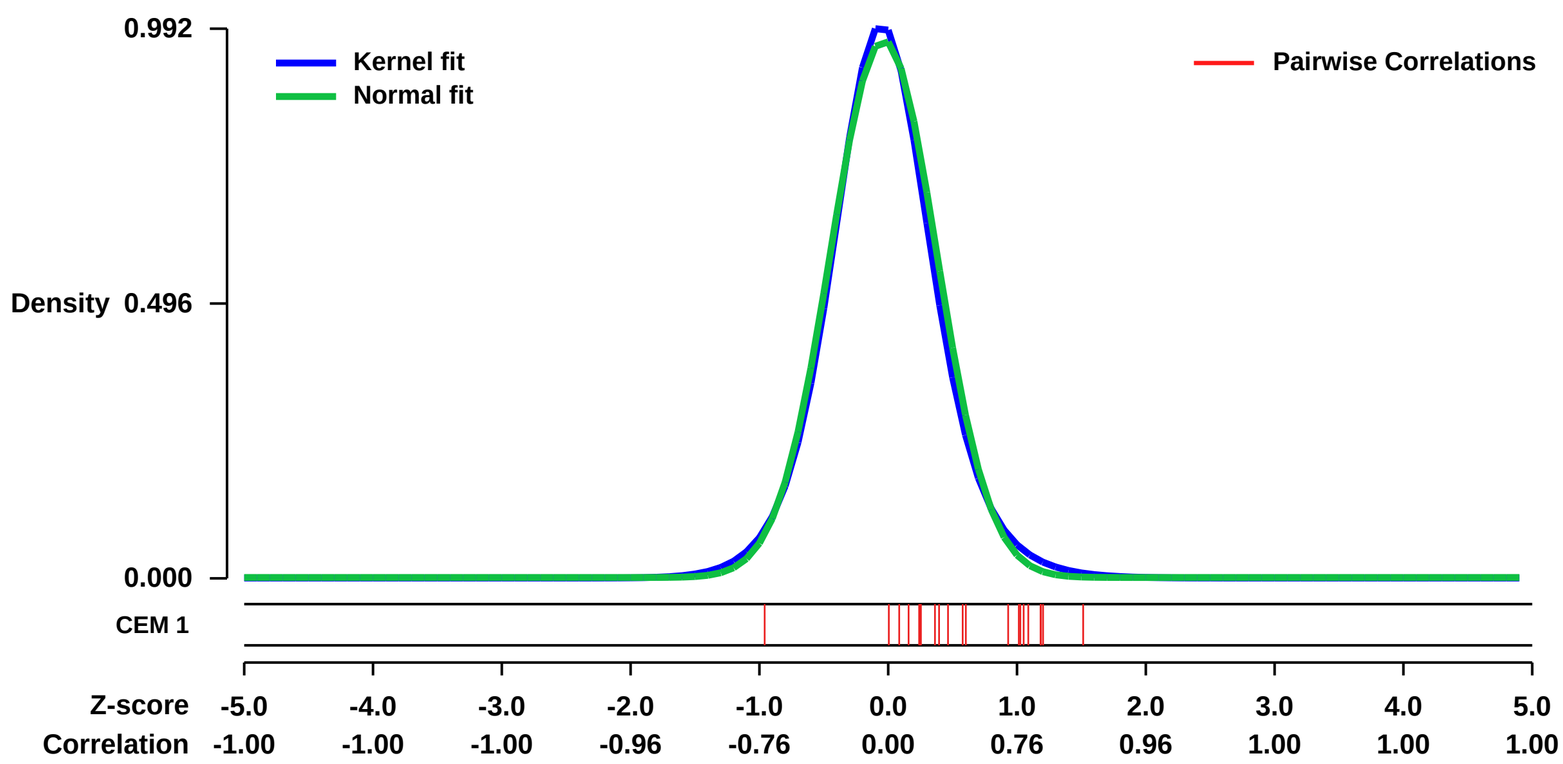

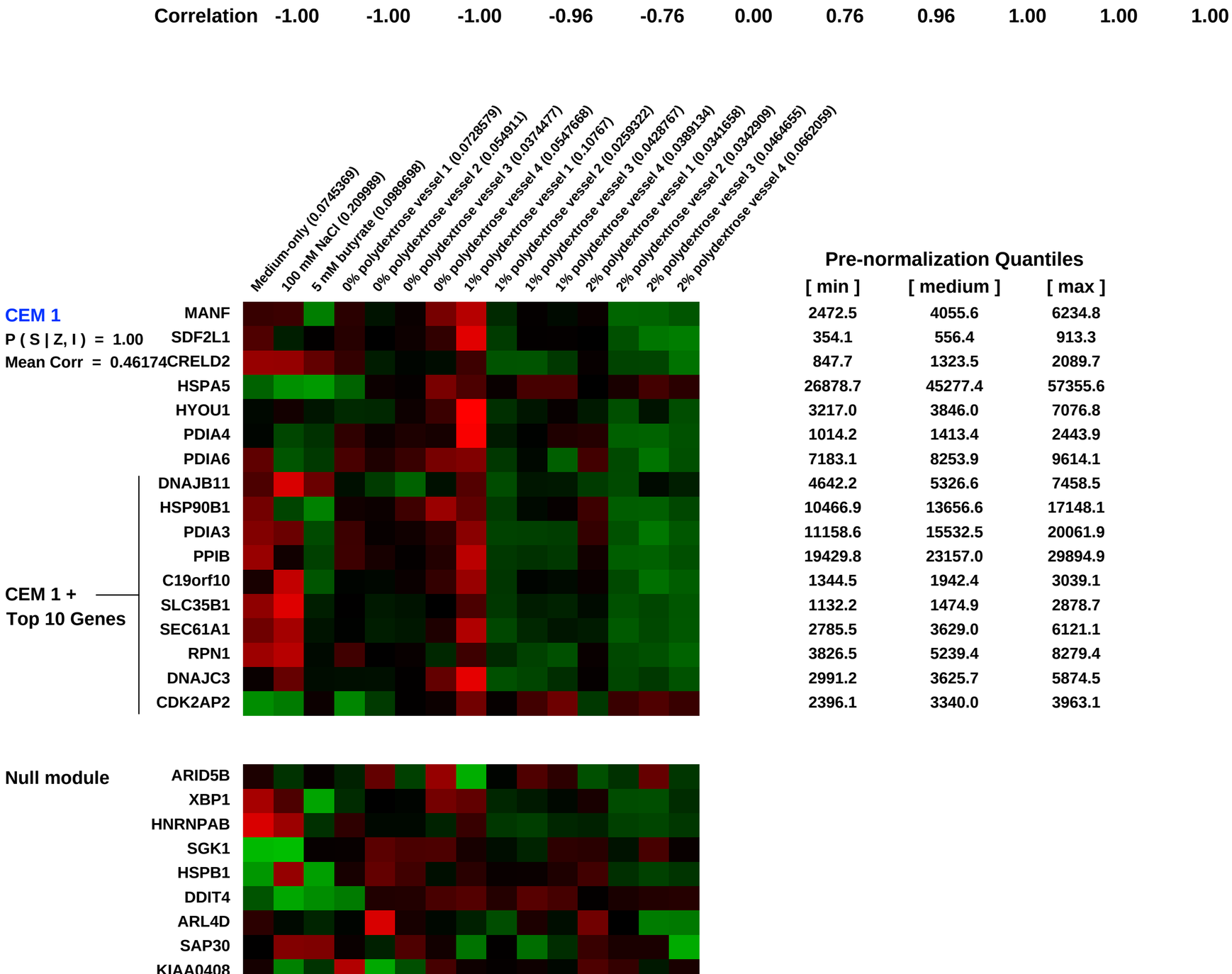

GEO Series "GSE12355" Expression Profiles

Num of samples in this series: 41

Scale of expression profile Z-scores

-3.0 -2.0 -1.0 0.0 1.0 2.0 3.0

GEO Link:	http://www.ncbi.nlm.nih.gov/geo/query/acc.cgi?acc=GSE12355
Status:	Public on Aug 06 2009
Title:	Detection of Notch1-IC, Notch2-IC and EBNA2 target genes in human B cells
Organism:	Homo sapiens
Experiment type:	Expression profiling by array
Platform:	GPL570
Pubmed ID:	19339697
Summary & Design:	**Summary:** Notch1-IC, Notch2-IC or EBNA2 have been induced in a conditionally immortalized human B cell line (EREB2-5) in order to identify similar and unique target genes in B cells. CAT was used as a control. **Keywords: time course** **Overall design:** RNA was isolated at different time points after induction of Notch1-IC, Notch2-IC or EBNA2 in EREB2-5 cells. Three independent experiments were performed (except Notch1-IC at 3day).

Background corr dist: KL-Divergence = 0.3698, L1-Distance = 0.0493, L2-Distance = 0.0056, Normal std = 0.2600

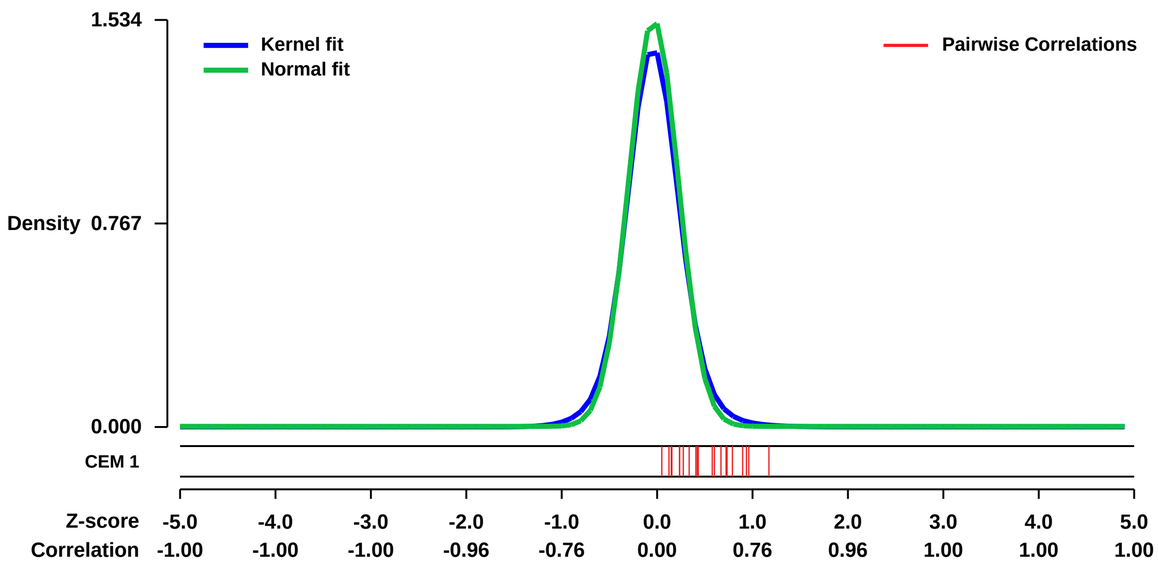

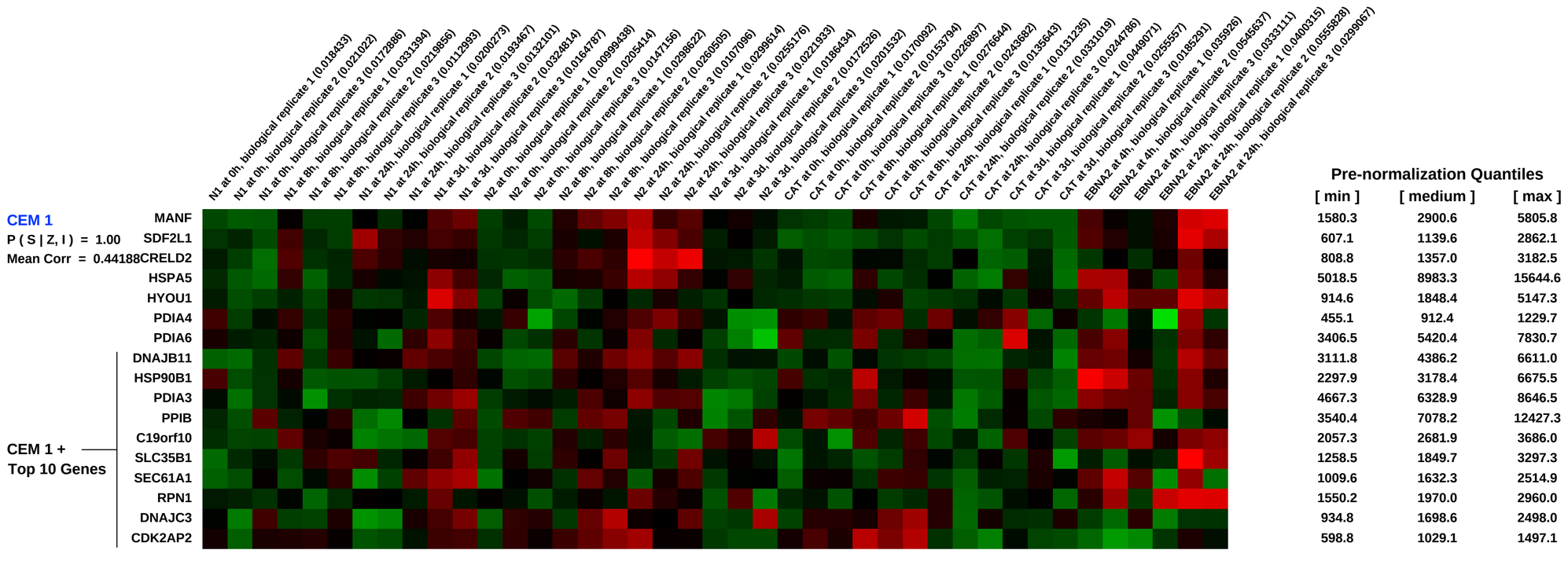

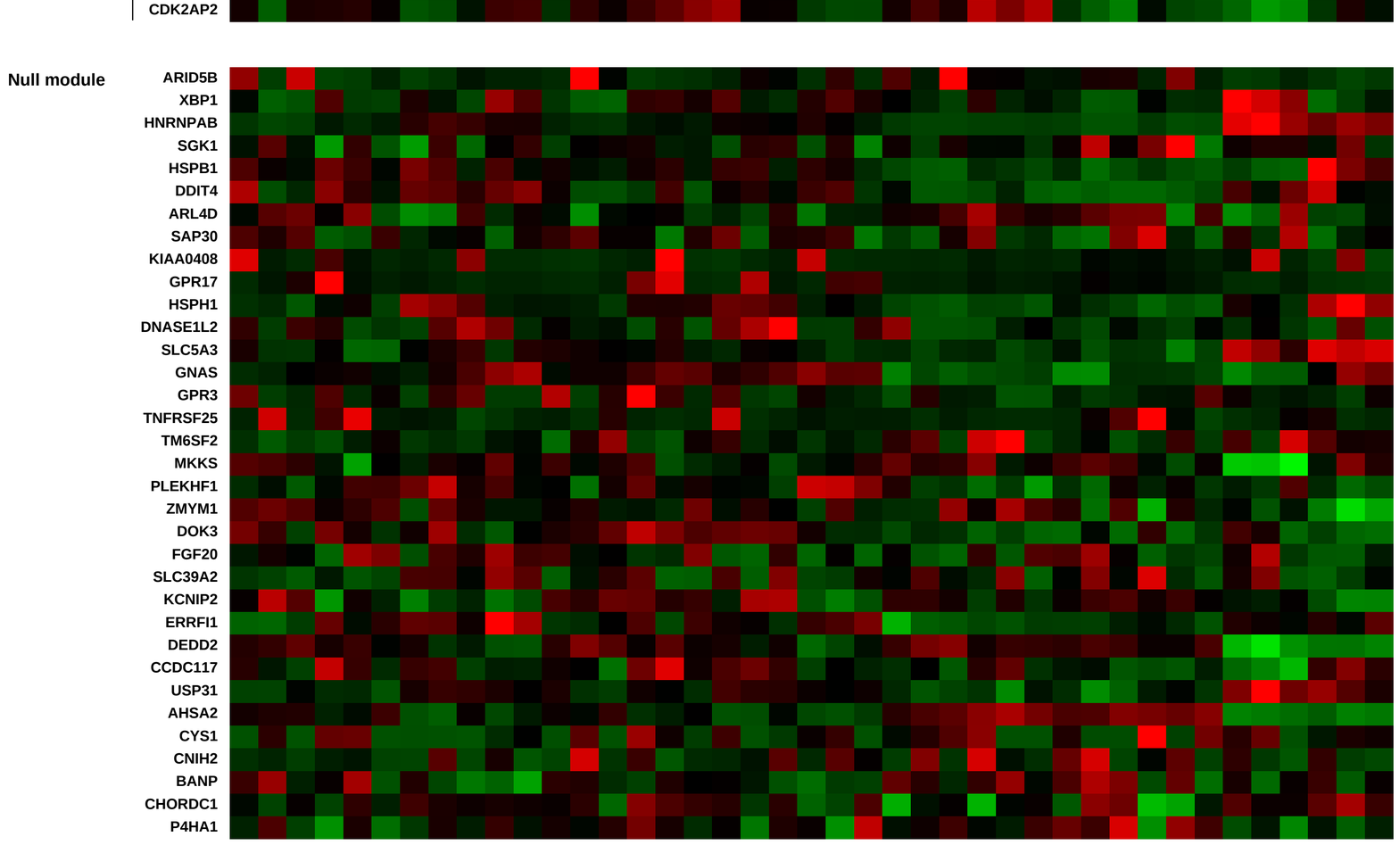

GEO Series "GSE30660" Expression Profiles

Num of samples in this series: 8

Scale of expression profile Z-scores

-3.0 -2.0 -1.0 0.0 1.0 2.0 3.0

GEO Link: http://www.ncbi.nlm.nih.gov/geo/query/acc.cgi?acc=GSE30660

Status: Public on Aug 31 2011

Title: The Effect of Repeated Whole Cigarette Smoke Challenge on Human Air-Liquid Interface Lung Epithelial Cultures

Organism: Homo sapiens

Experiment type: Expression profiling by array

Platform: GPL570

Pubmed ID:

Summary & Design:

Summary:
Airway epithelial cells are the first cells of the lungs to be exposed to the toxic agents contained within cigarette smoke. Accordingly, the response of these cells to this challenge is of considerable interest in the context of diseases in which cigarette smoke is a major aetiological factor.

We used Affymetrix microarrays to study the effects of repeated cigarette smoke challenge on three-dimensional human lung airway epithelial cultures.

Overall design:
We have used cultures from four individual donors, and compared the effects of repeated cigarette smoke challenge (30mins exposure on four separate days), with no challenge.

Background corr dist: KL-Divergence = 0.0674, L1-Distance = 0.0189, L2-Distance = 0.0005, Normal std = 0.5060

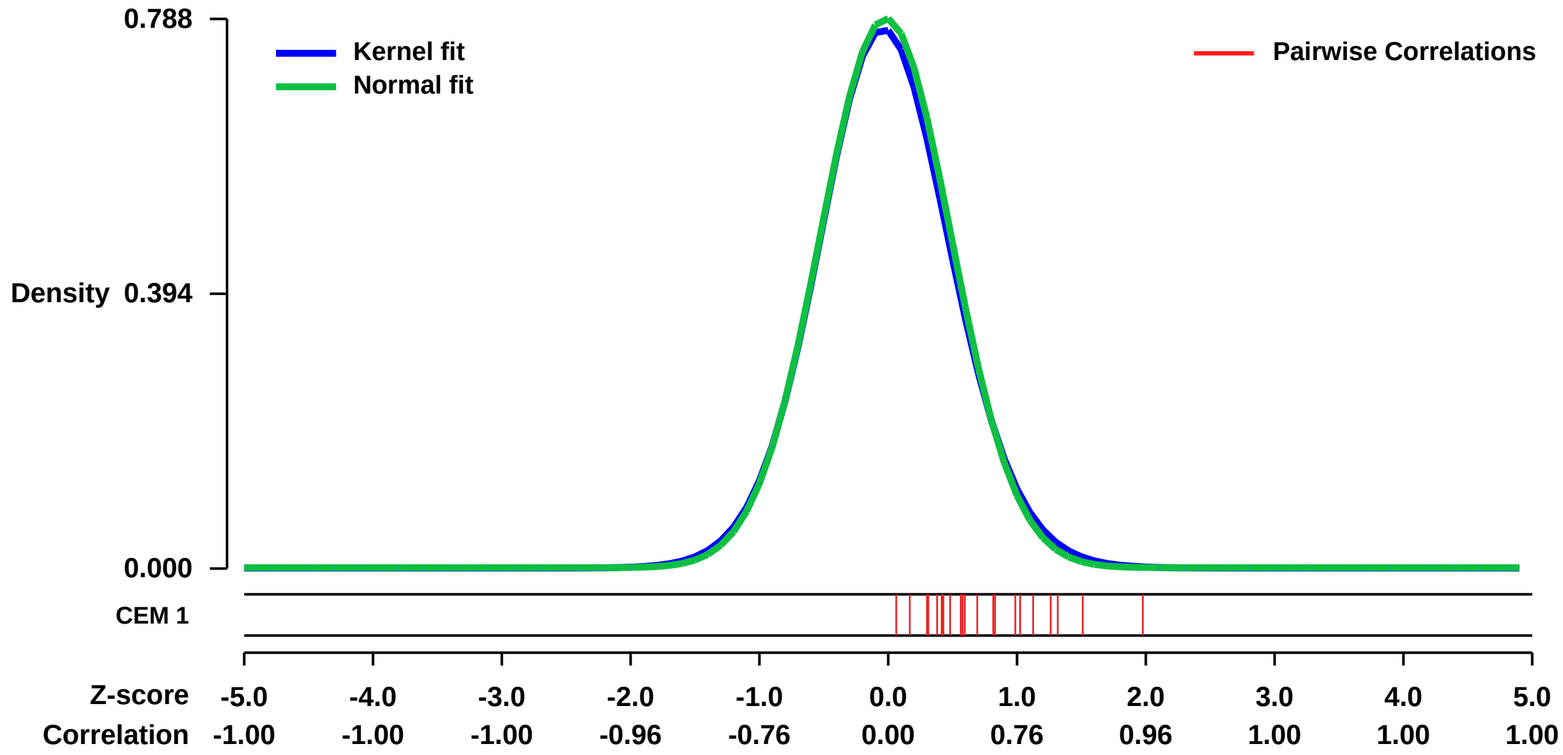

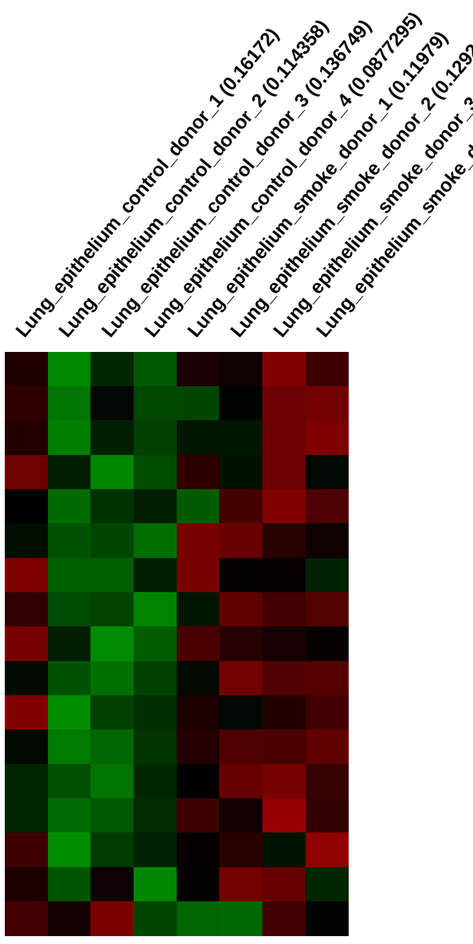

	Pre-normalization Quantiles		
	[min]	[medium]	[max]
MANF	1427.4	1995.2	2359.4
SDF2L1	449.7	554.6	659.6
CRELD2	1819.8	2033.5	2335.9
HSPA5	8291.5	9257.9	10136.7
HYOU1	1688.6	1998.7	2369.5
PDIA4	692.3	838.9	960.2
PDIA6	2895.1	3374.4	3986.7
DNAJB11	1833.9	2286.2	2407.5
HSP90B1	1290.0	1687.8	1920.3
PDIA3	6840.1	7524.8	8318.0
PPIB	6100.4	7443.6	8246.0
C19orf10	1136.0	1540.1	1695.5
SLC35B1	1465.8	1669.4	1878.3
SEC61A1	2237.5	2670.5	3135.6
RPN1	1914.0	2555.3	3143.3
DNAJC3	2129.7	2469.2	2707.5
CDK2AP2	954.9	1206.1	1417.2

GEO Series "GSE25725" Expression Profiles

Num of samples in this series: 8

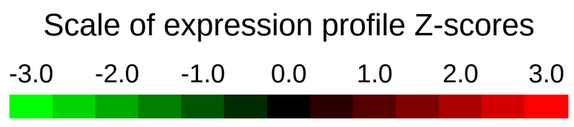

GEO Link:	http://www.ncbi.nlm.nih.gov/geo/query/acc.cgi?acc=GSE25725
Status:	Public on Jan 01 2011
Title:	gene expression data from cep701 treated HEL cells and shPRMT5 knocking down HEL cells
Organism:	Homo sapiens
Experiment type:	Expression profiling by array
Platform:	GPL570
Pubmed ID:	21316606
Summary & Design:	**Summary:** compare the gene expression profile between cep701 treated HEL cells with shPRMT5 knockingdown HEL cells. HEL cells contain homologous alells with mutation Jak2V617F. We found JAK2V617F can inactivate PRMT5 activity by directly phosphorylating PRMT5 through histone methylation. #!# **Overall design:** compare the gene expression profile between cep701 treated HEL cells with shPRMT5 knockingdown HEL cells

Background corr dist: KL-Divergence = 0.0462, L1-Distance = 0.0403, L2-Distance = 0.0021, Normal std = 0.6104

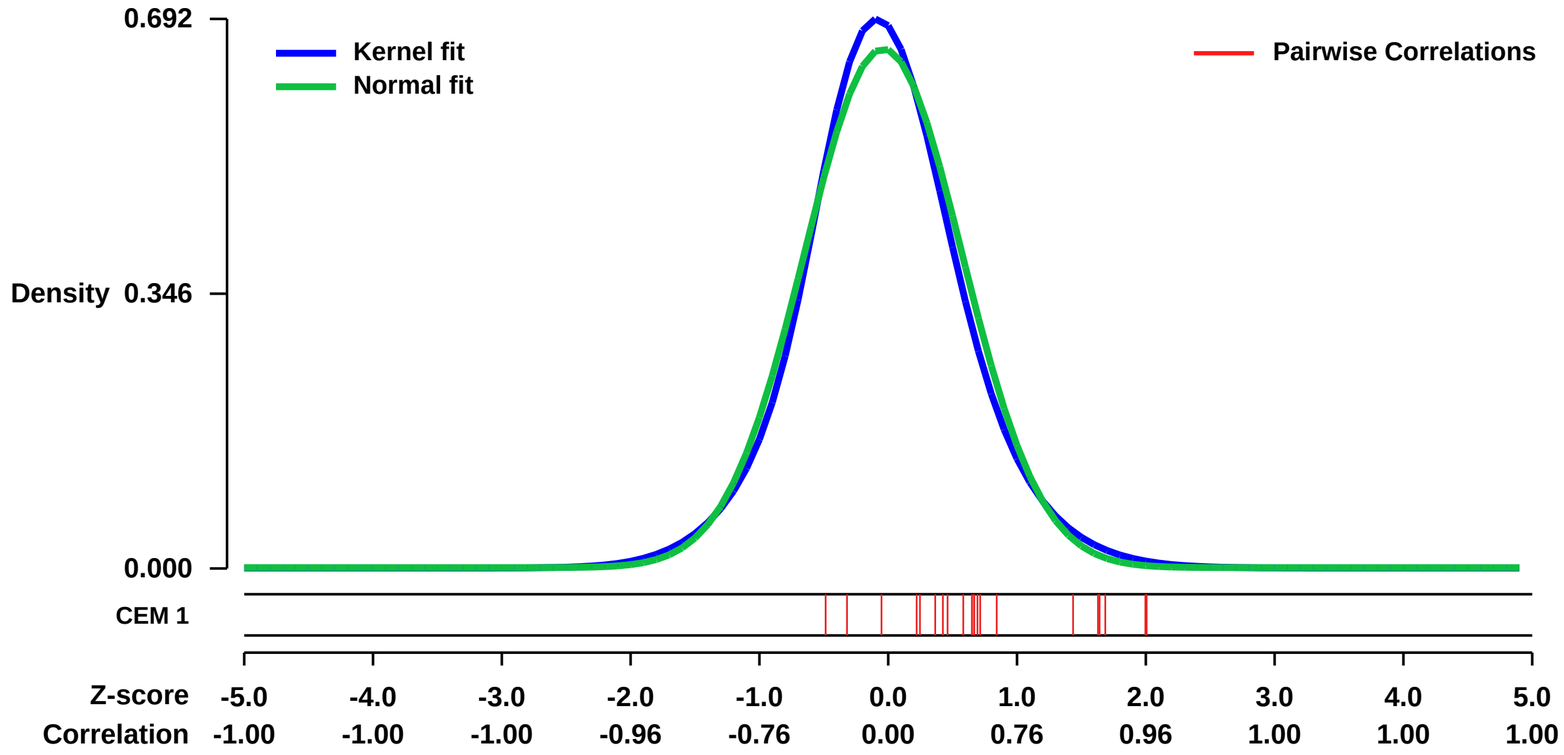

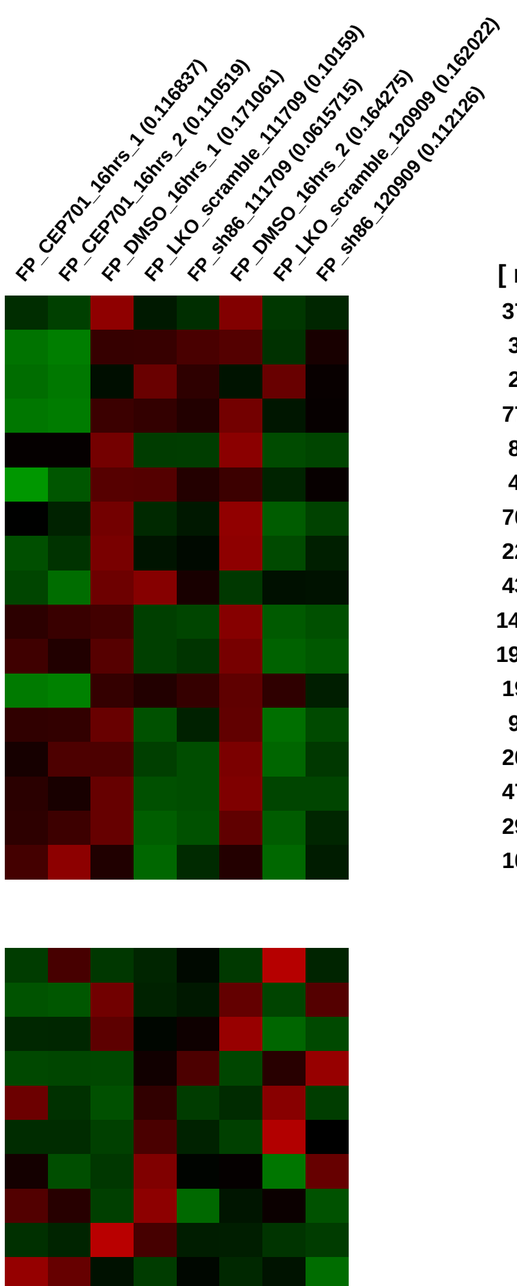

GEO Series "GSE9843" Expression Profiles

Num of samples in this series: 91

Scale of expression profile Z-scores

-3.0 -2.0 -1.0 0.0 1.0 2.0 3.0

GEO Link: http://www.ncbi.nlm.nih.gov/geo/query/acc.cgi?acc=GSE9843
Status: Public on Jun 22 2008
Title: Gene expression profiling of 91 hepatocellular carcinomas with hepatitis C virus etiology
Organism: Homo sapiens
Experiment type: Expression profiling by array
Platform: GPL570
Pubmed ID: 21324318

Summary & Design:

Summary:
To characterize the genetic alterations that instigate hepatitis C virus-induced hepatocellular carcinoma (HCC), we conducted an integrative genomic analysis of 103 HCCs. Most tumors harbored 1q gain, 8q gain or 8p loss, with occasional alterations in 13 additional chromosome arms. In addition to amplifications at 11q13 in 6 tumors, 4 tumors harbored focal gains at 6p21 incorporating VEGFA, which were confirmed in 4 of 113 HCC in an independent validation set. Strikingly, this locus overlapped with copy gains in 4 of 371 lung adenocarcinomas. Overexpression of VEGFA via 6p21 gain suggested a cell-nonautonomous mechanism of oncogene activation. Hierarchical clustering of gene expression among 91 tumors identified 5 classes, including â Wnt-CTNNB1â , â proliferationâ and â interferon-relatedâ gene classes. We also discovered a novel class defined by polysomy of chromosome 7, gains of which were associated with early tumor recurrence after resection. These findings reveal key alterations in HCC pathogenesis and implicate potential therapeutic targets.

Keywords: disease state analysis

Overall design:
91 hepatocellular carcinomas were obtained at the time of surgical resection or orthotopic transplantation.

Background corr dist: KL-Divergence = 0.3511, L1-Distance = 0.0931, L2-Distance = 0.0283, Normal std = 0.2698

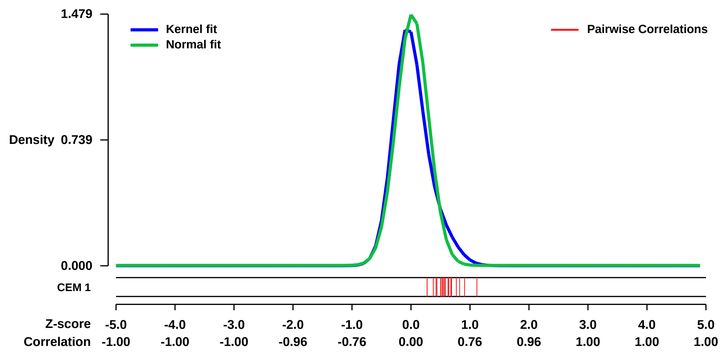

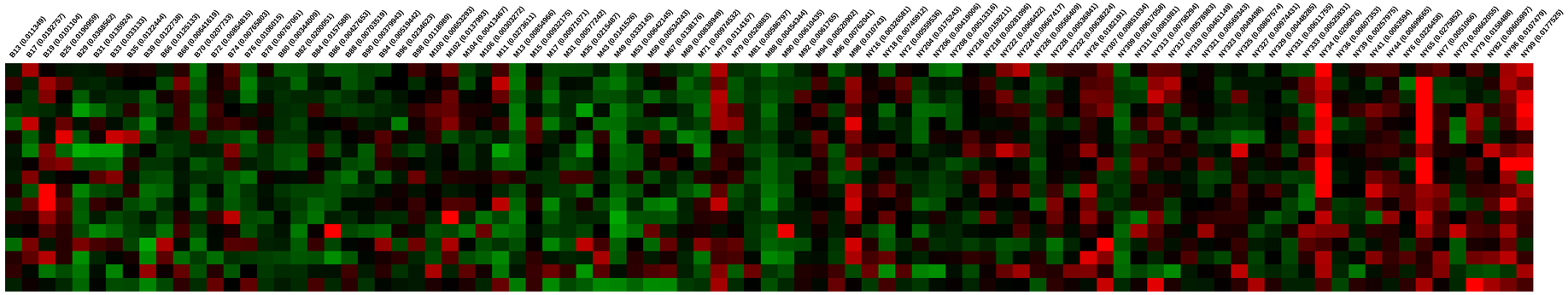

Pre-normalization Quantiles

	[min]	[medium]	[max]
MANF	803.9	2411.0	8329.7
SDF2L1	547.7	1551.3	4923.3
CRELD2	930.2	2374.2	8455.6
HSPA5	3961.0	16499.8	41956.3
HYOU1	1088.1	4304.1	11523.4
PDIA4	856.9	2367.2	6973.5
PDIA6	1330.5	8003.6	16167.6
DNAJB11	1886.5	3582.1	9488.9
HSP90B1	2386.9	5730.6	23351.1
PDIA3	4330.9	11883.3	30965.5
PPIB	10285.7	21756.3	49343.2
C19orf10	1141.3	2567.2	6456.6
SLC35B1	994.8	2286.8	4880.5
SEC61A1	1578.8	3457.3	7290.6
RPN1	2853.7	5082.7	8933.5
DNAJC3	1489.7	3244.8	5869.7
CDK2AP2	436.3	1139.8	3151.1

CEM 1
P (S | Z, I) = 1.00
Mean Corr = 0.51934

CEM 1 + Top 10 Genes

Null module

ARID5B
XBP1
HNRNPAB
SGK1
HSPB1
DDIT4
ARL4D
SAP30
KIAA0408
GPR17
HSPH1
DNASE1L2
SLC5A3
GNAS
GPR3
TNFRSF25
TM6SF2
MKKS
PLEKHF1
ZMYM1
DOK3
FGF20
SLC39A2
KCNIP2
ERRFI1
DEDD2
CCDC117
USP31
AHSA2
CYS1
CNIH2
BANP
CHORDC1
P4HA1

GEO Series "GSE44652" Expression Profiles

Num of samples in this series: 12

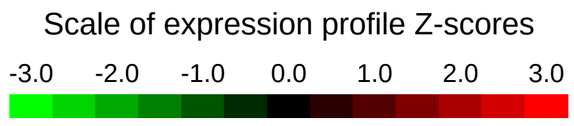

GEO Link:	http://www.ncbi.nlm.nih.gov/geo/query/acc.cgi?acc=GSE44652
Status:	Public on Mar 18 2013
Title:	Gene expression profile of the human T-ALL cell line JURKAT after TYK2 and STAT1 knockdown
Organism:	Homo sapiens
Experiment type:	Expression profiling by array
Platform:	GPL570
Pubmed ID:	23471820
Summary & Design:	**Summary:** Targeted molecular therapy has yielded remarkable outcomes in certain cancers, but specific therapeutic targets remain elusive for many others. As a result of two independent RNA interference (RNAi) screens, we identified pathway dependence on a member of the JAK tyrosine kinase family, TYK2, and its downstream effector STAT1 in T-cell acute lymphoblastic leukemia (T-ALL). Gene knockdown experiments consistently demonstrated TYK2 dependence in both T-ALL primary specimens and cell lines, and a small-molecule inhibitor of JAK kinase activity induced T-ALL cell death. Activation of this TYK2-STAT1 pathway in T-ALL cell lines occurs by gain-of-function TYK2 mutations or activation of IL-10 receptor signaling, and this pathway mediates T-ALL cell survival through upregulation of the anti-apoptotic protein BCL2. These findings indicate that in many T-ALL cases, the leukemic cells are dependent upon the TYK2-STAT1-BCL2 pathway for continued survival, supporting the development of molecular therapies targeting TYK2 and other components of this pathway. **Overall design:** Human T-ALL cell line JURKAT cells were transduced with TYK2 (TYK2#2 or #3), STAT1 (STAT1#2 or #3) or control shRNAs (GFP and Luc). Experiment was done in biological duplicate (""dup1"" and ""dup2"") . A total of 12 RNA samples (4 control, 4 TYK2 knockdown and 4 STAT1 knockdown) were used for microarray gene expression analysis.

Background corr dist: KL-Divergence = 0.1274, L1-Distance = 0.0259, L2-Distance = 0.0010, Normal std = 0.4008

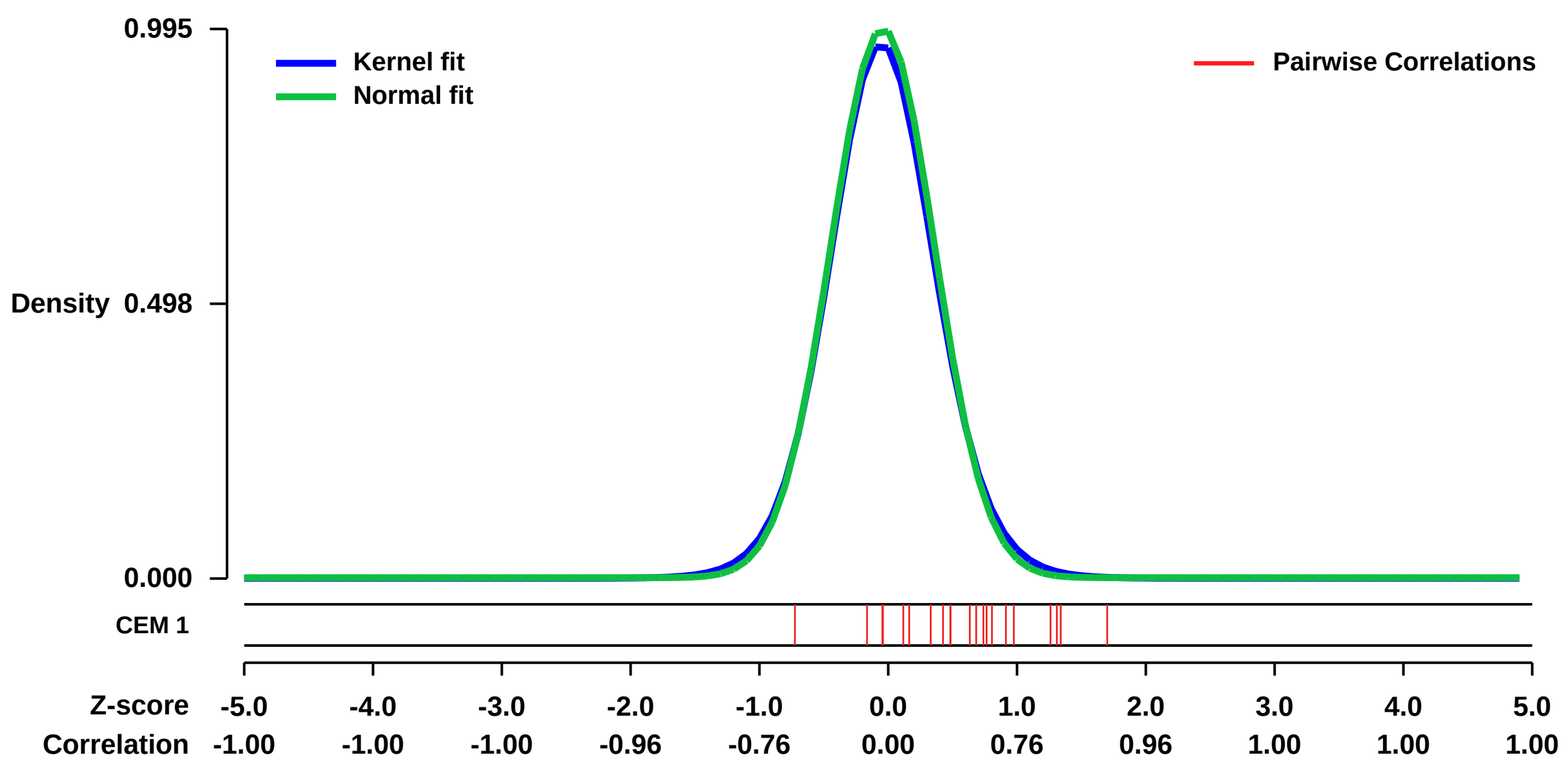

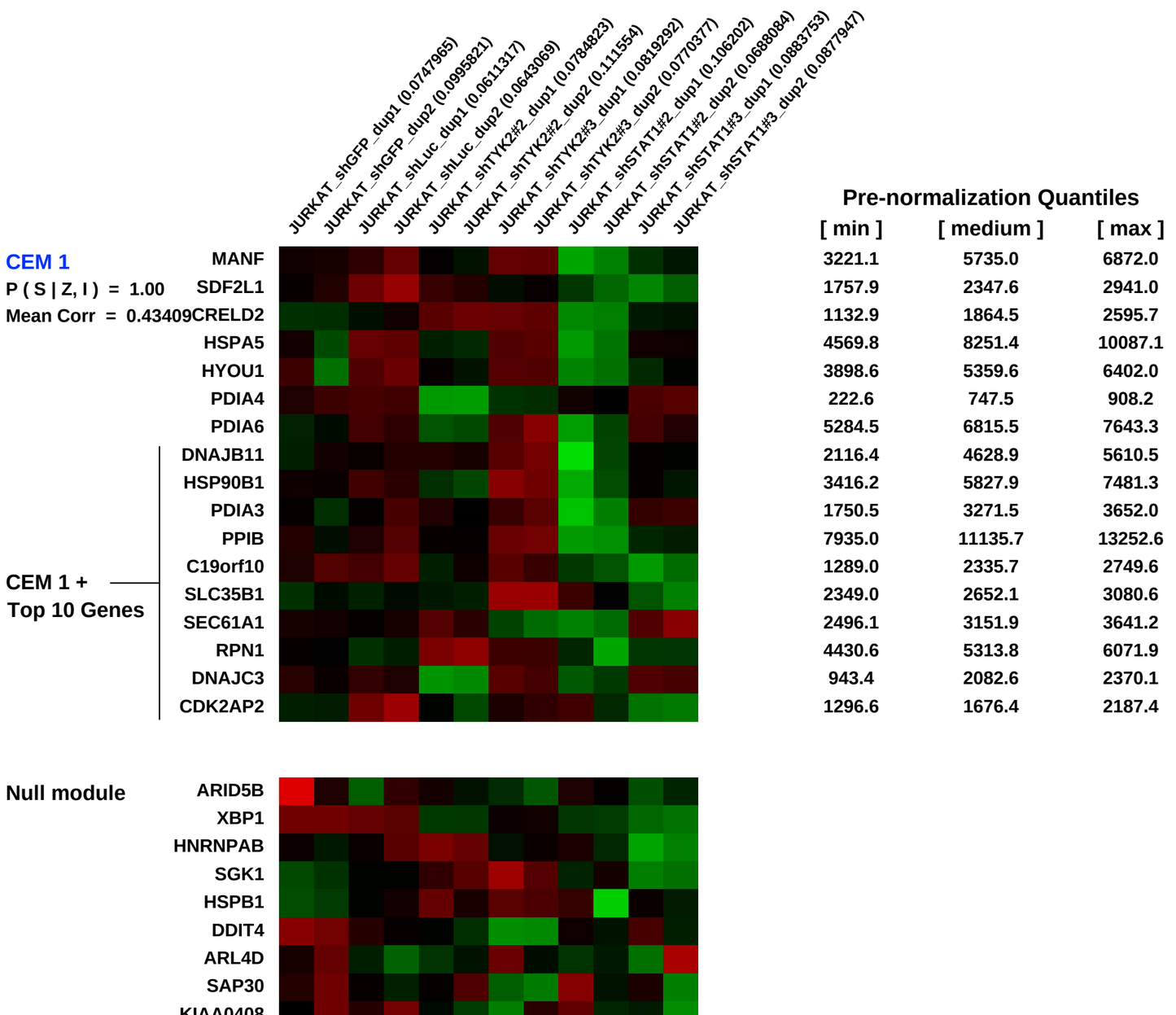

Pre-normalization Quantiles

	[min]	[medium]	[max]
JURKAT_shGFP_dup1 (0.0747965)	3221.1	5735.0	6872.0
JURKAT_shGFP_dup2 (0.0995821)	1757.9	2347.6	2941.0
JURKAT_shLuc_dup1 (0.0611317)	1132.9	1864.5	2595.7
JURKAT_shLuc_dup2 (0.0643069)	4569.8	8251.4	10087.1
JURKAT_shTYK2#2_dup1 (0.0784823)	3898.6	5359.6	6402.0
JURKAT_shTYK2#2_dup2 (0.111554)	222.6	747.5	908.2
JURKAT_shTYK2#3_dup1 (0.0819292)	5284.5	6815.5	7643.3
JURKAT_shTYK2#3_dup2 (0.0770377)	2116.4	4628.9	5610.5
JURKAT_shSTAT1#2_dup1 (0.106202)	3416.2	5827.9	7481.3
JURKAT_shSTAT1#2_dup2 (0.0688084)	1750.5	3271.5	3652.0
JURKAT_shSTAT1#3_dup1 (0.0883753)	7935.0	11135.7	13252.6
JURKAT_shSTAT1#3_dup2 (0.0877947)	1289.0	2335.7	2749.6
	2349.0	2652.1	3080.6
	2496.1	3151.9	3641.2
	4430.6	5313.8	6071.9
	943.4	2082.6	2370.1
	1296.6	1676.4	2187.4

GEO Series "GSE11118" Expression Profiles

Num of samples in this series: 12

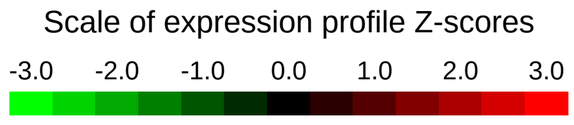

GEO Link:	http://www.ncbi.nlm.nih.gov/geo/query/acc.cgi?acc=GSE11118
Status:	Public on Dec 04 2009
Title:	Expression data following mitogen stimulation from Jurkat Cell
Organism:	Homo sapiens
Experiment type:	Expression profiling by array
Platform:	GPL570
Pubmed ID:	19880750
Summary & Design:	**Summary:** Gene expression analysis identified 27 of these 744 p300 and pol II associated genes as significantly increased (pâ∕0.05) within the first hour following mitogen stimulation **Keywords: time course** **Overall design:** Total RNA was purified from Jurkat T-cells treated 0, 30, and 60 min with phorbol ester and ionomycin. Antisense biotin-labeled RNA (aRNA) suitable for application to the Affymetrix microarray platform was generated using the Ambion MessageAmp 2-Biotin Enhanced kit as suggested by the manufacturer (www.Ambion.com). Purified biotin-labeled aRNA was fragmented and hybridized to U133 plus 2 GenechipsTM (Affymetrix), as recommended by the manufacturer. All samples were hybridized as technical replicates. Affymetrix U133 plus 2 GenechipsTM contain probe-sets corresponding to over 56,000 targets.

Background corr dist: KL-Divergence = 0.1437, L1-Distance = 0.0310, L2-Distance = 0.0017, Normal std = 0.3803

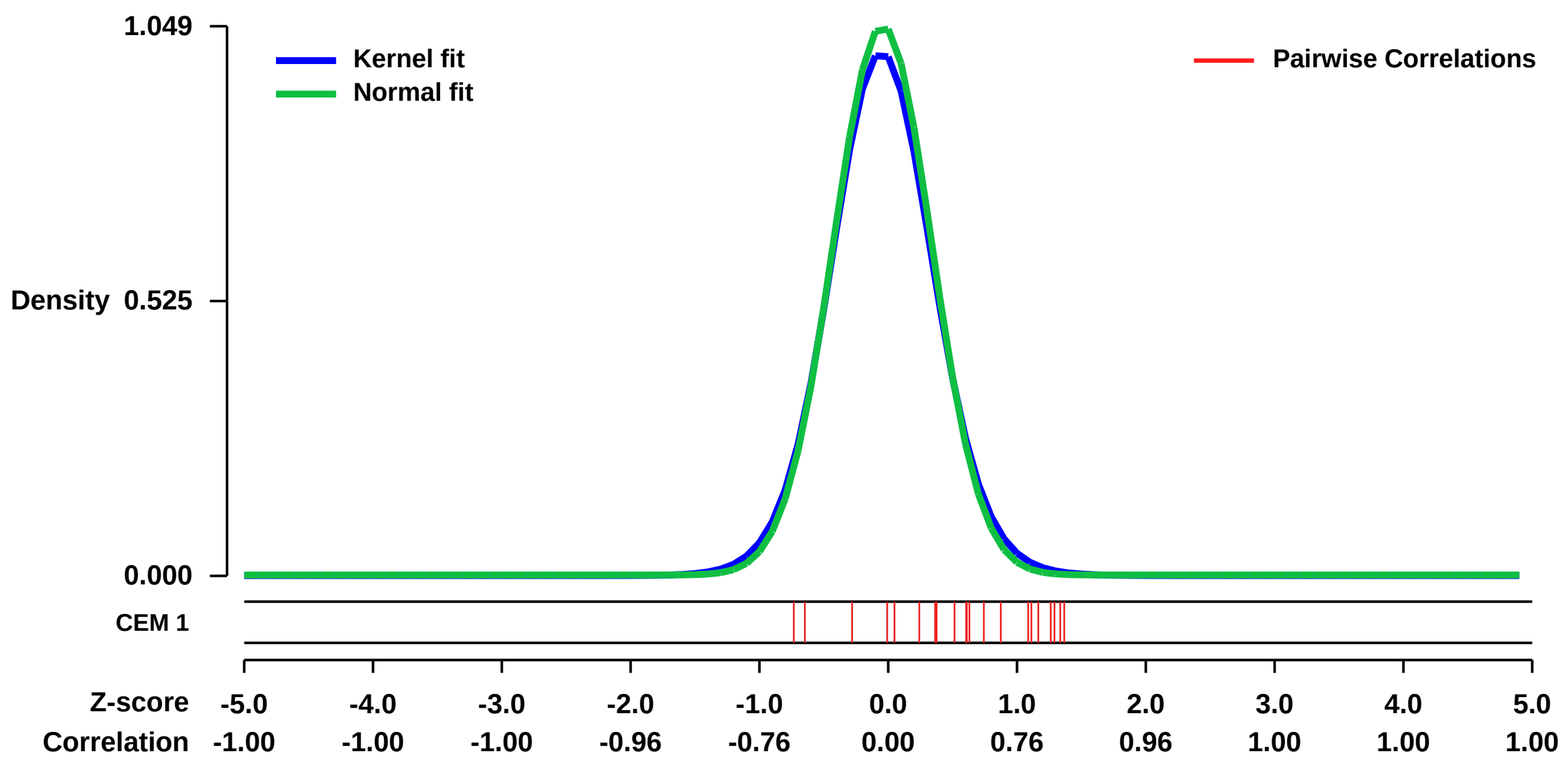

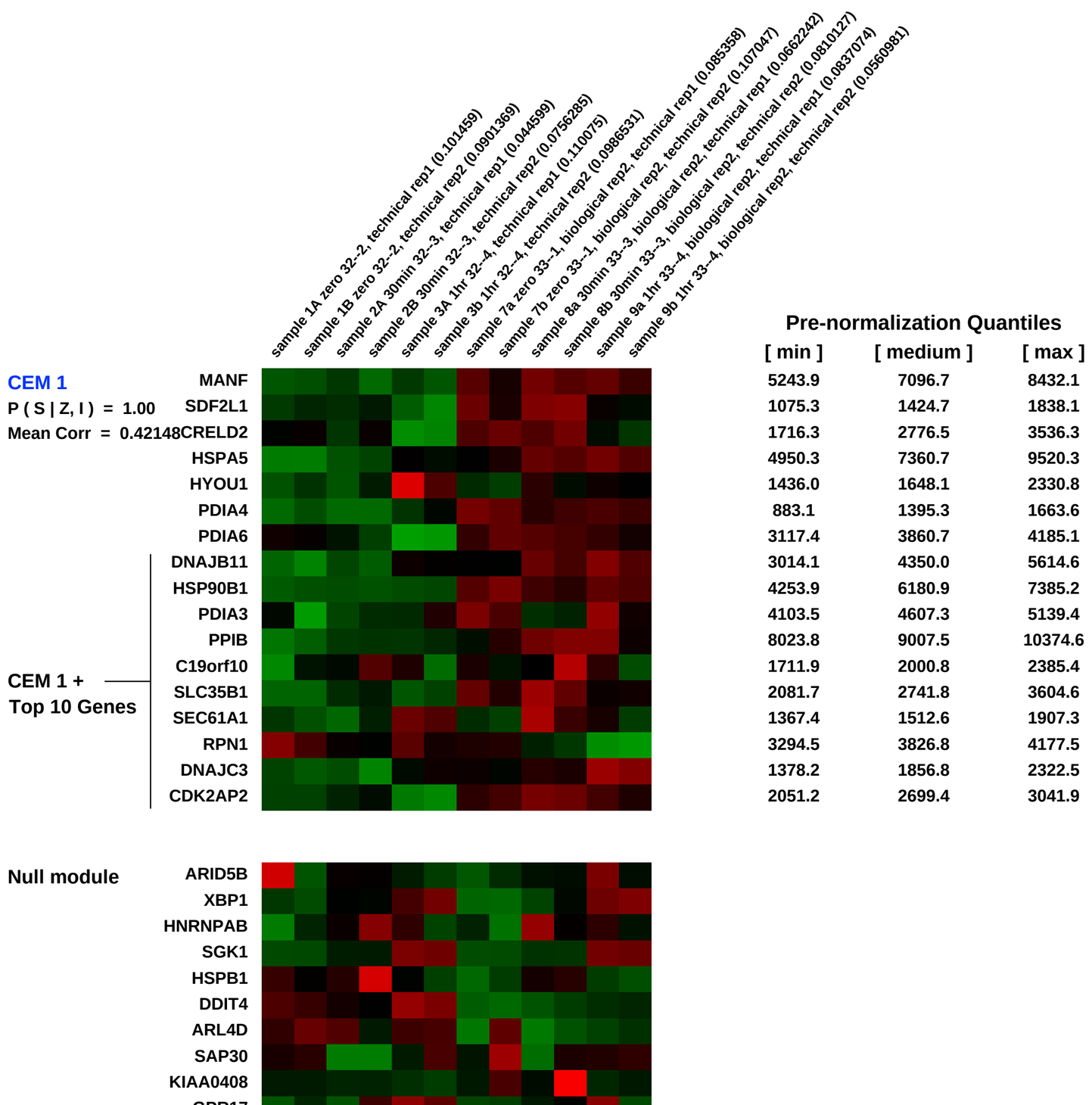

Pre-normalization Quantiles

	[min]	[medium]	[max]
MANF	5243.9	7096.7	8432.1
SDF2L1	1075.3	1424.7	1838.1
CRELD2	1716.3	2776.5	3536.3
HSPA5	4950.3	7360.7	9520.3
HYOU1	1436.0	1648.1	2330.8
PDIA4	883.1	1395.3	1663.6
PDIA6	3117.4	3860.7	4185.1
DNAJB11	3014.1	4350.0	5614.6
HSP90B1	4253.9	6180.9	7385.2
PDIA3	4103.5	4607.3	5139.4
PPIB	8023.8	9007.5	10374.6
C19orf10	1711.9	2000.8	2385.4
SLC35B1	2081.7	2741.8	3604.6
SEC61A1	1367.4	1512.6	1907.3
RPN1	3294.5	3826.8	4177.5
DNAJC3	1378.2	1856.8	2322.5
CDK2AP2	2051.2	2699.4	3041.9

GEO Series "GSE8023" Expression Profiles

Num of samples in this series: 12

Scale of expression profile Z-scores

-3.0 -2.0 -1.0 0.0 1.0 2.0 3.0

GEO Link:	http://www.ncbi.nlm.nih.gov/geo/query/acc.cgi?acc=GSE8023
Status:	Public on Dec 20 2007
Title:	AML1-ETO transduced human cord blood cells, CD34 selected, compared to normal cord blood cells, CD34 selected
Organism:	Homo sapiens
Experiment type:	Expression profiling by array
Platform:	GPL570
Pubmed ID:	17975013
Summary & Design:	**Summary:** AML1-ETO expression in normal human umbilical cord blood CD34+ cells leads to long-term proliferation of an early self-renewing primitive progenitor cell with multilineage potential and stem cell ability, but these cells do not induce leukemia in immunodeficient mice. This comparative microarray study was initiated to determine the differences in the transcriptome of AML-ETO-expressing CD34+ cells after extended culture in vitro, using normal cord blood cells expanded for 6-8 weeks in vitro and subsequently purified for the CD34+ population as the control comparison. Keywords: Disease state analysis; comparison of changes in transcriptome due to long-term AML1-ETO expression in normal human hematopoietic CD34+ progenitor cells **Overall design:** We have established a culture system whereby we retrovirally transduce human CD34+ cells, obtained from cord blood, with the leukemia fusion gene AML1-ETO. Cells expressing this fusion protein are able to proliferate long-term in vitro in a cytokine dependent manner. AML1-ETO-expressing cord blood cells have a large population of primitive self-renewing CD34+ cells with continued abnormal differentiation. We grow these cells in serum-free conditions using the BIT supplement from Stem Cell Technologies. For the current experiments we used cell cultures that had been proliferating in vitro for 8-12 weeks, in a cytokine cocktail of SCF, TPO, FLT3L, IL-6 all at 20 ng/mL and IL-3 at 10 ng/mL. Control cord blood samples that were CD34 purified were expanded for 5-8 weeks in the same culture media as used for AML1-ETO cells. All samples were magnetically selected for the CD34+ population, returned to culture, and one week later again selected for CD34+ cells and then lysed for RNA isolation.

Background corr dist: KL-Divergence = 0.1048, L1-Distance = 0.0328, L2-Distance = 0.0020, Normal std = 0.4301

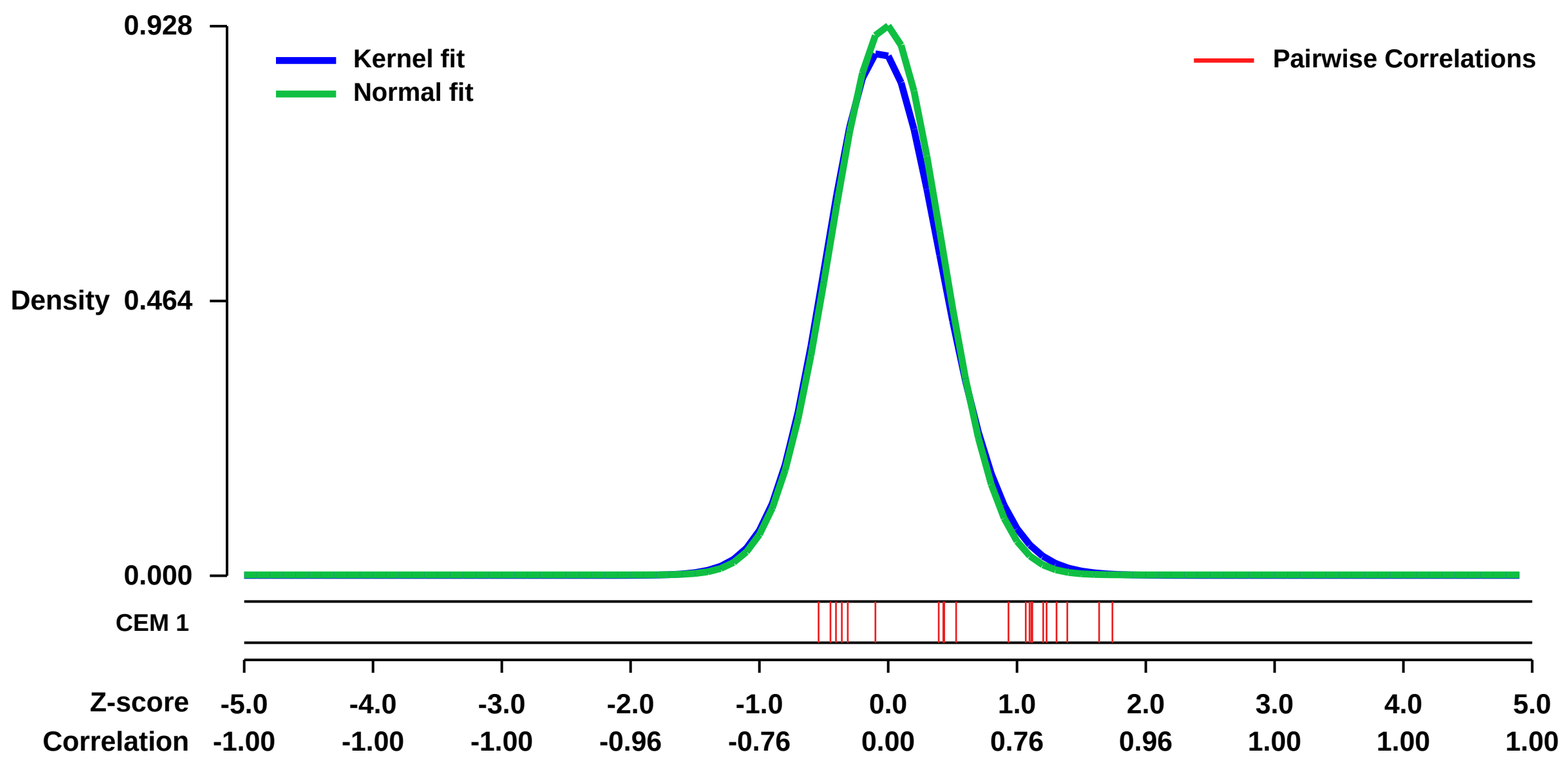

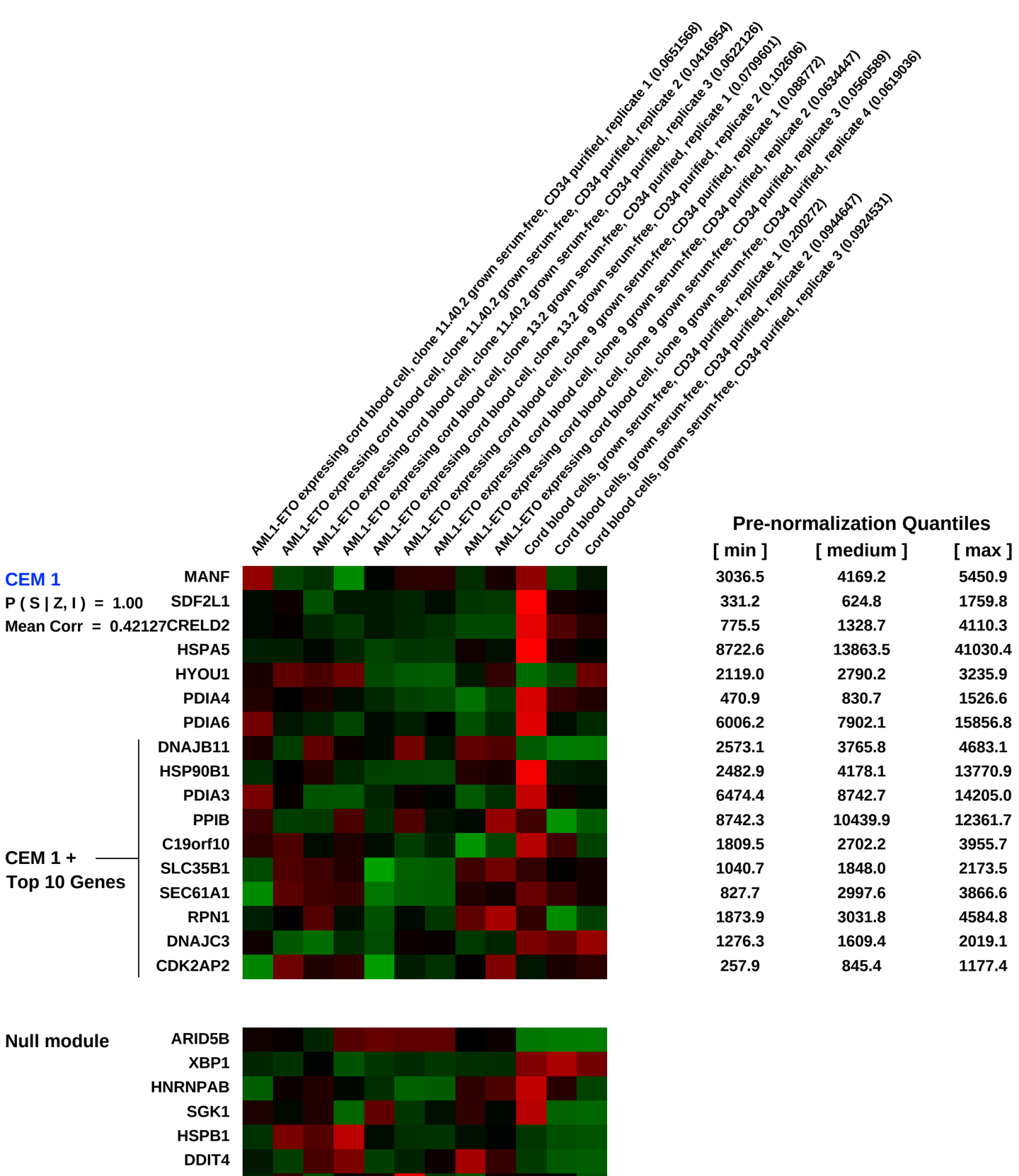

GEO Series "GSE20196" Expression Profiles

Num of samples in this series: 34

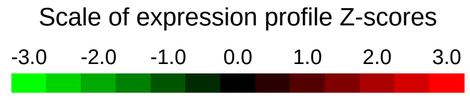

GEO Link:	http://www.ncbi.nlm.nih.gov/geo/query/acc.cgi?acc=GSE20196
Status:	Public on Sep 01 2010
Title:	Gene expression profile of poorly differentiated synovial sarcoma
Organism:	Homo sapiens
Experiment type:	Expression profiling by array
Platform:	GPL570
Pubmed ID:	20975339
Summary & Design:	**Summary:** Poorly differentiated type synovial sarcoma (PDSS) is a variant of synovial sarcoma characterized by predominantly round or short-spindled cells. Although accumulating evidence from clinicopathological studies suggests a strong association between this variant of synovial sarcoma and poor prognosis, little has been reported on the molecular basis of PDSS. To gain insight into the mechanism(s) that underlie the emergence of PDSS, we analyzed the gene expression profiles of 34 synovial sarcoma clinical samples, including 5 cases of PDSS, using an oligonucleotide microarray. In an unsupervised analysis, the 34 samples fell into 3 groups that correlated highly with histological subtype, namely, monophasic, biphasic, and poorly differentiated types. PDSS was characterized by down-regulation of genes associated with neuronal and skeletal development and cell adhesion, and up-regulation of genes on a specific chromosomal locus, 8q21.11. This locus-specific transcriptional activation in PDSS was confirmed by reverse transcriptase (RT)-PCR analysis of 9 additional synovial sarcoma samples. Our results indicate that PDSS tumors constitute a distinct genetic group based on expression profiles. **Overall design:** 34 SYT-SSX fusion transcript-positive SS samples, consisting of 21 MSS, 8 BSS and 5 PDSS cases, were analyzed using an oligonucleotide microarray using a GeneChip Human Genome U133 plus 2.0 array (Affymetrix).

Background corr dist: KL-Divergence = 0.5203, L1-Distance = 0.0987, L2-Distance = 0.0329, Normal std = 0.2214

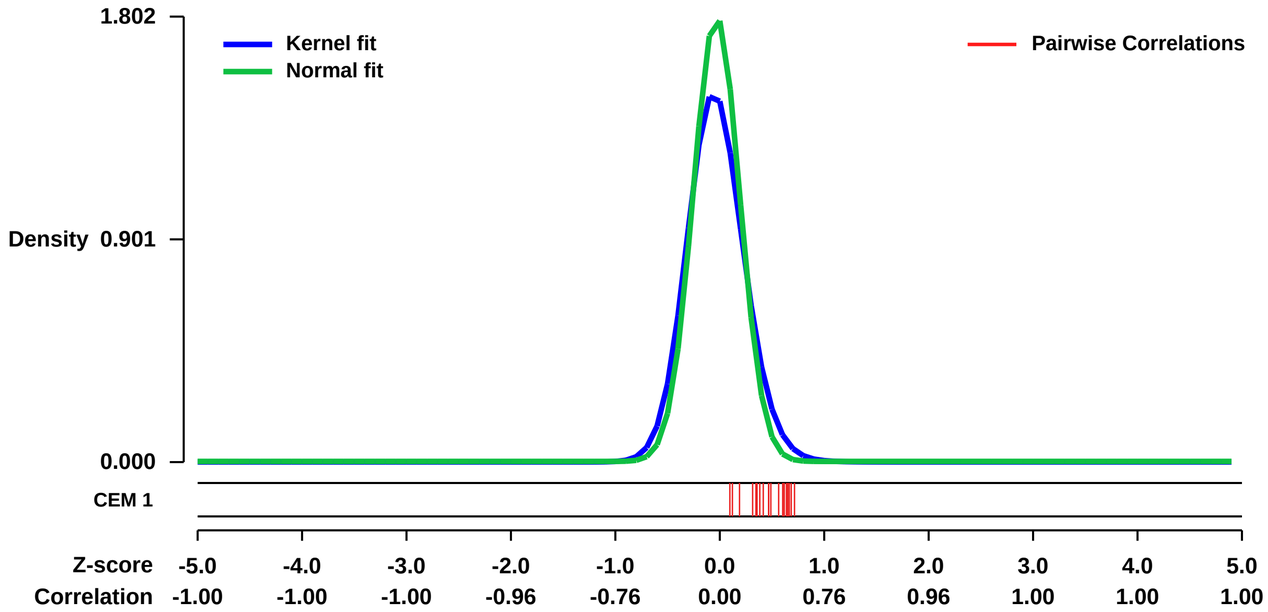

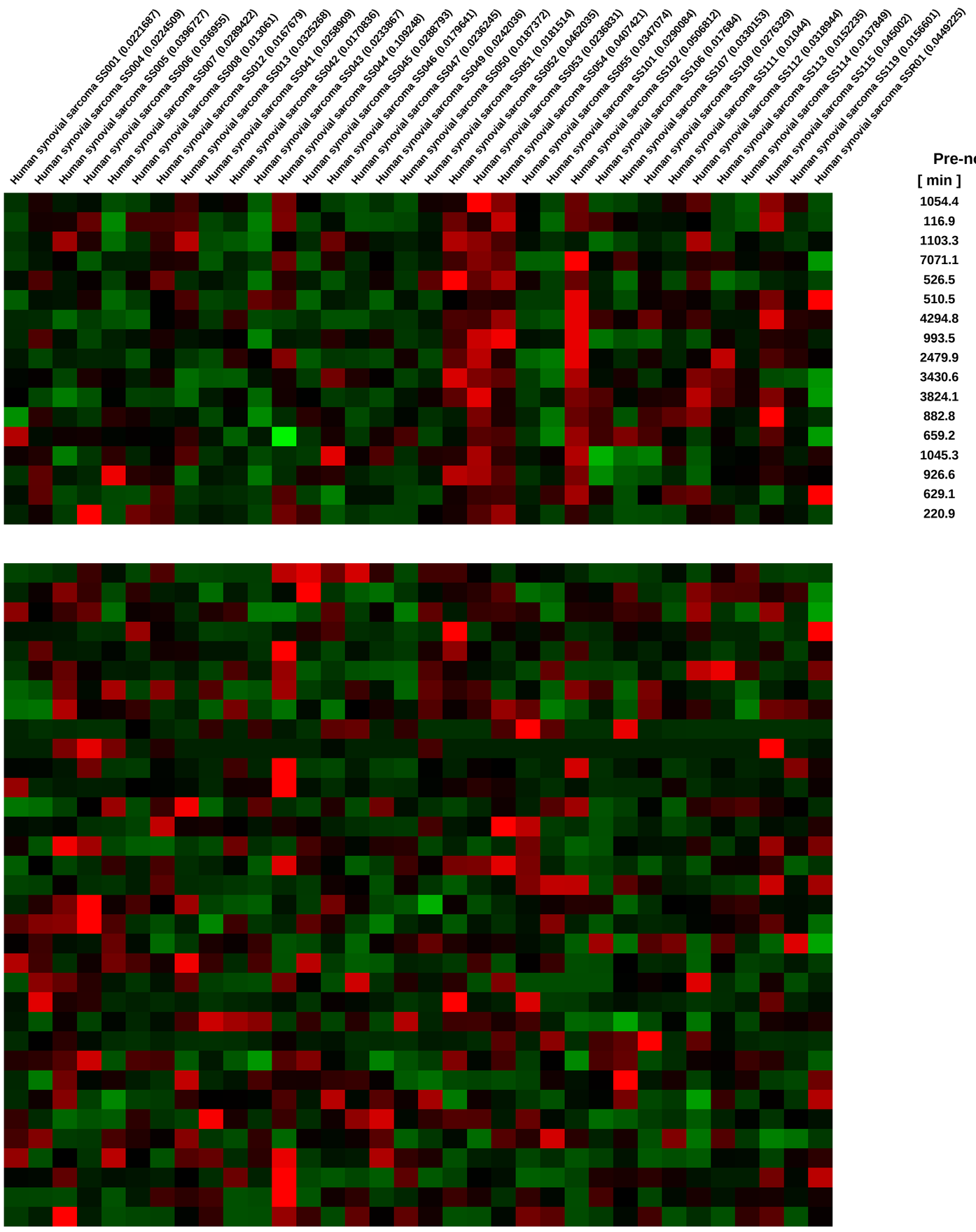

Pre-normalization Quantiles

	[min]	[medium]	[max]
MANF	1054.4	1818.3	4648.3
SDF2L1	116.9	393.4	853.4
CRELD2	1103.3	2524.1	5603.8
HSPA5	7071.1	12970.4	26496.2
HYOU1	526.5	1131.0	3034.3
PDIA4	510.5	788.3	1673.2
PDIA6	4294.8	6429.4	13069.4
DNAJB11	993.5	2002.3	4304.6
HSP90B1	2479.9	4583.1	9870.1
PDIA3	3430.6	6541.3	11326.1
PPIB	3824.1	9207.1	17204.0
C19orf10	882.8	1448.0	2782.1
SLC35B1	659.2	1602.5	2317.0
SEC61A1	1045.3	2413.6	4060.9
RPN1	926.6	1523.7	2855.0
DNAJC3	629.1	1256.9	3138.8
CDK2AP2	220.9	451.7	1710.5

GEO Series "GSE13142" Expression Profiles

Num of samples in this series: 6

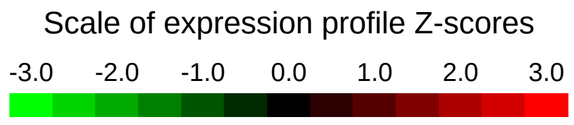

GEO Link:	http://www.ncbi.nlm.nih.gov/geo/query/acc.cgi?acc=GSE13142
Status:	Public on Nov 10 2008
Title:	HepG2/C3A cells cultured for 42 h in complete or leucine-devoid medium
Organism:	Homo sapiens
Experiment type:	Expression profiling by array
Platform:	GPL570
Pubmed ID:	20361218
Summary & Design:	**Summary:** HepG2/C3A cells cultured for 42 h in complete or leucine-devoid medium **Overall design:** Total of 6 Samples (Leu vs noLeu)

Background corr dist: KL-Divergence = 0.0362, L1-Distance = 0.0404, L2-Distance = 0.0019, Normal std = 0.6815

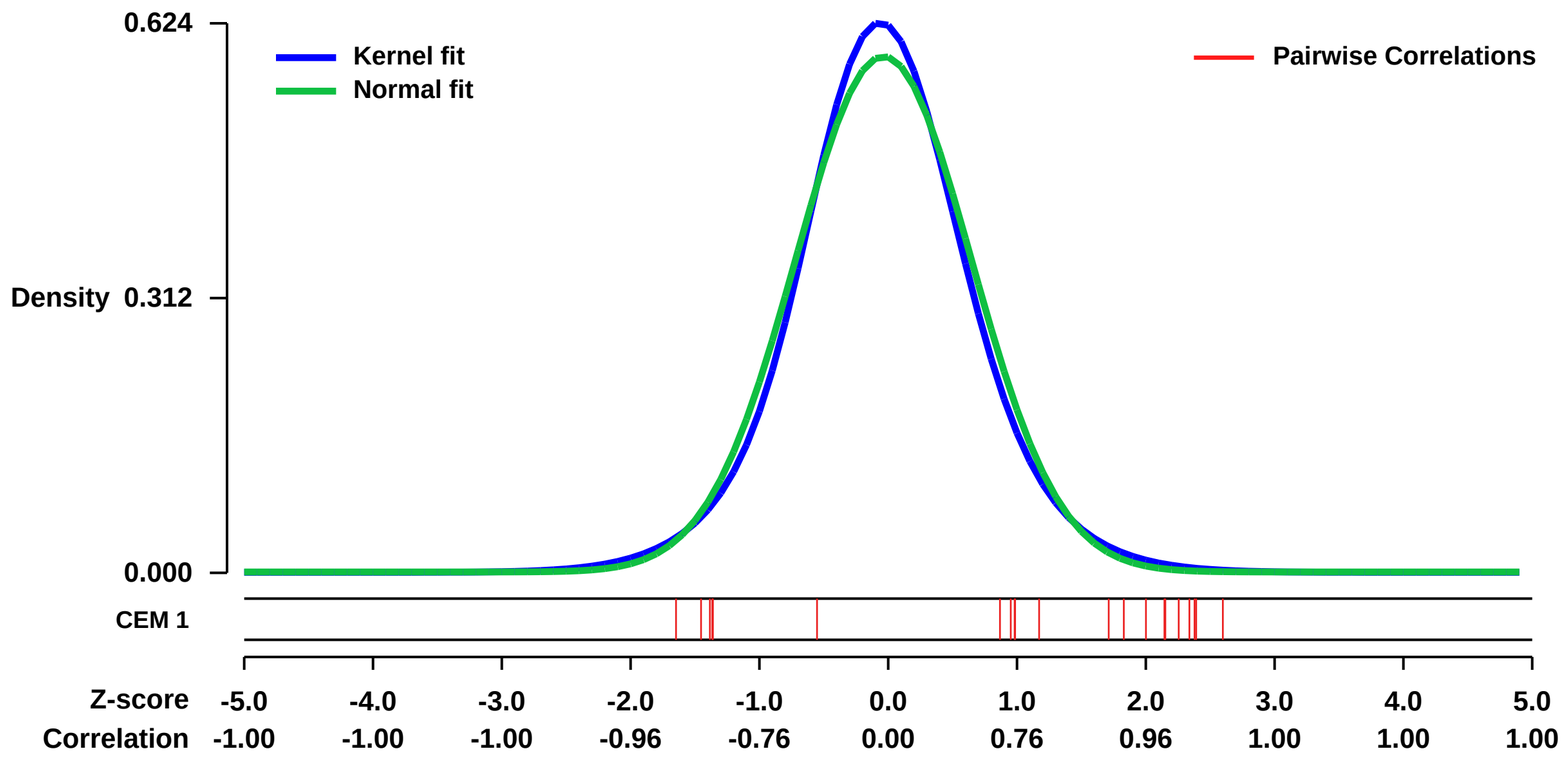

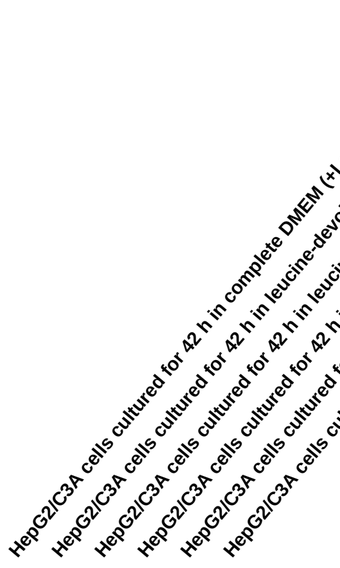

Pre-normalization Quantiles

		[min]	[medium]	[max]
CEM 1	MANF	3676.0	6922.1	7891.6
P (S | Z, I) = 1.00	SDF2L1	753.2	2040.4	2556.2
Mean Corr = 0.40586	CRELD2	1354.7	3847.5	4684.6
	HSPA5	14055.9	15983.2	17143.9
	HYOU1	1625.4	3059.5	3220.7
	PDIA4	1387.6	2231.0	2655.0
	PDIA6	8815.4	14290.7	14867.9
CEM 1 + Top 10 Genes	DNAJB11	3450.3	4327.6	4715.2
	HSP90B1	4632.8	6864.5	7649.6
	PDIA3	9976.5	13275.0	14128.6
	PPIB	12452.2	20137.8	22200.2
	C19orf10	4266.2	5464.6	5710.1
	SLC35B1	3895.3	4599.1	4975.6
	SEC61A1	2906.8	3119.5	3163.6
	RPN1	3237.4	4471.4	4627.3
	DNAJC3	2689.2	3049.4	3189.0
	CDK2AP2	840.3	1292.4	1323.3

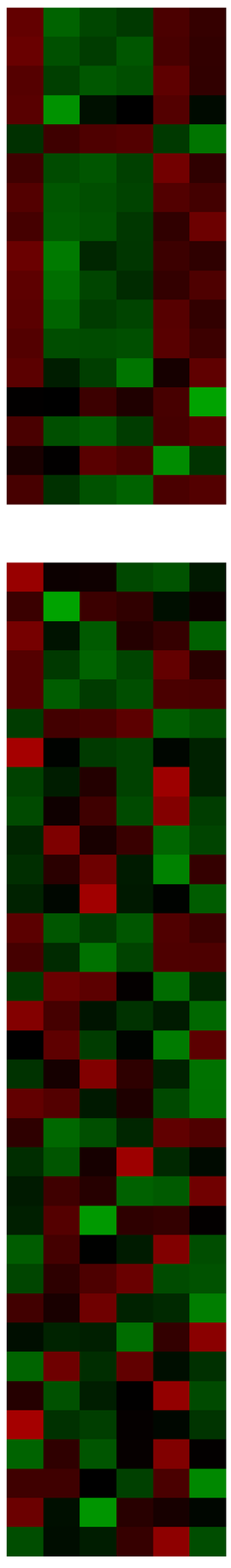

Null module	ARID5B	XBP1	HNRNPAB	SGK1	HSPB1	DDIT4	ARL4D	SAP30	KIAA0408	GPR17	HSPH1	DNASE1L2
	SLC5A3	GNAS	GPR3	TNFRSF25	TM6SF2	MKKS	PLEKHF1	ZMYM1	DOK3	FGF20	SLC39A2	KCNIP2
	ERRFI1	DEDD2	CCDC117	USP31	AHSA2	CYS1	CNIH2	BANP	CHORDC1	P4HA1		

GEO Series "GSE3151" Expression Profiles

Num of samples in this series: 55

Scale of expression profile Z-scores

-3.0 -2.0 -1.0 0.0 1.0 2.0 3.0

GEO Link:	http://www.ncbi.nlm.nih.gov/geo/query/acc.cgi?acc=GSE3151
Status:	Public on Nov 07 2005
Title:	Oncogene Signature Dataset
Organism:	Homo sapiens
Experiment type:	Expression profiling by array
Platform:	GPL570
Pubmed ID:	20516112
Summary & Design:	**Summary:** **Signatures of Oncogenic Pathway Deregulation in Human Cancers** **The ability to define cancer subtypes, recurrence of disease, and response to specific therapies using DNA microarray-based gene expression signatures has been demonstrated in multiple studies. Such data is also of substantial importance to the analysis of cellular signaling pathways central to the oncogenic process. With this focus, we have developed a series of gene expression signatures that reliably reflect the activation status of several oncogenic pathways. When evaluated in several large collections of human cancers, these gene expression signatures identify patterns of pathway deregulation in tumors, and clinically relevant associations with disease outcomes. Combining signature-based predictions across several pathways identifies coordinated patterns of pathway deregulation that distinguish between specific cancers and tumor sub-types. Clustering tumors based on pathway signatures further defines prognosis in respective patient subsets, demonstrating that patterns of oncogenic pathway deregulation underlie the development of the oncogenic phenotype and reflect the biology and outcome of specific cancers. Furthermore, predictions of pathway deregulation in cancer cell lines are shown to coincide with sensitivity to therapeutic agents that target components of the pathway, underscoring the potential for such pathway prediction to guide the use of targeted therapeutics.** **Keywords: other** **Overall design:** **RNA was extracted from human mammary epithelial cells expressing oncogenes (or GFP control) for gene array analysis. Experiment was performed in replicate.**

Background corr dist: **KL-Divergence = 0.5044, L1-Distance = 0.0740, L2-Distance = 0.0168, Normal std = 0.2258**

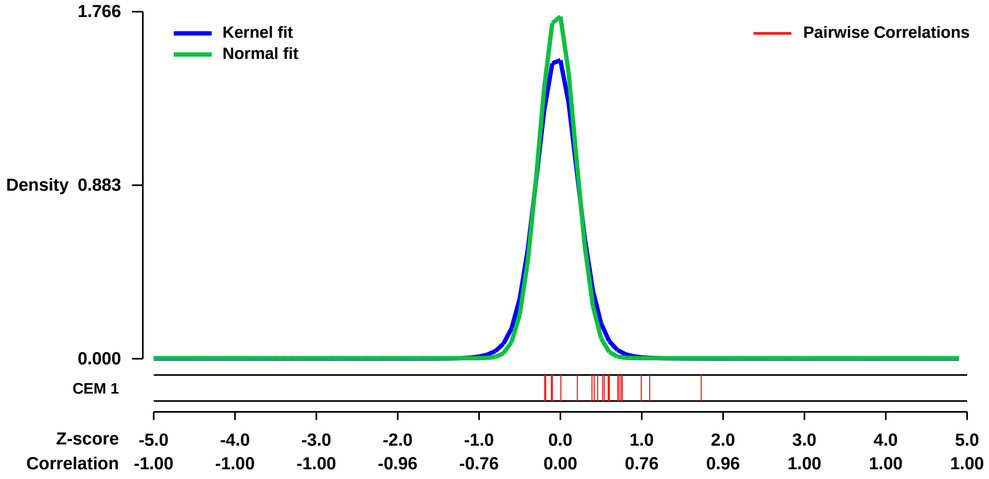

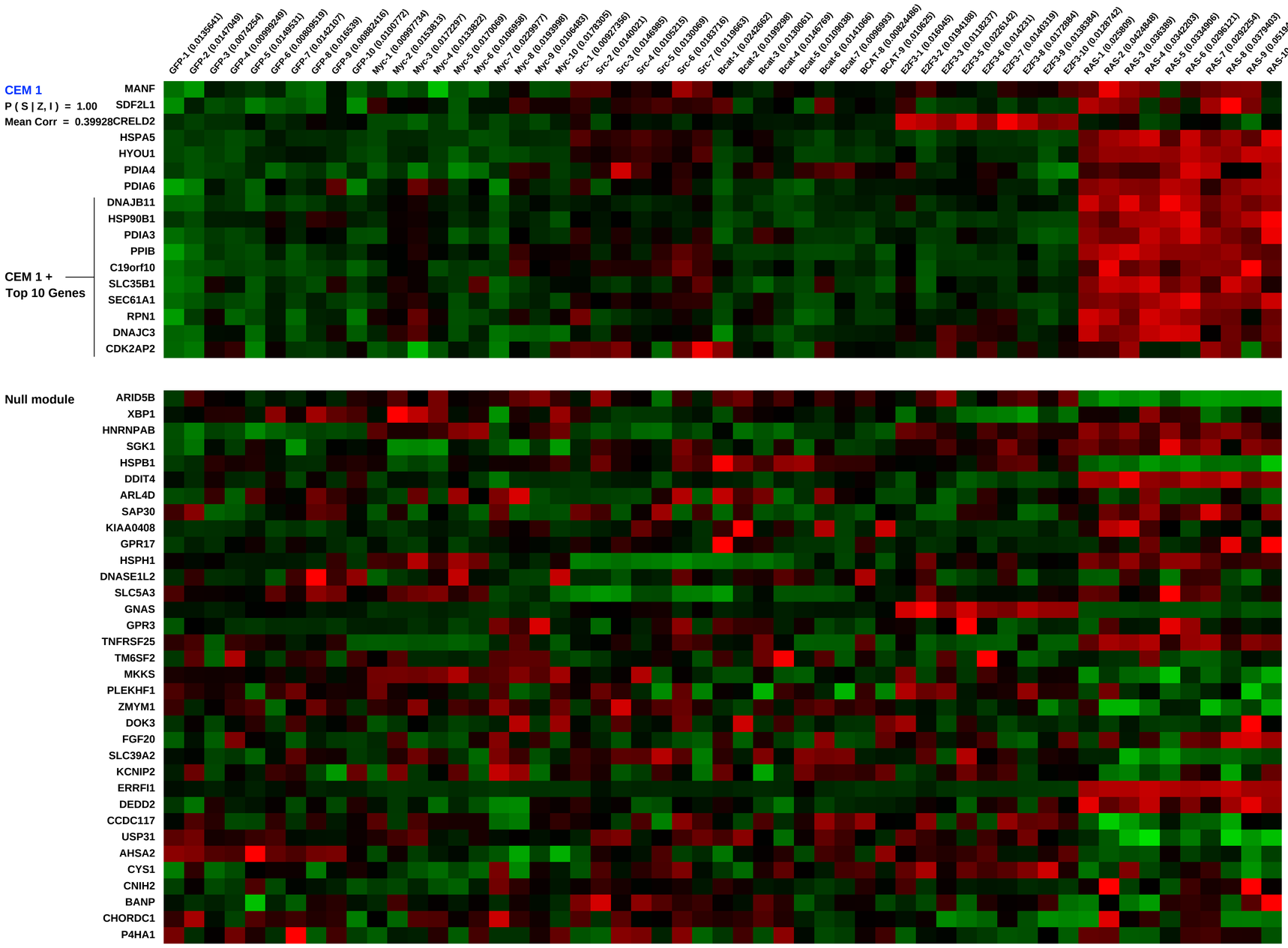

Pre-normalization Quantiles

[min]	[medium]	[max]
2326.7	3535.4	5199.1
397.2	654.3	1279.6
1570.8	2681.4	6114.2
22919.6	29325.8	67248.9
9097.4	12501.8	24950.9
1030.0	1442.1	2130.0
5942.9	8206.1	11466.6
2878.0	4681.1	11926.5
2956.9	3982.2	9395.0
12521.9	16008.3	26235.2
8838.1	14956.3	27502.5
3202.9	4525.5	9743.4
1502.9	2066.0	3592.4
7125.2	9458.1	17937.5
3095.0	4754.2	7717.1
3026.2	4365.8	6879.9
248.9	517.0	899.4

GEO Series "GSE8687" Expression Profiles

Num of samples in this series: 12

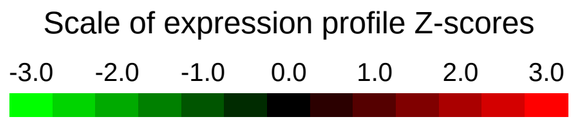

GEO Link:	http://www.ncbi.nlm.nih.gov/geo/query/acc.cgi?acc=GSE8687
Status:	Public on Feb 19 2008
Title:	Inhibition of activation of Sez-4 cell line with IL-2 by Jak kinase inhibitors.
Organism:	Homo sapiens
Experiment type:	Expression profiling by array
Platform:	GPL570
Pubmed ID:	18281483
Summary & Design:	**Summary:** In this study we compared the effects of IL-2, IL-15, and IL-21 on the gene expression, activation of cell signaling pathways, and functional properties of cells derived from the CD4+ cutaneous T-cell lymphoma (CTCL). Whereas both IL-2 and IL-15 that signal through receptors that share the common gamma chain and the beta chain modulated the expression of >1,000 genes, IL-21 that signals via the receptor also containing gamma chain up-regulated <40 genes. All three cytokines induced tyrosine phosphorylation of Jak1 and Jak3. However, only IL-2 and IL-15 strongly activated STAT5, PI3K/Akt, and MEK/ERK signaling pathways. In contrast, IL-21 selectively activated STAT3. Whereas all three cytokines protected CTCL cells from apoptosis, only IL-2 and IL-15 promoted their proliferation. The effects of the cytokine stimulation were Jak3- and Jak1-kinase dependent. These findings document the vastly different impact of IL-2 and IL-15 vs. IL-21 on malignant CD4+ T cells. They also suggest two novel therapeutic approaches to CTCL and, possibly, other CD4+ T cell lymphomas: inhibition of the Jak1/Jak3 kinase complex and, given the known strong immunostimulatory properties of IL-21 on CD8+ T, NK, and B cells, application of this cytokine to boost an immune response against malignant CD4+ T cells. **Keywords:** 3 replicates in each of 4 conditions **Overall design:** Sez-4 cell line was starved of IL-2 for 16h, washed twice and placed into 6-well plates in 10ml RPMI (10% FBS) for 2h followed by pre-treating for 30â with pan-Jak inhibitor (300 nM), Jak3 inhibitor (300 nM), or drig solvent and cultured with IL-2 (200U) or medium alone for 4 h.

Background corr dist: KL-Divergence = 0.1499, L1-Distance = 0.0292, L2-Distance = 0.0016, Normal std = 0.3769

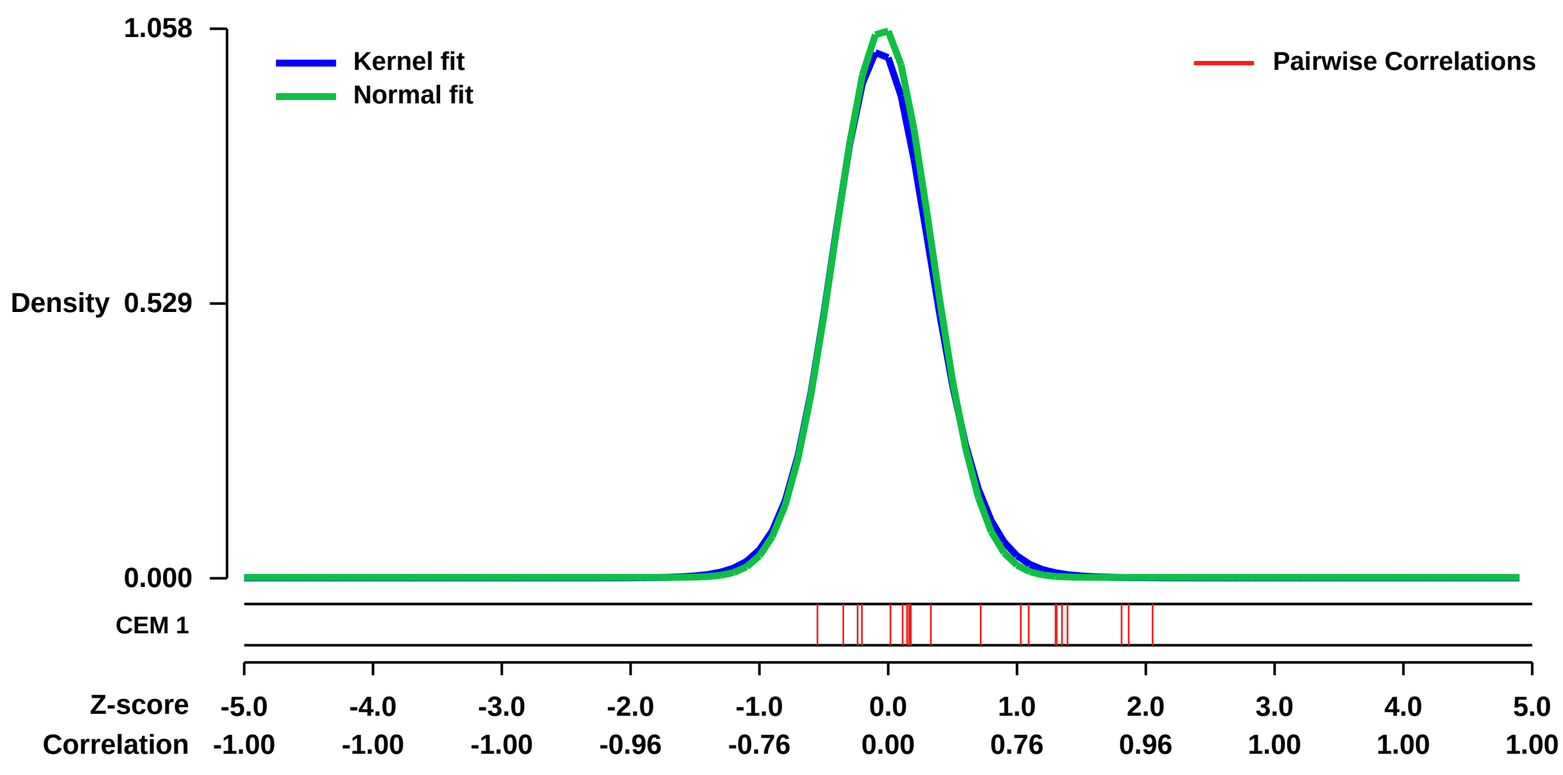

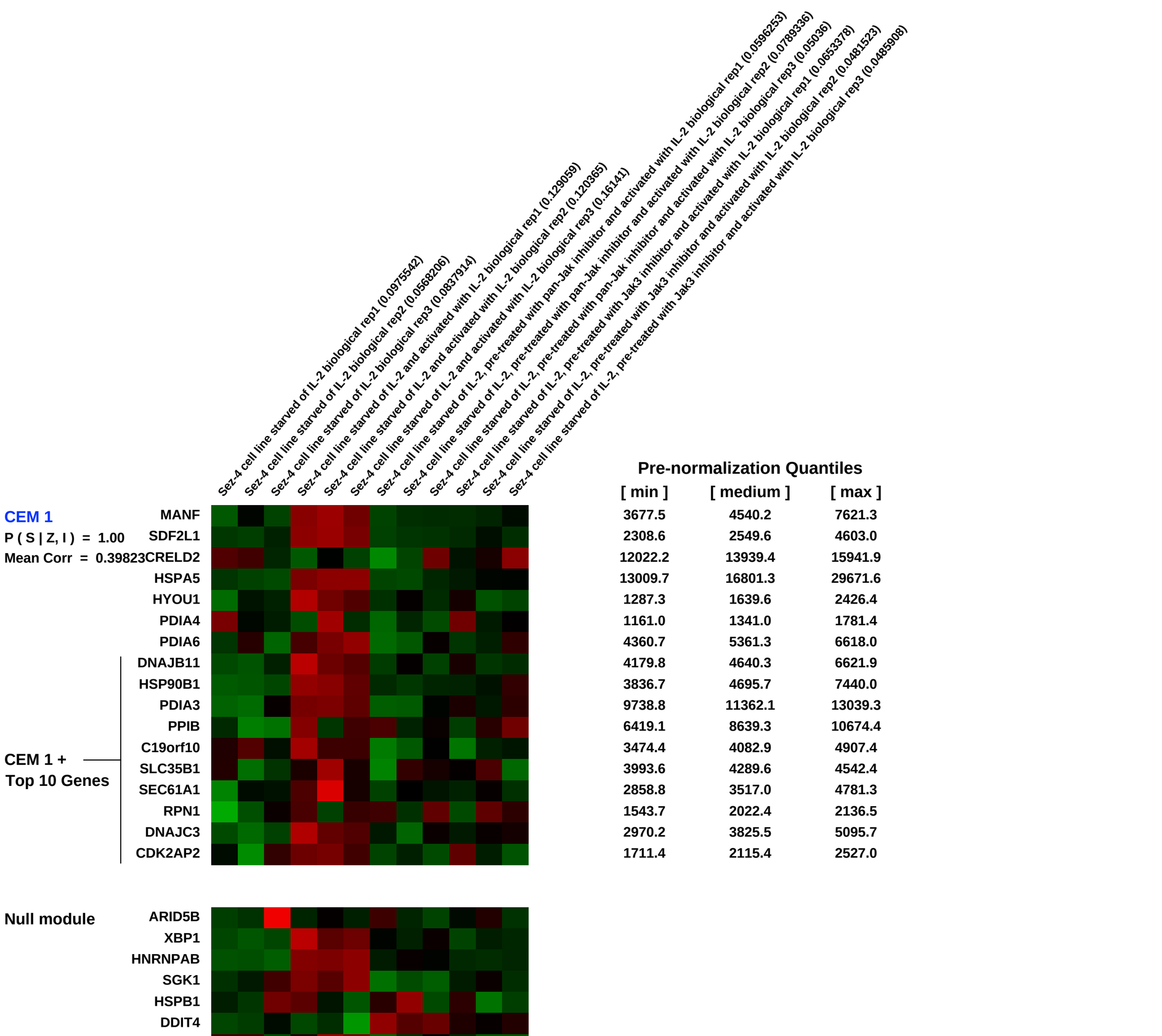

GEO Series "GSE25619" Expression Profiles

Num of samples in this series: 6

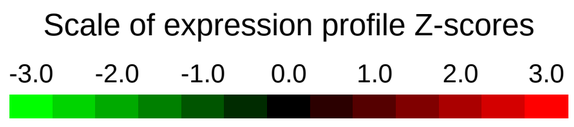

GEO Link:	http://www.ncbi.nlm.nih.gov/geo/query/acc.cgi?acc=GSE25619
Status:	Public on Nov 27 2010
Title:	Gene expression profiles of granulin- and control-treated normal human mammary fibroblasts
Organism:	Homo sapiens
Experiment type:	Expression profiling by array
Platform:	GPL570
Pubmed ID:	21266779
Summary & Design:	**Summary:** To examine the effects of recombinant granulin on human mammary stromal fibroblasts, we cultured normal human mammary fibroblasts in the presence of recombinant human granulin (1ug/ml) or PBS every 24h for 6 days. **Overall design:** We cultured normal human mammary fibroblasts in the presence human granulin (1ug/ml) or PBS control every 24h for 6 days. The analysis showen are for 3 control (control) and 3 granulin-treated (PGRN) fibrobast cultures.

Background corr dist: KL-Divergence = 0.0251, L1-Distance = 0.0282, L2-Distance = 0.0008, Normal std = 0.7386

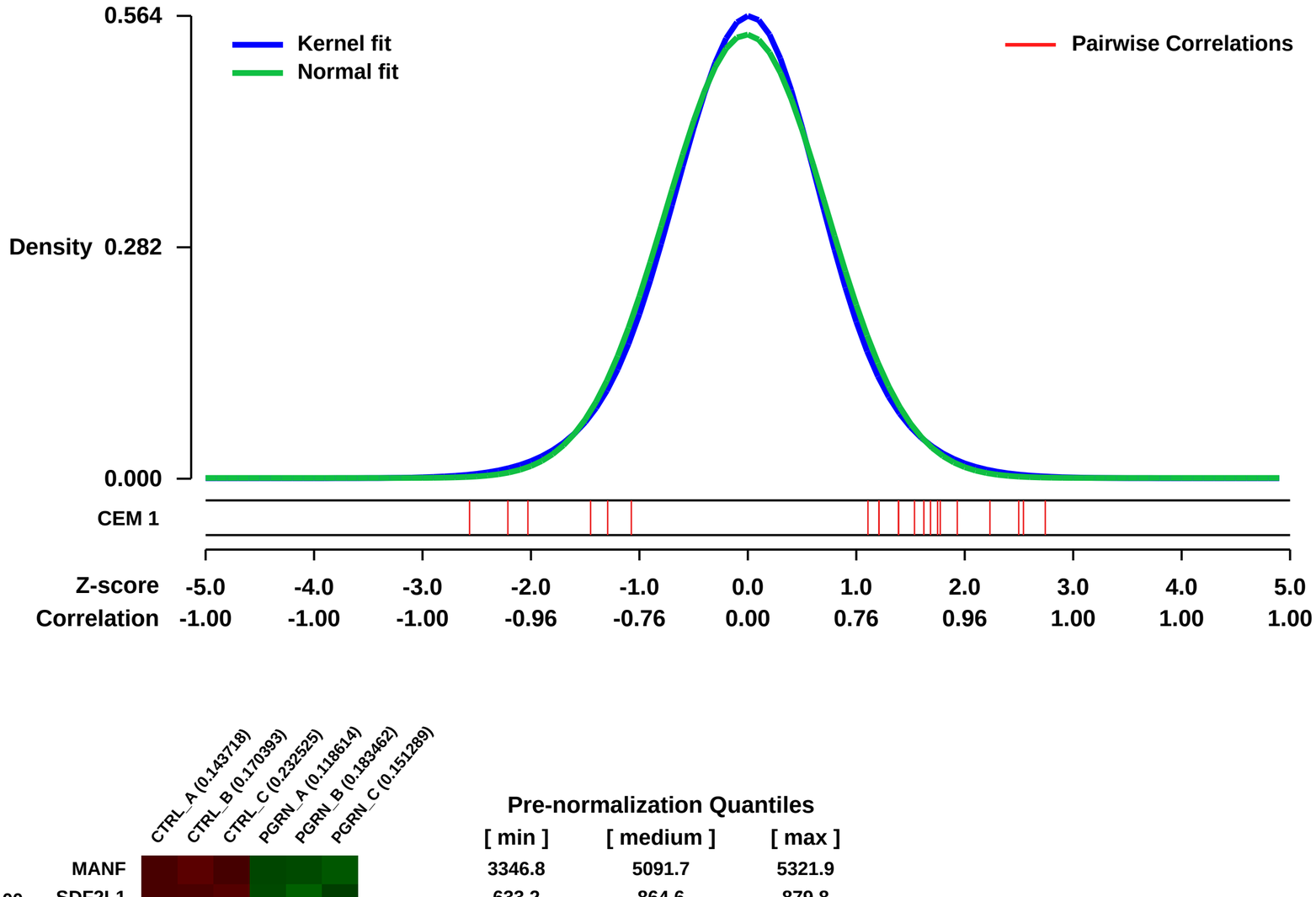

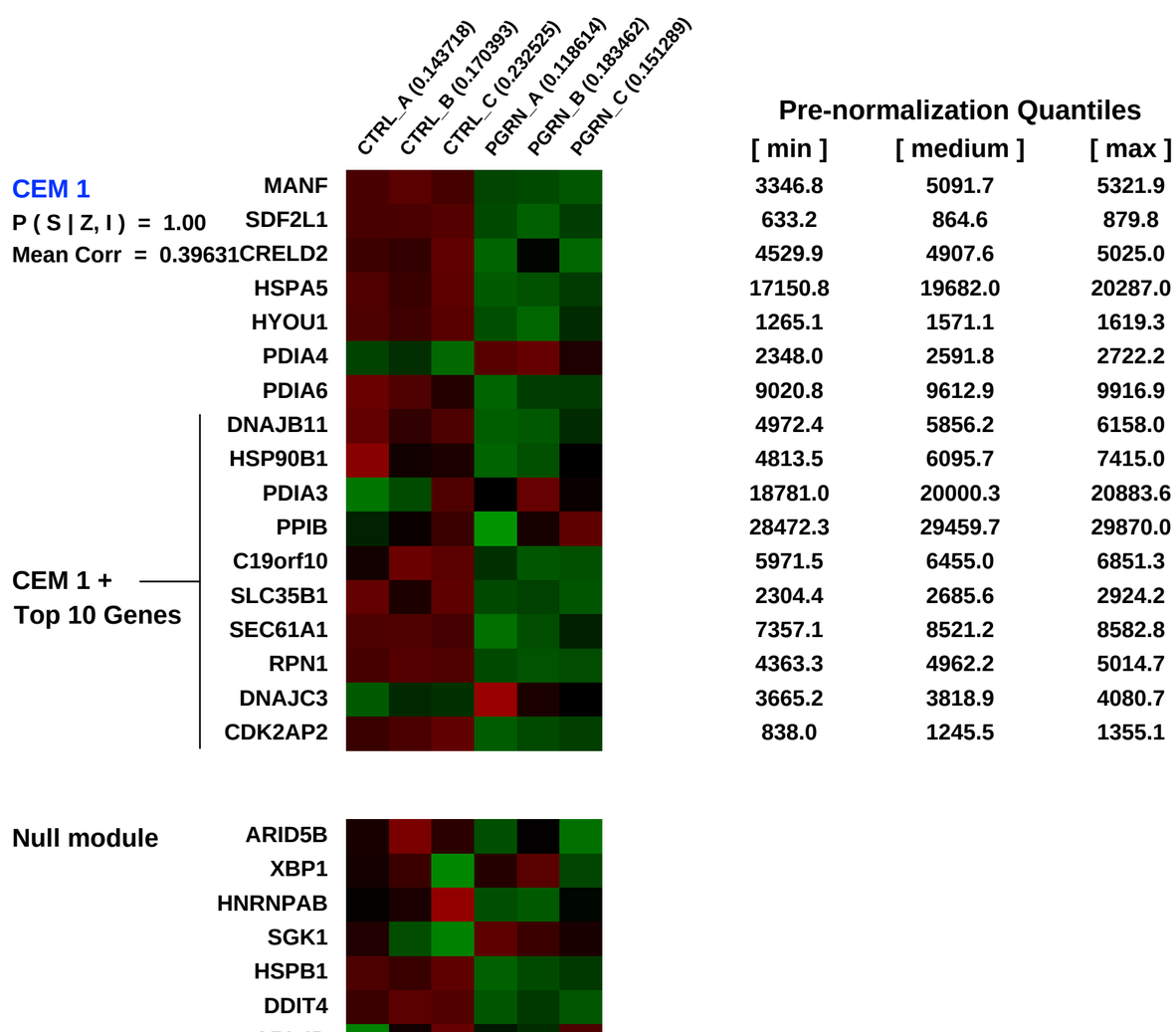

GEO Series "GSE18973" Expression Profiles

Num of samples in this series: 9

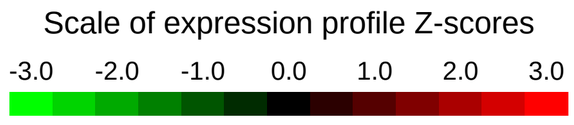

GEO Link:	http://www.ncbi.nlm.nih.gov/geo/query/acc.cgi?acc=GSE18973
Status:	Public on Dec 22 2010
Title:	Global expression analysis of HNF4alpha and HNFgamma-mediated transcriptional control
Organism:	Homo sapiens
Experiment type:	Expression profiling by array
Platform:	GPL570
Pubmed ID:	21047794
Summary & Design:	**Summary:** Hepatocyte nuclear factor-4ε– (HNF4ε–, NR2A1) is a nuclear receptor which has a critical role in hepatocyte differentiation and the maintenance of homeostasis in the adult liver. However, a detailed understanding of native HNF4ε– in the steady state remains to be elucidated. Here we report the native HNF4ε– isoforms, phosphorylation status and complexes in the steady state, as shown by shotgun proteomics in HepG2 hepatocarcinoma cells. Shotgun proteomic analysis revealed the complexity of native HNF4ε–, including multiple phosphorylation sites and inter-isoform heterodimerization. The associating complexes identified by label-free semi-quantitative proteomic analysis include the following: the DNA-dependent protein kinase catalytic subunit, histone acetyltransferase complexes, mRNA splicing complex, other nuclear receptor coactivator complexes, the chromatin remodeling complex, and the nucleosome remodeling and histone deacetylation complex. Among the associating proteins, GRB10 interacting GYF protein 2 (GIGYF2, PERQ2) is a new candidate cofactor in metabolic regulation. Moreover, an unexpected heterodimerization of HNF4ε– and Hepatocyte nuclear factor-4ε‡ was found. A biochemical and genome-wide analysis of transcriptional regulation showed that this heterodimerization activates gene transcription. The genes thus transcribed include the cell death-inducing DEF45-like effector b (CIDEB) gene, which is an important regulator of lipid metabolism in the liver. This suggests that the analysis of the distinctive stoichiometric balance of native HNF4ε– and its cofactor complexes described here is important for an accurate understanding of transcriptional regulation. **Overall design:** siRNA-mediated HNF4alpha and HNF4gamma double knockdown in HepG2 cells were analysed by using the Affymetrix GeneChip system in tripricate.

Background corr dist: KL-Divergence = 0.0785, L1-Distance = 0.0280, L2-Distance = 0.0010, Normal std = 0.4944

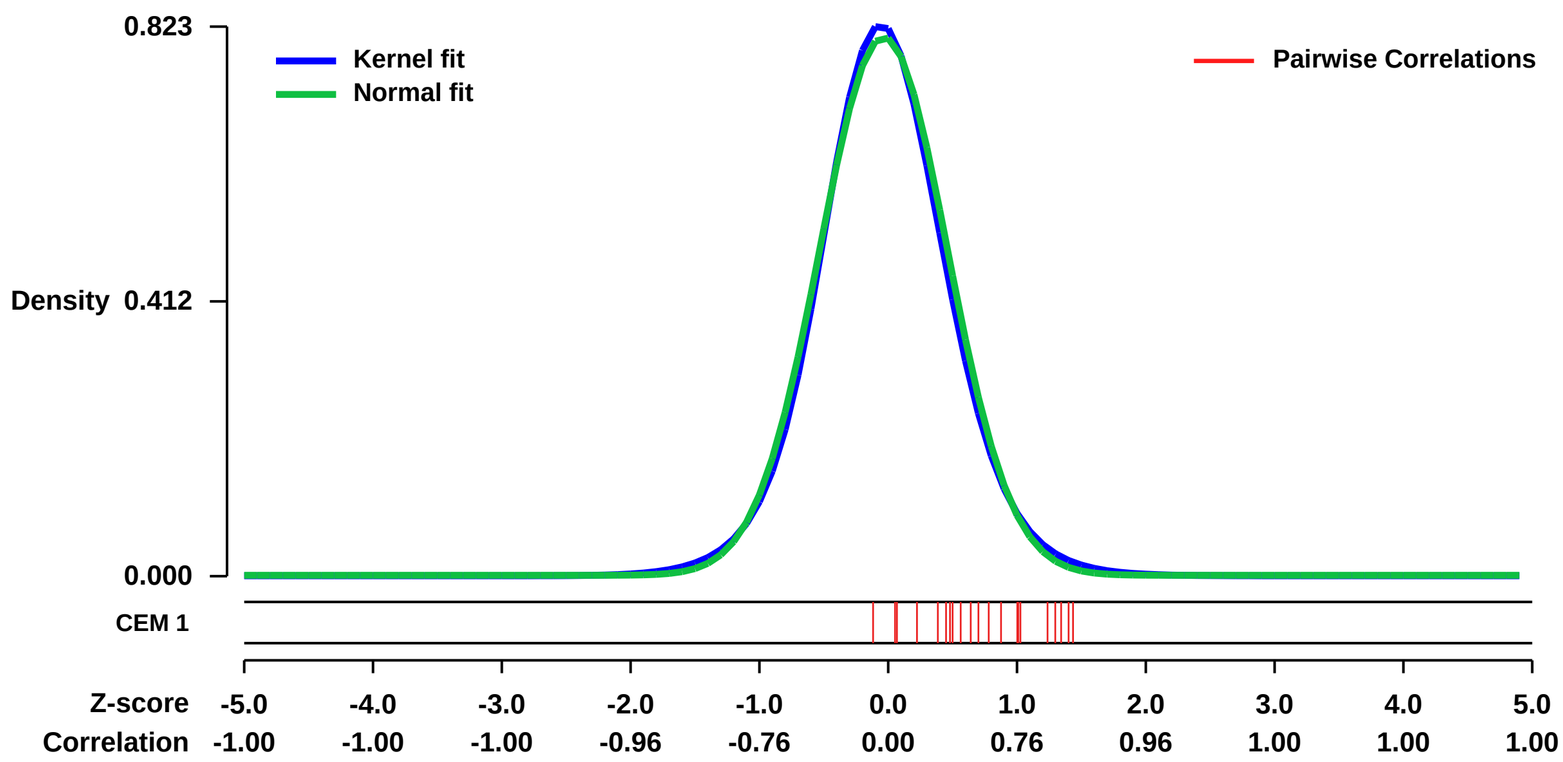

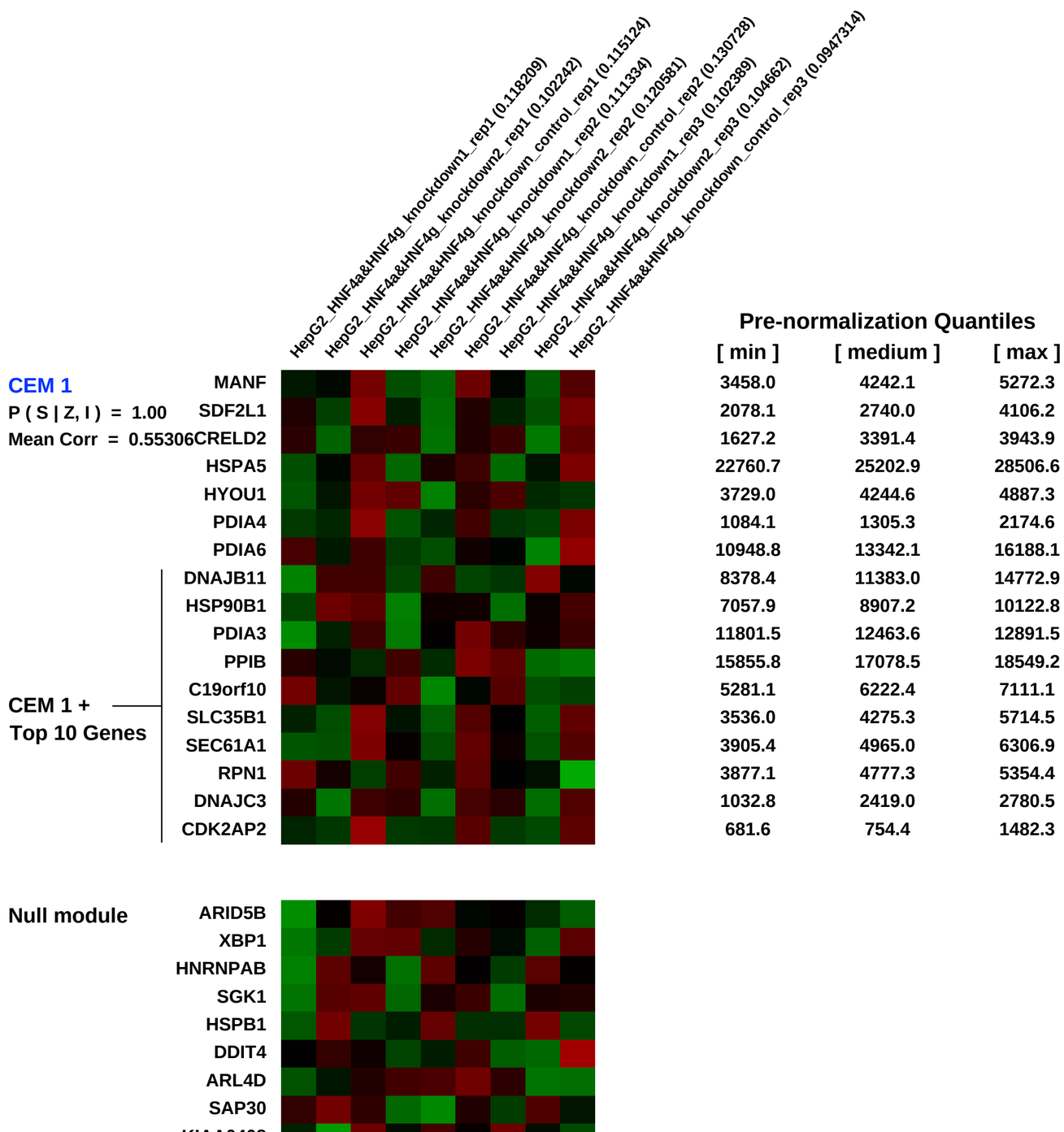

		Pre-normalization Quantiles [min]	[medium]	[max]
CEM 1	MANF	3458.0	4242.1	5272.3
	SDF2L1	2078.1	2740.0	4106.2
	CRELD2	1627.2	3391.4	3943.9
	HSPA5	22760.7	25202.9	28506.6
	HYOU1	3729.0	4244.6	4887.3
	PDIA4	1084.1	1305.3	2174.6
	PDIA6	10948.8	13342.1	16188.1
CEM 1 + Top 10 Genes	DNAJB11	8378.4	11383.0	14772.9
	HSP90B1	7057.9	8907.2	10122.8
	PDIA3	11801.5	12463.6	12891.5
	PPIB	15855.8	17078.5	18549.2
	C19orf10	5281.1	6222.4	7111.1
	SLC35B1	3536.0	4275.3	5714.5
	SEC61A1	3905.4	4965.0	6306.9
	RPN1	3877.1	4777.3	5354.4
	DNAJC3	1032.8	2419.0	2780.5
	CDK2AP2	681.6	754.4	1482.3
Null module	ARID5B			
	XBP1			
	HNRNPAB			
	SGK1			
	HSPB1			
	DDIT4			
	ARL4D			
	SAP30			
	KIAA0408			
	GPR17			
	HSPH1			
	DNASE1L2			
	SLC5A3			
	GNAS			
	GPR3			
	TNFRSF25			
	TM6SF2			
	MKKS			
	PLEKHF1			
	ZMYM1			
	DOK3			
	FGF20			
	SLC39A2			
	KCNIP2			
	ERRFI1			
	DEDD2			
	CCDC117			
	USP31			
	AHSA2			
	CYS1			
	CNIH2			
	BANP			
	CHORDC1			
	P4HA1			

GEO Series "GSE15091" Expression Profiles

Num of samples in this series: 7

Scale of expression profile Z-scores

-3.0 -2.0 -1.0 0.0 1.0 2.0 3.0

GEO Link:	http://www.ncbi.nlm.nih.gov/geo/query/acc.cgi?acc=GSE15091
Status:	Public on Mar 04 2009
Title:	PC3 cells transfected with androgen receptor treated with various concentration of androgens
Organism:	Homo sapiens
Experiment type:	Expression profiling by array
Platform:	GPL570
Pubmed ID:	19668381
Summary & Design:	**Summary:** We compared PC3 cells with or without harboring the wild-AR construct in the growth conditions of 1nM R1881, 10nM R1881 and ethanol (the solvent for R1881). The MOCK control is PC3 cells transfected with the empty vectors. **Overall design:** 2 PC3 Samples transfected with empty vector, without R1881, 2 PC3 Samples transfected with AR, treated with Ethanol, 2 PC3 Samples transfected with AR, treated with 1nM R1881, 1 PC3 transfected with AR, treated with 10nM R1881.

Background corr dist: KL-Divergence = 0.0125, L1-Distance = 0.0487, L2-Distance = 0.0036, Normal std = 0.9351

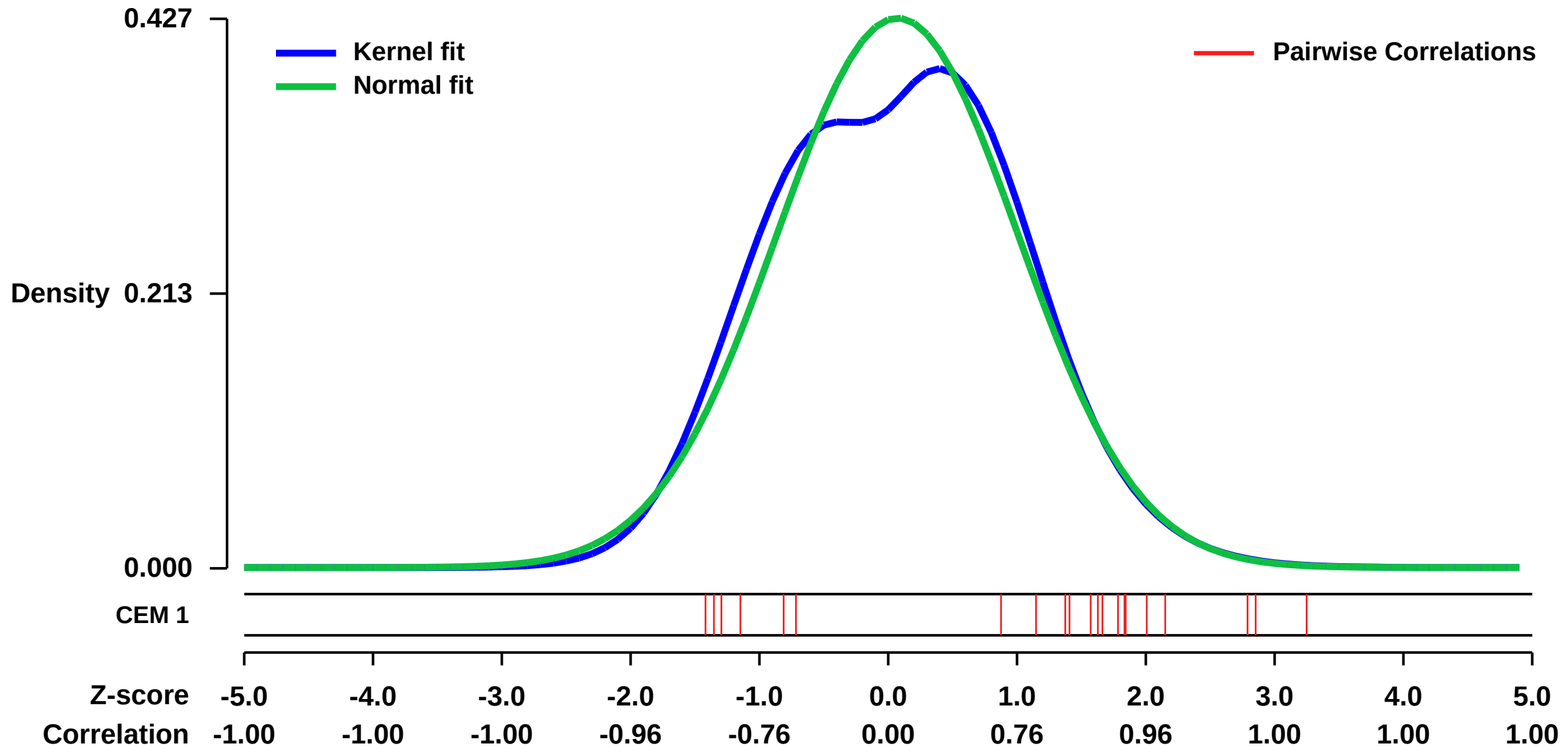

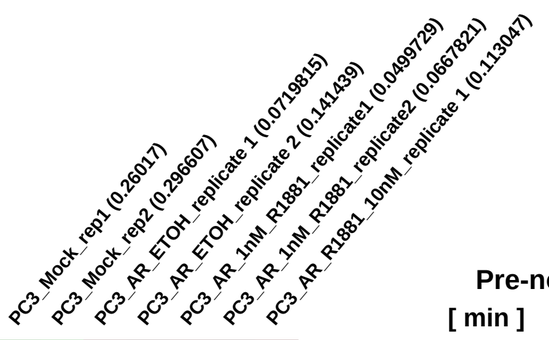

Pre-normalization Quantiles

[min] [medium] [max]

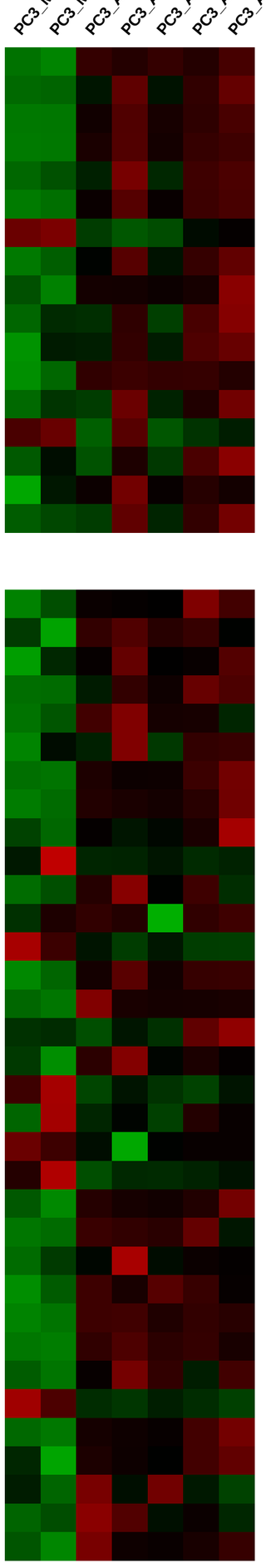

MANF	9958.7	16089.0	17306.3
SDF2L1	1128.8	1986.5	3158.9
CRELD2	1984.5	4147.3	5008.8
HSPA5	43953.3	93235.1	111377.6
HYOU1	4055.2	6627.0	12102.4
PDIA4	1842.7	4135.8	5426.6
PDIA6	17232.2	19395.1	23165.4
DNAJB11	7012.1	13157.8	18359.0
HSP90B1	14632.1	19894.8	24069.2
PDIA3	26727.7	31976.4	47173.0
PPIB	21392.4	29069.0	37374.9
C19orf10	6283.9	9729.6	9933.8
SLC35B1	6653.6	7255.5	8504.3
SEC61A1	2704.3	2957.1	3466.8
RPN1	3341.1	3867.0	4897.8
DNAJC3	1705.7	2275.9	2602.2
CDK2AP2	3453.5	3973.3	5380.7
ARID5B			
XBP1			
HNRNPAB			
SGK1			
HSPB1			
DDIT4			
ARL4D			
SAP30			
KIAA0408			
GPR17			
HSPH1			
DNASE1L2			
SLC5A3			
GNAS			
GPR3			
TNFRSF25			
TM6SF2			
MKKS			
PLEKHF1			
ZMYM1			
DOK3			
FGF20			
SLC39A2			
KCNIP2			
ERRFI1			
DEDD2			
CCDC117			
USP31			
AHSA2			
CYS1			
CNIH2			
BANP			
CHORDC1			
P4HA1			

GEO Series "GSE21644" Expression Profiles

Num of samples in this series: 10

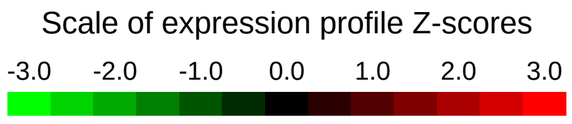

GEO Link:	http://www.ncbi.nlm.nih.gov/geo/query/acc.cgi?acc=GSE21644
Status:	Public on Jun 09 2011
Title:	FN1 expression is a marker of radioresistance in head and neck squamous cell carcinoma
Organism:	Homo sapiens
Experiment type:	Expression profiling by array
Platform:	GPL570
Pubmed ID:	20930522
Summary & Design:	**Summary:** The goal of this project was to analyze differential expression in head and neck cancer cells with various intrinsic radiosensitivity. The gene expression profiles of the cell lines were determined using the Human Genome U133 plus 2.0 Arrays (Affymetrix, Santa Clara, CA). **Overall design:** The UTSCC cells were cultured in DMEM (Gibco) supplemented with 2mM glutamine, 1% non-essential amino acids, 100 IU/ml penicillin-G, 50ug/ml streptomycin, and 5% fetal bovine serum (all from Gibco, Paisley, UK). Total RNA was prepared from 3 x 10^6 cells using the RNeasy Mini Protocol (Qiagen GmbH, Hilden, Germany). The study included a total of 10 samples with 2 seperate experiments from 5 cell lines respectivley.

Background corr dist: KL-Divergence = 0.0904, L1-Distance = 0.0398, L2-Distance = 0.0032, Normal std = 0.4661

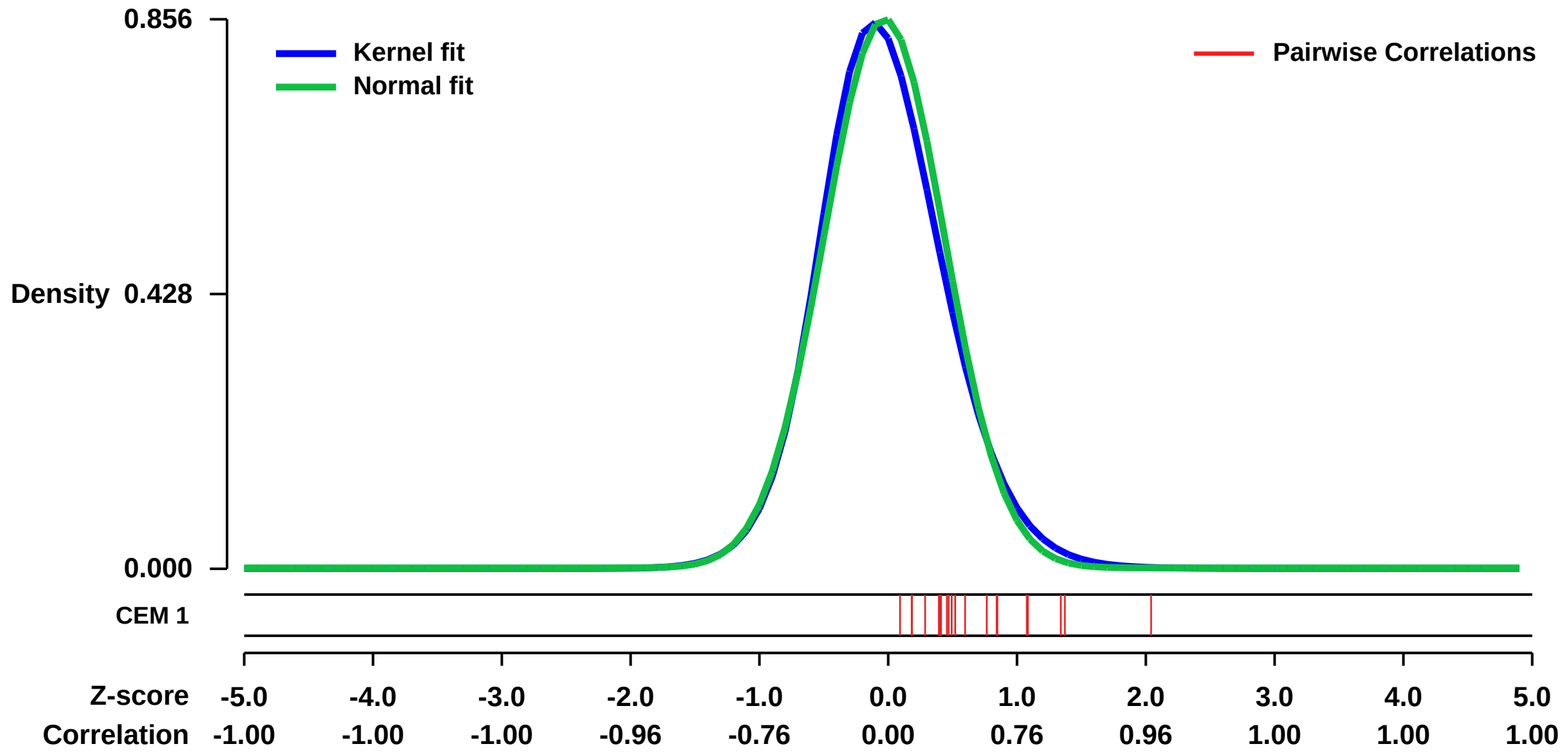

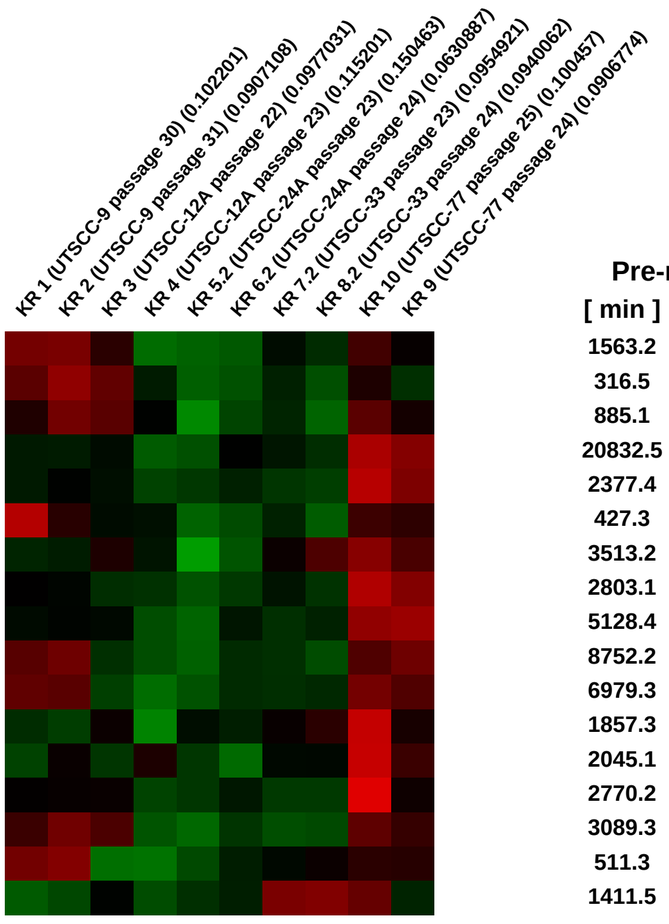

		Pre-normalization Quantiles [min]	[medium]	[max]
CEM 1	MANF	1563.2	2839.9	4139.5
P (S | Z, I) = 1.00	SDF2L1	316.5	807.7	2049.2
Mean Corr = 0.53460	CRELD2	885.1	2363.6	3247.2
	HSPA5	20832.5	25176.9	37093.8
	HYOU1	2377.4	3438.6	8727.5
	PDIA4	427.3	859.6	1791.7
	PDIA6	3513.2	6253.6	8264.3
CEM 1 + Top 10 Genes	DNAJB11	2803.1	4343.4	9163.0
	HSP90B1	5128.4	8654.6	15096.4
	PDIA3	8752.2	12362.6	22234.7
	PPIB	6979.3	10450.3	18253.3
	C19orf10	1857.3	2679.7	3789.4
	SLC35B1	2045.1	2515.2	3481.4
	SEC61A1	2770.2	3595.3	6229.7
	RPN1	3089.3	5008.3	5724.5
	DNAJC3	511.3	1793.9	3018.7
	CDK2AP2	1411.5	2031.9	3701.5
Null module	ARID5B			
	XBP1			
	HNRNPAB			
	SGK1			
	HSPB1			
	DDIT4			
	ARL4D			
	SAP30			
	KIAA0408			
	GPR17			
	HSPH1			
	DNASE1L2			
	SLC5A3			
	GNAS			
	GPR3			
	TNFRSF25			
	TM6SF2			
	MKKS			
	PLEKHF1			
	ZMYM1			
	DOK3			
	FGF20			
	SLC39A2			
	KCNIP2			
	ERRFI1			
	DEDD2			
	CCDC117			
	USP31			
	AHSA2			
	CYS1			
	CNIH2			
	BANP			
	CHORDC1			
	P4HA1			

GEO Series "GSE16237" Expression Profiles

Num of samples in this series: 51

Scale of expression profile Z-scores

-3.0 -2.0 -1.0 0.0 1.0 2.0 3.0

GEO Link:	http://www.ncbi.nlm.nih.gov/geo/query/acc.cgi?acc=GSE16237
Status:	Public on Sep 01 2009
Title:	Expression data of human neuroblastoma tissue samples
Organism:	Homo sapiens
Experiment type:	Expression profiling by array
Platform:	GPL570
Pubmed ID:	20380745
Summary & Design:	**Summary:** The prognosis of the patients with neuroblastoma largely depends on the biological characterisitics. Neuroblastoma tissues obtained before any treatments were analyzed for gene expression using Affymetrix array. We used microarrays to detail the global programme of gene expression distinguishing tumor biology of neuroblastoma tisses from the prognosis of the patients. **Overall design:** 51 neuroblastoma samples were selected those resected from the patients who died of tumor progression and those whose tumor regressed or matured spontaneously. Total RNA was extracted from these tissues samples and hybridized on Affymetrix microarrays. We sought to obtain genes to distinguish unfavorable tumors from favorable tumors.

Background corr dist: KL-Divergence = 0.3525, L1-Distance = 0.0724, L2-Distance = 0.0154, Normal std = 0.2657

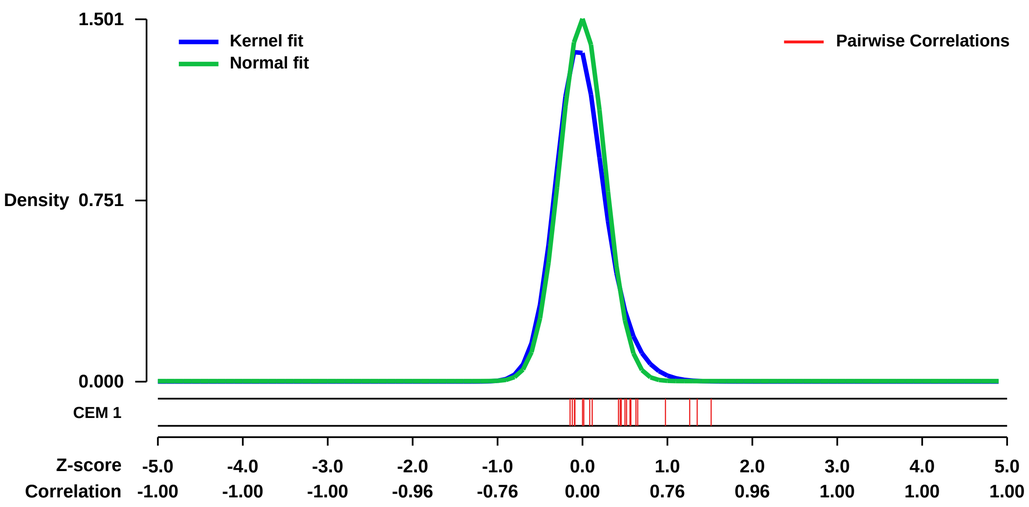

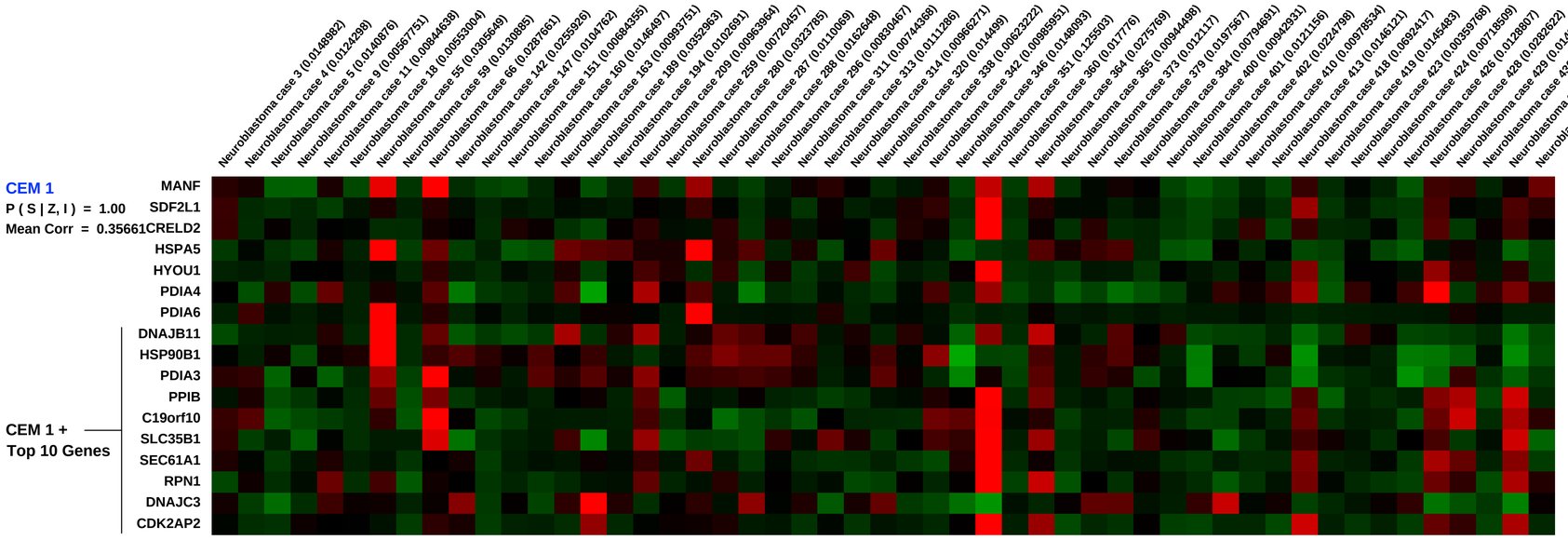

Pre-normalization Quantiles

[min]	[medium]	[max]
949.1	1573.1	4704.9
235.2	527.8	3706.8
1045.4	1817.9	8163.2
4599.0	7287.6	18042.0
541.2	1195.6	7414.4
308.0	768.0	1655.8
2320.8	4458.3	43686.3
969.1	1733.0	4711.1
235.1	2436.3	6828.3
2821.0	5081.5	10572.6
2696.1	4952.5	17932.5
660.8	1269.5	3568.8
835.1	1917.4	4704.6
903.7	1701.1	9566.8
795.9	1317.5	4360.8
307.6	971.9	2535.9
229.5	414.2	2281.6

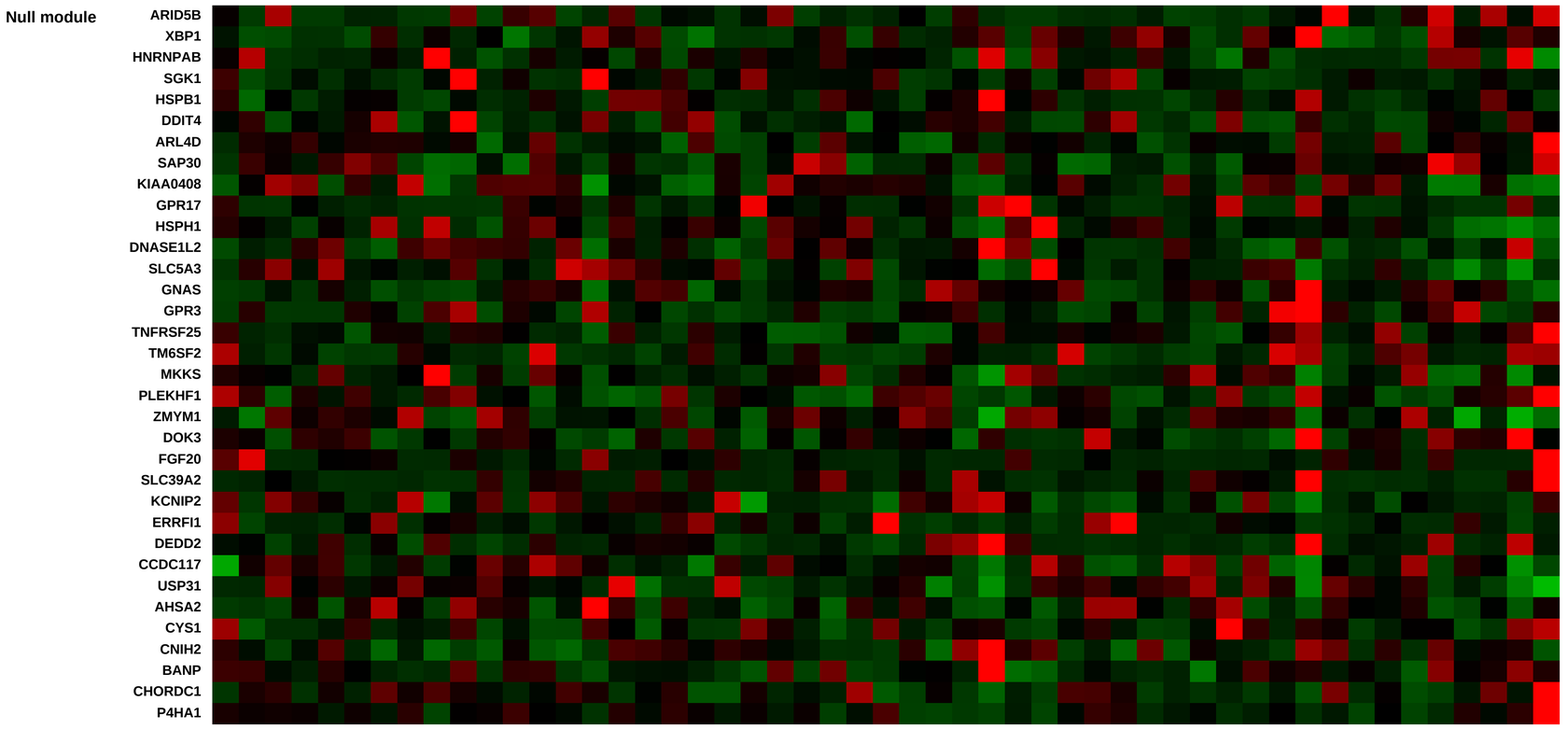

GEO Series "GSE50697" Expression Profiles

Num of samples in this series: 6

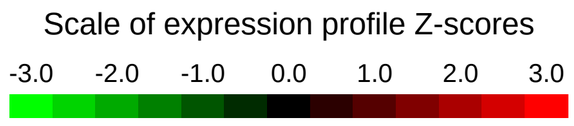

GEO Link:	http://www.ncbi.nlm.nih.gov/geo/query/acc.cgi?acc=GSE50697
Status:	Public on Sep 23 2013
Title:	Gene expression of SUM159 breast cancer cell line expressing microRNA--203
Organism:	Homo sapiens
Experiment type:	Expression profiling by array
Platform:	GPL570
Pubmed ID:	24045437
Summary & Design:	**Summary:** Determine the effect of miR-203 expression on the global mRNA expression in mesenchymal breast cancer cell line. **Overall design:** Generate control (pBabe puro) and miR-203 (pBabe puro miR-203) cells using retroviral transduction and puromycin selections. Extract total RNA using Trizol.

Background corr dist: KL-Divergence = 0.0444, L1-Distance = 0.0216, L2-Distance = 0.0005, Normal std = 0.5982

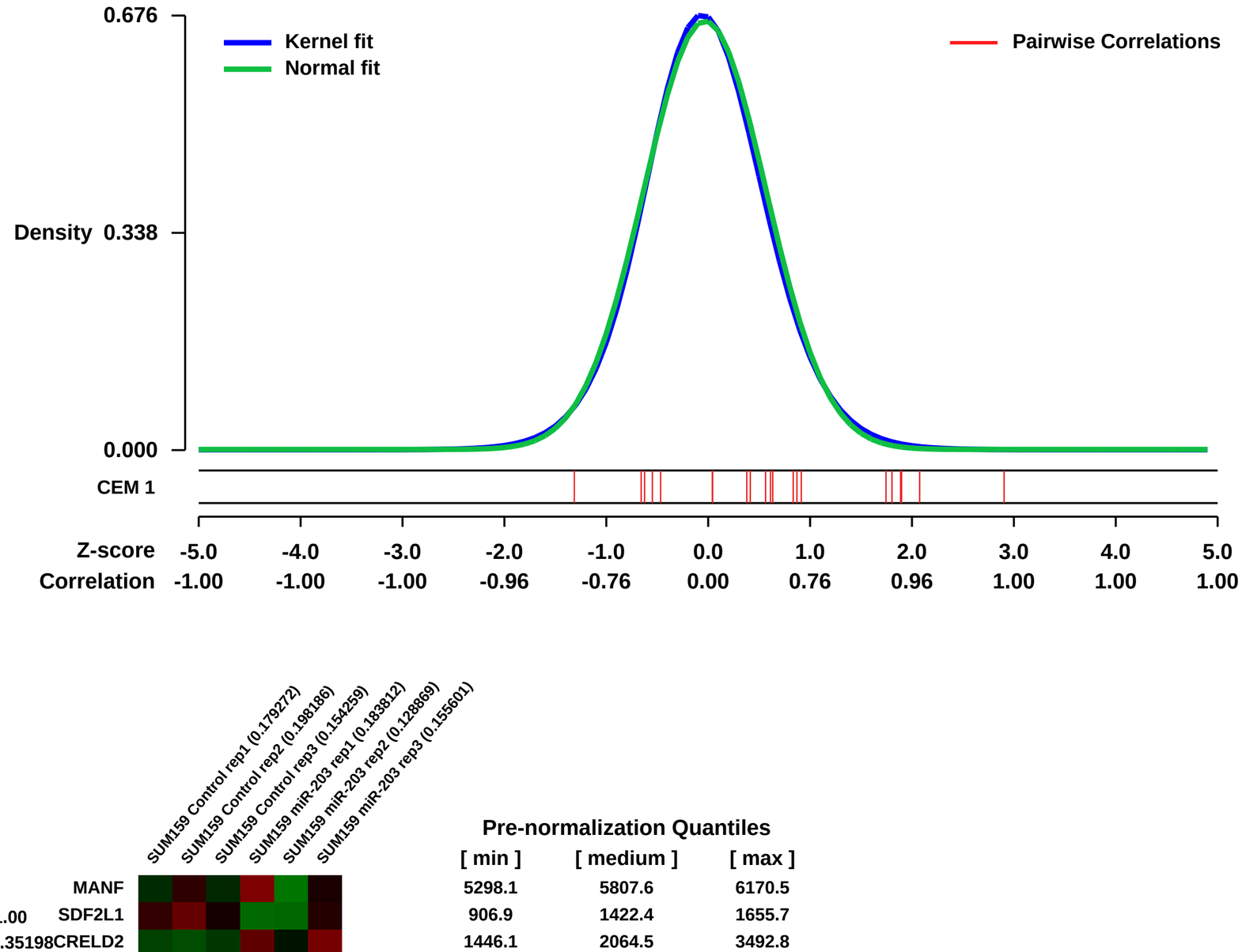

CEM 1
P (S | Z, I) = 1.00
Mean Corr = 0.35198

CEM 1 + Top 10 Genes

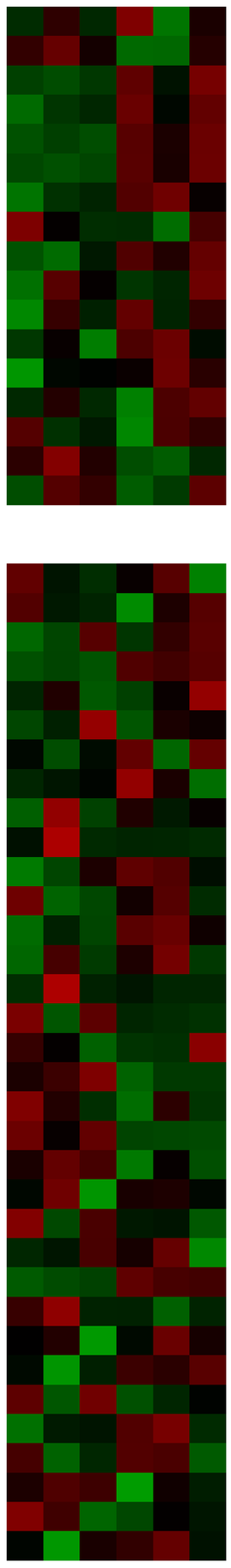

MANF	5298.1	5807.6	6170.5
SDF2L1	906.9	1422.4	1655.7
CRELD2	1446.1	2064.5	3492.8
HSPA5	11275.6	12779.9	14486.8
HYOU1	2071.5	2588.9	2966.0
PDIA4	882.4	1137.1	1338.1
PDIA6	6590.8	7269.5	7840.5
DNAJB11	5516.7	6246.0	7026.5
HSP90B1	3981.0	6474.3	7679.5
PDIA3	12092.6	13679.5	15088.4
PPIB	18749.4	21647.8	22405.4
C19orf10	4117.1	4567.2	4903.1
SLC35B1	2083.5	2331.0	2483.3
SEC61A1	1889.2	2443.5	2656.6
RPN1	3745.1	4234.5	4330.1
DNAJC3	780.4	1105.0	1354.2
CDK2AP2	776.2	920.1	961.0

Null module

ARID5B			
XBP1			
HNRNPAB			
SGK1			
HSPB1			
DDIT4			
ARL4D			
SAP30			
KIAA0408			
GPR17			
HSPH1			
DNASE1L2			
SLC5A3			
GNAS			
GPR3			
TNFRSF25			
TM6SF2			
MKKS			
PLEKHF1			
ZMYM1			
DOK3			
FGF20			
SLC39A2			
KCNIP2			
ERRFI1			
DEDD2			
CCDC117			
USP31			
AHSA2			
CYS1			
CNIH2			
BANP			
CHORDC1			
P4HA1			

GEO Series "GSE9517" Expression Profiles

Num of samples in this series: 15

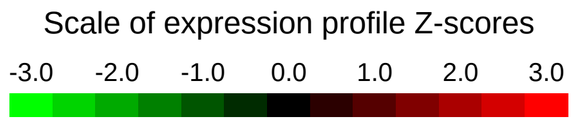

GEO Link:	http://www.ncbi.nlm.nih.gov/geo/query/acc.cgi?acc=GSE9517
Status:	Public on Dec 13 2007
Title:	Cysteine deprivation in liver cell line
Organism:	Homo sapiens
Experiment type:	Expression profiling by array
Platform:	GPL570
Pubmed ID:	18285520
Summary & Design:	**Summary:** First experiment: Cells were cultured in sulfur amino acid-free DMEM supplemented with 0.1 mM methionine + 0.1 mM cysteine (complete) or supplemented only with 0.1 mM methionine (cysteine-free). Cells were cultured in either medium for 42 h (Long + Cys; Long -Cys) or in cysteine-free medium for 36 h followed by 6 h in complete medium (Short +Cys) Second experiment: C3A/HepG2 cells were cultured in sulfur amino acid-free DMEM supplemented with 0.1 mM Met and 0.1 mM Cys (complete) or supplemented only with 0.1 mM Met (cysteine-devoid). Cells were cultured in complete medium for 42 h (Long +Cys) or in complete medium for 36 h followed by cysteine-devoid medium for 6 h (Short -Cys). Keywords: amino acid deprivation **Overall design:** Second experiment: C3A/HepG2 cells were cultured in sulfur amino acid-free DMEM supplemented with 0.1 mM Met and 0.1 mM Cys (complete) or supplemented only with 0.1 mM Met (cysteine-devoid). Cells were cultured in complete medium for 42 h (Long +Cys) or in complete medium for 36 h followed by cysteine-devoid medium for 6 h (Short -Cys).

Background corr dist: KL-Divergence = 0.1501, L1-Distance = 0.0255, L2-Distance = 0.0010, Normal std = 0.3829

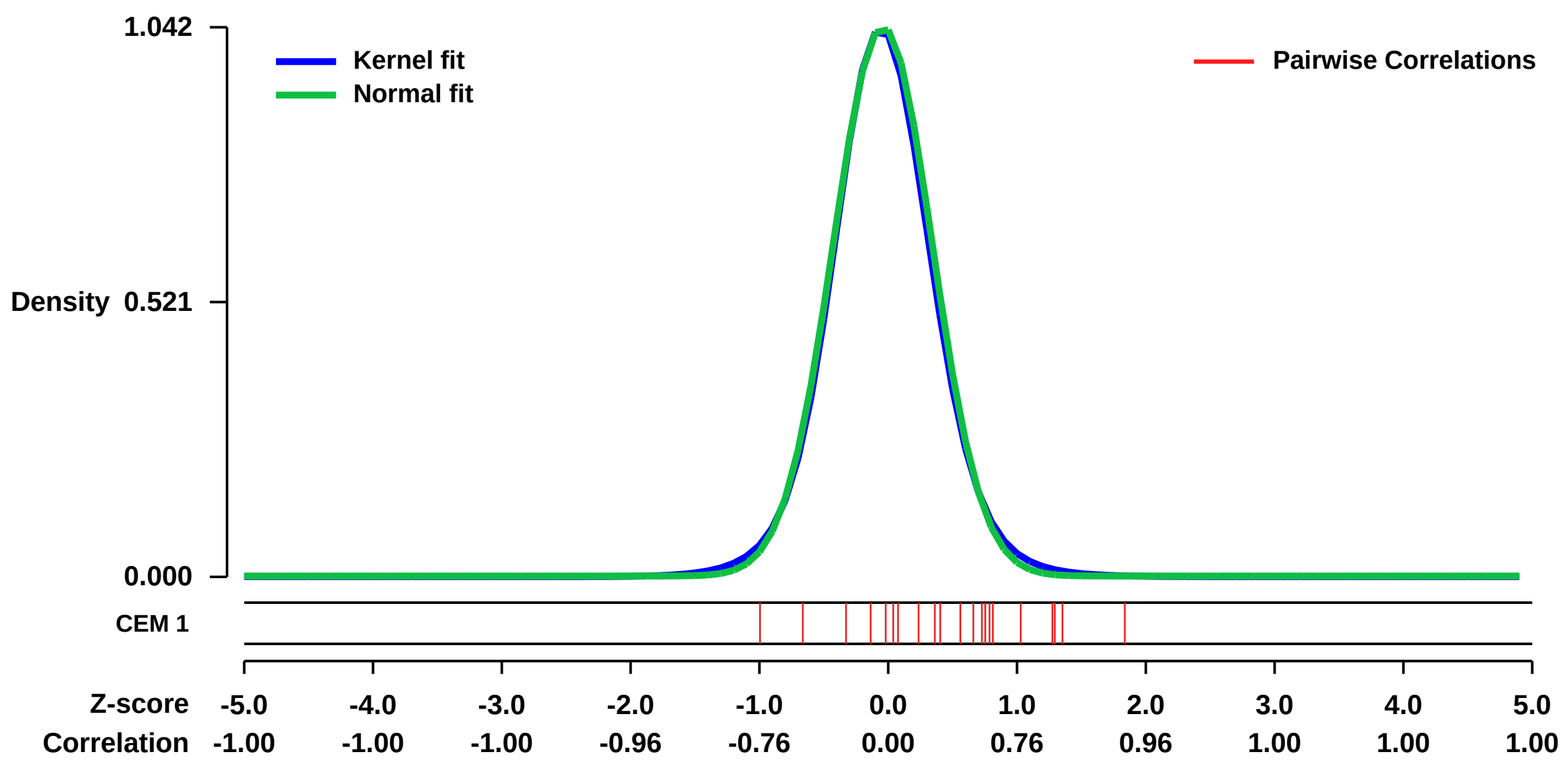

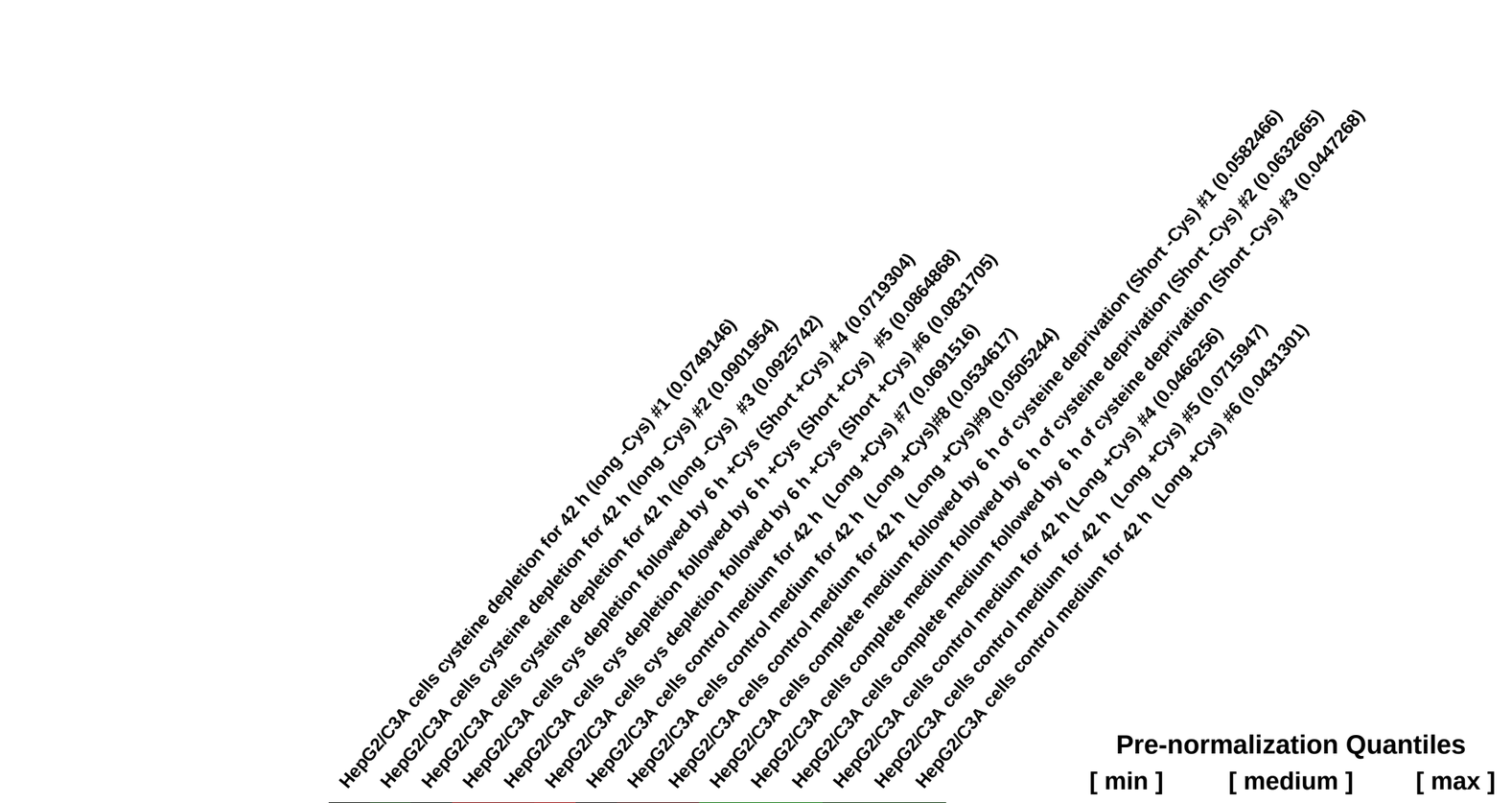

GEO Series "GSE11367" Expression Profiles

Num of samples in this series: 6

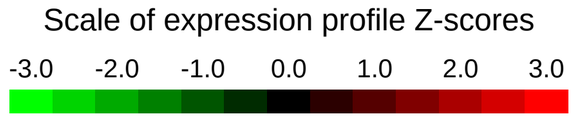

GEO Link:	http://www.ncbi.nlm.nih.gov/geo/query/acc.cgi?acc=GSE11367
Status:	Public on Jun 28 2008
Title:	Effect of IL-17 on human vascular smooth muscle cells
Organism:	Homo sapiens
Experiment type:	Expression profiling by array
Platform:	GPL570
Pubmed ID:	19075290
Summary & Design:	**Summary:** Investigate the effect of recombinant human IL-17A on vascular smooth muscle cells cultured from human aortas. **Keywords: Dose response** **Overall design:** SMCs from the aortas of three different donors were cultured in M199 media supplemented with 20% FCS and used at passage 3. The cells were either not treated or treated with IL-17 at 100 ng/ml for 6 hr. The six samples were labeled as Untreated or IL-17-treated from three independent experiments labeled A, B, and C.

Background corr dist: KL-Divergence = 0.0400, L1-Distance = 0.0273, L2-Distance = 0.0010, Normal std = 0.6211

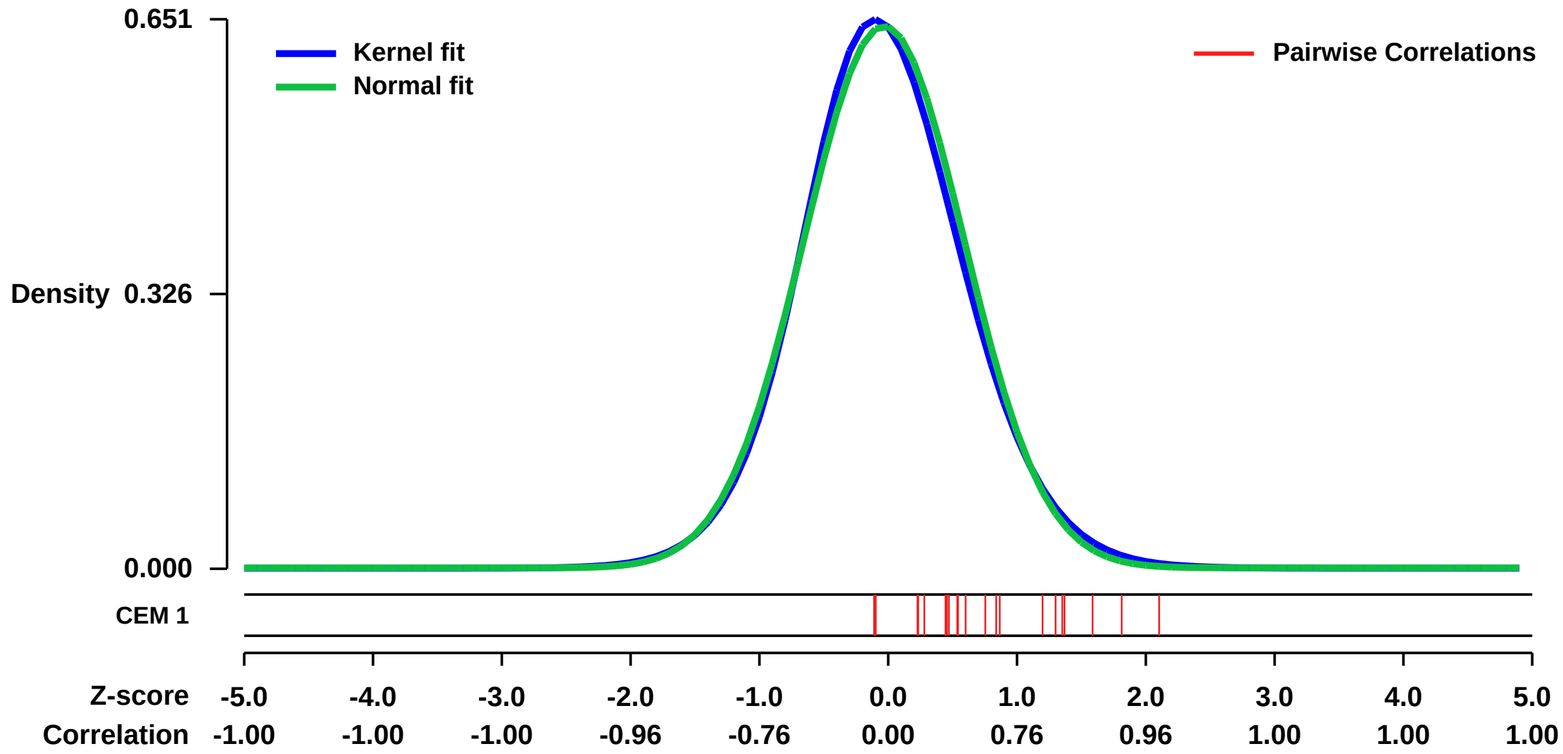

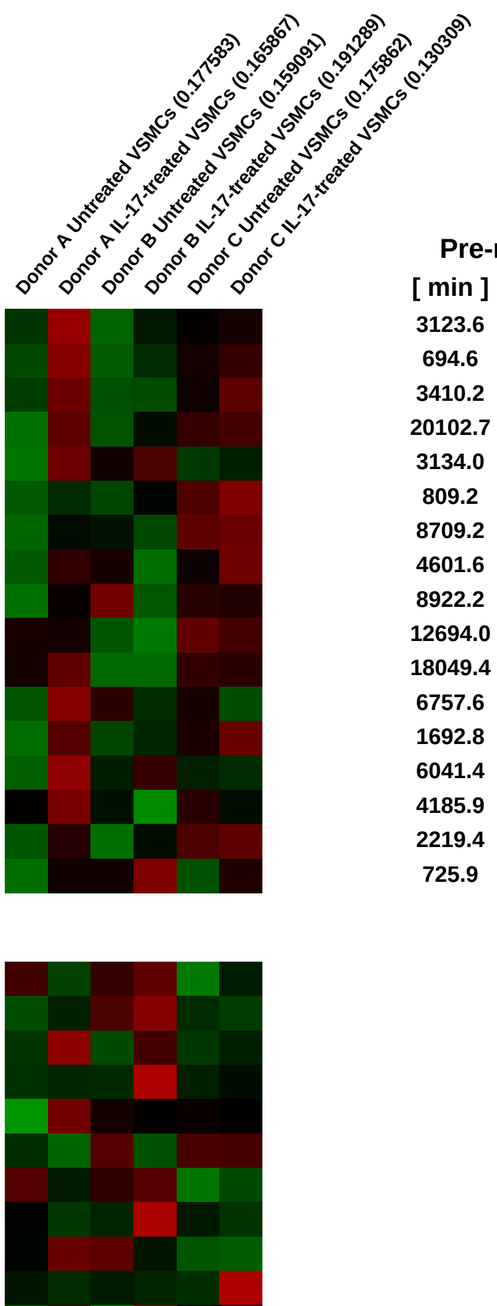

Pre-normalization Quantiles

		[min]	[medium]	[max]
CEM 1	MANF	3123.6	5162.1	7973.6
P (S | Z, I) = 1.00	SDF2L1	694.6	1216.0	1749.0
Mean Corr = 0.55401	CRELD2	3410.2	4952.4	6472.6
	HSPA5	20102.7	30971.2	33580.2
	HYOU1	3134.0	3995.1	4568.9
	PDIA4	809.2	1043.6	1405.8
	PDIA6	8709.2	9981.7	11582.6
CEM 1 + Top 10 Genes	DNAJB11	4601.6	6240.9	7362.0
	HSP90B1	8922.2	10300.7	11042.2
	PDIA3	12694.0	17872.8	20421.3
	PPIB	18049.4	27115.0	30392.6
	C19orf10	6757.6	8098.8	9550.0
	SLC35B1	1692.8	2185.7	2460.1
	SEC61A1	6041.4	6966.4	9426.5
	RPN1	4185.9	5341.5	6298.5
	DNAJC3	2219.4	3606.7	4137.0
	CDK2AP2	725.9	984.3	1205.1
Null module	ARID5B			
	XBP1			
	HNRNPAB			
	SGK1			
	HSPB1			
	DDIT4			
	ARL4D			
	SAP30			
	KIAA0408			
	GPR17			
	HSPH1			
	DNASE1L2			
	SLC5A3			
	GNAS			
	GPR3			
	TNFRSF25			
	TM6SF2			
	MKKS			
	PLEKHF1			
	ZMYM1			
	DOK3			
	FGF20			
	SLC39A2			
	KCNIP2			
	ERRFI1			
	DEDD2			
	CCDC117			
	USP31			
	AHSA2			
	CYS1			
	CNIH2			
	BANP			
	CHORDC1			
	P4HA1			

GEO Series "GSE8597" Expression Profiles

Num of samples in this series: 16

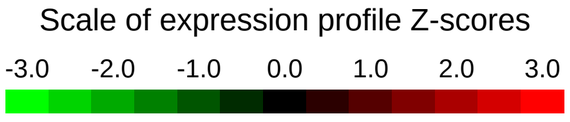

GEO Link:	http://www.ncbi.nlm.nih.gov/geo/query/acc.cgi?acc=GSE8597
Status:	Public on Sep 01 2007
Title:	Gene expression analysis of hormone treated MCF7 breast cancer cells in the presence or absence of cycloheximide
Organism:	Homo sapiens
Experiment type:	Expression profiling by array
Platform:	GPL570
Pubmed ID:	17986456
Summary & Design:	**Summary:** Estrogen receptors (ERs), which mediate the proliferative action of estrogens in breast cancer cells, are ligand-dependent transcription factors that regulate expression of their primary target genes through several mechanisms. In addition to direct binding to cognate DNA sequences, ERs can be recruited to DNA through other transcription factors (tethering), or affect gene transcription through modulation of signaling cascades by non-genomic mechanisms of action. To better characterize the mechanisms of gene regulation by estrogens, we have identified more than 700 putative primary and more than 1500 putative secondary target genes of estradiol in MCF7 cells through microarray analysis performed in the presence or absence of the translation inhibitor cycloheximide. **Keywords:** drug treatment **Overall design:** RNA samples were collected 24 h after treatment of MCF7 cells with vehicle or 17{beta}-estradiol (25 nM). Cells were pre-treated 1 h before E2 stimulation with cycloheximide (CHX, 10 microg/ml). Microarray analysis was performed with four replicates for each condition.

Background corr dist: KL-Divergence = 0.0630, L1-Distance = 0.0505, L2-Distance = 0.0037, Normal std = 0.5575

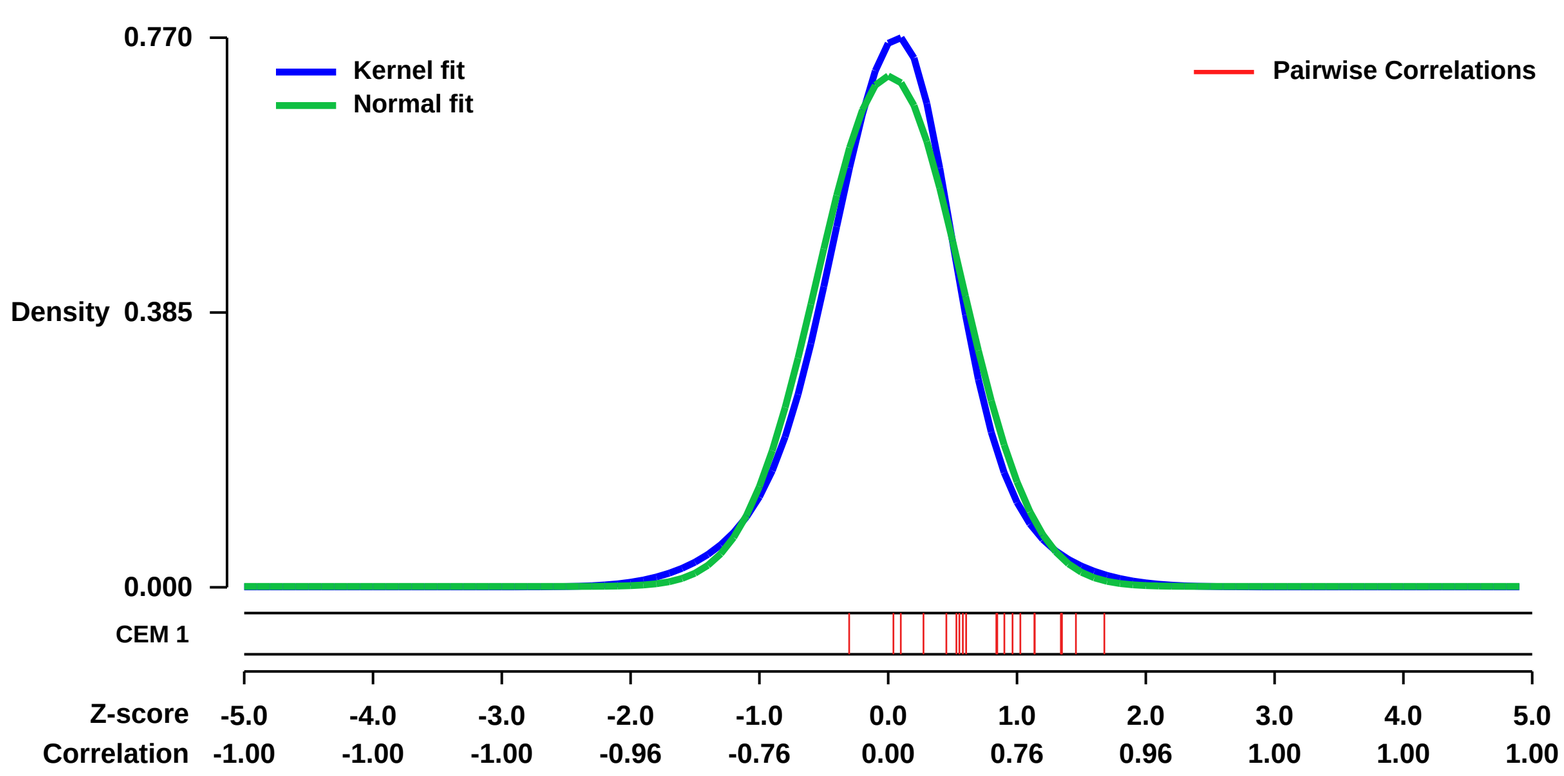

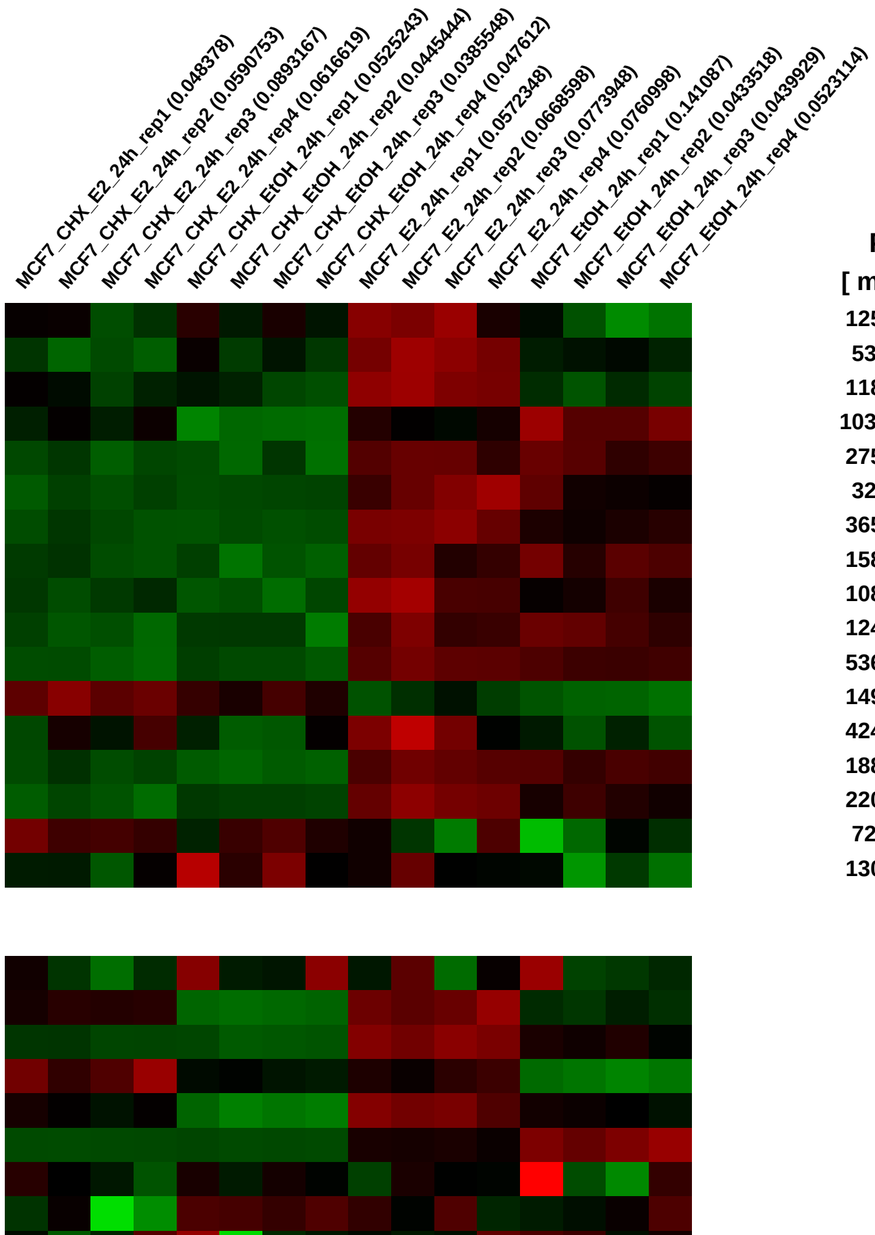

Pre-normalization Quantiles

	[min]	[medium]	[max]
CEM 1			
P (S | Z, I) = 0.99			
Mean Corr = 0.58430			
MANF	1250.4	1471.9	1699.2
SDF2L1	539.9	643.2	869.5
CRELD2	1184.2	1337.4	1901.4
HSPA5	10310.9	11873.2	13624.0
HYOU1	2756.4	3795.5	4174.0
PDIA4	320.9	488.8	762.3
PDIA6	3651.3	5283.3	7386.0
CEM 1 + Top 10 Genes			
DNAJB11	1583.0	2022.2	2271.3
HSP90B1	1088.2	1539.5	2163.2
PDIA3	1247.6	2525.3	3127.9
PPIB	5361.1	8930.0	10192.9
C19orf10	1499.6	2000.8	2400.3
SLC35B1	4247.2	4400.4	4839.1
SEC61A1	1885.4	3277.4	3820.5
RPN1	2203.9	3075.0	3938.1
DNAJC3	727.1	923.3	999.1
CDK2AP2	1305.4	1505.3	1750.9
Null module			
ARID5B			
XBP1			
HNRNPAB			
SGK1			
HSPB1			
DDIT4			
ARL4D			
SAP30			
KIAA0408			
GPR17			
HSPH1			
DNASE1L2			
SLC5A3			
GNAS			
GPR3			
TNFRSF25			
TM6SF2			
MKKS			
PLEKHF1			
ZMYM1			
DOK3			
FGF20			
SLC39A2			
KCNIP2			
ERRFI1			
DEDD2			
CCDC117			
USP31			
AHSA2			
CYS1			
CNIH2			
BANP			
CHORDC1			
P4HA1			

GEO Series "GSE34112" Expression Profiles

Num of samples in this series: 16

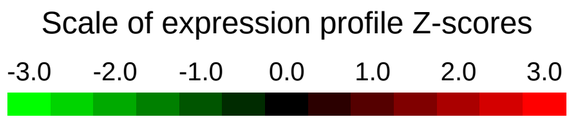

GEO Link: http://www.ncbi.nlm.nih.gov/geo/query/acc.cgi?acc=GSE34112
Status: Public on Dec 01 2012
Title: Effect of NO-sulindac treatment on hypoxic prostate cancer cells
Organism: Homo sapiens
Experiment type: Expression profiling by array
Platform: GPL570
Pubmed ID:

Summary & Design:

Summary:
The hypoxia response contributes to radio and chemo-resistance in cancer cells. Our previous work has shown that the nitric oxide donating non-steroidal anti-inflammatory drug (NO-NSAID) NO-sulindac is a potent inhibitor of the hypoxia response in prostate cancer cells and leads to increased susceptibilty to radiation. In this study we used microarrays to investigated the global impact of NO-sulindac on the hypoxia response in prostate cancer cells with a view to determining the mechanism of action.

Overall design:
PC3 hormone-insensitive prostate cancer cells were grown under normoxic or hypoxic conditions and treated with NO-sulindac, unnitrated sulindac or vehicle control. Global gene expression in response to treatment was examined using microarrays and the bioconductor software suite. Gene set enrichment analysis (GSEA), Gene ontology (GO) analysis and pathway analysis were used to examine the biological impact of treatments.

Background corr dist: KL-Divergence = 0.0912, L1-Distance = 0.0337, L2-Distance = 0.0016, Normal std = 0.4655

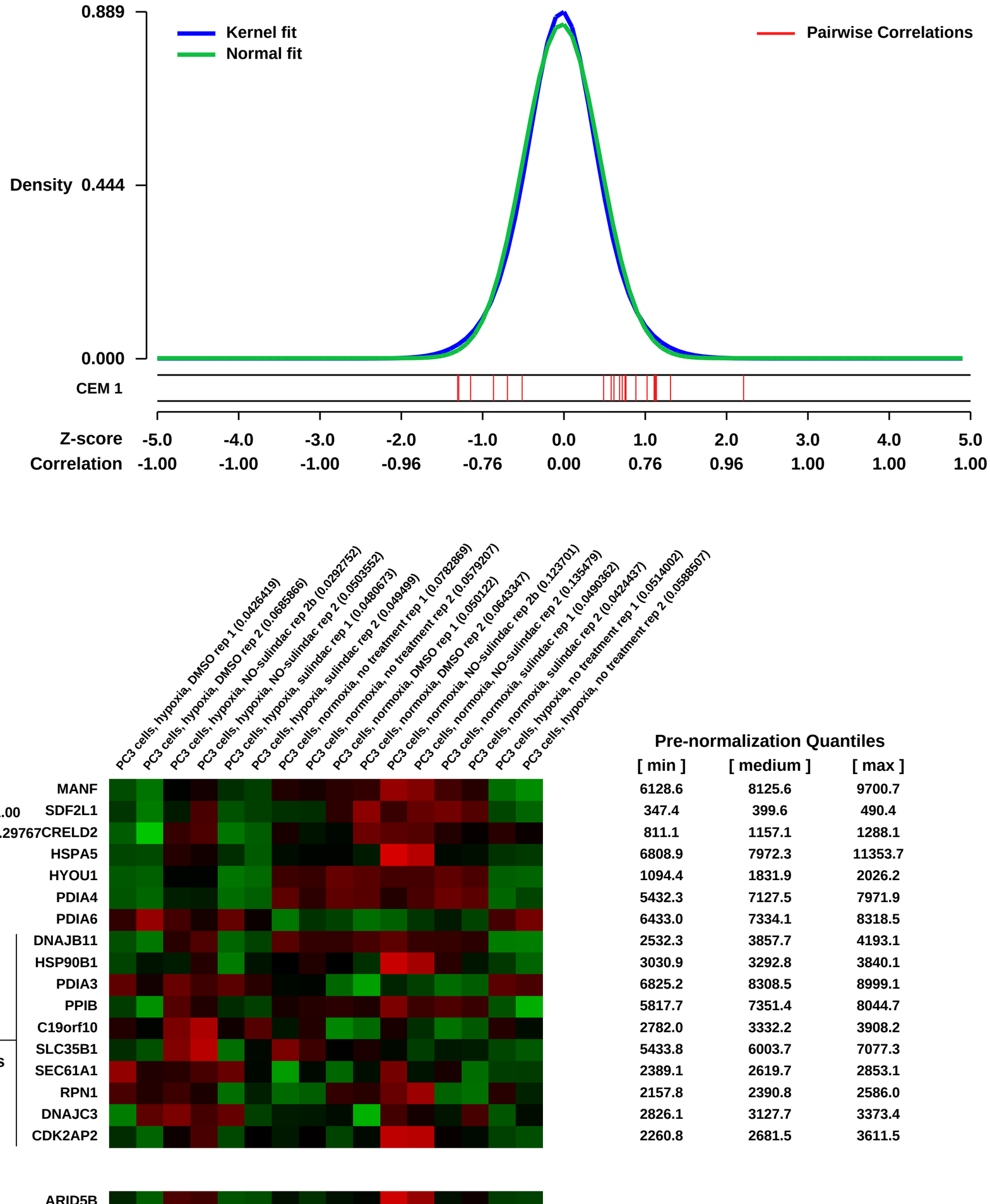

Pre-normalization Quantiles

	[min]	[medium]	[max]
MANF	6128.6	8125.6	9700.7
SDF2L1	347.4	399.6	490.4
CRELD2	811.1	1157.1	1288.1
HSPA5	6808.9	7972.3	11353.7
HYOU1	1094.4	1831.9	2026.2
PDIA4	5432.3	7127.5	7971.9
PDIA6	6433.0	7334.1	8318.5
DNAJB11	2532.3	3857.7	4193.1
HSP90B1	3030.9	3292.8	3840.1
PDIA3	6825.2	8308.5	8999.1
PPIB	5817.7	7351.4	8044.7
C19orf10	2782.0	3332.2	3908.2
SLC35B1	5433.8	6003.7	7077.3
SEC61A1	2389.1	2619.7	2853.1
RPN1	2157.8	2390.8	2586.0
DNAJC3	2826.1	3127.7	3373.4
CDK2AP2	2260.8	2681.5	3611.5

GEO Series "GSE11166" Expression Profiles

Num of samples in this series: 95

Scale of expression profile Z-scores

-3.0 -2.0 -1.0 0.0 1.0 2.0 3.0

GEO Link: http://www.ncbi.nlm.nih.gov/geo/query/acc.cgi?acc=GSE11166
Status: Public on Apr 16 2008
Title: Local regulation and clinical impact of complement gene expression in deceased and living donor kidney allografts
Organism: Homo sapiens
Experiment type: Expression profiling by array
Platform: GPL570
Pubmed ID: 19443638

Summary & Design:

Summary:
The biopsy samples obtained at implantation segregated in 2 distinct groups according to donor origin, with a cluster of 319 unique identified genes higher expressed in DD compared to LD kidneys, and 329 genes lower expressed (false discovery rate <5%). Using pathway analysis software a significant local renal overrepresentation of complement genes in DD implantation biopsies was identified. Complement gene expression in DD kidneys related both to donor death and cold ischemia duration, and was associated with a slower onset of renal allograft function. In post-transplantation protocol biopsies, there was a continued overexpression of complement genes, regardless of donor source. The local renal complement gene expression variability in post-transplantation biopsies correlated with renal graft function.

This study demonstrates a significant and clinically relevant local overexpression of complement genes in DD kidneys at engraftment and continuous functionally important regulation of complement gene expression after transplantation, regardless of donor source. Targeted therapy interfering with complement activation is an attractive therapeutic target that deserves further investigation in solid organ transplantation.

Keywords: time course, genomics gene expression

Overall design:
A total of 95 human renal allograft protocol biopsies were included in this study, 28 biopsies (14 DD, 14 LD) obtained at implantation prior to revascularization and 67 protocol biopsies obtained after transplantation. Whole genome expression profiles were assessed using microarrays.

Background corr dist: KL-Divergence = 0.5478, L1-Distance = 0.0902, L2-Distance = 0.0266, Normal std = 0.2171

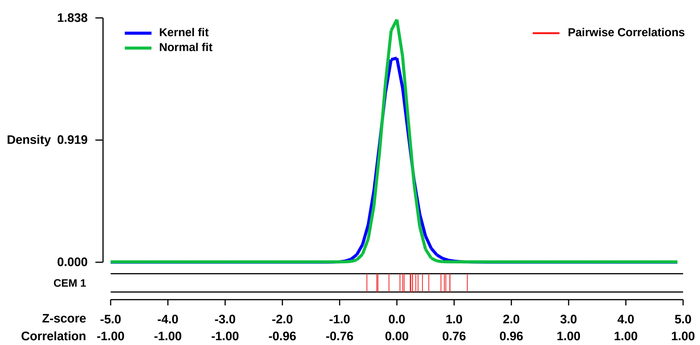

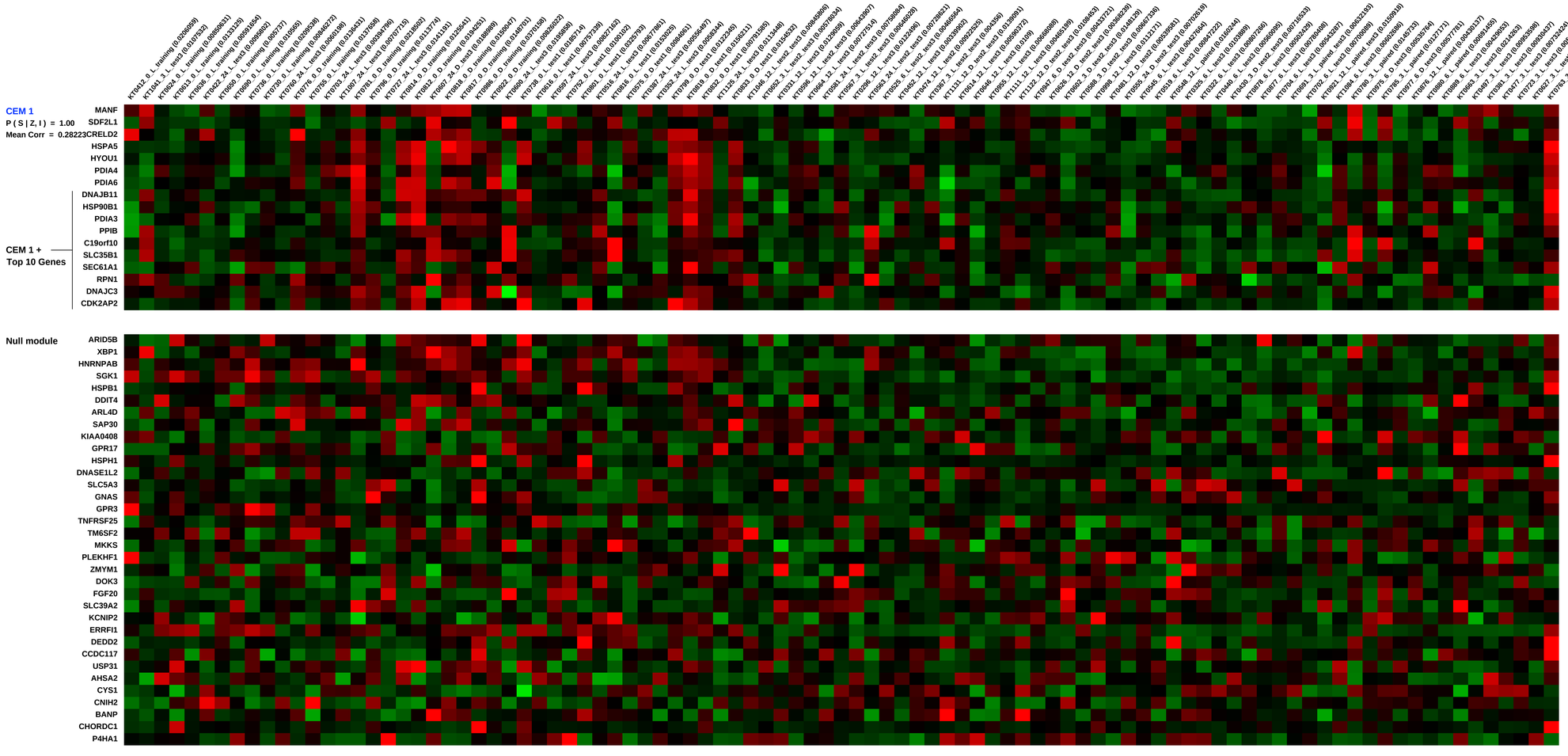

Pre-normalization Quantiles

[min]	[medium]	[max]
1440.9	3307.6	5967.7
81.3	183.4	499.6
151.5	437.9	1003.5
1502.0	3903.7	11282.4
39.6	287.6	1122.6
4170.6	7800.9	12868.3
3670.9	6392.1	9485.7
588.9	1142.3	3171.1
2488.6	5608.9	12623.1
2378.6	5048.0	9027.1
1573.5	2861.2	4918.7
199.5	350.1	1094.2
729.3	1346.9	3920.2
375.6	866.1	1584.3
1129.6	2534.1	4860.8
3985.9	6695.0	8772.5
86.2	324.2	1164.4

GEO Series "GSE11292" Expression Profiles

Num of samples in this series: 81

Scale of expression profile Z-scores

-3.0 -2.0 -1.0 0.0 1.0 2.0 3.0

GEO Link: http://www.ncbi.nlm.nih.gov/geo/query/acc.cgi?acc=GSE11292
Status: Public on Nov 23 2012
Title: High-time-resolution dynamic analysis of human regulatory T cell (Treg) / CD4+ T-effector cell (Teff) activation
Organism: Homo sapiens
Experiment type: Expression profiling by array
Platform: GPL570
Pubmed ID: 23169000

Summary & Design:

Summary:
Human FOXP3+CD25+CD4+ regulatory T cells (Tregs) play a dominant role in the maintenance of immune homeostasis. Several genes are known to be important for murine Tregs, but for human Tregs the genes and underlying molecular networks controlling the suppressor function still largely remain unclear. We here performed a high-time-resolution dynamic analysis of the transcriptome during the very early phase of human Treg/ CD4+ T-effector cell activation. After constructing a correlation network specific for Tregs based on these dynamic data, we described a strategy to identify key genes by directly analyzing the constructed undirected correlation network. Six out of the top 10 ranked key hubs are known to be important for Treg function or involved in autoimmune diseases. Surprisingly, PLAU (the plasminogen activator urokinase) was among the 4 new key hubs. We here show that PLAU was critical for expression regulation of FOXP3, EOS and several other important Treg genes and the suppressor function of human Tregs. Moreover, we found Plau inhibits murine Treg development and but promotes the suppressive function. Further analysis unveils that PLAU is particularly important for memory Tregs and that PLAU mediates Treg suppressor function via STAT5 and ERK signaling pathways. Our study shows the potential for identifying novel key genes for complex dynamic biological processes using a network strategy based on high-time-resolution data, and highlights a critical role of PLAU in both human and murine Tregs. The construction of a dynamic correlation network of human Tregs provides a useful resource for the understanding of Treg function and human autoimmune diseases.

The high-time-resolution time-series transcriptomic data during the very early phase of human Treg/Teff activation could be generally used for further mechanistic analysis of human Treg function. These data could be further used for biological network analysis, dynamic analysis, modeling by experimental researchers, bioinformaticians, computational biologists and systems biologists.

Overall design:
We have measured the genome-wide expression of 38,500 genes (probes) by performing a high-time-resolution time-series analysis during the activation process of human regulatory T cells /CD4+ T-effector cells at 19 time points for the first 6h with an equal interval of 20 min. We have also overexpressed the GARP gene in human effector T cells and measured the genome-scale expression for the GARP-overexpressed cells and ThGFP cells at time point 0, 100 and 360min following activation. The stimulation source used in this work is a combination of anti-CD3/-CD28 Dynal beads with IL2 100U/ml.

Background corr dist: KL-Divergence = 0.6505, L1-Distance = 0.0924, L2-Distance = 0.0285, Normal std = 0.2016

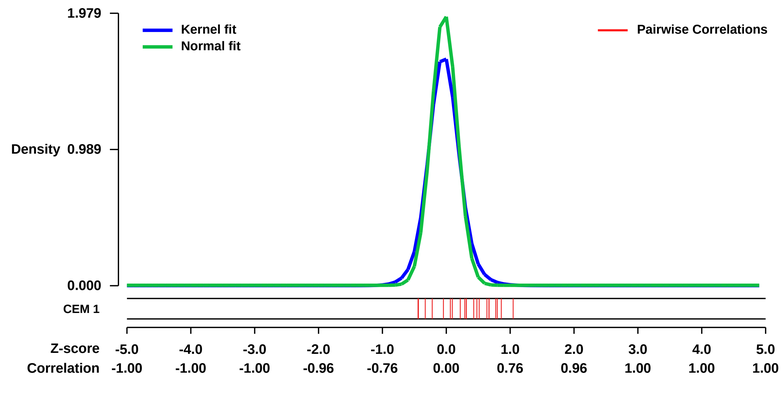

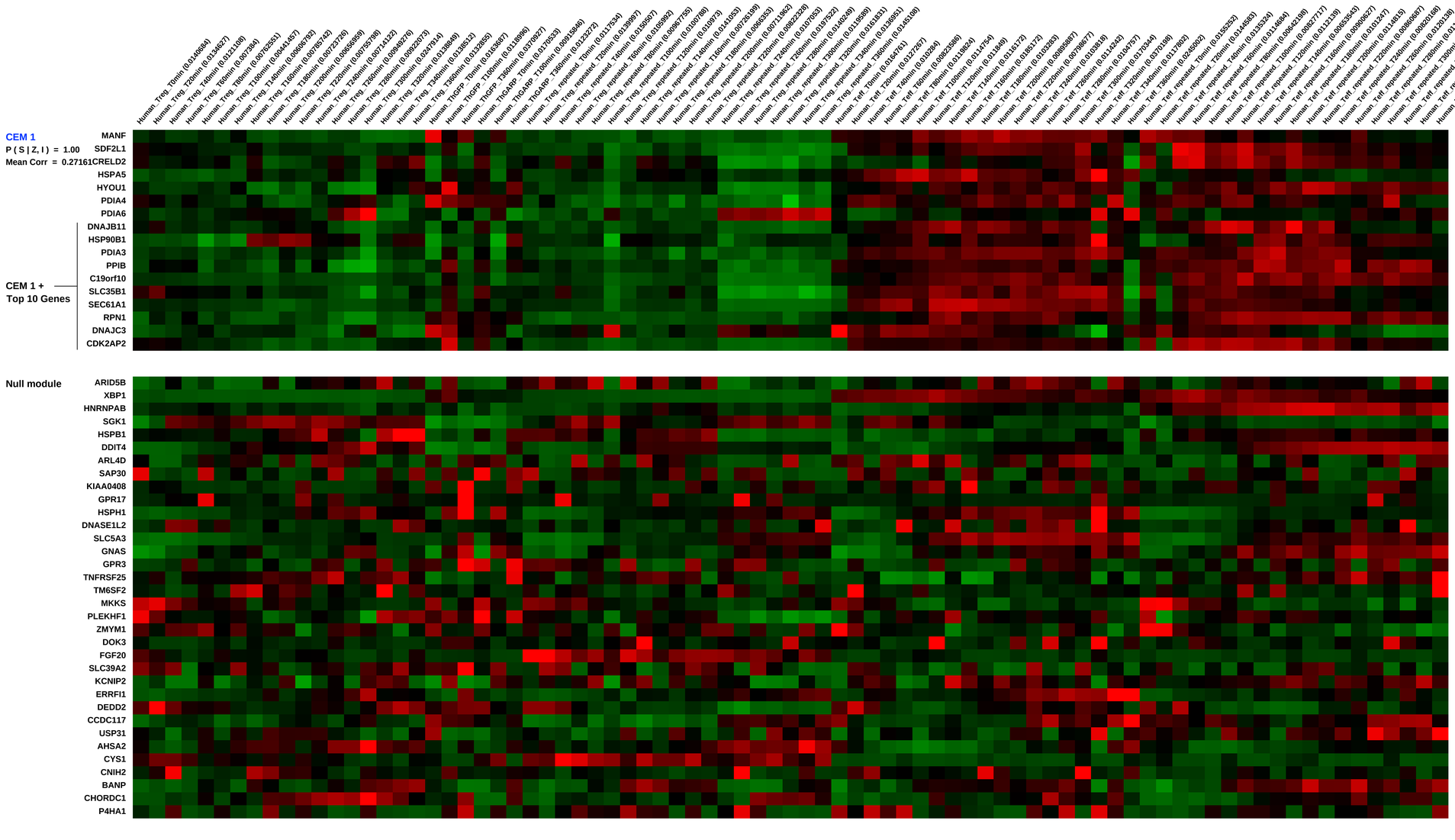

GEO Series "GSE13378" Expression Profiles

Num of samples in this series: 16

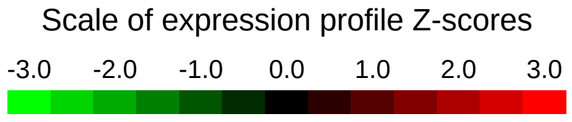

GEO Link:	http://www.ncbi.nlm.nih.gov/geo/query/acc.cgi?acc=GSE13378
Status:	Public on Feb 20 2010
Title:	Exposure of squamous esophageal cell line HET-1A to deoxycholic acid (DCA)
Organism:	Homo sapiens
Experiment type:	Expression profiling by array
Platform:	GPL570
Pubmed ID:	20139130
Summary & Design:	**Summary:** The involvment of bile acids such as deoxycholic acid (DCA) in gastro-esophageal reflux disease and subsequent Barrettâ s metaplsia has been postulated. This study examines gene expression induced by exposure to DCA in esophageal cells and may be utilised in cross-comparisions with data derived from gene expression studies of Barrettâ s esophagus and associated adenocarcinoma. Additionally this study may be used to assess divergence in response to bile acids by comparisons with similar study performed in SKGT4 barrett''s assocaited adenocarcinoma cell line. **Overall design:** HET-1A cells were exposed to 300um DCA over 24 hours in duplicate experiments including matched timepoint controls

Background corr dist: KL-Divergence = 0.1030, L1-Distance = 0.0466, L2-Distance = 0.0034, Normal std = 0.4551

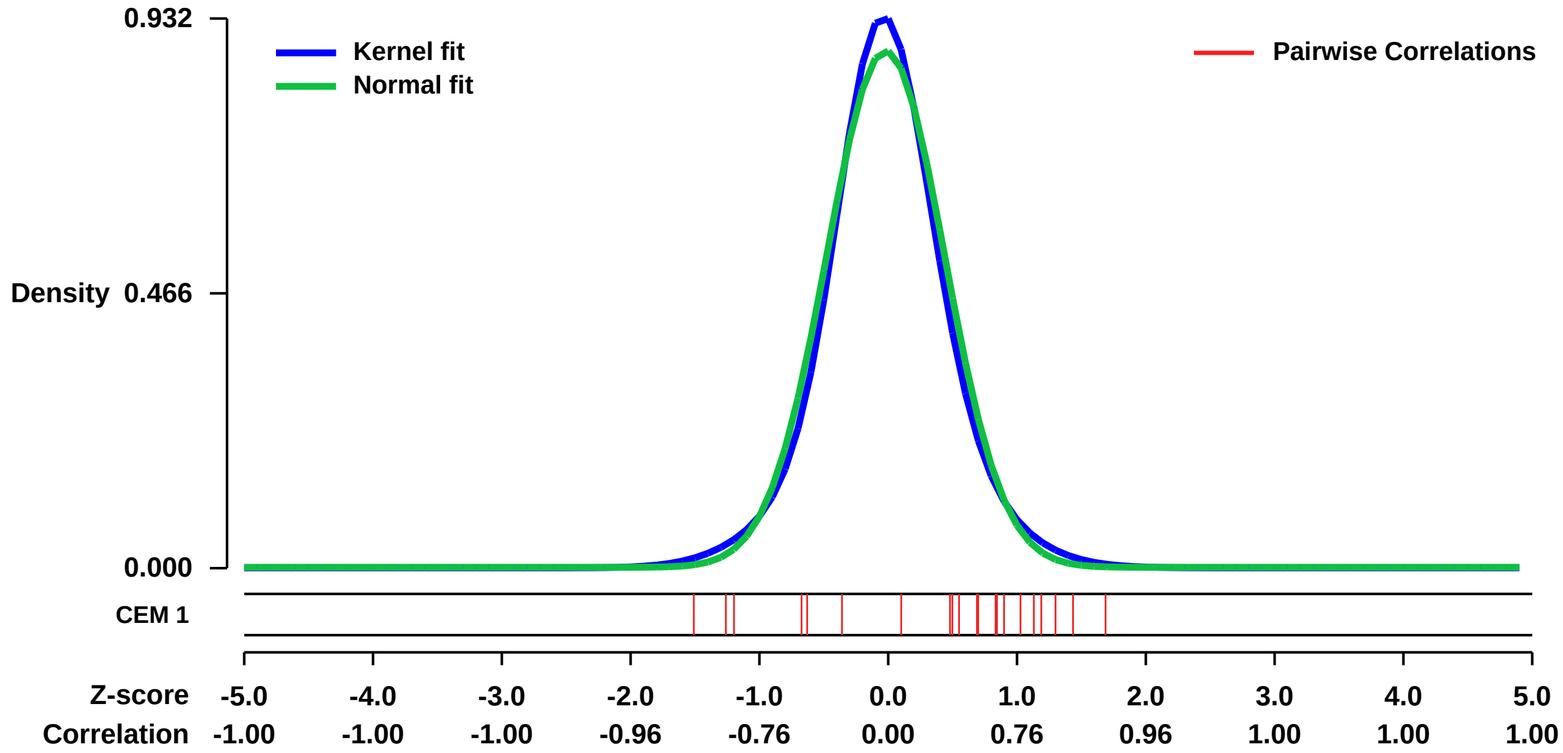

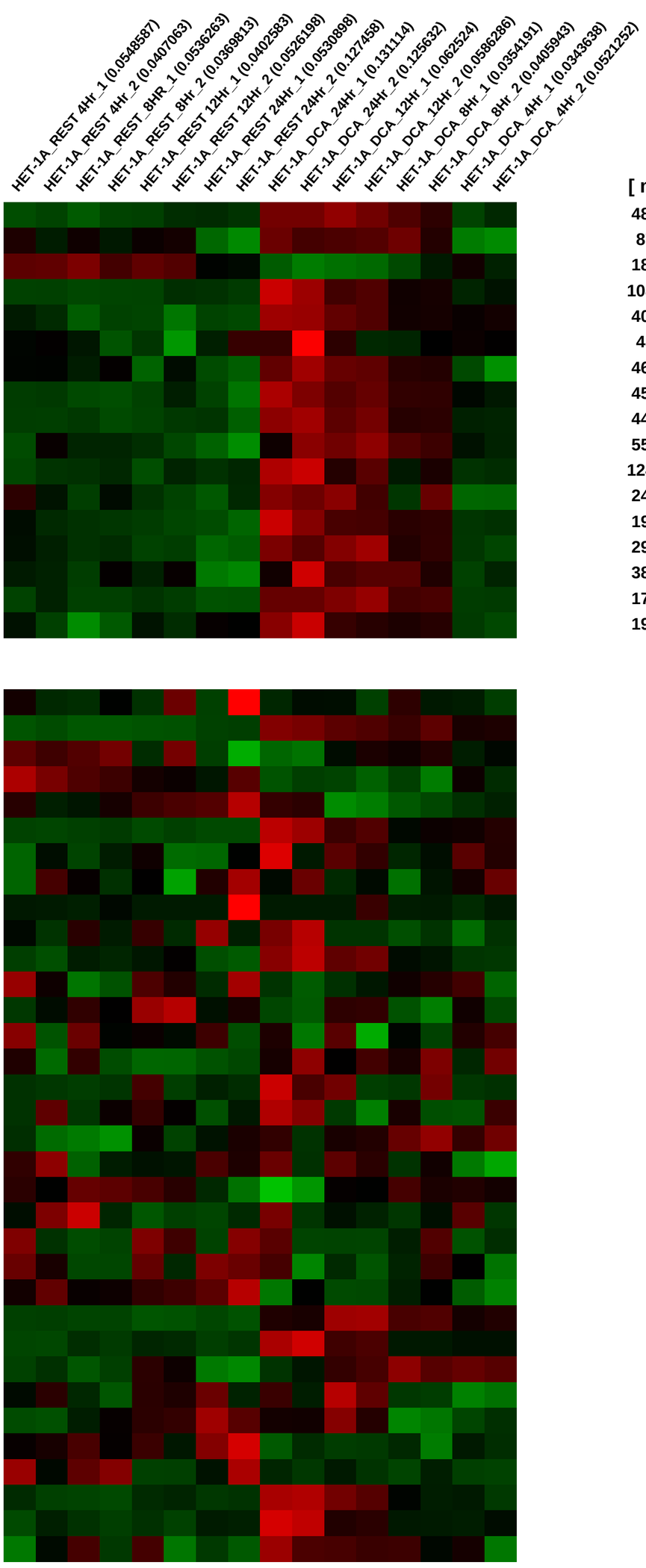

	Pre-normalization Quantiles		
	[min]	[medium]	[max]
MANF	4824.8	5595.2	8564.9
SDF2L1	870.4	1536.0	1912.9
CRELD2	1808.7	2803.1	3847.6
HSPA5	10853.8	16180.7	51863.5
HYOU1	4090.5	6858.7	10116.8
PDIA4	485.3	776.0	1260.0
PDIA6	4626.5	6171.0	7943.0
DNAJB11	4578.1	7362.2	13223.3
HSP90B1	4452.6	6967.8	15232.5
PDIA3	5589.6	7633.2	10260.8
PPIB	12422.2	14519.9	26940.8
C19orf10	2457.0	3198.7	4601.0
SLC35B1	1962.8	2604.9	5218.6
SEC61A1	2935.0	5243.7	11425.5
RPN1	3898.5	5826.9	8682.4
DNAJC3	1718.7	2073.0	4411.5
CDK2AP2	1976.6	2540.0	3364.2

GEO Series "GSE22467" Expression Profiles

Num of samples in this series: 9

Scale of expression profile Z-scores

-3.0 -2.0 -1.0 0.0 1.0 2.0 3.0

GEO Link: http://www.ncbi.nlm.nih.gov/geo/query/acc.cgi?acc=GSE22467
Status: Public on Jul 01 2010
Title: Impact of NRSF variant over-expression in SK-N-AS human neuroblastoma cells
Organism: Homo sapiens
Experiment type: Expression profiling by array
Platform: GPL570
Pubmed ID:

Summary & Design:

Summary:
Neuron-restrictive silencer factor (NRSF) and its isoforms are differentially regulated in rodent models of self-sustaining status epilepticus (SSSE). NRSF isoforms regulate genes associated with SSSE, including the proconvulsant tachykinins, brain-derived neurotrophic factor and multiple ion channels. NRSF isoforms may direct distinct gene expression patterns during SSSE and the ratio of each isoform may be a causative factor in traumatic damage to the CNS. Here we analysed global gene expression changes by microarray in human SK-N-AS neuroblastoma cells following the over expression of NRSF and a truncated isoform, HZ4.

We used bioinformatics software to analyse the microarray dataset and correlated these data with epilepsy candidate gene pathways. Findings were validated by RT-PCR. We demonstrated that NRSF and HZ4 direct overlapping as well as distinct gene expression patterns and that they differentially modulated gene expression patterns associated with epilepsy. Finally we revealed that NRSF gene expression may be modulated by the anticonvulsant, phenytoin. This study provides fundamental information on networks of genes that may be altered during SSSE, following altered NRSF expression, which may be important in future therapeutic research and clinical analysis of genetic variation predisposing to epilepsy.

Overall design:
Human SK-N-AS cells were treated with expression constructs over-expressing either the full length human transcription factor, NRSF, (via the RE-EX1 construct) or a truncated variant (via the HZ4 construct). Cells were treated for either 0hrs (base line controls), 24hrs or 48hrs, before being immediately processed for RNA extraction. An affymetrix microarray was employed to investigate gene expression patterns, comparing each time point (24hrs or 48hrs) againsts its baseline ()hrs) control. This experiment was performed in triplicate samples per batch, and over three batches.

Background corr dist: KL-Divergence = 0.1018, L1-Distance = 0.0300, L2-Distance = 0.0017, Normal std = 0.4365

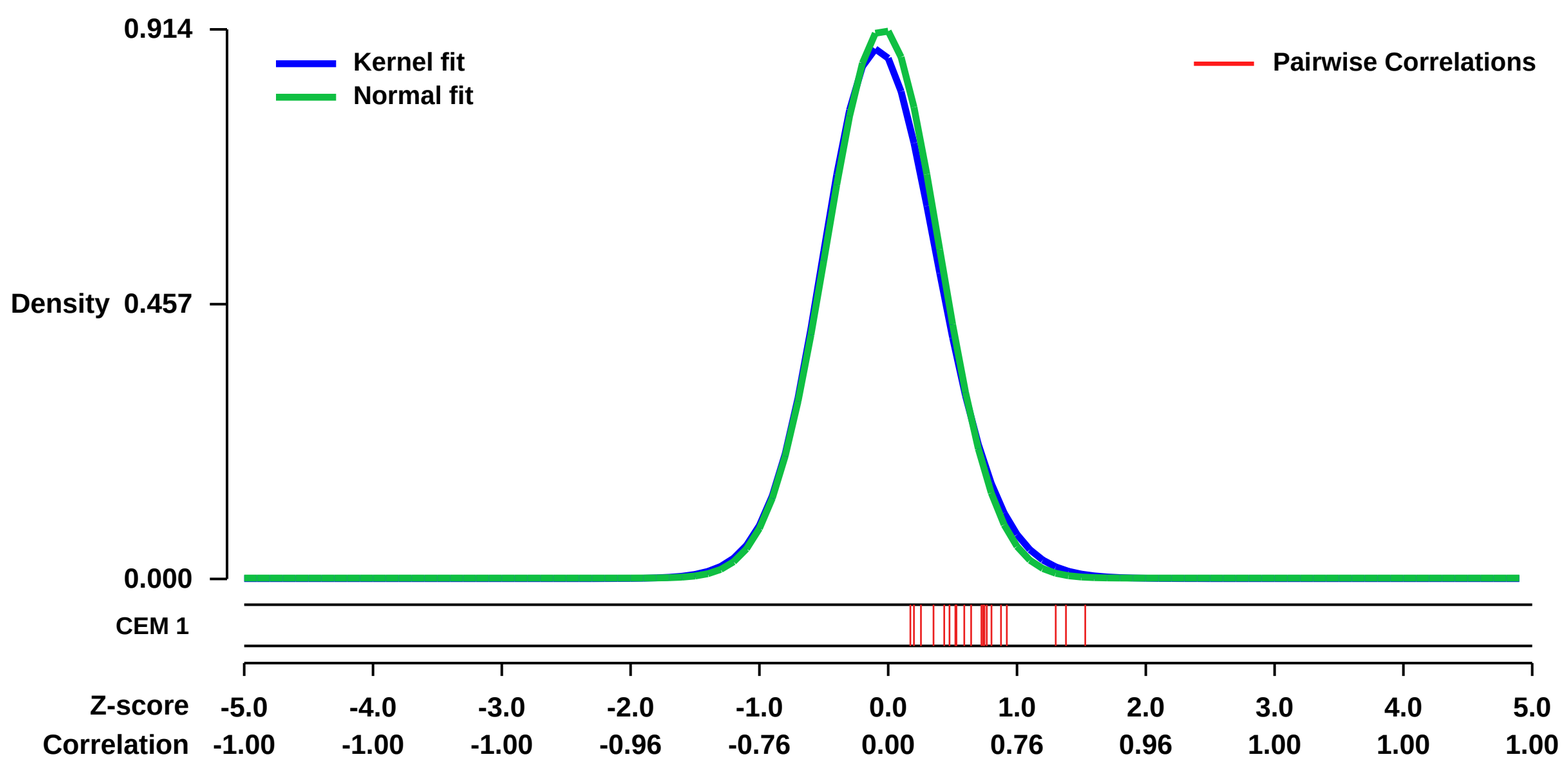

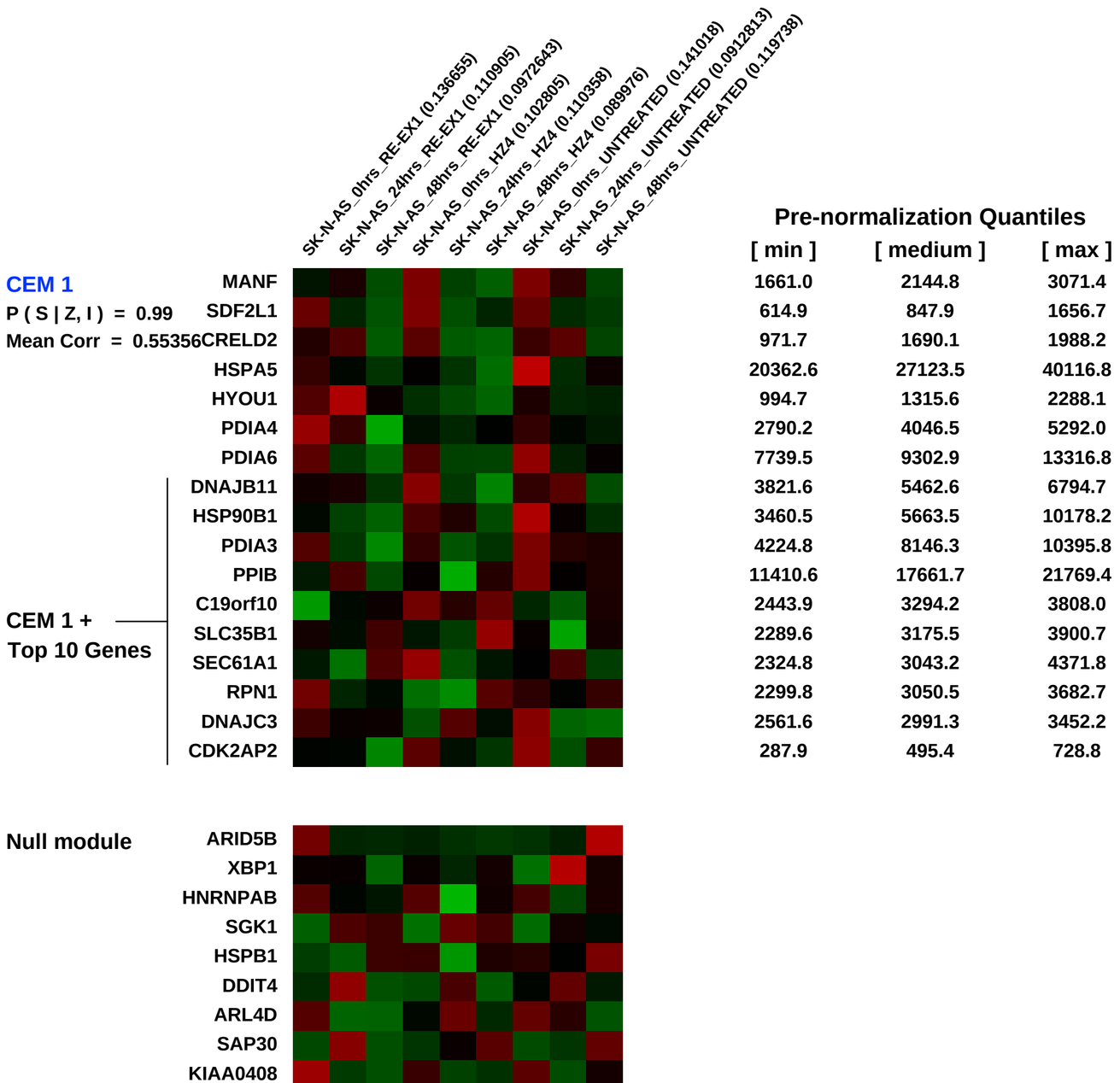

Pre-normalization Quantiles

	[min]	[medium]	[max]
MANF	1661.0	2144.8	3071.4
SDF2L1	614.9	847.9	1656.7
CRELD2	971.7	1690.1	1988.2
HSPA5	20362.6	27123.5	40116.8
HYOU1	994.7	1315.6	2288.1
PDIA4	2790.2	4046.5	5292.0
PDIA6	7739.5	9302.9	13316.8
DNAJB11	3821.6	5462.6	6794.7
HSP90B1	3460.5	5663.5	10178.2
PDIA3	4224.8	8146.3	10395.8
PPIB	11410.6	17661.7	21769.4
C19orf10	2443.9	3294.2	3808.0
SLC35B1	2289.6	3175.5	3900.7
SEC61A1	2324.8	3043.2	4371.8
RPN1	2299.8	3050.5	3682.7
DNAJC3	2561.6	2991.3	3452.2
CDK2AP2	287.9	495.4	728.8

GEO Series "GSE24044" Expression Profiles

Num of samples in this series: 6

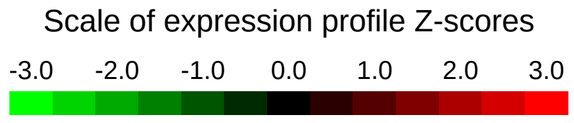

GEO Link:	http://www.ncbi.nlm.nih.gov/geo/query/acc.cgi?acc=GSE24044
Status:	Public on Jul 27 2011
Title:	KDM6B-induced gene expression changes in transfected CD10-positive GC B cells
Organism:	Homo sapiens
Experiment type:	Expression profiling by array
Platform:	GPL570
Pubmed ID:	21242977
Summary & Design:	**Summary:** In this study, we have investigated the effect of lysine-specific demethylase 6B (KDM6B) on gene expression in normal human germinal center (GC) B cells using a non-viral vector-based system. **Overall design:** Gene expression was compared between KDM6B-transfected and control vector-transfected GC B cells from three patients. RNA from the MACS-sorted transfected GC B cells was amplified. 10ug of fragmented cRNA was hybridized to HG-U133 Plus 2.0 microarrays. Differentially expressed genes were identified using Affymetrix GCOS pairwise analysis.

Background corr dist: KL-Divergence = 0.0460, L1-Distance = 0.0262, L2-Distance = 0.0009, Normal std = 0.5940

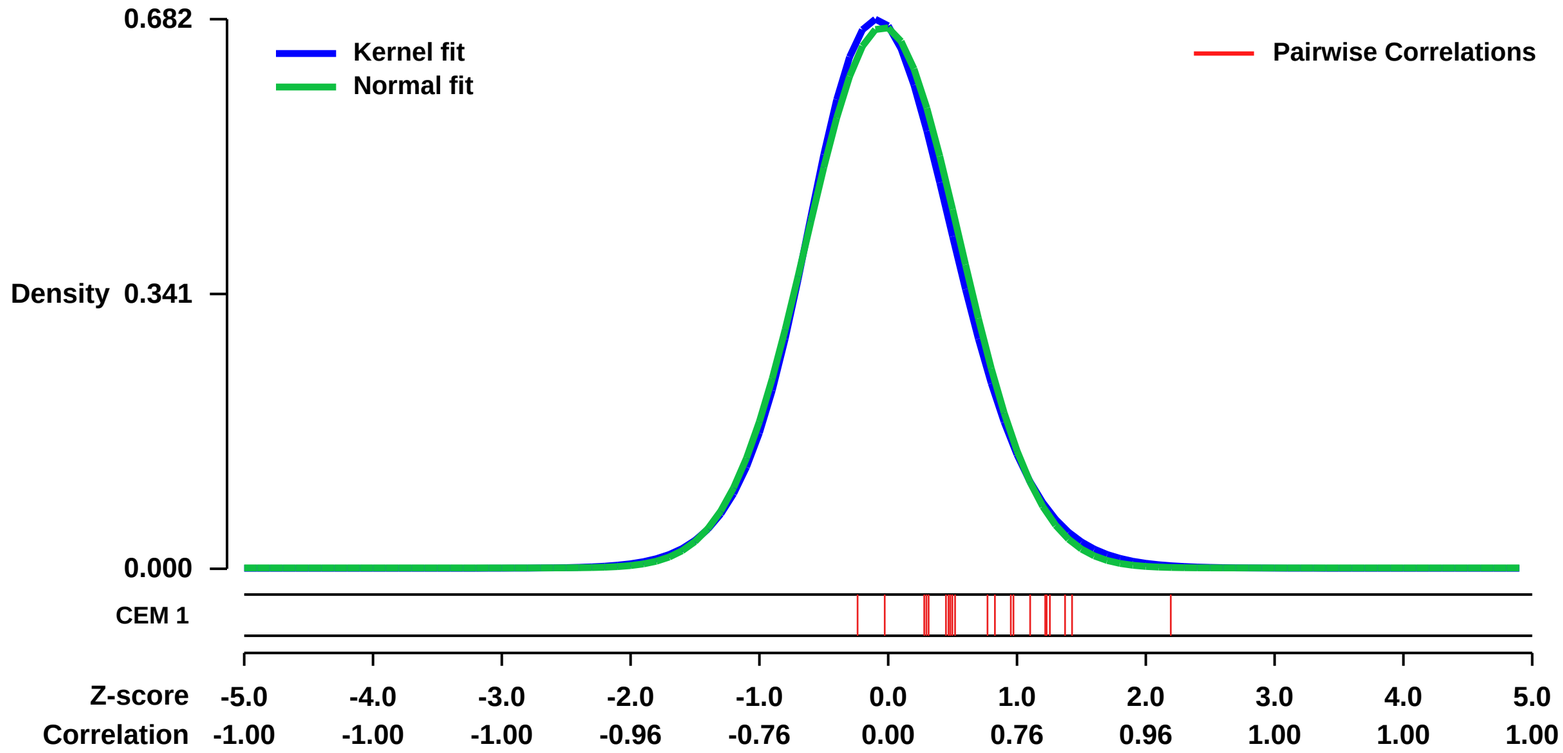

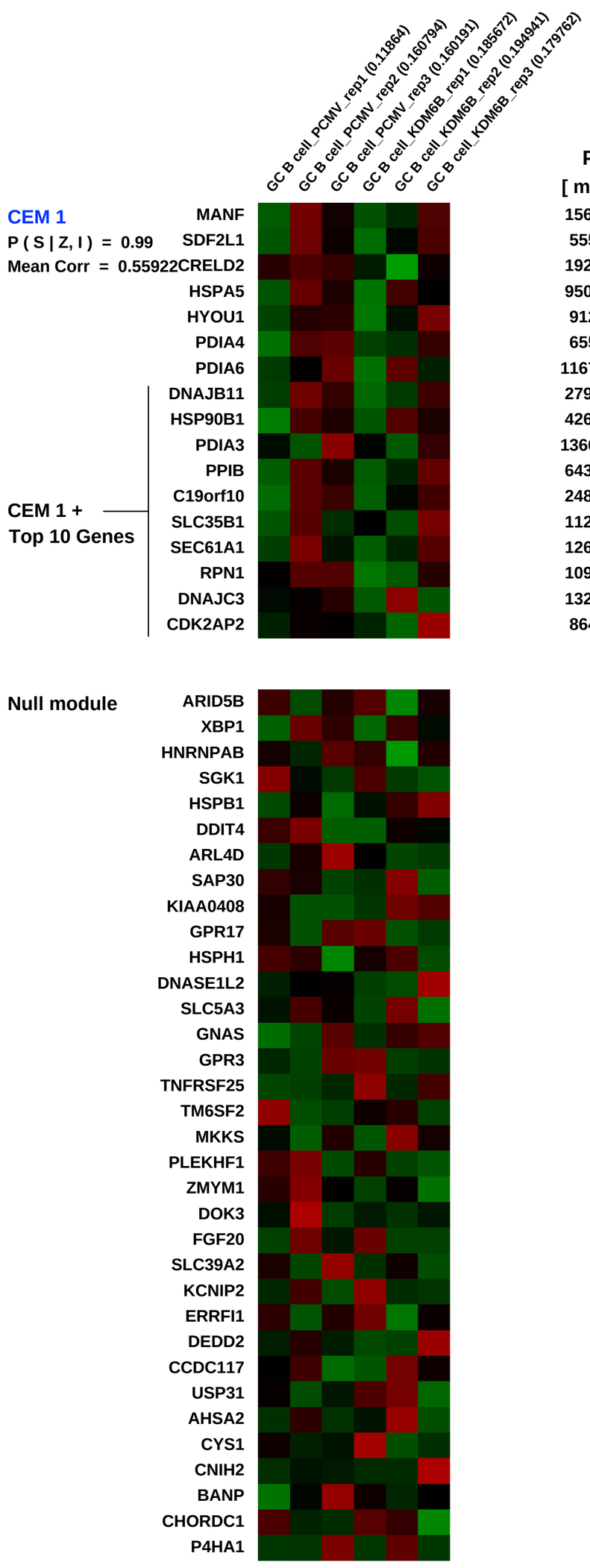

GEO Series "GSE17187" Expression Profiles

Num of samples in this series: 6

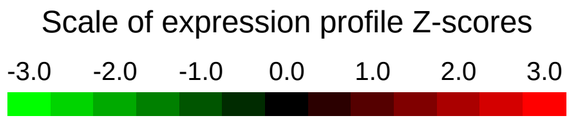

GEO Link:	http://www.ncbi.nlm.nih.gov/geo/query/acc.cgi?acc=GSE17187
Status:	Public on Jun 10 2010
Title:	Gene expression analysis of 3 node positive vs 3 node negative intestinal type gastric cancers by gene array technology.
Organism:	Homo sapiens
Experiment type:	Expression profiling by array
Platform:	GPL570
Pubmed ID:	20386750
Summary & Design:	**Summary:** Gastric cancer is one of the most common causes of cancer-related deaths worldwide. The lymph node status represents the strongest prognostic factor. Due to its extremely poor prognosis, the identification of novel therapeutic targets is urgently needed. Therefore, we aimed to assess differentially expressed genes in nodal negative versus nodal positive intestinal type gastric carcinoma by GeneChip array technique. The transcriptional profile of 6 gastric cancers with and without lymphatic dissemination was analyzed. A total of 115 transcripts were found to be up- and 219 to be down-regulated in node positive compared with node negative gastric cancers. Next we searched for differentially expressed GPCRs. We identified 52 GPCRs and GPCR-related genes, which were up- or down-regulated with a fold change factor greater 1.5. **Overall design:** Tissue samples of gastric cancer were obtained surgically at the Charitˆ' University Hospital Berlin. Tumours were classified by histology according to the WHO and Laurˆ'n classification. Fresh frozen tissue of 6 intestinal type gastric carcinoma cases was used for Affymetrix GeneChip analysis (nodal negative: 3 patients; nodal positive: 3 patients; female-male-ratio: 1:2). Total RNA was isolated from each sample. Subsequently to gene array analysis the transcription of candidate genes was validated by real-time RT-PCR on an independent series of 37 gastric cancers.

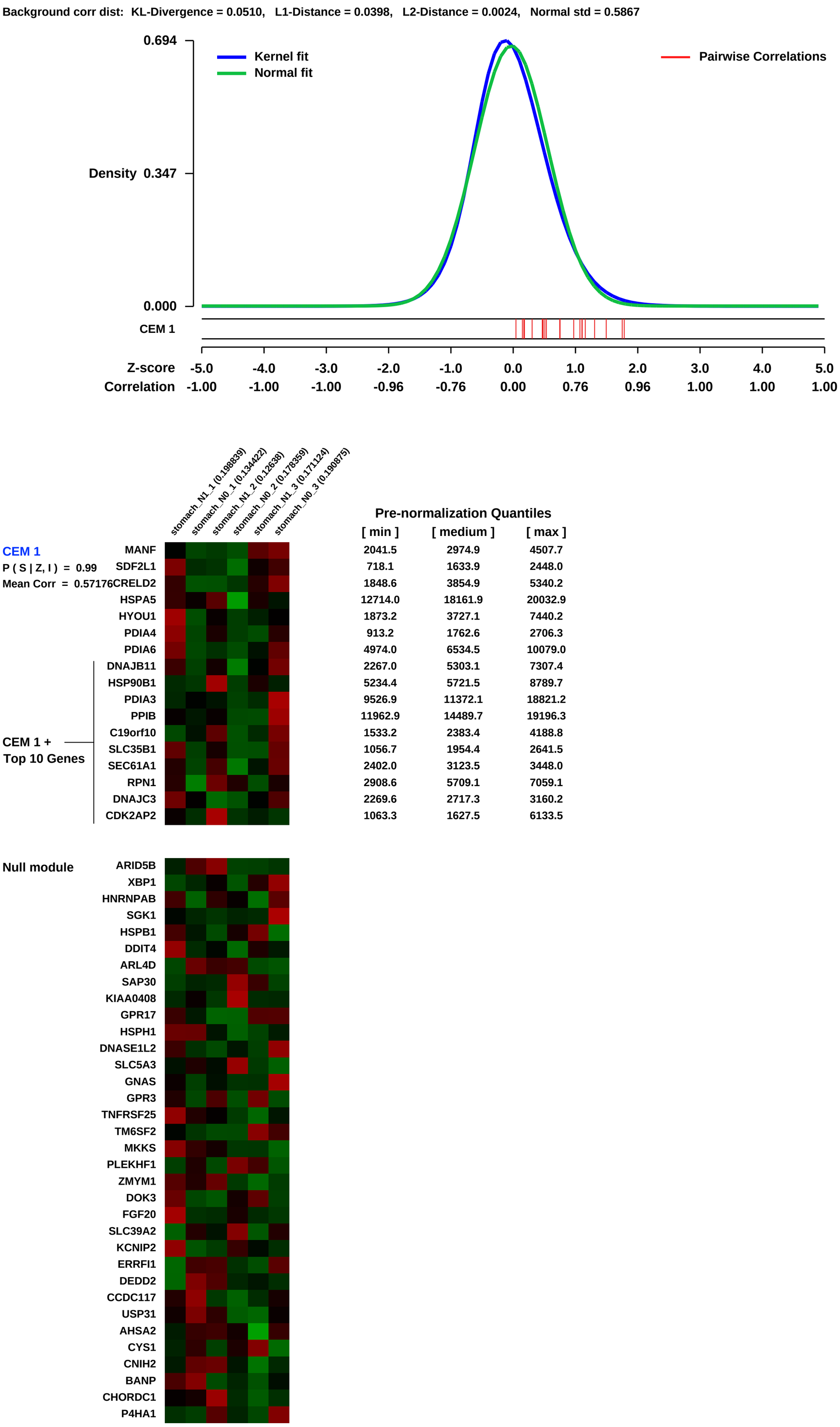

GEO Series "GSE18866" Expression Profiles

Num of samples in this series: 12

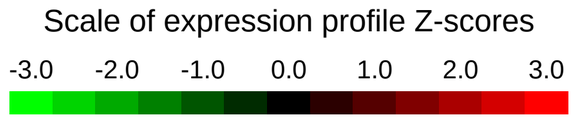

GEO Link:	http://www.ncbi.nlm.nih.gov/geo/query/acc.cgi?acc=GSE18866
Status:	Public on Dec 01 2009
Title:	Expression data from doxycylin-inducible miR-15a/16-1 and empty vector (EV) expression in a 13q14-\- cell line
Organism:	Homo sapiens
Experiment type:	Expression profiling by array
Platform:	GPL570
Pubmed ID:	20060366
Summary & Design:	**Summary:** Reexpression of microRNAs miR-15a/16-1 in a cell line deficient for these miRs (homozygous deletion of chromosomal region 13q14) results in the downregulation of certain mRNAs. **Overall design:** A doxycyclin-inducible expression vector containing miR-15a/16-1 was transfected into CLL-I83E95 cells that are deficient for those miRs. miR-expression was induced by addition of doxycyclin to the medium, and cell were harvested 48 hours later. Labeled cRNA was hybridized to microarrays and gene expression data were compared to CLL-I83U95 stably transfected with an empty vector.

Background corr dist: KL-Divergence = 0.1579, L1-Distance = 0.0393, L2-Distance = 0.0033, Normal std = 0.3663

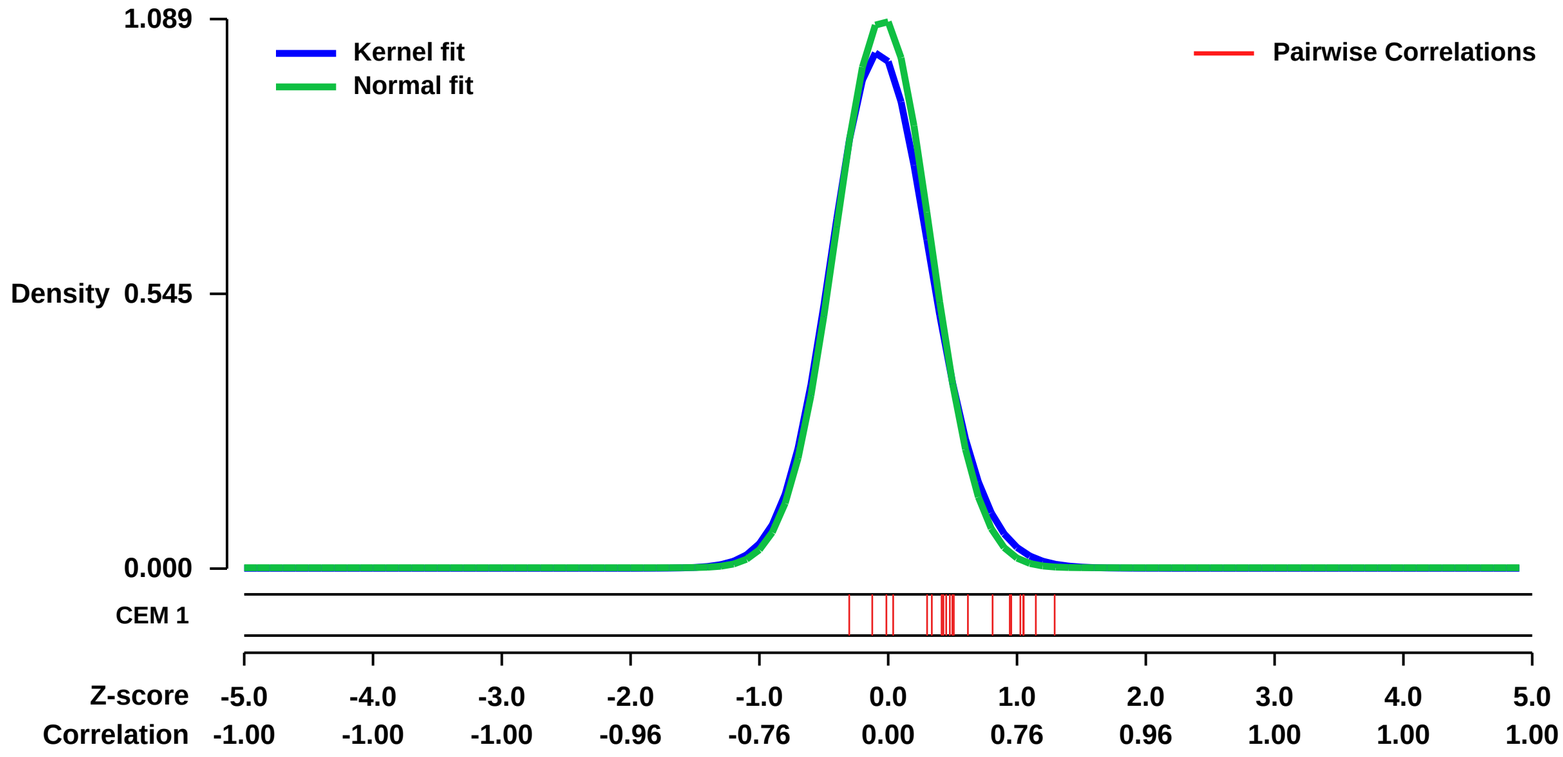

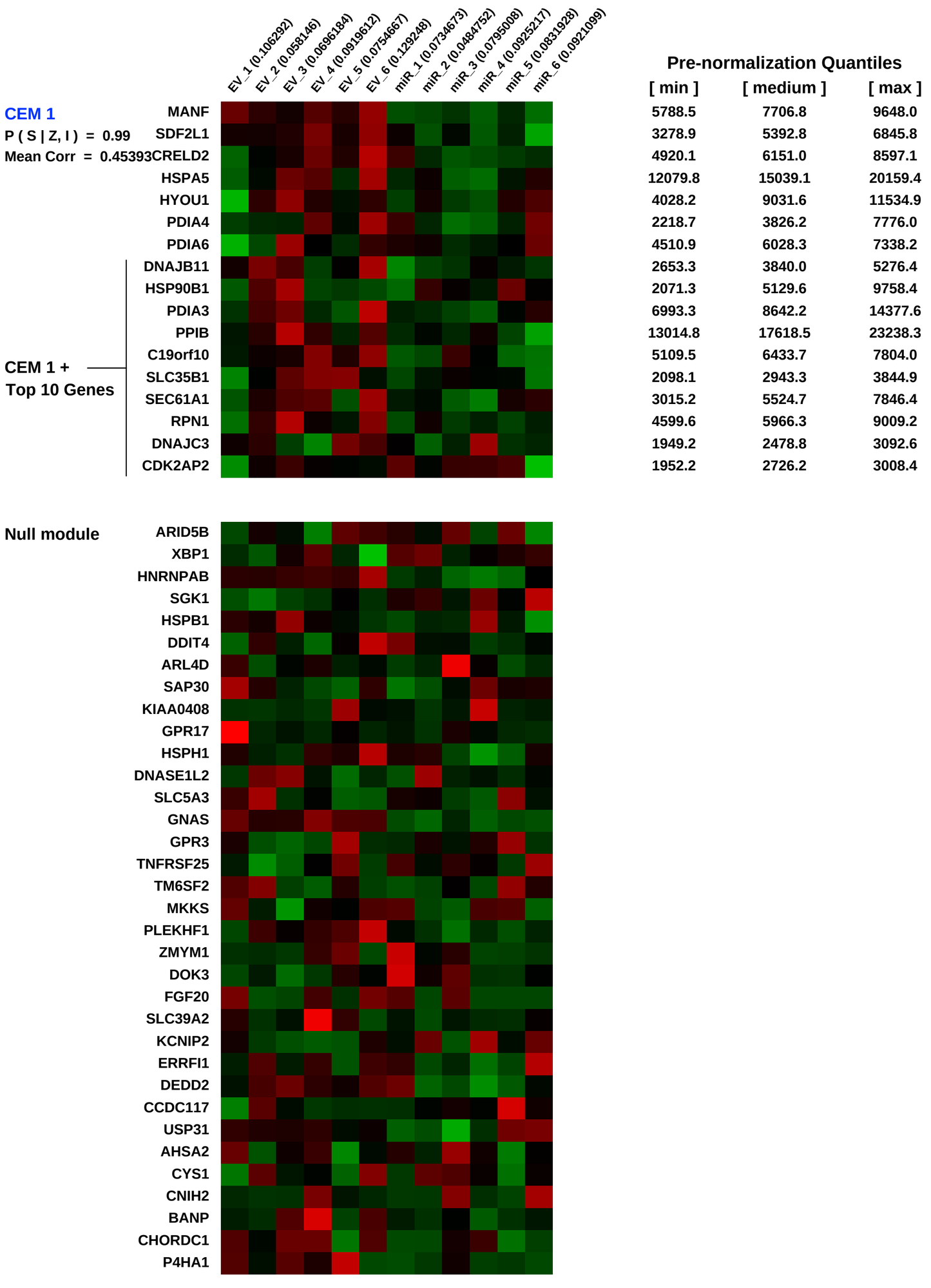

GEO Series "GSE40266" Expression Profiles

Num of samples in this series: 9

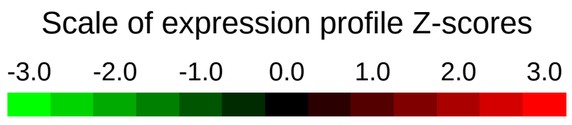

GEO Link:	http://www.ncbi.nlm.nih.gov/geo/query/acc.cgi?acc=GSE40266
Status:	Public on Dec 31 2013
Title:	Expression data from TGF-beta-treated human ovarian fibroblasts
Organism:	Homo sapiens
Experiment type:	Expression profiling by array
Platform:	GPL570
Pubmed ID:	23824740
Summary & Design:	**Summary:** Advanced ovarian cancer is the most lethal gynecologic malignancy in the United States. Ovarian cancer cells are known to have diminished response to TGF-beta, but it remains unclear whether TGF-beta can modulate ovarian cancer cell growth in an indirect manner through cancer-associated fibroblasts (CAFs). Using transcriptome profiling analyses on TGF-beta-treated ovarian fibroblasts, we identified a TGF-beta-responsive gene signature in ovarian fibroblasts. Identifying TGF-beta-regulated genes in the ovarian microenvironment helps in understanding the role of TGF-beta in ovarian cancer progression. **Overall design:** The human telomerase-immortalized ovarian fibroblast line NOF151 was treated with 5ng/mL of either TGF-beta-1 or TGF-beta-2. Total RNA was isolated from control samples and TGF-beta-treated fibroblasts samples at 48 hours post-treatment, followed by cDNA synthesis, IVT and biotin labeling. Samples were then hybridized onto Affymetrix Human Genome U133 Plus 2.0 microarrays. For each treatment group, three independent samples were prepared for the microarray experiment.

Background corr dist: KL-Divergence = 0.0786, L1-Distance = 0.0319, L2-Distance = 0.0013, Normal std = 0.5077

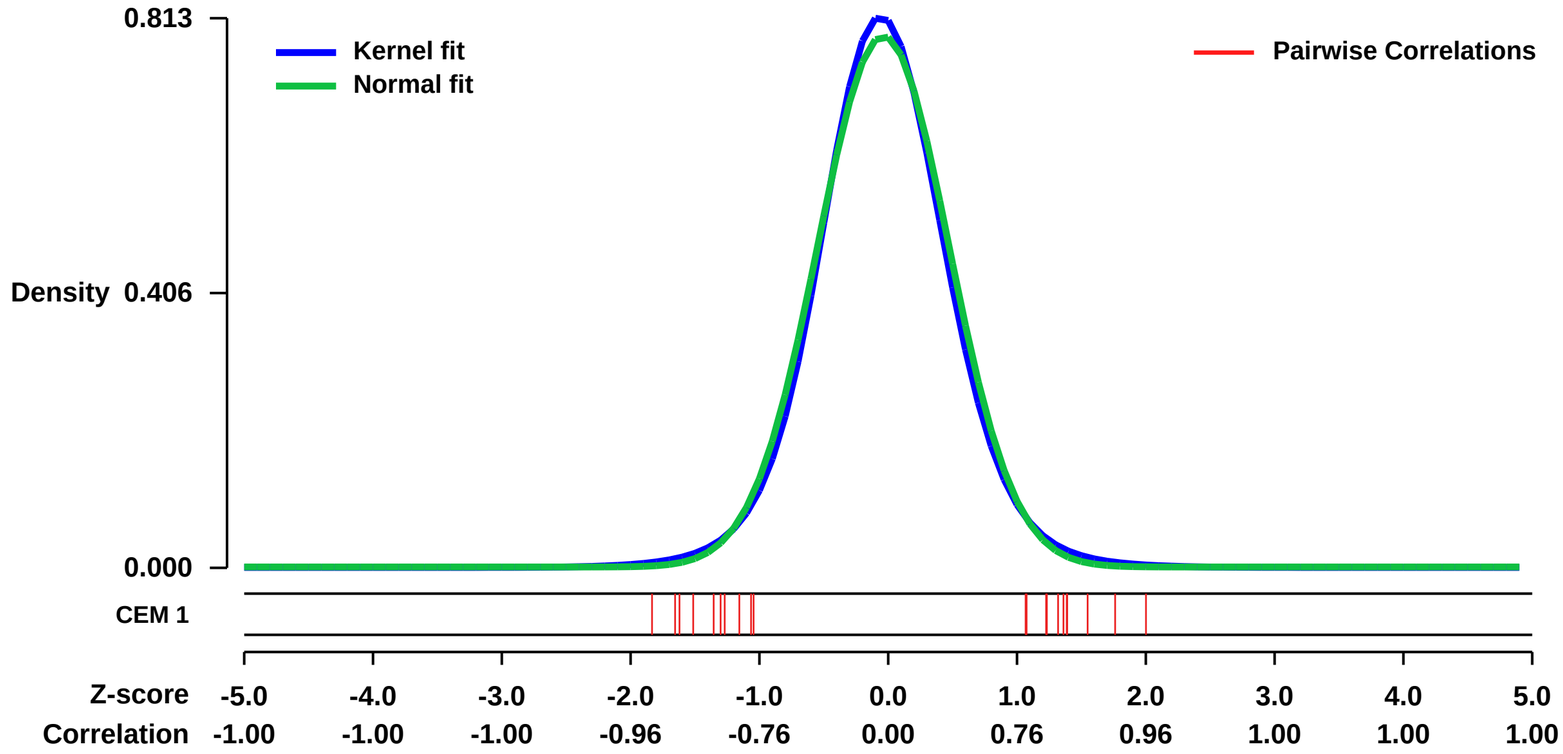

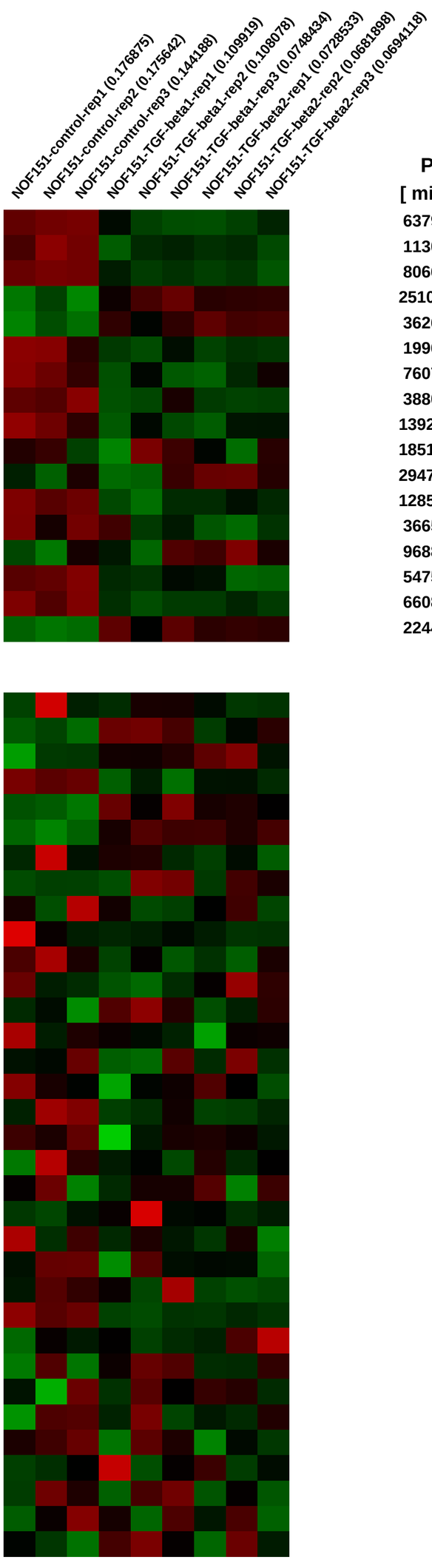

GEO Series "GSE15026" Expression Profiles

Num of samples in this series: 30

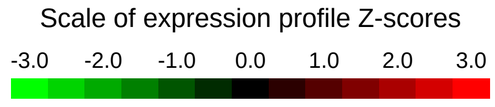

GEO Link:	http://www.ncbi.nlm.nih.gov/geo/query/acc.cgi?acc=GSE15026
Status:	Public on Apr 10 2009
Title:	Expression data from breast cancer cell lines with various colony-forming ability
Organism:	Homo sapiens
Experiment type:	Expression profiling by array
Platform:	GPL570
Pubmed ID:	19483725

Summary & Design:

Summary:
Cultured cancer cells exhibit substantial phenotypic heterogeneity when measured in a variety of ways such as sensitivity to drugs or the capacity to grow under various conditions. Among these, the ability to exhibit anchorage-independent cell growth (colony forming capacity in semisolid media), has been considered to be fundamental in cancer biology, because it has been connected with tumor cell aggressiveness in vivo such as tumorigenic and metastatic potentials, and also utilized as a marker for in vitro transformation. Although multiple genetic factors for anchorage-independence have been identified, the molecular basis for this capacity is still largely unknown. To investigate the molecular mechanisms underlying anchorage independent cell growth, we have used genome-wide DNA microarray studies to develop an expression signature associated with this phenotype. Using this signature, we identify a program of activated mitochondrial biogenesis associated with the phenotype of anchorage-independent growth and importantly, we demonstrate that this phenotype predicts potential for metastasis in primary breast and lung tumors.

Keywords: Breast cancer cell lines with various colony-forming ability

Overall design:
To develop an expression signature reflecting the capacity for anchorage-independent cell growth, we first carried out colony formation assays with 19 breast cancer cell lines in suspension culture dish with methyl-cellulose containing media. Starting with 20,000 plated cells, five cell lines (MDA-MB-361, HCC38, ZR75, Hs578T and BT483) gave rise to less than 20 colonies, while 8 cell lines (MCF7, MDA-MB-231, BT20, SKBR3, MDA-MB-435s, T47D and BT474) showed formation of more than 500 colonies. The rest of the cell lines showed an intermediate phenotype in colony forming ability (20-200 colonies; HCC1143, HCC1806, HCC1428, MDA-MB-453, CAMA1, BT549 and MDA-MB-157). Among 19 cell lines, 11 cell lines have duplicates of expression data in a different batch. We removed the batch effect of this Affymetrix expression data using ComBat according to the instruction of http://statistics.byu.edu/johnson/ComBat/Abstract.html. Therefore, this dataset is a combined and standardized data that are originally RMA formatted.

Background corr dist: KL-Divergence = 0.3069, L1-Distance = 0.0746, L2-Distance = 0.0169, Normal std = 0.2792

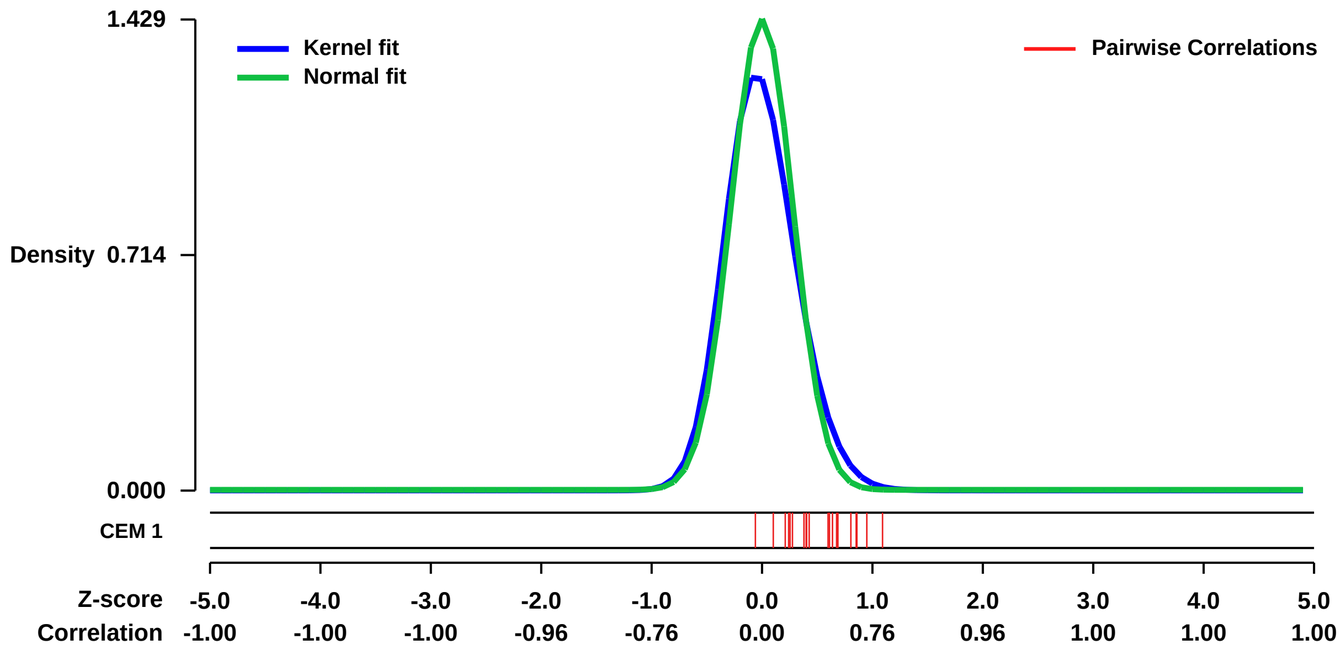

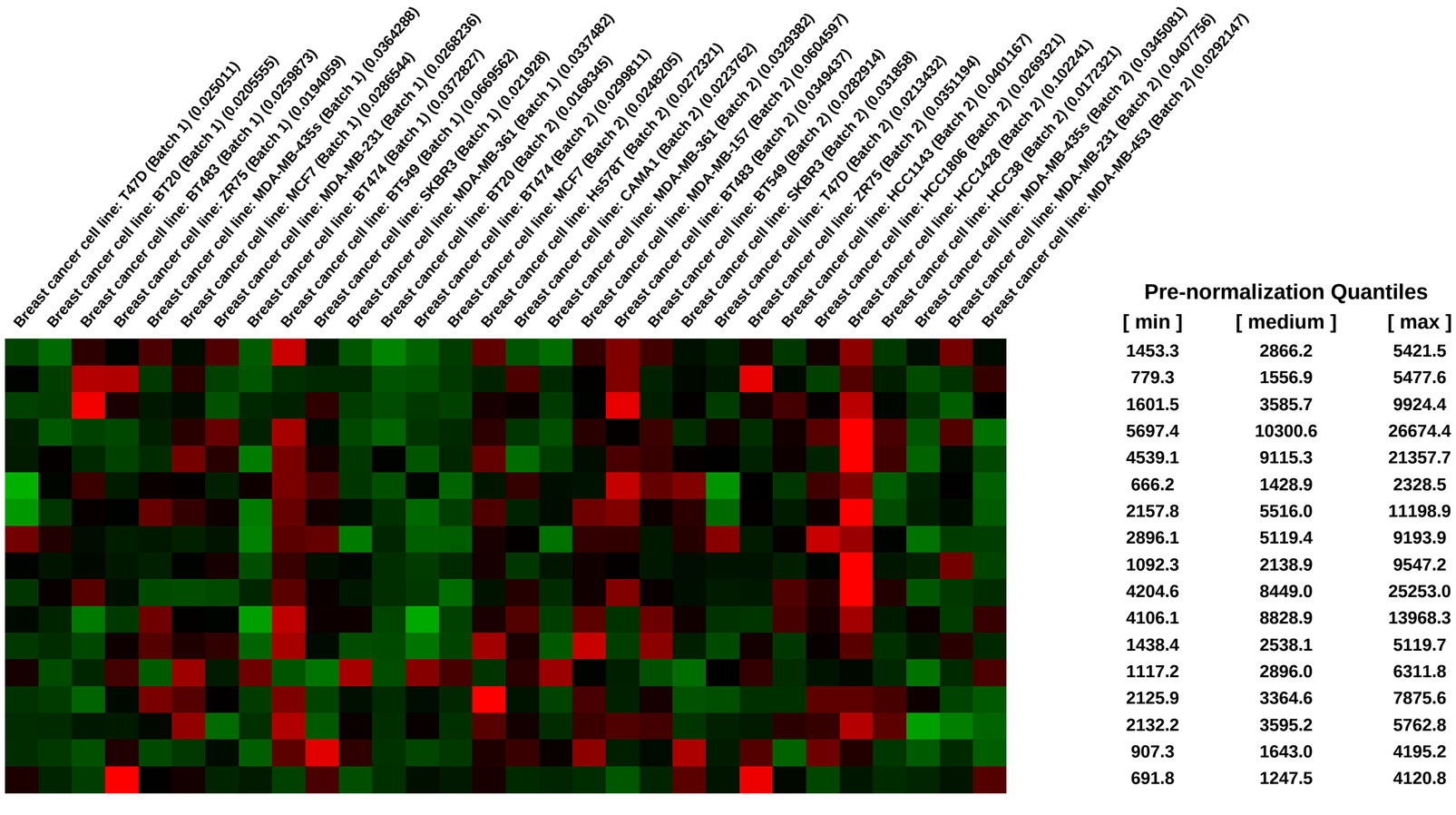

Pre-normalization Quantiles

	[min]	[medium]	[max]
MANF	1453.3	2866.2	5421.5
SDF2L1	779.3	1556.9	5477.6
CRELD2	1601.5	3585.7	9924.4
HSPA5	5697.4	10300.6	26674.4
HYOU1	4539.1	9115.3	21357.7
PDIA4	666.2	1428.9	2328.5
PDIA6	2157.8	5516.0	11198.9
DNAJB11	2896.1	5119.4	9193.9
HSP90B1	1092.3	2138.9	9547.2
PDIA3	4204.6	8449.0	25253.0
PPIB	4106.1	8828.9	13968.3
C19orf10	1438.4	2538.1	5119.7
SLC35B1	1117.2	2896.0	6311.8
SEC61A1	2125.9	3364.6	7875.6
RPN1	2132.2	3595.2	5762.8
DNAJC3	907.3	1643.0	4195.2
CDK2AP2	691.8	1247.5	4120.8

GEO Series "GSE52674" Expression Profiles

Num of samples in this series: 6

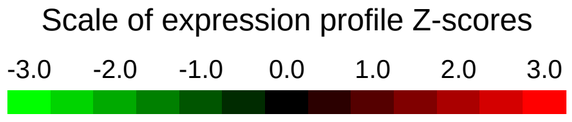

GEO Link:	http://www.ncbi.nlm.nih.gov/geo/query/acc.cgi?acc=GSE52674
Status:	Public on Mar 01 2014
Title:	expression data of miR-21 knockdown in MCF-7
Organism:	Homo sapiens
Experiment type:	Expression profiling by array
Platform:	GPL570
Pubmed ID:	
Summary & Design:	**Summary:** miR-21 is overexpressed in breast cancer cells. Knock-down of miR-21 cause apoptosis and decreased cell proliferation. To identify miR-21 regulated cancer-pathways in MCF-7 cells, we knocked-down miR-21 and performed microarray. **Overall design:** RNA was harvested from MCF-7 cells 24 hours transfection of anti-control, anti-21, or untreated cells. RNA was processed and hybridized into Affymetrix whole human genome arrays in duplicates.

Background corr dist: KL-Divergence = 0.0323, L1-Distance = 0.0127, L2-Distance = 0.0001, Normal std = 0.6479

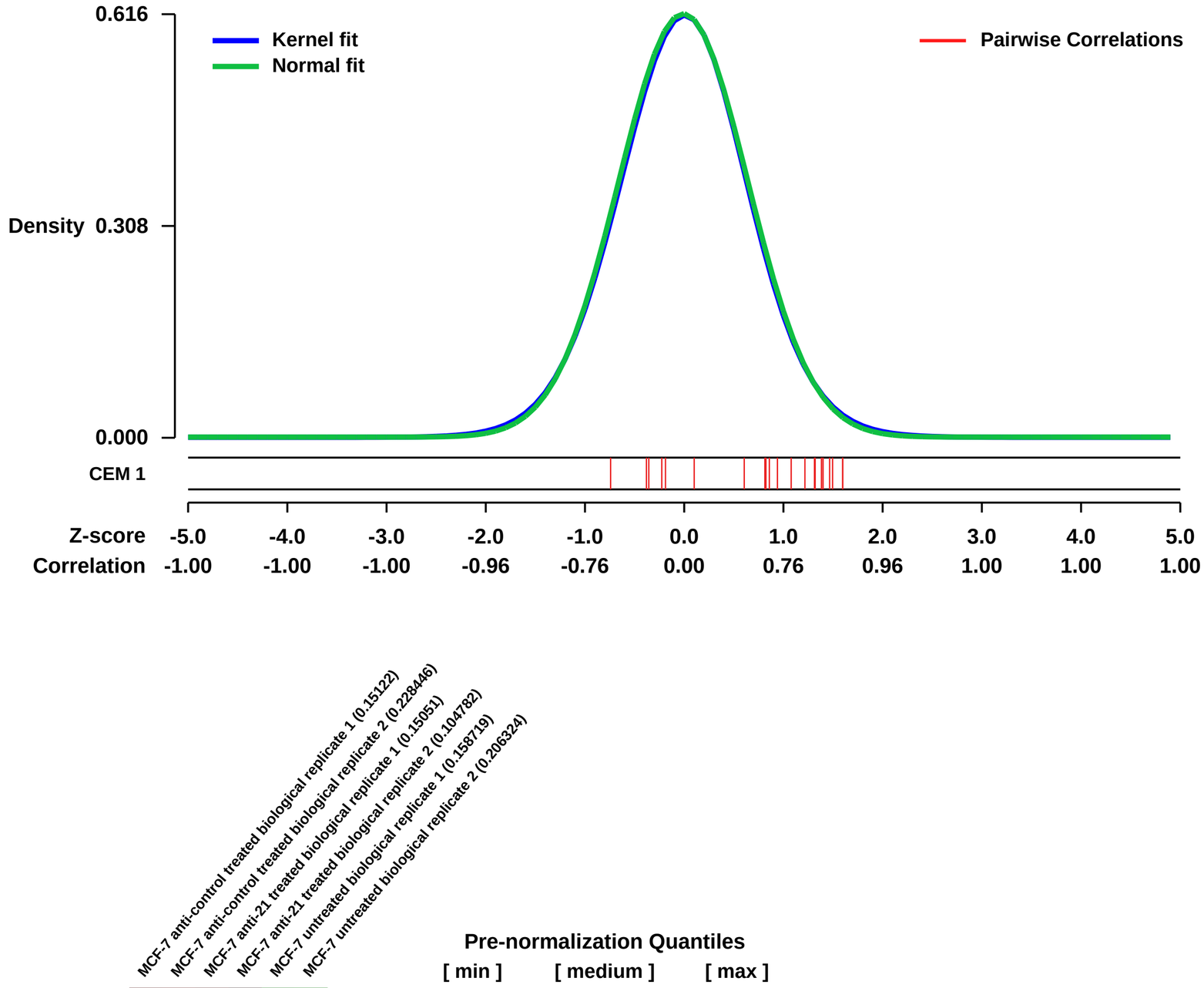

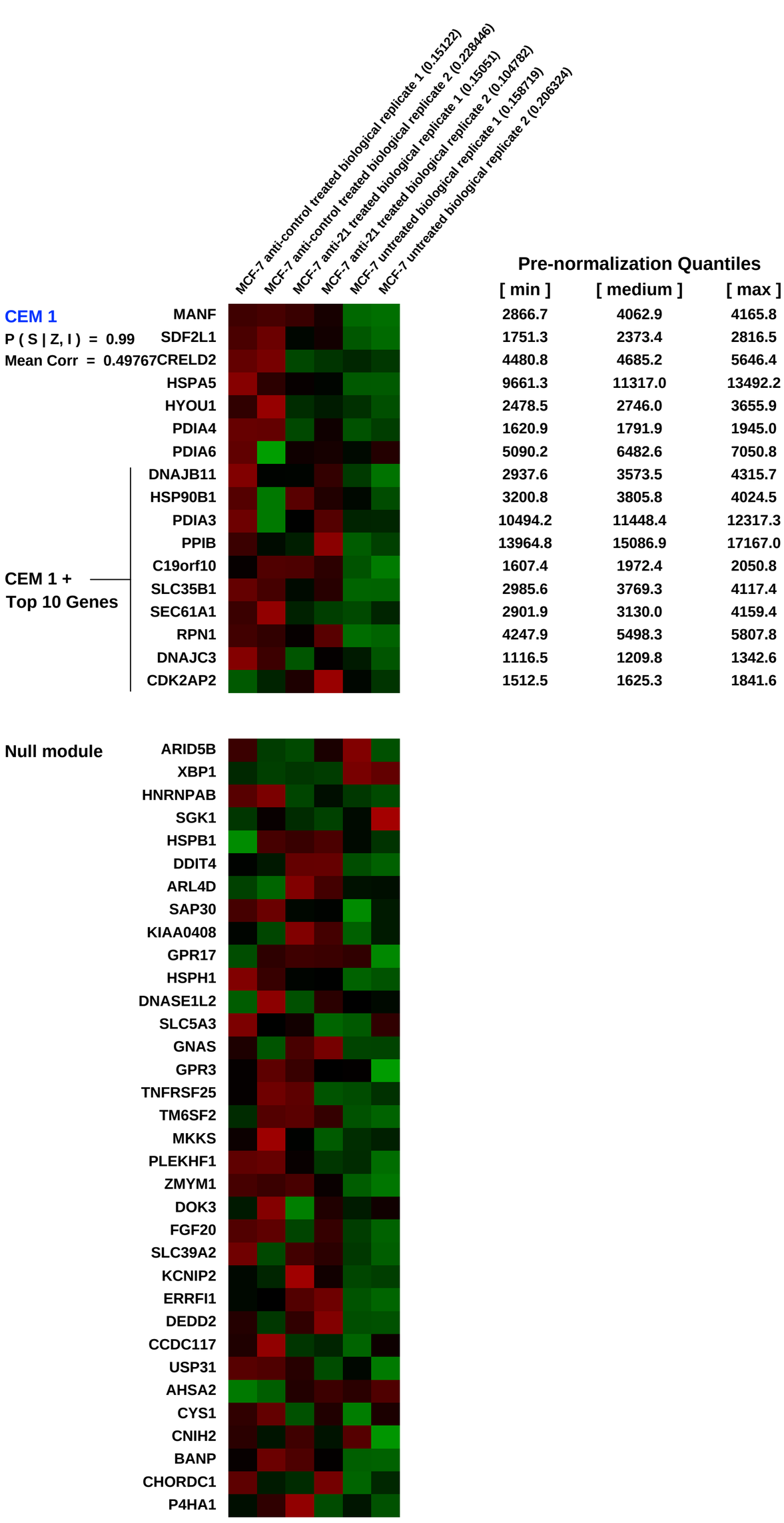

GEO Series "GSE22106" Expression Profiles

Num of samples in this series: 6

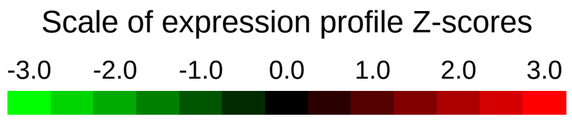

GEO Link:	http://www.ncbi.nlm.nih.gov/geo/query/acc.cgi?acc=GSE22106
Status:	Public on Jun 03 2010
Title:	Hydrocortisone induces changes in gene expression and differentiation of immature human enterocytes
Organism:	Homo sapiens
Experiment type:	Expression profiling by array
Platform:	GPL570
Pubmed ID:	21148402
Summary & Design:	**Summary:** It It is known that functional maturation of the small intestine occurring during the weaning period is facilitated by glucocorticoids (such as hydrocortisone, HC) including the increased expression of digestive hydrolases. However, the molecular mechanism(s) are not well understood, particularly in human gut. Here we report a microarray analysis of HC- induced changes in gene expression in H4 (a human fetal small intestinal epithelial cell line well-characterized in numerous previous studies). This study identified a large number of HC-affected genes, some involved in metabolism, cell cycle regulation, cell polarity, tight junction formation, and interactions with extracellular matrices. These effects could play an important role in HC-mediated enterocyte maturation in vivo and in vitro. **Overall design:** hydrocortisone effect on gene expression prlfile in H4 cells over time (no HC, HC_12h, HC_24h, HC_48h, HC_5d and T84). Six samples are analyzed. Control sample is H4 without HC.

Background corr dist: KL-Divergence = 0.0143, L1-Distance = 0.0229, L2-Distance = 0.0006, Normal std = 0.8752

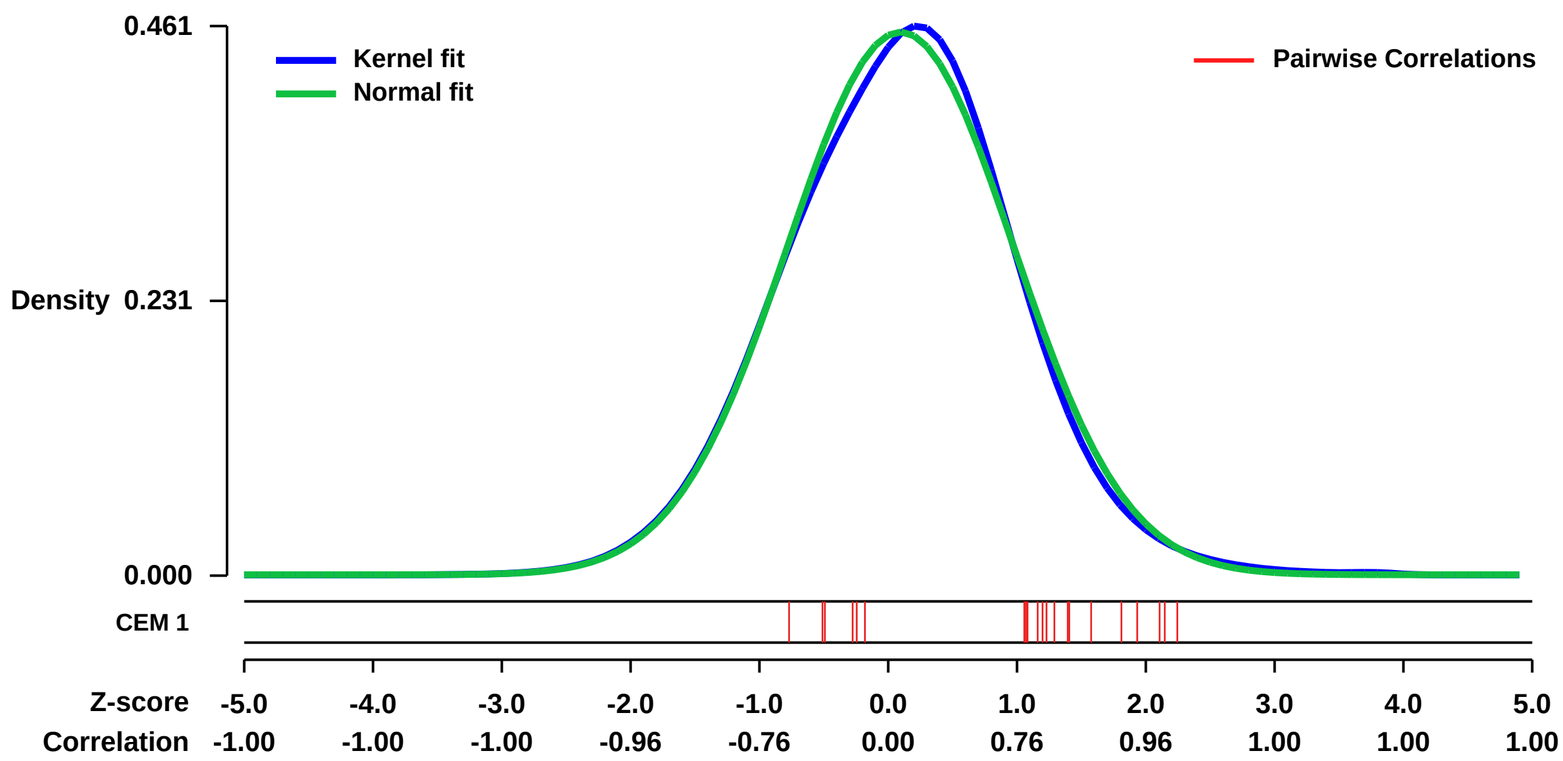

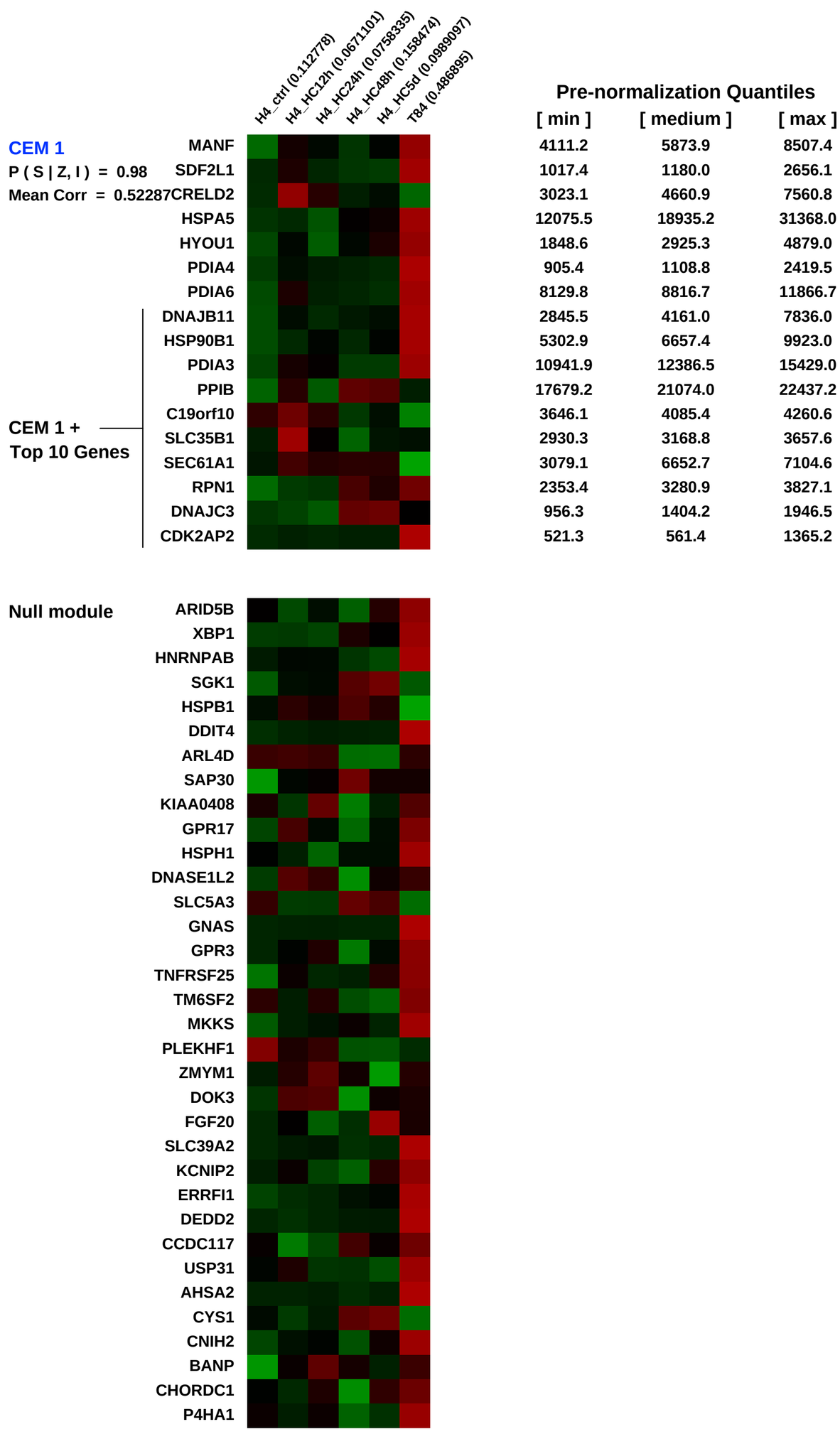

GEO Series "GSE34156" Expression Profiles

Num of samples in this series: 45

Scale of expression profile Z-scores

-3.0 -2.0 -1.0 0.0 1.0 2.0 3.0

GEO Link:	http://www.ncbi.nlm.nih.gov/geo/query/acc.cgi?acc=GSE34156
Status:	Public on Mar 15 2012
Title:	Human monocyte activation with NOD2L vs. TLR2/1L
Organism:	Homo sapiens
Experiment type:	Expression profiling by array
Platform:	GPL570
Pubmed ID:	22447076
Summary & Design:	**Summary:** **human blood monocytes were isolated, activated and harvested at several timepoints** **In this study, we identified genes that were differentially expressed in human monocytes activated with eiter NOD2L and/or TLR2/1L.** **Overall design:** **human blood monocytes were purified from healthy donors by Ficoll, Percoll and adherence. Monocytes were activated using NOD2L (MDP) and the TLR2/1L (19kD, triacylated peptide). Cells were harvested before activation (0h) and 6h and 24h after stimulation with ligands.**

Background corr dist: **KL-Divergence = 0.2245, L1-Distance = 0.0400, L2-Distance = 0.0041, Normal std = 0.3204**

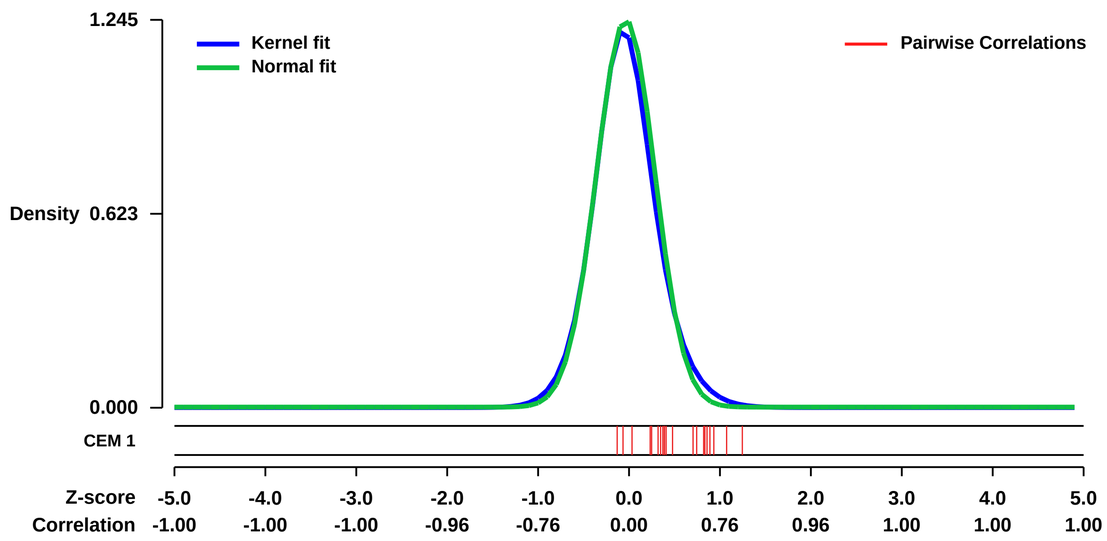

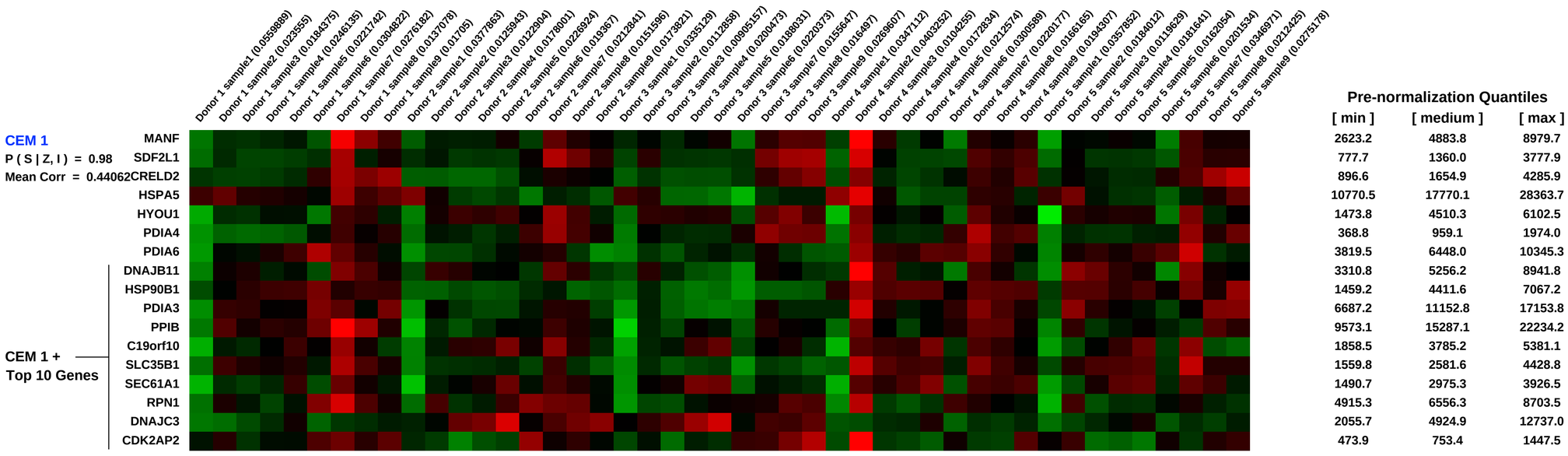

Pre-normalization Quantiles

[min]	[medium]	[max]
2623.2	4883.8	8979.7
777.7	1360.0	3777.9
896.6	1654.9	4285.9
10770.5	17770.1	28363.7
1473.8	4510.3	6102.5
368.8	959.1	1974.0
3819.5	6448.0	10345.3
3310.8	5256.2	8941.8
1459.2	4411.6	7067.2
6687.2	11152.8	17153.8
9573.1	15287.1	22234.2
1858.5	3785.2	5381.1
1559.8	2581.6	4428.8
1490.7	2975.3	3926.5
4915.3	6556.3	8703.5
2055.7	4924.9	12737.0
473.9	753.4	1447.5

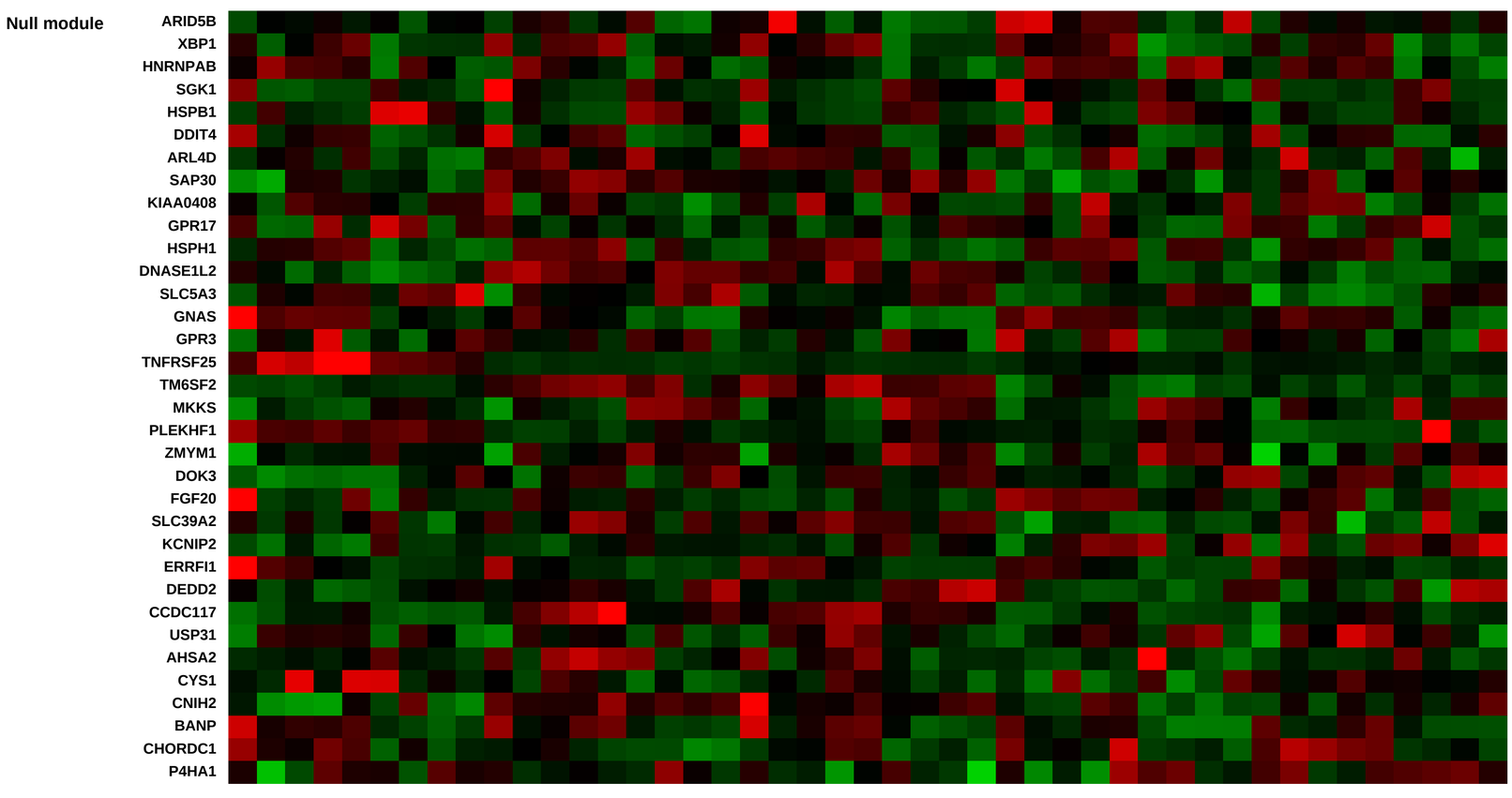

GEO Series "GSE28842" Expression Profiles

Num of samples in this series: 71

Scale of expression profile Z-scores

-3.0 -2.0 -1.0 0.0 1.0 2.0 3.0

GEO Link: http://www.ncbi.nlm.nih.gov/geo/query/acc.cgi?acc=GSE28842
Status: Public on Jan 09 2012
Title: Withdrawal of immunosuppressive therapy in stable liver transplant recipients
Organism: Homo sapiens
Experiment type: Expression profiling by array
Platform: GPL570
Pubmed ID: 22156196

Summary & Design:

Summary:
Complications due to long-term administration of immunosuppressive therapy increase the morbidity and mortality of liver transplant recipients. Discontinuation of immunosuppressive drugs in recipients spontaneously developing operational tolerance could substantially lessen this burden. However, this strategy results in the development of rejection in a high proportion of recipients who require lifelong immunosuppression. Thus, there is a need to identify predictive factors of successful drug withdrawal and to define the clinical and histological outcomes of operationally tolerant liver recipients. Methods. We enrolled 102 stable liver transplant recipients in an immunosuppression withdrawal trial in which drugs were gradually discontinued over a 6-9 month period. Patients with stable graft function and no signs of rejection in a liver biopsy conducted 12 months after cessation of immunosuppressive therapy were considered operationally tolerant. Results. Out of the 98 recipients who completed the study, immunosuppression discontinuation was successful in 41 recipients and rejection occurred in 57. Rejection episodes were mild and were resolved in all cases. Development of tolerance was independently associated with time elapsed since transplantation, recipient age, and male gender. No histological damage was apparent in protocol biopsies performed after successful drug withdrawal.

Overall design:
PBMC gene expression profiling was assessed by DNA microarray in liver trasplanted patients groups: A group of inmunetolerant patients (TOL ;n=20), a group of non inmunotolerant (NonTOL; n=25). Finally from these two groups (Tolerant pTOL=12 and Non Tolerant pNonTOL=14) a sample is obtained a year after weaning.

Background corr dist: KL-Divergence = 0.3536, L1-Distance = 0.0698, L2-Distance = 0.0140, Normal std = 0.2631

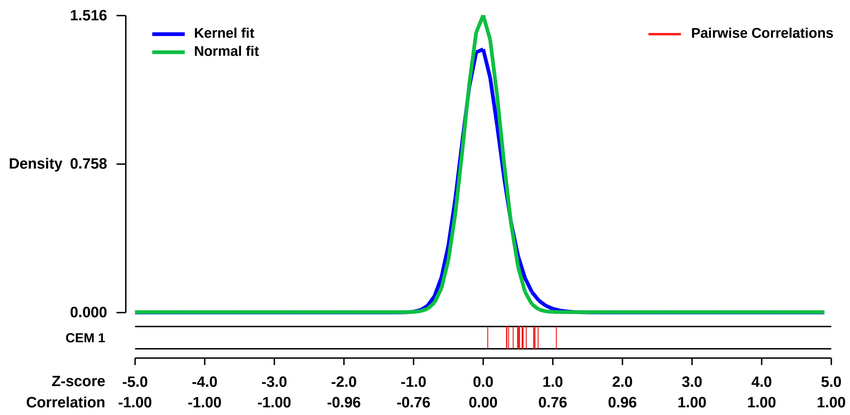

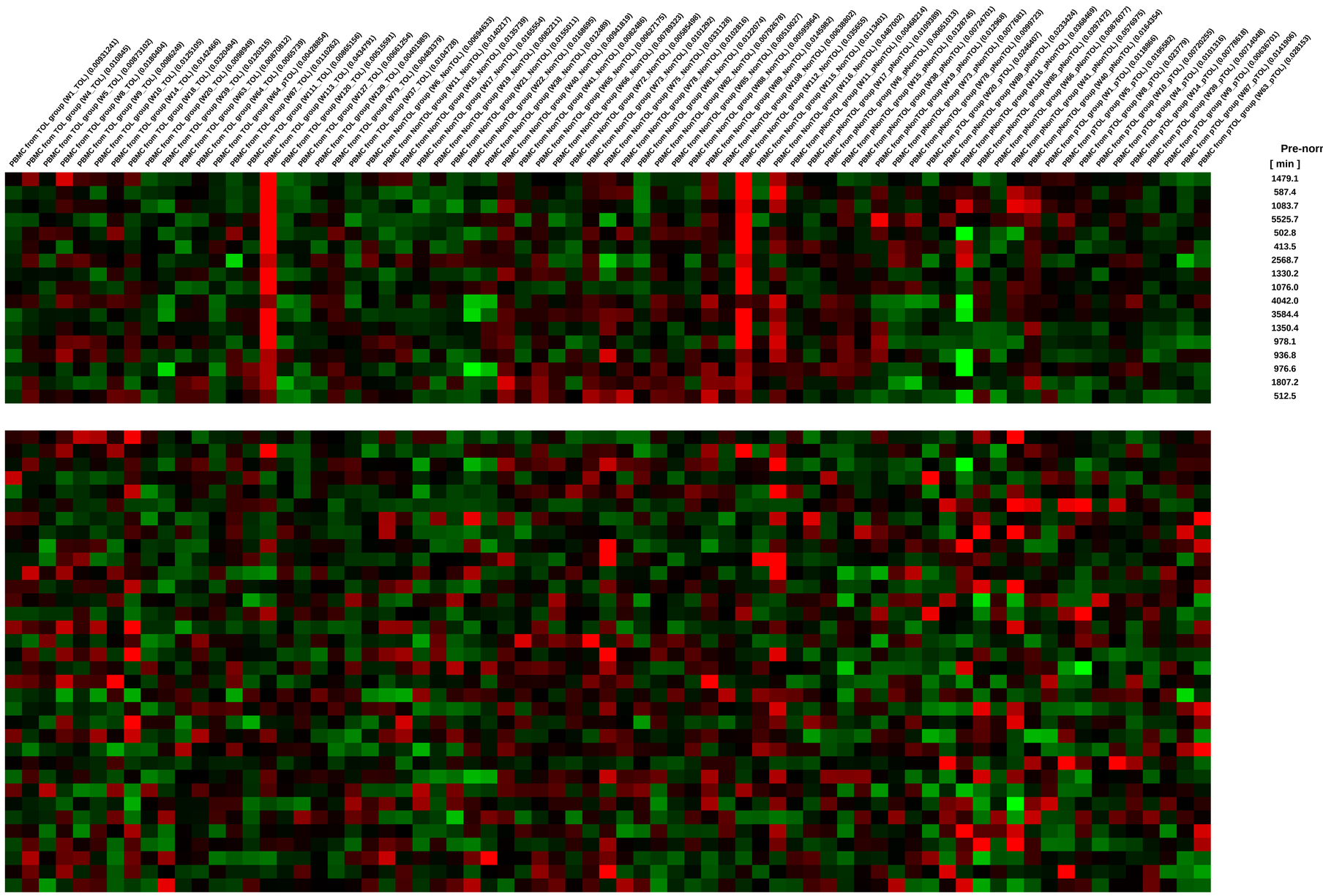

Pre-normalization Quantiles

[min]	[medium]	[max]
1479.1	1952.2	3447.9
587.4	820.3	1570.1
1083.7	1518.4	2588.9
5525.7	7113.1	10003.4
502.8	1241.2	2191.4
413.5	524.1	856.8
2568.7	3818.1	5073.8
1330.2	1714.5	3271.6
1076.0	1597.0	4343.1
4042.0	7256.1	9376.3
3584.4	8366.5	15907.5
1350.4	1614.9	3110.6
978.1	1140.0	1672.8
936.8	1855.4	2378.6
976.6	2881.0	4062.0
1807.2	2365.7	3155.6
512.5	1314.5	2039.6

GEO Series "GSE8685" Expression Profiles

Num of samples in this series: 12

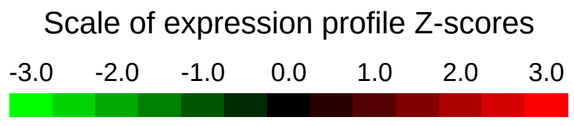

GEO Link:	http://www.ncbi.nlm.nih.gov/geo/query/acc.cgi?acc=GSE8685
Status:	Public on Feb 19 2008
Title:	Activation of Sez-4 cell line with IL-2, IL-15 or IL-21.
Organism:	Homo sapiens
Experiment type:	Expression profiling by array
Platform:	GPL570
Pubmed ID:	18281483
Summary & Design:	**Summary:** In this study we compared the effects of IL-2, IL-15, and IL-21 on the gene expression, activation of cell signaling pathways, and functional properties of cells derived from the CD4+ cutaneous T-cell lymphoma (CTCL). Whereas both IL-2 and IL-15 that signal through receptors that share the common gamma chain and the beta chain modulated the expression of >1,000 genes, IL-21 that signals via the receptor also containing gamma chain up-regulated <40 genes. All three cytokines induced tyrosine phosphorylation of Jak1 and Jak3. However, only IL-2 and IL-15 strongly activated STAT5, PI3K/Akt, and MEK/ERK signaling pathways. In contrast, IL-21 selectively activated STAT3. Whereas all three cytokines protected CTCL cells from apoptosis, only IL-2 and IL-15 promoted their proliferation. The effects of the cytokine stimulation were Jak3- and Jak1-kinase dependent. These findings document the vastly different impact of IL-2 and IL-15 vs. IL-21 on malignant CD4+ T cells. They also suggest two novel therapeutic approaches to CTCL and, possibly, other CD4+ T cell lymphomas: inhibition of the Jak1/Jak3 kinase complex and, given the known strong immunostimulatory properties of IL-21 on CD8+ T, NK, and B cells, application of this cytokine to boost an immune response against malignant CD4+ T cells. **Keywords:** 3 replicates in each of 4 conditions **Overall design:** Sez-4 cell line was starved of IL2 for 16h, washed twice and placed into 6-well plates in 10ml RPMI (10% FBS) for 2 h followed by addition of IL-2 (200U), IL-15 (20ng/mL), or IL-21 (100 ng/ml) or medium alone for 4 h.

Background corr dist: KL-Divergence = 0.1443, L1-Distance = 0.0276, L2-Distance = 0.0014, Normal std = 0.3822

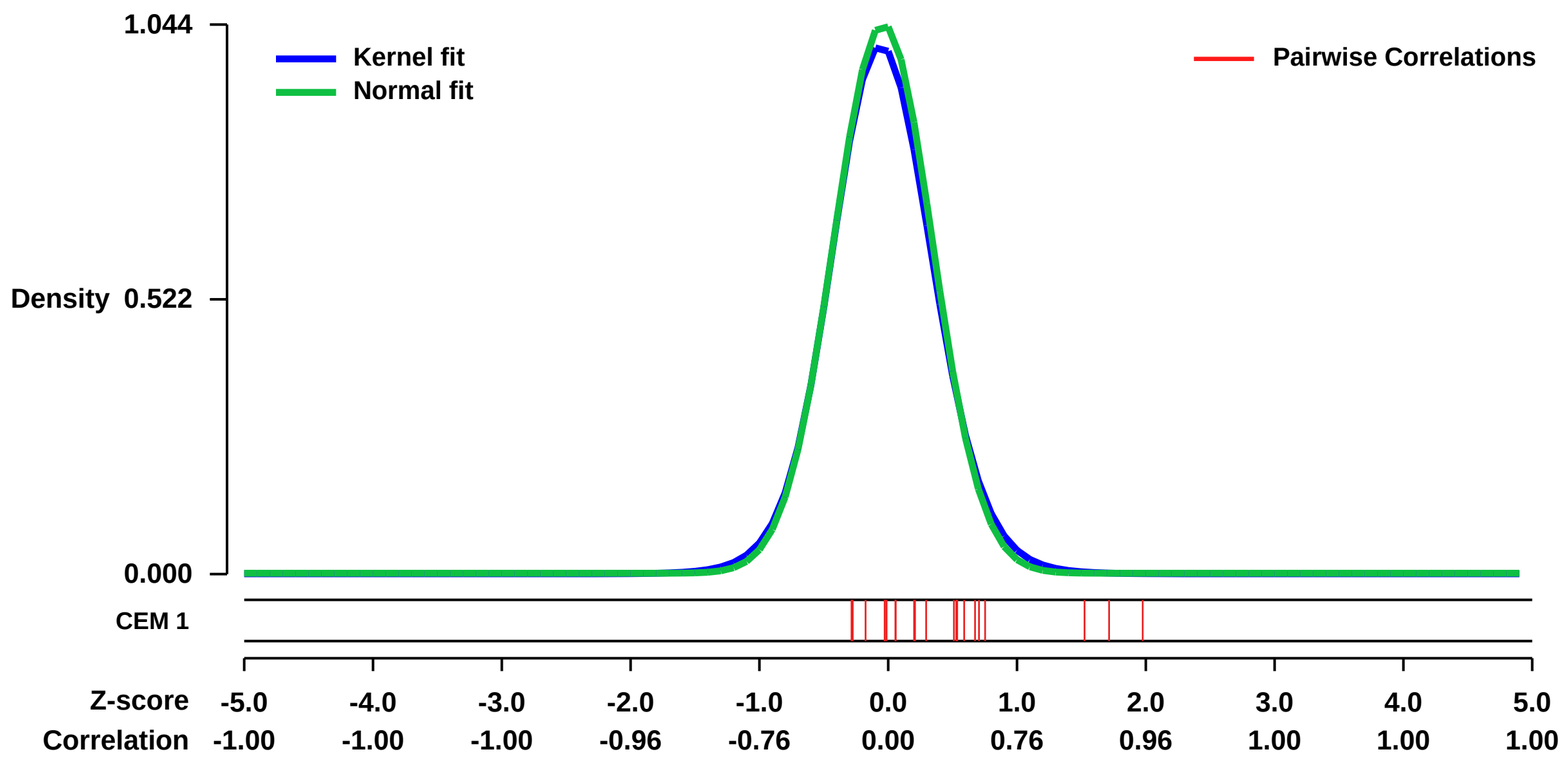

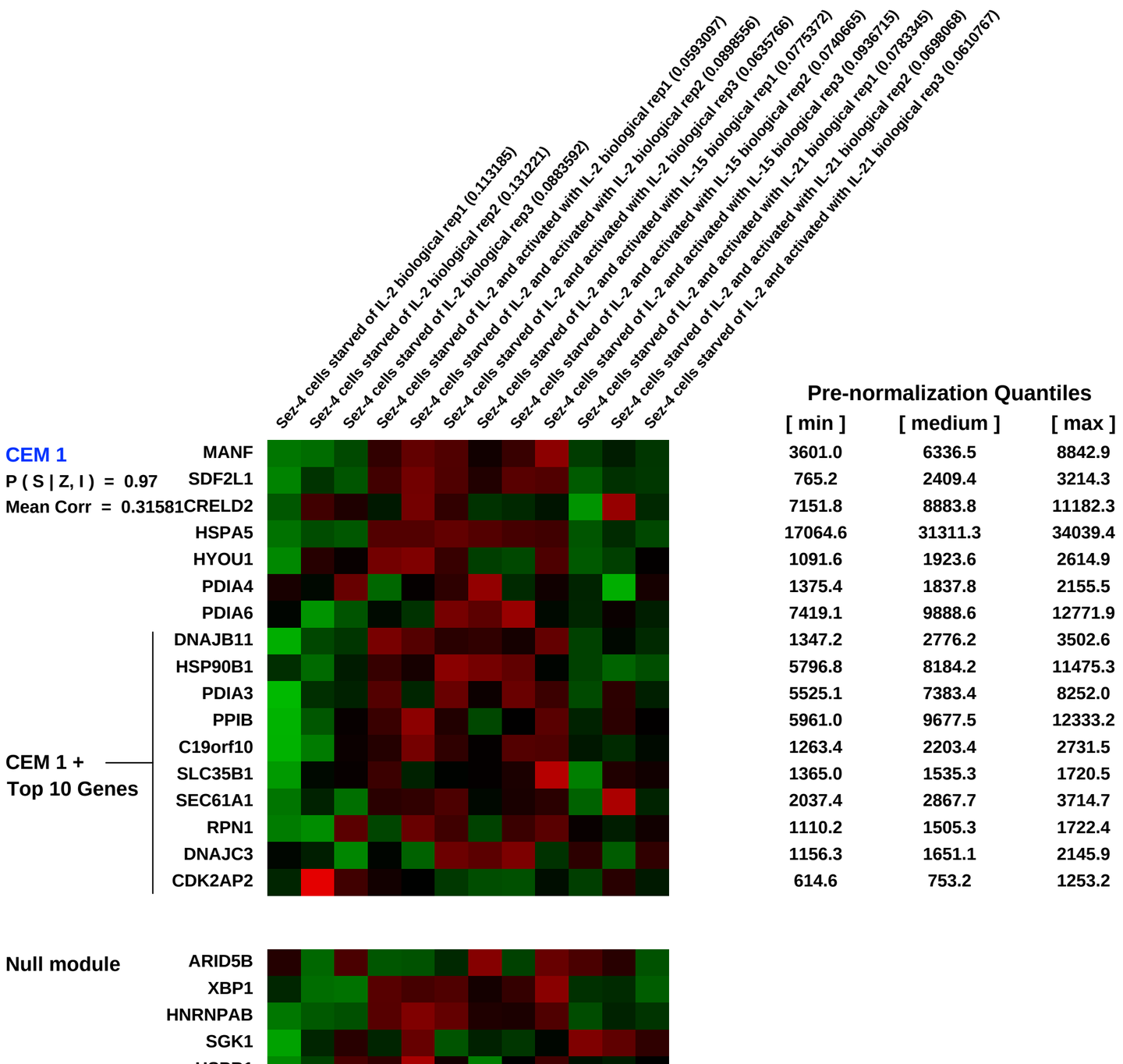

GEO Series "GSE32876" Expression Profiles

Num of samples in this series: 18

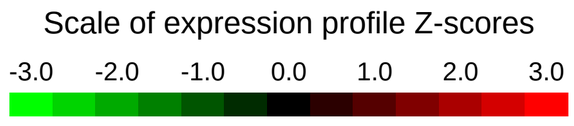

GEO Link:	http://www.ncbi.nlm.nih.gov/geo/query/acc.cgi?acc=GSE32876
Status:	Public on Oct 12 2011
Title:	Inferring transcriptional and microRNA-mediated regulatory programs in glioblastoma
Organism:	Homo sapiens
Experiment type:	Expression profiling by array
Platform:	GPL570
Pubmed ID:	22929615
Summary & Design:	**Summary:** Large-scale cancer genomics projects are profiling hundreds of tumors at multiple molecular layers, including copy number, mRNA and miRNA expression, but the mechanistic relationships between these layers are often excluded from computational models. We developed a supervised learning framework for integrating molecular profiles with regulatory sequence information to reveal regulatory programs in cancer, including miRNA-mediated regulation. We applied our approach to 320 glioblastoma profiles and identified key miRNAs and transcription factors as common or subtype-specific drivers of expression changes. We confirmed that predicted gene expression signatures for proneural subtype regulators were consistent with in vivo expression changes in a PDGF-driven mouse model. We tested two predicted proneural drivers, miR-124 and miR-132, both underexpressed in proneural tumors, by overexpression in neurospheres and observed a partial reversal of corresponding tumor expression changes. Computationally dissecting the role of miRNAs in cancer may ultimately lead to small RNA therapeutics tailored to subtype or individual. **Overall design:** miRNA mimetics were transfected to PDGFRA amplified neurosphere cell lines. Gene expression was measured 24 hours after transfection

Background corr dist: KL-Divergence = 0.2382, L1-Distance = 0.0498, L2-Distance = 0.0058, Normal std = 0.3088

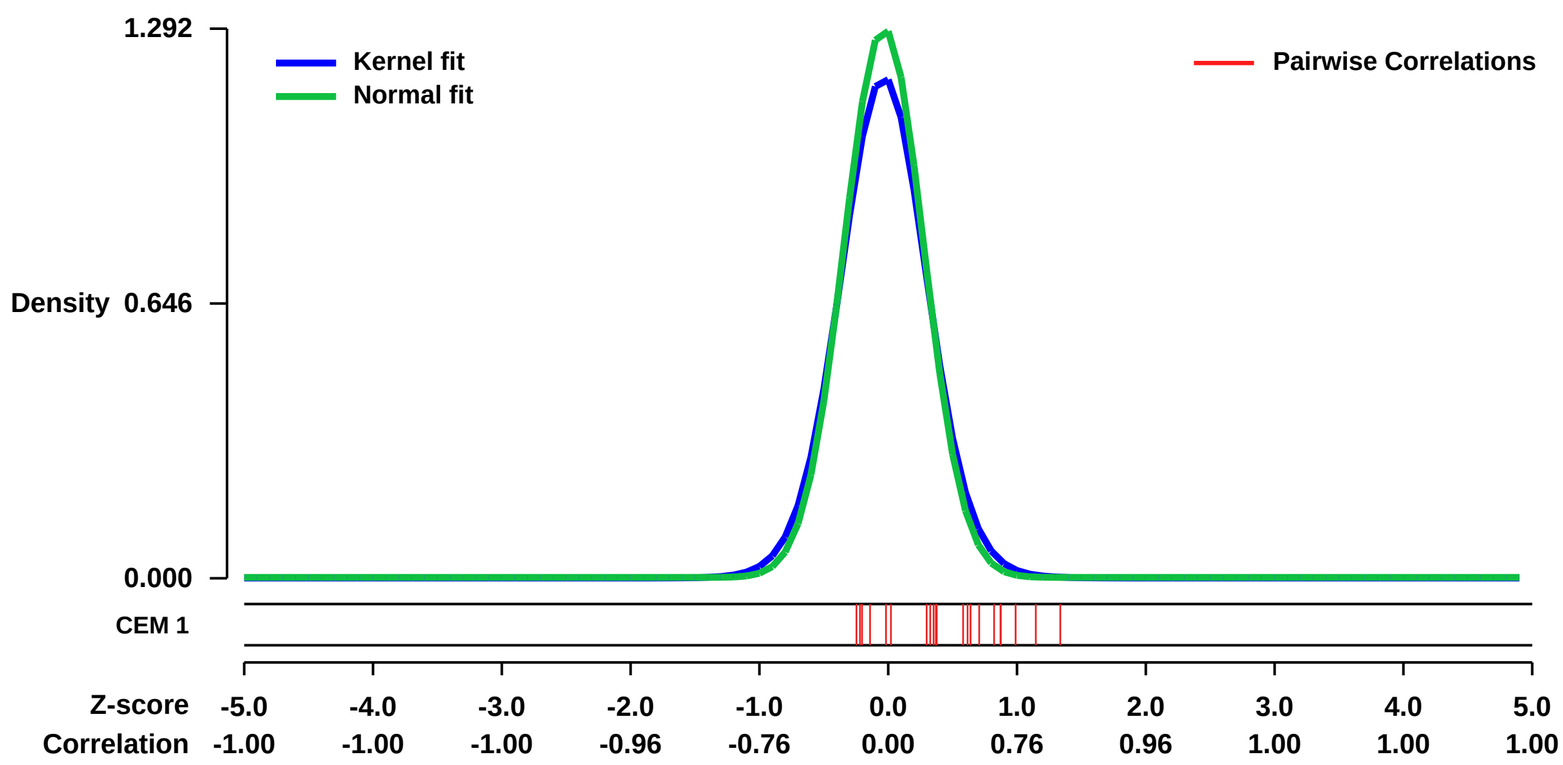

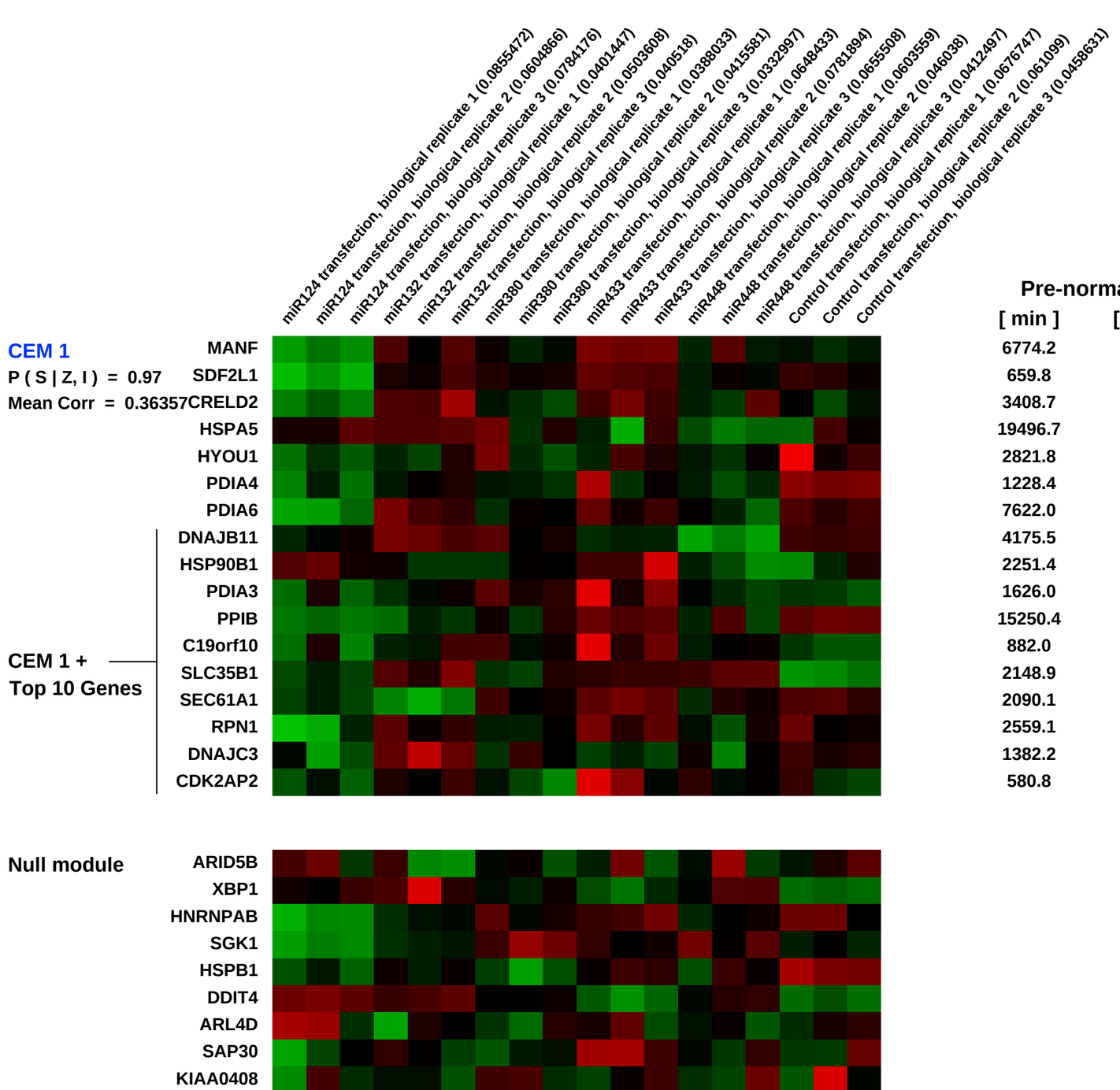

Pre-normalization Quantiles

	[min]	[medium]	[max]
MANF	6774.2	7417.0	8002.4
SDF2L1	659.8	1578.0	1896.2
CRELD2	3408.7	3786.4	4373.6
HSPA5	19496.7	22084.0	23251.8
HYOU1	2821.8	3024.9	3620.1
PDIA4	1228.4	1360.7	1590.7
PDIA6	7622.0	8729.7	9349.6
DNAJB11	4175.5	5345.7	5998.1
HSP90B1	2251.4	3002.5	4064.6
PDIA3	1626.0	1902.0	2505.0
PPIB	15250.4	16184.6	16866.9
C19orf10	882.0	1072.4	1393.4
SLC35B1	2148.9	2476.1	2649.7
SEC61A1	2090.1	2866.1	3266.1
RPN1	2559.1	3002.5	3242.1
DNAJC3	1382.2	1577.7	1801.8
CDK2AP2	580.8	638.3	742.4

GEO Series "GSE31980" Expression Profiles

Num of samples in this series: 6

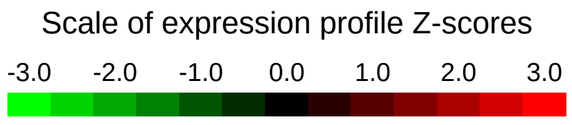

GEO Link:	http://www.ncbi.nlm.nih.gov/geo/query/acc.cgi?acc=GSE31980
Status:	Public on May 13 2012
Title:	Transcriptome profile in the human synovial MSC-aggregates
Organism:	Homo sapiens
Experiment type:	Expression profiling by array
Platform:	GPL570
Pubmed ID:	
Summary & Design:	**Summary:** One of strategies to regenerate cartilage defect is transplantation of mesenchymal stem cells (MSCs). Improvements of therapeutic potential of MSCs are needed to achieve successful cartilage regeneration by transplantation of a limited number of cells. Aggregated culture is a popular method in ES and iPS cells to maintain or enhance their potentials. Here we investigated gene expression profile of aggregated MSCs. 621 genes were up-regulated and 409 genes were down-regulated more than 5-fold in MSC-aggregates compared with the number in MSCs in a monolayer culture. The most up-regulated gene was BMP2, which is one of the genes involved in chondrogenesis. Anti-inflammatory genes were also up-regulated in MSC-aggregates. The microarray data for selected genes were confirmed by real-time PCR. **Overall design:** Human synovial MSCs was isolated from synovium of 3 distinct donors. The gene expression profile of MSC-aggregates cultured in hanging drop for 3days was compared with that of MSCs in a monolayer culture.

Background corr dist: KL-Divergence = 0.0292, L1-Distance = 0.0315, L2-Distance = 0.0012, Normal std = 0.6897

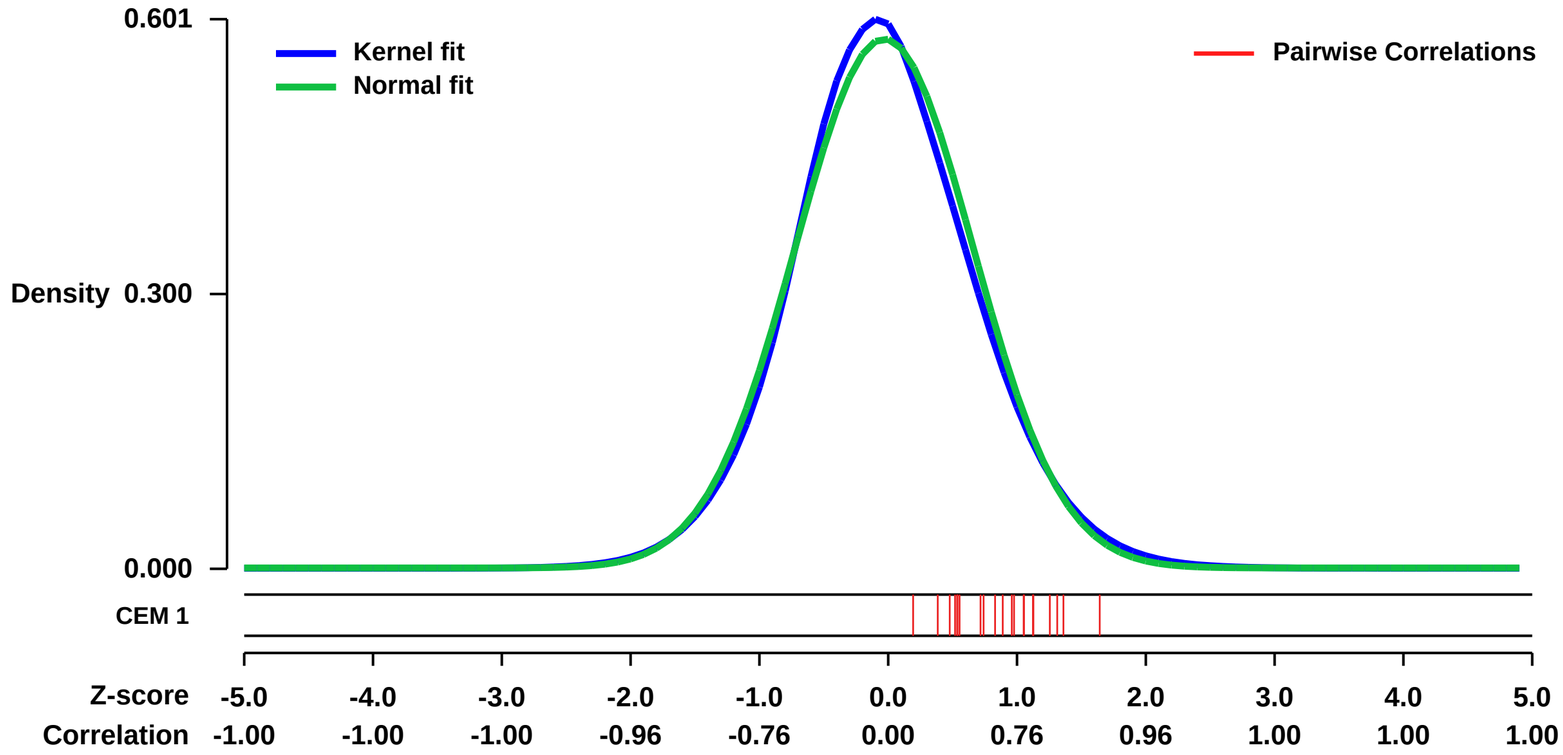

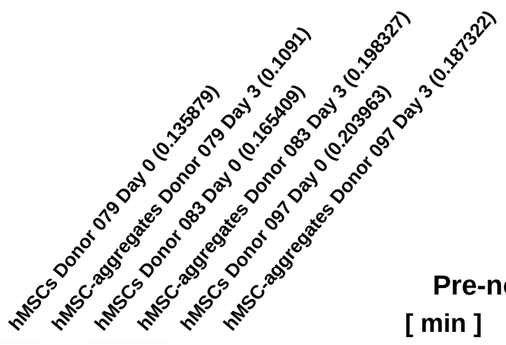

Pre-normalization Quantiles

		[min]	[medium]	[max]
CEM 1	MANF	1593.5	3400.1	3586.0
P (S | Z, I) = 0.97	SDF2L1	284.8	508.6	791.7
Mean Corr = 0.65708	CRELD2	1413.6	3679.5	4320.4
	HSPA5	13606.7	20889.6	22724.6
	HYOU1	979.0	2001.1	2571.2
	PDIA4	524.9	759.0	1378.3
	PDIA6	3592.6	5909.5	6683.5
CEM 1 + Top 10 Genes	DNAJB11	1401.8	2056.3	3383.7
	HSP90B1	4278.5	5403.0	8784.6
	PDIA3	5794.0	10403.4	11035.0
	PPIB	12874.3	17587.7	22268.3
	C19orf10	3012.6	3846.1	4772.4
	SLC35B1	1126.5	1392.4	1441.4
	SEC61A1	4606.1	6701.7	8921.8
	RPN1	1951.8	3198.1	3689.3
	DNAJC3	2289.4	3006.4	3653.0
	CDK2AP2	662.7	989.9	1141.1
Null module	ARID5B			
	XBP1			
	HNRNPAB			
	SGK1			
	HSPB1			
	DDIT4			
	ARL4D			
	SAP30			
	KIAA0408			
	GPR17			
	HSPH1			
	DNASE1L2			
	SLC5A3			
	GNAS			
	GPR3			
	TNFRSF25			
	TM6SF2			
	MKKS			
	PLEKHF1			
	ZMYM1			
	DOK3			
	FGF20			
	SLC39A2			
	KCNIP2			
	ERRFI1			
	DEDD2			
	CCDC117			
	USP31			
	AHSA2			
	CYS1			
	CNIH2			
	BANP			
	CHORDC1			
	P4HA1			

GEO Series "GSE50998" Expression Profiles

Num of samples in this series: 14

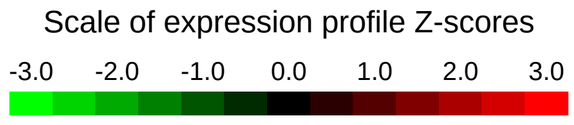

GEO Link:	http://www.ncbi.nlm.nih.gov/geo/query/acc.cgi?acc=GSE50998
Status:	Public on Jul 31 2014
Title:	Gene expression signature of T-ALL cell lines treated with the PI3K inhibitor AS605240
Organism:	Homo sapiens
Experiment type:	Expression profiling by array
Platform:	GPL570
Pubmed ID:	
Summary & Design:	**Summary:** The PI3K pathway is frequently hyperactivated in primary T-cell acute lymphoblastic leukemia (T-ALL) cells. Activation of the PI3K effector mTOR has been suggested to represent one mechanism of glucocorticoids resistance in T-ALL, and patients harboring mutations in the PI3K negative regulator PTEN may be at increased risk of induction failure and relapse. In this study, a PI3K gene expression signature allowed us to infer that higher PI3K activity is associated with glucocorticoid resistance and worst clinical outcome in T-ALL. The PI3K inhibitor AS605240 showed anti-leukemic activity and prevented leukemic progression in a xenograft model of T-ALL in NOD/SCID mice. Moreover, treatment of T-ALL cells with AS605240 downregulated Myc protein levels and Myc-dependent transcription in a Notch1-independent manner. Our data indicate that PI3K and Notch1 pathway converge at Myc, which was previously associated with glucocorticoids resistance in T-ALL. Accordingly, AS605240 showed strong synergism with glucocorticoids both in vitro and in T-ALL xenografted NOD/SCID mice. Surprisingly, PI3K inhibition showed antagonism with methotrexate and daunorubicin, drugs that preferentially target dividing cells. This antagonistic interaction could be circumvented by the use of correct drug scheduling schemes, which may be of major importance when considering introducing PI3K inhibitors in T-ALL treatment schemes. T-ALL cell lines were treated with the PI3K inhibitor AS605240 or vehicle for 6h in order to define a gene expression signature characteristic of PI3K activity in T-ALL cells. **Overall design:** Seven T-ALL cell lines (CCRF-CEM, HPB-ALL, Molt-4, ALL-SIL, P12-ICHIKAWA, TALL-1 and Jurkat) were cultured for 6h with the respective IC50 concentration of AS605240 or vehicle.

Background corr dist: KL-Divergence = 0.1216, L1-Distance = 0.0292, L2-Distance = 0.0016, Normal std = 0.4072

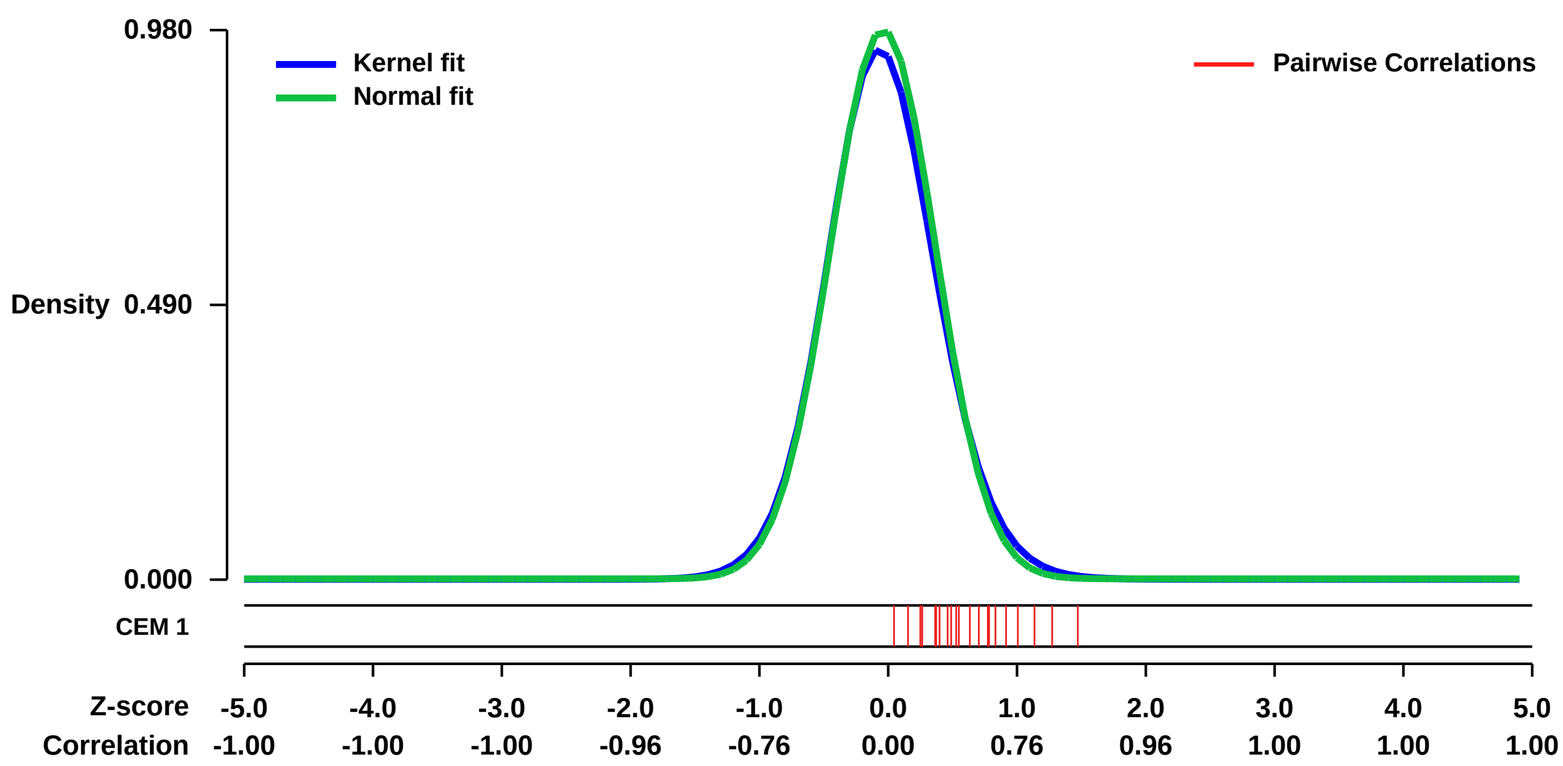

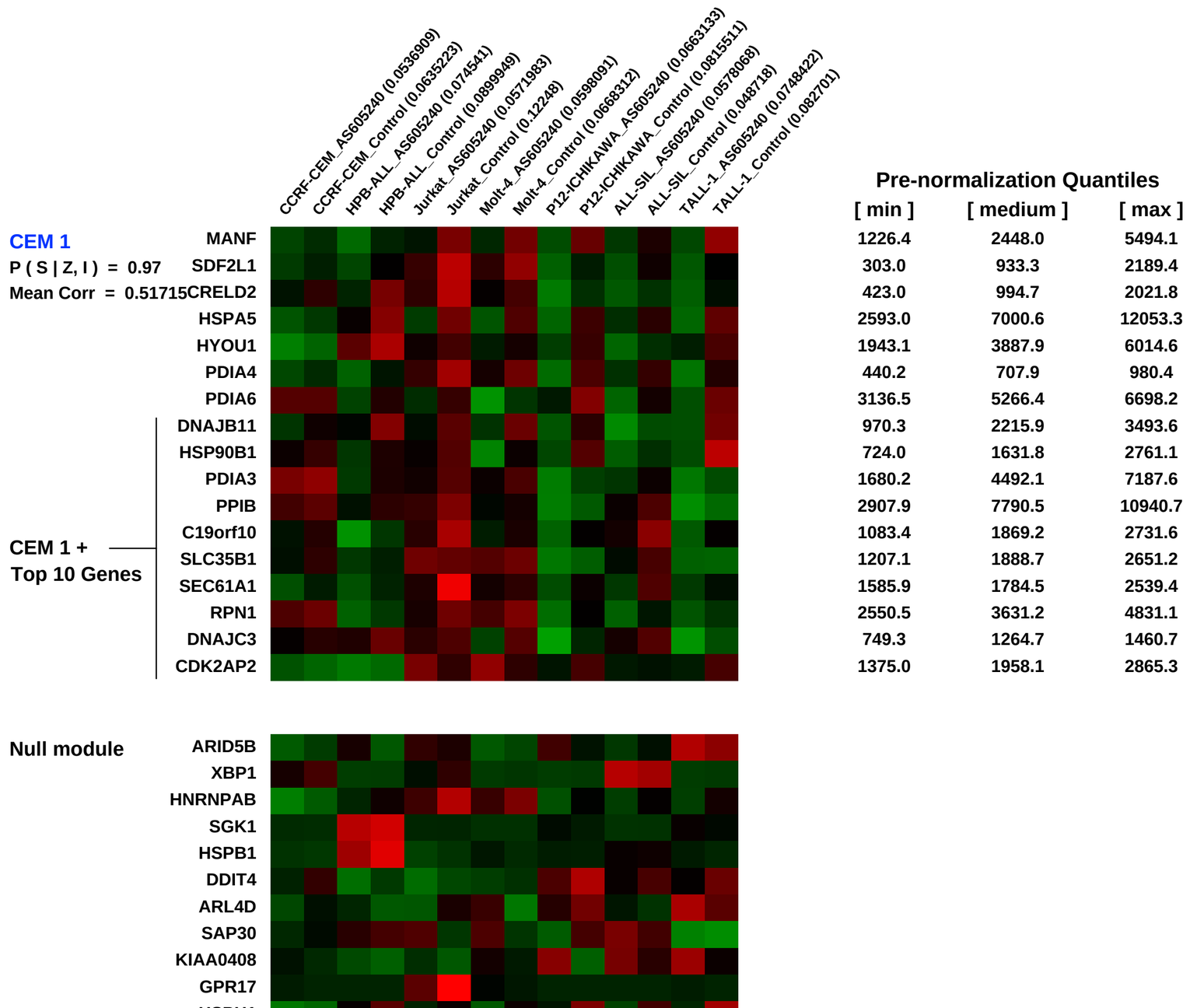

Pre-normalization Quantiles

	[min]	[medium]	[max]
MANF	1226.4	2448.0	5494.1
SDF2L1	303.0	933.3	2189.4
CRELD2	423.0	994.7	2021.8
HSPA5	2593.0	7000.6	12053.3
HYOU1	1943.1	3887.9	6014.6
PDIA4	440.2	707.9	980.4
PDIA6	3136.5	5266.4	6698.2
DNAJB11	970.3	2215.9	3493.6
HSP90B1	724.0	1631.8	2761.1
PDIA3	1680.2	4492.1	7187.6
PPIB	2907.9	7790.5	10940.7
C19orf10	1083.4	1869.2	2731.6
SLC35B1	1207.1	1888.7	2651.2
SEC61A1	1585.9	1784.5	2539.4
RPN1	2550.5	3631.2	4831.1
DNAJC3	749.3	1264.7	1460.7
CDK2AP2	1375.0	1958.1	2865.3

GEO Series "GSE17440" Expression Profiles

Num of samples in this series: 8

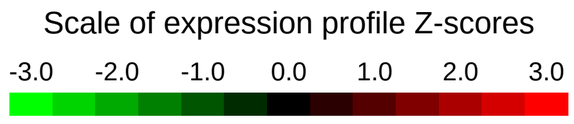

GEO Link:	http://www.ncbi.nlm.nih.gov/geo/query/acc.cgi?acc=GSE17440
Status:	Public on Feb 01 2010
Title:	Gene Expression in Frontal Cortex in Major Depression and HIV
Organism:	Homo sapiens
Experiment type:	Expression profiling by array
Platform:	GPL570
Pubmed ID:	20436668
Summary & Design:	**Summary:** Major depressive disorder (MDD) is a clinically defined entity with little understanding as to the underlying pathological substrate. Biologically, MDD is characterized by disruption of neurotransmitters, especially serotonin and noradrenaline, which are the main targets of antidepressants. We previously demonstrated significant reduction of glial cell number in the cingulate and dorsolateral prefrontal cortical regions. Unfortunately, individuals living with HIV still have very high rates of MDD, despite the fact that mortality rates have fallen sharply with effective antiretroviral treatment. It is possible that in this treatment era, living with chronic HIV infection may result in long-term neuropathological changes that predispose to MDD. For example, it is known that HIV is associated with a range of inflammatory pathologies, neuronal loss, and dendrite-synaptic damage. In HIV, these neurodegenerative changes have been linked to neurocognitive impairments, however it is also possible that these changes potentiate MDD. In the current study, we sought to determine whether there are changes in gene expression in the MDD brain in the frontal cortex in HIV-context. We identify a large number of genes dysregulated at p<0.05 significance. **Overall design:** Retrospective gene expression analysis of autopsy brain tissue. Four HIV/MDD subjects are identified and age-matched HIV patients without neuropsychiatric conditions are compared as controls.

Background corr dist: KL-Divergence = 0.0686, L1-Distance = 0.0289, L2-Distance = 0.0015, Normal std = 0.5071

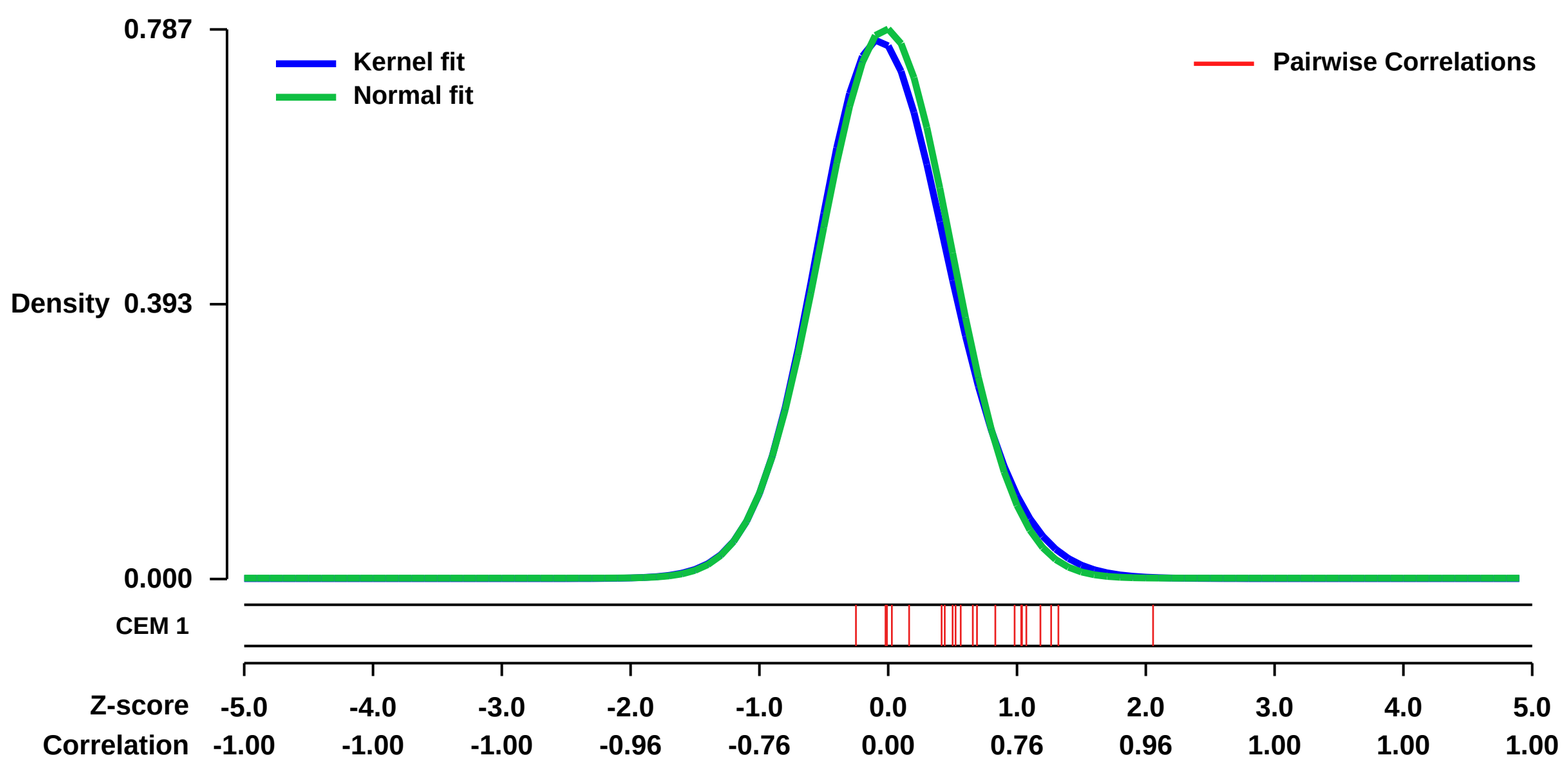

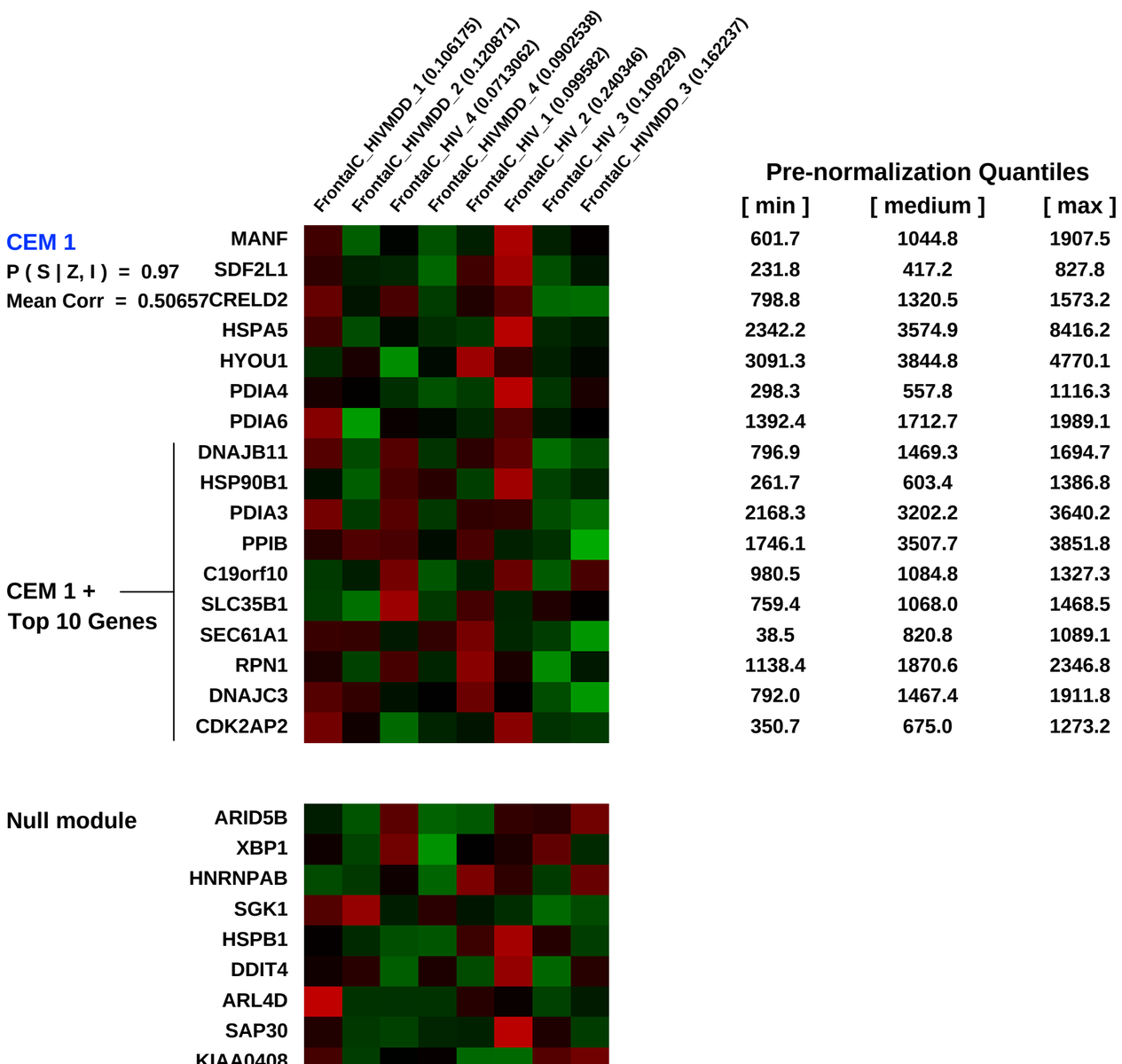

GEO Series "GSE11550" Expression Profiles

Num of samples in this series: 10

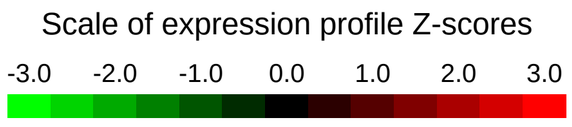

GEO Link:	http://www.ncbi.nlm.nih.gov/geo/query/acc.cgi?acc=GSE11550
Status:	Public on May 29 2008
Title:	Hs 294T Cells Treated with Elesclomol Alone or in Combination with Paclitaxel Compared to DMSO Treated
Organism:	Homo sapiens
Experiment type:	Expression profiling by array
Platform:	GPL570
Pubmed ID:	18723479
Summary & Design:	**Summary:** We used microarrays to detail gene expression changes in Hs 294T human melanoma cells after treatment with elesclomol alone, or in combination with paclitaxel, to aide in identifing the mechnism of action of elesclomol. **Keywords: treatment** **Overall design:** Hs 294T human melanoma cells were grown in vitro. They were seeded at a low density and were left untreated, treated with the vehicle, treated with elesclomol, treated with paclitaxel, or treated in combination with both elesclomol and paclitaxel. They were incubated for 6 hours before harvesting.

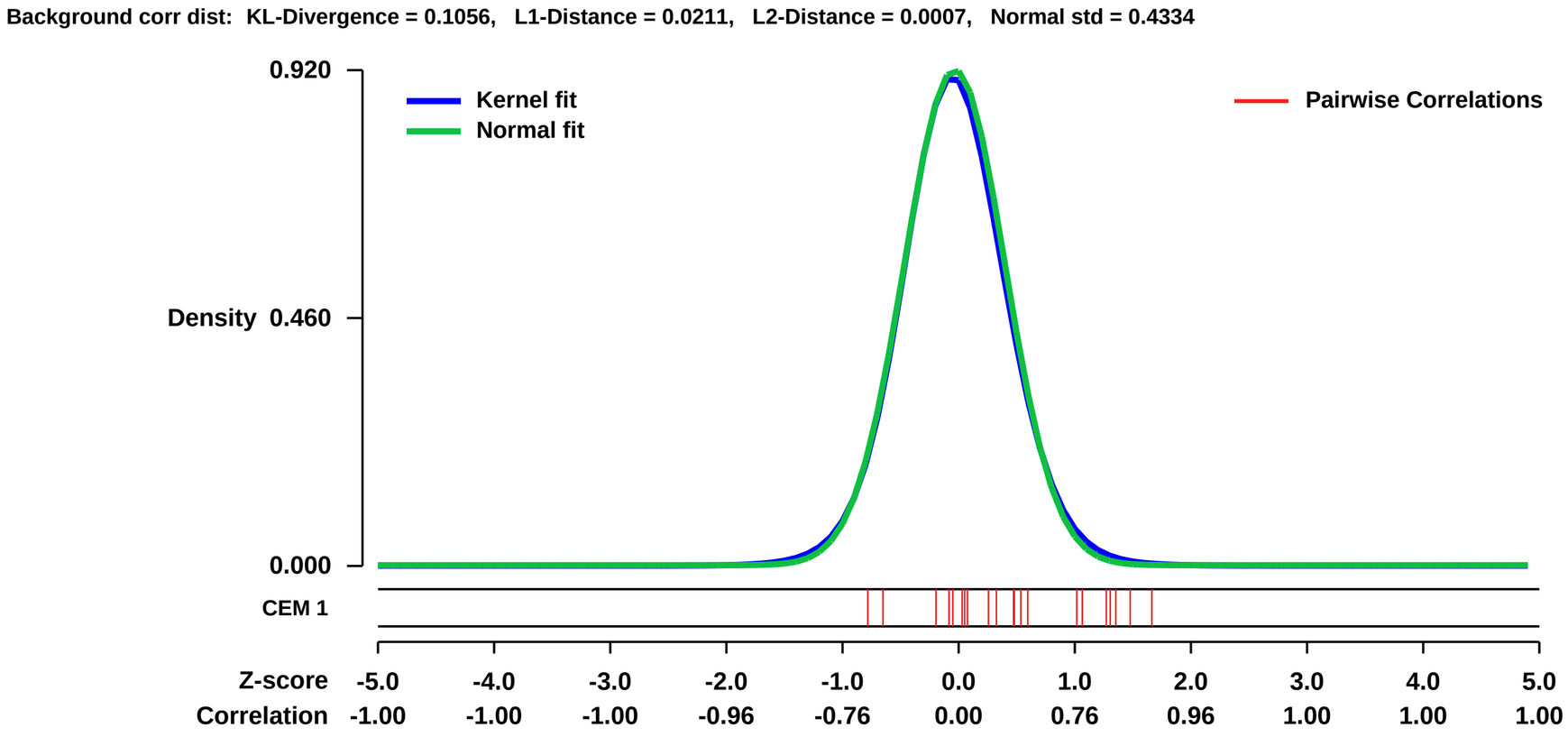

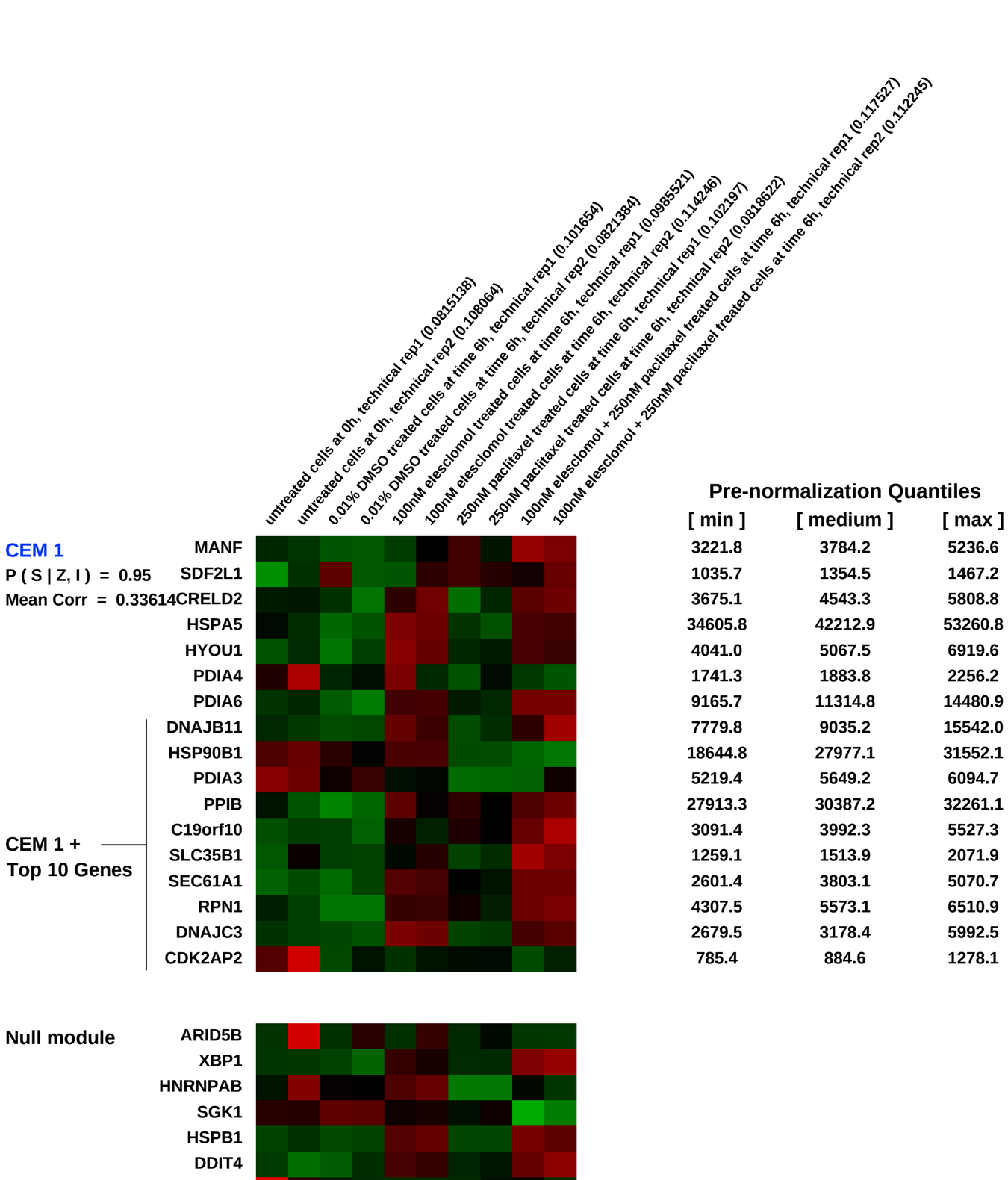

GEO Series "GSE38332" Expression Profiles

Num of samples in this series: 9

Scale of expression profile Z-scores

-3.0 -2.0 -1.0 0.0 1.0 2.0 3.0

GEO Link:	http://www.ncbi.nlm.nih.gov/geo/query/acc.cgi?acc=GSE38332
Status:	Public on Jul 04 2013
Title:	Identification of Nrf2-regulated genes in A549 lung cancer cells by oligonucleotide microarray
Organism:	Homo sapiens
Experiment type:	Expression profiling by array
Platform:	GPL570
Pubmed ID:	23921124
Summary & Design:	**Summary:** To elucidate the mechanisms by which Nrf2 regulates cell growth, we performed global gene expression profiling of A549 lung cancer cells with knockdown of Nrf2. Gene networks associated with carbohydrate metabolism and drug metabolism were significantly downregulated in Nrf2-depleted A549 cells. Gene Set Enrichment Analysis revealed significant enrichment of genes associated with carbohydrate catabolic processes, positive regulation of metabolic processes, PPP, and arachidonic acid metabolism. In summary, this analysis revealed that Nrf2 positively regulates transcription of genes that play key roles in central carbon metabolism. **Overall design:** A549 cells were transfected with non targeting NS siRNA or siRNA targeting Nrf2. Mock transfected A549 cells were treated with transfection reagent alone. We had 3 biological replicates for each of the 3 groups. Ninty six hours post transfection, cells were lysed and total RNA was isolated.

Background corr dist: KL-Divergence = 0.0321, L1-Distance = 0.0303, L2-Distance = 0.0014, Normal std = 0.6601

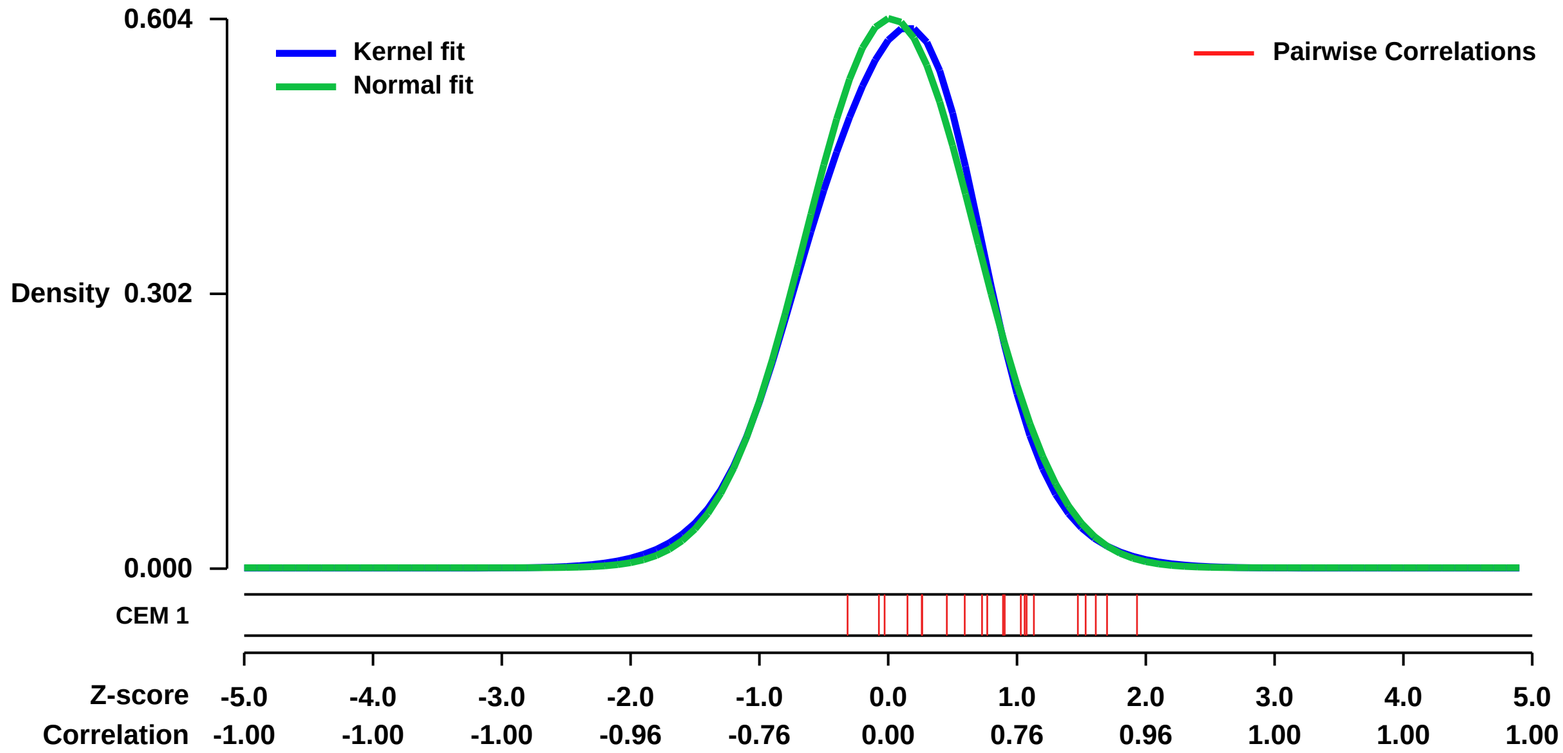

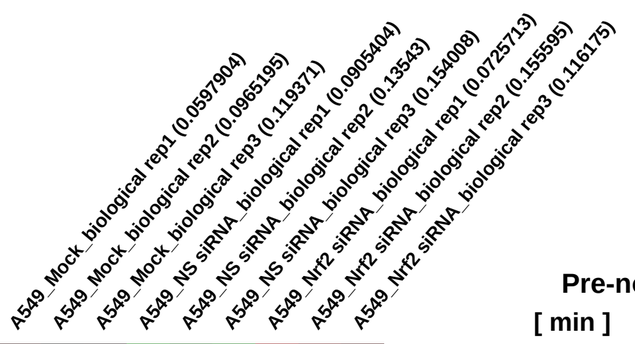

Pre-normalization Quantiles

[min] [medium] [max]

CEM 1
P (S | Z, I) = 0.94
Mean Corr = 0.55734

CEM 1 + Top 10 Genes

Null module

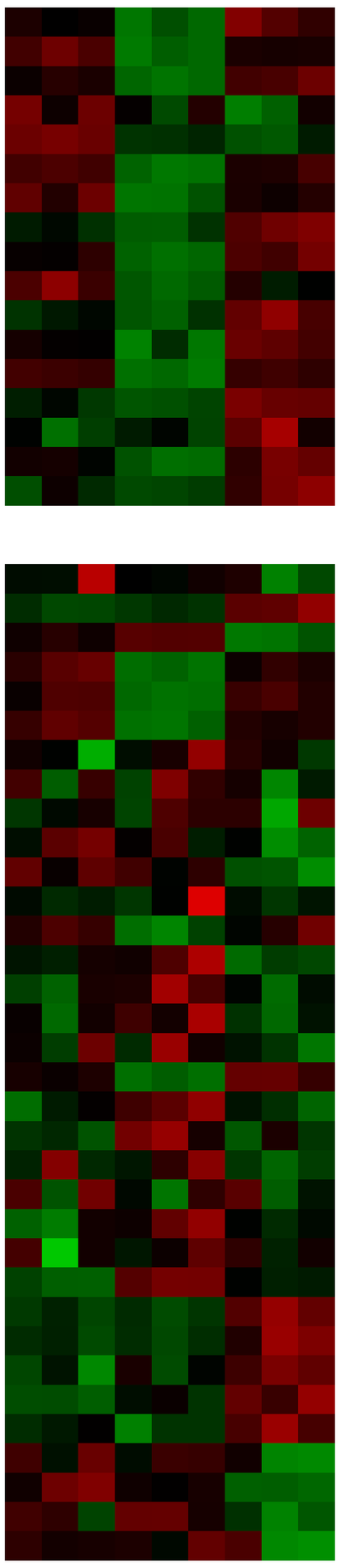

MANF	2224.9	2697.1	3146.8
SDF2L1	611.7	851.5	991.2
CRELD2	1156.8	1655.4	1944.6
HSPA5	10117.2	10583.6	10930.2
HYOU1	2259.1	2489.2	3177.5
PDIA4	901.4	1359.3	1498.4
PDIA6	5200.1	6183.0	6748.2
DNAJB11	2432.2	2565.0	2877.8
HSP90B1	2082.0	2534.2	2947.9
PDIA3	2179.7	2783.6	3610.8
PPIB	8346.4	9197.4	11132.6
C19orf10	1871.8	2200.0	2446.1
SLC35B1	1687.5	3796.5	3966.8
SEC61A1	2196.8	2404.2	2968.1
RPN1	2645.4	2952.8	3443.0
DNAJC3	1092.8	1390.7	1624.9
CDK2AP2	1331.7	1425.6	1891.3
ARID5B			
XBP1			
HNRNPAB			
SGK1			
HSPB1			
DDIT4			
ARL4D			
SAP30			
KIAA0408			
GPR17			
HSPH1			
DNASE1L2			
SLC5A3			
GNAS			
GPR3			
TNFRSF25			
TM6SF2			
MKKS			
PLEKHF1			
ZMYM1			
DOK3			
FGF20			
SLC39A2			
KCNIP2			
ERRFI1			
DEDD2			
CCDC117			
USP31			
AHSA2			
CYS1			
CNIH2			
BANP			
CHORDC1			
P4HA1			

GEO Series "GSE14334" Expression Profiles

Num of samples in this series: 38

Scale of expression profile Z-scores

-3.0 -2.0 -1.0 0.0 1.0 2.0 3.0

GEO Link:	http://www.ncbi.nlm.nih.gov/geo/query/acc.cgi?acc=GSE14334
Status:	Public on Sep 10 2009
Title:	Transcriptomic analysis of human lung development
Organism:	Homo sapiens
Experiment type:	Expression profiling by array
Platform:	GPL570
Pubmed ID:	19815808
Summary & Design:	**Summary:** We decompose the genome-wide expression patterns in 38 embryonic human lung (53-154 days post conception/dpc) into their independent, dominant directions of transcriptomic sample variation in order togain global insight of the developing human lung transcriptome.The characteristic genes and their corresponding bioâ ontologic attribute profile for the latter were identified. We noted the overâ representation of lung specific attributes (e.g., surfactant proteins) traditionally associated with later developmental stages, and highly ranked attributes (e.g., chemokineâ immunologic processes) not previously reported nor immediately apparent in an early lung development context. We defined the 3,223â gene union of the characteristic genes of the 3 most dominant sources of variation as the developing lung characteristic subâ transcriptome (DLCS). It may be regarded as the minimal gene set describing the essential biology of this process. The developing lung series in this transcriptomic variation perspectiveform a contiguous trajectory with critical time points that both correlate with the 2 traditional morphologic stages overlapping -154 dpc and suggest the existence of 2 novel phases within the pseudoglandular stage. To demonstrate that this characterization is robust, we showed that the model could be used to estimate the gestational age of independent human lung tissue samples with a median absolute error of 5 days, based on the DLCS of their lung profile alone. Repeating this procedure on the homologous transcriptome profiles of developing mouse lung 14â 19 dpc, we were able to recover their correct developmental chronology. **Whole human fetal lung gene expression profiling from estimated gestational ages 53 to 154 days post conception.** **Keywords: Whole lung gene expression profiling, lung development, human fetus.** **Overall design:** **Time series with biological replicates.**

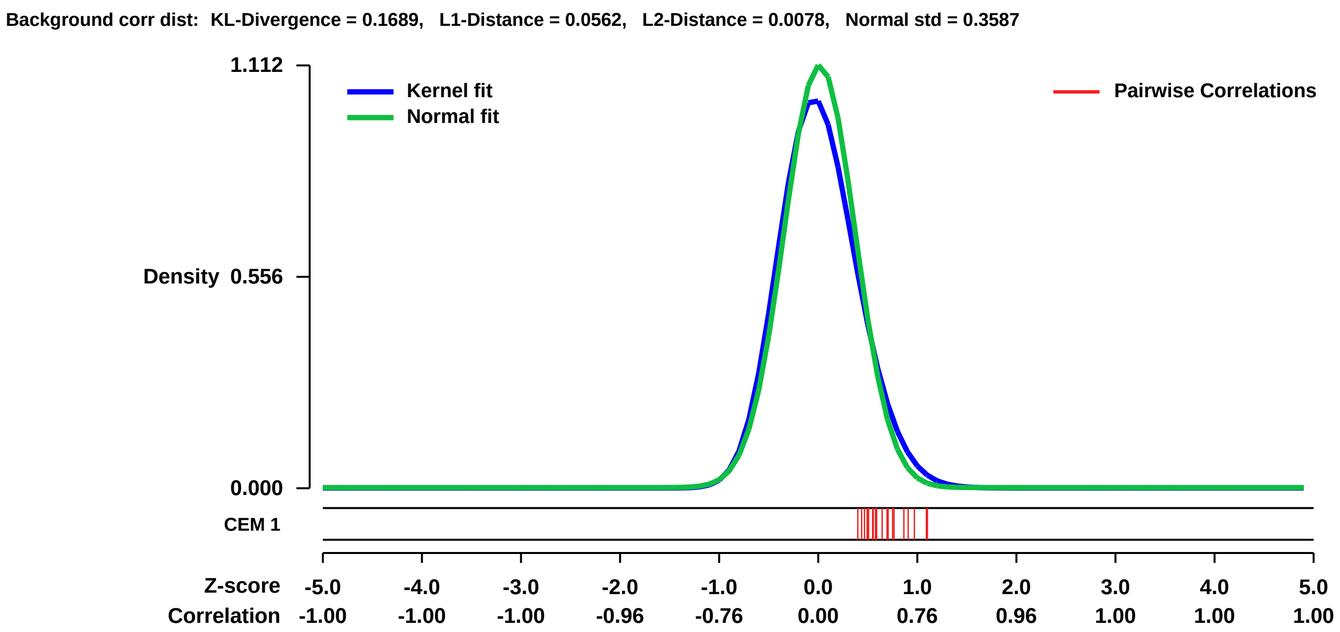

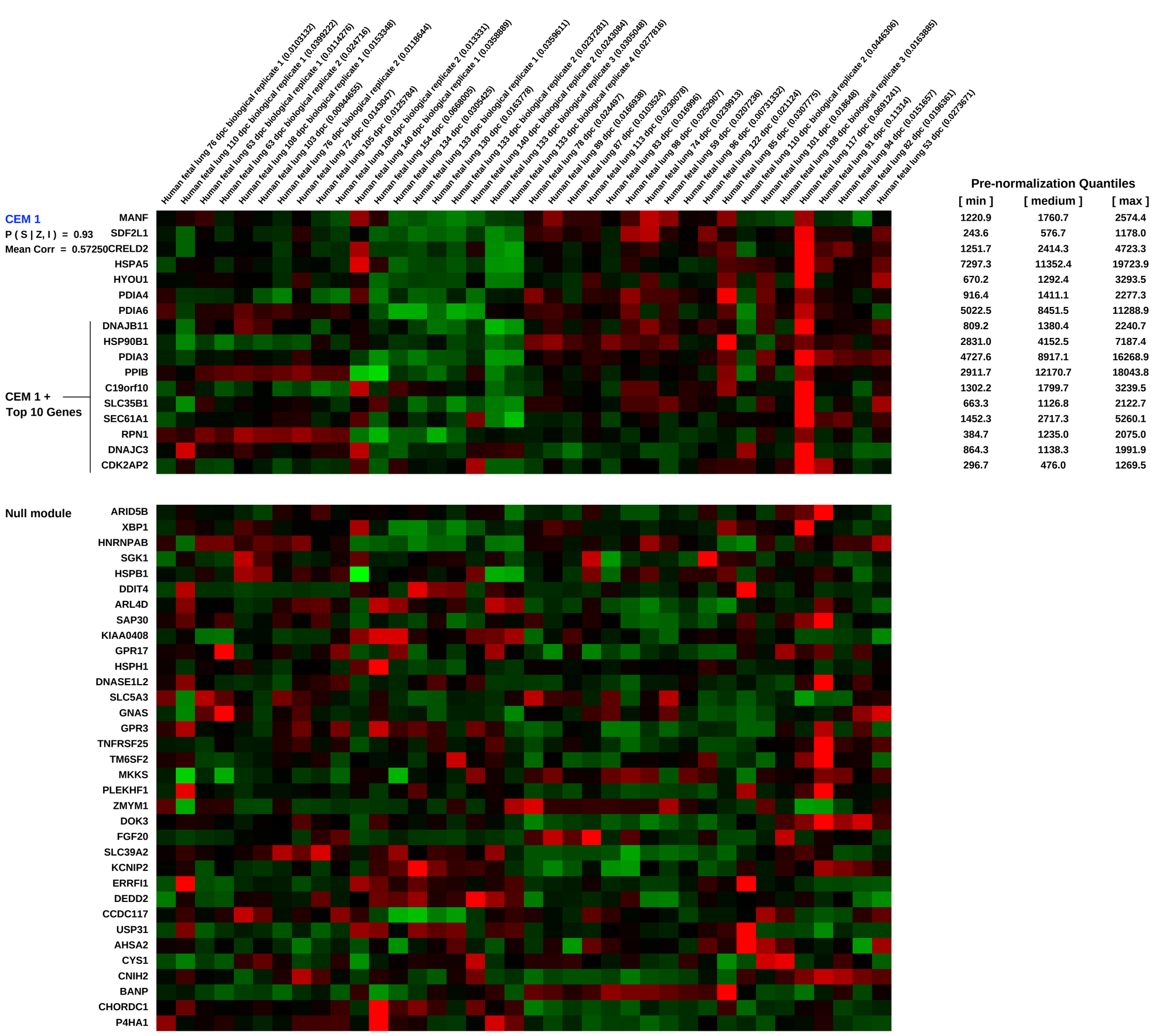

Pre-normalization Quantiles

[min]	[medium]	[max]
1220.9	1760.7	2574.4
243.6	576.7	1178.0
1251.7	2414.3	4723.3
7297.3	11352.4	19723.9
670.2	1292.4	3293.5
916.4	1411.1	2277.3
5022.5	8451.5	11288.9
809.2	1380.4	2240.7
2831.0	4152.5	7187.4
4727.6	8917.1	16268.9
2911.7	12170.7	18043.8
1302.2	1799.7	3239.5
663.3	1126.8	2122.7
1452.3	2717.3	5260.1
384.7	1235.0	2075.0
864.3	1138.3	1991.9
296.7	476.0	1269.5

GEO Series "GSE6518" Expression Profiles

Num of samples in this series: 9

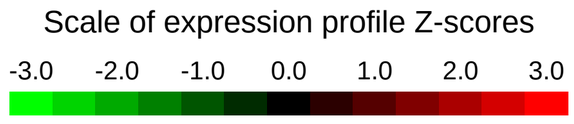

GEO Link:	http://www.ncbi.nlm.nih.gov/geo/query/acc.cgi?acc=GSE6518
Status:	Public on Dec 13 2007
Title:	Conjugated linoleic acid (CLA) and Caco-2 cells
Organism:	Homo sapiens
Experiment type:	Expression profiling by array
Platform:	GPL570
Pubmed ID:	17951470
Summary & Design:	**Summary:** The effect of CLA on gene expression in Caco-2 cells **Keywords: Human** **Overall design:** Caco-2 cells were treated with linoleic acid (LA; the parent and control fatty acid) trans-10, cis-12 CLA or cis-9, trans-11 CLA for 12 d.

Background corr dist: KL-Divergence = 0.0520, L1-Distance = 0.0423, L2-Distance = 0.0025, Normal std = 0.6116

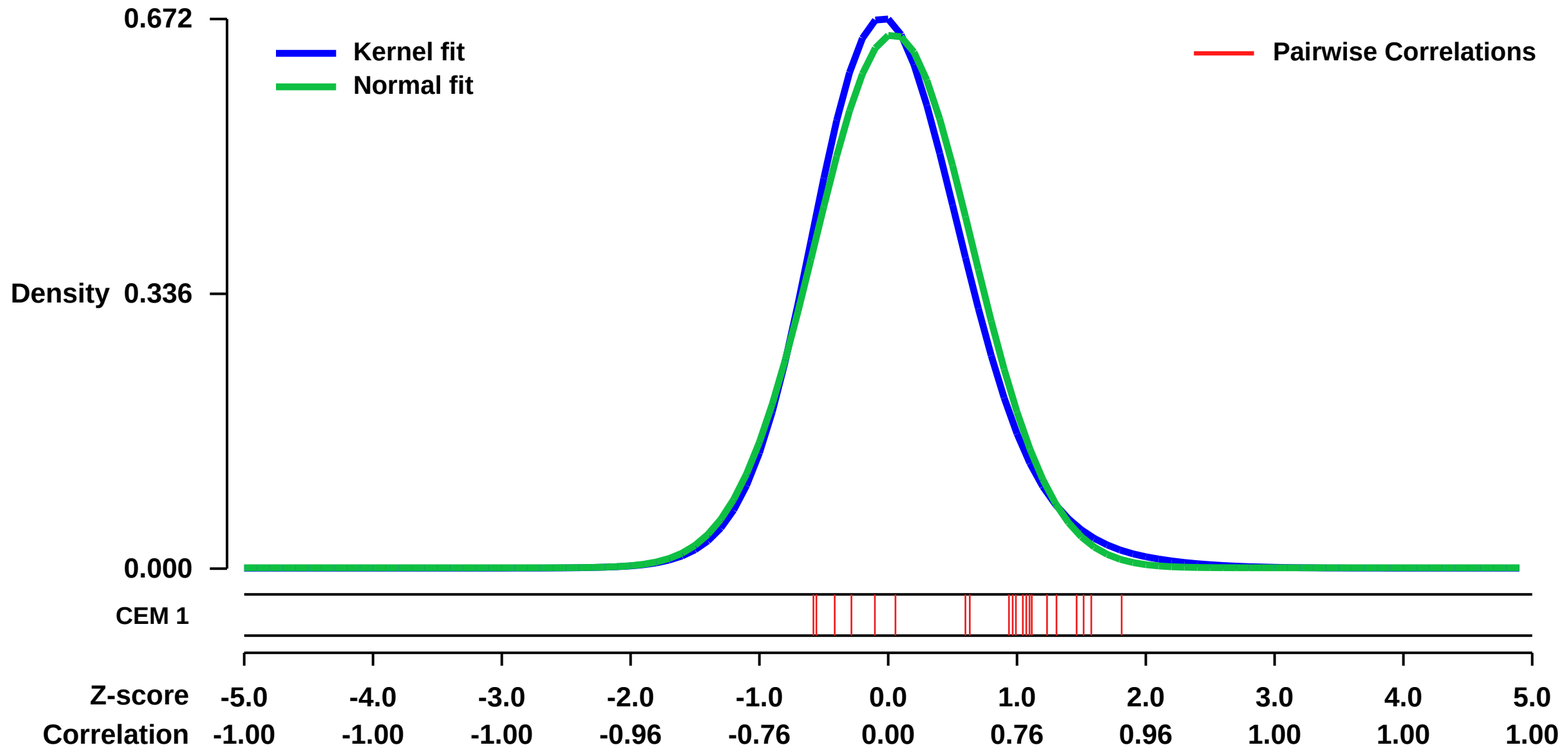

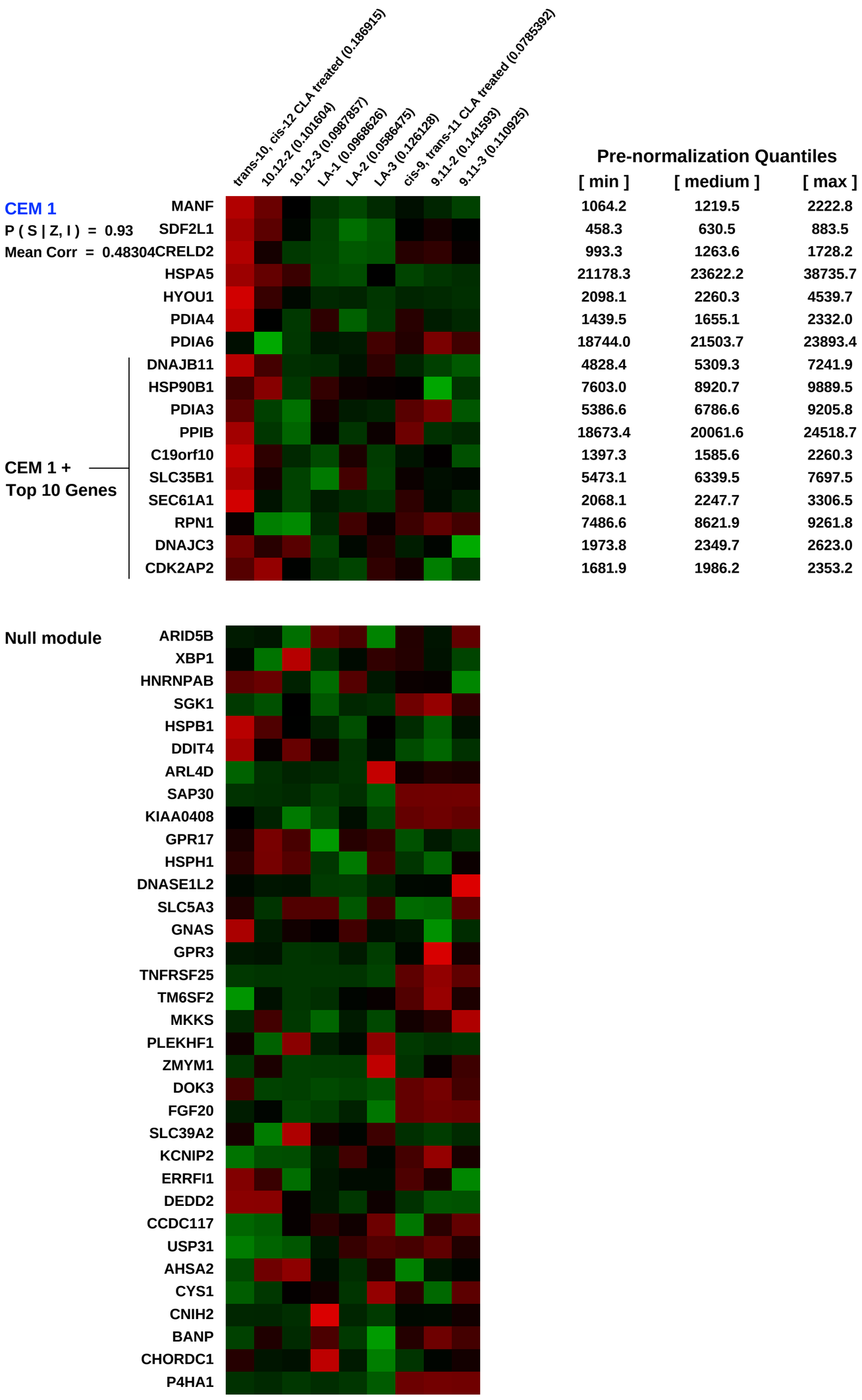

GEO Series "GSE33243" Expression Profiles

Num of samples in this series: 6

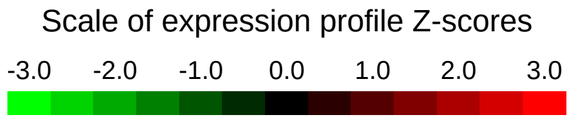

GEO Link:	http://www.ncbi.nlm.nih.gov/geo/query/acc.cgi?acc=GSE33243
Status:	Public on Nov 30 2011
Title:	Human acute myelogenous leukemia-initiating cells treated with fenretinide
Organism:	Homo sapiens
Experiment type:	Expression profiling by array
Platform:	GPL570
Pubmed ID:	23513221
Summary & Design:	**Summary:** Transcriptional profiling of human acute myelogenous leukemia (AML) CD34+ cells treated with 5 ¸…M fenretinide. Two timepoints included are 6h, 12h, covering the apoptosis-induction time window of AML CD34+ cells responsing to the fenretinide treatment. We studied gene expression series in human AML CD34+ cells with or without 5 ¸…M fenretinide treatment by cDNA microarray analysis. Several signal transduction pathways are involve, including stress response, NF-kappaB inhibition and p53 inhibition (p<0.05). These findings indicate fenretinide may represent a promising candidate for targeting AML-initiating cells. **Overall design:** 6-condition experiment, untreated AML CD34+ cells vs. fenretinide-treated AML CD34+ cells,including 2 time points, for each point the untreated and 5 ¸…M fenretinide treated, independently grown and harvested. Untreated was used to counteracting the background.

Background corr dist: KL-Divergence = 0.0482, L1-Distance = 0.0585, L2-Distance = 0.0053, Normal std = 0.6360

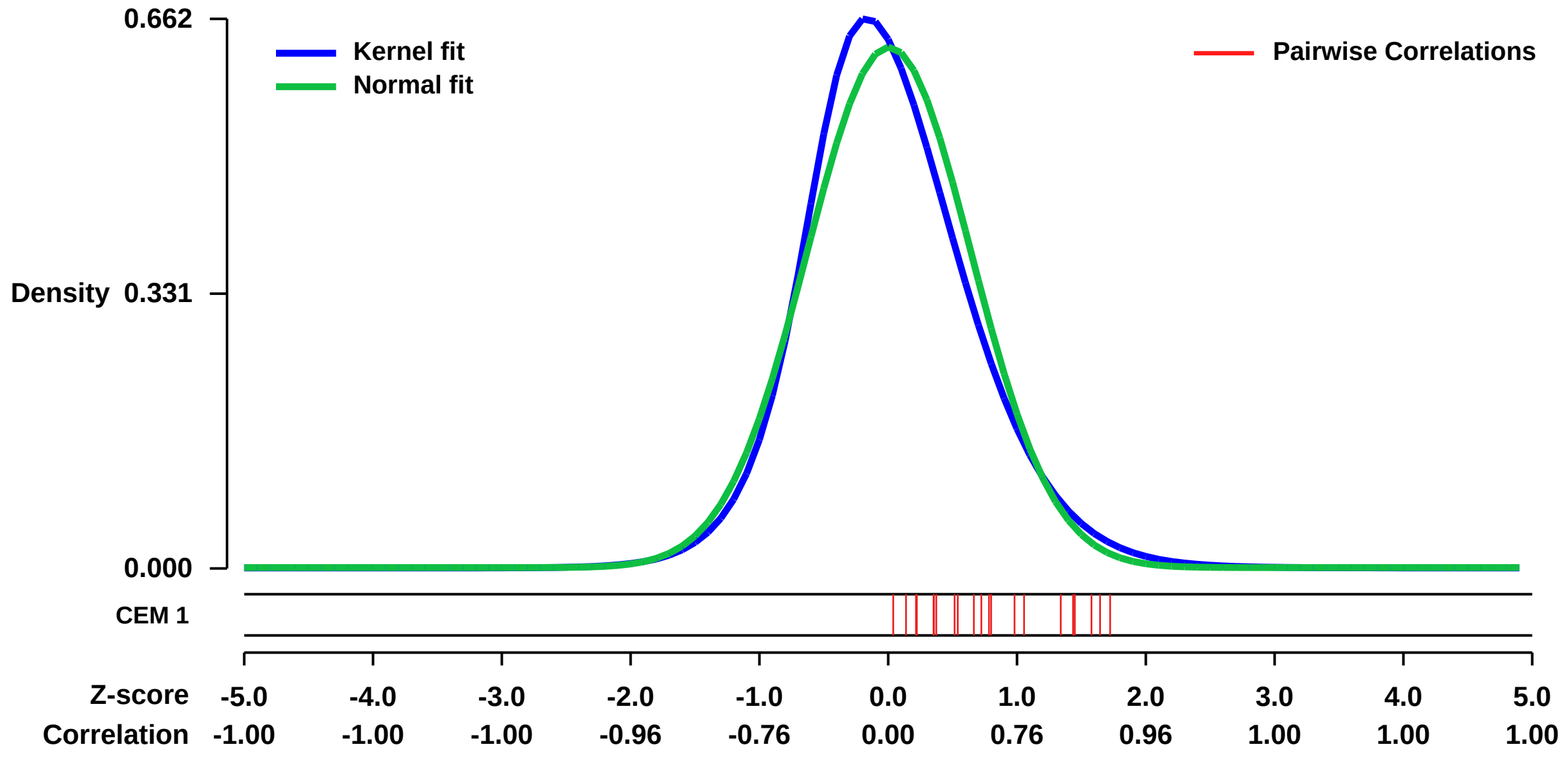

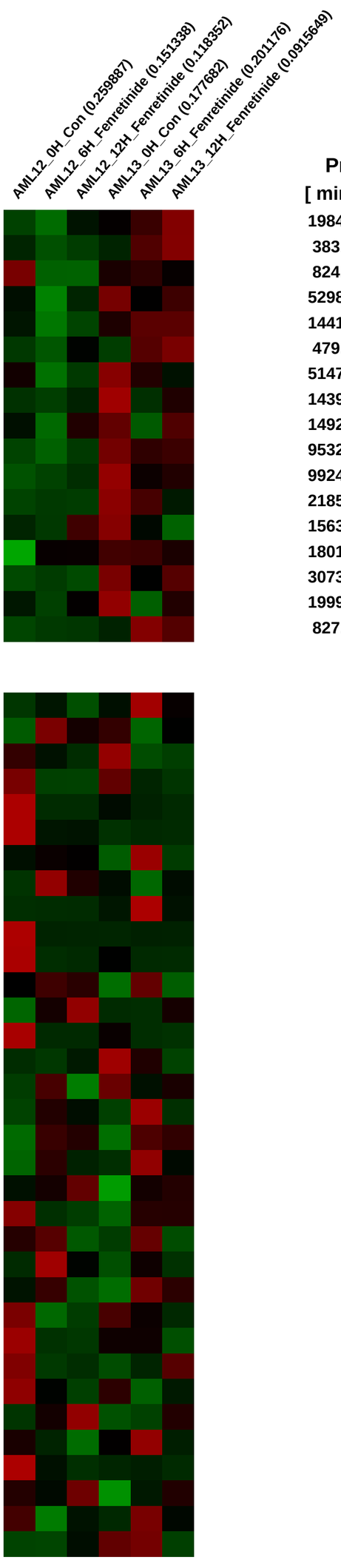

GEO Series "GSE15132" Expression Profiles

Num of samples in this series: 18

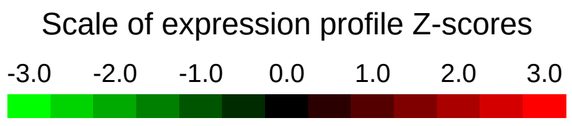

GEO Link:	http://www.ncbi.nlm.nih.gov/geo/query/acc.cgi?acc=GSE15132
Status:	Public on Mar 06 2009
Title:	Riboflavin depletion impairs cell proliferation in intestinal cells: Identification of mechanisms and consequences
Organism:	Homo sapiens
Experiment type:	Expression profiling by array
Platform:	GPL570
Pubmed ID:	20848206
Summary & Design:	**Summary:** Microarray analysis has been applied to the cell proliferation in a human colonic cel line, Caco-2. We have shown previously that a moderate riboflavin depletion around weaning has a profound impact on the structure and function of the small intestine of the rat, which is not reversible following riboflavin repletion. In this study we have modelled riboflavin deficiency in a human cell line, shown irreversible loss of cell viability associated with impaired mitosis and identified candidate effectors of riboflavin depletion in the cell. The aim of the present study is to develop a cell culture model of riboflavin depletion and analyse its behaviour using a using a combination of cell biology approaches including microarray analysis. **Overall design:** A human colonic cell line, Caco-2, was grown in culture and treated to riboflavin depletion. Treated and untreated cells were collected at appropriate time points and isolated RNA subjected to microarray analysis.

Background corr dist: KL-Divergence = 0.2062, L1-Distance = 0.0476, L2-Distance = 0.0054, Normal std = 0.3282

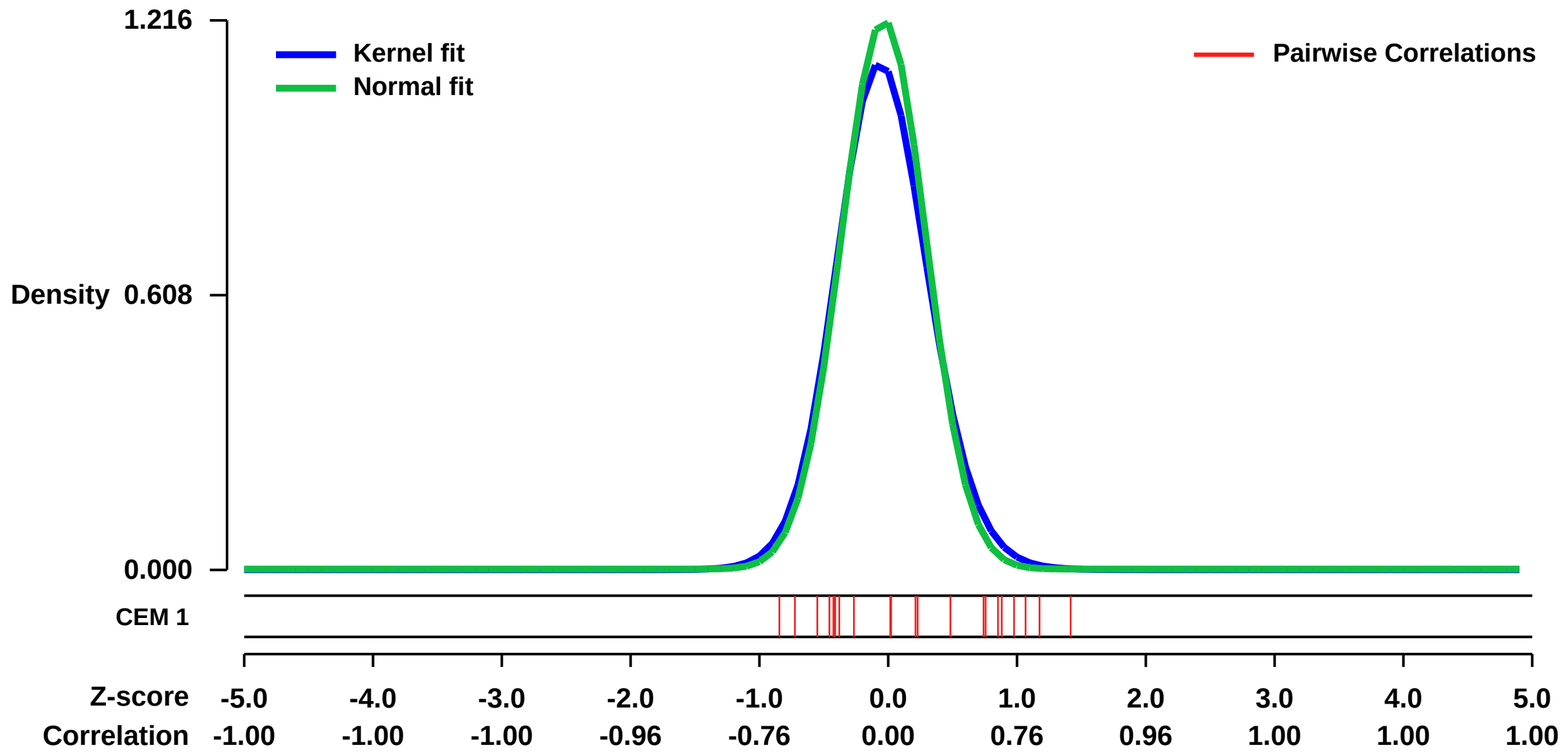

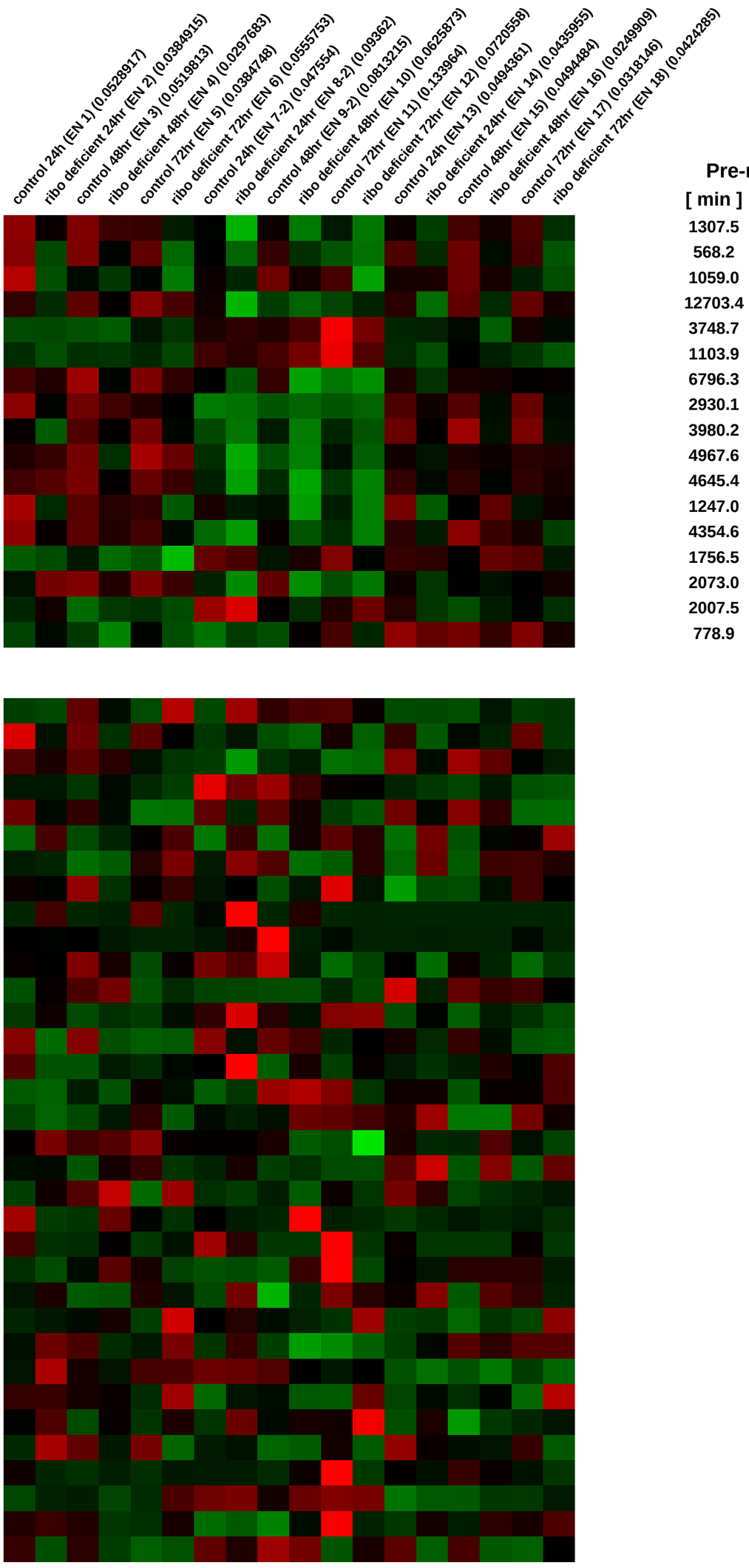

Pre-normalization Quantiles

	[min]	[medium]	[max]
control 24h (EN 1) (0.0528917)	1307.5	3139.8	4380.4
ribo deficient 24hr (EN 2) (0.0384915)	568.2	1328.5	2249.2
control 48hr (EN 3) (0.0519813)	1059.0	2819.0	4512.4
ribo deficient 48hr (EN 4) (0.0297683)	12703.4	19740.8	23838.3
control 72hr (EN 5) (0.0384748)	3748.7	6164.2	13629.3
ribo deficient 72hr (EN 6) (0.0555753)	1103.9	1674.5	4974.4
control 24h (EN 7-2) (0.047554)	6796.3	11206.9	14578.0
ribo deficient 24hr (EN 8-2) (0.09362)	2930.1	5471.7	8383.2
control 48hr (EN 9-2) (0.0813215)	3980.2	7838.7	13000.5
ribo deficient 48hr (EN 10) (0.0625873)	4967.6	11429.5	16614.0
control 72hr (EN 11) (0.133964)	4645.4	13721.5	18249.5
ribo deficient 72hr (EN 12) (0.0720558)	1247.0	2017.7	2846.6
control 24h (EN 13) (0.0494361)	4354.6	5465.2	6341.7
ribo deficient 24hr (EN 14) (0.0435955)	1756.5	3144.9	4093.6
control 48hr (EN 15) (0.0494484)	2073.0	3973.3	5680.0
ribo deficient 48hr (EN 16) (0.0249909)	2007.5	2417.6	3713.4
control 72hr (EN 17) (0.0318146)	778.9	1508.0	2370.3
ribo deficient 72hr (EN 18) (0.0424285)			

GEO Series "GSE31474" Expression Profiles

Num of samples in this series: 6

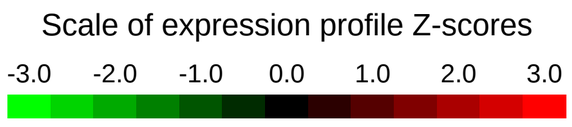

GEO Link:	http://www.ncbi.nlm.nih.gov/geo/query/acc.cgi?acc=GSE31474
Status:	Public on Jan 03 2013
Title:	Host cell gene expression in Influenza A/duck/Malaysia/F189/07/2004 (H5N2) infected A549 cells at 10 hour post infection
Organism:	Homo sapiens
Experiment type:	Expression profiling by array
Platform:	GPL570
Pubmed ID:	22470468
Summary & Design:	**Summary:** We used the microarray data to analyze host cells response on A549 cells infected with A/duck/Malaysia/F189/07/2004(H5N2) **Overall design:** A/duck/Malaysia/F189/07/2004(H5N2) infected A549 cells were harvested at 10 hpi and RNA extraction was performed using standard protocol as described by Affymetrix. The aim of this experiment is to analyze host response to Influenza A/duck/Malaysia/F189/07/2004(H5N2) infection.

Background corr dist: KL-Divergence = 0.0308, L1-Distance = 0.0389, L2-Distance = 0.0017, Normal std = 0.7146

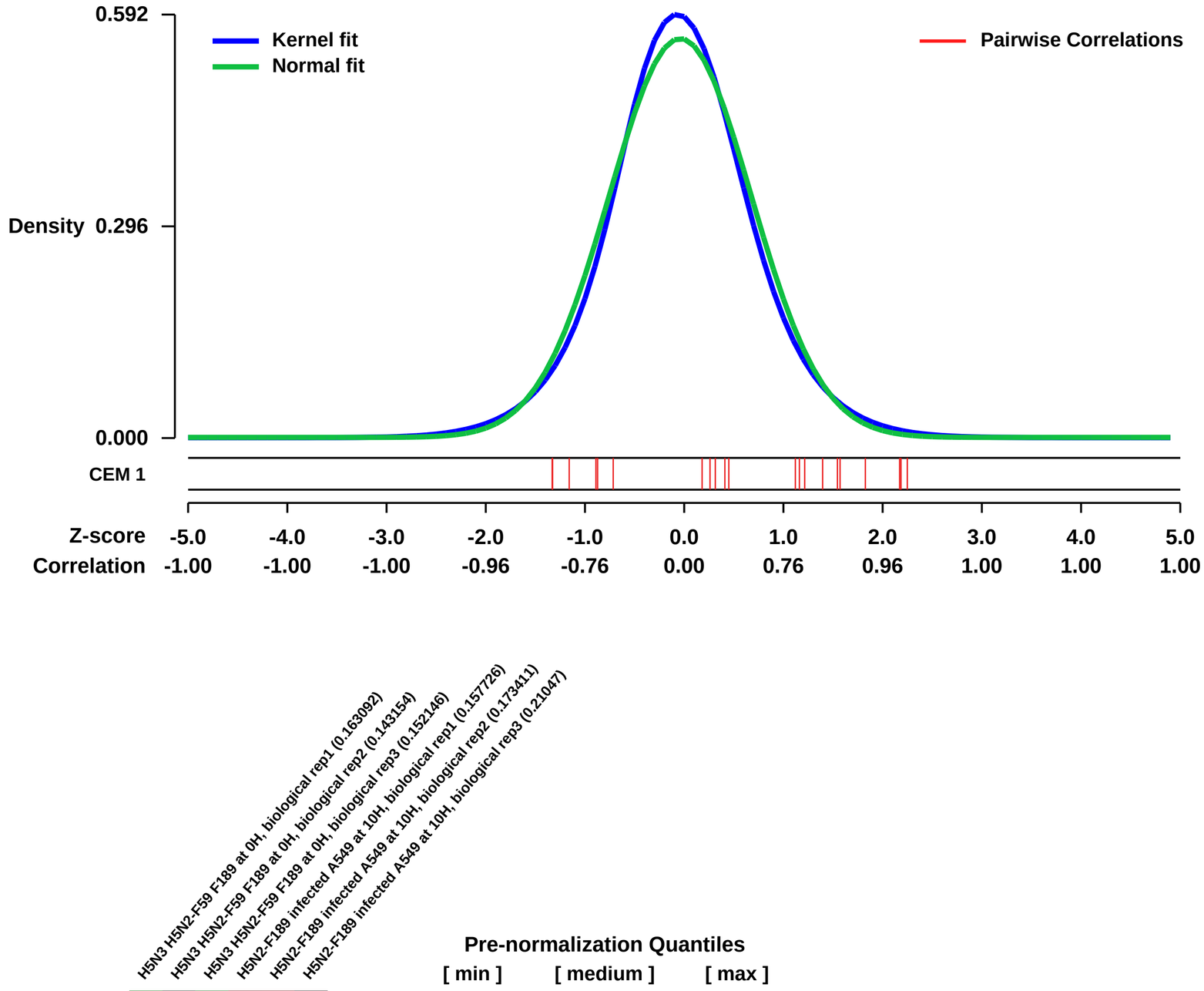

CEM 1		MANF	3473.5	4341.0	4929.3
P (S | Z, I) = 0.90		SDF2L1	1127.0	1510.7	1563.9
Mean Corr = 0.28659		CRELD2	2128.6	2289.9	2546.6
		HSPA5	7723.5	14452.1	15141.0
		HYOU1	657.0	1320.6	1406.1
		PDIA4	1631.5	2257.3	2342.2
		PDIA6	10926.9	11851.4	12467.1
CEM 1 + Top 10 Genes		DNAJB11	2494.4	3011.2	3198.4
		HSP90B1	9174.0	12076.2	12989.0
		PDIA3	8693.5	11704.7	12072.8
		PPIB	23478.9	29449.2	33662.4
		C19orf10	2711.5	3147.3	3558.1
		SLC35B1	2458.5	2886.9	3351.9
		SEC61A1	1682.7	2615.7	2786.3
		RPN1	2668.0	3863.6	4126.9
		DNAJC3	2490.9	3874.7	4146.4
		CDK2AP2	1566.7	2204.9	2432.3
Null module		ARID5B			
		XBP1			
		HNRNPAB			
		SGK1			
		HSPB1			
		DDIT4			
		ARL4D			
		SAP30			
		KIAA0408			
		GPR17			
		HSPH1			
		DNASE1L2			
		SLC5A3			
		GNAS			
		GPR3			
		TNFRSF25			
		TM6SF2			
		MKKS			
		PLEKHF1			
		ZMYM1			
		DOK3			
		FGF20			
		SLC39A2			
		KCNIP2			
		ERRFI1			
		DEDD2			
		CCDC117			
		USP31			
		AHSA2			
		CYS1			
		CNIH2			
		BANP			
		CHORDC1			
		P4HA1			

GEO Series "GSE2435" Expression Profiles

Num of samples in this series: 6

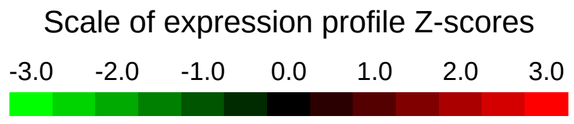

GEO Link:	http://www.ncbi.nlm.nih.gov/geo/query/acc.cgi?acc=GSE2435
Status:	Public on Apr 01 2005
Title:	Autophagy promotes MHC class II presentation of peptides from intracellular source proteins
Organism:	Homo sapiens
Experiment type:	Expression profiling by array
Platform:	GPL570
Pubmed ID:	15894616
Summary & Design:	**Summary:** Assessment of mRNA expression changes in the B-lymphoblastoid cell line Awells after 6 h and 24 h of starvation-induced autophagy **Keywords: ordered** **Overall design:**

Background corr dist: KL-Divergence = 0.0303, L1-Distance = 0.0298, L2-Distance = 0.0012, Normal std = 0.6807

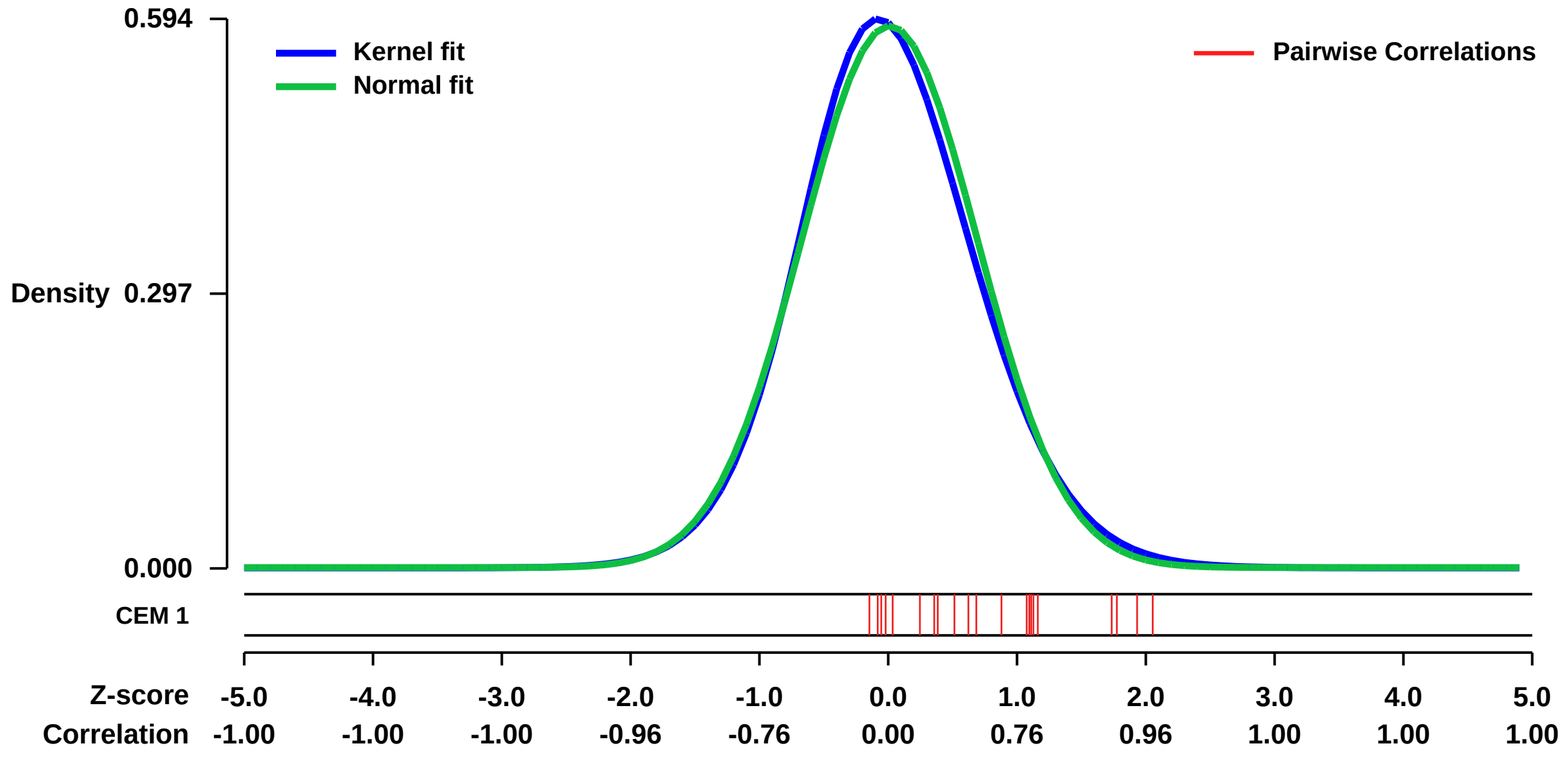

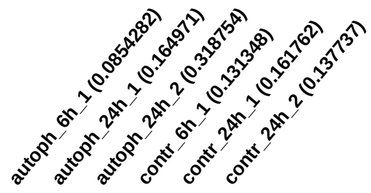

Pre-normalization Quantiles

		[min]	[medium]	[max]
CEM 1	MANF	868.3	3579.2	4417.5
P (S | Z, I) = 0.87	SDF2L1	240.3	1192.1	1712.1
Mean Corr = 0.51656	CRELD2	191.1	1790.9	2967.6
	HSPA5	9392.1	13214.9	18458.0
	HYOU1	4735.2	7255.4	9583.3
	PDIA4	608.5	1013.4	1124.4
	PDIA6	1750.6	6578.9	6706.0
CEM 1 + Top 10 Genes	DNAJB11	2500.5	4117.9	5400.0
	HSP90B1	3106.1	3587.0	5788.1
	PDIA3	3797.2	6519.3	8769.3
	PPIB	4911.2	8720.6	9850.5
	C19orf10	1943.8	2878.8	3290.0
	SLC35B1	1240.5	2300.9	2793.0
	SEC61A1	1905.2	3732.5	4162.2
	RPN1	2347.7	2476.9	2677.4
	DNAJC3	1970.2	2932.2	3399.5
	CDK2AP2	439.9	604.9	955.9
Null module	ARID5B			
	XBP1			
	HNRNPAB			
	SGK1			
	HSPB1			
	DDIT4			
	ARL4D			
	SAP30			
	KIAA0408			
	GPR17			
	HSPH1			
	DNASE1L2			
	SLC5A3			
	GNAS			
	GPR3			
	TNFRSF25			
	TM6SF2			
	MKKS			
	PLEKHF1			
	ZMYM1			
	DOK3			
	FGF20			
	SLC39A2			
	KCNIP2			
	ERRFI1			
	DEDD2			
	CCDC117			
	USP31			
	AHSA2			
	CYS1			
	CNIH2			
	BANP			
	CHORDC1			
	P4HA1			

GEO Series "GSE28603" Expression Profiles

Num of samples in this series: 12

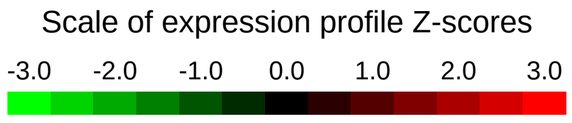

GEO Link:	**http://www.ncbi.nlm.nih.gov/geo/query/acc.cgi?acc=GSE28603**
Status:	**Public on Apr 14 2011**
Title:	**Expression data from human SGBS adipocytes under hypoxic conditions**
Organism:	**Homo sapiens**
Experiment type:	**Expression profiling by array**
Platform:	**GPL570**
Pubmed ID:	
Summary & Design:	**Summary:** **Hypoxia in adipose tissue is suggested to be involved in the development of a chronic mild inflammation, which in obesity can further lead to insulin-resistance. The effect of hypoxia on gene expression in adipocytes seems to play a central role in this inflammatory response observed in obesity. However, the global impact of hypoxia on transcriptional changes in human adipocytes is unclear. Therefore, we compared gene expression profiles of human Simpson-Golabi-Behmel syndrome (SGBS) adipocytes under normoxic or hypoxic conditions to detect hypoxia-responsive genes in adipocytes by using whole human genome microarrays.** **Overall design:** **Human SGBS adipocytes were cultured in a hypoxic environment (1% O2) for 3, 6 and 16 hours and the control group was cultured under normoxic conditions (21% O2). Total RNA was prepared from control and treated SGBS cells, in triplicate experiments, and probes were hybridized on â Human Genome U133 2.0â arrays (Affymetrix).**

Background corr dist: **KL-Divergence = 0.0802, L1-Distance = 0.0223, L2-Distance = 0.0006, Normal std = 0.4743**

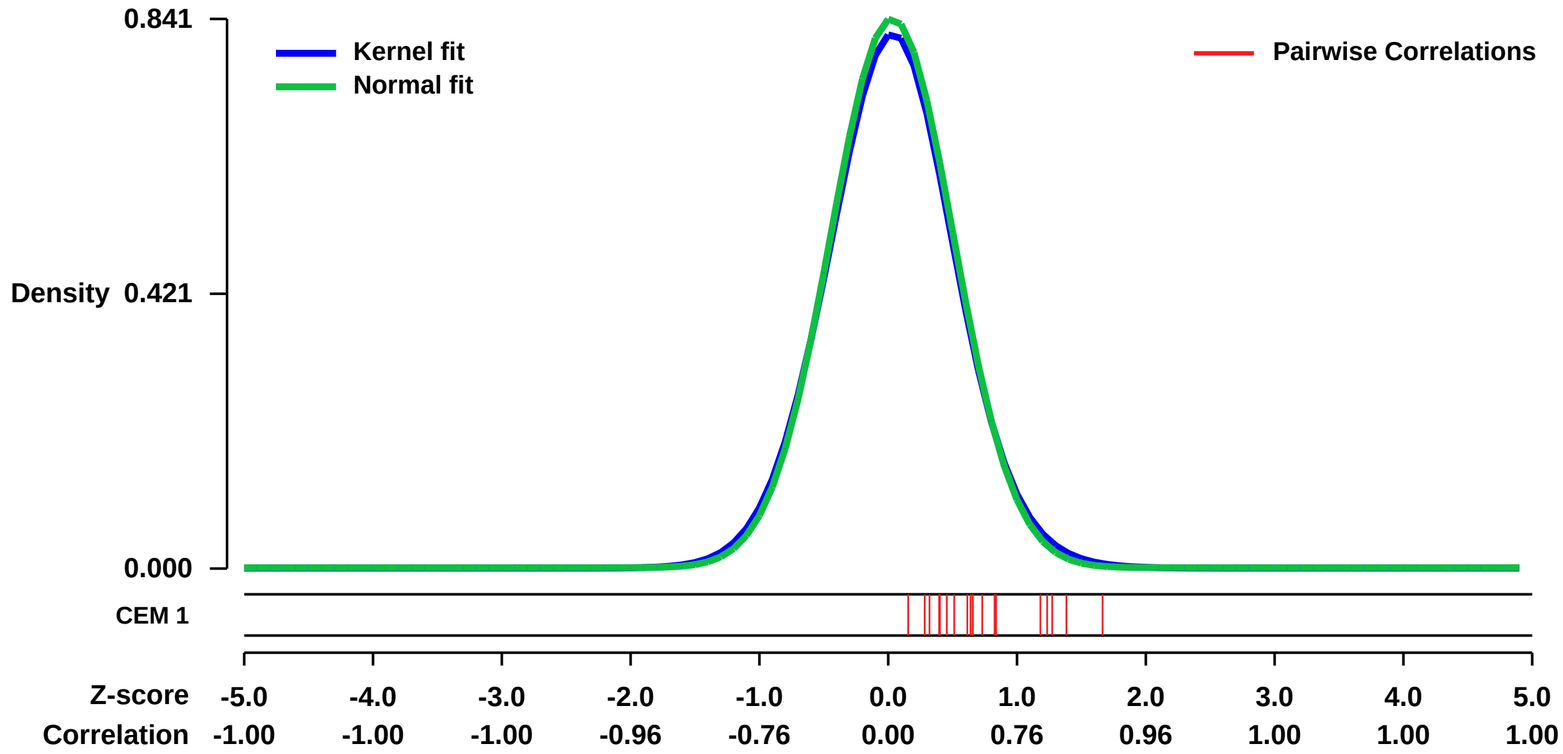

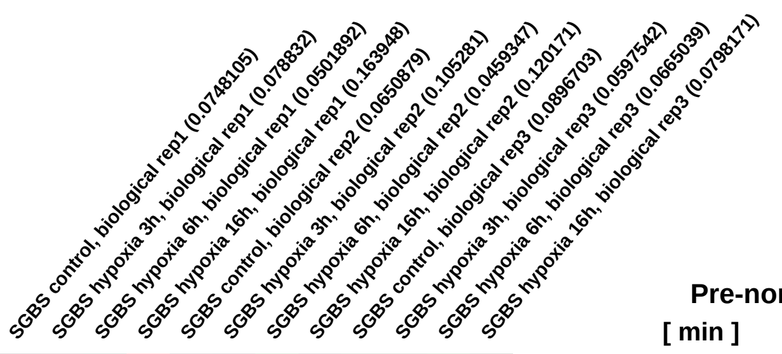

Pre-normalization Quantiles

	[min]	[medium]	[max]
CEM 1			
P (S | Z, I) = 0.86			
Mean Corr = 0.57360			
MANF	**1638.6**	**2268.9**	**3986.0**
SDF2L1	**33.9**	**83.3**	**130.4**
CRELD2	**534.3**	**1026.7**	**1335.8**
HSPA5	**12262.8**	**15025.8**	**33300.3**
HYOU1	**164.6**	**299.5**	**807.1**
PDIA4	**125.9**	**218.4**	**466.7**
PDIA6	**10750.5**	**13571.5**	**16864.7**
CEM 1 + Top 10 Genes			
DNAJB11	**2393.2**	**3224.1**	**3732.3**
HSP90B1	**743.9**	**2662.7**	**4793.1**
PDIA3	**4751.7**	**6106.5**	**11313.7**
PPIB	**17592.8**	**22909.3**	**27585.3**
C19orf10	**1600.2**	**2422.0**	**3613.1**
SLC35B1	**982.2**	**1995.0**	**3716.8**
SEC61A1	**3824.9**	**4822.9**	**8031.9**
RPN1	**4087.8**	**6387.3**	**8733.7**
DNAJC3	**1343.9**	**2970.6**	**3356.5**
CDK2AP2	**179.0**	**431.4**	**864.9**
Null module			
ARID5B			
XBP1			
HNRNPAB			
SGK1			
HSPB1			
DDIT4			
ARL4D			
SAP30			
KIAA0408			
GPR17			
HSPH1			
DNASE1L2			
SLC5A3			
GNAS			
GPR3			
TNFRSF25			
TM6SF2			
MKKS			
PLEKHF1			
ZMYM1			
DOK3			
FGF20			
SLC39A2			
KCNIP2			
ERRFI1			
DEDD2			
CCDC117			
USP31			
AHSA2			
CYS1			
CNIH2			
BANP			
CHORDC1			
P4HA1			

GEO Series "GSE25320" Expression Profiles

Num of samples in this series: 8

Scale of expression profile Z-scores

-3.0 -2.0 -1.0 0.0 1.0 2.0 3.0

GEO Link: http://www.ncbi.nlm.nih.gov/geo/query/acc.cgi?acc=GSE25320

Status: Public on Apr 16 2012

Title: Characterisation of mRNA and microRNA in human mast cell exosomes and their transfer to other mast cells and blood CD34 progenitor cells

Organism: Homo sapiens

Experiment type: Non-coding RNA profiling by array

Platform: GPL570

Pubmed ID:

Summary & Design:

Summary:
Background: Exosomes are nanovesicles of endocytic origin believed to be involved in communication between cells. Recently, it has been shown that mast cell exosomes contain RNA named ""exosomal shuttle RNA"". The aim of this study was to evaluate whether exosomal shuttle RNA could play a role in the communication between human mast cells and between human mast cells and human CD34 positive progenitor cells. Results: Exosomes from the human mast cell line HMC-1 contain RNA. The exosomes contain no or very little ribosomal RNA compared to their donor cells. The mRNA and microRNA content in exosomes and their donor cells was examined using microarray analyses. We found 116 microRNA in the exosomes and 134 microRNA in the cells, from which some were expressed at different level. DNA microarray experiments revealed the presence of approximately 1800 mRNAs in the exosomes, which represent 15% of the donor cell mRNA content. Transfer experiments revealed that exosomes and their RNA can transfer to other HMC-1 cells and to CD34 positive progenitors. Conclusions: To conclude, HMC-1 exosomes contain mRNA and microRNA that can be transferred to other mast cells and to CD34 progenitors. This shuttle of exosomal RNA may represent a powerful mode of communication between cells where cells send genetic information to other cells over a distance via exosomes.

[miRNA profiling] Identification of microRNA was performed by Exiqon (www.exiqon.com). Briefly, the quality of the total RNA was verified by an Agilent 2100 Bioanalyzer. Total RNA from the exosome and the HMC-1 cell samples were labelled with Hy3 and Hy5 fluorescent stain, respectively, using the miRCURY Hy3/Hy5 power labelling kit. The Hy3-labelled exosome samples and a Hy5-labeled mast cells were mixed pair-wise and hybridized to the miRCURY? LNA array (v9.2). The hybridization was performed according to the miRCURY? LNA array manual using a Tecan HS4800 hybridization station (Tecan Systems, Inc. San Jose, CA). The miRCURY? LNA array microarray slides were scanned by a ScanArray 4000 XL scanner (Packard Biochip Technologies, Billerica, MA ,USA) and the image analysis was carried out using the ImaGene 6.1.0 software (BioDiscovery, Inc, El Segundo, CA USA). The quantified signals were normalized using the global Lowess (LOcally WEighted Scatterplot Smoothing) regression algorithm. MicroRNA with signals equal to or below the background signal in 2 or more of the 4 replicate measurements were identified as absent in that slide. The limit for a miRNA to be listed as detectable was set to signal intensities higher than 3 x background (3 x median Hy3 or Hy5 for the total slide). In addition, where signals were detected for <3 of the slides, they were considered unreliable and excluded from sets of detected miRNAs. The experiment was performed in triplicate samples. The signal was calculated as the mean value of the log2MeanRatio Hy3/Hy5 for the triplicates ´– SD.

Overall design:
[miRNA profiling] Exosomes were prepared from the supernatant of HMC-1 cells by differential centrifugations and filtration. RNA was isolated from the exosomes and their parental cells using Trizol followed by RNeasy clean-up. The microarray experiments were performed by Exiqon.

Background corr dist: KL-Divergence = 0.0157, L1-Distance = 0.0499, L2-Distance = 0.0045, Normal std = 0.8719

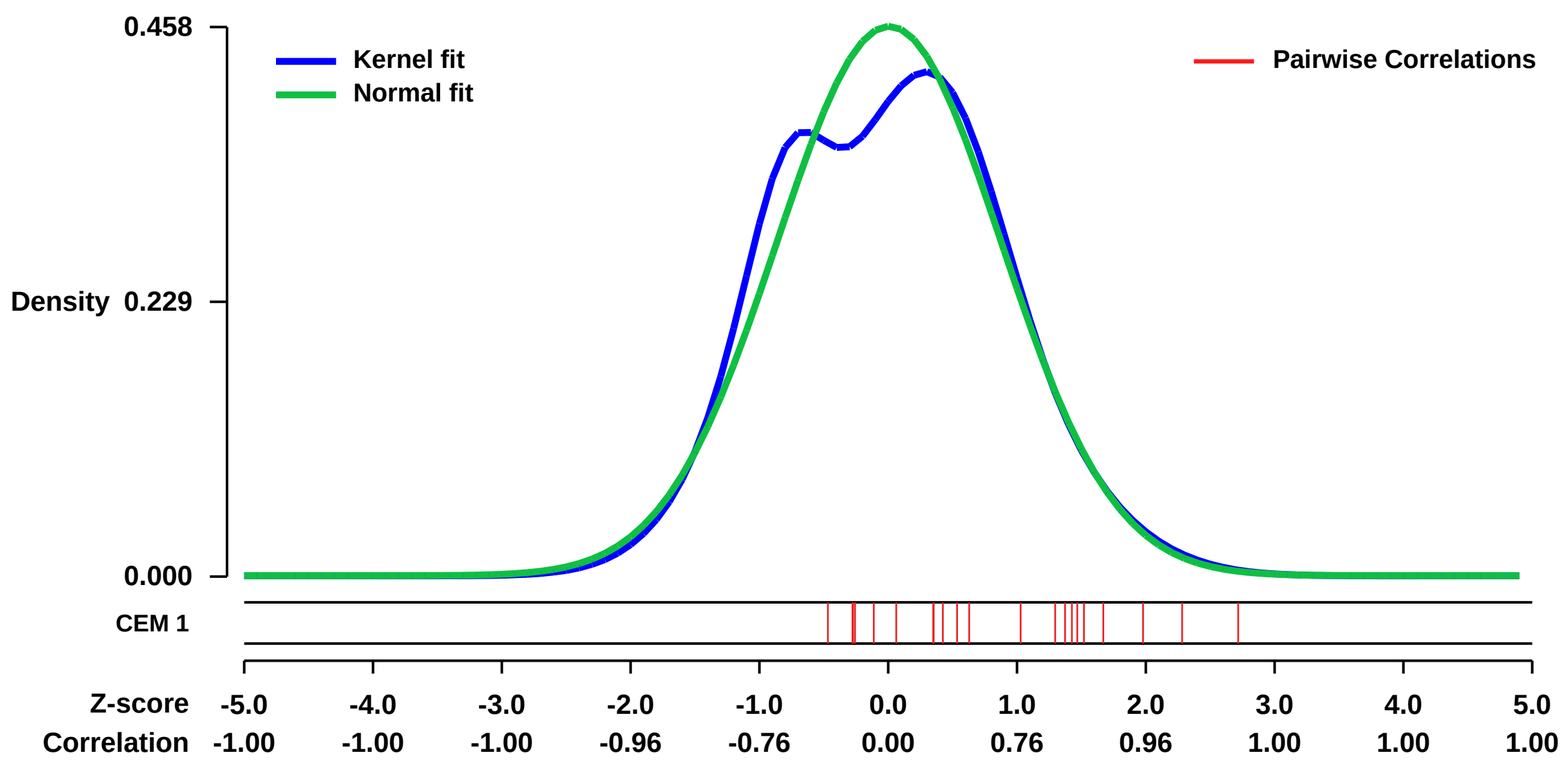

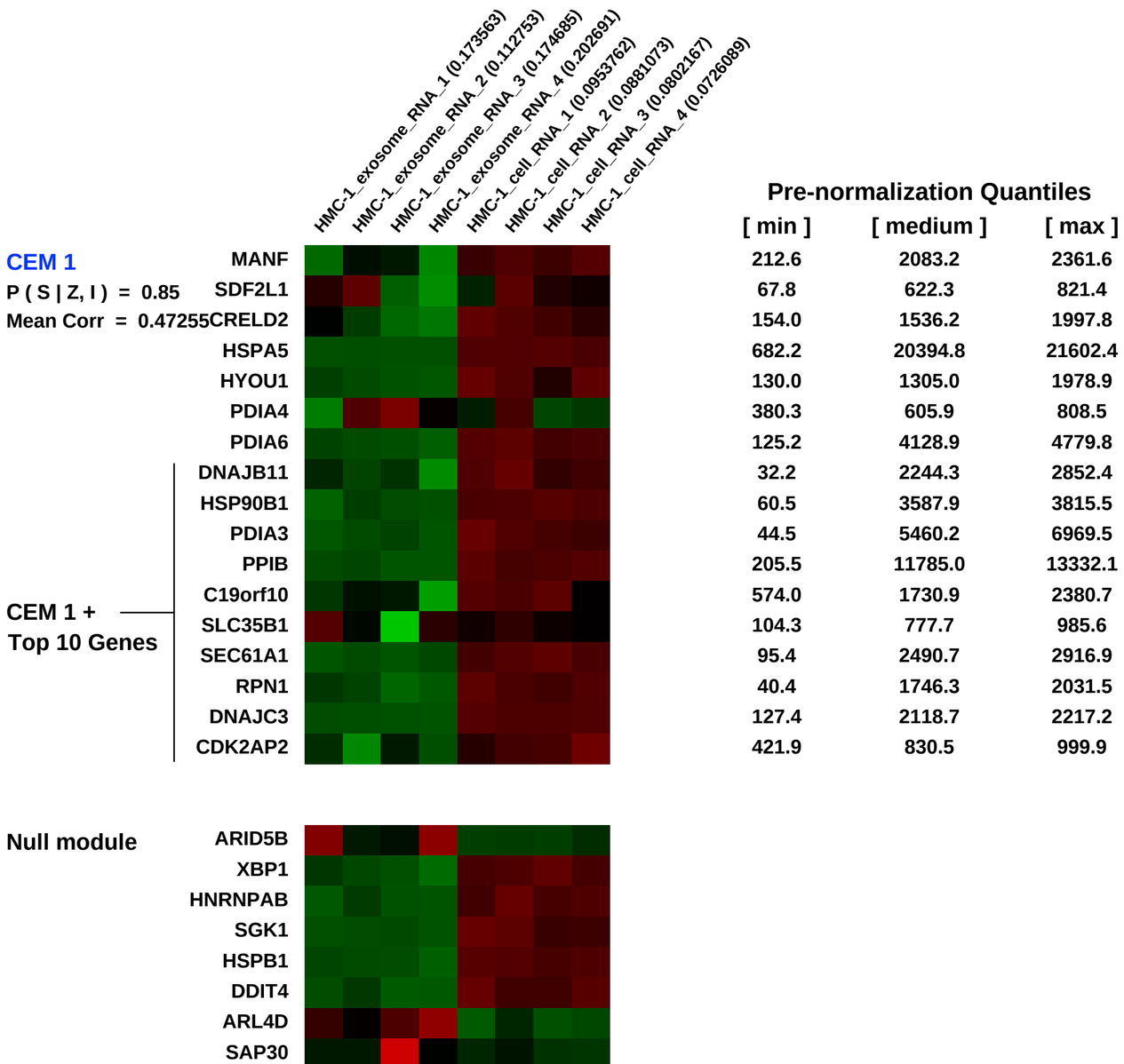

GEO Series "GSE15367" Expression Profiles

Num of samples in this series: 8

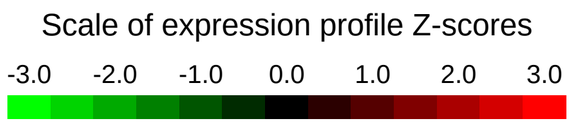

GEO Link:	http://www.ncbi.nlm.nih.gov/geo/query/acc.cgi?acc=GSE15367
Status:	Public on Apr 15 2009
Title:	Expression analysis of Saos-2 p53-null cells
Organism:	Homo sapiens
Experiment type:	Expression profiling by array
Platform:	GPL570
Pubmed ID:	
Summary & Design:	**Summary:** Our compound (PRIMA) selectively kills tumor cells expressing mutant p53. Here in our study we decided to investigate the impact of our compound on the transcriptome of Saos2 cells lacking p53. **Overall design:** We plated Saos-2 cells, and treated them with our compound for 6h or 12h. We then harvested the cells, extracted the RNA, and followed the protocol to run affymetrix array to analyse the impact of our drug on the whole transcriptome of cells lacking p53.

Background corr dist: KL-Divergence = 0.0270, L1-Distance = 0.0363, L2-Distance = 0.0017, Normal std = 0.7026

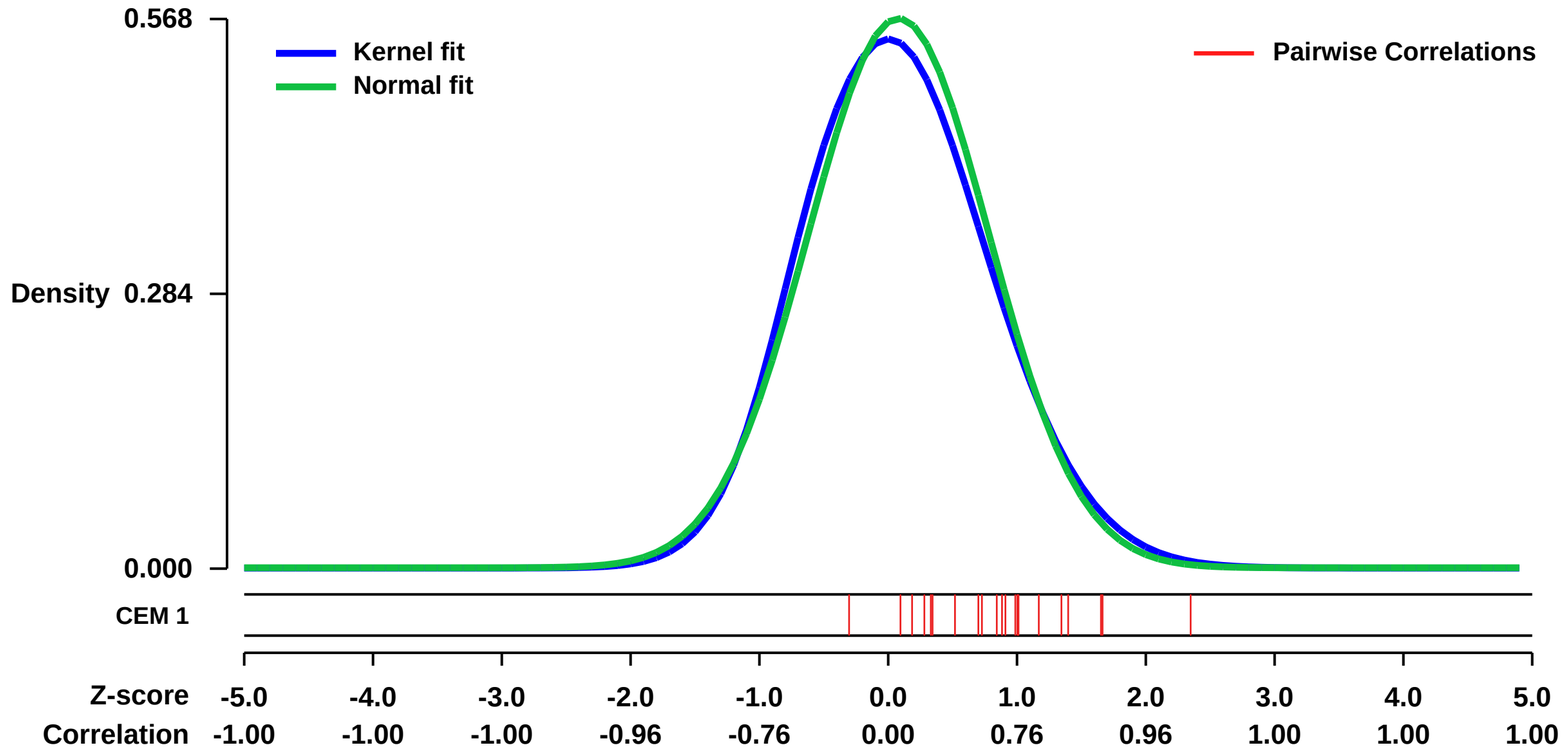

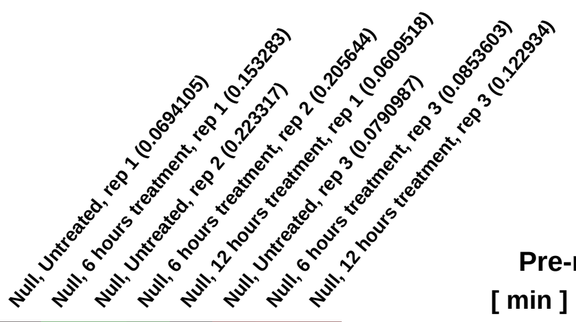

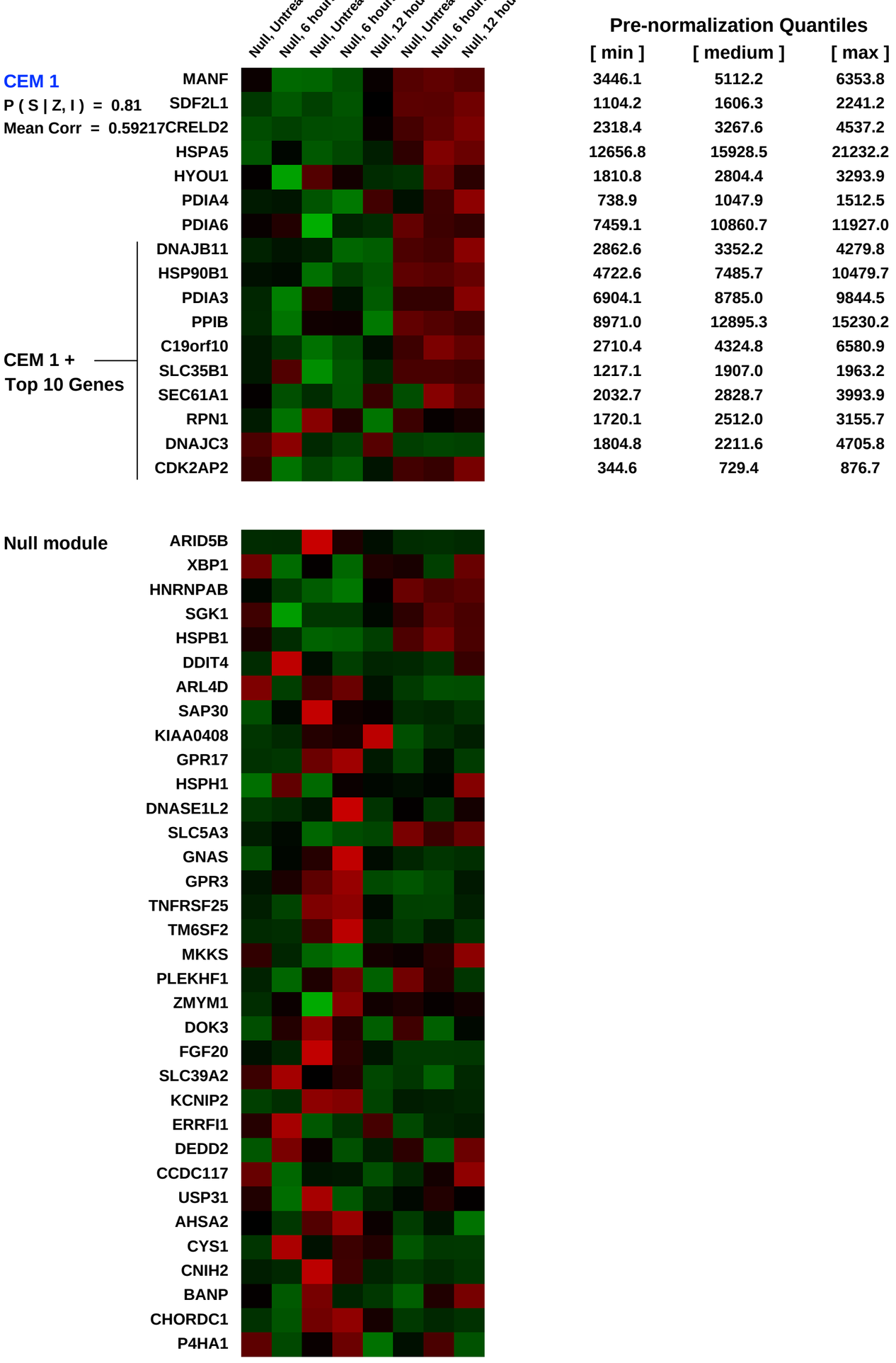

GEO Series "GSE52322" Expression Profiles

Num of samples in this series: 37

Scale of expression profile Z-scores

-3.0 -2.0 -1.0 0.0 1.0 2.0 3.0

GEO Link:	http://www.ncbi.nlm.nih.gov/geo/query/acc.cgi?acc=GSE52322
Status:	Public on Mar 31 2014
Title:	Novel linkages between DCE-MRI and genomic profiling in locally advanced and inflammatory breast cancer
Organism:	Homo sapiens
Experiment type:	Expression profiling by array
Platform:	GPL570
Pubmed ID:	16467094
Summary & Design:	**Summary:** Gene expression signatures have the capacity to identify clinically significant features of breast cancer and can predict which individual patients are likely to be resistant to neoadjuvant therapy, thus providing the opportunity to guide treatment decisions. Data used in publication: Clin Cancer Res. 2006;12:819â 826. 89. Dressman et.al., Gene Expression Profiles of Multiple Breast Cancer Phenotypes and Response to Neoadjuvant Chemotherapy Combining DCE-MRI imaging and genomics have identified putative genomic biomarkers that are associated with risk for pCR following neoadjuvant chemotherapy.´ Furthermore, IBC gene expression profiles were associated with long term overall survival.´ The genomic profiles identified in this pilot study are preliminary but novel, and thus of great interest to validate as biomarkers in independent datasets.´ **Overall design:** 37 breast tissue samples were collected under ultrasound guidance from patients with stage IIB/III breast cancer before four cycles of neoadjuvant liposomal doxorubicinpaclitaxel chemotherapy combined with local whole breast hyperthermia. Gene expression analysis was done using Affymetrix U133 Plus 2.0 GeneChip arrays.

Background corr dist: KL-Divergence = 0.0977, L1-Distance = 0.0989, L2-Distance = 0.0212, Normal std = 0.4862

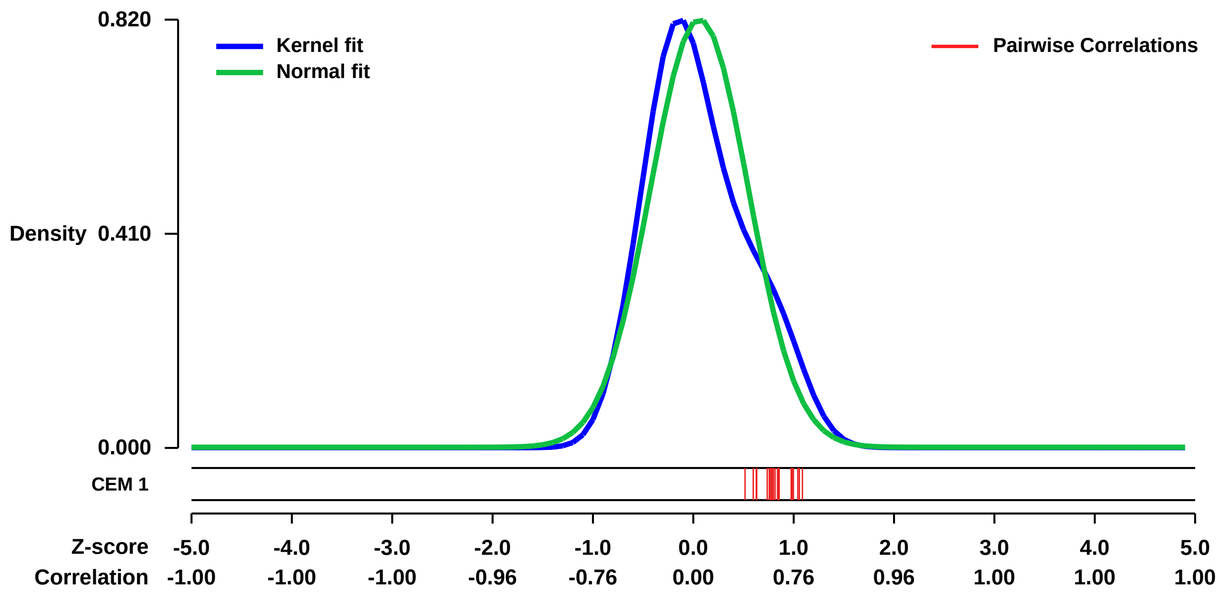

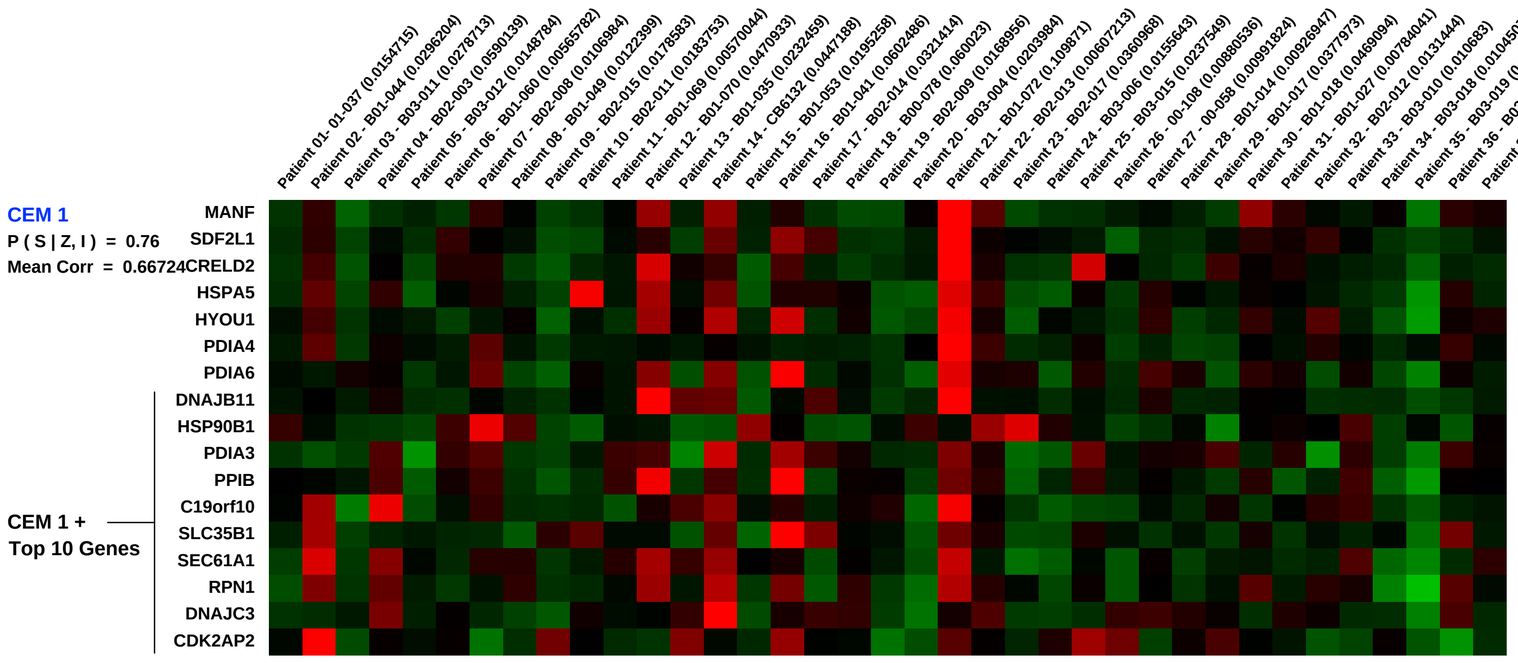

Pre-normalization Quantiles

[min]	[medium]	[max]
1689.9	2671.1	6535.0
464.1	1036.1	4046.1
1217.4	2099.9	6144.3
726.0	5364.2	14279.9
704.9	3580.2	8838.9
868.2	1326.4	5593.3
686.8	3214.8	8771.5
746.7	1237.2	3759.3
753.7	1339.2	2580.7
2577.8	7006.2	12541.1
1808.2	7044.4	16679.1
899.1	1561.3	3155.7
708.3	1313.2	3420.3
1203.4	2573.3	5544.1
770.1	2388.5	4211.2
117.7	940.4	3706.2
751.1	1252.4	2187.1

GEO Series "GSE42660" Expression Profiles

Num of samples in this series: 22

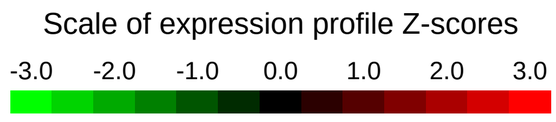

GEO Link:	http://www.ncbi.nlm.nih.gov/geo/query/acc.cgi?acc=GSE42660
Status:	Public on Feb 01 2013
Title:	BL2 cells stimulated with B cell specific paracrine stimuli
Organism:	Homo sapiens
Experiment type:	Expression profiling by array
Platform:	GPL570
Pubmed ID:	23253402
Summary & Design:	**Summary:** Expression data of BL2 Burkitt Lymphoma cell line (controls and samples treated with different B cell specific stimuli) **Overall design:** BL2 cells were cultured in RPMI and stimulated with the respective agents (rhCD40L, rhIL21, rhBAFF, LPS and antiIgM F(ab) fragments) for indicated timepoints. Cells were harvested and total RNA was isolated for gene expression profiling. The experiments were conducted in 2-3 biological replicates.

Background corr dist: KL-Divergence = 0.1872, L1-Distance = 0.0499, L2-Distance = 0.0059, Normal std = 0.3407

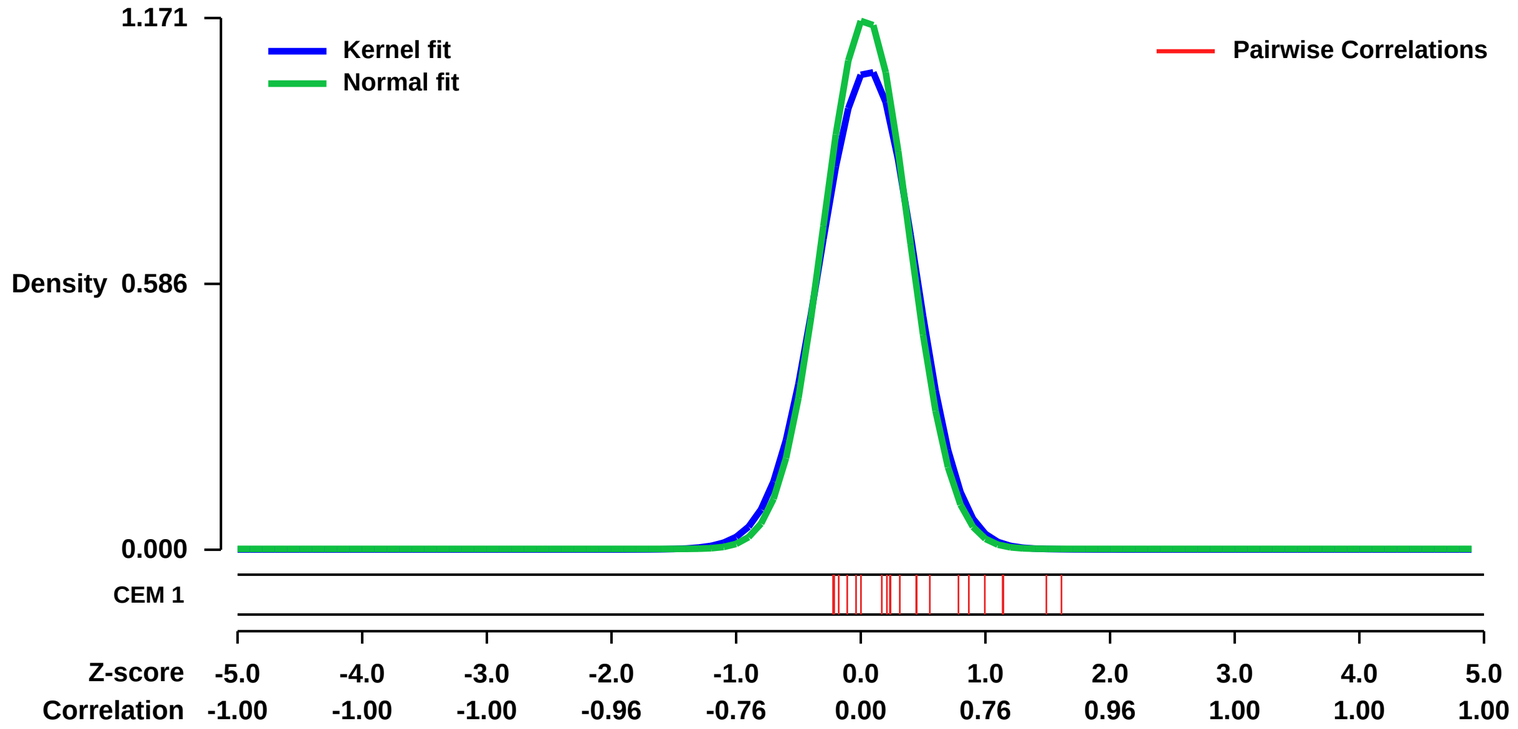

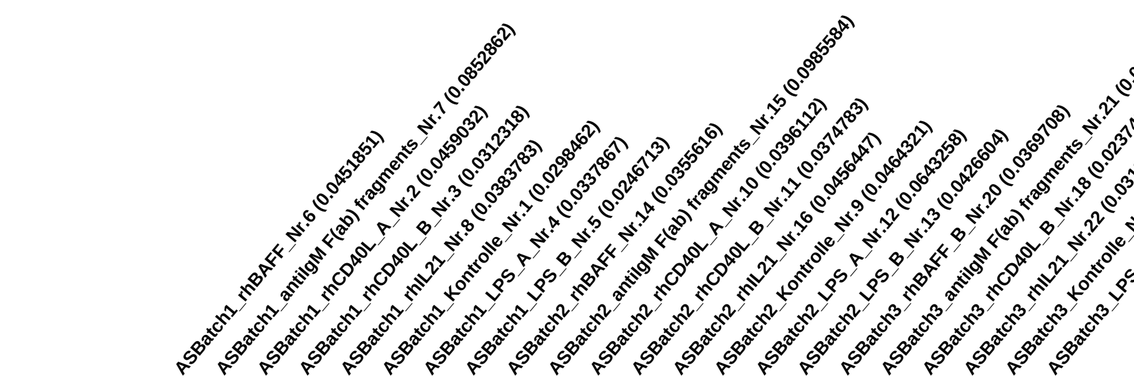

CEM 1
P (S | Z, I) = 0.76
Mean Corr = 0.34778

CEM 1 + Top 10 Genes

Null module

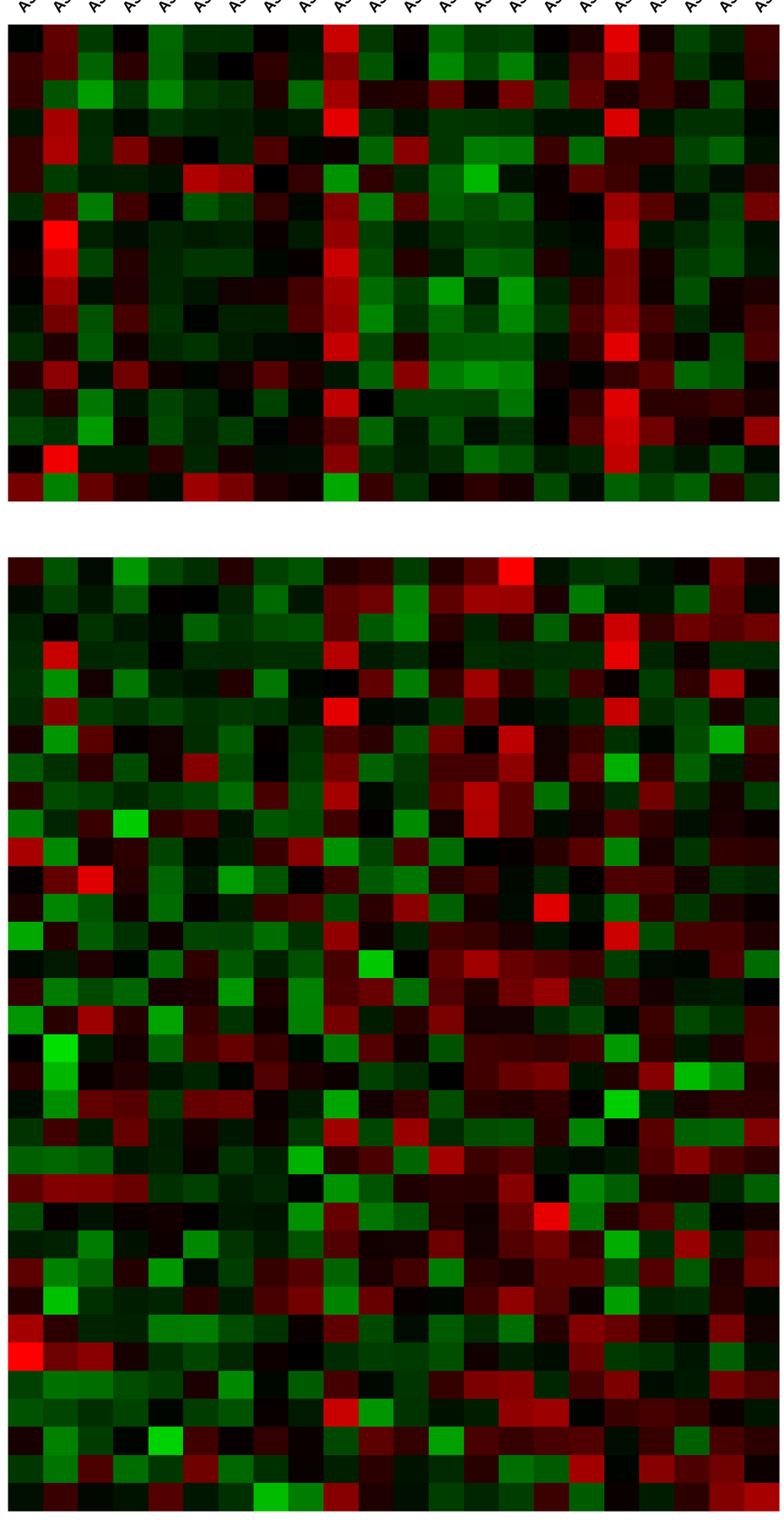

Pre-normalization Quantiles

[min]	[medium]	[max]
1664.0	2417.3	4132.7
874.4	1170.4	1571.7
1522.0	1737.7	1897.1
7363.4	9937.7	29308.2
915.3	1170.2	1526.1
985.8	1122.6	1272.7
4550.7	5949.8	7742.6
1686.5	2146.4	4617.6
1662.2	2326.0	4059.3
5083.5	6355.5	7438.8
6487.6	7844.6	9905.5
1461.4	1653.1	2221.3
1028.4	1263.3	1440.2
1837.8	2090.6	2582.8
2032.8	2435.5	2989.2
646.8	776.0	1191.4
818.6	1075.4	1277.3

GEO Series "GSE42853" Expression Profiles

Num of samples in this series: 9

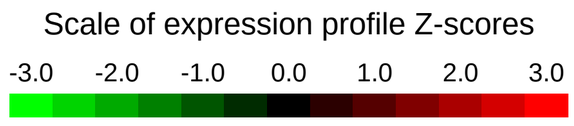

GEO Link:	http://www.ncbi.nlm.nih.gov/geo/query/acc.cgi?acc=GSE42853
Status:	Public on Dec 13 2012
Title:	Distinct gene expression profiles associated with the susceptibility of pathogen-specific CD4 T cells to HIV-1 infection
Organism:	Homo sapiens
Experiment type:	Expression profiling by array
Platform:	GPL570
Pubmed ID:	23258923
Summary & Design:	**Summary:** Analysis of global gene expression profiles of flow cytometry-sorted, different pathogen-specific CD4+ T cell populations from the same peripheral blood mononuclear cells (PBMC), to identify molecular parameters that regulate differential susceptibilities of these CD4+ T cells to HIV infection. The results reveal distinct gene expression profiles between CMV-specific and tetanus toxoid/Candida-specific CD4+ T cells that involved selective upregulation of comprehensive innate antiviral **Overall design:** Total RNA extracted from CFSE-low, flow-sorted pathogen-specific CD4+ T cells were analyzed for global gene expression. Changes in gene expression were compared between CMV to combined TT/Candida, or TT/CMV and Candida/CMV.

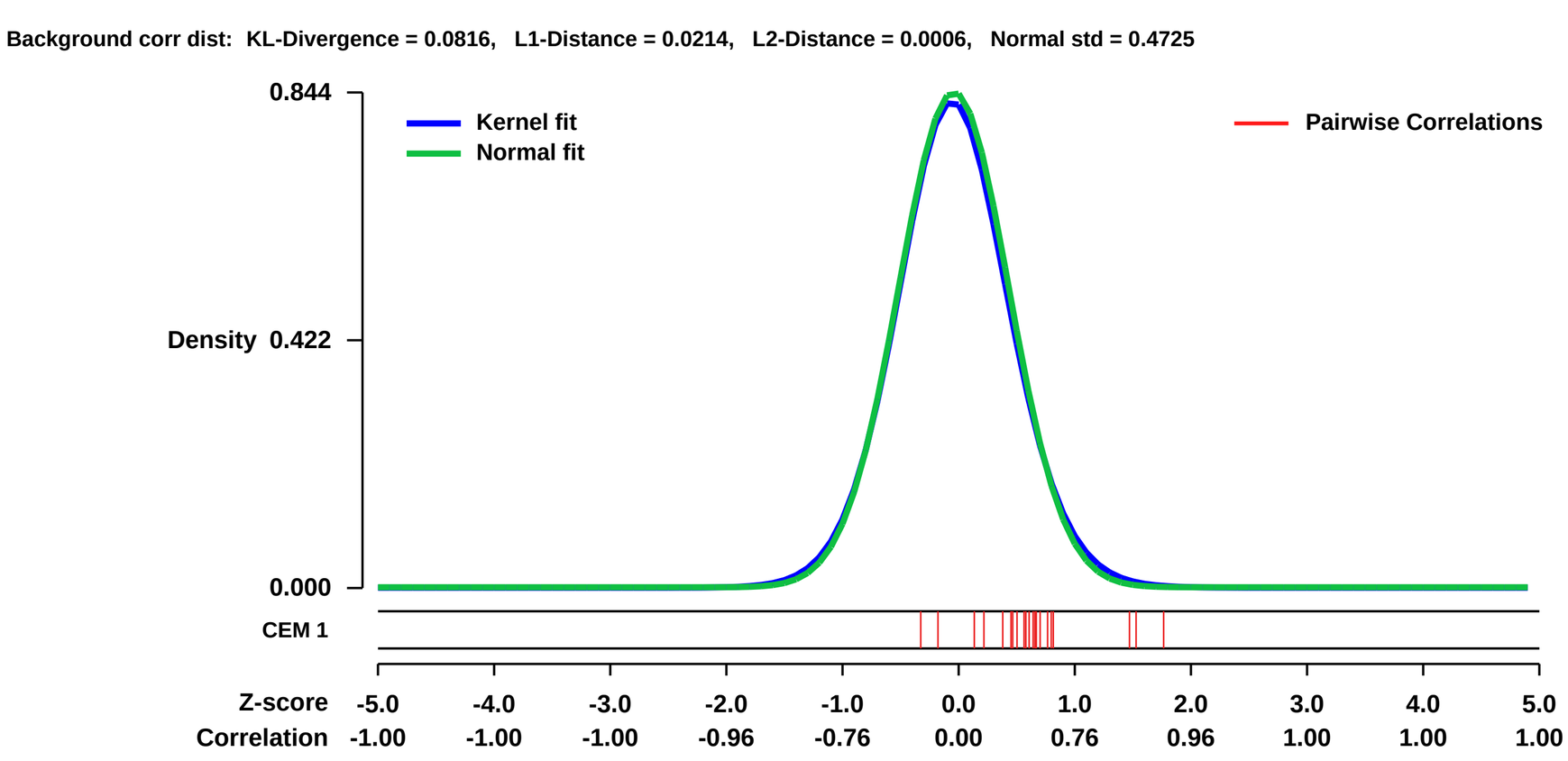

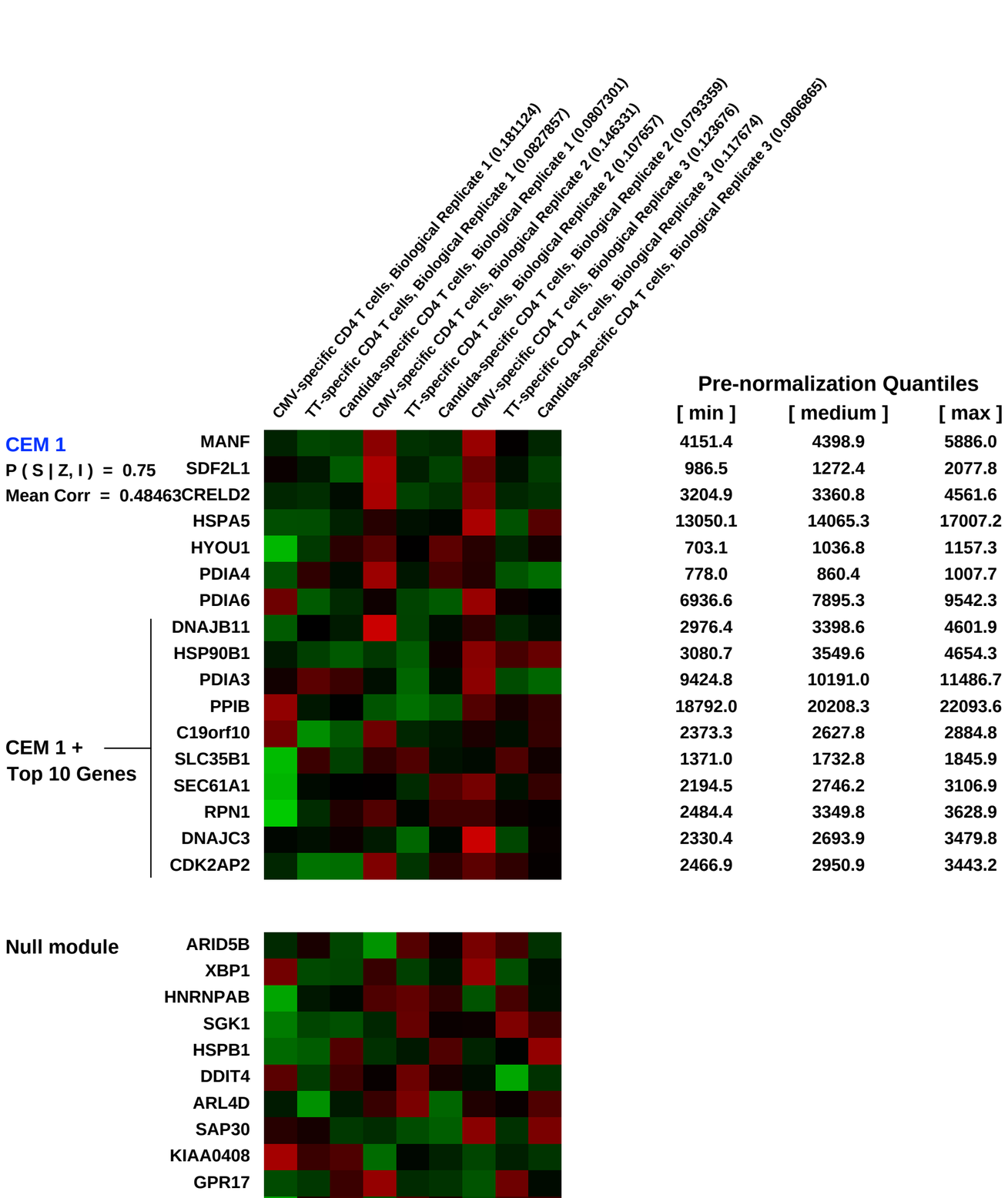

Pre-normalization Quantiles

	[min]	[medium]	[max]
MANF	4151.4	4398.9	5886.0
SDF2L1	986.5	1272.4	2077.8
CRELD2	3204.9	3360.8	4561.6
HSPA5	13050.1	14065.3	17007.2
HYOU1	703.1	1036.8	1157.3
PDIA4	778.0	860.4	1007.7
PDIA6	6936.6	7895.3	9542.3
DNAJB11	2976.4	3398.6	4601.9
HSP90B1	3080.7	3549.6	4654.3
PDIA3	9424.8	10191.0	11486.7
PPIB	18792.0	20208.3	22093.6
C19orf10	2373.3	2627.8	2884.8
SLC35B1	1371.0	1732.8	1845.9
SEC61A1	2194.5	2746.2	3106.9
RPN1	2484.4	3349.8	3628.9
DNAJC3	2330.4	2693.9	3479.8
CDK2AP2	2466.9	2950.9	3443.2

GEO Series "GSE56102" Expression Profiles

Num of samples in this series: 6

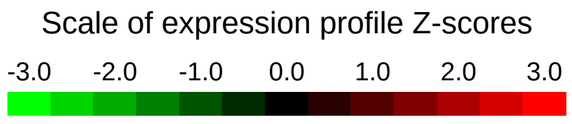

GEO Link:	http://www.ncbi.nlm.nih.gov/geo/query/acc.cgi?acc=GSE56102
Status:	Public on Jun 01 2014
Title:	siRNA-mediated knockdown of VAMP7 in NTERA2/D1 cells
Organism:	Homo sapiens
Experiment type:	Expression profiling by array
Platform:	GPL570
Pubmed ID:	
Summary & Design:	**Summary:** To unravel the function of VAMP7 in the male sexual differentiation, we carried out in vitro studies of VAMP7 knockdown using siRNA, in the human embryonal carcinoma NTERA2/D1 cells. **Overall design:** We knocked down VAMP7 expression in the testicular teratocarcinoma cell line, NTERA2/D1. By comparing the knockdown conditions with the control scrambled samples, we are able to dissect the cellular pathways affected by alteration of VAMP7 gene expression.

Background corr dist: KL-Divergence = 0.0461, L1-Distance = 0.0195, L2-Distance = 0.0004, Normal std = 0.5880

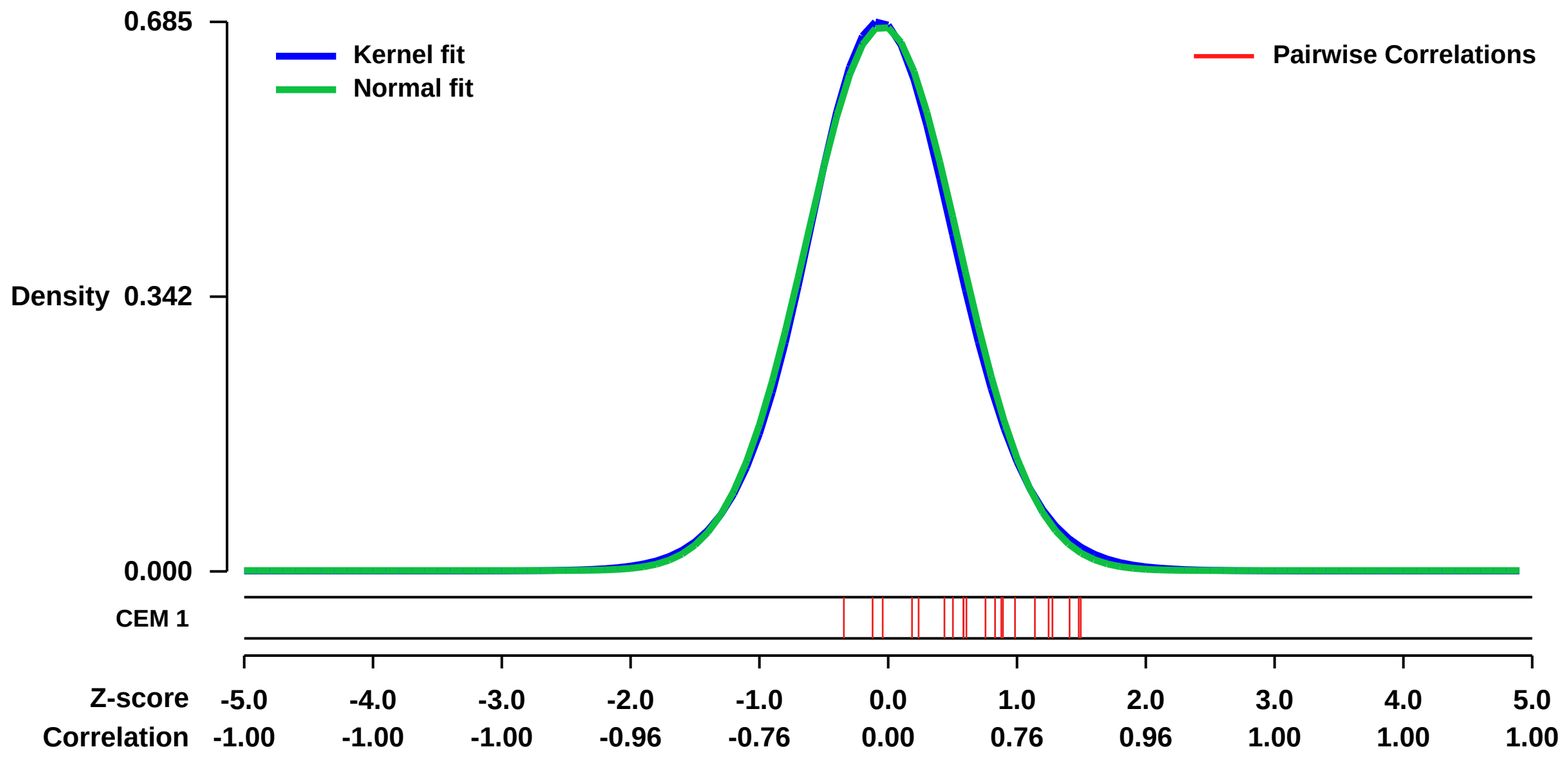

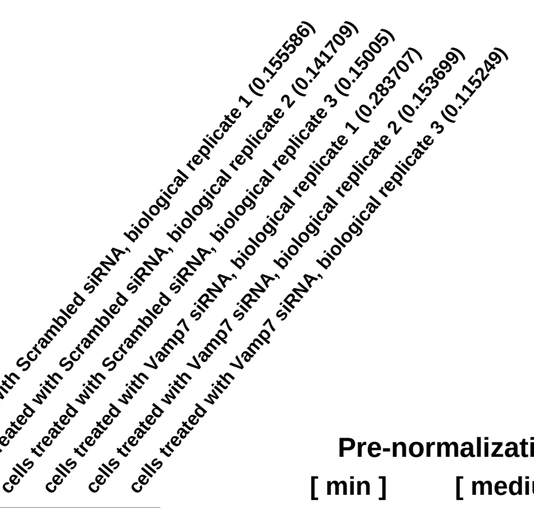

Pre-normalization Quantiles

		[min]	[medium]	[max]
CEM 1	MANF	4378.6	5139.1	5956.7
P (S | Z, I) = 0.72	SDF2L1	583.4	668.0	850.2
Mean Corr = 0.52804	CRELD2	1337.9	1560.3	1898.7
	HSPA5	19549.9	22975.6	25558.2
	HYOU1	4480.8	4895.2	5148.2
	PDIA4	2567.8	2721.3	2817.5
	PDIA6	11516.8	13054.0	13677.2
CEM 1 + Top 10 Genes	DNAJB11	5015.1	5756.6	6358.9
	HSP90B1	4491.9	6249.9	6640.0
	PDIA3	11255.7	12543.3	13657.8
	PPIB	15816.4	17272.6	21990.0
	C19orf10	1903.1	2000.9	2071.1
	SLC35B1	1352.1	1500.3	1679.0
	SEC61A1	2099.3	2169.0	2724.9
	RPN1	3423.1	3932.1	4064.4
	DNAJC3	1891.2	1960.0	2147.1
	CDK2AP2	1478.1	1638.1	1676.6
Null module	ARID5B			
	XBP1			
	HNRNPAB			
	SGK1			
	HSPB1			
	DDIT4			
	ARL4D			
	SAP30			
	KIAA0408			
	GPR17			
	HSPH1			
	DNASE1L2			
	SLC5A3			
	GNAS			
	GPR3			
	TNFRSF25			
	TM6SF2			
	MKKS			
	PLEKHF1			
	ZMYM1			
	DOK3			
	FGF20			
	SLC39A2			
	KCNIP2			
	ERRFI1			
	DEDD2			
	CCDC117			
	USP31			
	AHSA2			
	CYS1			
	CNIH2			
	BANP			
	CHORDC1			
	P4HA1			

GEO Series "GSE5716" Expression Profiles

Num of samples in this series: 40

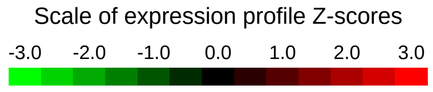

GEO Link:	http://www.ncbi.nlm.nih.gov/geo/query/acc.cgi?acc=GSE5716
Status:	Public on Aug 20 2008
Title:	Gene expression analysis of T-ALL cell lines treated with gamma-secretase inhibitor
Organism:	Homo sapiens
Experiment type:	Expression profiling by array
Platform:	GPL570
Pubmed ID:	17873882
Summary & Design:	**Summary:** Gain-of-function mutations in NOTCH1 are common in T-cell lymphoblastic leukemias making this receptor a promising target for drugs such as gamma-secretase inhibitors (GSI), which block a proteolytic cleavage required for NOTCH1 activation. However, the enthusiasm for these therapies has been tempered by tumor resistance and the paucity of information on the oncogenic programs regulated by oncogenic NOTCH1. Analysis of gene expression in GSI-responsive and GSI-resistant cell lines treated with Compound E identifies differential resopnses to GSI. **Keywords: Drug response** **Overall design:** Samples for microarray analysis were prepared and hybridized in Affymetrix Human U133 Plus 2.0 arrays according to the manufacturerâ s instructions and as previously described. RNA was extracted from duplicate cultures of GSI-sensitive (ALL-SIL, CUTLL1, DND41, HPB-ALL, KOPTK1) and GSI-resistant (CCRF-CEM, MOLT3, P12 ICHIKAWA, PF382 and RPMI8402) T-ALL cell lines treated for 24 h with vehicle (DMSO) or 500 nM CompE. Interarray intensity differences were normalized with Dchip.

Background corr dist: KL-Divergence = 0.1779, L1-Distance = 0.0384, L2-Distance = 0.0029, Normal std = 0.3463

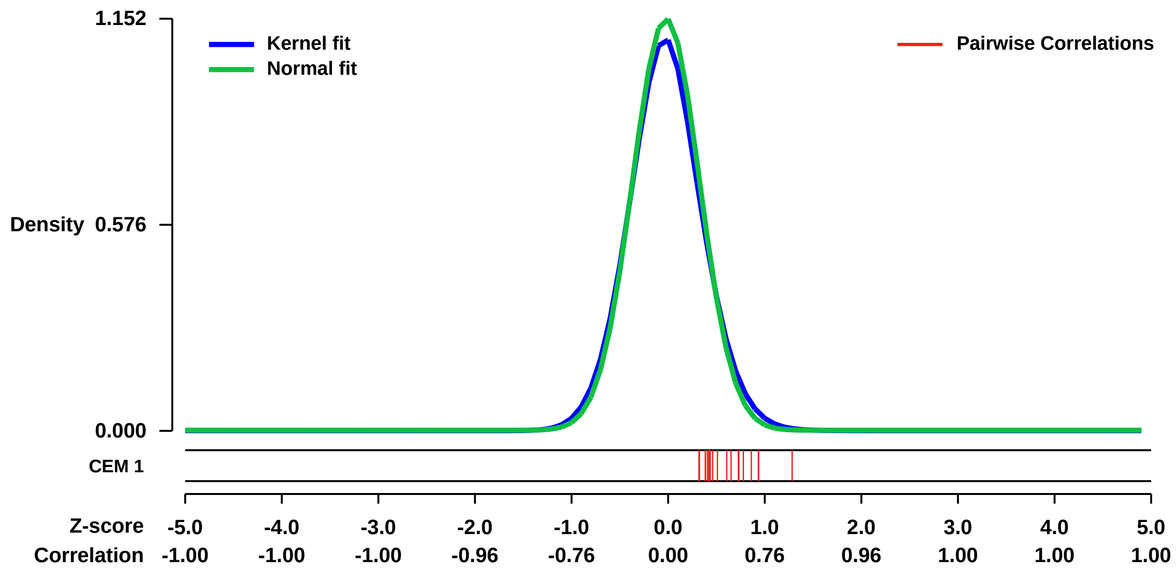

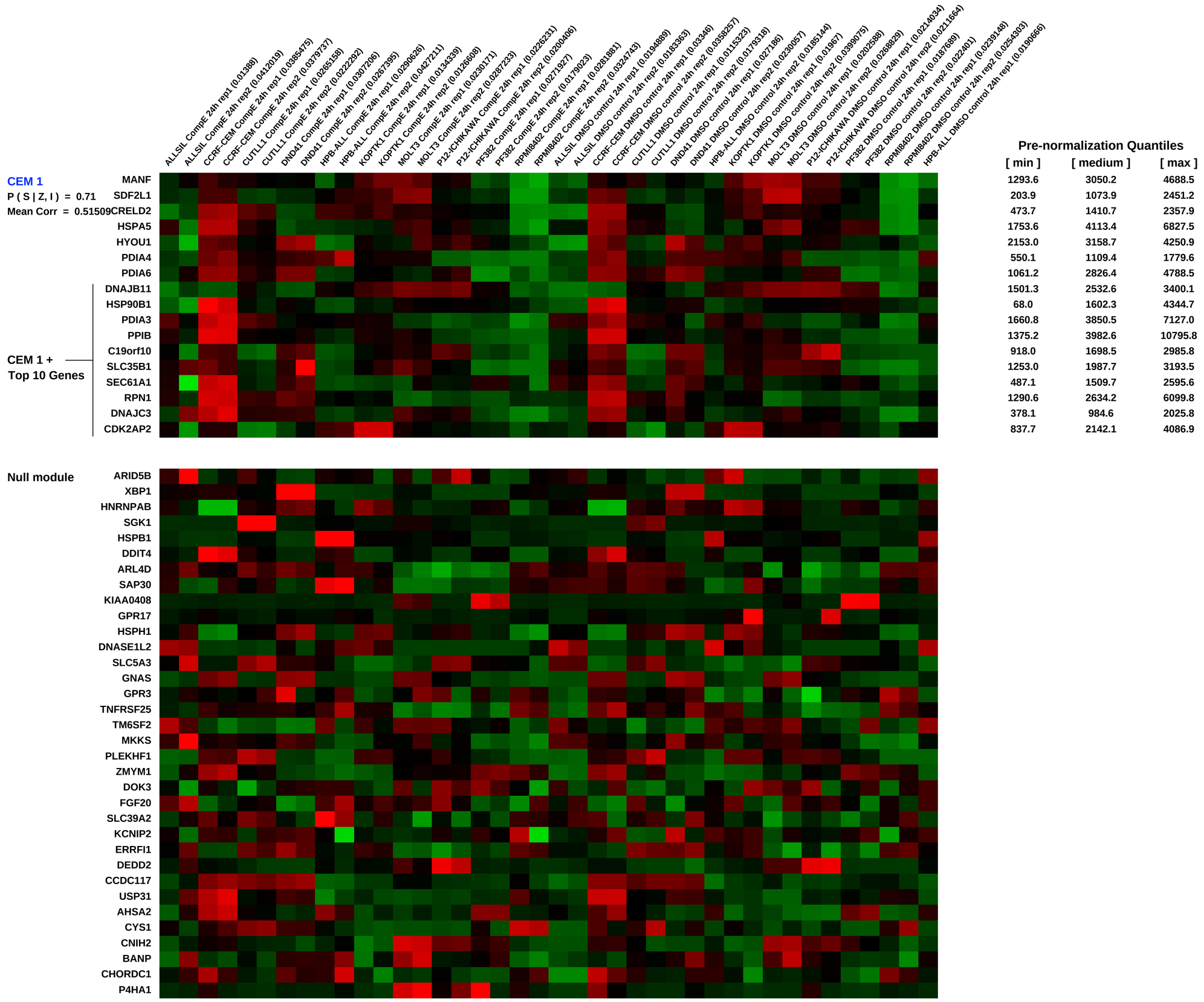

Pre-normalization Quantiles

	[min]	[medium]	[max]
MANF	1293.6	3050.2	4688.5
SDF2L1	203.9	1073.9	2451.2
CRELD2	473.7	1410.7	2357.9
HSPA5	1753.6	4113.4	6827.5
HYOU1	2153.0	3158.7	4250.9
PDIA4	550.1	1109.4	1779.6
PDIA6	1061.2	2826.4	4788.5
DNAJB11	1501.3	2532.6	3400.1
HSP90B1	68.0	1602.3	4344.7
PDIA3	1660.8	3850.5	7127.0
PPIB	1375.2	3982.6	10795.8
C19orf10	918.0	1698.5	2985.8
SLC35B1	1253.0	1987.7	3193.5
SEC61A1	487.1	1509.7	2595.6
RPN1	1290.6	2634.2	6099.8
DNAJC3	378.1	984.6	2025.8
CDK2AP2	837.7	2142.1	4086.9

GEO Series "GSE5809" Expression Profiles

Num of samples in this series: 14

Scale of expression profile Z-scores

-3.0 -2.0 -1.0 0.0 1.0 2.0 3.0

GEO Link: http://www.ncbi.nlm.nih.gov/geo/query/acc.cgi?acc=GSE5809
Status: Public on Sep 18 2006
Title: Decidual stromal cell response to paracrine signals from the trophoblast
Organism: Homo sapiens
Experiment type: Expression profiling by array
Platform: GPL570
Pubmed ID: 17021345

Summary & Design:

Summary:
During the invasive phase of implantation, trophoblasts and maternal decidual stromal cells secrete products that regulate trophoblast differentiation and migration into the maternal endometrium. Paracrine interactions between the extravillous trophoblast and the maternal decidua are important for successful embryonic implantation, including establishing the placental vasculature, anchoring the placenta to the uterine wall, and promoting immuno-acceptance of the fetal allograph. Global cross-talk between the trophoblast and the decidua has not been elucidated to date, and the current study used a functional genomics approach to investigate these paracrine interactions.

Our data demonstrate a significant induction of pro-inflammatory cytokines and chemokines, as well as angiogenic/static factors in decidualized endometrial stromal cells in response to trophoblast-secreted products. The data suggest that the trophoblast acts to alter the local immune environment of the decidua to facilitate the process of implantation and assure an enriched cytokine/chemokine environment, while limiting mitotic activity of the stromal cells during the invasive phase of implantation.

Keywords: Gene expression arrays in human stromal cells

Overall design:
Human endometrial stromal cells were decidualized with progesterone and were further treated with conditioned media (CM) from human trophoblasts (TCM) or, as a control, with conditioned media (CCM) from non-decidualized stromal cells for 0, 3 and 12 hr. Total RNA was isolated and processed for analysis on whole genome, high density oligonucleotide arrays, containing 54,600 genes.

Background corr dist: KL-Divergence = 0.1133, L1-Distance = 0.0460, L2-Distance = 0.0048, Normal std = 0.4271

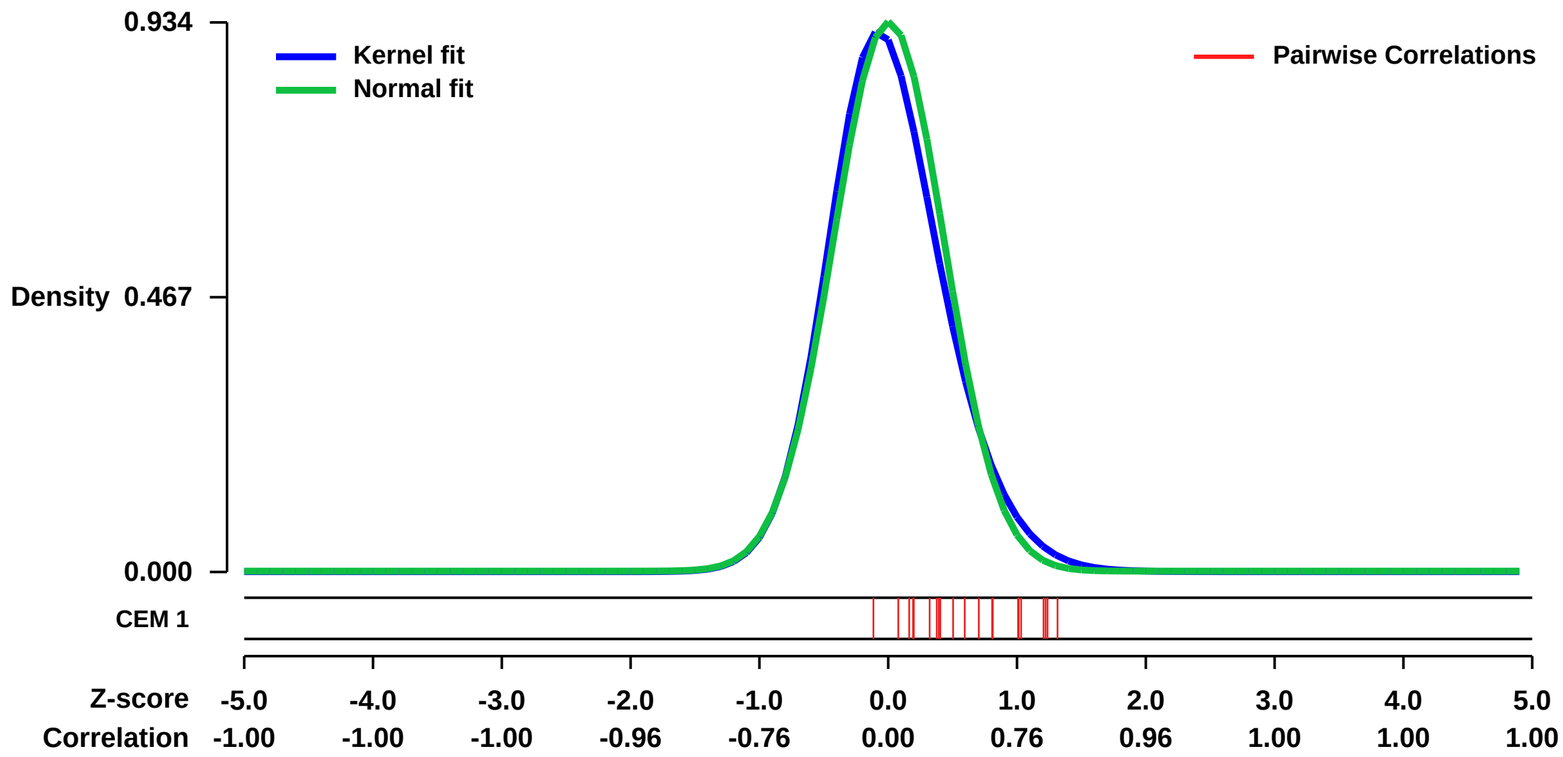

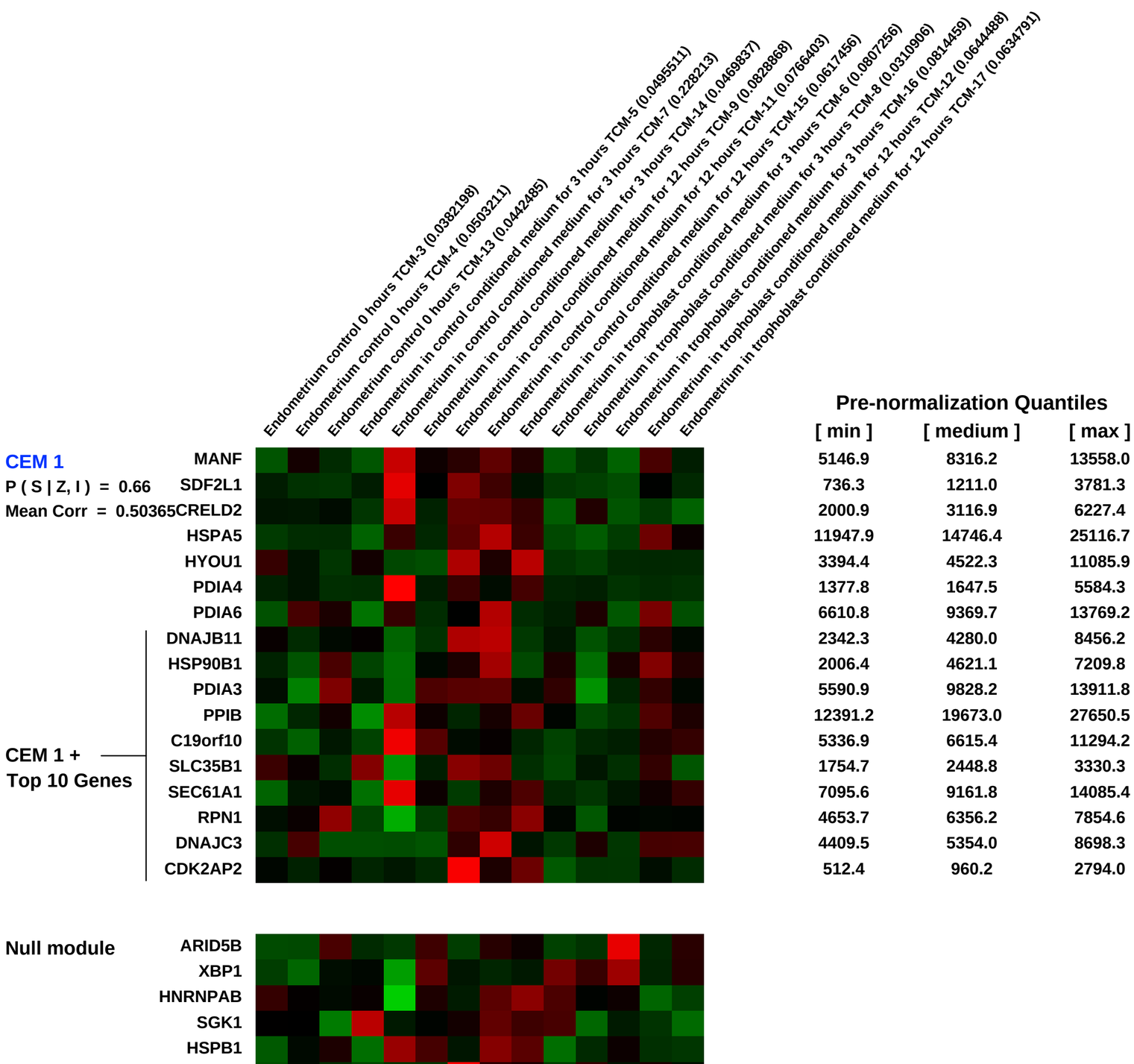

GEO Series "GSE28005" Expression Profiles

Num of samples in this series: 38

Scale of expression profile Z-scores

-3.0 -2.0 -1.0 0.0 1.0 2.0 3.0

GEO Link:	http://www.ncbi.nlm.nih.gov/geo/query/acc.cgi?acc=GSE28005
Status:	Public on Mar 05 2012
Title:	Charaterization of the initial molecular events of adipose tissue development and growth during overfeeding in humans
Organism:	Homo sapiens
Experiment type:	Expression profiling by array
Platform:	GPL570
Pubmed ID:	22162470
Summary & Design:	**Summary:** The adaptive mechanisms in response to excess energy supply are still poorly known in humans. Our aims were to define metabolic responses and changes in gene expression in adipose tissue of healthy volunteers during fat overfeeding. **Overall design:** Healthy lean and overweight subjects were submitted to a high fat diet during 56 days. Adipose tissue biopsies were taken at Day 0, Day 14 and Day 56.

Background corr dist: KL-Divergence = 0.2816, L1-Distance = 0.0541, L2-Distance = 0.0071, Normal std = 0.2882

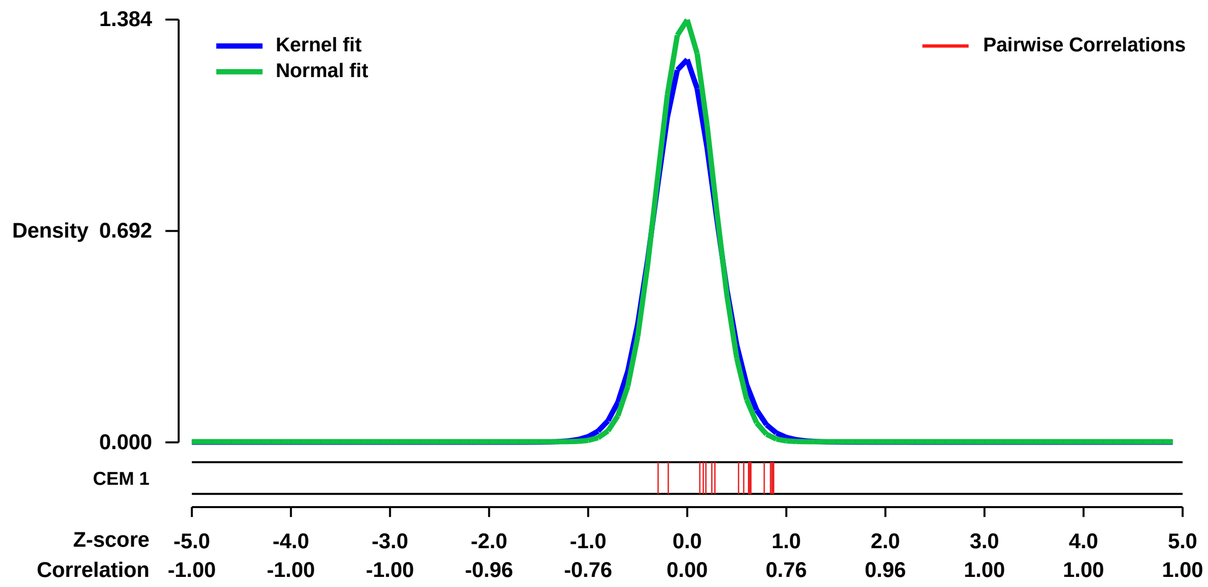

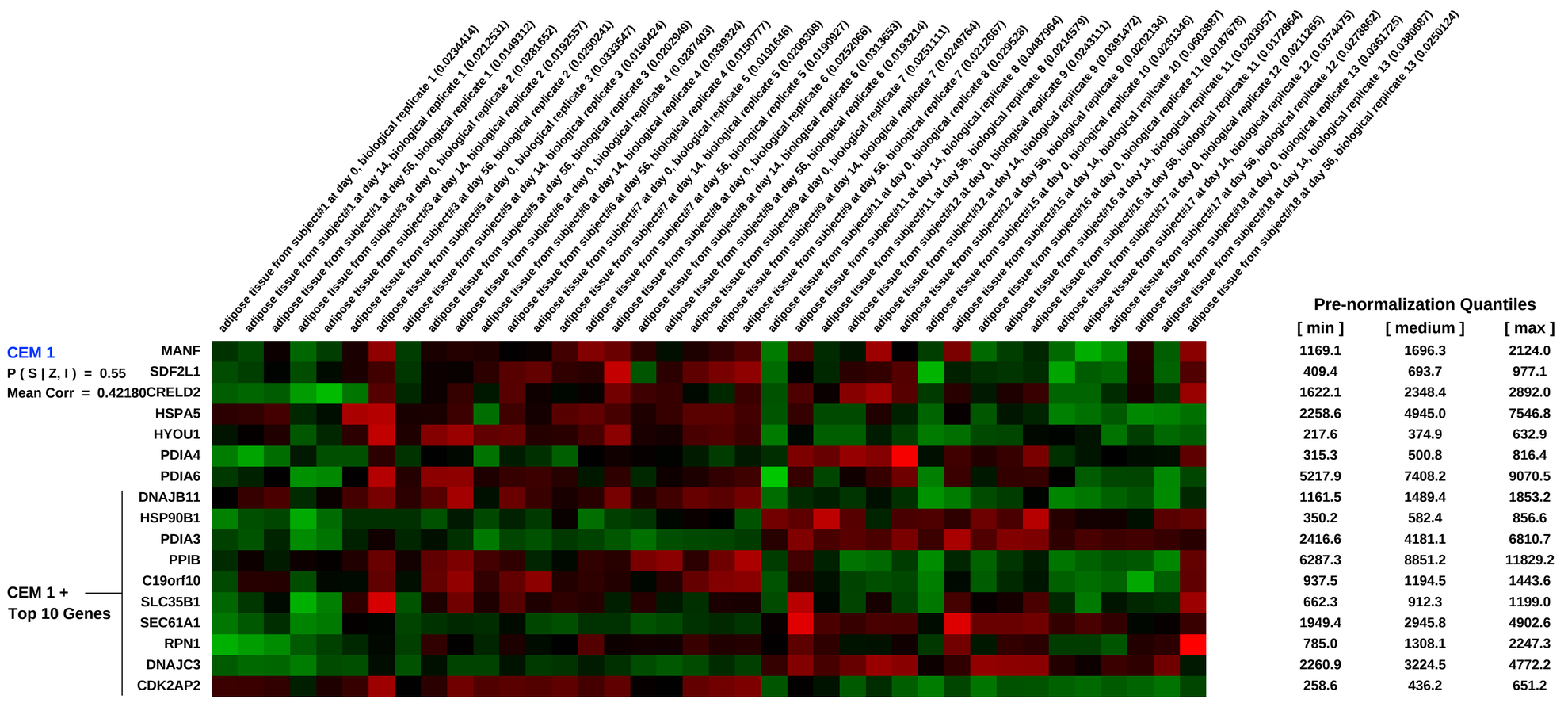

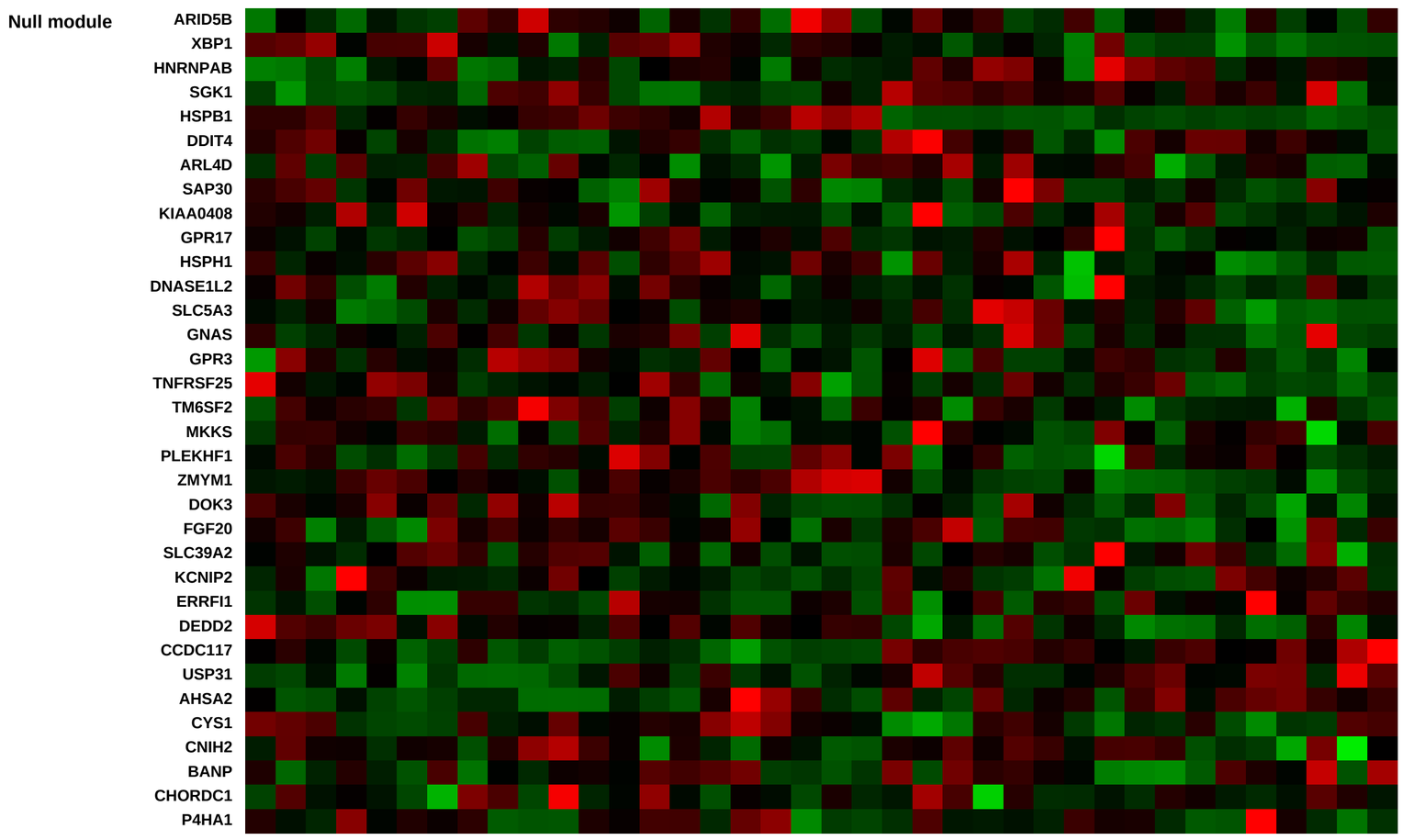

GEO Series "GSE23035" Expression Profiles

Num of samples in this series: 9

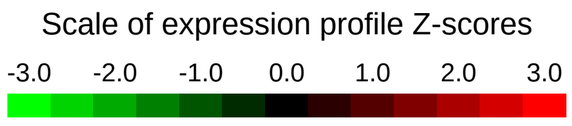

GEO Link:	http://www.ncbi.nlm.nih.gov/geo/query/acc.cgi?acc=GSE23035
Status:	Public on Nov 05 2010
Title:	Expression data from BAP1 depleted cells
Organism:	Homo sapiens
Experiment type:	Expression profiling by array
Platform:	GPL570
Pubmed ID:	20805357
Summary & Design:	**Summary:** The deubiquitinase BAP1 is a candidate tumor suppressor regulating cell proliferation in human and is required for development in Drosophila. BAP1 is assembled into high molecular weight transcriptional multi-protein complexes. In order to identify potential BAP1 target genes, global mRNA expression profiling using microarrays was conducted. **Overall design:** U2OS cells, transfected with a non-target control shRNA or shRNAs targeting BAP1, were selected with puromycin containing medium and then synchronized at the G1/S border to allow comparative analysis of gene expression.

Background corr dist: KL-Divergence = 0.0576, L1-Distance = 0.0326, L2-Distance = 0.0013, Normal std = 0.5571

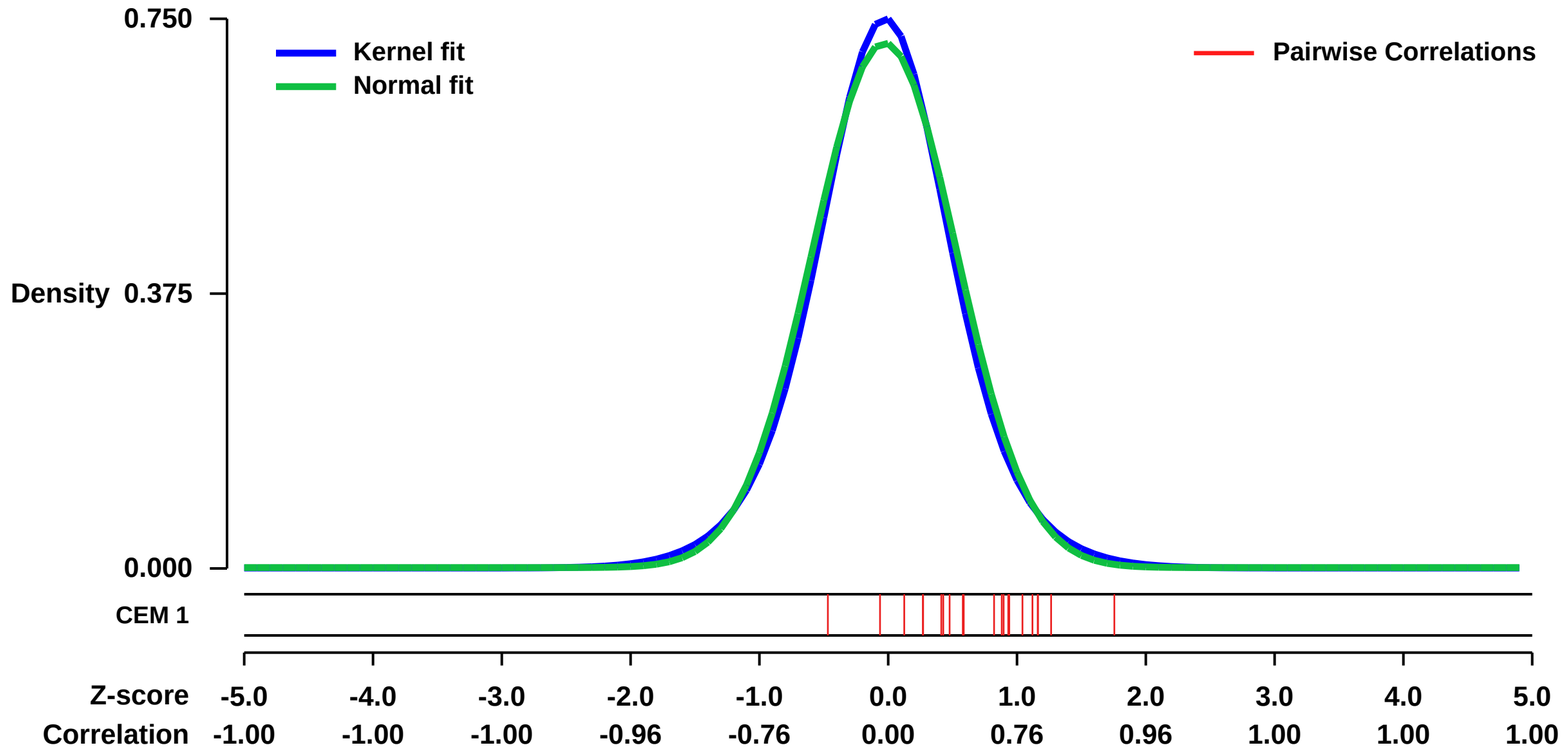

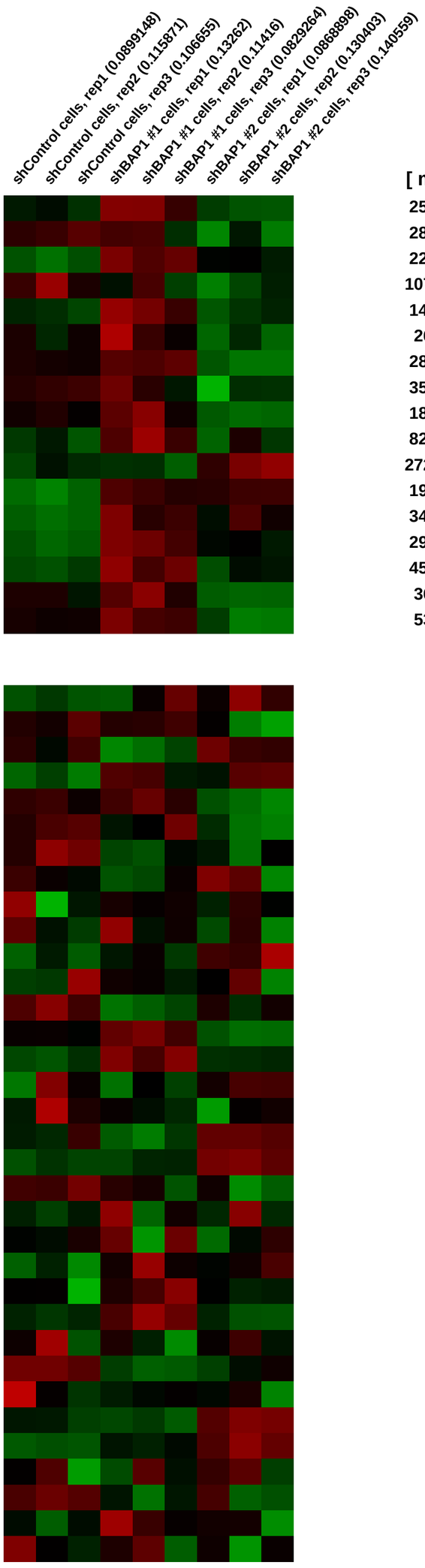

GEO Series "GSE16589" Expression Profiles

Num of samples in this series: 20

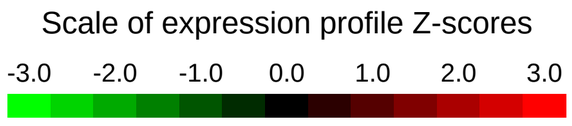

GEO Link:	http://www.ncbi.nlm.nih.gov/geo/query/acc.cgi?acc=GSE16589
Status:	Public on Jul 01 2009
Title:	Time course profile of umbilical cord blood cells in culture
Organism:	Homo sapiens
Experiment type:	Expression profiling by array
Platform:	GPL570
Pubmed ID:	20924352
Summary & Design:	**Summary:** Despite the importance of inter-cellular communication networks in regulating stem cell fate decisions, very little is known about the topology, dynamics, or functional significance. Using human blood stem cell cultures as an experimental paradigm, we present a novel bioinformatic approach to integrate genome-scale molecular profiles (transcriptome and secretome) and publicly available databases to reconstruct soluble factor-mediated inter-cellular signalling networks regulating blood stem cell fate decisions. **Overall design:** Umbilical cord blood UCB cells were lineage depleted via immuno-magnetic column and placed in serum free media, supplemented with SCF, FL, and TPO. At culture day 4, cells were either subject to Lin- cell re-selection + media exchange (S/E) or not (NS/NE) and cultured for an additional 4 days. At day-8, S/E cell sample was subject to another S/E procedure and cultured for an additional 4 days. At day-0, 4, 8, and 12, cells were separated into Lin- and Lin+ for independent profiling using Affymetrix HU133 v2.0 arrays.

Background corr dist: KL-Divergence = 0.2115, L1-Distance = 0.0409, L2-Distance = 0.0039, Normal std = 0.3285

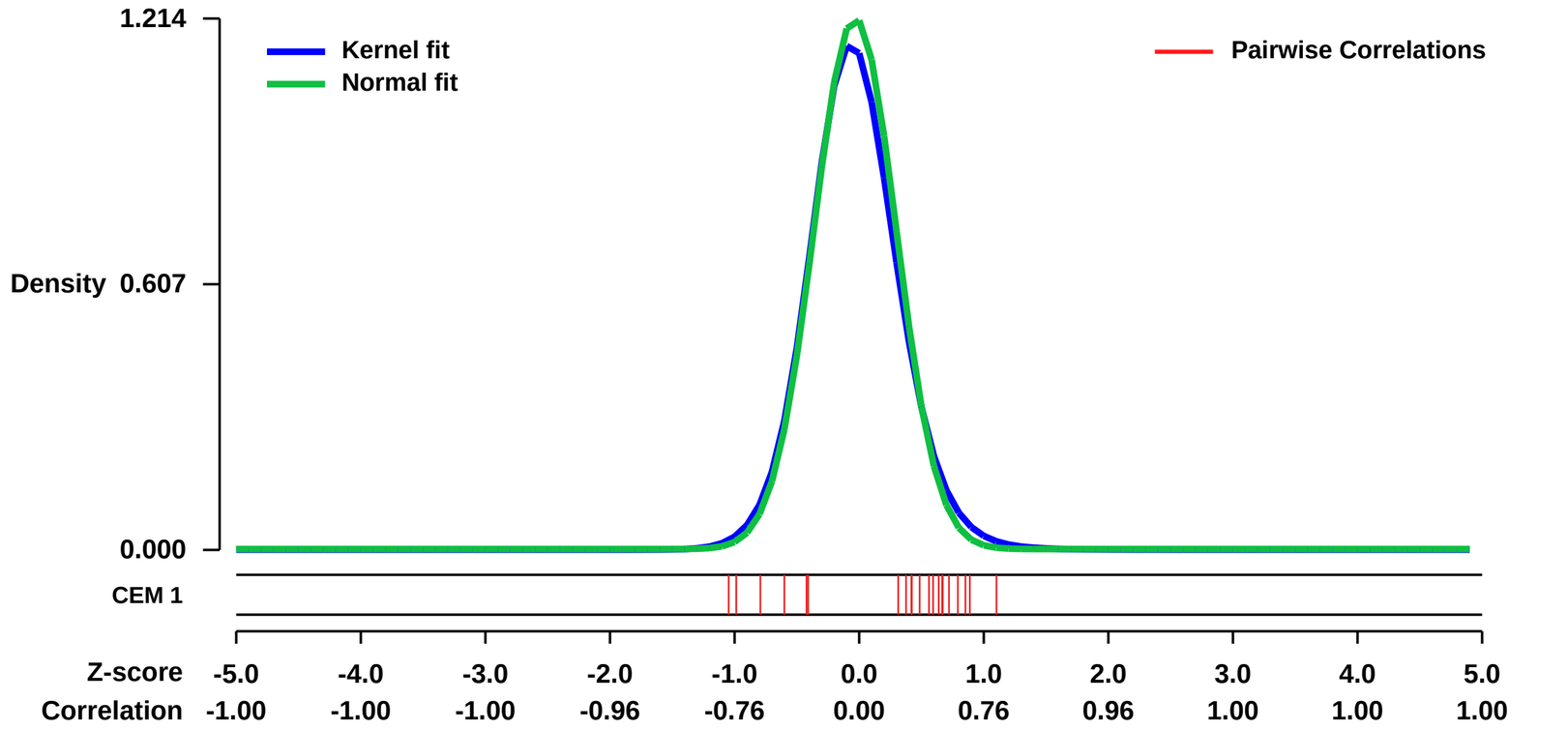

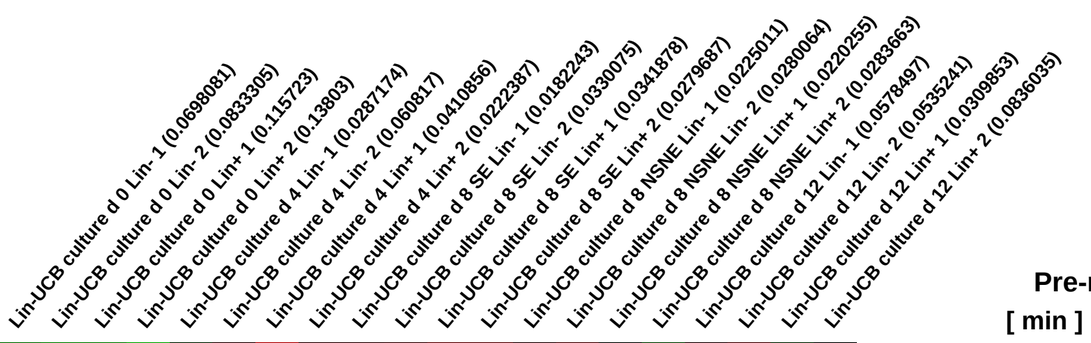

Pre-normalization Quantiles

	[min]	[medium]	[max]
CEM 1			
P (S | Z, I) = 0.48			
Mean Corr = 0.22101			
MANF	1028.9	7240.9	11889.9
SDF2L1	274.4	1046.8	1230.1
CRELD2	1323.4	2953.7	5715.4
HSPA5	5692.7	11187.2	18532.3
HYOU1	447.0	1921.2	2896.7
PDIA4	319.9	1472.6	3085.6
PDIA6	3486.8	13044.7	17611.9
CEM 1 + Top 10 Genes			
DNAJB11	1141.2	2016.9	3583.2
HSP90B1	655.7	1403.4	4403.9
PDIA3	4515.8	8050.2	12176.3
PPIB	4851.7	10947.4	16575.0
C19orf10	1720.2	2225.7	3538.4
SLC35B1	553.6	1370.3	1989.4
SEC61A1	1820.6	3718.0	5926.7
RPN1	1379.4	3458.5	6418.1
DNAJC3	1458.8	3282.8	4738.5
CDK2AP2	159.0	353.3	726.8
Null module			
ARID5B			
XBP1			
HNRNPAB			
SGK1			
HSPB1			
DDIT4			
ARL4D			
SAP30			
KIAA0408			
GPR17			
HSPH1			
DNASE1L2			
SLC5A3			
GNAS			
GPR3			
TNFRSF25			
TM6SF2			
MKKS			
PLEKHF1			
ZMYM1			
DOK3			
FGF20			
SLC39A2			
KCNIP2			
ERRFI1			
DEDD2			
CCDC117			
USP31			
AHSA2			
CYS1			
CNIH2			
BANP			
CHORDC1			
P4HA1			

GEO Series "GSE40904" Expression Profiles

Num of samples in this series: 26

Scale of expression profile Z-scores

-3.0 -2.0 -1.0 0.0 1.0 2.0 3.0

GEO Link:	http://www.ncbi.nlm.nih.gov/geo/query/acc.cgi?acc=GSE40904
Status:	Public on Jan 29 2014
Title:	Gene expression analysis for Il13Ra2-positive and IL13Ra2-negative glioma cell lines
Organism:	Homo sapiens
Experiment type:	Expression profiling by array
Platform:	GPL570
Pubmed ID:	24204956
Summary & Design:	**Summary:** Affymetrix expression profiling was used to evaluate the association between IL13R$_{\epsilon}$–2 expression, and mesenchymal, proneural, classical and neural signature genes expression for glioma subclasses defined by Verhaak et al (Cancer Cell; 2010). **Overall design:** The goal of this study is to compare gene expression patterns between IL13Ra2-postive and IL13Ra2-negative glioma cell lines. IL13Ra2 status was determined by flow cytometry and confirmed by qPCR.

Background corr dist: KL-Divergence = 0.1836, L1-Distance = 0.0328, L2-Distance = 0.0024, Normal std = 0.3508

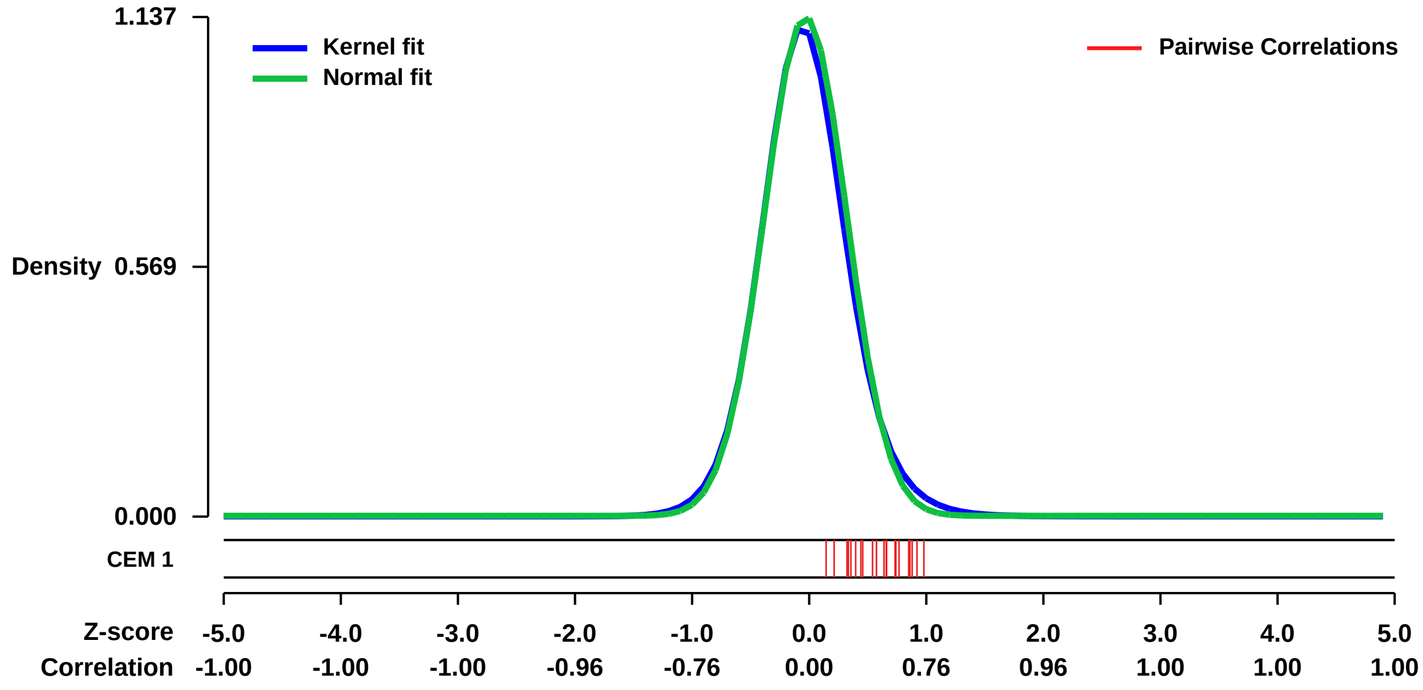

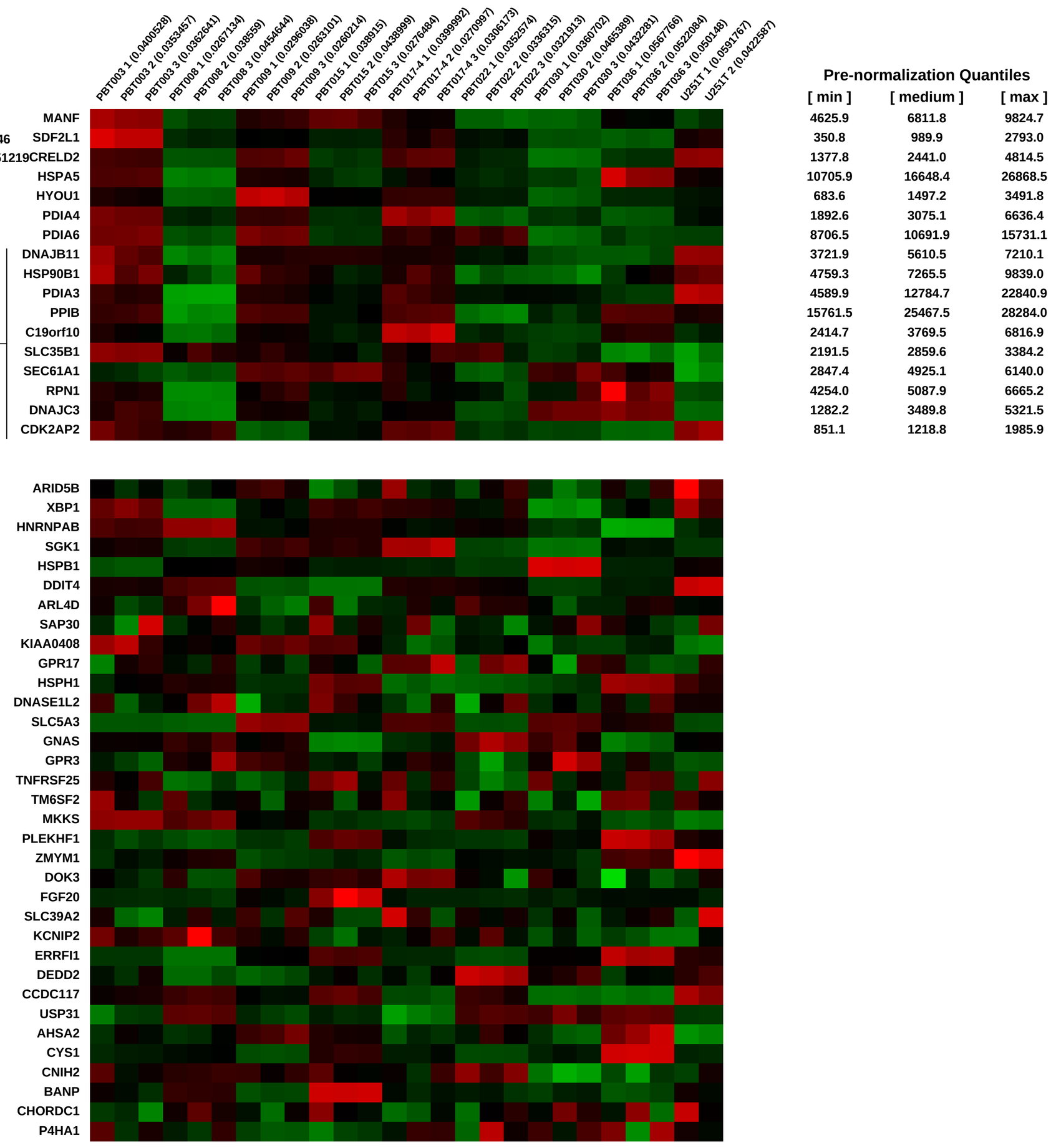

GEO Series "GSE27187" Expression Profiles

Num of samples in this series: 10

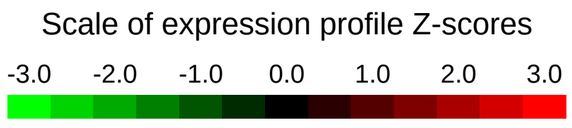

GEO Link:	http://www.ncbi.nlm.nih.gov/geo/query/acc.cgi?acc=GSE27187
Status:	Public on Feb 12 2011
Title:	Expression profile of acute monocytic leukemia patients
Organism:	Homo sapiens
Experiment type:	Expression profiling by array
Platform:	GPL570
Pubmed ID:	21399634
Summary & Design:	**Summary:** To understand the pathogenesis of DNMT3A in acute monocytic leukemia (AML-M5), we identified genes that are expressed differently in leukemia cells from AML-M5 patients collected at diagnosis with DNMT3A mutations (6 cases) compared to those without the mutations (4 cases). Differences of expression level were observed in 889 out of 20,723 (4.3%) annotated genes by using Affymetrix microarray with 469 genes upregulated and 420 genes downregulated. **Overall design:** Leukemia cells in bone marrow of acute monocytic leukemia patients were collected at diagnosis for RNA extraction and hybridization on Affymetrix microarrays. 6 cases of AML-M5 samples with DNMT3A mutations and 4 cases of AML-M5 samples wihtout DNMT3A mutations were used.

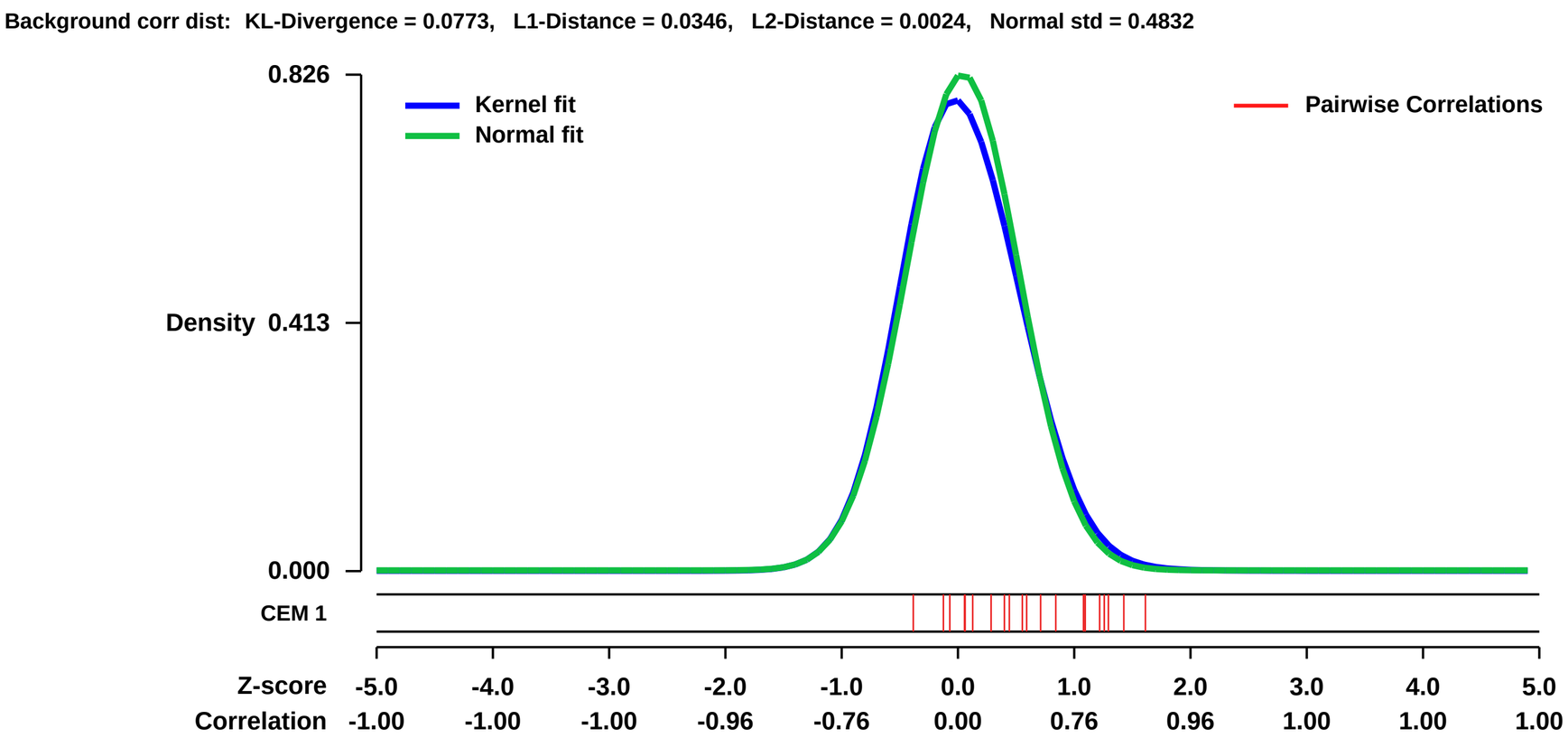

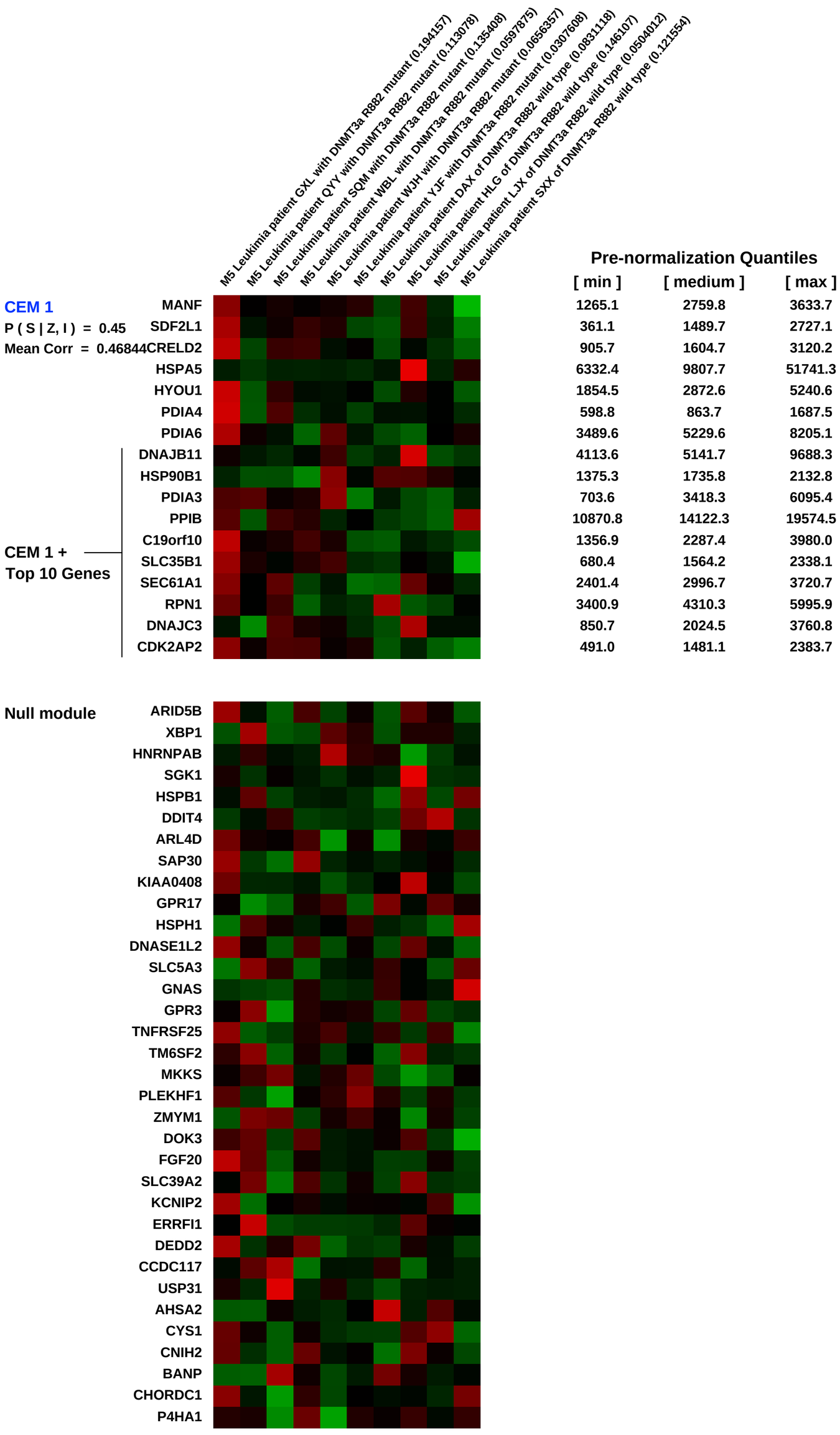

Pre-normalization Quantiles

	[min]	[medium]	[max]
MANF	1265.1	2759.8	3633.7
SDF2L1	361.1	1489.7	2727.1
CRELD2	905.7	1604.7	3120.2
HSPA5	6332.4	9807.7	51741.3
HYOU1	1854.5	2872.6	5240.6
PDIA4	598.8	863.7	1687.5
PDIA6	3489.6	5229.6	8205.1
DNAJB11	4113.6	5141.7	9688.3
HSP90B1	1375.3	1735.8	2132.8
PDIA3	703.6	3418.3	6095.4
PPIB	10870.8	14122.3	19574.5
C19orf10	1356.9	2287.4	3980.0
SLC35B1	680.4	1564.2	2338.1
SEC61A1	2401.4	2996.7	3720.7
RPN1	3400.9	4310.3	5995.9
DNAJC3	850.7	2024.5	3760.8
CDK2AP2	491.0	1481.1	2383.7

GEO Series "GSE8166" Expression Profiles

Num of samples in this series: 8

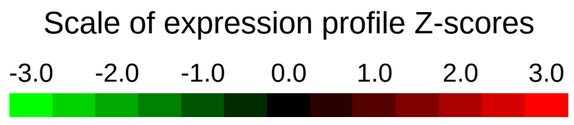

GEO Link:	http://www.ncbi.nlm.nih.gov/geo/query/acc.cgi?acc=GSE8166
Status:	Public on Dec 01 2007
Title:	Transcriptome Profile of the Vascular Endothelial Cell Response to Candida albicans
Organism:	Homo sapiens
Experiment type:	Expression profiling by array
Platform:	GPL570
Pubmed ID:	18500935
Summary & Design:	**Summary:** We perform microarray analysis of HUVECs upon stimulation with virulent wildtype C. albicans strain SC5314 or its efg1/efg1 cph1/cph1 hyphal-deficient derivative strain CAN34 to compare the gene expression profiles elicited from HUVECs in response to these strains. In addition, these responses are compared to that of TNF-alpha induced responses to determine which responses are Candida-specific. Keywords: comparison of host response to different Candida albicans morphologies **Overall design:** HUVECs are co-cultured for 3 or 8 hours in M199 medium alone or with CAN34, SC5314, or TNF-alpha. Total RNA is isolated, cRNA is synthesized and labeled, and labeled cRNA is hybridized onto Affymetrix chips. Each Candida and TNF sample is compared to its corresponding medium alone sample to determine fold changes in expression at each time point.

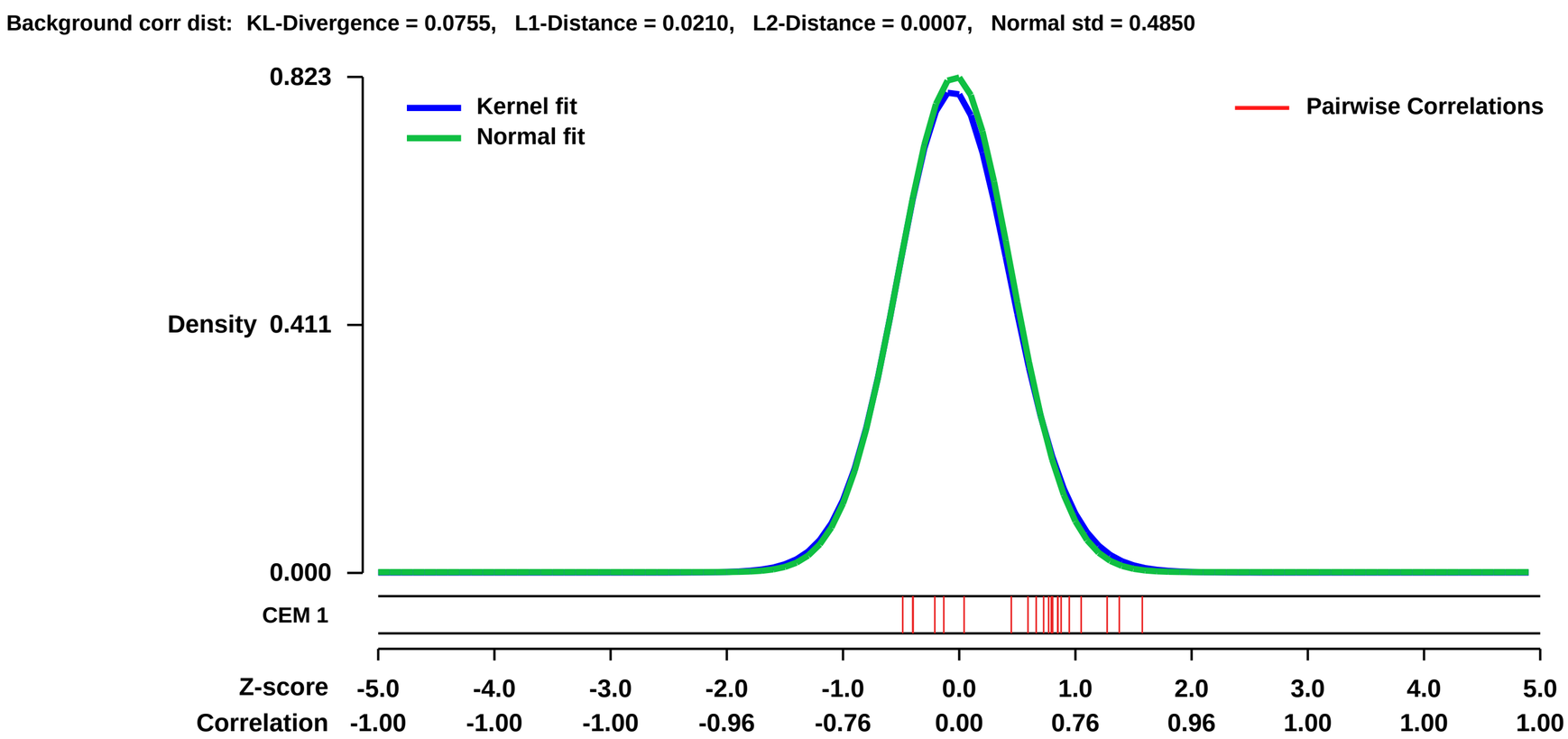

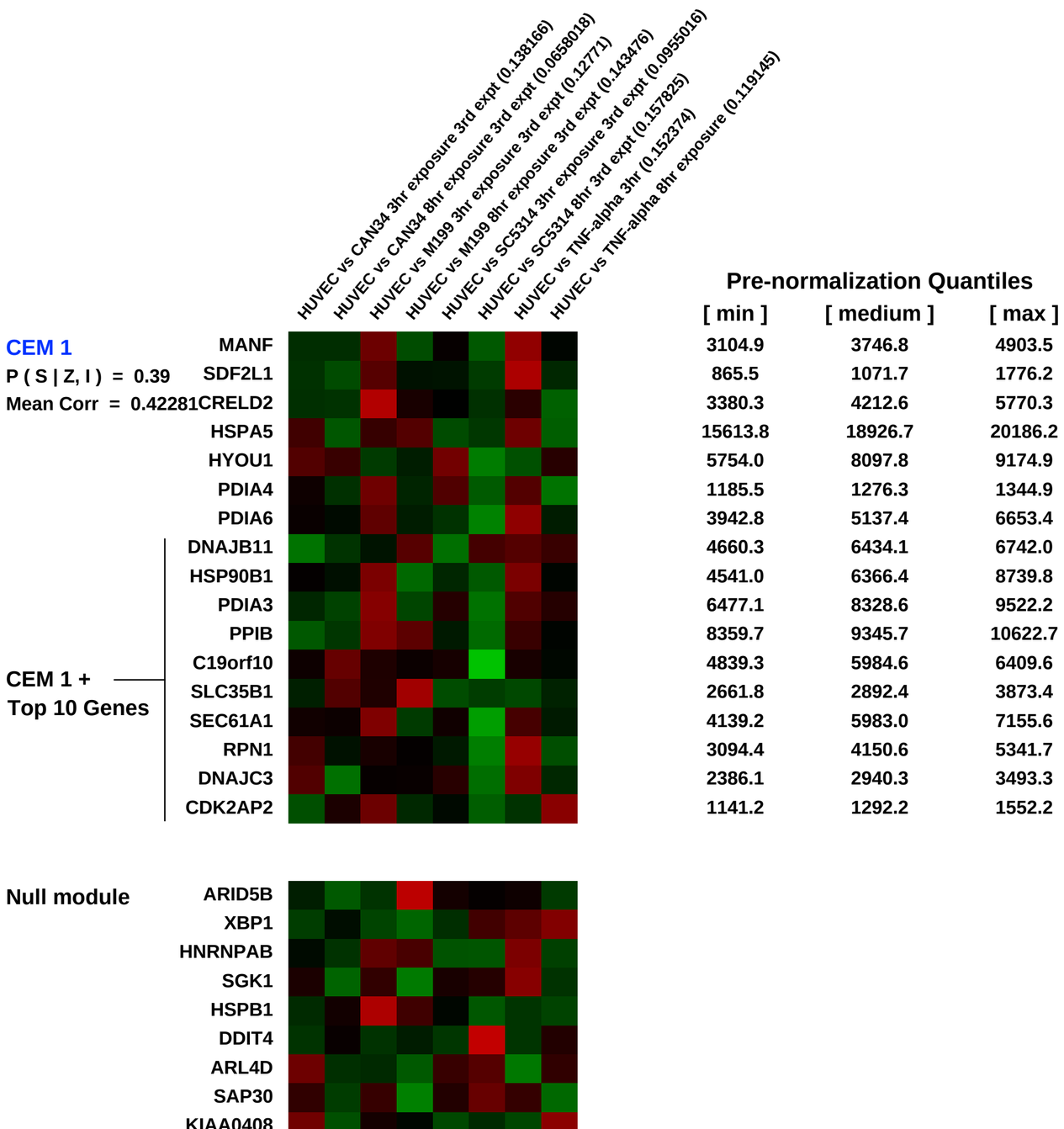

GEO Series "GSE32158" Expression Profiles

Num of samples in this series: 8

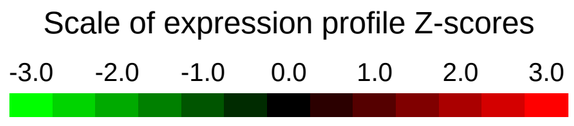

GEO Link:	http://www.ncbi.nlm.nih.gov/geo/query/acc.cgi?acc=GSE32158
Status:	Public on Sep 16 2011
Title:	Bisphenol A Regulates the Expression of DNA Repair Genes in Human Breast Epithelial Cells (expression data)
Organism:	Homo sapiens
Experiment type:	Expression profiling by array
Platform:	GPL570
Pubmed ID:	
Summary & Design:	**Summary:** Xenoestrogens are part of a group of agents termed endocrine disruptors because of their capacity to perturb normal hormonal actions. It has been suggested that xenoestrogens may contribute to the development of hormone-dependent cancers, such as breast and endometrial cancers. Bisphenol A (BPA) is polymerized to manufacture polycarbonate plastic and epoxy resins. Human exposure occurs when BPA leaches from plastic-lined food and beverage cans. In the present work we are aiming to determine if BPA has carcinogenic properties by using an in vitro system. For this purpose the human breast epithelial cells MCF-10F were treated with 10-3M to 10-9M BPA continuously for two weeks. The MCF-10F cells treated with 10-3M and 10-4M BPA died, indicating that these concentrations were toxic for the human breast epithelial cells. The cells treated with 10-5M to 10-9M BPA were evaluated for formation of solid masses in collagen and invasion capacity, both phenotypes that are indicators of cell transformation. MCF-10F treated with 10-5M, 10-6M, 10-7M, 10-8M and 10-9M BPA formed a high percentage of solid masses (34.6%, 20%, 42.4%, 31.8% and 32.2%, respectively). Ten passages after BPA treatments, the invasive capacities of the cells were evaluated using Boyden chambers. The invasion capacity was lower in the cells treated at high concentrations of BPA (10-5M and 10-6M), and there was an increased invasion for the cells treated at low BPA concentration (10-9M) although, in all the cases the differences were not significant to the controls. Expression and DNA methylation analyses were performed with the cells treated with 10-5M and 10-6M BPA. We found that these cells showed an increased expression of BRCA1, BARD1, CtIP, RAD51 and BRCC3, all genes involved in DNA repair, and downregulation of PDCD5 and BCL2L11 (also known as BIM), both involved in apoptosis. The upregulation of CtIP was related to hypomethylation of the promoter/exon1 of this gene. Furthermore, BPA induced silencing of BCL2L11 by hypermethylation. This is the first demonstration that BPA induces neoplastic transformation of breast epithelial cells and that aberrant DNA methylation of genes involved in DNA repair and apoptosis could be involved in the initiation of the neoplastic process. **Overall design:** MCF-10F, a normal-like human breast epithelial cell (HBEC) line that is ERalpha-negative PR-negative, was maintained in high-calcium medium at 37´℃ and 5% CO2 until confluent. These cells were treated with different concentrations of BPA continuously for two weeks, adding fresh media every day. As controls, MCF-10F cells were not treated and maintained in the regular media or treated with 0.284% DMSO (vehicle). The cells treated with 10-5M or 10-6M BPA after the invasion assay were collected and expanded during 6 passages. RNA was isolated from the cells using an RNA extraction kit (Qiagen).

Background corr dist: KL-Divergence = 0.0401, L1-Distance = 0.0390, L2-Distance = 0.0019, Normal std = 0.6499

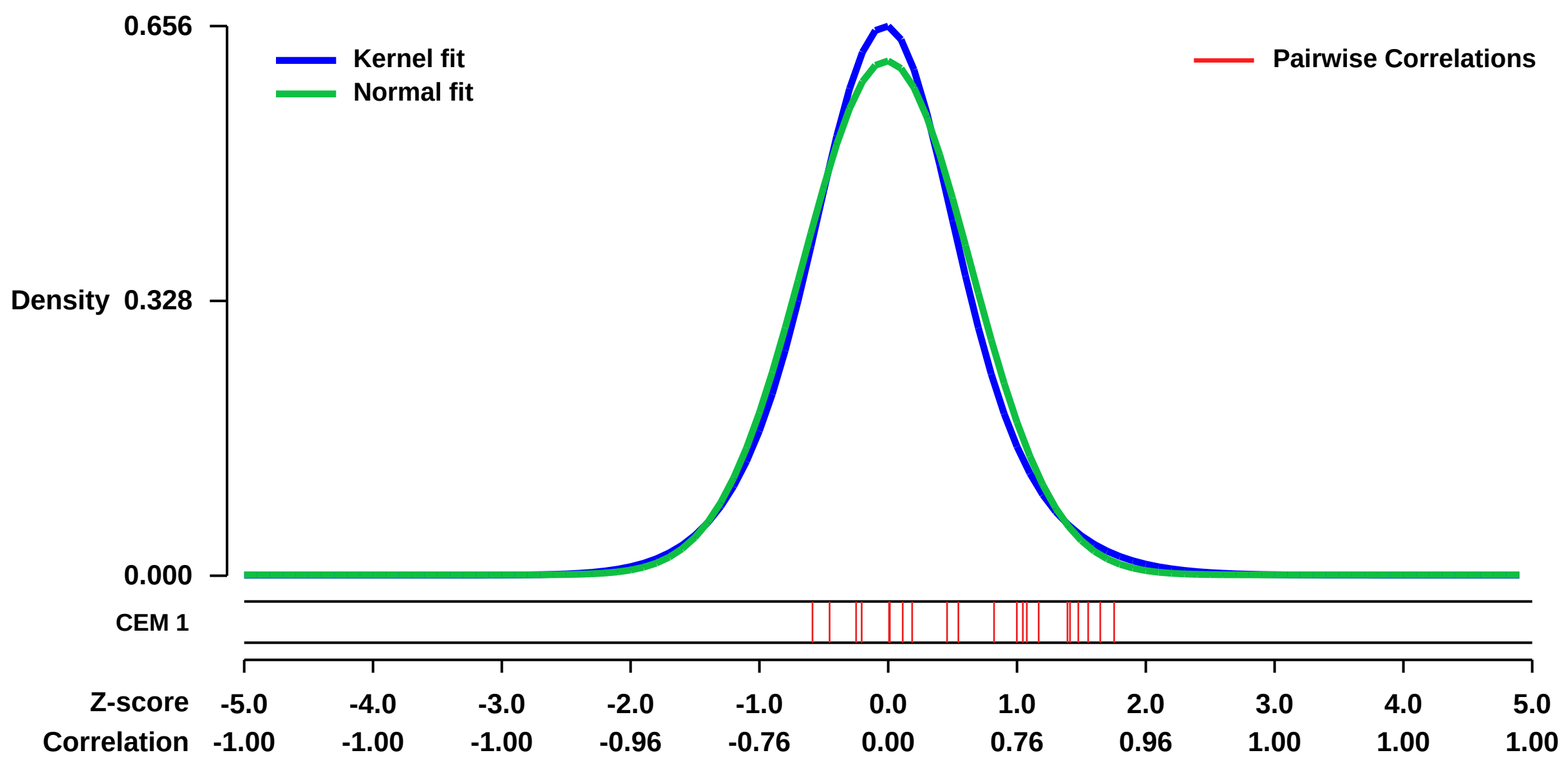

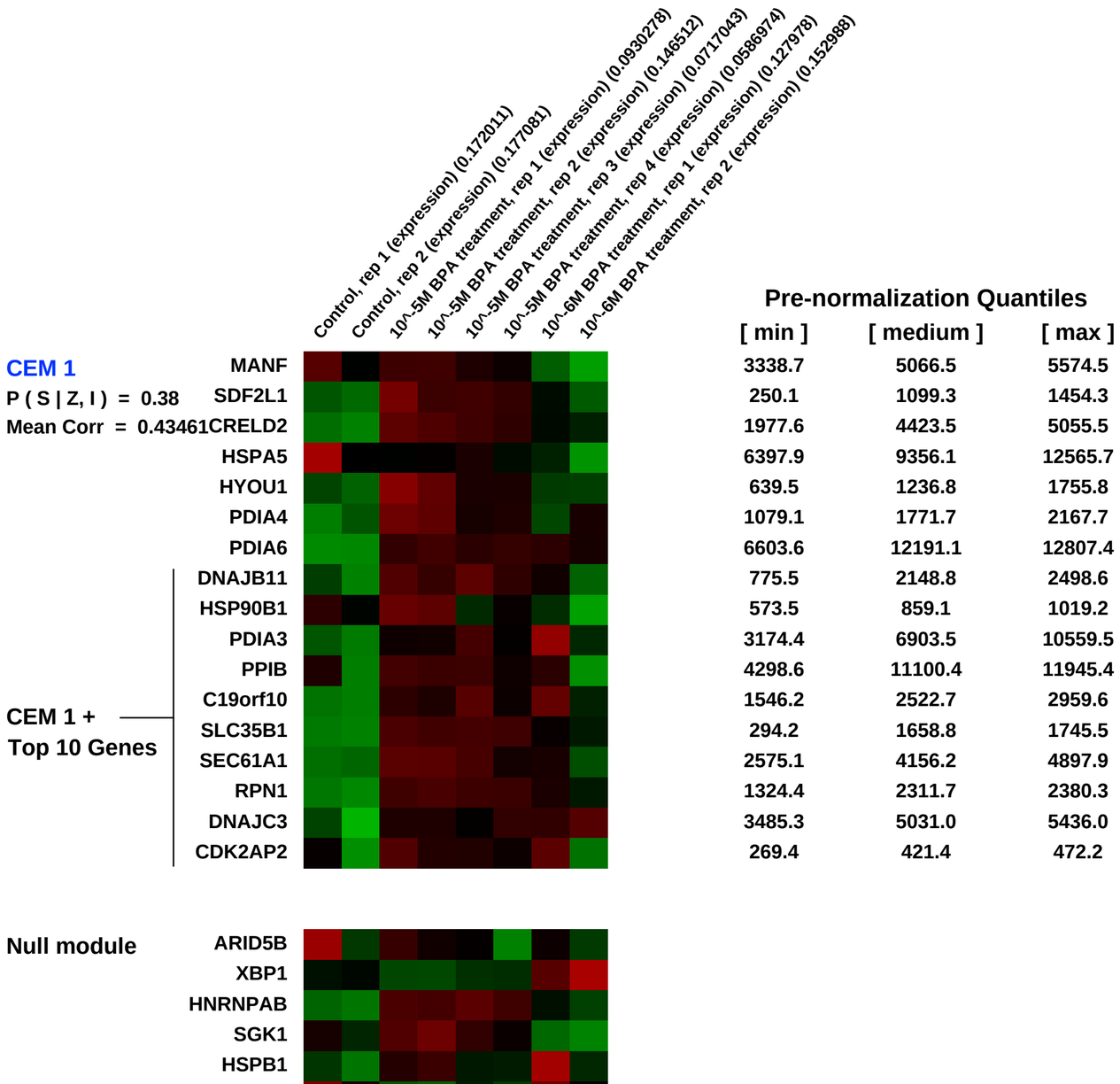

GEO Series "GSE4888" Expression Profiles

Num of samples in this series: 27

Scale of expression profile Z-scores

-3.0 -2.0 -1.0 0.0 1.0 2.0 3.0

GEO Link:	http://www.ncbi.nlm.nih.gov/geo/query/acc.cgi?acc=GSE4888
Status:	Public on May 24 2006
Title:	Molecular phenotyping of human endometrium
Organism:	Homo sapiens
Experiment type:	Expression profiling by array
Platform:	GPL570
Pubmed ID:	16306079
Summary & Design:	**Summary:** To examine the possibility that biochemical or molecular signatures of endometrium may prove to be more useful, we have investigated whole genome molecular phenotyping (54,600 genes/ESTs) of this tissue sampled across the cycle in 28 normo-ovulatory women, using high-density oligonucleotide microarrays. The results demonstrate that endometrial samples obtained by two different sampling techniques (biopsy and curetting hysterectomy specimens) from subjects who are as normal as possible in a human study and 4 including those with unknown histology, can be classified by their molecular signatures and correspond to known phases of the menstrual cycle with identical results using two independent analytical methods. Also, the results enable global identification of biological processes and molecular mechanisms that occur dynamically in the endometrium in the changing steroid hormone milieu across the menstrual cycle in normo-ovulatory women. The results underscore the potential of gene expression profiling for developing molecular diagnostics of endometrial normalcy and abnormalities and identifying molecular targets for therapeutic purposes in endometrial disorders. **Keywords:** Gene expression arrays human endometrium **Overall design:** Unsupervised principal component analysis (PCA) of all samples revealed that samples selfcluster into four groups consistent with histologic phenotypes of proliferative (PE), early secretory (ESE), mid-secretory (MSE), and late secretory (LSE) endometrium. Independent hierarchical clustering analysis revealed equivalent results, with 2 major dendrogram branches corresponding to PE/ESE and MSE/LSE and sub-branching into the 4 respective phases with heterogeneity among samples within each sub-branch. K-means clustering of genes revealed 4 major patterns of gene expression (high in PE, high in ESE, high in MSE, and high in LSE), and gene ontology analysis of these clusters demonstrated cycle-phase specific biological processes and molecular functions. Six samples with ambiguous histology were identically assignable to a cycle phase by both PCA and hierarchical clustering. Additionally, pair-wise comparisons of relative gene expression across the cycle revealed genes/families that clearly distinguish the transitions of PE to ESE, ESE to MSE, and MSE to LSE, including receptomes and signaling pathways. Select genes were validated by quantitative RT-PCR.

Background corr dist: KL-Divergence = 0.1592, L1-Distance = 0.0589, L2-Distance = 0.0089, Normal std = 0.3720

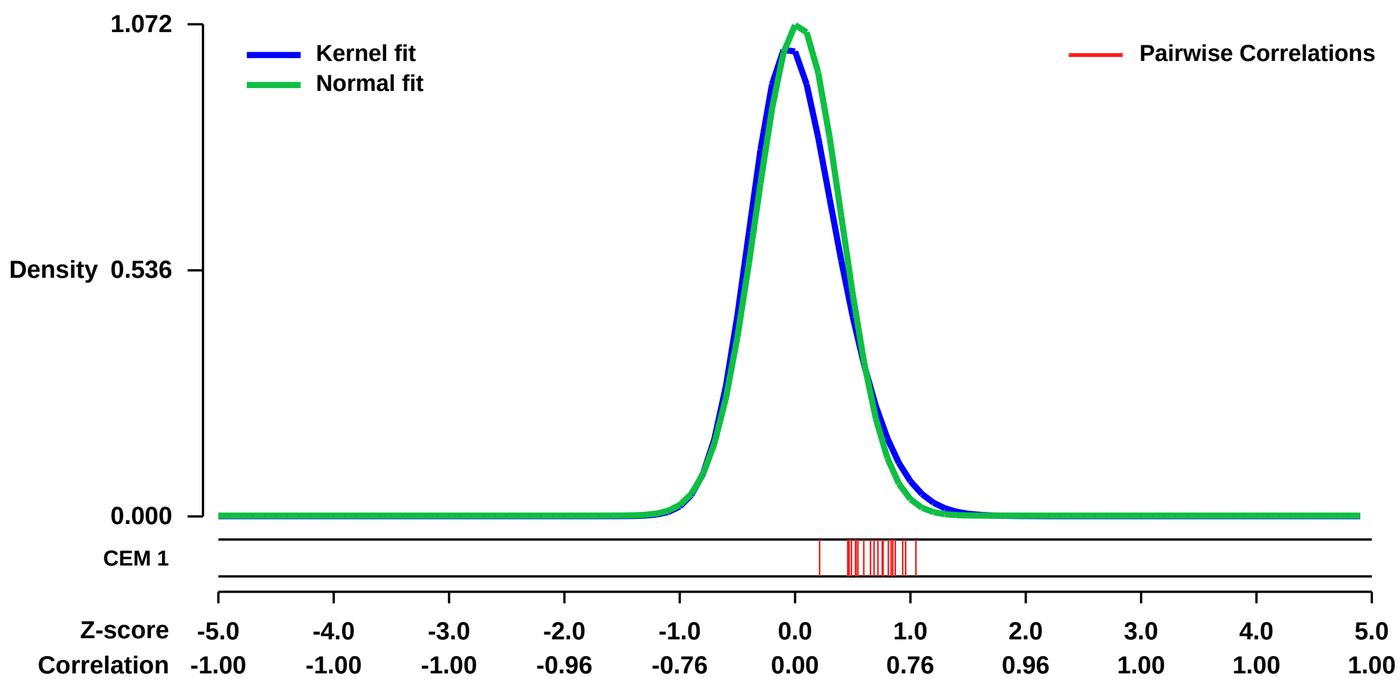

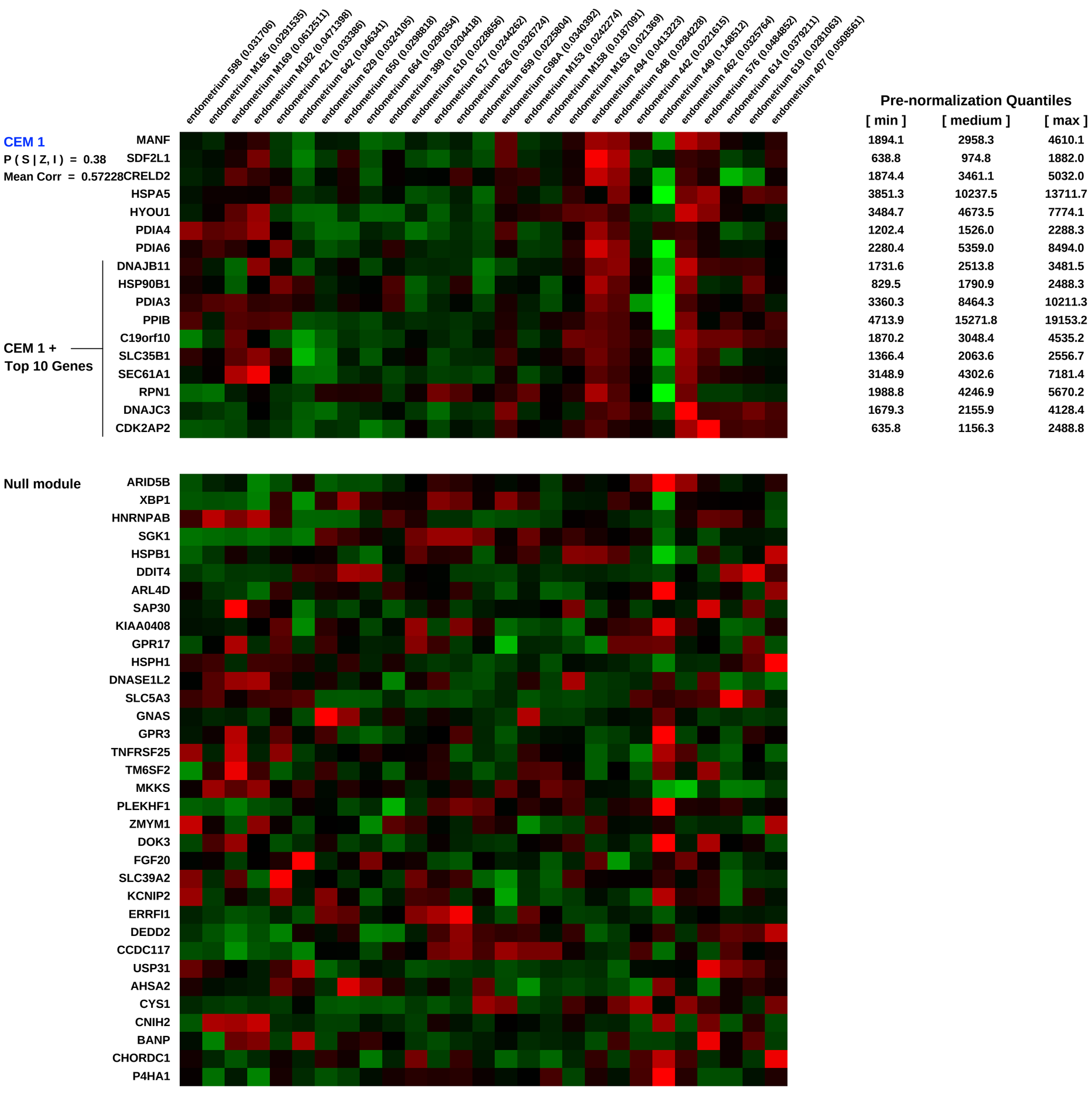

Pre-normalization Quantiles

	[min]	[medium]	[max]
endometrium 598 (0.031706)	1894.1	2958.3	4610.1
endometrium M165 (0.0291535)	638.8	974.8	1882.0
endometrium M169 (0.0612511)	1874.4	3461.1	5032.0
endometrium M182 (0.0471398)	3851.3	10237.5	13711.7
endometrium 421 (0.033386)	3484.7	4673.5	7774.1
endometrium 642 (0.046341)	1202.4	1526.0	2288.3
endometrium 629 (0.0324105)	2280.4	5359.0	8494.0
endometrium 650 (0.0298818)	1731.6	2513.8	3481.5
endometrium 664 (0.0290354)	829.5	1790.9	2488.3
endometrium 389 (0.0204418)	3360.3	8464.3	10211.3
endometrium 610 (0.0228656)	4713.9	15271.8	19153.2
endometrium 617 (0.0244262)	1870.2	3048.4	4535.2
endometrium 626 (0.0326724)	1366.4	2063.6	2556.7
endometrium 659 (0.0225804)	3148.9	4302.6	7181.4
endometrium G98A (0.0340392)	1988.8	4246.9	5670.2
endometrium M153 (0.0242274)	1679.3	2155.9	4128.4
endometrium M158 (0.0187091)	635.8	1156.3	2488.8
endometrium M163 (0.021369)			
endometrium 494 (0.0413223)			
endometrium 648 (0.0284228)			
endometrium 442 (0.0221615)			
endometrium 449 (0.148512)			
endometrium 462 (0.0325764)			
endometrium 576 (0.0484852)			
endometrium 614 (0.0379211)			
endometrium 619 (0.0281063)			
endometrium 407 (0.0508561)			

GEO Series "GSE17920" Expression Profiles

Num of samples in this series: 130

Details of this dataset are not shown due to large number of samples and the page size limit.

Find details in http://www.ncbi.nlm.nih.gov/geo/query/acc.cgi?acc=GSE17920

Background corr dist: KL-Divergence = 0.2274, L1-Distance = 0.0924, L2-Distance = 0.0276, Normal std = 0.3210

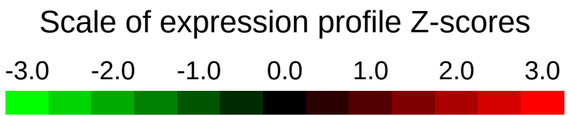

GEO Series "GSE15013" Expression Profiles

Num of samples in this series: 25

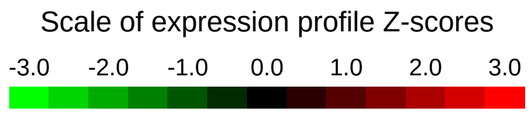

GEO Link:	http://www.ncbi.nlm.nih.gov/geo/query/acc.cgi?acc=GSE15013
Status:	Public on Jun 30 2011
Title:	Expression of HOXB genes is significantly different in acute myeloid leukemia with a partial tandem duplication of MLL vs. a MLL translocation: a cross-laboratory study
Organism:	Homo sapiens
Experiment type:	Expression profiling by array
Platform:	GPL570
Pubmed ID:	21665178
Summary & Design:	**Summary:** In acute myeloid leukemia (AML), the mixed lineage leukemia (MLL) gene may be rearranged to generate a partial tandem duplication (PTD), or fused to partner genes through a chromosomal translocation (tMLL). In this study, we first explored the differentially expressed genes between MLL-PTD and tMLL using gene expression profiling of our cohort (15 MLL-PTD and 10 tMLL) and one published data set. The top 250 probes were chosen from each set, resulting in 29 common probes (21 unique genes) to both sets. The selected genes include four HOXB genes, HOXB2, B3, B5, and B6. The expression values of these HOXB genes significantly differ between MLL-PTD and tMLL cases. Clustering and classification analyses were thoroughly conducted to support our gene selection results. Second, as MLL-PTD, FLT3-ITD, and NPM1 mutations are identified in AML with normal karyotypes, we briefly studied their impact on the HOXB genes. Another contribution of this study is to demonstrate that using public data from other studies enriches samples for analysis and yields more conclusive results. **Overall design:** 25 bone marrow samples of acute myeloid leukemia patients were hybridized to Affymetrix HG-U133 plus 2 GeneChips.

Background corr dist: KL-Divergence = 0.3714, L1-Distance = 0.0739, L2-Distance = 0.0163, Normal std = 0.2577

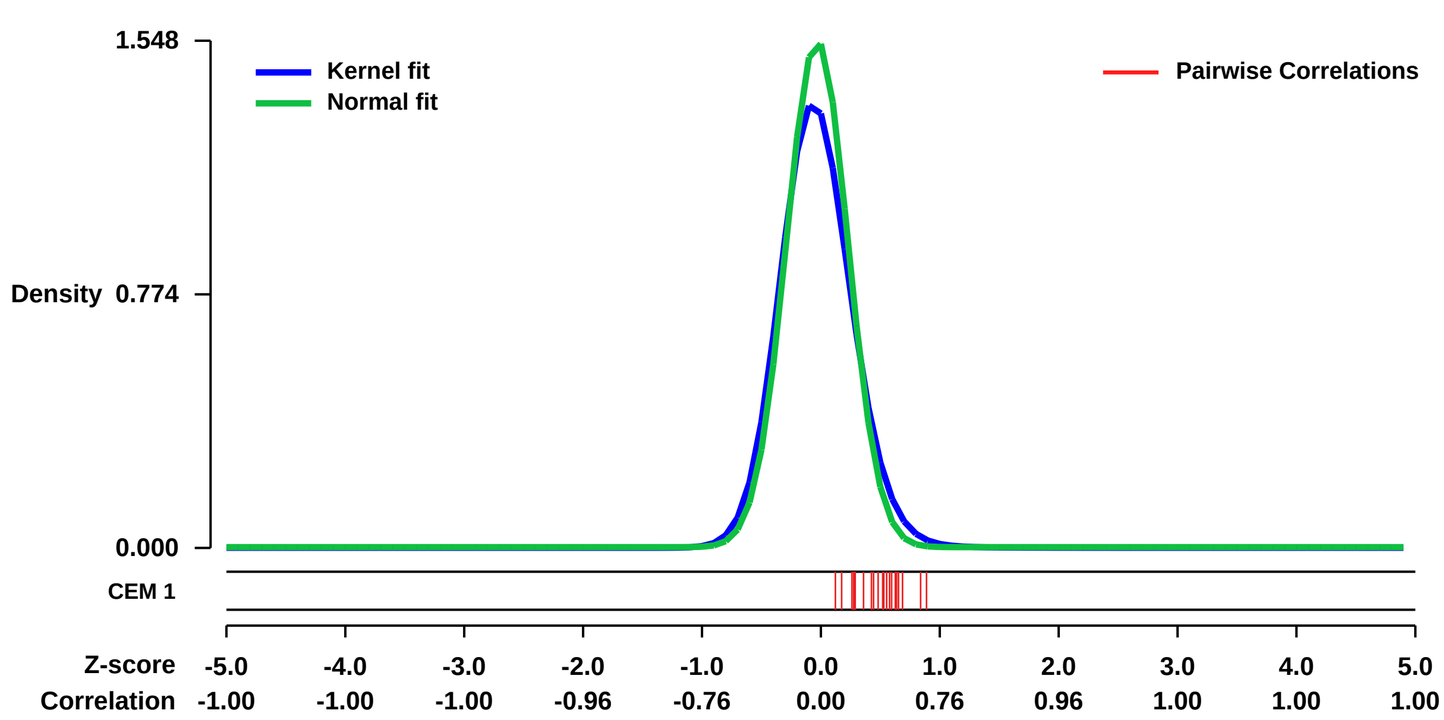

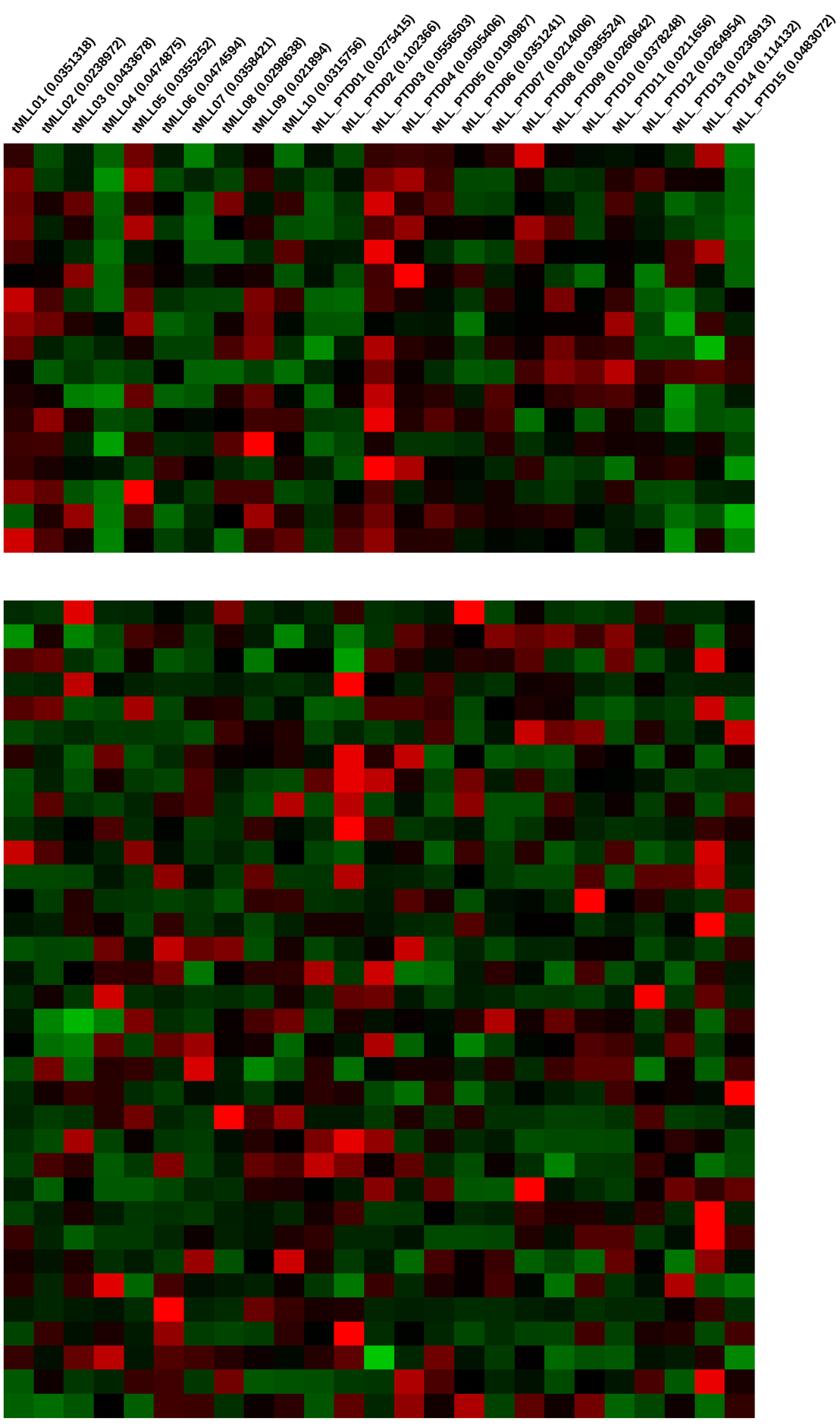

Pre-normalization Quantiles		
[min]	[medium]	[max]
1015.4	1932.8	3742.3
217.2	485.6	943.3
581.6	989.5	2097.4
7042.9	11639.9	19101.1
821.1	1373.3	2636.6
327.7	691.4	1438.1
3527.1	5704.1	9334.0
1403.0	2585.2	3802.8
910.4	3280.7	5252.3
1095.8	2804.3	5821.9
6892.3	13857.5	21401.0
1064.0	1927.1	3451.3
617.7	1190.0	2425.9
1378.5	2135.5	3601.2
1412.0	2216.7	4880.4
1074.7	2457.6	3487.0
511.3	949.7	1577.5

GEO Series "GSE50803" Expression Profiles

Num of samples in this series: 6

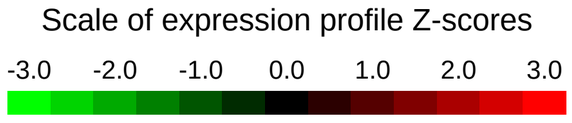

GEO Link:	http://www.ncbi.nlm.nih.gov/geo/query/acc.cgi?acc=GSE50803
Status:	Public on Oct 31 2013
Title:	Expression of SUDHL-1 cell line treated by ALK inhibitors
Organism:	Homo sapiens
Experiment type:	Expression profiling by array
Platform:	GPL570
Pubmed ID:	24218456
Summary & Design:	**Summary:** In this study we compared the effects of ALK inhibitor on the gene expression, activation of cell signaling pathways, and functional properties of cells derived from a patient with Anaplastic Large Cell Lymphoma. we used microarrays to map the genome-wide gene expression patterns in ALK+TCL cells in response to ALK inhibition. **Overall design:** The ALK+TCL Sudhl-1 cell line was treated in triplicates with the ALK inhibitor, CEP-14083, or the compound's solvent for 6 h. The isolated RNA was reverse-transcribed, biotin-labeled, and hybridized to the U133 Plus 2.0 array chips (Affymetrix). Microarray data were normalized using the MAS5 algorithm and analyzed using Partek GS (Partek).

Background corr dist: KL-Divergence = 0.0301, L1-Distance = 0.0472, L2-Distance = 0.0029, Normal std = 0.7358

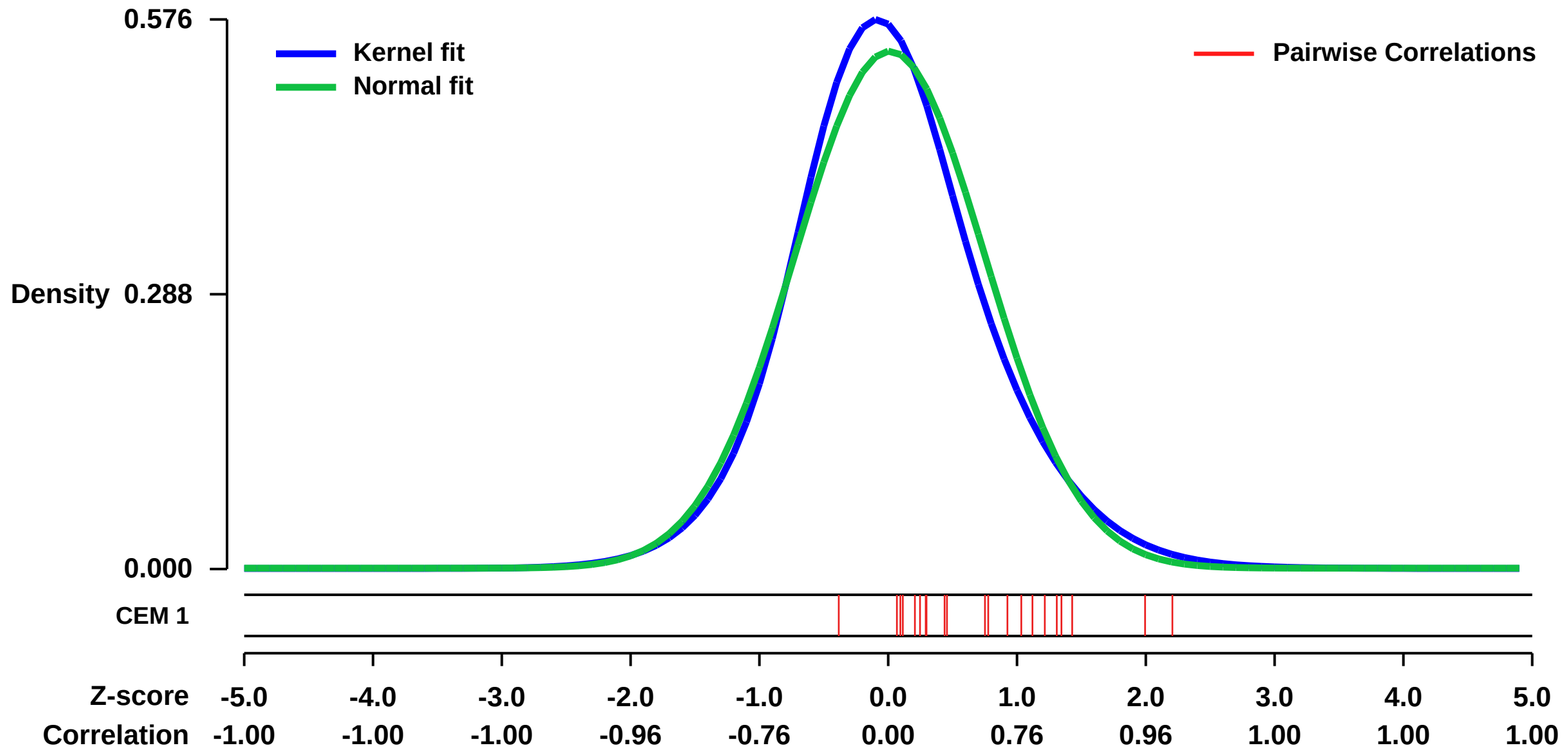

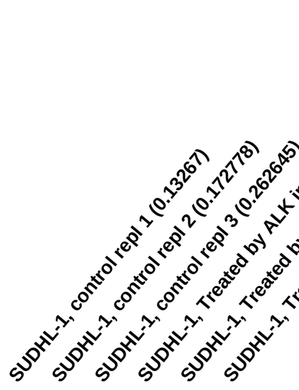

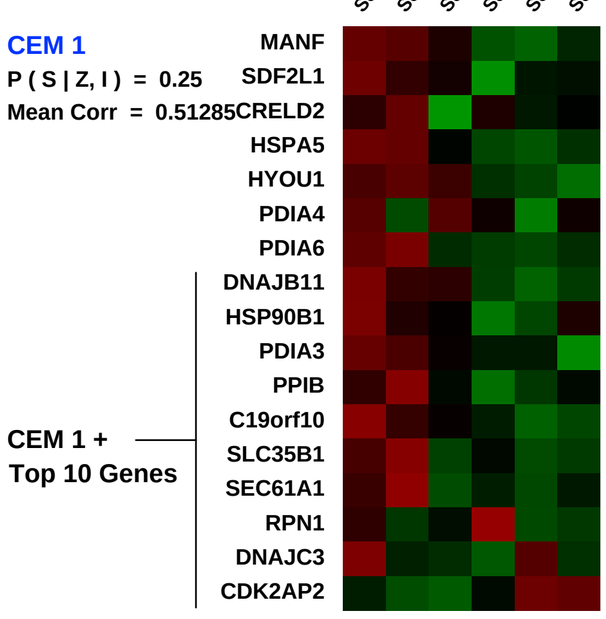

Pre-normalization Quantiles

	[min]	[medium]	[max]
MANF	3436.8	4368.7	4894.7
SDF2L1	682.4	1046.3	1251.1
CRELD2	1257.5	1708.0	1885.9
HSPA5	10269.0	11883.4	14069.9
HYOU1	1683.8	2263.3	2380.4
PDIA4	441.2	555.8	613.8
PDIA6	6339.1	6558.1	7922.0
DNAJB11	2723.1	3982.8	4669.8
HSP90B1	5579.2	6616.9	7278.4
PDIA3	5096.2	5586.7	5905.5
PPIB	9628.8	11176.7	13365.3
C19orf10	2456.4	2796.5	3221.8
SLC35B1	6703.9	6953.0	7479.2
SEC61A1	2256.0	2372.5	2747.9
RPN1	2355.9	2609.1	3296.2
DNAJC3	1058.8	1093.3	1190.5
CDK2AP2	704.6	876.3	1132.8

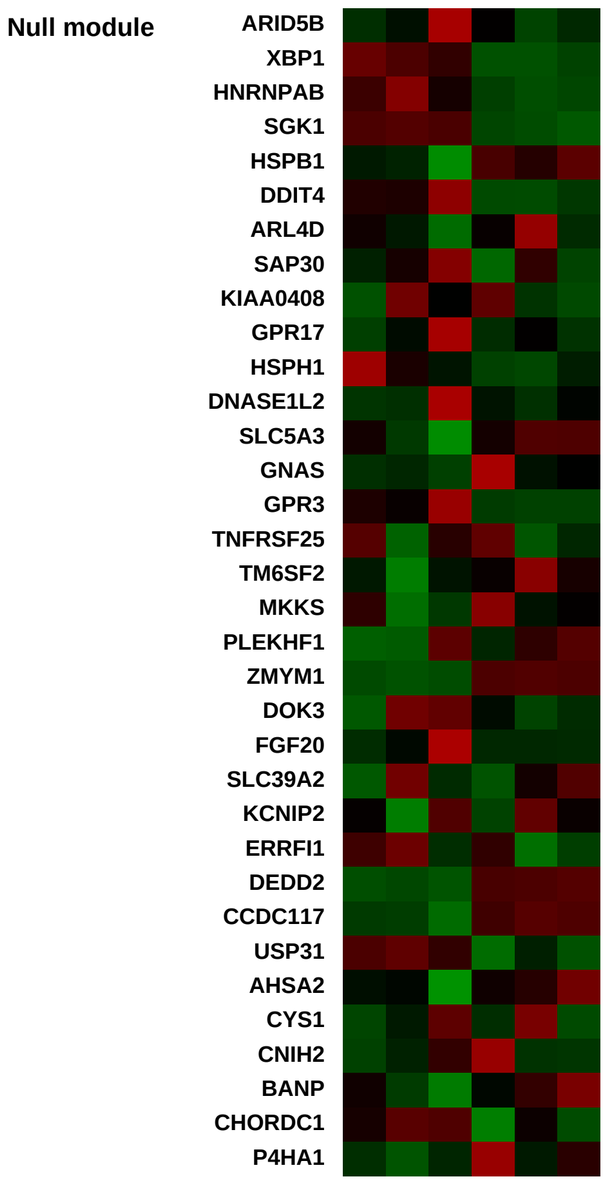

GEO Series "GSE5504" Expression Profiles

Num of samples in this series: 10

Scale of expression profile Z-scores

-3.0 -2.0 -1.0 0.0 1.0 2.0 3.0

GEO Link:	http://www.ncbi.nlm.nih.gov/geo/query/acc.cgi?acc=GSE5504
Status:	Public on Aug 10 2007
Title:	human peripheral blood derived monocytes, LPS stimulation time-series
Organism:	Homo sapiens
Experiment type:	Expression profiling by array
Platform:	GPL570
Pubmed ID:	17913878
Summary & Design:	**Summary:** To evaluate gene expression in human peripheral blood derived monocytes over the course of an LPS stimulation time-series. **Keywords: time course** **Overall design:** Blood samples from three individuals, each sample split into separate culture for each timepoint (0, 2, 4, 8, and 24 hours). RNA prepared from all, and analyzed with Bioanalyzer. Two best RNA samples from each timepoint analyzed by hybridization to a chip.

Background corr dist: KL-Divergence = 0.0324, L1-Distance = 0.0614, L2-Distance = 0.0062, Normal std = 0.6898

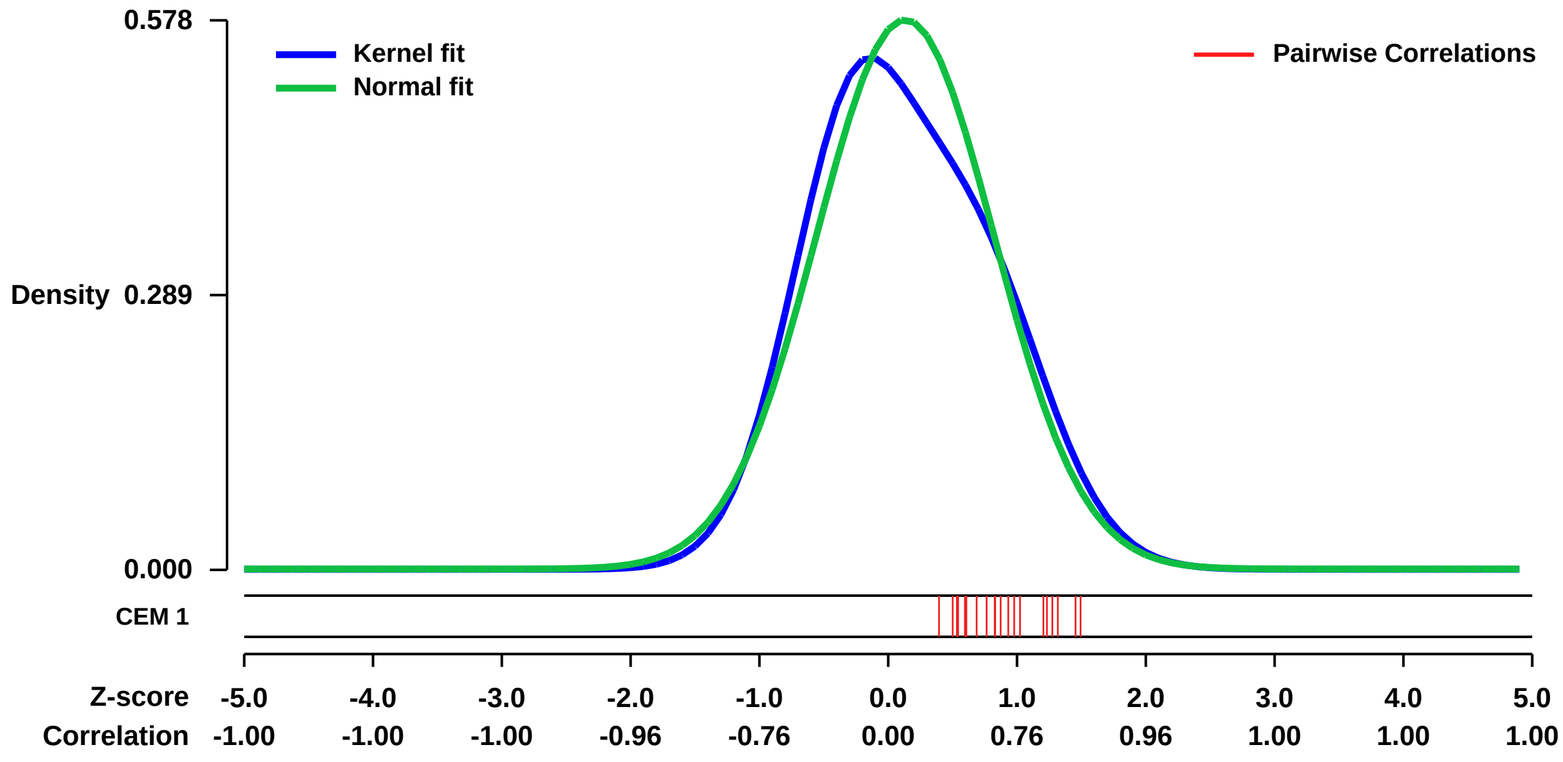

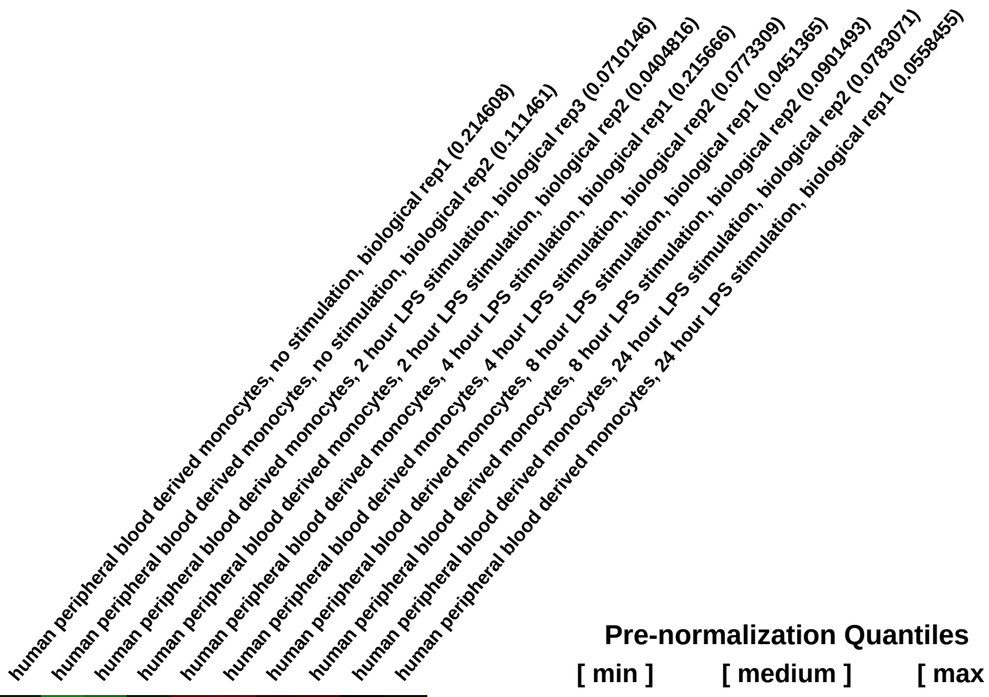

CEM 1
P (S | Z, I) = 0.17
Mean Corr = 0.67568

CEM 1 + Top 10 Genes

Null module

		Pre-normalization Quantiles		
		[min]	[medium]	[max]
CEM 1	MANF	1225.1	2579.5	3646.9
	SDF2L1	878.4	2473.1	5842.8
	CRELD2	754.1	1603.8	4912.0
	HSPA5	9467.0	27777.8	36673.3
	HYOU1	940.9	2434.3	4427.0
	PDIA4	1009.0	1832.1	2228.9
	PDIA6	5073.3	9042.5	10804.1
CEM 1 + Top 10 Genes	DNAJB11	2626.1	4567.8	7191.6
	HSP90B1	1662.0	3547.1	4511.2
	PDIA3	7905.8	13327.3	14689.6
	PPIB	12345.1	15527.2	16416.9
	C19orf10	3664.2	4397.6	5052.9
	SLC35B1	1673.6	2484.1	3044.7
	SEC61A1	3080.0	3749.4	4019.8
	RPN1	6530.1	7267.7	8294.3
	DNAJC3	2467.3	3672.4	5512.5
	CDK2AP2	713.8	950.2	1162.0
Null module	ARID5B			
	XBP1			
	HNRNPAB			
	SGK1			
	HSPB1			
	DDIT4			
	ARL4D			
	SAP30			
	KIAA0408			
	GPR17			
	HSPH1			
	DNASE1L2			
	SLC5A3			
	GNAS			
	GPR3			
	TNFRSF25			
	TM6SF2			
	MKKS			
	PLEKHF1			
	ZMYM1			
	DOK3			
	FGF20			
	SLC39A2			
	KCNIP2			
	ERRFI1			
	DEDD2			
	CCDC117			
	USP31			
	AHSA2			
	CYS1			
	CNIH2			
	BANP			
	CHORDC1			
	P4HA1			

GEO Series "GSE28305" Expression Profiles

Num of samples in this series: 8

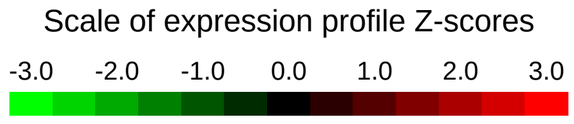

GEO Link:	http://www.ncbi.nlm.nih.gov/geo/query/acc.cgi?acc=GSE28305
Status:	Public on Jul 11 2011
Title:	Effect of 5a-dihydrotestosterone on breast cancer cell line MDA-MB-453
Organism:	Homo sapiens
Experiment type:	Expression profiling by array
Platform:	GPL570
Pubmed ID:	21741601
Summary & Design:	**Summary:** Analysis of MDA-MB-453 breast cancer cells treated with the androgen 5a-dihydrotestosterone (DHT) for 6h, 16h and 48h to define the genes that are differentially regulated in response to DHT. **Overall design:** MDA-MB-453 breast cancer cells were treated with 5a-dihydrotestosterone (DHT) for time course, followed by RNA extraction and hybridization on Affymetrix microarrays, in order to obtain the gene expression profiles at three time points. The vehicle treated samples are used as control.

Background corr dist: KL-Divergence = 0.0621, L1-Distance = 0.0191, L2-Distance = 0.0004, Normal std = 0.5186

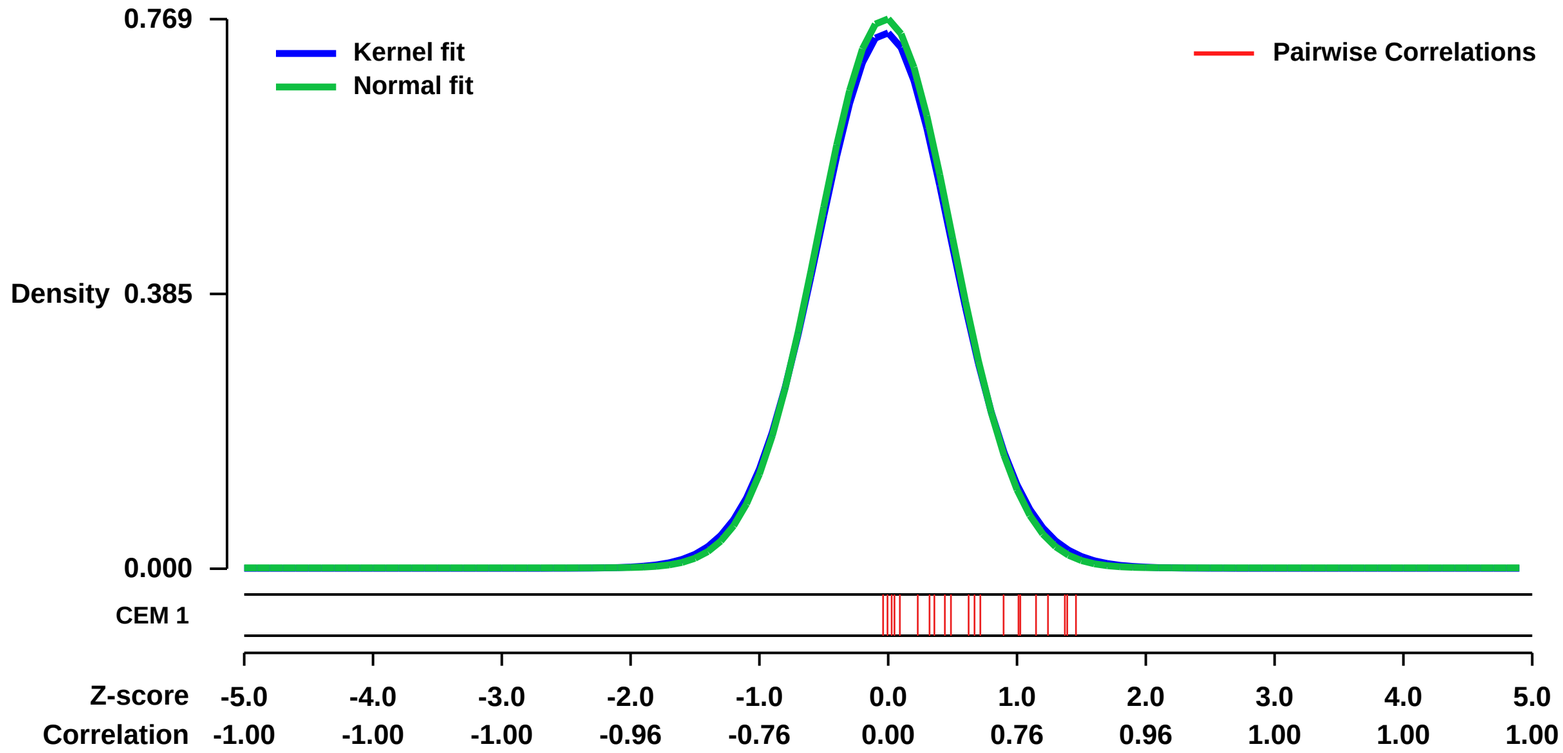

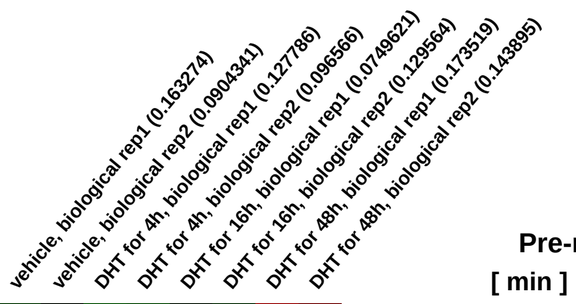

Pre-normalization Quantiles

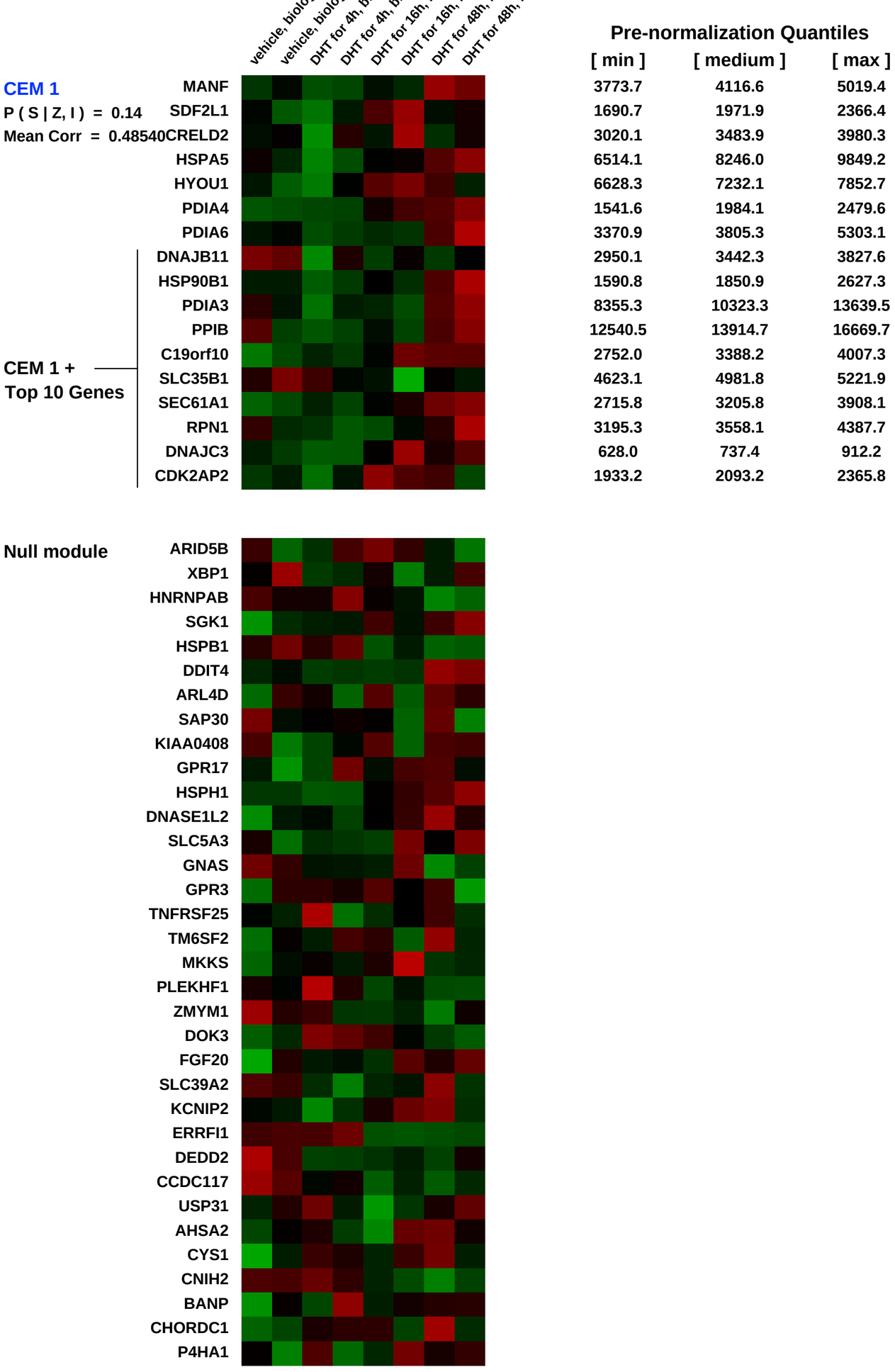

GEO Series "GSE48786" Expression Profiles

Num of samples in this series: 6

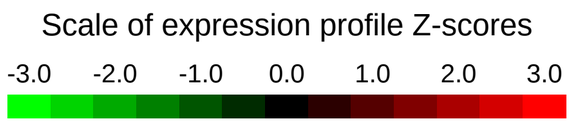

GEO Link:	http://www.ncbi.nlm.nih.gov/geo/query/acc.cgi?acc=GSE48786
Status:	Public on Dec 31 2013
Title:	Expression data from endothelial cells sorted from breast cancer cells MDA-MB231 as compared with normal endothelial cells
Organism:	Homo sapiens
Experiment type:	Expression profiling by array
Platform:	GPL570
Pubmed ID:	
Summary & Design:	**Summary:** We studied the crosstalk between tumor and endothelial cells to explore the role of tumor microenvironment on cancer growth and progression. As part of our investigation, we showed that contact-dependent interaction of endothelial cells with breast tumor cells triggered the differential expression of a large number of genes in endothelium. **Overall design:** WCMC-Q Genomics Core

Background corr dist: KL-Divergence = 0.0170, L1-Distance = 0.0347, L2-Distance = 0.0014, Normal std = 0.8125

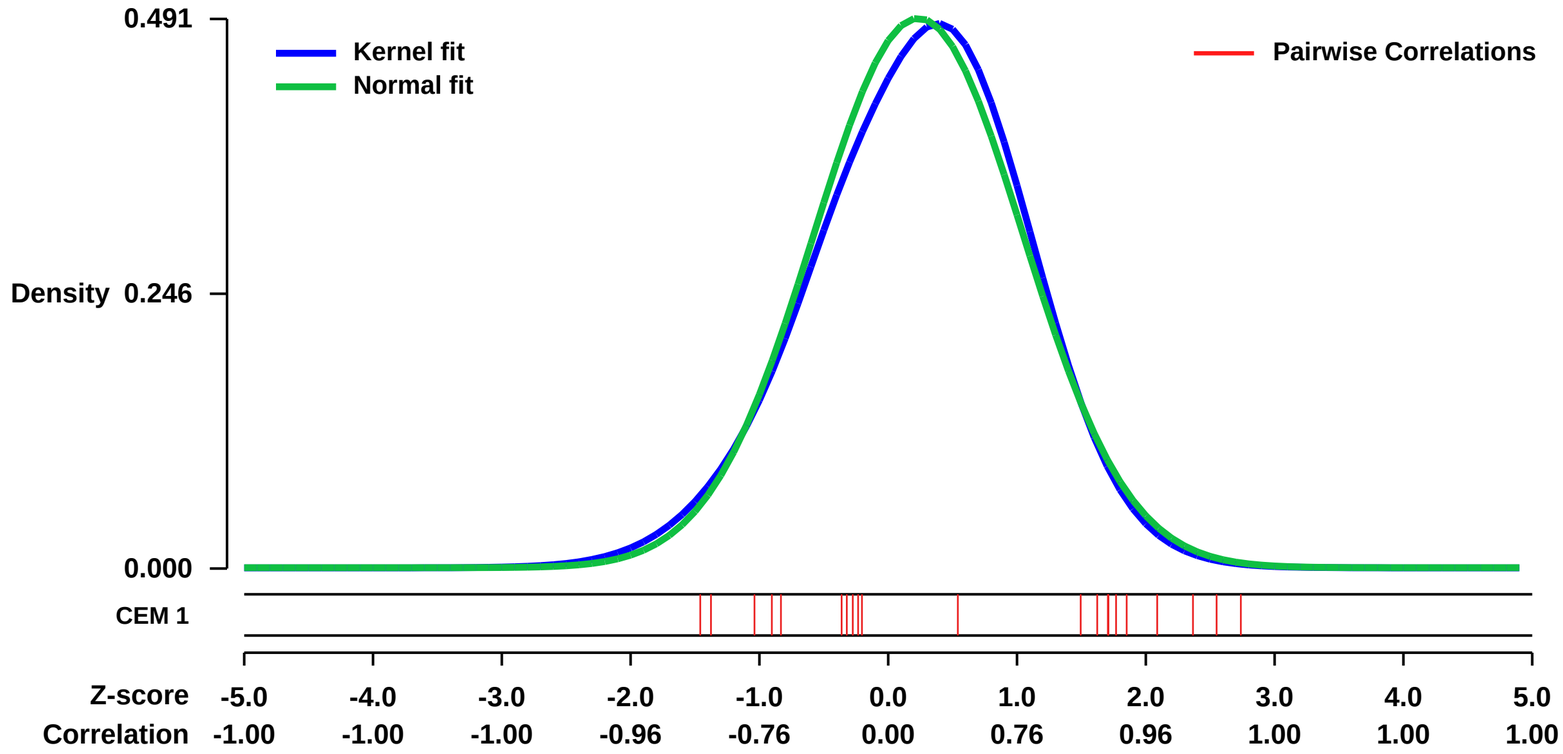

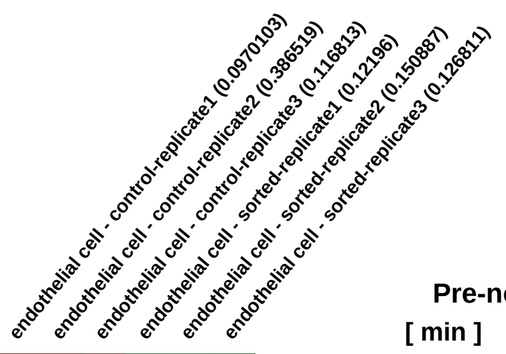

Pre-normalization Quantiles

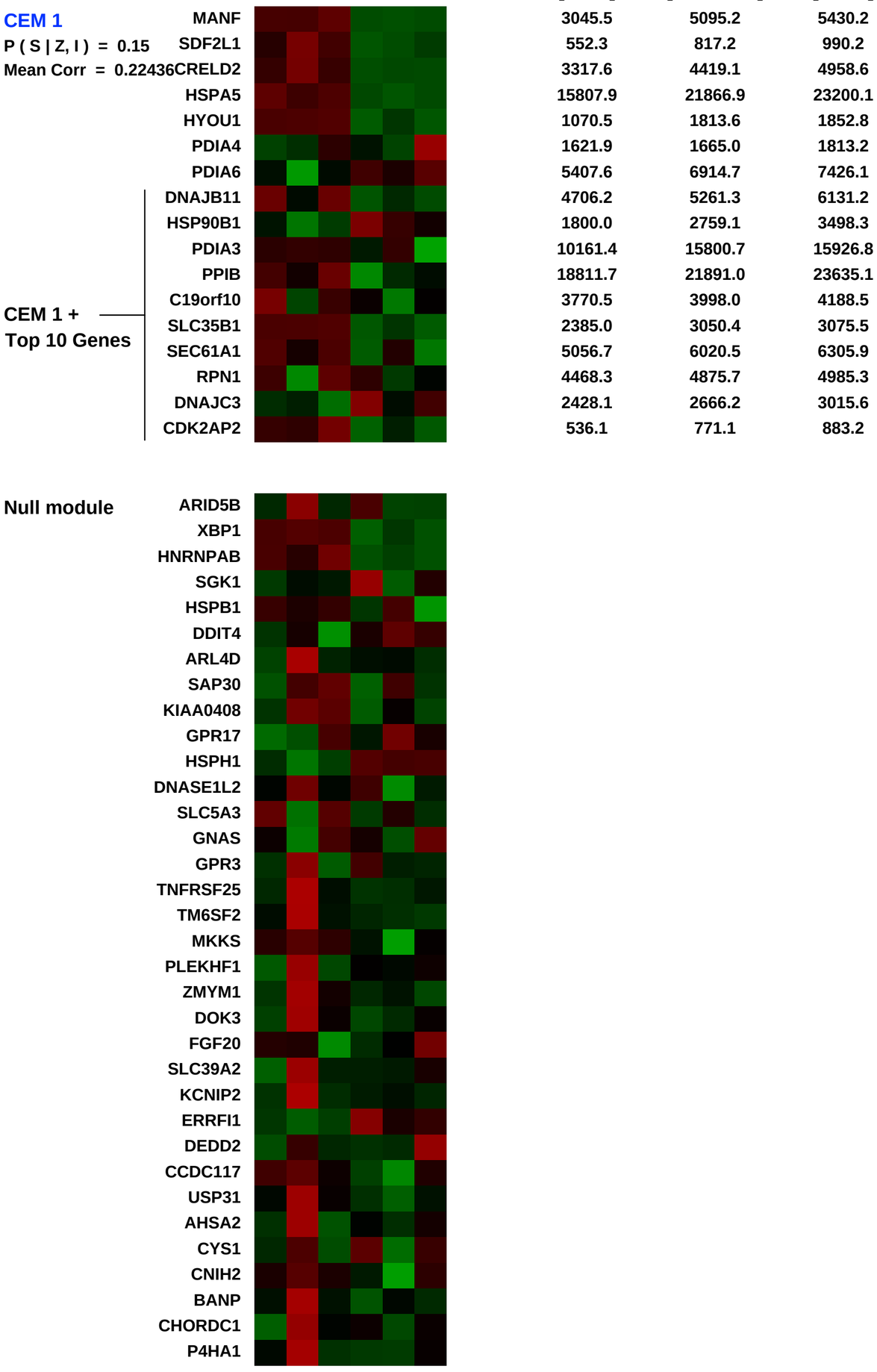

	[min]	[medium]	[max]
MANF	3045.5	5095.2	5430.2
SDF2L1	552.3	817.2	990.2
CRELD2	3317.6	4419.1	4958.6
HSPA5	15807.9	21866.9	23200.1
HYOU1	1070.5	1813.6	1852.8
PDIA4	1621.9	1665.0	1813.2
PDIA6	5407.6	6914.7	7426.1
DNAJB11	4706.2	5261.3	6131.2
HSP90B1	1800.0	2759.1	3498.3
PDIA3	10161.4	15800.7	15926.8
PPIB	18811.7	21891.0	23635.1
C19orf10	3770.5	3998.0	4188.5
SLC35B1	2385.0	3050.4	3075.5
SEC61A1	5056.7	6020.5	6305.9
RPN1	4468.3	4875.7	4985.3
DNAJC3	2428.1	2666.2	3015.6
CDK2AP2	536.1	771.1	883.2
ARID5B			
XBP1			
HNRNPAB			
SGK1			
HSPB1			
DDIT4			
ARL4D			
SAP30			
KIAA0408			
GPR17			
HSPH1			
DNASE1L2			
SLC5A3			
GNAS			
GPR3			
TNFRSF25			
TM6SF2			
MKKS			
PLEKHF1			
ZMYM1			
DOK3			
FGF20			
SLC39A2			
KCNIP2			
ERRFI1			
DEDD2			
CCDC117			
USP31			
AHSA2			
CYS1			
CNIH2			
BANP			
CHORDC1			
P4HA1			

GEO Series "GSE2600" Expression Profiles

Num of samples in this series: 6

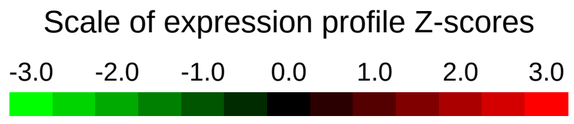

GEO Link:	**http://www.ncbi.nlm.nih.gov/geo/query/acc.cgi?acc=GSE2600**
Status:	**Public on Jul 29 2005**
Title:	**Anaplasma phagocytophilum infected NB4 cells**
Organism:	**Homo sapiens**
Experiment type:	**Expression profiling by array**
Platform:	**GPL570**
Pubmed ID:	**16005178**
Summary & Design:	**Summary:** **THREE INDEPENDENT REPLICATES AND ARE THE CONTROL NON-INFECTED CELLS:** **GSM49939, GSM49940, GSM49941** **THREE INFECTED INDEPEDENDENT REPLICATES:** **GSM49942, GSM49943, GSM49944** **Keywords: ordered** **Overall design:**

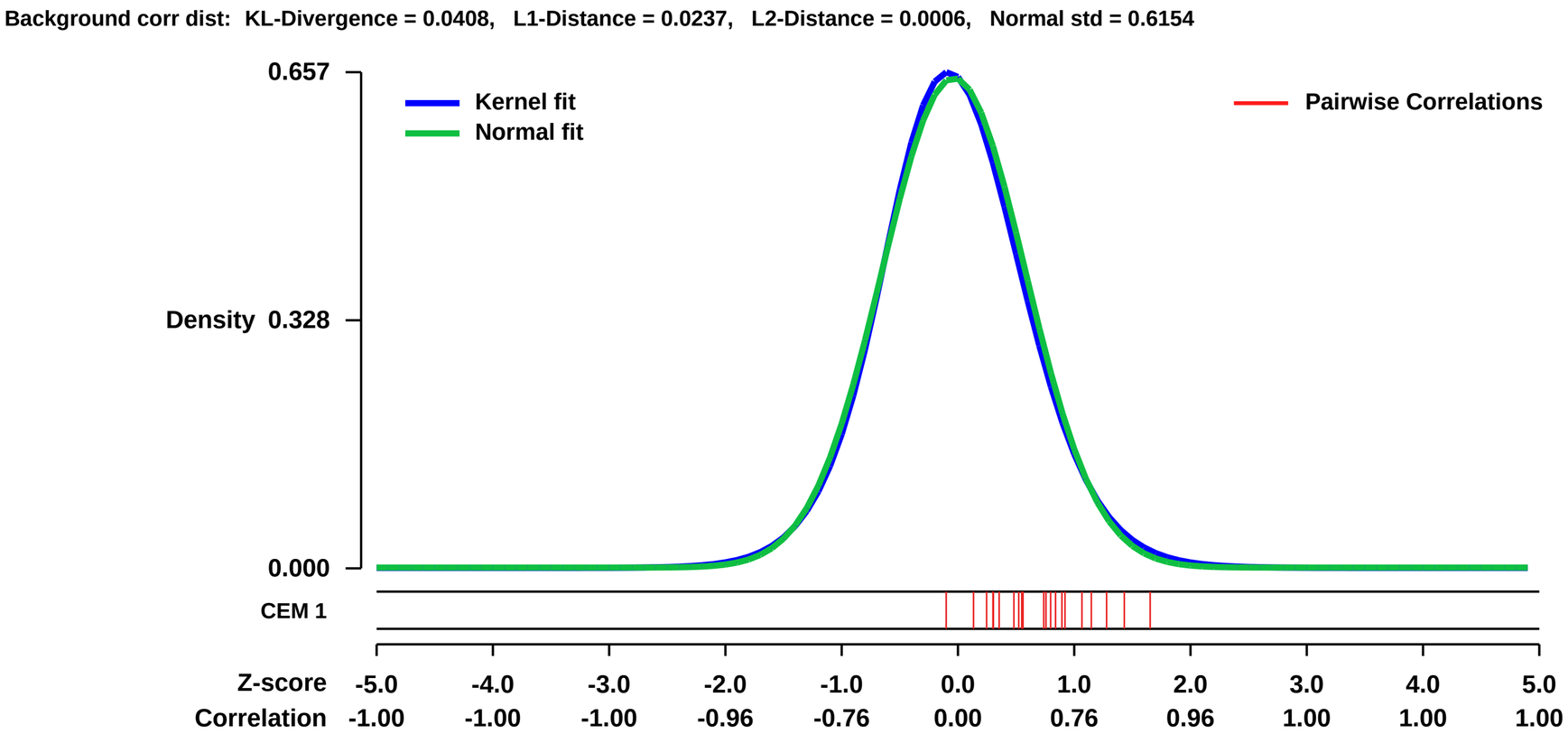

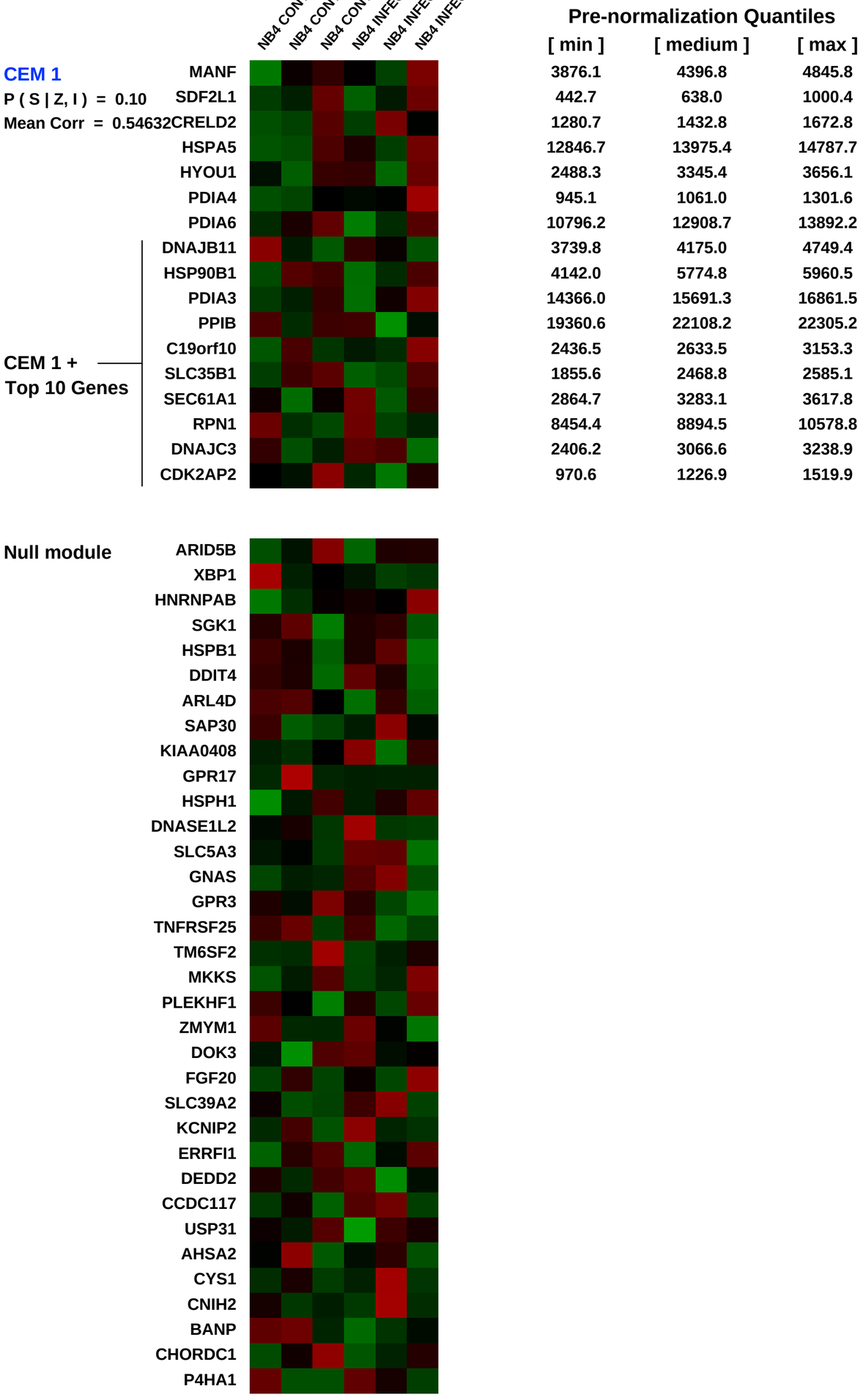

GEO Series "GSE6869" Expression Profiles

Num of samples in this series: 12

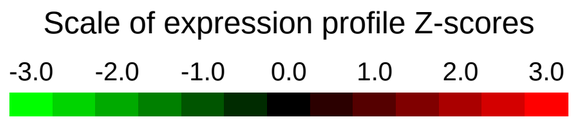

GEO Link:	http://www.ncbi.nlm.nih.gov/geo/query/acc.cgi?acc=GSE6869
Status:	Public on Jul 22 2010
Title:	Expression data from human liver cell line induced by PCB77
Organism:	Homo sapiens
Experiment type:	Expression profiling by array
Platform:	GPL570
Pubmed ID:	20638727
Summary & Design:	**Summary:** Exposure to Polychlorobiphenyls (PCBs) is known to cause serious health effects in human but the gene expression profiles leading to development of different diseases is not fully understood. The knowledge of global gene expression will help us to develop early diagnostic biomarkers for PCB induced health effects. We used microarrays to detail the global gene expression profile underlying the effects of PCB77 on human liver cells leading to identification of distinct classes of up-regulated and down-regulated genes and cellular processes. Keywords: time course **Overall design:** The HepG2 cells were grown for 48 hours in DMEM supplemented with 10% FBS and 1X Pennicillin-Streptromycin and treated with PCB77 for different times. Trizol extraction of total RNA was performed according to the manufacturer's instructions. Biotinylated cRNA were prepared according to the standard Affymetrix protocol from 6 microgram of total RNA (Expression Analysis Technical Manual, 2001, Affymetrix). Following fragmentation, 10 microgram of cRNA were hybridized for 16 hr at 45C on GeneChip Human Genome Array (HGU133 plus 2.0). GeneChips were washed and stained in the Affymetrix Fluidics Station 450 and scanned using the Affymetrix GeneArray Scanner 3000. The data were analyzed with Microarray Suite version 5.0 (MAS 5.0) using Affymetrix default analysis settings and global scaling as normalization method. The trimmed mean target intensity of each array was arbitrarily set to 150.

Background corr dist: KL-Divergence = 0.1071, L1-Distance = 0.0299, L2-Distance = 0.0017, Normal std = 0.4303

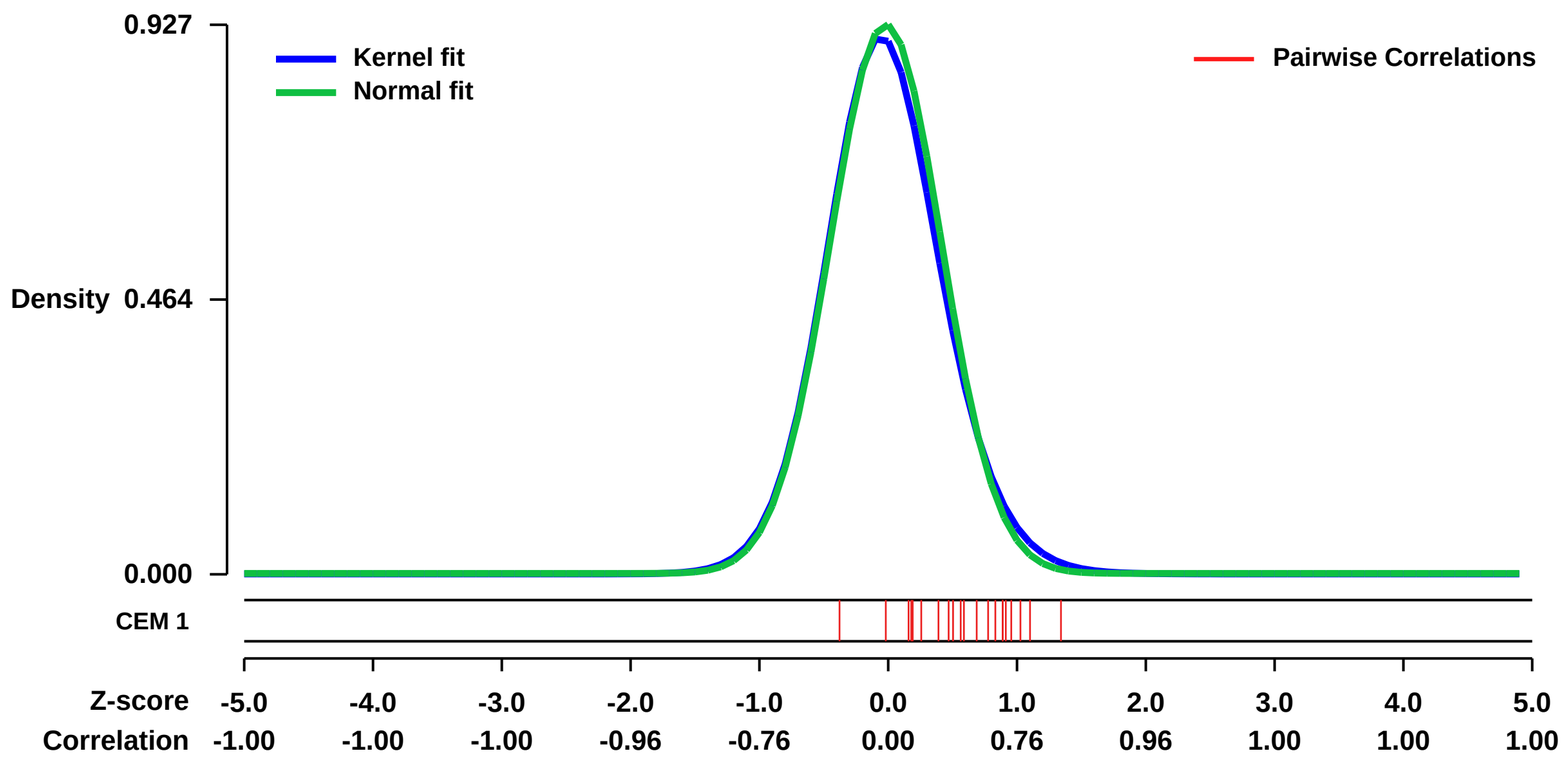

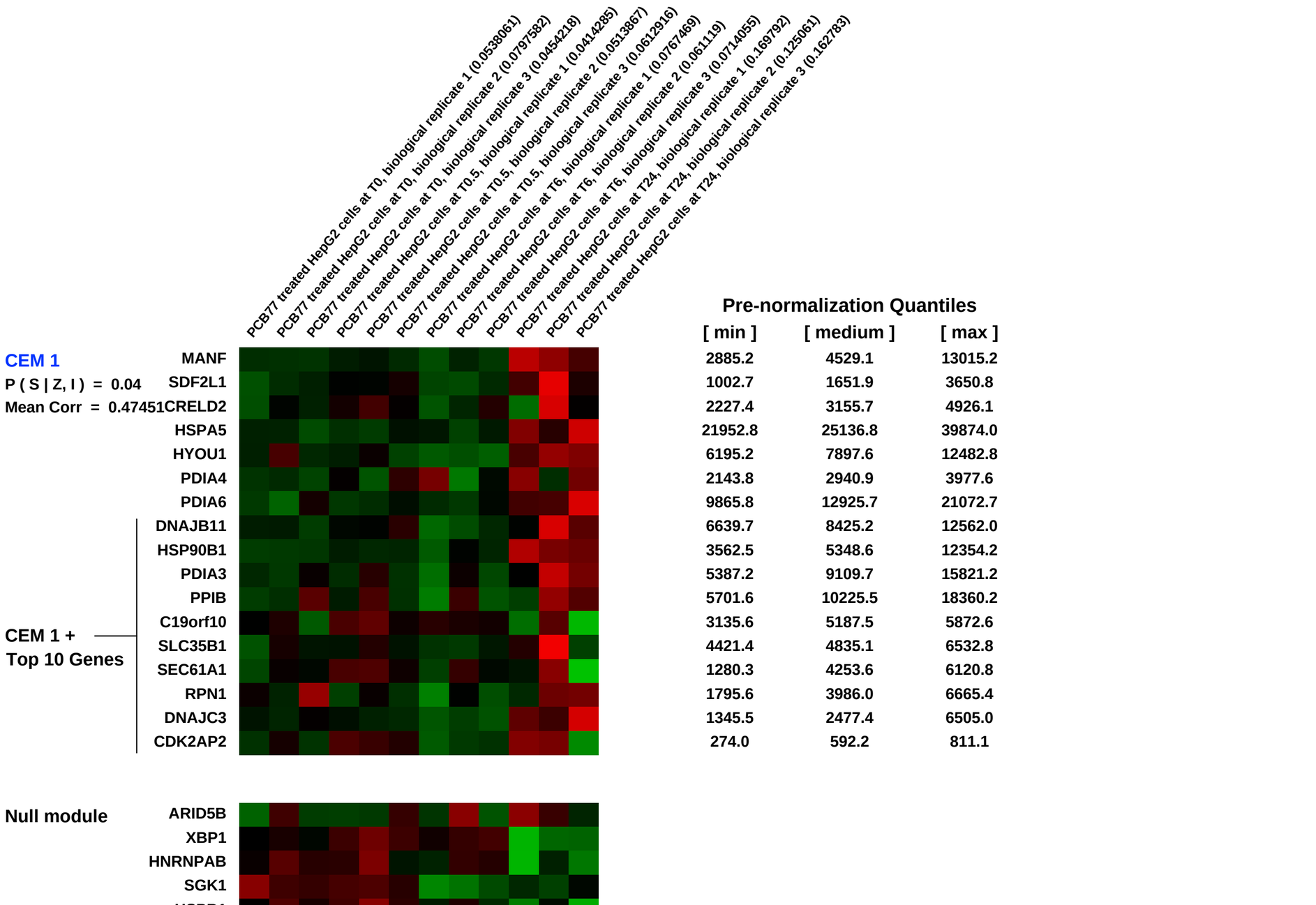

GEO Series "GSE12287" Expression Profiles

Num of samples in this series: 20

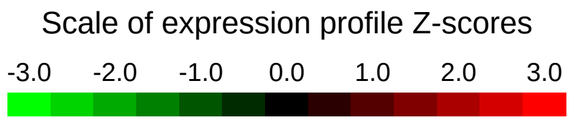

GEO Link:	http://www.ncbi.nlm.nih.gov/geo/query/acc.cgi?acc=GSE12287
Status:	Public on May 27 2009
Title:	Bioligical pathways of Hsp90 inhibitors in adult T cell leukemia cell lines
Organism:	Homo sapiens
Experiment type:	Expression profiling by array
Platform:	GPL570
Pubmed ID:	19464103
Summary & Design:	**Summary:** Heat shock protein 90 (Hsp90) is essential for the stability and the function of many client proteins, such as ERB2, C-RAF, CDK4, HIF-1 aplha and AKT. Recent reports demonstrated that inhibition of Hsp90 modulates multiple functions required for survival of human cancer, such as myeloma (Mitsiades et al, Blood:107, 1092, 2006), The aim of this study is evaluate the effect of Hsp90 inhibition, and to identify molecular pathways responsible for anti-proliferative effect on ATL cells. For Hsp90 inhibition, Geldanamycin derivates, 17AAG (17-allylamino -17-demethoxygeldanamycin) and 17DMAG (17-(dimethylaminoethylamino) 17-demethoxygeldanamycin) were used in this study. Interleukin 2-independent ATL cell lines (MT-2 and MT-4) and an interleukin 2-dependent ATL cell line (TaY-E10) were incubated, with or without Hsp90 inhibitors. **Overall design:** Three ATL cell lines(TaY-E10, MT-2, and MT-4) were cultured in the presence or absence of Hsp90 inhibitors(17-AAG and 17-DMAG).

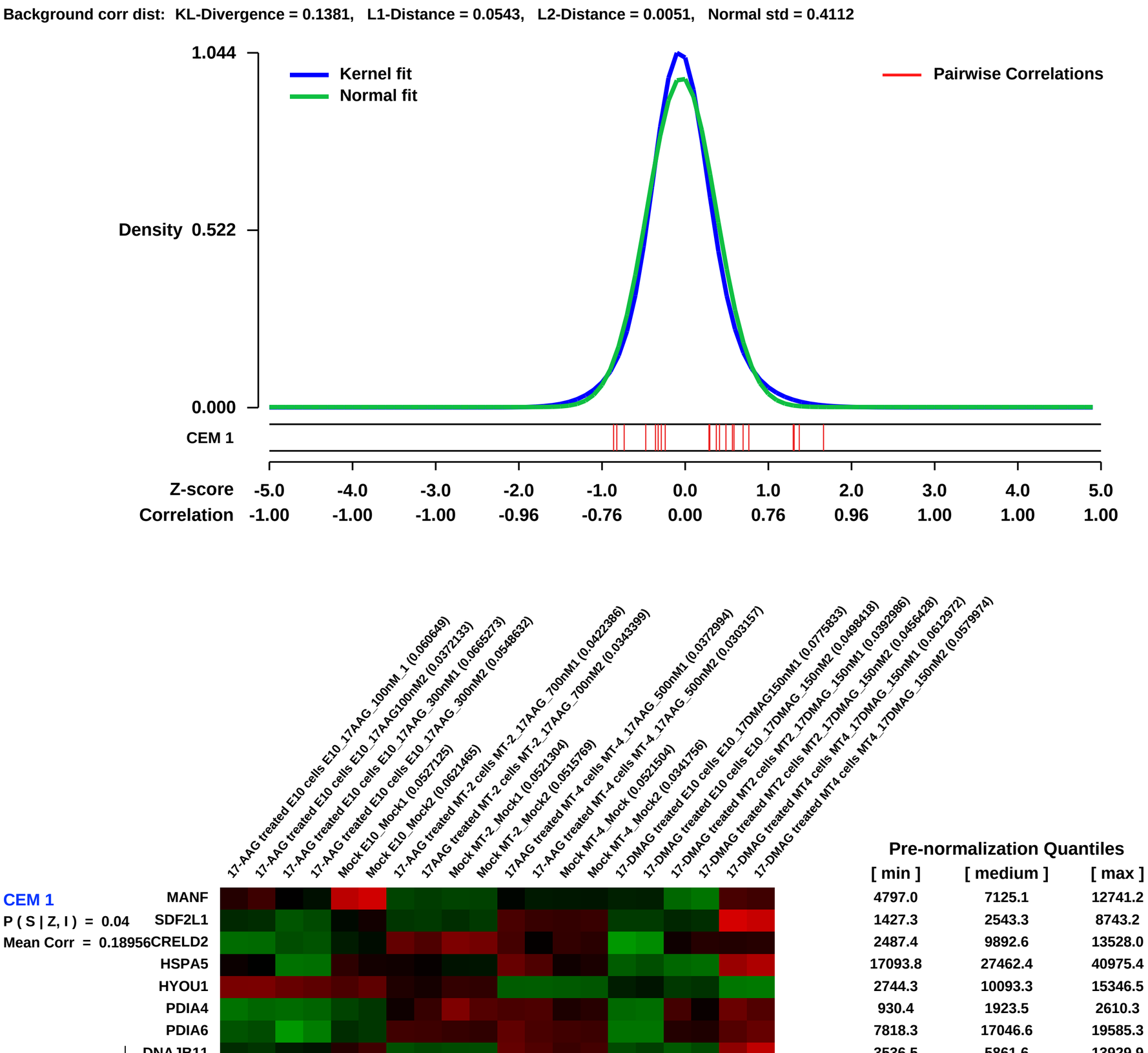

GEO Series "GSE18331" Expression Profiles

Num of samples in this series: 14

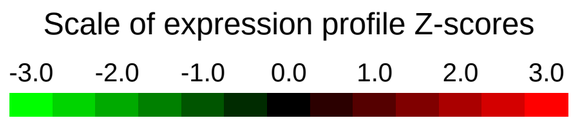

GEO Link:	http://www.ncbi.nlm.nih.gov/geo/query/acc.cgi?acc=GSE18331
Status:	Public on Jun 01 2011
Title:	A phenotype-based model for rational selection of novel targeted therapies in treating aggressive breast cancer
Organism:	Homo sapiens
Experiment type:	Expression profiling by array
Platform:	GPL570
Pubmed ID:	21772261
Summary & Design:	**Summary:** Treating unselected cancer patients with new drugs dilutes proof of efficacy when only a fraction of patients respond to therapy. We conducted a meta-analysis on eight primary breast cancer microarray datasets representing diverse breast cancer phenotypes. We present a high-throughput protocol which incorporates drug sensitivity signatures to guide preclinical testing for effective therapeutic agents. Specifically, we focus on drug classes currently undergoing early phase clinical testing. Our genomic and experimental results suggest that the majority of basal-like breast cancers should respond to inhibitors of the phosphatidylinositol-3-kinase pathway, and that a relatively low toxicity histone deacetylase inhibitor, valproic acid, may target aggressive breast cancers. For a subset of drugs, prediction of sensitivity associates with tumor recurrence, suggesting clinical relevance. Preclinical studies using both cell lines and patient tumors grown in 3-dimensional in vitro and orthotopic in vivo preclinical models provide an efficient and highly relevant assessment of drug sensitivity in tumor phenotypes, and validate our genomic analyses. Together, our results show that high-throughput transcriptional profiling can significantly impact drug selection for breast cancer patients. Pre-identification of patient response may not only improve therapeutic response rates, it can also assist in quickly identifying the optimal inclusion criteria for clinical trials. Our model facilitates personalized drug therapy for cancer patients and may be generalized for study of drug efficacy in other diseases. **Overall design:** Breast cancer pleural effusion samples from triple negative patients. Compared samples that are computationally predicted to be sensitive to valproic acid and those that are not predicted to be sensitive.

Background corr dist: KL-Divergence = 0.1808, L1-Distance = 0.0528, L2-Distance = 0.0071, Normal std = 0.3510

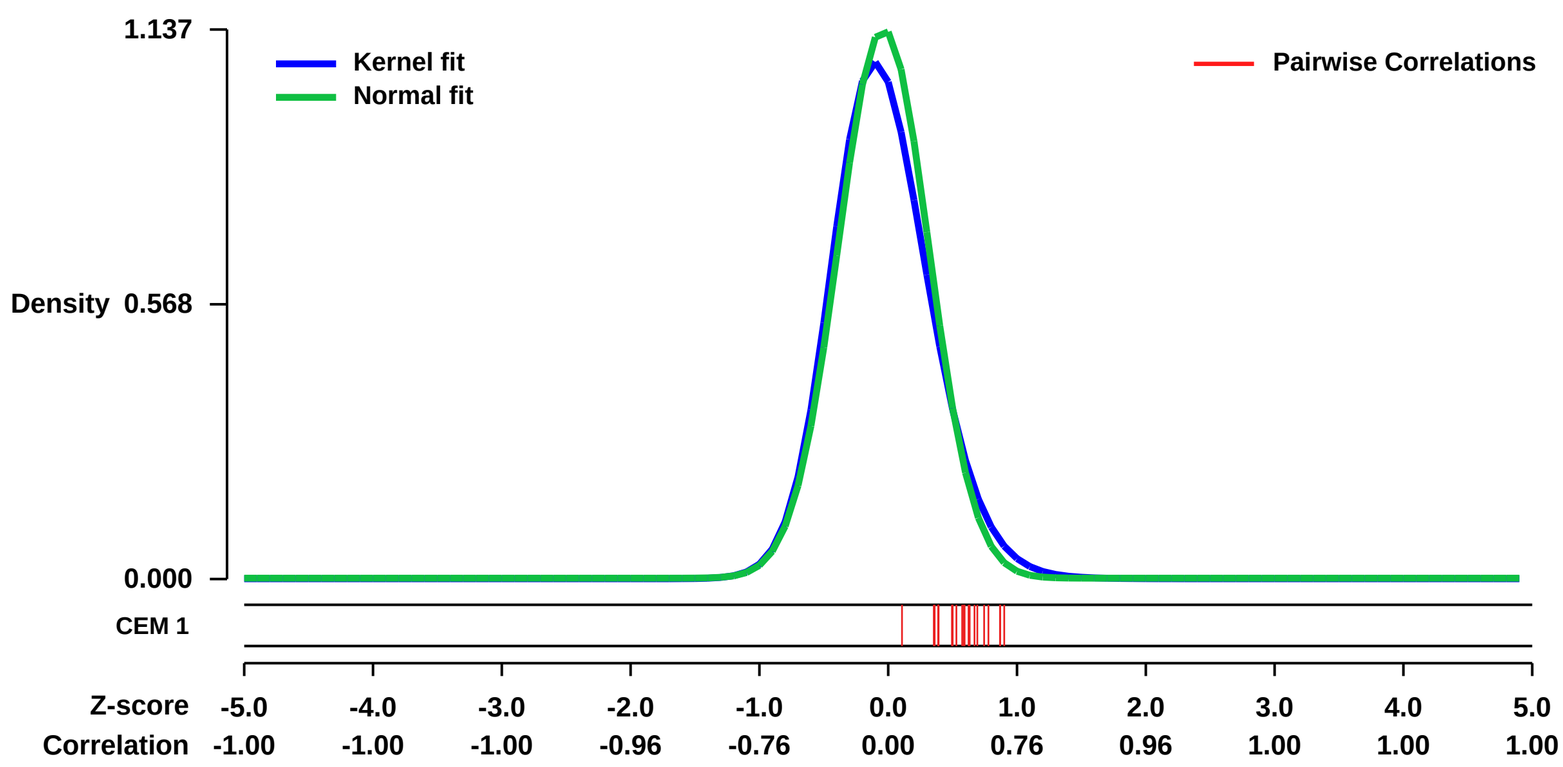

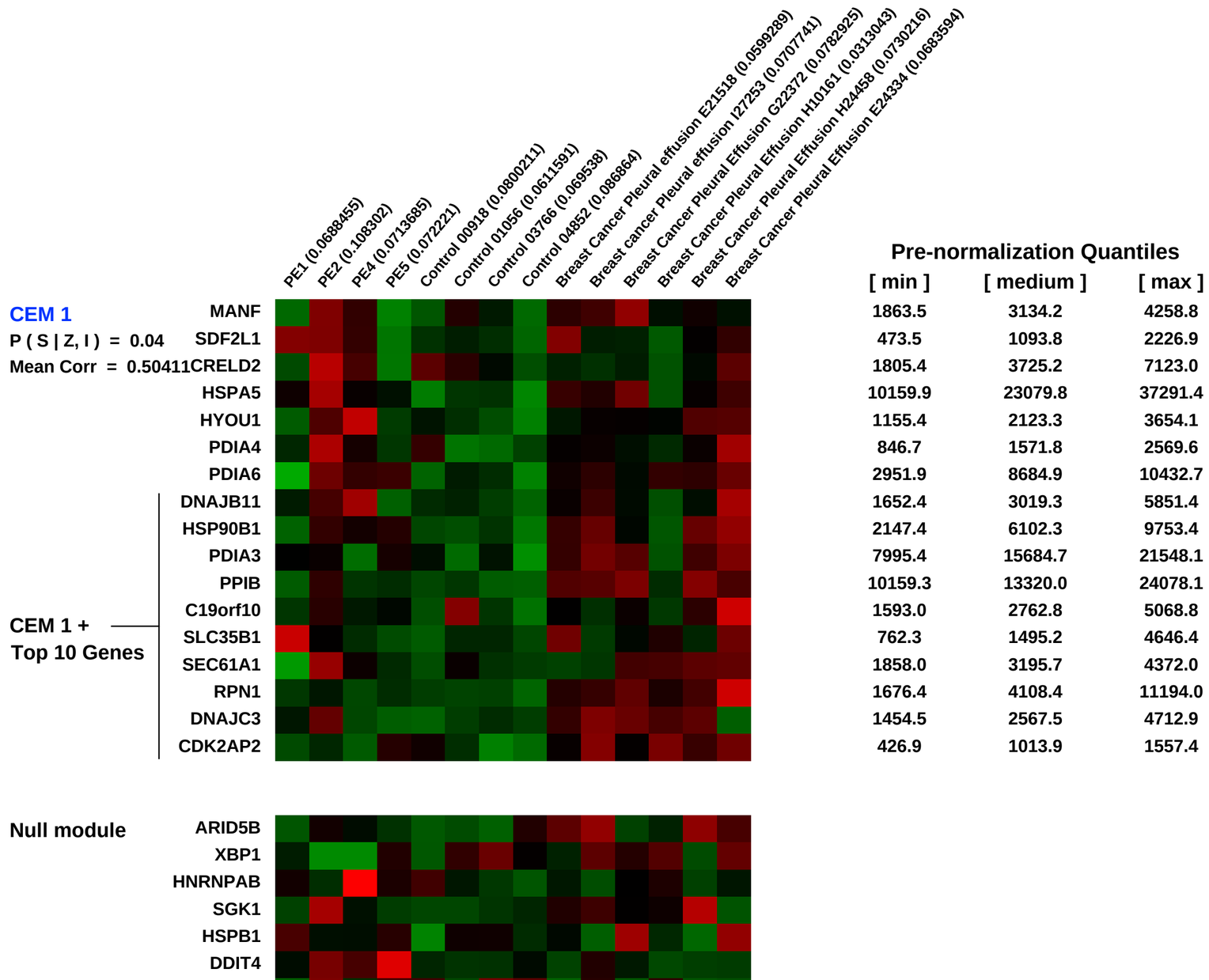

GEO Series "GSE8837" Expression Profiles

Num of samples in this series: 10

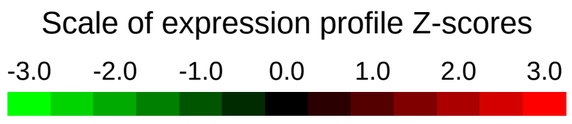

GEO Link:	http://www.ncbi.nlm.nih.gov/geo/query/acc.cgi?acc=GSE8837
Status:	Public on Aug 20 2008
Title:	Transcriptional regulation by the novel Rho GTPase RhoBTB2.
Organism:	Homo sapiens
Experiment type:	Expression profiling by array
Platform:	GPL570
Pubmed ID:	18762809
Summary & Design:	**Summary:** RhoBTB2 is a novel Rho GTPase that undergoes loss, underexpression and mutation in breast and lung cancer. We have shown that we can mimic loss of RhoBTB2 through siRNA treatment of primary cells. We propose to perform comparative microarray analysis of primary lung cells to establish the identification of the gene targets of RhoBTb2 regulation. **Keywords: Effects of siRNA expression** **Overall design:** Primary lung cells (NHBE) transfected with siRNA oligonucleotides against cyclophilin or Lamin A/C (controls) were compared to cells transfected with siRNA oligonucleotides against RhoBTB2. We used two siRNA oligonucleotides against RhoBTB2 (1 and 2) to determine any non-specific effects. Cells expressed the siRNA oligonucleotides for 72 hours before total RNA extraction. 10 samples have been analysed.

Background corr dist: KL-Divergence = 0.0527, L1-Distance = 0.0180, L2-Distance = 0.0004, Normal std = 0.5470

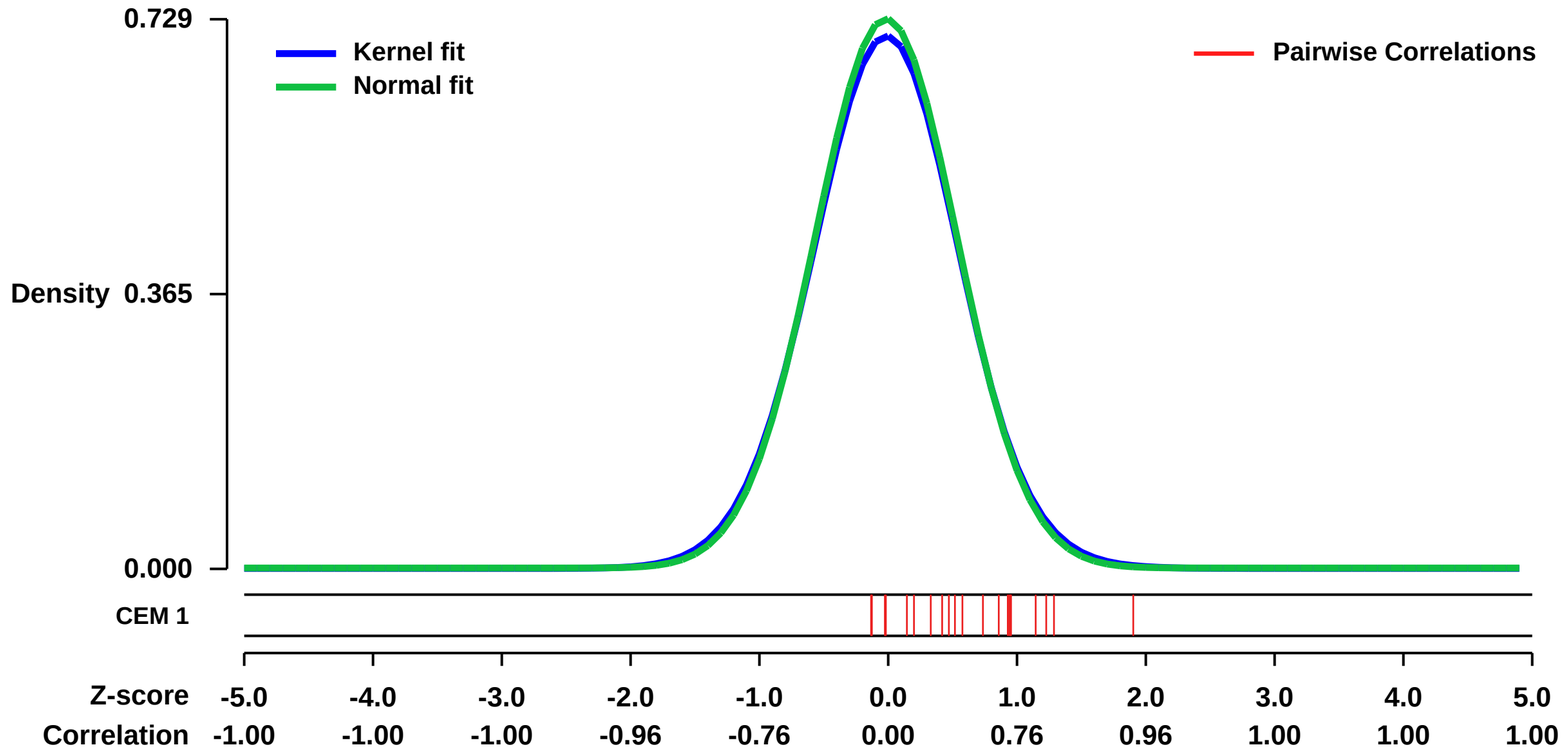

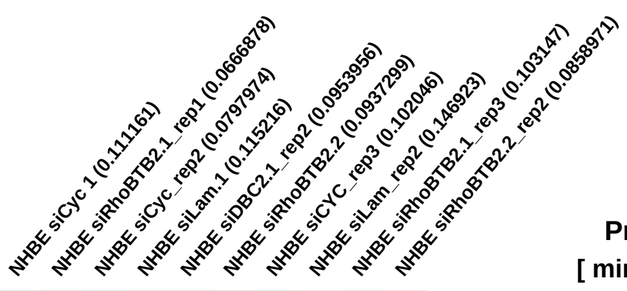

Pre-normalization Quantiles

[min] [medium] [max]

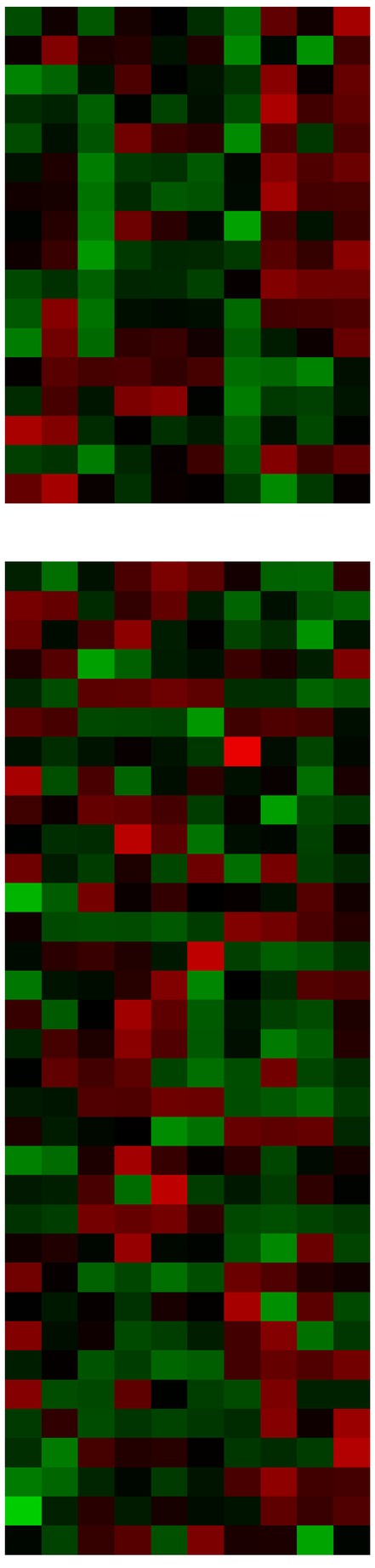

		[min]	[medium]	[max]
CEM 1	MANF	4024.4	5076.3	6297.0
P (S | Z, I) = 0.03	SDF2L1	954.3	1289.8	1484.0
Mean Corr = 0.47275	CRELD2	2351.2	3162.6	4034.8
	HSPA5	10110.3	12415.2	17820.3
	HYOU1	2037.8	2843.0	3140.1
	PDIA4	796.1	1133.9	1538.3
	PDIA6	5535.4	8279.6	11207.1
CEM 1 + Top 10 Genes	DNAJB11	1660.7	2372.4	2627.9
	HSP90B1	2061.9	4329.8	6023.8
	PDIA3	5655.9	7834.8	14106.3
	PPIB	514.7	8452.7	19356.1
	C19orf10	2560.4	2987.4	3266.9
	SLC35B1	1748.2	2675.2	2859.8
	SEC61A1	2018.4	2299.5	2729.8
	RPN1	2863.7	3356.2	4455.5
	DNAJC3	2206.5	2795.8	3339.3
	CDK2AP2	856.8	1426.3	2058.5

Null module	ARID5B
	XBP1
	HNRNPAB
	SGK1
	HSPB1
	DDIT4
	ARL4D
	SAP30
	KIAA0408
	GPR17
	HSPH1
	DNASE1L2
	SLC5A3
	GNAS
	GPR3
	TNFRSF25
	TM6SF2
	MKKS
	PLEKHF1
	ZMYM1
	DOK3
	FGF20
	SLC39A2
	KCNIP2
	ERRFI1
	DEDD2
	CCDC117
	USP31
	AHSA2
	CYS1
	CNIH2
	BANP
	CHORDC1
	P4HA1

GEO Series "GSE10138" Expression Profiles

Num of samples in this series: 68

Scale of expression profile Z-scores

-3.0 -2.0 -1.0 0.0 1.0 2.0 3.0

GEO Link: http://www.ncbi.nlm.nih.gov/geo/query/acc.cgi?acc=GSE10138
Status: Public on Oct 31 2009
Title: A Genomic Approach to Improve Prognosis and Predict Therapeutic Response in Chronic Lymphocytic Leukemia (Duke_VA)
Organism: Homo sapiens
Experiment type: Expression profiling by array
Platform: GPL570
Pubmed ID: 19861443

Summary & Design:

Summary:
Chronic lymphocytic leukemia (CLL) is a heterogeneous malignancy, characterized by a variable clinical course. While clinical and laboratory parameters are increasingly being used to refine prognosis, they do not accurately predict response to commonly used therapy. We used gene expression profiling to generate and further refine prognostic and predictive markers. Genomic signatures that reflect progressive disease and responses to chemotherapy or chemo-immunotherapy were created using cancer cell lines and patient leukemia samples. We validated these signatures using independent clinical data from four separate cohorts representing a total of 301 CLL patients. A prognostic genomic signature created from patient leukemic cell gene expression data coupled with clinical parameters could statistically differentiate patients with stable or progressive disease in the training dataset. The progression signature was then validated in two independent datasets, demonstrating a capacity to accurately identify patients at risk for progressive disease. In addition, two distinct genomic signatures that predict response to chlorambucil or pentostatin, cyclophosphamide, and rituximab were also generated and were shown to accurately distinguish responding and non-responding CLL patients. Microarray analysis of CLL patientsâ lymphocytes can be used to refine prognosis and predict response to different therapies. These results have direct implications for standard and investigational therapeutics in CLL patients.

Keywords: Gene Expression Profiling of two phenotypic states

Overall design:
For the prognostic genomic signature, 68 CLL leukemia samples were used (36 from patients with stable disease and 32 from patients with progressive disease).

Background corr dist: KL-Divergence = 0.4600, L1-Distance = 0.0765, L2-Distance = 0.0177, Normal std = 0.2345

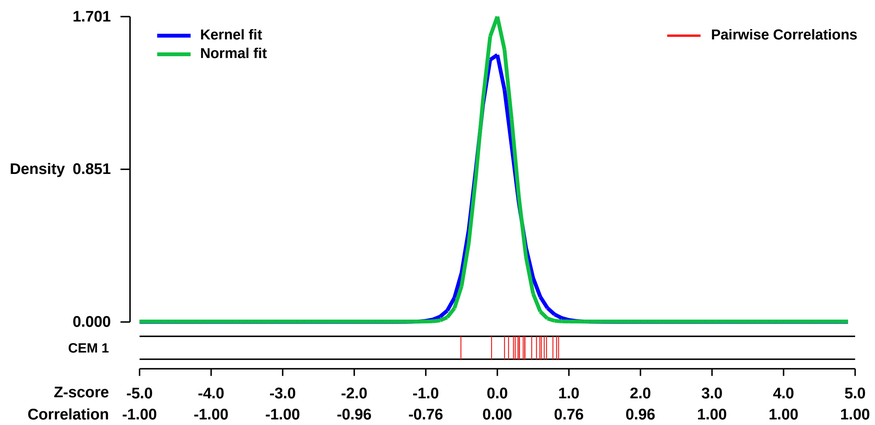

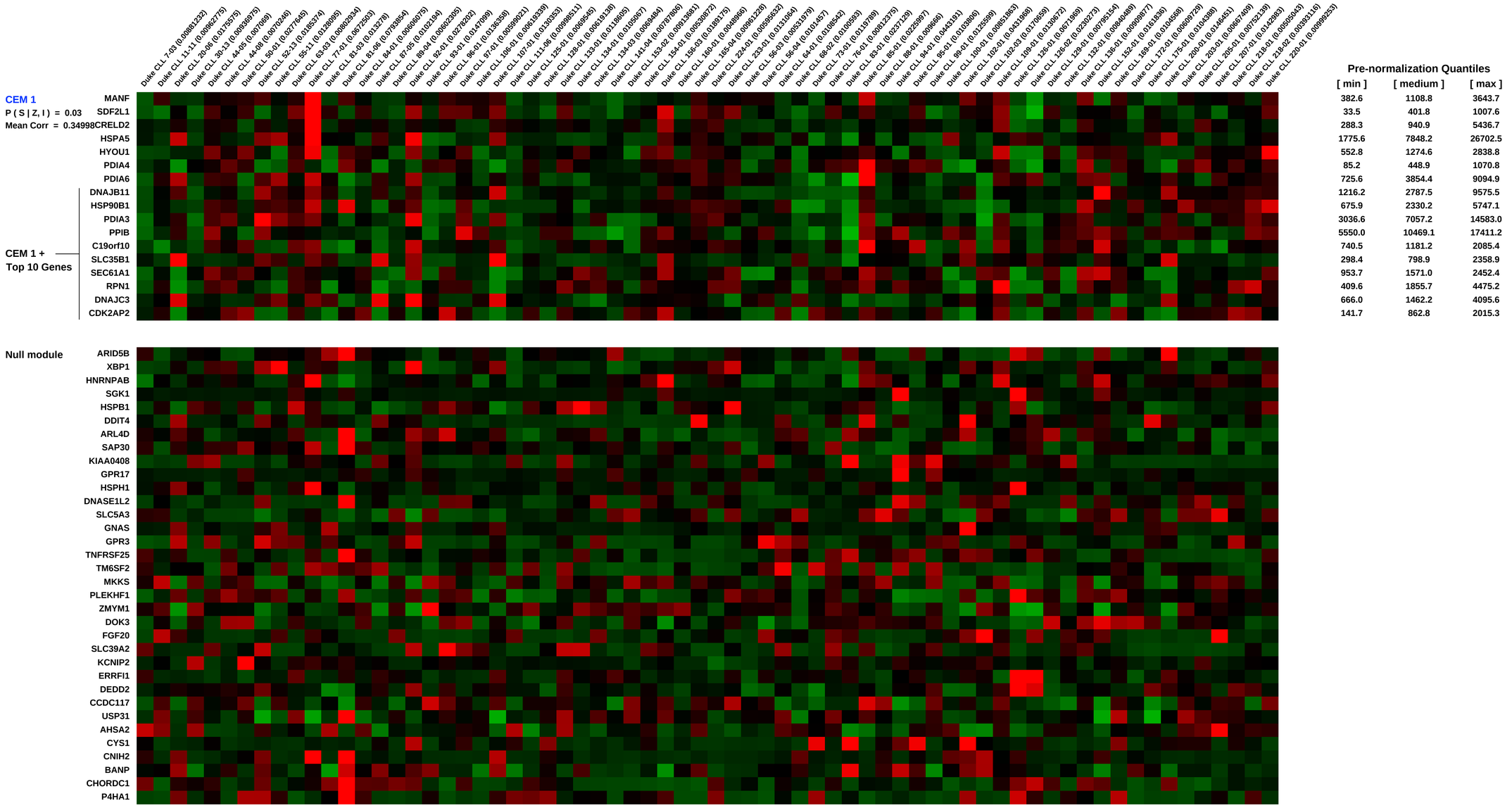

Pre-normalization Quantiles

[min]	[medium]	[max]
382.6	1108.8	3643.7
33.5	401.8	1007.6
288.3	940.9	5436.7
1775.6	7848.2	26702.5
552.8	1274.6	2838.8
85.2	448.9	1070.8
725.6	3854.4	9094.9
1216.2	2787.5	9575.5
675.9	2330.2	5747.1
3036.6	7057.2	14583.0
5550.0	10469.1	17411.2
740.5	1181.2	2085.4
298.4	798.9	2358.9
953.7	1571.0	2452.4
409.6	1855.7	4475.2
666.0	1462.2	4095.6
141.7	862.8	2015.3

GEO Series "GSE31255" Expression Profiles

Num of samples in this series: 11

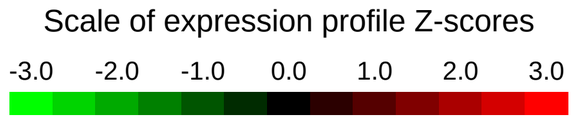

GEO Link:	http://www.ncbi.nlm.nih.gov/geo/query/acc.cgi?acc=GSE31255
Status:	Public on Nov 22 2011
Title:	Isolation and in vitro expansion of human colonic stem cells [Expression profile]
Organism:	Homo sapiens
Experiment type:	Expression profiling by array
Platform:	GPL570
Pubmed ID:	21892181
Summary & Design:	**Summary:** Using the surface marker EPHB2, we have FACS-purified and profiled stem cell-enriched cell fractions from normal human mucosa, crypt proliferative progenitors and late transient amplifying cells to define a gene expression program specific for normal human colon epithelial stem cells **Overall design:** We FACS purified human colonic crypt cells according to their EPHB2 surface abundance. We used Affymetrix chips to hybridize 3 samples from EPHB2-high, 3 samples from EPHB2-medium, 3 samples from EPHB2-low, and 2 samples from EPHB2-negative cells

Background corr dist: KL-Divergence = 0.0347, L1-Distance = 0.0244, L2-Distance = 0.0008, Normal std = 0.6382

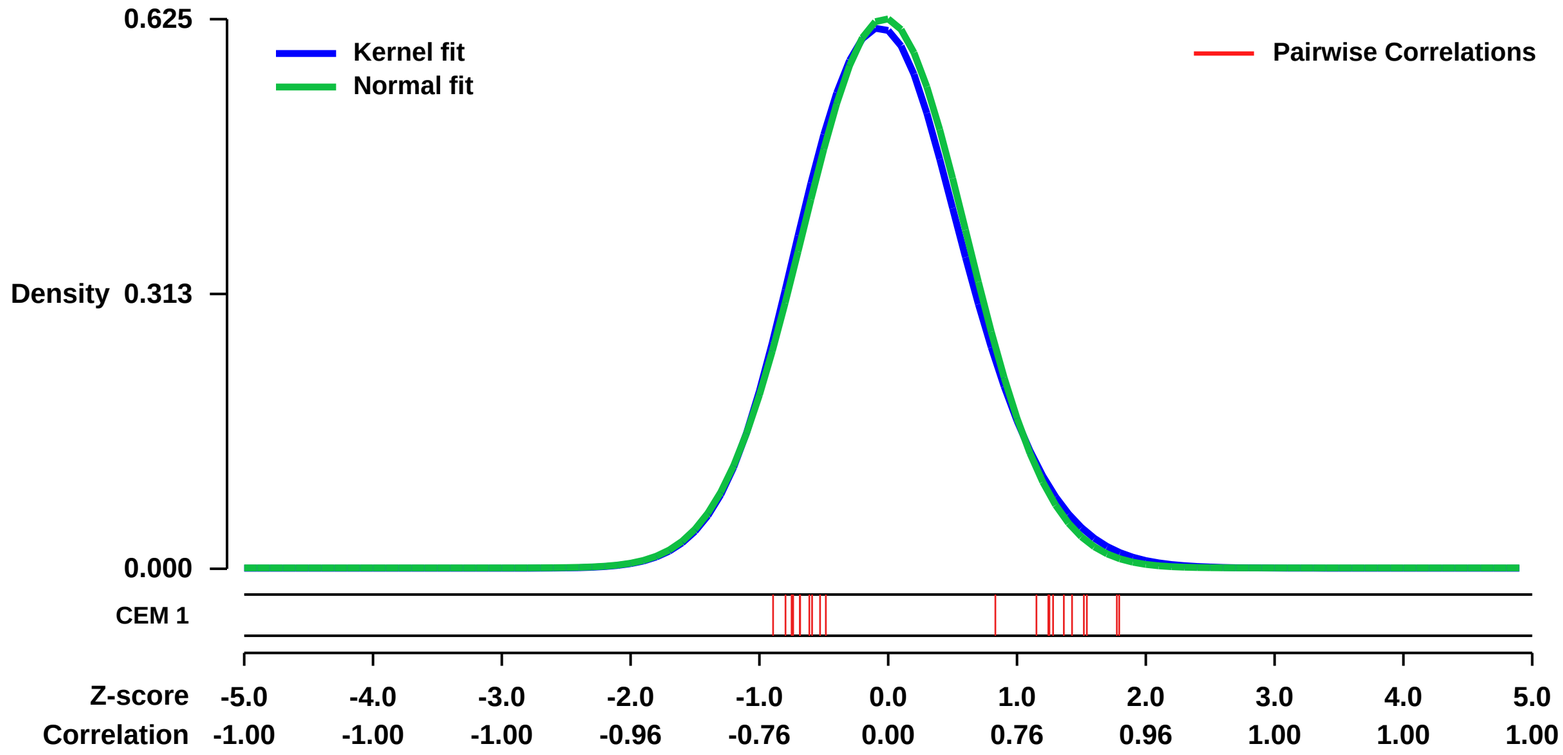

Pre-normalization Quantiles

[min] [medium] [max]

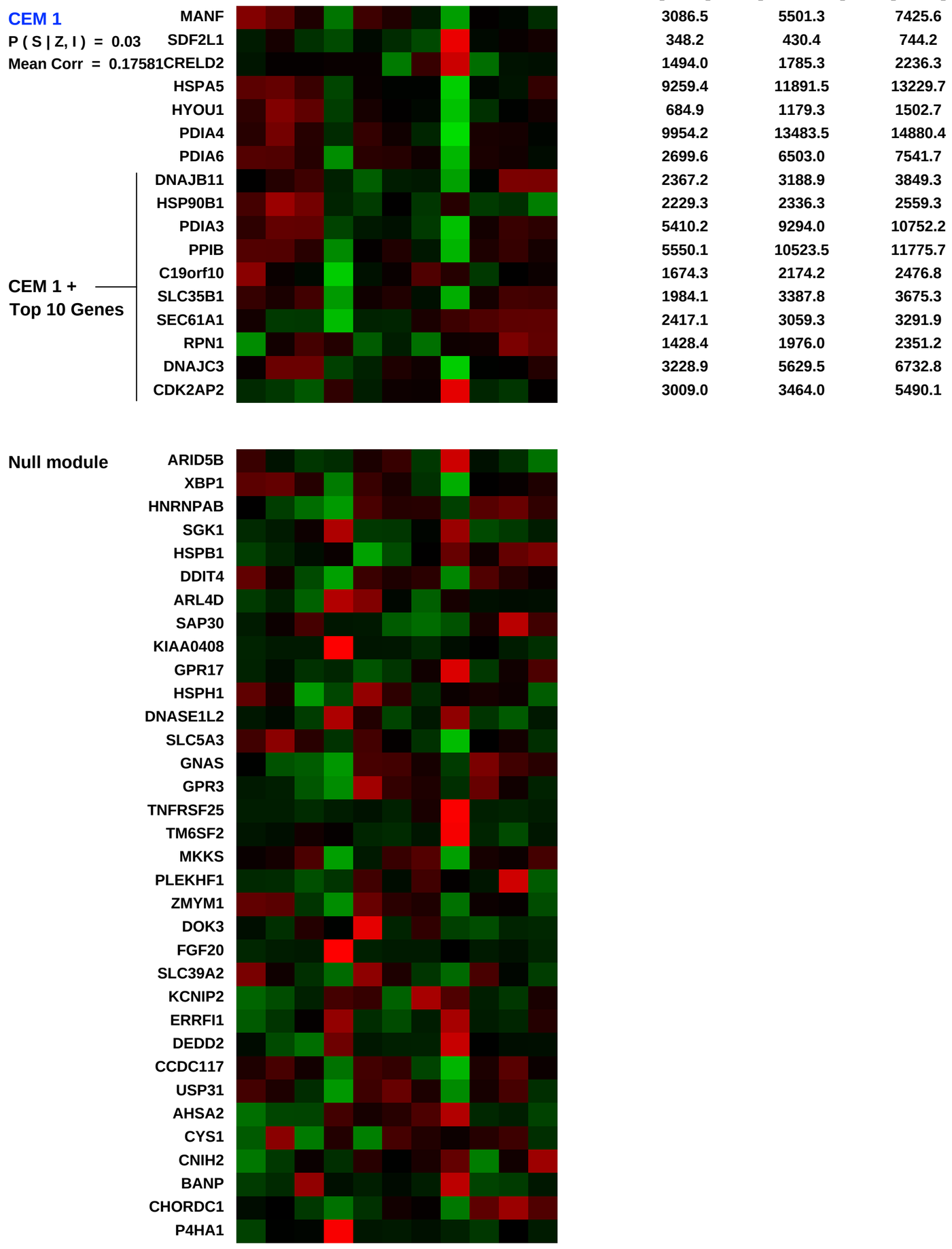

GEO Series "GSE10233" Expression Profiles

Num of samples in this series: 6

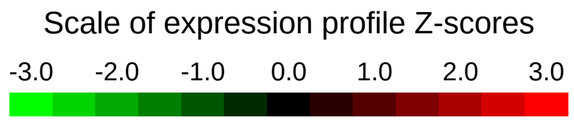

GEO Link:	http://www.ncbi.nlm.nih.gov/geo/query/acc.cgi?acc=GSE10233
Status:	Public on Jul 31 2008
Title:	CTDG in PMA-activated MM6 cells
Organism:	Homo sapiens
Experiment type:	Expression profiling by array
Platform:	GPL570
Pubmed ID:	18773076
Summary & Design:	**Summary:** **Cyclin T1-dependent genes in PMA-activated MM6 cells.** **HIV-1 is dependent upon cellular co-factors to mediate its replication cycle in CD4+ T cells and macrophages, the two major cell types infected by the virus in vivo. One critical co-factor is Cyclin T1, a subunit of a general RNA polymerase II elongation factor known as P-TEFb. Cyclin T1 is targeted directly by the viral Tat protein to activate proviral transcription. Cyclin T1 is up-regulated when resting CD4+ T cells are activated and during macrophage differentiation or activation, conditions that are also necessary for high levels of HIV-1 replication. Because Cyclin T1 is a subunit of a transcription factor, the up-regulation of Cyclin T1 in these cells results in the induction of cellular genes, some of which might be HIV-1 co-factors. Using shRNA depletions of Cyclin T1 and transcriptional profiling, we identified 54 cellular mRNAs that are Cyclin T1-dependent for their induction in activated CD4+ T cells and during macrophage differentiation and activation. The promoters for these Cyclin T1-dependent genes (CTDGs) are over-represented in two transcription factor binding sites, SREBP1 and ARP1. Notably, 10 of these CTDGs have been reported to be involved in HIV-1 replication, a significant over-representation of such genes when compared to randomly generated lists of 54 genes (p value < 0.00021). SiRNA depletions of two CTDGs identified here, CDK11 and Casein kinase1gamma1, suggest that these genes are also involved in HIV-1 replication. It is therefore likely that the 54 CTDGs identified here include novel HIV-1 co-factors. The presence of CTDGs in the protein space that was available for HIV-1 to sample during its evolution and acquisition of Tat function may provide an explanation for why CTDGs are enriched in viral co-factors.** **Keywords: shrna knockdown** **Overall design:** **Using shRNA knockdown of cyclin T1, cyclin T1-dependent genes were identified in PMA-activated MM6 cells.**

Background corr dist: KL-Divergence = 0.0418, L1-Distance = 0.0249, L2-Distance = 0.0007, Normal std = 0.6120

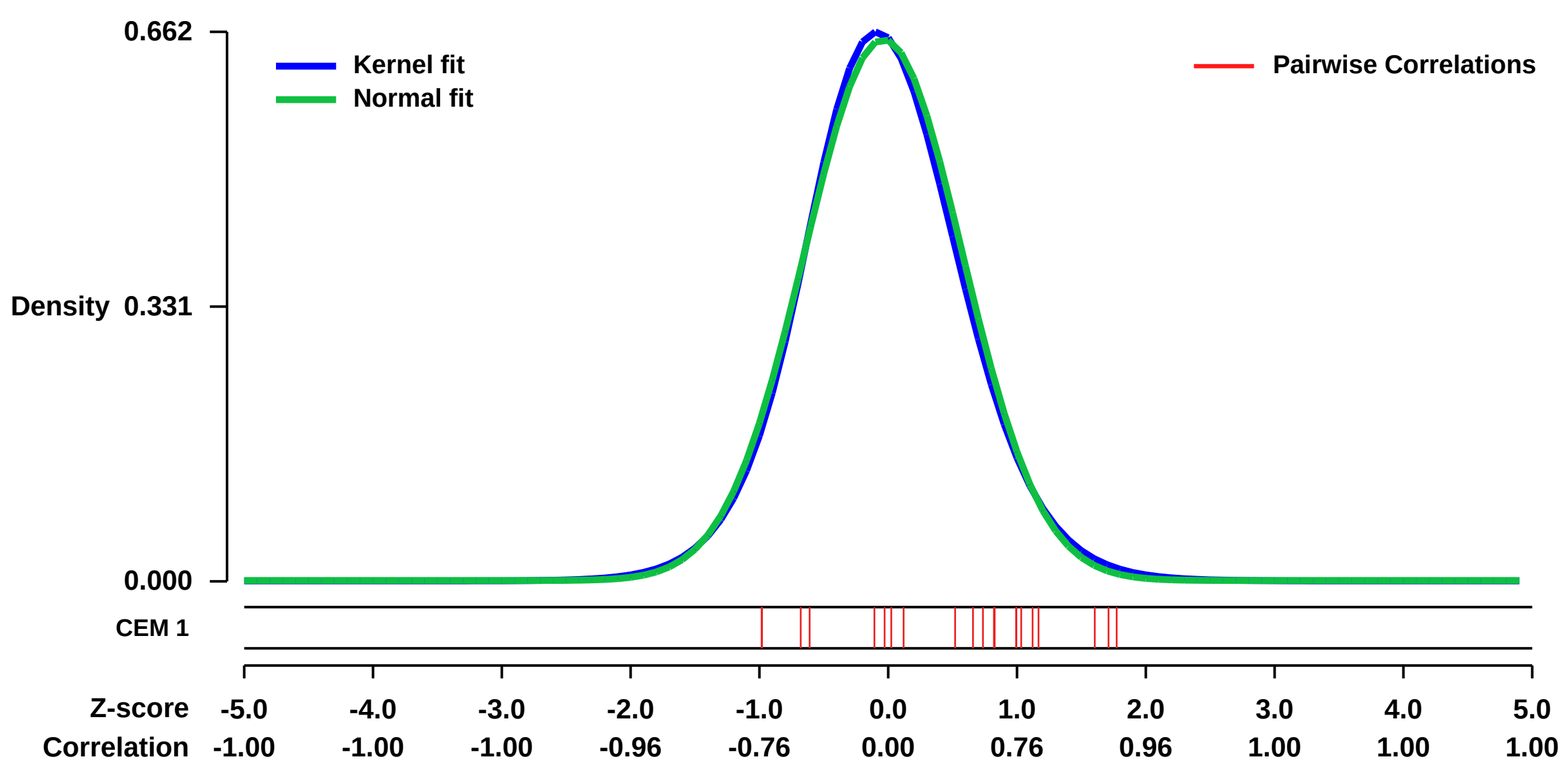

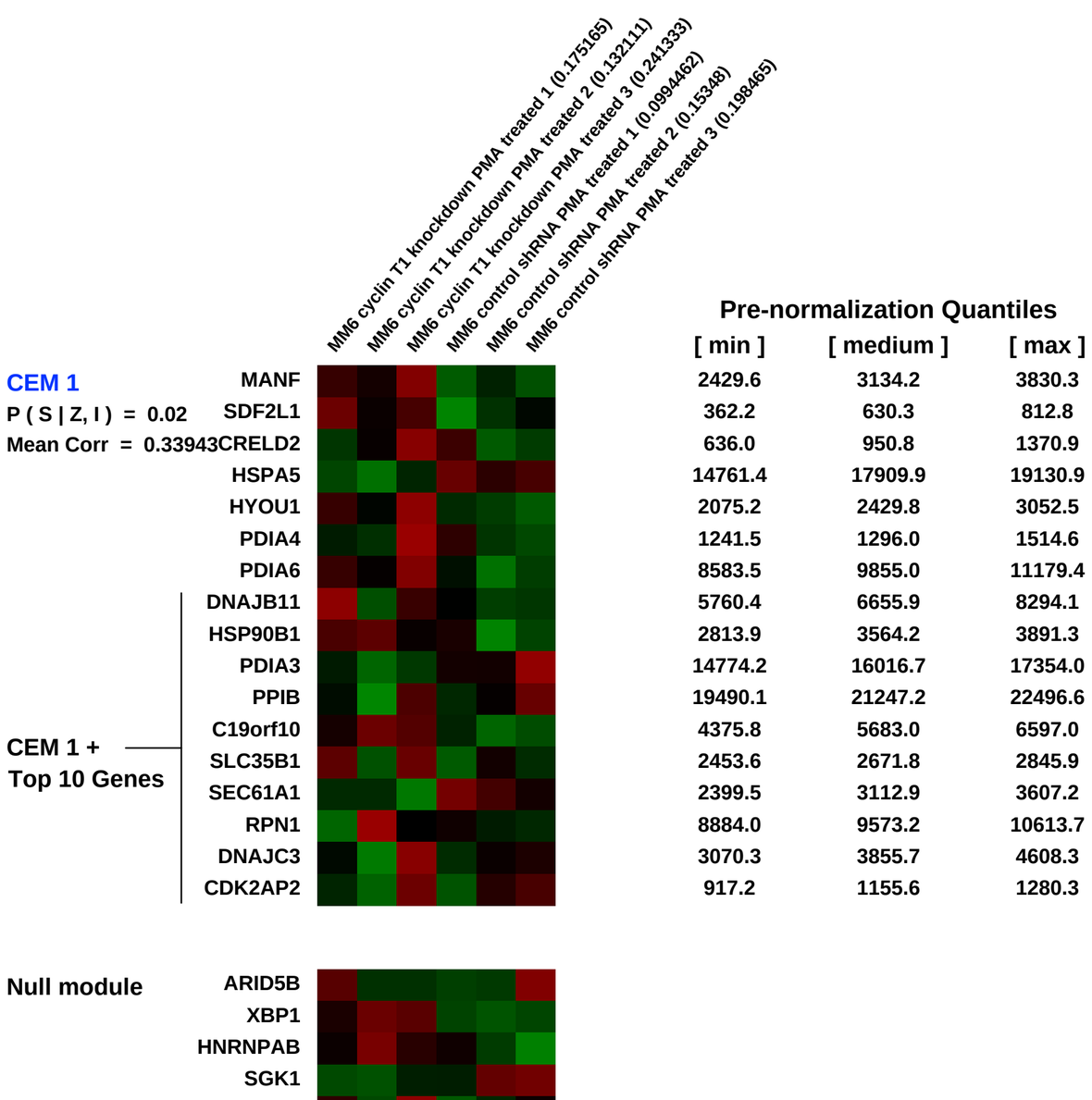

GEO Series "GSE35696" Expression Profiles

Num of samples in this series: 11

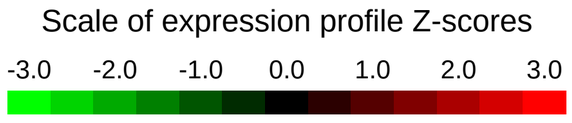

GEO Link:	http://www.ncbi.nlm.nih.gov/geo/query/acc.cgi?acc=GSE35696
Status:	Public on Aug 02 2012
Title:	SIN3A-regulated LIF-responsive genes in MCF7 cells
Organism:	Homo sapiens
Experiment type:	Expression profiling by array
Platform:	GPL570
Pubmed ID:	22783022
Summary & Design:	**Summary:** Tyrosine phosphorylation is a hallmark for activation of Signal Transducer and Activator of Transcription (STAT) proteins, but their transcriptional activity also depends on other secondary modifications. Type I interferons (IFNs) can activate both the ISGF3 (STAT1:STAT2:IRF9) complex and STAT3, but with cell-specific, selective triggering of only the ISGF3 transcriptional program. Following a genome-wide RNAi screen, we identified the Sin3a complex as an important mediator of this STAT3 transcriptional repression. Sin3a directly interacts with the DNA-binding domain of STAT3 and alters its acetylation status. SIN3A silencing enhances recruitment of STAT3 and enhanceosome components to the SOCS3 promoter, resulting in histone hyperacetylation and enhanced transcription. Conversely, Sin3a is required for ISGF3-dependent gene transcription and for an efficient IFN-mediated antiviral protection against Influenza A and hepatitis C viruses. The Sin3a complex therefore acts as a context-dependent STAT1/3 transcriptional switch. **Overall design:** MCF7 cells were transfected with 50nM Renilla luciferase (control) or SIN3A-specific siRNA. 72h later, cells were cultured for 4h in absence of FCS and left non-stimulated or stimulated with LIF (10ng/ml, 1h). Total RNA was extracted. For each of the 4 conditions, 3 biological replicates were included. Nevertheless, one sample (SIN3A_siRNA_LIF1h_rep3) was discarded. In total 11 samples were analyzed.

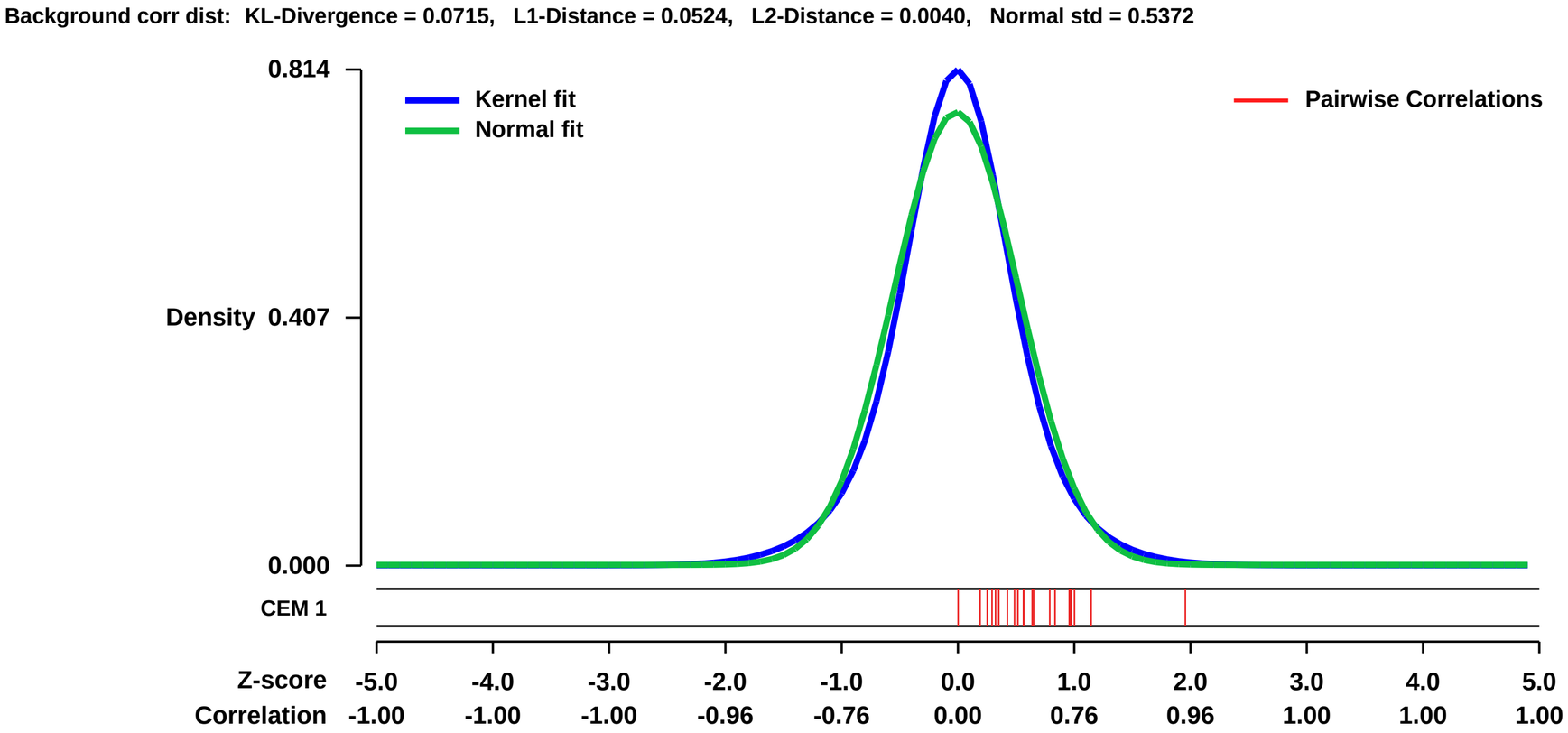

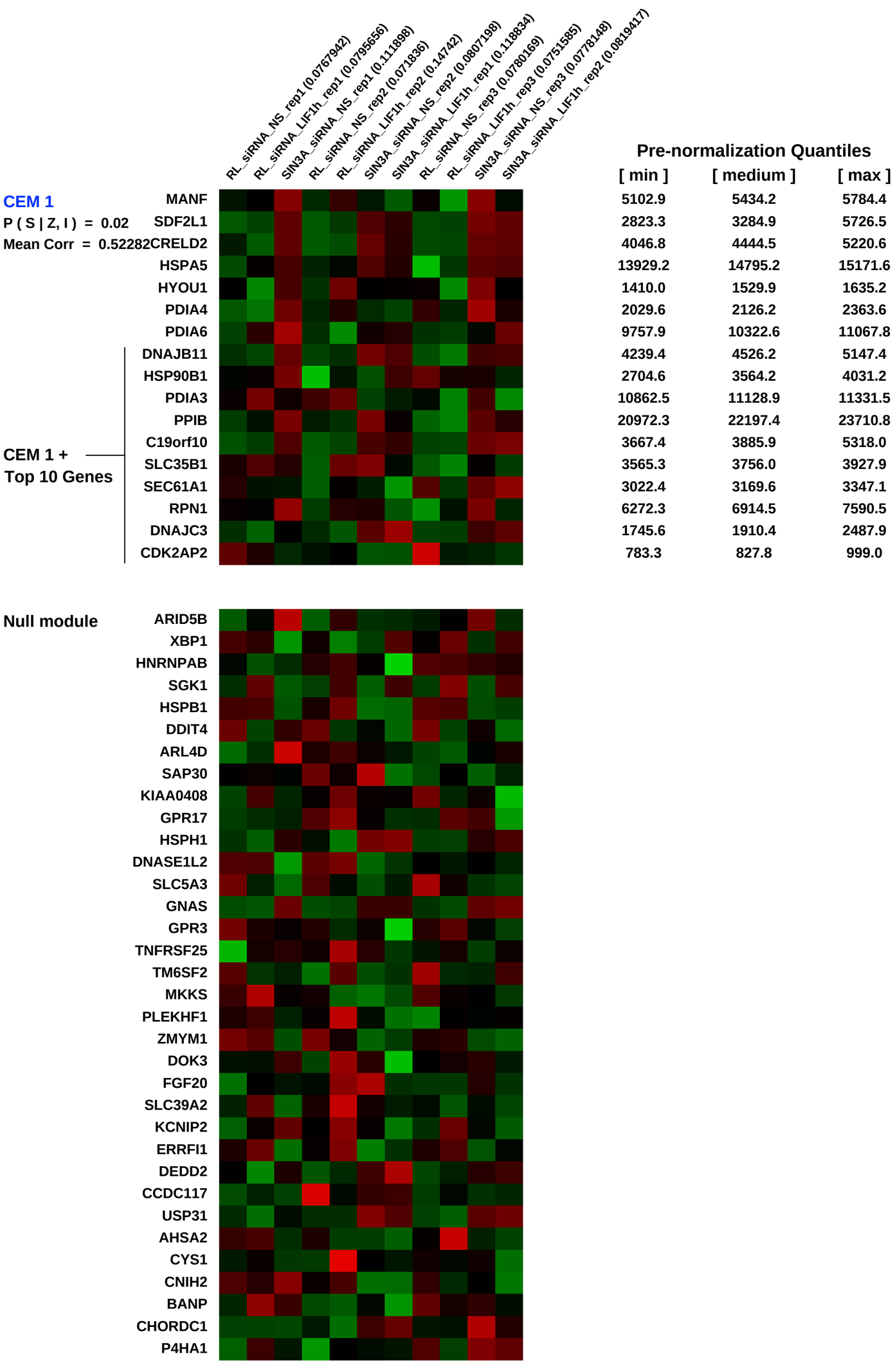

GEO Series "GSE7586" Expression Profiles

Num of samples in this series: 20

Scale of expression profile Z-scores

-3.0 -2.0 -1.0 0.0 1.0 2.0 3.0

GEO Link:	http://www.ncbi.nlm.nih.gov/geo/query/acc.cgi?acc=GSE7586
Status:	Public on Jul 01 2007
Title:	Genome wide analysis of placental malaria
Organism:	Homo sapiens
Experiment type:	Expression profiling by array
Platform:	GPL570
Pubmed ID:	17579077
Summary & Design:	**Summary:** Chronic inflammation during placental malaria (PM) caused by Plasmodium falciparum is most frequent in first-time mothers and is associated with poor maternal and fetal outcomes. In the first genome wide analysis of the local human response to sequestered malaria parasites, we identified genes associated with chronic PM, then localized the corresponding proteins and immune cell subsets in placental cryosections. **Keywords: Disease state analysis** **Overall design:** Placental samples from twenty first-time mothers were selected based on placental malaria (PM) status and RNA quality. Ten had active PM-episodes, seven of which had inflammatory cells on histology. Of the ten PM-negative women, five had histological evidence of a past PM-episode, including one with inflammatory cells.

Background corr dist: KL-Divergence = 0.1677, L1-Distance = 0.0501, L2-Distance = 0.0060, Normal std = 0.3551

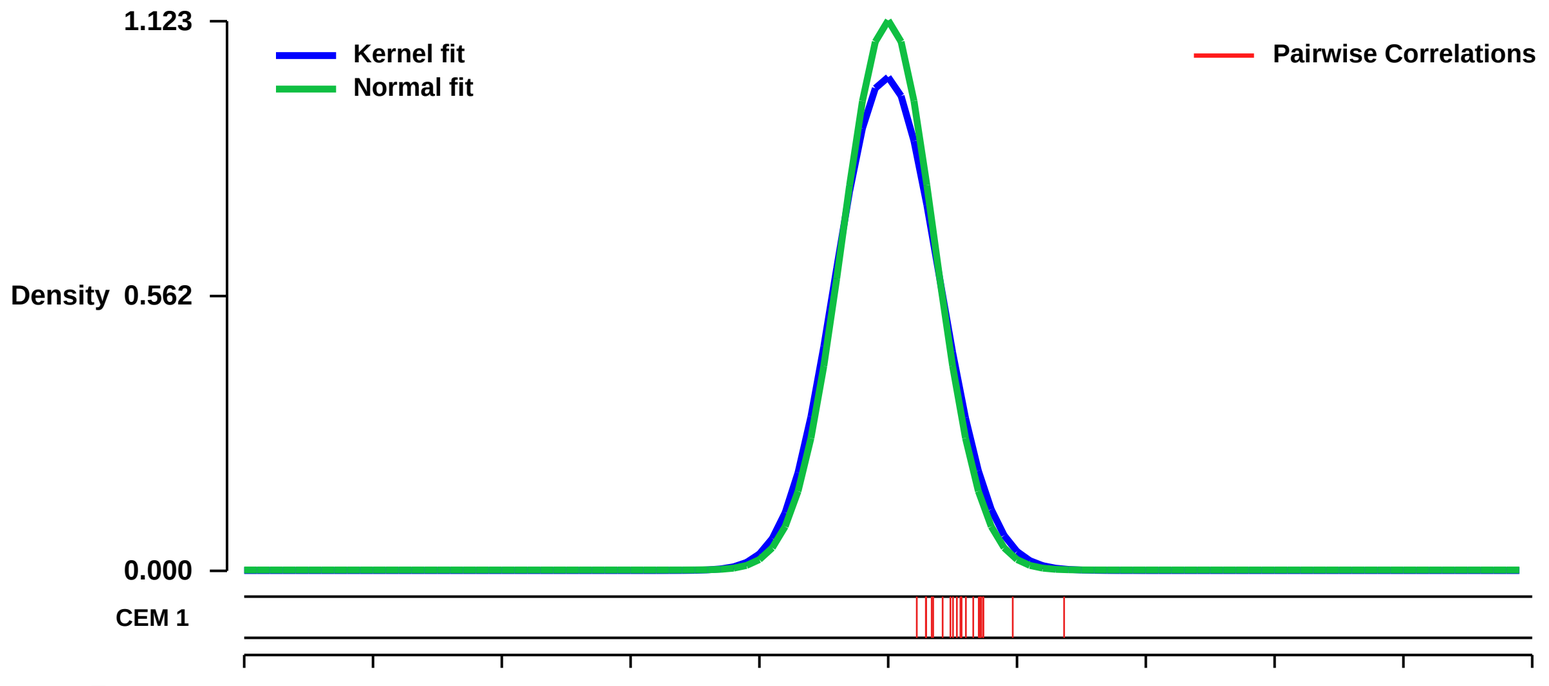

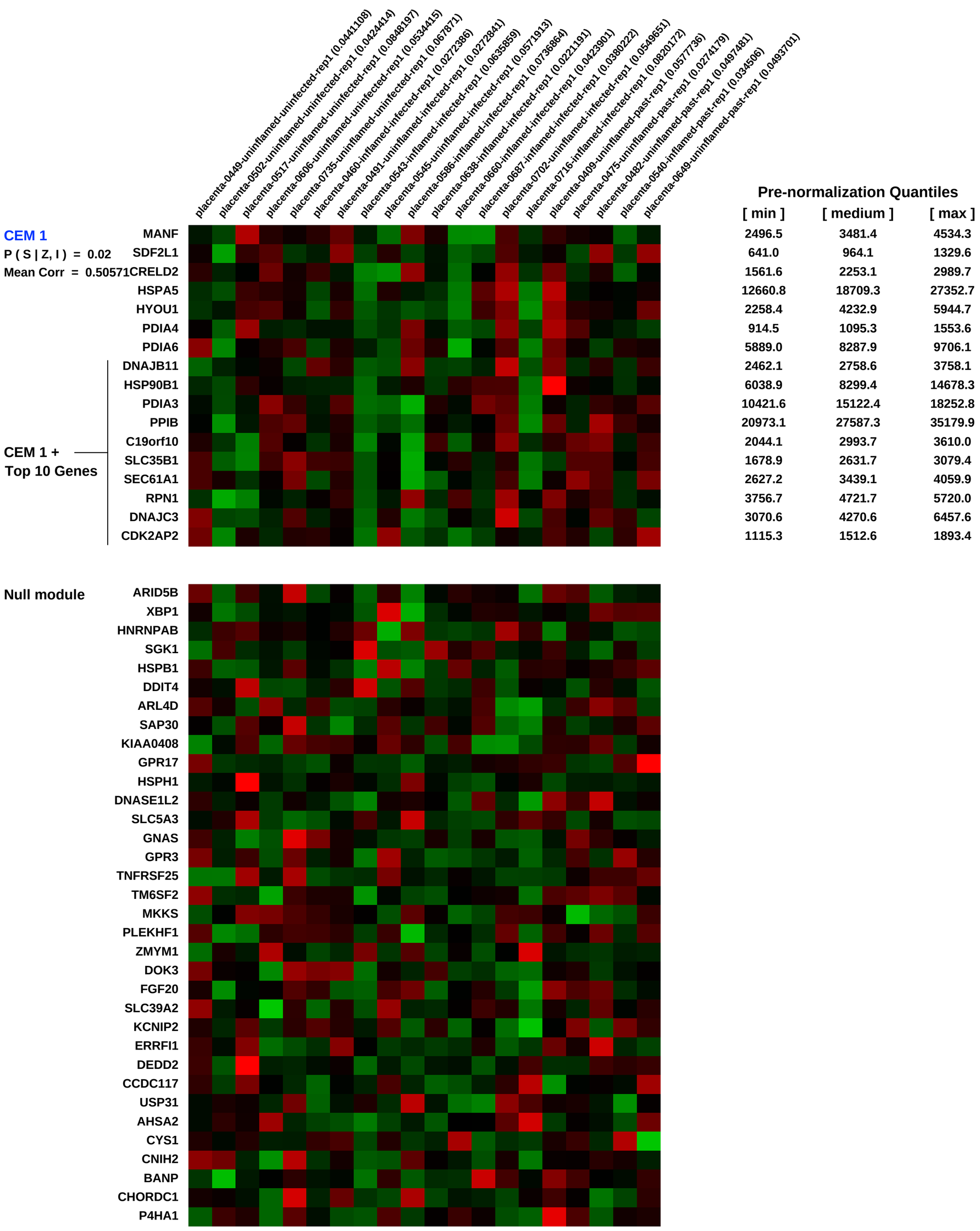

Pre-normalization Quantiles

	[min]	[medium]	[max]
CEM 1	2496.5	3481.4	4534.3
	641.0	964.1	1329.6
	1561.6	2253.1	2989.7
	12660.8	18709.3	27352.7
	2258.4	4232.9	5944.7
	914.5	1095.3	1553.6
	5889.0	8287.9	9706.1
CEM 1 + Top 10 Genes	2462.1	2758.6	3758.1
	6038.9	8299.4	14678.3
	10421.6	15122.4	18252.8
	20973.1	27587.3	35179.9
	2044.1	2993.7	3610.0
	1678.9	2631.7	3079.4
	2627.2	3439.1	4059.9
	3756.7	4721.7	5720.0
	3070.6	4270.6	6457.6
	1115.3	1512.6	1893.4

GEO Series "GSE17307" Expression Profiles

Num of samples in this series: 15

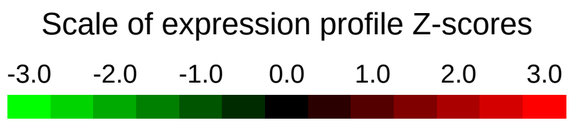

GEO Link:	http://www.ncbi.nlm.nih.gov/geo/query/acc.cgi?acc=GSE17307
Status:	Public on Sep 01 2009
Title:	GRE specific DNA-binding polyamide effect on dexamethasone-stimulated lung adenocarcinoma cell line
Organism:	Homo sapiens
Experiment type:	Expression profiling by array
Platform:	GPL570
Pubmed ID:	19805343
Summary & Design:	**Summary:** Analysis of dexamethasone-stimulated A549 lung adenocarcinoma epithelial cells treated with a glucocorticoid response (GR) element (GRE) specific DNA binding polyamide. Polyamide designed to target the sequence 5'-WGWWCW-3' and disrupt GR-mediated gene expression. Effects of the GR antagonist mifepristone also examined. **Overall design:** A549 cells were treated with compounds for 48 hours before RNA extraction and hybridization on Affymetrix microarrays.

Background corr dist: KL-Divergence = 0.1336, L1-Distance = 0.0318, L2-Distance = 0.0015, Normal std = 0.4040

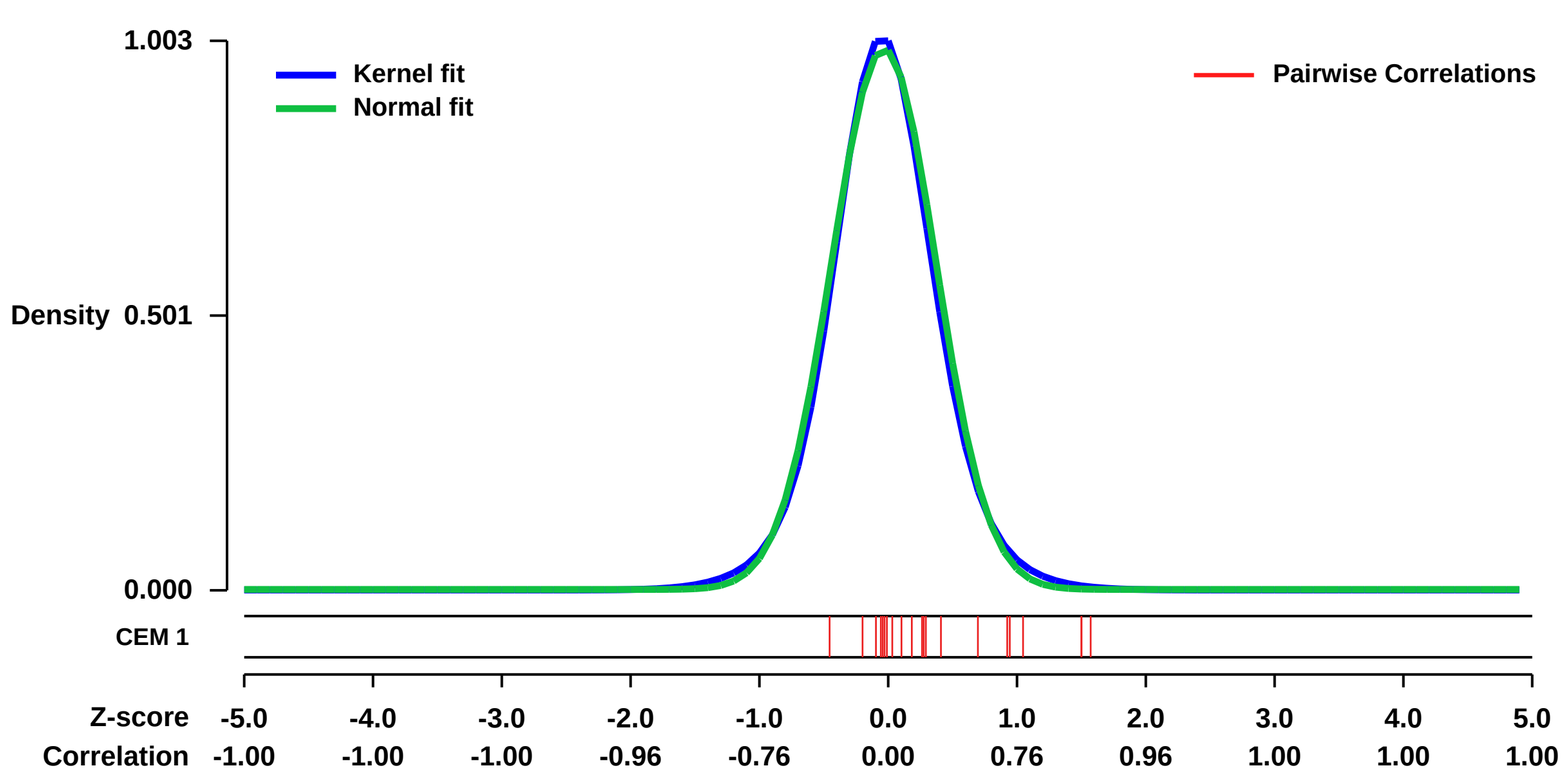

Pre-normalization Quantiles

	[min]	[medium]	[max]
MANF	2382.7	3212.5	3514.5
SDF2L1	587.5	958.2	1223.5
CRELD2	855.6	1117.6	1502.9
HSPA5	15804.2	18601.4	22136.9
HYOU1	1163.8	1432.8	1692.1
PDIA4	663.8	1145.0	1659.1
PDIA6	7764.2	11888.6	12650.7
DNAJB11	1993.2	2842.1	3887.8
HSP90B1	3666.0	5911.6	7353.2
PDIA3	4286.2	7362.3	9842.6
PPIB	12765.3	17831.3	23729.2
C19orf10	1888.1	2328.4	2861.7
SLC35B1	2726.5	3498.2	3736.5
SEC61A1	1445.4	1897.4	2128.5
RPN1	2949.7	3561.6	4281.9
DNAJC3	744.4	1424.1	1728.9
CDK2AP2	1588.3	1846.8	2851.1

GEO Series "GSE35283" Expression Profiles

Num of samples in this series: 12

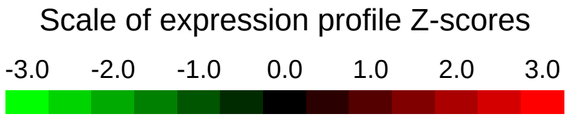

GEO Link:	http://www.ncbi.nlm.nih.gov/geo/query/acc.cgi?acc=GSE35283
Status:	Public on Jul 01 2013
Title:	Highly pathogenic influenza virus inhibit Inflammatory Responses in Monocytes via Activation of the Rar-Related Orphan Receptor Alpha (RORalpa)
Organism:	Homo sapiens
Experiment type:	Expression profiling by array
Platform:	GPL570
Pubmed ID:	
Summary & Design:	**Summary:** Highly pathogenic influenza virus inhibit Inflammatory Responses in Monocytes via Activation of the Rar-Related Orphan Receptor Alpha (RORalpha). Low (PR8) and high pathogenic influenza viruses (FPV and H5N1) were used. **Overall design:** Monocytes were infected with low (PR8) and high pathogenic influenza viruses (FPV and H5N1)

Background corr dist: KL-Divergence = 0.0748, L1-Distance = 0.0374, L2-Distance = 0.0028, Normal std = 0.4872

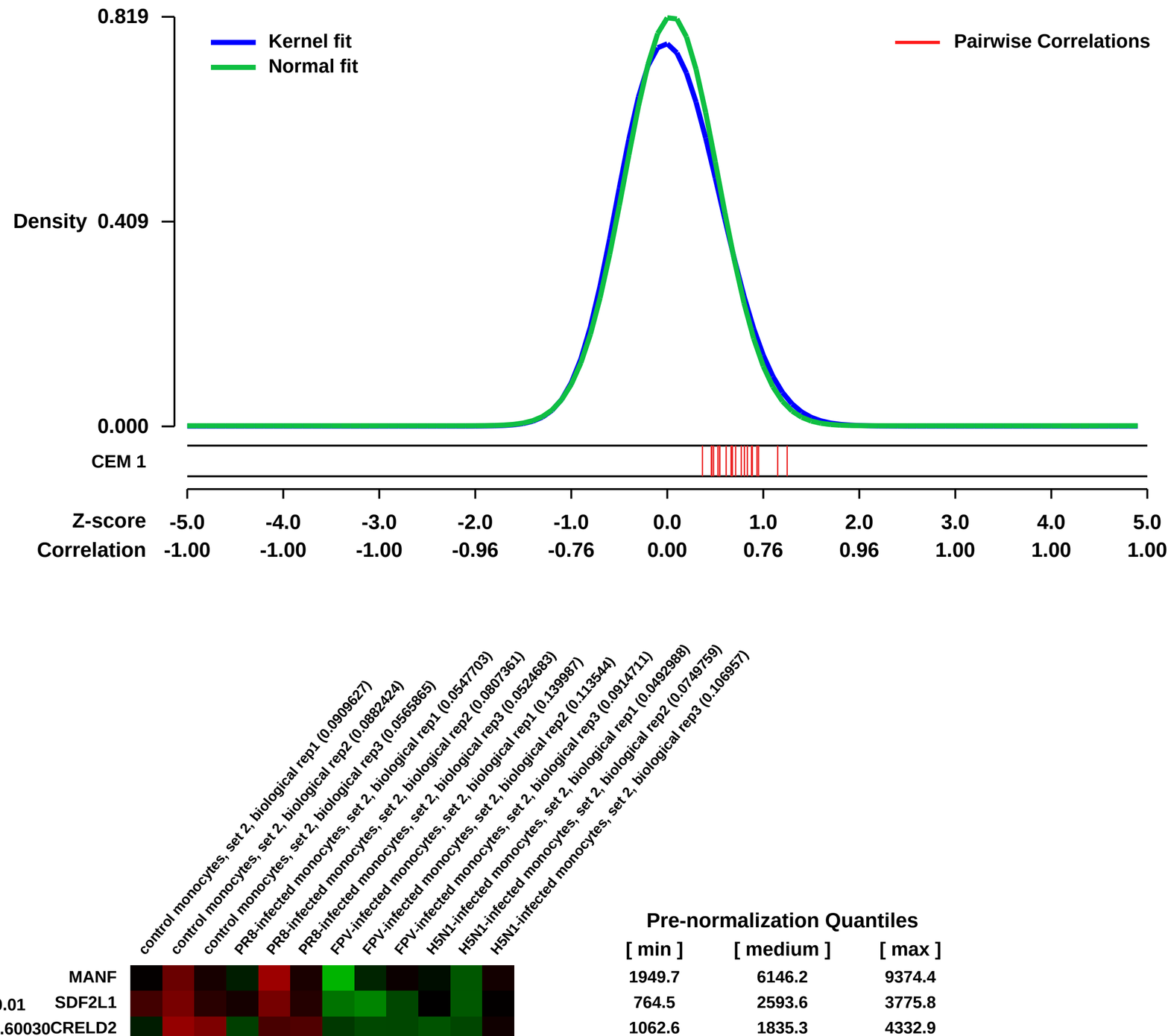

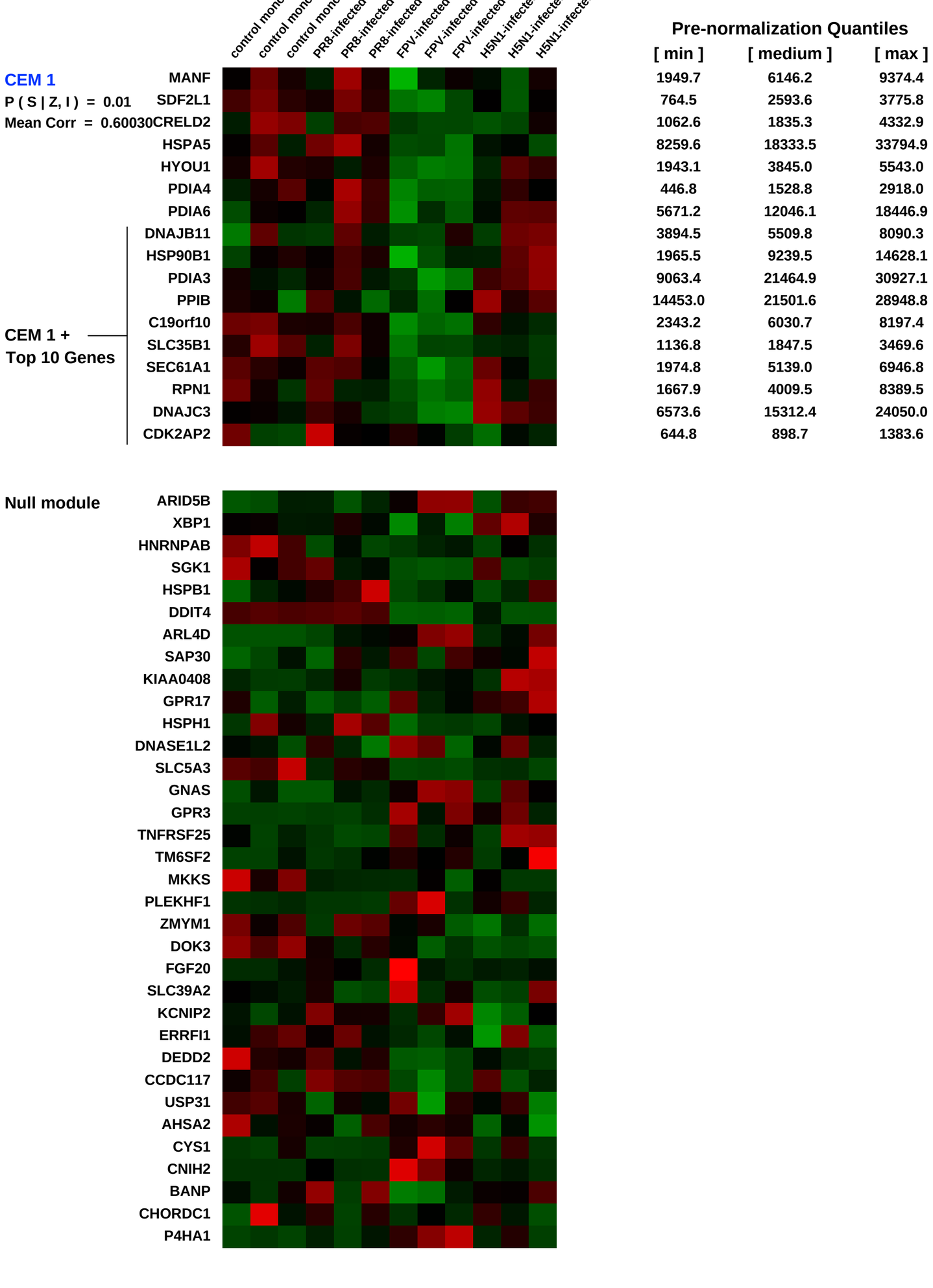

GEO Series "GSE5741" Expression Profiles

Num of samples in this series: 9

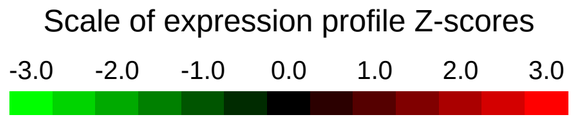

GEO Link:	http://www.ncbi.nlm.nih.gov/geo/query/acc.cgi?acc=GSE5741
Status:	Public on Sep 01 2006
Title:	Expression data from ARPE-19 cells treated with LDL or ox-LDL
Organism:	Homo sapiens
Experiment type:	Expression profiling by array
Platform:	GPL570
Pubmed ID:	18182060
Summary & Design:	**Summary:** LDL or Ox-LDL 200ug/ml, which showed no loss of viability after a 48 hour exposure, induced a physiological and pathological transcriptional response, respectively. LDL induced a downregulation of genes associated with cholesterol biosynthesis while ox-LDL induced transcriptional alterations in genes related to inflammation, matrix expansion, lipid metabolism and processing, and apoptosis. Pentraxin-3 was secreted into the culture medium after RPE cells were stimulated with ox-LDL, and immunohistochemically evident in Bruchâ s membrane of human macular samples with age-related macular degeneration. ARPE-19 cells exposed to 200?g/ml ox-LDL had a 38% apoptosis rate compared to less than 1% when exposed to LDL or untreated controls (p<0.0001). While LDL induced a physiologic response by RPE cells, a pathological phenotypic response was seen after treatment with oxidatively modified LDL. The transcriptional, biochemical, and functional data provide initial support of a role for the hypothesis that modified LDLs are one trigger for initiating events that contribute to the development of age-related macular degeneration. **Keywords:** treatment with non-treatment control **Overall design:** Human ARPE-19 cells were exposed to LDL or oxidatively modified LDL (ox-LDL) for 48 hours for RNA extraction and hybridization on Affymetrix microarrays. We sought to determine whether retina, pigment epithelial cells develop a pathologic phenotype after exposure to low density lipoproteins (LDL) that are oxidatively modified.We have made two comparsions: LDL treatment versus non-treatment; ox-LDL treatment versus non-treatment.

Background corr dist: KL-Divergence = 0.0914, L1-Distance = 0.0208, L2-Distance = 0.0006, Normal std = 0.4617

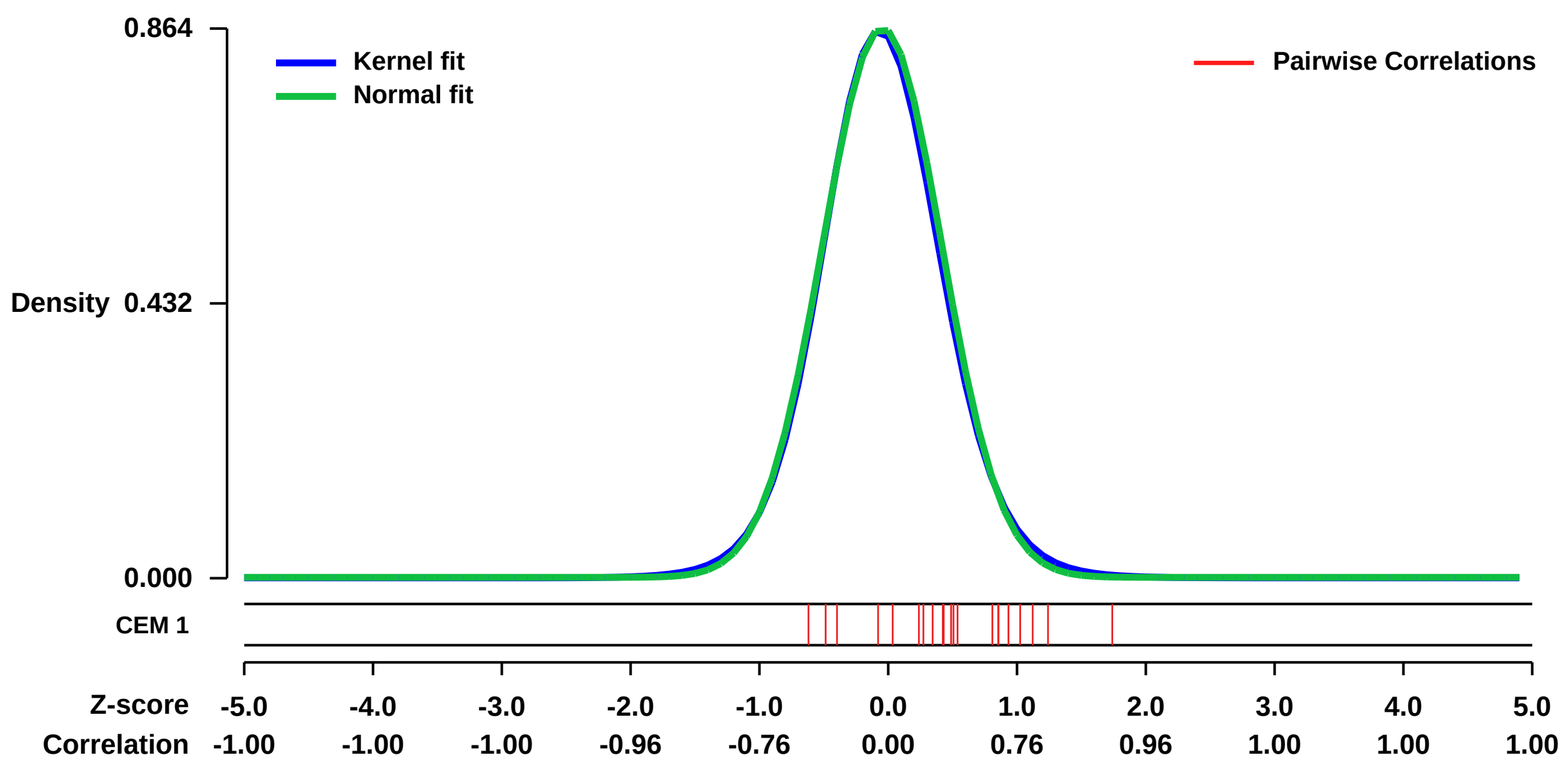

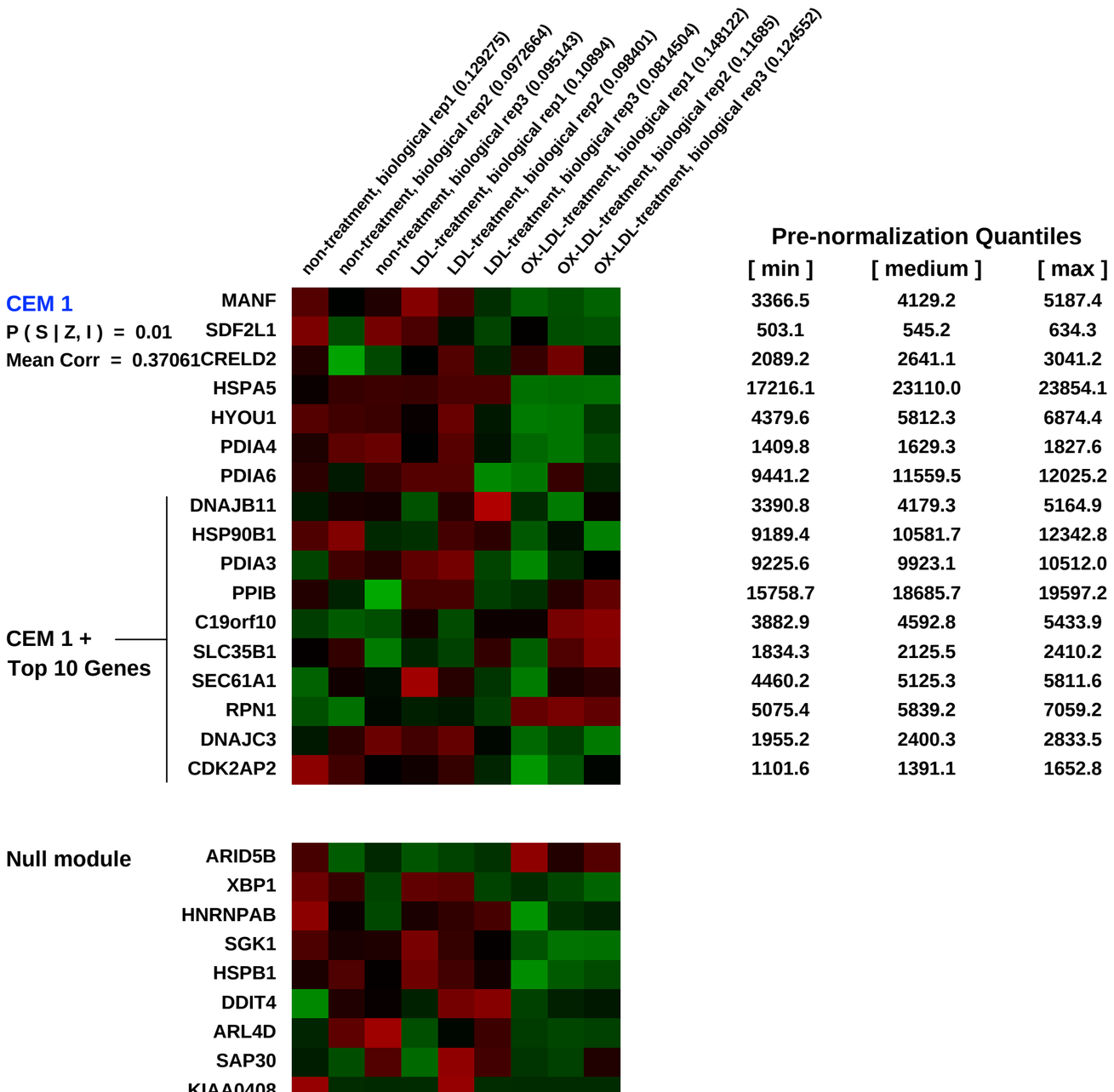

Pre-normalization Quantiles

	[min]	[medium]	[max]
MANF	3366.5	4129.2	5187.4
SDF2L1	503.1	545.2	634.3
CRELD2	2089.2	2641.1	3041.2
HSPA5	17216.1	23110.0	23854.1
HYOU1	4379.6	5812.3	6874.4
PDIA4	1409.8	1629.3	1827.6
PDIA6	9441.2	11559.5	12025.2
DNAJB11	3390.8	4179.3	5164.9
HSP90B1	9189.4	10581.7	12342.8
PDIA3	9225.6	9923.1	10512.0
PPIB	15758.7	18685.7	19597.2
C19orf10	3882.9	4592.8	5433.9
SLC35B1	1834.3	2125.5	2410.2
SEC61A1	4460.2	5125.3	5811.6
RPN1	5075.4	5839.2	7059.2
DNAJC3	1955.2	2400.3	2833.5
CDK2AP2	1101.6	1391.1	1652.8

GEO Series "GSE34515" Expression Profiles

Num of samples in this series: 9

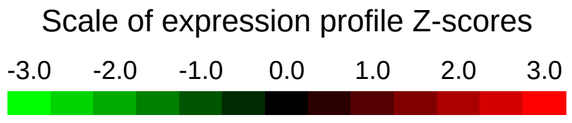

GEO Link:	http://www.ncbi.nlm.nih.gov/geo/query/acc.cgi?acc=GSE34515
Status:	Public on Dec 17 2011
Title:	Gene expression profiles of human blood classical monocytes (CD14++CD16-), CD16 positive monocytes (CD14+16++ and CD14++CD16+), and CD1c+ CD19- dendritic cells
Organism:	Homo sapiens
Experiment type:	Expression profiling by array
Platform:	GPL570
Pubmed ID:	
Summary & Design:	**Summary:** In this study gene expression of human blood classical monocytes (CD14++CD16-), CD16 positive monocytes (consisting of non-classical CD14+16++ and intermediate CD14++CD16+ monocytes) and CD1c+ CD19- dendritic cells from healthy subjects were investigated. **Keywords:** expression profiling by array **Overall design:** The two major monocyte subsets and the CD1+ blood dendritic cells (DCs CD1c+ CD19-) were isolated from venous heparinized blood of three apparently healthy human volunteers (donors 1, 2 and 3) using MACS technology with all reagents and tools from Miltenyi Biotec. RNA was isolated and 1 ´µg was labeled using the Affymetrix One-Cycle Target Labeling Kit and the biotinylated cRNA used to perform Affymetrix U133 Plus 2.0 expression arrays. The data sets for CD14++CD16- classical monocytes are tagged CD16neg, the data sets for CD16 positive monocytes are tagged CD16pos and the data sets for the CD1c+CD19- DCs are tagged CD1cpos.

Background corr dist: KL-Divergence = 0.0633, L1-Distance = 0.0189, L2-Distance = 0.0006, Normal std = 0.5179

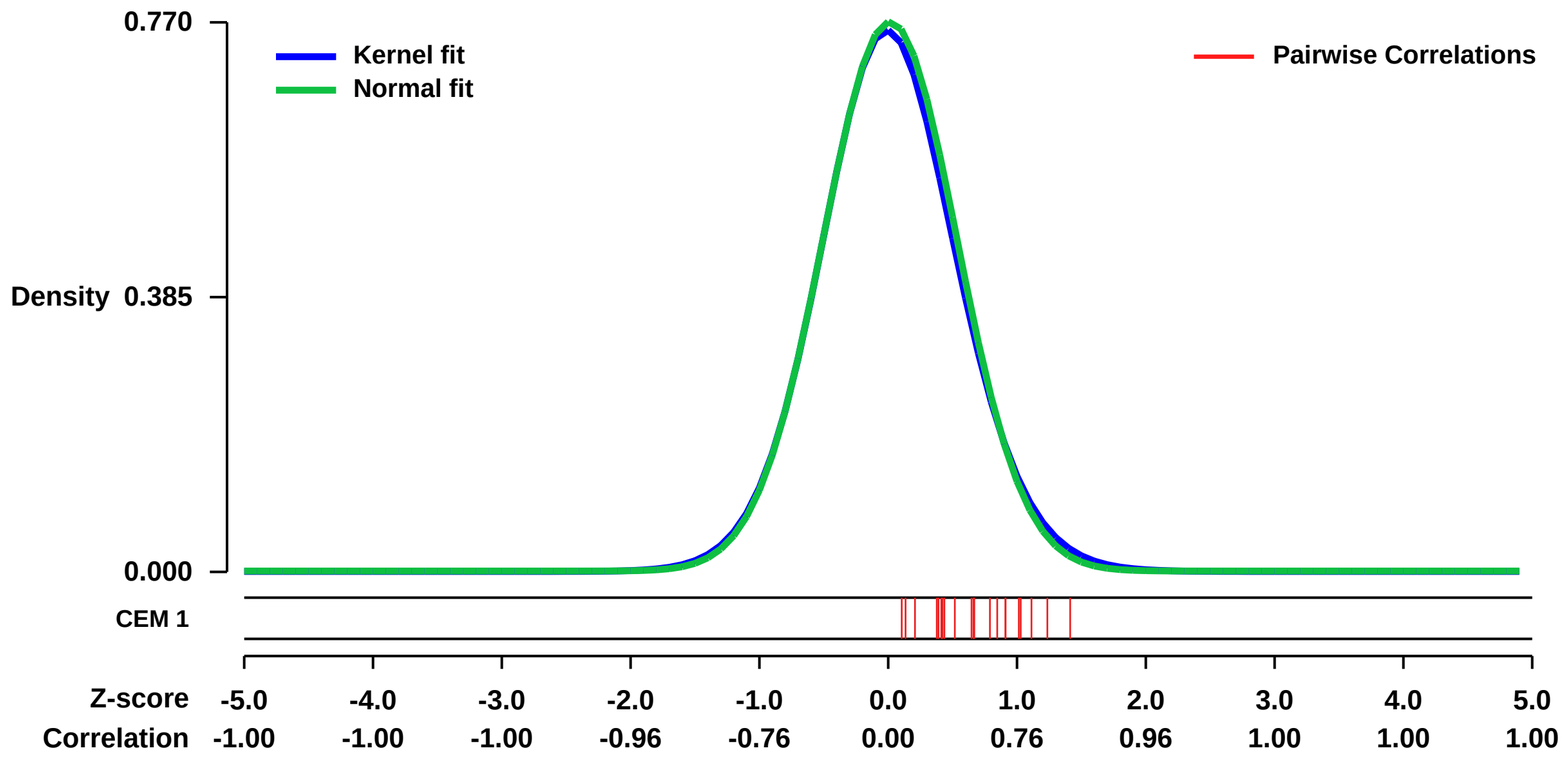

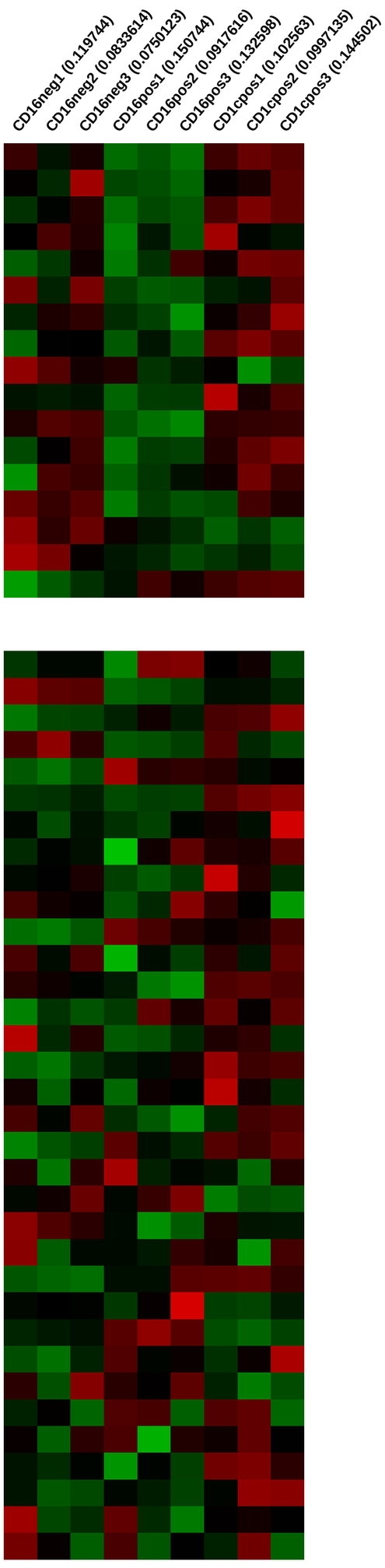

GEO Series "GSE27914" Expression Profiles

Num of samples in this series: 31

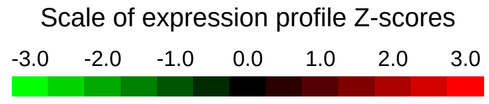

GEO Link:	http://www.ncbi.nlm.nih.gov/geo/query/acc.cgi?acc=GSE27914
Status:	Public on Apr 08 2011
Title:	Expression data from LNCap cell line treated with COP1 (RFWD2), ETV1, and JUN siRNAs
Organism:	Homo sapiens
Experiment type:	Expression profiling by array
Platform:	GPL570
Pubmed ID:	21572435
Summary & Design:	**Summary:** The proto-oncogenes ETV1, ETV4, and ETV5 encode members of the E26 transformation-specific (ETS) transcription factor family, which includes the most frequently rearranged and overexpressed genes in prostate cancer. Despite being critical regulators of development, little is known about their post-translational regulation. Here we identify the ubiquitin ligase COnstitutive Photomorphogenic-1 (COP1, also called RFWD2) as a tumor suppressor that negatively regulates ETV1, ETV4, and ETV5. ETV1, which is the member mutated more frequently in prostate cancer, was degraded after being ubiquitinated by COP1. Truncated ETV1 encoded by prostate cancer translocation TMPRSS2:ETV1 lacks the critical COP1 binding motifs (degrons) and was 50-fold more stable than wild-type ETV1. Almost all patient translocations eliminate these ETV1 degrons, implying that translocations rendering ETV1 insensitive to COP1 confer a significant selective advantage to prostate epithelial cells. Indeed, COP1 deficiency in mouse prostate elevated ETV1 levels and produced increased cell proliferation, hyperplasia, and early prostate intraepithelial neoplasia. The combined loss of COP1 and PTEN enhanced the invasiveness of mouse prostate adenocarcinomas. Finally, relatively rare human prostate cancer samples showed hemizygous loss of the COP1 gene, loss of COP1 protein expression, and abnormally elevated ETV1 protein while lacking a translocation event. These findings identify COP1 as a bona fide tumor suppressor whose down-regulation promotes prostatic epithelial cell proliferation and tumorigenesis. **Overall design:** LNCap prostate cancer cell line were treated with 5 different sets of siRNAs: (1) control siRNA; (2) COP1 (RFWD2) siRNA; (3) COP1 siRNA + ETV1 siRNA; (4) COP1 siRNA + c-JUN siRNA; (5) COP1 siRNA + ETV1 siRNA + c-JUN siRNA. The experiments were conducted in two batches; each batch has its own control siRNA group, so that the batch effect can be properly modelled. Each group has 4-6 replicates; there are 31 samples in total.

Background corr dist: KL-Divergence = 0.1450, L1-Distance = 0.0367, L2-Distance = 0.0025, Normal std = 0.3770

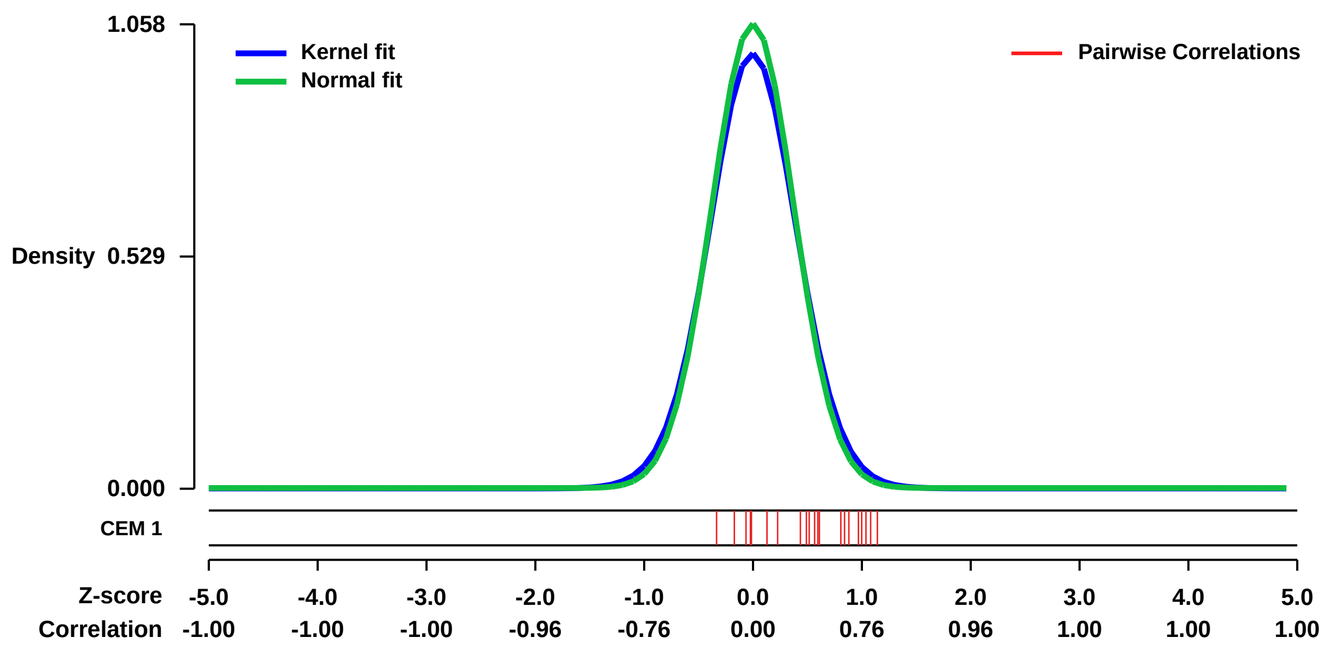

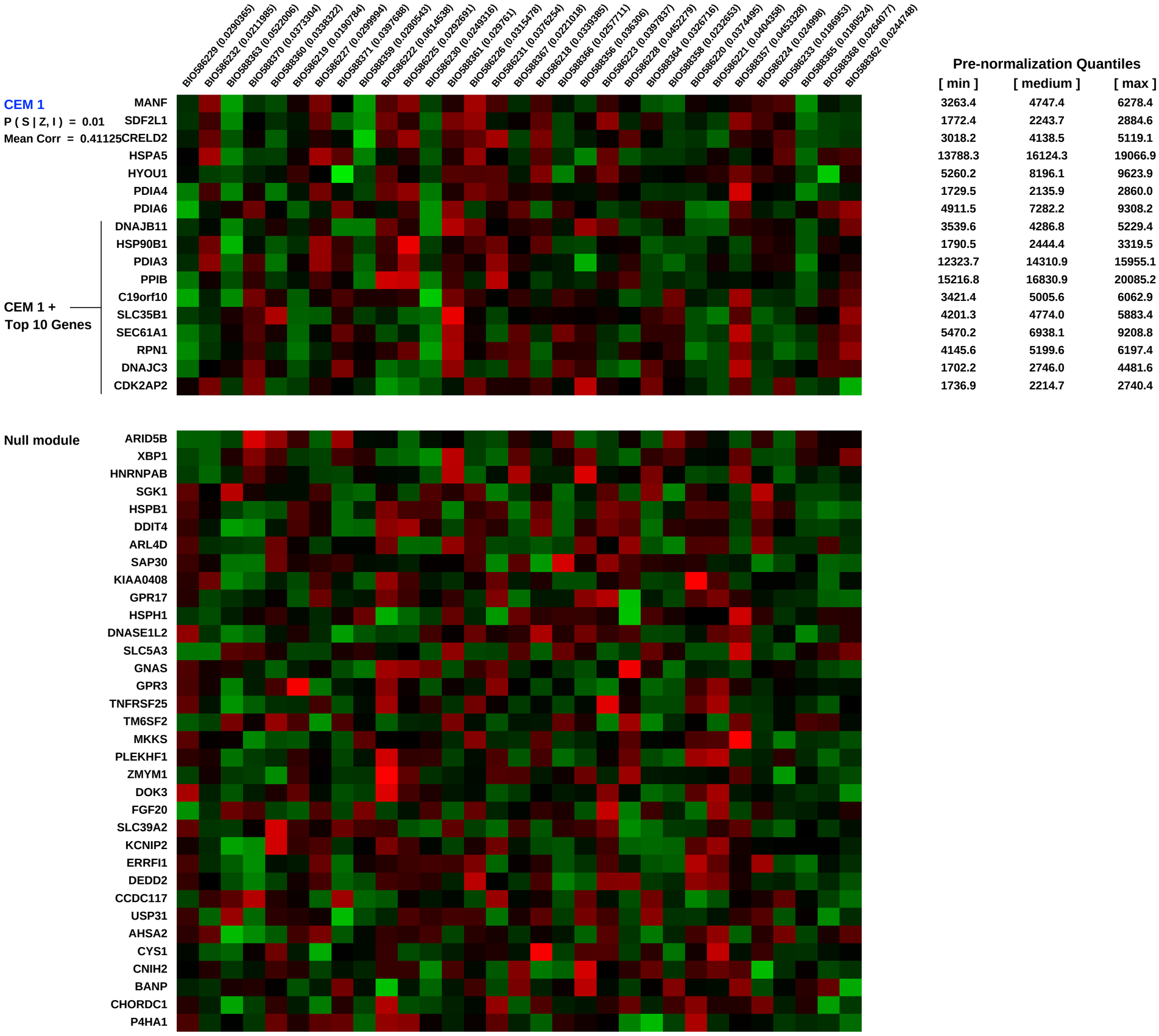

Pre-normalization Quantiles

[min]	[medium]	[max]
3263.4	4747.4	6278.4
1772.4	2243.7	2884.6
3018.2	4138.5	5119.1
13788.3	16124.3	19066.9
5260.2	8196.1	9623.9
1729.5	2135.9	2860.0
4911.5	7282.2	9308.2
3539.6	4286.8	5229.4
1790.5	2444.4	3319.5
12323.7	14310.9	15955.1
15216.8	16830.9	20085.2
3421.4	5005.6	6062.9
4201.3	4774.0	5883.4
5470.2	6938.1	9208.8
4145.6	5199.6	6197.4
1702.2	2746.0	4481.6
1736.9	2214.7	2740.4

GEO Series "GSE21912" Expression Profiles

Num of samples in this series: 42

Scale of expression profile Z-scores

-3.0 -2.0 -1.0 0.0 1.0 2.0 3.0

GEO Link: http://www.ncbi.nlm.nih.gov/geo/query/acc.cgi?acc=GSE21912
Status: Public on May 19 2010
Title: The Polycomb Group Protein Bmi-1 is essential for the growth of Multiple Myeloma cells
Organism: Homo sapiens
Experiment type: Expression profiling by array
Platform: GPL570
Pubmed ID:
Summary & Design:

Summary:
The RPMI-8226 human multiple myeloma cell line was stably infected with either a validated shRNA against BMI1 or a control shRNA. RNA was prepared from these lines, +/- doxycycline induction and at various time points post-induction. Samples were hybridized on the Affymetrix U133plus2 human genome expression microarray.

Overall design:
The RPMI-8226 human multiple myeloma cell line was stably infected with either a validated shRNA against BMI1 or a control shRNA. RNA was prepared from these lines, +/- doxycycline induction and at various time points post-induction. Samples were hybridized on the Affymetrix U133plus2 human genome expression microarray.

Background corr dist: KL-Divergence = 0.3656, L1-Distance = 0.0387, L2-Distance = 0.0027, Normal std = 0.2706

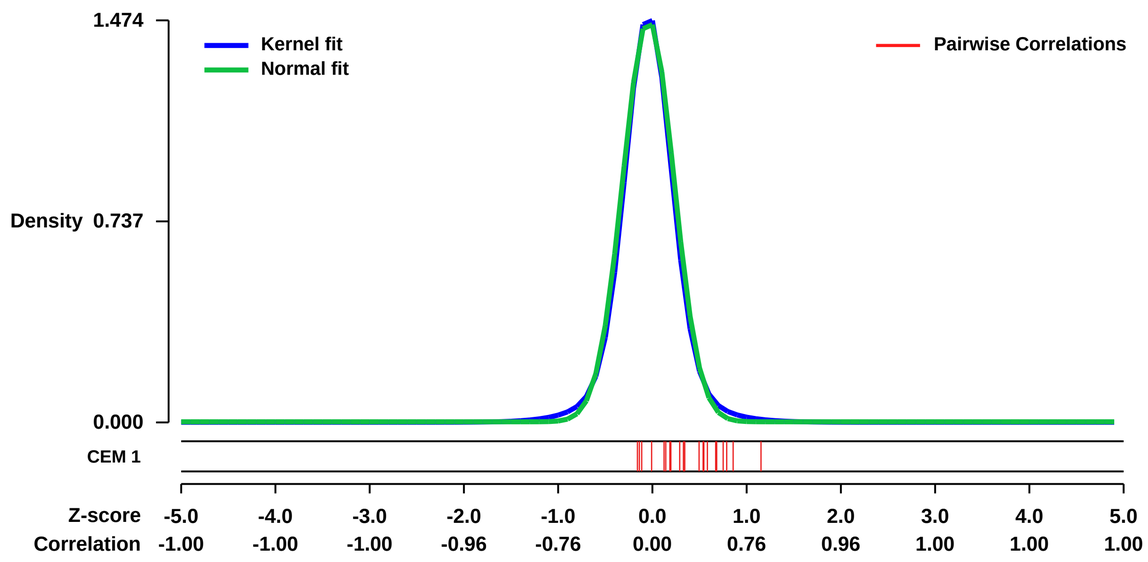

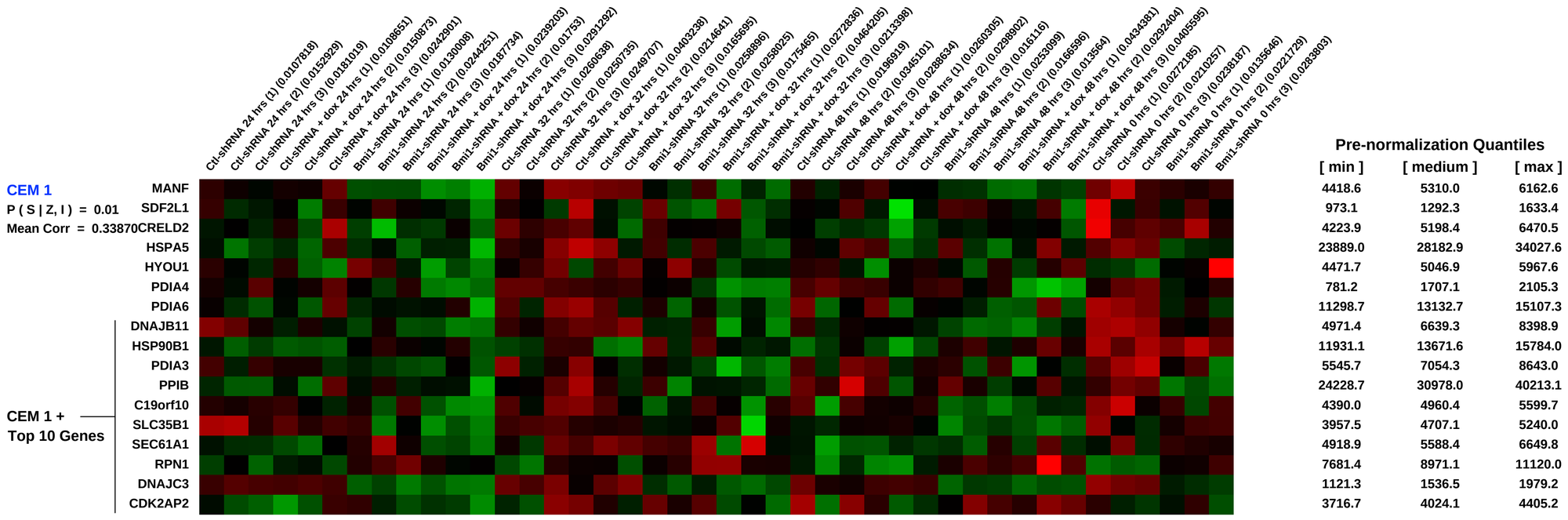

Pre-normalization Quantiles

[min]	[medium]	[max]
4418.6	5310.0	6162.6
973.1	1292.3	1633.4
4223.9	5198.4	6470.5
23889.0	28182.9	34027.6
4471.7	5046.9	5967.6
781.2	1707.1	2105.3
11298.7	13132.7	15107.3
4971.4	6639.3	8398.9
11931.1	13671.6	15784.0
5545.7	7054.3	8643.0
24228.7	30978.0	40213.1
4390.0	4960.4	5599.7
3957.5	4707.1	5240.0
4918.9	5588.4	6649.8
7681.4	8971.1	11120.0
1121.3	1536.5	1979.2
3716.7	4024.1	4405.2

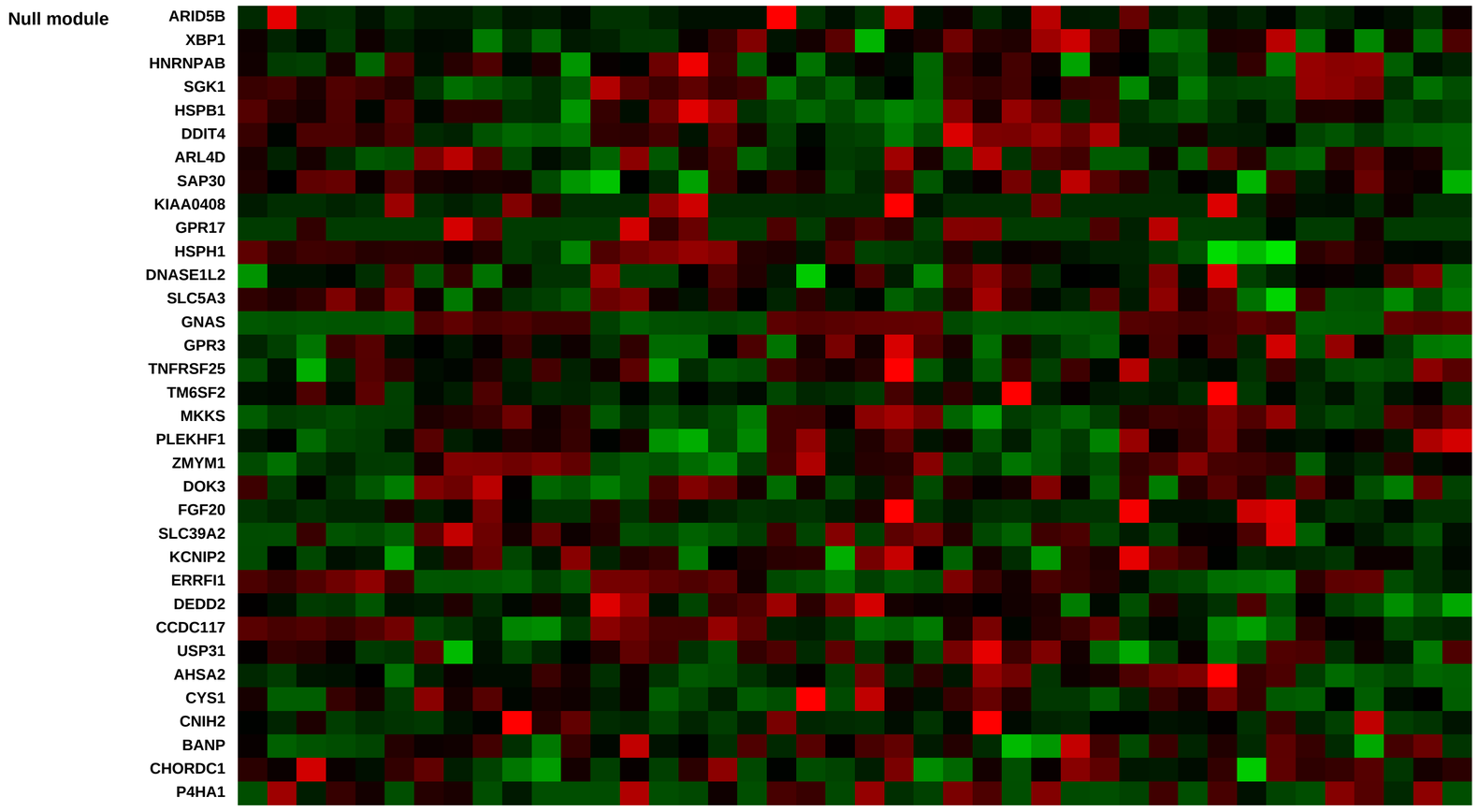

GEO Series "GSE7745" Expression Profiles

Num of samples in this series: 6

Scale of expression profile Z-scores

-3.0 -2.0 -1.0 0.0 1.0 2.0 3.0

GEO Link: http://www.ncbi.nlm.nih.gov/geo/query/acc.cgi?acc=GSE7745
Status: Public on May 10 2007
Title: Mapping of HNF4˛– binding sites, acetylation of histone H3 and expression in Caco2 cells
Organism: Homo sapiens
Experiment type: Genome binding/occupancy profiling by genome tiling array
Platform: GPL570
Pubmed ID:

Summary & Design:

Summary:
Background & Aims: The role of HNF4˛– has been extensively studied in hepatocytes and pancreatic ˛† cells, but emerging evidence indicates that HNF4˛– is a key regulator of intestinal epithelial cell differentiation as well. The aim of the present work is to identify HNF4˛– target genes in the intestine in order to elucidate the role of HNF4˛– in differentiation of the intestinal epithelial cells. Results: One thousand one hundred and seventy-six genes were identified as HNF4˛– targets, many of which have not previously been described as being regulated by HNF4˛–. The 1,176 genes contributed significantly to gene ontology (GO) pathways categorized by lipid and amino acid transport and metabolism. A thorough analysis of Cdx-2, trehalase, and cingulin promoters verified that these genes are regulated by HNF4˛–. In each case we were able to identify a functional HNF4˛– binding site in their promoters. Conclusions: HNF4˛– regulation of the Cdx-2 promoter unravels a transcription factor network also including HNF1˛– and ˛†, all of which are transcription factors involved in intestinal development and gene expression.

Keywords: ChIP-CHIP and expression data

Overall design:
Methods: We have performed a ChIP-chip analysis of the human intestinal cell line Caco-2 in order to make a genome-wide identification of HNF4˛– binding to promoter regions. The HNF4˛– ChIP-chip data was matched with gene expression and histone H3 acetylation status of the promoters in order to identify HNF4˛– binding to actively transcribed genes with an open chromatin structure.

Background corr dist: KL-Divergence = 0.0214, L1-Distance = 0.0627, L2-Distance = 0.0044, Normal std = 0.9025

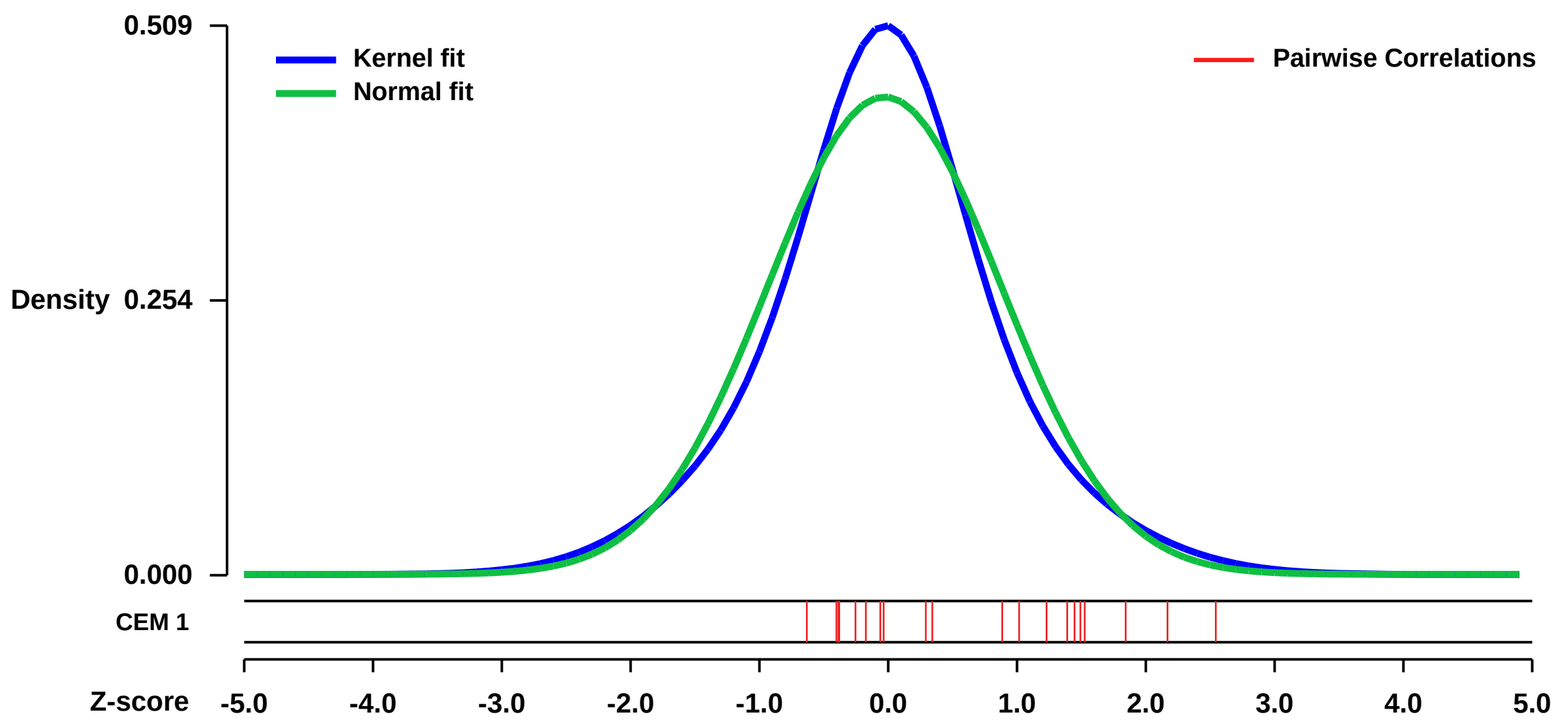

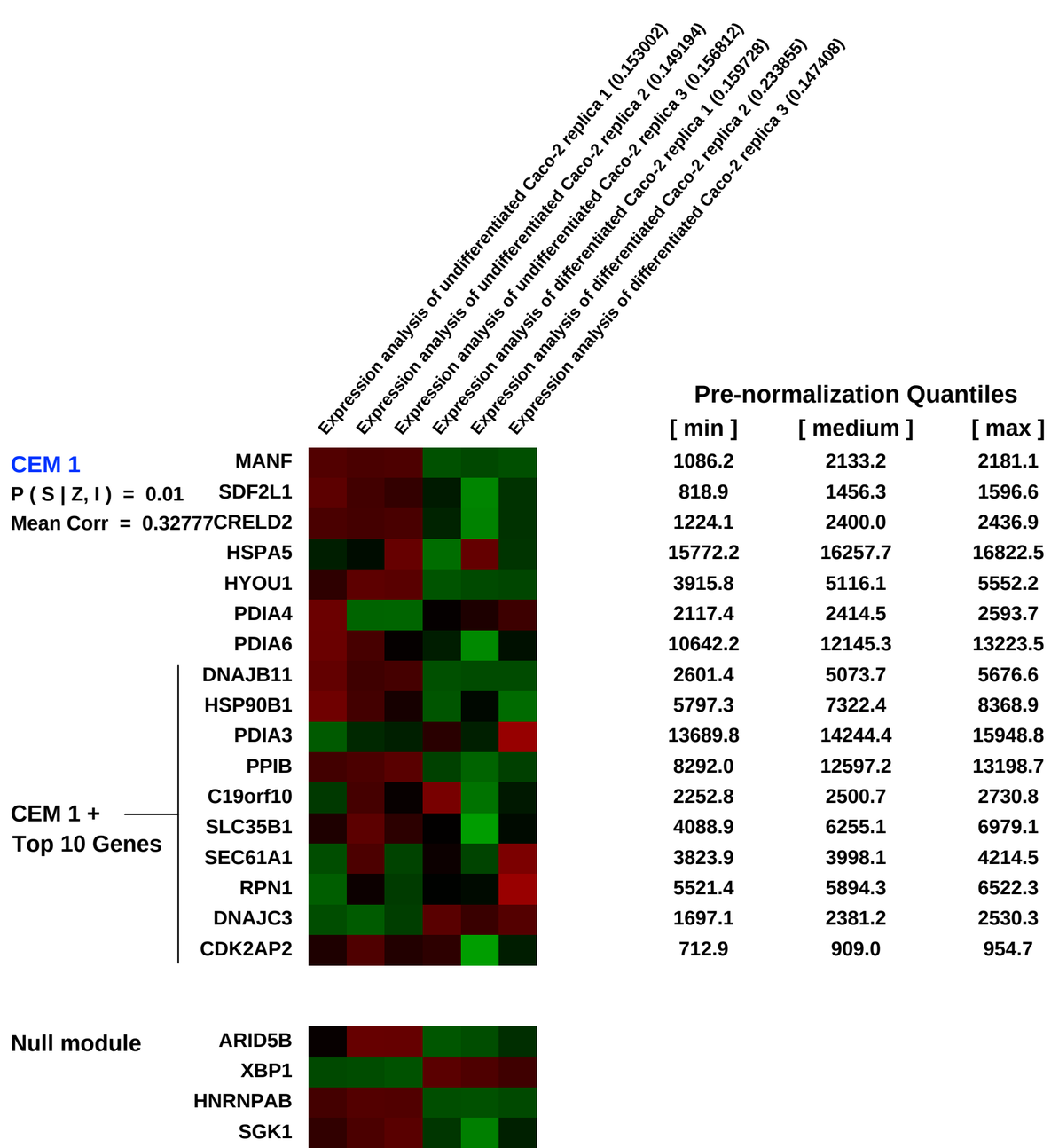

GEO Series "GSE13710" Expression Profiles

Num of samples in this series: 10

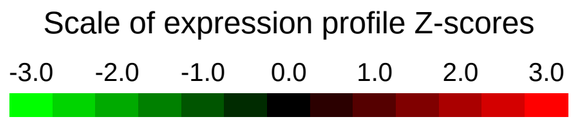

GEO Link:	http://www.ncbi.nlm.nih.gov/geo/query/acc.cgi?acc=GSE13710
Status:	Public on Dec 10 2008
Title:	MKL1 promotes megakaryocytic differentiation in HEL cells
Organism:	Homo sapiens
Experiment type:	Expression profiling by array
Platform:	GPL570
Pubmed ID:	19136660
Summary & Design:	**Summary:** Megakaryoblastic Leukemia 1 (MKL1) was identified as part of the t(1;22) translocation specific to acute megakaryoblastic leukemia, but nothing is known regarding its role in hematopoiesis. Here we show that overexpression of MKL1 enhances megakaryocytic differentiation of the Human Erythroleukemia cell line (HEL). Microarray analysis reveals that MKL1 promotes expression of megakaryocyte-specific genes such as glycoprotein V (GP5), as well as cytoskeletal and adhesion molecule genes relevant to megakaryocyte differentiation and proplatelet formation. MKL1 is a transcriptional coactivator of Serum Response Factor. In this study, MKL1 also upregulates known SRF targets. Results provide insight into the role of MKL1 in megakaryocytopoiesis. **Overall design:** Analysis of megakaryocytic human erythroleukemia (HEL) cells after 24 hours of TPA induced differentiation with MKL1 overexpression. Gene expression data for control/HEL cells and MKL1/HEL cells, which expresses high levels of MKL1 protein upon doxycycline addition, were determined. TPA, which was added to the samples to induce differentiation, was added together with doxycycline for 24 hours. The TPA differentiated MKL1/HEL samples with or without doxycyline induced MKL overexpression were done in duplicate and were used for both Affymetrix and Illumina platforms.

Background corr dist: KL-Divergence = 0.0769, L1-Distance = 0.0286, L2-Distance = 0.0010, Normal std = 0.4970

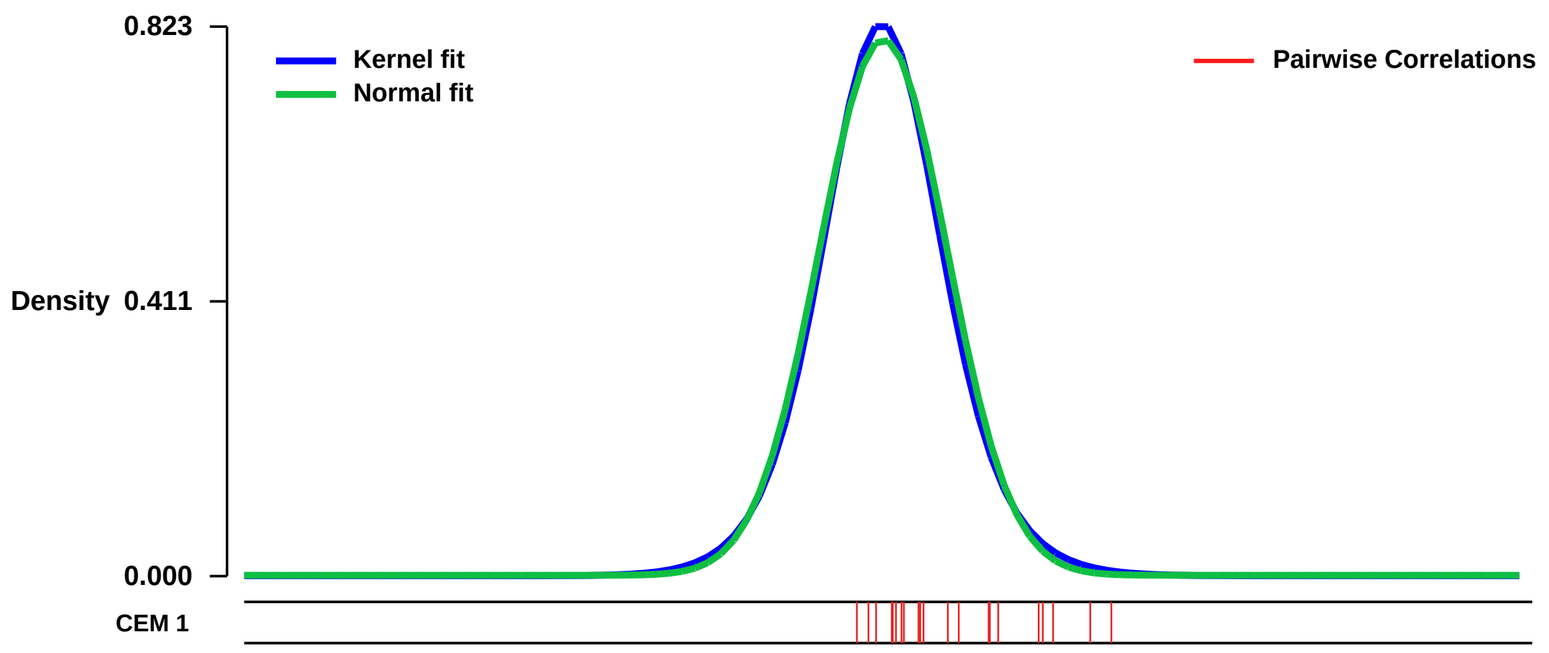

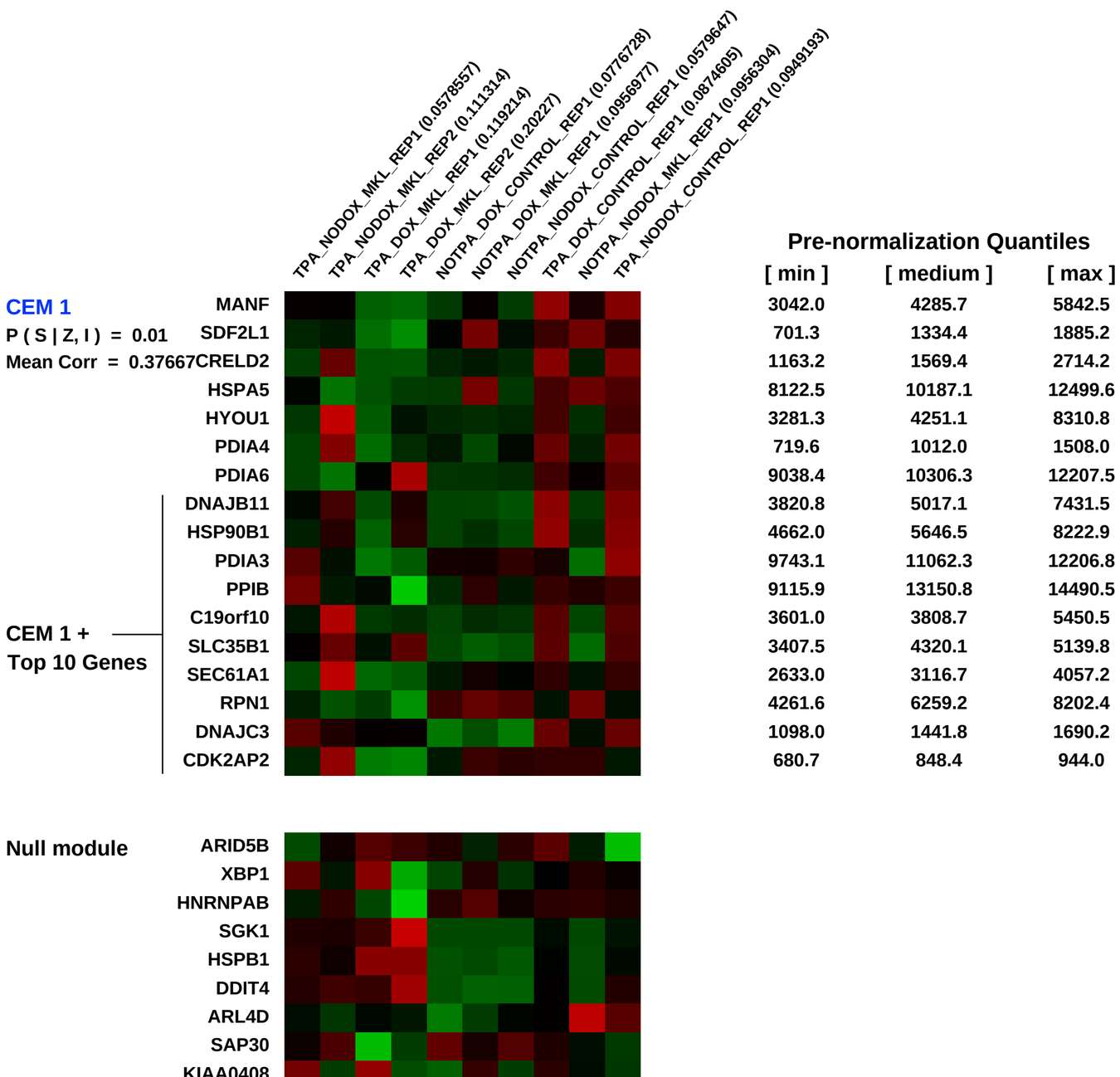

GEO Series "GSE41386" Expression Profiles

Num of samples in this series: 9

Scale of expression profile Z-scores

-3.0 -2.0 -1.0 0.0 1.0 2.0 3.0

GEO Link:	http://www.ncbi.nlm.nih.gov/geo/query/acc.cgi?acc=GSE41386
Status:	Public on Oct 06 2012
Title:	Role of REST in the pathogenesis of uterine fibroids
Organism:	Homo sapiens
Experiment type:	Expression profiling by array
Platform:	GPL570
Pubmed ID:	23284171
Summary & Design:	**Summary:** The loss of REST in uterine fibroids promotes aberrant gene expression and enables mTOR pathway activation **Overall design:** We used siRNA to knockdown REST/ NRSF in cultured primary myometrial smooth muscle cells (SMCs) and global gene expression was analyzed using microarrays.

Background corr dist: KL-Divergence = 0.0827, L1-Distance = 0.0209, L2-Distance = 0.0006, Normal std = 0.4728

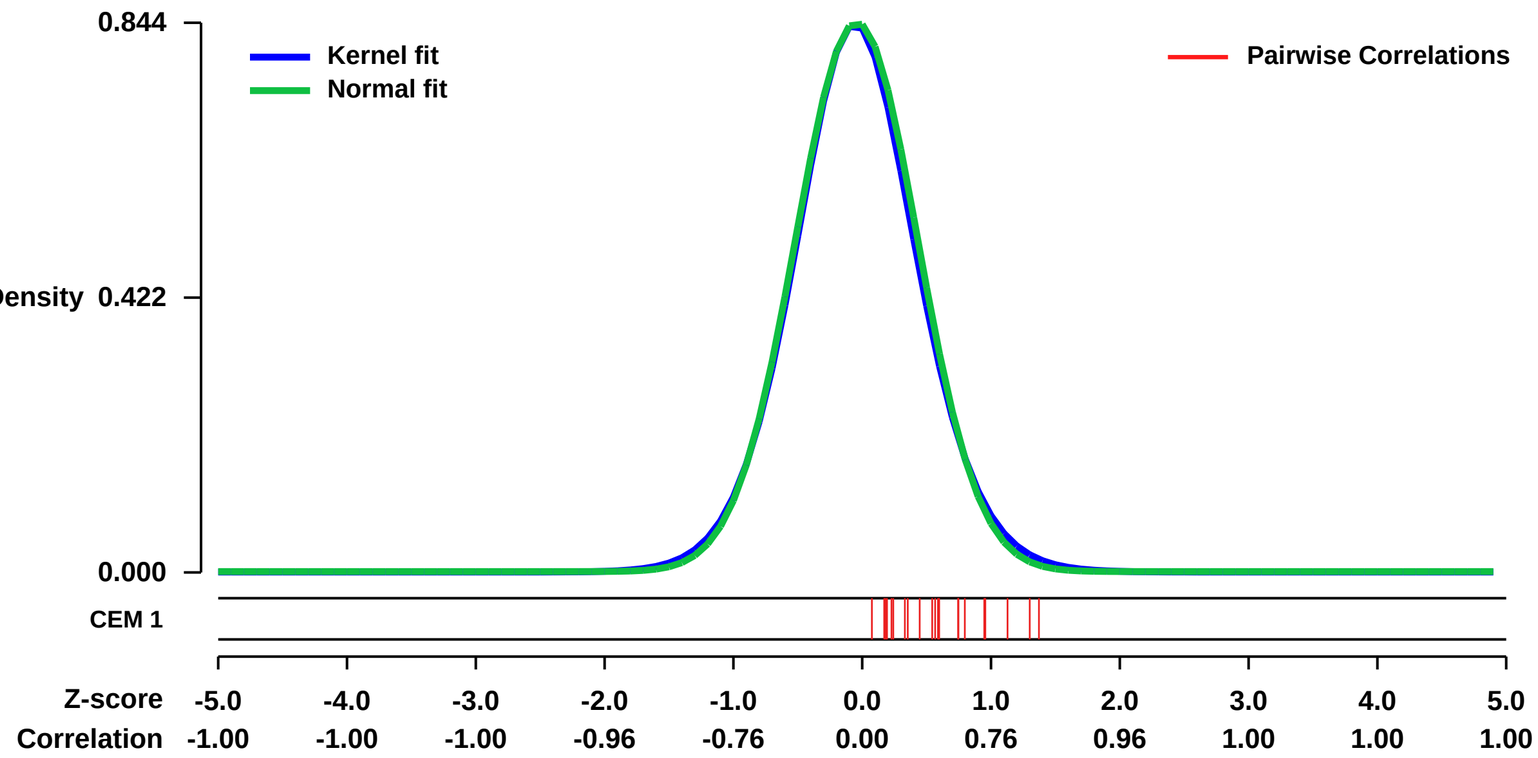

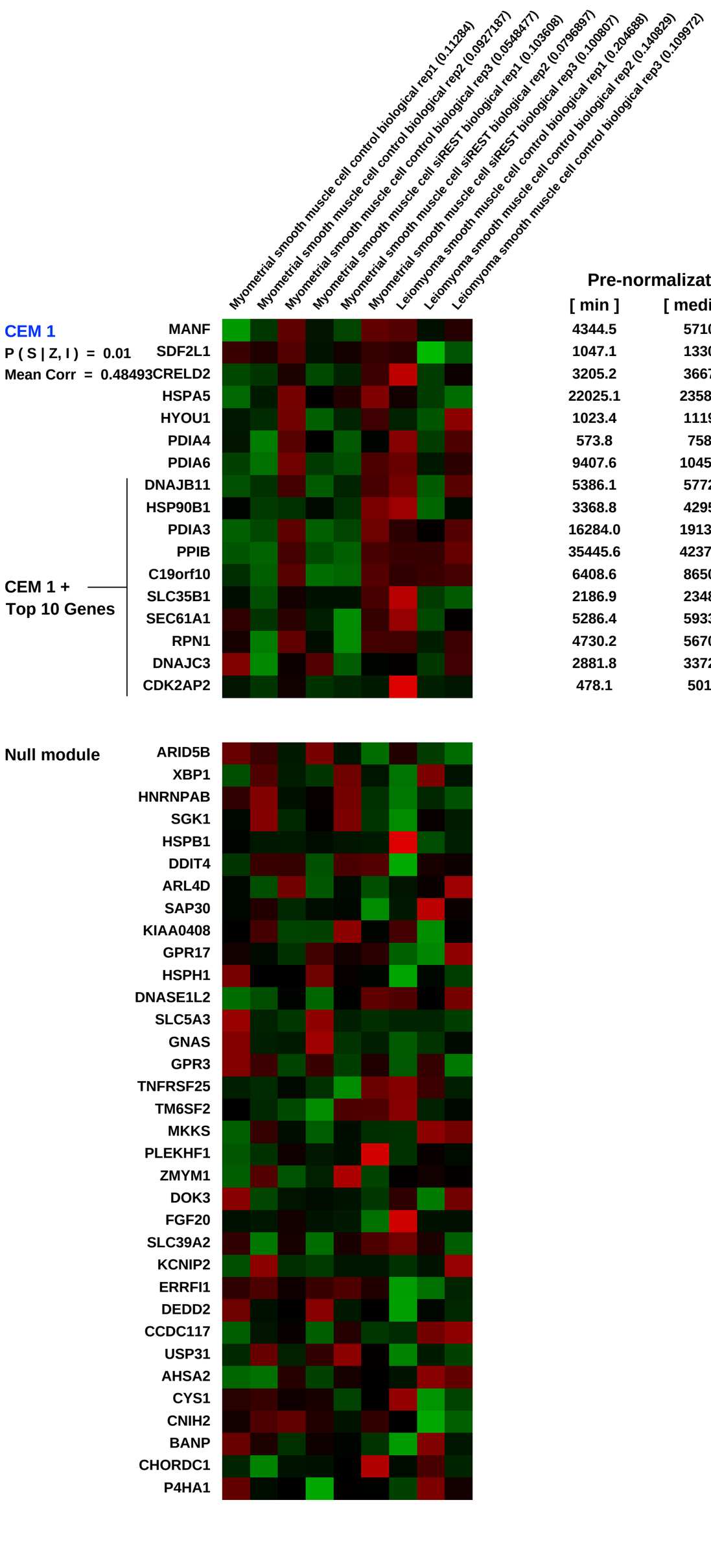

GEO Series "GSE23405" Expression Profiles

Num of samples in this series: 9

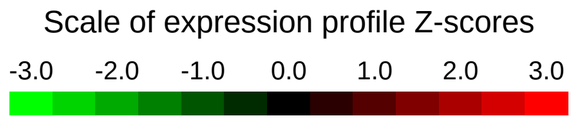

GEO Link:	http://www.ncbi.nlm.nih.gov/geo/query/acc.cgi?acc=GSE23405
Status:	Public on Aug 11 2010
Title:	Gene profiling of apoptosis induced by heat stress in U937 human lymphoma cells
Organism:	Homo sapiens
Experiment type:	Expression profiling by array
Platform:	GPL570
Pubmed ID:	21617838
Summary & Design:	**Summary:** Hyperthermia is widely used to treat patients with various cancers. 42.5¸ C is well known as the inflection point of hyperthermia and generally up to 42¸ C of hyperthermia is used in clinical cases combined with other therapies. Here, the effects of heat stress at 42 or 44¸ C for 15 min on the gene expression in human lymphoma U937 cells were investigated using an Affymetrix GeneChip system. The cells were treated with heat stress (42 or 44´℃ for 15 min), followed by incubation for 0, 1, 3 or 6 h at 37´℃. The percentage of DNA fragmentation was 8.4 ´– 2.2 (mean ´– SD) at 42´℃ for 6 h and 21.0 ´– 2.0 at 44´℃ for 6 h. Of approximately 47,000 probe sets analyzed, many genes that were differentially expressed by a factor 2.0 or greater were identified in the cells treated with heat stress at 42 and 44´℃. **Overall design:** U937 cells, a human lymphoma cell line, were treated with heat stress (42 or 44´℃ for 15 min), followed by incubation for 0, 1, 3 or 6 h at 37´℃. Non-treated cells served as the control. Total RNA samples were prepared from the cells. Gene expression was analyzed by an Affymetrix GeneChip´fi system with a Human Genome U133-plus 2.0 array for analysis of over 47,000 transcripts. Sample preparation for array hybridization was carried out as described in the manufacturerâ s instruction

Background corr dist: KL-Divergence = 0.0979, L1-Distance = 0.0267, L2-Distance = 0.0013, Normal std = 0.4427

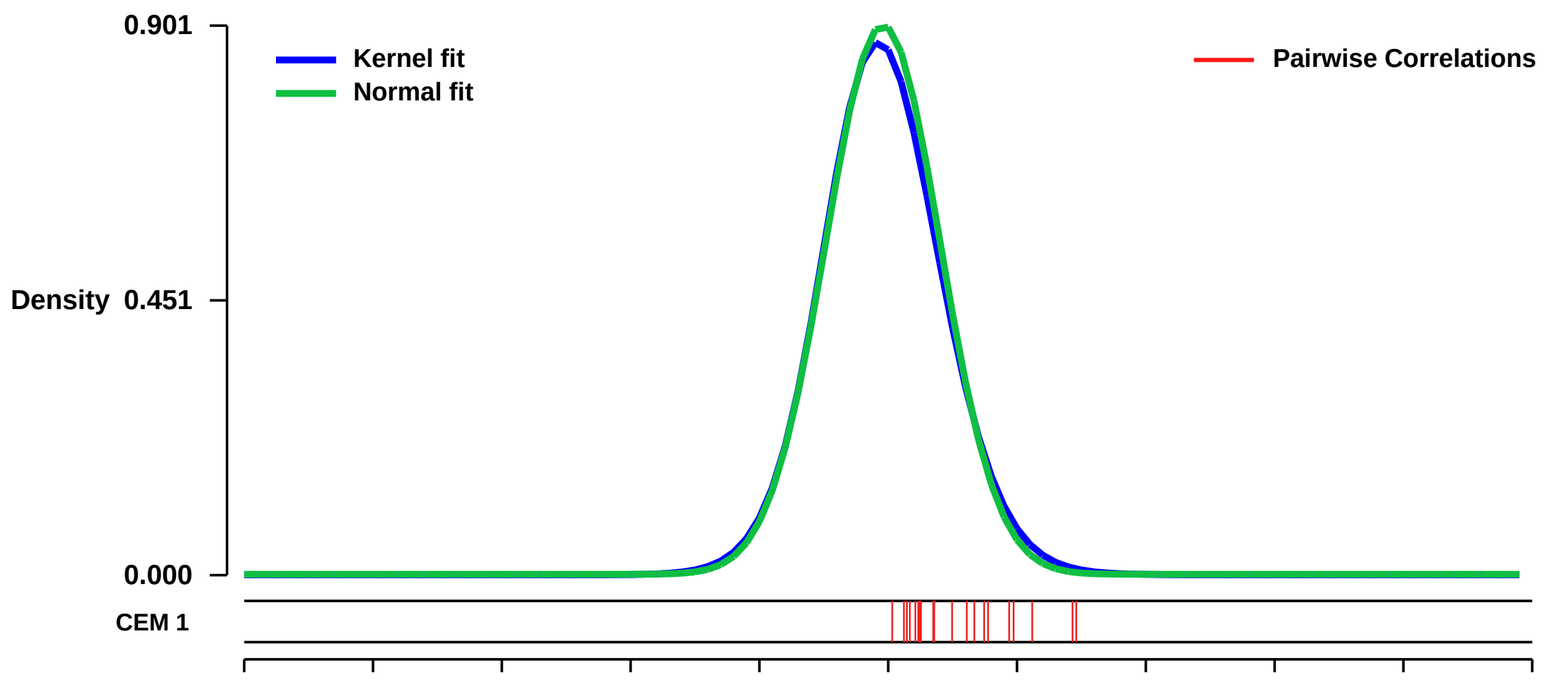

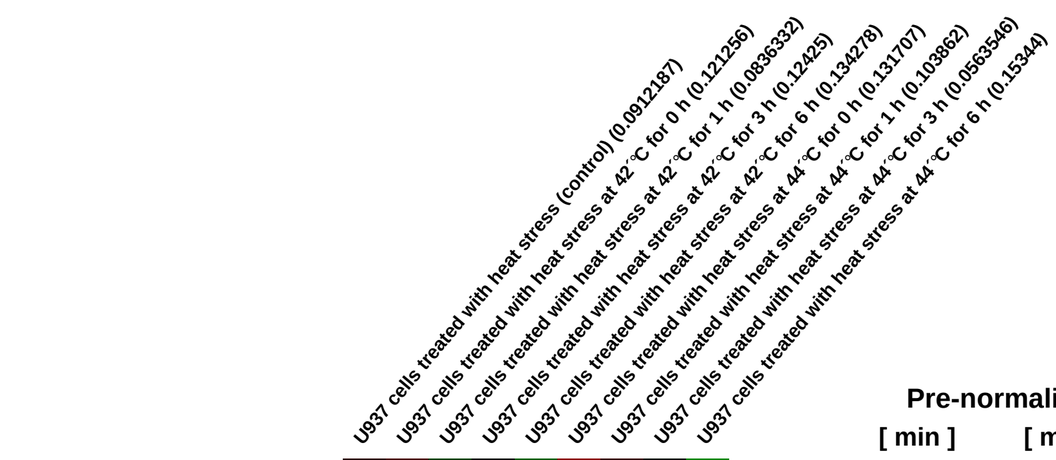

		Pre-normalization Quantiles [min]	[medium]	[max]
CEM 1	MANF	3449.5	4361.1	5333.1
P (S | Z, I) = 0.01	SDF2L1	1400.2	1787.2	2619.5
Mean Corr = 0.44114	CRELD2	2408.4	2546.0	4027.8
	HSPA5	13778.7	18297.9	21364.9
	HYOU1	2766.7	3168.1	3879.8
	PDIA4	1157.5	1609.9	2211.1
	PDIA6	11279.2	12044.1	15061.7
CEM 1 + Top 10 Genes	DNAJB11	2822.8	3834.3	4555.0
	HSP90B1	3188.7	3961.0	5972.5
	PDIA3	11213.5	12298.9	15719.8
	PPIB	24070.2	26566.3	32642.6
	C19orf10	7510.2	9021.7	9982.0
	SLC35B1	2616.6	3007.4	3894.0
	SEC61A1	3743.9	4390.9	5199.1
	RPN1	3796.4	4844.1	5318.5
	DNAJC3	2367.1	2585.9	3040.3
	CDK2AP2	838.0	975.2	1246.1
Null module	ARID5B			
	XBP1			
	HNRNPAB			
	SGK1			
	HSPB1			
	DDIT4			
	ARL4D			
	SAP30			
	KIAA0408			
	GPR17			
	HSPH1			
	DNASE1L2			
	SLC5A3			
	GNAS			
	GPR3			
	TNFRSF25			
	TM6SF2			
	MKKS			
	PLEKHF1			
	ZMYM1			
	DOK3			
	FGF20			
	SLC39A2			
	KCNIP2			
	ERRFI1			
	DEDD2			
	CCDC117			
	USP31			
	AHSA2			
	CYS1			
	CNIH2			
	BANP			
	CHORDC1			
	P4HA1			

GEO Series "GSE7513" Expression Profiles

Num of samples in this series: 29

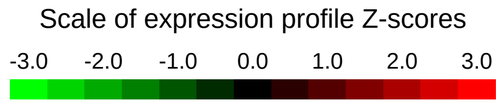

GEO Link:	http://www.ncbi.nlm.nih.gov/geo/query/acc.cgi?acc=GSE7513
Status:	Public on Aug 15 2009
Title:	Gene expression data from CD44+/CD24- cells sorted by flow cytometry
Organism:	Homo sapiens
Experiment type:	Expression profiling by array
Platform:	GPL570
Pubmed ID:	19666588

Summary & Design:

Summary:
Tumorigenic breast cancer cells characterized by CD44 expression and low or undetectable CD24 levels (CD44+/CD24-/low) may be resistant to chemotherapy and therefore responsible for cancer relapse. Paired breast cancer core biopsies before and after neoadjuvant chemotherapy or lapatinib were obtained and as single cell suspensions stained using antibodies against CD24, CD44, and lineage markers, and then analyzed by flow cytometry. Mammosphere (MS) formation in culture was compared before and after treatment. Global gene expression differences between cancer cells bearing CD44+/CD24-/low cells and all other sorted cells, and between cancer MS and the primary bulk invasive cancers were analyzed. We report that CD44+/CD24-/low tumorigenic breast cancer cells were intrinsically chemoresistant â chemotherapy led to increased CD44+/CD24-/low cells, increased self-renewal capacity on MS assays, and enhanced tumorigeneicity in immunocompromised SCID/Beige mice. Conversely, in patients with HER2 overexpressing tumors, the EGFR/HER2 tyrosine kinase inhibitor, lapatinib decreased CD44+/CD24-/low cells, with the majority of these patients after conventional therapy achieving pathologic complete response, a validated surrogate marker for long-term survival. Gene transcription pathways that underlie chemoresistant, MS-forming CD44+/CD24-/low cells involve genes belonging to stem cell self-renewal, Wnt signaling, and early development pathways.

Keywords: two group comparison

Overall design:
Core biopsies of primary breast tumors were taken and placed immediately in cold RPMI-1640 supplemented with 10% heat-inactivated newborn calf serum (HINCS, Invitrogen, Carlsbad, CA). Within an hour, the samples were minced and then digested in 10-15 mL of MEGM with 250-300 units/mL collagenase at 370C. The samples were filtered, washed, and then subjected to hypotonic shock to lyse red blood cells. About 106 single cells were re-suspended, incubated for 15 min at 40C with anti-CD44 (APC), anti-CD24 (FITC), and anti-lineage cocktail antibodies (PE-conjugated anti-CD2, CD3, CD10, CD16, CD18, CD31 and CD 140B) (Pharmingen, San Diego, CA) using the manufacturerâ s suggested concentrations. The cells were then washed twice, re-suspended with the viability dye propidium iodide, and analyzed using Dako MoFlo flow cytometry. Side- and forward- scatter were used to eliminate debris and cell doublets, and the Lin- cells were further analyzed by CD44 and CD24 markers.

Background corr dist: KL-Divergence = 0.3810, L1-Distance = 0.0828, L2-Distance = 0.0214, Normal std = 0.2538

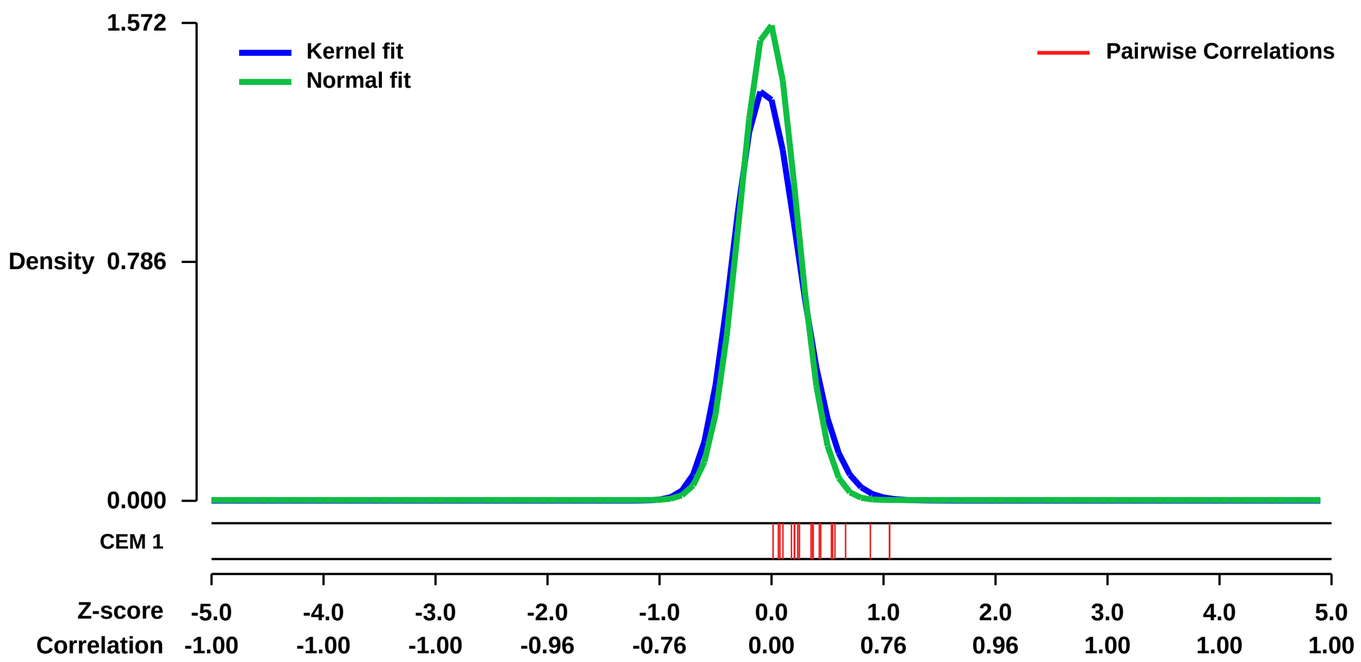

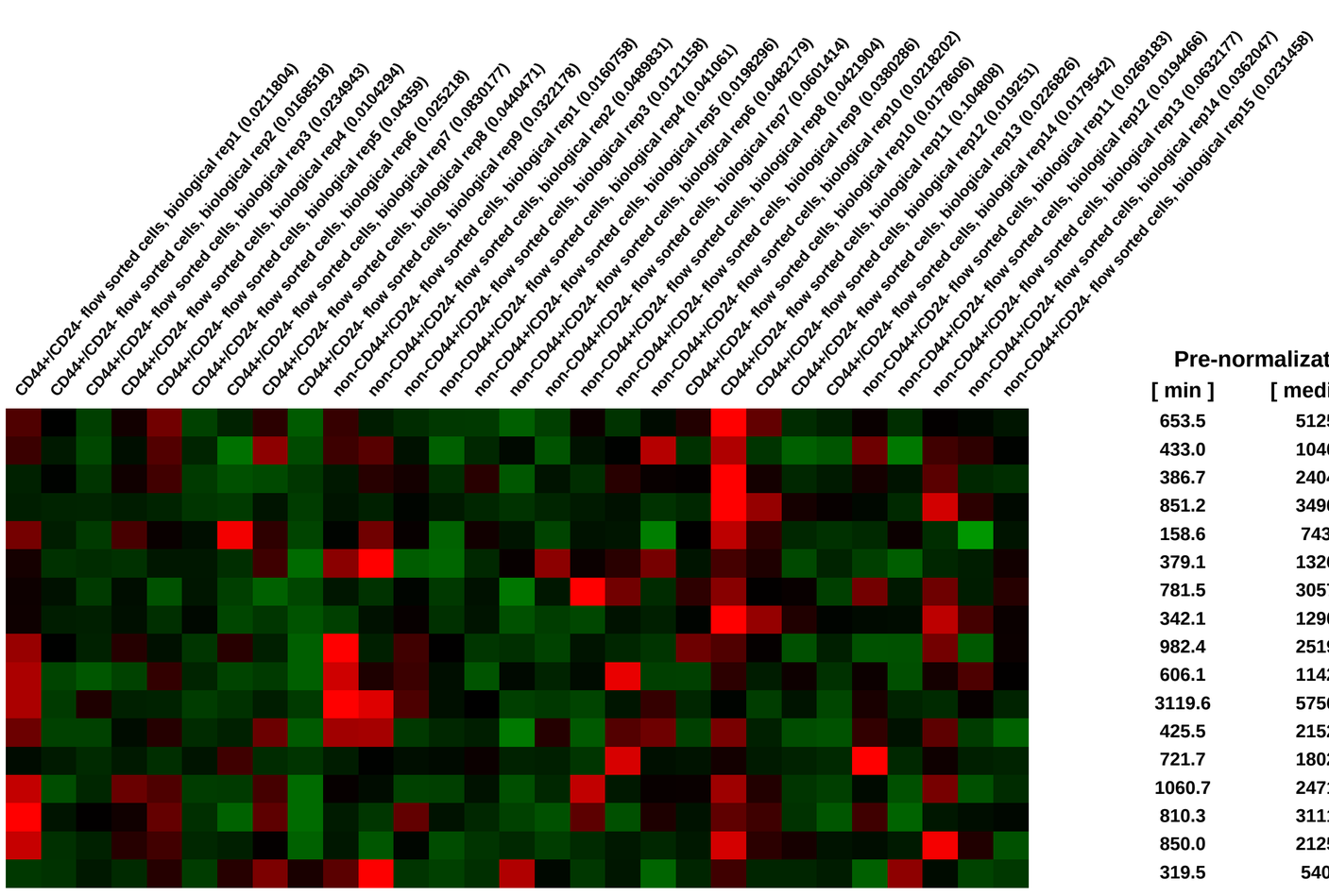

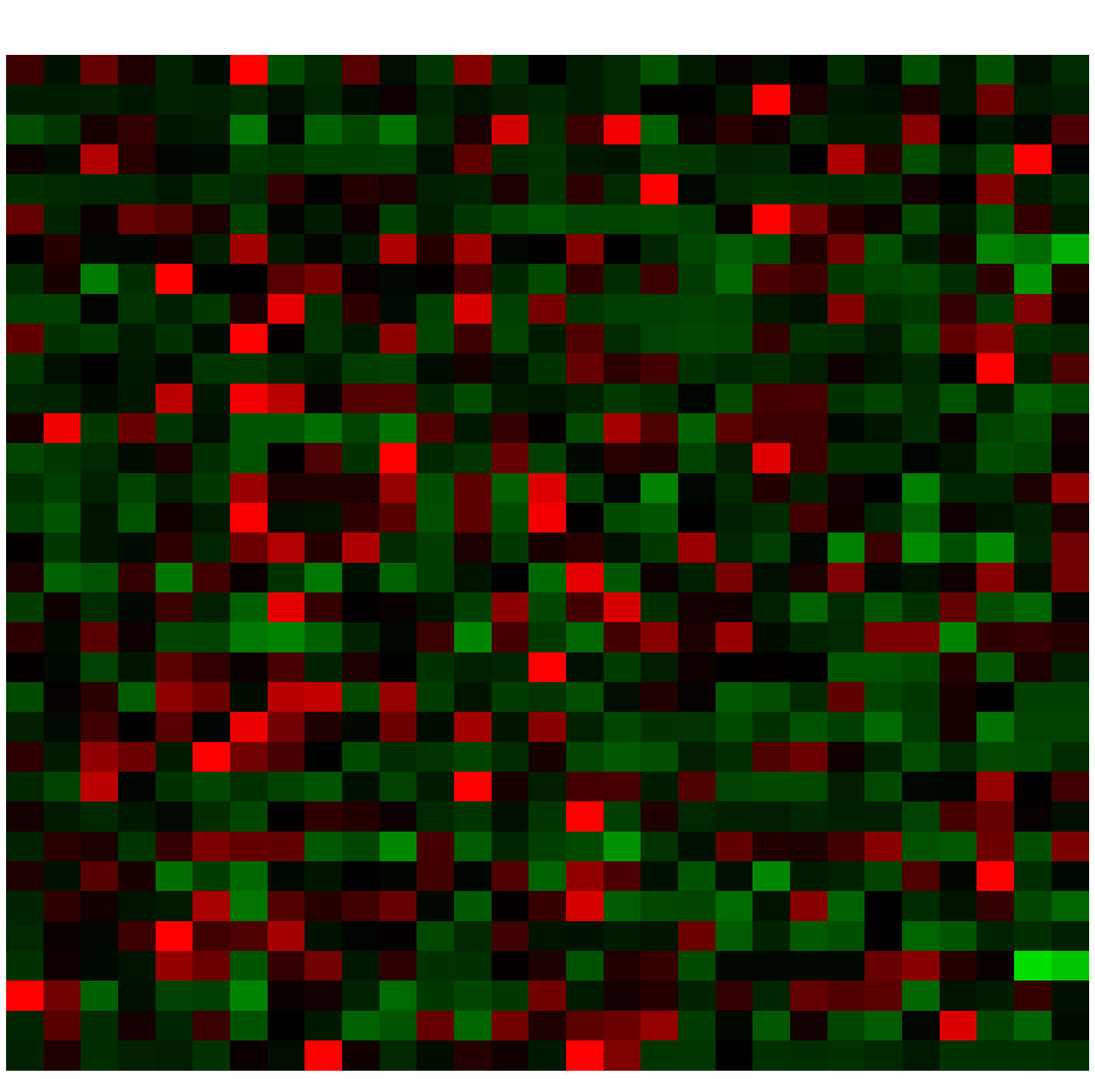

GEO Series "GSE52707" Expression Profiles

Num of samples in this series: 12

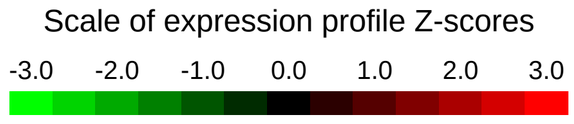

GEO Link:	http://www.ncbi.nlm.nih.gov/geo/query/acc.cgi?acc=GSE52707
Status:	Public on Feb 13 2014
Title:	Nuclear factor kappa B activation-induced anti-apoptosis renders HER2 positive cells drug resistant and accelerates tumor growth
Organism:	Homo sapiens
Experiment type:	Expression profiling by array
Platform:	GPL570
Pubmed ID:	24319068
Summary & Design:	**Summary:** Breast cancers with HER2 overexpression are sensitive to drugs targeting the receptor or its kinase activity. HER2-targeting drugs are initially effective against HER2- positive breast cancer, but resistance inevitably occurs. We previously found that nuclear factor kappa B is hyper-activated in the subset of HER-2 positive breast cancer cells and tissue specimens. In this study, we report that constitutively active NF-¸”B rendered HER2-positive cancer cells resistant to anti-HER2 drugs, and cells selected for Lapatinib resistance up-regulated NF-¸”B. In both circumstances, cells were anti-apoptotic and grew rapidly as xenografts. Lapatinib-resistant cells were refractory to HER2 and NF-¸”B inhibitors alone but were sensitive to their combination, suggesting a novel therapeutic strategy. A subset of NF-¸”B-responsive genes was overexpressed in HER2-positive and triple-negative breast cancers, and patients with this NF-¸”B signature had poor clinical outcome. Anti-HER2 drug resistance may be a consequence of NF-¸”B activation, and selection for resistance results in NF-¸”B activation, suggesting this transcription factor is central to oncogenesis and drug resistance. Clinically, the combined targeting of HER2 and NF-¸”B suggests a potential treatment paradigm for patients who relapse after anti-HER2 therapy. Patients with these cancers may be treated by simultaneously suppressing HER2 signaling and NF-¸”B activation. We used microarrays to detail the gene expression differences underlying the characterictic survival differences between the SKR6, SKR6-Vector, SKR6CA, and SKR6LR cell lines, which are defined as follows: SKR6: A clonal derivative of SKBR3 cells isolated by fluorescence-activated cell sorting (FACS) to enrich for elevated HER2 levels, SKR6CA: SKR6 cells retrovirally transduced with constitutively active NF-¸”B relA/p65 (CAp65) and selected with puromycin, SKR6 vector: SKR6 cells transduced with the pQCXIP empty retroviral vector and selected with puromycin, and SKR6LR: SKR6 cells treated with increasing lapatinib concentrations (0.2 to 5 ¸…M) for several months. **Overall design:** We sorted SKBR-3 cells by fluorescence-activated cell sorting (FACS) to enriched for cell population with elevated HER2 expression, which we termed SKR6. The following cell lines were then created from SKR6 cells: SKR6CA: SKR6 cells retrovirally transduced with constitutively active NF-¸”B relA/p65 (CAp65), SKR6 vector: SKR6 cells transduced with the pQCXIP empty retroviral vector and selected with puromycin, and SKR6LR: SKR6 cells treated with increasing lapatinib concentrations (0.2 to 5 ¸…M) for several months.

Background corr dist: KL-Divergence = 0.0550, L1-Distance = 0.0525, L2-Distance = 0.0039, Normal std = 0.5938

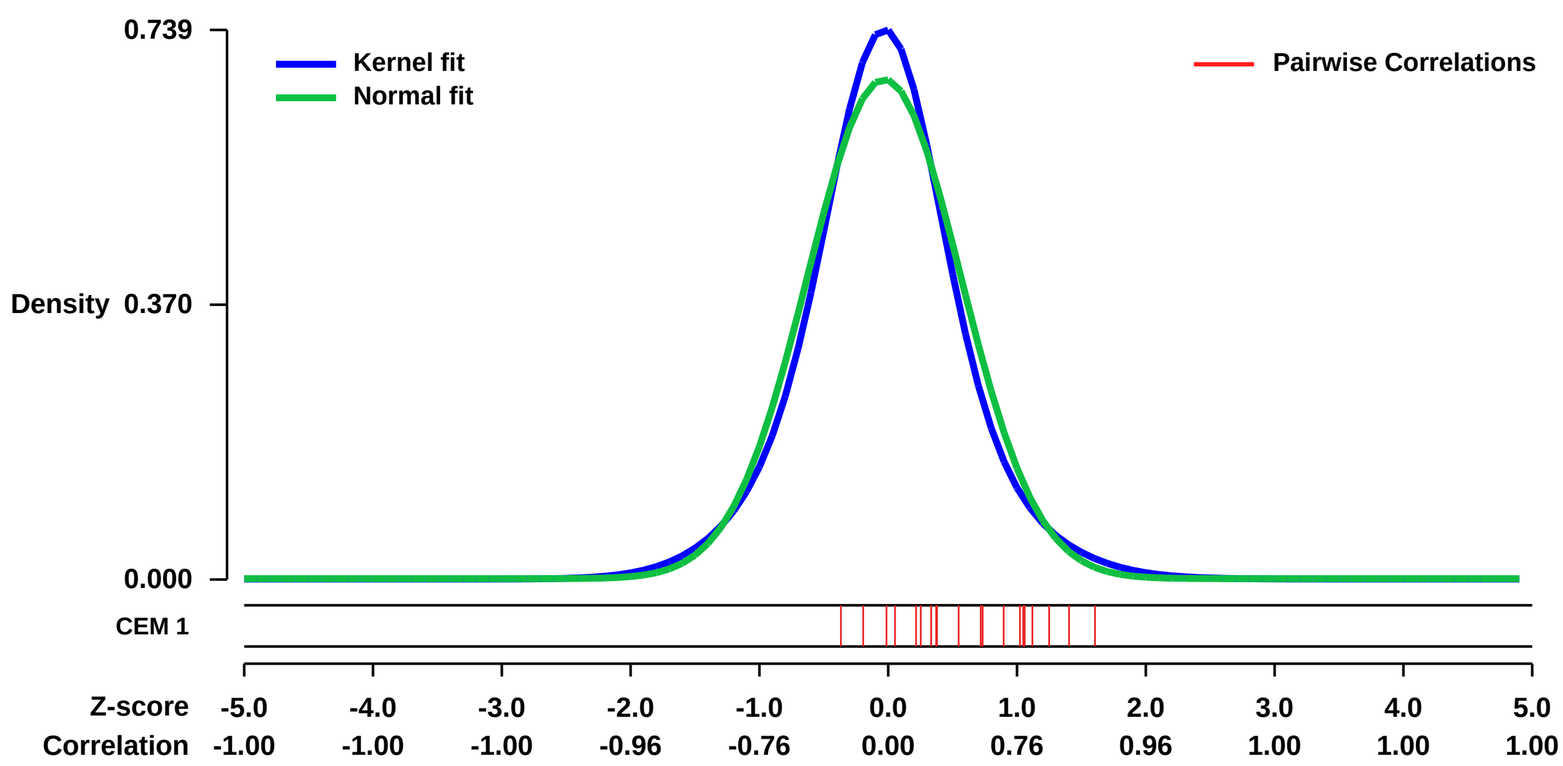

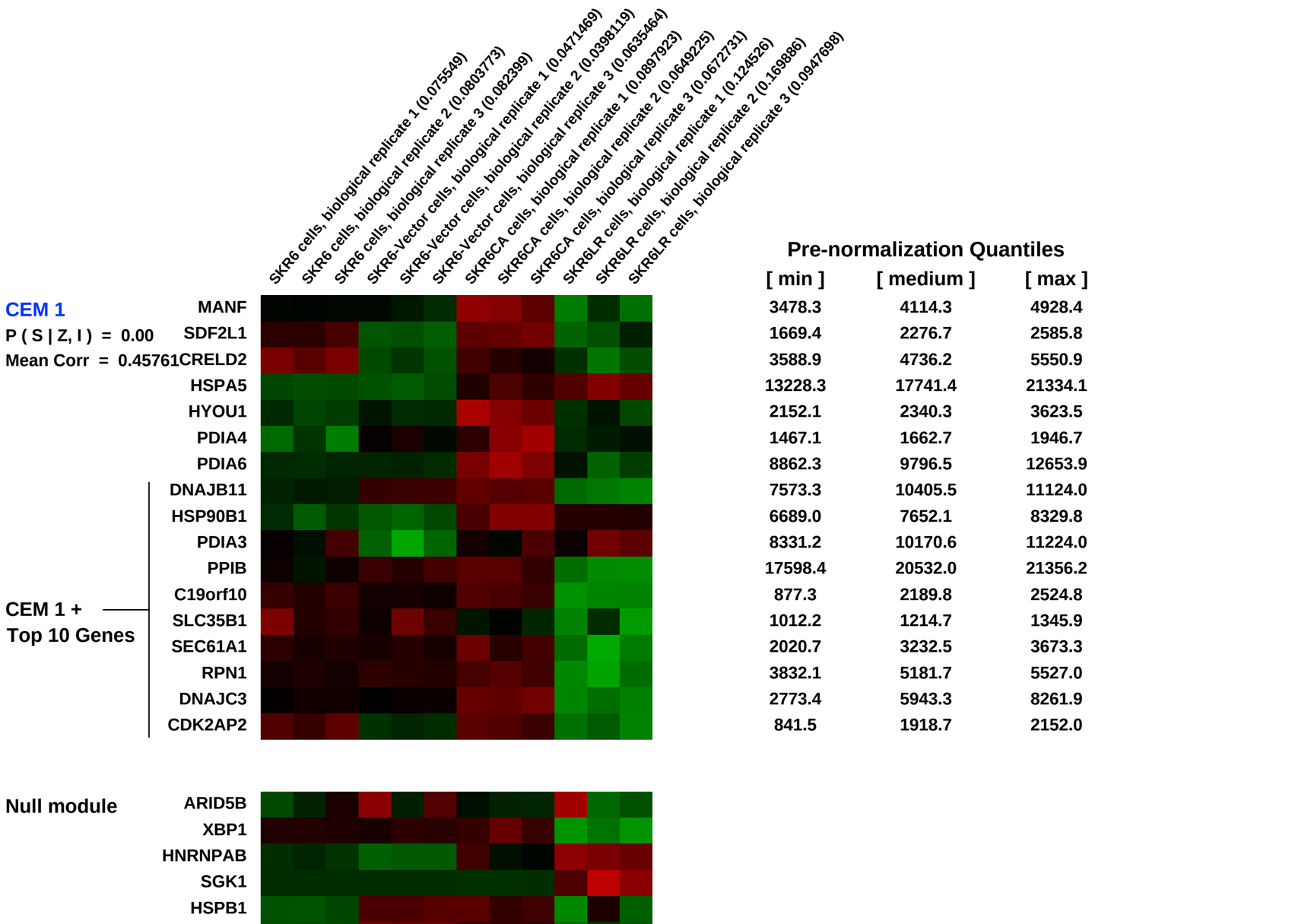

GEO Series "GSE24897" Expression Profiles

Num of samples in this series: 12

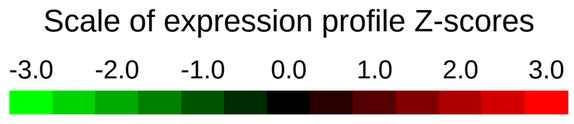

GEO Link:	http://www.ncbi.nlm.nih.gov/geo/query/acc.cgi?acc=GSE24897
Status:	Public on Oct 23 2010
Title:	Expression data from human macrophages treated with Porphyromonas gingivalis and its components
Organism:	Homo sapiens
Experiment type:	Expression profiling by array
Platform:	GPL570
Pubmed ID:	21203416
Summary & Design:	**Summary:** Periodontitis is the most common human infection affecting tooth-supporting structures. It was shown to play a role in aggravating atherosclerosis. To deepen our understanding of the pathogenesis of this disease, we exposed human macrophages to an oral bacteria Porphyromonas gingivalis (P. gingivalis) either as live bacteria, or its lipopolysaccharide (LPS) or fimbria. Microarray data from treated macrophages or control cells were analyzed to define molecular signatures. We focused our analysis on three important groups of genes. Group PG (genes differentially expressed by live bacteria only); Group LFG (genes differentially expressed in response to exposure to LPS and/or FimA); Group CG (core gene set jointly activated by all 3 stimulants). A total of 842 macrophage genes were differentially expressed in at least one of the three conditions compared to naˆflve cells. Using pathway analysis, we found that group CG activates the initial phagocytosis process and induces genes relevant to immune response, whereas group PG can de-activate the phagocytosis process associated with phagosome-lysosome fusion. LFG mostly affected RIG-I-like receptor signaling pathway. **Overall design:** 12 samples in total. 4 conditions (treatment with live P. gingivalis, P. gingivalis LPS, P. gingivalis fimbriae, or saline) were used, and triplicates were performed for each condition. We considered the following comparisons: PG vs. Control (saline), PG-LPS vs. Control, and PG-fimbriae vs. Control. Fold-change > 2.0 and FDR < 0.25 were used to select significantly expressed genes.

Background corr dist: KL-Divergence = 0.0574, L1-Distance = 0.0508, L2-Distance = 0.0055, Normal std = 0.5406

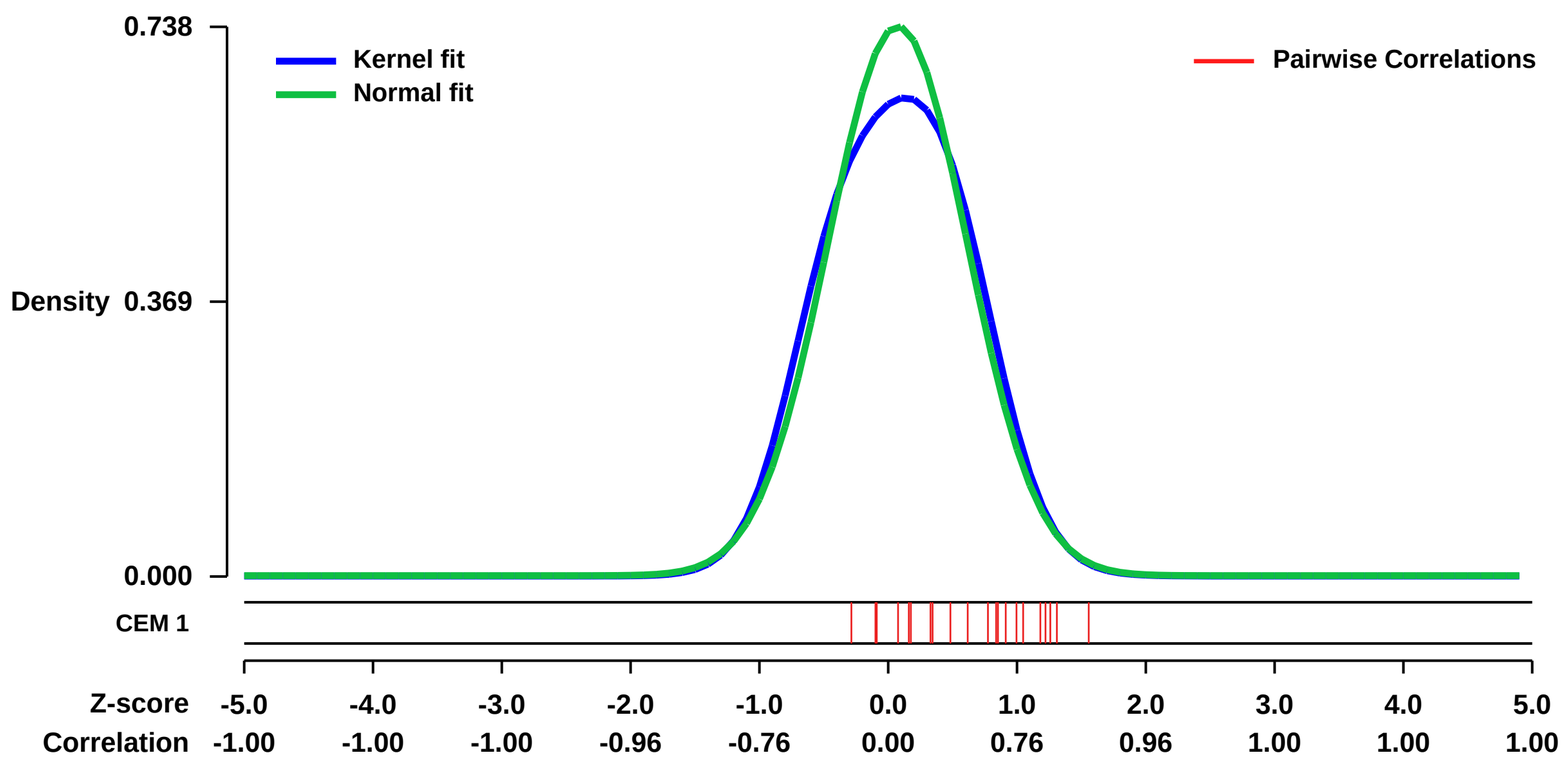

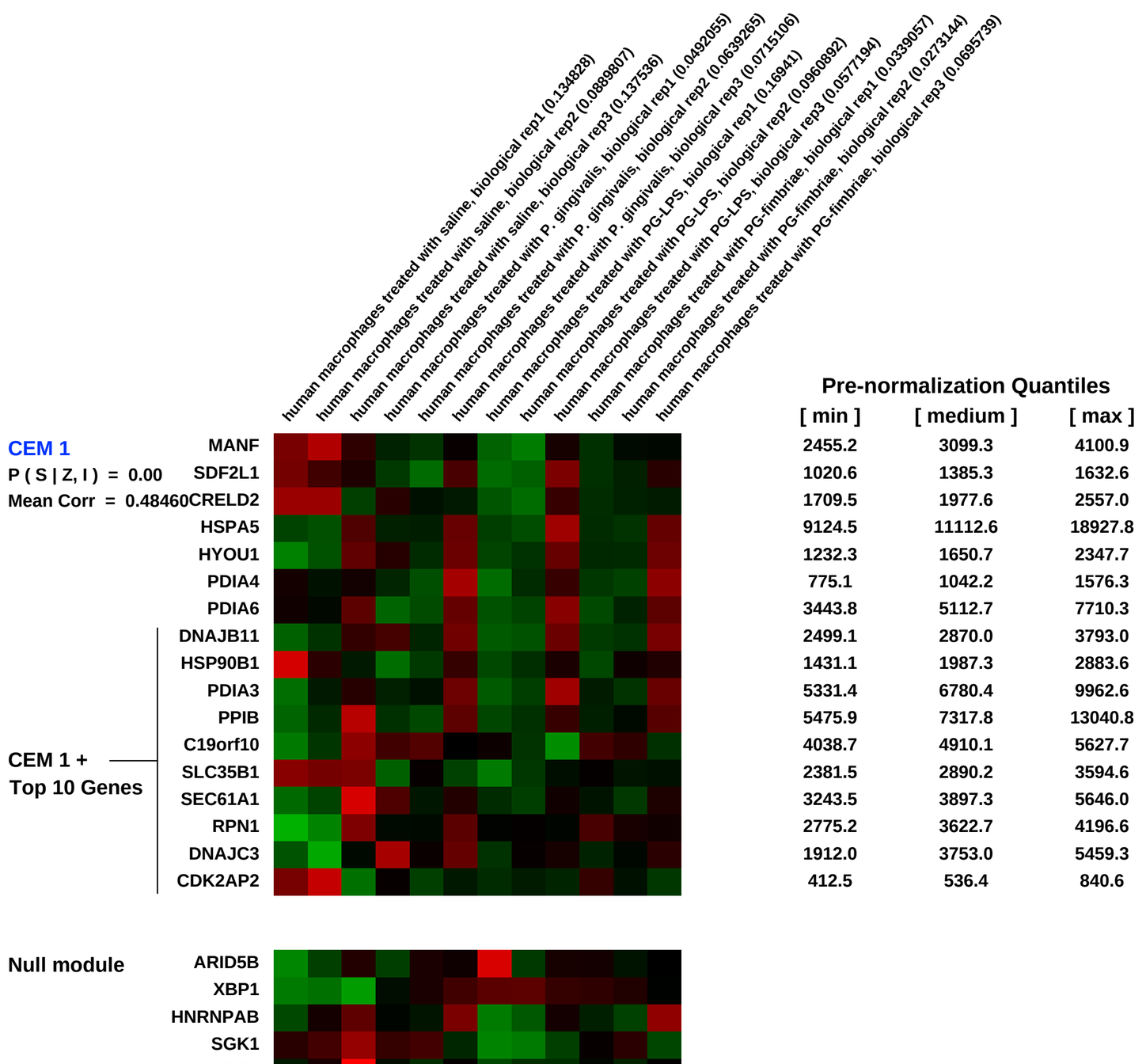

GEO Series "GSE33115" Expression Profiles

Num of samples in this series: 11

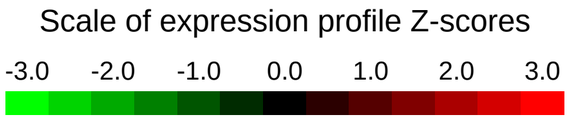

GEO Link:	http://www.ncbi.nlm.nih.gov/geo/query/acc.cgi?acc=GSE33115
Status:	Public on Sep 30 2013
Title:	Molecular changes induced by melanoma cell conditioned medium (MCM) in HUVEC cells.
Organism:	Homo sapiens
Experiment type:	Expression profiling by array
Platform:	GPL570
Pubmed ID:	
Summary & Design:	**Summary:** Malignant melanoma is a complex genetic disease and the most aggressive form of skin cancer. Melanoma progression and metastatic dissemination fundamentally relies on the process of angiogenesis. Melanomas produce an array of angiogenic modulators that mediate pathological angiogenesis. Such tumor-associated modulators arbitrate the enhanced proliferative, survival and migratory responses exhibited by endothelial cells, in the hypoxic tumor environment. The current study focuses on melanoma-induced survival of endothelial cells under hypoxic conditions. Melanoma conditioned media were capable of enabling prolonged endothelial cell survival under hypoxia, in contrast with the conditioned media derived from melanocytes, breast and pancreatic tumors. To identify the global changes in gene expression and further characterize the pro-survival pathway induced in endothelial cells, we performed microarray analysis on endothelial cells treated with melanoma conditioned medium under normoxic and hypoxic conditions. **Overall design:** Huvec cells were grown in melanoma conditioned medium or DMEM 10% FCS for 12 h under hypoxic or normoxic conditions. In order to identify the transcripts modulated by melanoma CM, samples treated with MCM were compared to those grown in DMEM alone.

Background corr dist: KL-Divergence = 0.0994, L1-Distance = 0.0288, L2-Distance = 0.0014, Normal std = 0.4358

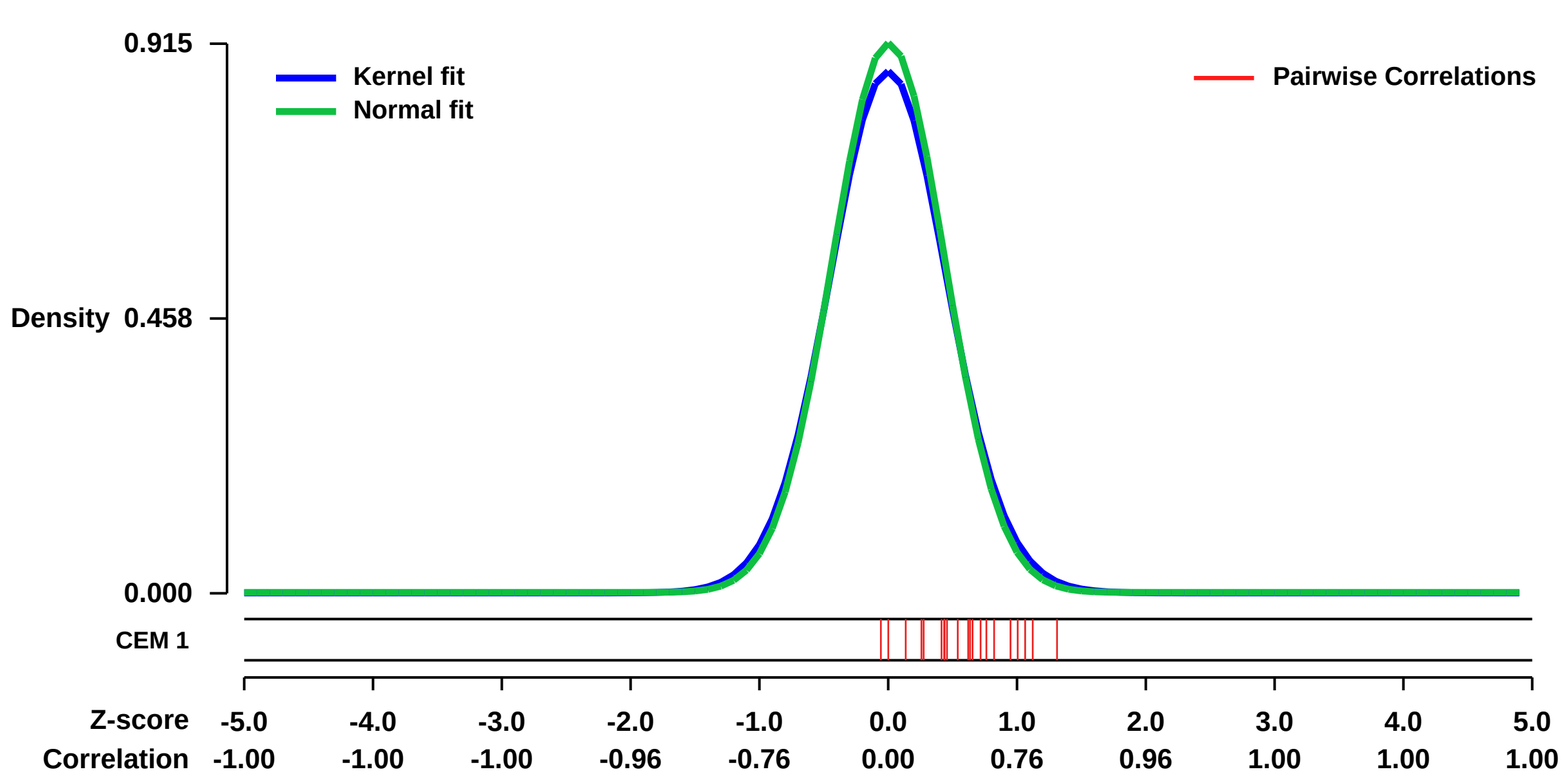

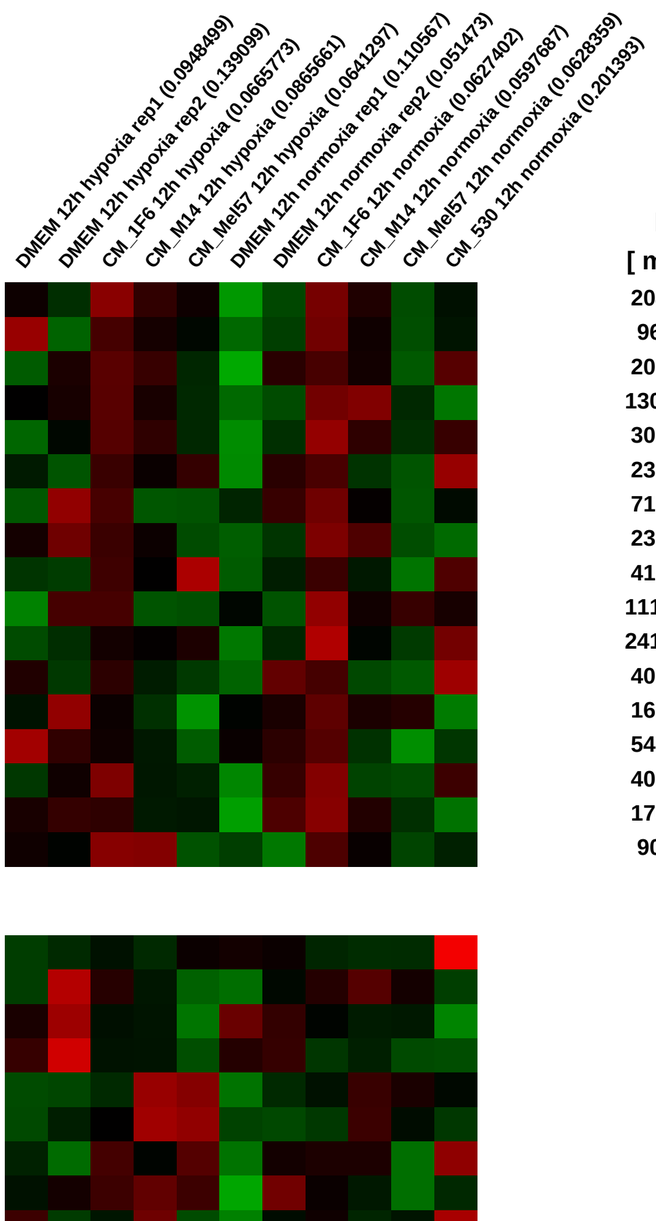

Pre-normalization Quantiles

	[min]	[medium]	[max]
CEM 1			
P (S | Z, I) = 0.00			
Mean Corr = 0.49135			
MANF	2040.8	3285.4	4224.9
SDF2L1	964.2	1244.0	1704.4
CRELD2	2014.1	3258.3	3649.9
HSPA5	13077.3	19216.5	25861.6
HYOU1	3069.1	4904.3	7029.9
PDIA4	2370.1	3820.1	5192.5
PDIA6	7171.8	8085.8	9913.2
CEM 1 + Top 10 Genes			
DNAJB11	2369.5	3062.6	3723.2
HSP90B1	4155.8	4953.0	6651.8
PDIA3	11100.6	15725.0	19785.5
PPIB	24110.1	27272.2	32303.4
C19orf10	4088.9	4564.2	5822.0
SLC35B1	1608.8	2102.8	2523.6
SEC61A1	5437.3	6921.4	8416.9
RPN1	4005.5	4805.1	5920.3
DNAJC3	1708.2	2582.2	3114.8
CDK2AP2	908.4	1238.8	1631.6
Null module			
ARID5B			
XBP1			
HNRNPAB			
SGK1			
HSPB1			
DDIT4			
ARL4D			
SAP30			
KIAA0408			
GPR17			
HSPH1			
DNASE1L2			
SLC5A3			
GNAS			
GPR3			
TNFRSF25			
TM6SF2			
MKKS			
PLEKHF1			
ZMYM1			
DOK3			
FGF20			
SLC39A2			
KCNIP2			
ERRFI1			
DEDD2			
CCDC117			
USP31			
AHSA2			
CYS1			
CNIH2			
BANP			
CHORDC1			
P4HA1			

GEO Series "GSE23952" Expression Profiles

Num of samples in this series: 6

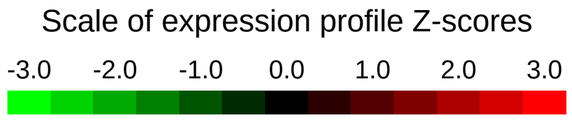

GEO Link:	http://www.ncbi.nlm.nih.gov/geo/query/acc.cgi?acc=GSE23952
Status:	Public on Sep 03 2010
Title:	Expression data from TGF-beta treated Panc-1 pancreatic adenocarcinoma cell line
Organism:	Homo sapiens
Experiment type:	Expression profiling by array
Platform:	GPL570
Pubmed ID:	20885998
Summary & Design:	**Summary:** TGF-beta treatment of Panc-1 pancreatic adenocarcinoma cell line on Affymetrix HG_U133_plus_2 arrays; triplicate experiments. The goal of the experiment is to profile temporal gene expression changes during TGF-beta-induced epithelial-mesenchymal transition (EMT). During EMT cancer cells lose their epithelial specifc proteins and gain mesenchymal proteins to acquire migratory and invasive phenotype essential for metastasis. Human Panc-1 pancreatic adenocarcinoma cell line was treated with 5 ng/mL TGF-beta for 48 h to induce EMT. The experiment was repeated 3 times. Samples were assayed using Affymetrix HG_U133_plus_2 arrays with 54675 probe-sets, using standard techniques. **Overall design:** Human Panc-1 pancreatic adenocarcinoma cell line was treated with 5 ng/mL TGF-beta for 48 h. The experiment was repeated 3 times. Samples were assayed using Affymetrix HG_U133_plus_2 arrays with 54675 probe-sets, using standard techniques.

Background corr dist: KL-Divergence = 0.0266, L1-Distance = 0.0463, L2-Distance = 0.0025, Normal std = 0.7662

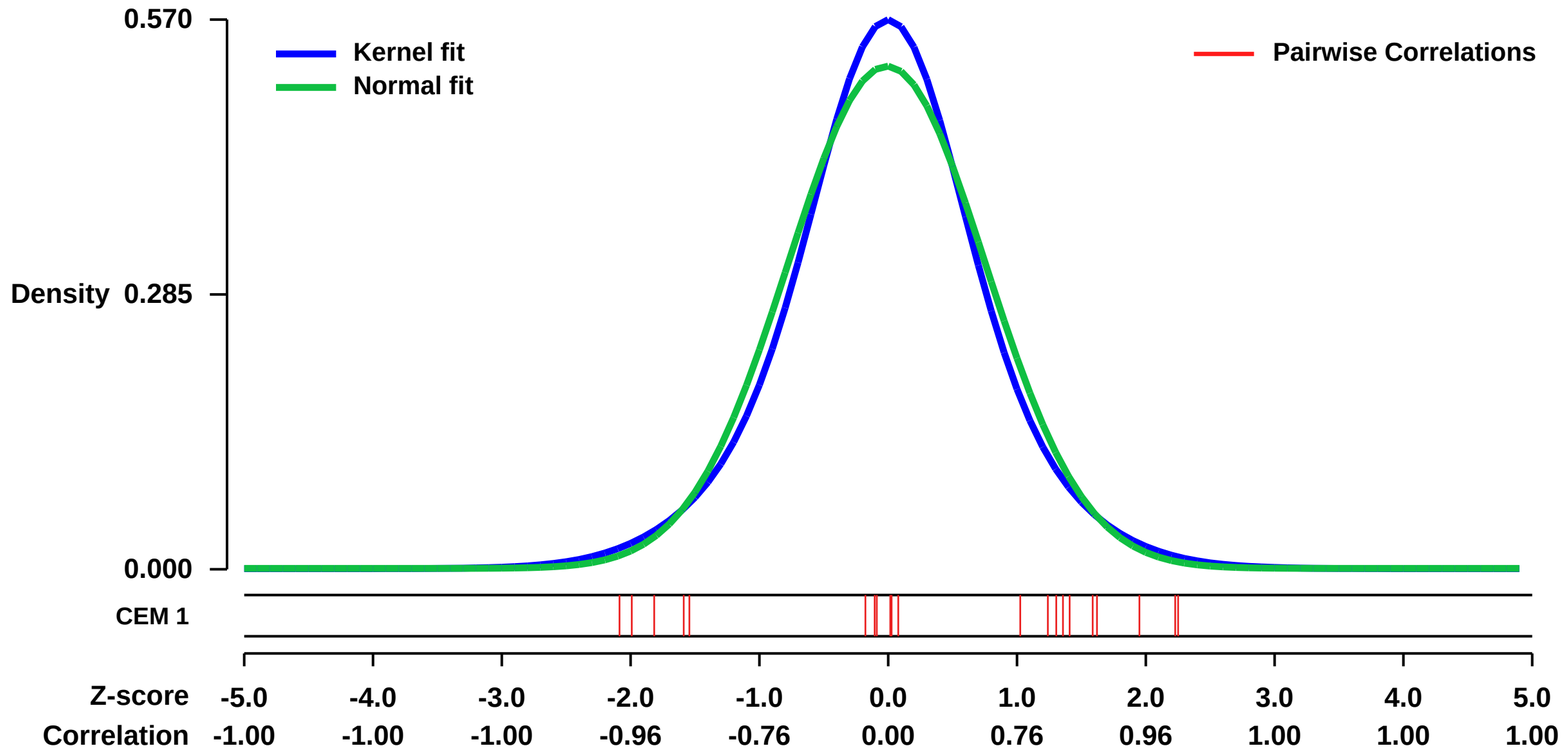

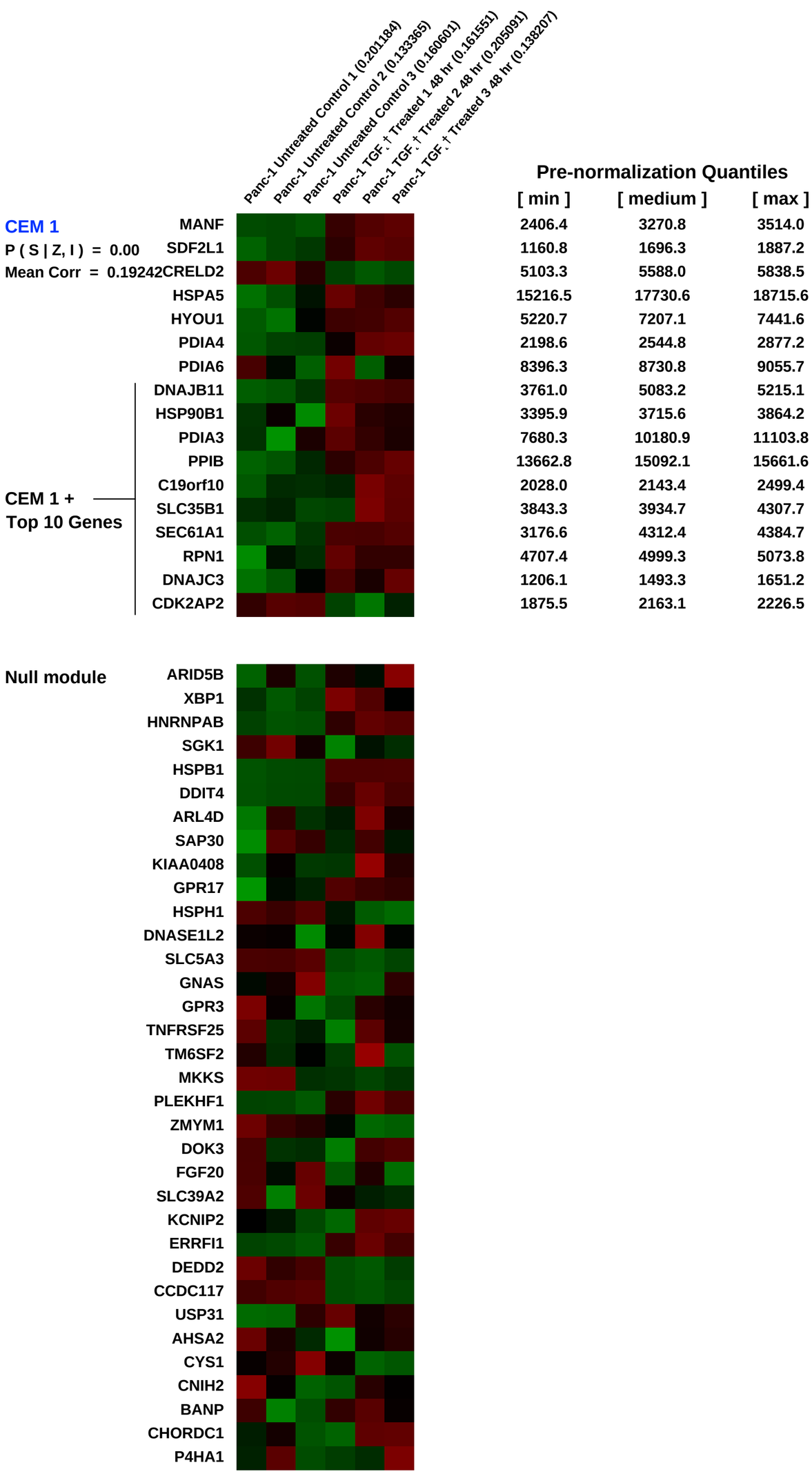

GEO Series "GSE13487" Expression Profiles

Num of samples in this series: 30

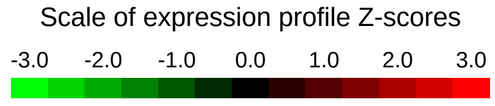

GEO Link:	http://www.ncbi.nlm.nih.gov/geo/query/acc.cgi?acc=GSE13487
Status:	Public on Oct 01 2009
Title:	Antitumor efficacy of RAF inhibitor GDC-0879 involving BRAFV600E mutational status and ERK/MAPK pathway suppression
Organism:	Homo sapiens
Experiment type:	Expression profiling by array
Platform:	GPL570
Pubmed ID:	19276360
Summary & Design:	**Summary:** Unsupervised hierarchical clustering revealed a strong similarity in gene modulation resulting from either compound treatment or BRAF ablation mediated by RNA interference relative to DMSO-treated control samples . **Keywords:** Expression Array **Overall design:** We have generated melanoma A375 cells stably expressing a shRNA construct for doxycycline-inducible knockdown of B-Raf (2 mg/ml Dox, 48h). Small molecule treatment was at 1000nM R341787, 24h.

Background corr dist: KL-Divergence = 0.2351, L1-Distance = 0.0362, L2-Distance = 0.0024, Normal std = 0.3171

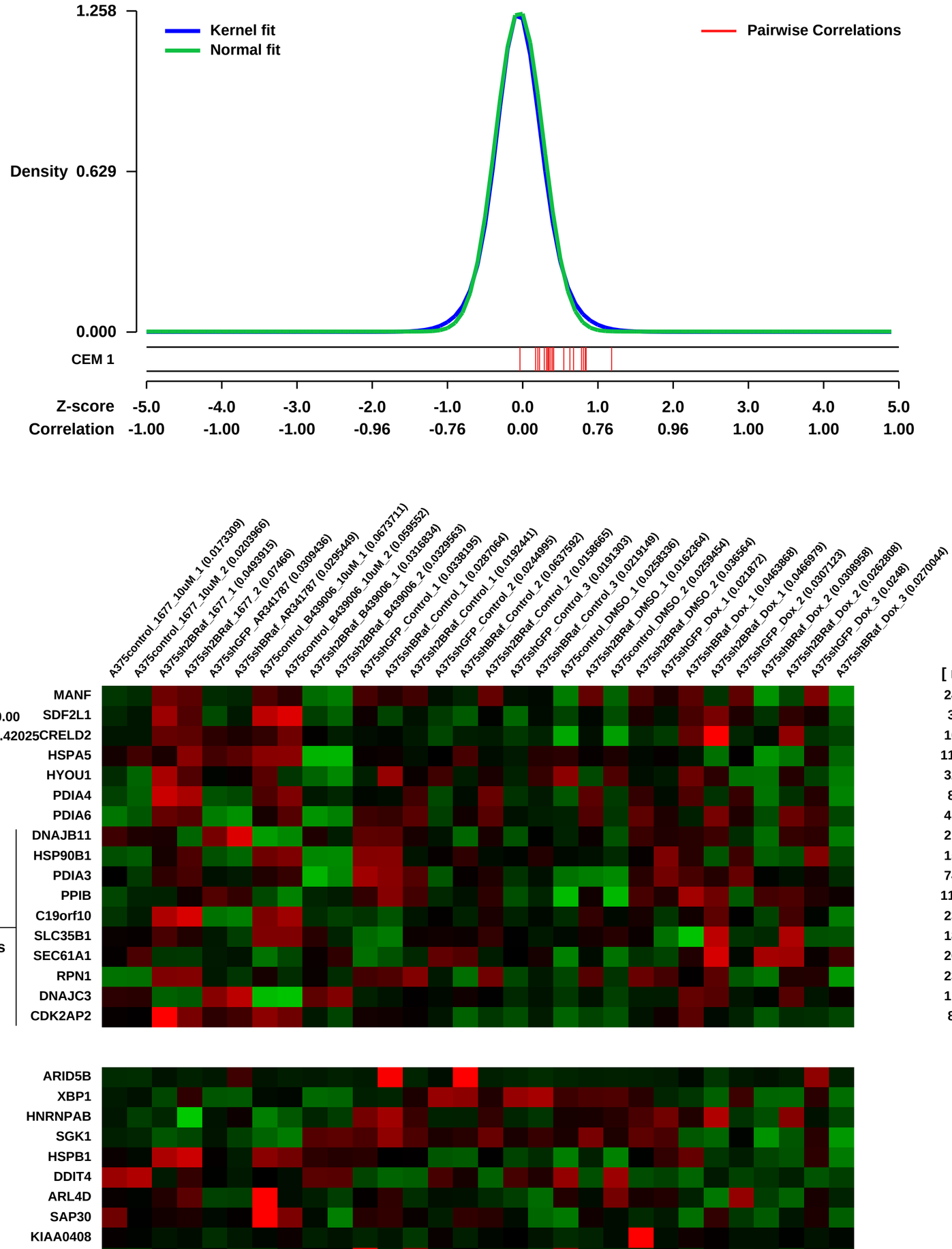

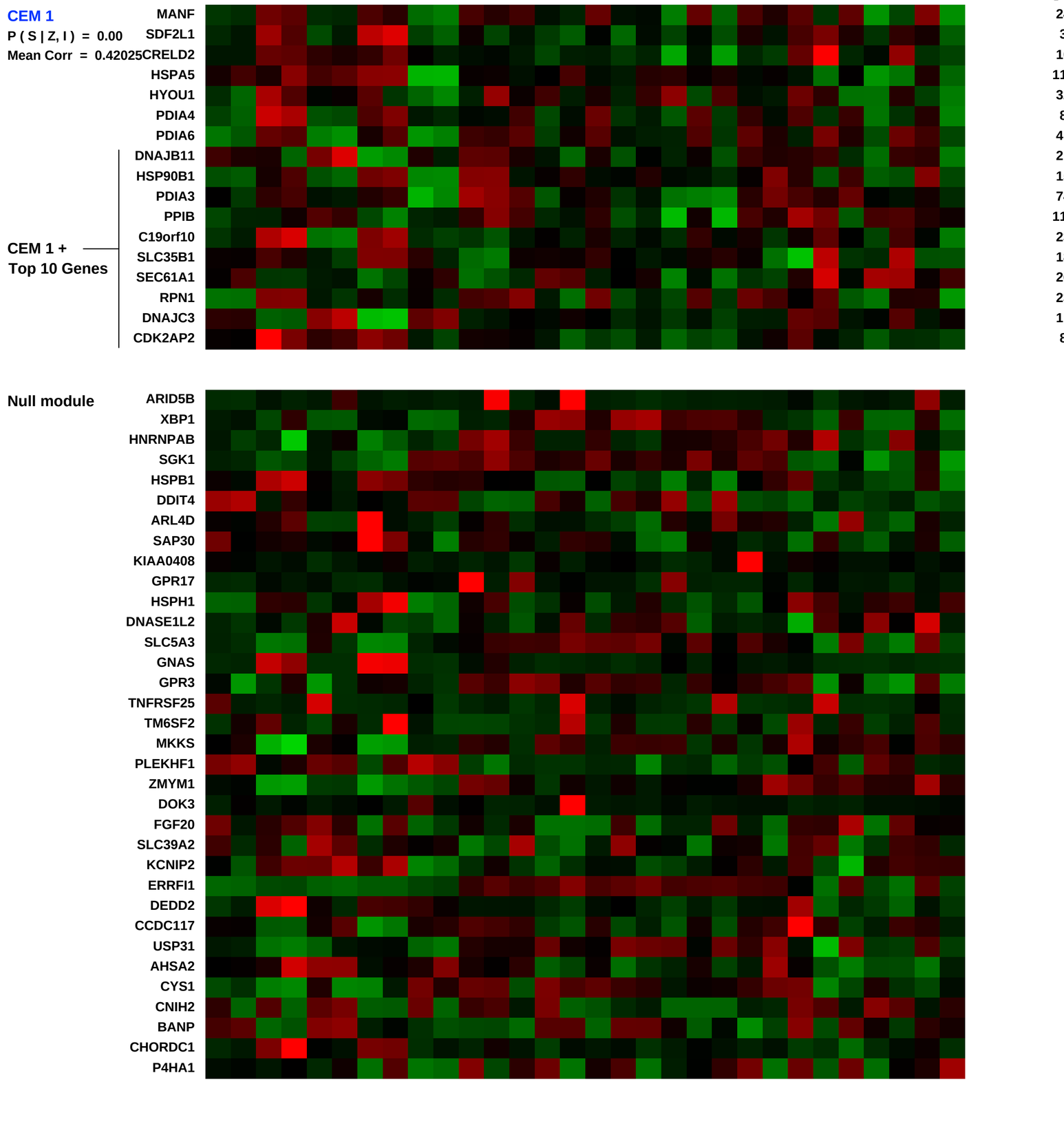

	Pre-normalization Quantiles		
	[min]	[medium]	[max]
MANF	2453.0	3678.4	4881.5
SDF2L1	397.5	567.6	1046.0
CRELD2	1035.3	1595.5	2639.3
HSPA5	11440.8	16496.8	19953.1
HYOU1	3213.8	4215.2	5550.1
PDIA4	838.3	1564.1	2868.8
PDIA6	4183.8	6553.3	7870.2
DNAJB11	2101.9	3018.4	4006.8
HSP90B1	1598.2	2731.3	3903.8
PDIA3	7447.1	9624.7	11454.2
PPIB	11607.3	14896.0	17249.2
C19orf10	2354.0	3238.7	4961.2
SLC35B1	1801.9	2558.2	3226.3
SEC61A1	2629.5	3581.6	5324.6
RPN1	2330.6	3951.8	5310.3
DNAJC3	1111.6	2820.1	4642.9
CDK2AP2	867.0	1078.5	1875.1

GEO Series "GSE15481" Expression Profiles

Num of samples in this series: 15

Scale of expression profile Z-scores

-3.0 -2.0 -1.0 0.0 1.0 2.0 3.0

GEO Link:	http://www.ncbi.nlm.nih.gov/geo/query/acc.cgi?acc=GSE15481
Status:	Public on Dec 14 2009
Title:	Gene expression data from AP-2‚ silenced MCF-7 cells
Organism:	Homo sapiens
Experiment type:	Expression profiling by array
Platform:	GPL570
Pubmed ID:	19798054
Summary & Design:	**Summary:** Overexpression of the AP-2‚ transcription factor in breast tumours has been identified as an independent predictor of poor outcome and failure of hormone therapy, even in ER positive, ErbB2 negative tumours; markers of a more favourable prognosis. To understand further the role of AP-2‚ in breast carcinoma, we have used an RNA interference and gene expression profiling strategy using the MCF-7 cell line as a model for ER positive, ErbB2 negative tumours with AP-2‚ overexpression. Gene expression changes between control and silenced cells implicate AP-2‚ in the control of cell cycle progression and developmental signalling. Keywords: RNA interference **Overall design:** We compared the expression profiles of MCF-7 cells separately transfected with three independent AP-2‚ targeting sequences with those from control cells treated with transfection reagent alone or a non-silencing control siRNA on Affymetrix arrays; each condition was examined in triplicate.

Background corr dist: KL-Divergence = 0.0552, L1-Distance = 0.0304, L2-Distance = 0.0016, Normal std = 0.5364

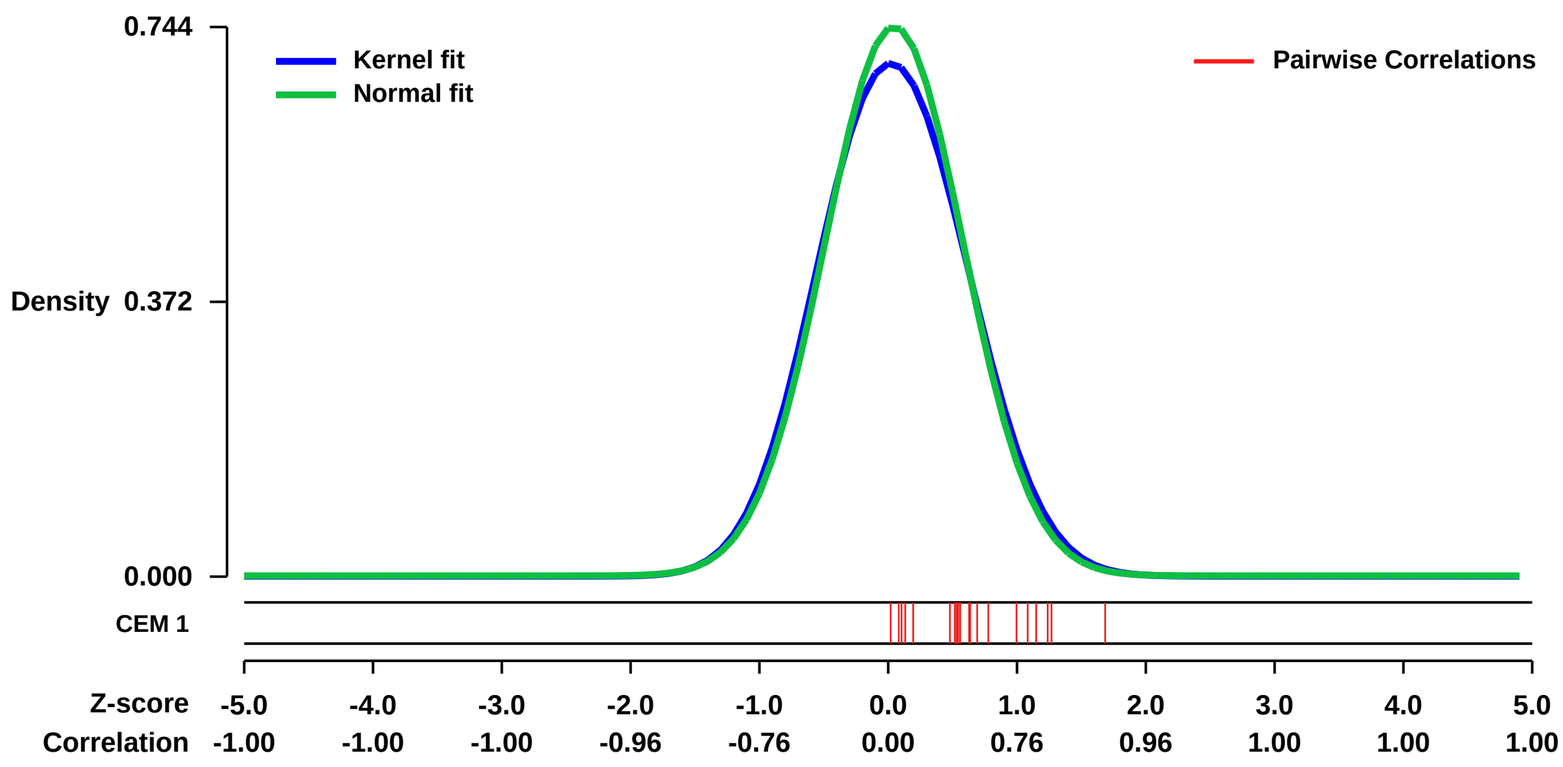

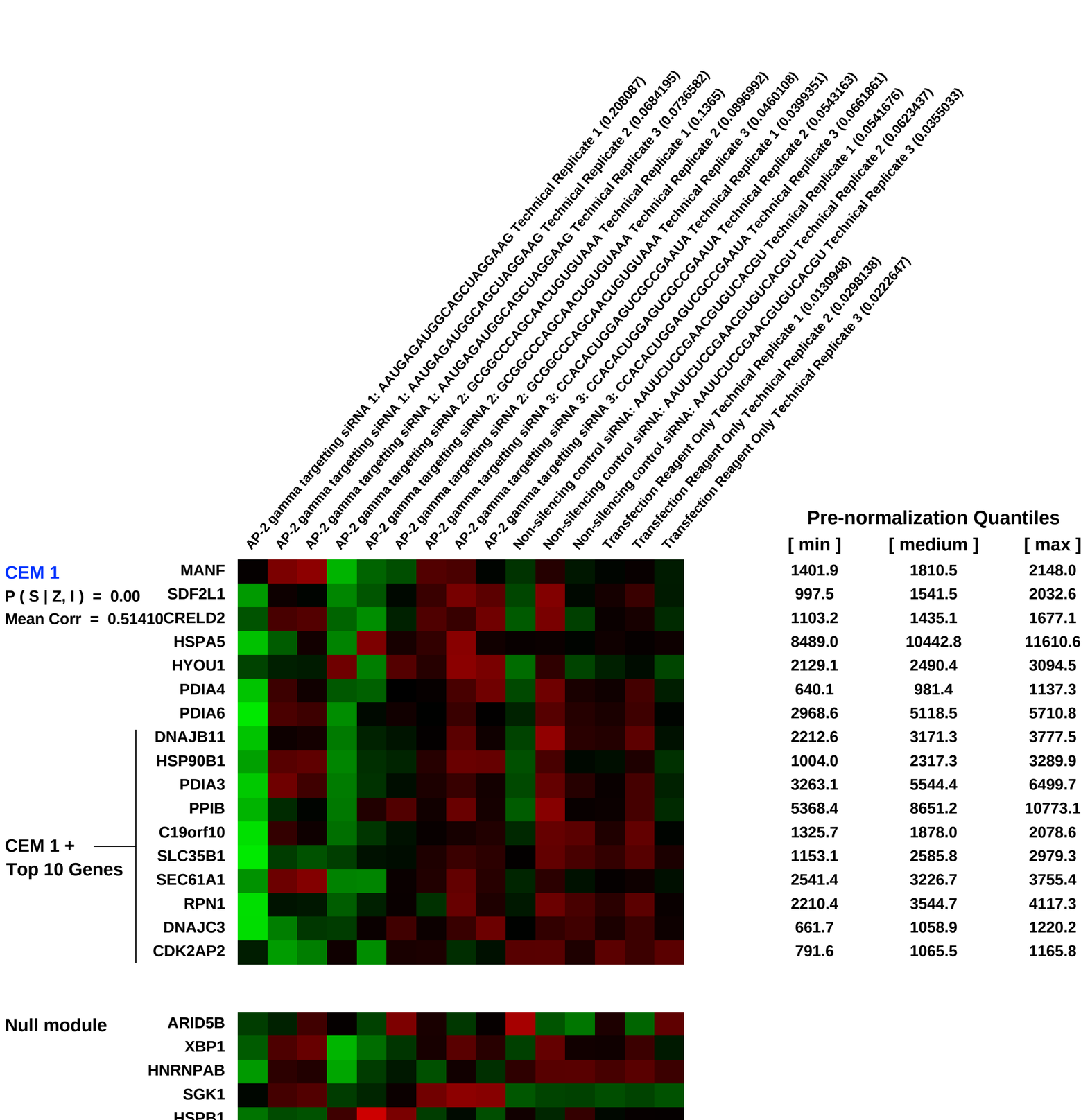

GEO Series "GSE55609" Expression Profiles

Num of samples in this series: 24

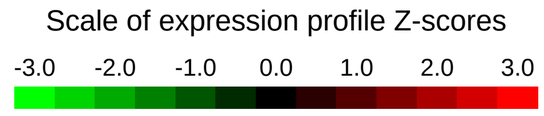

GEO Link:	**http://www.ncbi.nlm.nih.gov/geo/query/acc.cgi?acc=GSE55609**
Status:	**Public on Mar 06 2014**
Title:	**Human meningioma culture**
Organism:	**Homo sapiens**
Experiment type:	**Expression profiling by array**
Platform:	**GPL570**
Pubmed ID:	
Summary & Design:	**Summary:** **Comparison of the gene expression profiles with meningiomas of different grading.** **Overall design:** **24 primary meningioma cultures from surgical specimen were maintained to primary meningioma cultures.**

Background corr dist: **KL-Divergence = 0.3089, L1-Distance = 0.0617, L2-Distance = 0.0104, Normal std = 0.2778**

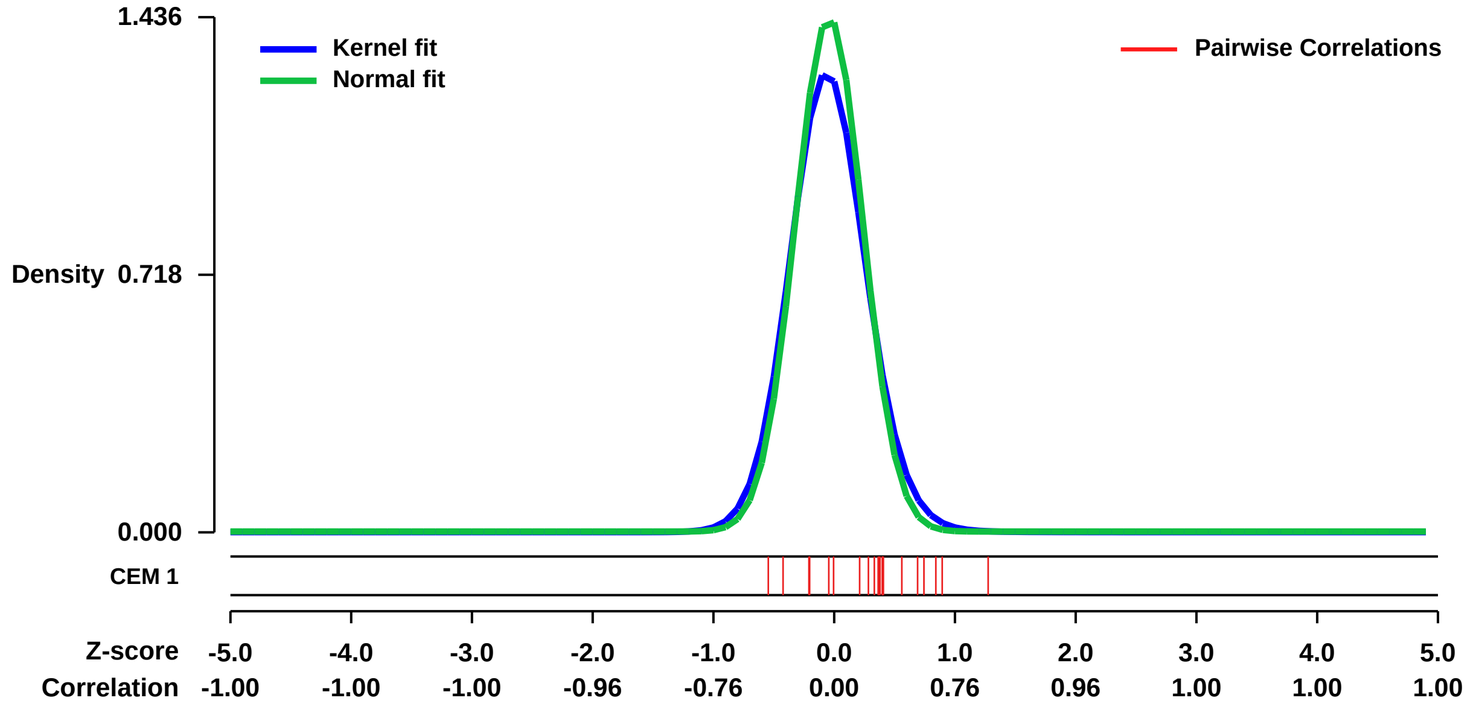

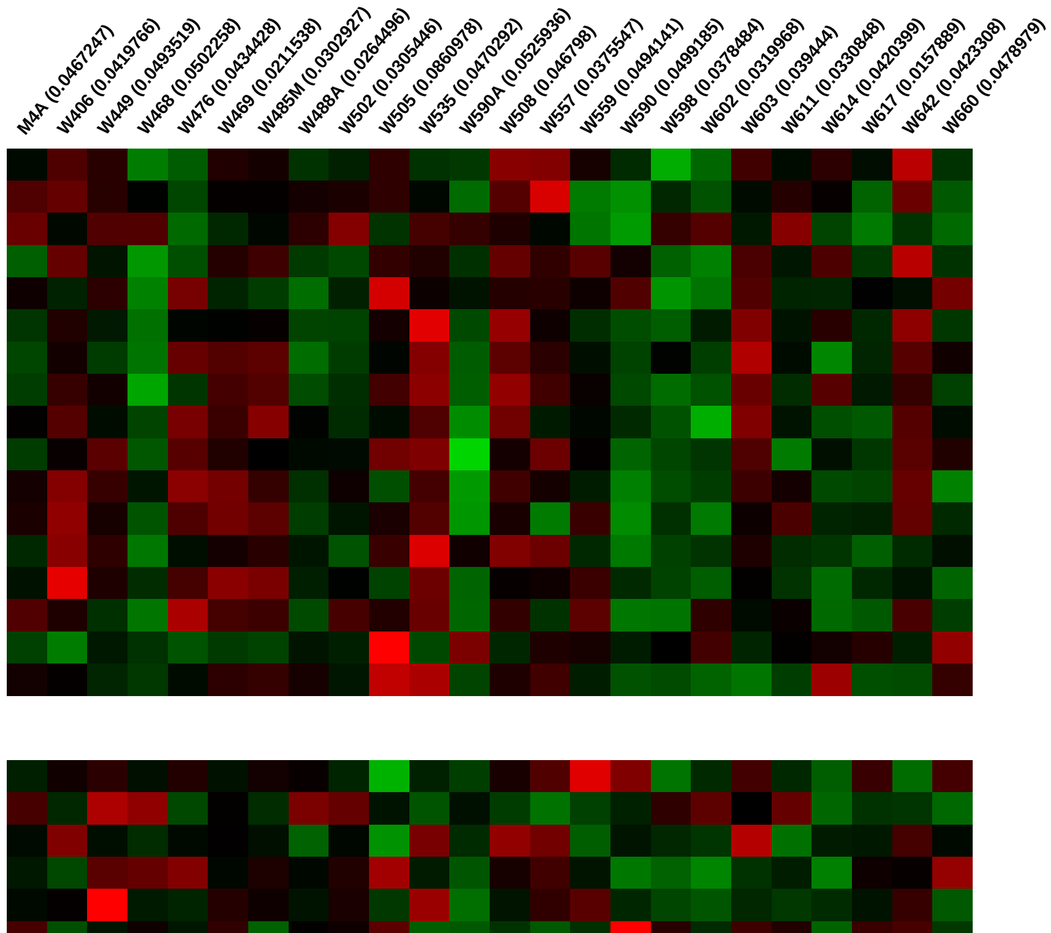

CEM 1
P (S | Z, I) = 0.00
Mean Corr = 0.26924

CEM 1 +
Top 10 Genes

Null module

Pre-normalization Quantiles	[min]	[medium]	[max]
MANF	1375.5	2933.5	4795.1
SDF2L1	258.8	575.6	1025.1
CRELD2	856.0	1659.8	2415.5
HSPA5	8069.2	11599.8	15027.5
HYOU1	3507.5	4263.8	5346.8
PDIA4	662.6	945.1	1685.1
PDIA6	5093.1	6660.9	8858.8
DNAJB11	1816.0	2975.6	3881.2
HSP90B1	1934.6	3332.6	4592.4
PDIA3	6091.1	8655.1	10120.8
PPIB	8523.8	11341.6	13265.6
C19orf10	2544.3	4403.7	5726.1
SLC35B1	1505.0	1928.3	2869.6
SEC61A1	3885.0	4808.8	7332.4
RPN1	3977.4	4853.8	5677.6
DNAJC3	2548.7	3538.3	6423.9
CDK2AP2	549.1	870.0	1491.2

GEO Series "GSE24795" Expression Profiles

Num of samples in this series: 30

Scale of expression profile Z-scores

-3.0 -2.0 -1.0 0.0 1.0 2.0 3.0

GEO Link:	http://www.ncbi.nlm.nih.gov/geo/query/acc.cgi?acc=GSE24795
Status:	Public on Oct 19 2010
Title:	Gene Expression differences between replication error deficient and proficient colorectal cancers: the dominant role of deletions in 3â UTR poly T sequences
Organism:	Homo sapiens
Experiment type:	Expression profiling by array
Platform:	GPL570
Pubmed ID:	21097699
Summary & Design:	**Summary:** 16 replication error proficient (RER-/MSI-) and 14 replication error deficient (RER+/MSI+) colorectal cancer cell lines Replication error deficient (RER+) colorectal cancers are a distinct subset of colorectal cancers, characterised by inactivation of the DNA mismatch repair system. They are typically pseudodiploid, accumulate mutations in repetitive sequences as a result of their mismatch repair deficiency, and have distinct pathologies. Regulatory sequences controlling all aspects of mRNA processing, including especially message stability are found in the 3â UTR sequence of most genes. The relevant sequences are typically A/U rich elements and/or U repeats. Microarray analysis of 14 RER+ (deficient) and 16 RER- (proficient) colorectal cancer (CRC) cell lines confirms a striking difference in expression profiles. Analysis of the incidence of mononucleotide repeat sequences in the 3â UTRs, 5â UTRs and coding sequences of those genes most differentially expressed in RER+ versus â cell lines has shown that much of this differential expression can be explained by the occurrence of a massive enrichment of genes with 3â UTR T repeats longer than 11 base pairs in the most differentially expressed genes. This enrichment was confirmed by analysis of two published consensus sets of RER differentially expressed probe sets for a large number of primary colorectal cancers. Sequence analysis of the 3â UTRs of a selection of the most differentially expressed genes shows that they all contain deletions in these repeats in all RER+ cell lines studied. These data strongly imply that deregulation of mRNA stability through accumulation of mutations in repetitive regulatory 3â UTR sequences underlies the striking difference in expression profiles between RER+ and RER- colorectal cancers. **Overall design:** 16 replication error proficient (RER-/MSI-) and 14 replication error deficient (RER+/MSI+) colorectal cancer cell lines.

Background corr dist: KL-Divergence = 0.2558, L1-Distance = 0.0782, L2-Distance = 0.0179, Normal std = 0.3102

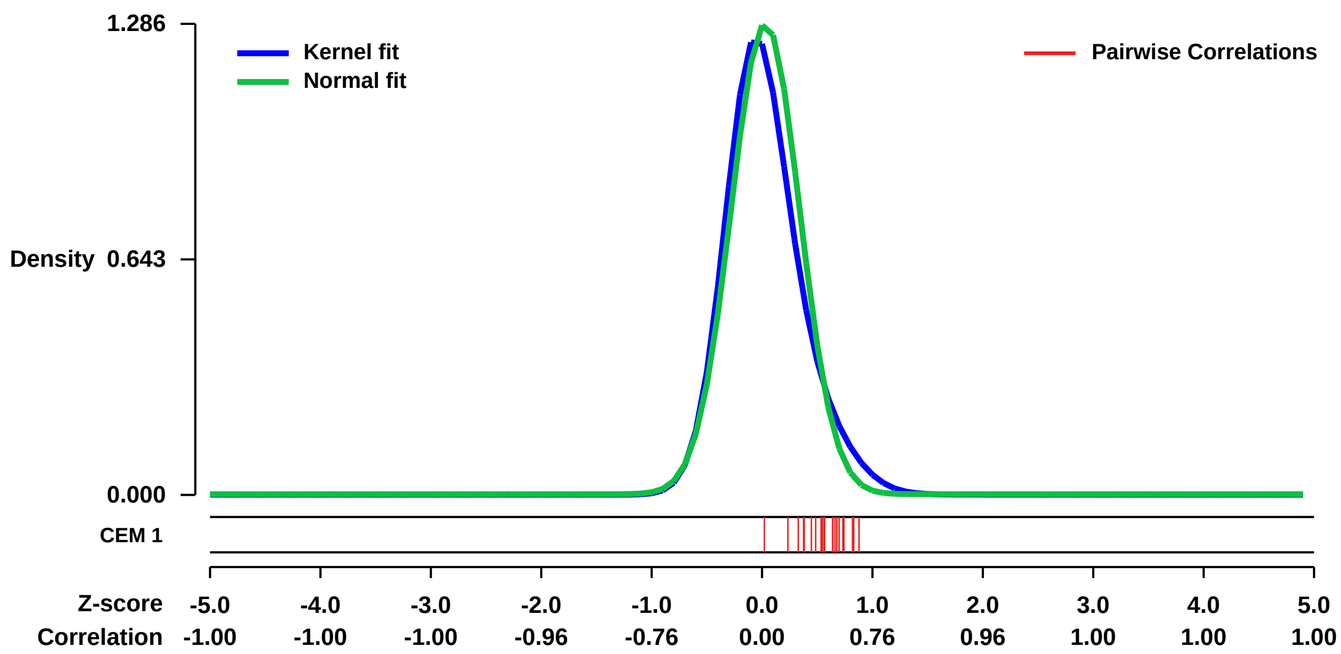

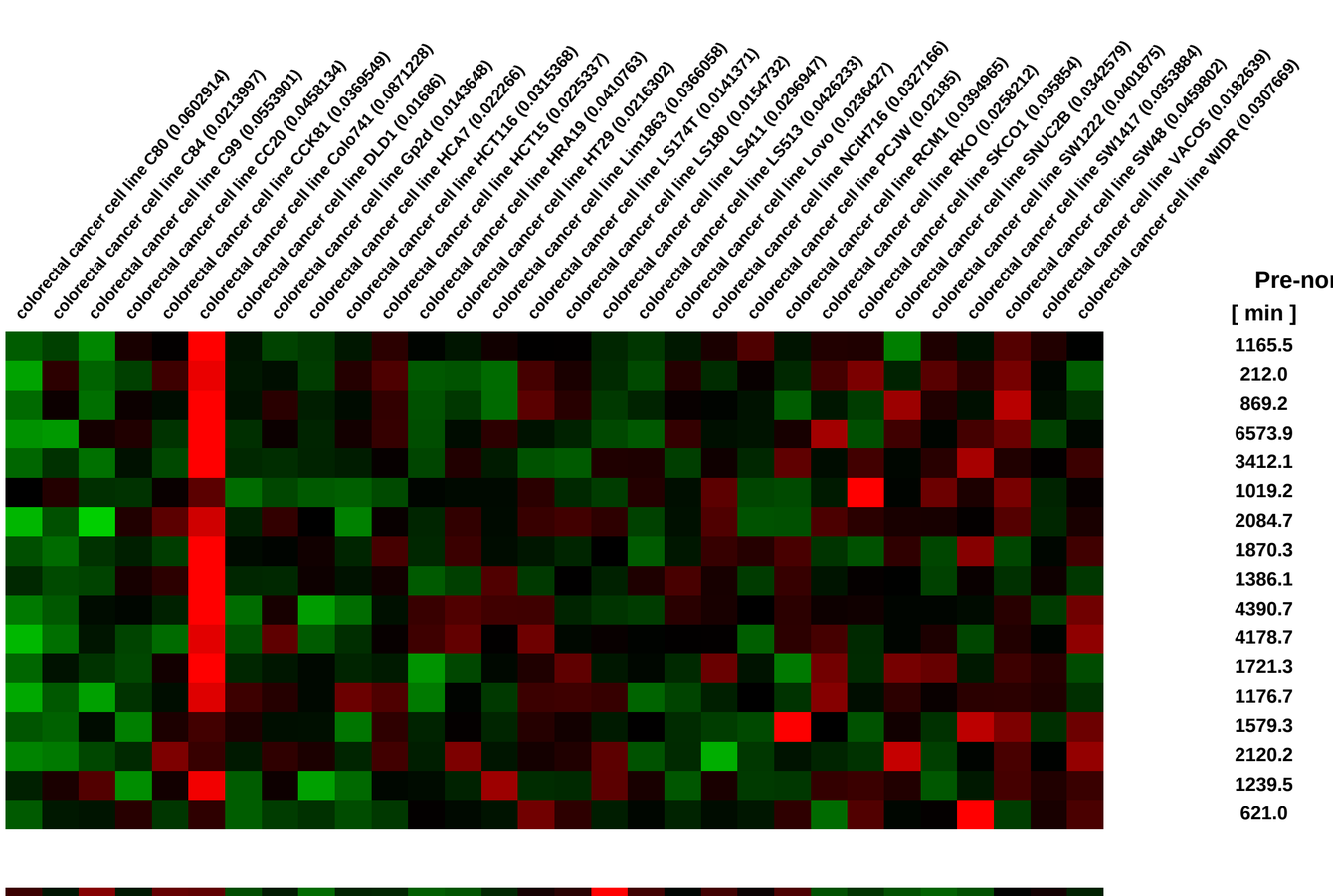

Pre-normalization Quantiles

	[min]	[medium]	[max]
MANF	1165.5	2503.5	6102.7
SDF2L1	212.0	1244.6	2821.9
CRELD2	869.2	2023.6	5283.7
HSPA5	6573.9	11254.0	20085.0
HYOU1	3412.1	6773.9	17596.9
PDIA4	1019.2	1802.6	4370.9
PDIA6	2084.7	7598.0	11991.6
DNAJB11	1870.3	3314.9	8526.5
HSP90B1	1386.1	2253.9	5987.1
PDIA3	4390.7	8717.5	17451.1
PPIB	4178.7	9840.0	16641.9
C19orf10	1721.3	2629.4	4651.0
SLC35B1	1176.7	3316.7	6138.8
SEC61A1	1579.3	2355.4	4132.4
RPN1	2120.2	3421.4	5226.8
DNAJC3	1239.5	3042.1	5430.4
CDK2AP2	621.0	1230.9	3554.8

GEO Series "GSE23882" Expression Profiles

Num of samples in this series: 9

Scale of expression profile Z-scores

-3.0 -2.0 -1.0 0.0 1.0 2.0 3.0

GEO Link:	http://www.ncbi.nlm.nih.gov/geo/query/acc.cgi?acc=GSE23882
Status:	Public on Aug 15 2011
Title:	Microarray analysis of gene expression profile in HCT116 colon cancer cells expressed the isoform A or isoform B of the Tazarotene-induced gene 1.
Organism:	Homo sapiens
Experiment type:	Expression profiling by array
Platform:	GPL570
Pubmed ID:	21575264
Summary & Design:	**Summary:** Tazarotene-induced gene 1 (TIG1), also named as retinoic acid receptor responder 1 (RARRES1), is a retinoid inducible type II tumor suppressor gene; the TIG1B isoform inhibits growth and invasion of cancer cells. Expression of TIG1B is frequently downregulated in various cancer tissues; however, the expression and activities of the TIG1A isoform has yet to be analyzed. This study investigated the effects of TIG1A and TIG1B isoforms on gene expression profiles of colon cancer cells. TIG1A, TIG1B and control stable clones derived from HCT116 colon cells were established using the GeneSwitch system. TIG1 isoform expression was induced upon 5 micro Molar of mifepristone (MFP) treatment for 24 hr. Biological triplicate samples were prepared and gene expression profiles were determined by microarray using human genome HGU133 plus 2 array (Affymatrix). Upon induction of TIG1A and TIG1B expression for 24 hr, a total of 129 and 55 genes were significantly altered, respectively. Of the genes analyzed, 23 and 6 genes were up- and downregulated, respectively in both TIG1A and TIG1B expressing cells. **Overall design:** TIG1A, TIG1B and control stable clones derived from HCT116 colon cells were established using the GeneSwitch system. Inducible stable clones were plated in 15-cm dishes overnight in maintaining medium free of hygromycin and zeocin. Cells were refreshed with medium containing 5 micro molar of mifepristone and then incubated overnight. Cells were washed with ice-cold PBS and then harvested. Total RNA was prepared. Biological triplicate samples were prepared for control, TIGA and TIG1B stable cells. Samples of cRNA were prepared, labeled with biotin, and then hybridized to Human Genome U133 Plus 2.0 Array.

Background corr dist: KL-Divergence = 0.0899, L1-Distance = 0.0244, L2-Distance = 0.0010, Normal std = 0.4566

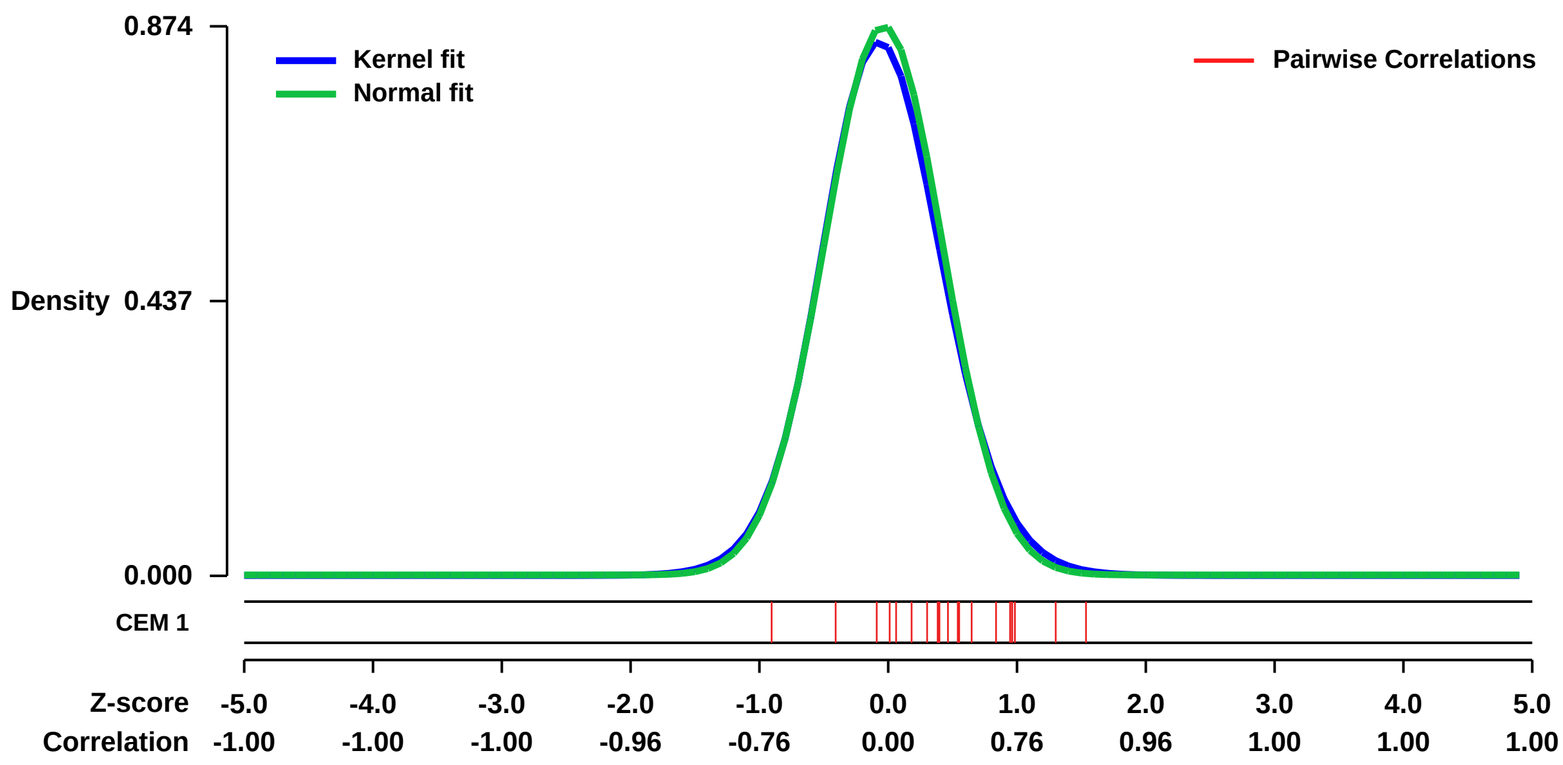

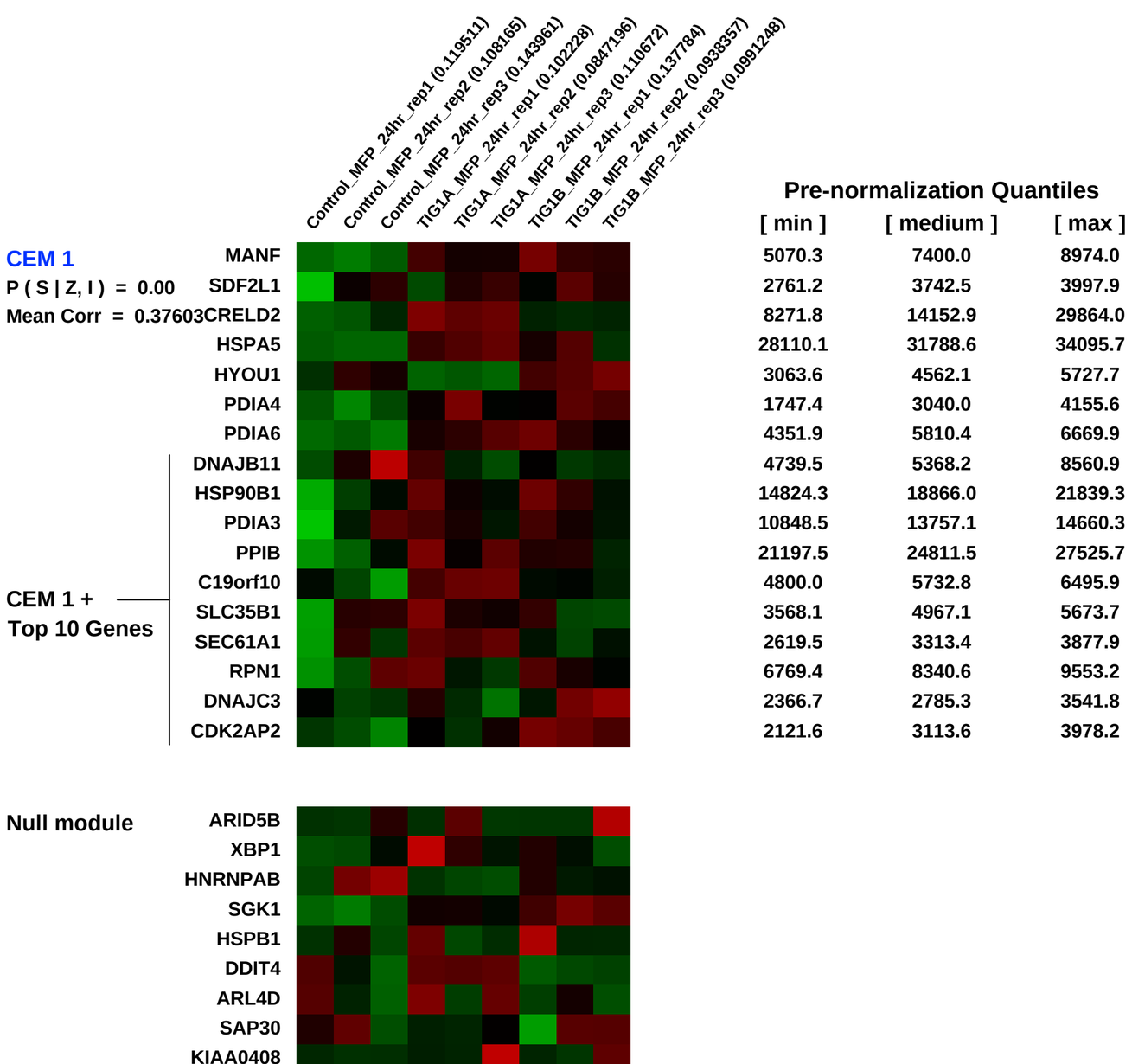

Pre-normalization Quantiles

	[min]	[medium]	[max]
MANF	5070.3	7400.0	8974.0
SDF2L1	2761.2	3742.5	3997.9
CRELD2	8271.8	14152.9	29864.0
HSPA5	28110.1	31788.6	34095.7
HYOU1	3063.6	4562.1	5727.7
PDIA4	1747.4	3040.0	4155.6
PDIA6	4351.9	5810.4	6669.9
DNAJB11	4739.5	5368.2	8560.9
HSP90B1	14824.3	18866.0	21839.3
PDIA3	10848.5	13757.1	14660.3
PPIB	21197.5	24811.5	27525.7
C19orf10	4800.0	5732.8	6495.9
SLC35B1	3568.1	4967.1	5673.7
SEC61A1	2619.5	3313.4	3877.9
RPN1	6769.4	8340.6	9553.2
DNAJC3	2366.7	2785.3	3541.8
CDK2AP2	2121.6	3113.6	3978.2

GEO Series "GSE10580" Expression Profiles

Num of samples in this series: 12

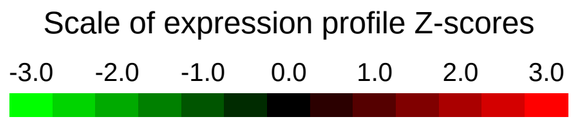

GEO Link:	http://www.ncbi.nlm.nih.gov/geo/query/acc.cgi?acc=GSE10580
Status:	Public on Jan 26 2009
Title:	Genes regulated by PRDM5 in U2OS cells.
Organism:	Homo sapiens
Experiment type:	Expression profiling by array
Platform:	GPL570
Pubmed ID:	19169355
Summary & Design:	**Summary:** PRDM5 is a recently identified member of the PRDM family of proteins, which functions as a transcriptional repressor by recruiting histone methyltransferase G9A to DNA, and behaves as a putative tumor suppressor in different types of cancer. We investigated PRDM5 function by identifying its target genes in U2OS cells at different time points after expression of PRDM5 protein. Keywords: Transcriptional regulation, time course **Overall design:** We analyzed gene expression profiles of a U2OS cell line conditionally expressing HA-tagged PRDM5 (U2OS-PRDM5), where PRDM5 is under the transcriptional control of a doxycycline-inducible promoter. Expression of PRDM5 protein is detectable after 8 hours of induction with 2ug/ml doxycycline, and increases steadily up to 48 hours, after which cells begin to undergo apoptosis. U2OS cells containing the empty cloning vector (U2OS-pSG213) were used as controls for each condition.

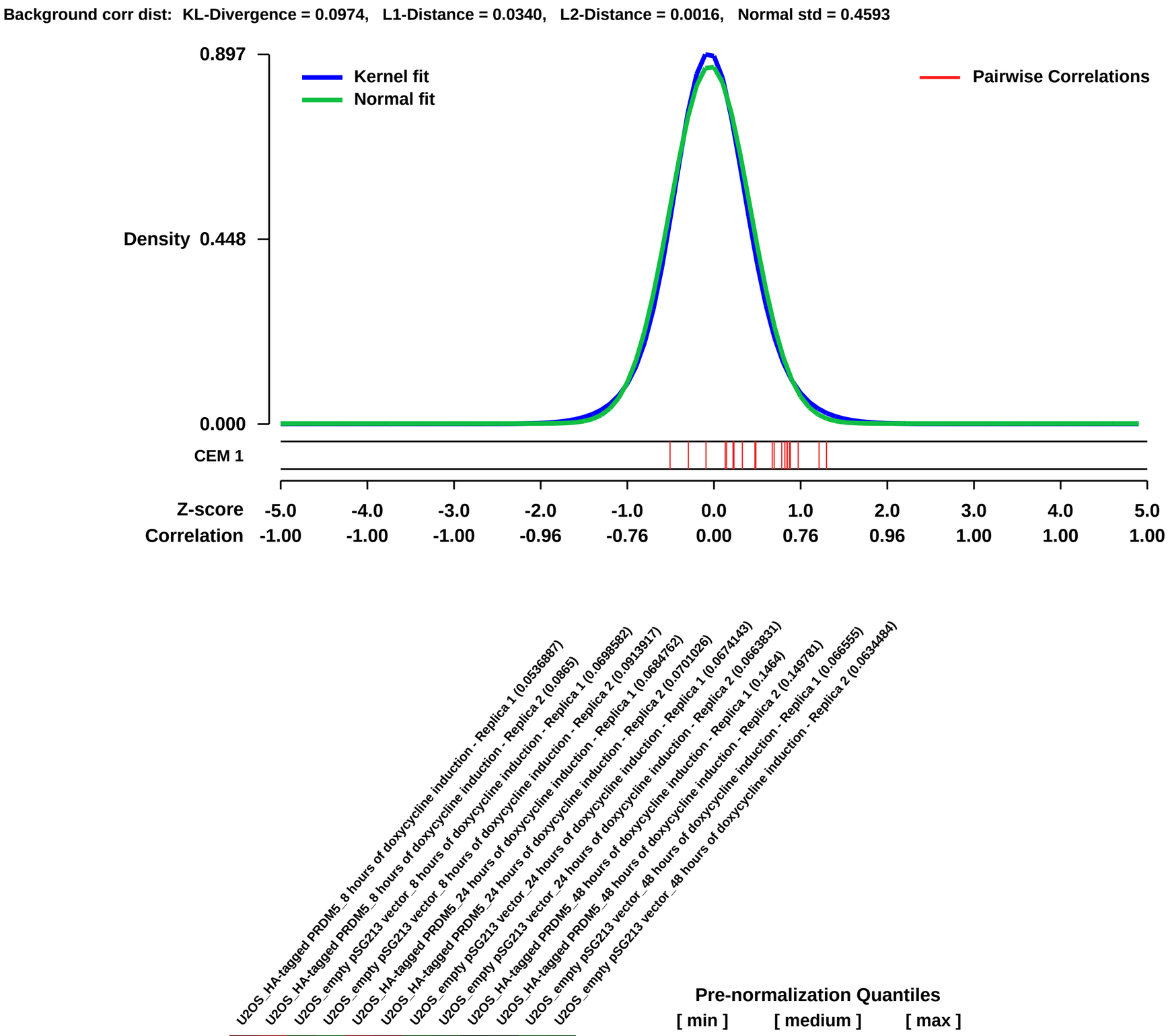

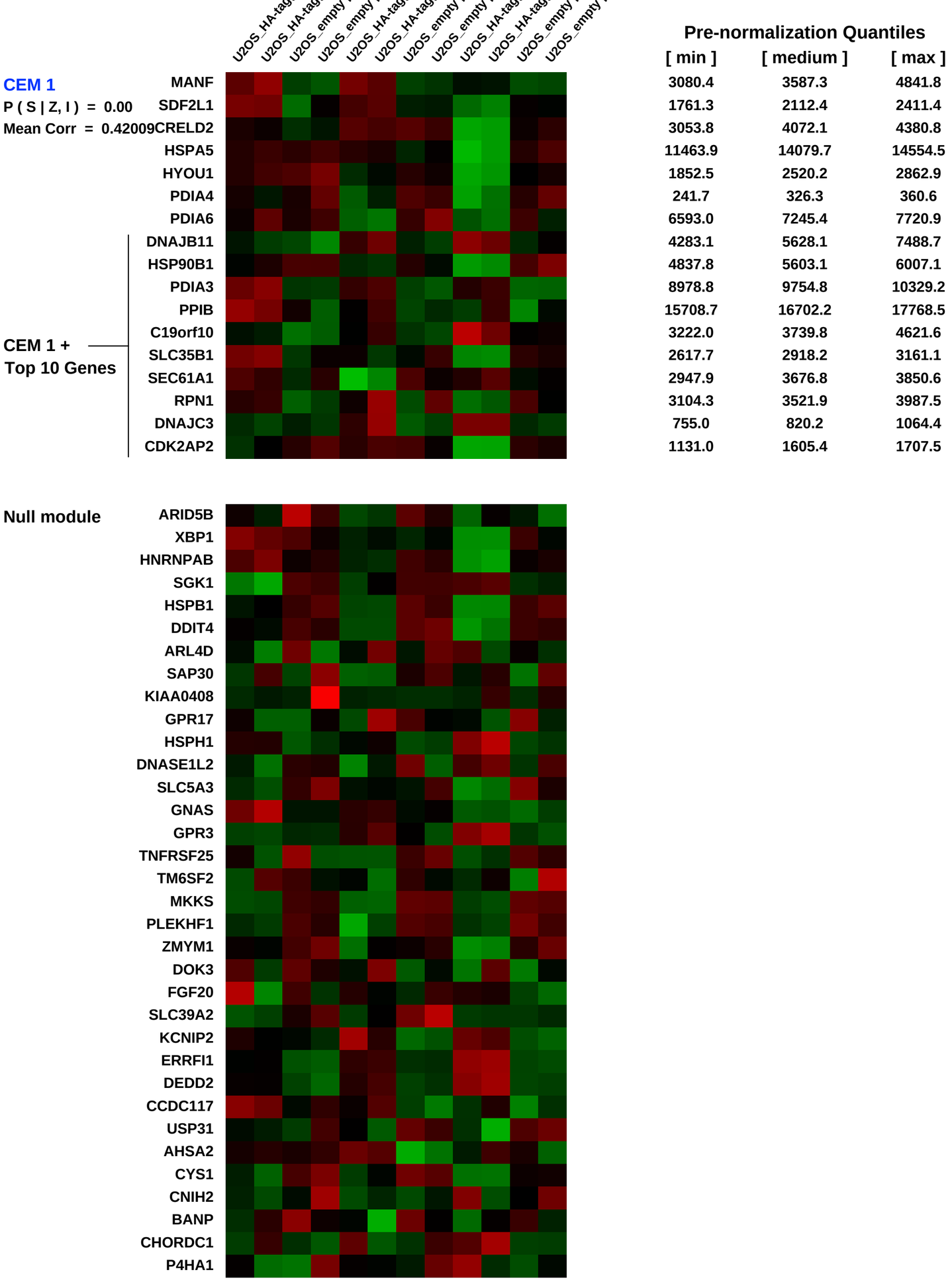

GEO Series "GSE39134" Expression Profiles

Num of samples in this series: 29

Scale of expression profile Z-scores

-3.0 -2.0 -1.0 0.0 1.0 2.0 3.0

GEO Link:	http://www.ncbi.nlm.nih.gov/geo/query/acc.cgi?acc=GSE39134
Status:	Public on Aug 31 2012
Title:	Gene expression profiling of microdissected HRS cells is correlated with primary treatment outcome
Organism:	Homo sapiens
Experiment type:	Expression profiling by array
Platform:	GPL570
Pubmed ID:	22955918
Summary & Design:	**Summary:** Hodgkin lymphoma is derived from germinal center / post-germinal center B cells. **Overall design:** Gene expression profilies of micodissected Hodkin Reed Sternberg cells (n=29) were dichotomized into primary treatment failure (n=14) and primary treatment succeses (n=15). Treament failure was defined as refractory disease or progression at any time after ABVD chemotherapy.

Background corr dist: KL-Divergence = 0.2035, L1-Distance = 0.0824, L2-Distance = 0.0196, Normal std = 0.3378

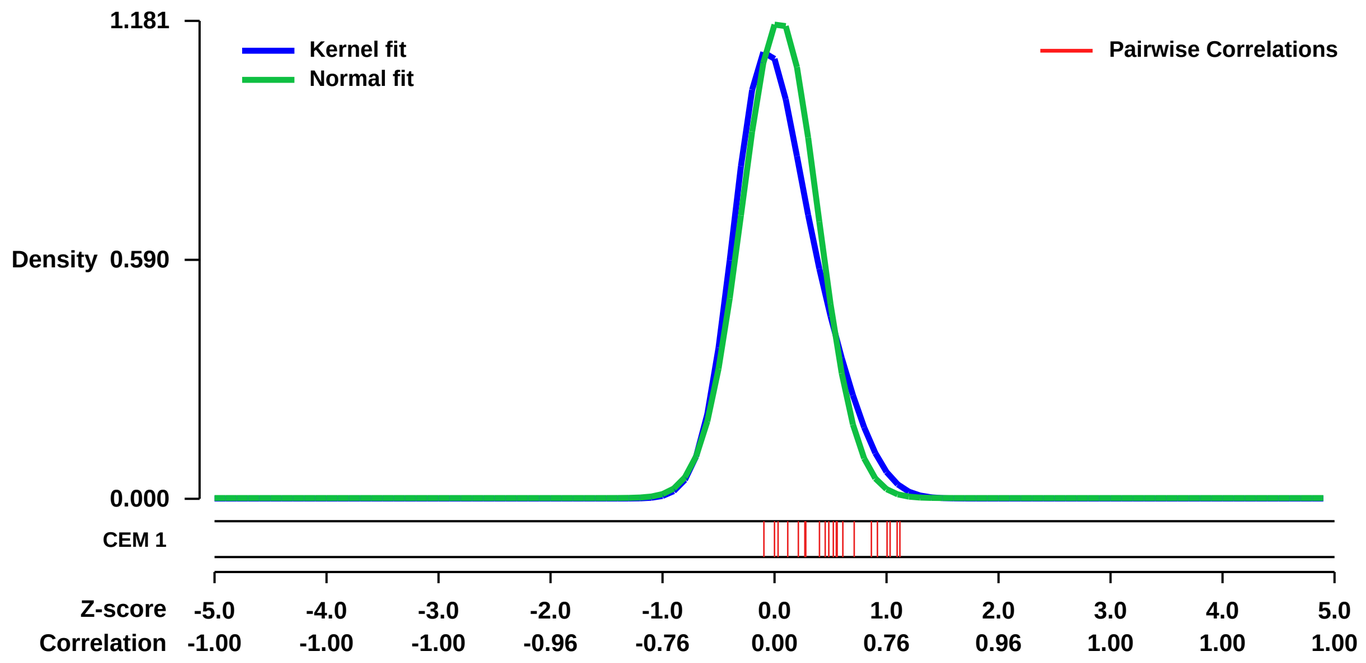

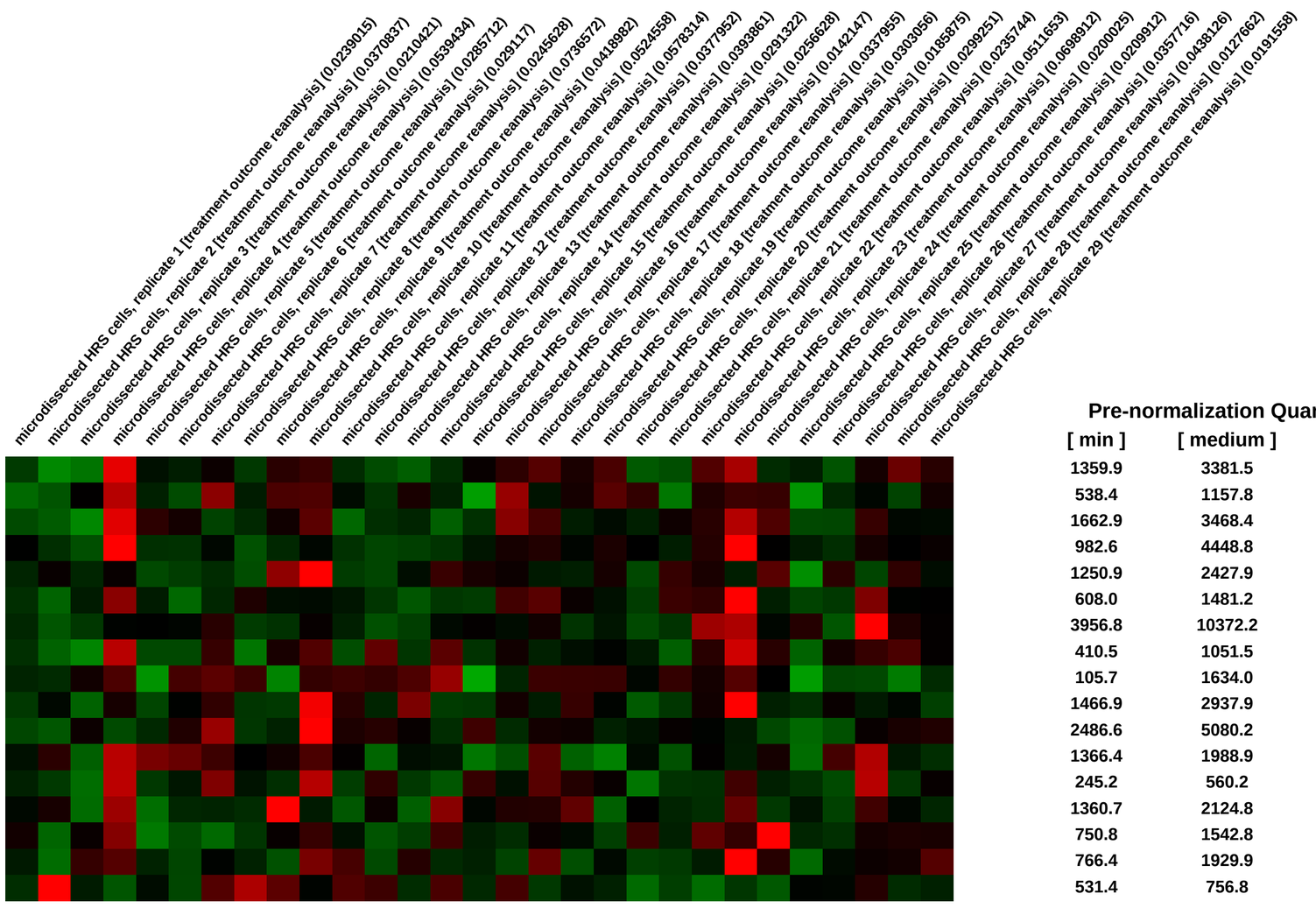

Pre-normalization Quantiles

	[min]	[medium]	[max]
MANF	1359.9	3381.5	7503.6
SDF2L1	538.4	1157.8	1928.0
CRELD2	1662.9	3468.4	6908.2
HSPA5	982.6	4448.8	18042.6
HYOU1	1250.9	2427.9	5459.0
PDIA4	608.0	1481.2	4907.3
PDIA6	3956.8	10372.2	37220.8
DNAJB11	410.5	1051.5	2087.7
HSP90B1	105.7	1634.0	2698.0
PDIA3	1466.9	2937.9	8761.8
PPIB	2486.6	5080.2	14036.3
C19orf10	1366.4	1988.9	3011.0
SLC35B1	245.2	560.2	1360.0
SEC61A1	1360.7	2124.8	4412.6
RPN1	750.8	1542.8	3794.4
DNAJC3	766.4	1929.9	6475.0
CDK2AP2	531.4	756.8	1584.0

GEO Series "GSE32169" Expression Profiles

Num of samples in this series: 12

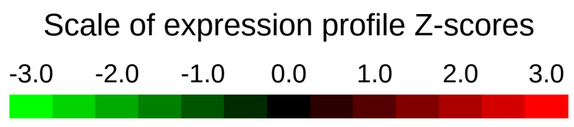

GEO Link:	**http://www.ncbi.nlm.nih.gov/geo/query/acc.cgi?acc=GSE32169**
Status:	**Public on Jun 30 2012**
Title:	**Gene expression profile of phagocyticially challenged human trabecular meshwork cells under physiolgical and oxidative stress conditions**
Organism:	**Homo sapiens**
Experiment type:	**Expression profiling by array**
Platform:	**GPL570**
Pubmed ID:	
Summary & Design:	**Summary:** **In theses experimetns we have analized the differential gene expression profile in human trabecular meshwork cells phagocytically challenged to E. coli and pigment under physiological and oxidative stress conditions using affymetrix microarrays** **Overall design:** **HTM cells grown for two weeks either at 5% oxygen concentration or 40% oxygen concentration were phagocytically challenged to either E.coli or pigment. Changes in gene profile were analyzed at day 2.**

Background corr dist: **KL-Divergence = 0.1455, L1-Distance = 0.0292, L2-Distance = 0.0015, Normal std = 0.3800**

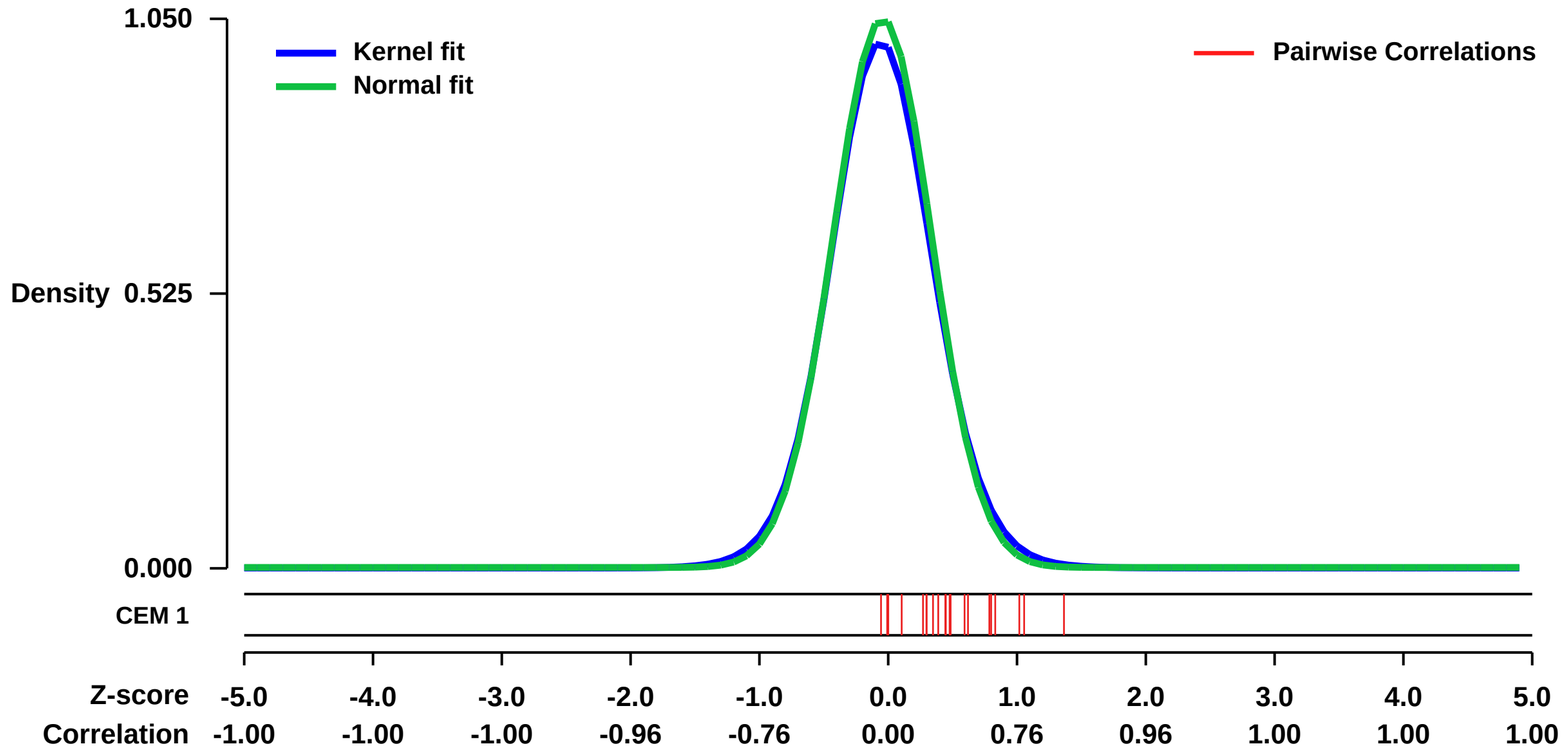

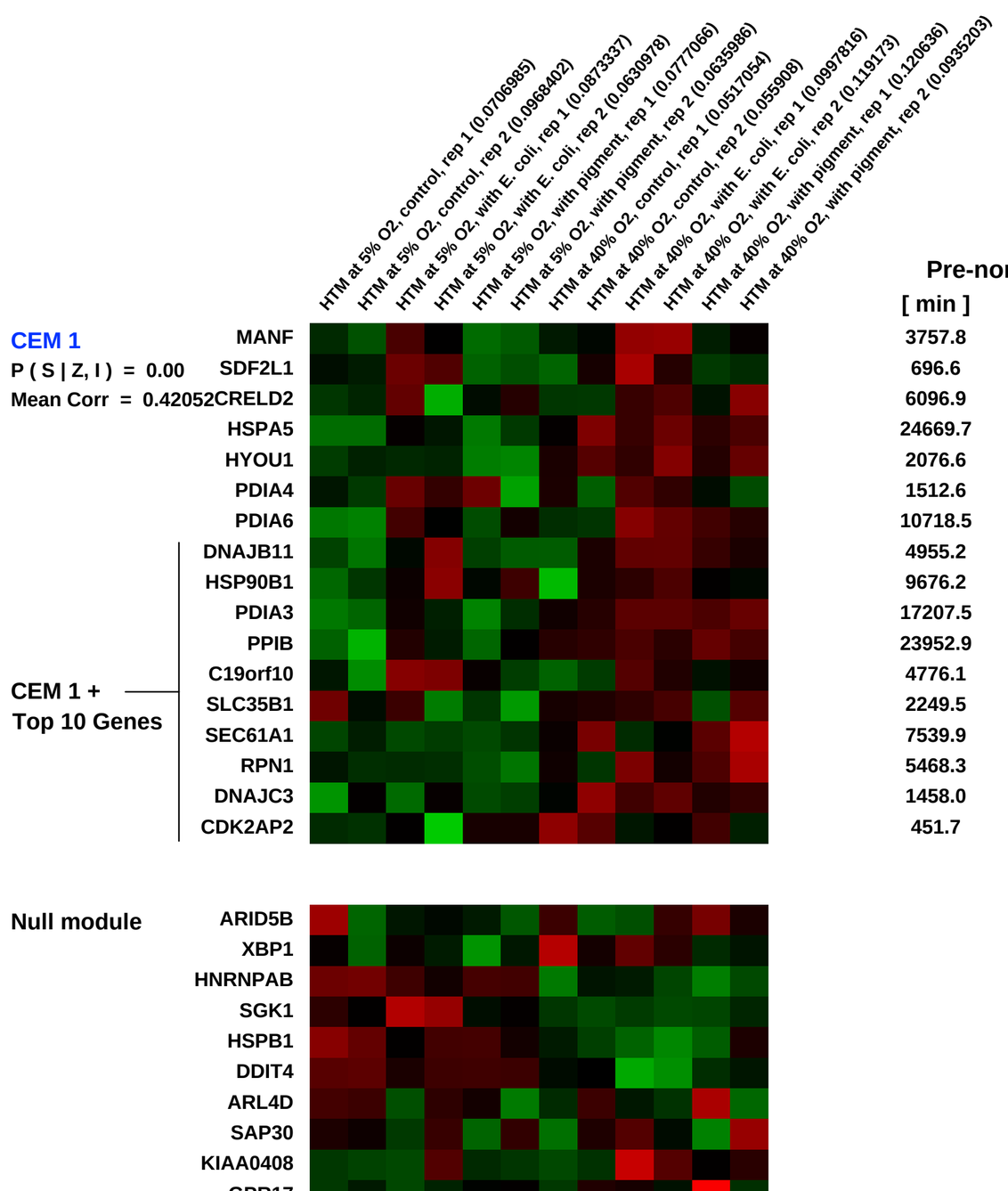

GEO Series "GSE38749" Expression Profiles

Num of samples in this series: 15

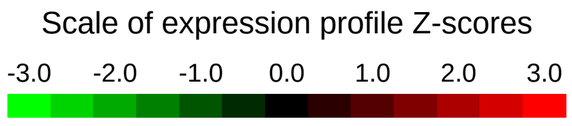

GEO Link:	http://www.ncbi.nlm.nih.gov/geo/query/acc.cgi?acc=GSE38749
Status:	Public on Sep 01 2012
Title:	Expression data of Human Gastric Adenocarcinoma
Organism:	Homo sapiens
Experiment type:	Expression profiling by array
Platform:	GPL570
Pubmed ID:	
Summary & Design:	**Summary:** Anatomical staging is a critical, although imperfect, instrument to assess gastric cancer prognosis and define indication for surgery and adjuvant therapy. Despite recent advances, treatment results, as a whole, remain less than satisfactory. Thus, biomarkers are sorely needed to improve risk categorization and define new molecular targets for therapy. We used microarrays to identify genes differentially expressed according to prognosis of the patients. **Overall design:** A cohort of 15 patients was prospectively identified with a histological diagnosis of gastric adenocarcinoma, submitted to surgery with curative intent. Two prognostic patient groups were defined, according to overall survival (short x long), with a 24 month cut-off. These groups were matched by known prognostic factors: TNM staging, histological subtype (intestinal/diffuse) and gender.

Background corr dist: KL-Divergence = 0.1669, L1-Distance = 0.0470, L2-Distance = 0.0052, Normal std = 0.3587

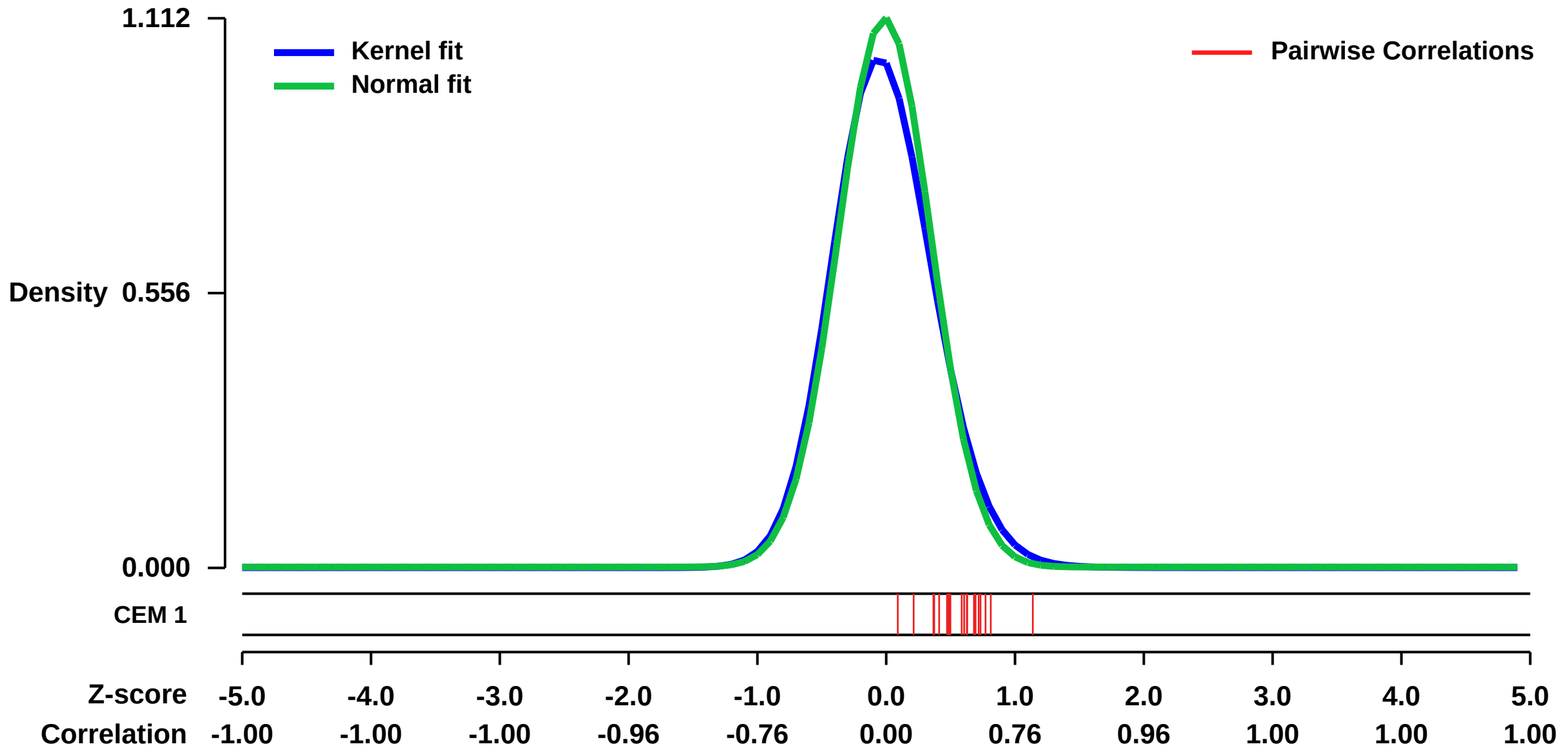

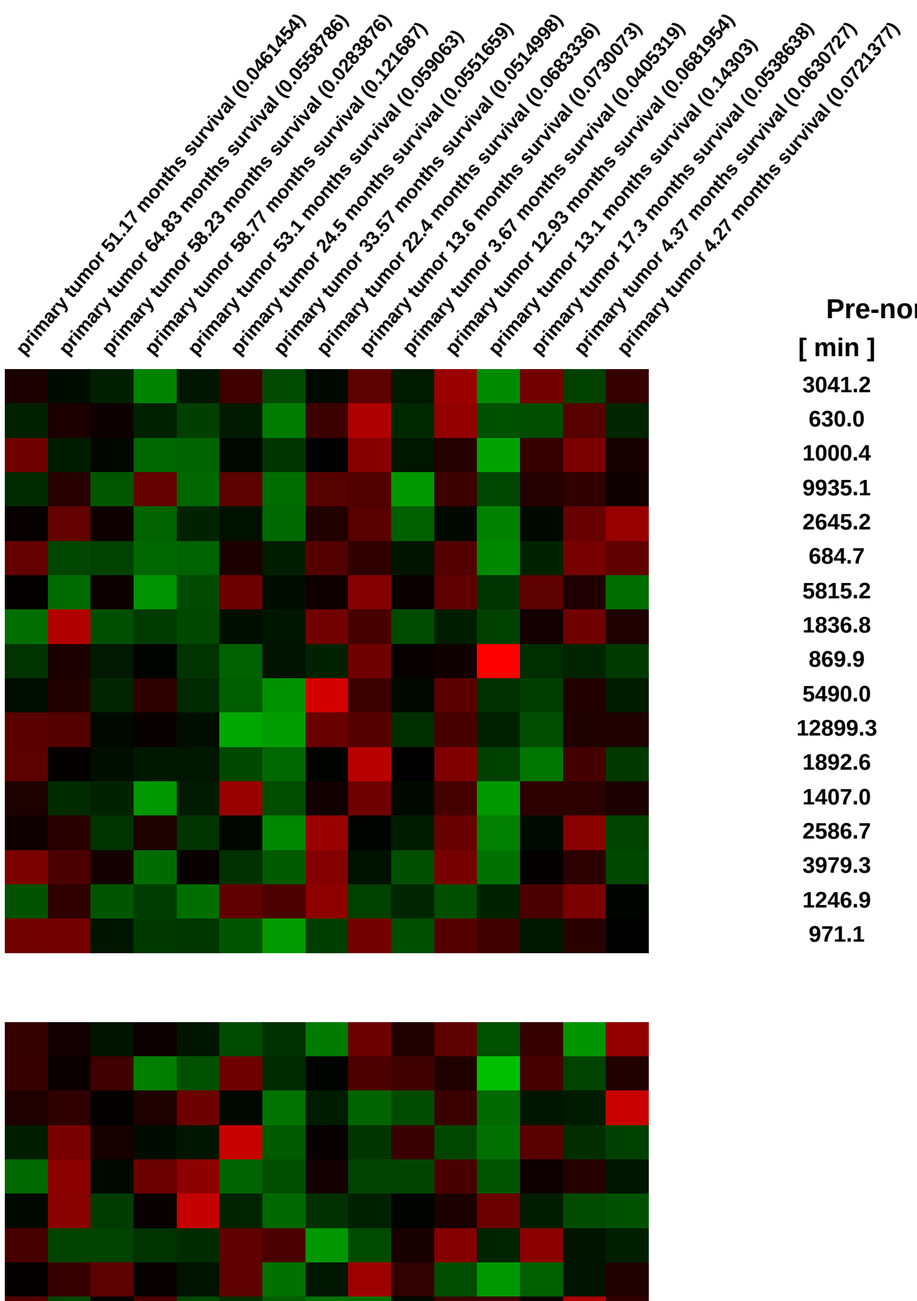

GEO Series "GSE15960" Expression Profiles

Num of samples in this series: 18

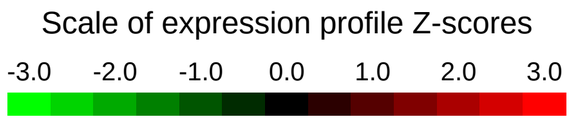

GEO Link:	http://www.ncbi.nlm.nih.gov/geo/query/acc.cgi?acc=GSE15960
Status:	Public on Mar 03 2010
Title:	Expression data from human colonic epithelial cells normal (N), adenoma (AD) or colorectal cancer (CRC) tissues
Organism:	Homo sapiens
Experiment type:	Expression profiling by array
Platform:	GPL570
Pubmed ID:	20087348
Summary & Design:	**Summary:** The whole-genome oligonucleotide microarray analysis of laser microdissected human colonic epithelial cells can contribute to determination of disease-specific expression alterations in colonic epithelial cells and to localize the origin the expression changes measured in whole biopsy samples. **Keywords: whole genomic expression** **Overall design:** Total RNA was extracted from laser microdissected human colon epithelial cells and hybridized on Affymetrix HGU133 Plus 2.0 microarrays

Background corr dist: KL-Divergence = 0.1729, L1-Distance = 0.0558, L2-Distance = 0.0077, Normal std = 0.3564

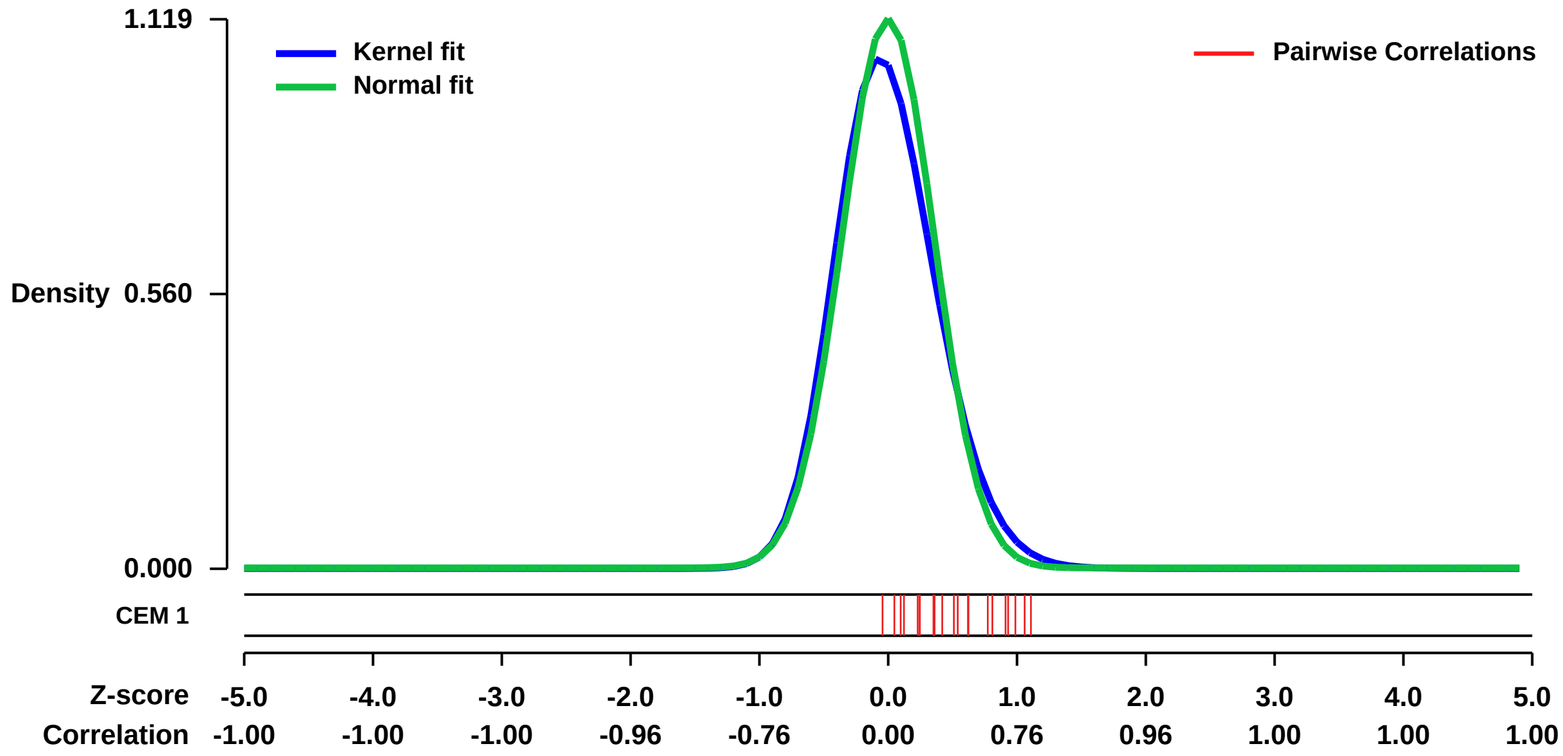

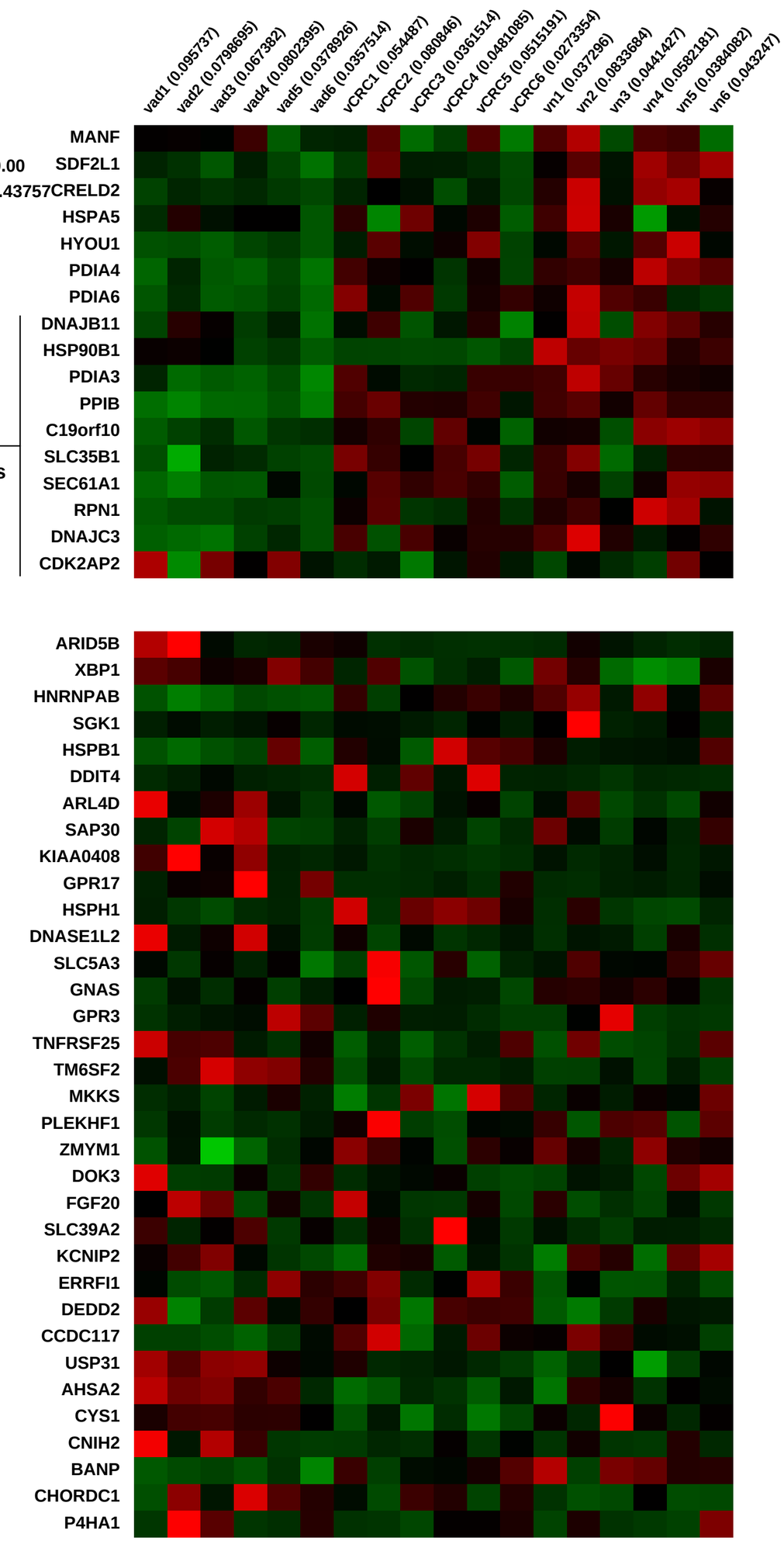

Pre-normalization Quantiles		
[min]	[medium]	[max]
2056.2	4023.3	6804.7
29.5	611.6	1908.8
1134.2	3273.9	12624.3
5464.2	12155.5	20889.0
555.4	1568.9	4278.5
813.3	3551.9	7238.1
12163.7	19419.5	35258.0
1315.4	3060.6	5576.9
1343.9	2959.3	6415.2
4347.0	15763.2	28778.8
3565.0	16764.6	22308.1
1873.1	2775.4	4327.6
59.5	1411.8	2455.0
888.8	2624.8	4227.8
1229.8	3037.8	8857.7
2664.2	5406.4	10086.1
155.4	347.6	658.2

GEO Series "GSE30336" Expression Profiles

Num of samples in this series: 6

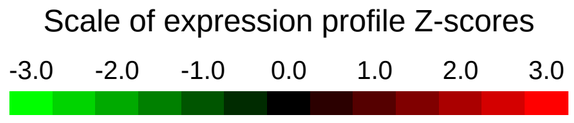

GEO Link:	http://www.ncbi.nlm.nih.gov/geo/query/acc.cgi?acc=GSE30336
Status:	Public on Feb 16 2012
Title:	Expression analysis of 52 glioma clinical samples (36 CIMP+ and 16 CIMP-) and 6 cell line samples
Organism:	Homo sapiens
Experiment type:	Expression profiling by array
Platform:	GPL570
Pubmed ID:	22343889
Summary & Design:	**Summary:** Glioma CIMP (G-CIMP) is a powerful determinant of tumor pathogenicity but the molecular cause of G-CIMP is a fundamental question that is unresolved. Here, we show that mutation of a single gene, isocitrate dehydrogenase 1 (IDH1), directly causes the G-CIMP in gliomas by remodeling the methylome. **Overall design:** In this study 52 glioma clinic samples (36 CIMP+ and 16 CIMP-) were analyzed. Parental IDH1 wild-type and IDH1 mutant cells were passaged 40 and passage 40 were cell line was sent for expression array.

Background corr dist: KL-Divergence = 0.0304, L1-Distance = 0.0224, L2-Distance = 0.0005, Normal std = 0.6749

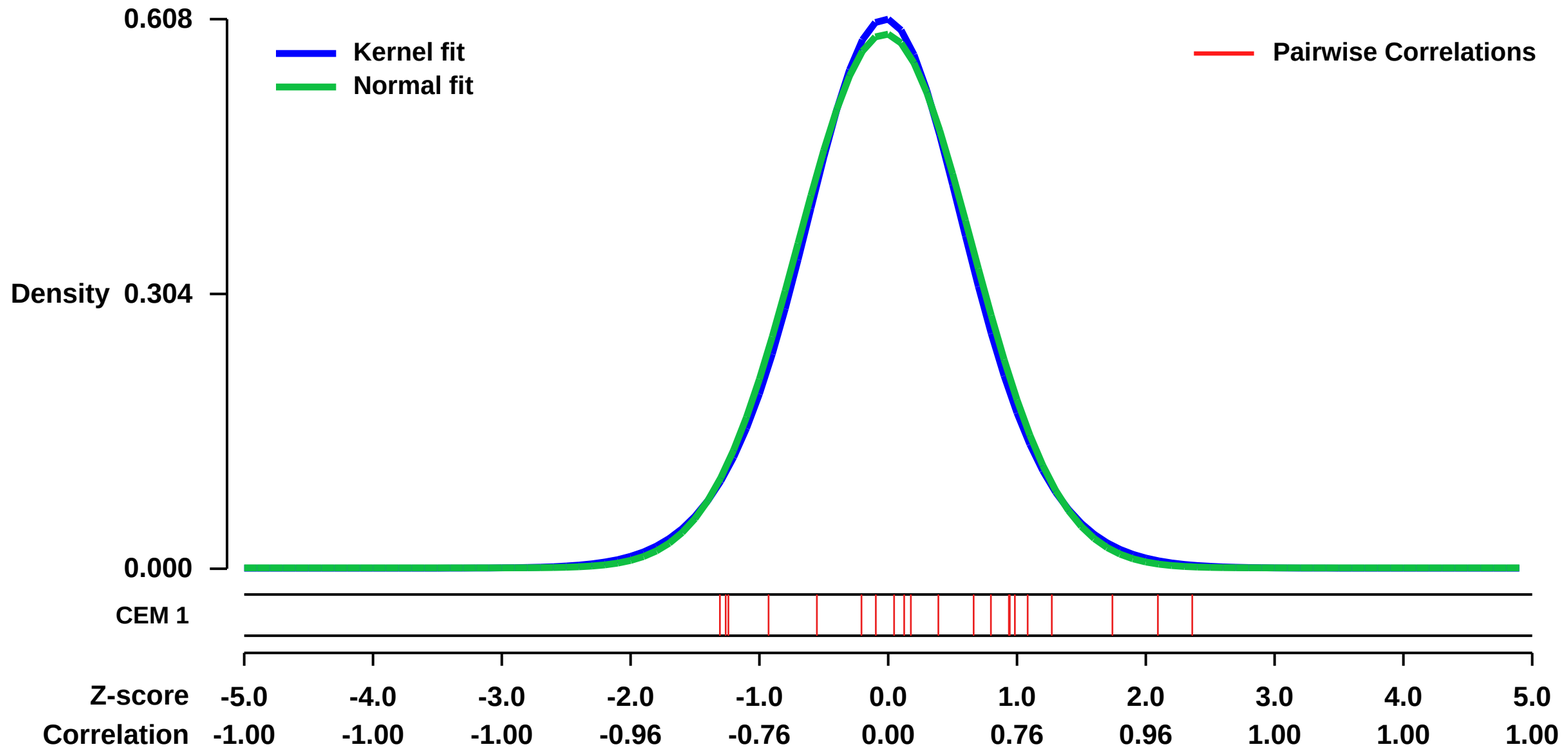

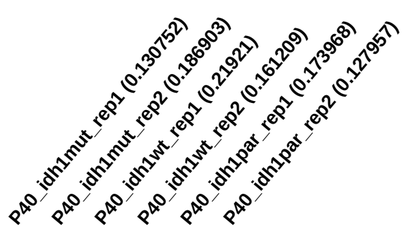

Pre-normalization Quantiles

			[min]	[medium]	[max]
CEM 1		MANF	5157.3	6203.6	6959.9
P (S | Z, I) = 0.00		SDF2L1	1255.0	1428.5	1479.7
Mean Corr = 0.22042		CRELD2	3061.8	3388.8	3754.1
		HSPA5	13995.3	22058.6	25044.3
		HYOU1	2114.4	3573.5	4291.9
		PDIA4	582.3	801.8	869.7
		PDIA6	6167.9	6502.4	7431.8
CEM 1 + Top 10 Genes		DNAJB11	3912.2	5314.5	6489.8
		HSP90B1	1425.4	2396.5	2644.6
		PDIA3	6281.3	9311.5	11208.5
		PPIB	19719.8	24950.0	25825.5
		C19orf10	3712.3	4042.7	5968.5
		SLC35B1	2816.2	2942.6	3059.7
		SEC61A1	4526.1	5437.0	5682.7
		RPN1	4752.2	6138.2	6732.6
		DNAJC3	715.3	1284.2	2276.0
		CDK2AP2	1312.5	2266.3	2468.0
Null module		ARID5B			
		XBP1			
		HNRNPAB			
		SGK1			
		HSPB1			
		DDIT4			
		ARL4D			
		SAP30			
		KIAA0408			
		GPR17			
		HSPH1			
		DNASE1L2			
		SLC5A3			
		GNAS			
		GPR3			
		TNFRSF25			
		TM6SF2			
		MKKS			
		PLEKHF1			
		ZMYM1			
		DOK3			
		FGF20			
		SLC39A2			
		KCNIP2			
		ERRFI1			
		DEDD2			
		CCDC117			
		USP31			
		AHSA2			
		CYS1			
		CNIH2			
		BANP			
		CHORDC1			
		P4HA1			

GEO Series "GSE46922" Expression Profiles

Num of samples in this series: 13

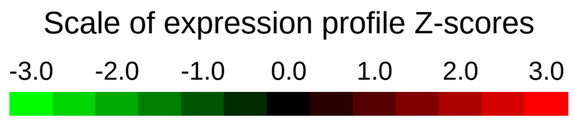

GEO Link:	http://www.ncbi.nlm.nih.gov/geo/query/acc.cgi?acc=GSE46922
Status:	Public on Aug 05 2013
Title:	Differences in gene expression and cytokines levels between newly diagnosed and chronic pediatric immune thrombocytopenia (ITP)
Organism:	Homo sapiens
Experiment type:	Expression profiling by array
Platform:	GPL570
Pubmed ID:	23869085
Summary & Design:	**Summary:** Immune thrombocytopenia (ITP) is an autoimmune disease where platelets are destroyed prematurely. In the majority of children the disease resolves but in some it becomes chronic. To investigate whether the two forms of the disease are similar or separate entities we performed DNA microarray analysis of T-cells from newly diagnosed children and children with chronic ITP. We found complete separation of the expression files between the two forms of the disease. Furthermore, the gene expression of several cytokines differed between the two forms of the disease. This was also reflected in plasma with increased levels of IL-16 and TWEAK and lower levels of IL-4 in newly diagnosed compared with chronic ITP. Thus, our data indicate that the two forms of the disease may be separate entities. **Overall design:** Microarray expression analysis of mRNA in peripheral blood T-cell of Newly diagnosed ITP vs Chronic ITP

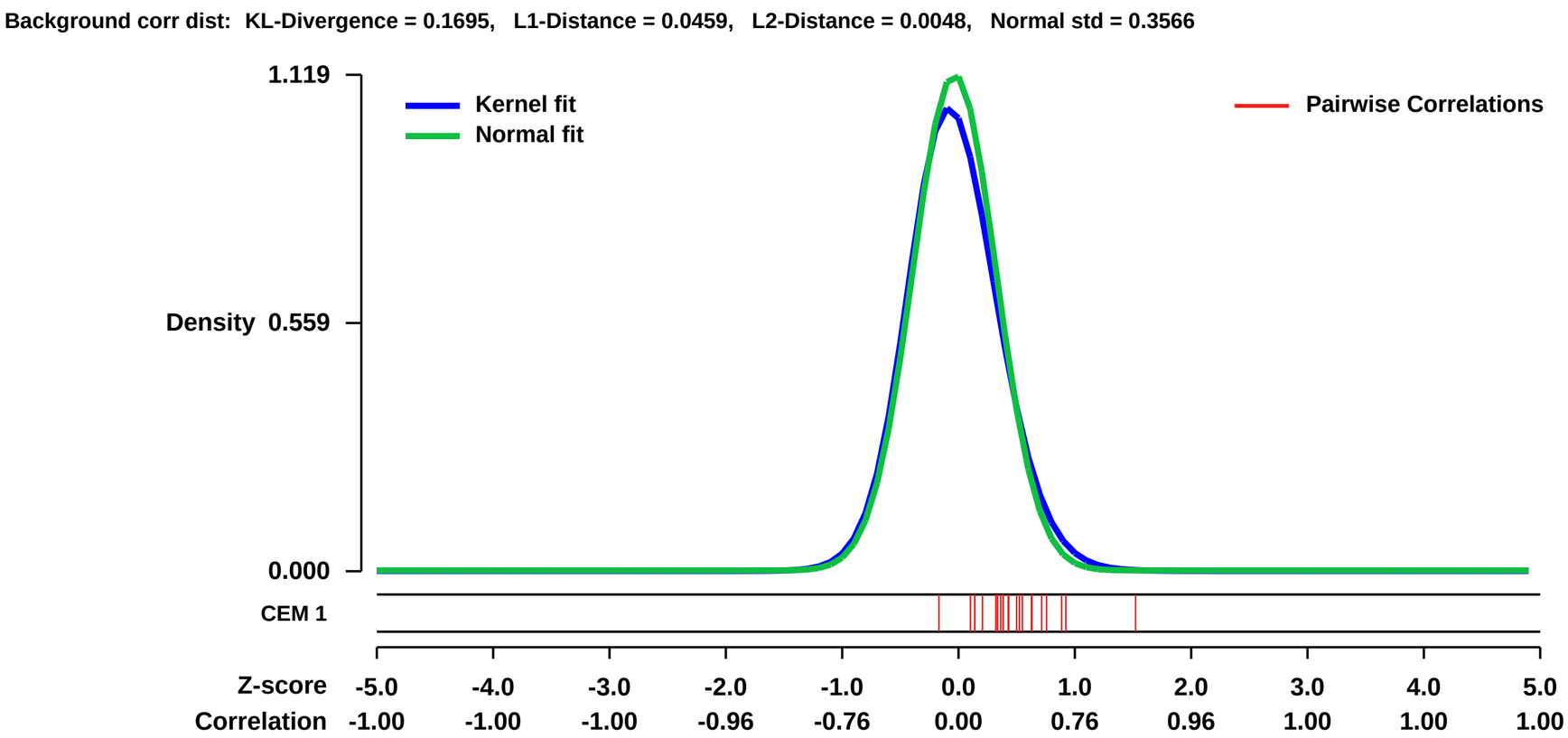

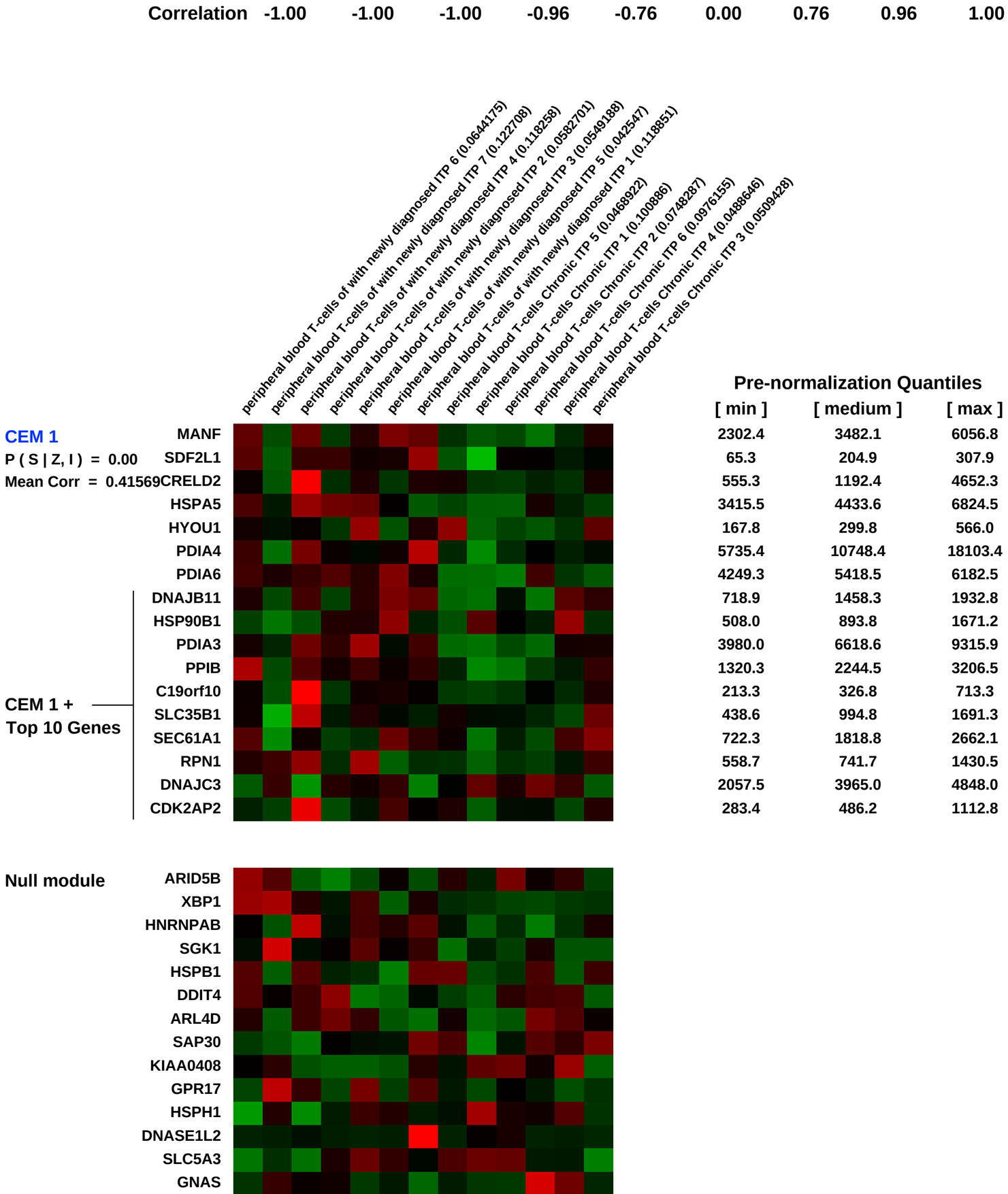

Pre-normalization Quantiles

	[min]	[medium]	[max]
MANF	2302.4	3482.1	6056.8
SDF2L1	65.3	204.9	307.9
CRELD2	555.3	1192.4	4652.3
HSPA5	3415.5	4433.6	6824.5
HYOU1	167.8	299.8	566.0
PDIA4	5735.4	10748.4	18103.4
PDIA6	4249.3	5418.5	6182.5
DNAJB11	718.9	1458.3	1932.8
HSP90B1	508.0	893.8	1671.2
PDIA3	3980.0	6618.6	9315.9
PPIB	1320.3	2244.5	3206.5
C19orf10	213.3	326.8	713.3
SLC35B1	438.6	994.8	1691.3
SEC61A1	722.3	1818.8	2662.1
RPN1	558.7	741.7	1430.5
DNAJC3	2057.5	3965.0	4848.0
CDK2AP2	283.4	486.2	1112.8

GEO Series "GSE29435" Expression Profiles

Num of samples in this series: 6

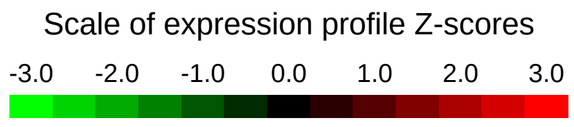

GEO Link:	http://www.ncbi.nlm.nih.gov/geo/query/acc.cgi?acc=GSE29435
Status:	Public on Jan 26 2012
Title:	Progesterone inhibits epithelial-to-mesenchymal transition in endometrial cancer: cell line data
Organism:	Homo sapiens
Experiment type:	Expression profiling by array
Platform:	GPL570
Pubmed ID:	
Summary & Design:	**Summary:** Every year more than 42,000 women die of endometrial cancer, mainly due to recurrent or metastatic disease. The presence of tumor infiltrating lymphocytes (TILs) as well as progesterone receptor (PR) positivity has been correlated with improved prognosis. This study describes two mechanisms by which progesterone inhibits metastatic spread of endometrial cancer: by stimulating T-cell infiltration and by inhibiting epithelial-to-mesenchymal cell transition (EMT). Paraffin sections from patients with (n=9) or without (n=10) progressive endometrial cancer (recurrent or metastatic disease) were assessed for the presence of CD4+ (helper), CD8+ (cytotoxic) and Foxp3+ (regulatory) T-lymphocytes and PR expression. Progressive disease was observed to be associated with significant loss of TILs and loss of PR expression. Frozen tumor samples, used for genome-wide expression analysis, showed significant regulation of pathways involved in immunosurveillance, EMT and metastasis. For a number of genes, such as CXCL14, DKK1, DKK4 and WIF1, quantitive RT-PCR was performed to verify down regulation in progressive disease. To corroborate the role of progesterone in regulating invasion, Ishikawa (IK) endometrial cancer cell lines stably transfected with PRA (IKPRA), PRB (IKPRB) and PRA+PRB (IKPRAB) were cultured in the presence/absence of progesterone (MPA) and used for genome-wide expression analysis, Boyden- and wound healing migration assays, and IHC for known EMT makers. IKPRB and IKPRAB cell lines showed MPA induced inhibition of migration and loss of the mesenchymal marker vimentin at the invasive front of the wound healing assay. Furthermore, pathway analysis of significantly MPA-regulated genes showed significant down regulation of important pathways involved in EMT, immunesuppression and metastasis: such as IL6-, TGF-¸† and Wnt/¸†-catenin signalling. Intact progesterone signaling in non-progressive endometrial cancer seems to be an important factor stimulating immunosurveillance and inhibiting transition from an epithelial to a more mesenchymal, more invasive phenotype. **Overall design:** The PRA- and PRB-expressing Ishikawa endometrial cancer cell line (IKPRAB36) was cultured for 48h in the absence or presence of 1nM MPA (n = 3). The RNA was isolated and used for hybridization on Affymetrix microarrays. Cells cultured in the presence of MPA were compared with cells cultured in the absence of MPA.

Background corr dist: KL-Divergence = 0.0249, L1-Distance = 0.0115, L2-Distance = 0.0001, Normal std = 0.6929

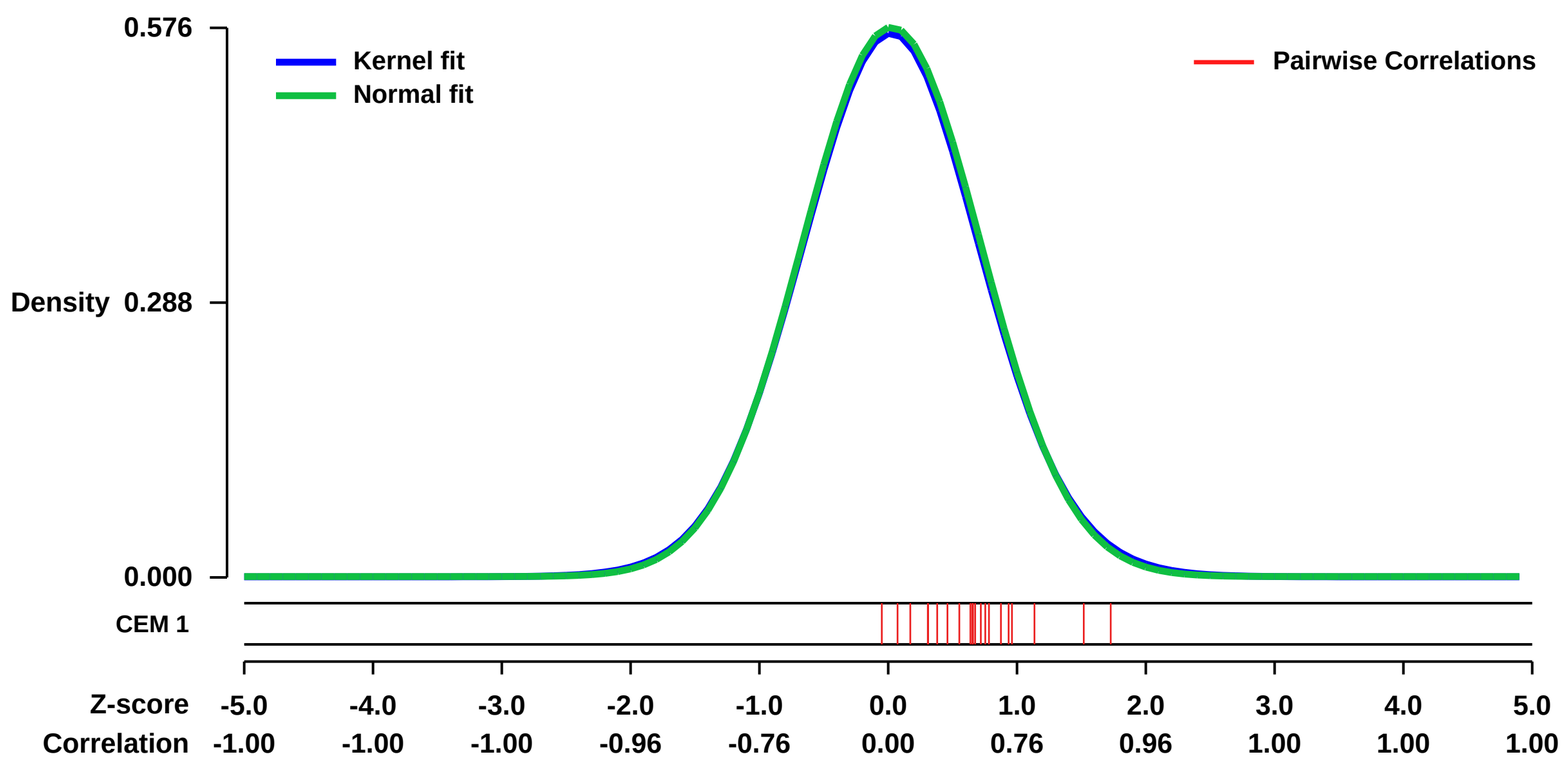

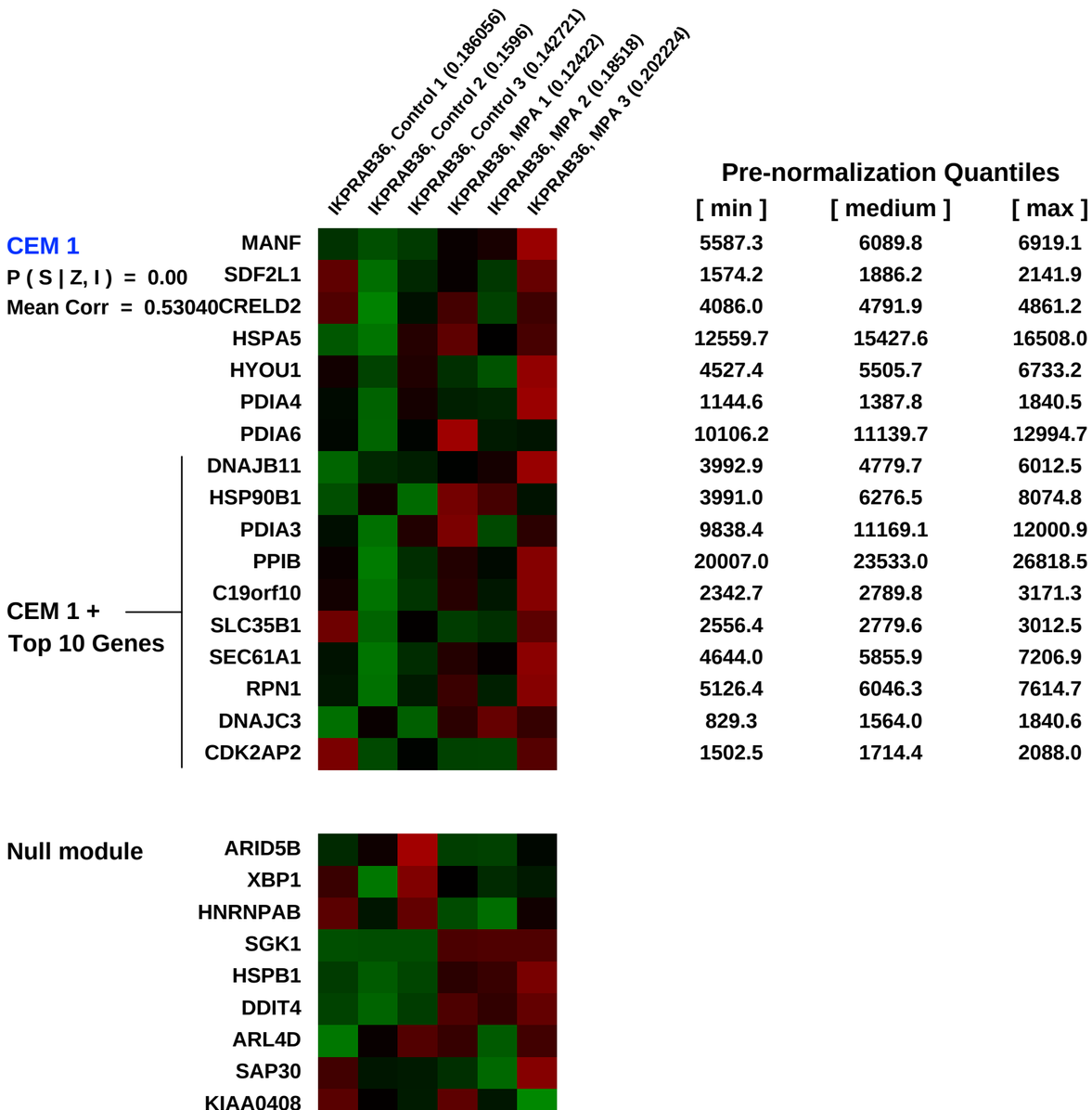

Pre-normalization Quantiles

	[min]	[medium]	[max]
MANF	5587.3	6089.8	6919.1
SDF2L1	1574.2	1886.2	2141.9
CRELD2	4086.0	4791.9	4861.2
HSPA5	12559.7	15427.6	16508.0
HYOU1	4527.4	5505.7	6733.2
PDIA4	1144.6	1387.8	1840.5
PDIA6	10106.2	11139.7	12994.7
DNAJB11	3992.9	4779.7	6012.5
HSP90B1	3991.0	6276.5	8074.8
PDIA3	9838.4	11169.1	12000.9
PPIB	20007.0	23533.0	26818.5
C19orf10	2342.7	2789.8	3171.3
SLC35B1	2556.4	2779.6	3012.5
SEC61A1	4644.0	5855.9	7206.9
RPN1	5126.4	6046.3	7614.7
DNAJC3	829.3	1564.0	1840.6
CDK2AP2	1502.5	1714.4	2088.0
ARID5B			
XBP1			
HNRNPAB			
SGK1			
HSPB1			
DDIT4			
ARL4D			
SAP30			
KIAA0408			
GPR17			
HSPH1			
DNASE1L2			
SLC5A3			
GNAS			
GPR3			
TNFRSF25			
TM6SF2			
MKKS			
PLEKHF1			
ZMYM1			
DOK3			
FGF20			
SLC39A2			
KCNIP2			
ERRFI1			
DEDD2			
CCDC117			
USP31			
AHSA2			
CYS1			
CNIH2			
BANP			
CHORDC1			
P4HA1			

GEO Series "GSE33143" Expression Profiles

Num of samples in this series: 6

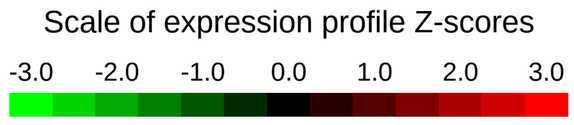

GEO Link:	http://www.ncbi.nlm.nih.gov/geo/query/acc.cgi?acc=GSE33143
Status:	Public on Aug 23 2012
Title:	Targeted disruption of the BCL9/beta-catenin complex in cancer
Organism:	Homo sapiens
Experiment type:	Expression profiling by array
Platform:	GPL570
Pubmed ID:	22914623
Summary & Design:	**Summary:** Stabilized Alpha-Helix peptides of BCL9 HD2 (SAH-BCL9) block BCL9 and B9L interactions with beta-catenin and specifically downregulate Wnt target gene expression. **Overall design:** RNA from triplicate SAH-BCL9B- and vehicle-treated DLD1 samples (10 ´µM each for 12 hours) was hybridized to Affymetrix Human U133 Plus 2.0 arrays to asses global gene expression changes.

Background corr dist: KL-Divergence = 0.0287, L1-Distance = 0.0132, L2-Distance = 0.0001, Normal std = 0.6717

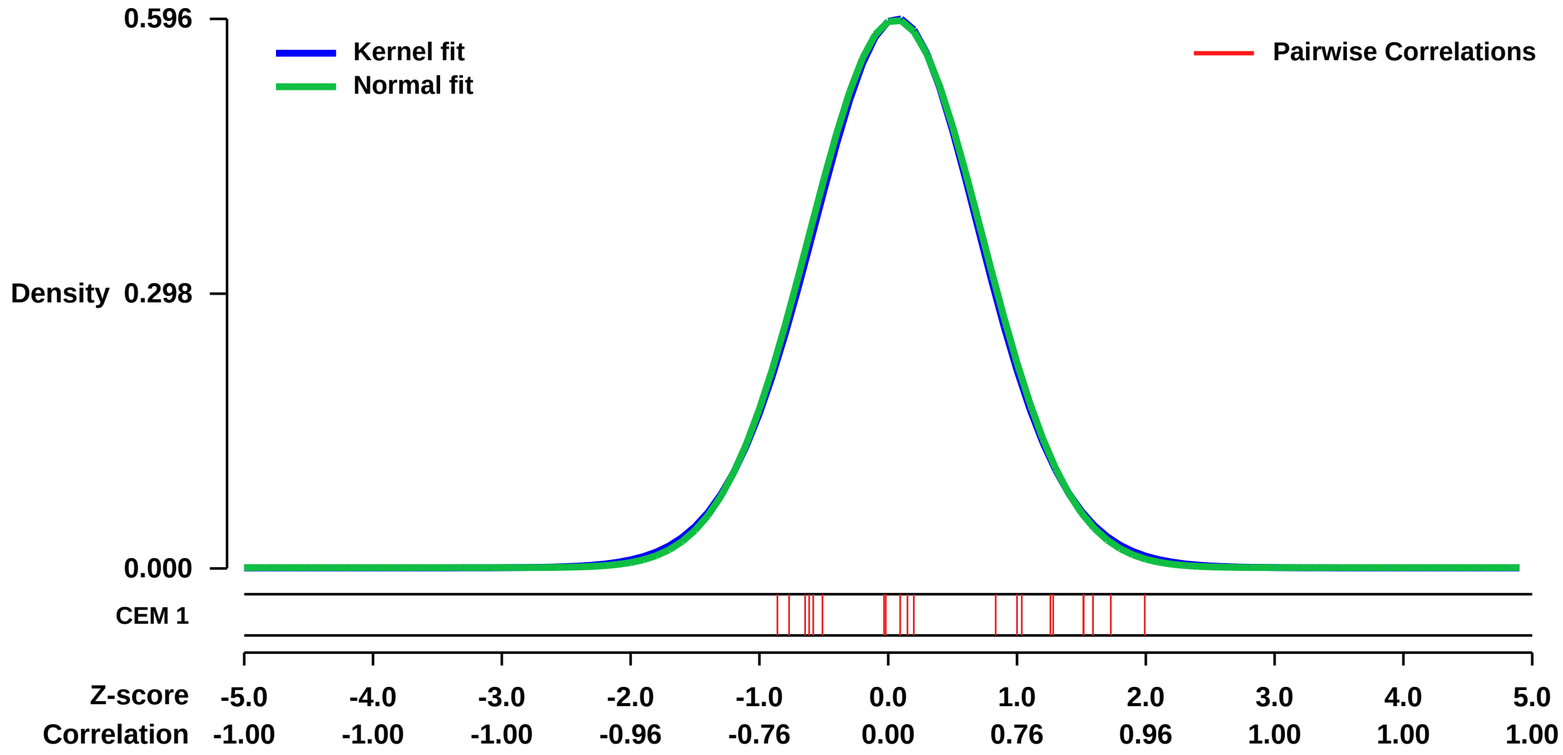

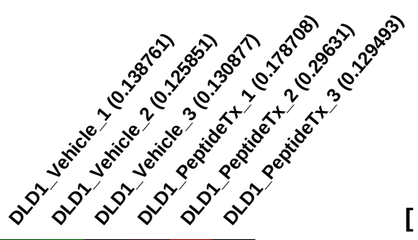

Pre-normalization Quantiles

			[min]	[medium]	[max]
CEM 1		MANF	2940.2	3457.8	4079.5
P (S | Z, I) = 0.00		SDF2L1	1068.6	1208.2	1619.7
Mean Corr = 0.26198		CRELD2	3920.8	4369.7	5336.1
		HSPA5	15769.8	16658.5	16984.7
		HYOU1	2518.5	2901.0	3588.3
		PDIA4	1269.0	1609.2	1978.0
		PDIA6	5865.8	6284.7	6426.5
CEM 1 + Top 10 Genes		DNAJB11	4849.5	5754.7	6285.3
		HSP90B1	4722.6	6409.3	7280.4
		PDIA3	2282.3	2547.2	2757.5
		PPIB	15160.6	16226.3	18061.8
		C19orf10	937.5	1014.1	1278.1
		SLC35B1	2523.8	2957.7	3079.6
		SEC61A1	2880.9	3373.0	3659.3
		RPN1	5284.9	5445.4	6442.8
		DNAJC3	2749.2	2989.9	3289.8
		CDK2AP2	856.7	936.9	964.5
Null module		ARID5B			
		XBP1			
		HNRNPAB			
		SGK1			
		HSPB1			
		DDIT4			
		ARL4D			
		SAP30			
		KIAA0408			
		GPR17			
		HSPH1			
		DNASE1L2			
		SLC5A3			
		GNAS			
		GPR3			
		TNFRSF25			
		TM6SF2			
		MKKS			
		PLEKHF1			
		ZMYM1			
		DOK3			
		FGF20			
		SLC39A2			
		KCNIP2			
		ERRFI1			
		DEDD2			
		CCDC117			
		USP31			
		AHSA2			
		CYS1			
		CNIH2			
		BANP			
		CHORDC1			
		P4HA1			

GEO Series "GSE18182" Expression Profiles

Num of samples in this series: 6

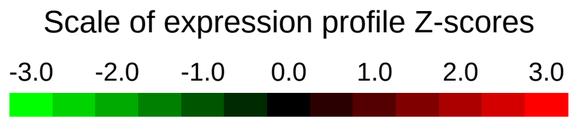

GEO Link:	http://www.ncbi.nlm.nih.gov/geo/query/acc.cgi?acc=GSE18182
Status:	Public on Feb 08 2011
Title:	Expression profile of lung adenocarcinoma, A549 cells following targeted depletion of non metastatic 2 (NME2/NM23 H2)
Organism:	Homo sapiens
Experiment type:	Expression profiling by array
Platform:	GPL570
Pubmed ID:	25081206
Summary & Design:	**Summary:** Non-metastatic 2 (NME2) is an established metastases suppressor in multiple human cancer types. However, the molecular mechanisms of NME2 action remain insufficiently resolved. We recently validated the transcription regulatory activity of NME2 with respect to control of proto-oncogene c-MYC expression. We hypothesized that large scale transcriptional potential of NME2 may be at the core of metastases suppression by NME2. Using a combination of high throughput genomic assays such as chromatin immunoprecipitation coupled to promoter array hybridization (ChIP-chip) and gene expression profiling, we characterized the transcriptional roles of NME2. Specifically, we found a set of NME2 target genes which changed expression upon selective depletion of NME2 in a lung cancer cell line, A549. The analysis of gene expression suggested control of various biological pathways esp. cell adhesion and apoptosis by NME2 target genes which could be important in regulation of metastases. **Overall design:** For transcriptome analysis, total RNA was purified from A549 cells transiently silenced for NME2 (siRNA duplex against NME2/ NM23 H2(Santa Cruz)) or transfected with control siRNA duplexes. Isolated RNA was converted to cDNA, transcribed in vitro to synthesize biotinylated cRNA, and hybridized to Affymetrix HG-U133 plus 2.0 GeneChip oligonucleotide microarrays, according to manufacturerâ s instructions. Three biological replicates were averaged and significance analysis performed using GCOS (P <0.005 of fold change).

Background corr dist: KL-Divergence = 0.0486, L1-Distance = 0.0191, L2-Distance = 0.0004, Normal std = 0.5779

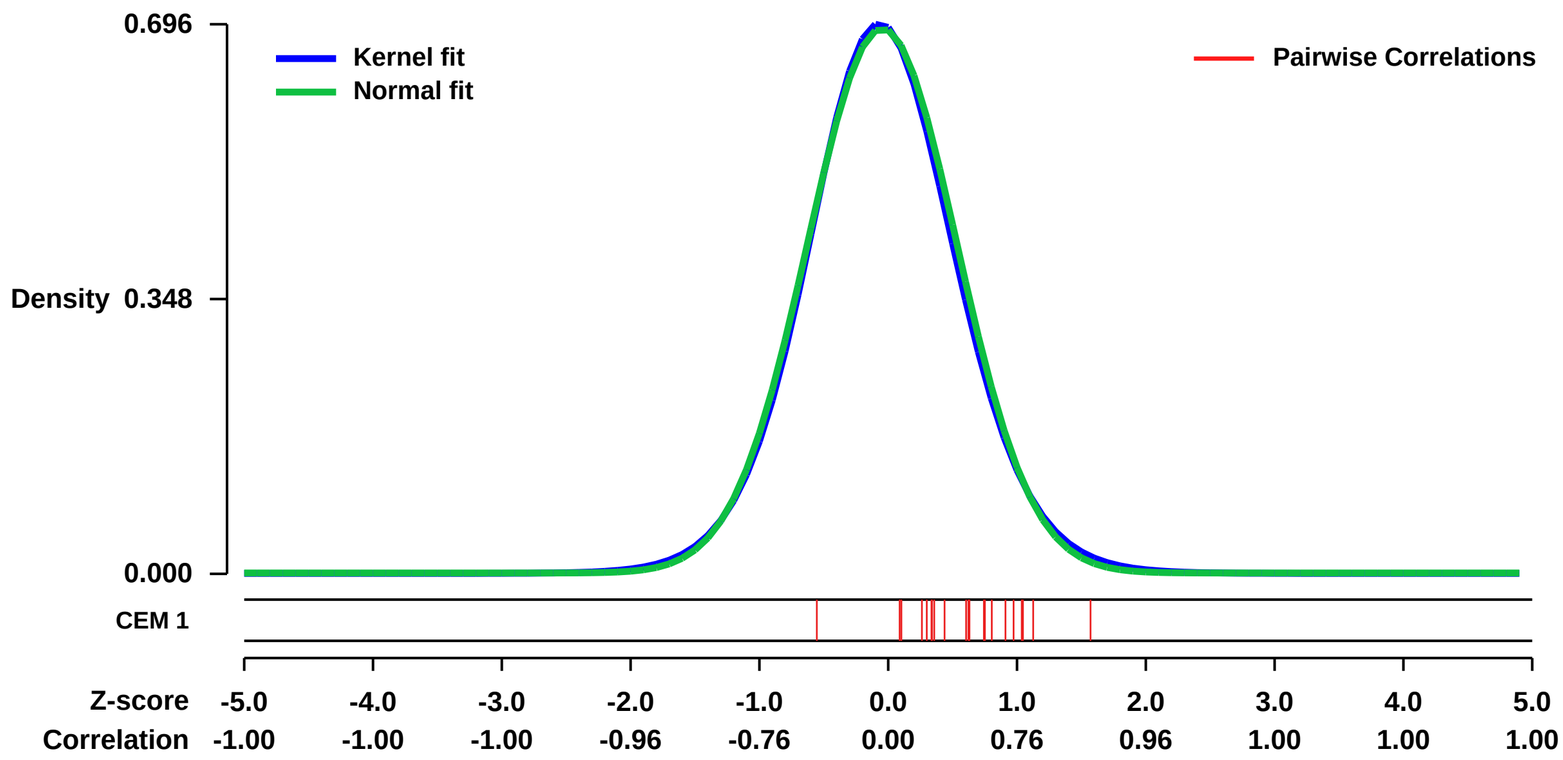

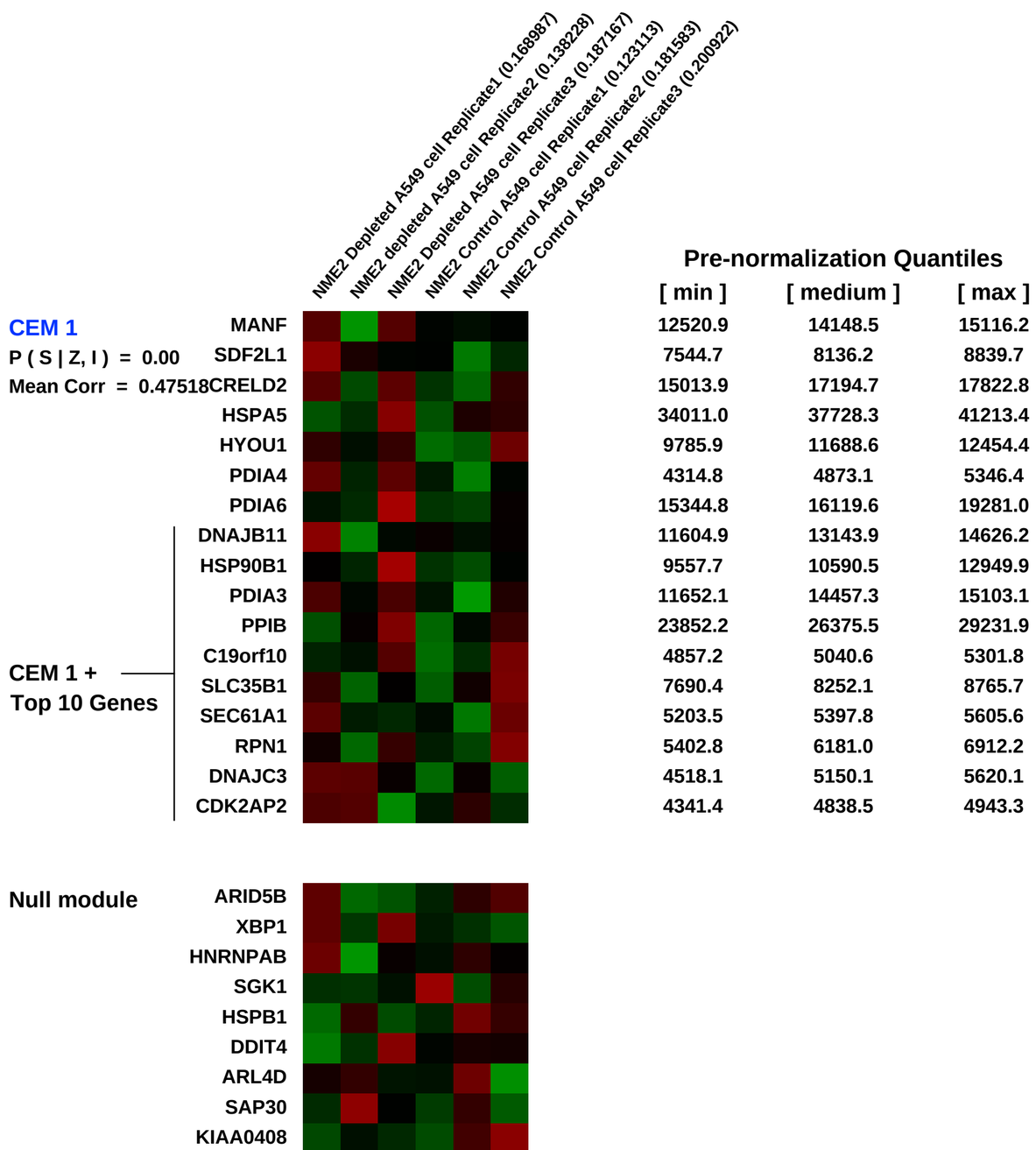

Pre-normalization Quantiles

	[min]	[medium]	[max]
MANF	12520.9	14148.5	15116.2
SDF2L1	7544.7	8136.2	8839.7
CRELD2	15013.9	17194.7	17822.8
HSPA5	34011.0	37728.3	41213.4
HYOU1	9785.9	11688.6	12454.4
PDIA4	4314.8	4873.1	5346.4
PDIA6	15344.8	16119.6	19281.0
DNAJB11	11604.9	13143.9	14626.2
HSP90B1	9557.7	10590.5	12949.9
PDIA3	11652.1	14457.3	15103.1
PPIB	23852.2	26375.5	29231.9
C19orf10	4857.2	5040.6	5301.8
SLC35B1	7690.4	8252.1	8765.7
SEC61A1	5203.5	5397.8	5605.6
RPN1	5402.8	6181.0	6912.2
DNAJC3	4518.1	5150.1	5620.1
CDK2AP2	4341.4	4838.5	4943.3

GEO Series "GSE22973" Expression Profiles

Num of samples in this series: 12

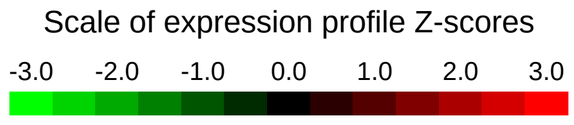

GEO Link:	**http://www.ncbi.nlm.nih.gov/geo/query/acc.cgi?acc=GSE22973**
Status:	**Public on Jan 01 2011**
Title:	**An Invasive Gene Expression Signature in Pancreas Cancer.**
Organism:	**Homo sapiens**
Experiment type:	**Expression profiling by array**
Platform:	**GPL570**
Pubmed ID:	
Summary & Design:	**Summary:** **Gene expression profiling has demonstrated clinical utility as a predictive tool in clinical oncology. We have identified genes associated with invasion of pancreatic cancer, and with potential for identifying early recurrence.** **We used Affymetrix Human U133 Plus 2.0 microarrays to identifiy specific predictive profiles in pancreatic cancer, and the evolution of gene expression. We identified distinct classes of up-regulated genes during this process.** **Overall design:** **Primary and metastatic pancreatic cancer cell lines (BxPC-3 and AsPC-1), were stimulated with with phorbol-12-myristate 13-acetate (PMA), a known inducer of invasion. Affymetrix gene expression microarray analysis was performed, comparing PMA stimulated BxPC-3 and AsPC-1 gene expression to unstimulated controls, and also PMA stimulated BxPC-3 verses stimulated AsPC-1 cell lines. Differential gene expression was identified using ArrayAssist bioinformatics software. Gene expression changes were confirmed using quantitative reverse transcription polymerase chain reaction (qRT-PCR) (Assays-on-demand, Taqman, ABI systems). Pathway Assist and GOstat were used to identify pathway and gene ontology changes.**

Background corr dist: KL-Divergence = 0.0862, L1-Distance = 0.0346, L2-Distance = 0.0019, Normal std = 0.4765

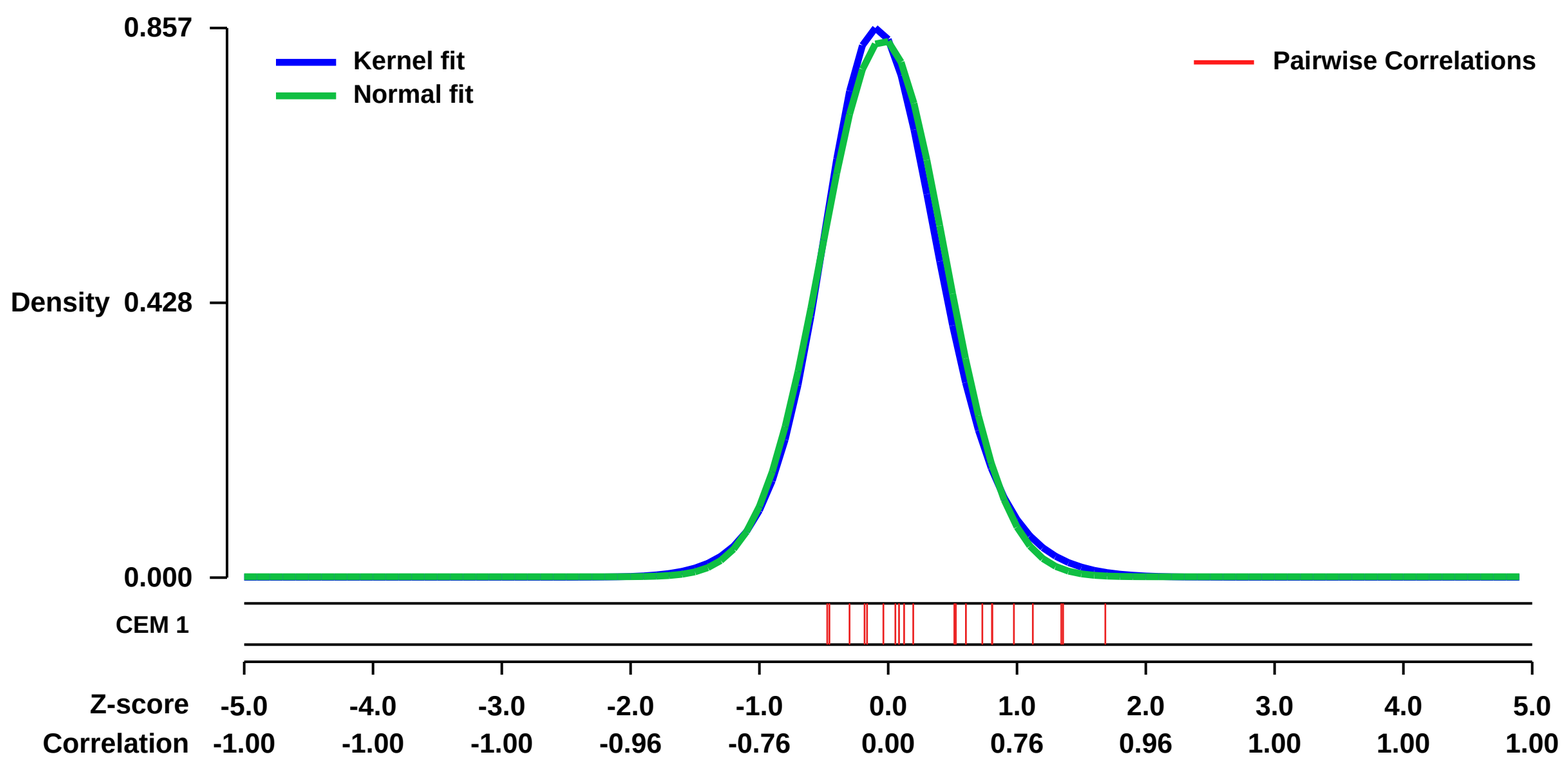

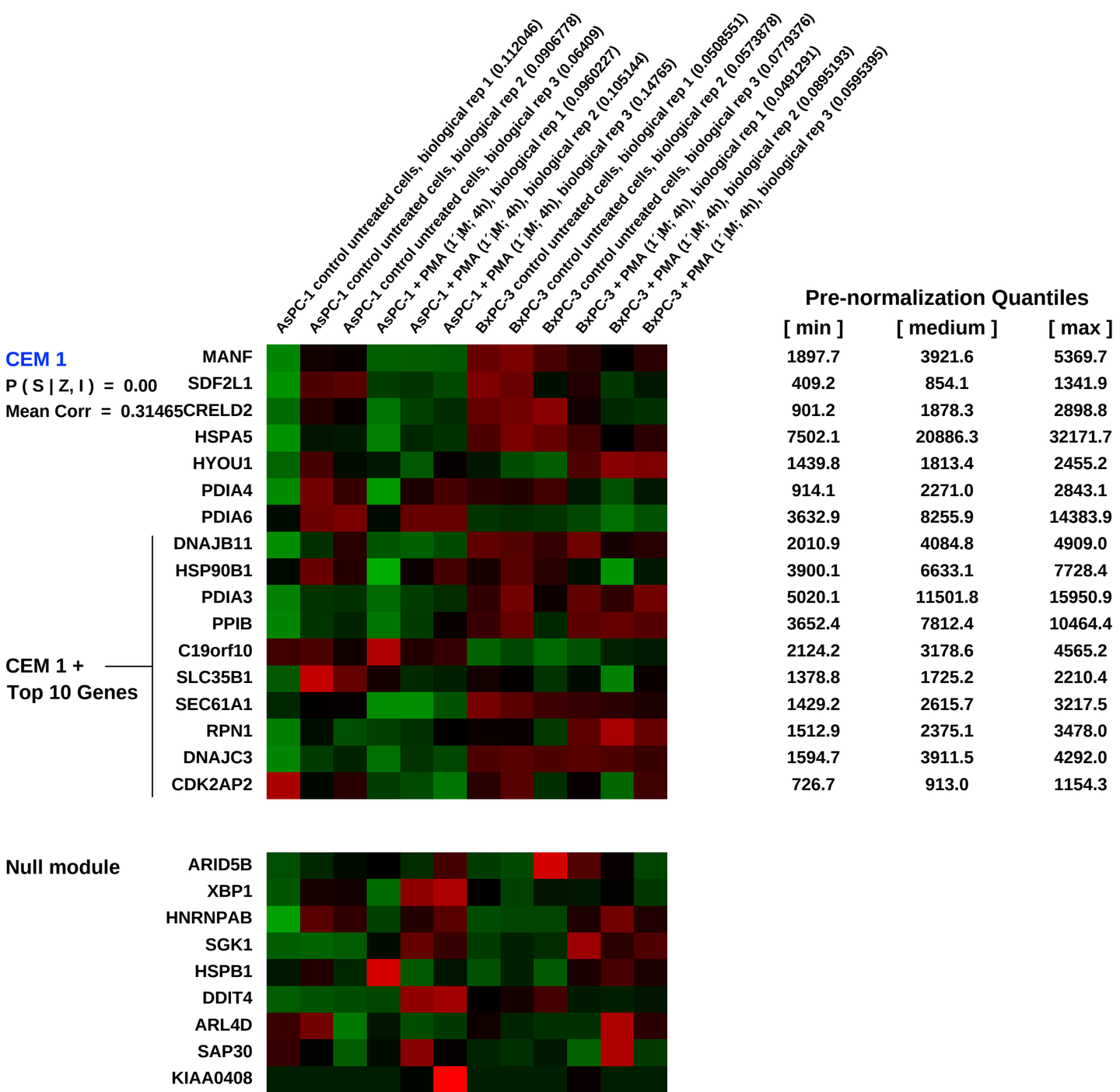

GEO Series "GSE47855" Expression Profiles

Num of samples in this series: 30

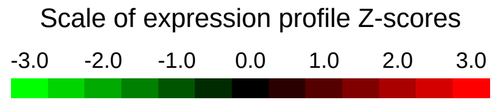

GEO Link:	http://www.ncbi.nlm.nih.gov/geo/query/acc.cgi?acc=GSE47855
Status:	Public on Jul 01 2013
Title:	Gene expression analysis for CD56- T, NK, CD56+ T cells, and iNKT cells
Organism:	Homo sapiens
Experiment type:	Expression profiling by array
Platform:	GPL570
Pubmed ID:	23858032
Summary & Design:	**Summary:** A small subset of T cells also expresses kiler-cell immunoglobulin-like receptors (KIRs). We find that KIR+ T cells primarily reside in the CD56+ T population. However, little is known on how these cells are different from the conventional CD56- T, NK, and iNKT cells. We used microarray profiling to compare and determine the distinctive differences of CD56+ T cell and its KIR subsets when compared to the conventional CD56- T, NK and iNKT cells. **Overall design:** Lymphocyte subsets were sorted from human peripheral blood mononuclear cells with FACSAriaII (BD Biosciences, San Jose, CA) using anti-CD3, anti-CD56, anti-CD14, anti-KIR2DL1, anti-KIR2DL2/3, anti-KIR3DL1 and anti-TCRValpha24 antibodies. The purity of CD3+CD56- T cells, CD3-CD56+ NK cells, CD3+CD56+ T cells, KIR-CD3+CD56+ T cells, and KIR+CD3+CD56+ T cells were more than 98% in all experiments. The purities of iNKT cells for TCRValpha24 and CD1d-tetramer were >95% and >90%, respectively. RNA pre-amplification, labeling and hybridization on Human Genome U133Plus 2.0 GeneChip array were performed in the St. Jude Hartwell Center for Bioinformatics & Biotechnology microarray core facility according to the manufacturerâ s instructions (Affymetrix, Santa Clara, CA).

Background corr dist: KL-Divergence = 0.3188, L1-Distance = 0.0569, L2-Distance = 0.0087, Normal std = 0.2766

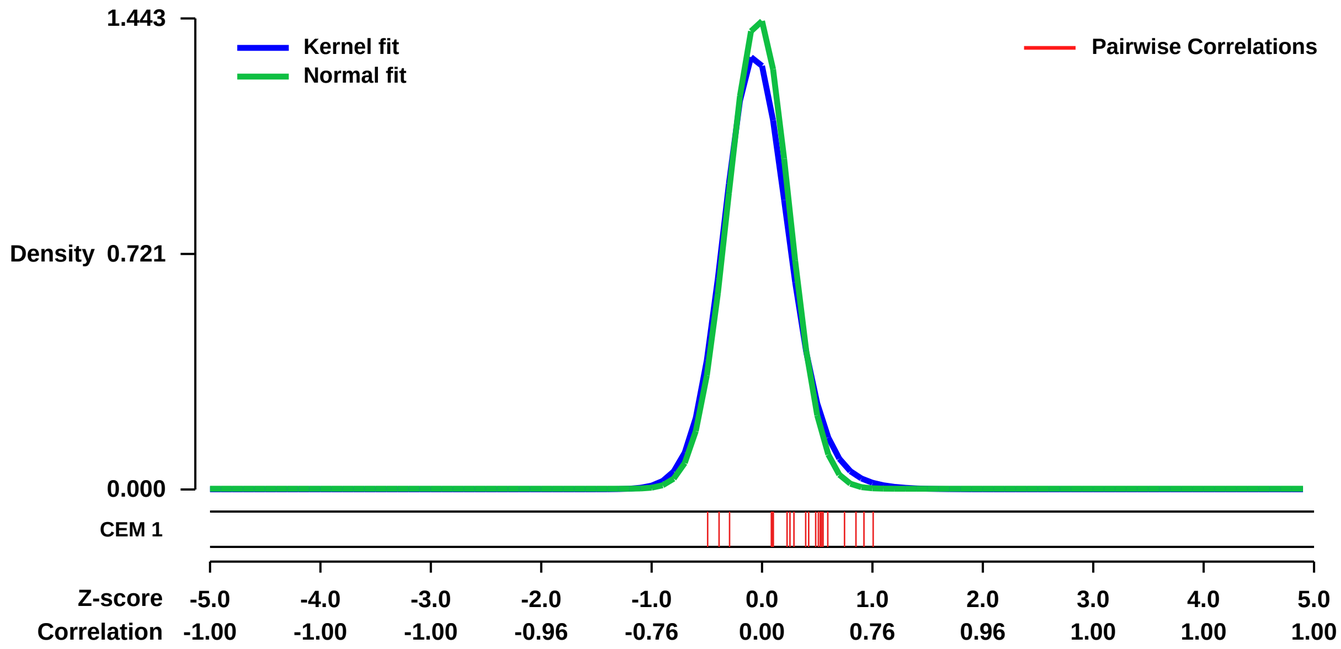

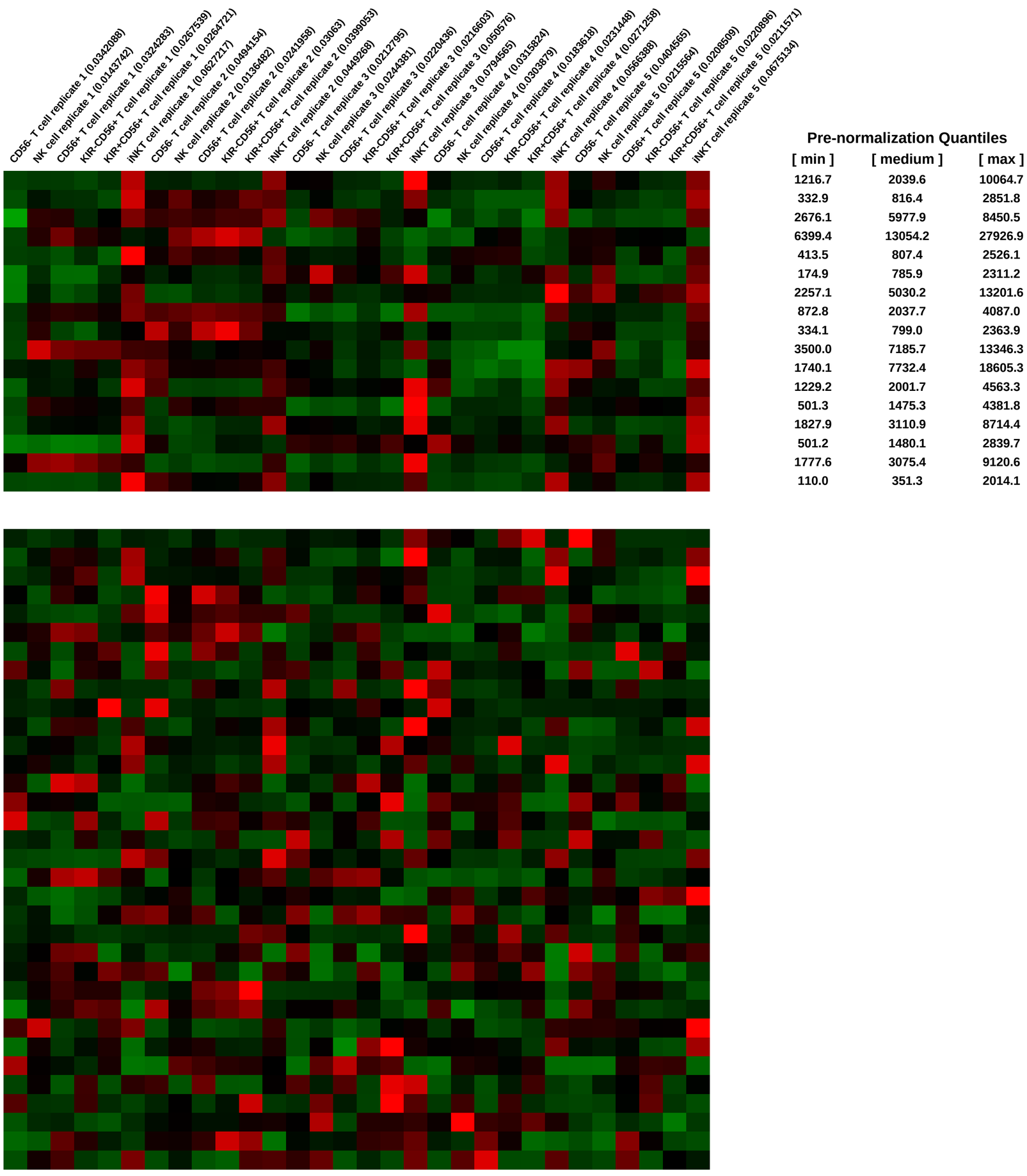

GEO Series "GSE39338" Expression Profiles

Num of samples in this series: 8

Scale of expression profile Z-scores

-3.0 -2.0 -1.0 0.0 1.0 2.0 3.0

GEO Link: http://www.ncbi.nlm.nih.gov/geo/query/acc.cgi?acc=GSE39338
Status: Public on Sep 01 2012
Title: Expression data from glucocorticoid-treated ALL (CCRF-CEM-C7-14 cells)
Organism: Homo sapiens
Experiment type: Expression profiling by array
Platform: GPL570
Pubmed ID: 22869147

Summary & Design: **Summary:**
The beneficial effects of glucocorticoids (GCs) in acute lymphoblastic leukemia (ALL) are based on their ability to induce apoptosis. Omics technologies such as DNA microarray analysis are widely used to study the changes in gene expression and have been successfully implemented in biomarker identification. In addition, time series studies of gene expression enable the identification of correlations between kinetic profiles of glucocorticoid receptor (GR) target genes and diverse modes of transcriptional regulation. This study presents a genome-wide microarray analysis of both our and published Affymetrix HG-U133 Plus 2.0 data in GCs-sensitive and -resistant ALL. GCs-sensitive CCRF-CEM-C7-14 cells were treated with dexamethasone at three time points (0 h, 2 h and 10 h). The treated samples were then compared to the control (0 h).

The published data used were as follows:

GSE2677:

GSM51674: B-ALL-24-24h

GSM51675: B-ALL-24-6h

GSM51676: B-ALL-24-0h

GSM51680: B-ALL-17-24h

GSM51681: B-ALL-17-8h

GSM51682: B-ALL-17-0h

GSM51677: B-ALL-13-24h

GSM51678: B-ALL-13-8h

GSM51679: B-ALL-13-0h

GSM51683: B-ALL-31-24h

GSM51684: B-ALL-31-6h

GSM51685: B-ALL-31-0h

GSM51686: B-ALL-32-24h

GSM51687: B-ALL-32-6h

GSM51688: B-ALL-32-0h

GSM51689: B-ALL-33-24h

GSM51690: B-ALL-33-6h

GSM51691: B-ALL-33-0h

GSM51692: B-ALL-37-24h

GSM51693: B-ALL-37-6h

GSM51694: B-ALL-37-0h

GSM51695: B-ALL-38-24h

GSM51696: B-ALL-38-6h

GSM51697: B-ALL-38-0h

GSM51698: B-ALL-40-24h

GSM51699: B-ALL-40-6h

GSM51700: B-ALL-40-0h

GSM51701: B-ALL-43-24h

GSM51702: B-ALL-43-6h

GSM51703: B-ALL-43-0h

GSM51707: T-ALL-25-24h

GSM51708: T-ALL-25-6h

GSM51709: T-ALL-25-0h

GSM51704: T-ALL-20-24h

GSM51705: T-ALL-20-8h

GSM51706: T-ALL-20-0h

GSM51710: T-ALL-2-24h

GSM51711: T-ALL-2-8h

GSM51712: T-ALL-2-0h

GSE2842

GSM60545: S-Line-PreB-6h-EtOH

GSM60546: S-Line-PreB-6h-GC

GSM60547: S-Line-PreB-24h-GC

GSM60542: S-Line-C7H2-6h-EtOH

GSM60543: S-Line-C7H2-6h-GC

GSM60544: S-Line-C7H2-24h-GC

GSM60560: R-Line-CEMC1-6h-EtOH

GSM60561: R-Line-CEMC1-6h-GC

GSM60562: R-Line-CEMC1-24h-GC

GSM60564: R-Line-C7R1-6h-EtOH

GSM60566: R-Line-C7R1-6h-GC

GSM60576: R-Line-C7R1dim-low-6h-EtOH

GSM60578: R-Line-C7R1dim-low-6h-GC

GSM60579: R-Line-C7R1dim-low-24h-GC

Background corr dist: KL-Divergence = 0.0724, L1-Distance = 0.0228, L2-Distance = 0.0008, Normal std = 0.4927

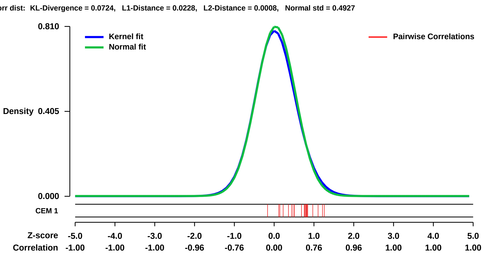

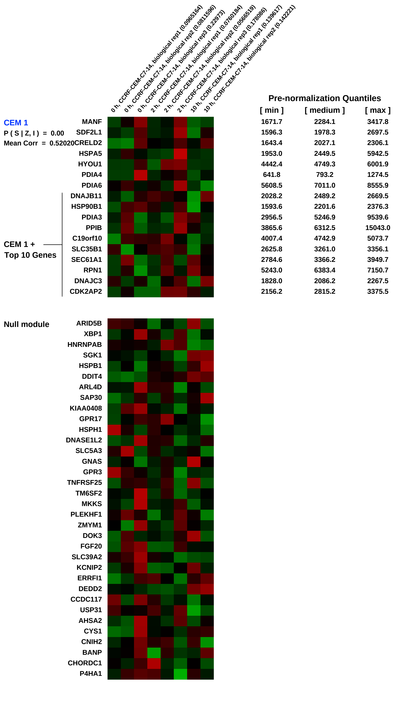

GEO Series "GSE2677" Expression Profiles

Num of samples in this series: 39

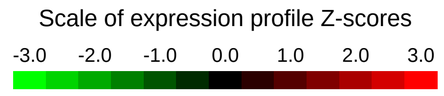

GEO Link:	http://www.ncbi.nlm.nih.gov/geo/query/acc.cgi?acc=GSE2677
Status:	Public on Nov 14 2005
Title:	Prednisolone treated childhood ALL samples
Organism:	Homo sapiens
Experiment type:	Expression profiling by array
Platform:	GPL570
Pubmed ID:	16293608
Summary & Design:	**Summary:** **Glucocorticoids (GC) are in most chemotherapy protocols for lymphoid malignancies, particularly childhood acute lymphoblastic leukaemia (ALL) for their ability to induce apoptosis in malignant blast. The underlying mechanism, however, has so far only been investigated in model systems. This study comprises Affymetrix hgu133 plus 2.0 analyses of** **Peripheral blood lymphoblasts purified at three time points (0h, 6-8h, 24h after treatment initiation) from 13 children under therapy for ALL . Treated samples were compared to untreated (0h). This series consists of this set of microarrays. For comparison, expression profiles were generated from an adult ALL patient, peripheral blood lymphocytes from GC-exposed healthy donors, GC-sensitive and -resistant ALL cell lines and mouse thymocytes treated with GC in vivo and in vitro.** **Findings. An essentially complete list of GC-regulated candidate genes in clinical settings experimental and was generated, enabling immediate analysis of any gene with respect to its potential significance for GC-induced apoptosis in these systems. Gene regulations previously thought responsible for cell death in experimental systems were reconfirmed in few children only. In contrast, a small number of genes, most not implicated in GC-induced apoptosis previously, were co-ordinately regulated in the majority of children.** **Keywords = ALL** **Keywords = apoptosis** **Keywords = glucocorticoid** **Keywords = leukemia** **Keywords = pediatric oncology** **Keywords: other** **Overall design:**

Background corr dist: KL-Divergence = 0.3018, L1-Distance = 0.0609, L2-Distance = 0.0100, Normal std = 0.2799

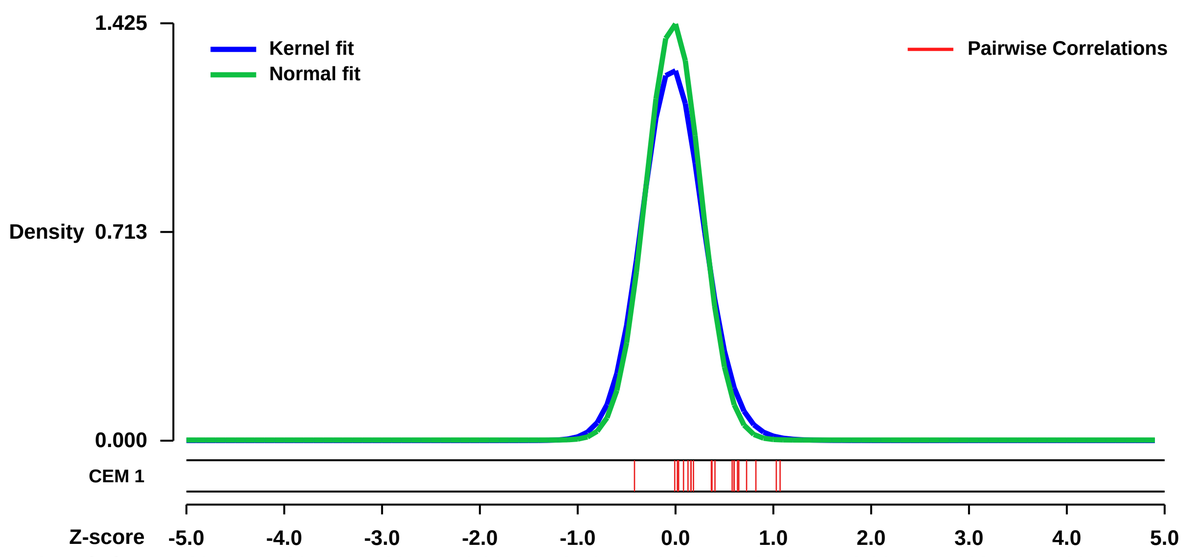

Correlation	-1.00	-1.00	-1.00	-0.96	-0.76	0.00	0.76	0.96	1.00	1.00	1.00

Pre-normalization Quantiles

[min]	[medium]	[max]
952.2	1621.1	3058.4
223.0	582.4	1381.5
813.1	1867.0	3300.9
2901.4	4678.0	16024.3
630.2	1250.8	3876.6
390.0	657.2	1090.5
1485.7	5111.3	11989.6
1912.1	2583.9	3916.0
351.5	1762.5	4136.0
2399.3	6266.3	10812.3
5969.7	11189.6	22026.3
739.9	1103.1	2131.9
950.6	1264.9	1826.3
1223.4	1514.5	2766.0
870.1	2820.5	3836.4
718.3	1084.4	2213.2
307.3	969.8	2423.7

GEO Series "GSE39353" Expression Profiles

Num of samples in this series: 10

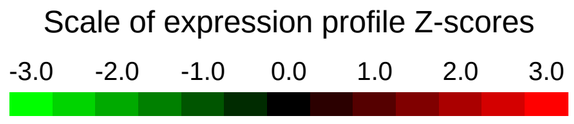

GEO Link:	http://www.ncbi.nlm.nih.gov/geo/query/acc.cgi?acc=GSE39353
Status:	Public on Mar 01 2013
Title:	Expression profiling of human prostate non-tumorigenic RWPE-1 cells after overexpressing ERG and ETV1, and ERG and ETV1 silencing on prostate cancer cells LNCaP ar
Organism:	Homo sapiens
Experiment type:	Expression profiling by array
Platform:	GPL570
Pubmed ID:	23512661
Summary & Design:	**Summary:** Chromosomal rearrangements involving ETS factors, ERG and ETV1, occur frequently in prostate cancer. We here examine human prostate non-tumorigenic RWPE-1 cells with ERG- or ETV1-expressing stable RWPE-1 cell. **Overall design:** RWPE-1 stable cell clones overexpressing ERG and ETV1 were grown under normal conditions. Total RNA was extracted from three biological replicates. This was used to hybridize to Affymetrix expression arrays using the HG-U133 Plus 2.0 platform.

Background corr dist: KL-Divergence = 0.0128, L1-Distance = 0.0358, L2-Distance = 0.0015, Normal std = 0.8515

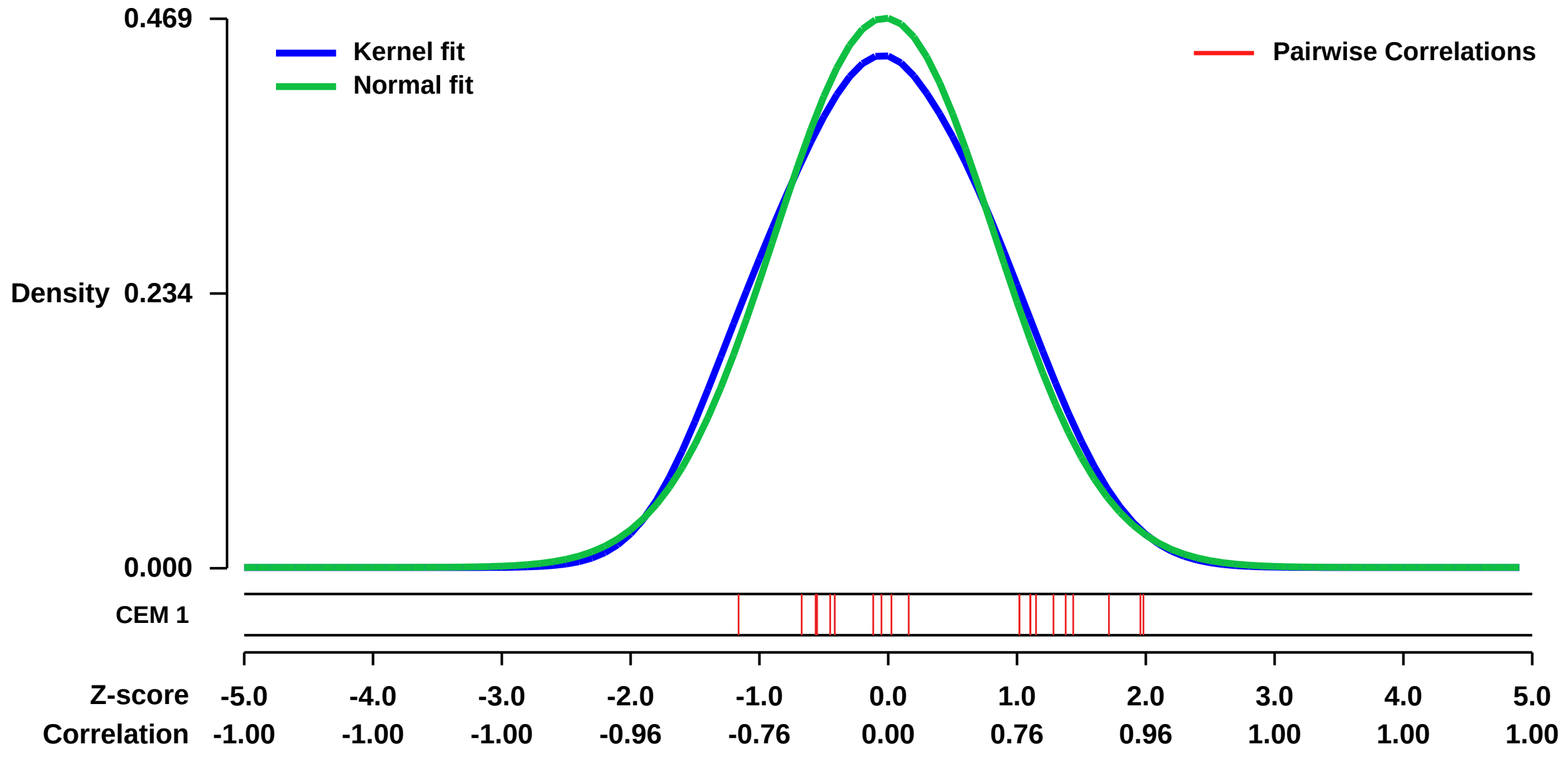

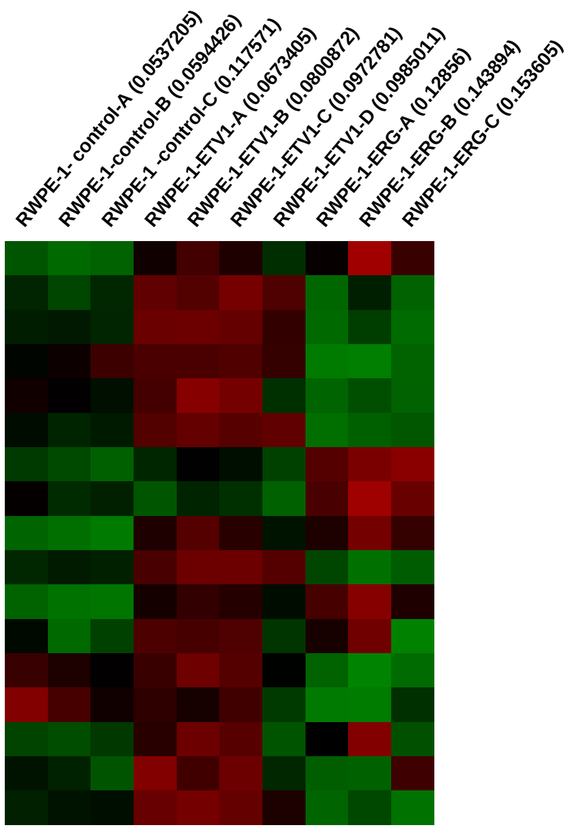

GEO Series "GSE14801" Expression Profiles

Num of samples in this series: 6

Scale of expression profile Z-scores

-3.0 -2.0 -1.0 0.0 1.0 2.0 3.0

GEO Link:	http://www.ncbi.nlm.nih.gov/geo/query/acc.cgi?acc=GSE14801
Status:	Public on Apr 17 2009
Title:	Expression data from ERG Si treated and Control HUVEC cells
Organism:	Homo sapiens
Experiment type:	Expression profiling by array
Platform:	GPL570
Pubmed ID:	19359602
Summary & Design:	**Summary:** ERG (Ets Related Gene) is an ETS transcription factor that was originally described for its role in a number of human cancers. Our preliminary data demonstrate that ERG exhibits a highly EC restricted pattern of expression in cultured primary cells and several adult tissues including the heart, lung, and brain. In response to inflammatory stimuli, such as TNF-alpha, we observed a marked reduction of ERG expression in EC. To further define the role of ERG in the regulation of normal EC function we used RNA interference to knockdown ERG. Knockdown of ERG in human umbilical vein EC (HUVEC) using siRNA was associated with the reduction of a number known ERG targets. Keywords: SIRNA Functional Role **Overall design:** The functional role of the ERG in the EC cellls was elucidated by comparing gene expression data from HUVEC cells trasfected with only vector (BERG) , non-sense SiRNA (CERG) vs ERG SiRNA (ERG).

Background corr dist: KL-Divergence = 0.0408, L1-Distance = 0.0288, L2-Distance = 0.0010, Normal std = 0.6250

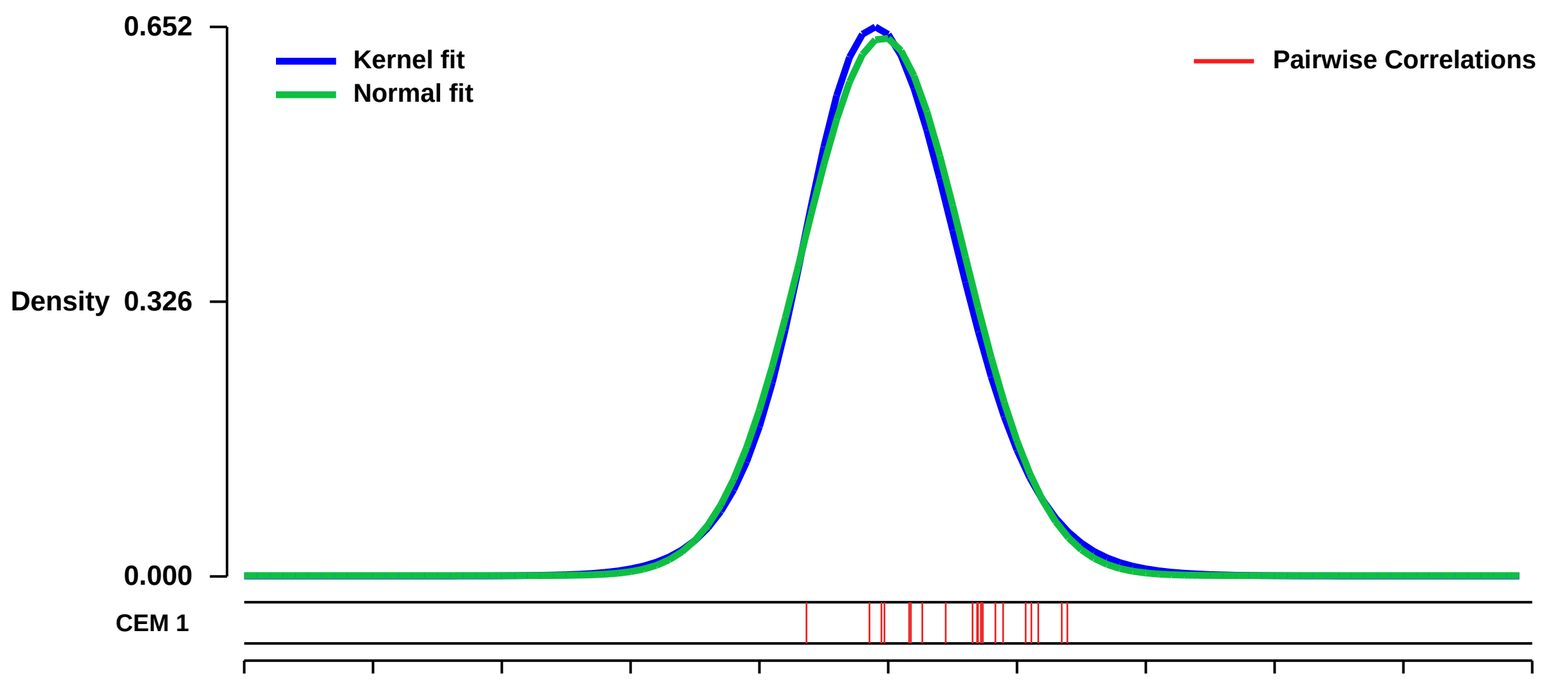

Z-score	-5.0	-4.0	-3.0	-2.0	-1.0	0.0	1.0	2.0	3.0	4.0	5.0
Correlation	-1.00	-1.00	-1.00	-0.96	-0.76	0.00	0.76	0.96	1.00	1.00	1.00

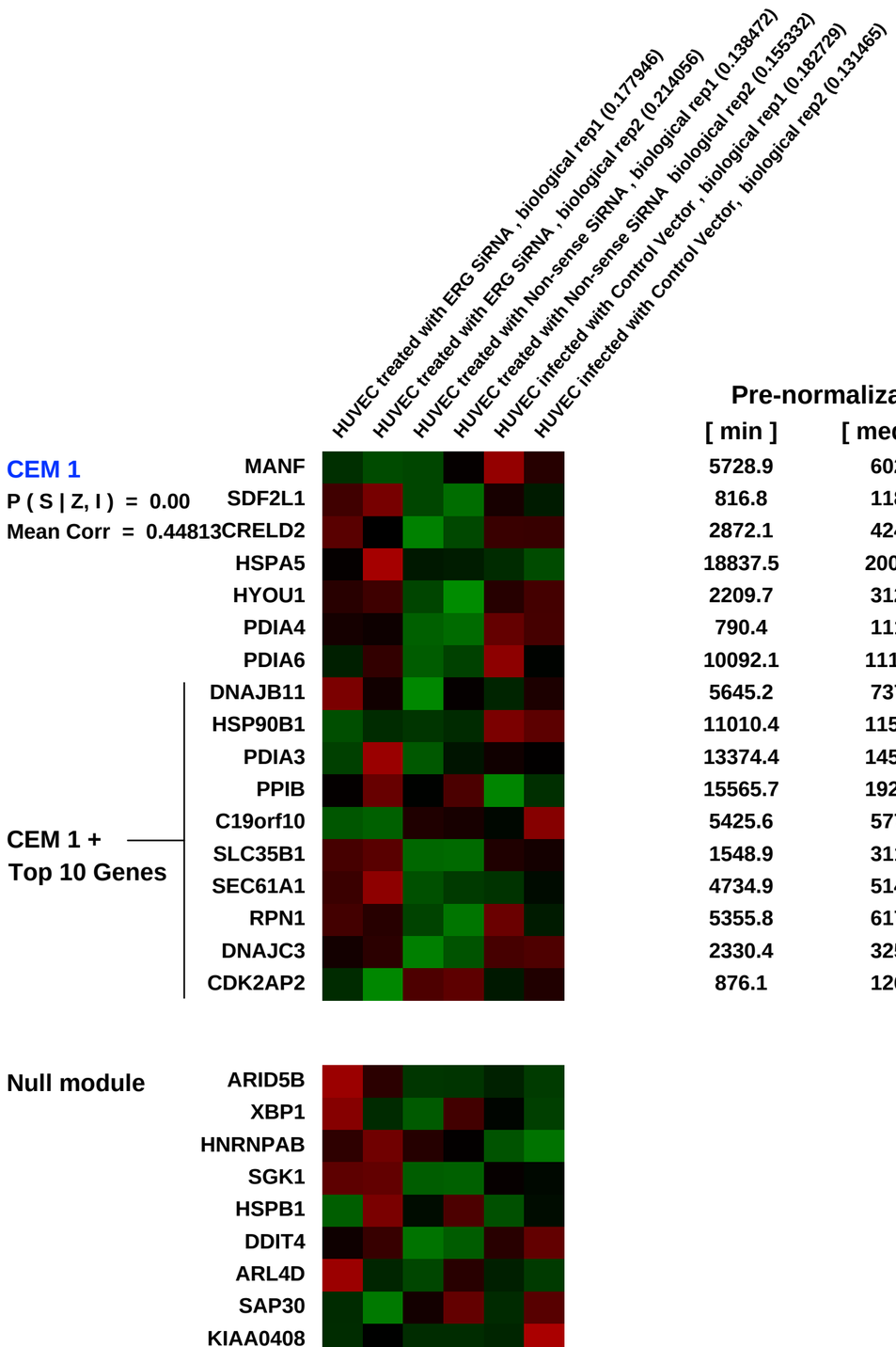

Pre-normalization Quantiles

	[min]	[medium]	[max]
MANF	5728.9	6026.6	6556.3
SDF2L1	816.8	1185.4	1455.3
CRELD2	2872.1	4244.9	4504.3
HSPA5	18837.5	20038.6	24523.3
HYOU1	2209.7	3126.2	3269.8
PDIA4	790.4	1119.7	1321.0
PDIA6	10092.1	11110.0	12749.3
DNAJB11	5645.2	7370.7	8570.5
HSP90B1	11010.4	11503.9	13772.0
PDIA3	13374.4	14531.3	16471.6
PPIB	15565.7	19211.7	21862.1
C19orf10	5425.6	5778.1	6107.1
SLC35B1	1548.9	3110.3	3777.8
SEC61A1	4734.9	5148.4	6064.4
RPN1	5355.8	6173.5	6523.5
DNAJC3	2330.4	3250.1	3435.4
CDK2AP2	876.1	1267.6	1410.6

GEO Series "GSE19510" Expression Profiles

Num of samples in this series: 14

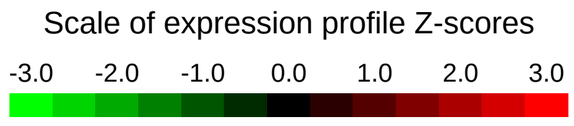

GEO Link:	http://www.ncbi.nlm.nih.gov/geo/query/acc.cgi?acc=GSE19510
Status:	Public on Jan 01 2010
Title:	Transcriptional response of normal human lung WI-38 fibroblasts to benzo[a]pyrene diol epoxide: a dose-response study
Organism:	Homo sapiens
Experiment type:	Expression profiling by array
Platform:	GPL570
Pubmed ID:	20382639
Summary & Design:	**Summary:** Cellular responses to carcinogens are typically studied in transformed cell lines, which do not reflect the physiological status of normal tissues. To address this question, we have characterized the transcriptional program and cellular responses of normal human lung WI-38 fibroblasts upon exposure to the ultimate carcinogen benzo[a]pyrene diol epoxide (BPDE). Exposure to BPDE induces a strong inflammatory response in WI-38 primary fibroblasts. Whole-genome microarray analysis shows induction of several genes related to the production of inflammatory factors, including those that encode interleukins (ILs), growth factors, and enzymes related to prostaglandin synthesis and signaling. This is the first demonstration that a strong inflammatory response is triggered in primary fibroblasts in response to a reactive diol epoxide derived from a polycyclic aromatic hydrocarbon. **Overall design:** Normal human lung WI-38 fibroblasts were exposed to vehicle control (DMSO) and increasing doses (0.1, 0.5 and 1 uM) of anti-BPDE, respectively. The genome wide transcriptional response of the three treatments were compared to that of the control, respectively, in quadruplicates (Control and 1 uM) and triplicates (0.1 and 0.5 uM).

Background corr dist: KL-Divergence = 0.0744, L1-Distance = 0.0289, L2-Distance = 0.0014, Normal std = 0.4834

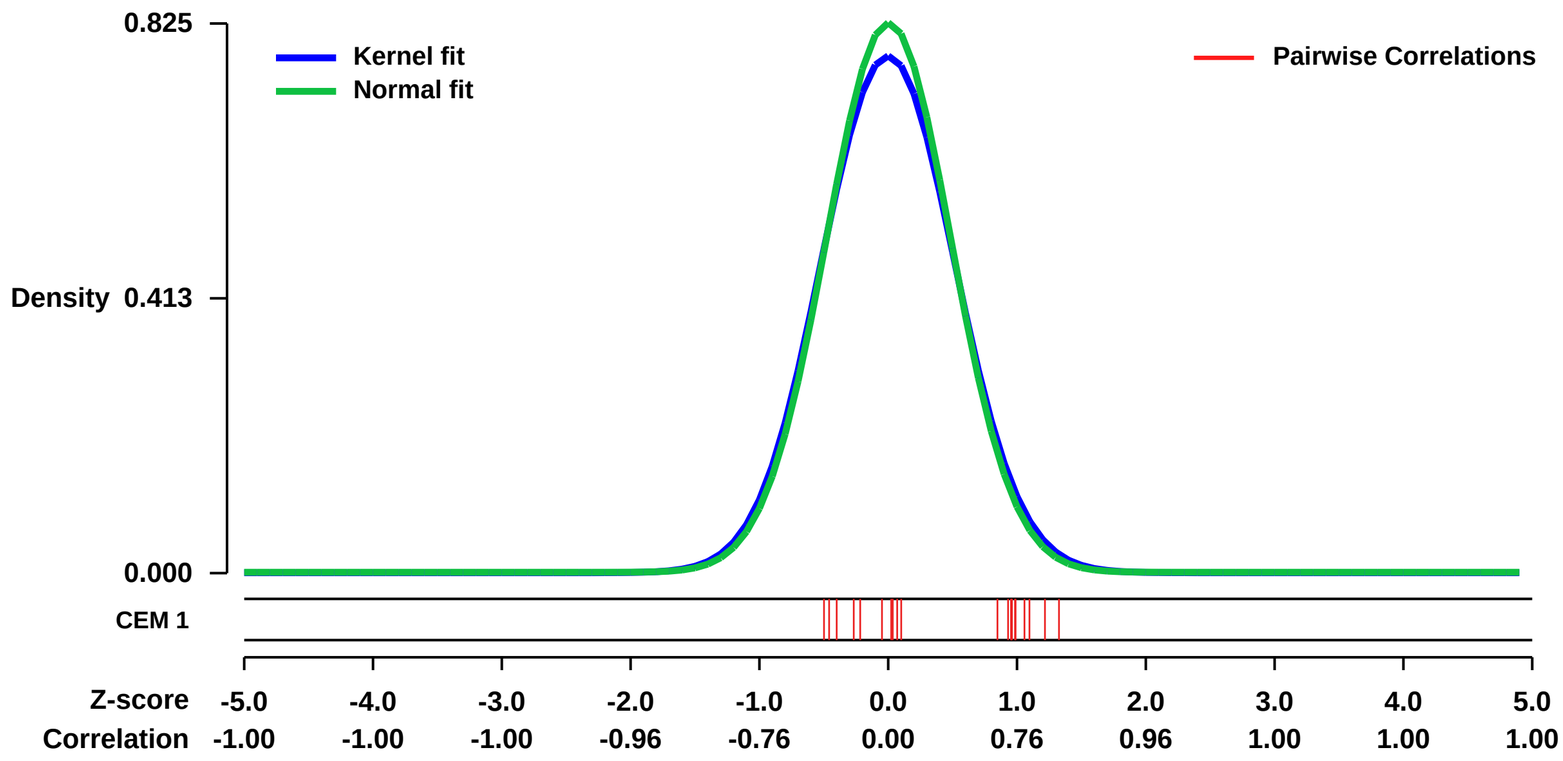

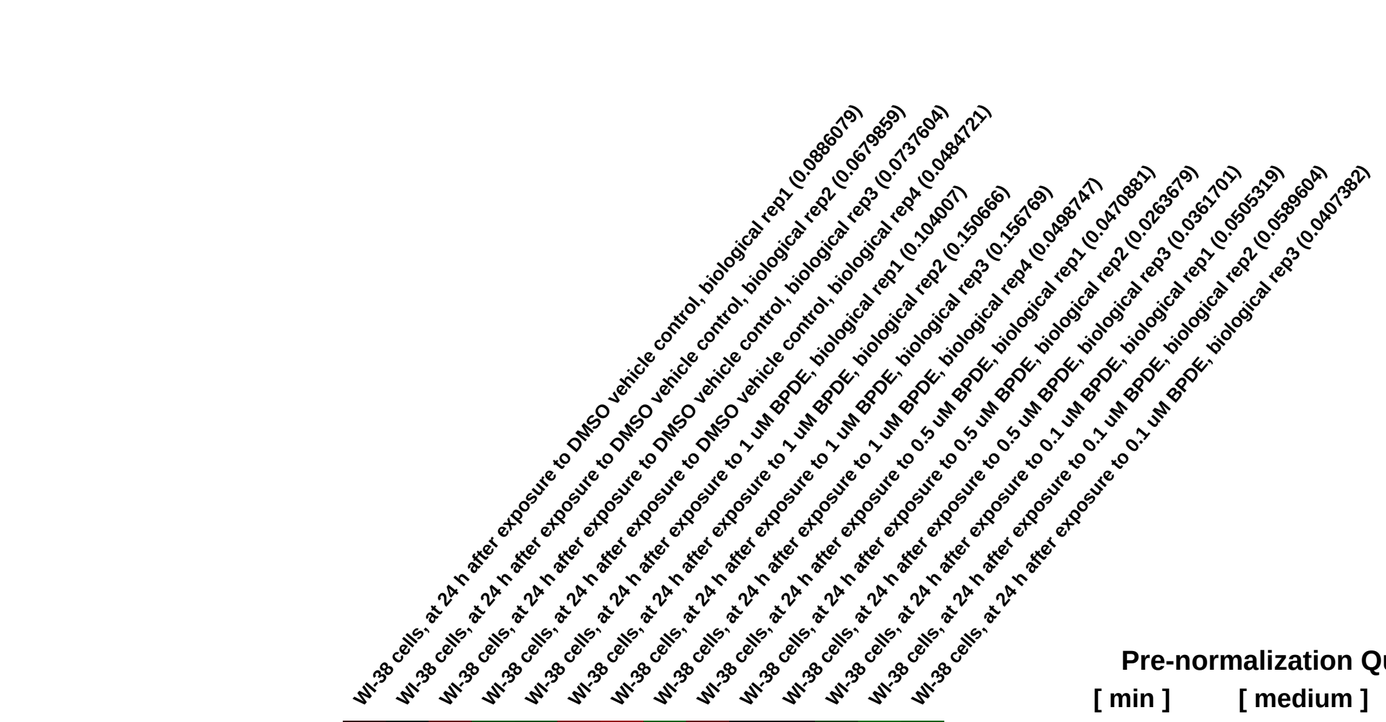

GEO Series "GSE58792" Expression Profiles

Num of samples in this series: 51

Scale of expression profile Z-scores

-3.0 -2.0 -1.0 0.0 1.0 2.0 3.0

GEO Link: http://www.ncbi.nlm.nih.gov/geo/query/acc.cgi?acc=GSE58792
Status: Public on Jul 01 2014
Title: Effects of soy supplementation on gene expression in breast cancer
Organism: Homo sapiens
Experiment type: Expression profiling by array
Platform: GPL570
Pubmed ID:

Summary & Design:

Summary:
Background There are conflicting reports on the impact of soy on breast carcinogenesis. This study examines the effects of soy supplementation on breast cancer-related genes and pathways. Methods Women (n = 140) with early-stage breast cancer were randomized to soy protein supplementation (n = 70) or placebo (n = 70) for 7 to 30 days, from diagnosis until surgery. Adherence was determined by plasma isoflavones: genistein and daidzein. Gene expression changes were evaluated by NanoString inin pre- and post-treatment tumor tissue. Genome-wide expression analysis was performed on post-treatment tissue. Proliferation (Ki67) and apoptosis (Cas3) were assessed by immunohistochemistry. Results Plasma isoflavones rose in the soy group (two-sided Wilcoxon rank-sum test, P < .001) and did not change in the placebo group. In paired analysis of pre- and post-treatment samples, 21 genes (out of 202) showed altered expression (two-sided Studentâ s t-test, P < .05). Several genes including FANCC and UGT2A1 revealed different magnitude and direction of expression changes between the two groups (two-sided Studentâ s t-test, P < .05). A high-genistein signature consisting of 126 differentially expressed genes was identified from microarray analysis of tumors. This signature was characterized by overexpression (>2 fold) of cell cycle transcripts, including those which promote cell proliferation, such as FGFR2, E2F5, BUB1, CCNB2, MYBL2, CDK1, and CDC20 (P < .01). Soy intake did not result in statistically significant changes in Ki67 or Cas3. Conclusions Gene expression associated with soy intake and high plasma genistein define a signature characterized by overexpression of FGFR2 and genes that drive cell cycle and proliferation pathways. These findings raise the concerns that in a subset of women soy could adversely affect gene expression in breast cancer.

Overall design:
Genome-wide expression analysis was performed on breast cancer tissue from women following treatment with soy (n=28) or placebo (n=23).

Background corr dist: KL-Divergence = 0.3313, L1-Distance = 0.0902, L2-Distance = 0.0254, Normal std = 0.2825

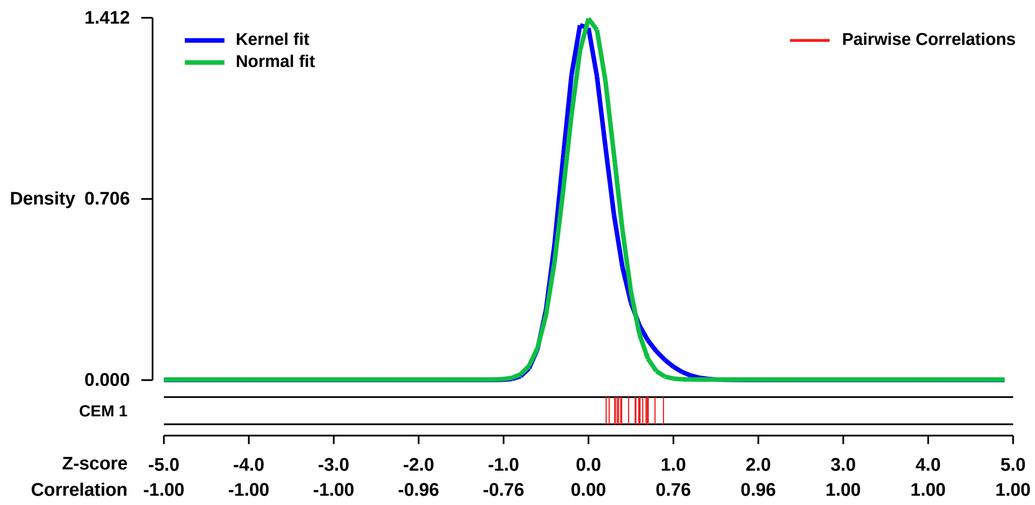

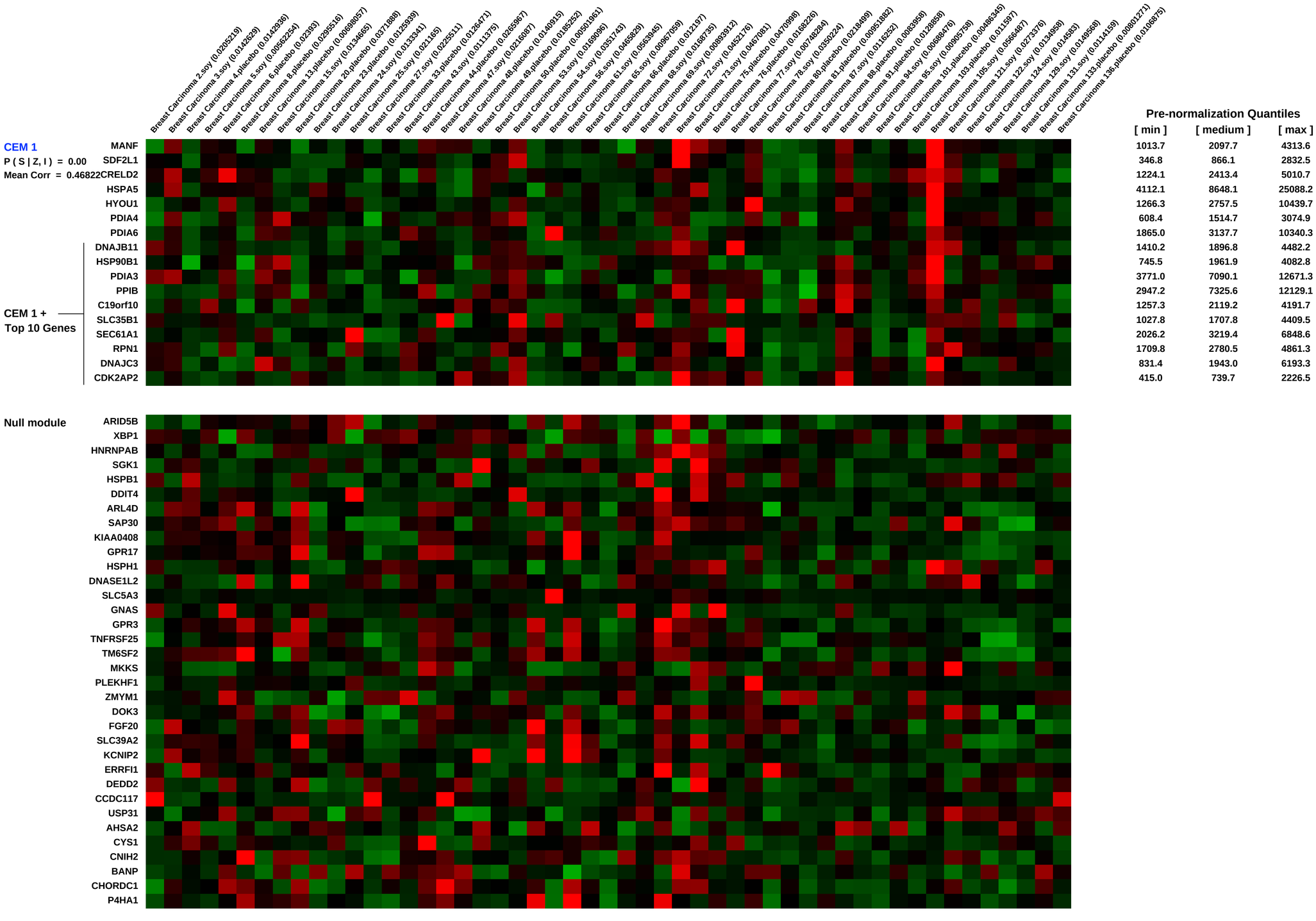

Pre-normalization Quantiles

[min]	[medium]	[max]
1013.7	2097.7	4313.6
346.8	866.1	2832.5
1224.1	2413.4	5010.7
4112.1	8648.1	25088.2
1266.3	2757.5	10439.7
608.4	1514.7	3074.9
1865.0	3137.7	10340.3
1410.2	1896.8	4482.2
745.5	1961.9	4082.8
3771.0	7090.1	12671.3
2947.2	7325.6	12129.1
1257.3	2119.2	4191.7
1027.8	1707.8	4409.5
2026.2	3219.4	6848.6
1709.8	2780.5	4861.3
831.4	1943.0	6193.3
415.0	739.7	2226.5

GEO Series "GSE10313" Expression Profiles

Num of samples in this series: 104

Details of this dataset are not shown due to large number of samples and the page size limit.

Find details in http://www.ncbi.nlm.nih.gov/geo/query/acc.cgi?acc=GSE10313

Background corr dist: KL-Divergence = 0.0652, L1-Distance = 0.0565, L2-Distance = 0.0053, Normal std = 0.5331

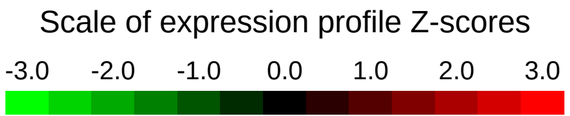

GEO Series "GSE22611" Expression Profiles

Num of samples in this series: 27

Scale of expression profile Z-scores

-3.0 -2.0 -1.0 0.0 1.0 2.0 3.0

GEO Link:	http://www.ncbi.nlm.nih.gov/geo/query/acc.cgi?acc=GSE22611
Status:	Public on Jan 01 2013
Title:	NOD2 and desease associated variant NOD2-L1007fsinsC dependent genomewide transcriptional regulation in stable Flp-In HEK cells
Organism:	Homo sapiens
Experiment type:	Expression profiling by array
Platform:	GPL570
Pubmed ID:	21335489
Summary & Design:	**Summary:** NOD2 is an intracellular receptor for the bacterial cell wall component muramyl dipeptide (MDP) and variants of NOD2 are associated with chronic inflammatory diseases of barrier organs e.g. Crohn disease, asthma and atopic eczema. It is known that activation of NOD2 induces a variety of inflammatory and antibacterial factors. The exact transcriptomal signatures that define the cellular programs downstream of NOD2 activation and the influence of the Crohn-associated variant L1007fsinsC are yet to be defined. To describe the MDP-induced activation program, we analyzed the transcriptomal reactions of isogenic HEK293 cells expressing NOD2wt or NOD2L1007fsinsC to stimulation with MDP. Importantly, a clear loss-of-function could be observed in the cells carrying the Crohn-associated variant L1007fsinsC, while the NOD2wt cells showed differential regulation of growth factors, chemokines and several antagonists of NF-¸”B, e.g. TNFAIP3 (A20) and IER3. **Overall design:** To elucidate the MDP-induced activation program we generated isogenic HEK293 cells stably expressing wildtype NOD2 or NOD2L1007fsinsC using a FRT-recombinase based approach. Cells carrying the inserted vector cassette were used as controls (mock-transfectant). To comprehensively analyze NOD2-mediated innate immune responses we analyzed transcriptomal signature patterns using genome-wide cDNA microarrays. Samples were harvested from cell cultures under normal growth conditions 0 h, 2 h and 6 h after MDPâ stimulation of the cells.

Background corr dist: KL-Divergence = 0.3786, L1-Distance = 0.0654, L2-Distance = 0.0118, Normal std = 0.2545

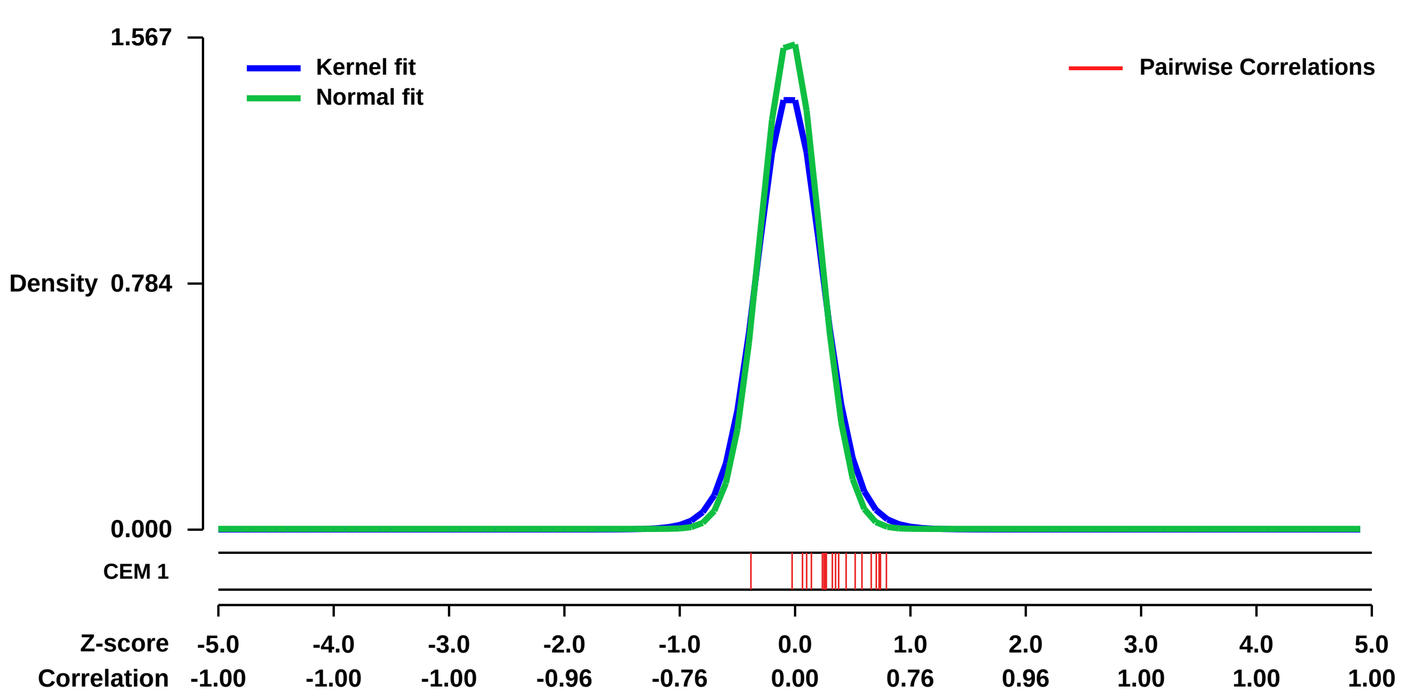

		Pre-normalization Quantiles		
		[min]	[medium]	[max]
CEM 1	MANF	3160.4	3999.4	4693.3
P (S | Z, I) = 0.00	SDF2L1	764.6	1184.7	1587.8
Mean Corr = 0.33641	CRELD2	1455.5	2357.3	3047.6
	HSPA5	10620.1	12179.4	14979.1
	HYOU1	804.2	1361.1	2349.0
	PDIA4	817.8	1077.2	1500.0
	PDIA6	9751.8	12244.7	14000.1
CEM 1 + Top 10 Genes	DNAJB11	3866.5	5264.7	8033.6
	HSP90B1	6915.0	8405.7	10317.5
	PDIA3	3837.3	6193.8	9545.9
	PPIB	9524.5	12620.2	14830.6
	C19orf10	2188.7	2654.5	3211.7
	SLC35B1	2178.3	2959.0	3893.4
	SEC61A1	1618.5	2205.9	4041.4
	RPN1	3344.9	4484.6	6953.3
	DNAJC3	1403.6	1613.3	1844.4
	CDK2AP2	214.2	353.8	499.3
Null module	ARID5B			
	XBP1			
	HNRNPAB			
	SGK1			
	HSPB1			
	DDIT4			
	ARL4D			
	SAP30			
	KIAA0408			
	GPR17			
	HSPH1			
	DNASE1L2			
	SLC5A3			
	GNAS			
	GPR3			
	TNFRSF25			
	TM6SF2			
	MKKS			
	PLEKHF1			
	ZMYM1			
	DOK3			
	FGF20			
	SLC39A2			
	KCNIP2			
	ERRFI1			
	DEDD2			
	CCDC117			
	USP31			
	AHSA2			
	CYS1			
	CNIH2			
	BANP			
	CHORDC1			
	P4HA1			

GEO Series "GSE28645" Expression Profiles

Num of samples in this series: 14

Scale of expression profile Z-scores

-3.0 -2.0 -1.0 0.0 1.0 2.0 3.0

GEO Link:	http://www.ncbi.nlm.nih.gov/geo/query/acc.cgi?acc=GSE28645
Status:	Public on Jan 11 2012
Title:	SRC1 gene regulation in endocrine resistant breast cancer cells
Organism:	Homo sapiens
Experiment type:	Expression profiling by array
Platform:	GPL570
Pubmed ID:	24648347
Summary & Design:	**Summary:** The development of breast cancer resistance to endocrine therapy results from an increase in cellular plasticity leading to the development of a steroid independent tumour. The p160 steroid coactivator protein SRC-1, through interactions with developmental proteins and other non-steroidal transcription factors drives this tumour adaptability. Here, using discovery studies we identify ADAM22, a non-protease member of the ADAMs family, as a direct target of SRC-1, independent of estrogen receptor(ER). Molecular, cellular, in vivo and clinical studies confirmed SRC-1 as a regulator of ADAM22 and established a role for ADAM22 in endocrine resistant tumour progression. ADAM22 has the potential to act as a therapeutic drug target and a companion predictive biomarker in the treatment of endocrine resistant breast cancer. **Overall design:** 14 samples representing 4 conditions were analysed. Samples were transfected with either a siRNA targetting SRC1 or a control scrambled siRNA. Samples were subject to tamoxifen treatment or untreated.

Background corr dist: KL-Divergence = 0.1238, L1-Distance = 0.0303, L2-Distance = 0.0015, Normal std = 0.4019

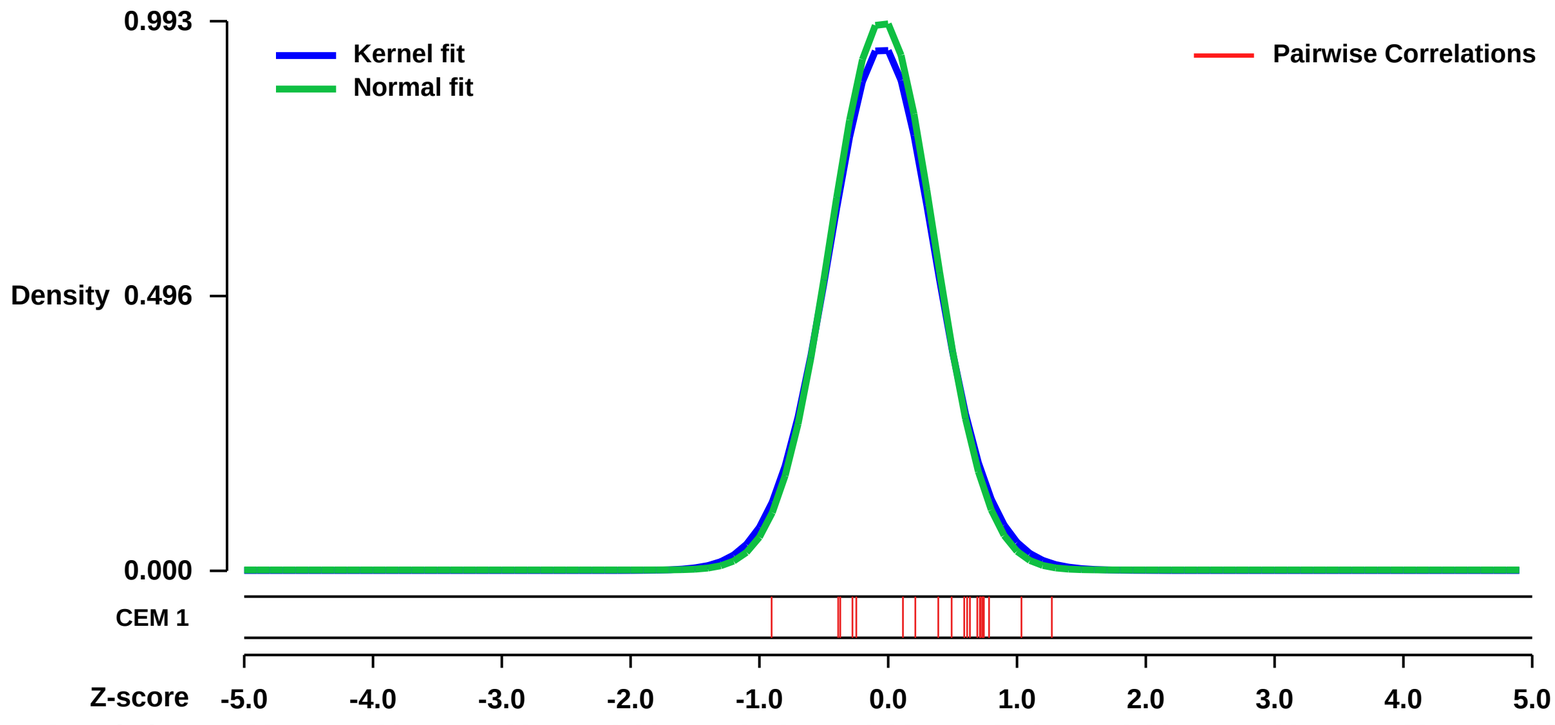

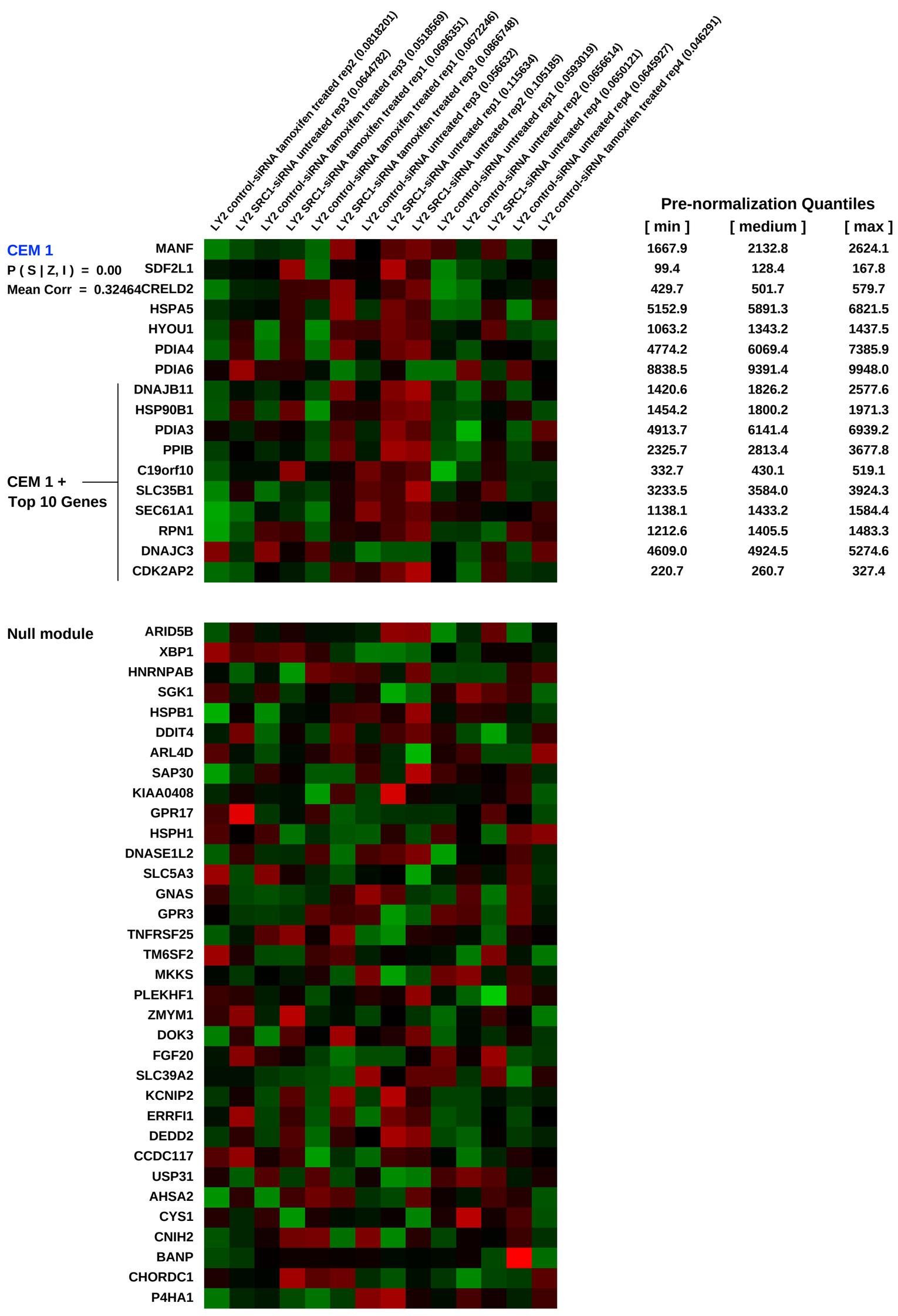

Pre-normalization Quantiles

	[min]	[medium]	[max]
MANF	1667.9	2132.8	2624.1
SDF2L1	99.4	128.4	167.8
CRELD2	429.7	501.7	579.7
HSPA5	5152.9	5891.3	6821.5
HYOU1	1063.2	1343.2	1437.5
PDIA4	4774.2	6069.4	7385.9
PDIA6	8838.5	9391.4	9948.0
DNAJB11	1420.6	1826.2	2577.6
HSP90B1	1454.2	1800.2	1971.3
PDIA3	4913.7	6141.4	6939.2
PPIB	2325.7	2813.4	3677.8
C19orf10	332.7	430.1	519.1
SLC35B1	3233.5	3584.0	3924.3
SEC61A1	1138.1	1433.2	1584.4
RPN1	1212.6	1405.5	1483.3
DNAJC3	4609.0	4924.5	5274.6
CDK2AP2	220.7	260.7	327.4

GEO Series "GSE21589" Expression Profiles

Num of samples in this series: 42

Scale of expression profile Z-scores

-3.0 -2.0 -1.0 0.0 1.0 2.0 3.0

GEO Link: http://www.ncbi.nlm.nih.gov/geo/query/acc.cgi?acc=GSE21589
Status: Public on Jun 01 2010
Title: The Relationship between Virus Replication and Host Gene Expression in Lymphatic Tissue during HIV-1 Infection
Organism: Homo sapiens
Experiment type: Expression profiling by array
Platform: GPL570
Pubmed ID: 20935203

Summary & Design:

Summary:
During HIV-1 infection, there is a massive perturbation of host gene expression, but as yet, genome-wide studies have not identified host genes affecting HIV-1 replication in lymphatic tissue, the primary site of virus-host interactions. In this study, we isolated RNA from the inguinal lymph nodes of 22 HIV-1-infected individuals and utilized a microarray approach to identify host genes critically important for viral replication in lymphatic tissue by examining gene expression associated with viral load. Strikingly, ~95% of the transcripts (558) in this data set (592 transcripts total) were negatively associated with HIV-1 replication. Genes in this subset (1) inhibit cellular activation/proliferation (ex.: TCFL5, SOCS5 and SCOS7, KLF10), (2) promote heterochromatin formation (ex.: HIC2, CREBZF, ZNF148/ZBP-89), (3) increase collagen synthesis (ex.: PLOD2, POSTN, CRTAP), and (4) reduce cellular transcription and translation. Potential anti-HIV-1 restriction factors were also identified (ex.: NR3C1, HNRNPU, PACT). Only ~5% of the transcripts (34) were positively associated with HIV-1 replication. Paradoxically, nearly all these genes function in innate and adaptive immunity, particularly highlighting a heightened interferon system. The predominance of negative correlations as well as the disconnect between host defenses and viral load point to the importance of genes that regulate target cell activation and genes that code for potentially new restriction factors as determinants of viral load rather than conventional host defenses.

Overall design:
Total RNA was isolated from the inguinal lymph nodes of 22 HIV-1-infected subjects at different clinical stages (and varying viral loads) and prepared for RNA extraction and hybridization on Affymetrix Human Genome U133 Plus 2.0 microarrays. Replicate arrays were performed for lymph node samples to minimize assay noise and host genes critically important for viral replication in lymphatic tissue were identified by examining gene expression and its association with viral load. Replicates were not performed for samples WB91 and TS35 due to limited amounts of biomaterial.

Background corr dist: KL-Divergence = 0.2207, L1-Distance = 0.0591, L2-Distance = 0.0088, Normal std = 0.3194

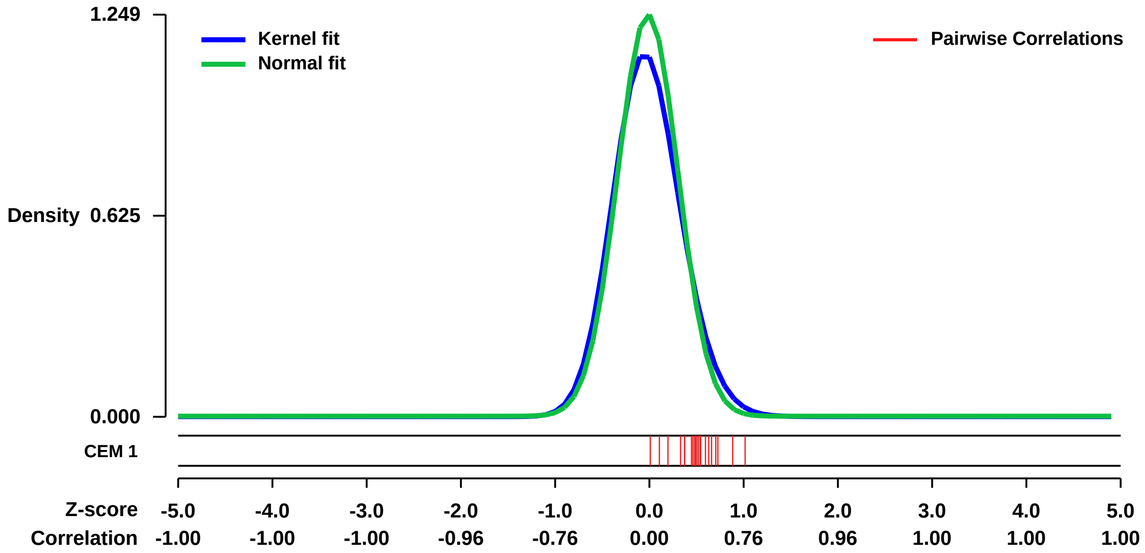

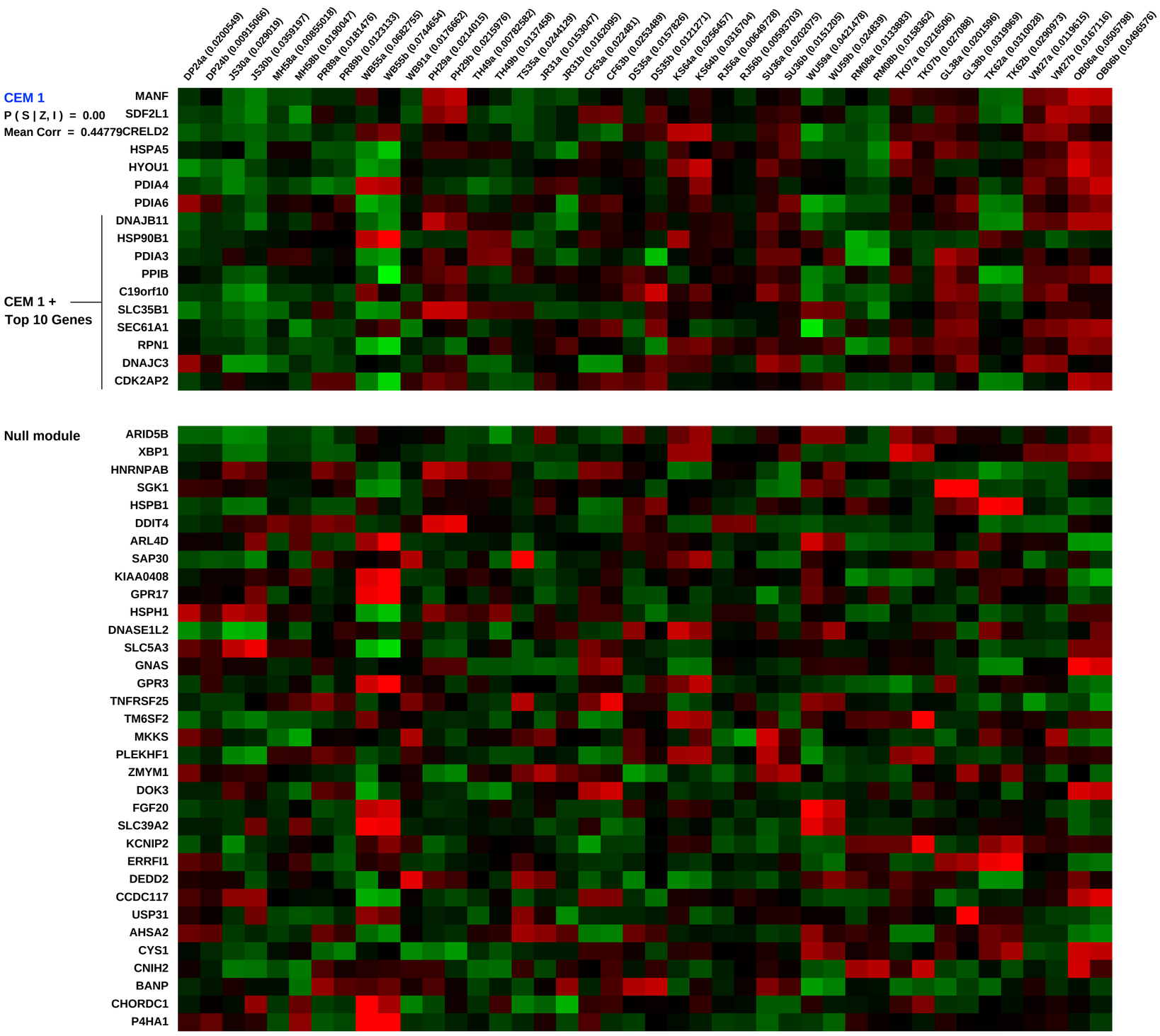

Pre-normalization Quantiles

[min]	[medium]	[max]
1409.5	1944.1	2836.4
426.3	590.6	818.3
1715.0	2381.1	3366.2
3280.4	4712.4	6037.7
1704.8	2321.8	3291.1
746.5	980.2	1393.9
1958.0	3070.8	3848.5
1494.5	1900.8	2455.4
468.3	1447.4	3262.9
2770.2	3992.9	5006.0
1993.2	3681.8	4587.1
1141.2	1621.8	2403.7
734.8	911.3	1161.4
758.4	1016.5	1211.4
864.8	1484.9	1855.5
1355.3	1998.2	2664.9
403.5	843.6	1242.2

GEO Series "GSE44946" Expression Profiles

Num of samples in this series: 9

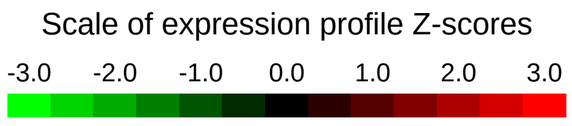

GEO Link:	http://www.ncbi.nlm.nih.gov/geo/query/acc.cgi?acc=GSE44946
Status:	Public on Mar 10 2013
Title:	Expression data by BRD7552 treatment in PANC-1 cells
Organism:	Homo sapiens
Experiment type:	Expression profiling by array
Platform:	GPL570
Pubmed ID:	24290880
Summary & Design:	**Summary:** Three master regulatory transcription factors Pdx1, MafA and Ngn3 have the ability to transdifferentiate pancreatic acinar cells to insulin-producing beta cells in mice. BRD7552 was identified as a small-molecule inducer that can upregulate the expression of Pdx1 in PANC-1 cells by high-throughput qPCR screening. We used microarrays to illustrate the mechnism of BRD7552 for PDX1 and insulin induction. **Overall design:** PANC-1 cells were treated with BRD7552 at 5uM, the mininal concentration for the maximal induction of Pdx1. The RNA was isloated at two time points 6-hour and 72-hour.

Background corr dist: KL-Divergence = 0.0666, L1-Distance = 0.0187, L2-Distance = 0.0004, Normal std = 0.5091

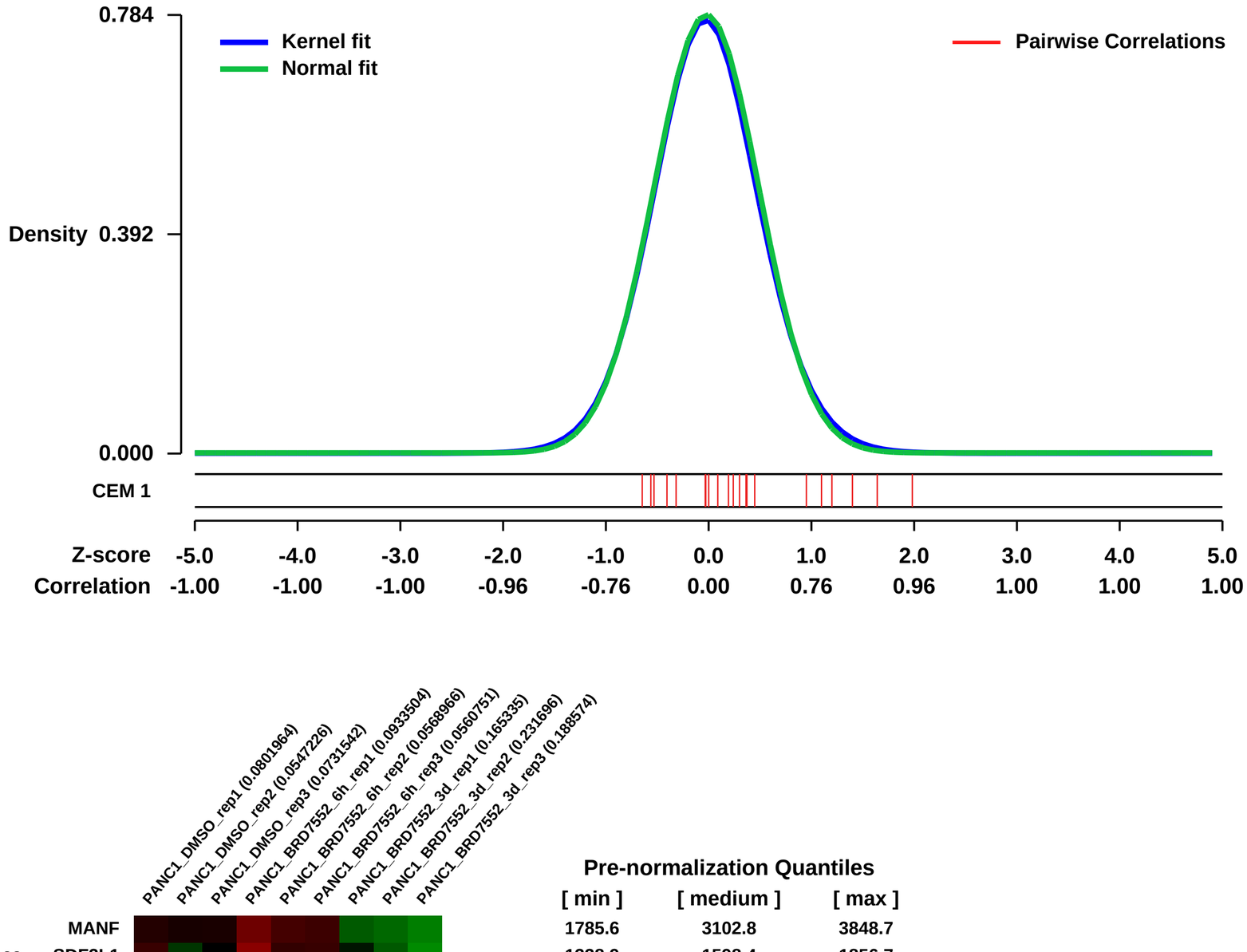

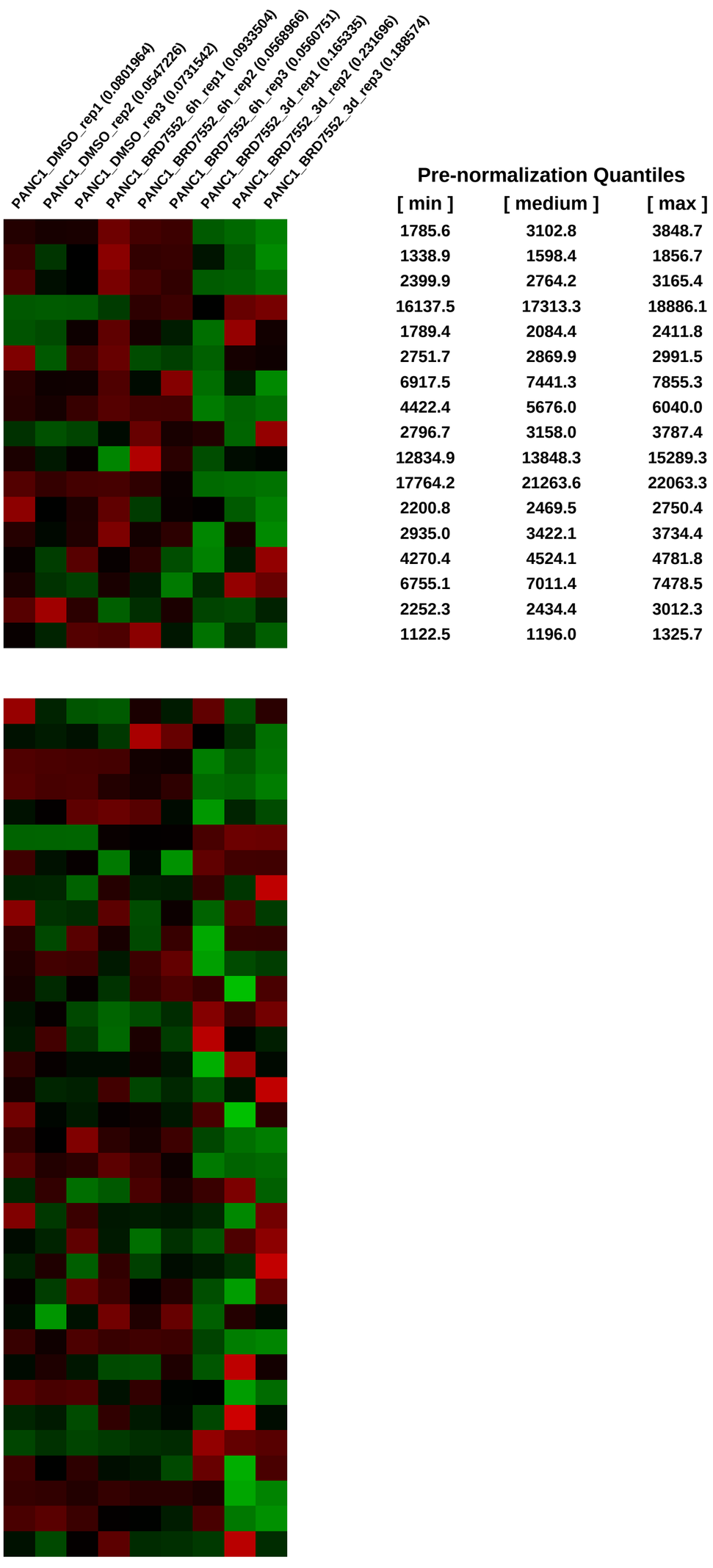

GEO Series "GSE27444" Expression Profiles

Num of samples in this series: 14

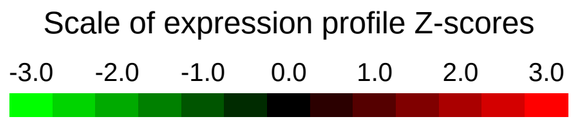

GEO Link:	http://www.ncbi.nlm.nih.gov/geo/query/acc.cgi?acc=GSE27444
Status:	Public on Jul 18 2011
Title:	Expression data from zinc-finger-transcription-factor-induced Fulvestrant-Resistant MCF7 Cell Lines
Organism:	Homo sapiens
Experiment type:	Expression profiling by array
Platform:	GPL570
Pubmed ID:	21818254
Summary & Design:	**Summary:** Multiple gene expression studies have demonstrated that breast cancer biological diversity is associated with distinct transcriptional programs. Transcription factors, because of their unique ability to coordinate the expression of multiple genes, are speculated to play a role in generating phenotypic plasticity associated with cancer progression including acquired drug resistance. Combinatorial libraries of artificial zinc-finger transcription factors (ZF-TFs) provide a robust means for inducing and understanding various functional components of the cancer phenotype. Herein, we utilized combinatorial ZF-TF library technology to better understand how breast cancer cells acquire resistance to a fulvestrant, a clinically important anti-endocrine therapeutic agent. We isolated six ZF-TF library members capable of inducing stable, long-term anti-endocrine drug-resistance in two independent estrogen receptor positive breast cancer cell lines. Comparative gene expression profile analysis of the ZF-TF-transduced breast cancer cell lines revealed a 72-gene cluster that constituted a common signature for the fulvestrant-resistance phenotype. Pathway enrichment-analysis of gene expression data revealed that the ZF-TF-induced fulvestrant resistance is associated with an estrogen receptor negative-like gene set and four unique myb-regulated gene sets. Furthermore, we identified a set of genes strongly expressed in the ZF-TF-induced fulvestrant-resistant cells that was correlated with a lower probability of distant metastasis-free or death-from-relapse-free survival of breast cancer patients. **Overall design:** MCF7-R73 cells, a monoclonal MCF7 subline that is highly sensitive to fulvestrant-induced cytocidal activity, underwent retroviral transduction with the zinc finger transcription factor (ZF-TF) activator library or with a control plasmid encoding only the NF-kB p65 activation domain. Both populations of cells were enriched for transduced cells by selecting for growth in puromycin and for fulvestrant-resistant cells by selecting with 100 nM fulvestrant. After 6 weeks of continuous treatment with fulvestrant, hundreds of drug-resistant colonies emerged from the population of cells infected with the ZF-TF activator library. By contrast, as expected, the control MCF7cell line transduced by NF-kB p65-only underwent massive cell death resulting in the complete absence of resistant colonies. DNA encoding the zinc-finger arrays was rescued by PCR from genomic DNA of pooled fulvestrant-resistant cells. The sequences of the ZF-TFs were determined and 46 unique ZF-TF clones identified. These 46 unique ZF-TFs were re-cloned into the retroviral vector and converted into clonal virus stocks that were used to transduce MCF7-R73 cells. These 46 retrovirally transduced cell populations were then challenged with fulvestrant. As compared with the control MCF-238 cells, MCF7-R73 cells transduced with six unique ZF-TFs demonstrated survival and growth in the presence of 100nM fulvestrant.

Background corr dist: KL-Divergence = 0.1698, L1-Distance = 0.0419, L2-Distance = 0.0037, Normal std = 0.3550

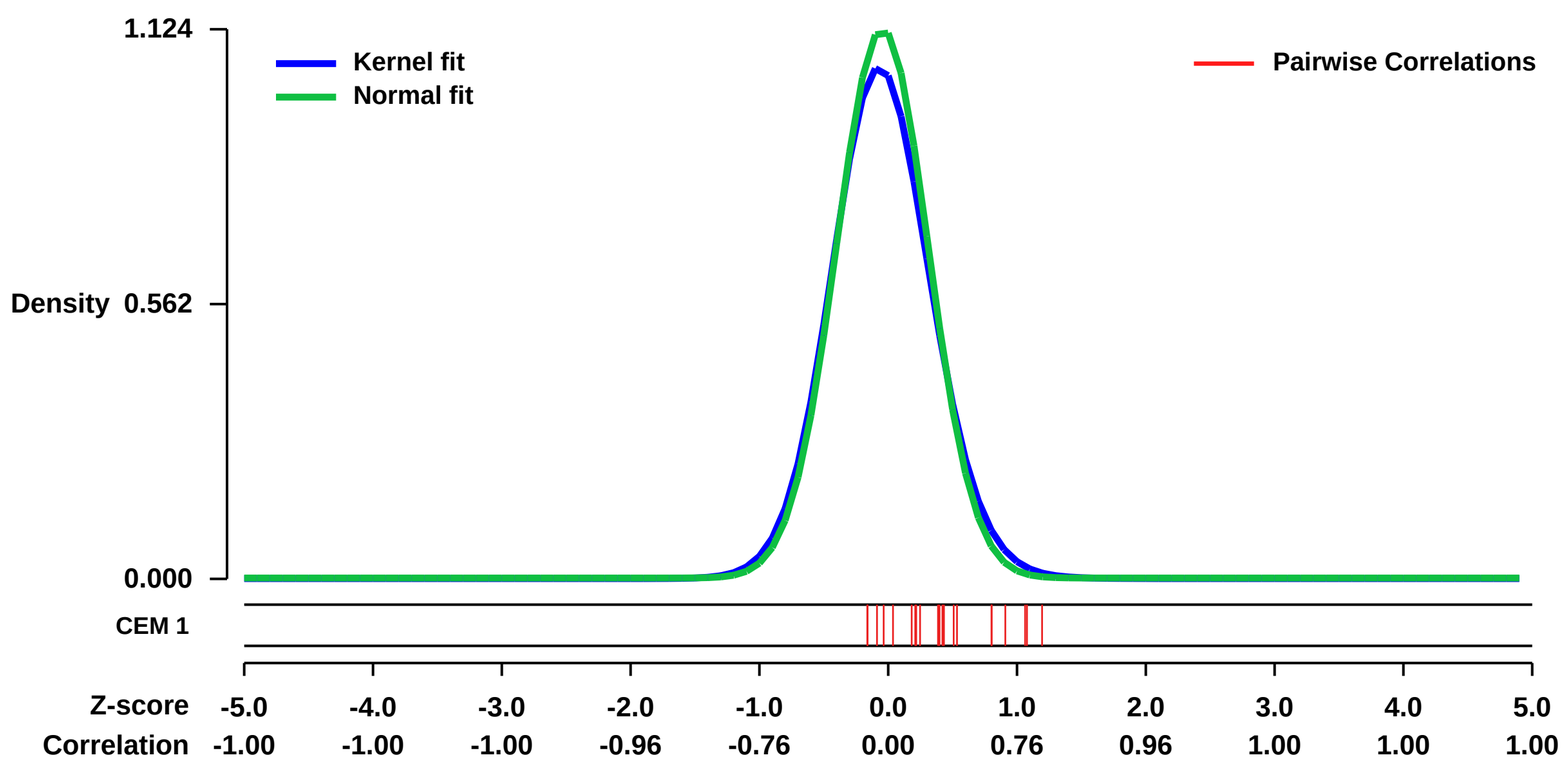

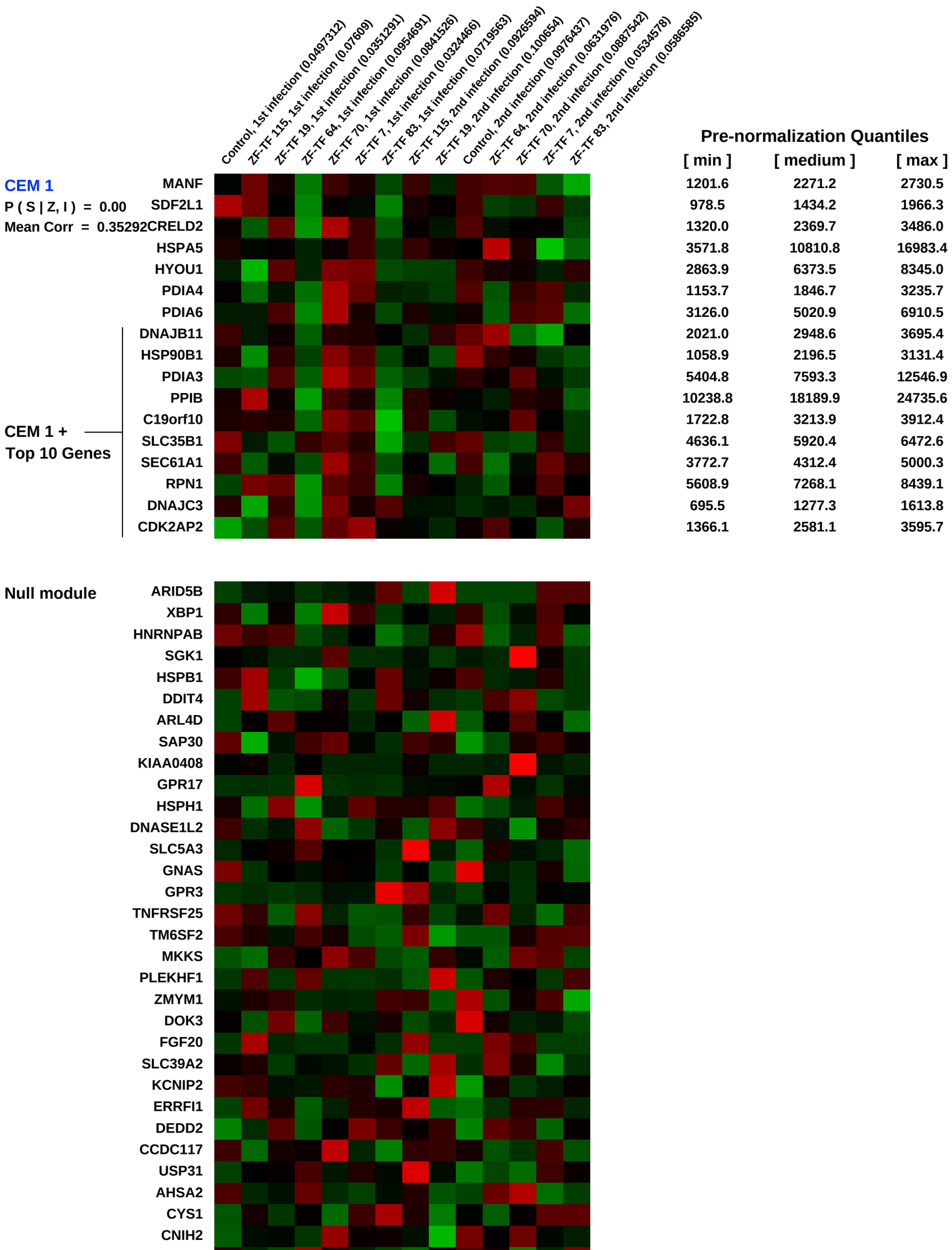

GEO Series "GSE31534" Expression Profiles

Num of samples in this series: 51

Scale of expression profile Z-scores

-3.0 -2.0 -1.0 0.0 1.0 2.0 3.0

GEO Link:	http://www.ncbi.nlm.nih.gov/geo/query/acc.cgi?acc=GSE31534
Status:	Public on Mar 15 2012
Title:	Gene expression profile in A375 melanoma cells after 45 functionally important molecules were knocked down using siRNA
Organism:	Homo sapiens
Experiment type:	Expression profiling by array
Platform:	GPL570
Pubmed ID:	22536322
Summary & Design:	**Summary:** Affymetrix microarray data were generated from A375 melanoma cells treated in vitro with siRNAs against 45 transcription factors and signalling molecules. **Overall design:** 45 functionally important molecules were knocked down in A375 melanoma cells by siRNA. Then the gene expression profiles of these A375 cells, along with untreated cells and sRNA control treated cells were analysed by microarrays.

Background corr dist: KL-Divergence = 0.2201, L1-Distance = 0.0351, L2-Distance = 0.0021, Normal std = 0.3281

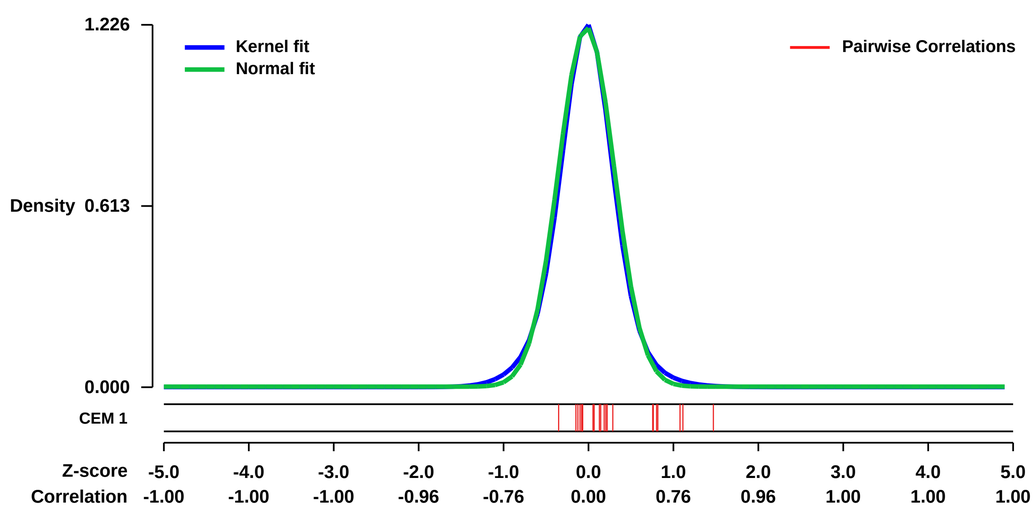

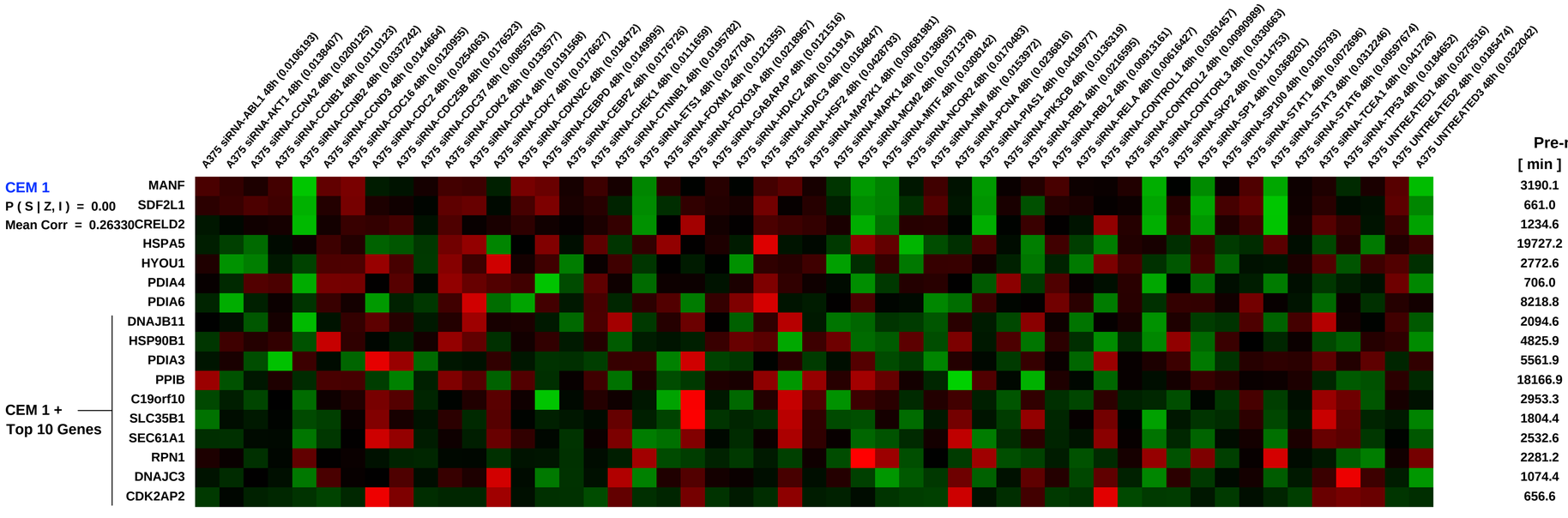

Pre-normalization Quantiles

[min]	[medium]	[max]
3190.1	5642.0	6744.3
661.0	1184.4	1420.4
1234.6	2460.4	3257.8
19727.2	23016.0	27440.8
2772.6	3870.8	5155.9
706.0	1104.7	1396.9
8218.8	9780.7	11618.4
2094.6	2615.7	3112.4
4825.9	6084.0	7572.4
5561.9	7439.1	9841.7
18166.9	23441.4	27192.2
2953.3	4057.3	5524.3
1804.4	2287.2	3247.2
2532.6	3552.0	5430.8
2281.2	2908.7	4703.0
1074.4	1507.0	2269.3
656.6	750.5	1440.3

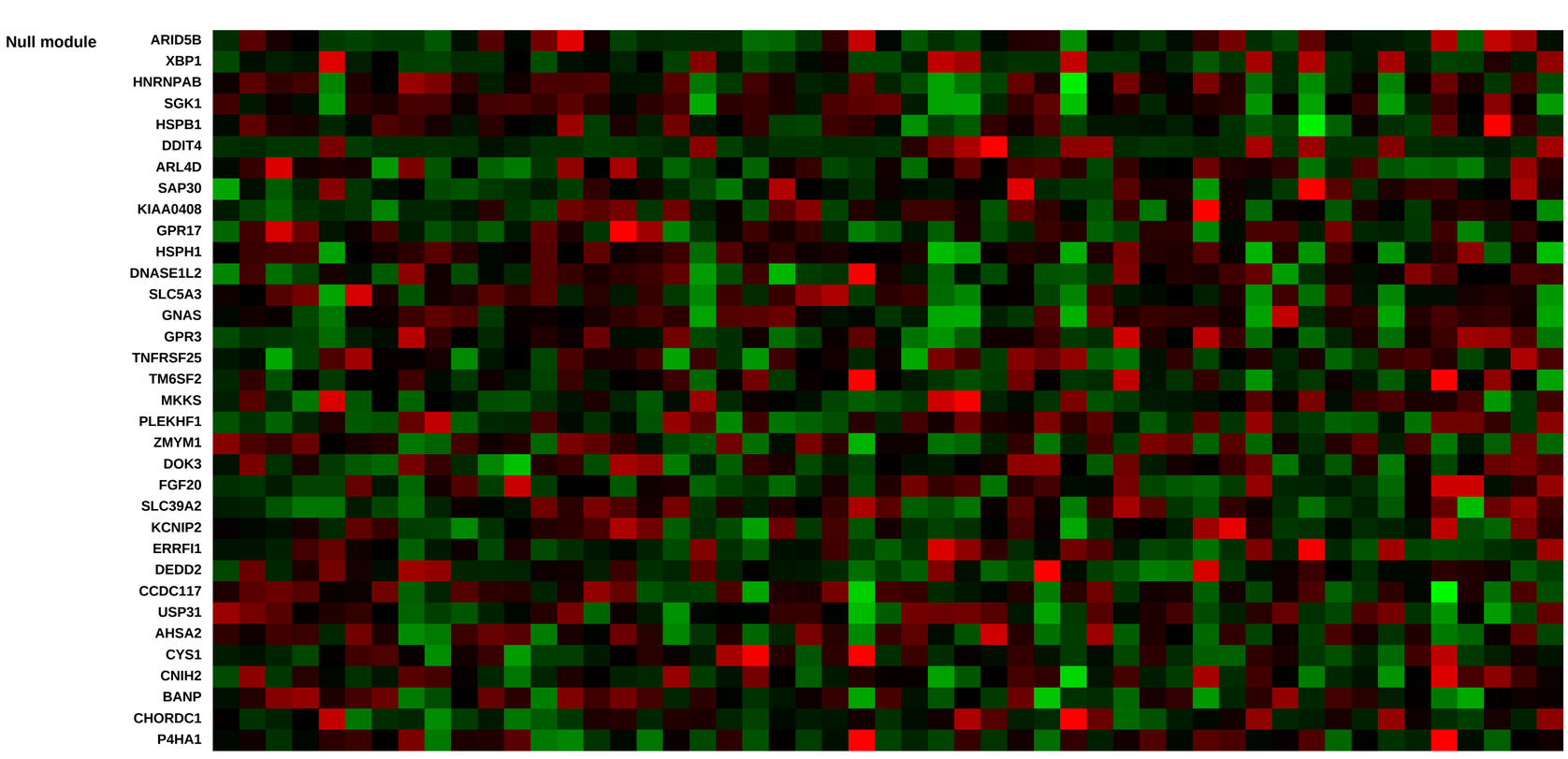

GEO Series "GSE59957" Expression Profiles

Num of samples in this series: 6

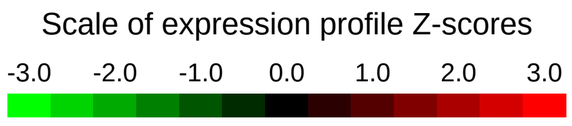

GEO Link:	http://www.ncbi.nlm.nih.gov/geo/query/acc.cgi?acc=GSE59957
Status:	Public on Aug 01 2014
Title:	Identification of lncRNA-NTT regulated genes using small interference RNA knockdown for cDNA microarray
Organism:	Homo sapiens
Experiment type:	Expression profiling by array
Platform:	GPL570
Pubmed ID:	
Summary & Design:	**Summary:** We used microarrays to detail the global programme of gene expression underlying lncRNA-NTT knockdown We employed small interference RNA (siRNA) and microarray techniques to investigate the effect of NTT silencing on gene expression in HepG2 cells. **Overall design:** HepG2 cells were transfected with NTT siRNA (siNTT) or control siRNA (siCon) for 120 h, and then RNA extraction and cDNA synthesis for hybridization on Affymetrix microarrays. We collect siRNA-transfection HepG2 cells and test knockdown efficiency. After comparison of the siCon group then we choose the best three sample for microarray.

Background corr dist: KL-Divergence = 0.0281, L1-Distance = 0.0239, L2-Distance = 0.0006, Normal std = 0.6892

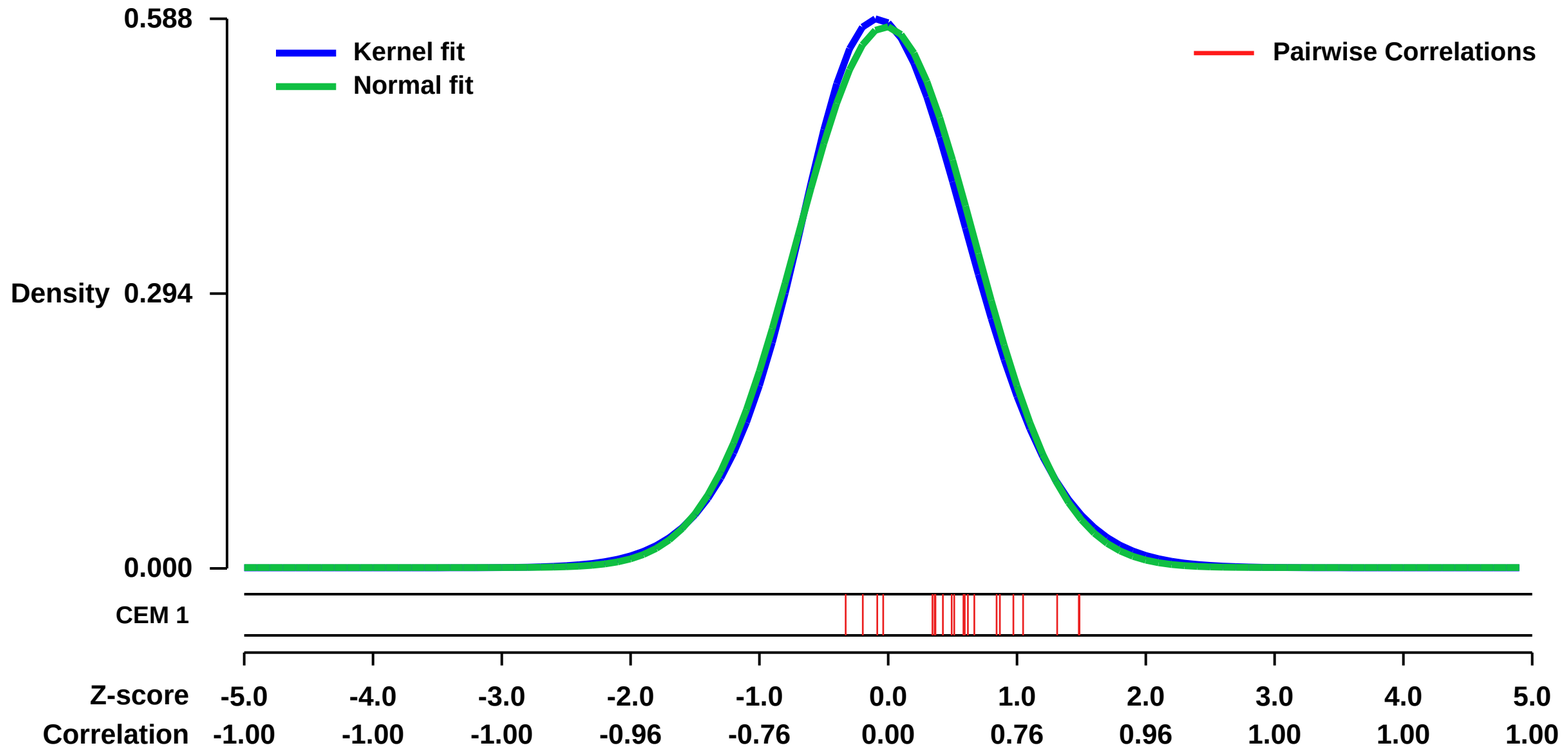

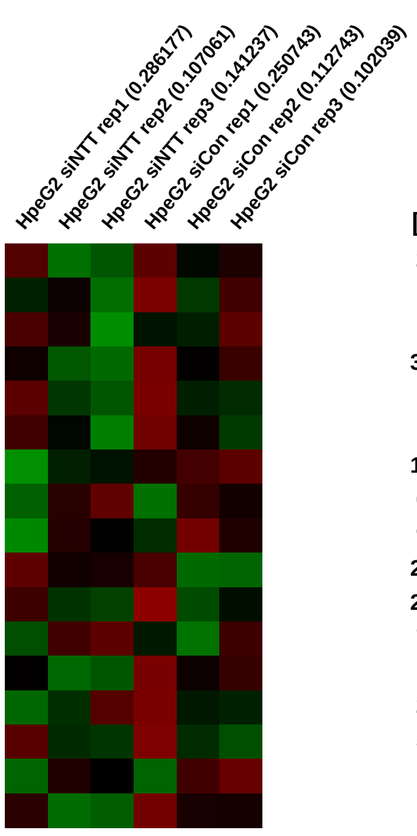

Pre-normalization Quantiles

		[min]	[medium]	[max]
CEM 1	MANF	2449.2	3094.8	3389.4
P (S | Z, I) = 0.00	SDF2L1	383.4	574.6	743.0
Mean Corr = 0.45227	CRELD2	391.0	623.4	715.3
	HSPA5	32265.4	34626.5	36631.2
	HYOU1	1872.2	2281.9	3415.1
	PDIA4	1863.6	2597.7	3110.0
	PDIA6	12104.9	15558.8	16672.2
CEM 1 + Top 10 Genes	DNAJB11	6596.0	11620.3	13504.2
	HSP90B1	9352.0	12506.8	14075.0
	PDIA3	20237.0	23376.7	25066.9
	PPIB	27693.7	31154.5	39943.5
	C19orf10	7887.5	8907.9	9084.9
	SLC35B1	1273.7	1652.5	2007.2
	SEC61A1	2127.6	2384.4	2856.7
	RPN1	5831.6	6231.7	7993.6
	DNAJC3	1265.6	1848.9	2149.4
	CDK2AP2	710.1	990.4	1187.1
Null module	ARID5B			
	XBP1			
	HNRNPAB			
	SGK1			
	HSPB1			
	DDIT4			
	ARL4D			
	SAP30			
	KIAA0408			
	GPR17			
	HSPH1			
	DNASE1L2			
	SLC5A3			
	GNAS			
	GPR3			
	TNFRSF25			
	TM6SF2			
	MKKS			
	PLEKHF1			
	ZMYM1			
	DOK3			
	FGF20			
	SLC39A2			
	KCNIP2			
	ERRFI1			
	DEDD2			
	CCDC117			
	USP31			
	AHSA2			
	CYS1			
	CNIH2			
	BANP			
	CHORDC1			
	P4HA1			

GEO Series "GSE11581" Expression Profiles

Num of samples in this series: 8

Scale of expression profile Z-scores

-3.0 -2.0 -1.0 0.0 1.0 2.0 3.0

GEO Link:	http://www.ncbi.nlm.nih.gov/geo/query/acc.cgi?acc=GSE11581
Status:	Public on Aug 17 2009
Title:	Role of FAK, dominant-negative FAK, FAK-CD and FAKsiRNA in MCF-7 human breast cancer cell tumorigenesis
Organism:	Homo sapiens
Experiment type:	Expression profiling by array
Platform:	GPL570
Pubmed ID:	19671193
Summary & Design:	**Summary:** Focal adhesion kinase (FAK) is a non-receptor tyrosine kinase that plays an important role in proliferation, motility, adhesion, invasion, angiogenesis, and survival signaling. Focal adhesion kinase has been shown to be overexpressed in many types of tumors, including breast cancer at early stages of tumorigenesis. To study the biological role of FAK in breast tumorigenesis, we used FAKsiRNA to down-regulate FAK in MCF-7 cell lines. **Overall design:** Eight samples were analyzed in MCF-7, MCF-7-Vector, MCF-7 control (luciferase) siRNA and FAKsiRNA#1, FAKsiRNA#2

Background corr dist: KL-Divergence = 0.0330, L1-Distance = 0.0148, L2-Distance = 0.0002, Normal std = 0.6341

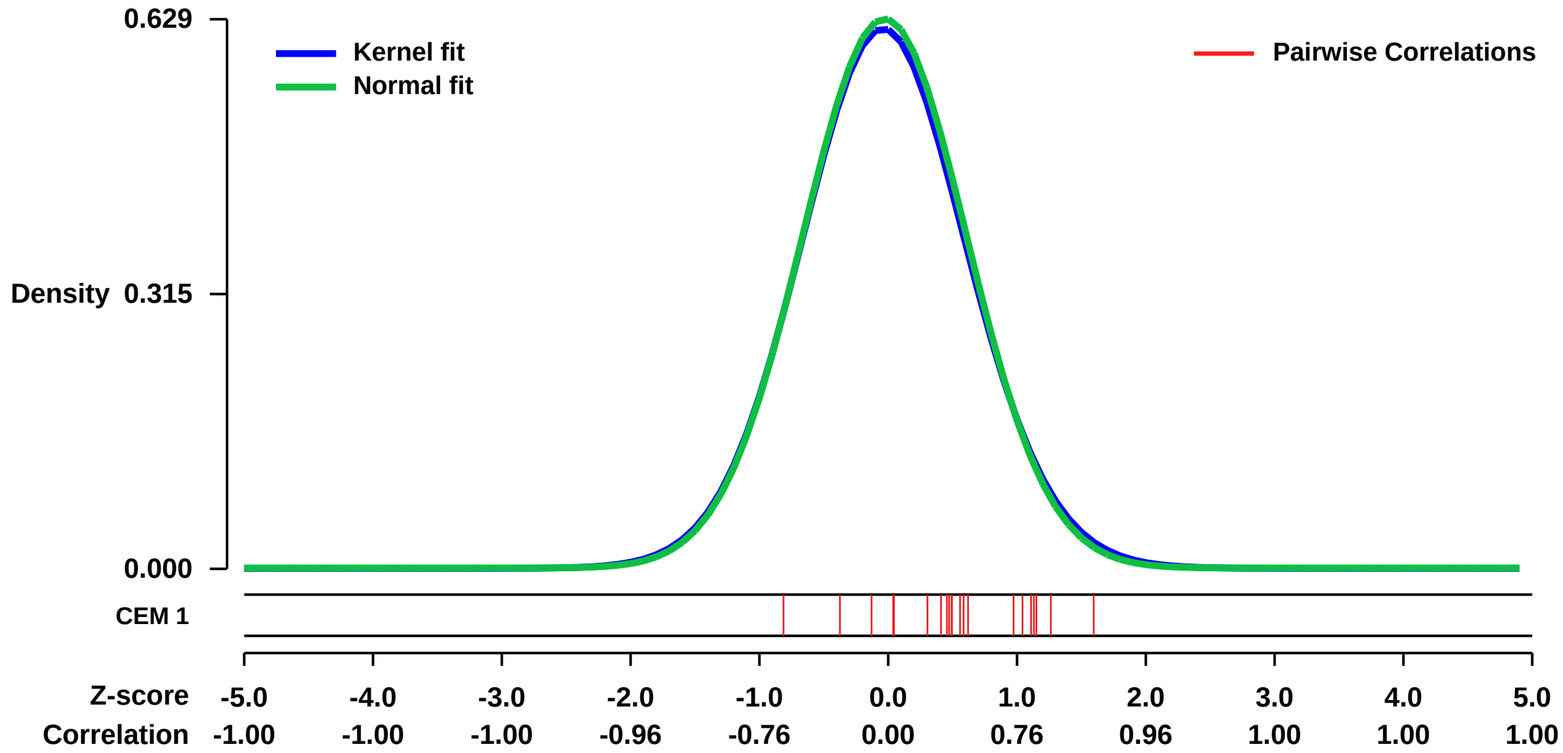

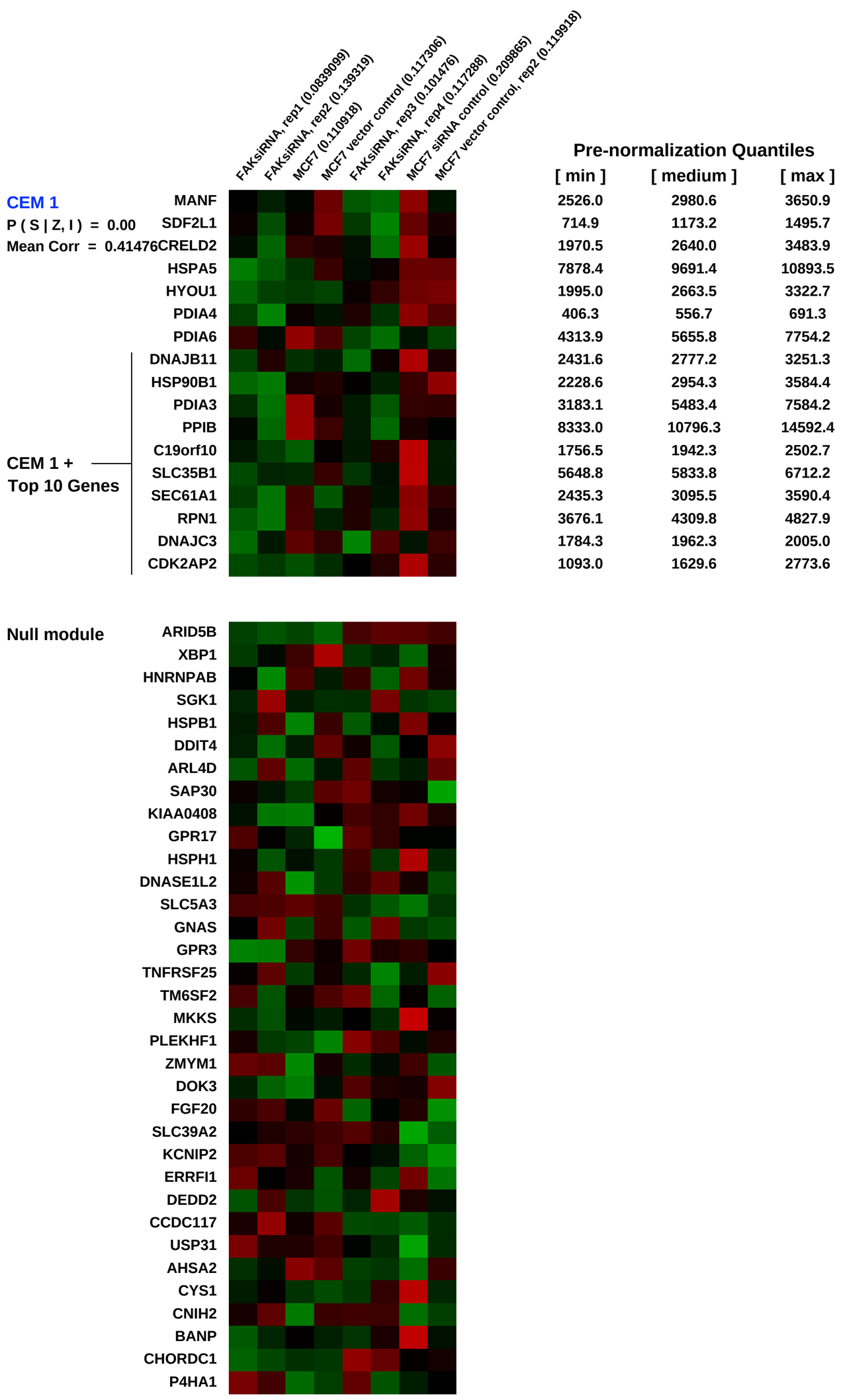

GEO Series "GSE16066" Expression Profiles

Num of samples in this series: 6

Scale of expression profile Z-scores

-3.0 -2.0 -1.0 0.0 1.0 2.0 3.0

GEO Link:	http://www.ncbi.nlm.nih.gov/geo/query/acc.cgi?acc=GSE16066
Status:	Public on Sep 08 2009
Title:	Networking of differentially expressed genes in CaCo2 human colon cancer cells resistant to methotrexate
Organism:	Homo sapiens
Experiment type:	Expression profiling by array
Platform:	GPL570
Pubmed ID:	19732436
Summary & Design:	**Summary:** **A summary of the work associated to these microarrays is the following:** **The need for an integrated view of all data obtained from high-throughput technologies gave rise to network analyses. These are especially useful to rationalize phenomena in terms of how external perturbations propagate through the expression of genes. To address this issue in the case of drug resistance, we constructed Biological Association Networks of genes differentially expressed in cell lines resistant to methotrexate (MTX). Seven cell lines representative of different types of cancer including colon cancer (HT29 and Caco2), breast cancer (MCF7 and MDA-MB-468), pancreatic cancer (MIA PaCa-2), erythroblastic leukemia (K562) and osteosarcoma (Saos-2), were used. The differential expression pattern between sensitive and MTX-resistant cells was determined by microarrays covering the whole human genome and analyzed with the GeneSpring GX software package, v.7.3.1. Genes deregulated in common in the two colon cancer cell lines studied, were subject of Biological Association Networks construction. Dikkopf homolog-1 (DKK1) was a clear node of this network, and functional validations of this target using a siRNA showed a chemosensitization toward MTX. Members of the UDP-glucuronosyltransferase 1A (UGT1A) family formed a network of differentially expressed genes in the two breast cancer cell lines studied. siRNA treatment against UGT1A showed also an increase in MTX sensitivity. Eukaryotic translation elongation factor 1 alpha 1 (EEF1A1) was a gene overexpressed in common among the pancreatic cancer, leukemia and osteosarcoma cell lines, and siRNA treatment against EEF1A1 produced a chemosensitization toward MTX. Biological Association Networks identified DKK1, UGT1As and EEF1A1 as important gene nodes in MTX-resistance. Treatments using iRNA technology against these three genes show chemosensitization toward MTX.** **Overall design:** **Two cell lines are compared, which are Caco2 colon cancer cells sensitive to methotrexate and Caco2 cells resistant to 10e-5M MTX. Six samples are provided, which correspond to triplicates of each cell line. The samples provided were analyzed using the specific software GeneSpring GX.**

Background corr dist: KL-Divergence = 0.0396, L1-Distance = 0.0303, L2-Distance = 0.0011, Normal std = 0.6307

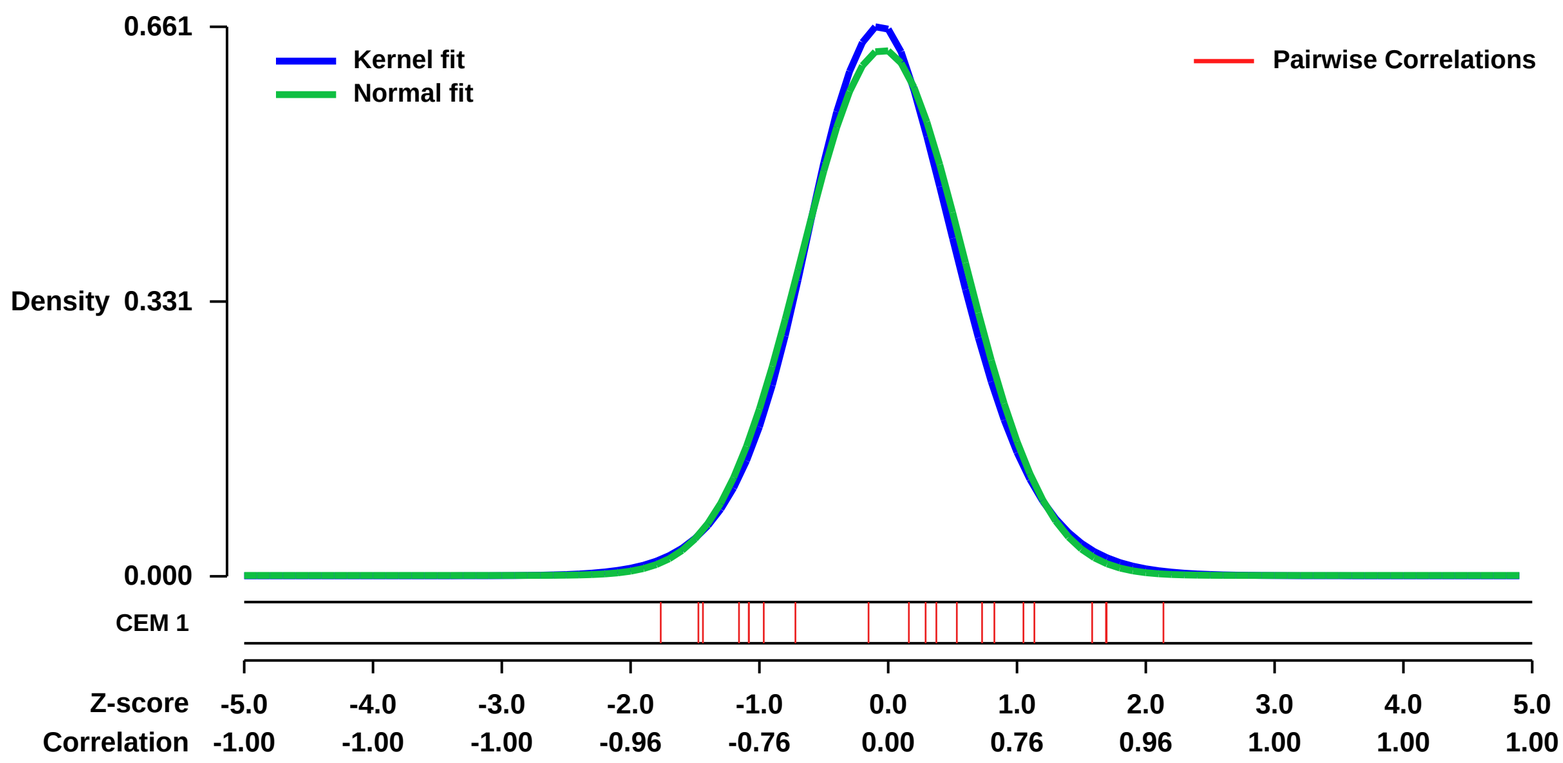

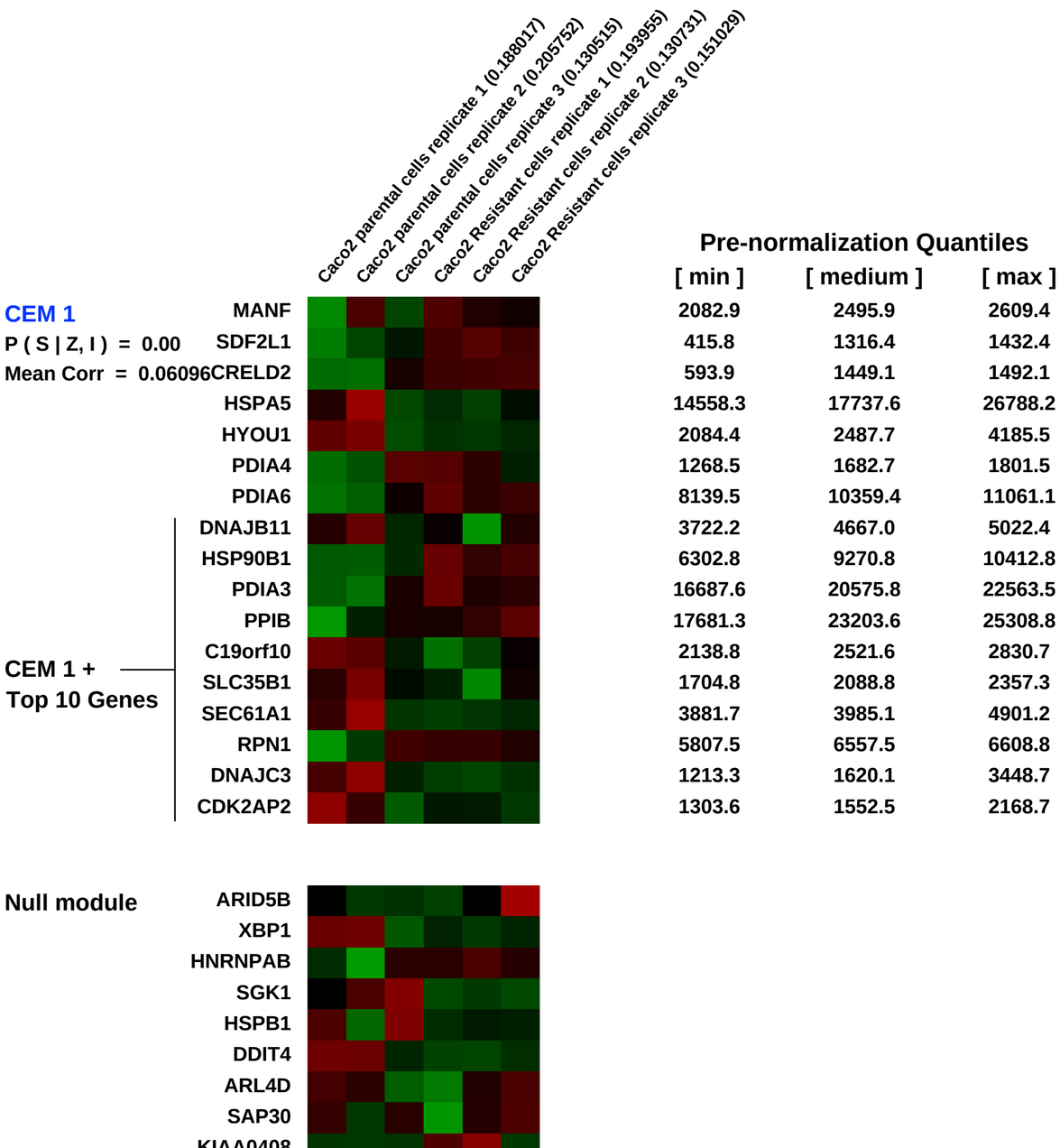

GEO Series "GSE9649" Expression Profiles

Num of samples in this series: 30

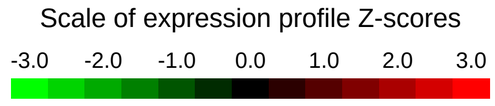

GEO Link:	http://www.ncbi.nlm.nih.gov/geo/query/acc.cgi?acc=GSE9649
Status:	Public on Dec 18 2008
Title:	Expression studies of HMEC exposed to lactic acidosis and hypoxia
Organism:	Homo sapiens
Experiment type:	Expression profiling by array
Platform:	GPL570
Pubmed ID:	19057672
Summary & Design:	**Summary:** Human Mammalian Epithelial Cells (HMEC) were exposed to different environmental stresses, including hypoxia, lactic acidosis, the combination of hypoxia and lactic acidosis, lactosis , as well as acidosis. We used microarrays to examine the genomic programs of cells incubated under different microenvironments. Keywords: different environmental stresses **Overall design:** HMEC cells were exposed to different environmental stresses and RNAs were extracted and put on Affymetrix microarrays. We gathered RNAs from cells grown in regular media (control), lactic acidosis, hypoxia, the combinatino of lactic acidosis and hypoxia, lactosis, as well as acidosis.

Background corr dist: KL-Divergence = 0.0326, L1-Distance = 0.0864, L2-Distance = 0.0094, Normal std = 0.8283

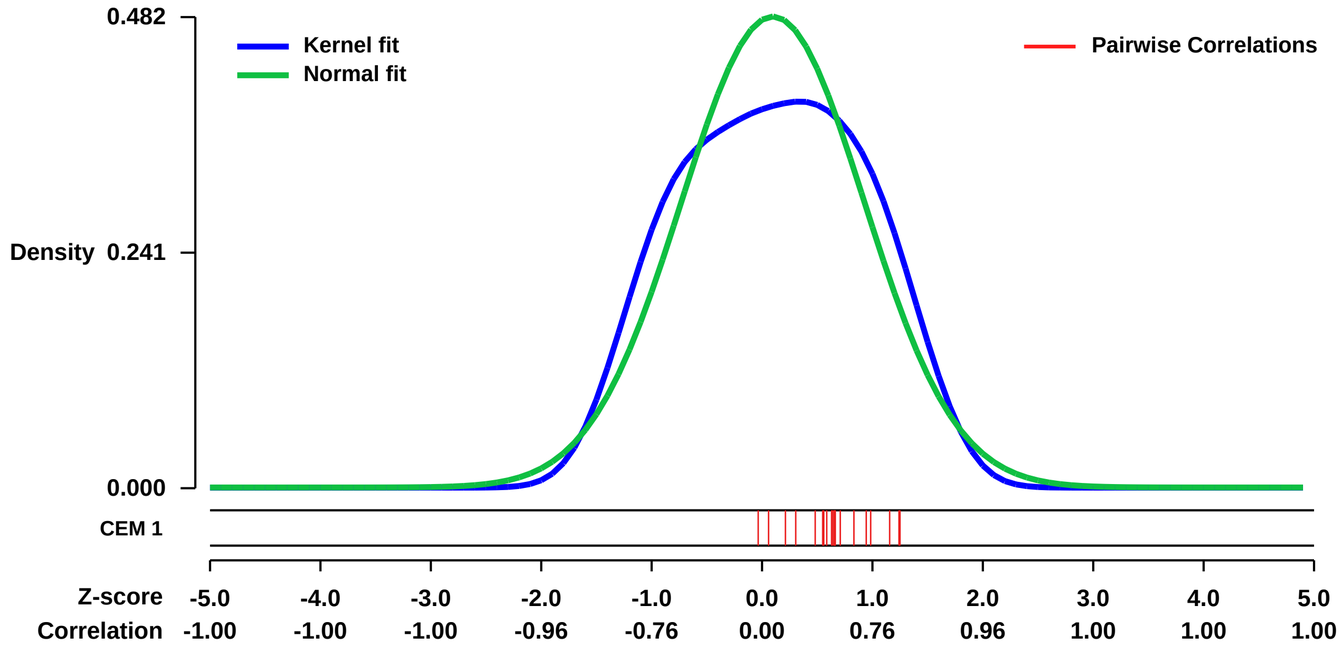

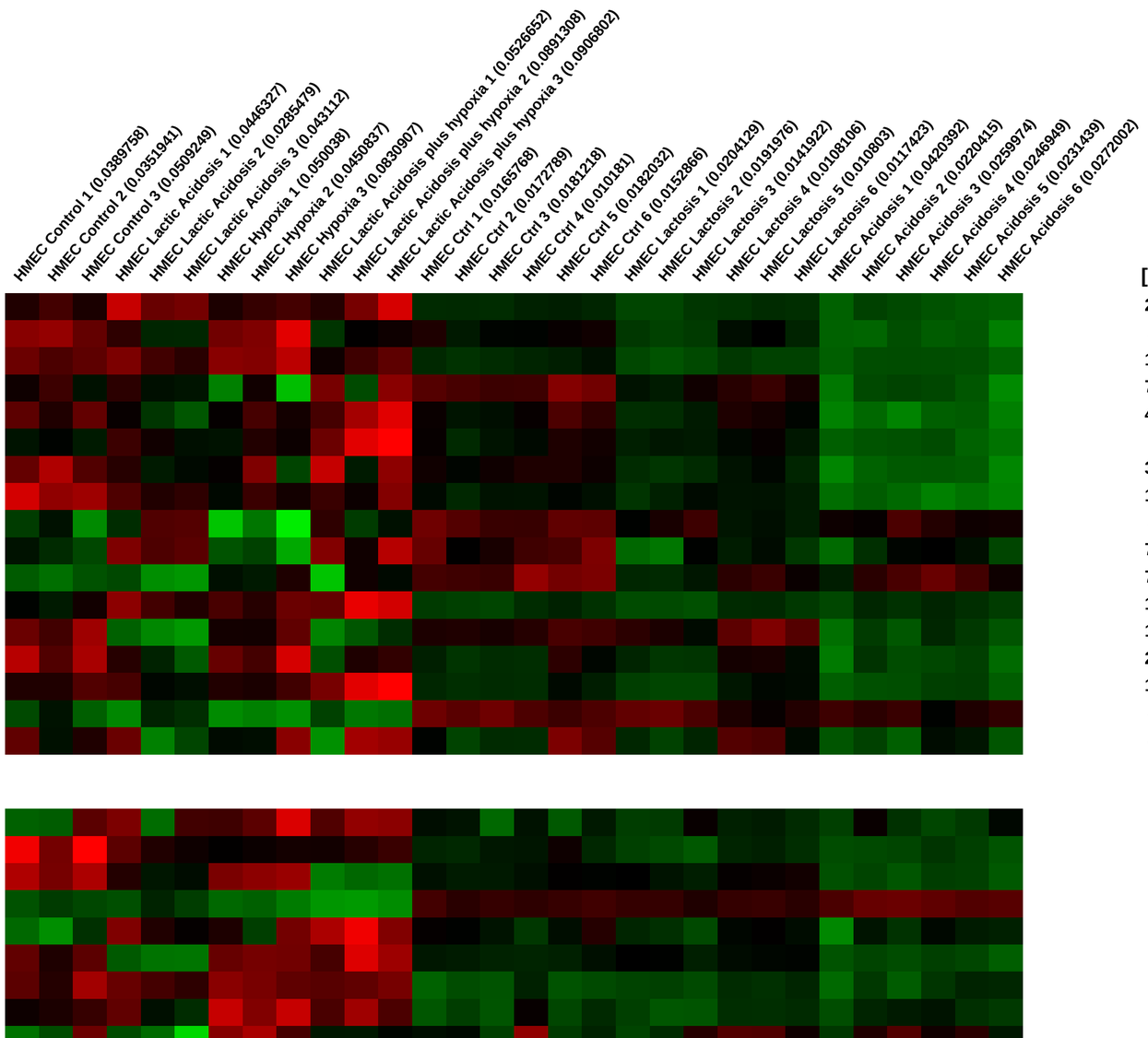

GEO Series "GSE18560" Expression Profiles

Num of samples in this series: 12

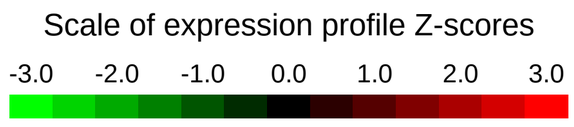

GEO Link:	http://www.ncbi.nlm.nih.gov/geo/query/acc.cgi?acc=GSE18560
Status:	Public on Nov 29 2011
Title:	Deciphering the Wnt-dependent gene signature in colorectal cancer cells
Organism:	Homo sapiens
Experiment type:	Expression profiling by array
Platform:	GPL570
Pubmed ID:	21914722
Summary & Design:	**Summary:** Microarray-based gene expression data were generated from RNA from Ls174T colorectal carcinoma cell lines in which Wnt-dependent transcriptional activity can be abrogated by inducible overexpression of a dominant-negative form of Tcf4 or siRNA against ¸†-catenin. **Overall design:** shRNA against ¸†-catenin, or a dominant-negative Tcf4 transgene, were induced in Ls174T cells for 72 or 24 hours, respectively. Uninduced cells were used as a control. Three replicates per condition.

Background corr dist: KL-Divergence = 0.1124, L1-Distance = 0.0298, L2-Distance = 0.0013, Normal std = 0.4299

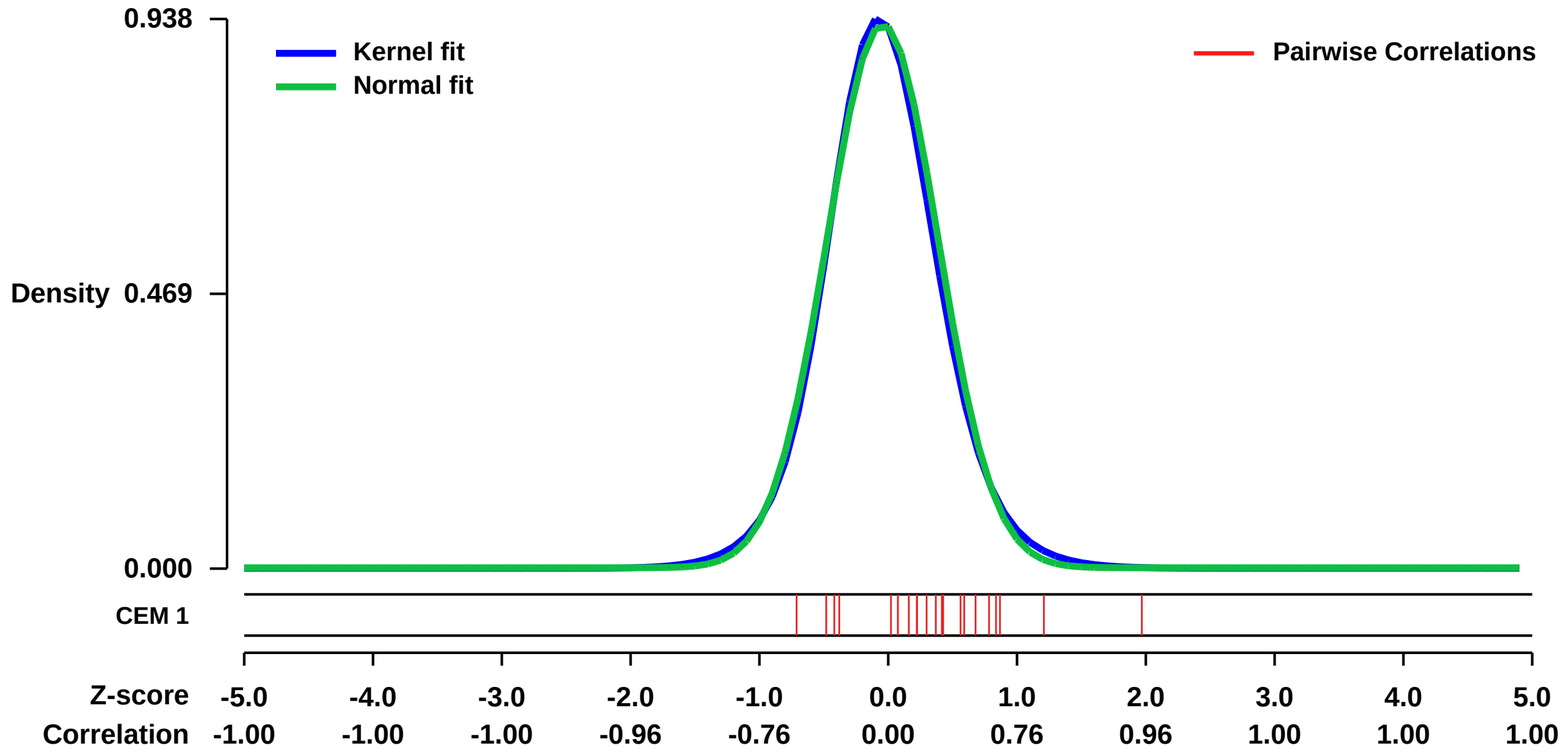

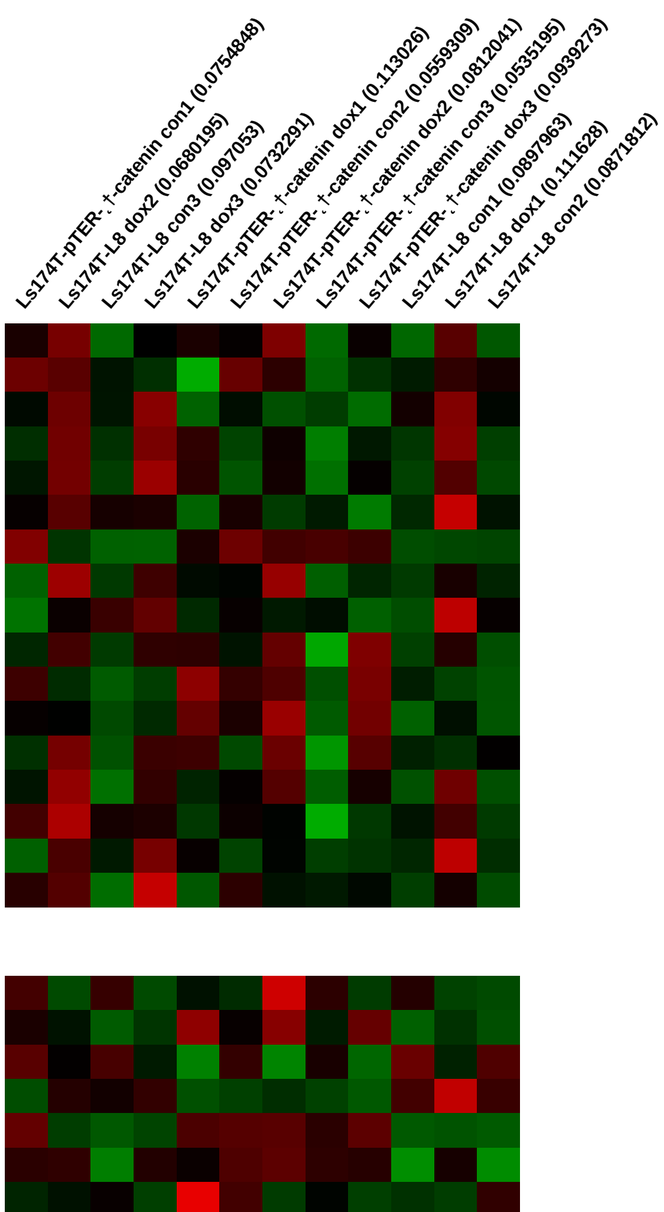

GEO Series "GSE56268" Expression Profiles

Num of samples in this series: 24

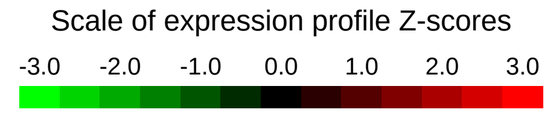

GEO Link:	http://www.ncbi.nlm.nih.gov/geo/query/acc.cgi?acc=GSE56268
Status:	Public on Jun 01 2014
Title:	miR-28 expression in the Burkitt lymphoma cell line P3HR1
Organism:	Homo sapiens
Experiment type:	Expression profiling by array
Platform:	GPL570
Pubmed ID:	24843176
Summary & Design:	**Summary:** Burkitt lymphoma (BL) is a highly aggressive B cell non-Hodgkin lymphoma (B-NHL), which originates from germinal center (GC) B cells and harbors translocations deregulating the MYC oncogene. A comparative analysis of microRNAs (miRNAs) expressed in normal and malignant GC B cells identified miR-28 as significantly down-regulated in BL, as well as in other GC-derived B-NHL. We show that re-expression of miR-28 impairs cell growth and clonogenic properties of BL cells by modulating several targets including MAD2L1, a component of the spindle checkpoint whose down-regulation is essential in mediating miR-28-induced growth-arrest, and BAG1, an activator of the ERK pathway. **Overall design:** P3HR1 Burkitt lymphoma cell line was engineered to display inducible expression of GFP alone or GFP in combination with the miR-28 precursor from the pRTS1 vector upon doxycycline treatment. Two bulk populations (A and B) were established for both the control (GFP alone) and the miR28-expressing (GFP and miR-28 precursor) cells. Cells were induced with 0.1ug/ml doxycycline for 12h or 24h. Induction was performed on each bulk population in triplicates.

Background corr dist: KL-Divergence = 0.4534, L1-Distance = 0.0908, L2-Distance = 0.0273, Normal std = 0.2343

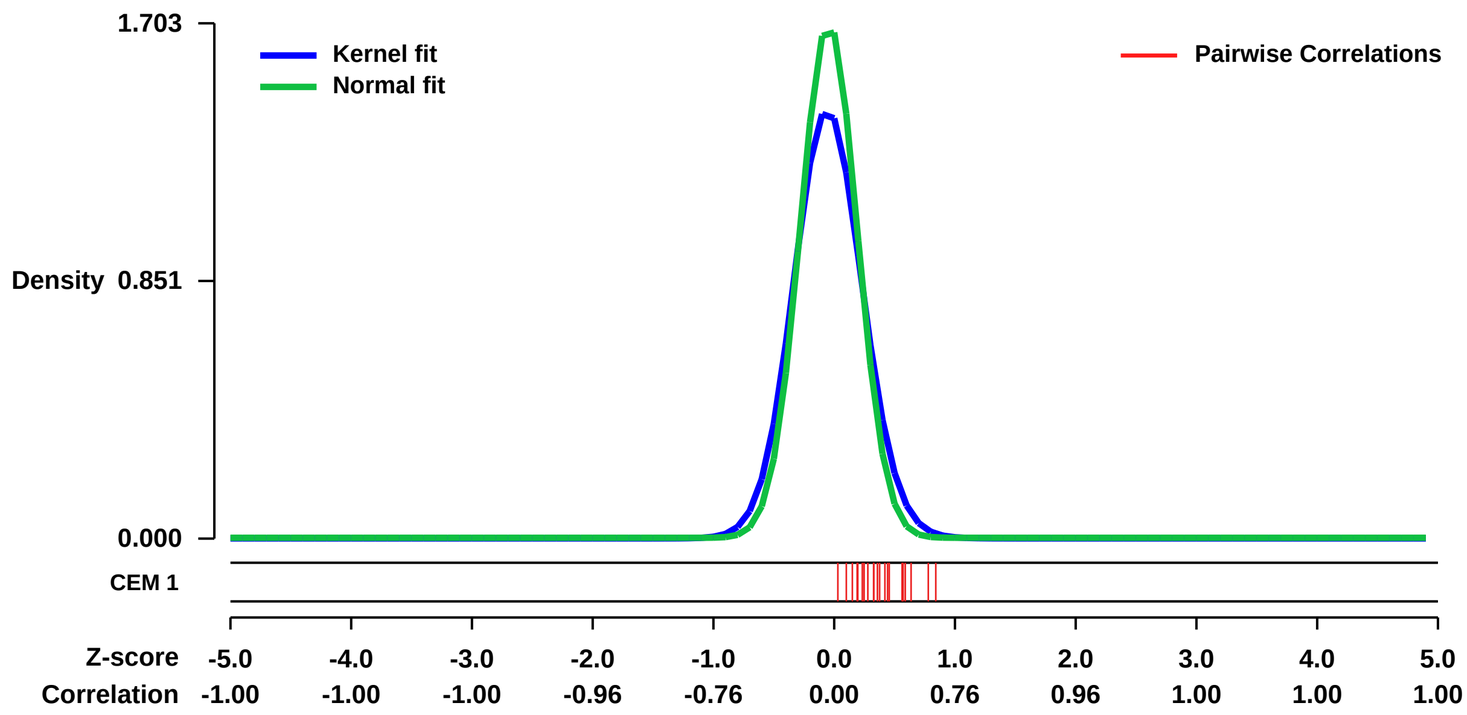

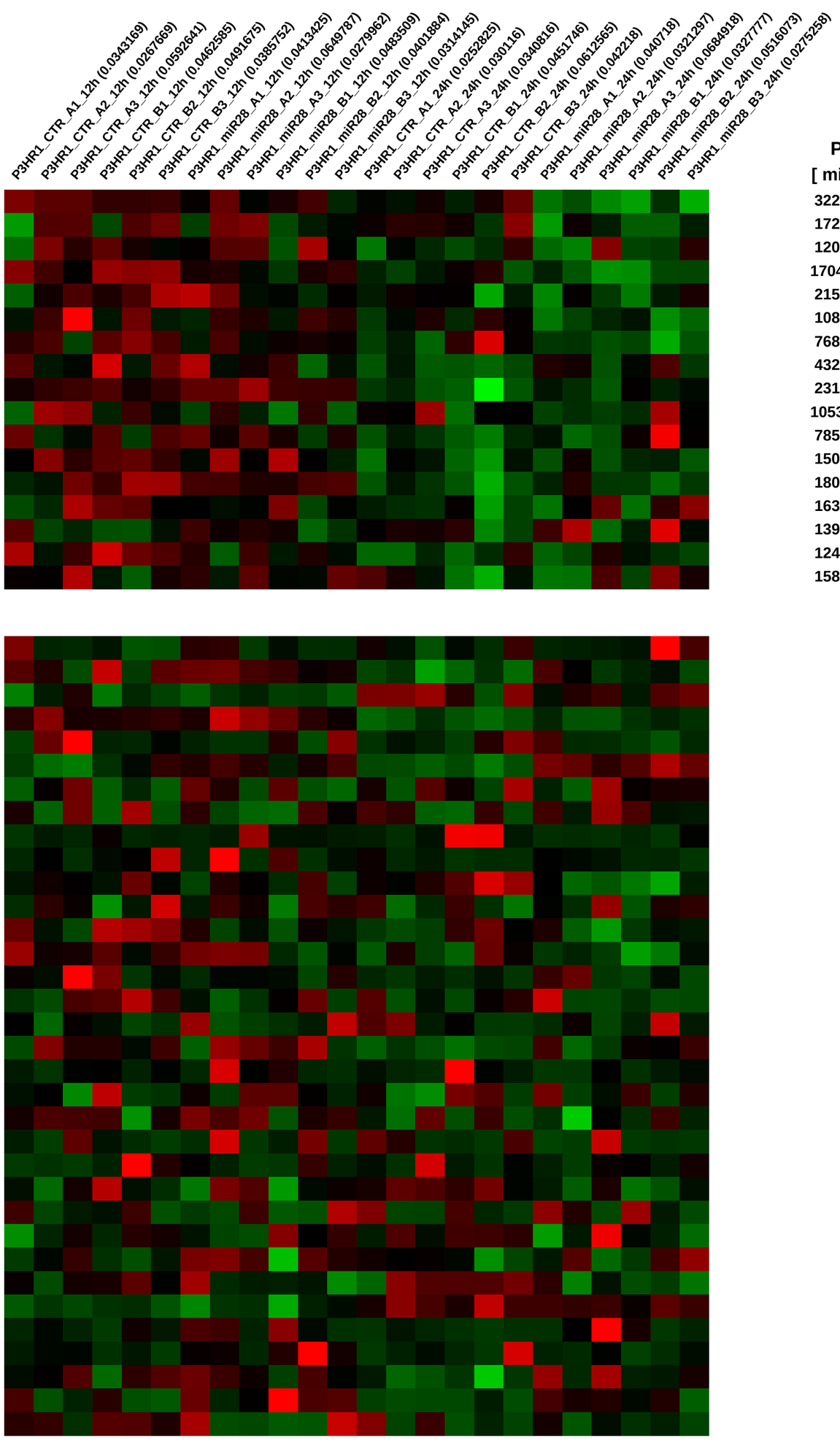

GEO Series "GSE15065" Expression Profiles

Num of samples in this series: 6

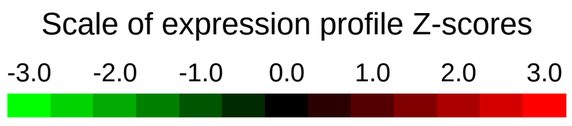

GEO Link:	**http://www.ncbi.nlm.nih.gov/geo/query/acc.cgi?acc=GSE15065**
Status:	**Public on Mar 02 2010**
Title:	**C/EBPbeta-2 regulation of gene expression in MCF10A cells**
Organism:	**Homo sapiens**
Experiment type:	**Expression profiling by array**
Platform:	**GPL570**
Pubmed ID:	
Summary & Design:	**Summary:** **C/EBPbeta-2 results in EMT and ErbB indpendence this project investigated the gene changes in related genes upon C/EBPbeta-2 overexpression in MCF10A cells.** **We used microarray analysis to detail the global gene expression mediated by C/EBPbeta-2 and identified changes in known EMT genes, however, known ErbB related genes were not altered.** **Overall design:** **MCF10A with or without C/EBPbeta-2 were compared.**

Background corr dist: **KL-Divergence = 0.0199, L1-Distance = 0.0237, L2-Distance = 0.0008, Normal std = 0.7429**

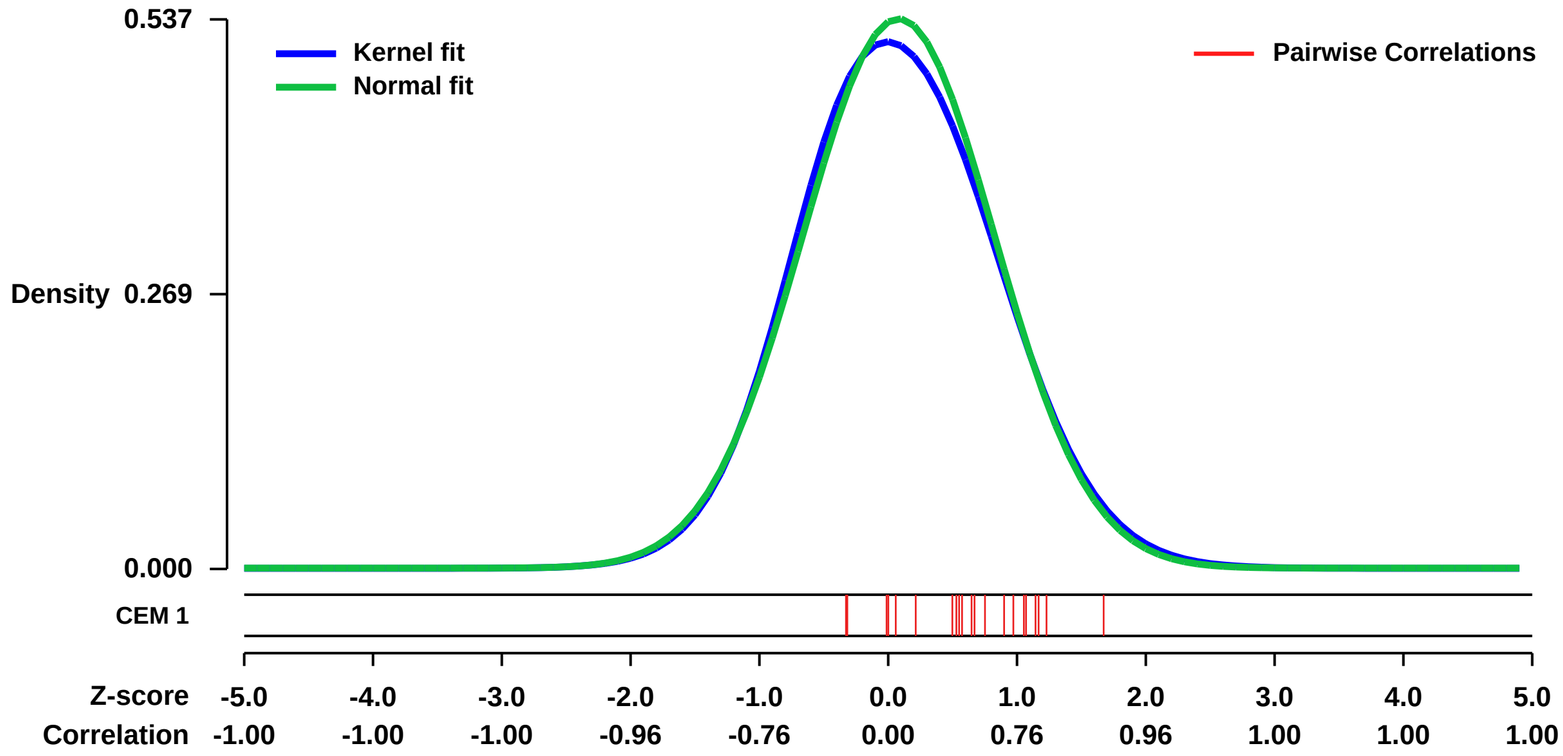

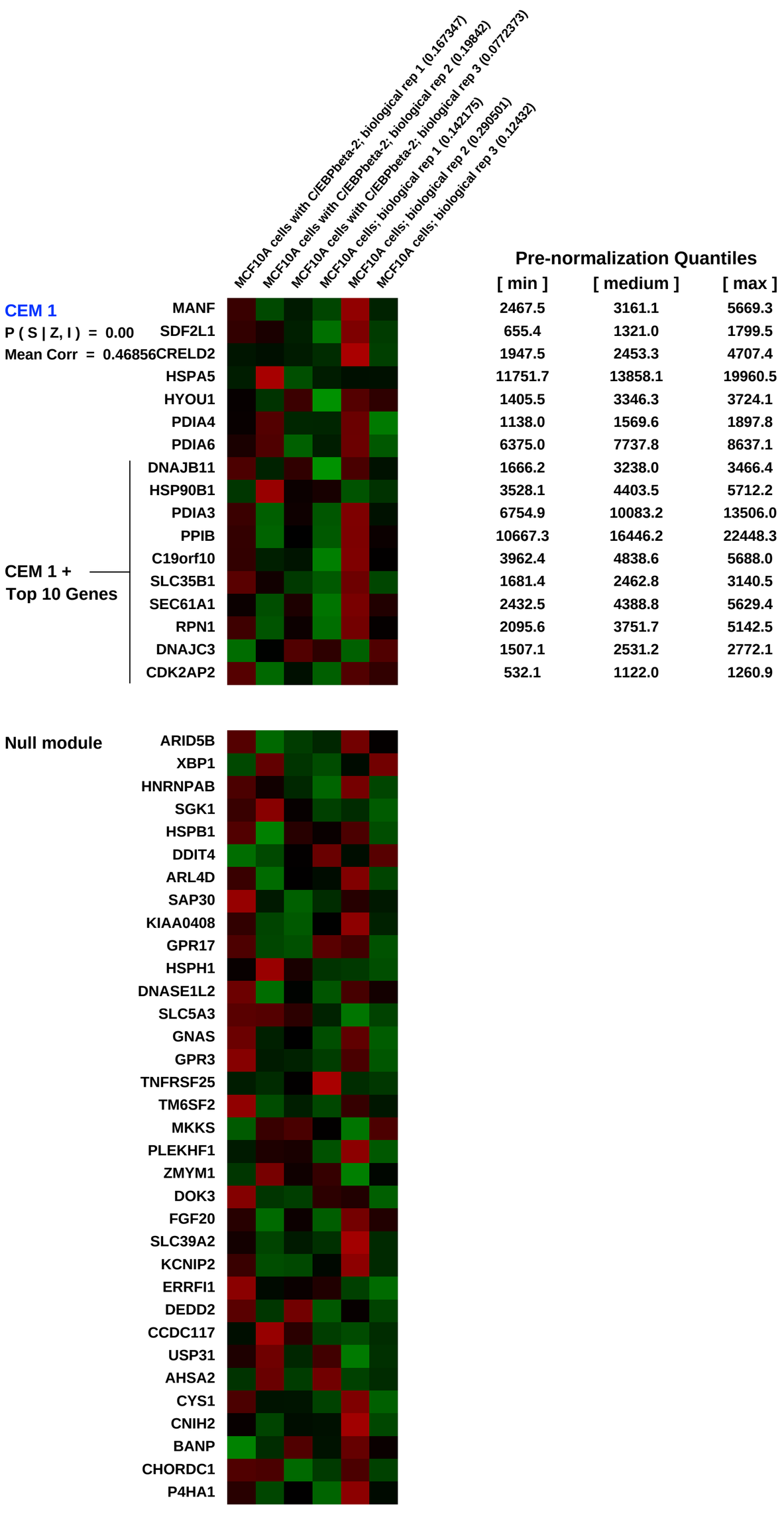

Pre-normalization Quantiles	[min]	[medium]	[max]
MANF	2467.5	3161.1	5669.3
SDF2L1	655.4	1321.0	1799.5
CRELD2	1947.5	2453.3	4707.4
HSPA5	11751.7	13858.1	19960.5
HYOU1	1405.5	3346.3	3724.1
PDIA4	1138.0	1569.6	1897.8
PDIA6	6375.0	7737.8	8637.1
DNAJB11	1666.2	3238.0	3466.4
HSP90B1	3528.1	4403.5	5712.2
PDIA3	6754.9	10083.2	13506.0
PPIB	10667.3	16446.2	22448.3
C19orf10	3962.4	4838.6	5688.0
SLC35B1	1681.4	2462.8	3140.5
SEC61A1	2432.5	4388.8	5629.4
RPN1	2095.6	3751.7	5142.5
DNAJC3	1507.1	2531.2	2772.1
CDK2AP2	532.1	1122.0	1260.9

GEO Series "GSE8832" Expression Profiles

Num of samples in this series: 6

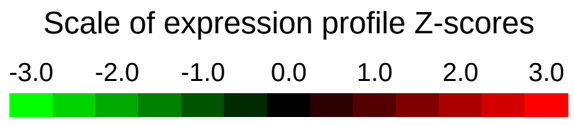

GEO Link:	http://www.ncbi.nlm.nih.gov/geo/query/acc.cgi?acc=GSE8832
Status:	Public on Aug 22 2007
Title:	K562 Gene Expression Control vs 1R-Chl treatments
Organism:	Homo sapiens
Experiment type:	Expression profiling by array
Platform:	GPL570
Pubmed ID:	18413791
Summary & Design:	**Summary:** To determine whether the polyamide-Chl conjugate 1R-Chl would cause similar changes in global gene expression in K562 cells, affymetrix gene chip analysis was performed using 1R-Chl. Through class comparison analysis, 1R-Chl affected the levels of transcription and genes of interest were determined. **Keywords: Treatment response** **Overall design:** K562 cells were incubated with 1R-Chl (at 250 nM) or in the absence of polyamide, in triplicate for 24 h before RNA purification and microarray analysis at The Scripps Research Institute microarray facility. Affymetrix U133A Plus 2.0 GeneChips were hybridized in groups of three for each of the two groups. The Affymetrix probe set data were imported into BRB Arraytools (3.5.0 Beta 2), selecting the U133 chips used in the experiment and leaving all filters off.

Background corr dist: KL-Divergence = 0.0508, L1-Distance = 0.0244, L2-Distance = 0.0007, Normal std = 0.5739

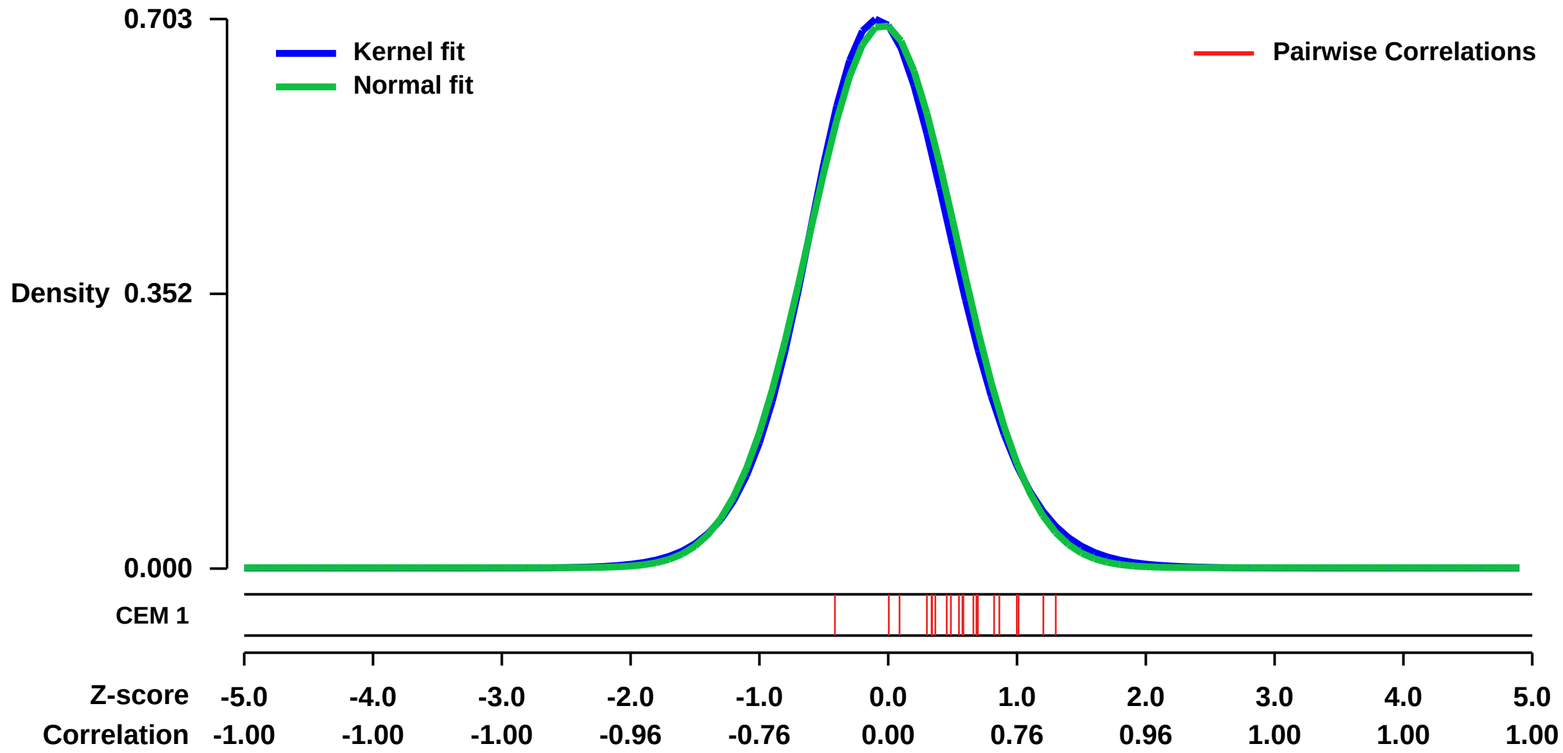

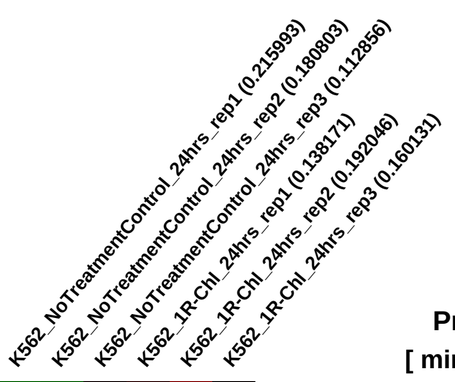

Pre-normalization Quantiles

[min] [medium] [max]

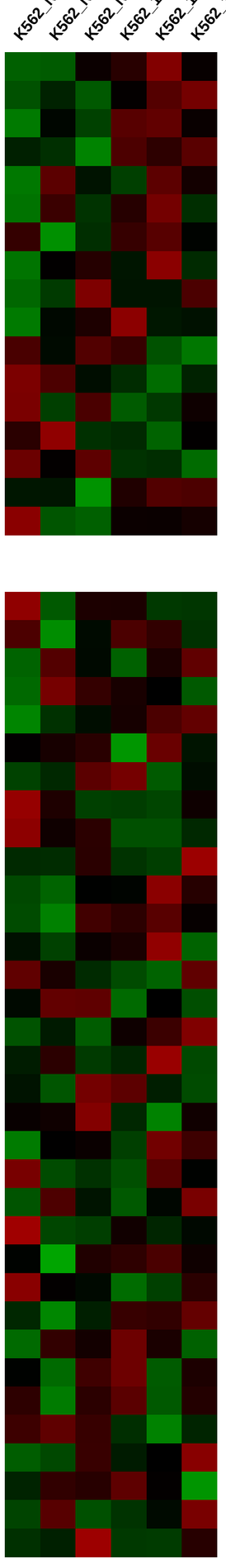

CEM 1	MANF	2144.2	2438.1	2763.1
P (S | Z, I) = 0.00	SDF2L1	9019.8	9805.1	10764.8
Mean Corr = 0.46632	CRELD2	1778.2	2228.1	2533.8
	HSPA5	9576.6	10690.8	10968.1
	HYOU1	2186.6	2409.9	2525.7
	PDIA4	746.6	1056.9	1213.2
	PDIA6	4697.0	5082.8	5149.8
CEM 1 + Top 10 Genes	DNAJB11	3973.6	4245.8	4562.7
	HSP90B1	2108.0	2531.3	3272.2
	PDIA3	9048.3	9524.5	10145.3
	PPIB	11441.5	13111.7	13375.2
	C19orf10	3629.3	4045.5	4645.8
	SLC35B1	3319.6	3638.9	3970.0
	SEC61A1	1995.5	2188.7	2461.6
	RPN1	3027.0	3340.9	3636.6
	DNAJC3	976.3	1181.1	1237.4
	CDK2AP2	1379.0	1494.1	1629.5
Null module	ARID5B			
	XBP1			
	HNRNPAB			
	SGK1			
	HSPB1			
	DDIT4			
	ARL4D			
	SAP30			
	KIAA0408			
	GPR17			
	HSPH1			
	DNASE1L2			
	SLC5A3			
	GNAS			
	GPR3			
	TNFRSF25			
	TM6SF2			
	MKKS			
	PLEKHF1			
	ZMYM1			
	DOK3			
	FGF20			
	SLC39A2			
	KCNIP2			
	ERRFI1			
	DEDD2			
	CCDC117			
	USP31			
	AHSA2			
	CYS1			
	CNIH2			
	BANP			
	CHORDC1			
	P4HA1			

GEO Series "GSE39890" Expression Profiles

Num of samples in this series: 15

Scale of expression profile Z-scores

-3.0 -2.0 -1.0 0.0 1.0 2.0 3.0

GEO Link: http://www.ncbi.nlm.nih.gov/geo/query/acc.cgi?acc=GSE39890

Status: Public on Nov 05 2012

Title: Gene knockdown and overexpression of 402C>G FOXL2 in COV434 and KGN cells

Organism: Homo sapiens

Experiment type: Expression profiling by array

Platform: GPL570

Pubmed ID: 23029457

Summary & Design:

Summary:
Despite their distinct biology, granulosa cell tumours (GCTs) are treated the same as other ovarian tumours. Intriguingly, a recurring somatic mutation in the transcription factor Forkhead Box L2 (FOXL2) 402C>G has been found in nearly all GCTs examined. This investigation aims to identify the pathogenicity of mutant FOXL2 by studying its altered transcriptional targets. The expression of mutant FOXL2 was reduced in the GCT cell line KGN, and wildtype and mutant FOXL2 were overexpressed in the GCT cell line COV434. Comparisons were made between the transcriptomes of control cells and cells altered by FOXL2 knockdown and overexpression, to detect potential transcriptional targets of mutant FOXL2. Comparisons were made between the transcriptomes of control cells and cells altered by FOXL2 knockdown and overexpression, to detect potential transcriptional targets of mutant FOXL2.

Overall design:
Mutant FOXL2 was silenced in KGN cells with the use of siRNA and a non-targetting siRNA control. Wildtype and mutant FOXL2 were overexpressed in COV434 cells with the use of overexpression plasmids and an empty plasmid control. Each experiment was performed in triplicate. Total RNA was harvested at 24h post transfection and hybridised to Affymetrix U133 plus 2.0 arrays.

Background corr dist: KL-Divergence = 0.0109, L1-Distance = 0.0164, L2-Distance = 0.0003, Normal std = 0.8531

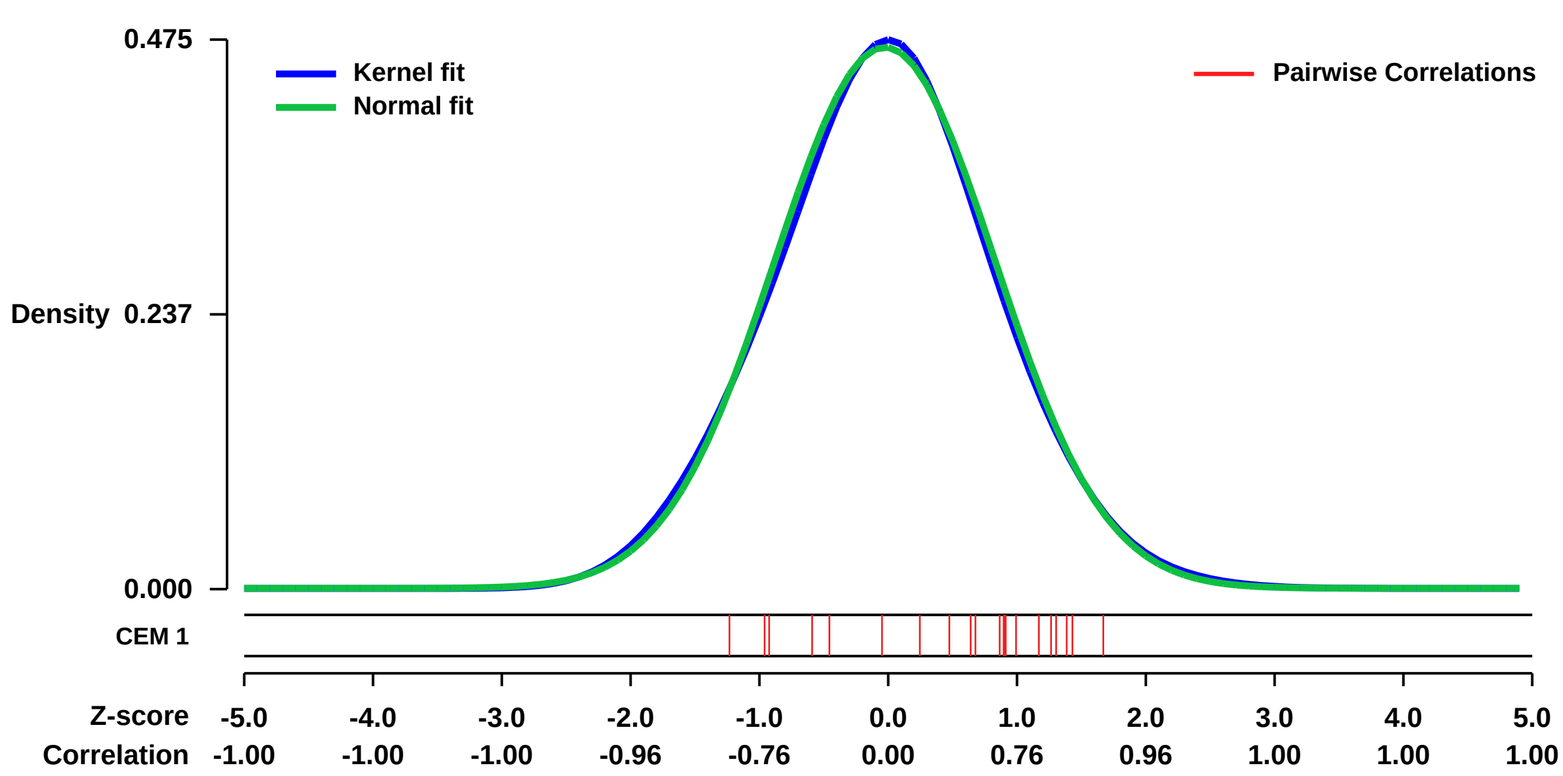

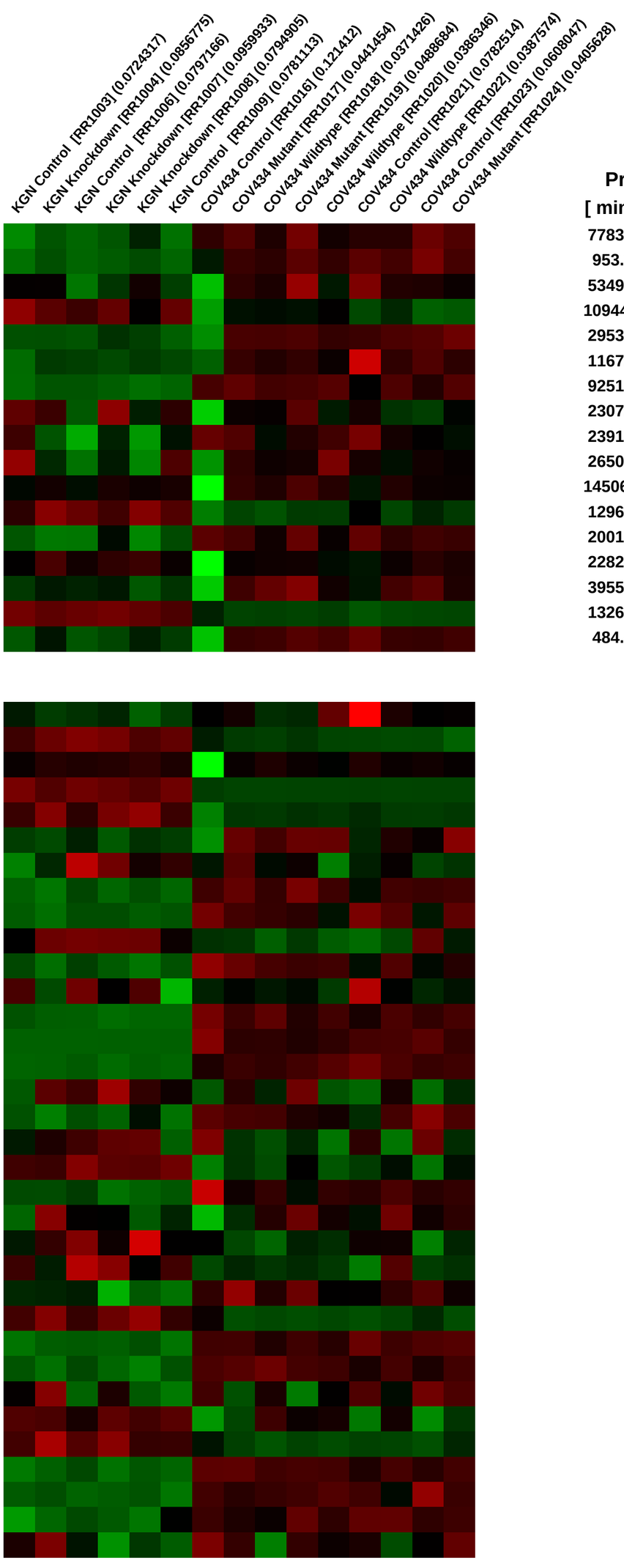

		Pre-normalization Quantiles [min]	[medium]	[max]
CEM 1	MANF	7783.1	9924.1	11001.8
P (S | Z, I) = 0.00	SDF2L1	953.3	2557.7	3341.1
Mean Corr = 0.35106	CRELD2	5349.2	6649.4	7538.7
	HSPA5	10944.0	18361.0	26125.5
	HYOU1	2953.1	5280.9	5974.4
	PDIA4	1167.4	1512.8	2082.8
	PDIA6	9251.1	12782.7	14253.3
CEM 1 + Top 10 Genes	DNAJB11	2307.8	3270.4	3886.7
	HSP90B1	2391.6	3887.3	4904.5
	PDIA3	2650.8	3181.7	3622.5
	PPIB	14506.6	25203.8	27115.3
	C19orf10	1296.7	1754.3	2606.7
	SLC35B1	2001.0	2756.7	3175.6
	SEC61A1	2282.5	4906.2	5391.3
	RPN1	3955.4	5045.7	5929.0
	DNAJC3	1326.0	1490.6	2630.9
	CDK2AP2	484.4	1276.9	1439.6
Null module	ARID5B			
	XBP1			
	HNRNPAB			
	SGK1			
	HSPB1			
	DDIT4			
	ARL4D			
	SAP30			
	KIAA0408			
	GPR17			
	HSPH1			
	DNASE1L2			
	SLC5A3			
	GNAS			
	GPR3			
	TNFRSF25			
	TM6SF2			
	MKKS			
	PLEKHF1			
	ZMYM1			
	DOK3			
	FGF20			
	SLC39A2			
	KCNIP2			
	ERRFI1			
	DEDD2			
	CCDC117			
	USP31			
	AHSA2			
	CYS1			
	CNIH2			
	BANP			
	CHORDC1			
	P4HA1			

GEO Series "GSE41040" Expression Profiles

Num of samples in this series: 14

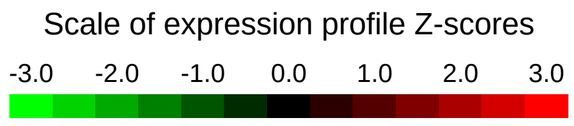

GEO Link:	http://www.ncbi.nlm.nih.gov/geo/query/acc.cgi?acc=GSE41040
Status:	Public on Sep 14 2013
Title:	Gene expresion changes following knockdown of KDM4C in primary fibroblasts
Organism:	Homo sapiens
Experiment type:	Expression profiling by array
Platform:	GPL570
Pubmed ID:	24285722
Summary & Design:	**Summary:** Epigenetic and genetic regulations are sometimes considered as separate mechanisms that influence gene expression and phenotypes. However, there are DNA sequence variants in epigenetic regulators that could affect gene regulation. The histone demethylase, KDM4C, promotes transcriptional activation by removing the repressive histone mark, tri-methylation of lysine 9 of histone H3 (H3K9me3), from its target genes. In this study, we uncovered cis-acting DNA sequence variants in KDM4C that contribute to individual differences in its expression. Utilizing this natural variation, we performed genetic analyses in B-cells in order to identify target genes that are regulated by KDM4C. We used microarrays to investigate gene expression changes in the target genes from our genetic analyses following knockdown of KDM4C in primary fibroblasts. **Overall design:** Primary fibroblasts with stable expression of shRNA targeting KDM4C or a control construct were selected for RNA extraction and hybridization to Affymetrix microarrays. Following selection for stable expression of the shRNA constructs we selected clones expressing 3 non-overlapping constructs targeting KDM4C (shKDM4C) and 2 clones expressing the control construct (shCtr) for analysis by microarray.

Background corr dist: KL-Divergence = 0.1330, L1-Distance = 0.0308, L2-Distance = 0.0019, Normal std = 0.3935

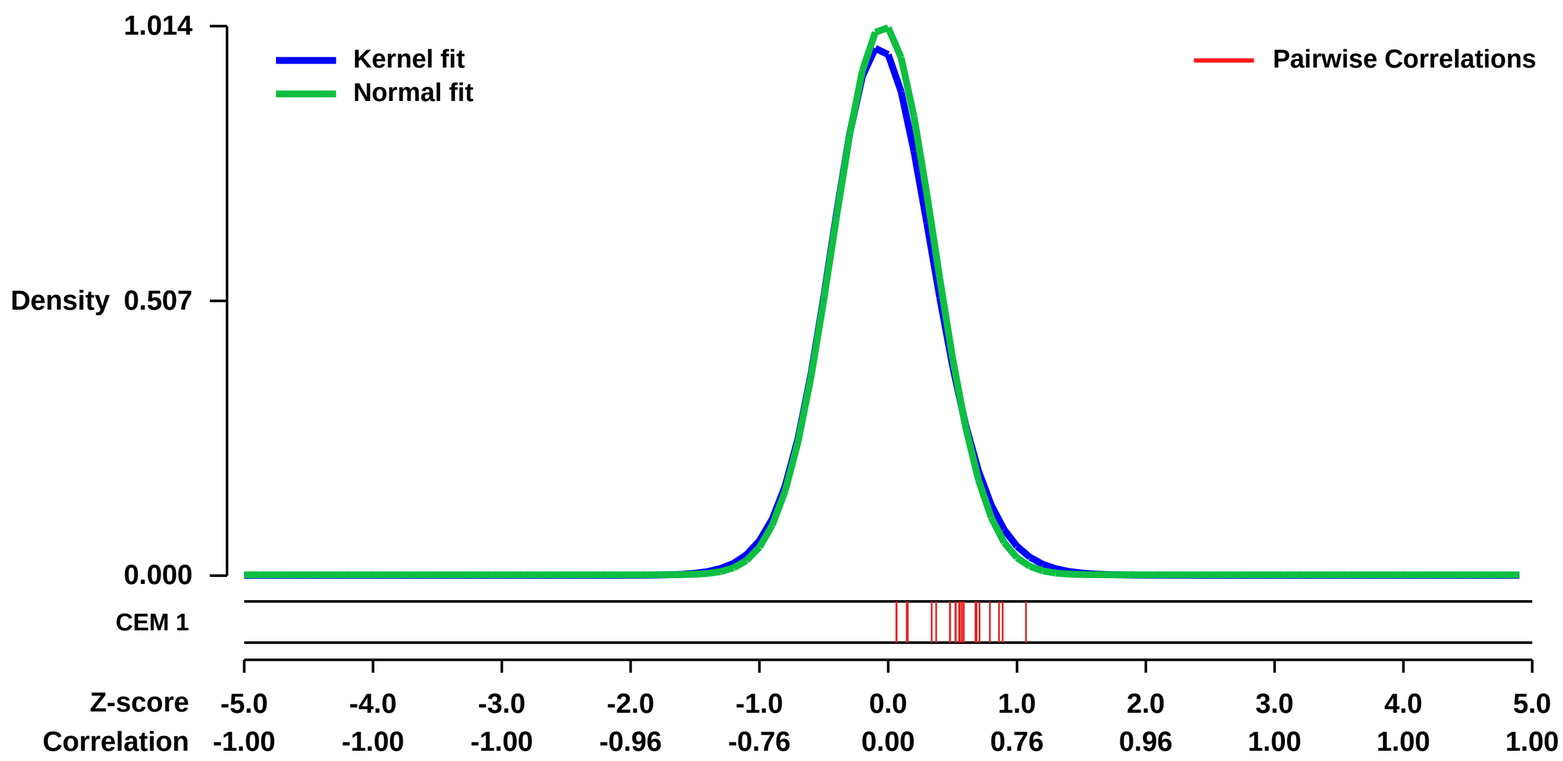

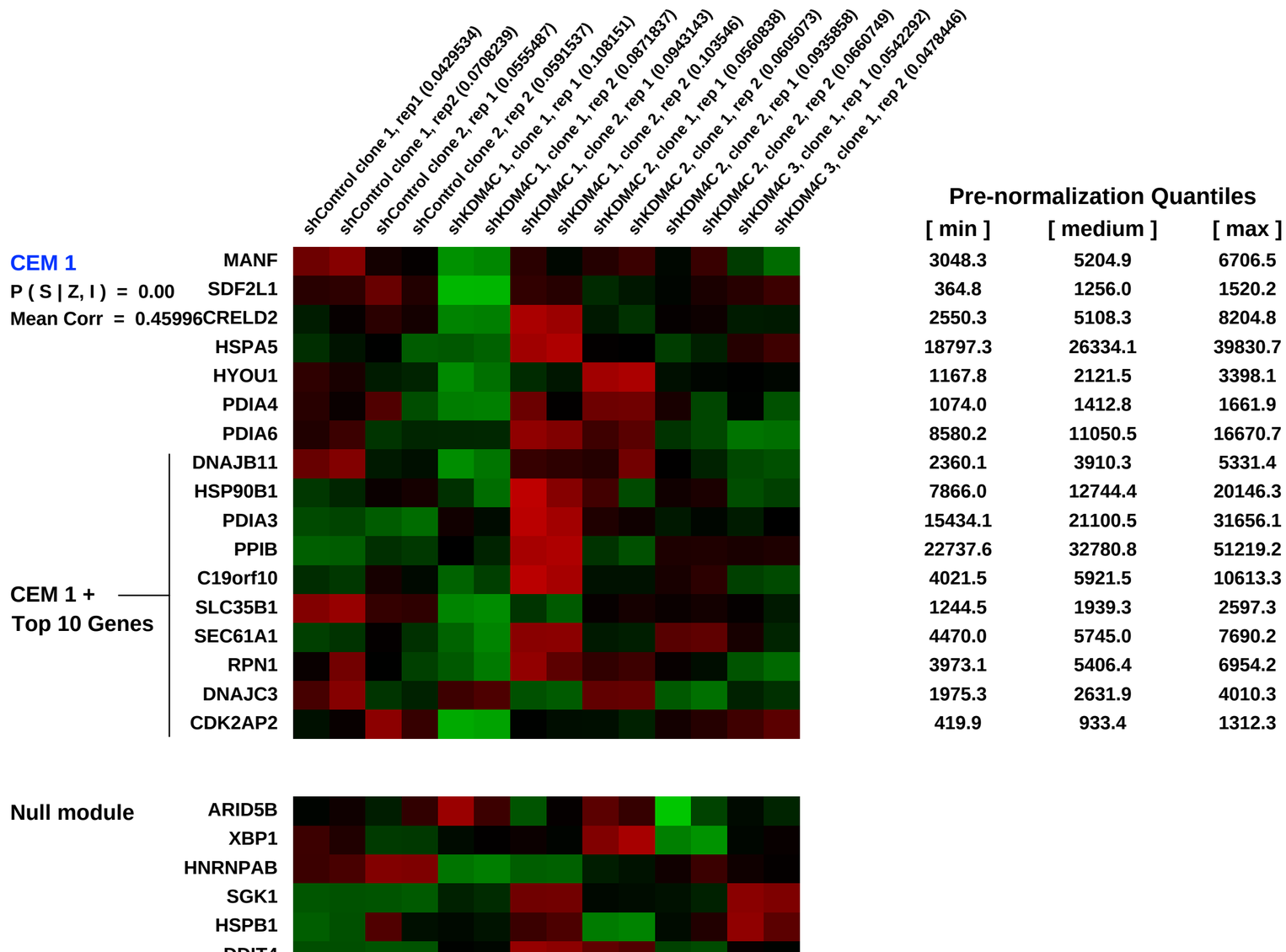

Pre-normalization Quantiles

	[min]	[medium]	[max]
MANF	3048.3	5204.9	6706.5
SDF2L1	364.8	1256.0	1520.2
CRELD2	2550.3	5108.3	8204.8
HSPA5	18797.3	26334.1	39830.7
HYOU1	1167.8	2121.5	3398.1
PDIA4	1074.0	1412.8	1661.9
PDIA6	8580.2	11050.5	16670.7
DNAJB11	2360.1	3910.3	5331.4
HSP90B1	7866.0	12744.4	20146.3
PDIA3	15434.1	21100.5	31656.1
PPIB	22737.6	32780.8	51219.2
C19orf10	4021.5	5921.5	10613.3
SLC35B1	1244.5	1939.3	2597.3
SEC61A1	4470.0	5745.0	7690.2
RPN1	3973.1	5406.4	6954.2
DNAJC3	1975.3	2631.9	4010.3
CDK2AP2	419.9	933.4	1312.3

GEO Series "GSE29061" Expression Profiles

Num of samples in this series: 6

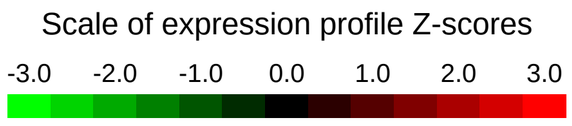

GEO Link:	http://www.ncbi.nlm.nih.gov/geo/query/acc.cgi?acc=GSE29061
Status:	Public on Dec 01 2012
Title:	Expression data from the hepatitis E virus capsid protein
Organism:	Homo sapiens
Experiment type:	Expression profiling by array
Platform:	GPL570
Pubmed ID:	21966512
Summary & Design:	**Summary:** The hepatitis E virus (HEV), a non enveloped RNA virus, causes viral hepatitis. The viral open reading frame 2 (ORF2) protein represents the capsid protein of HEV which is known to cause endoplasmic reticulum stress in ORF2 expressing cells. The initiation of endoplasmic reticulum stress induced apoptosis mainly involves the transcriptional activation of pro-apoptotic gene CHOP which will further trigger the major apoptotic pathways. However, the activation of CHOP by ORF2 protein in this study does not induce apoptotic markers such as Bax translocation to mitochondria. We have used the Affymetrix microarray platform to screen the pro-apoptotic effects induced by the expression of ORF2 protein in human hepatic cell lines (Huh7). The Huh7 cells were transduced either with recombinant adenovirus encoding the HEV ORF2 (Ad-ORF2) or an adenovirus encoding the green fluorescent protein (Ad-GFP). The array results consistently showed an ORF2 specific induction of mRNA corresponding to the chaperones Hsp72, Hsp70Bâ and co-chaperone Hsp40. These studies provide further mechanisms of the ER stress mediated pro apoptotic effects caused by the ORF2 protein and its potential role for the activation of anti-apoptotic activity of the host cell. **Overall design:** Huh7 cells transduced with Ad-GFP (control) or with Ad-HEV ORF2.

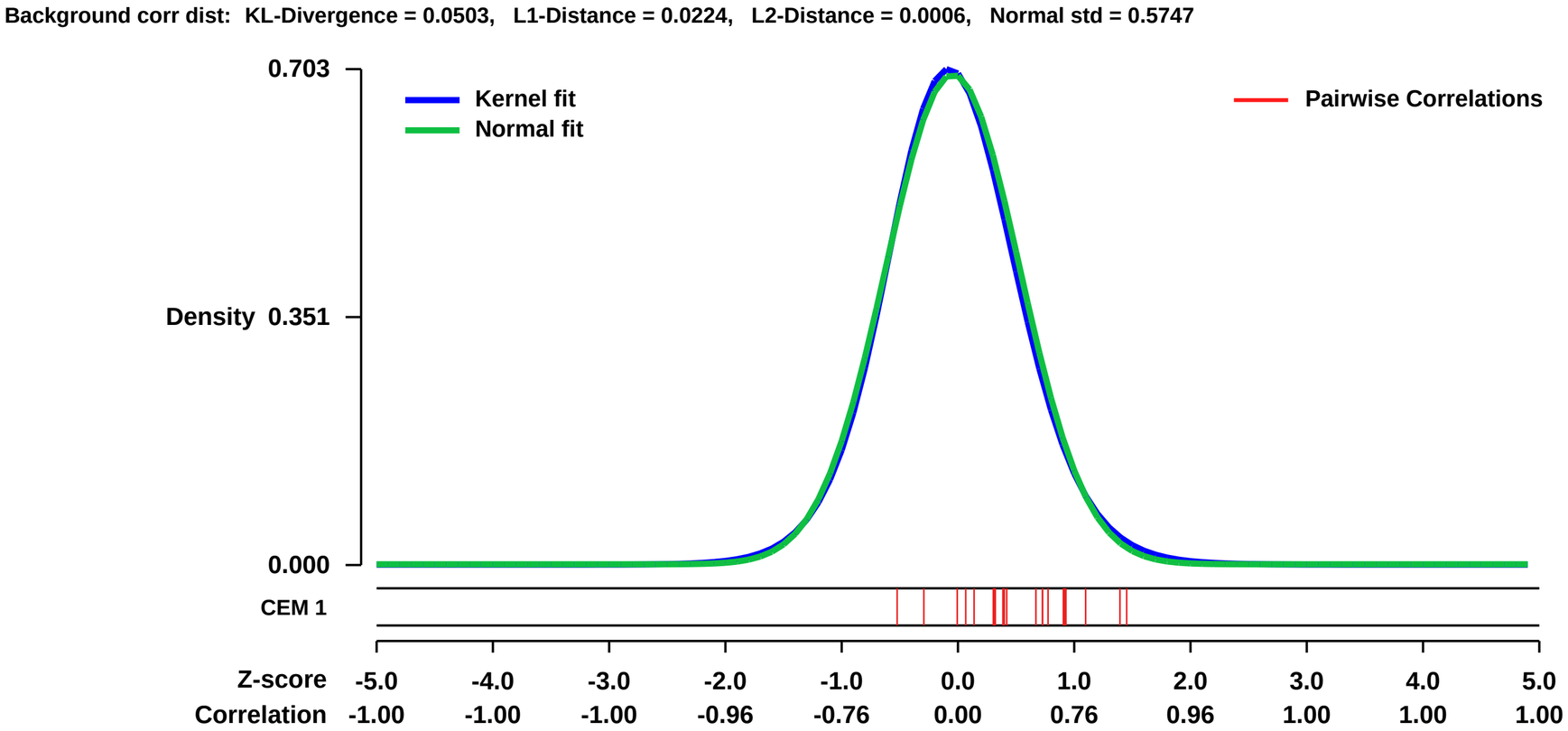

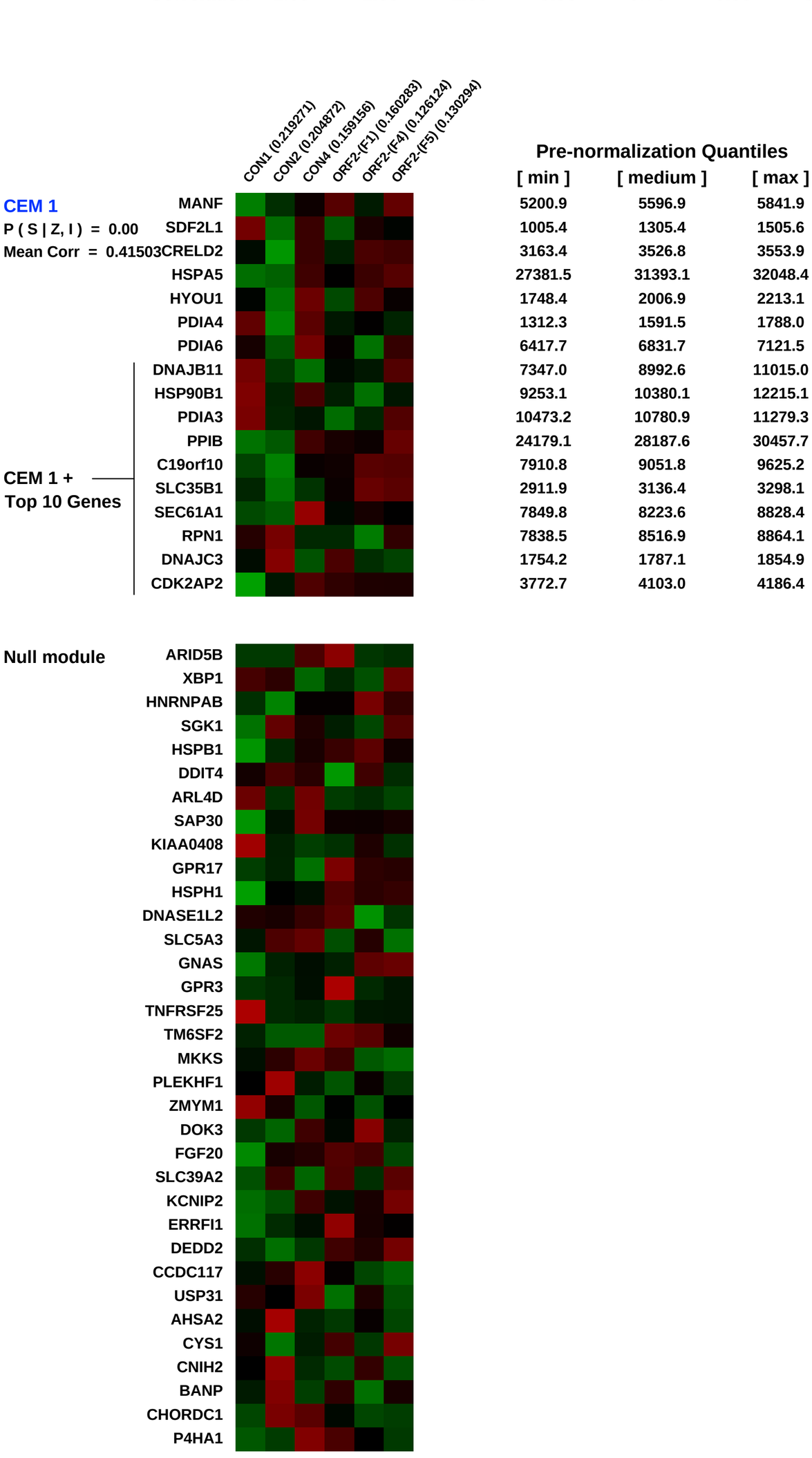

GEO Series "GSE55512" Expression Profiles

Num of samples in this series: 12

Scale of expression profile Z-scores

-3.0 -2.0 -1.0 0.0 1.0 2.0 3.0

GEO Link: http://www.ncbi.nlm.nih.gov/geo/query/acc.cgi?acc=GSE55512
Status: Public on Mar 04 2014
Title: Gene-expression profiles of ovarian cancer regarding its microenvironment
Organism: Homo sapiens
Experiment type: Expression profiling by array
Platform: GPL570
Pubmed ID:

Summary & Design:

Summary:
PD-L1 suppresses host immunity and promotes tumor growth. We investigated how IFN-¿‡ regulates PD-L1 in the ovarian cancer microenvironment. In clinical samples, the number of stromal CTLs in peritoneally disseminated tumors was correlated with PD-L1 expression on the tumor cells, and the lymphocyte number was significantly related to the IFN-¿‡ signature score. In mouse models, PD-L1 was induced in peritoneal disseminated tumors, where lymphocytes were prominent, but not in subcutaneous tumors. Depleting IFNGR1 resulted in lower PD-L1 expression and longer survival in peritoneal dissemination model. Injection of IFN-¿‡ into subcutaneous tumors increased PD-L1 expression and tumor size, and PD-L1 depletion abrogated tumor growth. These data suggest that IFN-¿‡ works as a tumor progressor through PD-L1 induction. The source of IFN-¿‡ in ovarian cancer microenvironment and its biological effect to the tumor cells is unclear. The immortalized human ovarian surface epithelial cell line, HOSE-E7/hTERT (HOSE) was treated with IFN-¿‡ and expression microarray analysis was performed, and probes showing significantly higher values in IFN-¿‡-added group were termed â IFN-¿‡ signature genes (295 probes)â . We then applied this signature to our ovarian cancer microarray data, which included 75 ovarian cancer clinical samples, by means of ss-GSEA. IFN-¿‡ signature score was strongly correlated to the number of infiltrating CD4-positive or CD8-positive lymphocytes in the tumors. These data suggest that the IFN-¿‡ in the ovarian cancer microenvironment is derived from lymphocytes, and an IFN-¿‡-rich microenvironment is strongly correlated to a lymphocyte-rich microenvironment.

Overall design:
Genome-wide transcriptional changes in human ovarian cancer tissue were observed in different tumor immunological microenvironment.

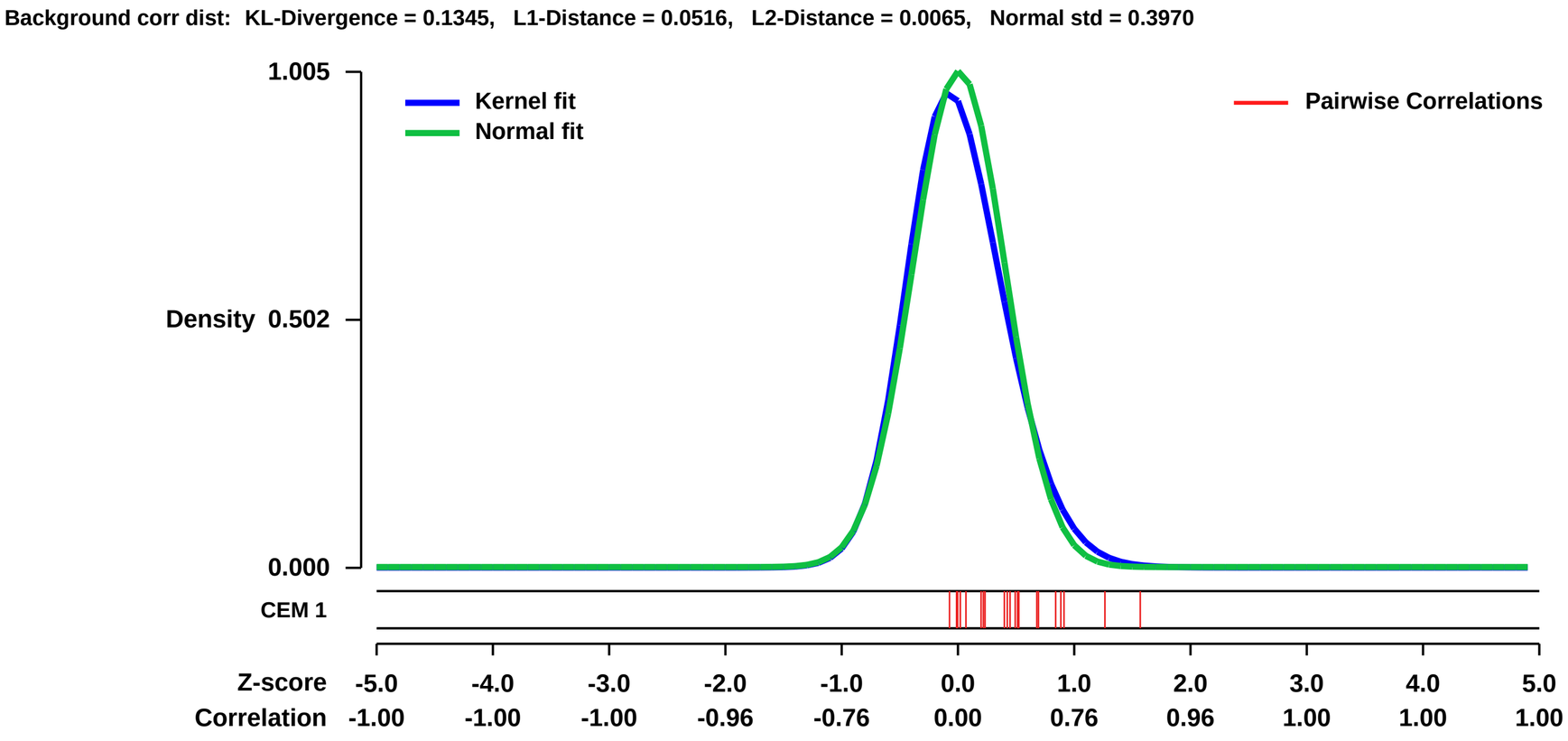

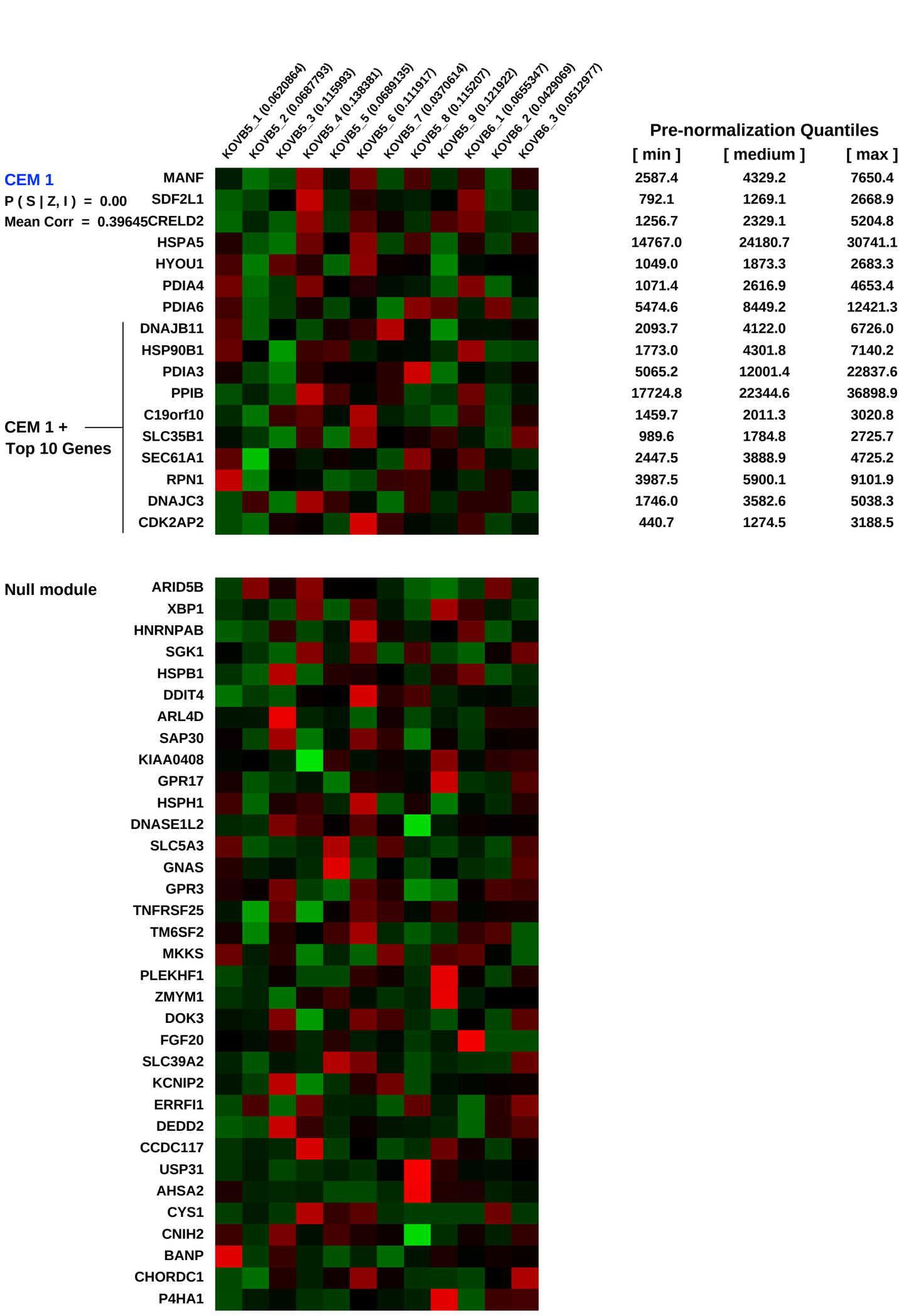

GEO Series "GSE47052" Expression Profiles

Num of samples in this series: 6

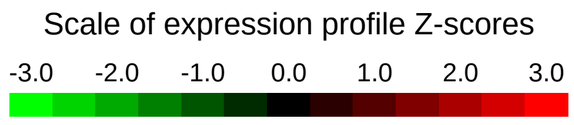

GEO Link:	http://www.ncbi.nlm.nih.gov/geo/query/acc.cgi?acc=GSE47052
Status:	Public on Jan 07 2014
Title:	COUP-TFII regulates human endometrial stromal genes involved in inflammation
Organism:	Homo sapiens
Experiment type:	Expression profiling by array
Platform:	GPL570
Pubmed ID:	24176914
Summary & Design:	**Summary:** Although the function of COUP-TFII in uterine decidualization has been described in mice, its role in the human uterus remains unknown.To interrogate the role of COUP-TFII in human endometrial function, we utilized a siRNA-mediated loss of function approach in primary human endometrial stromal cells. **Overall design:** Two group comparison

Background corr dist: KL-Divergence = 0.0116, L1-Distance = 0.0265, L2-Distance = 0.0006, Normal std = 0.9325

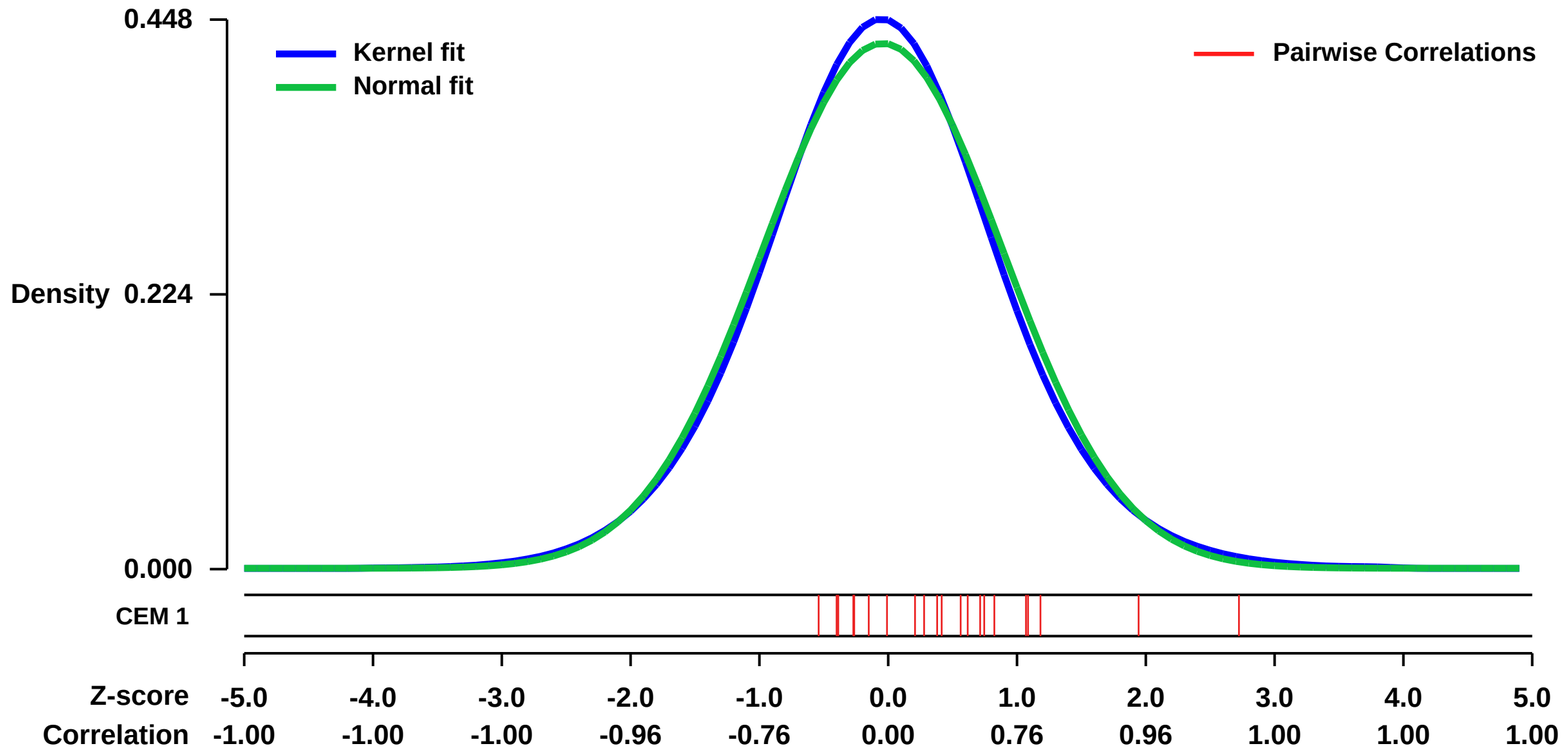

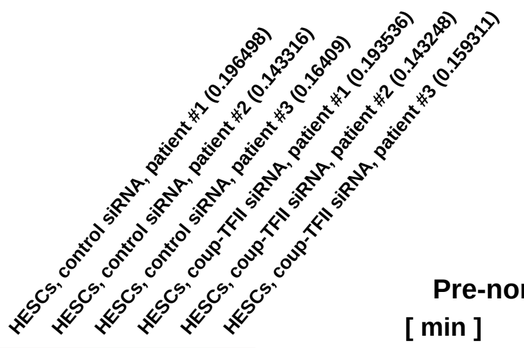

Pre-normalization Quantiles

		[min]	[medium]	[max]
CEM 1 P (S | Z, I) = 0.00 Mean Corr = 0.31684	MANF	4140.2	4255.5	4271.3
	SDF2L1	680.2	753.9	834.5
	CRELD2	2565.9	2785.8	2979.6
	HSPA5	17291.8	18162.3	18896.6
	HYOU1	1025.5	1135.8	1173.9
	PDIA4	2037.0	2155.8	2281.0
	PDIA6	12038.3	13110.4	13908.1
CEM 1 + Top 10 Genes	DNAJB11	4144.4	4301.8	4343.9
	HSP90B1	4882.0	5175.7	5294.2
	PDIA3	16257.7	16965.1	17341.5
	PPIB	20909.8	21453.5	22002.4
	C19orf10	4881.3	5455.3	5896.3
	SLC35B1	1740.7	1826.2	1876.1
	SEC61A1	7092.9	7248.0	7349.2
	RPN1	7296.1	7614.3	7800.3
	DNAJC3	5752.0	5844.7	5894.6
	CDK2AP2	391.2	436.5	451.8
Null module	ARID5B			
	XBP1			
	HNRNPAB			
	SGK1			
	HSPB1			
	DDIT4			
	ARL4D			
	SAP30			
	KIAA0408			
	GPR17			
	HSPH1			
	DNASE1L2			
	SLC5A3			
	GNAS			
	GPR3			
	TNFRSF25			
	TM6SF2			
	MKKS			
	PLEKHF1			
	ZMYM1			
	DOK3			
	FGF20			
	SLC39A2			
	KCNIP2			
	ERRFI1			
	DEDD2			
	CCDC117			
	USP31			
	AHSA2			
	CYS1			
	CNIH2			
	BANP			
	CHORDC1			
	P4HA1			

GEO Series "GSE36547" Expression Profiles

Num of samples in this series: 20

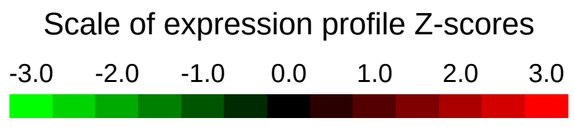

GEO Link:	http://www.ncbi.nlm.nih.gov/geo/query/acc.cgi?acc=GSE36547
Status:	Public on Apr 16 2012
Title:	Assessment of Ex Vivo Prostaglandin pathway activation in HSCs
Organism:	Homo sapiens
Experiment type:	Expression profiling by array
Platform:	GPL570
Pubmed ID:	23996087
Summary & Design:	**Summary:** Transplantation with low numbers of hematopoietic stem cells (HSCs), found in many of the publically accessible cryopreserved umbilical cord blood (UCB) units, leads to delayed time to engraftment, high graft failure rates, and early mortality in many patients. A chemical screen in zebrafish identified the prostaglandin compound, 16,16 dimethyl prostaglandin E2 (dmPGE2), to be a critical regulator of hematopoietic stem cell homeostasis. We hypothesized that an ex vivo modulation with dmPGE2 prior to transplantation would lead to enhanced engraftment by increasing the â effectiveâ dose of hematopoietic stem cells (HSCs) in cord blood. A phase I trial of reduced-intensity double UCB transplantation was performed to evaluate safety, rates of engraftment and fractional chimerism of dmPGE2 enhanced UCB units. To explore potential causes of the lack of enhanced efficacy in the first cohort, we characterized HSCs to determine whether the prostaglandin pathway was being activated under the ex vivo incubation conditions (4´℃, 10´μM dmPGE2, 60 minutes). Incubation conditions were identified (37´℃, 10´μM dmPGE2, 120 minutes) that maximize the activation of the prostaglandin pathway by dmPGE2 in human CD34+ cells. **Overall design:** Isolated human CD34+ from umbilical cord blood were incubated ex vivo in Stem Span media with 10uM 16,16-dmPGE2 or DMSO. Two treatment conditions were evaluated (4 deg C for 1 hour, 37 deg C for 2 hours) with either 3 or 7 biological replicates at each condition. Total RNA was isolated post incubation and analyzed on Affymetrix microarrays for pathway activation.

Background corr dist: KL-Divergence = 0.1142, L1-Distance = 0.0409, L2-Distance = 0.0034, Normal std = 0.4152

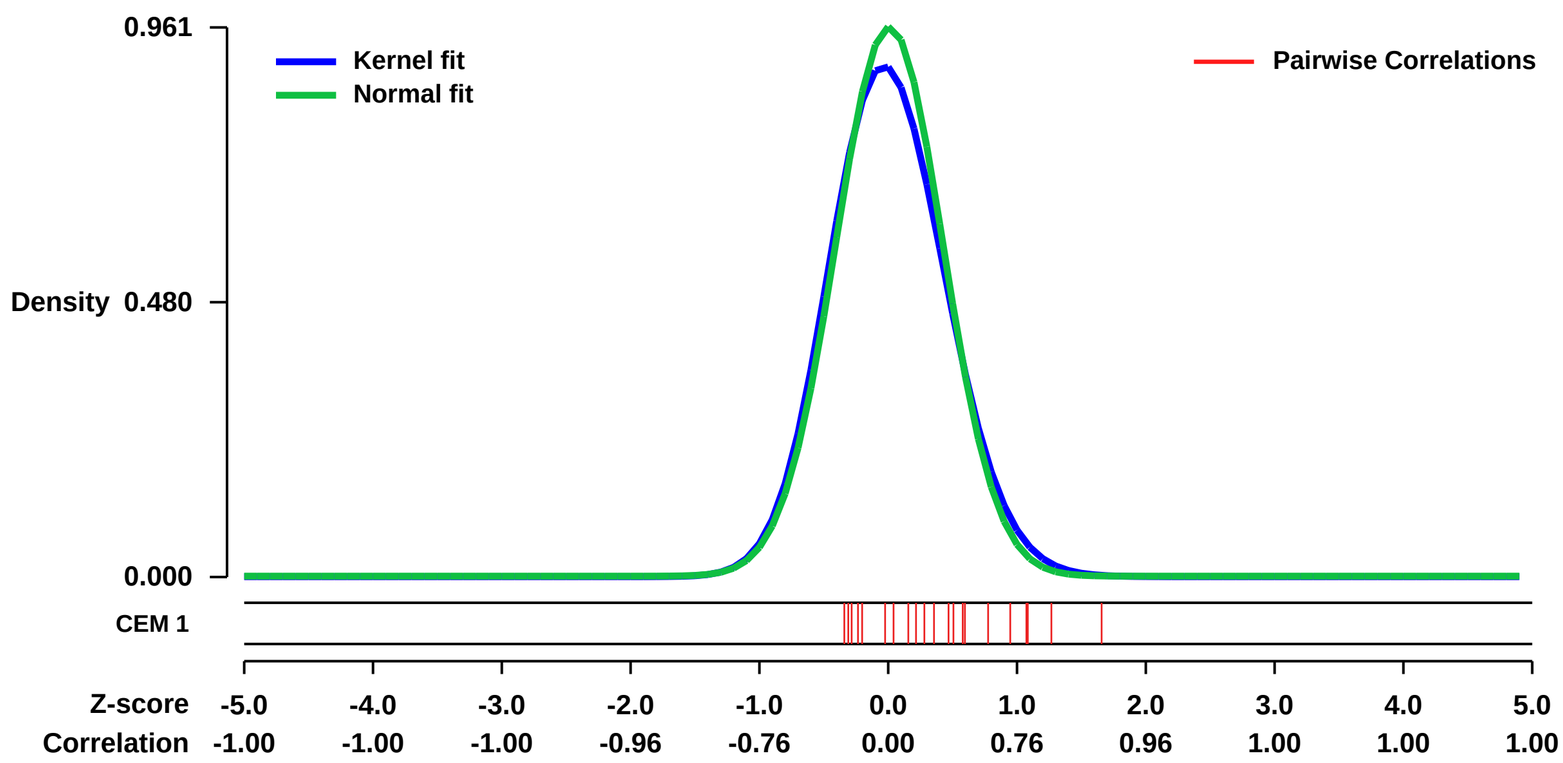

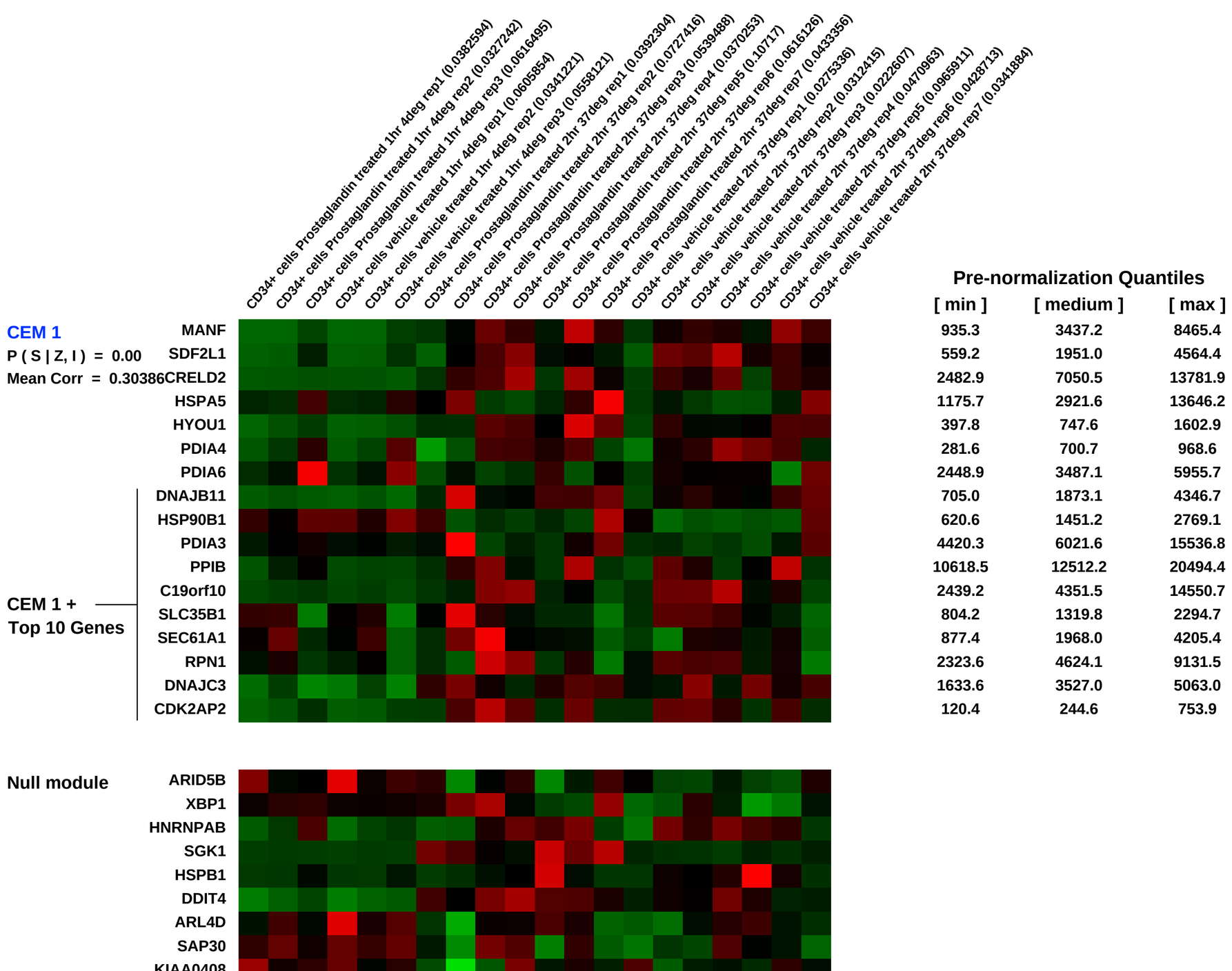

Pre-normalization Quantiles

	[min]	[medium]	[max]
MANF	935.3	3437.2	8465.4
SDF2L1	559.2	1951.0	4564.4
CRELD2	2482.9	7050.5	13781.9
HSPA5	1175.7	2921.6	13646.2
HYOU1	397.8	747.6	1602.9
PDIA4	281.6	700.7	968.6
PDIA6	2448.9	3487.1	5955.7
DNAJB11	705.0	1873.1	4346.7
HSP90B1	620.6	1451.2	2769.1
PDIA3	4420.3	6021.6	15536.8
PPIB	10618.5	12512.2	20494.4
C19orf10	2439.2	4351.5	14550.7
SLC35B1	804.2	1319.8	2294.7
SEC61A1	877.4	1968.0	4205.4
RPN1	2323.6	4624.1	9131.5
DNAJC3	1633.6	3527.0	5063.0
CDK2AP2	120.4	244.6	753.9

GEO Series "GSE21225" Expression Profiles

Num of samples in this series: 6

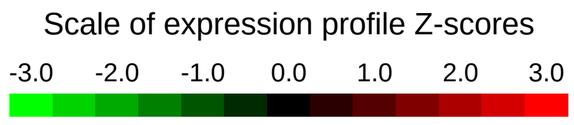

GEO Link:	http://www.ncbi.nlm.nih.gov/geo/query/acc.cgi?acc=GSE21225
Status:	Public on Sep 07 2010
Title:	Low dose hCG pregnant vs non-pregnant
Organism:	Homo sapiens
Experiment type:	Expression profiling by array
Platform:	GPL570
Pubmed ID:	20800227
Summary & Design:	**Summary:** Influence of ovarian stimulation with 200 IU of hCG, (administered in the late follicular phase among ICSI patients undergoing a GnRH-antagonist protocol), on the endometrium on the day of oocyte pick-up. The purpose of the present study is to assess the influence of the administration of low dose hCG on the endometrium. In addition, by analysing the correlation of the morphological pattern and gene expression profile of human endometrium on the day of oocyte retrieval in patients of both treatment groups, we want to study the implantation potential. Pregnant and non-pregnant patients were compared. **Overall design:** In total 6 samples were analyzed for gene expression analysis with microarrays, 3 pregnant and 3 non-pregnant patients were compared.

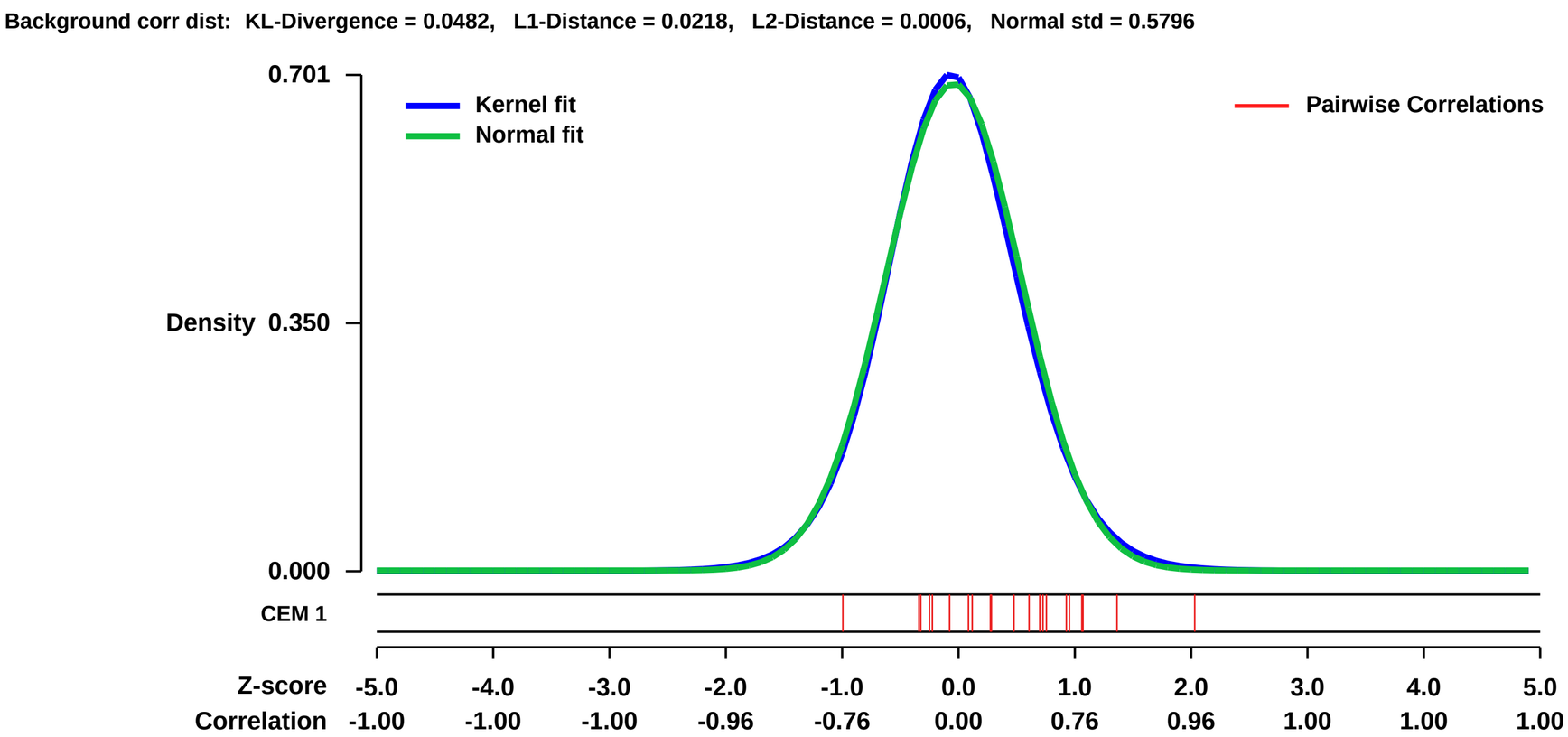

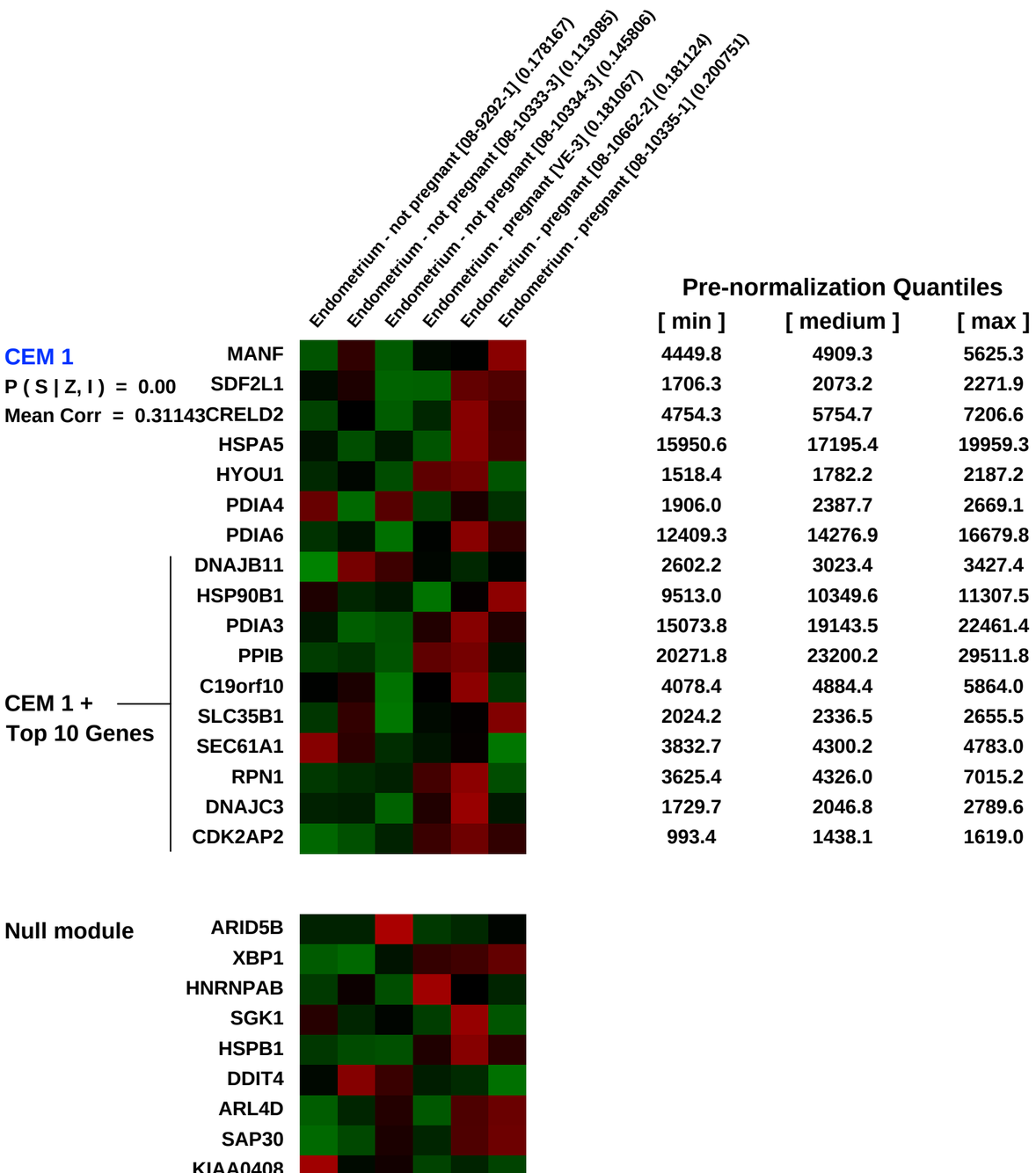

Pre-normalization Quantiles

	[min]	[medium]	[max]
MANF	4449.8	4909.3	5625.3
SDF2L1	1706.3	2073.2	2271.9
CRELD2	4754.3	5754.7	7206.6
HSPA5	15950.6	17195.4	19959.3
HYOU1	1518.4	1782.2	2187.2
PDIA4	1906.0	2387.7	2669.1
PDIA6	12409.3	14276.9	16679.8
DNAJB11	2602.2	3023.4	3427.4
HSP90B1	9513.0	10349.6	11307.5
PDIA3	15073.8	19143.5	22461.4
PPIB	20271.8	23200.2	29511.8
C19orf10	4078.4	4884.4	5864.0
SLC35B1	2024.2	2336.5	2655.5
SEC61A1	3832.7	4300.2	4783.0
RPN1	3625.4	4326.0	7015.2
DNAJC3	1729.7	2046.8	2789.6
CDK2AP2	993.4	1438.1	1619.0

GEO Series "GSE58004" Expression Profiles

Num of samples in this series: 8

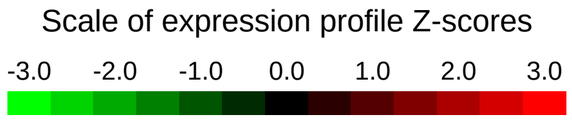

GEO Link:	http://www.ncbi.nlm.nih.gov/geo/query/acc.cgi?acc=GSE58004
Status:	Public on Sep 04 2014
Title:	Epigenetic silencing of miR-210 increases the proliferation of gastric epithelium during chronic Helicobacter pylori infection
Organism:	Homo sapiens
Experiment type:	Expression profiling by array
Platform:	GPL570
Pubmed ID:	
Summary & Design:	**Summary:** Persistent colonization of the gastric mucosa by Helicobacter pylori (Hp) elicits chronic inflammation and aberrant epithelial cell proliferation, which increases the risk of gastric cancer. We examined the ability of microRNAs to modulate gastric cell proliferation in response to persistent Hp infection and found that epigenetic silencing of miR-210 plays a key role in gastric disease progression. Importantly, DNA methylation of the miR-210 gene was increased in Hp-positive human gastric biopsies as compared to Hp-negative controls. Moreover silencing of miR-210 in gastric epithelial cells promoted proliferation. We identified STMN1 and DIMT1 as miR-210 target genes and demonstrated that inhibition of miR-210 expression augmented cell proliferation by activating STMN1 and DIMT1. Together, our results highlight inflammation-induced epigenetic silencing of miR-210 as a mechanism of induction of chronic gastric diseases, including cancer, during Hp infection. **Overall design:** To identify miR-210 targets in gastric cells, whole transcriptome analysis of AGS and MKN45 cells transfected with pre-miR-210 was conducted using Affymetrix GeneChip Human Genome U133 Plus 2.0 Array.

Background corr dist: KL-Divergence = 0.0397, L1-Distance = 0.0415, L2-Distance = 0.0022, Normal std = 0.6495

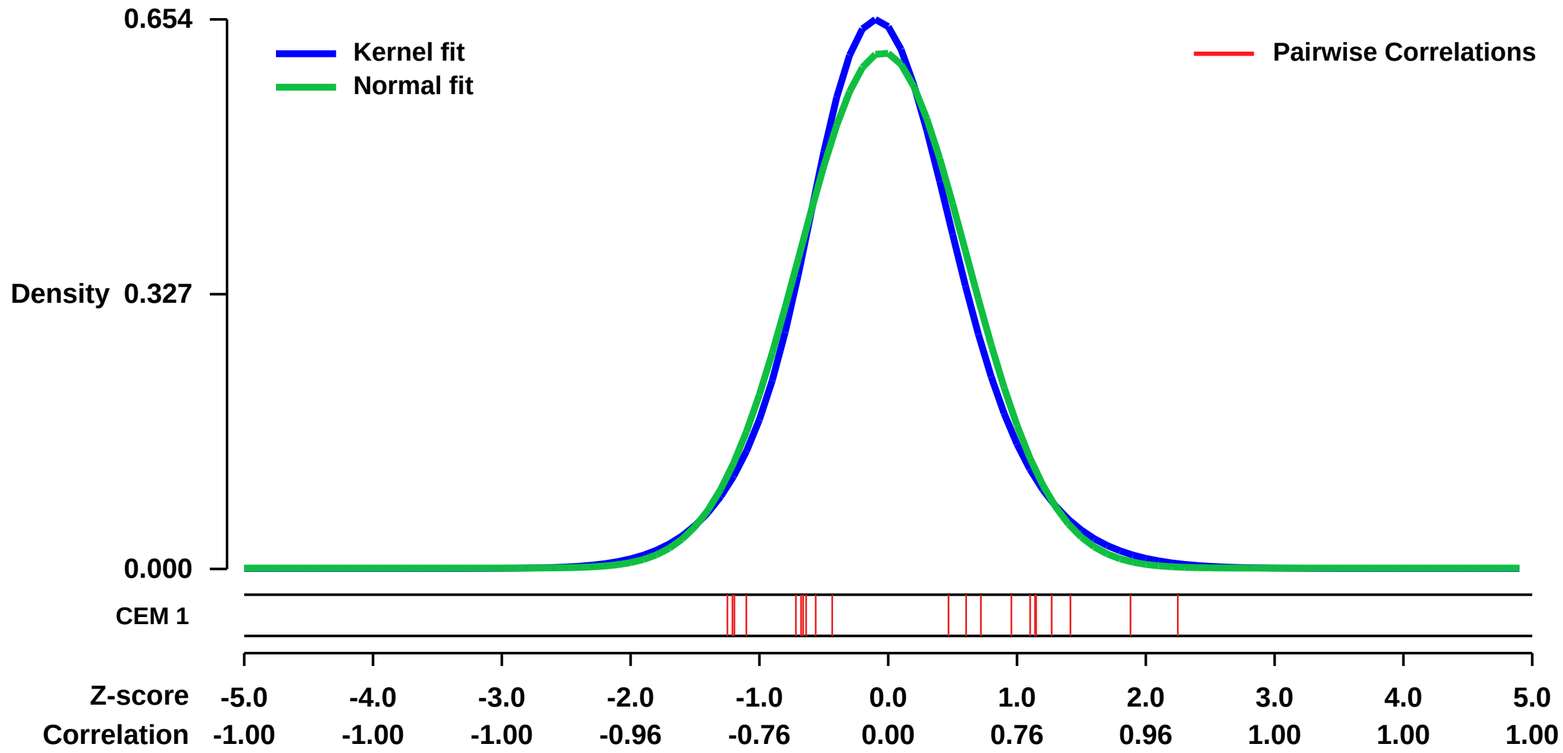

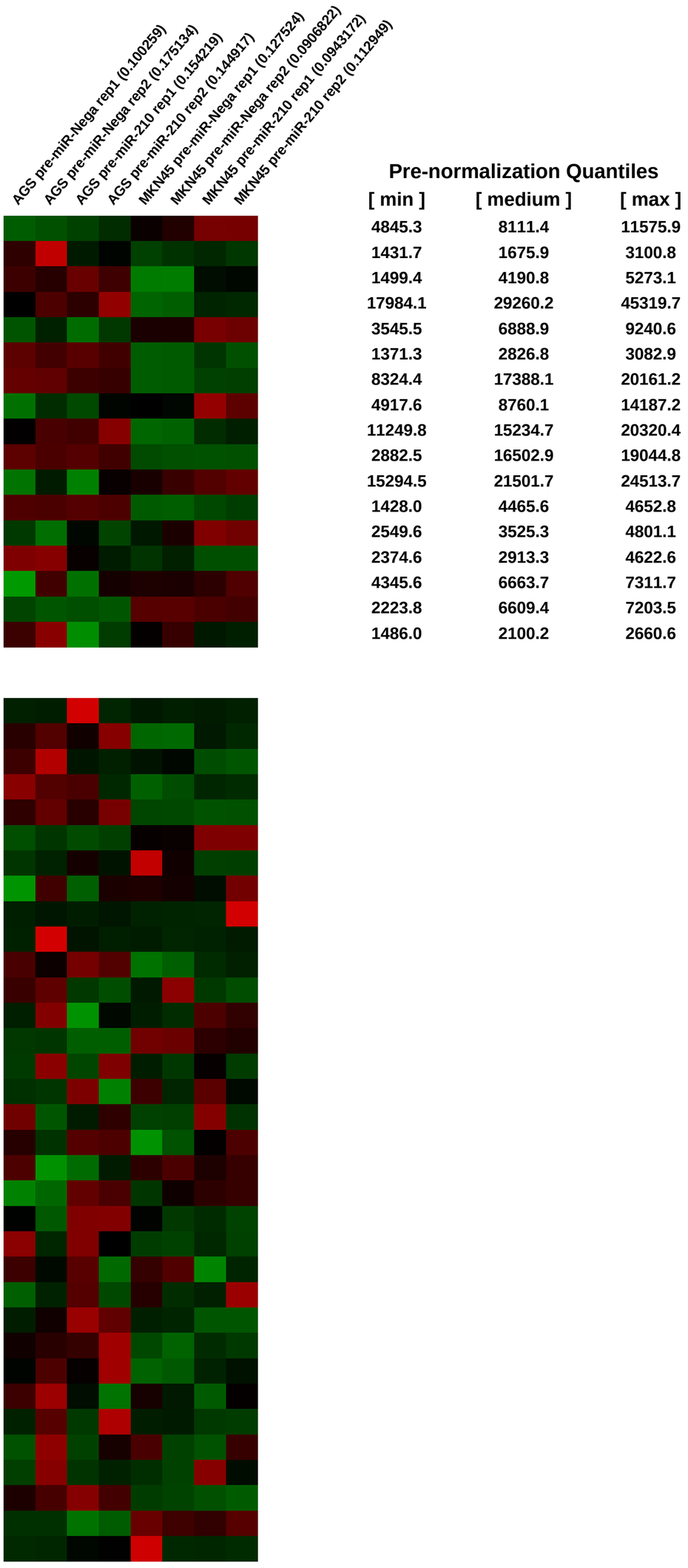

GEO Series "GSE11551" Expression Profiles

Num of samples in this series: 8

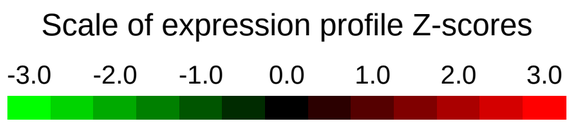

GEO Link:	http://www.ncbi.nlm.nih.gov/geo/query/acc.cgi?acc=GSE11551
Status:	Public on May 29 2008
Title:	Hs 294T Cells Treated with Elesclomol Alone or in Combination with NAC Compared to DMSO Treated
Organism:	Homo sapiens
Experiment type:	Expression profiling by array
Platform:	GPL570
Pubmed ID:	18723479
Summary & Design:	**Summary:** We used microarrays to detail gene expression changes in Hs 294T human melanoma cells after treatment with elesclomol alone, or in combination with NAC, to aide in identifing the mechnism of action of elesclomol. **Keywords: treatment** **Overall design:** Hs 294T human melanoma cells were grown in vitro. They were seeded at a low density and were left untreated, treated with the vehicle, treated with elesclomol, treated with NAC, or treated in combination with both elesclomol and NAC. The cells treated with NAC were given the NAC 30 minutes prior to additional treatments. They were incubated for 6 hours before harvesting.

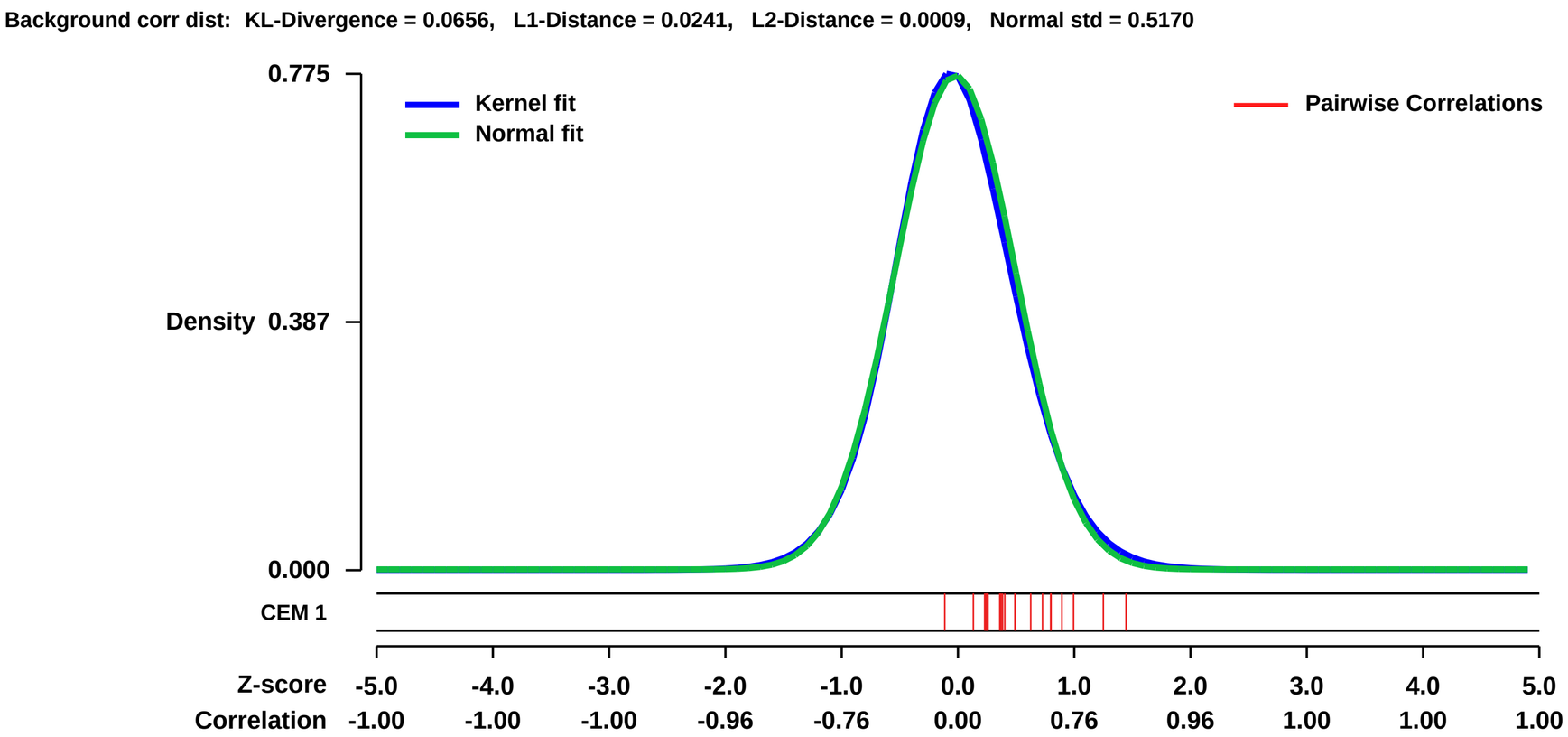

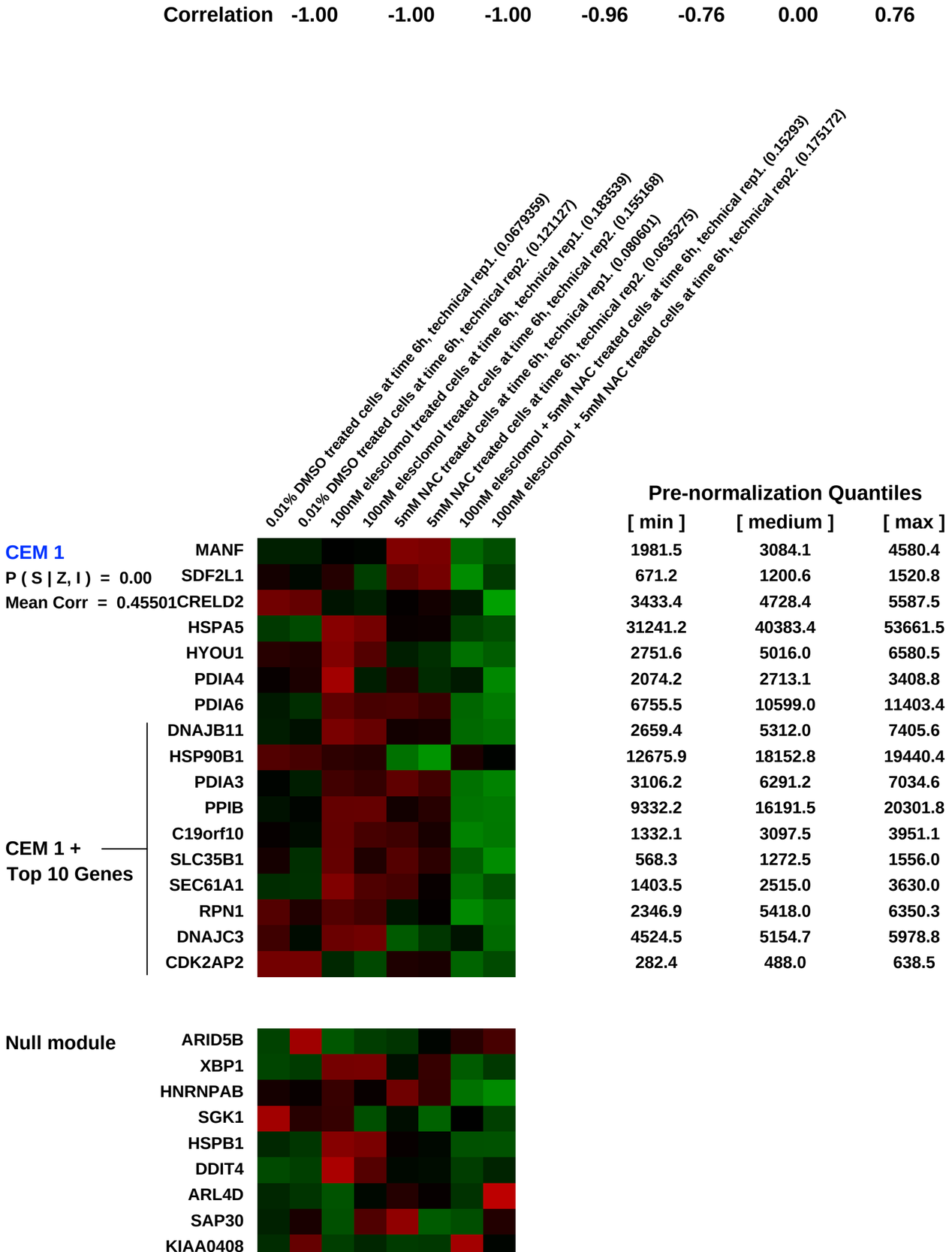

GEO Series "GSE7538" Expression Profiles

Num of samples in this series: 24

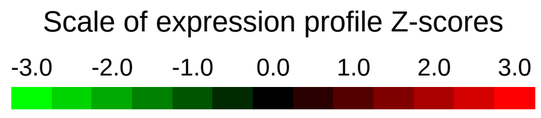

GEO Link:	http://www.ncbi.nlm.nih.gov/geo/query/acc.cgi?acc=GSE7538
Status:	Public on Feb 27 2008
Title:	Treatment of primary acute myelogenous leukemia (AML) specimens with parthenolide (PTL)
Organism:	Homo sapiens
Experiment type:	Expression profiling by array
Platform:	GPL570
Pubmed ID:	24934933
Summary & Design:	**Summary:** The effects of 7.5 micromolar parthenolide (PTL) were assessed on primary CD34+ acute myelogenous leukemia specimens obtained from 12 patients. **Keywords: drug response, gene expression search agent** **Overall design:** Acute myelogenous leukemia (AML) specimens were obtained from 12 patients and CD34+ cells were isolated. For each patient, cells were cultured in vitro and exposed to either 7.5 micromolar parthenolide (PTL) or left untreated (UT) for 6 h. Total RNA was then harvested for global gene expression analysis.

Background corr dist: KL-Divergence = 0.1711, L1-Distance = 0.0542, L2-Distance = 0.0074, Normal std = 0.3524

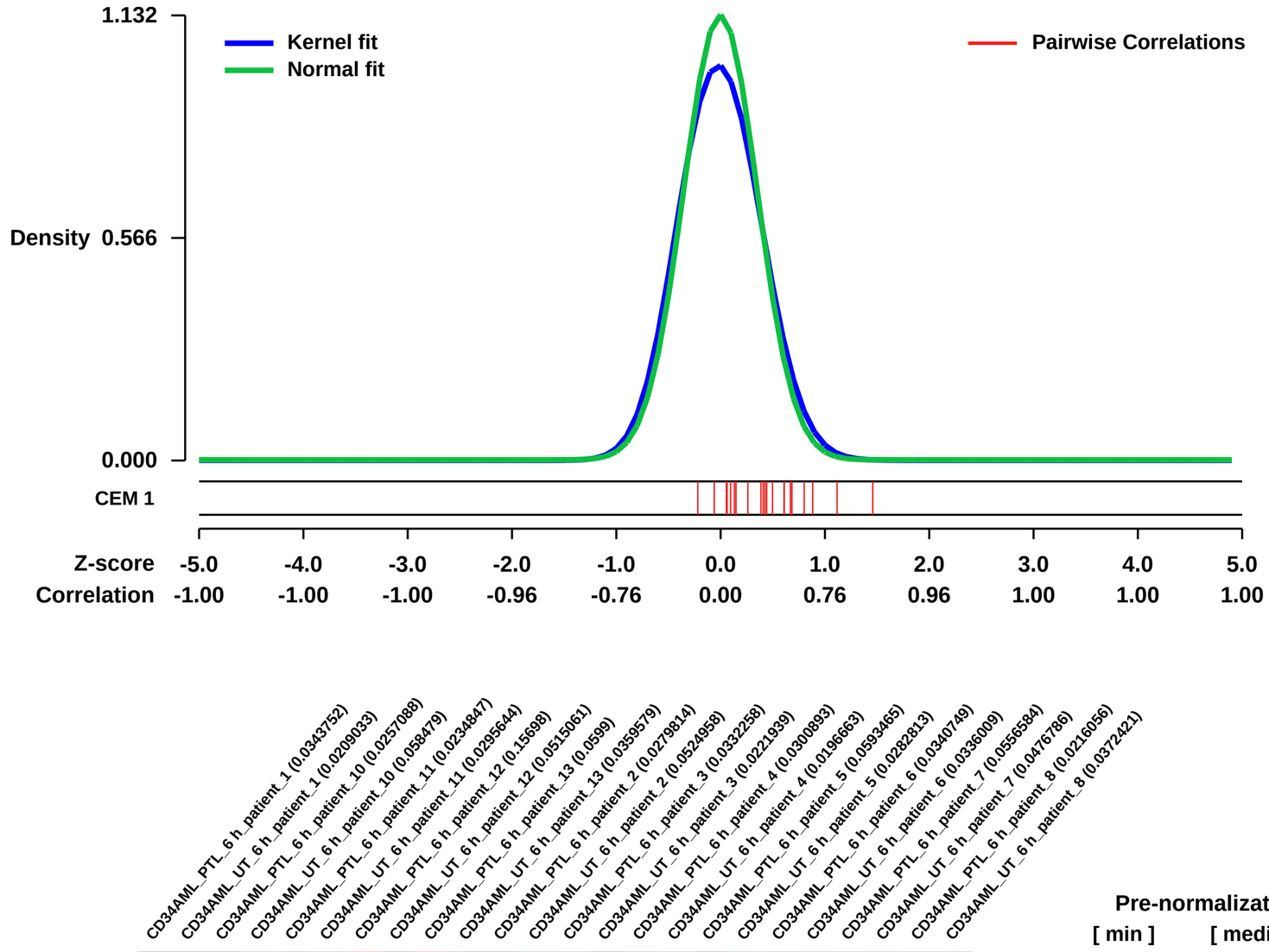

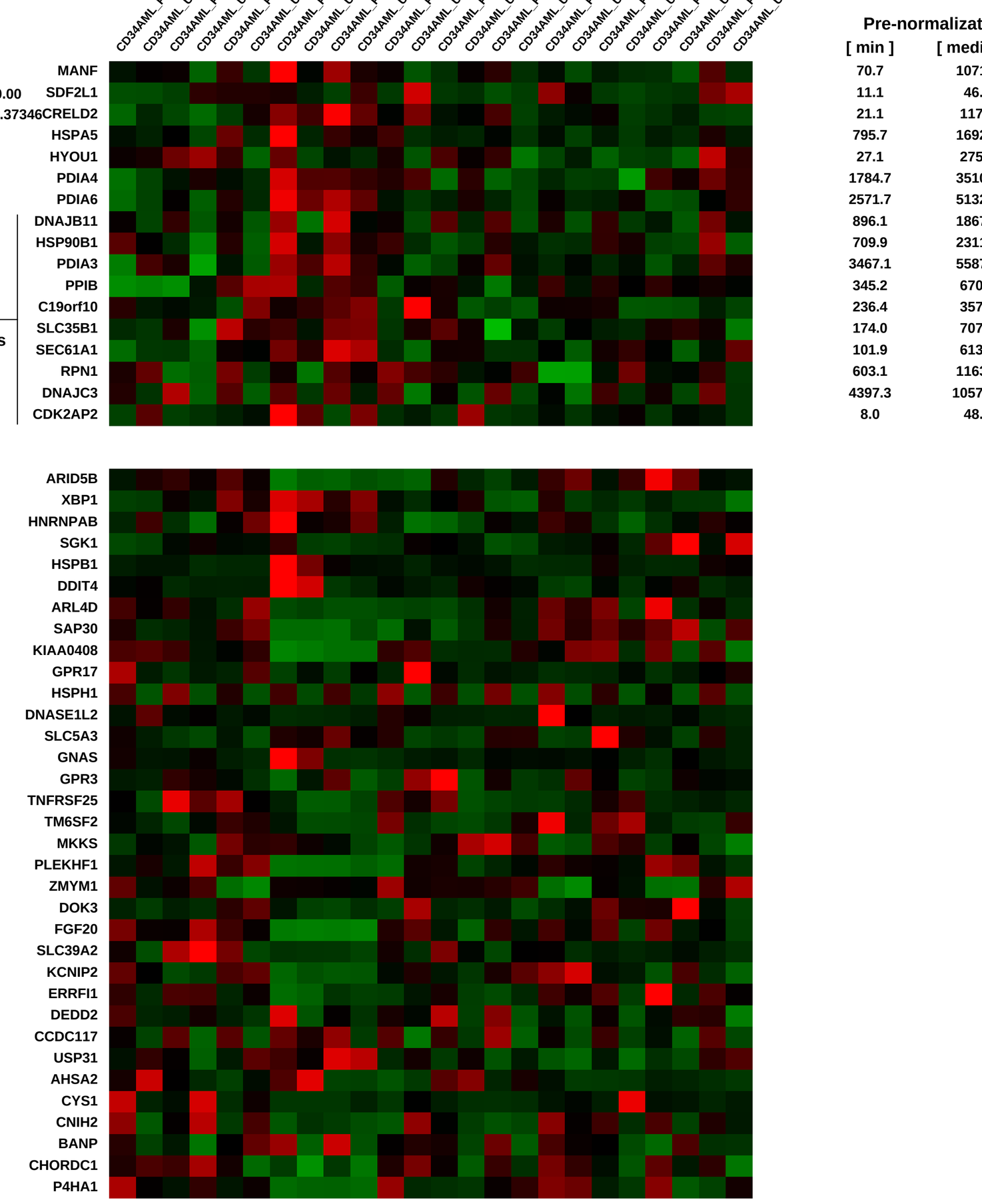

Pre-normalization Quantiles

[min]	[medium]	[max]
70.7	1071.2	4661.9
11.1	46.3	320.0
21.1	117.6	408.6
795.7	1692.9	9657.5
27.1	275.2	637.0
1784.7	3510.0	5474.0
2571.7	5132.3	12621.6
896.1	1867.7	3842.0
709.9	2311.9	5852.5
3467.1	5587.6	8219.8
345.2	670.8	1044.3
236.4	357.3	769.1
174.0	707.8	1154.6
101.9	613.1	1691.6
603.1	1163.9	1567.7
4397.3	10577.5	20270.6
8.0	48.2	306.6

GEO Series "GSE3397" Expression Profiles

Num of samples in this series: 12

Scale of expression profile Z-scores

-3.0 -2.0 -1.0 0.0 1.0 2.0 3.0

GEO Link:	http://www.ncbi.nlm.nih.gov/geo/query/acc.cgi?acc=GSE3397
Status:	Public on May 01 2006
Title:	RSV gene expression
Organism:	Homo sapiens
Experiment type:	Expression profiling by array
Platform:	GPL570
Pubmed ID:	19459069
Summary & Design:	**Summary:** Human bronchial epithelial cells (BEAS-2B cells) were treated with RSV at 1.0 MOI for 4 and 24 hours or control (vehicle-treated for 4 hours). Global gene expression was measured by Affy Hu133 plus 2.0 microarray chips. **Keywords: Inflammation, microtubules, RSV, time course** **Overall design:** 4 RSV-treated for 24 hours

Background corr dist: KL-Divergence = 0.1367, L1-Distance = 0.0322, L2-Distance = 0.0019, Normal std = 0.3877

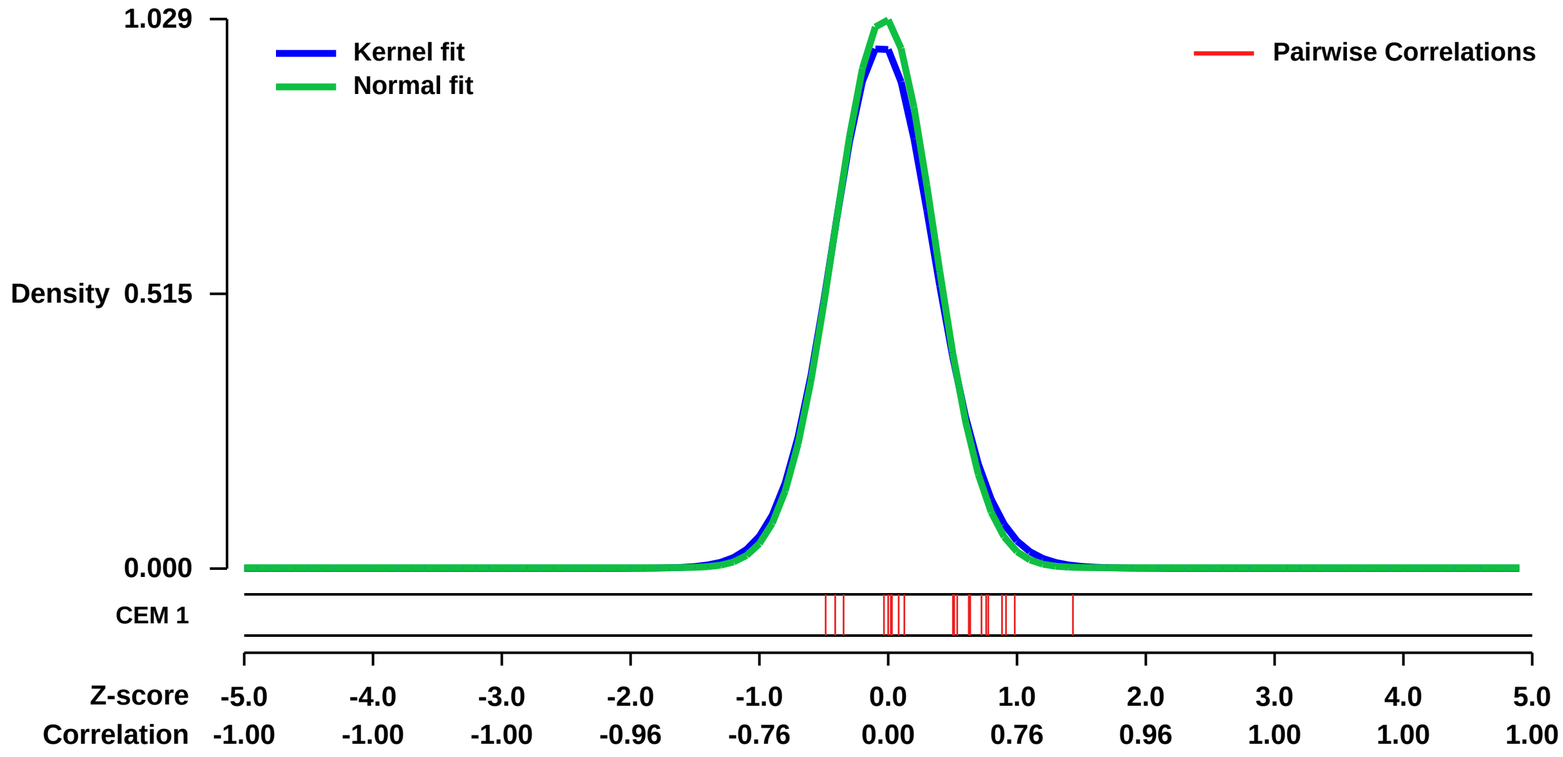

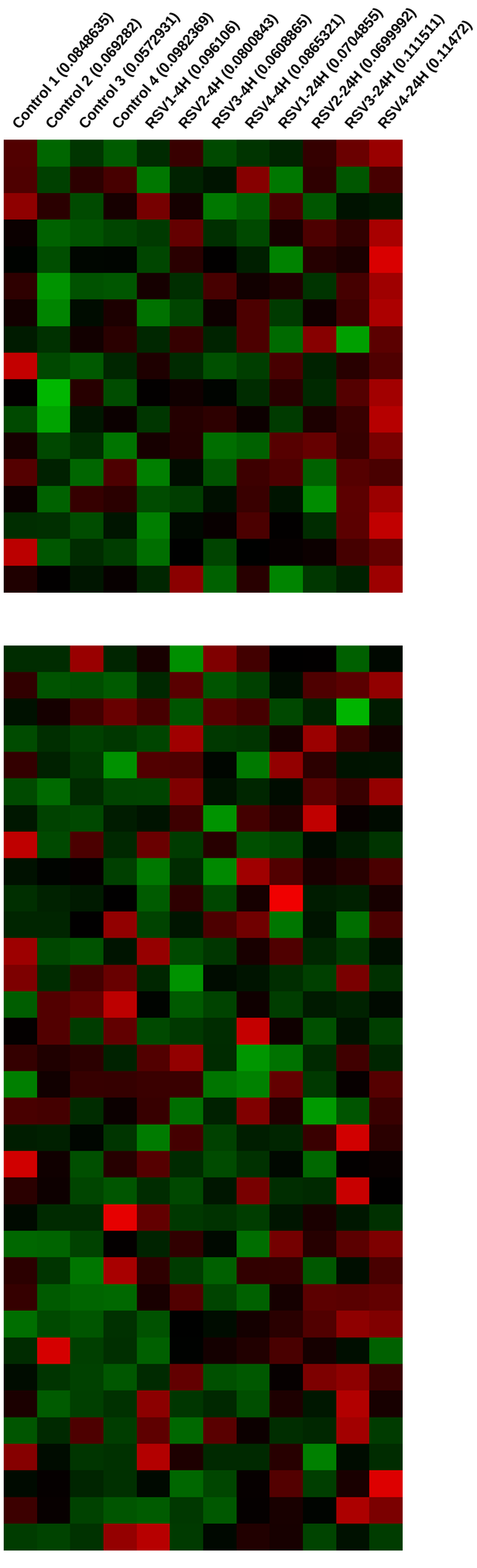

Pre-normalization Quantiles

	[min]	[medium]	[max]
CEM 1			
P (S | Z, I) = 0.00			
Mean Corr = 0.31339			
MANF	4362.8	5257.4	7769.0
SDF2L1	1043.9	1490.6	1736.7
CRELD2	2535.4	3873.4	5028.6
HSPA5	13215.0	18396.3	25820.2
HYOU1	5340.2	6786.8	9309.3
PDIA4	1420.5	1946.8	2377.7
PDIA6	6286.8	7394.7	8580.5
CEM 1 + Top 10 Genes			
DNAJB11	4568.8	5752.4	6542.4
HSP90B1	4817.7	5731.3	9486.5
PDIA3	9723.8	11663.2	13310.9
PPIB	10511.5	13107.2	15635.3
C19orf10	3095.6	3814.9	4327.7
SLC35B1	2336.3	2932.8	3007.1
SEC61A1	3166.9	3967.6	4731.1
RPN1	3204.8	3885.2	5055.5
DNAJC3	2339.9	2796.7	3574.5
CDK2AP2	1120.8	1380.4	1679.1
Null module			
ARID5B			
XBP1			
HNRNPAB			
SGK1			
HSPB1			
DDIT4			
ARL4D			
SAP30			
KIAA0408			
GPR17			
HSPH1			
DNASE1L2			
SLC5A3			
GNAS			
GPR3			
TNFRSF25			
TM6SF2			
MKKS			
PLEKHF1			
ZMYM1			
DOK3			
FGF20			
SLC39A2			
KCNIP2			
ERRFI1			
DEDD2			
CCDC117			
USP31			
AHSA2			
CYS1			
CNIH2			
BANP			
CHORDC1			
P4HA1			

GEO Series "GSE27220" Expression Profiles

Num of samples in this series: 15

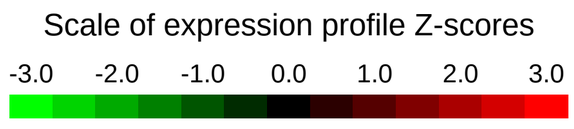

GEO Link: http://www.ncbi.nlm.nih.gov/geo/query/acc.cgi?acc=GSE27220

Status: Public on Feb 11 2011

Title: Transcriptional effects of 1,25 dihydroxi-vitamin D3 physiological and supra-physiological concentrations in breast cancer organotypic culture

Organism: Homo sapiens

Experiment type: Expression profiling by array

Platform: GPL570

Pubmed ID:

Summary & Design:

Summary:
Vitamin D may have anti-tumorigenic actions by influencing the gene expression profile of target tissues, which possess vitamin D receptors. We used a more physiological in vitro model, represented by short-term culture of breast cancer tissue slices, to study the transcriptional effects of a near physiological concentration of calcitriol. Methods. Breast cancer fragments were sliced and maintained in culture for 24 hours in the presence or absence (control) of calcitriol 0.5nM or 100nM (called physiological or supra-physiological concentrations). Five and 16 samples were included in a test or validation group and gene expression was analyzed by microarray (using SAM paired analysis) or qPCR, respectively. Results. Nine genes were regulated by calcitriol 0.5nM including CYP24A1, DPP4, EFTUD1 (FDR´£0.01), which were up-modulated. However, using a less stringent FDR value (0.25) 61 genes were differentially expressed. Among the down-regulated transcripts were members of the MHC class II complex (HLA-DPA1, HLA-DQA1, HLA-DQA2, HLA-DQB1, HLA-DRA, HLA-DRB1, HLA-DRB3) and IgG binding (FCGR2A, FCGR2B, FCGR2C). There was an enrichment of genes presenting transcription factor binding sites for vitamin D, among the up-regulated genes and for interferon regulatory factor IRF1, among the down-regulated genes. Analyzing calcitriol supra-physiological effects, a more impressive transcriptional modulation was identified and 136 and 60 genes (FDR 0.1) were more and less expressed in treated samples. Up-regulated genes were involved in vitamin metabolic process, regulation of leukocyte-mediated immunity and positive regulation of alpha-beta T cell activation. Many of the induced genes were already reported as vitamin D responsive genes, including CD14, which was also up-regulated in another set of 16 samples. Genes modulated by both calcitriol concentrations were CYP24A1, DPP4, CA2 (these three in both sets of samples), EFTUD1, TKTL1, KCNK3. Conclusion. Small increments in calcitriol concentration, within the physiological range, for a relatively short period of time may exert transcriptional effects in breast cancer samples. Further studies employing physiological concentrations of vitamin D for longer periods of time may help to elucidate the hormone effects in breast cancer treatment and prevention.

Overall design:
Breast cancer fragments were sliced and maintained in culture for 24 hours in the presence or absence (control) of calcitriol 0.5nM or 100nM (called physiological or supra-physiological concentrations). Five samples were included and were categorized according to treatment in three groups: control (A), 1,25(OH)2D3 0.5nM (B) and 1,25(OH)2D3 100nM (C).Total RNA was isolated using RNeasy kit and than was carried out according to microarray Affymetrix protocol. Data was then assessed with GeneSpring X software for background correction, normalization and summarization of raw data (CEL files) using the Robust Multi-Array Average (RMA). Five samples were included in a test and gene expression was analyzed by microarray (using SAM paired analysis). To establish a differential gene expression profile between vitamin D treated and untreated samples, SAM two class paired, provided on MEV (MultiExperiment Viewer â Boston, MA, USA) was used. Unsupervised hierarchical clustering based on Euclidean distance and average linkage was used to verify association patterns. The reliability of the clustering was assessed by the Bootstrap technique using MEV (MultiExperiment Viewer â Boston, MA, USA). Samples (16) were included in a validation group and was analyzed by qPCR.

Background corr dist: KL-Divergence = 0.0877, L1-Distance = 0.0364, L2-Distance = 0.0026, Normal std = 0.4631

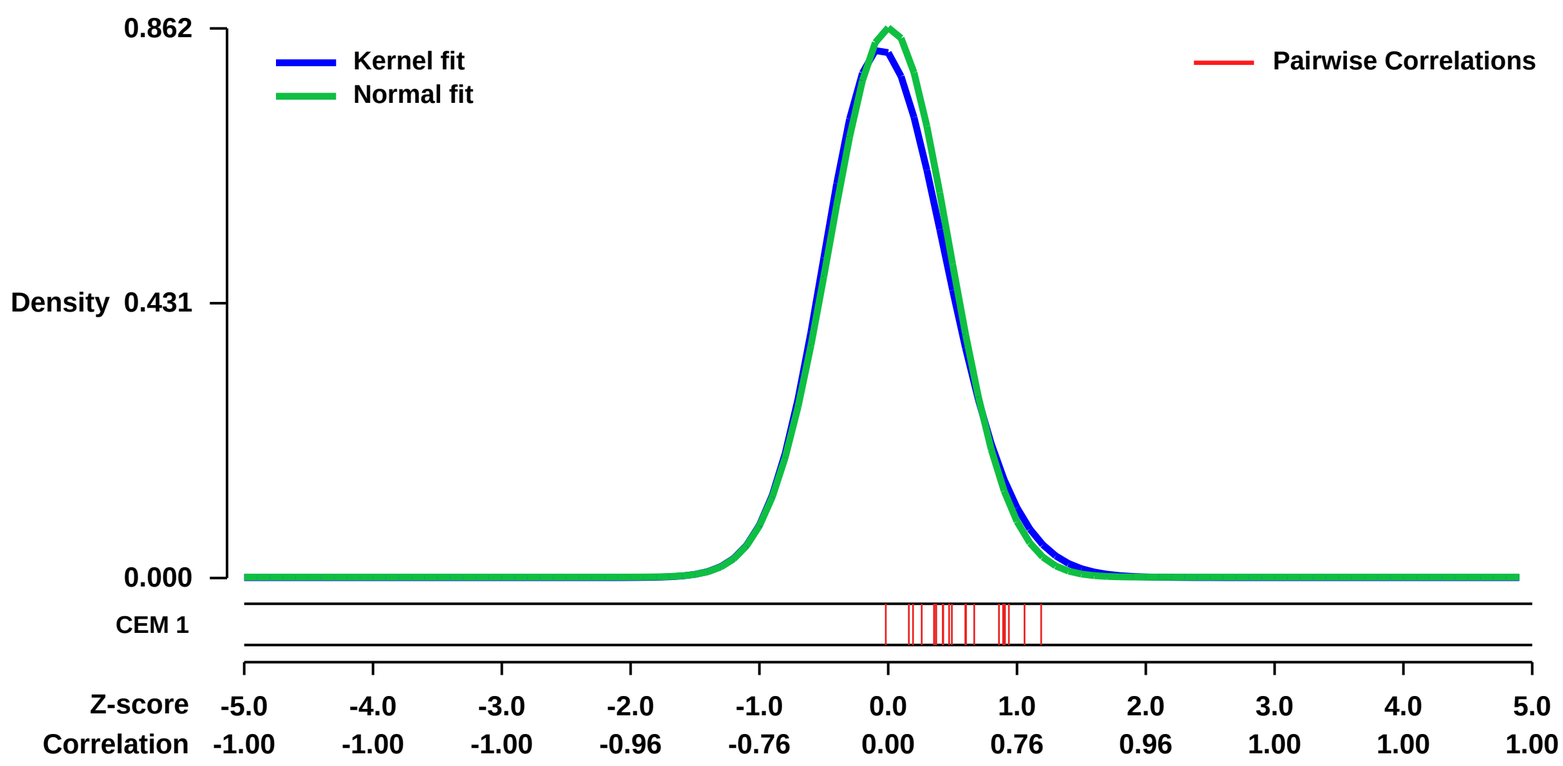

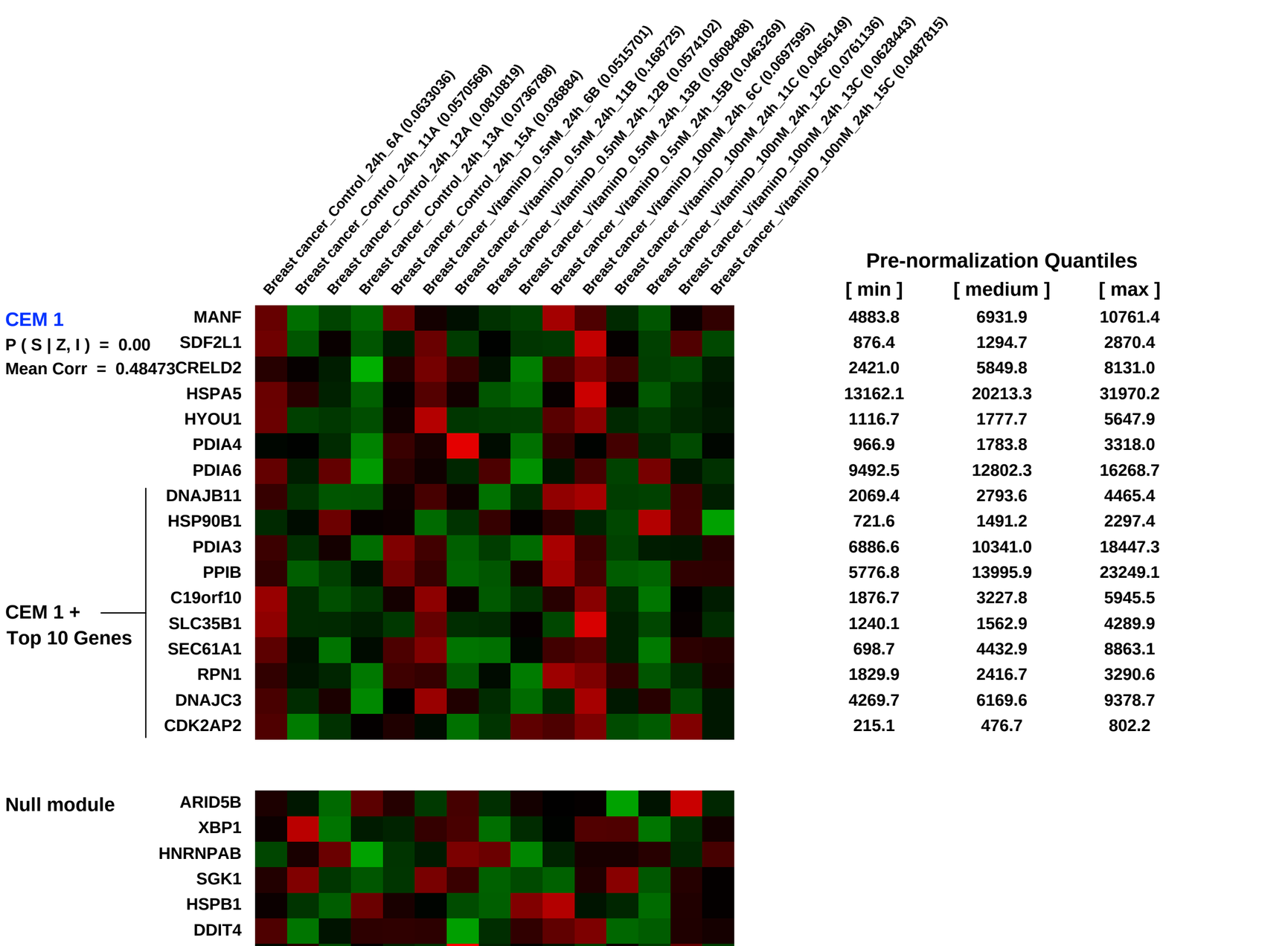

GEO Series "GSE32161" Expression Profiles

Num of samples in this series: 6

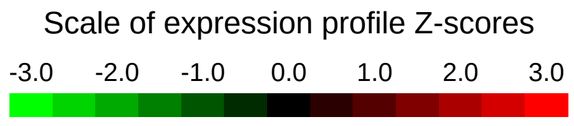

GEO Link:	http://www.ncbi.nlm.nih.gov/geo/query/acc.cgi?acc=GSE32161
Status:	Public on Sep 16 2011
Title:	Microarray analysis of genes associated with cell surface NIS protein levels in breast cancer
Organism:	Homo sapiens
Experiment type:	Expression profiling by array
Platform:	GPL570
Pubmed ID:	21989294
Summary & Design:	**Summary:** Na+/I- symporter (NIS)-mediated iodide uptake allows radioiodine therapy for thyroid cancer. NIS is also expressed in breast tumors, raising potential for radionuclide therapy of breast cancer. However, NIS expression in most breast cancers is low and may not be sufficient for radionuclide therapy. A better understanding of the mechanisms of NIS regulation in breast cancer may lead to strategies for increasing cell surface NIS and radioactive iodide uptake (RAIU) in breast cancer. The MCF-7 cell line is the only human breast cancer cell line with inducible endogenous NIS expression. Kogai et al. [2000] first reported that trans-retinoic acid (tRA) induces NIS mRNA expression in MCF-7 cells and it was later reported that a combination treatment of tRA and hydrocortisone (tRA/H) further increases tRA-induced NIS expression/function in MCF-7 cells (Kogai et al., 2005; Dohan et al., 2006). In this study, we used gene expression profiling to identify genes that correlate with NIS expression in MCF-7 cells such that mechanisms underlying NIS modulation may be elucidated. **Overall design:** MCF-7 cells were treated with DMSO vehicle, tRA (1´µM), or tRA(1´µM)/H(1´µM) for 12 hours and total RNA was extracted. There are two replicates for each treatment group.

Background corr dist: KL-Divergence = 0.0326, L1-Distance = 0.0144, L2-Distance = 0.0002, Normal std = 0.6487

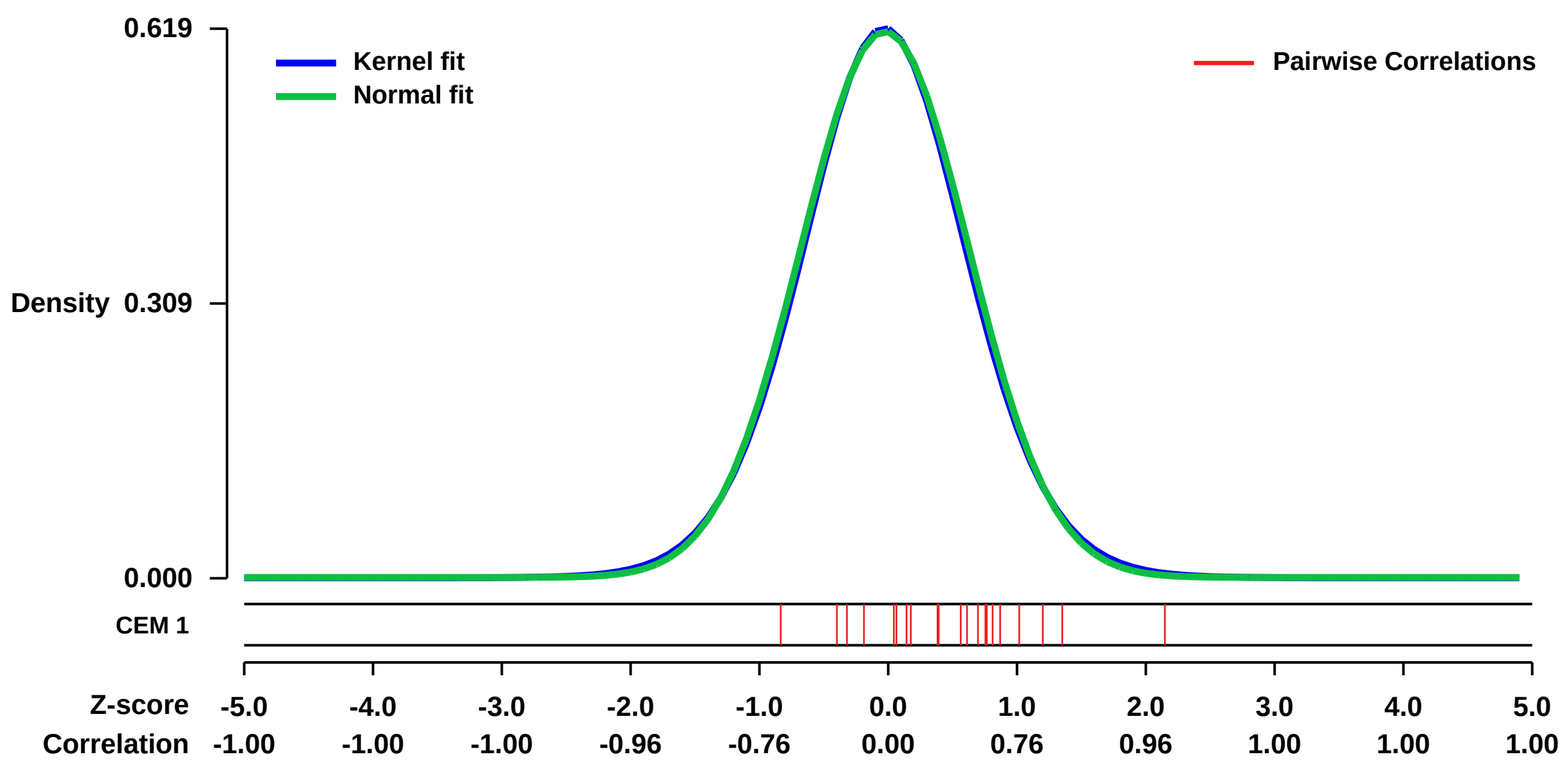

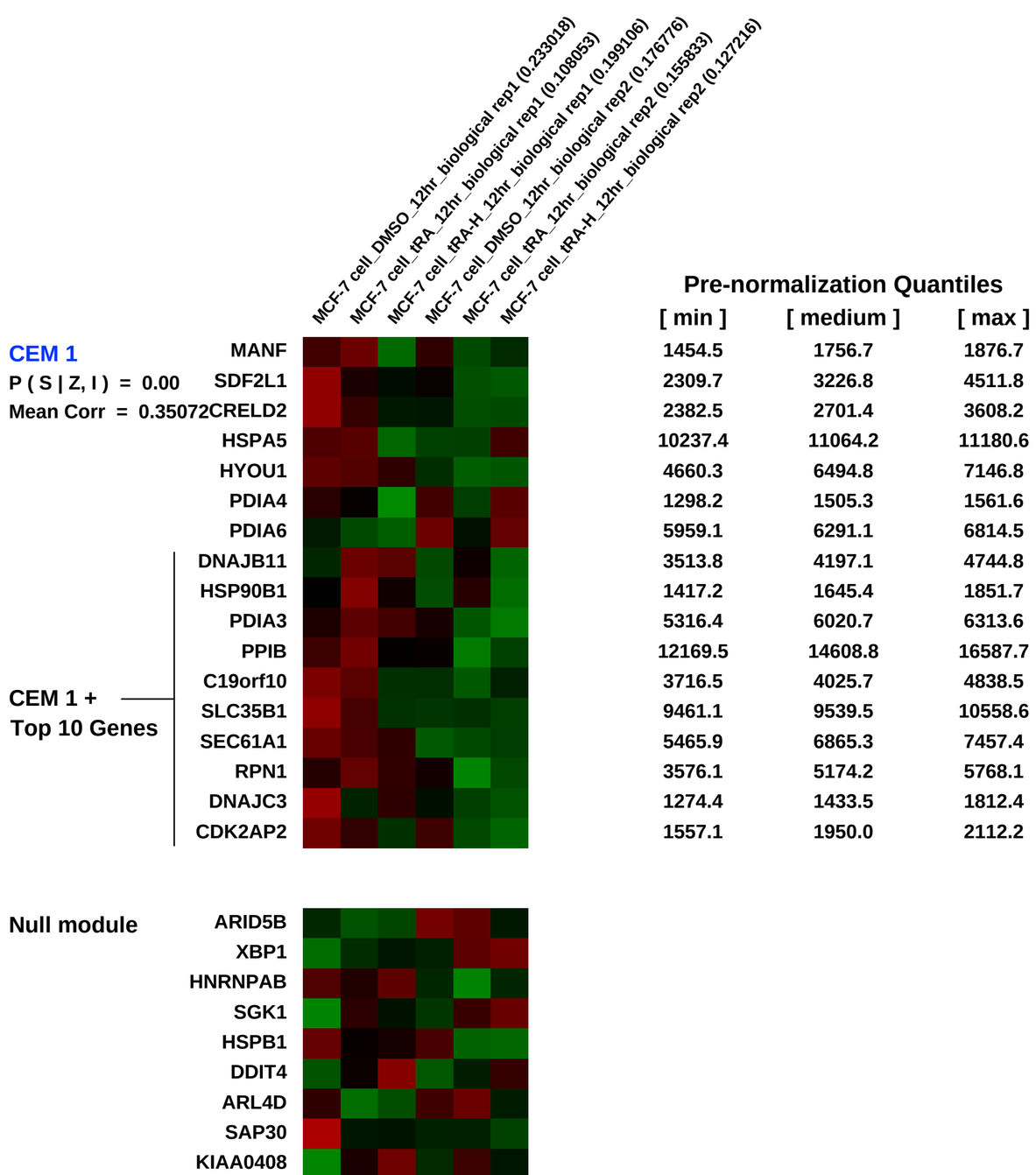

	Pre-normalization Quantiles		
	[min]	[medium]	[max]
MANF	1454.5	1756.7	1876.7
SDF2L1	2309.7	3226.8	4511.8
CRELD2	2382.5	2701.4	3608.2
HSPA5	10237.4	11064.2	11180.6
HYOU1	4660.3	6494.8	7146.8
PDIA4	1298.2	1505.3	1561.6
PDIA6	5959.1	6291.1	6814.5
DNAJB11	3513.8	4197.1	4744.8
HSP90B1	1417.2	1645.4	1851.7
PDIA3	5316.4	6020.7	6313.6
PPIB	12169.5	14608.8	16587.7
C19orf10	3716.5	4025.7	4838.5
SLC35B1	9461.1	9539.5	10558.6
SEC61A1	5465.9	6865.3	7457.4
RPN1	3576.1	5174.2	5768.1
DNAJC3	1274.4	1433.5	1812.4
CDK2AP2	1557.1	1950.0	2112.2
ARID5B			
XBP1			
HNRNPAB			
SGK1			
HSPB1			
DDIT4			
ARL4D			
SAP30			
KIAA0408			
GPR17			
HSPH1			
DNASE1L2			
SLC5A3			
GNAS			
GPR3			
TNFRSF25			
TM6SF2			
MKKS			
PLEKHF1			
ZMYM1			
DOK3			
FGF20			
SLC39A2			
KCNIP2			
ERRFI1			
DEDD2			
CCDC117			
USP31			
AHSA2			
CYS1			
CNIH2			
BANP			
CHORDC1			
P4HA1			

GEO Series "GSE8853" Expression Profiles

Num of samples in this series: 6

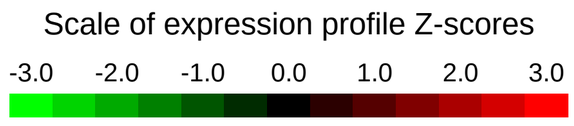

GEO Link:	http://www.ncbi.nlm.nih.gov/geo/query/acc.cgi?acc=GSE8853
Status:	Public on Dec 21 2007
Title:	IL-13 involvement in eosinophilic esophagitis: transcriptome analysis
Organism:	Homo sapiens
Experiment type:	Expression profiling by array
Platform:	GPL570
Pubmed ID:	20208004
Summary & Design:	**Summary:** 3 eosinophilic esophagitis biopsies, cultured and stimulated with IL-13 : each of them was either left unstimulated or stimulated (100ng for 48h) We used microarray to uncover the IL-13-induced genes in esophageal epithelial cells of the esophagus Keywords: treated vs non treated **Overall design:** 3 biopsies from EE patients were obtained and primary epithelial cell were cultured and either left unstimulated or stimulated with IL-13 followed by RNA extraction and hybridization on Affymetrix microarrays.

Background corr dist: KL-Divergence = 0.0295, L1-Distance = 0.0175, L2-Distance = 0.0003, Normal std = 0.6741

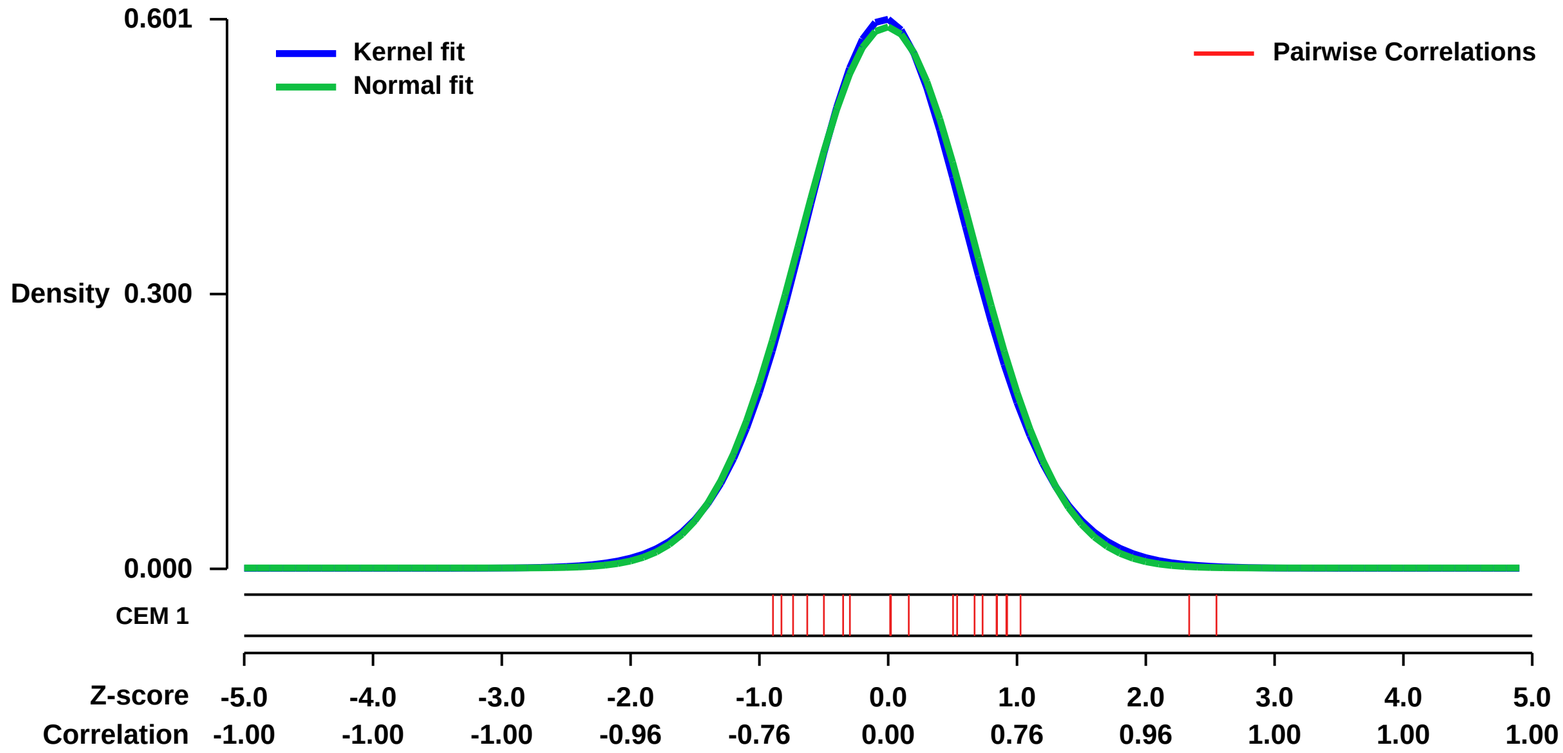

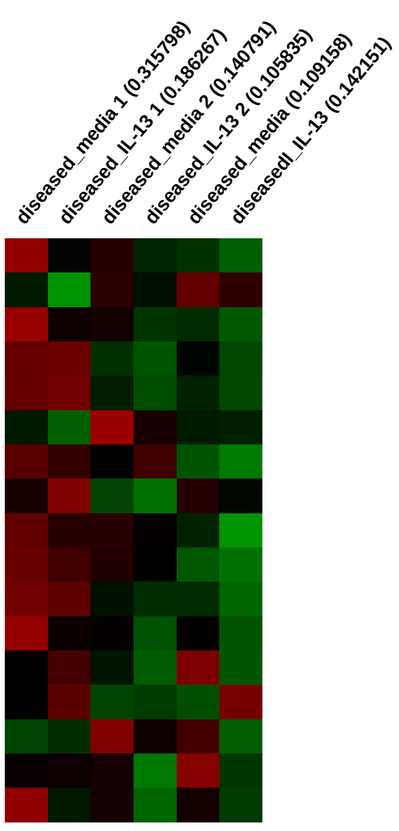

Pre-normalization Quantiles

		[min]	[medium]	[max]
CEM 1	MANF	2414.5	2825.3	3498.9
P (S | Z, I) = 0.00	SDF2L1	509.0	632.8	670.9
Mean Corr = 0.20298	CRELD2	2035.0	2424.9	2972.1
	HSPA5	14565.5	17937.6	22583.9
	HYOU1	1035.6	1235.4	1804.4
	PDIA4	554.3	636.5	847.6
	PDIA6	5229.5	5756.8	5867.9
CEM 1 + Top 10 Genes	DNAJB11	3162.3	3553.3	3855.6
	HSP90B1	3144.3	4324.4	4691.3
	PDIA3	3622.8	4822.2	5412.2
	PPIB	3916.1	4410.4	5157.2
	C19orf10	2129.0	2406.2	2861.4
	SLC35B1	2906.7	3113.4	3378.9
	SEC61A1	2198.7	2348.0	2573.3
	RPN1	2828.6	3017.4	3217.3
	DNAJC3	4081.7	4573.4	5026.5
	CDK2AP2	279.7	383.0	488.7
Null module	ARID5B			
	XBP1			
	HNRNPAB			
	SGK1			
	HSPB1			
	DDIT4			
	ARL4D			
	SAP30			
	KIAA0408			
	GPR17			
	HSPH1			
	DNASE1L2			
	SLC5A3			
	GNAS			
	GPR3			
	TNFRSF25			
	TM6SF2			
	MKKS			
	PLEKHF1			
	ZMYM1			
	DOK3			
	FGF20			
	SLC39A2			
	KCNIP2			
	ERRFI1			
	DEDD2			
	CCDC117			
	USP31			
	AHSA2			
	CYS1			
	CNIH2			
	BANP			
	CHORDC1			
	P4HA1			

GEO Series "GSE14973" Expression Profiles

Num of samples in this series: 28

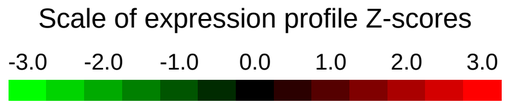

GEO Link:	http://www.ncbi.nlm.nih.gov/geo/query/acc.cgi?acc=GSE14973
Status:	Public on Aug 24 2009
Title:	Antileukemic activity of valproic acid in chronic lymphocytic leukemia cells defined by microarray analysis
Organism:	Homo sapiens
Experiment type:	Expression profiling by array
Platform:	GPL570
Pubmed ID:	19710697
Summary & Design:	**Summary:** Epigenetic code modifications by histone deacetylase inhibitors (HDACi) have recently been proposed as potential new therapies for hematological malignancies. Chronic Lymphocytic Leukemia (CLL) remains incurable despite the introduction of new treatments. CLL cells are characterized by an apoptosis defect rather than excessive proliferation, but proliferation centers have been found in organs such as bone marrow and lymph nodes. Here, we investigated gene expression modifications in CLL cells following treatment with valproic acid (VPA), a well-tolerated anti-epileptic drug with HDAC inhibitory activity. **Overall design:** CLL cells obtained from 14 patients were treated in vitro with a concentration of 1mM VPA for 4 hours. VPA effects on gene expression were thereafter studied using Affymetrix technology

Background corr dist: KL-Divergence = 0.2218, L1-Distance = 0.0605, L2-Distance = 0.0096, Normal std = 0.3176

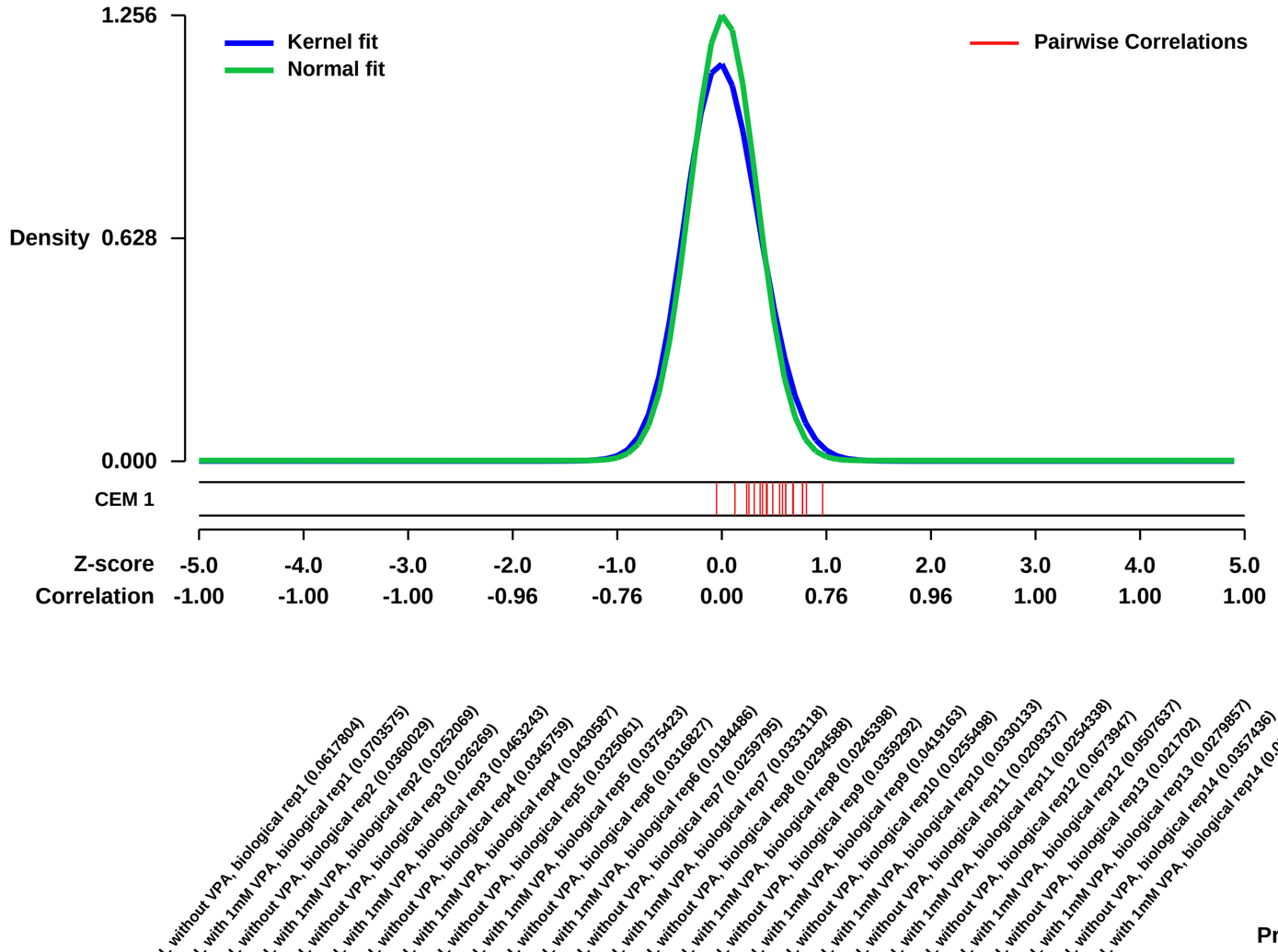

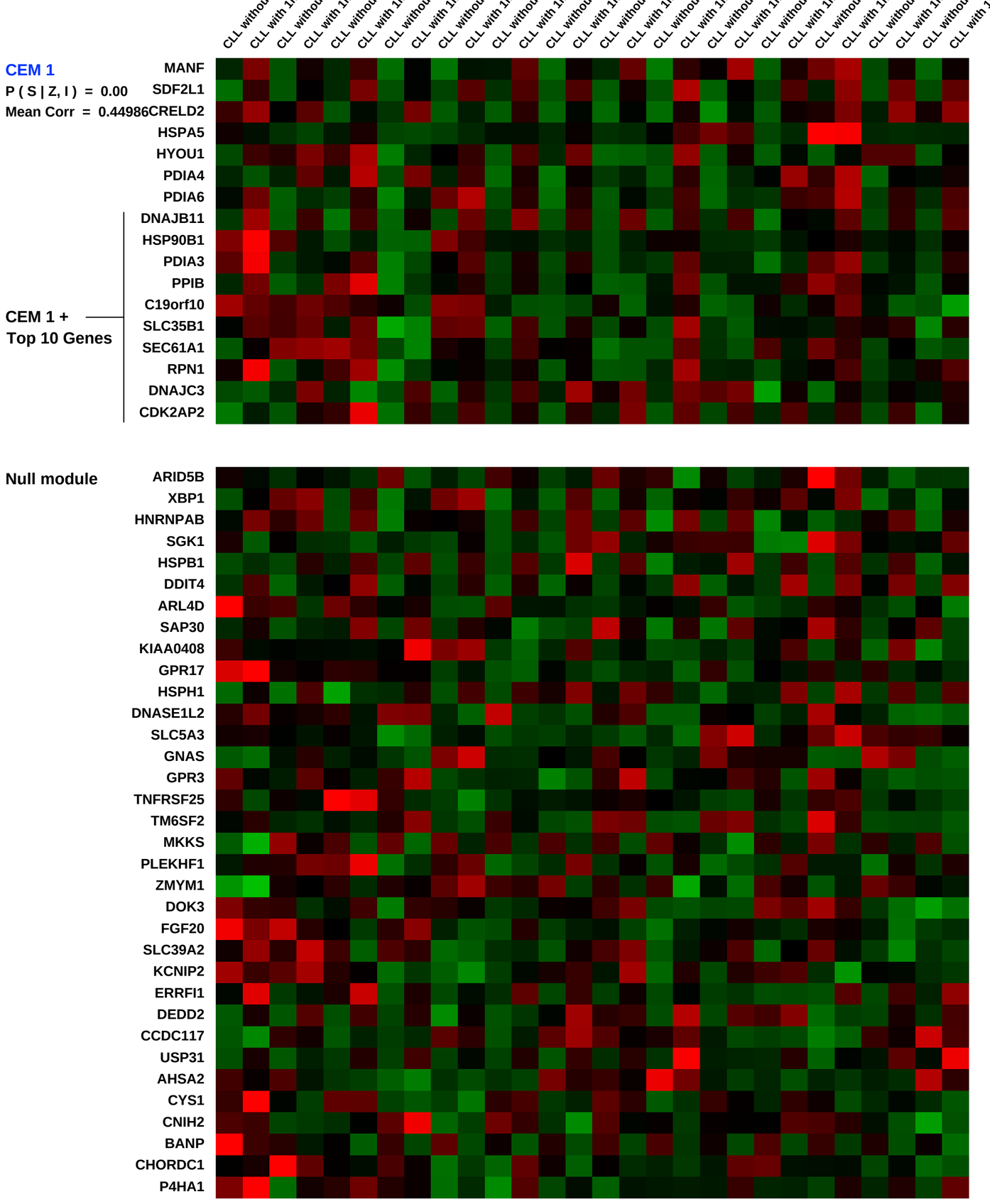

Pre-normalization Quantiles

	[min]	[medium]	[max]
CLL	1113.1	1758.5	2548.2
CLL	258.4	603.0	1182.9
CLL	1305.9	2671.3	4249.9
CLL	2835.8	3365.4	7534.8
CLL	966.8	1559.2	2373.6
CLL	203.7	297.6	462.0
CLL	1006.4	2460.8	4729.3
CLL	1424.9	2373.0	3613.5
CLL	927.2	1714.2	5223.0
CLL	3296.9	5642.1	11623.7
CLL	4186.1	6002.6	9997.1
CLL	828.4	1144.3	1416.0
CLL	696.8	923.8	1112.0
CLL	1393.5	1714.7	2089.8
CLL	1026.1	1414.6	2206.7
CLL	1042.4	1548.4	2002.4
CLL	579.0	1257.2	2228.1

GEO Series "GSE21351" Expression Profiles

Num of samples in this series: 6

Scale of expression profile Z-scores

-3.0 -2.0 -1.0 0.0 1.0 2.0 3.0

GEO Link:	http://www.ncbi.nlm.nih.gov/geo/query/acc.cgi?acc=GSE21351
Status:	Public on Apr 08 2013
Title:	Ubiquinol-induced gene expression signatures are translated into reduced erythropoiesis and LDL cholesterol levels in humans
Organism:	Homo sapiens
Experiment type:	Expression profiling by array
Platform:	GPL570
Pubmed ID:	21280176
Summary & Design:	**Summary:** Studies in vitro and in mice indicate a role for Coenzyme Q10 (CoQ10) in gene expression. To determine this function in relationship to physiological readouts, a 2-week supplementation study with the reduced form of CoQ10 (ubiquinol, Q10H2, 150 mg/d) was performed in 53 healthy males. Mean CoQ10 plasma levels increased 4.8-fold after supplementation. Transcriptomic and bioinformatic approaches identified a gene-gene interaction network in CD14-positive monocytes, which functions in inflammation, cell differentiation and PPAR-signaling. These Q10H2-induced gene expression signatures were also described previously in liver tissues of SAMP1 mice. Biochemical as well as NMR-based analyses showed a reduction of LDL cholesterol plasma levels after Q10H2 supplementation. This effect was especially pronounced in atherogenic small dense LDL particles (19-21 nm, 1.045 g/l). In agreement with gene expression signatures, Q10H2 reduces the number of erythrocytes but increases the concentration of reticulocytes. In conclusion, Q10H2 induces characteristic gene expression patterns, which are translated into reduced LDL cholesterol levels and erythropoiesis in humans. #!# **Overall design:** Whole genome expression profiles were analyzed in isolated monocytes of 3 Q10H2 supplemented subjects at the indicated time points (before (T0) and after (T14) Q10H2 supplementation. This results in a total of 6 microarrays.

Background corr dist: KL-Divergence = 0.0181, L1-Distance = 0.0393, L2-Distance = 0.0016, Normal std = 0.9022

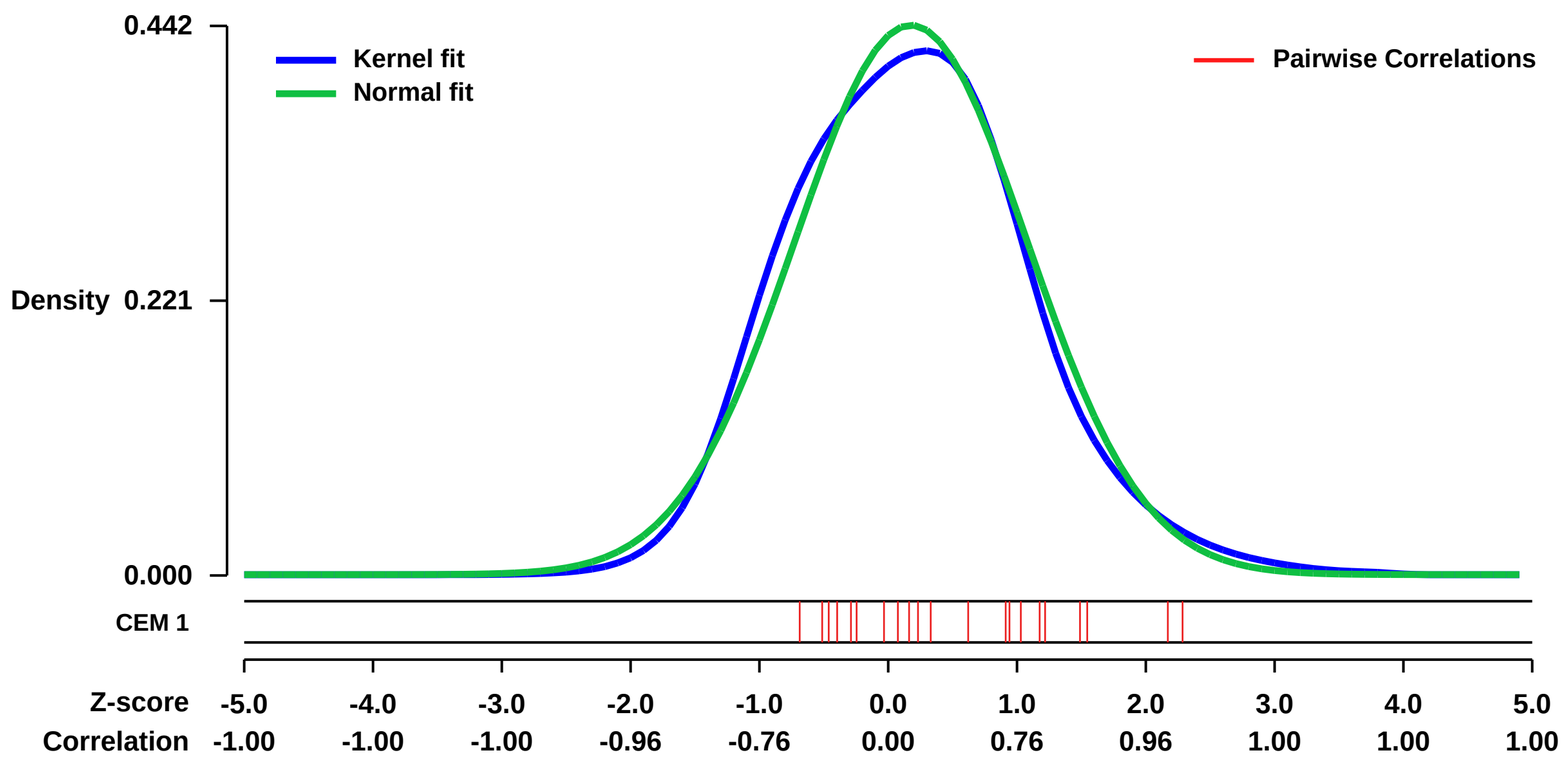

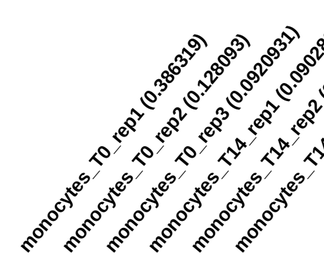

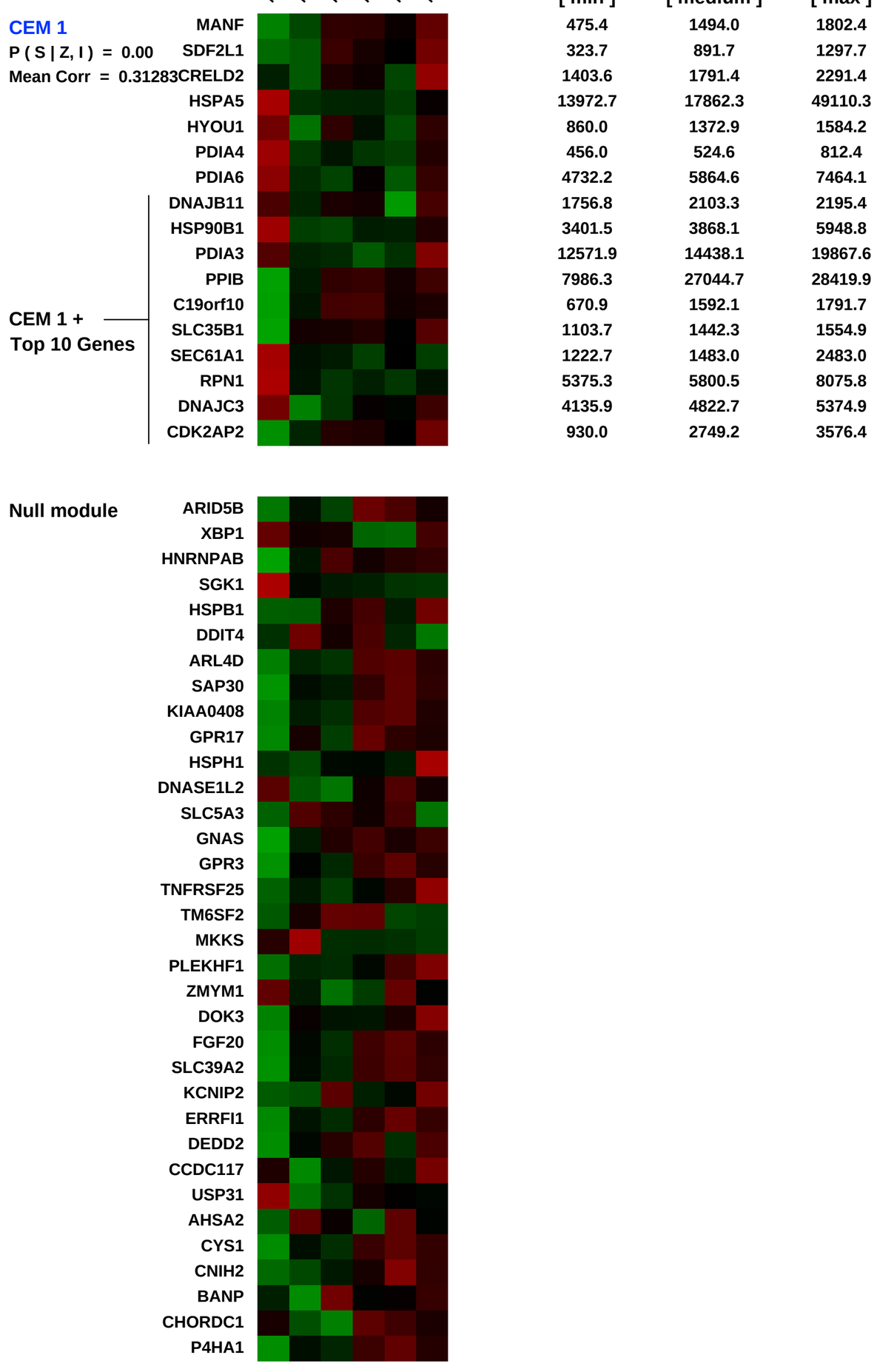

Pre-normalization Quantiles

	[min]	[medium]	[max]
MANF	475.4	1494.0	1802.4
SDF2L1	323.7	891.7	1297.7
CRELD2	1403.6	1791.4	2291.4
HSPA5	13972.7	17862.3	49110.3
HYOU1	860.0	1372.9	1584.2
PDIA4	456.0	524.6	812.4
PDIA6	4732.2	5864.6	7464.1
DNAJB11	1756.8	2103.3	2195.4
HSP90B1	3401.5	3868.1	5948.8
PDIA3	12571.9	14438.1	19867.6
PPIB	7986.3	27044.7	28419.9
C19orf10	670.9	1592.1	1791.7
SLC35B1	1103.7	1442.3	1554.9
SEC61A1	1222.7	1483.0	2483.0
RPN1	5375.3	5800.5	8075.8
DNAJC3	4135.9	4822.7	5374.9
CDK2AP2	930.0	2749.2	3576.4

GEO Series "GSE19959" Expression Profiles

Num of samples in this series: 14

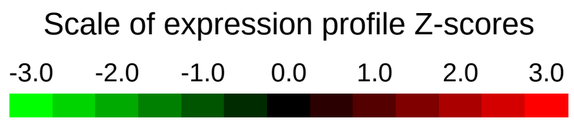

GEO Link:	http://www.ncbi.nlm.nih.gov/geo/query/acc.cgi?acc=GSE19959
Status:	Public on Dec 21 2010
Title:	Premature progesterone rise
Organism:	Homo sapiens
Experiment type:	Expression profiling by array
Platform:	GPL570
Pubmed ID:	21273126
Summary & Design:	**Summary:** Premature progesterone (P) rise during GnRH antagonist cycles for IVF is a frequent phenomenon and has been associated with lower pregnancy and implantation rates. Different thresholds of progesterone have been used so far to define its premature rise during the follicular phase of an IVF stimulated cycle. In this study, we evaluated endometrial gene expression on the day of oocyte retrieval according to the level of serum progesterone on the day of hCG administration in GnRH antagonist cycles.Endometrial biopsies from eleven patients were taken with a Pipelle de Cornier (Prodimed, Neuilly-en-Thelle, France) on the day of oocyte retrieval in a GnRH antagonist/rec-FSH stimulated IVF cycle with fresh embryo transfer. Biopsies were analysed for gene expression with Affymetrix Human Genome (HG) U133 Plus 2.0 Arrays and GCOS software (Affymetrix, Santa Clara, CA, USA). Patients were divided into three different groups according to their progesterone serum concentration on the day of hCG administration (A) P <= 0.9 ng/mL, (B) 1 < P < 1.5 ng/mL, and (C) P > 1.5 ng/mL. Serum P was measured with the automated Elecsys immunoanalyser (Roche Diagnostics, Mannheim, Germany). Selected differentially expressed genes were validated with quantitative real-time PCR (QPCR) with TaqMan Gene Expression Assays (Applied Biosystems, Foster City, CA, USA). **Keywords:** gene expression analysis, premature progesterone rise **Overall design:** Endometrial biopsies from fourteen patients were taken on the day of oocyte retrieval in a GnRH/rec-FSH stimulated IVF cycle with fresh embryo transfer and analyzed with microarrays. Patients were divided into three groups according to their progesterone serum concentration on day of hCG: A <=0.9ng/ml; B 1-1.5 ng/ml; C > 1.5ng/ml

Background corr dist: KL-Divergence = 0.1586, L1-Distance = 0.0374, L2-Distance = 0.0029, Normal std = 0.3653

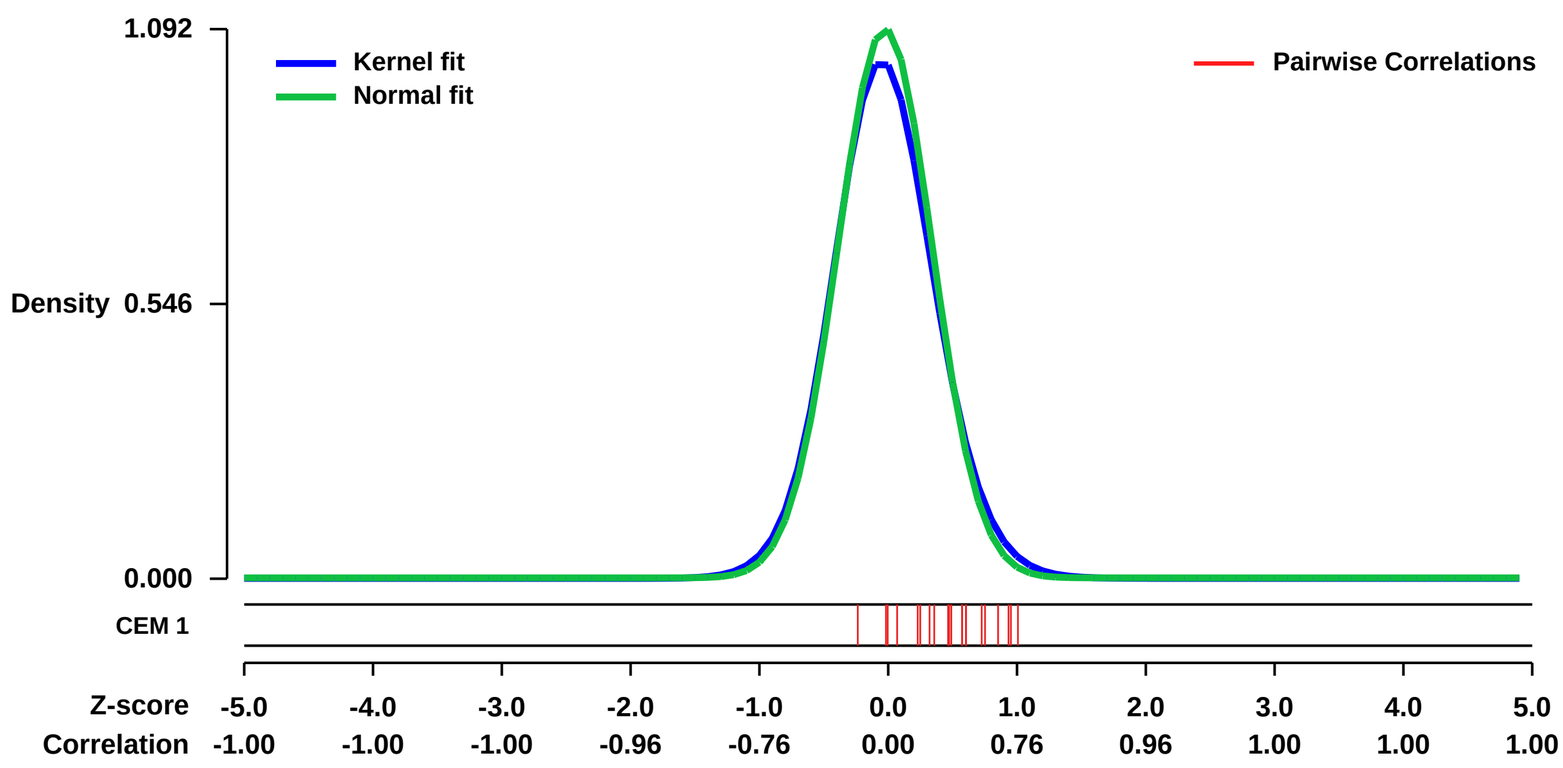

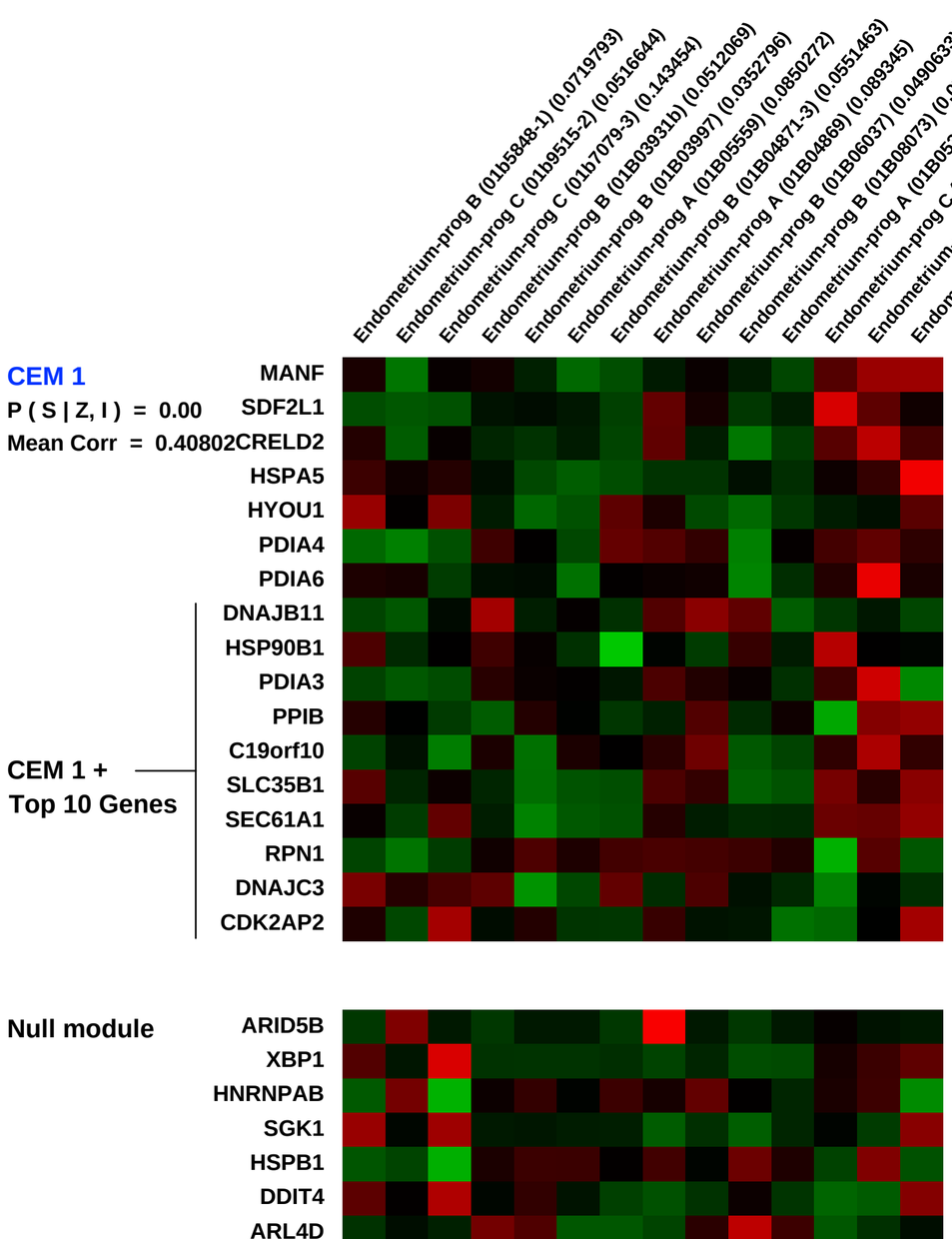

Pre-normalization Quantiles

	[min]	[medium]	[max]
MANF	2997.6	3937.5	5062.5
SDF2L1	655.7	939.9	1885.9
CRELD2	2625.1	3536.3	5646.8
HSPA5	14794.4	16797.1	23226.1
HYOU1	1411.2	1929.7	2891.0
PDIA4	1307.6	2076.5	2324.1
PDIA6	9938.8	12562.3	16650.9
DNAJB11	2685.8	3257.6	4762.9
HSP90B1	6203.2	8497.3	10576.6
PDIA3	10004.7	14480.1	20535.0
PPIB	18411.2	22773.0	26646.8
C19orf10	2575.9	3518.6	4410.2
SLC35B1	1489.1	1923.6	2367.4
SEC61A1	2961.4	3510.1	4443.9
RPN1	3574.6	6157.7	6790.7
DNAJC3	2322.3	2814.2	3249.0
CDK2AP2	990.0	1207.4	1585.7

GEO Series "GSE15602" Expression Profiles

Num of samples in this series: 11

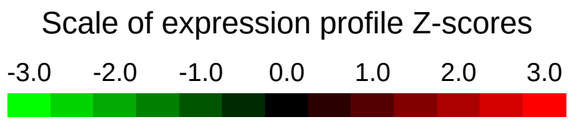

GEO Link:	http://www.ncbi.nlm.nih.gov/geo/query/acc.cgi?acc=GSE15602
Status:	Public on Apr 15 2009
Title:	Differential gene expression in RA synovial biopsies from responders versus non-responders to adalimumab therapy
Organism:	Homo sapiens
Experiment type:	Expression profiling by array
Platform:	GPL570
Pubmed ID:	19389237
Summary & Design:	**Summary:** TNF antagonists are routinely used in severe rheumatoid arthritis (RA) patients who failed conventional DMARD therapy. According to large clinical trials, the three available drugs (adalimumab, infliximab and etanercept) display similar effects in terms of efficacy, tolerability and side effects. These studies also indicate that about 25% of RA patients treated with TNF-antagonists do not display any significant clinical improvement. The aim of this study was to investigate global molecular patterns in synovial biopsies from RA patients obtained 12 weeks after initiation of adalimumab therapy. **Overall design:** Synovial biopsies were obtained by needle-arthroscopy of knee of the patients at T12. The aim of the study was to compare gene expression profiles in synovial tissue of RA patients who responded versus not responded to adalimumab therapy.

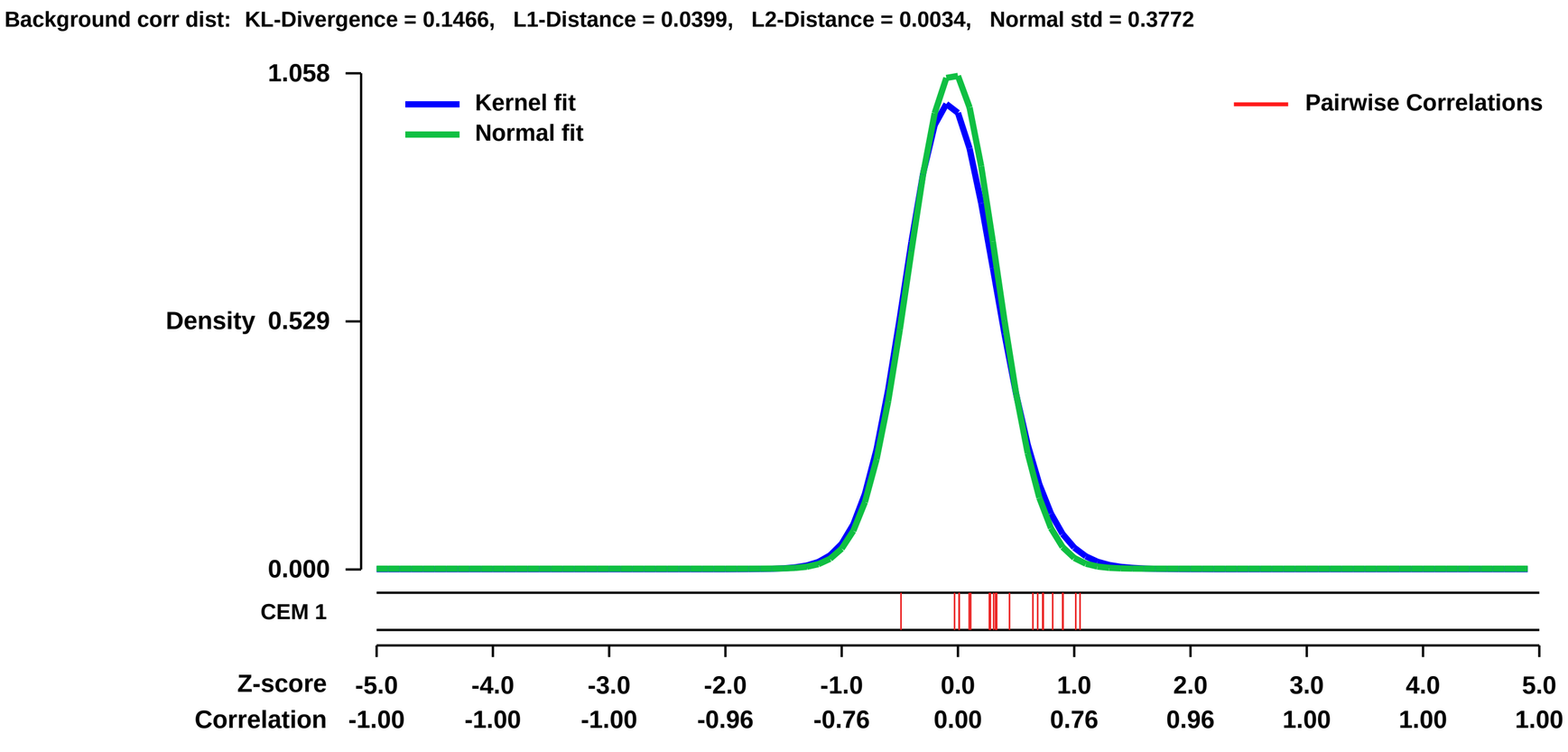

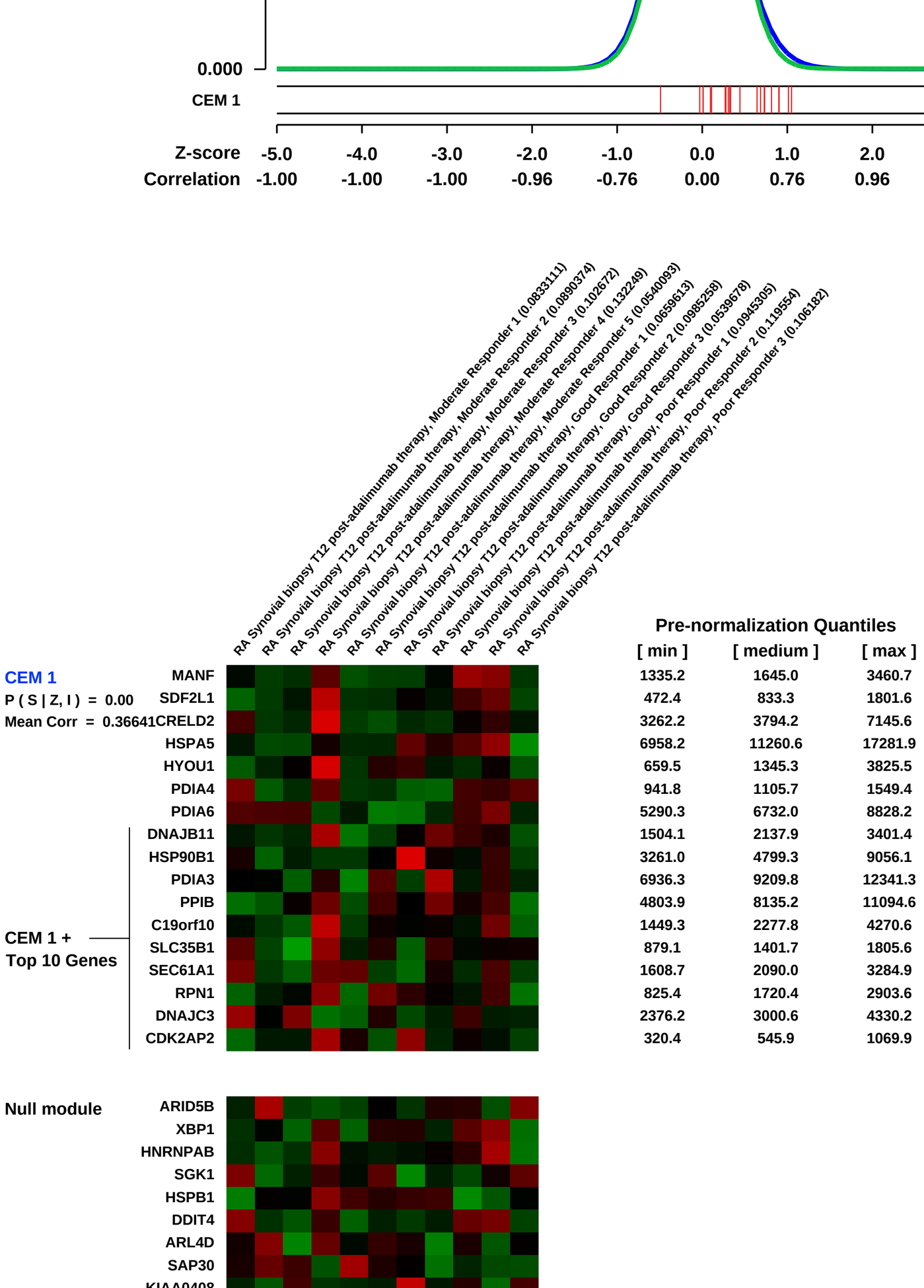

GEO Series "GSE12488" Expression Profiles

Num of samples in this series: 17

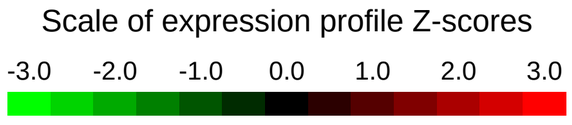

GEO Link:	http://www.ncbi.nlm.nih.gov/geo/query/acc.cgi?acc=GSE12488
Status:	Public on Sep 01 2008
Title:	Involvement of hCMV in the ontogeny of CD4+ T-LGL
Organism:	Homo sapiens
Experiment type:	Expression profiling by array
Platform:	GPL570
Pubmed ID:	18768393
Summary & Design:	**Summary:** Recent studies suggest the potential involvement of common antigenic stimuli on the ontogeny of monoclonal TCRalphabeta+/CD4+/NKa+/CD8-/+dim T-large granular lymphocyte (LGL) lymphocytosis. Since healthy individuals show (oligo)clonal expansions of hCMV-specific TCRVbeta+/CD4+/cytotoxic/memory T-cells, we investigate the potential involvement of hCMV in the origin and/or expansion of monoclonal CD4+ T-LGL. A detailed characterization of those genes that underwent changes in T-LGL cells responding to hCMV was performed by microarray gene expression profile (GEP) analysis. **Overall design:** In parallel, total RNA was also isolated from highly purified (â¥ 98% purity) hCMV-stimulated (specific) CD69+ CD4+ T-lymphocytes isolated from PB samples from hCMV-seropositive healthy donors (n=5, mean age of 36 years) using a FACSAria flow cytometer (BDB). To get pure and highly concentrated RNA, the silica membrane technology NucleoSpin´fi RNA XS (Macherey-Nagel, Dˆ…ren, Germany) was used. Total RNA was then amplified, labeled and hybridized to the Human Genome U133 Plus 2.0 Array (Affymetrix) as described above.

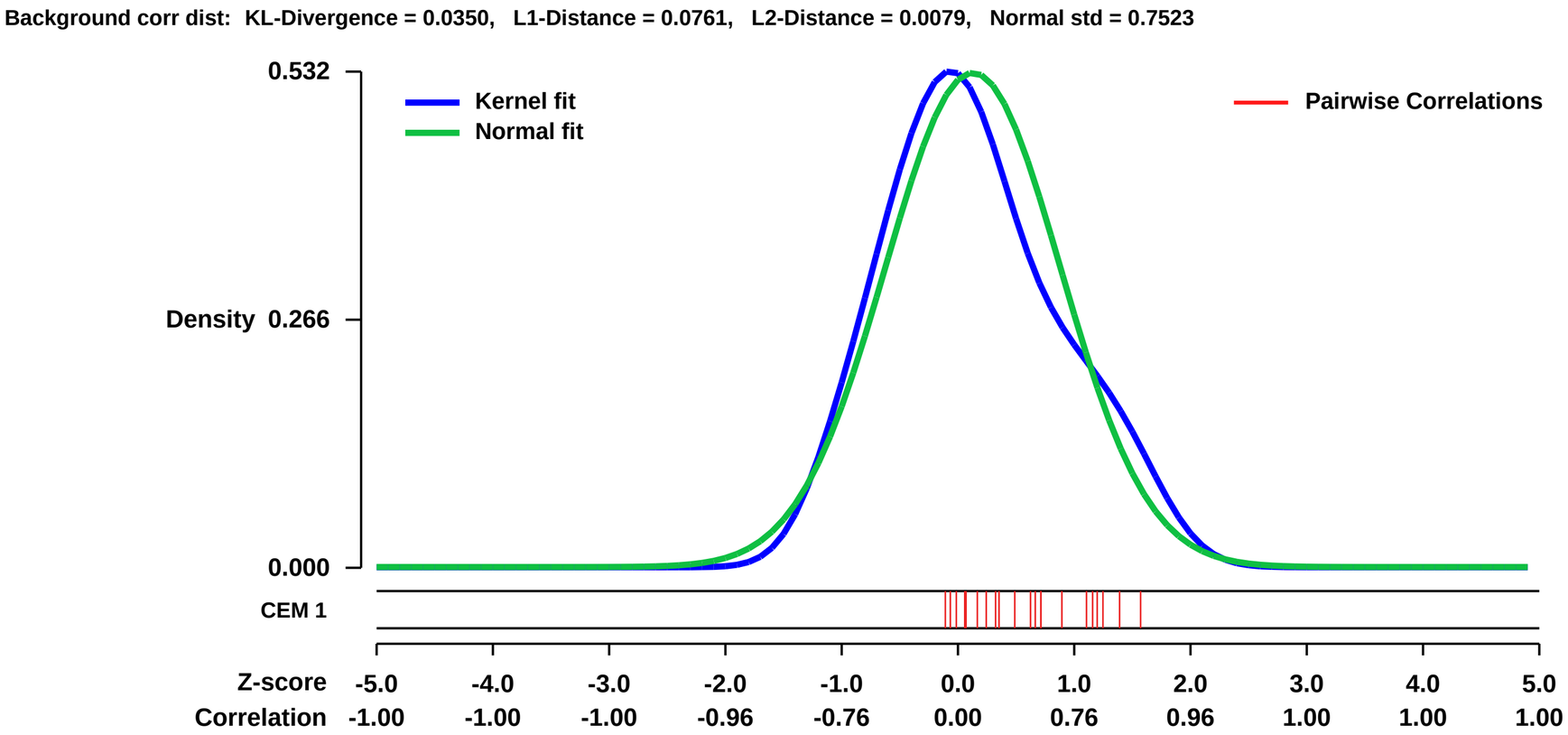

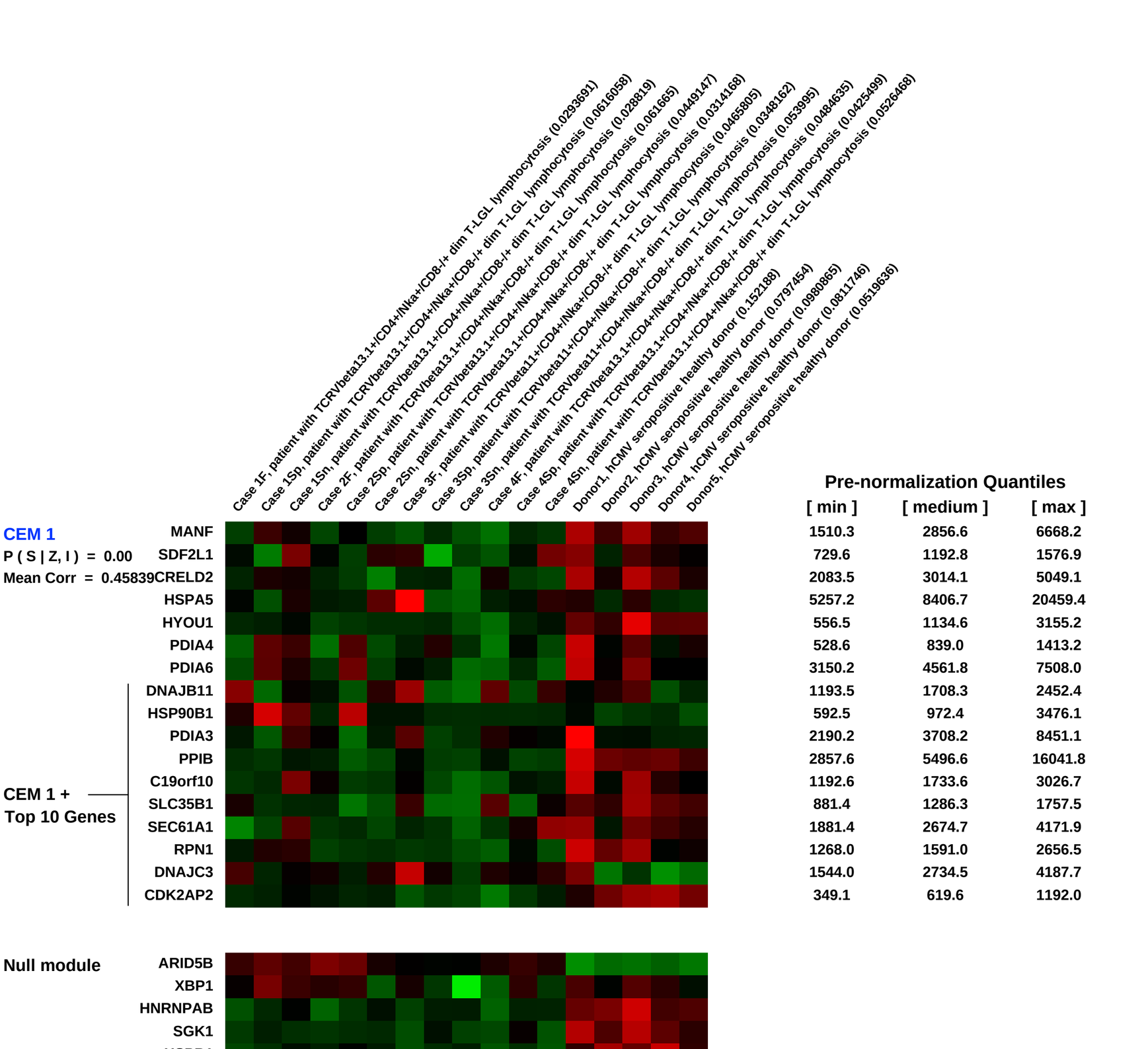

GEO Series "GSE15192" Expression Profiles

Num of samples in this series: 8

Scale of expression profile Z-scores

-3.0 -2.0 -1.0 0.0 1.0 2.0 3.0

GEO Link:	http://www.ncbi.nlm.nih.gov/geo/query/acc.cgi?acc=GSE15192
Status:	Public on Mar 01 2010
Title:	Differences between CD44+/CD24- and CD44-/CD24+ subpopulation of immortalized human mammary epithelial cells
Organism:	Homo sapiens
Experiment type:	Expression profiling by array
Platform:	GPL570
Pubmed ID:	20691079
Summary & Design:	**Summary:** CD44+/CD24- subpopulation of normal and cancerous breast epithelial cells are suggested to have stem cell properties. The goal of this study was to identify gene expression differences between CD44+/CD24- and CD44-/CD24+ subpopulation of cells from a same cell lines. We selected MCF-10A cells, which are immortalized derived from a fibrocystic breast disease. These cells are immortalized but not transformed and express basal cell markers. Cells were from a single sort but plated into four 100 mm plates. RNA was prepared from each plate separately for the analysis. **Overall design:** Comparison of gene expression between 2 groups (CD44+/CD24- and CD44-/CD24+) 4 replicates each.

Background corr dist: KL-Divergence = 0.0574, L1-Distance = 0.0817, L2-Distance = 0.0088, Normal std = 0.6740

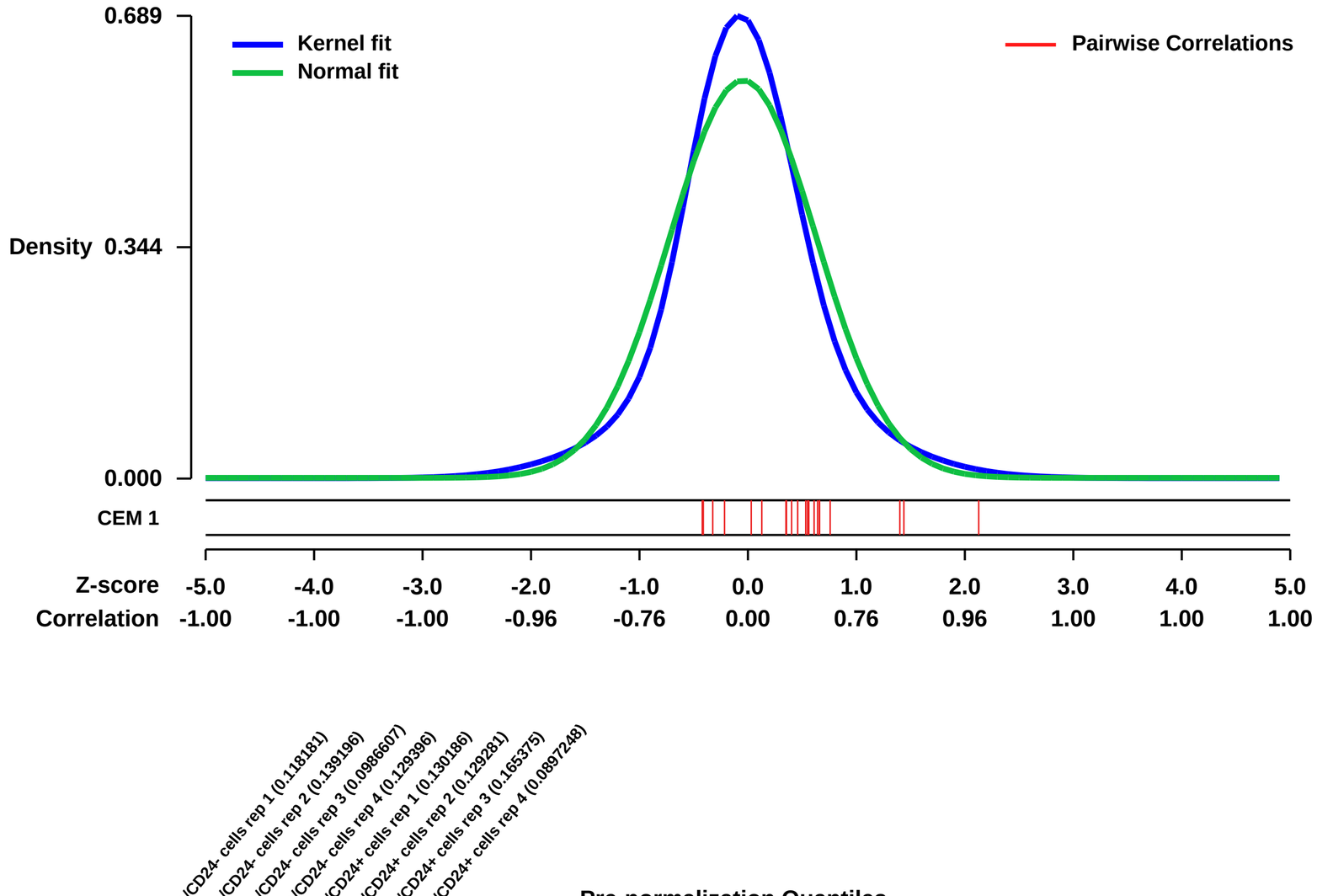

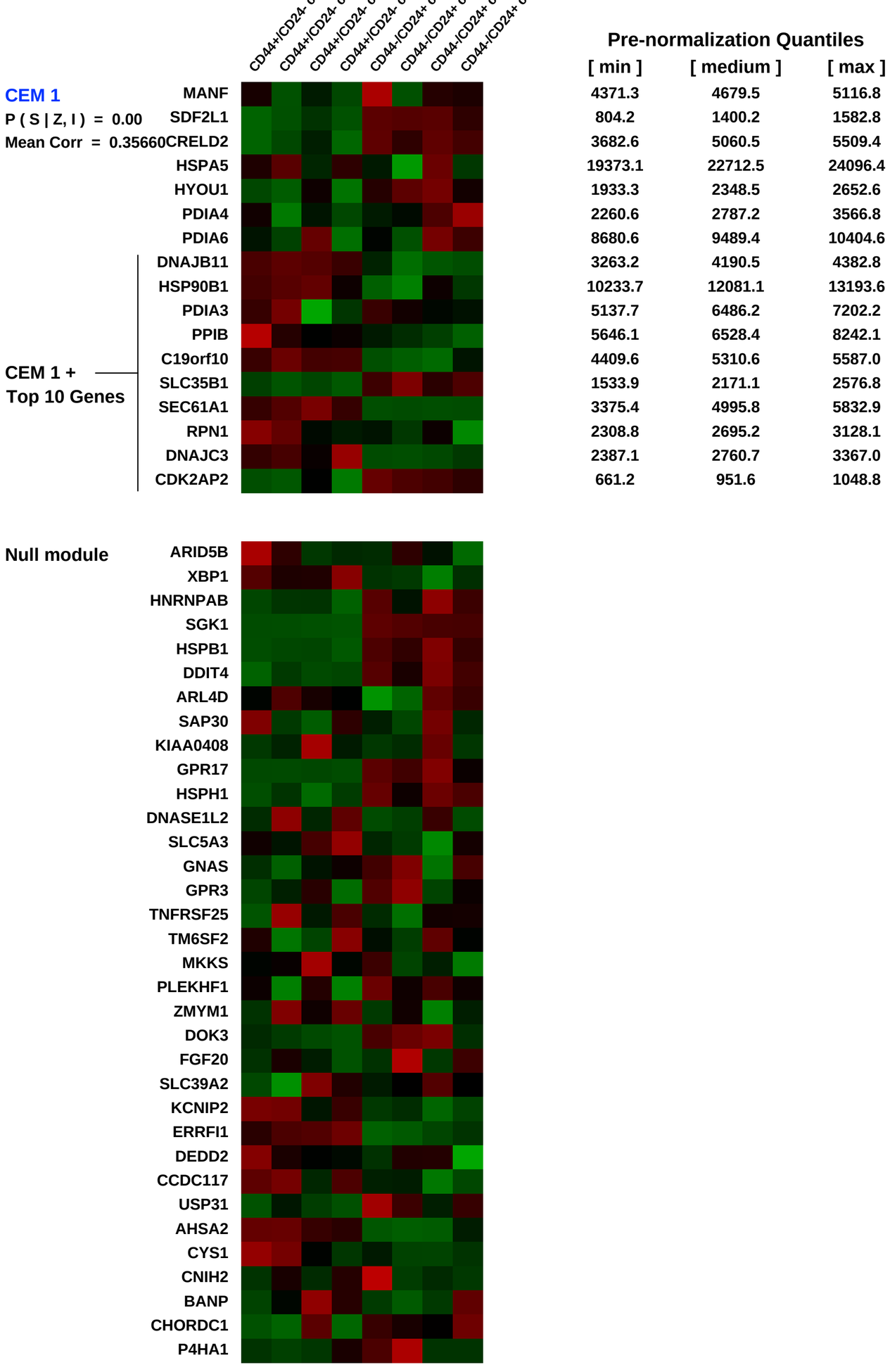

Pre-normalization Quantiles

	[min]	[medium]	[max]
MANF	4371.3	4679.5	5116.8
SDF2L1	804.2	1400.2	1582.8
CRELD2	3682.6	5060.5	5509.4
HSPA5	19373.1	22712.5	24096.4
HYOU1	1933.3	2348.5	2652.6
PDIA4	2260.6	2787.2	3566.8
PDIA6	8680.6	9489.4	10404.6
DNAJB11	3263.2	4190.5	4382.8
HSP90B1	10233.7	12081.1	13193.6
PDIA3	5137.7	6486.2	7202.2
PPIB	5646.1	6528.4	8242.1
C19orf10	4409.6	5310.6	5587.0
SLC35B1	1533.9	2171.1	2576.8
SEC61A1	3375.4	4995.8	5832.9
RPN1	2308.8	2695.2	3128.1
DNAJC3	2387.1	2760.7	3367.0
CDK2AP2	661.2	951.6	1048.8

GEO Series "GSE35712" Expression Profiles

Num of samples in this series: 12

Scale of expression profile Z-scores

-3.0 -2.0 -1.0 0.0 1.0 2.0 3.0

GEO Link:	http://www.ncbi.nlm.nih.gov/geo/query/acc.cgi?acc=GSE35712
Status:	Public on Sep 01 2012
Title:	Transcriptional Signatures as a Disease-Specific and Predictive Inflammatory Biomarker for Type 1 Diabetes [H1N1_S5_5Pre_5D0]
Organism:	Homo sapiens
Experiment type:	Expression profiling by array
Platform:	GPL570
Pubmed ID:	22972474
Summary & Design:	**Summary:** The complex milieu of inflammatory mediators associated with many diseases is often too dilute to directly measure in the periphery, necessitating development of more sensitive measurements suitable for mechanistic studies, earlier diagnosis, guiding selection of therapy, and monitoring interventions. Previously we determined that plasma of recent-onset (RO) Type 1 diabetes (T1D) patients induce a proinflammatory transcriptional signature in fresh peripheral blood mononuclear cells (PBMC) relative to that of unrelated healthy controls (HC). Here, using an optimized cryopreserved PBMC-based protocol, we compared the signature found in pre H1N1 samples to the signature associated with active H1N1 flu. **Overall design:** UPN727 cells were stimulated with plasma that was collected pre-H1N1 (healthy) or during active-H1N1 from 5 different individuals. Gene expression analysis was perfromed in order to evaluate the transcriptional signature associated with the H1N1 influenza virus.

Background corr dist: KL-Divergence = 0.0968, L1-Distance = 0.0289, L2-Distance = 0.0015, Normal std = 0.4422

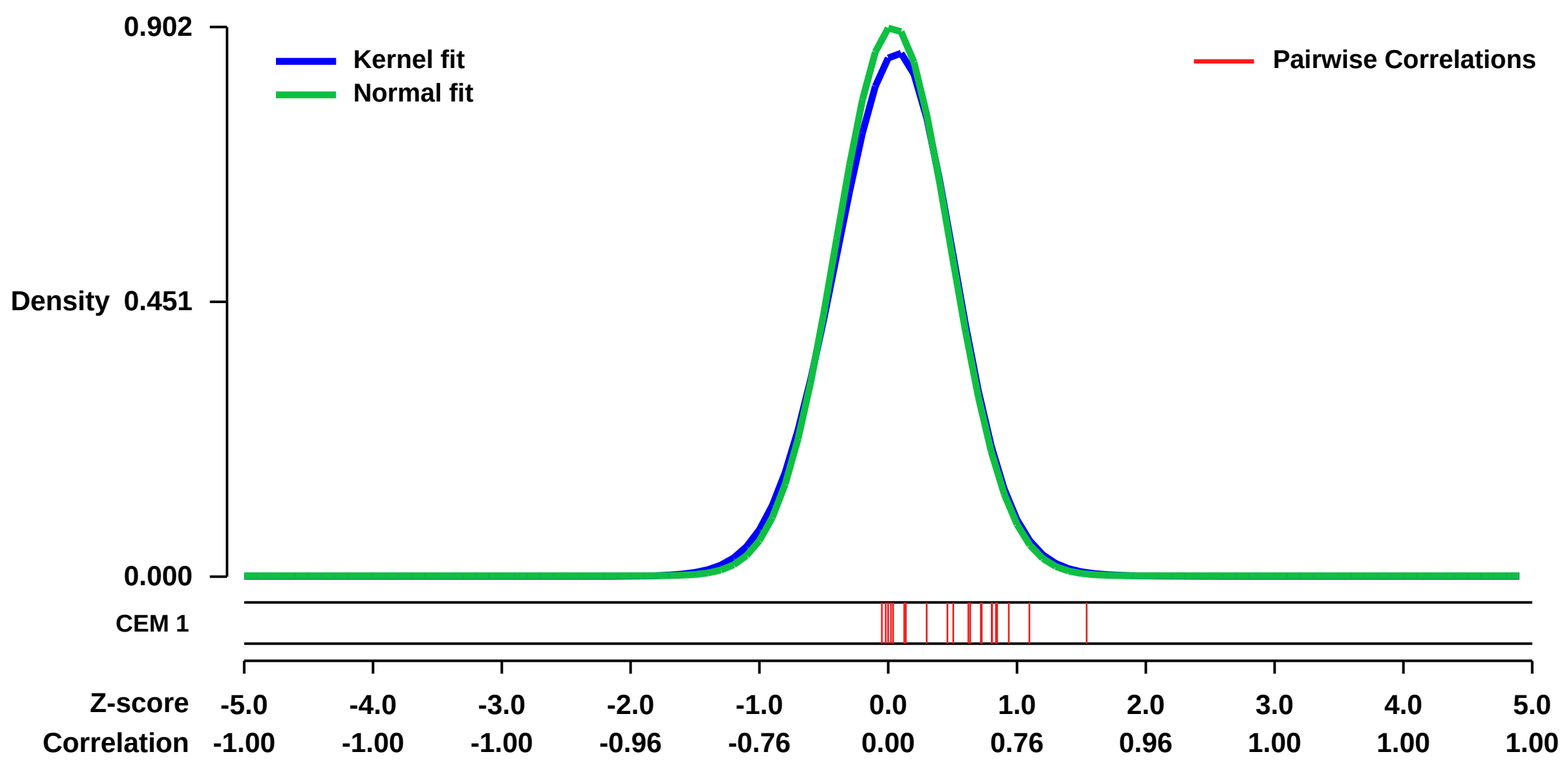

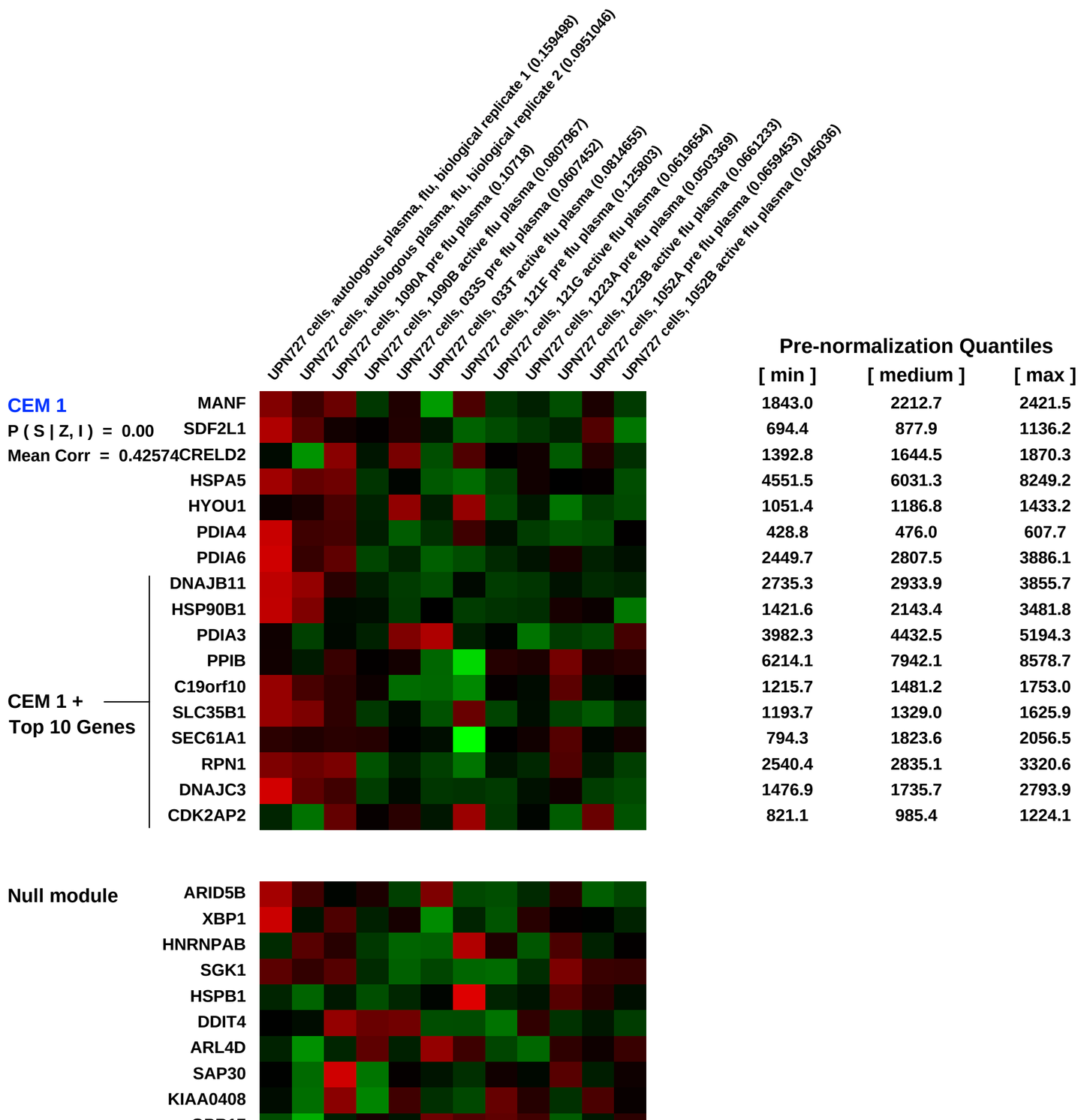

	Pre-normalization Quantiles		
	[min]	[medium]	[max]
MANF	1843.0	2212.7	2421.5
SDF2L1	694.4	877.9	1136.2
CRELD2	1392.8	1644.5	1870.3
HSPA5	4551.5	6031.3	8249.2
HYOU1	1051.4	1186.8	1433.2
PDIA4	428.8	476.0	607.7
PDIA6	2449.7	2807.5	3886.1
DNAJB11	2735.3	2933.9	3855.7
HSP90B1	1421.6	2143.4	3481.8
PDIA3	3982.3	4432.5	5194.3
PPIB	6214.1	7942.1	8578.7
C19orf10	1215.7	1481.2	1753.0
SLC35B1	1193.7	1329.0	1625.9
SEC61A1	794.3	1823.6	2056.5
RPN1	2540.4	2835.1	3320.6
DNAJC3	1476.9	1735.7	2793.9
CDK2AP2	821.1	985.4	1224.1

GEO Series "GSE18239" Expression Profiles

Num of samples in this series: 11

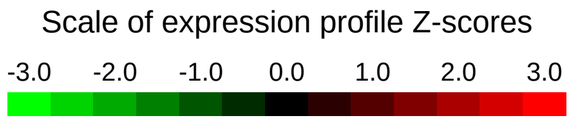

GEO Link:	http://www.ncbi.nlm.nih.gov/geo/query/acc.cgi?acc=GSE18239
Status:	Public on Sep 24 2009
Title:	Expression data from JAK1 wild-type and JAK1 mutation-positive T cell acute lymphoblastic leukemia blasts
Organism:	Homo sapiens
Experiment type:	Expression profiling by array
Platform:	GPL570
Pubmed ID:	20167706
Summary & Design:	**Summary:** Aberrant signal transduction contributes substantially to leukemogenesis. The Janus kinase 1 (JAK1) gene encodes a cytoplasmic tyrosine kinase that noncovalently associates with a variety of cytokine receptors and plays a nonredundant role in lymphoid cell precursor proliferation, survival, and differentiation. Somatic mutations in JAK1 occur in individuals with acute lymphoblastic leukemia (ALL). JAK1 mutations were more prevalent among adult subjects with the T cell precursor ALL, where they accounted for 18% of cases, and were associated with advanced age at diagnosis, poor response to therapy, and overall prognosis We used microarray to compare the gene expression profile of JAK1 mutation positive or negative ALL blasts **Overall design:** Thawed or freshly isolated T-ALL cells (>90% blasts) were homogenized, total RNA was extracted and hybridized on Affymetrix microarrays

Background corr dist: KL-Divergence = 0.0997, L1-Distance = 0.0797, L2-Distance = 0.0126, Normal std = 0.4842

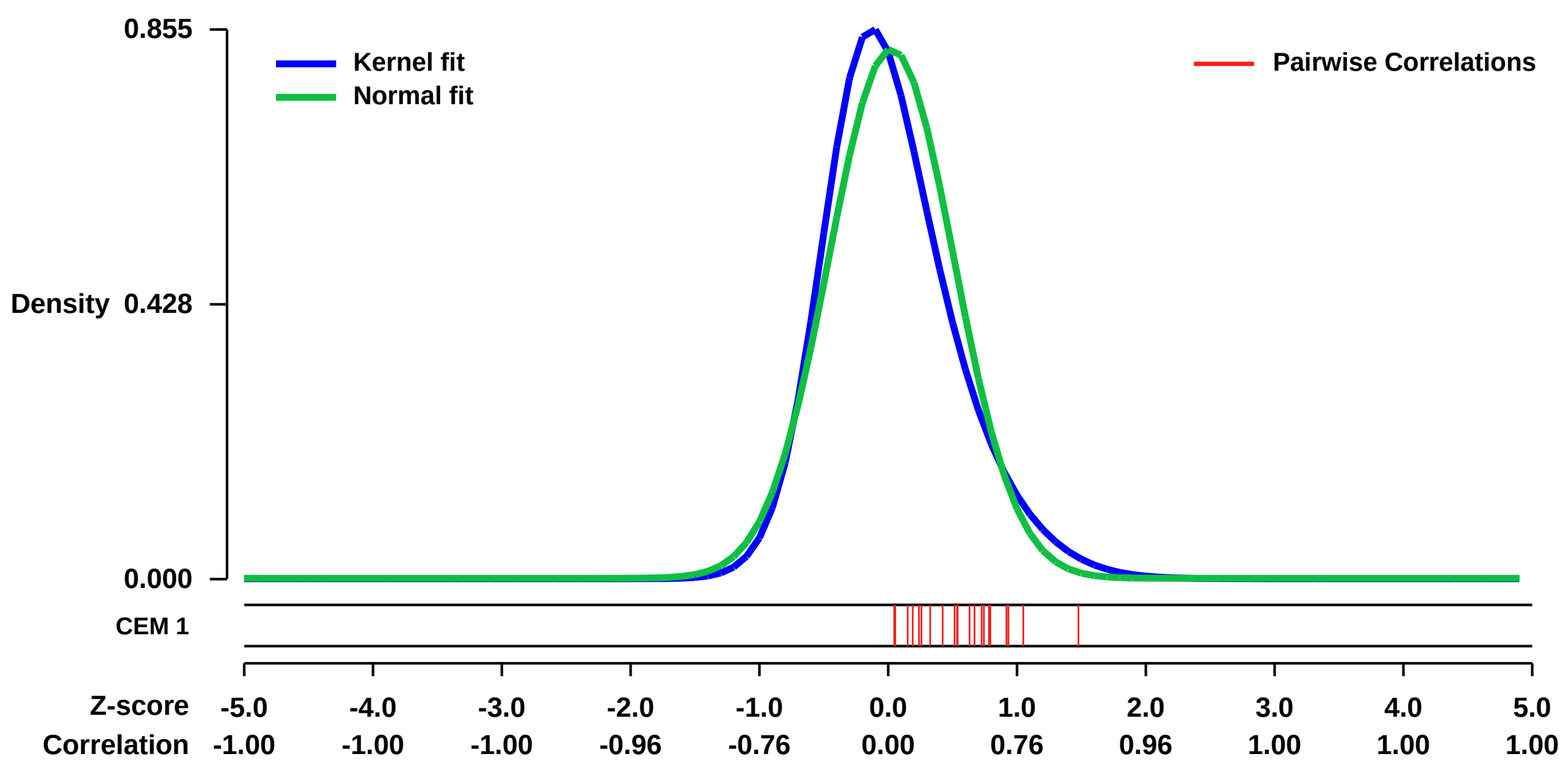

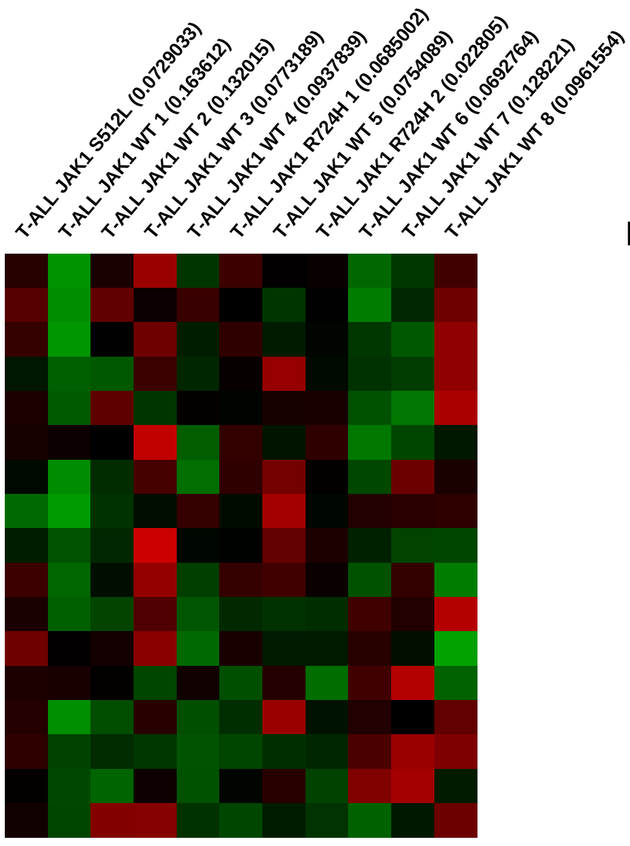

GEO Series "GSE12720" Expression Profiles

Num of samples in this series: 63

Scale of expression profile Z-scores

-3.0 -2.0 -1.0 0.0 1.0 2.0 3.0

GEO Link:	http://www.ncbi.nlm.nih.gov/geo/query/acc.cgi?acc=GSE12720
Status:	Public on Jun 11 2009
Title:	Unique early gene expression patterns in adult to adult living donor liver grafts compared to deceased donor grafts
Organism:	Homo sapiens
Experiment type:	Expression profiling by array
Platform:	GPL570
Pubmed ID:	19353763
Summary & Design:	**Summary:** Because of inherent differences between deceased donor (DD) and living donor (LD) liver grafts, we hypothesize that the molecular signatures will be unique, correlating with specific biologic pathways and clinical patterns. Following reperfusion, 579 genes in DD grafts and 1324 genes in LDs were differentially expressed (p<0.005). Many up-regulated LD genes were related to regeneration, biosynthesis and cell cycle, and a large number of down-regulated genes were linked to hepatic metabolism and energy pathways correlating with post-transplant clinical laboratory findings. There was significant up-regulation of inflammatory/immune genes in both DD and LD, each with a distinct pattern. Gene expression patterns of select genes associated with inflammation and regeneration in LD and DD grafts correlated with protein expression. Unique patterns of early gene expression are seen in LD and DD liver grafts, correlating with protein expression and clinical results, demonstrating distinct inflammatory profiles and significant down-regulation of metabolic pathways in LD grafts. Keywords: liver transplantation, live donor transplantation, liver regeneration, microarrays, mRNA expression, reperfusion injury **Overall design:** Microarray profiles of 63 biopsies in 13 DD and 8 LD liver grafts done at serial time points (procurement - No Manipulation, backbench - Cold Preservation, and 1-hour post-reperfusion - Post reperfusion) were compared between groups using class comparisons, network and biological function analyses. Specific genes were validated by quantitative PCR and immunopathology. Clinical findings were also compared.

Background corr dist: KL-Divergence = 0.0669, L1-Distance = 0.0833, L2-Distance = 0.0135, Normal std = 0.5571

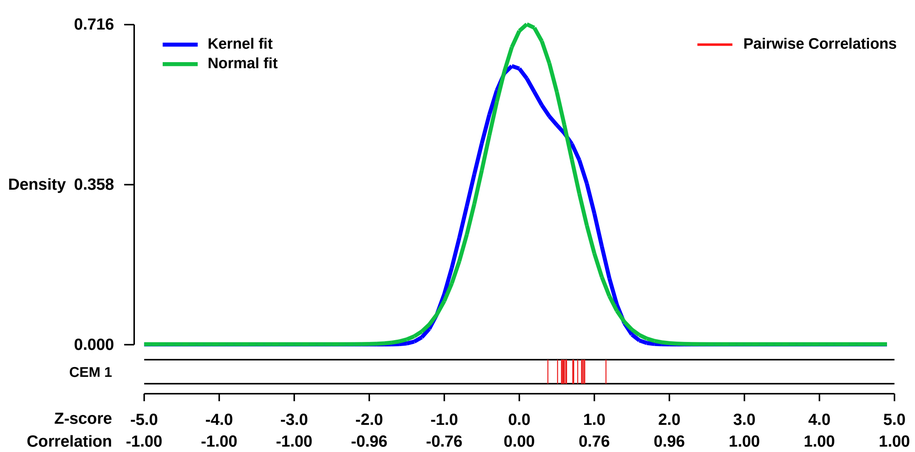

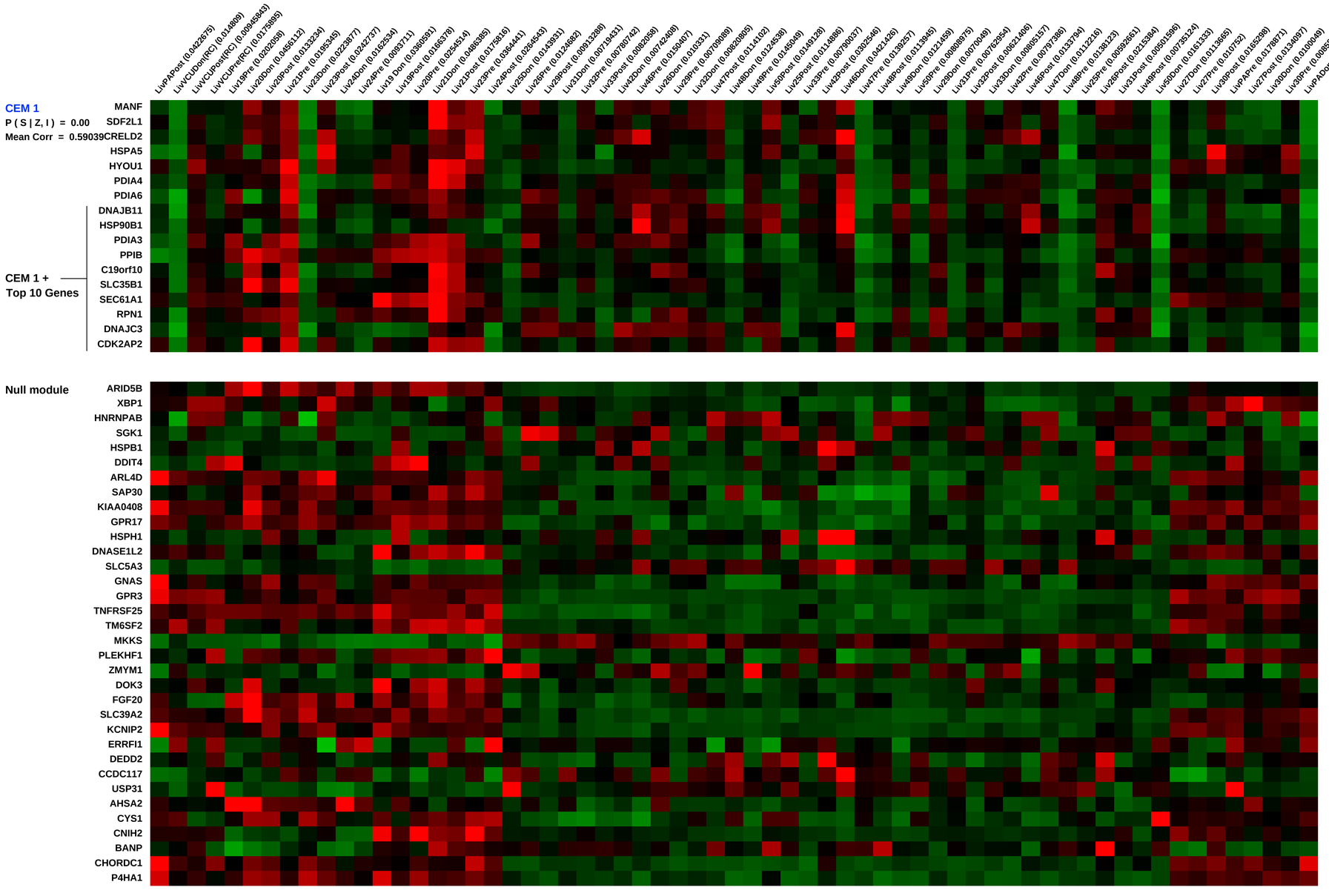

Pre-normalization Quantiles

[min]	[medium]	[max]
2076.3	7424.1	18600.7
541.4	2536.9	9079.0
2049.9	7084.1	20414.7
6968.2	18564.0	39312.6
739.8	4556.3	17328.1
1014.0	2760.0	7467.1
3847.8	9535.5	17028.5
2007.4	8823.0	18800.5
2953.8	6720.3	18603.7
5654.3	14179.3	24931.3
10001.1	19323.7	40151.3
1777.6	3595.5	9223.6
2094.5	4811.1	13489.7
1375.3	3499.2	13950.2
2560.4	4524.9	10179.0
3156.2	7339.6	14623.1
649.9	1471.5	3891.8

GEO Series "GSE31421" Expression Profiles

Num of samples in this series: 15

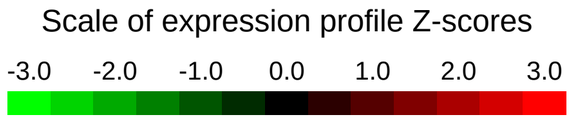

GEO Link:	http://www.ncbi.nlm.nih.gov/geo/query/acc.cgi?acc=GSE31421
Status:	Public on Oct 01 2011
Title:	Cereblon expression is required for the anti-myeloma activity of lenalidomide and pomalidomide [expression profiling]
Organism:	Homo sapiens
Experiment type:	Expression profiling by array
Platform:	GPL570
Pubmed ID:	21860026
Summary & Design:	**Summary:** The precise molecular mechanism of action and targets through which thalidomide and related immunomodulatory drugs (IMiDs) exert their anti-tumor effects remains unclear. We investigated the role of cereblon (CRBN), a primary teratogenic target of thalidomide, in the anti-myeloma activity of IMiDs. CRBN depletion is initially cytotoxic to human myeloma cells but surviving cells with stable CRBN depletion become highly resistant to both lenalidomide and pomalidomide, but not to the unrelated drugs bortezomib, dexamethasone and melphalan. Acquired deletion of CRBN was found to be the primary genetic event differentiating isogenic MM1.S cell lines cultured to be sensitive or resistant to lenalidomide and pomalidomide. Gene expression changes induced by lenalidomide were dramatically suppressed in the presence of CRBN depletion further demonstrating that CRBN is required for lenalidomide activity. Downstream targets of CRBN include interferon regulatory factor 4 (IRF4) previously reported to also be a target of lenalidomide. Patients exposed to and putatively resistant to lenalidomide had lower CRBN levels in paired samples before and after therapy. In summary, CRBN is an essential requirement for IMiD activity, and a possible biomarker for the clinical assessment of anti-myeloma efficacy. **Overall design:** We included 15 samples from multiple myeloma cell lines.

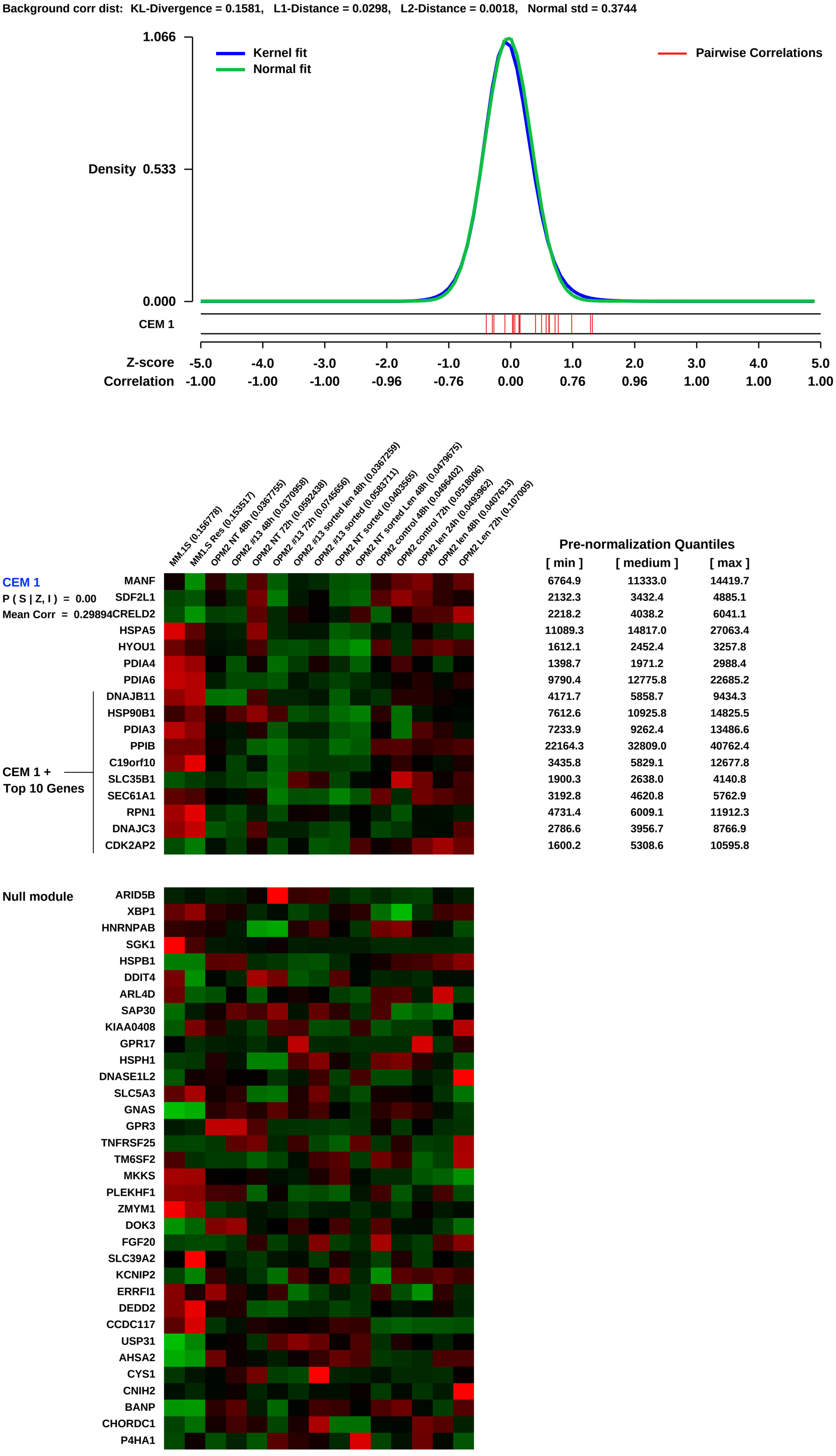

GEO Series "GSE18140" Expression Profiles

Num of samples in this series: 8

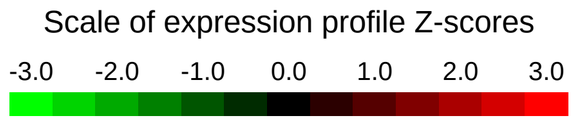

GEO Link:	http://www.ncbi.nlm.nih.gov/geo/query/acc.cgi?acc=GSE18140
Status:	Public on Sep 07 2010
Title:	COX-2 network as predictive molecular marker for clinical pregnancy in IVF
Organism:	Homo sapiens
Experiment type:	Expression profiling by array
Platform:	GPL570
Pubmed ID:	20800227
Summary & Design:	**Summary:** **CONTEXT Nowadays, the molecular mechanisms involved in endometrial receptivity and implantation are still not clear.** **OBJECTIVE The gene expression of human endometrium of patients undergoing an IVF treatment with GnRH antagonists/rec-FSH was studied.** **CONCLUSIONS COX-2 has been extensively studied as a crucial fertility element in both knock-out mice and human. It appears that increased expression of COX-2 and/or SCGB1D2 on the day of oocyte retrieval in GnRH antagonist/rec-FSH stimulated cycles coincides with a lower probability of achieving a clinical pregnancy in this cycle.** **Keywords: gene expression analysis, clinical pregnancy in IVF stimulated cycles** **Overall design:** **Endometrial biopsies taken from patients on day of oocyte retrieval in stimulated IVF cycles with 1 or 2 embryos replaced in the same cycle. Gene expression of pregnant patients (n=4) was compared with matched non-pregnant patients (n=4)**

Background corr dist: KL-Divergence = 0.0876, L1-Distance = 0.0250, L2-Distance = 0.0011, Normal std = 0.4623

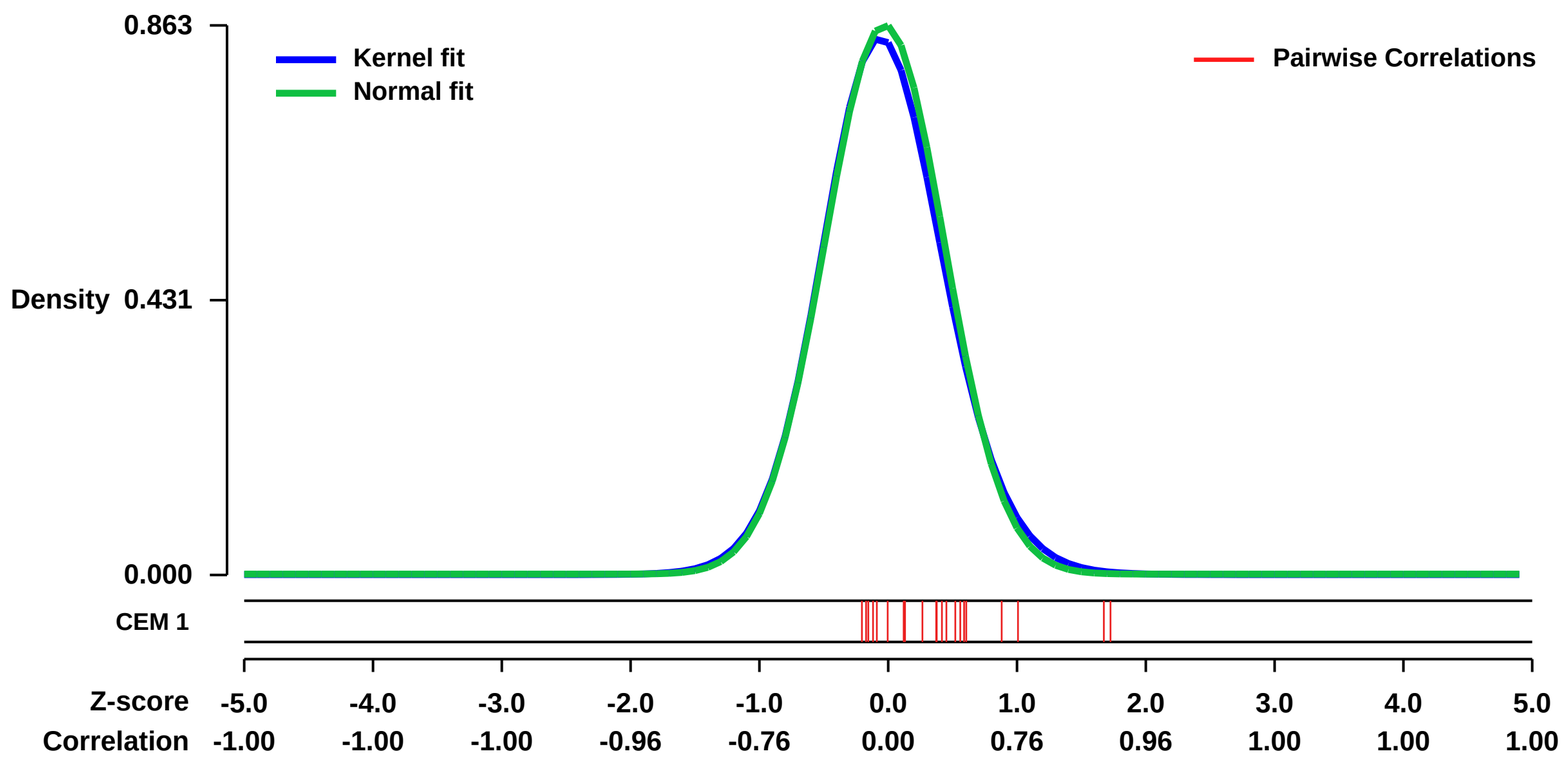

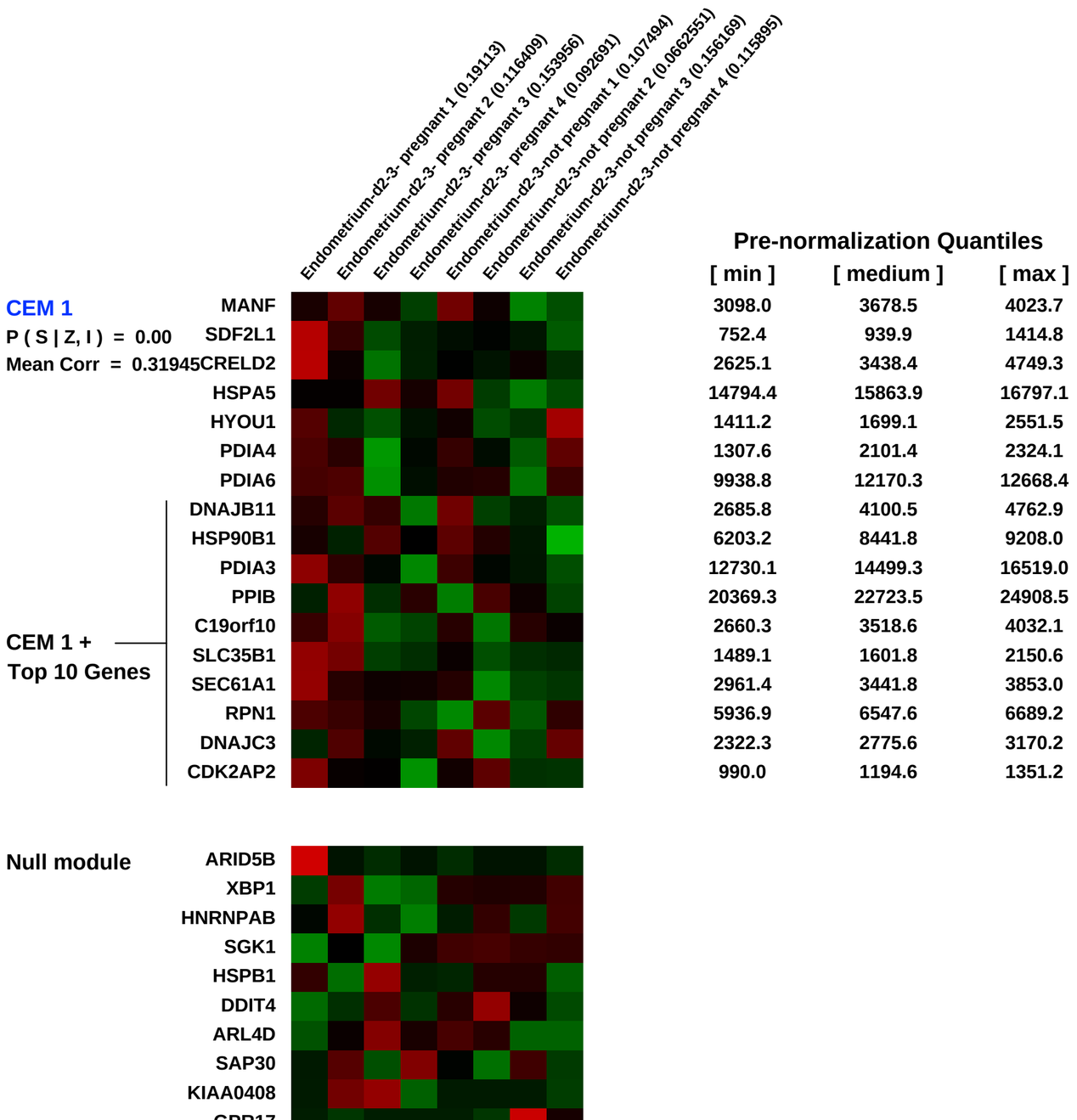

Pre-normalization Quantiles

	[min]	[medium]	[max]
MANF	3098.0	3678.5	4023.7
SDF2L1	752.4	939.9	1414.8
CRELD2	2625.1	3438.4	4749.3
HSPA5	14794.4	15863.9	16797.1
HYOU1	1411.2	1699.1	2551.5
PDIA4	1307.6	2101.4	2324.1
PDIA6	9938.8	12170.3	12668.4
DNAJB11	2685.8	4100.5	4762.9
HSP90B1	6203.2	8441.8	9208.0
PDIA3	12730.1	14499.3	16519.0
PPIB	20369.3	22723.5	24908.5
C19orf10	2660.3	3518.6	4032.1
SLC35B1	1489.1	1601.8	2150.6
SEC61A1	2961.4	3441.8	3853.0
RPN1	5936.9	6547.6	6689.2
DNAJC3	2322.3	2775.6	3170.2
CDK2AP2	990.0	1194.6	1351.2

GEO Series "GSE41972" Expression Profiles

Num of samples in this series: 6

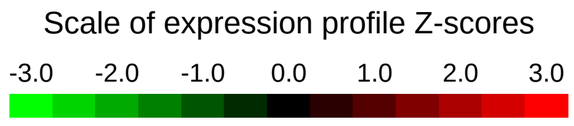

GEO Link:	http://www.ncbi.nlm.nih.gov/geo/query/acc.cgi?acc=GSE41972
Status:	Public on Nov 02 2012
Title:	In vivo NCL-targeting affects breast cancer aggressiveness through miRNA regulation [Affymetrix]
Organism:	Homo sapiens
Experiment type:	Expression profiling by array
Platform:	GPL570
Pubmed ID:	23610125
Summary & Design:	**Summary:** Numerous studies have described the altered expression and the causal role of miRNAs in human cancer. However, to date efforts to modulate miRNA levels for therapeutic purposes have been challenging to implement. Here, we find that Nucleolin (NCL), a major nucleolar protein, post-transcriptionally regulates the expression of a specific subset of miRNAs, including miR-21, miR-221, miR-222, and miR-103, causally involved in breast cancer initiation, progression and drug-resistance. We also show that NCL is commonly overexpressed in human breast tumors, and its expression correlates with that of NCL-dependent miRNAs. Finally, this study indicates that NCL-binding guanosine-rich aptamers affect the levels of NCL-dependent miRNAs and their target genes, reducing breast cancer cell aggressiveness, both in vitro and in vivo. These findings illuminate a path to novel therapeutic approaches based on NCL-targeting aptamers for the modulation of miRNA expression in the treatment of breast cancer. **Overall design:** MCF7 cells were treated with the control drug or AS1411 aptamer. After 72hours total RNA was collected and analyzed by Affymetrix U133 plus.

Background corr dist: KL-Divergence = 0.0175, L1-Distance = 0.0382, L2-Distance = 0.0016, Normal std = 0.8189

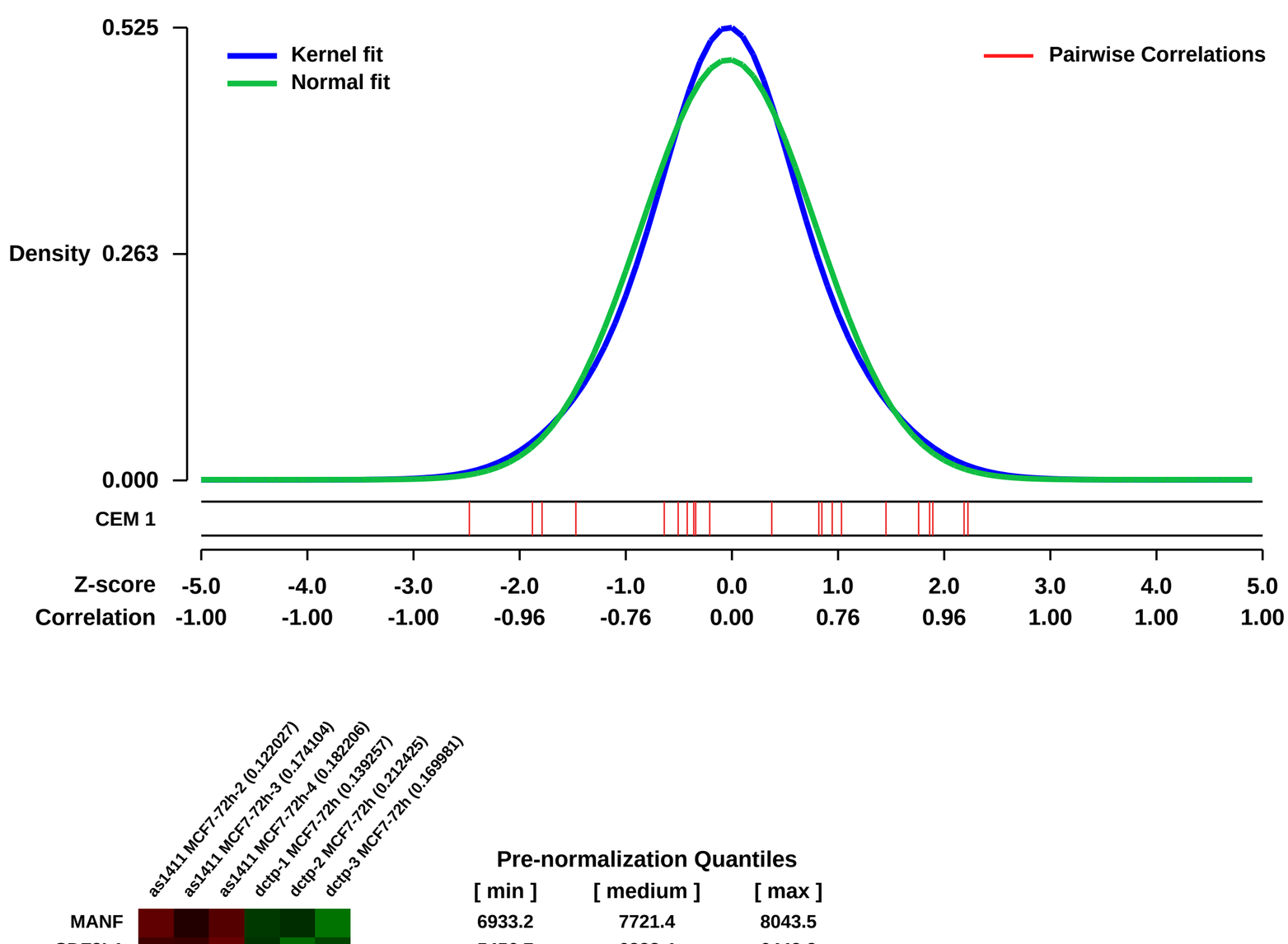

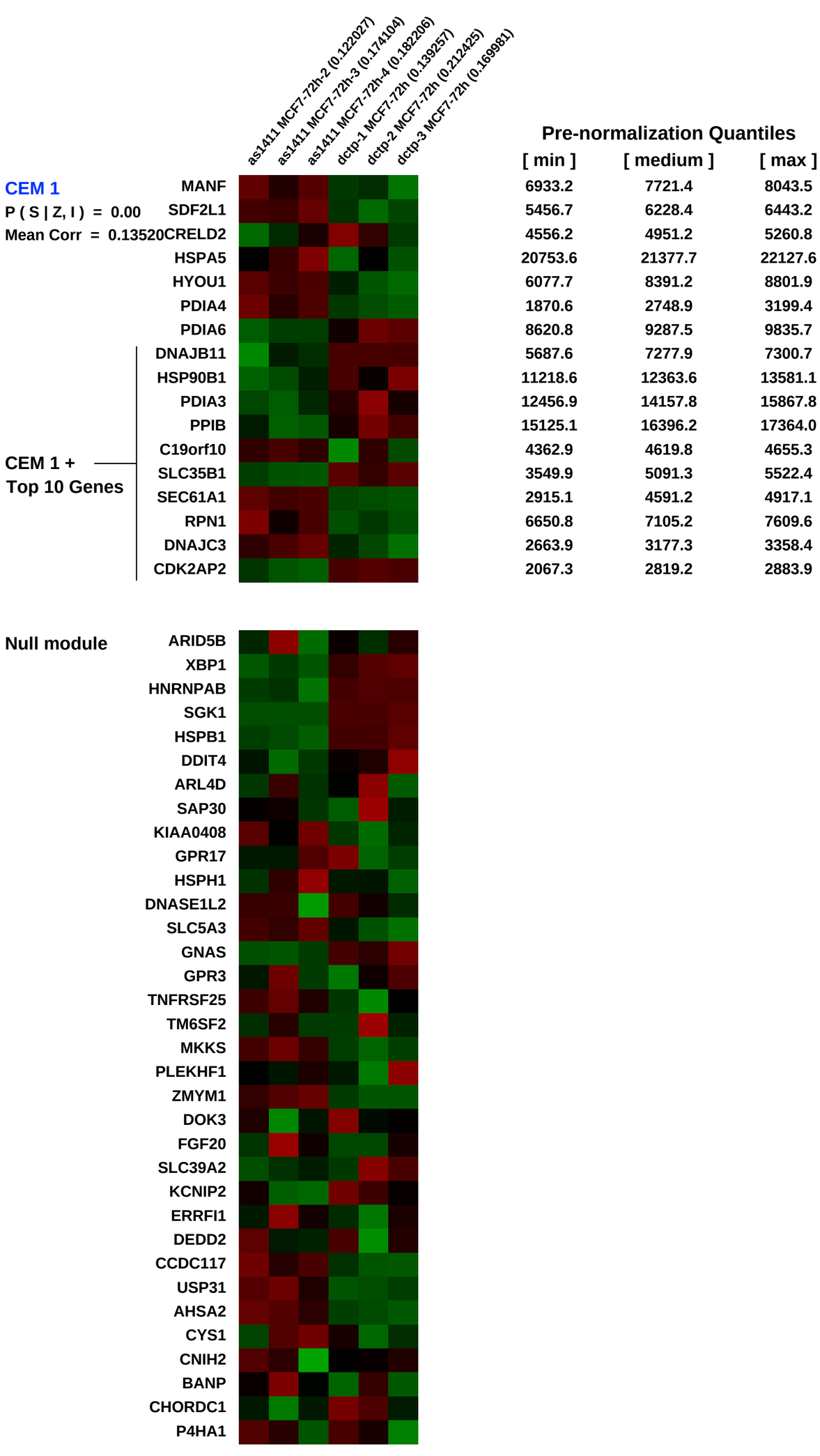

GEO Series "GSE21496" Expression Profiles

Num of samples in this series: 21

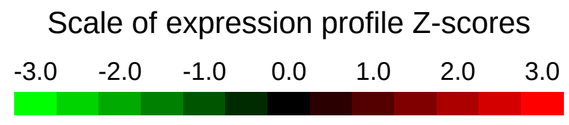

GEO Link:	http://www.ncbi.nlm.nih.gov/geo/query/acc.cgi?acc=GSE21496
Status:	Public on Oct 23 2010
Title:	Effects of 48h Lower Limb Unloading in Human Skeletal Muscle
Organism:	Homo sapiens
Experiment type:	Expression profiling by array
Platform:	GPL570
Pubmed ID:	20798274

Summary & Design:

Summary:
Although short-term disuse does not result in measurable muscle atrophy, studies suggest that molecular changes associated with protein degradation may be initiated within days of the onset of a disuse stimulus. We examined the global gene expression patterns in sedentary men (n = 7, mean age ´– S.D = 22.1 ´– 3.7 yr) following 48h unloading (UL) via unilateral lower limb suspension and 24h reloading (RL). Biopsy samples of the left vastus lateralis muscle were collected at baseline, 48h UL, and 24h RL. Expression changes were measured by microarray and gene clustering; identification of enriched functions and canonical pathways were performed using the Database for Annotation, Visualization and Integrated Discovery (DAVID) and Ingenuity Pathway Analysis (IPA). Four genes were validated with qRT-PCR, and protein levels were measured with Western blot. Of the upregulated genes after UL, the most enriched functional group and highest ranked canonical pathway were related to protein ubiquitination. The oxidative stress response pathway was the second highest ranked canonical pathway. Of the downregulated genes, functions related to mitochondrial metabolism were the mostly highly enriched. In general, gene expression patterns following UL persisted following RL. qRT-PCR confirmed increases in mRNA for UPP-related E3 ligase Atrogin1 (but not accompanying increases in protein products) and stress response gene heme oxygenase-1 (HMOX, which showed a trend towards increases in protein products at 48h UL) as well as extracellular matrix (ECM) component COL4.

The gene expression patterns were not readily reversed upon RL suggesting that molecular responses to short-term periods of skeletal muscle inactivity may persist after activity resumes.

Overall design:
Biopsies were taken of the left vastus lateralis of healthy, sedentary men (N = 7) at baseline, immediately following 48h UL and 24h RL. A 5mm Berstrom biopsy needle was used. Biopsy samples were immediately snap-frozen in liquid nitrogen upon excision. All samples were stored at -80´° C until analysis.

Background corr dist: KL-Divergence = 0.3544, L1-Distance = 0.0757, L2-Distance = 0.0173, Normal std = 0.2604

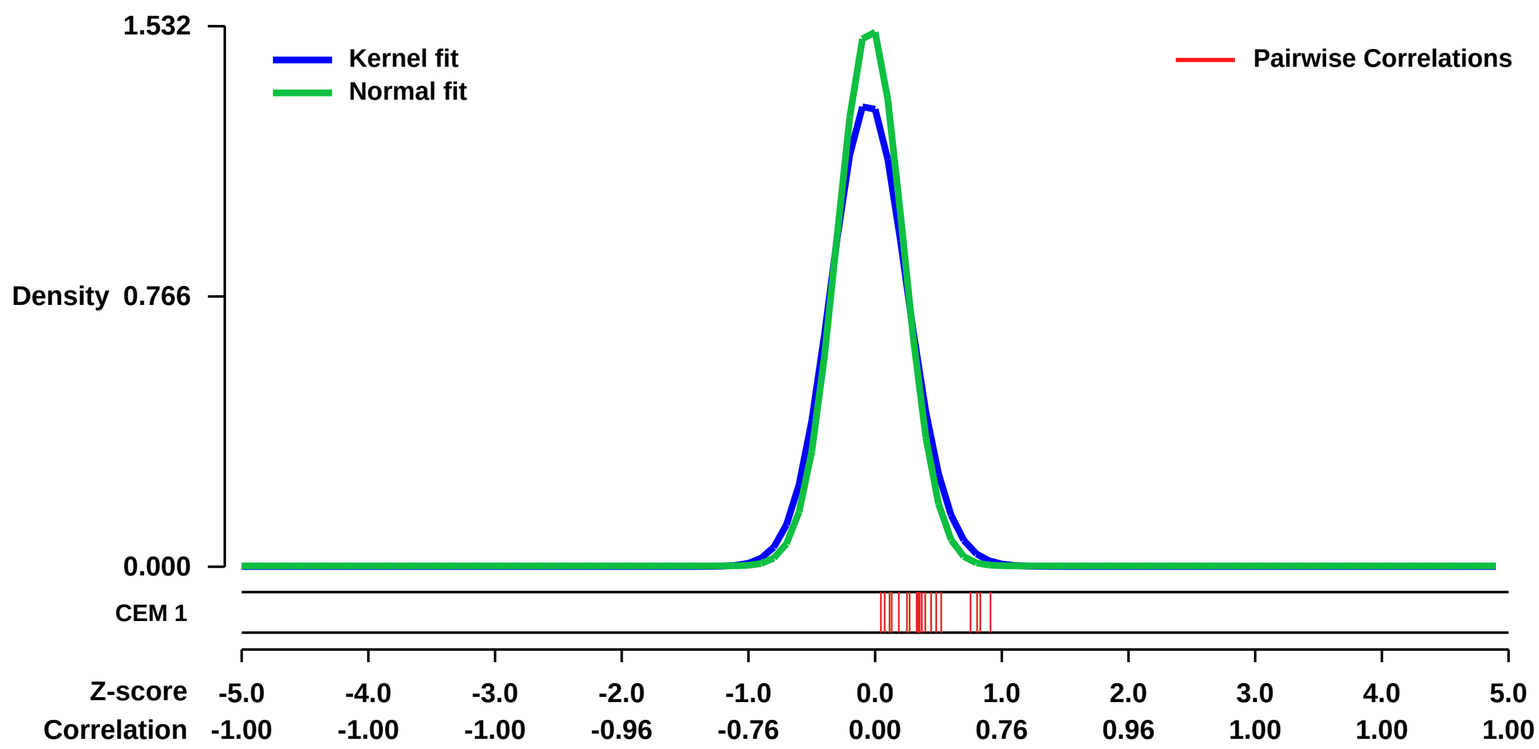

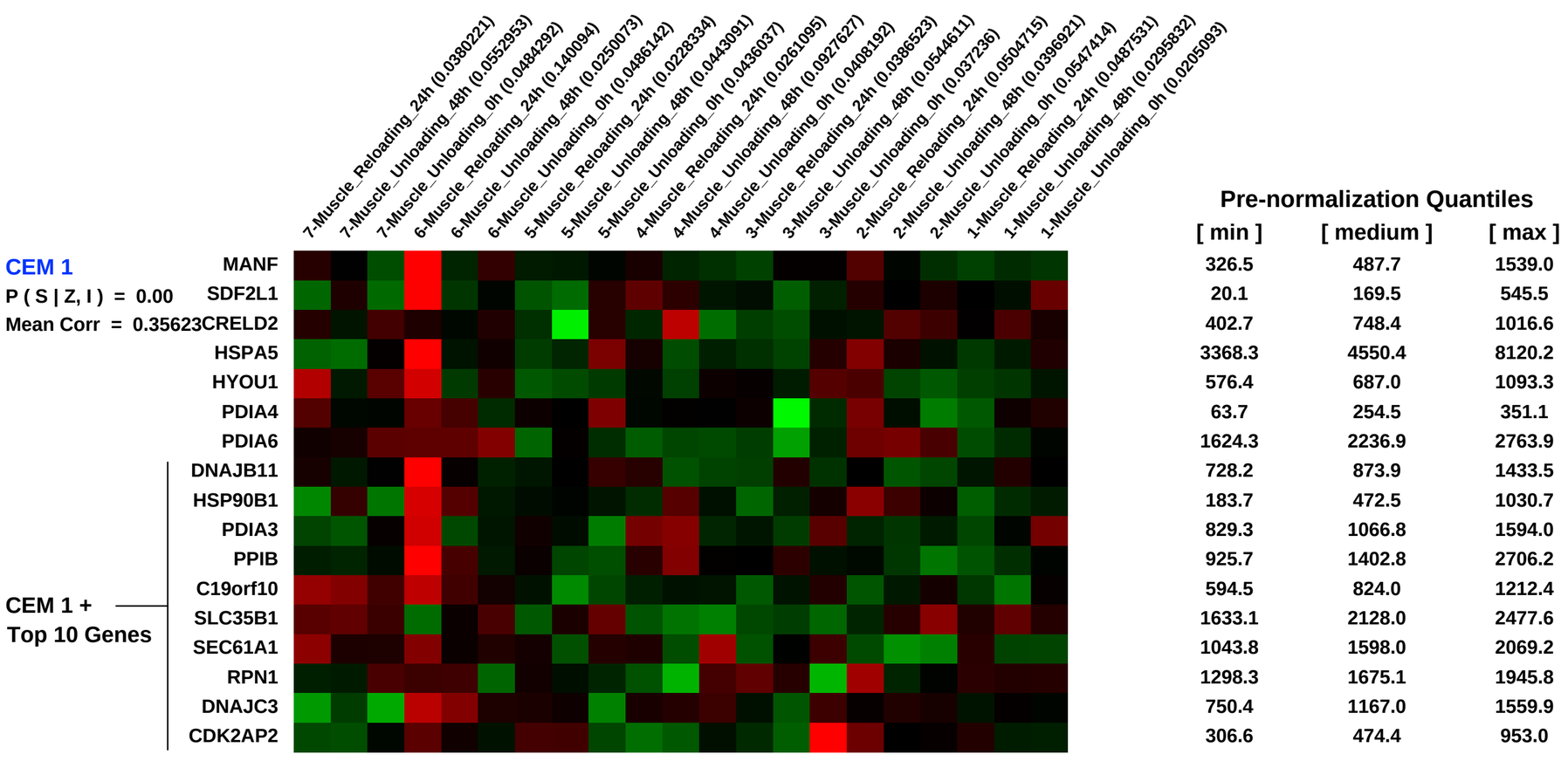

Pre-normalization Quantiles

	[min]	[medium]	[max]
MANF	326.5	487.7	1539.0
SDF2L1	20.1	169.5	545.5
CRELD2	402.7	748.4	1016.6
HSPA5	3368.3	4550.4	8120.2
HYOU1	576.4	687.0	1093.3
PDIA4	63.7	254.5	351.1
PDIA6	1624.3	2236.9	2763.9
DNAJB11	728.2	873.9	1433.5
HSP90B1	183.7	472.5	1030.7
PDIA3	829.3	1066.8	1594.0
PPIB	925.7	1402.8	2706.2
C19orf10	594.5	824.0	1212.4
SLC35B1	1633.1	2128.0	2477.6
SEC61A1	1043.8	1598.0	2069.2
RPN1	1298.3	1675.1	1945.8
DNAJC3	750.4	1167.0	1559.9
CDK2AP2	306.6	474.4	953.0

GEO Series "GSE43998" Expression Profiles

Num of samples in this series: 8

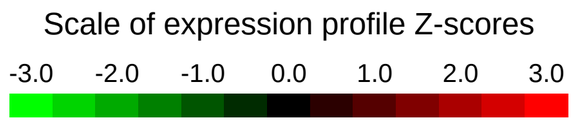

GEO Link:	http://www.ncbi.nlm.nih.gov/geo/query/acc.cgi?acc=GSE43998
Status:	Public on Apr 01 2013
Title:	C/EBPa gene signature
Organism:	Homo sapiens
Experiment type:	Expression profiling by array
Platform:	GPL570
Pubmed ID:	
Summary & Design:	**Summary:** We defined the C/EBPa signature characterized by a set of genes which are upregulated upon C/EBPa activation. In order to identify the C/EBPa signature, we performed microarray gene expression analysis of K562 cells stably expressing p42-C/EBPa-ER after activating the C/EBPa construct to translocate to the nucleus for 6 hours with beta-estradiol. **Overall design:** The gene expression profile was performed in K562 p42-C/EBPa-ER expressing cells treated with beta-estradiol (n=4) or EtOH vehicle control (n-4) for 6 hours. Induction of nuclear localization of C/EBPa-ER fusion protein was achieved by addition of 1 uM beta-estradiol as indicated into the culture medium.

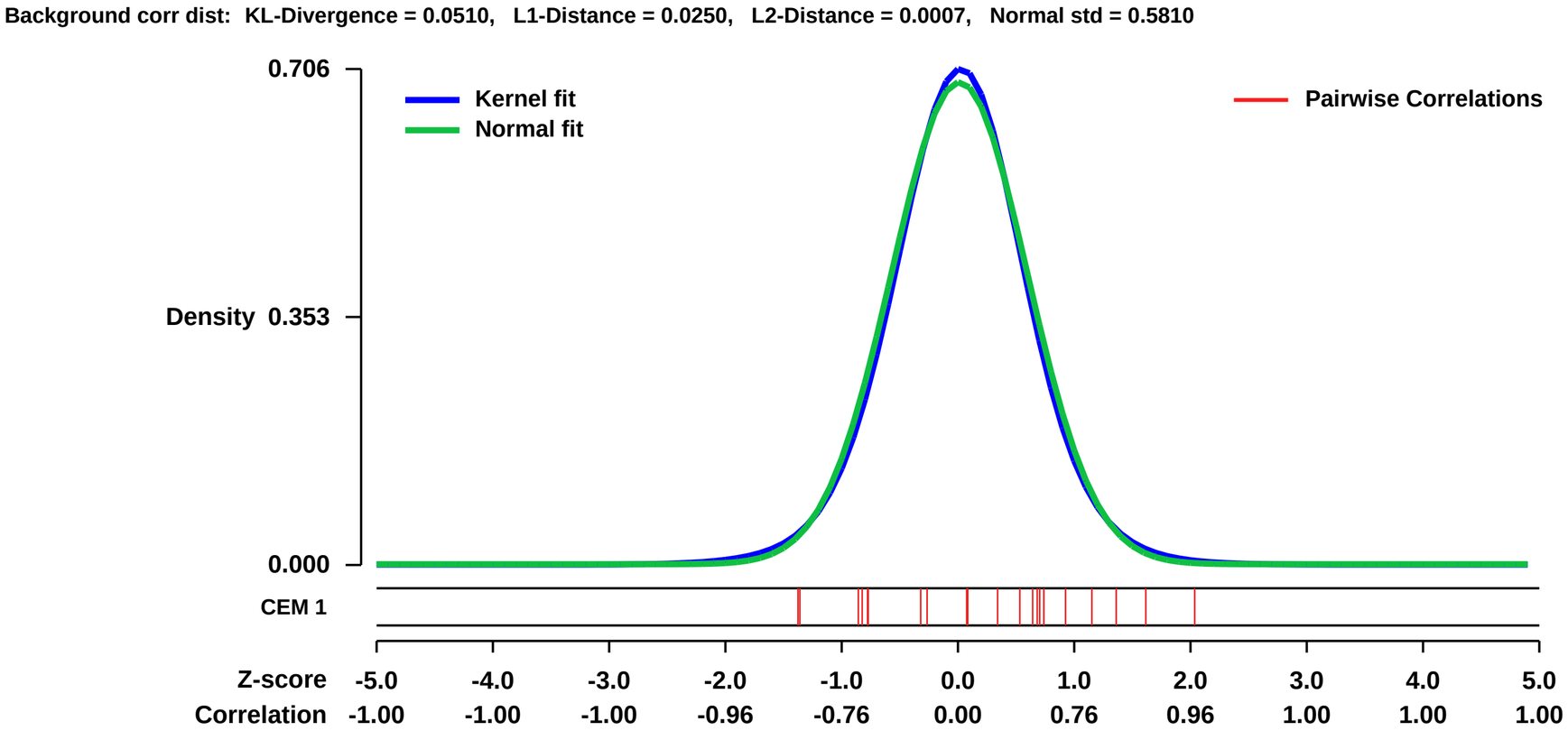

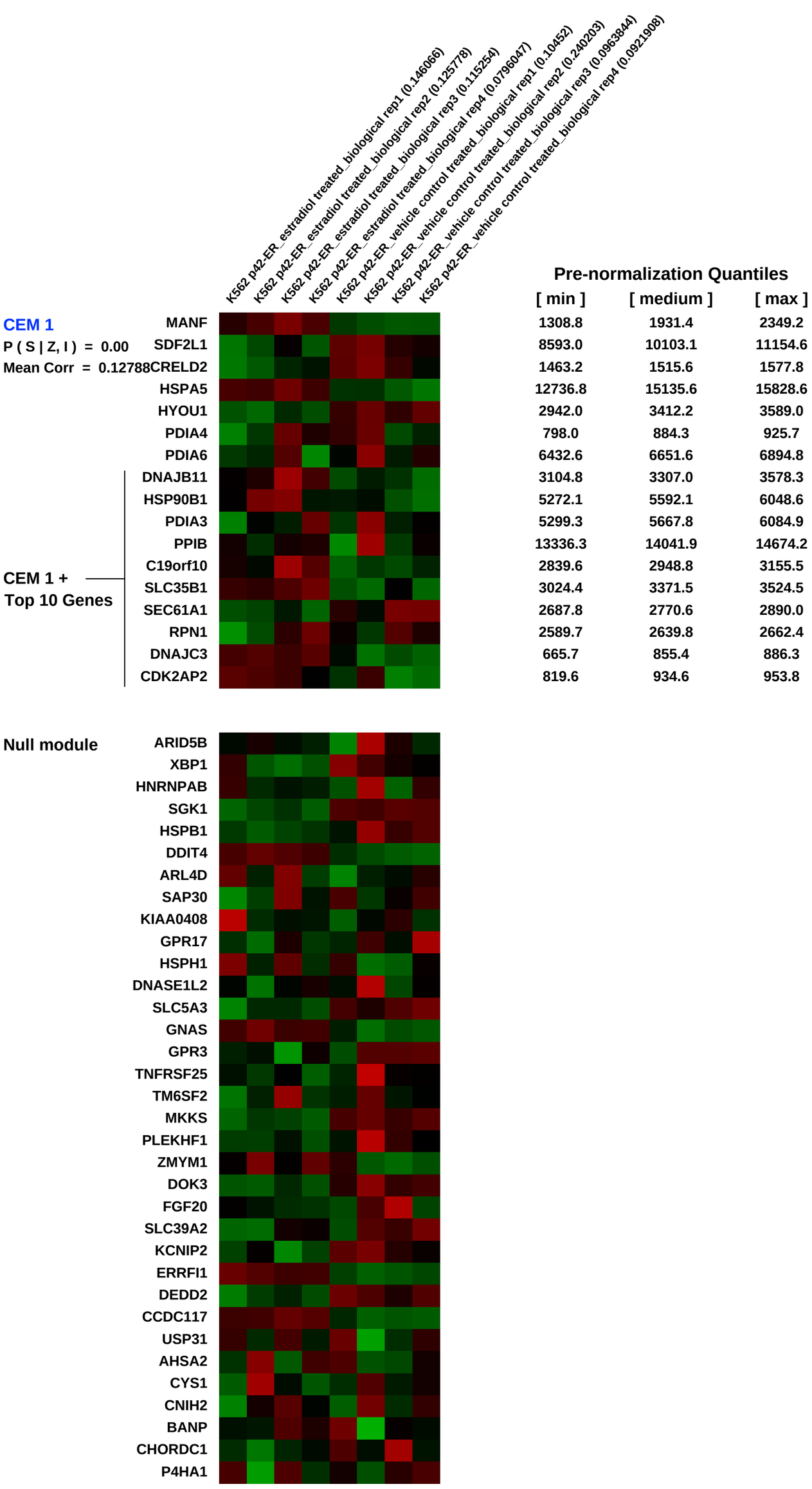

GEO Series "GSE16097" Expression Profiles

Num of samples in this series: 6

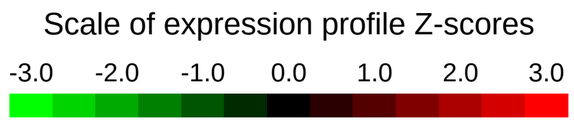

GEO Link:	http://www.ncbi.nlm.nih.gov/geo/query/acc.cgi?acc=GSE16097
Status:	Public on Jul 16 2009
Title:	Transcriptome of BAHD1 knock-down HEK293 cells with siRNA
Organism:	Homo sapiens
Experiment type:	Expression profiling by array
Platform:	GPL570
Pubmed ID:	19666599
Summary & Design:	**Summary:** Gene silencing via heterochromatin formation plays a major role in cell differentiation and maintenance of homeostasis. Here, we report the identification and characterization of a novel heterochromatinization factor in vertebrates, Bromo Adjacent Homology Domain-containing protein 1 (BAHD1). BAHD1 interacts with HP1, MBD1, HDAC5 and with several transcription factors. Through electron and immunofluorescence microscopy studies, we show that BAHD1 overexpression directs HP1 to specific nuclear sites and promotes formation of large heterochromatic domains, which lack acetyl histone H3 and are enriched in H3 trimethylated at lysine 27. Furthermore, ectopically expressed BAHD1 colocalizes with the heterochromatic X inactive chromosome. As highlighted by whole genome microarray analysis of BAHD1 knock down cells, BAHD1 represses several proliferation and survival genes and in particular, the insulin-like growth factor II gene (IGF2). BAHD1 specifically binds the CpG-rich P3 promoter of IGF2. This region contains DNA binding sequences for the transcription factor SP1, with which BAHD1 co-immunoprecipitates. Collectively, these findings provide evidence that BAHD1 acts as a silencer by recruiting proteins that coordinate heterochromatin assembly at specific sites in the genome. We used microarrays to identify BAHD1 gene targets. We compared the transcriptome profile of BAHD1 depleted cells with siRNA to that of cells treated with control siRNA. **Overall design:** Six samples were analysed, including three biological replicates of control cells and three biological replicates of BAHD1 KD cells.

Background corr dist: KL-Divergence = 0.0444, L1-Distance = 0.0219, L2-Distance = 0.0005, Normal std = 0.5966

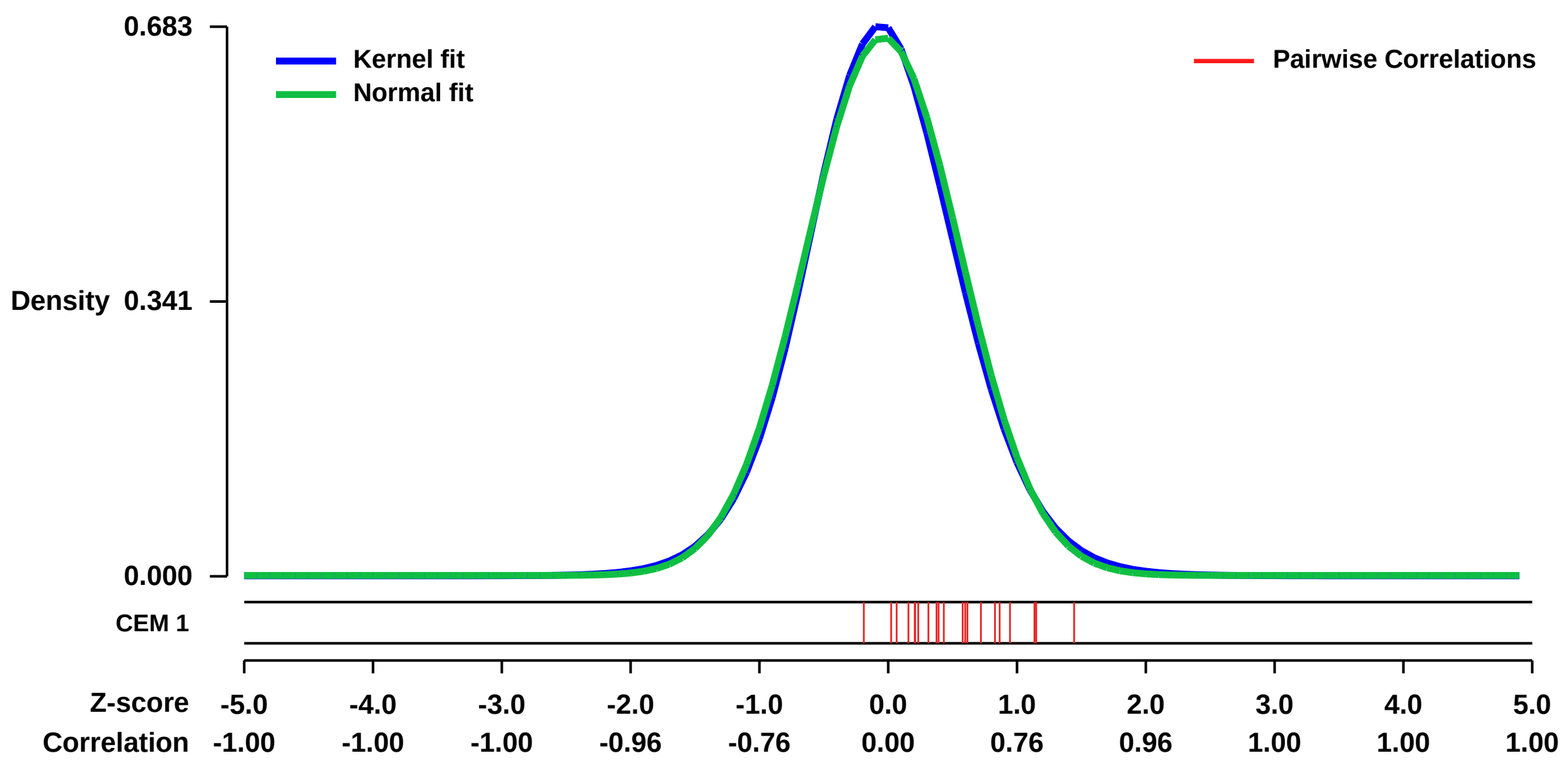

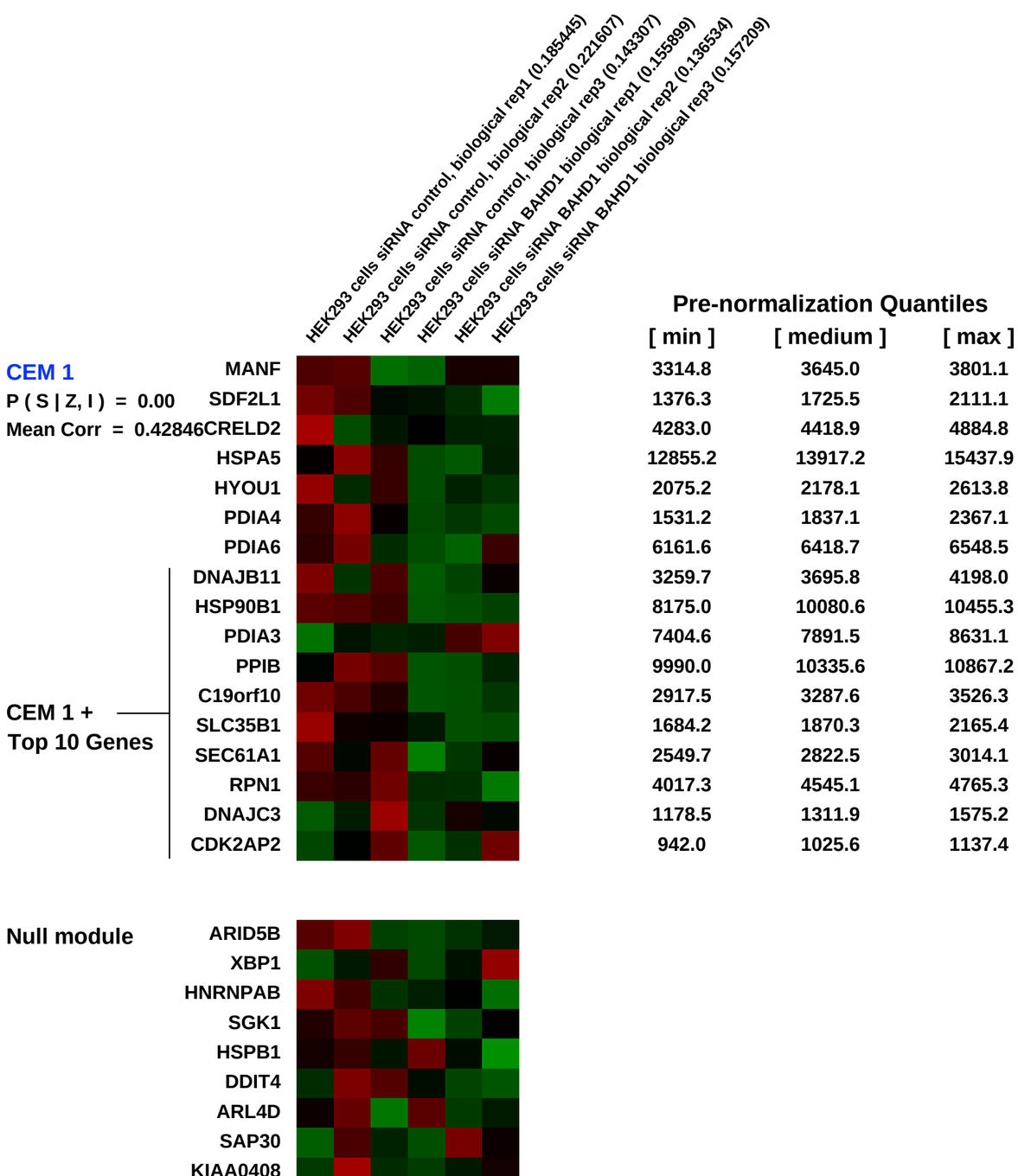

	Pre-normalization Quantiles		
	[min]	[medium]	[max]
MANF	3314.8	3645.0	3801.1
SDF2L1	1376.3	1725.5	2111.1
CRELD2	4283.0	4418.9	4884.8
HSPA5	12855.2	13917.2	15437.9
HYOU1	2075.2	2178.1	2613.8
PDIA4	1531.2	1837.1	2367.1
PDIA6	6161.6	6418.7	6548.5
DNAJB11	3259.7	3695.8	4198.0
HSP90B1	8175.0	10080.6	10455.3
PDIA3	7404.6	7891.5	8631.1
PPIB	9990.0	10335.6	10867.2
C19orf10	2917.5	3287.6	3526.3
SLC35B1	1684.2	1870.3	2165.4
SEC61A1	2549.7	2822.5	3014.1
RPN1	4017.3	4545.1	4765.3
DNAJC3	1178.5	1311.9	1575.2
CDK2AP2	942.0	1025.6	1137.4
ARID5B			
XBP1			
HNRNPAB			
SGK1			
HSPB1			
DDIT4			
ARL4D			
SAP30			
KIAA0408			
GPR17			
HSPH1			
DNASE1L2			
SLC5A3			
GNAS			
GPR3			
TNFRSF25			
TM6SF2			
MKKS			
PLEKHF1			
ZMYM1			
DOK3			
FGF20			
SLC39A2			
KCNIP2			
ERRFI1			
DEDD2			
CCDC117			
USP31			
AHSA2			
CYS1			
CNIH2			
BANP			
CHORDC1			
P4HA1			

GEO Series "GSE13433" Expression Profiles

Num of samples in this series: 16

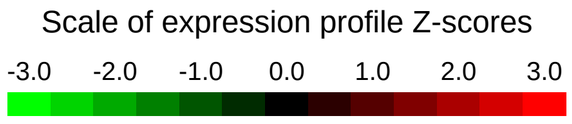

GEO Link:	http://www.ncbi.nlm.nih.gov/geo/query/acc.cgi?acc=GSE13433
Status:	Public on Jan 01 2009
Title:	Gene Expression Profiling of Alveolar Soft-Part Sarcoma (ASPS)
Organism:	Homo sapiens
Experiment type:	Expression profiling by array
Platform:	GPL570
Pubmed ID:	19146682
Summary & Design:	**Summary:** Alveolar soft-part sarcoma (ASPS) is an extremely rare, highly vascular soft tissue sarcoma affecting predominantly adolescents and young adults. In an attempt to gain insight into the pathobiology of this enigmatic tumor, we performed the first genome-wide gene expression profiling study. **Overall design:** For seven patients with confirmed primary or metastatic ASPS, RNA samples were isolated immediately following surgery, reverse transcribed to cDNA and each sample hybridized to duplicate high-density human U133 plus 2.0 microarrays. Array data was then analyzed relative to arrays hybridized to universal RNA to generate an unbiased transcriptome. Subsequent gene ontology analysis was used to identify transcripts with therapeutic or diagnostic potential. A subset of the most interesting genes was then validated using quantitative RT-PCR and immunohistochemistry.

Background corr dist: KL-Divergence = 0.1325, L1-Distance = 0.0662, L2-Distance = 0.0091, Normal std = 0.4502

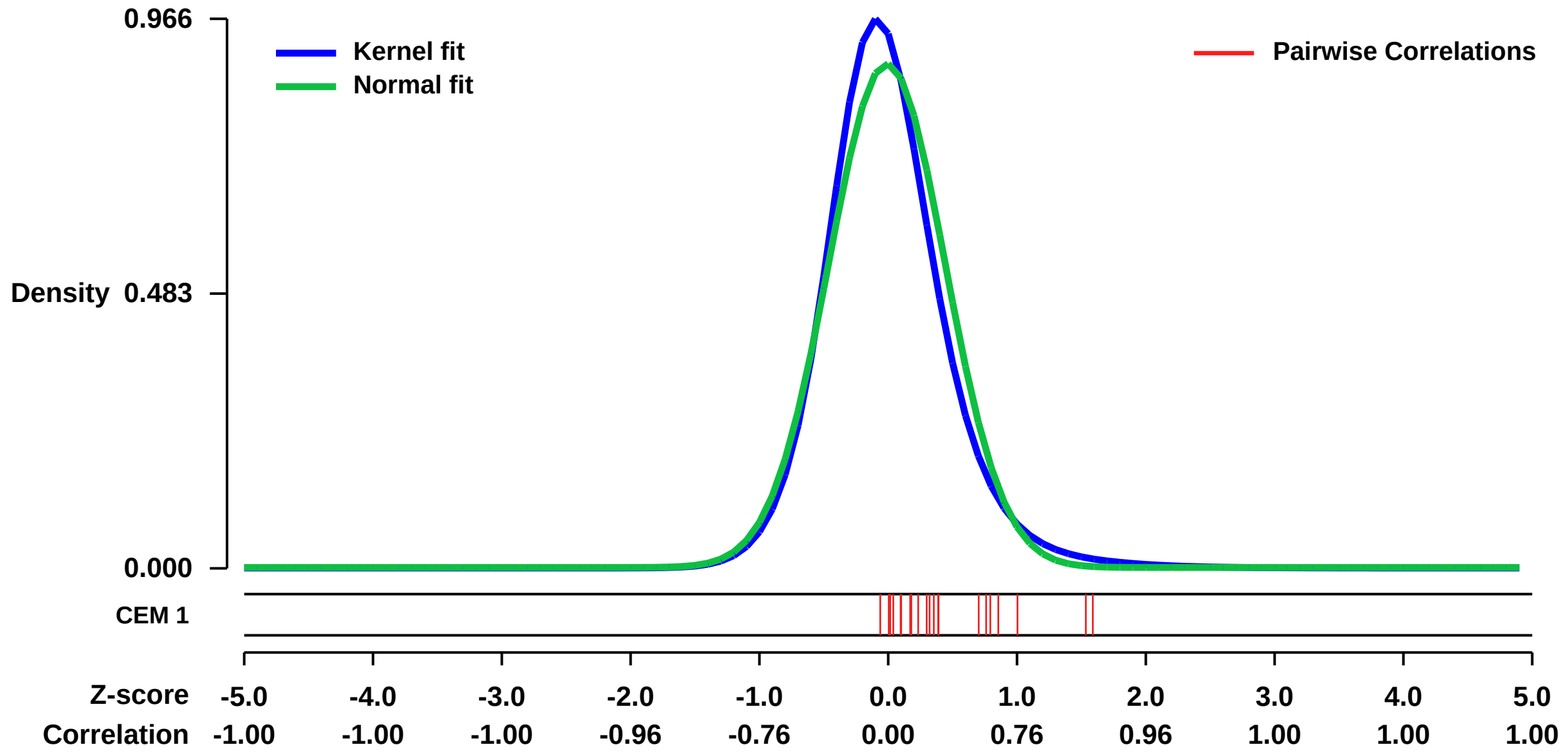

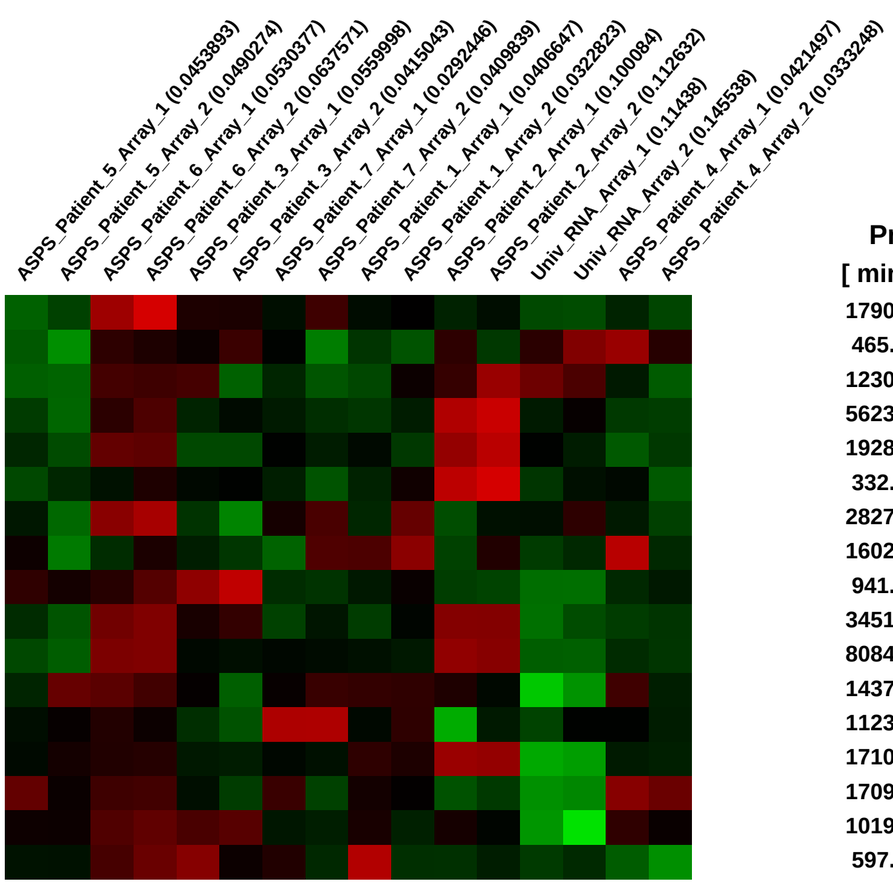

	Pre-normalization Quantiles		
	[min]	[medium]	[max]
MANF	1790.1	2287.2	3629.0
SDF2L1	465.6	760.8	973.4
CRELD2	1230.2	1813.5	2551.9
HSPA5	5623.1	9311.5	20319.5
HYOU1	1928.7	2622.6	5064.9
PDIA4	332.8	535.1	1158.3
PDIA6	2827.4	3441.8	4405.8
DNAJB11	1602.5	2054.6	3085.6
HSP90B1	941.2	2227.4	5406.2
PDIA3	3451.8	5366.3	8623.0
PPIB	8084.7	11834.2	19118.0
C19orf10	1437.1	3393.4	4013.1
SLC35B1	1123.2	1430.3	1747.9
SEC61A1	1710.6	3631.5	5534.3
RPN1	1709.5	2798.1	3681.5
DNAJC3	1019.5	2514.8	3033.1
CDK2AP2	597.8	769.7	1041.3

GEO Series "GSE34298" Expression Profiles

Num of samples in this series: 6

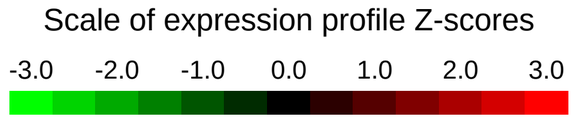

GEO Link:	http://www.ncbi.nlm.nih.gov/geo/query/acc.cgi?acc=GSE34298
Status:	Public on Dec 10 2011
Title:	Expression profile of shikonin resistant K562 cell line
Organism:	Homo sapiens
Experiment type:	Expression profiling by array
Platform:	GPL570
Pubmed ID:	23300986
Summary & Design:	**Summary:** After over 25cycle and 18month's induction of shikonin, K562 cell show maginal resistance to shikonin but great change in gene expression We use microarray to detect the global gene expression change of shikonin resistant cell **Overall design:** K562 cell was treated by 4uM shikonin for 4hours, then allowed to die and grow back in fresh medium. Once recovered, cells were immidiatly subjected to another treatment.

Background corr dist: KL-Divergence = 0.0321, L1-Distance = 0.0169, L2-Distance = 0.0003, Normal std = 0.6590

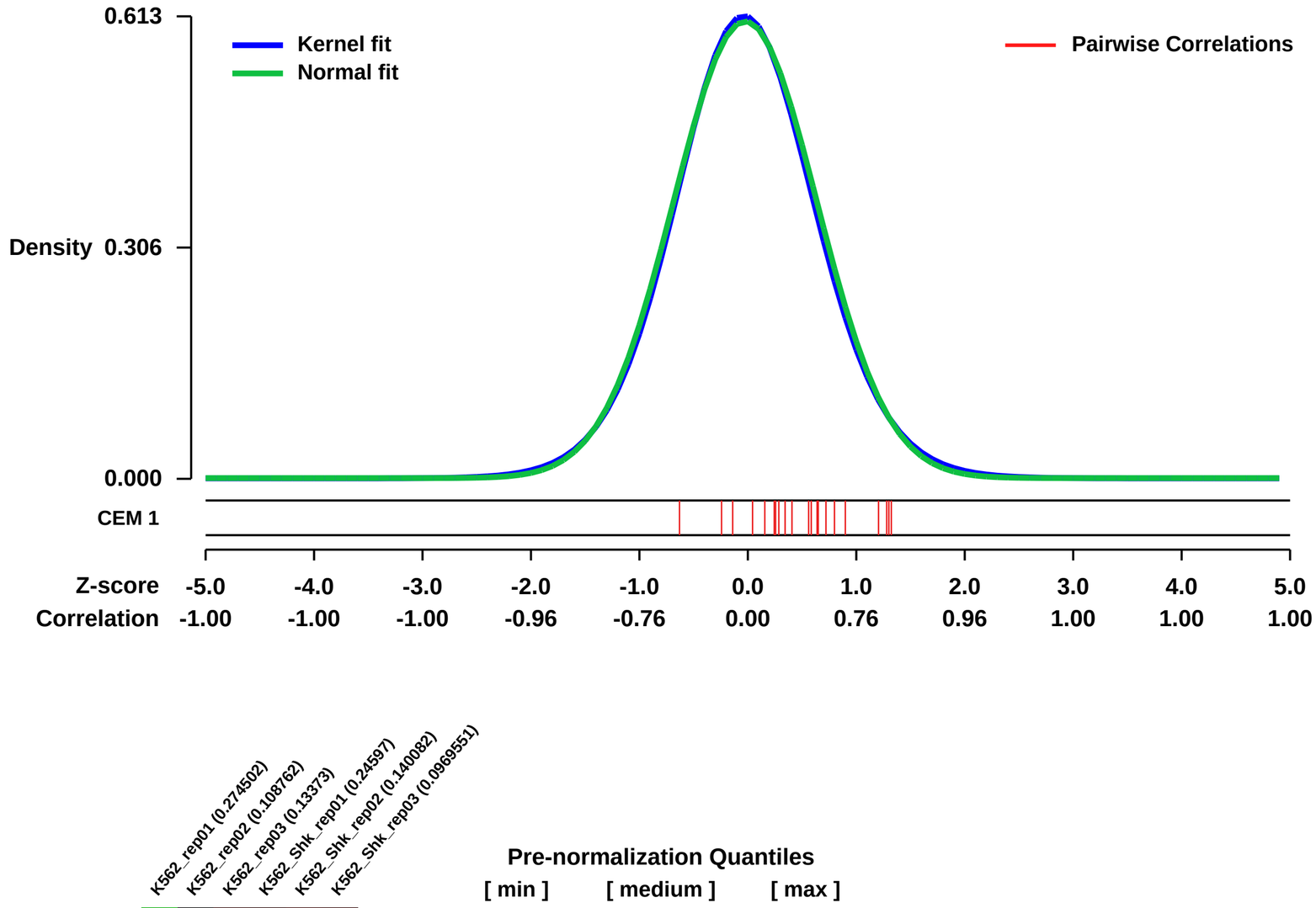

Pre-normalization Quantiles

			[min]	[medium]	[max]
CEM 1		MANF	820.1	1127.4	1139.2
P (S | Z, I) = 0.00		SDF2L1	4983.6	6590.6	7575.5
Mean Corr = 0.39687		CRELD2	1484.5	1796.1	2047.9
		HSPA5	8774.2	15415.8	15792.8
		HYOU1	2565.6	3569.8	4112.8
		PDIA4	1965.5	2178.0	2439.4
		PDIA6	7368.3	7655.1	9262.6
CEM 1 + Top 10 Genes		DNAJB11	2111.8	3023.0	3642.3
		HSP90B1	3479.1	4281.4	4949.7
		PDIA3	4586.8	6875.1	7818.6
		PPIB	8925.7	10294.4	14436.4
		C19orf10	3106.2	3246.1	3369.7
		SLC35B1	3129.1	4173.0	4284.2
		SEC61A1	2451.0	2802.7	2956.8
		RPN1	2275.1	2712.3	3320.2
		DNAJC3	555.8	758.7	775.8
		CDK2AP2	648.7	785.3	829.0
Null module		ARID5B			
		XBP1			
		HNRNPAB			
		SGK1			
		HSPB1			
		DDIT4			
		ARL4D			
		SAP30			
		KIAA0408			
		GPR17			
		HSPH1			
		DNASE1L2			
		SLC5A3			
		GNAS			
		GPR3			
		TNFRSF25			
		TM6SF2			
		MKKS			
		PLEKHF1			
		ZMYM1			
		DOK3			
		FGF20			
		SLC39A2			
		KCNIP2			
		ERRFI1			
		DEDD2			
		CCDC117			
		USP31			
		AHSA2			
		CYS1			
		CNIH2			
		BANP			
		CHORDC1			
		P4HA1			

GEO Series "GSE7117" Expression Profiles

Num of samples in this series: 8

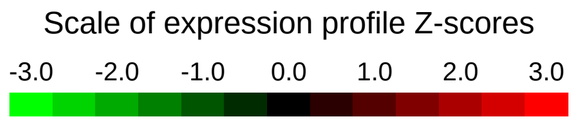

GEO Link:	http://www.ncbi.nlm.nih.gov/geo/query/acc.cgi?acc=GSE7117
Status:	Public on Jul 23 2008
Title:	Hepatic gene expression after a hypocaloric, low-fat diet in obese women and controls
Organism:	Homo sapiens
Experiment type:	Expression profiling by array
Platform:	GPL570
Pubmed ID:	18804985

Summary & Design:

Summary:
The prevalence of obesity has been increasing rapidly worldwide during the past two decades. This is alarming, since obesity has considerable effects on morbidity and mortality. The majority of gene expression studies about the effect of obesity and weight loss have been performed using the adipose tissue for mRNA extraction. However, also the liver plays a central role in maintaining energy balance. To our knowledge, no overall analysis of hepatic gene expression in response to changes in nutritional status has been made in humans Therefore, it is important to investigate how a short-time hypocaloric diet affects overall hepatic gene expression and the metabolic profile in a group of overweight and obese women. The subjects (n=31) were middle-aged, overweight (BMI>25 kg/m2) women with gallstone disease scheduled for an elective gallbladder operation. The intervention subjects were placed on a hypocaloric AHA step I diet with a recommended daily energy intake of 5.0 MJ. The objective was to reduce 0.5 kg of body weight per week. The control subjects were instructed to continue their habitual diet and not to lose weight. Basic clinical measurements and laboratory analyses were performed twice at baseline and at two week intervals during the weight reduction period. Surgical liver biopsies were obtained at the end of the weight reduction period. RNA samples of 4 individuals from the intervention group and 4 individuals from the control group were selected for the microarray analysis. The results from the microarray analysis were fairly surprising. Only one gene was up-regulated and the rest 142 down-regulated in the diet intervention group compared to the control group when a minimum of 2-fold change was set as the limit. The global decrease in hepatic gene expression was unexpected but the results are interesting, with several genes not previously linked to weight reduction. The decrease in triglyceride and fasting plasma insulin concentrations observed in our study is in accordance with results from many previous weight-loss trials.

Keywords: Overall hepatic gene expression associated with obesity and moderate weight loss in a group of overweight and obese middle-aged women.

Overall design:
Total RNA was extracted from liver tissue and RNA concentration and purity were assessed spectrophotometrically at wavelengths 260 and 280 nm. RNA integrity was checked by agarose gel electrophoresis. RNA samples of 4 individuals from the intervention group and 4 individuals from the control group were selected for the microarray analysis. The individuals from the diet intervention group were selected to represent the whole group, not just those who lost most weight. The microarray data was validated by performing relative quantitative real-time (RT) PCR using liver samples from 7 intervention subjects and 8 control subjects, including the samples used in the microarray analysis. 11 genes were selected on the basis of biological interest. The expression of these genes was concordant with the microarray data

Background corr dist: KL-Divergence = 0.0241, L1-Distance = 0.0620, L2-Distance = 0.0054, Normal std = 0.7837

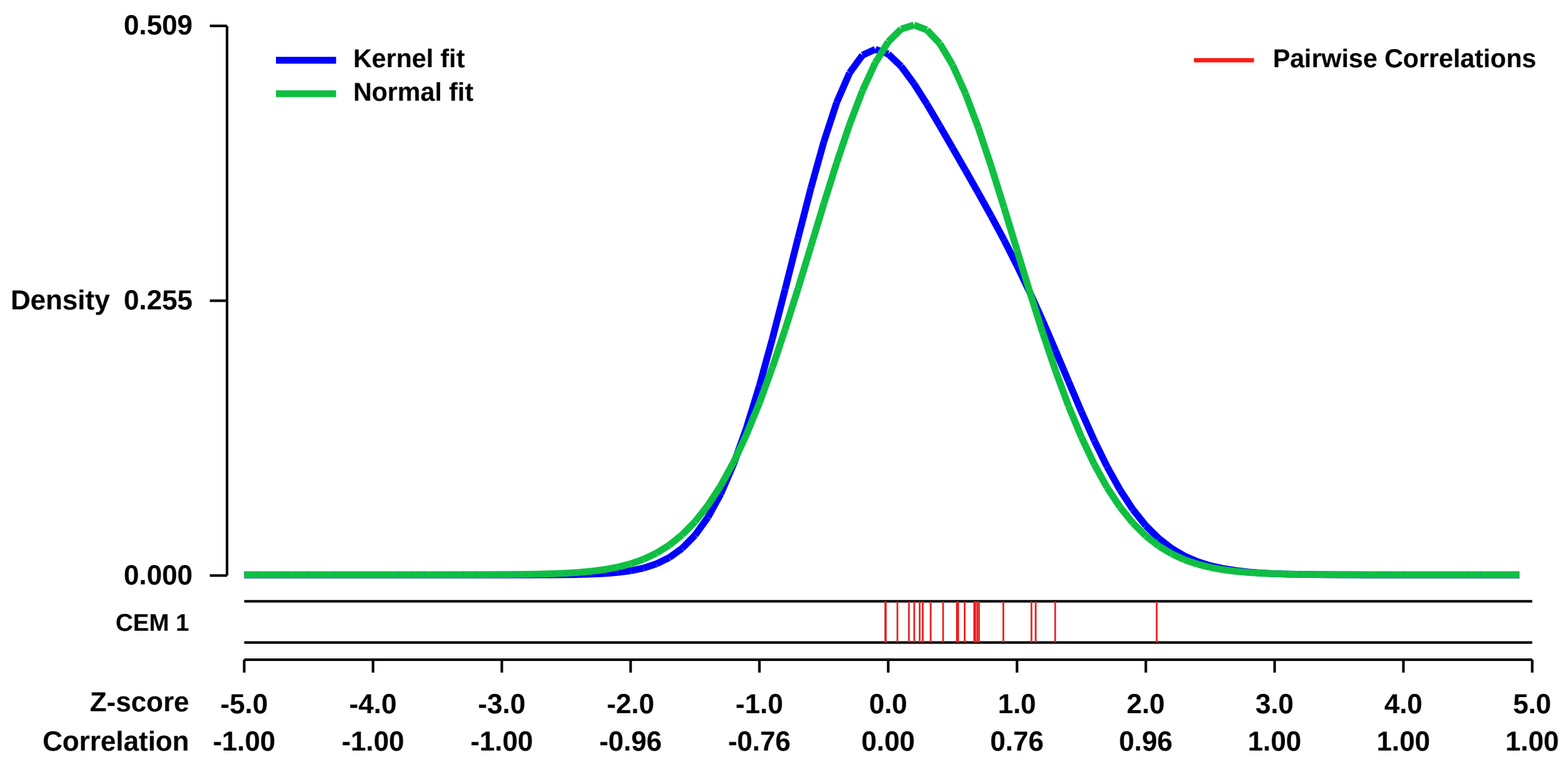

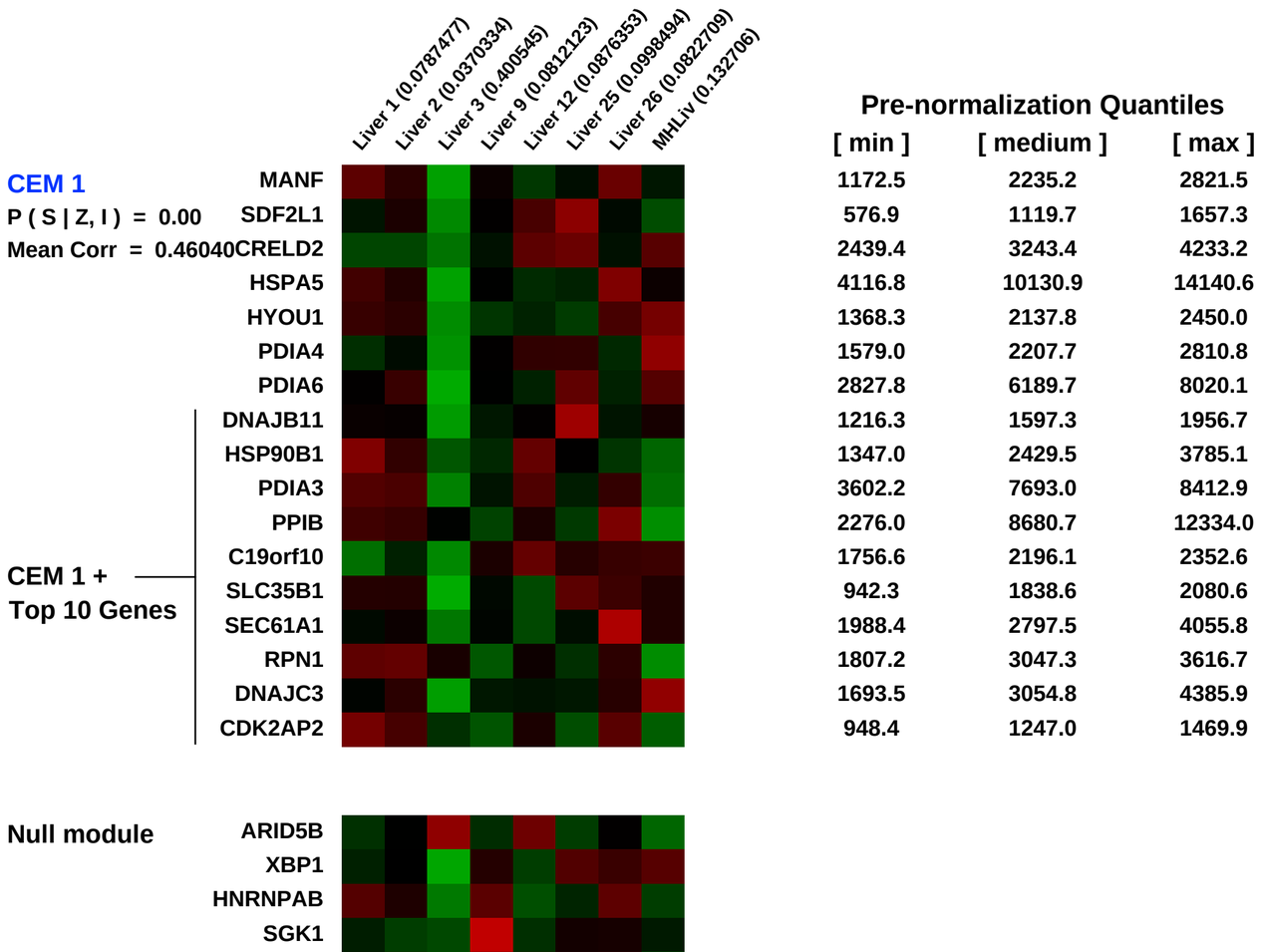

GEO Series "GSE6960" Expression Profiles

Num of samples in this series: 12

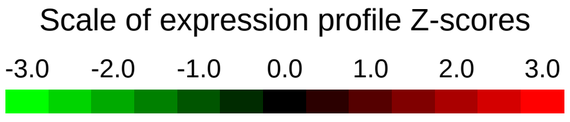

GEO Link:	http://www.ncbi.nlm.nih.gov/geo/query/acc.cgi?acc=GSE6960
Status:	Public on Feb 07 2007
Title:	Synthesis and Anticancer Properties of Water-Soluble Zinc Ionophores 1
Organism:	Homo sapiens
Experiment type:	Expression profiling by array
Platform:	GPL570
Pubmed ID:	18593933
Summary & Design:	**Summary:** We have shown that water solubilized versions of a zinc ionophore increase intracellular concentrations of free zinc and have antiproliferative activity in exponential phase A549 lung cancer cultures. The gene expression profiles of A549 lung cancer cultures treated with the lead compound PCI-5002 reveal the activation of stress response pathways. Medium supplementation with zinc (25 ¸…M) led to activation of additional oxidative stress response as well as apoptotic pathways. We propose that the pharmacologic delivery of zinc to tumors using water solubilized ionophores is a potential approach to cancer therapy. **Keywords: Dose response** **Overall design:** A549 human lung cancer cells (1 x 105 cells per T-25 flask in 7 mL complete RPMI 1640 medium) were seeded 8 days prior to treatment of non-cycling plateau phase cultures with drug. At 4 hours prior to RNA isolation, sapphyrin PCI-5002 (10 ¸…M final concentration), ZnOAc2 (25 ¸…M final concentration), the combination, or control (5% mannitol) solution was added to the cultures. Each experiment was performed in triplicate. After incubation, all cultures were washed twice with HBSS supplemented with 0.5% BSA and total RNA was isolated and subjected to analysis on Human Genome U133 Plus 2.0 Arrays (Affymetrix, Santa Clara, CA), as described. ArrayAssist software (Stratagene/Affymetrix) and the RMA (Robust Microarray Analysis) algorithm were used to generate scaled gene expression values.

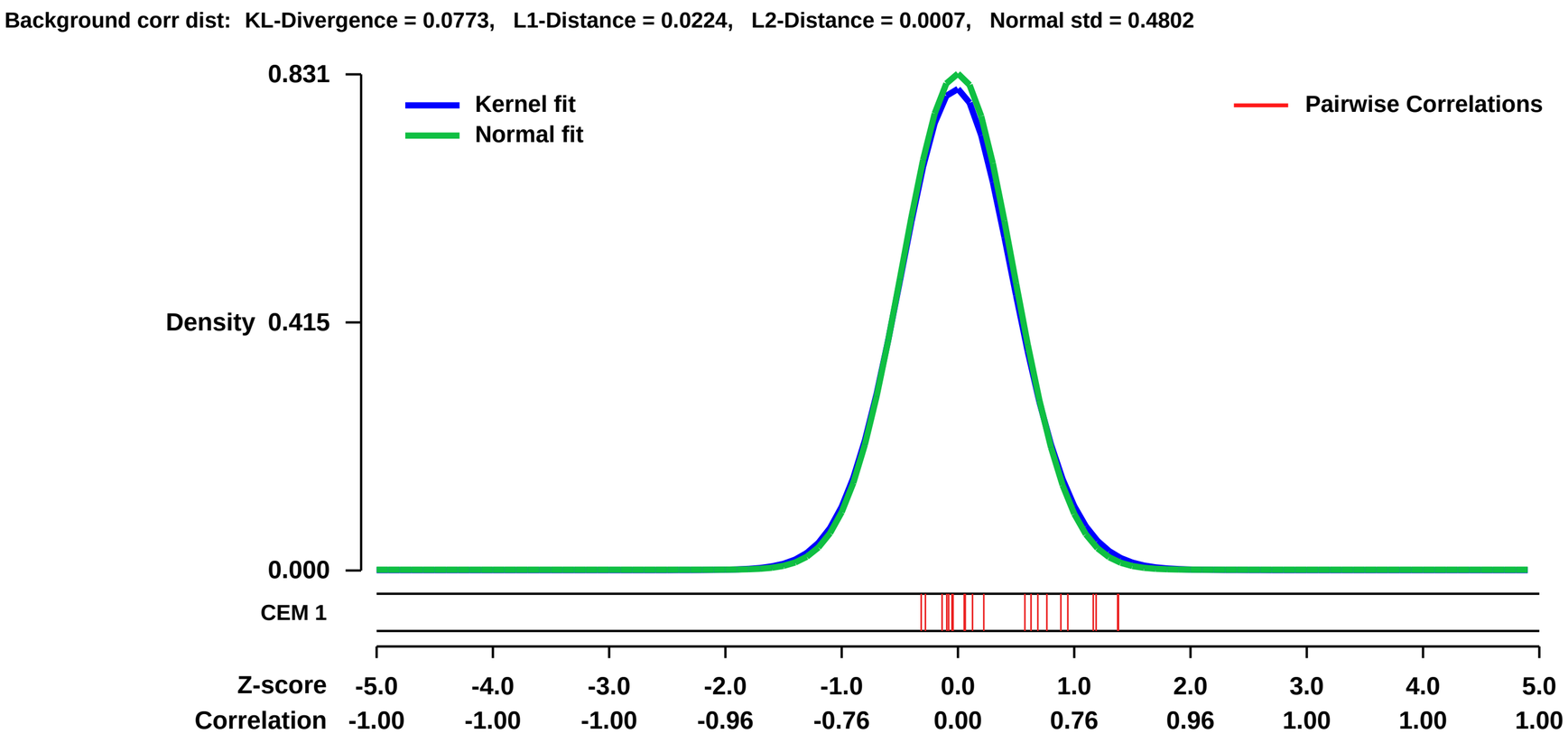

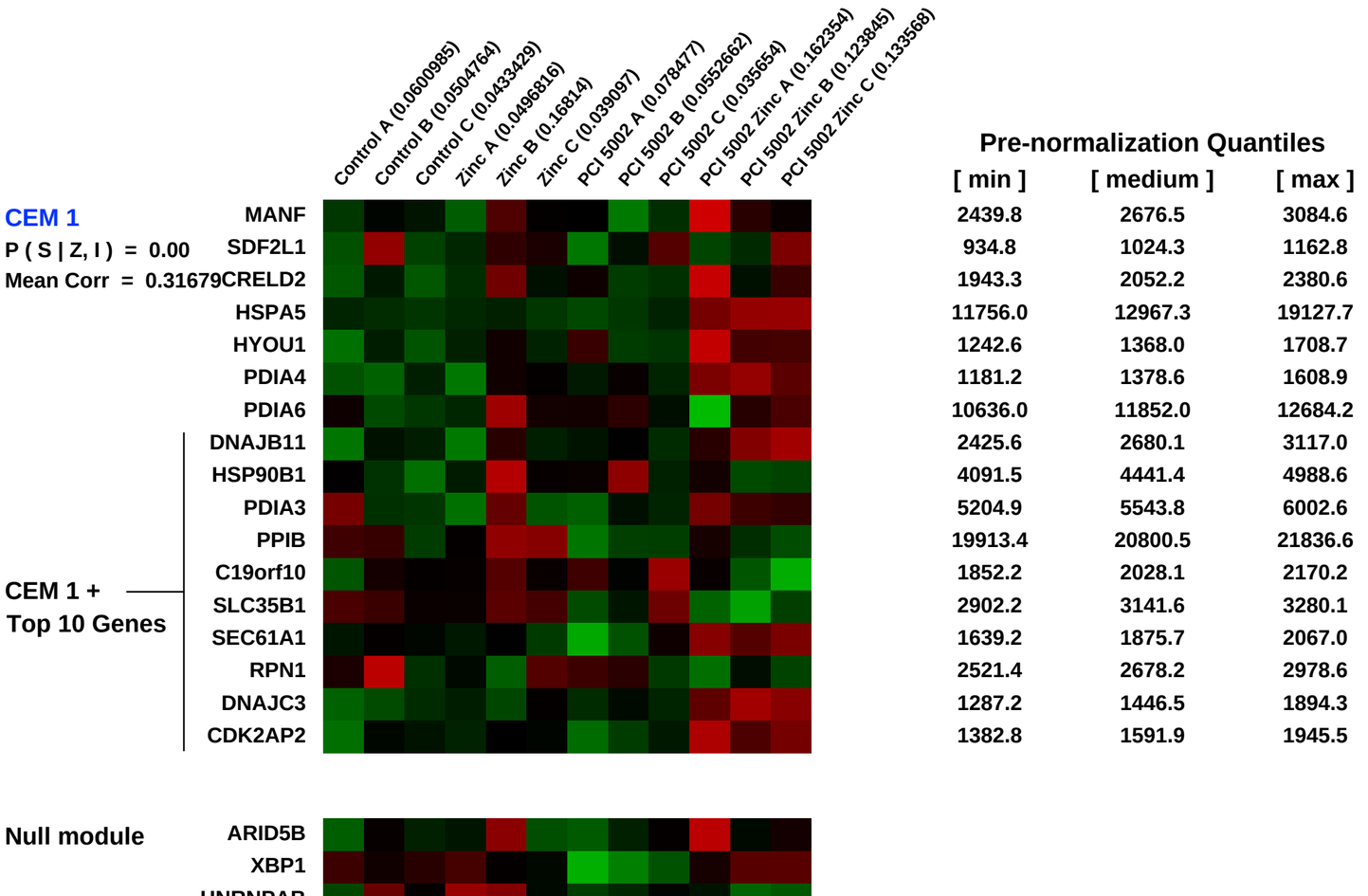

Pre-normalization Quantiles

	[min]	[medium]	[max]
MANF	2439.8	2676.5	3084.6
SDF2L1	934.8	1024.3	1162.8
CRELD2	1943.3	2052.2	2380.6
HSPA5	11756.0	12967.3	19127.7
HYOU1	1242.6	1368.0	1708.7
PDIA4	1181.2	1378.6	1608.9
PDIA6	10636.0	11852.0	12684.2
DNAJB11	2425.6	2680.1	3117.0
HSP90B1	4091.5	4441.4	4988.6
PDIA3	5204.9	5543.8	6002.6
PPIB	19913.4	20800.5	21836.6
C19orf10	1852.2	2028.1	2170.2
SLC35B1	2902.2	3141.6	3280.1
SEC61A1	1639.2	1875.7	2067.0
RPN1	2521.4	2678.2	2978.6
DNAJC3	1287.2	1446.5	1894.3
CDK2AP2	1382.8	1591.9	1945.5

GEO Series "GSE7874" Expression Profiles

Num of samples in this series: 15

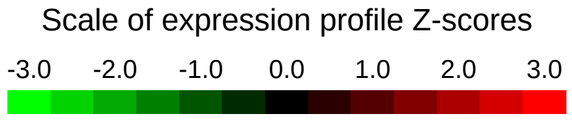

GEO Link:	http://www.ncbi.nlm.nih.gov/geo/query/acc.cgi?acc=GSE7874
Status:	Public on Aug 22 2007
Title:	Effects of EPO and EST on erythroid maturation
Organism:	Homo sapiens
Experiment type:	Expression profiling by array
Platform:	GPL570
Pubmed ID:	17721544
Summary & Design:	**Summary:** Transcriptional profiles of human CD34+ cells cultured in EPO and EST conditions. **Overall design:** After obtaining informed consent, human CD34+ cells were isolated in high purity from the peripheral blood of normal human volunteers. The cells were cultured at a concentration of 104 - 105 cells/mL in medium supplemented with 4 U/mL Erythropoietin (EPO) versus 4 U/mL Erythropoietin + 50 ng/mL Stem Cell Factor + 1.25 ng/mL Transforming Growth Factor Beta (EST) as described previously. Cells were sampled on culture Day 7, culture Day 14, or both culture days and enumerated using an electronic cell counter (Coulter, Hialeah, FL). Adult and fetal hemoglobin was analysed by HPLC. RNA was extracted using QIAshredder and Rneasy Minikit.

Background corr dist: KL-Divergence = 0.1185, L1-Distance = 0.0397, L2-Distance = 0.0024, Normal std = 0.4306

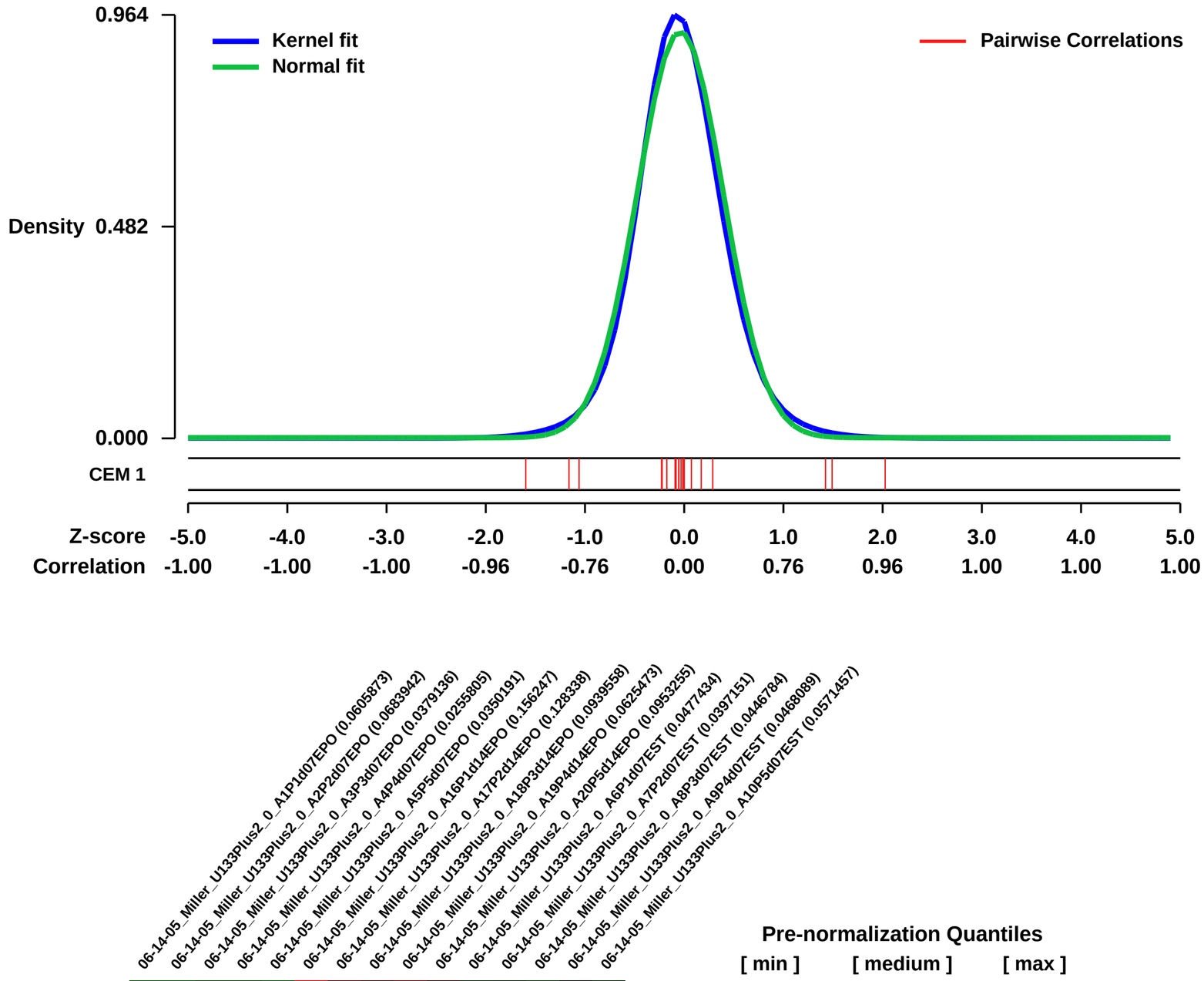

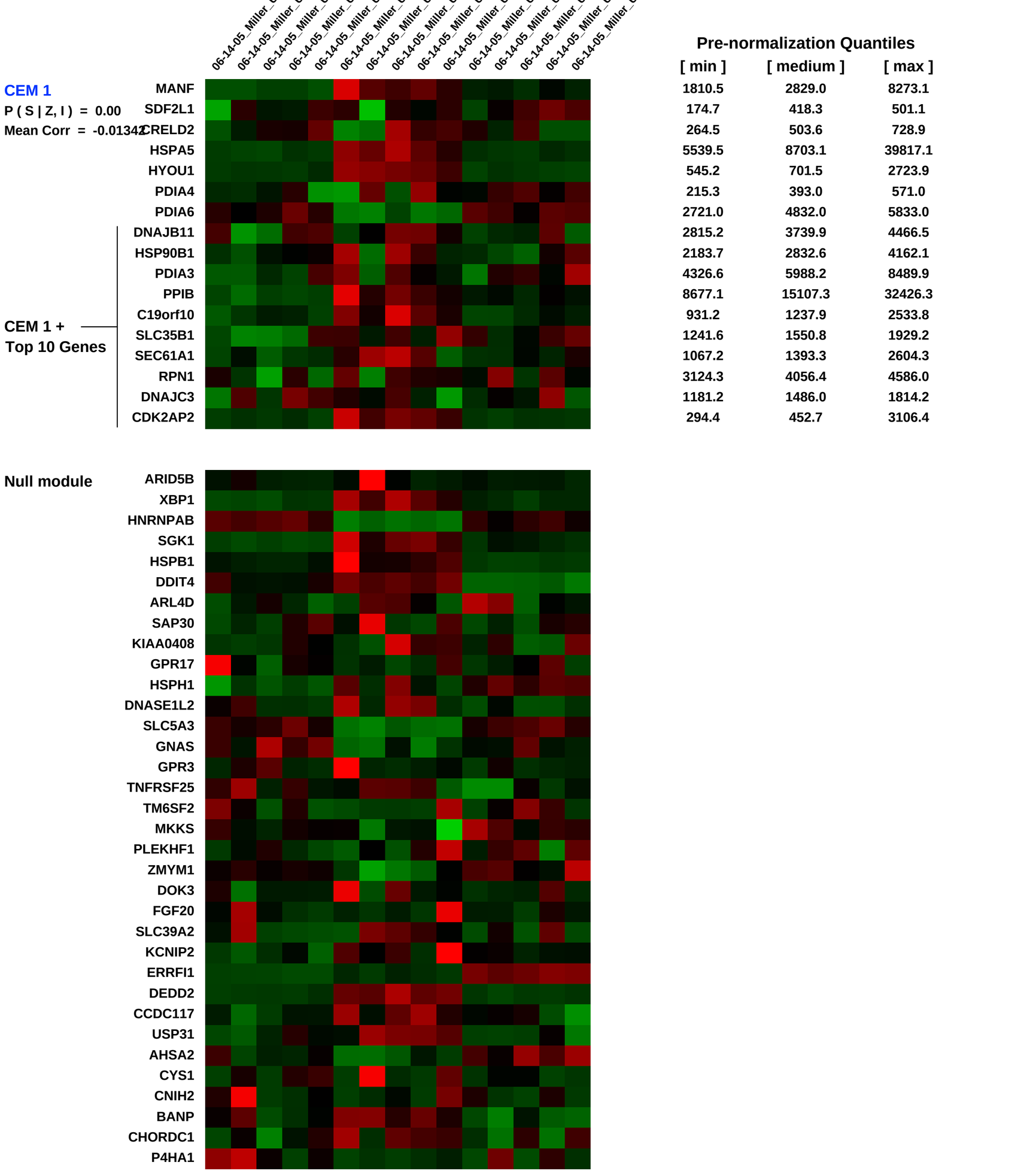

Pre-normalization Quantiles

	[min]	[medium]	[max]
MANF	1810.5	2829.0	8273.1
SDF2L1	174.7	418.3	501.1
CRELD2	264.5	503.6	728.9
HSPA5	5539.5	8703.1	39817.1
HYOU1	545.2	701.5	2723.9
PDIA4	215.3	393.0	571.0
PDIA6	2721.0	4832.0	5833.0
DNAJB11	2815.2	3739.9	4466.5
HSP90B1	2183.7	2832.6	4162.1
PDIA3	4326.6	5988.2	8489.9
PPIB	8677.1	15107.3	32426.3
C19orf10	931.2	1237.9	2533.8
SLC35B1	1241.6	1550.8	1929.2
SEC61A1	1067.2	1393.3	2604.3
RPN1	3124.3	4056.4	4586.0
DNAJC3	1181.2	1486.0	1814.2
CDK2AP2	294.4	452.7	3106.4

GEO Series "GSE16015" Expression Profiles

Num of samples in this series: 107

Details of this dataset are not shown due to large number of samples and the page size limit.

Find details in http://www.ncbi.nlm.nih.gov/geo/query/acc.cgi?acc=GSE16015

Background corr dist: KL-Divergence = 0.3126, L1-Distance = 0.0820, L2-Distance = 0.0209, Normal std = 0.2759

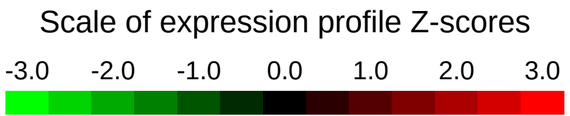

GEO Series "GSE34027" Expression Profiles

Num of samples in this series: 9

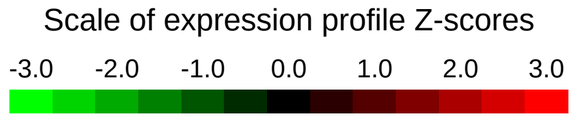

GEO Link:	http://www.ncbi.nlm.nih.gov/geo/query/acc.cgi?acc=GSE34027
Status:	Public on Oct 03 2012
Title:	EWS TC-71 cell lines: IGF-1R resistant
Organism:	Homo sapiens
Experiment type:	Expression profiling by array
Platform:	GPL570
Pubmed ID:	22798295
Summary & Design:	**Summary:** Ewing's Sarcoma cell lines were made resistant to different IGF-1R drugs to investigate mechanisms and pathways modulated by the resistance. **Overall design:** EWS TC-71 cell line was exposed to increasing concentration to three different anti-IGF-1R drugs (HAb AVE1642, TKI NVP-AEW541, HAb CP-751,871, cell lines named respectively as TC/AVE, TC/AEW or TC/CP) for at least six months. Expression profile of resistant cell variants was compared either singularly for each resistance or commonly vs. parental cell line. Two technical replicates for resistant variants and three biological replicated for parental cell were present.

Background corr dist: KL-Divergence = 0.0619, L1-Distance = 0.0209, L2-Distance = 0.0007, Normal std = 0.5248

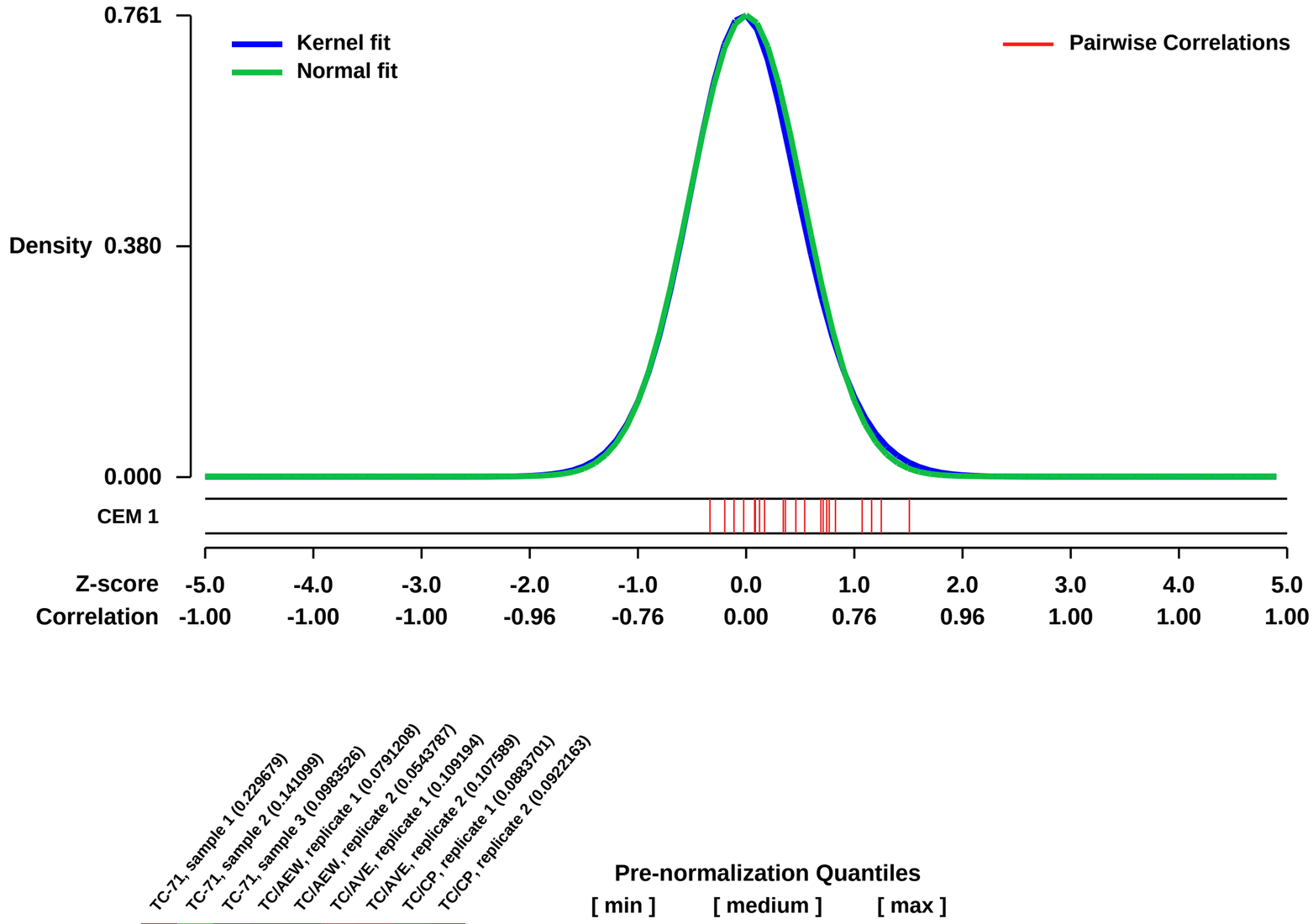

CEM 1
P (S | Z, I) = 0.00
Mean Corr = 0.37794

CEM 1 + Top 10 Genes

Null module

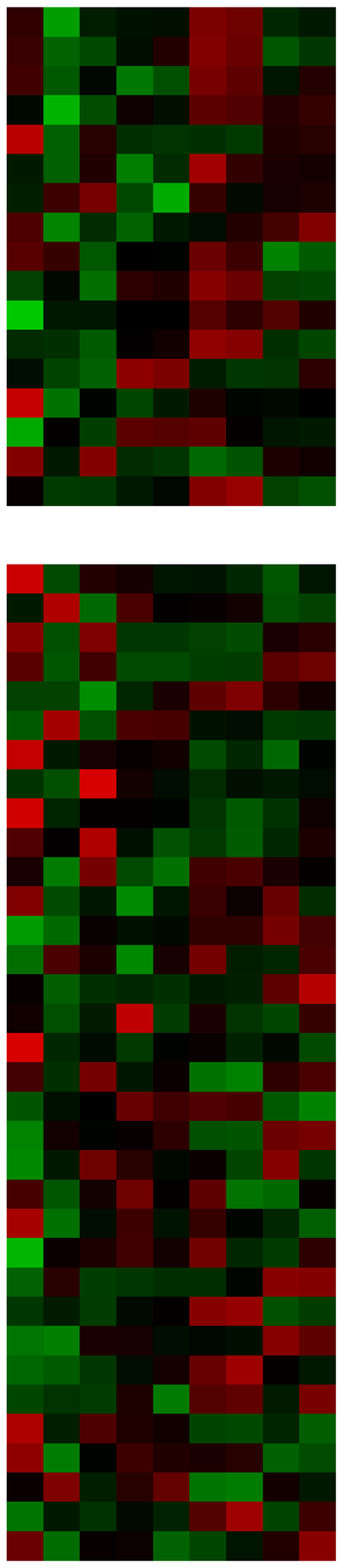

CEM 1 + Top 10 Genes	MANF	1660.6	2661.0	3671.9
	SDF2L1	1571.8	2040.7	2837.0
	CRELD2	2803.6	3415.7	4110.2
	HSPA5	7967.0	16908.6	20594.5
	HYOU1	4448.9	5110.7	8184.0
	PDIA4	951.9	1223.3	1482.6
	PDIA6	10119.3	11858.0	12698.6
	DNAJB11	4857.3	5534.6	6327.7
	HSP90B1	4243.7	5735.7	6960.9
	PDIA3	5721.7	7456.7	9836.9
	PPIB	11065.5	17730.2	20507.6
	C19orf10	4093.3	4438.8	5795.3
	SLC35B1	5099.9	5524.6	6570.9
	SEC61A1	2740.0	3382.2	4565.2
	RPN1	4090.2	5522.3	6279.4
	DNAJC3	1712.4	2077.6	2772.9
	CDK2AP2	860.4	1233.1	2406.3
Null module	ARID5B			
	XBP1			
	HNRNPAB			
	SGK1			
	HSPB1			
	DDIT4			
	ARL4D			
	SAP30			
	KIAA0408			
	GPR17			
	HSPH1			
	DNASE1L2			
	SLC5A3			
	GNAS			
	GPR3			
	TNFRSF25			
	TM6SF2			
	MKKS			
	PLEKHF1			
	ZMYM1			
	DOK3			
	FGF20			
	SLC39A2			
	KCNIP2			
	ERRFI1			
	DEDD2			
	CCDC117			
	USP31			
	AHSA2			
	CYS1			
	CNIH2			
	BANP			
	CHORDC1			
	P4HA1			

GEO Series "GSE41855" Expression Profiles

Num of samples in this series: 8

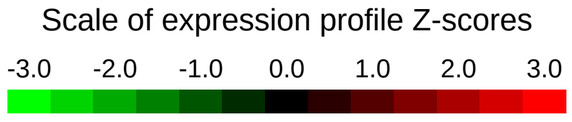

GEO Link:	http://www.ncbi.nlm.nih.gov/geo/query/acc.cgi?acc=GSE41855
Status:	Public on Oct 27 2012
Title:	Expression data from quiescent cells and cycling cells isolated from Multicellular aggregates of lymphoma cells (MALC)
Organism:	Homo sapiens
Experiment type:	Expression profiling by array
Platform:	GPL570
Pubmed ID:	
Summary & Design:	**Summary:** Follicular Lymphomas are blood tumors growing as spheres in patients. Before this study, there was no experimental model mimicking the 3D organization of these in vivo tumors. We develop such a model, called MALC, and observed a progressive enrichment in quiescent cells in these with time of culture; these cells were sorted, as their cycling counterparts, and their transcriptomes were compared. We used microarrays to detail the differential global gene expression profile between quiescent and cycling cells isolated from MALC. **Overall design:** 14 days-old MALC were stained with pyronin Y and quiescent and cycling subpopulations sorted were selected for RNA extraction and hybridization on Affymetrix U133+ 2.0 microarrays.

Background corr dist: KL-Divergence = 0.0633, L1-Distance = 0.0191, L2-Distance = 0.0004, Normal std = 0.5220

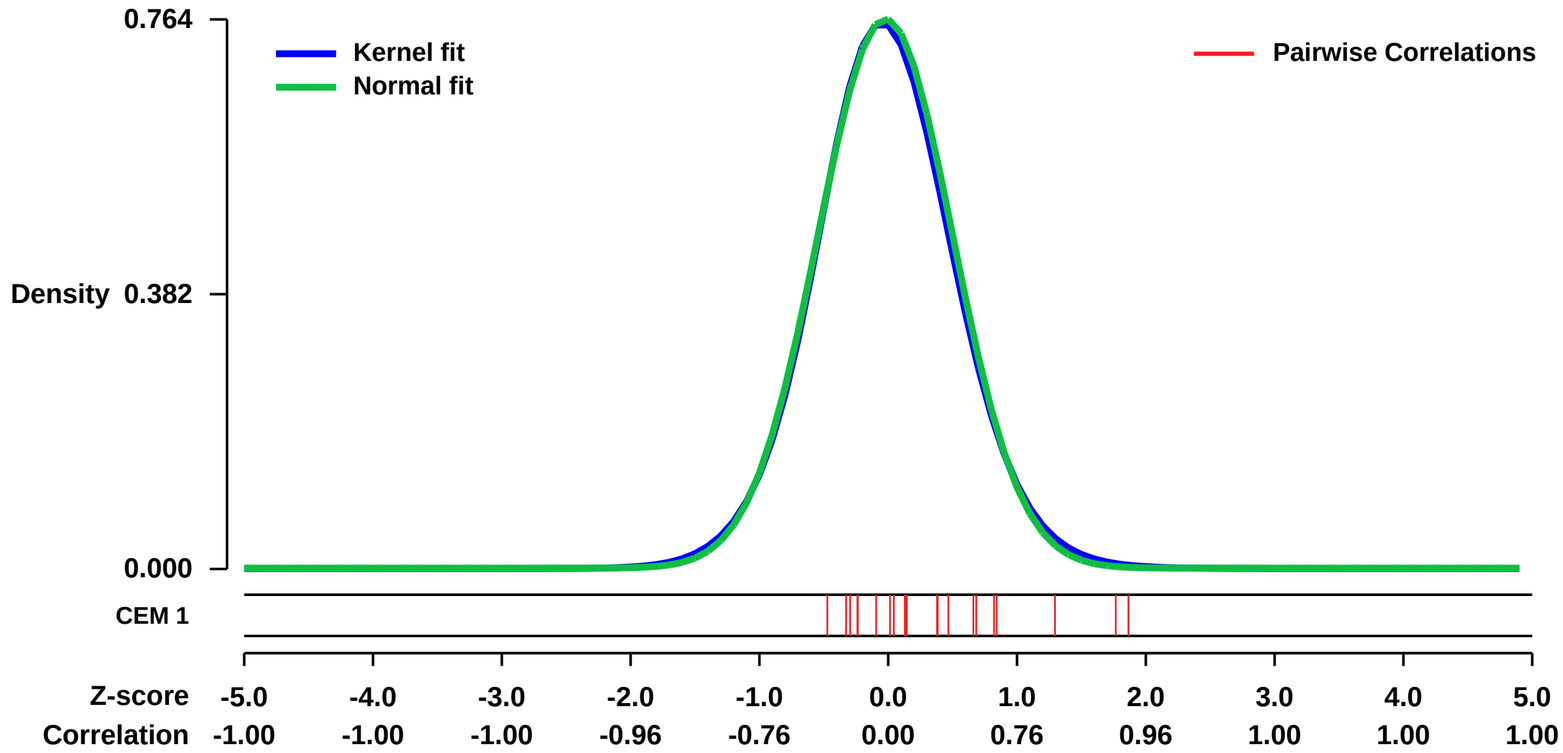

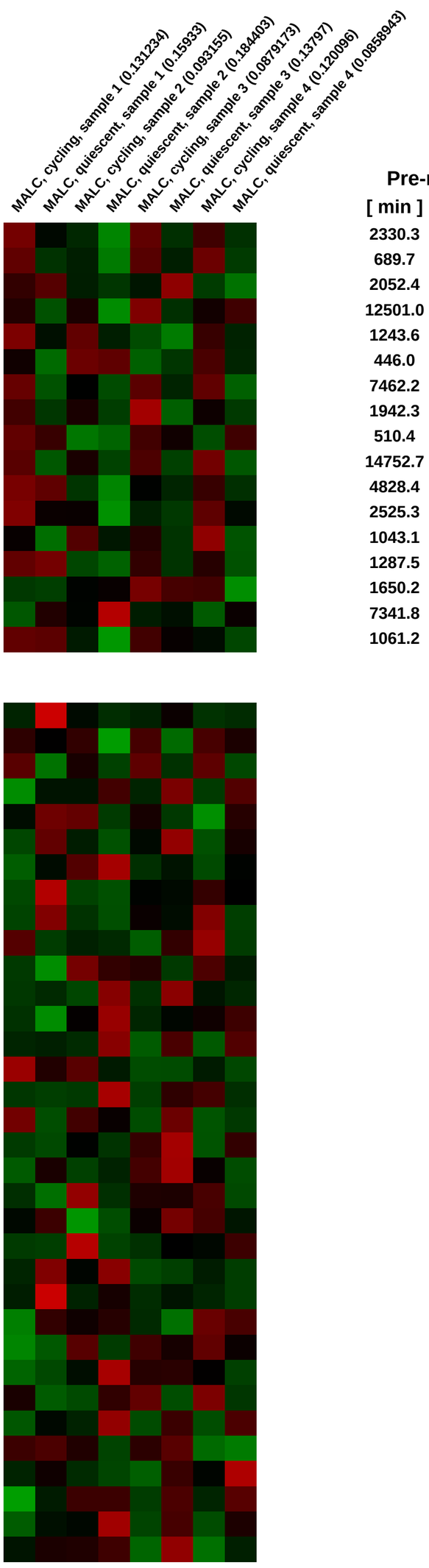

GEO Series "GSE16659" Expression Profiles

Num of samples in this series: 6

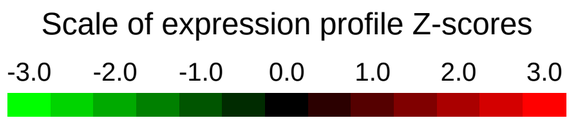

GEO Link:	http://www.ncbi.nlm.nih.gov/geo/query/acc.cgi?acc=GSE16659
Status:	Public on Dec 16 2011
Title:	Expression data of HGF/cMET pathway in prostate cancer DU145 cell line
Organism:	Homo sapiens
Experiment type:	Expression profiling by array
Platform:	GPL570
Pubmed ID:	22110593
Summary & Design:	**Summary:** DU145 prostate cancer cells were treated with 25 ng/ml hepatocyte growth factor (HGF) or vehicle for 2, 8, or 24 hours. HGF stimulates the cMET protein, a tyrosine kinase transmembrane protein. The aim of this study is to determine the role of the HGF/cMET pathway in immature cells of established prostate cancer. HGF stimulation of DU145 prostate cancer cell line led to cell migration in culture, formation of sprouts in Matrigel and inhibition of growth. These biological effects went together with induction of a stem-like phenotype as defined by up-regulation of CD49b, CD49f, CD44 and SOX9, and down-regulation of CD24 on gene-expression arrays and quantitative PCR. The shift towards a stem-like phenotype was reflected by protein modifications on FACS, Western blot, and enhanced rapid adhesion to collagen I. Small molecules SU11274 and PHA665752 were able to inhibit both morphologic and molecular HGF effects. **Overall design:** DU145 cells were stimulated for 2, 8 and 24 hours with 25 ng/ml HGF or vehicle. For each time point two arrays analyses were performed. One for cells stimulated with a vehicle and one for the HGF stimulated cells. Six arrays were performed in total in this study.

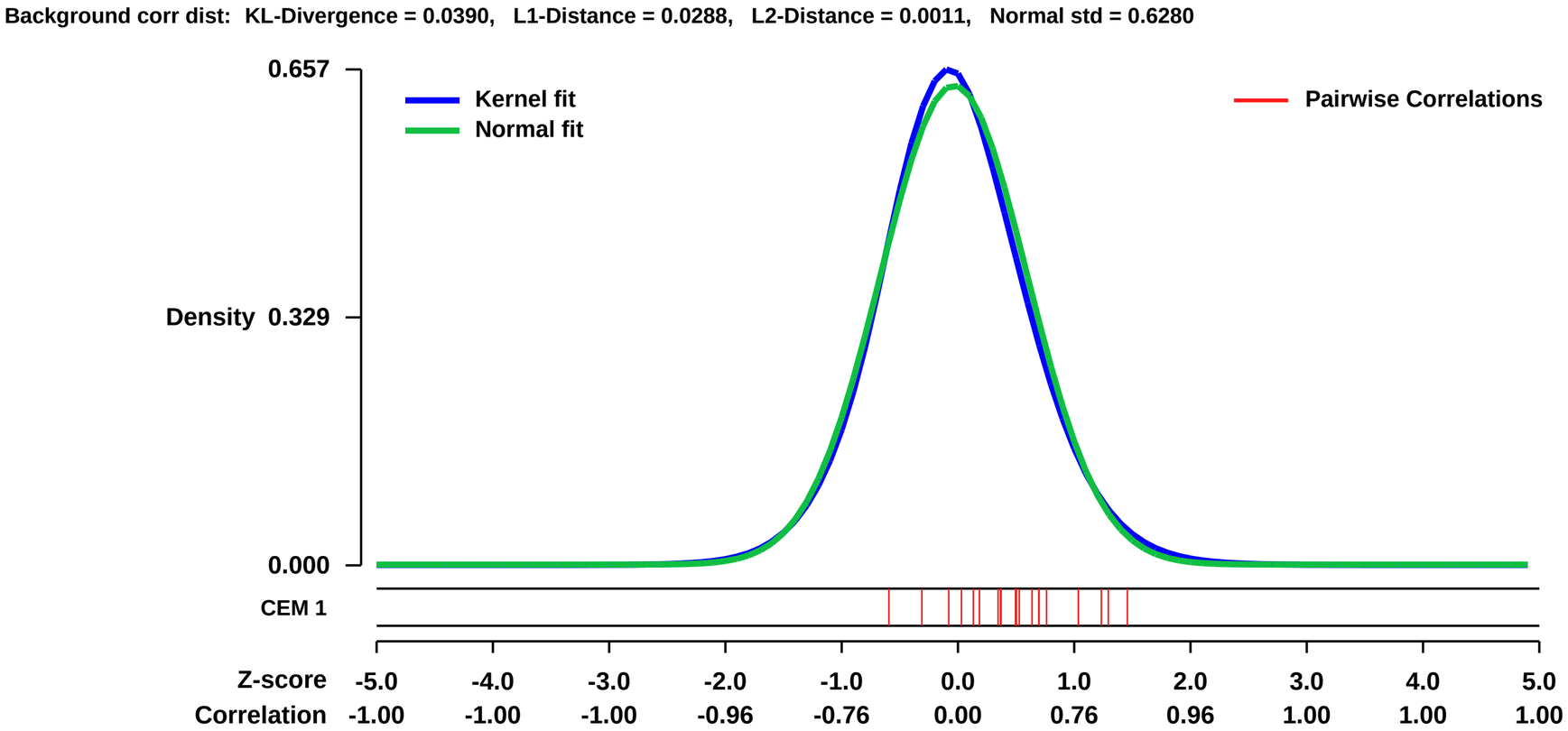

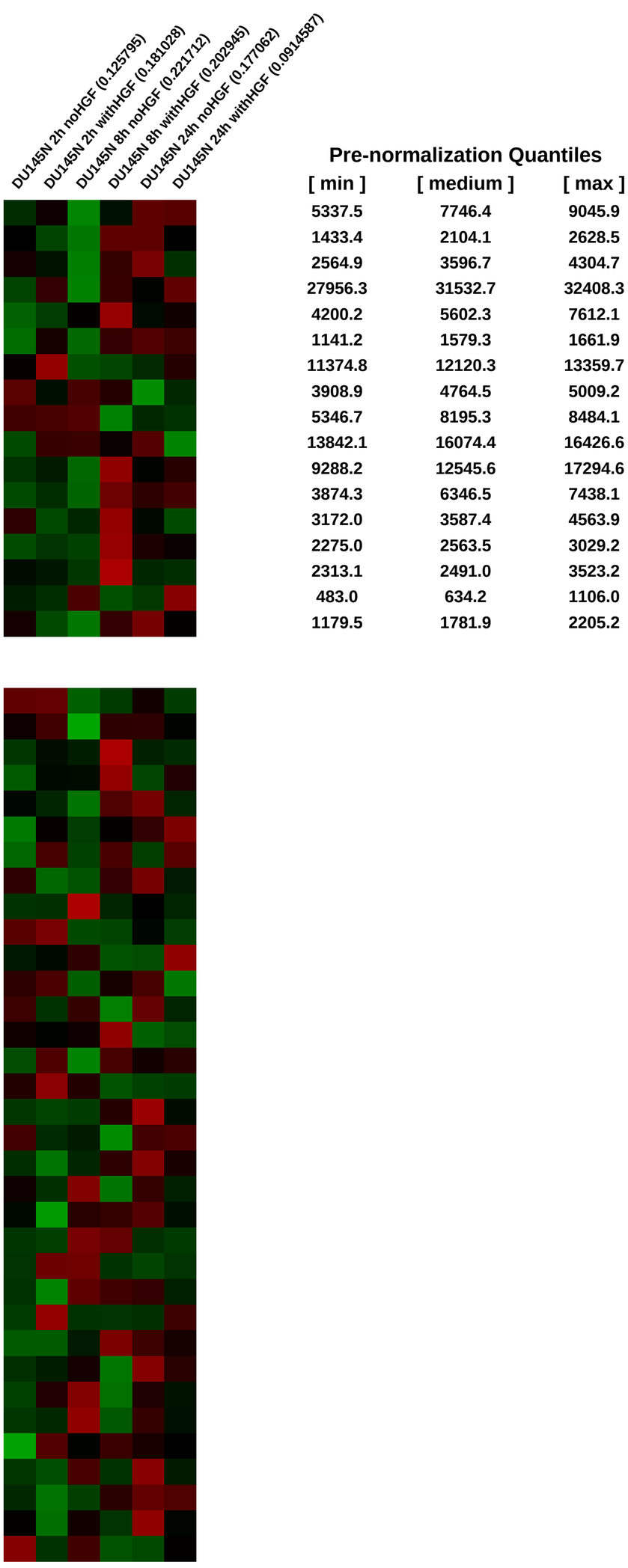

GEO Series "GSE28409" Expression Profiles

Num of samples in this series: 9

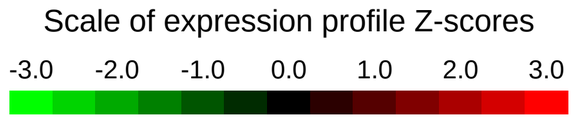

GEO Link:	http://www.ncbi.nlm.nih.gov/geo/query/acc.cgi?acc=GSE28409
Status:	Public on Oct 06 2013
Title:	EZH2 over-expression is associated with gain of chromosome arm 7q and essential for cell cycle progression and a marker of poor prognosis in neuroblastoma
Organism:	Homo sapiens
Experiment type:	Expression profiling by array
Platform:	GPL570
Pubmed ID:	
Summary & Design:	**Summary:** Neuroblastoma is an often aggressive childhood cancer with several large chromosomal regions showing recurrent gains or losses. Chromosome 7q is gained in 40-60% of neuroblastomas, but despite being the second most frequent genomic aberration, no oncogenes have been linked to 7q gain. **Overall design:** We performed expression profiling and array CGH on 88 primary neuroblastoma tumors to identify a 7q oncogene. We assayed neuroblastoma cell lines and combined bioinformatic analyses on the in vitro and in vivo data.

Background corr dist: KL-Divergence = 0.0703, L1-Distance = 0.0329, L2-Distance = 0.0020, Normal std = 0.5080

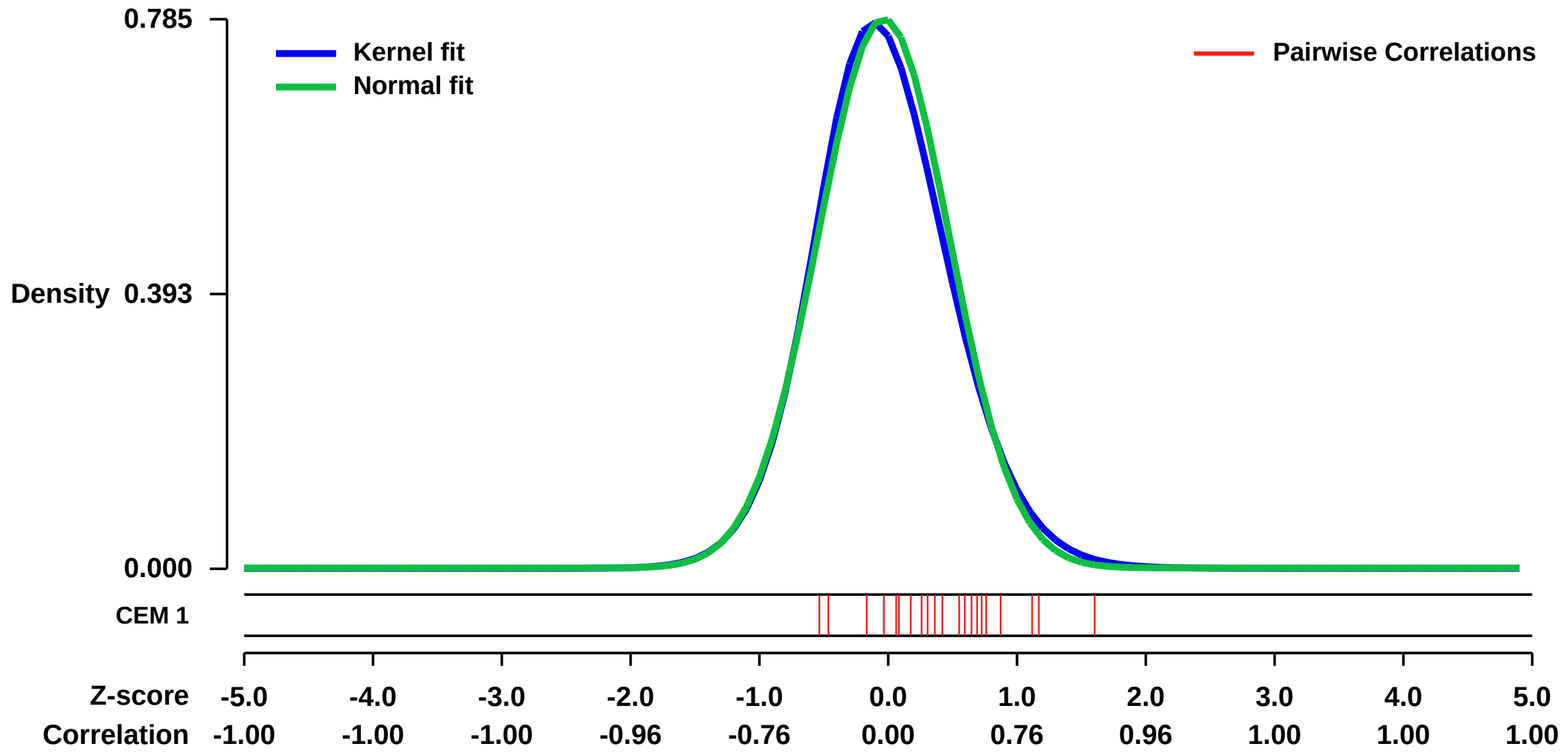

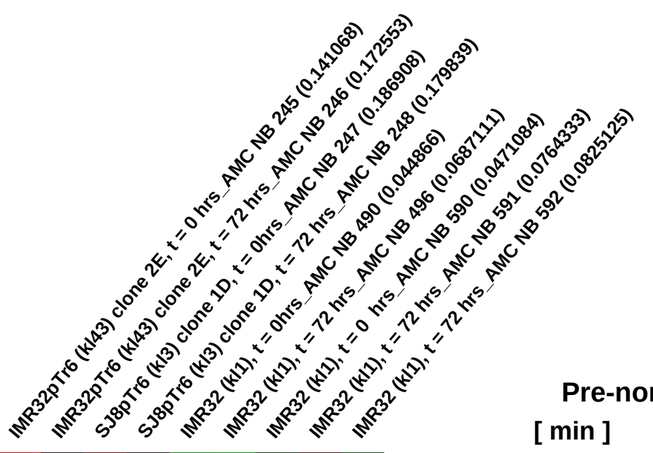

Pre-normalization Quantiles

		[min]	[medium]	[max]
CEM 1	MANF	3130.5	4635.5	6543.3
P (S | Z, I) = 0.00	SDF2L1	598.7	846.8	1649.4
Mean Corr = 0.34326	CRELD2	922.0	2071.0	4346.6
	HSPA5	9683.3	11760.8	15056.0
	HYOU1	923.0	2106.3	2325.0
	PDIA4	371.4	581.2	1211.5
	PDIA6	2752.4	6200.3	14511.3
CEM 1 + Top 10 Genes	DNAJB11	1991.2	5385.9	6334.5
	HSP90B1	1409.2	4312.4	5598.4
	PDIA3	3802.4	7185.4	8609.2
	PPIB	6325.4	12040.3	17508.8
	C19orf10	1676.0	1938.9	7089.4
	SLC35B1	1758.7	5158.8	6135.7
	SEC61A1	1470.0	3026.6	5233.5
	RPN1	1155.0	2705.9	4034.9
	DNAJC3	550.0	794.1	928.7
	CDK2AP2	570.7	751.4	845.5
Null module	ARID5B			
	XBP1			
	HNRNPAB			
	SGK1			
	HSPB1			
	DDIT4			
	ARL4D			
	SAP30			
	KIAA0408			
	GPR17			
	HSPH1			
	DNASE1L2			
	SLC5A3			
	GNAS			
	GPR3			
	TNFRSF25			
	TM6SF2			
	MKKS			
	PLEKHF1			
	ZMYM1			
	DOK3			
	FGF20			
	SLC39A2			
	KCNIP2			
	ERRFI1			
	DEDD2			
	CCDC117			
	USP31			
	AHSA2			
	CYS1			
	CNIH2			
	BANP			
	CHORDC1			
	P4HA1			

GEO Series "GSE4110" Expression Profiles

Num of samples in this series: 8

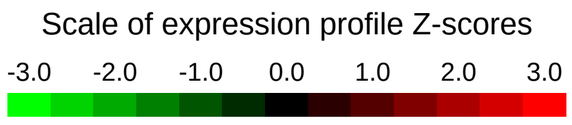

GEO Link:	http://www.ncbi.nlm.nih.gov/geo/query/acc.cgi?acc=GSE4110
Status:	Public on Jan 29 2006
Title:	Effect of ionizing radiation on procoagulant activity
Organism:	Homo sapiens
Experiment type:	Expression profiling by array
Platform:	GPL570
Pubmed ID:	17640852
Summary & Design:	**Summary:** Ionizing radiation (IR) is associated with thrombotic vascular occlusion. Thrombosis in malignancy predicts a poor clinical outcome. Tissue factor (TF) is the initiator of the extrinsic co-agulation system and induces thrombus formation. Our study examined whether IR induced TF expression and procoagulability in the myelomonocytic leukemia THP-1 cell model. We further investigated coordinated gene alterations associated with TF upregulation and IR-induced thrombogenicity. Gene expression profiling revealed IR to increase the expression of inflammatory and apoptosis-related pathways, contributing to TF upregulation and increased TF procoagulability on day 7 post IR. The upregulation of these pathways together with TF upregulation contributed to the increased thrombogenic potential of tissues post application of IR. **Keywords:** irridiation response **Overall design:** THP-1 cells were harvested on day 3 (1 sample) and day 7 (3 samples) post irradiation. For each time point untreated control samples were run.

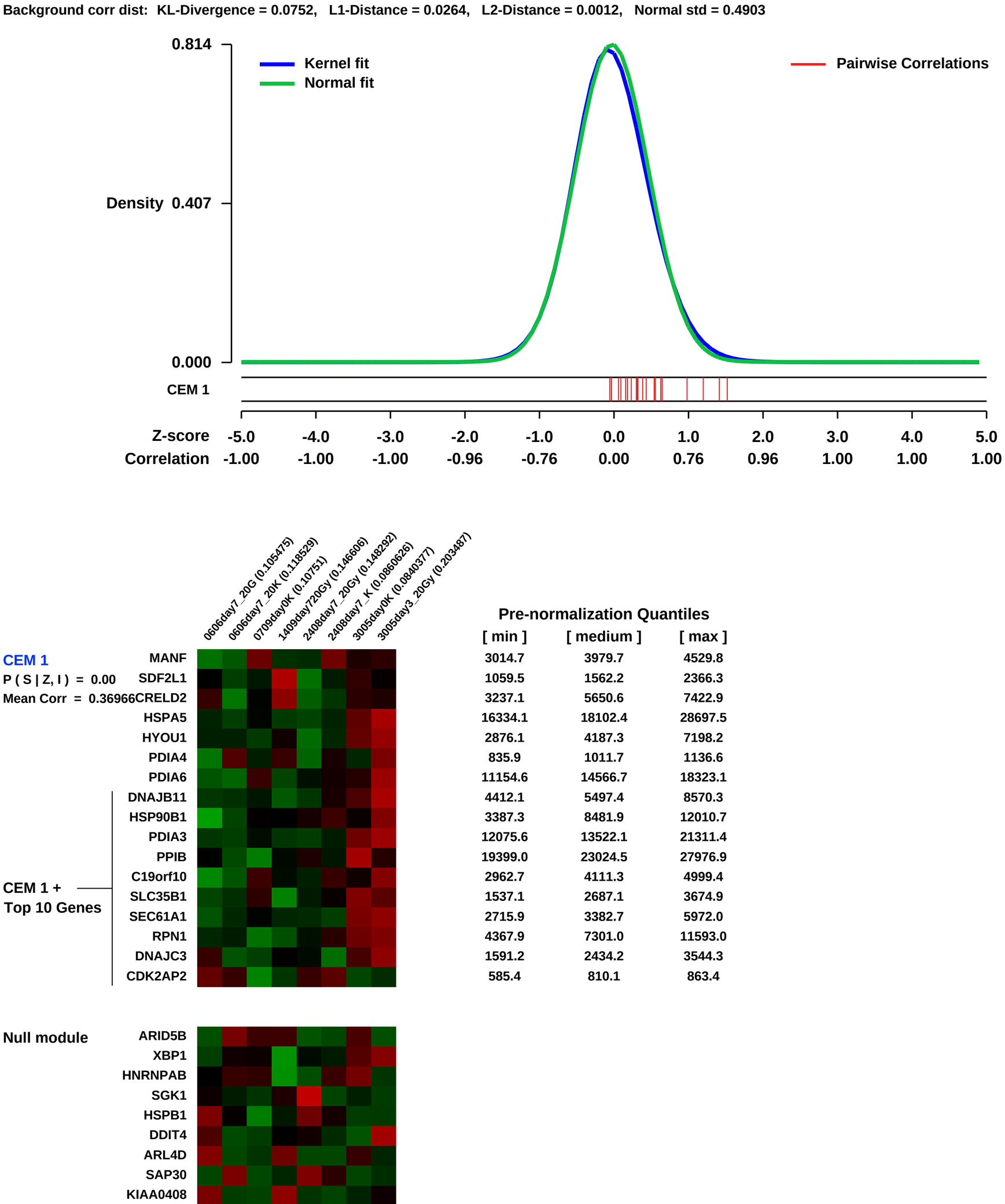

GEO Series "GSE41459" Expression Profiles

Num of samples in this series: 6

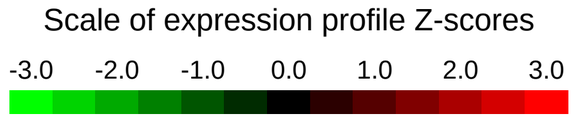

GEO Link:	http://www.ncbi.nlm.nih.gov/geo/query/acc.cgi?acc=GSE41459
Status:	Public on Oct 11 2012
Title:	Effect of PRR15 knockdown on human trophoblast cell gene expression
Organism:	Homo sapiens
Experiment type:	Expression profiling by array
Platform:	GPL570
Pubmed ID:	
Summary & Design:	**Summary:** Proline rich 15 (PRR15) is a small nuclear protein required for normal conceptus development in the sheep. We used microarrays to assess the changes in the trophoblast transcriptome when PRR15 expression was diminished. **Overall design:** The human first-trimester trophoblast cell line, ACH-3P, was infected with control lentivirus expressing no shRNA or lentivirus expressing shRNA to target PRR15 mRNA for degradation, with three biological replicates per treatment.

Background corr dist: KL-Divergence = 0.0393, L1-Distance = 0.0255, L2-Distance = 0.0008, Normal std = 0.6245

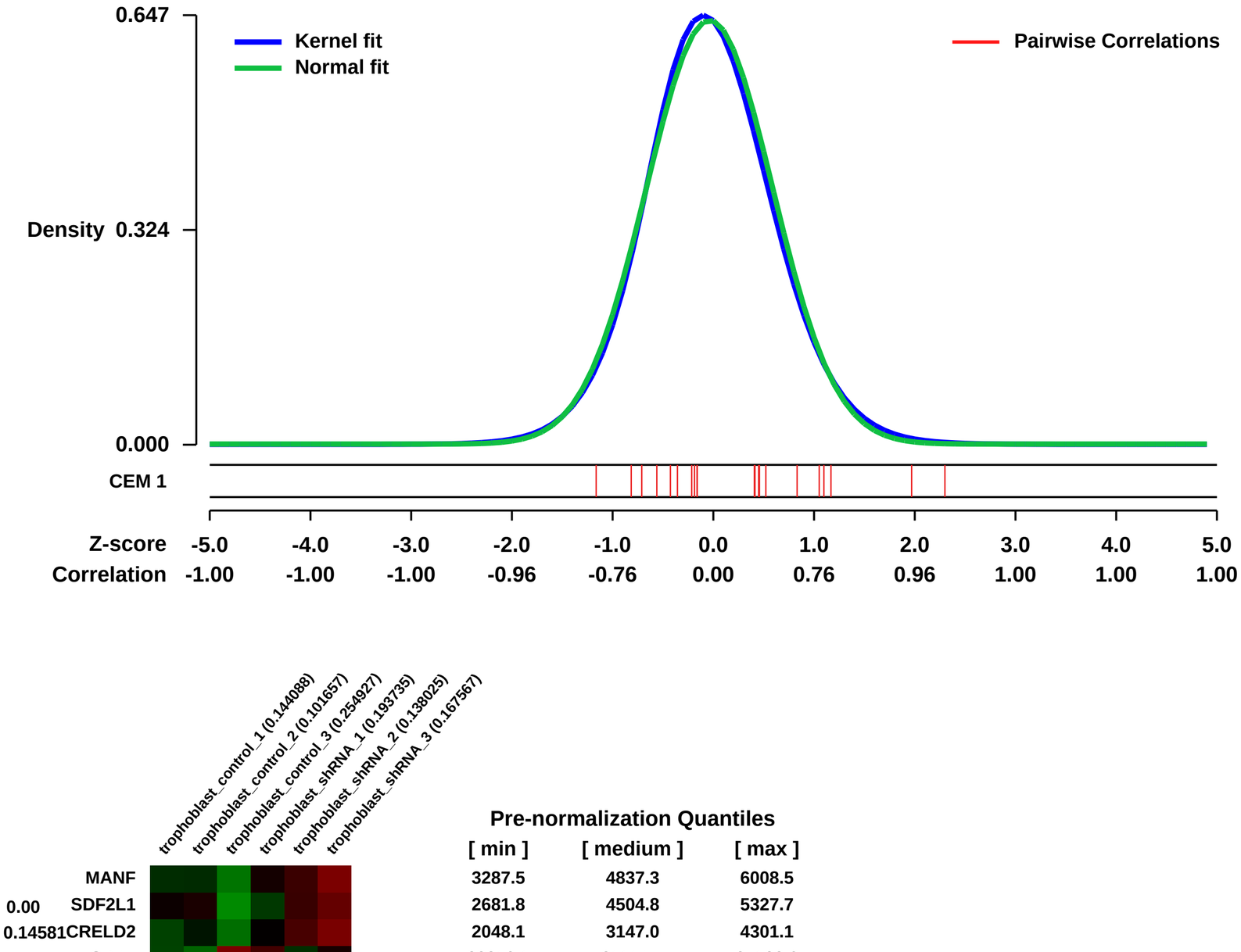

CEM 1
P (S | Z, I) = 0.00
Mean Corr = 0.14581

CEM 1 + Top 10 Genes

Null module

MANF	3287.5	4837.3	6008.5
SDF2L1	2681.8	4504.8	5327.7
CRELD2	2048.1	3147.0	4301.1
HSPA5	23819.1	31114.5	37122.0
HYOU1	888.8	1267.6	1380.4
PDIA4	1745.0	2074.1	2195.0
PDIA6	11696.9	13127.5	16142.6
DNAJB11	5173.4	6788.6	7467.3
HSP90B1	6545.9	8358.9	9331.4
PDIA3	14628.9	18878.7	21162.2
PPIB	11524.3	14665.4	17058.5
C19orf10	1610.3	2725.6	3171.3
SLC35B1	1394.4	1960.5	2491.0
SEC61A1	2037.5	2218.8	2370.3
RPN1	4066.2	4575.4	4819.3
DNAJC3	1776.3	2304.3	2452.7
CDK2AP2	656.2	1094.0	1183.0
ARID5B			
XBP1			
HNRNPAB			
SGK1			
HSPB1			
DDIT4			
ARL4D			
SAP30			
KIAA0408			
GPR17			
HSPH1			
DNASE1L2			
SLC5A3			
GNAS			
GPR3			
TNFRSF25			
TM6SF2			
MKKS			
PLEKHF1			
ZMYM1			
DOK3			
FGF20			
SLC39A2			
KCNIP2			
ERRFI1			
DEDD2			
CCDC117			
USP31			
AHSA2			
CYS1			
CNIH2			
BANP			
CHORDC1			
P4HA1			

GEO Series "GSE42046" Expression Profiles

Num of samples in this series: 24

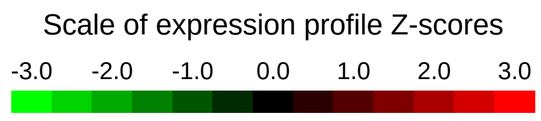

GEO Link:	http://www.ncbi.nlm.nih.gov/geo/query/acc.cgi?acc=GSE42046
Status:	Public on Oct 04 2013
Title:	TWEAK-treated time course in ACHN cells
Organism:	Homo sapiens
Experiment type:	Expression profiling by array
Platform:	GPL570
Pubmed ID:	23974006
Summary & Design:	**Summary:** Tumor necrosis factor-related weak inducer of apoptosis, TWEAK, is a TNF superfamily member that mediates signaling through its receptor fibroblast growth factor inducible-14, Fn14. In tumor cell lines, TWEAK induces proliferation, survival and NF-kappaB signaling and gene expression that promote tumor growth and suppress antitumor immune responses. Anti-TWEAK antibody, RG7212, inhibits tumor growth in vivo with decreases in pathway activation markers and modulation of tumor, blood and spleen immune cell composition. Candidate response prediction markers, including Fn14, have been identified in mouse models. Phase I pharmacodynamic data from patients are consistent with preclinical results. TWEAK:Fn14 signaling is upregulated in human cancer and pathway activation induces tumor proliferation and survival signaling. Blockade with anti-TWEAK mAb, RG7212, inhibits tumor growth in multiple models in mice. TWEAK induces changes that suppress anti-tumor immune responses and RG7212 blocks these effects resulting in changes in tumor immune cell composition and decreases in cytokines that promote immunosuppression. Antitumor efficacy in mice was observed in a range of Fn14 expressing models with pathway activation and expressing either wild-type or mutant p53, BRAF or KRAS suggesting both a patient selection strategy and potential broad clinical applicability. Preclinical mechanism of action hypotheses are supported by Phase I clinical data, with decreases in proliferation markers and increased tumor T cell infiltration. **Overall design:** ACHN cells untreated or treated with 1090-TW (TWEAK) for 4 hours, 8 hours, or 24 hours. Four replicates for each condition were performed.

Background corr dist: KL-Divergence = 0.2284, L1-Distance = 0.0332, L2-Distance = 0.0017, Normal std = 0.3206

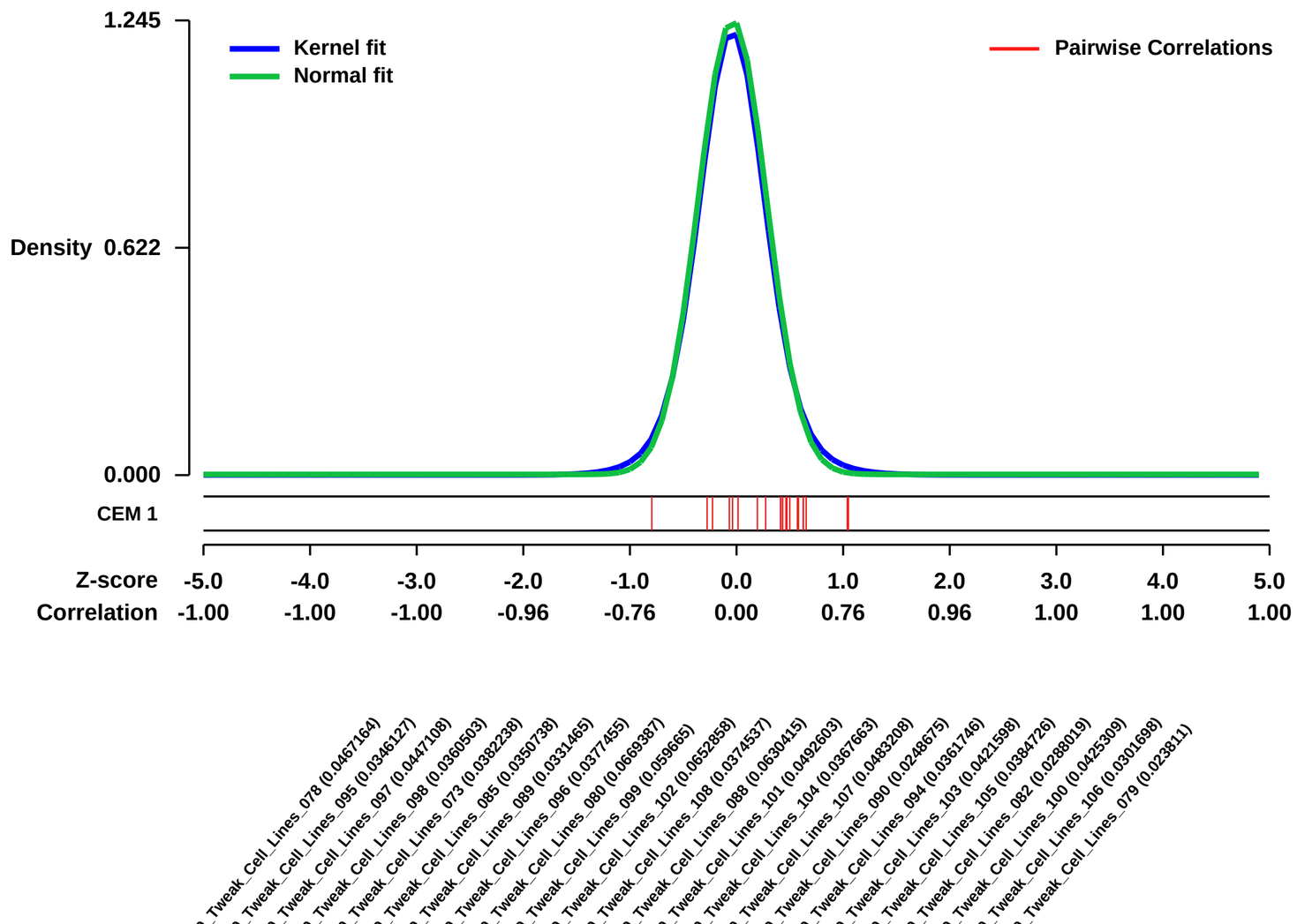

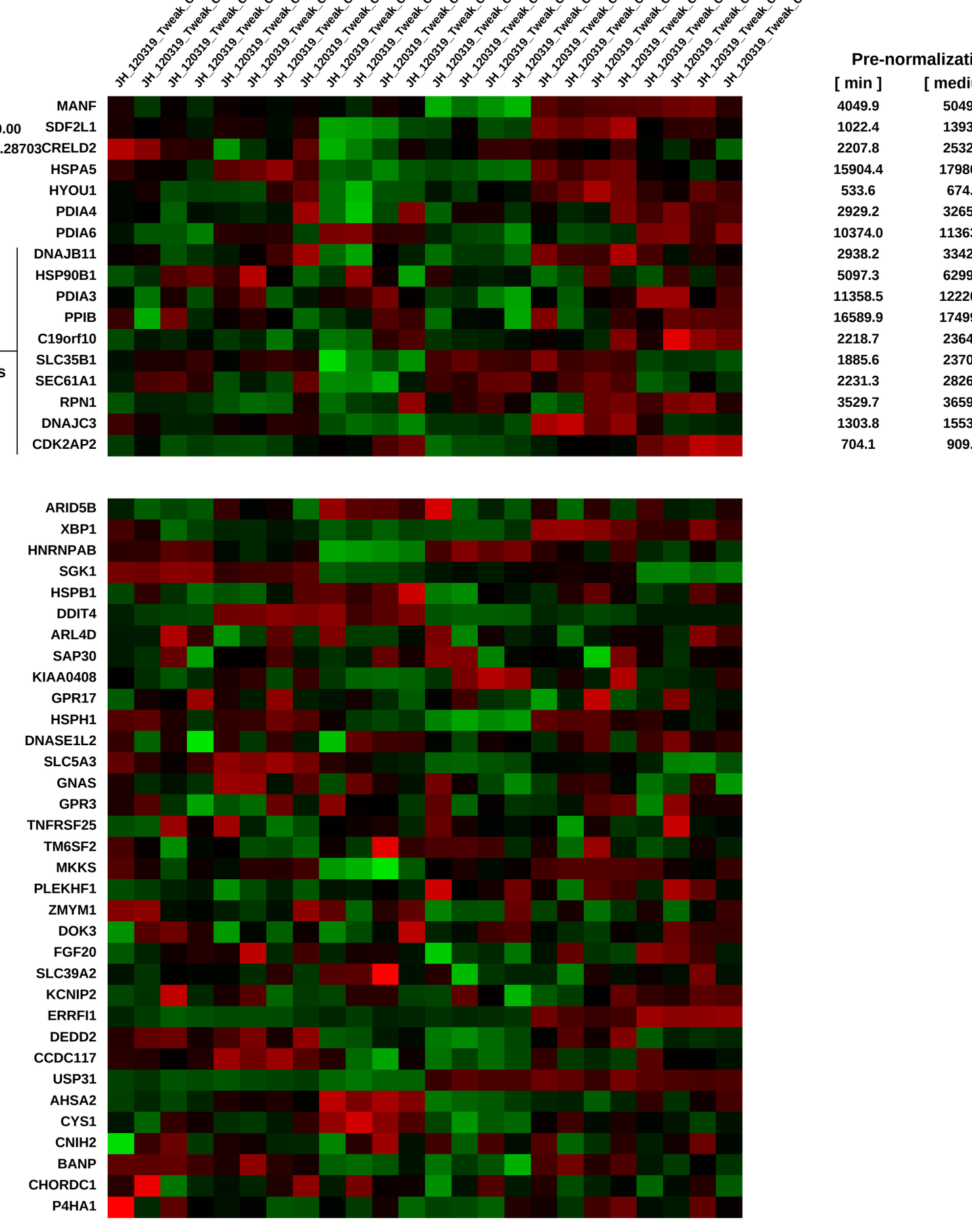

Pre-normalization Quantiles

[min]	[medium]	[max]
4049.9	5049.6	5564.8
1022.4	1393.6	1721.9
2207.8	2532.6	2815.3
15904.4	17980.3	19956.7
533.6	674.2	801.0
2929.2	3265.7	3559.0
10374.0	11363.6	12426.5
2938.2	3342.0	3732.3
5097.3	6299.4	7869.8
11358.5	12220.4	13014.5
16589.9	17499.6	18107.9
2218.7	2364.5	2729.1
1885.6	2370.0	2537.7
2231.3	2826.2	3092.6
3529.7	3659.2	3882.6
1303.8	1553.4	2077.6
704.1	909.9	1317.7

GEO Series "GSE15477" Expression Profiles

Num of samples in this series: 18

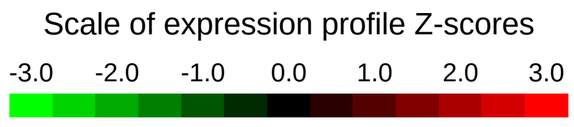

GEO Link:	http://www.ncbi.nlm.nih.gov/geo/query/acc.cgi?acc=GSE15477
Status:	Public on Apr 15 2009
Title:	Data integration from two microarray platforms identifies genetic inactivation of RIC8A in a breast cancer cell line
Organism:	Homo sapiens
Experiment type:	Genome variation profiling by array
Platform:	GPL570
Pubmed ID:	19432969
Summary & Design:	**Summary:** Using array comparative genomic hybridization (aCGH), a large number of deleted genomic regions have been identified in human cancers. However, subsequent efforts to identify target genes selected for inactivation in these regions have often been challenging. We integrated here genome-wide copy number data with gene expression data and non-sense mediated mRNA decay rates in breast cancer cell lines to prioritize gene candidates that are likely to be tumour suppressor genes inactivated by bi-allelic genetic events. The candidates were sequenced to identify potential mutations. This integrated genomic approach led to the identification of RIC8A at 11p15 as a putative candidate target gene for the genomic deletion in the ZR-75-1 breast cancer cell line. We identified a truncating mutation in this cell line, leading to loss of expression and rapid decay of the transcript. We screened 127 breast cancers for RIC8A mutations, but did not find any pathogenic mutations. No promoter hypermethylation in these tumours was detected either. However, analysis of gene expression data from breast tumours identified a small group of aggressive tumours that displayed low levels of RIC8A transcripts. Real-time PCR analysis of 38 breast tumours showed a strong association between low RIC8A expression and the presence of TP53 mutations (P=0.006). We demonstrate a data integration strategy leading to the identification of RIC8A as a gene undergoing a classical double-hit genetic inactivation in a breast cancer cell line, as well as in vivo evidence of loss of RIC8A expression in a subgroup of aggressive TP53 mutant breast cancers. **Overall design:** The experiment utilized six breast cancer cell lines; MDA-MB-468, MDA-MB-231, ZR-75-1, MCF7, BT-474 and T-47D. All cell lines were obtained from American Type Culture Collection and grown in accordance with the distributor's instructions. All samples were hybridized once on 44k Agilent Human Genome CGH microarrays according to manufacturers instructions. Genomic DNA pooled from healthy female donors was used as a reference in all hybridizations. DNA from cell line samples were labeled with Cy5 and DNA from reference were labeled with Cy3.

Background corr dist: KL-Divergence = 0.2218, L1-Distance = 0.0552, L2-Distance = 0.0079, Normal std = 0.3225

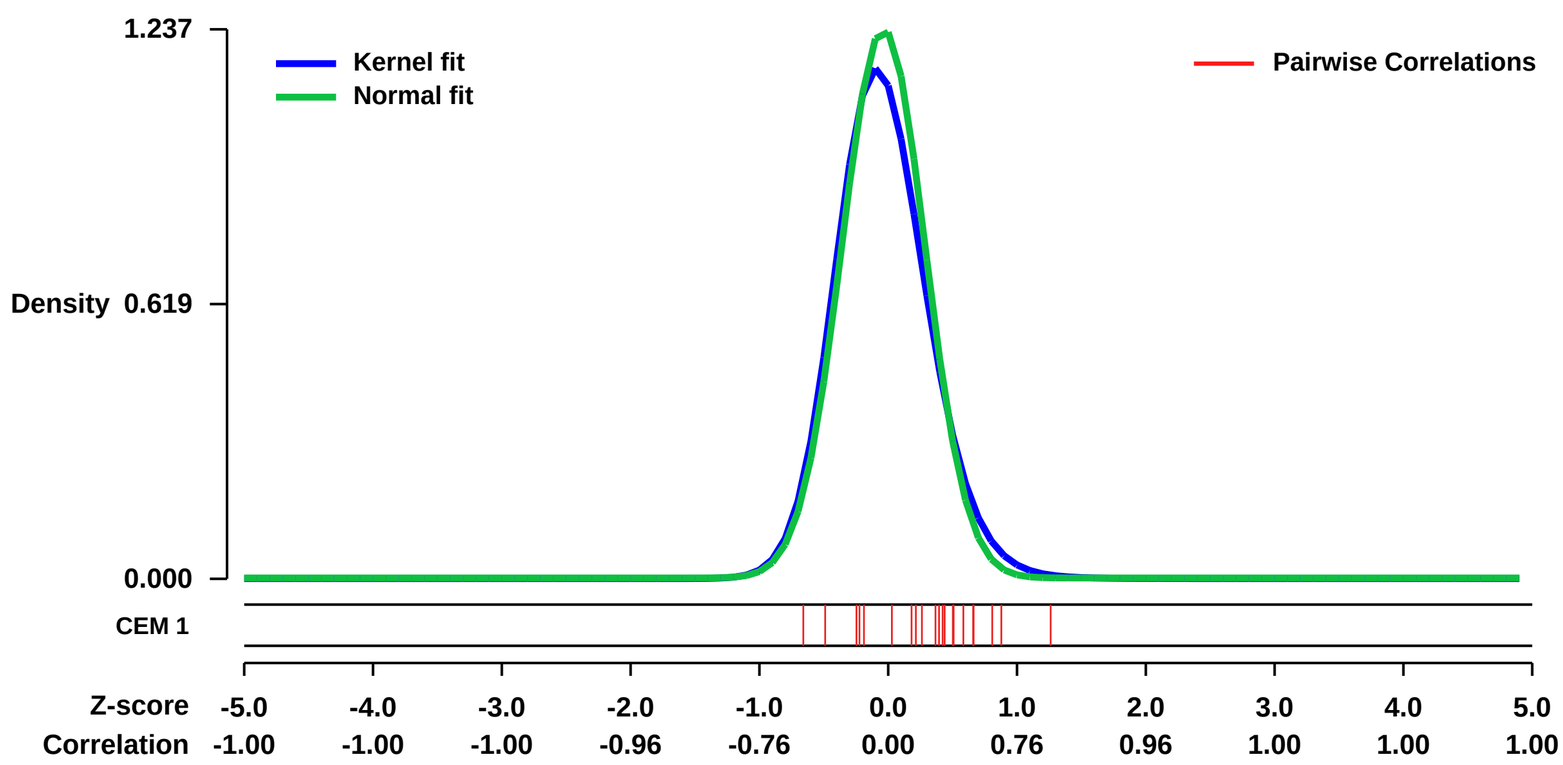

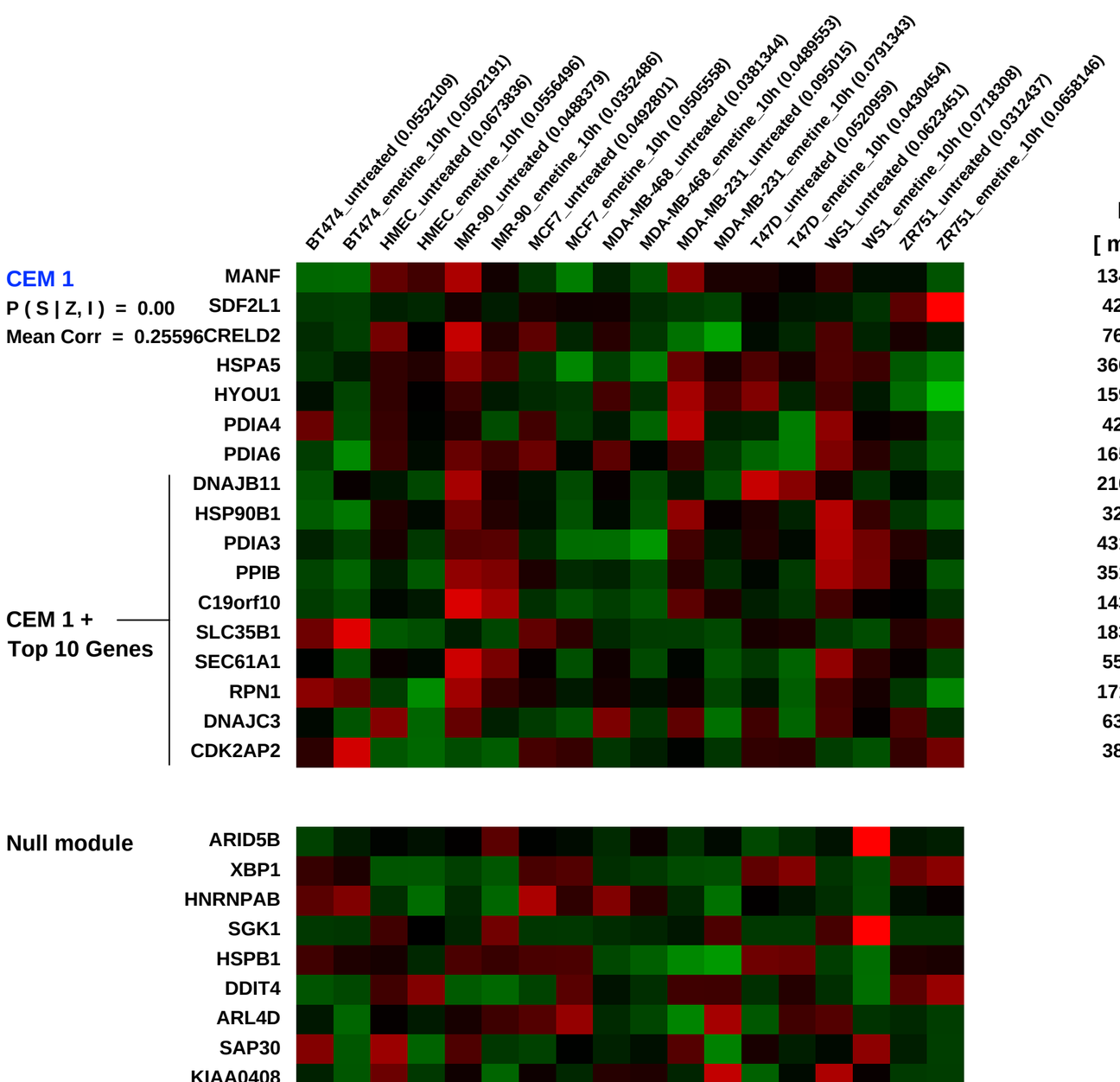

Pre-normalization Quantiles

	[min]	[medium]	[max]
MANF	1349.7	3904.8	7116.1
SDF2L1	425.8	1142.9	6960.2
CRELD2	764.3	2379.0	4646.6
HSPA5	3667.5	14019.6	21146.8
HYOU1	1594.5	4443.7	7405.3
PDIA4	425.1	1045.2	2002.1
PDIA6	1650.7	5879.4	10072.9
DNAJB11	2101.5	3049.7	6241.4
HSP90B1	324.9	2660.0	6650.7
PDIA3	4316.6	9218.0	15653.6
PPIB	3517.8	7372.6	17813.7
C19orf10	1438.8	3471.3	11511.4
SLC35B1	1836.6	3454.5	10243.0
SEC61A1	558.2	3723.3	10398.8
RPN1	1718.1	4633.9	7358.7
DNAJC3	630.3	1635.6	2978.2
CDK2AP2	384.9	1727.5	4561.2

GEO Series "GSE10821" Expression Profiles

Num of samples in this series: 6

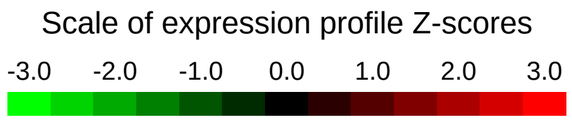

GEO Link:	http://www.ncbi.nlm.nih.gov/geo/query/acc.cgi?acc=GSE10821
Status:	Public on Oct 10 2008
Title:	LMP1 mediated gene expression changes in transfected CD10+ GC B cells
Organism:	Homo sapiens
Experiment type:	Expression profiling by array
Platform:	GPL570
Pubmed ID:	18566961
Summary & Design:	**Summary:** In this study, we have investigated the effect of LMP1 on gene expression in normal human GC B cells using a non-viral vector based system **Keywords: transfection of viral oncogene in normal human B cells** **Overall design:** Gene expression was compared between LMP1-transfected and control vector-transfected GC B cells from three patients. RNA from the FACS-sorted transfected GC B cells was amplified. 10ug of fragmented cRNA was hybridized to HG-U133 Plus 2.0 microarrays. Differentially expressed genes were identified using significance analysis of microarrays (SAM) with a 1.5 fold change threshold and the q-value threshold set to 5%.

Background corr dist: KL-Divergence = 0.0423, L1-Distance = 0.0166, L2-Distance = 0.0003, Normal std = 0.6005

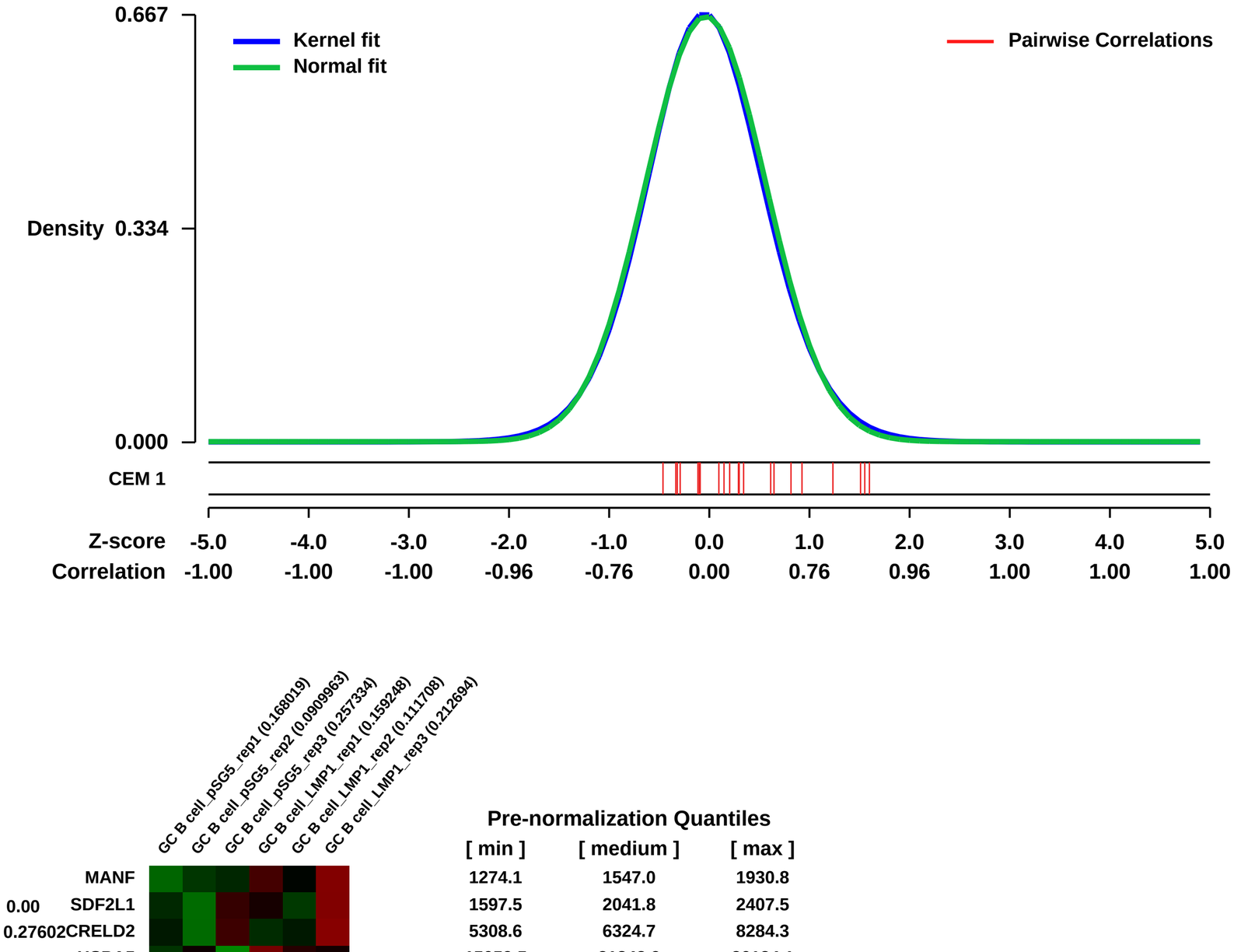

Pre-normalization Quantiles

		[min]	[medium]	[max]
CEM 1	MANF	1274.1	1547.0	1930.8
P (S | Z, I) = 0.00	SDF2L1	1597.5	2041.8	2407.5
Mean Corr = 0.27602	CRELD2	5308.6	6324.7	8284.3
	HSPA5	15059.5	21842.9	26124.1
	HYOU1	280.5	388.0	767.0
	PDIA4	532.4	650.3	855.1
	PDIA6	19906.4	21790.7	24140.1
CEM 1 + Top 10 Genes	DNAJB11	4337.9	4868.3	6788.0
	HSP90B1	872.9	1341.3	1474.1
	PDIA3	6743.6	9471.0	11031.6
	PPIB	1579.8	2585.2	3230.8
	C19orf10	1319.0	1636.2	2577.1
	SLC35B1	1402.5	1666.1	1735.8
	SEC61A1	1229.1	1322.0	2085.9
	RPN1	828.6	1583.0	2293.3
	DNAJC3	910.0	1623.4	1890.3
	CDK2AP2	359.9	441.8	533.1
Null module	ARID5B			
	XBP1			
	HNRNPAB			
	SGK1			
	HSPB1			
	DDIT4			
	ARL4D			
	SAP30			
	KIAA0408			
	GPR17			
	HSPH1			
	DNASE1L2			
	SLC5A3			
	GNAS			
	GPR3			
	TNFRSF25			
	TM6SF2			
	MKKS			
	PLEKHF1			
	ZMYM1			
	DOK3			
	FGF20			
	SLC39A2			
	KCNIP2			
	ERRFI1			
	DEDD2			
	CCDC117			
	USP31			
	AHSA2			
	CYS1			
	CNIH2			
	BANP			
	CHORDC1			
	P4HA1			

GEO Series "GSE19445" Expression Profiles

Num of samples in this series: 9

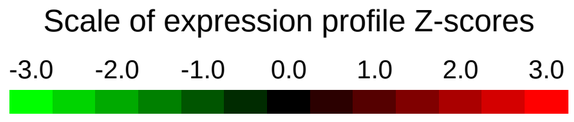

GEO Link:	http://www.ncbi.nlm.nih.gov/geo/query/acc.cgi?acc=GSE19445
Status:	Public on Jul 04 2010
Title:	LNCaP cells in response to DHT stimulation and inhibition/knockdown of TOPO2B
Organism:	Homo sapiens
Experiment type:	Expression profiling by array
Platform:	GPL570
Pubmed ID:	20601956
Summary & Design:	**Summary:** Microarray experiments were carried out to ascertain whether TOP2ς† is required for DHT induced androgen receptor target gene expression. We investigated the effect of pharmacological inhibition or RNA interference-mediated depletion of TOP2ς† on gene expression in androgen-dependent LNCaP prostate cancer cells. **Overall design:** Analysis of gene expression in LNCaP cells under various conditions including serum starvation, DHT treatment, and DHT treatment combined with TOPO2B pharmacological inhibitors (Merbarone and Etoposide) and TOPO2B-shRNA knockdown.

Background corr dist: KL-Divergence = 0.0161, L1-Distance = 0.0444, L2-Distance = 0.0026, Normal std = 0.8219

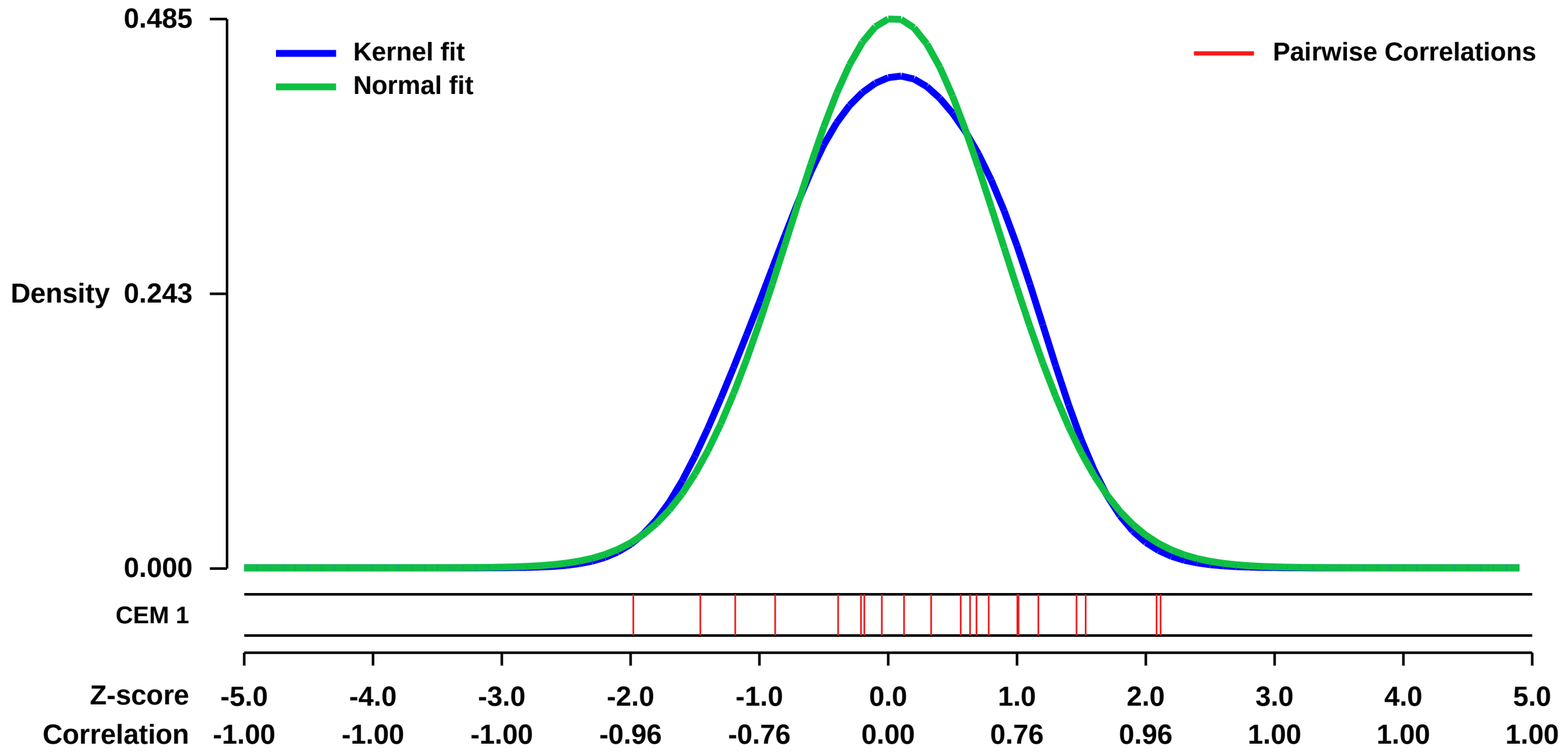

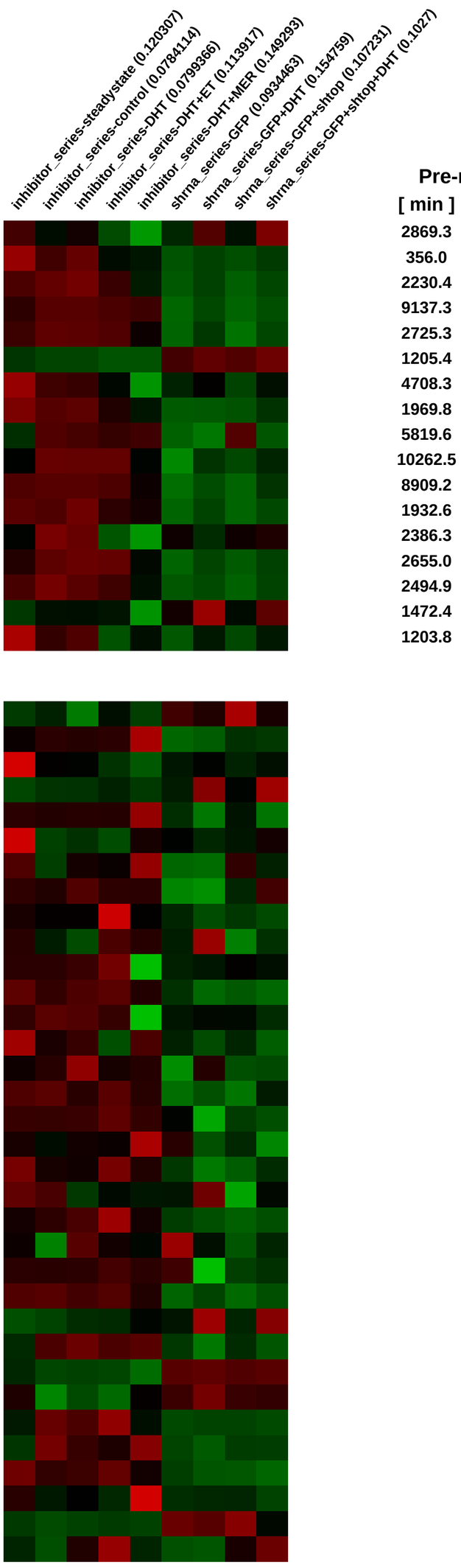

GEO Series "GSE59445" Expression Profiles

Num of samples in this series: 12

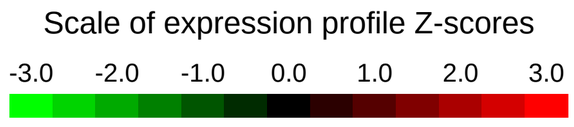

GEO Link:	http://www.ncbi.nlm.nih.gov/geo/query/acc.cgi?acc=GSE59445
Status:	Public on Jul 21 2014
Title:	Whole Genome Expression Profiling shows that BRG1 Transcriptionally Regulates UV Inducible Genes and other Novel Targets in Human Cells
Organism:	Homo sapiens
Experiment type:	Expression profiling by array
Platform:	GPL570
Pubmed ID:	
Summary & Design:	**Summary:** BRG1, an ATPase catalytic subunit of the SWI/SNF chromatin remodeling complex, has been identified as a tumor suppressor protein, as it has been shown to play a role in Nucleotide Excision Repair (NER) of CPDs, suppress apoptosis, and restore checkpoint deficiency, in response to UV exposure. Although BRG1 has been shown to regulate transcription of some genes that are instrumental in proper DNA damage repair and cell cycle maintenance in response to UV, its role in transcriptional regulation of the whole genome in response to UV has not yet been elucidated. With whole genome expression profiling in SW13 cells, we show that upon UV induction, BRG1 regulates transcriptional expression of many genes involved in cell stress response. Additionally, our results also highlight BRG1â s general role as a master regulator of the genome, as it transcriptionally regulates approximately 4.8% of the human genome, including expression of genes involved in many pathways. **Overall design:** SW13 cells without or with BRG1 protein exrpession were treated with UV-C (10 J/m2) or mock treated. Cells were incubated for 6 hrs after UV or mock treaments, total RNA was prepared using TRIZOL reagent (Invitrogen, Carlsbad, CA), followed by the RNeasy kit (Qiagen, Valencia, CA), according to the manufacturerâ s instructions. Three independent biological replicates of SW13+pREP7 and SW13+pREP7+BRG1 were subjected to microarray analysis using Affymetrix U133 plus 2.0 gene chip. Target synthesis and GeneChip hybridization, washing, staining, and scanning were performed at the Molecular Biology Core at Washington State University. Microarray output was examined visually for excessive background noise and physical anomalies. The default MAS statistical values were used for all analyses. All probe sets on each array were scaled to a mean target signal intensity of 125, with the signal correlating to the amount of transcript in the sample. An absolute analysis using MAS was performed to assess the relative abundance of the 47,000 represented transcripts and variants, including 38,500 human genes, based on signal and detection

Background corr dist: KL-Divergence = 0.1088, L1-Distance = 0.0332, L2-Distance = 0.0017, Normal std = 0.4385

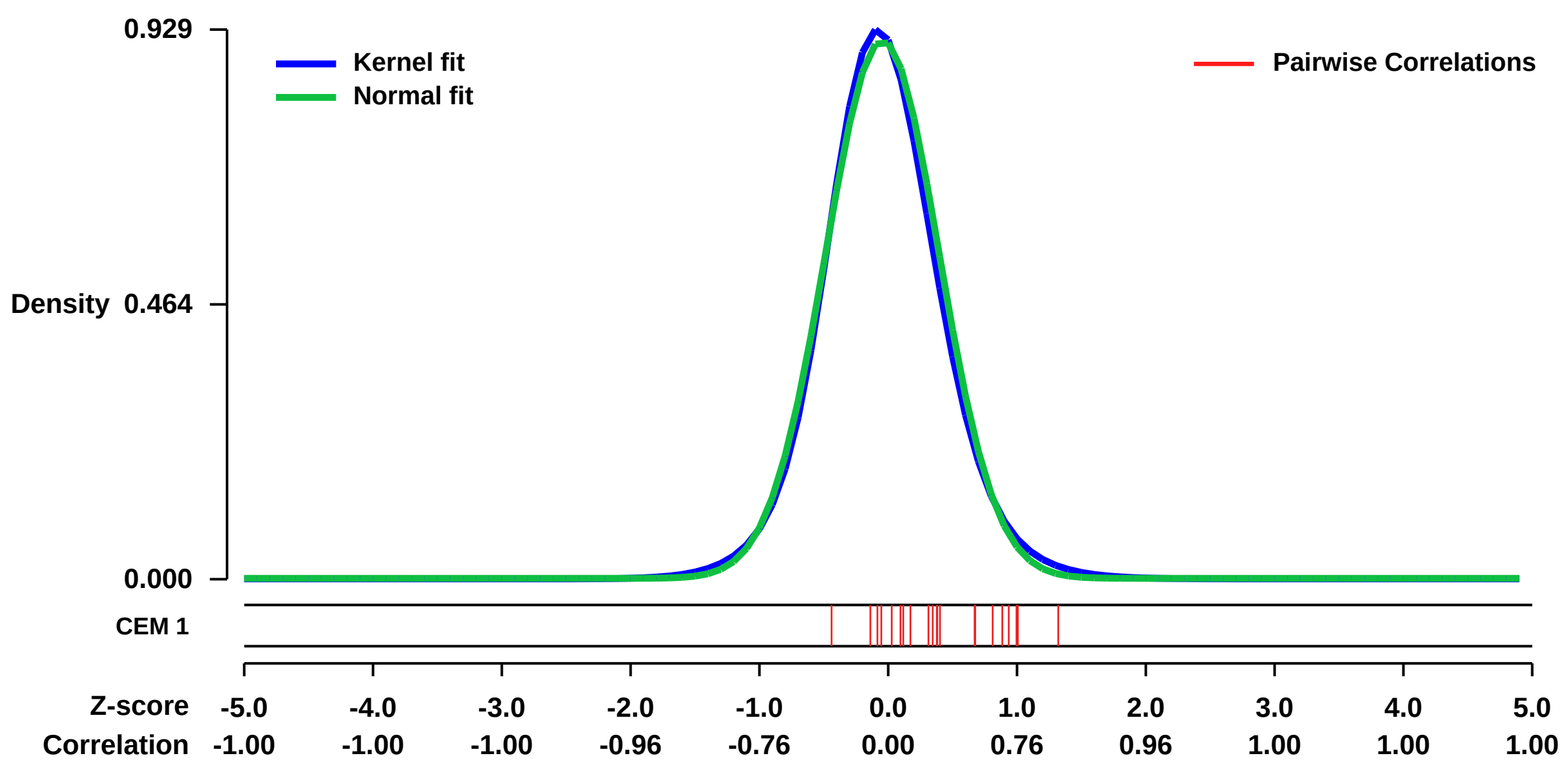

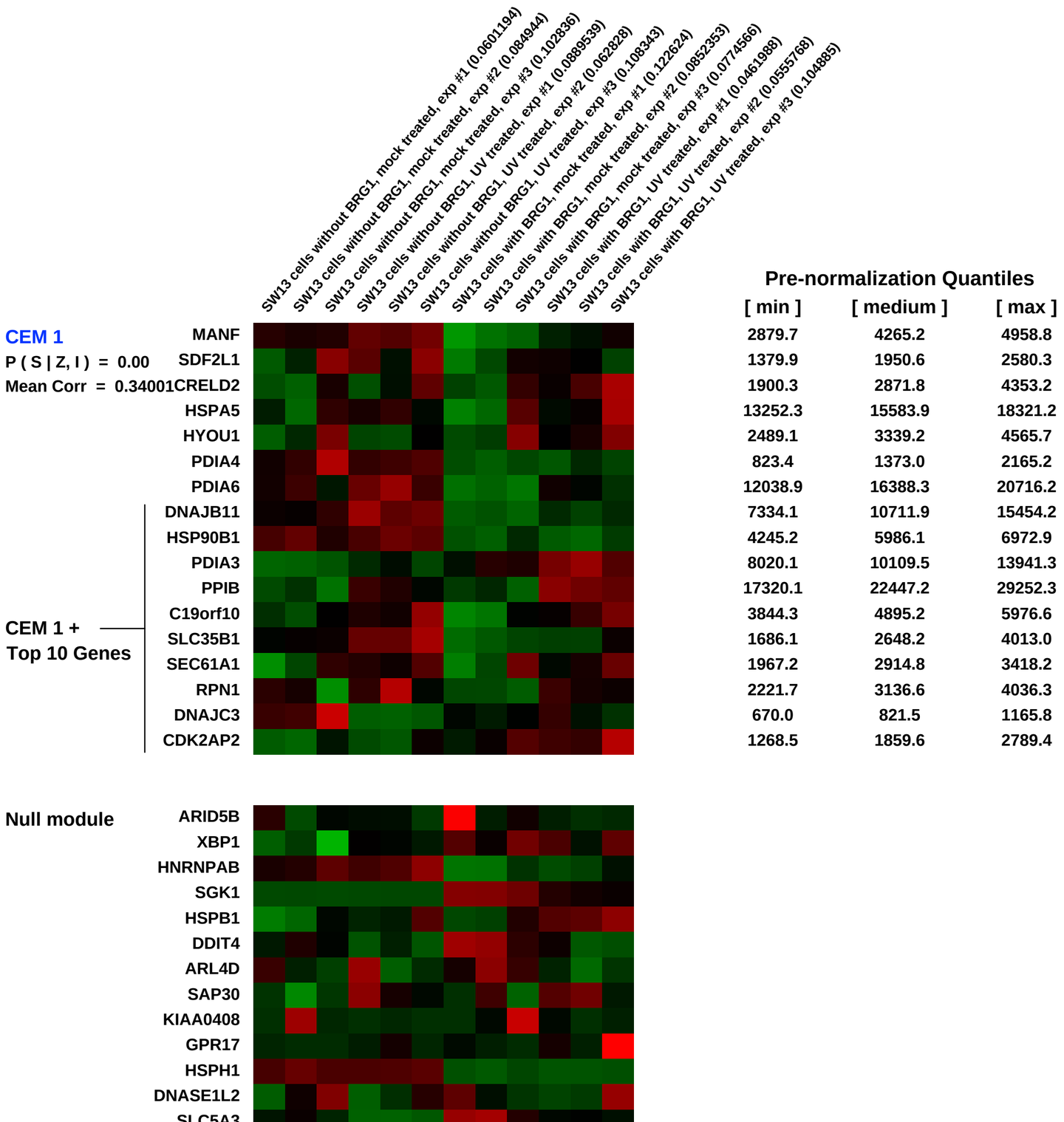

GEO Series "GSE31472" Expression Profiles

Num of samples in this series: 18

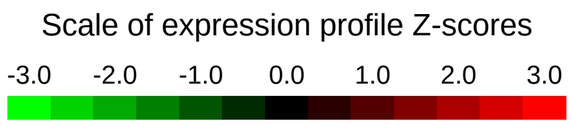

GEO Link:	http://www.ncbi.nlm.nih.gov/geo/query/acc.cgi?acc=GSE31472
Status:	Public on Jan 03 2013
Title:	Host cell gene expression in Influenza A/duck/Malaysia/F118/08/2004 (H5N2) infected A549 cells at 2, 4, 6, 8, and 10 hours post infection
Organism:	Homo sapiens
Experiment type:	Expression profiling by array
Platform:	GPL570
Pubmed ID:	22470468
Summary & Design:	**Summary:** We used the microarray data to analyze host cells response on A549 cells infected with A/duck/Malaysia/F118/08/2004(H5N2) **Overall design:** A/duck/Malaysia/F118/08/2004(H5N2) infected A549 cells were harvested at 2, 4, 6, 8 and 10 hpi and RNA extraction was performed using standard protocol as described by Affymetrix. The aim of this experiment is to analyze host response to Influenza A/duck/Malaysia/F118/08/2004(H5N2) infection.

Background corr dist: KL-Divergence = 0.1420, L1-Distance = 0.0350, L2-Distance = 0.0019, Normal std = 0.3942

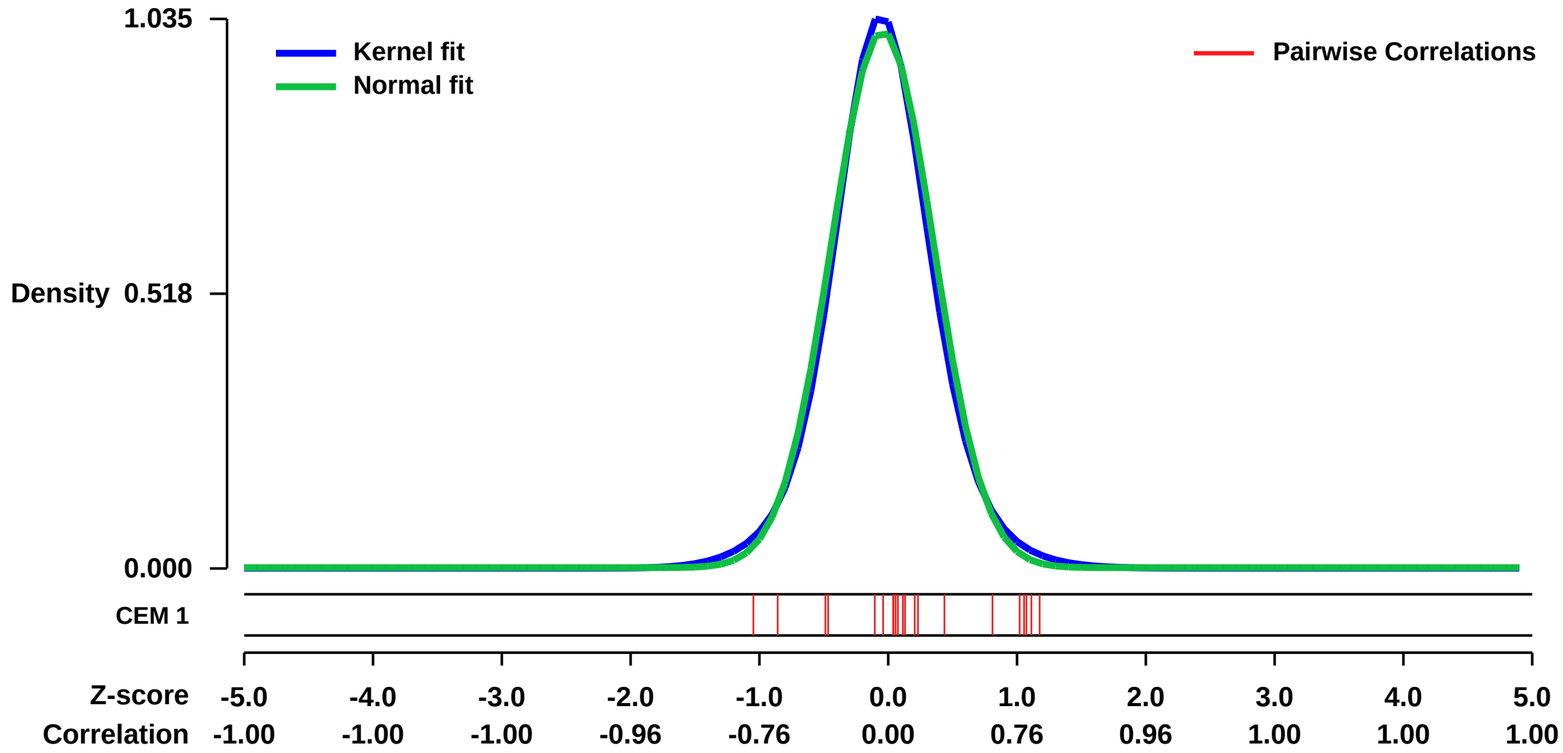

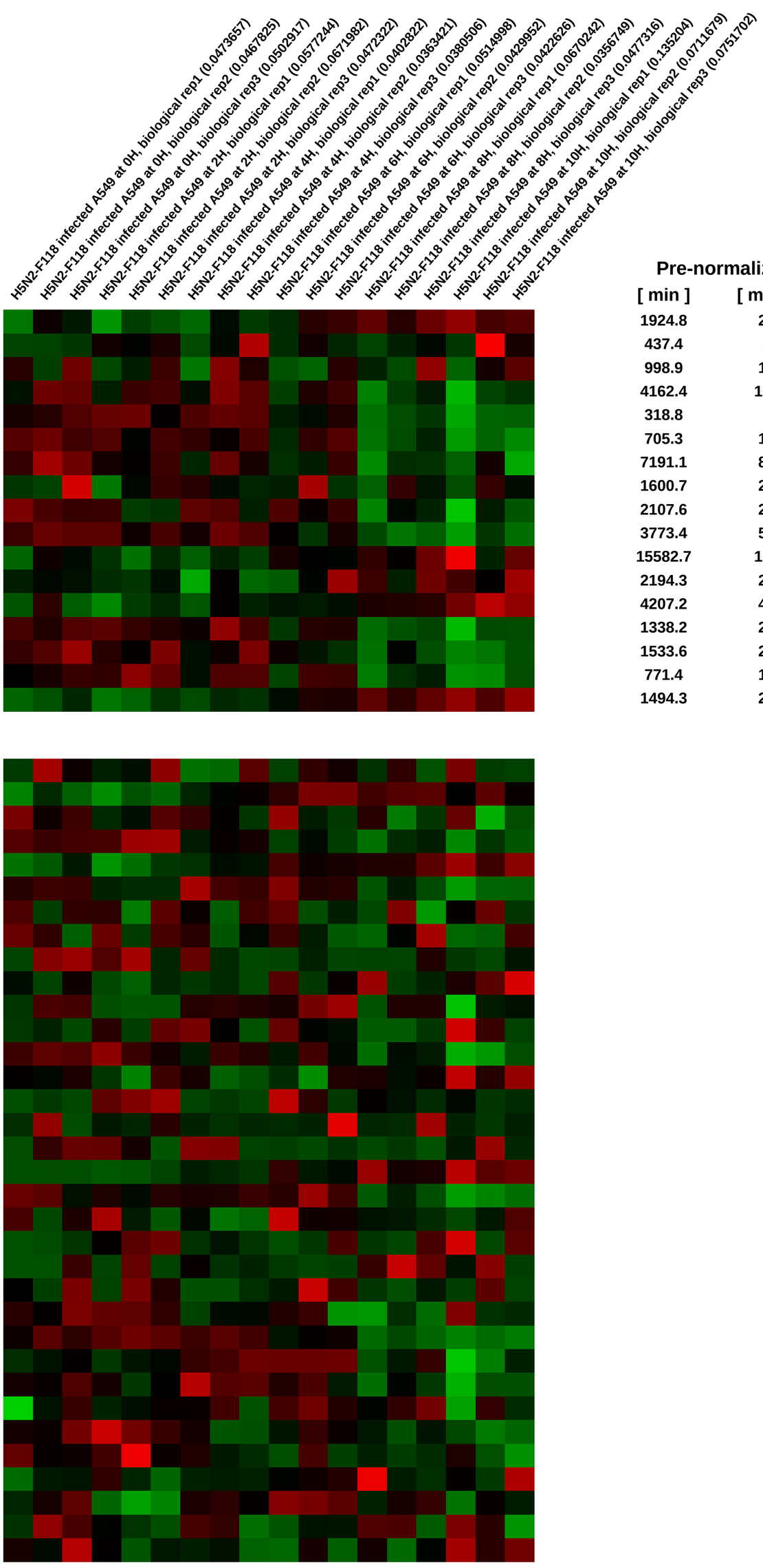

GEO Series "GSE37059" Expression Profiles

Num of samples in this series: 8

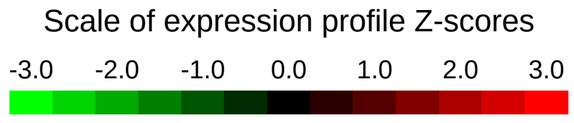

GEO Link:	**http://www.ncbi.nlm.nih.gov/geo/query/acc.cgi?acc=GSE37059**
Status:	**Public on Jul 03 2012**
Title:	**The role of SOX10 in human melanoma**
Organism:	**Homo sapiens**
Experiment type:	**Expression profiling by array**
Platform:	**GPL570**
Pubmed ID:	
Summary & Design:	**Summary:** **We have shown that Sox10 plays a crucial role in the initiation and maintenance of giant congenital nevi and melanoma in a mouse model of melanoma.To dissect the molecular mechanisms and analyze the role of SOX10 in the maintenance of human melanoma, we have performed microarray study.** **Overall design:** **Human melanoma cell line M010817 was transfected with either control shRNA or SOX10 shRNA. RNA was isolated at 48 hours and 96 hours after transfection and subjected to hybridization on Affymetrix microarrays.**

Background corr dist: **KL-Divergence = 0.0648, L1-Distance = 0.0189, L2-Distance = 0.0004, Normal std = 0.5174**

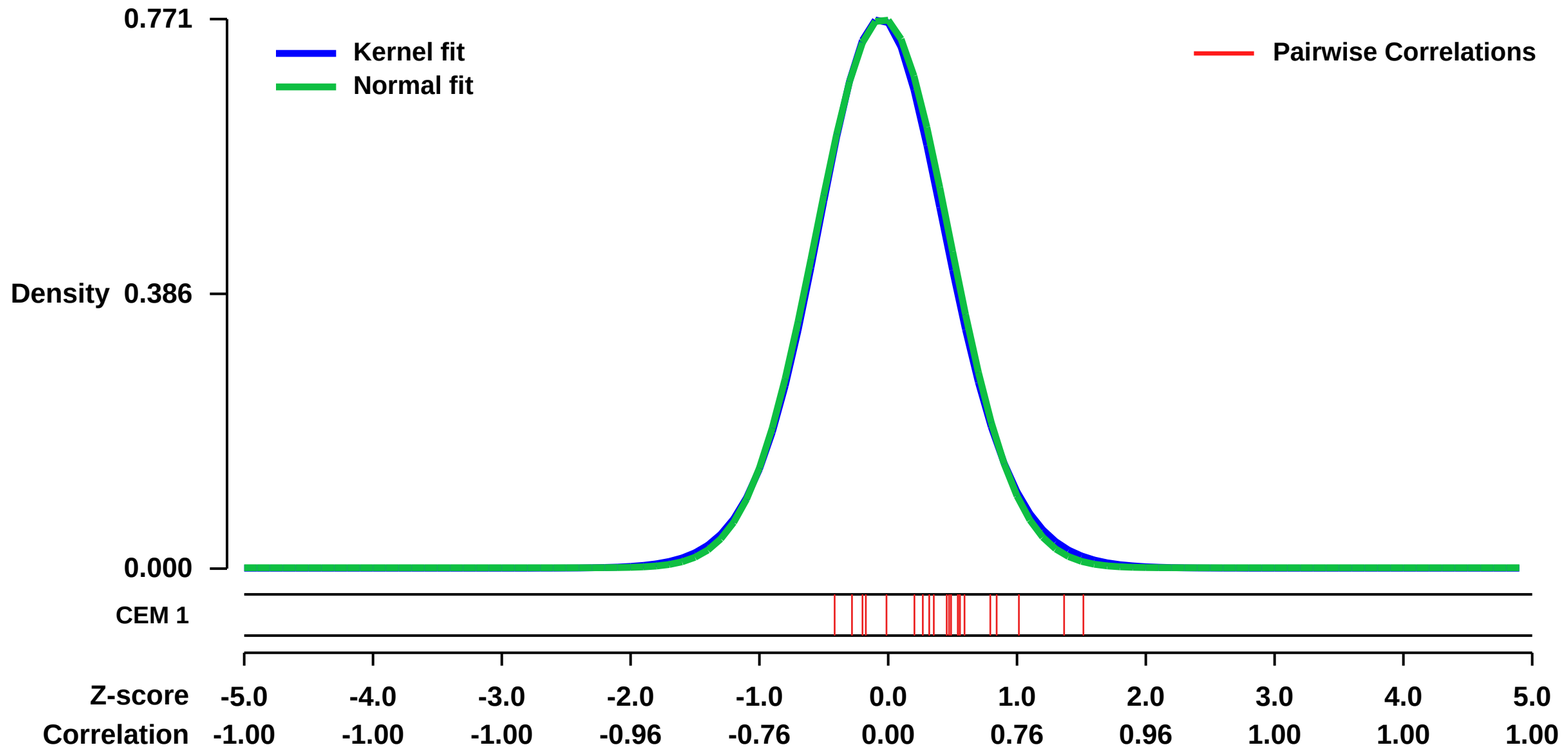

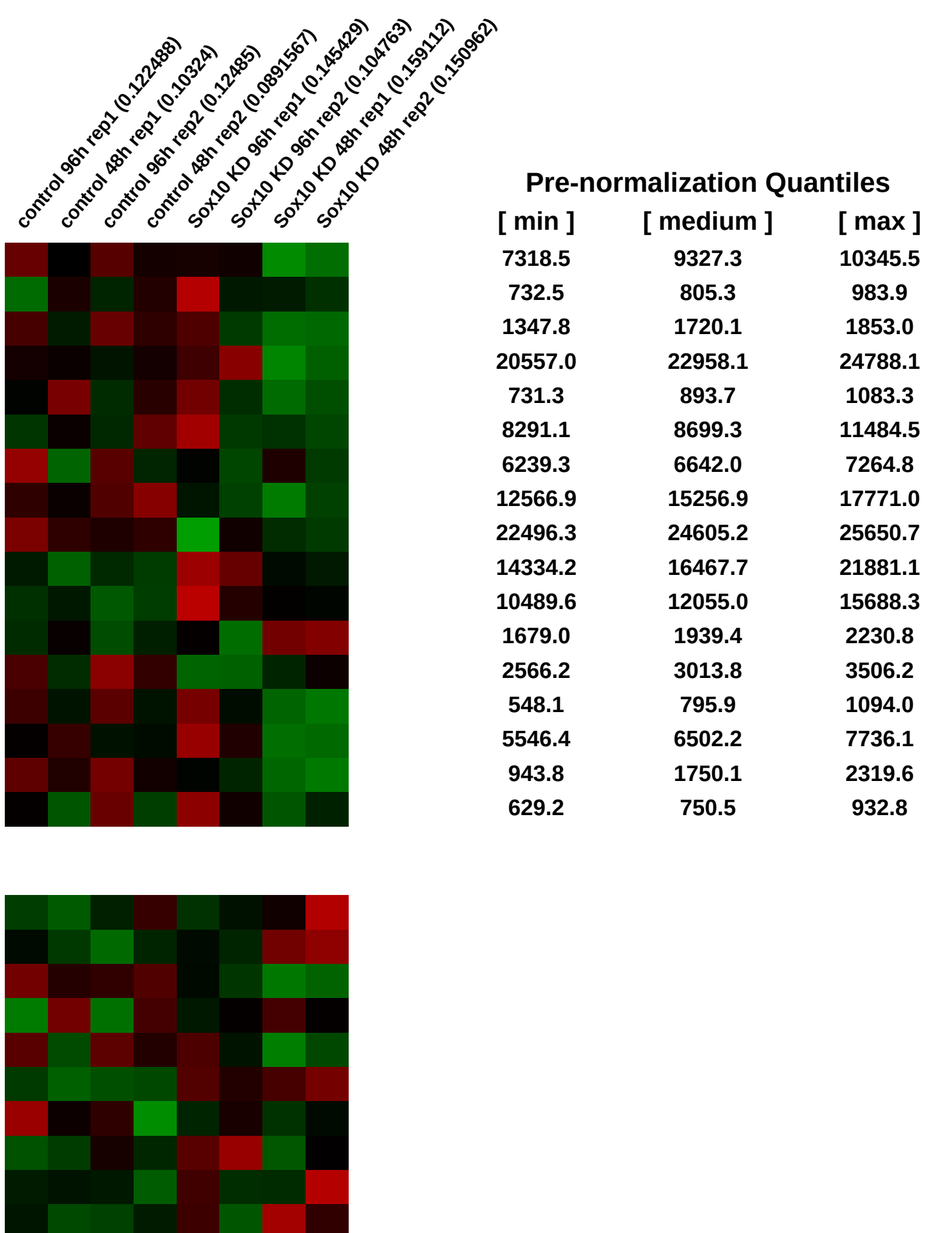

GEO Series "GSE20211" Expression Profiles

Num of samples in this series: 26

Scale of expression profile Z-scores

-3.0 -2.0 -1.0 0.0 1.0 2.0 3.0

GEO Link:	http://www.ncbi.nlm.nih.gov/geo/query/acc.cgi?acc=GSE20211
Status:	Public on Feb 01 2011
Title:	LMP-420: a novel purine nucleoside analogue with potent cytotoxic effects for chronic lymphocytic leukemia cells
Organism:	Homo sapiens
Experiment type:	Expression profiling by array
Platform:	GPL570
Pubmed ID:	20613784
Summary & Design:	**Summary:** **[original title] LMP-420: a novel purine nucleoside analogue with potent cytotoxic effects for chronic lymphocytic leukemia cells and minimal toxicity for normal hematopoietic cells.** **LMP-420 induces cytotoxicity and apoptosis to CLL cells in vitro without any negative effects to normal immune cells.** **This gene expression experiment compares CLL cells treated with LMP-420 versus media alone to investigate the mechanism of action of LMP-420.** **Overall design:** **CLL cells from 13 patients were treated with LMP-420 or media for 24 hours, then RNA was extracted and assayed on U133Plus2 GeneChips.**

Background corr dist: **KL-Divergence = 0.1436, L1-Distance = 0.0384, L2-Distance = 0.0031, Normal std = 0.3785**

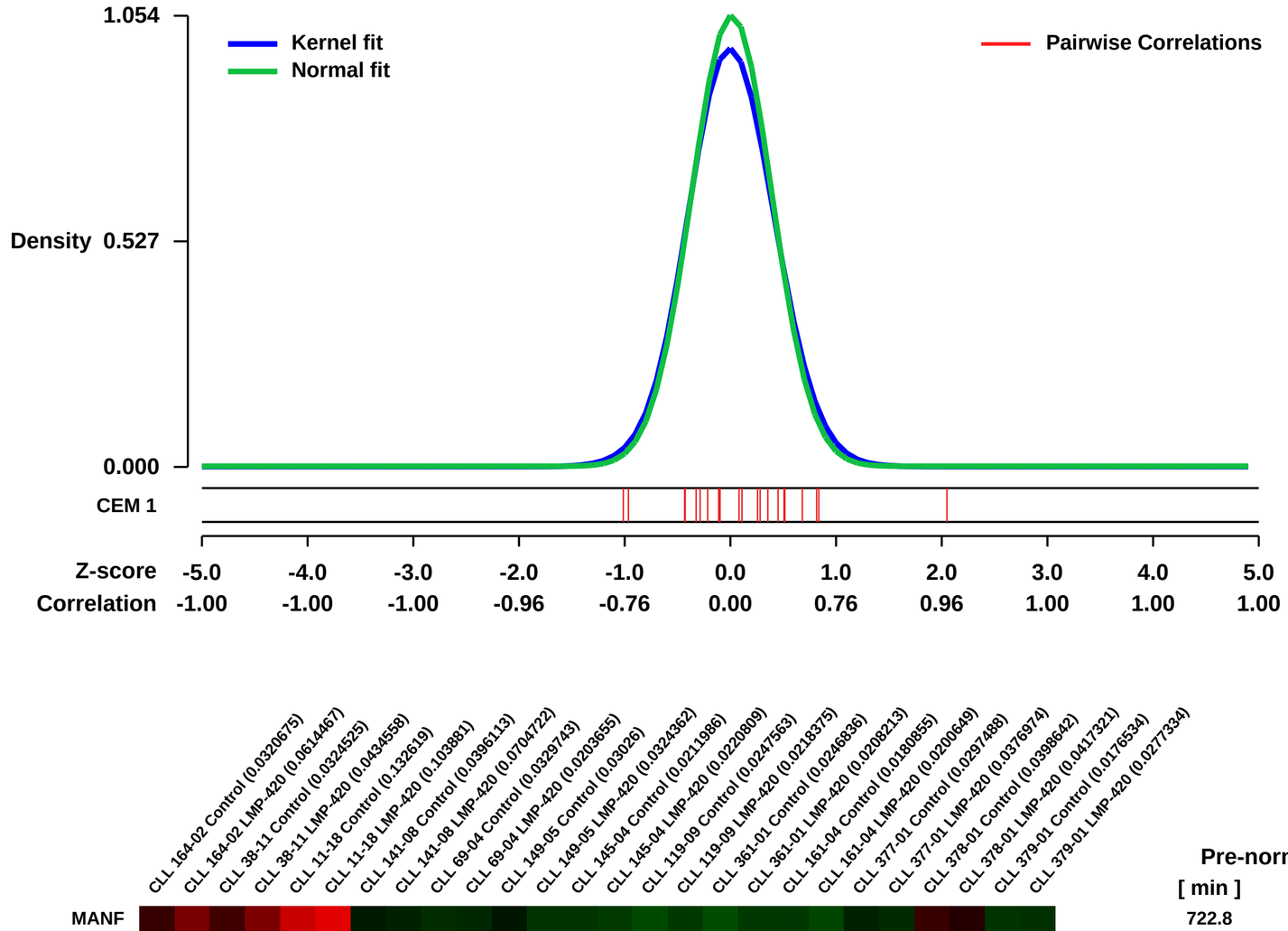

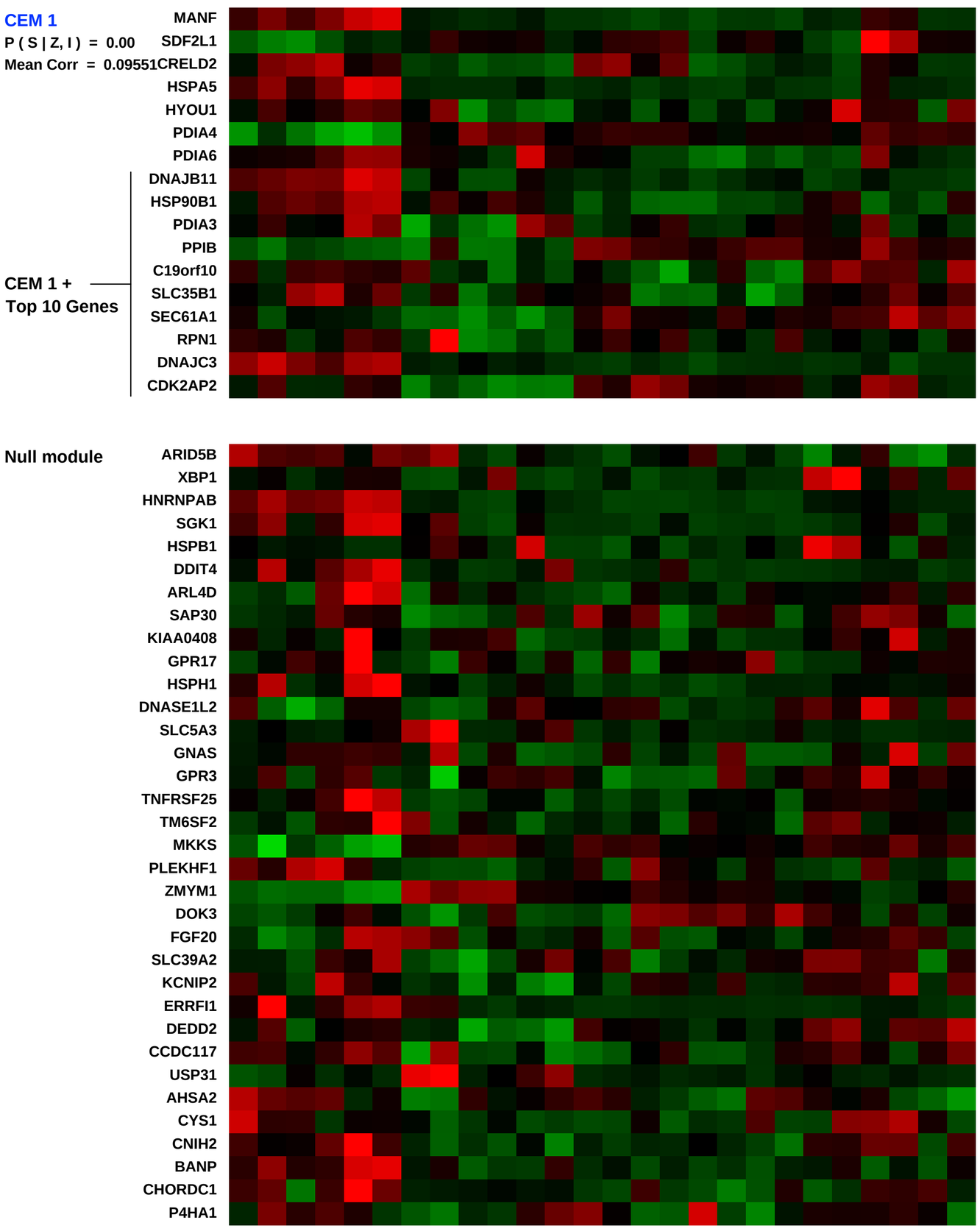

Pre-normalization Quantiles

[min]	[medium]	[max]
722.8	865.1	1846.6
321.6	458.2	681.6
1068.3	1450.7	2550.2
3585.8	4468.6	11726.5
651.0	1126.6	1879.8
176.9	381.4	487.8
1904.6	2788.7	4331.4
1107.8	1396.4	2893.6
1134.3	1810.9	3308.1
4031.2	5852.5	7920.0
5097.1	8209.8	10784.6
843.0	1045.6	1228.3
599.7	828.8	1063.6
1148.3	1505.8	1885.8
1035.3	1710.7	3349.7
627.0	822.8	2045.8
548.6	1081.6	1564.5

GEO Series "GSE13054" Expression Profiles

Num of samples in this series: 9

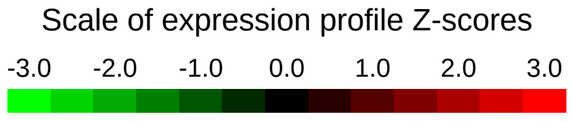

GEO Link:	http://www.ncbi.nlm.nih.gov/geo/query/acc.cgi?acc=GSE13054
Status:	Public on Feb 15 2011
Title:	Genes upregulated by HLX
Organism:	Homo sapiens
Experiment type:	Expression profiling by array
Platform:	GPL570
Pubmed ID:	21224470
Summary & Design:	**Summary:** HLX was found as a VEGF-A induced gene in HUVEC (B.Schweighofer, submitted). In order to detect genes regulated by HLX HUVEC were infected by recombinant adenovirus expressing HLX for 4, 8, 16 and 32h. RNA was isolated and subjected to microarray analysis using Affymetrix microarray. **Overall design:** HUVEC were infected with a MOI of 40 with either HLX expressing or empty adenovirus for 4, 8, 16 or 32 hours. HUVEC without an adenovirus infection were used as control.Total RNA was isolated with Trizol according to the instructions of the manufacturer. Gene expression was analysed with Affymetrix GeneChip Human Genome U133 Plus 2.0 Arrays according to the Affymetrix protocol.

Background corr dist: KL-Divergence = 0.0789, L1-Distance = 0.0211, L2-Distance = 0.0006, Normal std = 0.4862

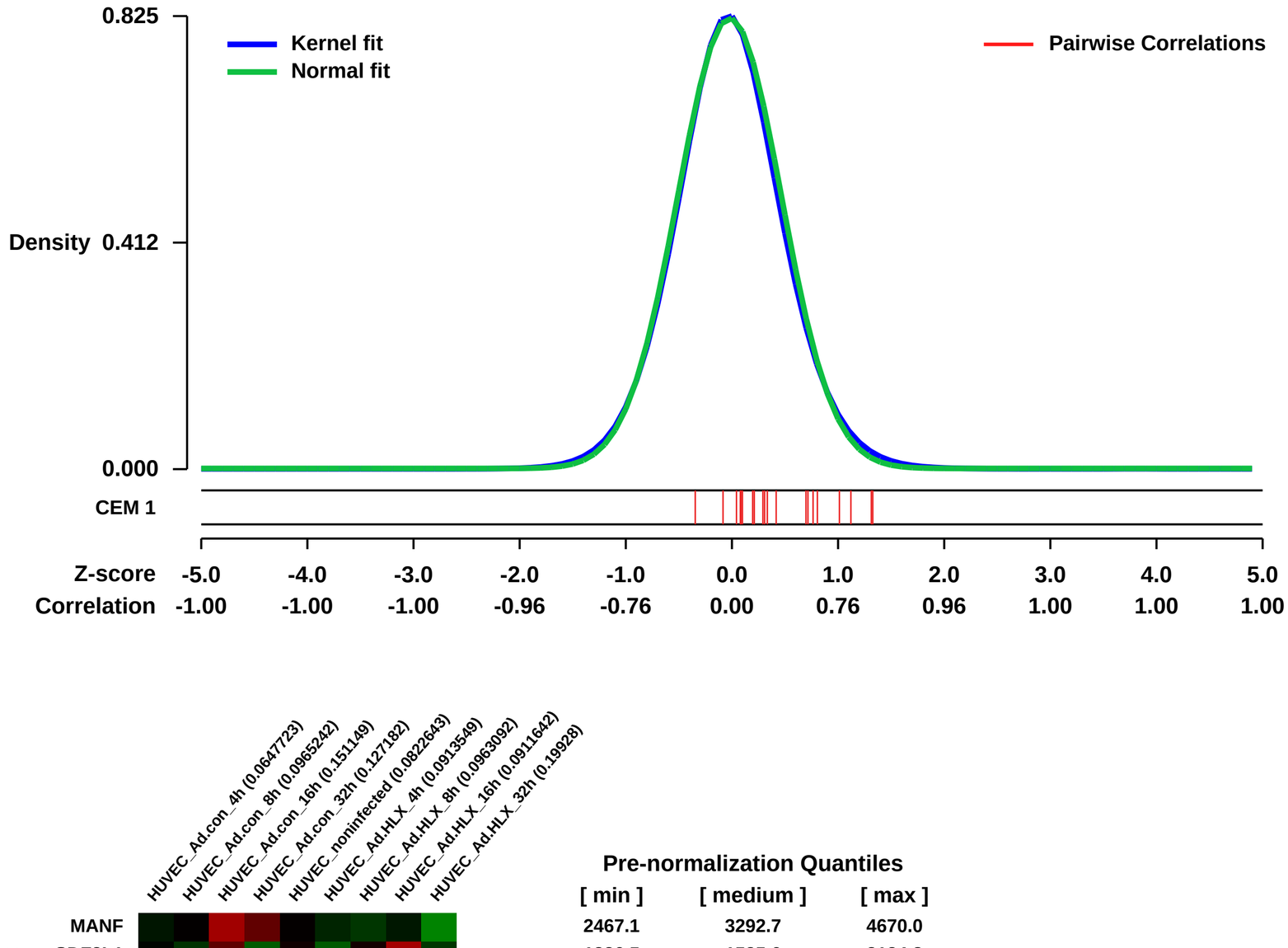

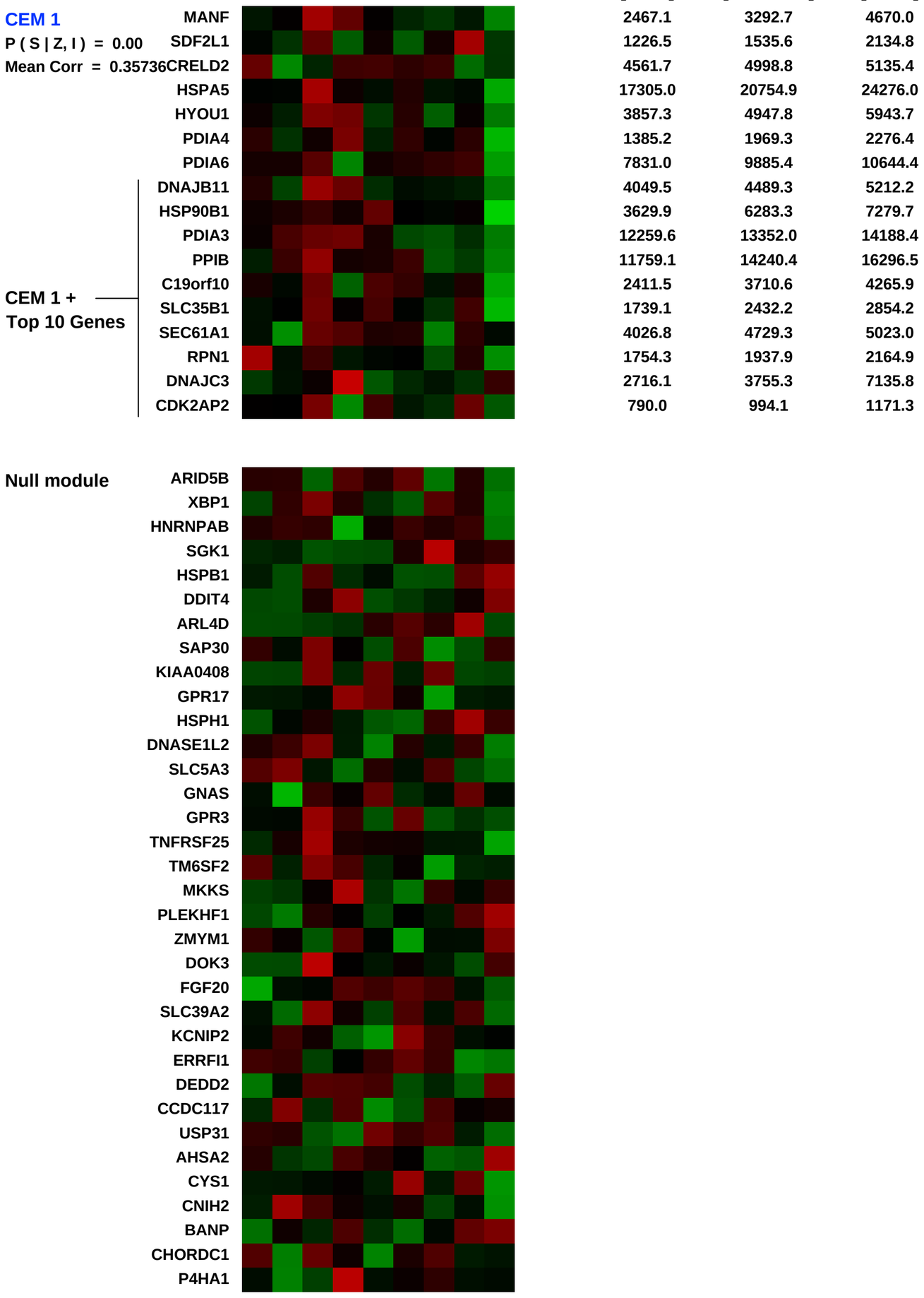

GEO Series "GSE29639" Expression Profiles

Num of samples in this series: 10

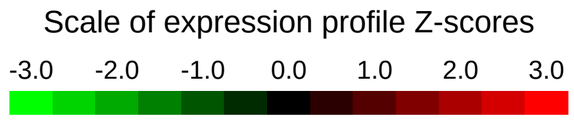

GEO Link:	http://www.ncbi.nlm.nih.gov/geo/query/acc.cgi?acc=GSE29639
Status:	Public on Nov 01 2011
Title:	The leukemia-specific fusion gene ETV6/RUNX1 perturbs distinct key biological functions primarily by gene repression
Organism:	Homo sapiens
Experiment type:	Expression profiling by array
Platform:	GPL570
Pubmed ID:	22028862
Summary & Design:	**Summary:** **Background: ETV6/RUNX1 (E/R) (also known as TEL/AML1) is the most frequent gene fusion in childhood acute lymphoblastic leukemia (ALL) and also most likely the crucial factor for disease initiation, whereas its role in leukemia propagation and maintenance remains largely elusive. To address this issue we performed a shRNA-mediated knock-down (KD) of the E/R fusion gene and investigated the ensuing consequences on genome-wide gene expression patterns and deducible regulatory functions in two E/R-positive leukemic cell lines. Findings: Microarray analyses identified 777 genes whose expression was substantially altered. Although approximately equal proportions were either up- (KD-UP) or down-regulated (KD-DOWN), the effects on biological processes and pathways differed considerably. The E/R KD-DOWN set was significantly enriched for genes included in the cell activation, immune response, apoptosis, signal transduction and development and differentiation categories, whereas in the E/R KD-UP set only the PI3K/AKT/mTOR signaling and hematopoietic stem cells categories became evident. Comparable expression signatures obtained from primary E/R-positive ALL samples underline the relevance of these pathways and molecular functions. We also validated six differentially expressed genes representing the categories stem cell properties, B-cell differentiation, immune response, cell adhesion and DNA damage with RT-qPCR. Conclusion: The results of our analyses provide the first preliminary evidence that the continuous expression of the E/R fusion gene interferes with regular B-cell development by repressing key functions that are necessary under physiological circumstances. E/R may thus constitute also the essential driving force for the propagation and maintenance of the leukemic process irrespective of potential consequences of associated secondary changes. Finally, these findings may also provide a valuable source of potentially attractive therapeutic targets.** **Overall design:** **Knockdown of ETV6/RUNX1 in two t(12;21) positive leukemic cell lines**

Background corr dist: KL-Divergence = 0.1105, L1-Distance = 0.0299, L2-Distance = 0.0015, Normal std = 0.4197

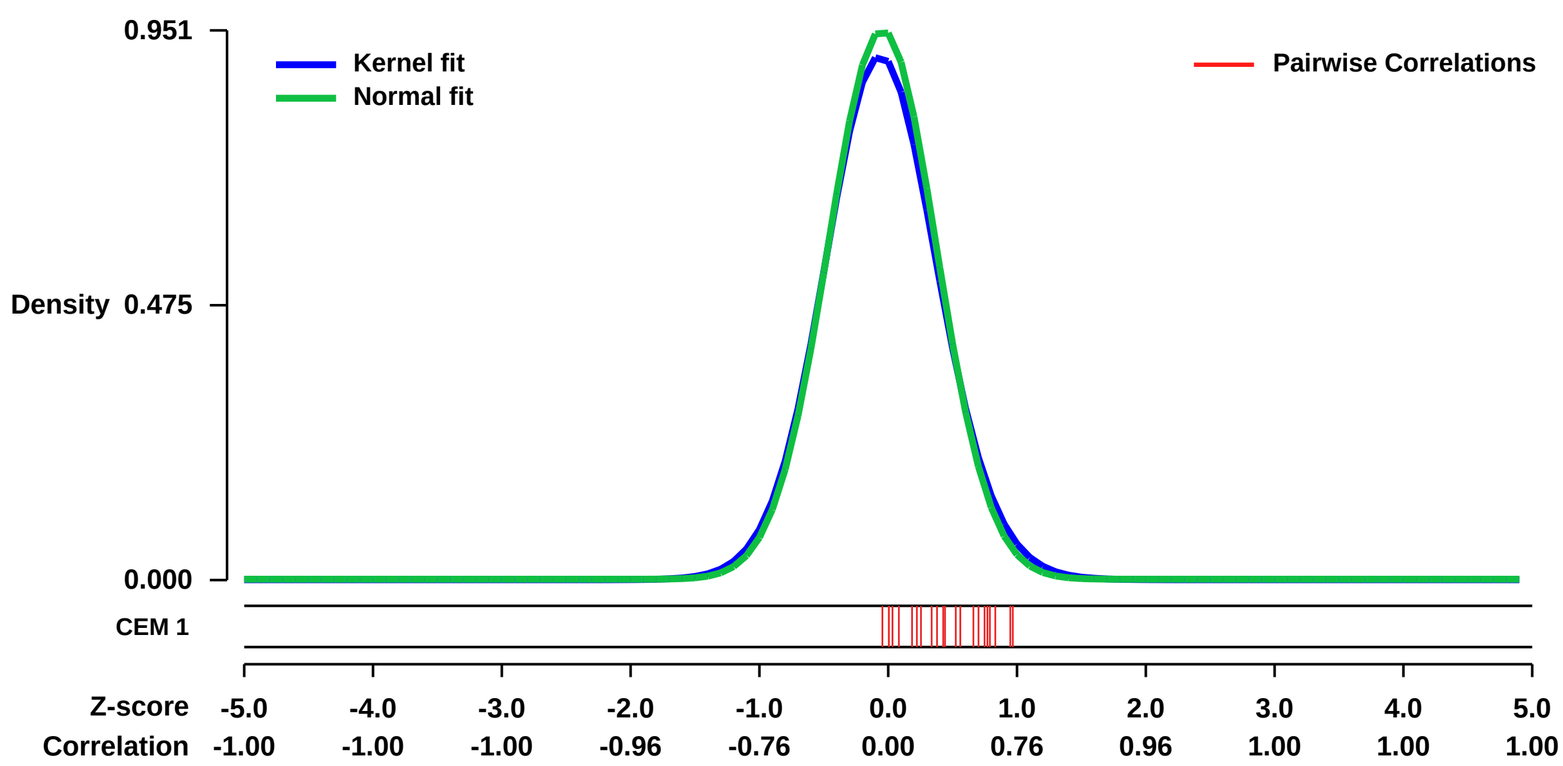

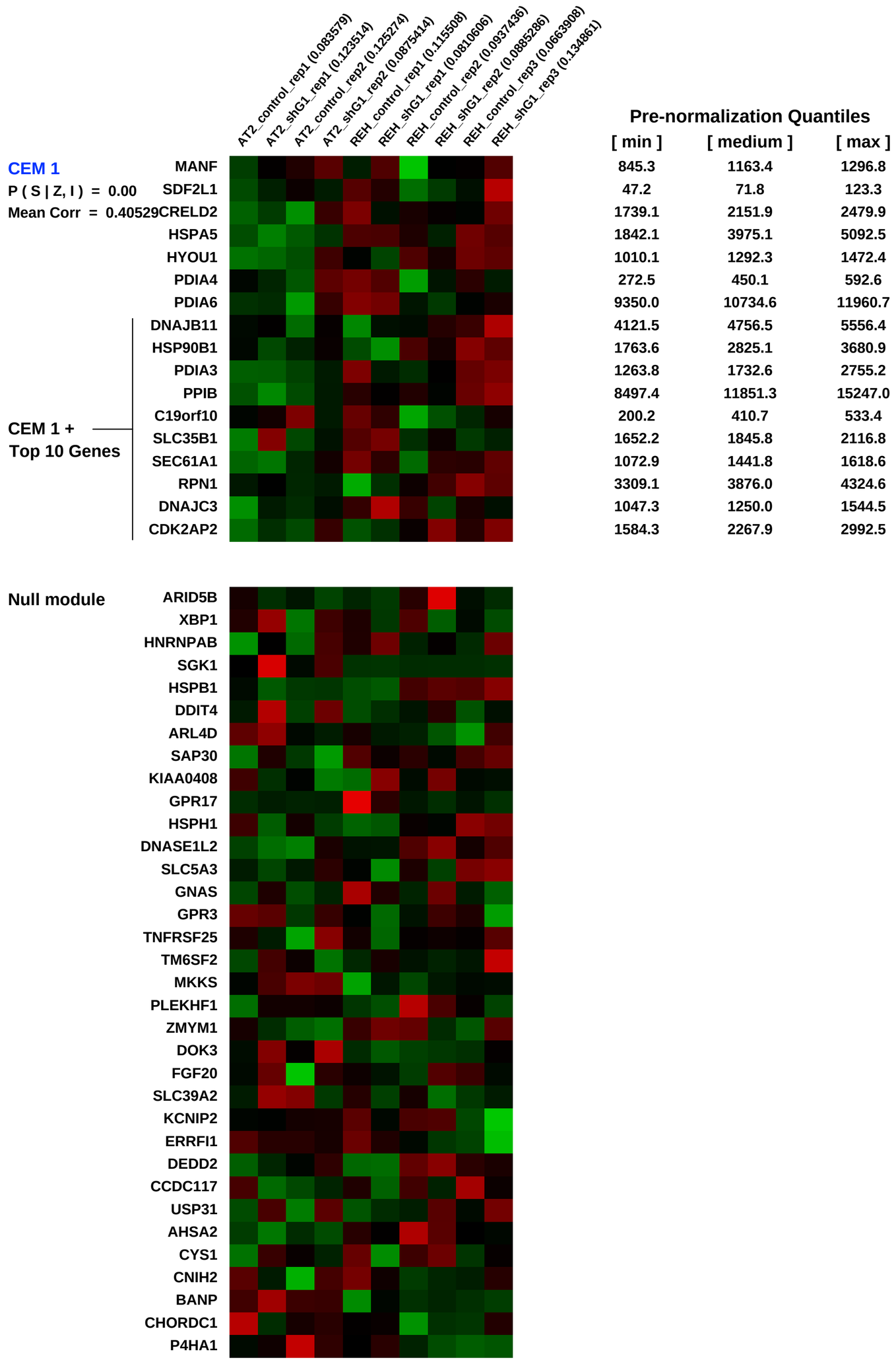

Pre-normalization Quantiles

	[min]	[medium]	[max]
MANF	845.3	1163.4	1296.8
SDF2L1	47.2	71.8	123.3
CRELD2	1739.1	2151.9	2479.9
HSPA5	1842.1	3975.1	5092.5
HYOU1	1010.1	1292.3	1472.4
PDIA4	272.5	450.1	592.6
PDIA6	9350.0	10734.6	11960.7
DNAJB11	4121.5	4756.5	5556.4
HSP90B1	1763.6	2825.1	3680.9
PDIA3	1263.8	1732.6	2755.2
PPIB	8497.4	11851.3	15247.0
C19orf10	200.2	410.7	533.4
SLC35B1	1652.2	1845.8	2116.8
SEC61A1	1072.9	1441.8	1618.6
RPN1	3309.1	3876.0	4324.6
DNAJC3	1047.3	1250.0	1544.5
CDK2AP2	1584.3	2267.9	2992.5

GEO Series "GSE37820" Expression Profiles

Num of samples in this series: 6

Scale of expression profile Z-scores

-3.0 -2.0 -1.0 0.0 1.0 2.0 3.0

GEO Link: http://www.ncbi.nlm.nih.gov/geo/query/acc.cgi?acc=GSE37820
Status: Public on May 07 2012
Title: Gene expression profile in MCF7 breast cancer cells after siRNA knock down of estrogen receptor alpha (ESR1)
Organism: Homo sapiens
Experiment type: Expression profiling by array
Platform: GPL570
Pubmed ID:

Summary & Design:

Summary:
Affymetrix microarray data was generated from MCF7 breast cancer cells treated in vitro with siRNAs against estrogen receptor alpha (ESR1).

Overall design:
Gene expresion of estrogen receptor alpha (ESR1) was knocked down in MCF7 breast cancer cells using siRNA. Then the gene expression profiles of these MCF7 cells, along with non-targetting control treated cells were analysed using Affymetrix Human Genome U133 Plus 2.0 microarrays.

Background corr dist: KL-Divergence = 0.0451, L1-Distance = 0.0177, L2-Distance = 0.0003, Normal std = 0.5897

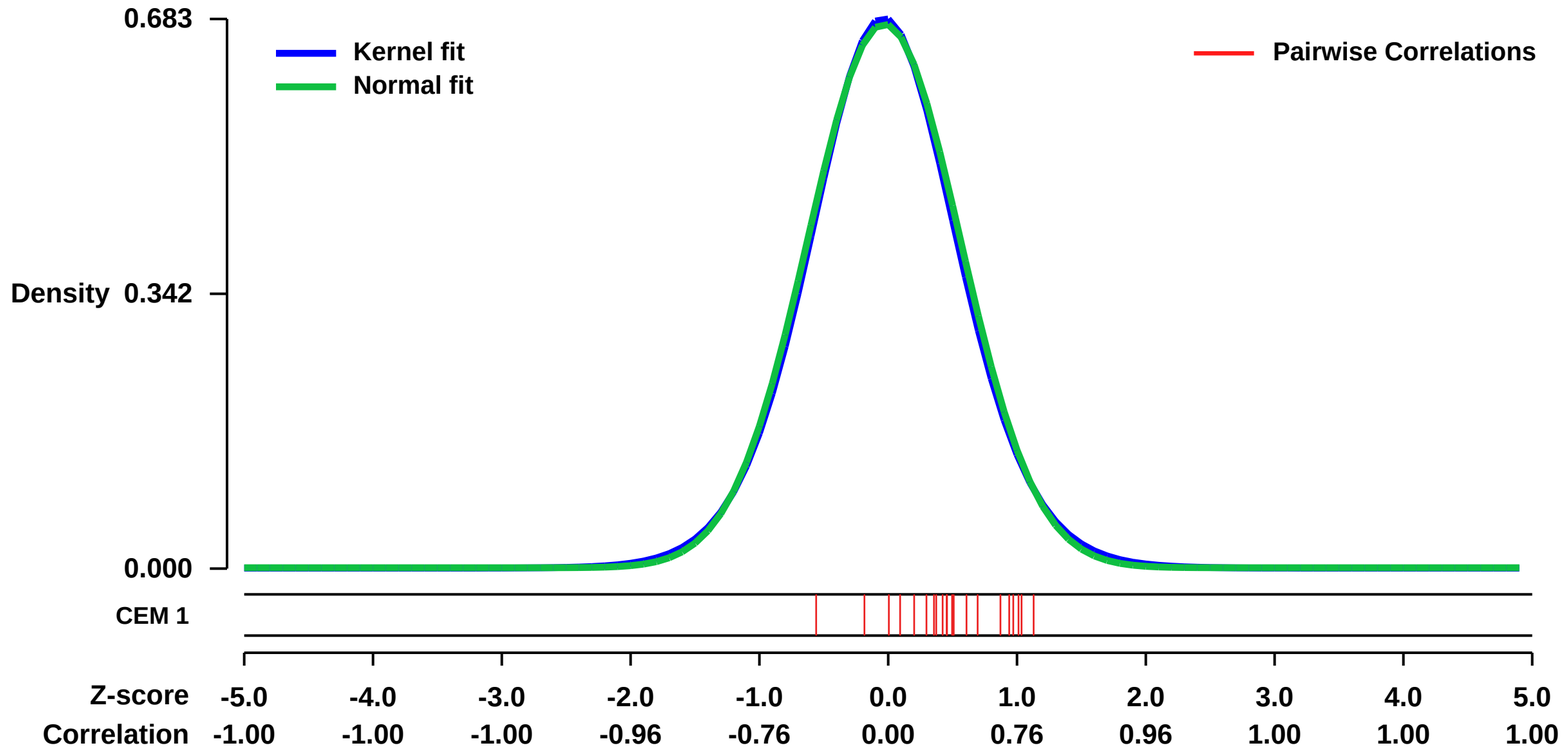

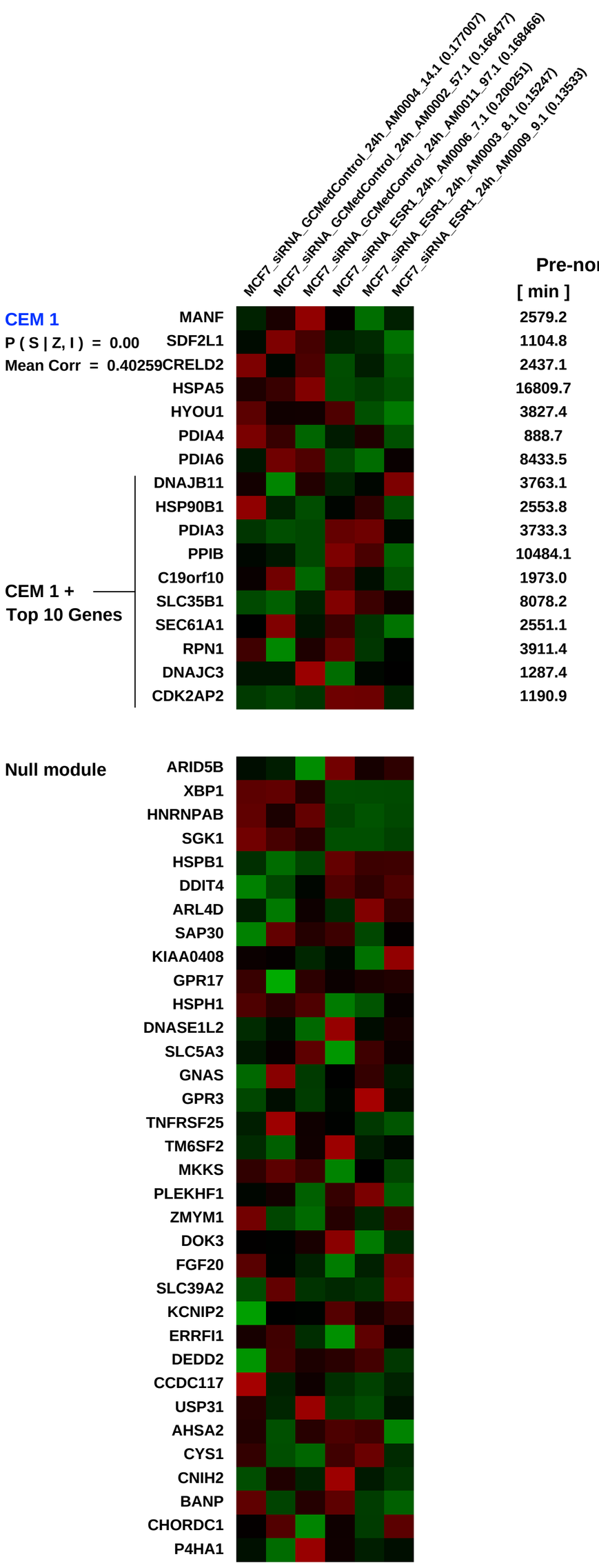

	Pre-normalization Quantiles		
	[min]	[medium]	[max]
MANF	2579.2	2747.8	2953.7
SDF2L1	1104.8	1379.3	1743.4
CRELD2	2437.1	2535.8	2696.4
HSPA5	16809.7	18957.9	20911.7
HYOU1	3827.4	4344.3	4620.9
PDIA4	888.7	971.2	1028.5
PDIA6	8433.5	9451.9	10352.3
DNAJB11	3763.1	4289.7	4658.2
HSP90B1	2553.8	2715.2	3042.4
PDIA3	3733.3	4122.0	4761.8
PPIB	10484.1	11218.8	12282.0
C19orf10	1973.0	2180.9	2373.4
SLC35B1	8078.2	8392.7	8722.7
SEC61A1	2551.1	3016.7	3543.6
RPN1	3911.4	4404.7	4613.4
DNAJC3	1287.4	1439.2	1680.3
CDK2AP2	1190.9	1268.0	1588.0

GEO Series "GSE45295" Expression Profiles

Num of samples in this series: 9

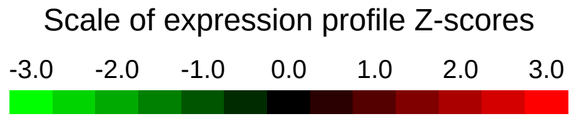

GEO Link:	http://www.ncbi.nlm.nih.gov/geo/query/acc.cgi?acc=GSE45295
Status:	Public on Mar 20 2013
Title:	Expression data from Control, HIRA and CABIN1 knockdown cells
Organism:	Homo sapiens
Experiment type:	Expression profiling by array
Platform:	GPL570
Pubmed ID:	21807893
Summary & Design:	**Summary:** The mammalian HIRA/UBN1/ASF1a complex is a histone chaperone complex that is conserved from yeast (Saccharomyces cerevisiae) to humans. This complex preferentially deposits the histone variant H3.3 into chromatin in a DNA replication-independent manner and is implicated in diverse chromatin regu- latory events from gene activation to heterochromatinization. In yeast, the orthologous complex consists of three Hir proteins (Hir1p, Hir2p, and Hir3p), Hpc2p, and Asf1p. Yeast Hir3p has weak homology to CABIN1, a fourth member of the human complex, suggesting that Hir3p and CABIN1 may be orthologs. Here we show that HIRA and CABIN1 interact at ectopic and endogenous levels of expression in cells, and we isolate the quaternary HIRA/UBN1/CABIN1/ASF1a (HUCA) complex, assembled from recombinant proteins. Mutational analyses support the view that HIRA acts as a scaffold to bring together UBN1, ASF1a, and CABIN1 into a quaternary complex. We show that, like HIRA, UBN1, and ASF1a, CABIN1 is involved in heterochromatinization of the genome of senescent human cells. Moreover, in proliferating cells, HIRA and CABIN1 regulate overlapping sets of genes, and these genes are enriched in the histone variant H3.3. In sum, these data demonstrate that CABIN1 is a functional member of the human HUCA complex and so is the likely ortholog of yeast Hir3p. We used microarrays to detail the global programme of gene expression after knockdown of HIRA and CABIN1 in 3 replicates **Overall design:** HeLa cells were nucleofacted with Dharmacon control siRNA and siRNA to HIRA and CABIN1 and RNA was isolated 72 hours after transfection.

Background corr dist: KL-Divergence = 0.0878, L1-Distance = 0.0224, L2-Distance = 0.0006, Normal std = 0.4607

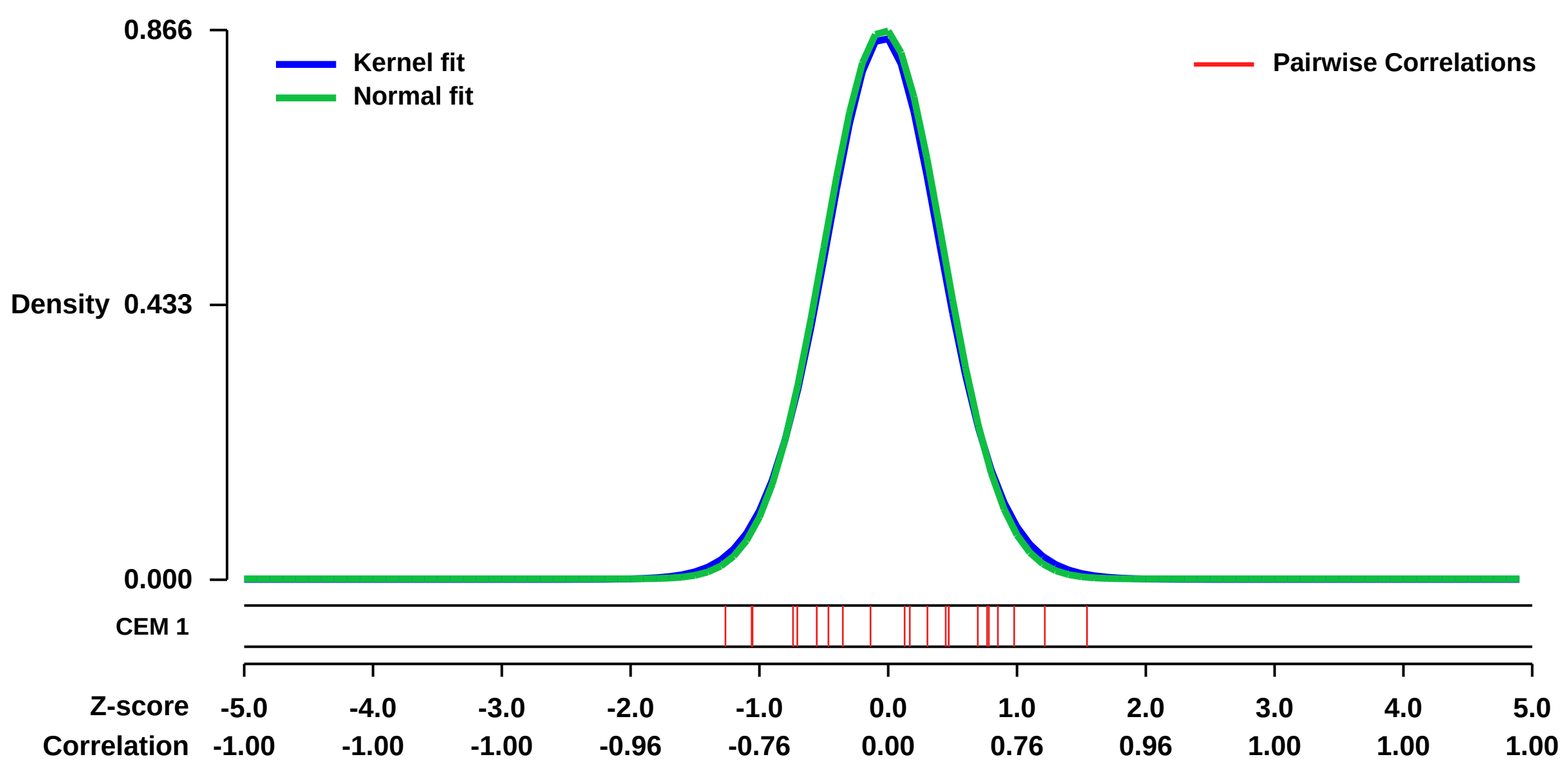

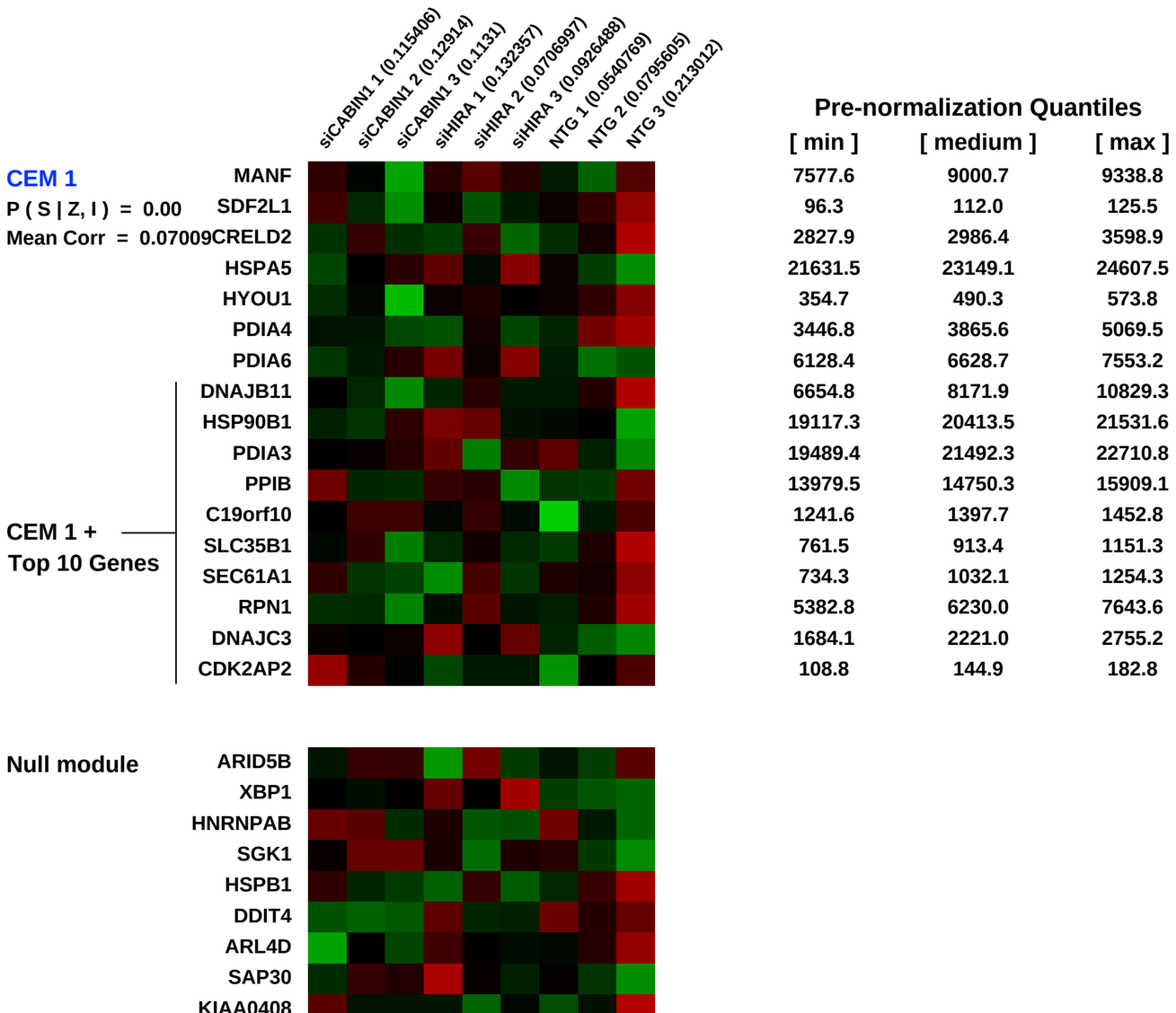

Pre-normalization Quantiles

	[min]	[medium]	[max]
MANF	7577.6	9000.7	9338.8
SDF2L1	96.3	112.0	125.5
CRELD2	2827.9	2986.4	3598.9
HSPA5	21631.5	23149.1	24607.5
HYOU1	354.7	490.3	573.8
PDIA4	3446.8	3865.6	5069.5
PDIA6	6128.4	6628.7	7553.2
DNAJB11	6654.8	8171.9	10829.3
HSP90B1	19117.3	20413.5	21531.6
PDIA3	19489.4	21492.3	22710.8
PPIB	13979.5	14750.3	15909.1
C19orf10	1241.6	1397.7	1452.8
SLC35B1	761.5	913.4	1151.3
SEC61A1	734.3	1032.1	1254.3
RPN1	5382.8	6230.0	7643.6
DNAJC3	1684.1	2221.0	2755.2
CDK2AP2	108.8	144.9	182.8

GEO Series "GSE12548" Expression Profiles

Num of samples in this series: 20

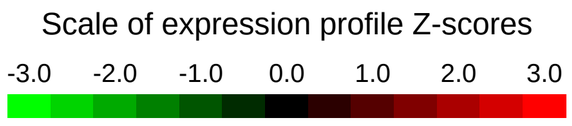

GEO Link:	http://www.ncbi.nlm.nih.gov/geo/query/acc.cgi?acc=GSE12548
Status:	Public on Aug 26 2009
Title:	EMT Time series in ARPE19
Organism:	Homo sapiens
Experiment type:	Expression profiling by array
Platform:	GPL570
Pubmed ID:	19965872
Summary & Design:	**Summary:** The purpose of this study is to determine the changes in gene expression by a human retinal pigment epithelium (RPE) cell line (ARPE-19) in response to combination treatment of TGF and TNF, which induces phenotypic changes in vitro that mimic the EMT (Epithelial-to-Mesenchymal Transition). For this purpose, total RNA was extracted from TGF and TNF-treated ARPE-19 cells and differential gene expression between each time point (0, 1, 6, 16, 24, 42, and 60 hours) was determined using genechip arrays (Affymetrix, Human Genome U133). Keywords: time course **Overall design:** ARPE19 cell lines treated with TGF and TNF for 0, 1, 6, 16, 24, 42, and 60 hour. Each experiment were repeated three times. But 1 hour experiment was repeated two times.

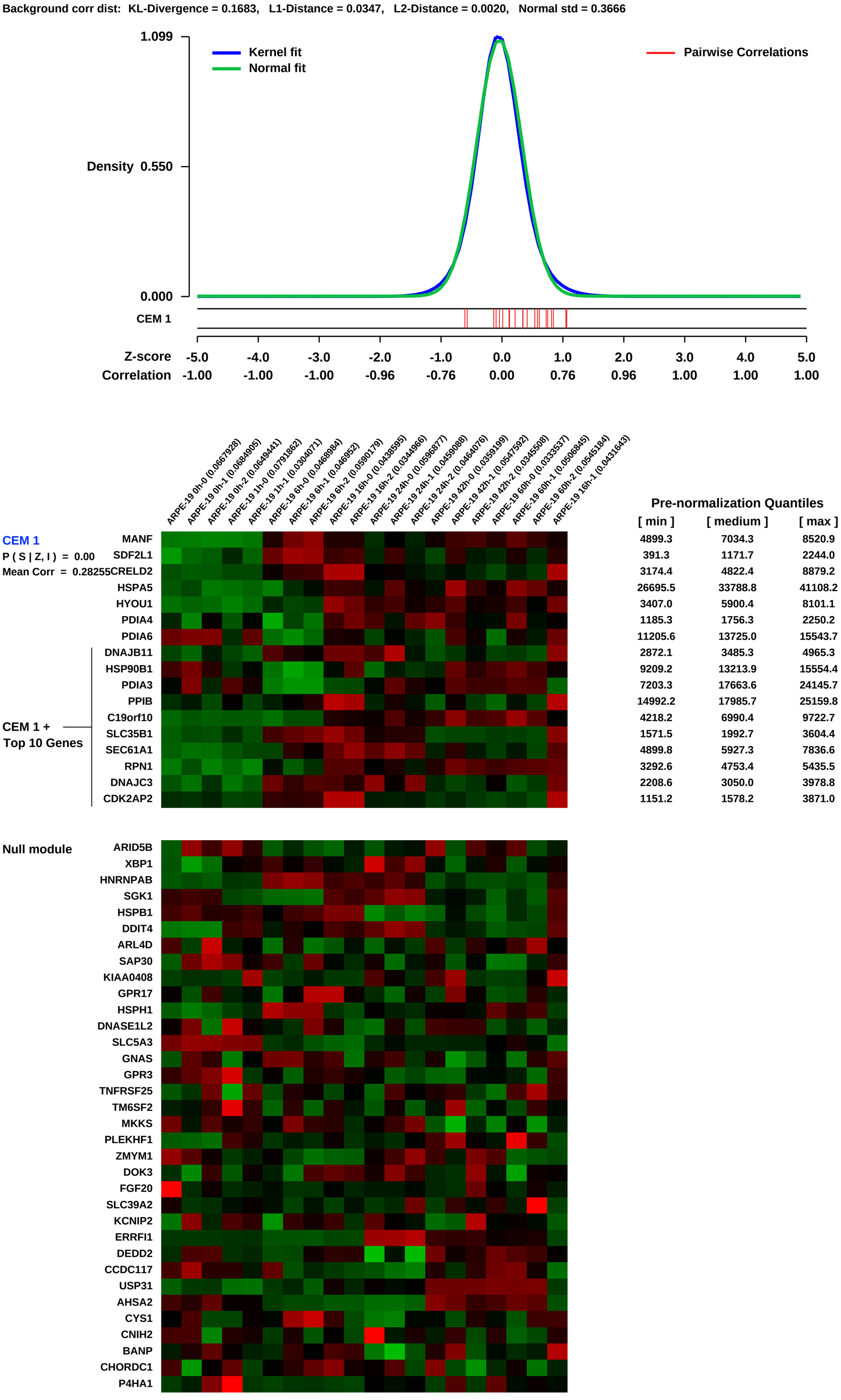

GEO Series "GSE33420" Expression Profiles

Num of samples in this series: 8

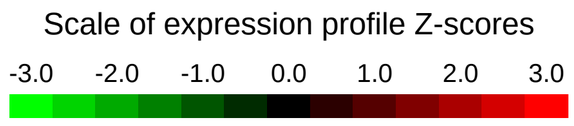

GEO Link:	**http://www.ncbi.nlm.nih.gov/geo/query/acc.cgi?acc=GSE33420**
Status:	**Public on May 02 2012**
Title:	**microRNA-143 downregulates Hexokinase 2 in colon cancer cells**
Organism:	**Homo sapiens**
Experiment type:	**Expression profiling by array**
Platform:	**GPL570**
Pubmed ID:	
Summary & Design:	**Summary:** **MicroRNAs (miRNAs) have emerged as important gene regulators and are recognized as key players in tumorigenesis. miR-143 is reported to be down-regulated in several cancers, but knowledge of its targets in colon cancer remains limited. To investigate the role of miR-143 in colon cancer, we have employed a microarray based approach to identify miR-143 targets. Based on seed site enrichment analyses and unbiased word analyses, we found a significant enrichment of miRNA binding sites in the 3â -untranslated regions (UTRs) of transcripts down-regulated upon miRNA overexpression. Here we identify Hexokinase 2 (HK2) as a direct target of miR-143 and show that re-introduction of miR-143 in the colon cancer cell line DLD-1 results in a decreased lactate secretion, indicating that miR-143 down-regulation of HK2 affects glucose metabolism in colon cancer cells.** **Overall design:** **DLD-1 cells were transfected with 50 nM miR-143 duplex or mock transfected. Total RNA was harvested 24 hours post-transfection and analyzed on Affymetrix HG-U133 Plus 2.0 human arrays.**

Background corr dist: **KL-Divergence = 0.0250, L1-Distance = 0.0668, L2-Distance = 0.0065, Normal std = 0.7861**

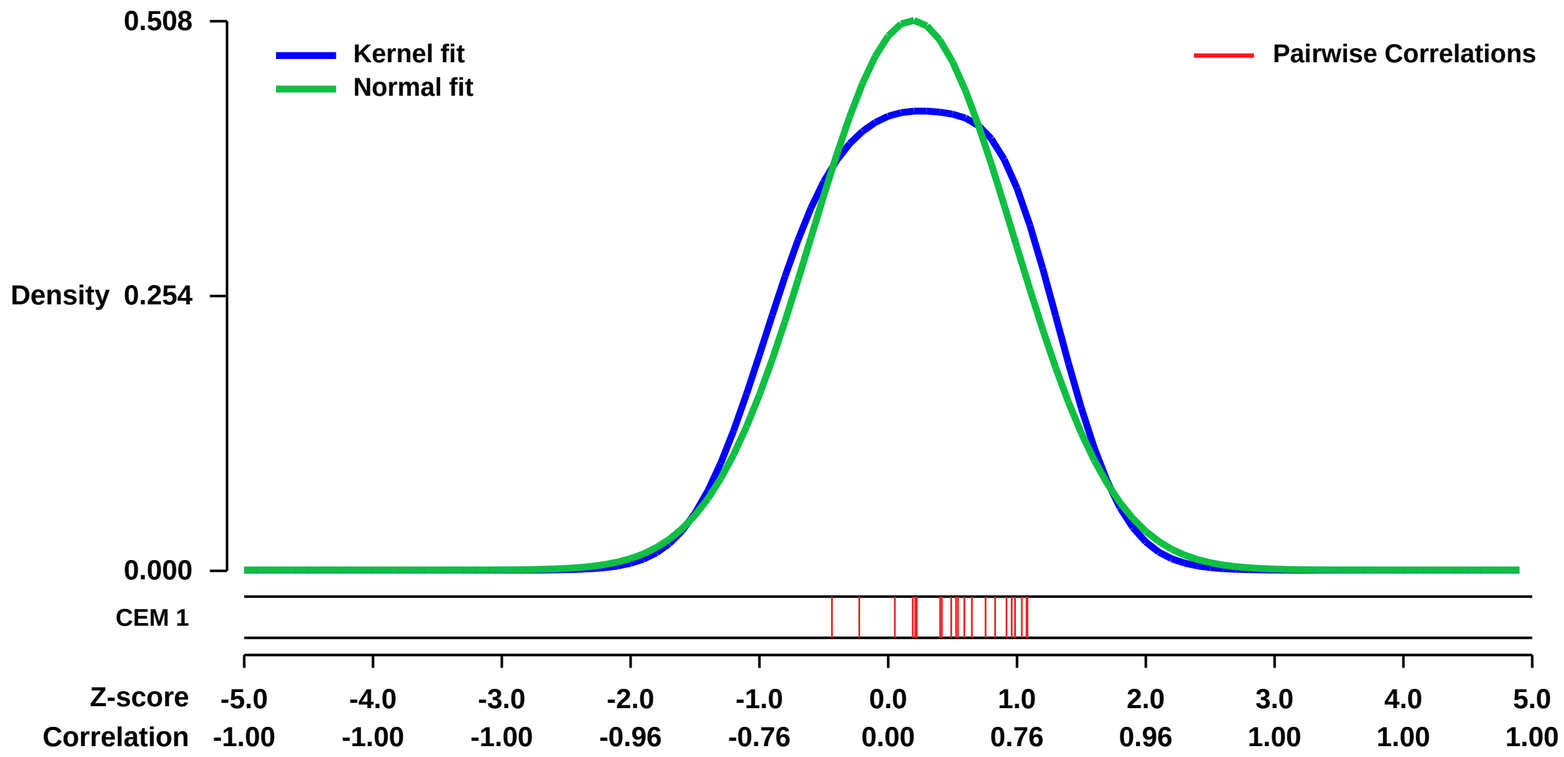

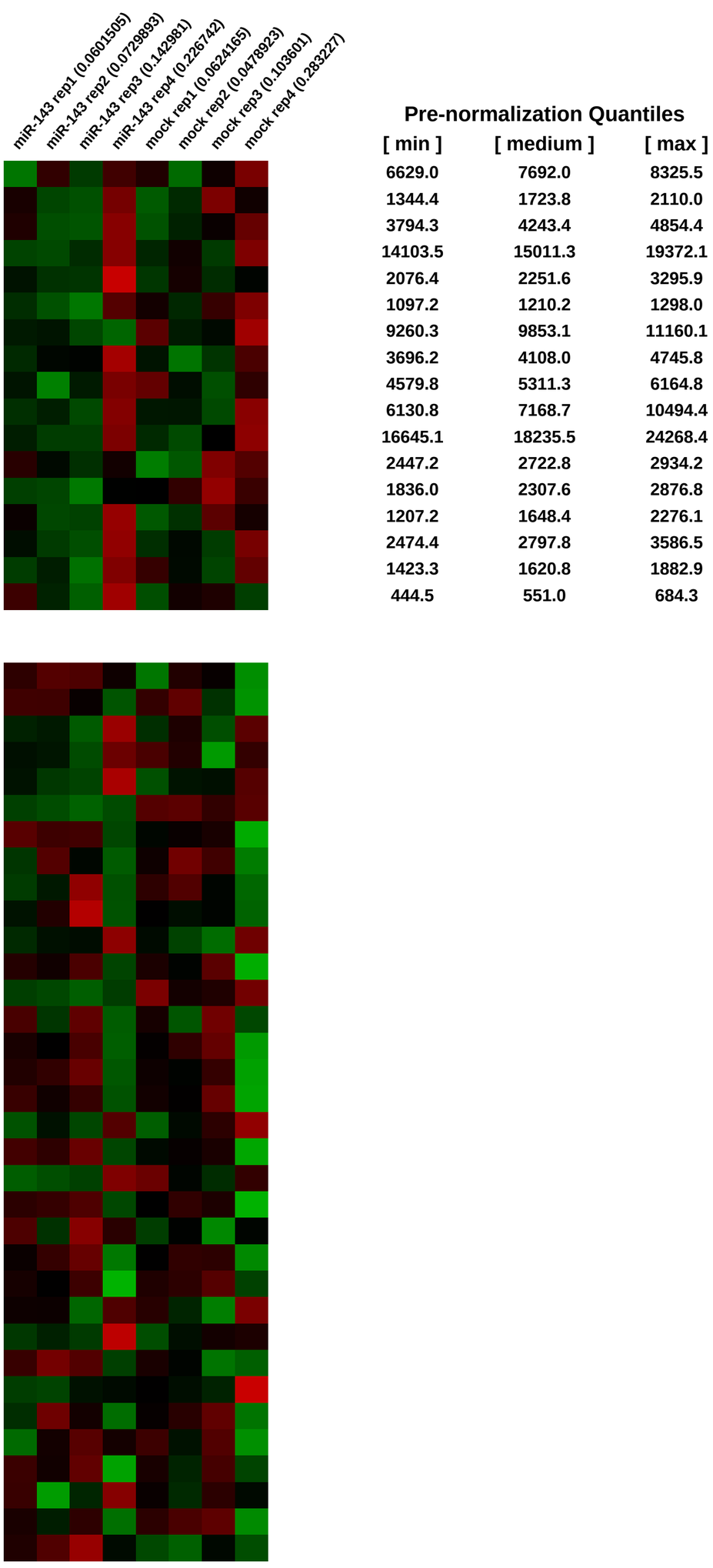

GEO Series "GSE45022" Expression Profiles

Num of samples in this series: 8

Scale of expression profile Z-scores

-3.0 -2.0 -1.0 0.0 1.0 2.0 3.0

GEO Link:	http://www.ncbi.nlm.nih.gov/geo/query/acc.cgi?acc=GSE45022
Status:	Public on Apr 18 2013
Title:	Expression data from Control and HIRA knockdown cells
Organism:	Homo sapiens
Experiment type:	Expression profiling by array
Platform:	GPL570
Pubmed ID:	23602572
Summary & Design:	**Summary:** The HIRA chaperone complex, comprised of HIRA, UBN1 and CABIN1, collaborates with histone-binding protein ASF1a to incorporate histone variant H3.3 into chromatin in a DNA replication-independent manner. To better understand its function and mechanism, we integrated HIRA, UBN1, ASF1a and histone H3.3 ChIP-seq and gene expression analyses. Most HIRA-binding sites co-localize with UBN1, ASF1a and H3.3 at active promoters and active and weak/poised enhancers. At promoters, binding of HIRA/UBN1/ASF1a correlates with the level of gene expression. HIRA is required for deposition of histone H3.3 at its binding sites. There are marked differences in nucleosome and co-regulator composition at different classes of HIRA-bound regulatory site. Underscoring this, we report novel physical interactions between the HIRA complex and transcription factors, a chromatin insulator and an ATP-dependent chromatin-remodelling complex. Our results map the distribution of the HIRA chaperone across the chromatin landscape and point to different interacting partners at functionally distinct regulatory sites. We used microarrays to detail the global programme of gene expression after knockdown of HIRA **Overall design:** HeLa cells were nucleofacted with Dharmacon control siRNA and siRNA to HIRA and RNA was isolated 72 hours after transfection in four biological replicates

Background corr dist: KL-Divergence = 0.0880, L1-Distance = 0.0231, L2-Distance = 0.0007, Normal std = 0.4582

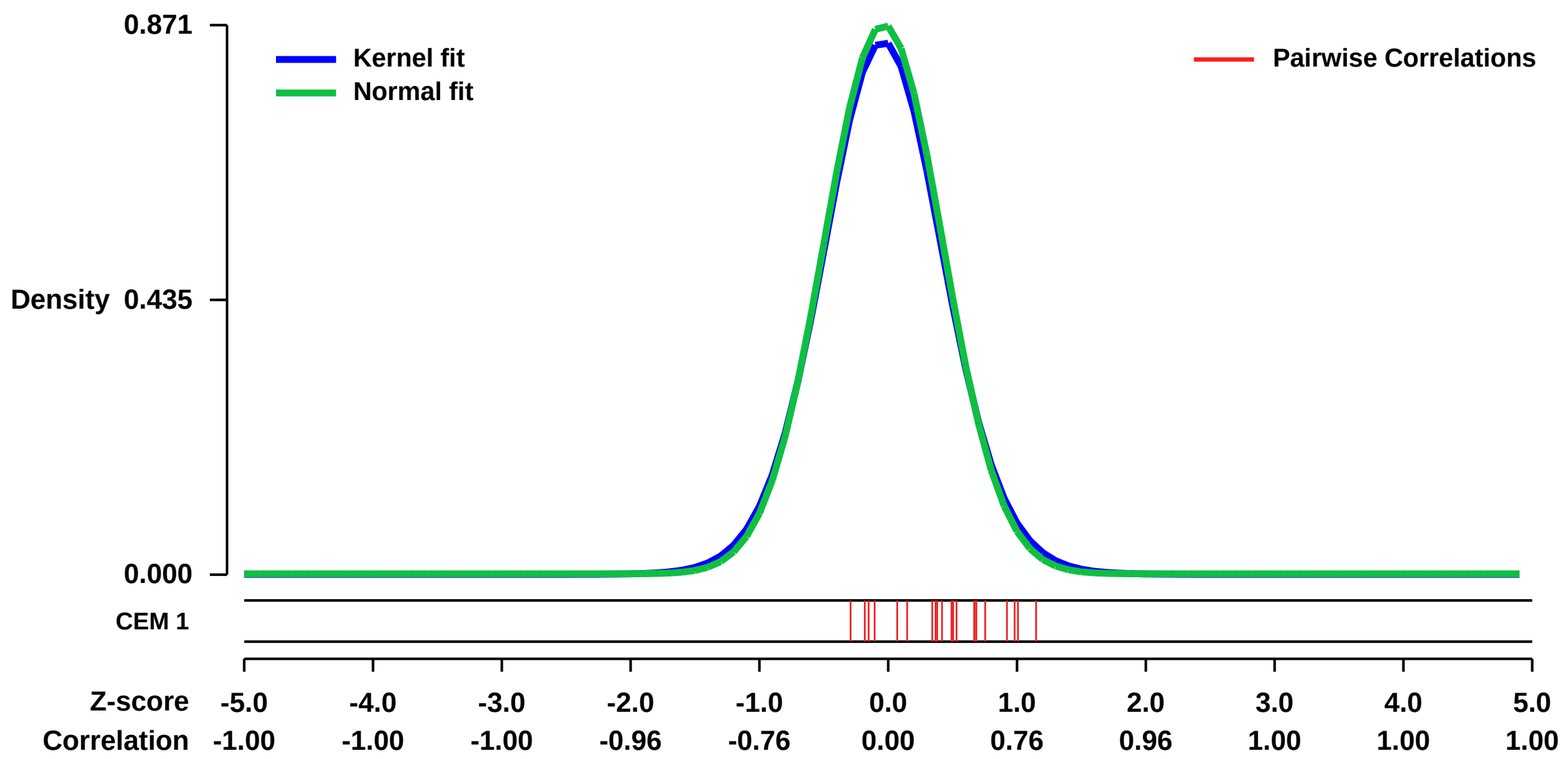

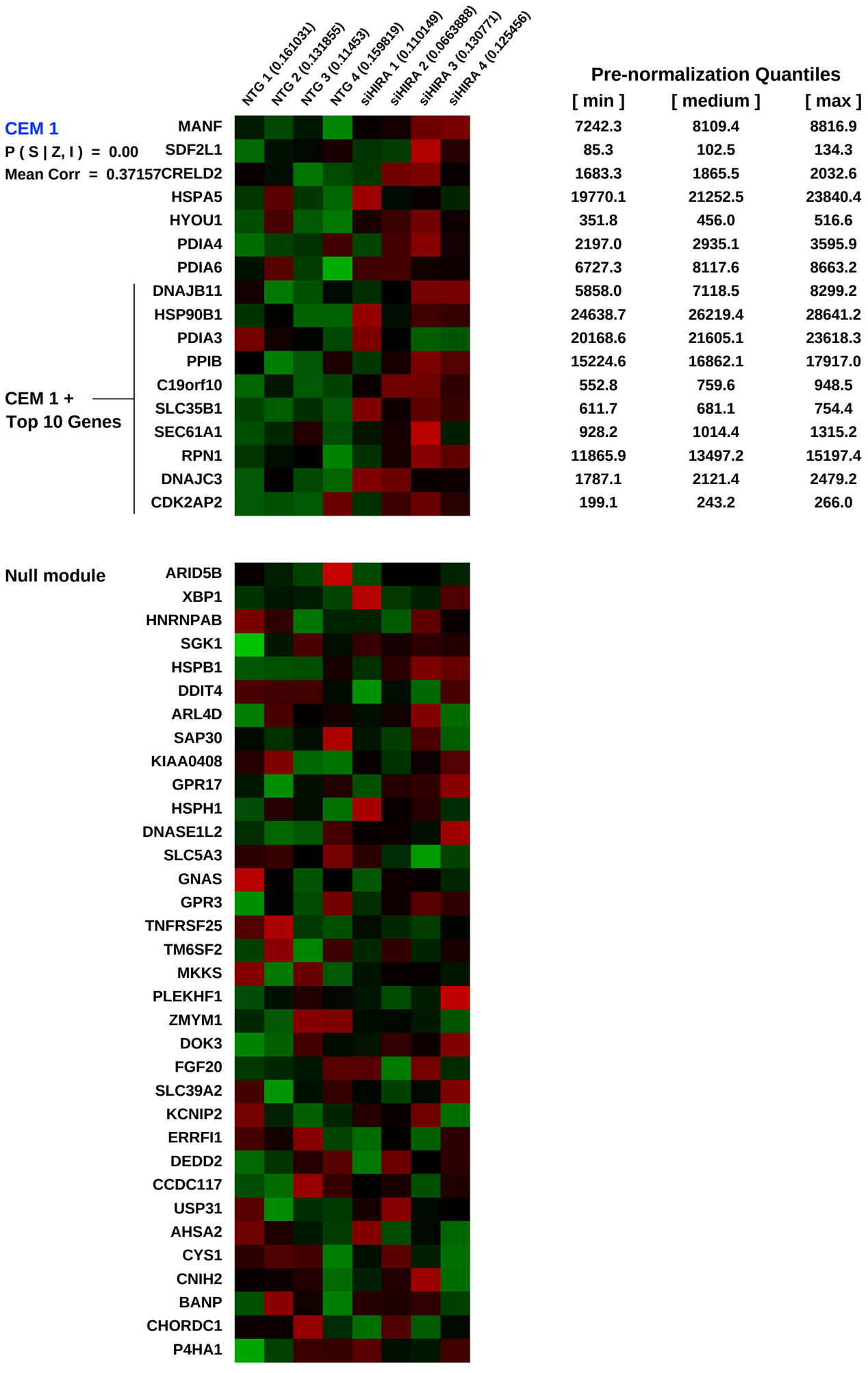

Pre-normalization Quantiles

	[min]	[medium]	[max]
MANF	7242.3	8109.4	8816.9
SDF2L1	85.3	102.5	134.3
CRELD2	1683.3	1865.5	2032.6
HSPA5	19770.1	21252.5	23840.4
HYOU1	351.8	456.0	516.6
PDIA4	2197.0	2935.1	3595.9
PDIA6	6727.3	8117.6	8663.2
DNAJB11	5858.0	7118.5	8299.2
HSP90B1	24638.7	26219.4	28641.2
PDIA3	20168.6	21605.1	23618.3
PPIB	15224.6	16862.1	17917.0
C19orf10	552.8	759.6	948.5
SLC35B1	611.7	681.1	754.4
SEC61A1	928.2	1014.4	1315.2
RPN1	11865.9	13497.2	15197.4
DNAJC3	1787.1	2121.4	2479.2
CDK2AP2	199.1	243.2	266.0

GEO Series "GSE18625" Expression Profiles

Num of samples in this series: 7

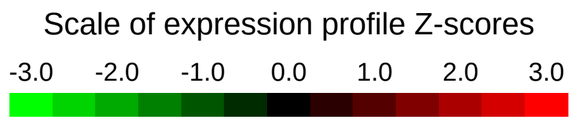

GEO Link:	**http://www.ncbi.nlm.nih.gov/geo/query/acc.cgi?acc=GSE18625**
Status:	**Public on Oct 01 2010**
Title:	**Identification of miR-145 targets involved in colon cancer**
Organism:	**Homo sapiens**
Experiment type:	**Expression profiling by array**
Platform:	**GPL570**
Pubmed ID:	
Summary & Design:	**Summary:** **MicroRNAs (miRNAs) have emerged as important gene regulators and are recognized as key players in tumorigenesis. miR-145 is reported to be down-regulated in several cancers, but knowledge of its targets in colon cancer remains limited. To investigate the role of miR-145 in colon cancer, we have employed a microarray based approach to identify miR-145 targets. Based on seed site enrichment analyses and unbiased word analyses, we found a significant enrichment of miRNA binding sites in the 3â -untranslated regions (UTRs) of transcripts down-regulated upon miRNA overexpression, which represent potential miR-145 targets. Gene Ontology analysis showed an overrepresentation of genes involved in cell death, gene expression, cancer, cell cycle, DNA replication, recombination and repair. A number of the identified miRNA targets have previously been implicated in cancer, including YES, FSCN1, ADAM17, BIRC2, VANGL1 as well as the transcription factor STAT1. Both YES and STAT1 were verified as direct miR-145 targets based on 3â UTR luciferase assays and western blots for endogenous proteins.** **Overall design:** **DLD-1 cells were transfected with 50 nM miR-145 duplex or mock transfected. Total RNA was harvested 24 hours post-transfection and analyzed on Affymetrix HG-U133 Plus 2.0 human arrays.**

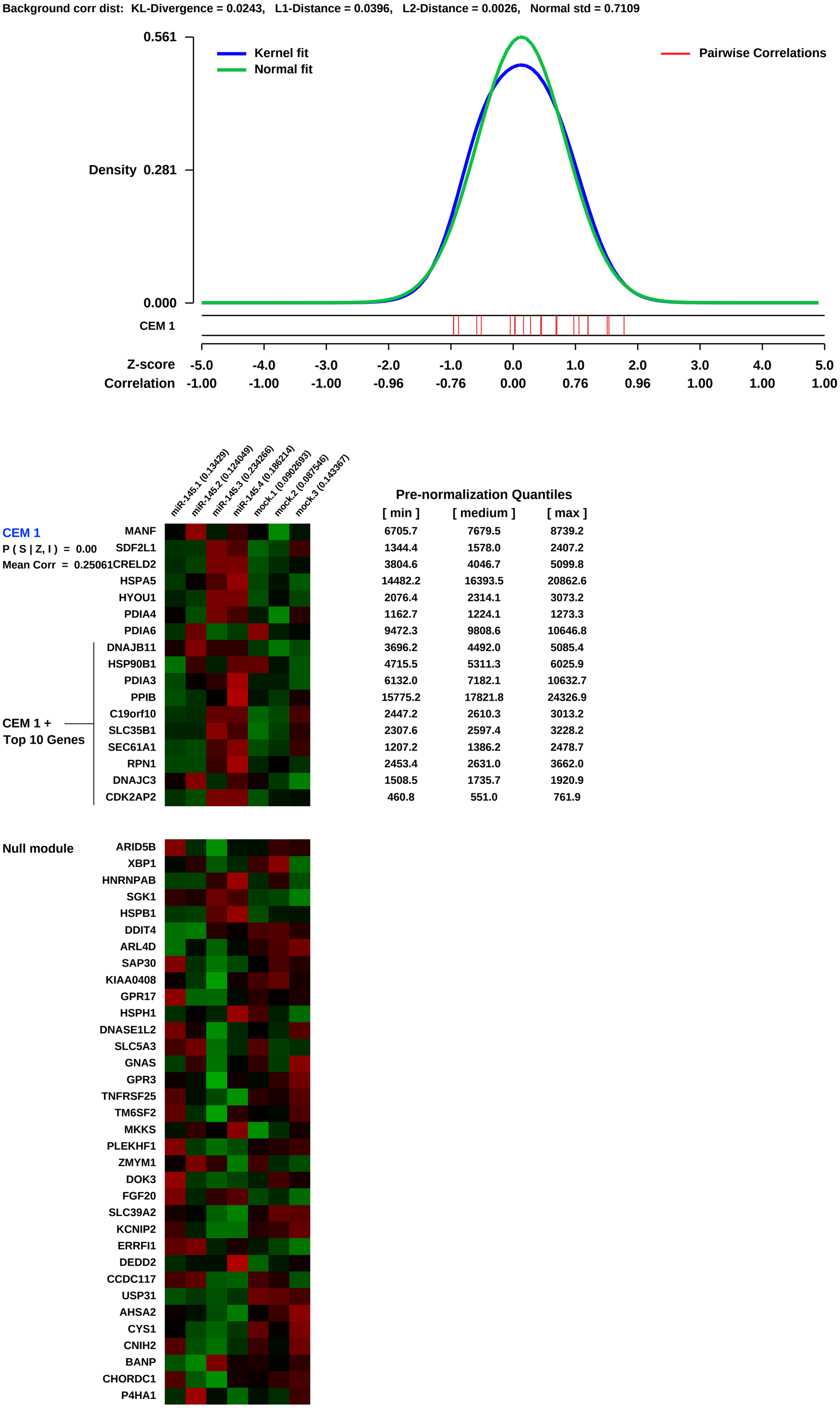

GEO Series "GSE21261" Expression Profiles

Num of samples in this series: 96

Scale of expression profile Z-scores

-3.0 -2.0 -1.0 0.0 1.0 2.0 3.0

GEO Link: http://www.ncbi.nlm.nih.gov/geo/query/acc.cgi?acc=GSE21261
Status: Public on Jan 01 2011
Title: Multilineage Dysplasia (MLD) in AML correlates with MDS-related cytogenetic abnormalities and a prior history of MDS or MDS/MPN but has no independent prognostic relevance
Organism: Homo sapiens
Experiment type: Expression profiling by array
Platform: GPL570
Pubmed ID: 20581309

Summary & Design:

Summary:
Full Title: Multilineage Dysplasia (MLD) in AML correlates with MDS-related cytogenetic abnormalities and a prior history of MDS or MDS/MPN but has no independent prognostic relevance: A comparison of 408 cases classified as â AML not otherwise specifiedâ or â AML with myelodysplasia-related changesâ

The WHO classification of acute myeloid leukemia (AML) is hierarchically structured and integrates genetic information, data on patientsâ history, and multilineage dysplasia (MLD). The category â AML with MDS-related changesâ (AML-MRC) is separated from AML not otherwise specified (AML-NOS) by the presence of either MLD, MDS-related cytogenetics or MDS history. To clarify whether MLD alone is clinically relevant, we analyzed 408 adult patients categorized as AML-MRC or AML-NOS. EFS (Median 13.8 months vs. 16.0 months) and 3-year-OS (45.8% vs. 53.9%) did not differ significantly between patients with MLD and without. However, MLD correlated with pre-existing MDS (p<0.001) and MDS-related cytogenetics (p=0.035). Patients with MLD as sole AML-MRC criterion (AML-MLD-sole; n=90) had less frequently FLT3-ITD (p=0.032), and a lower median age than AML-NOS (n=232), but EFS, OS, and WBC did not differ significantly. Contrarily, patients with AML-NOS plus AML-MLD-sole (n=323) versus patients with MDS history or MDS-related cytogenetics (n=85) had better EFS (16.9 vs. 10.7 months; p=0.005) and 3-year-OS (55.8% vs. 32.5%; p=0.001). Gene expression profiles were measured for a subset of 96 patients. Analysis of the expression data showed distinct clusters for AML-MLD-sole and AML-NOS versus AML with MDS-related cytogenetics or MDS history. Thus, MLD demonstrated no independent clinical impact, while cytogenetics and MDS history were of prognostic relevance. This data suggest modifications in a revised WHO proposal.

Overall design:
All 96 bone marrow samples were obtained from untreated patients at the time of diagnosis. Cells used for microarray analysis were collected from the purified fraction of mononuclear cells after Ficoll density centrifugation.

Background corr dist: KL-Divergence = 0.2603, L1-Distance = 0.0888, L2-Distance = 0.0249, Normal std = 0.3037

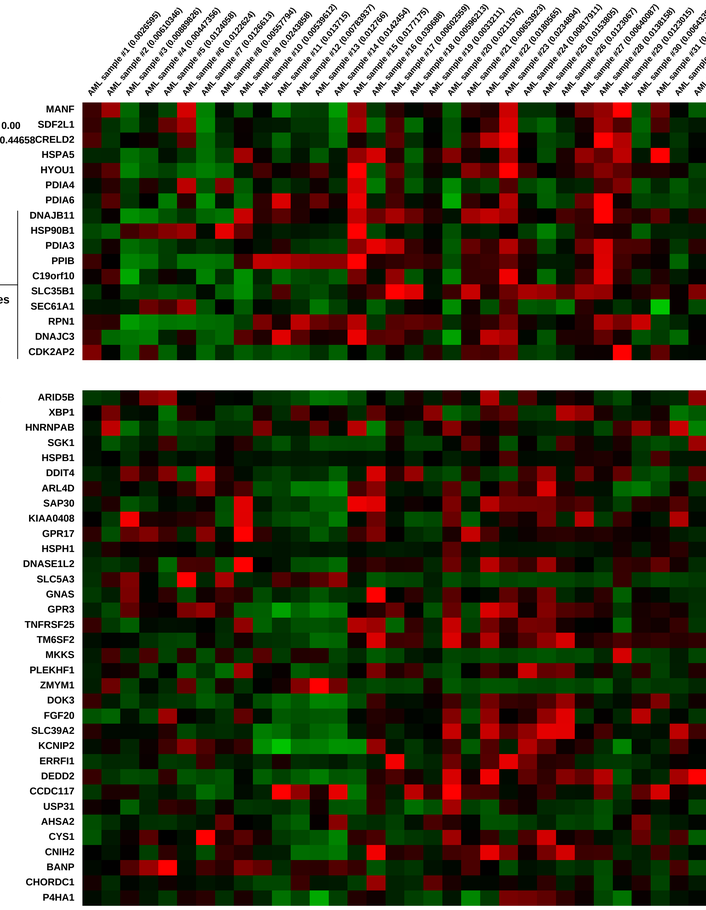

Pre-normalization Quantiles

	[min]	[medium]	[max]
MANF	875.9	2596.5	5878.0
SDF2L1	273.6	913.4	2285.5
CRELD2	1027.7	2295.4	7445.3
HSPA5	9405.4	24155.2	59213.4
HYOU1	321.4	1260.5	3595.3
PDIA4	230.4	771.3	2435.8
PDIA6	2230.4	5793.0	13355.4
DNAJB11	1258.0	2612.4	5518.6
HSP90B1	1817.4	4538.3	12916.0
PDIA3	6701.0	14683.6	25670.3
PPIB	932.9	8658.6	23287.5
C19orf10	1085.4	2624.2	4842.6
SLC35B1	952.3	2076.8	4852.2
SEC61A1	1678.9	3427.0	5345.1
RPN1	834.9	3605.9	6944.7
DNAJC3	873.7	3461.2	7601.6
CDK2AP2	277.5	1124.5	4010.7

GEO Series "GSE15615" Expression Profiles

Num of samples in this series: 6

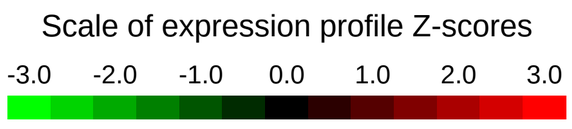

GEO Link:	http://www.ncbi.nlm.nih.gov/geo/query/acc.cgi?acc=GSE15615
Status:	Public on Apr 15 2009
Title:	Differential effects of TNFalpha and IL1beta on FLS global gene expression profile
Organism:	Homo sapiens
Experiment type:	Expression profiling by array
Platform:	GPL570
Pubmed ID:	19389237
Summary & Design:	**Summary:** TNFalpha and IL1beta play a pathogenic role in rheumatoid arthritis. Both cytokines are known to activate cytokine and metalloproteinase secretion by synovial fibroblasts. In the present study, we wanted to investigate whether TNFalpha and IL1beta displayed differential effects on cultured Fibroblast-like Synovial Cells derived from RA patients. Global gene expression analyses indicated that both cytokines induced similar genes in these cells. **Overall design:** Cells were seeded in 24-well plated at 25.000/well and incubated overnight with or without the following cytokines : TNF-¸– (R&D Systems, Minneapolis, MN) 10 ng/ml, IL-1¸† (R&D Systems) 10 ng/ml. After overnight incubation with the indicated cytokines, cells were harvested and total RNA was extracted using the Nucleospin´fi RNA II extraction kit (Macherey-Nagel, Dˆ…ren, Germany), in order to be labeled according to a standard Affymetrix procedure and hybridized on HGU133 Plus 2.0 Human Genome slides.

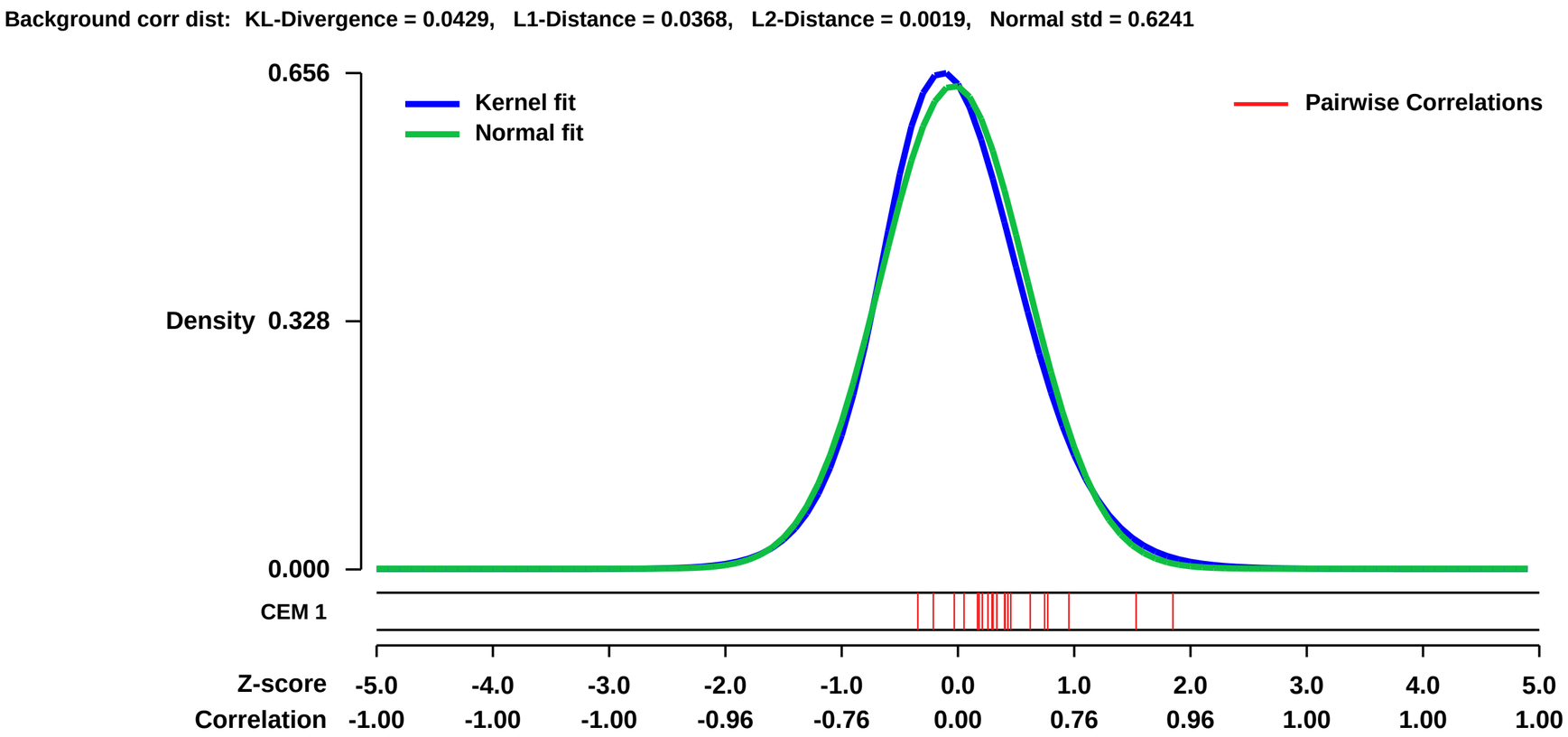

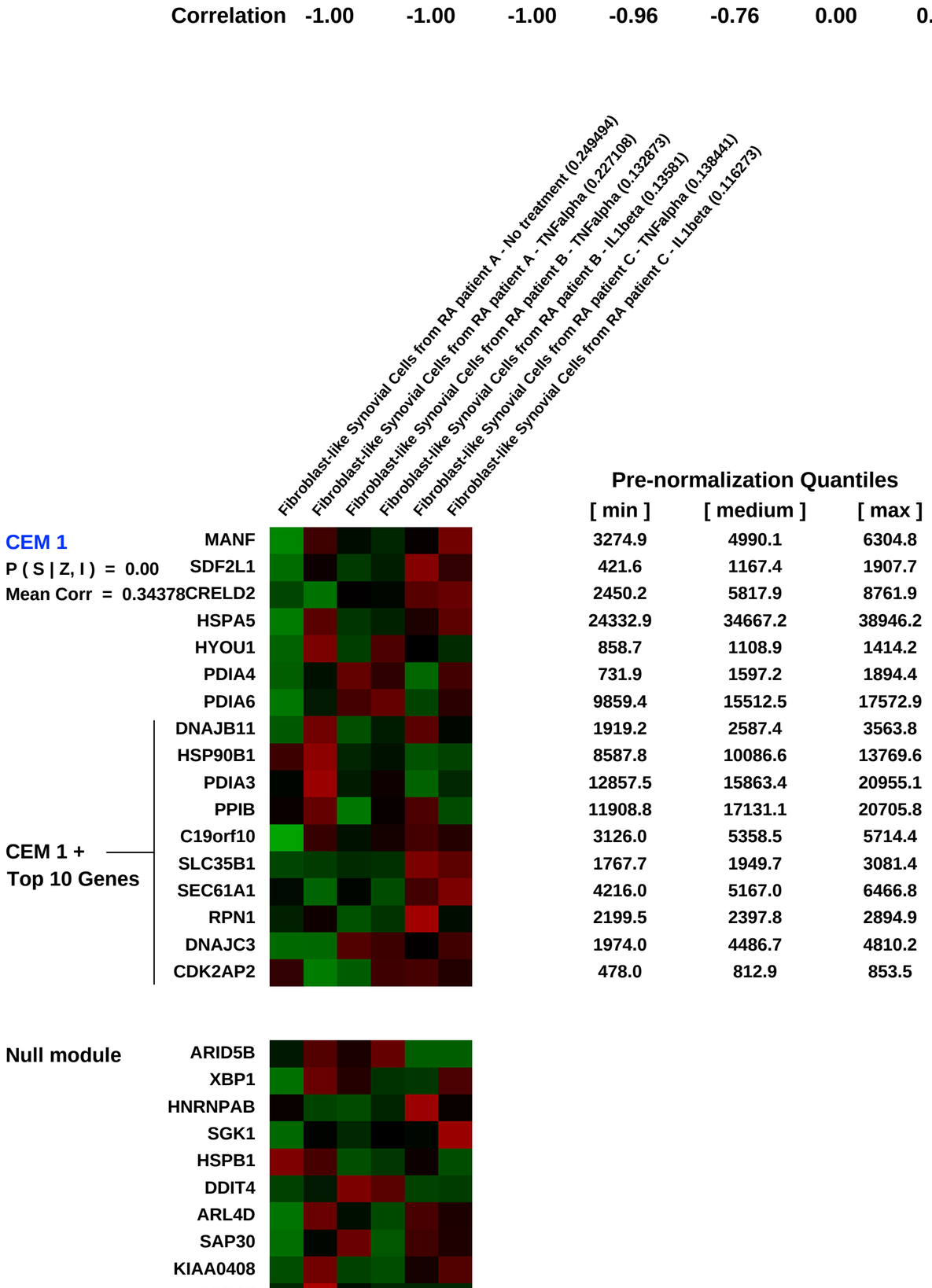

GEO Series "GSE12198" Expression Profiles

Num of samples in this series: 16

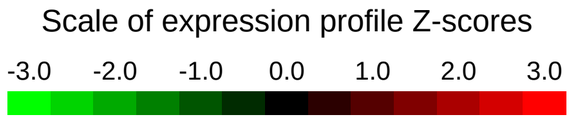

GEO Link:	http://www.ncbi.nlm.nih.gov/geo/query/acc.cgi?acc=GSE12198
Status:	Public on Mar 06 2010
Title:	Primary NKcells vs. NKAES-derived NK cells vs. NKcells stimulated by low/high dose IL2 after 7days of culture
Organism:	Homo sapiens
Experiment type:	Expression profiling by array
Platform:	GPL570
Pubmed ID:	19383914
Summary & Design:	**Summary:** Transcriptional profiling of NKAES-derived NK cells after 7 days of culture compared to primary human NK cells and NK cells stimulated by low or high dose IL2 after 7 days of culture. **Overall design:** Four-condition experiment, primary NK cells vs. NKAES-derived NK cells after 7 days of culture vs. NK cells stimulated by low/high dose IL2 after 7 days of culture. Biological replicates: 5 control, 5 NKAES-derived NK cells, 3 NK cells stimulated by low dose IL2, 3 NK cells stimulated by high dose IL2 independently grown and harvested. One replicate per array.

Background corr dist: KL-Divergence = 0.1598, L1-Distance = 0.0328, L2-Distance = 0.0022, Normal std = 0.3727

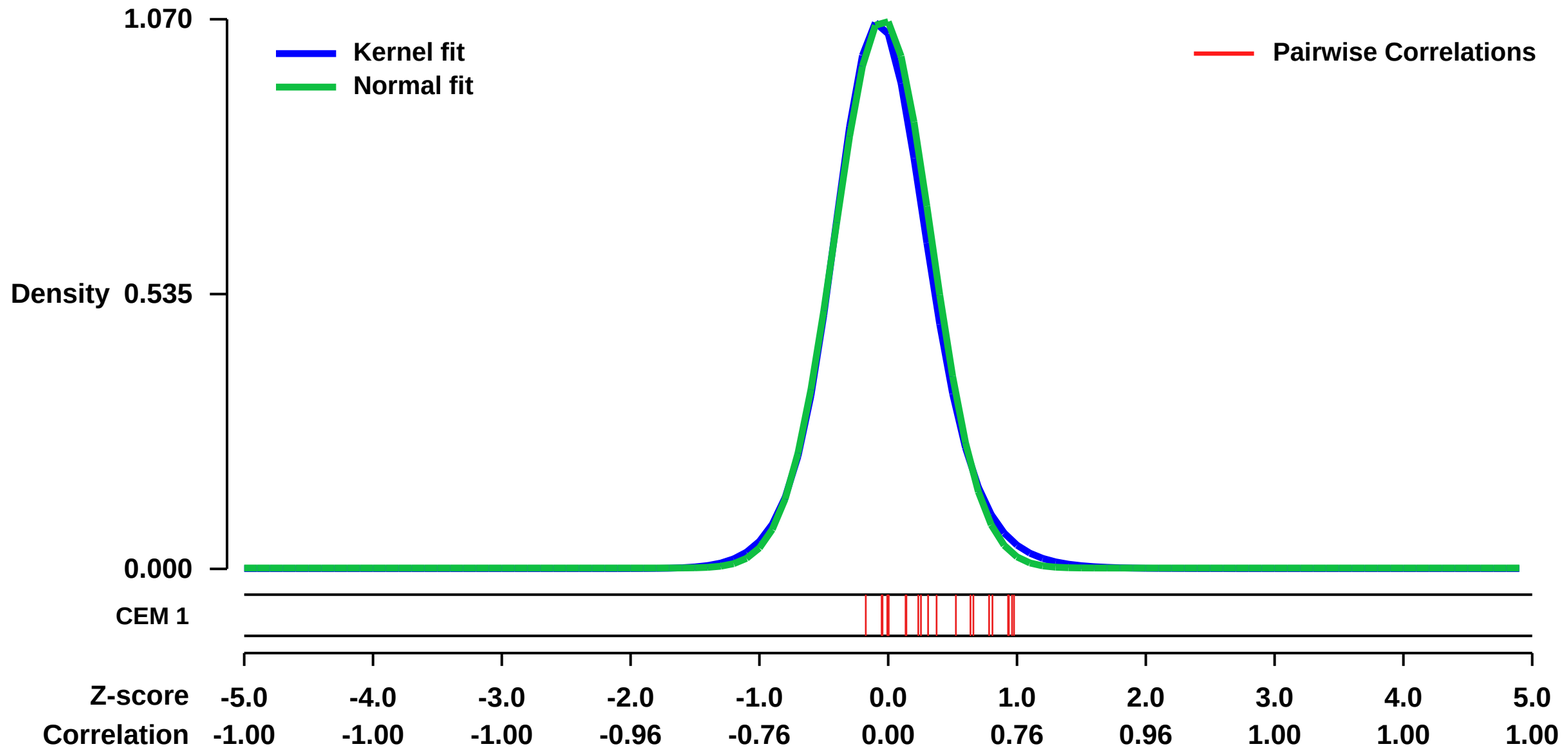

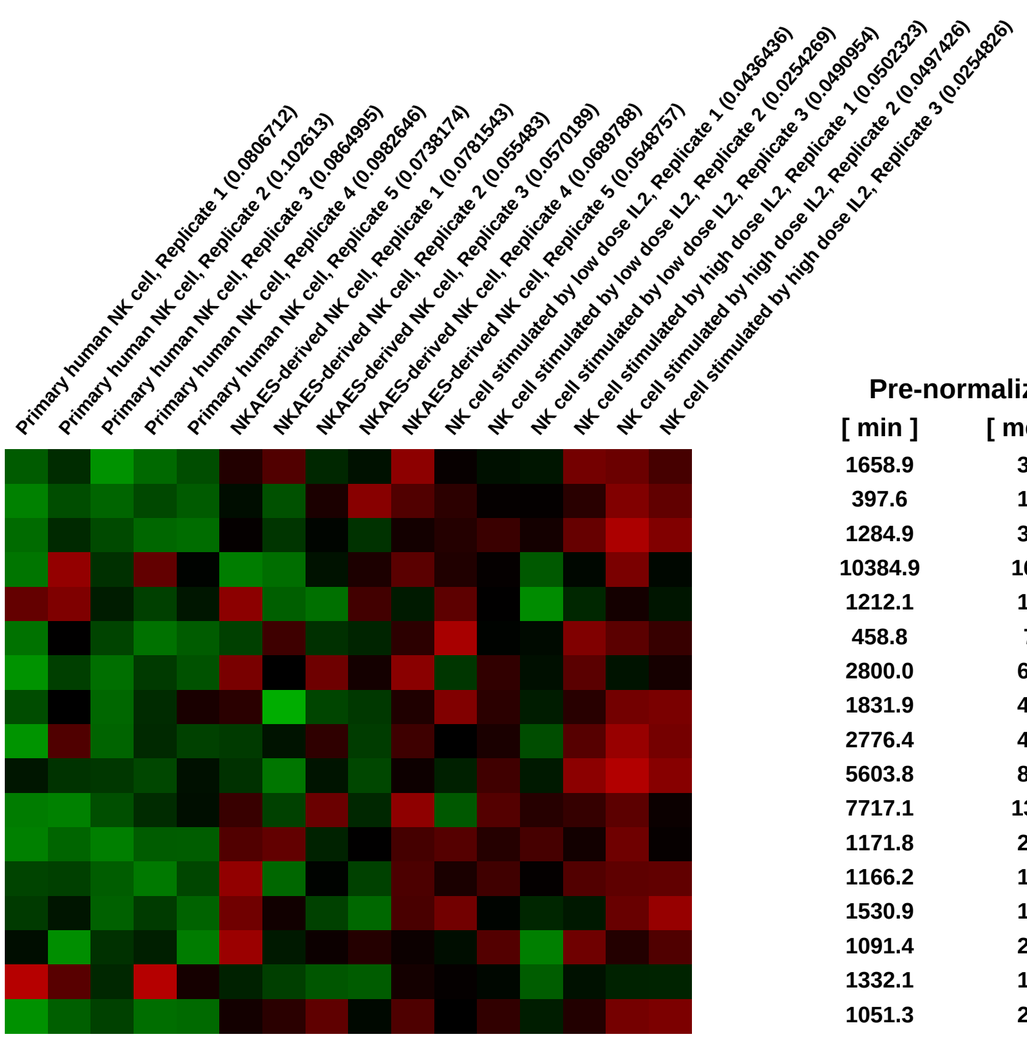

GEO Series "GSE38408" Expression Profiles

Num of samples in this series: 12

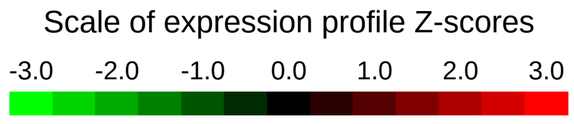

GEO Link:	http://www.ncbi.nlm.nih.gov/geo/query/acc.cgi?acc=GSE38408
Status:	Public on Jan 28 2013
Title:	Transcriptional profiles of TIMP-2 and Ala+TIMP-2 A549 overexpressing cells and in tumor xenografts.
Organism:	Homo sapiens
Experiment type:	Expression profiling by array
Platform:	GPL570
Pubmed ID:	23371049
Summary & Design:	**Summary:** TIMP-2 is an endogenous angiogenesis inhibitor, i.e. inhibits endothelial cell proliferation and tumor angiogenesis. As a result, TIMP-2 inhibits tumor growth and progression to metastasis. Understanding, therefore, the mechanisms of TIMP-2-mediated tumor growth inhibition would provide further support on the use of TIMP-2 as a novel biological agent for cancer therapy. We used microarray analysis to determine the TIMP-2 and Ala+TIMP-2 transcriptional profiles of A549 cancer cells in order to understand how TIMP-2 inhibits tumor growth and angiogenesis. **Overall design:** We overexpressed TIMP-2 and its mutant (does not inhibit MMP) in A549 human lung cancer cells and determined TIMP-2 and Ala+TIMP-2 transcriptional profiles, groups of genes and associated biological functions. We then injected the cells in NOD-SCID mice and RNA from tumors were isolated for further analysis to identify genes that are associated with tumor growth inhibition.

Background corr dist: KL-Divergence = 0.0944, L1-Distance = 0.0230, L2-Distance = 0.0008, Normal std = 0.4512

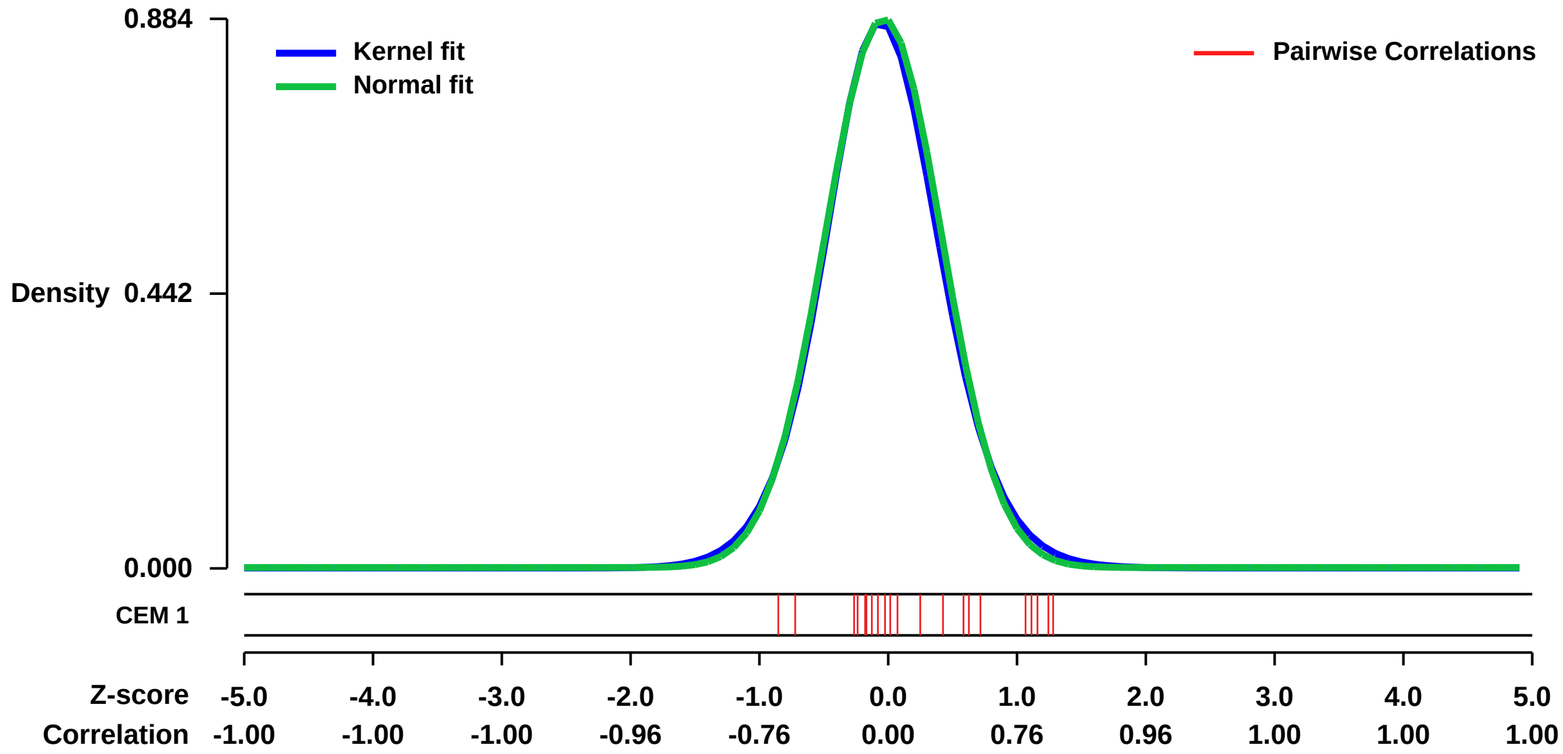

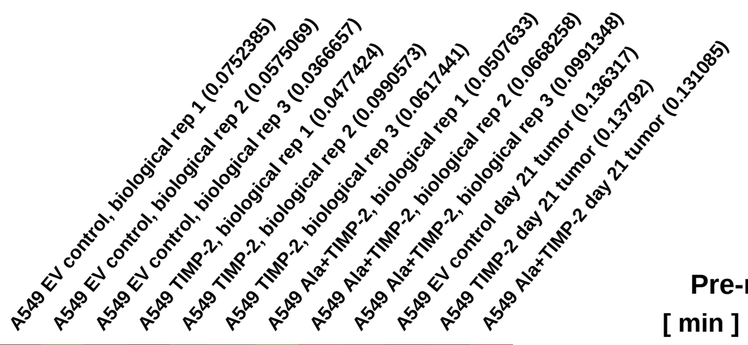

Pre-normalization Quantiles

	[min]	[medium]	[max]
CEM 1			
P (S | Z, I) = 0.00			
Mean Corr = 0.19843			
MANF	3234.0	4249.2	5082.9
SDF2L1	451.3	1068.0	2248.5
CRELD2	1349.9	2470.3	3612.7
HSPA5	17266.7	23855.8	30674.9
HYOU1	1274.7	1846.5	2139.0
PDIA4	1199.9	2201.6	2730.0
PDIA6	7525.7	11858.7	13867.0
CEM 1 + Top 10 Genes			
DNAJB11	2295.0	3161.7	4260.7
HSP90B1	4138.2	7311.9	8983.2
PDIA3	6616.0	7490.0	12498.5
PPIB	12580.5	19492.0	25818.4
C19orf10	1733.2	2248.9	3079.2
SLC35B1	2607.9	3516.7	3668.2
SEC61A1	2088.9	2488.9	3187.5
RPN1	1955.1	2441.1	4822.9
DNAJC3	1469.8	1893.1	3368.1
CDK2AP2	1025.7	1216.7	3555.4
Null module			
ARID5B			
XBP1			
HNRNPAB			
SGK1			
HSPB1			
DDIT4			
ARL4D			
SAP30			
KIAA0408			
GPR17			
HSPH1			
DNASE1L2			
SLC5A3			
GNAS			
GPR3			
TNFRSF25			
TM6SF2			
MKKS			
PLEKHF1			
ZMYM1			
DOK3			
FGF20			
SLC39A2			
KCNIP2			
ERRFI1			
DEDD2			
CCDC117			
USP31			
AHSA2			
CYS1			
CNIH2			
BANP			
CHORDC1			
P4HA1			

GEO Series "GSE43115" Expression Profiles

Num of samples in this series: 7

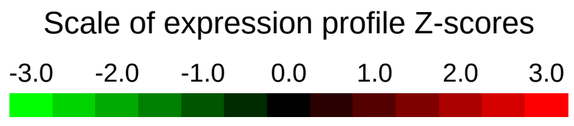

GEO Link:	http://www.ncbi.nlm.nih.gov/geo/query/acc.cgi?acc=GSE43115
Status:	Public on Feb 01 2013
Title:	Intrinsic glioma subtypes in EORTC 26951 (part 4)
Organism:	Homo sapiens
Experiment type:	Expression profiling by array
Platform:	GPL570
Pubmed ID:	24553142
Summary & Design:	**Summary:** **Background: Intrinsic glioma subtypes (IGS) are molecularly similar tumors that can be identified based on unsupervised gene-expression analysis. Here, we have evaluated the clinical relevance of these subtypes within EORTC26951, a randomized phase III clinical trial investigating adjuvant procarbazine, CCNU (lomustine) and vincristine (PCV) chemotherapy in anaplastic oligodendroglial tumors. Our study is the first to include gene-expression profiles of formalin-fixed and paraffin-embedded (FFPE) clinical trial samples. Methods: Gene-expression profiling was performed in 140 samples: 47 fresh frozen and 93 FFPE, on HU133_Plus_2.0 and HuEx_1.0_st arrays (Affymetrix), respectively. Results: All previously identified six intrinsic glioma subtypes are present in EORTC26951. This confirms that different molecular subtypes are present within a well-defined histological subtype. Intrinsic subtypes are highly prognostic for overall- (OS) and progression-free survival (PFS). They are prognostic for PFS independent of clinical (age, performance, tumor location), molecular (1p19qLOH, IDH1 mutation, MGMT methylation) and histological parameters. Combining known molecular (1p19LOH, IDH1) prognostic parameters with intrinsic subtypes improves outcome prediction (Proportion of Explained Variation 30% v 23%). Specific genetic changes (IDH1, 1p19qLOH and EGFR amplification) segregate into different subtypes. We identified one subtype, IGS-9 (characterized by a high percentage of 1p19qLOH and IDH1 mutations), that especially benefits from PCV chemotherapy. Median OS in this subtype was 5.5 years after radiotherapy (RT) alone v 12.8 years after RT/PCV; P=0.0349; HR 2.18, 95% CI [1.06, 4.50]. Conclusion: Intrinsic subtypes are highly prognostic in EORTC26951 and improve outcome prediction when combined with other prognostic factors. Tumors assigned to IGS-9 benefit from adjuvant PCV** **Overall design:** **A total of 140 samples were included in this study, profiles of 95 were FFPE derived samples run on exon arrays. 12 samples (part 2) can also be found in GSE16011 (PMID 19920198 and 16357140), and 6 from Oncomine (part 3).**

Background corr dist: KL-Divergence = 0.0642, L1-Distance = 0.0679, L2-Distance = 0.0082, Normal std = 0.5683

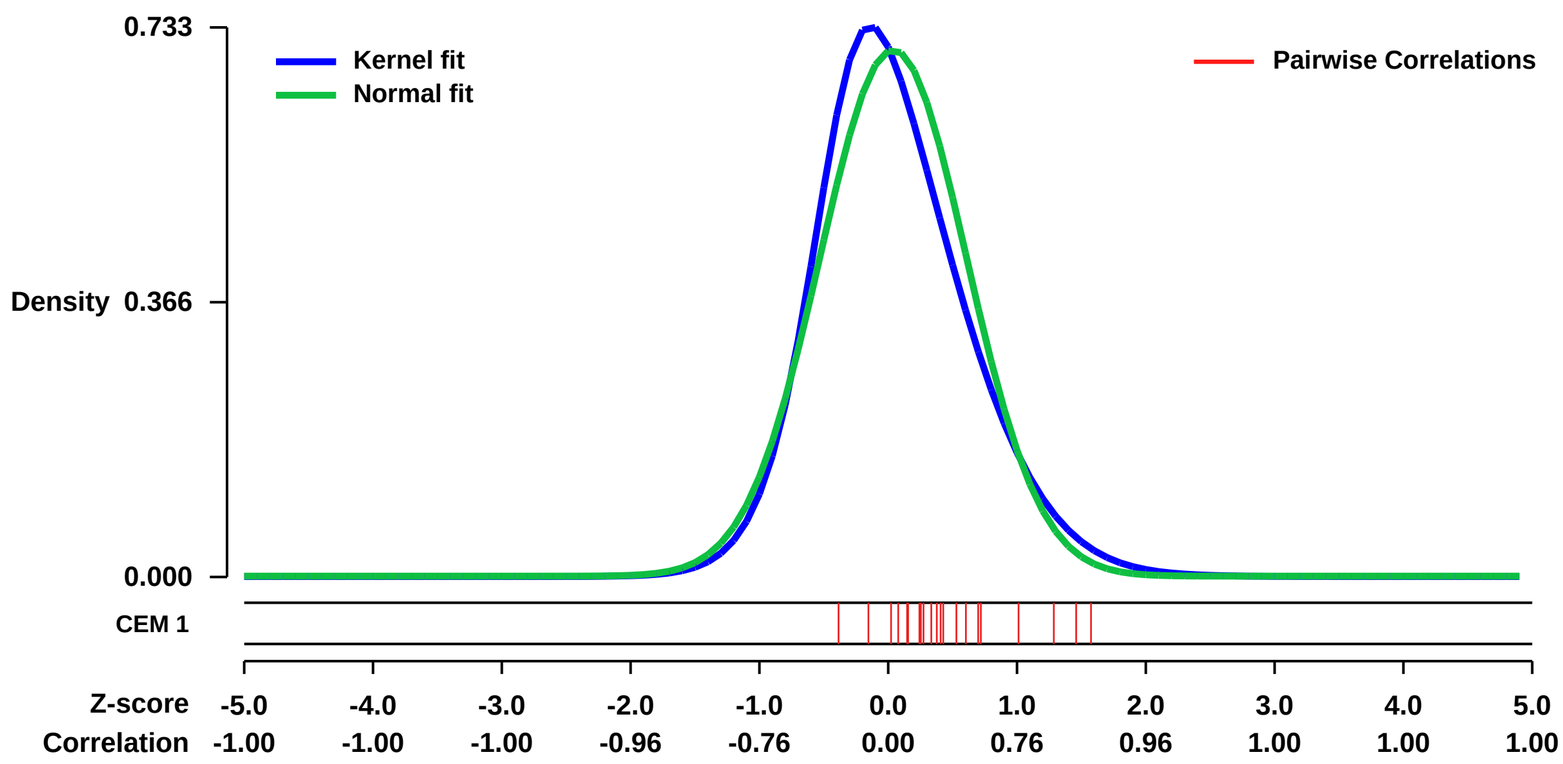

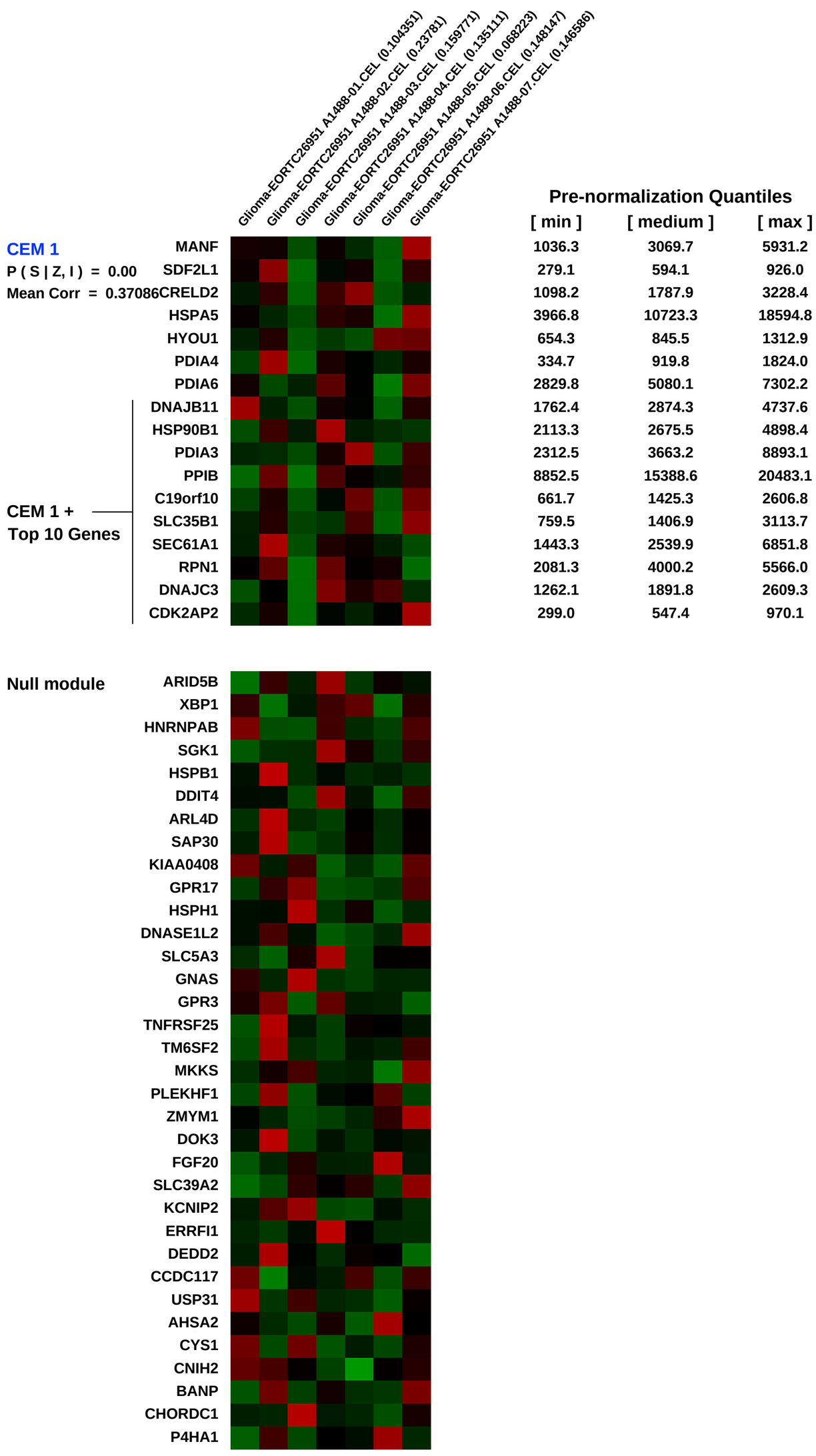

GEO Series "GSE11504" Expression Profiles

Num of samples in this series: 25

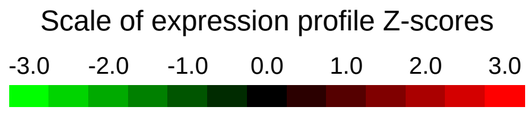

GEO Link:	http://www.ncbi.nlm.nih.gov/geo/query/acc.cgi?acc=GSE11504
Status:	Public on Dec 31 2009
Title:	Age-related expression data from composite bone marrow from healthy humans
Organism:	Homo sapiens
Experiment type:	Expression profiling by array
Platform:	GPL570
Pubmed ID:	20121553
Summary & Design:	**Summary:** Human bone marrow is a complex, diversified and well-organized hematopoietic network changing composition with age. The purpose of this study was to analyze variations in relative precursor B cell abundance in bone marrow with age by means of global gene expression profiling. RNA was isolated from composite bone marrow from 25 healthy children, adolescents and adults age 2 months to 28 years. As reference transcript for precursor B cells we used recombination activating gene RAG1 exploring the data for other transcripts showing the same profile as RAG1 with age. We identified 54 genes with correlated expression profiles to RAG1 (r â¥ 0.9, p = 0), characterized by high expression at 3 - 20 months followed by a fast decline to lower signal levels maintained until early adulthood. Immunophenotyping from a similar healthy age-matched cohort (n = 37) showed a comparable decrease of precursor B cells. Of the 54 genes 15 were characteristically B cell associated representing cell surface molecules (CD19, CD72, CD79A, CD79B, CD180, IGL@, IGLL1, VPREB1, VPREB3), a signal transduction molecule (BLNK) and transcription factors (DNTT, EBF1, PAX5, POU2AF1, RAG2). Of the remaining transcripts some may represent novel B cell transcripts or genes involved in control of B cells. Bone marrow was obtained from healthy children eligible for elective minor surgery and voluntary health care workers. The bone marrow samples (2.5ml) were immediately after aspiration transferred to PAXgene tubes for mRNA stabilization before RNA extraction and hybridization on Affymetrix microarrays. To that end, the study presents a picture of the total marrow activity with minimal manipulation that would otherwise influence gene expression results. **Overall design:** We used microarrays to determine age-related changes in precursor B cell transcripts in bone marrow from 25 healthy children and adults and searched for other transcripts showing the same expression profile with age.

Background corr dist: KL-Divergence = 0.1409, L1-Distance = 0.0657, L2-Distance = 0.0109, Normal std = 0.3911

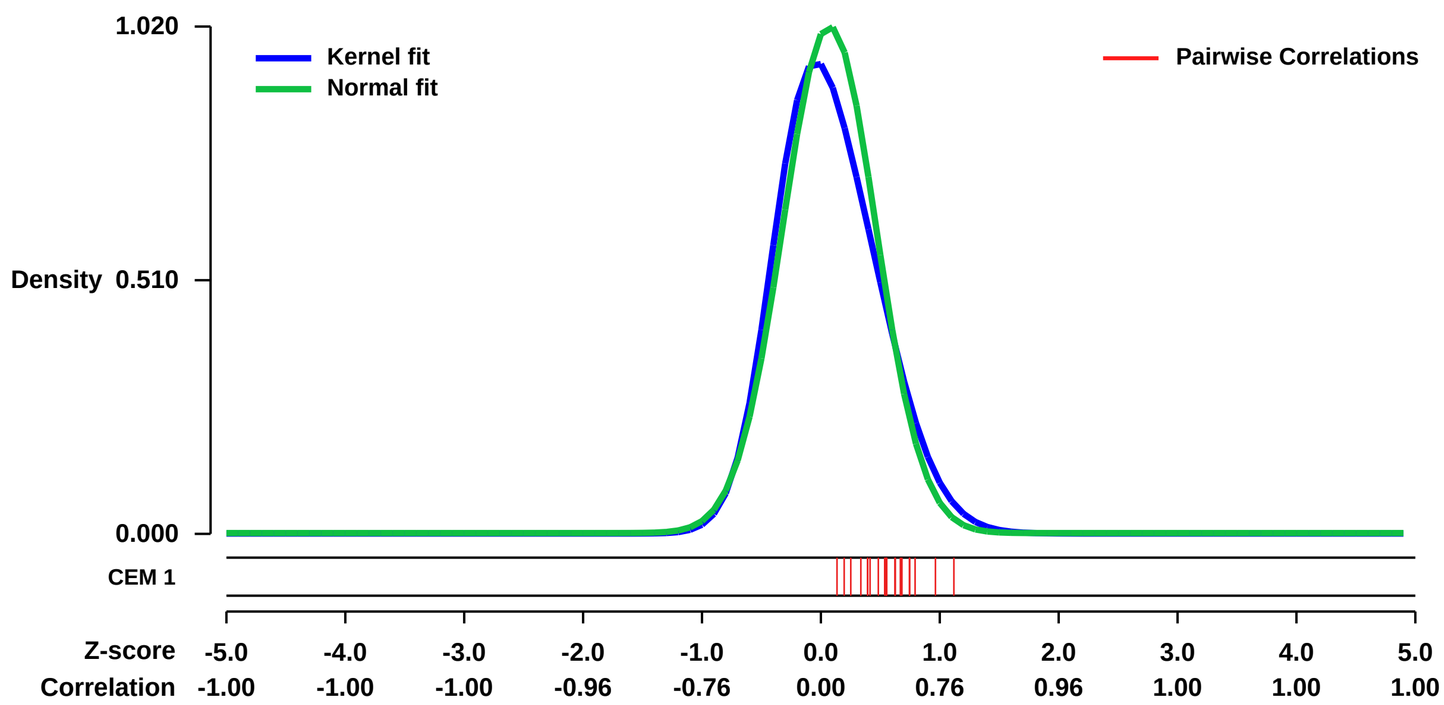

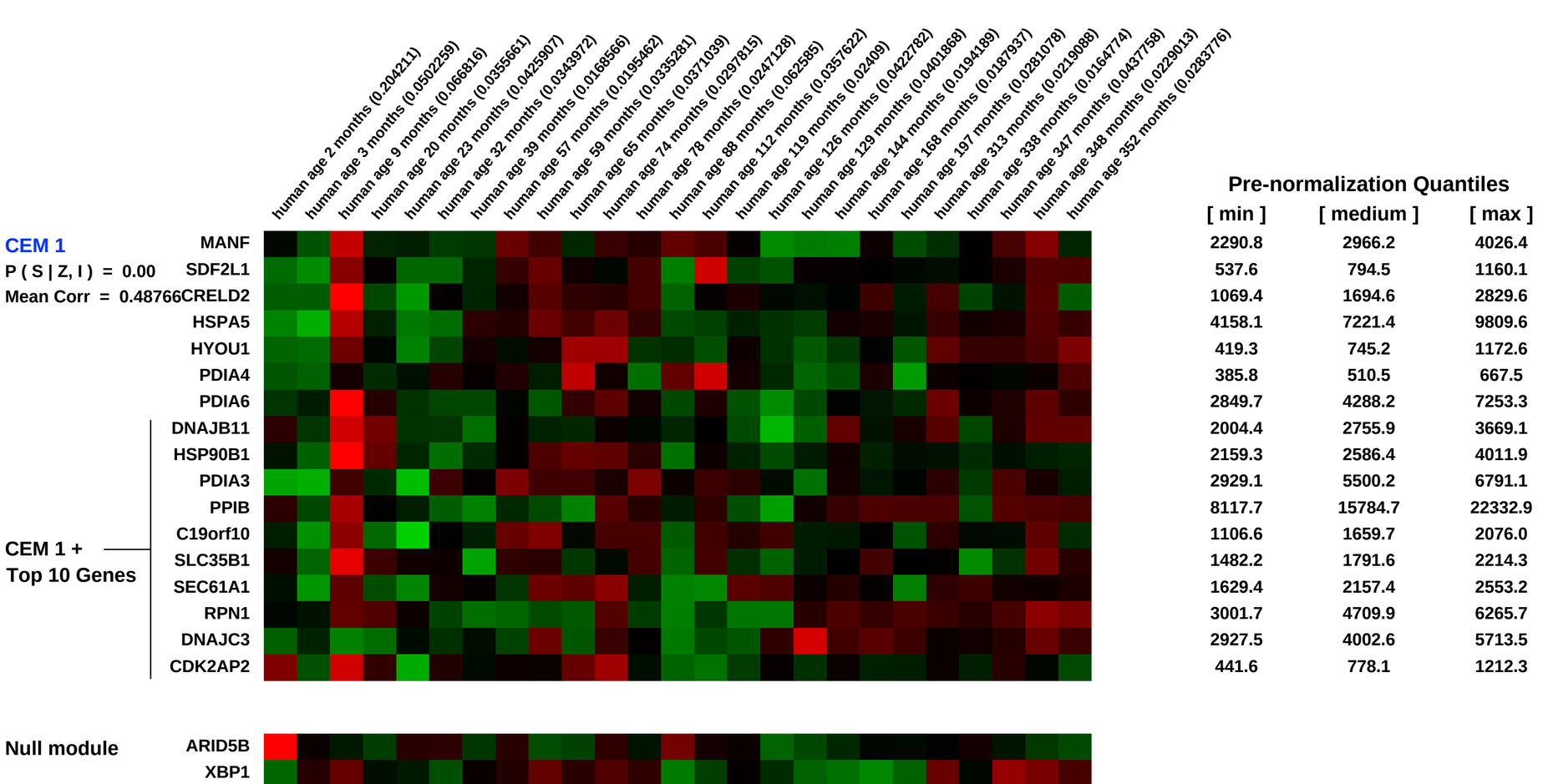

Pre-normalization Quantiles

[min]	[medium]	[max]
2290.8	2966.2	4026.4
537.6	794.5	1160.1
1069.4	1694.6	2829.6
4158.1	7221.4	9809.6
419.3	745.2	1172.6
385.8	510.5	667.5
2849.7	4288.2	7253.3
2004.4	2755.9	3669.1
2159.3	2586.4	4011.9
2929.1	5500.2	6791.1
8117.7	15784.7	22332.9
1106.6	1659.7	2076.0
1482.2	1791.6	2214.3
1629.4	2157.4	2553.2
3001.7	4709.9	6265.7
2927.5	4002.6	5713.5
441.6	778.1	1212.3

GEO Series "GSE11506" Expression Profiles

Num of samples in this series: 9

Scale of expression profile Z-scores

-3.0 -2.0 -1.0 0.0 1.0 2.0 3.0

GEO Link:	http://www.ncbi.nlm.nih.gov/geo/query/acc.cgi?acc=GSE11506
Status:	Public on May 20 2008
Title:	Novel Estrogen Receptor-{alpha} Binding Sites and Estradiol Target Genes Identified by ChIP Cloning in Breast Cancer.
Organism:	Homo sapiens
Experiment type:	Expression profiling by array
Platform:	GPL570
Pubmed ID:	17510434
Summary & Design:	**Summary:** Estrogen receptor-{alpha} (ER{alpha}) and its ligand estradiol play critical roles in breast cancer growth and are important therapeutic targets for this disease. Using chromatin immunoprecipitation (ChIP)-on-chip, ligand-bound ER{alpha} was recently found to function as a master transcriptional regulator via binding to many cis-acting sites genome-wide. Here, we used an alternative technology (ChIP cloning) and identified 94 ER{alpha} target loci in breast cancer cells. The ER{alpha}-binding sites contained both classic estrogen response elements and nonclassic binding sequences, showed specific transcriptional activity in reporter gene assay, and interacted with the key transcriptional regulators, including RNA polymerase II and nuclear receptor coactivator-3. The great majority of the binding sites were located in either introns or far distant to coding regions of genes. Forty-three percent of the genes that lie within 50 kb to an ER{alpha}-binding site were regulated by estradiol. Most of these genes are novel estradiol targets encoding receptors, signaling messengers, and ion binders/transporters. mRNA profiling in estradiol-treated breast cancer cell lines and tissues revealed that these genes are highly ER{alpha} responsive both in vitro and in vivo. Among estradiol-induced genes, Wnt11 was found to increase cell survival by significantly reducing apoptosis in breast cancer cells. Taken together, we showed novel genomic binding sites of ER{alpha} that regulate a novel set of genes in response to estradiol in breast cancer. Our findings suggest that at least a subset of these genes, including Wnt11, may play important in vivo and in vitro biological roles in breast cancer. **Keywords:** time course **Overall design:** This Series currently contains the gene expression data accompanying Zhihong Lin et al. Cancer Research 67,5017-5024(2007). MCF7 cells were treated with vehicle or E2 at a concentration of 10E-9 mol/L for 3 and 6 h. All experiments were performed in triplicate.

Background corr dist: KL-Divergence = 0.0262, L1-Distance = 0.0509, L2-Distance = 0.0040, Normal std = 0.7168

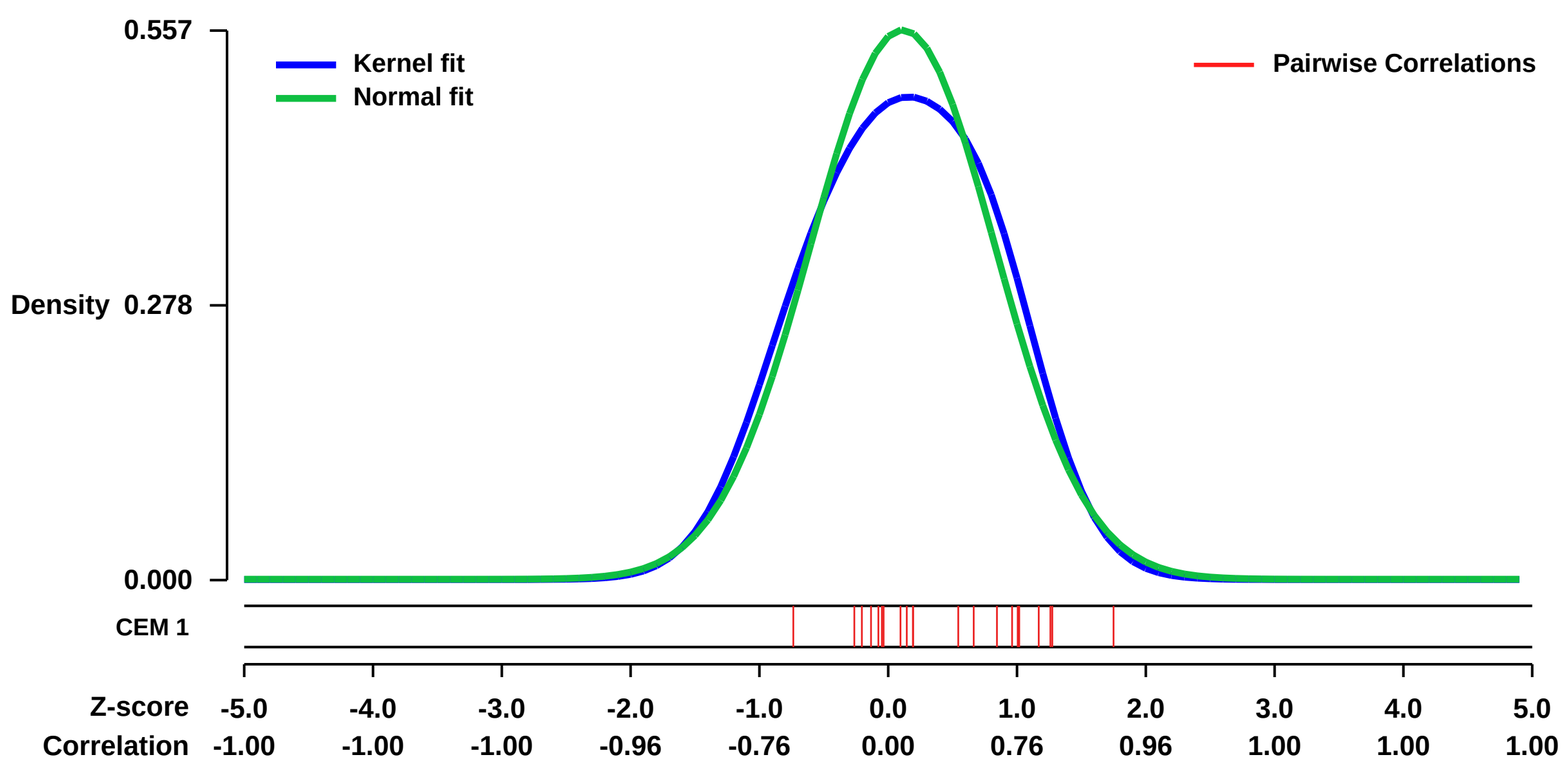

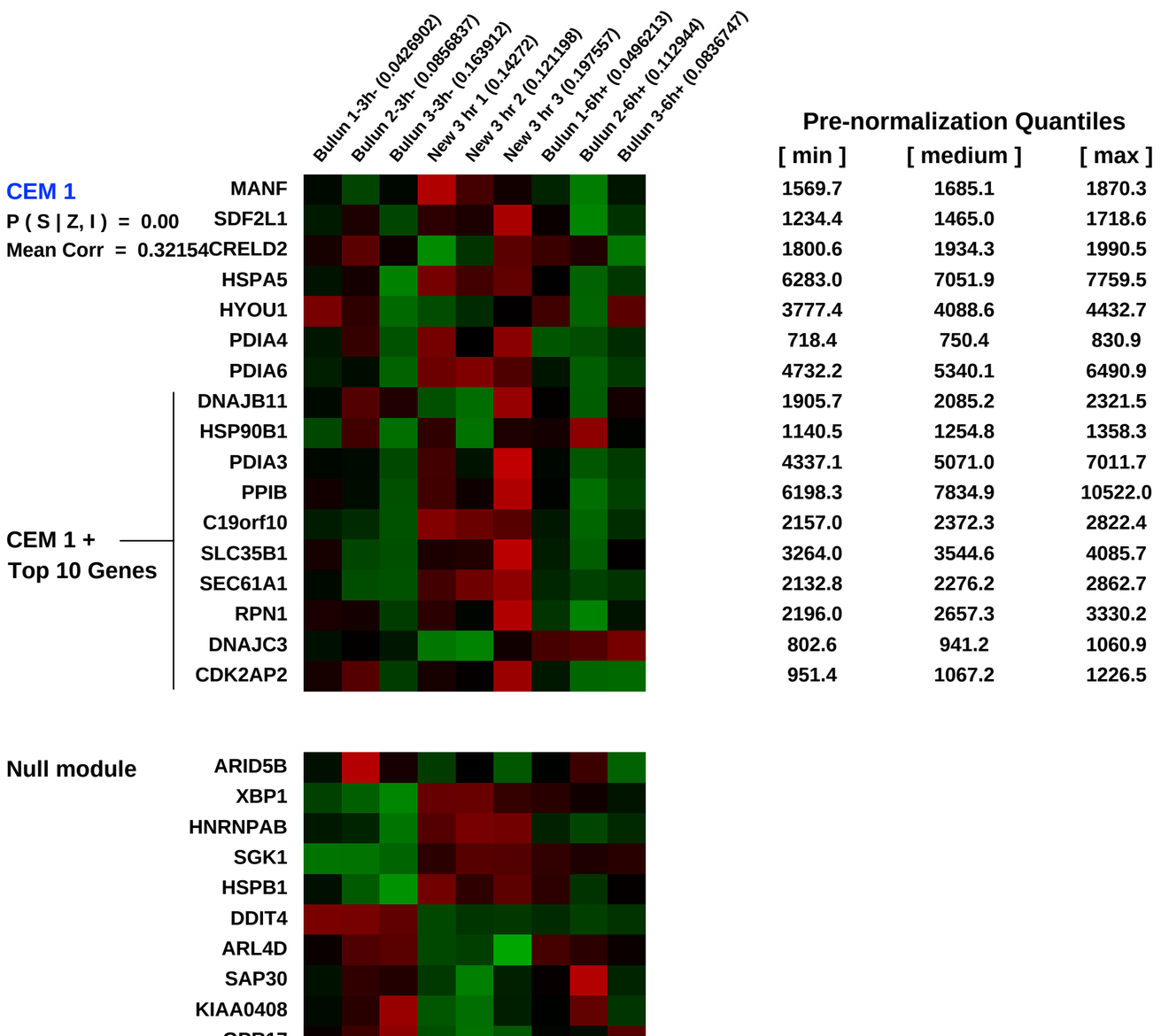

Pre-normalization Quantiles

	[min]	[medium]	[max]
MANF	1569.7	1685.1	1870.3
SDF2L1	1234.4	1465.0	1718.6
CRELD2	1800.6	1934.3	1990.5
HSPA5	6283.0	7051.9	7759.5
HYOU1	3777.4	4088.6	4432.7
PDIA4	718.4	750.4	830.9
PDIA6	4732.2	5340.1	6490.9
DNAJB11	1905.7	2085.2	2321.5
HSP90B1	1140.5	1254.8	1358.3
PDIA3	4337.1	5071.0	7011.7
PPIB	6198.3	7834.9	10522.0
C19orf10	2157.0	2372.3	2822.4
SLC35B1	3264.0	3544.6	4085.7
SEC61A1	2132.8	2276.2	2862.7
RPN1	2196.0	2657.3	3330.2
DNAJC3	802.6	941.2	1060.9
CDK2AP2	951.4	1067.2	1226.5

GEO Series "GSE57156" Expression Profiles

Num of samples in this series: 32

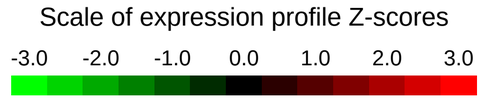

GEO Link:	http://www.ncbi.nlm.nih.gov/geo/query/acc.cgi?acc=GSE57156
Status:	Public on May 16 2014
Title:	Expression data from EGFR WT or EGFR mutant NSCLC with or without erlotinib
Organism:	Homo sapiens
Experiment type:	Expression profiling by array
Platform:	GPL570
Pubmed ID:	
Summary & Design:	**Summary:** Non-small cell lung cancers (NSCLCs) harboring activating EGFR mutants show dramatic responses to EGFR TKIs, such as erlotinib and geffitinib. However, nearly all patients show relapse within 1 year after initial treatment. We used microarrays to detail global gene expression changes in EGFR mutant cells vs. WT cells responding to erlotinib. **Overall design:** 4 EGFR mutant and 4 WT NSCLC cells were treated with or without erlotinib for 24 hr, followed by RNA extraction and hybridization on Affymetrix microarrays.

Background corr dist: KL-Divergence = 0.2093, L1-Distance = 0.0435, L2-Distance = 0.0044, Normal std = 0.3311

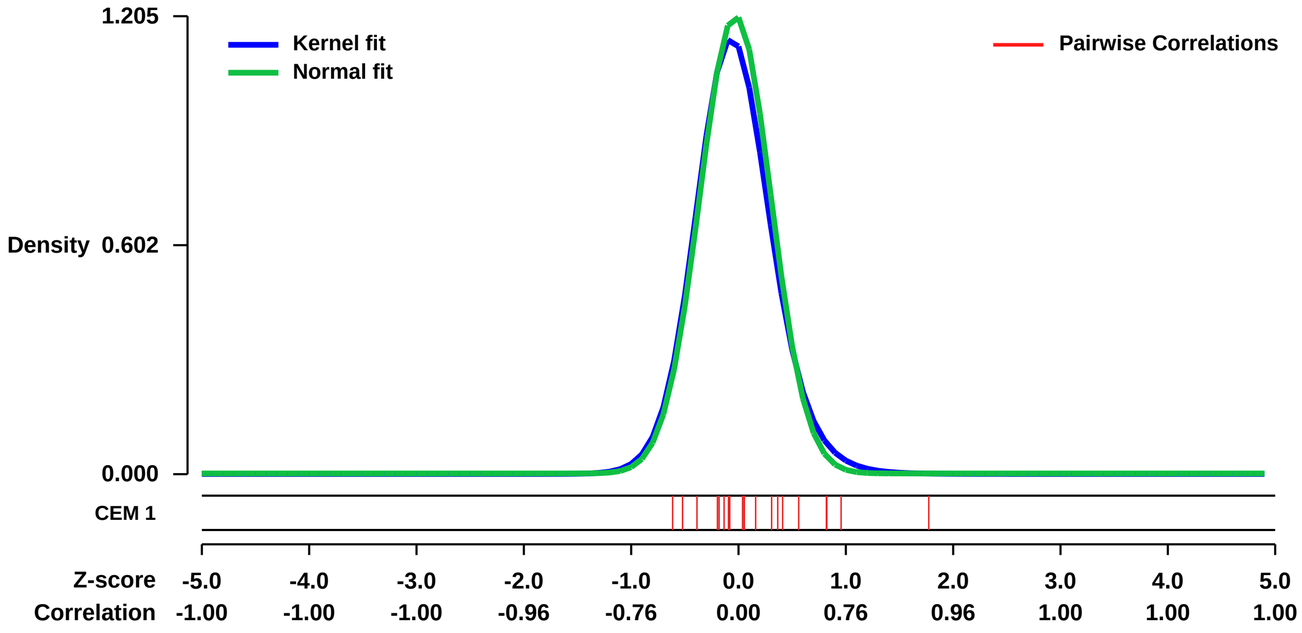

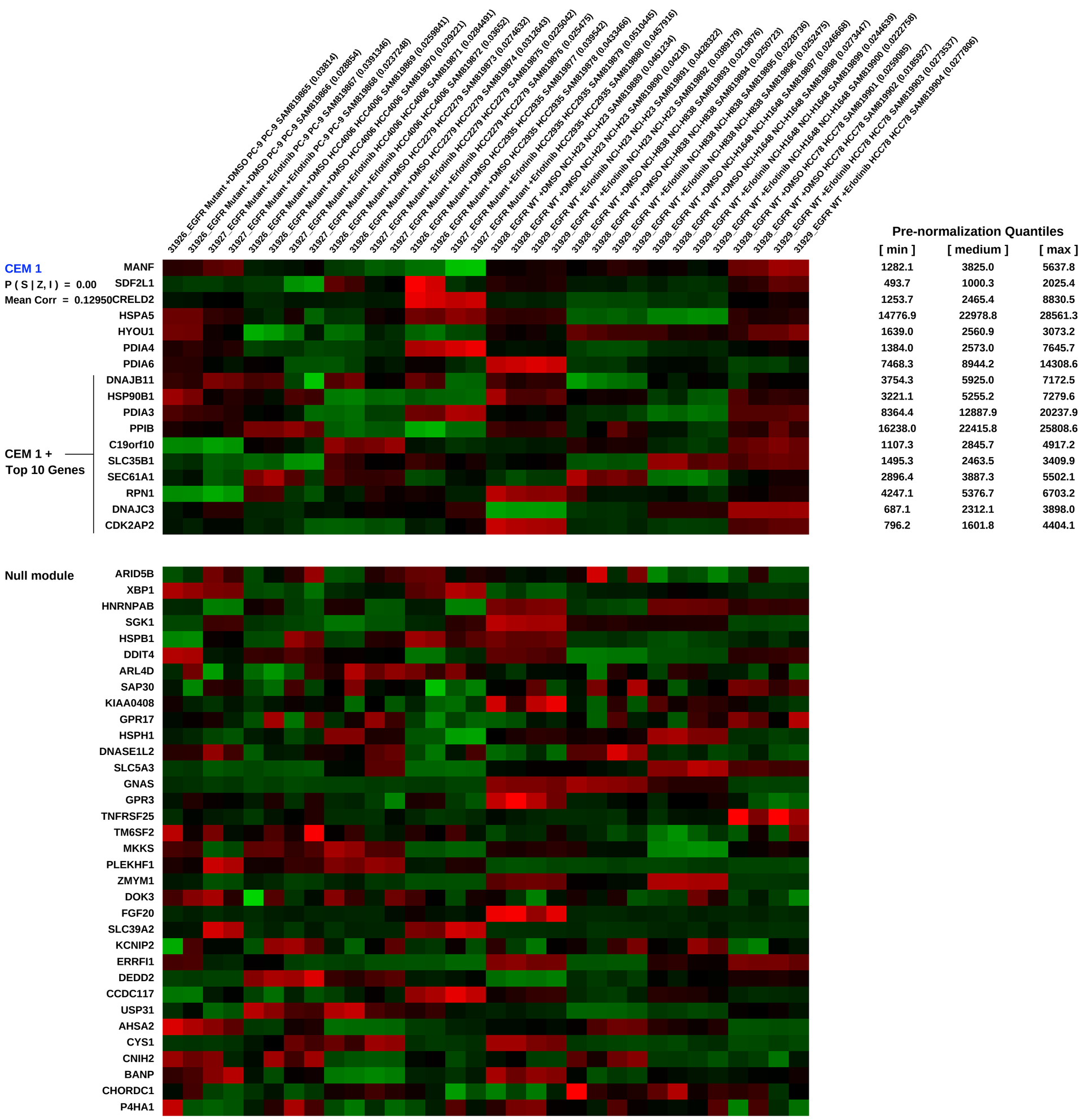

Pre-normalization Quantiles

	[min]	[medium]	[max]
MANF	1282.1	3825.0	5637.8
SDF2L1	493.7	1000.3	2025.4
CRELD2	1253.7	2465.4	8830.5
HSPA5	14776.9	22978.8	28561.3
HYOU1	1639.0	2560.9	3073.2
PDIA4	1384.0	2573.0	7645.7
PDIA6	7468.3	8944.2	14308.6
DNAJB11	3754.3	5925.0	7172.5
HSP90B1	3221.1	5255.2	7279.6
PDIA3	8364.4	12887.9	20237.9
PPIB	16238.0	22415.8	25808.6
C19orf10	1107.3	2845.7	4917.2
SLC35B1	1495.3	2463.5	3409.9
SEC61A1	2896.4	3887.3	5502.1
RPN1	4247.1	5376.7	6703.2
DNAJC3	687.1	2312.1	3898.0
CDK2AP2	796.2	1601.8	4404.1

GEO Series "GSE2816" Expression Profiles

Num of samples in this series: 6

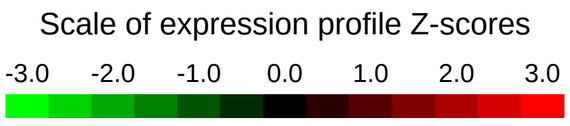

GEO Link:	http://www.ncbi.nlm.nih.gov/geo/query/acc.cgi?acc=GSE2816
Status:	Public on Jun 14 2005
Title:	cMyb and vMyb in human monocytes
Organism:	Homo sapiens
Experiment type:	Expression profiling by array
Platform:	GPL570
Pubmed ID:	16205643
Summary & Design:	**Summary:** The transcriptional activities of c-Myb and its oncogenic variant v-Myb were compared by expressing them in primary human monocytes using recombinant adenovirus vectors. All the samples were compared to cells infected with a control adenovirus expressing only GFP. The results showed that v-Myb, which differs from c-Myb only by N- and C-terminal deletions and eleven amino acid substitutions, has a qualitatively different transcriptional activity. **Keywords: repeat** **Overall design:** 2 replicates of each type were analyzed. Replicates were performed independently, more than a week apart.

Background corr dist: KL-Divergence = 0.0479, L1-Distance = 0.0384, L2-Distance = 0.0022, Normal std = 0.5960

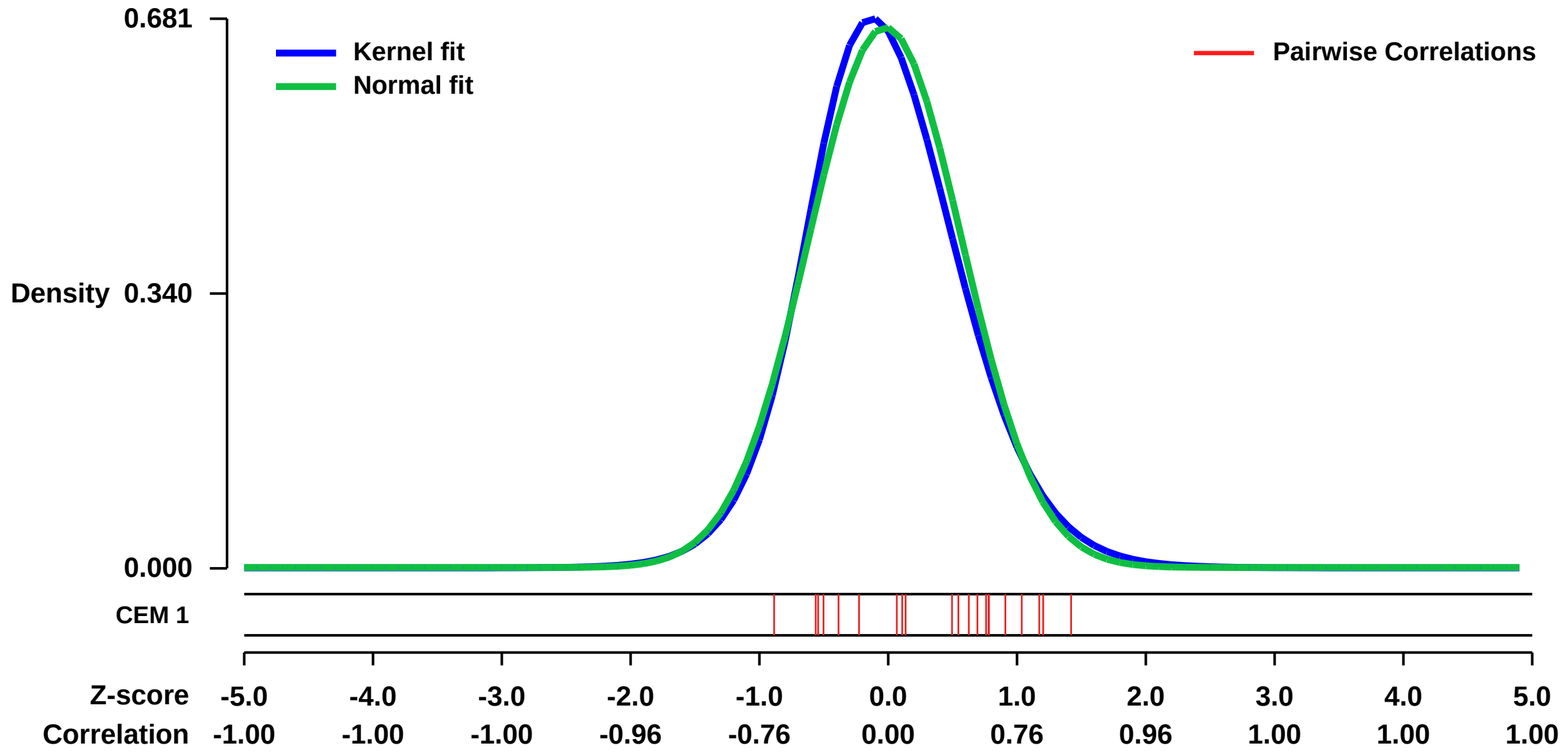

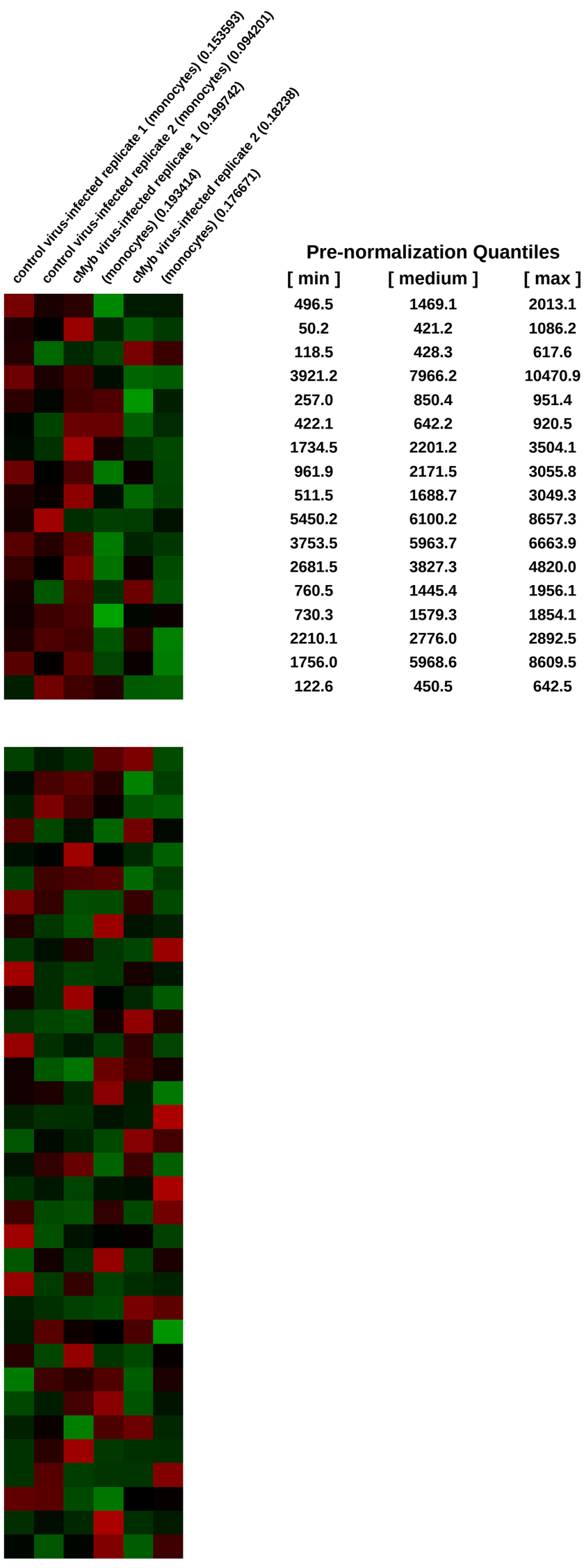

GEO Series "GSE30522" Expression Profiles

Num of samples in this series: 17

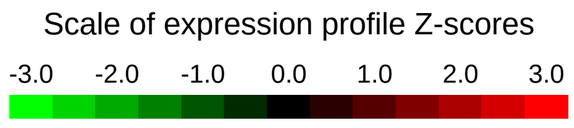

GEO Link:	**http://www.ncbi.nlm.nih.gov/geo/query/acc.cgi?acc=GSE30522**
Status:	**Public on Jul 09 2011**
Title:	**Transcriptomes of human bladder cells and cells in bladder cancer**
Organism:	**Homo sapiens**
Experiment type:	**Expression profiling by array**
Platform:	**GPL570**
Pubmed ID:	
Summary & Design:	**Summary:** **Characterization of the gene expression profiles of specific cell populations of the human urinary bladder provides an important set of research tools for the study of cellular differentiation and the cancer process. The transcriptome is a definitive identifier of each individual cell types. Surgically resected tissue was digested by collagenase and the different cell types were sorted by antibodies to cluster designation (CD) cell surface antigens. The sorted cells were analyzed by DNA microarrays. The transcriptome datasets were analyzed for differentially expressed genes and plotted on a principal components analysis space for cell lineage relationship. The following bladder cell types were analyzed: CD9+ urothelial, CD104+ basal, CD13+ stromal of lamina propria, CD9+ urothelial carcinoma cancer, and CD13+ urothelial carcinoma-associated stromal. Gene expression differences between the cell types of tumor and their respective non-cancer counterpart provide biomarker candidates. Basal cells of the bladder and prostate, although sharing CD cell surface markers, are quite different in overall gene expression. Furthermore, these cells lack transcript features of stem cell signature of embryonic stem or embryonal carcinoma cells. Cell type-specific transcriptomes are more informative than bulk tissue transcriptomes. The relatedness of different cell types can be determined by transcriptome dataset comparison.** **Overall design:** **Bladder cell types were sorted from tissue specimens, and analyzed by DNA microarrays. The various transcriptomes were compared by principal components analysis for cell lineage relationship.**

Background corr dist: KL-Divergence = 0.1425, L1-Distance = 0.0485, L2-Distance = 0.0057, Normal std = 0.3944

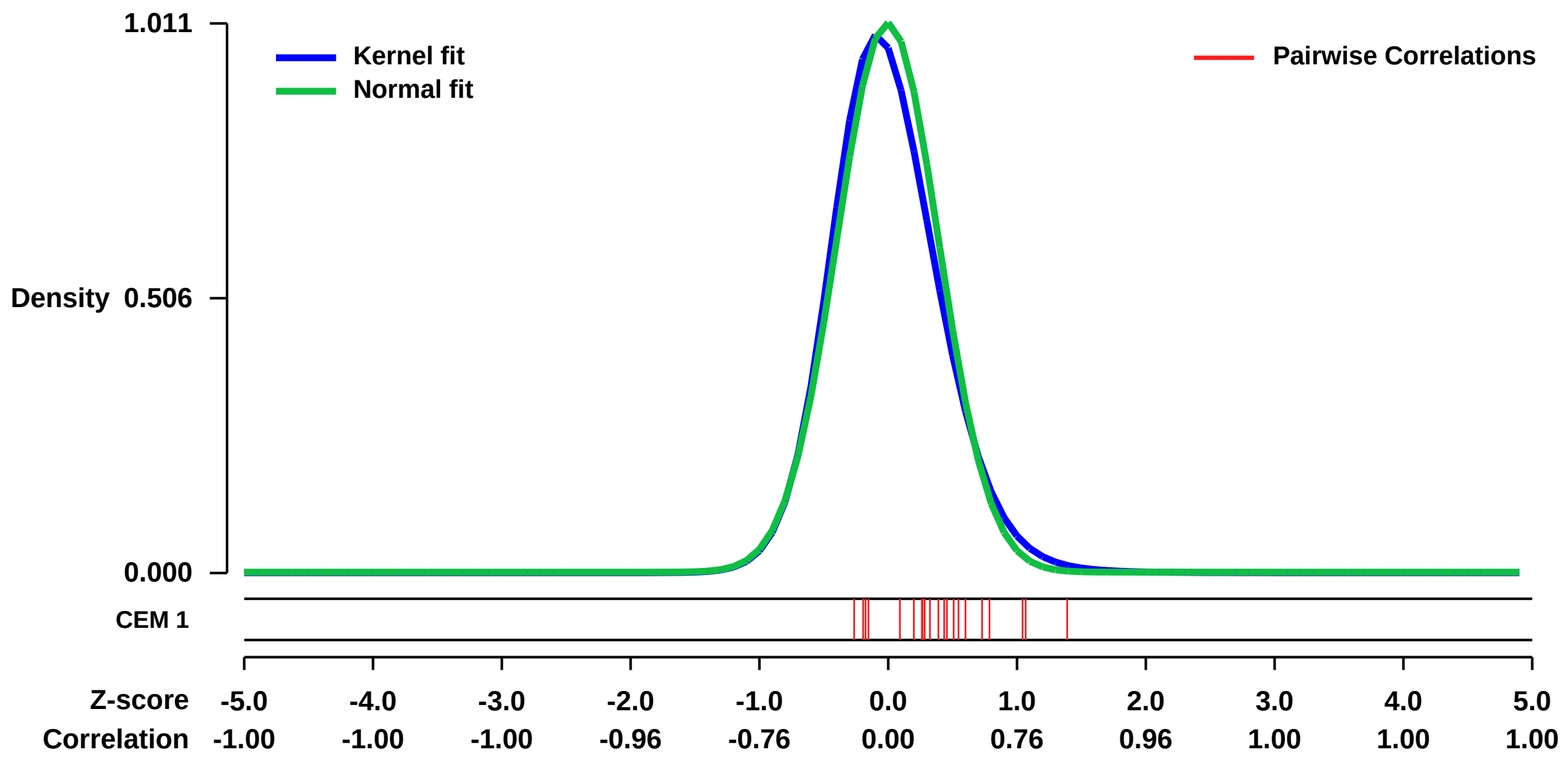

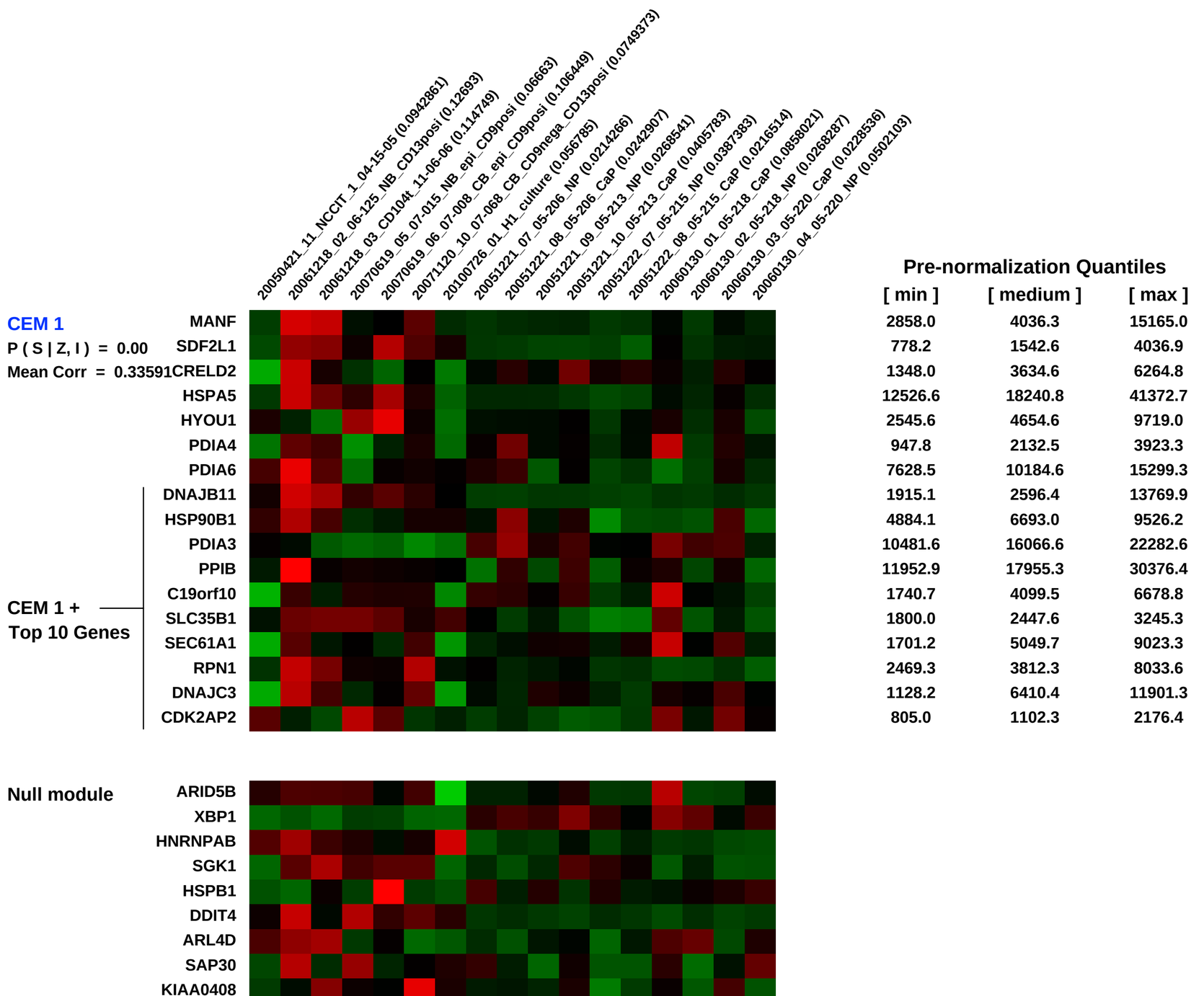

Pre-normalization Quantiles

	[min]	[medium]	[max]
MANF	2858.0	4036.3	15165.0
SDF2L1	778.2	1542.6	4036.9
CRELD2	1348.0	3634.6	6264.8
HSPA5	12526.6	18240.8	41372.7
HYOU1	2545.6	4654.6	9719.0
PDIA4	947.8	2132.5	3923.3
PDIA6	7628.5	10184.6	15299.3
DNAJB11	1915.1	2596.4	13769.9
HSP90B1	4884.1	6693.0	9526.2
PDIA3	10481.6	16066.6	22282.6
PPIB	11952.9	17955.3	30376.4
C19orf10	1740.7	4099.5	6678.8
SLC35B1	1800.0	2447.6	3245.3
SEC61A1	1701.2	5049.7	9023.3
RPN1	2469.3	3812.3	8033.6
DNAJC3	1128.2	6410.4	11901.3
CDK2AP2	805.0	1102.3	2176.4

GEO Series "GSE3893" Expression Profiles

Num of samples in this series: 14

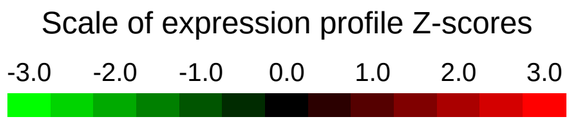

GEO Link:	http://www.ncbi.nlm.nih.gov/geo/query/acc.cgi?acc=GSE3893
Status:	Public on May 24 2006
Title:	Gene Expression Profiling of matched Ductal Carcinomas in Situ and Invasive Breast Tumors
Organism:	Homo sapiens
Experiment type:	Expression profiling by array
Platform:	GPL570
Pubmed ID:	16707453
Summary & Design:	**Summary:** This is a matched-pair analysis of ductal carcinoma in situ (DCIS) and invasive component (IDC) of nine breast ductal carcinoma to identify novel molecular markers characterizing the transition from DCIS to IDC for a better understanding of its molecular biology. **Keywords:** Affymetrix-based Microarrays in Mamma carcinoma **Overall design:** Absolute, one-channel, oligo-based microarrays used for whole-genome expression profiling of human mamma carcinoma

Background corr dist: KL-Divergence = 0.1729, L1-Distance = 0.0474, L2-Distance = 0.0051, Normal std = 0.3531

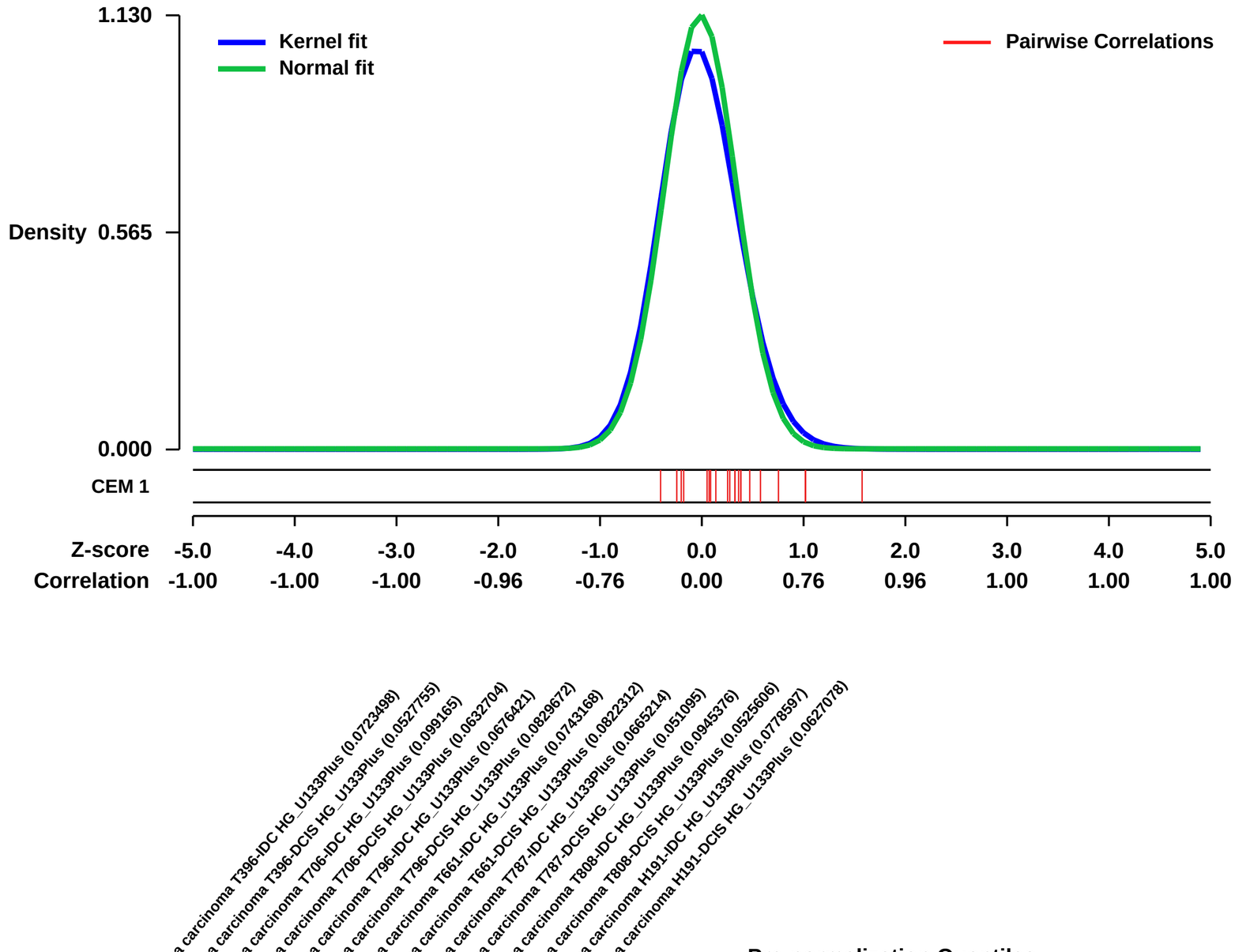

CEM 1
P (S | Z, I) = 0.00
Mean Corr = 0.26764

CEM 1 + Top 10 Genes

Null module

Pre-normalization Quantiles

	[min]	[medium]	[max]
MANF	1572.6	2335.5	3236.7
SDF2L1	782.9	1425.9	3375.3
CRELD2	1482.5	2472.2	4523.1
HSPA5	3523.7	4838.2	7284.3
HYOU1	801.0	1176.0	1928.3
PDIA4	504.4	921.0	1373.4
PDIA6	4828.6	7942.2	12100.2
DNAJB11	1124.1	1750.6	2820.5
HSP90B1	282.2	537.2	849.8
PDIA3	2917.6	4944.4	5810.4
PPIB	3098.9	5367.4	8413.6
C19orf10	2064.5	2396.4	7135.9
SLC35B1	1461.0	1977.1	10814.9
SEC61A1	1167.0	1586.6	3190.8
RPN1	689.4	1049.3	1854.2
DNAJC3	2890.9	4310.2	7015.9
CDK2AP2	438.4	722.2	1975.0
ARID5B			
XBP1			
HNRNPAB			
SGK1			
HSPB1			
DDIT4			
ARL4D			
SAP30			
KIAA0408			
GPR17			
HSPH1			
DNASE1L2			
SLC5A3			
GNAS			
GPR3			
TNFRSF25			
TM6SF2			
MKKS			
PLEKHF1			
ZMYM1			
DOK3			
FGF20			
SLC39A2			
KCNIP2			
ERRFI1			
DEDD2			
CCDC117			
USP31			
AHSA2			
CYS1			
CNIH2			
BANP			
CHORDC1			
P4HA1			

GEO Series "GSE42549" Expression Profiles

Num of samples in this series: 16

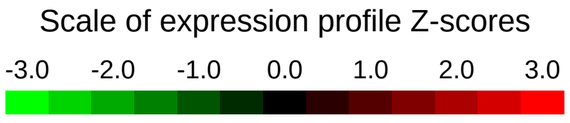

GEO Link:	http://www.ncbi.nlm.nih.gov/geo/query/acc.cgi?acc=GSE42549
Status:	Public on Dec 01 2013
Title:	Transcriptional responses of mantle cell lymphoma (MCL) lines to PKC inhibition
Organism:	Homo sapiens
Experiment type:	Expression profiling by array
Platform:	GPL570
Pubmed ID:	24362935
Summary & Design:	**Summary:** **MCL lines (biological replicates) were treated with DMSO or 2.5uM Sotrastaurin for 3hrs** **This experiment is designed to see if a common set of genes is affected by Sotrastaurin (STN) treatment in STN-sensitive and STN-insensitive MCL lines.** **Overall design:** **MCL cells were seeded in 6well dishes and treated for 3hrs with DMSO or 2.5uM Sotrastaurin**

Background corr dist: **KL-Divergence = 0.1125, L1-Distance = 0.0494, L2-Distance = 0.0043, Normal std = 0.4396**

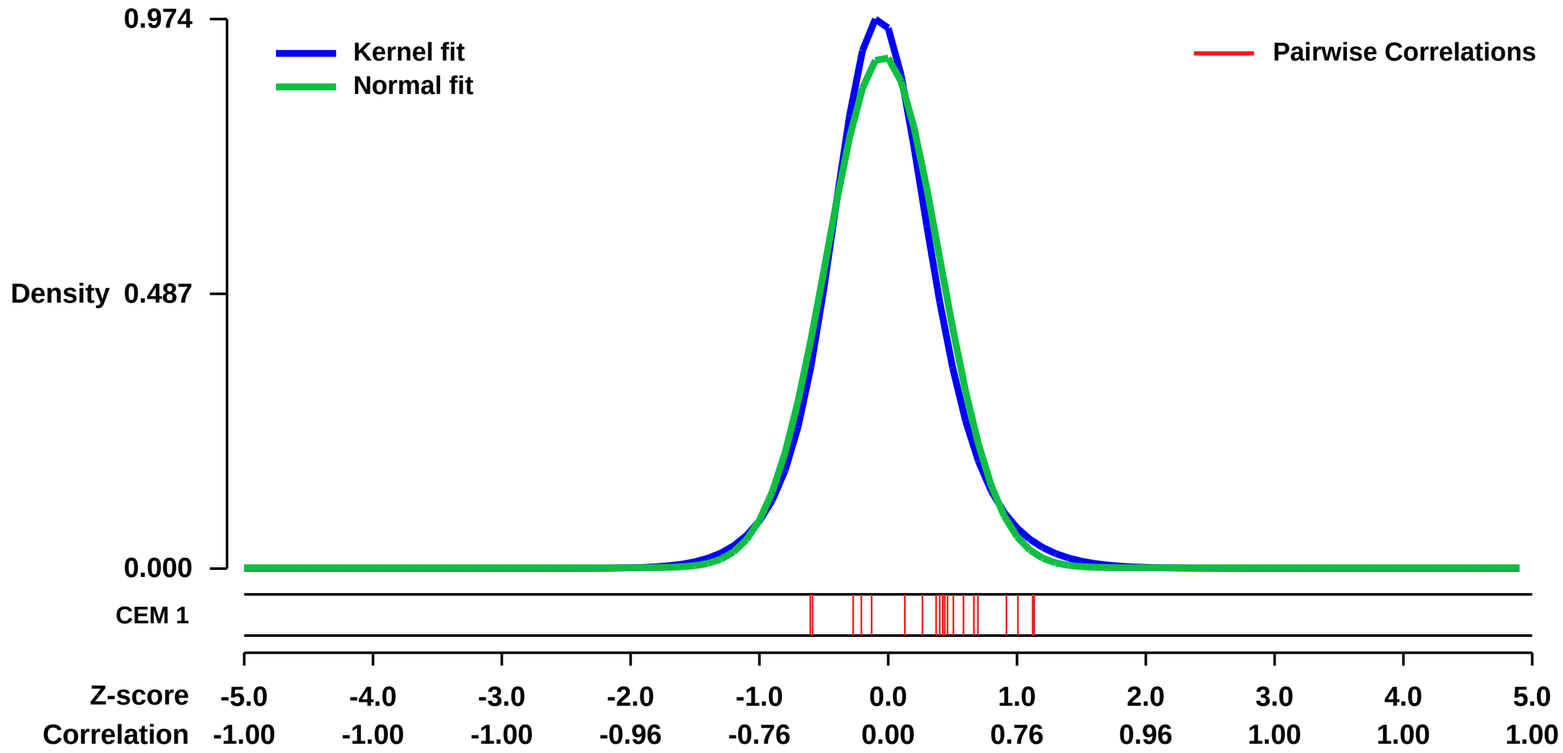

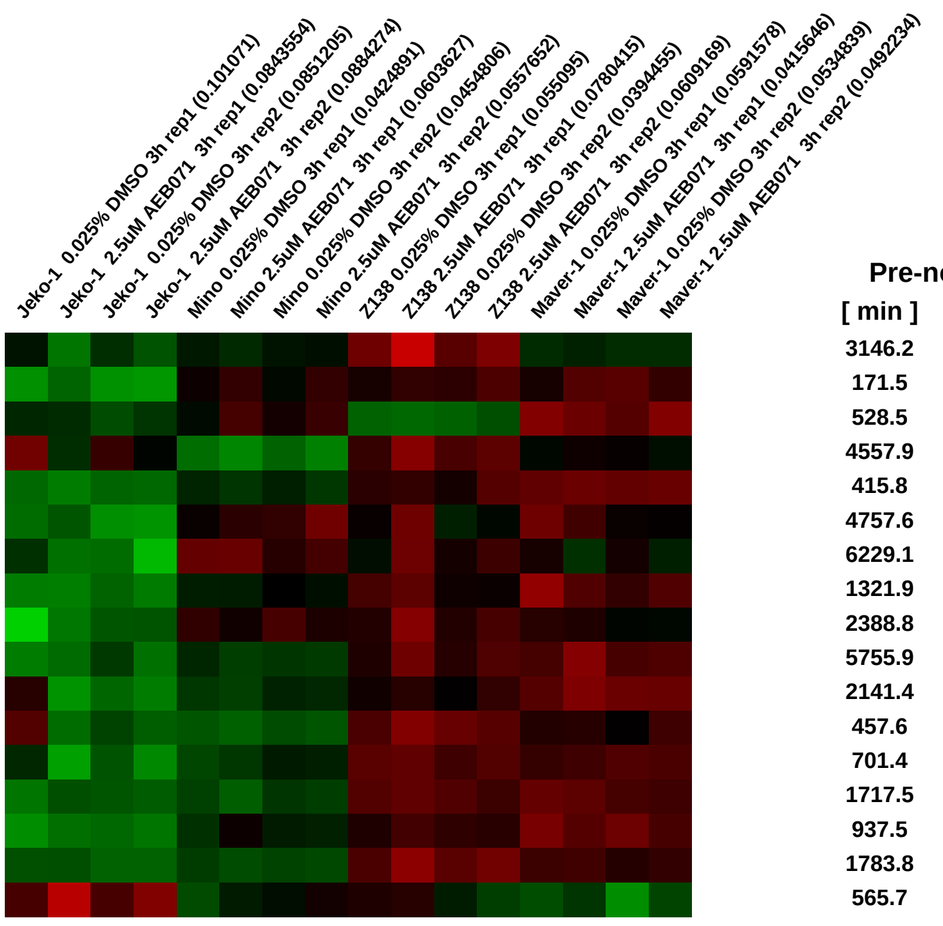

Pre-normalization Quantiles

	[min]	[medium]	[max]
MANF	3146.2	4399.6	7372.1
SDF2L1	171.5	428.6	486.1
CRELD2	528.5	955.9	1589.9
HSPA5	4557.9	6868.8	8964.0
HYOU1	415.8	825.8	1068.4
PDIA4	4757.6	6723.4	8022.0
PDIA6	6229.1	8023.9	8794.7
DNAJB11	1321.9	2178.5	3022.2
HSP90B1	2388.8	6251.4	7903.6
PDIA3	5755.9	7124.0	8029.0
PPIB	2141.4	4364.7	5837.4
C19orf10	457.6	748.4	942.6
SLC35B1	701.4	2007.0	2274.6
SEC61A1	1717.5	4507.8	5161.5
RPN1	937.5	2497.6	3305.4
DNAJC3	1783.8	4121.0	5925.0
CDK2AP2	565.7	803.2	1173.0
ARID5B			
XBP1			
HNRNPAB			
SGK1			
HSPB1			
DDIT4			
ARL4D			
SAP30			
KIAA0408			
GPR17			
HSPH1			
DNASE1L2			
SLC5A3			
GNAS			
GPR3			
TNFRSF25			
TM6SF2			
MKKS			
PLEKHF1			
ZMYM1			
DOK3			
FGF20			
SLC39A2			
KCNIP2			
ERRFI1			
DEDD2			
CCDC117			
USP31			
AHSA2			
CYS1			
CNIH2			
BANP			
CHORDC1			
P4HA1			

CEM 1
P (S | Z, I) = 0.00
Mean Corr = 0.30411

CEM 1 +
Top 10 Genes

Null module

GEO Series "GSE23102" Expression Profiles

Num of samples in this series: 12

Scale of expression profile Z-scores

-3.0 -2.0 -1.0 0.0 1.0 2.0 3.0

GEO Link:	http://www.ncbi.nlm.nih.gov/geo/query/acc.cgi?acc=GSE23102
Status:	Public on Jul 23 2011
Title:	Expression profiles from HEK293 cells by overexpression of TRPM7 channel
Organism:	Homo sapiens
Experiment type:	Expression profiling by array
Platform:	GPL570
Pubmed ID:	21471721
Summary & Design:	**Summary:** The functional activity of TRPM7 is essential for cell viability and growth, and its expression is up-regulated in certain pathological conditions. In order to assess the effects of TRPM7 activity on cellular gene expression, inducible HEK293 cell-lines harboring the wild-type mouse TRPM7 and a mutant lacking the kinase domain were established. By using microarray analysis, we identified genetic profiles altered in transcription significantly and specifically by the expression of the functional TRPM7 channel. **Overall design:** Overexpression of TRPM7 channel in HEK cells induce the cell damage and cell death. So we used tetracycline-inducible system for channel expression. However, since the treatment of inducer itself could also affect the transcription profile, we established another cell-line harboring a nonfunctional TRPM7 mutant (TRPM7DKD) as a control in which the entire kinase domain at the C-terminus was deleted. The wild-type and the non-functional TRPM7 channels were induced transiently, and the comparative changes in cellular transcription were investigated

Background corr dist: KL-Divergence = 0.1107, L1-Distance = 0.0245, L2-Distance = 0.0010, Normal std = 0.4236

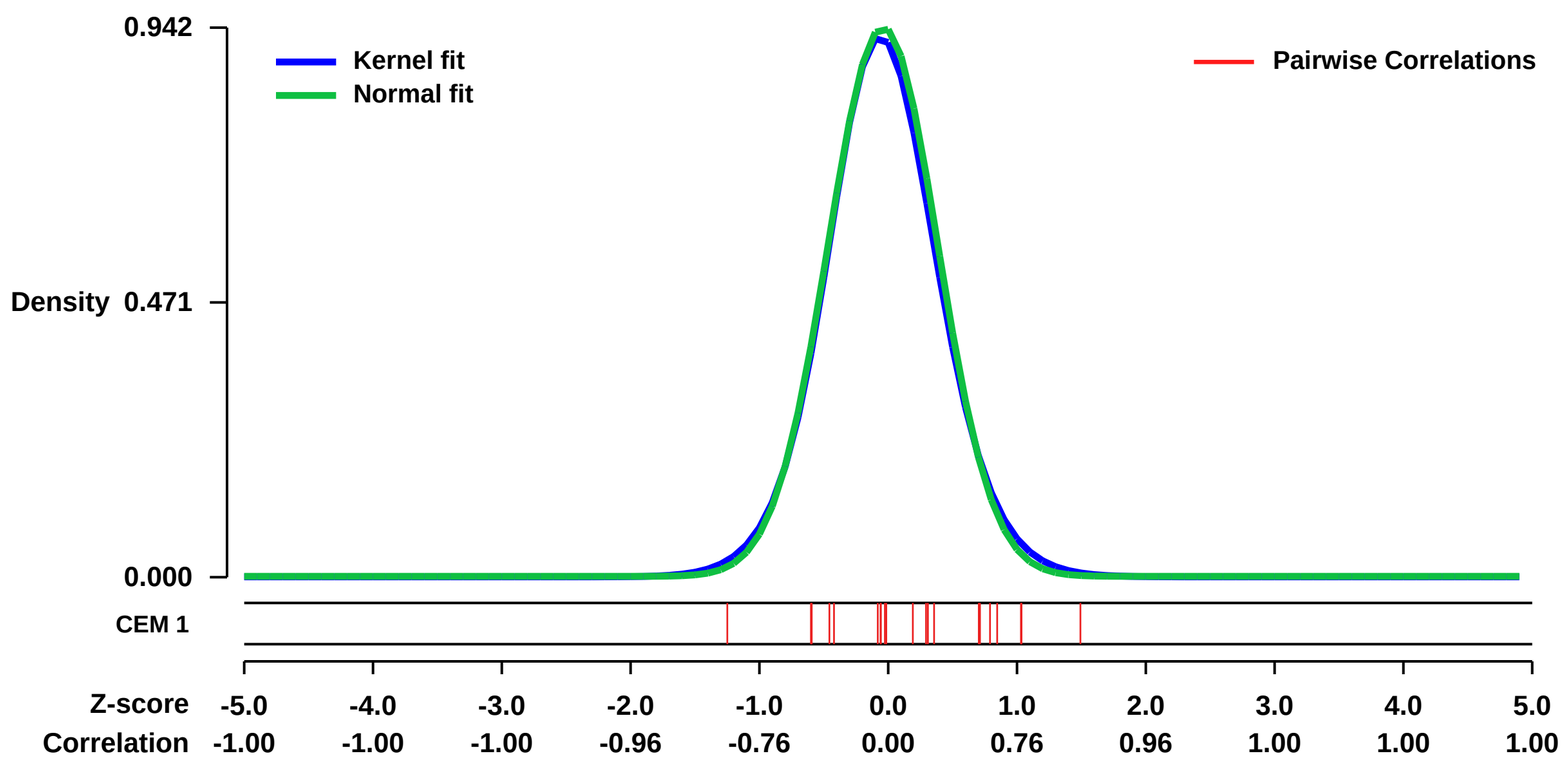

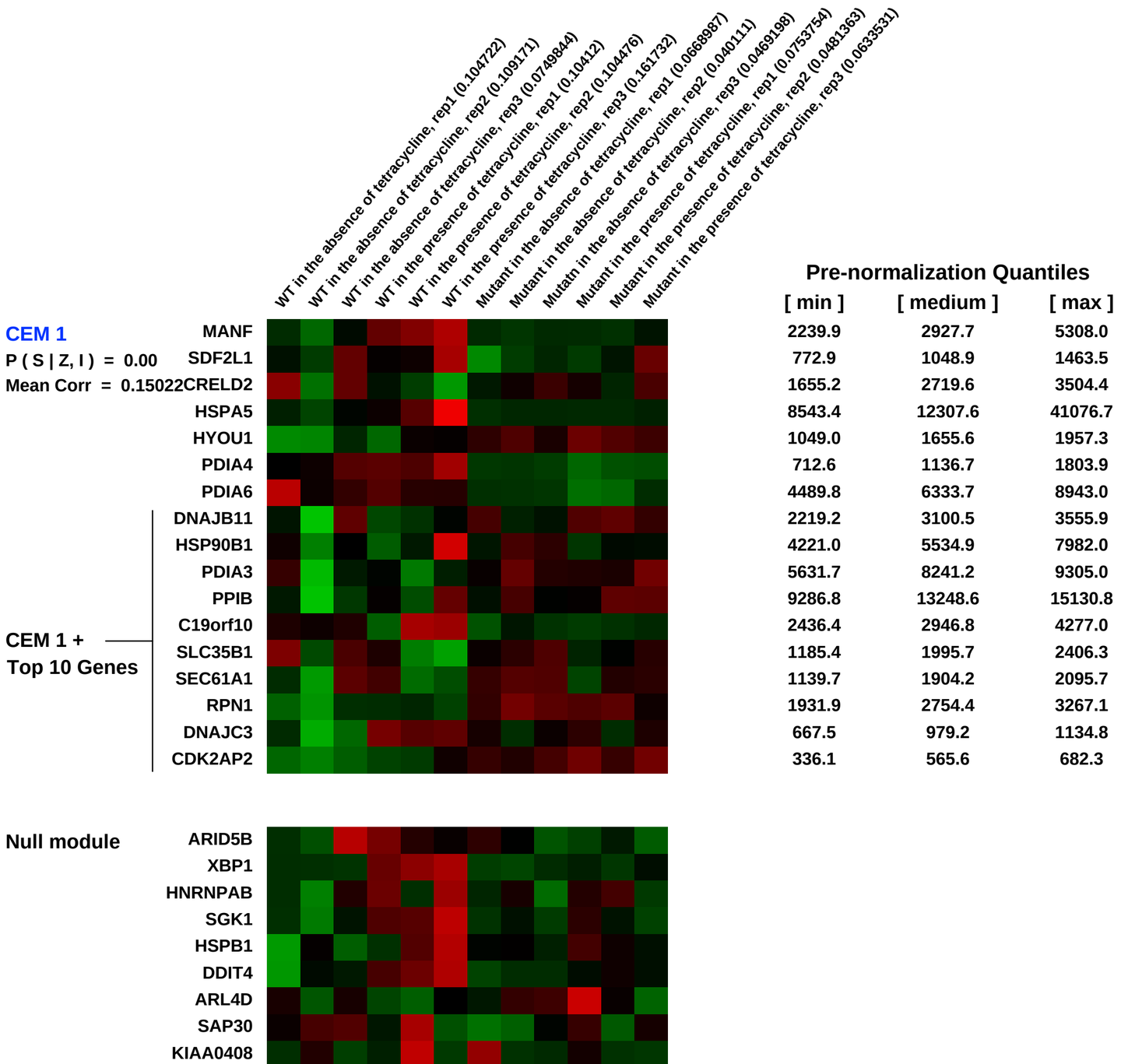

Pre-normalization Quantiles

	[min]	[medium]	[max]
MANF	2239.9	2927.7	5308.0
SDF2L1	772.9	1048.9	1463.5
CRELD2	1655.2	2719.6	3504.4
HSPA5	8543.4	12307.6	41076.7
HYOU1	1049.0	1655.6	1957.3
PDIA4	712.6	1136.7	1803.9
PDIA6	4489.8	6333.7	8943.0
DNAJB11	2219.2	3100.5	3555.9
HSP90B1	4221.0	5534.9	7982.0
PDIA3	5631.7	8241.2	9305.0
PPIB	9286.8	13248.6	15130.8
C19orf10	2436.4	2946.8	4277.0
SLC35B1	1185.4	1995.7	2406.3
SEC61A1	1139.7	1904.2	2095.7
RPN1	1931.9	2754.4	3267.1
DNAJC3	667.5	979.2	1134.8
CDK2AP2	336.1	565.6	682.3

GEO Series "GSE18018" Expression Profiles

Num of samples in this series: 48

Scale of expression profile Z-scores

-3.0 -2.0 -1.0 0.0 1.0 2.0 3.0

GEO Link:	http://www.ncbi.nlm.nih.gov/geo/query/acc.cgi?acc=GSE18018
Status:	Public on Jul 01 2010
Title:	Multilineage dysplasia and AML with mutated nucleophosmin
Organism:	Homo sapiens
Experiment type:	Expression profiling by array
Platform:	GPL570
Pubmed ID:	20203266
Summary & Design:	**Summary:** **Multilineage dysplasia (MLD) has no impact on biological, clinico-pathological and prognostic features of AML with mutated nucleophosmin (NPM1)** **NPM1-mutated AML is a provisional entity in the WHO-2008 classification of myeloid neoplasms. The significance of concomitant multilineage dysplasia (MLD) in NPM1-mutated AML is unclear. Thus, in the WHO-2008 classification, NPM1-mutated AML with MLD is classified as AML with myelodysplasia(MD)-related changes. We evaluated the MLD impact in 378 NPM1-mutated AML patients. MLD was found in about 25% cases. Except for a lower WBC and FLT3-ITD incidence in MLD+ group, no significant differences were observed in age, sex, cytogenetics and FLT3-TKD between NPM1-mutated AML with and without MLD. Notably, NPM1-mutated AML with/without MLD showed overlapping immunophenotype (CD34-negativity) and GEP (CD34 downregulation and HOX genes upregulation).** **Moreover, OS and EFS did not differ among NPM1-mutated AML patients, independently of whether they carried or not MLD, the NPM1-mutated/FLT3-ITD negative cases showing the better prognosis. Lack of MLD impact on survival was confirmed by multivariate analysis that highlighted FLT3-ITD as the most significant prognostic parameter in NPM1-mutated AML. Our findings indicate that NPM1 mutations rather than MLD dictate the distinctive features of NPM1-mutated AML. Thus, irrespective of MLD, NPM1-mutated AML should be considered as one disease entity clearly distinct from AML with MD-related changes. These findings have important diagnostic and prognostic implications in AML.** **Overall design:** **All bone marrow samples were obtained from untreated patients at the time of diagnosis. Cells used for microarray analysis were collected from the purified fraction of mononuclear cells after Ficoll density centrifugation. 48 samples**

Background corr dist: **KL-Divergence = 0.2271, L1-Distance = 0.0757, L2-Distance = 0.0166, Normal std = 0.3179**

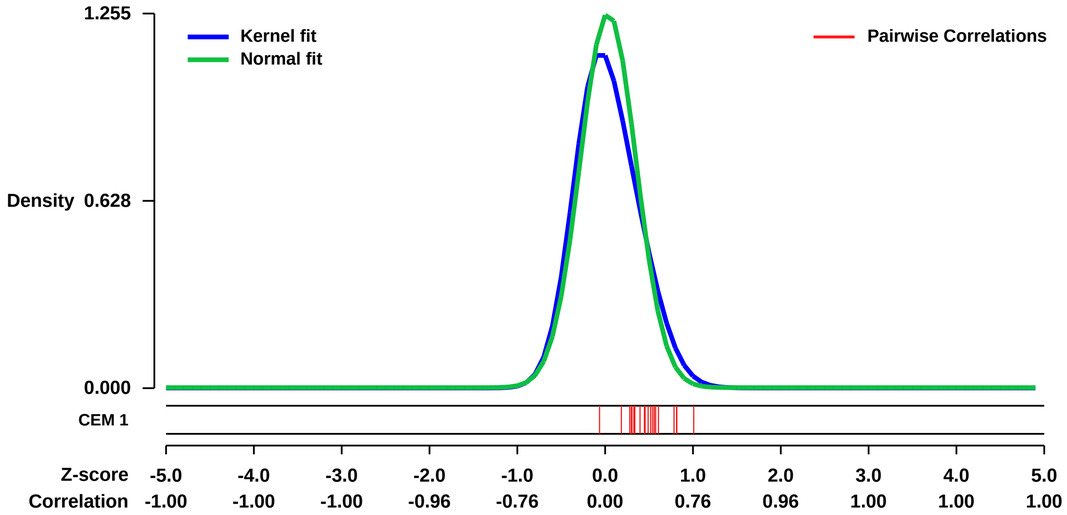

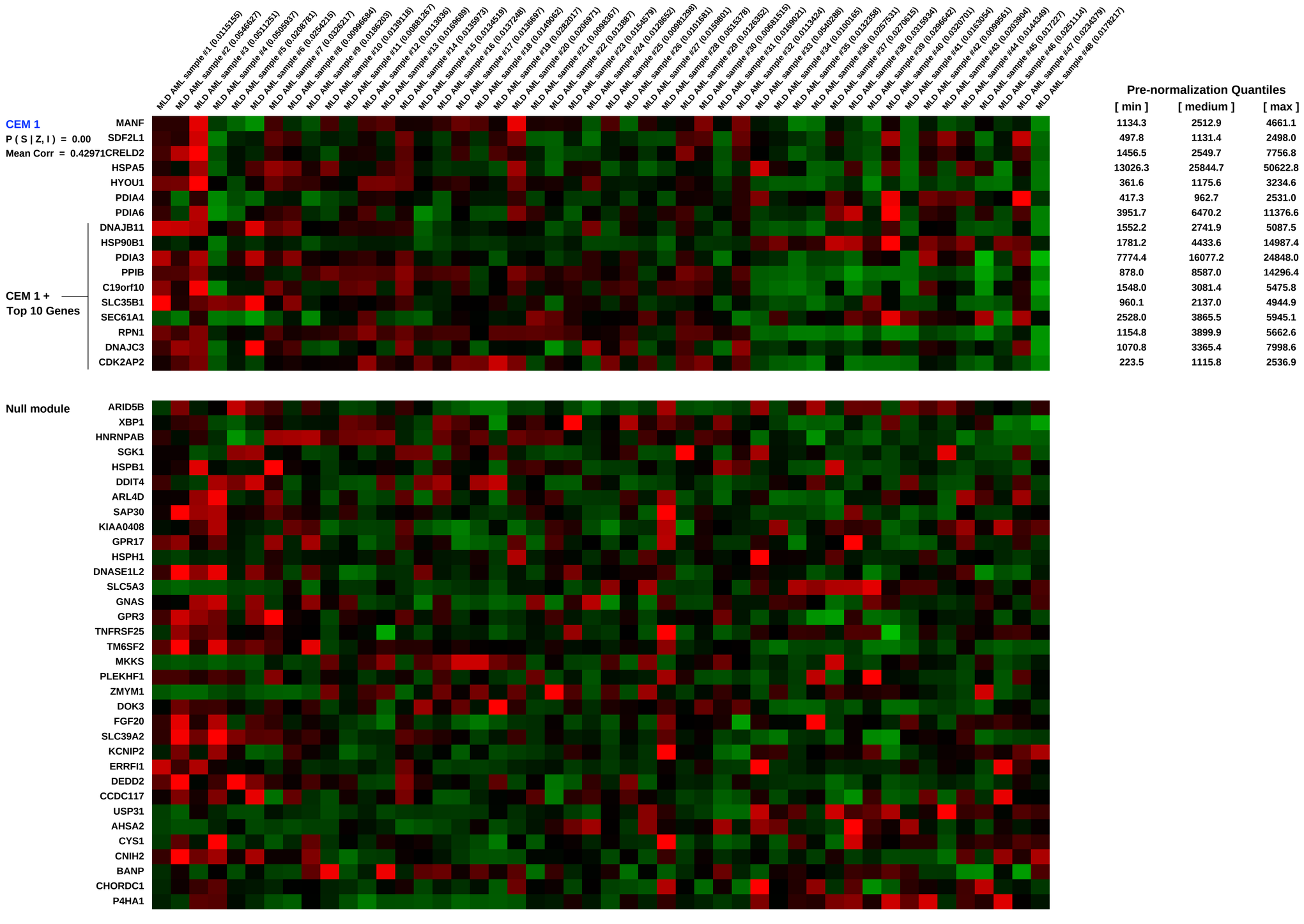

Pre-normalization Quantiles		
[min]	[medium]	[max]
1134.3	2512.9	4661.1
497.8	1131.4	2498.0
1456.5	2549.7	7756.8
13026.3	25844.7	50622.8
361.6	1175.6	3234.6
417.3	962.7	2531.0
3951.7	6470.2	11376.6
1552.2	2741.9	5087.5
1781.2	4433.6	14987.4
7774.4	16077.2	24848.0
878.0	8587.0	14296.4
1548.0	3081.4	5475.8
960.1	2137.0	4944.9
2528.0	3865.5	5945.1
1154.8	3899.9	5662.6
1070.8	3365.4	7998.6
223.5	1115.8	2536.9

GEO Series "GSE24752" Expression Profiles

Num of samples in this series: 6

Scale of expression profile Z-scores

-3.0 -2.0 -1.0 0.0 1.0 2.0 3.0

GEO Link:	http://www.ncbi.nlm.nih.gov/geo/query/acc.cgi?acc=GSE24752
Status:	Public on May 06 2013
Title:	Microarray Analysis of differential gene expression in peripheral blood cells of patients with human essential hypertension
Organism:	Homo sapiens
Experiment type:	Expression profiling by array
Platform:	GPL570
Pubmed ID:	21369372
Summary & Design:	**Summary:** The polygenic nature of essential hypertension and its dependence on environmental factors pose a challenge for biomedical research. We hypothesized that microarray analysis of differential gene expression in peripheral blood cells would distinguish patients with hypertension from normotensive controls. We utilized microaaray analysis of differential gene expression in peripheral blood cells to identify differences in transcription profile of human essential hypertension compared with normotensive volunteers. **Overall design:** Samples were pooled from participants who met with our recruitment criteria for RNA extraction and hybridization on Affymetrix Gene Chips Human Genome U133 Plus 2.0 Array. Experiments were performed at CapitalBio Corporation (Beijing, China)

Background corr dist: KL-Divergence = 0.0228, L1-Distance = 0.0199, L2-Distance = 0.0005, Normal std = 0.7122

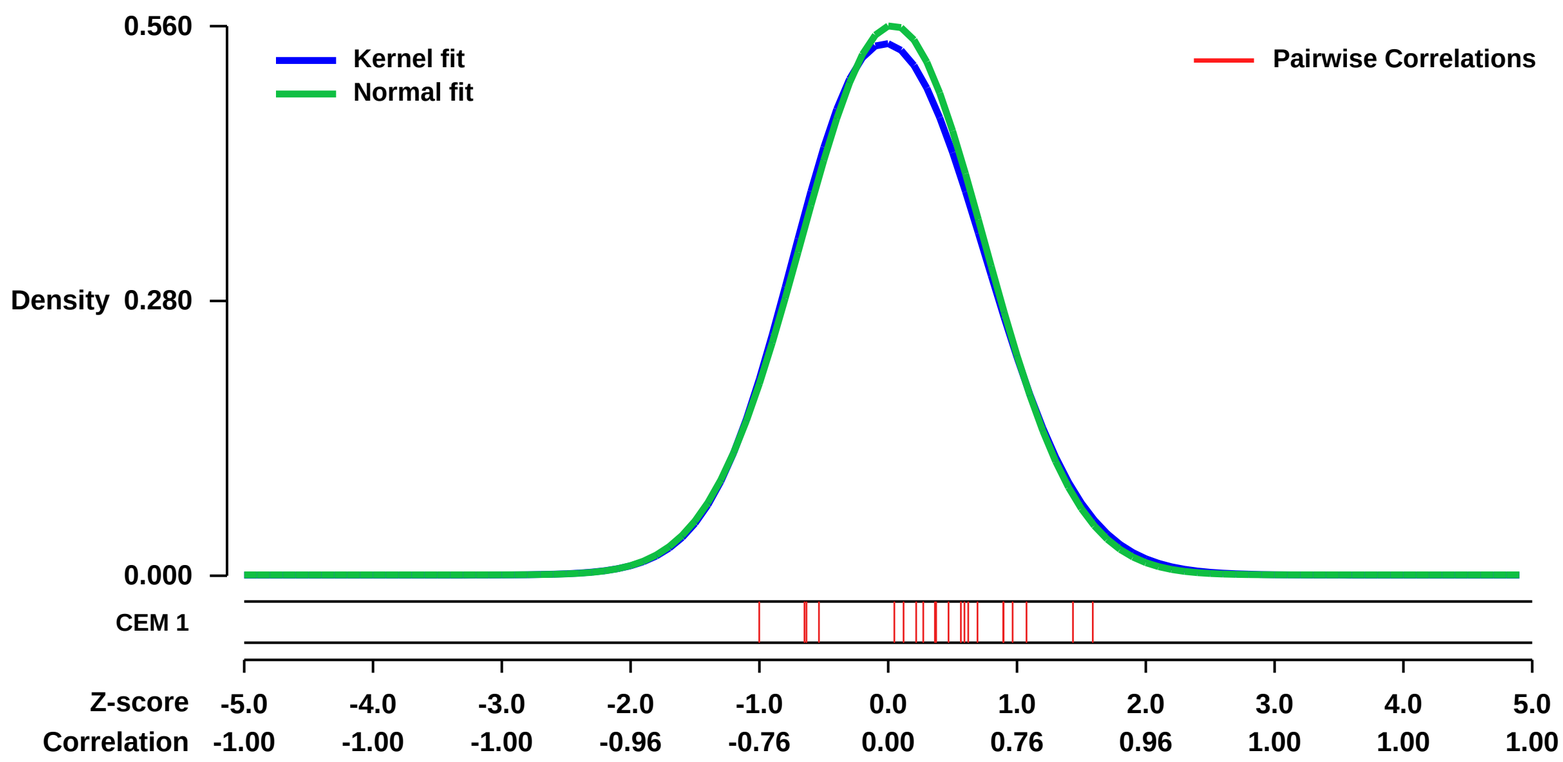

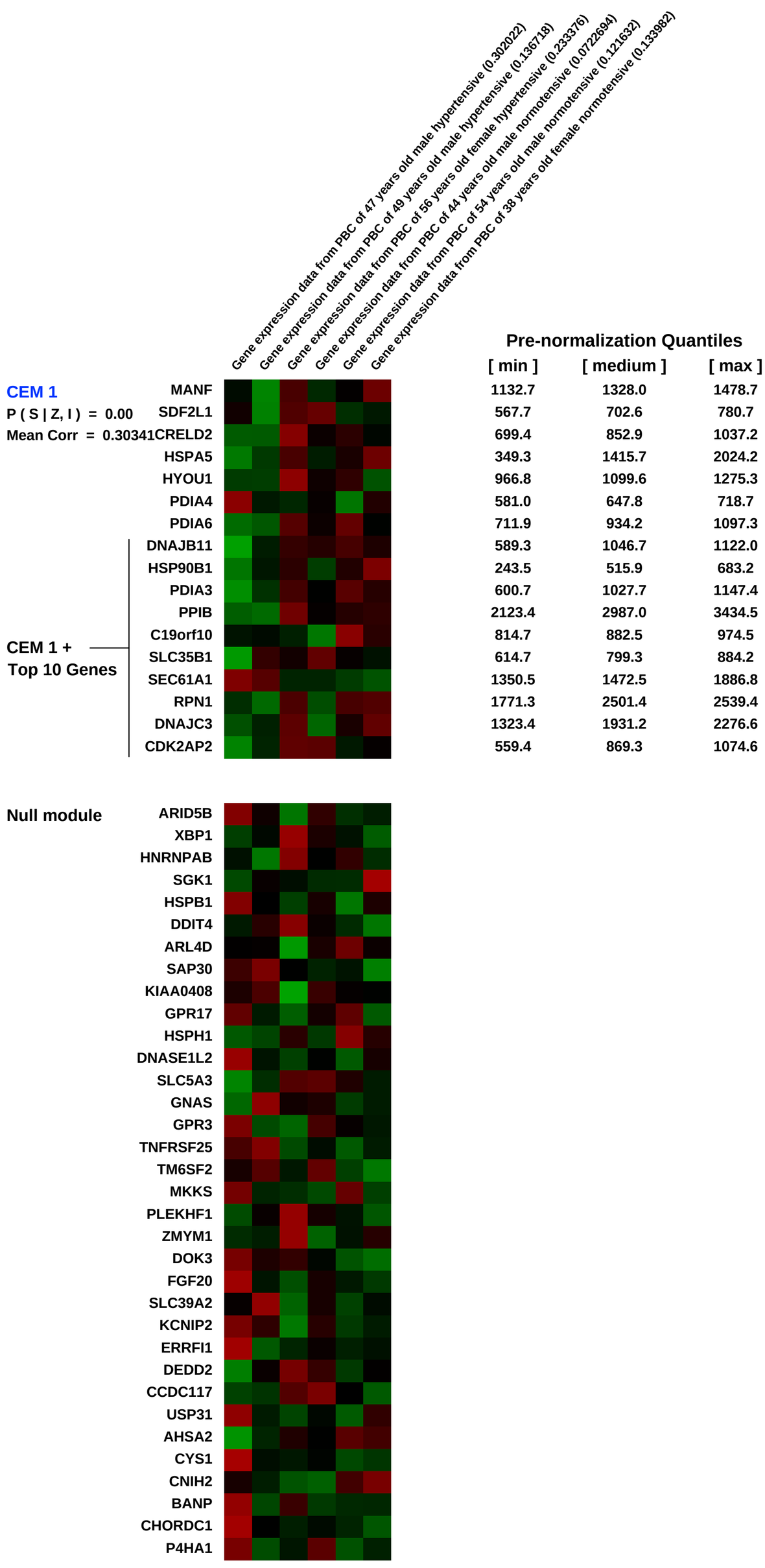

	Pre-normalization Quantiles		
	[min]	[medium]	[max]
MANF	1132.7	1328.0	1478.7
SDF2L1	567.7	702.6	780.7
CRELD2	699.4	852.9	1037.2
HSPA5	349.3	1415.7	2024.2
HYOU1	966.8	1099.6	1275.3
PDIA4	581.0	647.8	718.7
PDIA6	711.9	934.2	1097.3
DNAJB11	589.3	1046.7	1122.0
HSP90B1	243.5	515.9	683.2
PDIA3	600.7	1027.7	1147.4
PPIB	2123.4	2987.0	3434.5
C19orf10	814.7	882.5	974.5
SLC35B1	614.7	799.3	884.2
SEC61A1	1350.5	1472.5	1886.8
RPN1	1771.3	2501.4	2539.4
DNAJC3	1323.4	1931.2	2276.6
CDK2AP2	559.4	869.3	1074.6

GEO Series "GSE32062" Expression Profiles

Num of samples in this series: 10

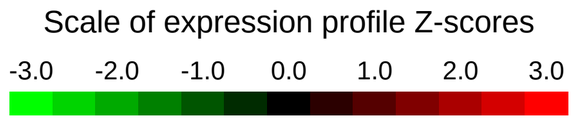

GEO Link:	http://www.ncbi.nlm.nih.gov/geo/query/acc.cgi?acc=GSE32062
Status:	Public on Mar 01 2012
Title:	Immune-activation as a therapeutic direction for patients with high-risk ovarian cancer based on gene expression signature (1)
Organism:	Homo sapiens
Experiment type:	Expression profiling by array
Platform:	GPL570
Pubmed ID:	22241791
Summary & Design:	**Summary:** **The Japanese Serous Ovarian Cancer Study Group** **Advanced-stage ovarian cancer is one of the most lethal gynecologic malignancies. To improve prognosis of patients with ovarian cancers, a predictive biomarkers leading to personalized treatments are required. In this large-scale cross-platform study of six microarray datasets consisting of 1054 ovarian cancer patients, we developed a novel risk classification system based on a 126-gene expression signature for predicting overall survival by applying elastic net7 and 10-fold cross validation to a Japanese dataset A (n = 260). We further validated its predictive ability with the five other datasets using multivariate analysis. Also, through gene ontology and pathway analyses of 1109 high-risk ovarian cancer specific transcripts, we identified a significant reduction of expression of immune-response related genes, especially on the antigen presentation pathway. Furthermore, an immunohistochemical analysis demonstrated that the number of CD8 T lymphocytes infiltrating into tumor tissue was significantly decreased in high-risk ovarian cancers. These predictive biomarkers based on the 126-gene expression signature will identify high-risk ovarian cancer patients who need novel immune-activating therapeutic approaches, leading to improved outcomes for such patients.** **Overall design:** **Microaray data from 10 patients who were diagnosed as advanced-stage high-grade serous ovarian cancer were analyzed to investigate coefficient of correlation in each probes between Agilent Whole Human Genome Oligo Microarray and Affymetrix HG-U133Plus2.0.**

Background corr dist: **KL-Divergence = 0.1252, L1-Distance = 0.0454, L2-Distance = 0.0047, Normal std = 0.4091**

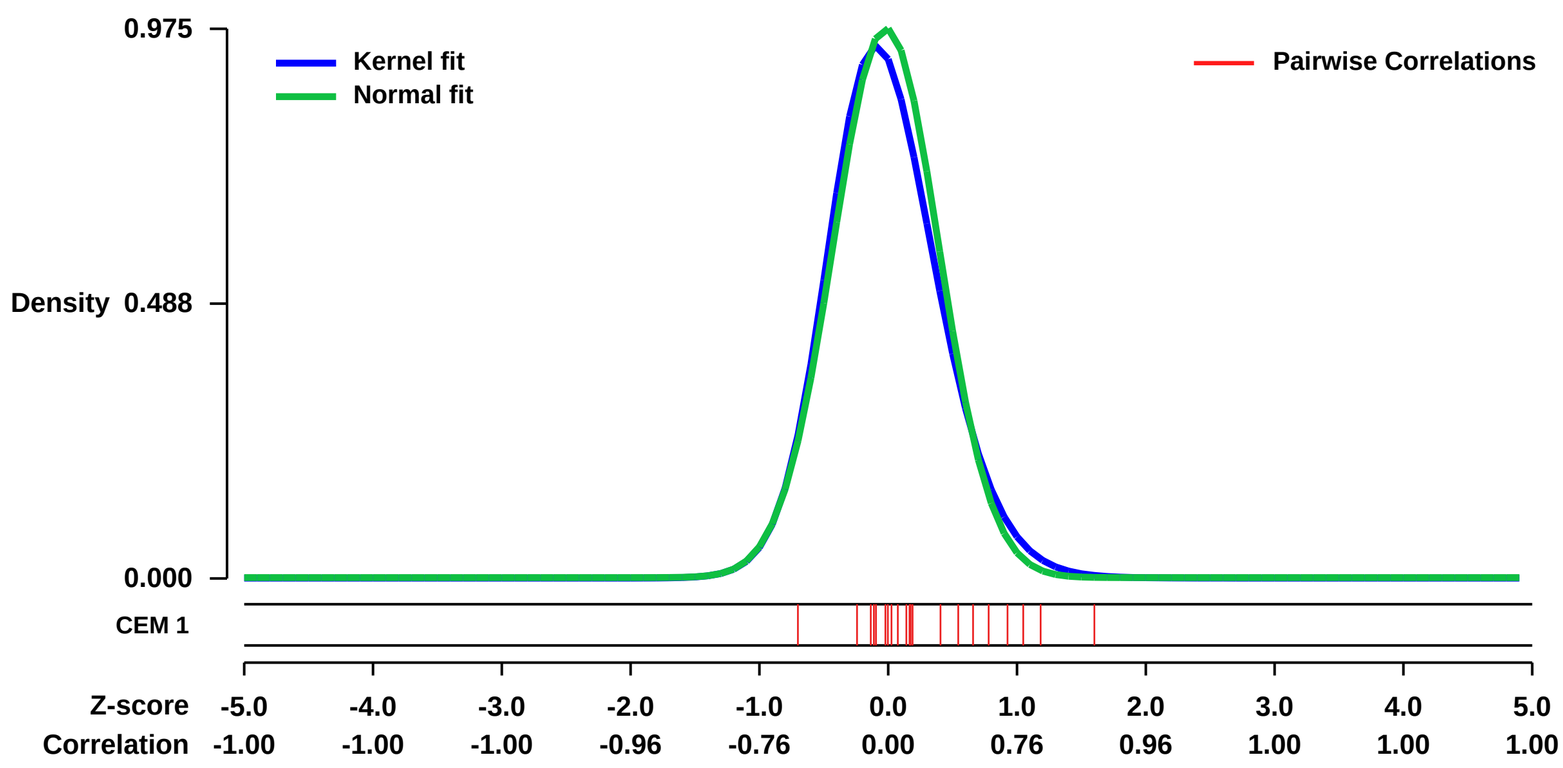

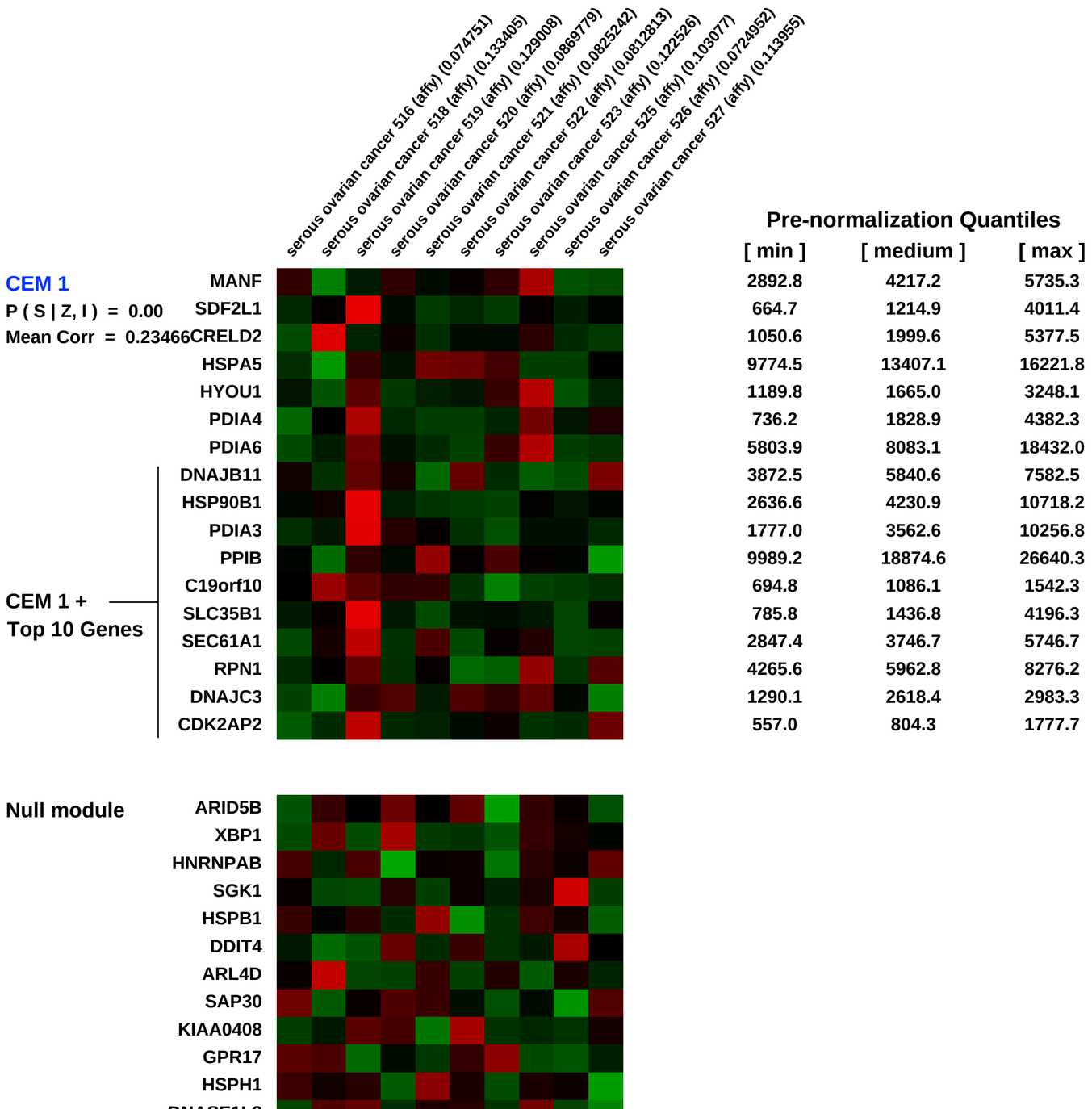

GEO Series "GSE16249" Expression Profiles

Num of samples in this series: 8

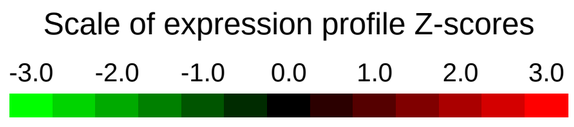

GEO Link:	http://www.ncbi.nlm.nih.gov/geo/query/acc.cgi?acc=GSE16249
Status:	Public on Jan 02 2010
Title:	siRNA-mediated knockdown of MITF and PAX3 in metastatic melanoma cell lines
Organism:	Homo sapiens
Experiment type:	Expression profiling by array
Platform:	GPL570
Pubmed ID:	

Summary & Design:

Summary:
The transcription factors PAX3 and MITF are required for the development of the neural crest and melanocyte lineage, and both proteins play important roles in melanoma cell growth and survival. PAX3 transcriptionally activates MITF expression during neural crest development, but the relationship between these transcription factors during melanocyte development and in melanoma cells is currently poorly understood. This study aimed to further our understanding of the interaction between transcriptional networks controlled by PAX3 and MITF by assessing the effect of siRNA-mediated knockdown of PAX3 and MITF in metastatic melanoma cell lines. The goals of this study were to determine (i) if PAX3 is required for maintaining expression of MITF in melanoma and melanocyte cell lines; (ii) whether PAX3 and MITF independently, or redundantly, influence growth and survival in melanoma cell lines; and (iii) to investigate the respective roles of PAX3 and MITF expression in melanoma cell differentiation.

Microarrays were used to measure global changes in transcript expression in response to siRNA-mediated knockdown of PAX3 or MITF compared to non-targeting controls in two metastatic melanoma cells lines.

Overall design:
RNA was isolated from two different metastatic melanoma cell lines 30 hours after one of four different treaments: (i) transfection with siRNA targeting PAX3; or (ii) transfection with siRNA targeting MITF; or (iii) or transfection with siRNA targeting luciferase (non-targeting negative control); or (iv) treatment with media only (control). Therefore, eight samples were used for gene expression profiling by using GeneChip arrays, with one replicate per cell line per treatment.

Background corr dist: KL-Divergence = 0.0287, L1-Distance = 0.0413, L2-Distance = 0.0021, Normal std = 0.7143

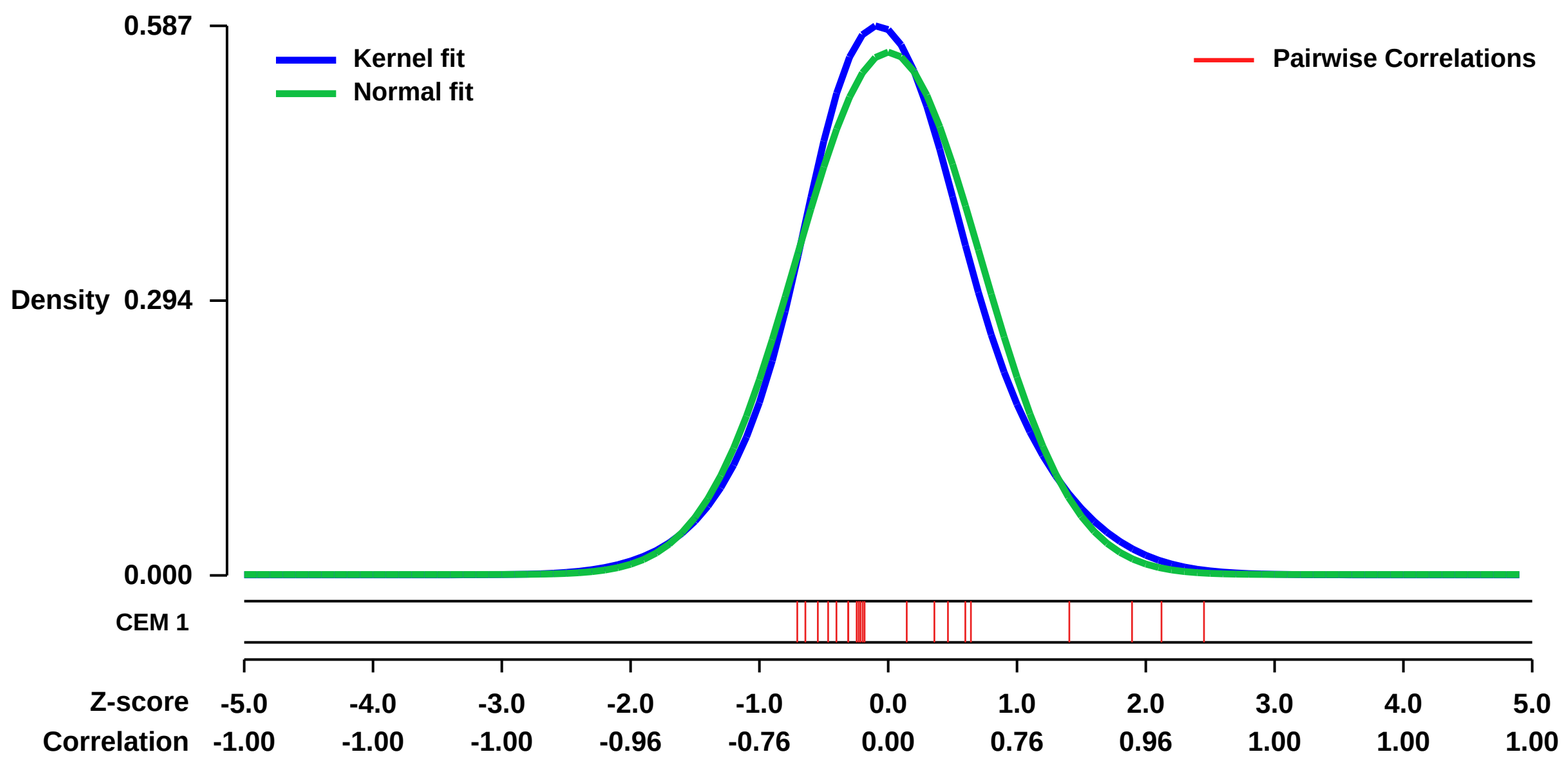

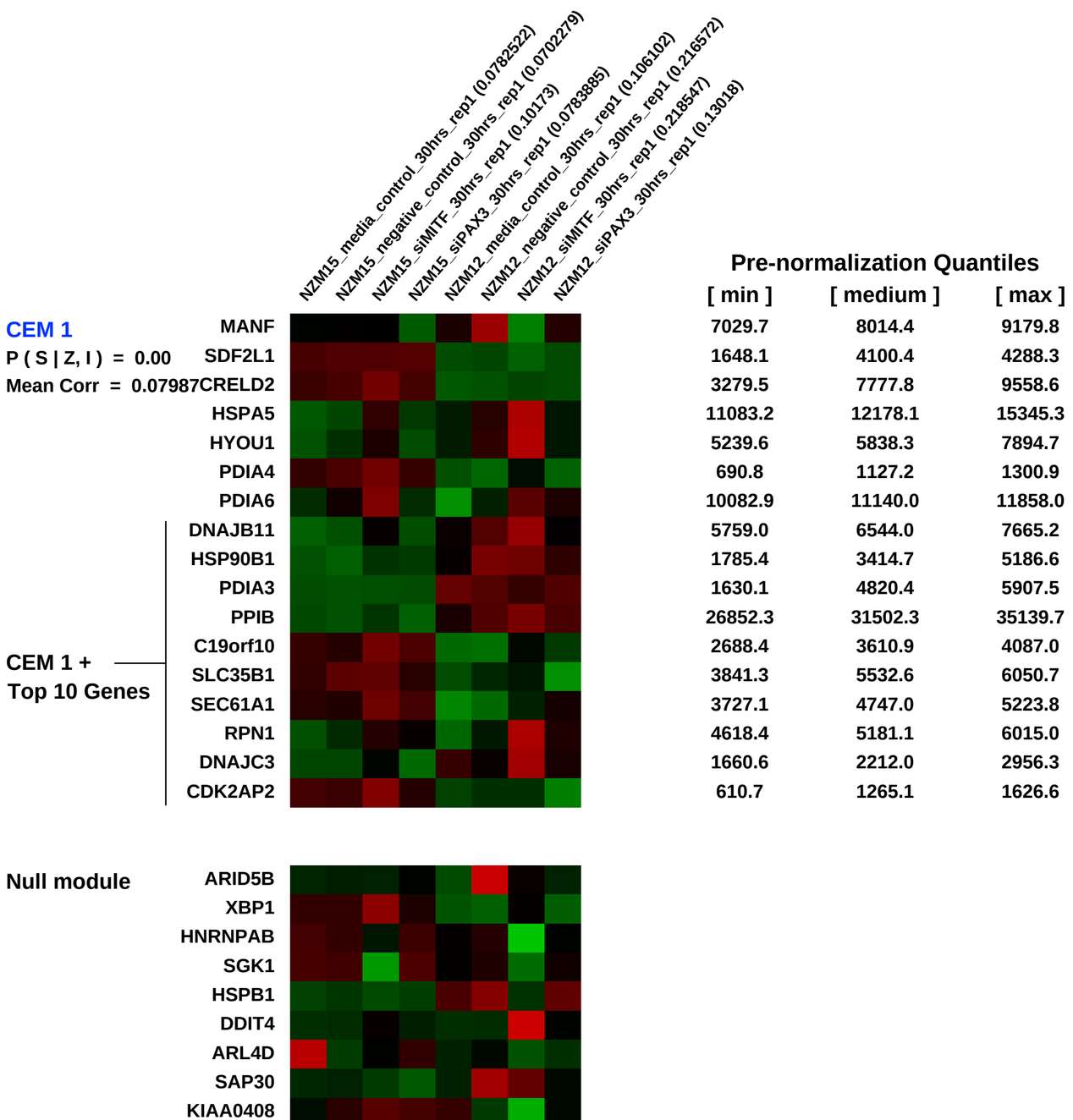

Pre-normalization Quantiles

	[min]	[medium]	[max]
MANF	7029.7	8014.4	9179.8
SDF2L1	1648.1	4100.4	4288.3
CRELD2	3279.5	7777.8	9558.6
HSPA5	11083.2	12178.1	15345.3
HYOU1	5239.6	5838.3	7894.7
PDIA4	690.8	1127.2	1300.9
PDIA6	10082.9	11140.0	11858.0
DNAJB11	5759.0	6544.0	7665.2
HSP90B1	1785.4	3414.7	5186.6
PDIA3	1630.1	4820.4	5907.5
PPIB	26852.3	31502.3	35139.7
C19orf10	2688.4	3610.9	4087.0
SLC35B1	3841.3	5532.6	6050.7
SEC61A1	3727.1	4747.0	5223.8
RPN1	4618.4	5181.1	6015.0
DNAJC3	1660.6	2212.0	2956.3
CDK2AP2	610.7	1265.1	1626.6

GEO Series "GSE10289" Expression Profiles

Num of samples in this series: 6

Scale of expression profile Z-scores

-3.0 -2.0 -1.0 0.0 1.0 2.0 3.0

GEO Link:	http://www.ncbi.nlm.nih.gov/geo/query/acc.cgi?acc=GSE10289
Status:	Public on Apr 01 2008
Title:	Cells silenced for SDHB expression and tumor phenotype
Organism:	Homo sapiens
Experiment type:	Expression profiling by array
Platform:	GPL570
Pubmed ID:	18519664
Summary & Design:	**Summary:** **Effect of SDHB silencing using siRNA methodologies in the tumor phenotype** **We used microarrays to detail the global programme of gene expression when SDHB is silenced.** **Keywords: siRNA experiment (loss of function)** **Overall design:** **Human hepatocellular carcinoma cell line Hep3B was stably silenced with control or SDHB-specific siRNAs**

Background corr dist: **KL-Divergence = 0.0303, L1-Distance = 0.0422, L2-Distance = 0.0020, Normal std = 0.7274**

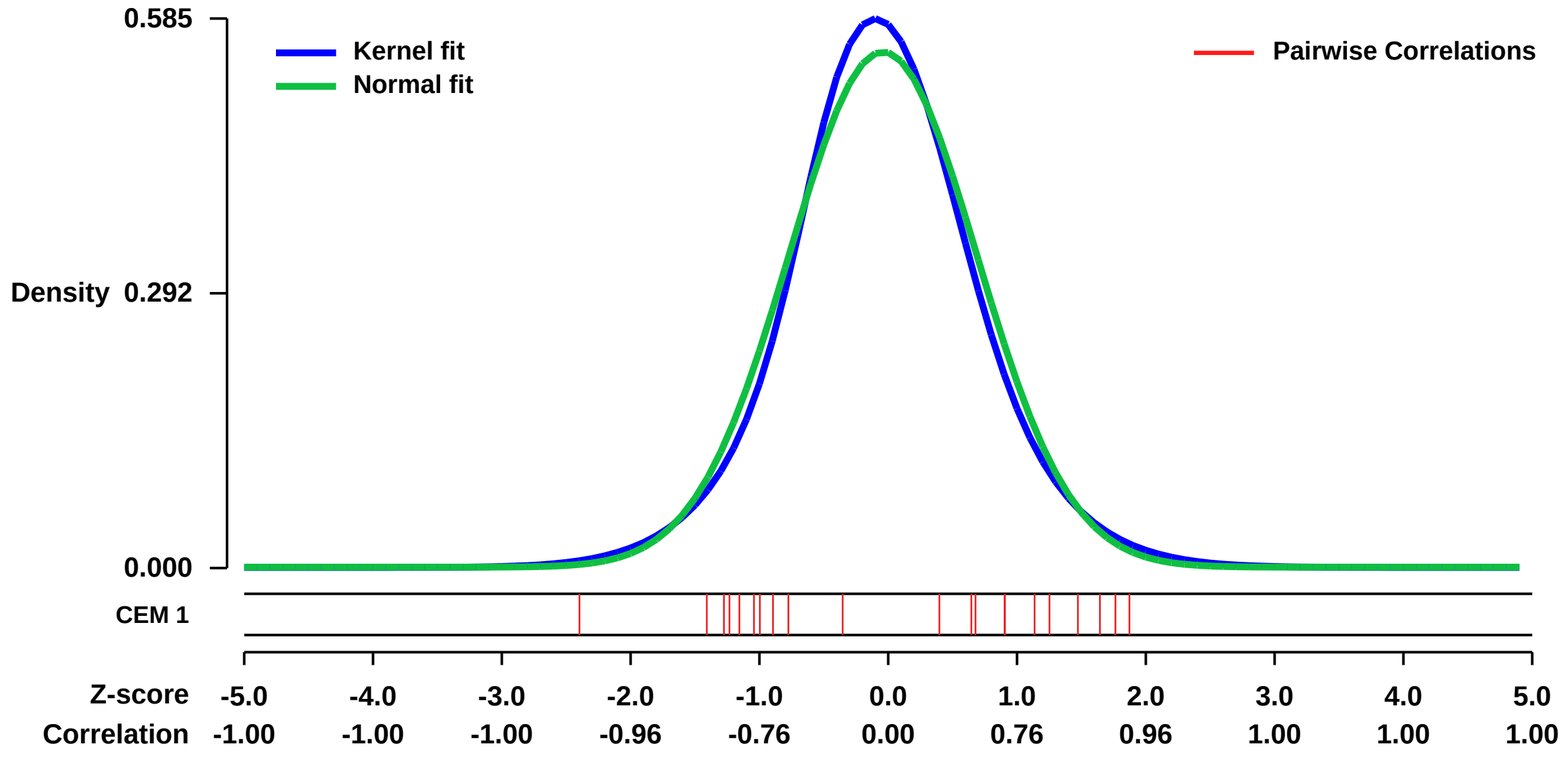

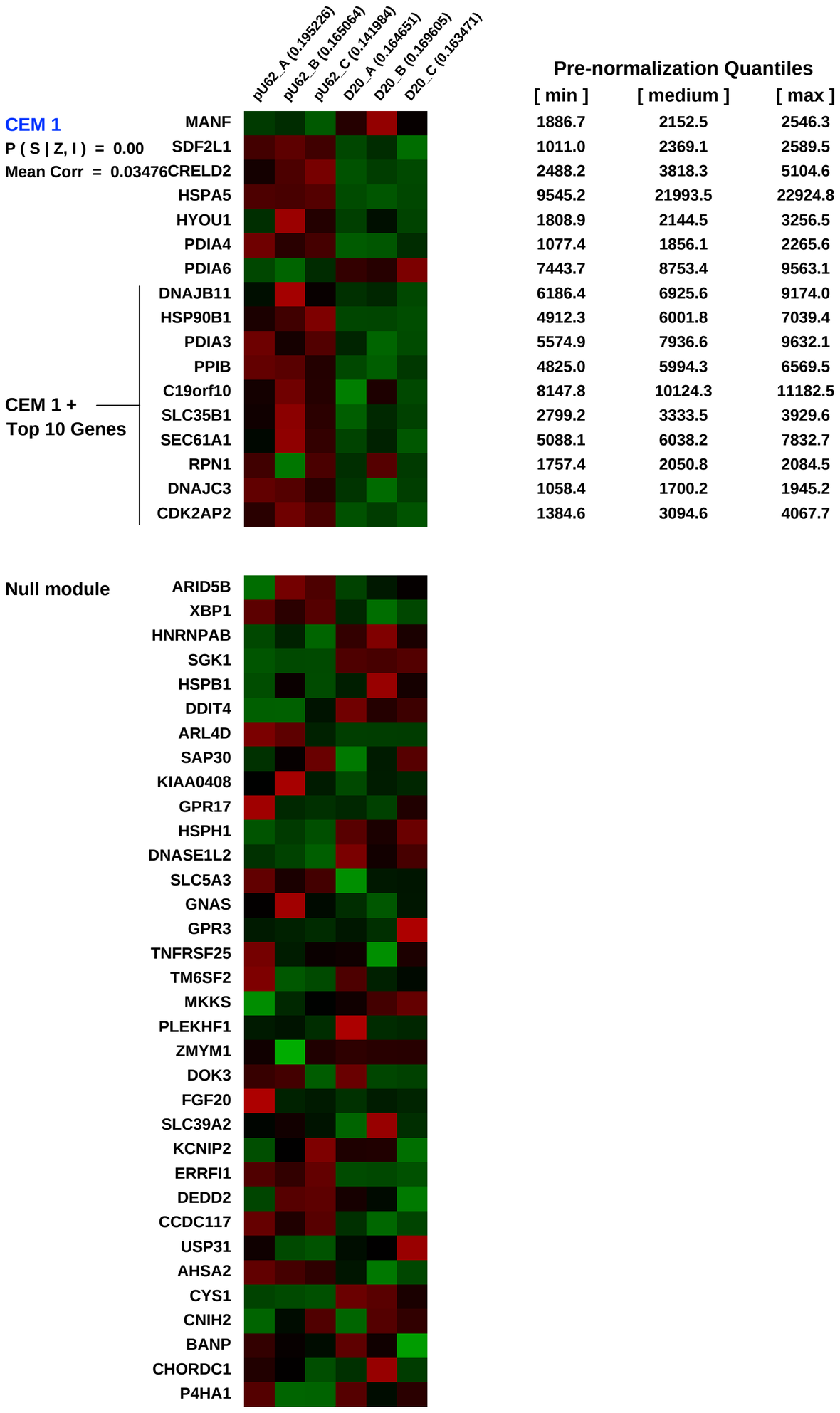

GEO Series "GSE17014" Expression Profiles

Num of samples in this series: 8

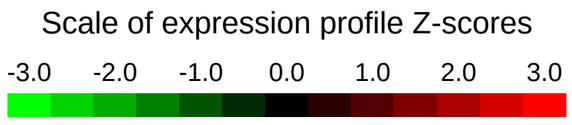

GEO Link:	http://www.ncbi.nlm.nih.gov/geo/query/acc.cgi?acc=GSE17014
Status:	Public on Oct 01 2009
Title:	Expression data from HD-1 bri and HD-1 dim cells
Organism:	Homo sapiens
Experiment type:	Expression profiling by array
Platform:	GPL570
Pubmed ID:	19652362
Summary & Design:	**Summary:** Pericytes derived from skin dermis can substantially enhance the short-term tissue-regenerative capacity of human epidermal cells already committed to differentiation; they also display both phenotypic and functional properties of mesenchymal stem cells. In this microarray analysis, we compared the gene expression profile of dermal pericytes to that of the remaining dermal cells of neonatal human foreskin. **Overall design:** Human neonatal foreskin was digested overnight in dispase II at 4˚C to separate the epidermis from the dermis. Subsequently the dermis was digested for 1-2 hours at 37˚C in a mixed dispase and collagenase solution and then fractionated into two populations, i.e. pericytes (HD-1bri) and the remaining dermal cells (HD-1dim), on the basis of differential VLA-1 expression using fluorescence-activated cell sorting. Total RNA from 15,000 cells of each population was extracted from 4 independent replicate sorts. mRNAs were amplified using a T7-primer-based-2-round linear RNA amplification protocol (GeneChip Two-Cycle cDNA synthesis kit). Fragmented and biotin-labelled cRNA from each individual sample was hybridised to Affymetrix HG-U133 plus 2.0 arrays and scanned on a Affymetrix GeneChip scanner. Probe intensities were RMA normalized and log2-transformed expression values were compared using moderated t statistics to quantify differences between individual samples.

Background corr dist: KL-Divergence = 0.0510, L1-Distance = 0.0164, L2-Distance = 0.0004, Normal std = 0.5555

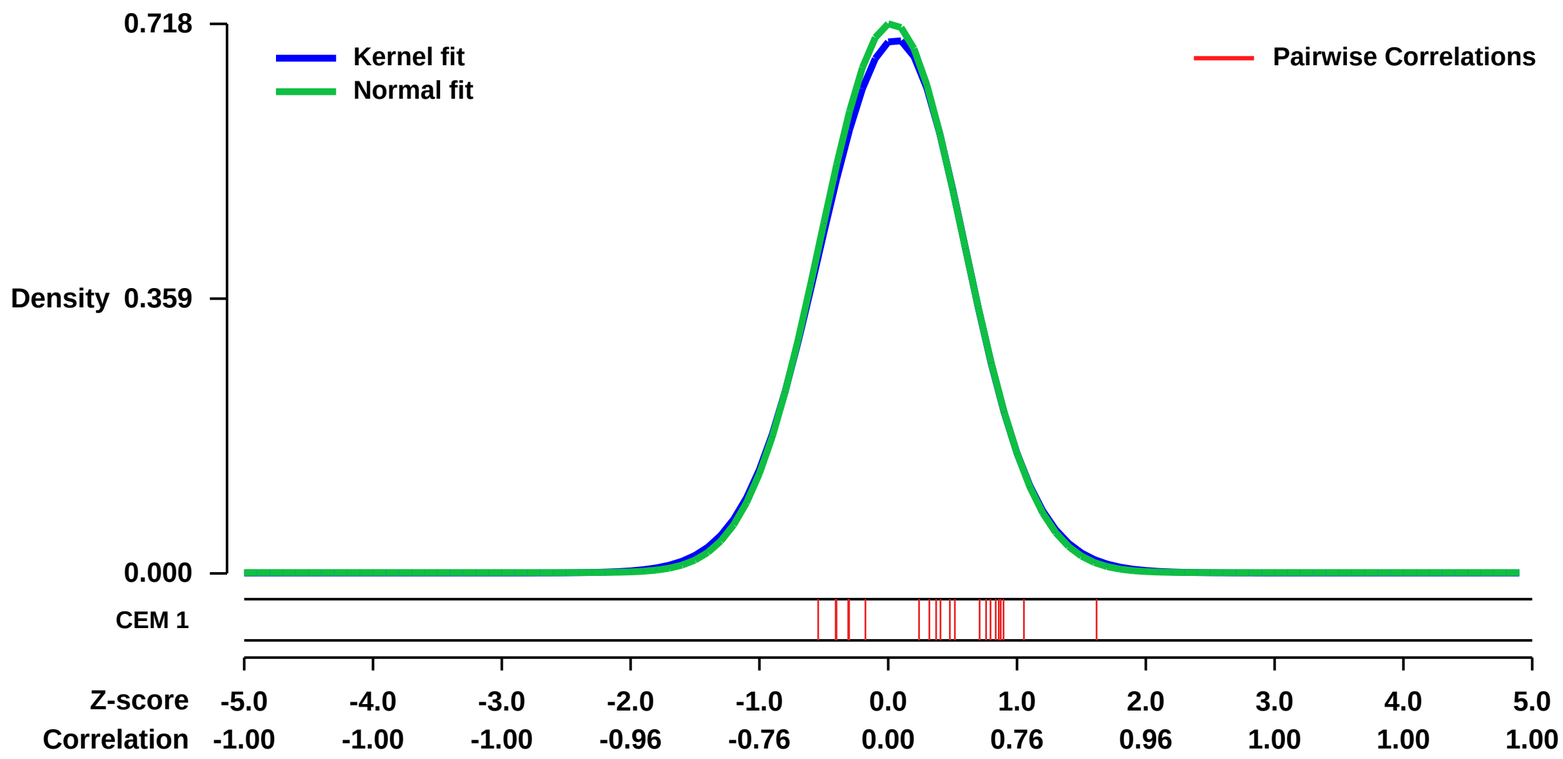

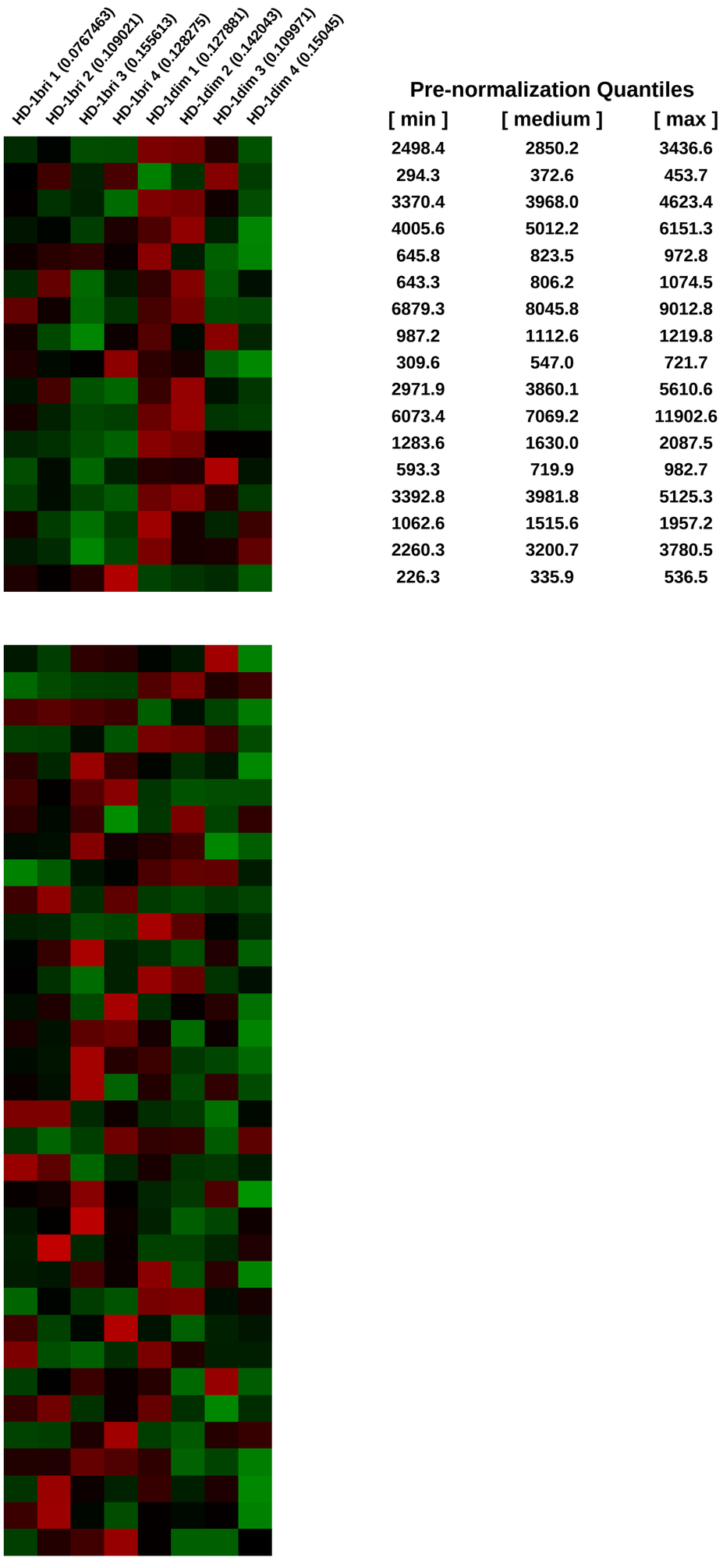

GEO Series "GSE16547" Expression Profiles

Num of samples in this series: 8

Scale of expression profile Z-scores

-3.0 -2.0 -1.0 0.0 1.0 2.0 3.0

GEO Link:	http://www.ncbi.nlm.nih.gov/geo/query/acc.cgi?acc=GSE16547
Status:	Public on Dec 01 2009
Title:	KSHV Manipulates Notch Signaling by Upregulating Dll4 and JAG1 to Alter Cell Cycle Gene Expression in LECs
Organism:	Homo sapiens
Experiment type:	Expression profiling by array
Platform:	GPL570
Pubmed ID:	19816565
Summary & Design:	**Summary:** Kaposi sarcoma is the most common cancer in AIDS patients and is typified by red skin lesions. The disease is caused by the KSHV virus (HHV8) and is recognizable by its distinctive red skin lesions. The lesions are KSHV infected spindle cells, most commonly the lymphatic endothelial and blood vessel endothelial cells (LEC and BEC), plus surrounding stroma. Here we examine KSHVs modulation of Notch signaling using wild-type LEC cells co-cultured with DLL4 and JAG1 expressing LEC cells. **Overall design:** There are 1) n=2 of LEC control cells co-cultured with pSIN expressing LEC, 2) n=3 of LEC co-cultured with pSIN-Dll4 expressing LEC, and 3) n=3 of LEC co-cultured with pSIN-JAG1 expressing LEC.

Background corr dist: KL-Divergence = 0.0510, L1-Distance = 0.0196, L2-Distance = 0.0006, Normal std = 0.5596

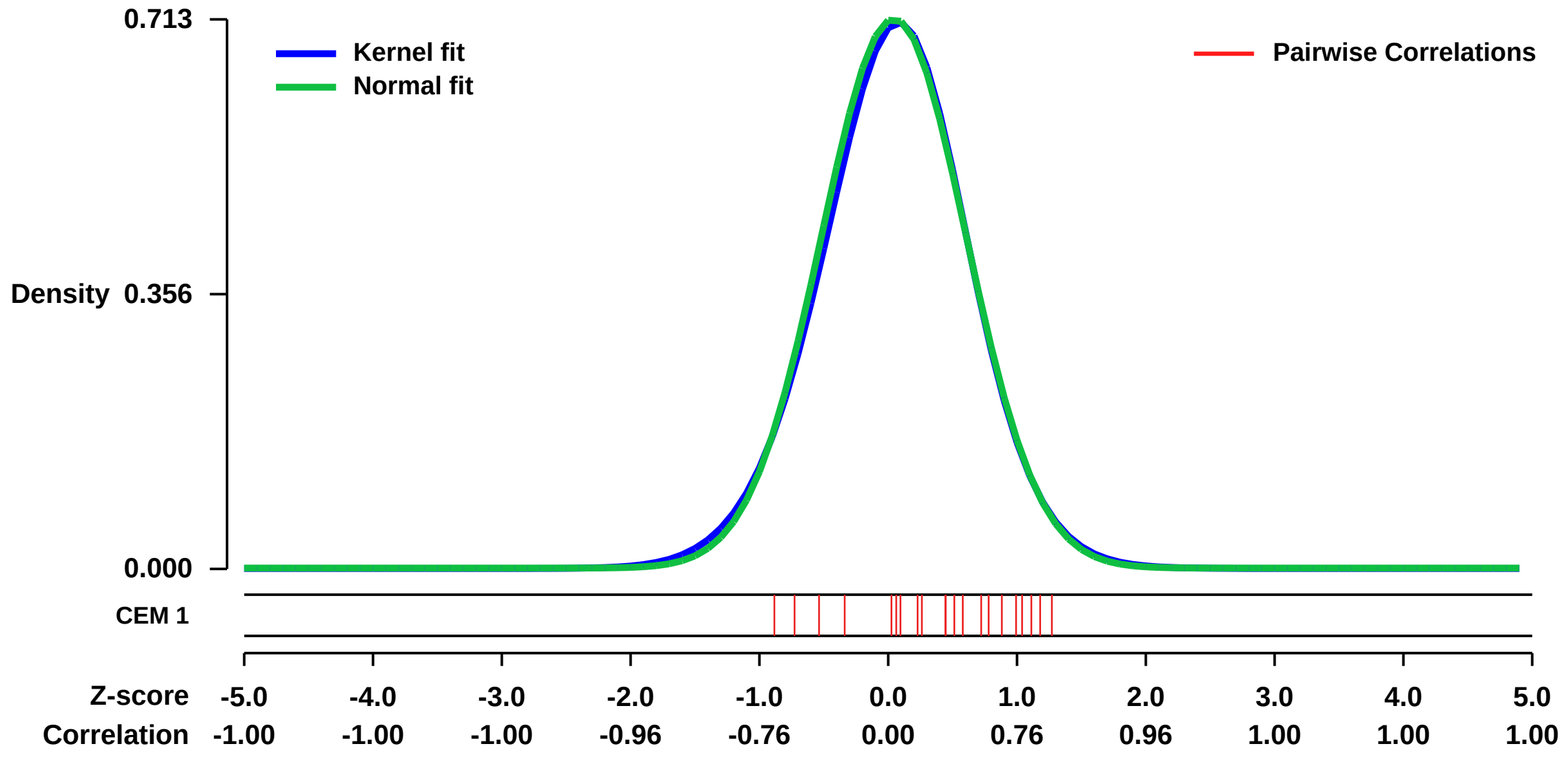

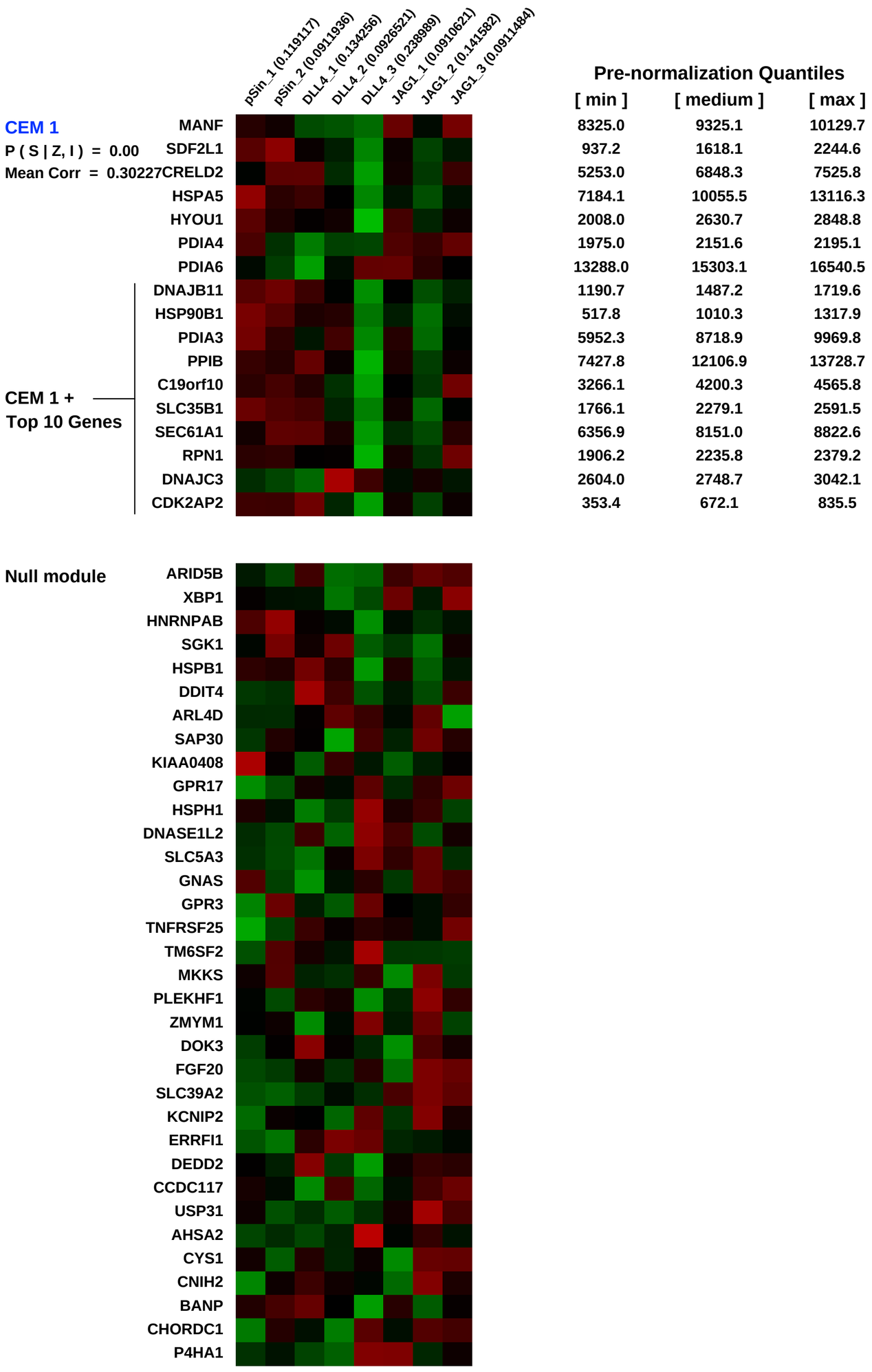

GEO Series "GSE21654" Expression Profiles

Num of samples in this series: 22

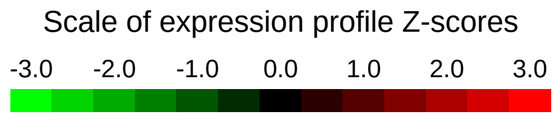

GEO Link:	http://www.ncbi.nlm.nih.gov/geo/query/acc.cgi?acc=GSE21654
Status:	Public on May 05 2010
Title:	Expression data from 22 Pancreatic Cancer Cell Lines
Organism:	Homo sapiens
Experiment type:	Expression profiling by array
Platform:	GPL570
Pubmed ID:	20885998
Summary & Design:	**Summary:** We used microarrays to analyze the global expression patterns for 22 commercially available pancreatic cancer cell lines **Overall design:** 22 pancreatic cancer cell lines were grown to 80% confluence in DMEM/FBS/PenStrep media and then harvested for total RNA

Background corr dist: KL-Divergence = 0.3978, L1-Distance = 0.0823, L2-Distance = 0.0215, Normal std = 0.2492

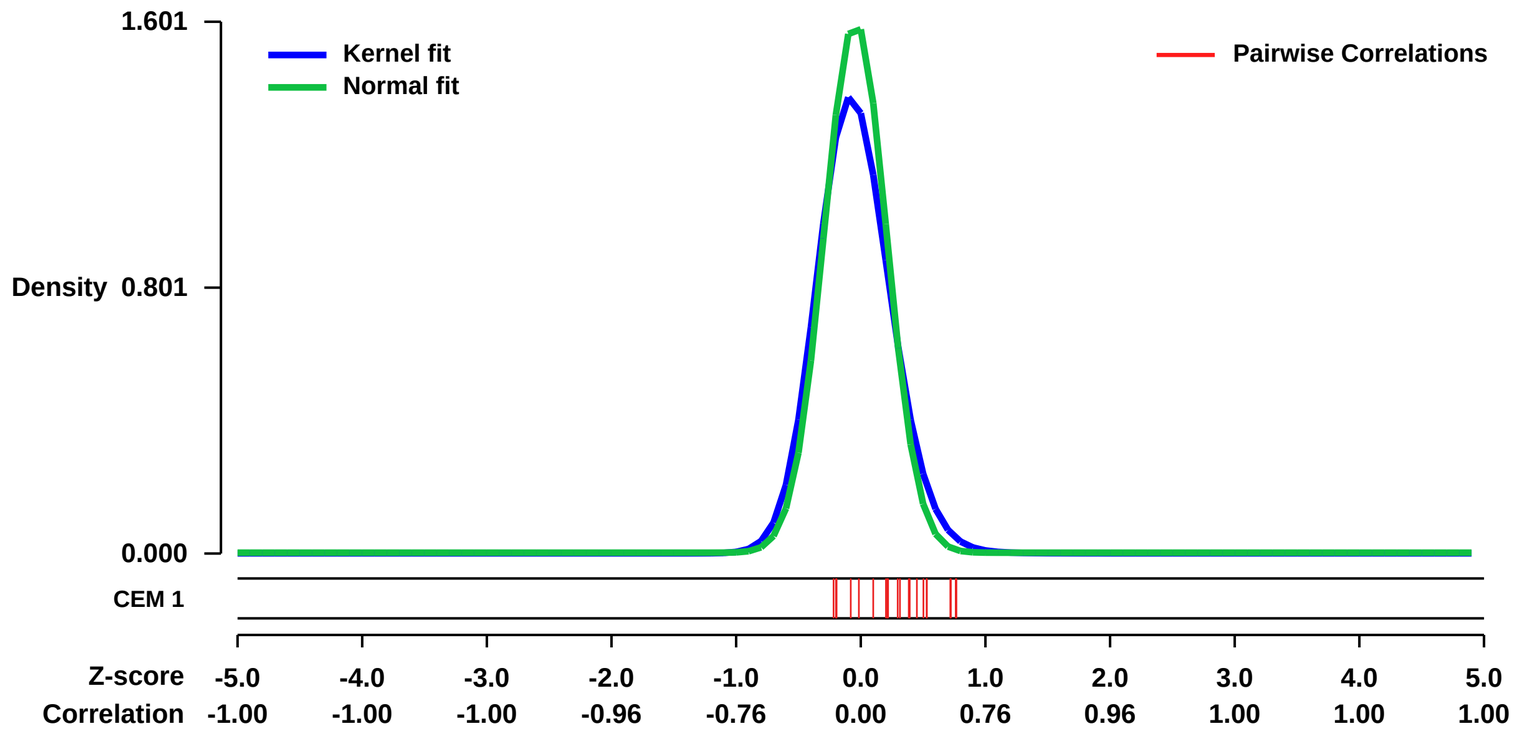

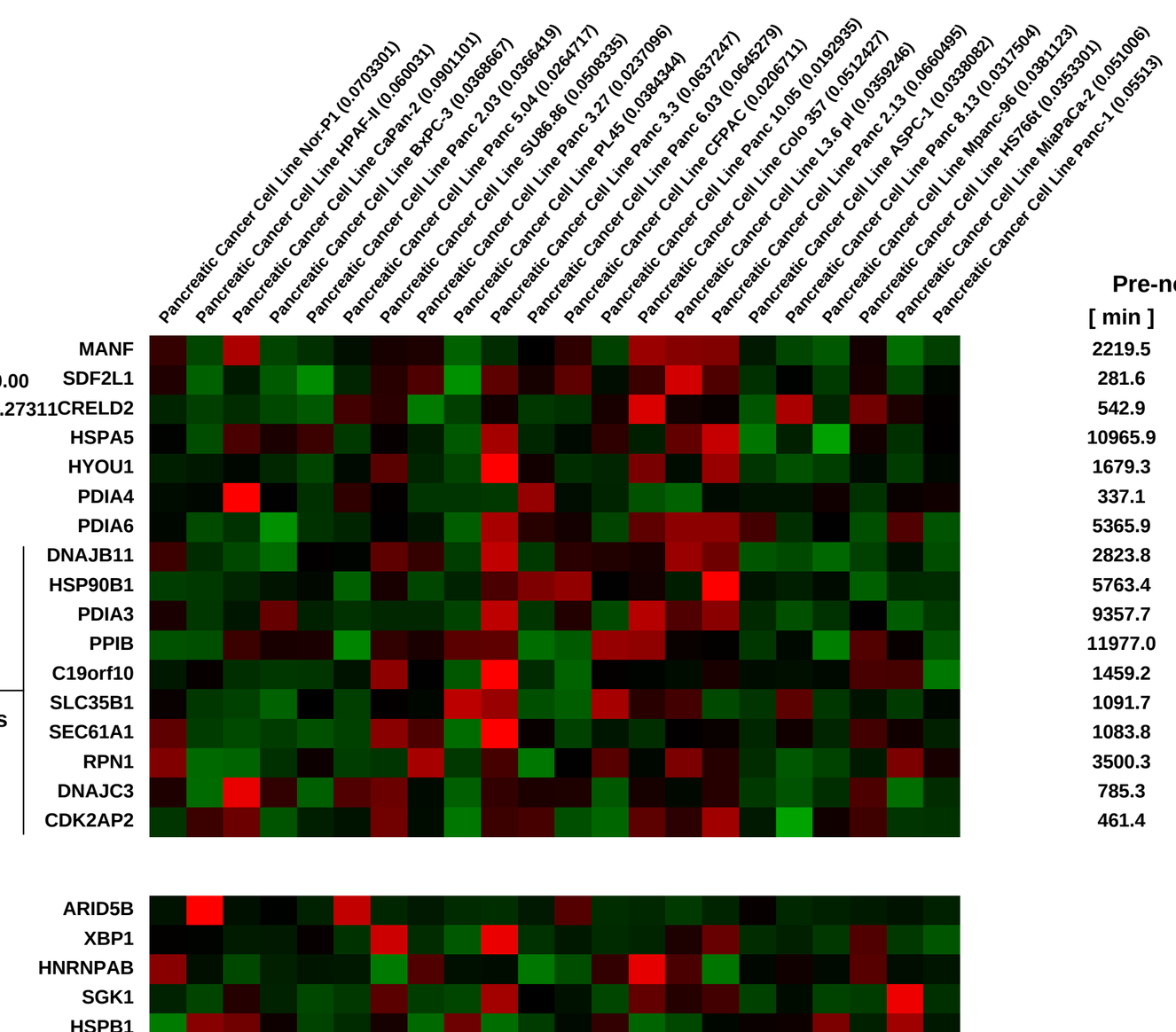

Pre-normalization Quantiles

[min]	[medium]	[max]
2219.5	3715.1	6675.2
281.6	954.3	1958.3
542.9	2194.0	5000.8
10965.9	24181.2	40890.4
1679.3	2820.5	8725.9
337.1	1235.9	4572.0
5365.9	11235.2	18635.8
2823.8	5203.3	9669.7
5763.4	9397.3	22754.8
9357.7	11649.6	21595.1
11977.0	20049.8	28102.6
1459.2	2729.8	6182.7
1091.7	2227.7	4638.4
1083.8	2046.0	5174.1
3500.3	5456.3	8447.6
785.3	2454.9	5061.1
461.4	1030.3	1687.4

GEO Series "GSE16683" Expression Profiles

Num of samples in this series: 6

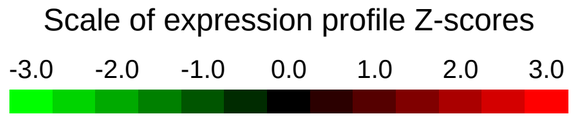

GEO Link:	http://www.ncbi.nlm.nih.gov/geo/query/acc.cgi?acc=GSE16683
Status:	Public on Jun 18 2009
Title:	Human endothelial gene expression under estradiol treatment
Organism:	Homo sapiens
Experiment type:	Expression profiling by array
Platform:	GPL570
Pubmed ID:	20011585
Summary & Design:	**Summary:** DNA microarrays were used to investigate global gene expression patterns in cultured human umbilical vein endothelial cells (HUVEC) exposed to 1 nmol/L estradiol for 24 hours, compared to control cells. **Overall design:** HUVEC from 9 separate cultures were exposed to control (0.1% ethanol) and 1nmol/L estradiol treatments for 24 h. Total cellular RNA was extracted. Equal amounts of RNA extracted from 3 control cells or 3 estradiol-treated cells obtained from three different cultures were pooled, achieving three biological replicates of the control and three that were treated with estradiol. Therefore, a total number of 6 microarrays were developed.

Background corr dist: KL-Divergence = 0.0208, L1-Distance = 0.0192, L2-Distance = 0.0005, Normal std = 0.7363

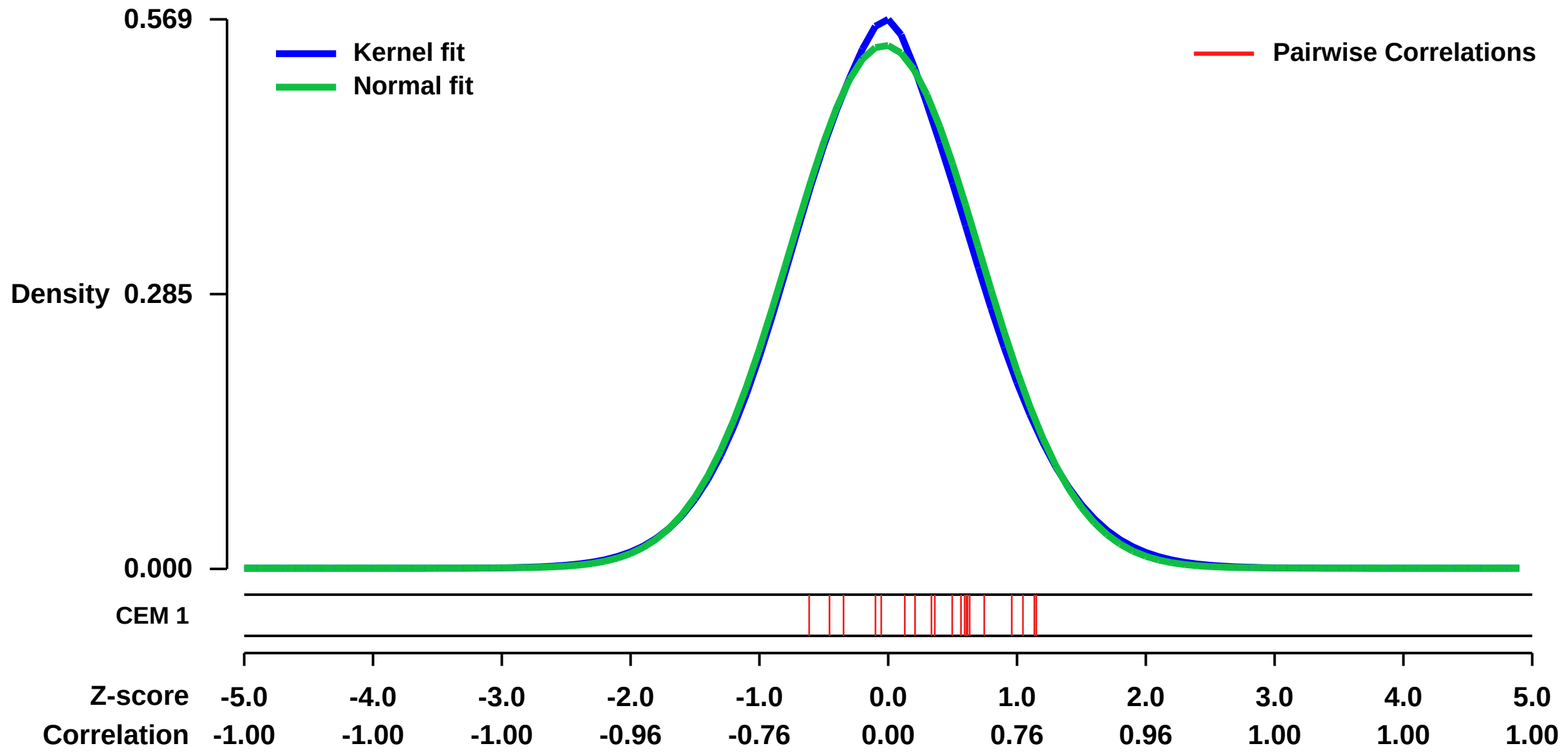

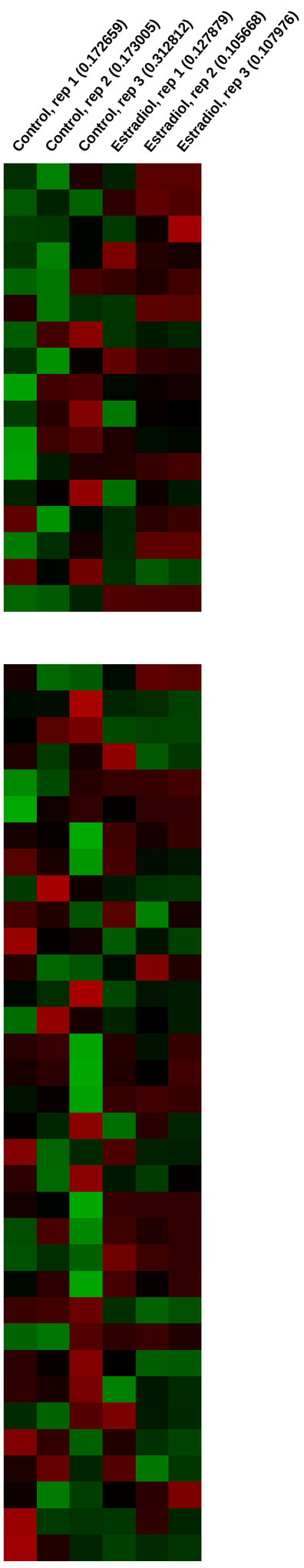

GEO Series "GSE29436" Expression Profiles

Num of samples in this series: 8

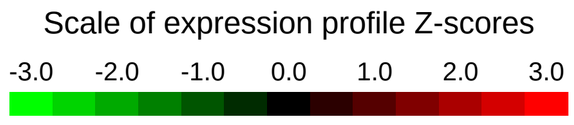

GEO Link:	http://www.ncbi.nlm.nih.gov/geo/query/acc.cgi?acc=GSE29436
Status:	Public on Jan 26 2012
Title:	Progesterone inhibits epithelial-to-mesenchymal transition in endometrial cancer: patient data
Organism:	Homo sapiens
Experiment type:	Expression profiling by array
Platform:	GPL570
Pubmed ID:	
Summary & Design:	**Summary:** Every year more than 42,000 women die of endometrial cancer, mainly due to recurrent or metastatic disease. The presence of tumor infiltrating lymphocytes (TILs) as well as progesterone receptor (PR) positivity has been correlated with improved prognosis. This study describes two mechanisms by which progesterone inhibits metastatic spread of endometrial cancer: by stimulating T-cell infiltration and by inhibiting epithelial-to-mesenchymal cell transition (EMT). Paraffin sections from patients with (n=9) or without (n=10) progressive endometrial cancer (recurrent or metastatic disease) were assessed for the presence of CD4+ (helper), CD8+ (cytotoxic) and Foxp3+ (regulatory) T-lymphocytes and PR expression. Progressive disease was observed to be associated with significant loss of TILs and loss of PR expression. Frozen tumor samples, used for genome-wide expression analysis, showed significant regulation of pathways involved in immunosurveillance, EMT and metastasis. For a number of genes, such as CXCL14, DKK1, DKK4 and WIF1, quantitive RT-PCR was performed to verify down regulation in progressive disease. To corroborate the role of progesterone in regulating invasion, Ishikawa (IK) endometrial cancer cell lines stably transfected with PRA (IKPRA), PRB (IKPRB) and PRA+PRB (IKPRAB) were cultured in the presence/absence of progesterone (MPA) and used for genome-wide expression analysis, Boyden- and wound healing migration assays, and IHC for known EMT makers. IKPRB and IKPRAB cell lines showed MPA induced inhibition of migration and loss of the mesenchymal marker vimentin at the invasive front of the wound healing assay. Furthermore, pathway analysis of significantly MPA-regulated genes showed significant down regulation of important pathways involved in EMT, immunesuppression and metastasis: such as IL6-, TGF-¸† and Wnt/¸†-catenin signalling. Intact progesterone signaling in non-progressive endometrial cancer seems to be an important factor stimulating immunosurveillance and inhibiting transition from an epithelial to a more mesenchymal, more invasive phenotype. **Overall design:** From 4 non-progressive and 4 progressive patients, snap-frozen endometrial cancer tumor specimens were used for microarray analysis. Gene expression data of progressive disease was compared with non-progressive disease.

Background corr dist: KL-Divergence = 0.0632, L1-Distance = 0.0310, L2-Distance = 0.0018, Normal std = 0.5234

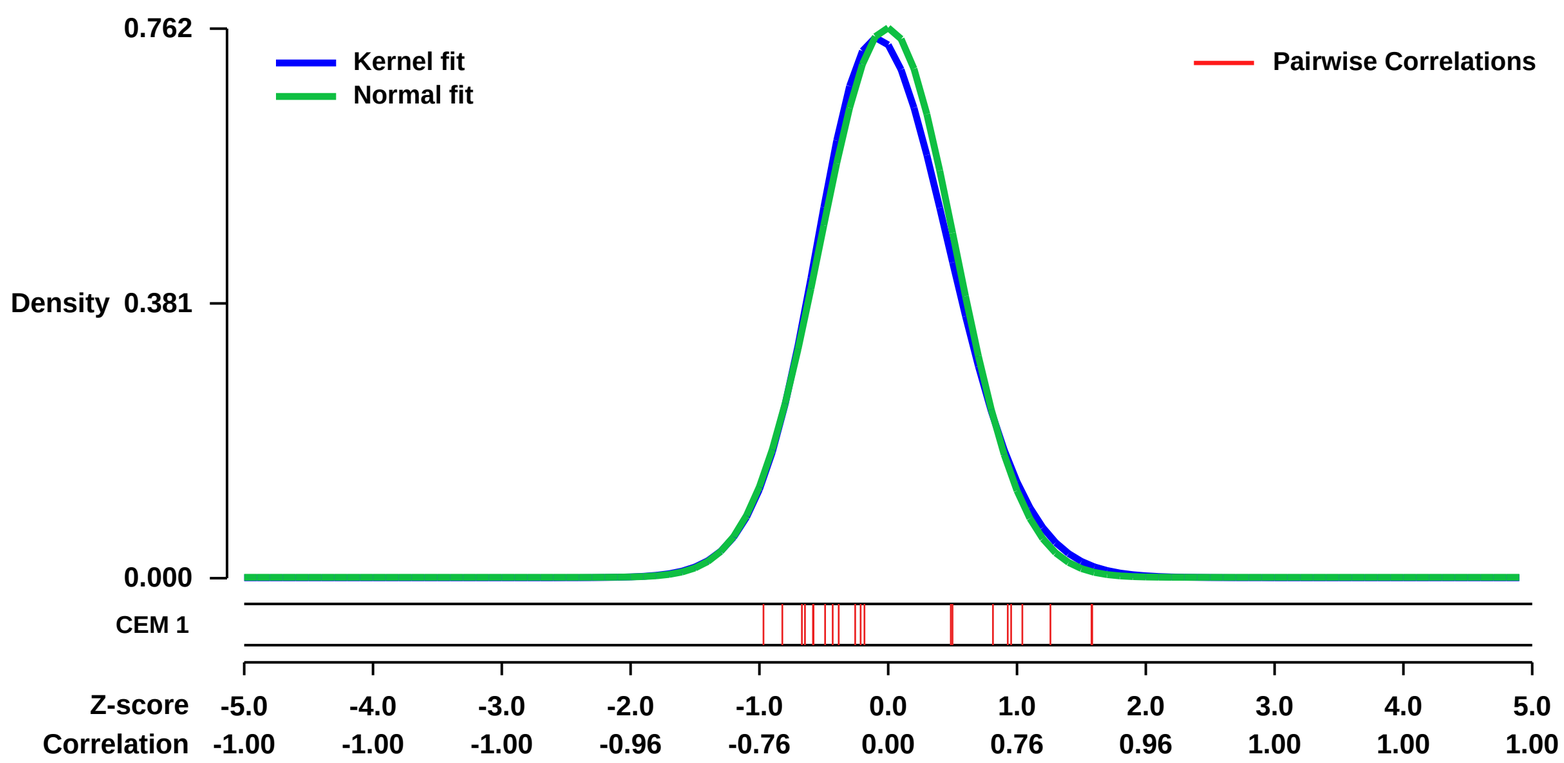

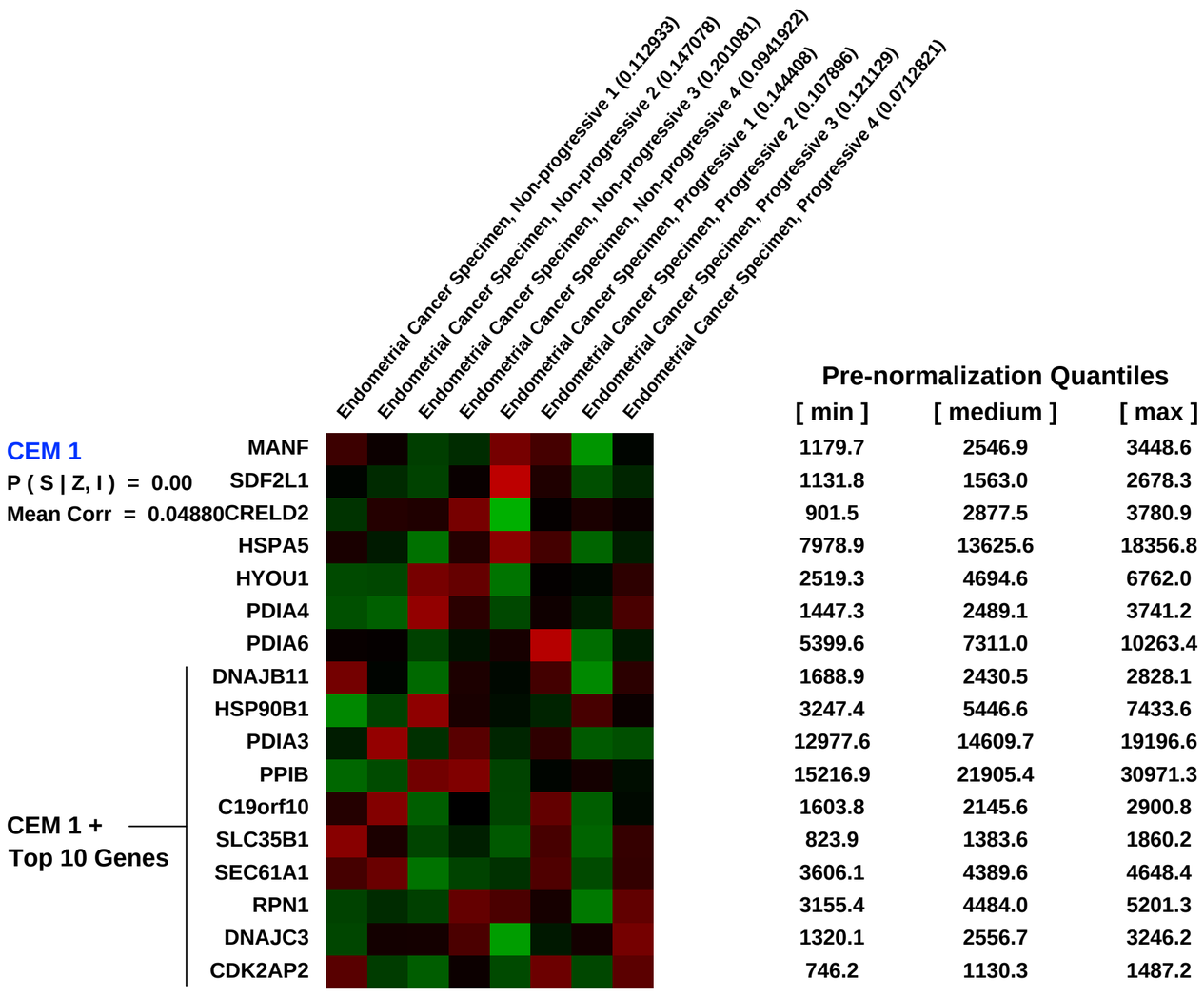

GEO Series "GSE13899" Expression Profiles

Num of samples in this series: 6

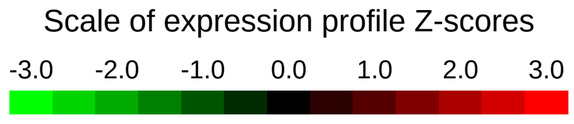

GEO Link:	http://www.ncbi.nlm.nih.gov/geo/query/acc.cgi?acc=GSE13899
Status:	Public on Dec 10 2009
Title:	Quercetin supplementation and CD14+ monocyte gene expression
Organism:	Homo sapiens
Experiment type:	Expression profiling by array
Platform:	GPL570
Pubmed ID:	20416132
Summary & Design:	**Summary:** Quercetin has been described to have a wide range of beneficial effects in humans, ranging from anti-carcinogenic properties to reduced risk of cardiovascular disease. We tested whether a daily supplementation of quercetin leads to reproducible changes in gene expression profiles of human monocytes. **Keywords: individual compound treatment** **Overall design:** CD14+ monocytes were isolated from three healthy volunteers before and after a 2 wk supplementation period of 150mg quercetin per day. With this design every subject served as his or her own control (baseline sample = control)

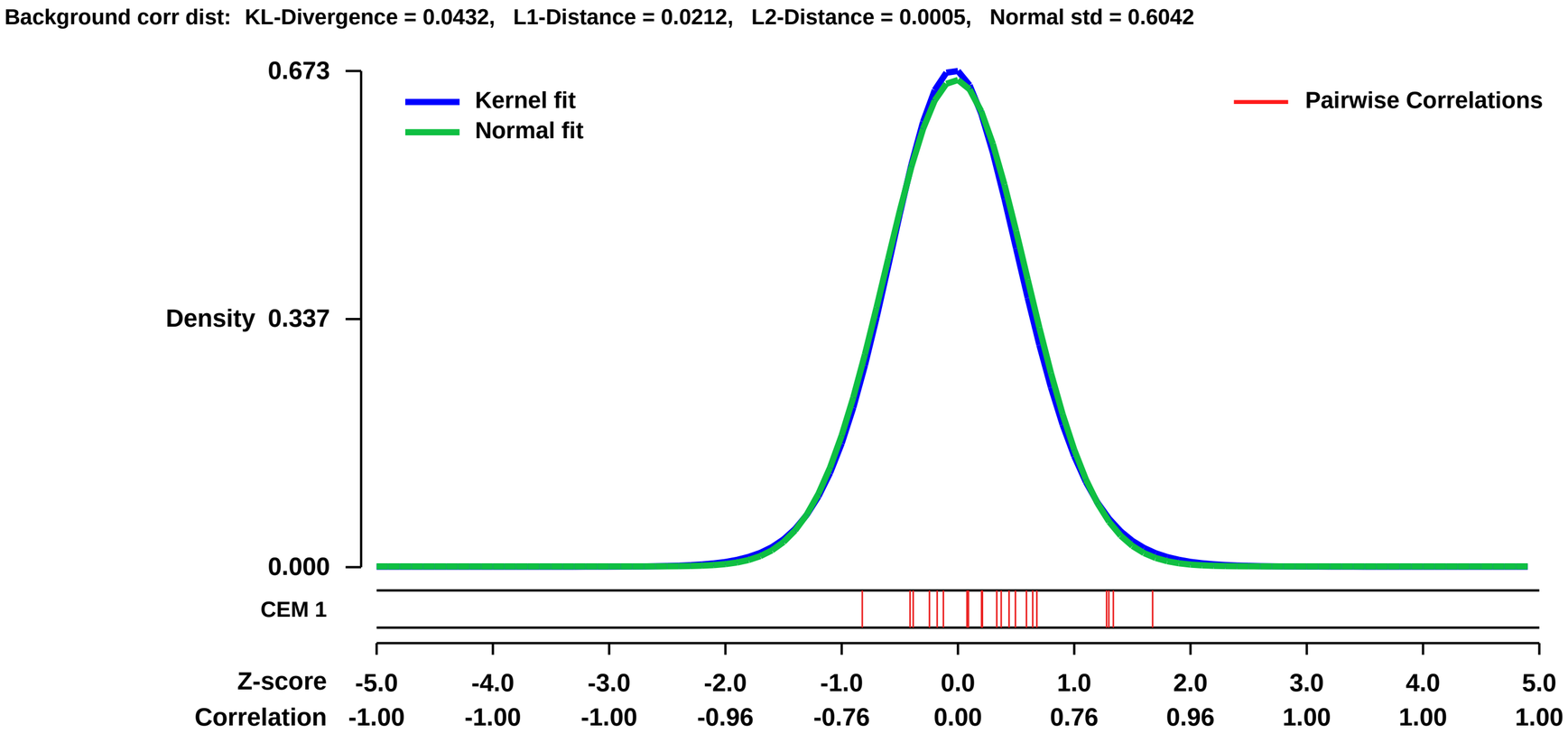

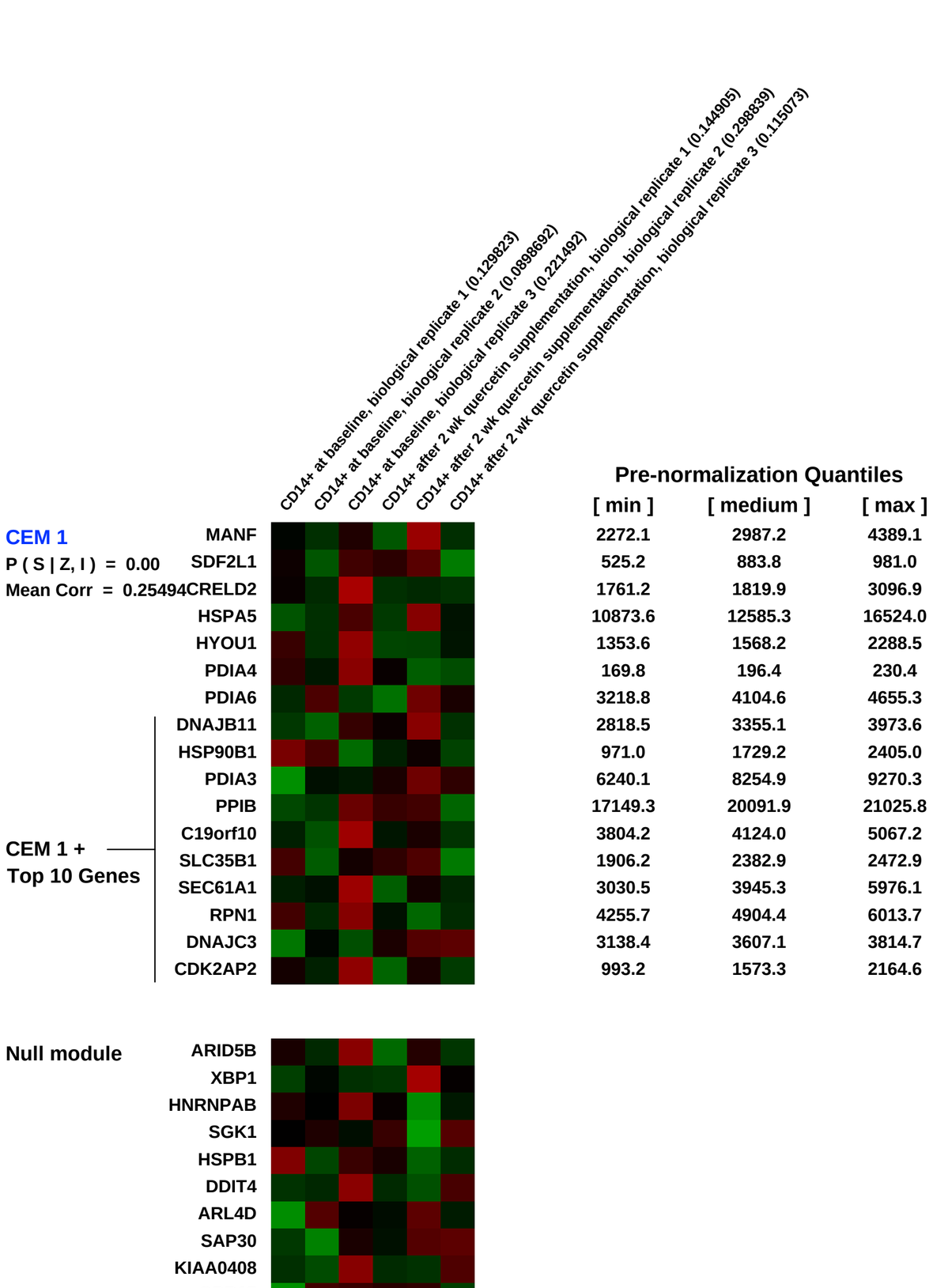

GEO Series "GSE15735" Expression Profiles

Num of samples in this series: 9

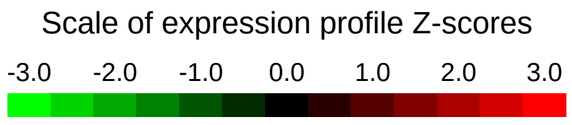

GEO Link:	http://www.ncbi.nlm.nih.gov/geo/query/acc.cgi?acc=GSE15735
Status:	Public on Aug 20 2009
Title:	Genome-wide mapping of HATs and HDACs in human CD4+ T cells
Organism:	Homo sapiens
Experiment type:	Expression profiling by array
Platform:	GPL570
Pubmed ID:	19698979
Summary & Design:	**Summary:** Histone acetyltransferases (HATs) and deacetylases (HDACs) function antagonistically to control histone acetylation. As acetylation is a histone mark for active transcription, HATs have been associated with active and HDACs with inactive genes. We describe here genome-wide mapping of HATs and HDACs binding on chromatin and ï‹ nd that both are found at active genes with acetylated histones. Our data provide evidence that HATs and HDACs are both targeted to transcribed regions of active genes by phosphorylated RNA Pol II. Furthermore, the majority of HDACs in the human genome function to reset chromatin by removing acetylation at active genes. Inactive genes that are primed by MLL-mediated histone H3K4 methylation are subject to a dynamic cycle of acetylation and deacetylation by transient HAT/HDAC binding, preventing Pol II from binding to these genes but poising them for future activation. Silent genes without any H3K4 methylation signal show no evidence of being bound by HDACs. **Overall design:** expression profiling: Global change in gene expression in human CD4+ T cells after HDAC inhibitor treatment for 2hours and 12 hours. (9 samples in total)

Background corr dist: KL-Divergence = 0.0645, L1-Distance = 0.0412, L2-Distance = 0.0024, Normal std = 0.5429

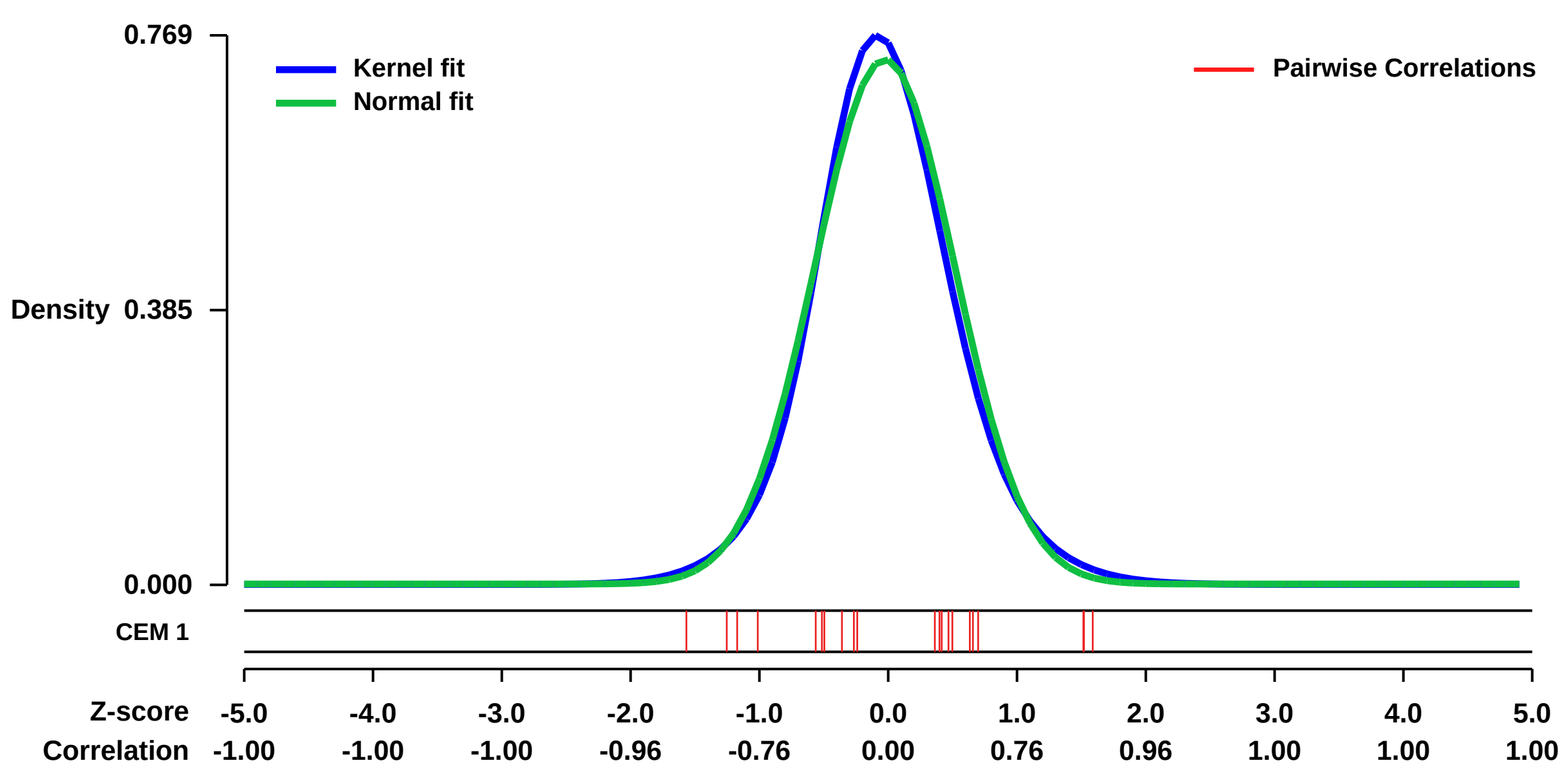

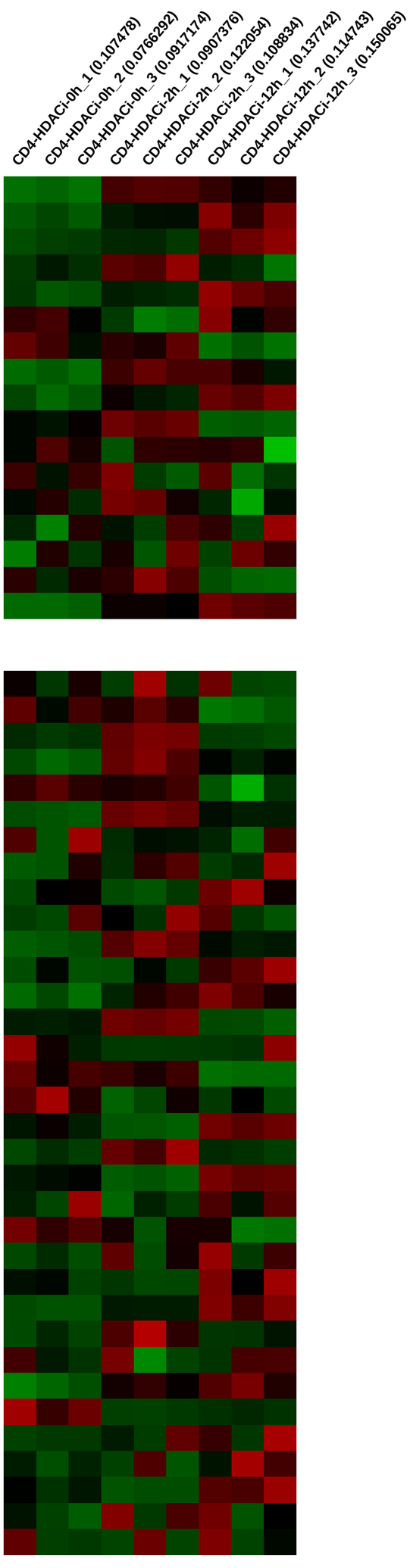

Pre-normalization Quantiles

		[min]	[medium]	[max]
CEM 1	MANF	1906.8	3168.8	3581.6
P (S | Z, I) = 0.00	SDF2L1	835.8	1258.9	2093.8
Mean Corr = 0.04053	CRELD2	2306.4	4311.9	13793.3
	HSPA5	7961.6	11960.5	19925.4
	HYOU1	1654.2	2389.0	4968.4
	PDIA4	585.2	740.0	915.4
	PDIA6	2757.6	4907.5	6024.4
CEM 1 + Top 10 Genes	DNAJB11	2376.8	6937.4	9408.3
	HSP90B1	6083.4	7581.5	10212.5
	PDIA3	5059.1	6714.7	8751.5
	PPIB	9428.9	17970.6	19492.7
	C19orf10	1267.4	1501.9	1879.7
	SLC35B1	916.7	1132.2	1306.1
	SEC61A1	2159.9	2436.3	2865.7
	RPN1	1704.6	2942.8	3649.0
	DNAJC3	1282.8	2150.6	2860.5
	CDK2AP2	1366.8	4641.5	7336.6
Null module	ARID5B			
	XBP1			
	HNRNPAB			
	SGK1			
	HSPB1			
	DDIT4			
	ARL4D			
	SAP30			
	KIAA0408			
	GPR17			
	HSPH1			
	DNASE1L2			
	SLC5A3			
	GNAS			
	GPR3			
	TNFRSF25			
	TM6SF2			
	MKKS			
	PLEKHF1			
	ZMYM1			
	DOK3			
	FGF20			
	SLC39A2			
	KCNIP2			
	ERRFI1			
	DEDD2			
	CCDC117			
	USP31			
	AHSA2			
	CYS1			
	CNIH2			
	BANP			
	CHORDC1			
	P4HA1			

GEO Series "GSE32975" Expression Profiles

Num of samples in this series: 58

Scale of expression profile Z-scores

-3.0 -2.0 -1.0 0.0 1.0 2.0 3.0

GEO Link: http://www.ncbi.nlm.nih.gov/geo/query/acc.cgi?acc=GSE32975
Status: Public on May 23 2012
Title: Gene expression signatures modulated by epidermal growth factor receptor activation and their relationship to cetuximab resistance in head and neck squamous cell carcinoma
Organism: Homo sapiens
Experiment type: Expression profiling by array
Platform: GPL570
Pubmed ID: 22549044

Summary & Design:

Summary:
Aberrant activation of signaling pathways controlled in normal epithelial cells by the epidermal growth factor receptor (EGFR) has been linked to cetuximab (a monoclonal antibody against EGFR) resistance in head and neck squamous cell carcinoma (HNSCC). To infer relevant and specific pathway activation downstream of EGFR from gene expression in HNSCC, we generated gene expression signatures using immortalized keratinocytes (HaCaT) subjected to either ligand stimulation or pharmacological inhibition of the signaling intermediaries PI-3-Kinase and MEK or transfected with EGFR, RELA/p65, or HRASVal12. The gene expression patterns that distinguished the various HaCaT variants and conditions were inferred using the Markov chain Monte Carlo (MCMC) matrix factorization algorithm Coordinated Gene Activity in Pattern Sets (CoGAPS). This approach inferred gene expression signatures with greater relevance to cell signaling pathway activation than the expression signatures inferred with standard linear models. Furthermore, the pathway signature generated using HaCaT-HRASVal12 further associated with the cetuximab treatment response in isogenic cetuximab-sensitive (UMSCC1) and -resistant (1CC8) cell lines. Our data suggest that the CoGAPS algorithm can generate gene expression signatures that are pertinent to downstream effects of receptor signaling pathway activation and potentially be useful in modeling resistance mechanisms to targeted therapies.

Overall design:
58 total RNA collected from HaCaT cell lines with combinations of the following experimental conditions: forced expression of EGFR, RELA/p65, and HRAS-VAL12D; grown in PBS, serum starve, and media stimulated with TNF or EGF; treated with gefitinib, LY294002, and U1026.

Background corr dist: KL-Divergence = 0.3556, L1-Distance = 0.0723, L2-Distance = 0.0154, Normal std = 0.2604

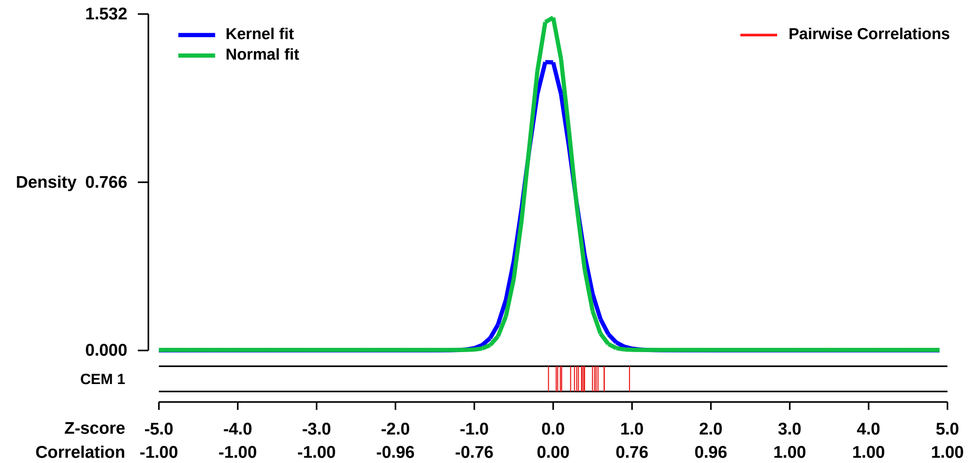

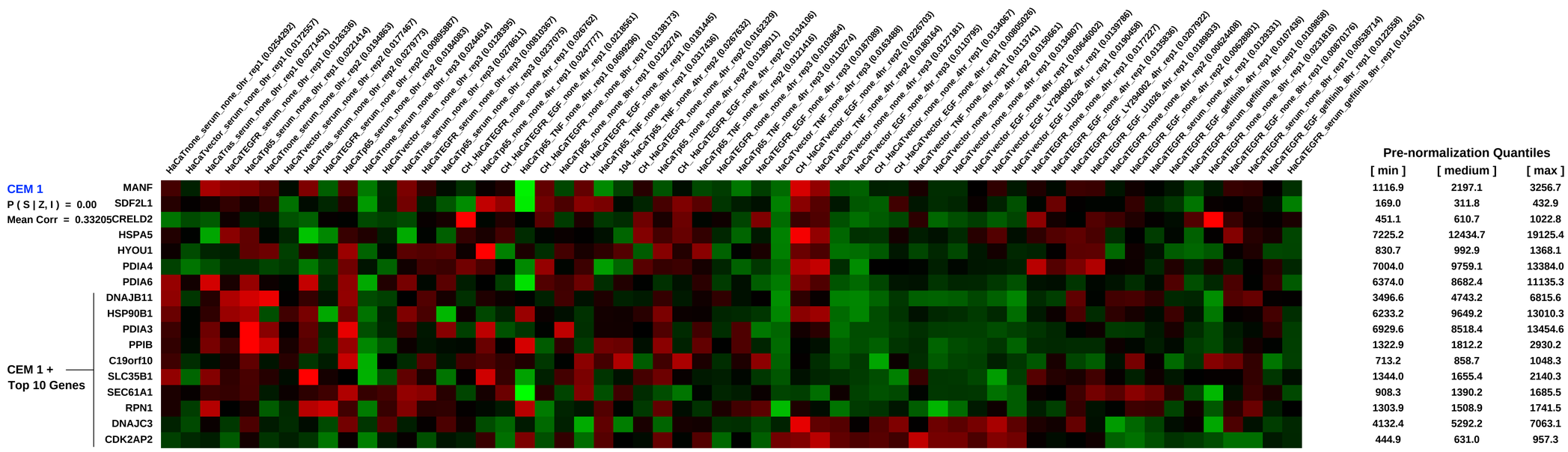

Pre-normalization Quantiles

[min]	[medium]	[max]
1116.9	2197.1	3256.7
169.0	311.8	432.9
451.1	610.7	1022.8
7225.2	12434.7	19125.4
830.7	992.9	1368.1
7004.0	9759.1	13384.0
6374.0	8682.4	11135.3
3496.6	4743.2	6815.6
6233.2	9649.2	13010.3
6929.6	8518.4	13454.6
1322.9	1812.2	2930.2
713.2	858.7	1048.3
1344.0	1655.4	2140.3
908.3	1390.2	1685.5
1303.9	1508.9	1741.5
4132.4	5292.2	7063.1
444.9	631.0	957.3

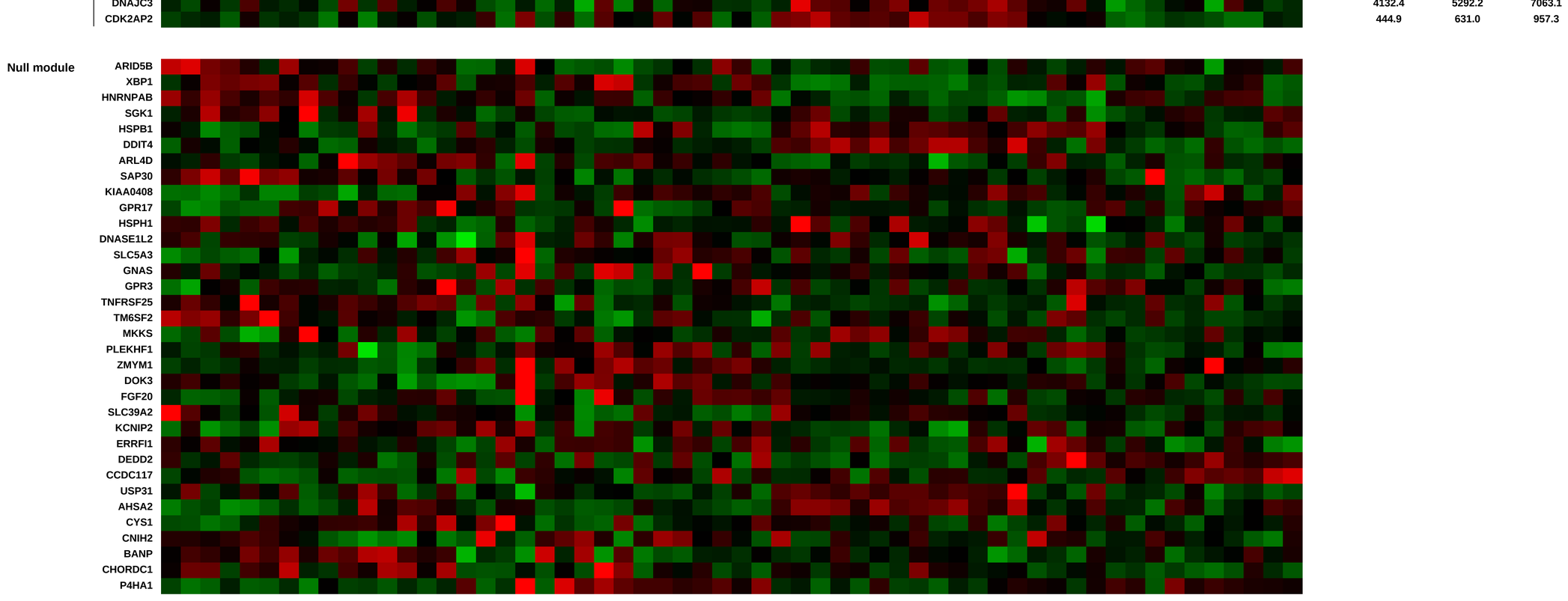

GEO Series "GSE44807" Expression Profiles

Num of samples in this series: 6

Scale of expression profile Z-scores

-3.0 -2.0 -1.0 0.0 1.0 2.0 3.0

GEO Link:	http://www.ncbi.nlm.nih.gov/geo/query/acc.cgi?acc=GSE44807
Status:	Public on May 08 2013
Title:	Gene expression data from primary human bronchial epithelial cells expressing EGFP or DN-GRHL2
Organism:	Homo sapiens
Experiment type:	Expression profiling by array
Platform:	GPL570
Pubmed ID:	23690579
Summary & Design:	**Summary:** The airways of the human lung are lined by an epithelium made up of ciliated and secretory luminal cells and undifferentiated p63+ Krt5+ progenitors. The integrity of this epithelium and its ability to act as a selective barrier are critical for normal lung function. In other epithelia there is evidence that transcription factors of the evolutionarily conserved grainyheadlike (GRHL) family play key roles in co-ordinating the expression of numerous proteins required for epithelial morphogenesis, differentiation, remodeling and repair. However, little is known about their function in the adult lung. We used Affymetrix microarray analysis to compare transcripts in lentivirus transfected primary human bronchial epithelial (HBE) cells expressing either EGFP or DN-GRHL2 to help identify GRHL2 target genes and their functions in HBE cells. **Overall design:** Primary HBE cells from three donors were infected with modified TripZ lentivirus designed to express EGFP or DN-GRHL2 in response to Dox. Dox was added to cells cultured at the air-liquid interface from day 7 to 14.

Background corr dist: KL-Divergence = 0.0221, L1-Distance = 0.0164, L2-Distance = 0.0004, Normal std = 0.7158

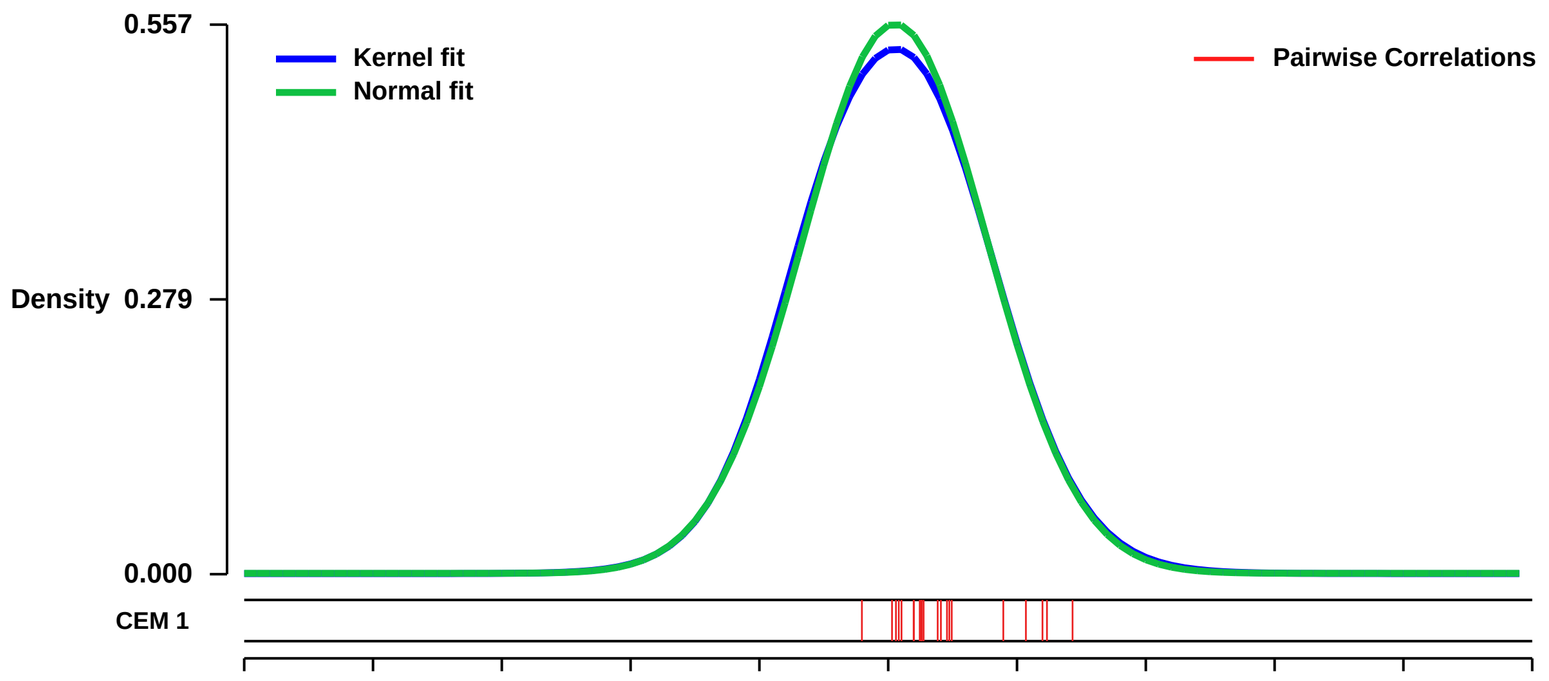

Z-score	-5.0	-4.0	-3.0	-2.0	-1.0	0.0	1.0	2.0	3.0	4.0	5.0
Correlation	-1.00	-1.00	-1.00	-0.96	-0.76	0.00	0.76	0.96	1.00	1.00	1.00

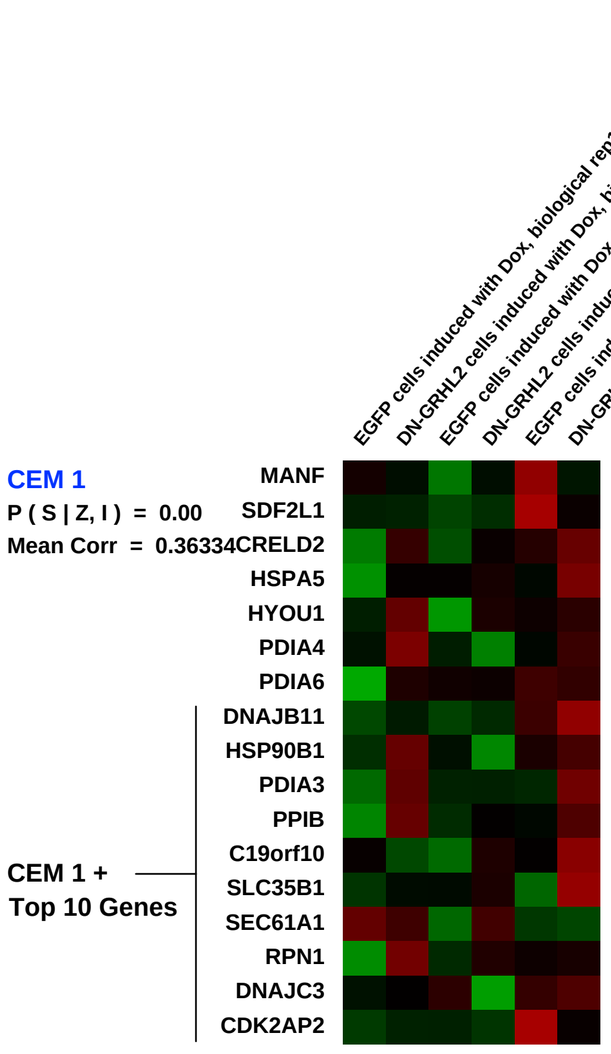

	Pre-normalization Quantiles		
	[min]	[medium]	[max]
MANF	2912.9	3261.1	3786.3
SDF2L1	591.1	629.0	826.6
CRELD2	1595.2	3192.3	3852.4
HSPA5	11548.4	15090.5	17805.7
HYOU1	1809.4	2577.1	2891.2
PDIA4	1193.4	1442.3	1704.4
PDIA6	4399.4	5466.7	5641.2
DNAJB11	2550.6	2784.8	3650.7
HSP90B1	3561.2	4584.6	5059.1
PDIA3	9289.6	10201.9	11993.4
PPIB	11899.4	13597.4	14836.4
C19orf10	2015.3	2103.8	2205.6
SLC35B1	1609.5	1762.1	2027.2
SEC61A1	2313.2	3105.2	3281.6
RPN1	3526.0	3834.6	4006.3
DNAJC3	3313.3	3681.5	3743.4
CDK2AP2	863.6	946.5	1582.2
ARID5B			
XBP1			
HNRNPAB			
SGK1			
HSPB1			
DDIT4			
ARL4D			
SAP30			
KIAA0408			
GPR17			
HSPH1			
DNASE1L2			
SLC5A3			
GNAS			
GPR3			
TNFRSF25			
TM6SF2			
MKKS			
PLEKHF1			
ZMYM1			
DOK3			
FGF20			
SLC39A2			
KCNIP2			
ERRFI1			
DEDD2			
CCDC117			
USP31			
AHSA2			
CYS1			
CNIH2			
BANP			
CHORDC1			
P4HA1			

GEO Series "GSE44905" Expression Profiles

Num of samples in this series: 18

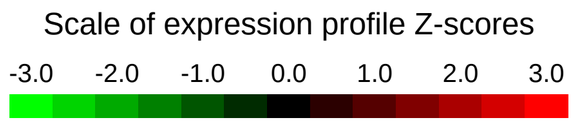

GEO Link:	http://www.ncbi.nlm.nih.gov/geo/query/acc.cgi?acc=GSE44905
Status:	Public on Apr 01 2013
Title:	Expression data from LNCaP cells treated with DHT and enzalutamide
Organism:	Homo sapiens
Experiment type:	Expression profiling by array
Platform:	GPL570
Pubmed ID:	23765603
Summary & Design:	**Summary:** Enzalutamide (formerly MDV3100 and available commercially as Xtandi), a novel androgen receptor (AR) signaling inhibitor, blocks the growth of castration-resistant prostate cancer (CRPC) in cellular model systems and was shown in a clinical study to increase survival in patients with metastatic CRPC. Enzalutamide inhibits multiple steps of AR signaling: (1) binding of androgens to AR, (2) AR nuclear translocation, and (3) association of AR with DNA. Here we used Affymetrix human genome microarray technology to investigate the global programme of gene expression of LNCaP cells in response to enzalutamide alone and in the context of DHT-stimulated androgen receptor gene expression. **Overall design:** LNCaP cells were grown in RPMI 1640 supplemented with 5% hormone depleted FBS and treated with vehicle (control sample) , DHT (100 nM), enzalutamide (1 or 10 ´µM) or DHT (100 nM) plus enzalutamide (1 or 10 ´µM)for 16 hours for RNA extraction and hybridization. Each condition was done in triplicate.

Background corr dist: KL-Divergence = 0.2164, L1-Distance = 0.0460, L2-Distance = 0.0047, Normal std = 0.3213

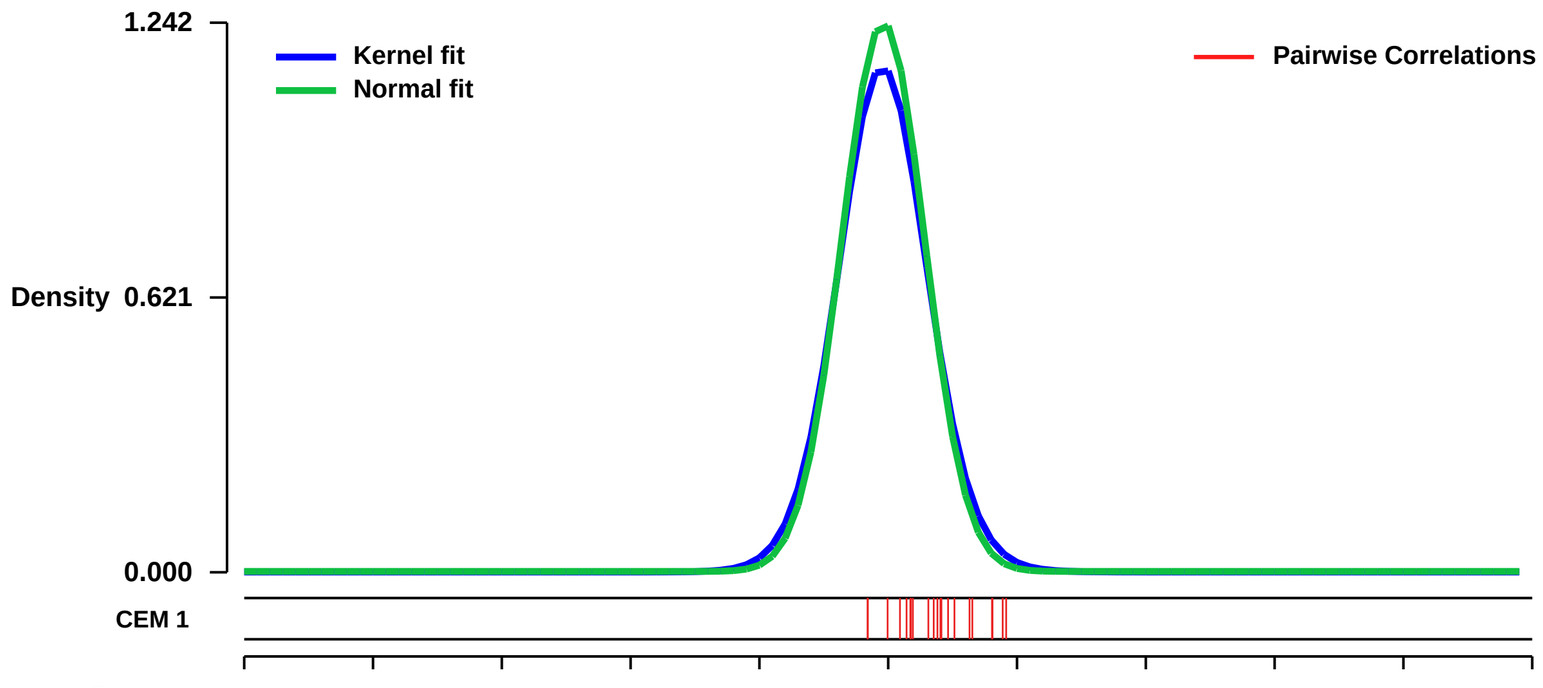

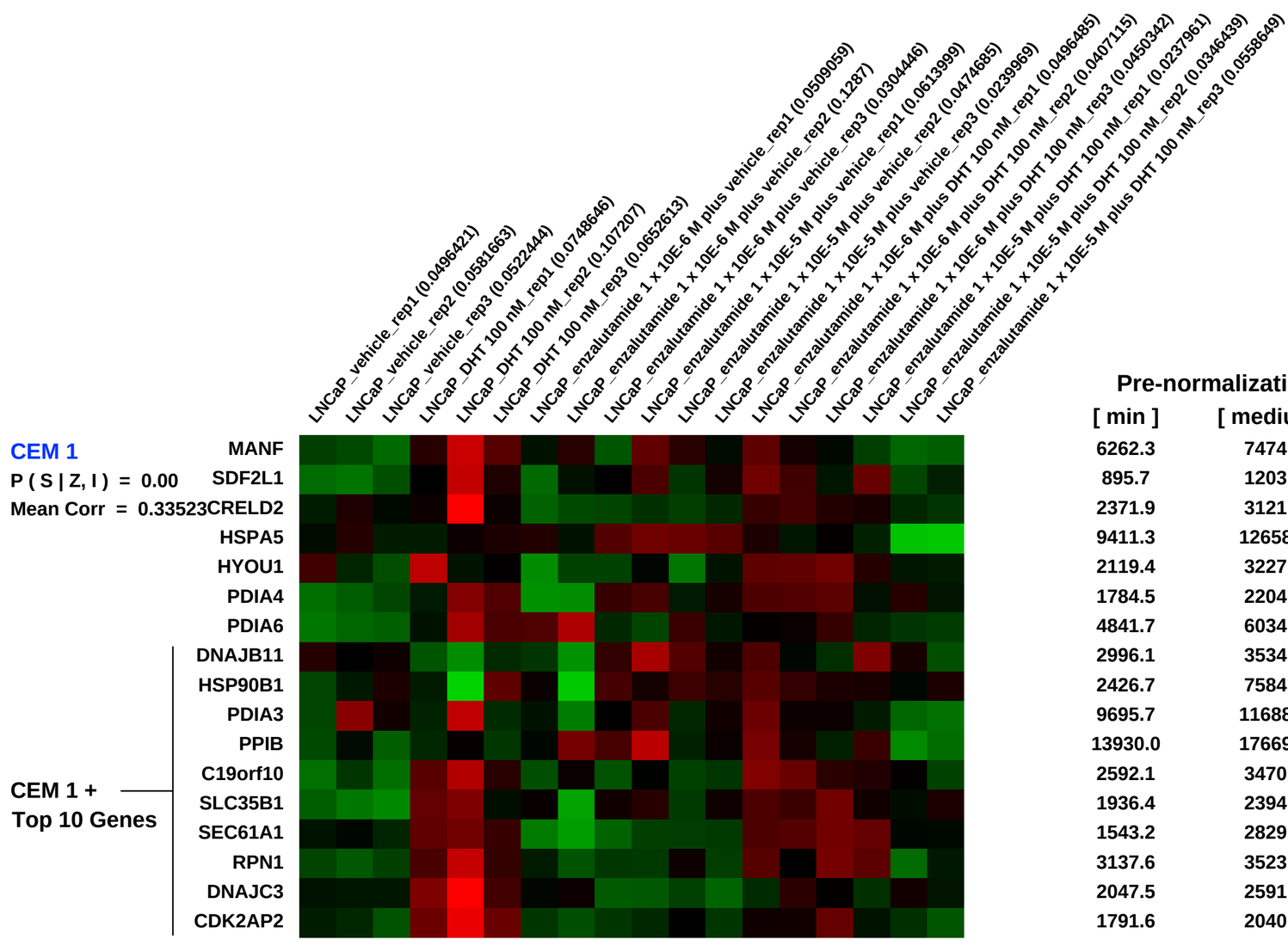

Pre-normalization Quantiles

	[min]	[medium]	[max]
MANF	6262.3	7474.9	10106.8
SDF2L1	895.7	1203.3	1721.9
CRELD2	2371.9	3121.9	5573.1
HSPA5	9411.3	12658.4	14174.2
HYOU1	2119.4	3227.3	5112.3
PDIA4	1784.5	2204.7	2478.9
PDIA6	4841.7	6034.2	8259.4
DNAJB11	2996.1	3534.0	4044.9
HSP90B1	2426.7	7584.9	9079.4
PDIA3	9695.7	11688.8	14813.0
PPIB	13930.0	17669.4	23119.0
C19orf10	2592.1	3470.0	4805.3
SLC35B1	1936.4	2394.2	2673.8
SEC61A1	1543.2	2829.2	3851.8
RPN1	3137.6	3523.5	4547.8
DNAJC3	2047.5	2591.0	4408.6
CDK2AP2	1791.6	2040.3	3199.0

GEO Series "GSE28117" Expression Profiles

Num of samples in this series: 13

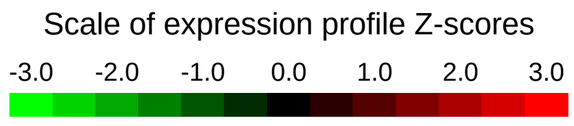

GEO Link:	http://www.ncbi.nlm.nih.gov/geo/query/acc.cgi?acc=GSE28117
Status:	Public on May 01 2011
Title:	IL-4 mediated gene expression profiles in vascular endothelial cells
Organism:	Homo sapiens
Experiment type:	Expression profiling by array
Platform:	GPL570
Pubmed ID:	21464207
Summary & Design:	**Summary:** Endothelial cell activation and dysfunction underlie many vascular disorders, including atherosclerosis and inflammation. Here, we show that interleukin (IL)-4 markedly induced vascular cell adhesion molecule (VCAM)-1, both in cultured endothelial cells and in the intact endothelium in mice. Combined treatment with IL-4 and tumor necrosis factor (TNF)- alpha resulted in further, sustained induction of VCAM-1 expression. IL-4-mediated induction of VCAM-1 and secondary monocyte adhesion was predominantly regulated by the transcription factor, STAT6. Genome-wide survey of IL-4-mediated STAT6 binding from sequential chromatin-immunoprecipitation with deep-sequencing (ChIP-seq) in endothelial cells revealed regions of transient and sustained transcription factor binding. By combining DNA microarrays and ChIP-seq at the same time points, the majority of IL-4-responsive genes were shown to be STAT6-dependent and associated with direct STAT6 binding to their promoter. IL-4-mediated stable binding of STAT6 led to sustained target gene expression. Moreover, our strategy led to the identification of a novel functionally important STAT6 binding site within -16 kb upstream of the VCAM-1 gene. Taken together, these findings support a critical role for STAT6 in mediating IL-4 signal transduction in endothelial cells. Identification of a novel IL-4-mediated VCAM-1 enhancer may provide a foundation for targeted therapy in vascular disease (ChIP-seq data not submitted to GEO). **Overall design:** Total 13 samples were derived from [1] HUVEC treated in the absence (0h) or presence of IL-4 (1,2,4,8, and 16h) to determine IL-4 regulated gene in endotherial cells, [2] control-siRNA or si-STAT6 transfected HUVEC cells treated in the absence or presenceof IL-4 [3] Ad-control or Ad-CA-STAT6 transfected HUVEC cells for the identification of STAT-6 dependent genes in endothelial cells.

Background corr dist: KL-Divergence = 0.1218, L1-Distance = 0.0303, L2-Distance = 0.0018, Normal std = 0.4121

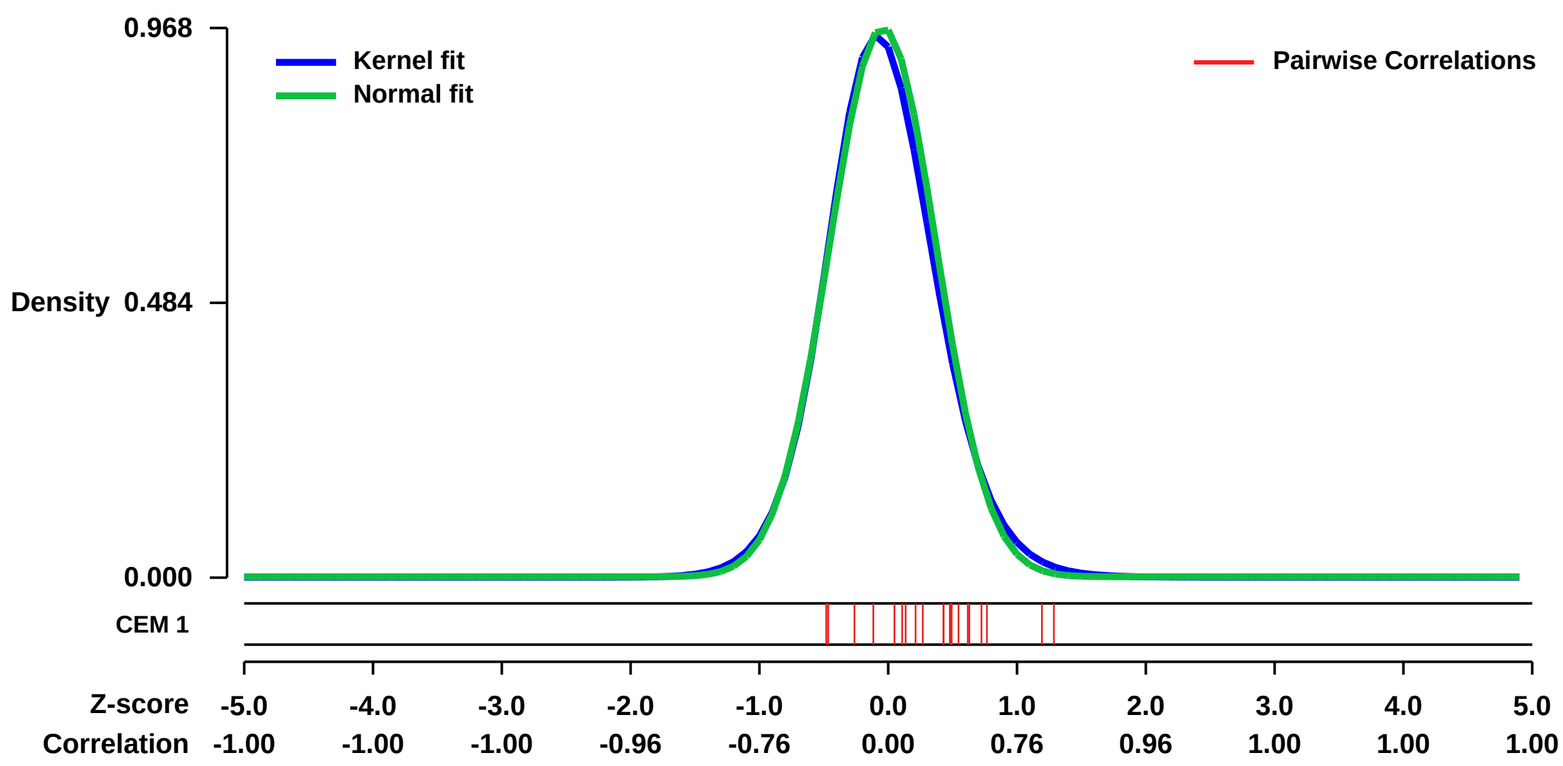

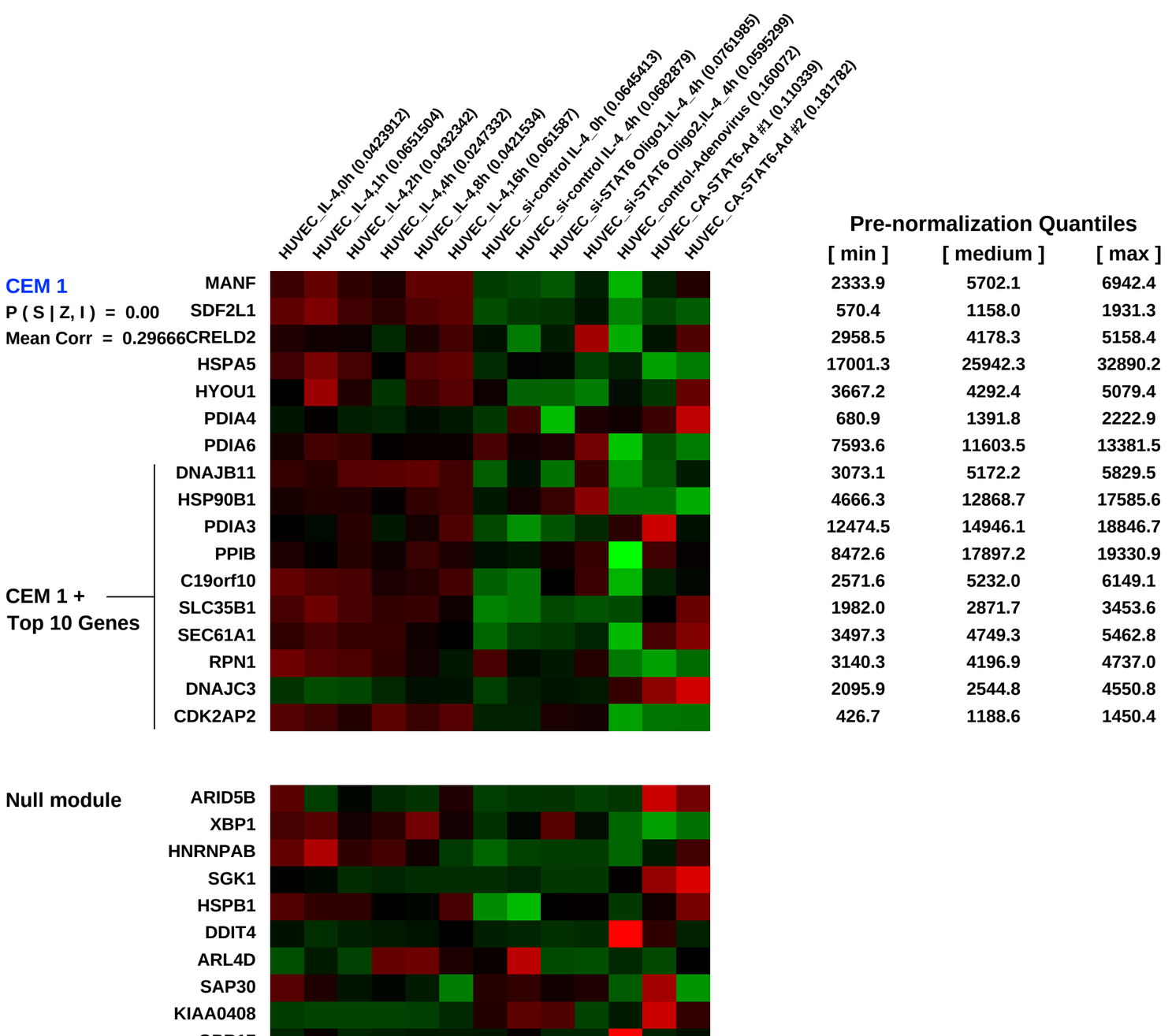

Pre-normalization Quantiles

	[min]	[medium]	[max]
MANF	2333.9	5702.1	6942.4
SDF2L1	570.4	1158.0	1931.3
CRELD2	2958.5	4178.3	5158.4
HSPA5	17001.3	25942.3	32890.2
HYOU1	3667.2	4292.4	5079.4
PDIA4	680.9	1391.8	2222.9
PDIA6	7593.6	11603.5	13381.5
DNAJB11	3073.1	5172.2	5829.5
HSP90B1	4666.3	12868.7	17585.6
PDIA3	12474.5	14946.1	18846.7
PPIB	8472.6	17897.2	19330.9
C19orf10	2571.6	5232.0	6149.1
SLC35B1	1982.0	2871.7	3453.6
SEC61A1	3497.3	4749.3	5462.8
RPN1	3140.3	4196.9	4737.0
DNAJC3	2095.9	2544.8	4550.8
CDK2AP2	426.7	1188.6	1450.4

GEO Series "GSE5230" Expression Profiles

Num of samples in this series: 16

Scale of expression profile Z-scores

-3.0 -2.0 -1.0 0.0 1.0 2.0 3.0

GEO Link:	http://www.ncbi.nlm.nih.gov/geo/query/acc.cgi?acc=GSE5230
Status:	Public on Aug 01 2006
Title:	Epigenetics of gene expression in human hepatoma cells
Organism:	Homo sapiens
Experiment type:	Expression profiling by array
Platform:	GPL570
Pubmed ID:	16854234
Summary & Design:	**Summary:** **Expression profiling the response to inhibition of DNA methylation and histone deacetylation.** **Comparison of expression in HepG2 cells treated with 5-aza-dC, Trichostatin A, both, or none (control) to change methylation and acetylation status.** **Background:DNA methylation and histone deacetylation are epigenetic mechanisms that play major roles in eukaryotic gene regulation. We hypothesize that many genes in the human hepatoma cell line HepG2 are regulated by DNA methylation and histone deacetylation. Treatment with 5-aza-2'-deoxycytidine (5-aza-dC) to inhibit DNA methylation with and/or Trichostatin A (TSA) to inhibit histone deacetylation should allow us to identify genes that are regulated epigenetically in hepatoma cells.** **Results:5-aza-dC had a much larger effect on gene expression in HepG2 cells than did TSA, as measured using Affymetrix´fi HG-U133A Plus 2.0 microarrays. The expression of 1504 probe sets was affected by 5-aza-dC (at p < 0.01), 535 probe sets by TSA, and 1929 probe sets by the combination of 5-aza-dC and TSA. 5-aza-dC treatment turned on the expression of 211 probe sets that were not detectably expressed in its absence. Expression of imprinted genes regulated by DNA methylation, such as H19 and NNAT, was turned on or greatly increased in response to 5-aza-dC. Genes involved in liver processes such as xenobiotic metabolism (CYP3A4, CYP3A5, and CYP3A7) and steroid biosynthesis (CYP17A1 and CYP19A1), and CCAAT element-binding proteins (CEBPA, CEBPB, and CEBPG) were affected by 5-aza-dC or the combination. Many of the genes that fall within these groups are also expressed in the developing fetal liver. Quantitative real-time RT-PCR assays confirmed selected gene expression changes seen in microarray analyses.** **Conclusions:Epigenetics play a role in regulating the expression of several genes involved in essential liver processes such as xenobiotic metabolism and steroid biosynthesis in HepG2 cells. Many genes whose expression is normally silenced in these hepatoma cells were re-expressed by 5-aza-dC treatment. Many genes that are expressed in the fetal liver are up-regulated by demethylation, indicating that DNA methylation is a major factor in restricting the expression of fetal genes during liver development.** **Keywords: comparison of treatments** **Overall design:** **4 cell culture replicates per treatment group.**

Background corr dist: KL-Divergence = 0.2136, L1-Distance = 0.0463, L2-Distance = 0.0048, Normal std = 0.3231

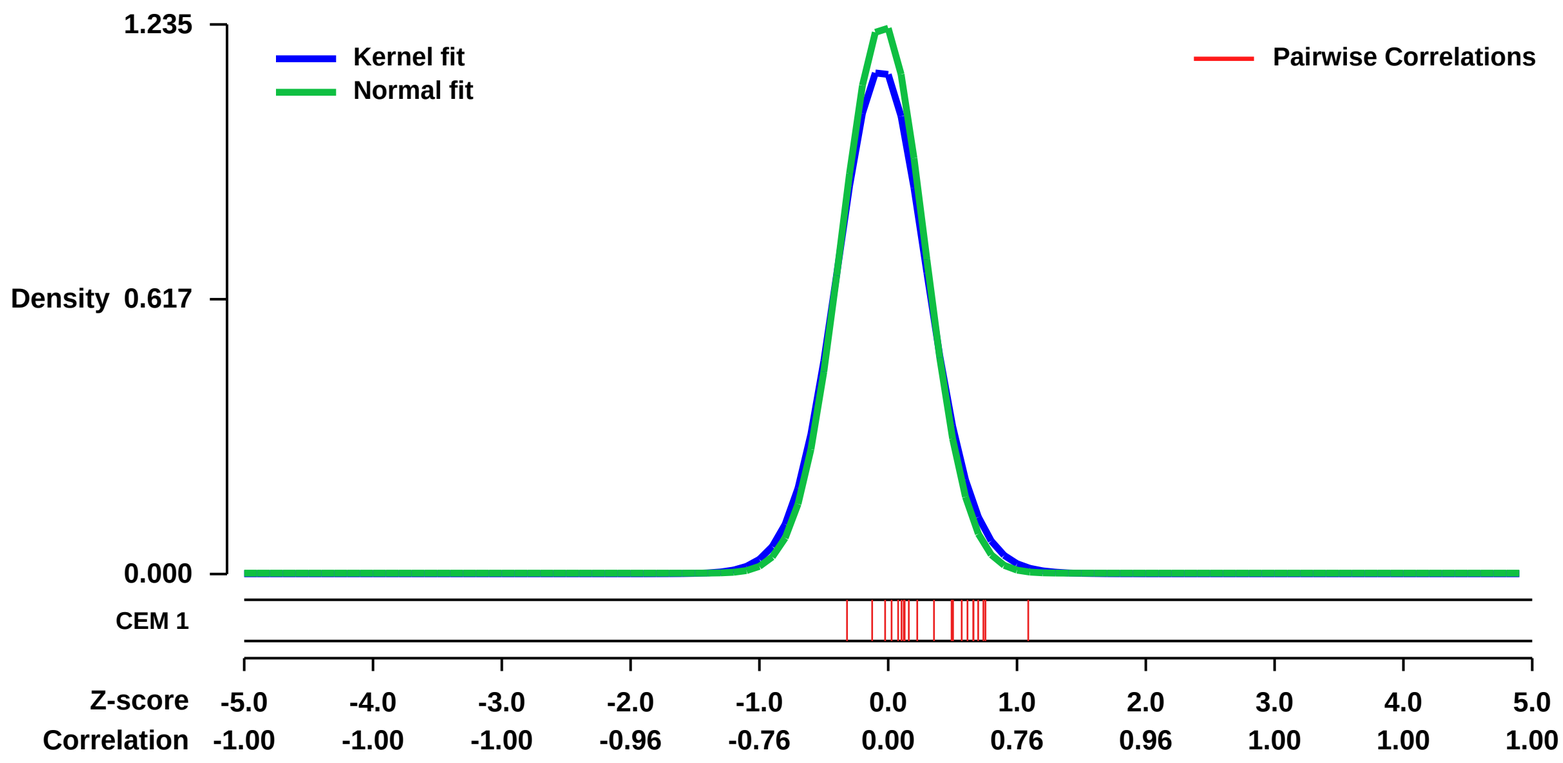

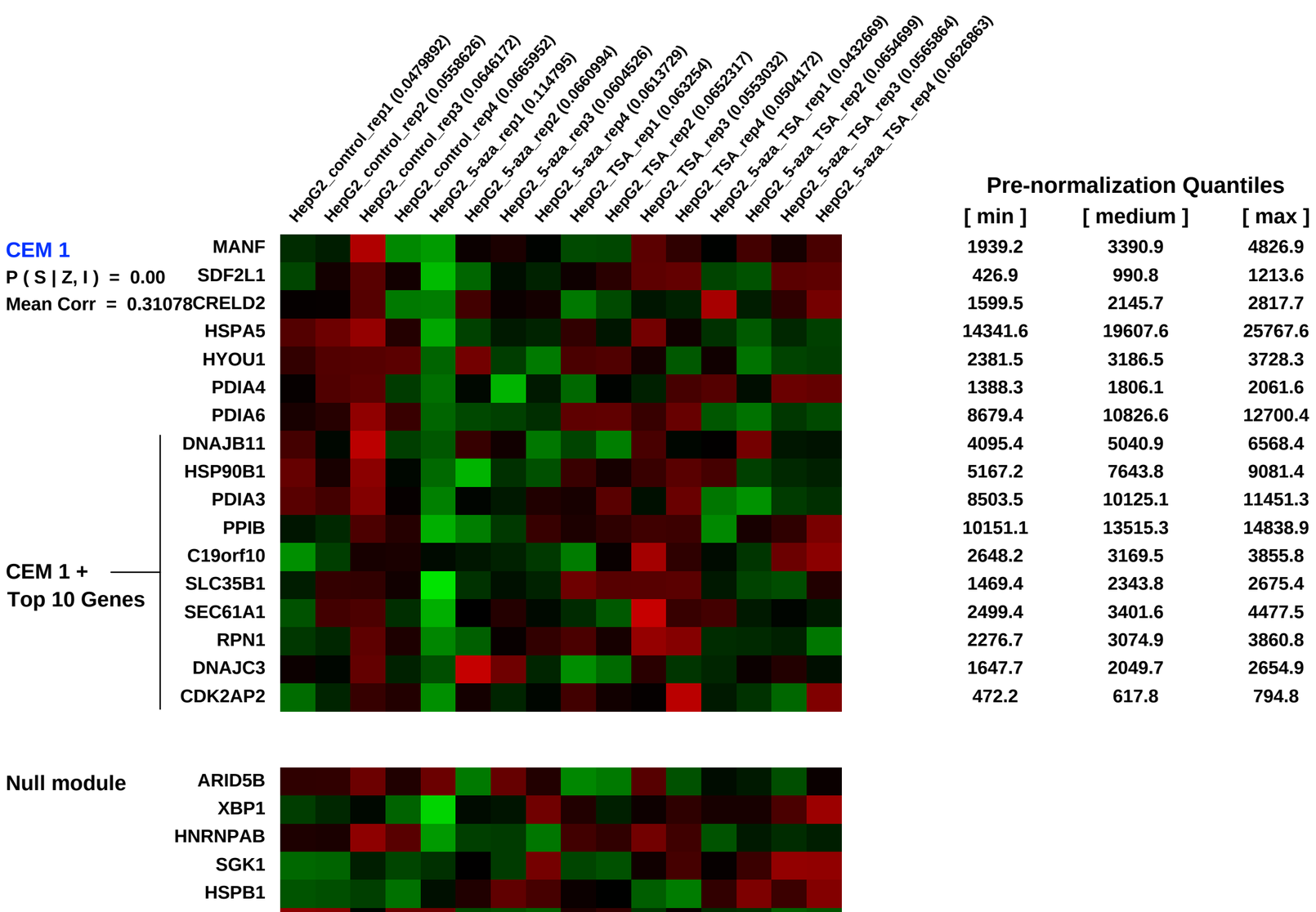

GEO Series "GSE38663" Expression Profiles

Num of samples in this series: 52

Scale of expression profile Z-scores

-3.0 -2.0 -1.0 0.0 1.0 2.0 3.0

GEO Link:	http://www.ncbi.nlm.nih.gov/geo/query/acc.cgi?acc=GSE38663
Status:	Public on Mar 08 2013
Title:	Effect of Ribavirin on Viral Kinetics and Liver Gene Expression in Chronic Hepatitis C
Organism:	Homo sapiens
Experiment type:	Expression profiling by array
Platform:	GPL570
Pubmed ID:	23396509
Summary & Design:	**Summary:** Background/Aims: Ribavirin improves treatment response to pegylated-interferon (PEG-IFN) in chronic hepatitis C but the mechanism remains controversial. We studied correlates of response and mechanism of action of ribavirin in treatment of hepatitis C. Methods: 70 treatment-naˆflve patients were randomized to 4 weeks of ribavirin (1000-1200 mg/d) or none, followed by PEG-IFN alfa-2a and ribavirin at standard doses and durations. Patients were randomized to undergo a liver biopsy either 24 hours before, or 6 hours after starting PEG-IFN. Hepatic gene expression was assessed by microarray and interferon-stimulated gene (ISG) expression quantified by the nCounter platform. Temporal changes in ISG expression were assessed by qPCR in peripheral-blood mononuclear cells (PBMC) and by serum levels of IP-10. Results: After four weeks of ribavirin monotherapy, HCV levels decreased by 0.5´–0.5 log10 (p=0.009 vs. controls) and ALT by 33% (p<0.001). Ribavirin pretreatment, while modestly augmenting the induction of ISGs by PEG-IFN, did not modify the virological response to subsequent PEG-IFN and ribavirin treatment. However, biochemical, but not virological response to ribavirin monotherapy predicted response to subsequent combination treatment (rapid virological response, 71% in biochemical responders vs. 22% non-responders, p=0.01; early virological response, 100% vs. 68%, p=0.03, sustained virological response 83% vs. 41%, p=0.053). Ribavirin monotherapy lowered serum IP-10 levels but had no effect on ISG expression in PBMC. Conclusion: Ribavirin is a weak antiviral but its clinical effect in combination with PEG-IFN seems to be mediated by a separate, indirect mechanism, which may act to reset the interferon responsiveness in HCV-infected liver. Ribavirin pretreatment does not alter the clinical outcome of subsequent combination therapy. **Overall design:** Analysis of liver biopsy samples from 52 patients under 4 different treatment conditions.

Background corr dist: KL-Divergence = 0.1215, L1-Distance = 0.0500, L2-Distance = 0.0060, Normal std = 0.4089

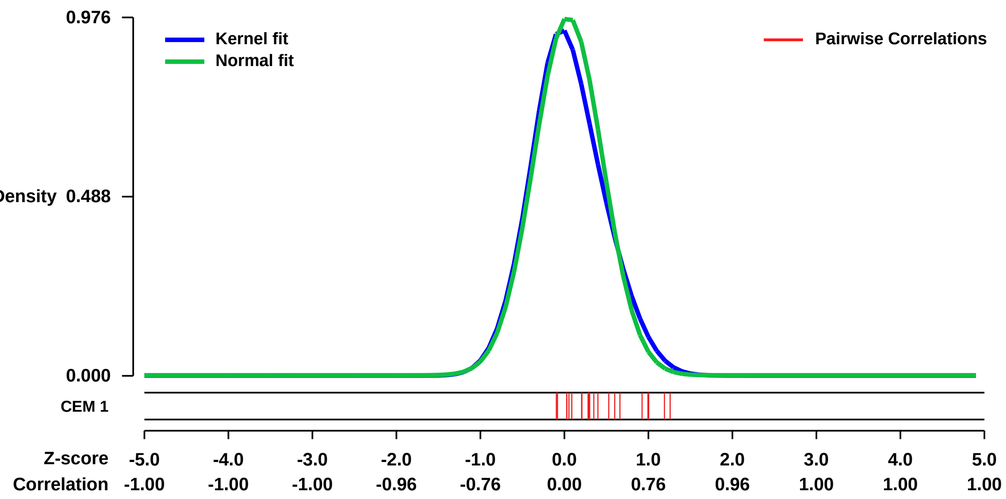

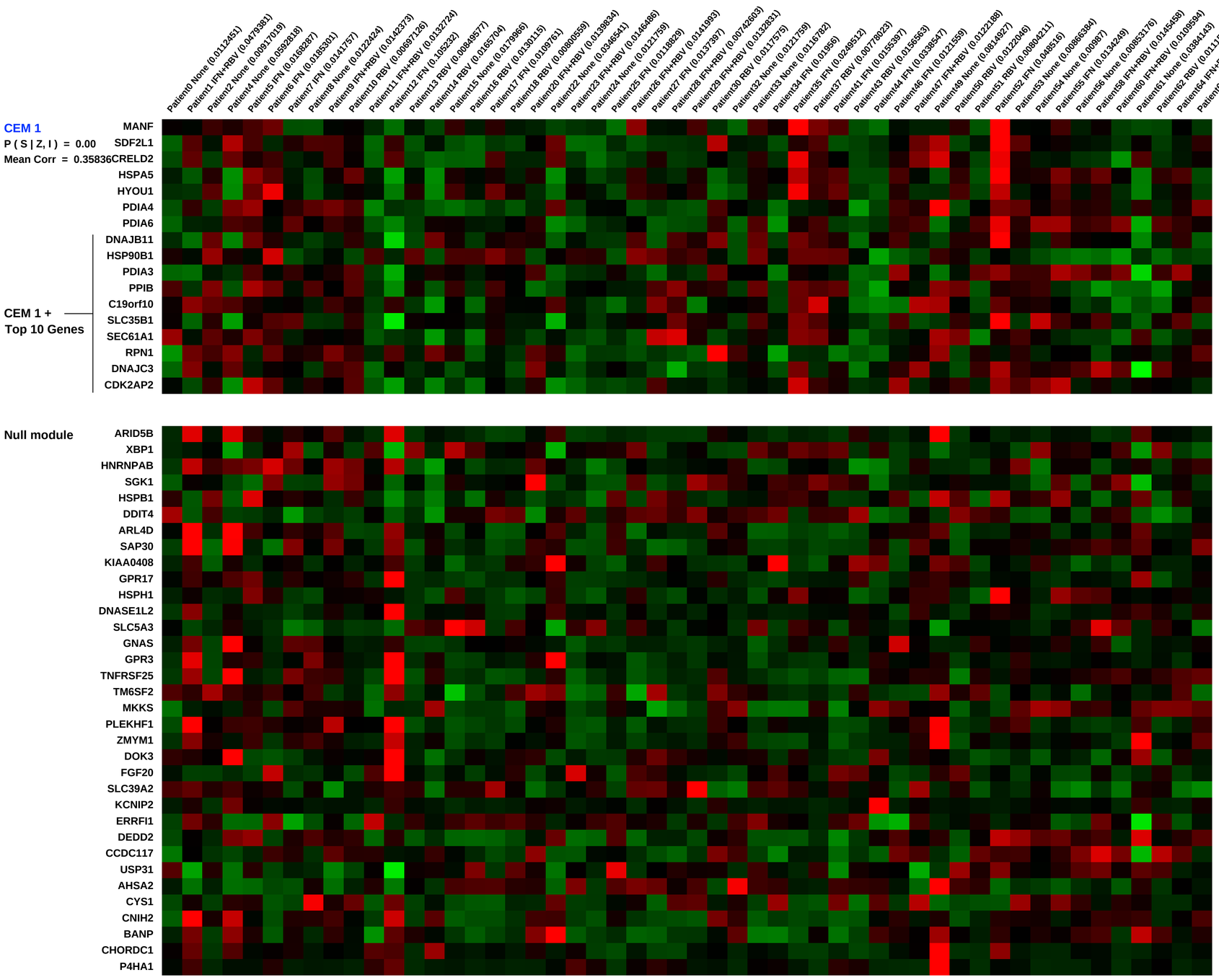

Pre-normalization Quantiles

[min]	[medium]	[max]
1888.5	3433.8	8729.4
262.8	591.3	1734.6
872.7	1480.8	2753.9
3110.0	7940.0	15675.1
241.4	902.8	2328.5
7025.4	10085.9	16072.5
4559.6	7032.2	10327.4
614.6	1897.8	3483.7
534.9	1048.1	1771.6
2309.5	5941.3	8902.7
3001.7	5748.7	8579.3
801.6	1377.1	2170.4
462.8	2436.1	4532.8
427.6	891.8	1689.1
867.2	1792.0	3742.2
2751.6	5236.1	7241.5
315.1	912.0	1839.5

GEO Series "GSE40496" Expression Profiles

Num of samples in this series: 6

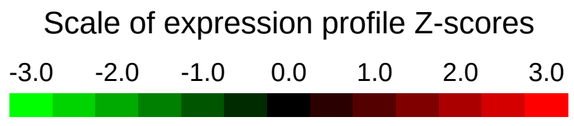

GEO Link:	http://www.ncbi.nlm.nih.gov/geo/query/acc.cgi?acc=GSE40496
Status:	Public on Jun 01 2013
Title:	Temporal induction of immunoregulatory processes coincides with age-dependent resistance to viral-induced type 1 diabetes [human]
Organism:	Homo sapiens
Experiment type:	Expression profiling by array
Platform:	GPL570
Pubmed ID:	23739610
Summary & Design:	**Summary:** A need exists for biomarkers in T1D that can 1) sensitively and specifically detect disease-related immune activity prior to, and independent of, measurement of auto-antibodies towards islet cell antigens; 2) define immunopathological mechanisms; and 3) monitor changes in the inflammatory state associated with disease progression or response to therapeutic intervention. In an effort to fill this gap, we have applied a novel bioassay to both human and BB rat T1D whereby the complex milieu of inflammatory mediators present in plasma can be indirectly detected through their ability to drive transcription in peripheral blood mononuclear cells drawn from healthy, unrelated donors. The resultant gene expressions are comprehensively measured with a microarray. In our human studies, we find that plasma of recent-onset T1D patients induces expression of a pro-inflammatory signature consisting in part of many interleukin-1 (IL-1) regulated genes related to immunological activation and immunocyte chemotaxis compared to unrelated healthy controls. This signature has been found to resolve in long-standing T1D subjects (>10 years post-onset), thus associating it with active autoimmunity. Importantly, this signature has been detected in pre-onset samples of progressors to T1D years prior to onset and prior to development of auto-antibodies directed towards islet antigens. **Overall design:** Fresh PBMCs of a healthy control donor were isolated by density gradient centrifugation. These cells were then stimulated with 20% plasma from a longitudinally monitored sibling of a T1D patient that progressed to T1D (n= 6 timepoints) at 37C in 5% CO2. Gene expression analysis was perfromed in order to evaluate the transcriptional signature associated with T1D pathogenesis.

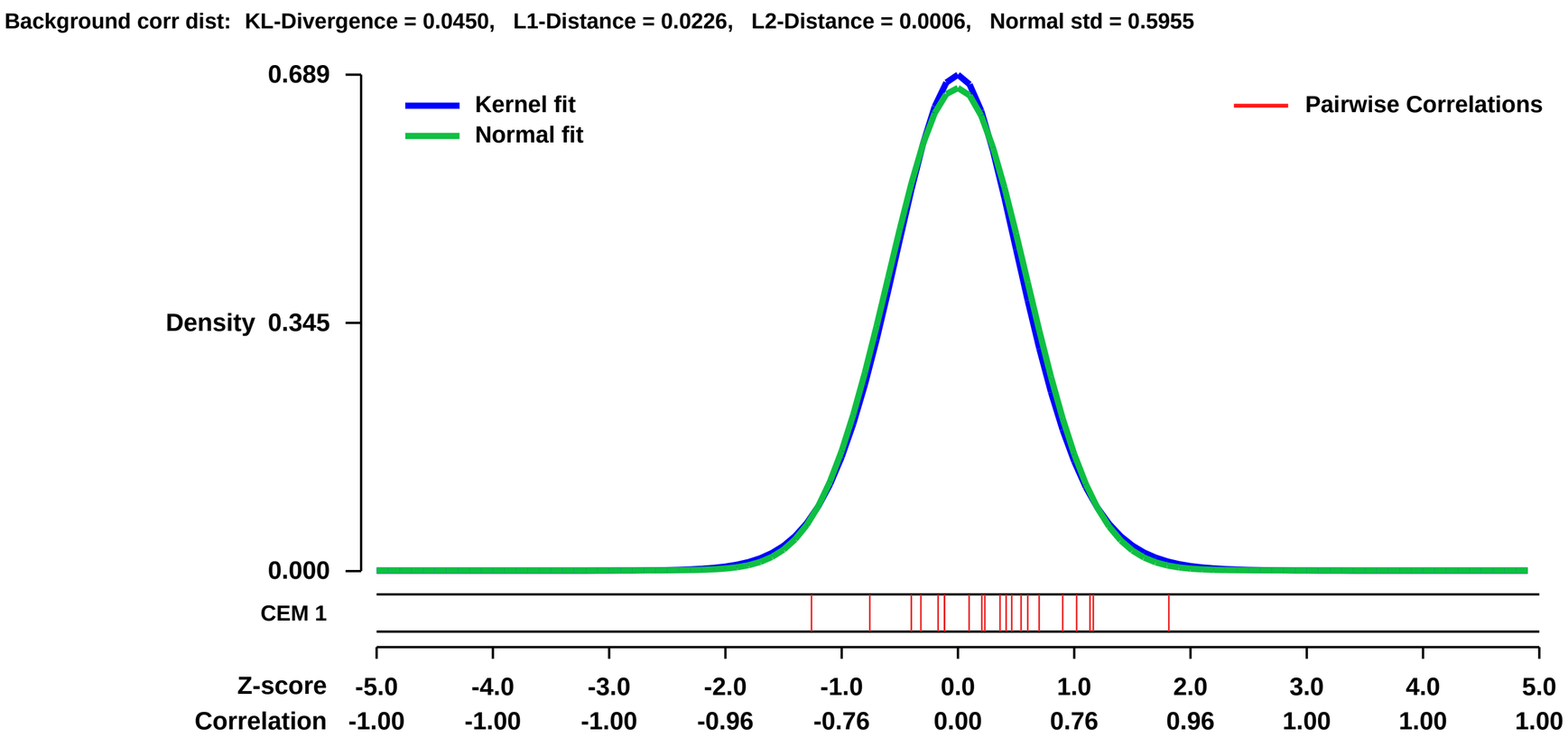

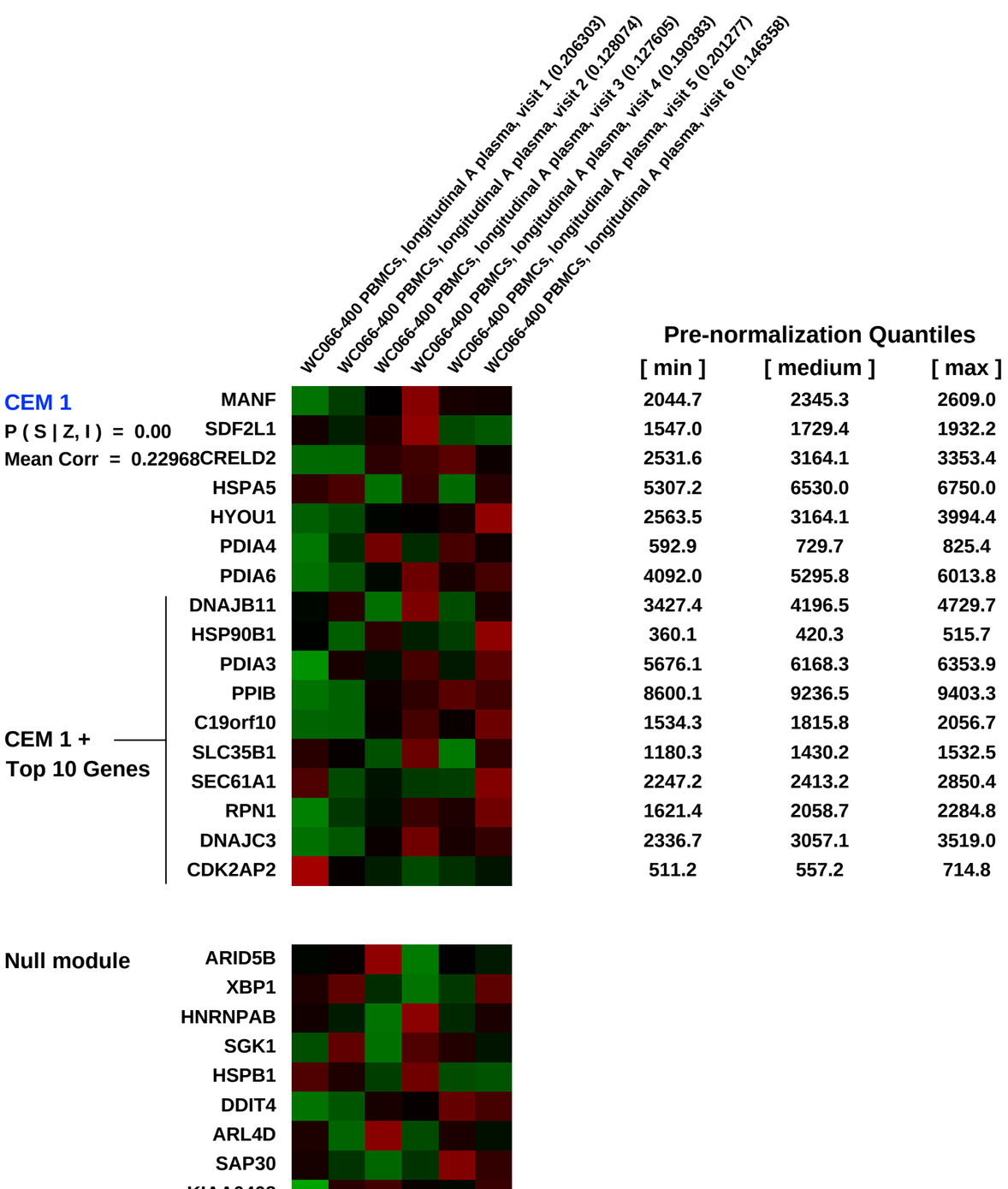

Pre-normalization Quantiles

	[min]	[medium]	[max]
MANF	2044.7	2345.3	2609.0
SDF2L1	1547.0	1729.4	1932.2
CRELD2	2531.6	3164.1	3353.4
HSPA5	5307.2	6530.0	6750.0
HYOU1	2563.5	3164.1	3994.4
PDIA4	592.9	729.7	825.4
PDIA6	4092.0	5295.8	6013.8
DNAJB11	3427.4	4196.5	4729.7
HSP90B1	360.1	420.3	515.7
PDIA3	5676.1	6168.3	6353.9
PPIB	8600.1	9236.5	9403.3
C19orf10	1534.3	1815.8	2056.7
SLC35B1	1180.3	1430.2	1532.5
SEC61A1	2247.2	2413.2	2850.4
RPN1	1621.4	2058.7	2284.8
DNAJC3	2336.7	3057.1	3519.0
CDK2AP2	511.2	557.2	714.8

GEO Series "GSE38836" Expression Profiles

Num of samples in this series: 9

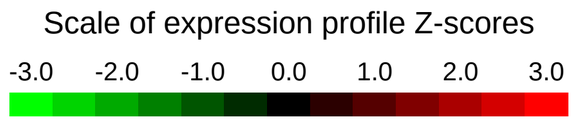

GEO Link:	http://www.ncbi.nlm.nih.gov/geo/query/acc.cgi?acc=GSE38836
Status:	Public on Jun 21 2012
Title:	T Cell Activation in Microgravity Compared to 1g (Earth's) Gravity
Organism:	Homo sapiens
Experiment type:	Expression profiling by array
Platform:	GPL570
Pubmed ID:	22750545
Summary & Design:	**Summary:** This study tested the hypothesis that transcription of immediate early genes is inhibited in T cells activated in microgravity (mg). Immunosuppression during spaceflight is a major barrier to safe long-term human space habitation and travel. The goals of these experiments were to prove that mg was the cause of impaired T cell activation during spaceflight as well as understand the mechanisms controlling early T cell activation. T cells from 4 human donors were stimulated with concanavalin A (ConA) and anti-CD28 onboard the International Space Station (ISS). An onboard centrifuge was used to generate a 1g simultaneous control to isolate the effects of mg from other variables of spaceflight. Microarray expression analysis after 1.5 hours of activation demonstrated that mg- and 1g-activated T cells had distinct patterns of global gene expression and identified 47 genes that were significantly differentially down-regulated in mg. Importantly, several key immediate early genes were inhibited in mg. **Overall design:** T cells were isolated from human volunteers. T cells from each donor were kept separate and loaded into individual chambers in separate cassettes for the following treatments: mg non-activated, mg activated, and 1g activated. Therefore, samples represent biological triplicates. Experimental units were launched into space and placed into the KUBIK facility onboard the International Space Station. The 1g units were placed in the central centrifuge positions and centrifuged with an applied 1g force. The mg units were place in the static positions for continued mg exposure. After 30 minutes of pre-incubation, mg non-activated units were fixed by addition of RNALater (QIAGEN, Valencia, CA), removed from the incubator, and stored in 4˚C. The mg and 1g activated units were injected with final concentration 10mg/ml Con A and 4mg/ml anti-CD28. These cassettes were replaced into KUBIK on either the centrifuge or static positions and activated for 1.5 hours. Activation was stopped with the addition of RNALater and the units were then moved to 4˚C storage. All units were returned to Earth for analysis.

Background corr dist: KL-Divergence = 0.0978, L1-Distance = 0.0267, L2-Distance = 0.0012, Normal std = 0.4399

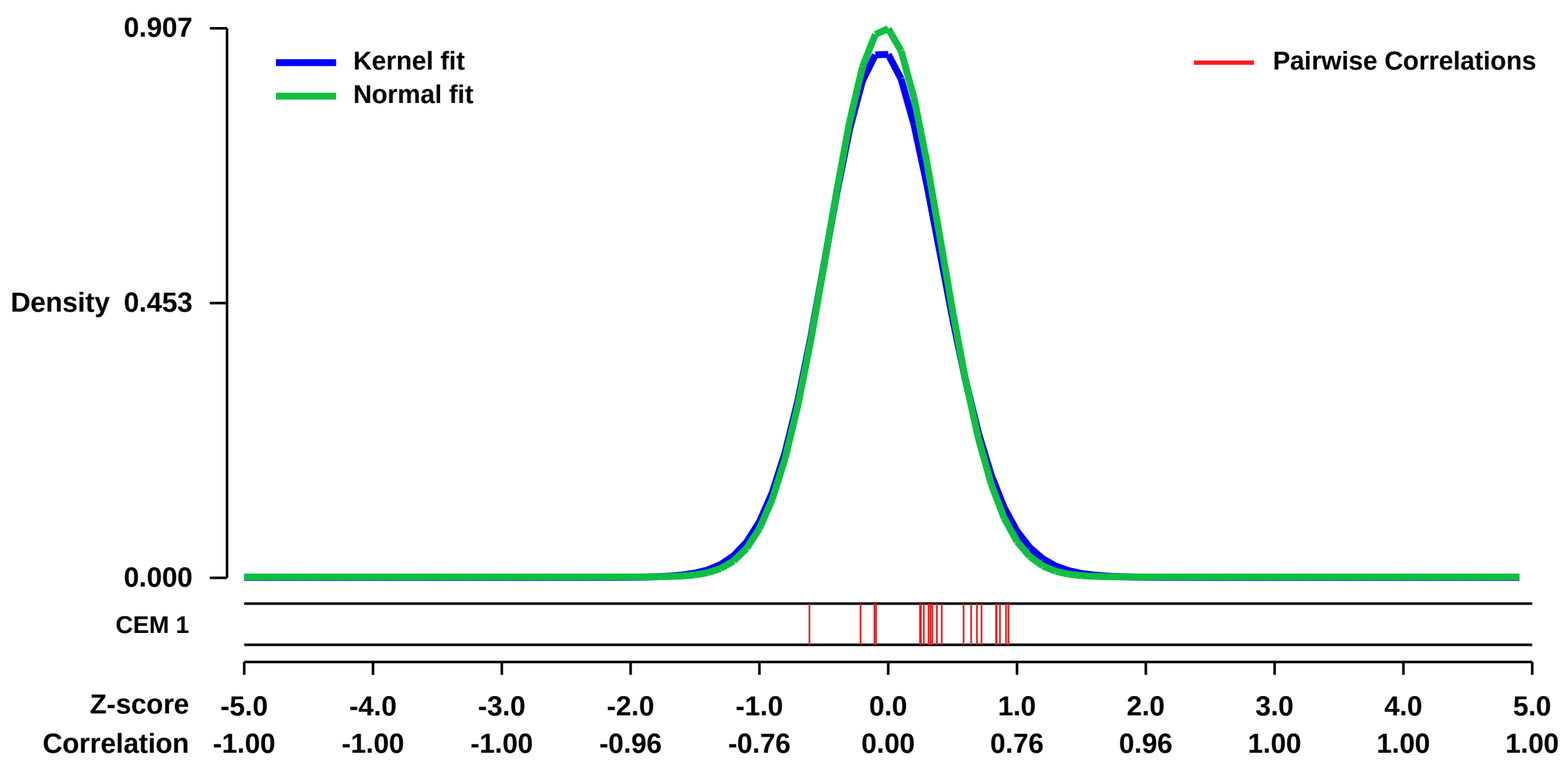

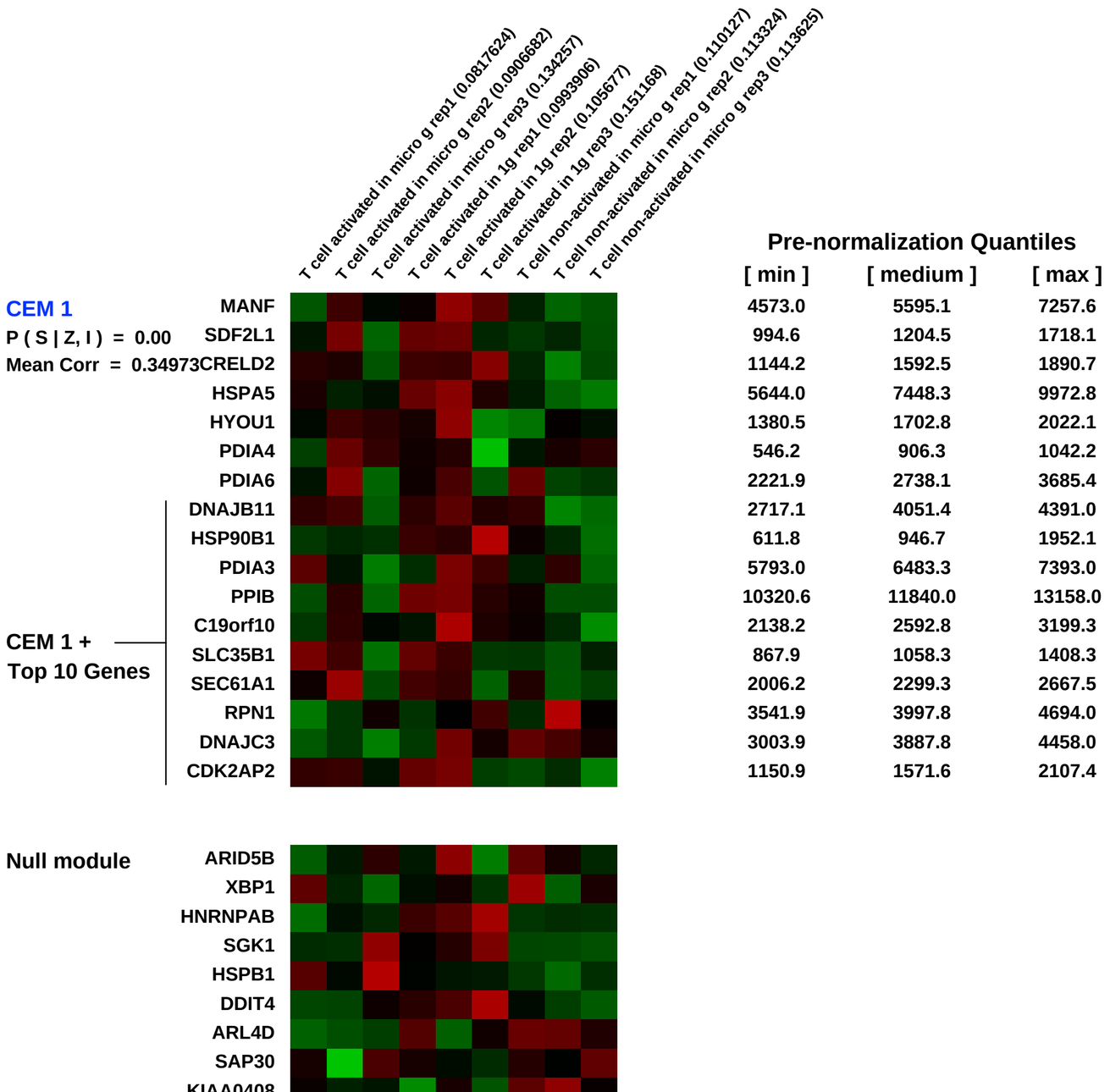

Pre-normalization Quantiles

	[min]	[medium]	[max]
MANF	4573.0	5595.1	7257.6
SDF2L1	994.6	1204.5	1718.1
CRELD2	1144.2	1592.5	1890.7
HSPA5	5644.0	7448.3	9972.8
HYOU1	1380.5	1702.8	2022.1
PDIA4	546.2	906.3	1042.2
PDIA6	2221.9	2738.1	3685.4
DNAJB11	2717.1	4051.4	4391.0
HSP90B1	611.8	946.7	1952.1
PDIA3	5793.0	6483.3	7393.0
PPIB	10320.6	11840.0	13158.0
C19orf10	2138.2	2592.8	3199.3
SLC35B1	867.9	1058.3	1408.3
SEC61A1	2006.2	2299.3	2667.5
RPN1	3541.9	3997.8	4694.0
DNAJC3	3003.9	3887.8	4458.0
CDK2AP2	1150.9	1571.6	2107.4

GEO Series "GSE44029" Expression Profiles

Num of samples in this series: 6

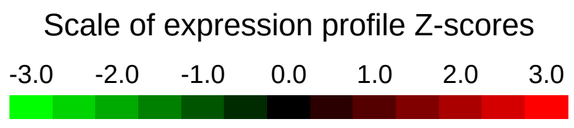

GEO Link:	http://www.ncbi.nlm.nih.gov/geo/query/acc.cgi?acc=GSE44029
Status:	Public on Feb 04 2013
Title:	Expression data from SW480 cells with Gankyrin knockdown
Organism:	Homo sapiens
Experiment type:	Expression profiling by array
Platform:	GPL570
Pubmed ID:	23576566
Summary & Design:	**Summary:** we performed genome-wide screening using SW480 cells with Gankyrin knockdown on an Affymetrix gene expression array to identify the transcriptional targets of Gankyrin **Overall design:** Transcriptional profiling with samples from SW480 cells that were infected with control or gankyrin shRNA. Two condition experiment: control shRNA (three replicates) and NFIL3 shRNA (three replicates)

Background corr dist: KL-Divergence = 0.0300, L1-Distance = 0.0237, L2-Distance = 0.0006, Normal std = 0.6800

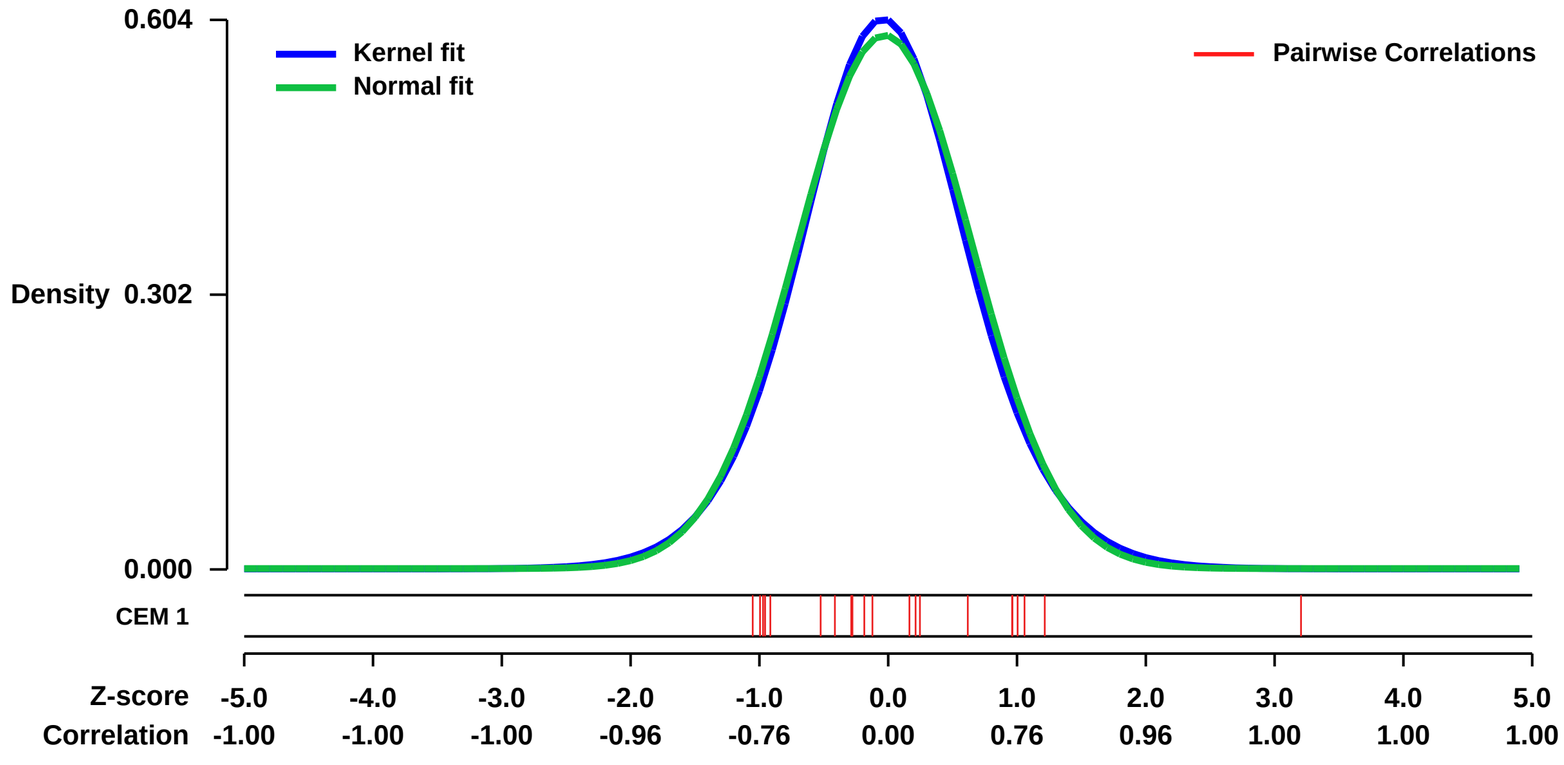

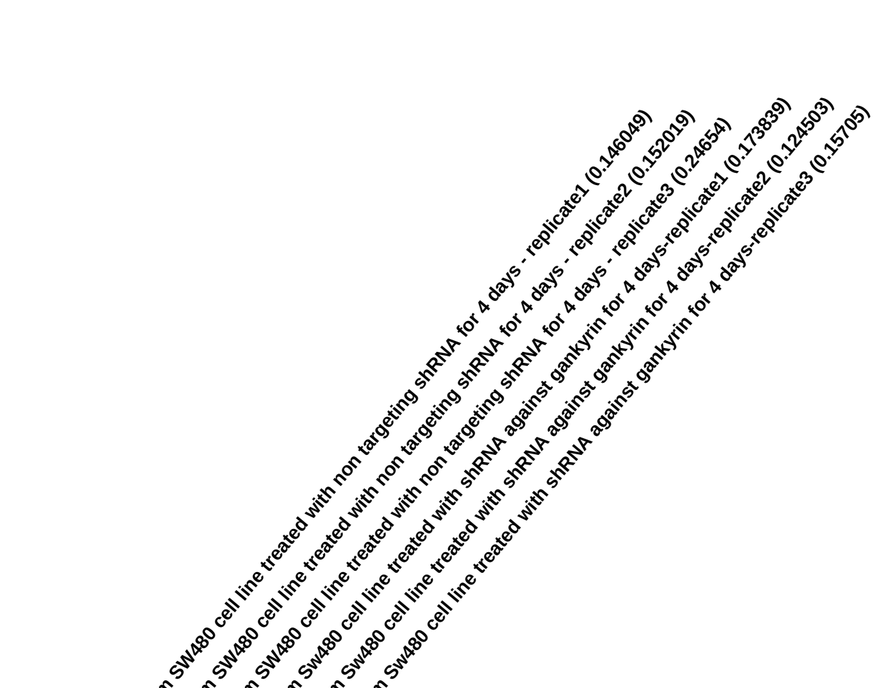

Pre-normalization Quantiles

[min] [medium] [max]

CEM 1	MANF	2475.1	3371.7	3975.1
P (S | Z, I) = 0.00	SDF2L1	789.5	953.3	1095.1
Mean Corr = 0.02629	CRELD2	1806.8	2043.4	2261.8
	HSPA5	17677.0	21421.6	23319.4
	HYOU1	4916.0	6291.7	7017.7
	PDIA4	1300.4	1360.2	1434.9
	PDIA6	8699.9	9520.3	10320.9
CEM 1 + Top 10 Genes	DNAJB11	5725.9	6119.7	6593.3
	HSP90B1	5328.8	5829.9	6067.1
	PDIA3	6547.8	7007.8	7607.9
	PPIB	18882.3	20692.0	21720.6
	C19orf10	2806.9	3162.3	3228.8
	SLC35B1	3012.6	3202.0	3303.1
	SEC61A1	4380.2	4887.1	5779.7
	RPN1	5739.8	6119.7	6404.0
	DNAJC3	977.7	1417.6	2550.9
	CDK2AP2	1084.8	1313.5	1592.2

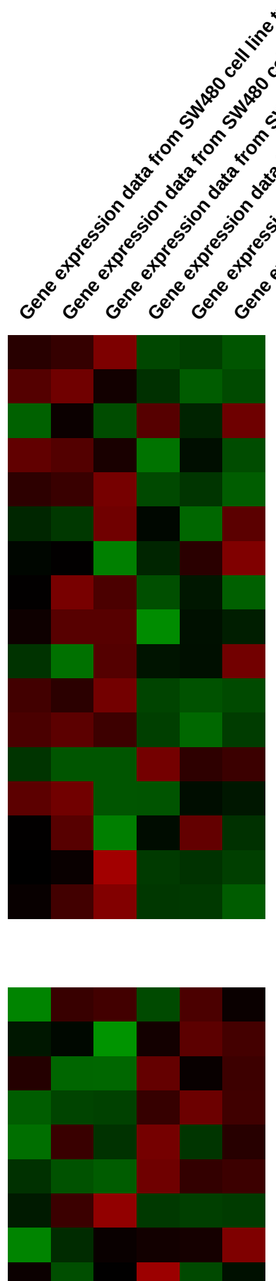

Null module	ARID5B			
	XBP1			
	HNRNPAB			
	SGK1			
	HSPB1			
	DDIT4			
	ARL4D			
	SAP30			
	KIAA0408			
	GPR17			
	HSPH1			
	DNASE1L2			
	SLC5A3			
	GNAS			
	GPR3			
	TNFRSF25			
	TM6SF2			
	MKKS			
	PLEKHF1			
	ZMYM1			
	DOK3			
	FGF20			
	SLC39A2			
	KCNIP2			
	ERRFI1			
	DEDD2			
	CCDC117			
	USP31			
	AHSA2			
	CYS1			
	CNIH2			
	BANP			
	CHORDC1			
	P4HA1			

GEO Series "GSE31215" Expression Profiles

Num of samples in this series: 8

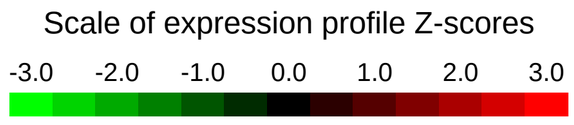

GEO Link:	http://www.ncbi.nlm.nih.gov/geo/query/acc.cgi?acc=GSE31215
Status:	Public on Aug 05 2011
Title:	Gene expression analysis of human pediatric mesenchymal stem cells (hpMSCs) upon expression of EWS-FLI-1
Organism:	Homo sapiens
Experiment type:	Expression profiling by array
Platform:	GPL570
Pubmed ID:	20382729
Summary & Design:	**Summary:** Cancer stem cells (CSCs) display plasticity and self-renewal properties reminiscent of normal tissue stem cells, but the events responsible for their emergence remain obscure. We recently identified CSCs in Ewing sarcoma family tumors (ESFTs) and showed that they retain mesenchymal stem cell (MSC) plasticity. In the present study, we addressed the mechanisms that underlie ESFT CSC development. We show that the EWS-FLI-1 fusion gene, associated with 85%-90% of ESFTs and believed to initiate their pathogenesis, induces expression of the embryonic stem cell (ESC) genes OCT4, SOX2, and NANOG in human pediatric MSCs (hpMSCs) but not in their adult counterparts. Moreover, under appropriate culture conditions, hpMSCs expressing EWS-FLI-1 generate a cell subpopulation displaying ESFT CSC features in vitro. We further demonstrate that induction of the ESFT CSC phenotype is the result of the combined effect of EWS-FLI-1 on its target gene expression and repression of microRNA-145 (miRNA145) promoter activity. Finally, we provide evidence that EWS-FLI-1 and miRNA-145 function in a mutually repressive feedback loop and identify their common target gene, SOX2, in addition to miRNA145 itself, as key players in ESFT cell differentiation and tumorigenicity. Our observations provide insight for the first time into the mechanisms whereby a single oncogene can reprogram primary cells to display a CSC phenotype. **Overall design:** 4 samples of hpMSCs expressing EWS-FLI-1 vs. 4 matched samples of empty-vector-infected cells.

Background corr dist: KL-Divergence = 0.0746, L1-Distance = 0.0251, L2-Distance = 0.0011, Normal std = 0.4923

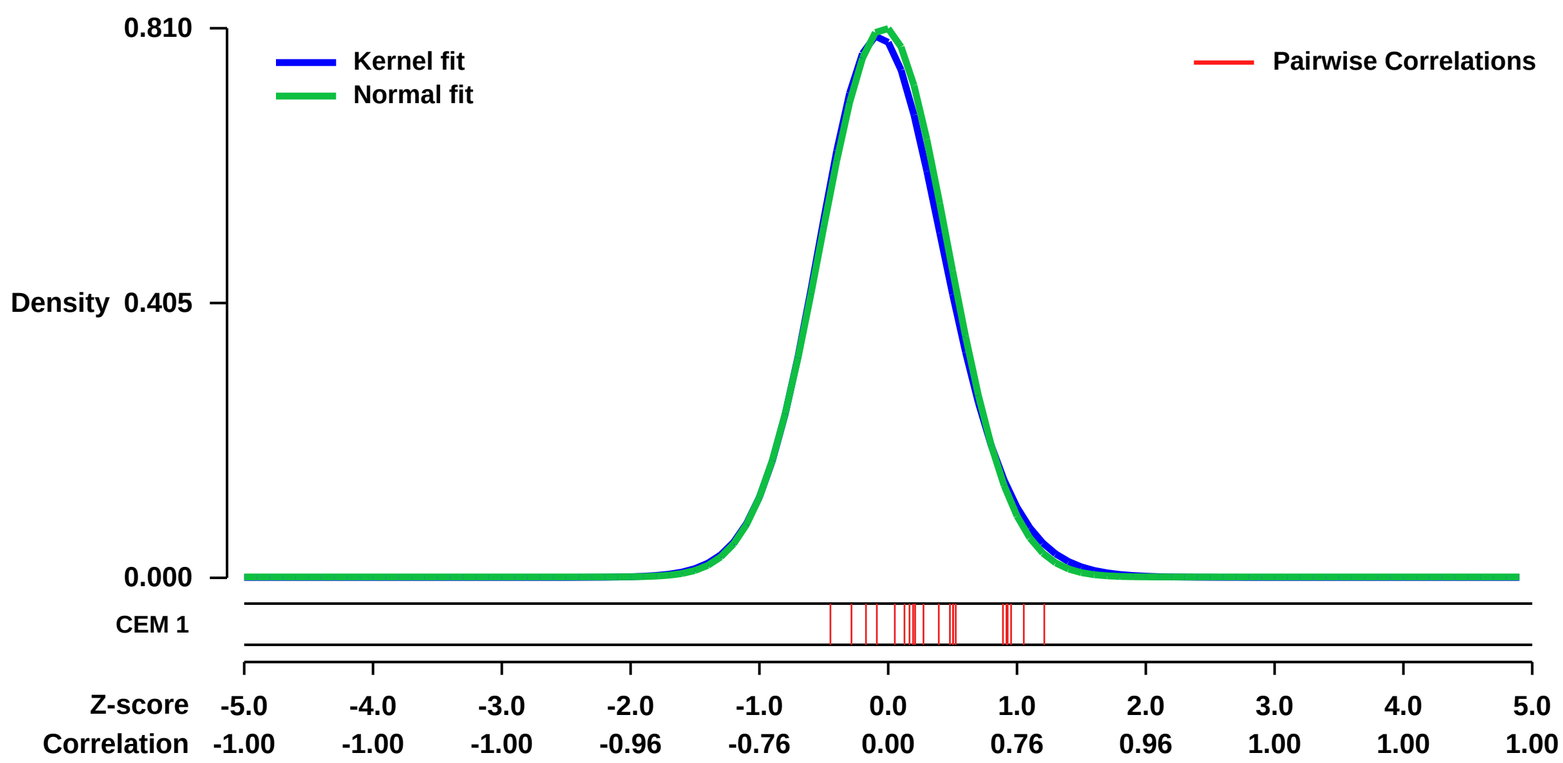

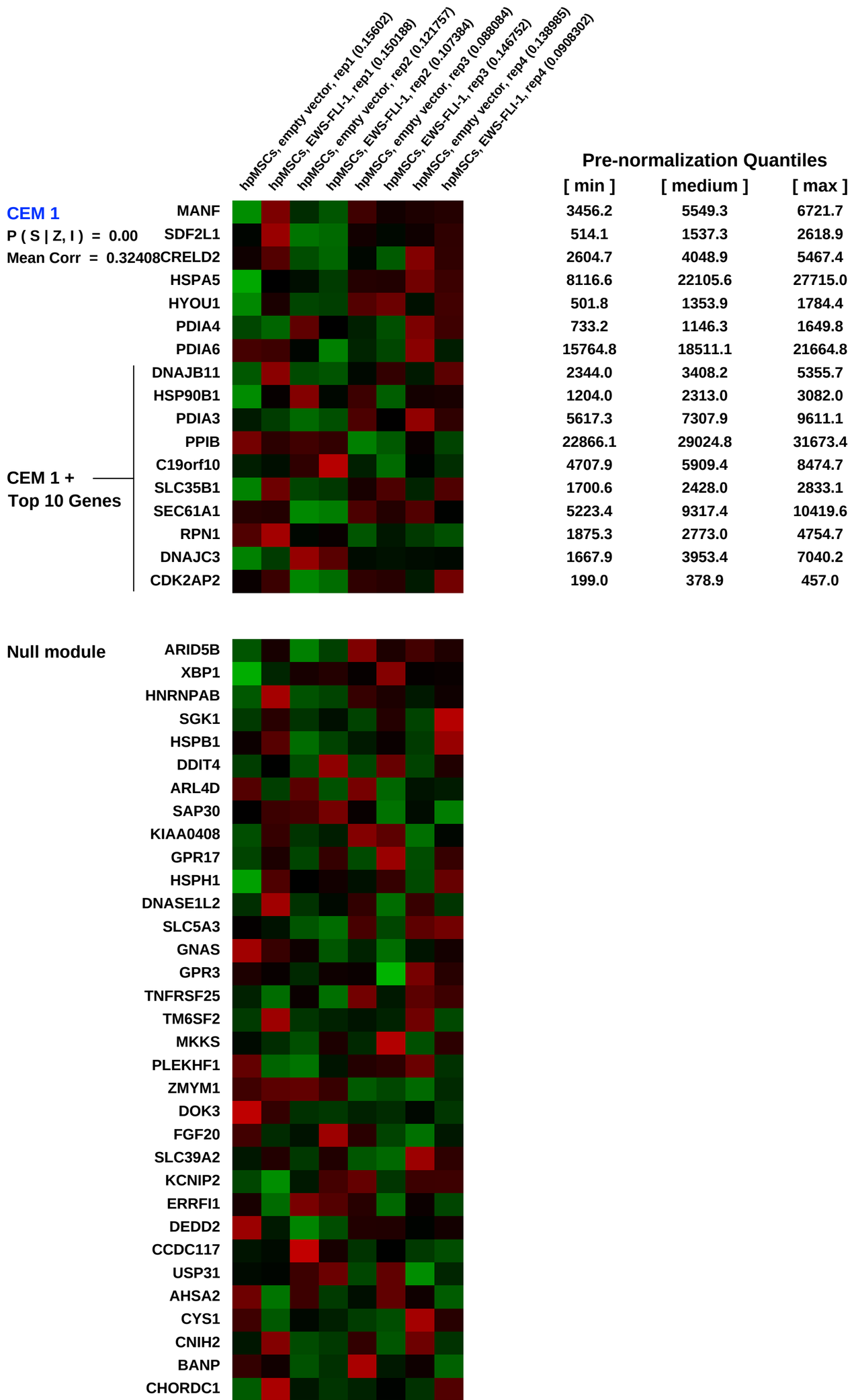

GEO Series "GSE17785" Expression Profiles

Num of samples in this series: 12

Scale of expression profile Z-scores

-3.0 -2.0 -1.0 0.0 1.0 2.0 3.0

GEO Link:	http://www.ncbi.nlm.nih.gov/geo/query/acc.cgi?acc=GSE17785
Status:	Public on Aug 10 2011
Title:	Endogenous expression of an oncogenic PI3K mutation leads to activated PI3K pathway signaling and an invasive phenotype
Organism:	Homo sapiens
Experiment type:	Expression profiling by array
Platform:	GPL570
Pubmed ID:	
Summary & Design:	**Summary:** The PTEN/PI3K pathway is commonly mutated in cancer and therefore represents a rational target for therapeutic intervention. In order to investigate the primary phenotype(s) mediated by mutant PIK3CA in a clean and highly patient-relevant context, we utilized a non-tumorigenic MCF10A parental and isogenic knock-in cell line that harbors a common activating PIK3CA kinase domain mutation (H1047R). We found that introduction of an endogenously mutated PIK3CA primarily results in a marked epithelial-mesenchymal transition (EMT) and invasive phenotype compared to isogenic wild-type cells. Moreover, a potent and selective inhibitor of PIK3CA (GDC-0941) was highly effective and selective on reversing this phenotype compared to cell-proliferation, highlighting a potential new paradigm for studying PI3K-pathway targeted agents. Keywords: Expression Array **Overall design:** Gene expression profiles from a parental MCF10A breast line and an MCF10A clone that has a PI3K activating mutation (H1047R) knocked-in. We plated the cells in 10cm dishes overnight in media with serum, but lacking EGF or insulin. DMSO or GDC-0941 (PI3K inhibitor) at an EC50 concentration were added to triplicate plates of cells in the morning. After 4 hours the RNA was harvested using the Qiagen RNeasy kit. There are 12 samples total.

Background corr dist: KL-Divergence = 0.0828, L1-Distance = 0.0451, L2-Distance = 0.0030, Normal std = 0.5007

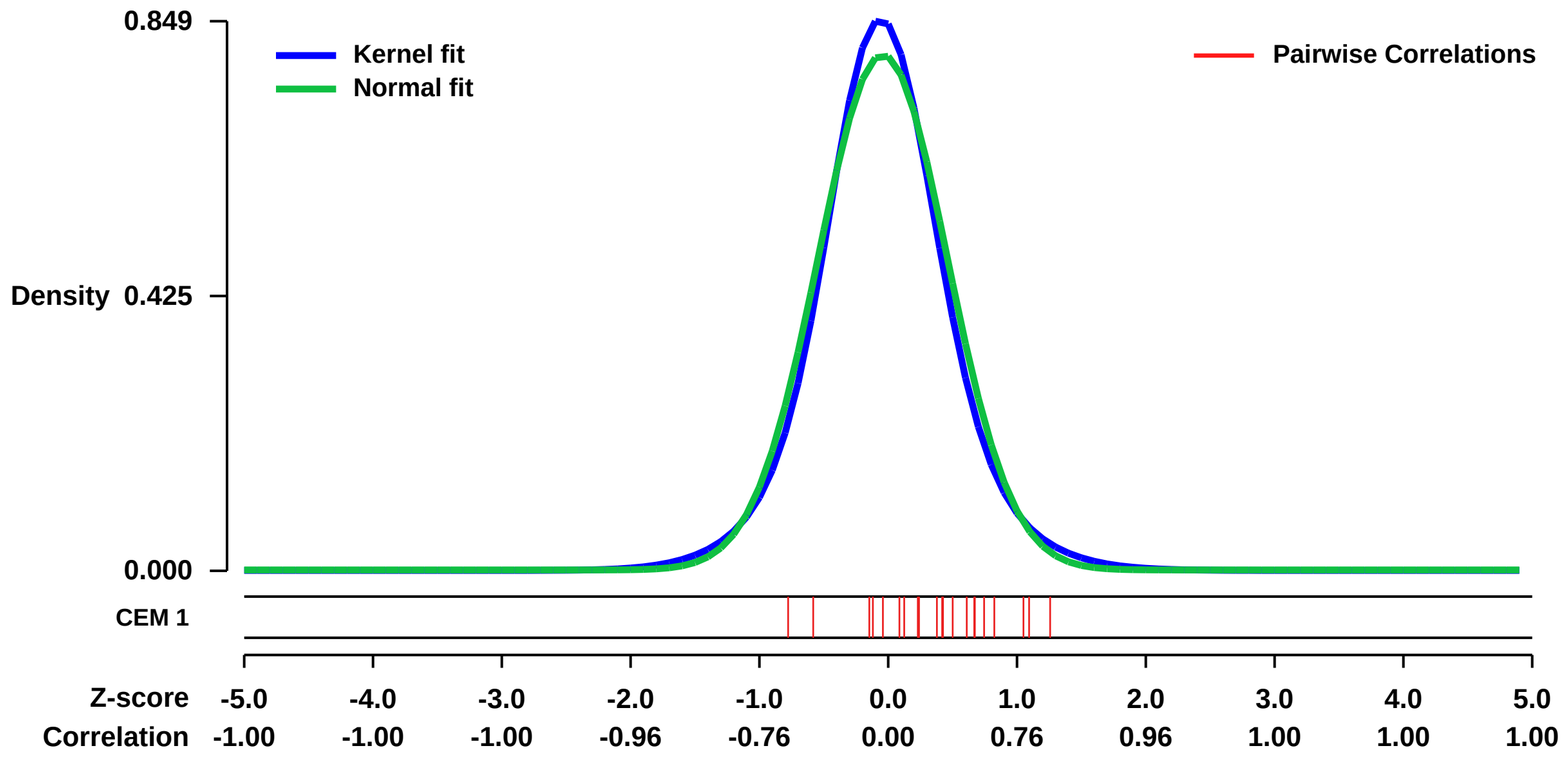

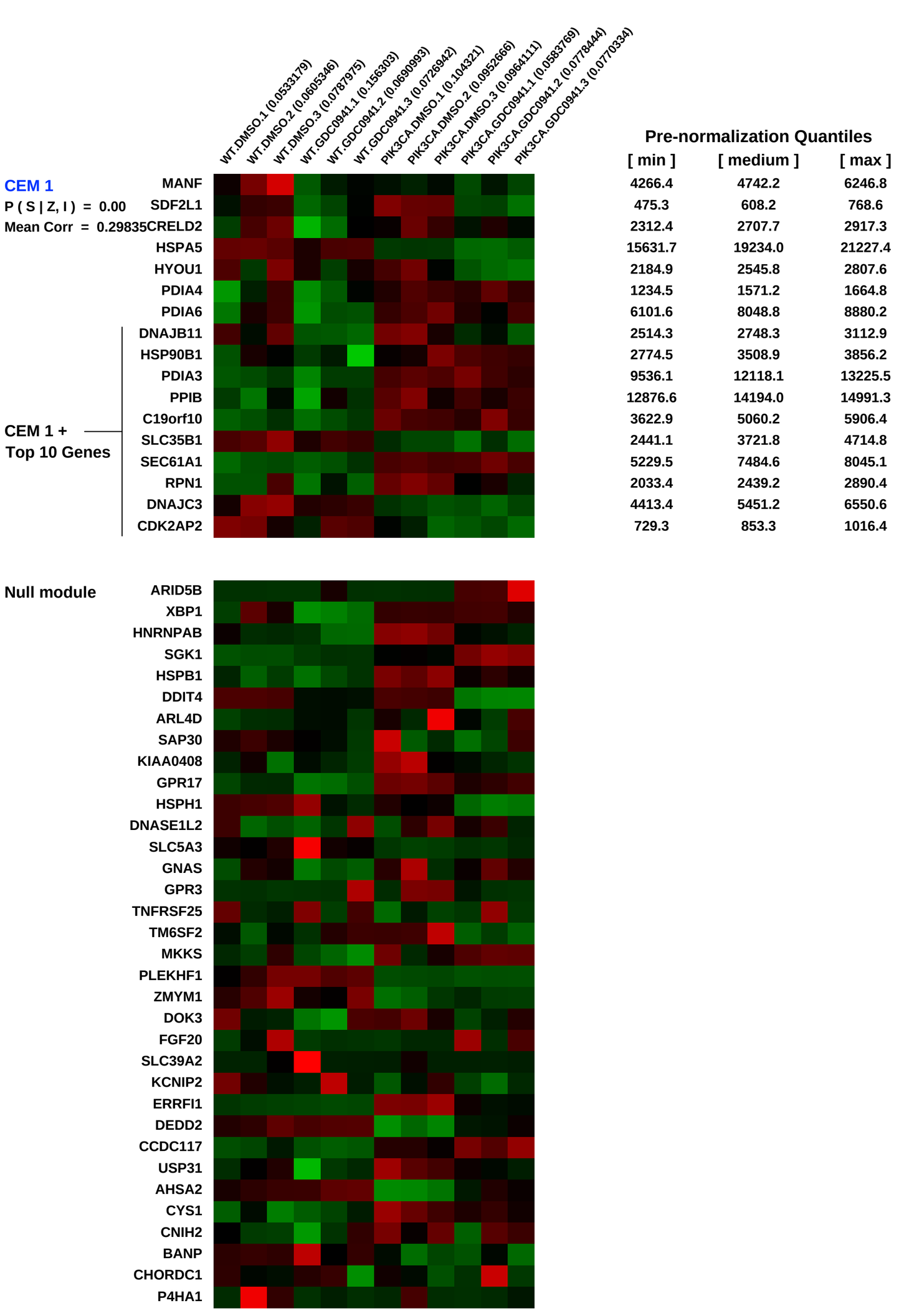

GEO Series "GSE5372" Expression Profiles

Num of samples in this series: 22

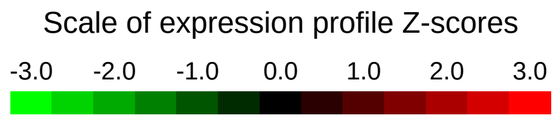

GEO Link:	http://www.ncbi.nlm.nih.gov/geo/query/acc.cgi?acc=GSE5372
Status:	Public on Dec 12 2006
Title:	airway epithelium, large airways, pre and post-mechanical injury
Organism:	Homo sapiens
Experiment type:	Expression profiling by array
Platform:	GPL570
Pubmed ID:	17164391
Summary & Design:	**Summary:** **Responses of the Human Airway Epithelium Transcriptome to In Vivo Injury** **To identify genes participating in repair of the human airway epithelium following injury, we used bronchoscopy and brushing to denude the airway epithelium of healthy individuals, sequentially sampled the same region 7 and 14 days later, and assessed the recovered epithelium for relative levels of gene expression using Affymetrix high-density oligonucleotide microarrays with TaqMan PCR confirmation. Histologic assessment showed that the epithelium was denuded immediately following injury, at 7 days the epithelium was completely covered but partially de-differentiated, and by 14 days there was close to normal proportions of differentiated cells. Gene expression analysis was carried out with both the Affymetrix Microarray Suite 5.0 and Robust Multi-array Average algorithms, applying a multiple test correction to identify bona fide changes in gene expression. At day 7, there were substantial differences in the gene expression pattern compared to the resting epithelium, with a distinctive airway epithelial â repair transcriptomeâ of actively proliferating cells in the process of re-differentiation. The repair transcriptome at 7 days was dominated by genes encoding proteins involved in cell cycle regulation, transcription, signal transduction, metabolism and transport. Interestingly, the majority of cell cycle genes differentially expressed at day 7 belonged to the G2 and M late phases of the cell cycle, suggesting that the proliferating cells are relatively synchronized 1 wk following injury. At 14 days post-injury, the majority of the gene expression changes observed at day 7 were no longer observed, with the expression profile similar to that of resting airway epithelium. Using a class prediction algorithm, a group of 50 genes dominated by cell cycle genes, that represent a human airway epithelial â repair signatureâ was identified. These observations provide a baseline of the functional gene categories participating in the process of normal human airway epithelial repair that can be used in future studies of injury and repair in human airway epithelial diseases.** **Keywords: response to airway injury** **Overall design:** **comparison of gene expression in airway epithelial cells of the large airways, before and after mechanical injury caused by airway brushing**

Background corr dist: KL-Divergence = 0.2949, L1-Distance = 0.0621, L2-Distance = 0.0103, Normal std = 0.2820

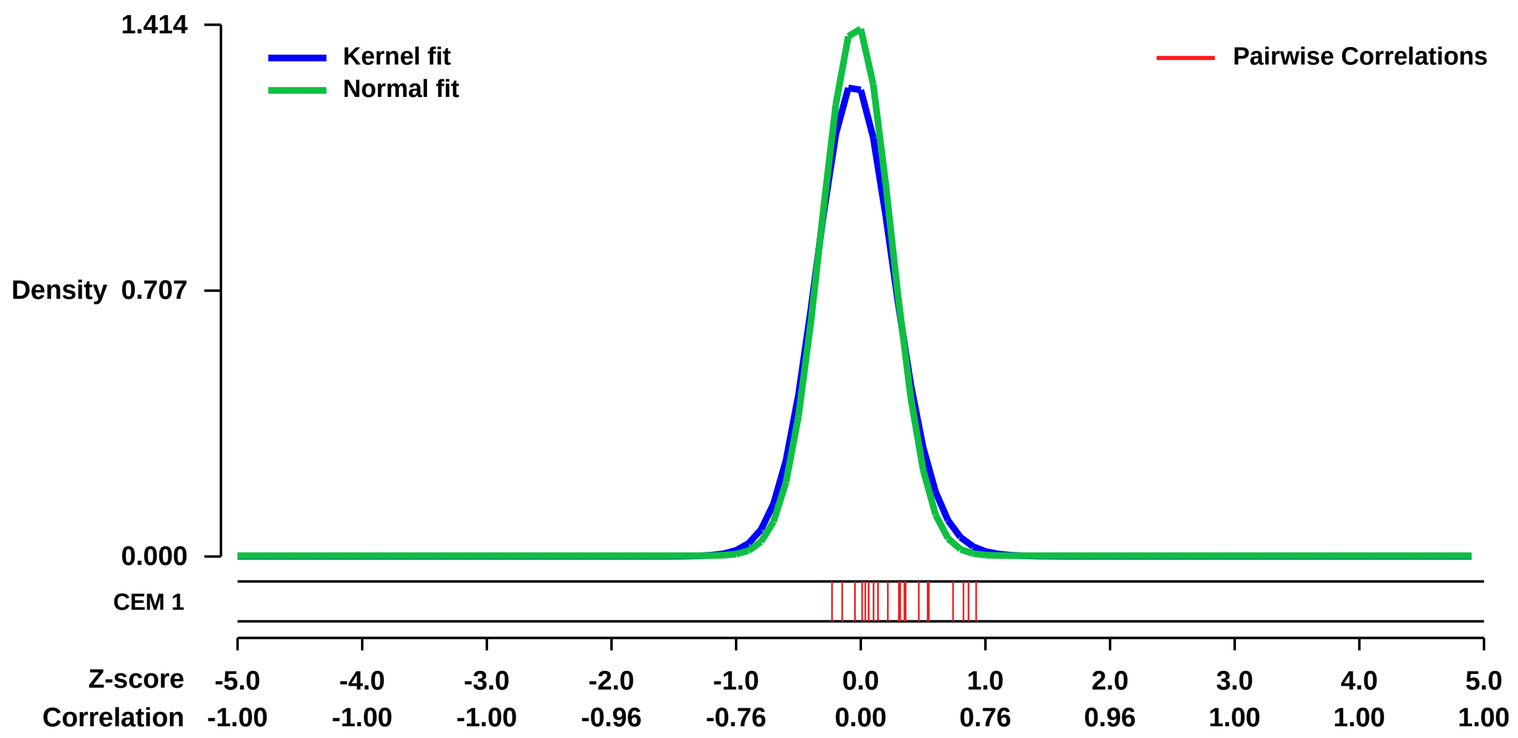

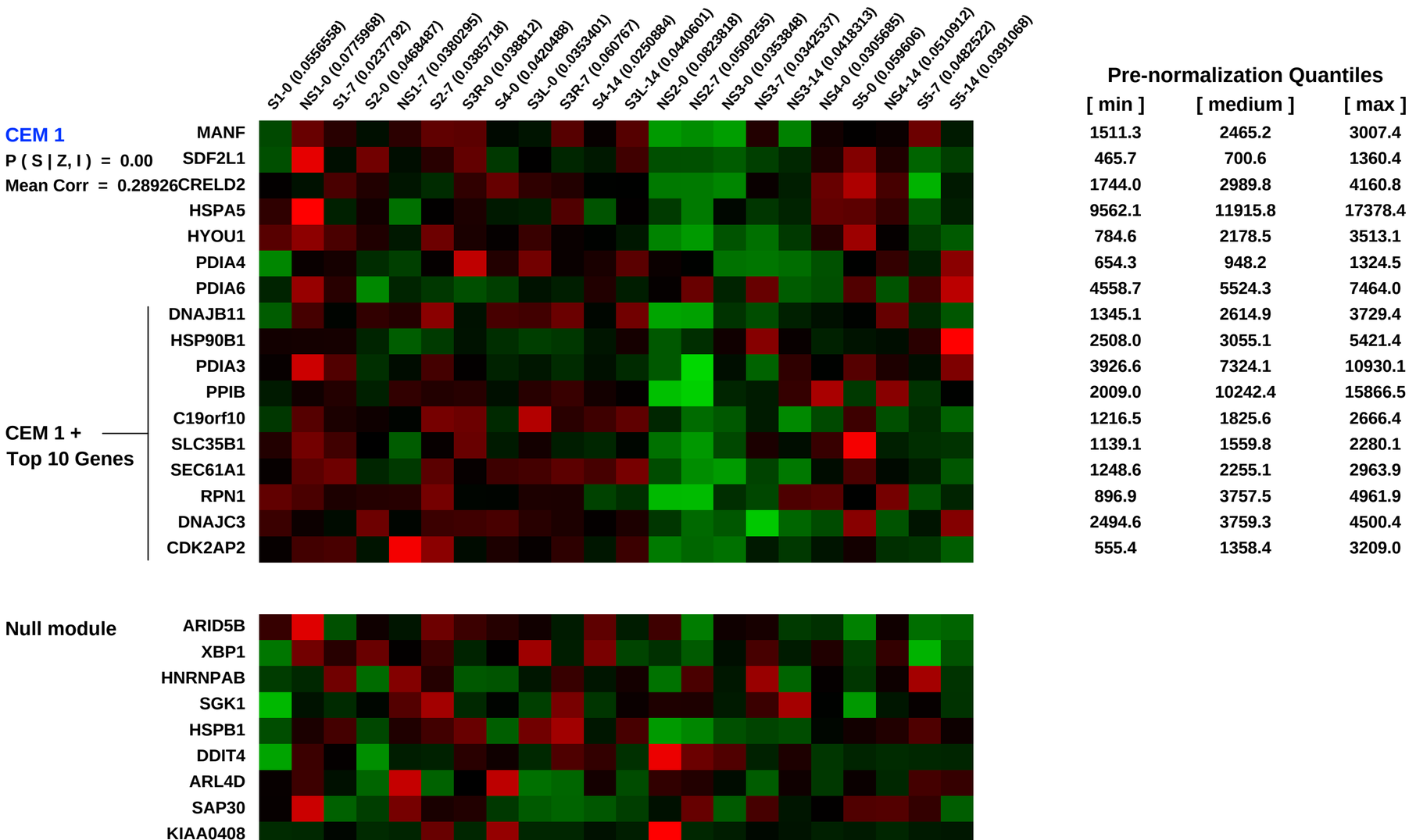

Pre-normalization Quantiles

[min]	[medium]	[max]
1511.3	2465.2	3007.4
465.7	700.6	1360.4
1744.0	2989.8	4160.8
9562.1	11915.8	17378.4
784.6	2178.5	3513.1
654.3	948.2	1324.5
4558.7	5524.3	7464.0
1345.1	2614.9	3729.4
2508.0	3055.1	5421.4
3926.6	7324.1	10930.1
2009.0	10242.4	15866.5
1216.5	1825.6	2666.4
1139.1	1559.8	2280.1
1248.6	2255.1	2963.9
896.9	3757.5	4961.9
2494.6	3759.3	4500.4
555.4	1358.4	3209.0

GEO Series "GSE21374" Expression Profiles

Num of samples in this series: 282

Details of this dataset are not shown due to large number of samples and the page size limit.

Find details in http://www.ncbi.nlm.nih.gov/geo/query/acc.cgi?acc=GSE21374

Background corr dist: KL-Divergence = 0.2005, L1-Distance = 0.0608, L2-Distance = 0.0097, Normal std = 0.3312

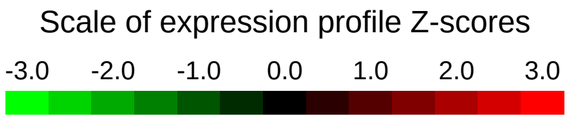

GEO Series "GSE27949" Expression Profiles

Num of samples in this series: 33

Scale of expression profile Z-scores

-3.0 -2.0 -1.0 0.0 1.0 2.0 3.0

GEO Link:	http://www.ncbi.nlm.nih.gov/geo/query/acc.cgi?acc=GSE27949
Status:	Public on May 31 2011
Title:	Gene-chip studies of adipogenesis-regulated microRNAs in mouse primary adipocytes and human obesity (Affymetrix)
Organism:	Homo sapiens
Experiment type:	Expression profiling by array
Platform:	GPL570
Pubmed ID:	21426570
Summary & Design:	**Summary:** Adipose tissue abundance relies partly on the factors that regulate adipogenesis, i.e. proliferation and differentiation of adipocytes. While the transcriptional program that initiates adipogenesis is well-known, the importance of microRNAs in adipogenesis is less well studied. We thus set out to investigate whether miRNAs would be actively modulated during adipogenesis and obesity. Several models exist to study adipogenesis in vitro, of which the cell line 3T3-L1 is probably the most well known, albeit not the most physiologically appropriate. We used a microarray strategy to provide a global profile of miRNAs in brown and white primary murine adipocytes (prior to and following differentiation) and evaluated the similarity of the responses to non-primary cell models, through literature data-mining. We found 65 miRNAs regulated during in vitro adipogenesis in primary adipocytes. When we compared our primary adipocyte profiles with those of cell lines reported in the literature, we found a high degree of difference in adipogenesis-regulated miRNAs. We evaluated the expression of 10 of our adipogenesis-regulated miRNAs using real-time qPCR and then selected 5 miRNAs that showed robust expression levels and profiled these by qPCR in subcutaneous adipose tissue of 20 humans with a range of body mass indices (BMI, range=21-48). Of the miRNAs tested, mir-21 was both highly expressed in human adipose tissue and positively correlated with BMI (R2=0.49, p<0.001). In conclusion, we provide the preliminary analysis of miRNAs important for primary cell in vitro adipogenesis and find that the inflammation-associated miRNA, mir-21, is up-regulated in subcutaneous adipose tissue in human obesity. **Overall design:** A global transcriptomic survey of subcutaneous adipose tissue from human subjects characterised as having normal glucose tolerance, glucose intolerance or frank type 2 diabetes.

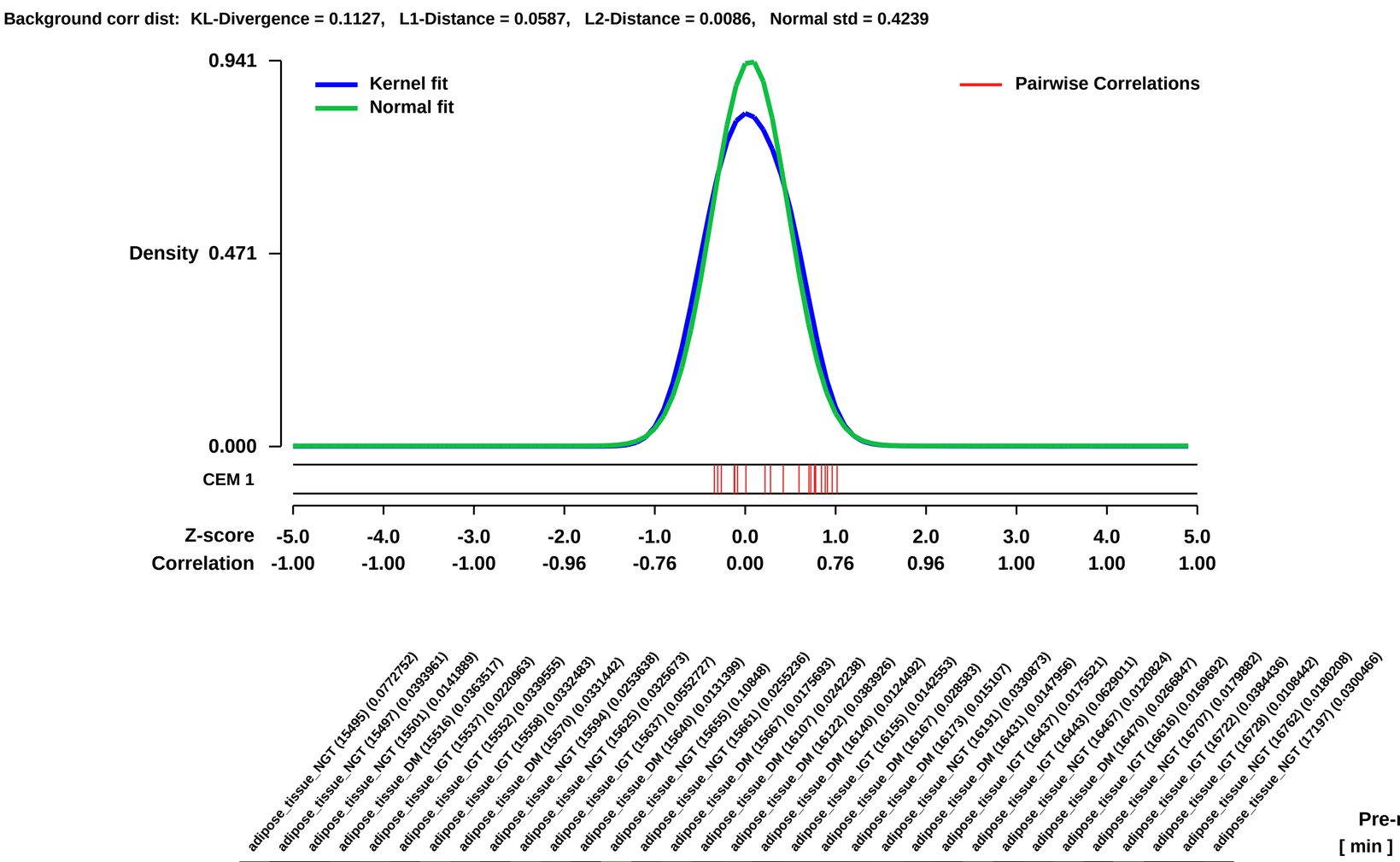

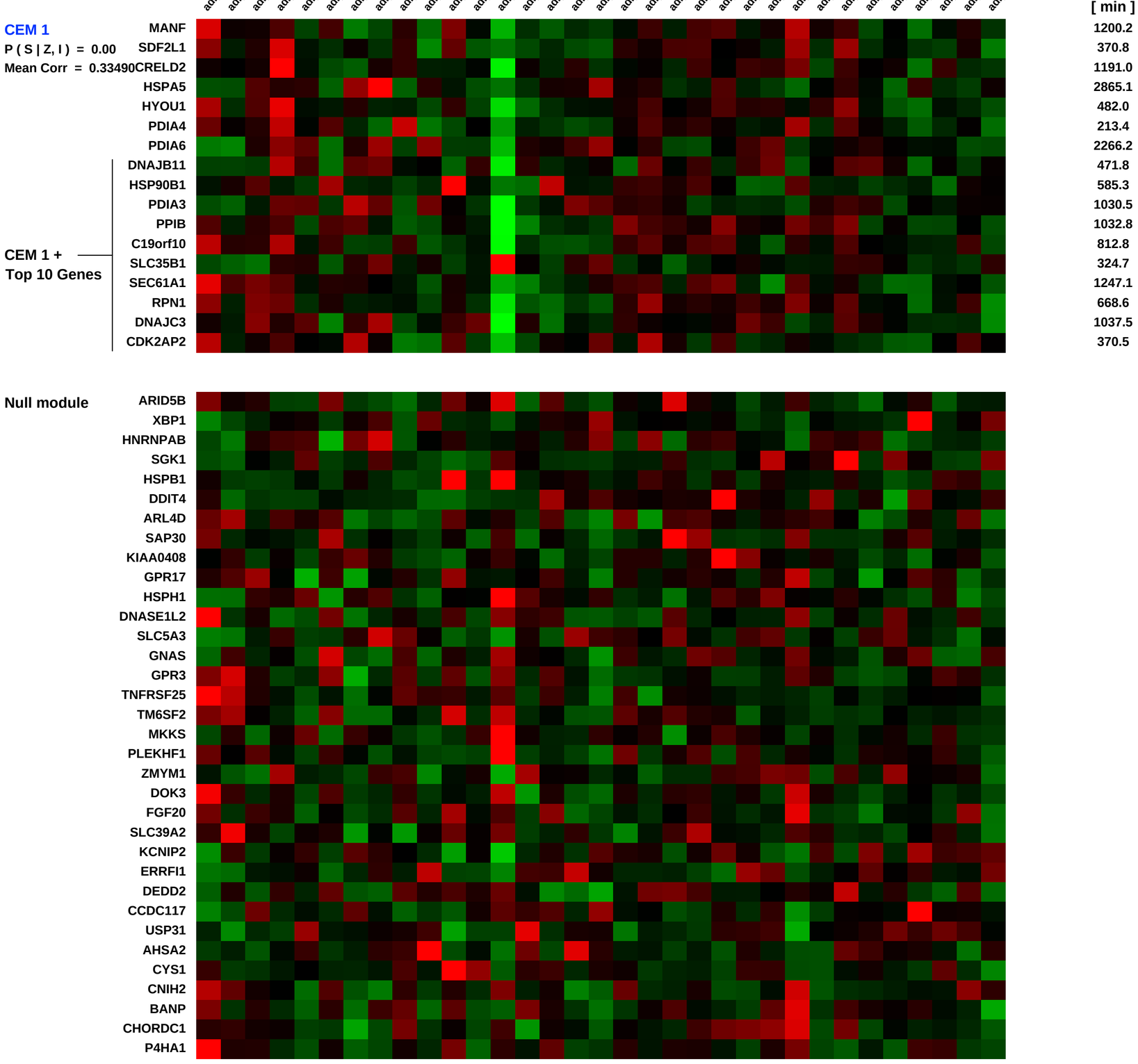

Pre-normalization Quantiles

[min]	[medium]	[max]
1200.2	2051.4	3199.0
370.8	595.8	1042.8
1191.0	2983.3	5245.8
2865.1	4429.7	8525.2
482.0	1219.5	2104.9
213.4	642.8	1240.8
2266.2	4310.3	6070.2
471.8	1297.5	1913.2
585.3	1308.8	3457.4
1030.5	4958.4	7617.9
1032.8	6898.8	9698.8
812.8	1957.9	2930.6
324.7	631.0	1717.7
1247.1	2119.2	3524.4
668.6	1793.8	2565.1
1037.5	2188.6	2947.9
370.5	663.4	955.1

GEO Series "GSE29621" Expression Profiles

Num of samples in this series: 65

Scale of expression profile Z-scores

-3.0 -2.0 -1.0 0.0 1.0 2.0 3.0

GEO Link:	http://www.ncbi.nlm.nih.gov/geo/query/acc.cgi?acc=GSE29621
Status:	Public on Jan 01 2014
Title:	mRNA and microRNA profile in colon cancer [mRNA data]
Organism:	Homo sapiens
Experiment type:	Expression profiling by array
Platform:	GPL570
Pubmed ID:	22362069
Summary & Design:	**Summary:** Compariosn of mRNA and miRNA profile in colon cancer **Overall design:** mRNA was extracted from colon tissues for microarray analysis

Background corr dist: KL-Divergence = 0.3933, L1-Distance = 0.0883, L2-Distance = 0.0258, Normal std = 0.2549

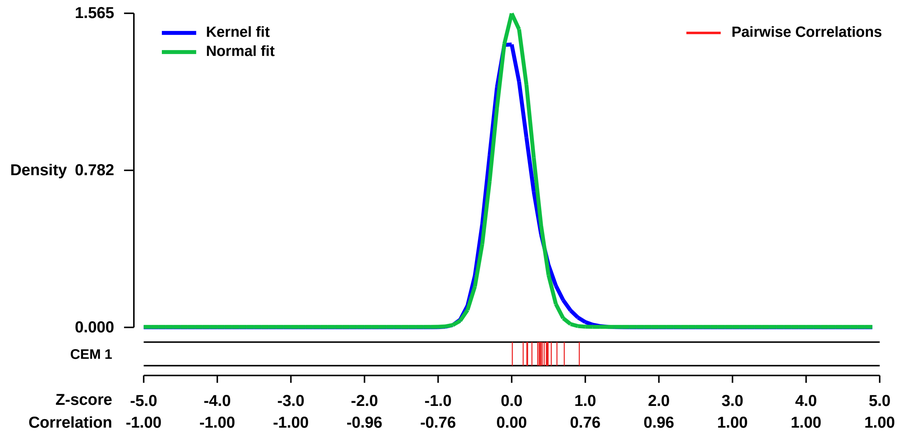

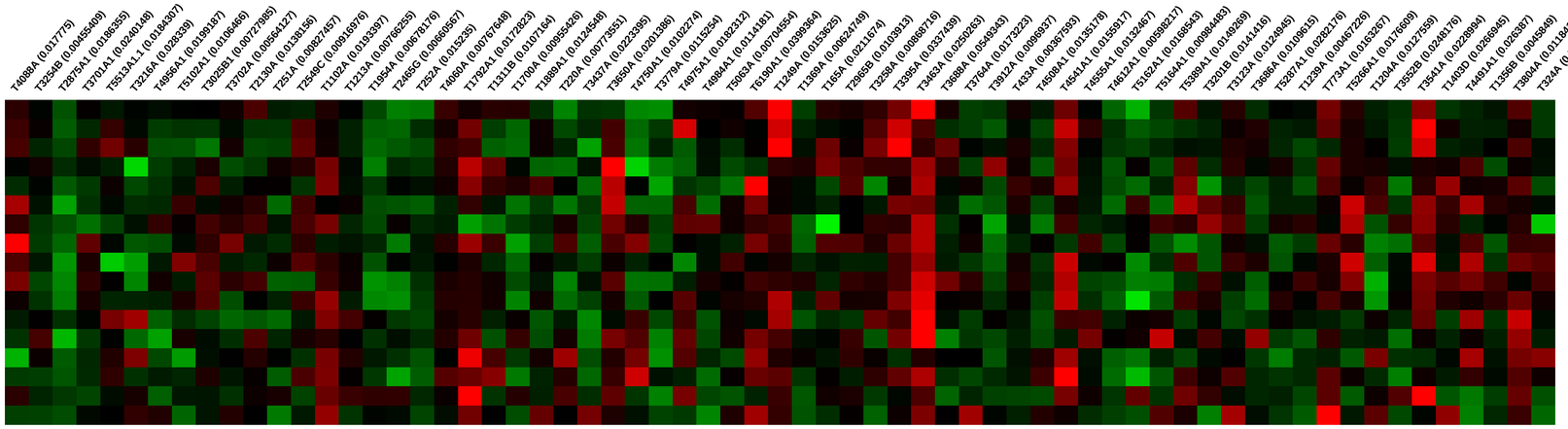

Pre-normalization Quantiles

[min]	[medium]	[max]
1413.1	2484.7	4657.3
660.1	1021.1	2599.6
1156.7	1898.9	3345.3
5753.0	8498.8	11963.9
2236.4	4003.0	6913.9
748.9	1511.5	2594.7
3367.2	5910.7	7725.0
1901.6	2943.8	4784.3
1077.1	2394.8	3960.6
4021.1	7688.8	11381.3
4384.7	7946.9	11251.5
1798.7	2479.6	4693.8
1226.7	2041.8	3321.9
1740.5	2689.3	4074.6
1722.5	2708.0	4303.9
1434.9	2264.1	4823.6
615.3	932.0	1706.1

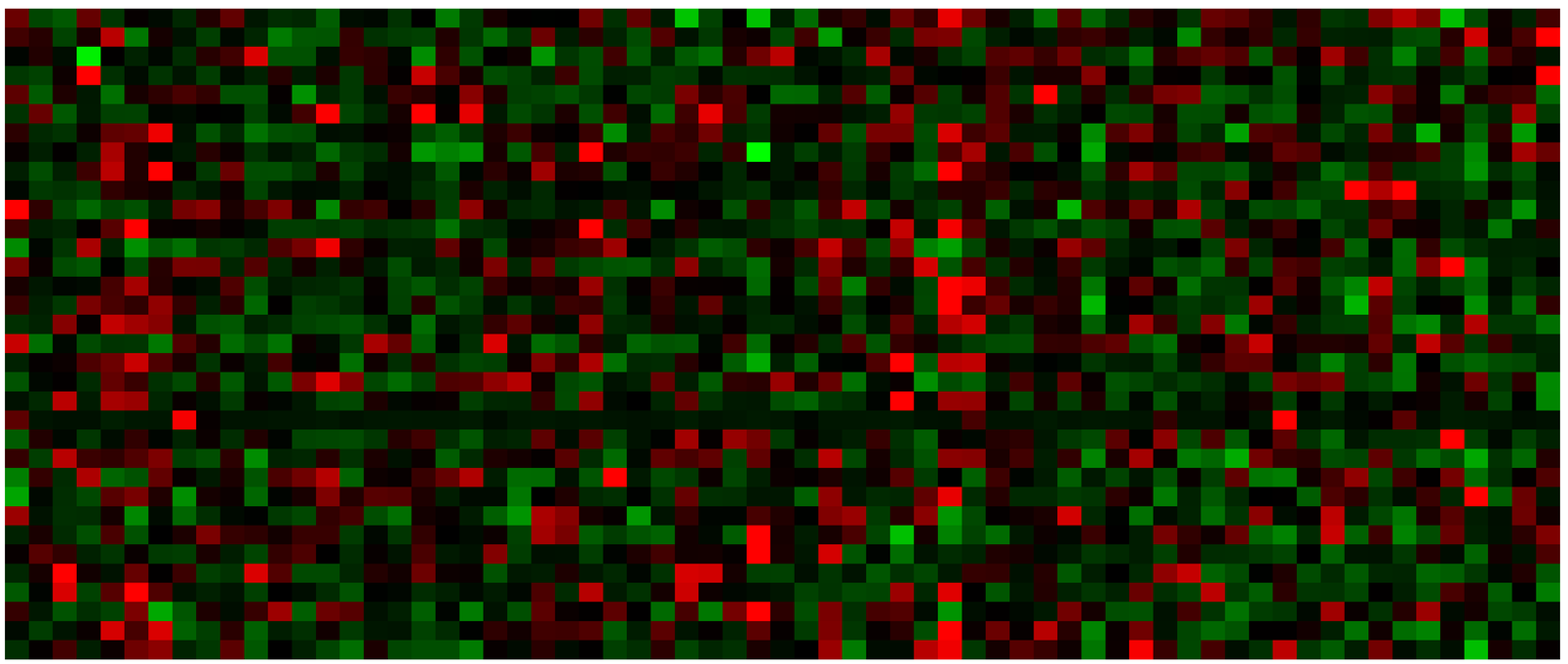

GEO Series "GSE14827" Expression Profiles

Num of samples in this series: 27

Scale of expression profile Z-scores

-3.0 -2.0 -1.0 0.0 1.0 2.0 3.0

GEO Link:	http://www.ncbi.nlm.nih.gov/geo/query/acc.cgi?acc=GSE14827
Status:	Public on Feb 01 2010
Title:	Gene expression profiles from osteosarcpma samples
Organism:	Homo sapiens
Experiment type:	Expression profiling by array
Platform:	GPL570
Pubmed ID:	24448647
Summary & Design:	**Summary:** Osteosarcoma patients with development of pulmonary metastasis have still poorer prognosis in spite of aggressive treatment. However, molecular mechanism of metastasis is still unknown. We analysed the expression levels of 54,613 probe sets in surgical 27 samples of osteosarcoma with GeneChip Human Genome U133 Plus 2.0 arrays. Keywords: gene expression array-based, count **Overall design:** Total RNA was extracted from 27 fresh frozen tumour specimens. We analysed the global gene exprssion profiles of these osteosarcoma cases in order to clarify the genomic basis behind the development of pulmonary metastasis.

Background corr dist: KL-Divergence = 0.2308, L1-Distance = 0.0848, L2-Distance = 0.0201, Normal std = 0.3273

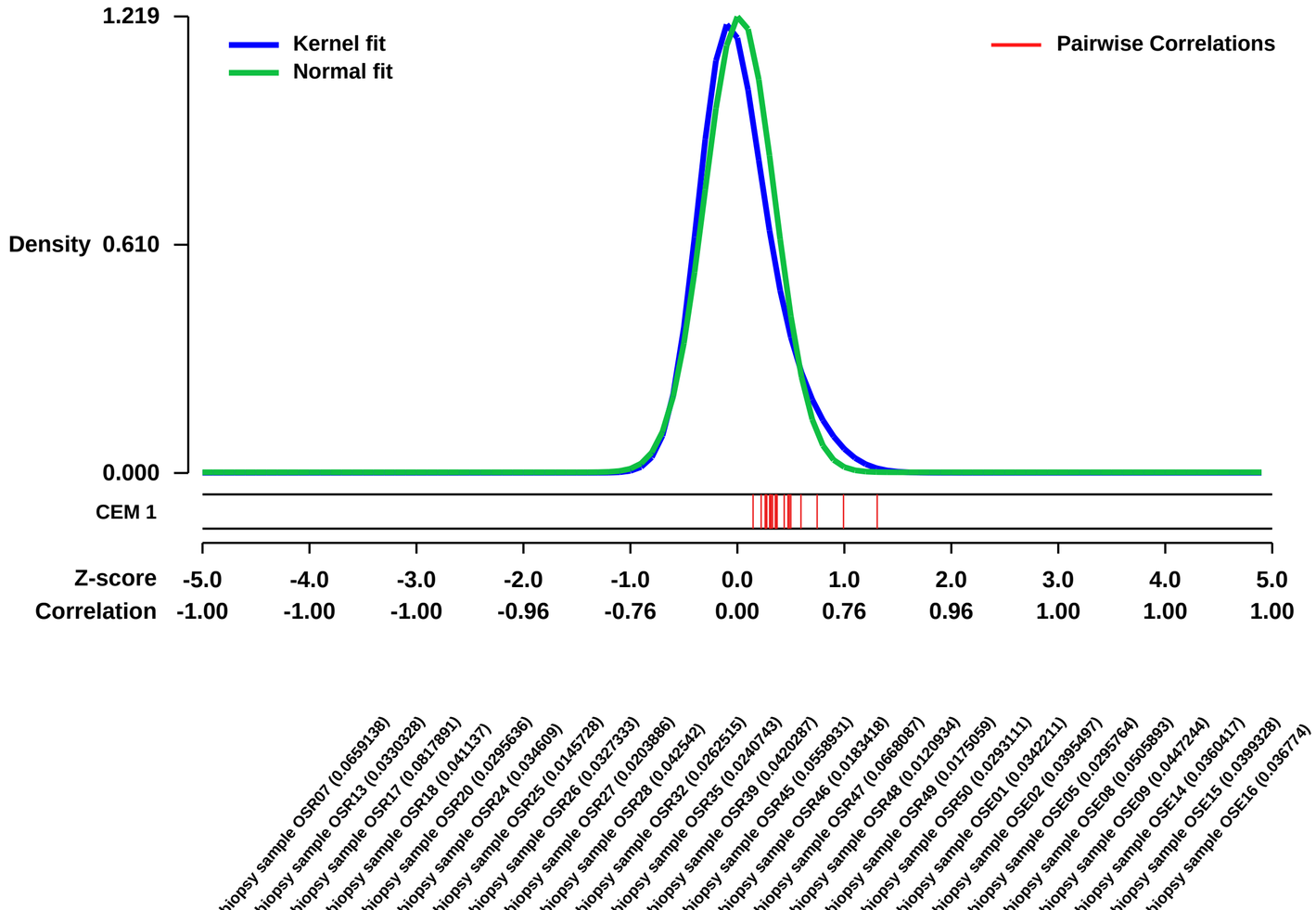

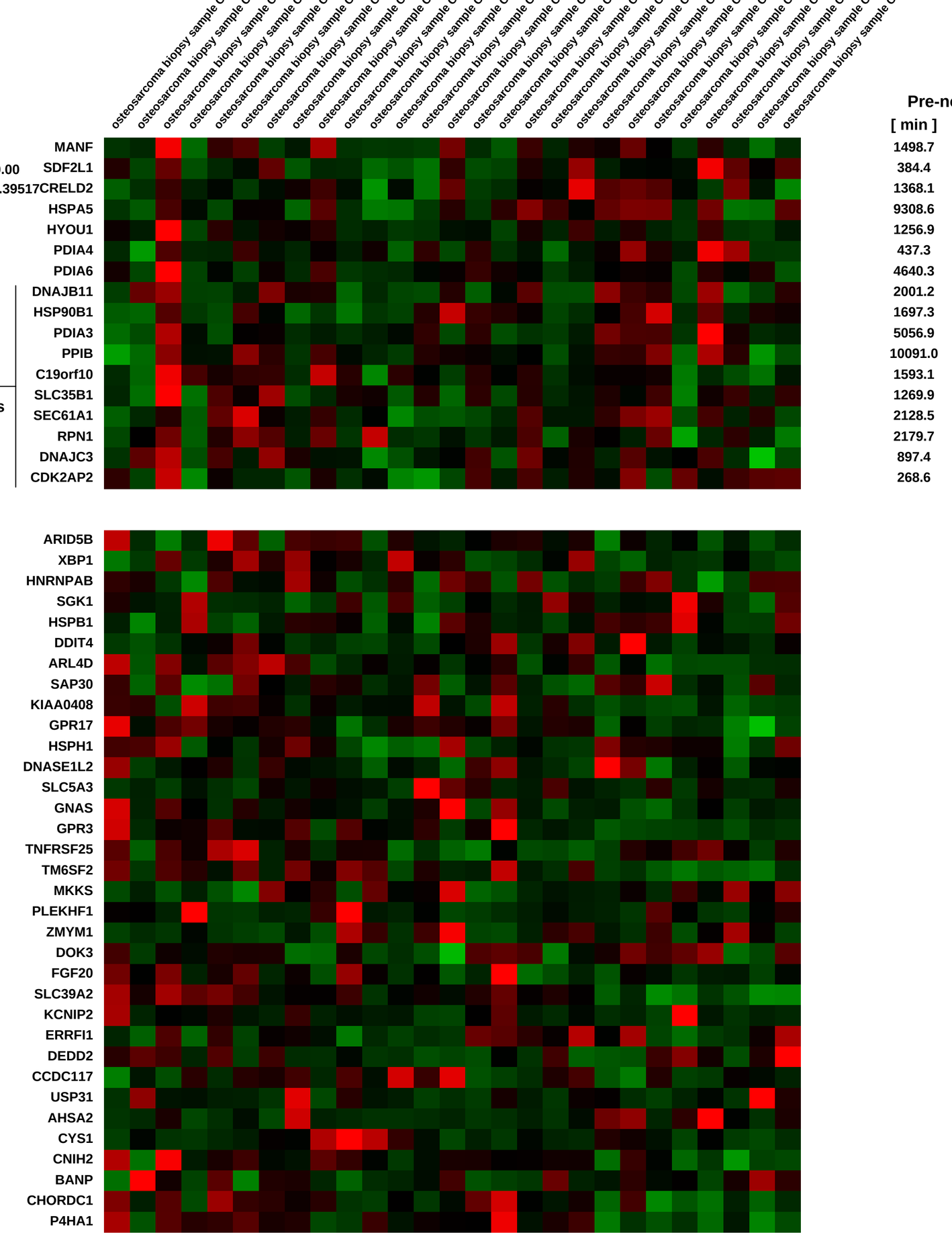

Pre-normalization Quantiles

	[min]	[medium]	[max]
MANF	1498.7	2417.1	5931.4
SDF2L1	384.4	715.5	1555.8
CRELD2	1368.1	2417.8	4269.0
HSPA5	9308.6	13806.5	18989.6
HYOU1	1256.9	2315.4	12084.6
PDIA4	437.3	877.4	1762.8
PDIA6	4640.3	7297.8	20038.1
DNAJB11	2001.2	3138.9	5800.5
HSP90B1	1697.3	2960.5	5382.3
PDIA3	5056.9	7736.0	17747.0
PPIB	10091.0	18485.2	28693.9
C19orf10	1593.1	2964.2	5478.2
SLC35B1	1269.9	2418.0	4412.8
SEC61A1	2128.5	3488.9	6386.6
RPN1	2179.7	3632.2	5925.1
DNAJC3	897.4	1859.7	2953.3
CDK2AP2	268.6	496.7	845.9

GEO Series "GSE12963" Expression Profiles

Num of samples in this series: 9

Scale of expression profile Z-scores

-3.0 -2.0 -1.0 0.0 1.0 2.0 3.0

GEO Link:	http://www.ncbi.nlm.nih.gov/geo/query/acc.cgi?acc=GSE12963
Status:	Public on Oct 02 2008
Title:	Gene expression in human CD4+ T-lymphocytes infected with VSVG-pseudotyped HIV-1 viruses lacking Env, Vpr, and Nef
Organism:	Homo sapiens
Experiment type:	Expression profiling by array
Platform:	GPL570
Pubmed ID:	19050264
Summary & Design:	**Summary:** The high mutation rate of HIV is linked to the generation of viruses expressing proteins with altered function whose impact on disease progression is unknown. We investigated the effects of HIV-1 viruses lacking Env, Vpr and Nef on CD4+ T cell gene expression using high-density DNA microarray analysis and functional assays. **Keywords:** three independent donors **Overall design:** Human activated CD4+ T-lymphocytes from three independent donors were infected with HIV-1 viruses that lack Env and Nef (pNL4-3.eGFP.R+E- or HIVD2GFP) or Env, Vpr and Nef. (pNL4-3.eGFP.R-E- or HIVD3GFP) were pseudotyped with VSVG envelope. As a control, CD4+ T-lymphocytes were infected with VSVG-pseudotyped eGFP. CD4+ T-cells were sorted 48 hours after infection using GFP as a marker of infectivity. RNA was isolated 10 hours after sorting, labeled, and prepared for microarray analysis.

Background corr dist: KL-Divergence = 0.0989, L1-Distance = 0.0274, L2-Distance = 0.0014, Normal std = 0.4407

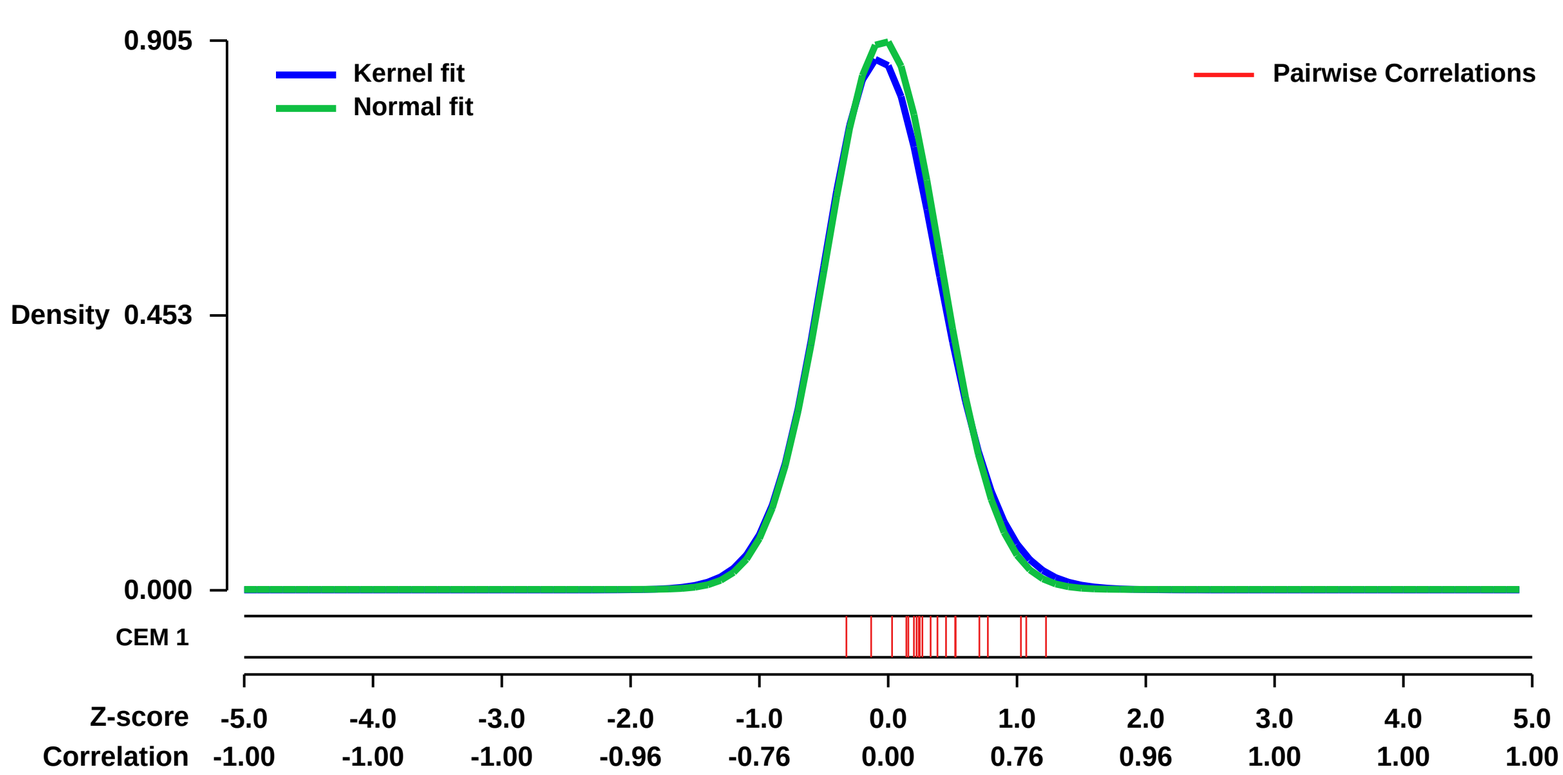

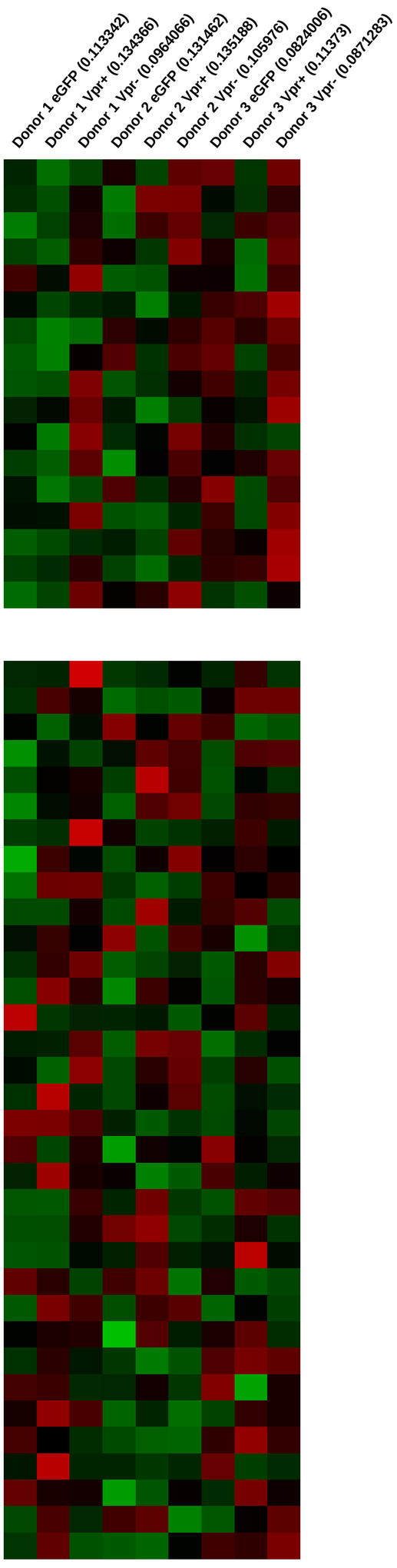

CEM 1
P (S | Z, I) = 0.00
Mean Corr = 0.34430

CEM 1 + Top 10 Genes

Null module

CEM 1 + Top 10 Genes	MANF	6417.9	7662.7	10105.3
	SDF2L1	2154.1	3192.5	4448.4
	CRELD2	6632.2	9180.0	10289.7
	HSPA5	8551.2	11291.9	13855.6
	HYOU1	1419.0	1749.4	2099.4
	PDIA4	648.8	1002.1	1638.6
	PDIA6	6654.2	11337.9	13058.6
	DNAJB11	3225.9	4557.8	5479.8
	HSP90B1	1489.3	1770.1	2690.3
	PDIA3	4886.6	6174.7	8291.9
	PPIB	14858.8	17366.6	20395.4
	C19orf10	2317.4	3430.9	4215.4
	SLC35B1	1834.6	2557.0	3637.2
	SEC61A1	3401.3	3922.0	4945.9
	RPN1	1827.1	2194.6	3235.9
	DNAJC3	2445.6	3187.2	5269.4
	CDK2AP2	721.5	1005.4	1350.2
Null module	ARID5B			
	XBP1			
	HNRNPAB			
	SGK1			
	HSPB1			
	DDIT4			
	ARL4D			
	SAP30			
	KIAA0408			
	GPR17			
	HSPH1			
	DNASE1L2			
	SLC5A3			
	GNAS			
	GPR3			
	TNFRSF25			
	TM6SF2			
	MKKS			
	PLEKHF1			
	ZMYM1			
	DOK3			
	FGF20			
	SLC39A2			
	KCNIP2			
	ERRFI1			
	DEDD2			
	CCDC117			
	USP31			
	AHSA2			
	CYS1			
	CNIH2			
	BANP			
	CHORDC1			
	P4HA1			

GEO Series "GSE9438" Expression Profiles

Num of samples in this series: 31

Scale of expression profile Z-scores

-3.0 -2.0 -1.0 0.0 1.0 2.0 3.0

GEO Link:	http://www.ncbi.nlm.nih.gov/geo/query/acc.cgi?acc=GSE9438
Status:	Public on Dec 01 2007
Title:	Gene Expression is associated with Progesterone Receptor Status in Meningioma
Organism:	Homo sapiens
Experiment type:	Expression profiling by array
Platform:	GPL570
Pubmed ID:	18172325
Summary & Design:	**Summary:** Examine gene expression for meningioma cases by hormone receptor status and indicate a stronger association with progesterone than with estrogen receptors **Keywords:** comparative gene expression **Overall design:** The data are surgical specimens from 31 meningioma patients undergoing neuro-surgical resection at Brigham and Womenâ s Hospital from 3/15/2004-5/10/2005. Progesterone (PR) and estrogen (ER) hormone receptors were measured via immunohistochemistry and compared with gene expression profiling results.

Background corr dist: KL-Divergence = 0.3907, L1-Distance = 0.0825, L2-Distance = 0.0210, Normal std = 0.2507

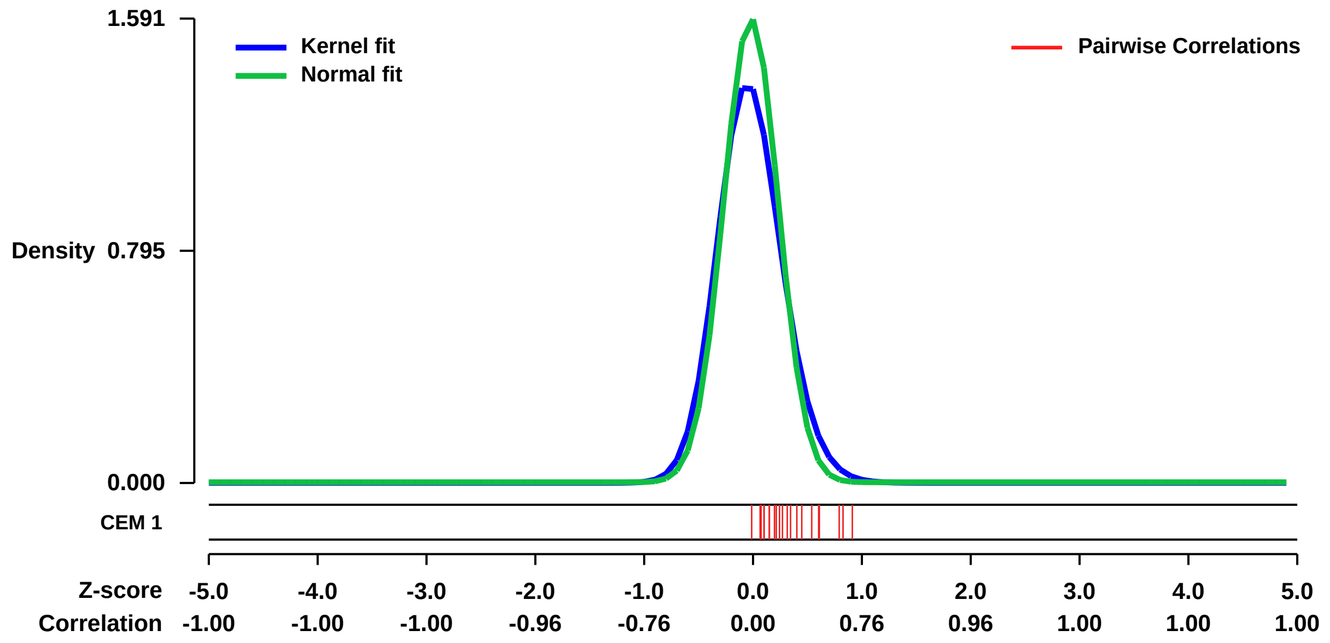

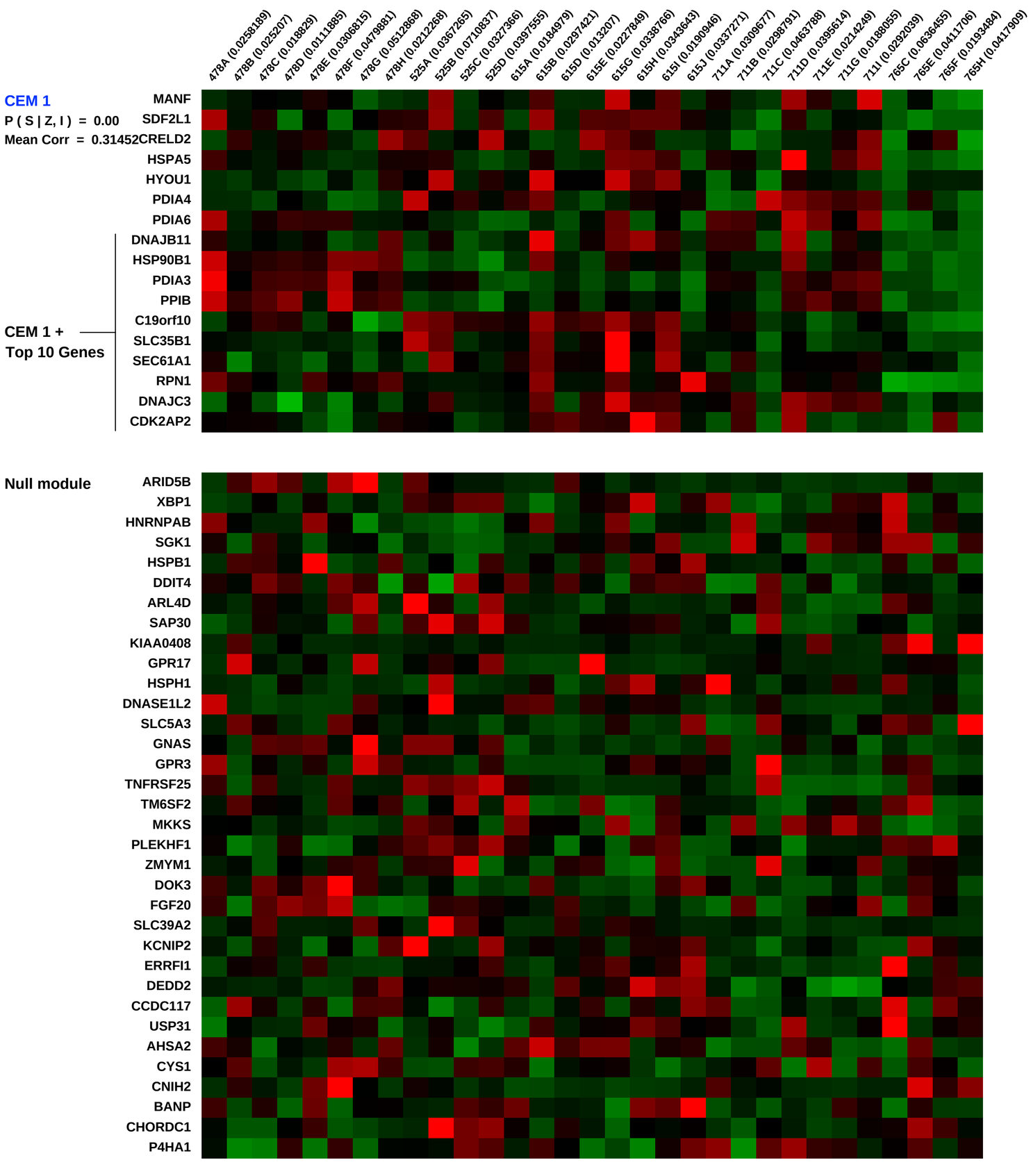

Pre-normalization Quantiles

[min]	[medium]	[max]
812.4	1481.5	2773.4
168.0	428.3	807.5
718.0	1389.1	2353.5
4163.7	8768.6	22056.2
1152.1	2337.4	4825.4
406.9	673.7	1179.5
1715.5	3060.0	5917.8
1250.2	2099.8	4665.3
665.9	2992.8	6803.7
3837.5	7853.4	16291.2
5862.8	10779.3	20088.3
781.8	1483.0	2082.2
704.2	1259.6	3497.6
1384.2	2670.9	5834.5
1381.4	3748.8	7280.4
1740.5	3434.2	5583.3
415.1	733.8	1526.3

GEO Series "GSE33135" Expression Profiles

Num of samples in this series: 24

Scale of expression profile Z-scores

-3.0 -2.0 -1.0 0.0 1.0 2.0 3.0

GEO Link:	http://www.ncbi.nlm.nih.gov/geo/query/acc.cgi?acc=GSE33135
Status:	Public on Dec 04 2012
Title:	Gene expression profile after dexamethasone in chronic lymphocytic leukemia cells according to IGHV/ZAP-70 status
Organism:	Homo sapiens
Experiment type:	Expression profiling by array
Platform:	GPL570
Pubmed ID:	22966019
Summary & Design:	**Summary:** Glucocorticoids are part of the therapeutic armamentarium of chronic lymphocytic leukemia where it has been suggested that cells with unmutated IGHV genes exhibit higher sensitivity. The mechanisms by which glucorticoids are active in CLL are not well elucidated. We used microarrays to detail the global programme of gene expression underlying dexamethasone differential activity according to the prognostic subgroups mutated IGHV genes / low ZAP-70 expression and unmutated IGHV genes / high ZAP-70 expression. We aimed to ascertain the molecular mechanisms that are influencing the diffferential response to this drug. **Overall design:** Peripheral blood mononuclear cells from chronic lymphocytic leukemia patients were obtained. Samples were split in two for control and incubation with dexamethasone for 6 hours. RNA was extracted and processed for further hybridization on Affymetrix microarrays.

Background corr dist: KL-Divergence = 0.3204, L1-Distance = 0.0711, L2-Distance = 0.0148, Normal std = 0.2717

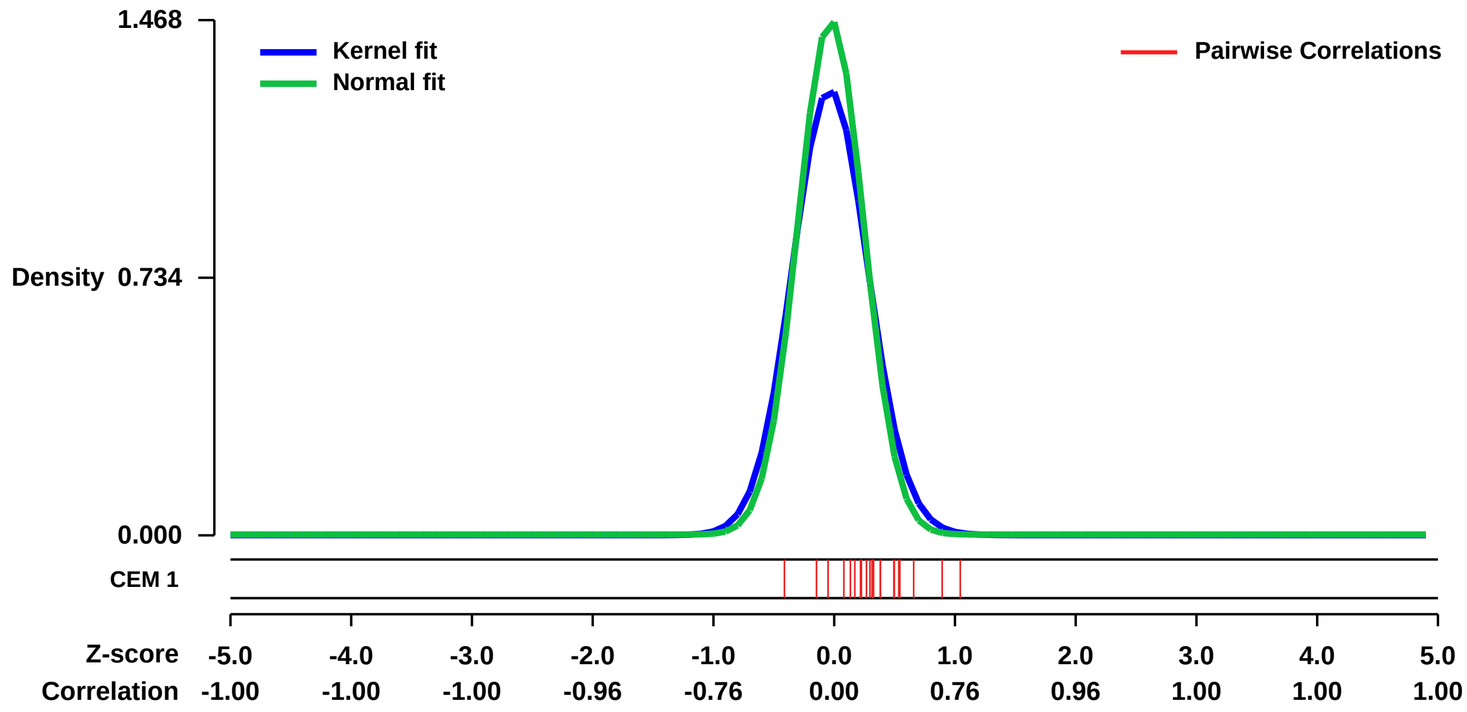

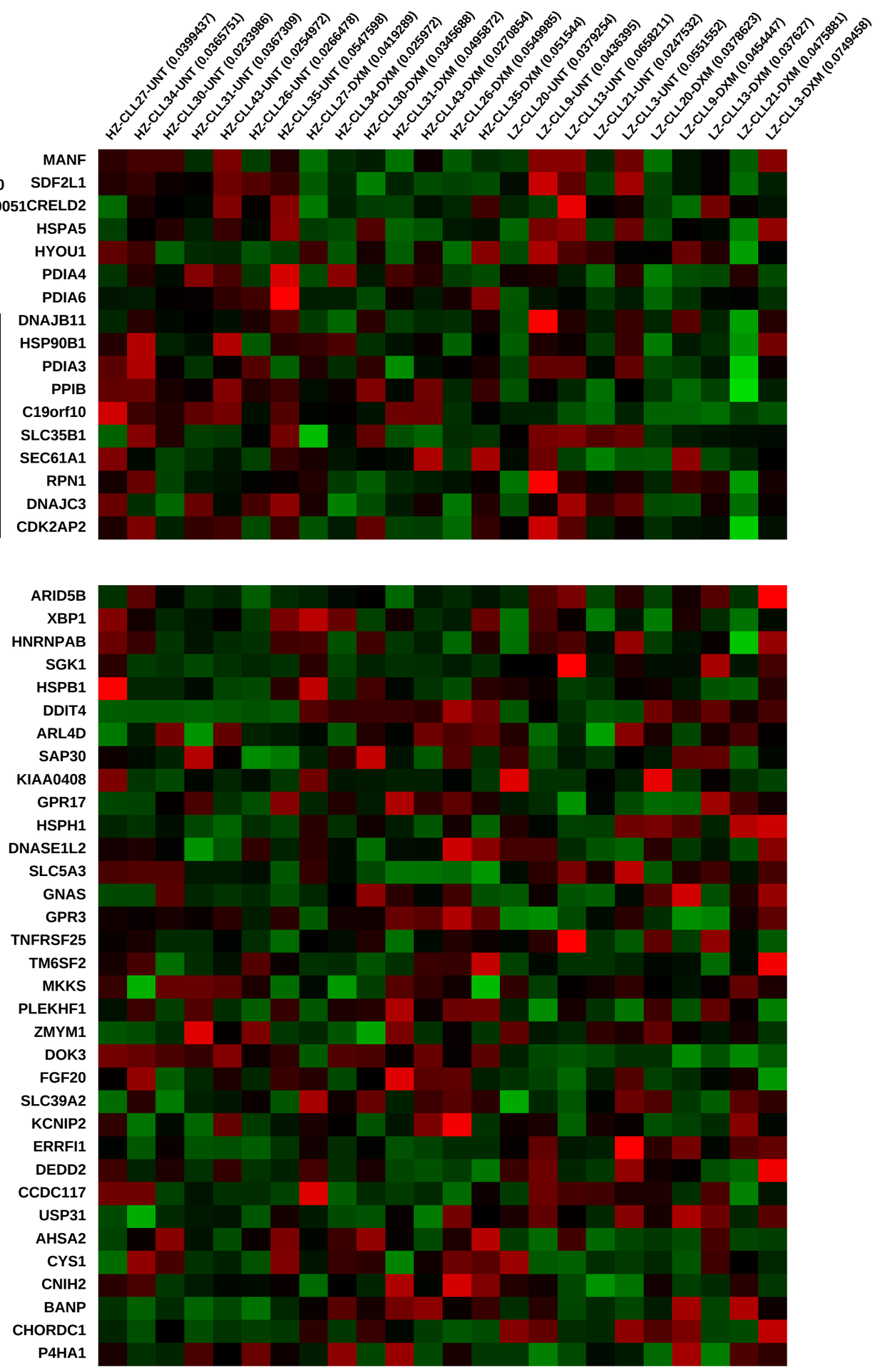

GEO Series "GSE40885" Expression Profiles

Num of samples in this series: 14

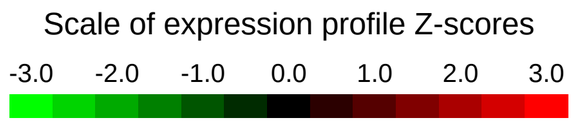

GEO Link:	http://www.ncbi.nlm.nih.gov/geo/query/acc.cgi?acc=GSE40885
Status:	Public on Sep 15 2012
Title:	Data expression in alveolar macrophages induced by lipopolysaccharide in humans
Organism:	Homo sapiens
Experiment type:	Expression profiling by array
Platform:	GPL570
Pubmed ID:	22952057
Summary & Design:	**Summary:** Rationale: Lipopolysaccharide (LPS) is ubiquitous in the environment. Inhalation of LPS has been implicated in the pathogenesis and/or severity of several lung diseases, including pneumonia, chronic obstructive pulmonary disease and asthma. Alveolar macrophages are the main resident leukocytes exposed to inhaled antigens. Objectives: To obtain insight into which innate immune pathways become activated within human alveolar macrophages upon exposure to LPS in vivo. **Overall design:** In seven healthy humans sterile saline was instilled into a lung segment by bronchoscope, followed by instillation of LPS into the contralateral lung. Six hours later a bilateral bronchoalveolar lavage was performed and whole-genome transcriptional profiling was done (Affymetrix HG-U133 Plus 2.0) on purified alveolar macrophages, comparing cells exposed to saline or LPS from the same individuals.

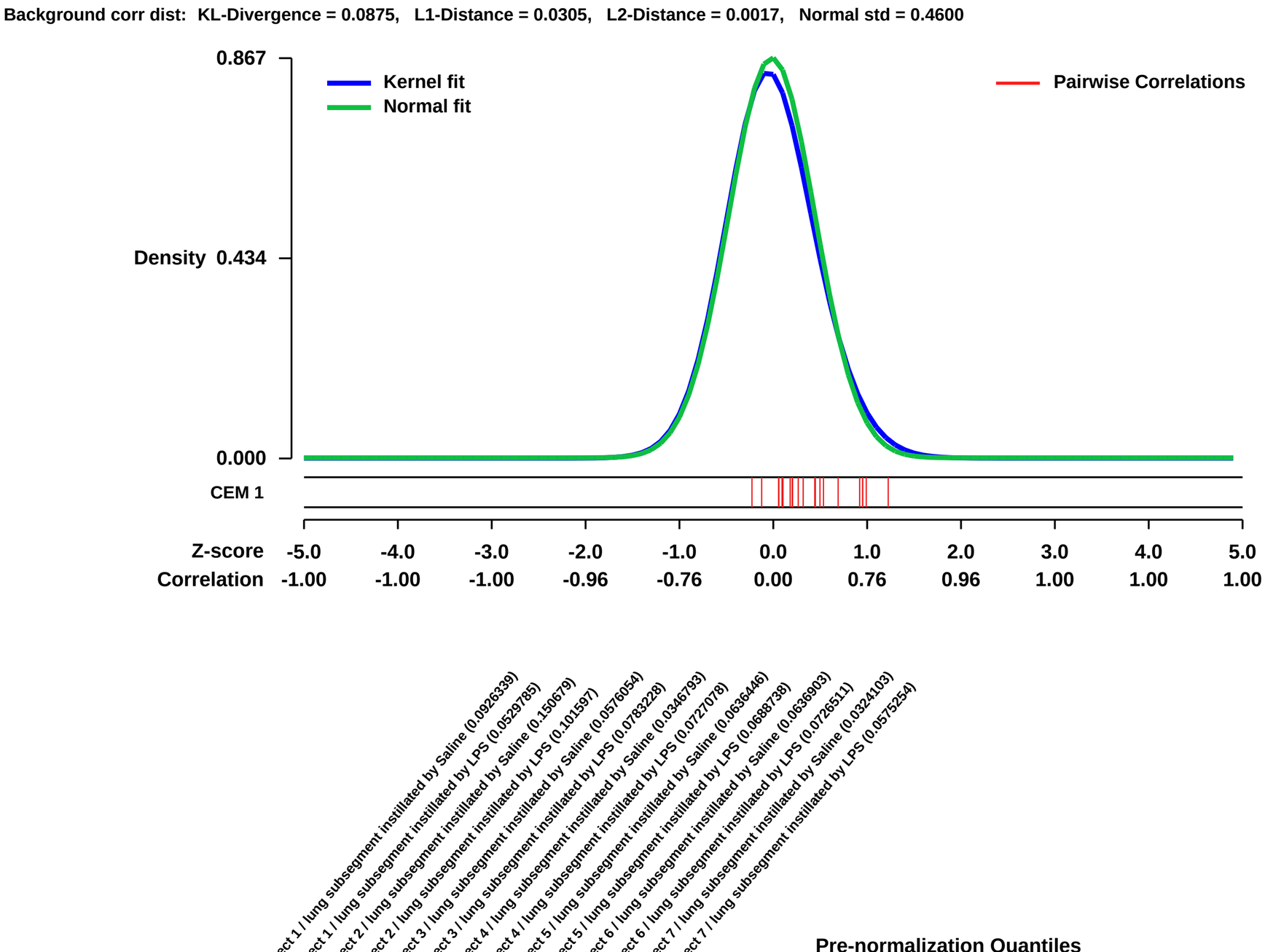

Pre-normalization Quantiles

	[min]	[medium]	[max]
MANF	1787.9	3207.8	3876.7
SDF2L1	491.9	623.5	843.7
CRELD2	1669.6	1910.0	2314.4
HSPA5	5770.4	6768.5	8339.5
HYOU1	723.5	994.4	1157.8
PDIA4	4452.3	5795.6	7570.5
PDIA6	3147.6	3767.3	4282.5
DNAJB11	7322.9	8457.9	10078.5
HSP90B1	6217.8	6667.7	7928.0
PDIA3	7816.0	9361.8	10562.1
PPIB	4322.7	5153.5	6937.9
C19orf10	1417.7	1675.0	1985.8
SLC35B1	1621.9	1929.6	2190.1
SEC61A1	854.6	1130.5	1586.4
RPN1	2438.2	2744.7	3233.9
DNAJC3	5703.3	6801.5	9967.0
CDK2AP2	412.2	544.7	916.1

GEO Series "GSE9526" Expression Profiles

Num of samples in this series: 16

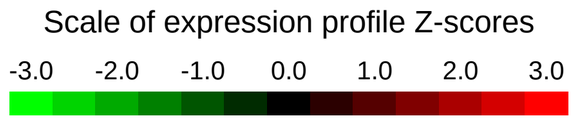

GEO Link:	http://www.ncbi.nlm.nih.gov/geo/query/acc.cgi?acc=GSE9526
Status:	Public on Nov 10 2007
Title:	Expression data from cumulus cells that surround oocytes resulting in early or late cleaving embryos
Organism:	Homo sapiens
Experiment type:	Expression profiling by array
Platform:	GPL570
Pubmed ID:	18204071
Summary & Design:	**Summary:** Besides the established selection criteria based on embryo morphology and blastomere number, new parameters for embryo viability are needed to improve the clinical outcome of in vitro fertilization (IVF) and more particular of elective single embryo transfer (eSET). The aim of the study was to analyse genome-wide whether the embryo viability was reflected by the expression of genes in the oocyte surrounding cumulus cells. Early cleavage (EC) was chosen as a parameter for embryo viability. Keywords: class comparison **Overall design:** Consenting patients visiting the IVF clinic underwent an IVF or ICSI treatment. Immediately following ultrasound-guided cumulus-oocyte-complex (COC) retrieval, a proportion of the cumulus cells surrounding the oocyte were removed. Gene expression in cumulus cells from eight oocytes resulting in an early cleavage embryo (EC-CC; n=8) and from eight oocytes resulting in a non-EC embryo (NEC-CC; n=8) derived from six patients were analysed using microarrays (n=16). To exclude a differential gene expression due to differences in patient characteristics, samples were paired. From four patients both an EC-CC and a NEC-CC sample were used. From two additional patients two EC-CC as well as two NEC-CC samples were used.

Background corr dist: KL-Divergence = 0.2614, L1-Distance = 0.0616, L2-Distance = 0.0101, Normal std = 0.2964

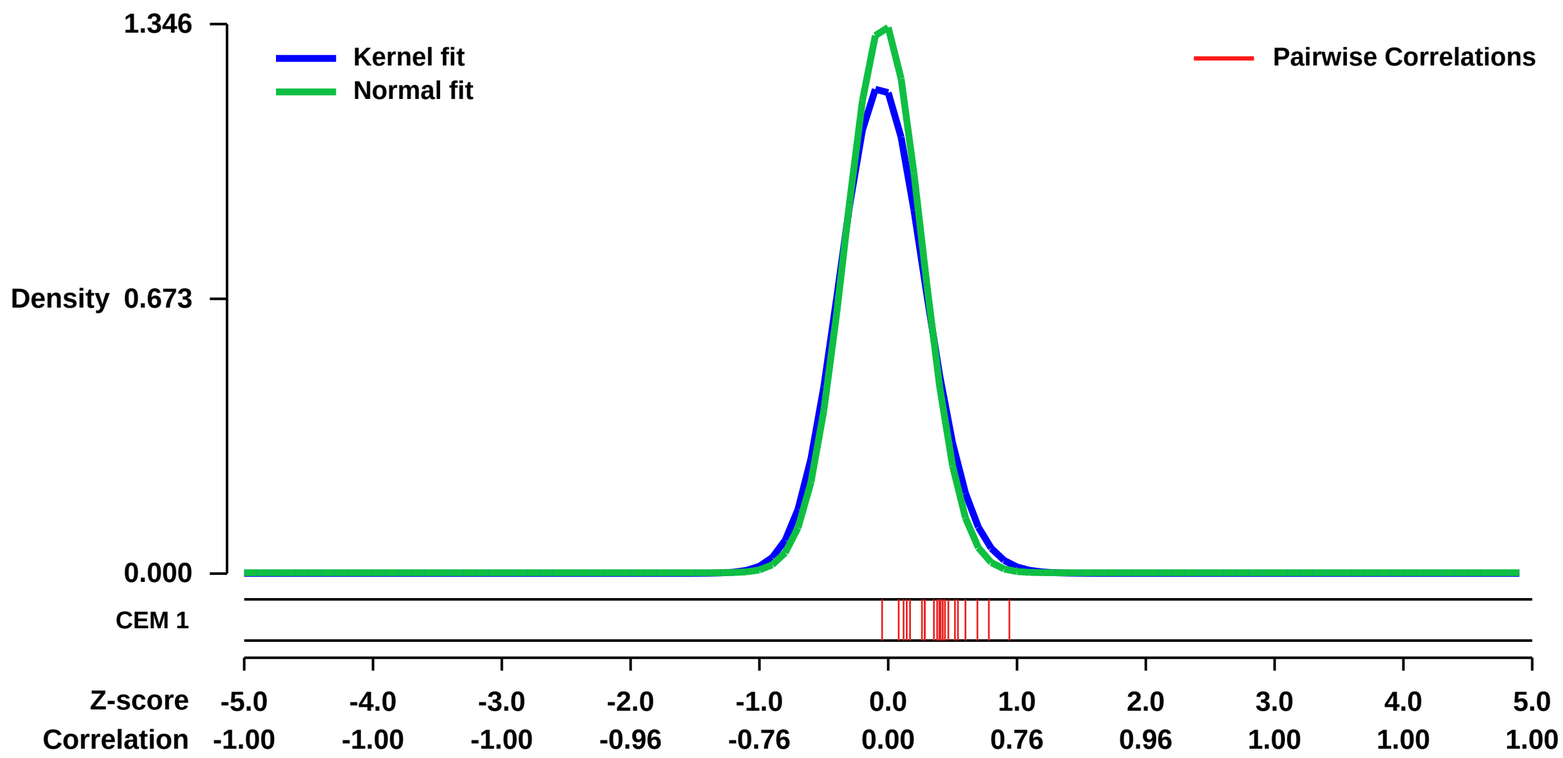

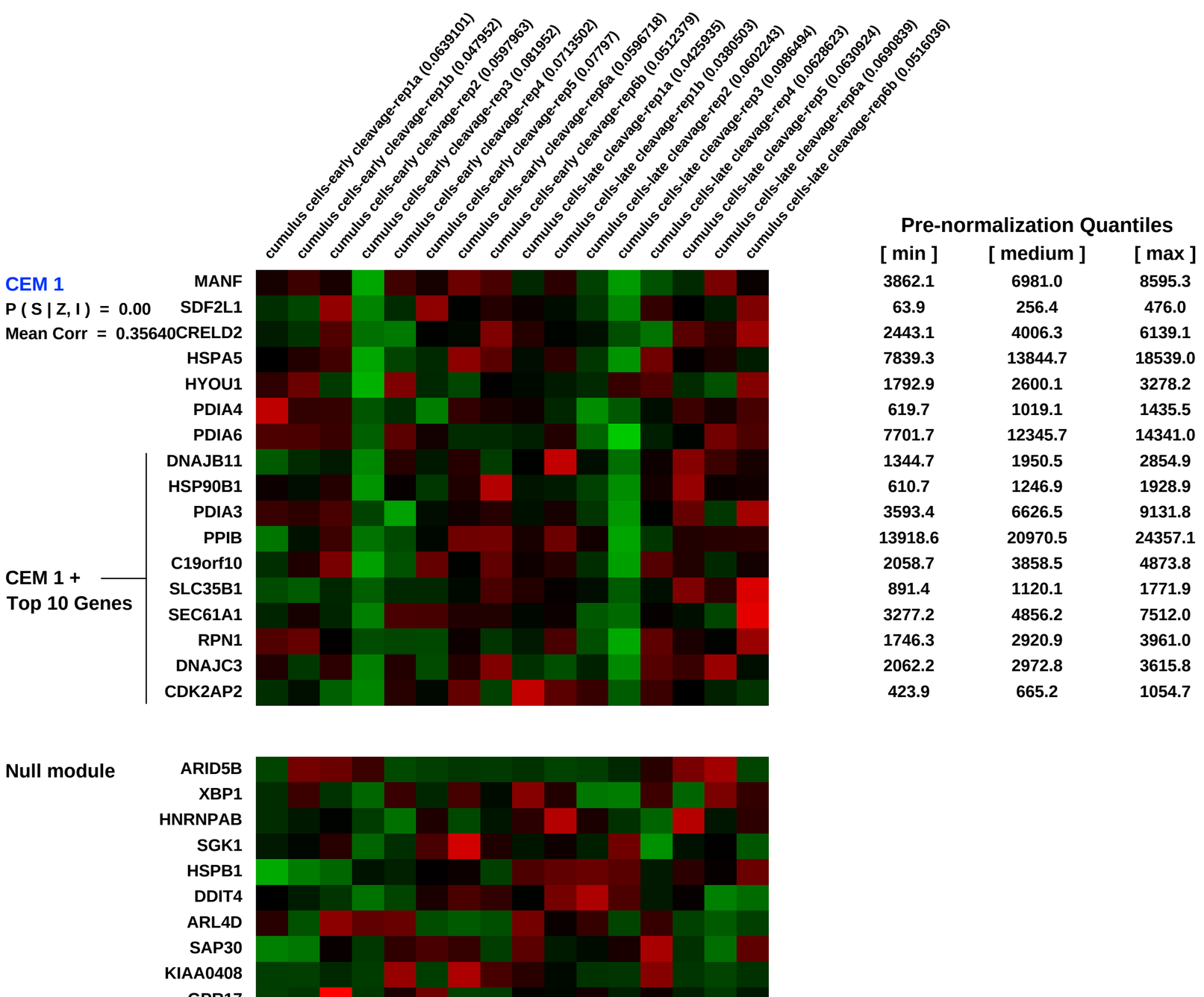

Pre-normalization Quantiles

	[min]	[medium]	[max]
MANF	3862.1	6981.0	8595.3
SDF2L1	63.9	256.4	476.0
CRELD2	2443.1	4006.3	6139.1
HSPA5	7839.3	13844.7	18539.0
HYOU1	1792.9	2600.1	3278.2
PDIA4	619.7	1019.1	1435.5
PDIA6	7701.7	12345.7	14341.0
DNAJB11	1344.7	1950.5	2854.9
HSP90B1	610.7	1246.9	1928.9
PDIA3	3593.4	6626.5	9131.8
PPIB	13918.6	20970.5	24357.1
C19orf10	2058.7	3858.5	4873.8
SLC35B1	891.4	1120.1	1771.9
SEC61A1	3277.2	4856.2	7512.0
RPN1	1746.3	2920.9	3961.0
DNAJC3	2062.2	2972.8	3615.8
CDK2AP2	423.9	665.2	1054.7

GEO Series "GSE41828" Expression Profiles

Num of samples in this series: 50

Scale of expression profile Z-scores

-3.0 -2.0 -1.0 0.0 1.0 2.0 3.0

GEO Link: http://www.ncbi.nlm.nih.gov/geo/query/acc.cgi?acc=GSE41828
Status: Public on Oct 04 2013
Title: TWEAK-treated time course in U2OS cells.
Organism: Homo sapiens
Experiment type: Expression profiling by array
Platform: GPL570
Pubmed ID: 23974006

Summary & Design:

Summary:
Tumor necrosis factor-related weak inducer of apoptosis, TWEAK, is a TNF superfamily member that mediates signaling through its receptor fibroblast growth factor inducible-14, Fn14. In tumor cell lines, TWEAK induces proliferation, survival and NF-kappaB signaling and gene expression that promote tumor growth and suppress antitumor immune responses. Anti-TWEAK antibody, RG7212, inhibits tumor growth in vivo with decreases in pathway activation markers and modulation of tumor, blood and spleen immune cell composition. Candidate response prediction markers, including Fn14, have been identified in mouse models. Phase I pharmacodynamic data from patients are consistent with preclinical results. TWEAK:Fn14 signaling is upregulated in human cancer and pathway activation induces tumor proliferation and survival signaling. Blockade with anti-TWEAK mAb, RG7212, inhibits tumor growth in multiple models in mice. TWEAK induces changes that suppress anti-tumor immune responses and RG7212 blocks these effects resulting in changes in tumor immune cell composition and decreases in cytokines that promote immunosuppression. Antitumor efficacy in mice was observed in a range of Fn14 expressing models with pathway activation and expressing either wild-type or mutant p53, BRAF or KRAS suggesting both a patient selection strategy and potential broad clinical applicability. Preclinical mechanism of action hypotheses are supported by Phase I clinical data, with decreases in proliferation markers and increased tumor T cell infiltration.

Overall design:
U2OS cells untreated or treated with 1090-TW (TWEAK) for 15 minutes, 1 hour, 4 hours, 8 hours, or 24 hours. Five replicates for each condition were performed.

Background corr dist: KL-Divergence = 0.3641, L1-Distance = 0.0627, L2-Distance = 0.0106, Normal std = 0.2589

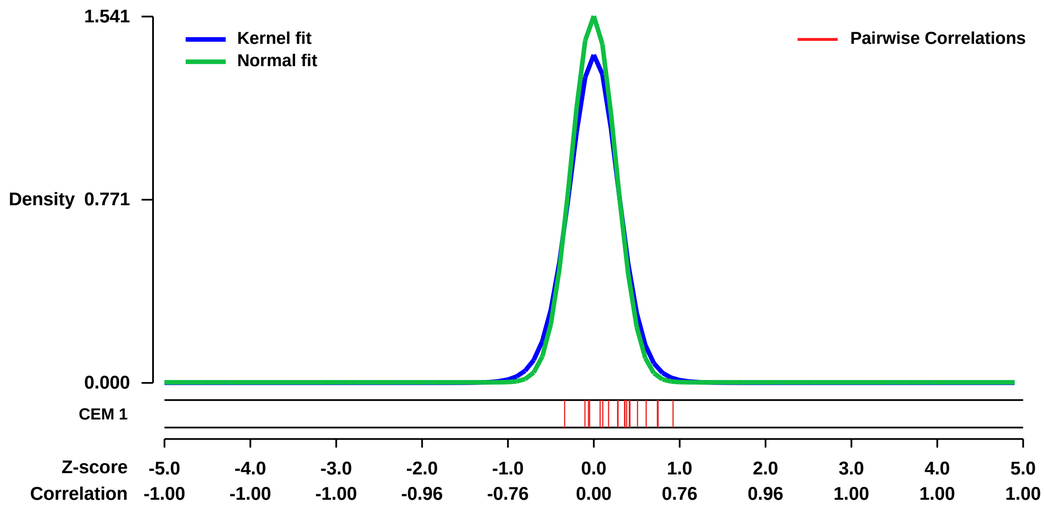

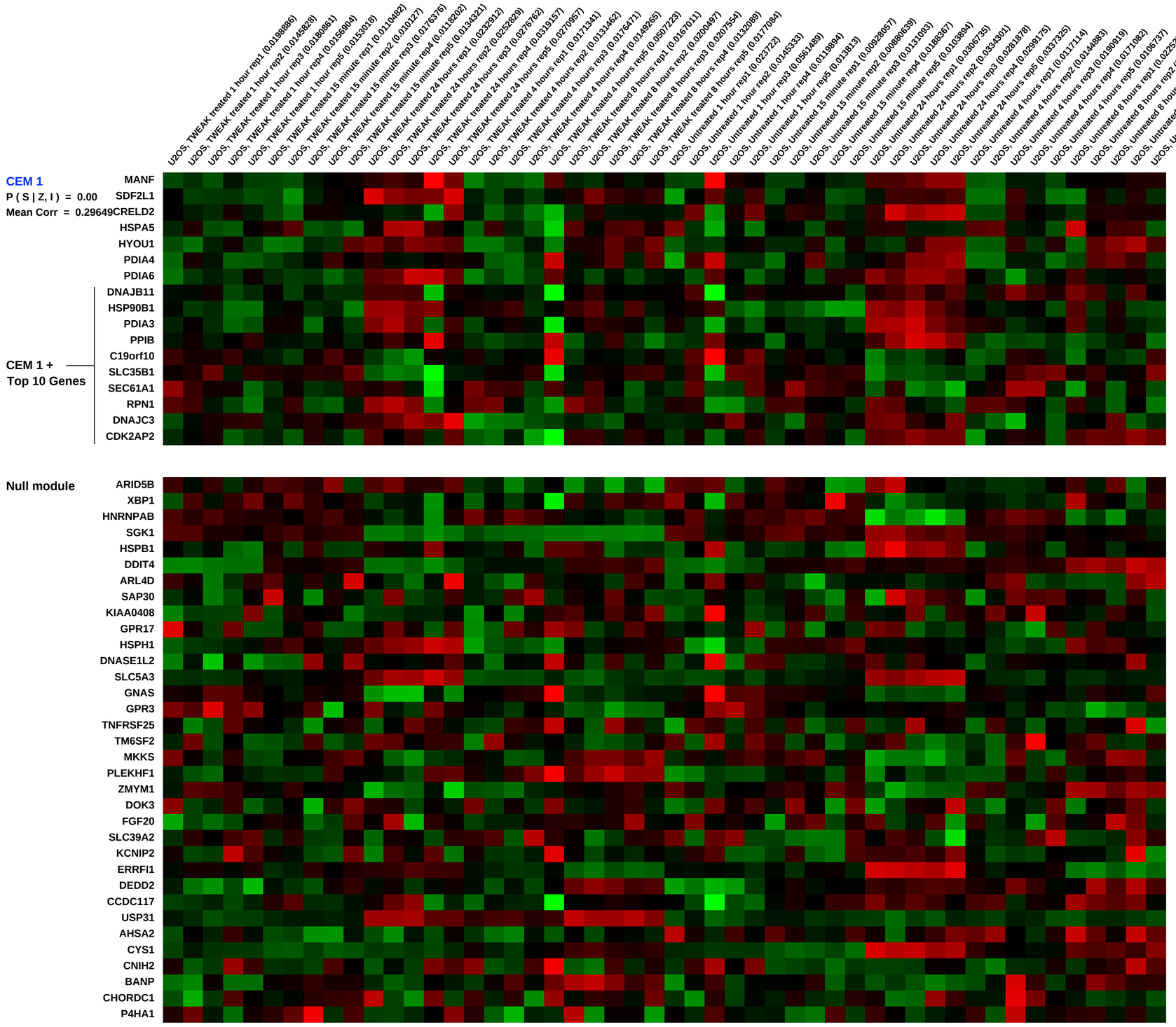

Pre-normalization Quantiles

[min]	[medium]	[max]
4967.5	5752.9	7953.0
2762.5	3366.0	4277.6
4130.1	4976.7	6095.6
13825.6	16817.1	19824.4
1008.9	1126.4	1293.5
626.0	721.6	855.8
8850.6	9959.2	11796.2
4277.0	6482.1	7258.5
5758.6	7484.3	9600.1
10900.8	14620.0	17961.6
26878.6	28646.7	32669.9
2463.8	2908.0	4092.0
1795.7	2386.6	2615.6
2906.1	3403.4	3695.5
3230.1	4066.5	5104.8
1085.3	1292.7	1545.3
1021.8	1447.9	1670.8

GEO Series "GSE17625" Expression Profiles

Num of samples in this series: 6

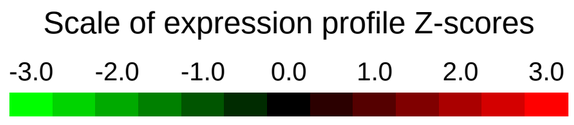

GEO Link:	http://www.ncbi.nlm.nih.gov/geo/query/acc.cgi?acc=GSE17625
Status:	Public on Mar 08 2010
Title:	Caco-2 cocultured with THP-1, time course
Organism:	Homo sapiens
Experiment type:	Expression profiling by array
Platform:	GPL570
Pubmed ID:	20139600
Summary & Design:	**Summary:** Previously, we constructed a coculture model to analyze the effect of macrophages on intestinal epithelial cells, and found that TNF-a secreted from human macrophage-like THP-1 cells induced cell damage to intestinal epithelial Caco-2 cells (Exp.Cell.Res. 2006, 312(19):3909-19). In this study, we present activation of NF-kB in Caco-2 cells within 15 min after coculturing. To reveal how TNF-a secreted from THP-1 cells affects Caco-2 cells in an early stage of coculture, we exhaustively analyzed the changes of gene expression in Caco-2 cells cocultured with THP-1 cells over the time periods of 0, 1, 3, 6, 24, and 48 h by using a DNA microarray. Differentially expressed genes extracted with maSigPro demonstrated that IEX-1 was the lowest p-value gene, that is, the most significantly changed gene among the up-regulated genes. The genes expressed in a similar pattern to IEX-1 involved immunity, apoptosis, and protein kinase cascade. These findings suggest that the stimuli of TNF-a from THP-1 cells activates NF-kB, leading induction of various gene expression. This pattern of gene expression indicates that not only early defense response but also cell death occurs at the same time, causing inflammatory condition. **Overall design:** Caco-2 cells were cultured for 14 days on a semi-permeable support, and THP-1 cells were differentiated with phorbol myristate acetate (PMA) for 4 days in 12-well plates. Then, the semi-permeable support membrane in which Caco-2 cells had been cultured was placed on the 12-well plates on which THP-1 has been cultured.

Background corr dist: KL-Divergence = 0.0445, L1-Distance = 0.0286, L2-Distance = 0.0011, Normal std = 0.6024

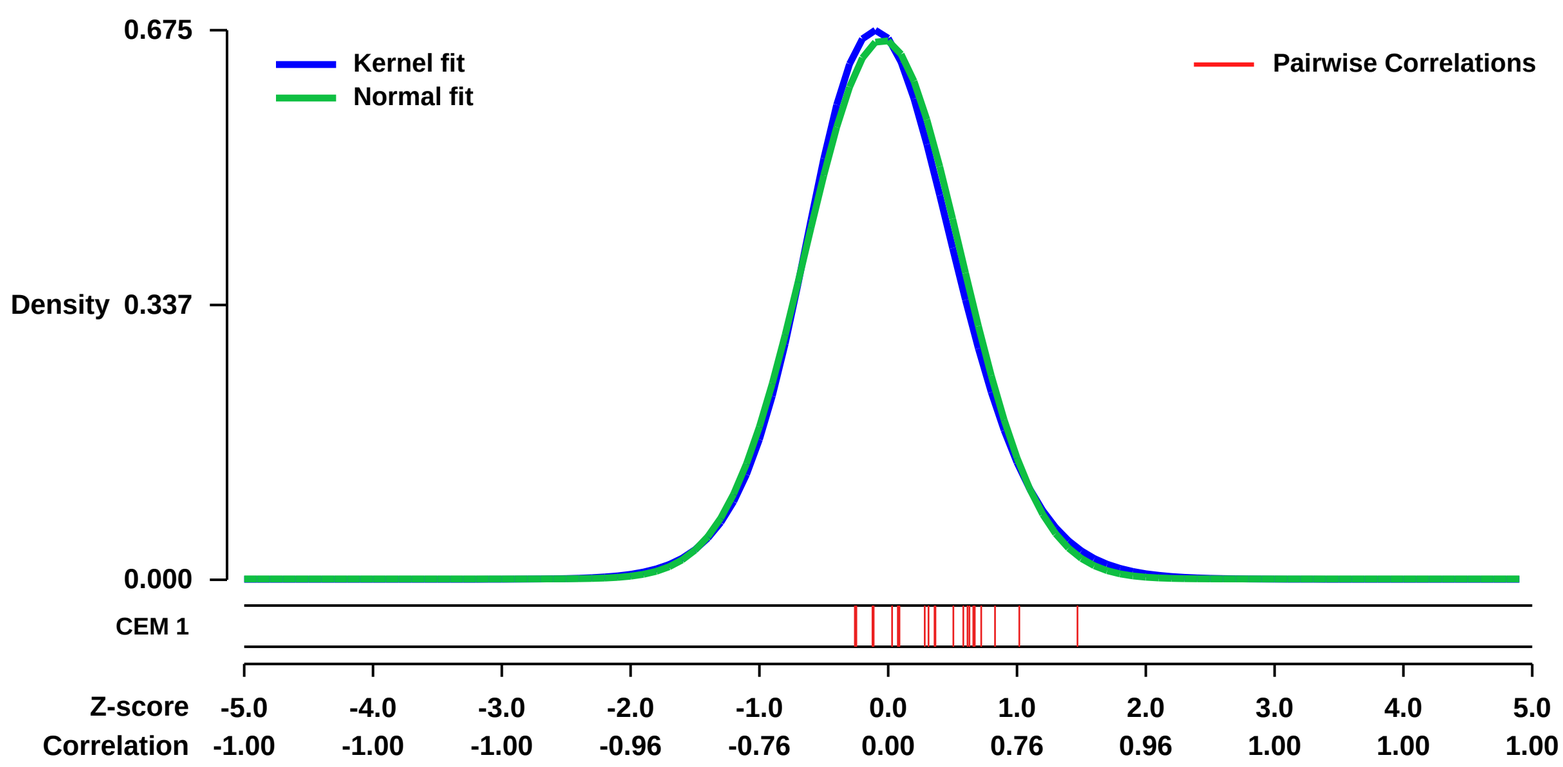

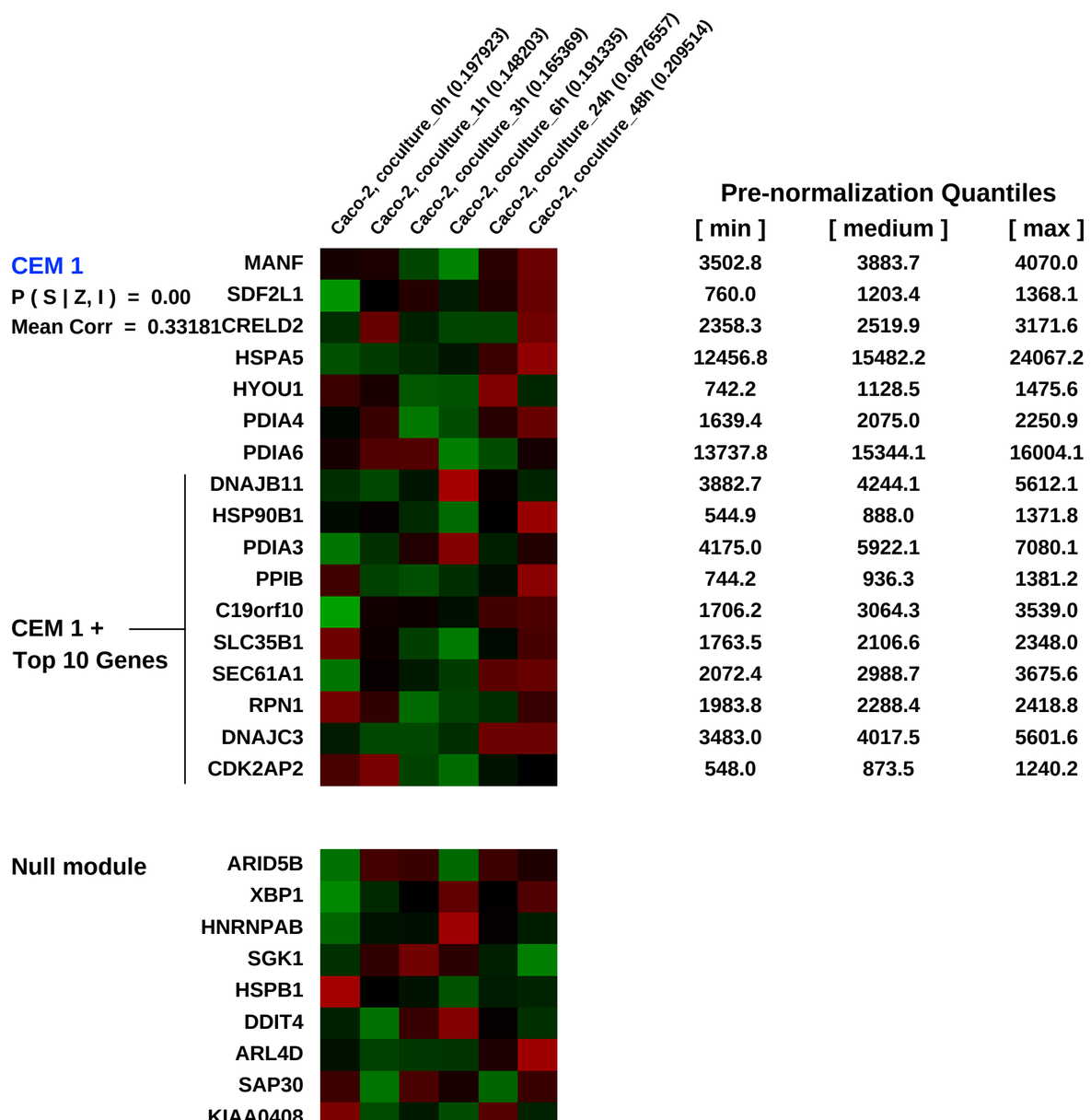

	Pre-normalization Quantiles		
	[min]	[medium]	[max]
MANF	3502.8	3883.7	4070.0
SDF2L1	760.0	1203.4	1368.1
CRELD2	2358.3	2519.9	3171.6
HSPA5	12456.8	15482.2	24067.2
HYOU1	742.2	1128.5	1475.6
PDIA4	1639.4	2075.0	2250.9
PDIA6	13737.8	15344.1	16004.1
DNAJB11	3882.7	4244.1	5612.1
HSP90B1	544.9	888.0	1371.8
PDIA3	4175.0	5922.1	7080.1
PPIB	744.2	936.3	1381.2
C19orf10	1706.2	3064.3	3539.0
SLC35B1	1763.5	2106.6	2348.0
SEC61A1	2072.4	2988.7	3675.6
RPN1	1983.8	2288.4	2418.8
DNAJC3	3483.0	4017.5	5601.6
CDK2AP2	548.0	873.5	1240.2
ARID5B			
XBP1			
HNRNPAB			
SGK1			
HSPB1			
DDIT4			
ARL4D			
SAP30			
KIAA0408			
GPR17			
HSPH1			
DNASE1L2			
SLC5A3			
GNAS			
GPR3			
TNFRSF25			
TM6SF2			
MKKS			
PLEKHF1			
ZMYM1			
DOK3			
FGF20			
SLC39A2			
KCNIP2			
ERRFI1			
DEDD2			
CCDC117			
USP31			
AHSA2			
CYS1			
CNIH2			
BANP			
CHORDC1			
P4HA1			

GEO Series "GSE49822" Expression Profiles

Num of samples in this series: 22

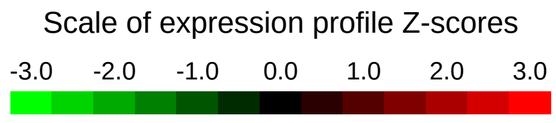

GEO Link:	http://www.ncbi.nlm.nih.gov/geo/query/acc.cgi?acc=GSE49822
Status:	Public on May 14 2014
Title:	Gene expression data of pHGG tumor samples
Organism:	Homo sapiens
Experiment type:	Expression profiling by array
Platform:	GPL570
Pubmed ID:	24183680
Summary & Design:	**Summary:** Pediatric high-grade gliomas (pHGGs) harboring the K27M mutation of H3F3A (histone H3.3) are characterized by global reduction of the repressive histone mark H3K27me3 and DNA hypomethylation. Analysis of K27M-induced changes on H3K27me3 occupancy and DNA methylation at differentially expresed genes (K27M vs. wild-type H3.3) in primary pHGG tumor samples. **Overall design:** 22 glioblastoma samples from pHGG patients were selected for RNA extraction and hybridization on Affymetrix Affymetrix Human Genome U133 Plus 2.0 Arrays. Expression profiling data of 17 pHHGs are part of our previous study (GSE36245 or GSE34824).

Background corr dist: KL-Divergence = 0.2796, L1-Distance = 0.0589, L2-Distance = 0.0103, Normal std = 0.3004

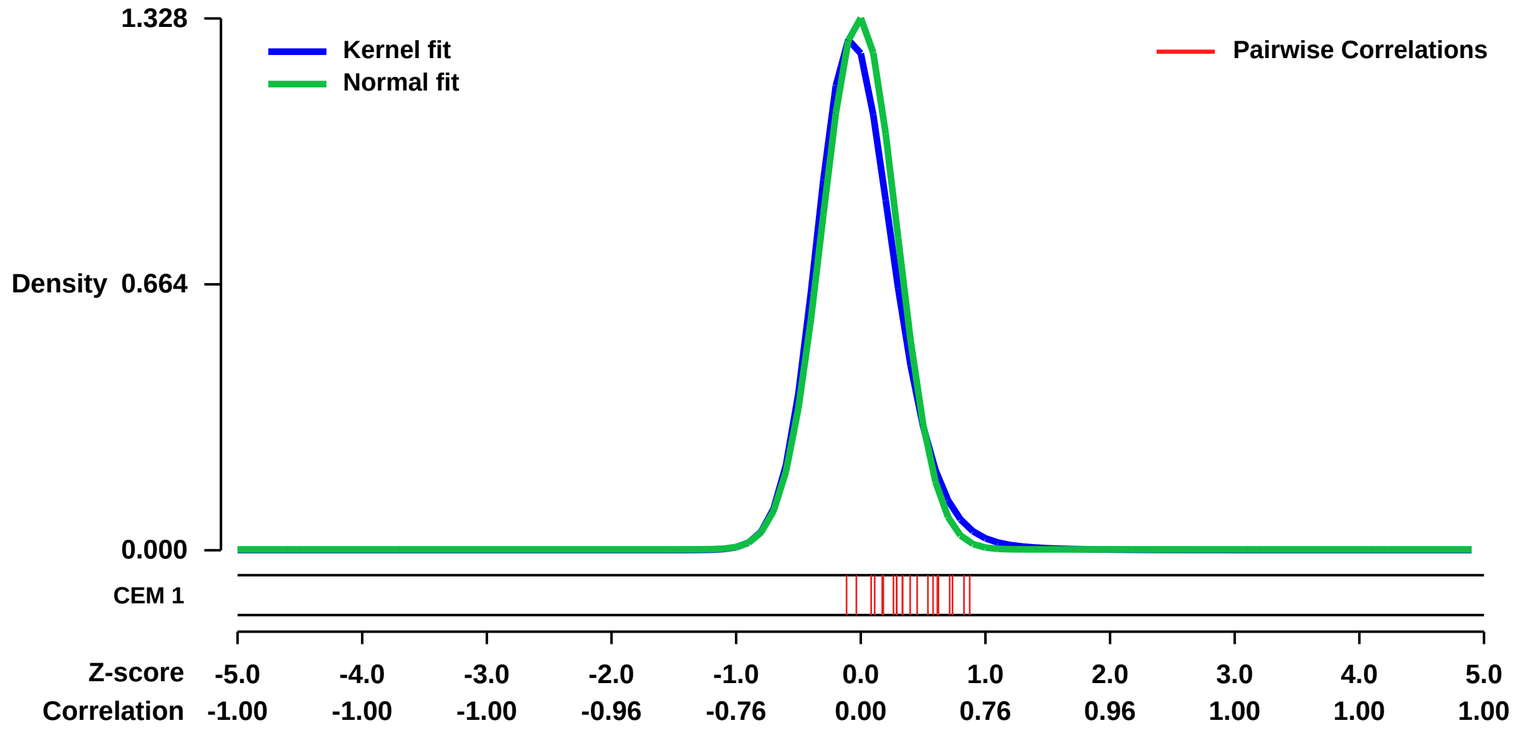

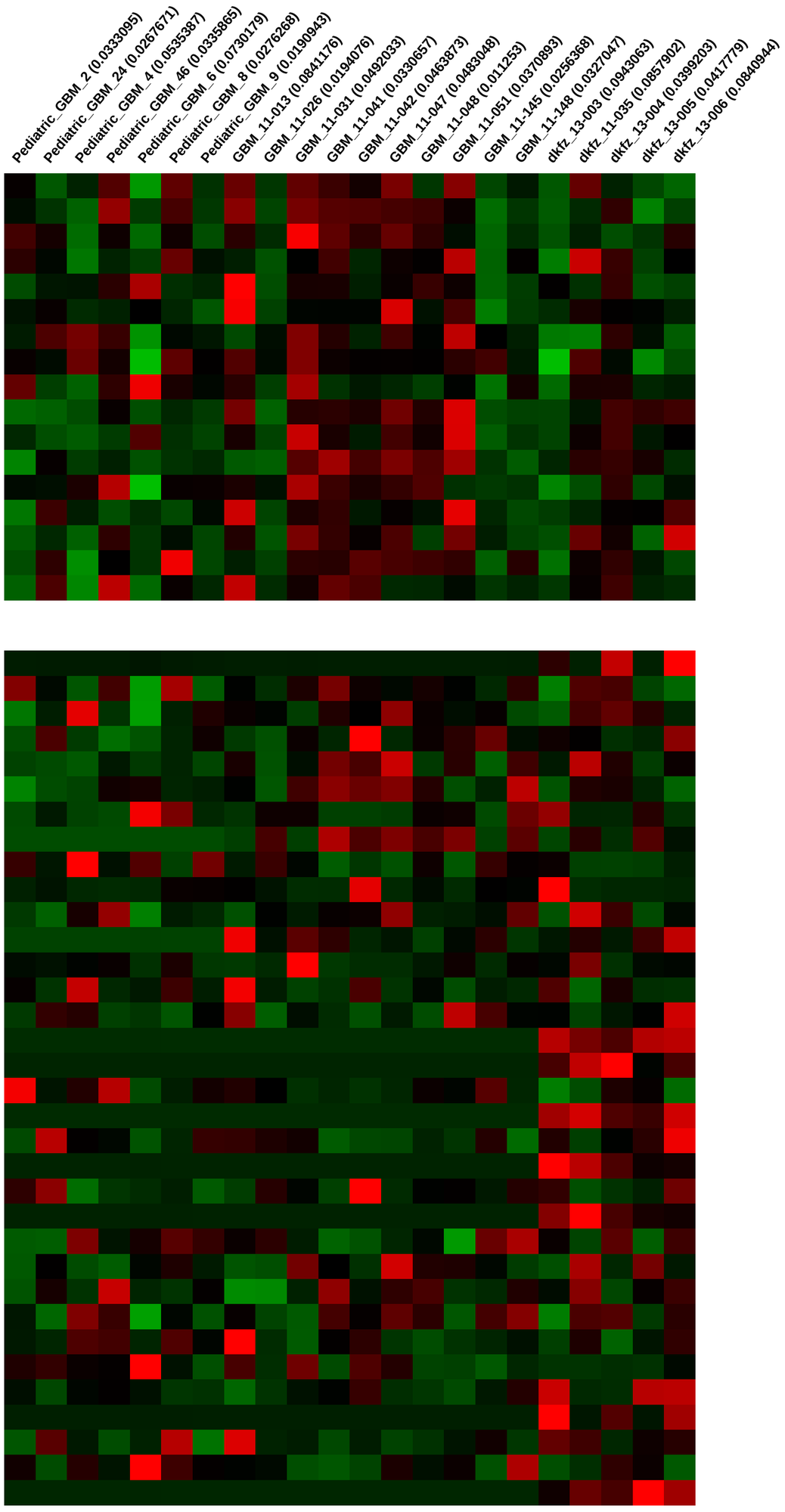

	Pre-normalization Quantiles		
	[min]	[medium]	[max]
MANF	950.0	2600.1	4644.9
SDF2L1	391.0	831.2	1438.2
CRELD2	1398.8	2483.3	4569.9
HSPA5	8139.7	14648.2	25333.4
HYOU1	823.9	1147.8	2316.9
PDIA4	204.7	1037.0	2788.6
PDIA6	3730.0	7020.6	11672.0
DNAJB11	1329.5	3331.5	4588.7
HSP90B1	2035.5	5341.1	12953.2
PDIA3	4188.6	8865.7	17687.9
PPIB	11379.6	14486.8	25341.1
C19orf10	667.1	1492.7	3066.9
SLC35B1	569.5	1660.5	2600.0
SEC61A1	1218.9	2457.7	5465.8
RPN1	2817.2	3925.1	6796.8
DNAJC3	1118.2	3330.5	6633.5
CDK2AP2	265.9	611.0	1381.2

GEO Series "GSE12486" Expression Profiles

Num of samples in this series: 10

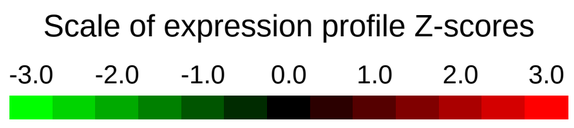

GEO Link:	http://www.ncbi.nlm.nih.gov/geo/query/acc.cgi?acc=GSE12486
Status:	Public on Jun 22 2010
Title:	Changes in cardiac transcription profiles following on-pump coronary artery bypass grafting
Organism:	Homo sapiens
Experiment type:	Expression profiling by array
Platform:	GPL570
Pubmed ID:	20332183
Summary & Design:	**Summary:** To investigate changes in cardiac transcription profiles caused by on-pump cardiac surgery, we collected myocardial samples, prior and after grafting, from patients undergoing on-pump coronary artery bypass grafting with cardiopulmonary bypass and cardiac arrest. The transcriptional profile of the mRNA in these samples was measured with gene array technology. Changes in transcriptional profiles can be correlated with the stress response of heart to surgery, cardiopulmonary bypass and cardiac arrest. Keywords: human, cardiac, CABG coronary surgery, gene expression, cardiopulmonary bypass. **Overall design:** Myocardial samples were collected, prior and after grafting, from patients undergoing on-pump coronary artery bypass grafting with cardiopulmonary bypass and cardiac arrest.

Background corr dist: KL-Divergence = 0.0499, L1-Distance = 0.0265, L2-Distance = 0.0011, Normal std = 0.5540

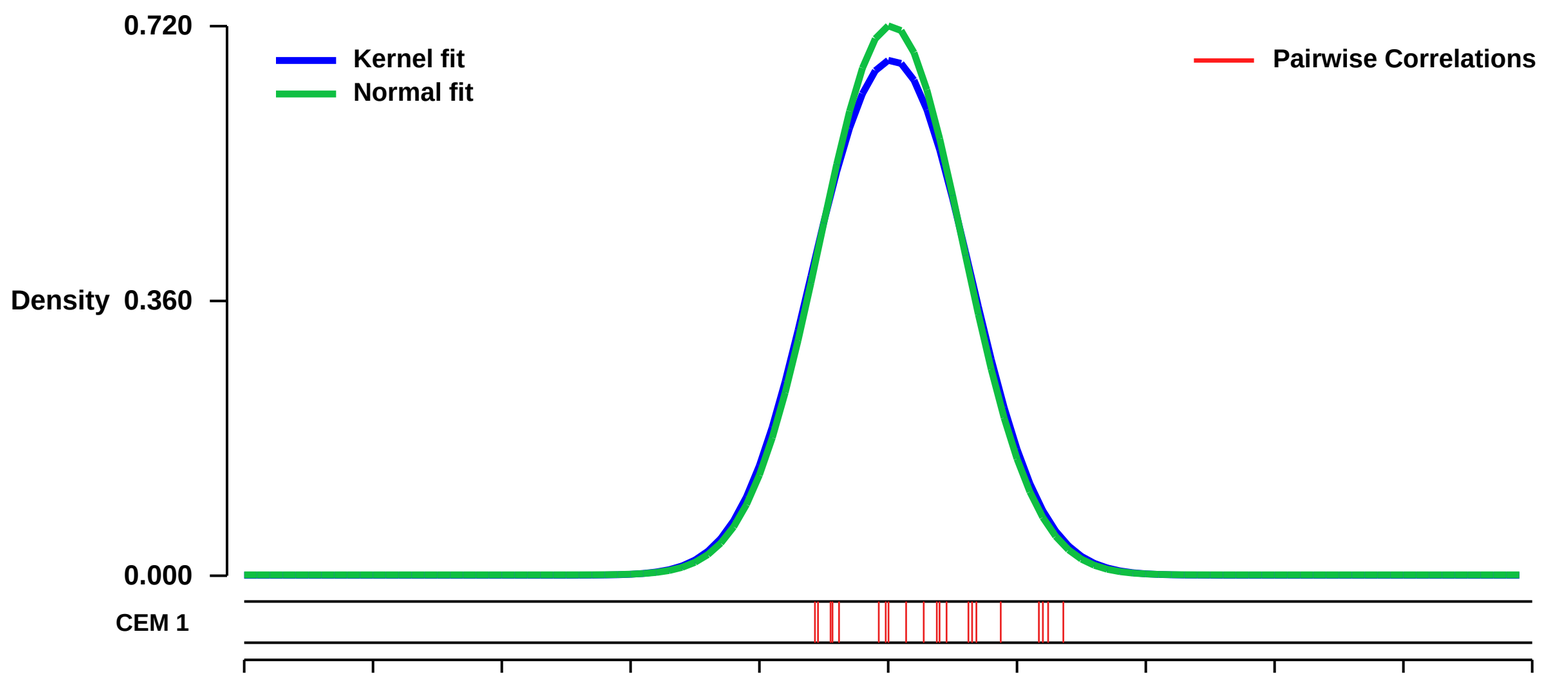

Z-score	-5.0	-4.0	-3.0	-2.0	-1.0	0.0	1.0	2.0	3.0	4.0	5.0
Correlation	-1.00	-1.00	-1.00	-0.96	-0.76	0.00	0.76	0.96	1.00	1.00	1.00

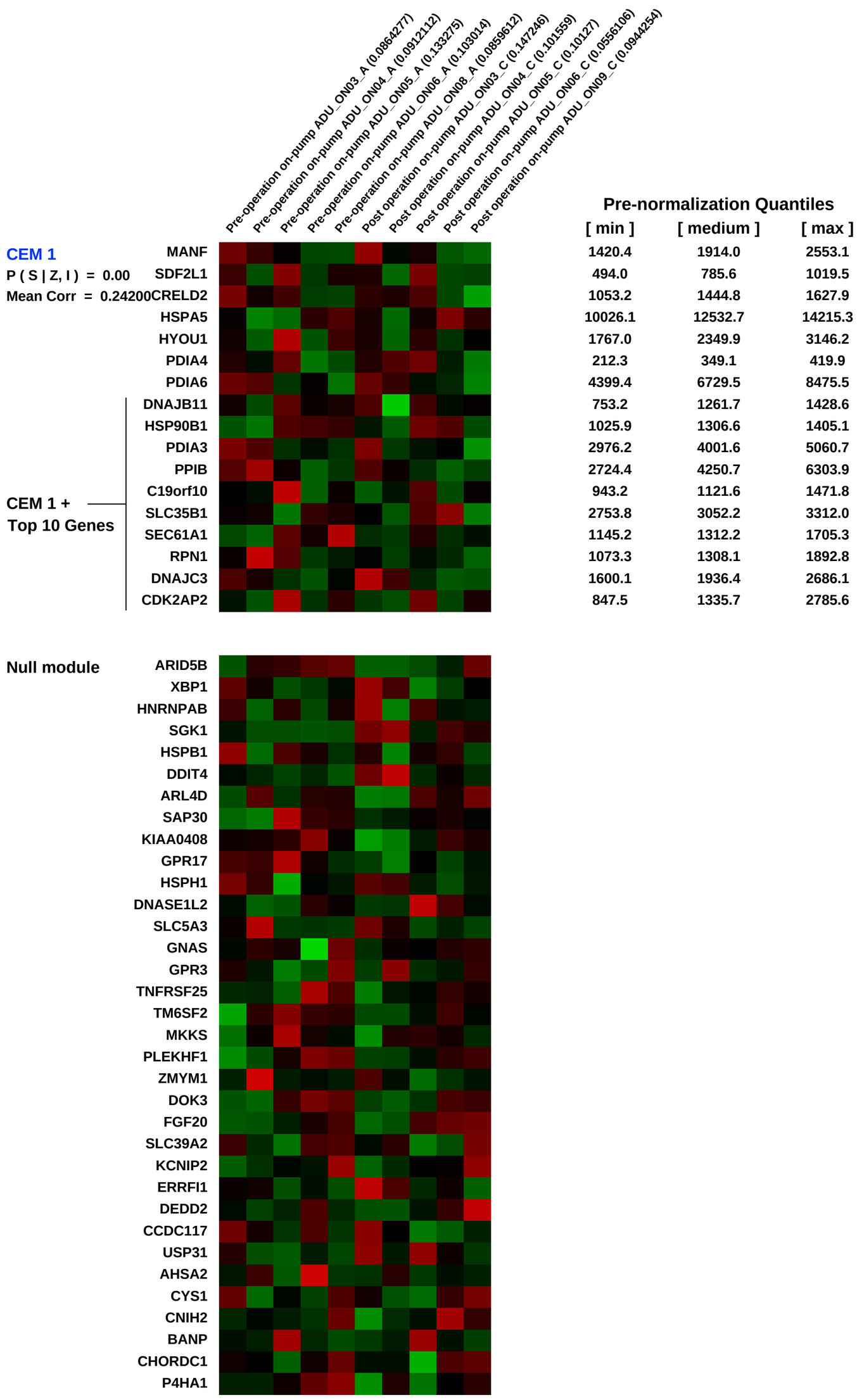

Pre-normalization Quantiles

	[min]	[medium]	[max]
MANF	1420.4	1914.0	2553.1
SDF2L1	494.0	785.6	1019.5
CRELD2	1053.2	1444.8	1627.9
HSPA5	10026.1	12532.7	14215.3
HYOU1	1767.0	2349.9	3146.2
PDIA4	212.3	349.1	419.9
PDIA6	4399.4	6729.5	8475.5
DNAJB11	753.2	1261.7	1428.6
HSP90B1	1025.9	1306.6	1405.1
PDIA3	2976.2	4001.6	5060.7
PPIB	2724.4	4250.7	6303.9
C19orf10	943.2	1121.6	1471.8
SLC35B1	2753.8	3052.2	3312.0
SEC61A1	1145.2	1312.2	1705.3
RPN1	1073.3	1308.1	1892.8
DNAJC3	1600.1	1936.4	2686.1
CDK2AP2	847.5	1335.7	2785.6

GEO Series "GSE8866" Expression Profiles

Num of samples in this series: 13

Scale of expression profile Z-scores

-3.0 -2.0 -1.0 0.0 1.0 2.0 3.0

GEO Link:	http://www.ncbi.nlm.nih.gov/geo/query/acc.cgi?acc=GSE8866
Status:	Public on Aug 20 2008
Title:	The undifferentiated phenotype in neuroblastoma depends on Cyclin D1 and CDK4 activity
Organism:	Homo sapiens
Experiment type:	Expression profiling by array
Platform:	GPL570
Pubmed ID:	18413728
Summary & Design:	**Summary:** Genomic aberrations of Cyclin D1 (CCND1) and CDK4 in neuroblastoma indicate that dysregulation of the G1 entry checkpoint is an important cell cycle aberration in this pediatric tumor. Here we report that analysis of Affymetrix expression data of primary neuroblastic tumors shows an extensive over-expression of Cyclin D1 and CDK4 which correlates with histological subgroups and prognosis respectively. Immunohistochemical analysis demonstrated an over-expression of Cyclin D1 in neuroblasts and a low Cyclin D1 expression in all cell types in ganglioneuroma. This suggests an involvement of G1 regulating genes in neuronal differentiation processes which we further evaluated using RNA interference against Cyclin D1 and its kinase partner CDK4 in several neuroblastoma cell lines. This resulted in pRb pathway inhibition as shown by an almost complete disappearance of CDK4 specific pRb phosphorylation; reduction of E2F transcriptional activity and a decrease of Cyclin A protein levels. The Cyclin D1 and CDK4 knock-down resulted in a significant reduction in cell proliferation, a G1 specific cell cycle arrest and moreover an extensive neuronal differentiation. Affymetrix microarray profiling of siRNA treated cells revealed a shift in expression profile towards a neuronal phenotype. Several new potential downstream players are identified. We conclude that neuroblastoma functionally depend on over-expression of G1 regulating genes to maintain their undifferentiated phenotype. **Keywords:** Neuroblastoma, CCND1, Cyclin D1, CDK4 **Overall design:** The Cell line IMR-32 at time point 0 and transiently transfected with siRNA against GFP, Cyclin D1 and CDK4 at time point 48 hours. All experiments are biological triplicates.

Background corr dist: KL-Divergence = 0.1277, L1-Distance = 0.0271, L2-Distance = 0.0014, Normal std = 0.4012

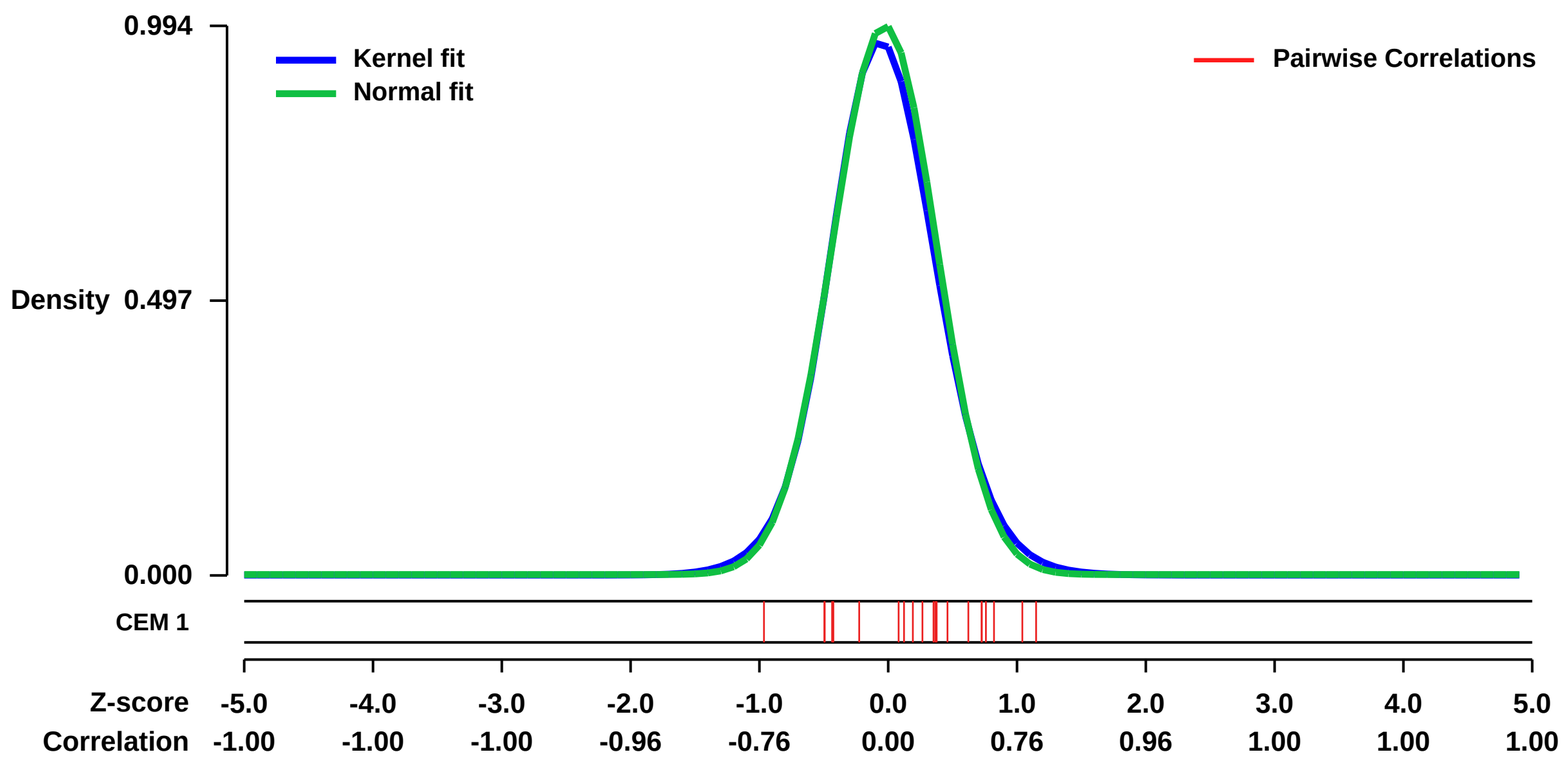

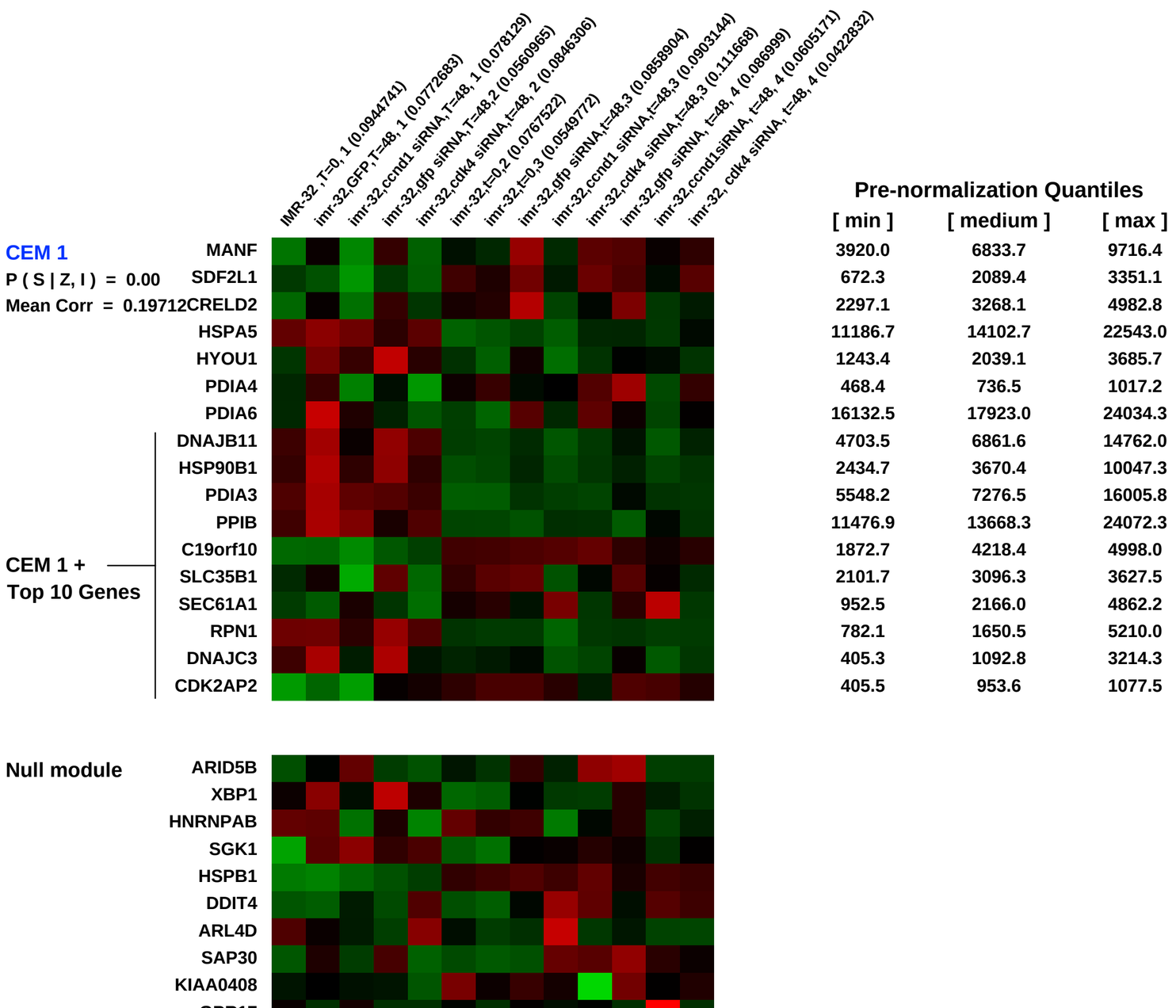

Pre-normalization Quantiles

	[min]	[medium]	[max]
MANF	3920.0	6833.7	9716.4
SDF2L1	672.3	2089.4	3351.1
CRELD2	2297.1	3268.1	4982.8
HSPA5	11186.7	14102.7	22543.0
HYOU1	1243.4	2039.1	3685.7
PDIA4	468.4	736.5	1017.2
PDIA6	16132.5	17923.0	24034.3
DNAJB11	4703.5	6861.6	14762.0
HSP90B1	2434.7	3670.4	10047.3
PDIA3	5548.2	7276.5	16005.8
PPIB	11476.9	13668.3	24072.3
C19orf10	1872.7	4218.4	4998.0
SLC35B1	2101.7	3096.3	3627.5
SEC61A1	952.5	2166.0	4862.2
RPN1	782.1	1650.5	5210.0
DNAJC3	405.3	1092.8	3214.3
CDK2AP2	405.5	953.6	1077.5

GEO Series "GSE8192" Expression Profiles

Num of samples in this series: 56

Scale of expression profile Z-scores

-3.0 -2.0 -1.0 0.0 1.0 2.0 3.0

GEO Link:	http://www.ncbi.nlm.nih.gov/geo/query/acc.cgi?acc=GSE8192
Status:	Public on Jan 01 2008
Title:	The DExH-box RNA helicase RHAU is a Nuclear Protein Involved in Transcription and mRNA Decay
Organism:	Homo sapiens
Experiment type:	Expression profiling by array
Platform:	GPL570
Pubmed ID:	18279852
Summary & Design:	**Summary:** RHAU (RNA helicase-associated with AU-rich element) is a DExH protein that was originally identified as a factor accelerating AU-rich element-mediated mRNA degradation. The finding that RHAU is predominantly localized in the nucleus, despite that mRNA degradation occurs in cytoplasm, prompted us to consider nuclear functions of RHAU. In HeLa cells, RHAU was localized throughout the nucleoplasm with some concentration in nuclear speckles in a manner dependent on ATPase activity. Transcriptional arrest altered its localization to nucleolar caps where it was colocalized with other RNA helicases, p68 and p72, suggesting that RHAU is involved in transcription-related RNA metabolism in the nucleus. To see whether RHAU affects global gene expression either transcriptionally or posttranscriptionally, we performed microarray analysis using total RNA prepared from RHAU-depleted HeLa cell lines, measuring both steady-state mRNA levels and mRNA half-lives by ActinomycinD-chase. We found that most transcripts whose steady-state levels were affected by RHAU knockdown did not show changes in their half-lives, suggesting the involvement of transcriptional regulation for these transcripts. We propose that RHAU has dual functions involved in synthesis and degradation of mRNA in different subcellular compartments. **Keywords: mRNA decay study using HeLa cells expressing shRNA** **Overall design:** Total RNA (5 ¸…g) from each replicate was reverse transcribed and labelled using the Affymetrix 1-cycle labelling kit according to manufacturerâ s instructions. Biotinylated cRNA (20 ¸…g) was fragmented by heating with magnesium (as per Affymetrixâ s instructions) and 15 ¸…g of this fragmentated cRNA was hybridized to Human U133 plus 2.0 GeneChipsTM. GC-RMA expression values and detection P-values were estimated using Refiner 4.0 from Genedata AG (Basel, Switzerland). Data analysis was performed using Analyst 4.0 from Genedata AG (Basel, Switzerland). The chip distributions were standardized by quantile normalization and they were scaled to make the median expression value, of genes with a detection P-value < 0.04, equal to 500. For the analysis of steady-state RNA levels, genes were required to have a detection P-value < 0.04 (Affymetrix default) in at least two replicates of at least one condition. The objective was to exclude genes that are not expressed in any condition. They were then subjected to a student t-test (P<0.05) and have a median fold change of 1.5 or 2 greater between samples dox+ and dox- or with and without starvation. Multiple testing errors were dealt with using a Benjamini and Hochberg false discovery correction.

Background corr dist: KL-Divergence = 0.4243, L1-Distance = 0.0539, L2-Distance = 0.0068, Normal std = 0.2452

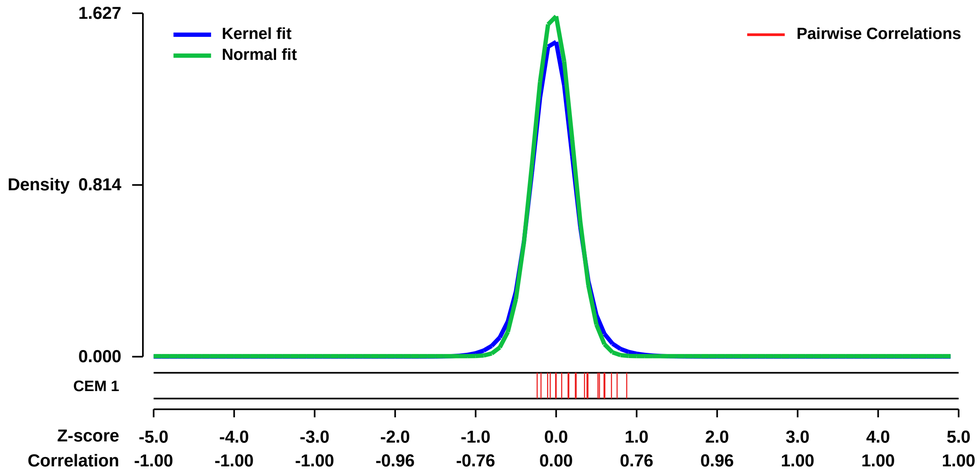

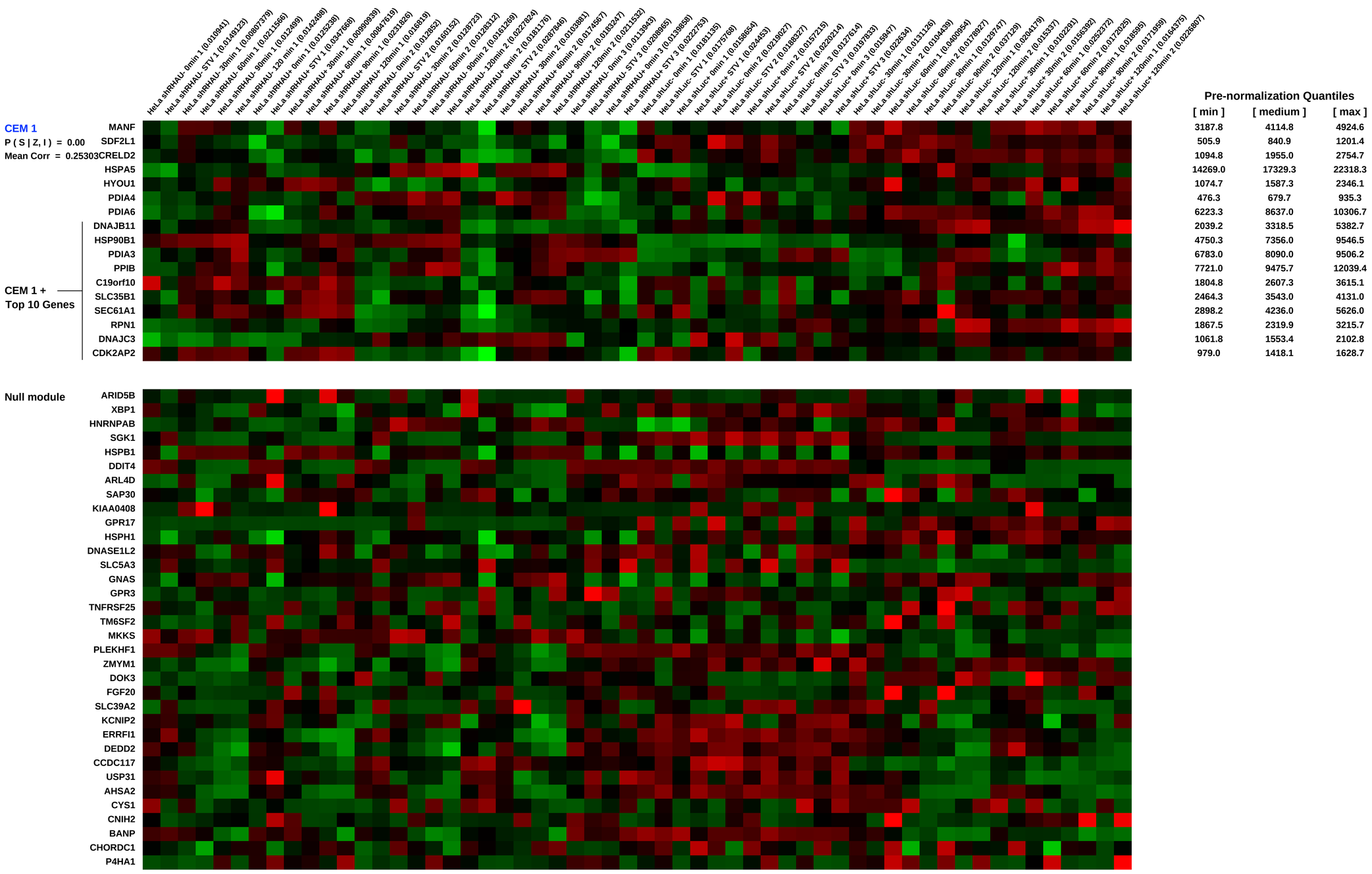

Pre-normalization Quantiles		
[min]	[medium]	[max]
3187.8	4114.8	4924.6
505.9	840.9	1201.4
1094.8	1955.0	2754.7
14269.0	17329.3	22318.3
1074.7	1587.3	2346.1
476.3	679.7	935.3
6223.3	8637.0	10306.7
2039.2	3318.5	5382.7
4750.3	7356.0	9546.5
6783.0	8090.0	9506.2
7721.0	9475.7	12039.4
1804.8	2607.3	3615.1
2464.3	3543.0	4131.0
2898.2	4236.0	5626.0
1867.5	2319.9	3215.7
1061.8	1553.4	2102.8
979.0	1418.1	1628.7

GEO Series "GSE6090" Expression Profiles

Num of samples in this series: 6

Scale of expression profile Z-scores

-3.0 -2.0 -1.0 0.0 1.0 2.0 3.0

GEO Link: http://www.ncbi.nlm.nih.gov/geo/query/acc.cgi?acc=GSE6090

Status: Public on Apr 24 2007

Title: DC-SIGN initiates an immature dendritic cell phenotype triggering Rho activation that is utilised by HIV-1

Organism: Homo sapiens

Experiment type: Expression profiling by array

Platform: GPL570

Pubmed ID: 17496896

Summary & Design:

Summary:
DC-SIGN is a C-type lectin expressed by dendritic cells (DCs) that binds HIV-1, sequestering it within multivesicular bodies to facilitate transmission to CD4+ T cells. Here we characterize the molecular basis of signalling through DC-SIGN by large-scale gene expression profiling and phosphoproteome analysis. Solitary DC-SIGN activation leads to a phenotypically disparate transcriptional program from Toll-like receptor (TLR) triggering with downregulation of MHC II, CD86, and interferon response genes and with induction of the TLR negative regulator ATF3. Phosphoproteome analysis reveals DC-SIGN signals through the leukemia-associated Rho guanine nucleotide exchange factor (LARG) to induce Rho activity. This LARG activation also occurs on DC HIV exposure and is required for effective HIV viral synapse formation. Taken together HIV mediated DC-SIGN signalling provides a mechanism by which HIV evades the immune response yet induces viral spread.

Keywords: Activation state, signalling, Toll-like Receptor (TLR)

Overall design:
Circulating monocyte derived DCs were isolated from buffy coats by adherence and culture in IL-4 and granulocyte-macrophage colony-stimulating factor (GM-CSF). DC preparations analyzed were more than 98% pure. At day four 10 million immature DCs were either left unstimulated or stimulated using plate bound anti-DC-SIGN antibody for 2 hr. Three replicates of non-stimulated or stimulated cells were taken and used to extract total RNA.

Background corr dist: KL-Divergence = 0.0505, L1-Distance = 0.0948, L2-Distance = 0.0130, Normal std = 0.7429

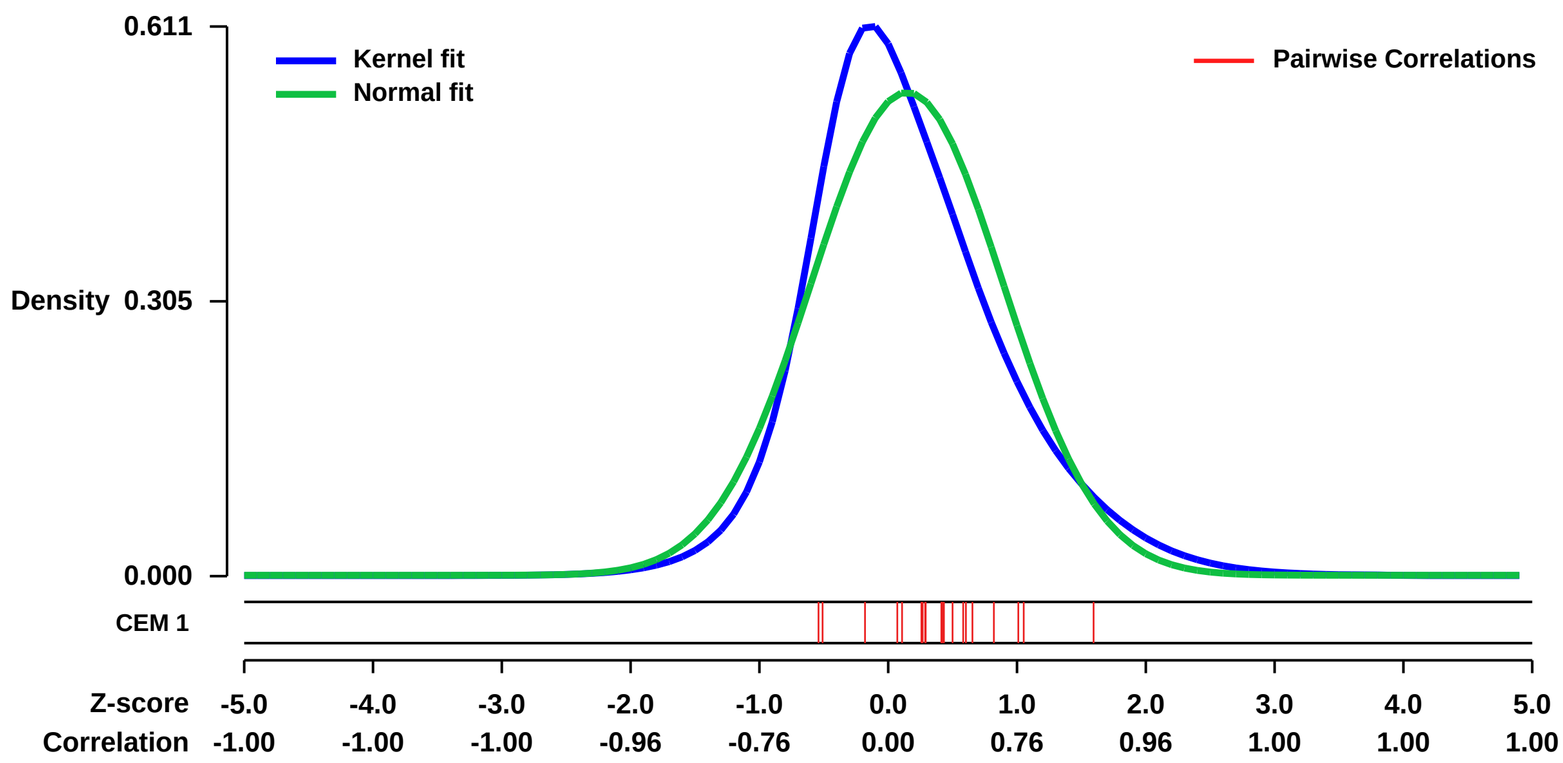

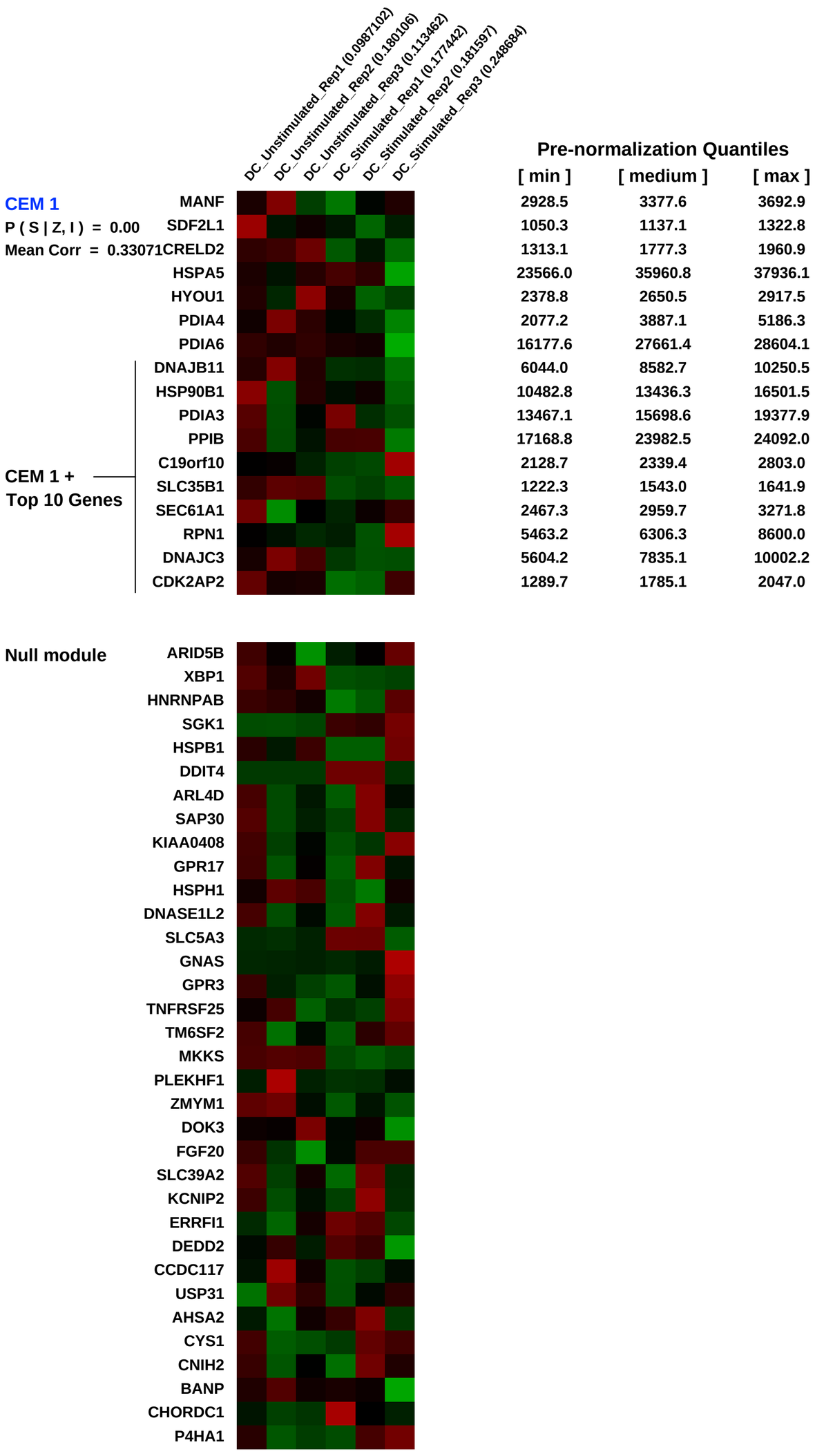

Pre-normalization Quantiles

	[min]	[medium]	[max]
MANF	2928.5	3377.6	3692.9
SDF2L1	1050.3	1137.1	1322.8
CRELD2	1313.1	1777.3	1960.9
HSPA5	23566.0	35960.8	37936.1
HYOU1	2378.8	2650.5	2917.5
PDIA4	2077.2	3887.1	5186.3
PDIA6	16177.6	27661.4	28604.1
DNAJB11	6044.0	8582.7	10250.5
HSP90B1	10482.8	13436.3	16501.5
PDIA3	13467.1	15698.6	19377.9
PPIB	17168.8	23982.5	24092.0
C19orf10	2128.7	2339.4	2803.0
SLC35B1	1222.3	1543.0	1641.9
SEC61A1	2467.3	2959.7	3271.8
RPN1	5463.2	6306.3	8600.0
DNAJC3	5604.2	7835.1	10002.2
CDK2AP2	1289.7	1785.1	2047.0

GEO Series "GSE14519" Expression Profiles

Num of samples in this series: 28

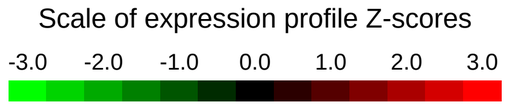

GEO Link:	http://www.ncbi.nlm.nih.gov/geo/query/acc.cgi?acc=GSE14519
Status:	Public on Jan 23 2009
Title:	Expression data from multiple myeloma cells treated with arsenic
Organism:	Homo sapiens
Experiment type:	Expression profiling by array
Platform:	GPL570
Pubmed ID:	19417148
Summary & Design:	**Summary:** We used microarrays to examine changes in gene expression in multiple myeloma cell lines following treatment with arsenic trioxide and darinaparsin **Keywords: Time course** **Overall design:** Four multiple myeloma cell lines (U266, MM.1s, KMS11, 8226/S) were treated with either arsenic trioxide (ATO) for 6, 24, or 48 hours or darinaparsin (DAR) for 6 or 24 hours; RNA was extracted from treated and control cells for microarray analysis

Background corr dist: KL-Divergence = 0.1944, L1-Distance = 0.0416, L2-Distance = 0.0040, Normal std = 0.3375

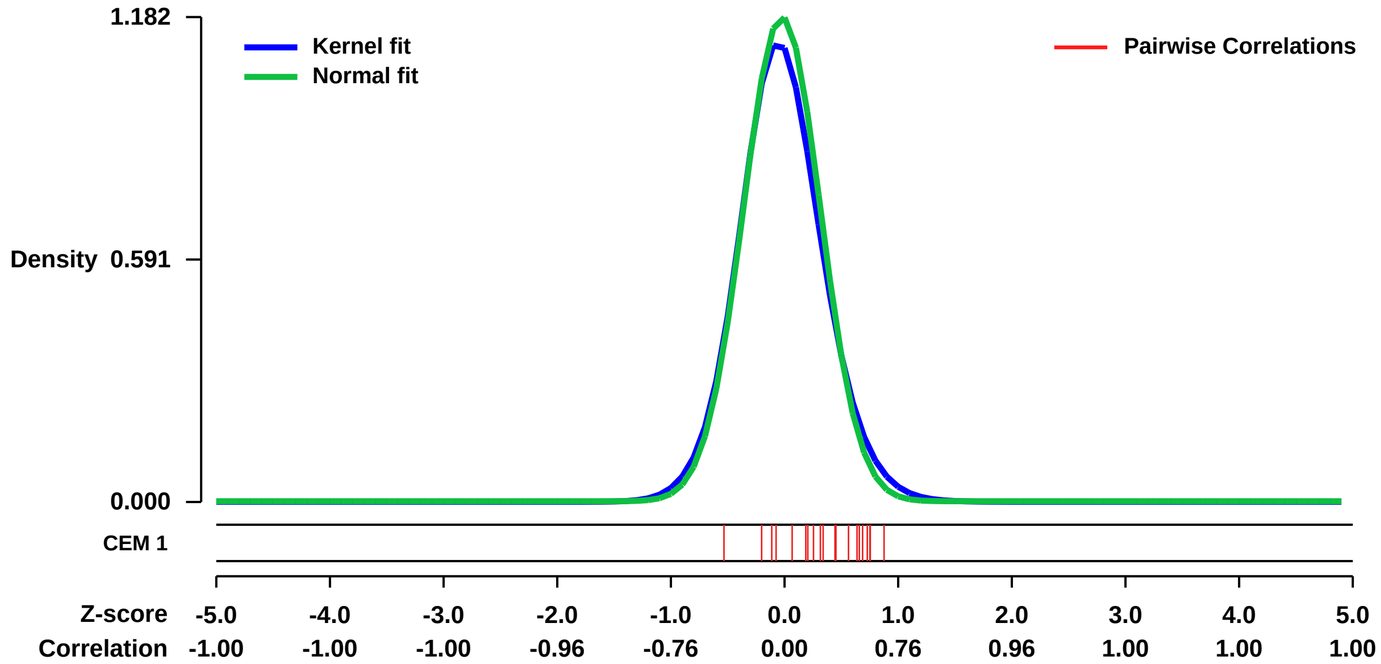

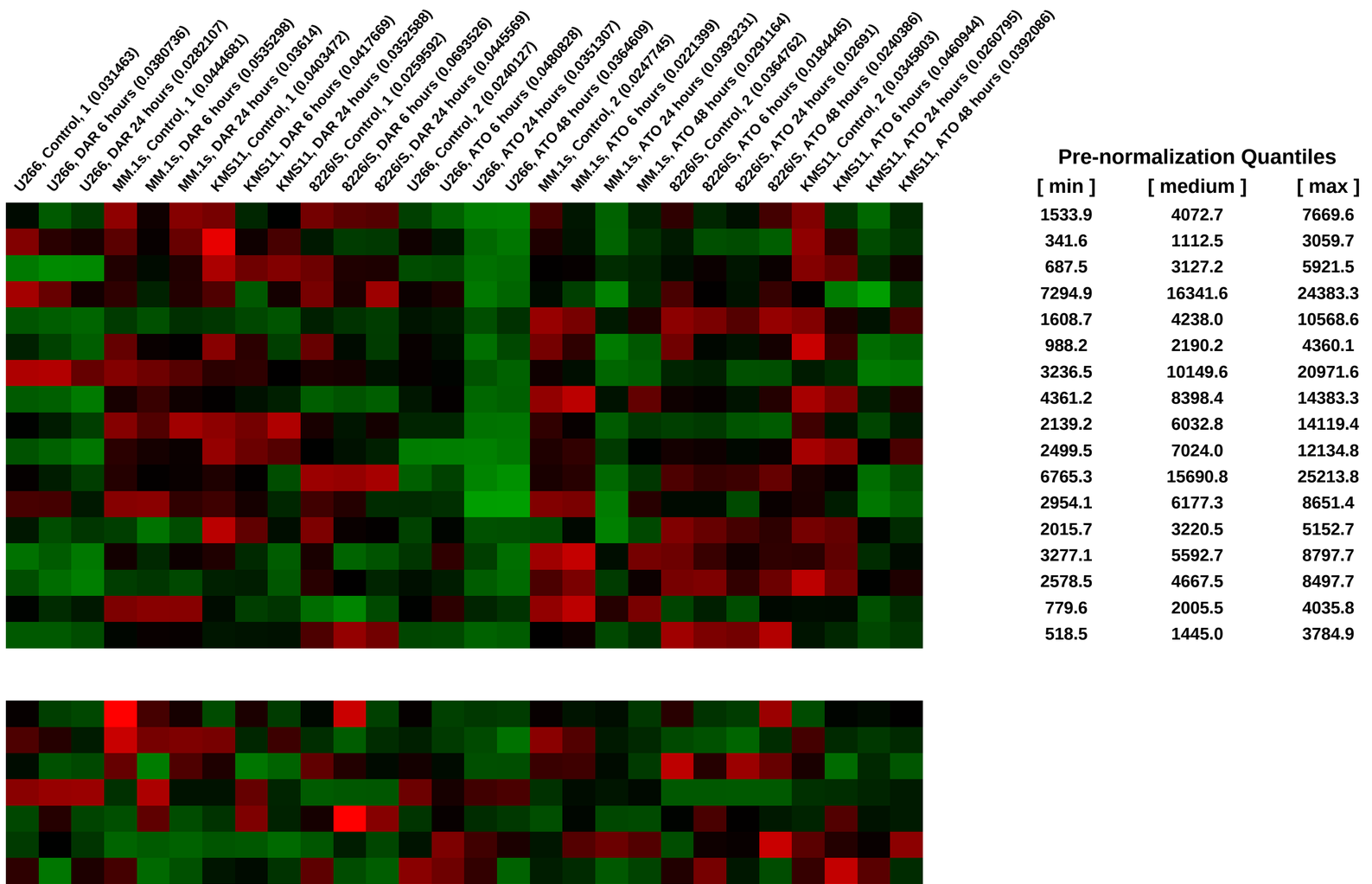

GEO Series "GSE16089" Expression Profiles

Num of samples in this series: 6

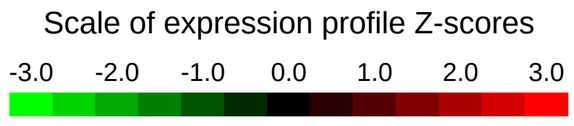

GEO Link:	http://www.ncbi.nlm.nih.gov/geo/query/acc.cgi?acc=GSE16089
Status:	Public on Sep 08 2009
Title:	Networking of differentially expressed genes in human Saos-2 osteosarcoma cells resistant to methotrexate
Organism:	Homo sapiens
Experiment type:	Expression profiling by array
Platform:	GPL570
Pubmed ID:	19732436
Summary & Design:	**Summary:** **A summary of the work associated to these microarrays is the following:** **The need for an integrated view of all data obtained from high-throughput technologies gave rise to network analyses. These are especially useful to rationalize phenomena in terms of how external perturbations propagate through the expression of genes. To address this issue in the case of drug resistance, we constructed Biological Association Networks of genes differentially expressed in cell lines resistant to methotrexate (MTX). Seven cell lines representative of different types of cancer including colon cancer (HT29 and Caco2), breast cancer (MCF7 and MDA-MB-468), pancreatic cancer (MIA PaCa-2), erythroblastic leukemia (K562) and osteosarcoma (Saos-2), were used. The differential expression pattern between sensitive and MTX-resistant cells was determined by microarrays covering the whole human genome and analyzed with the GeneSpring GX software package, v.7.3.1. Genes deregulated in common in the two colon cancer cell lines studied, were subject of Biological Association Networks construction. Dikkopf homolog-1 (DKK1) was a clear node of this network, and functional validations of this target using a siRNA showed a chemosensitization toward MTX. Members of the UDP-glucuronosyltransferase 1A (UGT1A) family formed a network of differentially expressed genes in the two breast cancer cell lines studied. siRNA treatment against UGT1A showed also an increase in MTX sensitivity. Eukaryotic translation elongation factor 1 alpha 1 (EEF1A1) was a gene overexpressed in common among the pancreatic cancer, leukemia and osteosarcoma cell lines, and siRNA treatment against EEF1A1 produced a chemosensitization toward MTX. Biological Association Networks identified DKK1, UGT1As and EEF1A1 as important gene nodes in MTX-resistance. Treatments using iRNA technology against these three genes show chemosensitization toward MTX.** **Overall design:** **Two cell lines are compared, which are Saos-2 osteosarcoma cells sensitive to methotrexate and Saos-2 cells resistant to 10e-6M methotrexate. Six samples are provided which correspond to triplicates of each cell line. The samples provided were analyzed using the specific software GeneSpring GX.**

Background corr dist: KL-Divergence = 0.0303, L1-Distance = 0.0370, L2-Distance = 0.0016, Normal std = 0.7046

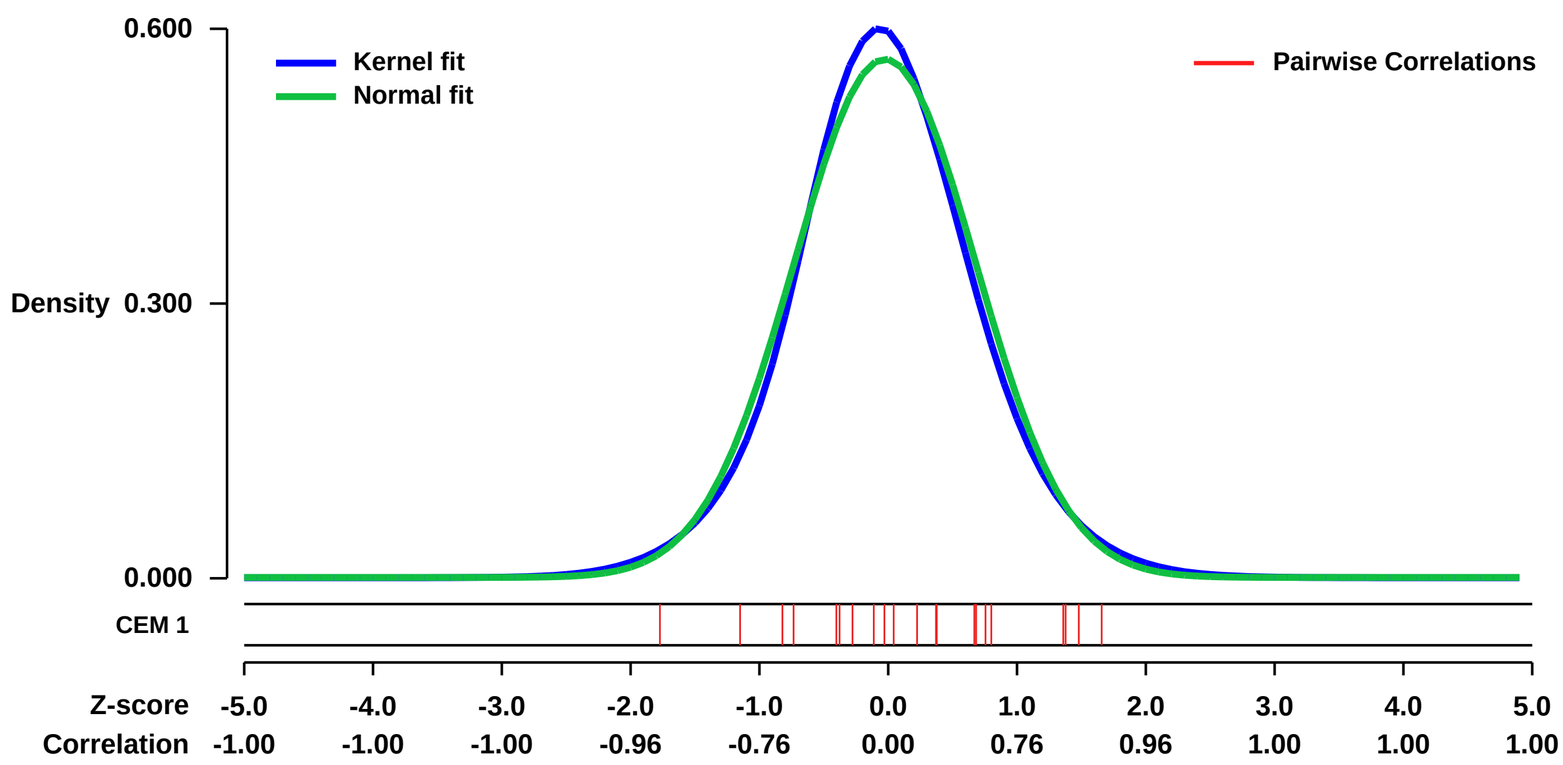

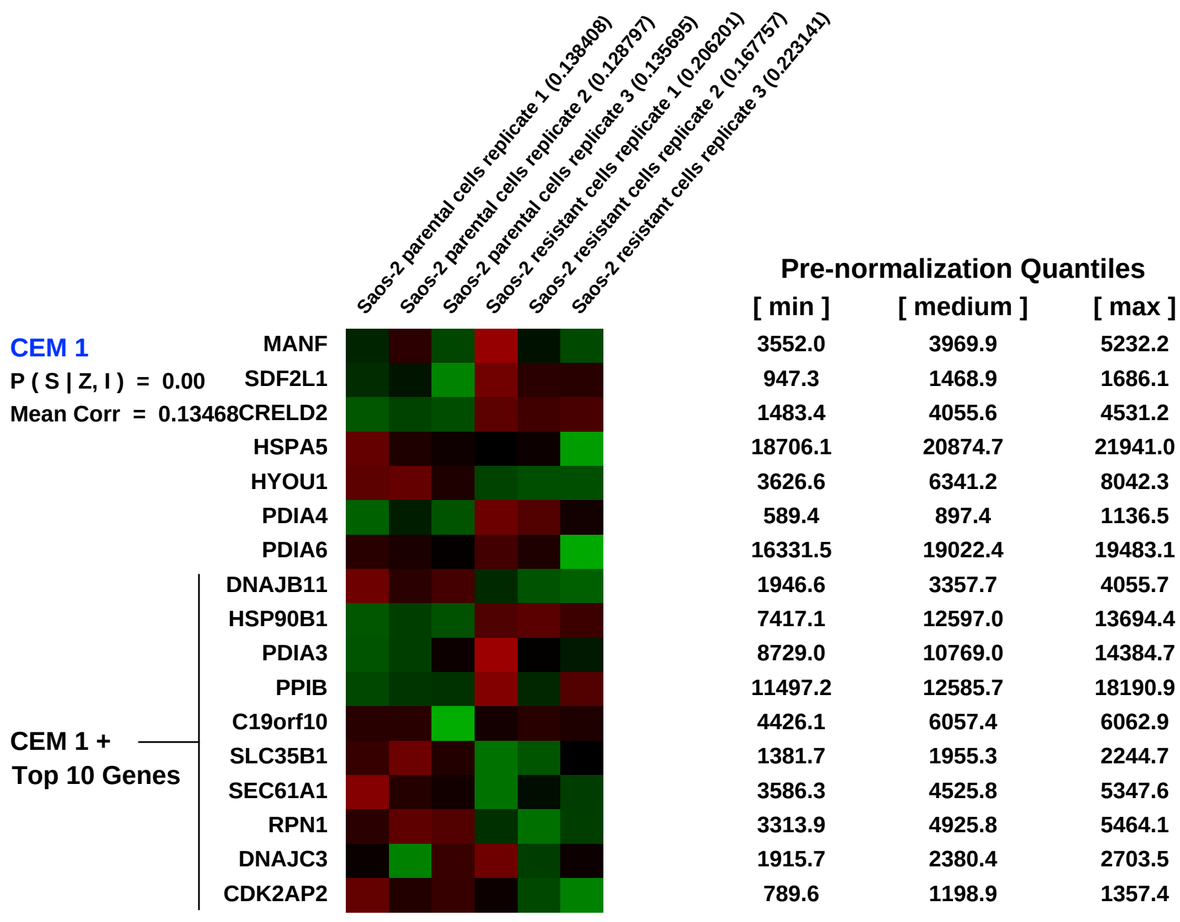

Pre-normalization Quantiles

	[min]	[medium]	[max]
MANF	3552.0	3969.9	5232.2
SDF2L1	947.3	1468.9	1686.1
CRELD2	1483.4	4055.6	4531.2
HSPA5	18706.1	20874.7	21941.0
HYOU1	3626.6	6341.2	8042.3
PDIA4	589.4	897.4	1136.5
PDIA6	16331.5	19022.4	19483.1
DNAJB11	1946.6	3357.7	4055.7
HSP90B1	7417.1	12597.0	13694.4
PDIA3	8729.0	10769.0	14384.7
PPIB	11497.2	12585.7	18190.9
C19orf10	4426.1	6057.4	6062.9
SLC35B1	1381.7	1955.3	2244.7
SEC61A1	3586.3	4525.8	5347.6
RPN1	3313.9	4925.8	5464.1
DNAJC3	1915.7	2380.4	2703.5
CDK2AP2	789.6	1198.9	1357.4

GEO Series "GSE29133" Expression Profiles

Num of samples in this series: 6

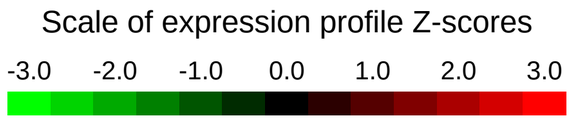

GEO Link:	http://www.ncbi.nlm.nih.gov/geo/query/acc.cgi?acc=GSE29133
Status:	Public on Oct 11 2012
Title:	Transcriptome in alveolar epithelial type II cells isolated from normal and COPD lungs of adult human
Organism:	Homo sapiens
Experiment type:	Expression profiling by array
Platform:	GPL570
Pubmed ID:	23117565
Summary & Design:	**Summary:** Alveolar epithelial type II (ATII) cells play a critical role in homeostasis and repair process of the lungs. In lung diseases such as chronic obstructive pulmonary disease (COPD), ATII cells are damaged and fall into apoptosis or senescence. Until to date, global gene expression of ATII cells in COPD lungs has not been analyzed. We isolated ATII cells from three non-COPD and three COPD patients using a FACS method. Then, we performed microarray analysis to compare gene expression profiles of ATII cells between non-COPD and COPD patients. **Overall design:** Primary ATII cells were isolated from lung tissues obtained from thoracic surgery using FACS. We profiled the gene expression of ATII cells from three non-COPD and three COPD patients. This study was approved by the Ethics Committee at Tohoku University School of Medicine and Ishinomaki Red Cross Hospital. All subjects gave informed consent.

Background corr dist: KL-Divergence = 0.0482, L1-Distance = 0.0257, L2-Distance = 0.0008, Normal std = 0.5834

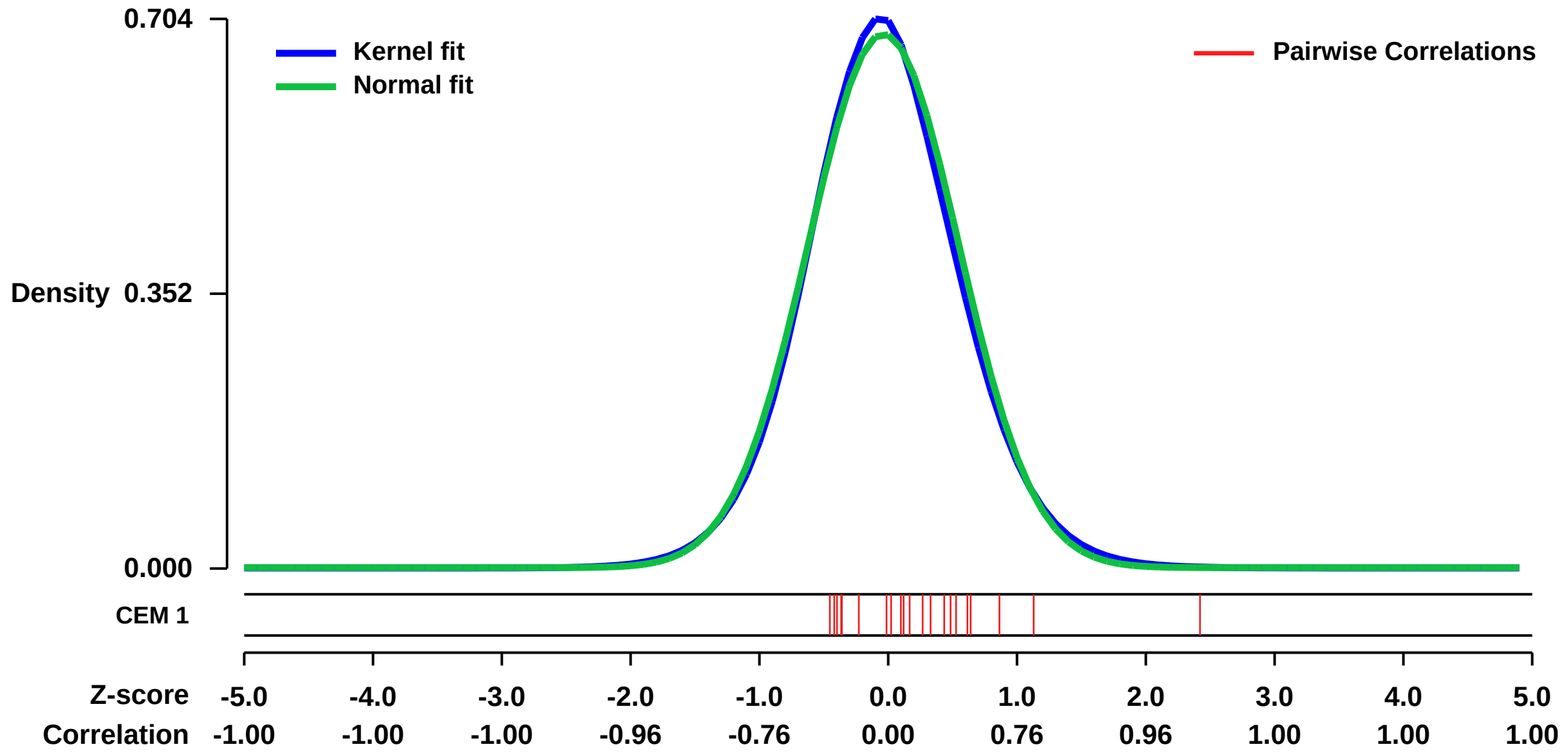

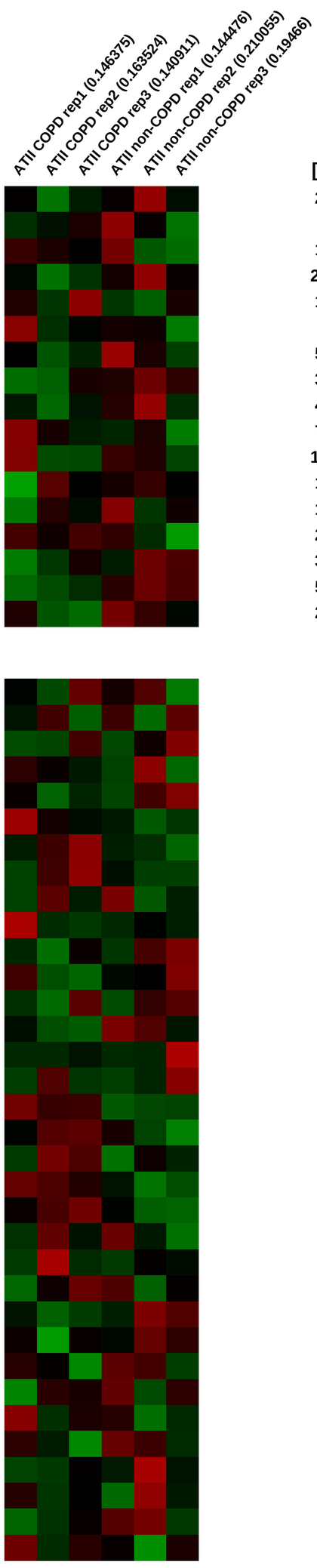

GEO Series "GSE13376" Expression Profiles

Num of samples in this series: 16

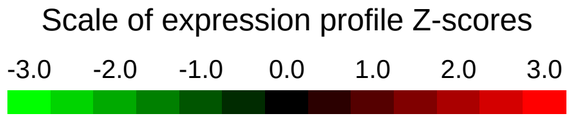

GEO Link:	http://www.ncbi.nlm.nih.gov/geo/query/acc.cgi?acc=GSE13376
Status:	Public on Feb 20 2010
Title:	Exposure of Barrett's associated adenocarcinoma cell lines SKGT4 to deoxycholic acid (DCA)
Organism:	Homo sapiens
Experiment type:	Expression profiling by array
Platform:	GPL570
Pubmed ID:	20139130
Summary & Design:	**Summary:** The involvment of bile acids such as deoxycholic acid (DCA) in gastro-esophageal reflux disease and subsequent Barrettâ s metaplsia has been postulated. This study examines gene expression induced by exposure to DCA in esophageal cells and may be utilised in cross-comparisons with data derived from gene expression studies of Barrettâ s esophagus and associated adenocarcinoma. **Overall design:** SKGT4 cells were exposed to 300um DCA over 24 hours in duplicate experiments including matched timepoint controls. RNA samples were taken at 4, 8, 12 and 24 hours from DCA (DCA) exposed and resting (REST) timepoint controls.

Background corr dist: KL-Divergence = 0.1309, L1-Distance = 0.0354, L2-Distance = 0.0020, Normal std = 0.4055

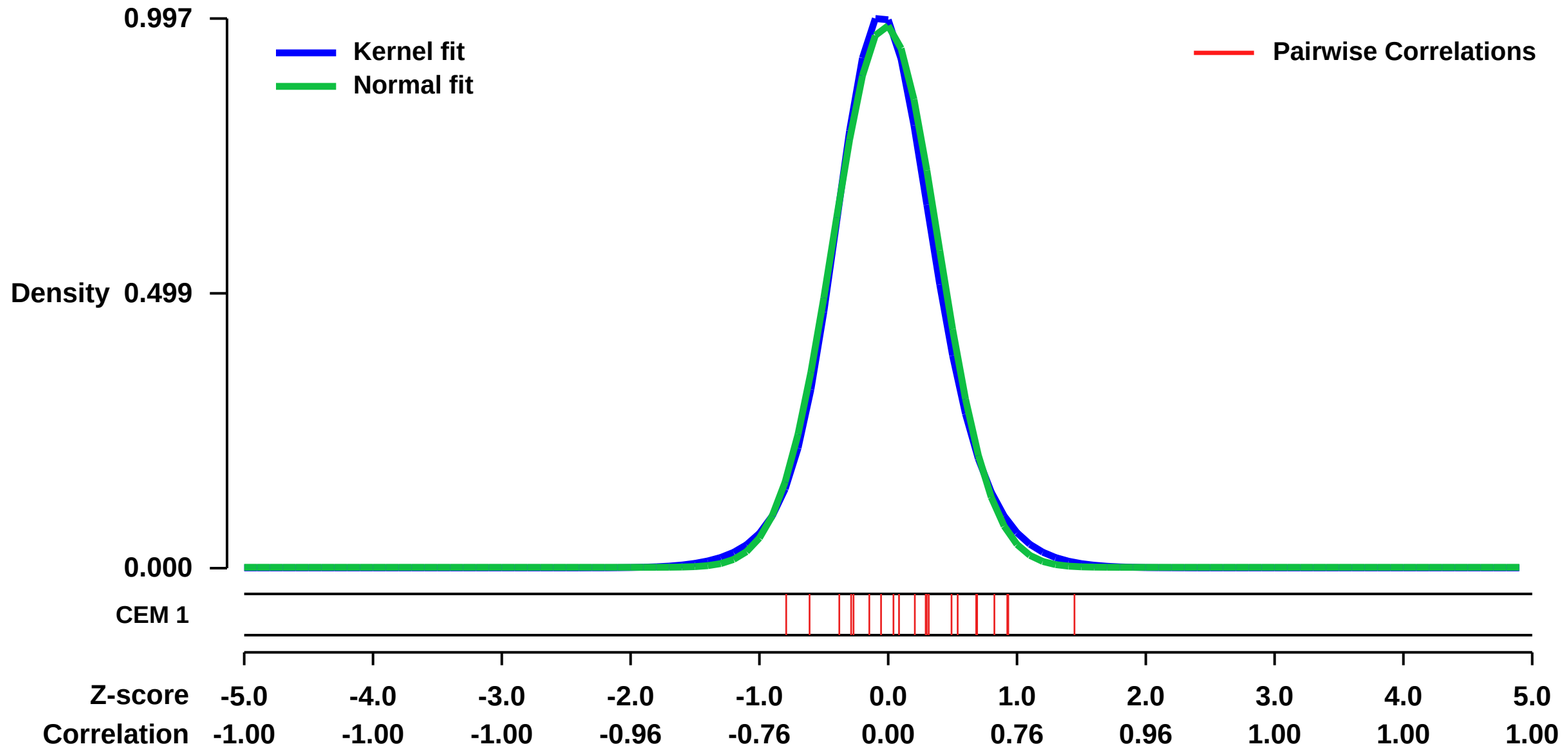

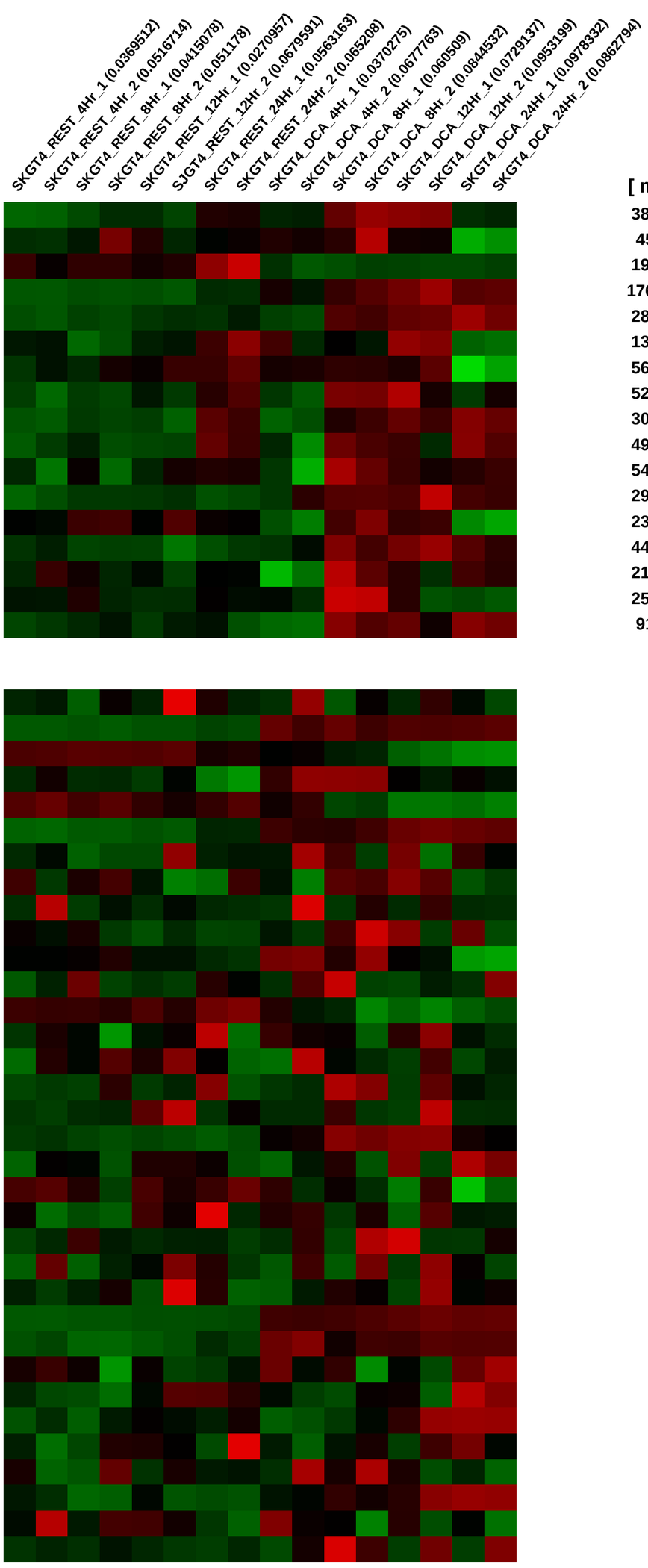

Pre-normalization Quantiles

	[min]	[medium]	[max]
MANF	3816.9	4801.8	7526.8
SDF2L1	453.1	1009.1	1513.0
CRELD2	1904.4	2464.5	3619.3
HSPA5	17614.4	25154.1	45195.3
HYOU1	2826.8	4009.8	9800.1
PDIA4	1335.5	1737.8	2481.8
PDIA6	5668.1	8363.9	9113.3
DNAJB11	5242.4	6593.1	9874.7
HSP90B1	3025.0	4633.3	5869.2
PDIA3	4915.0	6336.6	8487.1
PPIB	5499.1	8689.6	11074.4
C19orf10	2924.3	3425.3	5614.5
SLC35B1	2349.7	3082.0	3561.2
SEC61A1	4488.9	6055.2	9313.1
RPN1	2173.1	3118.2	4078.6
DNAJC3	2577.3	3181.6	5097.2
CDK2AP2	911.9	1214.6	1727.1

GEO Series "GSE13811" Expression Profiles

Num of samples in this series: 18

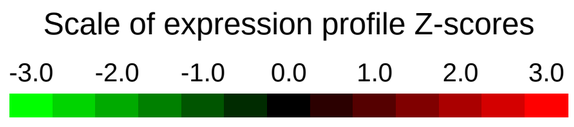

GEO Link:	http://www.ncbi.nlm.nih.gov/geo/query/acc.cgi?acc=GSE13811
Status:	Public on Dec 11 2008
Title:	Analysis of gene expression response of CLL cells to co-culture with Nurse like cells
Organism:	Homo sapiens
Experiment type:	Expression profiling by array
Platform:	GPL570
Pubmed ID:	19074730

Summary & Design:

Summary:
In the marrow and lymphatic tissues, chronic lymphocytic leukemia (CLL) cells interact with accessory cells that constitute the leukemia microenvironment. In lymphatic tissues, CLL cells are interspersed with CD68+ nurselike cells (NLC) and T cells. However, the mechanism regulating co-localization of CLL cells and these accessory cells are largely unknown. To dissect the molecular cross-talk between CLL and NLC, we profiled the gene expression of CD19-purified CLL cells before and after co-culture with NLC. NLC co-culture induced high-level expression of B cell maturation antigen (BCMA) and two chemoattractants (CCL3, CCL4) by CLL cells. Supernatants from CLL-NLC co-cultures revealed high CCL3/CCL4 protein levels. B cell receptor triggering also induced a robust induction of CCL3 and CCL4 expression by CLL cells, which was almost completely abrogated by a specific Syc inhibitor, R406. High CCL3 and CCL4 plasma levels in CLL patients suggest that activation of this pathway plays a role in vivo. These studies reveal a novel mechanism of cross-talk between CLL cells and their microenvironment, namely the secretion of two T cell chemokines by CLL-NLC interaction and in response to BCR stimulation. Through these chemokines, CLL cells can recruit accessory cells, and thereby actively create a microenvironment that favors their growth and survival.

Overall design:
In detail, RNA was isolated from CD19-purified CLL cells from 9 different patientsâ peripheral blood mononuclear cells (PBMC) after Ficoll separation and subsequent purification with CD19 MicroBeads and the MACS´fi technology according to the manufacturerâ s instructions (Miltenyi Biotec, Bergisch Gladbach, Germany). For comparison, the same CLL cell samples were co-cultured for 14 days with NLC (""14d NLC""). For co-culture with NLC, PBMC from patients with CLL were suspended in complete RPMI medium (RPMI1640 with 10% FCS, penicillin-streptomycin-glutamine, Gibco-BRL, Grand Island, NY) to a concentration of 1 x 107/ml (total 20 ml) and incubated for 14 days in 75 cm2 tissue culture flasks (Techno Plastic Products AG) as described previously3. Nonadherent lymphoid cells then were removed and the NLC layer was washed two times with phosphate-buffered saline (PBS). The complete removal of lymphocytes was verified by phase-contrast microscopy. The nonadherent cells together with the wash-fractions were then used for RNA preparation. In order to purify the CLL B cells prior to RNA isolation, CLL PBMC were passed through a 30 ´µm nylon mesh to obtain a single-cell suspension. Then CLL B cells were purified with CD19 MicroBeads. Subsequently RNA was extracted.

Background corr dist: KL-Divergence = 0.2773, L1-Distance = 0.0616, L2-Distance = 0.0102, Normal std = 0.2902

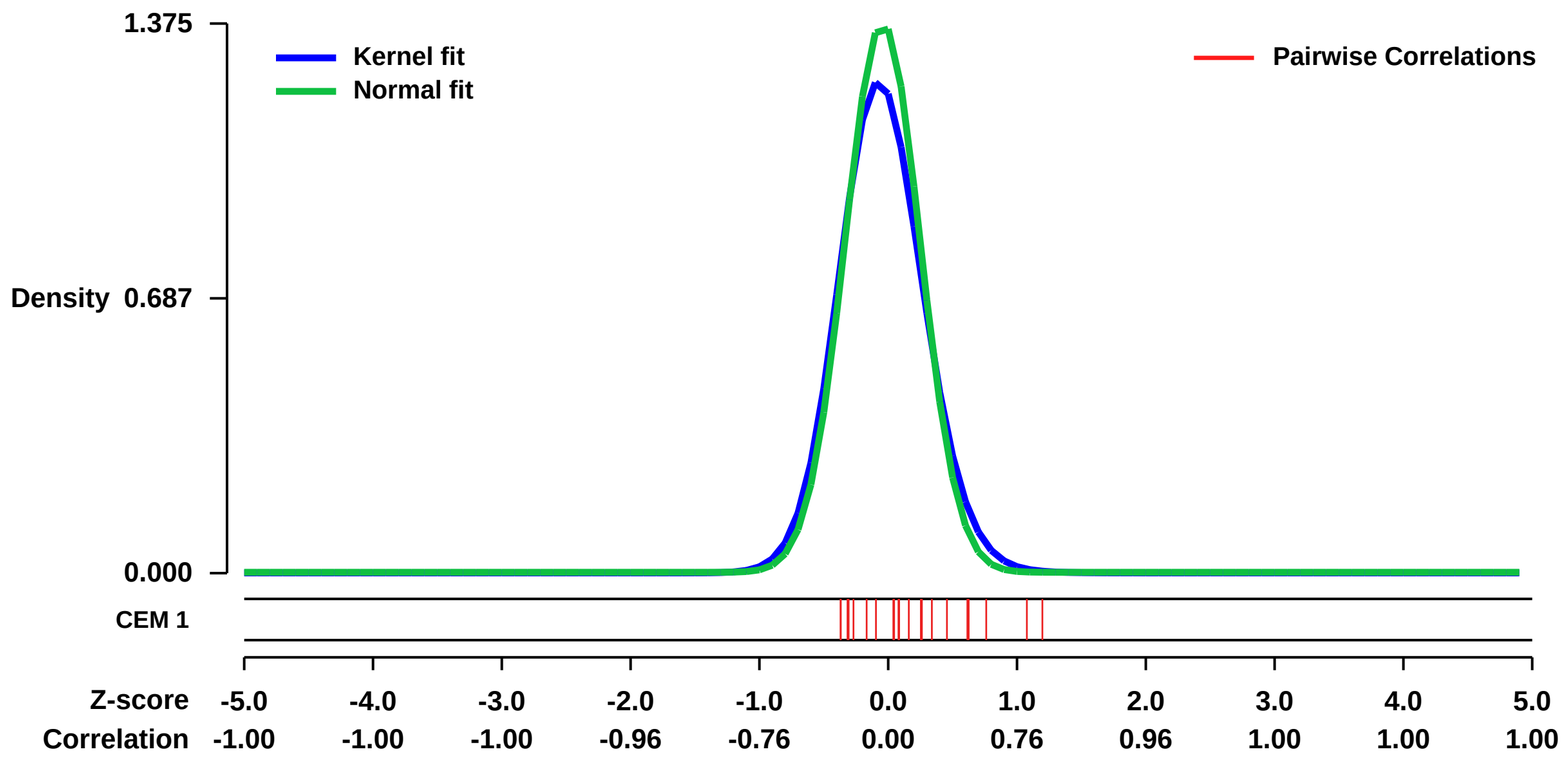

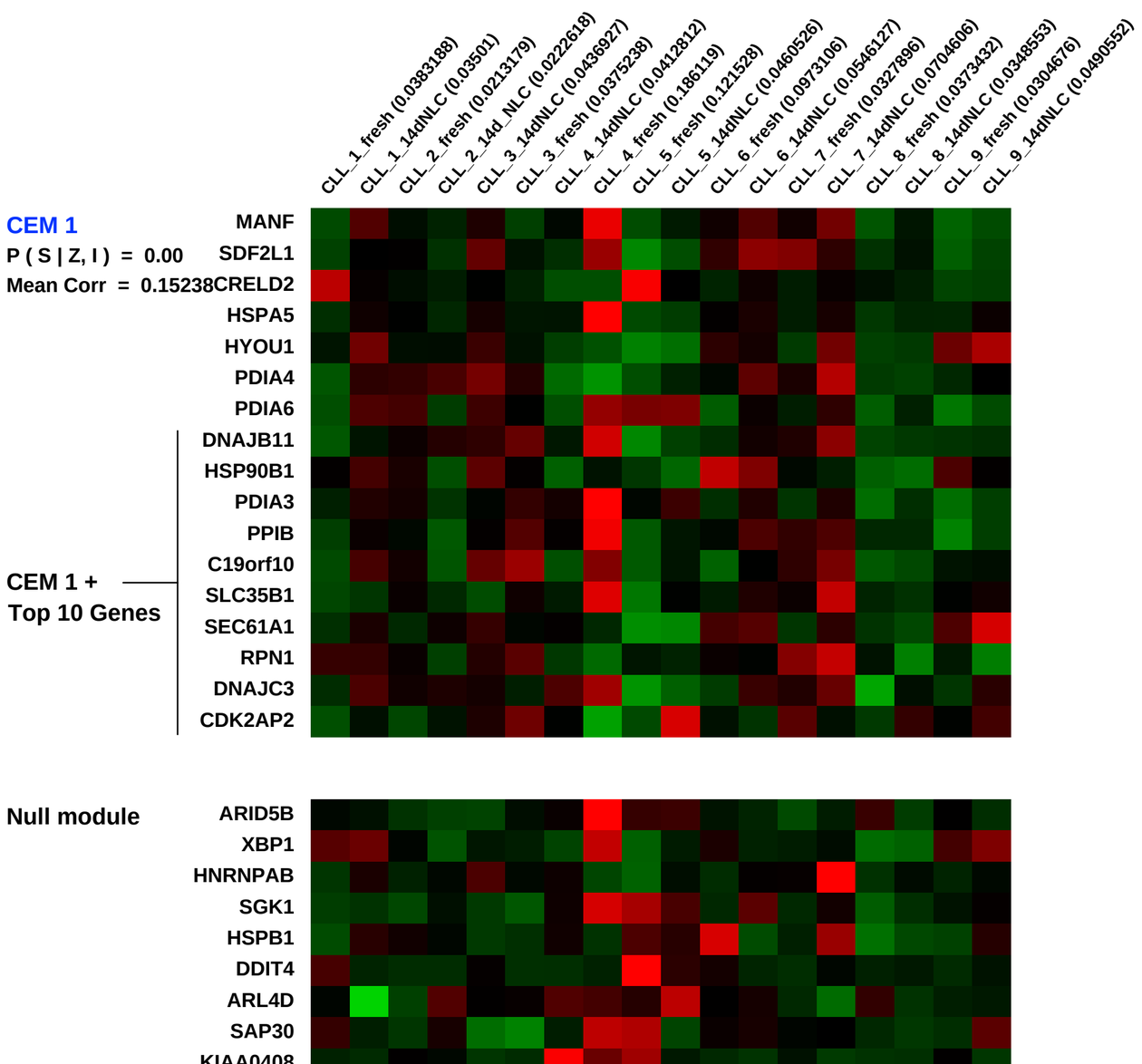

Pre-normalization Quantiles

	[min]	[medium]	[max]
MANF	818.8	1272.1	2580.2
SDF2L1	218.2	477.1	850.8
CRELD2	510.0	1020.2	3156.7
HSPA5	3979.8	8129.4	34298.6
HYOU1	270.2	726.7	1450.9
PDIA4	212.7	366.8	554.7
PDIA6	2419.1	3824.3	5624.4
DNAJB11	758.6	1828.8	3972.1
HSP90B1	2179.2	4274.8	7865.5
PDIA3	3520.9	6334.6	13833.7
PPIB	3946.7	9055.0	19481.3
C19orf10	1124.7	1342.1	1776.6
SLC35B1	393.4	711.5	1319.5
SEC61A1	784.4	1219.0	1841.1
RPN1	741.2	1309.0	2218.4
DNAJC3	606.5	1126.3	1518.2
CDK2AP2	446.1	1071.0	2052.0

GEO Series "GSE32540" Expression Profiles

Num of samples in this series: 9

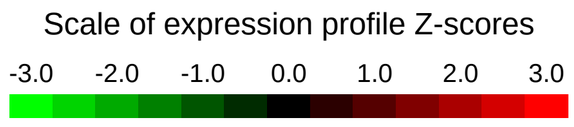

GEO Link:	http://www.ncbi.nlm.nih.gov/geo/query/acc.cgi?acc=GSE32540
Status:	Public on Aug 02 2012
Title:	Identification of novel tissue-specific transcription arising from E-cadherin/CDH1 intron2: a novel protein isoform increases gastric cancer cell invasion and angiogenesis.
Organism:	Homo sapiens
Experiment type:	Expression profiling by array
Platform:	GPL570
Pubmed ID:	22752307

Summary & Design:

Summary:
E-cadherin, a protein encoded by the CDH1 gene is the dominant epithelial cell adhesion molecule playing a crucial role in epithelial tissue polarity and structural integrity. The progression of 90% or more carcinomas is believed to be mediated by disruption of normal E-cadherin expression, subcellular localization or function. Despite the strong correlation between E-cadherin loss and malignancy the mechanism through how this occurs is not known in most sporadic and hereditary epithelial carcinomas. Previous works have shown the importance of CDH1 intron 2 sequences for proper gene and protein expression supporting the possibility of these being cis-modulators of E-cadherin expression/function. but when co-expressed it led to reduced cell-cell adhesiveness, increased invasion and angiogenesis. By expression array analysis, IFITM1 and IFI27 levels were found to be increased upon CDH1a overexpression. Importantly, CDH1a was found to be de novo expressed in gastric cancer cell lines when compared to normal stomach.

Results: In this sense we have searched for additional CDH1 transcripts arising from intron 2. From the four found, one (CDH1a) was demonstrated to be tissue specific and to be translated in vivo. When overexpressed in an E-cadherin negative context CDH1a replaced the canonic protein functions

Conclusions: We have demonstrated, for the first time, transcripts arising from CDH1 intron 2. One of these, CDH1a, was found to modulate E-cadherin function representing a novel mechanism underlying invasion and angiogenesis in epithelial cancers and opening the way for novel therapeutic approaches.

Overall design:
Total RNA obtained from human gastric tubular adenocarcinoma Mkn28 cell line. Three independent replicas of each conditions(i.e pLenti transduced cell lines overexpressing CDH1a , pLenti with empty vector and pLenti transduced cell lines overexpressing wild type CDH1) has been employed.

Background corr dist: KL-Divergence = 0.0810, L1-Distance = 0.0206, L2-Distance = 0.0005, Normal std = 0.4753

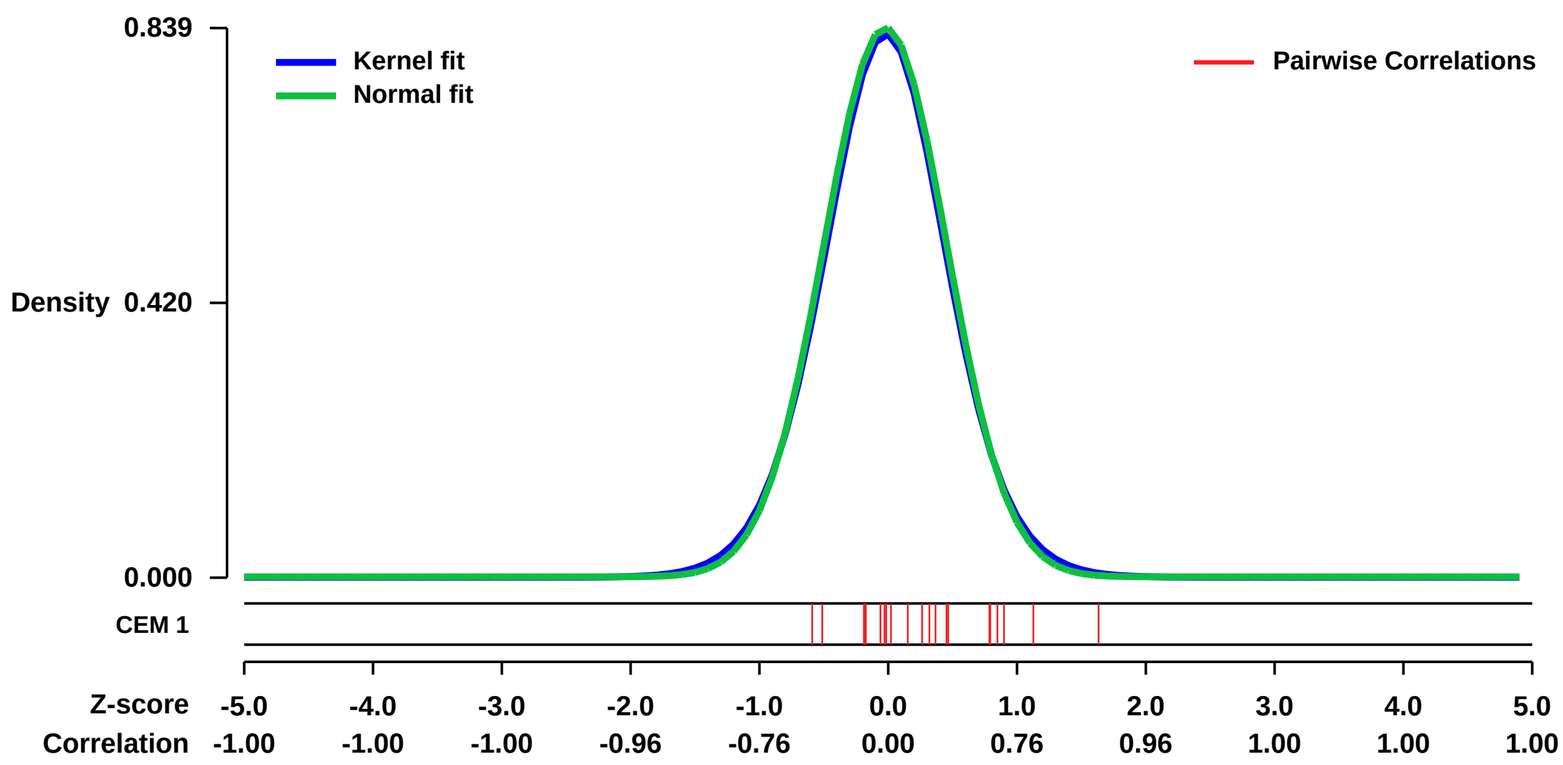

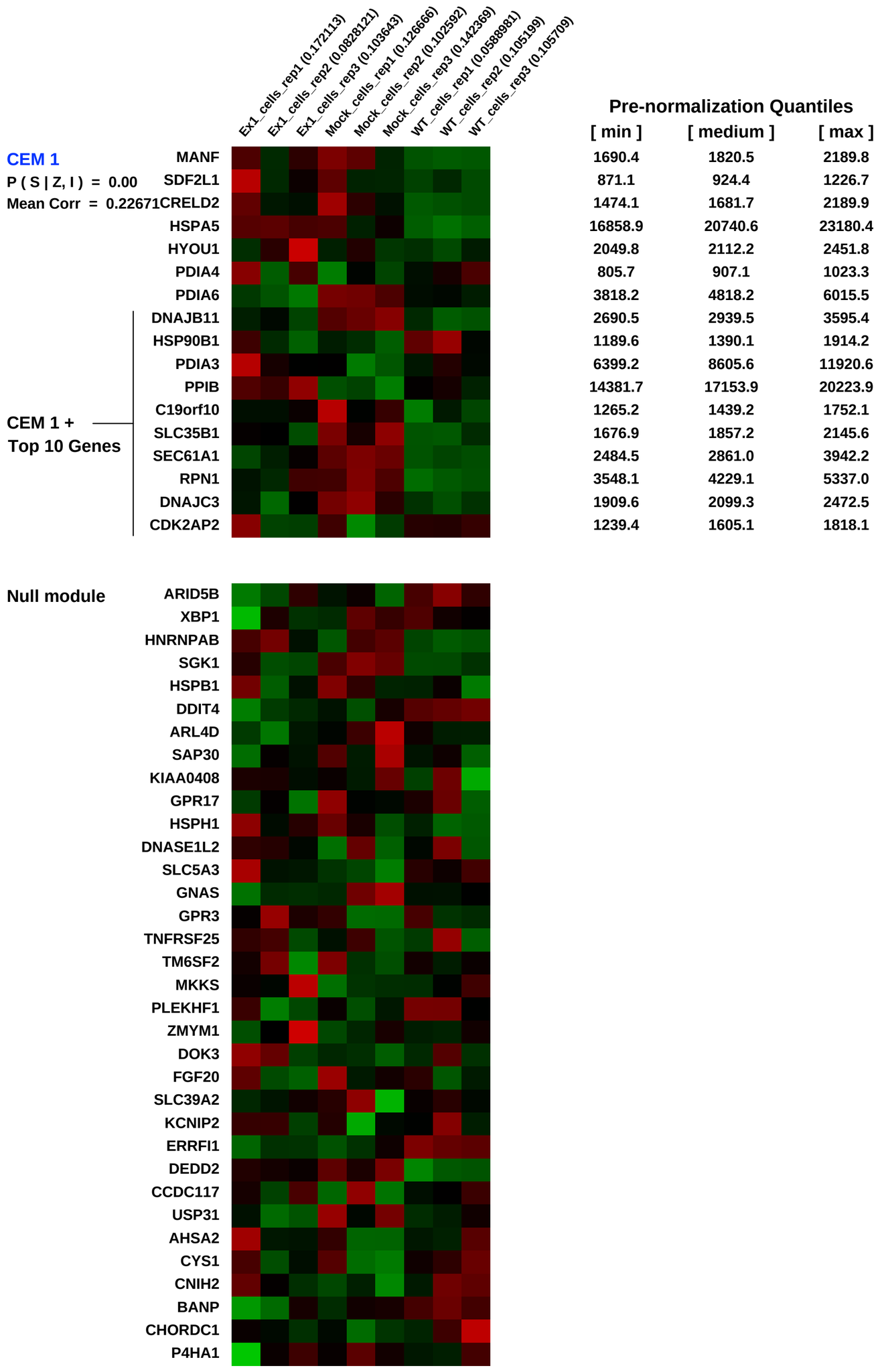

	Pre-normalization Quantiles		
	[min]	[medium]	[max]
MANF	1690.4	1820.5	2189.8
SDF2L1	871.1	924.4	1226.7
CRELD2	1474.1	1681.7	2189.9
HSPA5	16858.9	20740.6	23180.4
HYOU1	2049.8	2112.2	2451.8
PDIA4	805.7	907.1	1023.3
PDIA6	3818.2	4818.2	6015.5
DNAJB11	2690.5	2939.5	3595.4
HSP90B1	1189.6	1390.1	1914.2
PDIA3	6399.2	8605.6	11920.6
PPIB	14381.7	17153.9	20223.9
C19orf10	1265.2	1439.2	1752.1
SLC35B1	1676.9	1857.2	2145.6
SEC61A1	2484.5	2861.0	3942.2
RPN1	3548.1	4229.1	5337.0
DNAJC3	1909.6	2099.3	2472.5
CDK2AP2	1239.4	1605.1	1818.1
ARID5B			
XBP1			
HNRNPAB			
SGK1			
HSPB1			
DDIT4			
ARL4D			
SAP30			
KIAA0408			
GPR17			
HSPH1			
DNASE1L2			
SLC5A3			
GNAS			
GPR3			
TNFRSF25			
TM6SF2			
MKKS			
PLEKHF1			
ZMYM1			
DOK3			
FGF20			
SLC39A2			
KCNIP2			
ERRFI1			
DEDD2			
CCDC117			
USP31			
AHSA2			
CYS1			
CNIH2			
BANP			
CHORDC1			
P4HA1			

GEO Series "GSE25330" Expression Profiles

Num of samples in this series: 15

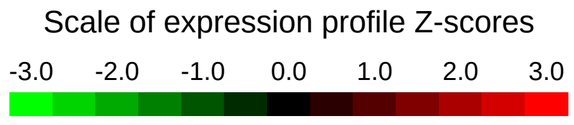

GEO Link:	http://www.ncbi.nlm.nih.gov/geo/query/acc.cgi?acc=GSE25330
Status:	Public on Jan 01 2011
Title:	Expression data from In vitro induced C2 M cells in the presence of commensal bacteria
Organism:	Homo sapiens
Experiment type:	Expression profiling by array
Platform:	GPL570
Pubmed ID:	22385384
Summary & Design:	**Summary:** M cells are the main site of bacterial translocation in the intestine. We used the in vitro M cell model to study the effect of the commensal bacteria; Lactobacillus salivarius, Eschericha coli and Bacteroides fragilis, on M cell gene expression. Bacterial translocation across the gut mucosa has traditionally been based on the detection of commensals in the mesenteric lymph node. Differential rates of commensal translocation have been reported in vivo, however fewer studies have examined translocation of commensals at the level of the gut epithelial M cell. In this study we employed an in vitro M cell model to quantify translocation of various bacteria. C2BBe1 cells were differentiated into M cells and the gene expression profile and transport kinetics of different bacterial strains, namely Lactobacillus salivarius, Escherichia coli, and Bacteroides fragilis, was assessed. For comparison with M cell uptake, the THP-1 monocytic cell line was used to analyze bacterial internalization and resulting cytokine production. The commensal bacterial strains were translocated across M cells with different efficiencies; E. coli and B. fragilis translocated with equal efficiency while L. salivarius translocated with less efficiency. In contrast, L. salivarius was internalized by THP-1 cells to a higher degree than B. fragilis or E. coli and was associated with a different cytokine profile. Microarray analysis showed both common and differential gene expression amongst the bacteria and control polystyrene beads. In the presence of bacteria, but not beads, upregulated genes were mainly involved in transcription regulation and dephosphorylation, e.g. EGR1, JUN; whereas proinflammatory and stress response genes were primarily upregulated by E. coli and B. fragilis, but not L. salivarius nor beads, e.g. IL8, TNFAIP3. These results demonstrate that M cells have the ability to discriminate between different commensal bacteria and modify subsequent immune responses. **Overall design:** C2bbe1 cells were converted to M cells (C2M) following 21 days of culture on Transwells in the presence of Raji B cells. C2M cells were co-cultured alone, Lactobacillus salivarius, Eschericha coli, Bacteroides fragilis and control beads. Total RNA was extracted and processed for Affymetrix array hybridisation

Background corr dist: KL-Divergence = 0.1808, L1-Distance = 0.0356, L2-Distance = 0.0024, Normal std = 0.3478

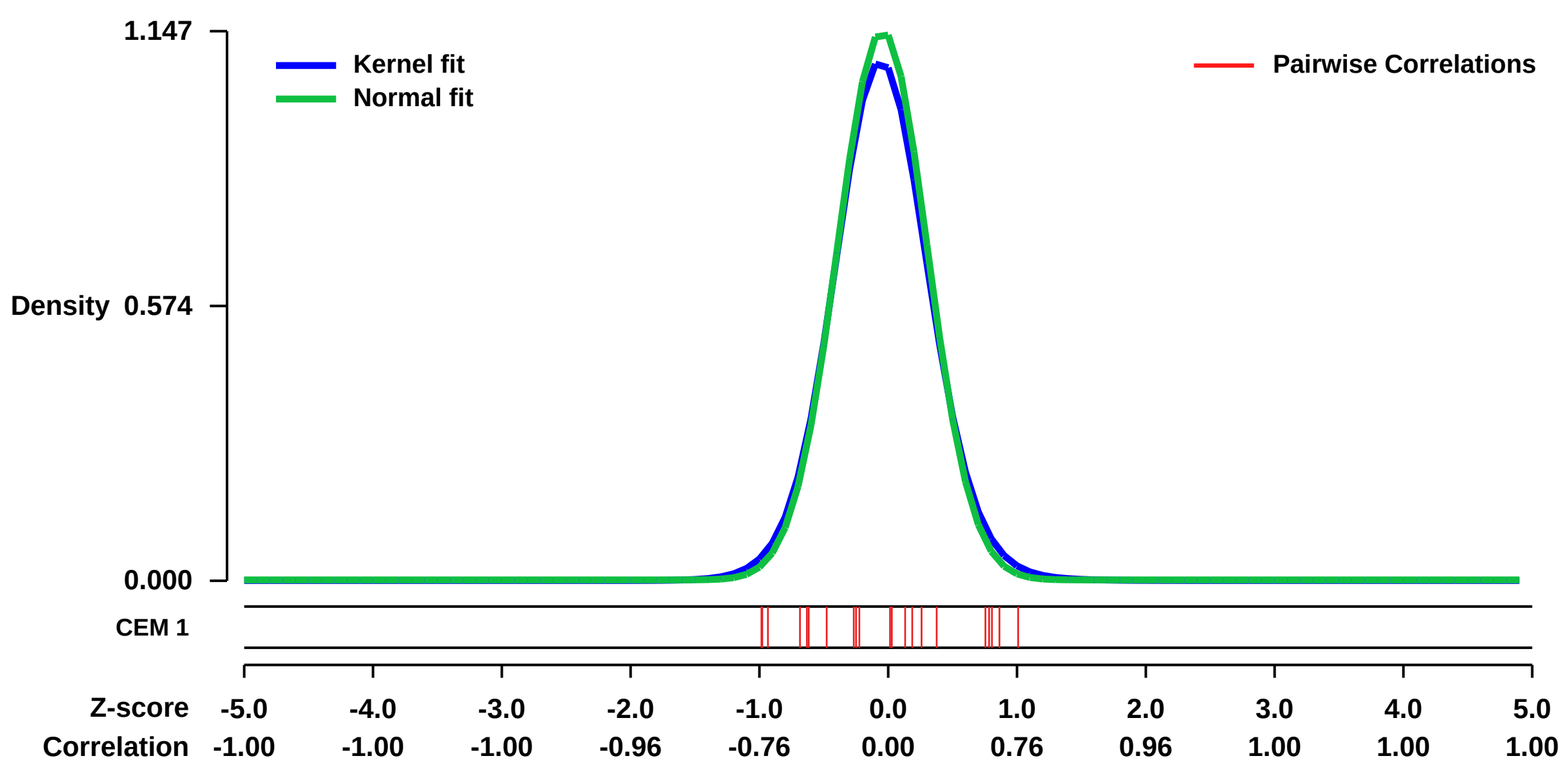

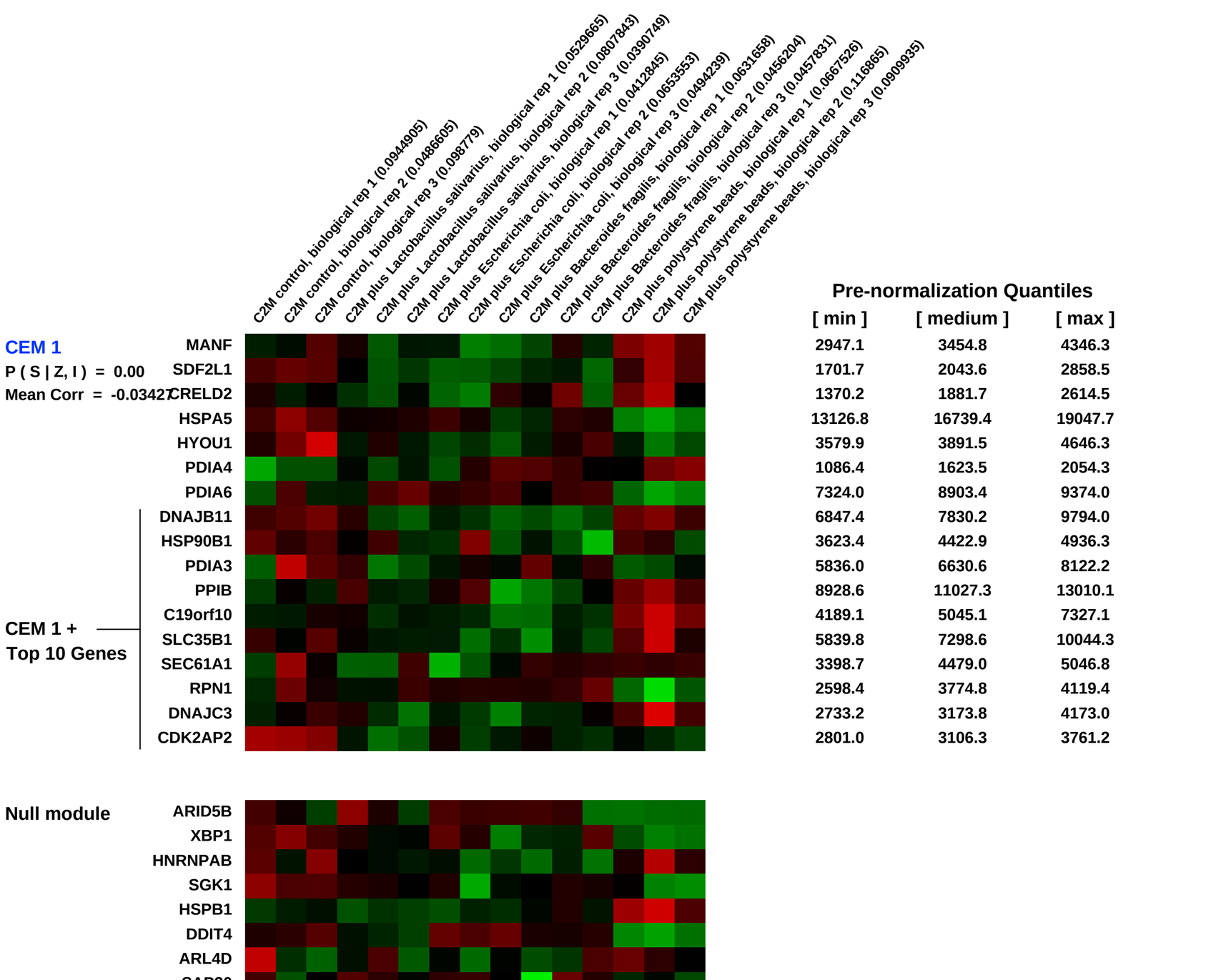

GEO Series "GSE19128" Expression Profiles

Num of samples in this series: 11

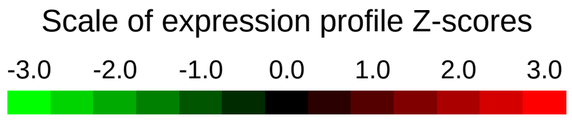

GEO Link:	http://www.ncbi.nlm.nih.gov/geo/query/acc.cgi?acc=GSE19128
Status:	Public on Nov 21 2009
Title:	Regulation of Inflammatory Gene Expression by Immunostimulatory Botanicals
Organism:	Homo sapiens
Experiment type:	Expression profiling by array
Platform:	GPL570
Pubmed ID:	
Summary & Design:	**Summary:** Using herbogenomics, this study provides novel insight into putative genes which may be involved in physiological responses. **Overall design:** PBMCs were treated with 5uL herbal extract for indicated times, followed by RNA isolation with Rneasy kit (Qiagen). Microarray analysis was performed using Affymetrix Human Genome U133 Plus 2.0 Array.

Background corr dist: KL-Divergence = 0.0598, L1-Distance = 0.0295, L2-Distance = 0.0015, Normal std = 0.5256

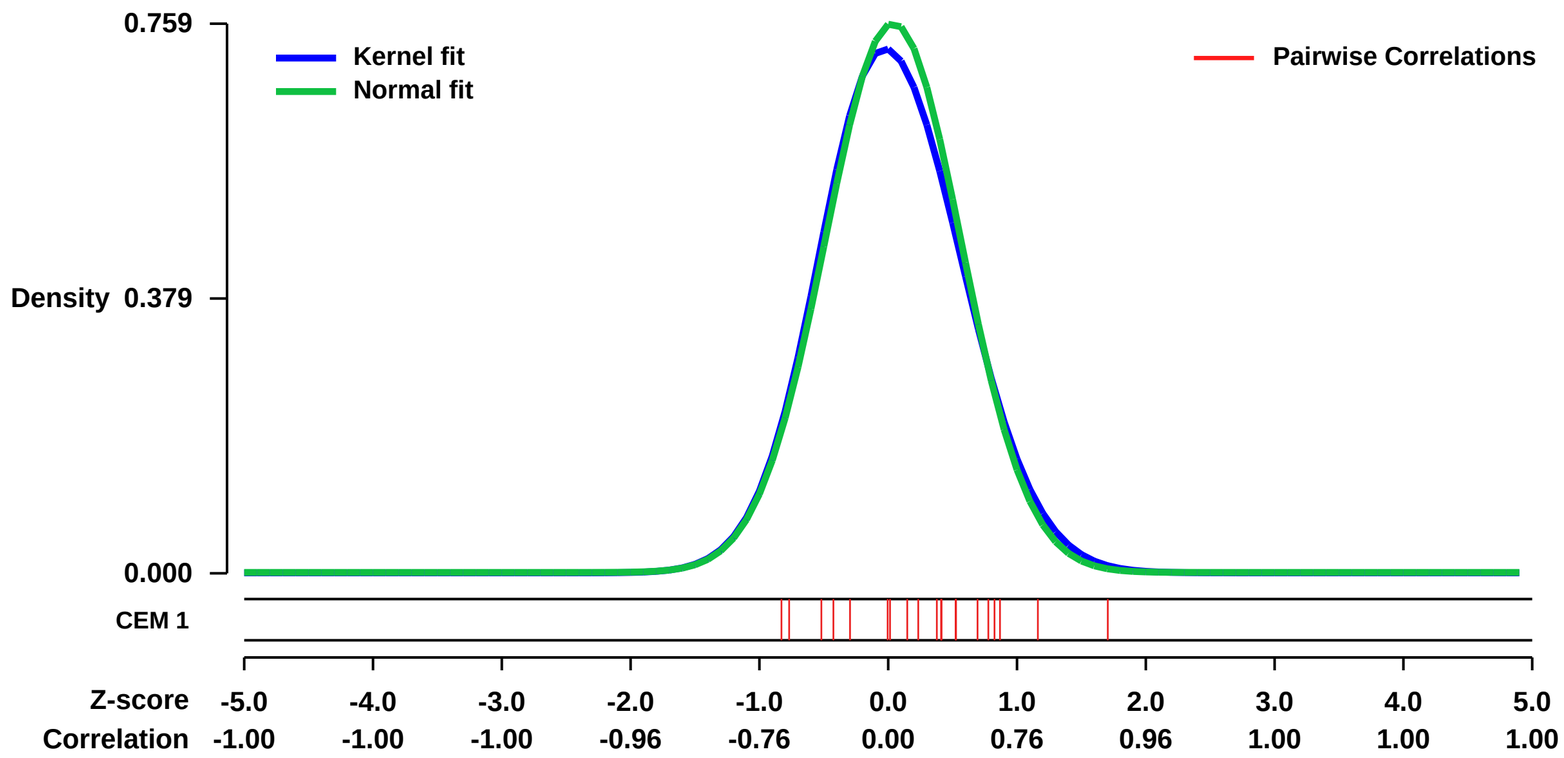

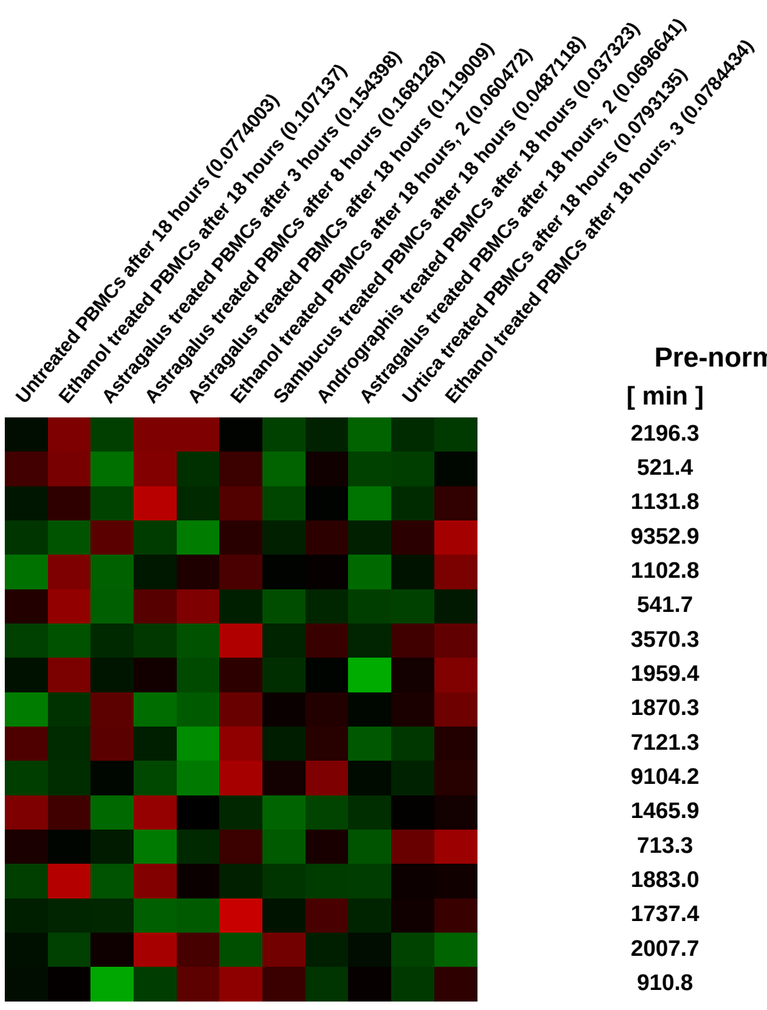

Pre-normalization Quantiles

	[min]	[medium]	[max]
CEM 1			
P (S | Z, I) = 0.00			
Mean Corr = 0.22738			
MANF	2196.3	2714.9	4000.5
SDF2L1	521.4	1231.7	2160.0
CRELD2	1131.8	1783.0	3207.8
HSPA5	9352.9	13353.8	21801.8
HYOU1	1102.8	1564.8	2104.4
PDIA4	541.7	898.0	1895.4
PDIA6	3570.3	4370.5	8226.9
CEM 1 + Top 10 Genes			
DNAJB11	1959.4	2625.3	3146.6
HSP90B1	1870.3	4438.2	6351.2
PDIA3	7121.3	9178.7	12390.2
PPIB	9104.2	12558.4	18134.3
C19orf10	1465.9	2543.1	4069.9
SLC35B1	713.3	1126.5	1700.3
SEC61A1	1883.0	2266.7	3875.7
RPN1	1737.4	1990.2	2897.2
DNAJC3	2007.7	2774.5	4453.7
CDK2AP2	910.8	1321.3	1651.7
Null module			
ARID5B			
XBP1			
HNRNPAB			
SGK1			
HSPB1			
DDIT4			
ARL4D			
SAP30			
KIAA0408			
GPR17			
HSPH1			
DNASE1L2			
SLC5A3			
GNAS			
GPR3			
TNFRSF25			
TM6SF2			
MKKS			
PLEKHF1			
ZMYM1			
DOK3			
FGF20			
SLC39A2			
KCNIP2			
ERRFI1			
DEDD2			
CCDC117			
USP31			
AHSA2			
CYS1			
CNIH2			
BANP			
CHORDC1			
P4HA1			

GEO Series "GSE43552" Expression Profiles

Num of samples in this series: 6

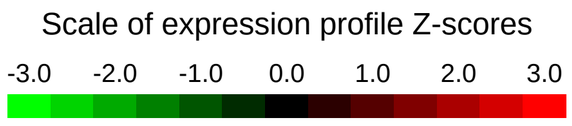

GEO Link:	http://www.ncbi.nlm.nih.gov/geo/query/acc.cgi?acc=GSE43552
Status:	Public on Aug 01 2013
Title:	Expression profiling of human medulloblastoma cell line ONS76 upon siRNA-mediated knockdown of KDM5A/LSD1
Organism:	Homo sapiens
Experiment type:	Expression profiling by array
Platform:	GPL570
Pubmed ID:	24252778
Summary & Design:	**Summary:** KDM5A/LSD1 is an important epigenetic regulator in medulloblastoma, the most frequent brain tumor of childhood. Here, the response of ONS76 medulloblastoma cells upon siRNA-mediated knockdown of KDM5A is analysed. **Overall design:** The expression profile of ONS76 cells upon KDM5A knockdown was compared to mock control. Both conditions were run in triplicate.

Background corr dist: KL-Divergence = 0.0311, L1-Distance = 0.0148, L2-Distance = 0.0002, Normal std = 0.6610

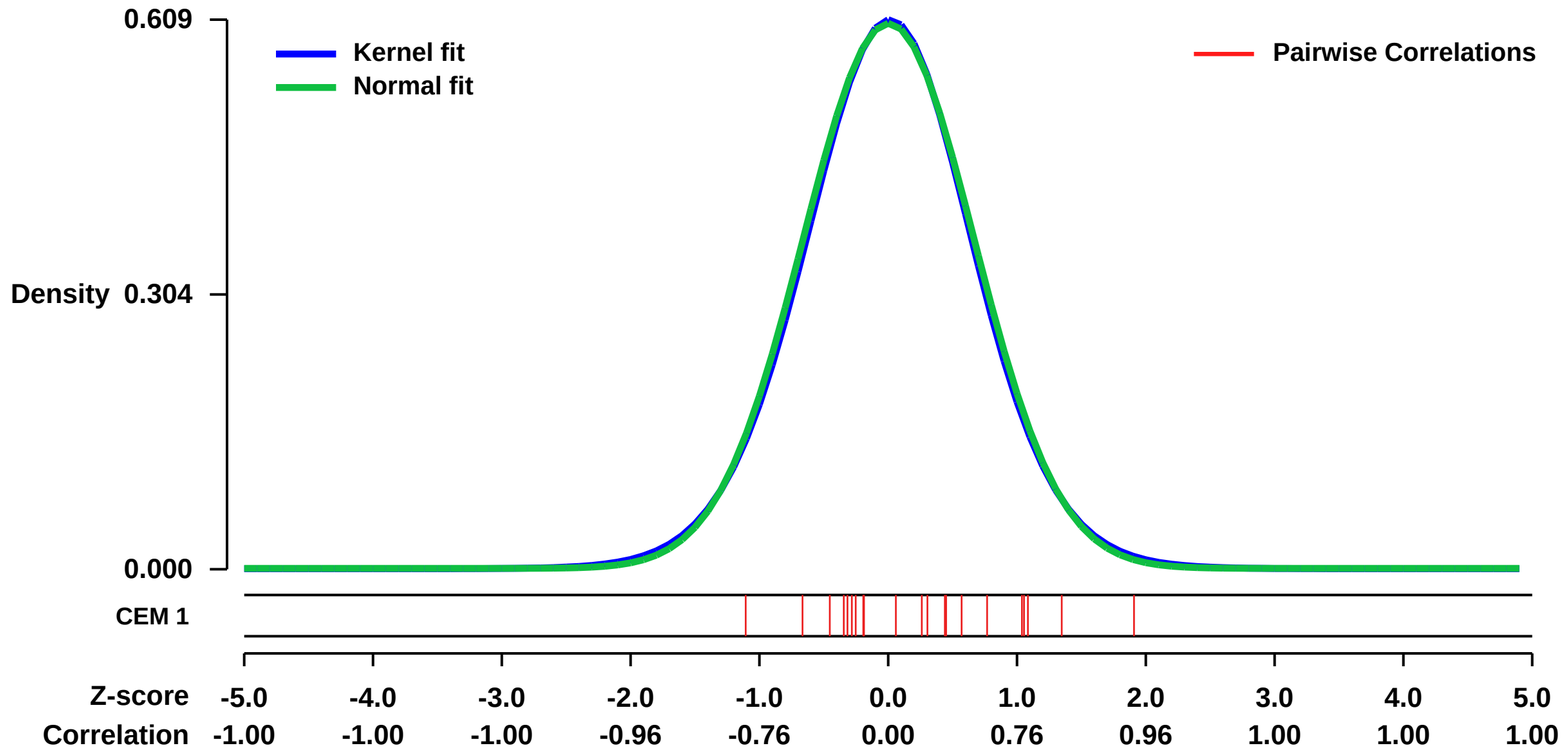

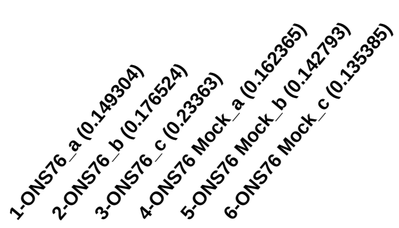

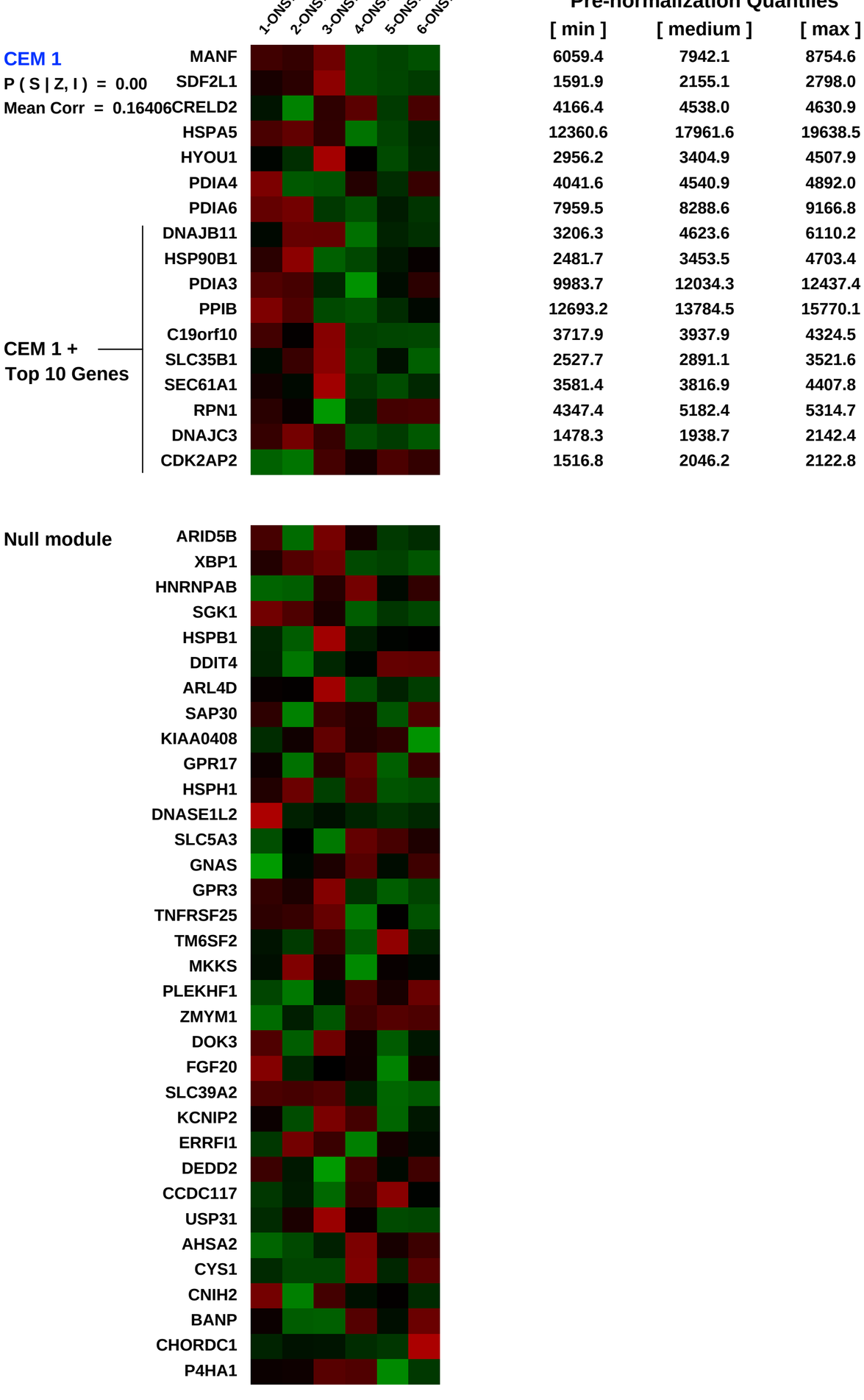

GEO Series "GSE18015" Expression Profiles

Num of samples in this series: 16

Scale of expression profile Z-scores

-3.0 -2.0 -1.0 0.0 1.0 2.0 3.0

GEO Link:	http://www.ncbi.nlm.nih.gov/geo/query/acc.cgi?acc=GSE18015
Status:	Public on Sep 09 2009
Title:	Molecular analysis of ex-vivo CD133+ GBM cells revealed a common invasive and angiogenic profile but different proliferative signatures among high grade gliomas.
Organism:	Homo sapiens
Experiment type:	Expression profiling by array
Platform:	GPL570
Pubmed ID:	20735813
Summary & Design:	**Summary:** **Background: Gliomas are the most common type of primary brain tumours, and in this group glioblastomas (GBMs) are the higher-grade gliomas with fast progression and unfortunate prognosis. Two major aspects of glioma biology that contributes to its awful prognosis are the formation of new blood vessels through the process of angiogenesis and the invasion of glioma cells. Despite of advances, two-year survival for GBM patients with optimal therapy is less than 30%. Even in those patients with low-grade gliomas, that imply a moderately good prognosis, treatment is almost never curative. Recent studies have demonstrated the existence of a small fraction of glioma cells with characteristics of neural stem cells which are able to grow in vitro forming neurospheres and that can be isolated in vivo using surface markers such as CD133. The aim of this study was to define the molecular signature of GBM cells expressing CD133 in comparison with non expressing CD133 cells. This molecular classification could lead to the finding of new potential therapeutic targets for the rationale treatment of high grade GBM.** **Methods: Eight fresh, primaries and non cultured GBMs were used in order to study the gene expression signatures from its CD133 positive and negative populations isolated by FACS-sorting. Dataset was generated with Affymetrix U133 Plus 2 arrays and analysed using the software of the Affymetrix Expression Console. In addition, genomic analysis of these tumours was carried out by CGH arrays, FISH studies and MLPA.** **Results: Gene expression analysis of CD133+ vs. CD133- cell population from each tumour showed that CD133+ cells presented common characteristics in all glioblastoma samples (up-regulation of genes involved in angiogenesis, permeability and down-regulation of genes implicated in cell assembly, neural cell organization and neurological disorders). Furthermore, unsupervised clustering of gene expression led us to distinguish between two groups of samples: those discriminated by tumour location and, the most importantly, the group discriminated by their proliferative potential.** **Conclusions: Primary glioblastomas could be sub-classified according to the properties of their CD133+ cells. The molecular characterization of these potential stem cell populations could be critical to find new therapeutic targets and to develop an effective therapy for these tumours with very dismal prognosis.** **Overall design:** **We studied a dataset generated with Affymetrix U133 Plus 2 arrays (Affymetrix, Santa Clara, CA, USA) in 8 gliomas. The collected cells (CD133+ and CD133- from each tumor) were sorted into separated vials containing RNA Later (Qiagen, Chatsworth, CA, USA), making a total of 16 samples (8 positives and 8 negatives).**

Background corr dist: KL-Divergence = 0.2218, L1-Distance = 0.0789, L2-Distance = 0.0177, Normal std = 0.3318

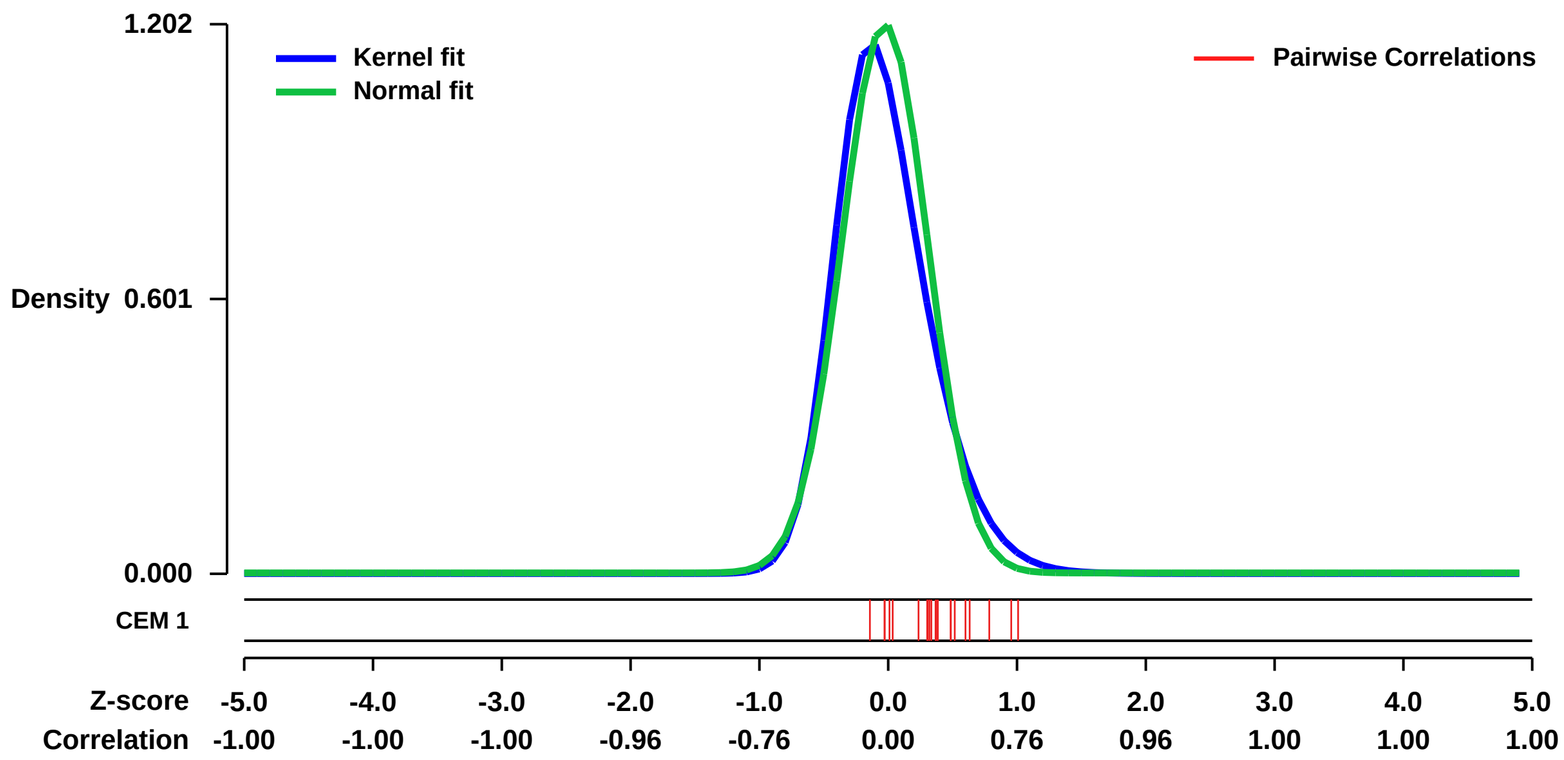

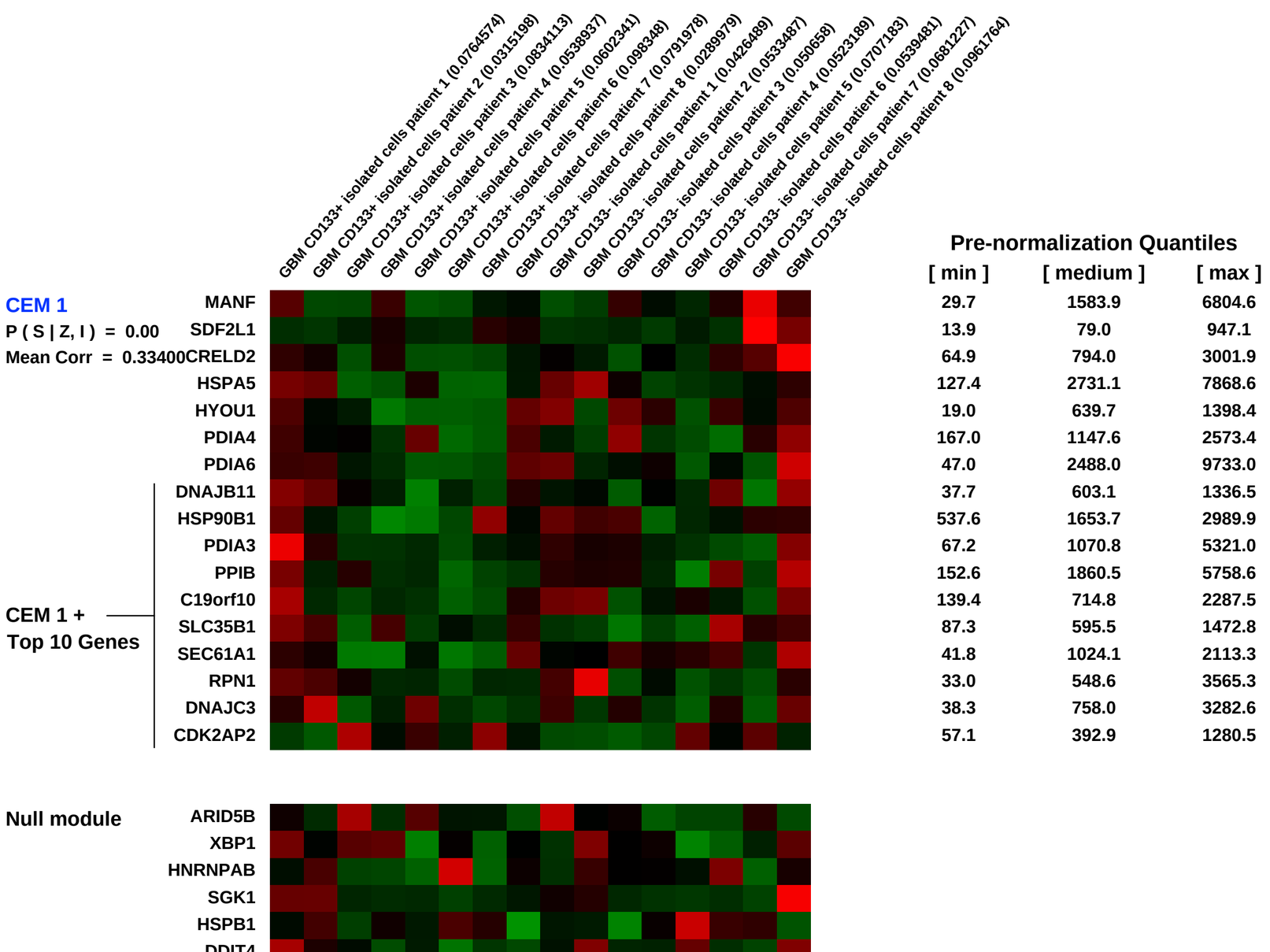

GEO Series "GSE17939" Expression Profiles

Num of samples in this series: 6

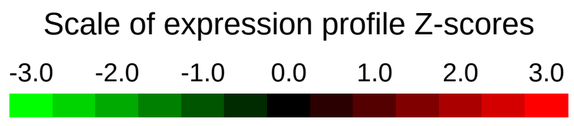

GEO Link:	http://www.ncbi.nlm.nih.gov/geo/query/acc.cgi?acc=GSE17939
Status:	Public on Jun 16 2010
Title:	MEK5D-transfected HUVEC
Organism:	Homo sapiens
Experiment type:	Expression profiling by array
Platform:	GPL570
Pubmed ID:	20551324
Summary & Design:	**Summary:** We expressed a constitutively active mutant of MEK5 (MEK5D) in human primary endothelial cells (EC) to study the transcriptional and functional responses to Erk5 activation under static conditions. **Overall design:** HUVEC were infected with either empty vector or constitutively active MEK5D and RNA was processed for microarray analysis 40 h post infection.

Background corr dist: KL-Divergence = 0.0365, L1-Distance = 0.0331, L2-Distance = 0.0014, Normal std = 0.6505

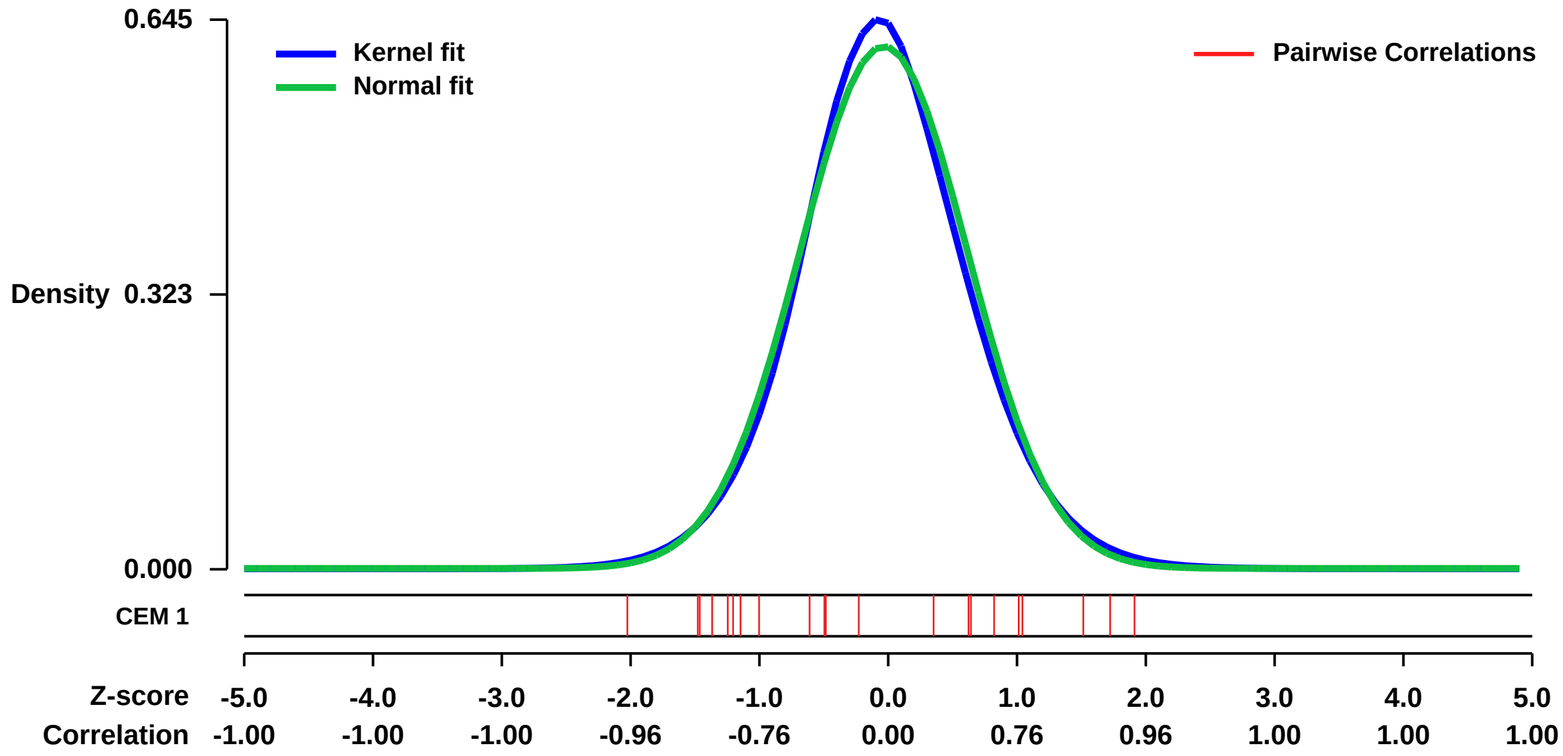

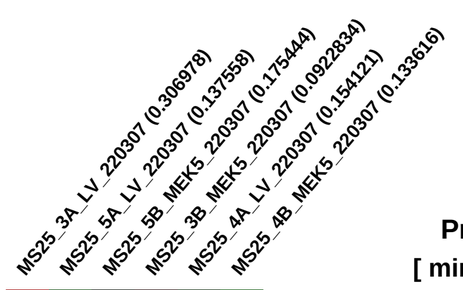

Pre-normalization Quantiles

		[min]	[medium]	[max]
CEM 1	MANF	6411.5	7046.1	8533.9
P (S | Z, I) = 0.00	SDF2L1	400.5	1458.0	1697.4
Mean Corr = -0.09989	CRELD2	4377.3	5104.7	6128.6
	HSPA5	24016.5	26079.3	32108.0
	HYOU1	2451.3	5552.2	5990.6
	PDIA4	1736.8	2358.5	2565.5
	PDIA6	10515.8	11904.8	19310.0
CEM 1 + Top 10 Genes	DNAJB11	4422.3	5121.1	7082.0
	HSP90B1	9841.4	11272.7	14579.6
	PDIA3	15606.2	17208.3	21630.7
	PPIB	16631.8	18221.7	25773.1
	C19orf10	5822.8	6481.5	6841.7
	SLC35B1	1830.5	2972.6	3056.2
	SEC61A1	1356.7	5492.2	5635.3
	RPN1	3699.7	4432.1	5246.9
	DNAJC3	3326.4	4141.4	4466.7
	CDK2AP2	557.2	1986.8	2312.5
Null module	ARID5B			
	XBP1			
	HNRNPAB			
	SGK1			
	HSPB1			
	DDIT4			
	ARL4D			
	SAP30			
	KIAA0408			
	GPR17			
	HSPH1			
	DNASE1L2			
	SLC5A3			
	GNAS			
	GPR3			
	TNFRSF25			
	TM6SF2			
	MKKS			
	PLEKHF1			
	ZMYM1			
	DOK3			
	FGF20			
	SLC39A2			
	KCNIP2			
	ERRFI1			
	DEDD2			
	CCDC117			
	USP31			
	AHSA2			
	CYS1			
	CNIH2			
	BANP			
	CHORDC1			
	P4HA1			

GEO Series "GSE57194" Expression Profiles

Num of samples in this series: 30

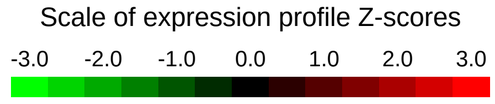

GEO Link:	http://www.ncbi.nlm.nih.gov/geo/query/acc.cgi?acc=GSE57194
Status:	Public on May 01 2014
Title:	In Vitro Transformation of Primary Human CD34+ Cells by AML Fusion Oncogenes: Early Gene Expression Profiling Reveals Possible Drug Target in AML
Organism:	Homo sapiens
Experiment type:	Expression profiling by array
Platform:	GPL570
Pubmed ID:	20805992
Summary & Design:	**Summary:** Different fusion oncogenes in acute myeloid leukemia (AML) have distinct clinical and laboratory features suggesting different modes of malignant transformation. Here we compare the in vitro effects of representatives of major groups of AML fusion oncogenes on primary human CD34+ cells. **Overall design:** For the 3 d and 8 d time points, the oncogenes were retrovirally expressed in primary human CD34+ cells, with cells transduced with empty retroviral vector as controls. As retroviral transduction requires days, for the 6 h time point the oncogenes were expressed from a pTracer-CMV/Bsd plasmid using nucleofection. Cells nucleofected with empty pTracer-CMV/Bsd vector were used as a control.

Background corr dist: KL-Divergence = 0.0998, L1-Distance = 0.0318, L2-Distance = 0.0021, Normal std = 0.4365

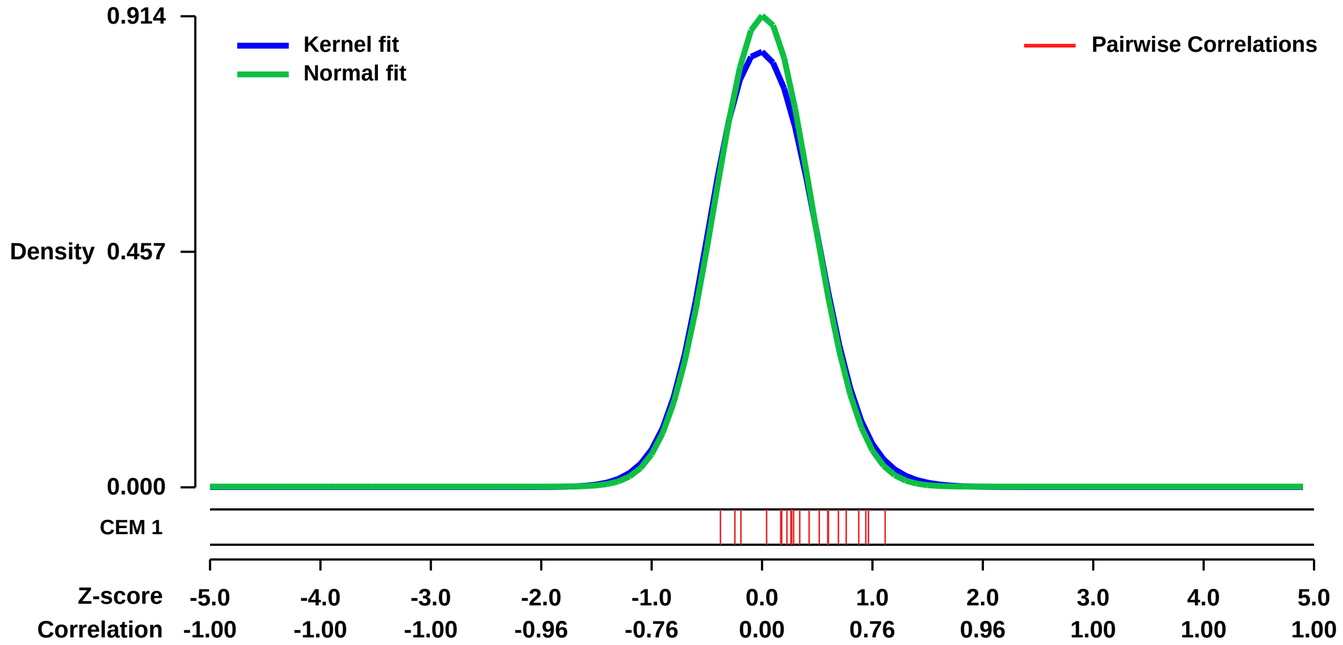

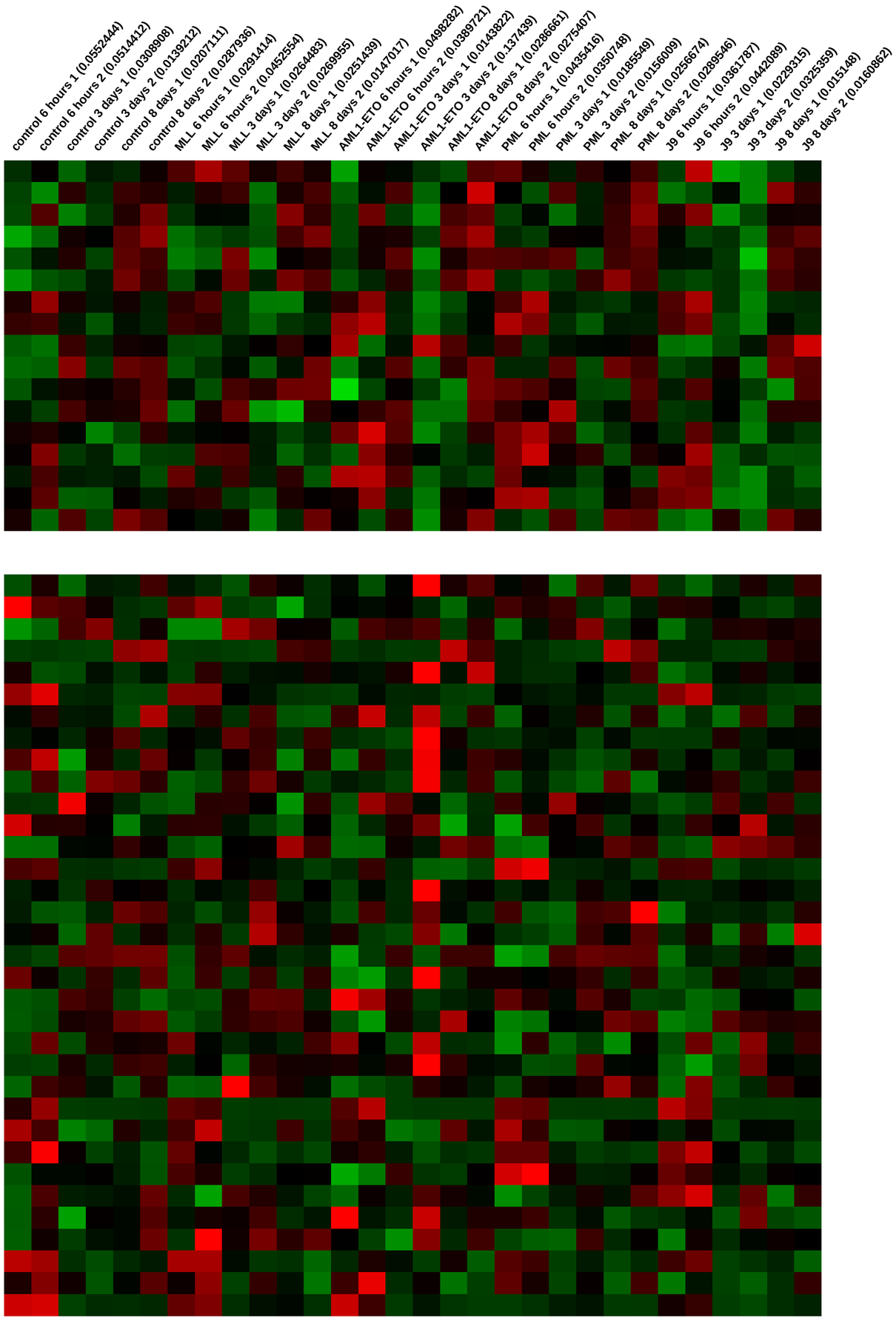

GEO Series "GSE26525" Expression Profiles

Num of samples in this series: 15

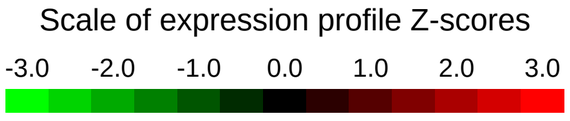

GEO Link:	http://www.ncbi.nlm.nih.gov/geo/query/acc.cgi?acc=GSE26525
Status:	Public on Jan 11 2011
Title:	Expression data analyzed with LPIA in A549 lung carcinoma cells treated with geldanamycin.
Organism:	Homo sapiens
Experiment type:	Expression profiling by array
Platform:	GPL570
Pubmed ID:	21788508
Summary & Design:	**Summary:** The statsitcal model, latent pathway identification analysis (LPIA), was implemented for the analysis of A549 lung carcinoma cells treated with geldanamycin. Control and treated samples were assayed with Affymetrix HG_U133_plus_2 arrays and analyzed using LPIA. LPIA looks for statistically signï‹ cant evidence of dysregulation in a network of pathways constructed in a manner that explicitly links pathways through their common function in the cell. Geldanamycin (geld) is known to inhibit the molecular chaperone protein, Hsp90, and plays a role in preventing the malignant transformation and proliferation of healthy cells during oncogenesis. LPIA successfully identified pathways specific to geldanamycin effects at the gene transcription level. **Overall design:** A549 lung carcinoma cells were allowed to adhere for 24h and further incubated in the presence of geldanamycin at a concentration equivalent to the determined IC50 of 40 nM or IC20 of 10 nM, or with vehicle DMSO (final concentration 0.4%). After 24h and 48 h, cells were harvested and total RNA was purified and processed for Affymetrix HG_U133_Plus_2.0 microarray analysis. Raw probe intensities were RMA-normalized and avereaged for three replicates for each condition. Probe sets for 54,120-annotated open reading frames were included in LPIA analysis.

Background corr dist: KL-Divergence = 0.0782, L1-Distance = 0.0217, L2-Distance = 0.0005, Normal std = 0.4781

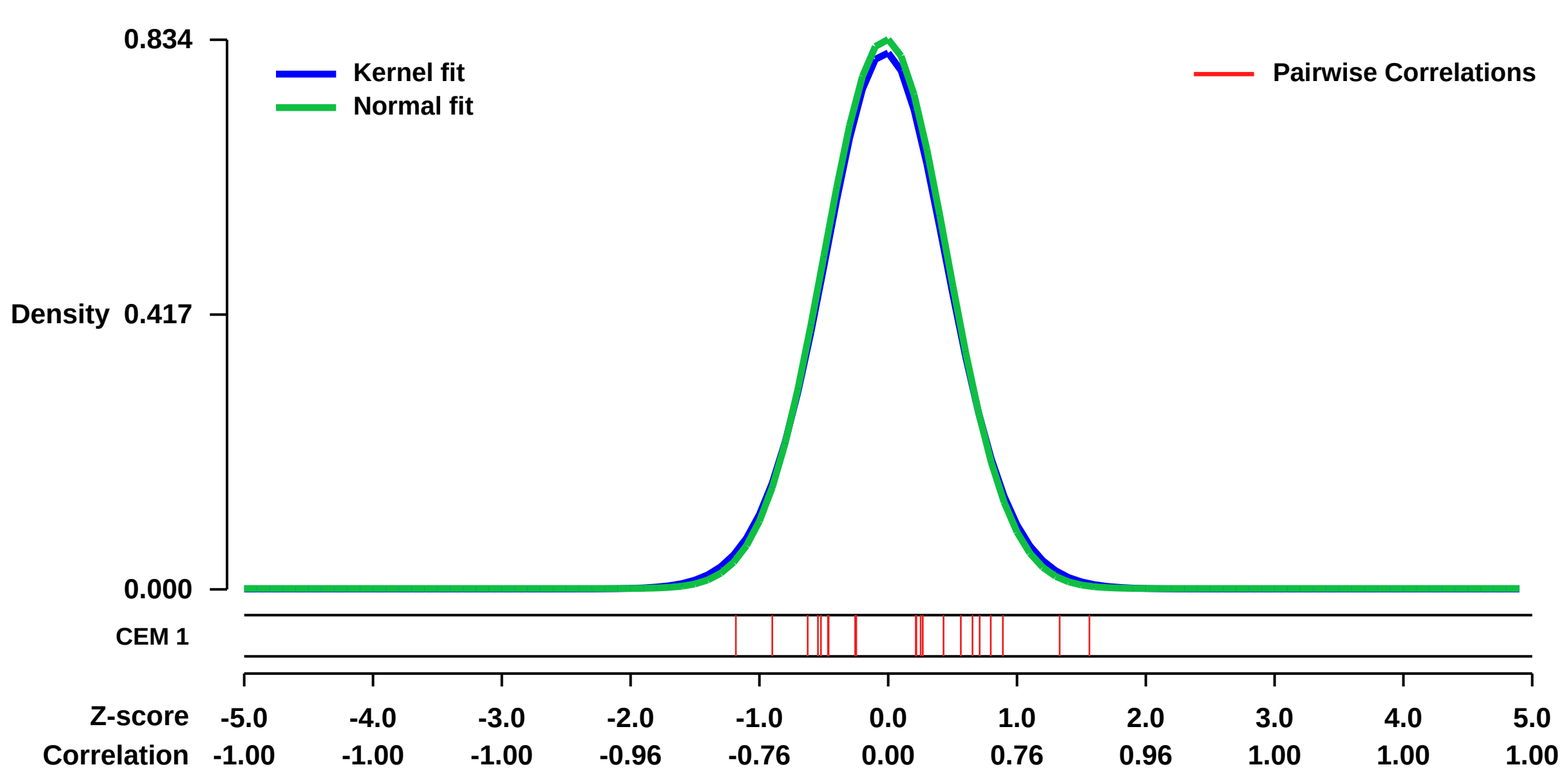

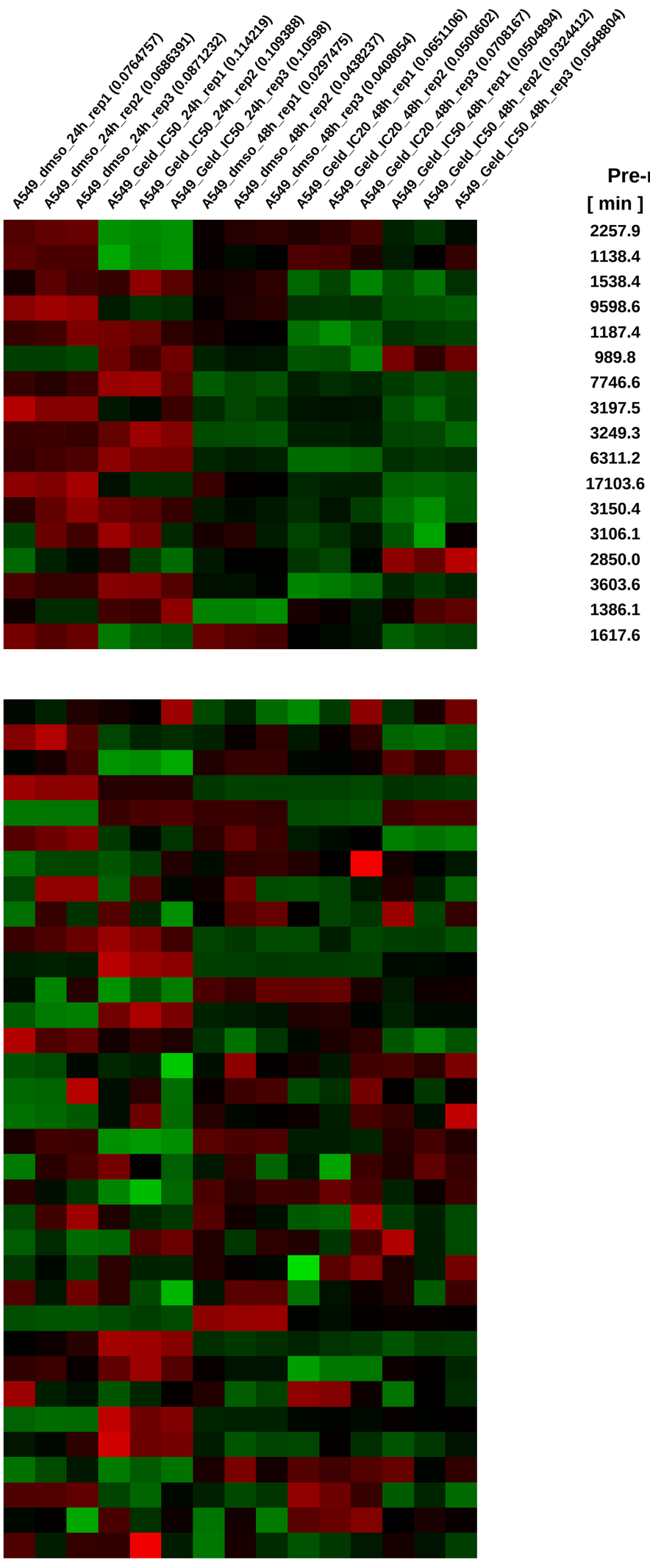

GEO Series "GSE4737" Expression Profiles

Num of samples in this series: 8

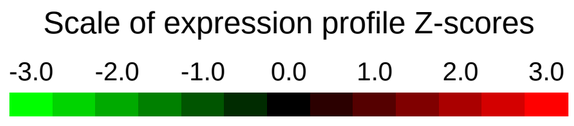

GEO Link:	http://www.ncbi.nlm.nih.gov/geo/query/acc.cgi?acc=GSE4737
Status:	Public on Oct 27 2006
Title:	HCaRG vs NEO
Organism:	Homo sapiens
Experiment type:	Expression profiling by array
Platform:	GPL570
Pubmed ID:	16033922
Summary & Design:	Summary: Summary: HEK293 cells were transfected with control plasmid (pcDNA1/Neo; Invitrogen) or with the plasmid encoding HCaRG by a standard calcium phosphate co-precipitation method. The clones expressing the highest levels of HCaRG, HCaRG clone 8 and 9 were used in this experiment, while clone transfected with vector alone, Neo clone, served as control. Stable transfectants were synchronized and grown in the presence of 10% FBS for 48 h. Total RNAs were purified with the mini RNeasy kit (Qiagen). Keywords: parallel sample Overall design: - Normalization: Employing GCOS software, chips were normalized using all probe sets scaling option and target signal at 500.

Background corr dist: KL-Divergence = 0.0495, L1-Distance = 0.0339, L2-Distance = 0.0015, Normal std = 0.5809

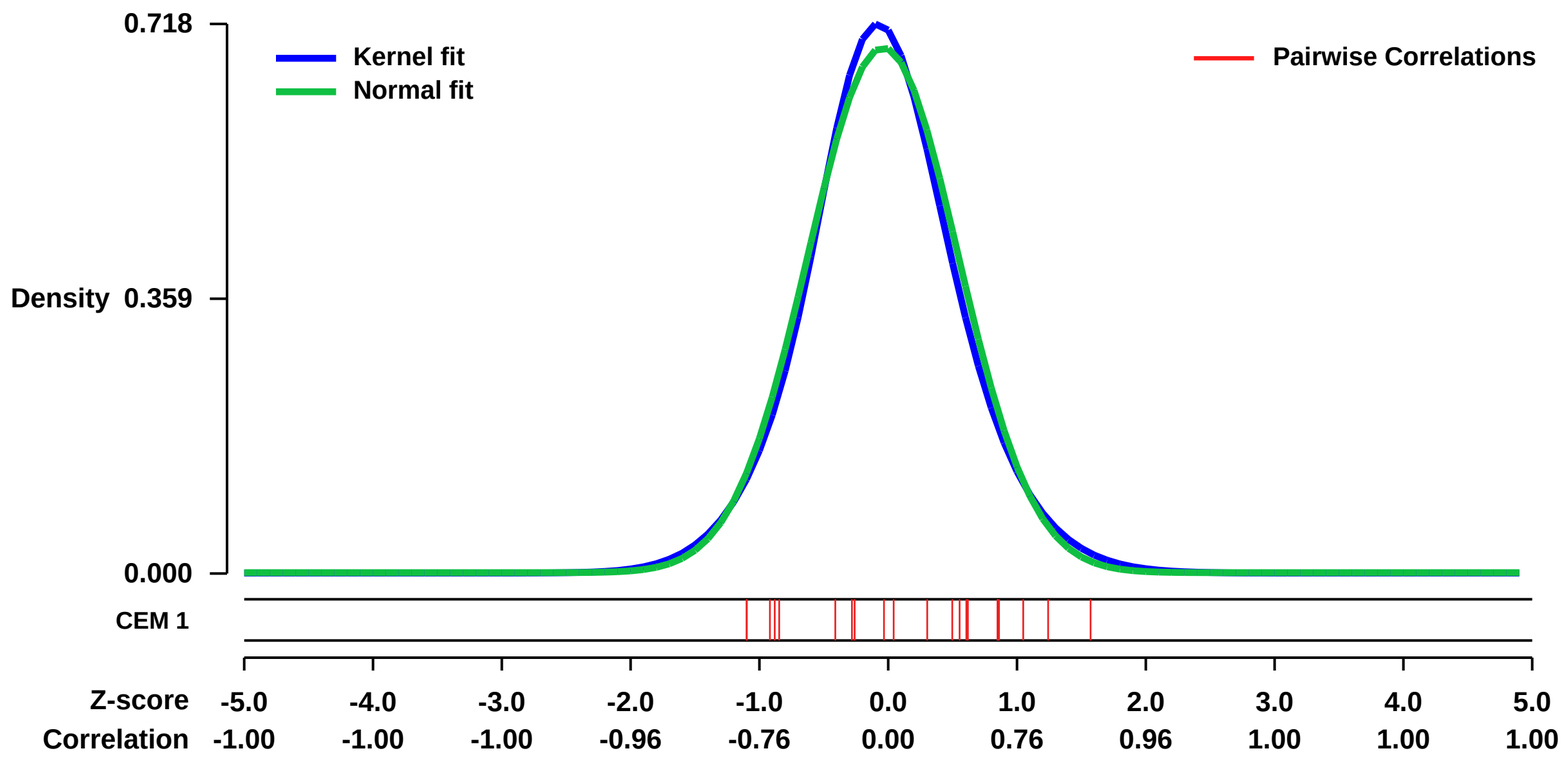

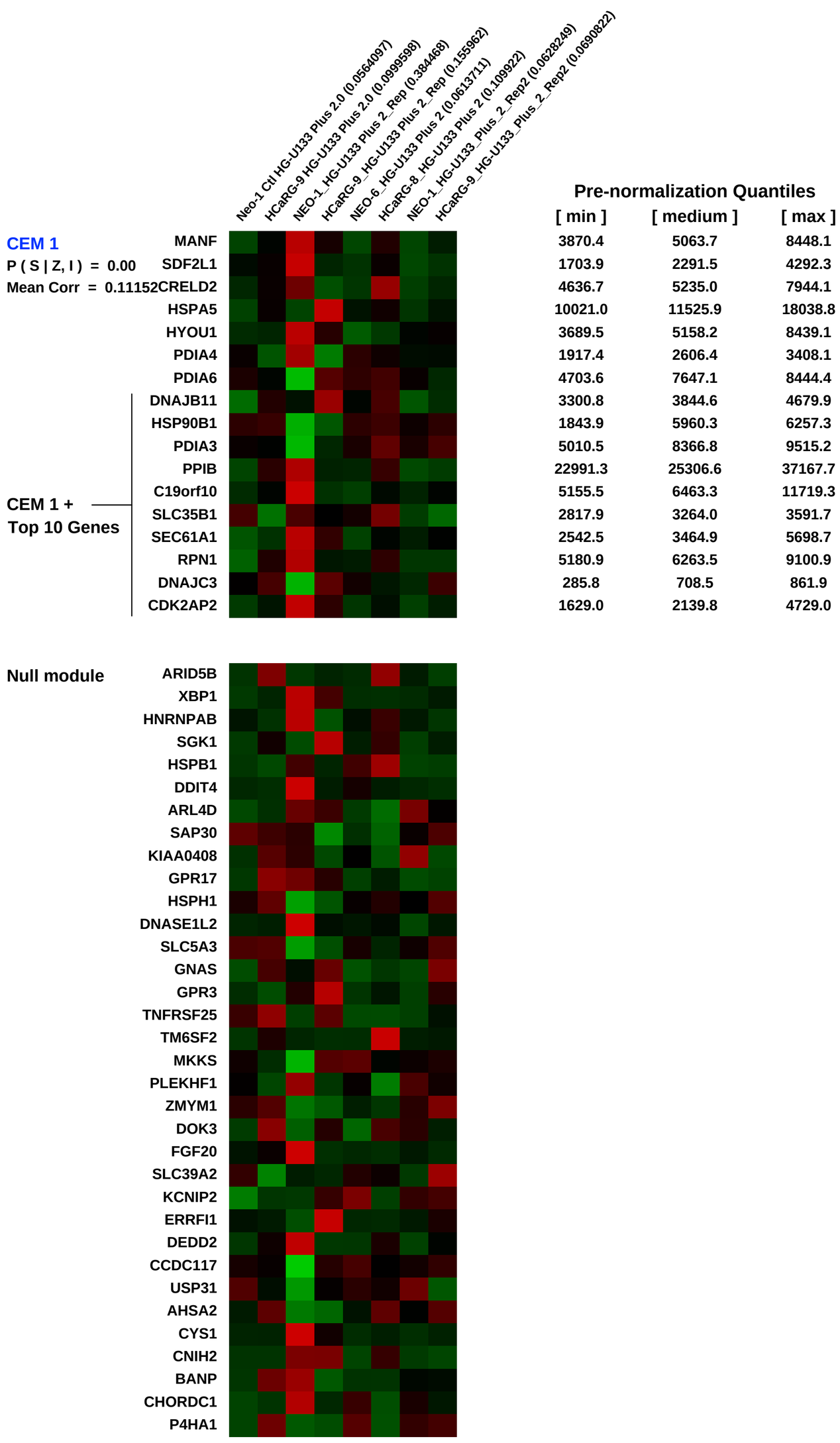

GEO Series "GSE12320" Expression Profiles

Num of samples in this series: 9

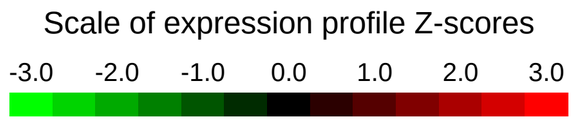

GEO Link:	http://www.ncbi.nlm.nih.gov/geo/query/acc.cgi?acc=GSE12320
Status:	Public on May 31 2009
Title:	Differential gene expression in GBS6 cells after EWS-POU5F1 knockdown
Organism:	Homo sapiens
Experiment type:	Expression profiling by array
Platform:	GPL570
Pubmed ID:	20203285
Summary & Design:	**Summary:** **Our objective is to clarify the function of EWS-POU5F1 chimera.** **Specifially, GBS6 cells were established from an undifferentiated bone sarcoma carrying translocation t(6;22)(p21;q12). The translocation resulted in a gene fusion between EWS and POU5F1. Gene expression analysis of t(6;22) undifferentiated sarcoma cell line GBS6 transfected with POU5F1 specific siRNA to investigate the function of EWS-POU5F1.** **Overall design:** **Knockdown of EWS-POU5F1 using POU5F1 specific siRNAs. 3 control and 6 experimental replicates representing the same experiment repeated 3 times (1st, 2nd, 3rd).**

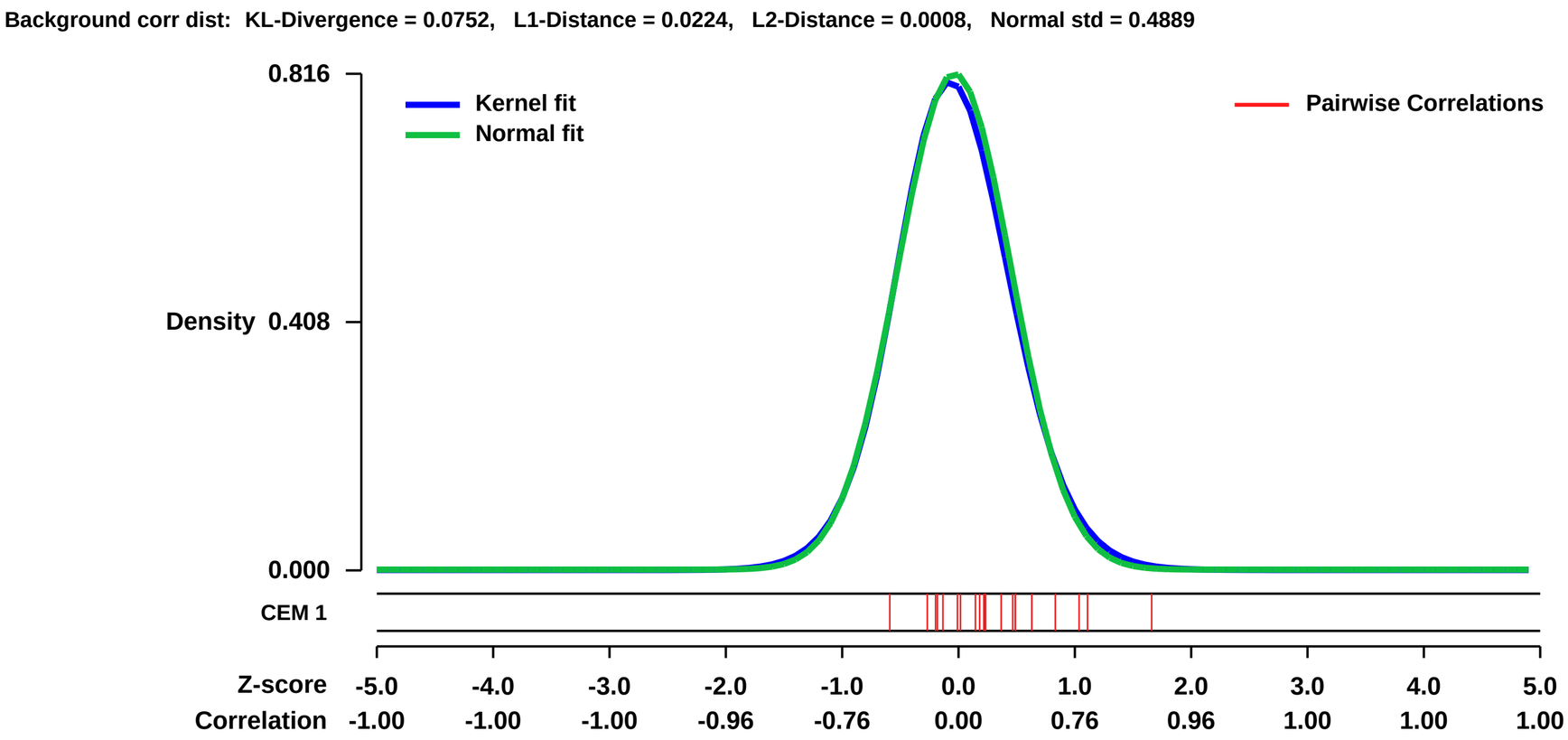

Pre-normalization Quantiles

	[min]	[medium]	[max]
MANF	3880.3	4317.1	5884.6
SDF2L1	638.2	1203.3	1588.6
CRELD2	2097.9	3093.7	4222.7
HSPA5	12733.7	18174.4	22447.7
HYOU1	2303.1	3192.8	3607.7
PDIA4	692.8	893.0	1009.4
PDIA6	10485.3	13657.7	16644.1
DNAJB11	1639.1	2815.8	5294.2
HSP90B1	571.4	2835.9	7757.6
PDIA3	13378.2	15389.6	17688.4
PPIB	21935.7	26318.9	30708.9
C19orf10	3316.7	3700.7	4859.8
SLC35B1	2278.5	2768.1	3411.6
SEC61A1	5240.3	5577.9	6262.3
RPN1	4704.6	7589.2	8767.9
DNAJC3	208.9	419.5	716.3
CDK2AP2	867.4	1280.4	1564.2

GEO Series "GSE20433" Expression Profiles

Num of samples in this series: 14

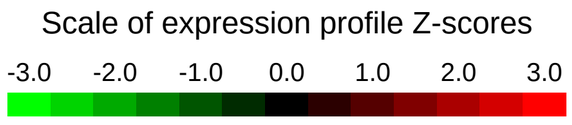

GEO Link:	http://www.ncbi.nlm.nih.gov/geo/query/acc.cgi?acc=GSE20433
Status:	Public on Nov 02 2010
Title:	Effects of T350 phospho- on gene repression activity of EZH2
Organism:	Homo sapiens
Experiment type:	Expression profiling by array
Platform:	GPL570
Pubmed ID:	20935635
Summary & Design:	**Summary:** The Polycomb group (PcG) protein enhancer of zeste homolog 2 (EZH2) plays an essential role in histone methylation-mediated epigenetic gene silencing. We demonstrate that under physiological conditions, cyclin-dependent kinase 1 (CDK1) and 2 (CDK2) bind to and phosphorylate EZH2 at threonine 350 (T350) in an evolutionally conserved motif. T350 phosphorylation is required for EZH2 function in silencing of genes that promote differentiation and inhibit proliferation and migration. Blockage of T350 phosphorylation by generating a T350A mutation largely diminishes the global effect of EZH2 on gene silencing. **Overall design:** Seven experiments have been designed. LNCaP cells were transfected with si-Control, si-EZH2, si-EZH2 plus RNAi resistant EZH2 plasmid, or si-EZH2 plus RNAi resistant T350A mutated EZH2 plsamid for 60 hours, or treated with DMSO, 5 uM TSA, or 10 uM Roscovitine for 24 hours. Two replicates per experiment.

Background corr dist: KL-Divergence = 0.0859, L1-Distance = 0.0728, L2-Distance = 0.0088, Normal std = 0.5319

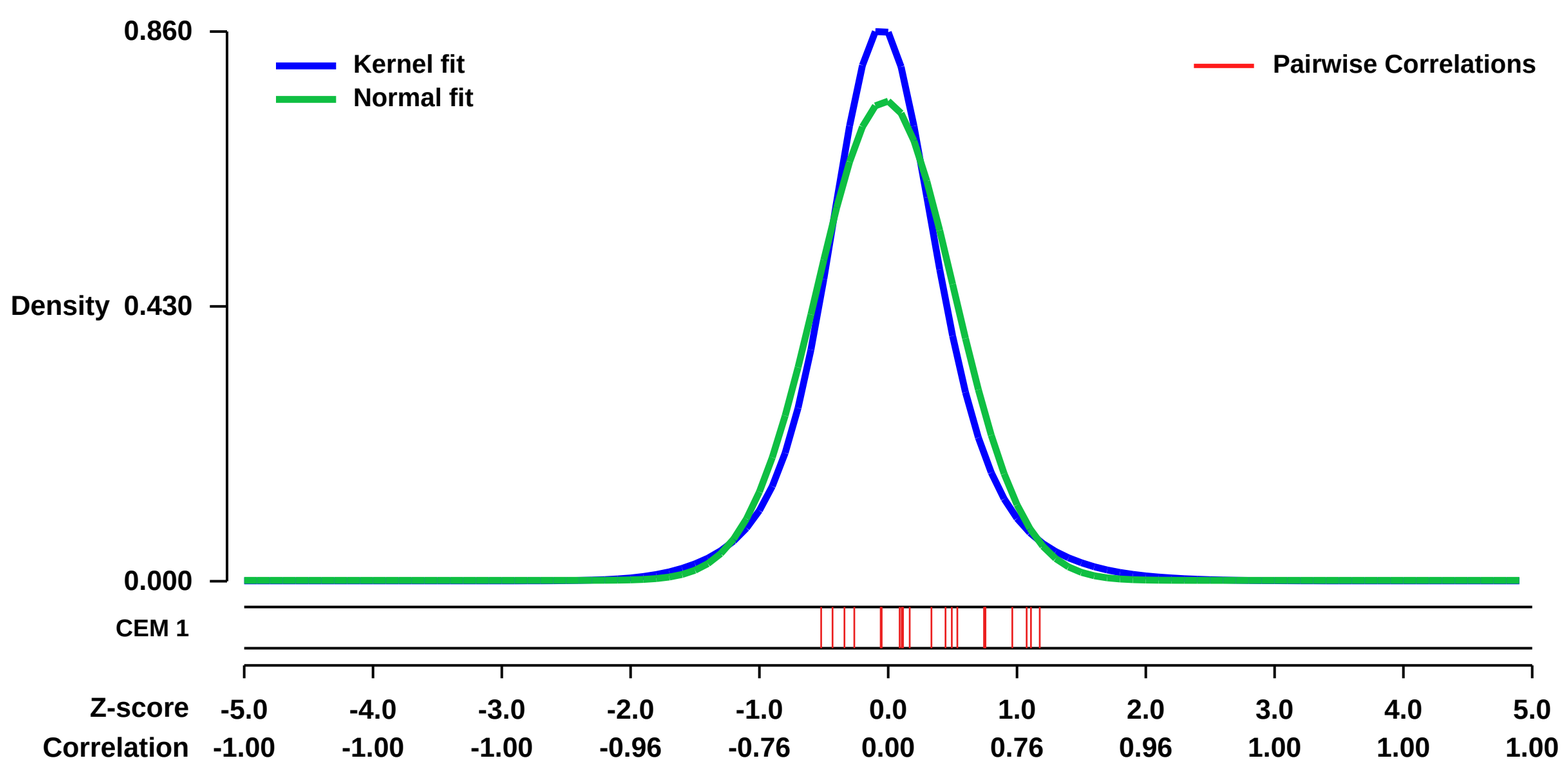

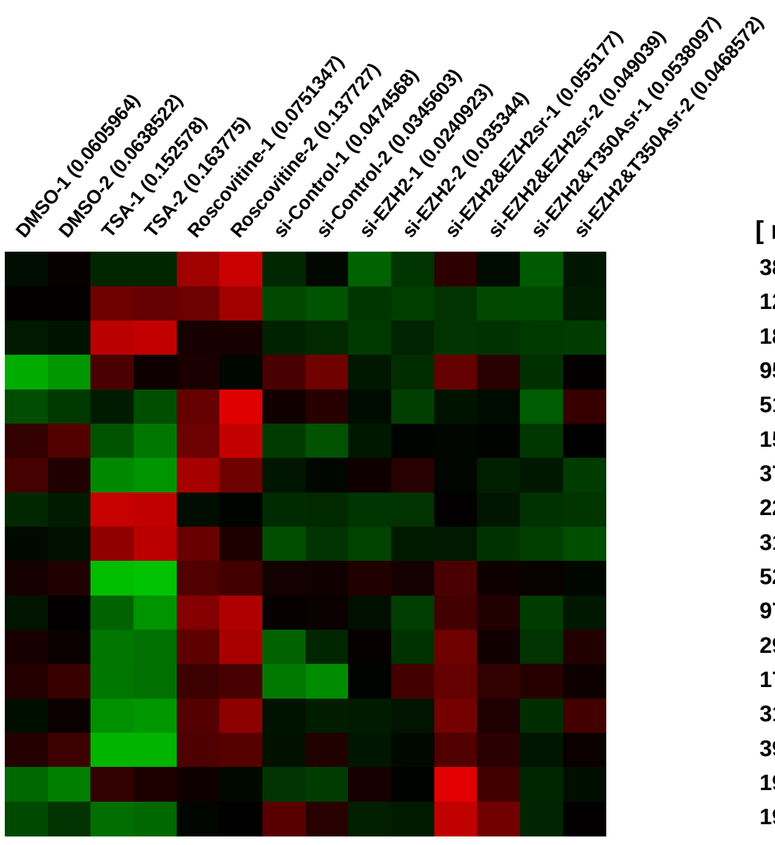

	Pre-normalization Quantiles [min]	[medium]	[max]
MANF	3809.4	4313.0	5561.2
SDF2L1	1275.0	1700.4	3148.1
CRELD2	1859.4	2187.3	5030.4
HSPA5	9570.6	10852.7	11524.7
HYOU1	5168.9	5713.9	7302.0
PDIA4	1500.1	1934.6	2672.7
PDIA6	3775.7	5079.2	6634.6
DNAJB11	2286.3	2554.4	4867.3
HSP90B1	3103.1	3399.2	4583.5
PDIA3	5264.8	7956.5	8713.8
PPIB	9765.5	10838.1	12067.8
C19orf10	2924.1	3482.8	4167.0
SLC35B1	1771.1	2477.4	2728.2
SEC61A1	3169.2	4086.9	5116.1
RPN1	3919.0	5268.1	5605.1
DNAJC3	1900.7	2290.2	3006.2
CDK2AP2	1901.7	2292.9	3024.8
ARID5B			
XBP1			
HNRNPAB			
SGK1			
HSPB1			
DDIT4			
ARL4D			
SAP30			
KIAA0408			
GPR17			
HSPH1			
DNASE1L2			
SLC5A3			
GNAS			
GPR3			
TNFRSF25			
TM6SF2			
MKKS			
PLEKHF1			
ZMYM1			
DOK3			
FGF20			
SLC39A2			
KCNIP2			
ERRFI1			
DEDD2			
CCDC117			
USP31			
AHSA2			
CYS1			
CNIH2			
BANP			
CHORDC1			
P4HA1			

GEO Series "GSE16356" Expression Profiles

Num of samples in this series: 6

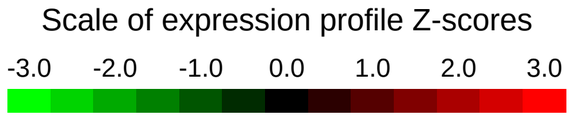

GEO Link:	http://www.ncbi.nlm.nih.gov/geo/query/acc.cgi?acc=GSE16356
Status:	Public on Sep 30 2009
Title:	Lymphatic endothelial cells (LEC) treated with a MAF-targeted siRNA
Organism:	Homo sapiens
Experiment type:	Expression profiling by array
Platform:	GPL570
Pubmed ID:	20080955
Summary & Design:	**Summary:** Kaposi sarcoma is the most common cancer in AIDS patients and is typified by red skin lesions. The disease is caused by the KSHV virus (HHV8) and is recognisable by its distinctive red skin lesions. The lesions are KSHV-infected spindle cells, most commonly the lymphatic endothelial and blood vessel endothelial cells (LEC and BEC), plus surrounding stroma. The KSHV virus expresses multiple MAF-downregulating microRNA. Here we test the effects of MAF silencing by siRNA in LEC cells using Affymetrix hgu133plus2 chips. **Overall design:** There are n=3 of 1. LEC control cells transfected with a non-targeting siRNA, 2. LEC transfected with a MAF-targeting siRNA

Background corr dist: KL-Divergence = 0.0371, L1-Distance = 0.0150, L2-Distance = 0.0002, Normal std = 0.6273

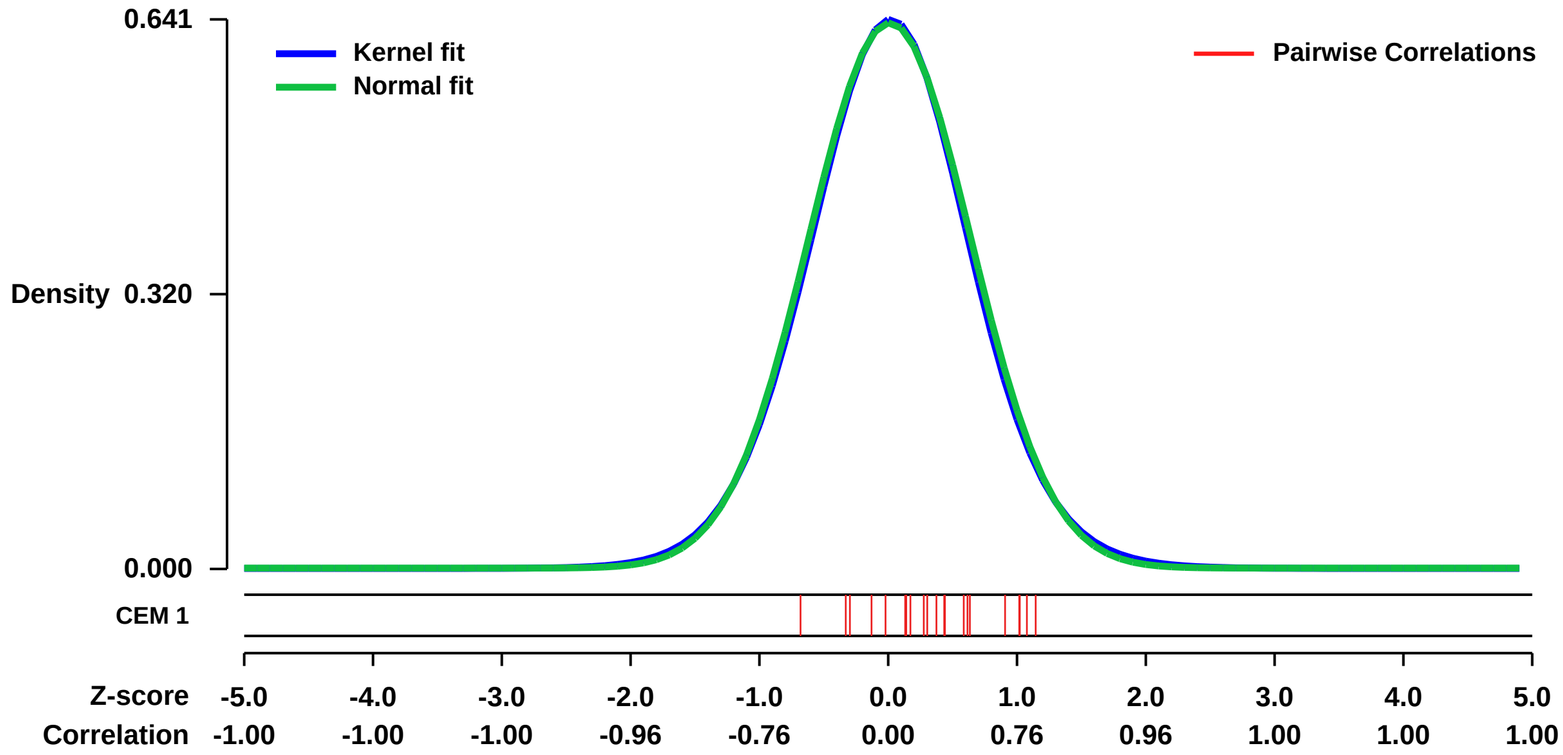

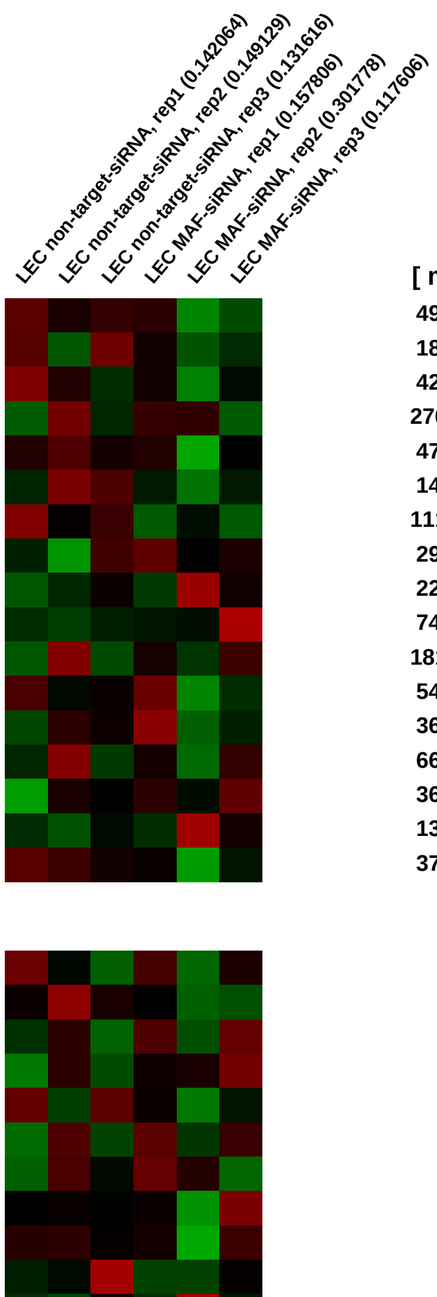

Pre-normalization Quantiles

		[min]	[medium]	[max]
CEM 1	MANF	4960.1	5978.4	6259.9
P (S | Z, I) = 0.00	SDF2L1	1858.8	2101.2	2311.4
Mean Corr = 0.30191	CRELD2	4207.5	4935.3	5474.7
	HSPA5	27614.9	29867.7	30955.8
	HYOU1	4718.0	5533.3	5716.7
	PDIA4	1413.1	1763.3	2344.5
	PDIA6	11128.2	11736.4	12562.1
CEM 1 + Top 10 Genes	DNAJB11	2969.0	3409.9	3578.1
	HSP90B1	2281.4	3226.8	4642.0
	PDIA3	7458.7	7967.6	10448.9
	PPIB	18190.7	21720.7	25265.0
	C19orf10	5446.2	6156.6	6619.3
	SLC35B1	3695.6	4156.6	4685.3
	SEC61A1	6655.5	7885.6	8976.5
	RPN1	3632.2	4135.0	4335.2
	DNAJC3	1307.1	1765.9	2839.5
	CDK2AP2	3740.1	4881.4	5331.1
Null module	ARID5B			
	XBP1			
	HNRNPAB			
	SGK1			
	HSPB1			
	DDIT4			
	ARL4D			
	SAP30			
	KIAA0408			
	GPR17			
	HSPH1			
	DNASE1L2			
	SLC5A3			
	GNAS			
	GPR3			
	TNFRSF25			
	TM6SF2			
	MKKS			
	PLEKHF1			
	ZMYM1			
	DOK3			
	FGF20			
	SLC39A2			
	KCNIP2			
	ERRFI1			
	DEDD2			
	CCDC117			
	USP31			
	AHSA2			
	CYS1			
	CNIH2			
	BANP			
	CHORDC1			
	P4HA1			

GEO Series "GSE60123" Expression Profiles

Num of samples in this series: 6

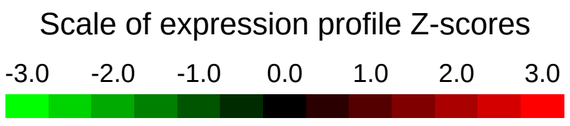

GEO Link:	**http://www.ncbi.nlm.nih.gov/geo/query/acc.cgi?acc=GSE60123**
Status:	**Public on Sep 01 2014**
Title:	**Examination of gene expression in response to ING2 knockdown by siRNA in human breast cancer cells**
Organism:	**Homo sapiens**
Experiment type:	**Expression profiling by array**
Platform:	**GPL570**
Pubmed ID:	
Summary & Design:	**Summary:** **The Sin3/HDAC multi-protein complex consists of at least 17 subunits and is known to have roles in diverse biological and cellular processes including transcription, chromatin structure, and the cell cycle. ING2 is a non-catalytic component of this complex. To obtain a better mechanistic understanding of the Sin3/HDAC complex in cancer, we extended its protein-protein interaction network and identified a mutually exclusive pair within the complex. Suberoylanilide hydroxamic acid (SAHA) is an FDA approved HDAC inhibitor used for the treatment of cutaneous T-cell lymphoma. We assessed the effects of SAHA on the disruption of the complex network through six homologous baits. SAHA perturbs multiple protein interactions and therefore compromises the composition of large parts of the Sin3/HDAC network. A comparison of the effect of SAHA treatment on gene expression in breast cancer cells to a knockdown of the ING2 subunit indicated that a portion of the anticancer effects of SAHA may be attributed to the disruption of ING2â s association with the complex.** **Overall design:** **ING2 siRNA knockdowns in human breast cancer cell line MDA-MB-231 were compared to a non-targeting control in triplicate, for a total of 6 samples.**
Background corr dist:	**KL-Divergence = 0.0190, L1-Distance = 0.0492, L2-Distance = 0.0037, Normal std = 0.7938**

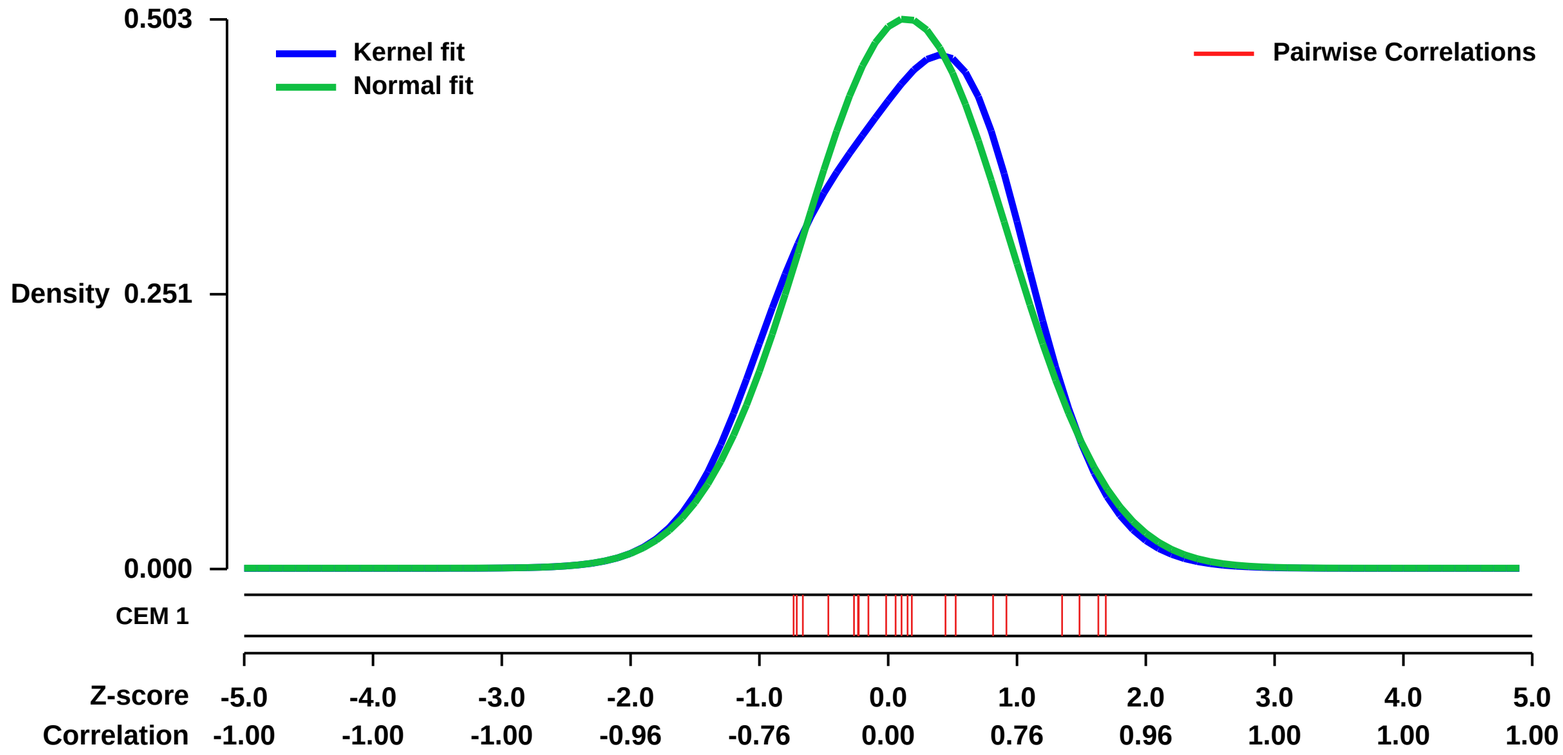

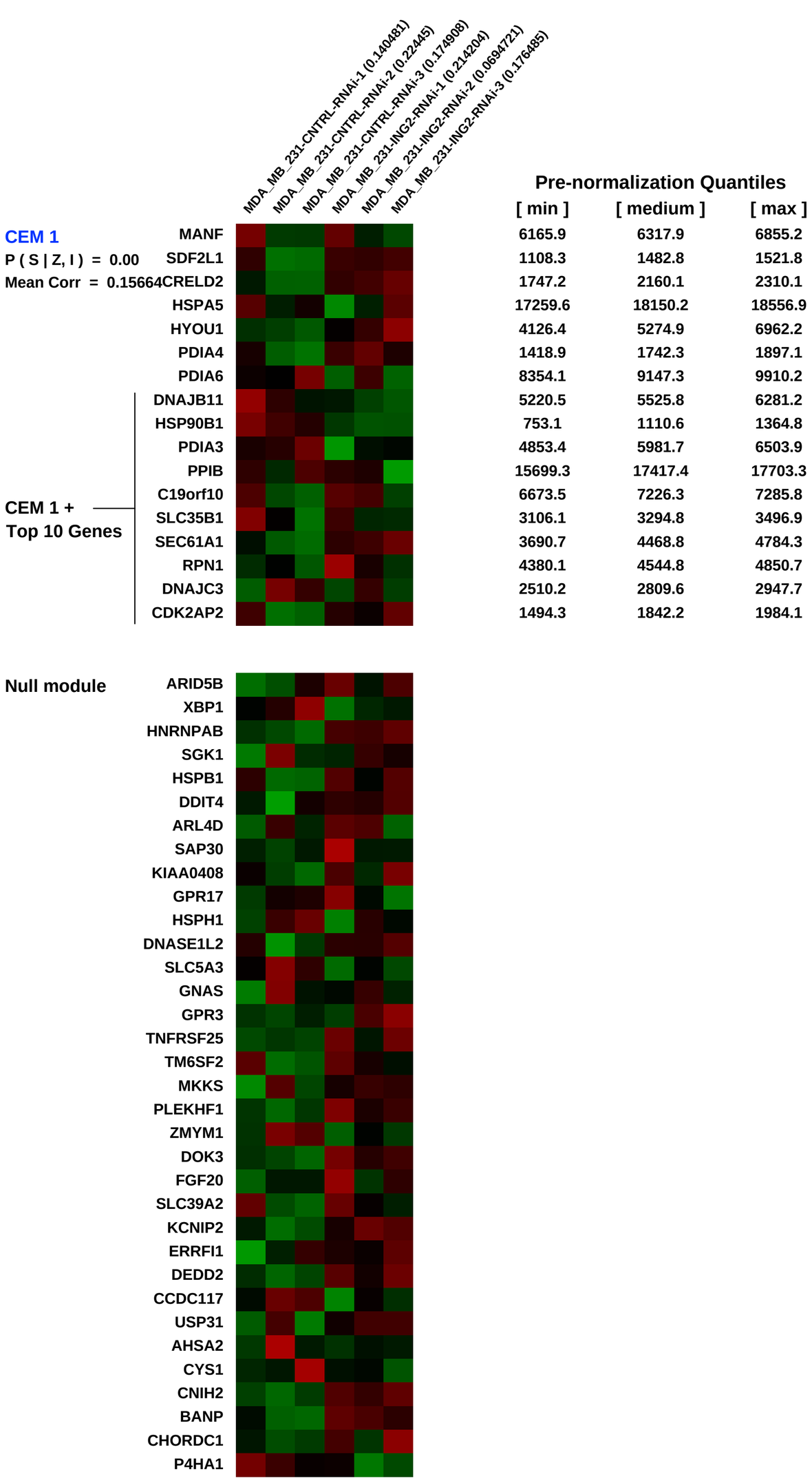

Pre-normalization Quantiles

	[min]	[medium]	[max]
MANF	6165.9	6317.9	6855.2
SDF2L1	1108.3	1482.8	1521.8
CRELD2	1747.2	2160.1	2310.1
HSPA5	17259.6	18150.2	18556.9
HYOU1	4126.4	5274.9	6962.2
PDIA4	1418.9	1742.3	1897.1
PDIA6	8354.1	9147.3	9910.2
DNAJB11	5220.5	5525.8	6281.2
HSP90B1	753.1	1110.6	1364.8
PDIA3	4853.4	5981.7	6503.9
PPIB	15699.3	17417.4	17703.3
C19orf10	6673.5	7226.3	7285.8
SLC35B1	3106.1	3294.8	3496.9
SEC61A1	3690.7	4468.8	4784.3
RPN1	4380.1	4544.8	4850.7
DNAJC3	2510.2	2809.6	2947.7
CDK2AP2	1494.3	1842.2	1984.1

GEO Series "GSE32727" Expression Profiles

Num of samples in this series: 12

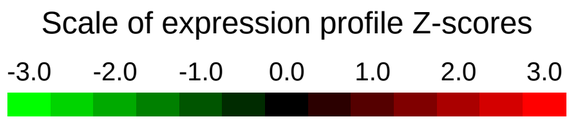

GEO Link:	http://www.ncbi.nlm.nih.gov/geo/query/acc.cgi?acc=GSE32727
Status:	Public on Jul 24 2012
Title:	EMT inducers catalyze malignant transformation of mammary epithelial cells and drive tumorigenesis towards claudin-low tumors [human]
Organism:	Homo sapiens
Experiment type:	Expression profiling by array
Platform:	GPL570
Pubmed ID:	22654675
Summary & Design:	**Summary:** The newly identified claudin-low subtype of cancer is believed to represent the most primitive breast malignancies, having arisen from transformation of an early epithelial precursor with inherent stemness properties and metaplastic features. Challenging this hypothesis, we show both in vitro and in vivo that transcription factors inducing epithelial-mesenchymal transition can drive the development of claudin-low tumors from differentiated mammary epithelial cells, by playing a dual role in cell transformation and dedifferentiation. **Overall design:** Human mammary epithelial cells (HMEC) were sequentially immortalized by hTert (HMEC-hTert), transduced with Twist1 or Zeb2 or Zeb1 and then with H-RasG12V. The gene expression profiles of the resulting HMEC-hTert-Twist1+Ras, HMEC-hTert-Zeb1+Ras and HMEC-hTert-Zeb2+Ras cell lines were defined. HMEC-hTert-Twist1+Ras and HMEC-hTert-Zeb2+Ras cell lines were additionally cultured in presence of TGFˆ ? and their gene expression profiles were determined. The parental HMEC-hTert, the luminal MCF7 and the basal B MDMB157cell lines were used as controls.

Background corr dist: KL-Divergence = 0.0662, L1-Distance = 0.0276, L2-Distance = 0.0013, Normal std = 0.5221

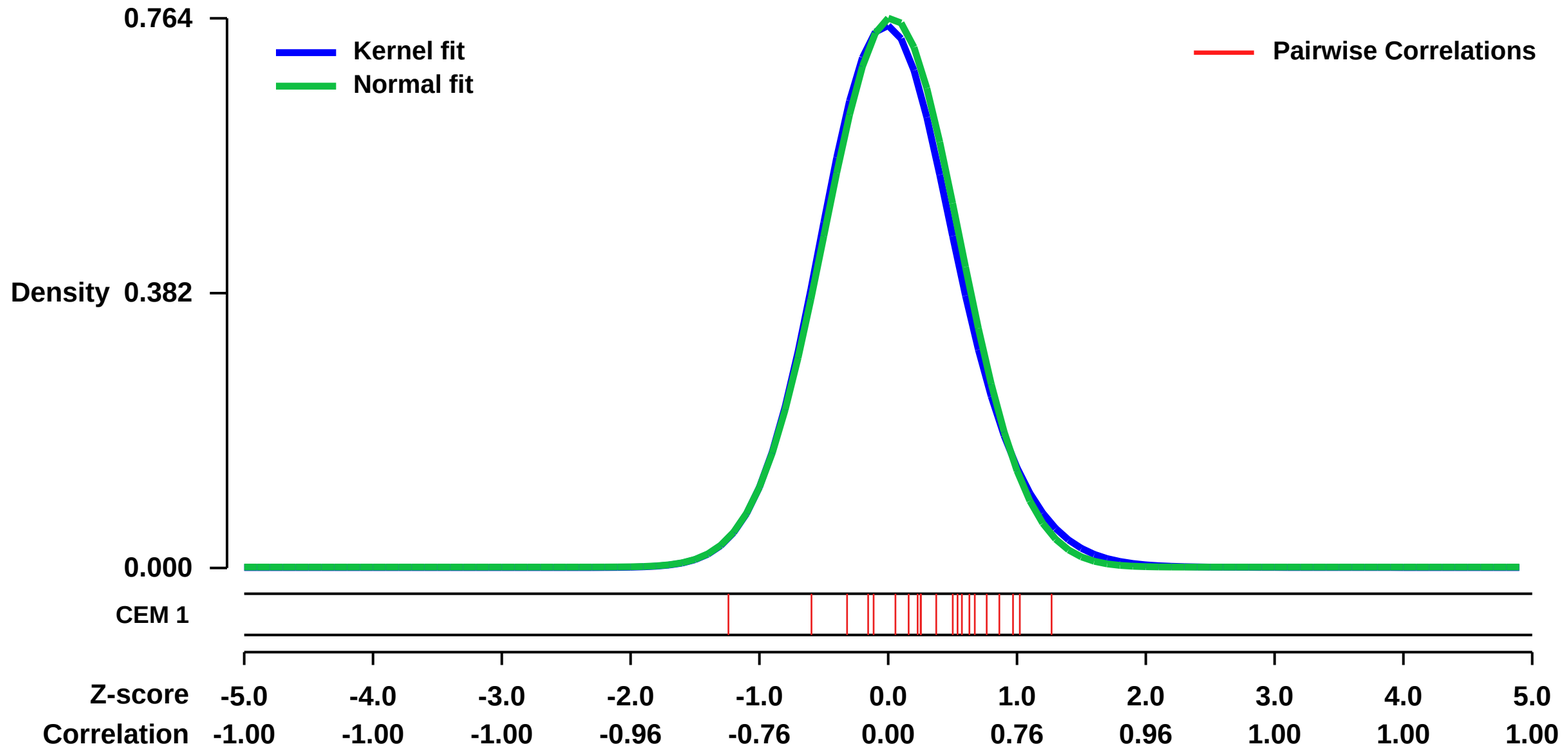

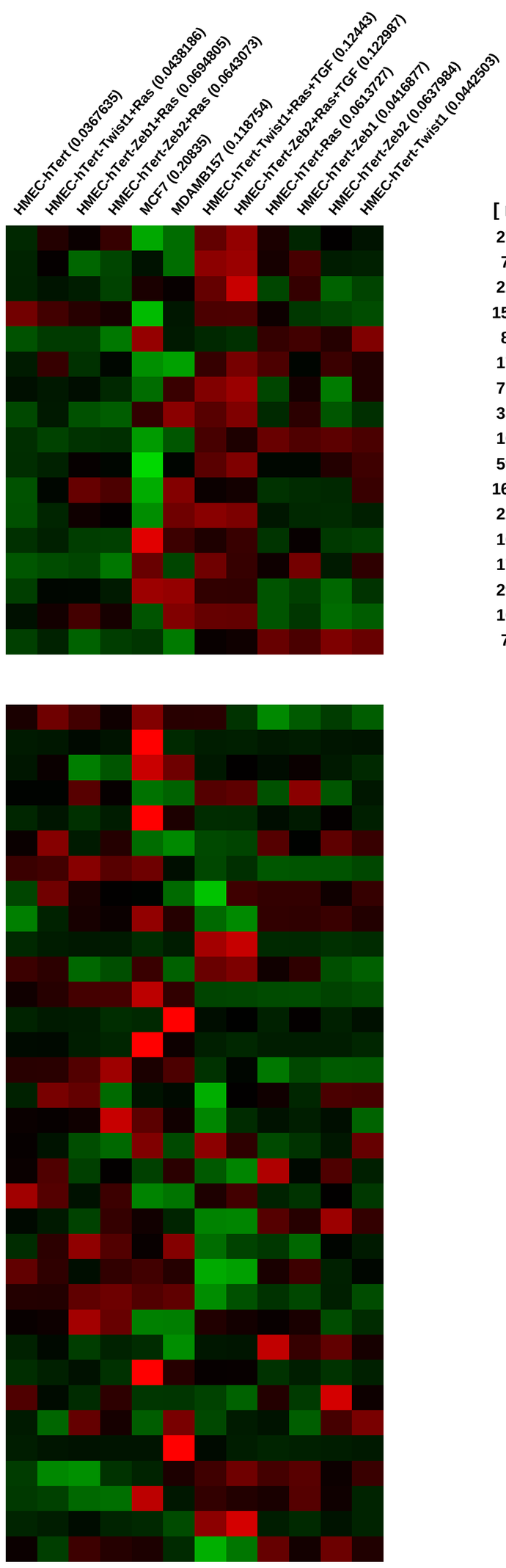

GEO Series "GSE9973" Expression Profiles

Num of samples in this series: 9

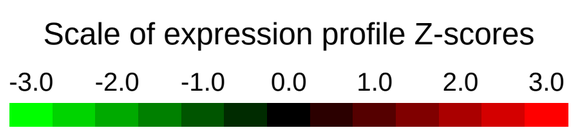

GEO Link:	**http://www.ncbi.nlm.nih.gov/geo/query/acc.cgi?acc=GSE9973**
Status:	**Public on Sep 30 2009**
Title:	**Half-life determination for human B-cells (BL41)**
Organism:	**Homo sapiens**
Experiment type:	**Expression profiling by array**
Platform:	**GPL570**
Pubmed ID:	**19561200**
Summary & Design:	**Summary:** **RNA was labeled in BL41 cells by culturing cells for 60 min in media containing 100´µM 4sU. Tc-RNA was separated into nt- and p-RNA. All three RNA subsets were subjected to microarray analysis. Only probe sets providing present calls in all RNA samples/subsets were included into the analysis** **We used microarrays to determine half-lives of mRNAs expressed in BL41 cells** **Keywords: Determination of mRNA half-life in human B-cells** **Overall design:** **RNA was labeled in BL41 cells by culturing cells for 60 min in media containing 100´µM 4sU. Tc-RNA was separated into nt- and p-RNA. All three RNA subsets were subjected to microarray analysis.**

Background corr dist: **KL-Divergence = 0.0679, L1-Distance = 0.0847, L2-Distance = 0.0104, Normal std = 0.7716**

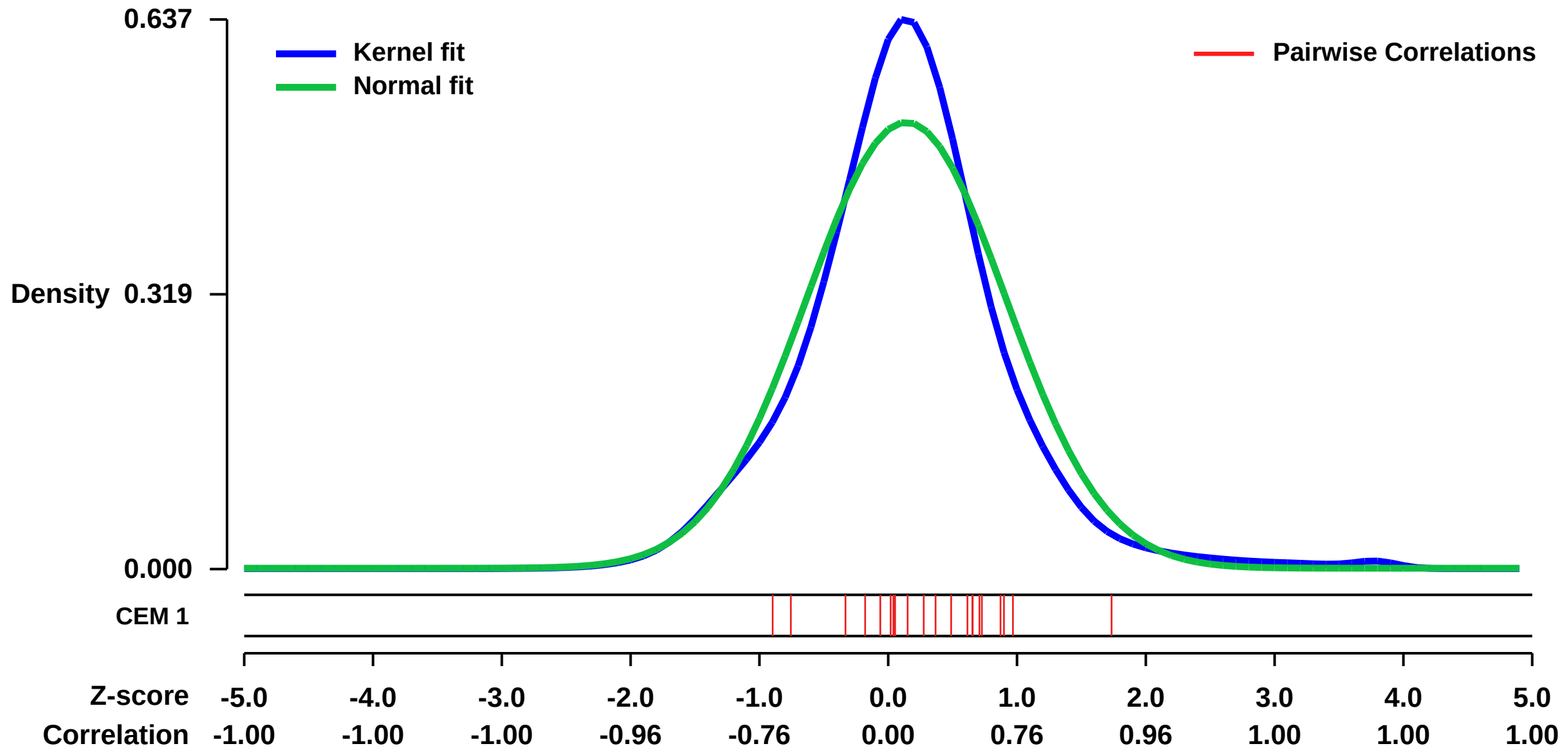

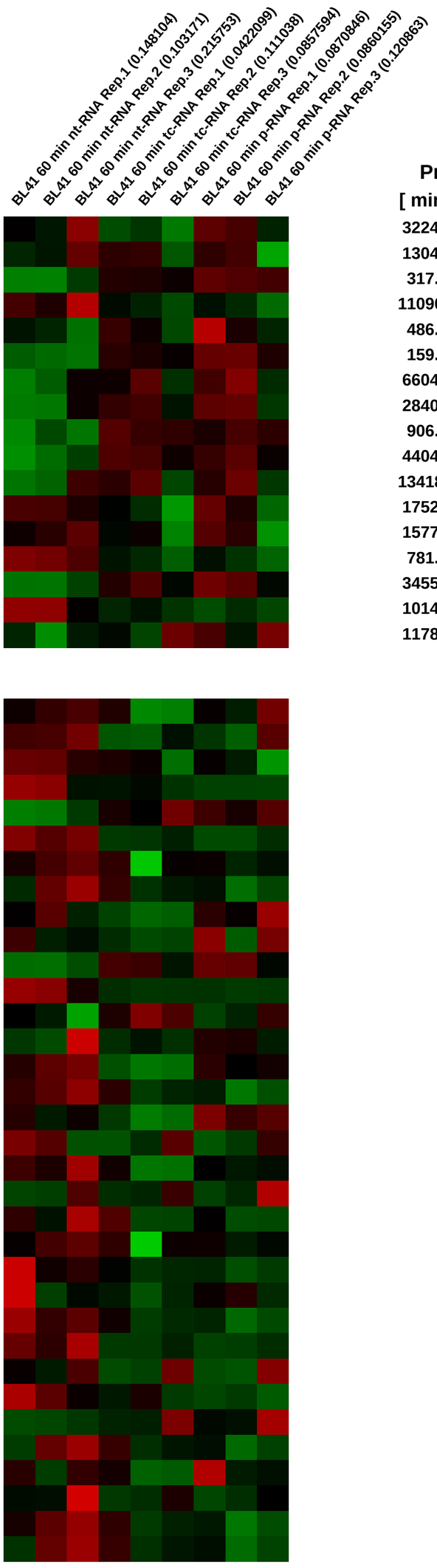

GEO Series "GSE15205" Expression Profiles

Num of samples in this series: 12

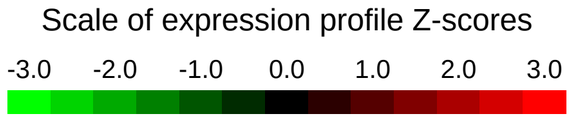

GEO Link:	http://www.ncbi.nlm.nih.gov/geo/query/acc.cgi?acc=GSE15205
Status:	Public on Mar 11 2010
Title:	TGF or TNF Time series in ARPE19
Organism:	Homo sapiens
Experiment type:	Expression profiling by array
Platform:	GPL570
Pubmed ID:	
Summary & Design:	**Summary:** Aberrant epithelial-mesenchymal transition (EMT) is involved in[a] pathological processes including fibrotic disorders and cancer invasion and metastasis. Alterations of the cell-extracellular matrix[a] (ECM) interaction also contribute to those pathological settings.[a] However, the functional interplay between EMT and cell-ECM[a] interaction is poorly understood. Here, we show that tumor necrosis factor (TNF)-¿–, a potent mediator of inflammation, induces[a] EMT-associated fibrosis in retinal pigment epithelial cells, and that this is regulated by hyaluronan (HA)-CD44-Moesin interaction. TNF-¿– elicits both HA synthesis and Moesin phosphorylation through protein kinase C activation, promoting binding of CD44 to the newly synthesized HA. The HA-CD44-Moesin interaction leads to cell-cell dissociation through actin remodeling and increased cellular motility associated with mesenchymal phenotype. Furthermore, we[a] established an in vivo model of TNF-¿–-induced fibrosis in the mouse eye, and the ocular fibrosis was completely suppressed in CD44-null mice. Therefore, HA production and its interaction with CD44 plays essential role in TNF-¿–-induced-EMT, and the interference of the complex formation can be a new strategy for the fibrotic disorders. **Overall design:** For this submission, total RNA was extracted from TGF- or TNF-treated ARPE-19 cells and differential gene expression between each time point (6 and 42 hours) was determined using genechip arrays (Affymetrix, Human Genome U133).

Background corr dist: KL-Divergence = 0.0967, L1-Distance = 0.0324, L2-Distance = 0.0015, Normal std = 0.4588

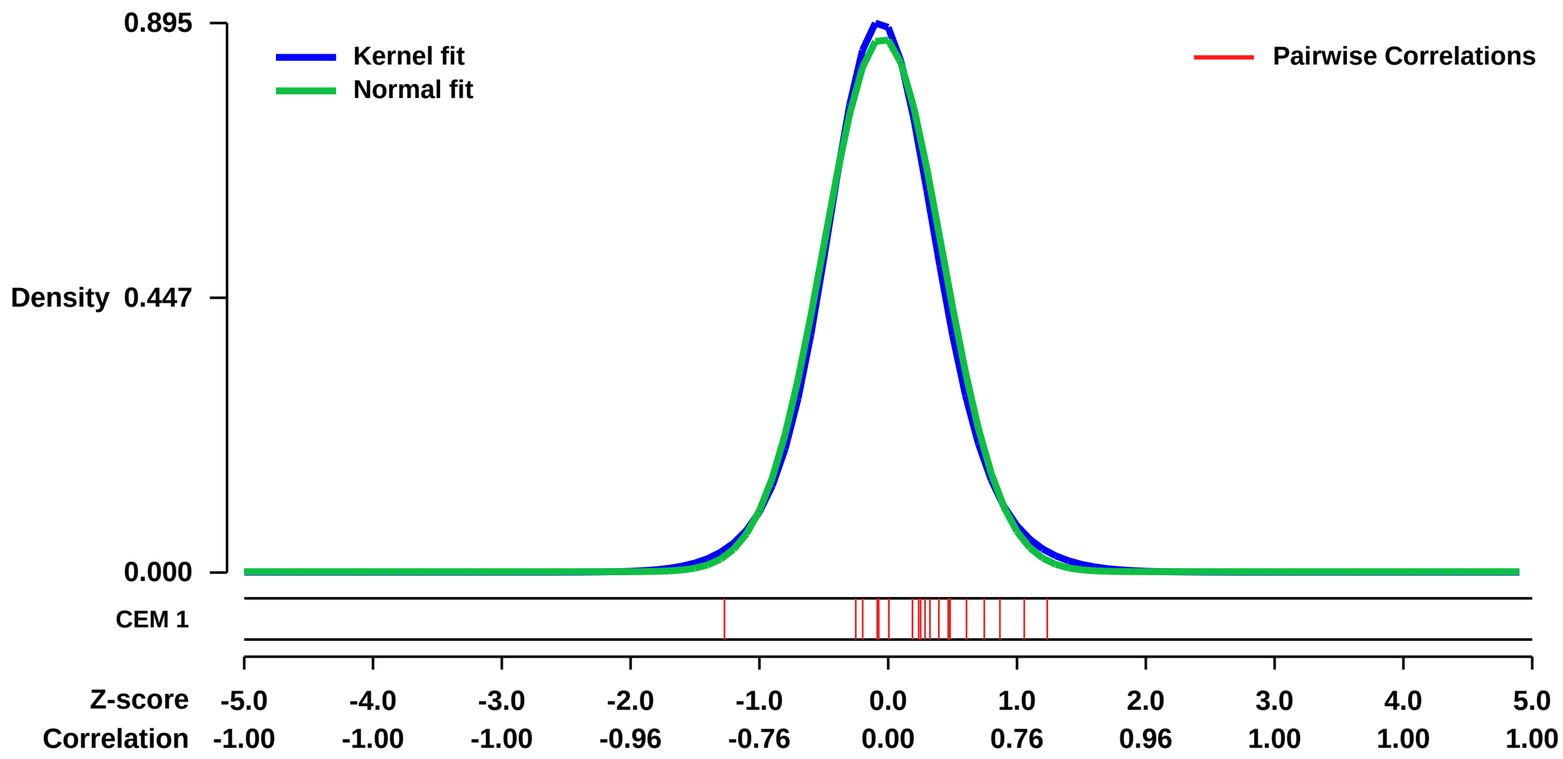

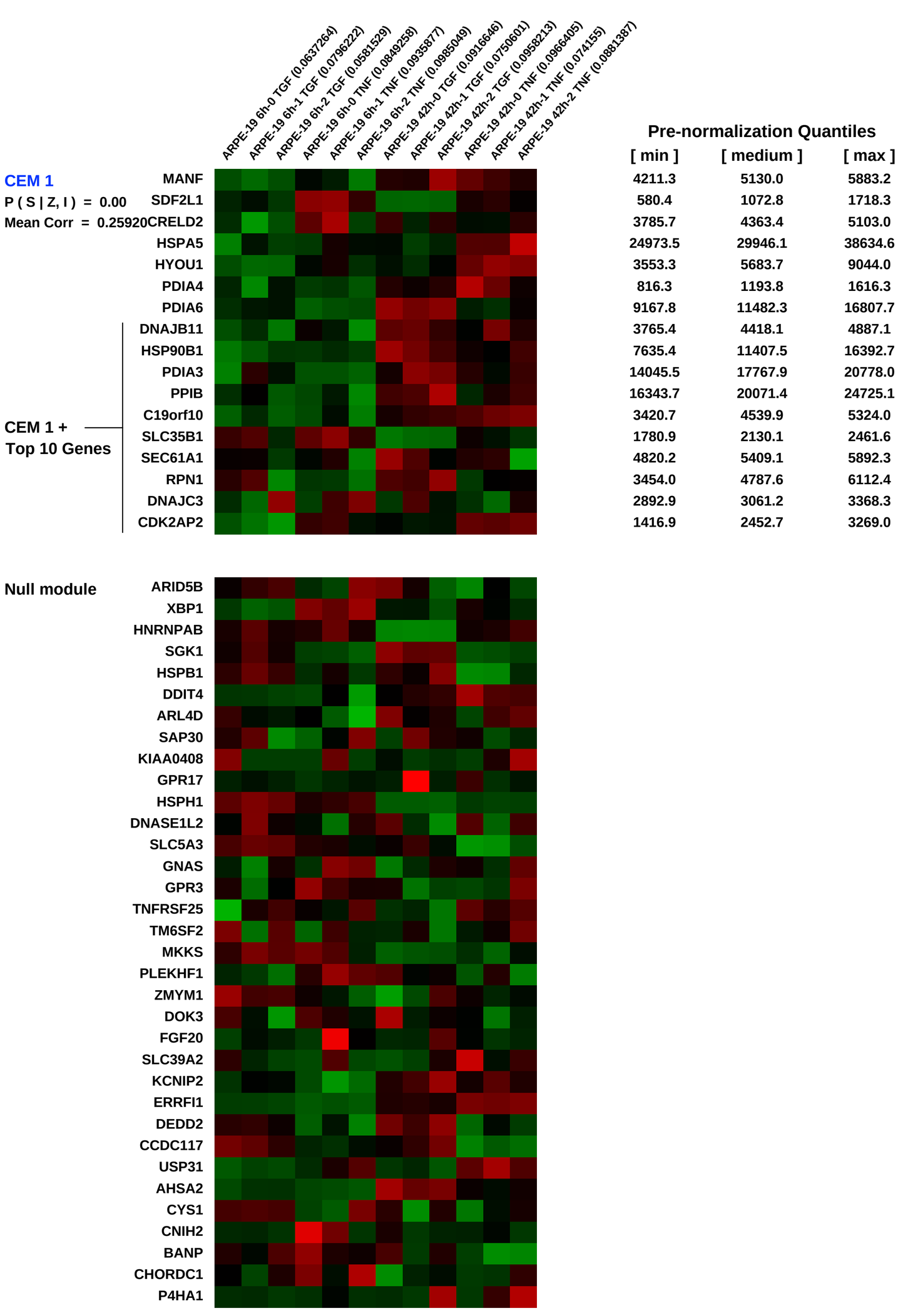

Pre-normalization Quantiles

	[min]	[medium]	[max]
MANF	4211.3	5130.0	5883.2
SDF2L1	580.4	1072.8	1718.3
CRELD2	3785.7	4363.4	5103.0
HSPA5	24973.5	29946.1	38634.6
HYOU1	3553.3	5683.7	9044.0
PDIA4	816.3	1193.8	1616.3
PDIA6	9167.8	11482.3	16807.7
DNAJB11	3765.4	4418.1	4887.1
HSP90B1	7635.4	11407.5	16392.7
PDIA3	14045.5	17767.9	20778.0
PPIB	16343.7	20071.4	24725.1
C19orf10	3420.7	4539.9	5324.0
SLC35B1	1780.9	2130.1	2461.6
SEC61A1	4820.2	5409.1	5892.3
RPN1	3454.0	4787.6	6112.4
DNAJC3	2892.9	3061.2	3368.3
CDK2AP2	1416.9	2452.7	3269.0

GEO Series "GSE28548" Expression Profiles

Num of samples in this series: 24

Scale of expression profile Z-scores

-3.0 -2.0 -1.0 0.0 1.0 2.0 3.0

GEO Link:	**http://www.ncbi.nlm.nih.gov/geo/query/acc.cgi?acc=GSE28548**
Status:	**Public on Jul 31 2011**
Title:	**The effect of sirtuin 6 overexpression on TNFa stimulation.**
Organism:	**Homo sapiens**
Experiment type:	**Expression profiling by array**
Platform:	**GPL570**
Pubmed ID:	
Summary & Design:	**Summary:** **SIRT6 has been implicated in a range of biological processes including inflammation, aging and the control of metabolism. Hence inhibitors or activators of SIRT6 have the potential to be therapeutics for a number of indications.** **Genome wide expression studies were used to investigate the effect of overexpression of SIRT6 and mutant SIRT6 on a wide range of NF¸"B dependent gene expression** **Overall design:** **HEK293 cells were transfected with expression vectors encoding wild type SIRT6 or the H133W mutant followed by stimulation with TNF¸– for one hour.**

Background corr dist: **KL-Divergence = 0.1526, L1-Distance = 0.0302, L2-Distance = 0.0018, Normal std = 0.3736**

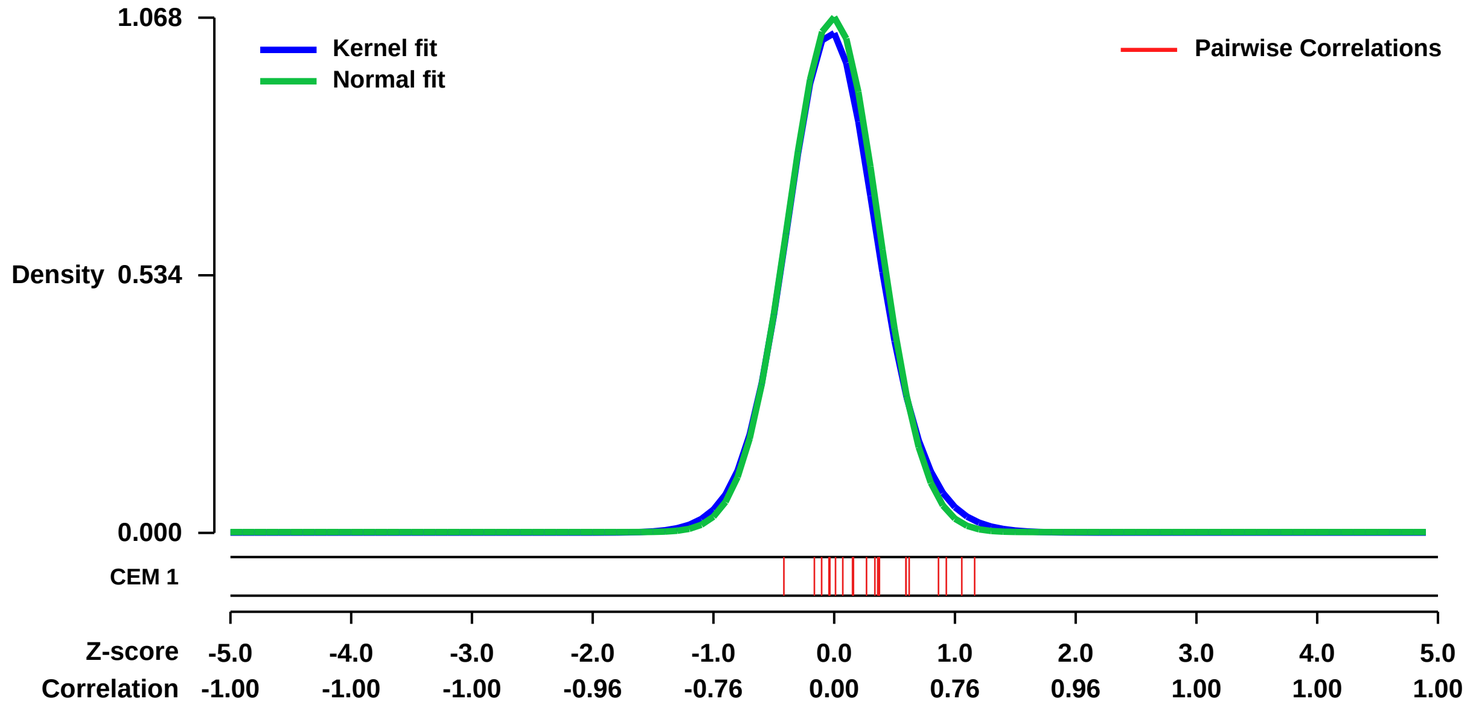

CEM 1
P (S | Z, I) = 0.00
Mean Corr = 0.28330

CEM 1 +
Top 10 Genes

Null module

Pre-normalization Quantiles

	[min]	[medium]	[max]
MANF	4974.8	5342.7	5756.3
SDF2L1	321.7	373.6	447.5
CRELD2	994.8	1239.7	2005.7
HSPA5	4324.6	4573.8	5720.8
HYOU1	1051.8	1126.0	1515.9
PDIA4	6079.6	6356.8	6772.5
PDIA6	6374.2	6731.9	7145.9
DNAJB11	2325.5	2680.7	2928.7
HSP90B1	3393.3	3679.9	4058.6
PDIA3	5026.4	5568.3	5874.4
PPIB	6481.3	6771.5	7291.0
C19orf10	1511.8	1653.7	2026.7
SLC35B1	3403.8	3650.0	3933.2
SEC61A1	1905.8	2426.6	2695.4
RPN1	1875.0	2263.7	3128.0
DNAJC3	2719.0	3232.9	3428.1
CDK2AP2	657.5	818.7	1014.5
ARID5B			
XBP1			
HNRNPAB			
SGK1			
HSPB1			
DDIT4			
ARL4D			
SAP30			
KIAA0408			
GPR17			
HSPH1			
DNASE1L2			
SLC5A3			
GNAS			
GPR3			
TNFRSF25			
TM6SF2			
MKKS			
PLEKHF1			
ZMYM1			
DOK3			
FGF20			
SLC39A2			
KCNIP2			
ERRFI1			
DEDD2			
CCDC117			
USP31			
AHSA2			
CYS1			
CNIH2			
BANP			
CHORDC1			
P4HA1			

GEO Series "GSE9093" Expression Profiles

Num of samples in this series: 6

Scale of expression profile Z-scores

-3.0 -2.0 -1.0 0.0 1.0 2.0 3.0

GEO Link:	http://www.ncbi.nlm.nih.gov/geo/query/acc.cgi?acc=GSE9093
Status:	Public on Nov 17 2008
Title:	MCF-7 6A-SA5 and WT-WB1 cells untreated
Organism:	Homo sapiens
Experiment type:	Expression profiling by array
Platform:	GPL570
Pubmed ID:	18316594
Summary & Design:	**Summary:** **Keywords: cell type comparison** **Overall design:** **MCF-7 cells were stably transfected with pIRES-TGFBR1-HA-FLAG or pIRES-TGFBR1*6A-HA-FLAG. Clones were picked up and named 6A-SA5 and WT-WB1 referring to the *6A and TGFBR1 clones, respectively. We have found that the *6A mutation causes an increase in migration and invasion of MCF-7 cells which is independent of TGF-beta. We used the gene array to identify genes that were differentially regulated between the two cell lines that could lead to this phenotype. We collected RNA from samples that were serum-deprived overnight prior to being fed with complete media to mimic the conditions in the migration experiment. No exogenous growth factors were added to the media besides the normal 10% heat inactivated FBS. Samples were collected and run in triplicate (referred to in this data set as sample 1, sample 2, and sample 3). The â untreatedâ refers to the fact that samples were grown in complete media alone with no exogenously added growth factors.**

Background corr dist: KL-Divergence = 0.0340, L1-Distance = 0.0335, L2-Distance = 0.0013, Normal std = 0.6740

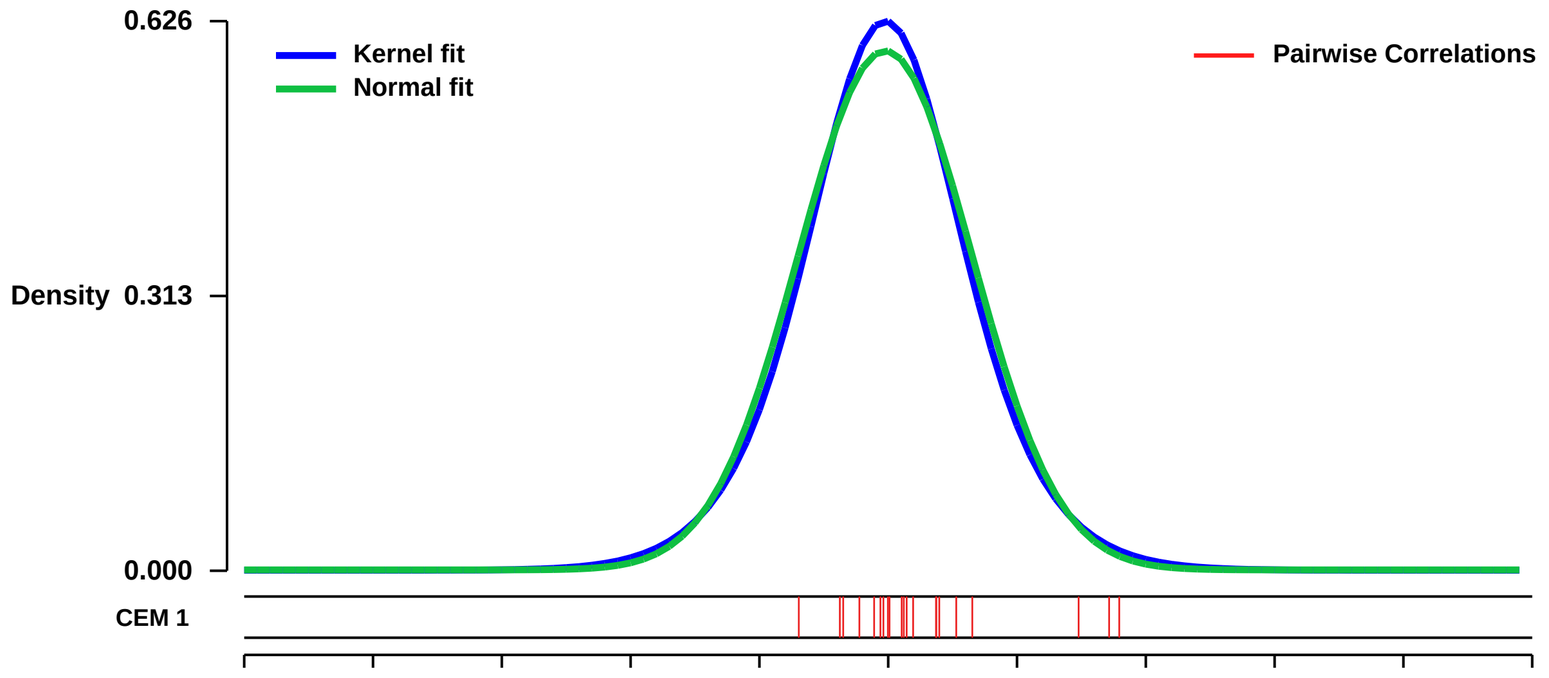

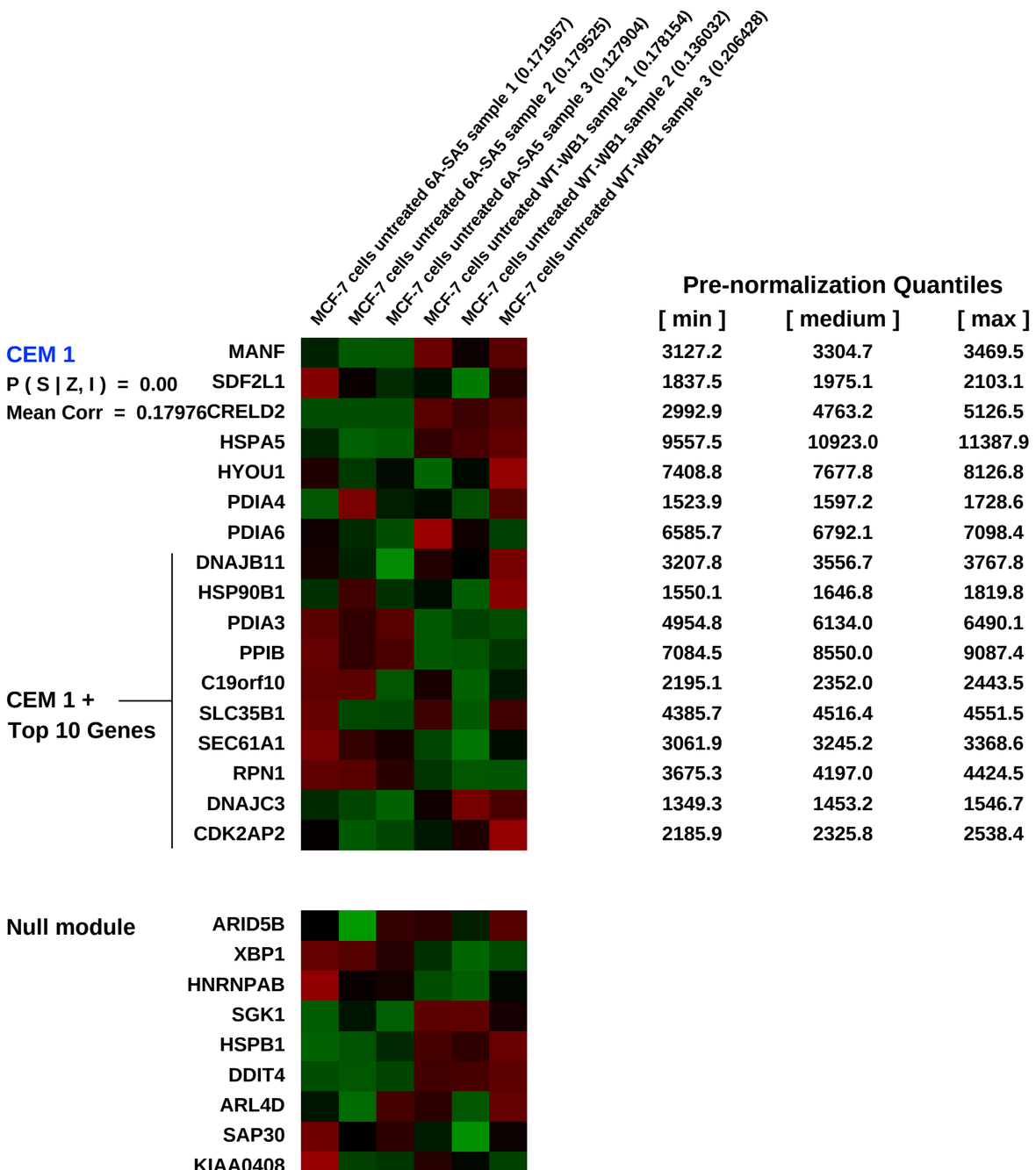

GEO Series "GSE33950" Expression Profiles

Num of samples in this series: 12

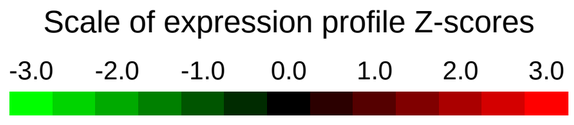

GEO Link:	http://www.ncbi.nlm.nih.gov/geo/query/acc.cgi?acc=GSE33950
Status:	Public on Jul 19 2012
Title:	SHARP1 suppresses breast cancer metastasis by promoting degradation of hypoxia-inducible factors
Organism:	Homo sapiens
Experiment type:	Expression profiling by array
Platform:	GPL570
Pubmed ID:	22801492
Summary & Design:	**Summary:** Triple Negative Breast cancer accounts for some of the most aggressive types of breast cancer. By interrogating clinical datasets, we found that the activities of p63 and Hypoxia-Inducible-Factors (HIFs), two master regulators of the invasive and metastatic cancer cell phenotype are linked in TNBC through the p63-target Sharp1. Mechanistically, Sharp1 promotes HIF-1$_{\alpha}$–/HIF-2$_{\alpha}$– proteasomal degradation by serving as HIFs presenting factor to the proteasome independently from oxygen levels and prior ubiquitination. To investigate unbiasedly if Sharp1 is a general inhibitor of HIF induced transcriptional program, we compared the transcriptomic profile of cells either overexpressing Sharp1 or depleted of HIF1a and HIF2a. **Overall design:** We collected RNA from control MDA-MB-231 cells (shGFP) or MDA-MB-231 cells overexpressing Sharp1 or MDA-MB-231 cells depleted of HIF1a and HIF2a (shHIF). Cells were left untreated in normal culturing conditions before harvesting. Samples were then processed for total RNA extraction and hybridization on Affymetrix microarrays. Four biological replicas (A, B, C, D) were used for each of the 4 conditions (1: shGFP, control cells; 2: shHIF cells; 3: Sharp1-overexpressing cells) for a total of 12 samples.

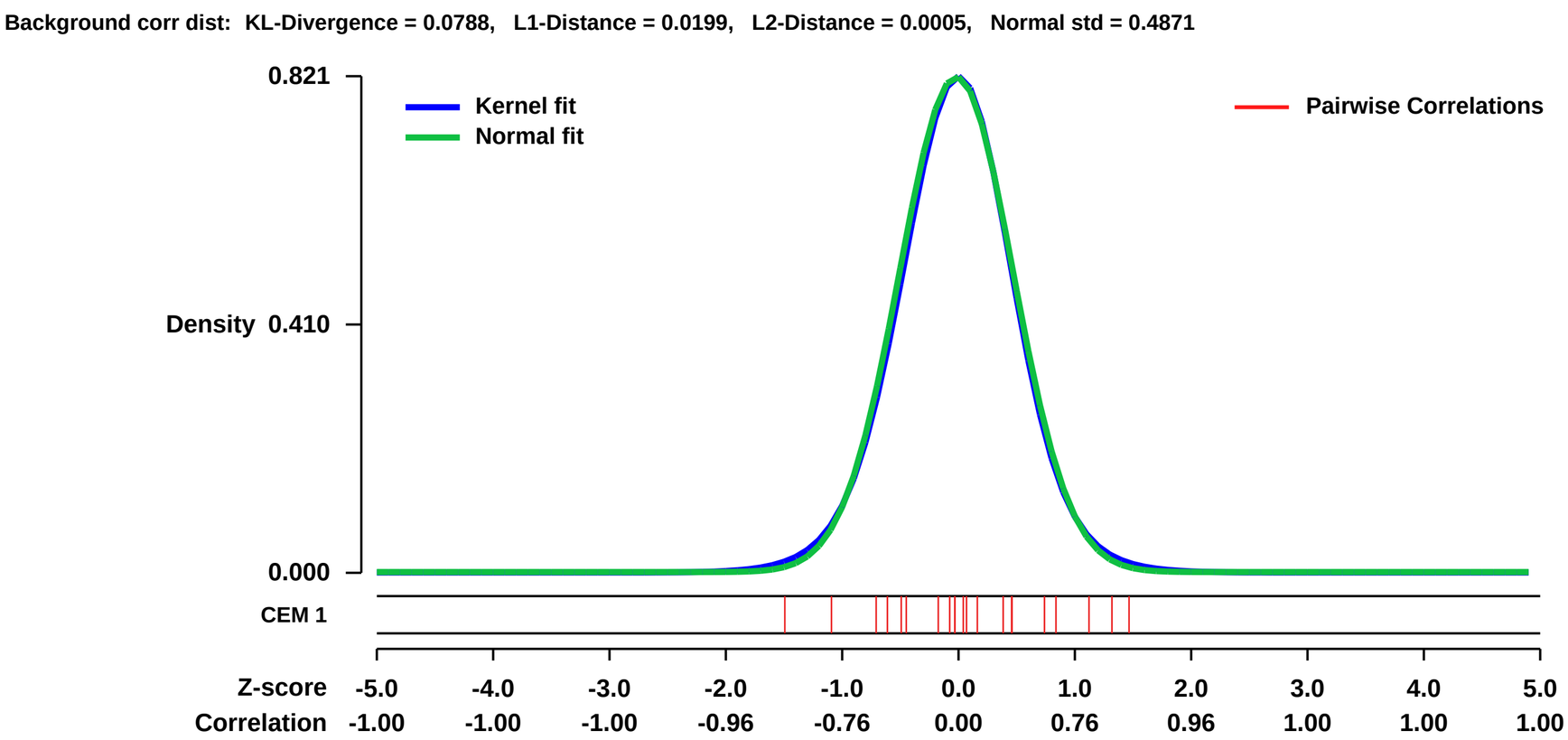

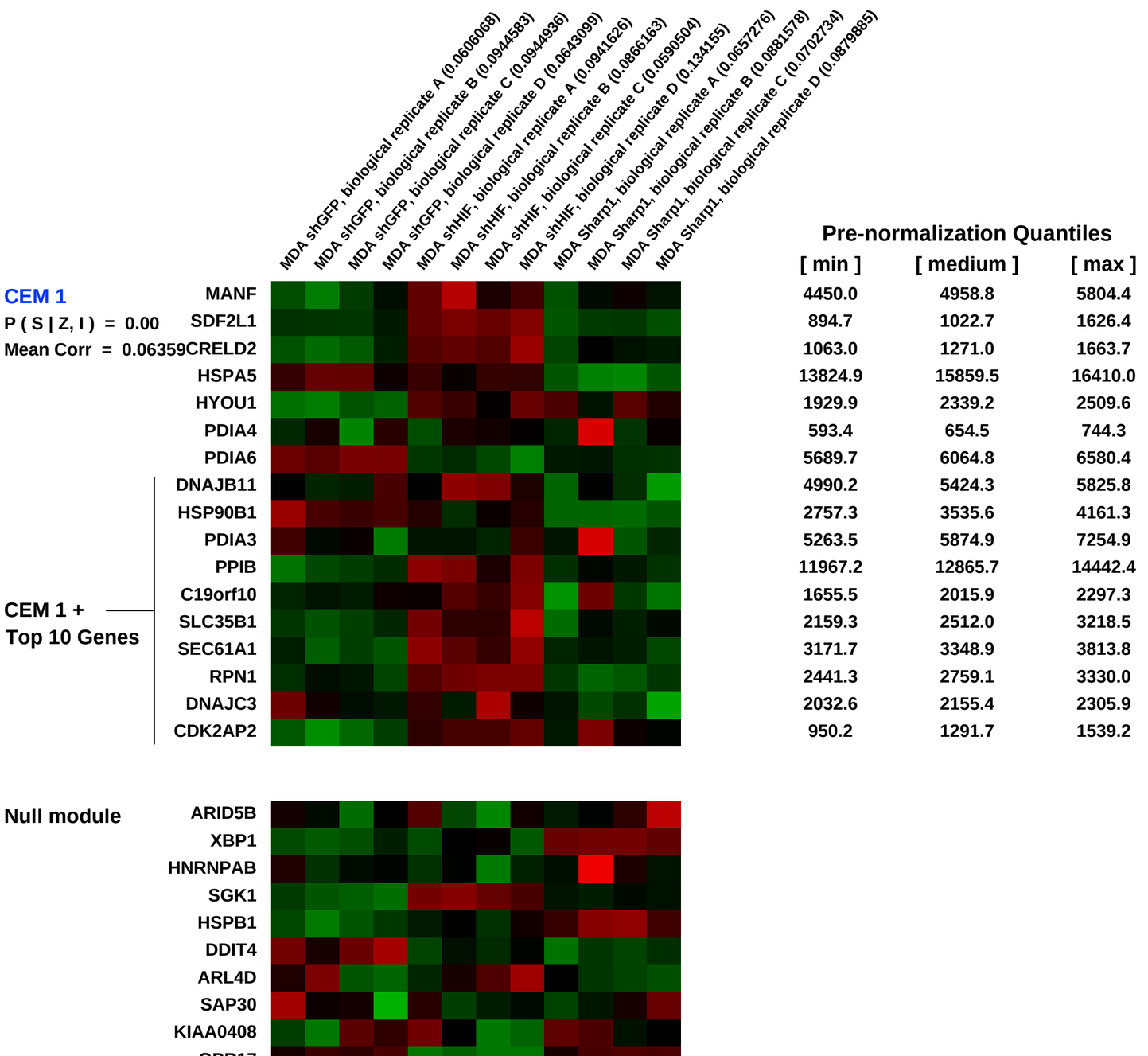

GEO Series "GSE30543" Expression Profiles

Num of samples in this series: 6

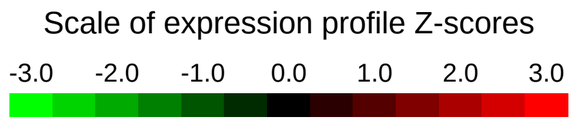

GEO Link:	http://www.ncbi.nlm.nih.gov/geo/query/acc.cgi?acc=GSE30543
Status:	Public on Dec 03 2013
Title:	Differential gene expression profiles between SUM149 cells transfected with control siRNA and SUM149 cells transfected with siRNA targeting tarzarotene-induced gene 1 (
Organism:	Homo sapiens
Experiment type:	Expression profiling by array
Platform:	GPL570
Pubmed ID:	24014597
Summary & Design:	**Summary:** We identified tazarotene-induced gene 1 (TIG1) as a potential tumorigenic gene in IBC. To investigate the underlying mechanism by which TIG1 promotes tumor growth and invasiveness of IBC cells, we first sought to identify TIG1 functional partners by using DNA microarray analysis to compare gene expression profiles between SUM149 cells transfected with control siRNA and SUM149 cells transfected with siRNA targeting TIG1. We identified receptor tyrosine kinase Axl as a functional partner of TIG1. **Overall design:** SUM149 cells transiently transfected with control siRNA or siRNA targeting TIG1 were used. Total RNA was extracted and purified using RNeasy mini kit (Qiagen, Inc.) according to the manufacturerâ s instructions. The integrity of the obtained RNA was assessed using an Agilent 2100 BioAnalyzer (Agilent Technologies). The Affymetrix HGU133 plus platform was used for hybridization, staining, and imaging of the arrays by following the manufacturerâ s instructions. Gene expression analysis was performed in triplicate.

Background corr dist: KL-Divergence = 0.0227, L1-Distance = 0.0219, L2-Distance = 0.0004, Normal std = 0.7403

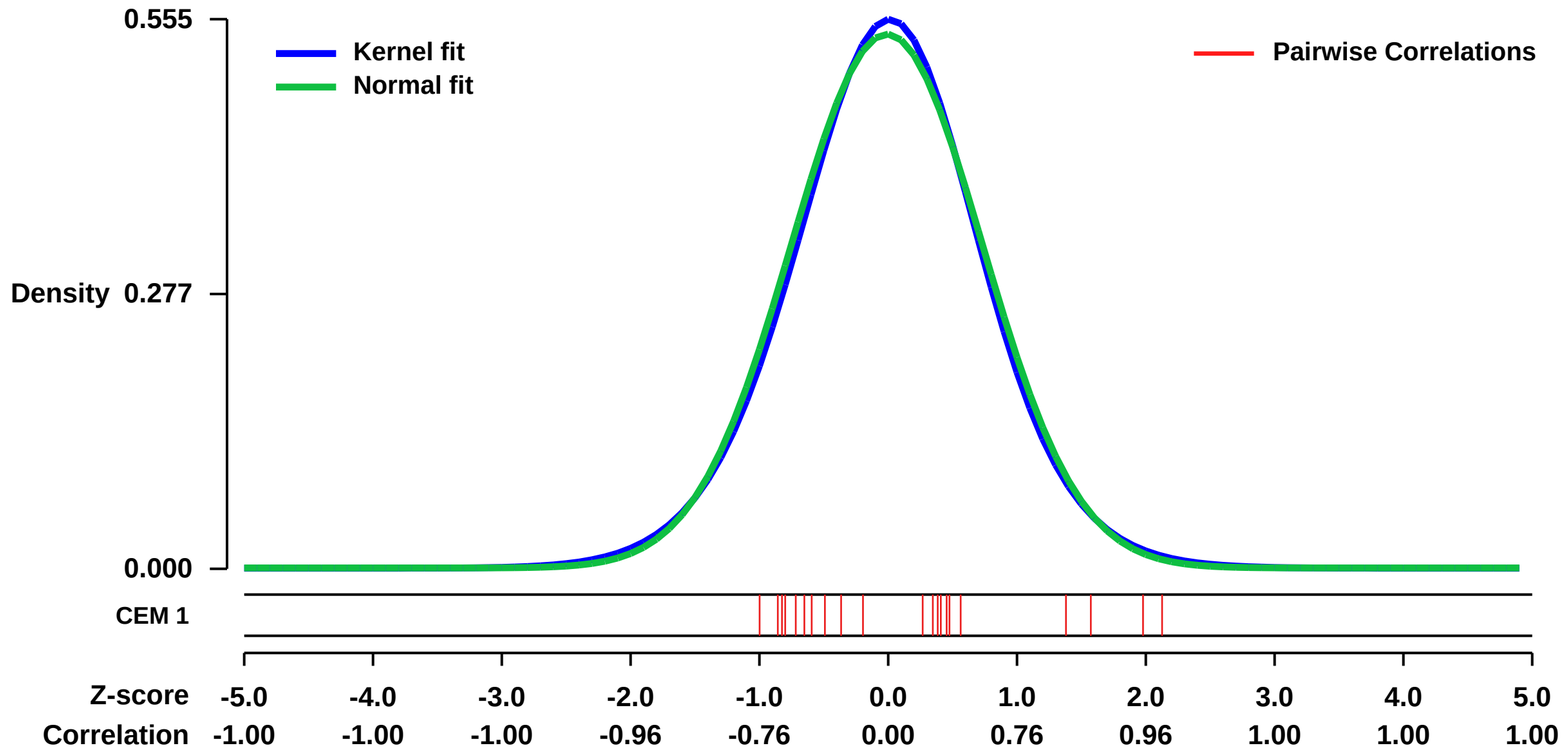

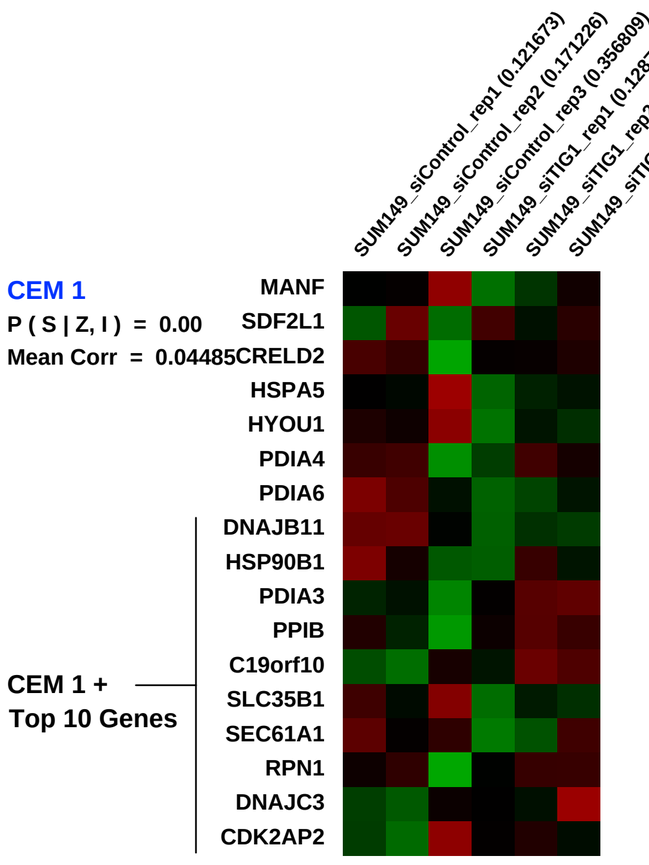

	Pre-normalization Quantiles		
	[min]	[medium]	[max]
MANF	2564.6	2843.7	3175.8
SDF2L1	1146.2	1505.7	1656.9
CRELD2	1489.0	2473.2	2689.0
HSPA5	11135.8	13361.6	17272.8
HYOU1	3045.0	3888.2	4706.5
PDIA4	735.5	978.3	988.4
PDIA6	13293.0	14133.4	15567.0
DNAJB11	3019.0	3604.7	4291.4
HSP90B1	1273.1	1609.4	1913.5
PDIA3	7808.6	9581.0	10786.0
PPIB	6089.0	7539.5	7956.4
C19orf10	2643.2	2939.9	3123.4
SLC35B1	2216.3	2374.8	2602.5
SEC61A1	2268.3	2526.8	2597.9
RPN1	1455.8	2005.9	2026.1
DNAJC3	2033.4	2203.7	2494.8
CDK2AP2	493.5	581.1	693.3
ARID5B			
XBP1			
HNRNPAB			
SGK1			
HSPB1			
DDIT4			
ARL4D			
SAP30			
KIAA0408			
GPR17			
HSPH1			
DNASE1L2			
SLC5A3			
GNAS			
GPR3			
TNFRSF25			
TM6SF2			
MKKS			
PLEKHF1			
ZMYM1			
DOK3			
FGF20			
SLC39A2			
KCNIP2			
ERRFI1			
DEDD2			
CCDC117			
USP31			
AHSA2			
CYS1			
CNIH2			
BANP			
CHORDC1			
P4HA1			

GEO Series "GSE36287" Expression Profiles

Num of samples in this series: 24

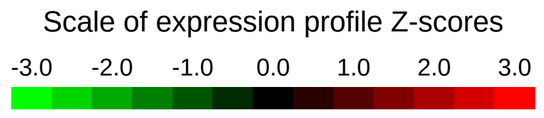

GEO Link:	http://www.ncbi.nlm.nih.gov/geo/query/acc.cgi?acc=GSE36287
Status:	Public on Mar 07 2012
Title:	Expression data from primary human keratinocytes exposed to cytokines in vitro (IL-4, IL-13, IL-17A, IFN-alpha, IFN-gamma, TNF)
Organism:	Homo sapiens
Experiment type:	Expression profiling by array
Platform:	GPL570
Pubmed ID:	22479649
Summary & Design:	**Summary:** The clinical features of psoriasis, characterized by sharply demarcated scaly erythematous plaques, are typically so distinctive that a diagnosis can easily be made on these grounds alone. However, there is great variability in treatment response between individual patients, and this may reflect heterogeneity of inflammatory networks driving the disease. In this study, whole-genome transcriptional profiling was used to characterize inflammatory and cytokine networks in 62 lesional skin samples obtained from patients with stable chronic plaque psoriasis. We were able to stratify lesions according to their inflammatory gene expression signatures, identifying those associated with strong (37% of patients), moderate (39%) and weak inflammatory infiltrates (24%). Additionally, we identified differences in cytokine signatures with heightened cytokine-response patterns in one sub-group of lesions (IL-13-strong; 50%) and attenuation of these patterns in a second sub-group (IL-13-weak; 50%). These sub-groups correlated with the composition of the inflammatory infiltrate, but were only weakly associated with increased risk allele frequency at some psoriasis susceptibility loci (e.g., REL, TRAF3IP2 and NOS2). Our findings highlight variable points in the inflammatory and cytokine networks known to drive chronic plaque psoriasis. Such heterogeneous aspects may shape clinical course and treatment responses, and can provide avenues for development of personalized treatments. We used Affymetrix microarrays to evaluate genome-wide expression in primary human keratinocytes exposed to cytokines. Cytokine activity signatures were used to interpret the shifts in gene expression that occur in psoriasis plaques relative to normal uninvolved skin. **Overall design:** Primary keratinocytes from three donors (subjects 1, 2, and 3) were obtained and were either untreated (control) or exposed to cytokines (IL-4, IL-13, IFN-alpha, IFN-gamma and TNF). For the IL17A samples, primary keratinocytes were obtained from six donors, with cells derived from three donors treated with IL-17A and cells derived from the other three donors left untreated (i.e., unpaired control samples).

Background corr dist: KL-Divergence = 0.1678, L1-Distance = 0.0322, L2-Distance = 0.0021, Normal std = 0.3603

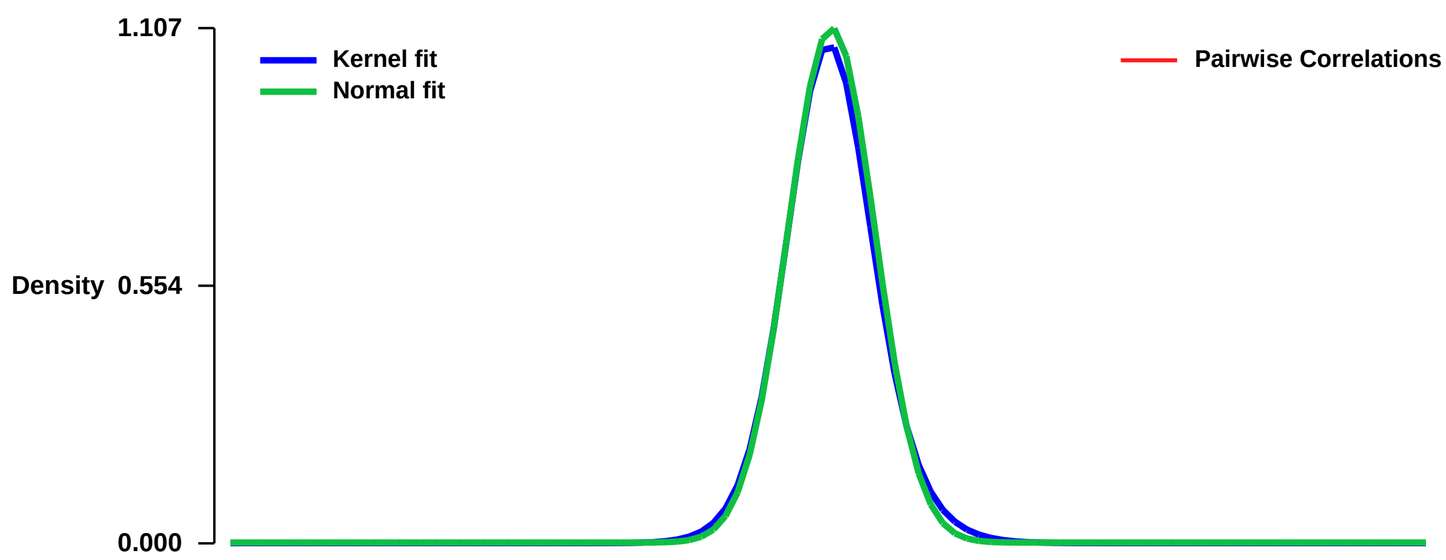

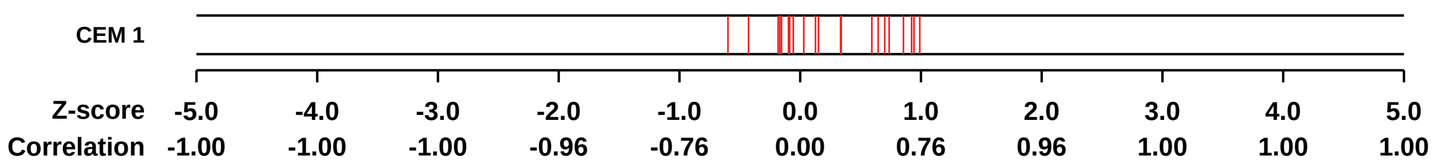

GEO Series "GSE31412" Expression Profiles

Num of samples in this series: 6

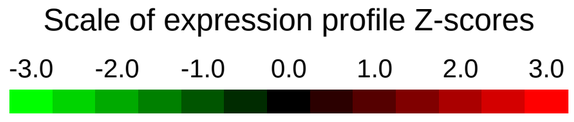

GEO Link:	http://www.ncbi.nlm.nih.gov/geo/query/acc.cgi?acc=GSE31412
Status:	Public on Jul 31 2012
Title:	Expression changes in HeLa cells treated with siRNA against HCFC1 or control luciferase
Organism:	Homo sapiens
Experiment type:	Expression profiling by array
Platform:	GPL570
Pubmed ID:	23539139
Summary & Design:	**Summary:** We compared in triplicate mRNA levels from cells treated with siRNA against either HCF-1 or, as a negative control, luciferase. We observed that 19% of Refseq annotated genes are differentially expressed (either up or down regulated with a multiple testing corrected p value of â∕0.05) upon depletion of HCF-1. This large number of differentially expressed genes upon HCF-1 depletion demonstrates a broad role of HCF-1 in the regulation of gene expression. **Overall design:** The experiment includes biological triplicates of the expression changes between cycling HeLa cells treated with a control siRNA or siRNA against HCFC1.

Background corr dist: KL-Divergence = 0.0319, L1-Distance = 0.0248, L2-Distance = 0.0006, Normal std = 0.6713

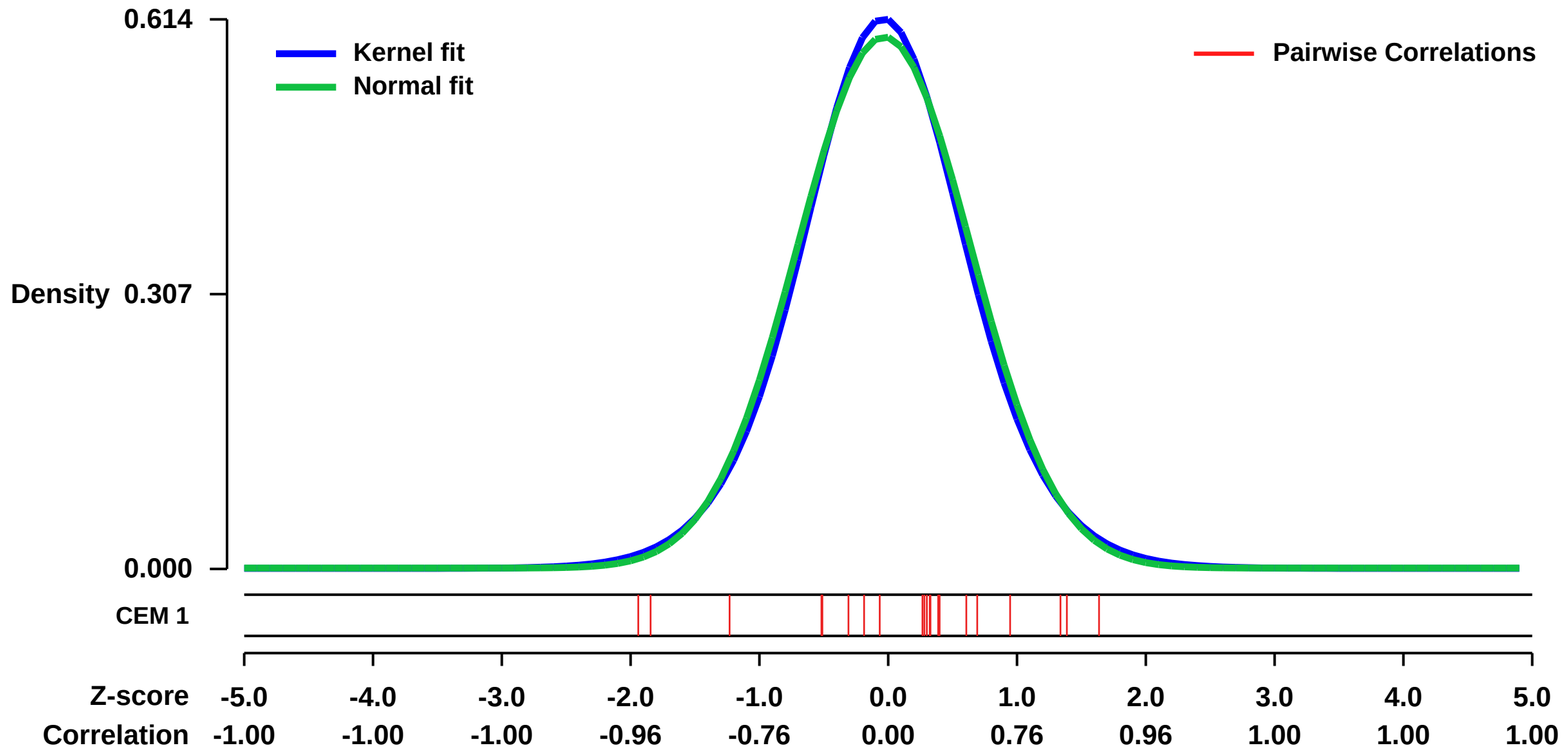

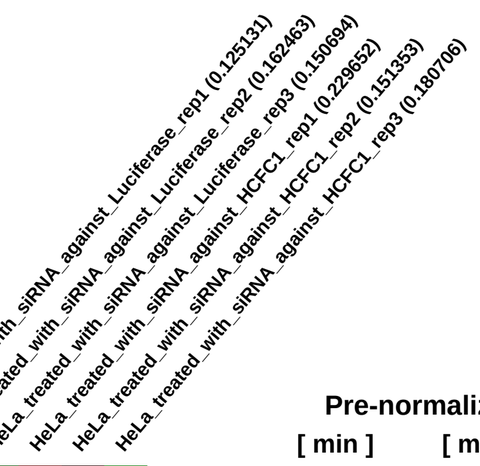

Pre-normalization Quantiles

		[min]	[medium]	[max]
CEM 1	MANF	9399.9	10276.6	10619.7
P (S | Z, I) = 0.00	SDF2L1	4140.8	4541.0	4732.6
Mean Corr = 0.11950	CRELD2	3763.3	4715.0	4978.5
	HSPA5	28593.8	30963.0	31494.0
	HYOU1	5512.2	6908.1	7505.9
	PDIA4	1395.0	1734.0	1801.2
	PDIA6	7952.3	8417.4	9092.4
CEM 1 + Top 10 Genes	DNAJB11	12348.9	12841.5	12932.2
	HSP90B1	3374.8	3811.1	3846.9
	PDIA3	14213.7	15685.9	16165.4
	PPIB	24327.8	25444.9	27087.6
	C19orf10	5755.5	6859.3	7401.1
	SLC35B1	3293.5	3758.5	4110.2
	SEC61A1	4379.6	4750.7	5076.6
	RPN1	4752.2	5694.6	6044.7
	DNAJC3	2423.8	2949.4	3151.0
	CDK2AP2	1471.2	1637.3	1736.6
Null module	ARID5B			
	XBP1			
	HNRNPAB			
	SGK1			
	HSPB1			
	DDIT4			
	ARL4D			
	SAP30			
	KIAA0408			
	GPR17			
	HSPH1			
	DNASE1L2			
	SLC5A3			
	GNAS			
	GPR3			
	TNFRSF25			
	TM6SF2			
	MKKS			
	PLEKHF1			
	ZMYM1			
	DOK3			
	FGF20			
	SLC39A2			
	KCNIP2			
	ERRFI1			
	DEDD2			
	CCDC117			
	USP31			
	AHSA2			
	CYS1			
	CNIH2			
	BANP			
	CHORDC1			
	P4HA1			

GEO Series "GSE14017" Expression Profiles

Num of samples in this series: 29

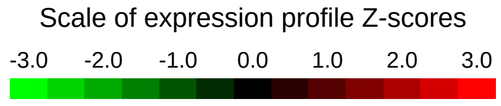

GEO Link:	http://www.ncbi.nlm.nih.gov/geo/query/acc.cgi?acc=GSE14017
Status:	Public on May 01 2009
Title:	Metastases of breast cancer (U133plus2)
Organism:	Homo sapiens
Experiment type:	Expression profiling by array
Platform:	GPL570
Pubmed ID:	19573813
Summary & Design:	**Summary:** Comparisons among breast cancer metastases at different organs revealed distinct microenvironments as characterized by cytokine content. Such microenvironment distinction might be important to dictate how the cancer cells adapt to survival before they successfully colonize. **Keywords: Disease state analyses** **Overall design:** 58 breast cancer metastases from different organs were profiled and compared by the expression level of over 400 cytokines. 29 samples were incuded in this series. 29 others as well as 7 in the present series were profiled on U133A platforms and included in series GSE14018.

Background corr dist: **KL-Divergence = 0.3565, L1-Distance = 0.0819, L2-Distance = 0.0212, Normal std = 0.2658**

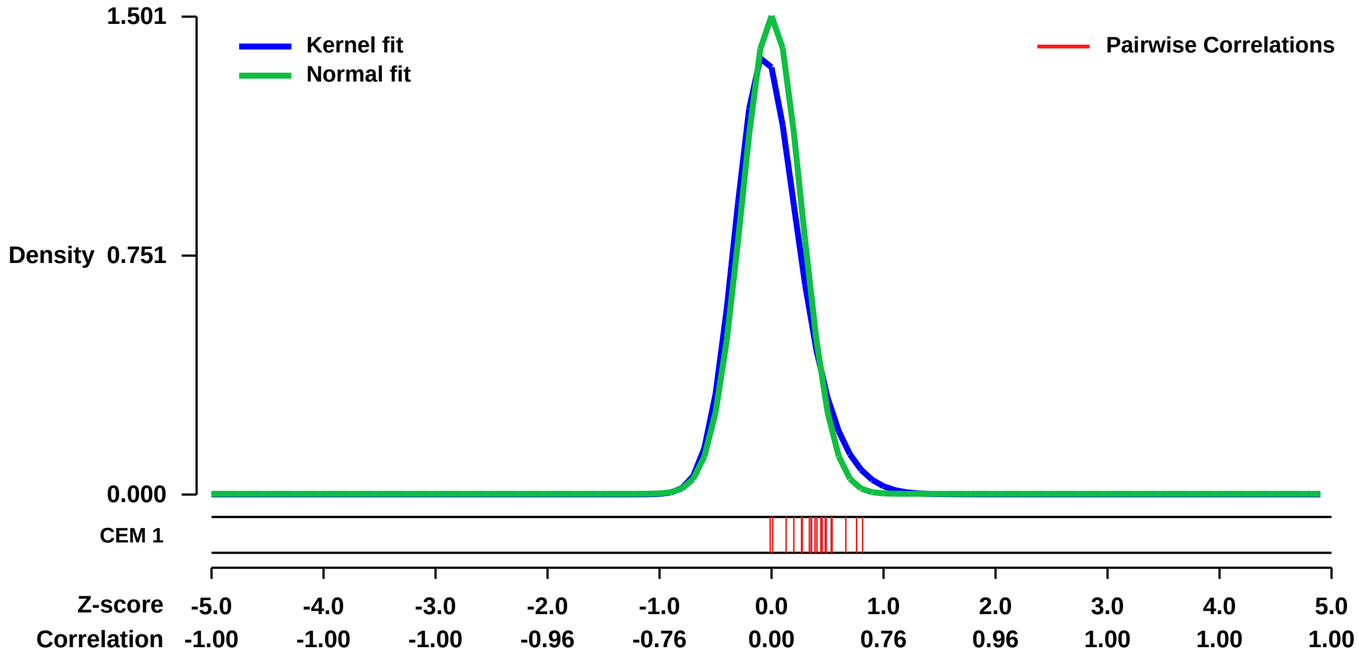

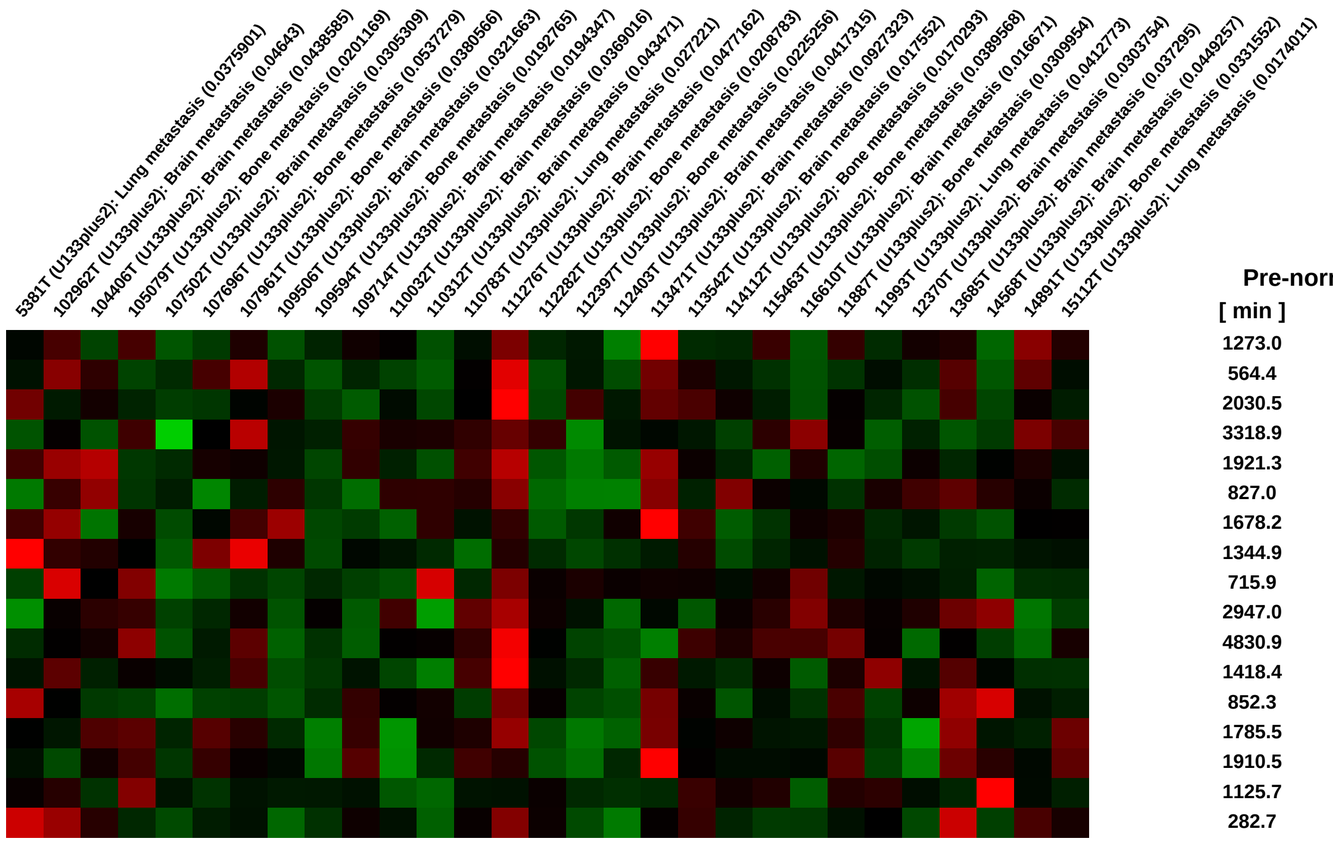

GEO Series "GSE51978" Expression Profiles

Num of samples in this series: 9

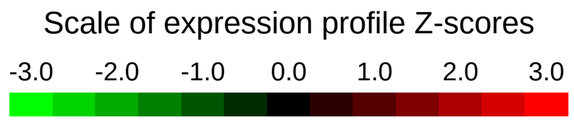

GEO Link:	http://www.ncbi.nlm.nih.gov/geo/query/acc.cgi?acc=GSE51978
Status:	Public on Nov 01 2013
Title:	Gene expression profiling in neuroblastoma cells upon CHAF1A silencing
Organism:	Homo sapiens
Experiment type:	Expression profiling by array
Platform:	GPL570
Pubmed ID:	24335960
Summary & Design:	**Summary:** We used an inducible ShRNA system and microarrays to detail the global programme of gene expression underlying neuroblastoma differentiation upon CHAF1A silencing . CHAF1A is a subunit of the Chromatin Assembly Factor-1 (CAF1) and regulates H3K9-trimethylation. High expression of CHAF1A strongly correlates with neuroblastoma poor prognosis and loss-of-function drives neuronal differentiation in vitro and in vivo. **Overall design:** Total RNA was isolated using RNAeasy kit from IMR32 cells transduced with inducible CHAF1A ShRNA. Gene expression profiling was performed in neuroblastoma cells upon CHAF1A silencing over time course (0, 5, and 10 days) in triplicate.

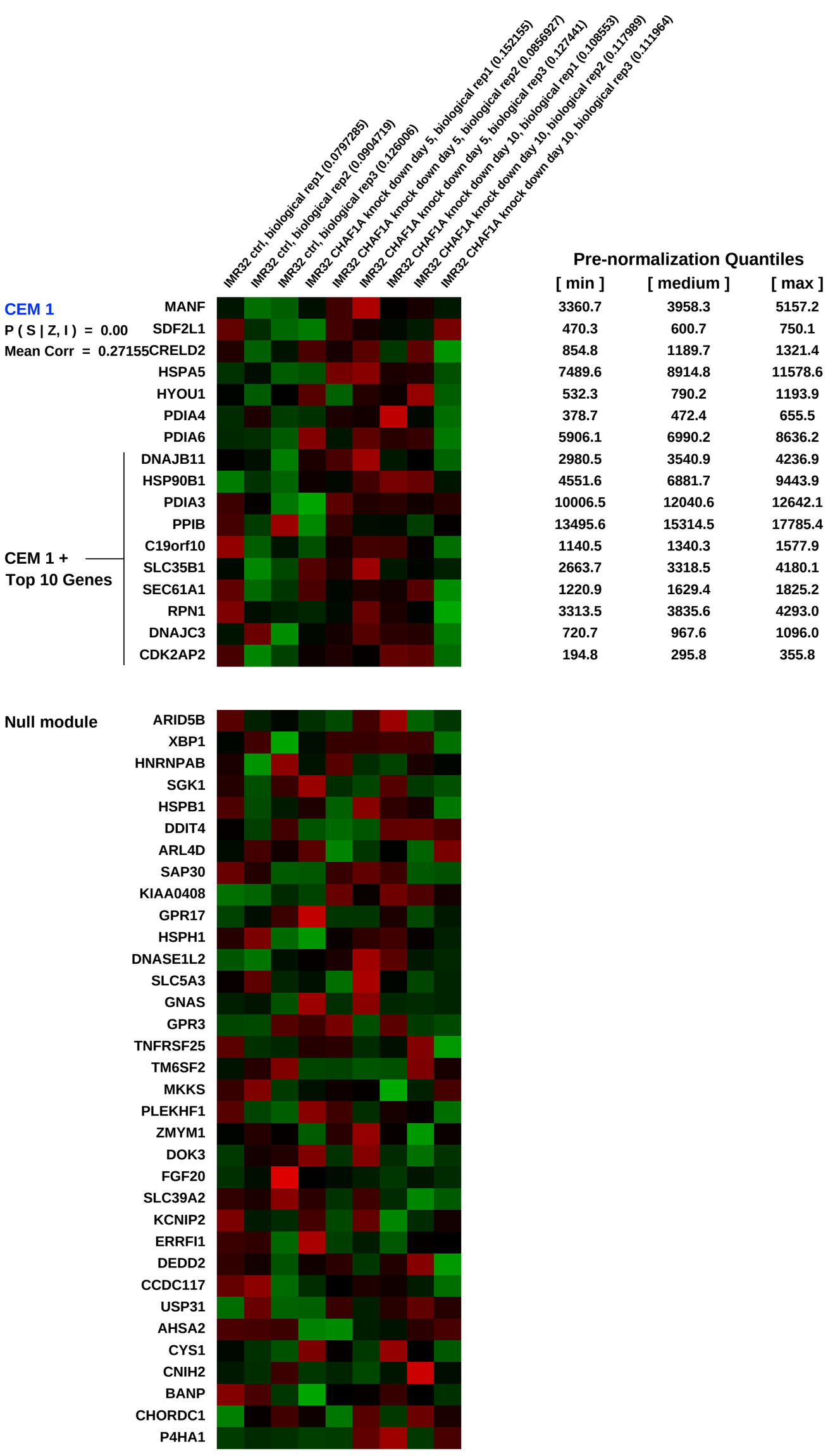

GEO Series "GSE13606" Expression Profiles

Num of samples in this series: 6

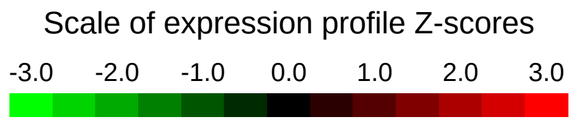

GEO Link:	http://www.ncbi.nlm.nih.gov/geo/query/acc.cgi?acc=GSE13606
Status:	Public on Oct 22 2009
Title:	UV- or oxidized lipid treated dermal skin fibroblasts
Organism:	Homo sapiens
Experiment type:	Expression profiling by array
Platform:	GPL570
Pubmed ID:	19720622

Summary & Design:

Summary:
Long wavelength Ultraviolet (UVA-1) radiation causes oxidative stress that leads to the formation of noxious substances within the skin. As a defensive mechanism skin cells produce detoxifying enzymes and antioxidants when they detect modified molecules. We have recently shown that UVA-1 irradiation oxidizes the abundant membrane phospholipid 1-palmitoyl-2-arachidonoyl-sn-glycero-3-phosphorylcholine (PAPC), which then induced the synthesis of the stress response protein heme oxygenase 1 (HO-1) in dermal fibroblasts. Here we examined the effects of UVA-1 and (UV-) oxidized phospholipids on the global gene expression in human dermal fibroblasts. We identified a cluster of genes that were co-induced by UVA-1-oxidized PAPC and UVA-1 radiation. The cluster included HO-1, glutamate-cysteine ligase modifier subunit (GCLM), aldo-keto reductases-1-C1 and -C2 (AKR1C1, AKR1C2), and interleukin 8 (IL8). These genes are members of the cellular stress response system termed â antioxidant responseâ or â Phase II detoxificationâ . Accordingly, the regulatory regions of all these genes contain binding sites for NF-E2-related factor 2 (Nrf2), a major regulator of the antioxidant response.
Both UVA-1 irradiation and treatment with oxidized lipids led to increased nuclear accumulation of Nrf2. Silencing expression of Nrf2 using siRNA or using cells and tissue from Nrf2-deficient mice, we show that the induction of the co-regulated genes was suppressed. Expression of other canonical UVA-1-induced genes, including cyclooxygenase 2 (Cox2) and interleukin 6 (IL6) was unaltered in the absence of Nrf2. Together, our data show that UVA-1-mediated lipid oxidation induces induction of antioxidant response genes, which is dependent on the redox-regulated transcription factor Nrf2. To activate Nrf2 is a major strategy for novel antioxidant drugs, the skin photo-adaptation (SPA) inducers. Our finding that specific uv-oxidized lipids act similar sheds a new (ultraviolet) light on the usually detrimental â imageâ of UV generated lipid mediators.

Overall design:
we profiled global mRNA expression levels in human dermal fibroblasts that had been treated with either UVA-1 or oxidized lipids. To investigate the effect of oxidized phospholipids on gene regulation, we used two preparations, which differed in their degree of oxidation; the minimally oxidized UV-PAPC resulting from UVA-1 irradiation of PAPC, and air-oxidized PAPC (OxPAPC), which represents the full spectrum of oxidation products (Gruber 07) (Reis et al., 2005). We irradiated dermal fibroblasts with UVA-1 (40J/cm´†) or treated them with UV-PAPC, OxPAPC or native PAPC (100´µg/ml each). We analyzed global gene expression four hours after stimulation with gene arrays (Affymetrix U133A Plus 2.0 Gene Chips).

Background corr dist: KL-Divergence = 0.0441, L1-Distance = 0.0222, L2-Distance = 0.0006, Normal std = 0.5987

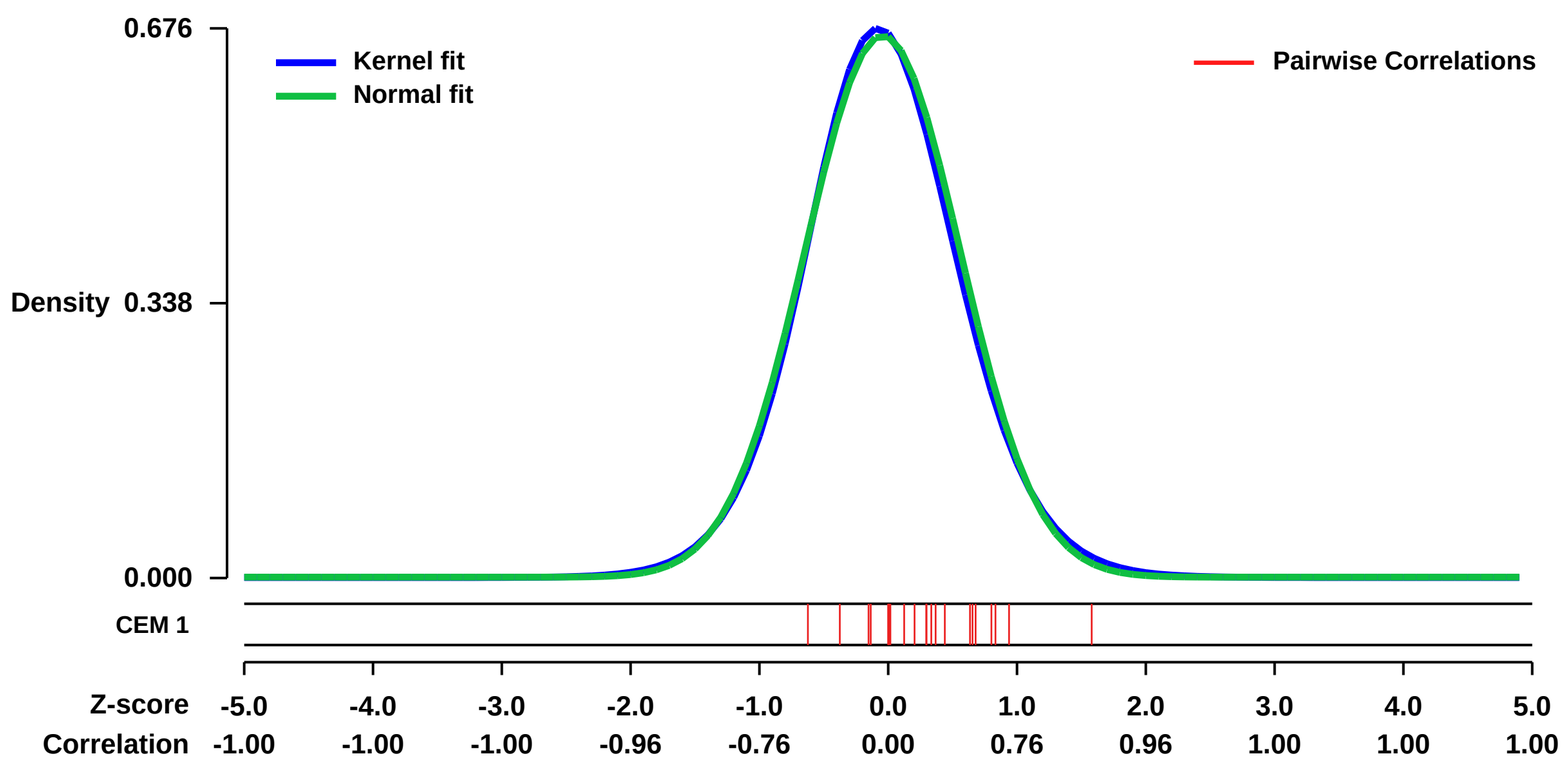

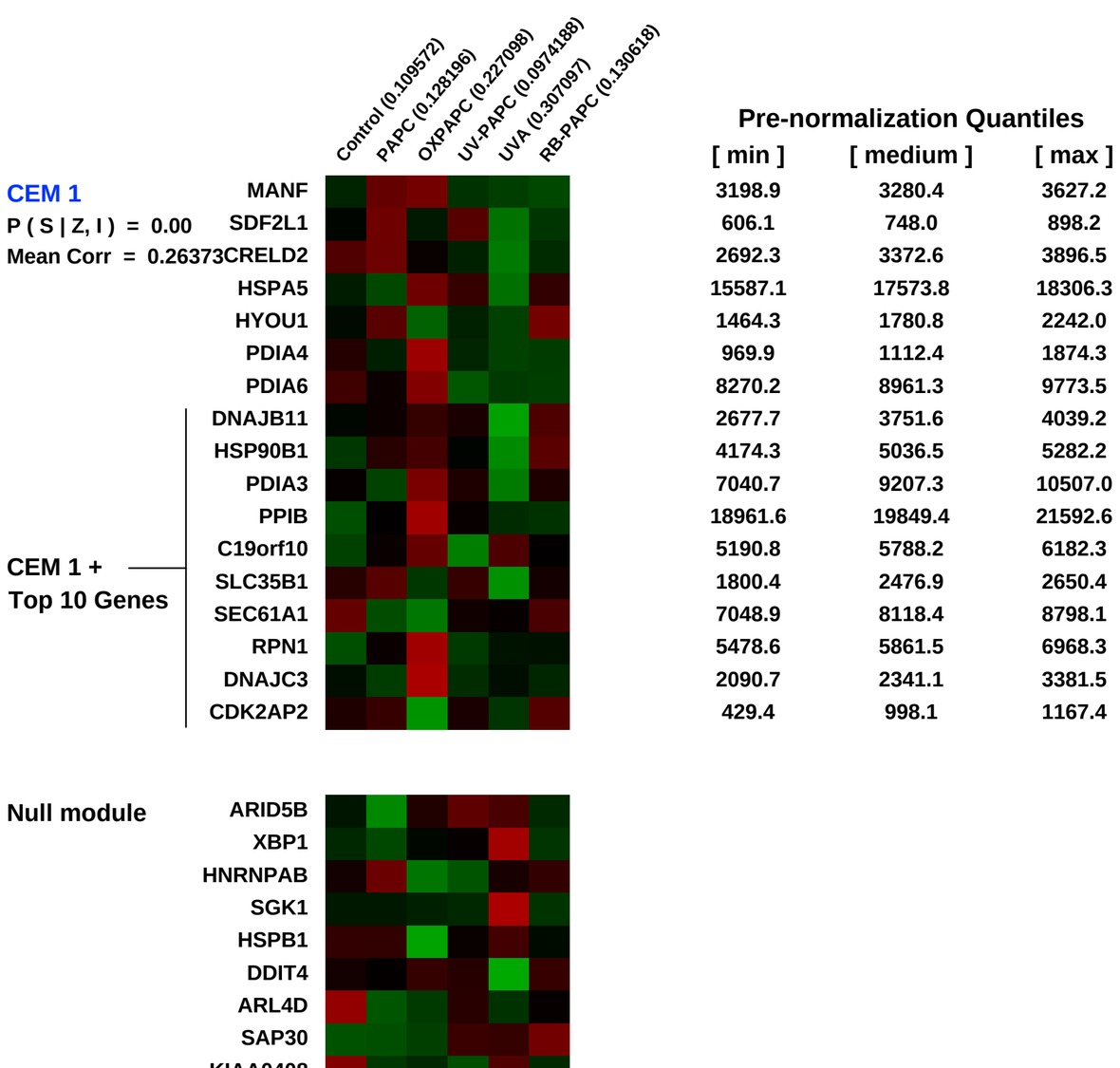

Pre-normalization Quantiles

	[min]	[medium]	[max]
MANF	3198.9	3280.4	3627.2
SDF2L1	606.1	748.0	898.2
CRELD2	2692.3	3372.6	3896.5
HSPA5	15587.1	17573.8	18306.3
HYOU1	1464.3	1780.8	2242.0
PDIA4	969.9	1112.4	1874.3
PDIA6	8270.2	8961.3	9773.5
DNAJB11	2677.7	3751.6	4039.2
HSP90B1	4174.3	5036.5	5282.2
PDIA3	7040.7	9207.3	10507.0
PPIB	18961.6	19849.4	21592.6
C19orf10	5190.8	5788.2	6182.3
SLC35B1	1800.4	2476.9	2650.4
SEC61A1	7048.9	8118.4	8798.1
RPN1	5478.6	5861.5	6968.3
DNAJC3	2090.7	2341.1	3381.5
CDK2AP2	429.4	998.1	1167.4

GEO Series "GSE16194" Expression Profiles

Num of samples in this series: 6

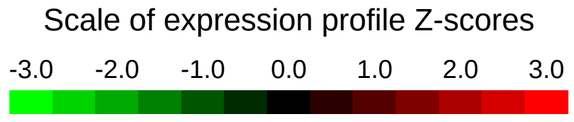

GEO Link:	http://www.ncbi.nlm.nih.gov/geo/query/acc.cgi?acc=GSE16194
Status:	Public on May 21 2010
Title:	Expression data from Snail over-expressing non-small cell lung cancer cell lines
Organism:	Homo sapiens
Experiment type:	Expression profiling by array
Platform:	GPL570
Pubmed ID:	19887480
Summary & Design:	**Summary:** Snail is a zinc-finger transcription factor best known for its ability to down-regulate E-cadherin. Its established significance in embryology and organogenesis has been expanded to include a role in the tumor progression of a number of human cancers. In addition to E-cadherin, it has more recently been associated with the down-regulation and up-regulation of a number of other genes that affect important malignant phenotypes. After establishing the presence of up-regulated Snail in human non-small cell lung cancer specimens, we used microarrays to detail the global programme of gene expression in non-small cell lung cancer cell lines stably transduced to over-express Snail as compared to vector control cell lines. **Overall design:** Non-small cell lung cancer cell lines (H441, H292, H1437) were stably transduced with a retroviral vector to over-express Snail. Elevated Snail and a corresponding down-regulation of E-cadherin was verified in the Snail over-expressing cell lines as compared to vector control cell lines by Western analysis. RNA extraction was performed and samples submitted to the UCLA Clinical Microarray Core for hybridization to Affymetrix arrays.

Background corr dist: KL-Divergence = 0.0383, L1-Distance = 0.0289, L2-Distance = 0.0011, Normal std = 0.6338

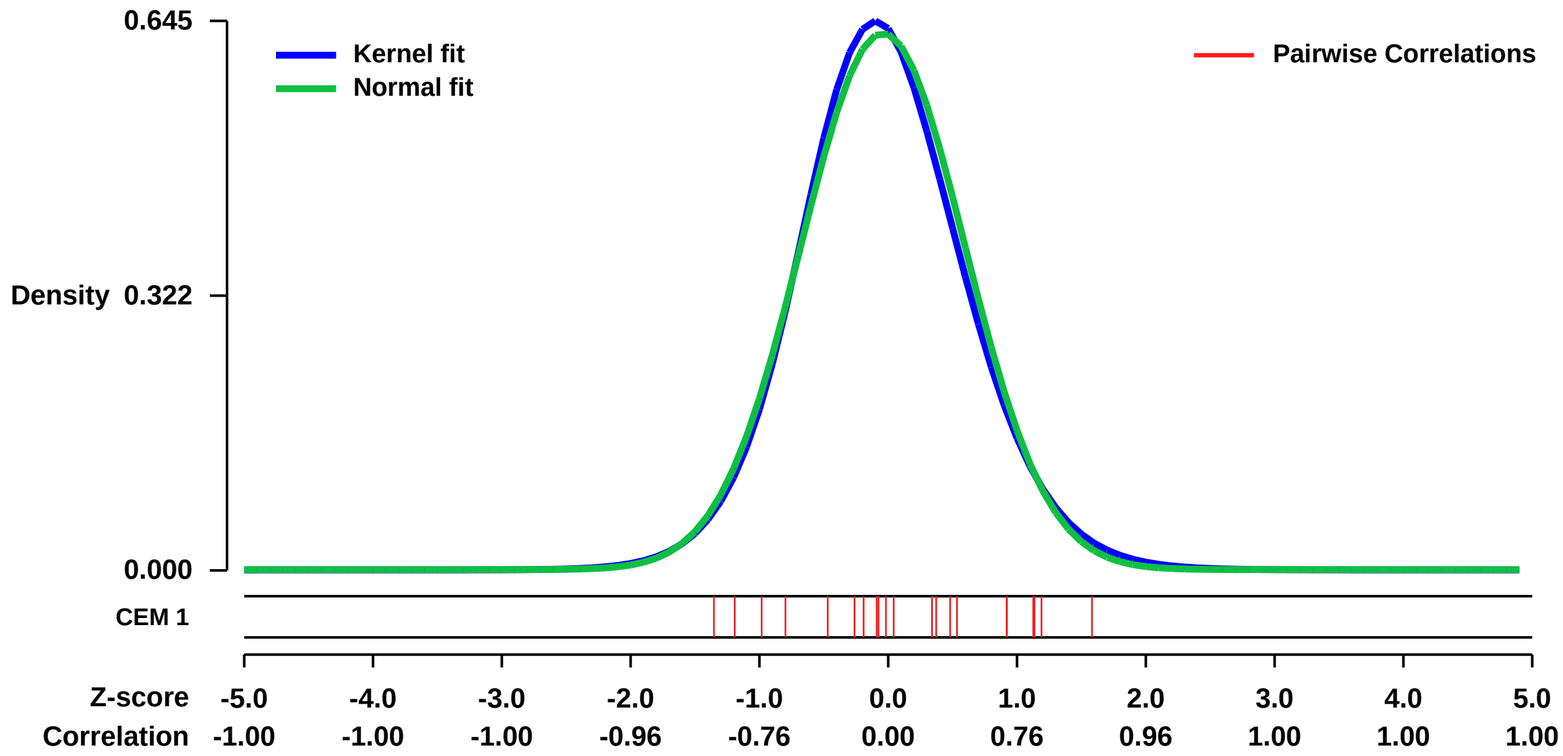

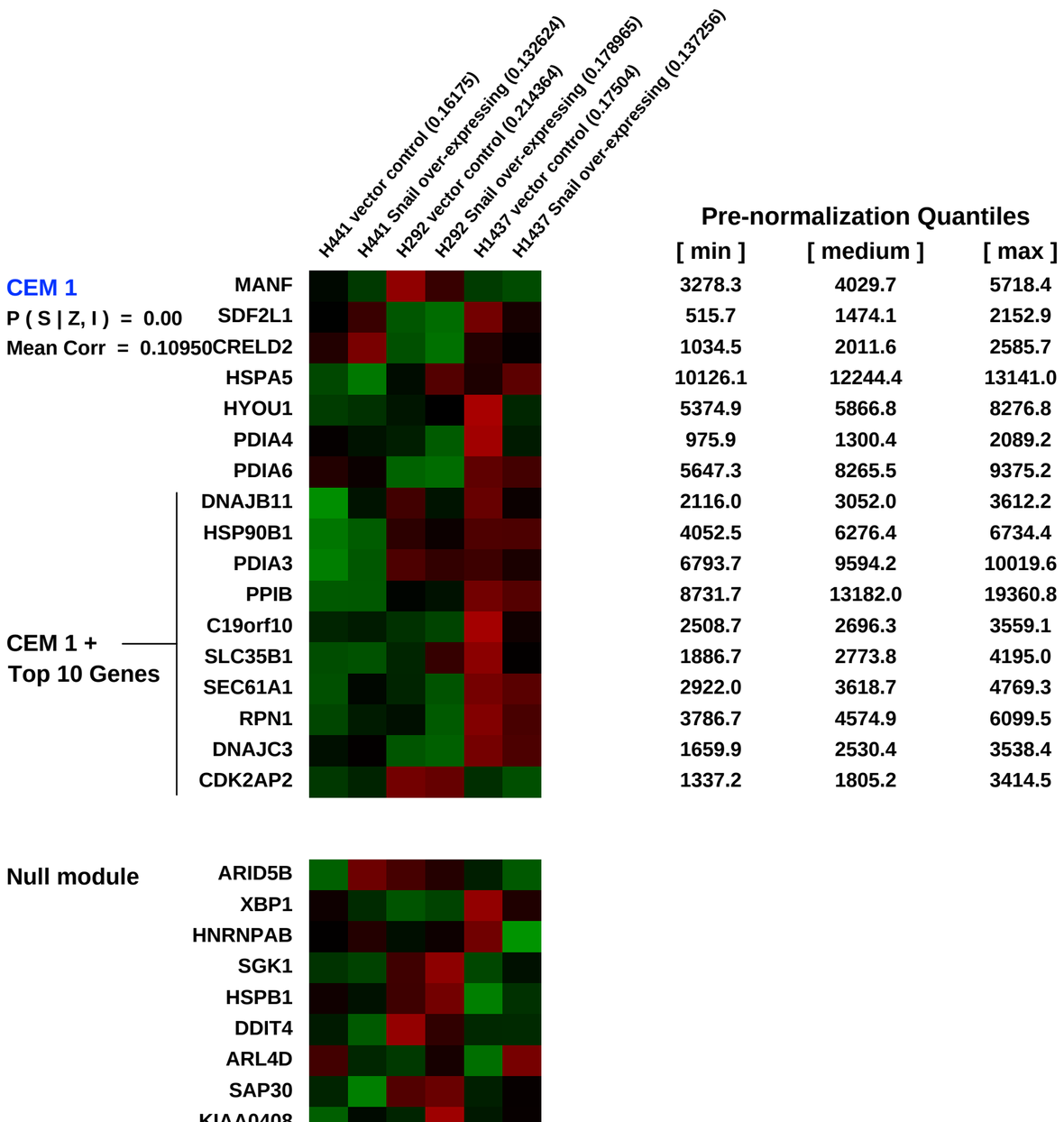

Pre-normalization Quantiles

	[min]	[medium]	[max]
MANF	3278.3	4029.7	5718.4
SDF2L1	515.7	1474.1	2152.9
CRELD2	1034.5	2011.6	2585.7
HSPA5	10126.1	12244.4	13141.0
HYOU1	5374.9	5866.8	8276.8
PDIA4	975.9	1300.4	2089.2
PDIA6	5647.3	8265.5	9375.2
DNAJB11	2116.0	3052.0	3612.2
HSP90B1	4052.5	6276.4	6734.4
PDIA3	6793.7	9594.2	10019.6
PPIB	8731.7	13182.0	19360.8
C19orf10	2508.7	2696.3	3559.1
SLC35B1	1886.7	2773.8	4195.0
SEC61A1	2922.0	3618.7	4769.3
RPN1	3786.7	4574.9	6099.5
DNAJC3	1659.9	2530.4	3538.4
CDK2AP2	1337.2	1805.2	3414.5

GEO Series "GSE11618" Expression Profiles

Num of samples in this series: 18

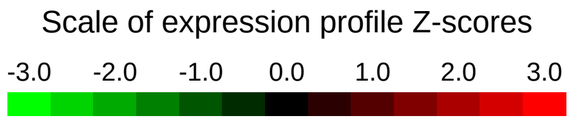

GEO Link:	http://www.ncbi.nlm.nih.gov/geo/query/acc.cgi?acc=GSE11618
Status:	Public on Dec 01 2008
Title:	Stable XIAP knockdown in HCT116 colon cancer cells
Organism:	Homo sapiens
Experiment type:	Expression profiling by array
Platform:	GPL570
Pubmed ID:	19034449
Summary & Design:	**Summary:** X-linked inhibitor of apoptosis (XIAP) is the most potent endogenous caspase inhibitor preventing cell death via caspase-9, -7 and -3 (initiator and executioner caspase pathways). Using short hairpin RNA (shRNA) against XIAP, stably expressed in a parent HCT116 human colon cancer cell line, a series of clones have been developed. XIAP mRNA levels were established by RT-PCR, the four X (XIAP knockdown) clonal cell lines show 82-93% reduction in XIAP mRNA when compared to the four L (luciferase control) cell lines. Immunoblot analysis showed a 67-89% reduction in XIAP protein in X cell lines compared to L. RNA was analysed by microarray and XIAP knockdown was confirmed in 7 probe sets, there was no significant compensation of other IAP family members. XIAP knockdown induced a 2-fold increase in the basal level of apoptosis without modification of caspase 3/7 activity. Finally, XIAP knockdown sensitises cells to radiotherapy by 20%, to recombinant TRAIL by a 3-fold factor, and to paclitaxel and docetaxel by >2 fold factor. Future work should focus on targeted agents such as rhTRAIL in combination with strategies to down regulate XIAP. XIAP antisense is now in clinical development in oncology. **Overall design:** Human HCT116 colon cancer cell lines were transfected with either XIAP (X) or luciferase (L) shRNA. The expression profiles of both were compared at early (p4) and late (p8) passage.

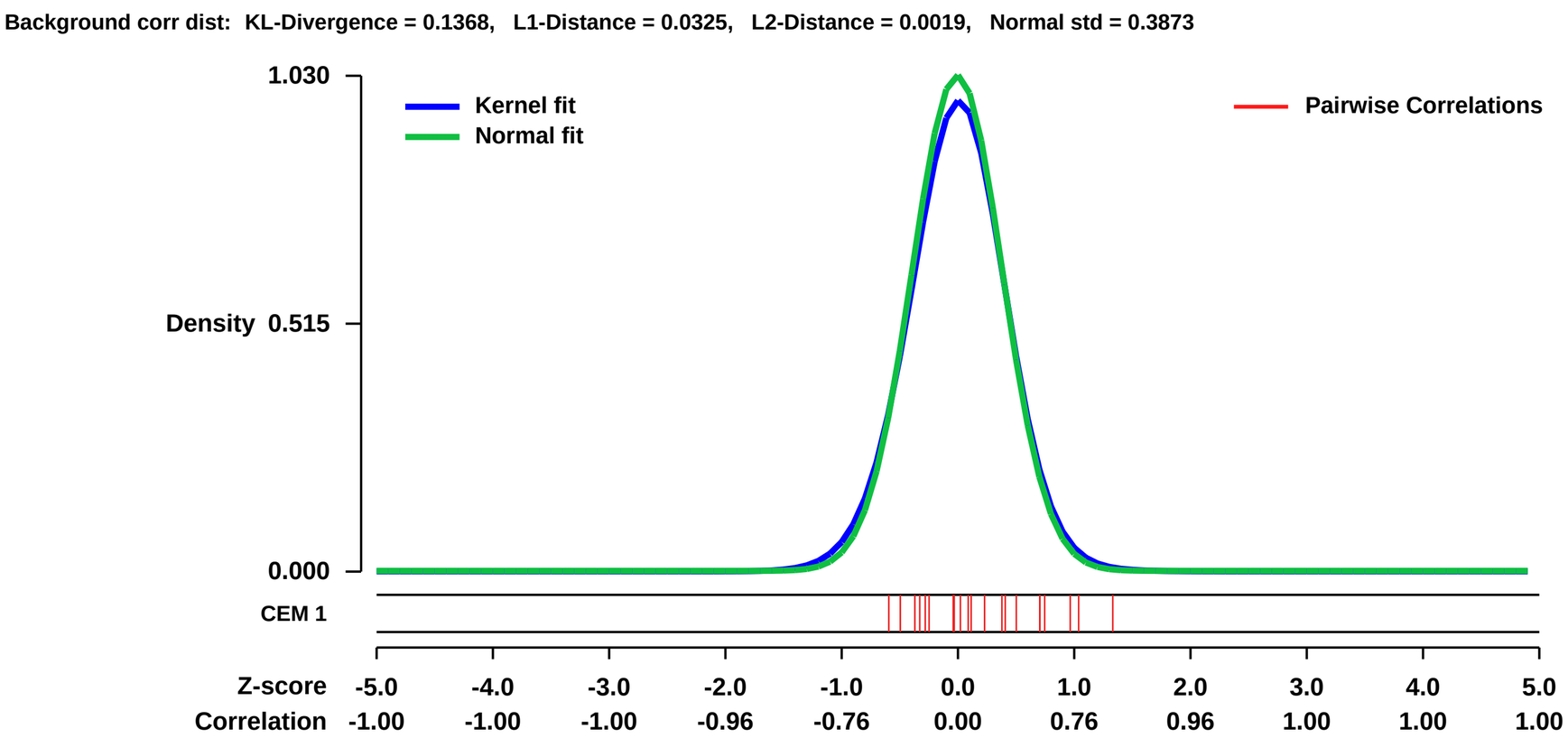

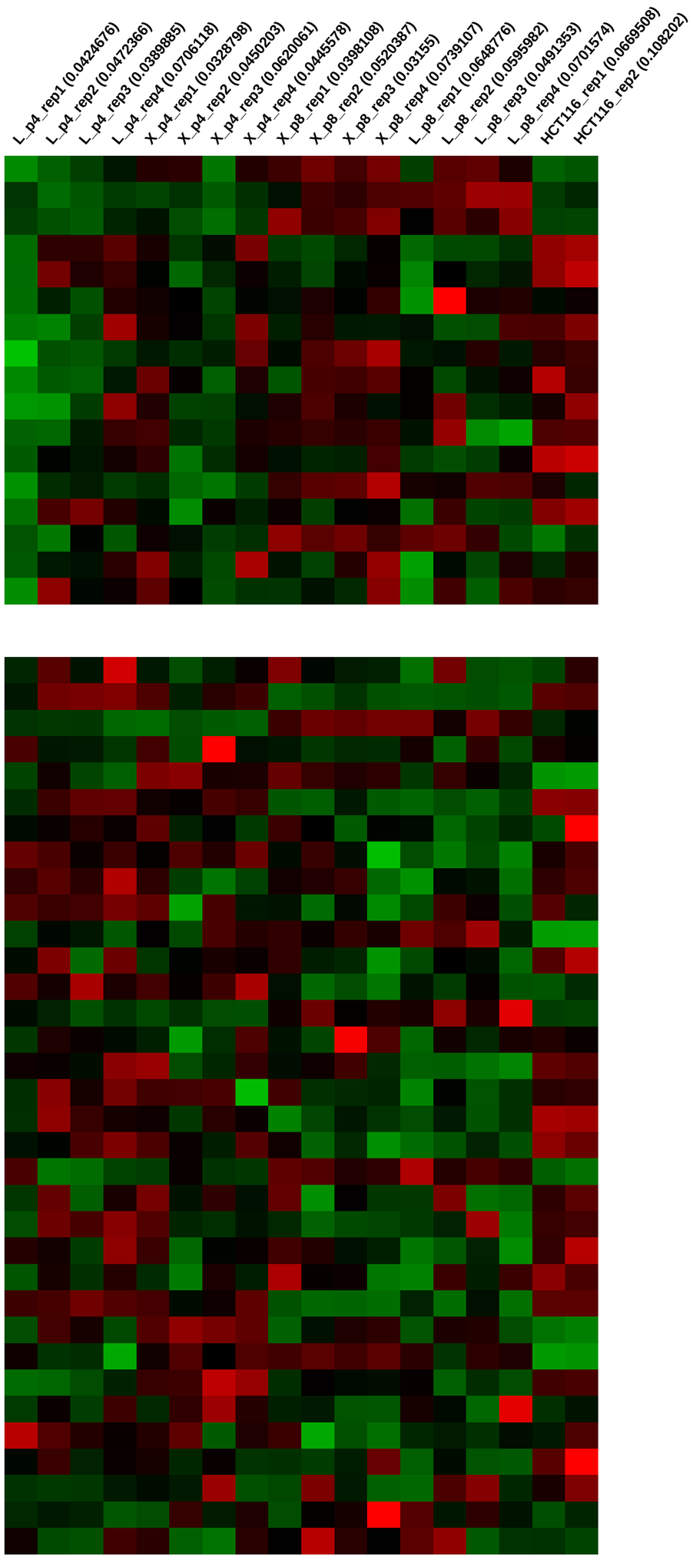

GEO Series "GSE40281" Expression Profiles

Num of samples in this series: 9

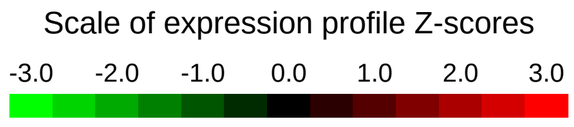

GEO Link:	http://www.ncbi.nlm.nih.gov/geo/query/acc.cgi?acc=GSE40281
Status:	Public on May 31 2013
Title:	Signaling pathways of HPAIV
Organism:	Homo sapiens
Experiment type:	Expression profiling by array
Platform:	GPL570
Pubmed ID:	24189062

Summary & Design:

Summary:
Highly pathogenic avian influenza viruses (HPAIV) induce severe inflammation in poultry and men. There is still an ongoing threat that these viruses may acquire the capability to freely spread as novel pandemic virus strains that may cause major morbidity and mortality. One characteristic of HPAIV infections is the induction of a cytokine burst that strongly contributes to viral pathogenicity. It has been suggested, that this cytokine overexpression is an intrinsic feature of infected cells and involves hyperinduction of p38 mitogen activated protein kinase (MAPK). Here we investigate the role of MAPK p38 signaling in the antiviral response against HPAIV in mice as well as in endothelial cells, the latter a primary source for cytokines during systemic infections.

Global gene expression profiling of HPAIV infected endothelial cells in the presence of the MAP kinase p38-specific inhibitor SB202190 revealed, that inhibition of MAPK p38 leads to reduced expression of interferon (IFN) and other cytokines after A/Thailand/1(KAN-1)/2004 (H5N1) and A/FPV/Bratislava/79 (H7N7) infection. Furthermore, the expression of interferon stimulated genes (ISGs) after treatment with IFN or conditioned media from HPAIV infected cells was decreased when the target cells were preincubated with SB202190. Finally, promoter analysis confirmed a direct impact of p38 MAPK on the IFN-enhanceosome and ISG-promoter activity. In vivo inhibition of MAP kinase p38 greatly diminishes virus induced cytokine expression concomitant with reduced viral titers, thereby protecting mice from lethal infection.

These observations show, that MAPK p38 acts on two levels of the antiviral IFN response: Initially the kinase regulates IFN induction and at a later stage MAPK p38 controls IFN signaling and thereby expression of IFN-stimulated genes. Thus, inhibition of MAP kinase p38 may be an antiviral strategy that significantly protects mice from lethal influenza via suppression of overshooting cytokine expression.

Overall design:
HUVEC were infected with FPV in the presence or absence of a p38 MAP kinase inhibitor

Background corr dist: KL-Divergence = 0.0743, L1-Distance = 0.0376, L2-Distance = 0.0025, Normal std = 0.5012

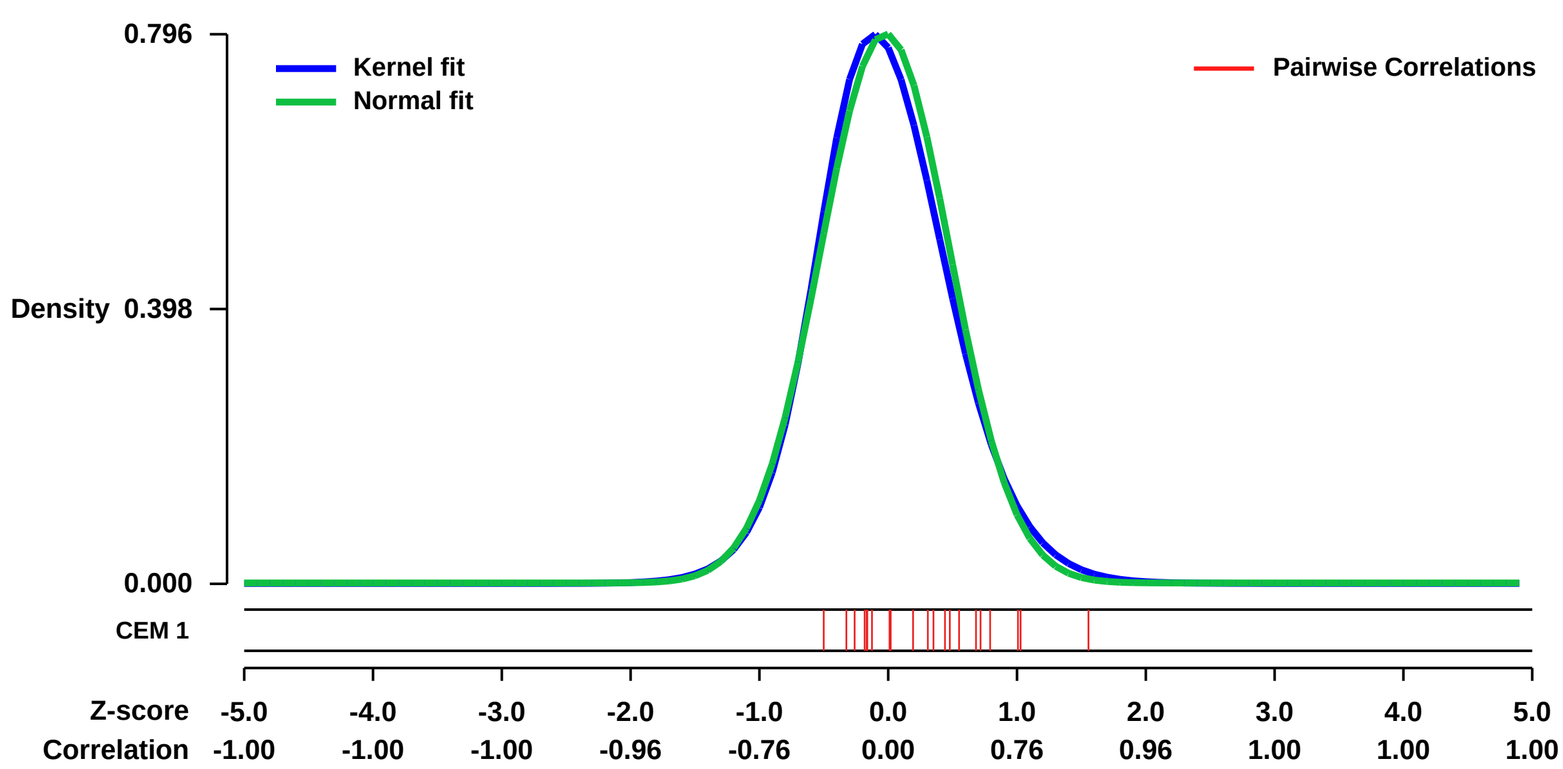

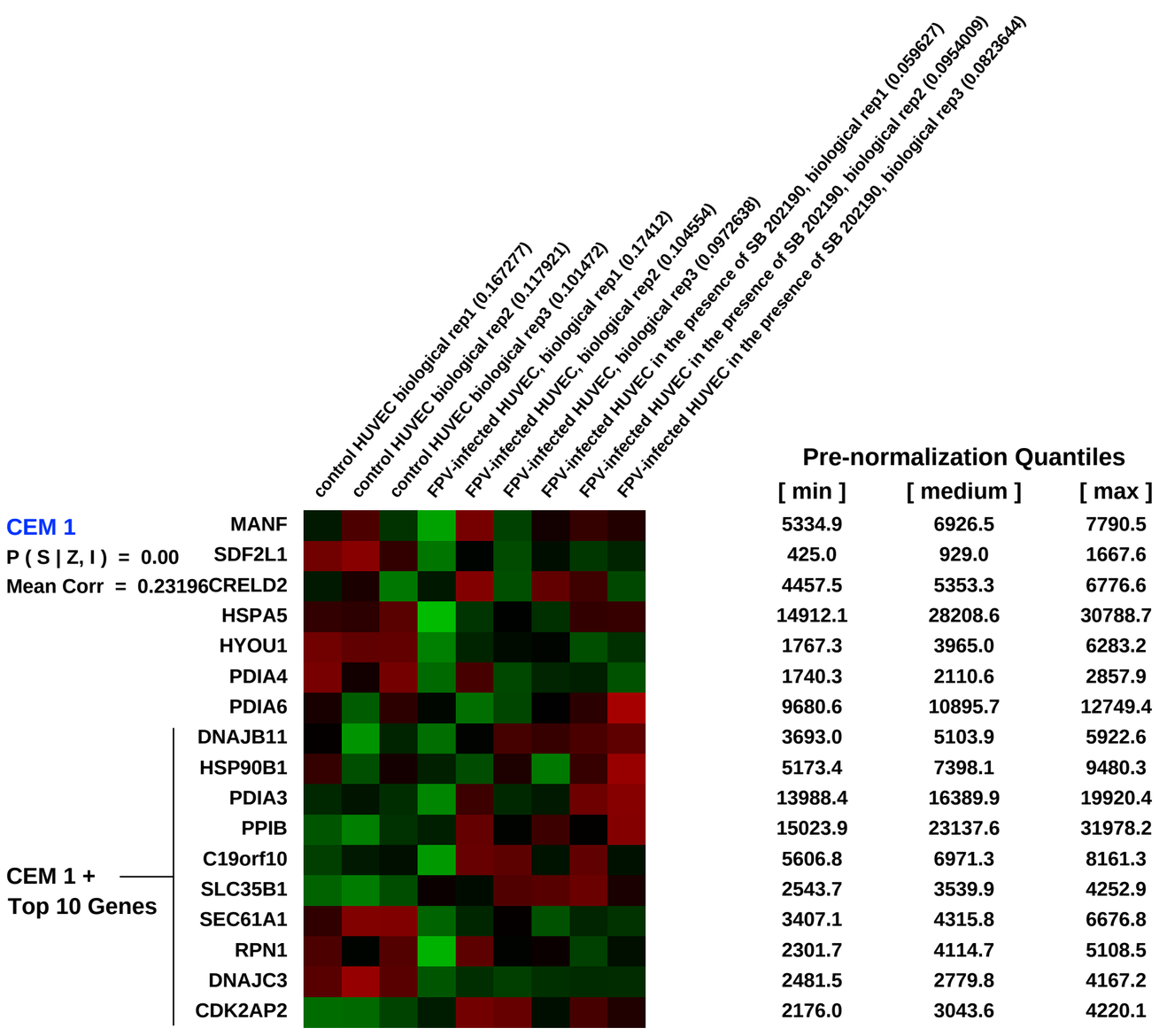

GEO Series "GSE58049" Expression Profiles

Num of samples in this series: 9

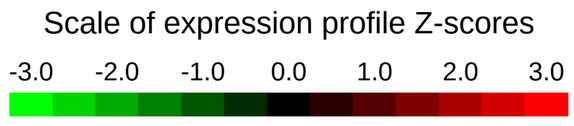

GEO Link:	http://www.ncbi.nlm.nih.gov/geo/query/acc.cgi?acc=GSE58049
Status:	Public on Jul 07 2014
Title:	Genome-wide analysis in human colorectal cancer cells reveals ischemia-mediated expression of motility genes via DNA hypomethylation (expression)
Organism:	Homo sapiens
Experiment type:	Expression profiling by array
Platform:	GPL570
Pubmed ID:	25079072
Summary & Design:	**Summary:** DNA hypomethylation is an important epigenetic modification found to occur in many different cancer types, leading to the upregulation of previously silenced genes and loss of genomic stability. We previously demonstrated that hypoxia and hypoglycaemia (ischemia), two common micro-environmental changes in solid tumors, decrease DNA methylation through the downregulation of DNMTs in human colorectal cancer cells. Here, we utilized a genome-wide cross-platform approach to identify genes hypomethylated and upregulated by ischemia. Following exposure to hypoxia or hypoglycaemia, methylated DNA from human colorectal cancer cells (HCT116) was immunoprecipitated and analysed with an Affymetrix promoter array. Additionally, RNA was isolated and analysed in parallel with an Affymetrix expression array. Ingenuity pathway analysis software revealed that a significant proportion of the genes hypomethylated and upregulated were involved in cellular movement, including PLAUR and CYR61. A Matrigel invasion assay revealed that indeed HCT116 cells grown in hypoxic or hypoglycaemic conditions have increased mobility capabilities. Confirmation of upregulated expression of cellular movement genes was performed with qPCR. The correlation between ischemia and metastasis is well established in cancer progression, but the molecular mechanisms responsible for this common observation have not been clearly identified. Our novel results suggest that hypoxia and hypoglycaemia may be driving changes in DNA methylation through downregulation of DNMTs. This is the first report to our knowledge that provides an explanation for the increased metastatic potential seen in ischemic cells; i.e. that ischemia could be driving DNA hypomethylation and increasing expression of cellular movement genes. **Overall design:** HCT116 cells were grown in either Hypoxic or Hypoglycaemic conditions, and compared to cells grown under normal conditions

Background corr dist: KL-Divergence = 0.0383, L1-Distance = 0.0319, L2-Distance = 0.0019, Normal std = 0.6074

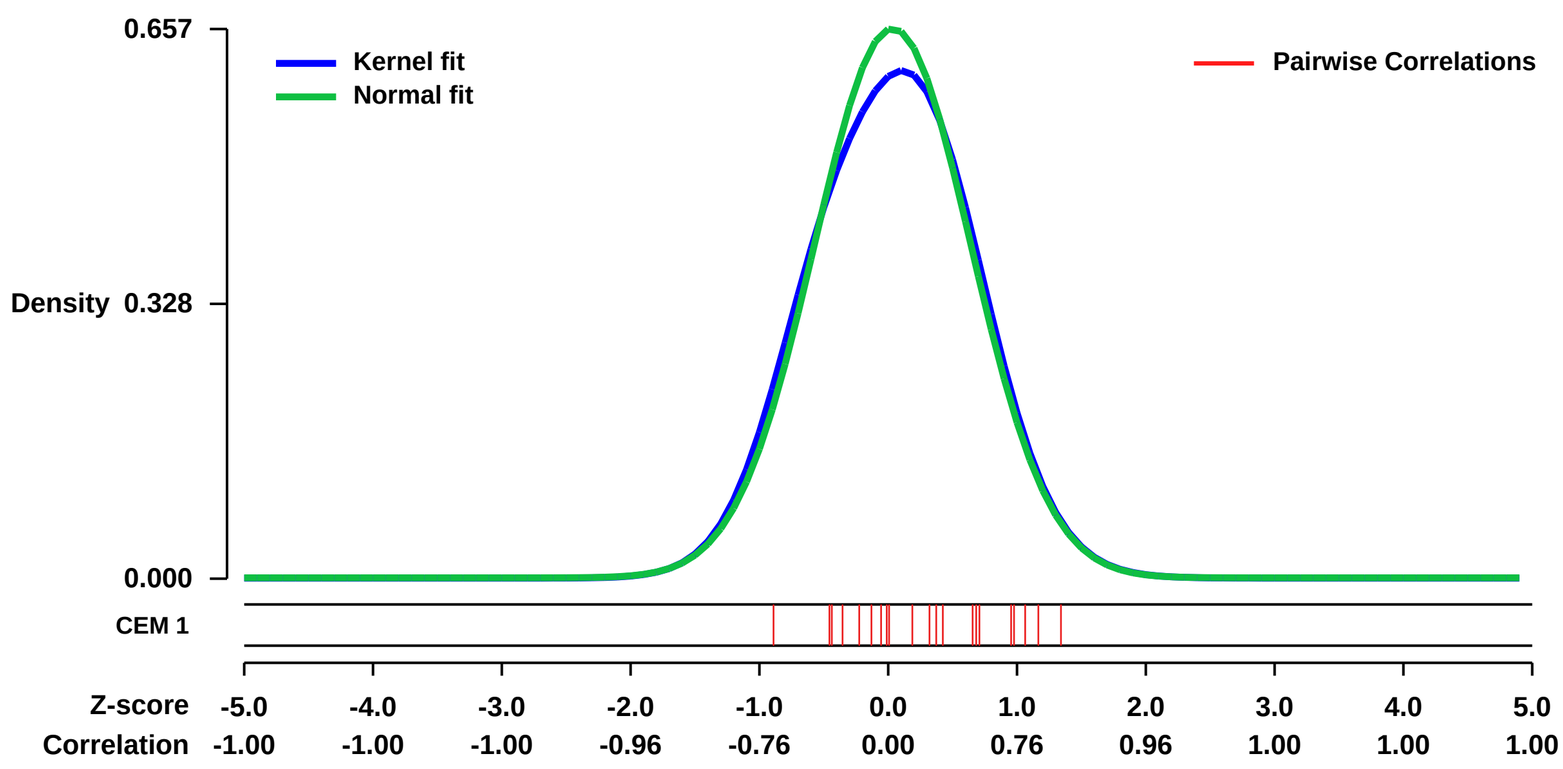

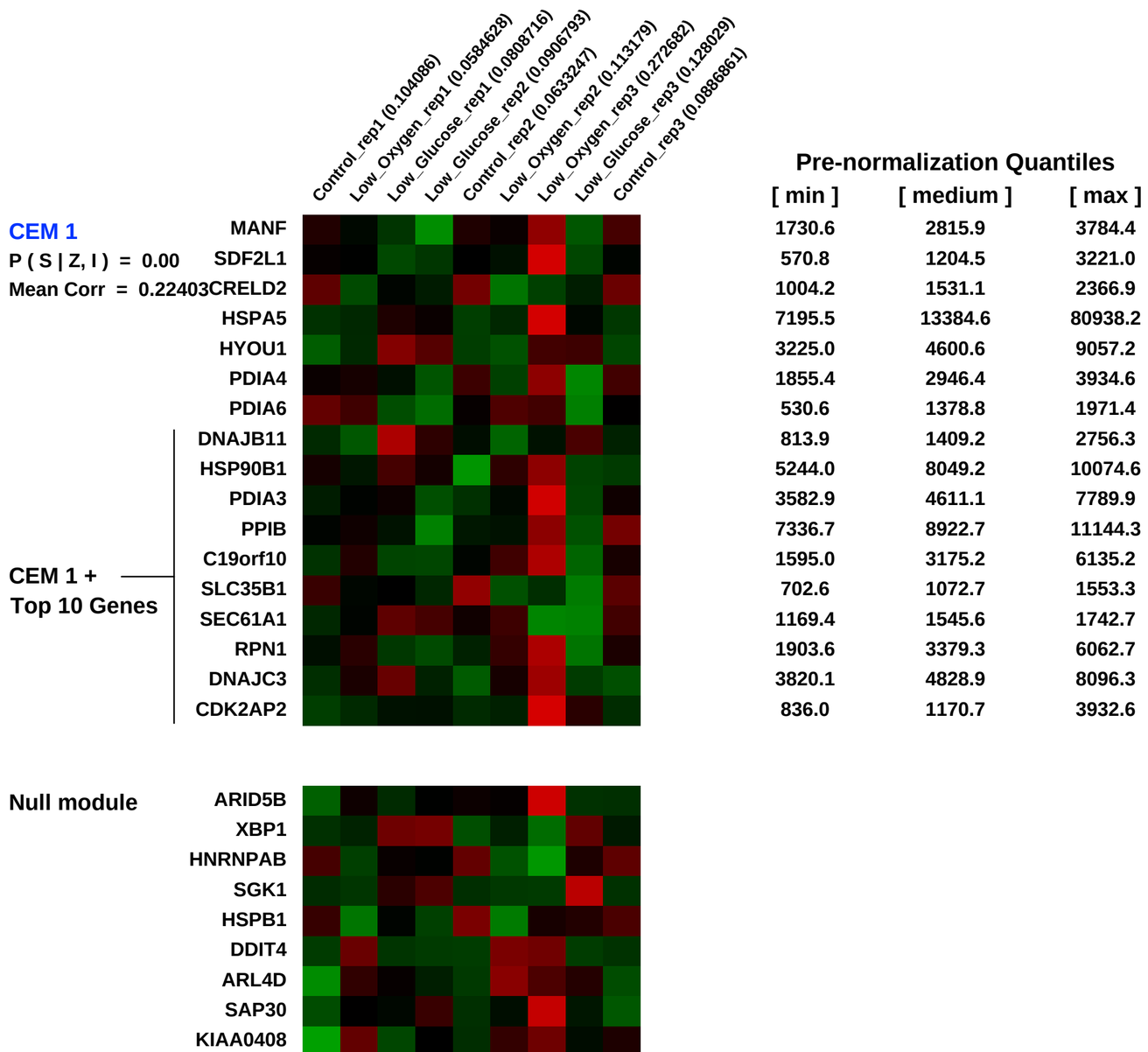

Pre-normalization Quantiles

	[min]	[medium]	[max]
MANF	1730.6	2815.9	3784.4
SDF2L1	570.8	1204.5	3221.0
CRELD2	1004.2	1531.1	2366.9
HSPA5	7195.5	13384.6	80938.2
HYOU1	3225.0	4600.6	9057.2
PDIA4	1855.4	2946.4	3934.6
PDIA6	530.6	1378.8	1971.4
DNAJB11	813.9	1409.2	2756.3
HSP90B1	5244.0	8049.2	10074.6
PDIA3	3582.9	4611.1	7789.9
PPIB	7336.7	8922.7	11144.3
C19orf10	1595.0	3175.2	6135.2
SLC35B1	702.6	1072.7	1553.3
SEC61A1	1169.4	1545.6	1742.7
RPN1	1903.6	3379.3	6062.7
DNAJC3	3820.1	4828.9	8096.3
CDK2AP2	836.0	1170.7	3932.6

GEO Series "GSE34454" Expression Profiles

Num of samples in this series: 9

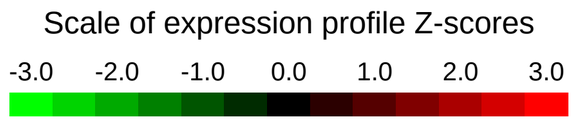

GEO Link:	http://www.ncbi.nlm.nih.gov/geo/query/acc.cgi?acc=GSE34454
Status:	Public on Jun 01 2012
Title:	Expression data from transfection of SW1783 glioma cells with microRNA-376a* for 24 hours
Organism:	Homo sapiens
Experiment type:	Expression profiling by array
Platform:	GPL570
Pubmed ID:	23093778
Summary & Design:	**Summary:** Enforced expression of miRNAs in cells leads to down-regulation of several mRNAs which harbour binding sites in their 3'UTRs for the overexpressed miRNA and represent potential target genes of the miRNA We transfected unedited miR-376a* (376a*A) and edited miR-376a* (376a*G) into SW1783 cells to identify transcripts down-regulated by each in comparison to control miRNA transfection. The aim was to identify target genes subject to direct regulation by miR-376a*A and by miR-376a*G. **Overall design:** SW1783 cells (100,000) were transfected with 50 nM of miR-376a*A, miR-376a*G or miR-control. Following incubation for 24 hours, total RNA was isolated from transfected cells. For each (miR-376a*A or miR-376a*G), genes differentially expressed upon miRNA transfection were determined based on comparison with miR-control-transfected samples. Biological triplicates were used for each sample type.

Background corr dist: KL-Divergence = 0.0547, L1-Distance = 0.0248, L2-Distance = 0.0009, Normal std = 0.5479

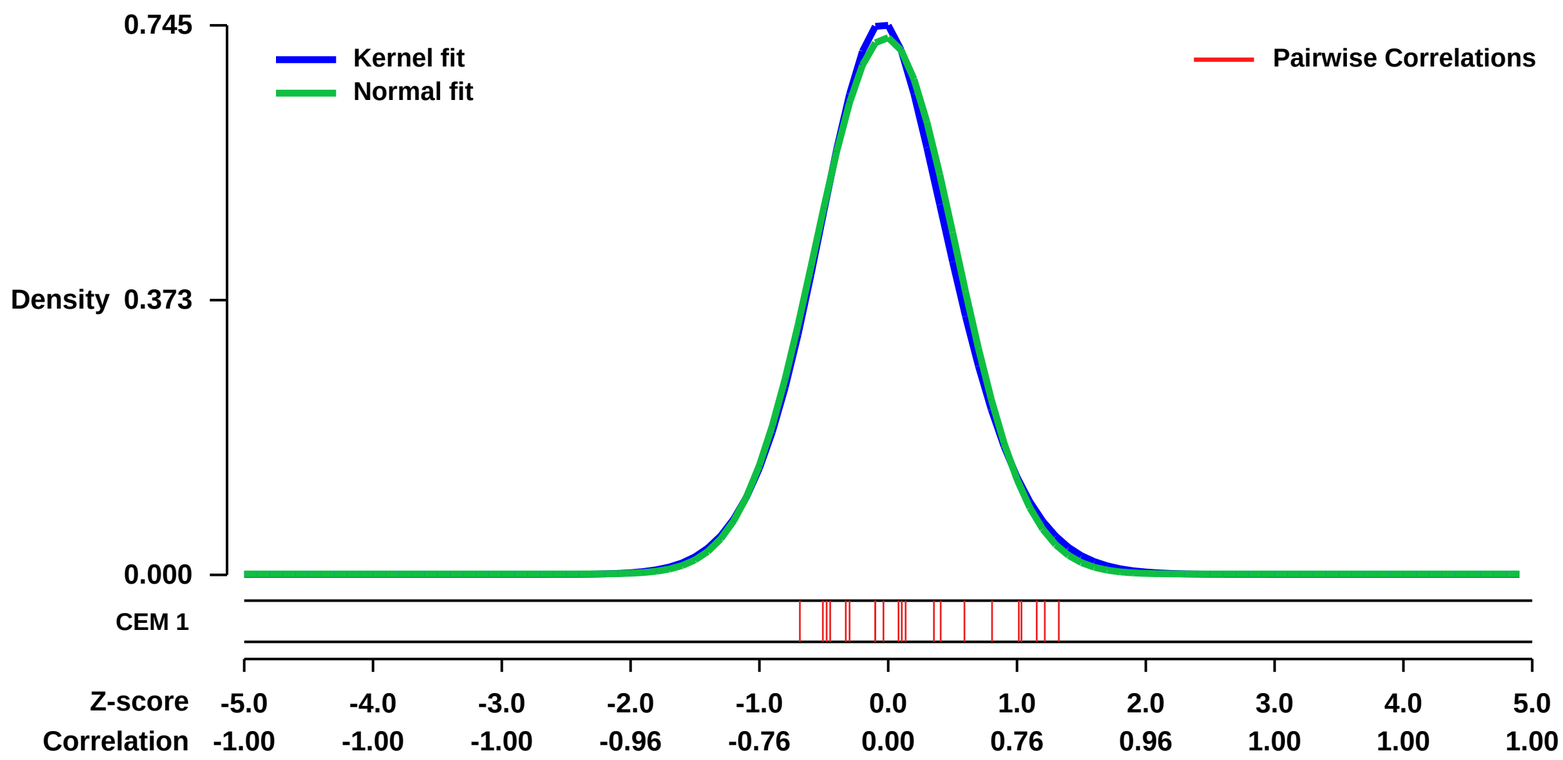

Z-score	-5.0	-4.0	-3.0	-2.0	-1.0	0.0	1.0	2.0	3.0	4.0	5.0
Correlation	-1.00	-1.00	-1.00	-0.96	-0.76	0.00	0.76	0.96	1.00	1.00	1.00

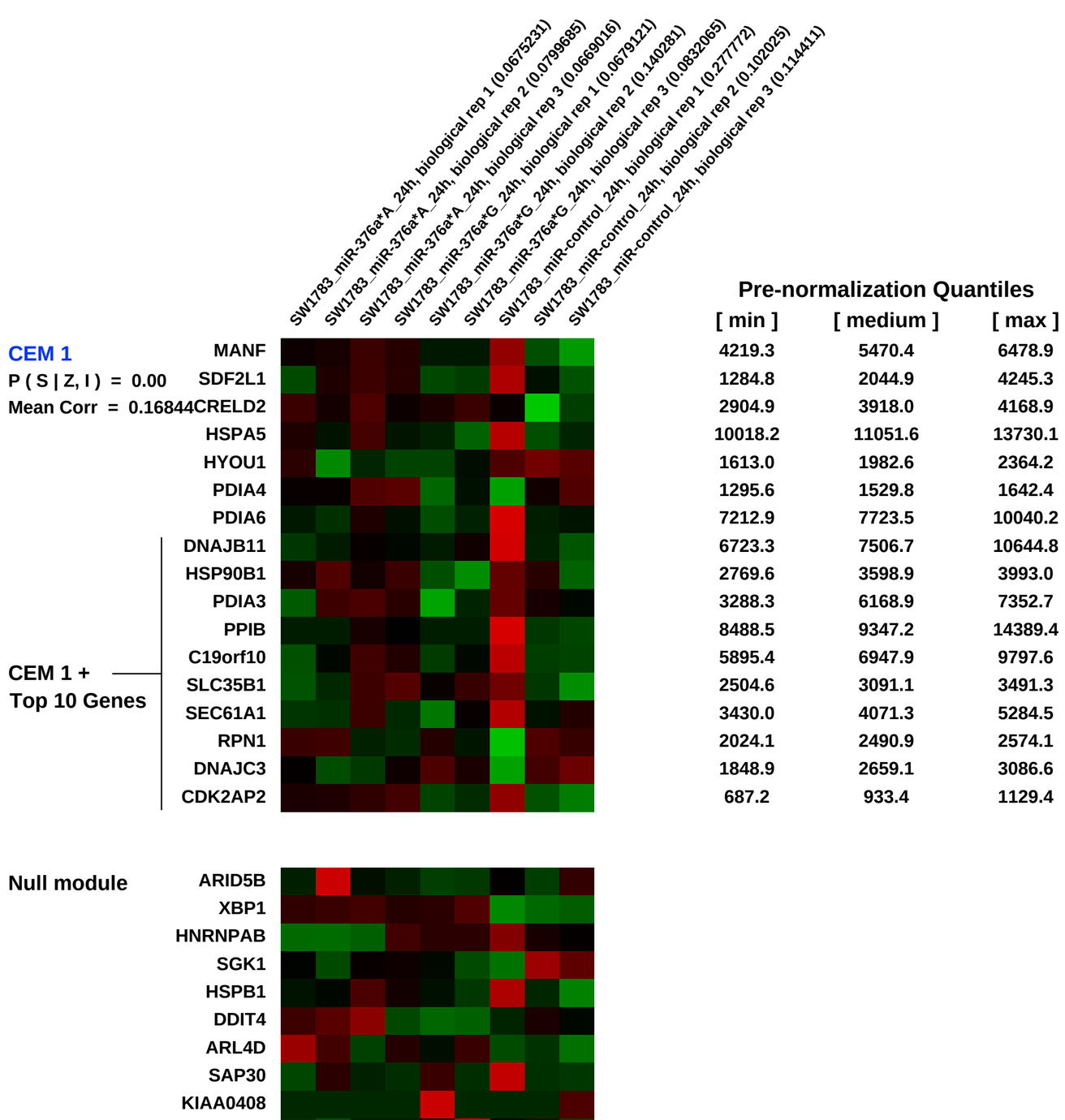

	Pre-normalization Quantiles		
	[min]	[medium]	[max]
MANF	4219.3	5470.4	6478.9
SDF2L1	1284.8	2044.9	4245.3
CRELD2	2904.9	3918.0	4168.9
HSPA5	10018.2	11051.6	13730.1
HYOU1	1613.0	1982.6	2364.2
PDIA4	1295.6	1529.8	1642.4
PDIA6	7212.9	7723.5	10040.2
DNAJB11	6723.3	7506.7	10644.8
HSP90B1	2769.6	3598.9	3993.0
PDIA3	3288.3	6168.9	7352.7
PPIB	8488.5	9347.2	14389.4
C19orf10	5895.4	6947.9	9797.6
SLC35B1	2504.6	3091.1	3491.3
SEC61A1	3430.0	4071.3	5284.5
RPN1	2024.1	2490.9	2574.1
DNAJC3	1848.9	2659.1	3086.6
CDK2AP2	687.2	933.4	1129.4
ARID5B			
XBP1			
HNRNPAB			
SGK1			
HSPB1			
DDIT4			
ARL4D			
SAP30			
KIAA0408			
GPR17			
HSPH1			
DNASE1L2			
SLC5A3			
GNAS			
GPR3			
TNFRSF25			
TM6SF2			
MKKS			
PLEKHF1			
ZMYM1			
DOK3			
FGF20			
SLC39A2			
KCNIP2			
ERRFI1			
DEDD2			
CCDC117			
USP31			
AHSA2			
CYS1			
CNIH2			
BANP			
CHORDC1			
P4HA1			

GEO Series "GSE51880" Expression Profiles

Num of samples in this series: 19

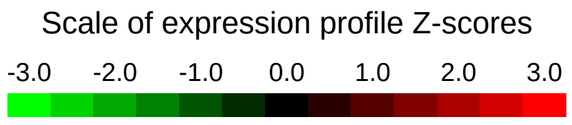

GEO Link:	http://www.ncbi.nlm.nih.gov/geo/query/acc.cgi?acc=GSE51880
Status:	Public on Nov 18 2013
Title:	Expression data from Uveal Melanoma
Organism:	Homo sapiens
Experiment type:	Expression profiling by array
Platform:	GPL570
Pubmed ID:	23849826
Summary & Design:	**Summary:** Despite advances in surgery and radiotherapy of uveal melanoma (UM), many patients develop distant metastases that poorly respond to therapy. Improved therapies for the metastatic disease are therefore urgently needed. Expression of the epidermal growth factor receptor (EGFR), a target of kinase inhibitors and humanized antibodies in use for several cancers, had been reported. 48 human UMs were analyzed by expression profiling. Evidence for signaling in tumors was obtained through the application of a UM-specific EGF signature. The EGFR specific kinase inhibitor, Gefitinib, and the humanized monoclonal antibody, Cetuximab, were tested for their effect on EGFR signaling. Natural killer cell mediated antibody-dependent cellular cytotoxicity (ADCC) and TNF-alpha release was analyzed for Cetuximab. EGFR appears suited as a novel molecular drug target for therapy of uveal melanoma. **Overall design:** Gene expression profiles of 19 unique samples from uveal melanoma patients were measured.

Background corr dist: KL-Divergence = 0.0675, L1-Distance = 0.0522, L2-Distance = 0.0051, Normal std = 0.5250

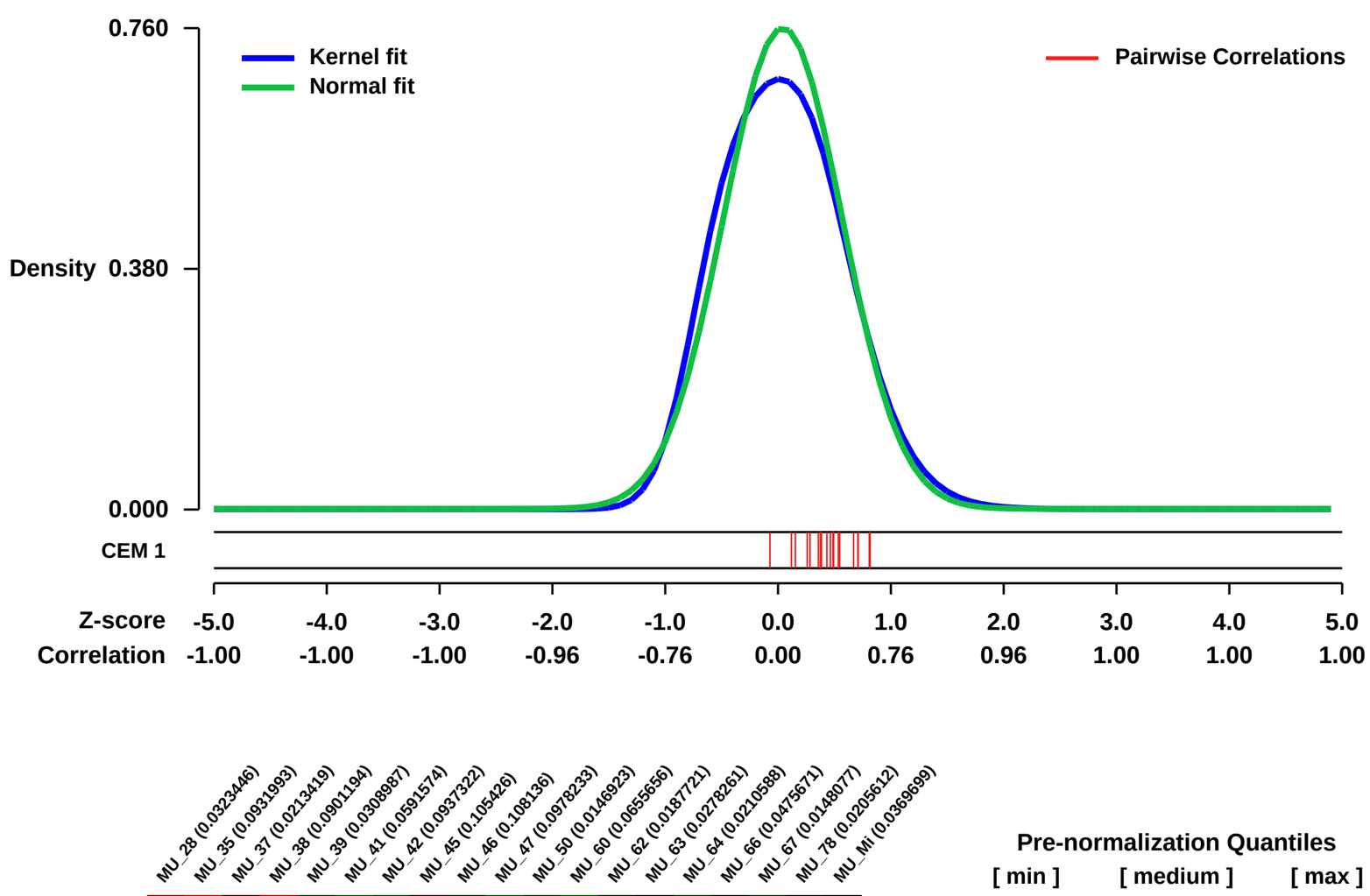

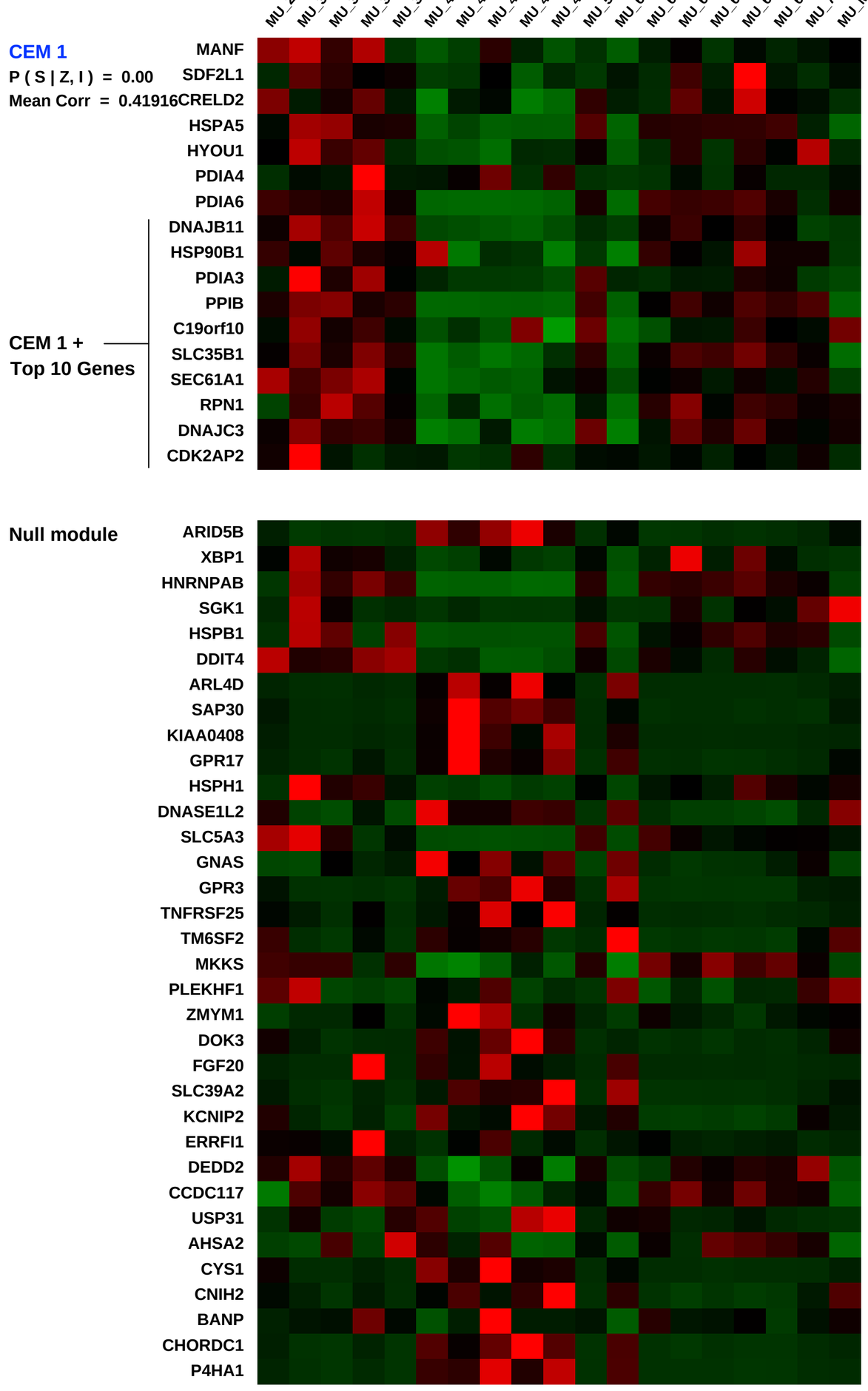

	Pre-normalization Quantiles		
	[min]	[medium]	[max]
MANF	372.8	1351.9	4788.9
SDF2L1	241.7	666.2	2596.9
CRELD2	293.1	1796.8	4907.5
HSPA5	197.8	5992.3	12280.7
HYOU1	138.2	934.1	3444.5
PDIA4	440.1	785.5	4134.6
PDIA6	238.9	5734.8	12695.1
DNAJB11	252.6	2215.1	6260.6
HSP90B1	295.3	2045.0	4454.7
PDIA3	300.0	1716.0	10220.7
PPIB	254.0	12006.2	21878.9
C19orf10	329.4	902.8	1529.7
SLC35B1	274.0	1430.9	2487.7
SEC61A1	165.3	1402.5	3319.4
RPN1	254.2	2336.4	5507.4
DNAJC3	325.9	3033.3	5421.3
CDK2AP2	267.0	679.8	5025.7

GEO Series "GSE22282" Expression Profiles

Num of samples in this series: 6

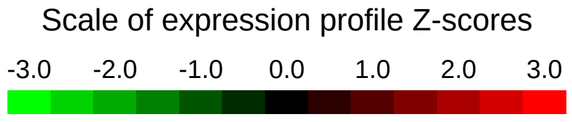

GEO Link:	http://www.ncbi.nlm.nih.gov/geo/query/acc.cgi?acc=GSE22282
Status:	Public on Dec 31 2010
Title:	Mature dendritic cells under hypoxic condition
Organism:	Homo sapiens
Experiment type:	Expression profiling by array
Platform:	GPL570
Pubmed ID:	21148811
Summary & Design:	**Summary:** Dendritic cells (DCs) are professional antigen-presenting cells whose activity is intrinsically linked to the microenvironment. Hypoxia is a condition of low oxygen tension occurring in inflammatory tissues that creates a special microenvironment conditioning cell physiology. We studied the effects of hypoxia on the differentiation of human monocytes into DCs and maturation into mature DCs. Mature DCs were differentiated in vitro from human monocytes under normoxic or hypoxic conditions and the gene expression profile was determined. **Overall design:** The expression profile of mature dendritic cells under normoxia vs hypoxia was studied. Three healthy donors were used as biologial replicates.

Background corr dist: KL-Divergence = 0.0340, L1-Distance = 0.0332, L2-Distance = 0.0015, Normal std = 0.6585

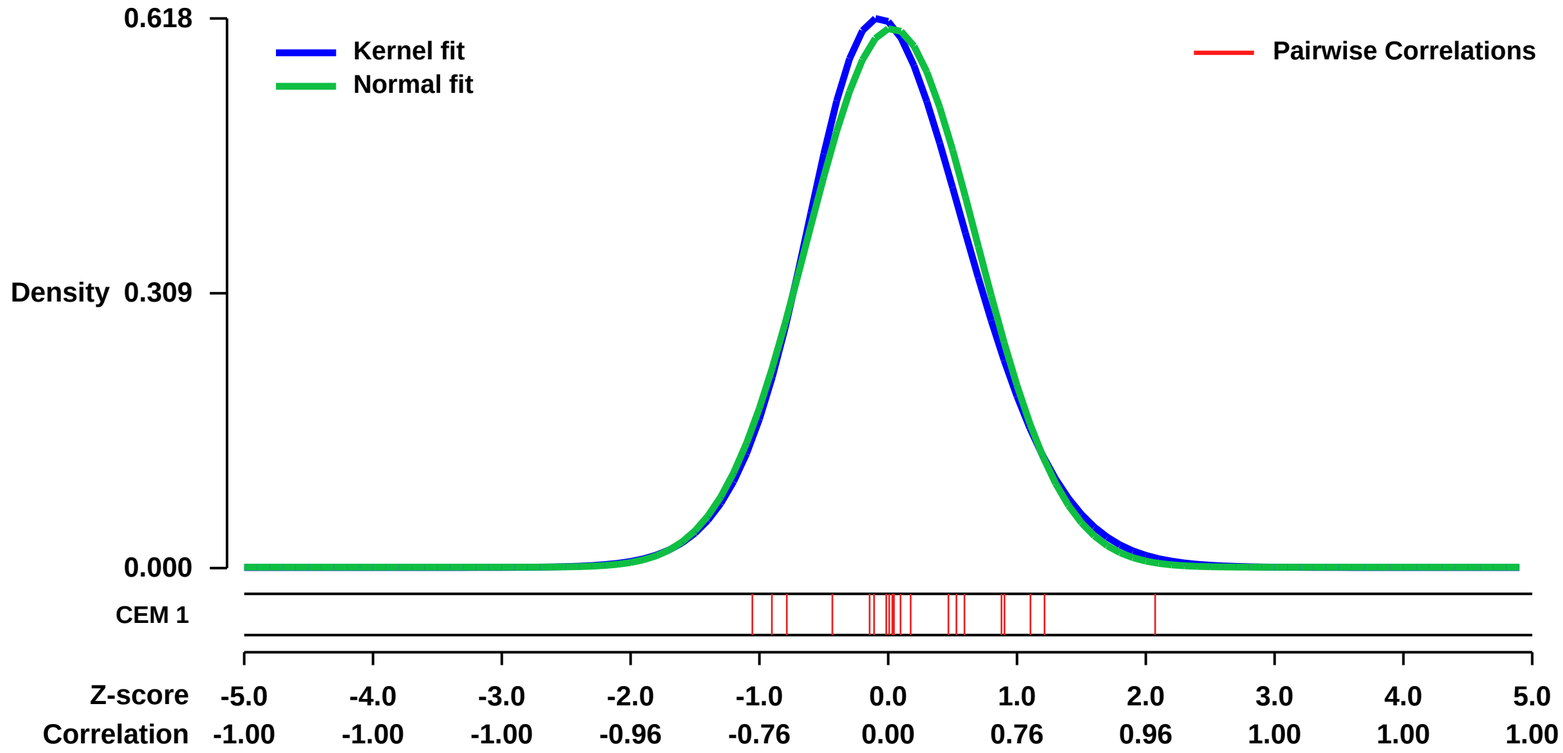

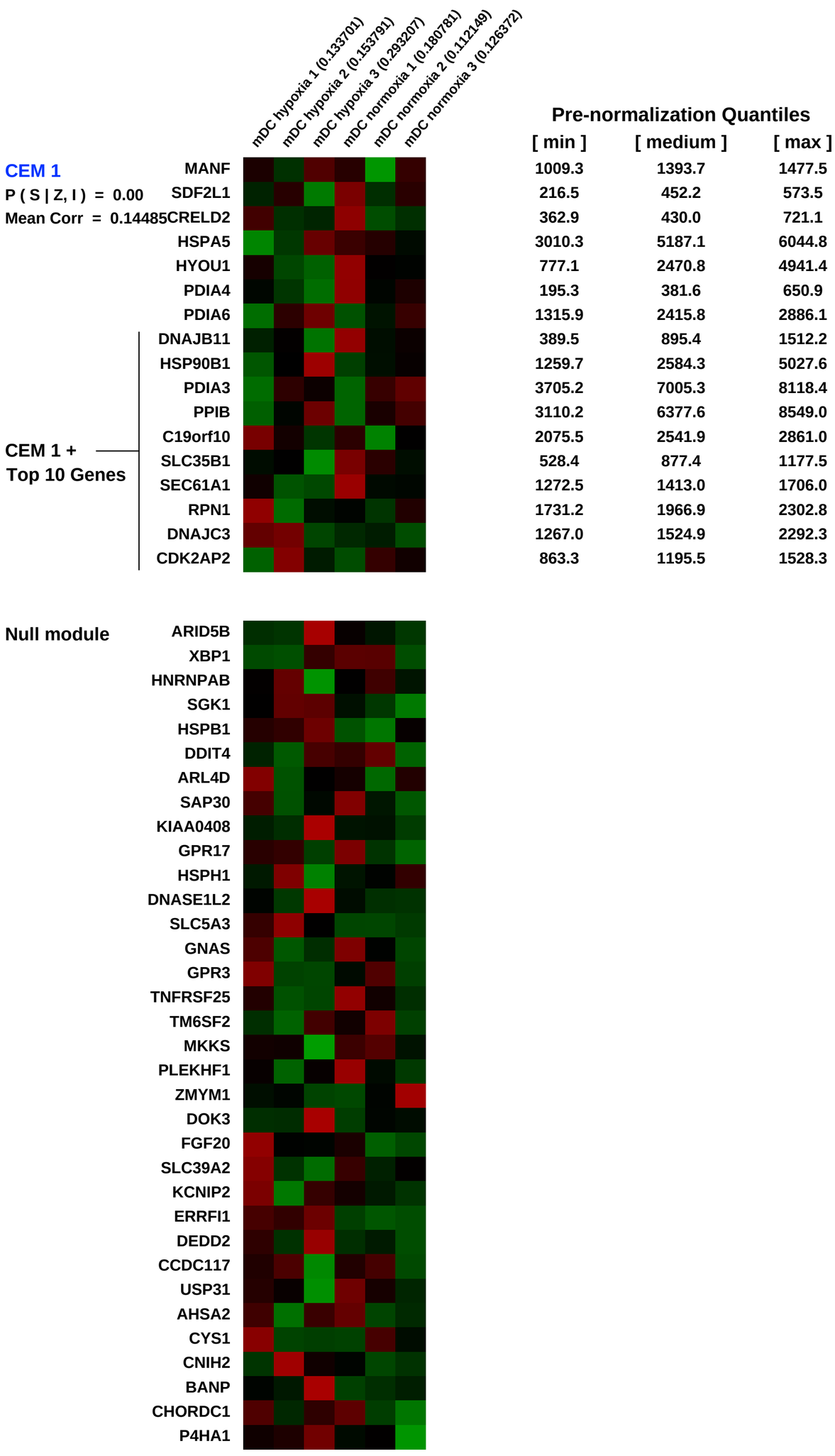

GEO Series "GSE21989" Expression Profiles

Num of samples in this series: 12

Scale of expression profile Z-scores

-3.0 -2.0 -1.0 0.0 1.0 2.0 3.0

GEO Link: http://www.ncbi.nlm.nih.gov/geo/query/acc.cgi?acc=GSE21989

Status: Public on May 26 2010

Title: Transcriptional response in human umbilical vein endothelial cells exposed to insulin

Organism: Homo sapiens

Experiment type: Expression profiling by array

Platform: GPL570

Pubmed ID:

Summary & Design:

Summary:
Background: In diabetes chronic hyperinsulinemia is responsible for the instability of the atherosclerotic plaque and stimulates cellular proliferation through the activation of the MAP kinases, which in turn regulate cellular proliferation. However, it is not known whether insulin itself could increase the transcription of specific genes for cellular proliferation in the endothelium. Hence, the characterization of transcriptional modifications in endothelium is an important step for a better understanding of the mechanism of insulin action and the relationship between endothelial cell dysfunction and insulin resistance.

Methodology and principal findings: The transcriptional response of endothelial cells in the 440 minutes following insulin stimulation was monitored using microarrays and compared to a control condition. About 1700 genes were selected as differentially expressed based on their treated minus control profile, thus allowing the detection of even small but systematic changes in gene expression. Genes were clustered in 7 groups according to their time expression profile and classified into 15 functional categories that can support the biological effects of insulin, based on Gene Ontology enrichment analysis. In terms of endothelial function, the most prominent processes affected were NADH dehydrogenase activity, N-terminal myristoylation domain binding, nitric-oxide synthase regulator activity and growth factor binding. Pathway-based enrichment analysis revealed â Electron Transport Chainâ significantly enriched.

Results were validated on genes belonging to â Electron Transport Chainâ pathway, using quantitative RT-PCR.

Conclusions: As far as we know, this is the first systematic study in the literature monitoring transcriptional response to insulin in endothelial cells, in a time series microarray experiment. Since chronic hyperinsulinemia is responsible for the instability of the atherosclerotic plaque and stimulates cellular proliferation, some of the genes identified in the present work are potential novel candidates in diabetes complications related to endothelial dysfunction.

Overall design:
Experiments were carried on human umbilical venous endothelial cells (HUVEC) to elucidate the regulatory aspects of insulin from dynamic gene expression data. HUVEC incubated with or without insulin were collected at times 0', 40', 100', 200', 340' and 440'. RNA was extracted and quantified for high-density oligonucleotide microarrays Human Genome U133 Plus 2.0 GeneChip (Affymetrix, Santa Clara, CA).

Background corr dist: KL-Divergence = 0.1436, L1-Distance = 0.0363, L2-Distance = 0.0025, Normal std = 0.3785

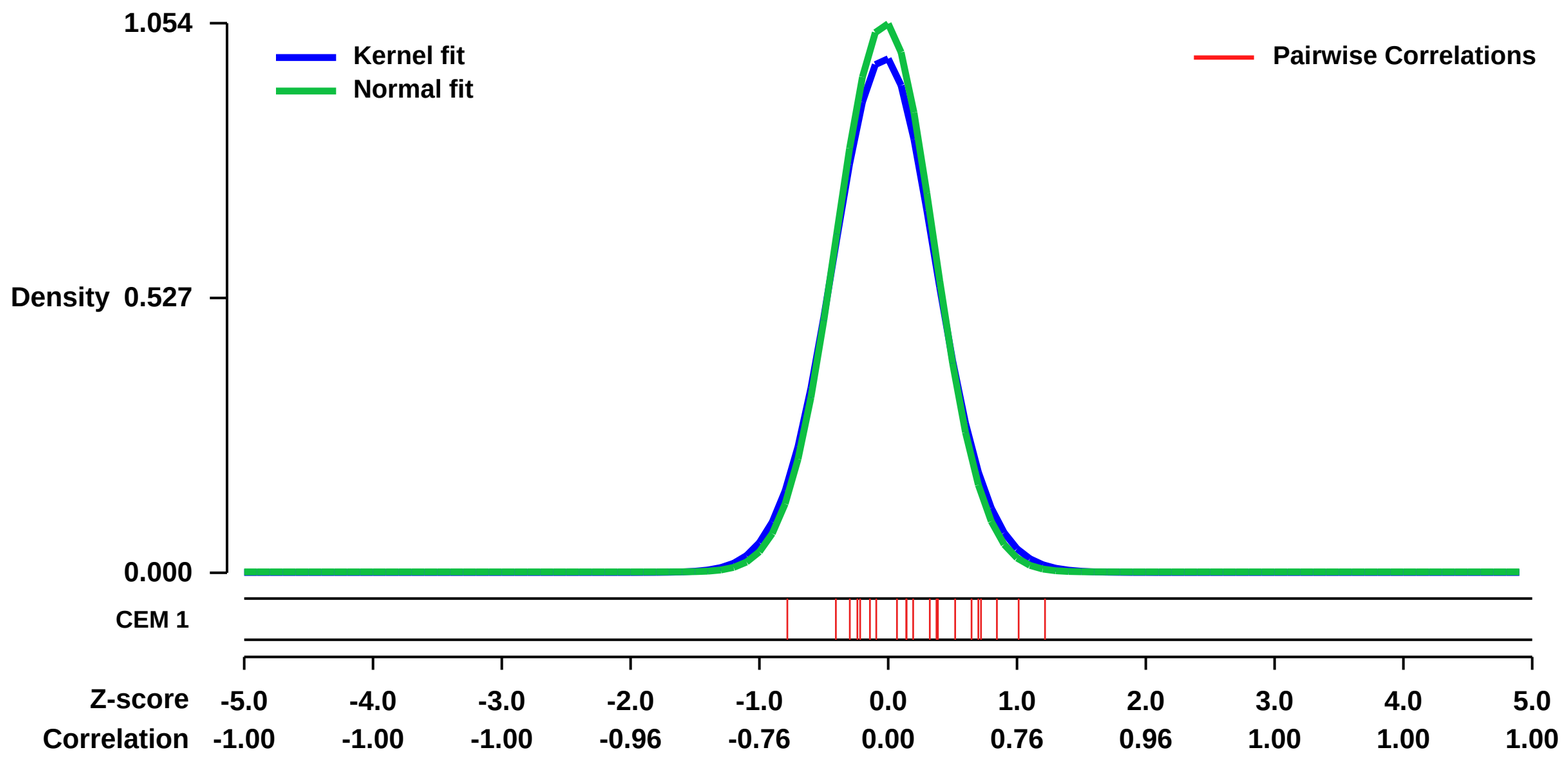

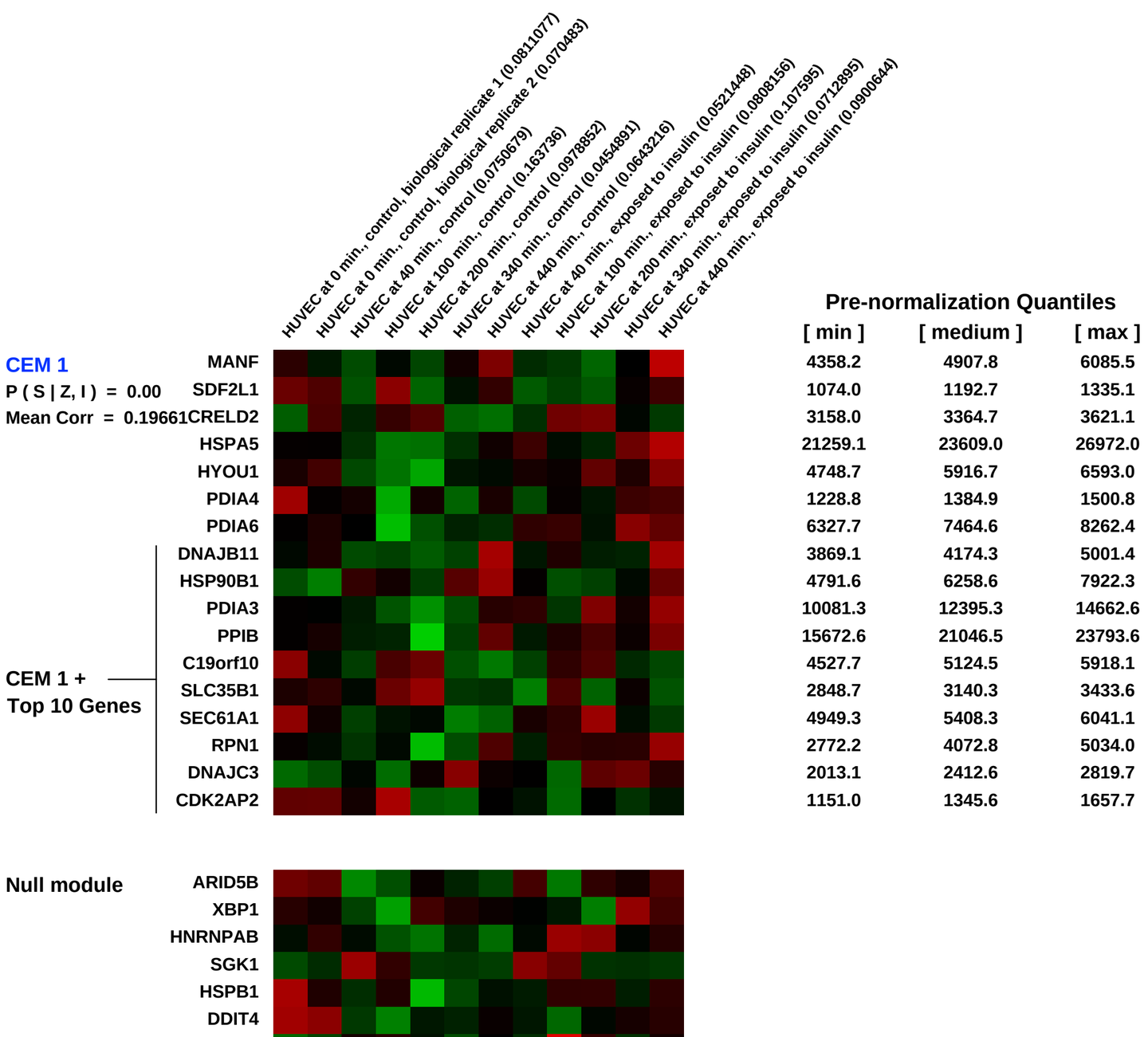

GEO Series "GSE29060" Expression Profiles

Num of samples in this series: 6

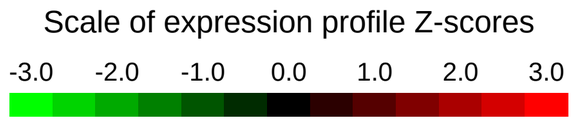

GEO Link:	http://www.ncbi.nlm.nih.gov/geo/query/acc.cgi?acc=GSE29060
Status:	Public on Jan 01 2012
Title:	Expression data from human HT-29 immortalized colorectal adenocarcinoma cell line
Organism:	Homo sapiens
Experiment type:	Expression profiling by array
Platform:	GPL570
Pubmed ID:	
Summary & Design:	**Summary:** Gene expression profiling for identification of genes regulated by DNA methylation **Overall design:** Total RNA was extracted from HT-29 cell line was hybridized on Affymetrix HGU133 Plus 2.0 microarrays

Background corr dist: KL-Divergence = 0.0472, L1-Distance = 0.0212, L2-Distance = 0.0005, Normal std = 0.5848

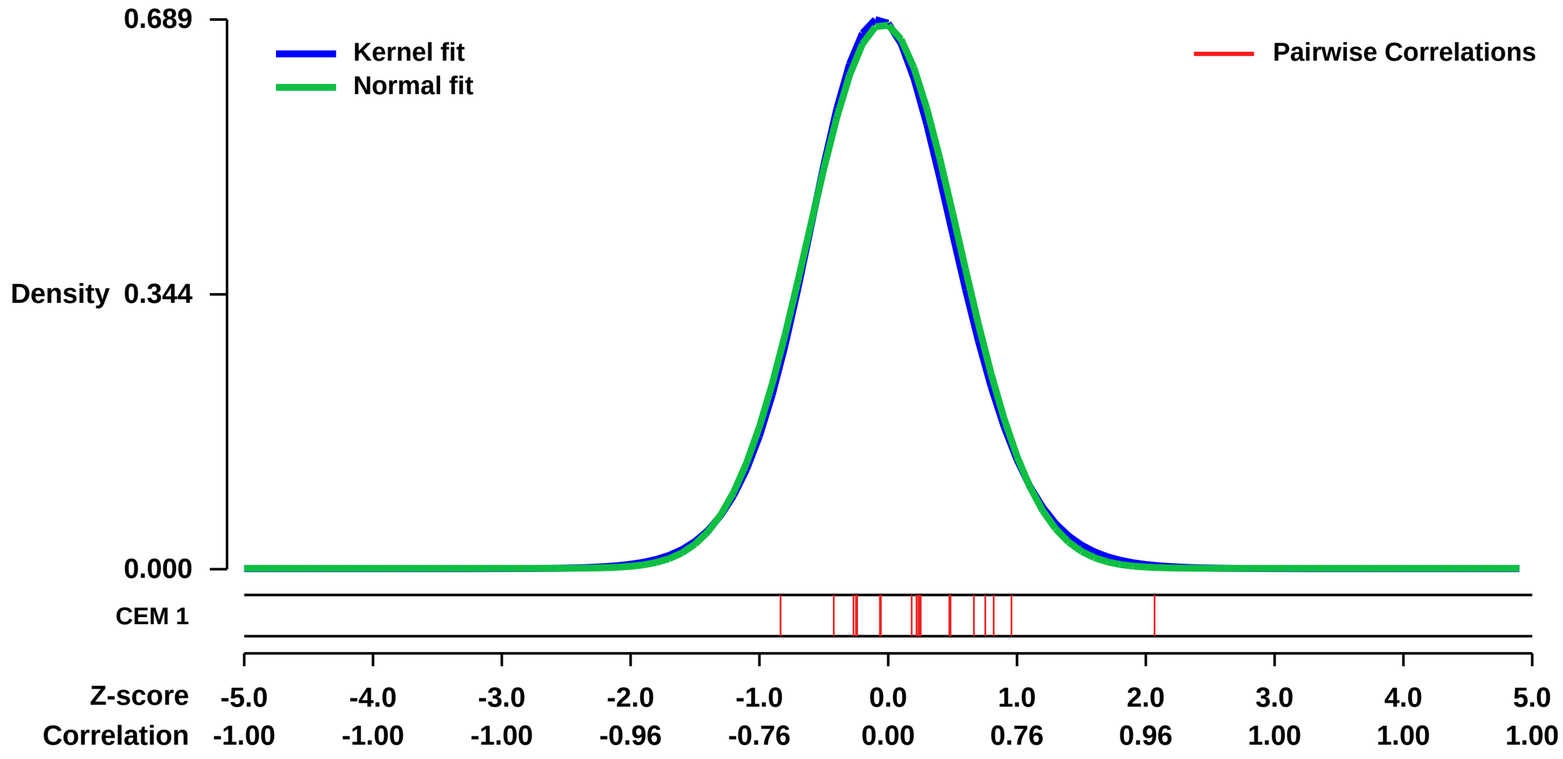

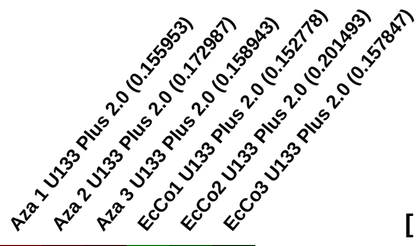

Pre-normalization Quantiles

		[min]	[medium]	[max]
CEM 1	MANF	3665.5	4358.3	4649.3
P (S | Z, I) = 0.00	SDF2L1	791.9	963.9	1056.8
Mean Corr = 0.19248	CRELD2	1819.4	1987.7	2172.9
	HSPA5	17296.3	21021.6	22047.4
	HYOU1	6429.5	7526.0	8268.3
	PDIA4	2161.4	2463.2	2719.9
	PDIA6	9442.4	11879.1	12603.1
CEM 1 + Top 10 Genes	DNAJB11	5196.3	6346.6	6373.5
	HSP90B1	5613.5	7730.1	8184.3
	PDIA3	20941.7	25173.7	27625.5
	PPIB	25975.2	30809.8	33636.2
	C19orf10	2102.9	2376.9	2976.2
	SLC35B1	1923.5	2119.0	2240.1
	SEC61A1	4439.2	4749.2	5108.0
	RPN1	5400.9	6057.6	6916.8
	DNAJC3	2809.1	3118.9	3727.8
	CDK2AP2	2085.4	2147.8	2206.0
Null module	ARID5B			
	XBP1			
	HNRNPAB			
	SGK1			
	HSPB1			
	DDIT4			
	ARL4D			
	SAP30			
	KIAA0408			
	GPR17			
	HSPH1			
	DNASE1L2			
	SLC5A3			
	GNAS			
	GPR3			
	TNFRSF25			
	TM6SF2			
	MKKS			
	PLEKHF1			
	ZMYM1			
	DOK3			
	FGF20			
	SLC39A2			
	KCNIP2			
	ERRFI1			
	DEDD2			
	CCDC117			
	USP31			
	AHSA2			
	CYS1			
	CNIH2			
	BANP			
	CHORDC1			
	P4HA1			

GEO Series "GSE12161" Expression Profiles

Num of samples in this series: 6

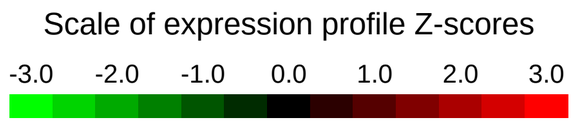

GEO Link:	http://www.ncbi.nlm.nih.gov/geo/query/acc.cgi?acc=GSE12161
Status:	Public on Mar 04 2010
Title:	Transcriptome profiling of control and TNFalpha treated HepG2 cells
Organism:	Homo sapiens
Experiment type:	Expression profiling by array
Platform:	GPL570
Pubmed ID:	20140224
Summary & Design:	**Summary:** The proinflammatory cytokine, TNFalpha is critical in maintaining liver homeostasis since it is a major determiner of hepatocyte life and death. Considering this, gene transcription profiling was examined in control and TNFalpha treated HepG2 cells. Results indicated that TNFalpha could significantly alter the expression of a significant number of genes; most of them were functionally distributed among molecular functions like catalytic activity, binding, molecular transducer activity, transporter activity, translation and transcription regulator activities or enzyme regulator activity. Also, within genes up-regulated by TNFalpha, several GO terms related to lipid and fat metabolism were significantly overrepresented indicating global dysregulation of fat metabolism within the hepatocyte and those within the down-regulated dataset included genes involved in immunoglobulin receptor activity and IgE binding thereby indicating a compromise in immune defense mechanism(s) apart from those involved the DNA binding and protein binding categories. The interacting network of â lipid metabolism, small molecule biochemistryâ was derived to be significantly affected that correlated well with the top canonical pathway of â biosynthesis of steroidsâ and molecular and cellular function of â lipid metabolismâ . All these indicate TNFalpha to be significantly altering the transcriptome profiling within HepG2 cells with genes involved in lipid and steroid metabolism being the most favoured. This study suitably addresses the genes that determine TNFalpha mediated alterations within the hepatocyte mainly the phenotypes of hepatic steatosis and fatty liver that are associated with several hepatic pathological states. **Overall design:** HepG2 cells were maintained in DMEM supplemented with 10% fetal calf serum with 1% antibiotic-antimycotic. On attaining confluency, cells were serum starved overnight and incubated in the absence (control) and presence of TNFalpha (0.5nM, 12h). On termination of incubation, total RNA was isolated, reverse transcribed to cDNA and subjected to in vitro transcription to produce biotinylated cRNA that was hybridized to the human array chip (Human Genome U133 Plus 2.0, Affymetrix) according to the manufacturer's instructions. Images were scanned using the GeneChip 3000 7G scanner (Affymetrix) and analysed. The experiment was performed with triplicates of each set (Control and TNF alpha treated).

Background corr dist: KL-Divergence = 0.0325, L1-Distance = 0.0474, L2-Distance = 0.0033, Normal std = 0.6985

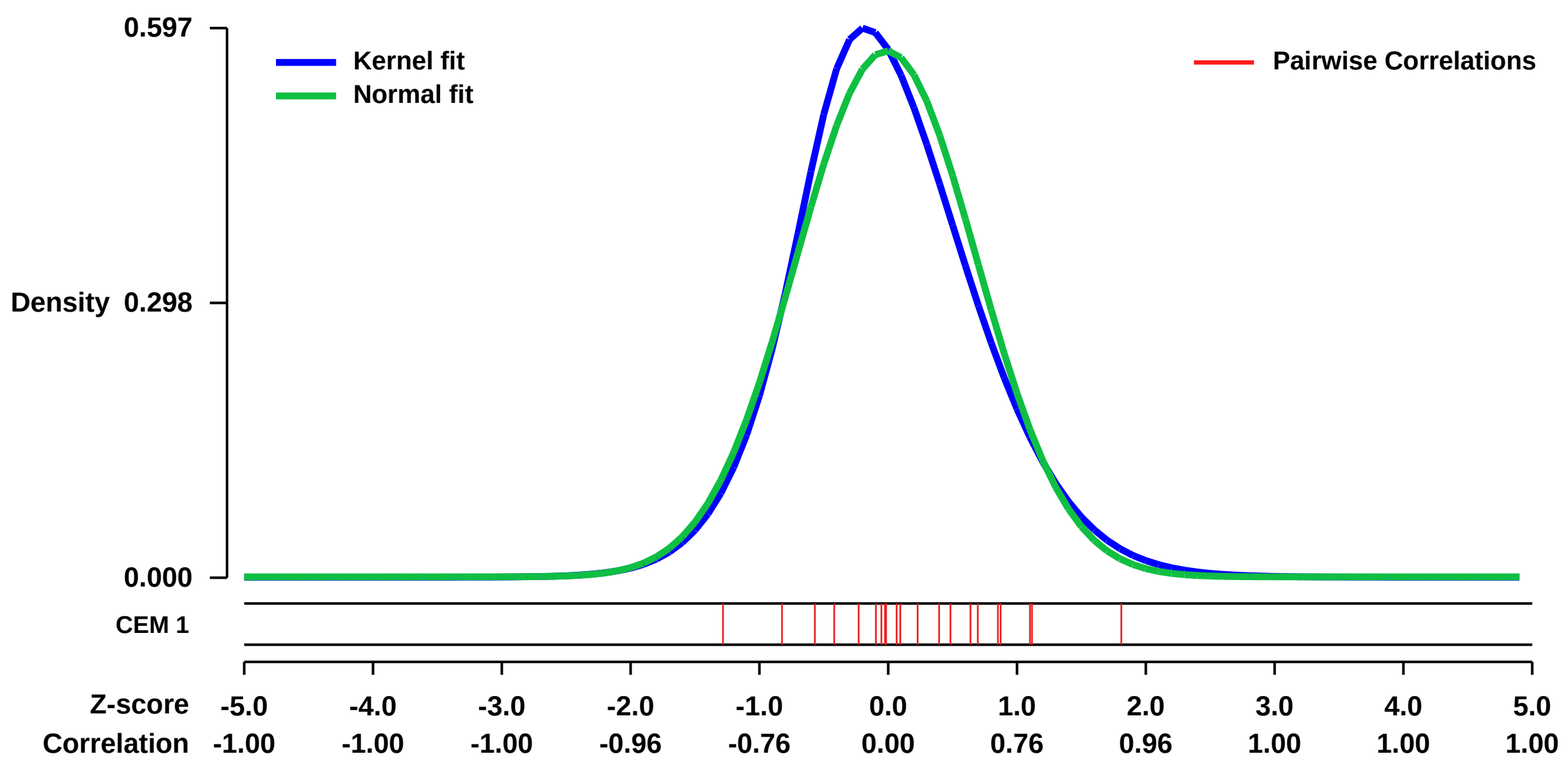

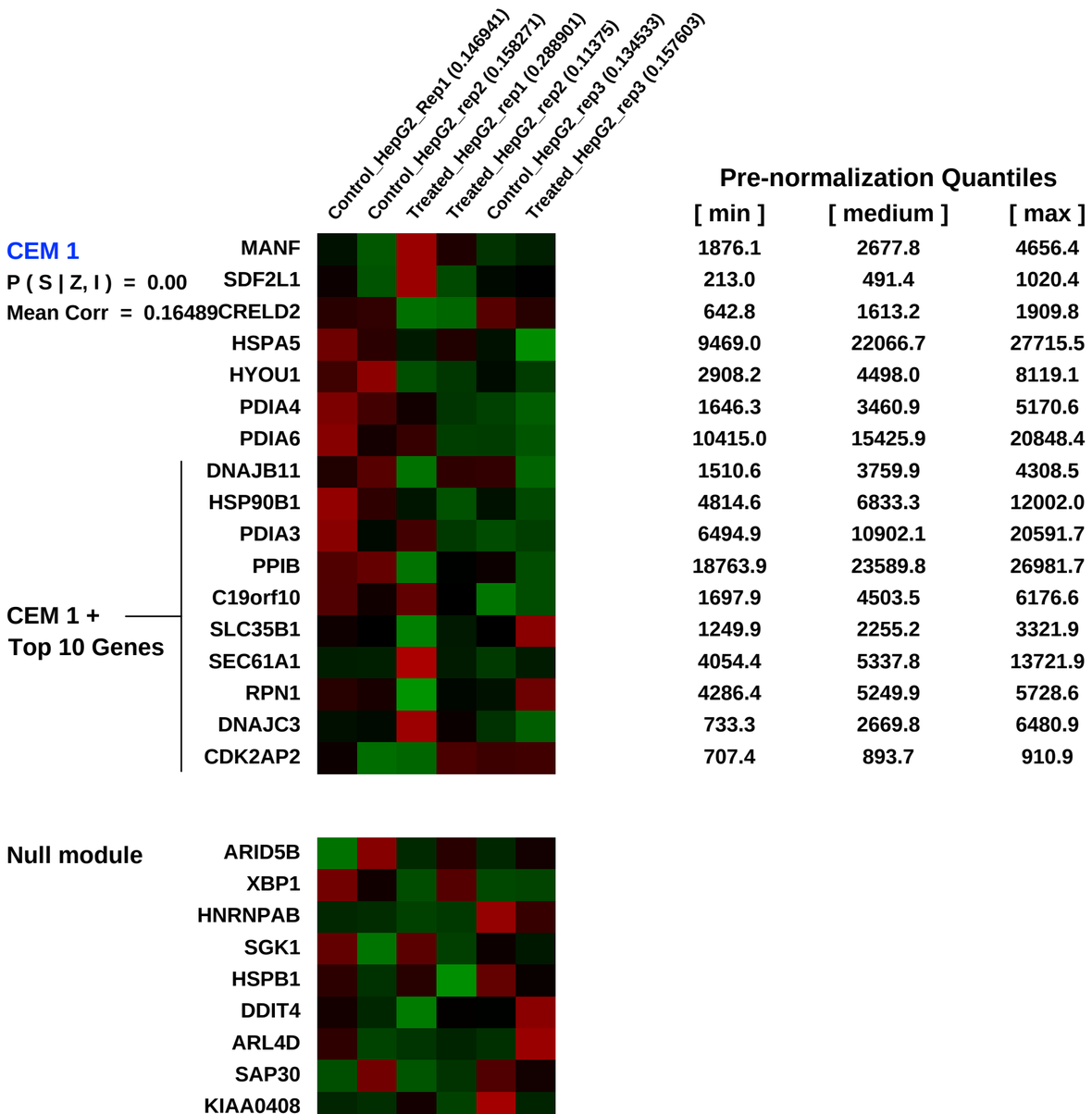

Pre-normalization Quantiles

	[min]	[medium]	[max]
MANF	1876.1	2677.8	4656.4
SDF2L1	213.0	491.4	1020.4
CRELD2	642.8	1613.2	1909.8
HSPA5	9469.0	22066.7	27715.5
HYOU1	2908.2	4498.0	8119.1
PDIA4	1646.3	3460.9	5170.6
PDIA6	10415.0	15425.9	20848.4
DNAJB11	1510.6	3759.9	4308.5
HSP90B1	4814.6	6833.3	12002.0
PDIA3	6494.9	10902.1	20591.7
PPIB	18763.9	23589.8	26981.7
C19orf10	1697.9	4503.5	6176.6
SLC35B1	1249.9	2255.2	3321.9
SEC61A1	4054.4	5337.8	13721.9
RPN1	4286.4	5249.9	5728.6
DNAJC3	733.3	2669.8	6480.9
CDK2AP2	707.4	893.7	910.9

GEO Series "GSE37935" Expression Profiles

Num of samples in this series: 6

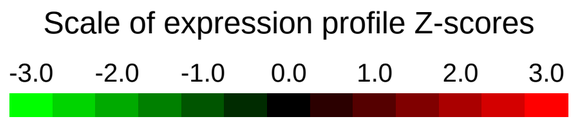

GEO Link:	http://www.ncbi.nlm.nih.gov/geo/query/acc.cgi?acc=GSE37935
Status:	Public on May 29 2013
Title:	Identification of Sp1 targets involved in proliferation and cancer
Organism:	Homo sapiens
Experiment type:	Expression profiling by array
Platform:	GPL570
Pubmed ID:	23018034
Summary & Design:	**Summary:** Sp1 is a transcription factor able to regulate many genes through its DNA binding domain, containing three zinc fingers. We were interested in identifying target genes regulated by Sp1, with a special emphasis to those involved in proliferation and cancer. Our approach was to treat HeLa cells with a siRNA directed against Sp1 mRNA (siSp1) to decrease the expression of Sp1 and, in turn, the genes activated by this transcription factor. Sp1 siRNA treatment led to a great number of differentially expressed genes as determined by whole genome cDNA microarray analysis. Underexpressed genes were selected since they represent putative genes activated by Sp1. These underexpressed genes were classified in six Gene Onthology categories, namely proliferation and cancer, mRNA processing, lipidic metabolism, glucidic metabolism, transcription and translation. Putative Sp1 binding sites were found in the promoters of the selected genes using the MatchTM software. After literature mining, 11 genes were selected for further validation of their expression levels using RT-real time PCR. Underexpression was confirmed for the 11 genes plus Sp1 in HeLa cells after siSp1 treatment. Additionally, EMSA and chromatin immunoprecipitation assays were performed to test for binding between Sp1 and the promoters of these genes. We observed binding of Sp1 to the promoters of RAB20, FGF21, IHPK2, ARHGAP18, NPM3, SRSF7, CALM3, PGD and Sp1 itself. Finally, the mRNA levels of RAB20, FGF21 and IHPK2, three genes related with proliferation and cancer, were determined after overexpression of Sp1 in HeLa cells, to confirm their relationship with Sp1. **Overall design:** The aim of our study was to evaluate, by using whole genome microarrays, the effects of a siRNA against the transcription factor of Sp1 in HeLa cells. Using this methodology genes activated by Sp1 could be downregulated. The obtective was to determine new genes regulated at the cellular level. Triplicate samples were hybridized for each experimental condition (6 samples in total). The samples provided were analyzed using the specific software GeneSpring GX.

Background corr dist: KL-Divergence = 0.0278, L1-Distance = 0.0280, L2-Distance = 0.0008, Normal std = 0.7080

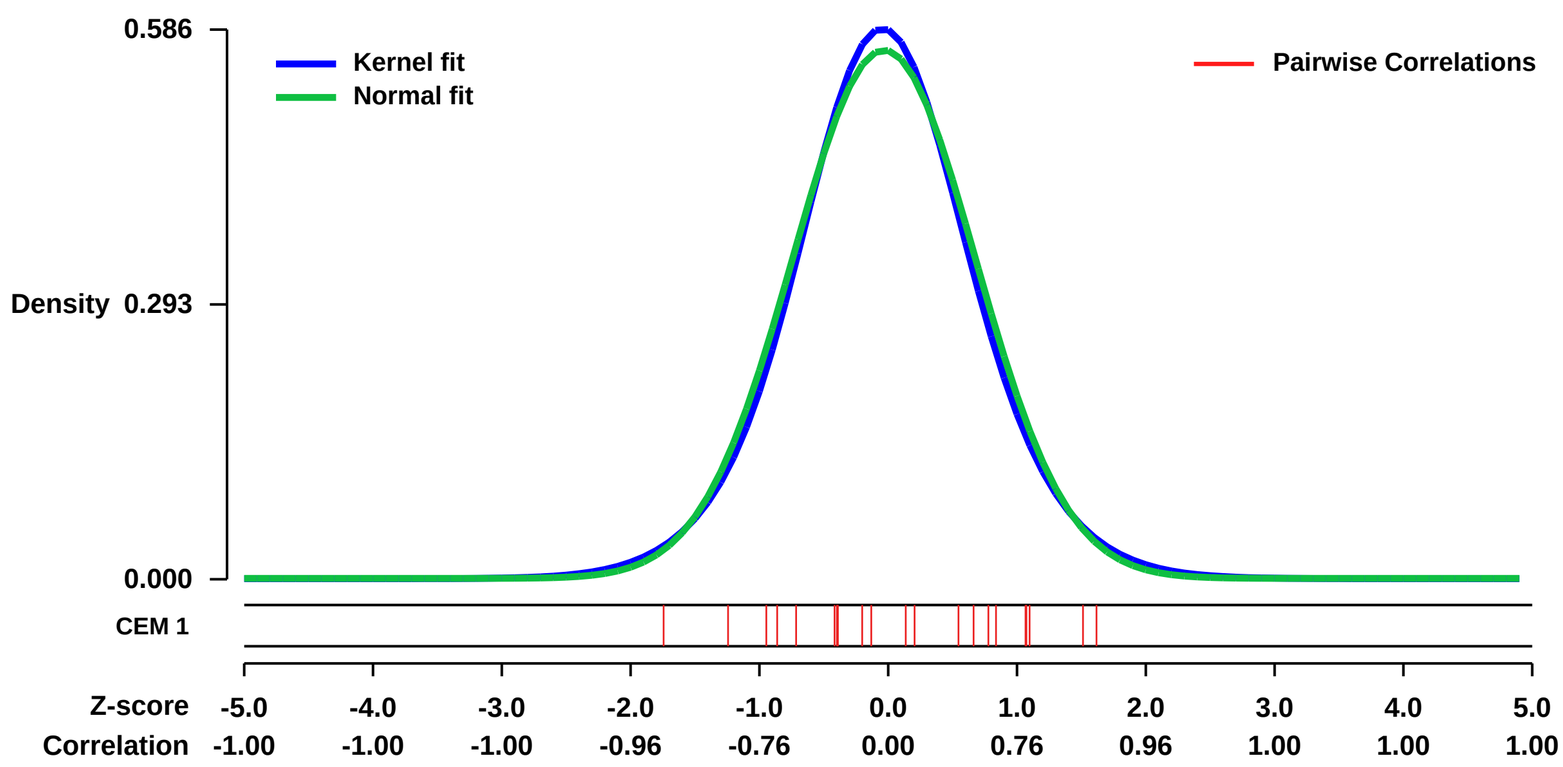

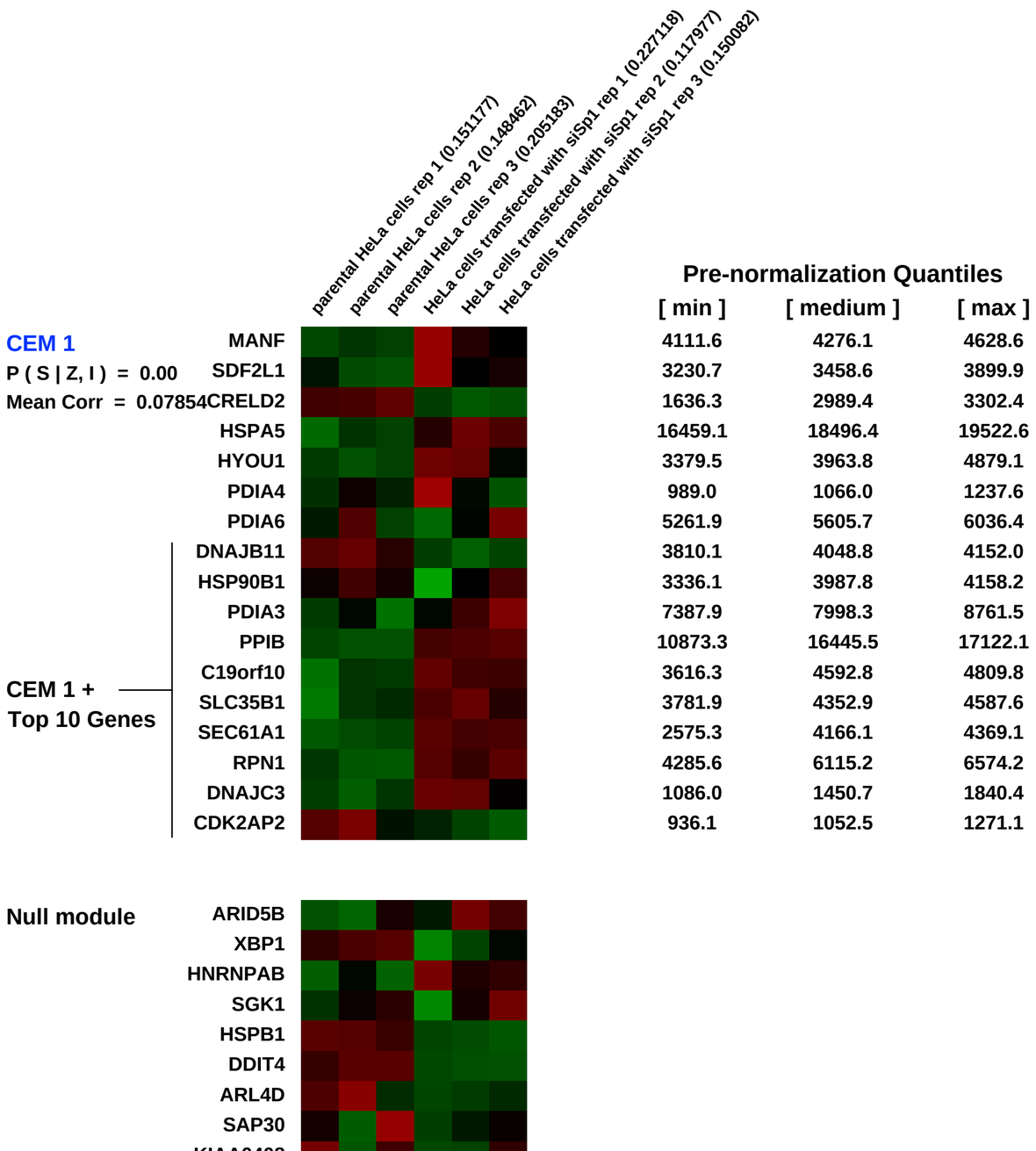

Pre-normalization Quantiles

	[min]	[medium]	[max]
MANF	4111.6	4276.1	4628.6
SDF2L1	3230.7	3458.6	3899.9
CRELD2	1636.3	2989.4	3302.4
HSPA5	16459.1	18496.4	19522.6
HYOU1	3379.5	3963.8	4879.1
PDIA4	989.0	1066.0	1237.6
PDIA6	5261.9	5605.7	6036.4
DNAJB11	3810.1	4048.8	4152.0
HSP90B1	3336.1	3987.8	4158.2
PDIA3	7387.9	7998.3	8761.5
PPIB	10873.3	16445.5	17122.1
C19orf10	3616.3	4592.8	4809.8
SLC35B1	3781.9	4352.9	4587.6
SEC61A1	2575.3	4166.1	4369.1
RPN1	4285.6	6115.2	6574.2
DNAJC3	1086.0	1450.7	1840.4
CDK2AP2	936.1	1052.5	1271.1

GEO Series "GSE29544" Expression Profiles

Num of samples in this series: 45

Scale of expression profile Z-scores

-3.0 -2.0 -1.0 0.0 1.0 2.0 3.0

GEO Link:	http://www.ncbi.nlm.nih.gov/geo/query/acc.cgi?acc=GSE29544
Status:	Public on Jul 06 2011
Title:	Expression profiling of human T-LL cell line CUTLL1
Organism:	Homo sapiens
Experiment type:	Expression profiling by array
Platform:	GPL570
Pubmed ID:	21737748
Summary & Design:	**Summary:** Notch is normally activated by cleavage and nuclear translocation of its intracellular domain (ICN1), which turns on downstream target genes. Human T cell acute lymphoblastic leukemia (T-ALL), an aggressive immature T cell malignancy, is associated with Notch 1 gain-of-function mutations in more than 50% of the cases. Efforts to date to identify direct Notch1 targets have been confounded by the lack of a method to turn Notch1 on in a controlled fashion in T-ALL cells that are poised to respond to Notch signals. Of note, because Notch signaling activates transcriptional repressors that feedback to dampen the expression of many target genes (a process referred to as incoherent logic), it is likely that many direct targets are missed in Notch off analyses, which are further complicated by an inability to identify direct targets in a clear-cut fashion. We have overcome this limitation by developing a GSI washout method that results in the rapid translocation of activated Notch1 to the nucleus. We intend to use this method to study the assembly and loading of transcriptional complexes onto downstream targets, the kinetics of target activation. To date, our efforts have been devoted to comparing the gene expression signature of Notch-on and Notch-off in the human T-ALL cell line CUTLL. In addition to previously identified Notch1 target genes, we have also identified a series of novel genes upregulated by GSI washout in the presence of cycloheximide, suggesting that they are likely to be direct targets. Additional controls included transduction of cells with dominant negative MAML1, a specific antagonist of canonical Notch1 signaling, prior to Notch1 reactivation, and a mock GSI washout to control for cycloheximide effects. **Overall design:** CUTLL1 cells are cultured in triplicates with different treatments. Total RNA was prepared and hybridized to Affymetrix human U133 plus 2.0 microarrays

Background corr dist: KL-Divergence = 0.0280, L1-Distance = 0.0586, L2-Distance = 0.0048, Normal std = 0.7342

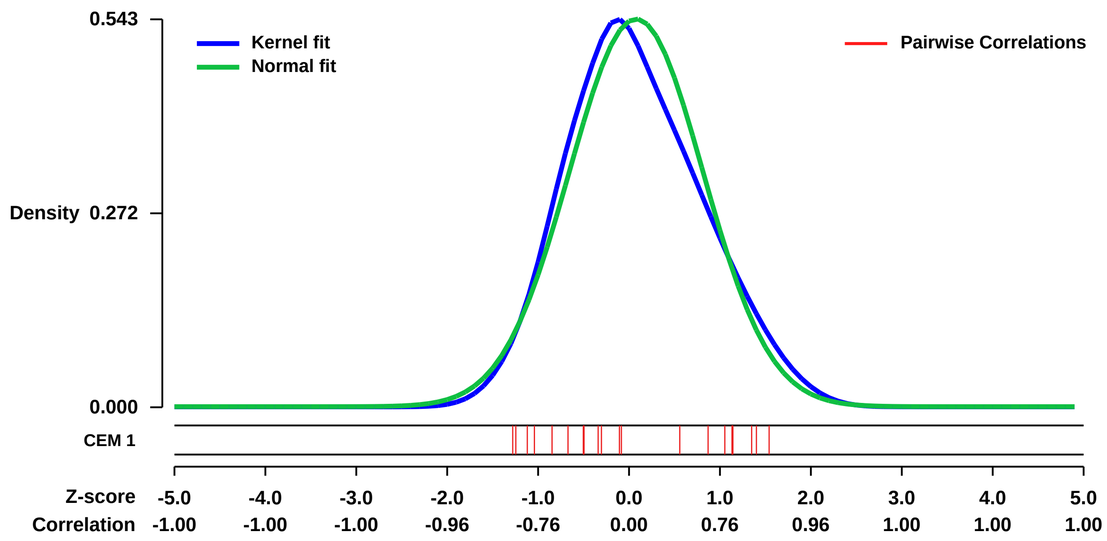

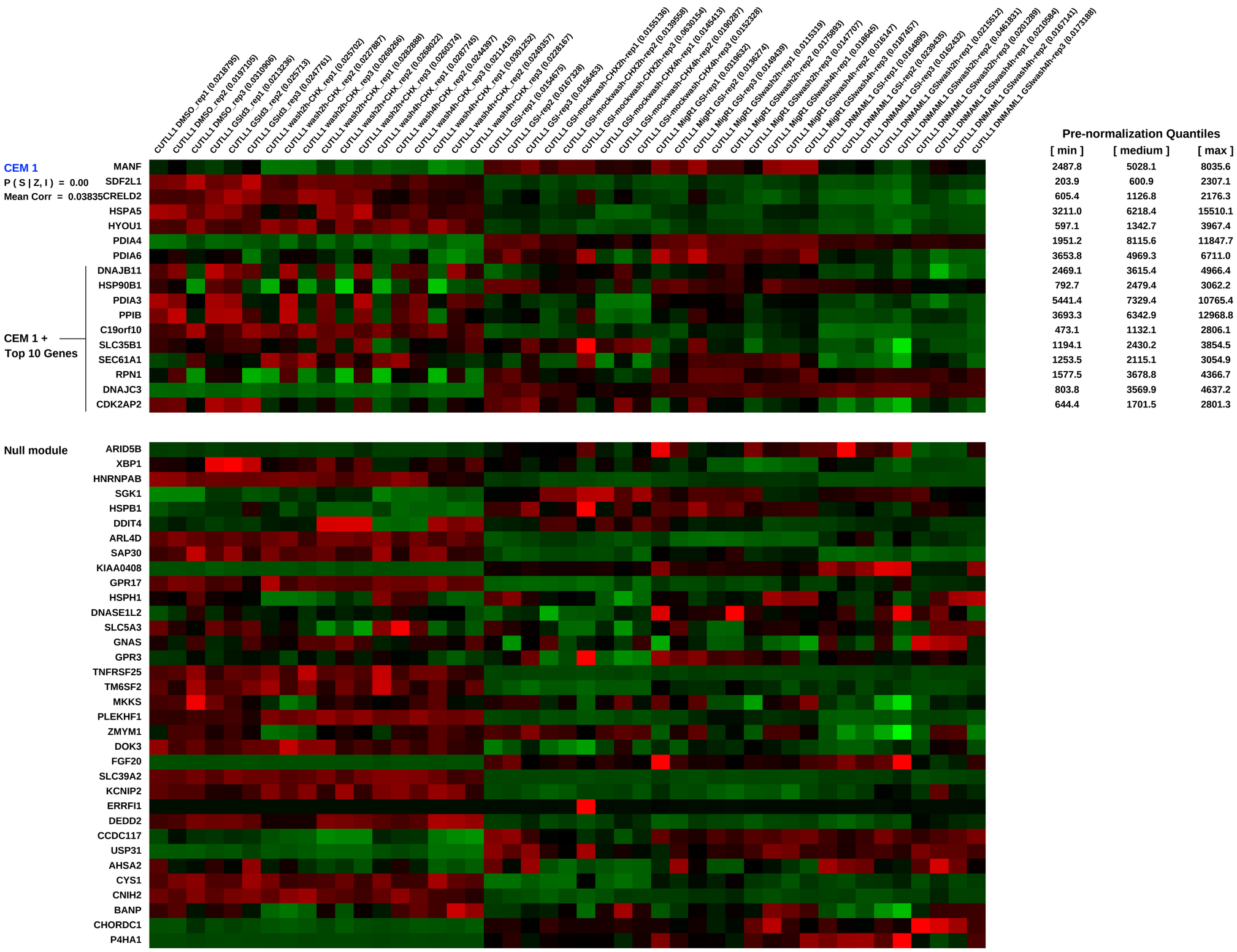

Pre-normalization Quantiles

[min]	[medium]	[max]
2487.8	5028.1	8035.6
203.9	600.9	2307.1
605.4	1126.8	2176.3
3211.0	6218.4	15510.1
597.1	1342.7	3967.4
1951.2	8115.6	11847.7
3653.8	4969.3	6711.0
2469.1	3615.4	4966.4
792.7	2479.4	3062.2
5441.4	7329.4	10765.4
3693.3	6342.9	12968.8
473.1	1132.1	2806.1
1194.1	2430.2	3854.5
1253.5	2115.1	3054.9
1577.5	3678.8	4366.7
803.8	3569.9	4637.2
644.4	1701.5	2801.3

GEO Series "GSE22035" Expression Profiles

Num of samples in this series: 43

Scale of expression profile Z-scores

-3.0 -2.0 -1.0 0.0 1.0 2.0 3.0

GEO Link: http://www.ncbi.nlm.nih.gov/geo/query/acc.cgi?acc=GSE22035
Status: Public on Jan 10 2011
Title: Gene expression data in estrogen receptor alpha positive breast tumors with and without PIK3CA mutations.
Organism: Homo sapiens
Experiment type: Expression profiling by array
Platform: GPL570
Pubmed ID: 21209903

Summary & Design:

Summary:
PI3K/AKT pathway plays one of pivotal roles in breast cancer development and maintenance. PIK3CA, coding PIK3 catalytic subunit, is the oncogene which shows the high frequency of gain-of-function mutations leading to the PI3K/AKT pathway activation in breast cancer. In particular in the ER$_{\alpha}$--positive breast tumors PIK3CA mutations have been observed in 30% to 40%. However, genes expressed in connection to the pathway activation in breast tumorigenesis remain largely unknown.

To identify downstream relevant target genes (and signaling pathways) turned on by the aberrant PI3K/AKT signal in breast tumors, we analyzed gene expression by pangenomic oligonucleotide microarray in a series of 43 ER$_{\alpha}$--positive tumors with and without PIK3CA mutations.

Overall design:
43 ER$_{\alpha}$--positive breast tumors including 14 tumors with PIK3CA mutations and 29 tumors without PIK3CA mutattions were used as screening set for microarray.

Background corr dist: KL-Divergence = 0.5217, L1-Distance = 0.0993, L2-Distance = 0.0365, Normal std = 0.2212

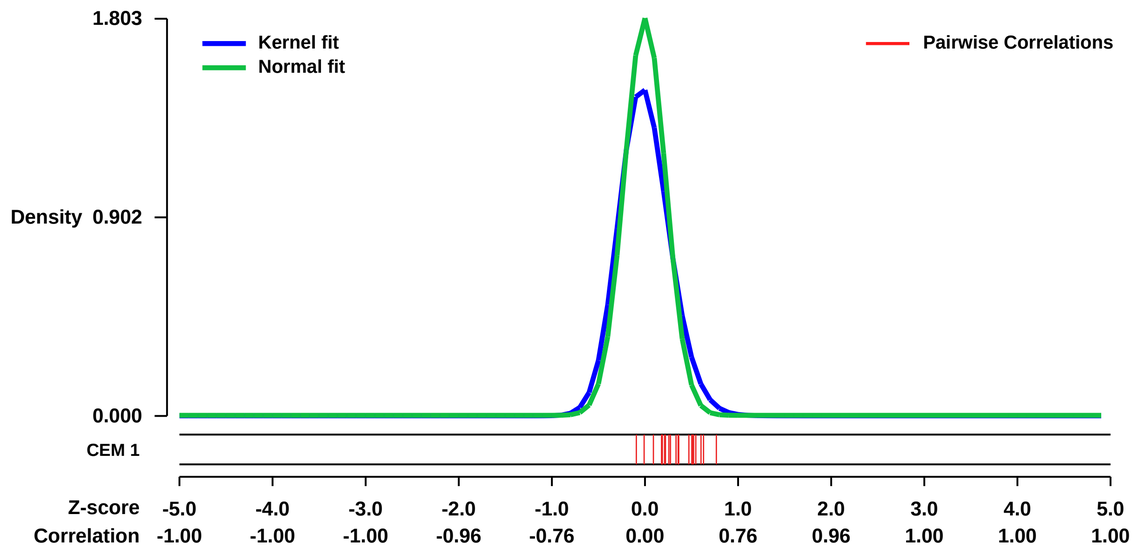

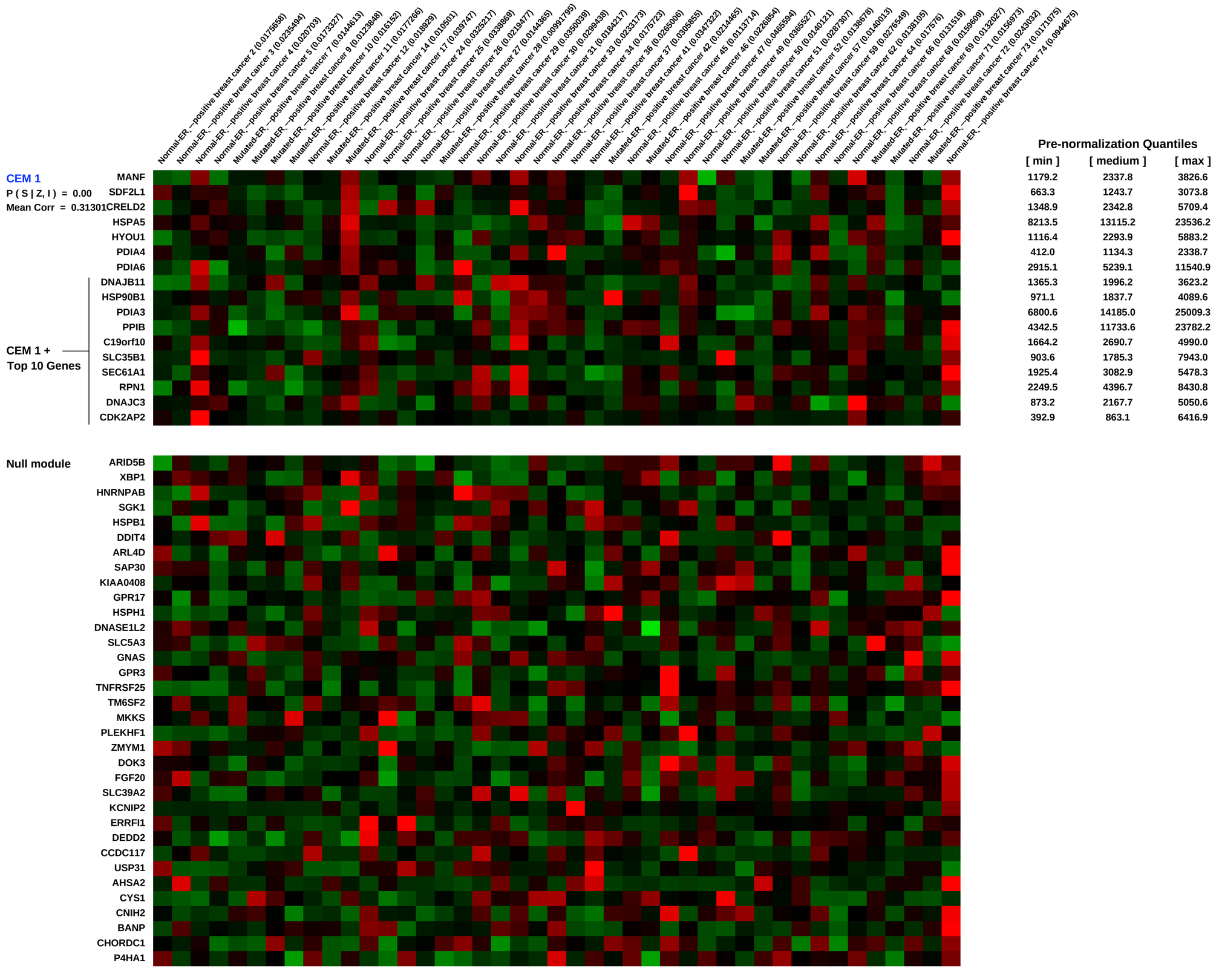

Pre-normalization Quantiles

[min]	[medium]	[max]
1179.2	2337.8	3826.6
663.3	1243.7	3073.8
1348.9	2342.8	5709.4
8213.5	13115.2	23536.2
1116.4	2293.9	5883.2
412.0	1134.3	2338.7
2915.1	5239.1	11540.9
1365.3	1996.2	3623.2
971.1	1837.7	4089.6
6800.6	14185.0	25009.3
4342.5	11733.6	23782.2
1664.2	2690.7	4990.0
903.6	1785.3	7943.0
1925.4	3082.9	5478.3
2249.5	4396.7	8430.8
873.2	2167.7	5050.6
392.9	863.1	6416.9

GEO Series "GSE10847" Expression Profiles

Num of samples in this series: 6

Scale of expression profile Z-scores

-3.0 -2.0 -1.0 0.0 1.0 2.0 3.0

GEO Link: http://www.ncbi.nlm.nih.gov/geo/query/acc.cgi?acc=GSE10847
Status: Public on Mar 18 2008
Title: H522 lung cancer cells' TGFbeta response was restored by putting back BRG1 and TGFbRII
Organism: Homo sapiens
Experiment type: Expression profiling by array
Platform: GPL570
Pubmed ID:

Summary & Design:

Summary:
The transcription factors Smad2 and Smad3 mediate a large set of genes responses induced by the cytokine TGF¸†, but the extent to which their function depends on chromatin remodeling remains to be defined. We observed interactions between these two Smads and BRG1, BAF250b, BAF170 and BAF155, which are core components of the SWI/SNF chromatin-remodeling complex. Smad2 and Smad3 have a similar affinity for these components in vitro, and their interactions are primarily mediated by BRG1. In vivo, however, BRG1 predominantly interacts with Smad3, and this interaction is enhanced by TGF¸† stimulation. Our results suggest that BRG1 is incorporated into transcriptional complexes that are formed by activated Smads in the nucleus, on target promoters. Using BRG1-deficient cell systems(H522 lung cancer cells), we defined the BRG1 dependence of the TGF¸† transcriptional program genome-wide. Most TGF¸† gene responses in human epithelial cells are dependent on BRG1 function. Remarkably, BRG1 is not required for the TGF¸†-mediated induction of SMAD7 and SNON, which encode key mediators of negative feedback in this pathway. Our results provide a genome-wide scope of the participation of BRG1 in TGF¸† action and suggest a widespread yet differential involvement of BRG1 SWI/SNF remodeler in the transcriptional response of many genes to this cytokine.

Keywords: comparative genomic hybridization

Overall design:
NCI-H522 cells that were transduced with BRG1, T¸†R-II, or both vectors combined were incubated with TGF¸† and subjected to transcriptomic analysis. Totally 6 samples.

Background corr dist: KL-Divergence = 0.0269, L1-Distance = 0.0449, L2-Distance = 0.0023, Normal std = 0.7559

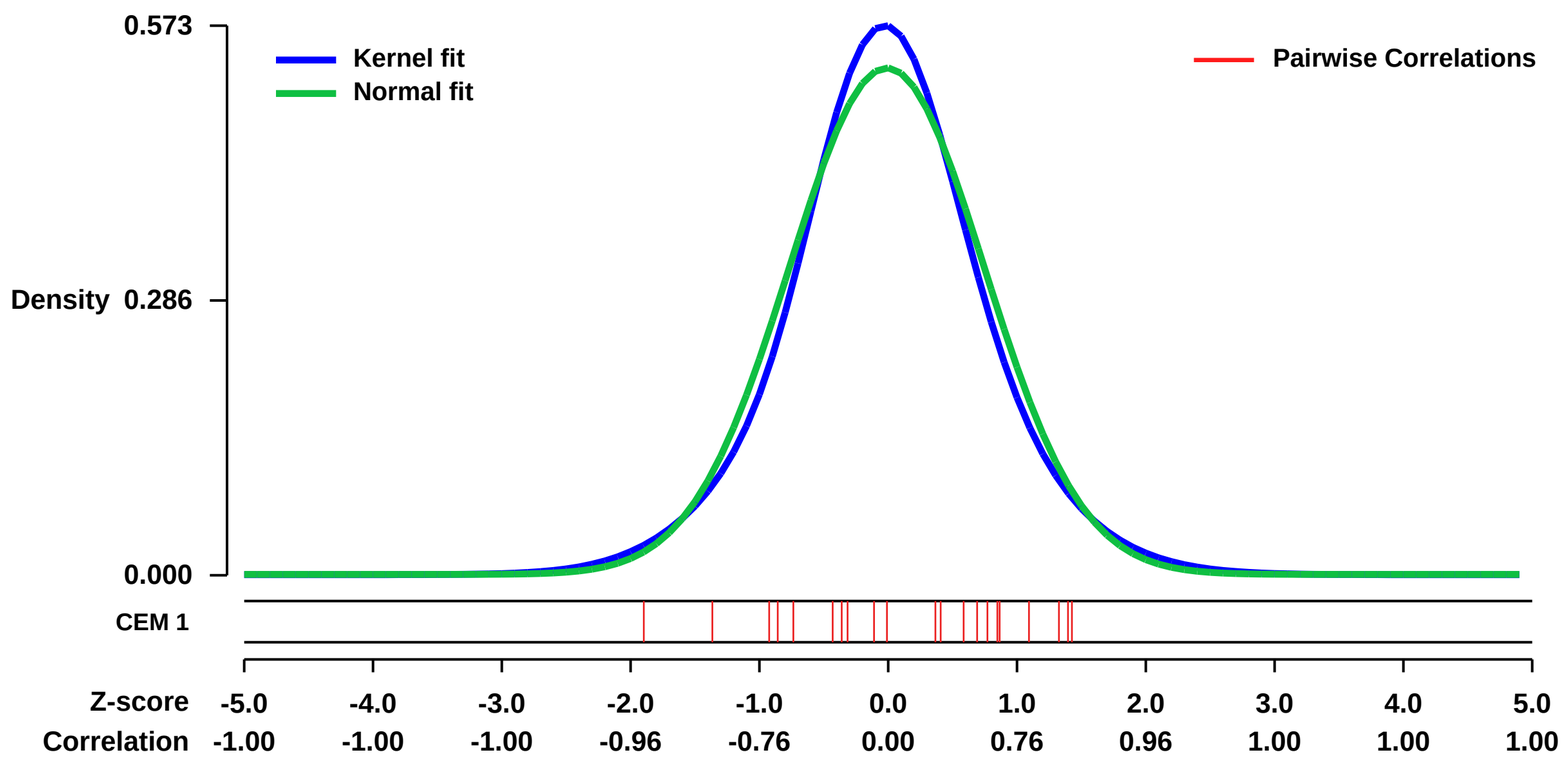

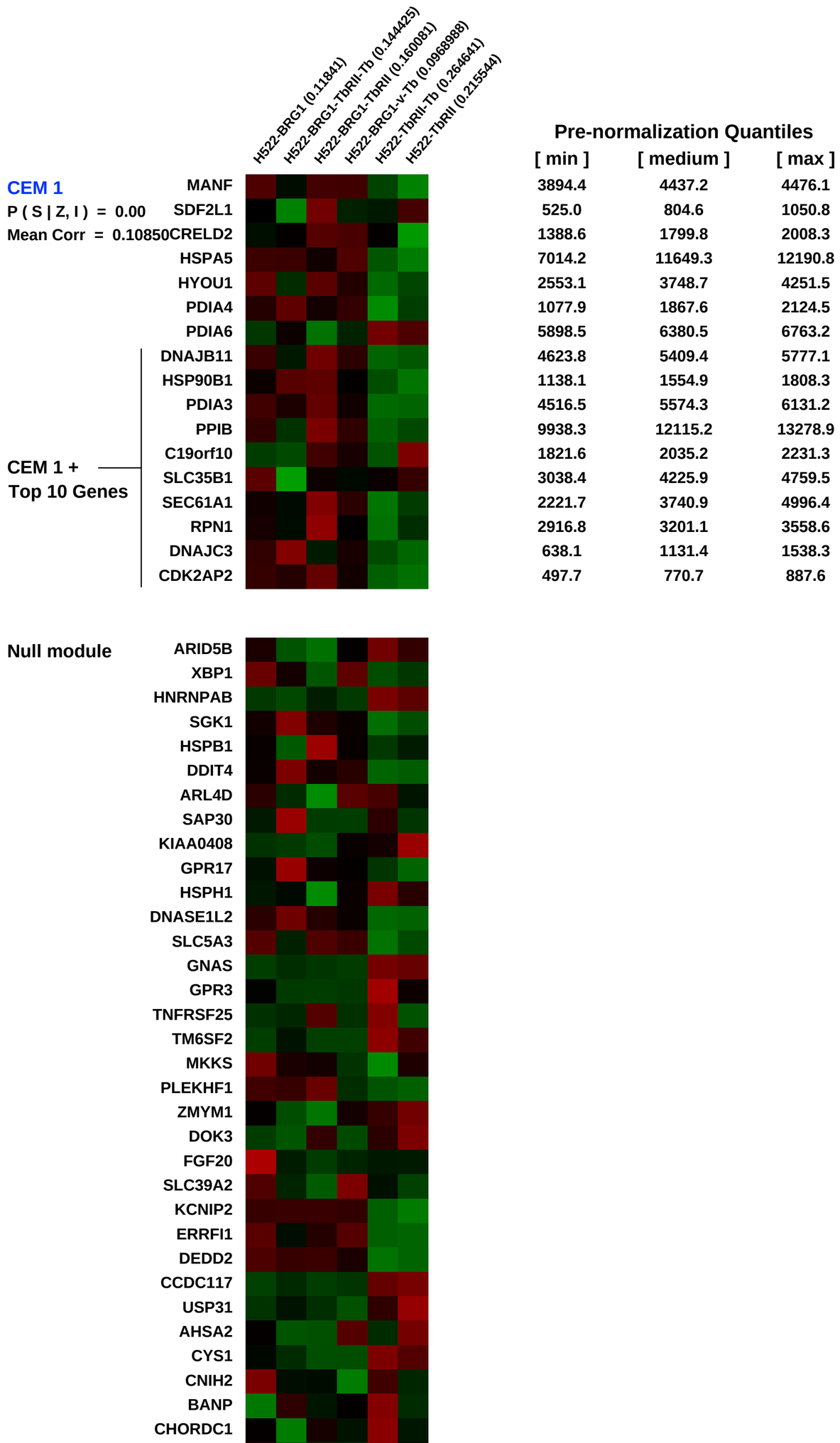

Pre-normalization Quantiles

	[min]	[medium]	[max]
MANF	3894.4	4437.2	4476.1
SDF2L1	525.0	804.6	1050.8
CRELD2	1388.6	1799.8	2008.3
HSPA5	7014.2	11649.3	12190.8
HYOU1	2553.1	3748.7	4251.5
PDIA4	1077.9	1867.6	2124.5
PDIA6	5898.5	6380.5	6763.2
DNAJB11	4623.8	5409.4	5777.1
HSP90B1	1138.1	1554.9	1808.3
PDIA3	4516.5	5574.3	6131.2
PPIB	9938.3	12115.2	13278.9
C19orf10	1821.6	2035.2	2231.3
SLC35B1	3038.4	4225.9	4759.5
SEC61A1	2221.7	3740.9	4996.4
RPN1	2916.8	3201.1	3558.6
DNAJC3	638.1	1131.4	1538.3
CDK2AP2	497.7	770.7	887.6
ARID5B			
XBP1			
HNRNPAB			
SGK1			
HSPB1			
DDIT4			
ARL4D			
SAP30			
KIAA0408			
GPR17			
HSPH1			
DNASE1L2			
SLC5A3			
GNAS			
GPR3			
TNFRSF25			
TM6SF2			
MKKS			
PLEKHF1			
ZMYM1			
DOK3			
FGF20			
SLC39A2			
KCNIP2			
ERRFI1			
DEDD2			
CCDC117			
USP31			
AHSA2			
CYS1			
CNIH2			
BANP			
CHORDC1			
P4HA1			

GEO Series "GSE15947" Expression Profiles

Num of samples in this series: 24

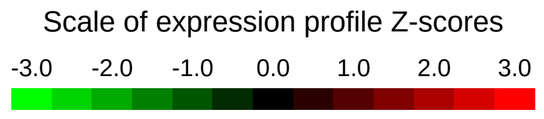

GEO Link:	http://www.ncbi.nlm.nih.gov/geo/query/acc.cgi?acc=GSE15947
Status:	Public on Dec 18 2009
Title:	Time course of 1,25(OH)2D treated RWPE1 cells.
Organism:	Homo sapiens
Experiment type:	Expression profiling by array
Platform:	GPL570
Pubmed ID:	20070897
Summary & Design:	**Summary:** **Background: Prostate cancer is the second leading cause of cancer mortality among US men. Epidemiological evidence suggests that high vitamin D status protects men from prostate cancer and the active form of vitamin D, 1¸–,25 dihydroxyvitamin D3 (1,25(OH)2D) has anti-cancer effects in cultured prostate cells. Still, the molecular mechanisms and the gene targets for vitamin D-mediated prostate cancer prevention are unknown.** **Results: We examined the effect of 1,25(OH)2D (+/- 100 nM, 6, 24, 48 h) on the transcript profile of proliferating RWPE1 cells, an immortalized, non-tumorigenic prostate epithelial cell line that is growth arrested by 1,25(OH)2D (Affymetrix U133 Plus 2.0, n=4/treatment per time and dose). Our analysis revealed many transcript level changes at a 5% false detection rate: 6 h, 1571 (61% up), 24 h, 1816 (60 % up), 48 h, 3566 (38 % up). 288 transcripts were regulated similarly at all time points (182 up, 80 down) and many of the promoters for these transcripts contained putative vitamin D response elements. Functional analysis by pathway or Gene Set Analysis revealed early suppression of WNT, Notch, NF-kB, and IGF1 signaling. Transcripts related to inflammation were suppressed at 6 h (e.g. IL-1 pathway) and suppression of proinflammatory pathways continued at later time points (e.g. IL-17 and IL-6 pathways). There was also evidence for induction of anti-angiogenic pathways and induction of transcripts for protection from oxidative stress or maintenance of cell redox homeostasis at 6 h.** **Conclusions: Our data reveal of large number of potential new, direct vitamin D target genes relevant to prostate cancer prevention. In addition, our data suggests that rather than having a single strong regulatory effect, vitamin D orchestrates a pattern of changes within prostate epithelial cells that limit or slow carcinogenesis.** **Overall design:** **RWPE1 cells were treated with medium containing 100 nM of 1,25(OH)2D or vehicle (0.1% ethanol) for 6, 24 or 48 hours (n=4 per treatment, 24 total samples). The transcripts levels in each sample were measured by using the Affymetrix HU133 plus 2.0 GeneChip (Affymetrix, Santa Clara, CA).**

Background corr dist: KL-Divergence = 0.0461, L1-Distance = 0.0843, L2-Distance = 0.0082, Normal std = 0.8784

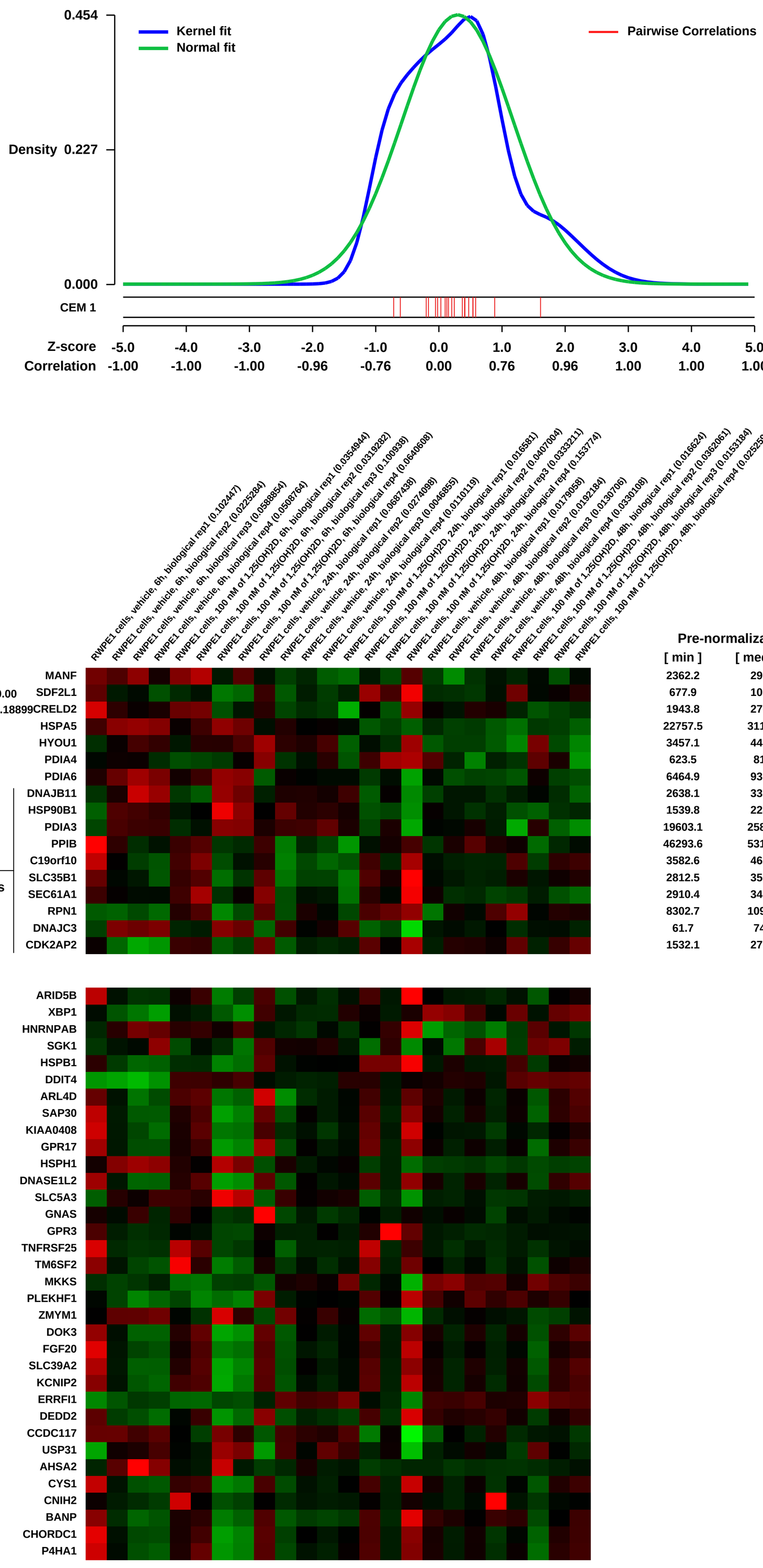

GEO Series "GSE15368" Expression Profiles

Num of samples in this series: 9

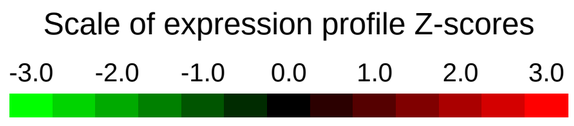

GEO Link:	http://www.ncbi.nlm.nih.gov/geo/query/acc.cgi?acc=GSE15368
Status:	Public on Apr 15 2009
Title:	Expression analysis of Saos-2 cells expressing p53-His273
Organism:	Homo sapiens
Experiment type:	Expression profiling by array
Platform:	GPL570
Pubmed ID:	
Summary & Design:	**Summary:** Our compound (PRIMA) selectively kills tumor cells expressing mutant p53. Here in our study we decided to investigate the impact of our compound on the transcriptome of p53 mutant-expressing cells, Saos2-His273. **Overall design:** We plated Saos-2-His273 cells and treated them with our compound for 6h or 12h. We then harvested the cells, extracted the RNA, and followed the protocol to run affymetrix array to analyse the impact of our drug on the whole transcriptome of cells expressing mutant p53.

Background corr dist: KL-Divergence = 0.0537, L1-Distance = 0.0477, L2-Distance = 0.0039, Normal std = 0.5909

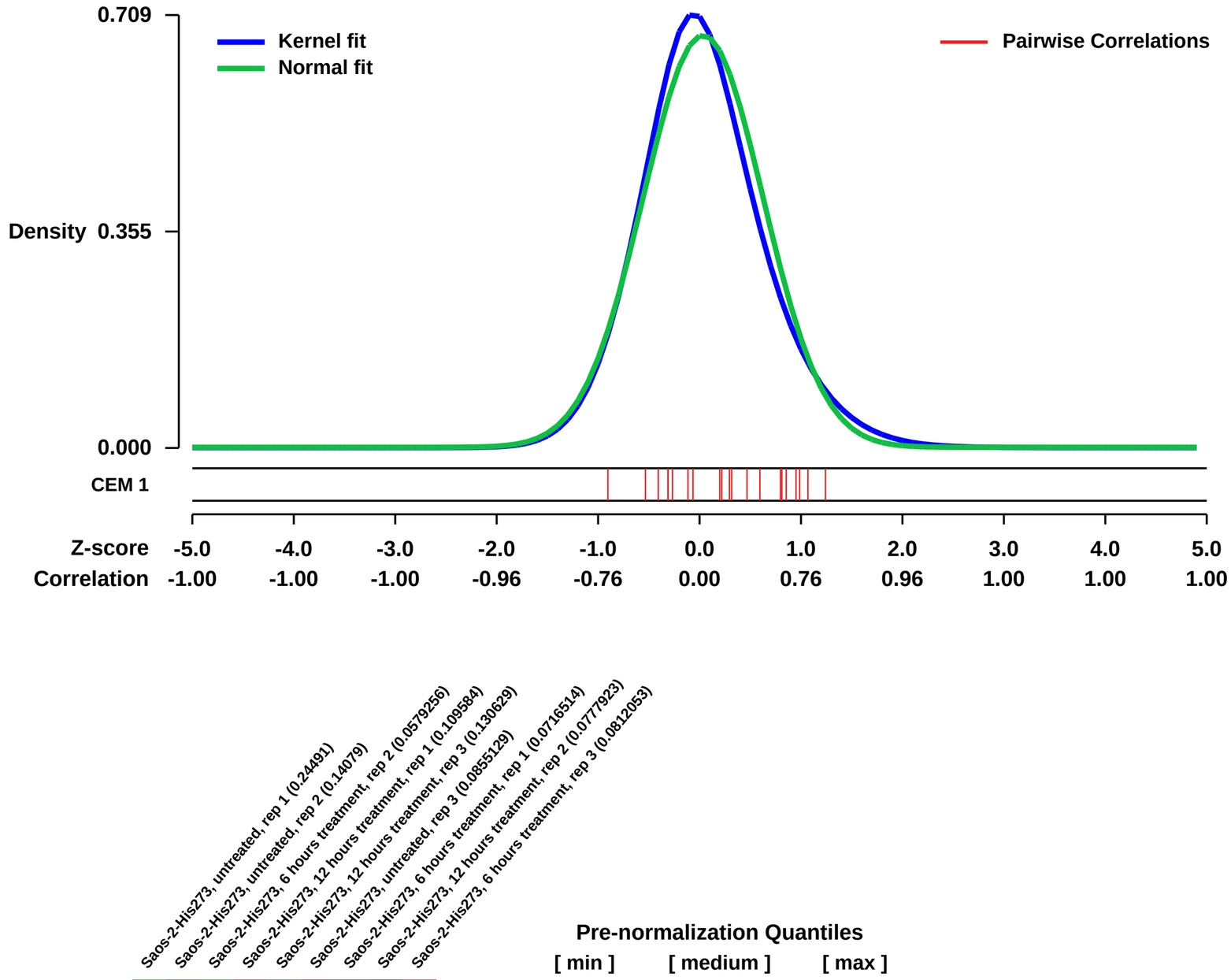

CEM 1
P (S | Z, I) = 0.00
Mean Corr = 0.21423

CEM 1 + Top 10 Genes

Null module

	Pre-normalization Quantiles		
	[min]	[medium]	[max]
MANF	2177.1	3262.6	4251.7
SDF2L1	956.6	1188.7	1918.1
CRELD2	1919.7	3356.0	4080.2
HSPA5	12892.5	20505.6	23929.3
HYOU1	1247.8	3314.4	4349.5
PDIA4	775.0	1080.1	1345.7
PDIA6	9052.9	12516.7	16879.8
DNAJB11	1661.0	4162.4	5226.7
HSP90B1	3269.4	8325.9	12223.0
PDIA3	6037.5	8587.7	11565.8
PPIB	3068.4	12552.4	17466.8
C19orf10	1756.8	3718.3	5392.4
SLC35B1	1405.1	1757.1	2148.4
SEC61A1	1114.4	2709.4	3218.9
RPN1	1065.1	2357.4	5390.3
DNAJC3	2515.3	3975.9	6071.6
CDK2AP2	283.9	464.1	664.9
ARID5B			
XBP1			
HNRNPAB			
SGK1			
HSPB1			
DDIT4			
ARL4D			
SAP30			
KIAA0408			
GPR17			
HSPH1			
DNASE1L2			
SLC5A3			
GNAS			
GPR3			
TNFRSF25			
TM6SF2			
MKKS			
PLEKHF1			
ZMYM1			
DOK3			
FGF20			
SLC39A2			
KCNIP2			
ERRFI1			
DEDD2			
CCDC117			
USP31			
AHSA2			
CYS1			
CNIH2			
BANP			
CHORDC1			
P4HA1			

GEO Series "GSE29881" Expression Profiles

Num of samples in this series: 20

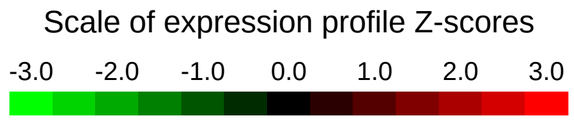

GEO Link: http://www.ncbi.nlm.nih.gov/geo/query/acc.cgi?acc=GSE29881
Status: Public on Jun 10 2011
Title: Human endothelial gene expression under estradiol and oxLDL treatments
Organism: Homo sapiens
Experiment type: Expression profiling by array
Platform: GPL570
Pubmed ID:

Summary & Design:

Summary:
DNA microarrays were used to investigate global gene expression patterns in cultured human umbilical artery endothelial cells (HUAECs) exposed to 1 nmol/L estradiol and/or 100 ´µg/ml oxidized low density lipoprotein (oxLDL) for 24 hours compared to control cells.

Overall design:
HUAECs from 15 separate cultures were exposed to control (0.1% ethanol), 1nmol/L estradiol, 100 ´µg/ml oxLDL, or 1nmol/L estradiol + 100 ´µg/ml oxLDL treatments for 24 h. Total cellular RNA was extracted. Equal amounts of RNA extracted from 3 control cells or 3 estradiol-treated cells obtained from three different cultures were pooled, achieving five biological replicates of the control, five replicates that were treated with estradiol, five replicates that were treated with oxLDL and five replicates that were treated with estradiol+oxLDL . Therefore, a total number of 20 microarrays were developed.

Background corr dist: KL-Divergence = 0.1378, L1-Distance = 0.0282, L2-Distance = 0.0012, Normal std = 0.3901

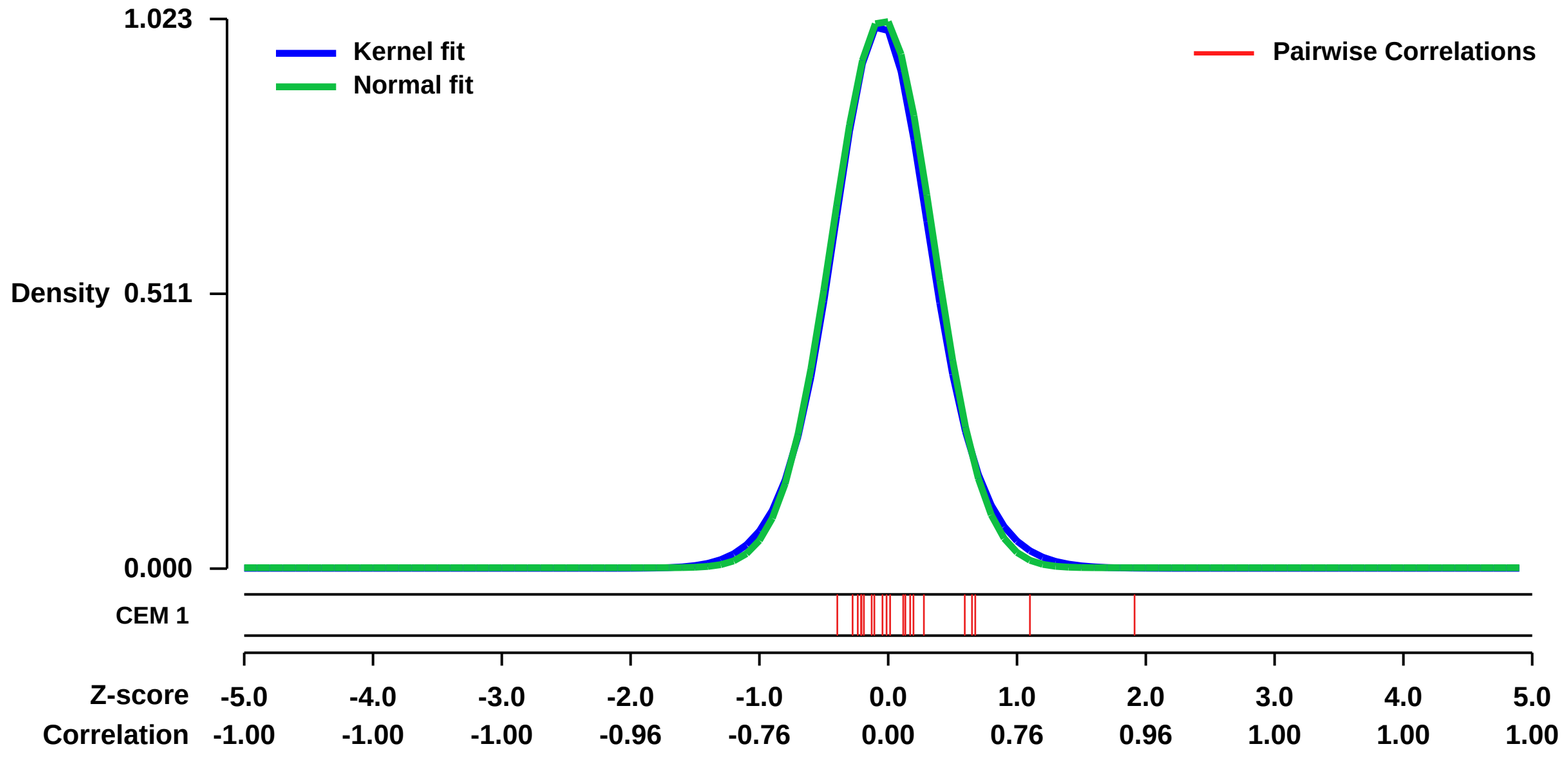

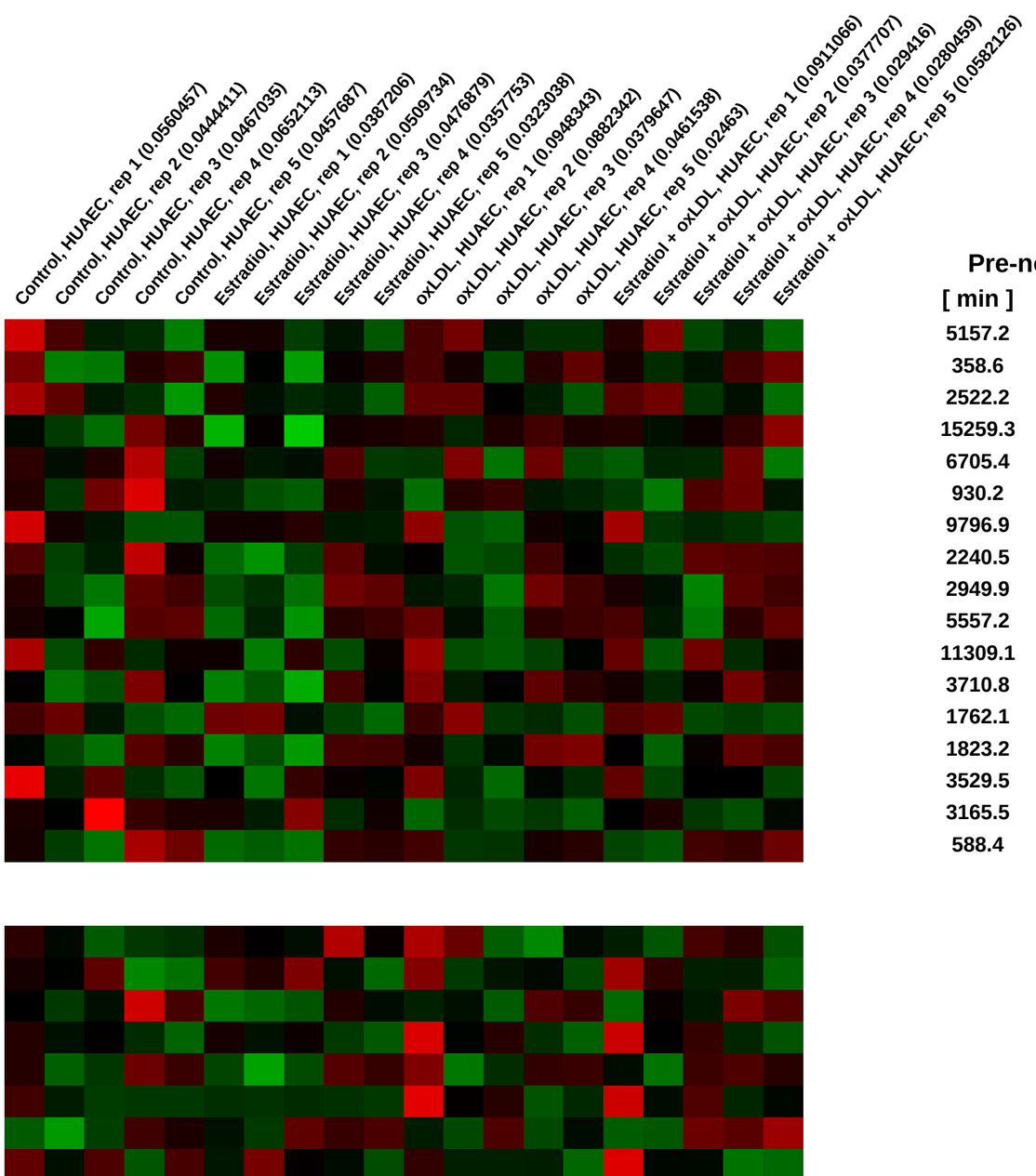

CEM 1
P (S | Z, I) = 0.00
Mean Corr = 0.12285

CEM 1 + Top 10 Genes

Null module

	Pre-normalization Quantiles [min]	[medium]	[max]
MANF	5157.2	6099.4	8116.1
SDF2L1	358.6	847.8	1110.9
CRELD2	2522.2	3183.9	4083.5
HSPA5	15259.3	18531.8	20149.6
HYOU1	6705.4	7301.4	8373.2
PDIA4	930.2	1104.6	1516.8
PDIA6	9796.9	10529.7	12775.6
DNAJB11	2240.5	3045.1	4066.3
HSP90B1	2949.9	5947.3	7573.1
PDIA3	5557.2	14117.6	16727.1
PPIB	11309.1	15245.7	19904.0
C19orf10	3710.8	4981.4	5876.5
SLC35B1	1762.1	2506.6	3889.1
SEC61A1	1823.2	3131.6	4057.9
RPN1	3529.5	4672.5	7088.9
DNAJC3	3165.5	3633.6	4884.4
CDK2AP2	588.4	1220.3	1869.3
ARID5B			
XBP1			
HNRNPAB			
SGK1			
HSPB1			
DDIT4			
ARL4D			
SAP30			
KIAA0408			
GPR17			
HSPH1			
DNASE1L2			
SLC5A3			
GNAS			
GPR3			
TNFRSF25			
TM6SF2			
MKKS			
PLEKHF1			
ZMYM1			
DOK3			
FGF20			
SLC39A2			
KCNIP2			
ERRFI1			
DEDD2			
CCDC117			
USP31			
AHSA2			
CYS1			
CNIH2			
BANP			
CHORDC1			
P4HA1			

GEO Series "GSE18826" Expression Profiles

Num of samples in this series: 6

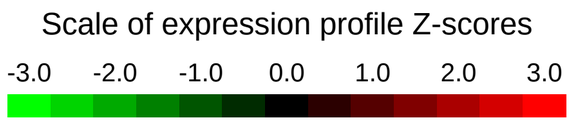

GEO Link:	http://www.ncbi.nlm.nih.gov/geo/query/acc.cgi?acc=GSE18826
Status:	Public on Mar 01 2010
Title:	3D culture of AIDS-NHL cells influences gene expression related to B-cell development, proliferation and survival
Organism:	Homo sapiens
Experiment type:	Expression profiling by array
Platform:	GPL570
Pubmed ID:	
Summary & Design:	**Summary:** **Full title: Three-dimensional culture of AIDS-NHL cells influences gene expression related to B-cell development, proliferation and survival** **The AIDS-NHL-derived cell line, UMCL01-101, representing diffuse large B-cell lymphoma of immunoblastic morphology (AIDS-IBL), was grown in conventional, static suspension culture or three-dimensionally (3D) in the Rotating Wall Vessel (RWV) bioreactor. The objective was to assess the impact on gene expression of growth as a three-dimensional tissue assembly.** **Global gene expression analysis was performed on UMCL01-101 cells grown under either condition using Affymetrix microarray.** **Overall design:** **UMCL01-101 cells were cultured in the Rotating Wall Vessel bioreactor to form 3D assemblies, or in conventional suspension culture, for 15 days. RNA was prepared from triplicate samples under each growth condition and submitted for microarray analysis.**

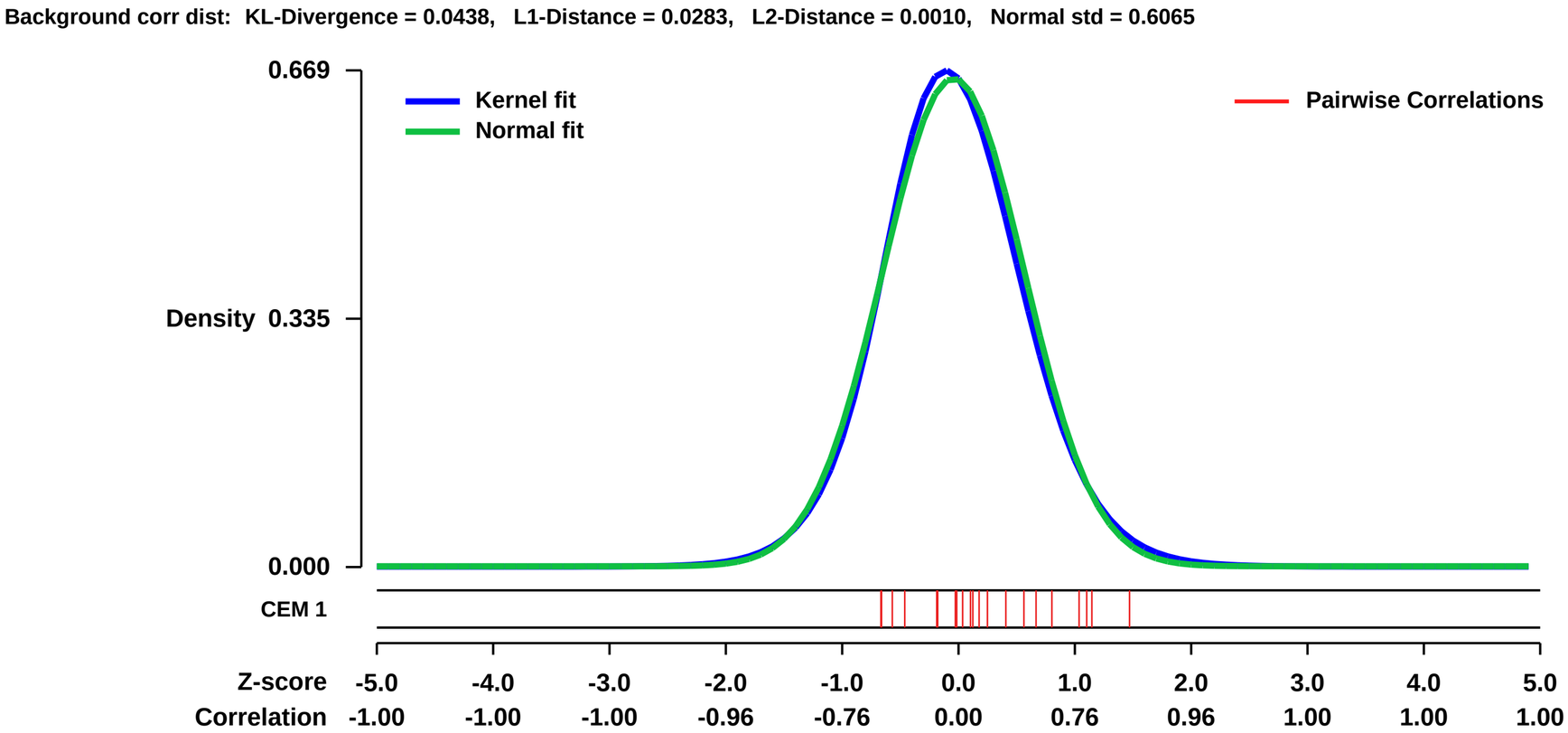

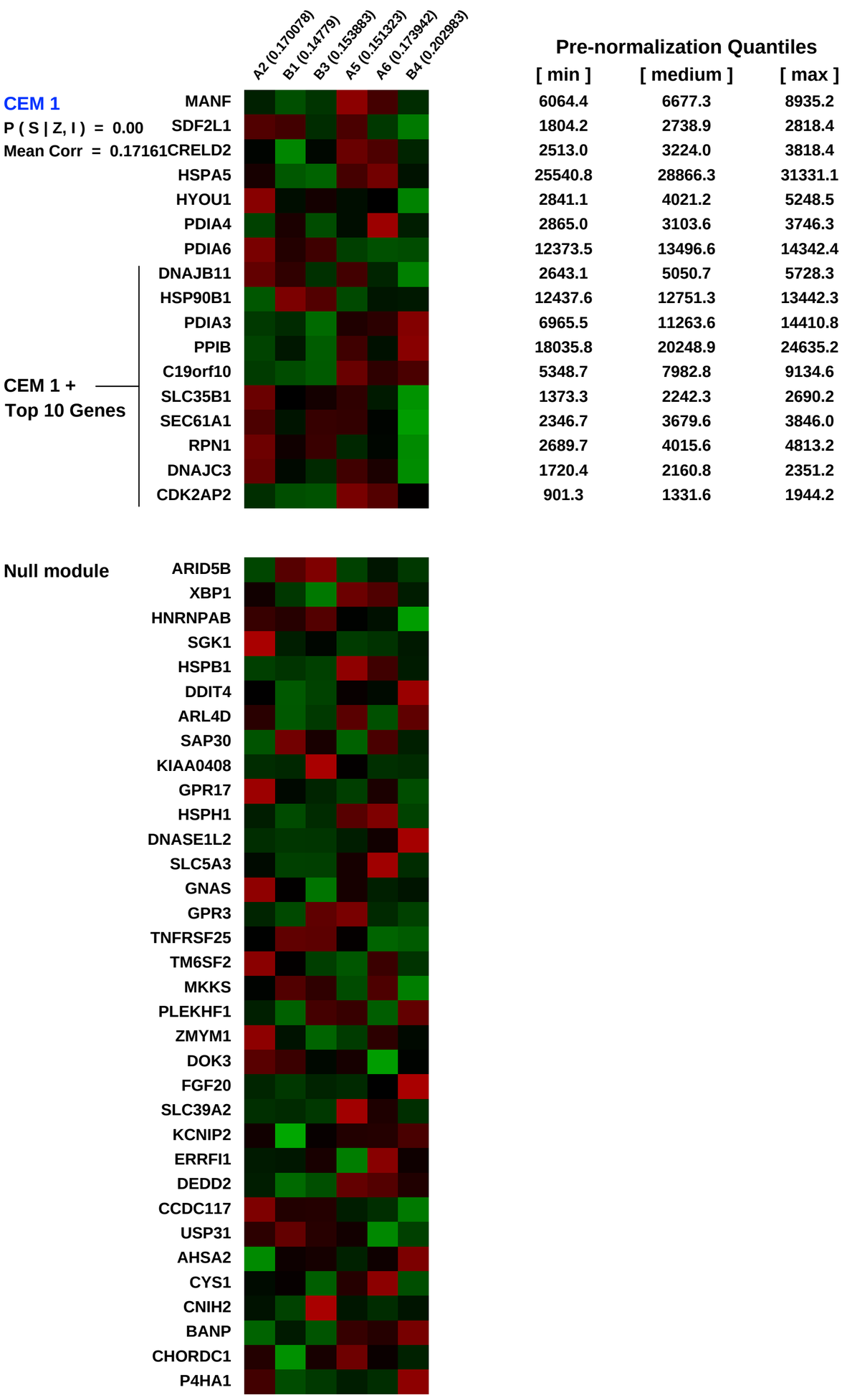

GEO Series "GSE40512" Expression Profiles

Num of samples in this series: 6

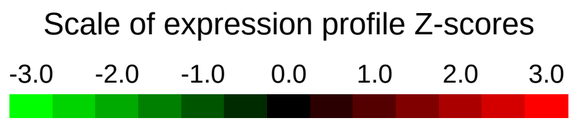

GEO Link:	http://www.ncbi.nlm.nih.gov/geo/query/acc.cgi?acc=GSE40512
Status:	Public on Oct 16 2012
Title:	Gene expression profile of human T-ALL cell line KOPTK1 treated with vehicle or PD 0332991
Organism:	Homo sapiens
Experiment type:	Expression profiling by array
Platform:	GPL570
Pubmed ID:	23079655
Summary & Design:	**Summary:** D-cyclins represent components of cell cycle machinery. To test the efficacy of targeting D-cyclins in cancer treatment, we engineered mouse strains which allow acute and global ablation of individual D-cyclins in a living animal. Ubiquitous shutdown of cyclin D1 or inhibition of cyclin D associated kinase activity in mice bearing ErbB2-driven mammary carcinomas halted cancer progression and triggered tumor-specific senescence, without compromising the animals' health. Ablation of cyclin D3 in mice bearing T-cell acute lymphoblastic leukemias (T-ALL) triggered tumorspecific apoptosis. Such selective killing of leukemic cells can be also achieved by inhibiting cyclin D associated kinase activity in mouse and human T-ALL models. Hence, contrary to what one might expect from ablation of a cell cycle protein, acute shutdown of a D-cyclin leads not only to cell cycle arrest, but it also triggers tumor cell senescence or apoptosis, and it affects different tumor types through distinct cellular mechanisms. Inhibiting cyclin D-activity represents a highly-selective anticancer strategy which specifically targets cancer cells without significantly affecting normal tissues. **Overall design:** A human T-ALL cell line KOPTK1 cells were cultured in the presence of the CDK4/6 inhibitor PD 0332991 (PD; 1 microM) or vehicle (VO) for 48 hrs. Experiment was done in biological triplicate. A total of 6 RNA samples (3 vehicle treated and 3 PD 0332991 treated samples) were used for microarray expression analysis.

Background corr dist: KL-Divergence = 0.0306, L1-Distance = 0.0585, L2-Distance = 0.0041, Normal std = 0.7823

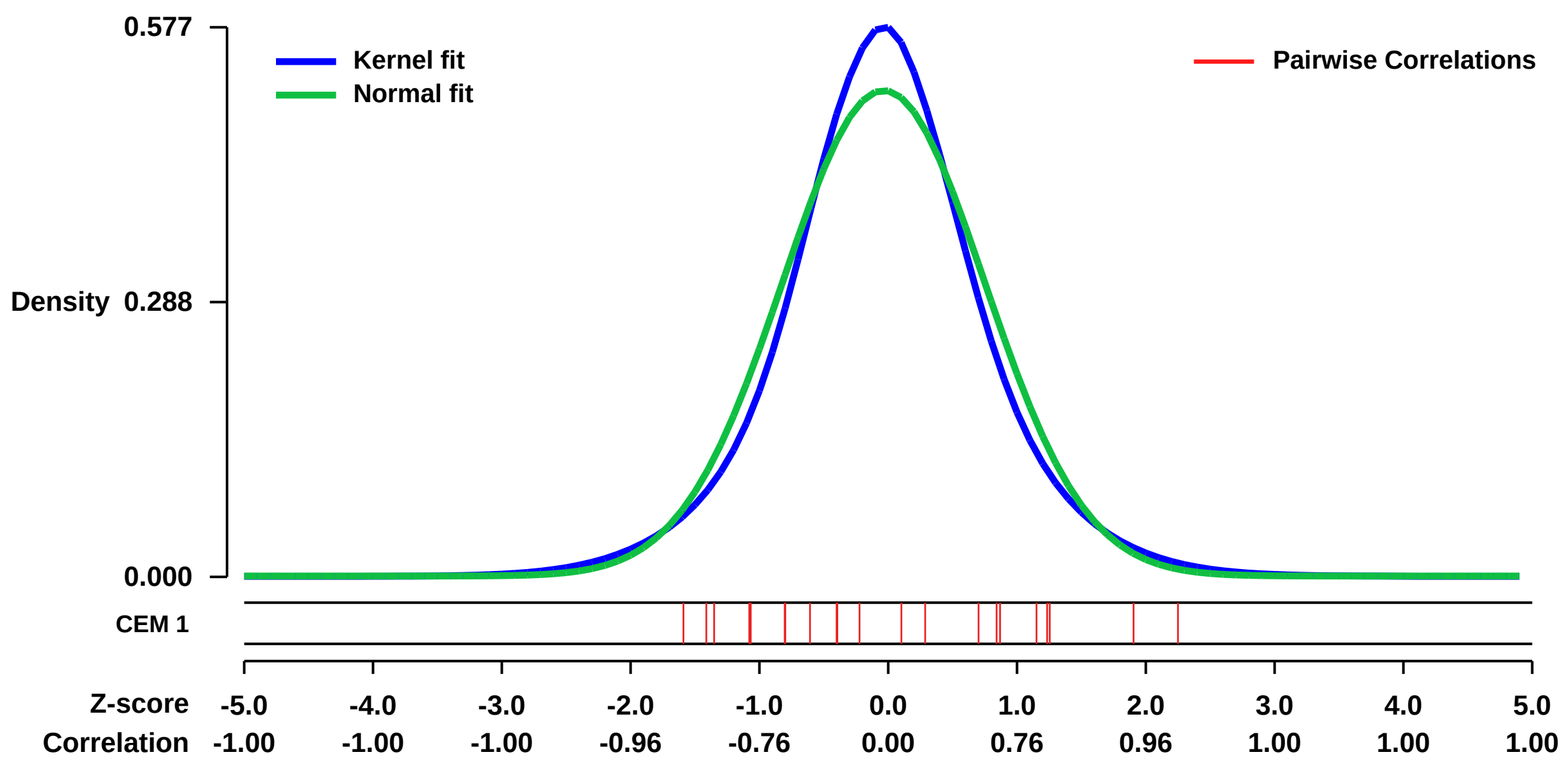

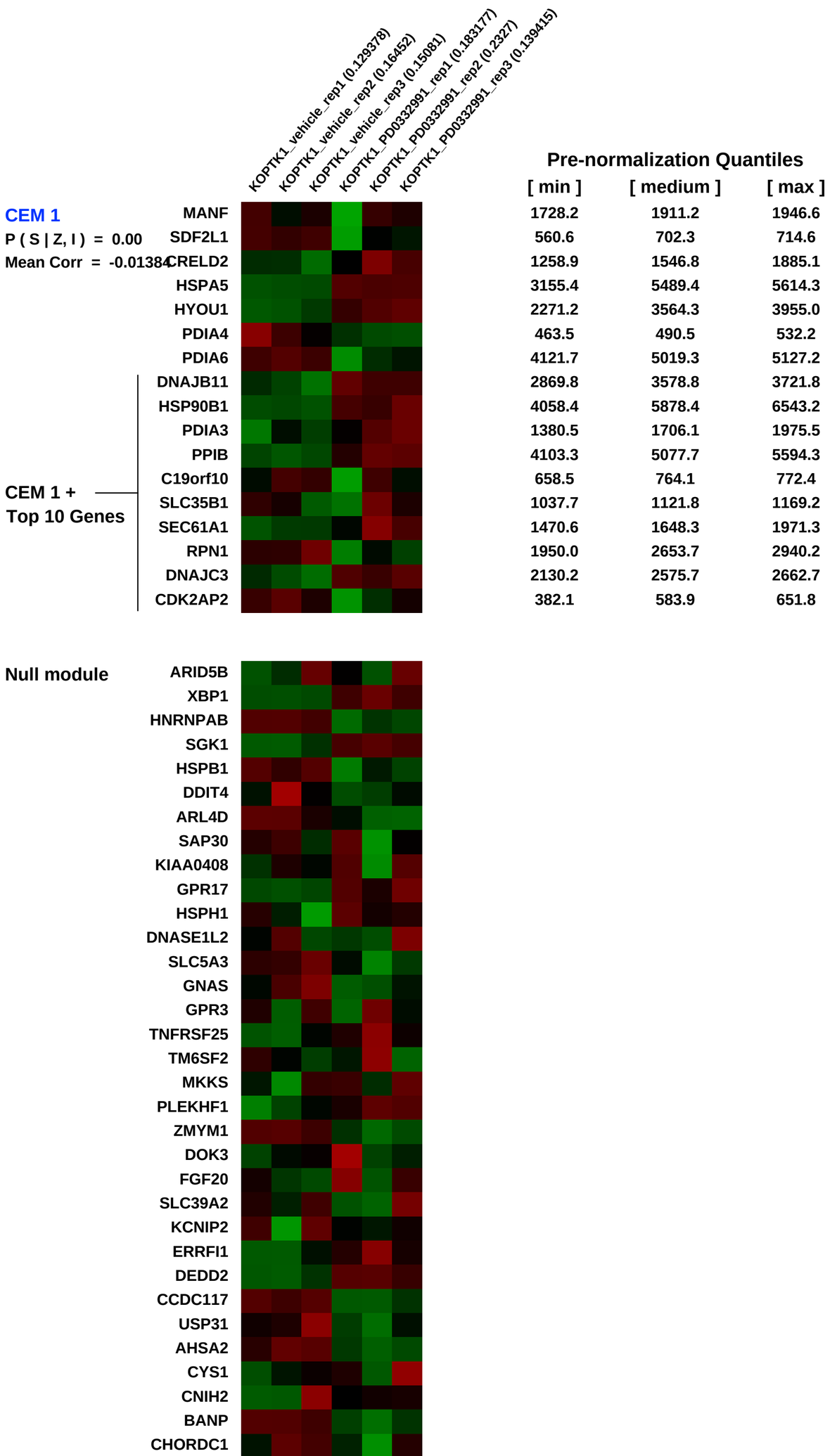

	Pre-normalization Quantiles [min]	[medium]	[max]
MANF	1728.2	1911.2	1946.6
SDF2L1	560.6	702.3	714.6
CRELD2	1258.9	1546.8	1885.1
HSPA5	3155.4	5489.4	5614.3
HYOU1	2271.2	3564.3	3955.0
PDIA4	463.5	490.5	532.2
PDIA6	4121.7	5019.3	5127.2
DNAJB11	2869.8	3578.8	3721.8
HSP90B1	4058.4	5878.4	6543.2
PDIA3	1380.5	1706.1	1975.5
PPIB	4103.3	5077.7	5594.3
C19orf10	658.5	764.1	772.4
SLC35B1	1037.7	1121.8	1169.2
SEC61A1	1470.6	1648.3	1971.3
RPN1	1950.0	2653.7	2940.2
DNAJC3	2130.2	2575.7	2662.7
CDK2AP2	382.1	583.9	651.8
ARID5B			
XBP1			
HNRNPAB			
SGK1			
HSPB1			
DDIT4			
ARL4D			
SAP30			
KIAA0408			
GPR17			
HSPH1			
DNASE1L2			
SLC5A3			
GNAS			
GPR3			
TNFRSF25			
TM6SF2			
MKKS			
PLEKHF1			
ZMYM1			
DOK3			
FGF20			
SLC39A2			
KCNIP2			
ERRFI1			
DEDD2			
CCDC117			
USP31			
AHSA2			
CYS1			
CNIH2			
BANP			
CHORDC1			
P4HA1			

GEO Series "GSE16080" Expression Profiles

Num of samples in this series: 6

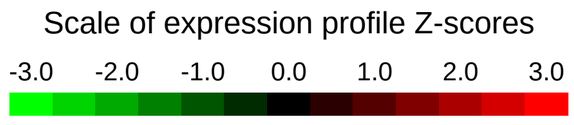

GEO Link:	http://www.ncbi.nlm.nih.gov/geo/query/acc.cgi?acc=GSE16080
Status:	Public on Sep 08 2009
Title:	Networking of differentially expressed genes in human MDA-MB-468 breast cancer cells resistant to methotrexate
Organism:	Homo sapiens
Experiment type:	Expression profiling by array
Platform:	GPL570
Pubmed ID:	19732436

Summary & Design:

Summary:
A summary of the work associated to these microarrays is the following:

The need for an integrated view of all data obtained from high-throughput technologies gave rise to network analyses. These are especially useful to rationalize phenomena in terms of how external perturbations propagate through the expression of genes. To address this issue in the case of drug resistance, we constructed Biological Association Networks of genes differentially expressed in cell lines resistant to methotrexate (MTX). Seven cell lines representative of different types of cancer including colon cancer (HT29 and Caco2), breast cancer (MCF7 and MDA-MB-468), pancreatic cancer (MIA PaCa-2), erythroblastic leukemia (K562) and osteosarcoma (Saos-2), were used. The differential expression pattern between sensitive and MTX-resistant cells was determined by microarrays covering the whole human genome and analyzed with the GeneSpring GX software package, v.7.3.1. Genes deregulated in common in the two colon cancer cell lines studied, were subject of Biological Association Networks construction. Dikkopf homolog-1 (DKK1) was a clear node of this network, and functional validations of this target using a siRNA showed a chemosensitization toward MTX. Members of the UDP-glucuronosyltransferase 1A (UGT1A) family formed a network of differentially expressed genes in the two breast cancer cell lines studied. siRNA treatment against UGT1A showed also an increase in MTX sensitivity. Eukaryotic translation elongation factor 1 alpha 1 (EEF1A1) was a gene overexpressed in common among the pancreatic cancer, leukemia and osteosarcoma cell lines, and siRNA treatment against EEF1A1 produced a chemosensitization toward MTX. Biological Association Networks identified DKK1, UGT1As and EEF1A1 as important gene nodes in MTX-resistance. Treatments using iRNA technology against these three genes show chemosensitization toward MTX.

Overall design:
Two cell lines are compared, which are MDA-MB-468 breast cancer cells sensitive to methotrexate and MDA-MB-468 cells resistant to 10e-6M methotrexate. Six samples are provided which correspond to tripicates of each cell line. The sample provided were analyzed using the specific software GeneSpring GX.

Background corr dist: KL-Divergence = 0.0392, L1-Distance = 0.0310, L2-Distance = 0.0013, Normal std = 0.6326

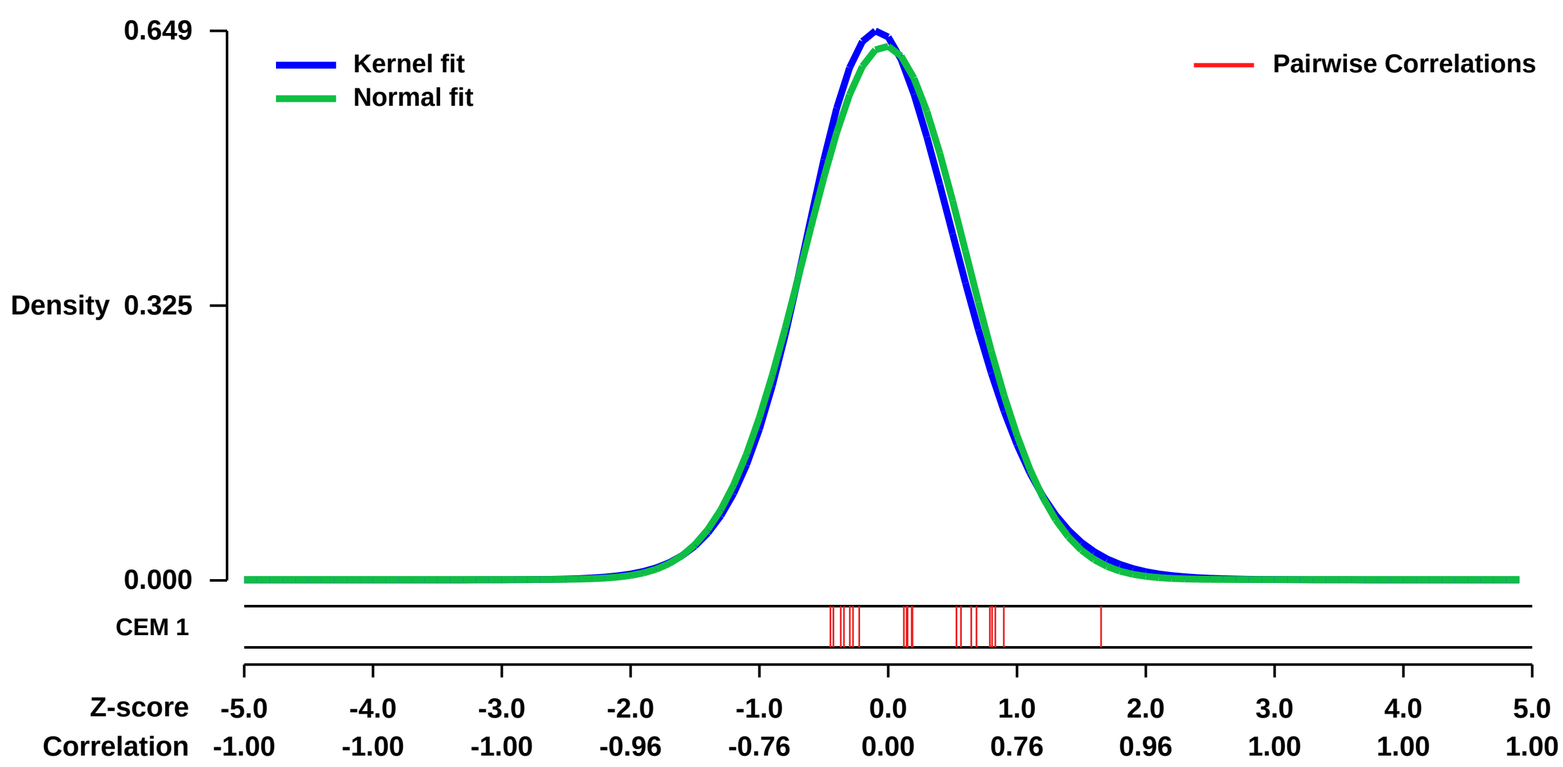

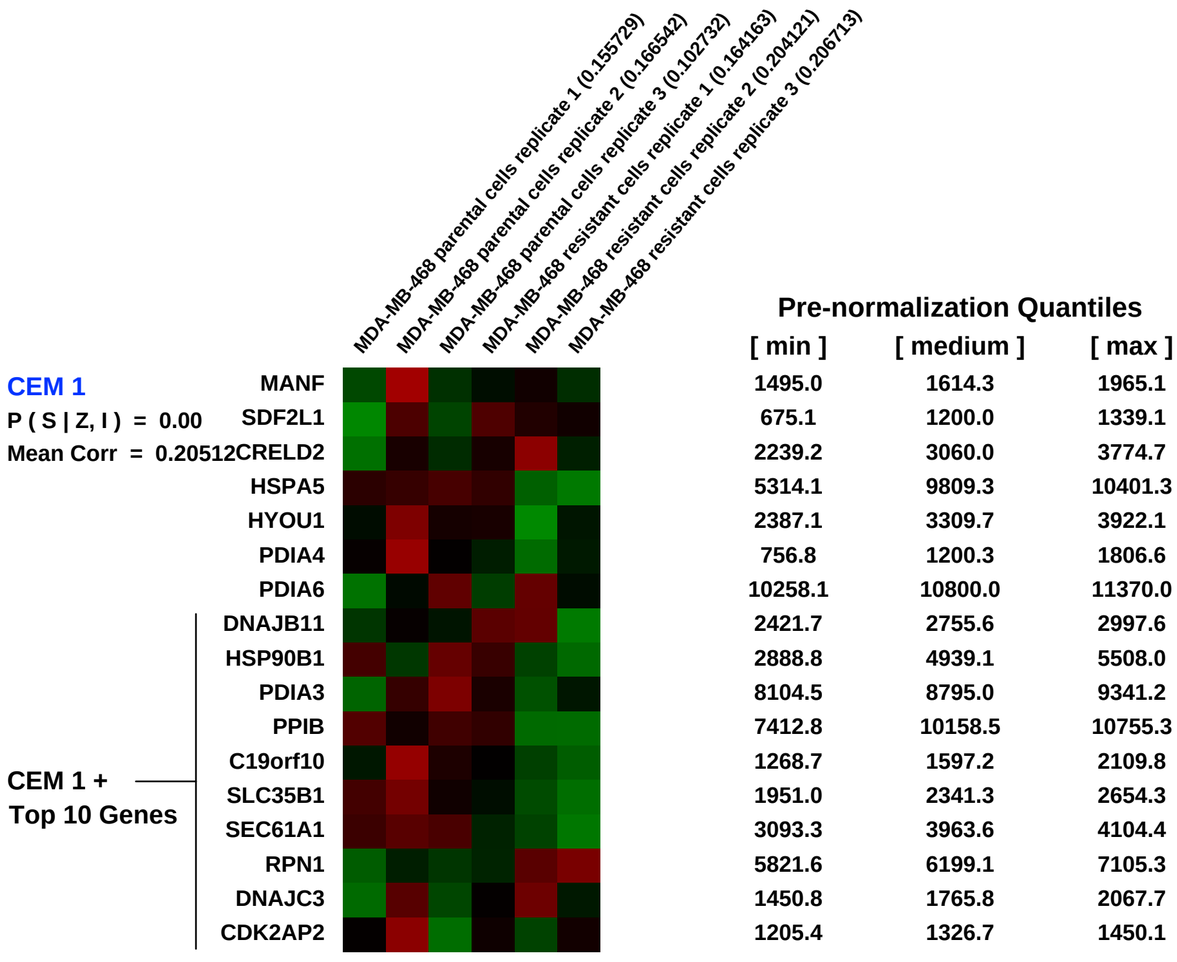

GEO Series "GSE29232" Expression Profiles

Num of samples in this series: 12

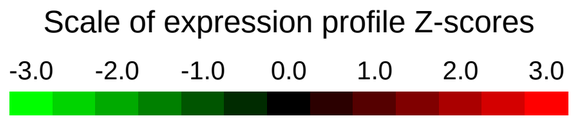

GEO Link:	http://www.ncbi.nlm.nih.gov/geo/query/acc.cgi?acc=GSE29232
Status:	Public on May 12 2011
Title:	Identification of androgen-regulated genes in RWPE-1-AR cells
Organism:	Homo sapiens
Experiment type:	Expression profiling by array
Platform:	GPL570
Pubmed ID:	
Summary & Design:	**Summary:** Transcriptional profiling of RWPE-1 cells stably expressing human androgen receptor (as described in Altintas et al., Mol Cell Endocrinol 2011) treated with a non-metabolisable androgen, R1881 **Overall design:** RWPE-1-AR cells were treated with R1881 during 3h or 24h and compared to control not treated cells. Three independent cell culture experiments for each treatment condition (vehicle or R1881 for 3h and 24h).

Background corr dist: KL-Divergence = 0.1325, L1-Distance = 0.0274, L2-Distance = 0.0012, Normal std = 0.3940

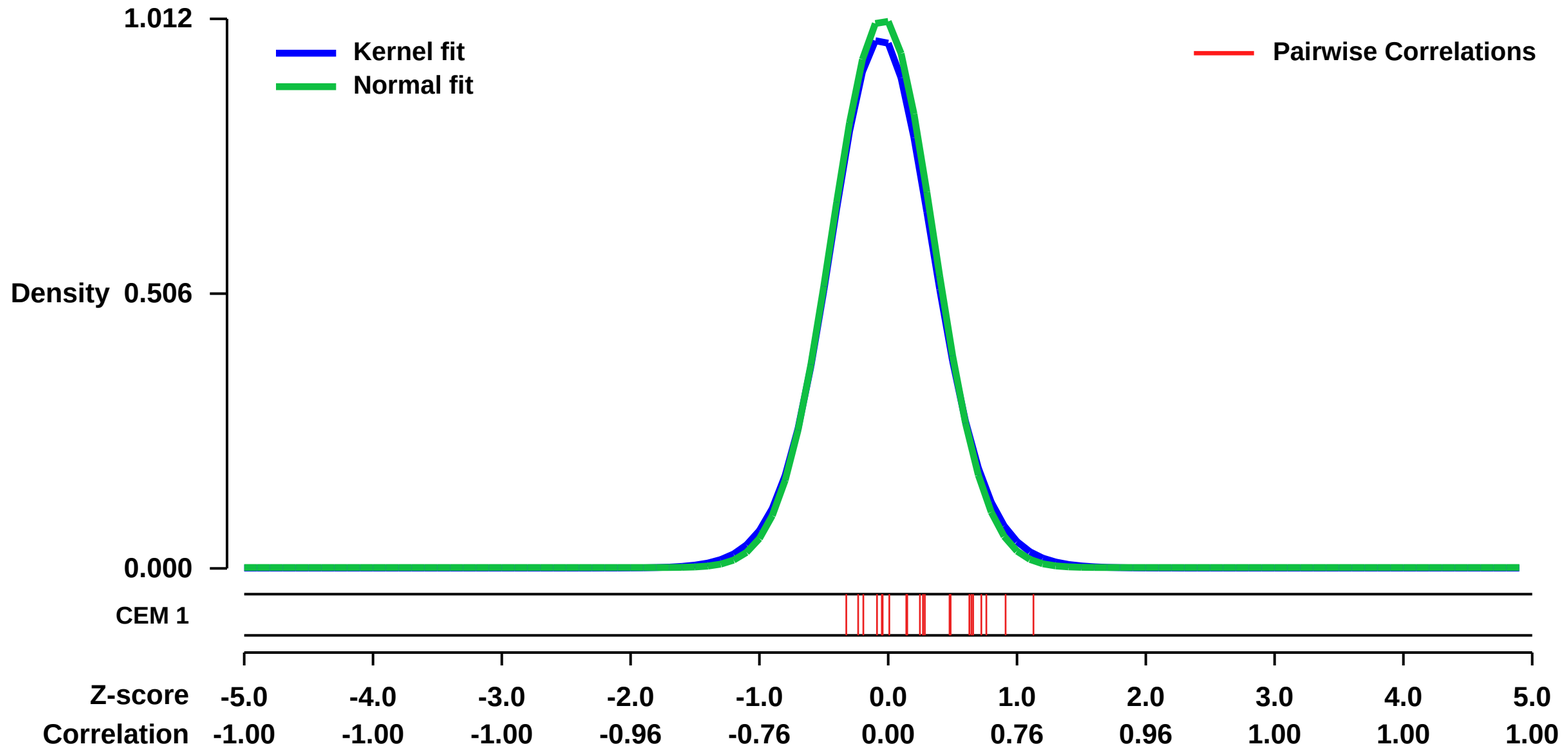

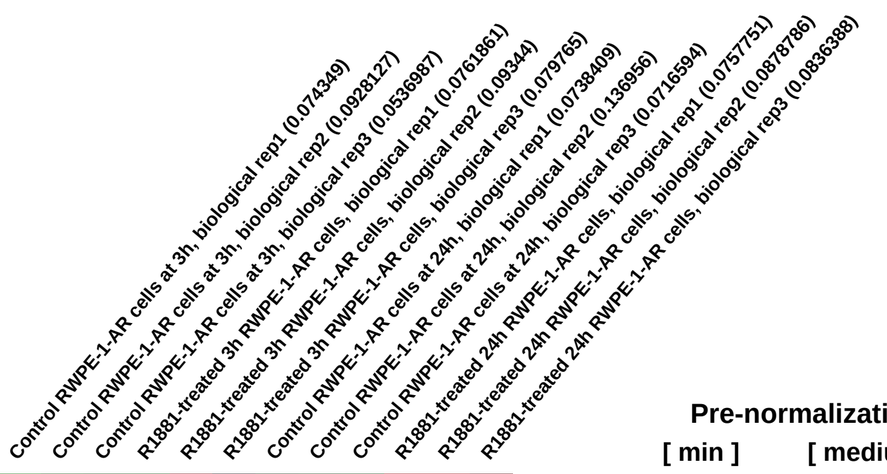

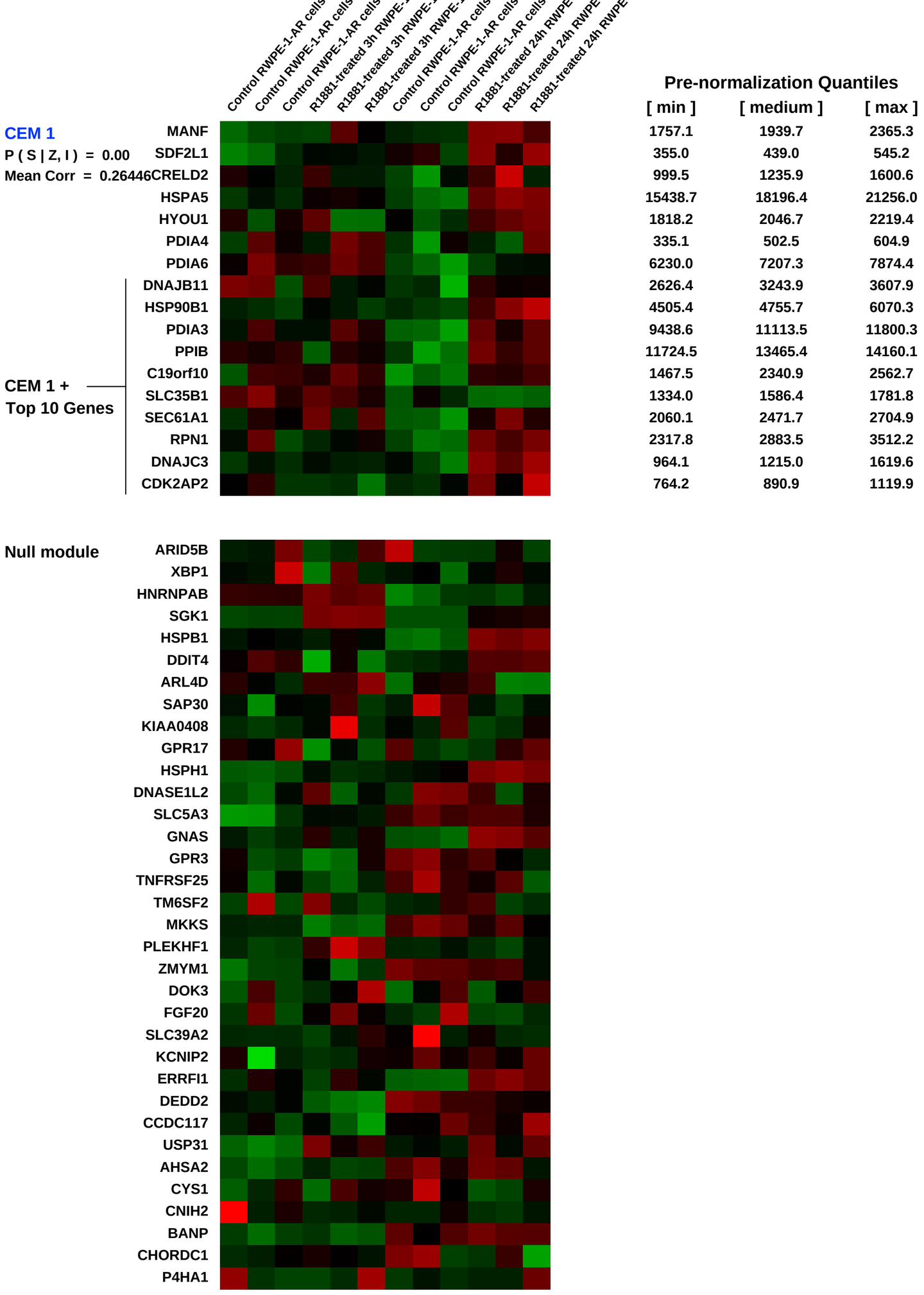

GEO Series "GSE4465" Expression Profiles

Num of samples in this series: 6

Scale of expression profile Z-scores

-3.0 -2.0 -1.0 0.0 1.0 2.0 3.0

GEO Link:	http://www.ncbi.nlm.nih.gov/geo/query/acc.cgi?acc=GSE4465
Status:	Public on Dec 17 2008
Title:	HDACI treatment of hepG2 cells
Organism:	Homo sapiens
Experiment type:	Expression profiling by array
Platform:	GPL570
Pubmed ID:	18959802
Summary & Design:	**Summary:** This study compares HEPG2 cells treated with either ethanol(control) or TSA (0.5uM) for 24 hrs. Gene Expression was profiled on HU-133 plus 2.0 arrays **Keywords: Treaded vs untreated** **Overall design:** 3 controls vs 3 TSA treated

Background corr dist: KL-Divergence = 0.0157, L1-Distance = 0.0192, L2-Distance = 0.0003, Normal std = 0.8100

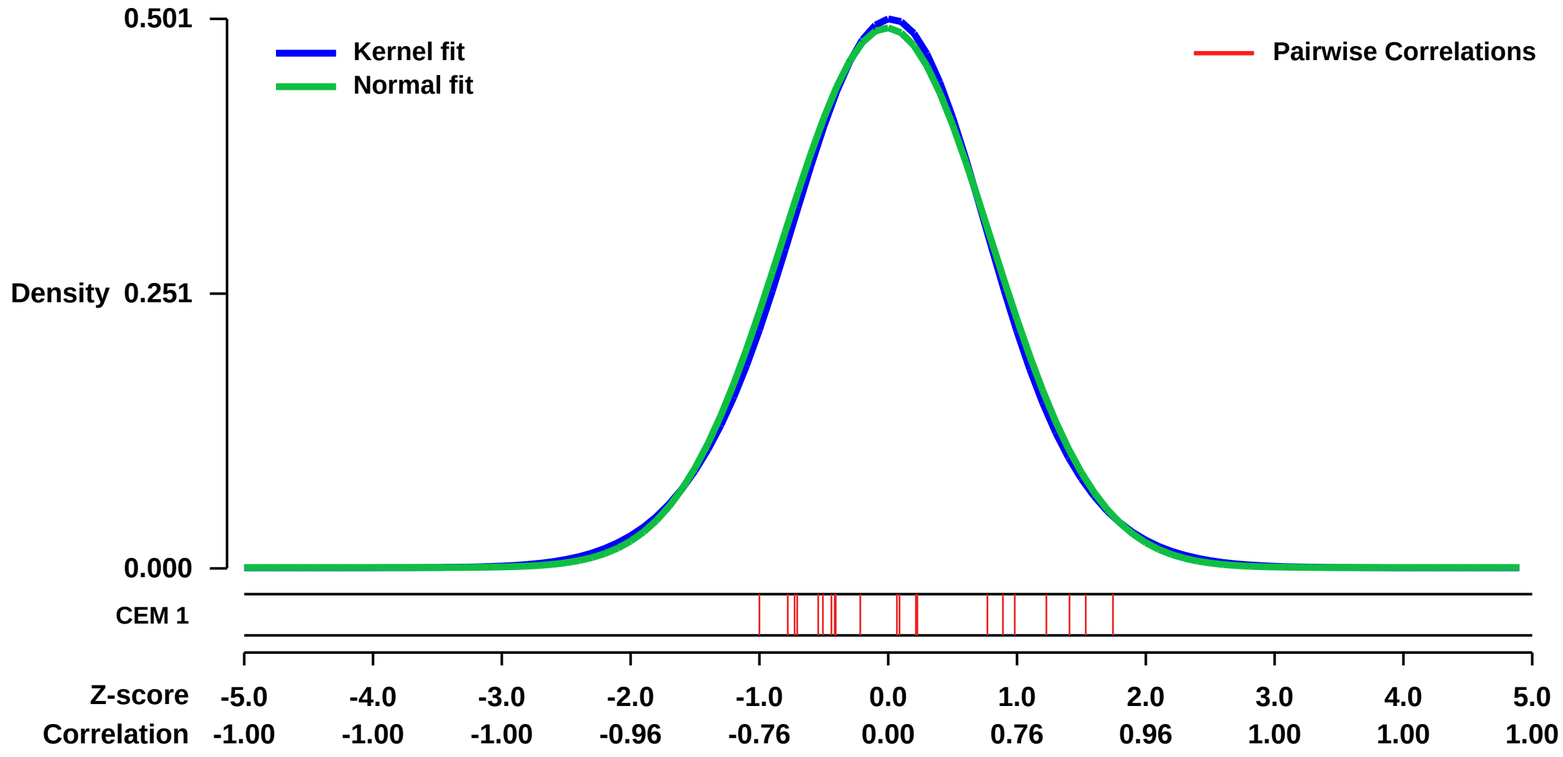

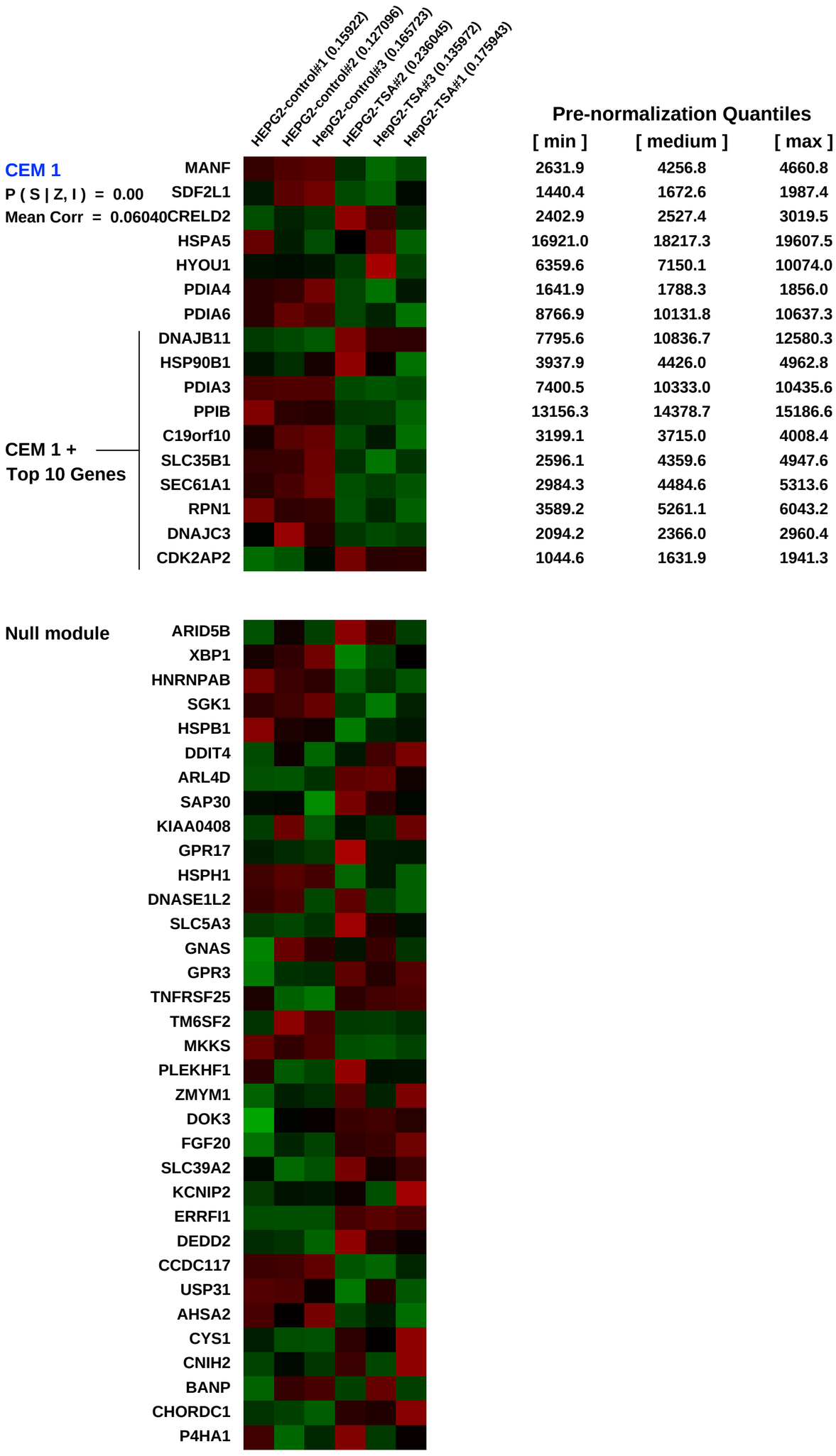

GEO Series "GSE18810" Expression Profiles

Num of samples in this series: 6

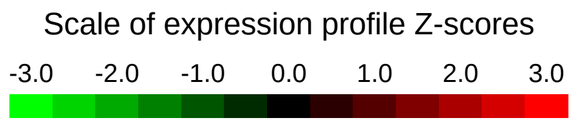

GEO Link:	http://www.ncbi.nlm.nih.gov/geo/query/acc.cgi?acc=GSE18810
Status:	Public on Mar 01 2010
Title:	Expression data from human neutrophils exposed to uropathogenic and commensal Esherichia coli.
Organism:	Homo sapiens
Experiment type:	Expression profiling by array
Platform:	GPL570
Pubmed ID:	

Summary & Design:

Summary:
The establishment of bacterial infections at epithelial surfaces is determined by the balance of virulence attributes of the pathogen with the activity of innate host defenses. Polymorphonuclear leukocytes (PMN) are key responders in many bacterial infections, but the mechanisms by which pathogens subvert these early responses to establish infection are largely undefined. Here, we model these early interactions between human PMN and the primary cause of urinary tract infections, namely uropathogenic Escherichia coli (UPEC). Our objective was to define virulence phenotypes of uropathogens (as compared with laboratory and commensal E. coli strains) that permit evasion of PMN activity. We found that UPEC strains resist phagocytic killing and dampen the production of antimicrobial reactive oxygen species by PMNs. Analysis of the global transcriptional responses of PMN to E. coli strains revealed that UPEC exposure downregulates the expression of PMN genes involved in proinflammatory signaling and PMN chemotaxis, adhesion, and migration. Consistent with these data, UPEC attenuated transepithelial neutrophil recruitment in an in vitro model of acute infection. We propose that these UPEC strategies are important in the establishment of epithelial infection, and that the findings are germane to a range of bacterial infections at epithelial surfaces.

We used microarrays to detail the global program of gene expression in human neutrophils in response to a uropathogenic bacteria compared to a closely related non-pathogenic strain relative to control samples with no bacteria. Our goal was to elucidate a pathogen-specific response. We chose an early time point of 60 minutes to evaluate the accute response to infection.

Overall design:
Human neutrophils were exposed to pathogenic or commensal Escherichia coli for RNA extraction and hybridization on Affymetrix microarrays

Background corr dist: KL-Divergence = 0.0423, L1-Distance = 0.0432, L2-Distance = 0.0028, Normal std = 0.6298

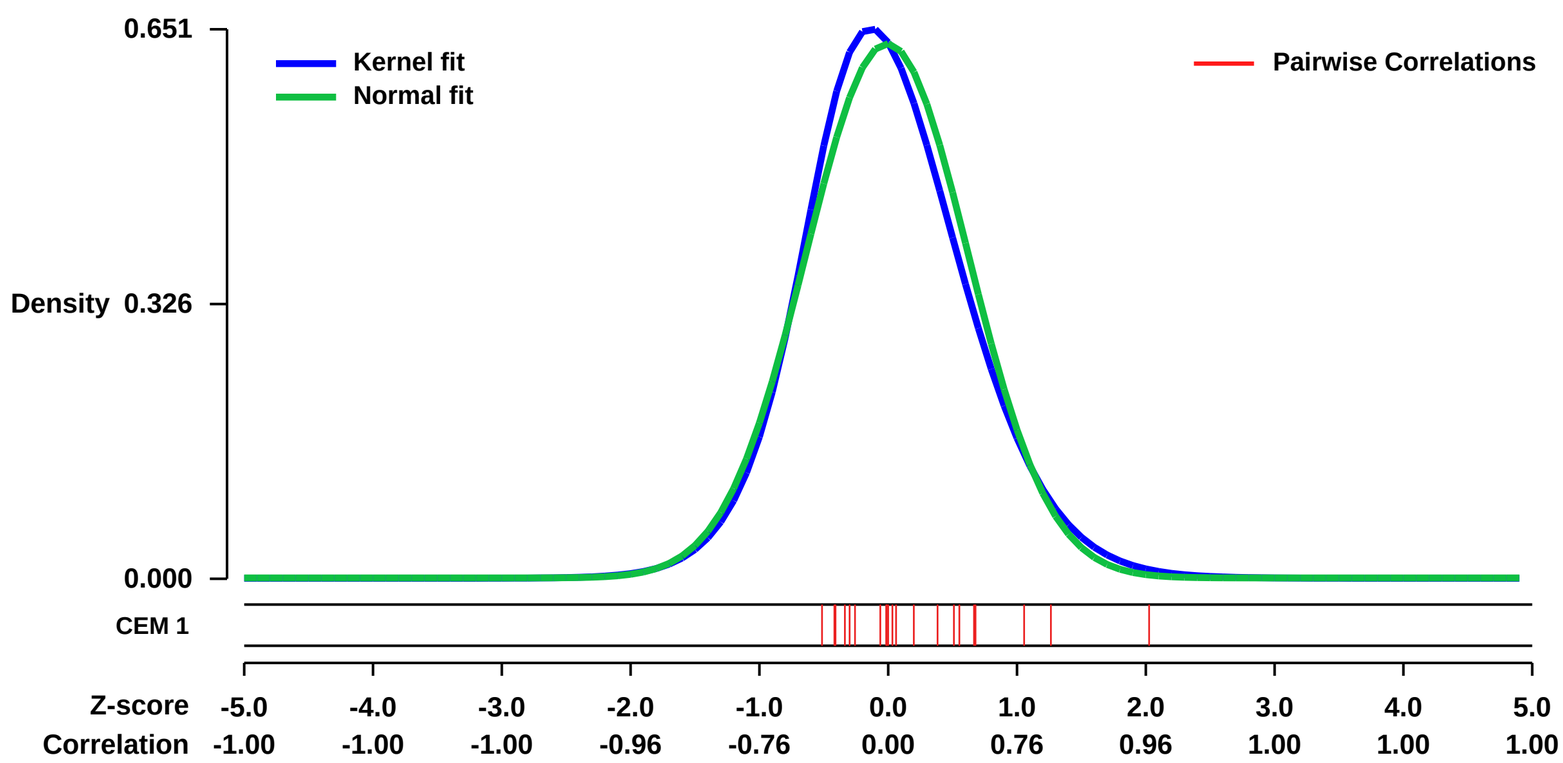

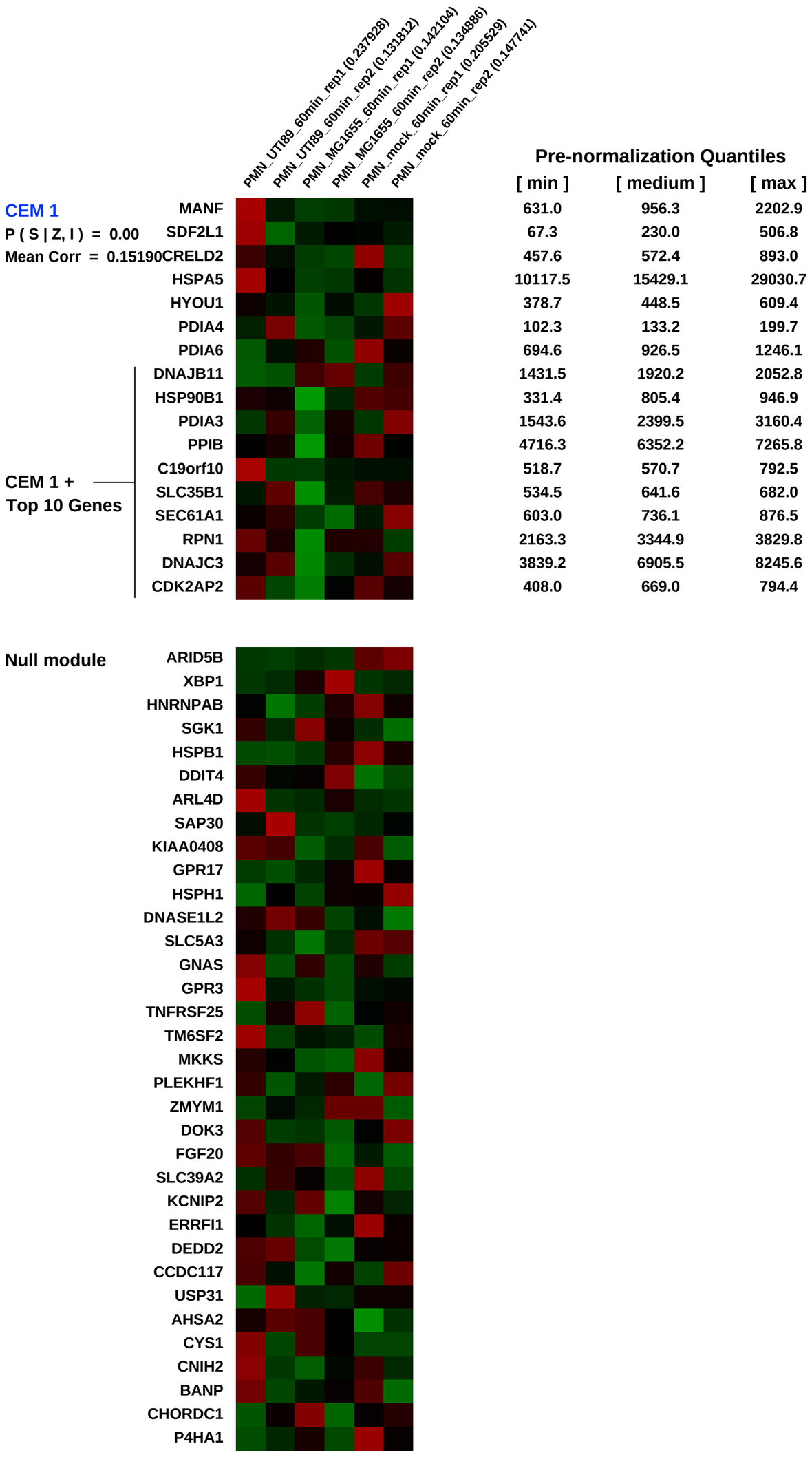

Pre-normalization Quantiles

	[min]	[medium]	[max]
MANF	631.0	956.3	2202.9
SDF2L1	67.3	230.0	506.8
CRELD2	457.6	572.4	893.0
HSPA5	10117.5	15429.1	29030.7
HYOU1	378.7	448.5	609.4
PDIA4	102.3	133.2	199.7
PDIA6	694.6	926.5	1246.1
DNAJB11	1431.5	1920.2	2052.8
HSP90B1	331.4	805.4	946.9
PDIA3	1543.6	2399.5	3160.4
PPIB	4716.3	6352.2	7265.8
C19orf10	518.7	570.7	792.5
SLC35B1	534.5	641.6	682.0
SEC61A1	603.0	736.1	876.5
RPN1	2163.3	3344.9	3829.8
DNAJC3	3839.2	6905.5	8245.6
CDK2AP2	408.0	669.0	794.4
ARID5B			
XBP1			
HNRNPAB			
SGK1			
HSPB1			
DDIT4			
ARL4D			
SAP30			
KIAA0408			
GPR17			
HSPH1			
DNASE1L2			
SLC5A3			
GNAS			
GPR3			
TNFRSF25			
TM6SF2			
MKKS			
PLEKHF1			
ZMYM1			
DOK3			
FGF20			
SLC39A2			
KCNIP2			
ERRFI1			
DEDD2			
CCDC117			
USP31			
AHSA2			
CYS1			
CNIH2			
BANP			
CHORDC1			
P4HA1			

GEO Series "GSE27291" Expression Profiles

Num of samples in this series: 12

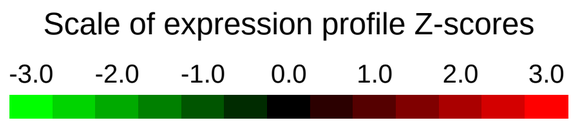

GEO Link:	http://www.ncbi.nlm.nih.gov/geo/query/acc.cgi?acc=GSE27291
Status:	Public on Feb 15 2011
Title:	Expression data from human TCRVg9-positive gamma delta T lymphocytes
Organism:	Homo sapiens
Experiment type:	Expression profiling by array
Platform:	GPL570
Pubmed ID:	21968650
Summary & Design:	**Summary:** We used microarrays to detail the global programme of gene expression by circulating TCRVgamma9+ gamma delta T cells isolated from healthy individuals,tested either as resting cells or cells activated by phosphoantigen BrHPP and IL-2at an early(+6hrs) and a late (+7days) timepoint. We find that with more â NK cellâ genes than alphabeta T cells and more â T cellâ genes than NK cells, the circulating TCRVgamma9+ gamma delta T cells cells have a hybrid transcriptome. The gene signature of the activated cells recapitulates their physiological functions: Th1 cytokine, chemokine and cytotoxic activities at first and mitotic activity at later time points. The gene expression pattern of activated normal gamma delta T cells is nevertheless clearly distinctive from that of NK/T and peripheral T cell lymphomas of the gamma delta subtype. **Overall design:** Human TCRVg9positive gamma delta T cells were isolated from PBMC by cell sorting (>98% purity) and activated for RNA extraction and hybridization on Affymetrix microarrays. Samples comprise cells before activation (control time 0), early after activation with BrHPP/IL2 (+6 hours) and at a later timepoint of the activated in vitro culture with BrHPP/IL2 (day 7).

Background corr dist: KL-Divergence = 0.1129, L1-Distance = 0.0340, L2-Distance = 0.0024, Normal std = 0.4258

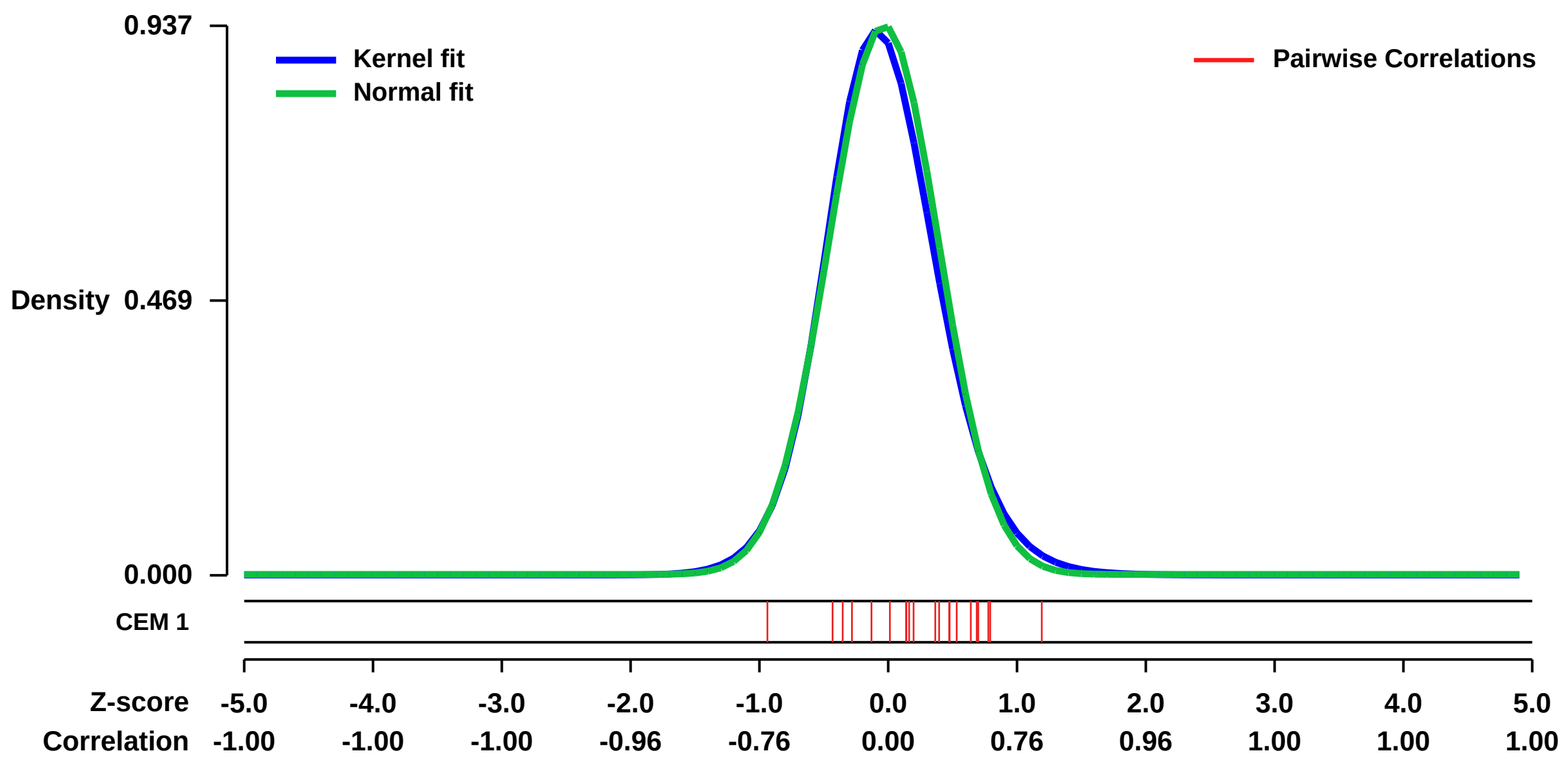

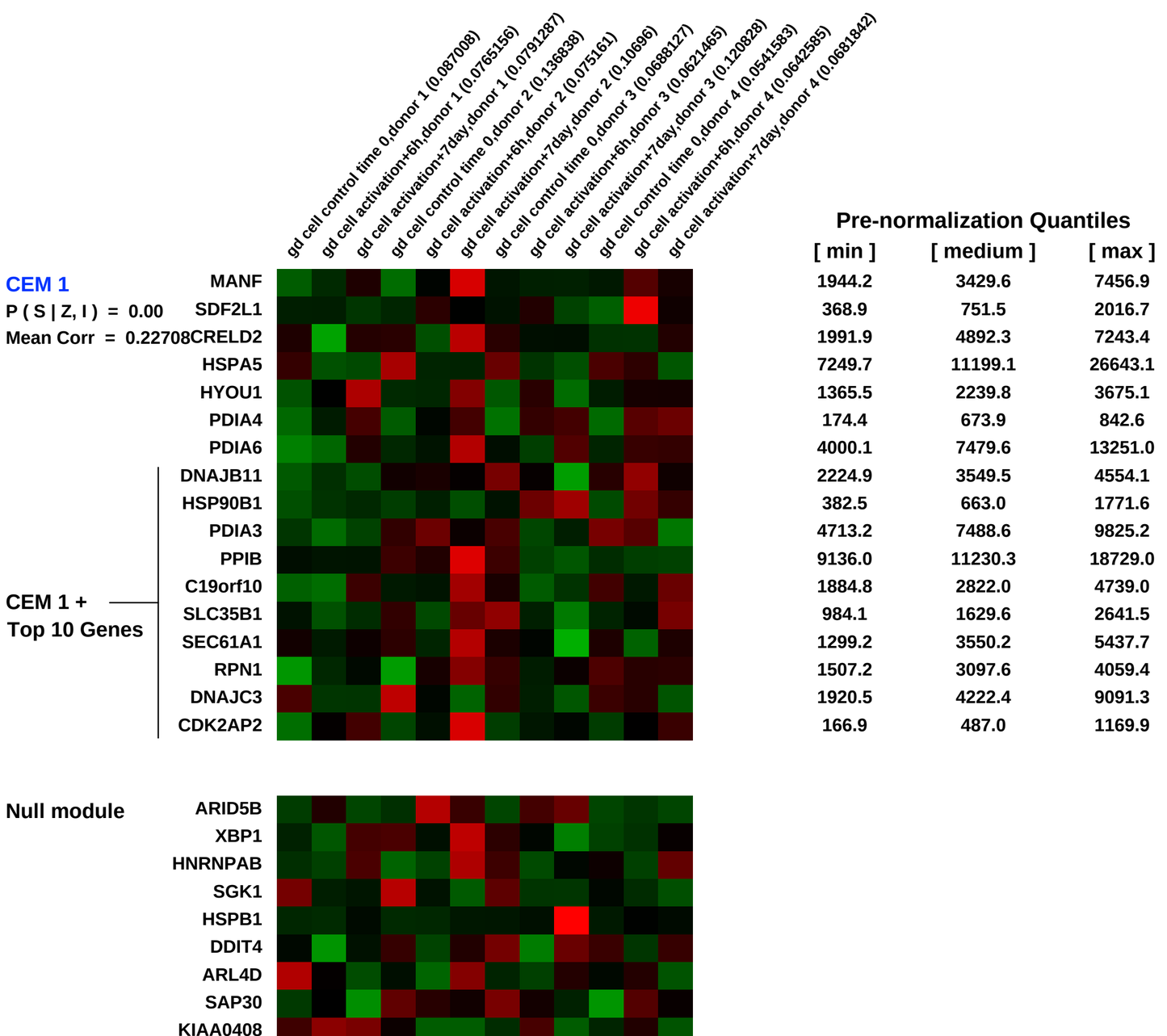

Pre-normalization Quantiles

	[min]	[medium]	[max]
MANF	1944.2	3429.6	7456.9
SDF2L1	368.9	751.5	2016.7
CRELD2	1991.9	4892.3	7243.4
HSPA5	7249.7	11199.1	26643.1
HYOU1	1365.5	2239.8	3675.1
PDIA4	174.4	673.9	842.6
PDIA6	4000.1	7479.6	13251.0
DNAJB11	2224.9	3549.5	4554.1
HSP90B1	382.5	663.0	1771.6
PDIA3	4713.2	7488.6	9825.2
PPIB	9136.0	11230.3	18729.0
C19orf10	1884.8	2822.0	4739.0
SLC35B1	984.1	1629.6	2641.5
SEC61A1	1299.2	3550.2	5437.7
RPN1	1507.2	3097.6	4059.4
DNAJC3	1920.5	4222.4	9091.3
CDK2AP2	166.9	487.0	1169.9

GEO Series "GSE15792" Expression Profiles

Num of samples in this series: 6

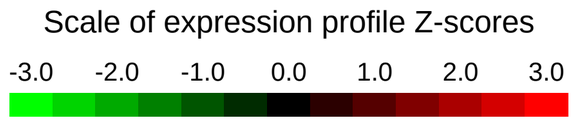

GEO Link:	**http://www.ncbi.nlm.nih.gov/geo/query/acc.cgi?acc=GSE15792**
Status:	**Public on Dec 31 2009**
Title:	**Expression profiles in PCARNEQ ncRNA depletion in prostate cancer cells**
Organism:	**Homo sapiens**
Experiment type:	**Expression profiling by array**
Platform:	**GPL570**
Pubmed ID:	
Summary & Design:	**Summary:** **To globally address the function of a novel ncRNA PCARNEQ located in chromosome 8q24, microarray analysis was performed on RNA isolated from prostate cancer cell line LNCaP cells treated with siRNA to PCARNEQ and the control siRNA to EGFP (siEGFP).** **Overall design:** **LNCaP cells were treated with siRNA to PCARNEQ or the control siRNA to EGFP and total RNA from each experiment was analyzed in triplicate by microarray.**

Background corr dist: **KL-Divergence = 0.0188, L1-Distance = 0.0297, L2-Distance = 0.0009, Normal std = 0.8031**

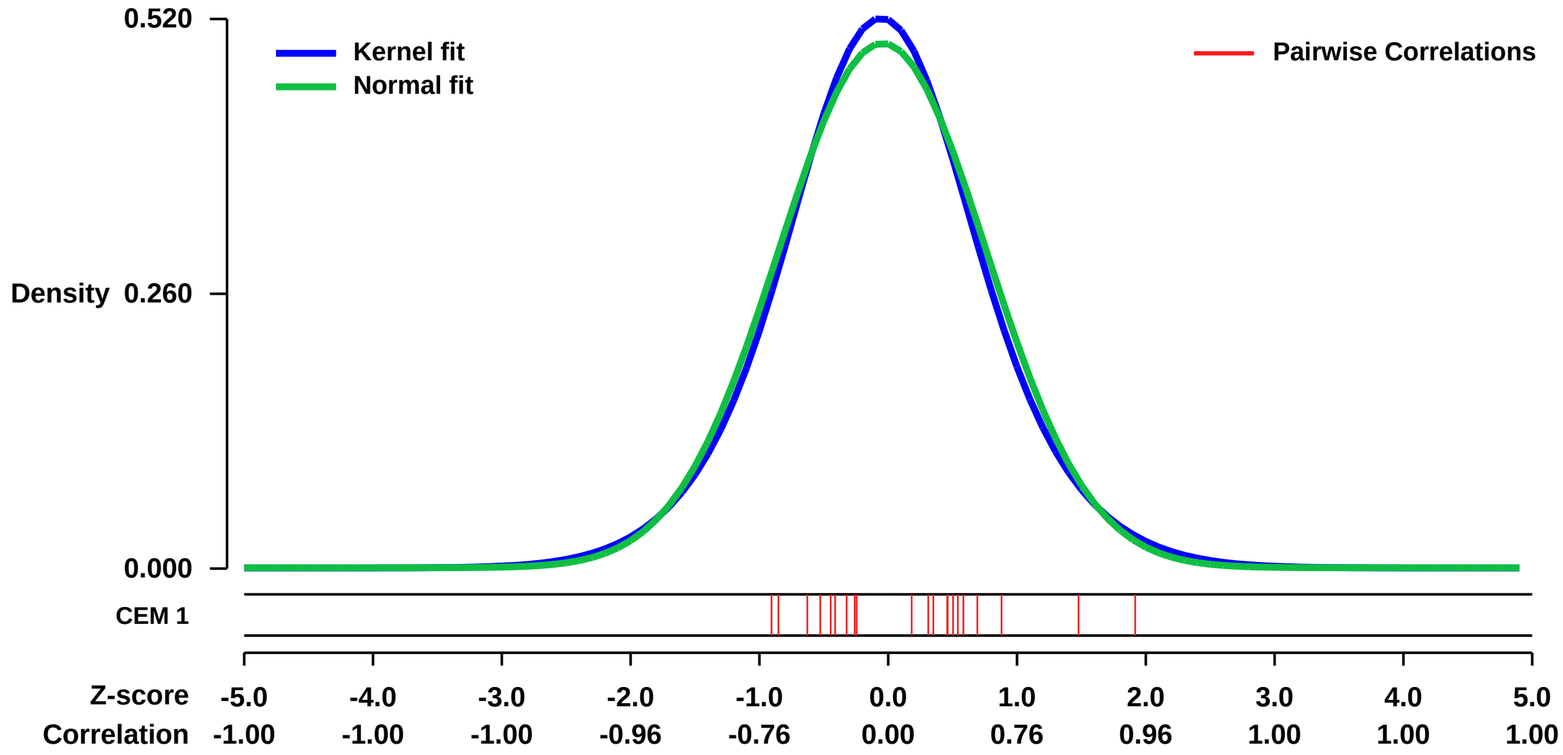

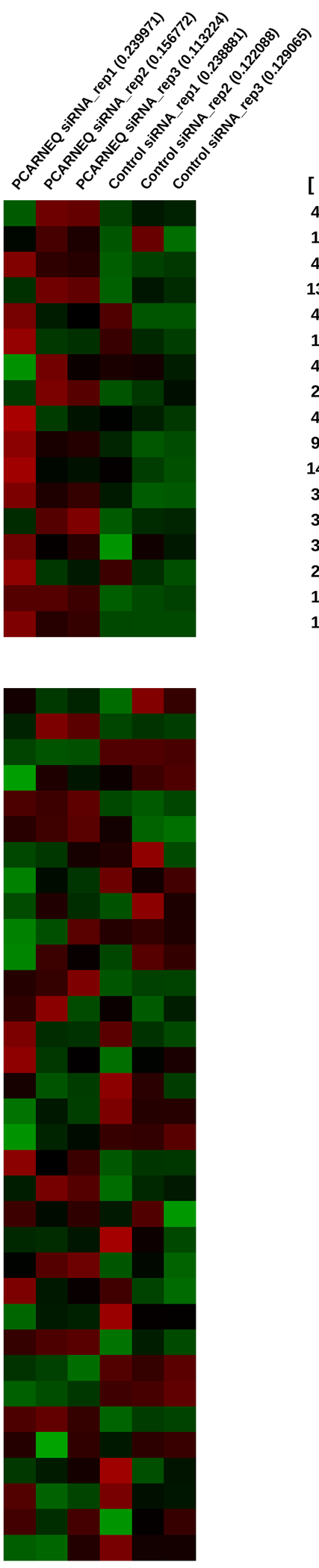

GEO Series "GSE43591" Expression Profiles

Num of samples in this series: 20

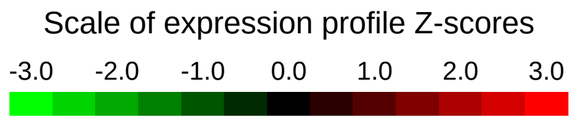

GEO Link:	http://www.ncbi.nlm.nih.gov/geo/query/acc.cgi?acc=GSE43591
Status:	Public on Aug 02 2013
Title:	MicroRNA regulate immune pathways in T-cells in multiple sclerosis (MS) mRNA
Organism:	Homo sapiens
Experiment type:	Expression profiling by array
Platform:	GPL570
Pubmed ID:	23895517
Summary & Design:	**Summary:** MicroRNAs are small noncoding RNA molecules that are involved in the control of gene expression. To investigate the role of microRNA in multiple sclerosis (MS), we performed global microarray analyses of mRNA and microRNA in peripheral blood T-cells from relapsing-remitting MS patients and controls. We identified 2,452 regulated genes and 21 regulated microRNA that differed between MS patients and controls. By Kolmogorov-Smirnov test, 20 of 21 regulated microRNA were shown to affect the expression of their target genes, many of which are involved in the immune system. LIGHT (TNFSF14) was a microRNA target gene significantly decreased in MS. The down-regulation of mir-494 and predicted mRNA-target LIGHT was verified by real-time PCR and we could demonstrate decreased serum levels of LIGHT in MS. Thus, regulated microRNA were significantly associated with both gene and protein expression of a molecule in immunological pathways. These findings indicate that microRNA may be important regulatory molecules in T-cells in MS. **Overall design:** Microarray expression analysis of mRNA and miRNA in peripheral blood T-cell of control andMS patients

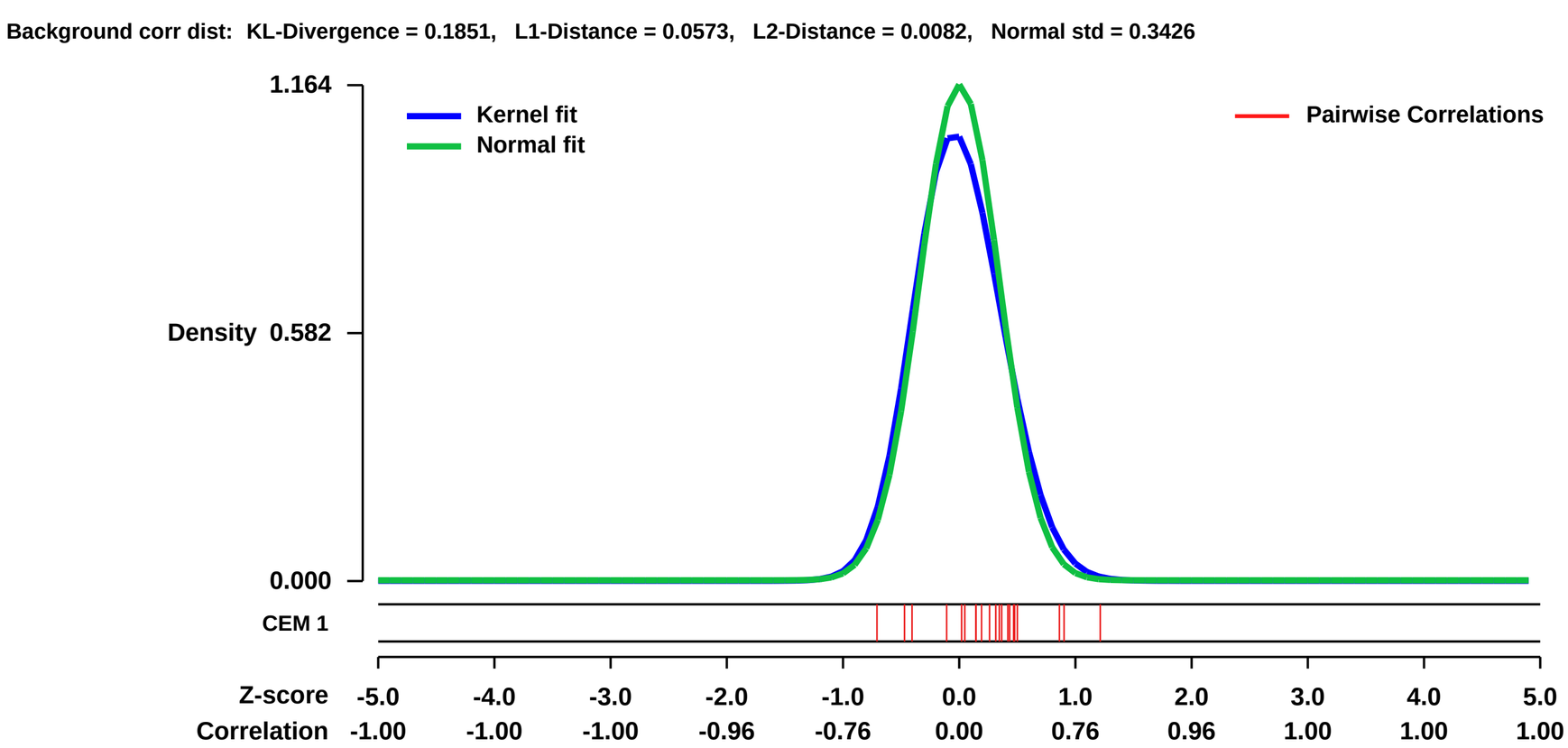

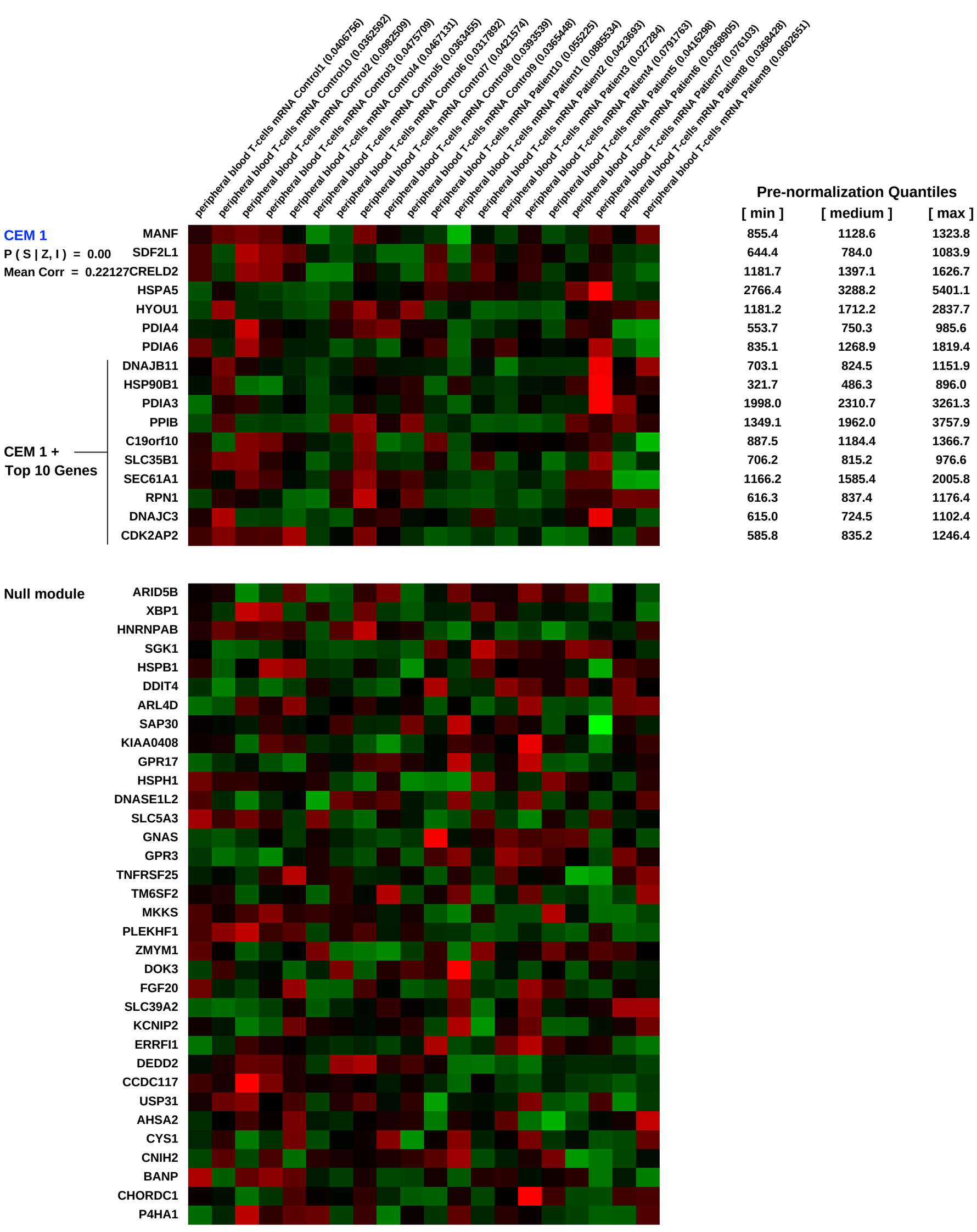

GEO Series "GSE5225" Expression Profiles

Num of samples in this series: 6

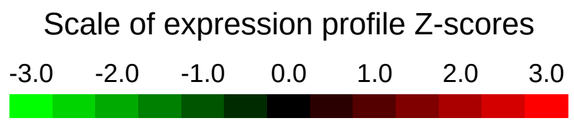

GEO Link:	**http://www.ncbi.nlm.nih.gov/geo/query/acc.cgi?acc=GSE5225**
Status:	**Public on Jun 30 2009**
Title:	**Expression data from OCUBM cells trasfected with IGF1R**
Organism:	**Homo sapiens**
Experiment type:	**Expression profiling by array**
Platform:	**GPL570**
Pubmed ID:	
Summary & Design:	**Summary:** **To investigate genes that might influence resistance to infection through IGF1R, we screened human breast cancer-derived OCUB-M cells transfected with expression vector encoding IGF1R using microarray analysis.** **Keywords: overexpression comparison** **Overall design:** **OCUBM cells were transfected with/without IGF1R for RNA extraction and hybridization on Affymetrix microarrays.**

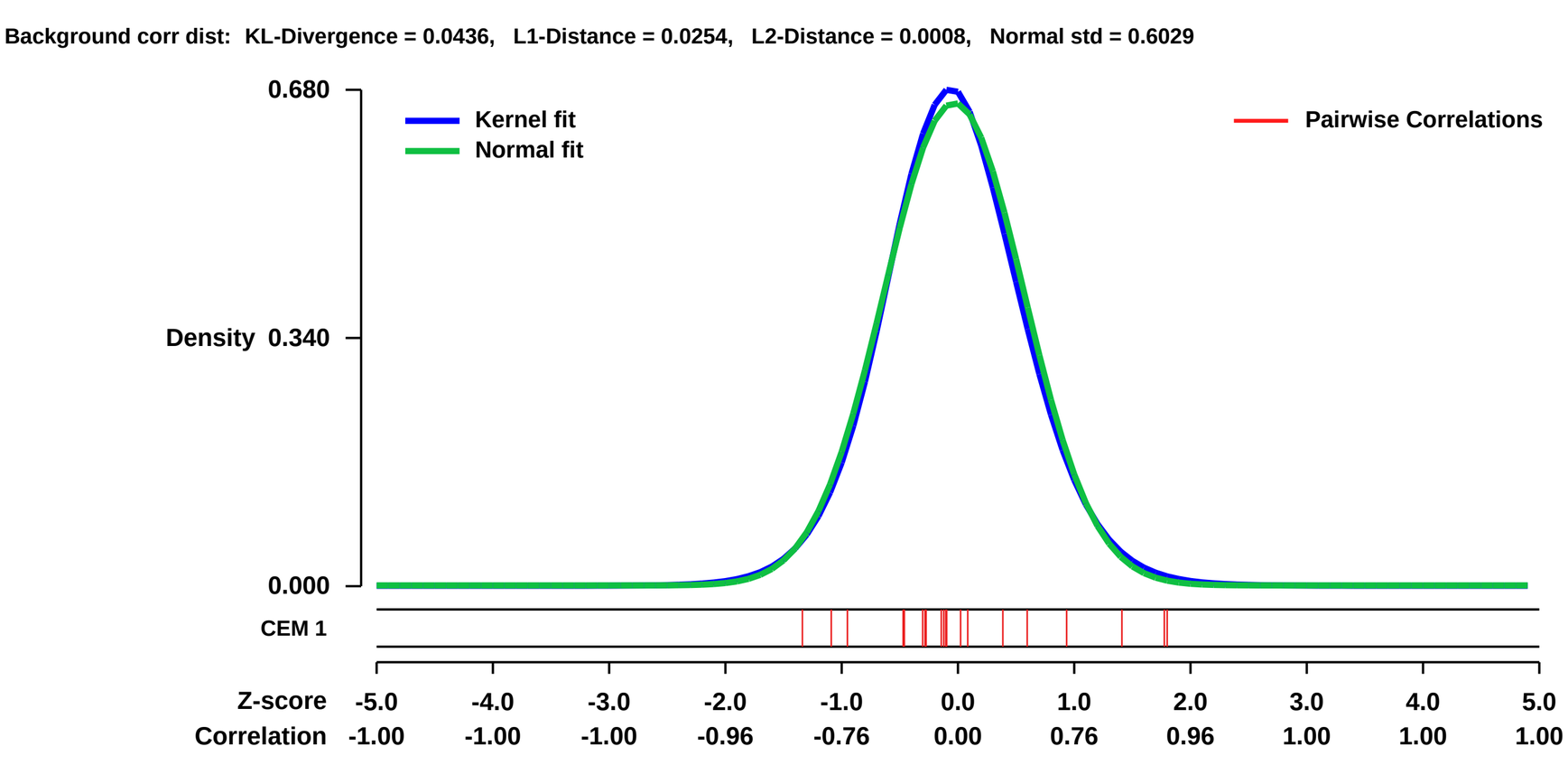

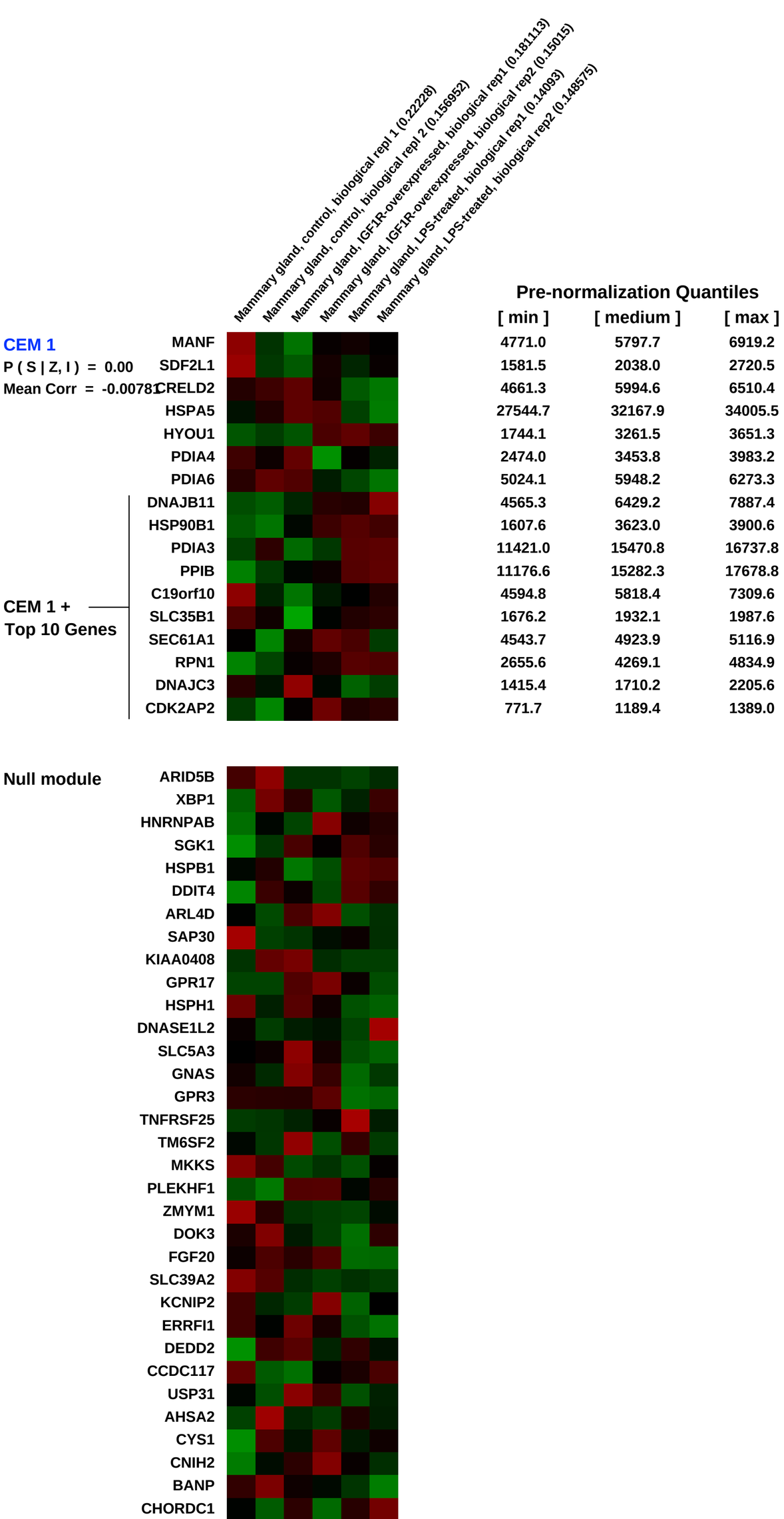

GEO Series "GSE15893" Expression Profiles

Num of samples in this series: 12

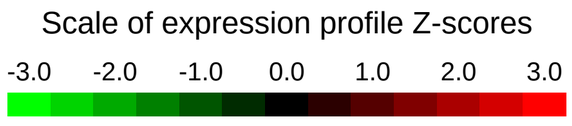

GEO Link:	http://www.ncbi.nlm.nih.gov/geo/query/acc.cgi?acc=GSE15893
Status:	Public on Apr 20 2010
Title:	Gene expression pattern in CXCR4+ and CXCR4- subpopulation of breast cancer cells
Organism:	Homo sapiens
Experiment type:	Expression profiling by array
Platform:	GPL570
Pubmed ID:	20603605
Summary & Design:	**Summary:** The goal of this study was to identify signaling molecules downstream of CXCR4 in breast cancer cells. For this purpose, we sorted CXCR4-positive and CXCR4-negative cells from MDA-MB-231 breast cancer cell line by flow cytometry and performed microarrays analysis. **Overall design:** Three sets of samples, each in quadrupicate, were analyzed. These include CXCR4-positive subpopulation, CXCR4-positive subpopulation treated with SDF-1 (ligand for CXCR4, also called CXCL12) for one hour and CXCR4-negative subpopulation.

Background corr dist: KL-Divergence = 0.1409, L1-Distance = 0.0272, L2-Distance = 0.0013, Normal std = 0.3859

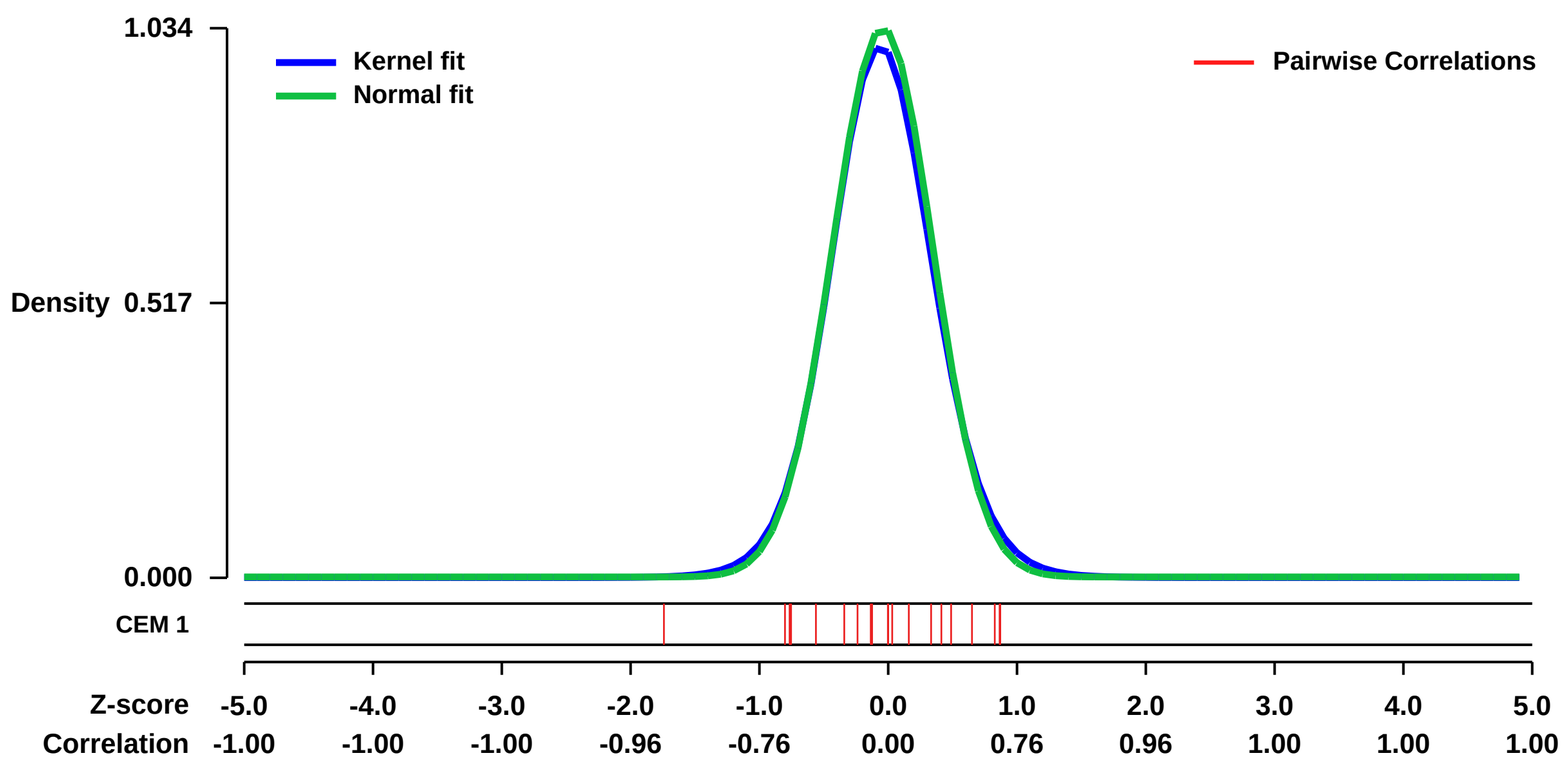

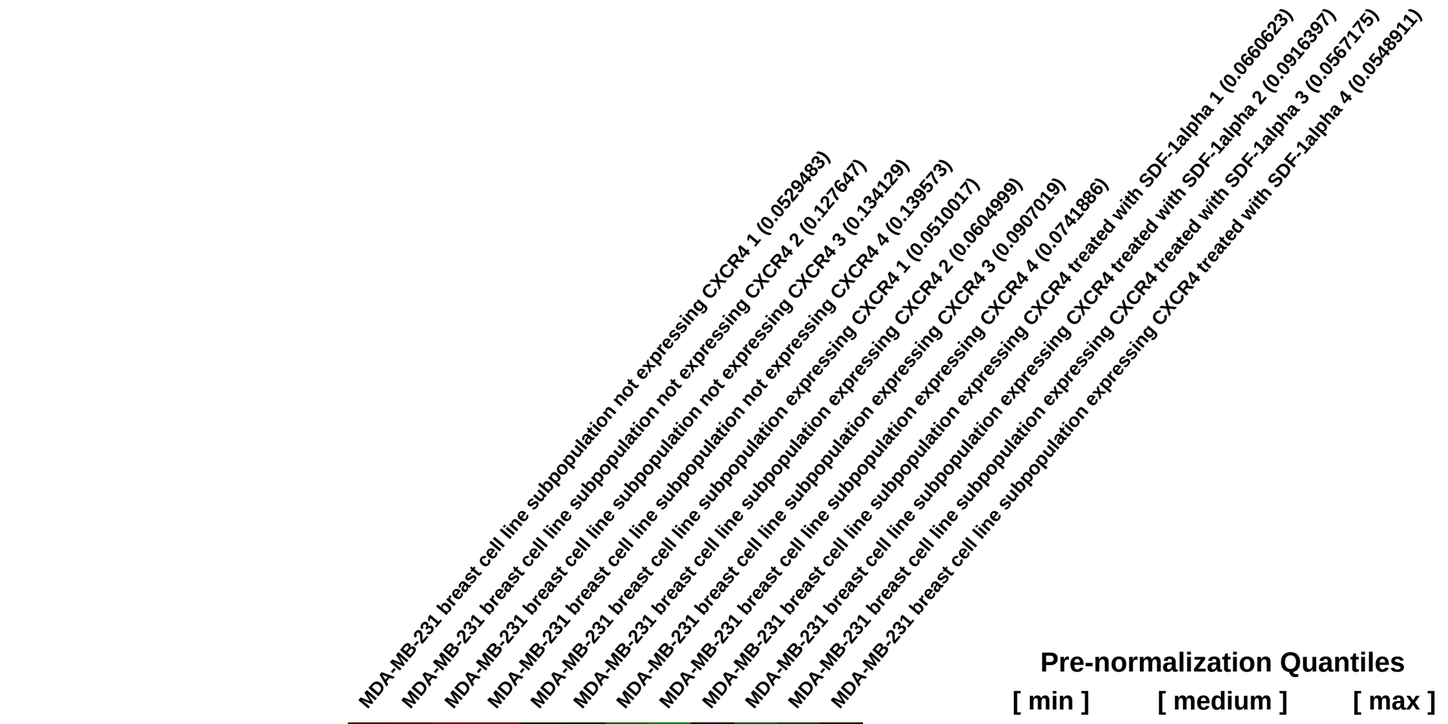

		Pre-normalization Quantiles		
		[min]	[medium]	[max]
CEM 1	MANF	3211.3	3774.5	4311.5
	SDF2L1	624.3	950.5	1151.5
	CRELD2	914.8	1228.2	1490.1
	HSPA5	14406.5	15787.9	17899.2
	HYOU1	3468.6	4599.1	5288.7
	PDIA4	1298.2	1492.7	1839.1
	PDIA6	6964.8	8540.6	9390.4
CEM 1 + Top 10 Genes	DNAJB11	2032.2	2980.4	3637.0
	HSP90B1	7248.0	7805.3	8472.1
	PDIA3	6408.5	7061.4	7805.0
	PPIB	9378.8	10841.7	11174.8
	C19orf10	3316.5	3620.3	5098.0
	SLC35B1	1859.8	2199.7	2635.3
	SEC61A1	3655.4	4502.7	5179.5
	RPN1	2729.1	3095.0	3362.8
	DNAJC3	1363.3	1753.0	2070.6
	CDK2AP2	1230.7	1533.1	1662.5
Null module	ARID5B			
	XBP1			
	HNRNPAB			
	SGK1			
	HSPB1			
	DDIT4			
	ARL4D			
	SAP30			
	KIAA0408			
	GPR17			
	HSPH1			
	DNASE1L2			
	SLC5A3			
	GNAS			
	GPR3			
	TNFRSF25			
	TM6SF2			
	MKKS			
	PLEKHF1			
	ZMYM1			
	DOK3			
	FGF20			
	SLC39A2			
	KCNIP2			
	ERRFI1			
	DEDD2			
	CCDC117			
	USP31			
	AHSA2			
	CYS1			
	CNIH2			
	BANP			
	CHORDC1			
	P4HA1			

GEO Series "GSE23764" Expression Profiles

Num of samples in this series: 18

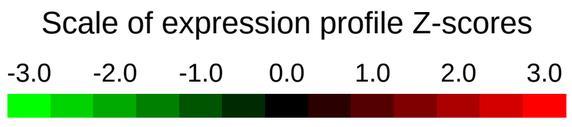

GEO Link:	http://www.ncbi.nlm.nih.gov/geo/query/acc.cgi?acc=GSE23764
Status:	Public on Aug 24 2010
Title:	Expression data from actomyosin contractility regulated genes
Organism:	Homo sapiens
Experiment type:	Expression profiling by array
Platform:	GPL570
Pubmed ID:	
Summary & Design:	**Summary:** Actomyosin contractility regulates cell morphology and movement. The objective of this study was to identify whether actomyosin contractility regulates gene expression in tumour cells and whether such genes are involved in cell morphology and movement. Gene expression analysis was carried out on highly contractile melanoma cell line A375M2 plated on a deformable collagen matrix under conditions where actomyosin contractility could be altered following treatment with blebbistatin, a direct inhibitor of myosin II, or Rho-kinase inhibitors Y27632 or H1152 that interfere with signalling to myosin II. **Overall design:** 18 samples (6 x 3 biological replicates). Cells were plated on rigid or deformable matrices. Rounded cells (A375M2 melanoma cells) plated on deformable matrices were left untreated or treated with Rho-kinase inhibitors Y27632, H1152 or blebbistatin an inhibitor of mysoin II.

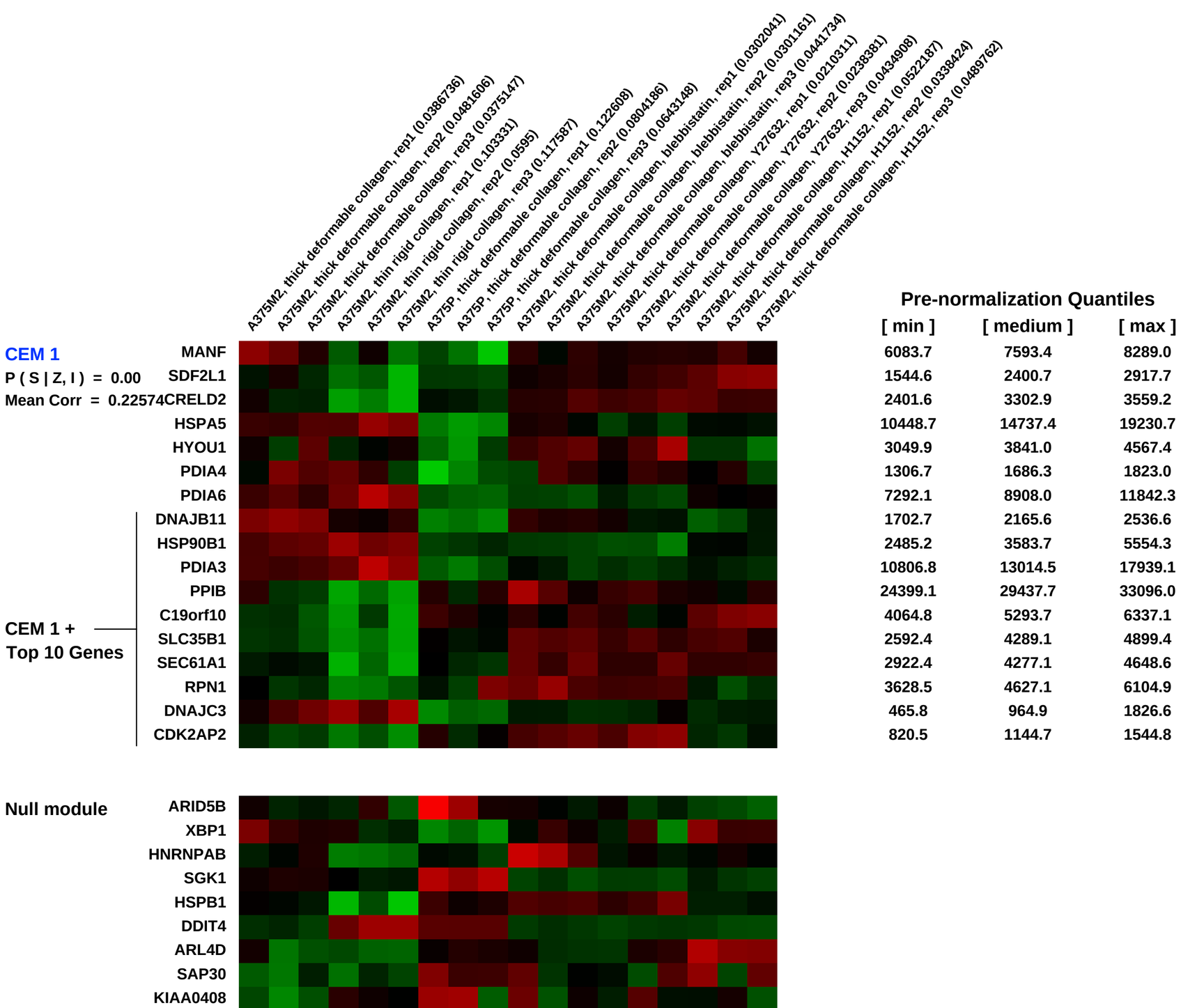

Pre-normalization Quantiles

	[min]	[medium]	[max]
MANF	6083.7	7593.4	8289.0
SDF2L1	1544.6	2400.7	2917.7
CRELD2	2401.6	3302.9	3559.2
HSPA5	10448.7	14737.4	19230.7
HYOU1	3049.9	3841.0	4567.4
PDIA4	1306.7	1686.3	1823.0
PDIA6	7292.1	8908.0	11842.3
DNAJB11	1702.7	2165.6	2536.6
HSP90B1	2485.2	3583.7	5554.3
PDIA3	10806.8	13014.5	17939.1
PPIB	24399.1	29437.7	33096.0
C19orf10	4064.8	5293.7	6337.1
SLC35B1	2592.4	4289.1	4899.4
SEC61A1	2922.4	4277.1	4648.6
RPN1	3628.5	4627.1	6104.9
DNAJC3	465.8	964.9	1826.6
CDK2AP2	820.5	1144.7	1544.8

GEO Series "GSE27328" Expression Profiles

Num of samples in this series: 18

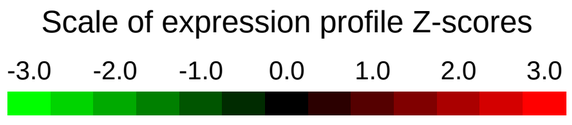

GEO Link:	http://www.ncbi.nlm.nih.gov/geo/query/acc.cgi?acc=GSE27328
Status:	Public on Mar 01 2011
Title:	Transcriptome analysis on ovarian cancer
Organism:	Homo sapiens
Experiment type:	Expression profiling by array
Platform:	GPL570
Pubmed ID:	21765906
Summary & Design:	**Summary:** We are studying signaling pathways and growth properties of cultured human ovarian cancer cells that are expressing the G protein-coupled receptor, luteinizing hormone receptor (LHR),particularly interested in the changes that occur when the receptor is activated by its cognate ligand, gonadotropin (LH). To investigate these questions, we have employed the SKOV3 ovarian cancer cell line that has been stably transfected with LHR, and can then test the response of these cells in culture following exposure to LH. **Overall design:** The parent SKOV-3 ovarian cancer cell line was chosen as a control in this study since it does not express LHR, and, following transfection, the LHR+ cells serve to determine the alterations in gene expression elicited by LH. The LHR+ cells bound human chorionic gonadotropin with a Kd of 0.3 nM (human chorionic gonadotropin and LH utilize the same G protein-coupled receptor, LHR), consistent with the binding affinity using ovarian reproductive cells, and responded to LH with increased intracellular levels of cAMP and inositol phosphates. In total, six groups of SKOV-3 cells (LHR-, LHR+, and LHR+ incubated with LH for various times: 1, 4, 8, and 20 h), each with three independent replicates, were used for examining the cell response.

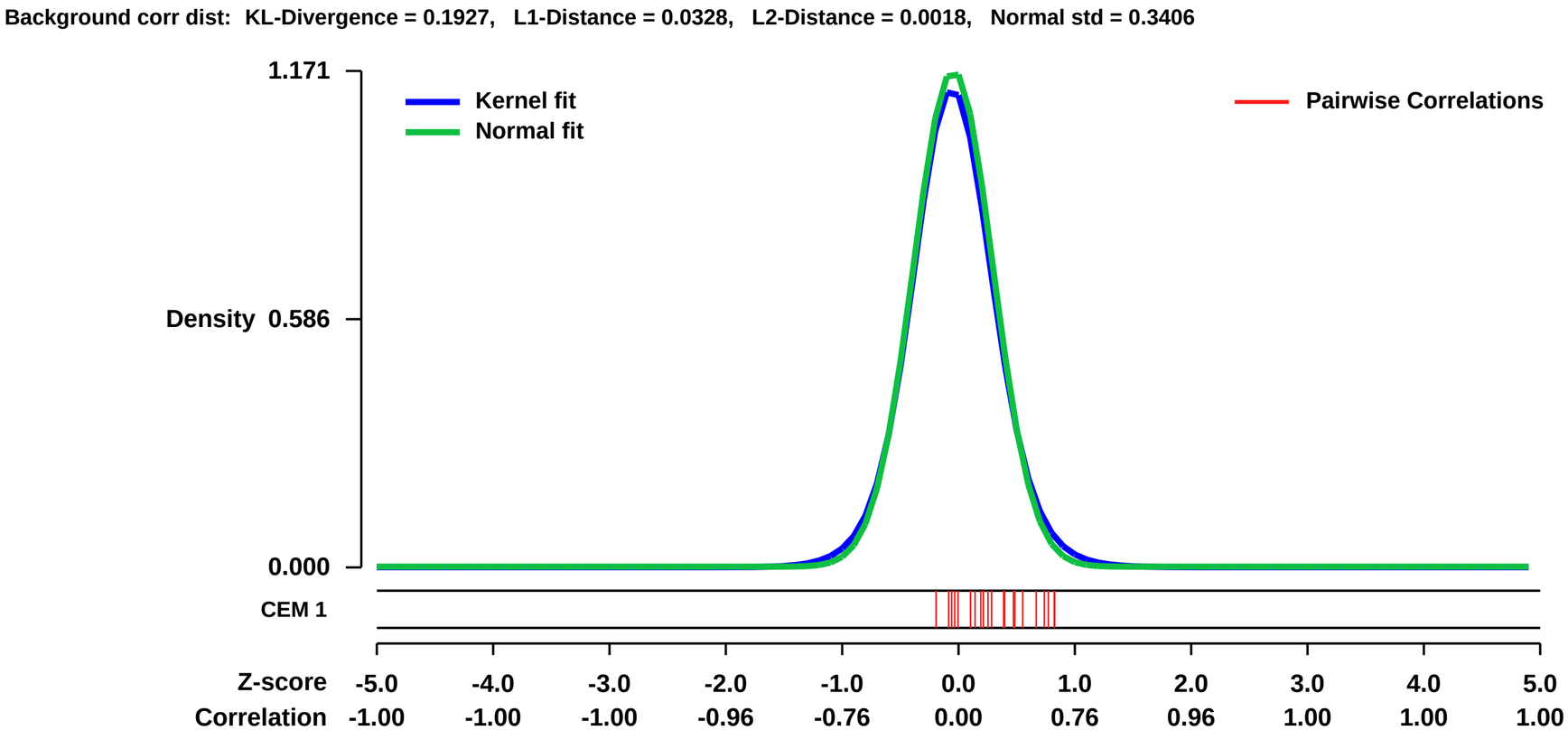

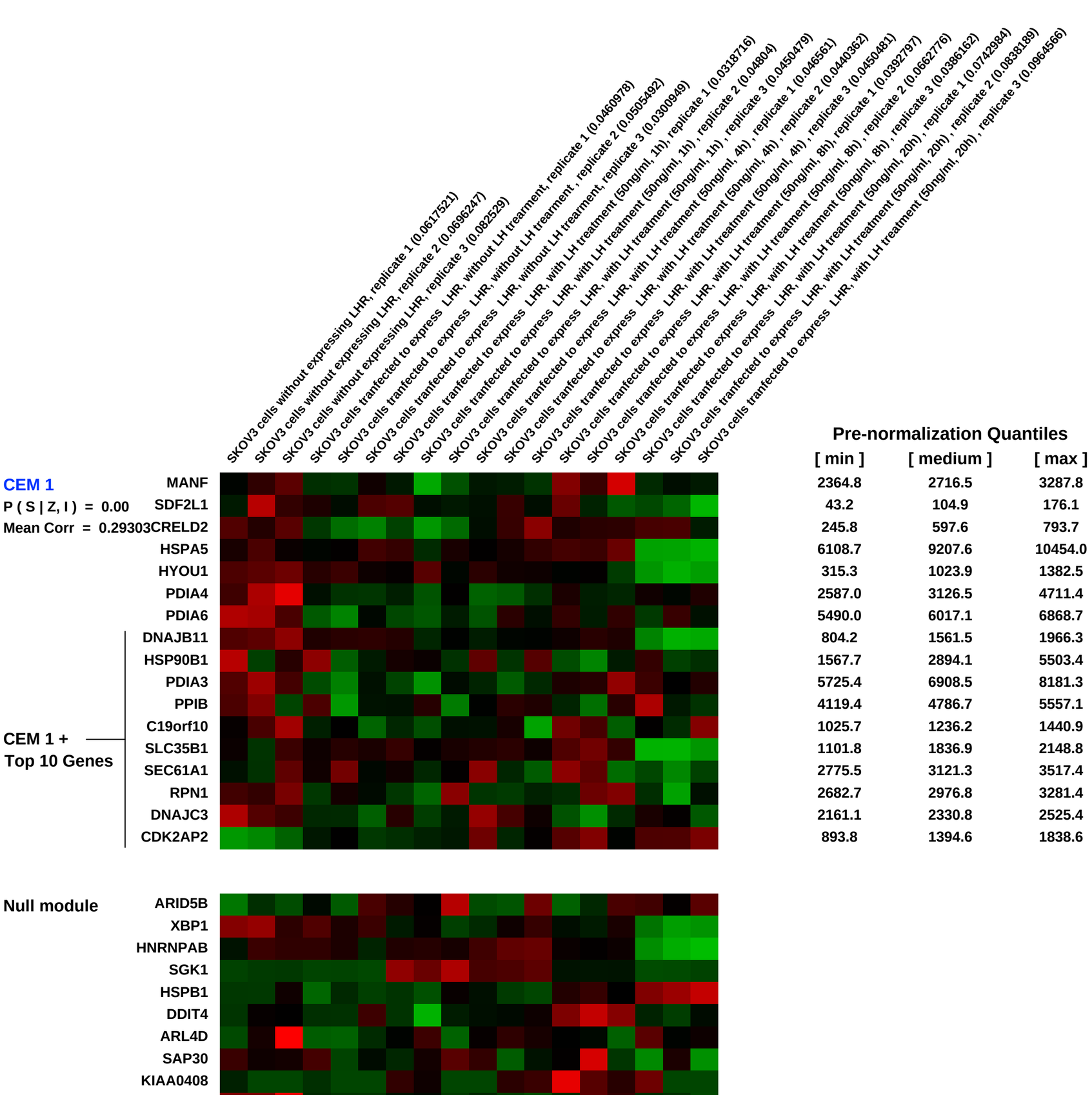

GEO Series "GSE49953" Expression Profiles

Num of samples in this series: 8

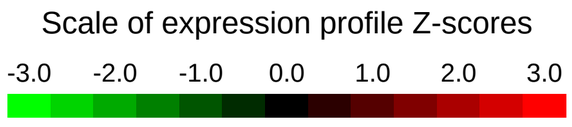

GEO Link:	http://www.ncbi.nlm.nih.gov/geo/query/acc.cgi?acc=GSE49953
Status:	Public on Sep 26 2013
Title:	Expression data from two breast cancer cell lines
Organism:	Homo sapiens
Experiment type:	Expression profiling by array
Platform:	GPL570
Pubmed ID:	24670641
Summary & Design:	**Summary:** During cancer progression, carcinoma cells encounter a variety of cytotoxic stresses such as hypoxia, nutrient deprivation, and low pH as a result of inadequate vascularization. To maintain survival and growth in the face of these physiologic stressors, a set of adaptive response pathways are induced. One adaptive pathway well studied in other contexts is the unfolded protein response (UPR), of which XBP1 is an important component. We used microarrays to detect transcriptome profile changes after XBP1 knockdown in breast cancer cell lines, and identify genes and pathways regulated by XBP1, which could help elucidate how XBP1 mediates the adaptive response of breast cancer to cytotoxic stresses. **Overall design:** We extracted RNA and hybridized it to Affymetrix microarrays in two breast cancer cell lines (T47D and MDA-MB-231) under treated (hypoxia and glucose deprivation) or untreated conditions with XBP1 knockdown or not.

Background corr dist: KL-Divergence = 0.0310, L1-Distance = 0.0481, L2-Distance = 0.0027, Normal std = 0.7290

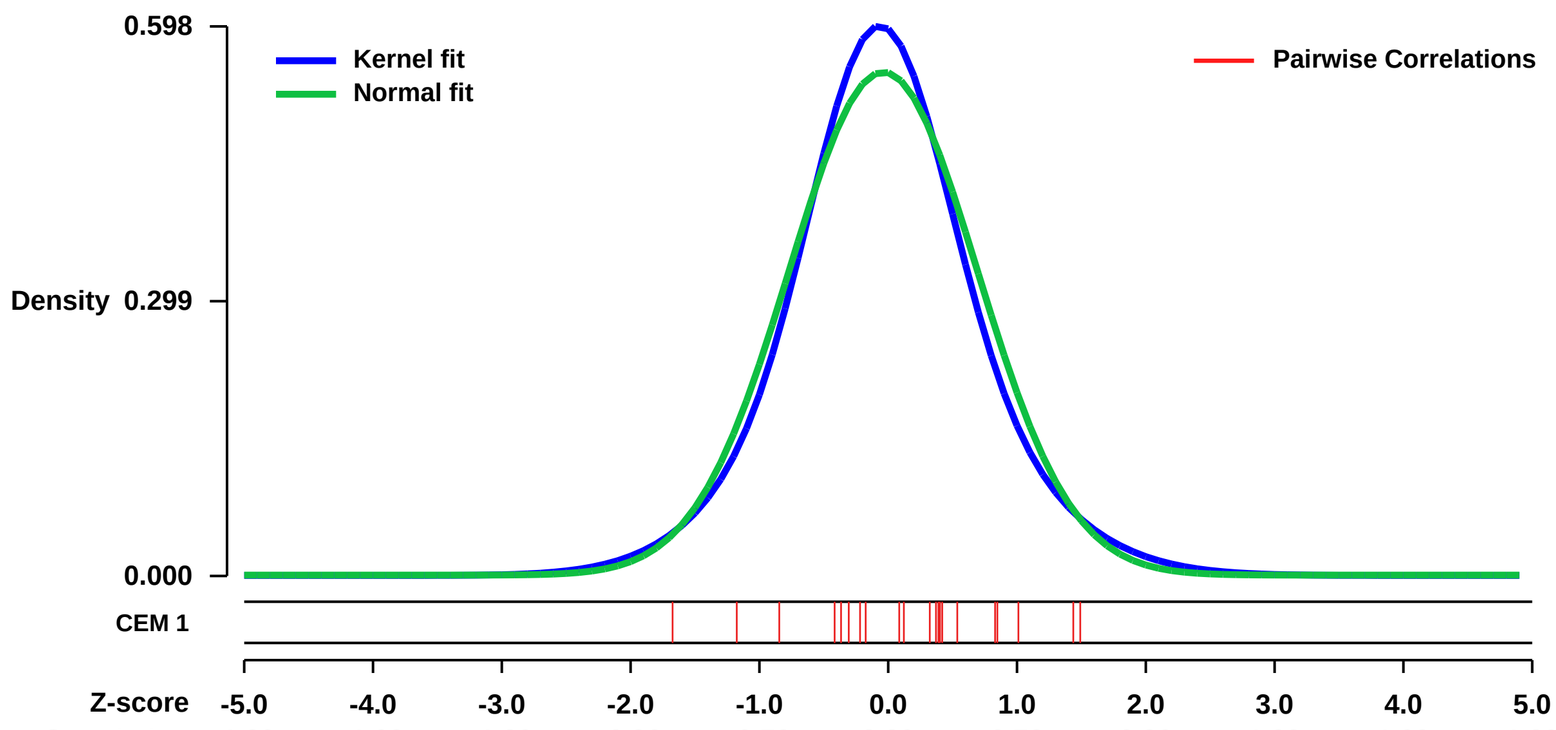

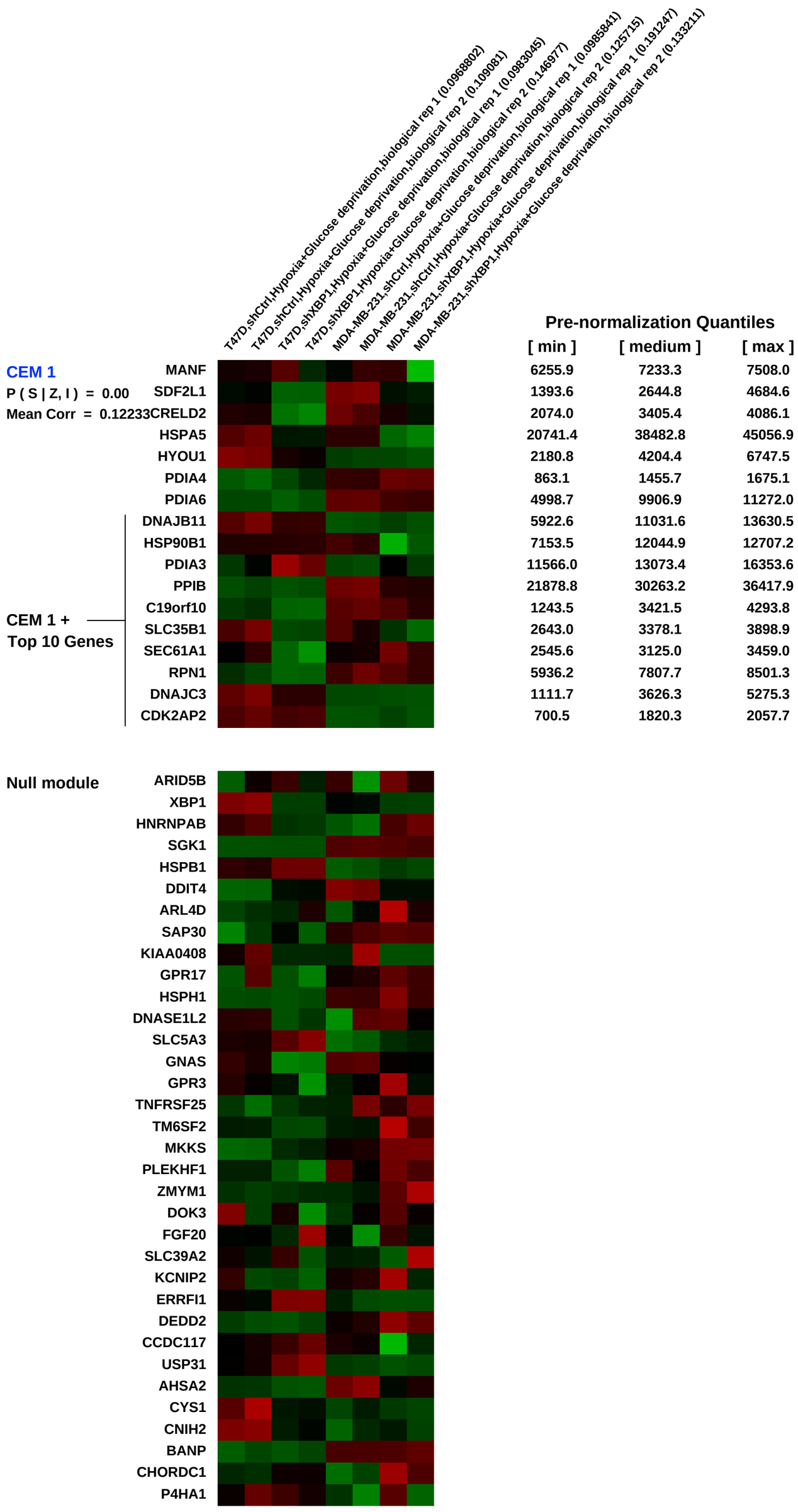

	Pre-normalization Quantiles		
	[min]	[medium]	[max]
MANF	6255.9	7233.3	7508.0
SDF2L1	1393.6	2644.8	4684.6
CRELD2	2074.0	3405.4	4086.1
HSPA5	20741.4	38482.8	45056.9
HYOU1	2180.8	4204.4	6747.5
PDIA4	863.1	1455.7	1675.1
PDIA6	4998.7	9906.9	11272.0
DNAJB11	5922.6	11031.6	13630.5
HSP90B1	7153.5	12044.9	12707.2
PDIA3	11566.0	13073.4	16353.6
PPIB	21878.8	30263.2	36417.9
C19orf10	1243.5	3421.5	4293.8
SLC35B1	2643.0	3378.1	3898.9
SEC61A1	2545.6	3125.0	3459.0
RPN1	5936.2	7807.7	8501.3
DNAJC3	1111.7	3626.3	5275.3
CDK2AP2	700.5	1820.3	2057.7

GEO Series "GSE37136" Expression Profiles

Num of samples in this series: 6

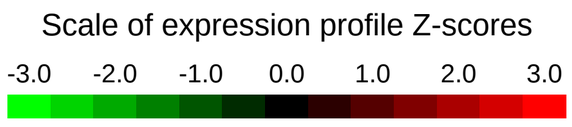

GEO Link:	http://www.ncbi.nlm.nih.gov/geo/query/acc.cgi?acc=GSE37136
Status:	Public on Jan 08 2013
Title:	Gene expression profiling of enforced HOXA1 expression in melanoma cell line
Organism:	Homo sapiens
Experiment type:	Expression profiling by array
Platform:	GPL570
Pubmed ID:	23435427
Summary & Design:	**Summary:** We recently reported an oncogenomics-guided screening approach designed to identify genetic drivers of early stage melanoma metastasis, and in this study we functionally validate the top-scoring candidate, homeobox transcription factor A1 (HOXA1), by demonstrating HOXA1â s robust effects on melanoma cell invasion, metastasis and tumorigenicity. Transcriptome and pathway profiling analyses of cells expressing HOXA1 reveal up-regulation of factors involved in diverse cytokine pathways that include the TGF‚† signaling axis, which we further demonstrate to be required for HOXA1-mediated cell invasion. Transcriptome profiling also informed HOXA1â s ability to potently down-regulate expression of microphthalmia-associated transcription factor (MITF) and other genes required for melanocyte differentiation, suggesting a mechanism by which HOXA1 expression de-differentiates cells into a pro-invasive precursor cell state concomitant with TGF‚† activation. Our analysis of publicly available datasets indicate that the HOXA1-induced gene signature successfully categorizes melanoma specimens based on their metastatic potential and, importantly, is capable of stratifying melanoma patient risk for metastasis based on expression in primary tumors. **Overall design:** The HOXA1-induced transcription analysis was conducted using RNAs extracted from WM115 cells transduced with either control or HOXA1, followed by hybridization of labeled cDNA onto Affymetrix GeneChips (Human Genome U133Plus2.0).

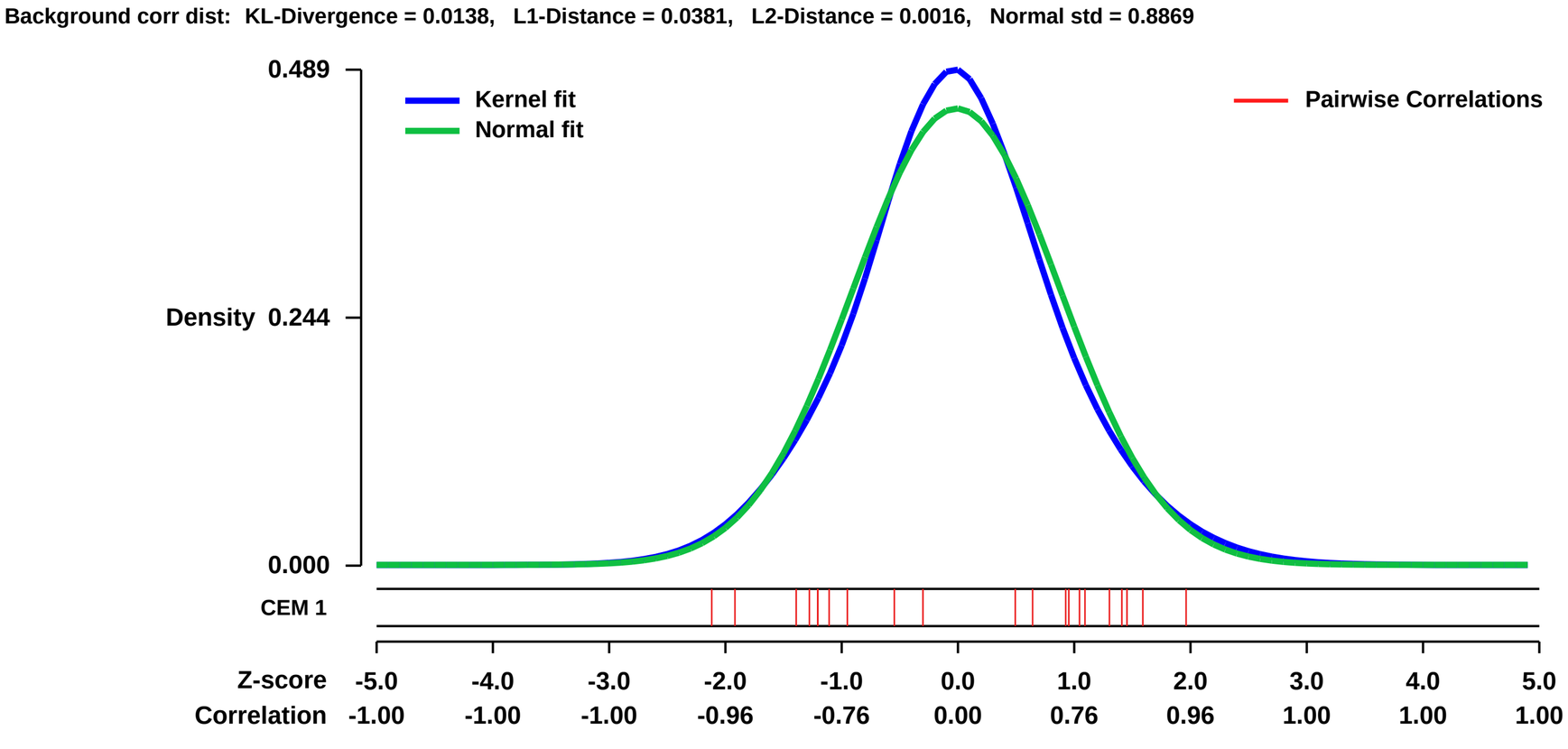

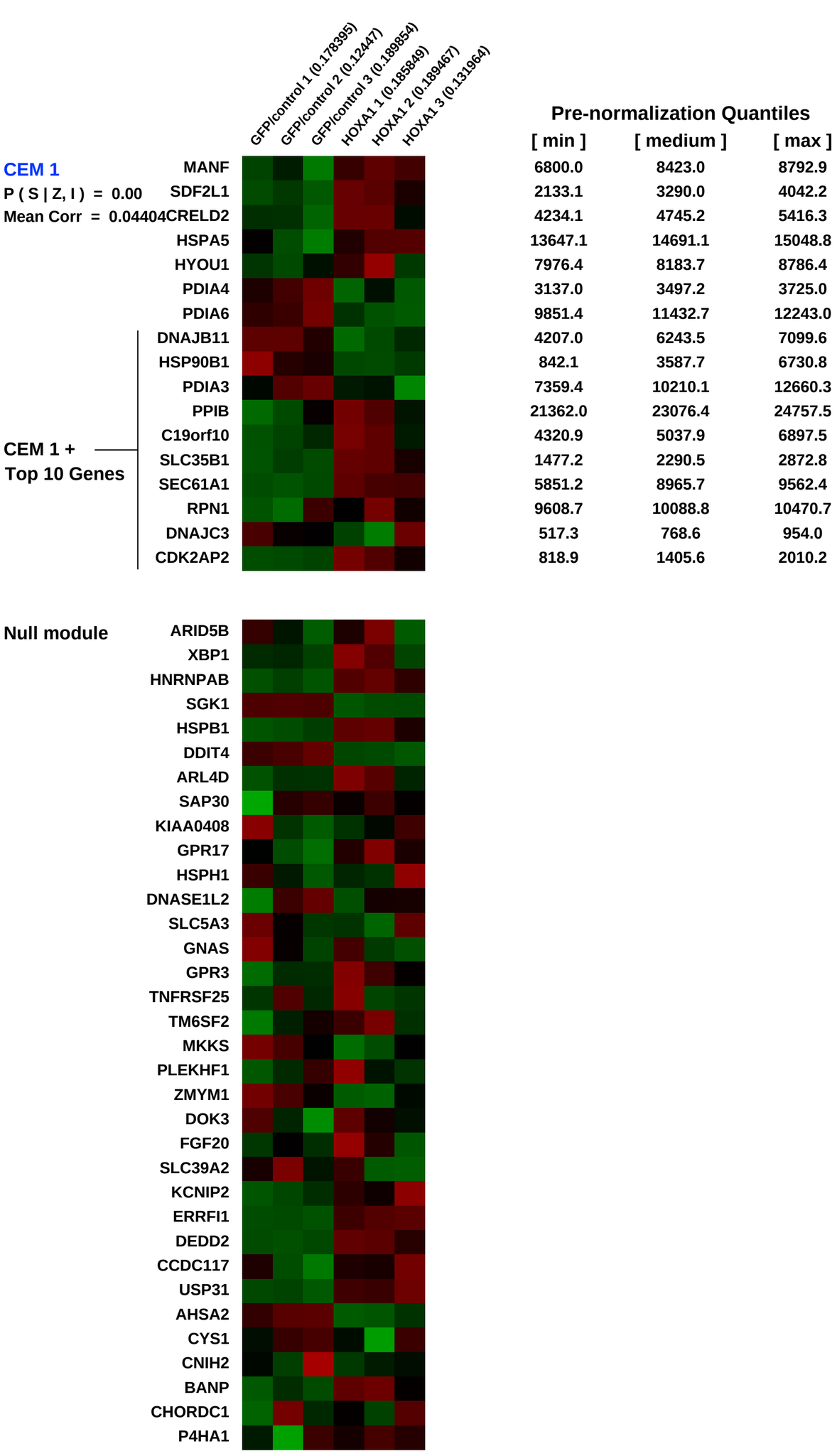

GEO Series "GSE12513" Expression Profiles

Num of samples in this series: 12

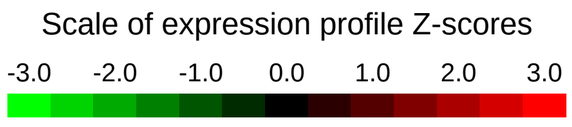

GEO Link:	http://www.ncbi.nlm.nih.gov/geo/query/acc.cgi?acc=GSE12513
Status:	Public on Jul 28 2013
Title:	Genes regulated by AGR2 in pancreatic cancer cell lines FA6 and MiaPaCa2
Organism:	Homo sapiens
Experiment type:	Expression profiling by array
Platform:	GPL570
Pubmed ID:	
Summary & Design:	**Summary:** We and others have shown that AGR2 is frequently upregulated during the development of pancreatic cancer. We used microarray to look at the target genes regulated by AGR2 in pancreatic cancer cell lines FA6 and MiaPaCa2. Keywords: gene knock-down, overexpression **Overall design:** We generated stable cell lines by introducing control vector pCEP4 or AGR2 overexpressing vector pCEP4-AGR2 into the pancreatic cancer cell line MiaPaCa2, single cell clones were then isolated. RNA was extracted and hybridized on Affymetrix microarrays.We looked for new target genes regulated by AGR2.

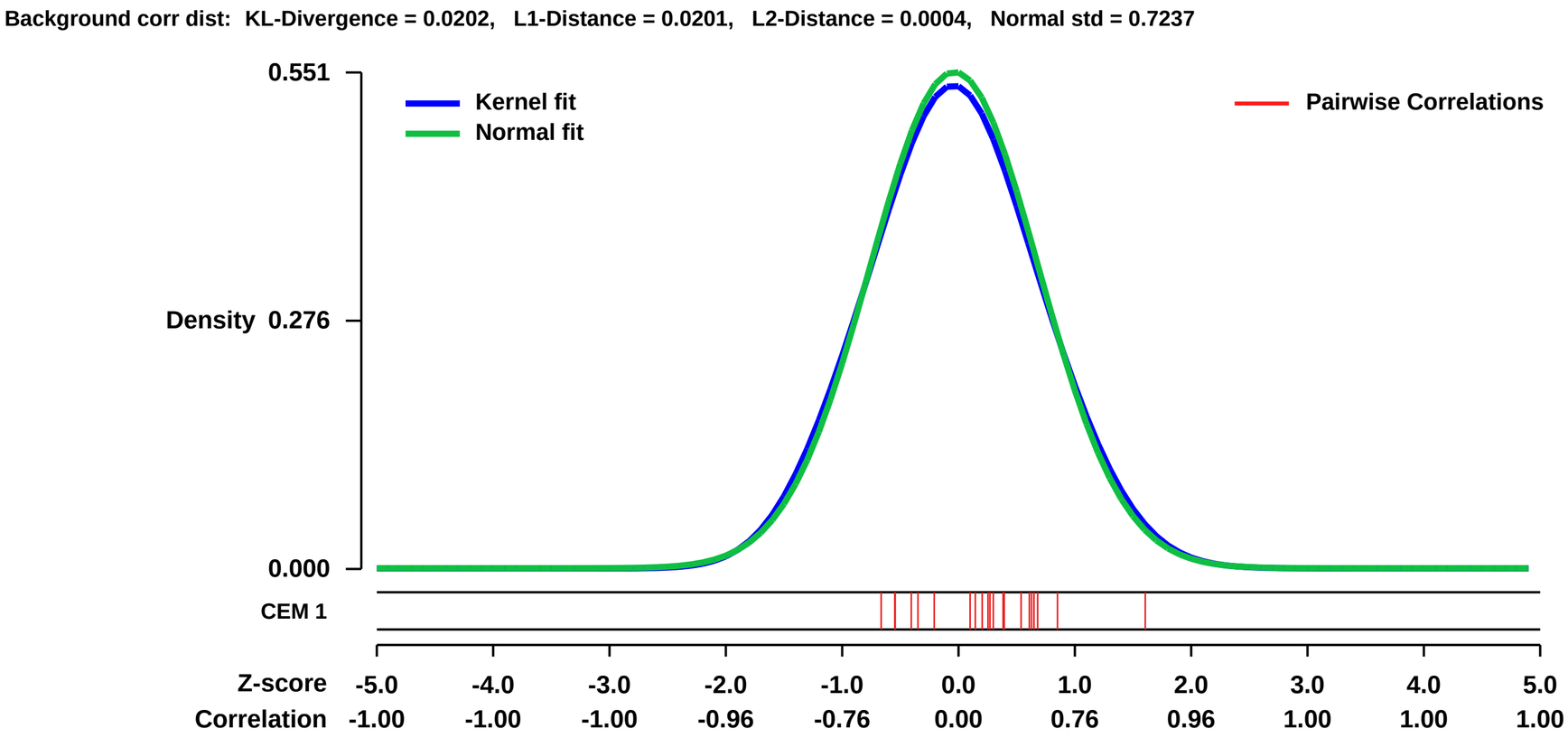

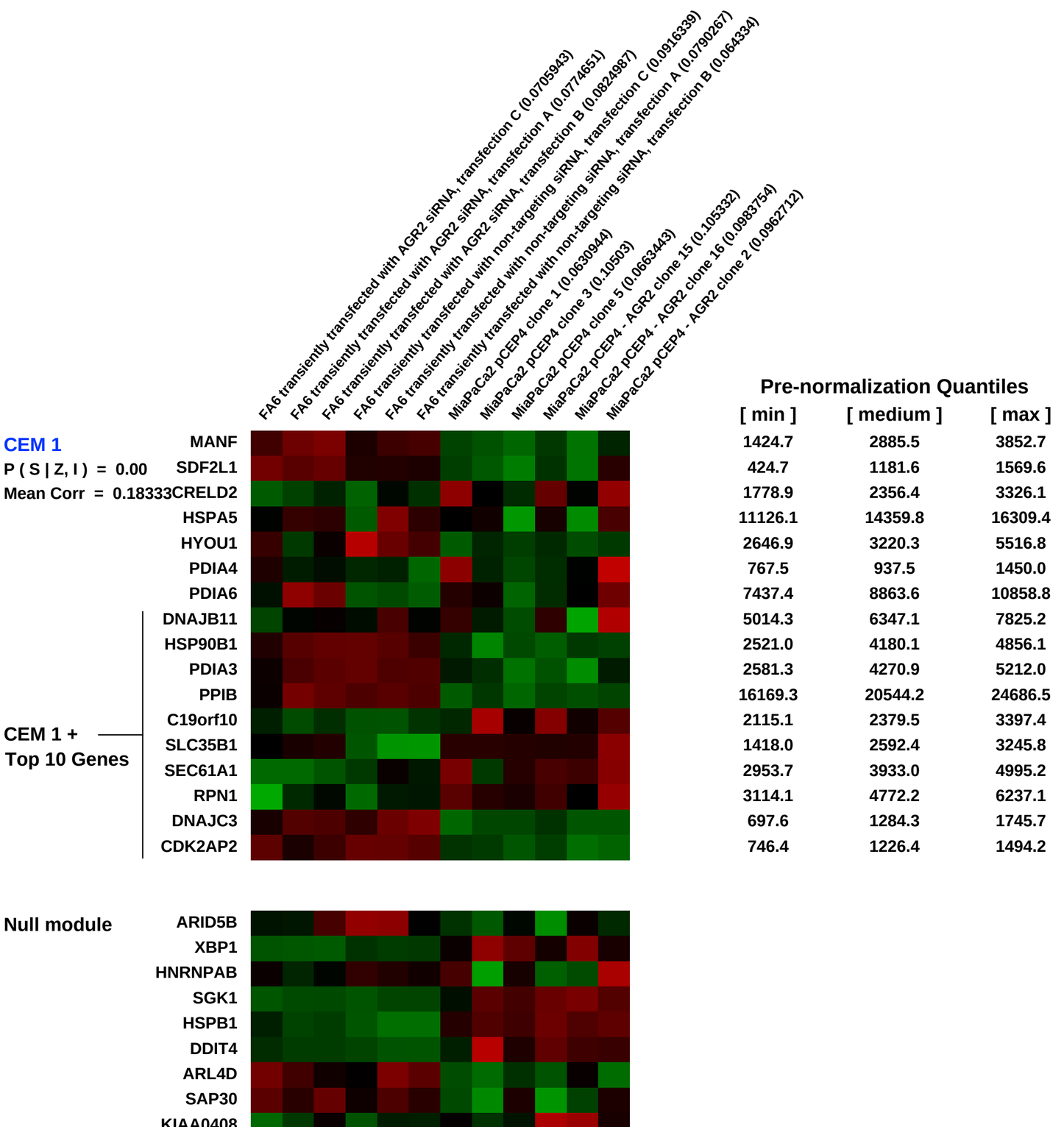

	Pre-normalization Quantiles		
	[min]	[medium]	[max]
MANF	1424.7	2885.5	3852.7
SDF2L1	424.7	1181.6	1569.6
CRELD2	1778.9	2356.4	3326.1
HSPA5	11126.1	14359.8	16309.4
HYOU1	2646.9	3220.3	5516.8
PDIA4	767.5	937.5	1450.0
PDIA6	7437.4	8863.6	10858.8
DNAJB11	5014.3	6347.1	7825.2
HSP90B1	2521.0	4180.1	4856.1
PDIA3	2581.3	4270.9	5212.0
PPIB	16169.3	20544.2	24686.5
C19orf10	2115.1	2379.5	3397.4
SLC35B1	1418.0	2592.4	3245.8
SEC61A1	2953.7	3933.0	4995.2
RPN1	3114.1	4772.2	6237.1
DNAJC3	697.6	1284.3	1745.7
CDK2AP2	746.4	1226.4	1494.2
ARID5B			
XBP1			
HNRNPAB			
SGK1			
HSPB1			
DDIT4			
ARL4D			
SAP30			
KIAA0408			
GPR17			
HSPH1			
DNASE1L2			
SLC5A3			
GNAS			
GPR3			
TNFRSF25			
TM6SF2			
MKKS			
PLEKHF1			
ZMYM1			
DOK3			
FGF20			
SLC39A2			
KCNIP2			
ERRFI1			
DEDD2			
CCDC117			
USP31			
AHSA2			
CYS1			
CNIH2			
BANP			
CHORDC1			
P4HA1			

GEO Series "GSE14886" Expression Profiles

Num of samples in this series: 8

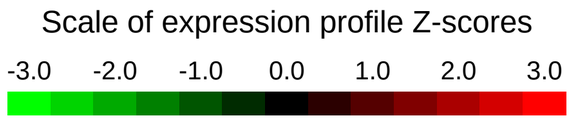

GEO Link:	http://www.ncbi.nlm.nih.gov/geo/query/acc.cgi?acc=GSE14886
Status:	Public on Feb 19 2009
Title:	Expression data in HTETOP cells following tetracycline or dexrazoxane treatment
Organism:	Homo sapiens
Experiment type:	Expression profiling by array
Platform:	GPL570
Pubmed ID:	19417146
Summary & Design:	**Summary:** HTETOP cells, derived from the human fibrosarcoma cell line HT1080, express human topoisomearse II ¸– (TOP2A) exclusively from a tetracycline (TET)-regulated transgene, we used HTETOP cells to differentiate between TOP2A-dependent and â independent apoptotic effects of doxorubicin and dexrazoxane. We used microarrays to detect global transcriptional changes in HTETOP cells following tetracycline doxycycline or dexrazoxane treatment. Keywords: Drug treatment comparison **Overall design:** HTETOP cells were treated with 100 ´µM dexrazoxane to inhibit TOP2A activity or vehicle for 24 hours, global trascriptional changes were identified by comparison of the two groups.

Background corr dist: KL-Divergence = 0.0236, L1-Distance = 0.0450, L2-Distance = 0.0032, Normal std = 0.7268

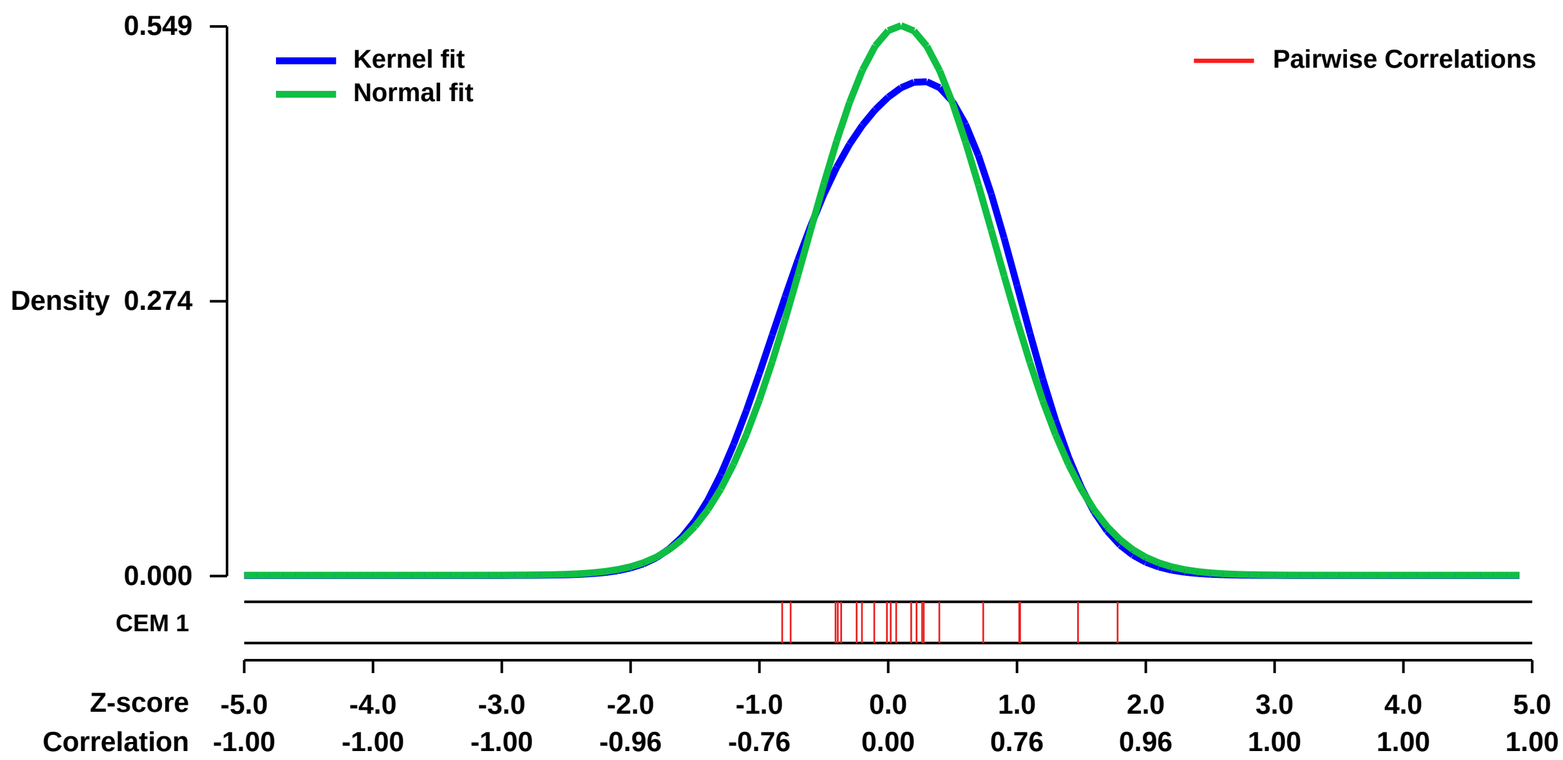

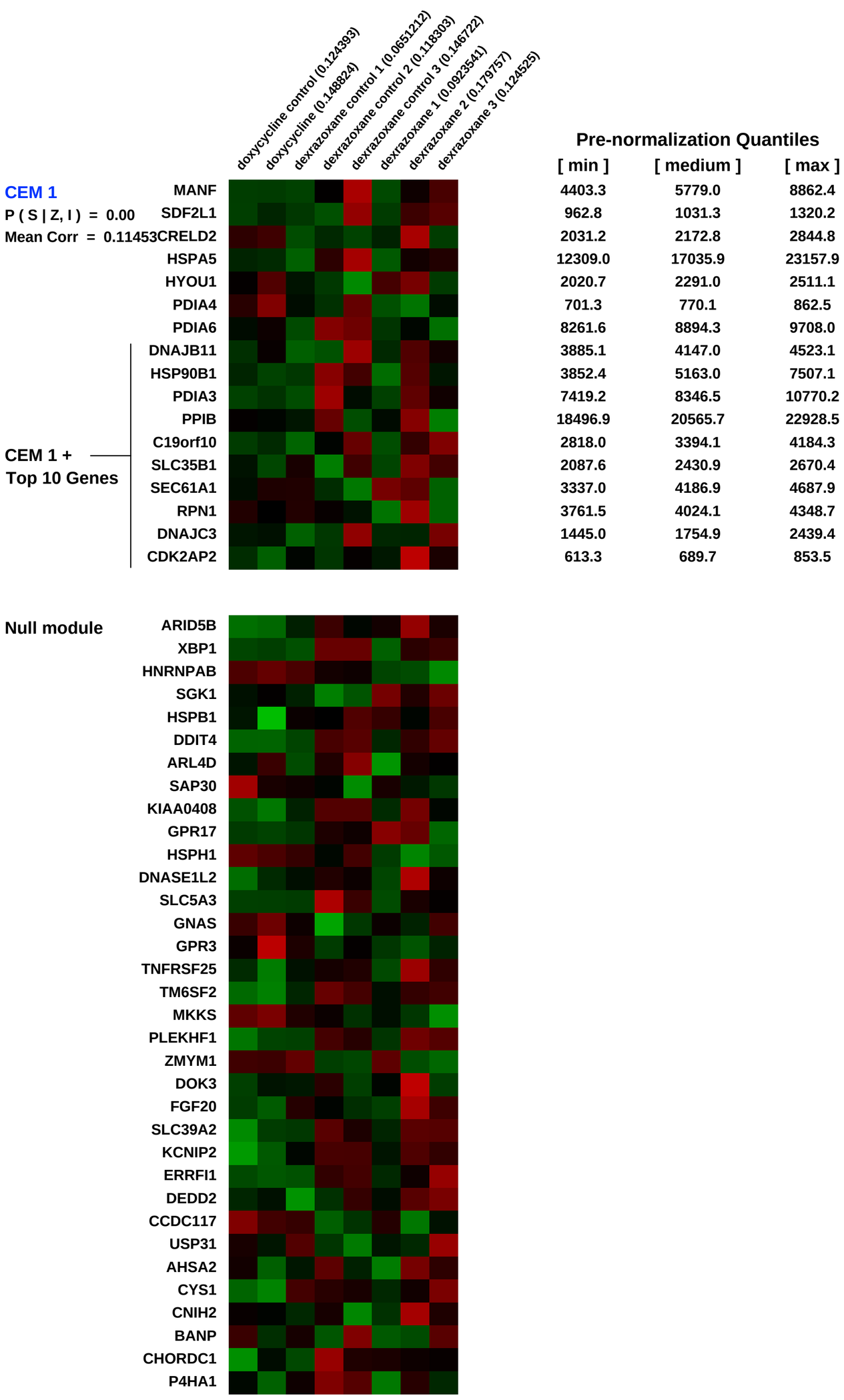

GEO Series "GSE20505" Expression Profiles

Num of samples in this series: 21

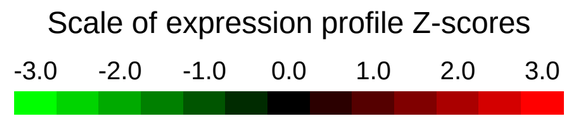

GEO Link:	**http://www.ncbi.nlm.nih.gov/geo/query/acc.cgi?acc=GSE20505**
Status:	**Public on Feb 24 2010**
Title:	**Expression data from CD34+ hematopoietic progenitor cells**
Organism:	**Homo sapiens**
Experiment type:	**Expression profiling by array**
Platform:	**GPL570**
Pubmed ID:	
Summary & Design:	**Summary:** **Gene transfer vectors based on gamma-retroviruses target actively transcribing genes indicating that the cellular gene expression profile can be predictive of their integration pattern. Therefore, different culture conditions leading to different transcriptional activity may translate into differences in the profile of targeted genes in cells transduced with these vectors. Recent data from two gene therapy trials for SCID-X1 conducted in France and the UK suggested that small differences between in vitro stimulation conditions could explain the disparity in the frequency of common integrations sites observed in the two studies.** **We set out to compare the transcriptional activity of human CD34+ bone marrow-derived cells cultured under the French (S1) or British (S2) culture conditions.** **Overall design:** **RNA was extracted from human CD34+ bone marrow-derived cells from 3 donors stimulated under the French (S1) conditions (X-vivo 10, 4% fetal calf serum, 300 ng/ml stem cell factor [SCF], 100 ng/ml thrombopoietin [TPO], 60 ng/ml interleukin-3 [IL3], and 300 ng/ml Flt3 ligand [FL]) and under the British (S2) conditions (X-vivo 10, 1% human serum albumin, 300 ng/ml SCF, 100 ng/ml TPO, 20 ng/ml IL3, and 300 ng/ml FL). Extracted RNA was amplified with random hexamer primer reverse transcription strategy. Lastly, amplified RNA was labeled and hybridized to HG U133 Plus 2.0 Affymetrix microarrays. Four time points during cytokine stimulation were analyzed, corresponding to 0 hr and three transduction time points in the French and British SCID-X1 gene therapy clinical trials (48 h, 72 h, and 96 h). Samples are referred to as donor, stimulation condition, and time point (e.g., Don 1 S1-48 for donor 1 of 3, S1 stimulation conditions, and 48 h after stimulation was begun).**

Background corr dist: KL-Divergence = 0.0656, L1-Distance = 0.0817, L2-Distance = 0.0130, Normal std = 0.5551

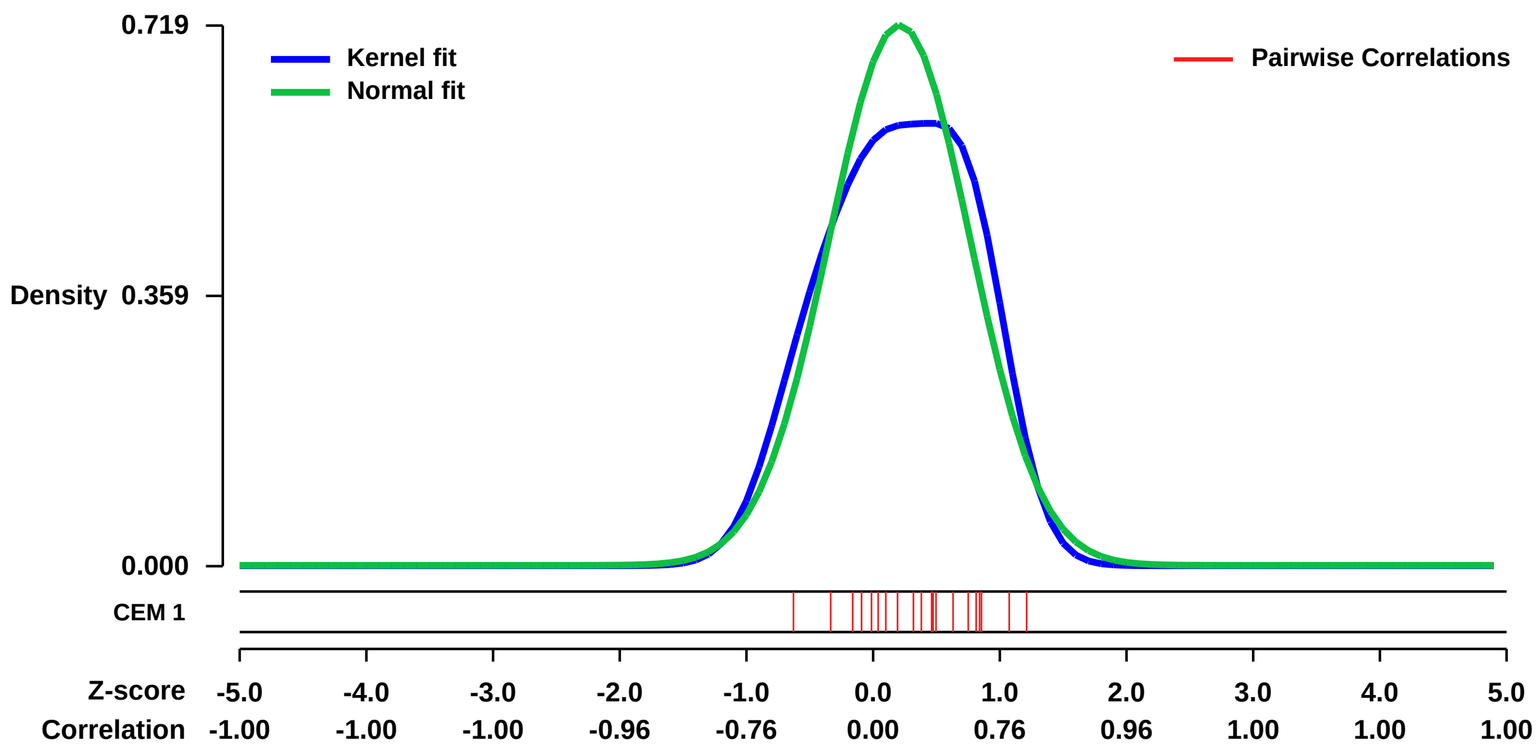

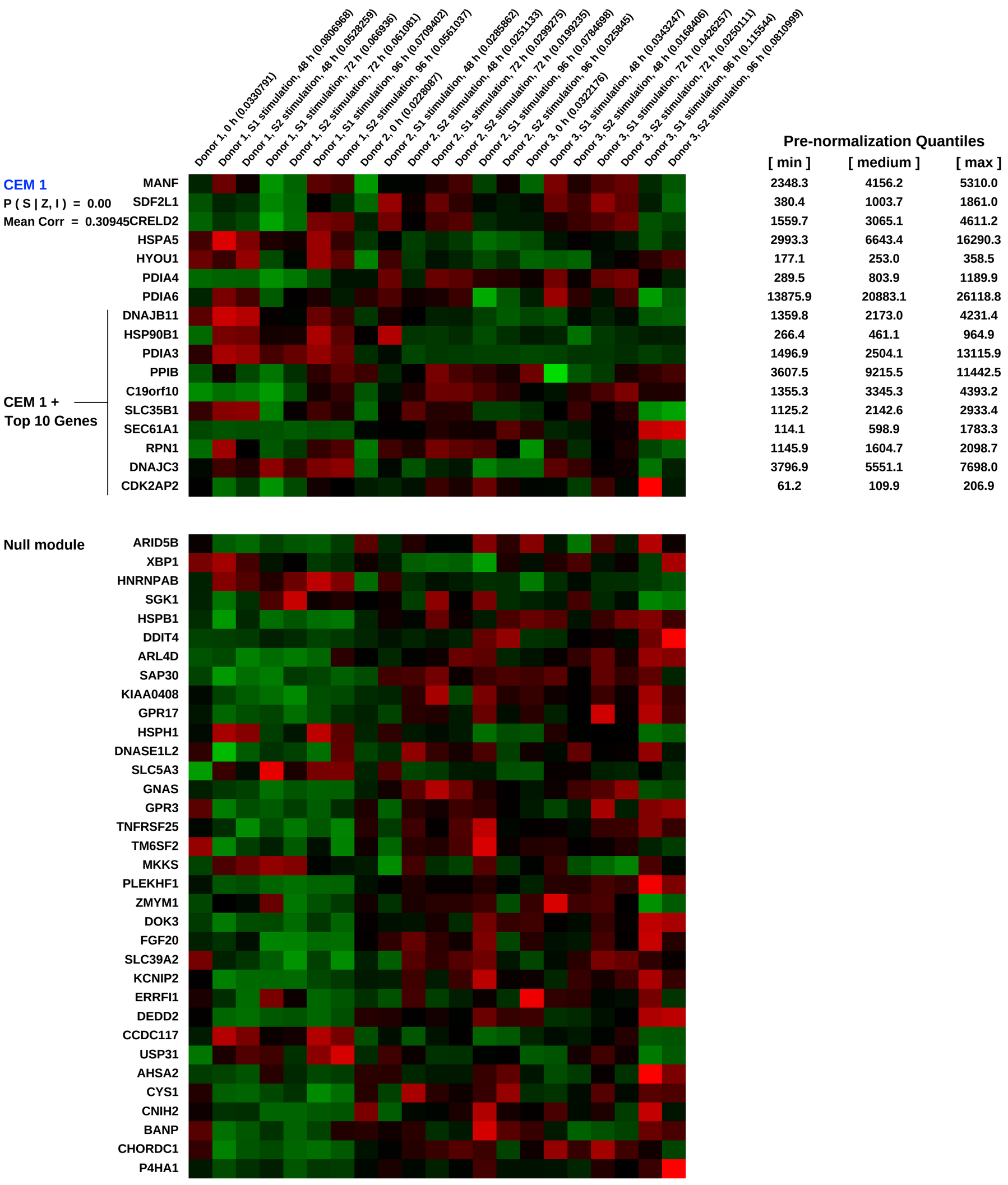

Pre-normalization Quantiles

	[min]	[medium]	[max]
MANF	2348.3	4156.2	5310.0
SDF2L1	380.4	1003.7	1861.0
CRELD2	1559.7	3065.1	4611.2
HSPA5	2993.3	6643.4	16290.3
HYOU1	177.1	253.0	358.5
PDIA4	289.5	803.9	1189.9
PDIA6	13875.9	20883.1	26118.8
DNAJB11	1359.8	2173.0	4231.4
HSP90B1	266.4	461.1	964.9
PDIA3	1496.9	2504.1	13115.9
PPIB	3607.5	9215.5	11442.5
C19orf10	1355.3	3345.3	4393.2
SLC35B1	1125.2	2142.6	2933.4
SEC61A1	114.1	598.9	1783.3
RPN1	1145.9	1604.7	2098.7
DNAJC3	3796.9	5551.1	7698.0
CDK2AP2	61.2	109.9	206.9

GEO Series "GSE37588" Expression Profiles

Num of samples in this series: 6

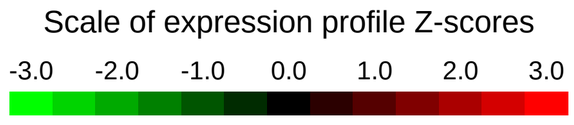

GEO Link:	http://www.ncbi.nlm.nih.gov/geo/query/acc.cgi?acc=GSE37588
Status:	Public on Jun 01 2012
Title:	New insights into key genes and pathways involved in the pathogenesis of HLA-B27-associated acute anterior uveitis
Organism:	Homo sapiens
Experiment type:	Expression profiling by array
Platform:	GPL570
Pubmed ID:	
Summary & Design:	**Summary:** HLA-B27-associated inflammatory diseases remains one of the strongest HLA-disease known to date. HLA-B27-associated acute anterior uveitis has wide-ranging medical significance due to its ocular, systemic, immunologic, and genetic features. To investigate the genes and signalling pathways located upstream of the inflammatory processes in HLA-B27-associated acute anterior uveitis will help to know the mechanism of this disease. HLA-B27-positive and -negative monocytes isolated from human peripheral blood were stimulated with Vibrio cholera lipopolysaccharide (LPS). Gene expression microarrays were used to identify the differentially expressed genes, and they were analysed by a series of bioinformatics-based techniques. Gene expression microarray analysis revealed marked differences between B27-positive monocytes in the genes that are upregulated in response to LPS stimulation. Gene Ontology enrichment (GO) and pathway analysis indicated that genes participating in protein transport and folding were essential to the inflammatory process. The LPS receptor, TLR4, induced the Toll-like receptor signalling pathway and pathways related to Vibrio cholerae infection, which are located upstream of the network and contribute to the overall response. Among the DE genes, PIK3CA, PIK3CB, AKT3, and MAPK1 may play critical roles in inflammation.Equivalent LPS stimulation induces a different response in HLA-B27-positive monocytes compared to monocytes lacking this HLA protein, suggesting that the TLR pathway is involved in the pathogenesis of HLA-B27-associated AAU. Blocking this pathway and other pathways by siRNA interference of candidate genes may contribute to the development of a treatment for this type of AAU. **Overall design:** HLA-B27-positive monocytes isolated from human peripheral blood were stimulated with Vibrio cholera lipopolysaccharide (LPS) for 12 hours.

Background corr dist: KL-Divergence = 0.0536, L1-Distance = 0.0886, L2-Distance = 0.0119, Normal std = 0.6853

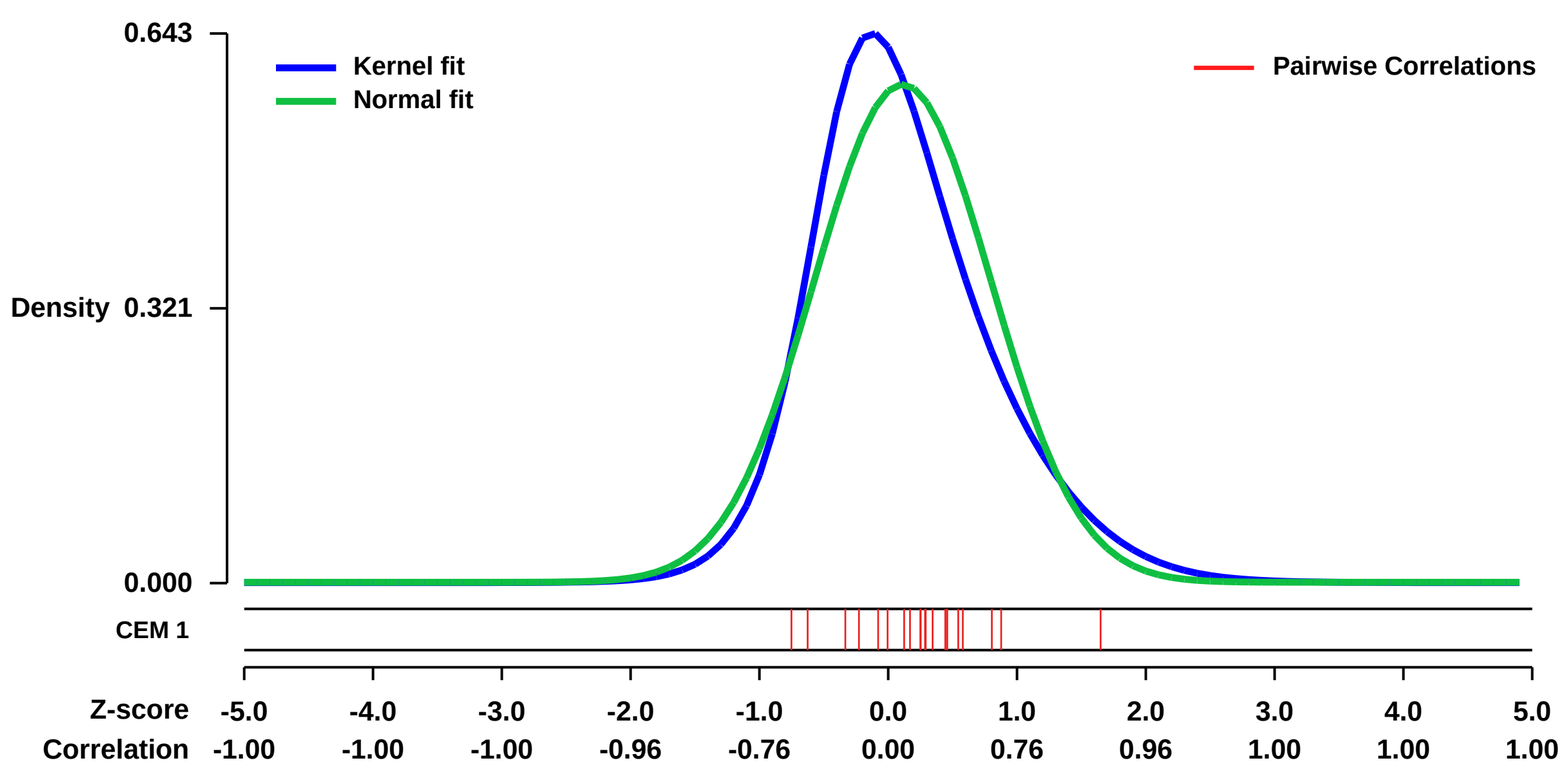

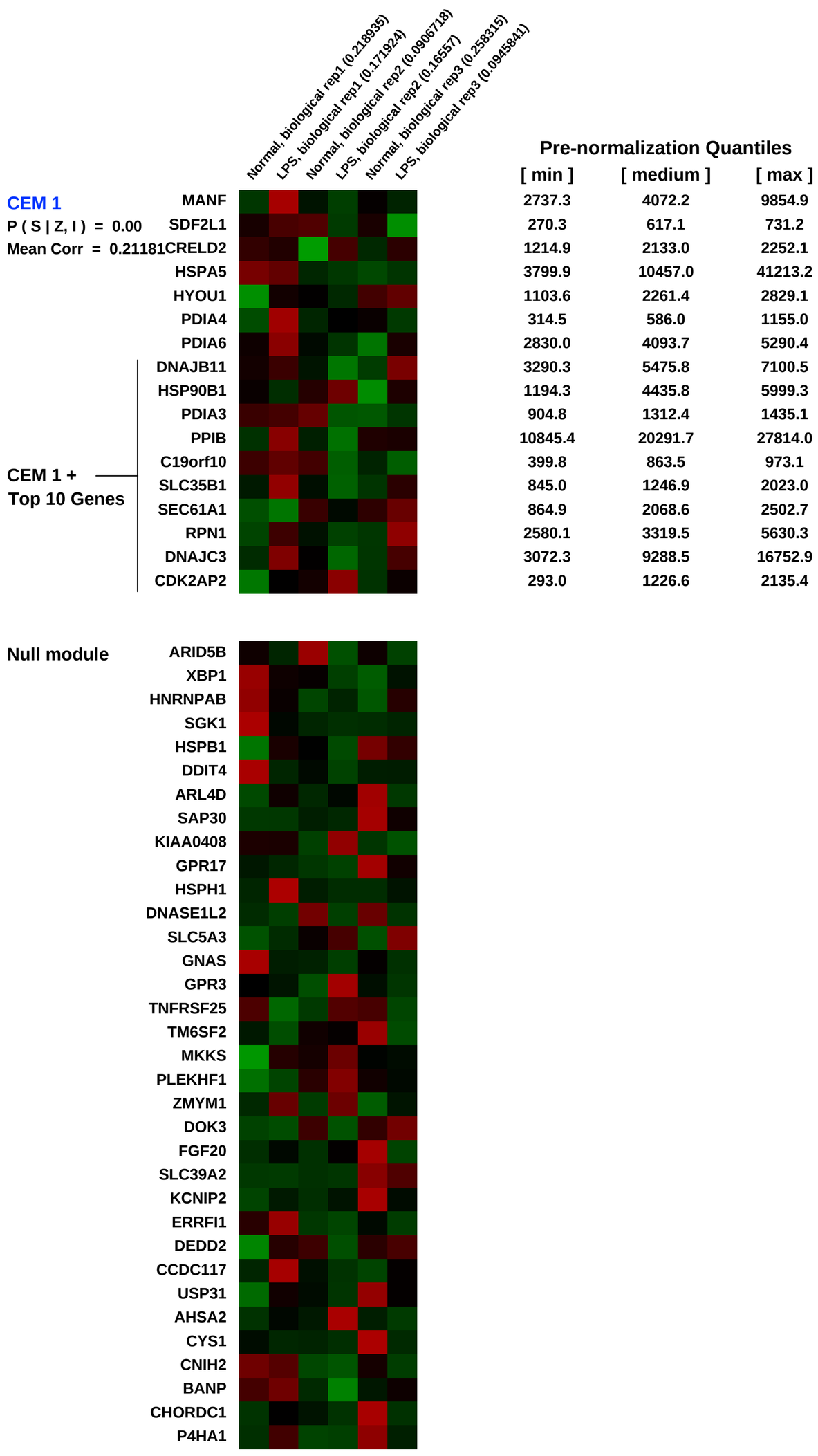

Pre-normalization Quantiles

	[min]	[medium]	[max]
MANF	2737.3	4072.2	9854.9
SDF2L1	270.3	617.1	731.2
CRELD2	1214.9	2133.0	2252.1
HSPA5	3799.9	10457.0	41213.2
HYOU1	1103.6	2261.4	2829.1
PDIA4	314.5	586.0	1155.0
PDIA6	2830.0	4093.7	5290.4
DNAJB11	3290.3	5475.8	7100.5
HSP90B1	1194.3	4435.8	5999.3
PDIA3	904.8	1312.4	1435.1
PPIB	10845.4	20291.7	27814.0
C19orf10	399.8	863.5	973.1
SLC35B1	845.0	1246.9	2023.0
SEC61A1	864.9	2068.6	2502.7
RPN1	2580.1	3319.5	5630.3
DNAJC3	3072.3	9288.5	16752.9
CDK2AP2	293.0	1226.6	2135.4

GEO Series "GSE43596" Expression Profiles

Num of samples in this series: 24

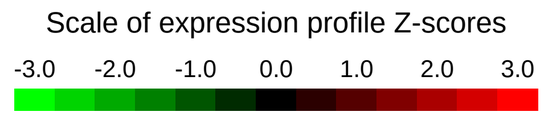

GEO Link:	http://www.ncbi.nlm.nih.gov/geo/query/acc.cgi?acc=GSE43596
Status:	Public on May 21 2014
Title:	Global gene expression analysis in macrophages treated with Nutlin-3
Organism:	Homo sapiens
Experiment type:	Expression profiling by array
Platform:	GPL570
Pubmed ID:	24737129
Summary & Design:	**Summary:** The goal of the study is to identify p53 target genes specific to macrophages using the p53 stabilizer, Nutlin-3. **Overall design:** Macrophages were differentiated x-vivo from monocytes obtained from healthy volunteers either left untreated or treated for 2 hours with 100 ng/mL of lipopolysaccharide (LPS), 0.1%v/v of DMSO (vehicle control for Nutlin-3) or 10 micromolar Nutlin-3. Three replicates were included for each treatment group.

Background corr dist: KL-Divergence = 0.2956, L1-Distance = 0.0411, L2-Distance = 0.0037, Normal std = 0.2865

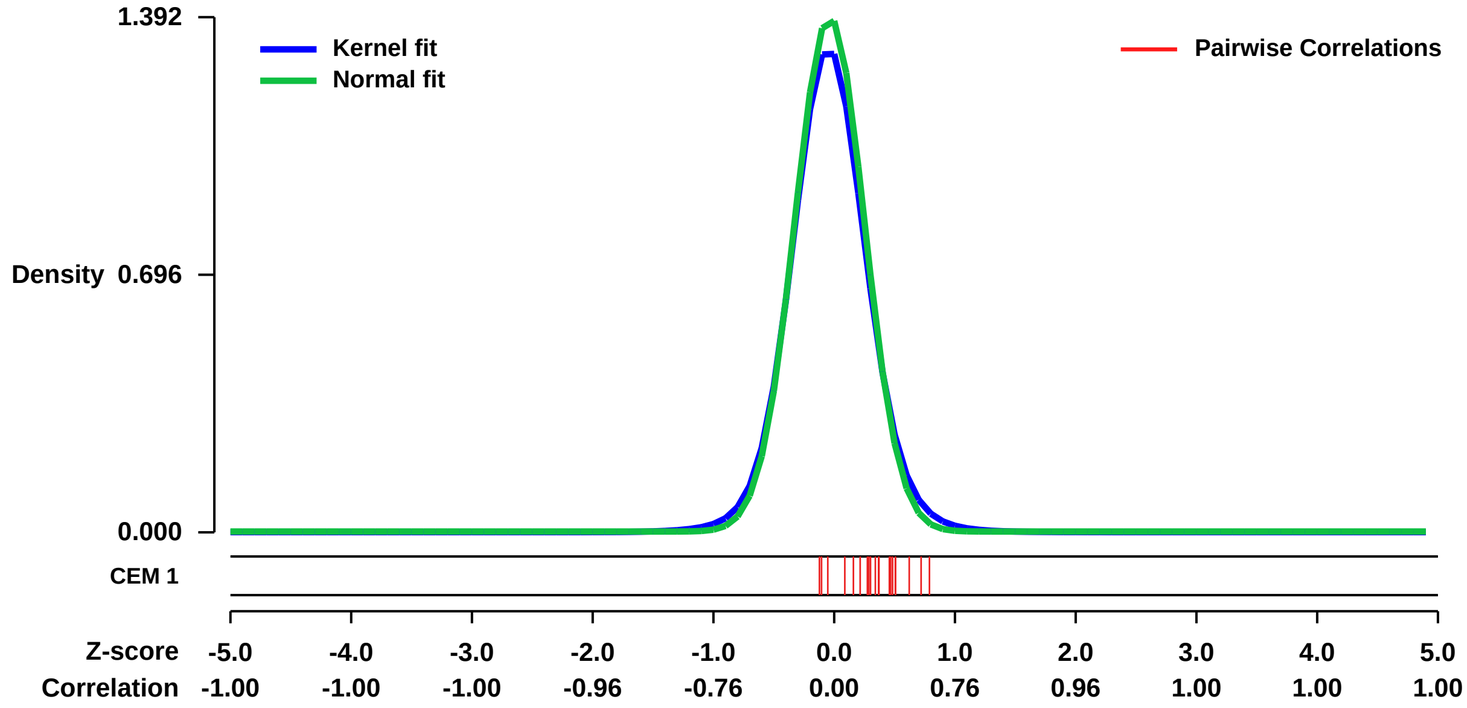

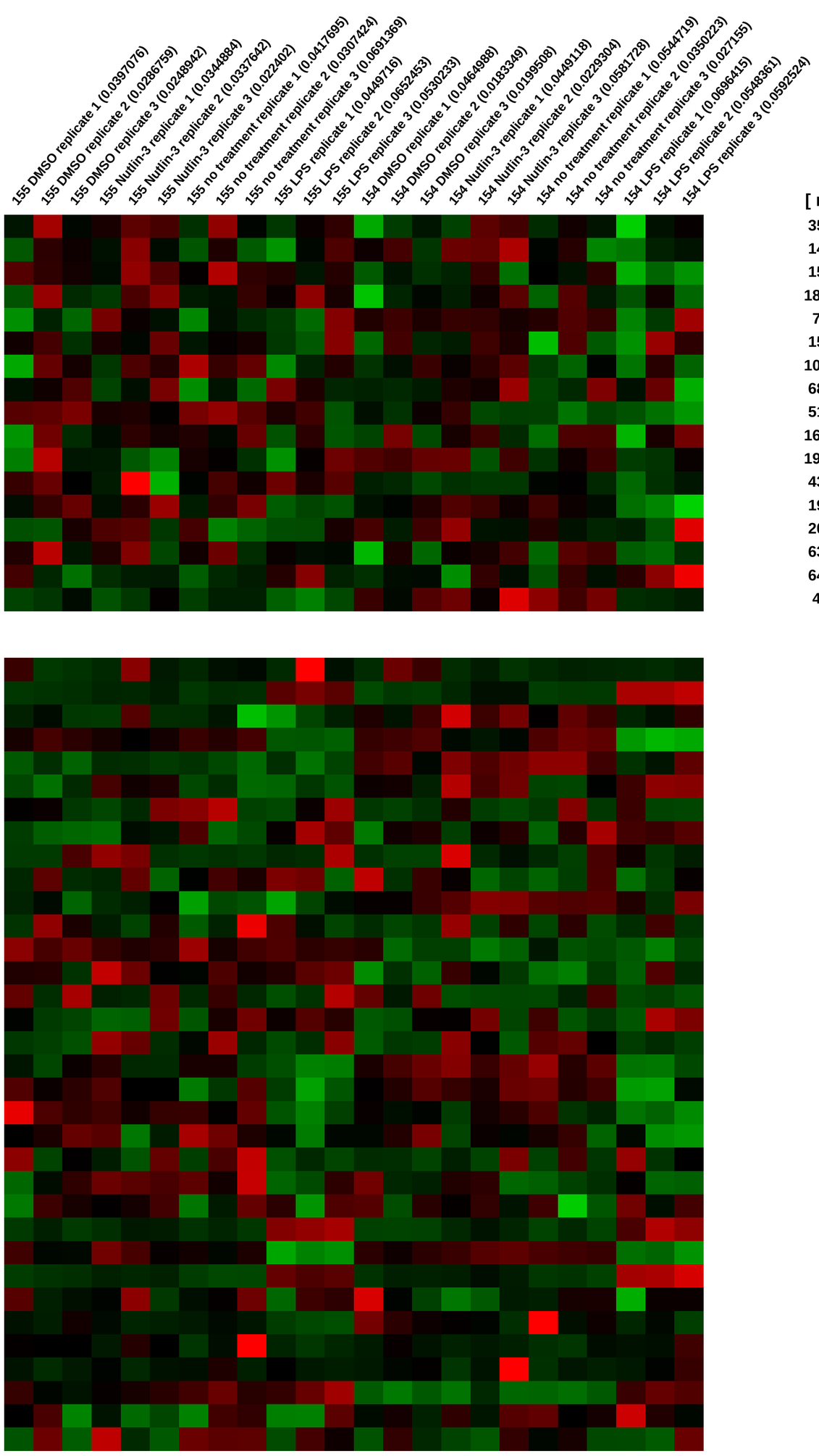

GEO Series "GSE16677" Expression Profiles

Num of samples in this series: 18

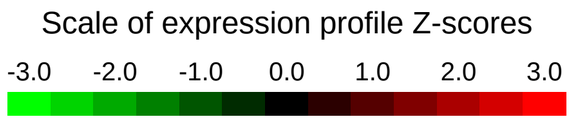

GEO Link:	http://www.ncbi.nlm.nih.gov/geo/query/acc.cgi?acc=GSE16677
Status:	Public on Aug 01 2010
Title:	Gene expression profiling of Down Syndrome (DS)-AMKL and non-DS AMKL samples
Organism:	Homo sapiens
Experiment type:	Expression profiling by array
Platform:	GPL570
Pubmed ID:	20679399
Summary & Design:	**Summary:** The goal of this study is to define a gene expression signature unique to DS-AMKL (acute megakaryoblastic leukemia or FAB M7 leukemia). A similar study was done previously, but using unfractionated patient leukemic samples. In this study, we sorted megakaryocytic leukemia blasts from patients and then compared their gene expression signatures to those from similarly sorted blasts from patients with non-DS AMKL. This allowed us to identify a gene expression signature more unique to DS-AMKL samples. **Overall design:** The leukemic blasts were sorted based on CD41, CD7, CD117, CD33, and CD34 antibodies as previously described (Klin. Padiatr. 217, 126-134).

Background corr dist: KL-Divergence = 0.1050, L1-Distance = 0.0748, L2-Distance = 0.0120, Normal std = 0.4549

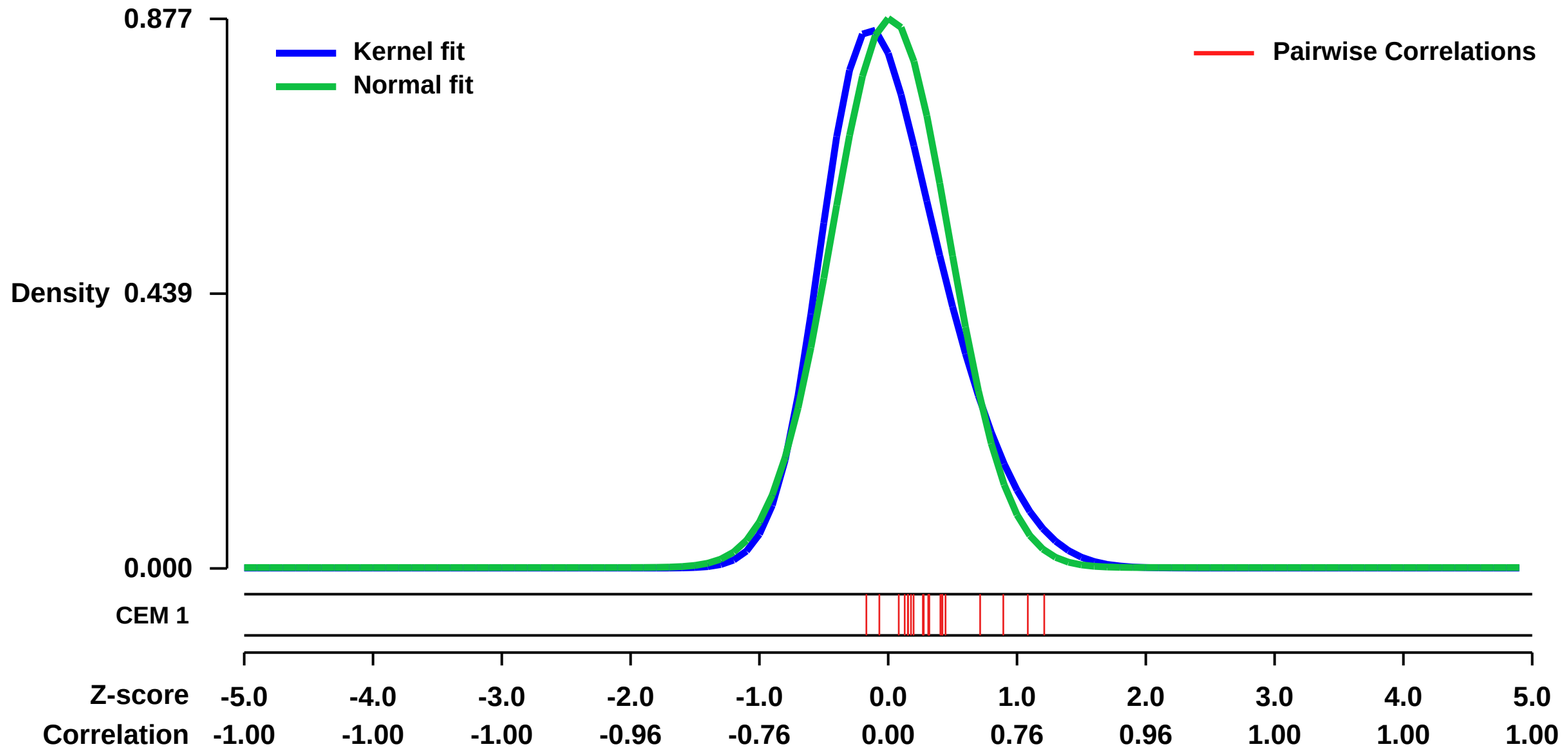

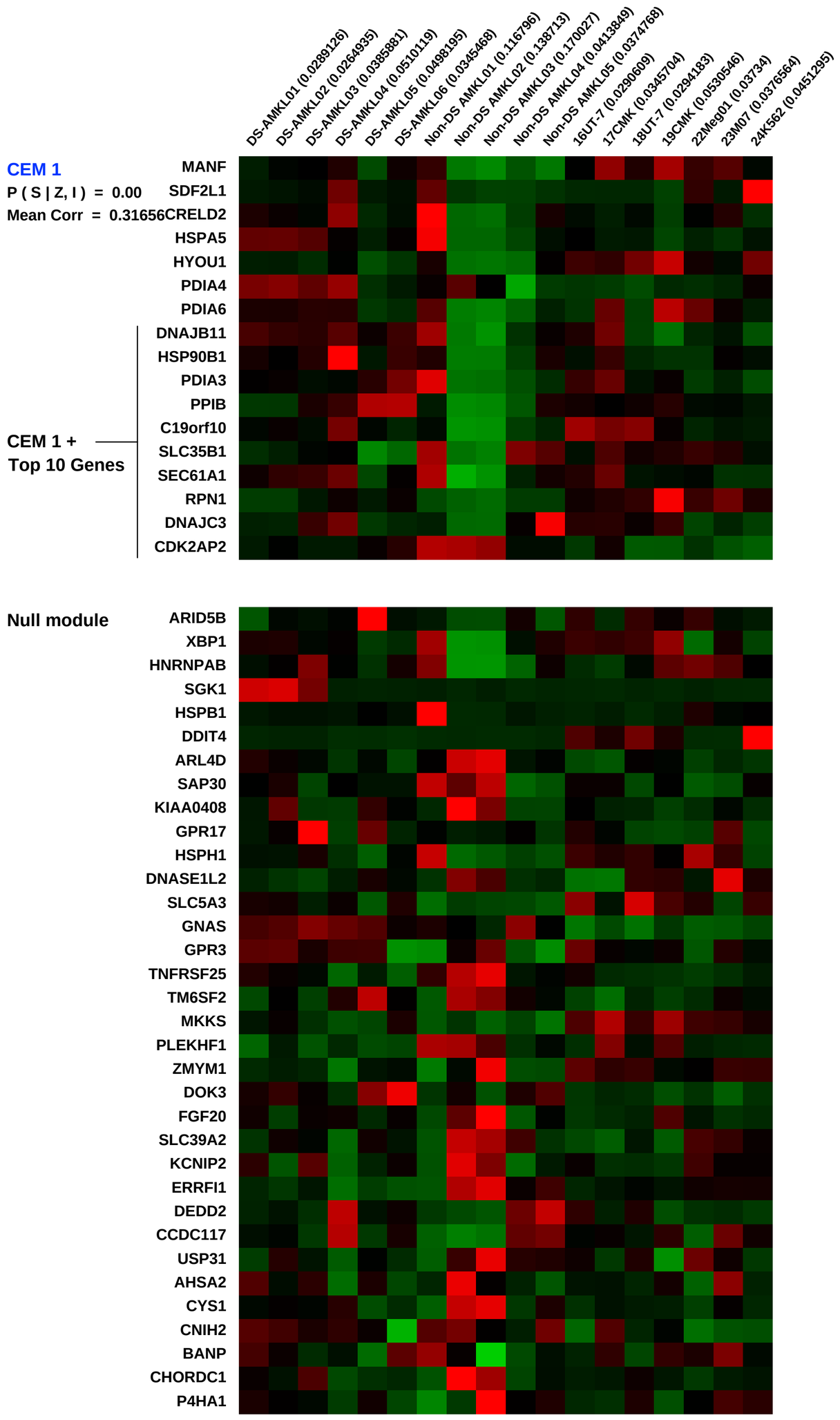

Pre-normalization Quantiles	[min]	[medium]	[max]
	95.5	1651.7	3507.4
	310.4	629.2	2927.7
	236.3	1072.8	3236.0
	134.6	7548.8	30648.8
	137.8	3962.9	10597.3
	500.9	1028.4	1675.4
	659.4	4791.5	9777.4
	462.7	1810.3	3056.7
	15.3	1383.8	4306.7
	877.1	4350.2	11796.0
	334.2	4695.4	10213.7
	369.4	1896.5	3713.4
	987.3	2399.7	4082.0
	213.7	1557.0	2830.0
	63.6	2724.4	8165.1
	219.4	963.6	3685.5
	264.2	575.4	1289.9

GEO Series "GSE49583" Expression Profiles

Num of samples in this series: 9

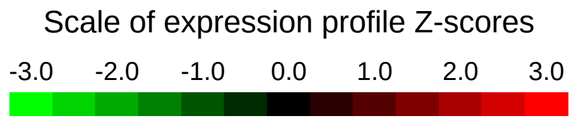

GEO Link:	http://www.ncbi.nlm.nih.gov/geo/query/acc.cgi?acc=GSE49583
Status:	Public on Aug 09 2013
Title:	Expression data from pancreatic stellate cells
Organism:	Homo sapiens
Experiment type:	Expression profiling by array
Platform:	GPL570
Pubmed ID:	
Summary & Design:	**Summary:** **tumor-stroma crosstalk drives pancreatic carcinogenesis** **we used time-resolved genome-wide transcriptional profiling to analyse changes caused by co-exposure of pancreatic tumor and stellate cells** **Overall design:** **The 8 tumor cell lines are pancreatic ductal adenocarcinoma lines: AsPC1, BxPC3, Capan1, Colo357, MiaPaca2, Panc1, Su8686, and T3M4**

Background corr dist: **KL-Divergence = 0.0951, L1-Distance = 0.0233, L2-Distance = 0.0006, Normal std = 0.4468**

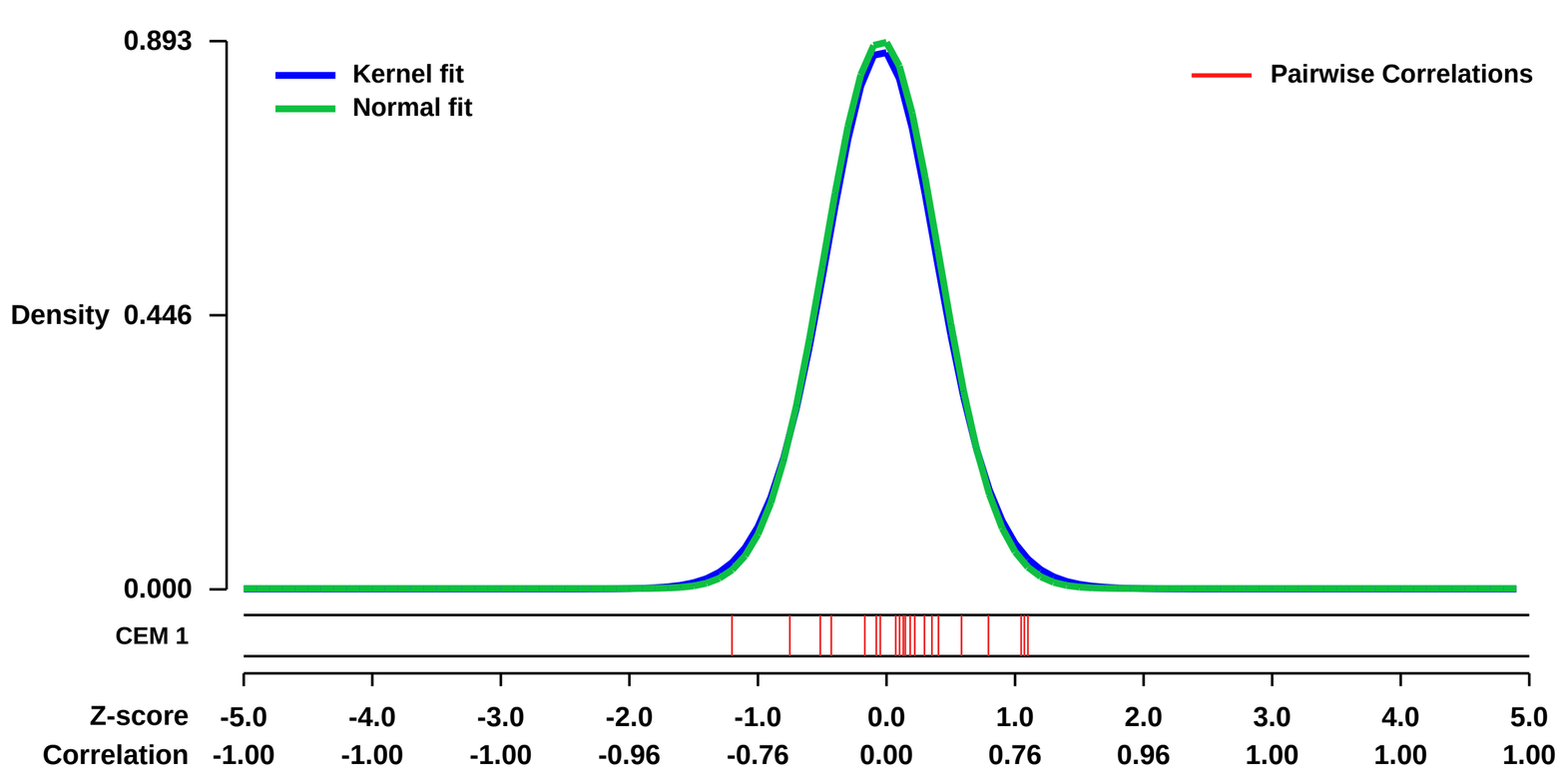

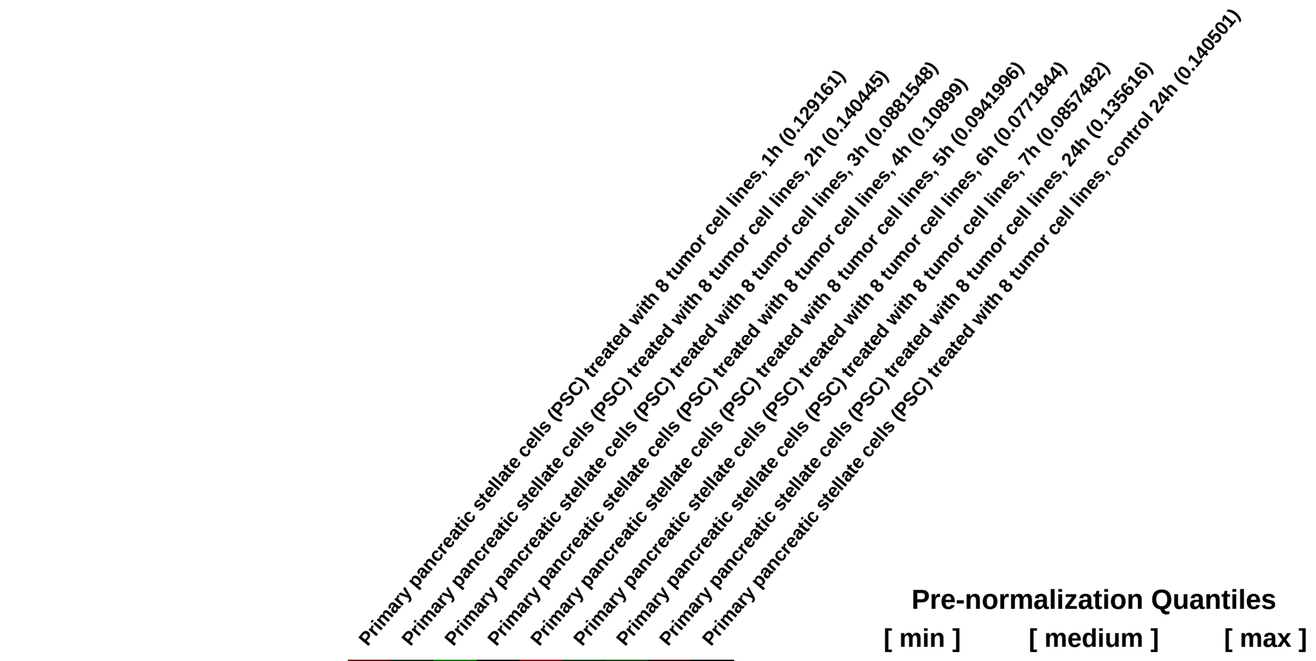

CEM 1
P (S | Z, I) = 0.00
Mean Corr = 0.13184

CEM 1 + Top 10 Genes

Null module

	Pre-normalization Quantiles [min]	[medium]	[max]
MANF	3114.9	3267.1	3437.0
SDF2L1	718.5	759.6	872.9
CRELD2	2311.2	2528.9	2648.5
HSPA5	18209.9	19955.6	22142.1
HYOU1	2137.8	2432.5	2836.4
PDIA4	888.2	1039.0	1163.9
PDIA6	7215.6	7656.3	8256.3
DNAJB11	2513.4	2844.5	3110.2
HSP90B1	4599.3	5072.0	5608.7
PDIA3	9655.1	10298.9	11462.8
PPIB	16718.5	17629.2	19569.4
C19orf10	5109.6	5553.5	5781.1
SLC35B1	2066.9	2193.7	2265.1
SEC61A1	7274.0	7564.3	8099.7
RPN1	1339.2	1498.4	1607.1
DNAJC3	2260.6	2422.3	2626.8
CDK2AP2	587.3	634.2	788.0
ARID5B			
XBP1			
HNRNPAB			
SGK1			
HSPB1			
DDIT4			
ARL4D			
SAP30			
KIAA0408			
GPR17			
HSPH1			
DNASE1L2			
SLC5A3			
GNAS			
GPR3			
TNFRSF25			
TM6SF2			
MKKS			
PLEKHF1			
ZMYM1			
DOK3			
FGF20			
SLC39A2			
KCNIP2			
ERRFI1			
DEDD2			
CCDC117			
USP31			
AHSA2			
CYS1			
CNIH2			
BANP			
CHORDC1			
P4HA1			

GEO Series "GSE34456" Expression Profiles

Num of samples in this series: 9

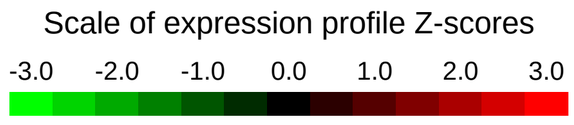

GEO Link:	http://www.ncbi.nlm.nih.gov/geo/query/acc.cgi?acc=GSE34456
Status:	Public on Jun 01 2012
Title:	Expression data from transfection of U87 glioma cells with miR-376a* for 72 hours
Organism:	Homo sapiens
Experiment type:	Expression profiling by array
Platform:	GPL570
Pubmed ID:	23093778
Summary & Design:	**Summary:** Several biological pathways can be under the regulation of miRNAs. These pathways can be indentified by the enforced expression of a miRNA and analysing the expression data for enrichment of specific pathways represented among the genes differentially expressed upon miRNA overexpression. We transfected unedited miR-376a* (376a*A) and edited miR-376a* (376a*G) into U87 cells to identify differentially regulated transcripts. List of differentially expressed genes were subject to pathway enrichment analysis to identify specific biological processes regulated by each of miR-376a*A and miR-376a*G. **Overall design:** U87 cells (100,000) were transfected with 50 nM of miR-376a*A, miR-376a*G or miR-control. Following incubation for 72 hours, total RNA was isolated from transfected cells. For each (miR-376a*A or miR-376a*G), genes differentially expressed upon miRNA transfection were determined based on comparison with miR-control-transfected samples. Biological triplicates were used for each sample type.

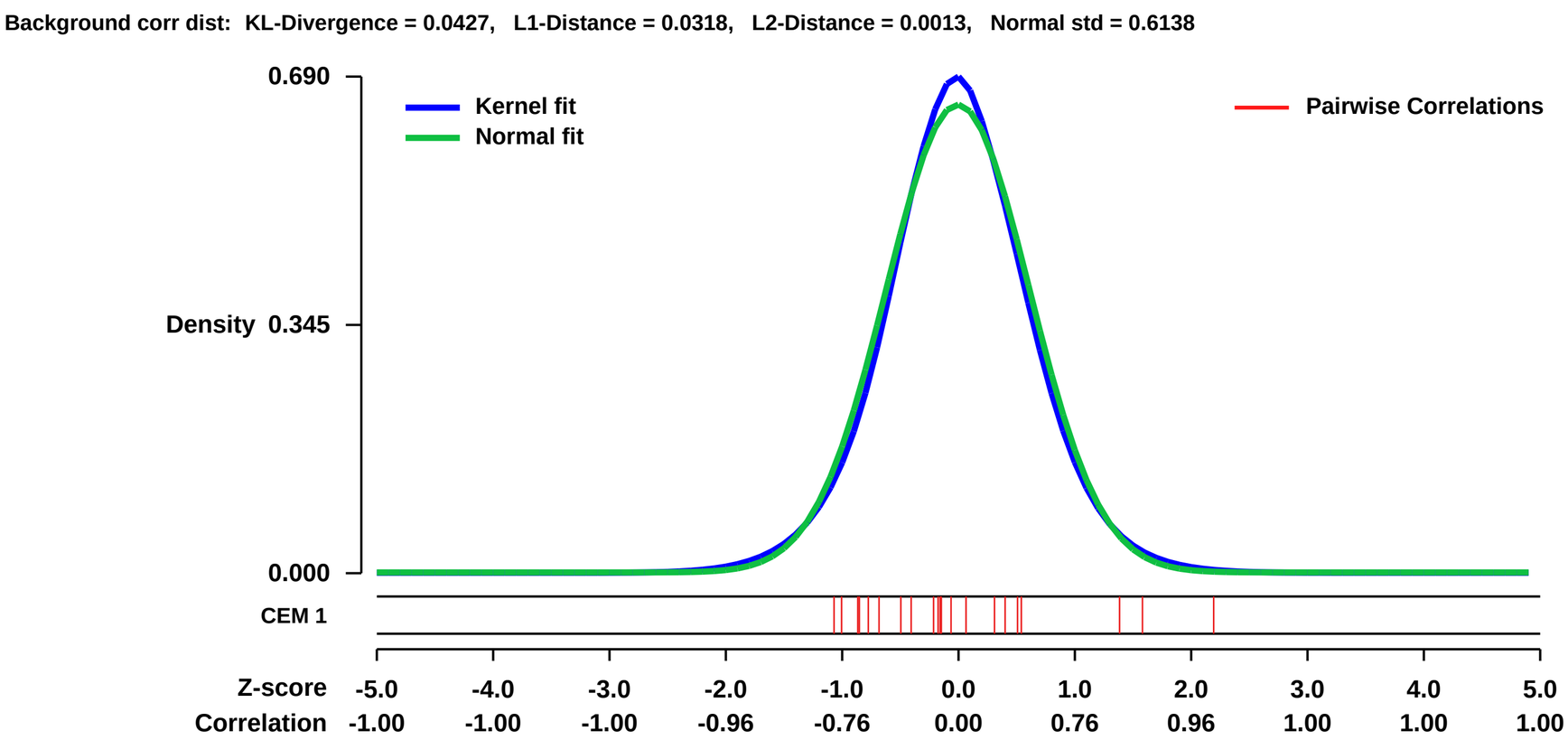

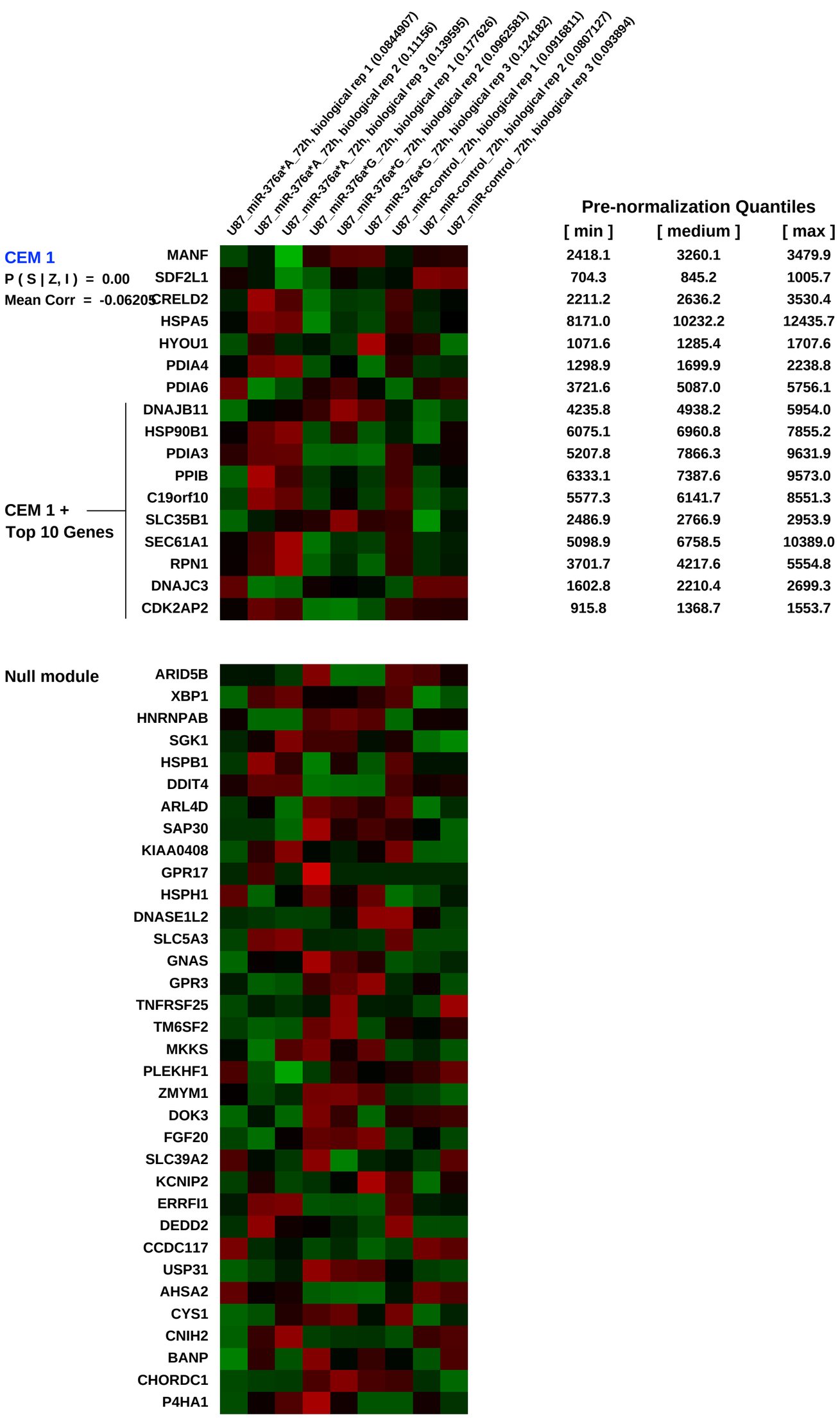

Pre-normalization Quantiles

	[min]	[medium]	[max]
MANF	2418.1	3260.1	3479.9
SDF2L1	704.3	845.2	1005.7
CRELD2	2211.2	2636.2	3530.4
HSPA5	8171.0	10232.2	12435.7
HYOU1	1071.6	1285.4	1707.6
PDIA4	1298.9	1699.9	2238.8
PDIA6	3721.6	5087.0	5756.1
DNAJB11	4235.8	4938.2	5954.0
HSP90B1	6075.1	6960.8	7855.2
PDIA3	5207.8	7866.3	9631.9
PPIB	6333.1	7387.6	9573.0
C19orf10	5577.3	6141.7	8551.3
SLC35B1	2486.9	2766.9	2953.9
SEC61A1	5098.9	6758.5	10389.0
RPN1	3701.7	4217.6	5554.8
DNAJC3	1602.8	2210.4	2699.3
CDK2AP2	915.8	1368.7	1553.7

GEO Series "GSE16085" Expression Profiles

Num of samples in this series: 6

Scale of expression profile Z-scores

-3.0 -2.0 -1.0 0.0 1.0 2.0 3.0

GEO Link:	http://www.ncbi.nlm.nih.gov/geo/query/acc.cgi?acc=GSE16085
Status:	Public on Sep 08 2009
Title:	Networking of differentially expressed genes in human K562 erythtoblastic leukemia cells resistant to methotrexate
Organism:	Homo sapiens
Experiment type:	Expression profiling by array
Platform:	GPL570
Pubmed ID:	19732436
Summary & Design:	**Summary:** **A summary of the work associated to these microarrays is the following:** **The need for an integrated view of all data obtained from high-throughput technologies gave rise to network analyses. These are especially useful to rationalize phenomena in terms of how external perturbations propagate through the expression of genes. To address this issue in the case of drug resistance, we constructed Biological Association Networks of genes differentially expressed in cell lines resistant to methotrexate (MTX). Seven cell lines representative of different types of cancer including colon cancer (HT29 and Caco2), breast cancer (MCF7 and MDA-MB-468), pancreatic cancer (MIA PaCa-2), erythroblastic leukemia (K562) and osteosarcoma (Saos-2), were used. The differential expression pattern between sensitive and MTX-resistant cells was determined by microarrays covering the whole human genome and analyzed with the GeneSpring GX software package, v.7.3.1. Genes deregulated in common in the two colon cancer cell lines studied, were subject of Biological Association Networks construction. Dikkopf homolog-1 (DKK1) was a clear node of this network, and functional validations of this target using a siRNA showed a chemosensitization toward MTX. Members of the UDP-glucuronosyltransferase 1A (UGT1A) family formed a network of differentially expressed genes in the two breast cancer cell lines studied. siRNA treatment against UGT1A showed also an increase in MTX sensitivity. Eukaryotic translation elongation factor 1 alpha 1 (EEF1A1) was a gene overexpressed in common among the pancreatic cancer, leukemia and osteosarcoma cell lines, and siRNA treatment against EEF1A1 produced a chemosensitization toward MTX. Biological Association Networks identified DKK1, UGT1As and EEF1A1 as important gene nodes in MTX-resistance. Treatments using iRNA technology against these three genes show chemosensitization toward MTX.** **Overall design:** **Two cell lines are compared, which are K562 erythroblastic leukemia cells sensitive to methotrexate and K562 cells resistant to 10e-5M methotrexate. Six samples are provided which correspond to triplicates of each cell line. The samples provided were analyzed using the specific software GeneSpring GX.**

Background corr dist: KL-Divergence = 0.0441, L1-Distance = 0.0358, L2-Distance = 0.0017, Normal std = 0.6161

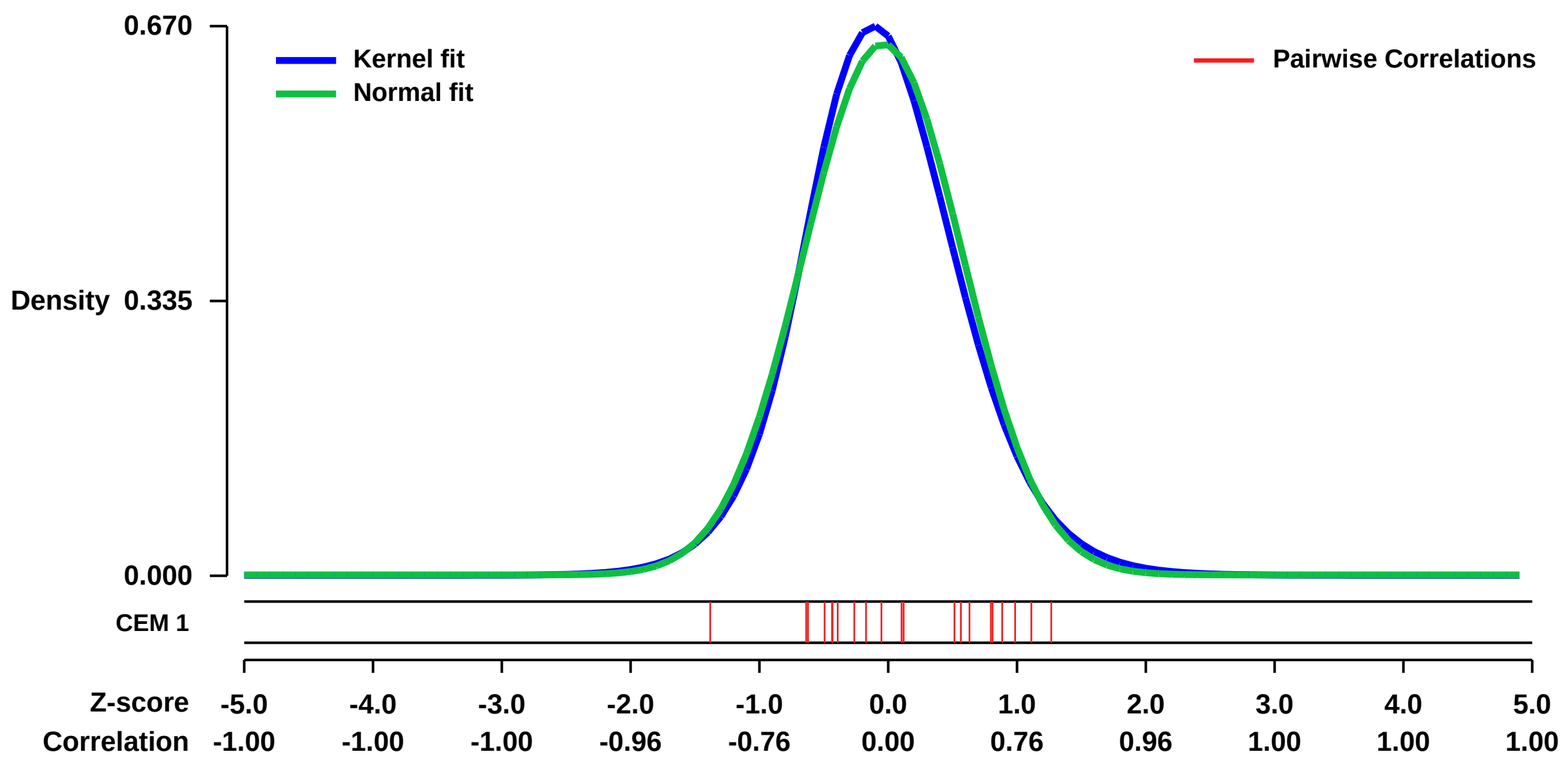

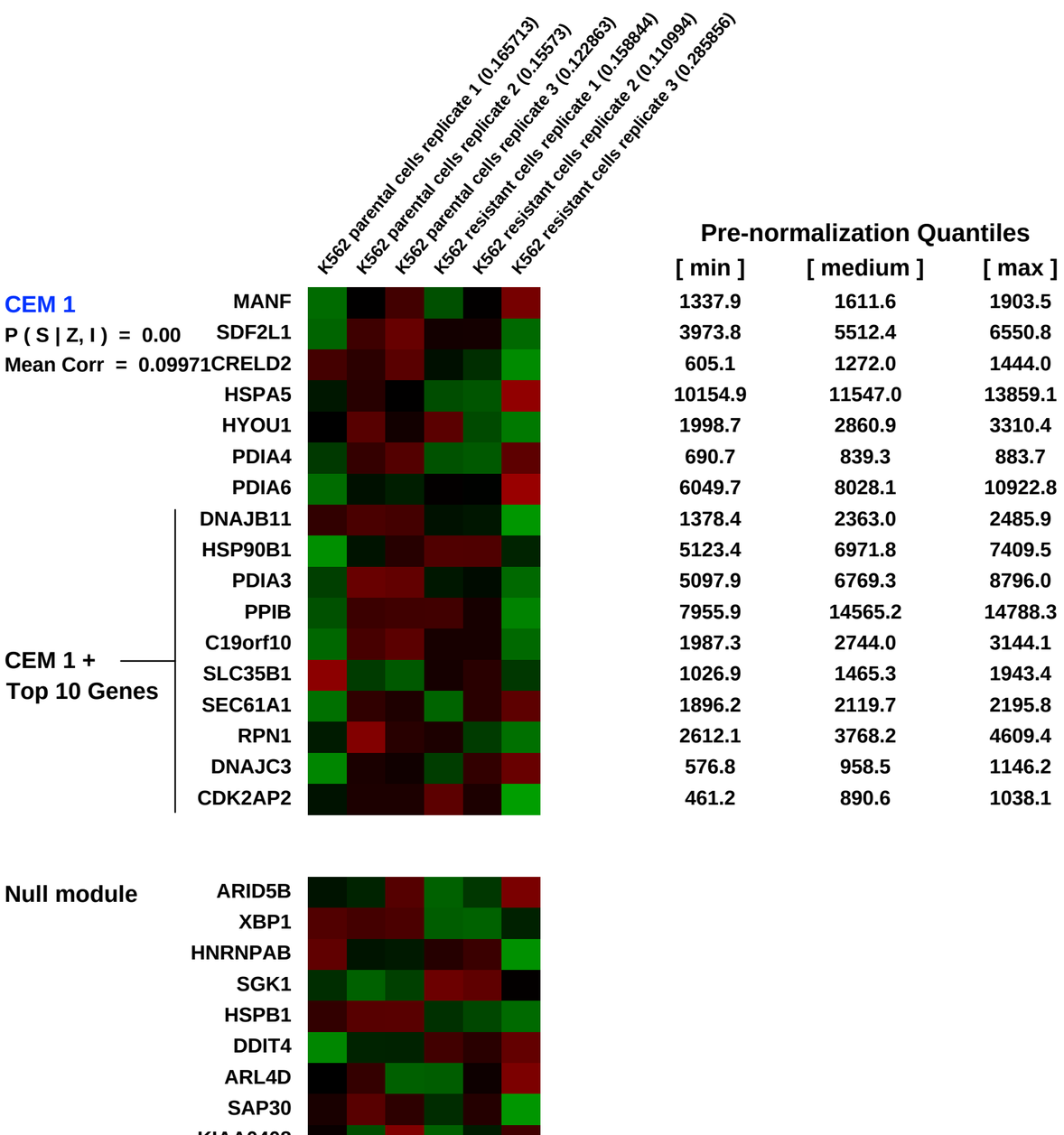

GEO Series "GSE38043" Expression Profiles

Num of samples in this series: 6

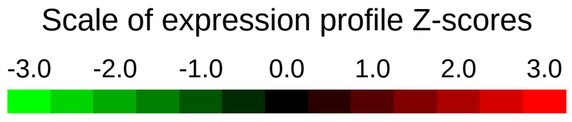

GEO Link:	http://www.ncbi.nlm.nih.gov/geo/query/acc.cgi?acc=GSE38043
Status:	Public on Mar 05 2013
Title:	Dysregulated expression of genes in regulatory T cells from metastatic castration-resistant prostate cancer patients
Organism:	Homo sapiens
Experiment type:	Expression profiling by array
Platform:	GPL570
Pubmed ID:	23319273
Summary & Design:	**Summary:** We analyzed the global gene expression pattern of Tregs between healthy donors and prostate cancer patients. We found that genes related to cell cycle, cellular proliferation, immune responses, hematological system development and function were differentially expressed in Tregs from prostate cancer patients. **Overall design:** Total RNA samples of Tregs, isolated from peripheral blood, were obtained from three separate healthy donors and three metastatic castration-resistant prostate cancer patients. Global gene expression pattern was examined by performing GeneChip microarray hybridization. Genes differentially expressed between the two groups of donors were sorted and categorized based on their biological functions.

Background corr dist: KL-Divergence = 0.0443, L1-Distance = 0.0281, L2-Distance = 0.0010, Normal std = 0.6027

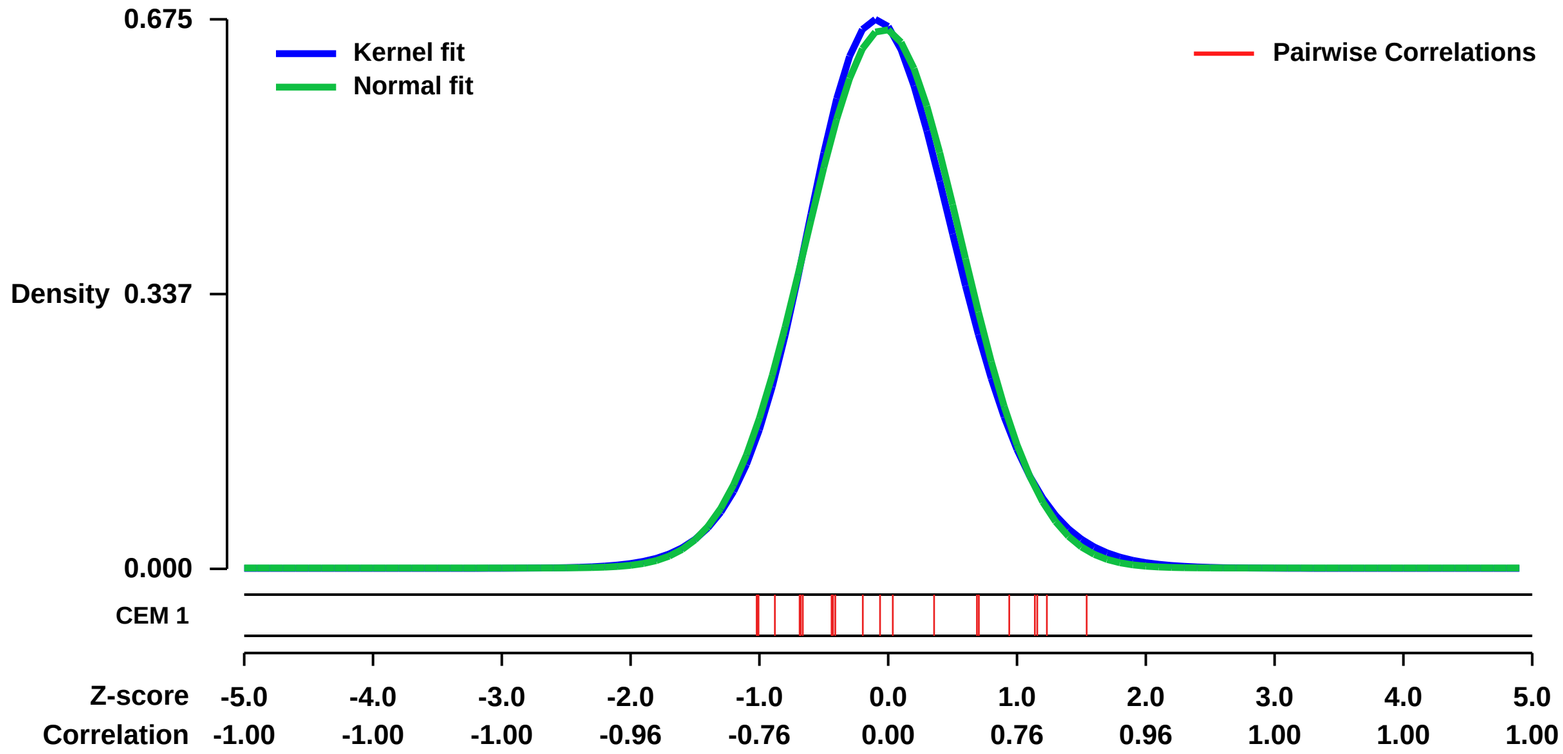

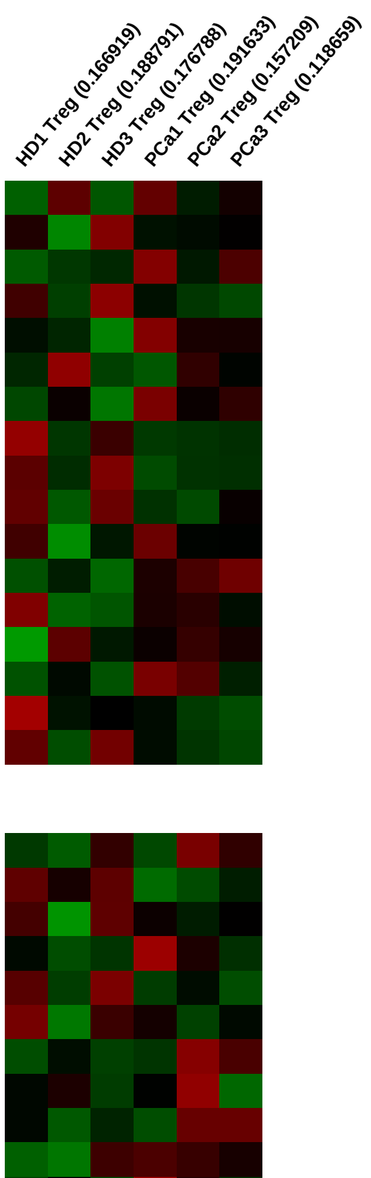

Pre-normalization Quantiles

		[min]	[medium]	[max]
CEM 1	MANF	1548.1	2129.7	2531.6
P (S | Z, I) = 0.00	SDF2L1	348.4	627.0	891.4
Mean Corr = -0.02540	CRELD2	3049.5	3491.4	4518.9
	HSPA5	3949.6	6716.1	14497.4
	HYOU1	576.2	834.3	1018.3
	PDIA4	413.2	591.9	907.8
	PDIA6	4241.6	5820.2	7192.2
CEM 1 + Top 10 Genes	DNAJB11	967.0	1128.0	3799.4
	HSP90B1	302.3	403.5	946.7
	PDIA3	1761.1	2885.1	4035.9
	PPIB	4200.2	5591.7	6678.5
	C19orf10	967.8	1133.5	1237.8
	SLC35B1	860.3	1062.5	1224.9
	SEC61A1	1765.7	2674.4	3039.9
	RPN1	1079.0	1651.3	2682.3
	DNAJC3	2017.8	2342.8	3219.6
	CDK2AP2	308.4	423.3	646.7
Null module	ARID5B			
	XBP1			
	HNRNPAB			
	SGK1			
	HSPB1			
	DDIT4			
	ARL4D			
	SAP30			
	KIAA0408			
	GPR17			
	HSPH1			
	DNASE1L2			
	SLC5A3			
	GNAS			
	GPR3			
	TNFRSF25			
	TM6SF2			
	MKKS			
	PLEKHF1			
	ZMYM1			
	DOK3			
	FGF20			
	SLC39A2			
	KCNIP2			
	ERRFI1			
	DEDD2			
	CCDC117			
	USP31			
	AHSA2			
	CYS1			
	CNIH2			
	BANP			
	CHORDC1			
	P4HA1			

GEO Series "GSE6092" Expression Profiles

Num of samples in this series: 8

Scale of expression profile Z-scores

-3.0 -2.0 -1.0 0.0 1.0 2.0 3.0

GEO Link: http://www.ncbi.nlm.nih.gov/geo/query/acc.cgi?acc=GSE6092

Status: Public on Jan 05 2007

Title: IFN-gamma alters the response of Borrelia burgdorferi-activated endothelium to favor chronic inflammation

Organism: Homo sapiens

Experiment type: Expression profiling by array

Platform: GPL570

Pubmed ID: 17202382

Summary & Design:

Summary:
Borrelia burgdorferi, the agent of Lyme disease, promotes pro-inflammatory changes in endothelium that lead to the recruitment of leukocytes. The host immune response to infection results in increased levels of IFN-gamma in the serum and lesions of Lyme disease patients that correlate with greater severity of disease. Therefore, the effect of IFN-gamma on the gene expression profile of primary human endothelial cells exposed to B. burgdorferi was determined. B. burgdorferi and IFN-gamma synergistically augmented the expression of 34 genes, seven of which encode chemokines. Six of these (CCL7, CCL8, CX3CL1, CXCL9, CXCL10, and CXCL11) attract T lymphocytes, and one (CXCL2) is specific for neutrophils. Synergistic production of the attractants for T cells was confirmed at the protein level. IL-1beta, TNF-alpha, and LPS also cooperated with IFN-gamma to induce synergistic production of CXCL10 by endothelium, indicating that IFN-gamma potentiates inflammation in concert with a variety of mediators. An in vitro model of the blood vessel wall revealed that an increased number of human T lymphocytes traversed endothelium exposed to B. burgdorferi and IFN-gamma, as compared to unstimulated endothelial monolayers. In contrast, addition of IFN-gamma diminished the migration of neutrophils across B. burgdorferi-activated endothelium. IFN-gamma thus alters gene expression by endothelium exposed to B. burgdorferi in a manner that promotes recruitment of T cells and suppresses that of neutrophils. This modulation may facilitate the development of chronic inflammatory lesions in Lyme disease.

Keywords: Cell response to inflammatory stimuli

Overall design:
Human umbilical vein endothelial cells (HUVEC) were stimulated with Interferon-gamma (IFN-g), Borrelia burgdorferi or both IFN-g and Borrelia or were left unstimulated. Affymetrix HGU133 plus 2.0 slides were used in duplicate for each condition.

Background corr dist: KL-Divergence = 0.0267, L1-Distance = 0.0393, L2-Distance = 0.0026, Normal std = 0.6928

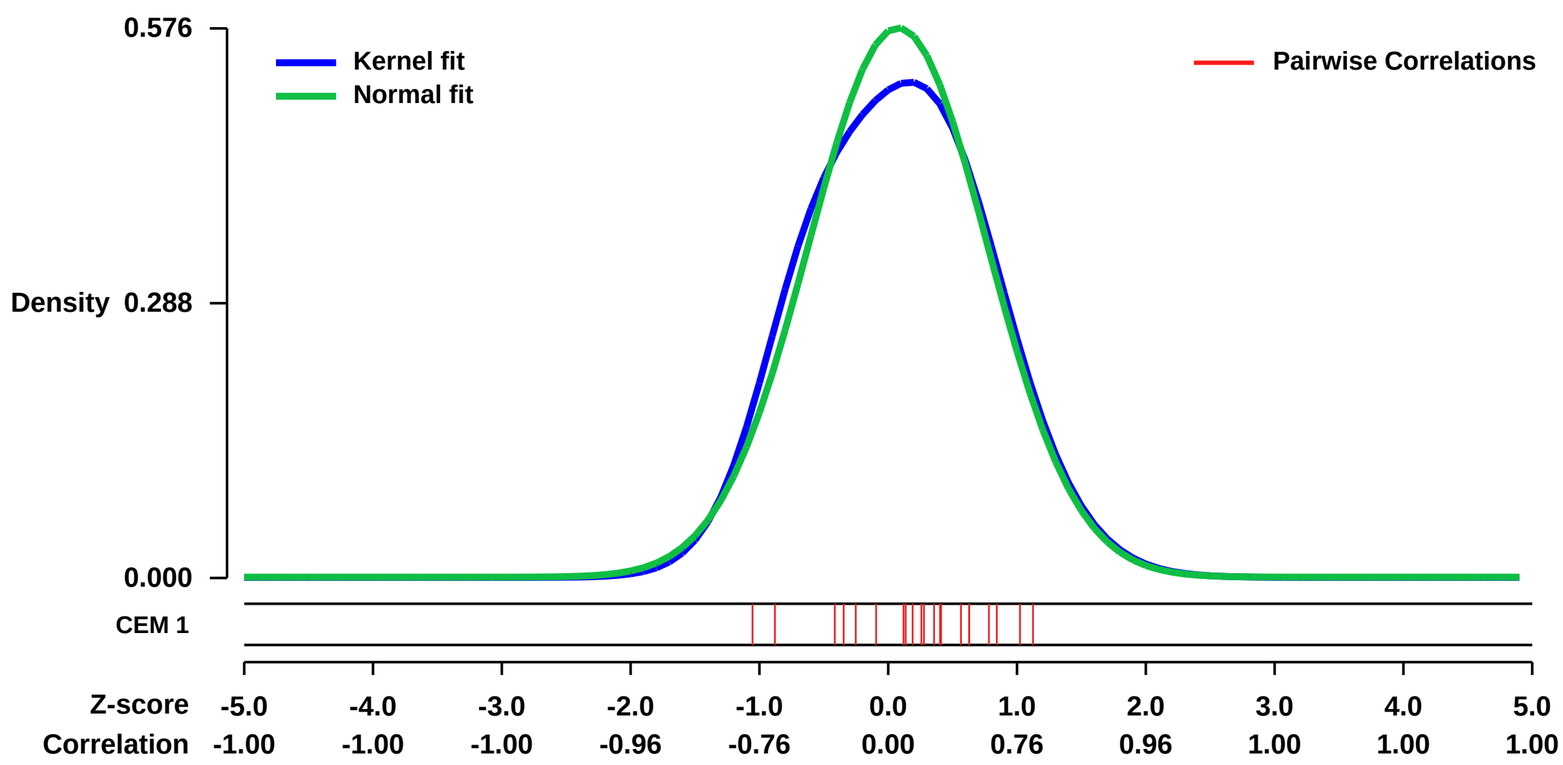

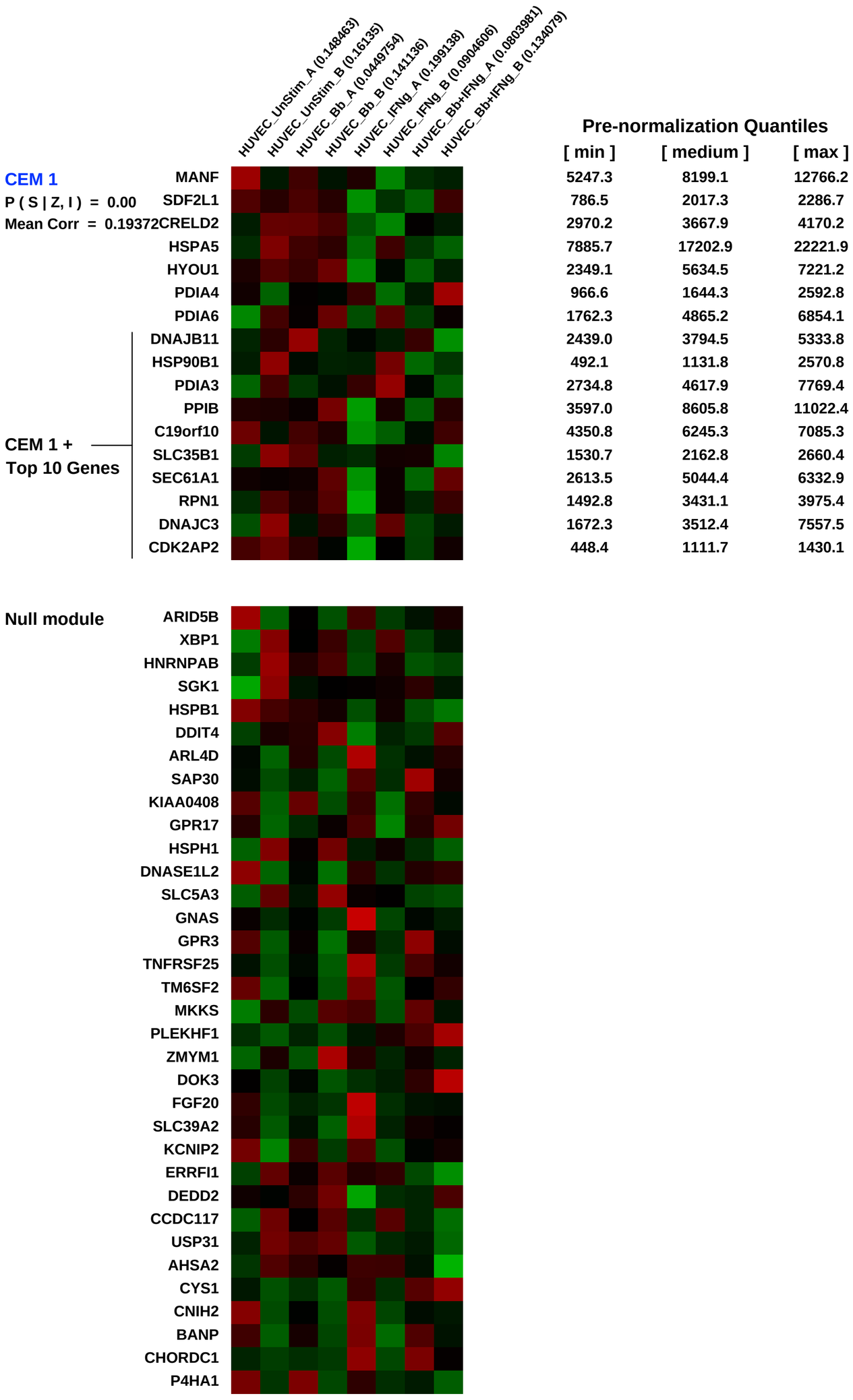

GEO Series "GSE17714" Expression Profiles

Num of samples in this series: 22

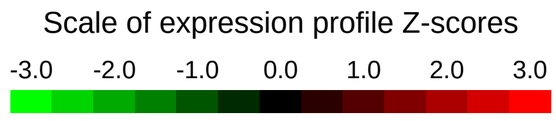

GEO Link:	http://www.ncbi.nlm.nih.gov/geo/query/acc.cgi?acc=GSE17714
Status:	Public on Sep 30 2009
Title:	11 Neuroblastoma cell lines under normoxic and hypoxic conditions
Organism:	Homo sapiens
Experiment type:	Expression profiling by array
Platform:	GPL570
Pubmed ID:	20624283
Summary & Design:	**Summary:** Hypoxia is a low oxygen condition that occurs in the developing tumor mass and that is associated with poor prognosis and resistance to chemo- and radio-therapy. The definition of the hypoxia gene signature is fundamental for the understanding of tumor biology, as in the case of neuroblastoma, the most common pediatric solid tumor. The issue of identifying a significant group of variables in microarray gene expression experiments is particularly difficult due to the typical high dimensional nature of the data and great effort has been spent in the development of feature selection techniques. Our main goal is to define a robust hypoxia gene signature in neuroblastoma cell lines. A set of 11 neuroblastoma cell lines were cultured under normoxic and hypoxic conditions for 18 hours, and their gene expression profiles were measured with Affymetrix GeneChip HG-U133 Plus 2.0. We used the l1-l2 regularization framework in order to select the significant probesets defining hypoxic versus normoxic cell lines. **Overall design:** The expression profiles of 11 neuroblastoma cell lines under normoxia vs hypoxia were studied.

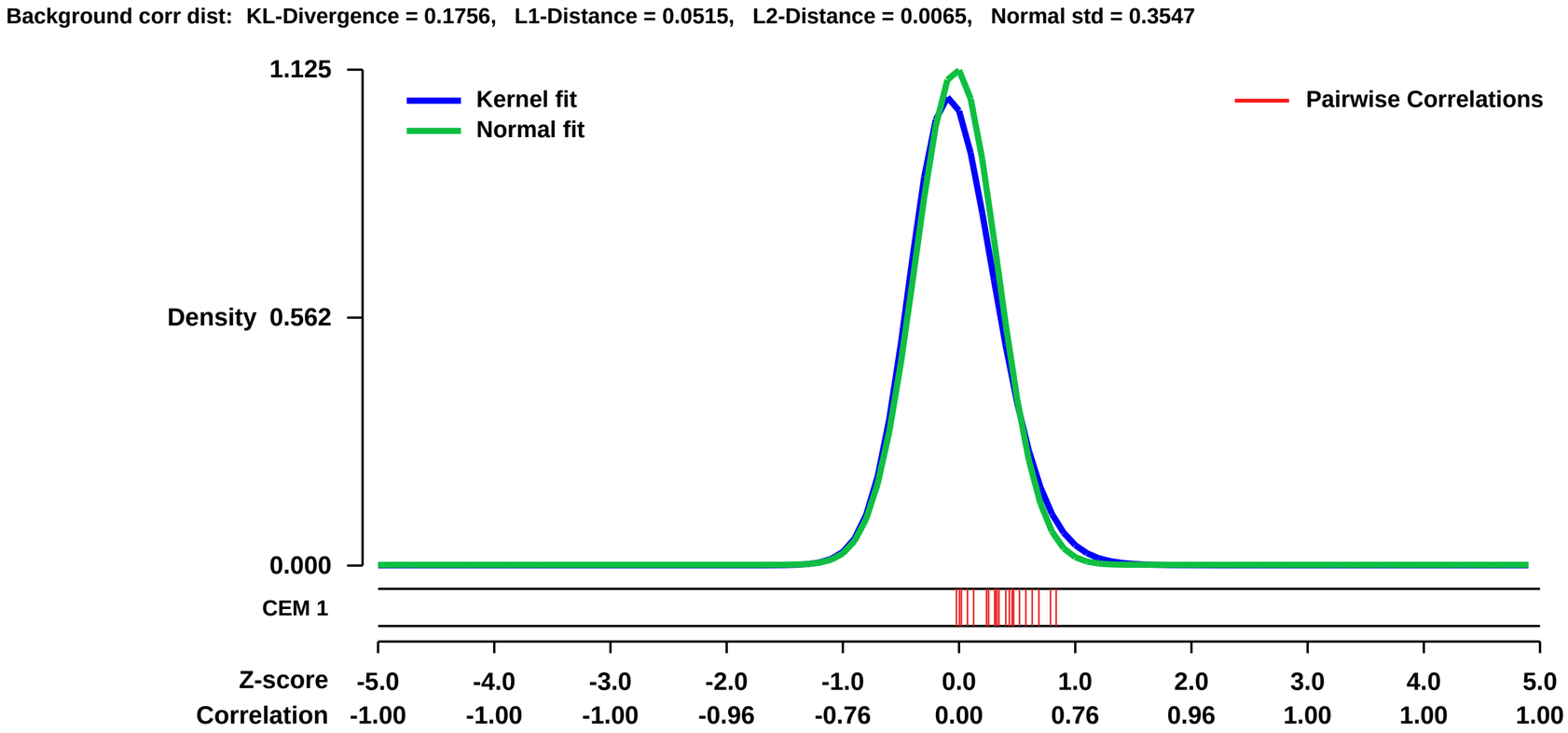

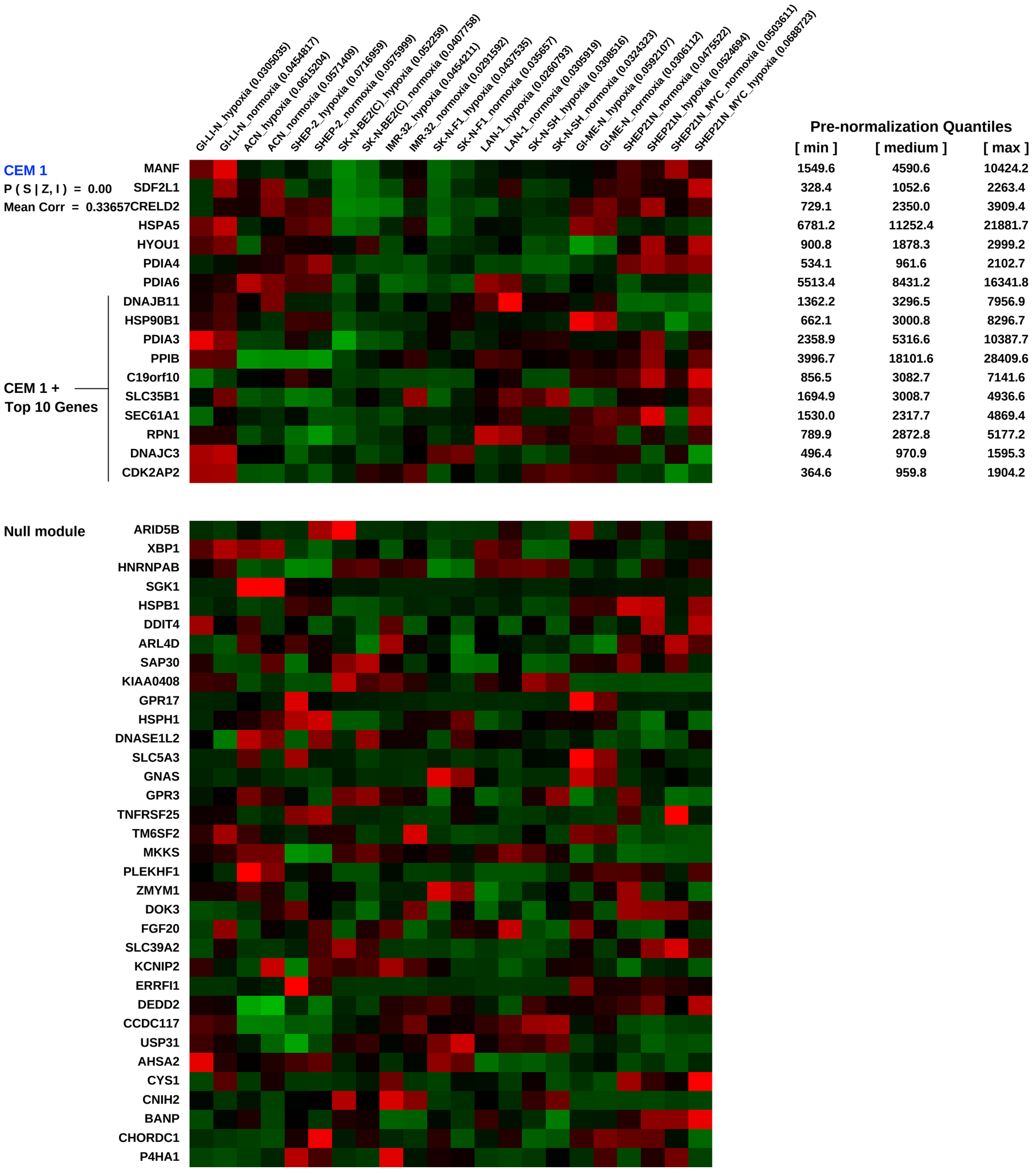

GEO Series "GSE20115" Expression Profiles

Num of samples in this series: 8

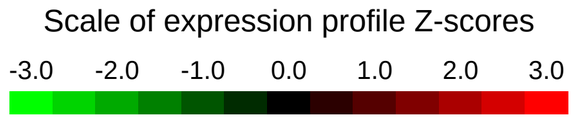

GEO Link:	http://www.ncbi.nlm.nih.gov/geo/query/acc.cgi?acc=GSE20115
Status:	Public on Apr 23 2010
Title:	Expression analysis of Reh cells after transfection with shRNA targeting CBFA2T3 and/or constitutively active IKK¸†(EE)
Organism:	Homo sapiens
Experiment type:	Expression profiling by array
Platform:	GPL570
Pubmed ID:	20436485
Summary & Design:	**Summary:** Genome-wide gene expression analysis of Reh cells following transfection with shRNA targeting CBFA2T3, constitutively active IKK¸†(EE), or both in combination. **Overall design:** Affymetrix U133 Plus 2.0 oligonucleotide arrays were hybridized to determine the gene expression profile of acute lymphoblastic leukemia-derived Reh cells following transfection with i) control shRNA construct, ii) shRNA construct targeting CBFA2T3, iii) a constitutively active variant of the IkB kinase ¸† (IKK¸†(EE)), or iv) shRNA targeting CBFA2T3 in combination with IKK¸†(EE). All hybridizations were done in biological duplicates.

Background corr dist: KL-Divergence = 0.0625, L1-Distance = 0.0179, L2-Distance = 0.0003, Normal std = 0.5208

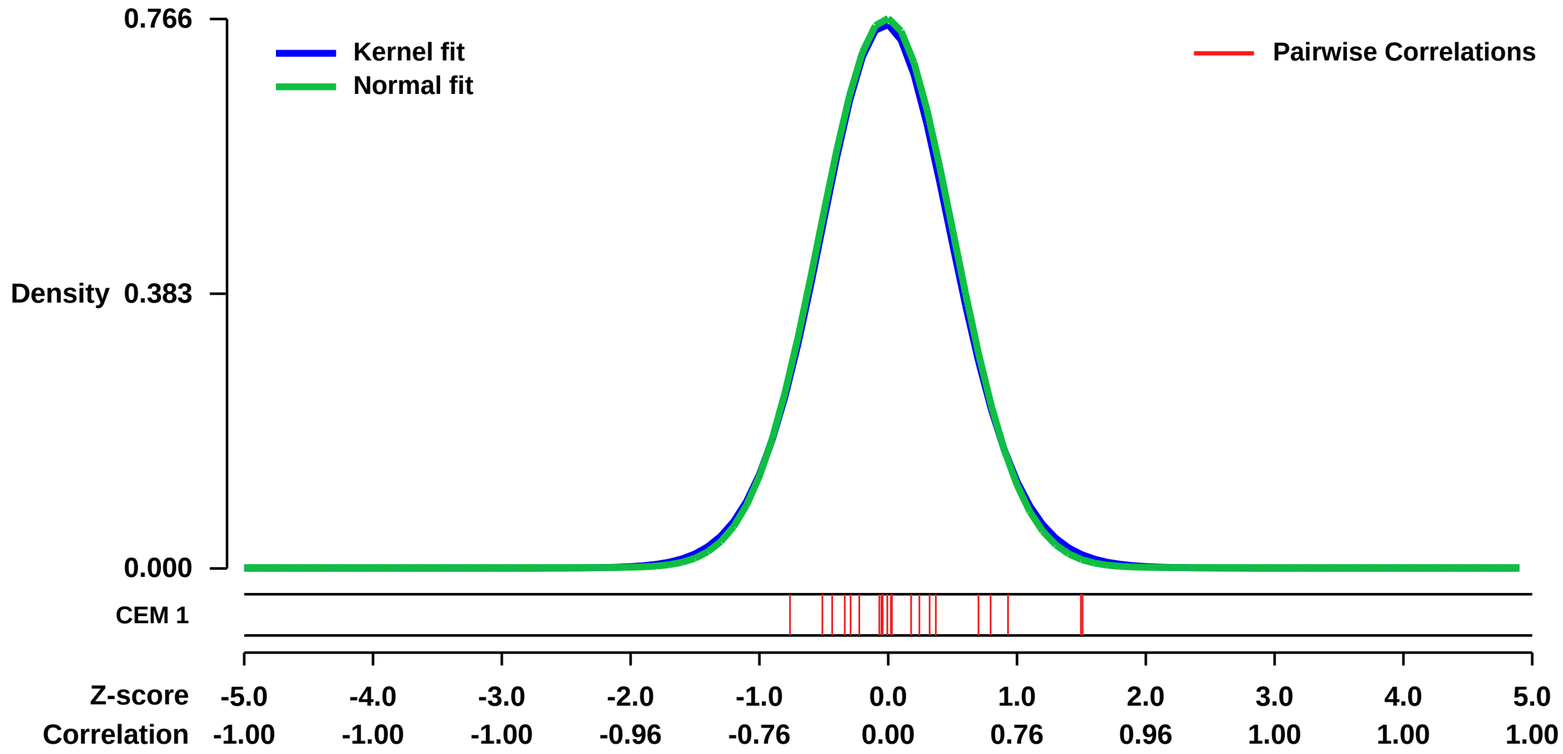

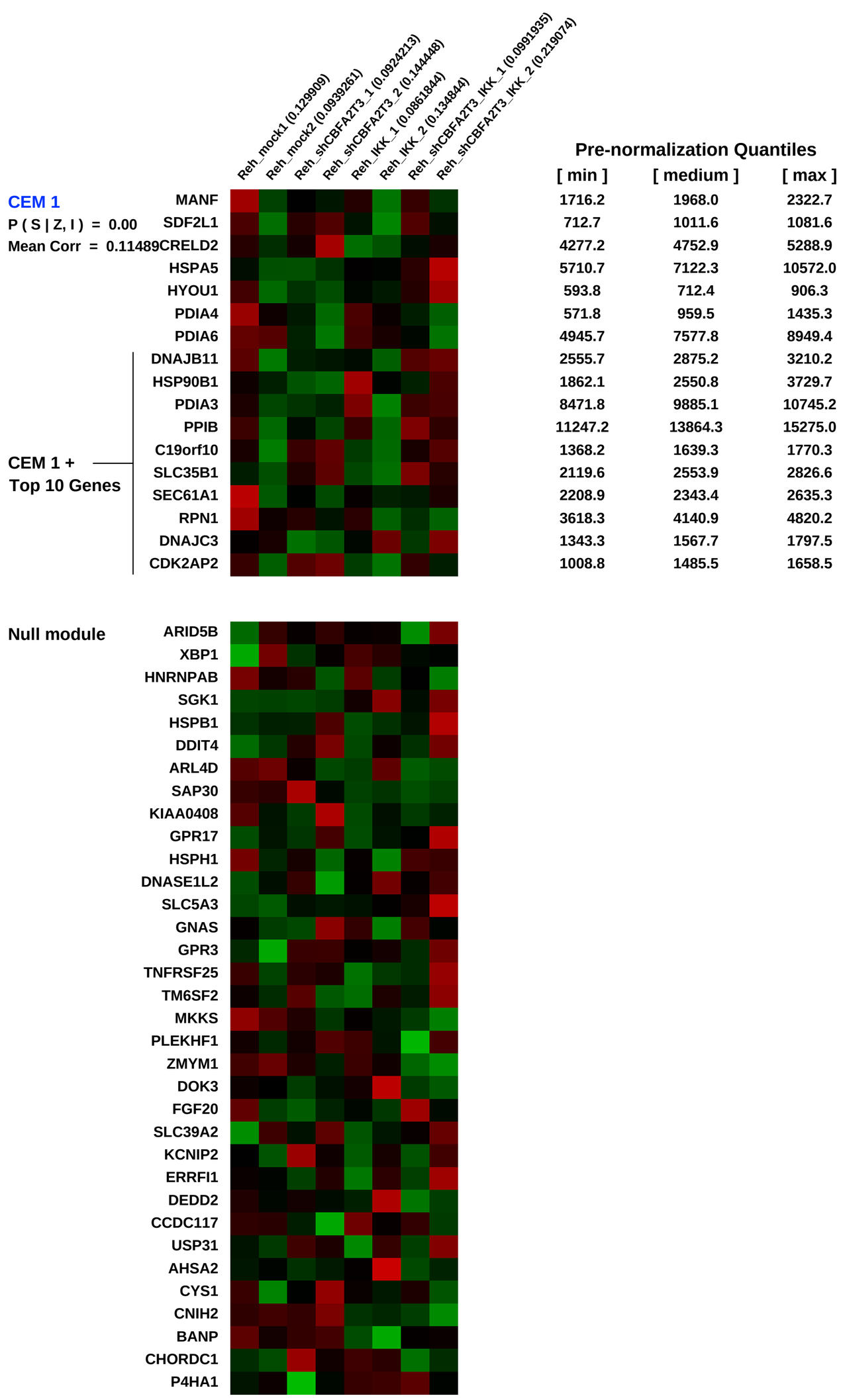

GEO Series "GSE19625" Expression Profiles

Num of samples in this series: 9

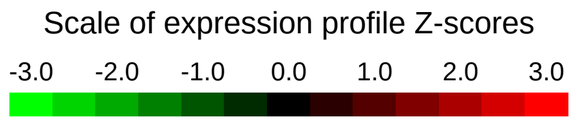

GEO Link:	http://www.ncbi.nlm.nih.gov/geo/query/acc.cgi?acc=GSE19625
Status:	Public on Dec 22 2010
Title:	Identification of LPS-inducible genes down-regulated by ubiquinone in human THP-1 cells
Organism:	Homo sapiens
Experiment type:	Expression profiling by array
Platform:	GPL570
Pubmed ID:	20533395
Summary & Design:	**Summary:** Coenzyme Q10 (CoQ10) is an obligatory element in the respiratory chain and functions as a potent antioxidant of lipid membranes. More recently, anti-inflammatory effects as well as an impact of CoQ10 on gene expression have been observed. To reveal putative effects of Q10 on LPS-induced gene expression, whole genome expression analysis was performed in the monocytic cell line THP-1. 1129 probe sets have been identified to be significantly up-regulated ($p < 0.05$) in LPS-treated cells when compared to controls. Text mining analysis of the top 50 LPS up-regulated genes revealed a functional connection in the NF$_{\kappa}$”B pathway and confirmed our applied in vitro stimulation model. Moreover, 33 LPS-sensitive genes have been identified to be significantly down-regulated by Q10-treatment between a factor of 1.32 and 1.85. GeneOntology (GO) analysis revealed for the Q10-sensitve genes a primary involvement in protein metabolism, cell proliferation and transcriptional processes. Three genes were either related to NF$_{\kappa}$”B transcription factor activity, cytokinesis or modulation of oxidative stress. In conclusion, our data provide evidence that Q10 down-regulates LPS-inducible genes in the monocytic cell line THP-1. Thus, the previously described effects of Q10 on the reduction of pro-inflammatory mediators might be due to its impact on gene expression. **Overall design:** Whole genome expression profiles were analysed from monocytes pre-incubated with ubiquinone (Q10) before subsequent stimulation with LPS. Stimulated (+LPS) and unstimulated (-LPS) monocytes were used as positive and negative controls, respectively. For every experimental group (3 groups in total), three Affymetrix Human Genome U133 Plus 2.0 arrays were used, thus resulting in the analysis of 9 microarrays.

Background corr dist: KL-Divergence = 0.0614, L1-Distance = 0.0482, L2-Distance = 0.0036, Normal std = 0.5689

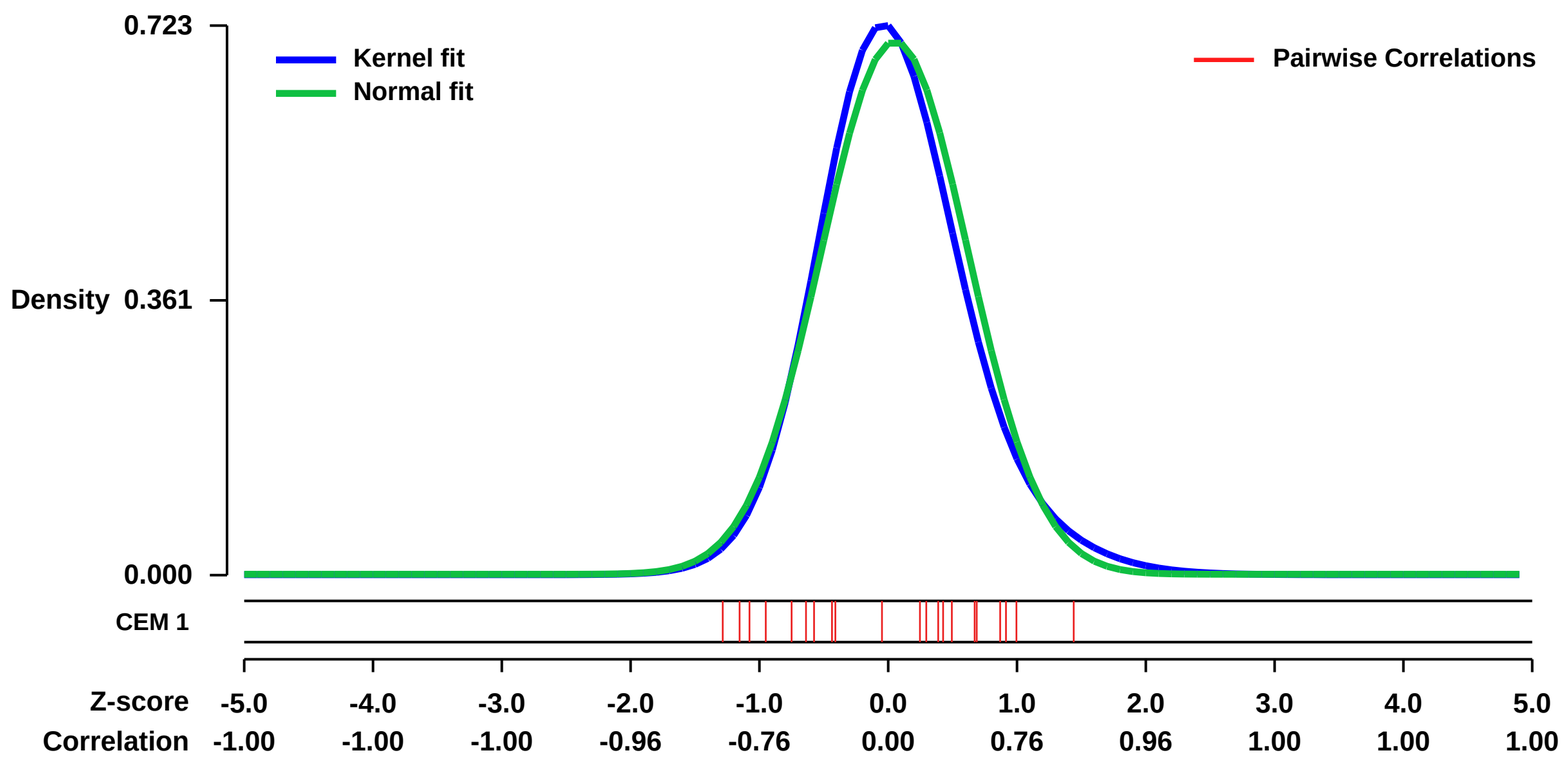

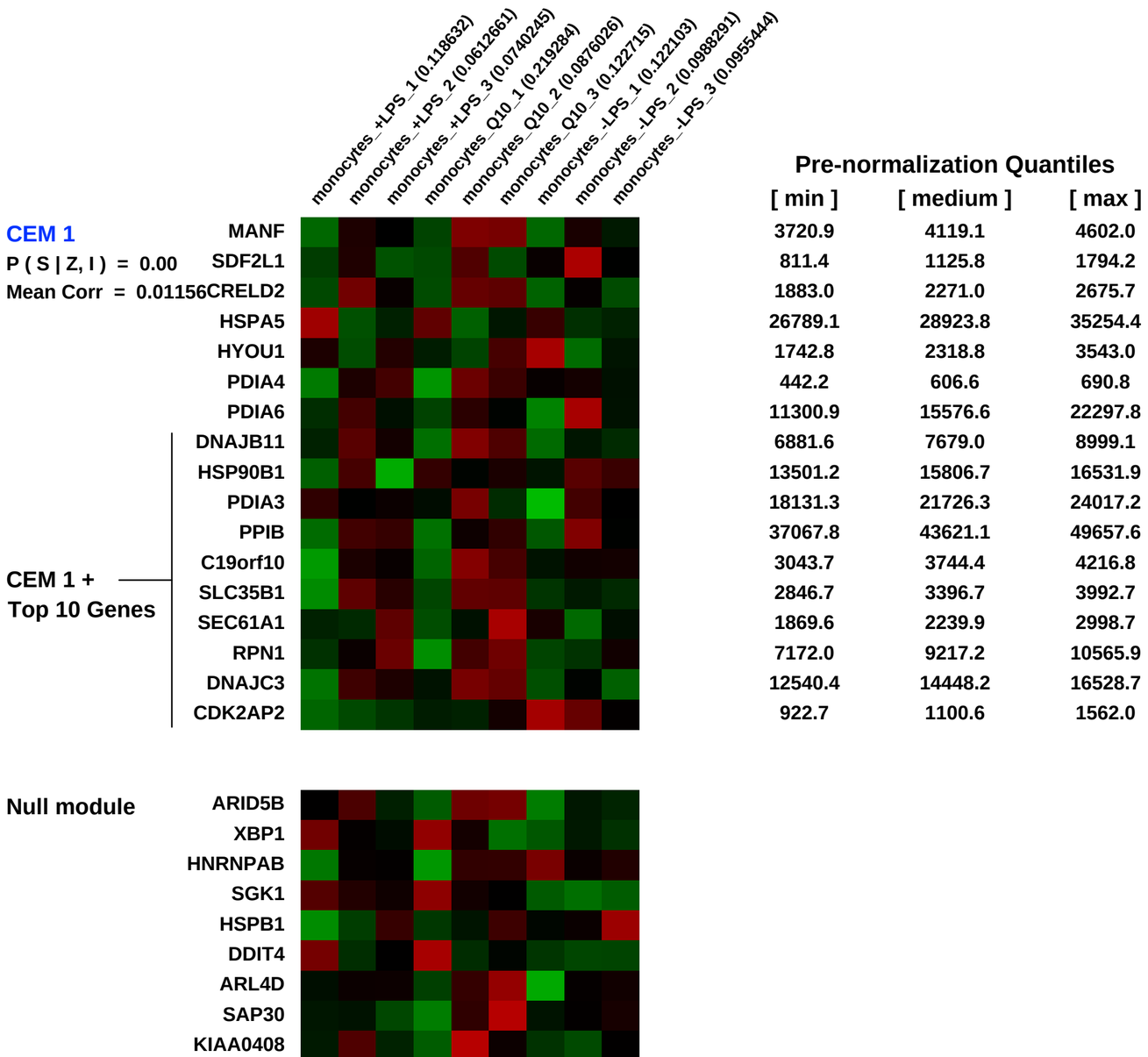

Pre-normalization Quantiles

	[min]	[medium]	[max]
MANF	3720.9	4119.1	4602.0
SDF2L1	811.4	1125.8	1794.2
CRELD2	1883.0	2271.0	2675.7
HSPA5	26789.1	28923.8	35254.4
HYOU1	1742.8	2318.8	3543.0
PDIA4	442.2	606.6	690.8
PDIA6	11300.9	15576.6	22297.8
DNAJB11	6881.6	7679.0	8999.1
HSP90B1	13501.2	15806.7	16531.9
PDIA3	18131.3	21726.3	24017.2
PPIB	37067.8	43621.1	49657.6
C19orf10	3043.7	3744.4	4216.8
SLC35B1	2846.7	3396.7	3992.7
SEC61A1	1869.6	2239.9	2998.7
RPN1	7172.0	9217.2	10565.9
DNAJC3	12540.4	14448.2	16528.7
CDK2AP2	922.7	1100.6	1562.0

GEO Series "GSE47436" Expression Profiles

Num of samples in this series: 6

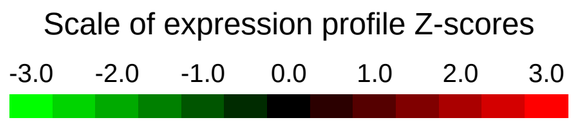

GEO Link:	http://www.ncbi.nlm.nih.gov/geo/query/acc.cgi?acc=GSE47436
Status:	Public on May 29 2013
Title:	Expression data from immortalized human lung small airway epithelial cells
Organism:	Homo sapiens
Experiment type:	Expression profiling by array
Platform:	GPL570
Pubmed ID:	
Summary & Design:	**Summary:** In lung cancer progression, p53 mutations are more often observed in invasive tumors than in non-invasive tumors, suggesting that p53 is involved in tumor invasion and metastasis. To understand the nature of p53 function as a tumor suppressor, it is crucial to elucidate the detailed mechanism of the alteration in epithelial cells, the main origin of solid tumors, following p53 inactivation. To elucidate the mechanism by which p53 loss enhances invasive and motile activities in human lung small airway epithelial cells (SAECs), we performed comprehensive expression profiling analyses between p53 knockdown and control cells using GeneChip Human Genome U133 plus 2.0 arrays. **Overall design:** SAECs were infected with lentiviruses for the expressions of CDK4 devoid of binding ability to p16INK4A, Cyclin D1 and TERT to generate immotalized SAECs. At 18 population doublings, immortalized SAECs were transfected with the siRNAs (si-control, si-p53-#1 or si-p53-#2) and used for RNA extraction and hybridization on Affymetrix microarrays.

Background corr dist: KL-Divergence = 0.0382, L1-Distance = 0.0255, L2-Distance = 0.0007, Normal std = 0.6353

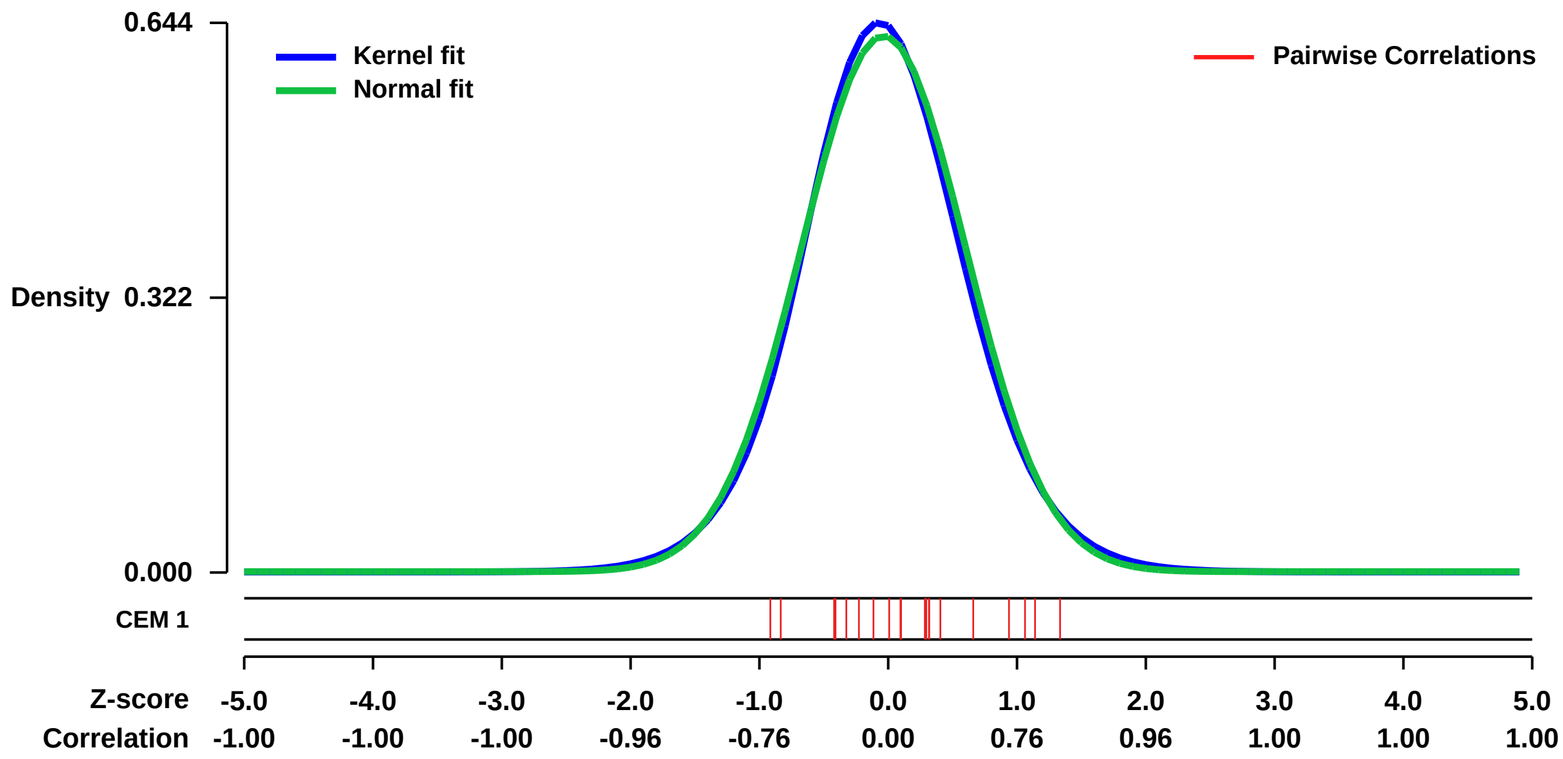

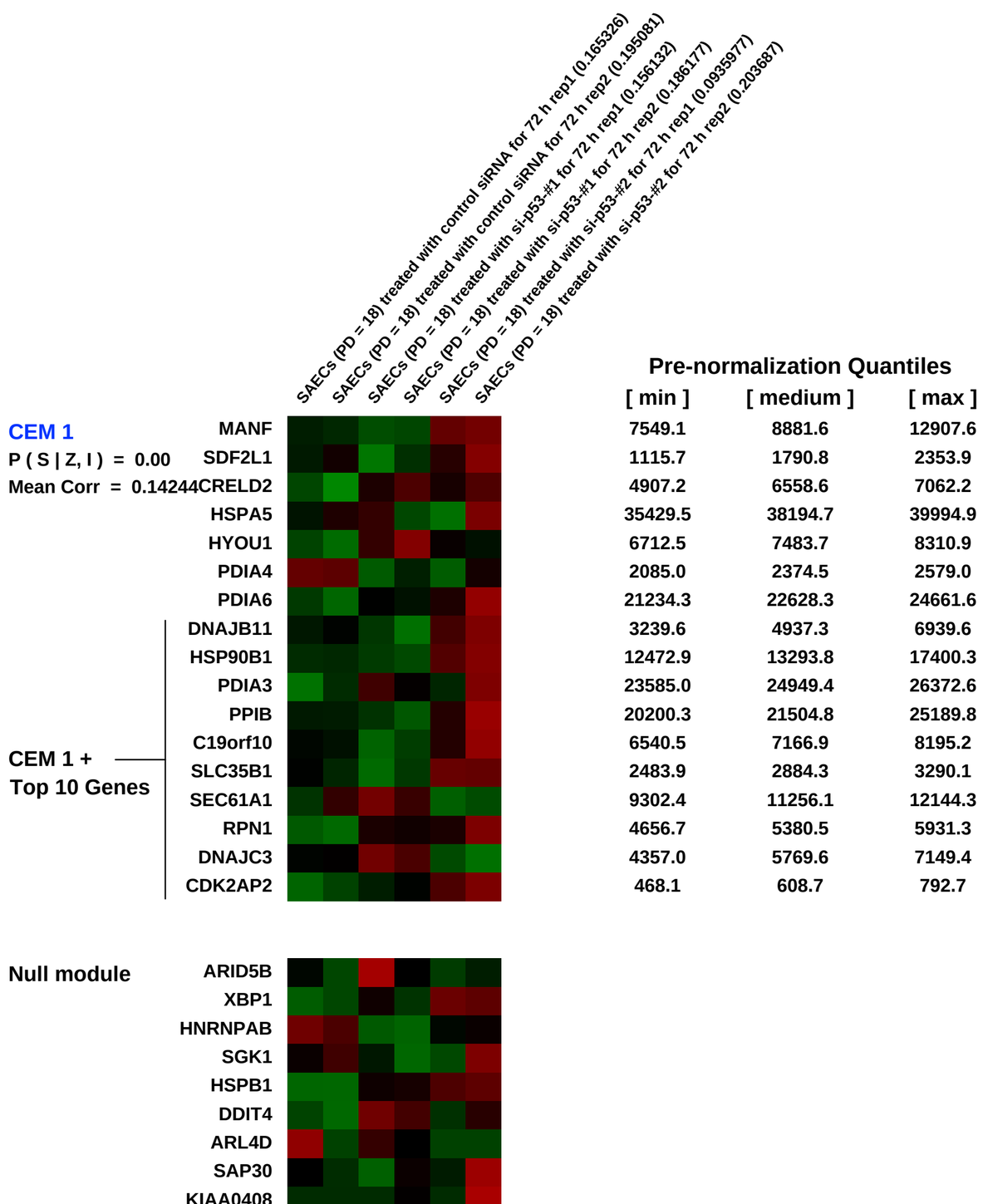

	Pre-normalization Quantiles [min]	[medium]	[max]
MANF	7549.1	8881.6	12907.6
SDF2L1	1115.7	1790.8	2353.9
CRELD2	4907.2	6558.6	7062.2
HSPA5	35429.5	38194.7	39994.9
HYOU1	6712.5	7483.7	8310.9
PDIA4	2085.0	2374.5	2579.0
PDIA6	21234.3	22628.3	24661.6
DNAJB11	3239.6	4937.3	6939.6
HSP90B1	12472.9	13293.8	17400.3
PDIA3	23585.0	24949.4	26372.6
PPIB	20200.3	21504.8	25189.8
C19orf10	6540.5	7166.9	8195.2
SLC35B1	2483.9	2884.3	3290.1
SEC61A1	9302.4	11256.1	12144.3
RPN1	4656.7	5380.5	5931.3
DNAJC3	4357.0	5769.6	7149.4
CDK2AP2	468.1	608.7	792.7
ARID5B			
XBP1			
HNRNPAB			
SGK1			
HSPB1			
DDIT4			
ARL4D			
SAP30			
KIAA0408			
GPR17			
HSPH1			
DNASE1L2			
SLC5A3			
GNAS			
GPR3			
TNFRSF25			
TM6SF2			
MKKS			
PLEKHF1			
ZMYM1			
DOK3			
FGF20			
SLC39A2			
KCNIP2			
ERRFI1			
DEDD2			
CCDC117			
USP31			
AHSA2			
CYS1			
CNIH2			
BANP			
CHORDC1			
P4HA1			

GEO Series "GSE20847" Expression Profiles

Num of samples in this series: 14

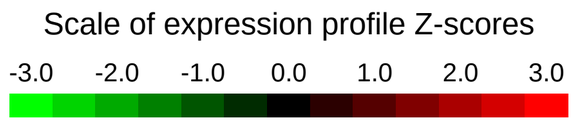

GEO Link:	http://www.ncbi.nlm.nih.gov/geo/query/acc.cgi?acc=GSE20847
Status:	Public on Mar 13 2010
Title:	Mitochondrial and nuclear genomic response to loss of LRPPRC expression
Organism:	Homo sapiens
Experiment type:	Expression profiling by array
Platform:	GPL570
Pubmed ID:	20220140

Summary & Design:

Summary:
Rapid advances in genotyping and sequencing technology have dramatically accelerated the discovery of genes underlying human disease. Elucidating the function of such genes and understanding their role in pathogenesis, however, remains challenging. Here, we introduce a genomic strategy to functionally characterize such genes, and apply it to LRPPRC (leucine-rich PPR-motif containing), a poorly studied gene that is mutated in Leigh Syndrome, French Canadian type (LSFC).

We utilize RNAi to engineer an allelic series of cellular models in which LRPPRC has been stably silenced to different levels of knockdown efficiency. Using expression profiling, we discovered a specific role for LRPPRC in the expression of all mitochondrial DNA (mtDNA)-encoded mRNAs, but not the rRNAs, without affecting nuclear genes encoding mitochondrial proteins.

Overall design:
We designed seven shRNAs targeting the LRPPRC cDNA sequence to silence its expression in MCH58 immortalized human fibroblasts. The LRPPRC expression level in these cells ranged from 9% to 100%. We demonstrated that knockdown cells carried stable silencing of the target gene and associated biochemical phenotypes. Our goal was to engineer stable knockdown cells which recapitulate the LSFC disease phenotype and subject them to expression profiling using Affymetric microarrays to identify genesets and biochemical pathways that are altered.

Background corr dist: KL-Divergence = 0.1655, L1-Distance = 0.0385, L2-Distance = 0.0029, Normal std = 0.3580

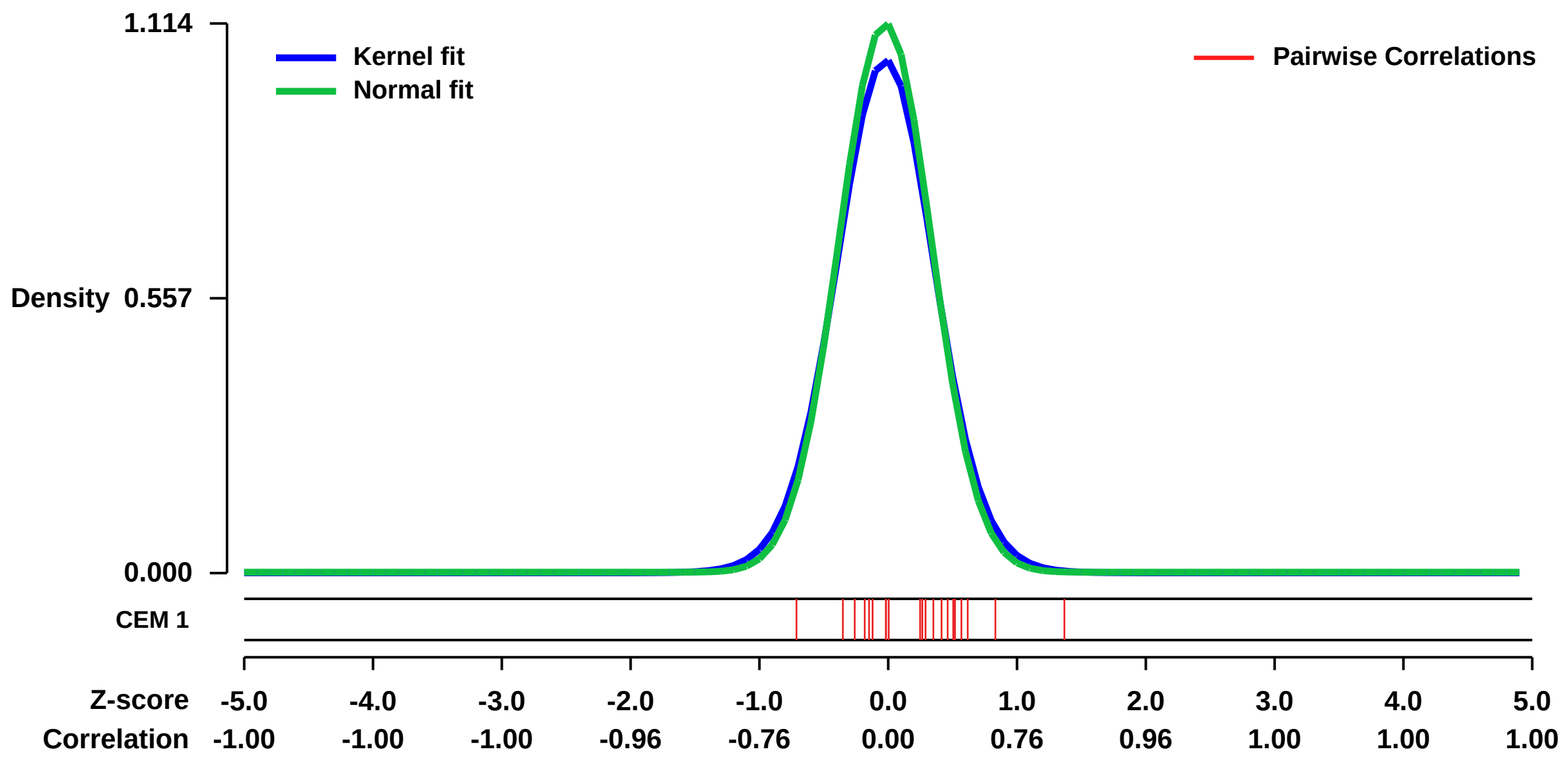

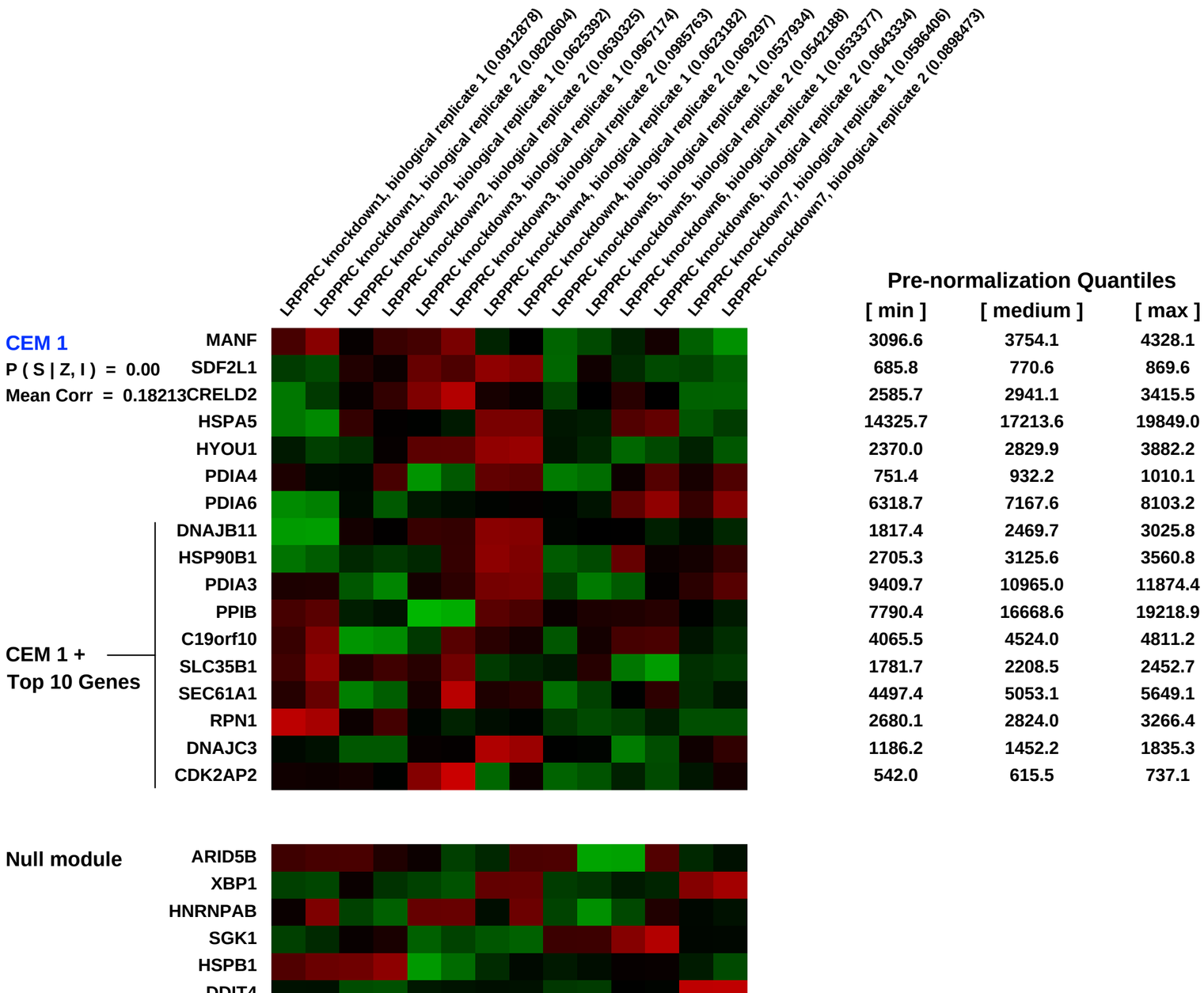

Pre-normalization Quantiles

	[min]	[medium]	[max]
MANF	3096.6	3754.1	4328.1
SDF2L1	685.8	770.6	869.6
CRELD2	2585.7	2941.1	3415.5
HSPA5	14325.7	17213.6	19849.0
HYOU1	2370.0	2829.9	3882.2
PDIA4	751.4	932.2	1010.1
PDIA6	6318.7	7167.6	8103.2
DNAJB11	1817.4	2469.7	3025.8
HSP90B1	2705.3	3125.6	3560.8
PDIA3	9409.7	10965.0	11874.4
PPIB	7790.4	16668.6	19218.9
C19orf10	4065.5	4524.0	4811.2
SLC35B1	1781.7	2208.5	2452.7
SEC61A1	4497.4	5053.1	5649.1
RPN1	2680.1	2824.0	3266.4
DNAJC3	1186.2	1452.2	1835.3
CDK2AP2	542.0	615.5	737.1

GEO Series "GSE40968" Expression Profiles

Num of samples in this series: 18

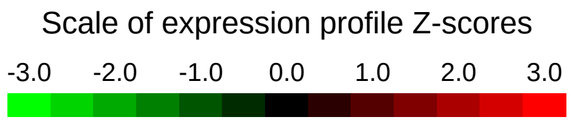

GEO Link: http://www.ncbi.nlm.nih.gov/geo/query/acc.cgi?acc=GSE40968

Status: Public on Sep 19 2012

Title: The effect of ACSL4 expression on overall gene expression in breast cancer cell lines

Organism: Homo sapiens

Experiment type: Expression profiling by array

Platform: GPL570

Pubmed ID:

Summary & Design:

Summary:
ACSL4 expression appears to be inversely associated with steroid hormone and growth factor receptor expression in breast cancer and positively correlated with an aggressive breast cancer phenotype. Neither MCF-7 nor SKBr3 cells normally express ACSL4, and when manipulated to do so, develop basal-like characteristics, including increased proliferation, migration and anchorage independent growth. We used an Affymetrix array platform to assess changes in individual gene expression as a function of conditional and stable expression of ACSL4 in MCF-7 and SKBr3 cells.

Overall design:
In experiment 1, MCF-7 Tet-ON cells were transfected with ACSL4 cDNA and induced to express ACSL4 by addition of 1ug/ml of doxycycline (A) or vehicle (C) for 72 hours. Three controls (C) and three doxycycline-induced (A) samples were evaluated for gene expression. In experiment 2, MCF-7 cells were stably transfected with either an empty vector (C) or Lenti-ORF-ACSL4 (A). In experiment 3, SKBr3 cells were stably transfected with either an empty vector (C) or Lenti-ORF-ACSL4 (A).

Background corr dist: KL-Divergence = 0.0741, L1-Distance = 0.0183, L2-Distance = 0.0003, Normal std = 0.4955

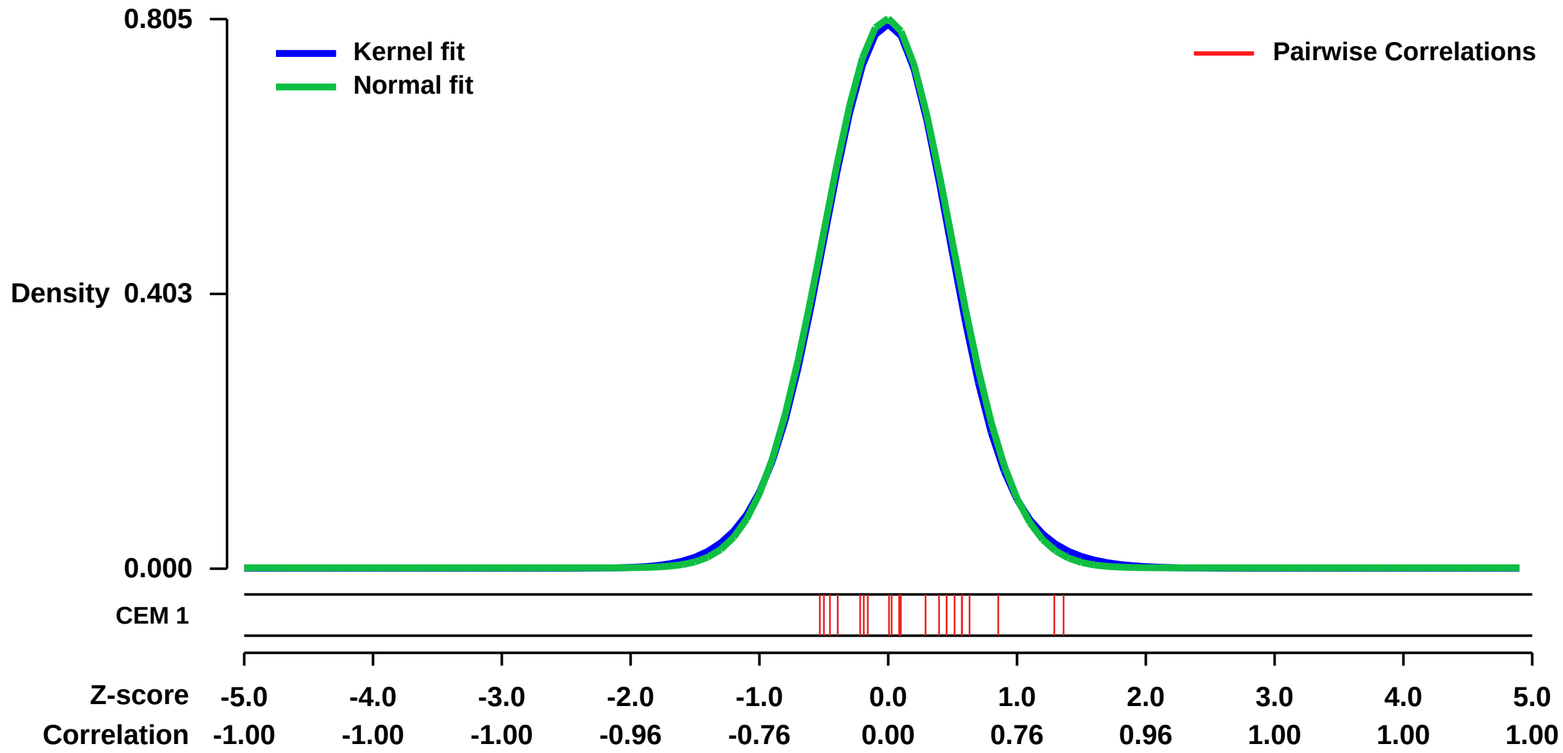

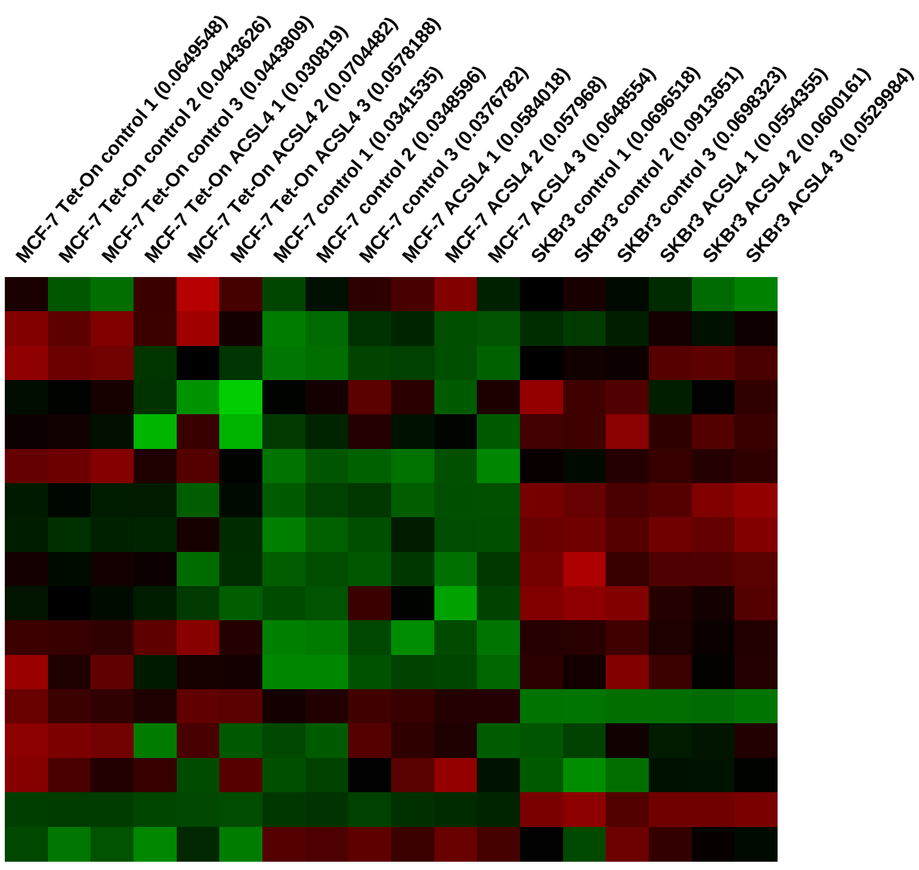

CEM 1
P (S | Z, I) = 0.00
Mean Corr = 0.16626

CEM 1 + Top 10 Genes

Null module

	Pre-normalization Quantiles [min]	[medium]	[max]
MANF	4053.2	4679.6	5551.8
SDF2L1	825.9	1626.0	2940.1
CRELD2	1797.0	3490.9	5525.5
HSPA5	8187.0	13042.1	15780.3
HYOU1	1071.5	2252.2	2976.1
PDIA4	824.2	1492.7	1905.3
PDIA6	7617.2	9481.0	14229.7
DNAJB11	4247.3	6320.5	9742.4
HSP90B1	2198.3	4945.1	8485.4
PDIA3	1324.0	3011.9	4567.5
PPIB	17598.7	23443.4	26743.9
C19orf10	603.4	1472.0	2220.5
SLC35B1	1469.1	6281.7	8386.4
SEC61A1	2583.5	3145.8	3641.8
RPN1	4565.0	5820.9	7174.6
DNAJC3	1329.7	2287.8	8406.4
CDK2AP2	1033.2	1745.7	2247.3
ARID5B			
XBP1			
HNRNPAB			
SGK1			
HSPB1			
DDIT4			
ARL4D			
SAP30			
KIAA0408			
GPR17			
HSPH1			
DNASE1L2			
SLC5A3			
GNAS			
GPR3			
TNFRSF25			
TM6SF2			
MKKS			
PLEKHF1			
ZMYM1			
DOK3			
FGF20			
SLC39A2			
KCNIP2			
ERRFI1			
DEDD2			
CCDC117			
USP31			
AHSA2			
CYS1			
CNIH2			
BANP			
CHORDC1			
P4HA1			

GEO Series "GSE27071" Expression Profiles

Num of samples in this series: 13

Scale of expression profile Z-scores

-3.0 -2.0 -1.0 0.0 1.0 2.0 3.0

GEO Link: http://www.ncbi.nlm.nih.gov/geo/query/acc.cgi?acc=GSE27071
Status: Public on May 01 2011
Title: pcaGoPromoter - An R package for functional interpretation of principal component analysis of genome-wide gene expression data
Organism: Homo sapiens
Experiment type: Expression profiling by array
Platform: GPL570
Pubmed ID:

Summary & Design:

Summary:
Background and aim: Analysis of data obtained from genome wide gene expression experiments is challenging, due to the huge amount of variables, management of the data and the need for multivariate analysis. We here present the R package: pcaGoPromoter that facilitates the interpretation of genome wide expression data to overcome these problems. In a first step principal component analysis is applied to overview any differences between the observations and possible groupings. The next step is interpretation of the principal components with respect to both biological function and involvement of predicted transcription factor binding sites. The robustness of the results is evaluated using cross validation. Illustrative plots of PCA score plots and Gene Ontology terms are available. To illustrate the functionality of the R package, we designed a serum stimulation experiment, where the main biological outcome is well documented.
Results: Samples from the serum stimulation experiment were analyzed using the Affymetrix Human Genome U133 Plus 2.0 chip. The array data were analyzed by the tools of the pcaGoPromoter package, which resulted in a clear separation of the observations into the three experimental groups - controls, serum only and serum with inhibitor. The functional annotation of the axes in the PCA score plot showed the expected serum promoted biological processes such as cell cycle progression and the predicted involvement of the expected transcription factors including E2F. In addition unexpected results, e.g. the cholesterol synthesis in serum depleted cells and NF-¸”B activation in inhibitor treated cells were uncovered. Conclusion: The pcaGoPromoter R package provides a collection of tools for analyzing gene expression data. It works with any platform using gene symbols or Entrez Ids as probe identifiers. In addition support for several popular Affymetrix GeneChip platforms is provided. The tools give an overview of the data via principal component analysis, functional interpretation by Gene Ontology terms (biological processes), and indication of involvement of possible transcription factors. Thus, pcaGoPromoter structures the high-dimensional data of gene expression experiments and can be applied to generate hypotheses for further exploration.

Overall design:
A serum starved human monocyte cell line (ATCC´fi Number: CRL-9853) was stimulated by serum in the presence or absence of the specific Erk-1/2 inhibitor U0126.

Background corr dist: KL-Divergence = 0.1291, L1-Distance = 0.0274, L2-Distance = 0.0011, Normal std = 0.3977

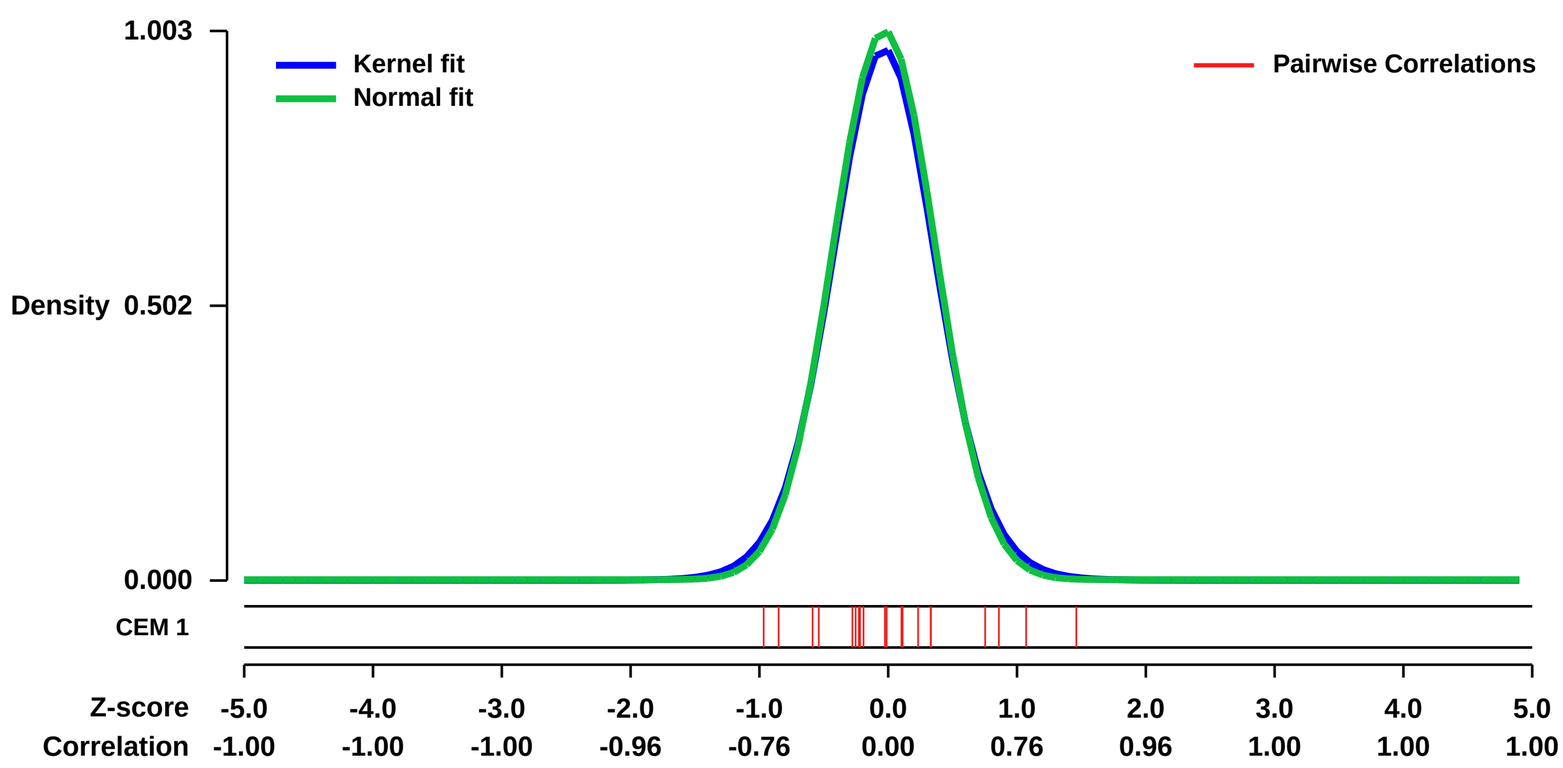

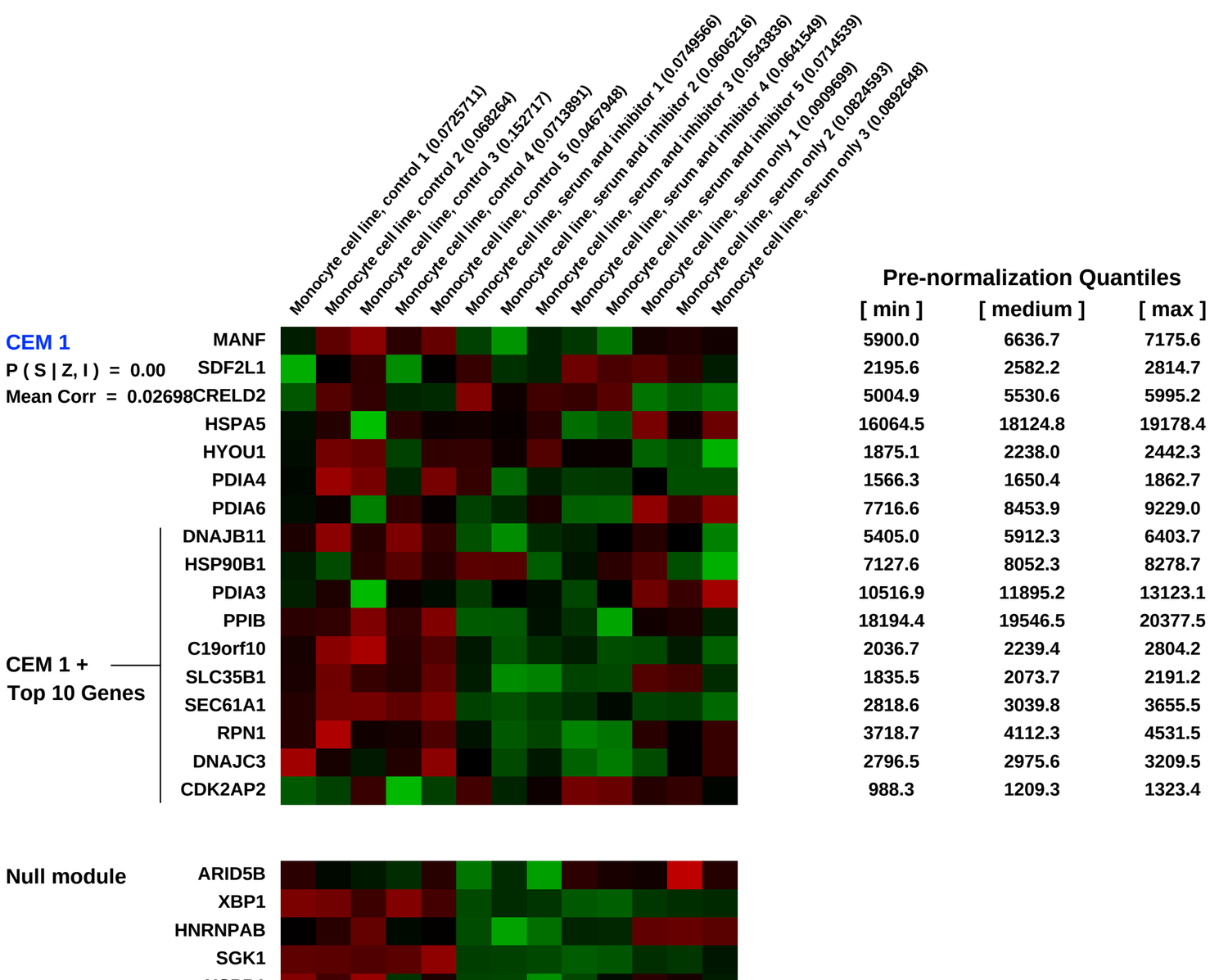

GEO Series "GSE26884" Expression Profiles

Num of samples in this series: 6

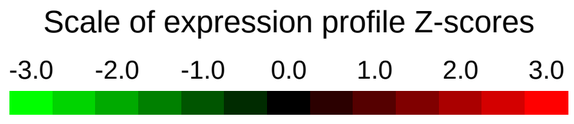

GEO Link:	http://www.ncbi.nlm.nih.gov/geo/query/acc.cgi?acc=GSE26884
Status:	Public on Feb 28 2011
Title:	Bisphenol A Induced the Expression of DNA Repair Genes in Human Breast Epithelial Cells
Organism:	Homo sapiens
Experiment type:	Expression profiling by array
Platform:	GPL570
Pubmed ID:	
Summary & Design:	**Summary:** Xenoestrogens are part of a group of agents termed endocrine disruptors because of their capacity to perturb normal hormonal actions. It has been suggested that xenoestrogens may contribute to the development of hormone-dependent cancers, such as breast and endometrial cancers. Bisphenol A (BPA) is polymerized to manufacture polycarbonate plastic and epoxy resins. Human exposure occurs when BPA leaches from plastic-lined food and beverage cans. In the present work we are aiming to determine if BPA has carcinogenic properties by using an in vitro system. For this purpose, the human breast epithelial cells MCF-10F were treated with 10-3M to 10-9M BPA continuously for two weeks. The MCF-10F cells treated with 10-3M and 10-4M BPA died, indicating that these concentrations were toxic for the human breast epithelial cells. The cells treated with 10-5M to 10-9M BPA were evaluated for formation of solid masses in collagen and invasion capacity, both phenotypes that are indicators of cell transformation. MCF-10F treated with 10-5M, 10-6M, 10-7M, 10-8M and 10-9M BPA formed a high percentage of solid masses (34.6%, 20%, 42.4%, 31.8% and 32.2%, respectively). Ten passages after BPA treatments, the invasive capacities of the cells were evaluated using Boyden chambers. The invasion capacity was lower in the cells treated at high concentrations of BPA (10-5M and 10-6M), and there was an increased invasion for the cells treated at low BPA concentration (10-9M), although in all the cases the differences were not significant to the controls. Expression and DNA methylation analysis were performed with the cells treated with 10-5M and 10-6M BPA. We found that these cells showed an increased expression of BRCA1, BARD1, CtIP, RAD51 and BRCC3, all genes involved in DNA repair, and downregulation of PDCD5 and BCL2L11 (also known as BIM), both involved in apoptosis. The upregulation of CtIP was related to hypomethylation of the promoter/exon1 of this gene. Furthermore, BPA induced silencing of BCL2L11 by hypermethylation. This is the first demonstration that BPA induces neoplastic transformation of breast epithelial cells and that aberrant DNA methylation of genes involved in DNA repair and apoptosis could be involved in the initiation of the neoplastic process. **Overall design:** MCF-10F, a normal-like Homo sapiens breast epithelial cell (HBEC) line that is ERa-negative PR-negative, was maintained in high calcium medium at 37´℃ and 5% CO2 until confluent. These cells were treated with different concentrations of BPA continuously for two weeks, adding fresh media every day. As controls, MCF-10F cells were not treated and maintained in the regular media or treated with 0.284% DMSO (vehicle). The cells treated with 10-5M or 10-6M BPA after the invasion assay were collected and expanded during 6 passages. RNA was isolated from the cells using an RNA extraction kit (Qiagen).

Background corr dist: KL-Divergence = 0.0192, L1-Distance = 0.0224, L2-Distance = 0.0007, Normal std = 0.7534

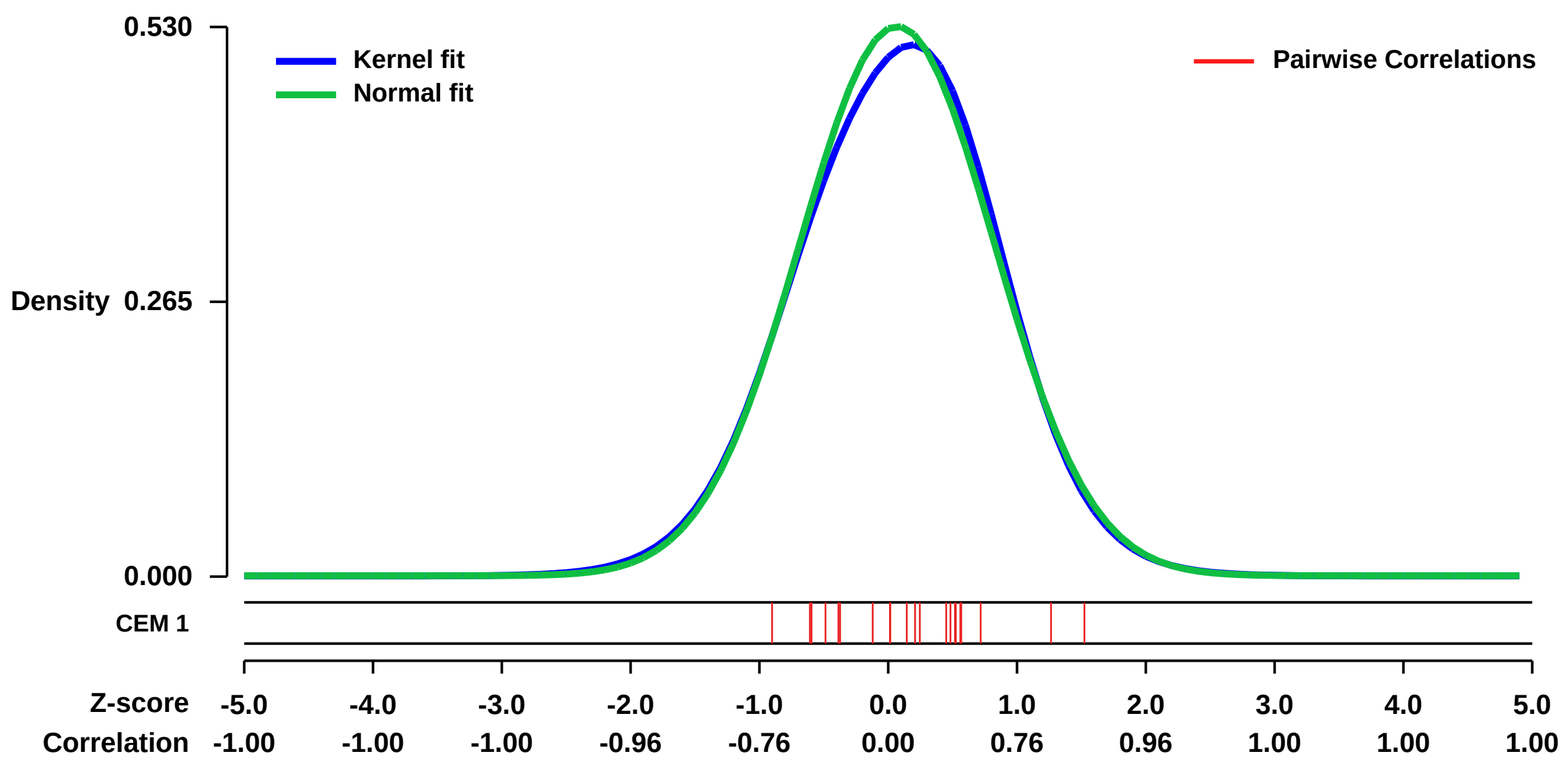

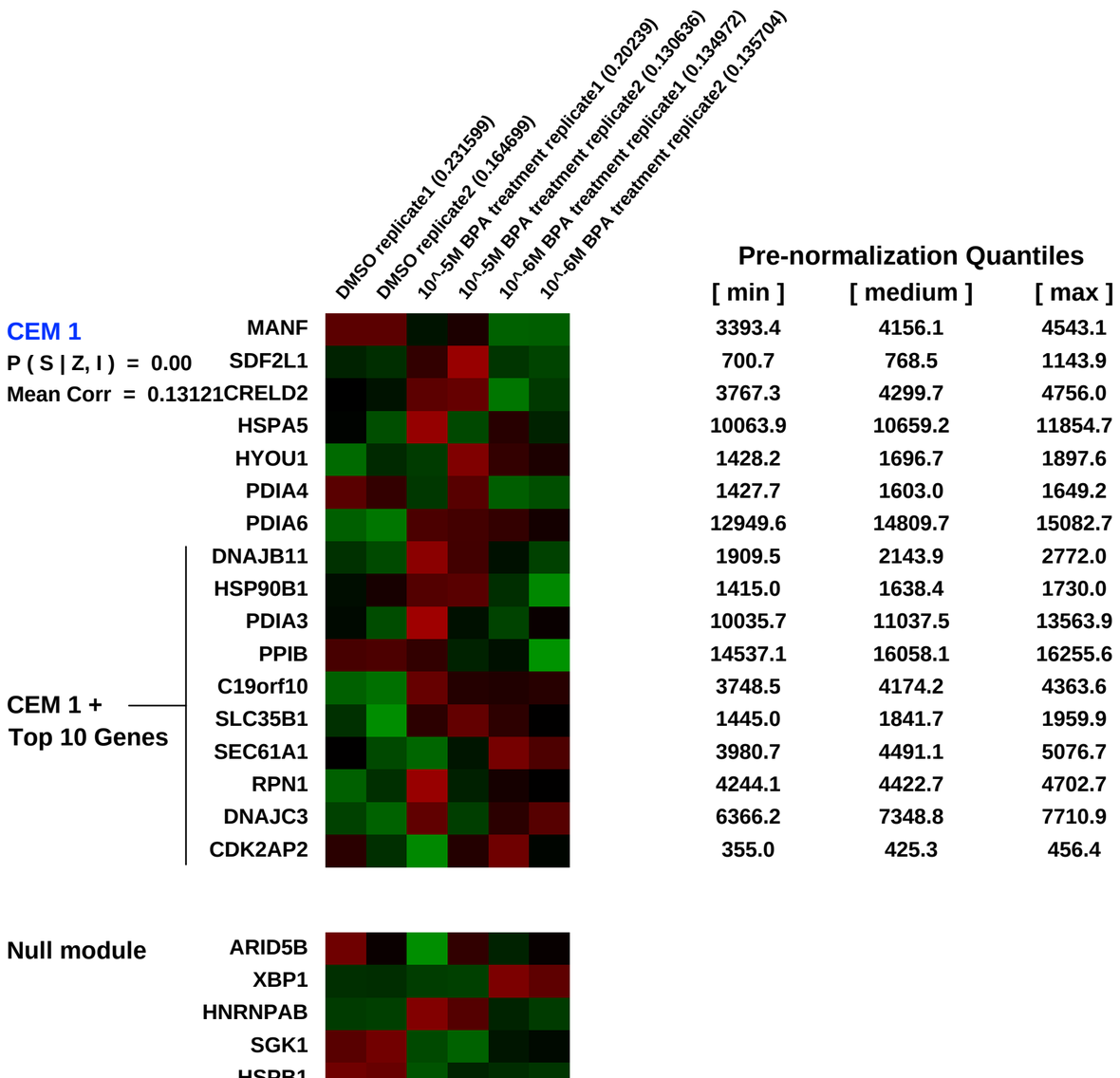

GEO Series "GSE4567" Expression Profiles

Num of samples in this series: 8

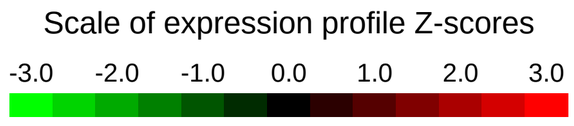

GEO Link:	http://www.ncbi.nlm.nih.gov/geo/query/acc.cgi?acc=GSE4567
Status:	Public on Jan 26 2007
Title:	Endothelial cell culture with Chapel Hill Ultrafine particle
Organism:	Homo sapiens
Experiment type:	Expression profiling by array
Platform:	GPL570
Pubmed ID:	17450221

Summary & Design:

Summary:
Epidemiology studies have linked exposure to pollutant particles to increased cardiovascular mortality and morbidity, however, the mechanism remains unknown. In this study, we hypothesized that the ultrafine fraction of ambient pollutant particles would cause endothelial cells dysfunction. We profiled gene expression of human pulmonary artery endothelial cells (HPAEC) exposed to ultrafine Chapel Hill particles (UFP) (100¸…g/ml) or vehicle for 4h with Affymetrix HG U133 Plus 2.0 chips (N = 4 each). Using an unpaired t-test (p <0.01, 5% false discovery rate) we found 426 unique genes to be differentially expressed with 320 upregulated genes and 106 downregulated genes. Among these genes, we noted upregulation of genes related to coagulation-inflammation circuitry including tissue factor (F3), coagulation factor II receptor-like 2 (F2RL2, PAR3), interleukin (IL)-6 and IL-8. Upregulation of these genes were independently confirmed by RT-PCR and/or protein release. Genes related to the CXC chemokine family that have been implicated in the pathogenesis of vascular disease were upregulated, including MCP-1 (2.60 fold), IL-8 (2.47 fold), CXCL1 (1.41 fold), CXCL2 (1.95 fold), CXCL3 (2.28 fold) and CXCR4 (1.30 fold). In addition, genes related to clotting independent signaling of F3 were also differentially expressed, including FOS, JUN and NFKBIA. Treatment of HPAEC with UFP for 16 hours increased the release of IL6 and IL8 by 1.9-fold and 1.8-fold respectively. Pretreatment of HPAEC with a blocking antibody against F3 attenuated IL6 and IL8 release by 30% and 70% respectively. Thus using gene profiling, we uncovered that UFP may induce vascular endothelial cells to express genes related to clotting and angiogenesis. These results provide a novel hypothesis that PM may cause cardiovascular adverse health effects via induction of tissue factor in vascular endothelial cells which then triggers clotting dependent and independent downstream signaling.

Keywords: particle treatment

Overall design:
Human pulmonary artery endothelial cell cultures were treated with Chapel Hill Ultrafine particles or with vehicle control for 4h. 4 bological replicates each for treatment (100ug/ml) and control. 8 affy chips total.

Background corr dist: KL-Divergence = 0.0892, L1-Distance = 0.0223, L2-Distance = 0.0007, Normal std = 0.4568

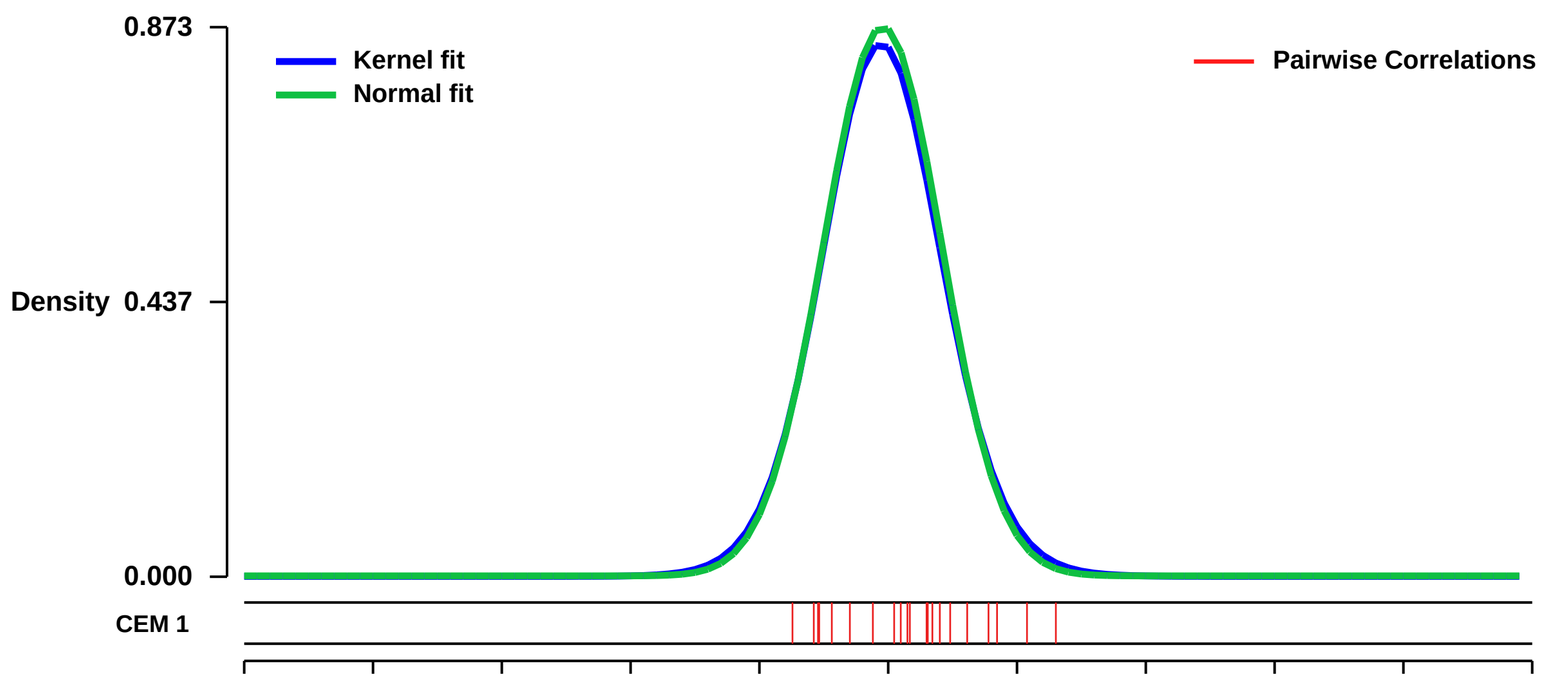

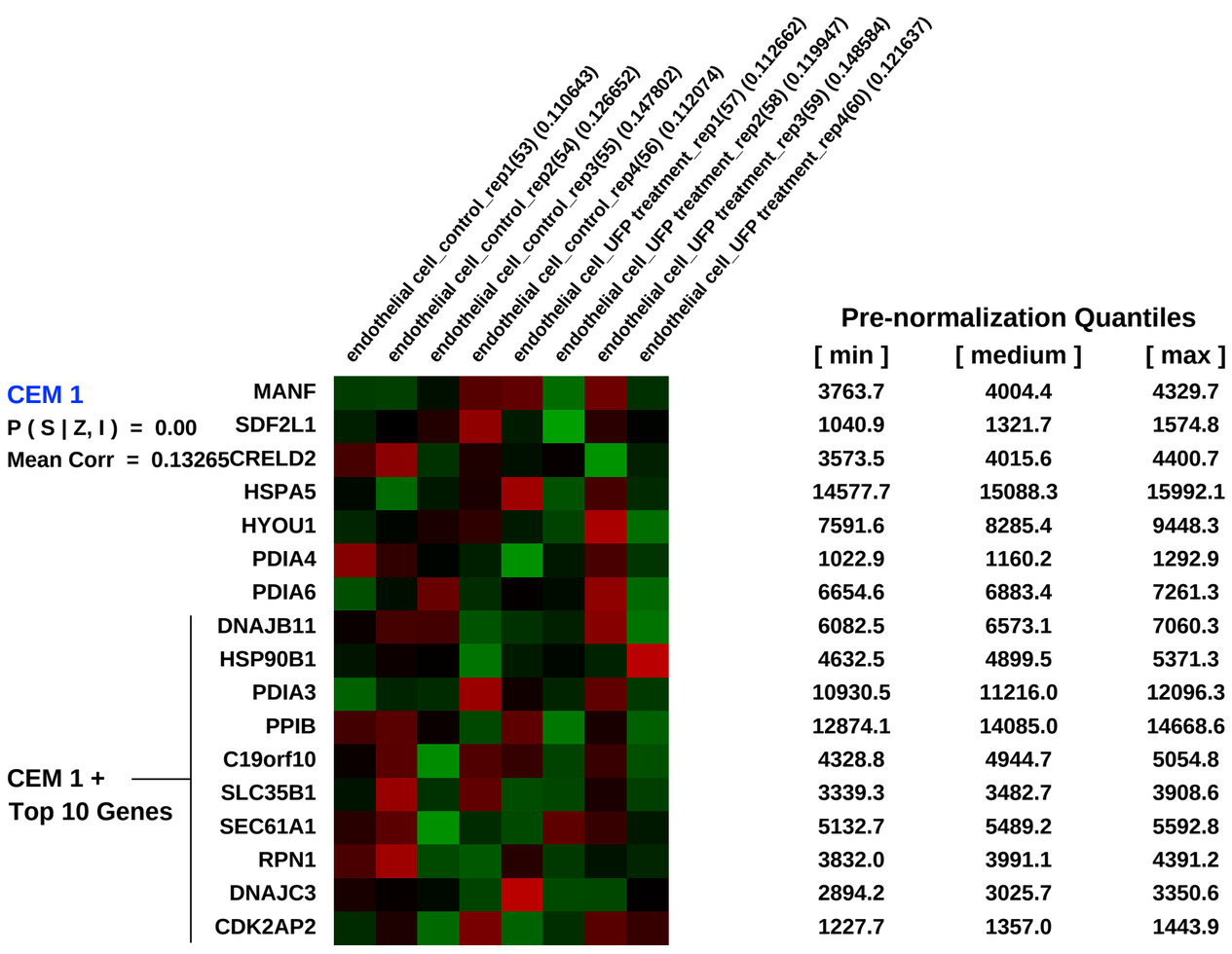

GEO Series "GSE12444" Expression Profiles

Num of samples in this series: 6

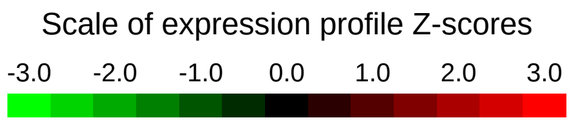

GEO Link:	http://www.ncbi.nlm.nih.gov/geo/query/acc.cgi?acc=GSE12444
Status:	Public on Nov 01 2008
Title:	FOXF2-regulated genes in human primary prostate stromal cells
Organism:	Homo sapiens
Experiment type:	Expression profiling by array
Platform:	GPL570
Pubmed ID:	19562724
Summary & Design:	**Summary:** To identify the genes and pathways regulated by FOXF2, we investigated potential FOXF2 gene targets by microarray analyses of primary prostate stromal cells (PrSC) in which FOXF2 was knocked down by siRNA. 190 differentially expressed genes were selected, of which 104 genes were more highly expressed in PrSC cells treated with FOXF2 siRNA and 86 were more highly expressed in PRSC cells treated with negative control siRNA. **Overall design:** In each experiment, we compared gene expression of PrSC cells treated with FOXF2 siRNA versus PrSC cells treated with negative control siRNA, in a total of 6 affymetrix arrays. 190 differentially expressed genes were selected (ratio negative control siRNA/siRNA â¥ 2log |0.8| as average in all arrays).

Background corr dist: KL-Divergence = 0.0385, L1-Distance = 0.0229, L2-Distance = 0.0006, Normal std = 0.6261

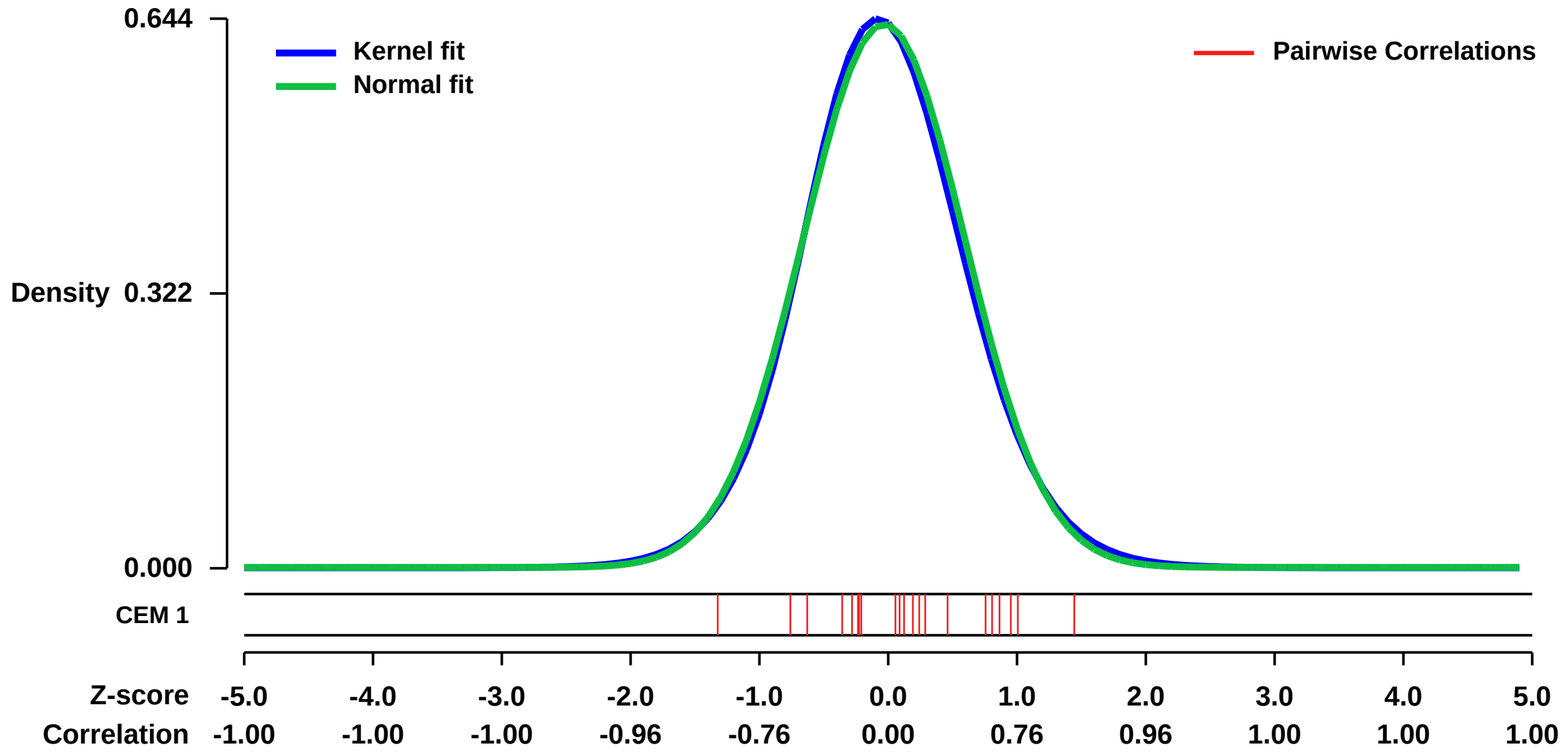

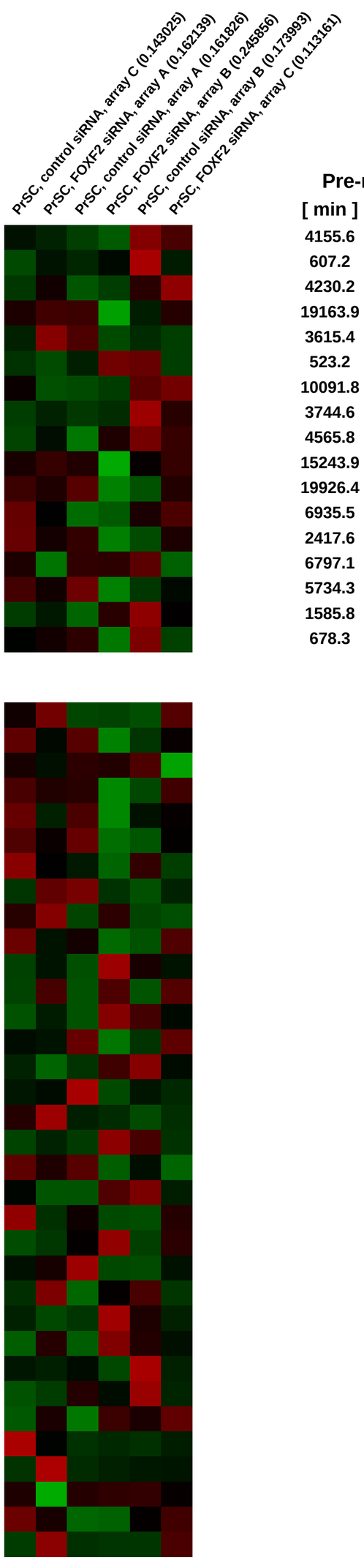

GEO Series "GSE26656" Expression Profiles

Num of samples in this series: 24

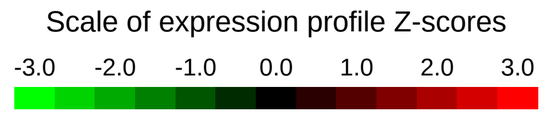

GEO Link:	http://www.ncbi.nlm.nih.gov/geo/query/acc.cgi?acc=GSE26656
Status:	Public on Jun 05 2012
Title:	Gene expression profiles of Wnt-1 overexpressing melanoma
Organism:	Homo sapiens
Experiment type:	Expression profiling by array
Platform:	GPL570
Pubmed ID:	22572818
Summary & Design:	**Summary:** We aimed to analyze the effects of Wnt-1 overexpression on the mRNA expression profile of human melanoma in a mouse xenograft model and correlated the results with then presence or absence of lymphangiogenesis and metastasis. Affymetrix gene expression analysis revealed activation of canonical and non-canonical targets genes in response to Wnt-1 as compared with controls. In regard to lymphangiogenic factors, the amount of VEGF-C was the single best marker to correlate with the amount of lymph-angiogenesis. **Overall design:** mRNA expression array of human melanoma orthotopically grown in SCID mice. Comparison includes mRNA expression profile of two melanoma cell-lines (A375 and M24met) stably overexpressing control vector or Wnt-1 treated with or without CsA. Comparison #1 comprised Wnt-1 versus control in A375 and M24met melanoma, respectively. Comparison #2 comprised Wnt-1 + Cyclosporine A (CsA) versus Wnt-1 without CsA.

Background corr dist: KL-Divergence = 0.0546, L1-Distance = 0.0287, L2-Distance = 0.0015, Normal std = 0.5446

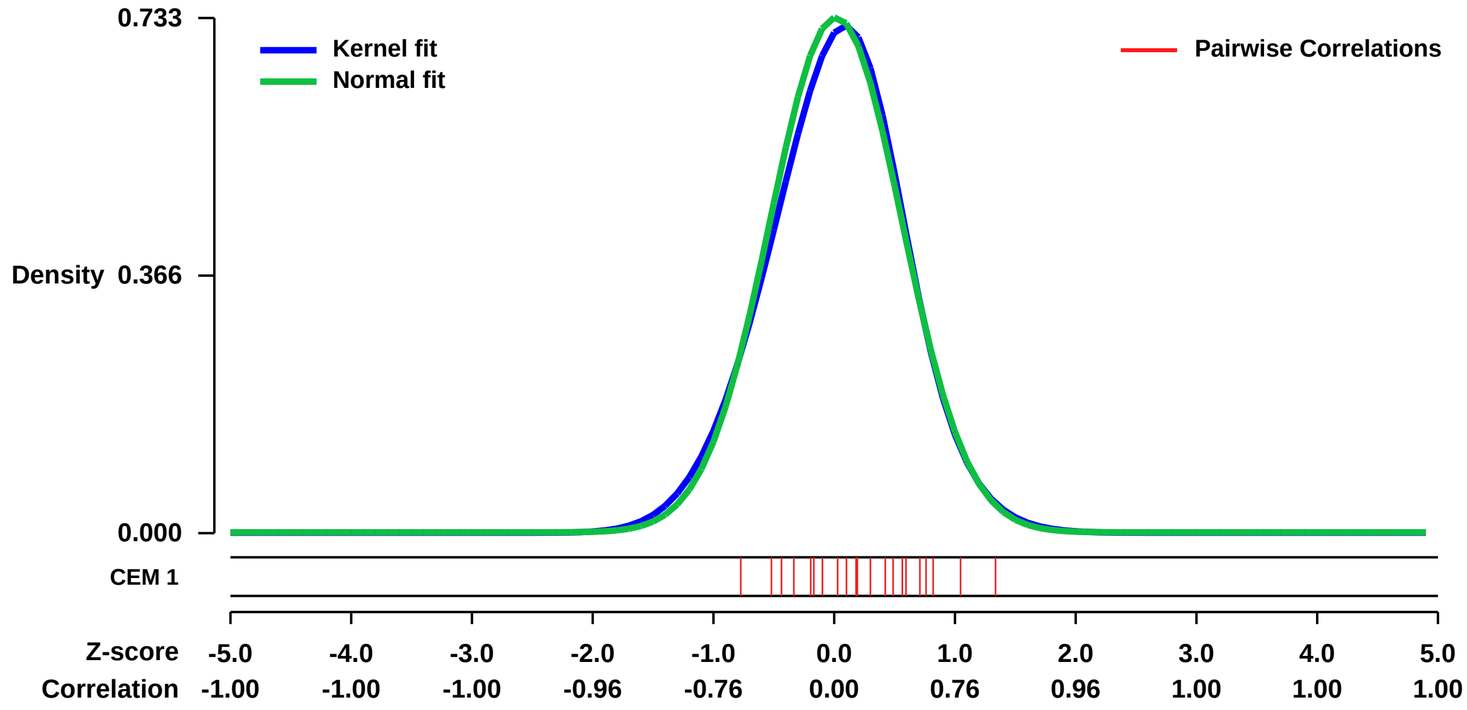

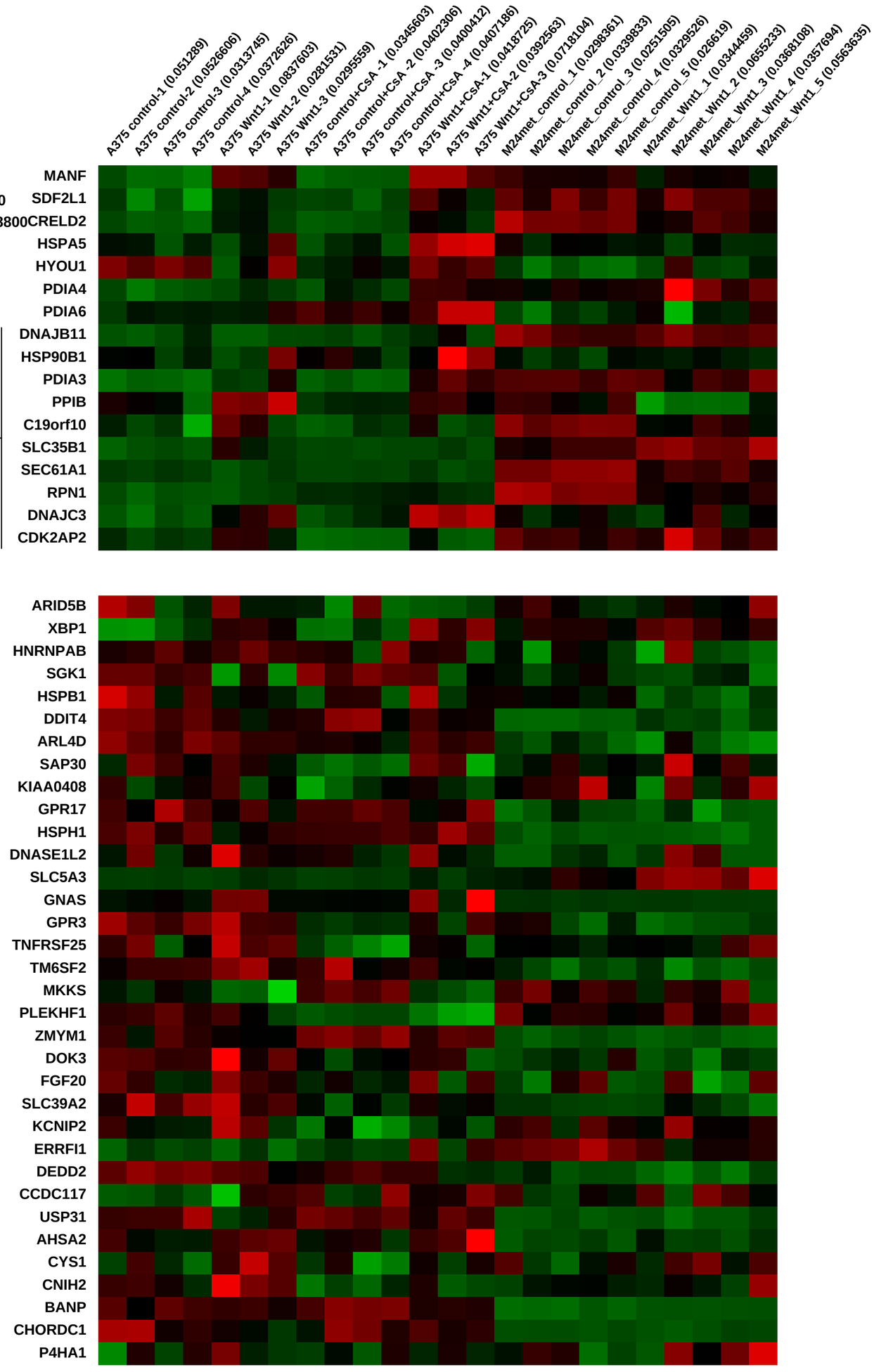

GEO Series "GSE31518" Expression Profiles

Num of samples in this series: 18

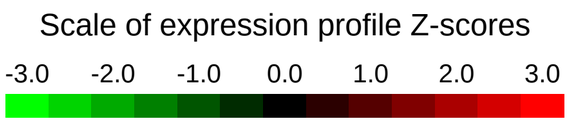

GEO Link:	http://www.ncbi.nlm.nih.gov/geo/query/acc.cgi?acc=GSE31518
Status:	Public on Jan 03 2013
Title:	Host cell gene expression in Influenza A virus (A/Singapore/478/2009 (pH1N1)) infected A549 cells at 2, 4, 6, 8 and 10 hours post infection
Organism:	Homo sapiens
Experiment type:	Expression profiling by array
Platform:	GPL570
Pubmed ID:	22470468
Summary & Design:	**Summary:** We used the microarray data to analyze host cells response on A549 cells infected with Influenza A virus (A/Singapore/478/2009 (pH1N1)) **Overall design:** The Influenza A virus (A/Singapore/478/2009 (pH1N1)) infected A549 cells were harvested at 2, 4, 6, 8 and 10 hpi and RNA extraction was performed using standard protocol as described by Affymetrix. The aim of this experiment is to analyze host response to Influenza A virus (A/Singapore/478/2009 (pH1N1)) infection.

Background corr dist: KL-Divergence = 0.1720, L1-Distance = 0.0292, L2-Distance = 0.0014, Normal std = 0.3584

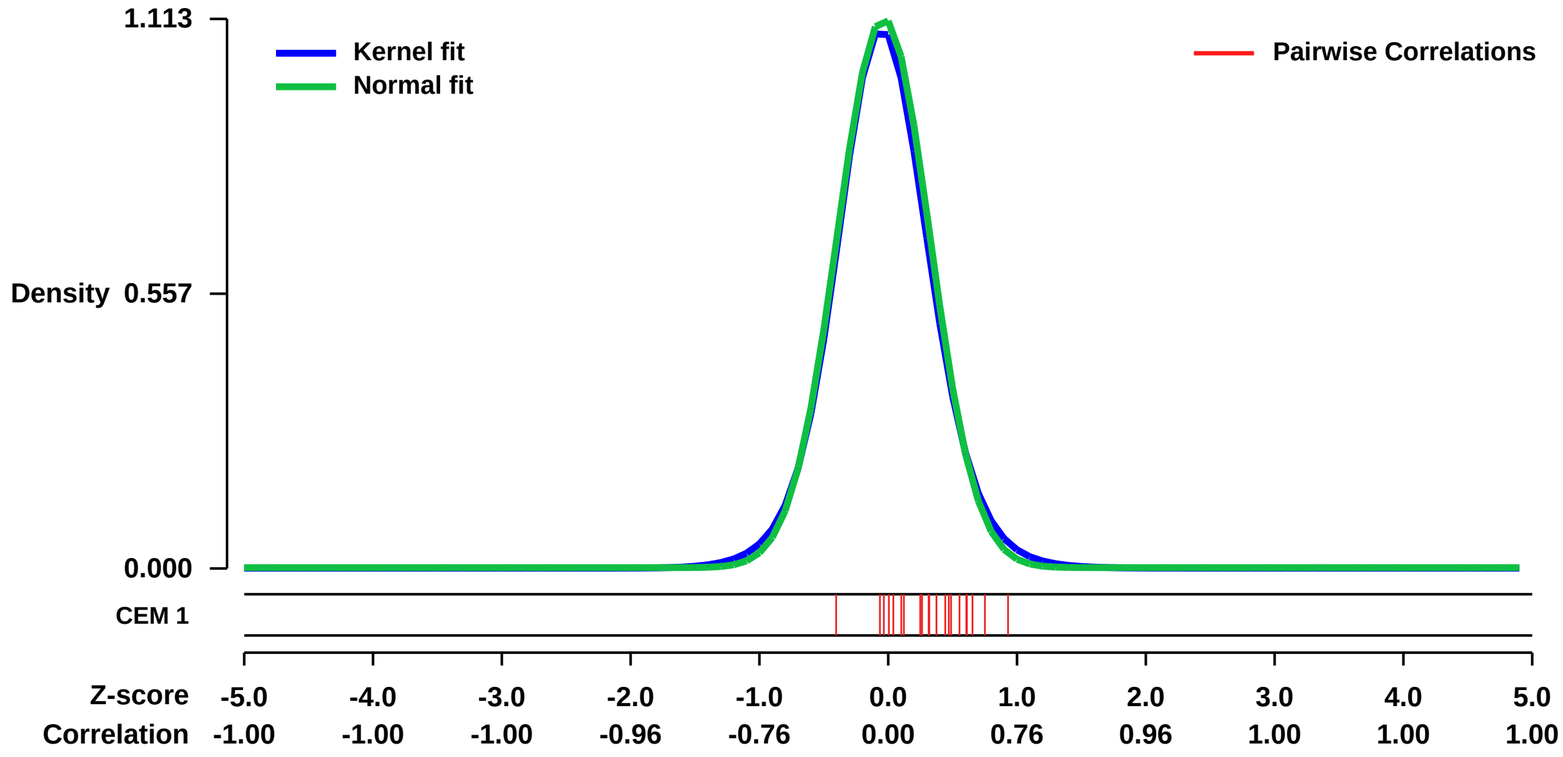

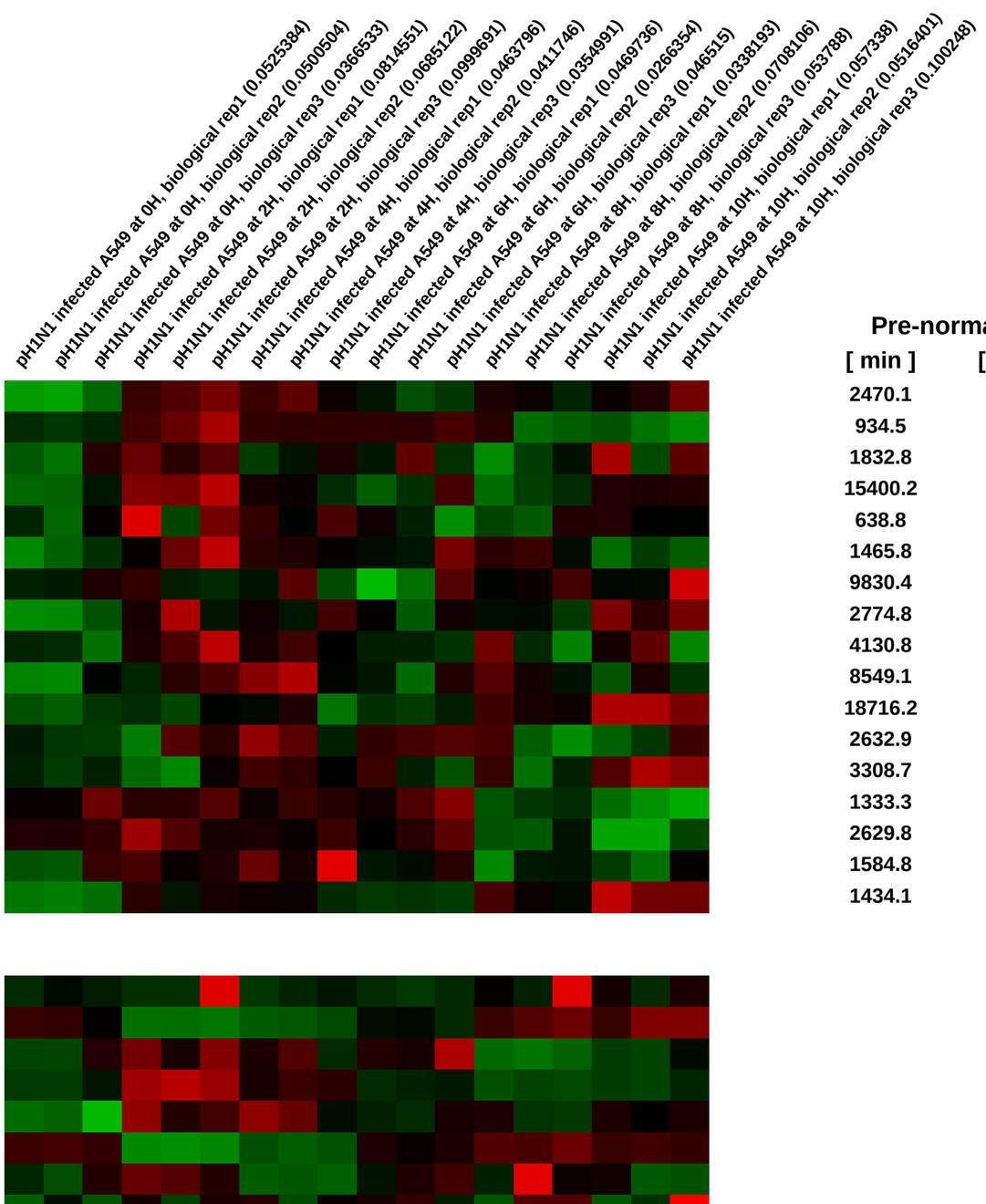

GEO Series "GSE13506" Expression Profiles

Num of samples in this series: 49

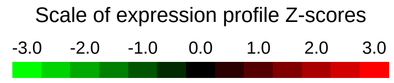

GEO Link:	http://www.ncbi.nlm.nih.gov/geo/query/acc.cgi?acc=GSE13506
Status:	Public on Jan 13 2009
Title:	Galanin preproprotein is associated with elevated plasma triglycerides
Organism:	Homo sapiens
Experiment type:	Expression profiling by array
Platform:	GPL570
Pubmed ID:	18988886
Summary & Design:	**Summary:** Assessment of mRNA expression levels in fat biopsies from subcutaneous adipose tissue from unrelated individuals. **Keywords: Subcutaneous adipose tissue.** **Overall design:** Subcutaneous adipose tissue from 49 unrelated individuals.

Background corr dist: KL-Divergence = 0.1345, L1-Distance = 0.0952, L2-Distance = 0.0215, Normal std = 0.4235

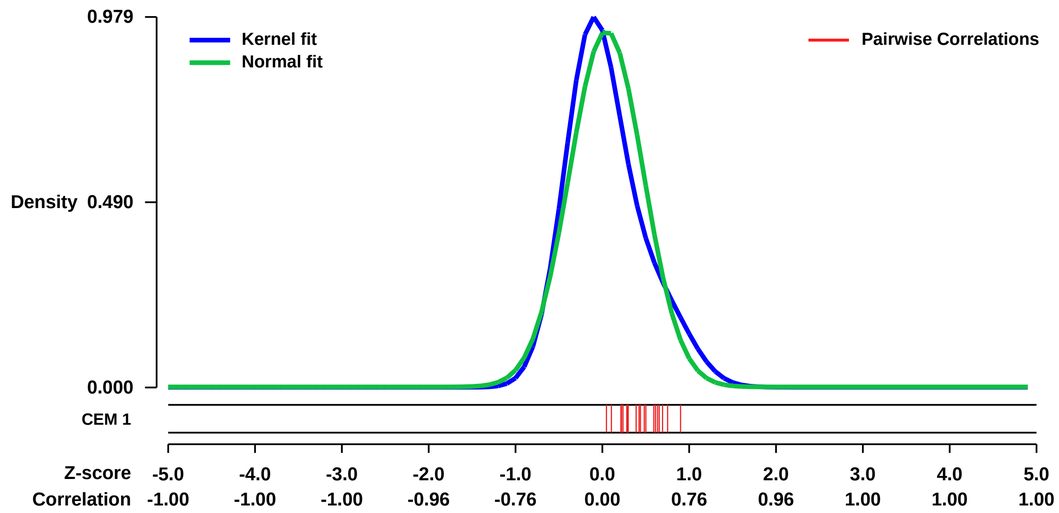

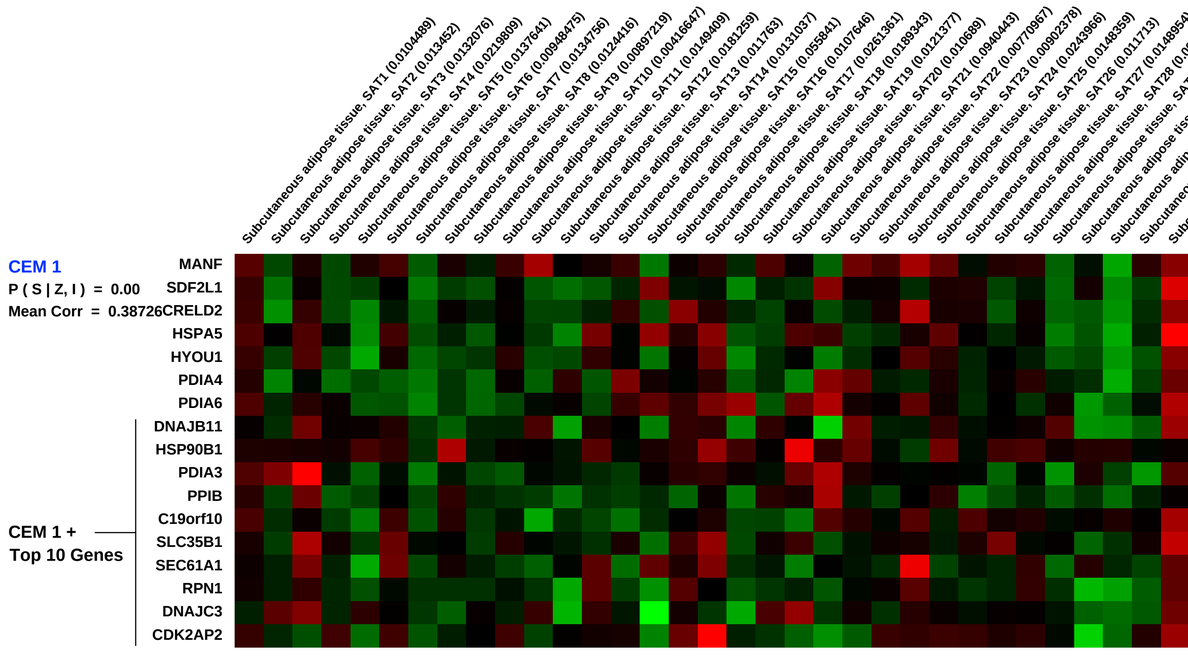

Pre-normalization Quantiles

[min]	[medium]	[max]
1183.9	1581.0	1926.6
221.3	351.9	569.7
1208.0	1486.2	1930.7
3159.5	4335.9	6256.1
648.5	1123.9	1636.7
235.4	348.1	493.7
3315.6	3975.4	4773.5
1087.5	1676.5	2083.1
2107.7	3211.4	4763.5
3785.1	5041.0	7303.7
10699.3	12693.0	16211.4
739.5	1118.4	1422.4
441.9	952.2	1267.2
1758.1	2120.6	2720.9
1952.1	2551.5	3221.6
1284.4	1960.5	2367.2
266.7	620.8	1082.9

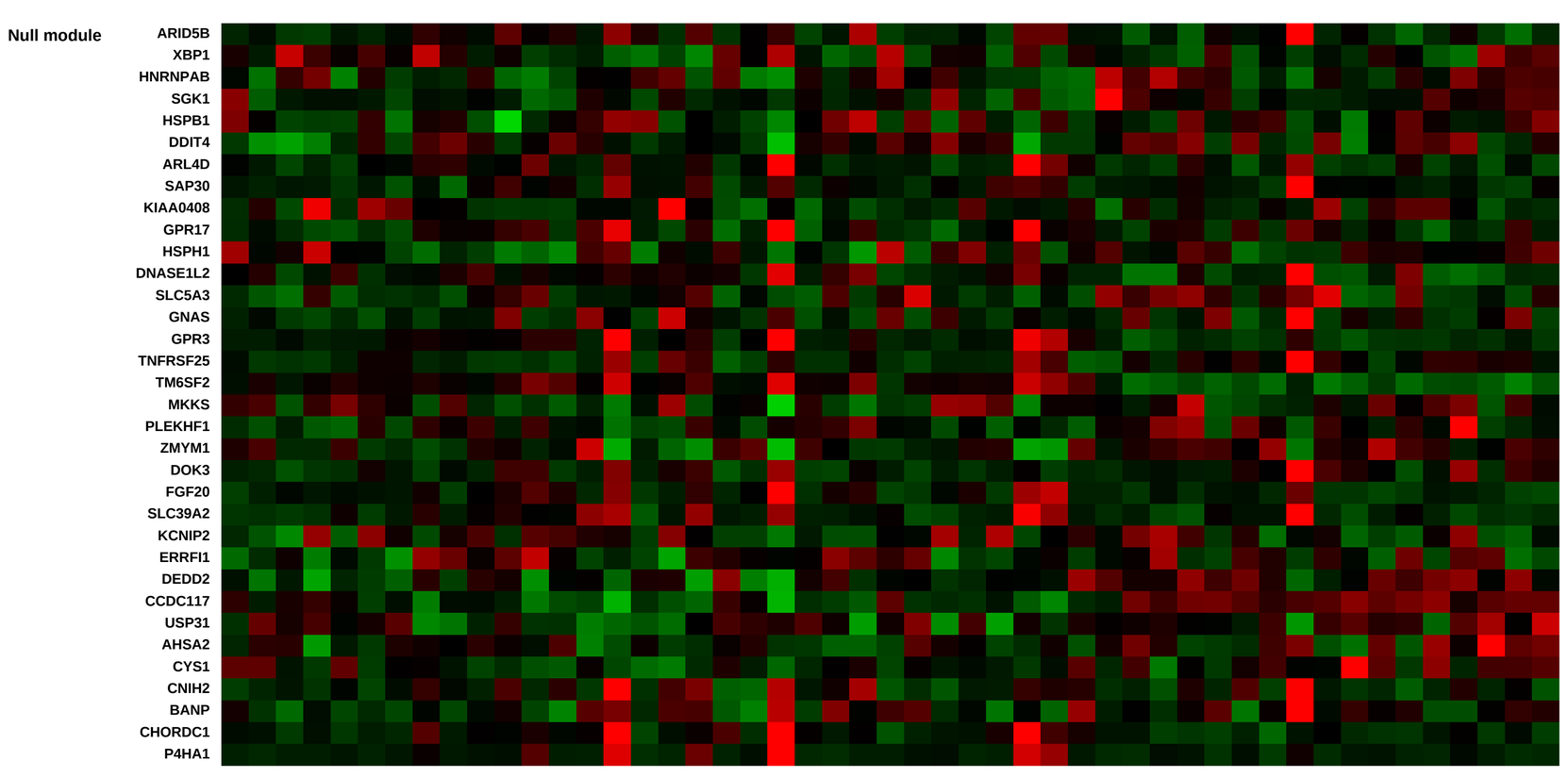

GEO Series "GSE22336" Expression Profiles

Num of samples in this series: 6

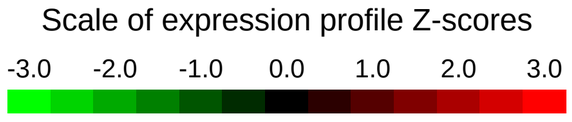

GEO Link:	http://www.ncbi.nlm.nih.gov/geo/query/acc.cgi?acc=GSE22336
Status:	Public on Aug 01 2010
Title:	UDP-GlcNAc 2-epimerase/ManNAc kinase (GNE) is an inducer of apoptotic processes in Capan-1 pancreatic carcinoma cells: GNE silencing
Organism:	Homo sapiens
Experiment type:	Expression profiling by array
Platform:	GPL570
Pubmed ID:	22049060
Summary & Design:	**Summary:** Early invasive growth and metastasis are features of pancreatic cancer that rely on resistance to anoikis, an apoptosis program activated upon loss of adequate matrix anchorage. Re-expression of the tumor suppressor p16 reversed anoikis resistance of pancreatic cancer cells. This conversion to an anoikis-susceptible phenotype was found to be associated with a striking loss of GNE mRNA expression, prompting us to address the role of GNE in pancreatic cancer in more detail. GNE catalyzes a rate-limiting key step of the sialic acid biosynthesis and may have additional functions in the nucleus. **Overall design:** Pancreatic cancer cells Capan-1. Three GNE-silencing samples and three control samples.

Background corr dist: KL-Divergence = 0.0195, L1-Distance = 0.0389, L2-Distance = 0.0016, Normal std = 0.8225

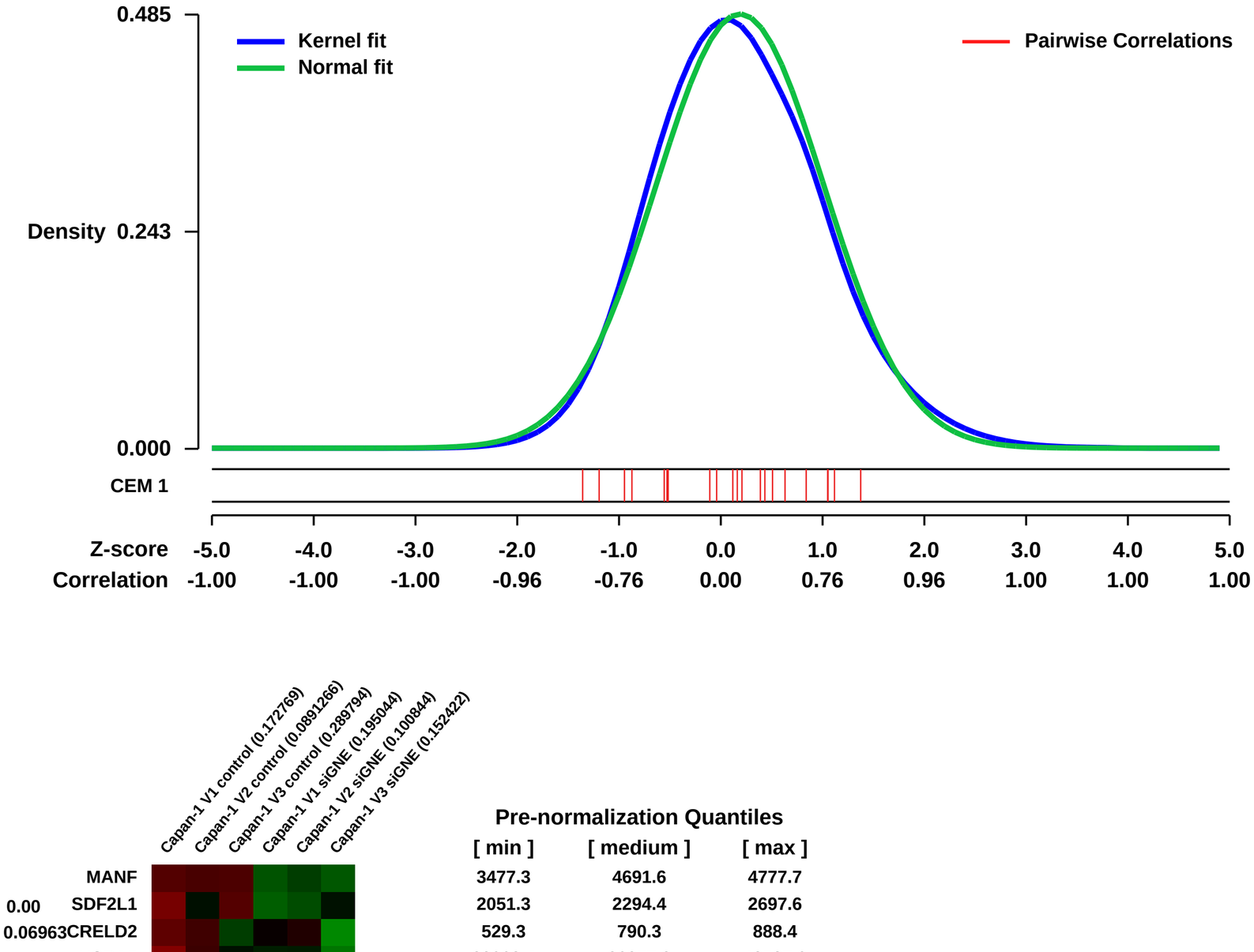

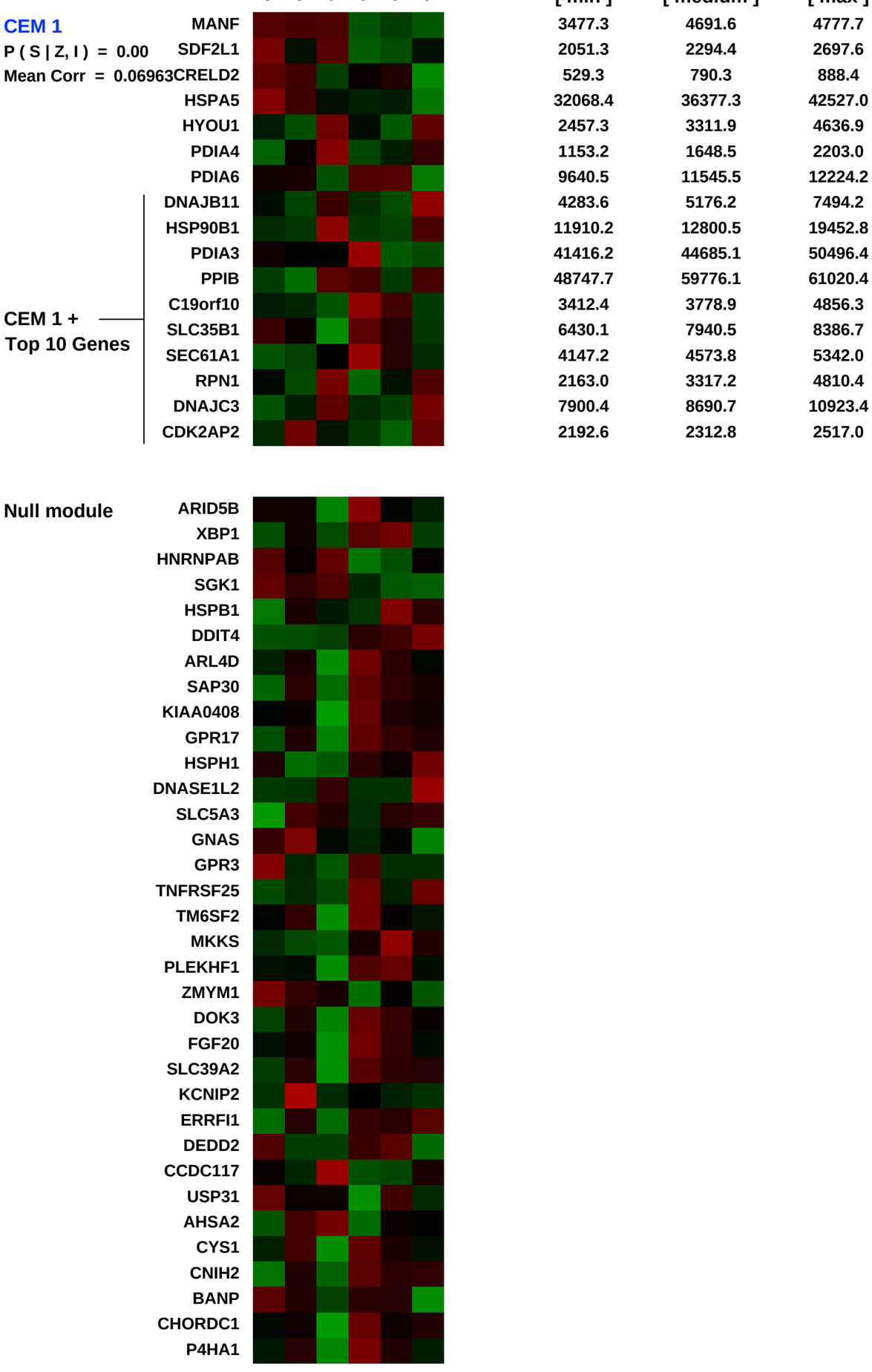

GEO Series "GSE35725" Expression Profiles

Num of samples in this series: 114

Details of this dataset are not shown due to large number of samples and the page size limit.

Find details in http://www.ncbi.nlm.nih.gov/geo/query/acc.cgi?acc=GSE35725

Background corr dist: KL-Divergence = 0.2327, L1-Distance = 0.0804, L2-Distance = 0.0198, Normal std = 0.3128

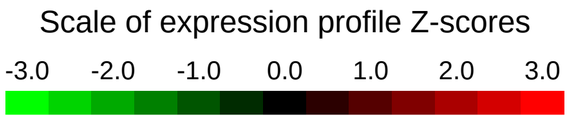

GEO Series "GSE38833" Expression Profiles

Num of samples in this series: 9

Scale of expression profile Z-scores

-3.0 -2.0 -1.0 0.0 1.0 2.0 3.0

GEO Link:	http://www.ncbi.nlm.nih.gov/geo/query/acc.cgi?acc=GSE38833
Status:	Public on Jun 20 2012
Title:	Transcription profiling of human colon Caco-2 cells treated with hydroxytyrosol (HTy) and hydroxytyrosyl ethyl ether (HTy-Et)
Organism:	Homo sapiens
Experiment type:	Expression profiling by array
Platform:	GPL570
Pubmed ID:	23411228
Summary & Design:	**Summary:** **The anticarcinogenic activity of hydroxytyrosyl ethyl ether (HTy-Et) compared to its precursor hydroxytyrosol (HTy) has been studied in human Caco-2 colon adenocarcinoma cells.** **Changes in global gene expression in Caco-2 cells exposed to HTy and HTy-Et for 24 h were evaluated using Affymetrix array.** **Microarray analysis showed that after exposure to HTy and HTy-Et, 451 and 977 genes respectively were differentially expressed compared with untreated cells (P < 0.005; FDR=0). Results show that HTy and its lipophilic ether derivative alter genes related with cancer prevention, which includes inducing cell cycle arrest, promoting apoptosis and enhancing xenobiotic metabolism.** **Overall design:** **Caco-2 cells were treated with 10 ¿…M of HTy and HTy-Et for 24 h, and total RNA from 3 biological replicates of each treatment together with the control cells, were isolated using a QIAGEN´fi RNeasy Mini Kit according to the manufacturerâ s instructions (Qiagen). RNA samples of each of the replicates were processed using Affymetrix Human HG-U133 Plus 2.0 microarrays (Affymetrix).**

Background corr dist: KL-Divergence = 0.0755, L1-Distance = 0.0192, L2-Distance = 0.0004, Normal std = 0.4887

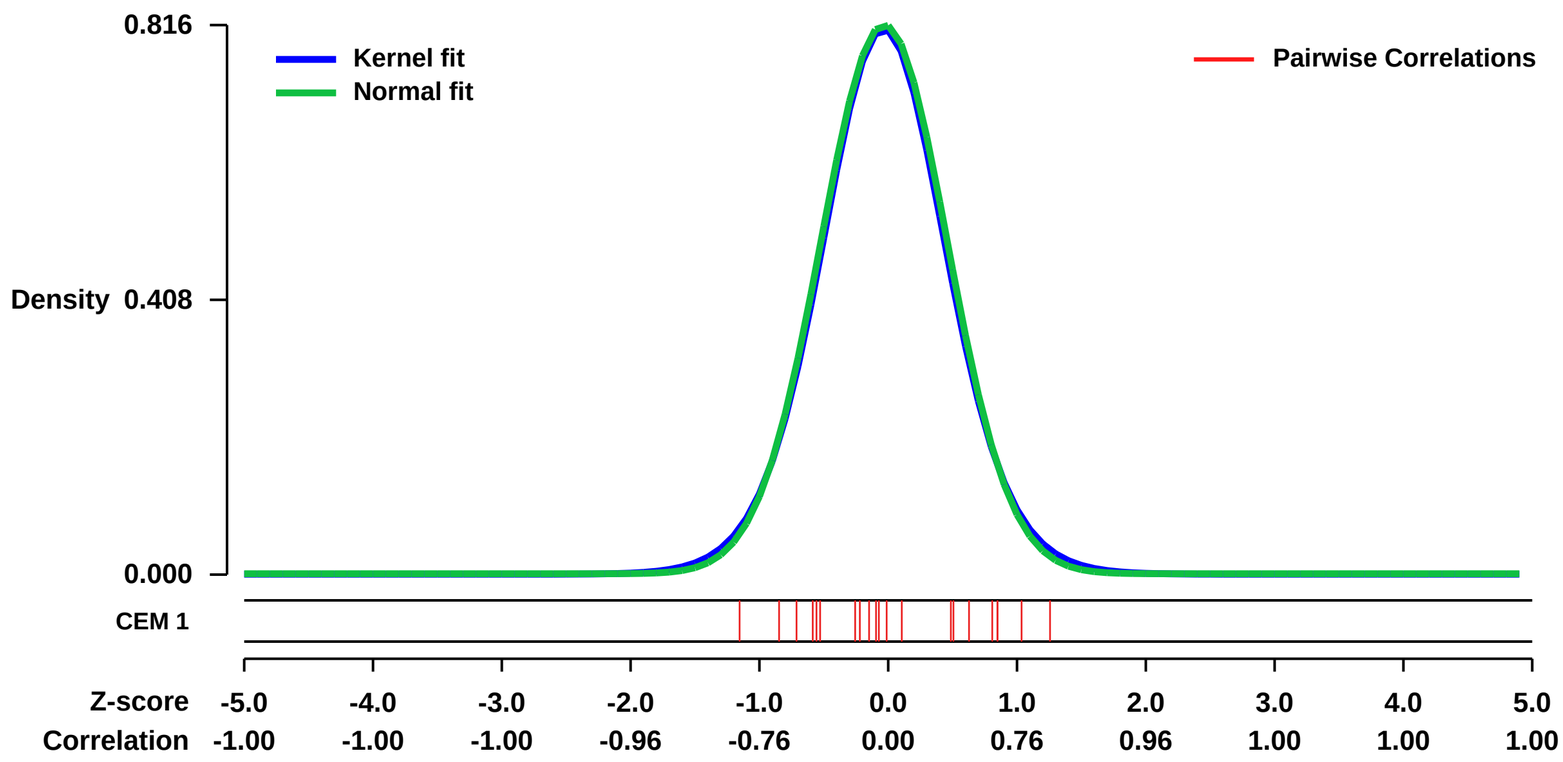

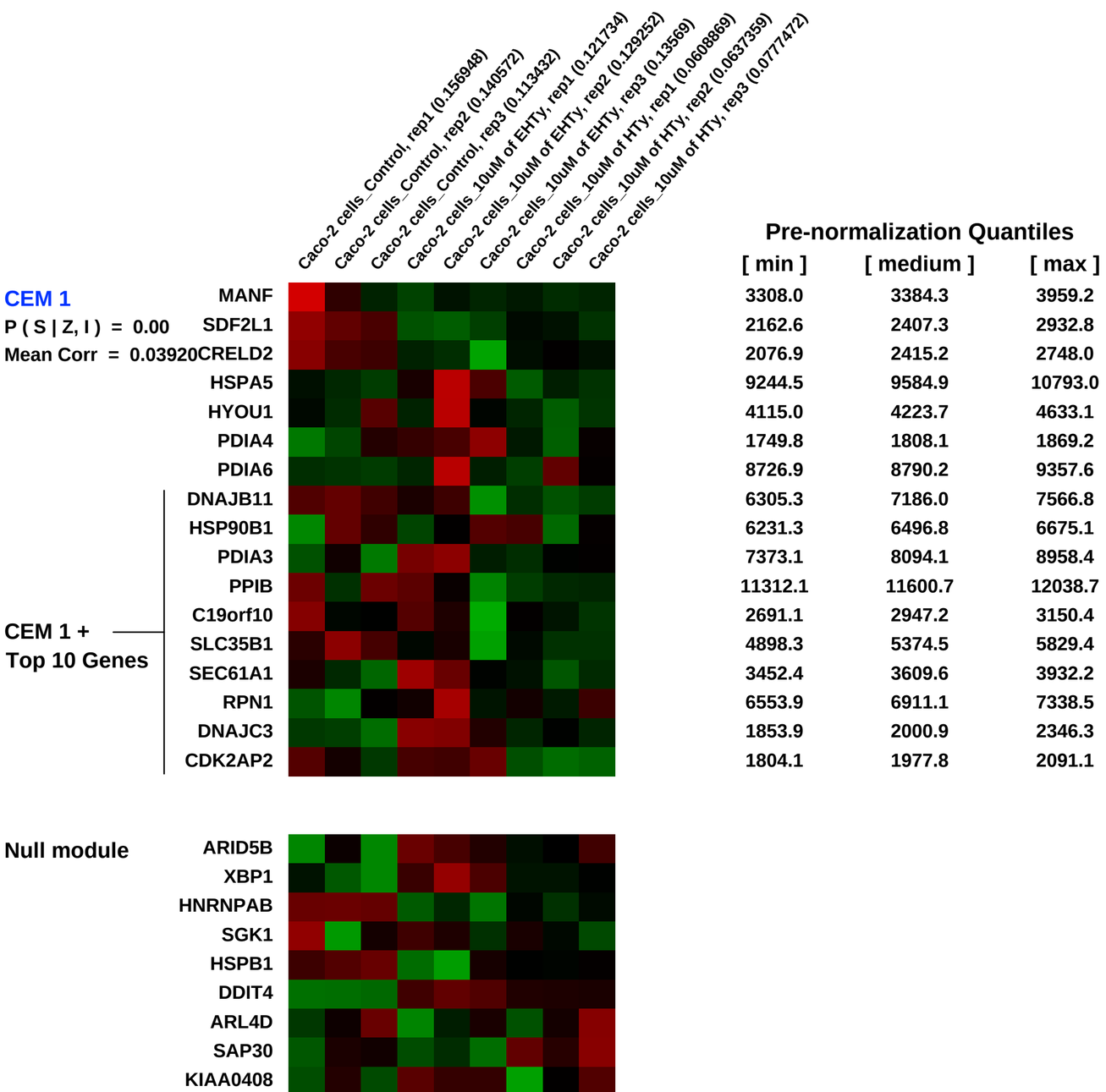

Pre-normalization Quantiles

	[min]	[medium]	[max]
MANF	3308.0	3384.3	3959.2
SDF2L1	2162.6	2407.3	2932.8
CRELD2	2076.9	2415.2	2748.0
HSPA5	9244.5	9584.9	10793.0
HYOU1	4115.0	4223.7	4633.1
PDIA4	1749.8	1808.1	1869.2
PDIA6	8726.9	8790.2	9357.6
DNAJB11	6305.3	7186.0	7566.8
HSP90B1	6231.3	6496.8	6675.1
PDIA3	7373.1	8094.1	8958.4
PPIB	11312.1	11600.7	12038.7
C19orf10	2691.1	2947.2	3150.4
SLC35B1	4898.3	5374.5	5829.4
SEC61A1	3452.4	3609.6	3932.2
RPN1	6553.9	6911.1	7338.5
DNAJC3	1853.9	2000.9	2346.3
CDK2AP2	1804.1	1977.8	2091.1

GEO Series "GSE33495" Expression Profiles

Num of samples in this series: 10

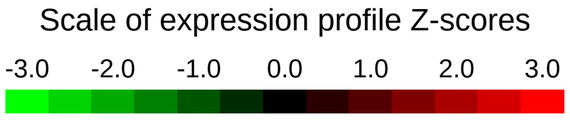

GEO Link:	http://www.ncbi.nlm.nih.gov/geo/query/acc.cgi?acc=GSE33495
Status:	Public on Jun 18 2012
Title:	Disrupted transcripitonal network in ΔNp63 AEC tissue model [gene expression]
Organism:	Homo sapiens
Experiment type:	Expression profiling by array
Platform:	GPL570
Pubmed ID:	
Summary & Design:	**Summary:** The transcriptional basis for disrupted epidermal differentiation arising from TP63 AEC mutations remains to be elucidated. Here we present an organotypic model of AEC dysfunction that phenocopies differentiation defects observed in AEC patient skin. Transcriptional analysis of model AEC tissue revealed impaired induction of differentiation regulators, including OVOL1, GRHL3, KLF4, PRDM1 and ZNF750. Genome wide binding analyses of TP63 during epidermal differentiation showed direct binding of OVOL1, GRHL3, and ZNF750 promoters suggesting AEC mutants prevent normal activation of these targets by direct transcriptional interference. Remarkably, exogenous ZNF750 restores impaired epidermal differentiation caused by AEC mutation. Thus, repression of ZNF750 is central to disrupted epidermal differentiation in model AEC tissue. **Overall design:** Gene expression analysis: To establish a differentiation signature for primary human keratinocytes, with p63i-depleted, and ΔNp63+– AEC mutants overexpressed, total RNA was isolated in biologic duplicate from cells in different conditions and hybridized to Affymetrix HG-U133 2.0 Plus arrays.

Background corr dist: KL-Divergence = 0.0437, L1-Distance = 0.0242, L2-Distance = 0.0010, Normal std = 0.5817

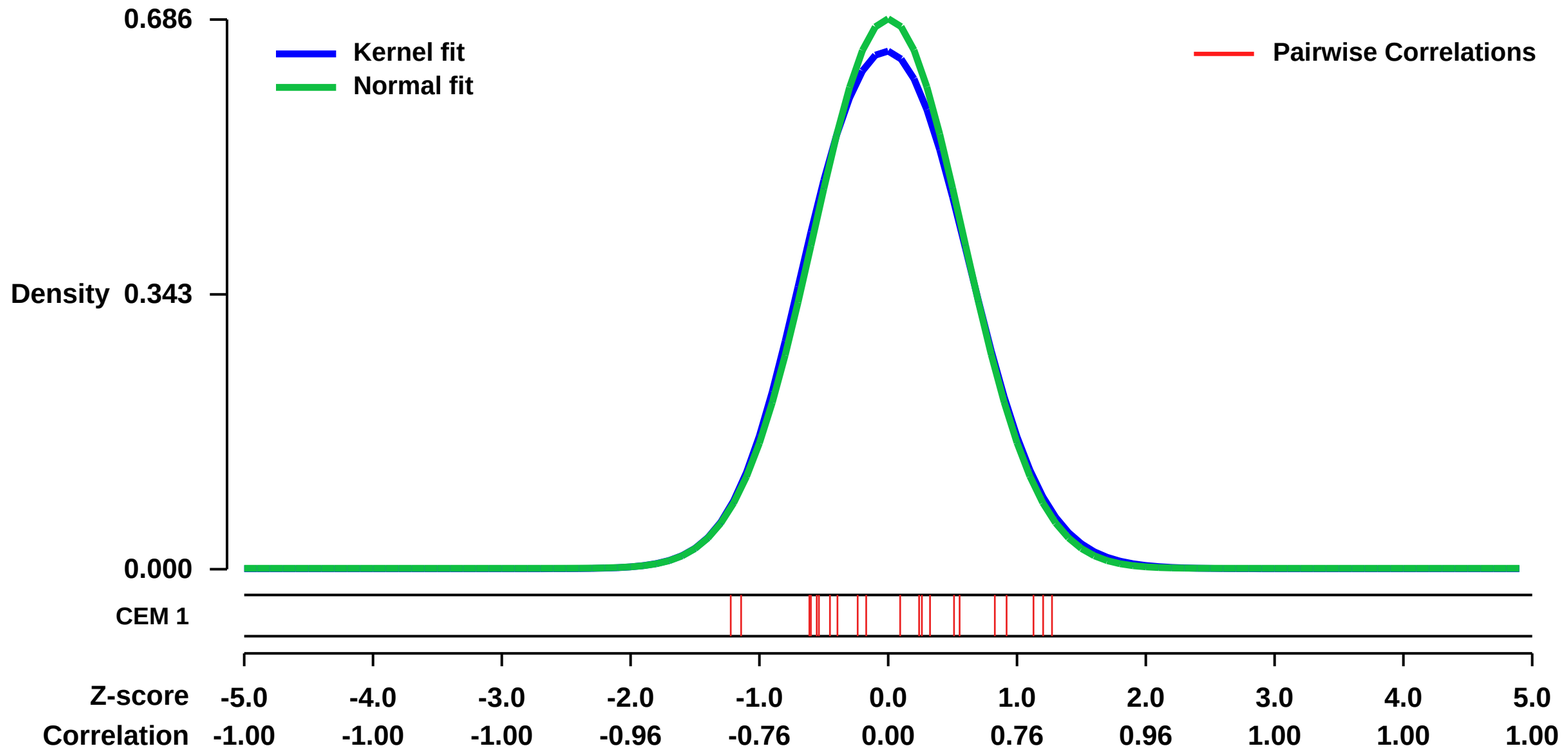

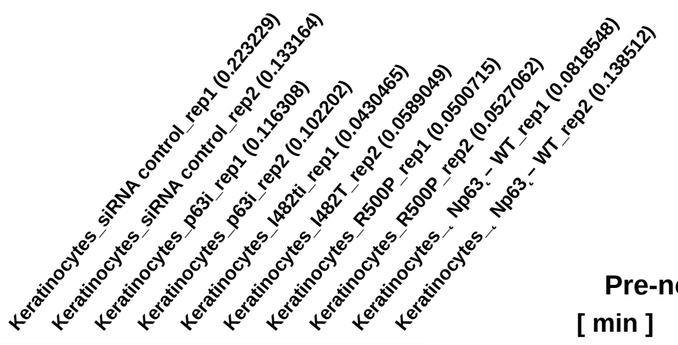

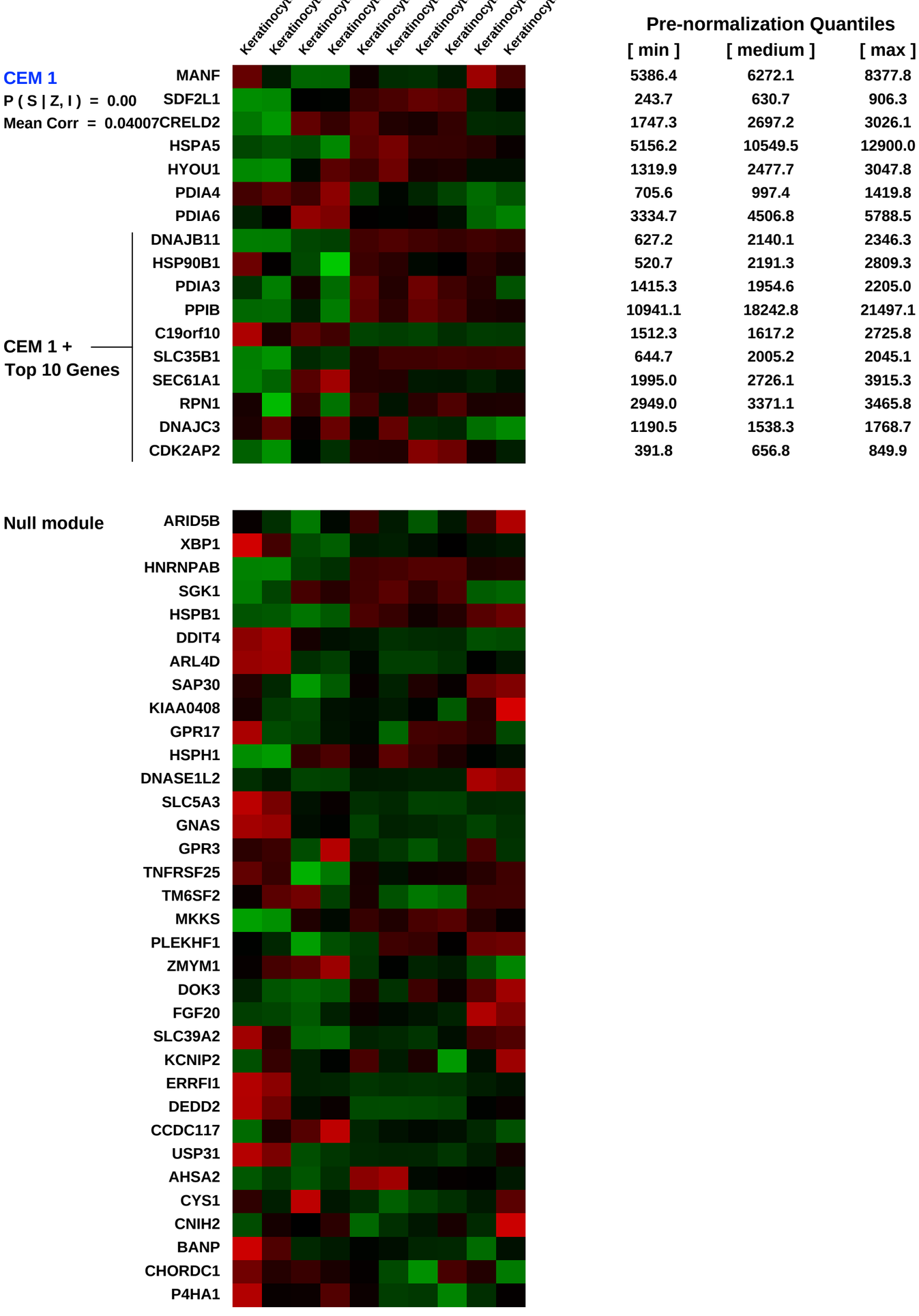

GEO Series "GSE6241" Expression Profiles

Num of samples in this series: 8

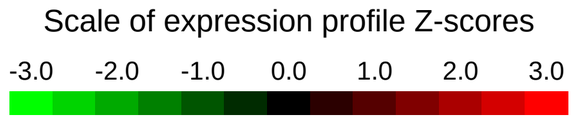

GEO Link:	http://www.ncbi.nlm.nih.gov/geo/query/acc.cgi?acc=GSE6241
Status:	Public on Nov 09 2006
Title:	The effects of Serum Amyloid A on gene expression profile in HUVECs
Organism:	Homo sapiens
Experiment type:	Expression profiling by array
Platform:	GPL570
Pubmed ID:	18552508
Summary & Design:	**Summary:** This study attemps to study the global effects of Serum Amyloid A (SAA) on human endothelial gene expression profile in different time points. **Keywords: time course** **Overall design:** HUVECs were cultured to confluence in 6-well plates and stimulated with 20 ¸…g/ml of SAA (PeproTech) for 0, 4, 24 and 48 h. To determine the cellular transcript profile in Control (0h) and 3 different SAA groups (S4h, S24h and S48h), the relative abundance of mRNAs in SAA groups were compared with Control by use of Human Genome U133 Plus 2.0 Array (HG-U133 Plus 2.0, Affymetrix)). Each group had 2 individual samples. . In order to obtain the 3 group comparison datasets (S4h/C, S24h/C and S48h/C), expression patterns for each individual SAA sample (4h, 24h and 48h) were compared to each individual control sample. Hence, each group comparison has 4 individual sample comparisons. The robust increased or decreased cut-off was use the Affymetrix recommending ""1"" or ""-1"" of the signal log ratio. . If the gene is robust â increasedâ or â decreasedâ in 4 individual sample comparisons of the total 4 comparisons, it was selected as the final robust changed in group comparison. Each gene we were interested, real time PCR was carried out to validate the microarray results.

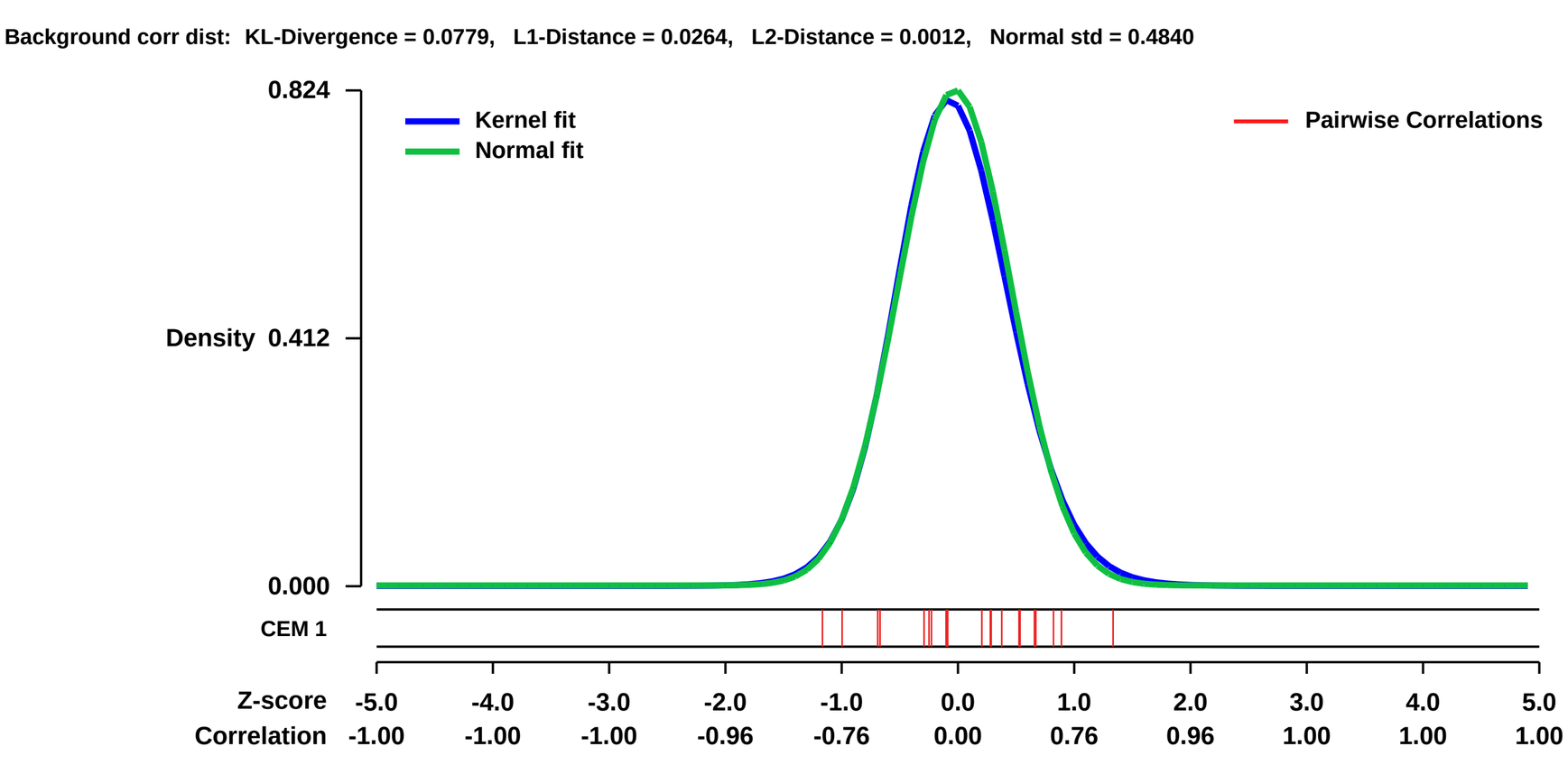

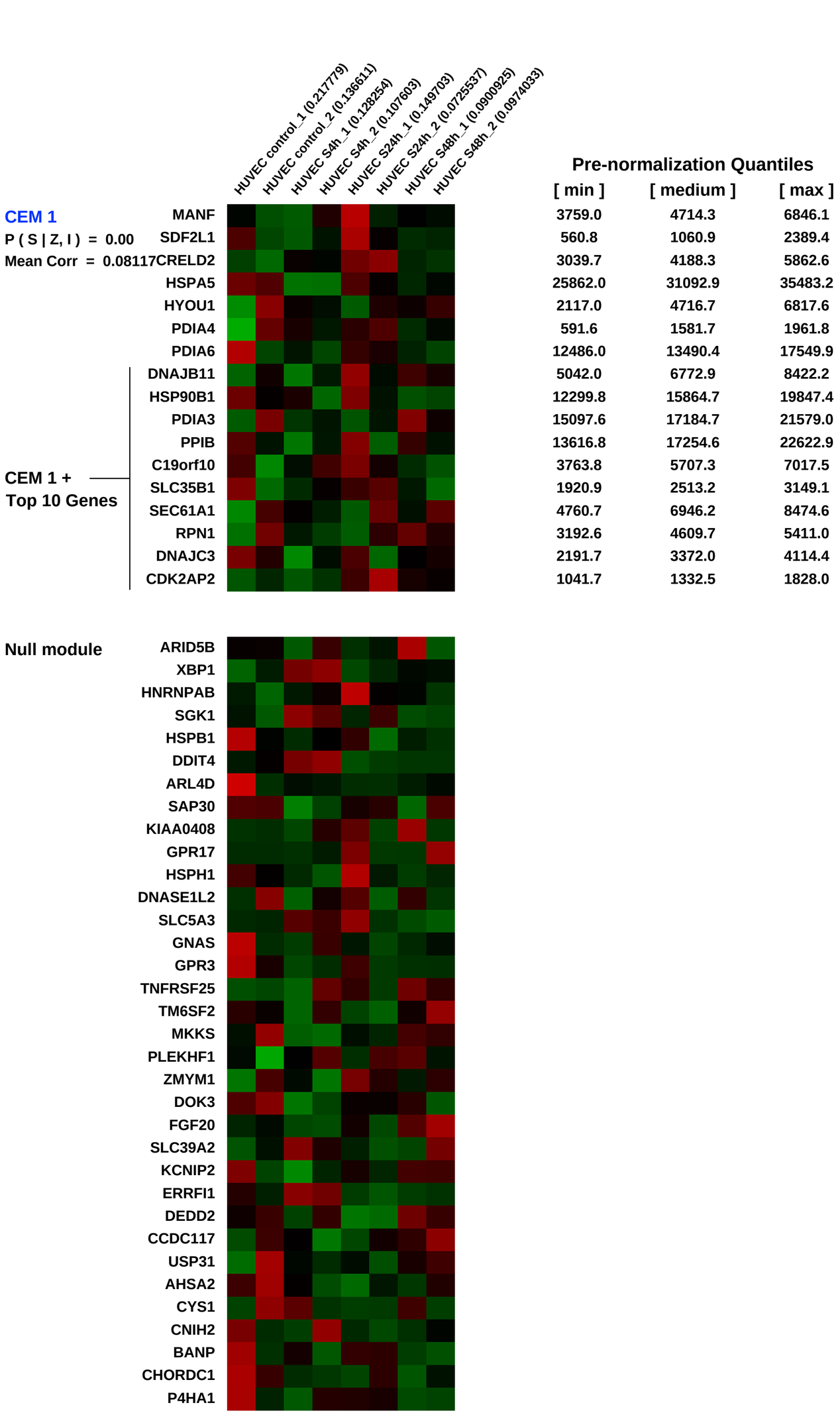

GEO Series "GSE2864" Expression Profiles

Num of samples in this series: 6

Scale of expression profile Z-scores

-3.0 -2.0 -1.0 0.0 1.0 2.0 3.0

GEO Link: http://www.ncbi.nlm.nih.gov/geo/query/acc.cgi?acc=GSE2864
Status: Public on Jul 06 2005
Title: tourt-affy-human-131547
Organism: Homo sapiens
Experiment type: Expression profiling by array
Platform: GPL570
Pubmed ID:

Summary & Design:

Summary:
Nerve growth factor (NGF) is a neurotrophin that plays an important role in regulating the survival, growth, and differentiation of sympathetic neurons. Many in vitro studies indicate that Egr transcription factors are coupled to NGF signaling and are essential signaling mediators of NGF-dependent differentiation of sympathetic neurons, such as neuroblastoma cells and pheochromocytoma cells. Mice that are deficient for both Egr1 and Egr3 have profound sympathetic nerve system defects, including abnormal neuron degeneration and impaired differentiation (unpublished observations). To further understand the role of Egr genes in sympathetic neuron development, it is necessary to examine the signal transduction pathways involved in NGF-mediated Egr-dependent gene regulation. The results will be helpful in understanding the pathobiology of those diseases related to aberrant sympathetic neuron differentiation, such as neuroblastoma and dysautonomias, and may provide new insights into therapies for these refractory diseases.

To identify NGF-mediated Egr-dependent target genes in human SH-SY5Y/TrkA neuroblastoma cells: Many potential Egr target genes have been described over the years. However, very few have been characterized to be involved in NGF-mediated sympathetic neuron differentiation. In order to further understand the role of Egr genes in sympathetic neuron development, it is necessary to examine the signal transduction pathways involved in NGF-mediated Egr-dependent gene regulation. Egr1 and Egr3 are rapidly induced after NGF treatment and Egr1 is involved in activation of the differentiation marker gene NPY in SH-SY5Y/TrkA cells. Therefore, SH-SY5Y/TtrkA cells appear to be an excellent model system to study the role of Egr transcription factors in sympathetic neuron differentiation in vitro. A dominant negative Egr molecule that specifically blocks transcriptional activity mediated by Egr transcription factors will be used in this study to identify Egr-dependent target genes.

Egr1 and Egr3 are rapidly induced after NGF treatment in human SH-SY5Y/TrkA neuroblastoma cells, which in turn differentiate into sympathetic-like neurons. We hypothesize that Egr transcription factors are involved in activating downstream signaling pathways during NGF mediated differentiation of SH-SY5Y/TrkA cells. Moreover, we hypothesize that by using a dominant negative Egr (dnEgr) molecule that blocks all Egr mediated gene transcription and Affymetrix microarray analysis, it will be possible to identify NGF-mediated Egr transcription dependent gene regulatory networks that may be involved in growth and differentiation of neuroblastoma. An unbiased approach to understanding these gene regulatory networks may lead to new insights relating to NGF signaling involved in neuronal growth and differentiation.

Human neuroblastoma SH-SY5Y/TrkA cells will be infected with either dnEgr-expressing adenovirus (SH-SY5Y/TrkA-dnEgr) or with EGFP-expressing control adenovirus (SH-SY5Y/TrkA-EGFP). Equivalent infection efficiency and lack of viral toxicity will be verified by EGFP fluorescence microscopy 24 hours after infection and the cells will be treated with NGF (100 ng/ml). Total RNA will be extracted from SH-SY5Y/TrkA (uninfected), SH-SY5Y/TrkA-dnEgr, and SH-SY5Y/TrkA-EGFP cells treated with NGF for 0, 1 hour and 3 hours. Total RNA will be prepared from all of the samples and a portion subjected to real-time PCR analysis to ensure that NGF mediated Egr gene induction was not altered by the context of viral infection. Pilot experiments demonstrate that Egr genes are still induced in the context of viral infection greater than 100-fold. Egr1 mRNA peak expression is known to occur at 1 hour and decrease by 3 hours after NGF treatment in all of the samples. The peak expression of Egr target genes is expected to occur later than Egr1 peak expression since Egr1 proteins need to be expressed first to initiate the transcription of target promoters. Therefore, the RNA samples from SH-SY5Y/TrkA-dnEgr and SH-SY5Y/TrkA-EGFP treated with NGF for 3 hours will be used to probe Affymetrix high-density human genome U133 Plus 2.0 Arrays to identify differentially expressed genes. RNA amplification for probe synthesis should not be necessary since we will provide 10 ug of intact total RNA for each sample. We will provide three sets of samples to perform the comparative microarray analysis twice from different starting materials and a nine-way comparative analysis of the data will be performed. We expect that cells containing high levels of dnEgr will inhibit NGF mediated Egr-dependent target gene expression and that these gene networks should be identifiable when compared to EGFP infected cells that have normal Egr gene transcriptional activity.

Keywords: time-course

Overall design:
as above

Background corr dist: KL-Divergence = 0.0463, L1-Distance = 0.0245, L2-Distance = 0.0007, Normal std = 0.5914

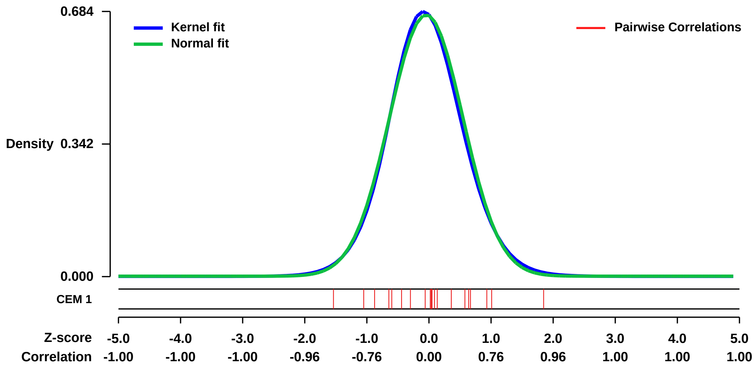

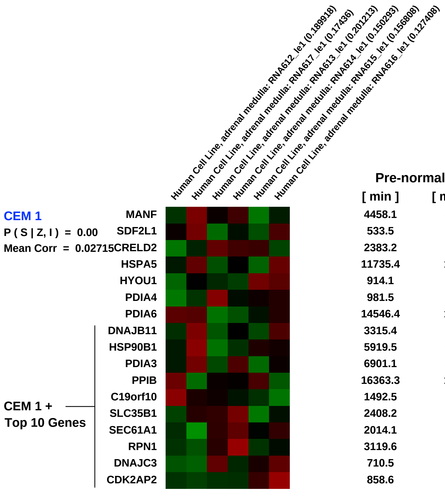

	Pre-normalization Quantiles		
	[min]	[medium]	[max]
MANF	4458.1	4755.8	5016.0
SDF2L1	533.5	895.5	1226.5
CRELD2	2383.2	2776.9	2866.6
HSPA5	11735.4	14424.0	17195.6
HYOU1	914.1	1275.6	1688.2
PDIA4	981.5	1173.4	1341.8
PDIA6	14546.4	16694.2	17487.7
DNAJB11	3315.4	3665.8	4164.3
HSP90B1	5919.5	6561.3	7142.6
PDIA3	6901.1	8210.1	9363.5
PPIB	16363.3	18902.1	20937.0
C19orf10	1492.5	1791.7	2072.6
SLC35B1	2408.2	2854.8	3073.4
SEC61A1	2014.1	3015.3	3272.0
RPN1	3119.6	3466.3	4256.1
DNAJC3	710.5	750.6	774.9
CDK2AP2	858.6	873.7	1054.4

Null module

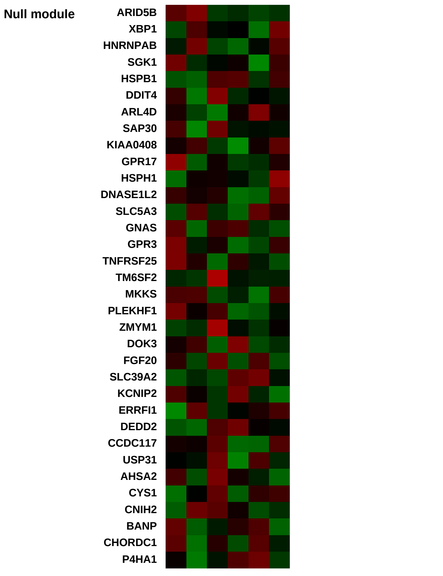

GEO Series "GSE13712" Expression Profiles

Num of samples in this series: 12

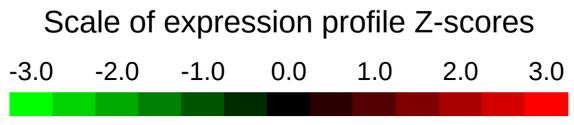

GEO Link:	http://www.ncbi.nlm.nih.gov/geo/query/acc.cgi?acc=GSE13712
Status:	Public on May 23 2009
Title:	Differential gene expression of young and senescent HUVECs under static and laminar shear stress conditions
Organism:	Homo sapiens
Experiment type:	Expression profiling by array
Platform:	GPL570
Pubmed ID:	20382854
Summary & Design:	**Summary:** Laminar shear stress due to constant blood flow is known to play a critical role in maintaining vascular health. In contrast, endothelial cell senescence appears to be closely associated with the incidence of vascular disorder. In an attempt to identify functional biomarkers for age-related vascular health/disease, the present study investigated differential gene expression of young and senescent human umbilical vein endothelial cells (HUVECs) under static and laminar shear stress. We used a cDNA microarray method to compare gene expression profiles of young and senescent HUVECs under static and laminar shear stress conditions. Keywords: stress response, age state analysis **Overall design:** Senescent cells were prepared by continuous subculture in vitro, and a cone-and-plate device was used to impose laminar shear stress onto cells. Young and senescent cells were exposed to laminar shear stress or maintained under static conditions. Total mRNA was extracted and gene expression profiles were analyzed by cDNA microarray.

Background corr dist: KL-Divergence = 0.1050, L1-Distance = 0.0363, L2-Distance = 0.0027, Normal std = 0.4367

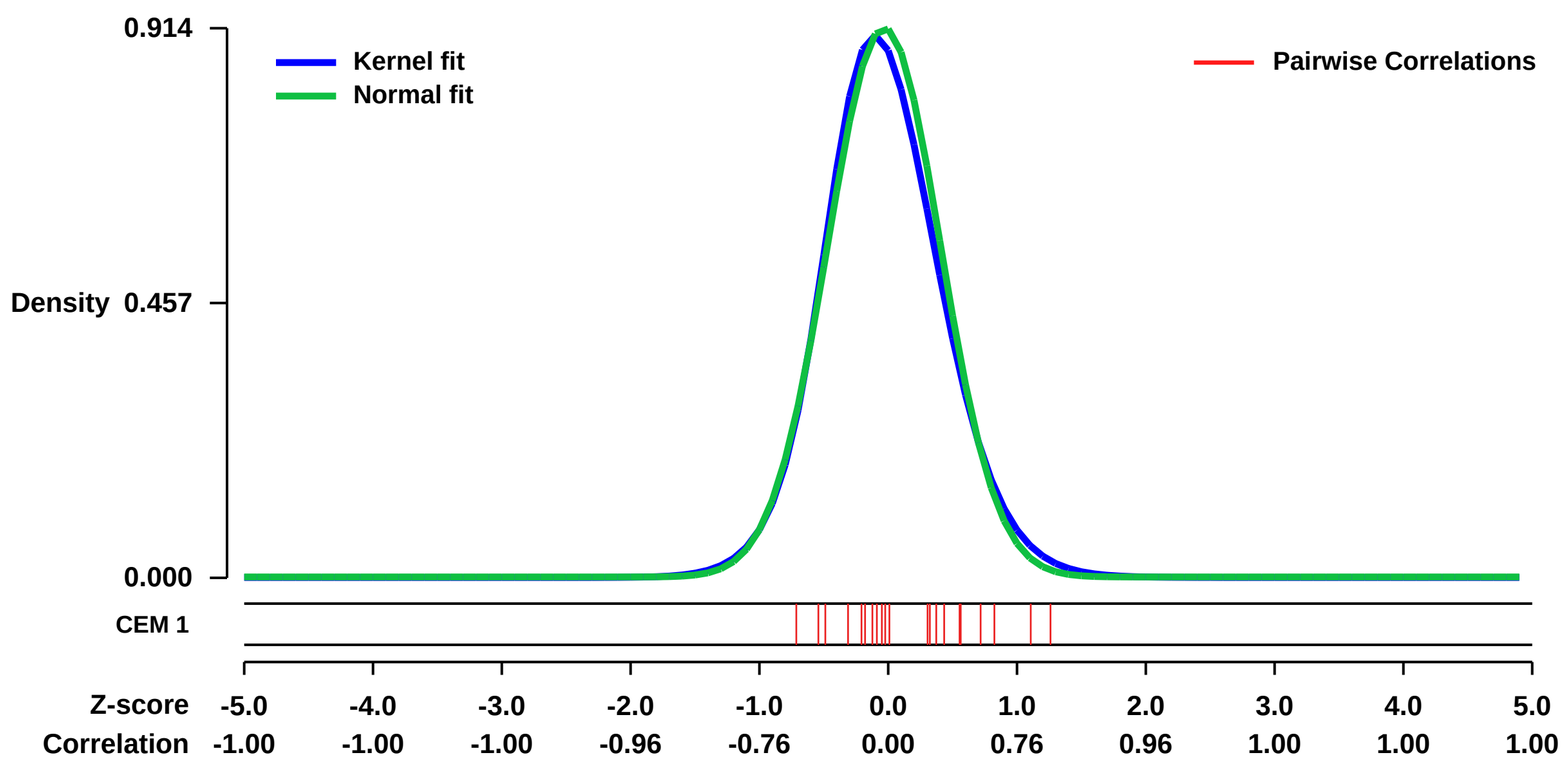

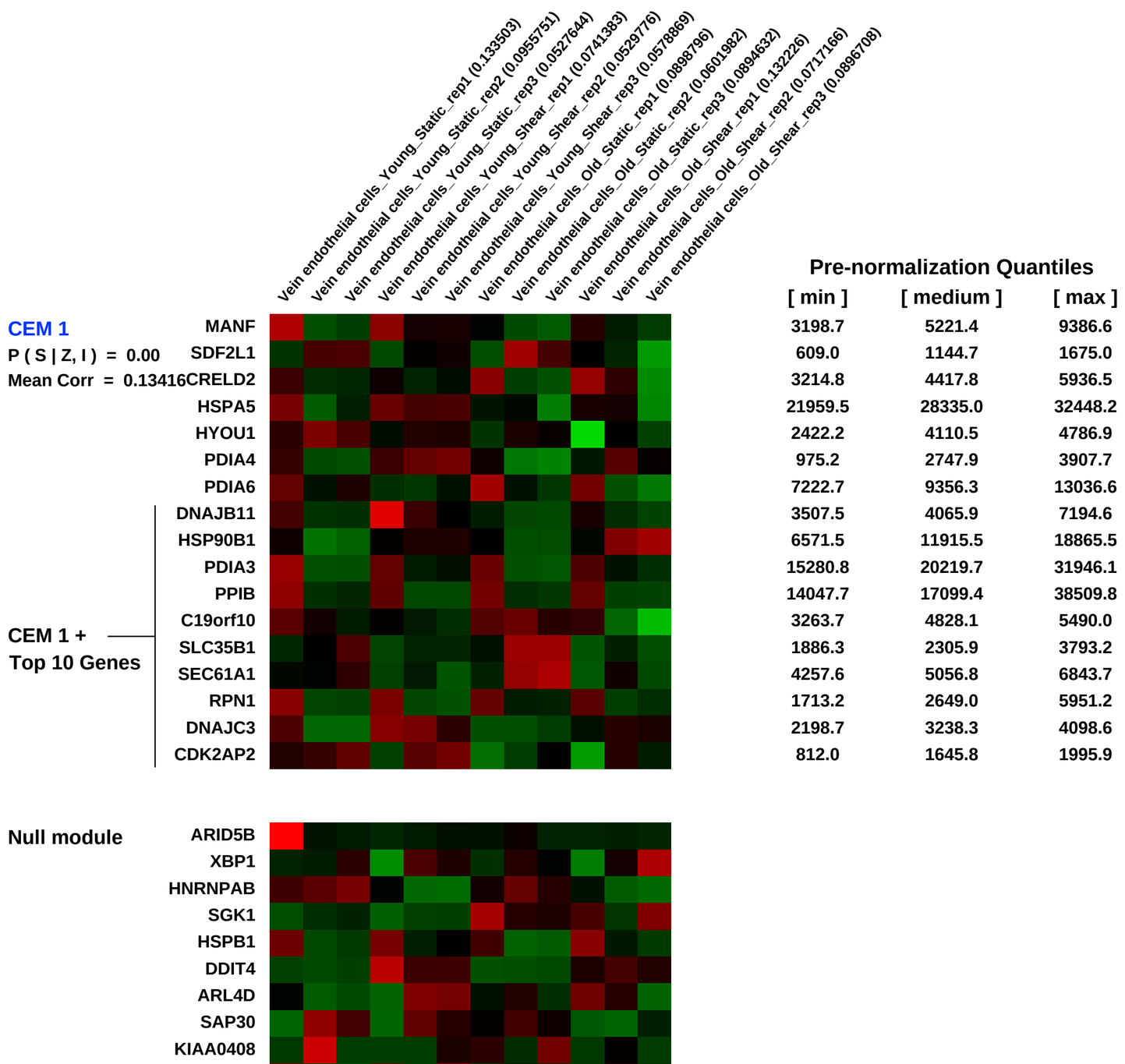

Pre-normalization Quantiles

	[min]	[medium]	[max]
MANF	3198.7	5221.4	9386.6
SDF2L1	609.0	1144.7	1675.0
CRELD2	3214.8	4417.8	5936.5
HSPA5	21959.5	28335.0	32448.2
HYOU1	2422.2	4110.5	4786.9
PDIA4	975.2	2747.9	3907.7
PDIA6	7222.7	9356.3	13036.6
DNAJB11	3507.5	4065.9	7194.6
HSP90B1	6571.5	11915.5	18865.5
PDIA3	15280.8	20219.7	31946.1
PPIB	14047.7	17099.4	38509.8
C19orf10	3263.7	4828.1	5490.0
SLC35B1	1886.3	2305.9	3793.2
SEC61A1	4257.6	5056.8	6843.7
RPN1	1713.2	2649.0	5951.2
DNAJC3	2198.7	3238.3	4098.6
CDK2AP2	812.0	1645.8	1995.9

GEO Series "GSE10696" Expression Profiles

Num of samples in this series: 6

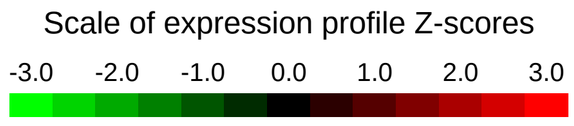

GEO Link:	http://www.ncbi.nlm.nih.gov/geo/query/acc.cgi?acc=GSE10696
Status:	Public on Mar 05 2008
Title:	Expression analysis in A431_wt vs A431_GR cells
Organism:	Homo sapiens
Experiment type:	Expression profiling by array
Platform:	GPL570
Pubmed ID:	18568074
Summary & Design:	**Summary:** A431 wild-type (wt) cancer cell line is sensitive to treatment with EGFR tyrosine kinase inhibitors (TKIs). By culturing it chronically under gefitinib, it eventually becomes resistant (A431_GR cell). We know of a few proteins involved in this mechanism of drug resistance, but a cDNA exprssion array would add information to other genes that might be involved in this resistance mechanism. We used microarrays to identify the differences in the global gene expression between A431_wt (wild-type) cells and A431_GR cells. Keywords: comparison of two cell lines **Overall design:** Total RNA was isolated from parental (wild-type) and GR (gefitinib-resistant) A431 cells using TRIzol reagent (Invitrogen, Carlsbad, CA), followed by RNeasy Mini Kit column purification (Qiagen, Valencia, CA) including an in column DNAse clean-up using RNAse-free DNAse Set (Qiagen). Synthesis of cRNA target, its hybridization to Human Genome U133 Plus 2.0 microarrays and scanning of those arrays was performed using Affymetrix GeneChip products and reagents in accordance with the manufacturerâ s recommendations at the Vanderbilt Microarray Shared Resource.

Background corr dist: KL-Divergence = 0.0287, L1-Distance = 0.0512, L2-Distance = 0.0029, Normal std = 0.7732

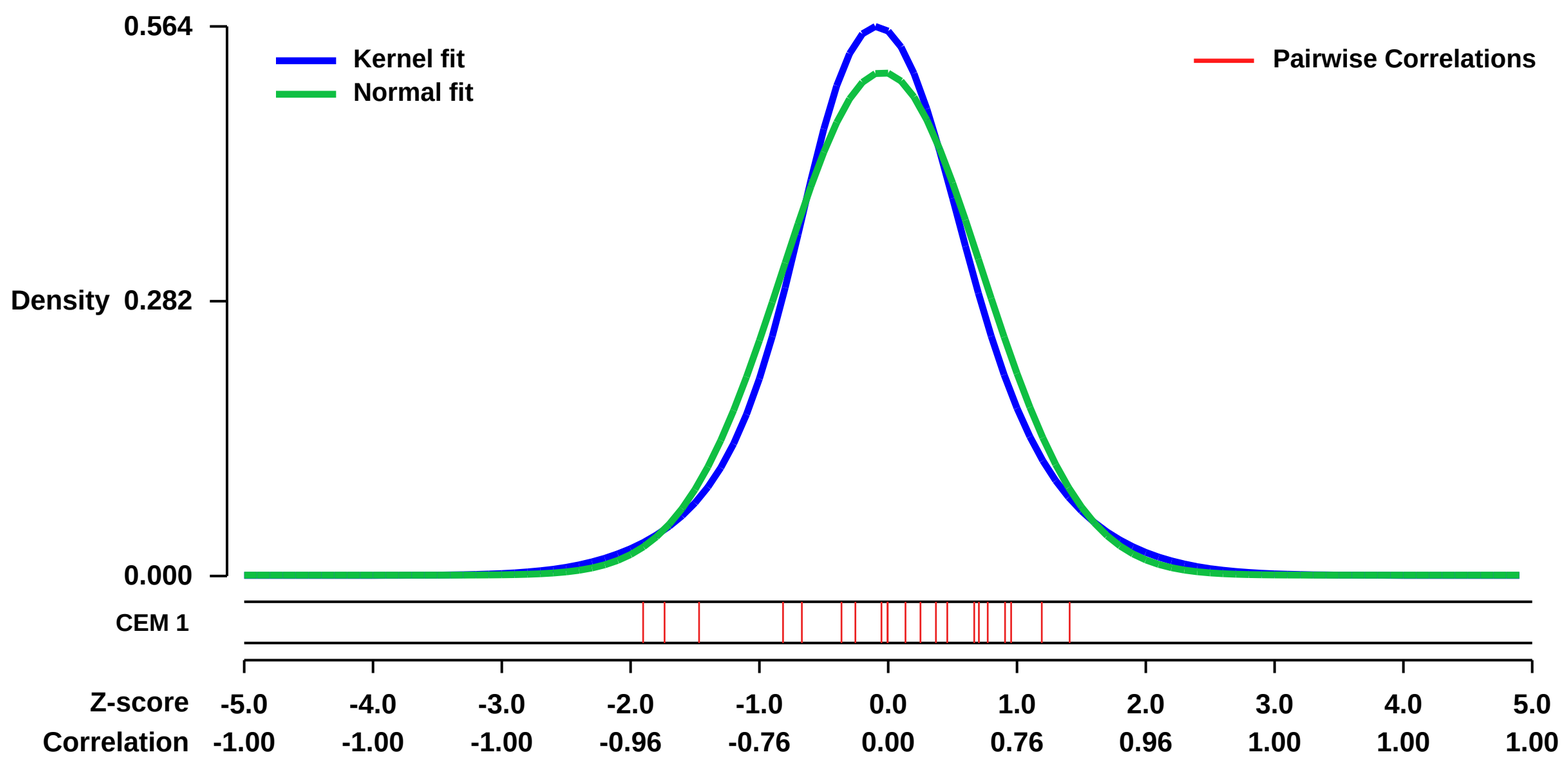

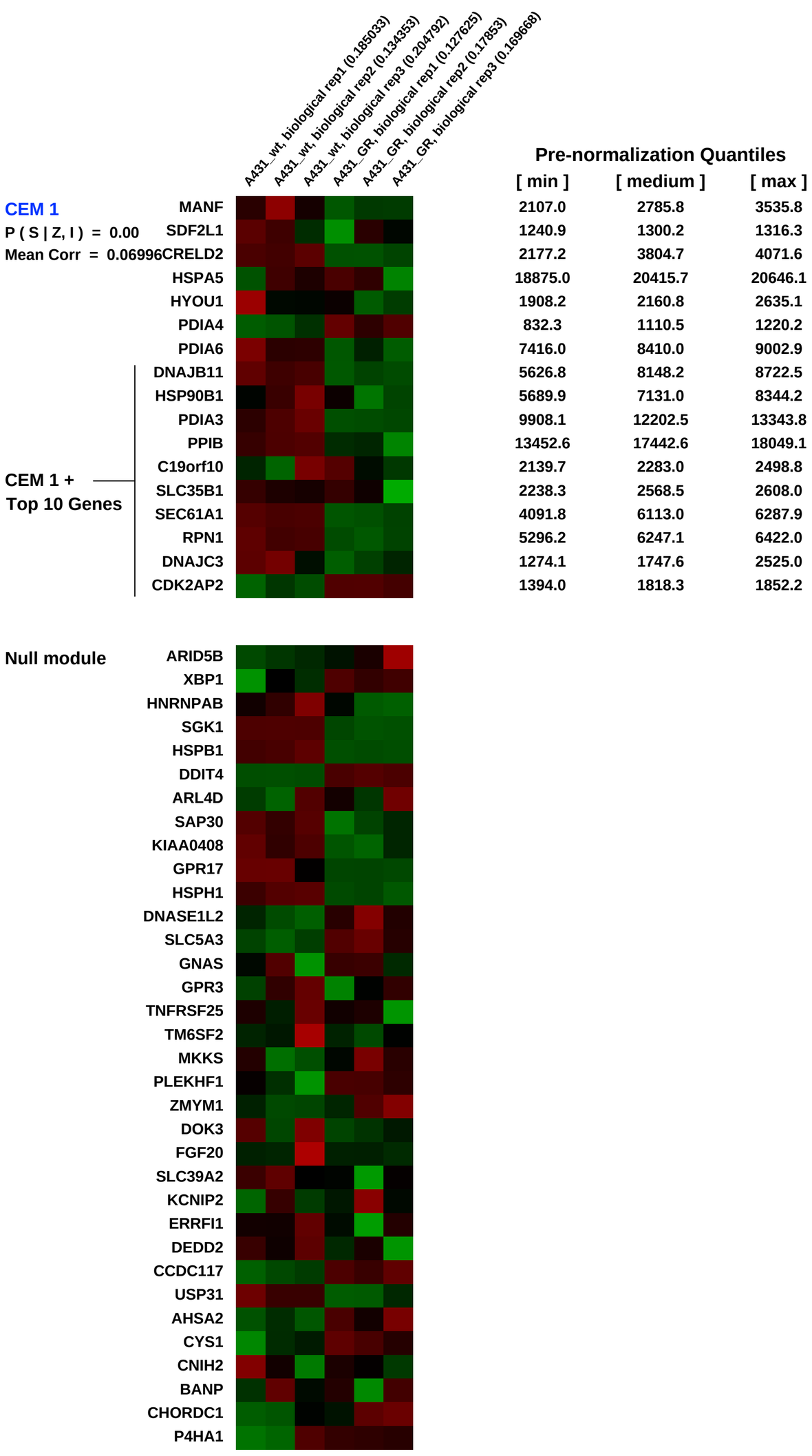

Pre-normalization Quantiles

	[min]	[medium]	[max]
MANF	2107.0	2785.8	3535.8
SDF2L1	1240.9	1300.2	1316.3
CRELD2	2177.2	3804.7	4071.6
HSPA5	18875.0	20415.7	20646.1
HYOU1	1908.2	2160.8	2635.1
PDIA4	832.3	1110.5	1220.2
PDIA6	7416.0	8410.0	9002.9
DNAJB11	5626.8	8148.2	8722.5
HSP90B1	5689.9	7131.0	8344.2
PDIA3	9908.1	12202.5	13343.8
PPIB	13452.6	17442.6	18049.1
C19orf10	2139.7	2283.0	2498.8
SLC35B1	2238.3	2568.5	2608.0
SEC61A1	4091.8	6113.0	6287.9
RPN1	5296.2	6247.1	6422.0
DNAJC3	1274.1	1747.6	2525.0
CDK2AP2	1394.0	1818.3	1852.2

GEO Series "GSE8640" Expression Profiles

Num of samples in this series: 6

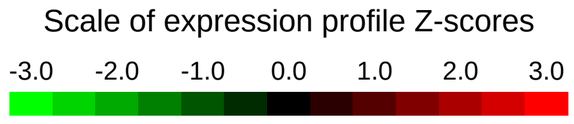

GEO Link:	http://www.ncbi.nlm.nih.gov/geo/query/acc.cgi?acc=GSE8640
Status:	Public on Dec 17 2007
Title:	TFAP2C regulates multiple pathways of estrogen signaling
Organism:	Homo sapiens
Experiment type:	Expression profiling by array
Platform:	GPL570
Pubmed ID:	17875680
Summary & Design:	**Summary:** We were interested in determining what genes might be controlled by TFAP2C and/or TFAP2A, either directly or indirectly through regulation of ER-alpha and potentially other signaling pathways. We performed an microarray analysis in MCF7 cells with elimination of either TFAP2C or TFAP2A. The patterns of gene expression with alteration of TFAP2 activity were compared to changes in expression induced by estrogen exposure. Knock-down of TFAP2C in the presence of estrogen altered the pattern of several known ERalpha-regulated genes and a number of genes outside the estrogen-regulated pathways. **Keywords:** Various siRNA treatments **Overall design:** 6.MCF7 cells with no siRNA treatment, with the presence of estrogen.

Background corr dist: KL-Divergence = 0.0414, L1-Distance = 0.0233, L2-Distance = 0.0006, Normal std = 0.6124

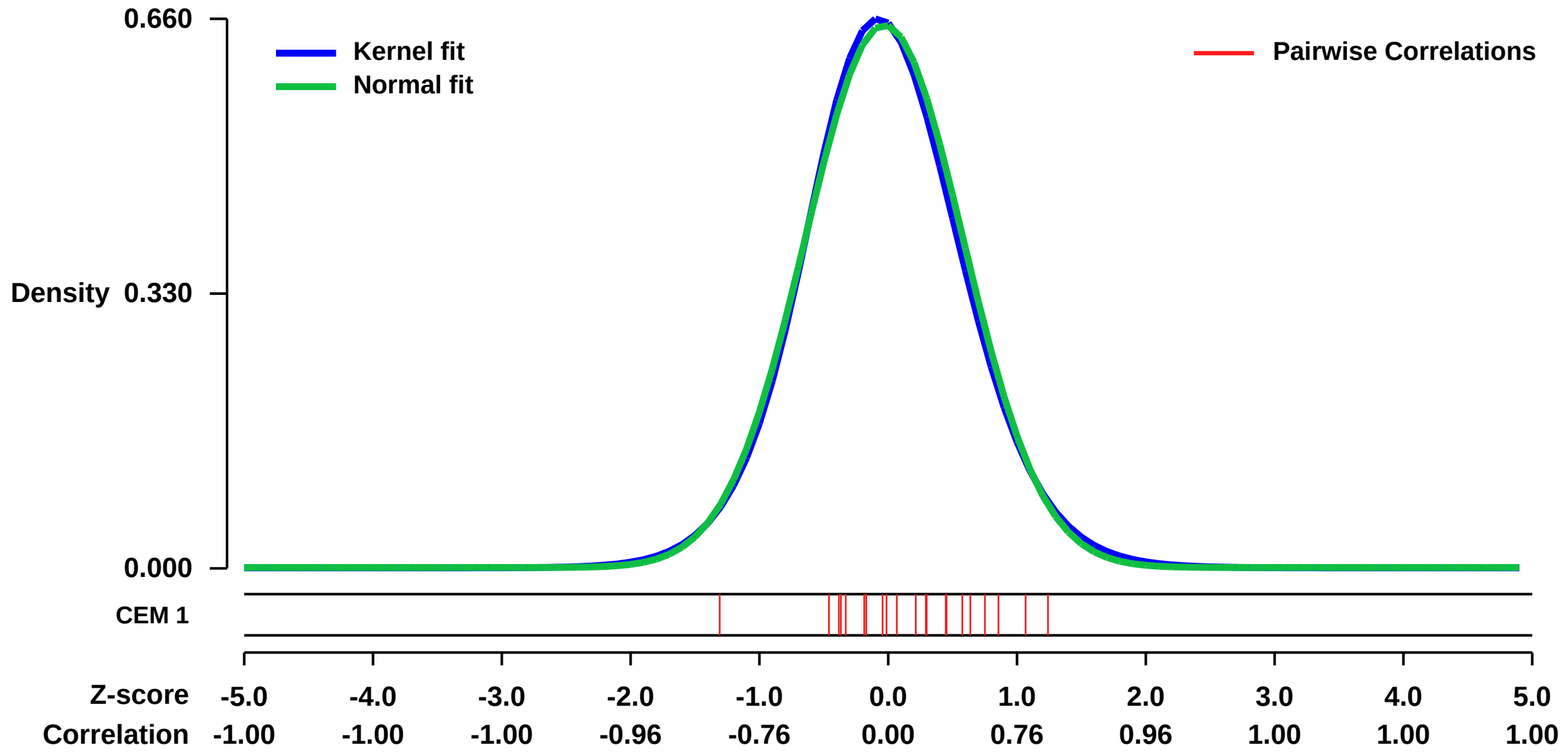

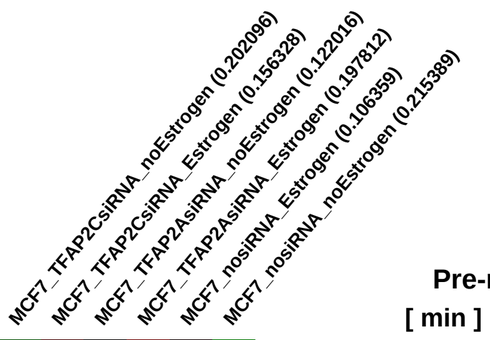

Pre-normalization Quantiles

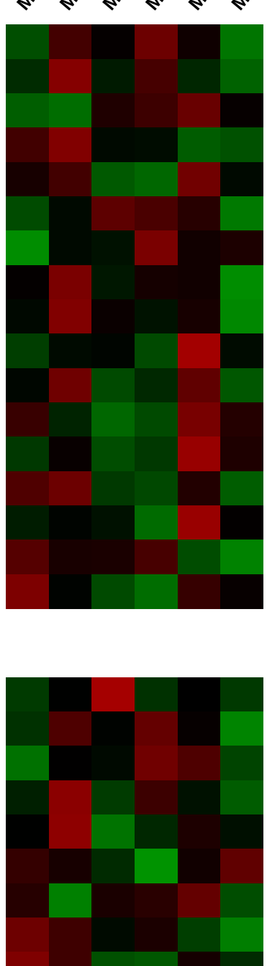

		[min]	[medium]	[max]
CEM 1	MANF	2630.9	3310.0	3784.8
P (S | Z, I) = 0.00	SDF2L1	1092.3	1359.4	1950.0
Mean Corr = 0.14302	CRELD2	1108.0	2044.2	2531.6
	HSPA5	18335.1	20527.5	24147.6
	HYOU1	2232.7	3139.6	3791.3
	PDIA4	768.8	915.2	965.0
	PDIA6	6031.3	7798.6	8977.5
CEM 1 + Top 10 Genes	DNAJB11	3625.1	4803.9	5589.0
	HSP90B1	2900.1	4177.6	5213.2
	PDIA3	6437.1	6776.3	7688.7
	PPIB	13066.5	14598.2	16773.7
	C19orf10	2137.1	2435.9	2618.4
	SLC35B1	5265.7	5767.3	6623.1
	SEC61A1	3394.3	4971.8	5901.4
	RPN1	3418.8	4492.9	6126.1
	DNAJC3	1550.4	1752.7	1828.5
	CDK2AP2	1099.9	1229.4	1360.2
Null module	ARID5B			
	XBP1			
	HNRNPAB			
	SGK1			
	HSPB1			
	DDIT4			
	ARL4D			
	SAP30			
	KIAA0408			
	GPR17			
	HSPH1			
	DNASE1L2			
	SLC5A3			
	GNAS			
	GPR3			
	TNFRSF25			
	TM6SF2			
	MKKS			
	PLEKHF1			
	ZMYM1			
	DOK3			
	FGF20			
	SLC39A2			
	KCNIP2			
	ERRFI1			
	DEDD2			
	CCDC117			
	USP31			
	AHSA2			
	CYS1			
	CNIH2			
	BANP			
	CHORDC1			
	P4HA1			

GEO Series "GSE15490" Expression Profiles

Num of samples in this series: 50

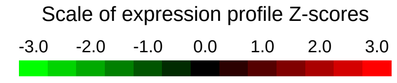

GEO Link:	http://www.ncbi.nlm.nih.gov/geo/query/acc.cgi?acc=GSE15490
Status:	Public on Mar 01 2011
Title:	Sequential gene expression profiling in CLL during treatment
Organism:	Homo sapiens
Experiment type:	Expression profiling by array
Platform:	GPL570
Pubmed ID:	20966934
Summary & Design:	**Summary:** **Purpose:** **Accurate prediction of clinical response is the prerequisite for individualized therapy in chronic lymphocytic leukemia (CLL). We hypothesized that sequential assessment of gene expression changes early during therapy may well reflect behaviour of the leukemic clone in response to specific drugs.** **Patients and Methods: Gene expression profiles (GEP) were determined in CD19+ selected B-cells from 20 patients treated with fludarabine and cyclophosphamide (FC) (N=10) or FC plus rituximab (FCR) (N=10). Samples were collected in the first cycle before and within 48hours after initiation of treatment. GEP analysis was stratified by clinical response 3 months after start of therapy.** **Results: GEP before treatment detected high expression of 34 genes correlated with response and 32 genes correlated with resistance to therapy. These genes were related to regulation of apoptosis, cell cycle, cell adhesion, and signal transduction. Different results were obtained with sequential GEP: Sixteen genes were up-regulated after rituximab infusion in non-responders. Rituximab therapy resulted in down-regulation of AKT1 indicating involvement of the PI3-kinase pathway in CD20-signaling. Up-regulation of 24 genes after FC (including ITPKB (inositol 1,4,5-trisphosphate 3-kinase) and CD44) and of 36 genes after FCR (including CD49d) was associated with resistance. Down-regulation of CTLA4 correlated with poor response to FC. CD44, CD49d and the PI3-kinase signaling pathway were confirmed as potential therapeutic targets to overcome resistance by (protein analysis) or functional experiments. Conclusion Sequential GEP provides rapid and relevant information for prediction of response and resistance. This approach could be used to guide and adapt individualized therapy in CLL.** **Overall design:** **50 Samples from CD19 selected B-cells, three treatments (rituximab, FC and RFC), 10 replicates for each treatment, 20 replicates for control condition**

Background corr dist: **KL-Divergence = 0.1711, L1-Distance = 0.0533, L2-Distance = 0.0071, Normal std = 0.3538**

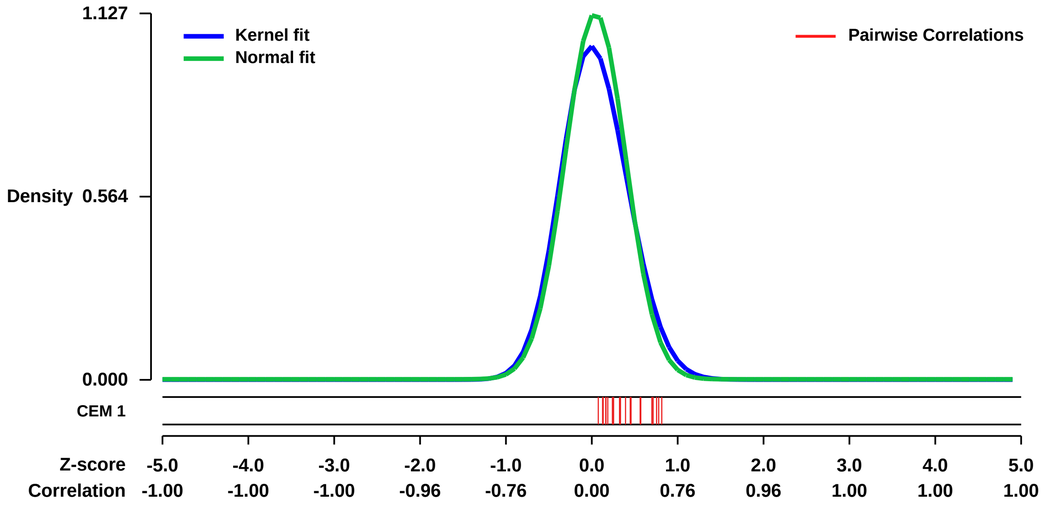

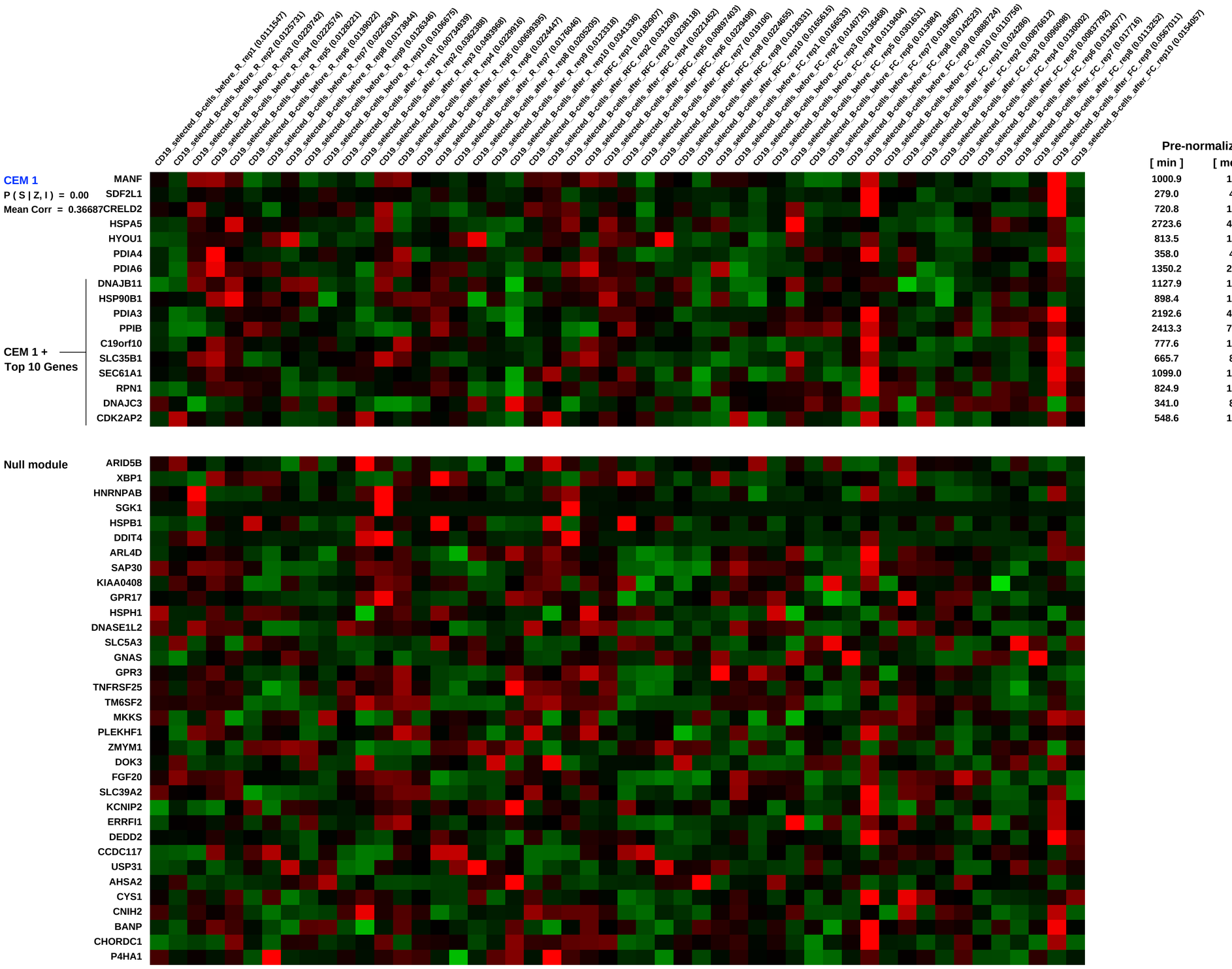

Pre-normalization Quantiles

[min]	[medium]	[max]
1000.9	1435.5	2516.9
279.0	448.6	1491.1
720.8	1218.8	2670.6
2723.6	4666.0	11573.9
813.5	1407.5	3068.0
358.0	486.8	903.5
1350.2	2878.7	6129.5
1127.9	1861.9	2447.6
898.4	1657.9	2771.2
2192.6	4620.1	10583.7
2413.3	7000.1	12327.5
777.6	1260.1	3219.4
665.7	860.6	1353.1
1099.0	1656.8	2649.6
824.9	1819.1	3327.4
341.0	889.7	1672.8
548.6	1114.2	2450.1

GEO Series "GSE30442" Expression Profiles

Num of samples in this series: 24

Scale of expression profile Z-scores

-3.0 -2.0 -1.0 0.0 1.0 2.0 3.0

GEO Link:	http://www.ncbi.nlm.nih.gov/geo/query/acc.cgi?acc=GSE30442
Status:	Public on Dec 16 2011
Title:	Whole-exome sequencing identifies mutations of BCOR in acute myeloid leukemia with normal karyotype
Organism:	Homo sapiens
Experiment type:	Expression profiling by array
Platform:	GPL570
Pubmed ID:	22012066
Summary & Design:	**Summary:** Among acute myeloid leukemias (AML) with normal karyotype (CN-AML), NPM1 and CEBPA mutations define WHO provisional entities accounting for ~60% of cases, but the remaining ~40% remains poorly characterized. By whole exome-sequencing (WES) of one CN-AML patient lacking mutations in NPM1, CEBPA, FLT3, MLL-PTD and IDH1, we newly identified a clonal somatic mutation in BCOR (BCL6 co-repressor), a gene located in chromosome X. Further analyses showed that BCOR mutations occurred in 11/262 (4.2%) CN-AML cases and represented a substantial fraction (14/82, 17.1%) of CN-AML patients showing the same genetic background as the index patient subjected to WES. BCOR somatic mutations were: i) disruptive events similar to germline BCOR mutations causing the oculo-cranio-facial-dental (OCFD) genetic syndrome; ii) associated with markedly decreased BCOR mRNA levels, absence of full-length BCOR and absent or low expression of a truncated BCOR protein; iii) almost mutually exclusive with NPM1 mutations and frequently associated with DNMT3A and RUNX1 mutations, pointing to a cooperation between these events. Finally, BCOR mutations correlated with poor outcome among a cohort of 160 CN-AML patients (28% versus 66% overall survival at 2 yrs, P=0.024). Our results implicate for the first time BCOR in the pathogenesis of CN-AML without NPM1 mutations. **Overall design:** AML samples with normal karyotype were studied. Molecular analyses were performed for BCOR mutations. 12 BCOR wild-type cases and 12 BCOR mutated cases were hybridized to gene expression micro-arrays.

Background corr dist: KL-Divergence = 0.2203, L1-Distance = 0.0727, L2-Distance = 0.0153, Normal std = 0.3236

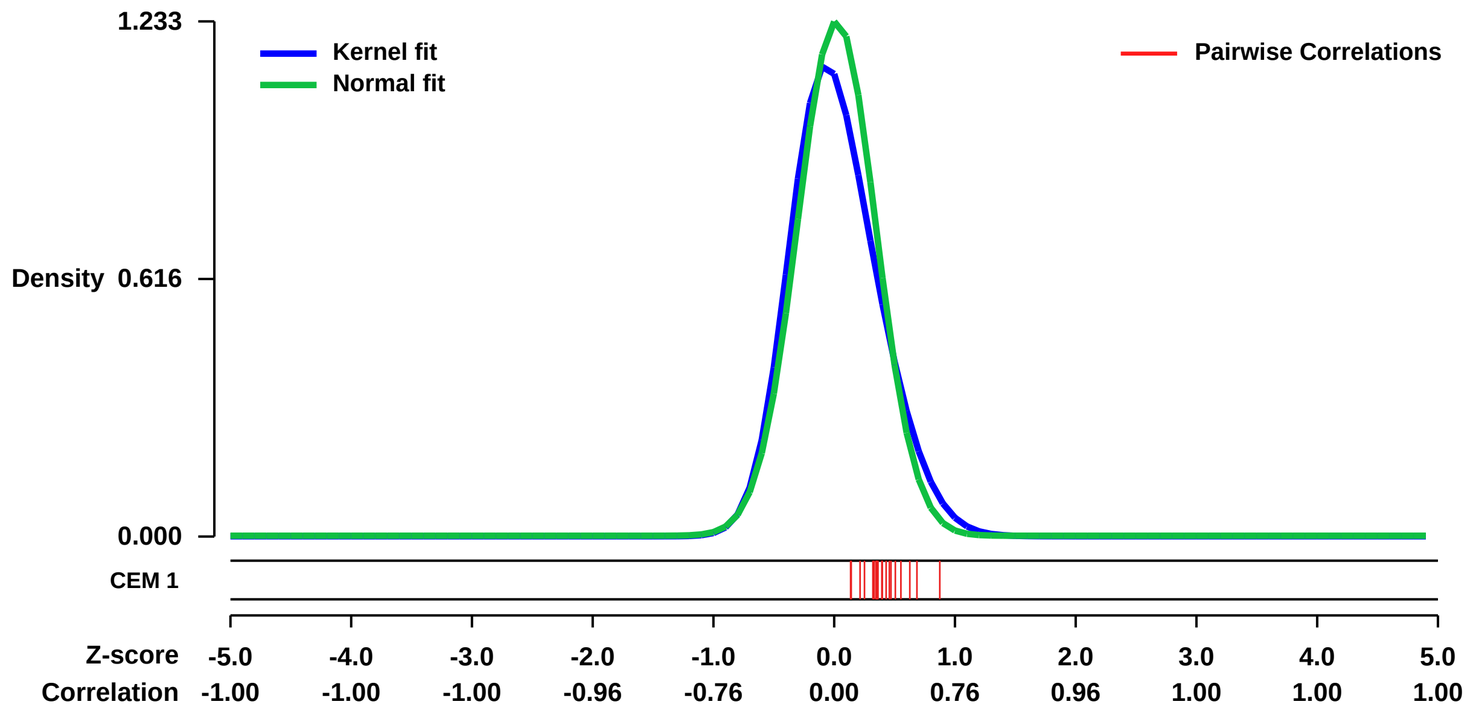

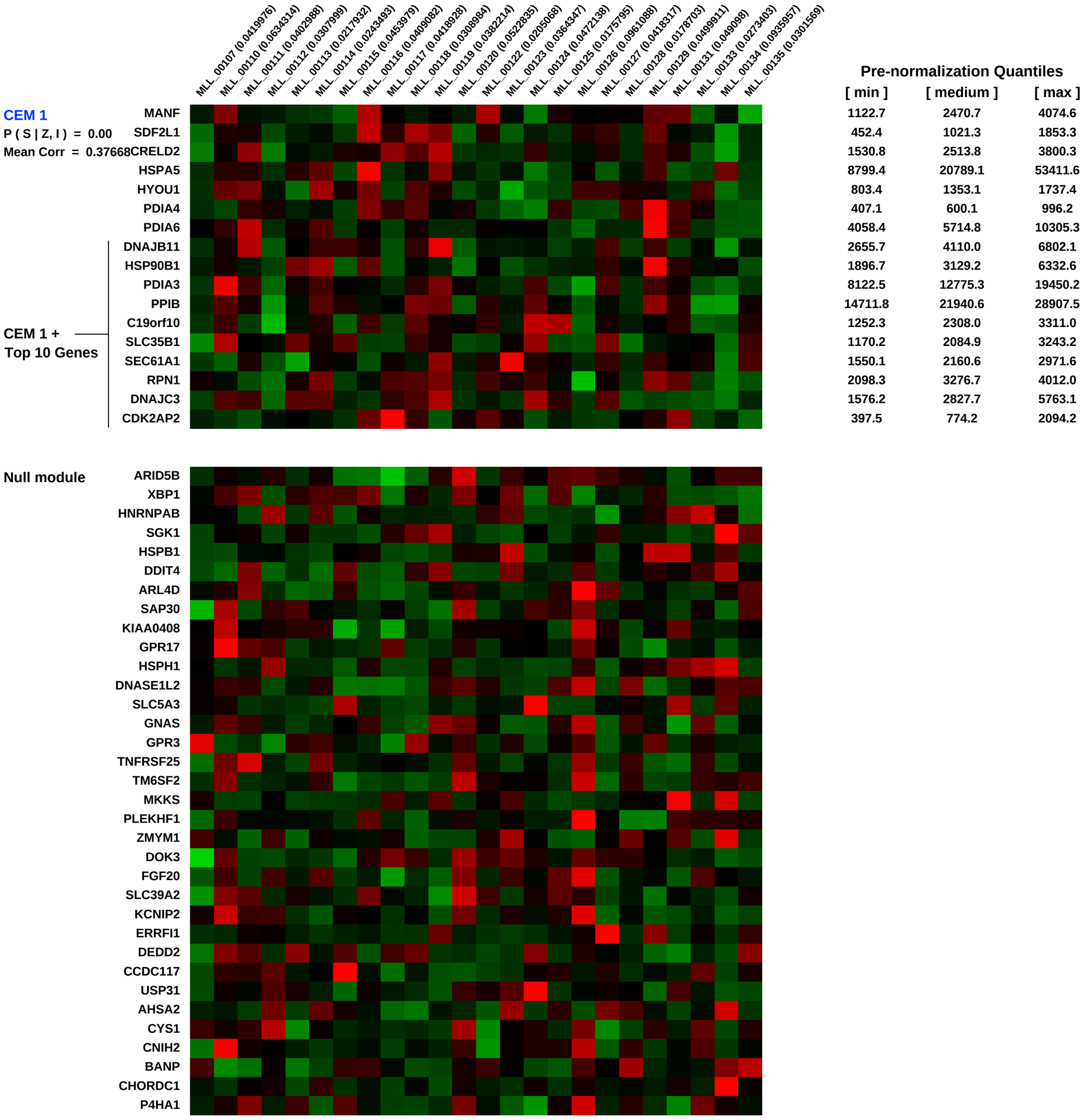

Pre-normalization Quantiles

	[min]	[medium]	[max]
MANF	1122.7	2470.7	4074.6
SDF2L1	452.4	1021.3	1853.3
CRELD2	1530.8	2513.8	3800.3
HSPA5	8799.4	20789.1	53411.6
HYOU1	803.4	1353.1	1737.4
PDIA4	407.1	600.1	996.2
PDIA6	4058.4	5714.8	10305.3
DNAJB11	2655.7	4110.0	6802.1
HSP90B1	1896.7	3129.2	6332.6
PDIA3	8122.5	12775.3	19450.2
PPIB	14711.8	21940.6	28907.5
C19orf10	1252.3	2308.0	3311.0
SLC35B1	1170.2	2084.9	3243.2
SEC61A1	1550.1	2160.6	2971.6
RPN1	2098.3	3276.7	4012.0
DNAJC3	1576.2	2827.7	5763.1
CDK2AP2	397.5	774.2	2094.2
ARID5B			
XBP1			
HNRNPAB			
SGK1			
HSPB1			
DDIT4			
ARL4D			
SAP30			
KIAA0408			
GPR17			
HSPH1			
DNASE1L2			
SLC5A3			
GNAS			
GPR3			
TNFRSF25			
TM6SF2			
MKKS			
PLEKHF1			
ZMYM1			
DOK3			
FGF20			
SLC39A2			
KCNIP2			
ERRFI1			
DEDD2			
CCDC117			
USP31			
AHSA2			
CYS1			
CNIH2			
BANP			
CHORDC1			
P4HA1			

GEO Series "GSE33845" Expression Profiles

Num of samples in this series: 12

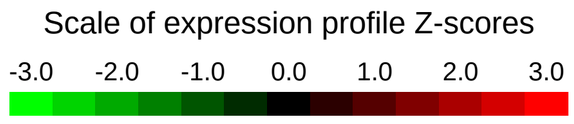

GEO Link:	http://www.ncbi.nlm.nih.gov/geo/query/acc.cgi?acc=GSE33845
Status:	Public on Jan 01 2013
Title:	dcEF-regulated gene expression of human lung cancer cells
Organism:	Homo sapiens
Experiment type:	Expression profiling by array
Platform:	GPL570
Pubmed ID:	
Summary & Design:	**Summary:** Highly metastatic cancer cells have been observed to move directionally in response to direct current (dc) electric fields (EFs) of physiological strength. The phenomenon, which is called electrotaxis or galvanotaxis, suggests the involvement of physiological EF in cancer metastasis. To explore this conjecture, we compared the influence of dcEF on gene expressions of a highly invasive (CL1-5) and a low invasive (CL1-0) lung cancer cell lines. **Overall design:** Gene expression of human lung cancer cells with (experimental samples) or without (control samples) dcEF stimulation in physiological strength was analyzed. Two cell lines, CL1-0 and CL1-5, were treated with the same condition and compared in this study. Each condition has three biological replicates for each cell line.

Background corr dist: KL-Divergence = 0.0835, L1-Distance = 0.0333, L2-Distance = 0.0017, Normal std = 0.4799

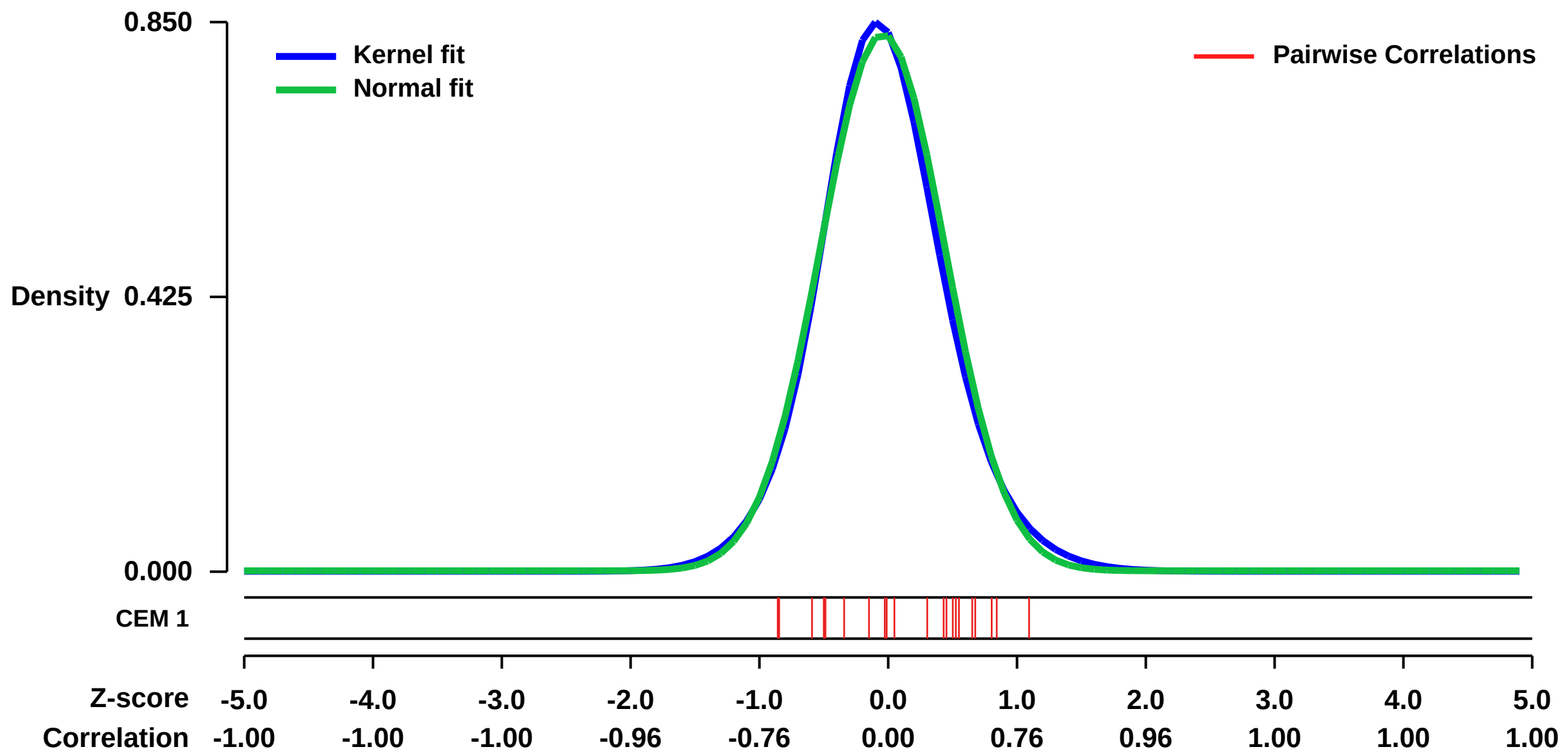

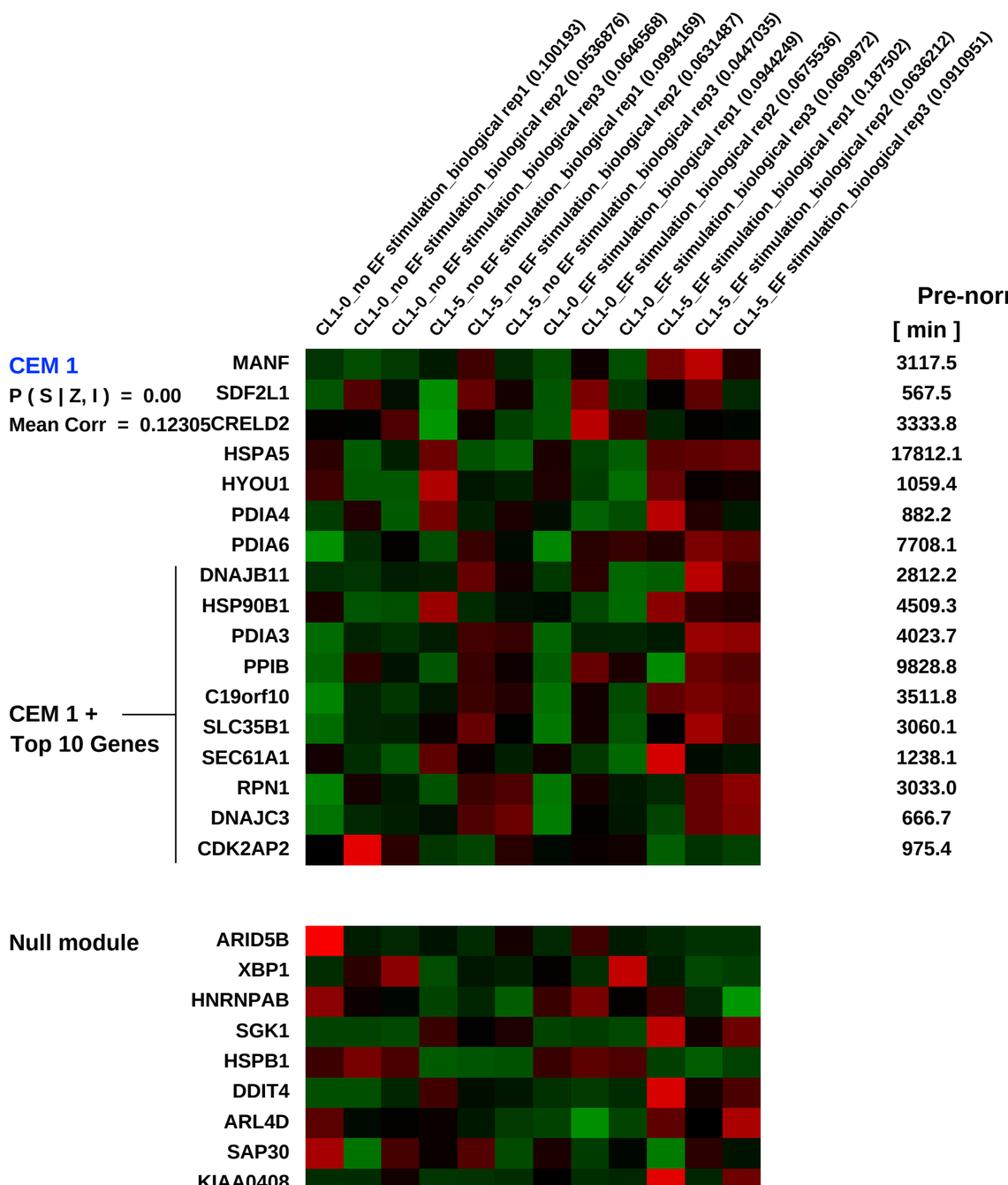

Pre-normalization Quantiles

	[min]	[medium]	[max]
MANF	3117.5	3627.1	5681.6
SDF2L1	567.5	1046.1	1428.9
CRELD2	3333.8	5073.2	7149.0
HSPA5	17812.1	23165.3	26421.6
HYOU1	1059.4	2545.9	4682.4
PDIA4	882.2	1097.2	1592.3
PDIA6	7708.1	12082.1	14257.0
DNAJB11	2812.2	3593.0	5837.6
HSP90B1	4509.3	6794.7	10808.8
PDIA3	4023.7	6634.5	12471.5
PPIB	9828.8	16317.8	19398.5
C19orf10	3511.8	5901.6	7516.5
SLC35B1	3060.1	3986.2	5178.0
SEC61A1	1238.1	2469.7	5442.1
RPN1	3033.0	5820.6	7956.2
DNAJC3	666.7	1140.0	1761.2
CDK2AP2	975.4	1332.4	2196.8

GEO Series "GSE11285" Expression Profiles

Num of samples in this series: 18

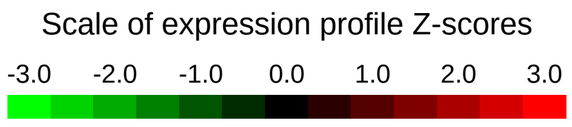

GEO Link:	http://www.ncbi.nlm.nih.gov/geo/query/acc.cgi?acc=GSE11285
Status:	Public on Jan 01 2009
Title:	GSK3 inhibition Induces Glioma Cell Death through c-MYC, NF-kB and Glucose Regulation
Organism:	Homo sapiens
Experiment type:	Expression profiling by array
Platform:	GPL570
Pubmed ID:	
Summary & Design:	**Summary:** We identified GSK3 as a regulator of GBM cell survival using microarray analysis, small molecule and genetic inhibitors of GSK3 activity. Various molecular and genetic approaches were then employed to dissect out the molecular mechanisms responsible for GSK3 inhibition-induced cytotoxicity. **Keywords: time course** **Overall design:** RNA extracted from U251 cells treated with DMSO or Enzastaurin for indicated time were hybridized to Affymetrix expression arrays (HG_U133-Plus_2) to detect changes in gene expression caused by Enzastaurin. Three replicates per sample were used.

Background corr dist: KL-Divergence = 0.2541, L1-Distance = 0.0522, L2-Distance = 0.0065, Normal std = 0.3007

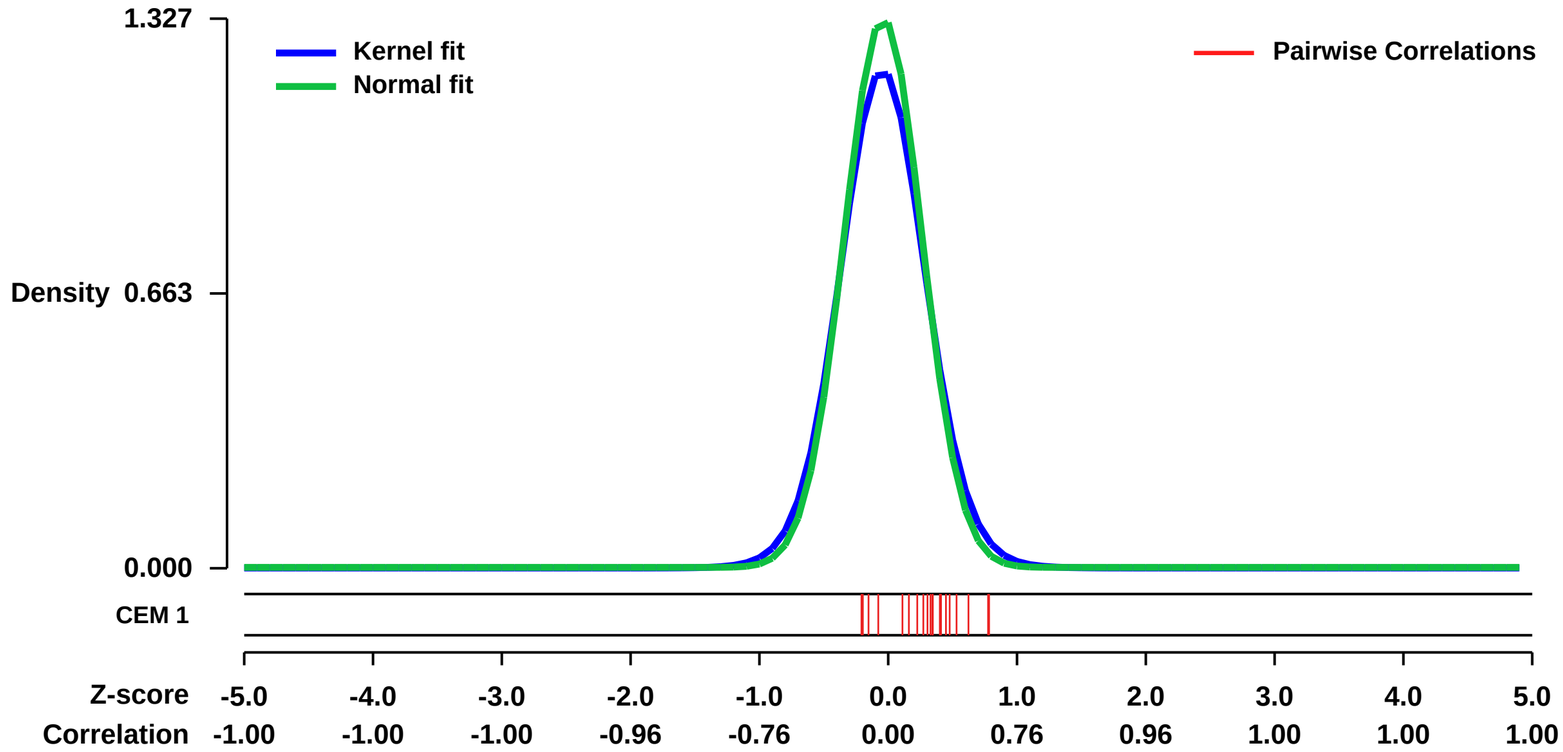

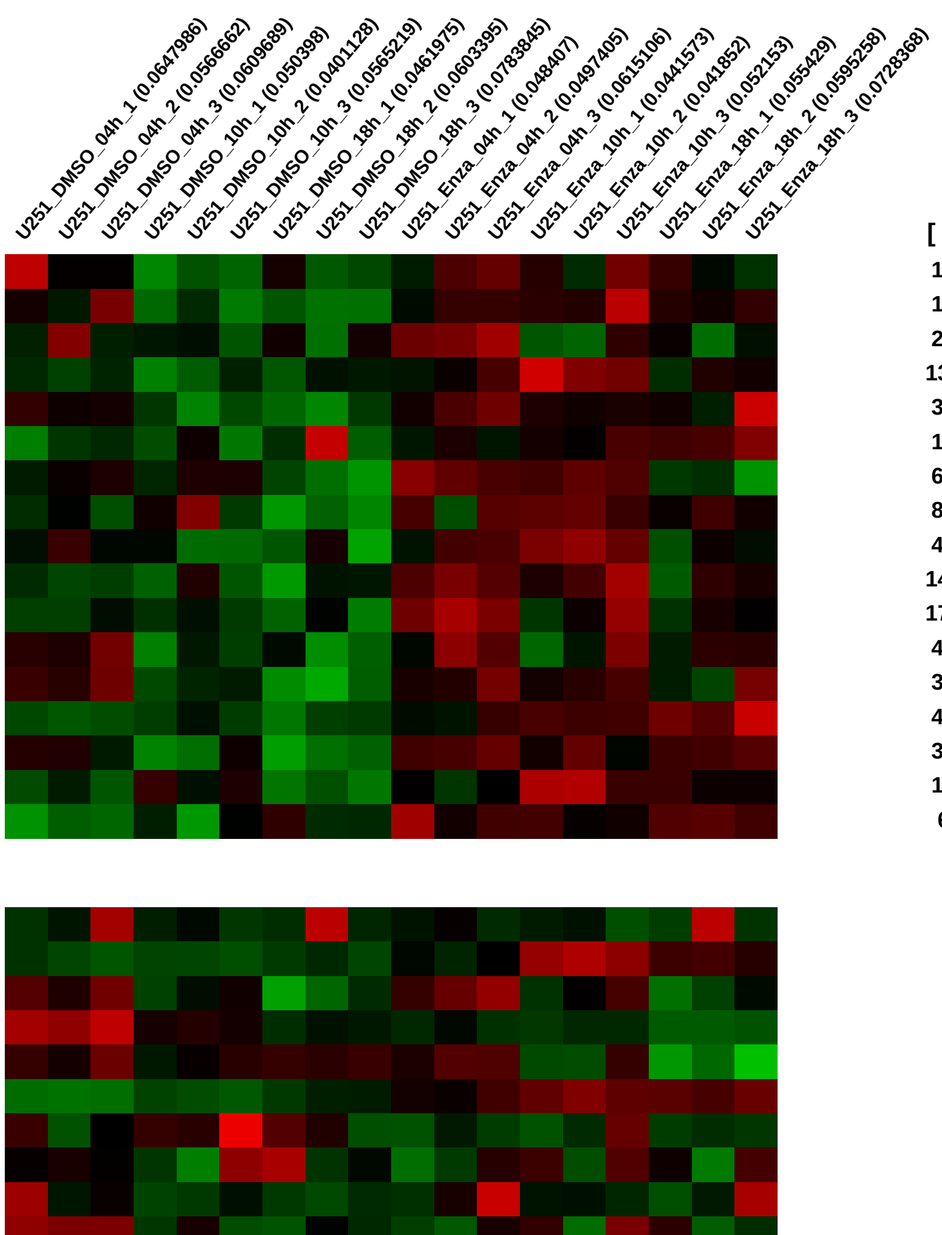

Pre-normalization Quantiles

	[min]	[medium]	[max]
CEM 1			
P (S | Z, I) = 0.00			
Mean Corr = 0.27457			
MANF	1640.8	1995.0	2466.7
SDF2L1	1494.5	1958.3	2490.4
CRELD2	2805.9	3317.4	4224.0
HSPA5	13334.9	16063.6	21890.3
HYOU1	3769.3	5514.7	7703.4
PDIA4	1240.9	1415.8	1674.3
PDIA6	6877.5	8116.1	8865.7
CEM 1 + Top 10 Genes			
DNAJB11	8283.0	10059.0	11267.6
HSP90B1	4349.9	5042.7	5704.3
PDIA3	14166.0	16255.8	17878.8
PPIB	17770.4	19629.6	22624.1
C19orf10	4944.1	5812.1	6772.2
SLC35B1	3301.3	3966.4	4289.5
SEC61A1	4026.3	5002.7	7068.8
RPN1	3569.5	4315.5	4578.4
DNAJC3	1251.8	1741.4	2455.8
CDK2AP2	609.2	816.5	994.0
Null module			
ARID5B			
XBP1			
HNRNPAB			
SGK1			
HSPB1			
DDIT4			
ARL4D			
SAP30			
KIAA0408			
GPR17			
HSPH1			
DNASE1L2			
SLC5A3			
GNAS			
GPR3			
TNFRSF25			
TM6SF2			
MKKS			
PLEKHF1			
ZMYM1			
DOK3			
FGF20			
SLC39A2			
KCNIP2			
ERRFI1			
DEDD2			
CCDC117			
USP31			
AHSA2			
CYS1			
CNIH2			
BANP			
CHORDC1			
P4HA1			

GEO Series "GSE13477" Expression Profiles

Num of samples in this series: 8

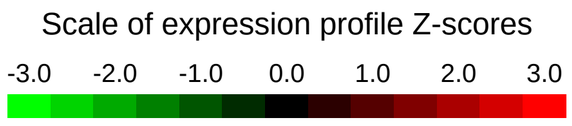

GEO Link:	http://www.ncbi.nlm.nih.gov/geo/query/acc.cgi?acc=GSE13477
Status:	Public on Nov 11 2008
Title:	Gene Expression Analysis of ARC (NSC 188491) Treated MCF7 cells
Organism:	Homo sapiens
Experiment type:	Expression profiling by array
Platform:	GPL570
Pubmed ID:	19232100
Summary & Design:	**Summary:** ARC (NSC 188491, SMA-491), 4-amino-6-hydrazino-7-beta-d-ribofuranosyl-7H-pyrrolo-(2,3-d)-pyrimidine-5-carboxamide, is a nucleoside analog with profound in vitro anti-cancer activity. First identified in a high-throughput screen for inhibitors of p21 mRNA expression, subsequent experiments showed that ARC also repressed expression of hdm2 and survivin, leading to its classification as a global inhibitor of transcription 1. The following Hu U133 plus 2.0 arrays represent single time point (24 hour) gene expression analysis of transcripts altered by ARC treatment. Arrays for the other compounds (sangivamycin and doxorubicin) are included as comparators. **Overall design:** MCF7 cells treated with ARC, Sangivamycin or Doxorubicin for 24 hours.

Background corr dist: KL-Divergence = 0.0518, L1-Distance = 0.0371, L2-Distance = 0.0019, Normal std = 0.5798

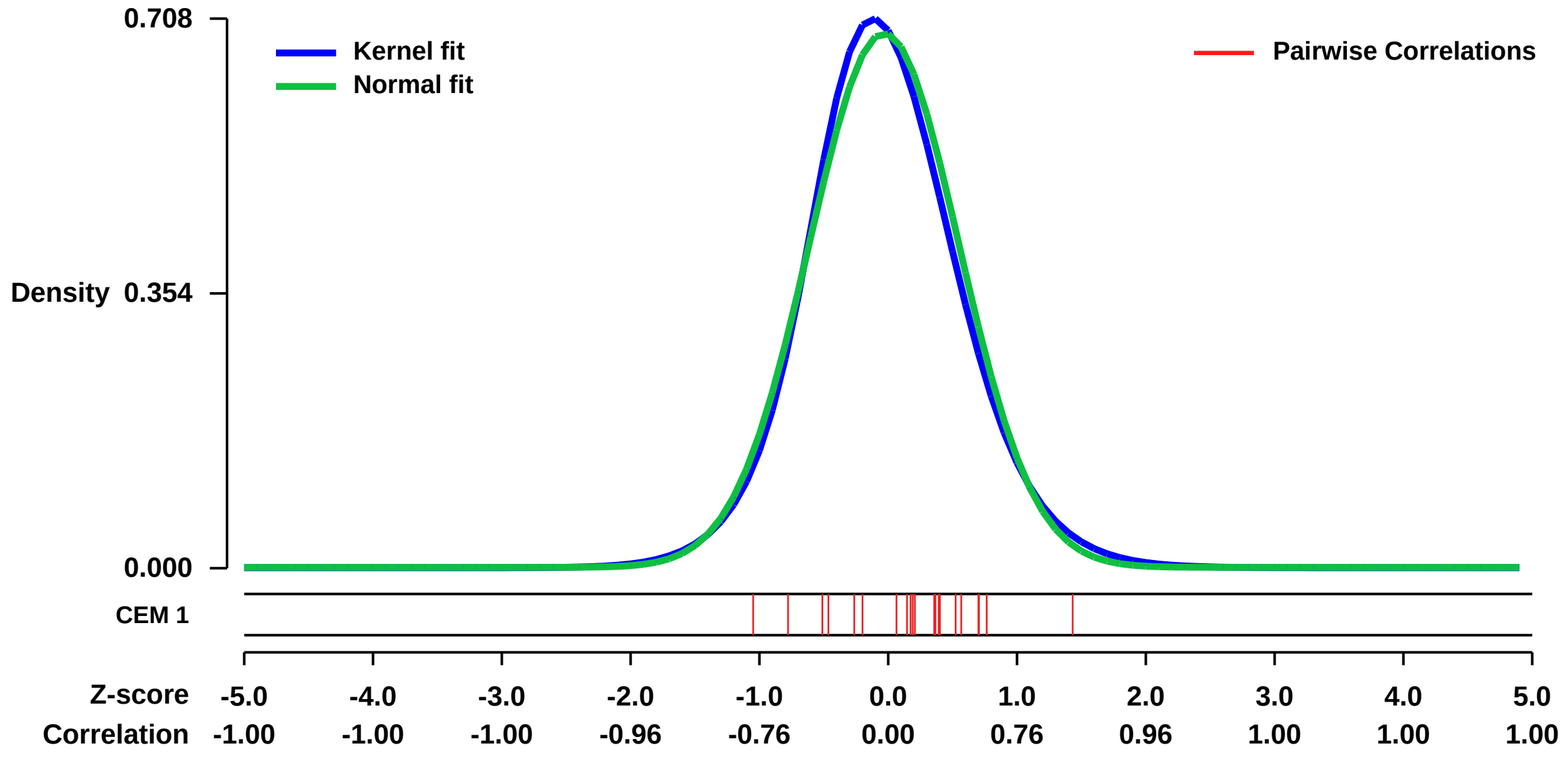

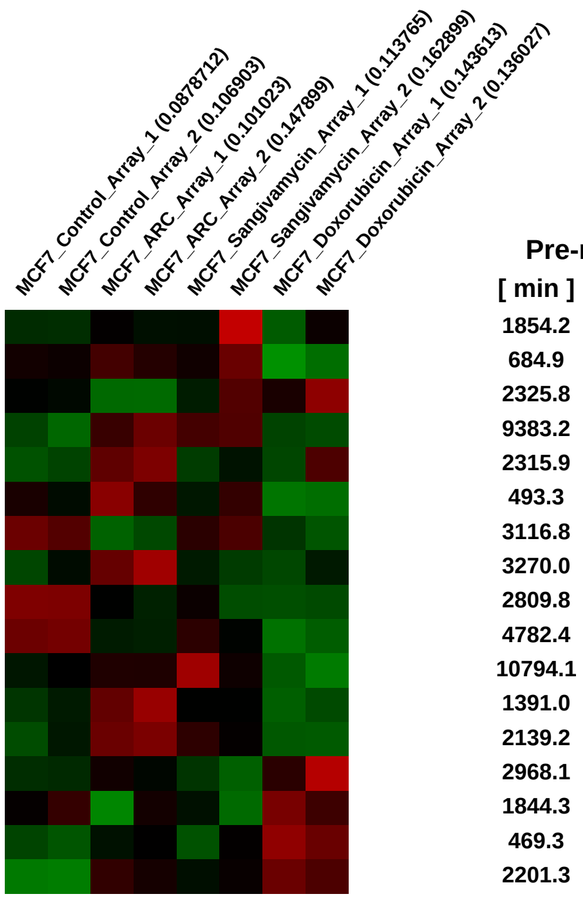

GEO Series "GSE51725" Expression Profiles

Num of samples in this series: 10

Scale of expression profile Z-scores

-3.0 -2.0 -1.0 0.0 1.0 2.0 3.0

GEO Link: http://www.ncbi.nlm.nih.gov/geo/query/acc.cgi?acc=GSE51725

Status: Public on Oct 26 2013

Title: EGFR expression status associated with lymph node ratio

Organism: Homo sapiens

Experiment type: Expression profiling by array

Platform: GPL570

Pubmed ID:

Summary & Design:

Summary:
We have tried to identify molecules associated with lymph node ratio expression by microarray. Expression microarray data prioritized gene candidates according to average expression ratio and its frequency.

Among these genes, we examined particular EGFR expression by immunohistochemistry (IHC) in 167 advanced gastric cancer.

Overall design:
We compared tumor specimens with high LNR (n=4) with those with low one (n=4) at mRNA level by Affymetrix microarray (harboring 54,675 genes) in stage III gastric cancer. We then prioritized the expression data, and enriched genes correlated with LNR, and finally validated EGFR as such candidates in primary advanced gastric cancer who underwent standard treatment (n=167).

Background corr dist: KL-Divergence = 0.1052, L1-Distance = 0.0613, L2-Distance = 0.0080, Normal std = 0.4521

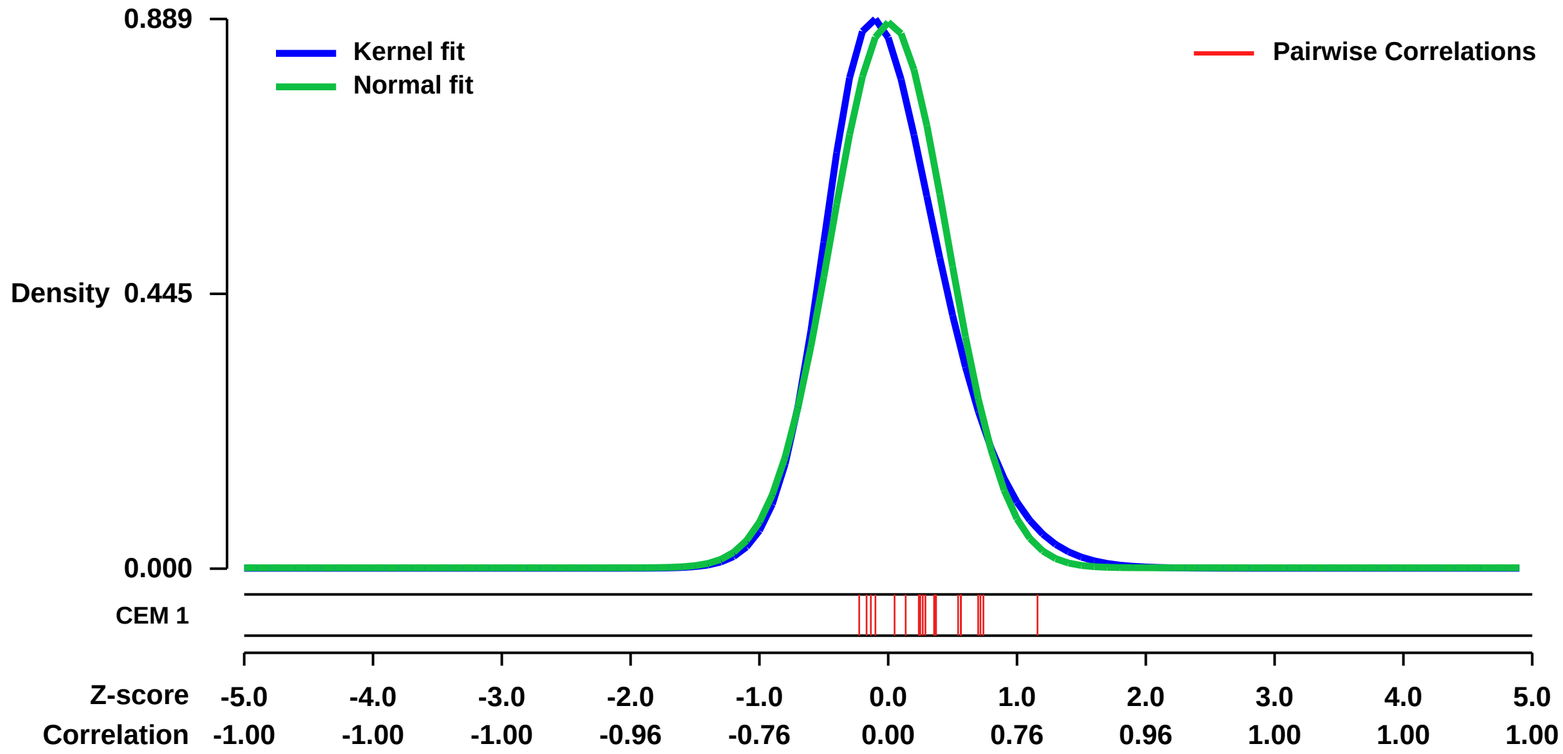

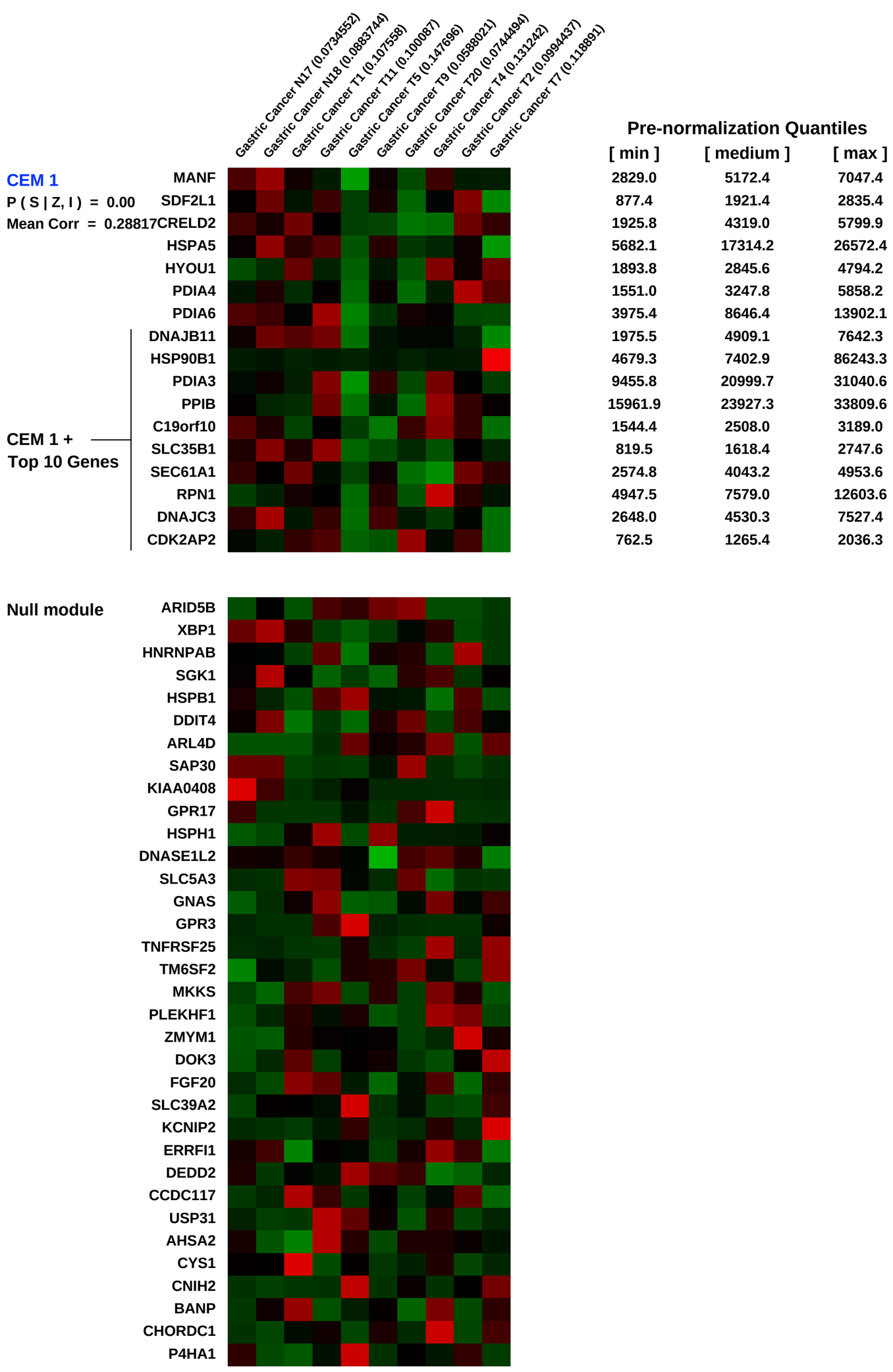

GEO Series "GSE16082" Expression Profiles

Num of samples in this series: 6

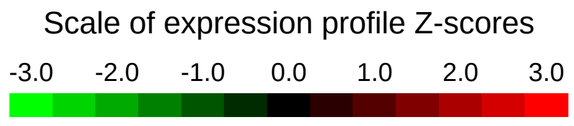

GEO Link:	http://www.ncbi.nlm.nih.gov/geo/query/acc.cgi?acc=GSE16082
Status:	Public on Sep 08 2009
Title:	Networking of differentially expressed genes in human MIA PaCa2 pancreatic cancer cells resistant to methotrexate
Organism:	Homo sapiens
Experiment type:	Expression profiling by array
Platform:	GPL570
Pubmed ID:	19732436
Summary & Design:	**Summary:** **A summary of the work associated to these microarrays is the following:** **The need for an integrated view of all data obtained from high-throughput technologies gave rise to network analyses. These are especially useful to rationalize phenomena in terms of how external perturbations propagate through the expression of genes. To address this issue in the case of drug resistance, we constructed Biological Association Networks of genes differentially expressed in cell lines resistant to methotrexate (MTX). Seven cell lines representative of different types of cancer including colon cancer (HT29 and Caco2), breast cancer (MCF7 and MDA-MB-468), pancreatic cancer (MIA PaCa-2), erythroblastic leukemia (K562) and osteosarcoma (Saos-2), were used. The differential expression pattern between sensitive and MTX-resistant cells was determined by microarrays covering the whole human genome and analyzed with the GeneSpring GX software package, v.7.3.1. Genes deregulated in common in the two colon cancer cell lines studied, were subject of Biological Association Networks construction. Dikkopf homolog-1 (DKK1) was a clear node of this network, and functional validations of this target using a siRNA showed a chemosensitization toward MTX. Members of the UDP-glucuronosyltransferase 1A (UGT1A) family formed a network of differentially expressed genes in the two breast cancer cell lines studied. siRNA treatment against UGT1A showed also an increase in MTX sensitivity. Eukaryotic translation elongation factor 1 alpha 1 (EEF1A1) was a gene overexpressed in common among the pancreatic cancer, leukemia and osteosarcoma cell lines, and siRNA treatment against EEF1A1 produced a chemosensitization toward MTX. Biological Association Networks identified DKK1, UGT1As and EEF1A1 as important gene nodes in MTX-resistance. Treatments using iRNA technology against these three genes show chemosensitization toward MTX.** **Overall design:** **Two cell lines are compared, which are MIA PaCa2 pancreatic cancer cells sensitive to methotrexate and MIA PaCa2 cells resistant to 10e-6M MTX. Six samples are provided which correspond to triplicates of each cell line. The samples provided were analyzed using the specific software GeneSpring GX.**

Background corr dist: KL-Divergence = 0.0286, L1-Distance = 0.0379, L2-Distance = 0.0016, Normal std = 0.7244

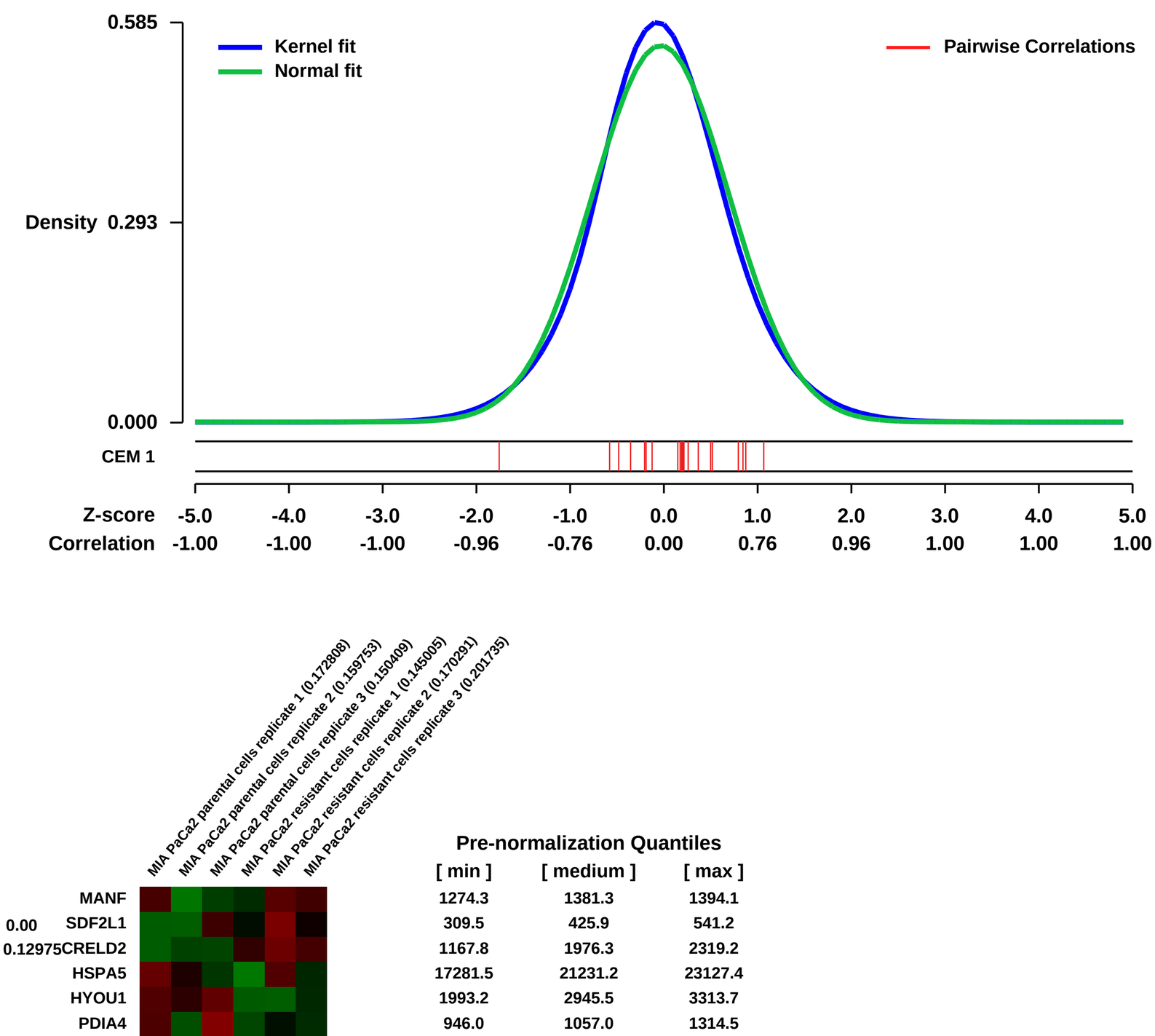

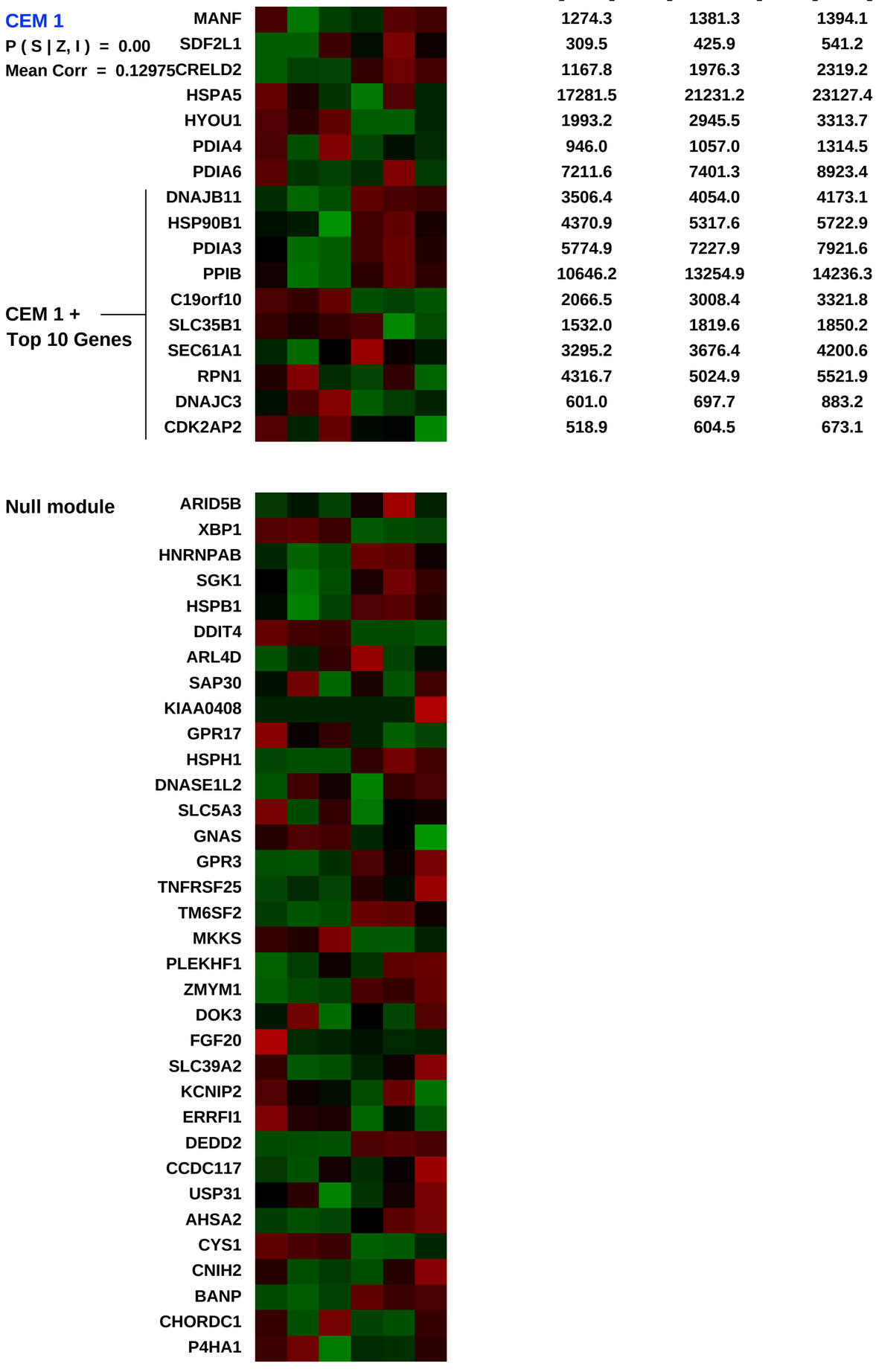

GEO Series "GSE38718" Expression Profiles

Num of samples in this series: 22

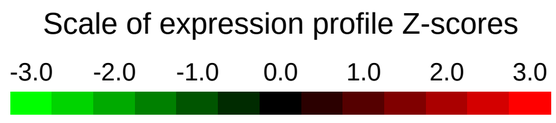

GEO Link:	http://www.ncbi.nlm.nih.gov/geo/query/acc.cgi?acc=GSE38718
Status:	Public on Feb 28 2013
Title:	Sex and aging effect on skeletal muscle transcriptome in humans
Organism:	Homo sapiens
Experiment type:	Expression profiling by array
Platform:	GPL570
Pubmed ID:	23418191
Summary & Design:	**Summary:** The aim of this investigation was to develop a global view of muscle transcriptional differences between older men and women and with aging for each sex. **Overall design:** Muscle biopsies were obtained from the biceps brachii of young (age 19~28yrs) and older (age 65~76 yrs) men (7 young, 4 older) and women (7 young, 4 older). Total RNA was extracted and gene expression profiling was performed using the Affymetrix Human Genome U133 Plus 2 chip.

Background corr dist: KL-Divergence = 0.1759, L1-Distance = 0.0552, L2-Distance = 0.0078, Normal std = 0.3516

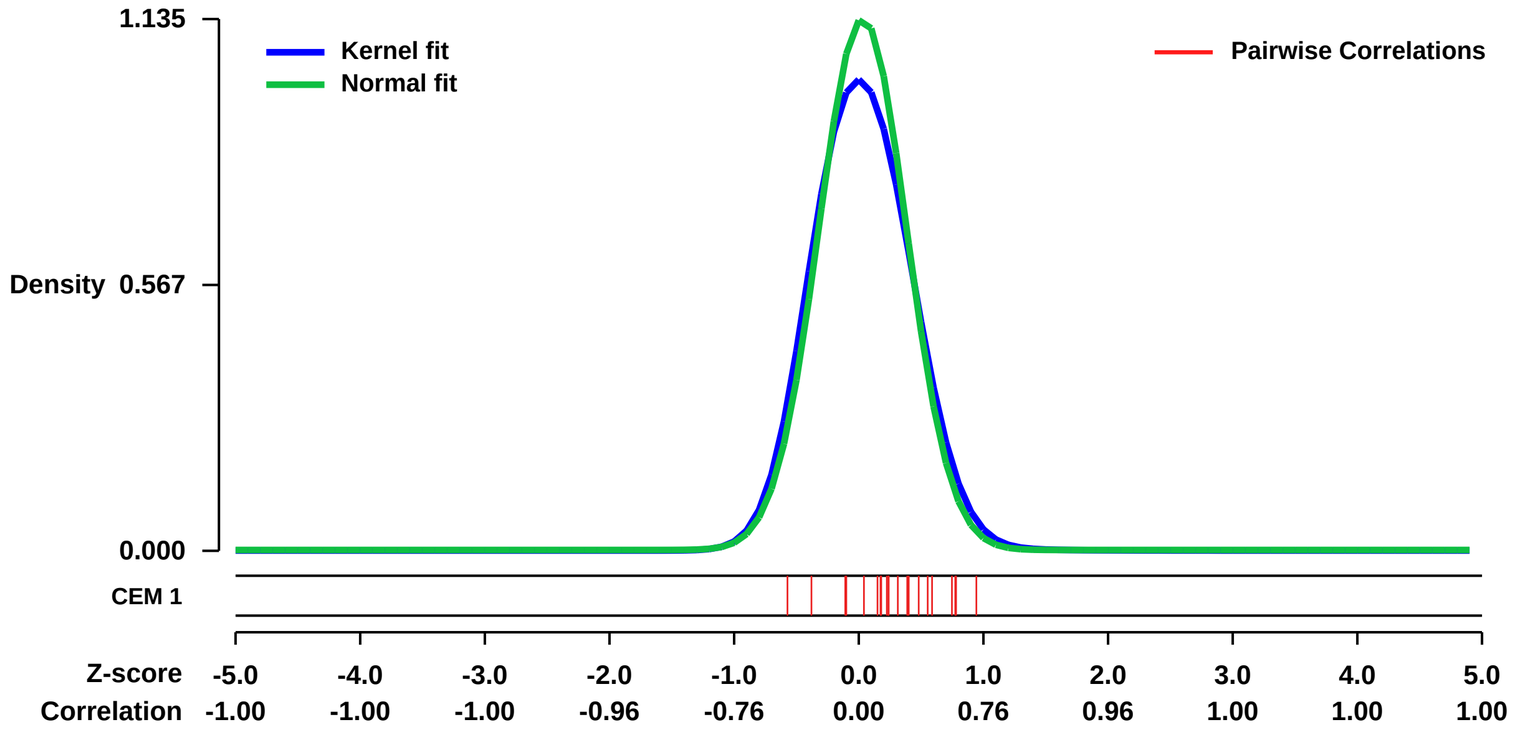

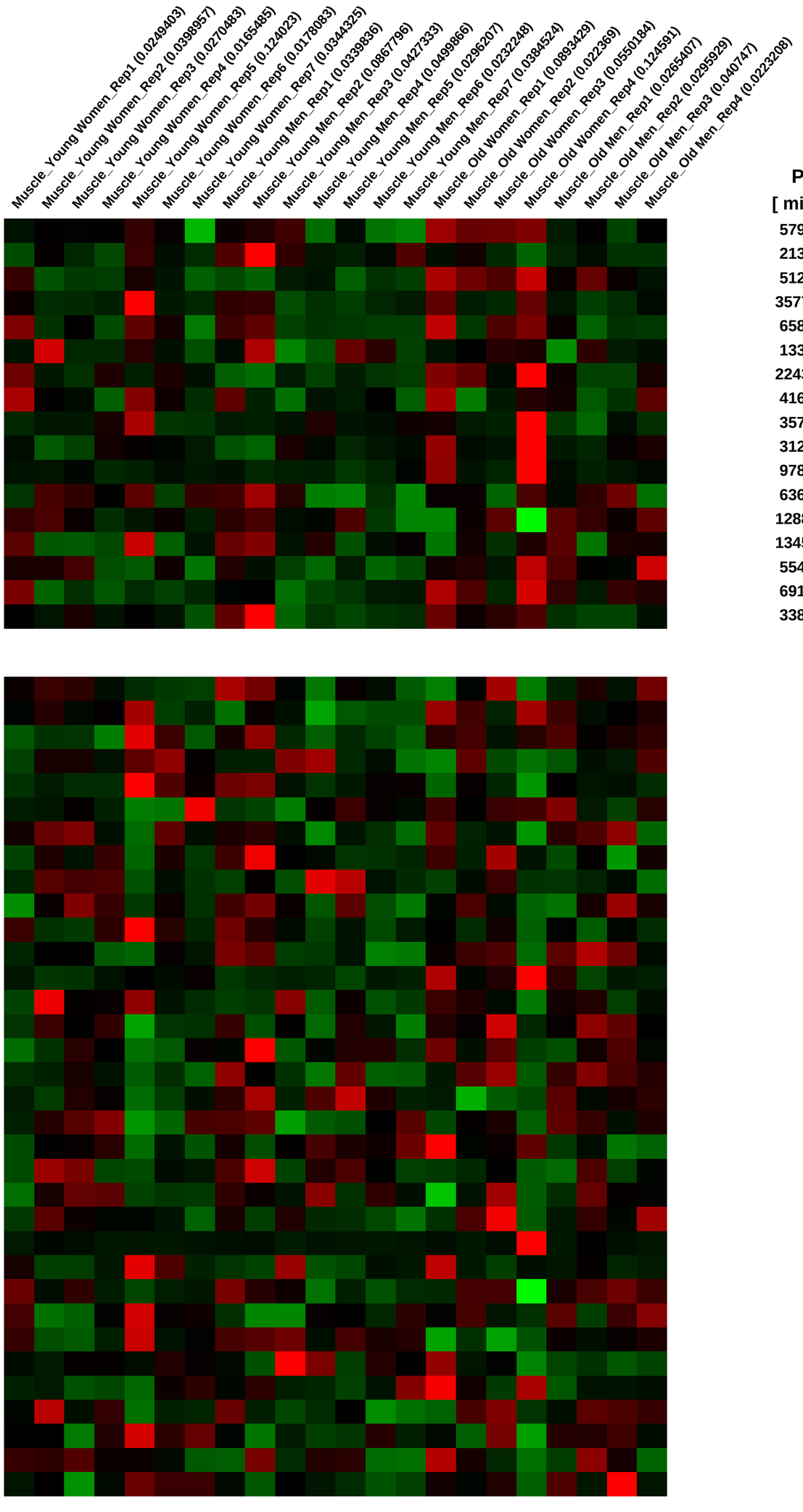

Pre-normalization Quantiles

[min]	[medium]	[max]
579.6	1092.4	1524.7
213.5	274.6	505.3
512.0	623.9	937.5
3577.2	4301.4	9421.0
658.8	845.2	1441.4
133.6	174.8	247.1
2243.7	2913.7	5097.7
416.8	604.6	903.0
357.1	533.2	1245.3
312.2	879.0	2994.4
978.7	1719.2	9184.2
636.4	795.2	963.7
1288.6	2265.7	2566.5
1345.7	1890.1	2742.1
554.3	1082.8	1981.9
691.4	986.2	1796.0
338.1	504.4	1107.6

GEO Series "GSE16149" Expression Profiles

Num of samples in this series: 18

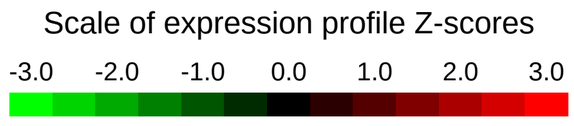

GEO Link:	http://www.ncbi.nlm.nih.gov/geo/query/acc.cgi?acc=GSE16149
Status:	Public on Mar 01 2010
Title:	Examining smoking-induced differential gene expression changes in buccal mucosa
Organism:	Homo sapiens
Experiment type:	Expression profiling by array
Platform:	GPL570
Pubmed ID:	20576139
Summary & Design:	**Summary:** A tissue like buccal mucosa (from cheek swabs) would be an ideal sample material for rapid, easy collection for testing of biomarkers as an alternative to blood. A limited number of studies, primarily in the smoker/oral cancer literature, address this tissue's efficacy for quantitative PCR or microarray gene expression analysis. In this study both qPCR and microarray analyses were used to evaluate gene expression in buccal cells. An initial study comparing blood and buccal cells from the same individuals looked at relative amounts of four genes. The RNA isolated from buccal cells was degraded but was of sufficient quality to be used with RT-qPCR to detect expression of specific genes. Second, buccal cell RNA was used for microarray-based differential gene expression studies by comparing gene expression between smokers and nonsmokers. The isolation and amplification protocol allowed use of 150-fold less buccal cell RNA than had been reported previously with human microarrays. We report here the finding of a small number of significant gene expression differences between smokers and nonsmokers, using buccal cells as target material. Additionally, Gene Set Enrichment Analysis confirmed that these genes were changing expression in the same pattern as seen in an earlier buccal cell study performed by another group. Our results suggest that in spite of a high degree of RNA degradation, buccal cells from cheek mucosa could be used to detect differential gene expression between smokers and nonsmokers. However the RNA degradation, increase in sample variability and microarray failure rate show that buccal samples should be used with caution as source material in expression studies. **Overall design:** Samples were collected from eight subjects, four smokers (Sm)and four nonsmokers (NS). Each cheek was sampled creating an a and b sample for each subject which is reflected in the array name. All samples were isolated separately for total RNA. Each was hybridzed to microarrays to examine for differential gene expression between smokers and nonsmokers. There are 14 total samples in the main dataset (Set 2). One cheek sample failed in microarray analysis for two individuals, 08BCNS23 a and 08BCSm27 a, and so are not included here. A sample set (Set 1) was created which contains the four samples shown in this file. They represent repeated sampling of both cheeks for two individuals to test for reproducibility. There is a separate RMA file and metadata file (this file) for these data. These included samples 08BC11Sm a and b, a smoker, and 08BC12NSa and b a nonsmoker.

Background corr dist: KL-Divergence = 0.1006, L1-Distance = 0.0560, L2-Distance = 0.0066, Normal std = 0.4464

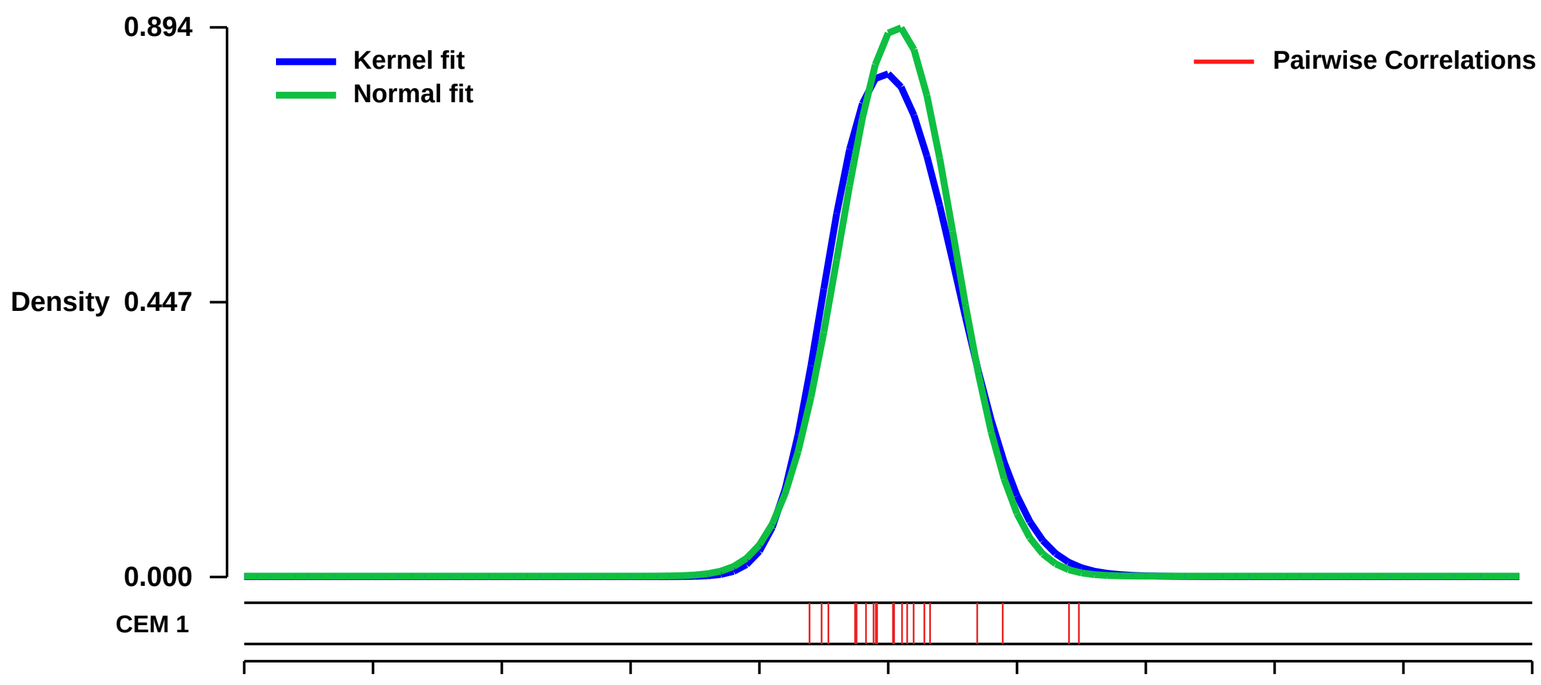

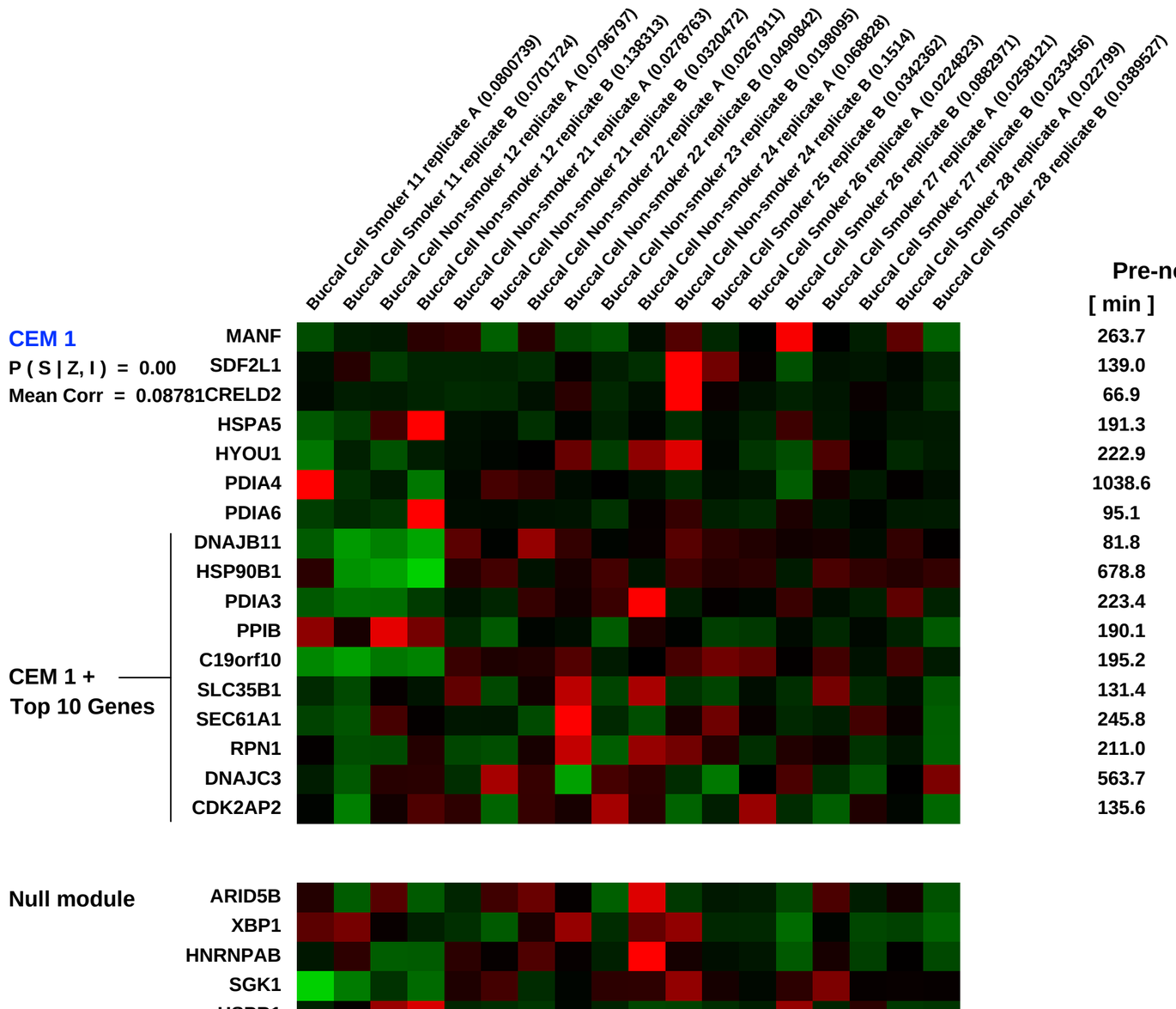

GEO Series "GSE26104" Expression Profiles

Num of samples in this series: 32

Scale of expression profile Z-scores

-3.0 -2.0 -1.0 0.0 1.0 2.0 3.0

GEO Link:	http://www.ncbi.nlm.nih.gov/geo/query/acc.cgi?acc=GSE26104
Status:	Public on Dec 18 2010
Title:	Search for specific biomarkers of IFN-beta bioactivity in patients with MS
Organism:	Homo sapiens
Experiment type:	Expression profiling by array
Platform:	GPL570
Pubmed ID:	21886806
Summary & Design:	**Summary:** We aimed to identify specific biomarkers of IFN-beta bioactivity in order to compare their gene expression induction by type I IFNs with the MxA, and to investigate their potential role in MS pathogenesis. Gene expression microarrays were performed in PBMC from MS patients who developed neutralizing antibodies (NAB) to IFN-beta. Nine genes followed patterns in gene expression over time similar to the MX1 and were selected for further experiments: IFI6, IFI27, IFI44L, IFIT1, HERC5, LY6E, RSAD2, SIGLEC1, and USP18. In vitro experiments revealed specific induction of selected biomarkers by IFN-beta but not IFN-gamma, and several markers, in particular USP18 and HERC5, were significantly induced at lower IFN-beta concentrations and more selective than the MX1 as biomarkers of IFN-beta bioactivity. In addition, USP18 expression was deficient in MS patients compared with healthy controls (p=0.0004). We propose specific biomarkers that may be considered in addition to the MxA to evaluate IFN-beta bioactivity, and to further explore their implication in MS pathogenesis. **Overall design:** Number of samples: 32. We analyzed PBMC from 8 patients at baseline and after 3, 12 and 24 months of IFN-beta treatment

Background corr dist: KL-Divergence = 0.1107, L1-Distance = 0.0268, L2-Distance = 0.0014, Normal std = 0.4208

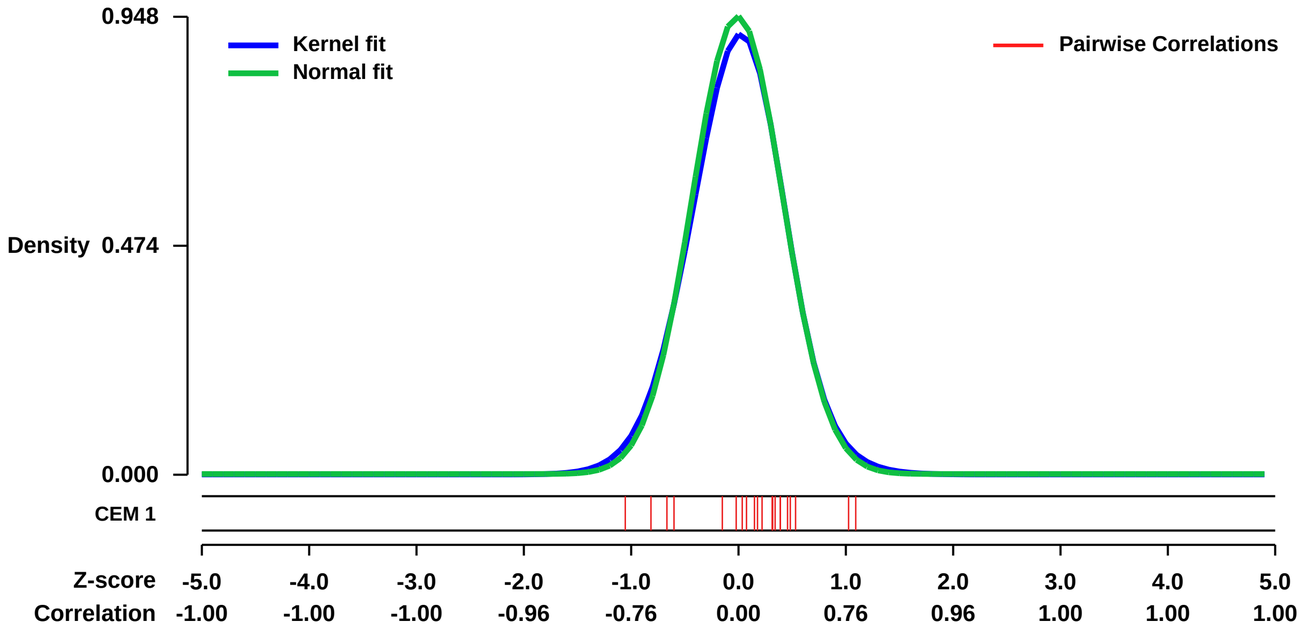

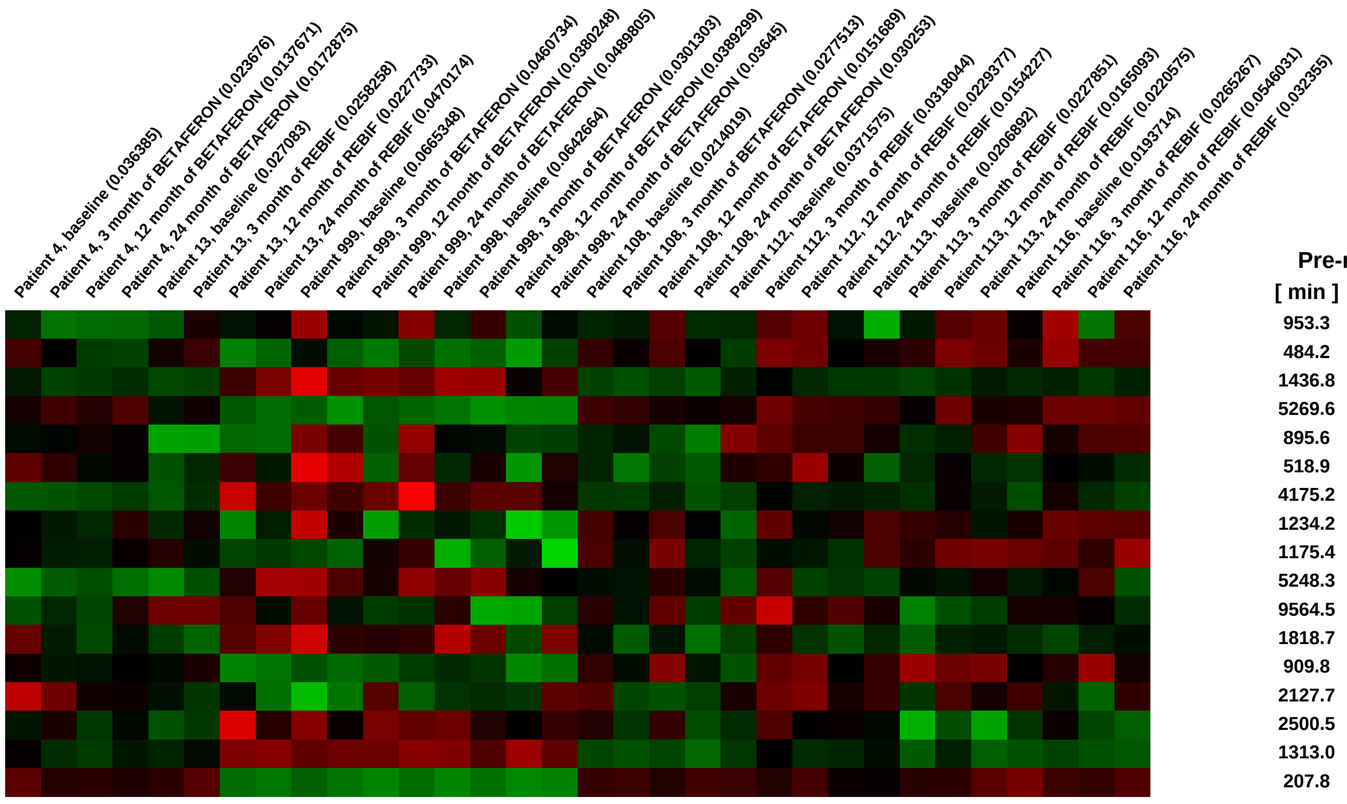

GEO Series "GSE41802" Expression Profiles

Num of samples in this series: 18

Scale of expression profile Z-scores

-3.0 -2.0 -1.0 0.0 1.0 2.0 3.0

GEO Link:	http://www.ncbi.nlm.nih.gov/geo/query/acc.cgi?acc=GSE41802
Status:	Public on Oct 25 2012
Title:	Isocitrata Dehydrogenase (IDH) Mutations Promote a Reversible ZEB1/mir-200-Dependent Epithelial Mesenchymal Transition (EMT)
Organism:	Homo sapiens
Experiment type:	Expression profiling by array
Platform:	GPL570
Pubmed ID:	23038259
Summary & Design:	**Summary:** Mutations in the genes encoding isocitrate dehydrogenase 1 and 2 (IDH1/2) occur in a variety of tumor types, resulting in production of the proposed oncometabolite, 2-hydroxyglutarate (2-HG). How mutant IDH and 2-HG alter signaling pathways to promote cancer, though, remains unclear. Additionally, there exist relatively few cell lines with IDH mutations. To examine the effect of endogenous IDH mutations and 2-HG, we created a panel of isogenic epithelial cell lines with either wild-type IDH1/2 or clinically relevant IDH1/2 mutations. Differences were noted in the ability of IDH mutations to cause robust 2-HG accumulation. IDH1/2 mutants that produce high levels of 2-HG cause an epithelial-mesenchymal transition (EMT)-like phenotype, characterized by changes in EMT-related gene expression and cellular morphology. 2-HG is sufficient to recapitulate aspects of this phenotype in the absence of an IDH mutation. In the cells types examined, mutant IDH-induced EMT is dependent on upregulation of the transcription factor ZEB1 and downregulation of the mir-200 family of microRNAs. Furthermore, sustained knockdown of IDH1 in IDH1 R132H mutant cells is sufficient to reverse many characteristics of EMT, demonstrating that continued expression of mutant IDH is required to maintain this phenotype. These results suggest mutant IDH proteins can reversibly deregulate discrete signaling pathways that contribute to tumorigenesis **Overall design:** 9 HCT116 isogenic clones with wild-type or IDH1/2 mutations. Samples were analyzed in duplicate.

Background corr dist: KL-Divergence = 0.2222, L1-Distance = 0.0441, L2-Distance = 0.0044, Normal std = 0.3175

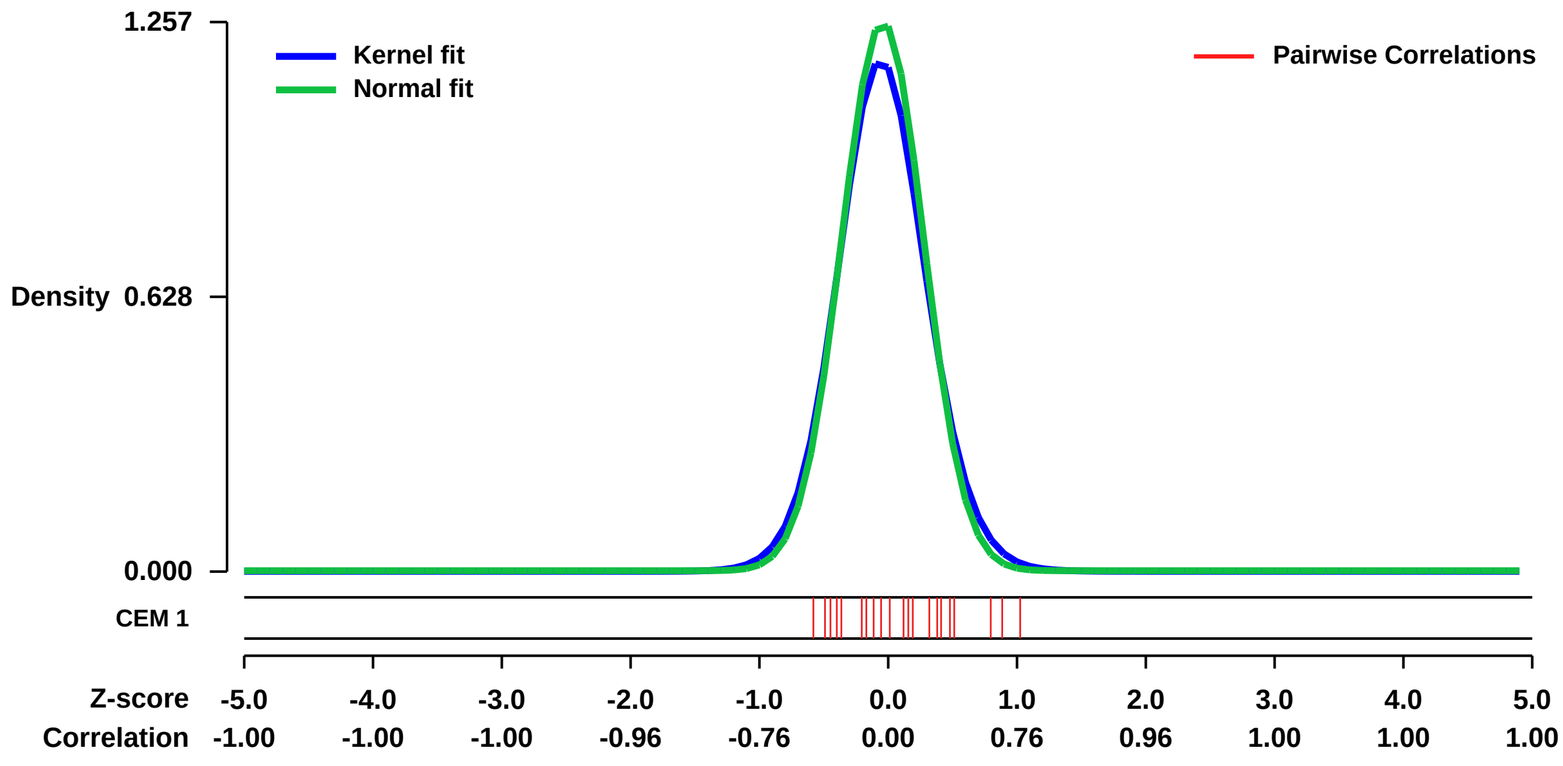

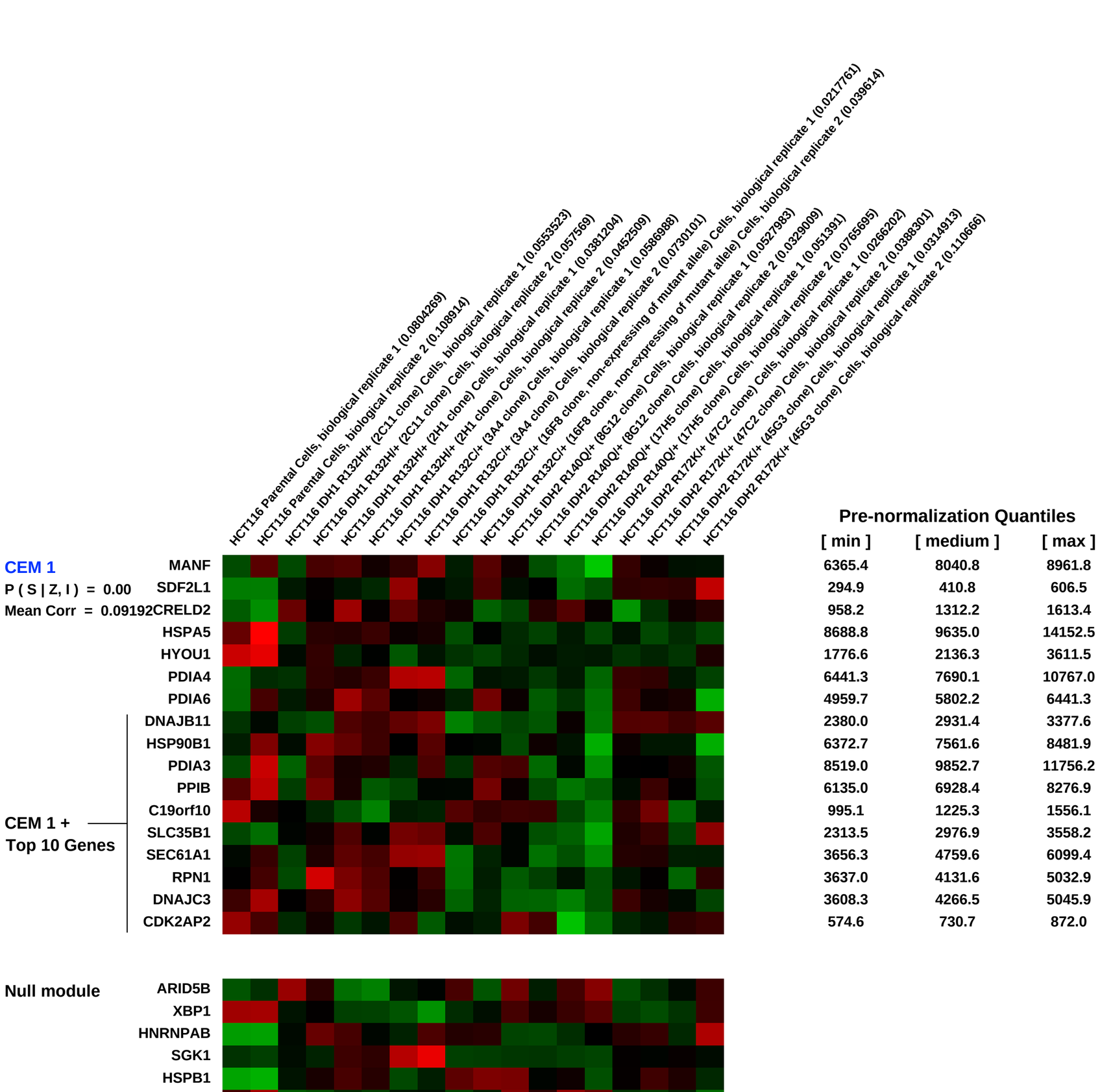

	Pre-normalization Quantiles		
	[min]	[medium]	[max]
MANF	6365.4	8040.8	8961.8
SDF2L1	294.9	410.8	606.5
CRELD2	958.2	1312.2	1613.4
HSPA5	8688.8	9635.0	14152.5
HYOU1	1776.6	2136.3	3611.5
PDIA4	6441.3	7690.1	10767.0
PDIA6	4959.7	5802.2	6441.3
DNAJB11	2380.0	2931.4	3377.6
HSP90B1	6372.7	7561.6	8481.9
PDIA3	8519.0	9852.7	11756.2
PPIB	6135.0	6928.4	8276.9
C19orf10	995.1	1225.3	1556.1
SLC35B1	2313.5	2976.9	3558.2
SEC61A1	3656.3	4759.6	6099.4
RPN1	3637.0	4131.6	5032.9
DNAJC3	3608.3	4266.5	5045.9
CDK2AP2	574.6	730.7	872.0

GEO Series "GSE17009" Expression Profiles

Num of samples in this series: 6

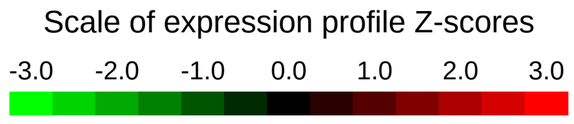

GEO Link:	http://www.ncbi.nlm.nih.gov/geo/query/acc.cgi?acc=GSE17009
Status:	Public on Jul 09 2009
Title:	Onconase Responsive Genes in Human Mesothelioma Cells: Implications for an RNA Damaging Therapeutic Agent
Organism:	Homo sapiens
Experiment type:	Expression profiling by array
Platform:	GPL570
Pubmed ID:	20137089
Summary & Design:	**Summary:** Onconase represents a new class of RNA-damaging drugs. Mechanistically, Onconase is thought to internalize, where it degrades intracellular RNAs such as tRNA and double-stranded RNA, and thereby suppresses protein synthesis. However, there may be additional or alternative mechanism(s) of action. Microarray analysis was used to compare gene expression profiles in untreated human malignant mesothelioma (MM) cell lines and cells exposed to 5 ug/ml Onconase for 24 h. **Overall design:** In this study, microarray analysis was used to compare gene expression profiles in untreated human malignant mesothelioma (MM) cell lines and cells exposed to 5 ug/ml Onconase for 24 h.

Background corr dist: KL-Divergence = 0.0348, L1-Distance = 0.0393, L2-Distance = 0.0022, Normal std = 0.6712

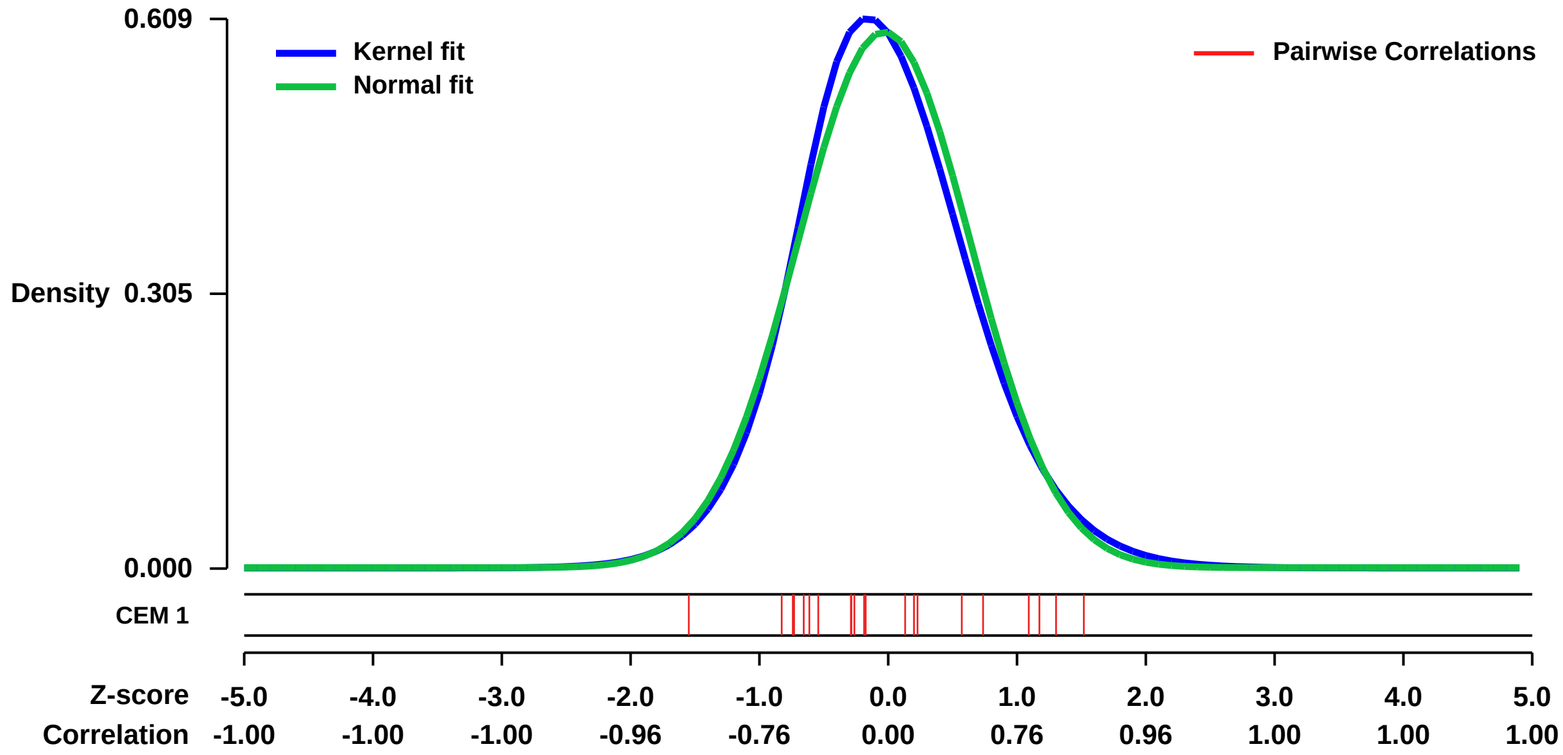

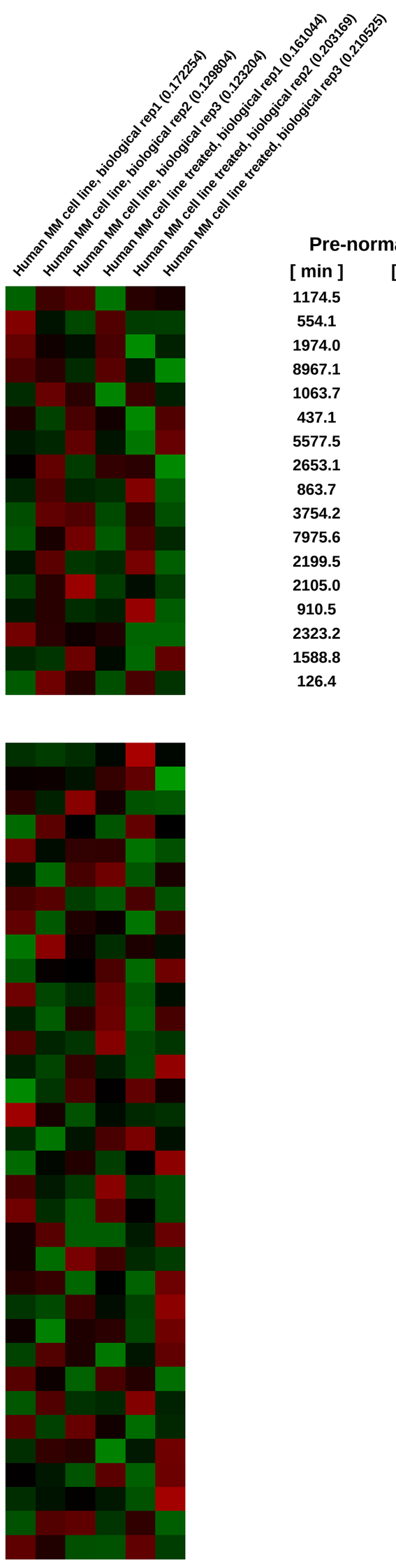

		Pre-normalization Quantiles		
		[min]	[medium]	[max]
CEM 1	MANF	1174.5	2799.2	3264.2
P (S | Z, I) = 0.00	SDF2L1	554.1	1143.8	2796.0
Mean Corr = -0.02610	CRELD2	1974.0	4349.7	5596.7
	HSPA5	8967.1	20729.0	23739.6
	HYOU1	1063.7	2942.2	3584.6
	PDIA4	437.1	1360.4	1636.7
	PDIA6	5577.5	8843.4	12955.5
CEM 1 + Top 10 Genes	DNAJB11	2653.1	5596.7	6511.4
	HSP90B1	863.7	2063.0	5347.0
	PDIA3	3754.2	7595.2	8819.5
	PPIB	7975.6	11603.5	14491.1
	C19orf10	2199.5	3040.5	4696.5
	SLC35B1	2105.0	2550.6	4076.0
	SEC61A1	910.5	2014.0	4847.5
	RPN1	2323.2	2925.4	3295.2
	DNAJC3	1588.8	2480.6	3615.9
	CDK2AP2	126.4	650.8	941.2
Null module	ARID5B			
	XBP1			
	HNRNPAB			
	SGK1			
	HSPB1			
	DDIT4			
	ARL4D			
	SAP30			
	KIAA0408			
	GPR17			
	HSPH1			
	DNASE1L2			
	SLC5A3			
	GNAS			
	GPR3			
	TNFRSF25			
	TM6SF2			
	MKKS			
	PLEKHF1			
	ZMYM1			
	DOK3			
	FGF20			
	SLC39A2			
	KCNIP2			
	ERRFI1			
	DEDD2			
	CCDC117			
	USP31			
	AHSA2			
	CYS1			
	CNIH2			
	BANP			
	CHORDC1			
	P4HA1			

GEO Series "GSE22483" Expression Profiles

Num of samples in this series: 6

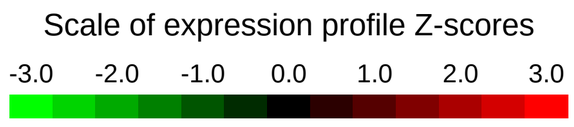

GEO Link:	http://www.ncbi.nlm.nih.gov/geo/query/acc.cgi?acc=GSE22483
Status:	Public on Jan 28 2011
Title:	Hormone-Independence of Prostate Cancer Cells is Supported by the Androgen Receptor without Binding to Classical Response Elements
Organism:	Homo sapiens
Experiment type:	Expression profiling by array
Platform:	GPL570
Pubmed ID:	21330406
Summary & Design:	**Summary:** Treatment of late passage (LP50) LNCaP cells with R1881 (androgen) and AR shRNA identified a gene program controlled by androgen receptor in the absence of androgen. **Overall design:** Gene expression in late passage (LP50) LNCaP cells that had enhanced androgen-independent growth was determined in androgen-depleted medium in response to R1881 or AR knock down via AR shRNA

Background corr dist: KL-Divergence = 0.0290, L1-Distance = 0.0486, L2-Distance = 0.0027, Normal std = 0.7522

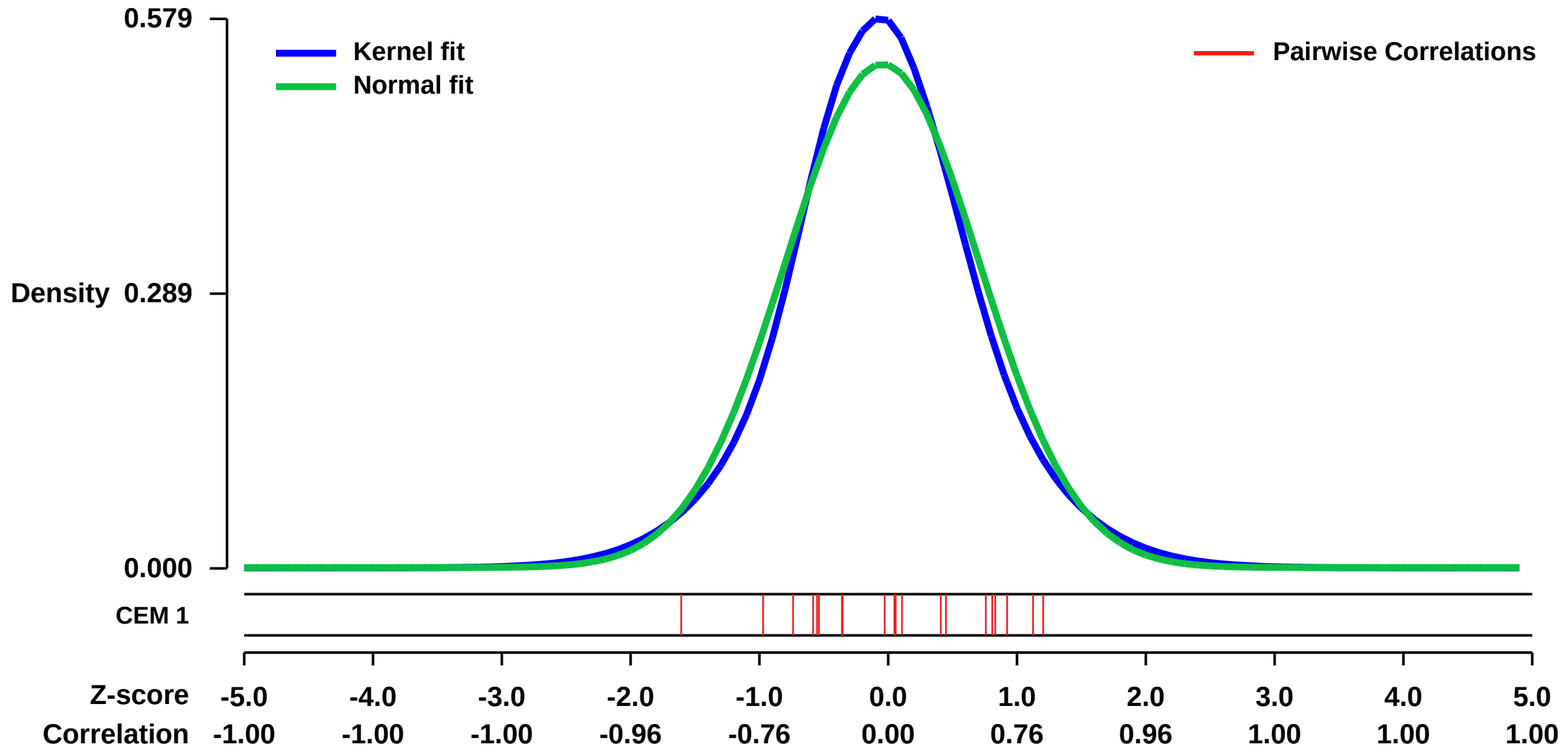

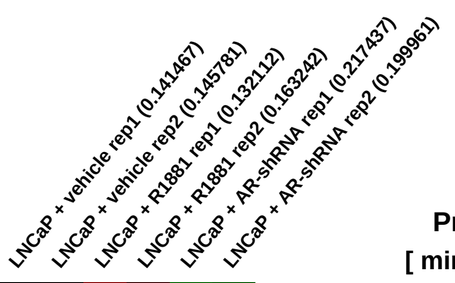

Pre-normalization Quantiles

		[min]	[medium]	[max]
CEM 1	MANF	3017.3	3471.0	3959.4
P (S | Z, I) = 0.00	SDF2L1	766.2	855.4	1121.7
Mean Corr = 0.04283	CRELD2	3542.4	3792.3	4112.7
	HSPA5	15971.5	18728.0	21025.6
	HYOU1	2862.3	3714.2	4116.5
	PDIA4	1227.2	1416.6	1485.1
	PDIA6	6029.8	6327.4	6838.4
CEM 1 + Top 10 Genes	DNAJB11	2305.1	3019.9	3670.9
	HSP90B1	7487.3	8616.2	9171.9
	PDIA3	13707.7	14648.0	18314.8
	PPIB	12356.2	17719.6	18318.9
	C19orf10	2821.3	3214.6	4861.2
	SLC35B1	2235.8	2459.4	2645.0
	SEC61A1	5792.2	6018.4	7437.4
	RPN1	3395.4	3629.2	3900.8
	DNAJC3	2330.2	2567.8	2831.5
	CDK2AP2	1235.2	1533.4	1746.7
Null module	ARID5B			
	XBP1			
	HNRNPAB			
	SGK1			
	HSPB1			
	DDIT4			
	ARL4D			
	SAP30			
	KIAA0408			
	GPR17			
	HSPH1			
	DNASE1L2			
	SLC5A3			
	GNAS			
	GPR3			
	TNFRSF25			
	TM6SF2			
	MKKS			
	PLEKHF1			
	ZMYM1			
	DOK3			
	FGF20			
	SLC39A2			
	KCNIP2			
	ERRFI1			
	DEDD2			
	CCDC117			
	USP31			
	AHSA2			
	CYS1			
	CNIH2			
	BANP			
	CHORDC1			
	P4HA1			

GEO Series "GSE28059" Expression Profiles

Num of samples in this series: 9

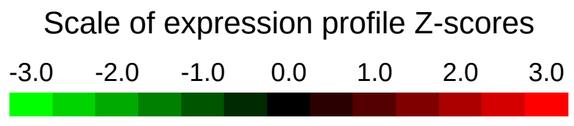

GEO Link:	http://www.ncbi.nlm.nih.gov/geo/query/acc.cgi?acc=GSE28059
Status:	Public on Jun 30 2011
Title:	Expression in Huh7 cells 72 hours after treatment with scramble, SPTLC123, or DEGS siRNA
Organism:	Homo sapiens
Experiment type:	Expression profiling by array
Platform:	GPL570
Pubmed ID:	22628619
Summary & Design:	**Summary:** Dysregulation of ceramide synthesis has been associated with metabolic disorders such as atherosclerosis and diabetes mellitus. Using a human hepatoma cell line (Huh7), we investigated the changes in lipid homeostasis and gene expression when the synthesis of ceramide is perturbed by knocking down serine transferases subunits 1, 2 and 3 (SPTLC123) or dihydroceramide desaturase (DEGS1). While the inhibition of serine palmitoyl transferase (SPTLC) affects ceramide production differently at the subspecies level depending upon which SPTLC subunit is silenced; depleting DEGS1 is sufficient to produce a similar outcome as knocking down all SPTLC subunits. Both the distribution of multiple lipid classes, especially at the subspecies level, and the global transcriptional profile is altered differently when either SPTLC123 or DEGS1 were silenced. The overall transcriptional changes indicate a negative regulation in biosynthetic processes and a down-regulation of genes involved in general endomembrane trafficking for both DEGS1 and SPTLC123 siRNA treated cells, but also the up-regulation of genes involved with cell migration function in DEGS1 siRNA cells. Pathway analysis indicate changes in amino acid, sugar and nucleotide metabolisms as well as vesicle trafficking between organelles occurred more robustly in DEGS1 silenced cells. Although either SPTLC123 or DEGS1 siRNA treatment positively regulated numerous genes involved with endocytosis and endosomal recycling, depleting SPTLC123 caused transcriptional changes in genes primarily involved with lipid metabolism. The alterations reflect how SPTLC or DEGS1 silenced cells respond differently to disruption in lipid flux, but also maintain cellular lipid pools through increasing endocytotic processes and down-regulating metabolic biosynthesis without developing endoplasmic reticulum stress. Also, these results are the first to demonstrate that reducing ceramide synthesis by decreasing the function of either SPTLC or DEGS1 affects cellular function differently at the level of lipid synthesis and gene expression. **Overall design:** Differential gene expression was assessed by Affymetrix microarray experiments for 9 Huh7 cell samples across 3 siRNA treatment groups (scramble siRNA conrol had 3 samples, SPTLC123 siRNA had 3 samples, DEGS1 siRNA had 3 samples)

Background corr dist: KL-Divergence = 0.0684, L1-Distance = 0.0195, L2-Distance = 0.0004, Normal std = 0.5033

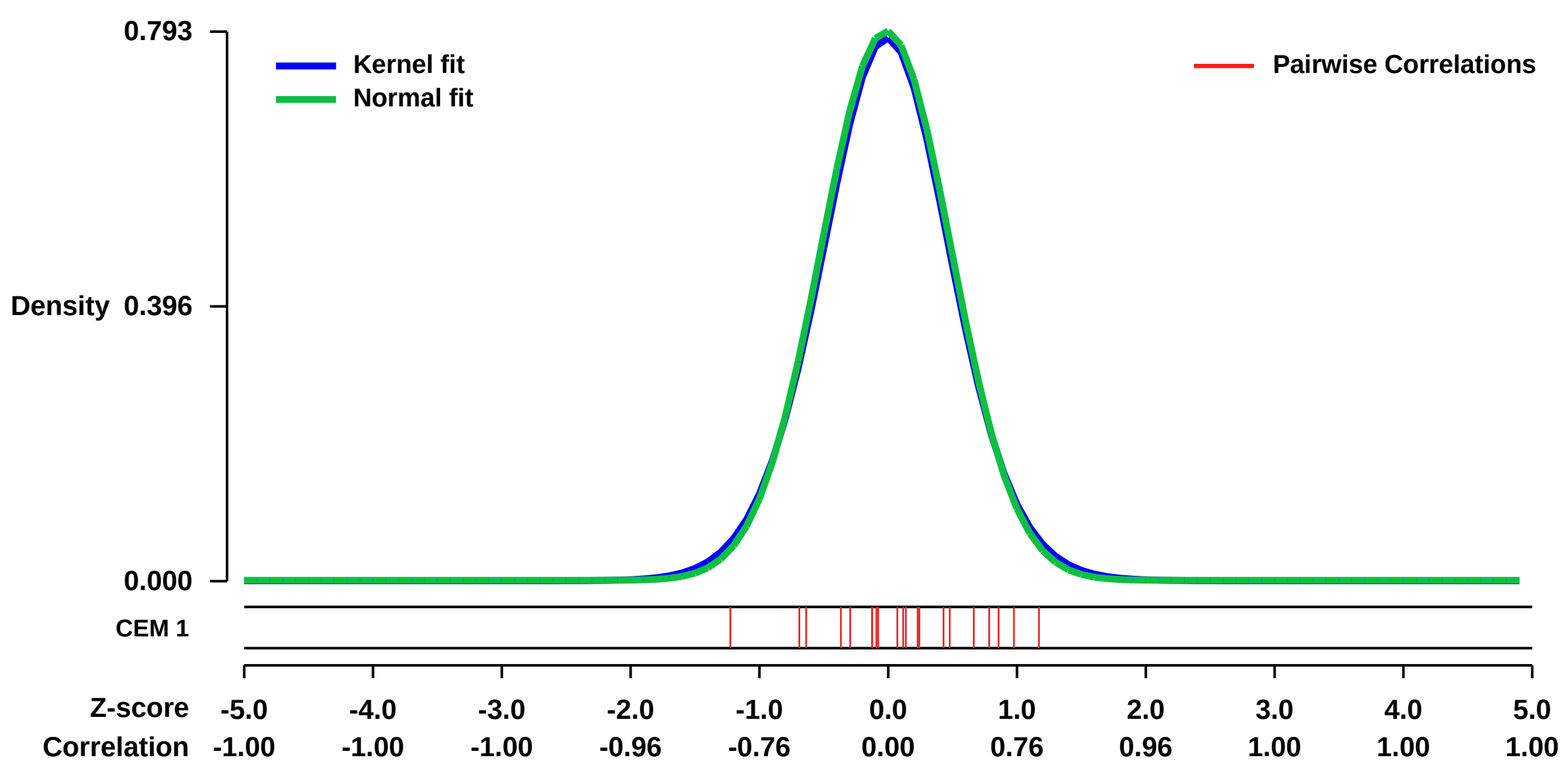

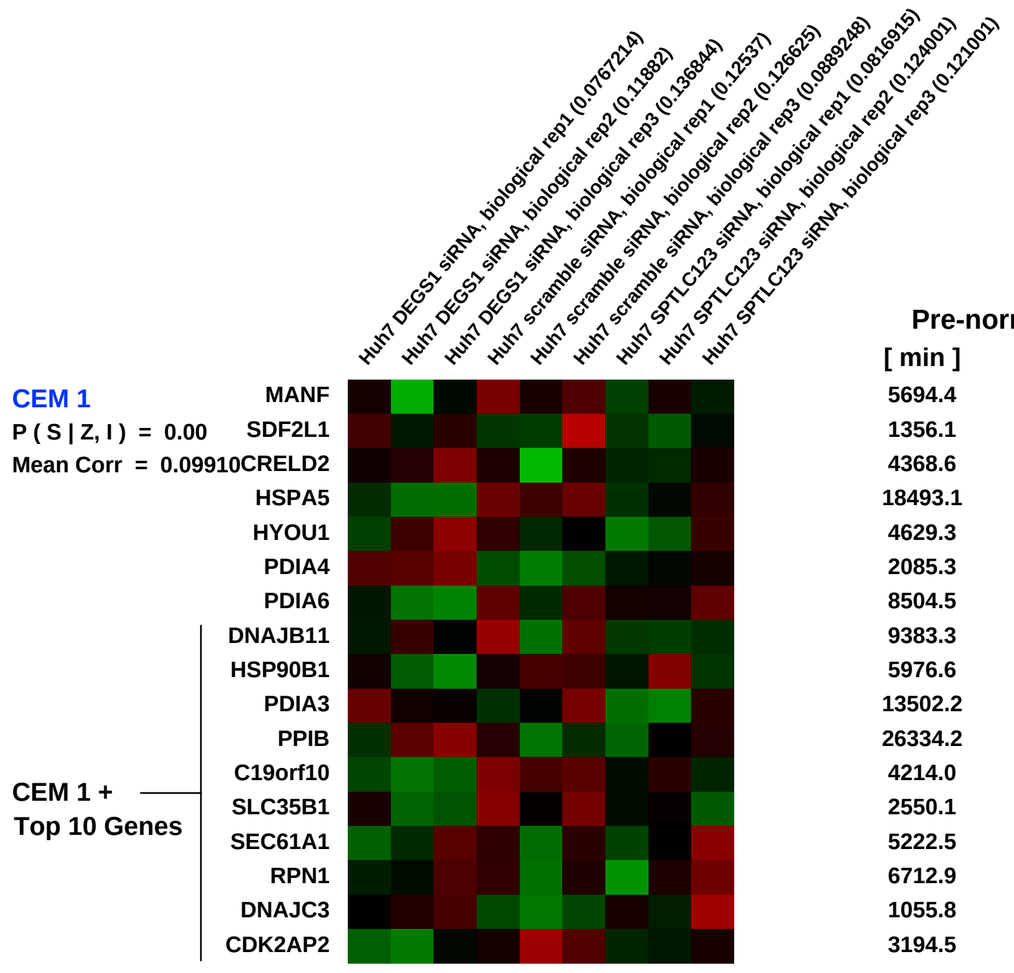

GEO Series "GSE2964" Expression Profiles

Num of samples in this series: 18

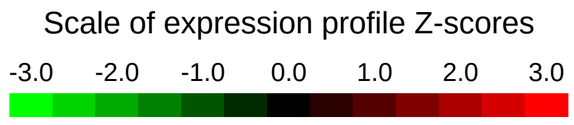

GEO Link:	http://www.ncbi.nlm.nih.gov/geo/query/acc.cgi?acc=GSE2964
Status:	Public on Jan 01 2006
Title:	Motexafin Gadolinium and Zinc Induce Oxidative Stress Responses and Apoptosis in B-Cell Lymphoma Lines
Organism:	Homo sapiens
Experiment type:	Expression profiling by array
Platform:	GPL570
Pubmed ID:	16357179
Summary & Design:	**Summary:** We report the effect of motexafin gadolinium (MGd) and exogenous zinc on intracellular levels of free zinc, oxidative stress, proliferation, cell cycle, and cell death in exponential phase human B-cell lymphoma and other hematologic cell lines. We find that increased levels of oxidative stress and intracellular free zinc precede and correlate with cell cycle arrest and apoptotic response. Treatment with exogenous zinc increased oxidative stress and, conversely, oxidative stress resulted in increased intracellular free zinc levels. To better understand the molecular basis of these results, gene expression profiling analyses were conducted on Ramos cell cultures treated with MGd and/or zinc acetate. Cultures treated with MGd or zinc acetate alone elicited transcriptional responses characterized by induction of MTF-1 and HIF-1 regulated genes. Cultures co-treated with MGd and zinc acetate displayed further increases in the levels of MTF-1 and HIF-1 regulated transcripts as well as additional transcripts regulated by NRF-2. Overall, these studies suggest that co-treatment of Ramos cells with MGd and zinc acetate increase intracellular zinc levels with a concomitant rise in oxidative stress levels that activate adaptive survival responses but eventually lead to cell death. **Keywords:** Dose response **Overall design:** Ramos cells were treated with MGd alone or along with different concentrations of zinc acetate. Each treatment was done in triplicates. Expression was compared to that of cells treated with mannitol.

Background corr dist: KL-Divergence = 0.2437, L1-Distance = 0.0444, L2-Distance = 0.0044, Normal std = 0.3075

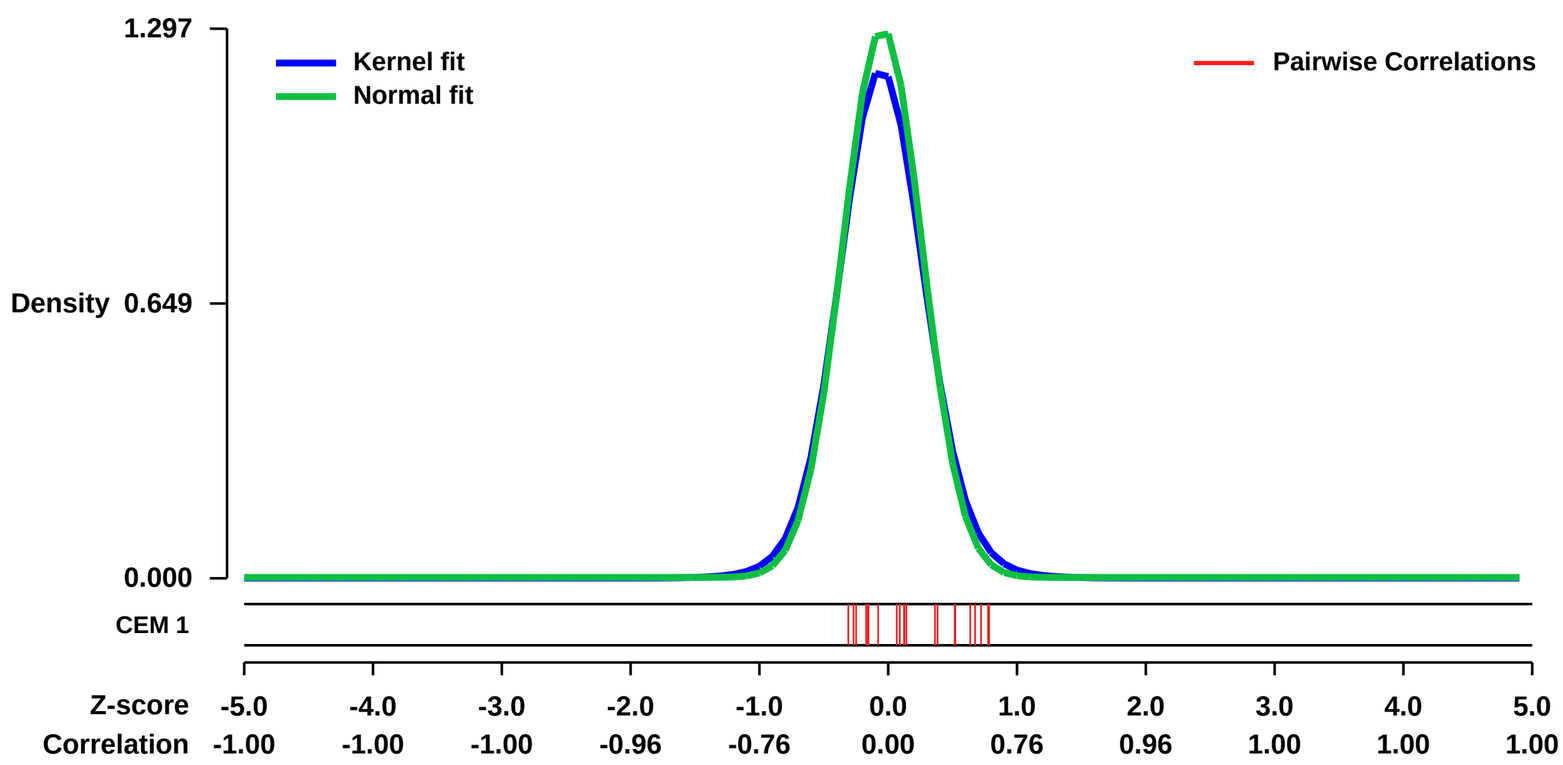

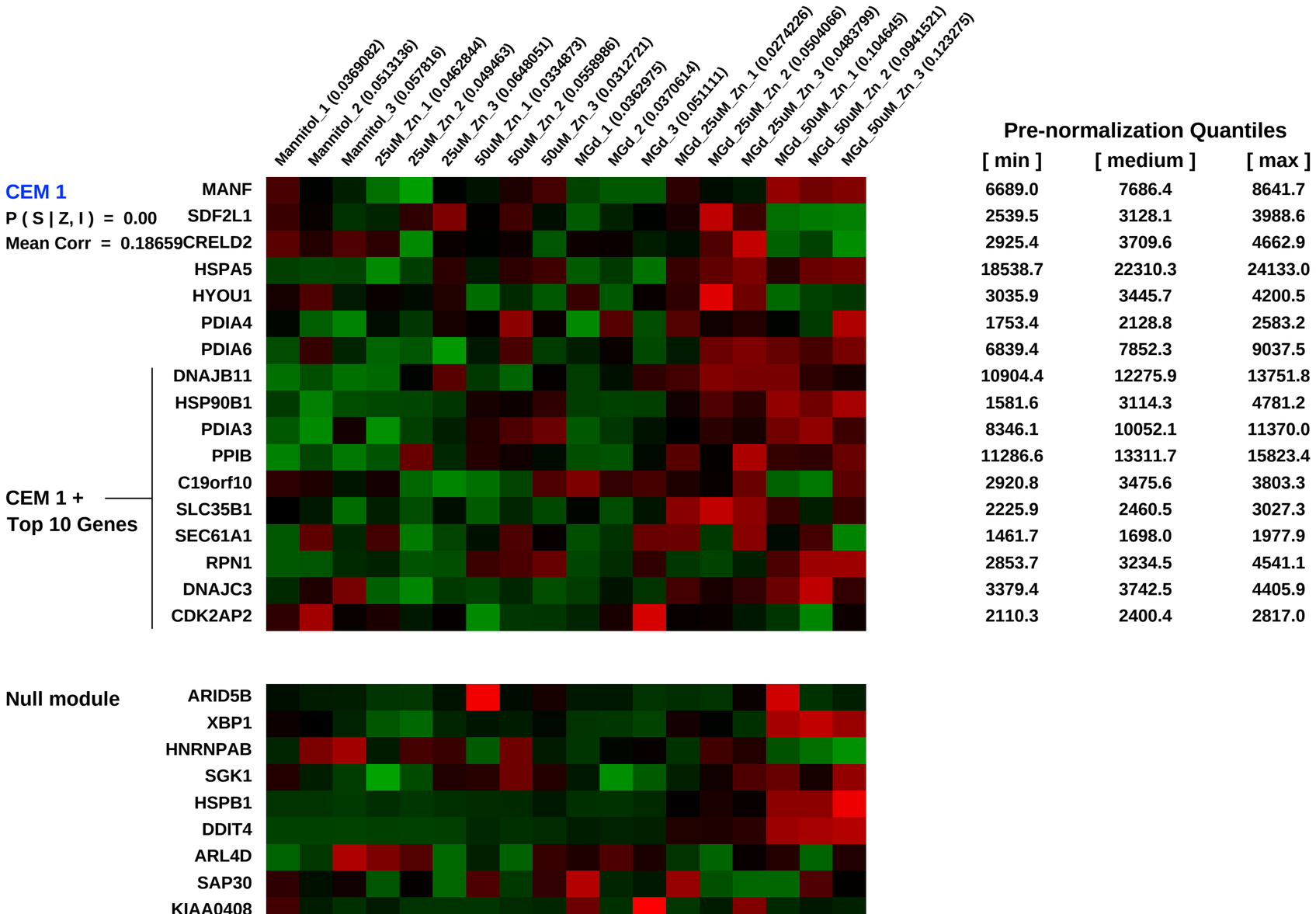

Pre-normalization Quantiles

	[min]	[medium]	[max]
MANF	6689.0	7686.4	8641.7
SDF2L1	2539.5	3128.1	3988.6
CRELD2	2925.4	3709.6	4662.9
HSPA5	18538.7	22310.3	24133.0
HYOU1	3035.9	3445.7	4200.5
PDIA4	1753.4	2128.8	2583.2
PDIA6	6839.4	7852.3	9037.5
DNAJB11	10904.4	12275.9	13751.8
HSP90B1	1581.6	3114.3	4781.2
PDIA3	8346.1	10052.1	11370.0
PPIB	11286.6	13311.7	15823.4
C19orf10	2920.8	3475.6	3803.3
SLC35B1	2225.9	2460.5	3027.3
SEC61A1	1461.7	1698.0	1977.9
RPN1	2853.7	3234.5	4541.1
DNAJC3	3379.4	3742.5	4405.9
CDK2AP2	2110.3	2400.4	2817.0

GEO Series "GSE10809" Expression Profiles

Num of samples in this series: 8

Scale of expression profile Z-scores

-3.0 -2.0 -1.0 0.0 1.0 2.0 3.0

GEO Link:	http://www.ncbi.nlm.nih.gov/geo/query/acc.cgi?acc=GSE10809
Status:	Public on Aug 11 2008
Title:	Global gene expression from SOX7 and SOX17 over-expressing human embryonic stem cells (CA1 and CA2 lines)
Organism:	Homo sapiens
Experiment type:	Expression profiling by array
Platform:	GPL570
Pubmed ID:	18682240
Summary & Design:	**Summary:** This study aimed to understand the transcriptional networks regulating endoderm specification from HESC and therefore explored the phenotype of CA1 and CA2 HESC constitutively over-expressing SOX7 or SOX17. Cell lines were created using an inducible construct whereby clonal populations containing transgene integration are selected by Neomycin resistance without expressing of the gene of interest (NoCre controls). Transgene expression is induced via Cre-mediated recombination and selected for puromycin resistance (SOX O/E). The phenotype of the resulting cells suggests that SOX7 expressing HESC represent stable extraembryonic endoderm progenitors, while SOX17 expressing HESC represent early definitive endoderm progenitors. Both in vitro and in vivo SOX7 expressing HESC are restricted to the extraembryonic endoderm lineage, while SOX17 expressing HESC demonstrate mesendodermal specificity. In vitro, SOX17 expressing HESC efficiently produce mature definitive endoderm derivatives. The molecular phenotype of the resulting SOX7 and SOX17 expressing HESC was characterized by microarray analysis **Keywords:** cell line comparison **Overall design:** Total RNA was extracted from confluent monolayer cultures of SOX7 over-expressing HESC, SOX17 over-expressing HESC, and their respective control parental HESC lines (designated NoCre Sox7 and NoCre Sox17).

Background corr dist: KL-Divergence = 0.0769, L1-Distance = 0.0259, L2-Distance = 0.0012, Normal std = 0.4845

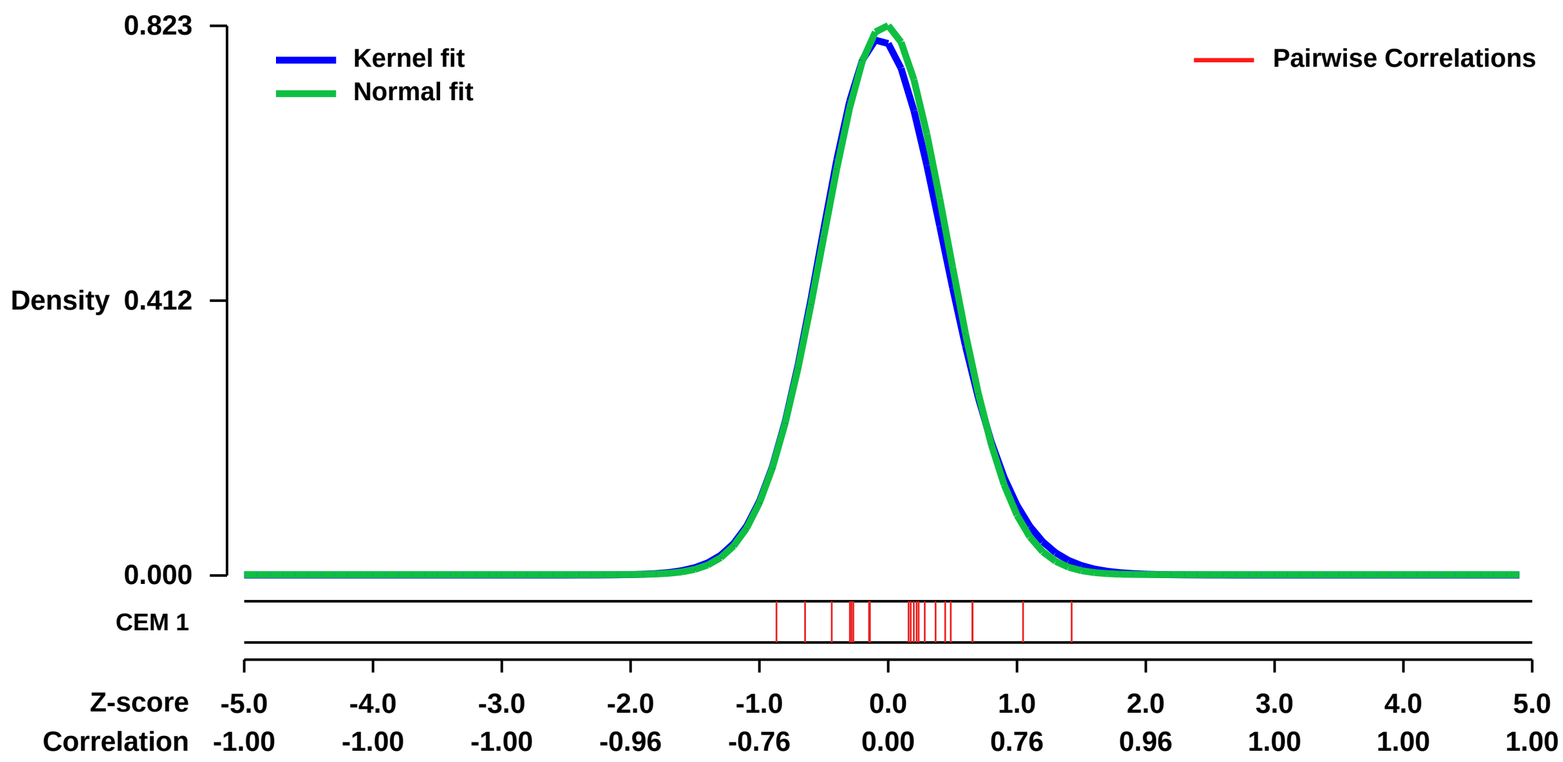

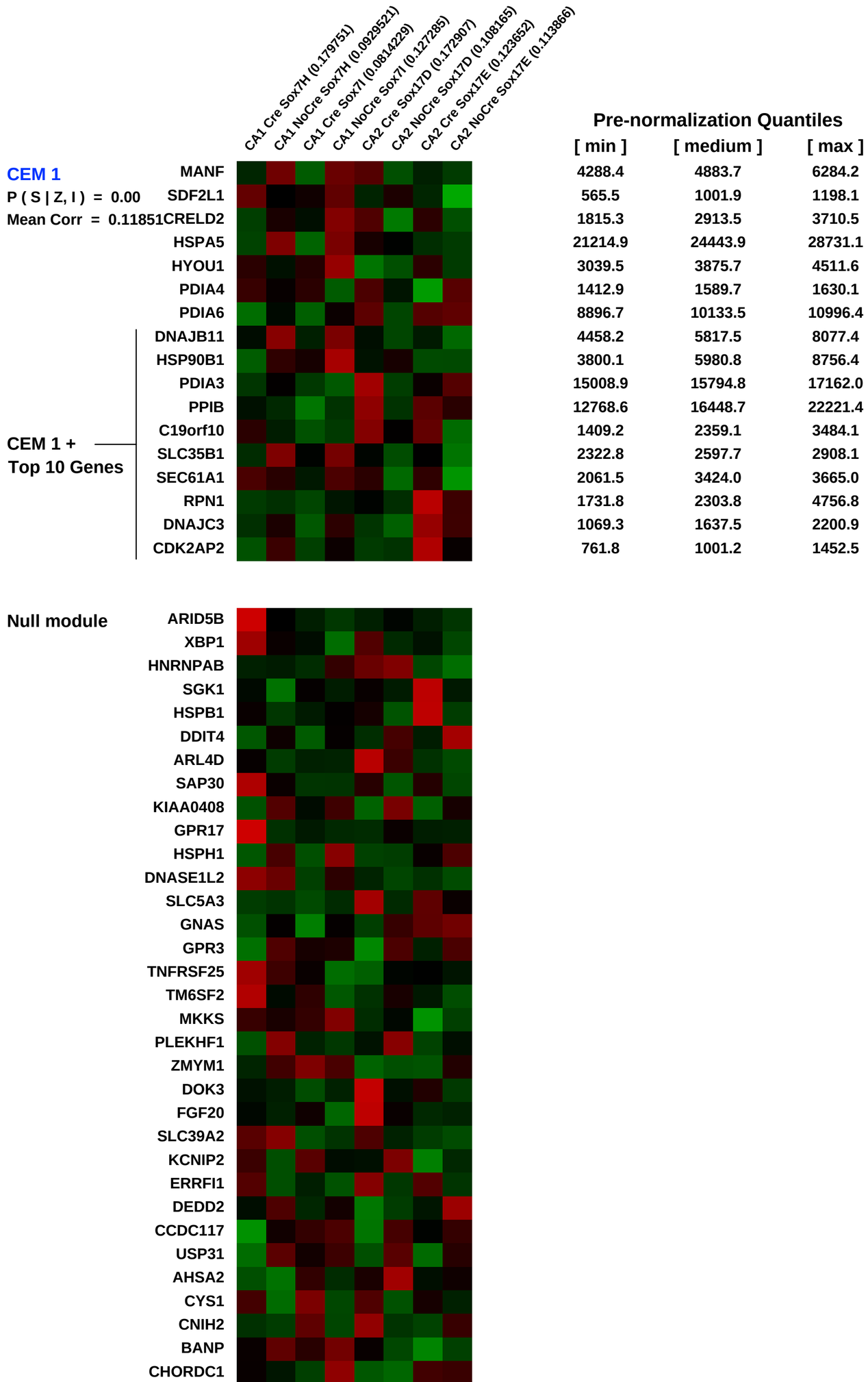

Pre-normalization Quantiles

	[min]	[medium]	[max]
MANF	4288.4	4883.7	6284.2
SDF2L1	565.5	1001.9	1198.1
CRELD2	1815.3	2913.5	3710.5
HSPA5	21214.9	24443.9	28731.1
HYOU1	3039.5	3875.7	4511.6
PDIA4	1412.9	1589.7	1630.1
PDIA6	8896.7	10133.5	10996.4
DNAJB11	4458.2	5817.5	8077.4
HSP90B1	3800.1	5980.8	8756.4
PDIA3	15008.9	15794.8	17162.0
PPIB	12768.6	16448.7	22221.4
C19orf10	1409.2	2359.1	3484.1
SLC35B1	2322.8	2597.7	2908.1
SEC61A1	2061.5	3424.0	3665.0
RPN1	1731.8	2303.8	4756.8
DNAJC3	1069.3	1637.5	2200.9
CDK2AP2	761.8	1001.2	1452.5

GEO Series "GSE2125" Expression Profiles

Num of samples in this series: 45

Scale of expression profile Z-scores

-3.0 -2.0 -1.0 0.0 1.0 2.0 3.0

GEO Link:	http://www.ncbi.nlm.nih.gov/geo/query/acc.cgi?acc=GSE2125
Status:	Public on Oct 04 2005
Title:	isolated alveolar macrophages
Organism:	Homo sapiens
Experiment type:	Expression profiling by array
Platform:	GPL570
Pubmed ID:	16166618
Summary & Design:	Summary: This series represents isolated alveolar macrophages from human subjects. Keywords: parallel sample Overall design:

Background corr dist: KL-Divergence = 0.0653, L1-Distance = 0.0794, L2-Distance = 0.0123, Normal std = 0.5529

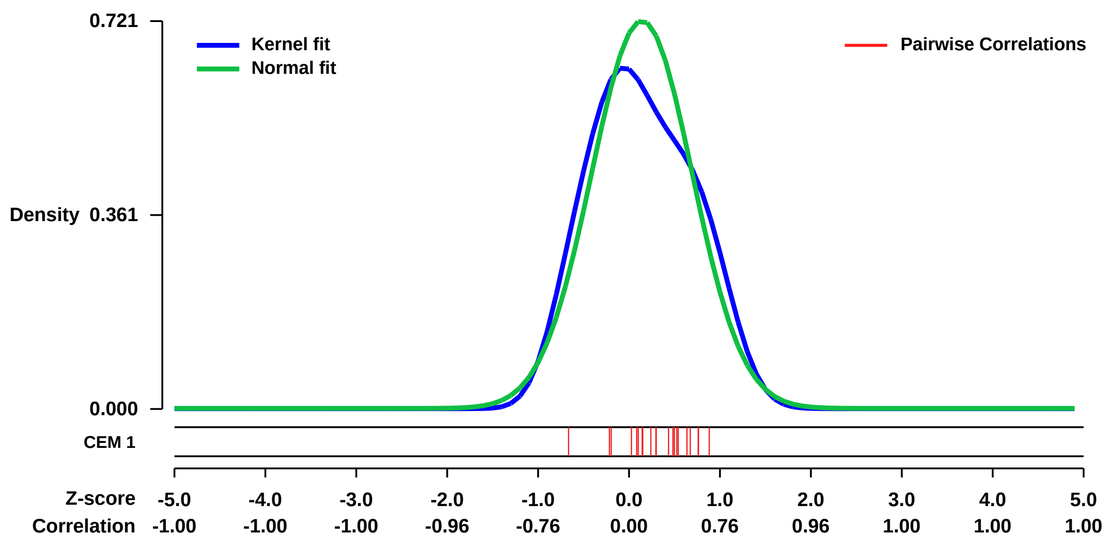

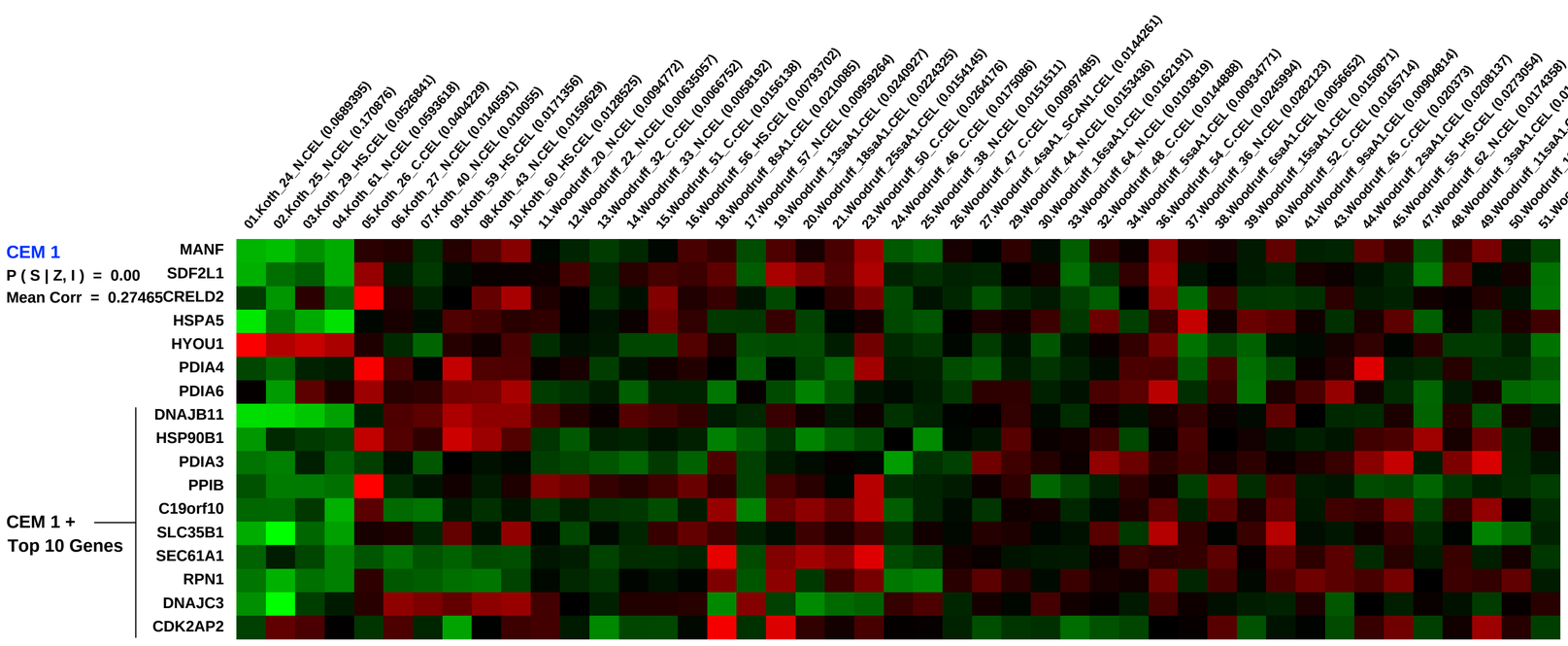

Pre-normalization Quantiles

[min]	[medium]	[max]
986.3	1772.7	2342.3
371.4	742.9	1156.3
2443.5	3337.7	5598.2
827.4	3055.2	4678.0
623.8	769.9	1164.6
1145.3	1536.2	2853.7
4190.5	6264.6	9287.5
764.4	1678.0	2310.5
379.7	624.8	1036.6
2379.6	4087.4	6773.8
897.6	1448.0	3290.2
2359.3	4219.1	6682.9
907.7	1747.2	2384.1
408.2	831.3	1883.0
939.4	1533.8	2034.5
3015.1	6682.4	8607.3
190.4	271.4	397.3

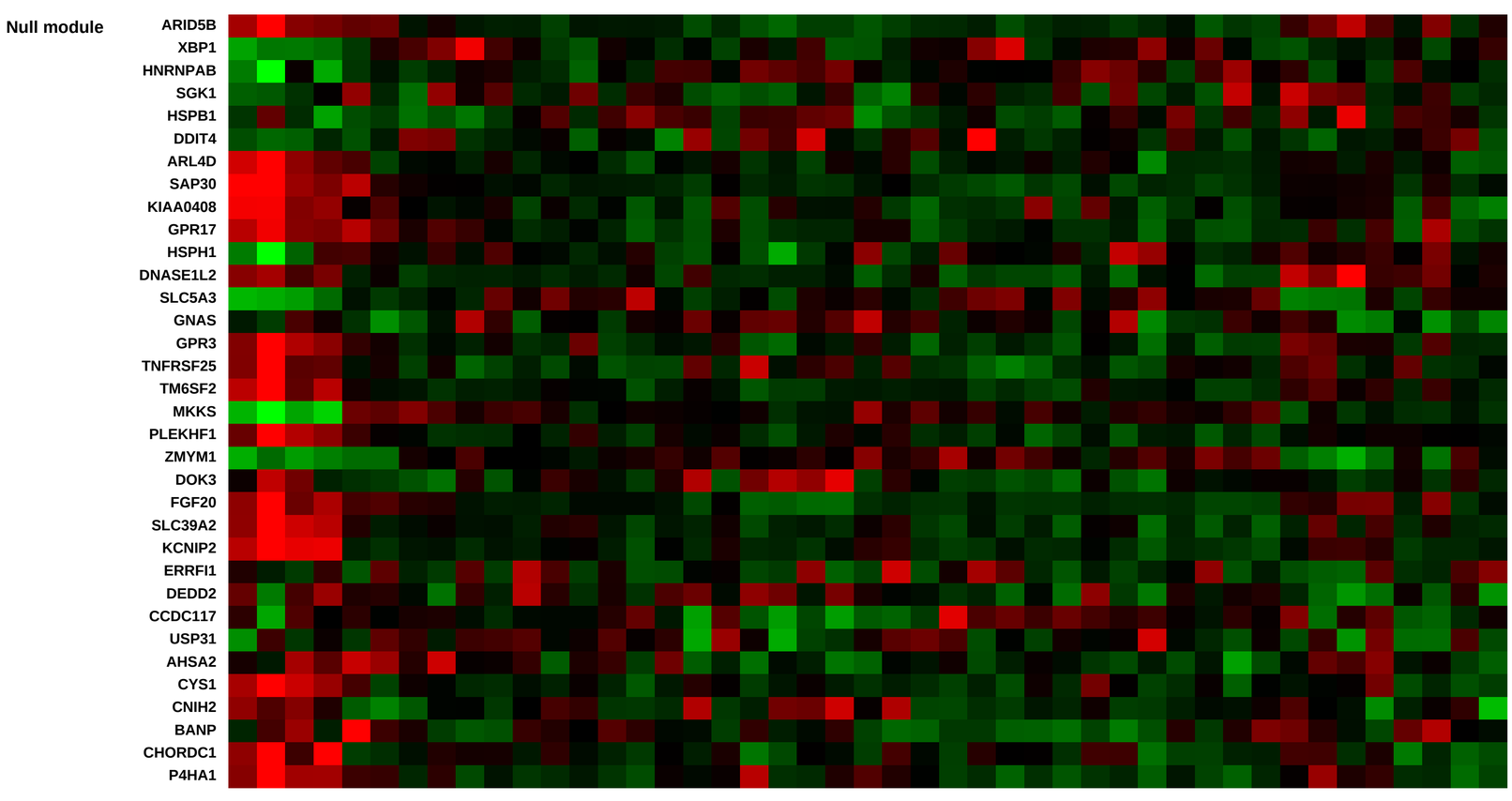

GEO Series "GSE43881" Expression Profiles

Num of samples in this series: 6

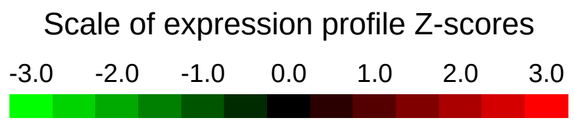

GEO Link:	http://www.ncbi.nlm.nih.gov/geo/query/acc.cgi?acc=GSE43881
Status:	Public on Jan 30 2013
Title:	HIPK2 and MED19 are new regulators of androgen receptor in prostate cancer cells
Organism:	Homo sapiens
Experiment type:	Expression profiling by array
Platform:	GPL570
Pubmed ID:	23403032

Summary & Design:

Summary:
The androgen receptor (AR) is a mediator of both androgen-dependent and castration- resistant prostate cancers. Identification of cellular factors affecting AR transcriptional activity could in principle yield new targets that reduce AR activity and combat prostate cancer, yet a comprehensive analysis of the genes required for AR-dependent transcriptional activity has not been determined. Using an unbiased genetic approach that takes advantage of the evolutionary conservation of AR signaling, we have conducted a genome-wide RNAi screen in Drosophila cells for genes required for AR transcriptional activity and applied the results to human prostate cancer cells. We identified 45 AR-regulators, which include known pathway components and genes with functions not previously linked to AR regulation, such as HIPK2 (a protein kinase) and MED19 (a subunit of the Mediator complex). Depletion of HIPK2 and MED19 in human prostate cancer cells decreased AR target gene expression and, importantly, reduced the proliferation of androgen-dependent and castration-resistant prostate cancer cells. We also systematically analyzed additional Mediator subunits and uncovered a small subset of Mediator subunits that interpret AR signaling and affect AR-dependent transcription and prostate cancer cell proliferation. Importantly, targeting of HIPK2 by an FDA approved kinase inhibitor phenocopied the effect of depletion by RNAi and reduced the growth of AR-positive, but not AR negative, treatment-resistant prostate cancer cells. Thus, our screen has yielded new AR regulators including drugable targets that reduce the proliferation of castration-resistant prostate cancer cells.

HIPK2 and MED19 were identified via a genome-wide RNAi screen as new androgen receptor (AR) reulators. Our goal in performing this microarray was to identify the gene regulated by HIPK2 and MED19 in a late stage prostate cancer cell line (LNCaP-abl), and to see what genes are in common with known genes to be regulated by AR, and what genes are unique to HIPK2 or MED19.

Overall design:
Knockdown of HIPK2 and MED19 was tested in LNCaP-abl cells against control. Each was performed in duplicates. Six samples were analyzed

Background corr dist: **KL-Divergence = 0.0490, L1-Distance = 0.0176, L2-Distance = 0.0003, Normal std = 0.5741**

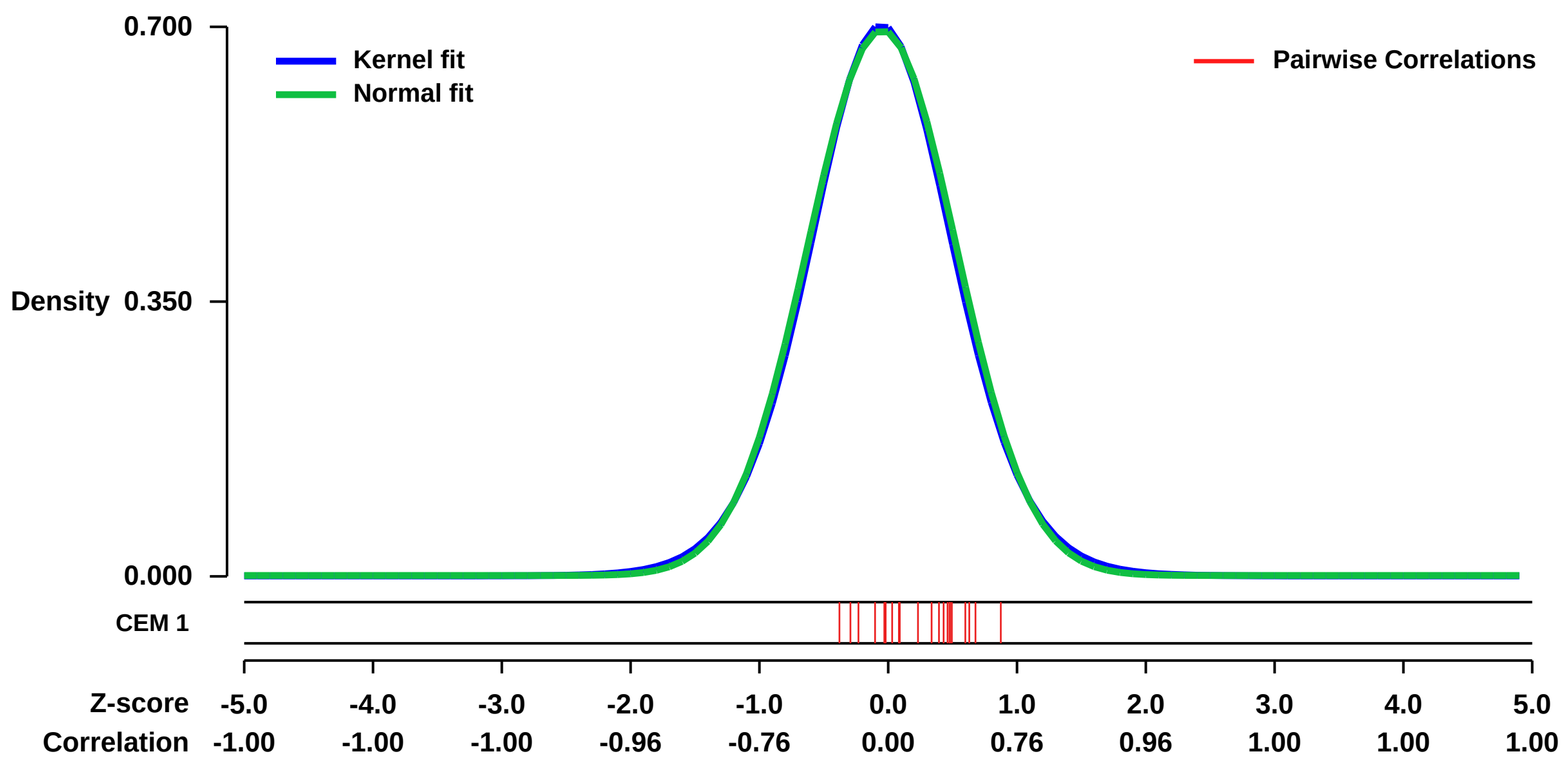

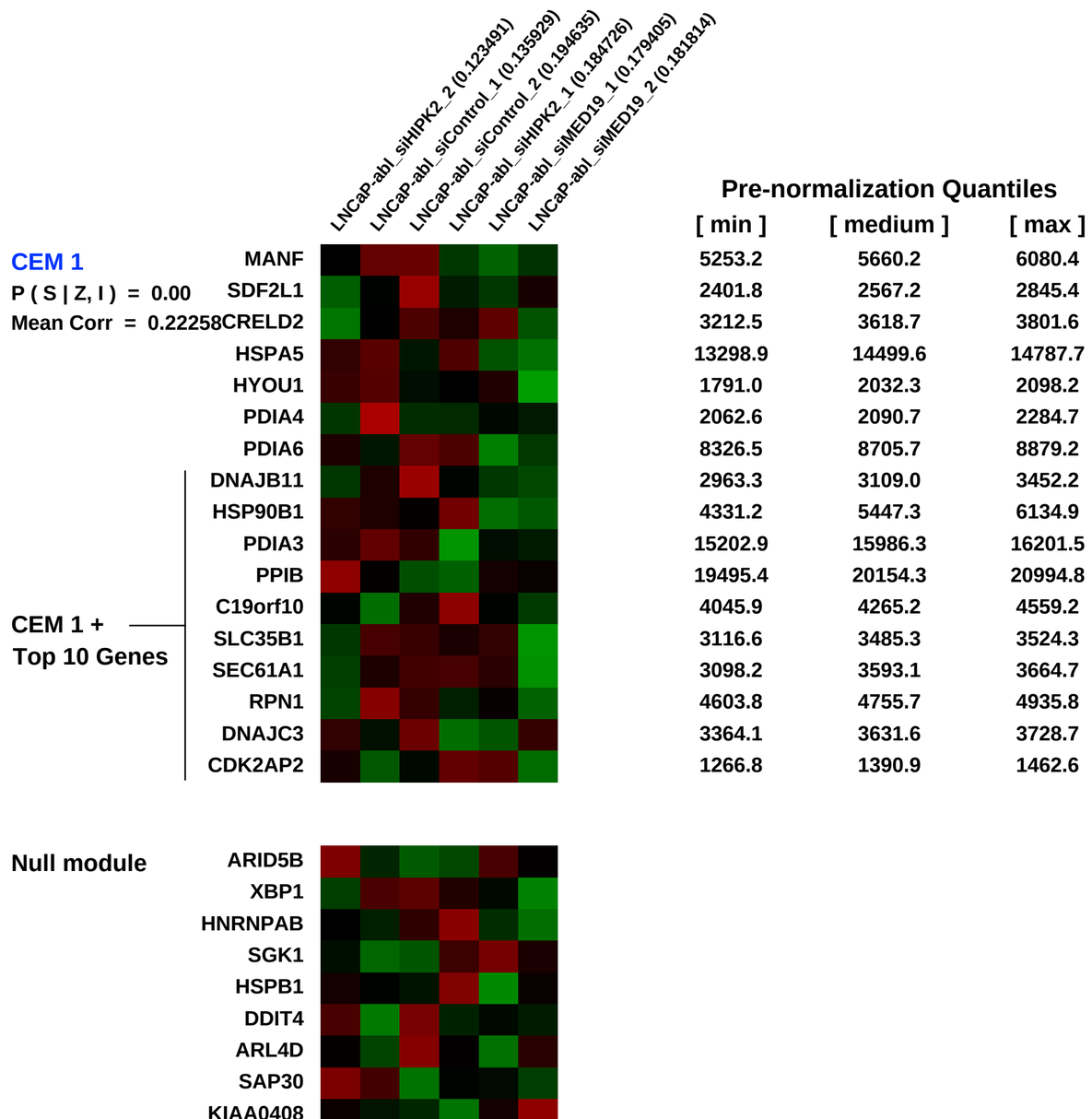

	Pre-normalization Quantiles		
	[min]	[medium]	[max]
MANF	5253.2	5660.2	6080.4
SDF2L1	2401.8	2567.2	2845.4
CRELD2	3212.5	3618.7	3801.6
HSPA5	13298.9	14499.6	14787.7
HYOU1	1791.0	2032.3	2098.2
PDIA4	2062.6	2090.7	2284.7
PDIA6	8326.5	8705.7	8879.2
DNAJB11	2963.3	3109.0	3452.2
HSP90B1	4331.2	5447.3	6134.9
PDIA3	15202.9	15986.3	16201.5
PPIB	19495.4	20154.3	20994.8
C19orf10	4045.9	4265.2	4559.2
SLC35B1	3116.6	3485.3	3524.3
SEC61A1	3098.2	3593.1	3664.7
RPN1	4603.8	4755.7	4935.8
DNAJC3	3364.1	3631.6	3728.7
CDK2AP2	1266.8	1390.9	1462.6
ARID5B			
XBP1			
HNRNPAB			
SGK1			
HSPB1			
DDIT4			
ARL4D			
SAP30			
KIAA0408			
GPR17			
HSPH1			
DNASE1L2			
SLC5A3			
GNAS			
GPR3			
TNFRSF25			
TM6SF2			
MKKS			
PLEKHF1			
ZMYM1			
DOK3			
FGF20			
SLC39A2			
KCNIP2			
ERRFI1			
DEDD2			
CCDC117			
USP31			
AHSA2			
CYS1			
CNIH2			
BANP			
CHORDC1			
P4HA1			

GEO Series "GSE40636" Expression Profiles

Num of samples in this series: 6

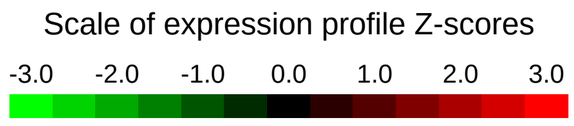

GEO Link:	http://www.ncbi.nlm.nih.gov/geo/query/acc.cgi?acc=GSE40636
Status:	Public on Sep 04 2013
Title:	PGN induced transcriptional changes in human neonatal neutrophils
Organism:	Homo sapiens
Experiment type:	Expression profiling by array
Platform:	GPL570
Pubmed ID:	23986550
Summary & Design:	**Summary:** We have employed whole genome microarray expression profiling to identify genes differentially expressed in cord blood purified neutrophils after a short-term exposure to peptidoglycan (PGN). **Overall design:** PGN induced gene expressions of neonatal neutrophils were measured at 4 hours. Three biological replicates were performed for each treatment group.

Background corr dist: KL-Divergence = 0.0263, L1-Distance = 0.0895, L2-Distance = 0.0111, Normal std = 0.9174

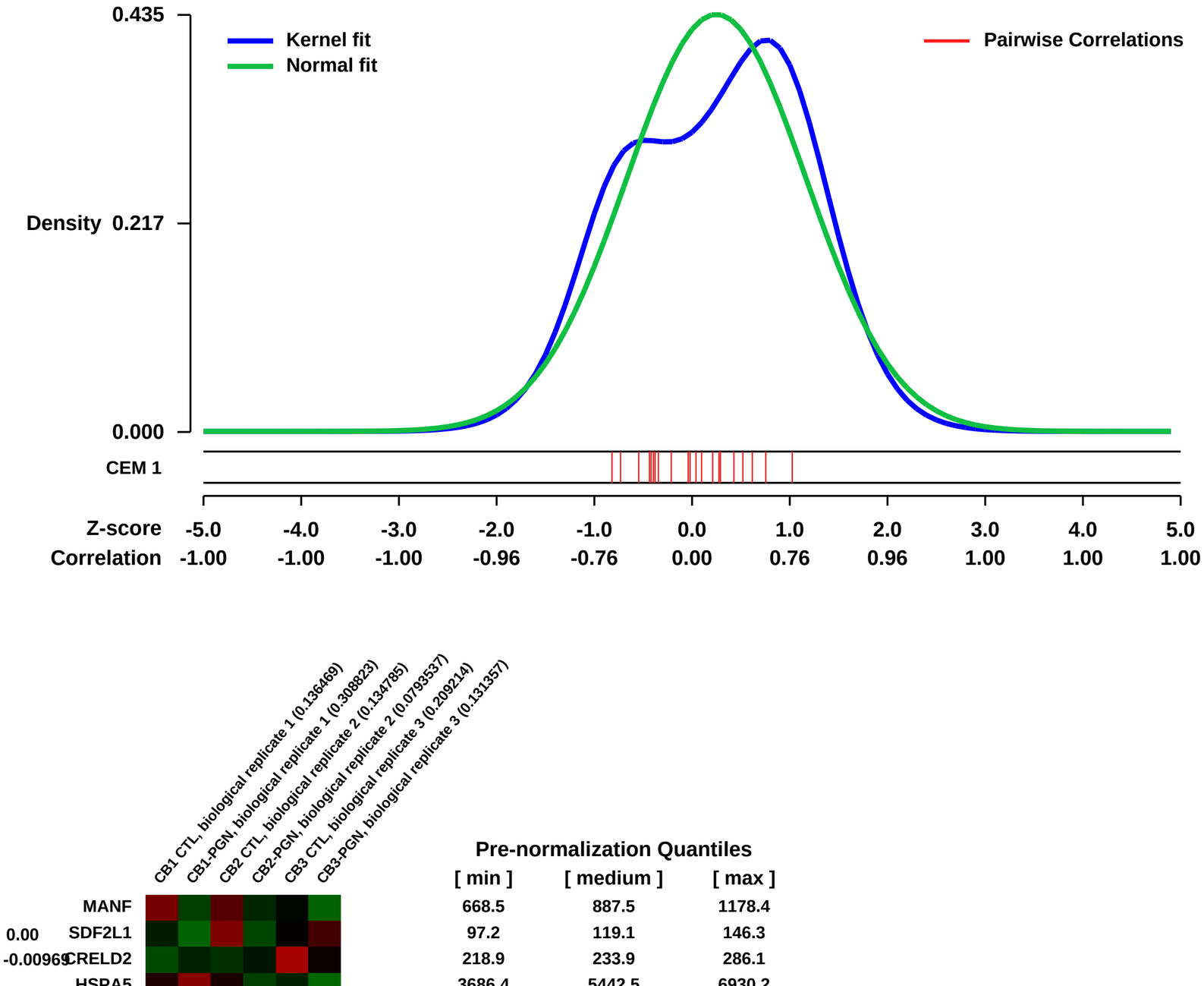

CEM 1
P (S | Z, I) = 0.00
Mean Corr = -0.00969

CEM 1 + Top 10 Genes

Null module

MANF	668.5	887.5	1178.4
SDF2L1	97.2	119.1	146.3
CRELD2	218.9	233.9	286.1
HSPA5	3686.4	5442.5	6930.2
HYOU1	204.9	290.3	398.8
PDIA4	125.7	154.9	160.6
PDIA6	399.8	787.4	883.1
DNAJB11	869.6	1052.9	1342.8
HSP90B1	181.8	285.2	349.2
PDIA3	890.7	2131.8	2865.6
PPIB	408.8	1642.4	2296.8
C19orf10	191.4	326.2	393.0
SLC35B1	289.2	454.6	525.0
SEC61A1	941.6	1126.1	1562.1
RPN1	918.3	1797.0	1962.6
DNAJC3	15804.6	16855.0	23571.2
CDK2AP2	112.8	118.1	139.8
ARID5B			
XBP1			
HNRNPAB			
SGK1			
HSPB1			
DDIT4			
ARL4D			
SAP30			
KIAA0408			
GPR17			
HSPH1			
DNASE1L2			
SLC5A3			
GNAS			
GPR3			
TNFRSF25			
TM6SF2			
MKKS			
PLEKHF1			
ZMYM1			
DOK3			
FGF20			
SLC39A2			
KCNIP2			
ERRFI1			
DEDD2			
CCDC117			
USP31			
AHSA2			
CYS1			
CNIH2			
BANP			
CHORDC1			
P4HA1			

GEO Series "GSE23610" Expression Profiles

Num of samples in this series: 24

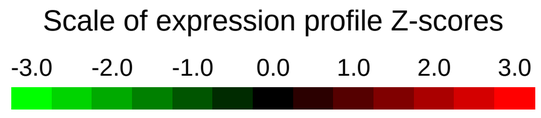

GEO Link:	http://www.ncbi.nlm.nih.gov/geo/query/acc.cgi?acc=GSE23610
Status:	Public on May 18 2011
Title:	Gene expression profiles of MCF-7 cells treated with Si-Wu-Tang, estradiol and ferulic acid
Organism:	Homo sapiens
Experiment type:	Expression profiling by array
Platform:	GPL570
Pubmed ID:	21464939
Summary & Design:	**Summary:** Traditional Chinese medicines (TCM), usually composed of a mixture of components, may simultaneously target multiple genes/pathways and thus achieve superior efficacy for complex diseases such as cancer. To identify novel mechanisms of action and potential health benefits for a TCM formula Si-Wu-Tang (SWT) widely used for womenâ s health, we obtained the DNA microarray expression profiles for SWT, its active component ferulic acid, and estradiol in human breast cancer cell line MCF-7 and analyzed the gene expression signatures associated with each treatment using the â Connectivity Mapâ (cMAP). This study indicates that DNA microarray profiling analysis and cMAP data mining provide a powerful approach to discover unknown mechanisms of actions and identify potential new health benefits for TCM. **Overall design:** We profiled the gene expression of MCF-7 cell lines to SWT, its active component FA, as well as estradiol using Affymetrix human genome U133 plus 2.0 arrays. The data set includes profiles for 24 samples, divided into eight groups of treatment: 0.001% DMSO used as the vehicle control (C), 0.1 ´µM estradiol (EM), FA at three concentrations (0.1, 1, and 10 ´µM) (FL, FM and FH) and SWT at three concentrations (0.0256, 0.256, and 2.56 mg/ml) (SL, SM and SH). For each treatment group, 3 biological replicates were included, resulting in 24 (8 groups ^ 3 replicates/group) RNA samples.

Background corr dist: KL-Divergence = 0.1747, L1-Distance = 0.0411, L2-Distance = 0.0027, Normal std = 0.3675

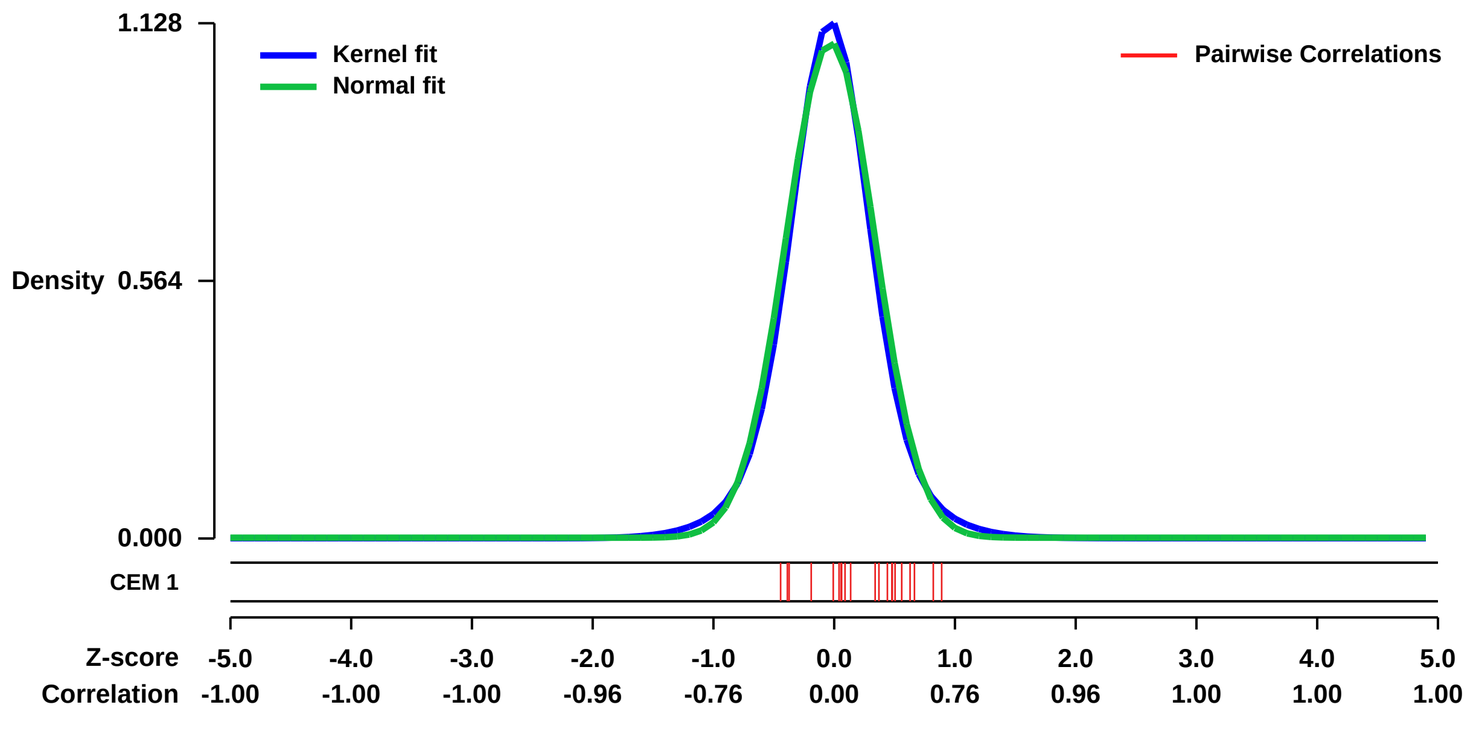

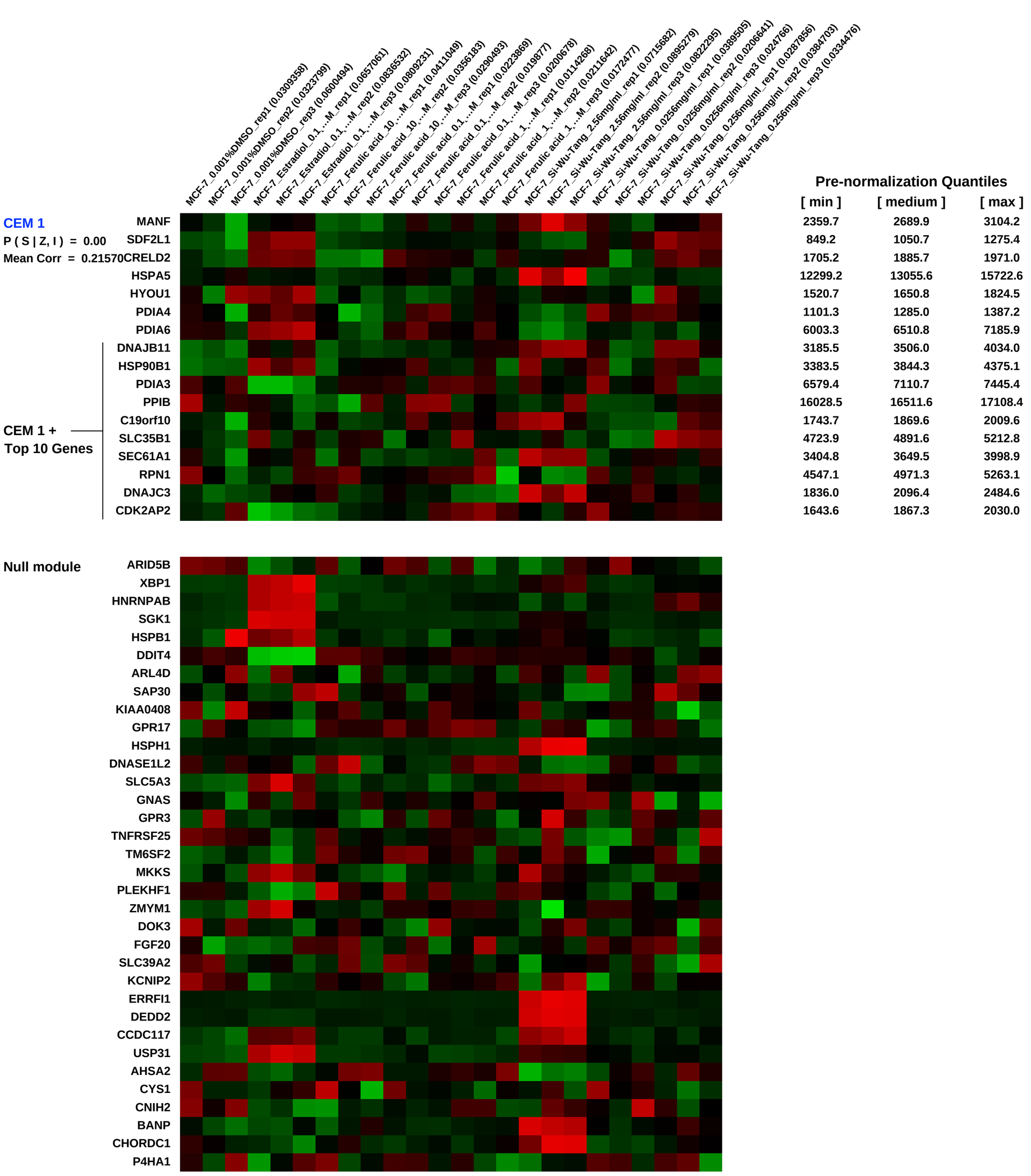

Pre-normalization Quantiles

	[min]	[medium]	[max]
MANF	2359.7	2689.9	3104.2
SDF2L1	849.2	1050.7	1275.4
CRELD2	1705.2	1885.7	1971.0
HSPA5	12299.2	13055.6	15722.6
HYOU1	1520.7	1650.8	1824.5
PDIA4	1101.3	1285.0	1387.2
PDIA6	6003.3	6510.8	7185.9
DNAJB11	3185.5	3506.0	4034.0
HSP90B1	3383.5	3844.3	4375.1
PDIA3	6579.4	7110.7	7445.4
PPIB	16028.5	16511.6	17108.4
C19orf10	1743.7	1869.6	2009.6
SLC35B1	4723.9	4891.6	5212.8
SEC61A1	3404.8	3649.5	3998.9
RPN1	4547.1	4971.3	5263.1
DNAJC3	1836.0	2096.4	2484.6
CDK2AP2	1643.6	1867.3	2030.0

GEO Series "GSE60135" Expression Profiles

Num of samples in this series: 12

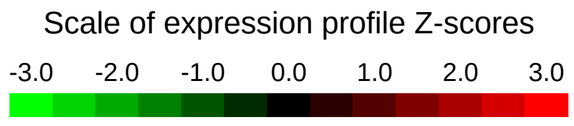

GEO Link:	**http://www.ncbi.nlm.nih.gov/geo/query/acc.cgi?acc=GSE60135**
Status:	**Public on Aug 07 2014**
Title:	**Gene-expression profiles of BMP signaling-affected SK-OV-3 cells**
Organism:	**Homo sapiens**
Experiment type:	**Expression profiling by array**
Platform:	**GPL570**
Pubmed ID:	
Summary & Design:	**Summary:** **Bone morphogenetic proteins (BMPs) are extracellular signaling molecules that belong to the transforming growth factor beta (TGF-¸†) superfamily. By regulating target gene transcription, BMPs control various cellular processes, such as proliferation, differentiation, apoptosis and migration.** **In addition, rBMP2 was used to observe BMP signaling in treatment of ovarian cancer cell line SK-OV-3. We attempted to address the possible roles of BMP signaling by inhibiting a wide-range of downstream pathways using a small molecule inhibitor of type I BMPRs, dorsomorphin. The potential utility of this molecule as a molecular inhibitor of BMP signaling in treatment of ovarian cancer cell line SK-OV-3 was also evaluated.** **Overall design:** **SK-OV-3 cells were incubated in 12 separate culture dishes, 3 dishes with PBS, 3 dishes with recombinant BMP2 (rBMP2) (100 ng/ml), 3 dishes with DM (5 ¸…M) and 3 dishes with recombinant BMP2 (rBMP2) (100 ng/ml) plus DM (5 ¸…M) in the culture medium for 24 hours prior to the analysis.**

Background corr dist: **KL-Divergence = 0.1764, L1-Distance = 0.0440, L2-Distance = 0.0043, Normal std = 0.3490**

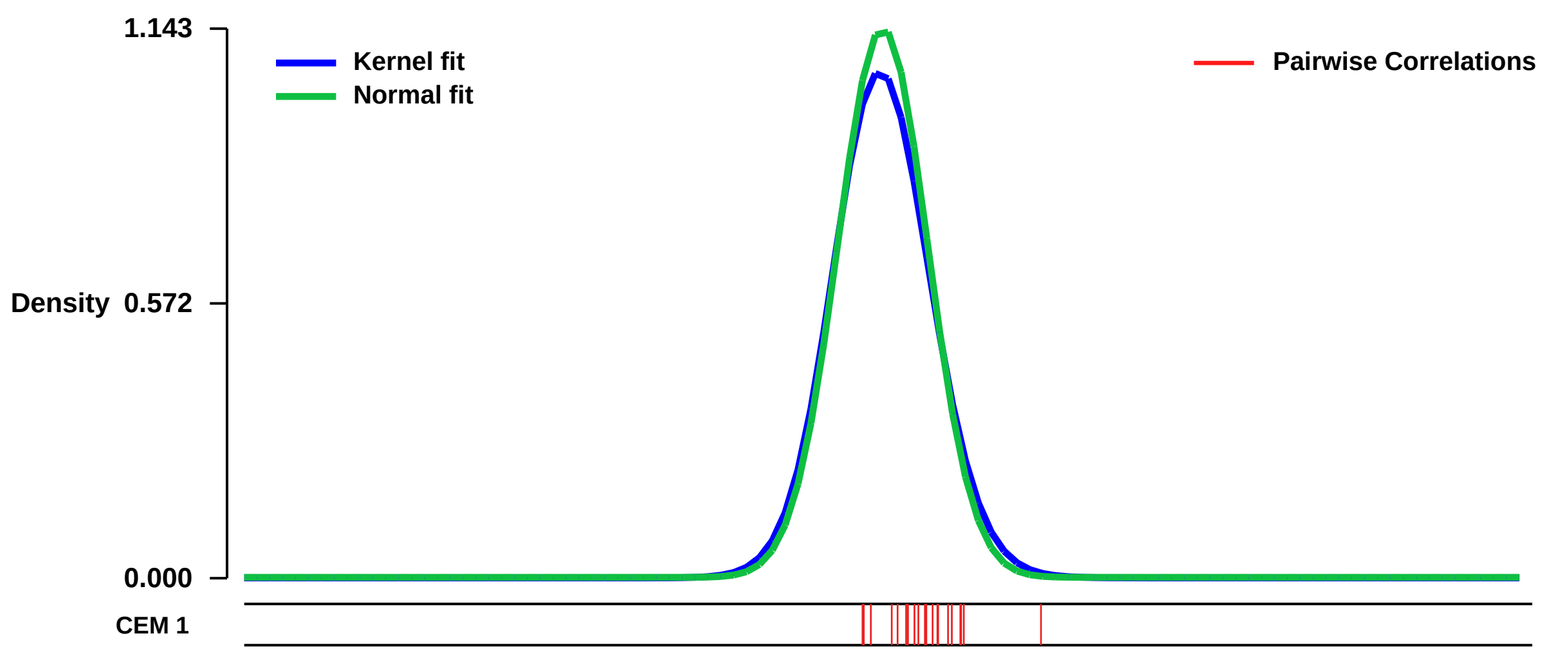

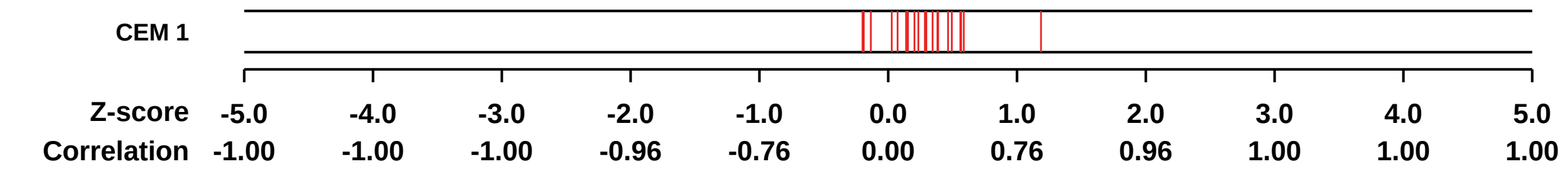

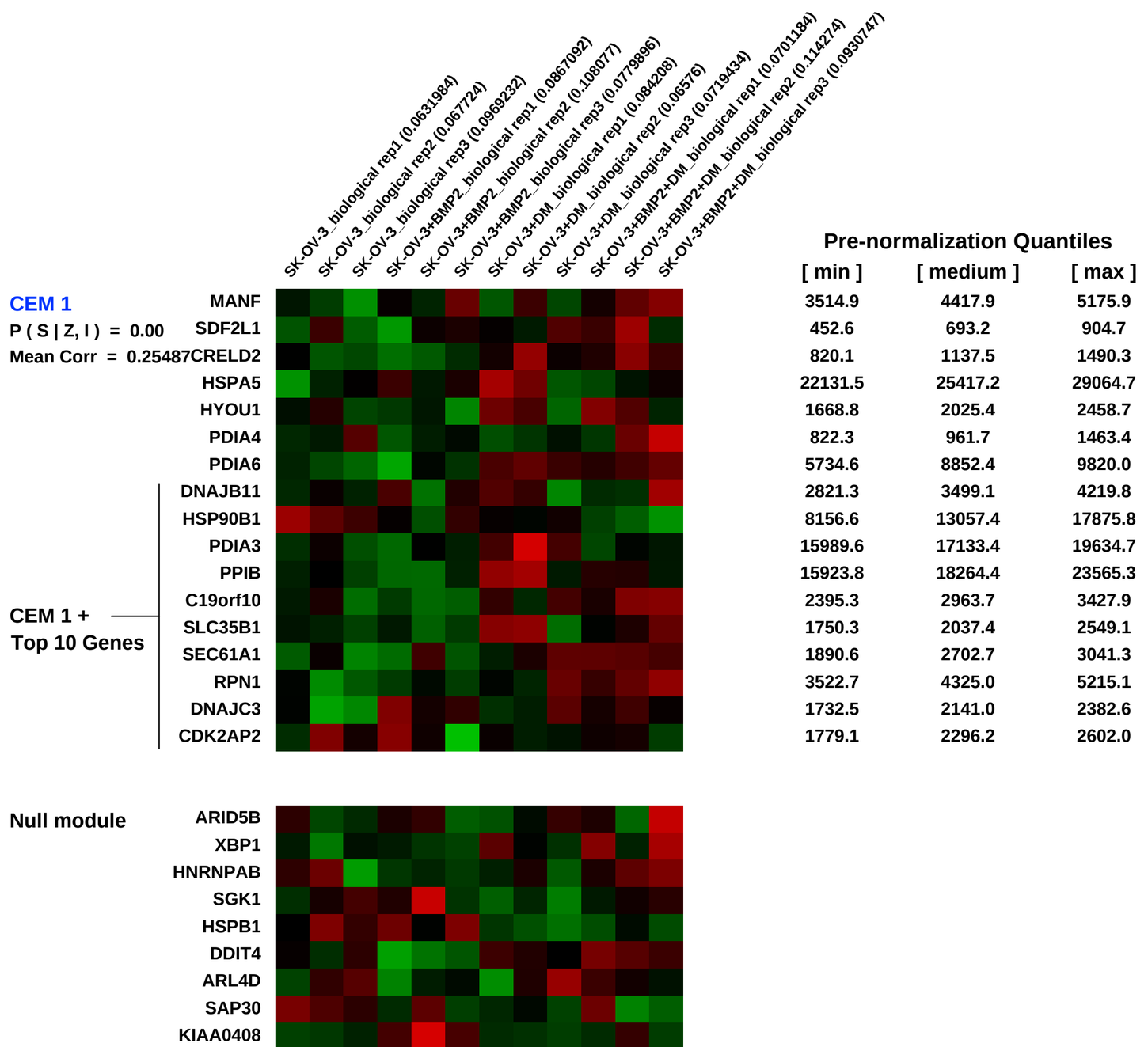

Pre-normalization Quantiles

	[min]	[medium]	[max]
MANF	3514.9	4417.9	5175.9
SDF2L1	452.6	693.2	904.7
CRELD2	820.1	1137.5	1490.3
HSPA5	22131.5	25417.2	29064.7
HYOU1	1668.8	2025.4	2458.7
PDIA4	822.3	961.7	1463.4
PDIA6	5734.6	8852.4	9820.0
DNAJB11	2821.3	3499.1	4219.8
HSP90B1	8156.6	13057.4	17875.8
PDIA3	15989.6	17133.4	19634.7
PPIB	15923.8	18264.4	23565.3
C19orf10	2395.3	2963.7	3427.9
SLC35B1	1750.3	2037.4	2549.1
SEC61A1	1890.6	2702.7	3041.3
RPN1	3522.7	4325.0	5215.1
DNAJC3	1732.5	2141.0	2382.6
CDK2AP2	1779.1	2296.2	2602.0
ARID5B			
XBP1			
HNRNPAB			
SGK1			
HSPB1			
DDIT4			
ARL4D			
SAP30			
KIAA0408			
GPR17			
HSPH1			
DNASE1L2			
SLC5A3			
GNAS			
GPR3			
TNFRSF25			
TM6SF2			
MKKS			
PLEKHF1			
ZMYM1			
DOK3			
FGF20			
SLC39A2			
KCNIP2			
ERRFI1			
DEDD2			
CCDC117			
USP31			
AHSA2			
CYS1			
CNIH2			
BANP			
CHORDC1			
P4HA1			

GEO Series "GSE26704" Expression Profiles

Num of samples in this series: 8

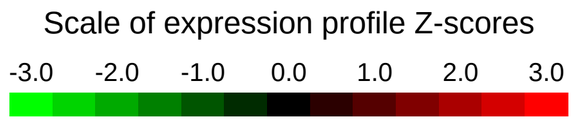

GEO Link: http://www.ncbi.nlm.nih.gov/geo/query/acc.cgi?acc=GSE26704

Status: Public on Jan 01 2012

Title: p38alfa and ATF2 act differentially depending on DUSP1 expression in NCSCL in response to cisplatin

Organism: Homo sapiens

Experiment type: Expression profiling by array

Platform: GPL570

Pubmed ID:

Summary & Design:

Summary:
DUSP1 is involved in different cellular pathways including cancer cell proliferation, angiogenesis, invasion and resistance to chemotherapy. To gain insight into the cellular signaling pathways involving DUSP1 actions and the response to Cisplatin (CDDP) in non small cell lung cancer (NSCLC), we have used a double strategy that combines microarray and SiRNA technology. This strategy provided a differential expression profile of genes involved in CDDP response in NSCLC cell line regulated by DUSP1 using H460 and H460cri and a time course to CDDP.

KEYWORDS: Expression profiling by array in cells with genetic modification in response to CCDP treatment

Overall design:
The human non small lung cancer cell line H460 used in this study was from ATCC (American Type Culture Collection). The cell line was maintained in RPMI (Gibco, Invitrogen) supplemented with 10% bovine serum and transfected by Lipofectamine Plus Reagent from Life Technologies as directed by the manufacturer. The DUSP1 pSuperRetro-derived vectors were constructed as described (Chattoppadhyay et al., 2006). Clones expressing siRNA for DUSP1 were selected for their ability to grow in the presence of puromycin and kept for selection. Stable transfection was confirmed by Western blotting. We analyzed the differences in expression of 47000 genes in H460 cells expressing DUSP1SiRNA (H460cri) compared with the parental cell line H460pSuperRetro vector (H460v) after 0, 1, 3 and 6 hours of CDDP exposure, in order to know the different pathways that were activated by CDDP treatment dependent on expression of DUSP1. RNA was extracted and quality control was checked before hybridization on Affymetrix microarrays.

Background corr dist: KL-Divergence = 0.0374, L1-Distance = 0.0265, L2-Distance = 0.0012, Normal std = 0.6097

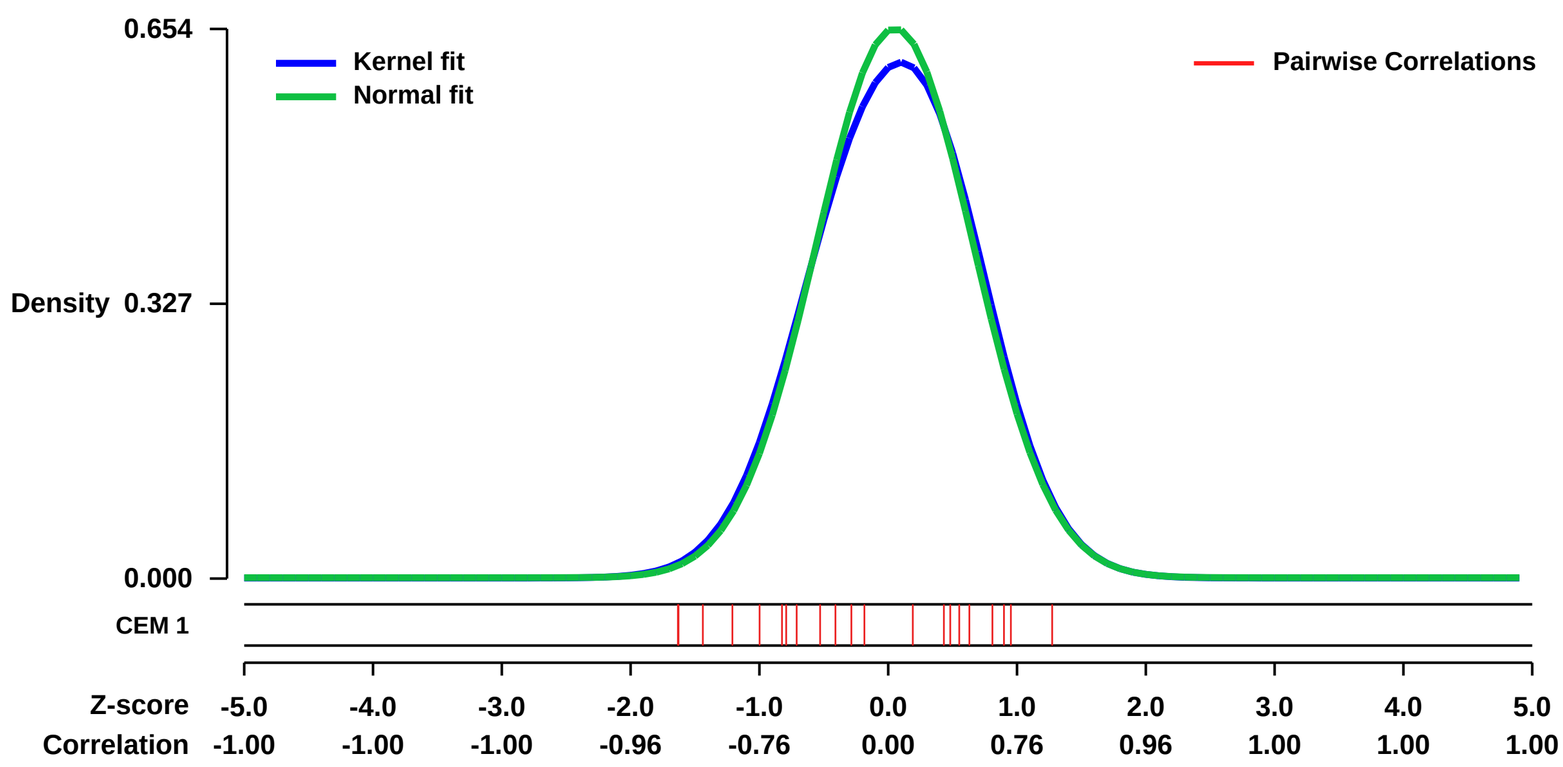

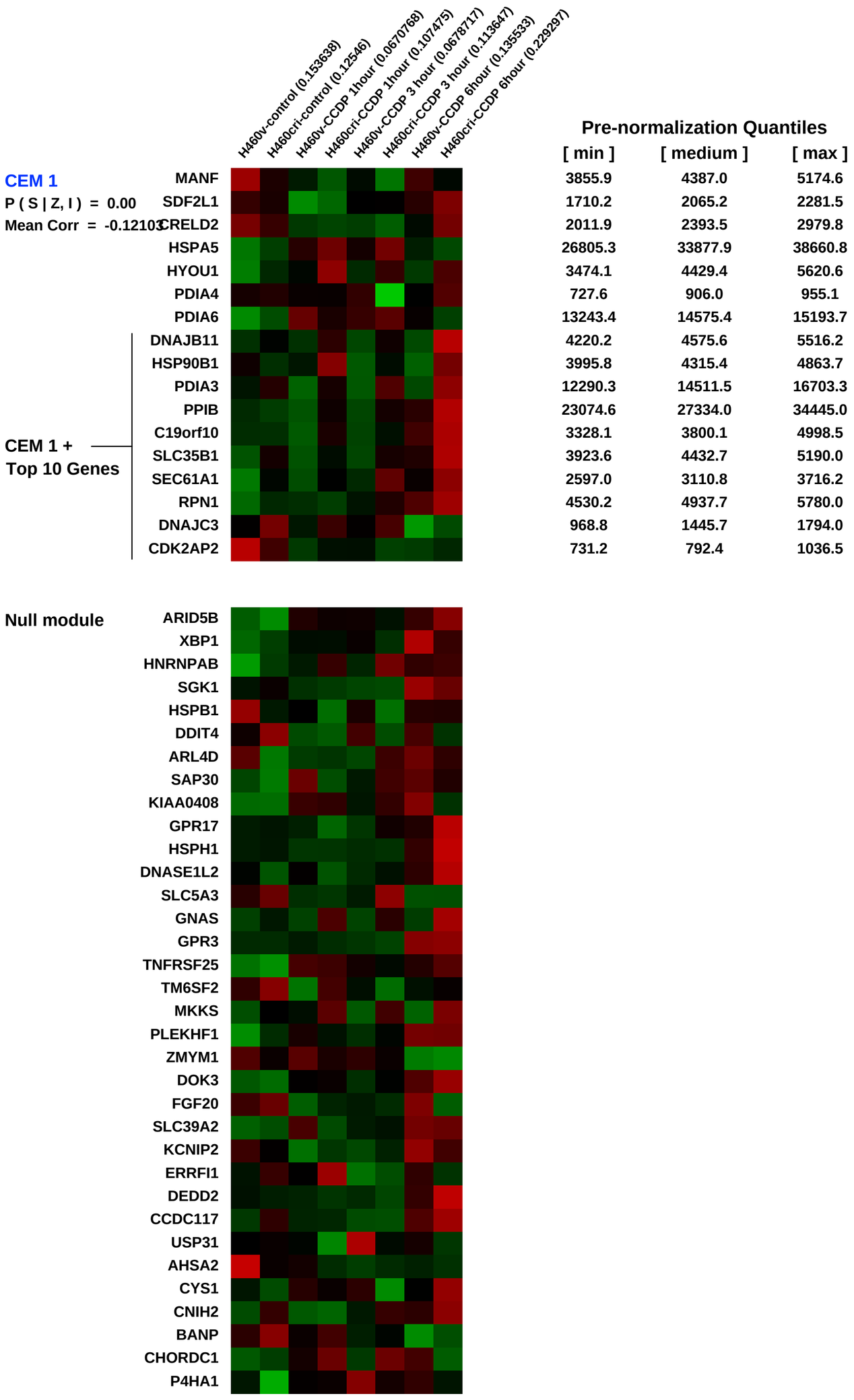

Pre-normalization Quantiles

	[min]	[medium]	[max]
MANF	3855.9	4387.0	5174.6
SDF2L1	1710.2	2065.2	2281.5
CRELD2	2011.9	2393.5	2979.8
HSPA5	26805.3	33877.9	38660.8
HYOU1	3474.1	4429.4	5620.6
PDIA4	727.6	906.0	955.1
PDIA6	13243.4	14575.4	15193.7
DNAJB11	4220.2	4575.6	5516.2
HSP90B1	3995.8	4315.4	4863.7
PDIA3	12290.3	14511.5	16703.3
PPIB	23074.6	27334.0	34445.0
C19orf10	3328.1	3800.1	4998.5
SLC35B1	3923.6	4432.7	5190.0
SEC61A1	2597.0	3110.8	3716.2
RPN1	4530.2	4937.7	5780.0
DNAJC3	968.8	1445.7	1794.0
CDK2AP2	731.2	792.4	1036.5

GEO Series "GSE2748" Expression Profiles

Num of samples in this series: 34

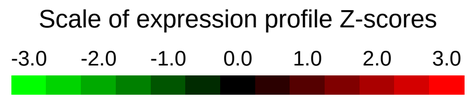

GEO Link:	http://www.ncbi.nlm.nih.gov/geo/query/acc.cgi?acc=GSE2748
Status:	Public on Jul 01 2005
Title:	A molecular classification of papillary renal cell carcinoma
Organism:	Homo sapiens
Experiment type:	Expression profiling by array
Platform:	GPL570
Pubmed ID:	15994935
Summary & Design:	Summary: BACKGROUND: Despite the moderate incidence of papillary renal cell carcinoma (PRCC), there is a disproportionately limited understanding of its underlying genetic programs. There is no effective therapy for metastatic PRCC, and patients are often excluded from kidney cancer trials. A morphological classification of PRCC into Type 1 and Type 2 tumors has been recently proposed, but its biological relevance remains uncertain. PATIENTS AND METHODS. We studied the gene expression profiles of 34 cases of PRCC using Affymetrix HGU133 Plus 2.0 arrays (54,675 probe sets) using both unsupervised and supervised analysis. Comparative genomic microarray analysis (CGMA) was used to infer cytogenetic aberrations, and pathways were ranked with a curated database. Expression of selected genes was validated by immunohistochemistry in 34 samples, with 15 independent tumors. RESULTS. We identified 2 highly distinct molecular PRCC subclasses with morphologic correlation. The first class, with excellent survival, corresponded to 3 histological subtypes: Type 1, low-grade Type 2 and mixed Type 1/low-grade Type 2 tumors. The second class, with poor survival, corresponded to high-grade Type 2 tumors (n=11). Dysregulation of G1/S and G2/M checkpoint genes were found in Class 1 and Class 2 tumors respectively, alongside characteristic chromosomal aberrations. We identified a 7-transcript predictor that classified samples on cross-validation with 97% accuracy. Immunohistochemistry confirmed high expression of cytokeratin 7 in Class 1 tumors, and of topoisomerase II¸– in Class 2 tumors. CONCLUSIONS. We report 2 molecular subclasses of PRCC, which are biologically and clinically distinct, which may be readily distinguished in a clinical setting. Keywords: survival, prognostic classification, disease state analysis Overall design: 34 individual samples analyzed, no technical replicates.

Background corr dist: KL-Divergence = 0.2034, L1-Distance = 0.0838, L2-Distance = 0.0191, Normal std = 0.3453

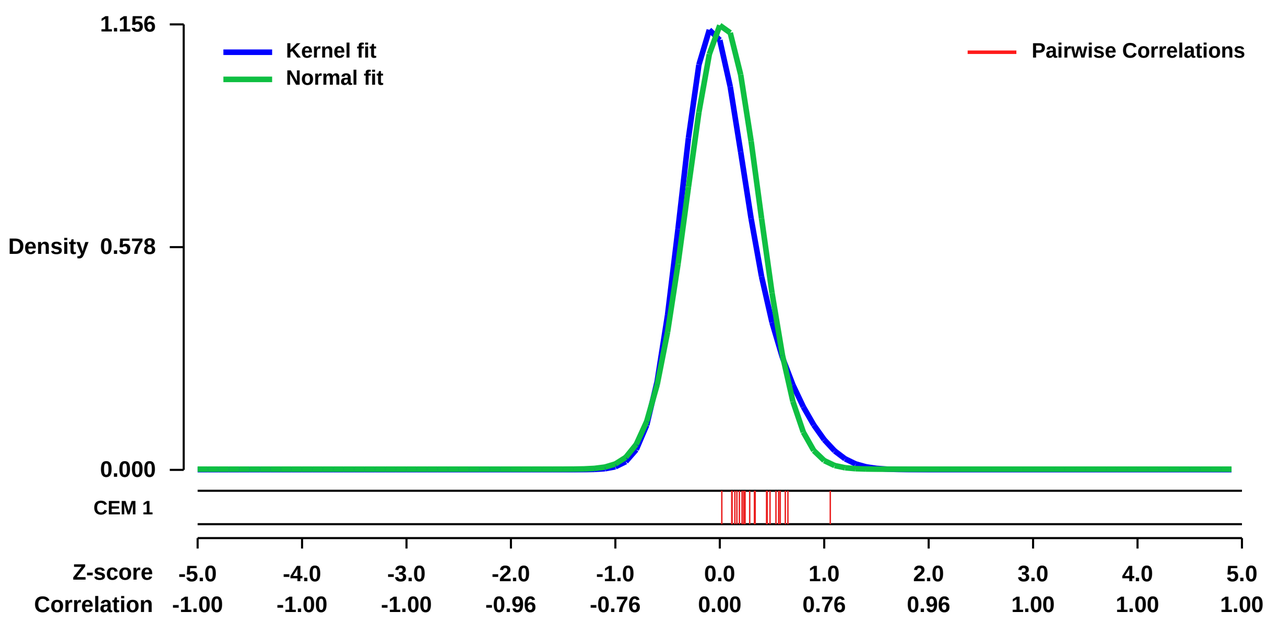

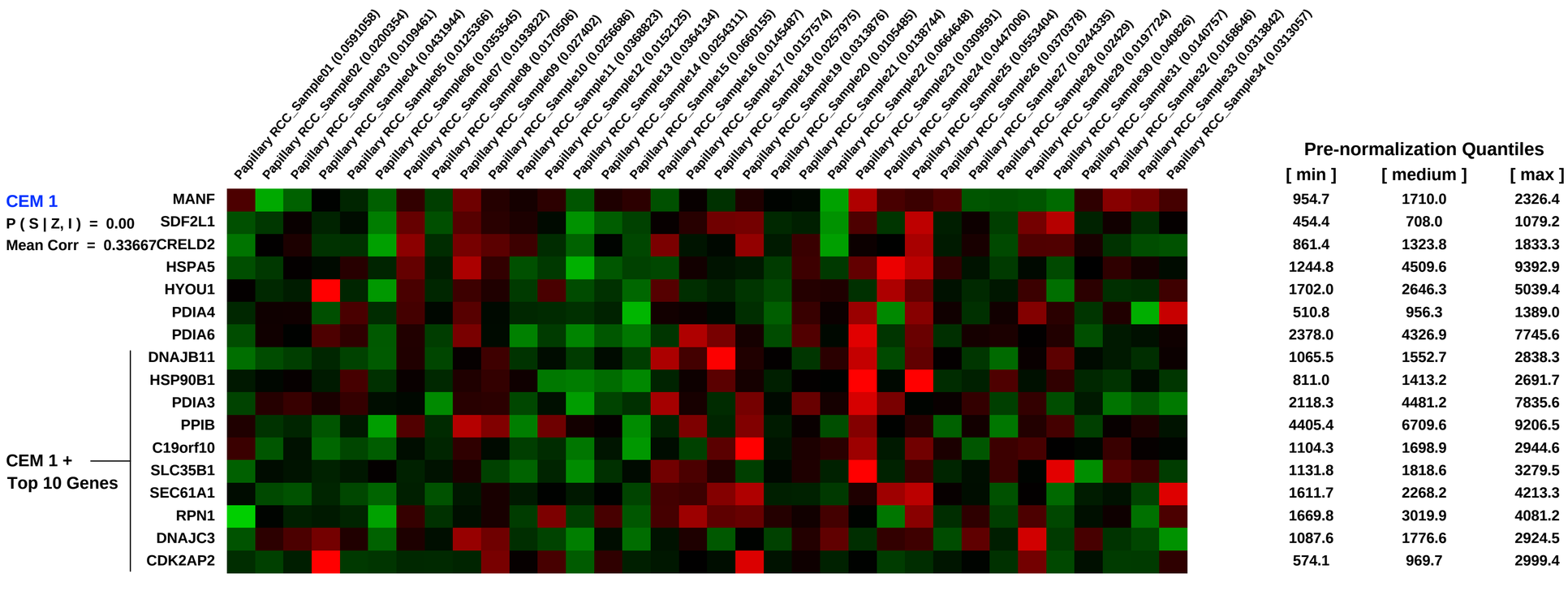

Pre-normalization Quantiles

[min]	[medium]	[max]
954.7	1710.0	2326.4
454.4	708.0	1079.2
861.4	1323.8	1833.3
1244.8	4509.6	9392.9
1702.0	2646.3	5039.4
510.8	956.3	1389.0
2378.0	4326.9	7745.6
1065.5	1552.7	2838.3
811.0	1413.2	2691.7
2118.3	4481.2	7835.6
4405.4	6709.6	9206.5
1104.3	1698.9	2944.6
1131.8	1818.6	3279.5
1611.7	2268.2	4213.3
1669.8	3019.9	4081.2
1087.6	1776.6	2924.5
574.1	969.7	2999.4

GEO Series "GSE29246" Expression Profiles

Num of samples in this series: 6

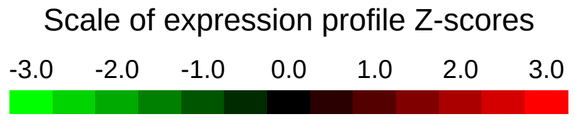

GEO Link:	http://www.ncbi.nlm.nih.gov/geo/query/acc.cgi?acc=GSE29246
Status:	Public on May 13 2011
Title:	RAP1A signaling in Leishmania donovani infected macrophages
Organism:	Homo sapiens
Experiment type:	Expression profiling by array
Platform:	GPL570
Pubmed ID:	23292345
Summary & Design:	**Summary:** Monastrol treatment of Leishmania donovani infected macrophages **Overall design:** Macrophages were infected with Leishmania donovani and treated with monastrol to look for signalling molecules

Background corr dist: KL-Divergence = 0.0607, L1-Distance = 0.0622, L2-Distance = 0.0068, Normal std = 0.6074

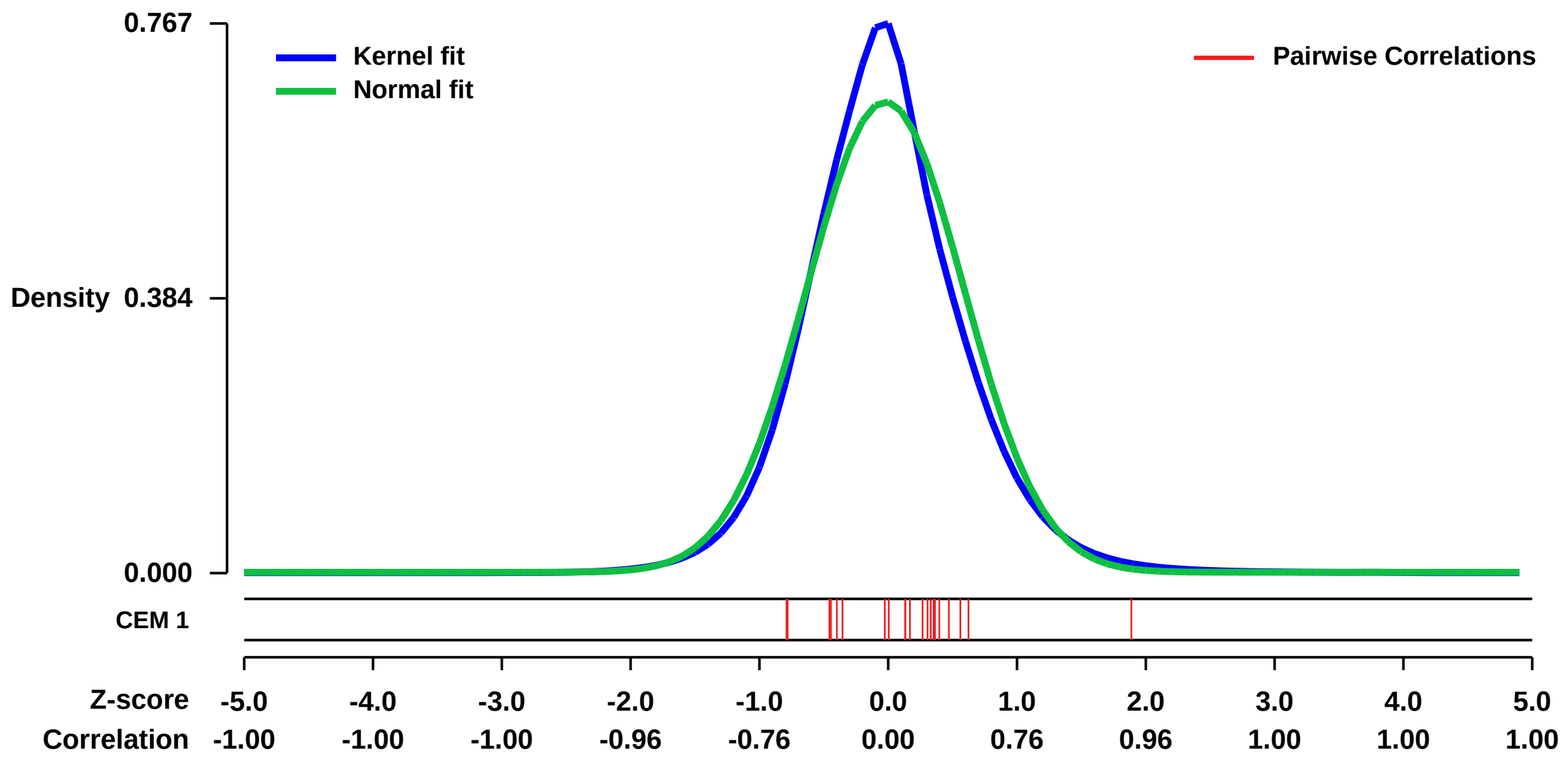

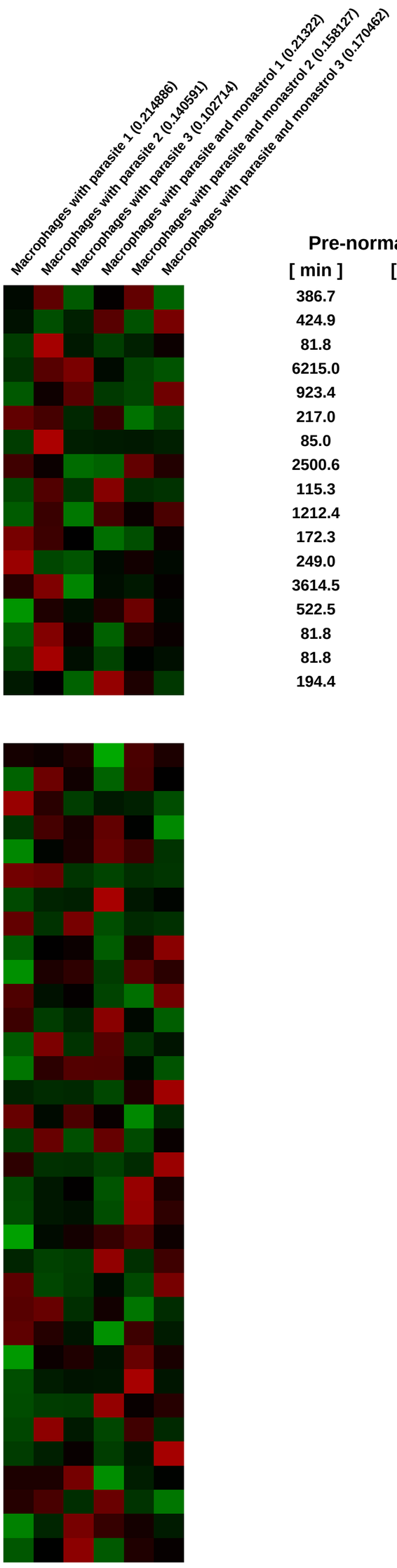

GEO Series "GSE39733" Expression Profiles

Num of samples in this series: 12

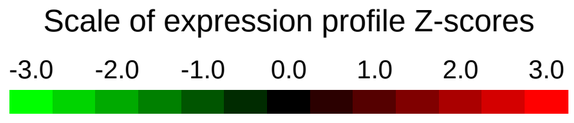

GEO Link:	http://www.ncbi.nlm.nih.gov/geo/query/acc.cgi?acc=GSE39733
Status:	Public on Sep 15 2012
Title:	Microarray analysis of gene expression changes in human A549 lung cancer cells upon siRNA knockdown of FAM60A and SDS3
Organism:	Homo sapiens
Experiment type:	Expression profiling by array
Platform:	GPL570
Pubmed ID:	22984288

Summary & Design:

Summary:
The Sin3 histone deacetylase (HDAC) complex is a 1.2 MDa chromatin modifying complex that can repress transcription by binding to gene promoters and deacetylating histones. The Sin3/HDAC complex can affect cell cycle progression through multiple mechanisms and is among the targets of anticancer drugs, called HDAC inhibitors. We describe the identification of a new subunit of the Sin3 complex named family with sequence similarity 60 member A (FAM60A). We show that FAM60A/Sin3 complexes normally suppress the epithelial-to-mesenchymal transition (EMT) and cell migration. This occurs through transcriptional repression of genes that encode components of the TGF-beta signaling pathway. This work reveals that FAM60A and the Sin3 complex are upstream repressors of TGF-beta signaling, EMT and cell migration and extends the known biological roles of the Sin3 complex. This experiment investigates the role of FAM60A in gene expression by comparing A549 lung cancer cells treated with or without siRNA against FAM60A.

The Sin3 histone deacetylase (HDAC) complex is a 1.2 MDa chromatin modifying complex that can repress transcription by binding to gene promoters and deacetylating histones. SDS3 is a core component of the Sin3 complex. The Sin3/HDAC complex can affect cell cycle progression through multiple mechanisms and is among the targets of anticancer drugs, called HDAC inhibitors. We describe the identification of a new subunit of the Sin3 complex named family with sequence similarity 60 member A (FAM60A). We show that FAM60A/Sin3 complexes normally suppress the epithelial-to-mesenchymal transition (EMT) and cell migration. This occurs through transcriptional repression of genes that encode components of the TGF-beta signaling pathway. This work reveals that FAM60A and the Sin3 complex are upstream repressors of TGF-beta signaling, EMT and cell migration and extends the known biological roles of the Sin3 complex. As a base line to better understand the relationship between FAM60A and the Sin3 complex, this experiment investigates the gene expression changes which occur in A549 lung cancer cells when the Sin3 complex is perturbed by knockdown of a core component via siRNA against SDS3.

Overall design:
SDS3 siRNA knockdowns were compared to a non-targeting control in triplicate, for a total of 6 samples.

Background corr dist: KL-Divergence = 0.0168, L1-Distance = 0.0380, L2-Distance = 0.0019, Normal std = 0.7917

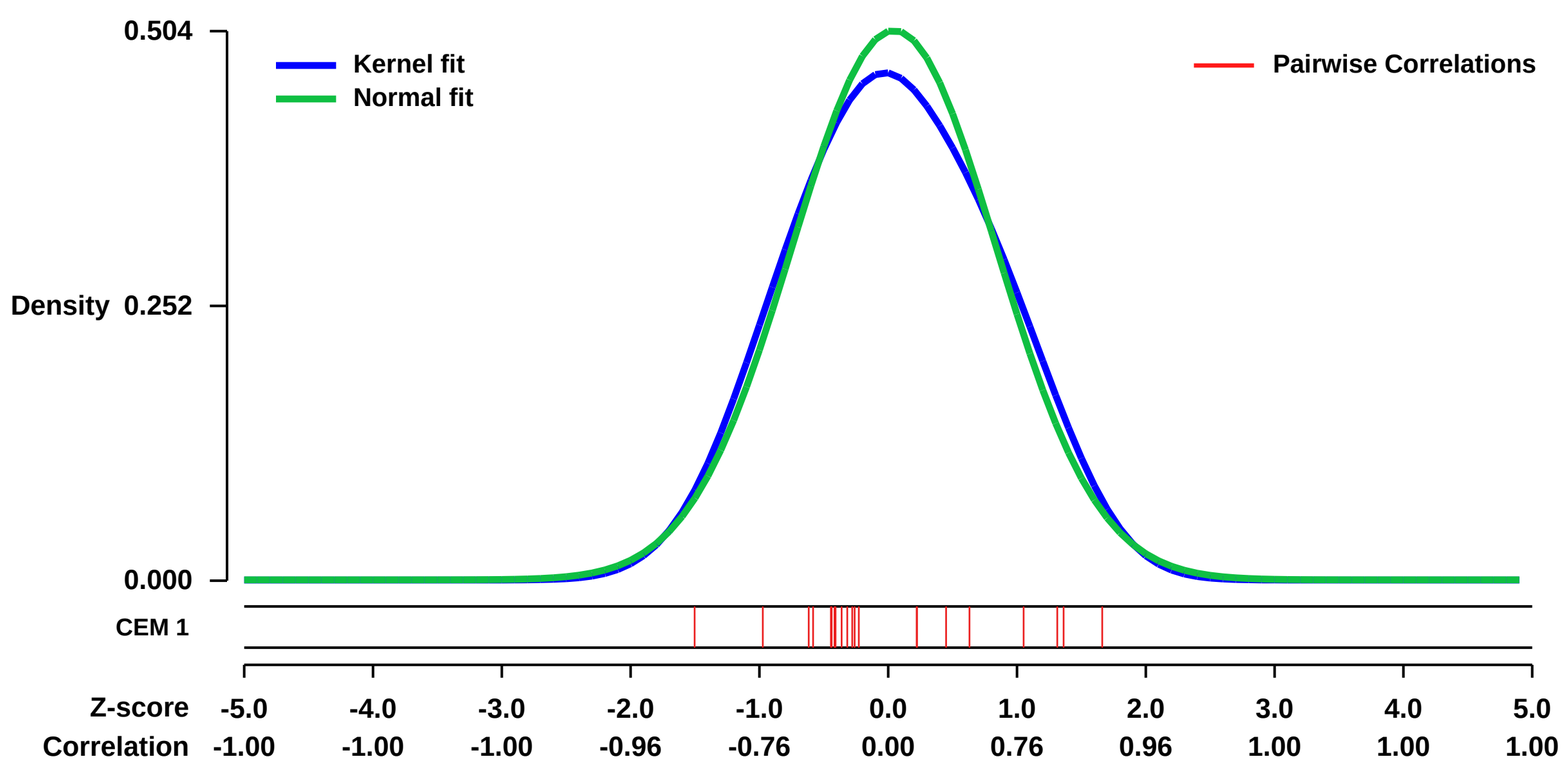

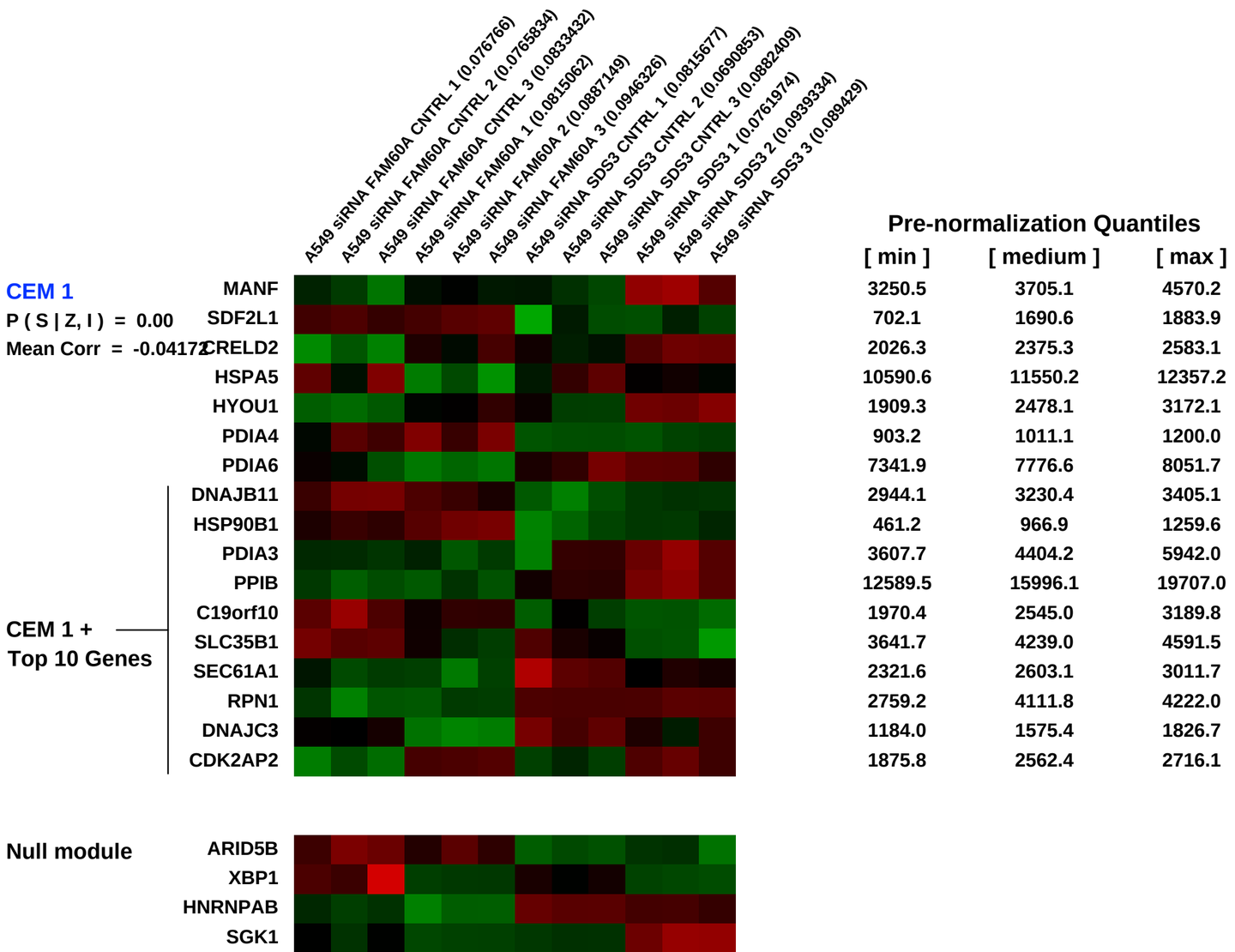

GEO Series "GSE58209" Expression Profiles

Num of samples in this series: 6

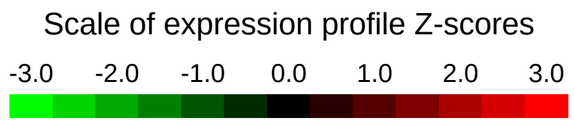

GEO Link:	http://www.ncbi.nlm.nih.gov/geo/query/acc.cgi?acc=GSE58209
Status:	Public on Jun 05 2014
Title:	SSEA-4 labels a subset of poor prognosis-associated osteosarcoma-initiating cells that respond to differentiation induction
Organism:	Homo sapiens
Experiment type:	Expression profiling by array
Platform:	GPL570
Pubmed ID:	
Summary & Design:	**Summary:** Osteosarcoma is thought of arising from the malignant transformation of osteogenic progenitors. The stage-specific embryonic antigen-4 (SSEA-4) labels a subset of TICs specially present in the high-risk subgroup. **Overall design:** SSEA-4+ AND SSEA-4-

Background corr dist: KL-Divergence = 0.0444, L1-Distance = 0.0204, L2-Distance = 0.0004, Normal std = 0.5979

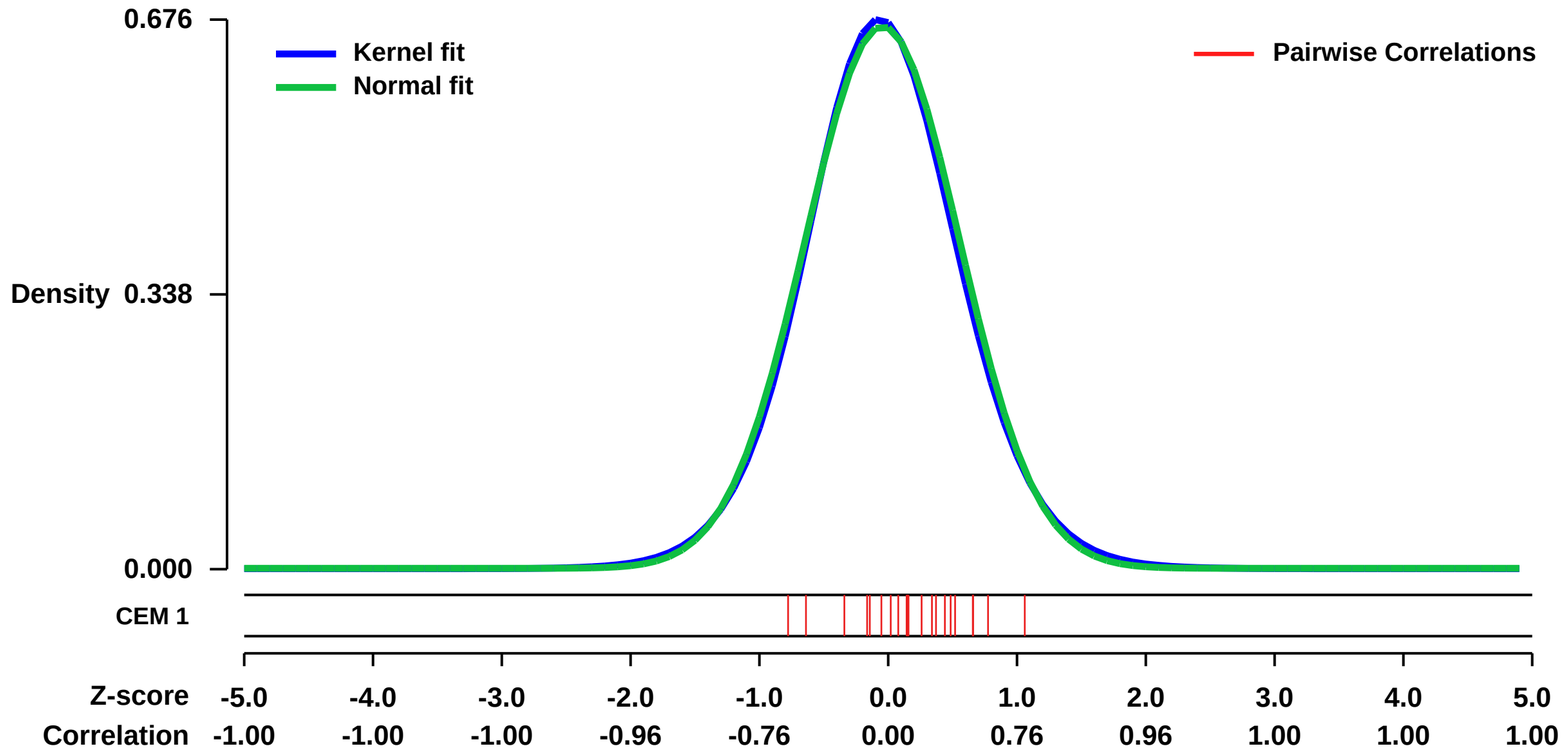

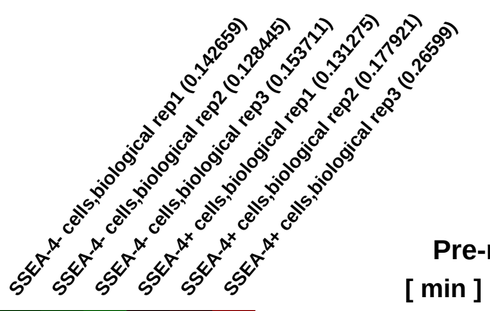

Pre-normalization Quantiles

		[min]	[medium]	[max]
CEM 1	MANF	6772.6	7373.5	7992.7
P (S | Z, I) = 0.00	SDF2L1	905.6	1087.0	1155.8
Mean Corr = 0.16719	CRELD2	2598.3	2819.1	2990.6
	HSPA5	30880.1	33581.1	34883.1
	HYOU1	1451.0	1573.0	1750.8
	PDIA4	567.1	650.8	706.3
	PDIA6	6157.4	6380.0	6767.2
CEM 1 + Top 10 Genes	DNAJB11	4698.3	5679.9	6803.3
	HSP90B1	3184.3	3752.8	3994.1
	PDIA3	8473.5	9909.8	11085.0
	PPIB	28364.5	32598.3	34425.3
	C19orf10	18121.1	20659.0	21598.0
	SLC35B1	3301.7	3845.5	3930.9
	SEC61A1	4822.2	5392.9	5629.8
	RPN1	8062.0	9292.2	10327.7
	DNAJC3	2575.2	2780.2	3044.3
	CDK2AP2	561.3	788.7	878.9
Null module	ARID5B			
	XBP1			
	HNRNPAB			
	SGK1			
	HSPB1			
	DDIT4			
	ARL4D			
	SAP30			
	KIAA0408			
	GPR17			
	HSPH1			
	DNASE1L2			
	SLC5A3			
	GNAS			
	GPR3			
	TNFRSF25			
	TM6SF2			
	MKKS			
	PLEKHF1			
	ZMYM1			
	DOK3			
	FGF20			
	SLC39A2			
	KCNIP2			
	ERRFI1			
	DEDD2			
	CCDC117			
	USP31			
	AHSA2			
	CYS1			
	CNIH2			
	BANP			
	CHORDC1			
	P4HA1			

GEO Series "GSE19816" Expression Profiles

Num of samples in this series: 12

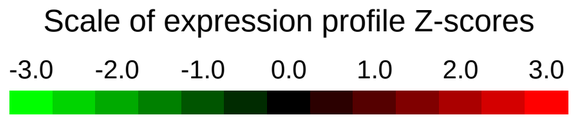

GEO Link:	http://www.ncbi.nlm.nih.gov/geo/query/acc.cgi?acc=GSE19816
Status:	Public on Nov 10 2010
Title:	Effect of von Willebrand factor on gene expression in HUVECs
Organism:	Homo sapiens
Experiment type:	Expression profiling by array
Platform:	GPL570
Pubmed ID:	21083900
Summary & Design:	**Summary:** Von Willebrand factor is a paracrine/autocrine regulator of human mesenchymal stem cell adhesion to distressed/apoptotic endothelial cells. This data set examines effect of vWF on gene expression in HUVECs. **Overall design:** HUVECs were maintained in EGM2 media and treated with vWF in Hank's buffered salt solution (HBSS).

Background corr dist: KL-Divergence = 0.0415, L1-Distance = 0.0259, L2-Distance = 0.0010, Normal std = 0.5880

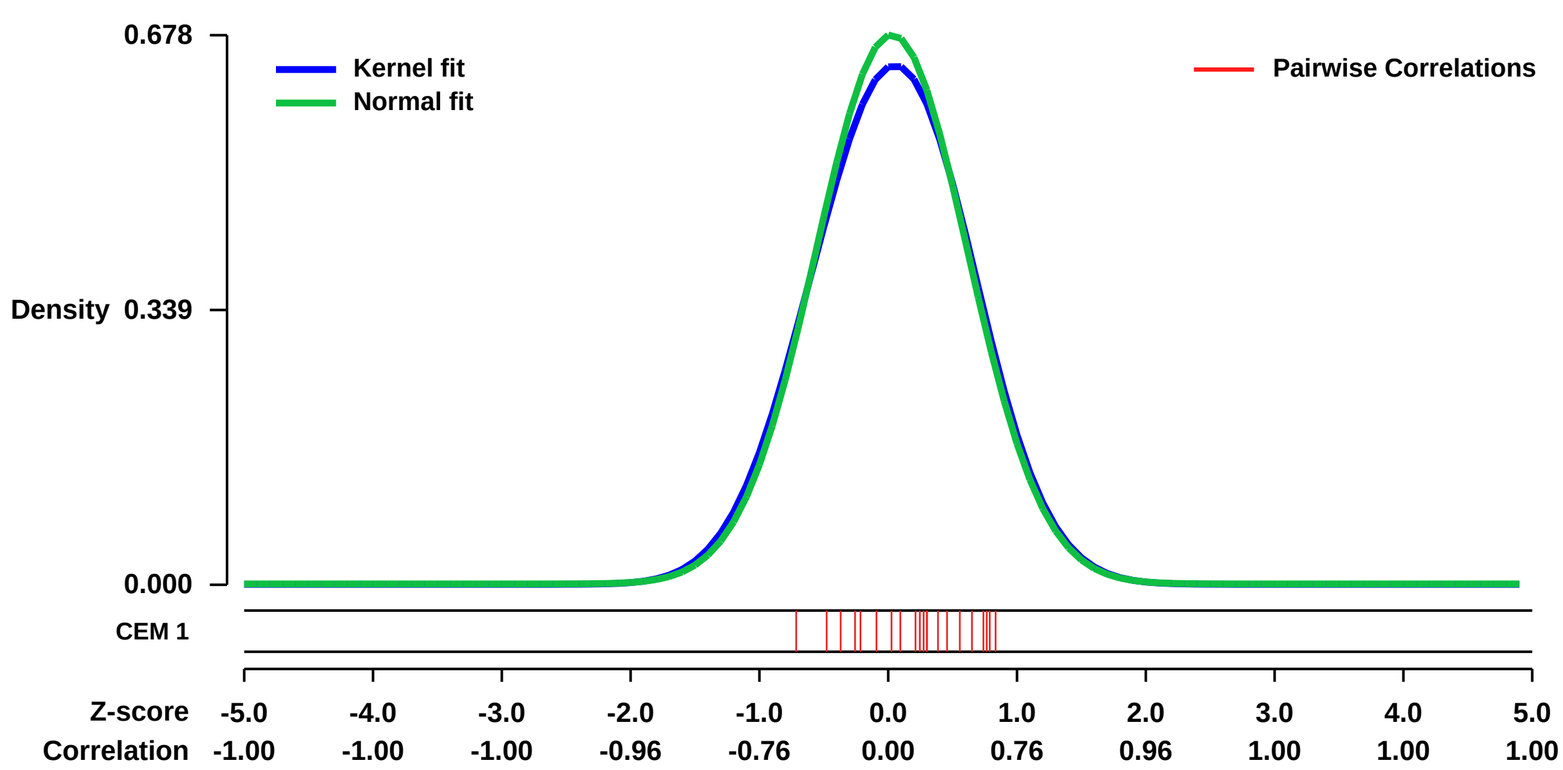

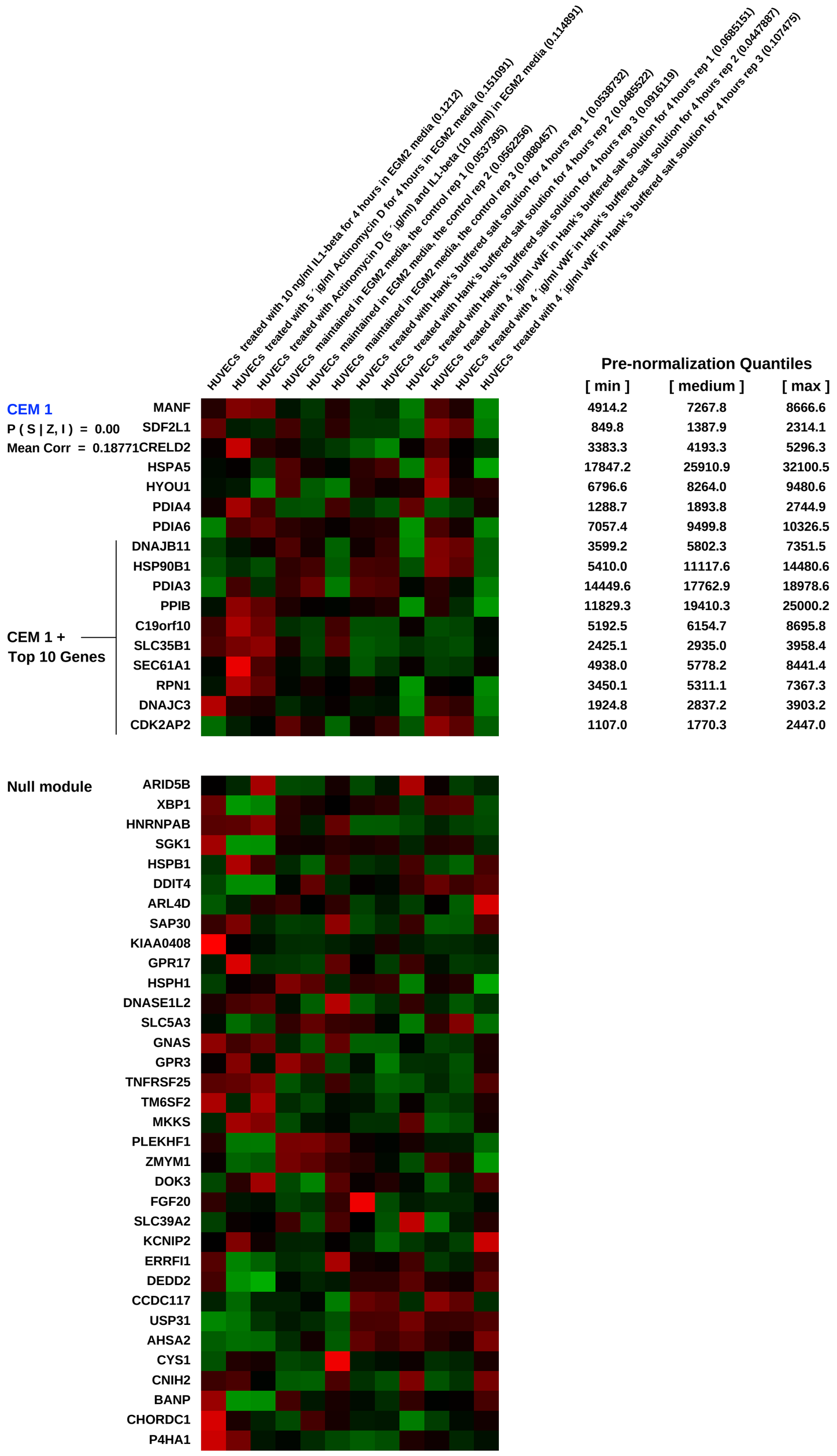

Pre-normalization Quantiles

	[min]	[medium]	[max]
MANF	4914.2	7267.8	8666.6
SDF2L1	849.8	1387.9	2314.1
CRELD2	3383.3	4193.3	5296.3
HSPA5	17847.2	25910.9	32100.5
HYOU1	6796.6	8264.0	9480.6
PDIA4	1288.7	1893.8	2744.9
PDIA6	7057.4	9499.8	10326.5
DNAJB11	3599.2	5802.3	7351.5
HSP90B1	5410.0	11117.6	14480.6
PDIA3	14449.6	17762.9	18978.6
PPIB	11829.3	19410.3	25000.2
C19orf10	5192.5	6154.7	8695.8
SLC35B1	2425.1	2935.0	3958.4
SEC61A1	4938.0	5778.2	8441.4
RPN1	3450.1	5311.1	7367.3
DNAJC3	1924.8	2837.2	3903.2
CDK2AP2	1107.0	1770.3	2447.0

GEO Series "GSE36768" Expression Profiles

Num of samples in this series: 6

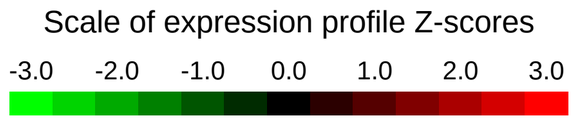

GEO Link:	http://www.ncbi.nlm.nih.gov/geo/query/acc.cgi?acc=GSE36768
Status:	Public on Jun 17 2013
Title:	Effect of human breast tumor supernatant on normal CD4+ T cells (Preliminary Experiment)
Organism:	Homo sapiens
Experiment type:	Expression profiling by array
Platform:	GPL570
Pubmed ID:	23778140
Summary & Design:	**Summary:** CD4+ helper T (Th) cells are critical regulators of immune responses but their role in breast cancer is currently unknown. This work aims to characterize Th cells infiltrating invasive primary human breast tumors, analyze the influence by the tumor microenvironment and identify Th cell specific prognostic gene signatures. CD4+ T cells isolated from the tumor (TIL), axillary lymph node (LN) and blood (PB) of 10 patients were analyzed on Affymetrix U133 Plus 2.0 arrays. A confirmation set of 60 patients were studied by flow cytometry, qRT-PCR or immunohistochemistry and analyzed according to the extent of the tumor immune infiltrate. Gene expression profiles of freshly isolated TIL were also compared with TIL that had been rested overnight or with CD4+ T cells [non-stimulated (NS) or stimulated (S)] from healthy donor PB treated with tumor supernatant (SN). Comparing gene expression profiles of donor blood derived total CD4+ T cells [non-stimulated (NS)] with and without tumor supernatant (SN) treatment **Overall design:** Total CD4+ T cells from a healthy donor blood (NS) were treated (and as control: untreated samples in biological triplicate) with SN from fresh breast tumor homogenates of 3 patients and analyzed on Affymetrix U133 Plus 2.0 arrays

Background corr dist: KL-Divergence = 0.0439, L1-Distance = 0.0208, L2-Distance = 0.0004, Normal std = 0.5985

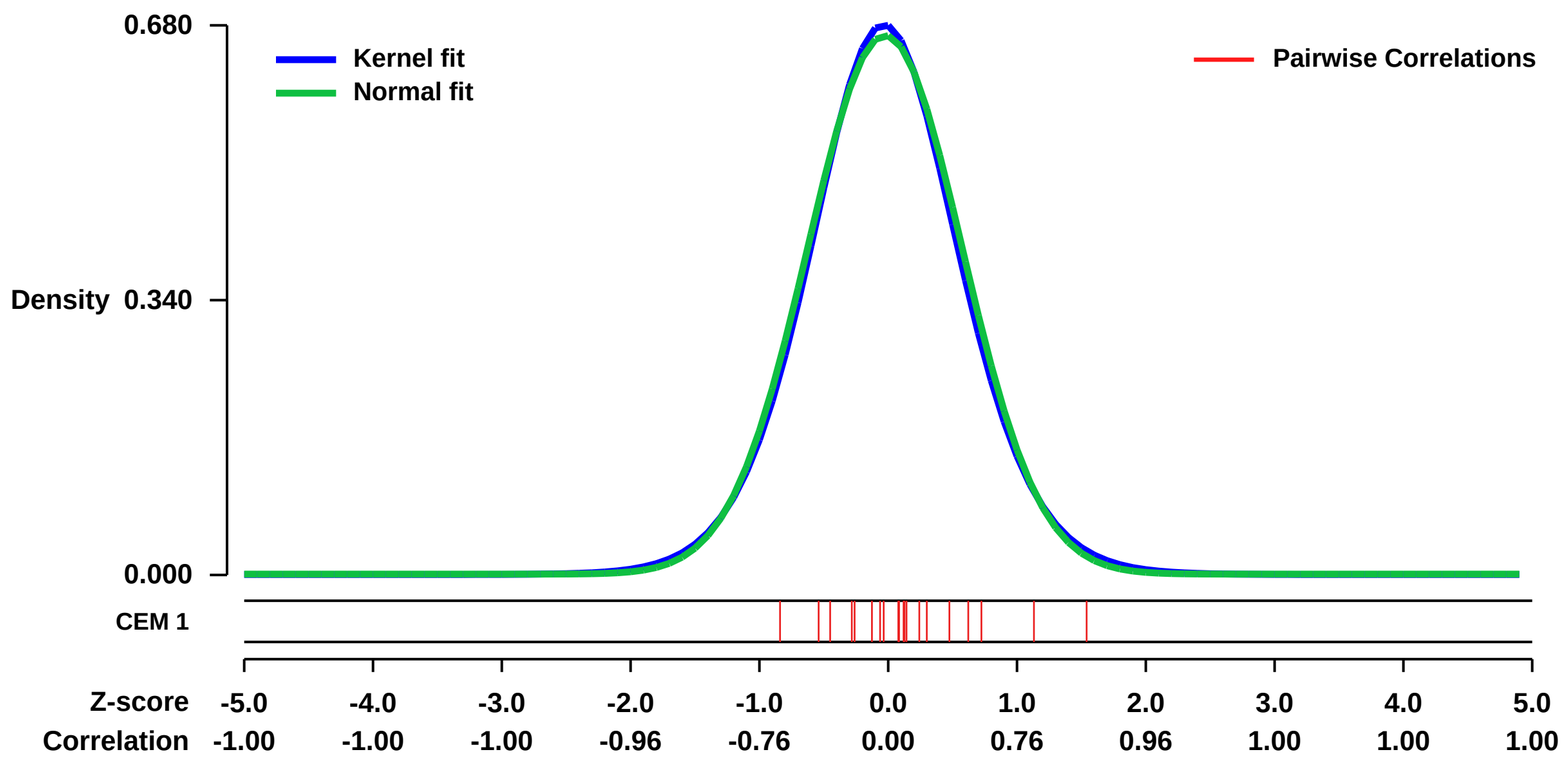

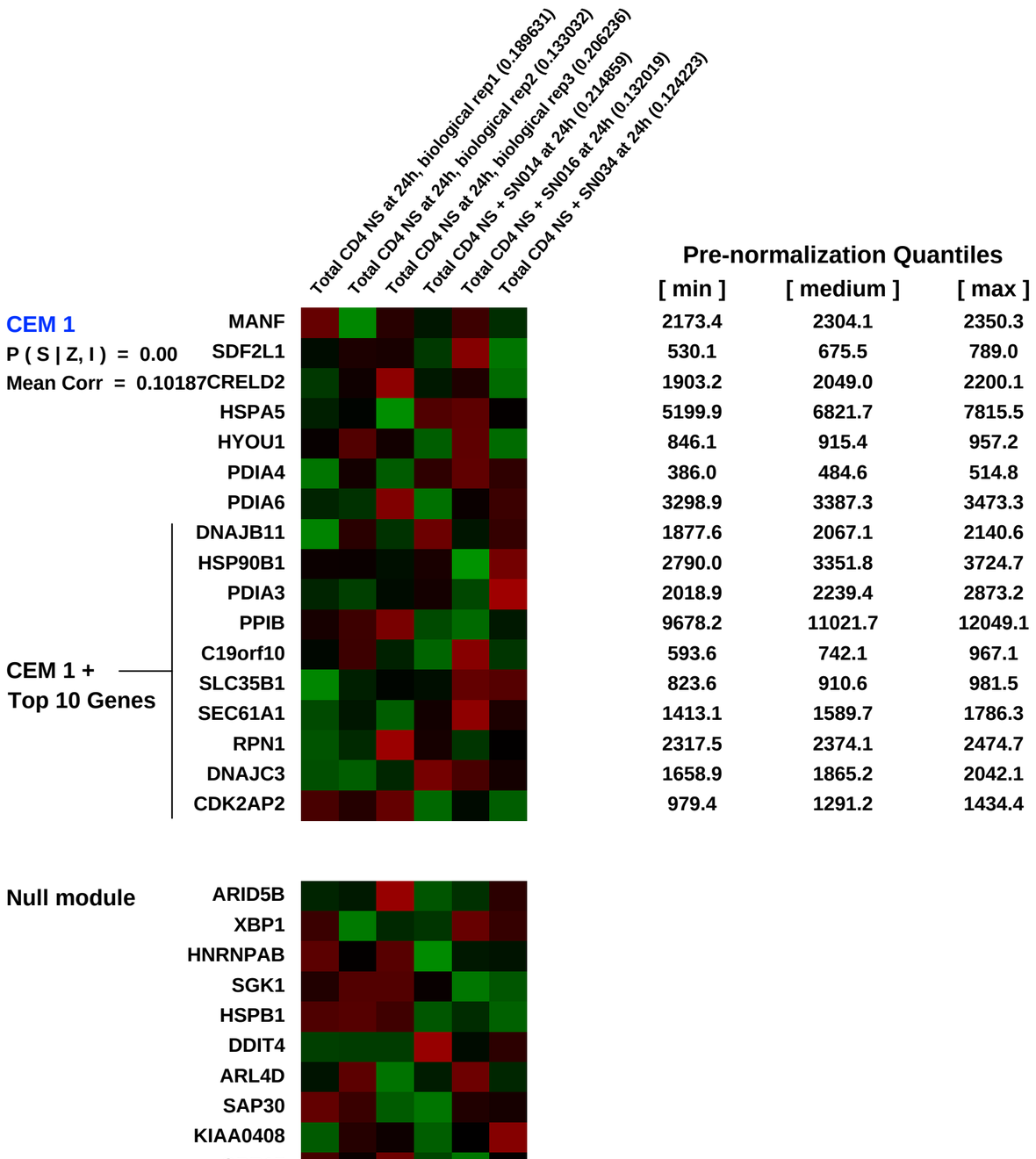

Pre-normalization Quantiles

	[min]	[medium]	[max]
MANF	2173.4	2304.1	2350.3
SDF2L1	530.1	675.5	789.0
CRELD2	1903.2	2049.0	2200.1
HSPA5	5199.9	6821.7	7815.5
HYOU1	846.1	915.4	957.2
PDIA4	386.0	484.6	514.8
PDIA6	3298.9	3387.3	3473.3
DNAJB11	1877.6	2067.1	2140.6
HSP90B1	2790.0	3351.8	3724.7
PDIA3	2018.9	2239.4	2873.2
PPIB	9678.2	11021.7	12049.1
C19orf10	593.6	742.1	967.1
SLC35B1	823.6	910.6	981.5
SEC61A1	1413.1	1589.7	1786.3
RPN1	2317.5	2374.1	2474.7
DNAJC3	1658.9	1865.2	2042.1
CDK2AP2	979.4	1291.2	1434.4

GEO Series "GSE9055" Expression Profiles

Num of samples in this series: 25

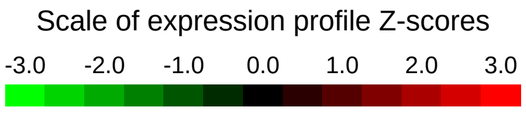

GEO Link:	http://www.ncbi.nlm.nih.gov/geo/query/acc.cgi?acc=GSE9055
Status:	Public on Sep 13 2008
Title:	Time course gene expression of HUVEC after TNF-alpha treatment
Organism:	Homo sapiens
Experiment type:	Expression profiling by array
Platform:	GPL570
Pubmed ID:	19826084
Summary & Design:	**Summary:** The many steps involved in the production of a mature mammalian mRNA are extensively coupled, and levels of both precursors and products can be measured using expression and genomic tiling microarrays. Different probes in these arrays targeting the same transcript often give different signals; then, precursor (nascent) RNA â which is present transiently at low concentrations â is difficult to detect. **Keywords:** TNFa stimulation time course of HUVEC **Overall design:** Using tumor necrosis factor a (TNF-alpha) to switch on transcription of selected human genes rapidly and synchronously, we apply samples collected every 15 min to arrays

Background corr dist: KL-Divergence = 0.3381, L1-Distance = 0.0543, L2-Distance = 0.0075, Normal std = 0.2685

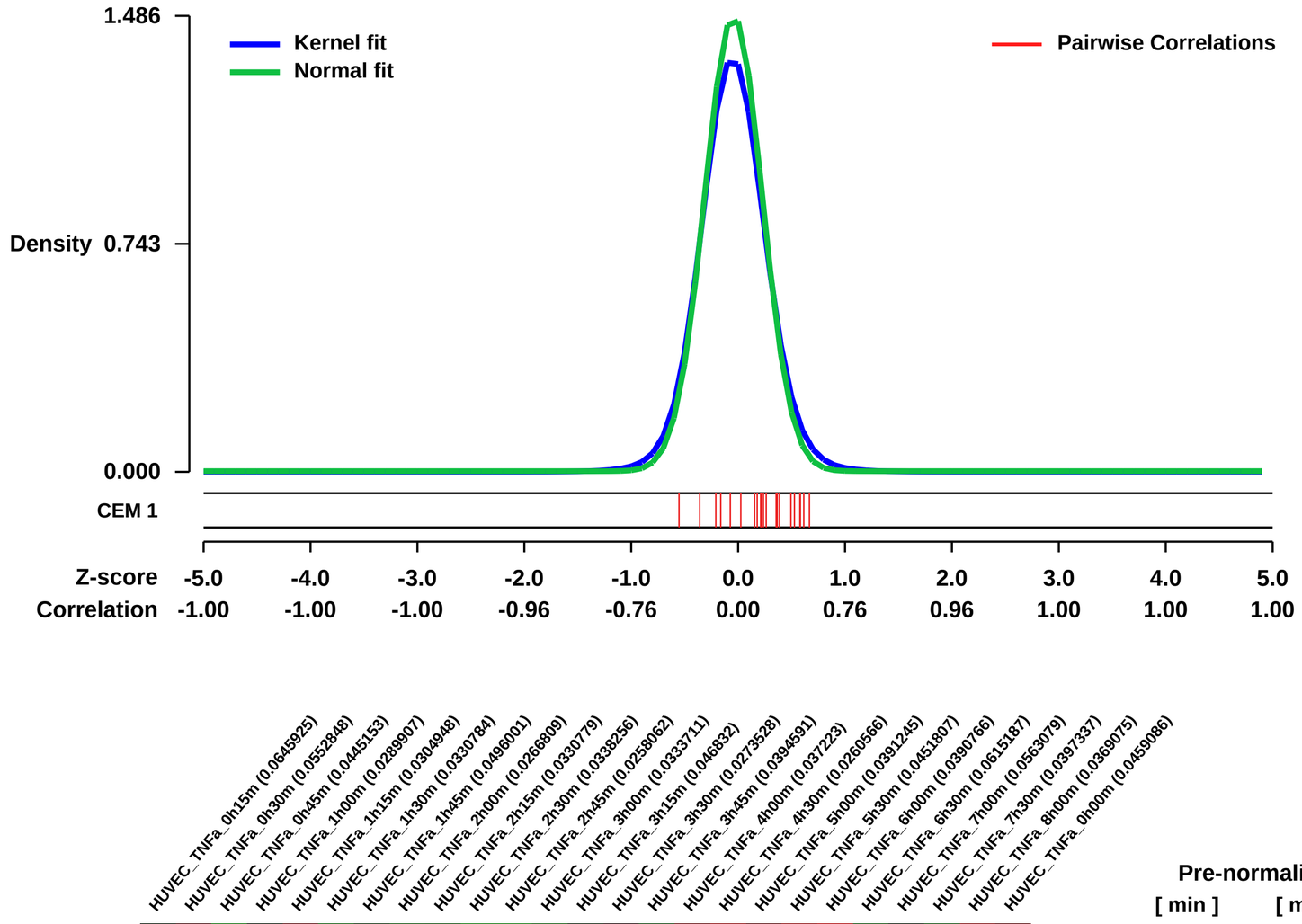

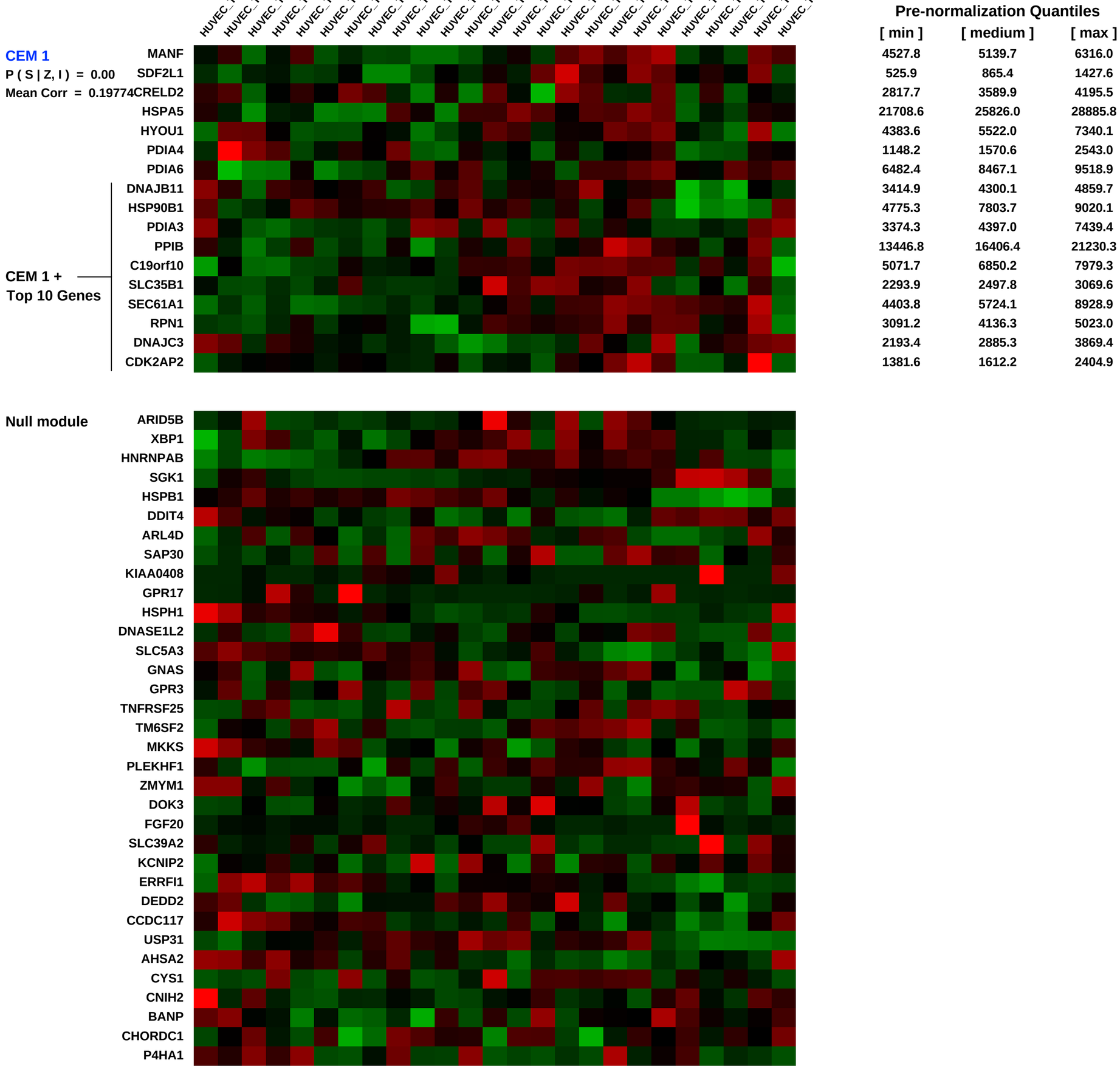

Pre-normalization Quantiles

[min]	[medium]	[max]
4527.8	5139.7	6316.0
525.9	865.4	1427.6
2817.7	3589.9	4195.5
21708.6	25826.0	28885.8
4383.6	5522.0	7340.1
1148.2	1570.6	2543.0
6482.4	8467.1	9518.9
3414.9	4300.1	4859.7
4775.3	7803.7	9020.1
3374.3	4397.0	7439.4
13446.8	16406.4	21230.3
5071.7	6850.2	7979.3
2293.9	2497.8	3069.6
4403.8	5724.1	8928.9
3091.2	4136.3	5023.0
2193.4	2885.3	3869.4
1381.6	1612.2	2404.9

GEO Series "GSE21550" Expression Profiles

Num of samples in this series: 12

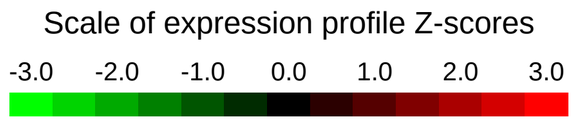

GEO Link:	http://www.ncbi.nlm.nih.gov/geo/query/acc.cgi?acc=GSE21550
Status:	Public on Sep 01 2010
Title:	Effect of Protease-resistant PML-RAR$_{\zeta}$– on the leukemogenic potential in a mouse model of Acute Promyelocytic Leukemia
Organism:	Homo sapiens
Experiment type:	Expression profiling by array
Platform:	GPL570
Pubmed ID:	20647568
Summary & Design:	**Summary:** Previous studies in our laboratory demonstrated that the azurophil granule protease neutrophil elastase (NE) cleaves PML-RARA (PR), the fusion protein that initiates acute promyelocytic leukemia (APL). Further, NE deficiency reduces the penetrance of APL in a murine model of this disease. We therefore predicted that NE-mediated PR cleavage might be important for its ability to initiate APL. To test this hypothesis, we generated a mouse expressing NE-resistant PR. These mice developed APL indistinguishable from wild type PR, but with significantly reduced latency (median leukemia-free survival of 274 days versus 473 days for wild type PR, p<0.001). Resistance to proteolysis may increase the abundance of full length PR protein in early myeloid cells, and our previous data suggested that non-cleaved PR may be less toxic to early myeloid cells. Together, these effects appear to increase the leukemogenicity of NE-resistant PR, contrary to our previous prediction. We conclude that NE deficiency may reduce APL penetrance via indirect mechanisms that are still NE dependent. **Keywords:** Time course **Overall design:** U937 cells were transfected with one of three tagged constructs GFP,GFP-PR,GFP-PR-2VR sorted for GFP positivity at the indicated time points and harvested for RNA.

Background corr dist: KL-Divergence = 0.1143, L1-Distance = 0.0380, L2-Distance = 0.0030, Normal std = 0.4180

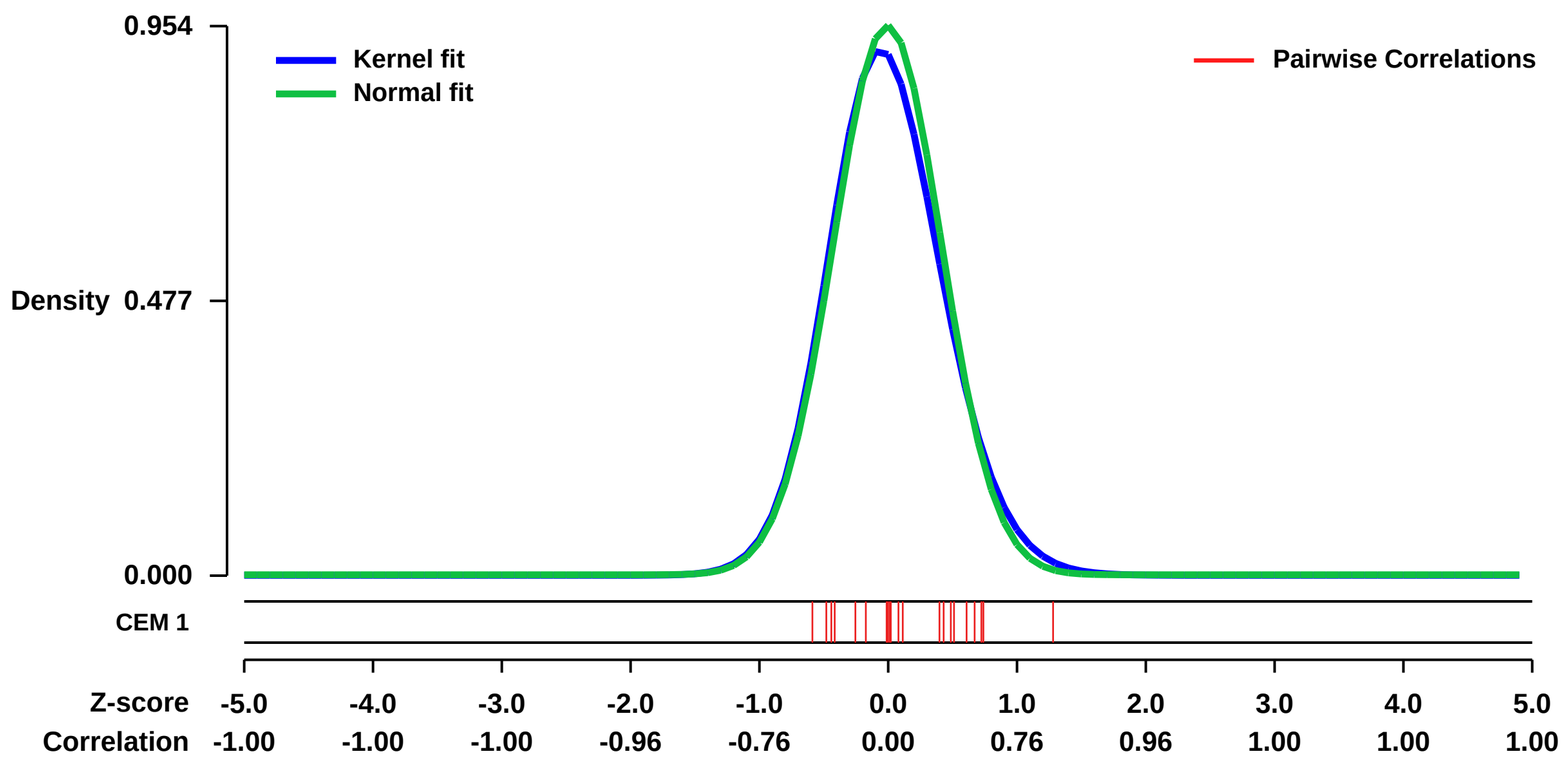

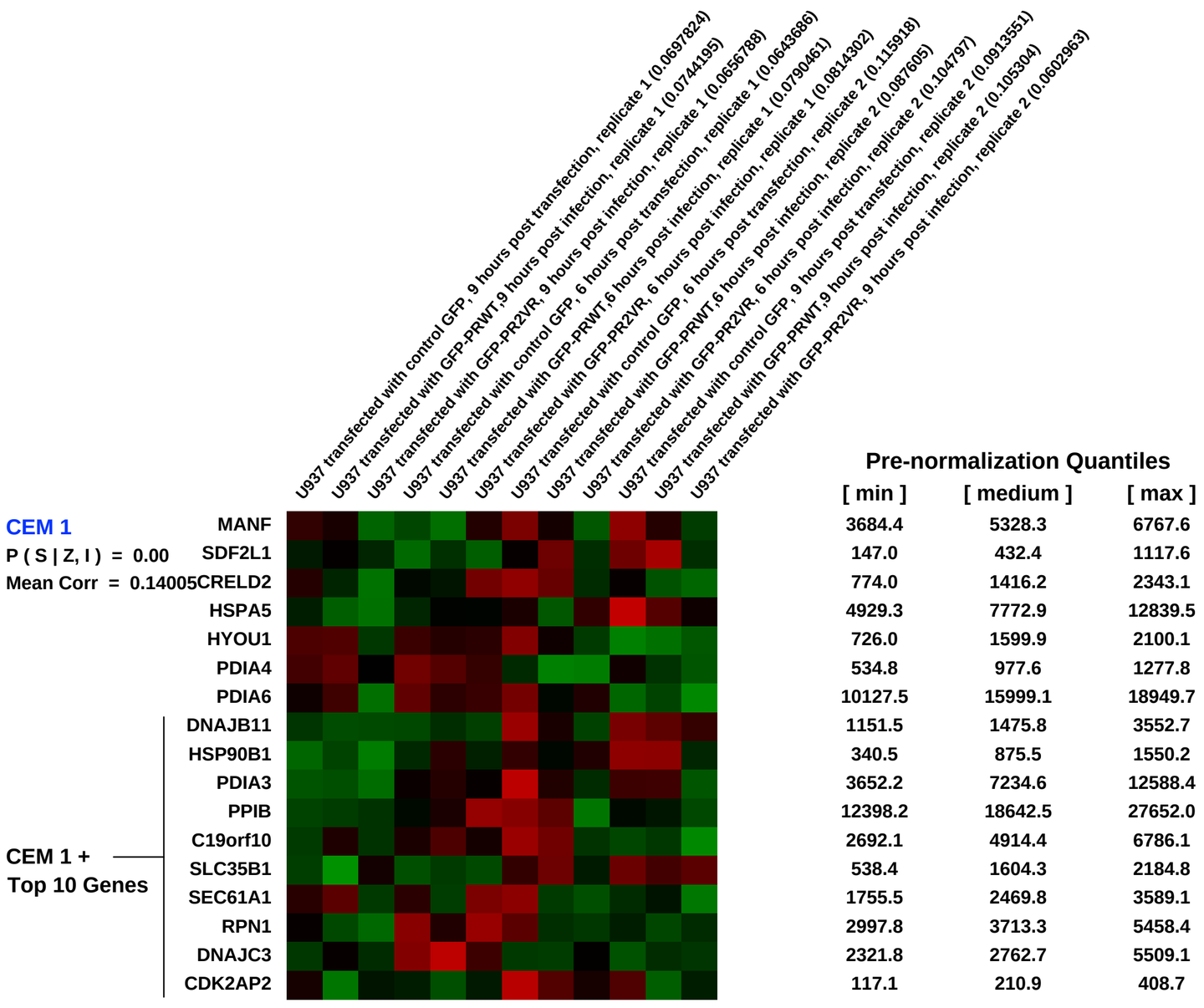

GEO Series "GSE28724" Expression Profiles

Num of samples in this series: 34

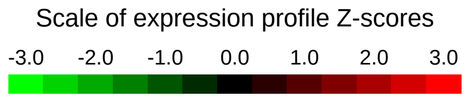

GEO Link:	http://www.ncbi.nlm.nih.gov/geo/query/acc.cgi?acc=GSE28724
Status:	Public on May 21 2013
Title:	Expression data from cultured human ovarian carcinoma cell lines
Organism:	Homo sapiens
Experiment type:	Expression profiling by array
Platform:	GPL570
Pubmed ID:	23666744
Summary & Design:	**Summary:** The hallmark of human cancer is heterogeneity, mirroring the complexity of genetic and epigenetic alterations acquired during oncogenesis. We extracted RNA of 34 cultured human ovarian carcinoma cell lines and performed expression microarrays so that cultured cell lines can represent in vivo human tumors. **Overall design:** 34 ovarian carcinoma cell lines expression data.

Background corr dist: KL-Divergence = 0.5261, L1-Distance = 0.0942, L2-Distance = 0.0301, Normal std = 0.2210

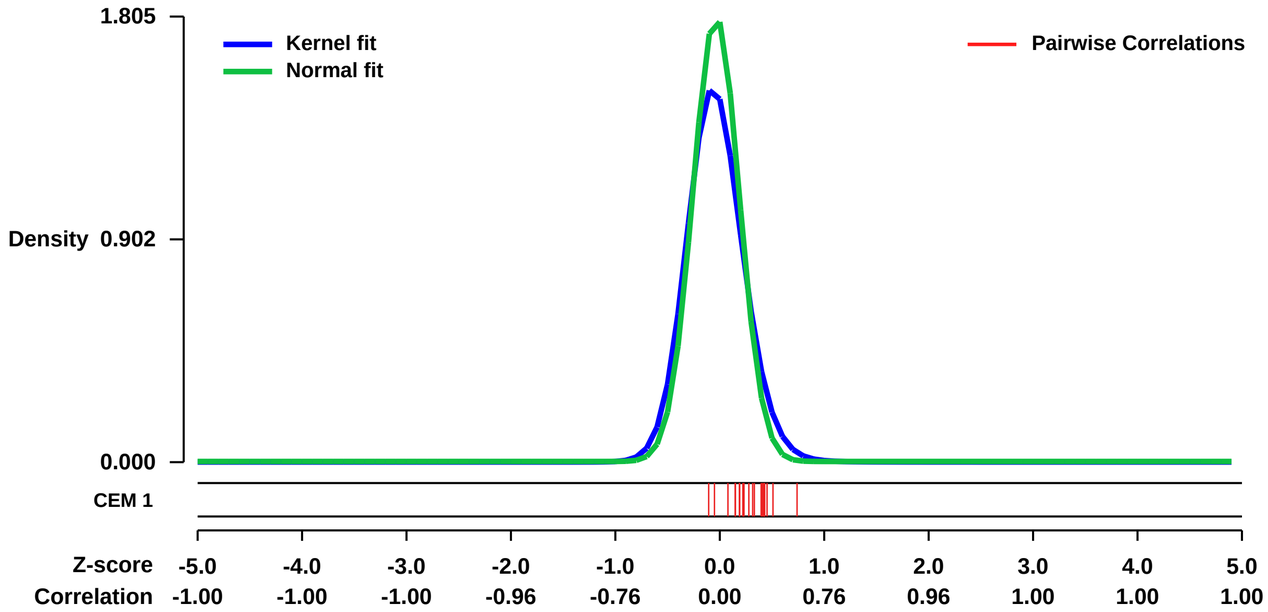

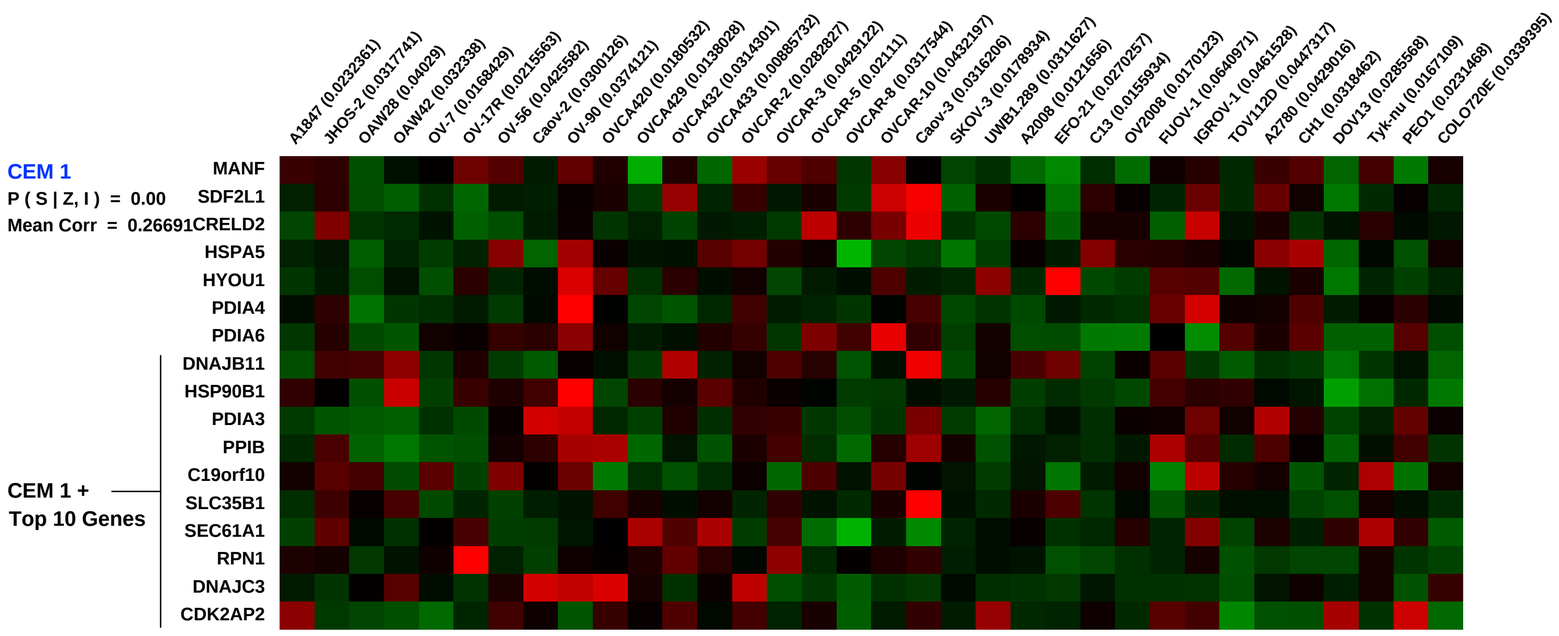

Pre-normalization Quantiles

	[min]	[medium]	[max]
MANF	2482.8	5357.4	7498.3
SDF2L1	494.6	1384.3	3934.4
CRELD2	1211.0	2316.3	6174.6
HSPA5	8984.3	17723.3	26492.8
HYOU1	1071.0	2221.9	5659.2
PDIA4	365.0	1237.4	4657.8
PDIA6	6067.6	10868.7	17531.7
DNAJB11	2588.3	6134.4	15095.2
HSP90B1	3292.6	5827.7	10324.1
PDIA3	3468.3	5498.4	12587.0
PPIB	12646.8	18494.1	29851.5
C19orf10	1148.0	2004.6	3303.6
SLC35B1	1672.4	2535.6	8041.2
SEC61A1	1595.5	3250.3	5073.5
RPN1	4148.1	6362.0	19456.4
DNAJC3	845.4	1942.1	6142.8
CDK2AP2	706.5	1337.8	2675.8

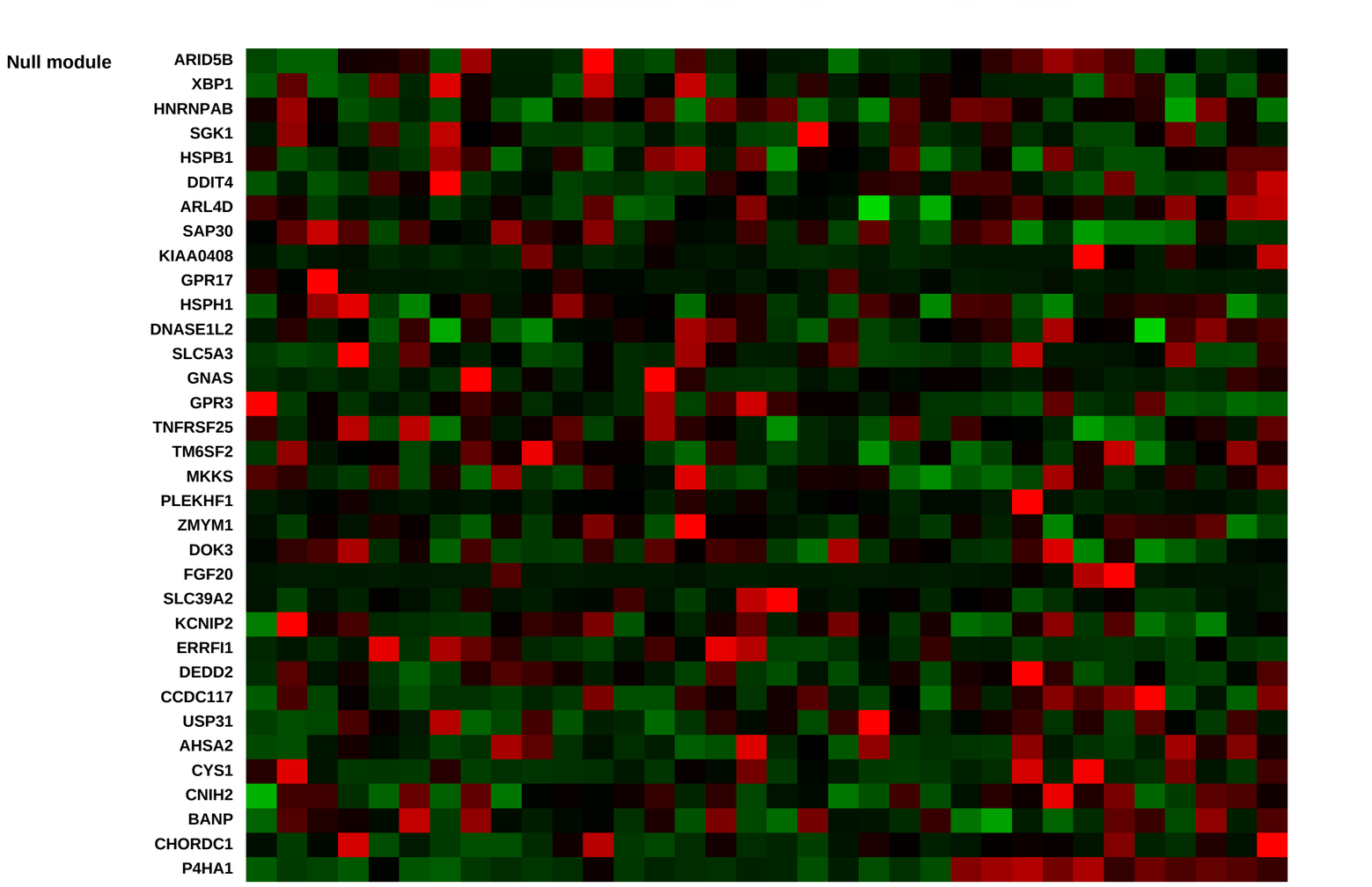

GEO Series "GSE21164" Expression Profiles

Num of samples in this series: 16

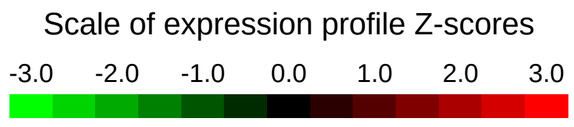

GEO Link:	http://www.ncbi.nlm.nih.gov/geo/query/acc.cgi?acc=GSE21164
Status:	Public on Apr 02 2010
Title:	Expression data from total knee arthroplasty patients
Organism:	Homo sapiens
Experiment type:	Expression profiling by array
Platform:	GPL570
Pubmed ID:	20459731
Summary & Design:	**Summary:** Ischaemic preconditioning is a method of protecting tissue against ischaemia-reperfusion injury. It is an innate protective mechanism that increases a tissue's tolerance to prolonged ischaemia when it is first subjected to short burst of ischaemia and reperfusion. It is thought to provide this protection by increasing the tissue's tolerance to ischaemia, therby reducing oxidative stress, inflammation and apoptosis in the preconditioned tissue. We used microarrays to investigate the genomic response induced by ischaemic preconditioning in muscle biopsies taken from the operative leg of total knee arthroplasty patients in order to gain insight into the ischaemic preconditioning mechanism. **Overall design:** Patients undergoing primary knee arthroplasty were randomised to control and treatment (ischaemic preconditioning) groups. Patients in the treatment group received a preconditioning stimulus immediately prior to surgery. The ischaemic preconditioning stimulus consisted of three five-minute periods of tourniquet insufflation on the lower operative limb, interrupted by five minute periods of reperfusion. All patients had a tourniquet applied to the lower limb after the administration of spinal anaesthesia, as per normal protocol for knee arthroplasty surgery. Muscle biopsies were taken from the quadriceps muscle of the operative knee at the immediate onset of surgery (T0) and at 1 hour into surgery (T1). Total RNA was extracted from biospies of four control and four treatment patients and hybridised to the Affymetrix Human U133 2.0 chip.

Background corr dist: KL-Divergence = 0.1692, L1-Distance = 0.0299, L2-Distance = 0.0018, Normal std = 0.3556

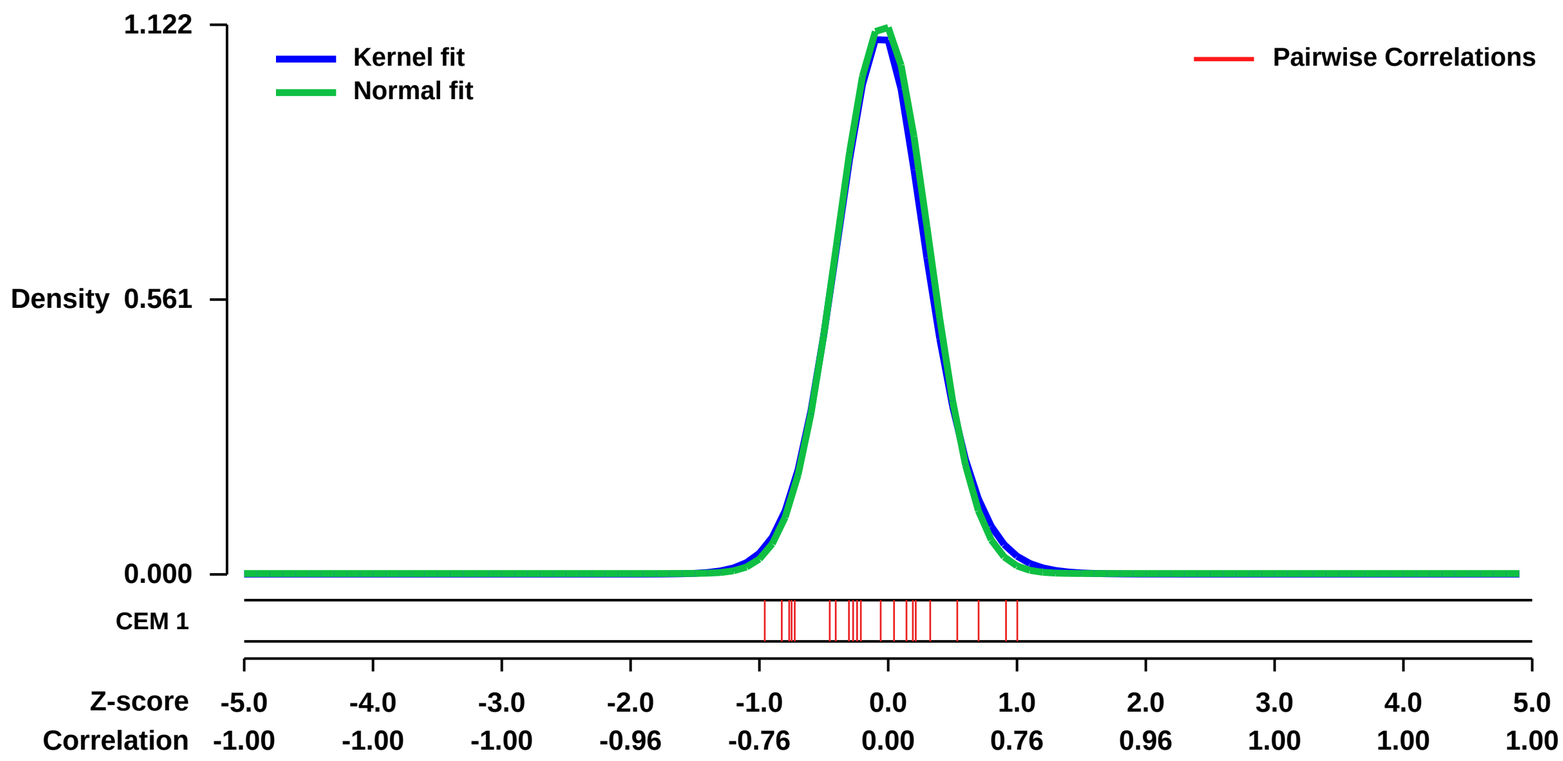

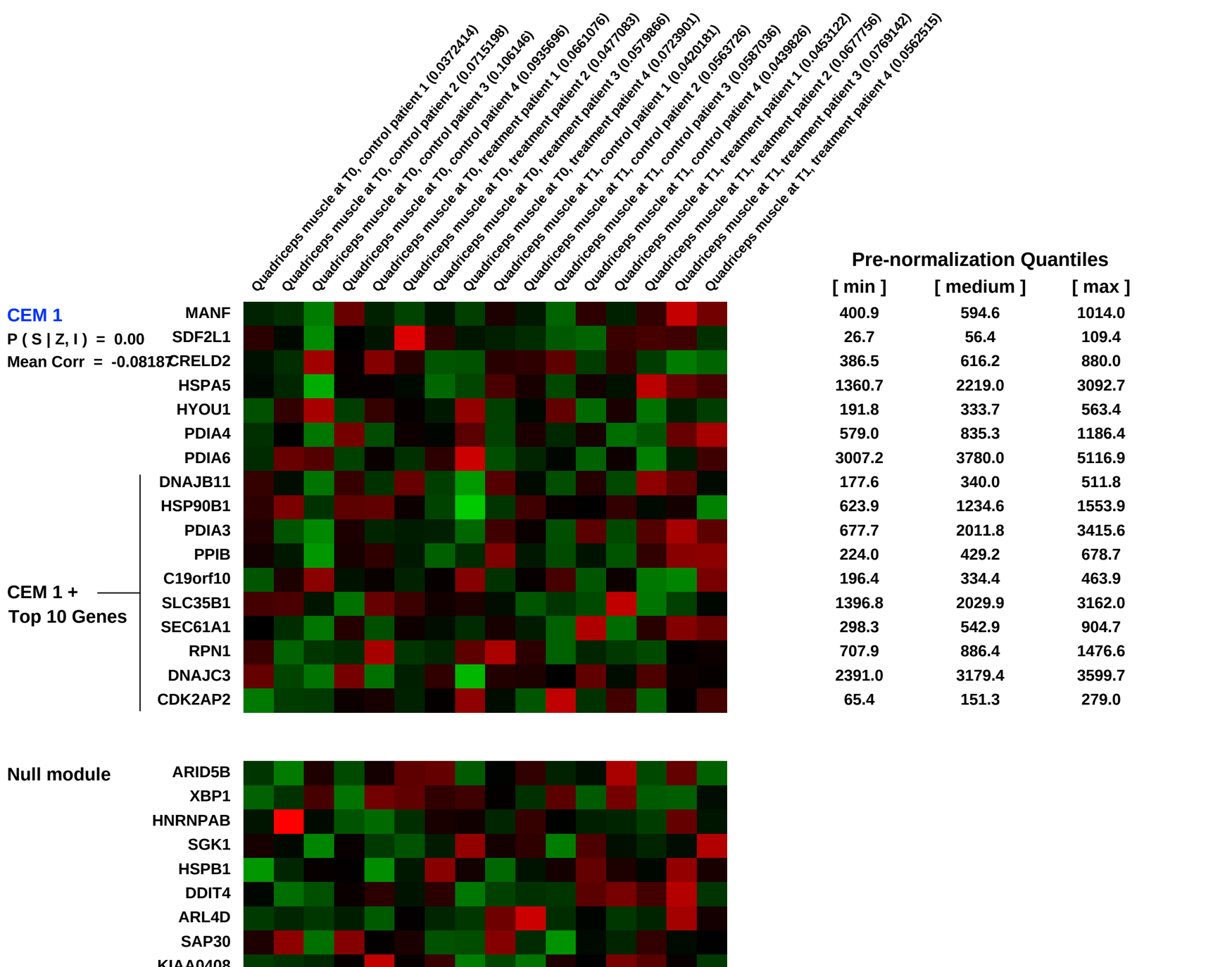

Pre-normalization Quantiles

	[min]	[medium]	[max]
MANF	400.9	594.6	1014.0
SDF2L1	26.7	56.4	109.4
CRELD2	386.5	616.2	880.0
HSPA5	1360.7	2219.0	3092.7
HYOU1	191.8	333.7	563.4
PDIA4	579.0	835.3	1186.4
PDIA6	3007.2	3780.0	5116.9
DNAJB11	177.6	340.0	511.8
HSP90B1	623.9	1234.6	1553.9
PDIA3	677.7	2011.8	3415.6
PPIB	224.0	429.2	678.7
C19orf10	196.4	334.4	463.9
SLC35B1	1396.8	2029.9	3162.0
SEC61A1	298.3	542.9	904.7
RPN1	707.9	886.4	1476.6
DNAJC3	2391.0	3179.4	3599.7
CDK2AP2	65.4	151.3	279.0

GEO Series "GSE31470" Expression Profiles

Num of samples in this series: 6

Scale of expression profile Z-scores

-3.0 -2.0 -1.0 0.0 1.0 2.0 3.0

GEO Link:	http://www.ncbi.nlm.nih.gov/geo/query/acc.cgi?acc=GSE31470
Status:	Public on Jan 03 2013
Title:	Host cell gene expression in Influenza A/WSN/33 (H1N1) infected A549 cells at 10 hour post infection
Organism:	Homo sapiens
Experiment type:	Expression profiling by array
Platform:	GPL570
Pubmed ID:	22470468
Summary & Design:	**Summary:** We used the microarray data to analyze host cells response on A549 cells infected with A/WSN/33 (H1N1) **Overall design:** The A/WSN/33 (H1N1) infected A549 cells were harvested at 10 hpi and RNA extraction was performed using standard protocol as described by Affymetrix. The aim of this experiment is to analyze host response to Influenza A/WSN/33 (H1N1) infection.

Background corr dist: KL-Divergence = 0.0211, L1-Distance = 0.0229, L2-Distance = 0.0005, Normal std = 0.7571

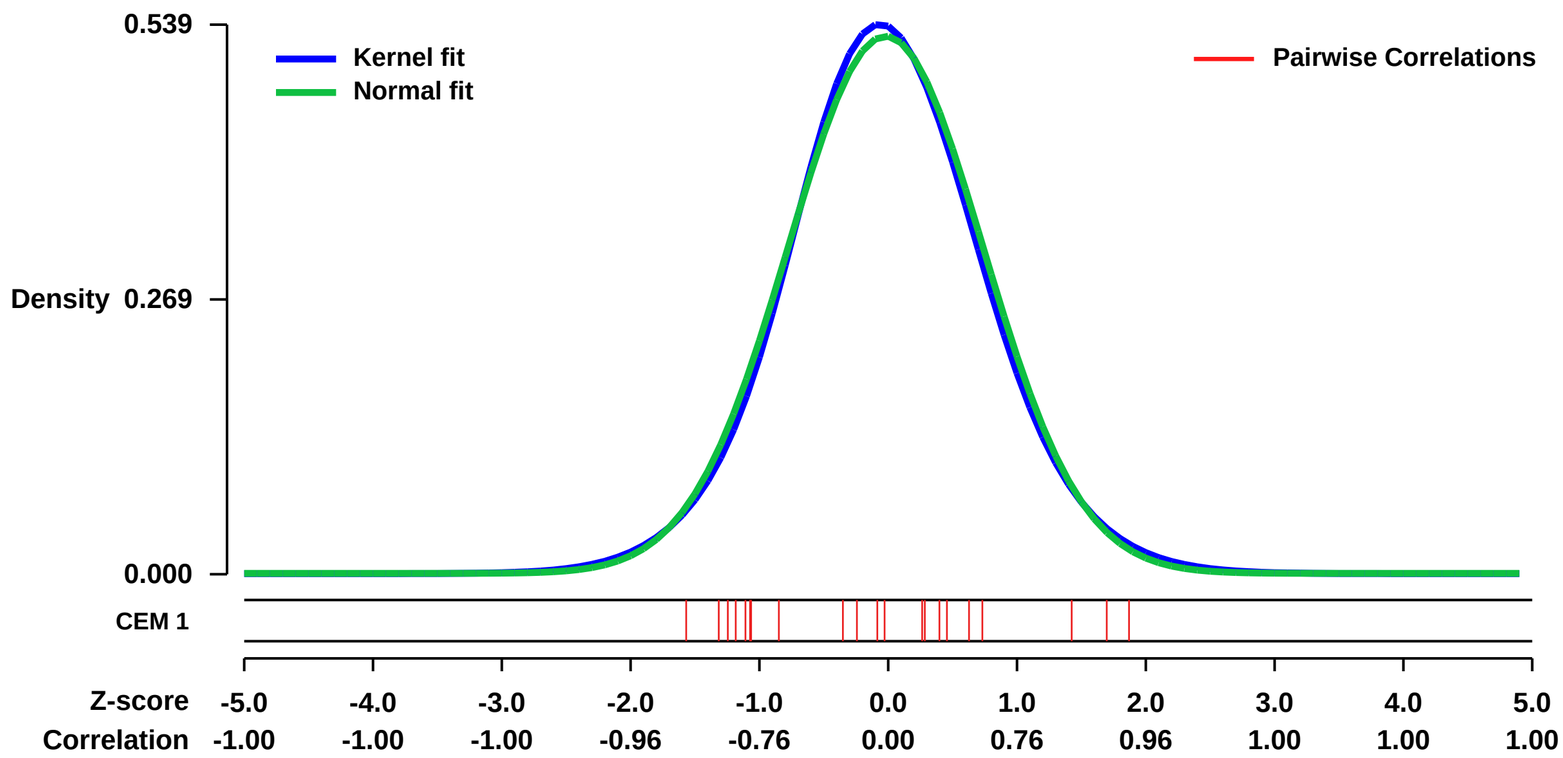

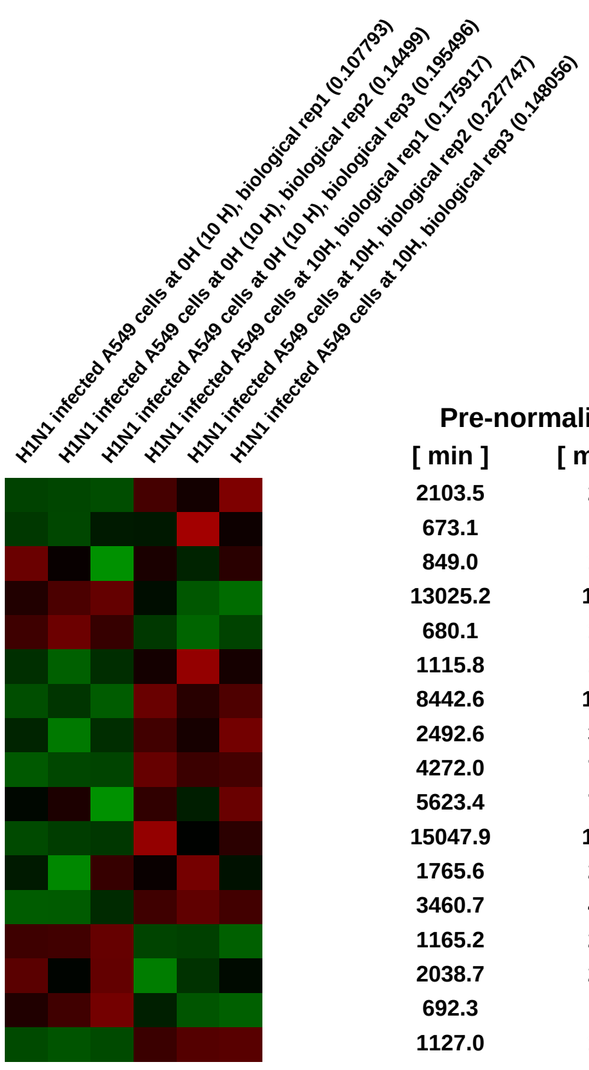

CEM 1
P (S | Z, I) = 0.00
Mean Corr = -0.09144

CEM 1 + Top 10 Genes

Null module

MANF	2103.5	2496.7	2936.3
SDF2L1	673.1	816.4	1391.9
CRELD2	849.0	1272.8	1470.9
HSPA5	13025.2	16470.1	18103.7
HYOU1	680.1	1201.9	1385.3
PDIA4	1115.8	1661.9	2259.9
PDIA6	8442.6	10704.7	11834.5
DNAJB11	2492.6	3152.7	3578.3
HSP90B1	4272.0	7089.9	7888.8
PDIA3	5623.4	7278.1	8013.1
PPIB	15047.9	19469.3	28663.4
C19orf10	1765.6	2147.3	2430.6
SLC35B1	3460.7	4572.2	4809.5
SEC61A1	1165.2	2144.4	2382.8
RPN1	2038.7	2395.9	2700.9
DNAJC3	692.3	881.0	1003.6
CDK2AP2	1127.0	1837.7	1989.1
ARID5B			
XBP1			
HNRNPAB			
SGK1			
HSPB1			
DDIT4			
ARL4D			
SAP30			
KIAA0408			
GPR17			
HSPH1			
DNASE1L2			
SLC5A3			
GNAS			
GPR3			
TNFRSF25			
TM6SF2			
MKKS			
PLEKHF1			
ZMYM1			
DOK3			
FGF20			
SLC39A2			
KCNIP2			
ERRFI1			
DEDD2			
CCDC117			
USP31			
AHSA2			
CYS1			
CNIH2			
BANP			
CHORDC1			
P4HA1			

GEO Series "GSE15799" Expression Profiles

Num of samples in this series: 6

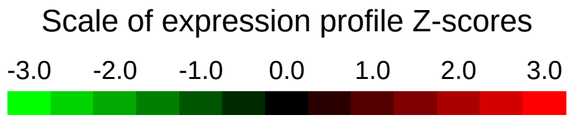

GEO Link:	http://www.ncbi.nlm.nih.gov/geo/query/acc.cgi?acc=GSE15799
Status:	Public on Mar 03 2010
Title:	Expression data from NS398-treated and control HT29 colon adenocarcinoma cell line samples
Organism:	Homo sapiens
Experiment type:	Expression profiling by array
Platform:	GPL570
Pubmed ID:	20087348
Summary & Design:	**Summary:** The whole-genome oligonucleotide microarray analysis of NS398-treated HT29 colon adenocarcinoma cells samples can give an insight into global molecular background of selective COX2 inhibitor administration in order to find other target molecules and pathways influenced by NS398 selective COX2 inhibitor treatment in the epithelial cells. **Overall design:** Total RNA was extracted from NS398-treated and control HT29 colon adenocarcinoma cells and hybridized on Affymetrix HGU133 Plus 2.0 microarrays

Background corr dist: KL-Divergence = 0.0386, L1-Distance = 0.0255, L2-Distance = 0.0007, Normal std = 0.6326

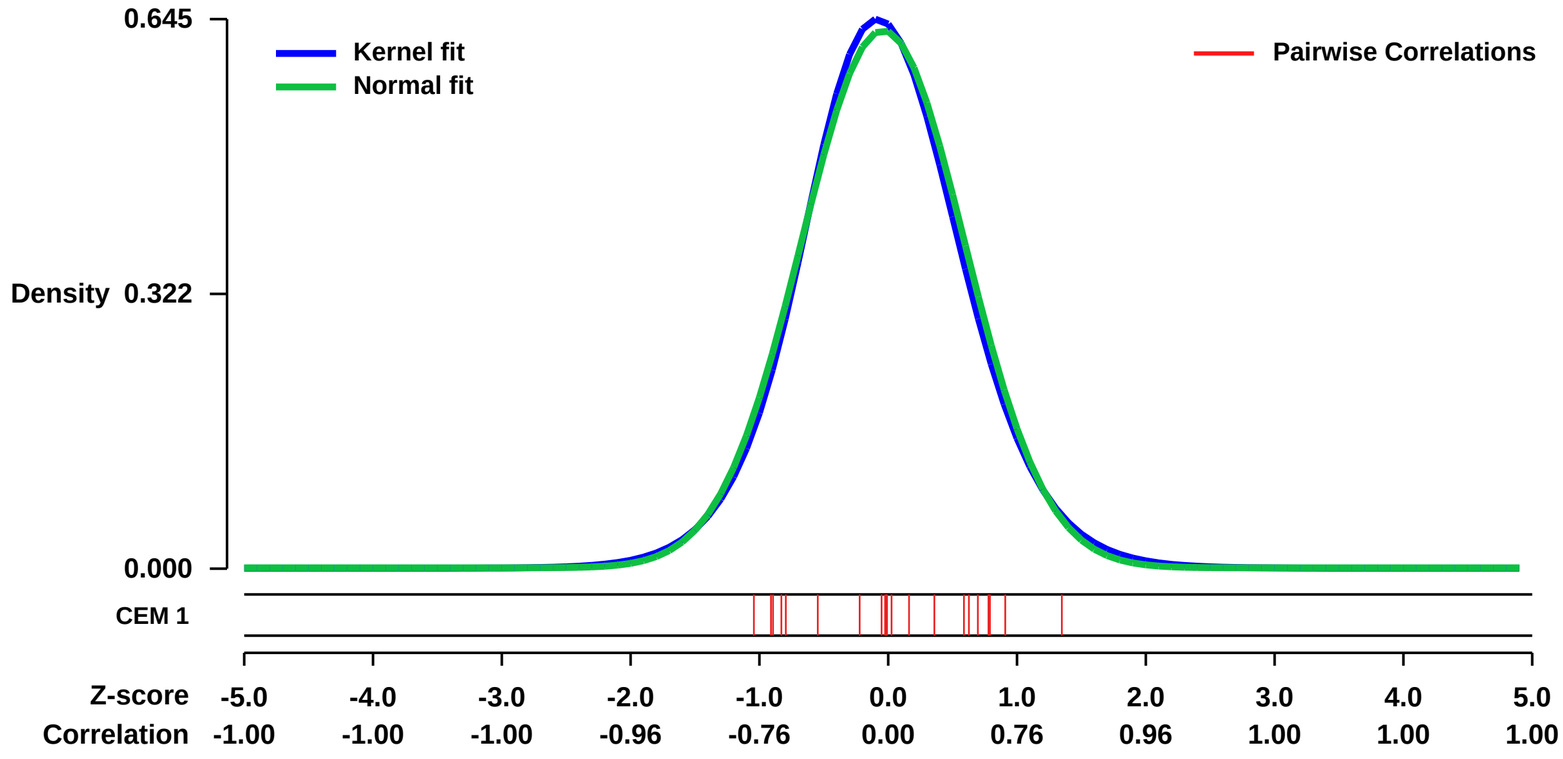

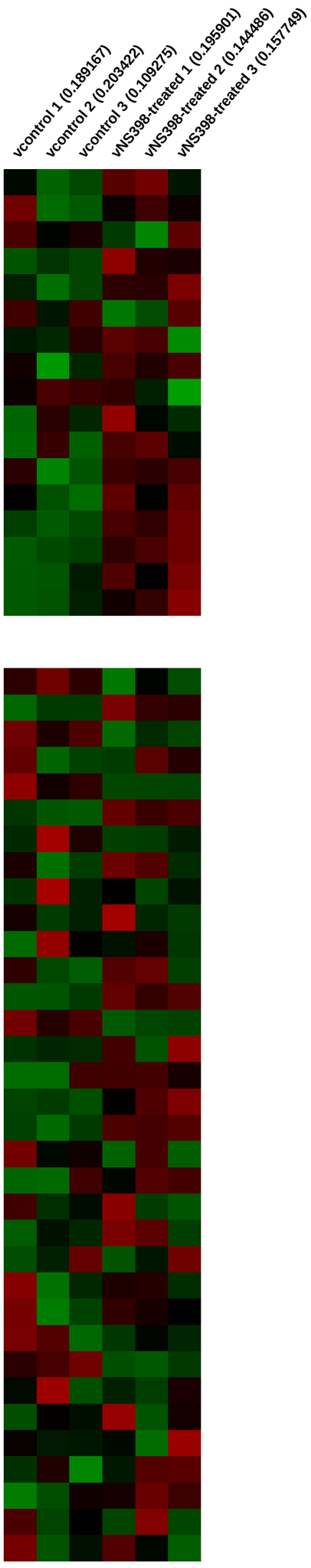

		Pre-normalization Quantiles [min]	[medium]	[max]
CEM 1	MANF	4002.2	4261.8	4614.6
P (S | Z, I) = 0.00	SDF2L1	812.7	1070.8	1278.6
Mean Corr = 0.03573	CRELD2	1659.2	2025.8	2178.2
	HSPA5	19176.0	27173.2	35341.0
	HYOU1	5480.1	9556.1	11768.2
	PDIA4	2030.4	2538.7	2599.5
	PDIA6	10120.7	11451.8	11807.1
CEM 1 + Top 10 Genes	DNAJB11	5298.8	6856.5	7194.1
	HSP90B1	5911.4	8784.9	9115.5
	PDIA3	23443.7	25113.5	27794.6
	PPIB	28875.8	35301.5	36762.7
	C19orf10	2042.0	2844.2	2971.7
	SLC35B1	2259.4	2483.2	2685.9
	SEC61A1	4374.5	7504.5	8834.4
	RPN1	5599.9	7268.2	8057.5
	DNAJC3	2503.9	3152.4	3979.9
	CDK2AP2	2069.0	2338.5	2645.5
Null module	ARID5B			
	XBP1			
	HNRNPAB			
	SGK1			
	HSPB1			
	DDIT4			
	ARL4D			
	SAP30			
	KIAA0408			
	GPR17			
	HSPH1			
	DNASE1L2			
	SLC5A3			
	GNAS			
	GPR3			
	TNFRSF25			
	TM6SF2			
	MKKS			
	PLEKHF1			
	ZMYM1			
	DOK3			
	FGF20			
	SLC39A2			
	KCNIP2			
	ERRFI1			
	DEDD2			
	CCDC117			
	USP31			
	AHSA2			
	CYS1			
	CNIH2			
	BANP			
	CHORDC1			
	P4HA1			

GEO Series "GSE14825" Expression Profiles

Num of samples in this series: 6

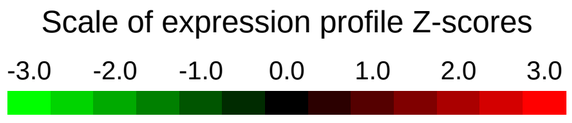

GEO Link:	http://www.ncbi.nlm.nih.gov/geo/query/acc.cgi?acc=GSE14825
Status:	Public on Feb 14 2009
Title:	Expression data from rhabdomyosarcoma cells expressing Myod and E-protein heterodimer and controls
Organism:	Homo sapiens
Experiment type:	Expression profiling by array
Platform:	GPL570
Pubmed ID:	19299559
Summary & Design:	**Summary:** Rhabdomyosarcomas (RMS) are characterized by expression of myogenic specification genes, such as MyoD and/or Myf5, as well as their bHLH partners for heterodimerization, the E-proteins. We have shown that expression of a forced heterodimer of MyoD with one of the E2A proteins, E12, leads to differentiation in a RMS cell culture model when exposed to low serum conditions. **Keywords: RD expressing Myod~E heterodimers and controls** **Overall design:** RD cells (a type of RMS) were retrovirally infected with either the MyoD~E heterodimer or an empty control vector, differentiated for 24 hours and then RNA collected.

Background corr dist: KL-Divergence = 0.0221, L1-Distance = 0.0472, L2-Distance = 0.0026, Normal std = 0.8055

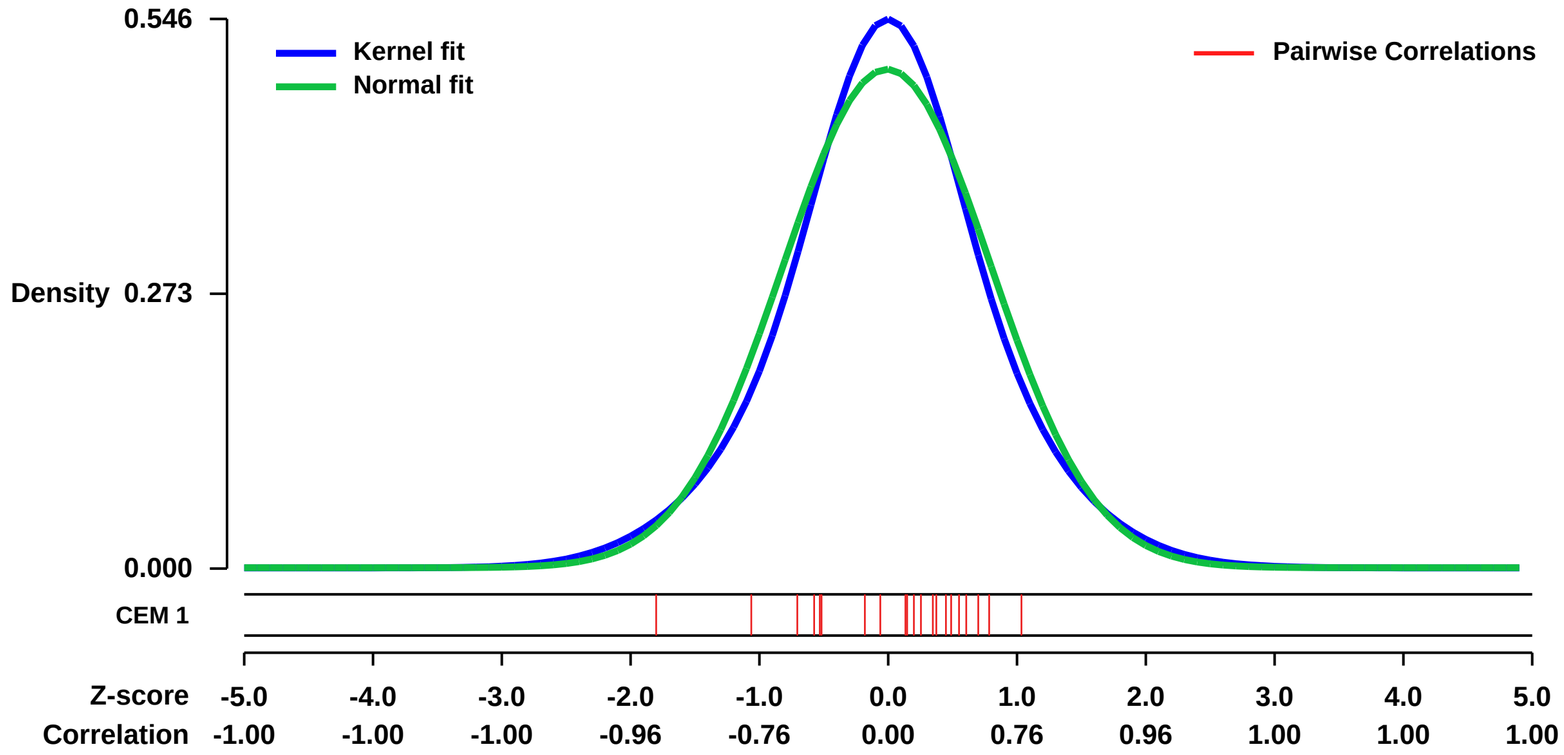

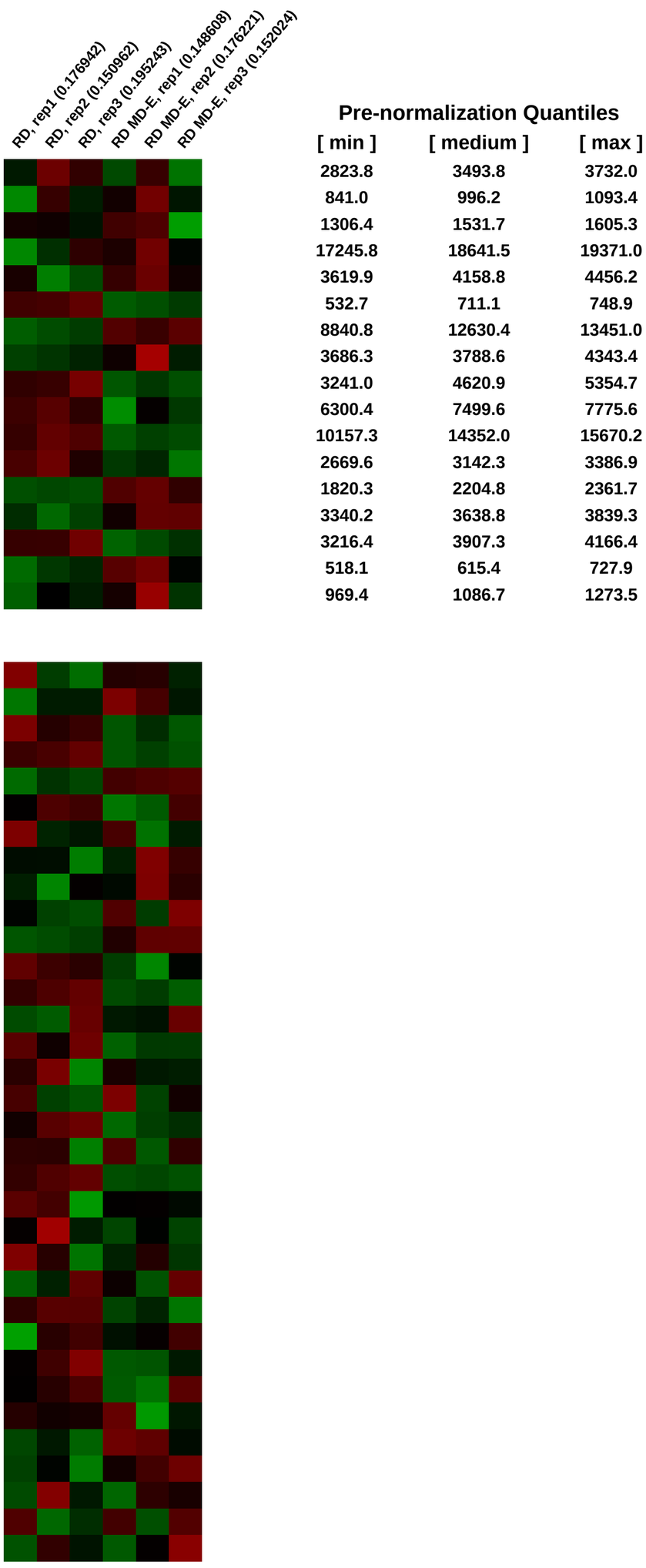

GEO Series "GSE20272" Expression Profiles

Num of samples in this series: 6

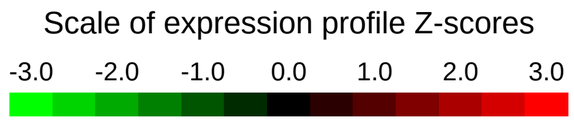

GEO Link:	http://www.ncbi.nlm.nih.gov/geo/query/acc.cgi?acc=GSE20272
Status:	Public on Feb 11 2010
Title:	Expression data from human ovarian cancer cells induced by IL-6 and CNTO328
Organism:	Homo sapiens
Experiment type:	Expression profiling by array
Platform:	GPL570
Pubmed ID:	20699329
Summary & Design:	**Summary:** The SKOV-3 and Caov-3 ovarian cancer cell lines where seeded onto the 100mm cell culture plate for overnight. The cells were then incubated with IL-6 (30ng/ml) alone for one hour or pre-treated with siltuximab for four hours and then treated with IL-6 for one hour. Total RNA was collected from these cells using TRIzol´fi Reagent (GIBCO Grand Island, NY) according to the manufacturerâ s instructions. To account for and eliminate biologic noise, RNA was isolated from three distinct flasks of each cell line and pooled together. RNA quality was determined via ethidium bromide staining following agarose/formaldehyde gel electrophoresis. Total RNA was processed and hybridized to Affymetrix Genechip HG-U95Av2 arrays (Affymetrix, Santa Clara, CA) by the Gene Array Technology Center at Harvard Medical School (http://genome.med.harvard.edu). Affymetrix Gene Chip U133 Plus 2.0 in the first and most comprehensive whole human genome expression array. This array completes coverage of the whole human Genome with over 47,000 transcripts. The expression level of each mRNA is quantified by measuring its hybridization to these 23-mers in comparison to its hybridization to a one-base mismatch oligonucleotide. GeneSifter was used to analyze the microarray data (http://www.genesifter.net/web/). Fold change in expression between sensitive and resistant cell lines was evaluated using the Mann-Whitney test. A tenfold or greater change in intensity combined with a Mann-Whitney associated P value less than 0.05 was used as the criterion for inclusion in our filtered data set. **Overall design:** Evalutate the effect of CNTO328 on IL-6 induced gene expression in ovarian cancer cells

Background corr dist: KL-Divergence = 0.0194, L1-Distance = 0.0587, L2-Distance = 0.0038, Normal std = 0.9000

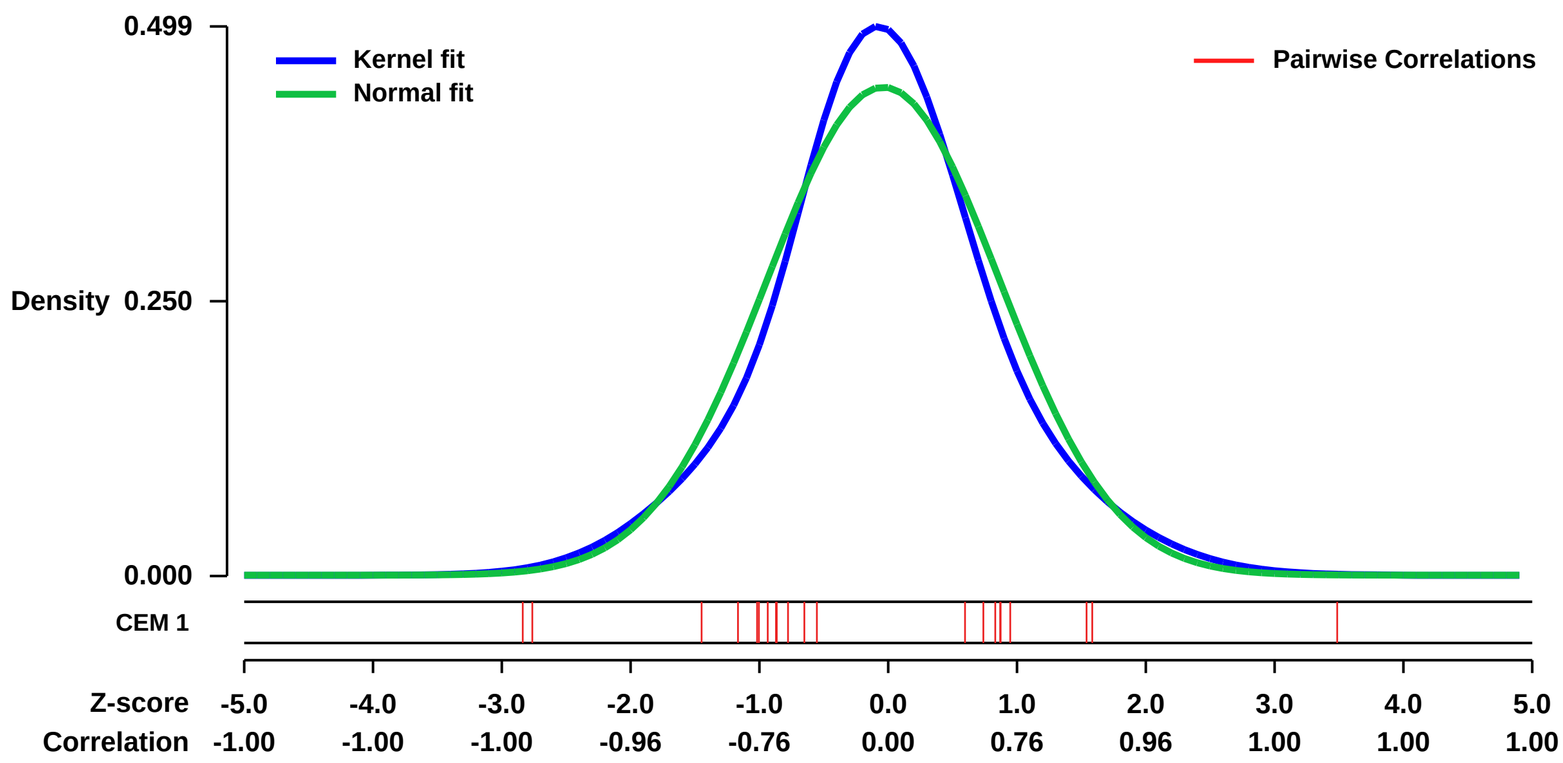

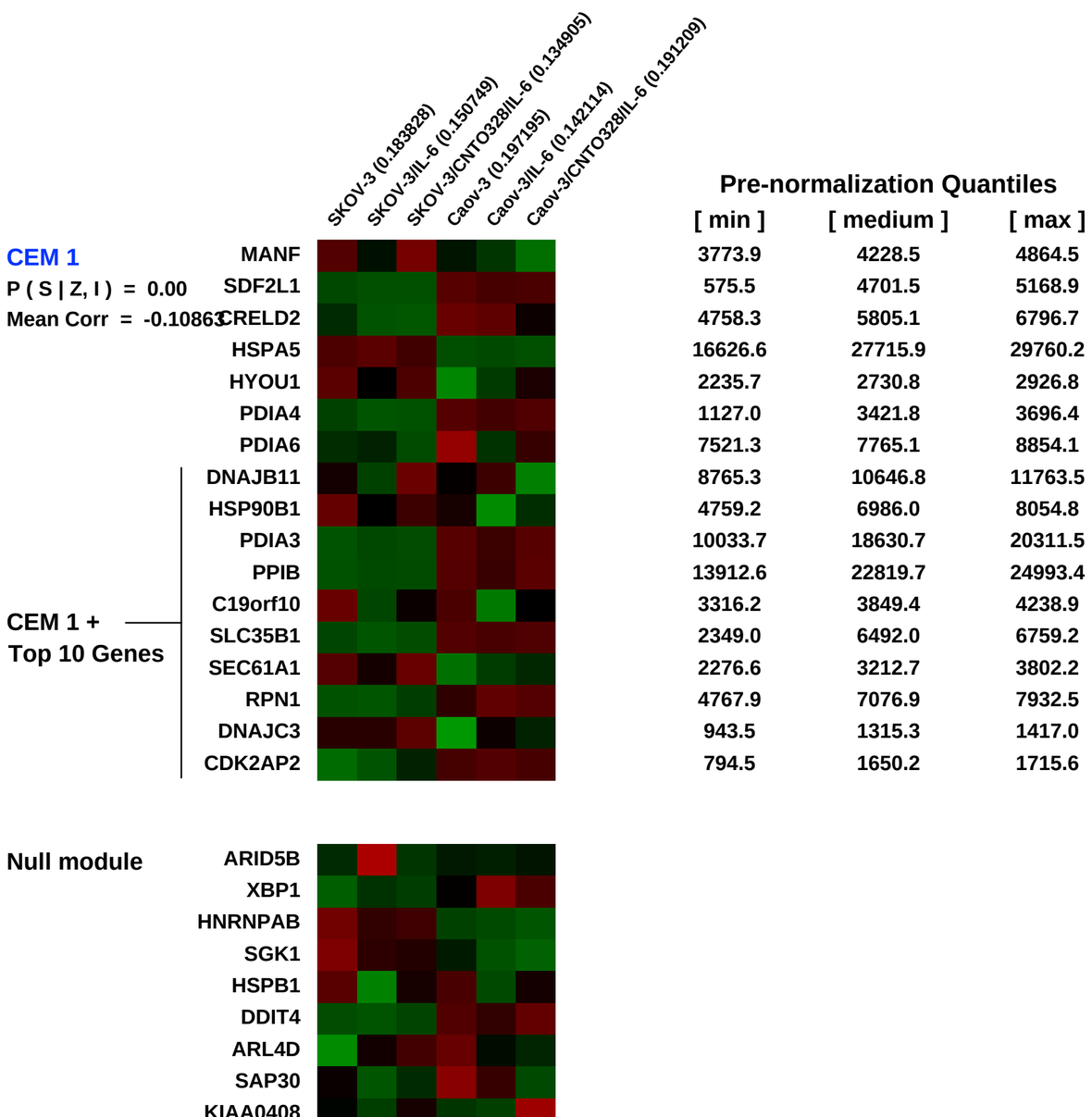

	Pre-normalization Quantiles		
	[min]	[medium]	[max]
MANF	3773.9	4228.5	4864.5
SDF2L1	575.5	4701.5	5168.9
CRELD2	4758.3	5805.1	6796.7
HSPA5	16626.6	27715.9	29760.2
HYOU1	2235.7	2730.8	2926.8
PDIA4	1127.0	3421.8	3696.4
PDIA6	7521.3	7765.1	8854.1
DNAJB11	8765.3	10646.8	11763.5
HSP90B1	4759.2	6986.0	8054.8
PDIA3	10033.7	18630.7	20311.5
PPIB	13912.6	22819.7	24993.4
C19orf10	3316.2	3849.4	4238.9
SLC35B1	2349.0	6492.0	6759.2
SEC61A1	2276.6	3212.7	3802.2
RPN1	4767.9	7076.9	7932.5
DNAJC3	943.5	1315.3	1417.0
CDK2AP2	794.5	1650.2	1715.6
ARID5B			
XBP1			
HNRNPAB			
SGK1			
HSPB1			
DDIT4			
ARL4D			
SAP30			
KIAA0408			
GPR17			
HSPH1			
DNASE1L2			
SLC5A3			
GNAS			
GPR3			
TNFRSF25			
TM6SF2			
MKKS			
PLEKHF1			
ZMYM1			
DOK3			
FGF20			
SLC39A2			
KCNIP2			
ERRFI1			
DEDD2			
CCDC117			
USP31			
AHSA2			
CYS1			
CNIH2			
BANP			
CHORDC1			
P4HA1			

GEO Series "GSE52434" Expression Profiles

Num of samples in this series: 16

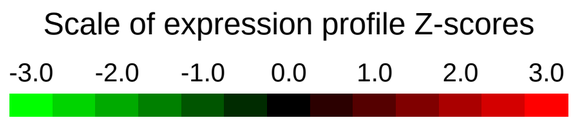

GEO Link:	http://www.ncbi.nlm.nih.gov/geo/query/acc.cgi?acc=GSE52434
Status:	Public on Dec 01 2013
Title:	Transcriptional responses of mantle cell lymphoma (MCL) lines to IKKB inhibition
Organism:	Homo sapiens
Experiment type:	Expression profiling by array
Platform:	GPL570
Pubmed ID:	24362935
Summary & Design:	**Summary:** MCL cell lines were treated with DMSO or 5uM AFN700 for 20hrs This experiment is designed to see if NFKB-target genes are downregulated by inhibition of IKKB in MCL cell lines that are insensitive to ibrutinib (BTK inhibitor) or sotrastaurin (PKC inhibitor) **Overall design:** MCL cells were seeded in 6well dishes and treated for 20hrs with DMSO or 5uM AFN700

Background corr dist: KL-Divergence = 0.1989, L1-Distance = 0.0472, L2-Distance = 0.0053, Normal std = 0.3361

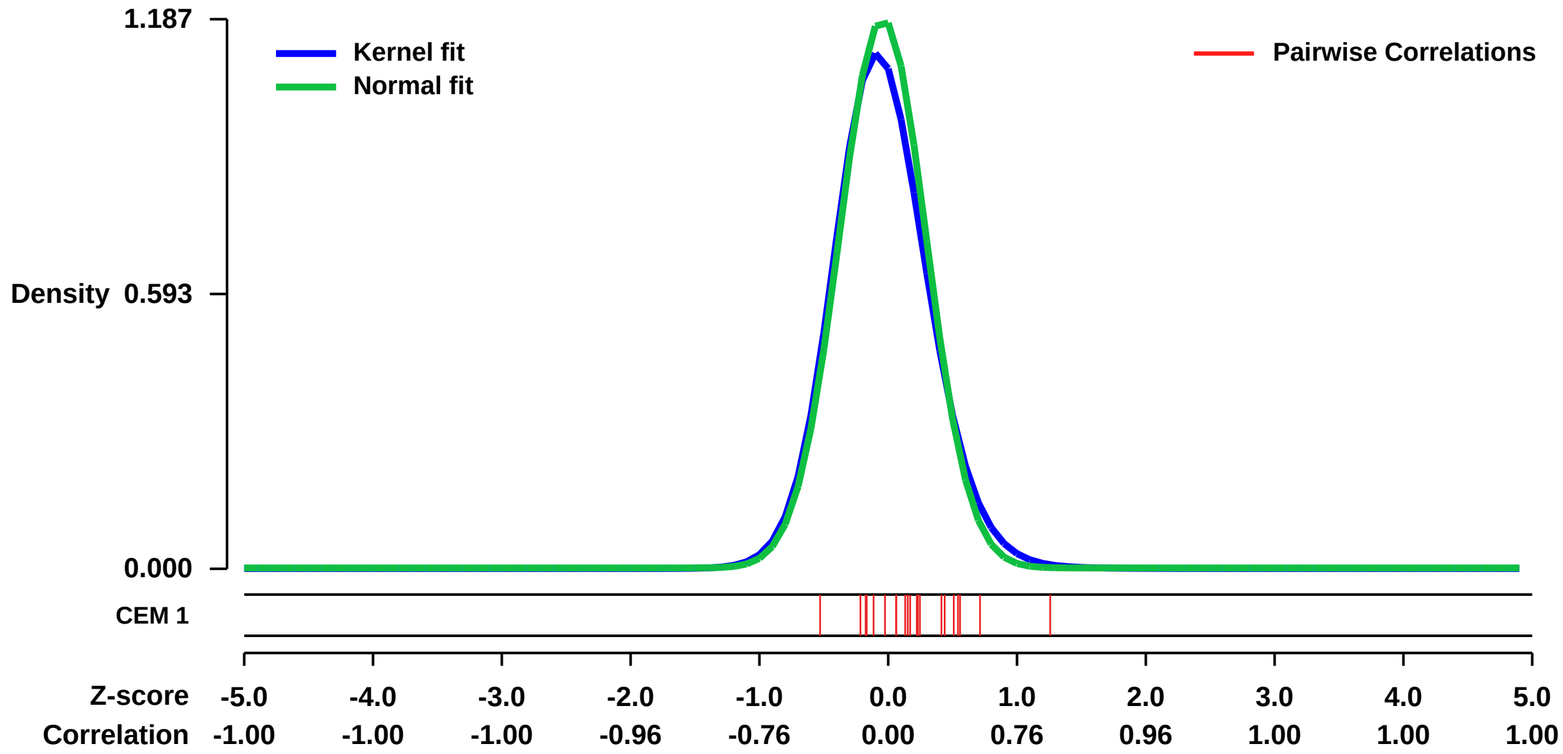

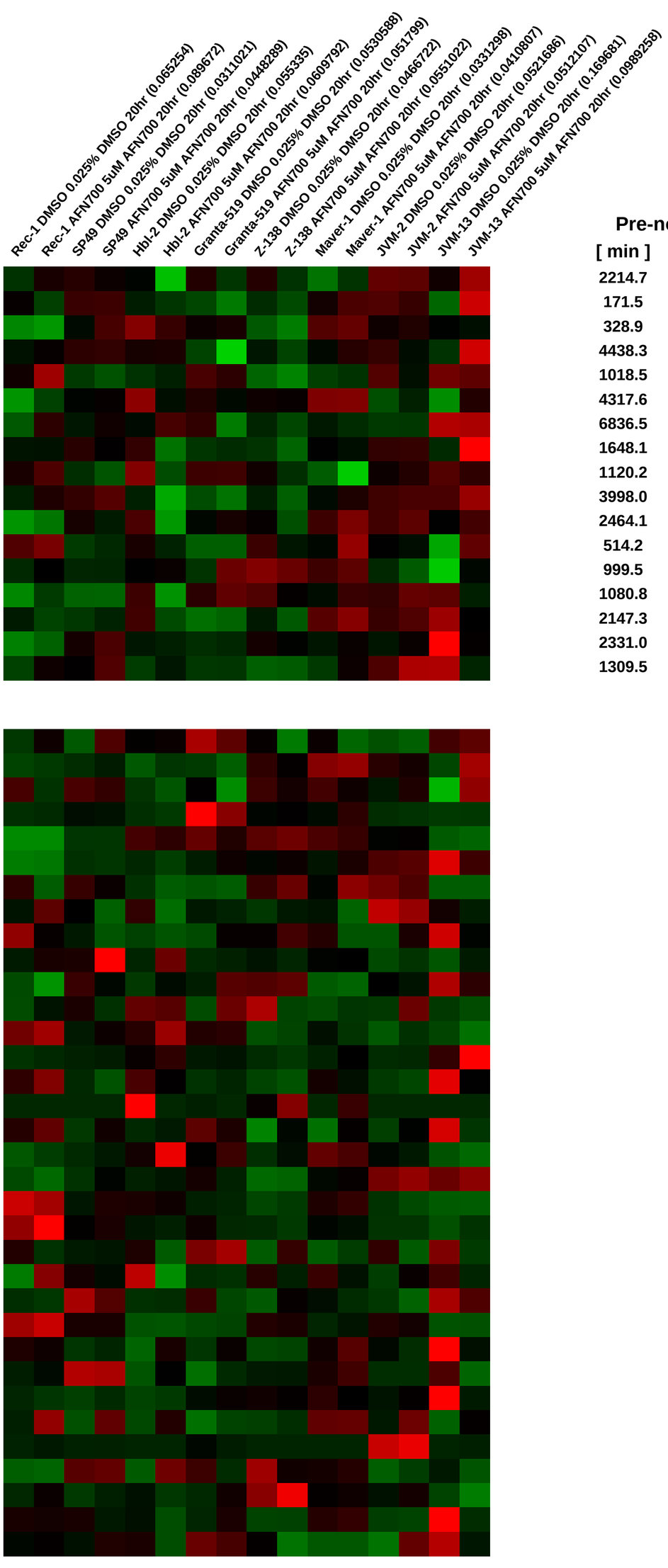

GEO Series "GSE31912" Expression Profiles

Num of samples in this series: 89

Scale of expression profile Z-scores

-3.0 -2.0 -1.0 0.0 1.0 2.0 3.0

GEO Link: http://www.ncbi.nlm.nih.gov/geo/query/acc.cgi?acc=GSE31912

Status: Public on Mar 15 2012

Title: Gene expression profile in MCF7 breast cancer cells after 78 functionallly important molecules were knocked down using siRNA.

Organism: Homo sapiens

Experiment type: Expression profiling by array

Platform: GPL570

Pubmed ID: 22536322

Summary & Design:

Summary:
Affymetrix microarray data was generated from MCF7 breast cancer cells treated in vitro with siRNAs against 78 transcription factors and signalling molecules.

Overall design:
Gene expresion of 78 functionally important molecules were knocked down in MCF7 breast cancer cells using siRNA. Then the gene expression profiles of these MCF7 cells, along with untreated cells and non-targetting control (SICONTROL) treated cells were analysed using microarrays.

Background corr dist: KL-Divergence = 0.3023, L1-Distance = 0.0655, L2-Distance = 0.0120, Normal std = 0.2786

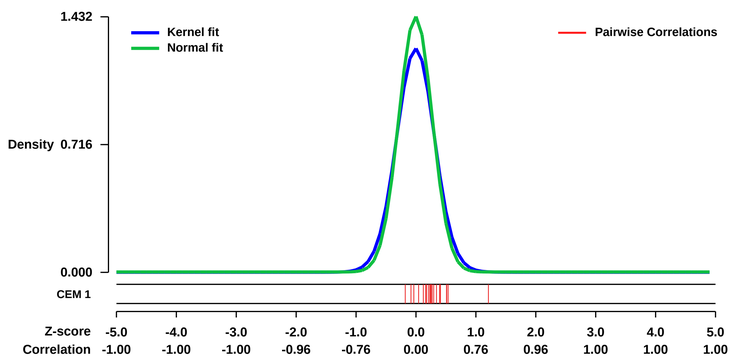

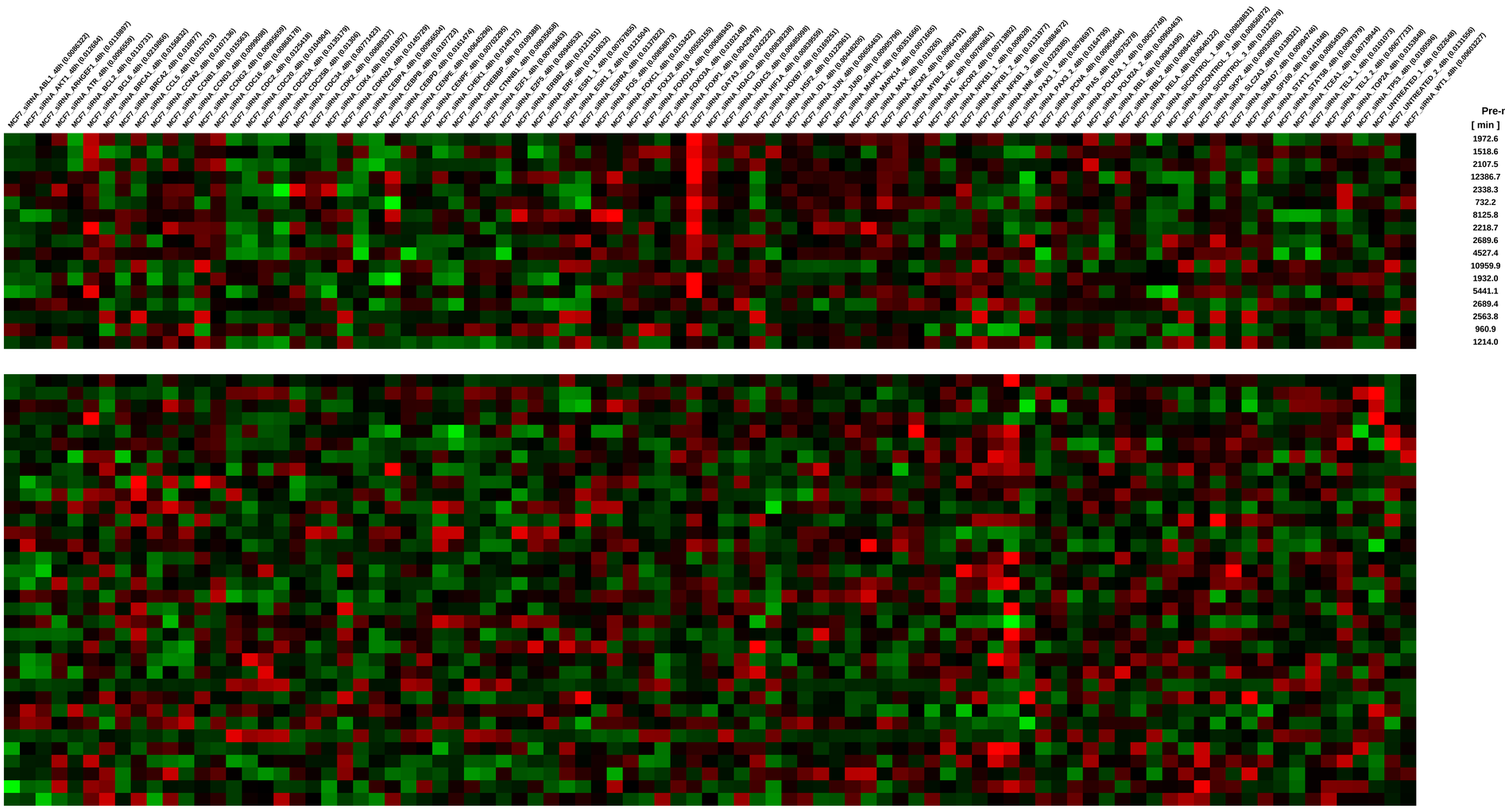

Pre-normalization Quantiles		
[min]	[medium]	[max]
1972.6	2451.0	3355.8
1518.6	2008.5	2657.7
2107.5	2638.4	3763.3
12386.7	16729.2	22897.5
2338.3	3800.8	5110.8
732.2	1201.7	1658.9
8125.8	9896.7	12614.2
2218.7	2679.7	3604.5
2689.6	3411.9	4315.4
4527.4	8075.3	10166.2
10959.9	14231.9	22932.8
1932.0	2848.9	3648.1
5441.1	6749.3	8431.2
2689.4	3626.5	4522.3
2563.8	3410.7	7053.1
960.9	1356.1	1786.3
1214.0	1600.5	2187.4

GEO Series "GSE35525" Expression Profiles

Num of samples in this series: 8

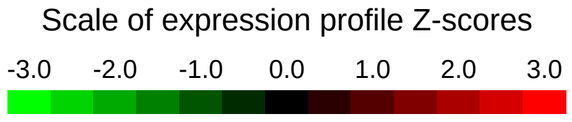

GEO Link:	http://www.ncbi.nlm.nih.gov/geo/query/acc.cgi?acc=GSE35525
Status:	Public on Dec 10 2013
Title:	Pivotal role of HMGA1 gene signature in highly metastatic breast cancer
Organism:	Homo sapiens
Experiment type:	Expression profiling by array
Platform:	GPL570
Pubmed ID:	23945276
Summary & Design:	**Summary:** Analysis of MDA-MB-231 breast cancer cells depleted for High Mobility Group A1 (HMGA1) using siRNA. HMGA1 is involved in invasion and metastasis in breast cancer cells. Results identify the specific transcriptional program induced by HMGA1 in highly metastatic breast cancer cells. **Overall design:** MDA-MB-231 cells were transfected with HMGA1-specific siRNA or a control siRNA. Transfections were performed by using Lipofectamin RNAiMAX (Invitrogen) according to the manufacturer's procedure. Seventy-two hours after transfection, samples were processed for total RNA extraction and hybridization on Affymetrix microarrays. Four biological replicas (A, B, C, D) were used for each of the two conditions, for a total of 8 samples.

Background corr dist: KL-Divergence = 0.0471, L1-Distance = 0.0447, L2-Distance = 0.0026, Normal std = 0.6229

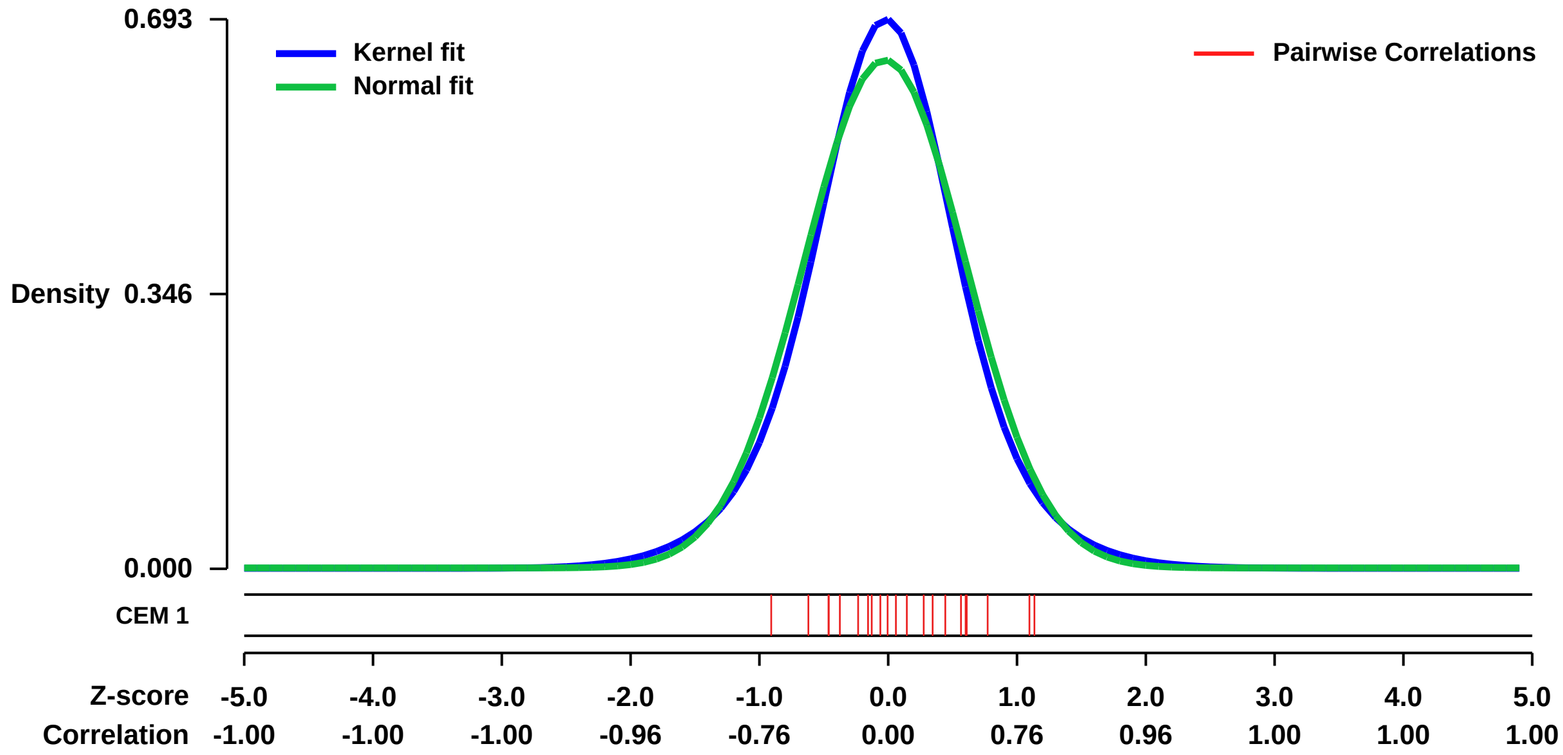

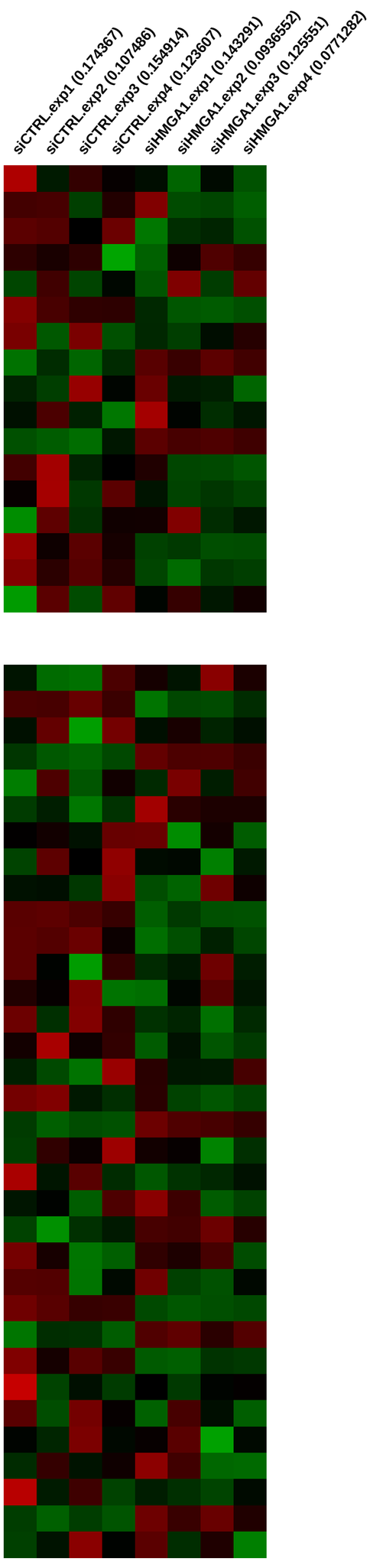

		Pre-normalization Quantiles [min]	[medium]	[max]
CEM 1				
P (S | Z, I) = 0.00	MANF	4215.7	4451.2	4939.0
Mean Corr = 0.09532	SDF2L1	716.0	780.2	828.5
	CRELD2	1438.7	1514.1	1582.4
	HSPA5	12073.4	13218.0	13406.3
	HYOU1	1476.4	1615.0	1850.3
	PDIA4	629.2	823.8	949.1
	PDIA6	7084.7	7341.6	7796.8
CEM 1 + Top 10 Genes	DNAJB11	4003.8	4704.8	4853.6
	HSP90B1	2226.6	2572.3	3361.8
	PDIA3	2182.3	2489.7	3024.8
	PPIB	14195.4	17207.0	17699.2
	C19orf10	1494.1	1794.3	2369.8
	SLC35B1	2540.8	2652.1	3084.8
	SEC61A1	2967.0	3375.9	3668.9
	RPN1	2804.0	3359.7	4184.4
	DNAJC3	2192.4	3061.7	3633.4
	CDK2AP2	638.1	860.6	961.1
Null module	ARID5B			
	XBP1			
	HNRNPAB			
	SGK1			
	HSPB1			
	DDIT4			
	ARL4D			
	SAP30			
	KIAA0408			
	GPR17			
	HSPH1			
	DNASE1L2			
	SLC5A3			
	GNAS			
	GPR3			
	TNFRSF25			
	TM6SF2			
	MKKS			
	PLEKHF1			
	ZMYM1			
	DOK3			
	FGF20			
	SLC39A2			
	KCNIP2			
	ERRFI1			
	DEDD2			
	CCDC117			
	USP31			
	AHSA2			
	CYS1			
	CNIH2			
	BANP			
	CHORDC1			
	P4HA1			

GEO Series "GSE39452" Expression Profiles

Num of samples in this series: 12

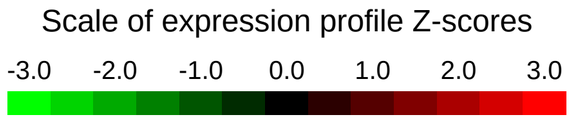

GEO Link:	http://www.ncbi.nlm.nih.gov/geo/query/acc.cgi?acc=GSE39452
Status:	Public on Nov 30 2012
Title:	Expression data of EZH2-dependent genes in prostate cancer cell lines
Organism:	Homo sapiens
Experiment type:	Expression profiling by array
Platform:	GPL570
Pubmed ID:	23239736
Summary & Design:	**Summary:** EZH2 is frequently over-expressed in aggressive and metastatic solid tumors, including castration resistant prostate cancer (CRPC). We sought to determine EZH2-dependent gene expression programmes in prostate cancer progression, and found an intriguing functional switch of EZH2 from a repressor to an activator during CRPC development. We used microarrays to detail the global profiling of gene expression that are differentially regulated upon EZH2 depletion in two different prostate cancer cell lines. **Overall design:** The androgen-dependent prostate cancer cell line LNCaP and the LNCaP-derived androgen-independent cell line LNCaP-abl (abl) were used for this study, as their transcription profiles strongly resemble that of clinical androgen-dependent and castration resistant prostate tumors, respectively. EZH2 was silenced by specific siRNAs in both cell lines, and total RNA was extracted and hybridized on Affymetrix microarrays.

Background corr dist: KL-Divergence = 0.0284, L1-Distance = 0.0712, L2-Distance = 0.0072, Normal std = 0.7692

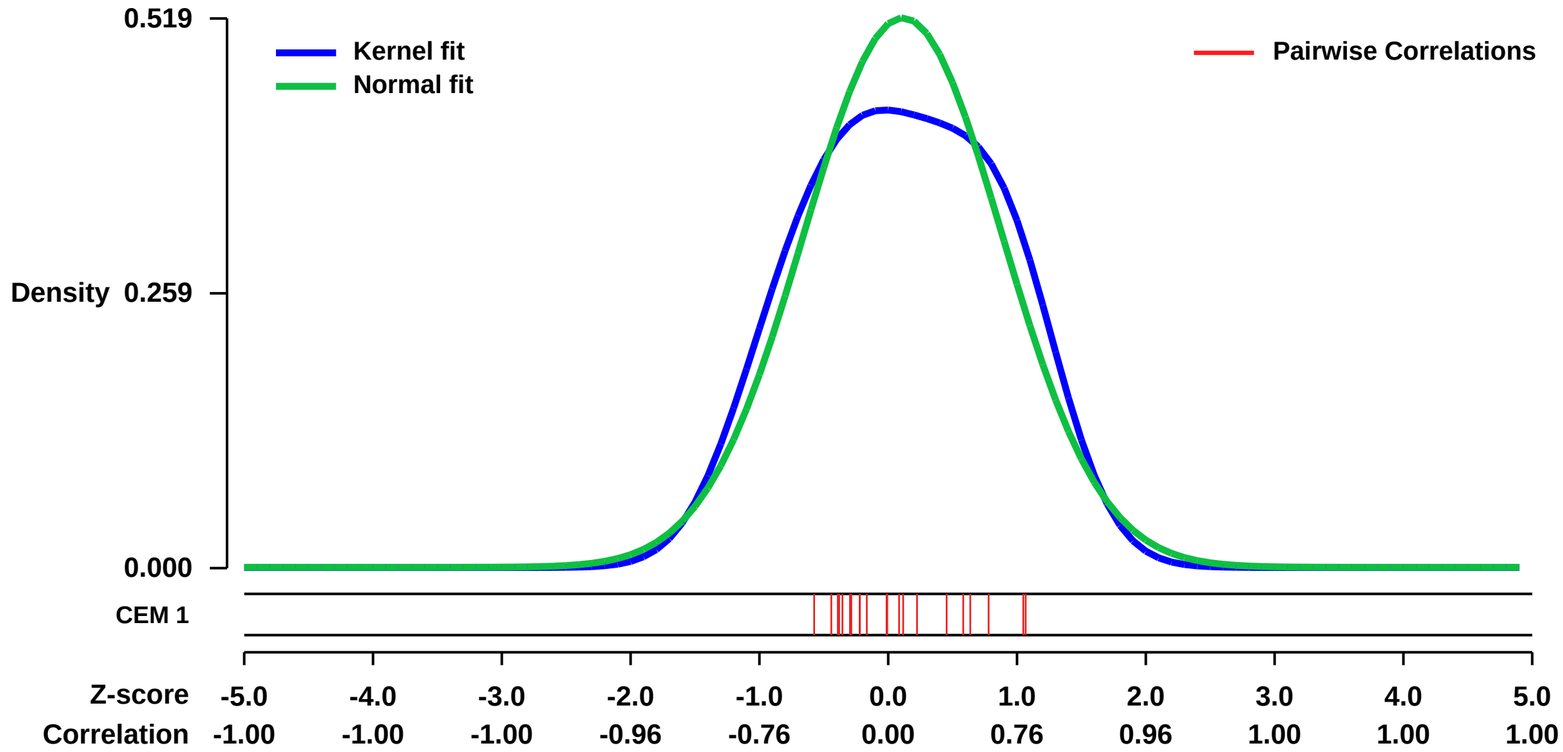

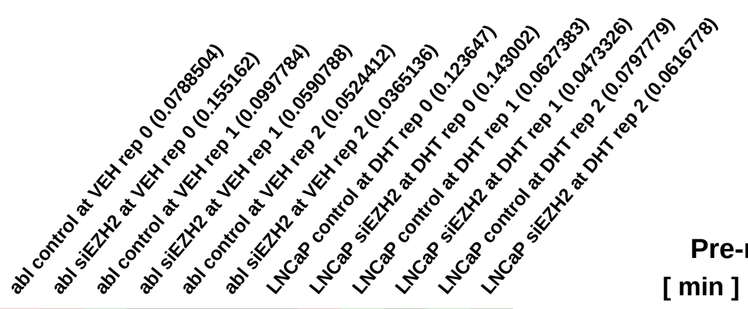

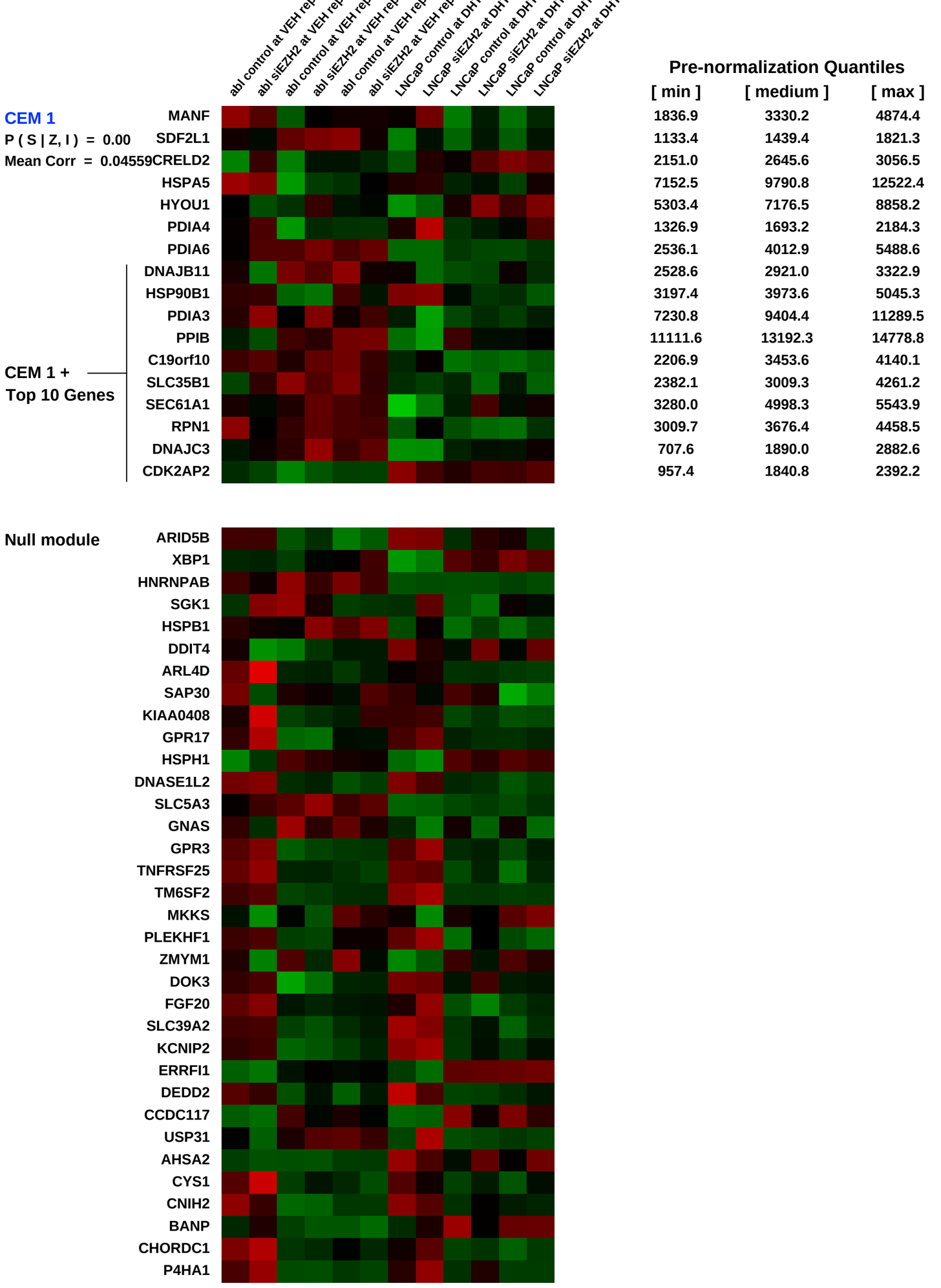

GEO Series "GSE9103" Expression Profiles

Num of samples in this series: 40

Scale of expression profile Z-scores

-3.0 -2.0 -1.0 0.0 1.0 2.0 3.0

GEO Link:	http://www.ncbi.nlm.nih.gov/geo/query/acc.cgi?acc=GSE9103
Status:	Public on Nov 01 2007
Title:	Skeletal Muscle Transcript Profiles in Trained or Sedentary Young and Old Subjects
Organism:	Homo sapiens
Experiment type:	Expression profiling by array
Platform:	GPL570
Pubmed ID:	
Summary & Design:	**Summary:** Aging is associated with mitochondrial dysfunction and insulin resistance. We conducted a study to determine the role of long-term vigorous endurance exercise on age-related changes in insulin sensitivity and various indices of mitochondrial functions. **Keywords:** The effect of excises in young and old human subjects by transcription profiling **Overall design:** Skeletal muscle transcript profiling was done using Vastus Lateralis muscle biopsy samples from 10 young sedentary (YS), 10 older sedentary (OS), 10 young trained (YT) and 10 older trained (OT) men and women. Note that YT2, YS1, and OT1 didn't pass the Quality Control Step of dChip (high array/single outliers). Sedentary subjects exercised less than 30 min/day, twice per week. Trained subjects performed â¥ 1 hour cycling or running 6 days/week over the past 4 years.

Background corr dist: KL-Divergence = 0.1432, L1-Distance = 0.0411, L2-Distance = 0.0034, Normal std = 0.3833

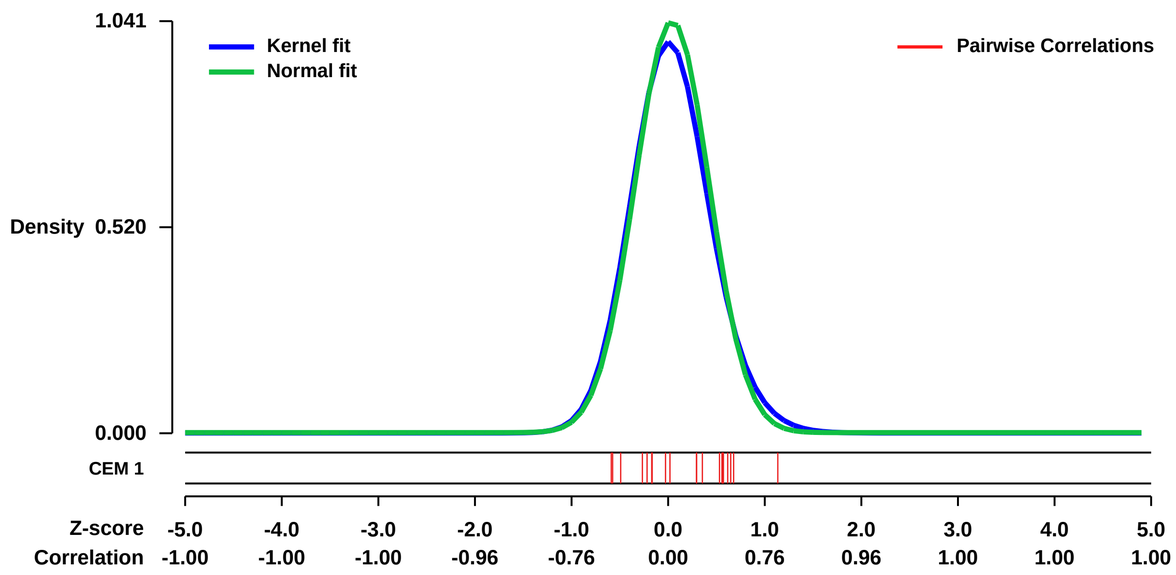

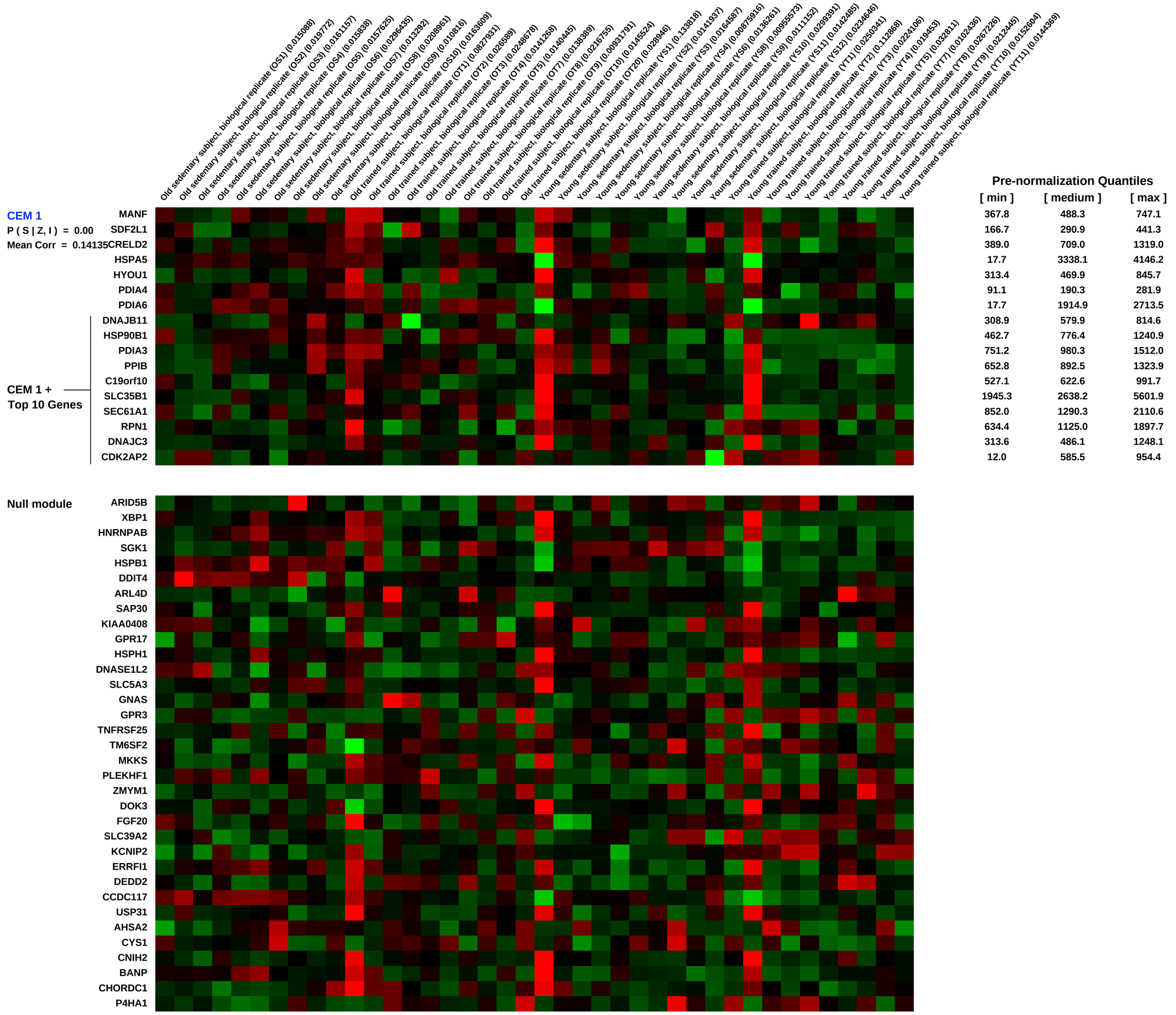

Pre-normalization Quantiles		
[min]	[medium]	[max]
367.8	488.3	747.1
166.7	290.9	441.3
389.0	709.0	1319.0
17.7	3338.1	4146.2
313.4	469.9	845.7
91.1	190.3	281.9
17.7	1914.9	2713.5
308.9	579.9	814.6
462.7	776.4	1240.9
751.2	980.3	1512.0
652.8	892.5	1323.9
527.1	622.6	991.7
1945.3	2638.2	5601.9
852.0	1290.3	2110.6
634.4	1125.0	1897.7
313.6	486.1	1248.1
12.0	585.5	954.4

GEO Series "GSE8045" Expression Profiles

Num of samples in this series: 12

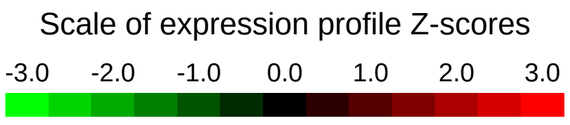

GEO Link:	http://www.ncbi.nlm.nih.gov/geo/query/acc.cgi?acc=GSE8045
Status:	Public on Oct 29 2008
Title:	Gene Expression Profiling in A549 Lung Cancer Cell Line Following siRNA Mediated Knock-down of ALDH1A1 and ALDH3A1
Organism:	Homo sapiens
Experiment type:	Expression profiling by array
Platform:	GPL570
Pubmed ID:	
Summary & Design:	**Summary:** Aldehyde dehydrogenase isozymes ALDH1A1 and ALDH3A1 are highly expressed in non small cell cell lung cancer. Neither the mechanism nor the biological significance for such over expression have been studied. We used microarrays to analyze changes in A549 lung cancer cell line in which ALDH activity was reduced using lentiviral mediated expression of siRNA against both isozymes (Lenti 1+3) Keywords: Gene Profiling after ALDH Knock Down **Overall design:** A549 lung cancer cell lines were transduced with lentiviral vectors containing specific siRNA sequences against ALDH1A1, ALDH3A1, both vectors (Lenti 1+3 cells), and against the green flourescent protein (GFP) gene (GFP cells, used as control).

Background corr dist: KL-Divergence = 0.0257, L1-Distance = 0.0372, L2-Distance = 0.0020, Normal std = 0.6988

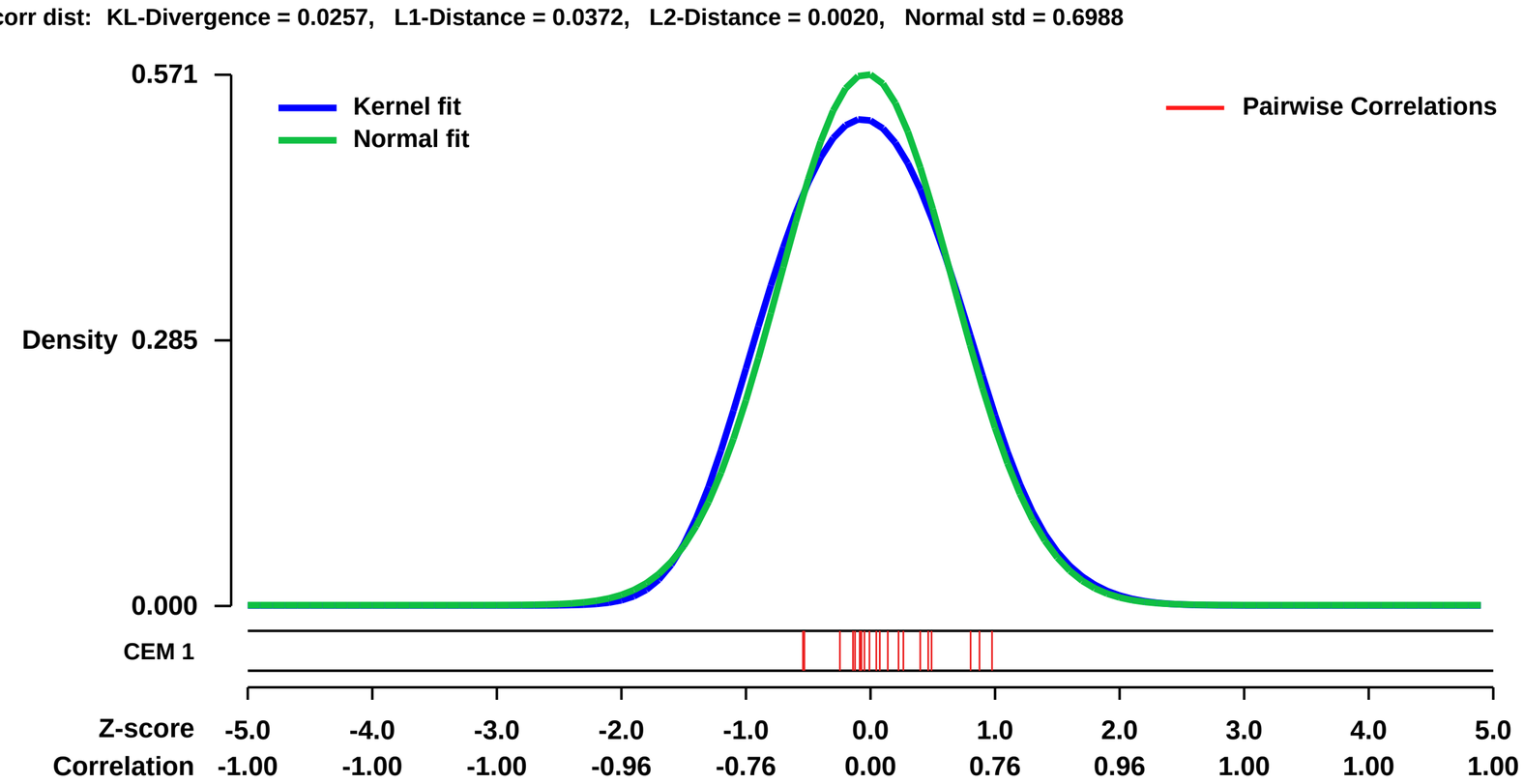

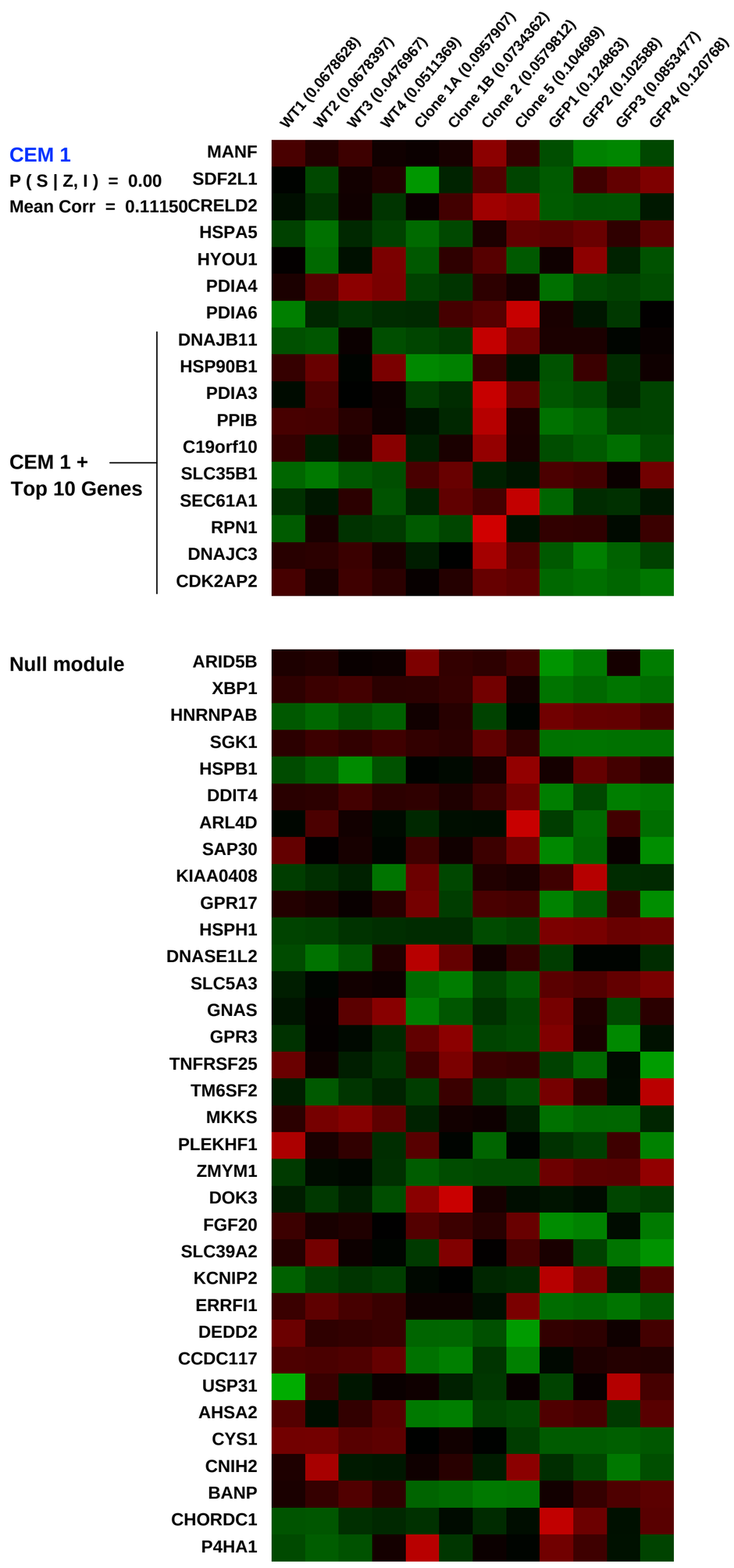

GEO Series "GSE52435" Expression Profiles

Num of samples in this series: 12

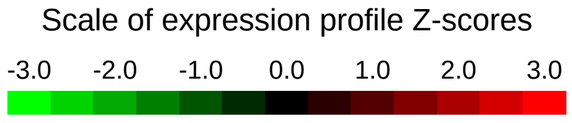

GEO Link:	http://www.ncbi.nlm.nih.gov/geo/query/acc.cgi?acc=GSE52435
Status:	Public on Dec 01 2013
Title:	Transcriptional responses of mantle cell lymphoma (MCL) after NIK knockdown
Organism:	Homo sapiens
Experiment type:	Expression profiling by array
Platform:	GPL570
Pubmed ID:	24362935
Summary & Design:	**Summary:** MCL lines were treated with or without 100ng/ml doxycycline for 7 days This experiment is designed to see if shRNA-mediated knockdown of NIK downregulates NFKB signaling in MCL lines with mutations in upstream regulators of the alternative pathway (TRAF2 & TRAF3) **Overall design:** MCL cells carrying inducible non-targeting control (NTC) shRNA, NIKshRNA#1 (NIKsh#1), or NIKshRNA#2 (NIKsh#2) were seeded in 6well dishes and treated for 7 days with or without 100ng/ml doxycycline.

Background corr dist: KL-Divergence = 0.0840, L1-Distance = 0.0443, L2-Distance = 0.0030, Normal std = 0.4923

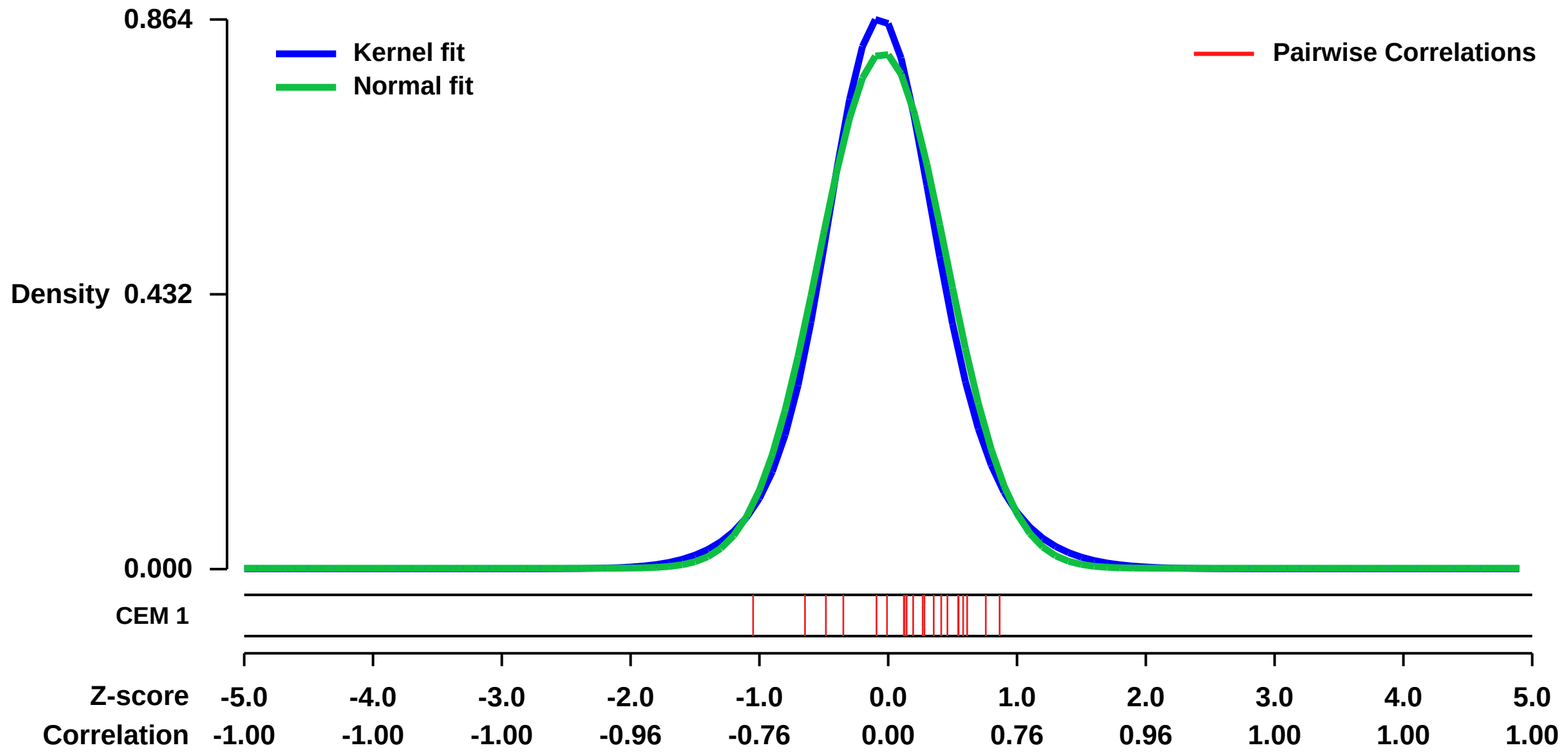

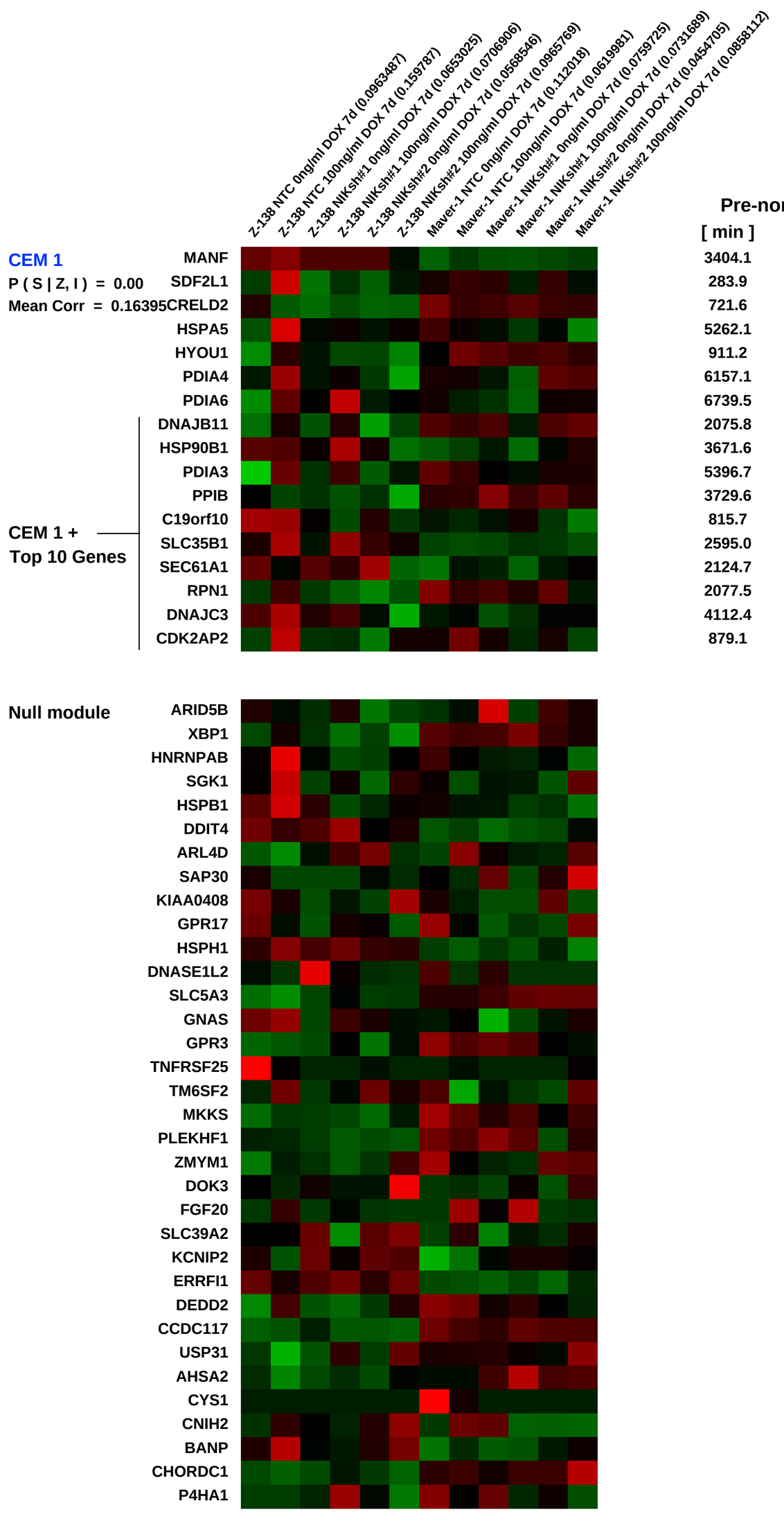

GEO Series "GSE19686" Expression Profiles

Num of samples in this series: 9

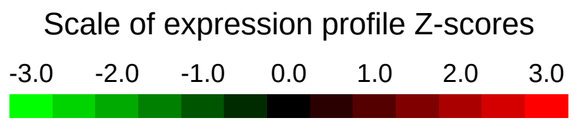

GEO Link:	http://www.ncbi.nlm.nih.gov/geo/query/acc.cgi?acc=GSE19686
Status:	Public on Dec 30 2009
Title:	shGFP- and shQK-transduced human Hs683 cells
Organism:	Homo sapiens
Experiment type:	Expression profiling by array
Platform:	GPL570
Pubmed ID:	
Summary & Design:	**Summary:** Identify potential QK-regulated mRNAs and linked pathways by comparing the transcriptional profiles of shGFP- and shQK-transduced human Hs683 cells **Overall design:** Hs683 cells infected with shQk-2, shQk-5 and Hs683 cells infected with shGFP as control

Background corr dist: KL-Divergence = 0.1146, L1-Distance = 0.0274, L2-Distance = 0.0013, Normal std = 0.4148

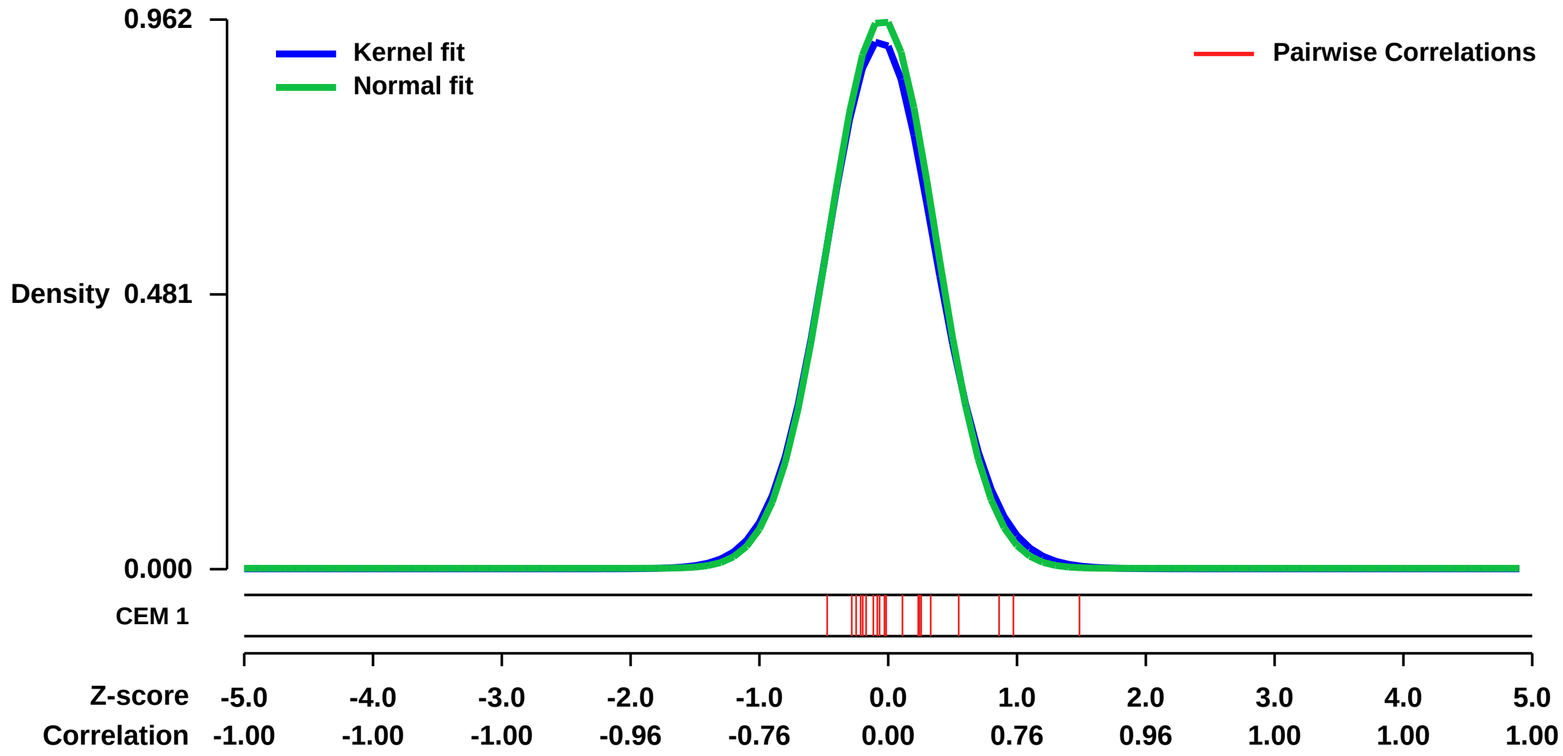

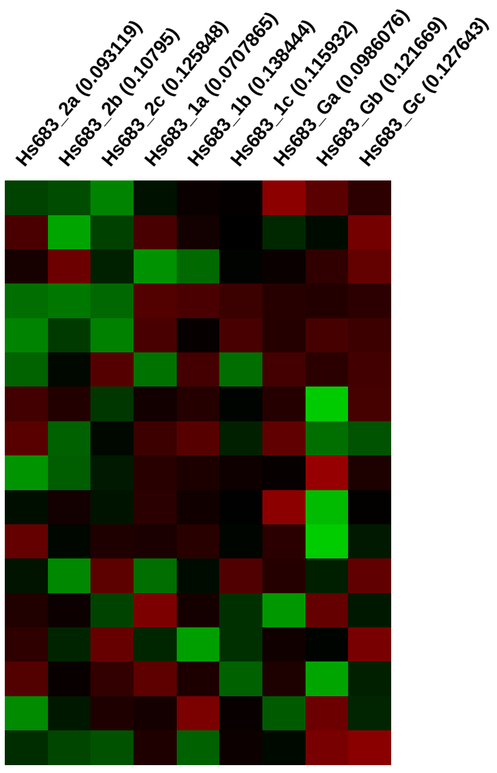

Pre-normalization Quantiles

		[min]	[medium]	[max]
CEM 1	MANF	3038.8	3944.4	4843.2
P (S | Z, I) = 0.00	SDF2L1	645.2	878.5	1041.1
Mean Corr = 0.11328	CRELD2	3605.2	4903.0	5702.8
	HSPA5	15572.7	19993.5	21252.4
	HYOU1	5883.0	6755.8	6952.0
	PDIA4	1897.4	2171.4	2244.4
	PDIA6	6152.8	7549.1	7743.7
CEM 1 + Top 10 Genes	DNAJB11	8916.0	9504.7	10101.4
	HSP90B1	2882.4	3838.6	4645.6
	PDIA3	7309.0	8770.7	9823.9
	PPIB	12465.0	14861.4	15648.9
	C19orf10	5737.8	6371.0	6918.5
	SLC35B1	3313.3	3858.5	4235.2
	SEC61A1	5224.1	5877.5	6398.7
	RPN1	5197.3	5953.7	6215.5
	DNAJC3	1577.5	1948.5	2240.8
	CDK2AP2	767.8	936.6	1217.2

Null module

ARID5B	
XBP1	
HNRNPAB	
SGK1	
HSPB1	
DDIT4	
ARL4D	
SAP30	
KIAA0408	
GPR17	
HSPH1	
DNASE1L2	
SLC5A3	
GNAS	
GPR3	
TNFRSF25	
TM6SF2	
MKKS	
PLEKHF1	
ZMYM1	
DOK3	
FGF20	
SLC39A2	
KCNIP2	
ERRFI1	
DEDD2	
CCDC117	
USP31	
AHSA2	
CYS1	
CNIH2	
BANP	
CHORDC1	
P4HA1	

GEO Series "GSE26298" Expression Profiles

Num of samples in this series: 12

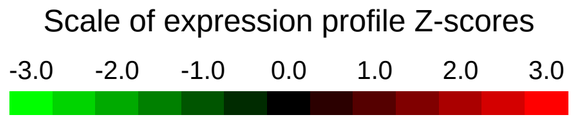

GEO Link:	http://www.ncbi.nlm.nih.gov/geo/query/acc.cgi?acc=GSE26298
Status:	Public on May 13 2011
Title:	Under conditions of hormonal adjuvant treatment the estrogen receptor apoprotein supports breast cancer cell cycling through the retinoic acid receptor ¸–1 apoprotein
Organism:	Homo sapiens
Experiment type:	Expression profiling by array
Platform:	GPL570
Pubmed ID:	21299862
Summary & Design:	**Summary:** Under conditions of hormonal adjuvant treatment the estrogen receptor apoprotein supports breast cancer cell cycling through the retinoic acid receptor ¸–1 apoprotein. Basal proliferation persisted in estrogen-sensitive breast cancer cells grown in hormone depleted conditioned media without or with 4-hydroxytamoxifen (OH-Tam). Downregulating ER using siRNA inhibited basal proliferation by promoting cell cycle arrest. The basal expression of RAR¸–1, the only RAR¸– isoform that was expressed in breast cancer cell lines and in most breast tumors, was supported by apo-ER but was unaffected by OH-Tam. The overlapping tamoxifen-insensitive gene regulation by apo-ER and apo-RAR¸–1 comprised activation of mainly genes promoting cell cycle and mitosis and suppression of genes involved in growth inhibition. **Overall design:** Cells were plated at 20% confluence in low glucose phenol red free medium supplemented with 5% charcoal stripped FBS and glutamine 24h-48h prior to transfection. Treatment with vehicle, OH-Tam (100nM), or OH-Tam (500nM) was begun an additional 24h later. Cells were transfected with control siRNA, ER¸– siRNA or RAR¸– siRNA.

Background corr dist: KL-Divergence = 0.1597, L1-Distance = 0.0373, L2-Distance = 0.0028, Normal std = 0.3637

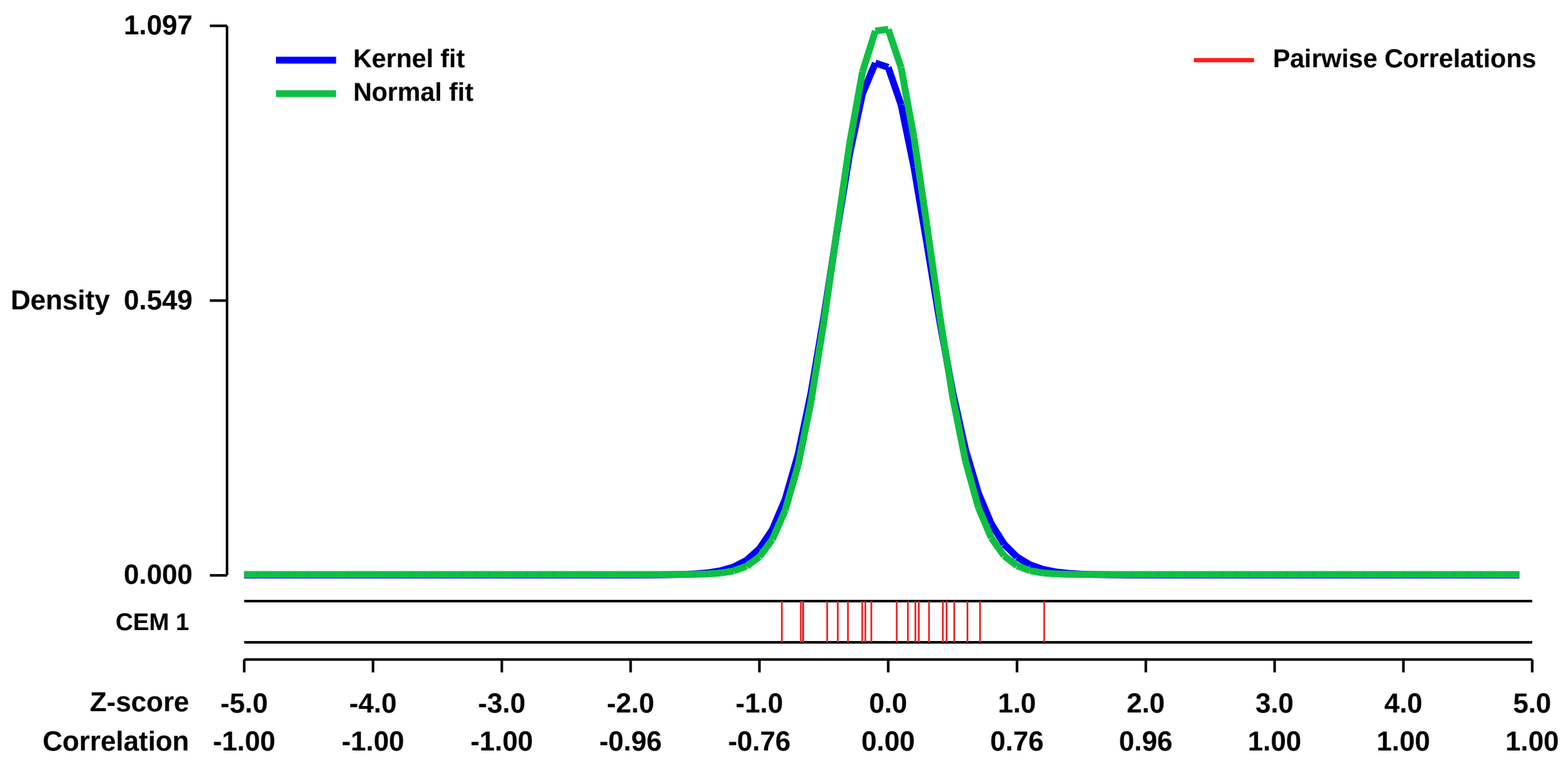

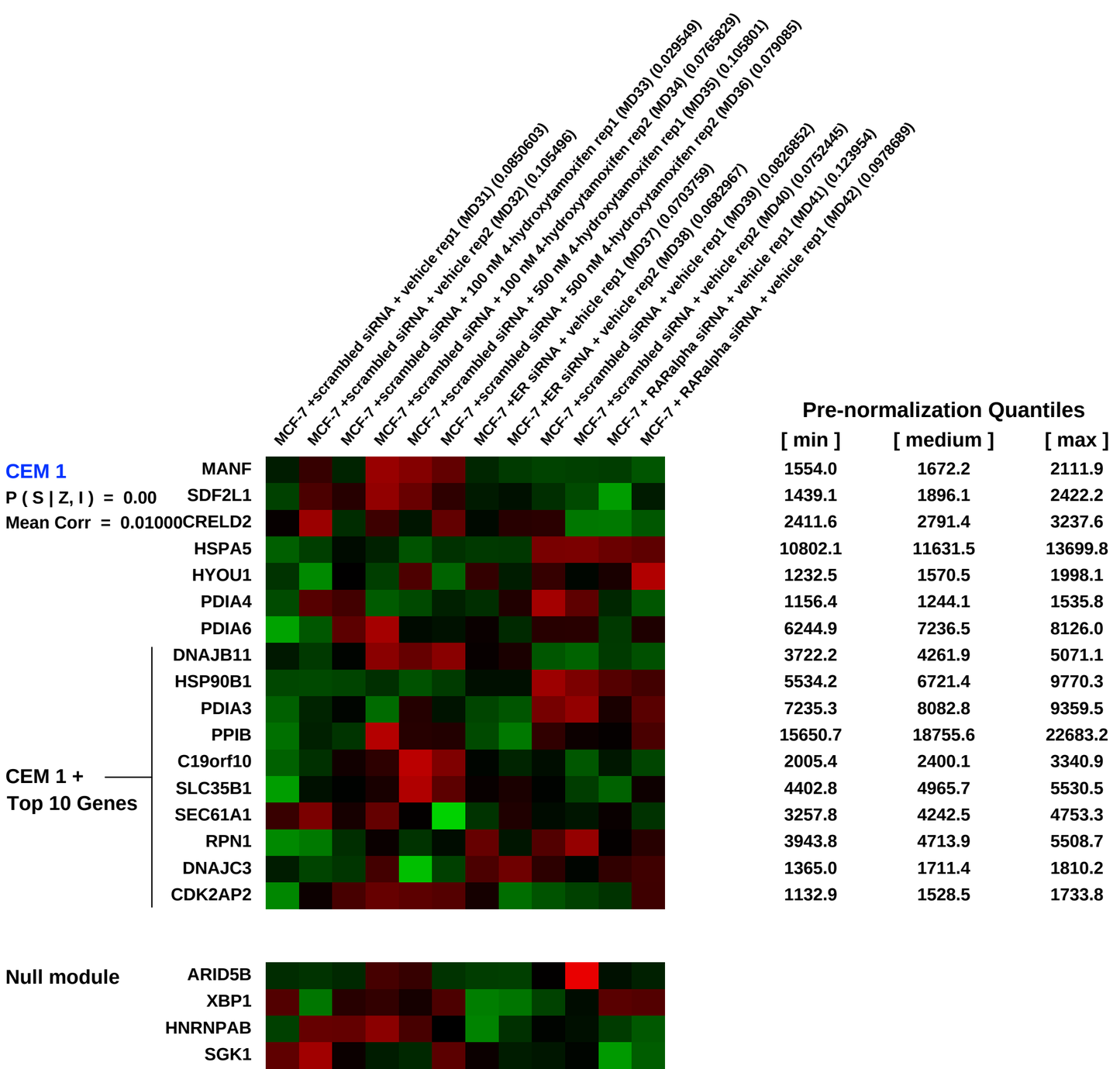

GEO Series "GSE31397" Expression Profiles

Num of samples in this series: 6

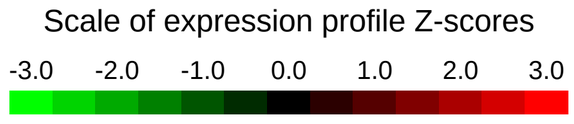

GEO Link:	http://www.ncbi.nlm.nih.gov/geo/query/acc.cgi?acc=GSE31397
Status:	Public on Aug 20 2011
Title:	Expression profile of miR-101 transfection in MCF-7 cells compared with scramble control
Organism:	Homo sapiens
Experiment type:	Expression profiling by array
Platform:	GPL570
Pubmed ID:	
Summary & Design:	**Summary:** Autophagy is an evolutionarily conserved mechanism of cellular self-digestion in which proteins and organelles are degraded through delivery to lysosomes. Defects in this process are implicated in numerous human diseases including cancer. To further elucidate regulatory mechanisms of autophagy, we performed a functional screen in search of microRNAs (miRNAs), which regulate the autophagic flux in breast cancer cells. In this study we identified the tumor suppressive miRNA, miR-101, as a potent inhibitor of basal, etoposide- and rapamycin-induced autophagy. Through transcriptome profiling, we identified three novel miR-101 targets, STMN1, RAB5A and ATG4D. siRNA-mediated depletion of these genes phenocopied the effect of miR-101 overexpression, demonstrating their importance in autophagy regulation. Importantly, overexpression of STMN1 could partially rescue cells from miR-101-mediated inhibition of autophagy, indicating a functional importance for this target. Finally, we show that miR-101-mediated inhibition of autophagy can sensitize breast cancer cells to 4-hydroxytamoxifen (4-OHT) mediated cell death. Collectively, these data establish a novel link between two highly important and rapidly growing research fields and present a new role for miR-101 as a key regulator of autophagy. **Overall design:** MCF-7 cells were seeded in 6-cm plates and independent triplicate transfections were performed the following day with 50 nM miR-101 or scramble control using Lipofectamine 2000. Total RNA was harvested 24 h after transfection using Trizol reagent. There are a total of six arrays included in this experiment, including three biological replicates of mRNA expression after miR-101 over-expression and three scramble controls in MCF-7 cells.

Background corr dist: KL-Divergence = 0.0391, L1-Distance = 0.0139, L2-Distance = 0.0002, Normal std = 0.6137

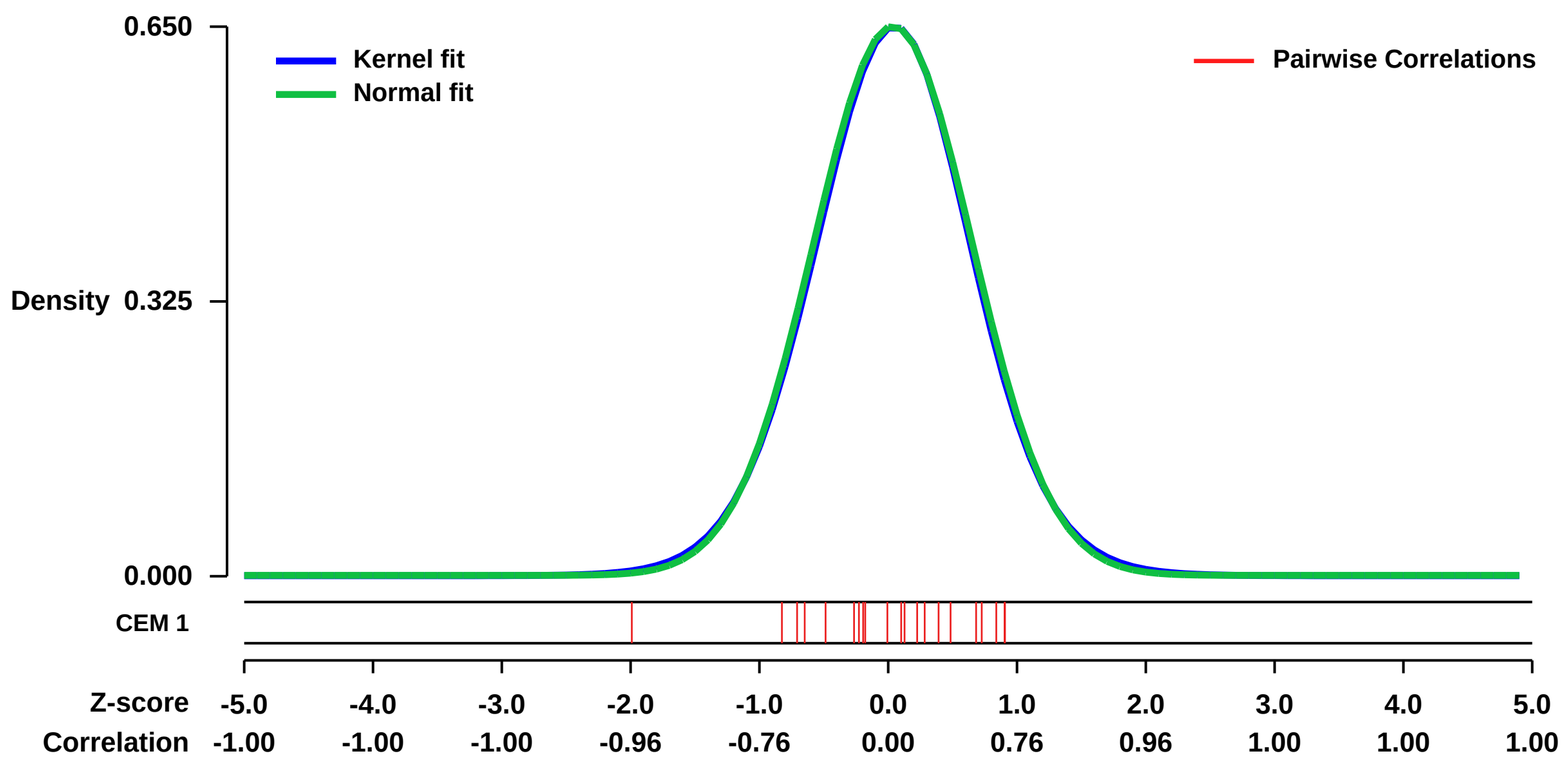

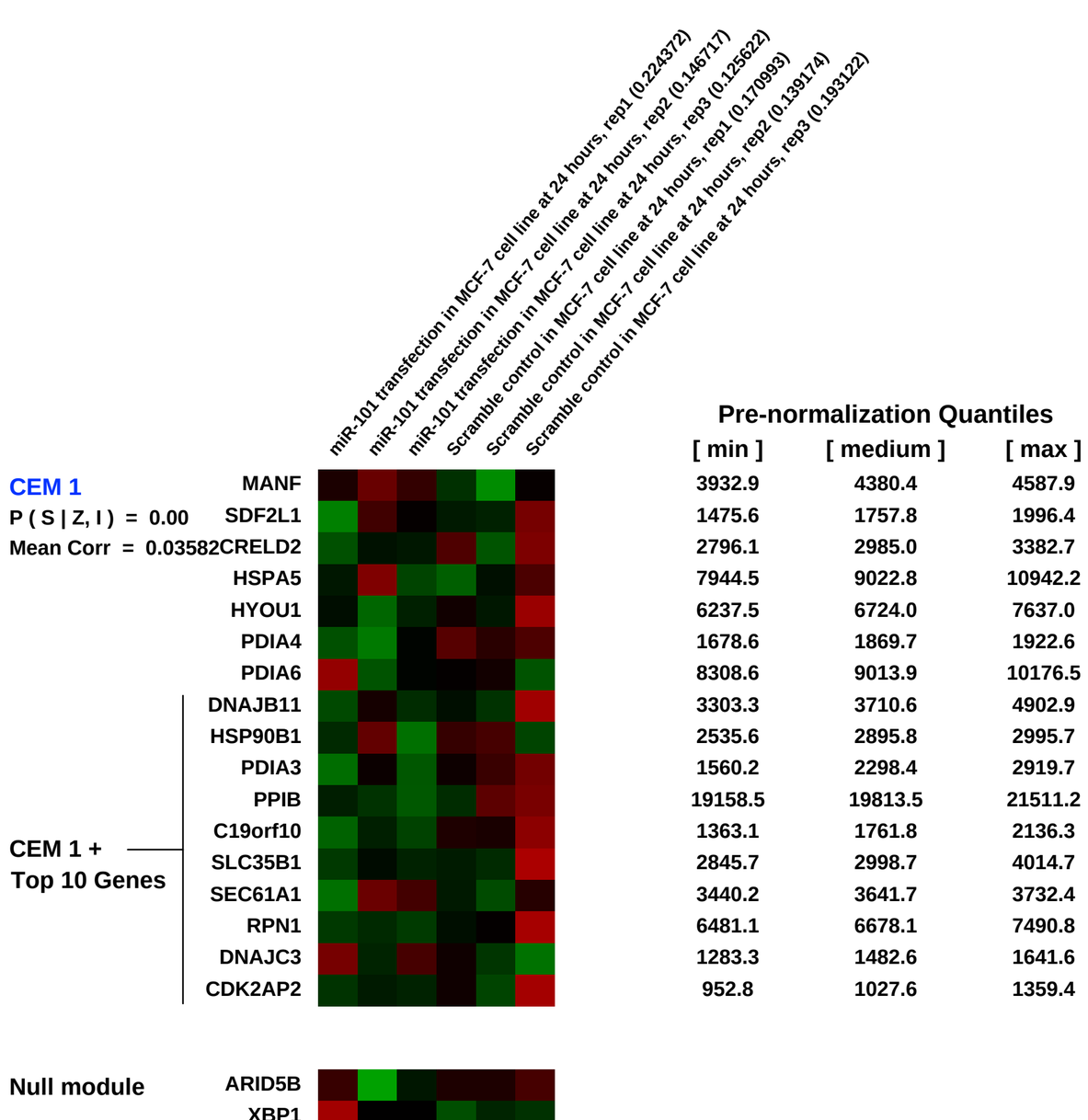

GEO Series "GSE5145" Expression Profiles

Num of samples in this series: 6

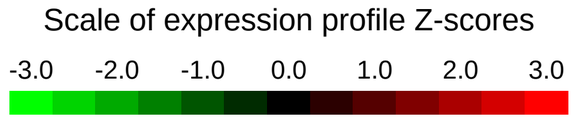

GEO Link:	http://www.ncbi.nlm.nih.gov/geo/query/acc.cgi?acc=GSE5145
Status:	Public on Feb 20 2007
Title:	Genes regulated by vitamin D in bronchial smooth muscle cells
Organism:	Homo sapiens
Experiment type:	Expression profiling by array
Platform:	GPL570
Pubmed ID:	17213369
Summary & Design:	**Summary:** Studied gene regulation in bronchial smooth muscle cells following vitamin D stimulation. **Keywords: comparison** **Overall design:** Human primary bronchial smooth muscle cells were from the same patient in all hybridization. Cells were treated for 24 hours with 100 nM of 1alpha,25-Dihydroxyvitamin D3 or with the same concentration of vehicle (ethanol at 0.05%). The experiment was done in triplicates (a total of 6 samples were analyzed).

Background corr dist: KL-Divergence = 0.0362, L1-Distance = 0.0147, L2-Distance = 0.0002, Normal std = 0.6293

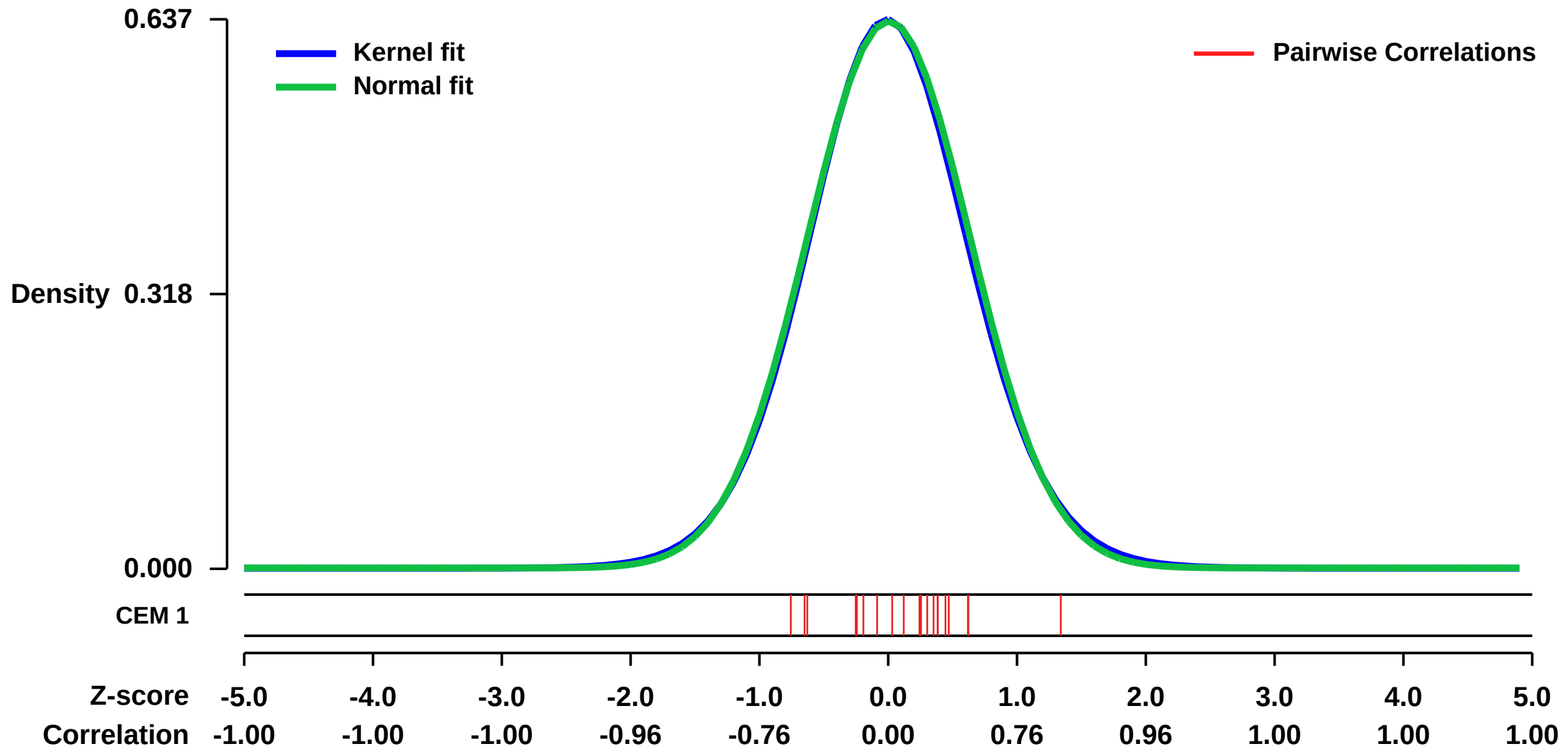

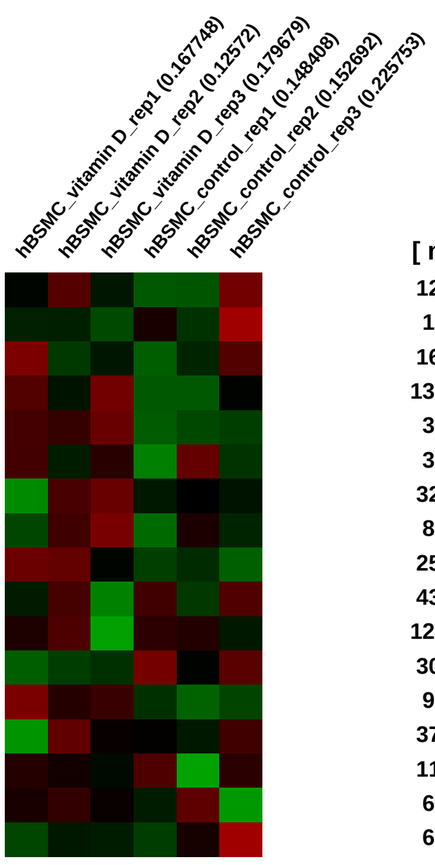

GEO Series "GSE38783" Expression Profiles

Num of samples in this series: 24

Scale of expression profile Z-scores

-3.0 -2.0 -1.0 0.0 1.0 2.0 3.0

GEO Link:	http://www.ncbi.nlm.nih.gov/geo/query/acc.cgi?acc=GSE38783
Status:	Public on Dec 04 2013
Title:	Acute venous hypertension induces local release of inflammatory cytokines and endothelial activation in humans
Organism:	Homo sapiens
Experiment type:	Expression profiling by array
Platform:	GPL570
Pubmed ID:	24265434
Summary & Design:	**Summary:** Background: Venous hypertension is often present in advanced and in acute decompensated heart failure (HF). However, it is unclear whether high intravenous pressure can cause alterations in homeostasis by promoting inflammation and endothelial cell (EC) activation. We used an experimental model of acute, local venous hypertension to study the changes in circulating inflammatory mediators and EC phenotype that occur in response to biomechanical stress. Methods and Results: Twenty-four healthy subjects (14 men, age 35´–2 years) were studied. Venous arm pressure was increased to ~30 mmHg above baseline level by inflating a tourniquet cuff around the dominant arm (test arm). Blood and endothelial cells (ECs) were sampled from test and control arm (lacking an inflated cuff) before and after 75 minutes of venous hypertension, using angiocatheters and endovascular wires. Magnetic beads coated with EC specific antibodies were used for EC separation; amplified mRNA was analyzed by Affymetrix HG-U133 2.0 Microarray. Plasma endothelin-1 (ET-1), interleukin-6 (IL-6), vascular cell adhesion molecule-1 (VCAM-1) and chemokine (C-X-C motif) ligand 2 (CXCL2) were significantly increased in the congested arm. 5,332 probe sets were differentially expressed in venous ECs before vs. after testing. Among the 143 probe sets that exhibited a significant absolute fold change >2, we identified several inflammatory mediators including ET-1, VCAM-1, and CXCL2. Conclusions: Acute experimental venous hypertension is sufficient to cause local increase in circulating inflammatory mediators and to activate venous ECs in healthy human subjects. Additional work is needed to determine the effect of venous hypertension in patients with established HF. **Overall design:** 24 samples were analyzed from 12 patients. Each patient contributed 2 samples (1 prior to intervention and 1 after intervention). The pre-intervention sample serves as the control.

Background corr dist: KL-Divergence = 0.0554, L1-Distance = 0.0945, L2-Distance = 0.0148, Normal std = 0.6471

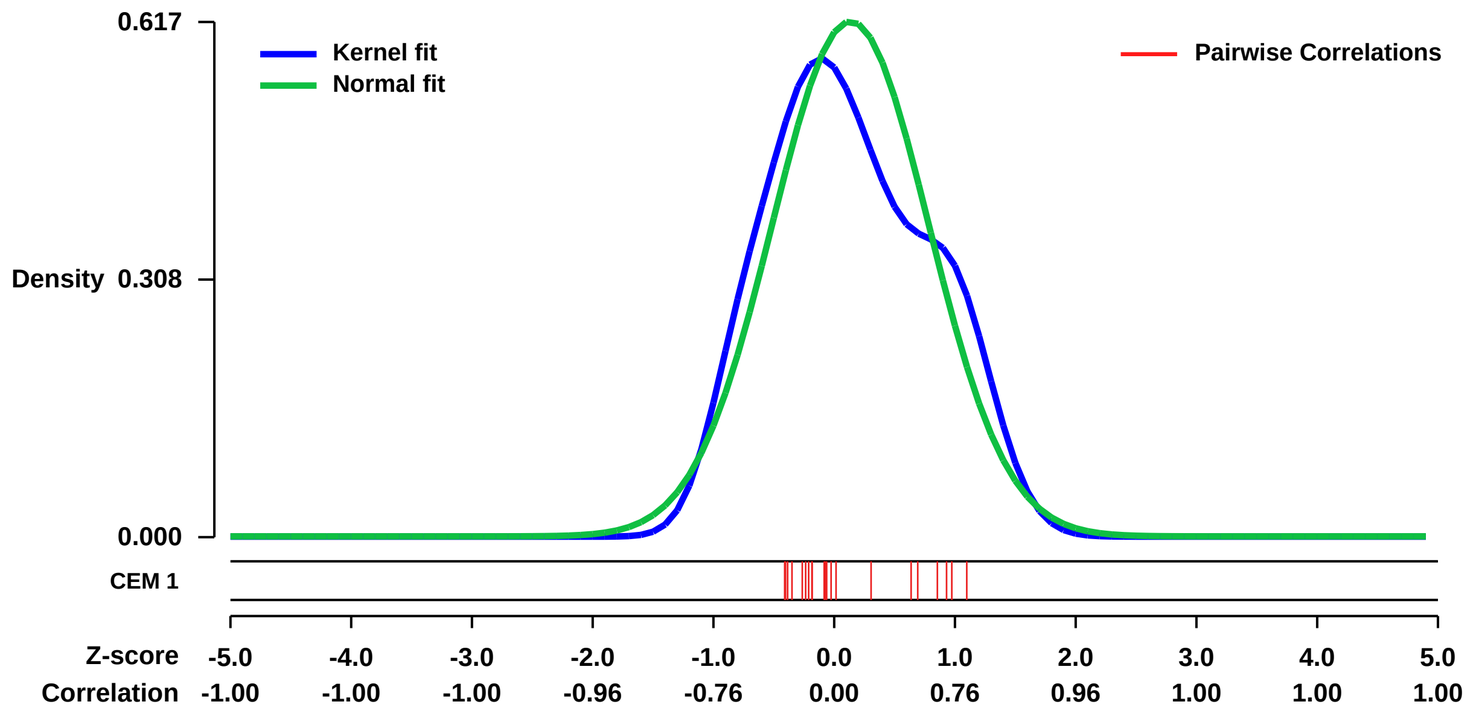

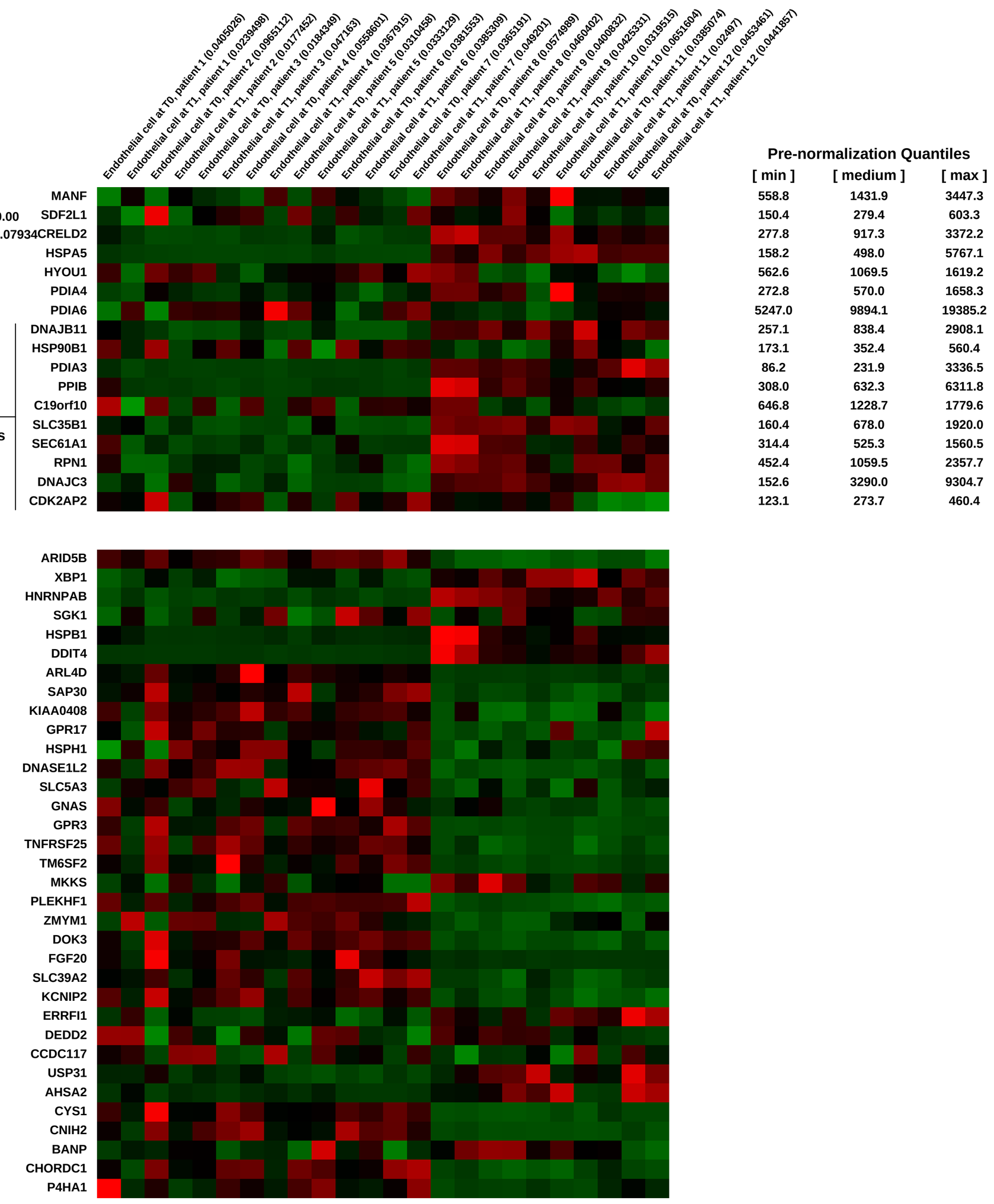

Pre-normalization Quantiles

[min]	[medium]	[max]
558.8	1431.9	3447.3
150.4	279.4	603.3
277.8	917.3	3372.2
158.2	498.0	5767.1
562.6	1069.5	1619.2
272.8	570.0	1658.3
5247.0	9894.1	19385.2
257.1	838.4	2908.1
173.1	352.4	560.4
86.2	231.9	3336.5
308.0	632.3	6311.8
646.8	1228.7	1779.6
160.4	678.0	1920.0
314.4	525.3	1560.5
452.4	1059.5	2357.7
152.6	3290.0	9304.7
123.1	273.7	460.4

GEO Series "GSE39904" Expression Profiles

Num of samples in this series: 16

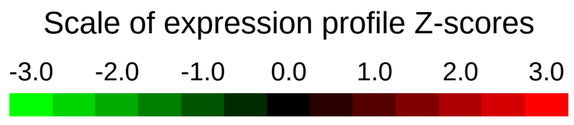

GEO Link:	http://www.ncbi.nlm.nih.gov/geo/query/acc.cgi?acc=GSE39904
Status:	Public on Dec 21 2012
Title:	Role of TAZ as mediator of Wnt signaling (SW480)
Organism:	Homo sapiens
Experiment type:	Expression profiling by array
Platform:	GPL570
Pubmed ID:	23245942
Summary & Design:	**Summary:** To investigate the role of TAZ downstream of the abberrant Wnt signaling in CRC cells, we compared the expression profiles of parental SW480 cells (empty vector) transfected with siControl, siTAZ, sibeta-catenin or reconstituted with wild type APC and transfected with siControl **Keywords: expression profiling by array** **Overall design:** We collected RNA from parental SW480 cells (empty vector) transfected with siControl, siTAZ, sibeta-catenin or from SW480 cells reconstituted with wild type APC and transfected with siControl. Cells were left untreated in normal culturing conditions before harvesting. Samples were then processed for total RNA extraction and hybridization on Affymetrix microarrays. Four biological replicas (A, B, C, D) were used for each of the 4 conditions (1: siControl, control cells; 2: siTAZ cells; 3: sibeta-catenin (sibcat) cells; 4.APC reconstituted cells) for a total of 16 samples.

Background corr dist: KL-Divergence = 0.1177, L1-Distance = 0.0365, L2-Distance = 0.0020, Normal std = 0.4284

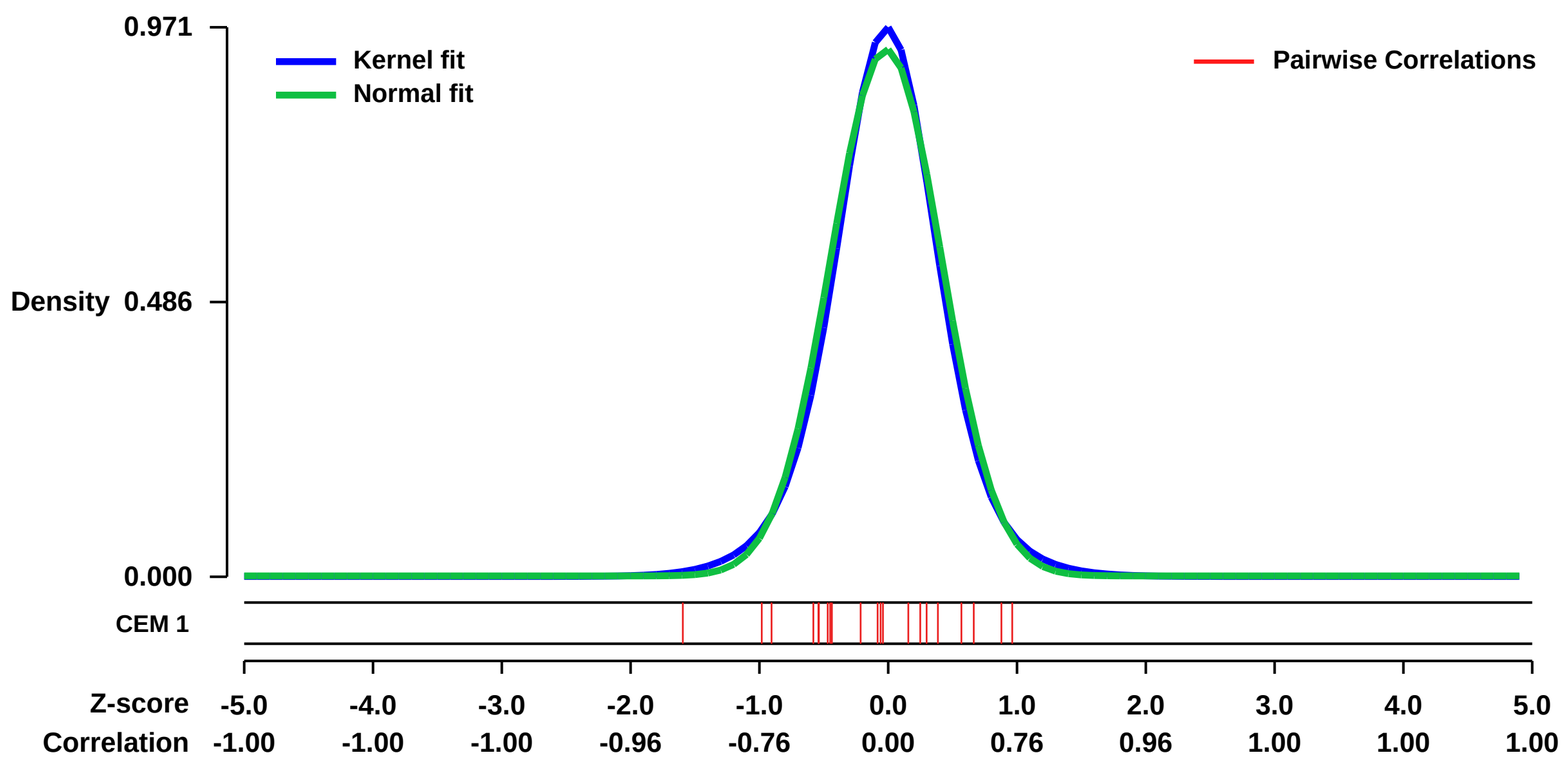

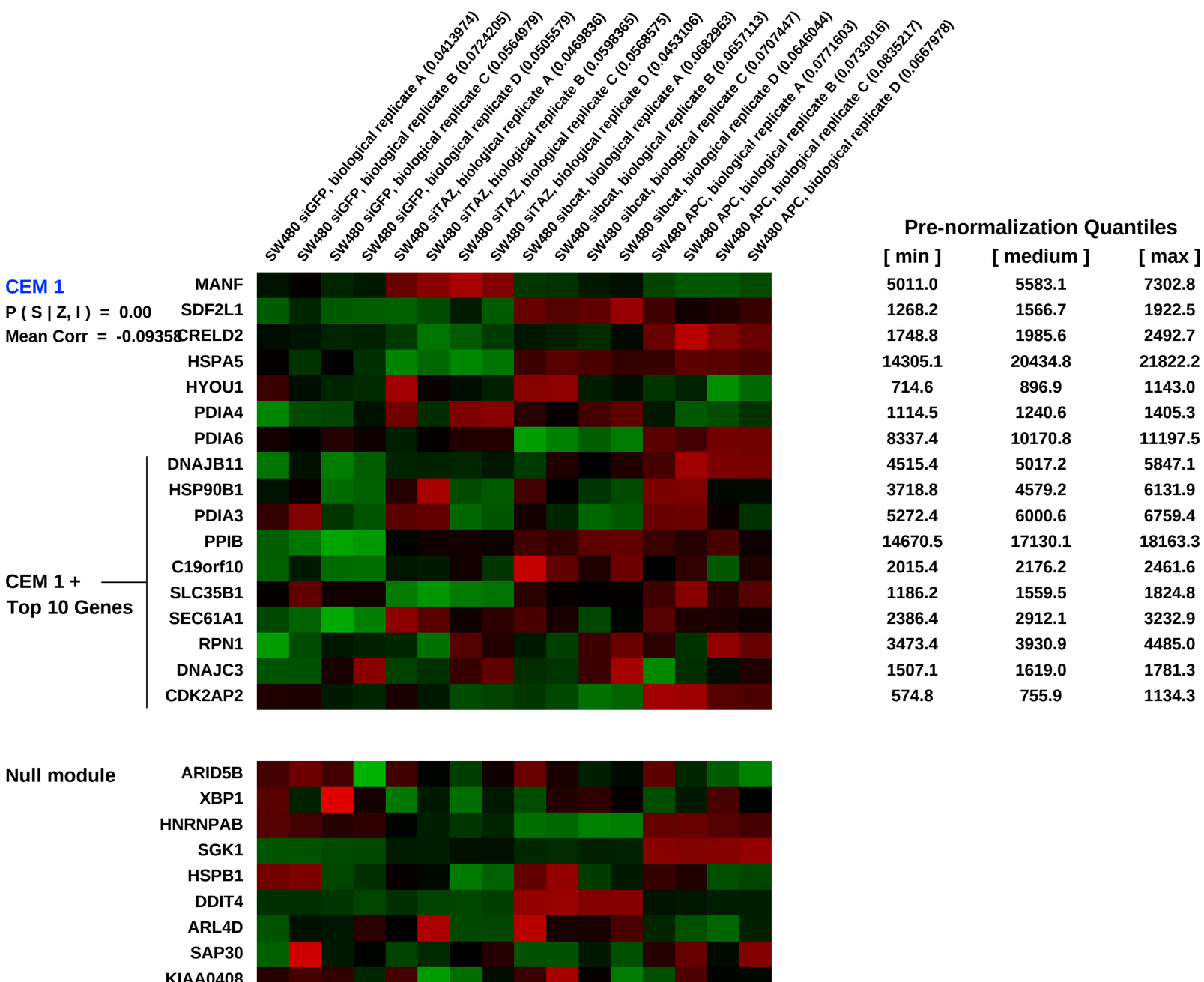

Pre-normalization Quantiles

	[min]	[medium]	[max]
MANF	5011.0	5583.1	7302.8
SDF2L1	1268.2	1566.7	1922.5
CRELD2	1748.8	1985.6	2492.7
HSPA5	14305.1	20434.8	21822.2
HYOU1	714.6	896.9	1143.0
PDIA4	1114.5	1240.6	1405.3
PDIA6	8337.4	10170.8	11197.5
DNAJB11	4515.4	5017.2	5847.1
HSP90B1	3718.8	4579.2	6131.9
PDIA3	5272.4	6000.6	6759.4
PPIB	14670.5	17130.1	18163.3
C19orf10	2015.4	2176.2	2461.6
SLC35B1	1186.2	1559.5	1824.8
SEC61A1	2386.4	2912.1	3232.9
RPN1	3473.4	3930.9	4485.0
DNAJC3	1507.1	1619.0	1781.3
CDK2AP2	574.8	755.9	1134.3

GEO Series "GSE28339" Expression Profiles

Num of samples in this series: 6

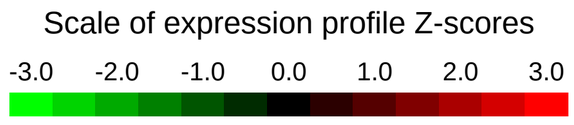

GEO Link:	http://www.ncbi.nlm.nih.gov/geo/query/acc.cgi?acc=GSE28339
Status:	Public on Aug 03 2011
Title:	Gene expression data following Cyclin T2 and Cyclin T1 depletion by shRNA in HeLa cells
Organism:	Homo sapiens
Experiment type:	Expression profiling by array
Platform:	GPL570
Pubmed ID:	21791050
Summary & Design:	**Summary:** We have characterized gene expression changes in HeLa cells following long term depletion of Cyclin T2 or Cyclin T1 using shRNA **Overall design:** HeLa cells were transduced with VSV-G pseudotyped lentiviral vectors expressing shRNA against either Cyclin T2 or Cyclin T1. As a control, cells were transduced with shRNA vector with four nucleotides mismatch in the Cyclin T1 mRNA that has been previously shown to have minimal effects on mRNA expression levels. The vectors have a GFP reporter that can be used to estimate transduction efficiency. Five days post-transduction, cells were harvested and total RNA extracted. Transcriptional profiling was carried out on these RNA samples. Two independent biological replicate experiments were carried out in this analysis and the xpression values normalized by GC-RMA and averaged. The following comparisons were made: MM to Cyclin T2 and MM to Cyclin T1.

Background corr dist: KL-Divergence = 0.0265, L1-Distance = 0.0113, L2-Distance = 0.0001, Normal std = 0.6817

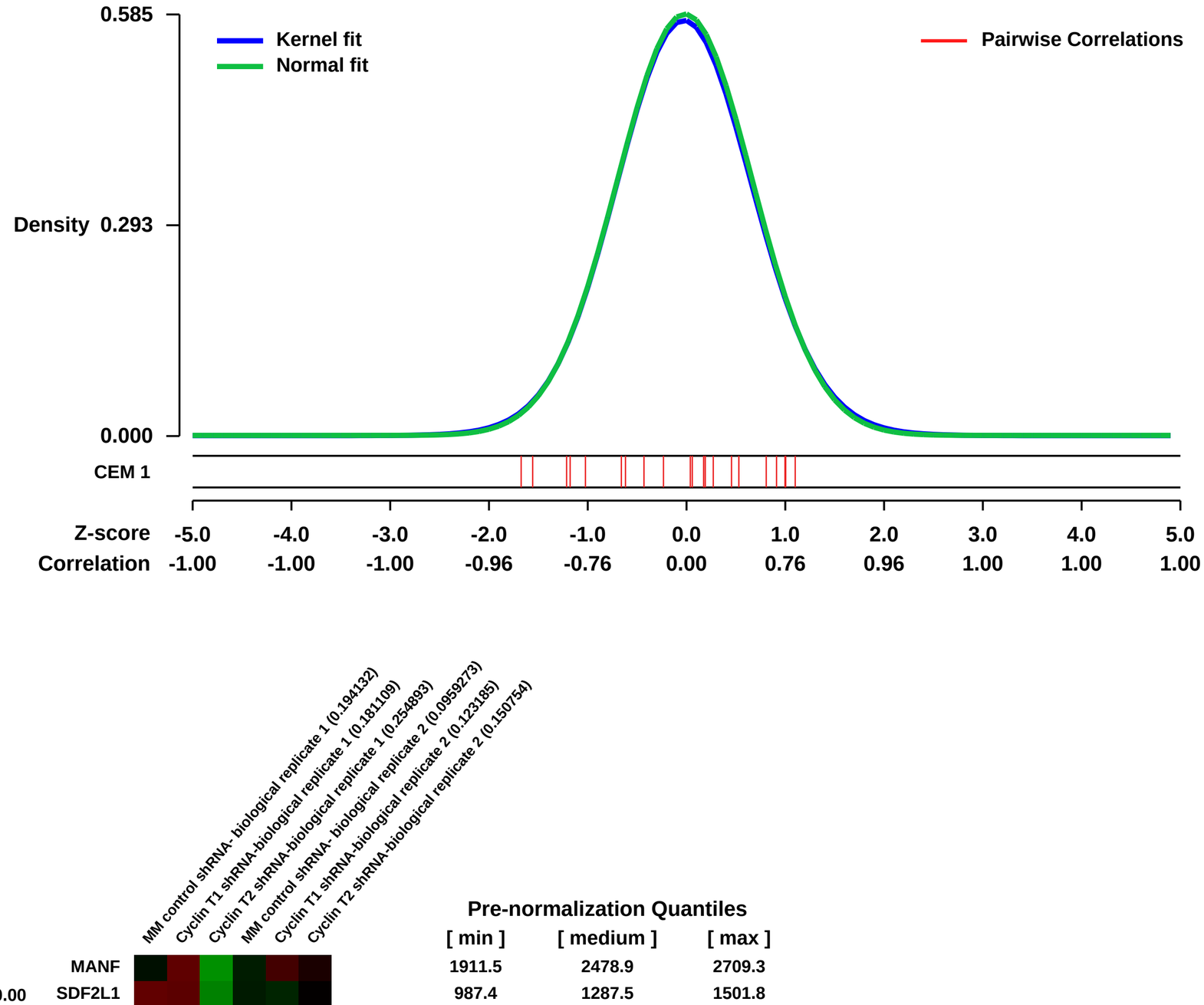

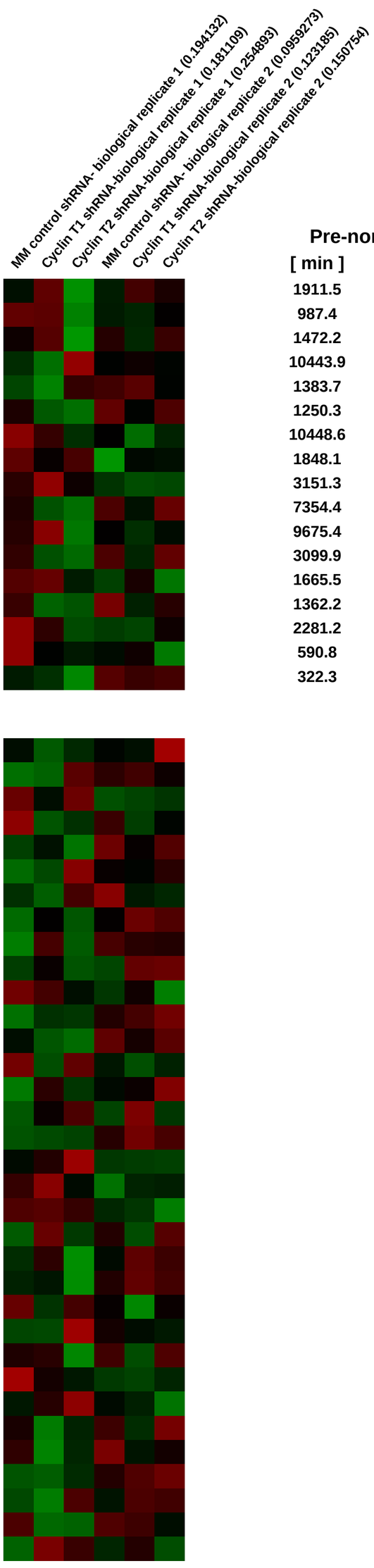

GEO Series "GSE26272" Expression Profiles

Num of samples in this series: 8

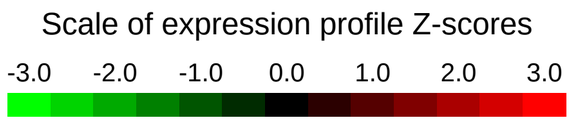

GEO Link:	http://www.ncbi.nlm.nih.gov/geo/query/acc.cgi?acc=GSE26272
Status:	Public on Dec 22 2010
Title:	Expression data from control and ZNF145-overexpressing human mesenchymal stem cells (MSCs)
Organism:	Homo sapiens
Experiment type:	Expression profiling by array
Platform:	GPL570
Pubmed ID:	21547890
Summary & Design:	**Summary:** ZNF145 is shown to be upregulated during three linage differentiation of MSCs especially in chondrogenesis. To understand the molecular basis of ZNF145 underlying MSCs, targets of ZNF145 in MSCs are determined by microarray We used microarrays to detail the change in gene expression profile upon overexpression of ZNF145 compared with control in undifferentiated MSCs **Overall design:** Control MSCs and ZNF145-overexpressing MSCs are processed for RNA extraction and hybridization on Affymetrix microarrays. To that end, we overexpressed ZNF145 in two patient-derived human MSCs.

Background corr dist: KL-Divergence = 0.0848, L1-Distance = 0.0266, L2-Distance = 0.0013, Normal std = 0.4728

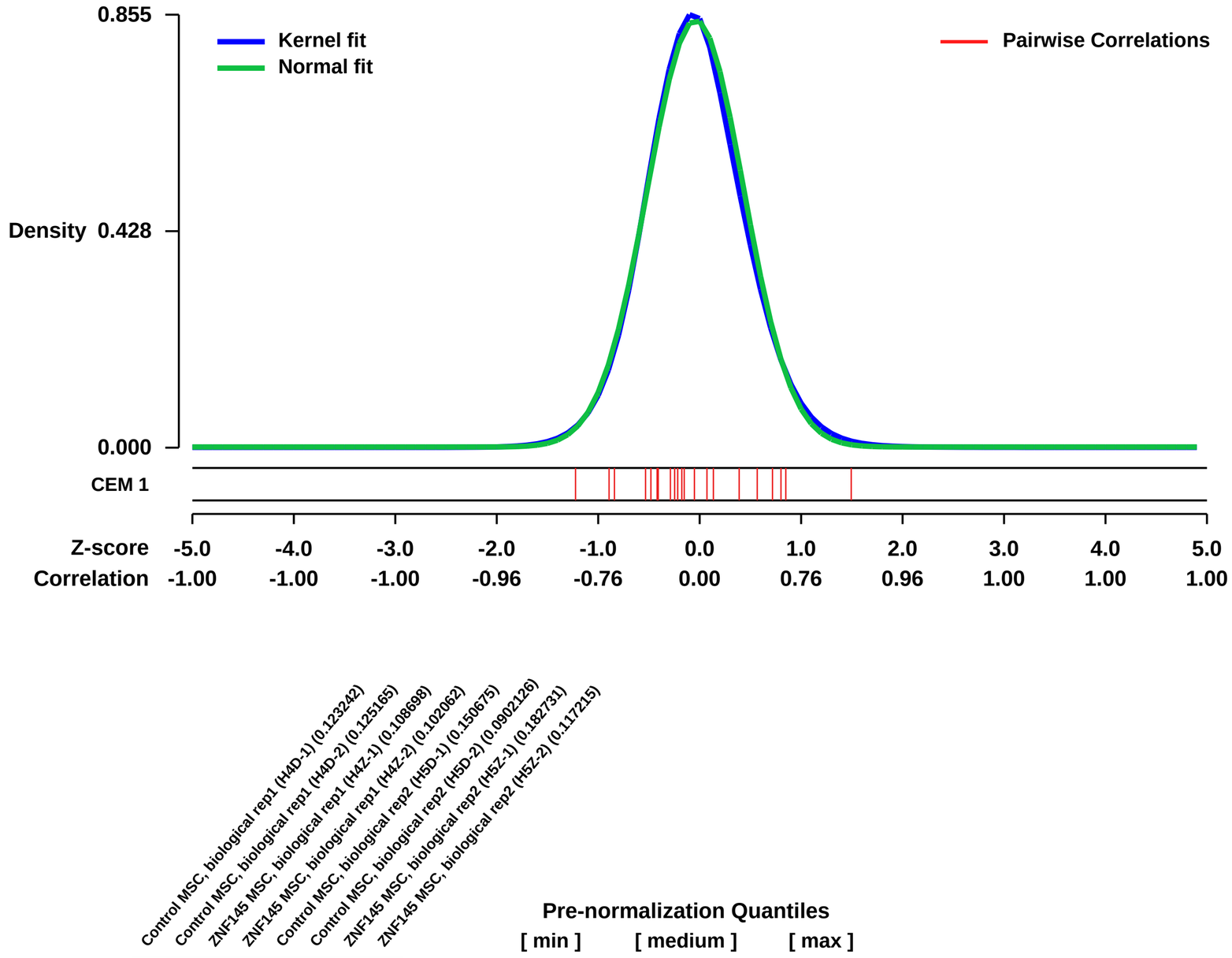

CEM 1
P (S | Z, I) = 0.00
Mean Corr = -0.05259

CEM 1 + Top 10 Genes

Null module

	Pre-normalization Quantiles [min]	[medium]	[max]
MANF	4090.5	4882.0	5644.2
SDF2L1	658.5	849.7	1146.8
CRELD2	4305.9	4911.5	6188.6
HSPA5	26215.8	30016.4	33150.7
HYOU1	1867.4	2028.3	2420.2
PDIA4	463.3	674.8	910.7
PDIA6	13469.6	14718.1	15592.6
DNAJB11	3526.9	3931.4	4610.8
HSP90B1	8218.8	9274.5	11072.8
PDIA3	12991.9	15179.8	17009.1
PPIB	26498.9	28577.5	29652.1
C19orf10	8754.6	9999.3	12476.3
SLC35B1	2188.6	2496.6	2697.6
SEC61A1	7566.9	10865.9	11169.4
RPN1	3154.0	3417.4	3904.2
DNAJC3	1922.0	2925.4	3123.6
CDK2AP2	763.5	922.5	1002.1
ARID5B			
XBP1			
HNRNPAB			
SGK1			
HSPB1			
DDIT4			
ARL4D			
SAP30			
KIAA0408			
GPR17			
HSPH1			
DNASE1L2			
SLC5A3			
GNAS			
GPR3			
TNFRSF25			
TM6SF2			
MKKS			
PLEKHF1			
ZMYM1			
DOK3			
FGF20			
SLC39A2			
KCNIP2			
ERRFI1			
DEDD2			
CCDC117			
USP31			
AHSA2			
CYS1			
CNIH2			
BANP			
CHORDC1			
P4HA1			

GEO Series "GSE51524" Expression Profiles

Num of samples in this series: 18

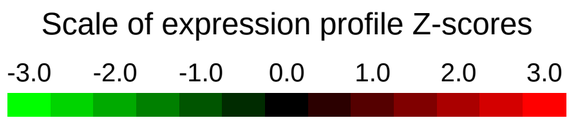

GEO Link:	http://www.ncbi.nlm.nih.gov/geo/query/acc.cgi?acc=GSE51524
Status:	Public on Feb 18 2014
Title:	LNCaP prostate cancer cell lines overexpressing wild-type or GARRPR-mutant Bag-1L
Organism:	Homo sapiens
Experiment type:	Expression profiling by array
Platform:	GPL570
Pubmed ID:	24523409
Summary & Design:	**Summary:** The BF-3 pocket of the androgen receptor (AR) has been identified as an allosteric modulator of the transactivation function of the AR. We now demonstrate that a duplicated GARRPR motif at the N-terminus of the cochaperone Bag-1L functions through this BF-3 domain. Amino acid exchanges in these two motifs impair binding of Bag-1L to the AR but increase the androgen-dependent activation of a subset of AR-target genes. We have therefore identified GARRPR as a novel BF-3 regulatory sequence important for fine-tuning the activity of the receptor. **Overall design:** LNCaP cells stably expressing the empty vector construct (=control), or wild-type or N-terminal GARRPR mutant Bag-1L were cultured under hormone-starvation conditions for 72 h and then treated with vehicle or 10 nM DHT for 4 h. Biological triplicate samples were analyzed for each cell line.

Background corr dist: KL-Divergence = 0.0699, L1-Distance = 0.0399, L2-Distance = 0.0023, Normal std = 0.5141

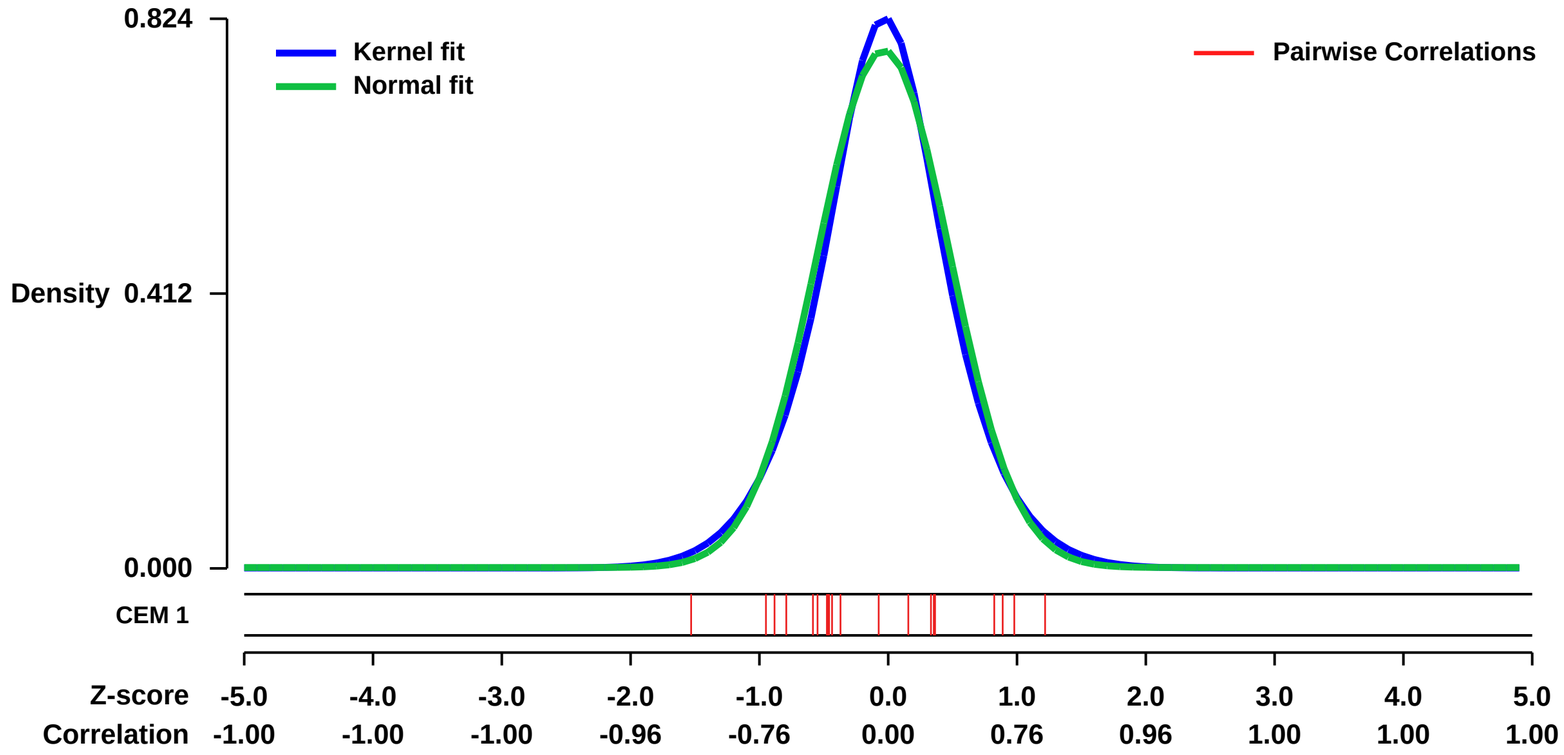

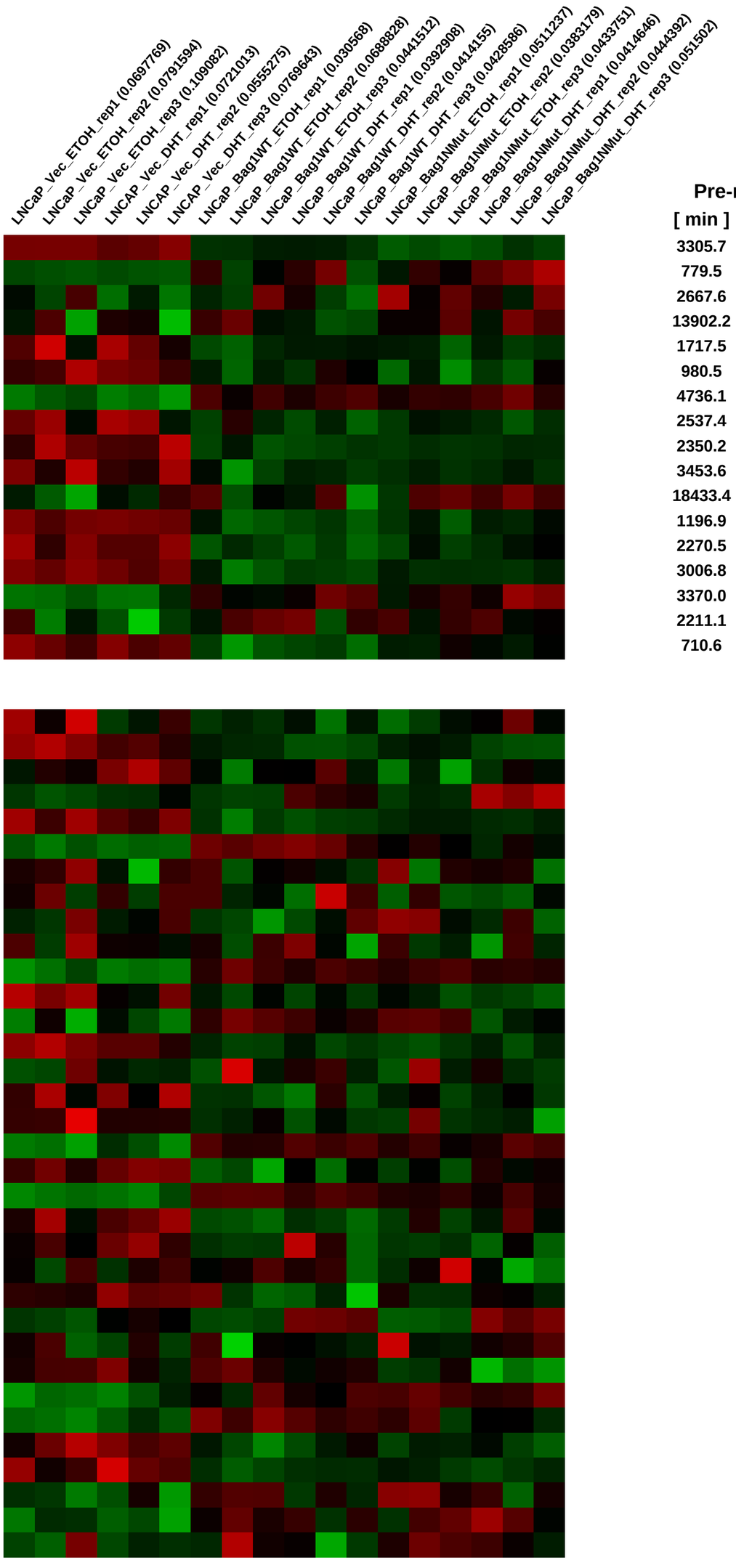

GEO Series "GSE40215" Expression Profiles

Num of samples in this series: 6

Scale of expression profile Z-scores

-3.0 -2.0 -1.0 0.0 1.0 2.0 3.0

GEO Link:	http://www.ncbi.nlm.nih.gov/geo/query/acc.cgi?acc=GSE40215
Status:	Public on Dec 31 2012
Title:	shRNA knockdown of the transcription factor NF-YA (NFYA)
Organism:	Homo sapiens
Experiment type:	Expression profiling by array
Platform:	GPL570
Pubmed ID:	23595228
Summary & Design:	**Summary:** NF-Y, a trimeric transcription factor (TF) composed of two histone-like subunits (NF-YB (NFYB) and NF-YC (NFYC)) and a sequence-specific subunit (NF-YA), binds to the CCAAT motif, a common promoter element. Genome-wide mapping reveals 5,000-15,000 NF-Y binding sites depending on the cell type, with the NF-YA and NF-YB subunits binding asymmetrically with respect to the CCAAT motif. Despite being characterized as a proximal promoter TF, only 25% of NF-Y sites map to promoters. A comparable number of NF-Y sites are located at enhancers, many of which are tissue specific, and nearly half of NF-Y sites are in select subclasses of HERV LTR repeats. Unlike most TFs, NF-Y can access its target DNA motif in inactive (non-modified) or polycomb-repressed chromatin domains. Unexpectedly, NF-Y extensively co-localizes with FOS in all genomic contexts, and at promoters and enhancers this often occurs in the absence of JUN and the AP-1 motif. NF-Y also co-associates with a select cluster of growth-controlling and oncogenic TFs, consistent with the abundance of CCAAT motifs in the promoters of genes overexpressed in cancer. Interestingly, NF-Y and several growth-controlling TFs bind in a stereo-specific manner, suggesting a mechanism for cooperative action at promoters and enhancers. Our results indicate that NF-Y is not merely a commonly-used, proximal promoter TF, but rather performs a more diverse set of biological functions, many of which are likely to involve co-association with FOS. Scrambled control (shSCM) and NF-YA pLKO.1-shRNAs were designed by Sigma-Aldrich. The puromycin resistance cassette was replaced with an EGFP cassette. Viral production and transduction were carried out as previously described (Benatti et al. 2011). HeLaS3 cells were transduced with shSCM or shNF-YA viral supernatants, in triplicate, and cells collected after 48 hr of incubation. Total RNA was prepared by Trizol extraction and Qiagen RNeasy kit purification, converted to biotinylated aRNA and hybridized to U133 Plus 2.0 GeneChip expression arrays using the 3â IVT Express Kit (Affymetrix, USA) following the manufacturerâ s protocol. Arrays were RMA normalized (Irizarry et al. 2003), gene expression levels calculated, differential expression determined using the following R packages from the Bioconductor project: affy (Gautier et al. 2004), limma (Smyth 2004). **Overall design:** HelaS3 cells were transduced with shSCM or shNF-YA in triplicate for 48hrs.

Background corr dist: KL-Divergence = 0.0355, L1-Distance = 0.0203, L2-Distance = 0.0004, Normal std = 0.6387

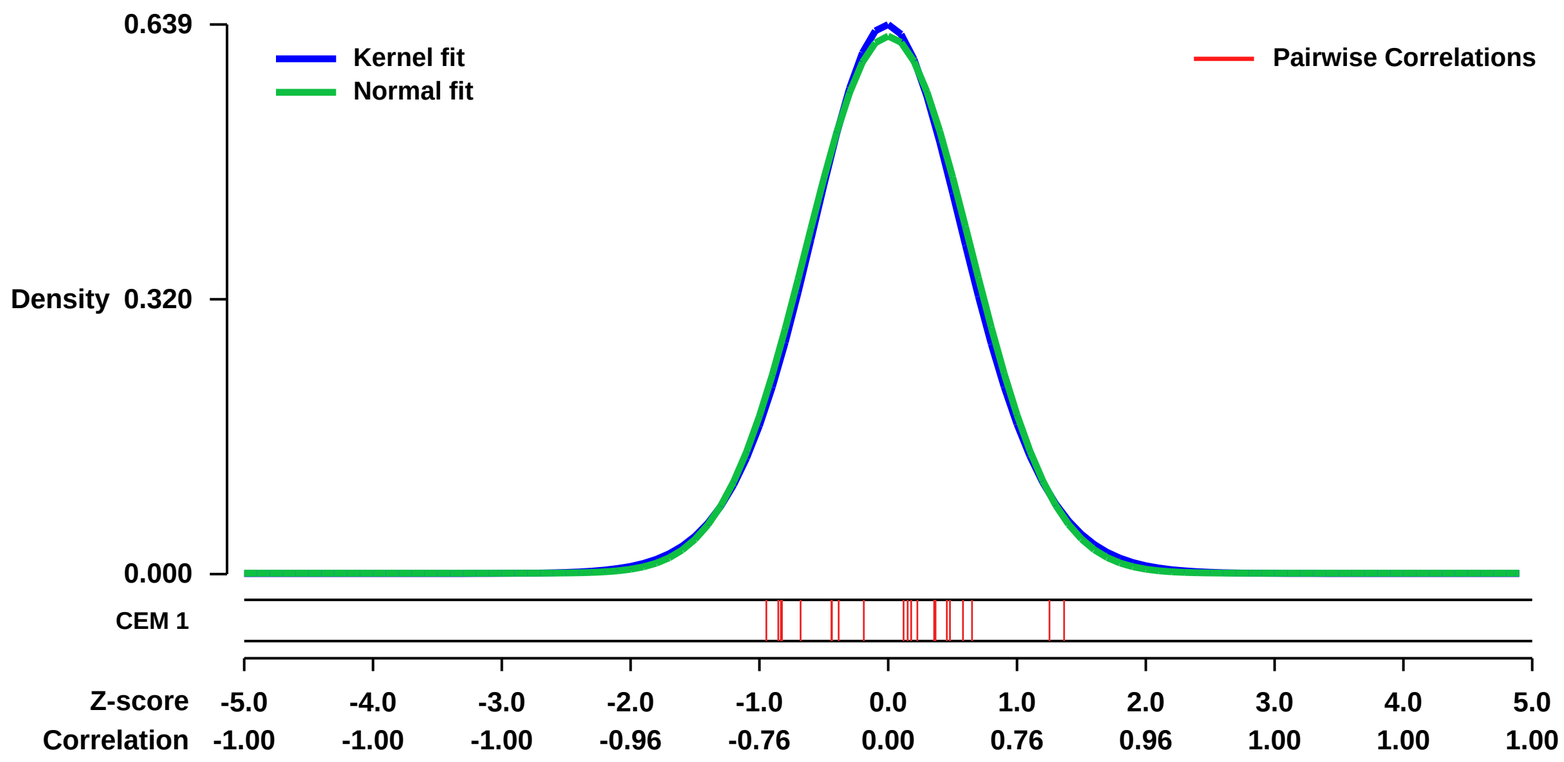

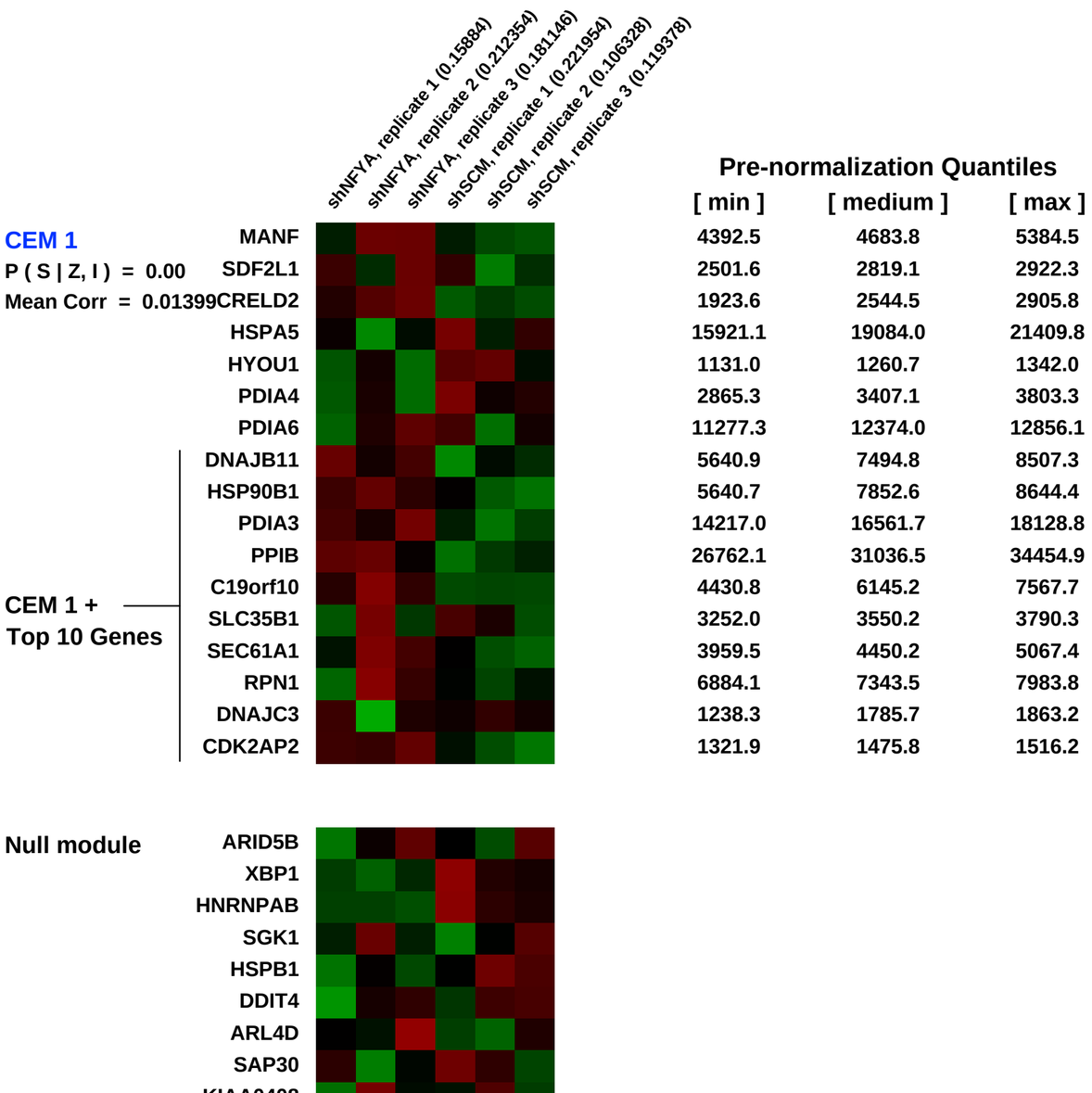

	Pre-normalization Quantiles		
	[min]	[medium]	[max]
MANF	4392.5	4683.8	5384.5
SDF2L1	2501.6	2819.1	2922.3
CRELD2	1923.6	2544.5	2905.8
HSPA5	15921.1	19084.0	21409.8
HYOU1	1131.0	1260.7	1342.0
PDIA4	2865.3	3407.1	3803.3
PDIA6	11277.3	12374.0	12856.1
DNAJB11	5640.9	7494.8	8507.3
HSP90B1	5640.7	7852.6	8644.4
PDIA3	14217.0	16561.7	18128.8
PPIB	26762.1	31036.5	34454.9
C19orf10	4430.8	6145.2	7567.7
SLC35B1	3252.0	3550.2	3790.3
SEC61A1	3959.5	4450.2	5067.4
RPN1	6884.1	7343.5	7983.8
DNAJC3	1238.3	1785.7	1863.2
CDK2AP2	1321.9	1475.8	1516.2
ARID5B			
XBP1			
HNRNPAB			
SGK1			
HSPB1			
DDIT4			
ARL4D			
SAP30			
KIAA0408			
GPR17			
HSPH1			
DNASE1L2			
SLC5A3			
GNAS			
GPR3			
TNFRSF25			
TM6SF2			
MKKS			
PLEKHF1			
ZMYM1			
DOK3			
FGF20			
SLC39A2			
KCNIP2			
ERRFI1			
DEDD2			
CCDC117			
USP31			
AHSA2			
CYS1			
CNIH2			
BANP			
CHORDC1			
P4HA1			

GEO Series "GSE29316" Expression Profiles

Num of samples in this series: 6

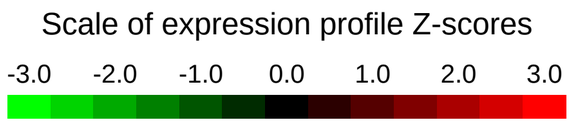

GEO Link:	http://www.ncbi.nlm.nih.gov/geo/query/acc.cgi?acc=GSE29316
Status:	Public on May 17 2011
Title:	Expression data from colon fibroblasts treated with Sonic hedgehog homolog (SHH)
Organism:	Homo sapiens
Experiment type:	Expression profiling by array
Platform:	GPL570
Pubmed ID:	21597001
Summary & Design:	**Summary:** Canonical Hedgehog (Hh) signaling regulates the expression of genes that are critical to the patterning and development of a variety of organ systems. In adult, both ligand-dependent and ligand-independent Hh pathway activation are known to promote tumorigenesis. Recent studies have shown that in tumors promoted by Hh ligand, activation occurs within the stromal microenvironment (Yauch et al., 2009). In situ hybridization of the pathway target gene, Ptch1, shows that signaling is located at stromal perivascular fibroblast-like cells in xenograft tumor sections derived from Hh-expressing colorectal cancer cell lines. To study the downstream genes regulated by Hh signaling, we treated a primary human colon myofibroblast, CCD-18Co, with SHH (1 ug/ml) or no treatment (control) in serum-free medium supplemented with 0.1% BSA for 72 hrs and performed microarray analysis (Affymetrix U133P) on these samples. **Overall design:** Three biological replicates of SHH stimulated and three replicates of unstimulated primary colon myofibroblast cells CCD-18Co were used in the experiment to analyze their gene expression.

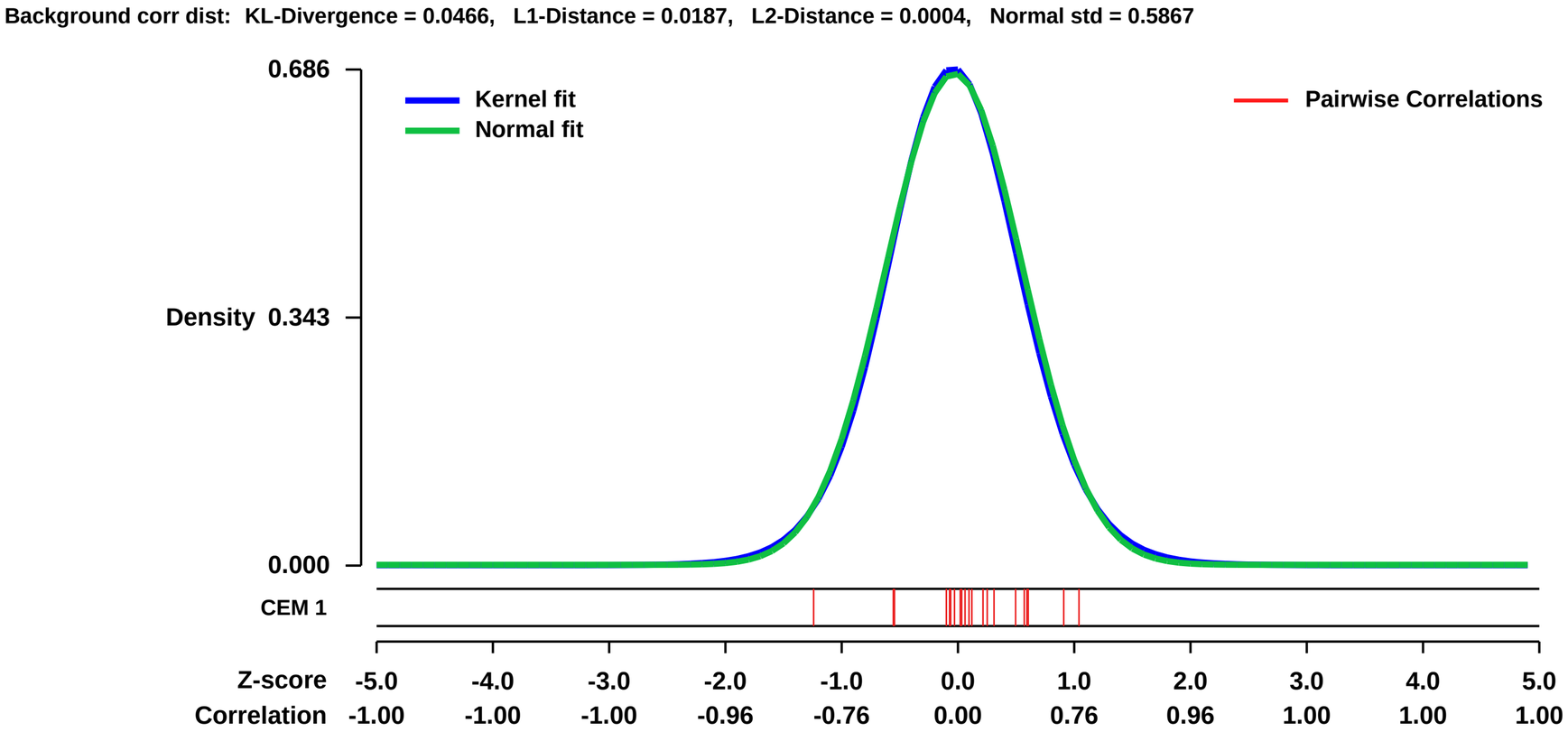

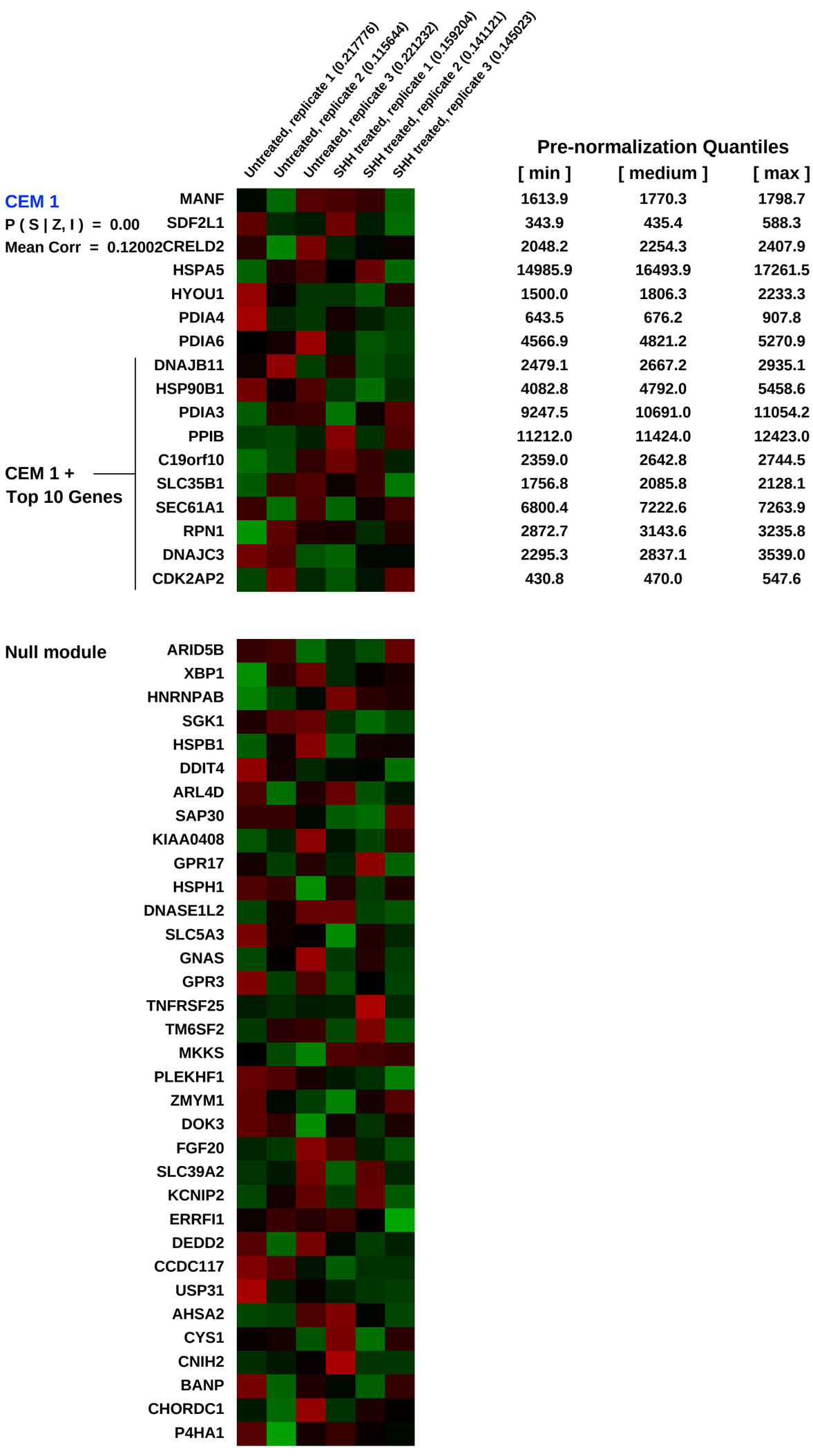

GEO Series "GSE45636" Expression Profiles

Num of samples in this series: 6

Scale of expression profile Z-scores

-3.0 -2.0 -1.0 0.0 1.0 2.0 3.0

GEO Link:	http://www.ncbi.nlm.nih.gov/geo/query/acc.cgi?acc=GSE45636
Status:	Public on Aug 12 2014
Title:	eIF3a in Urinary Bladder Cancer â in vivo and in vitro insights
Organism:	Homo sapiens
Experiment type:	Expression profiling by array
Platform:	GPL570
Pubmed ID:	25070653
Summary & Design:	**Summary:** The eukaryotic translation initiation factor (eIF) 3a is described in various tumor entities as potential tumor marker involved in development and progression of cancer. eIF3a is the largest subunit of the eIF3 complex, a key functional entity in 80S establishment and translation initiation. We hypothesize that eIF3a is more a specific than global translation initiator and involved in signalling pathways that are frequently targeted in UBC therapy. Methods: In FFPE samples of UBC patients eIF3a expression was analysed together with overall survival. In cell culture we investigated proliferation, migration, clonogenicity and tumorgenicity of UBC cell lines with and without knockdown of eIF3a and compared the cytotoxicity of eIF3a knockdown with other translational inhibitors, including the chemotherapeutic Rapamycine. Detailed information on changed gene expression and global translation initiation were gathered by mRNA expresssion and polysomal profiling. Results: and Conclusion eIF3a is upregulated in UBC and high expression of eIF3a corresponds with longer overall survival in low grade tumors. Knockdown of eIF3a in UBC cell lines reduces their malignant phenotype, including reduced tumor growth in xenotransplanted mice. eIF3a regulates DNA damage response (ATM, ATR, CDC25A) on a translational level and we show that reduction in eIF3a expression does not hamper global translation initiation. Overall design: Differential expression of genes between eIF3a knock-down and control samples was assessed with the moderated t-test (Bioconductor's limma package). Raw p-values were adjusted for multiple hypothesis testing using the method from Benjamini and Hochberg for a strong control of the false discovery rate.

Background corr dist: KL-Divergence = 0.0270, L1-Distance = 0.0229, L2-Distance = 0.0005, Normal std = 0.7005

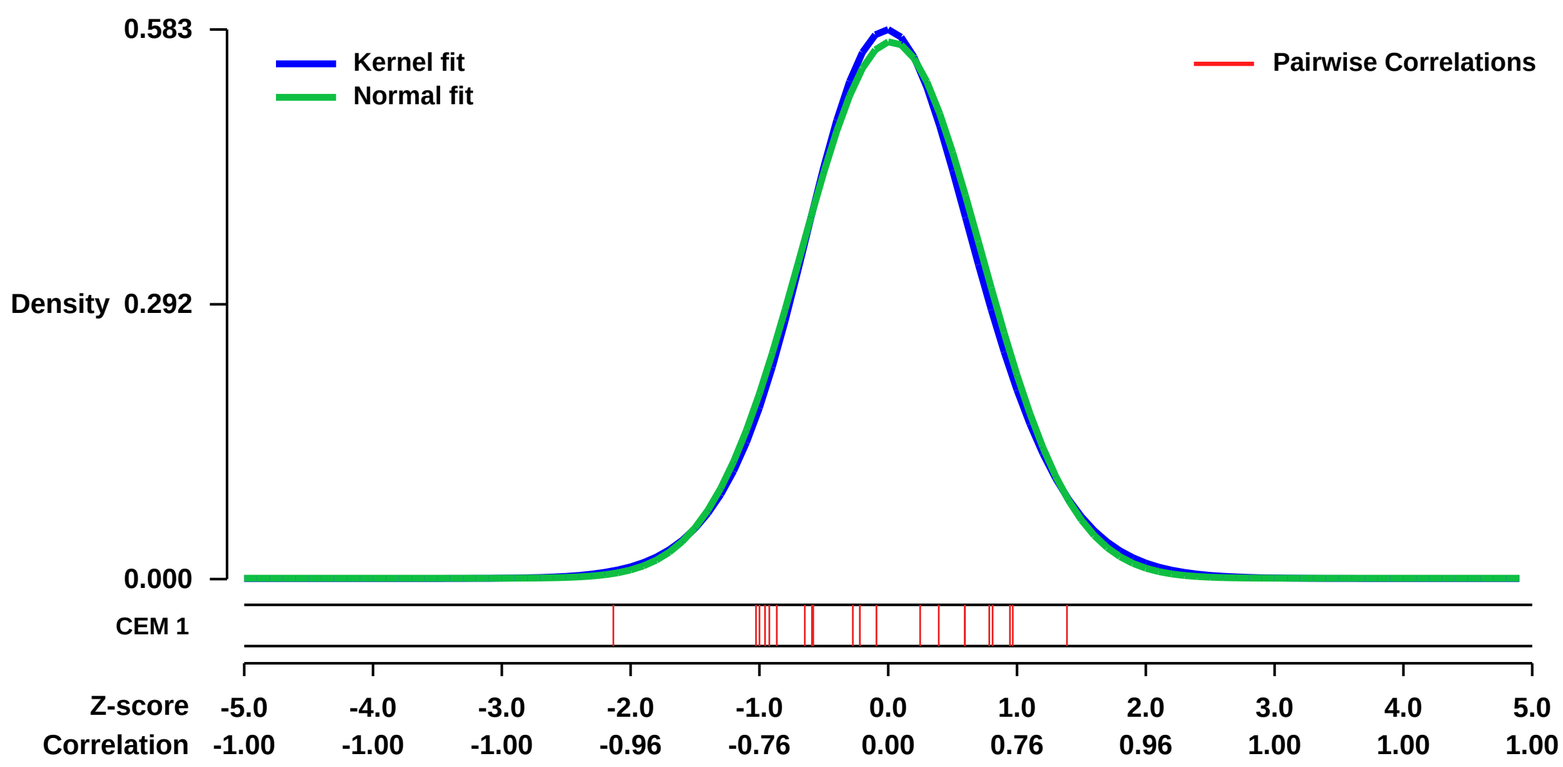

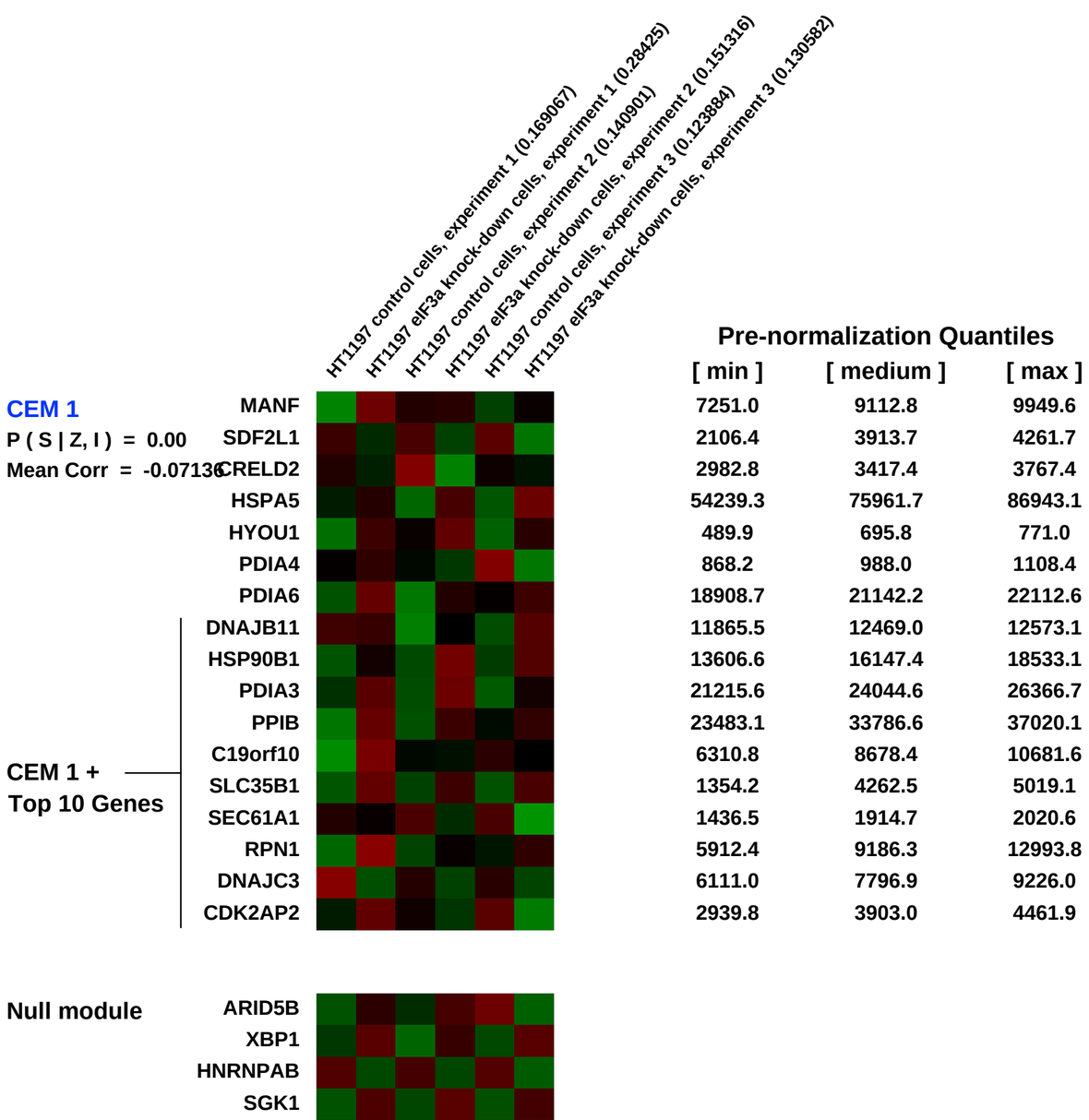

GEO Series "GSE16355" Expression Profiles

Num of samples in this series: 6

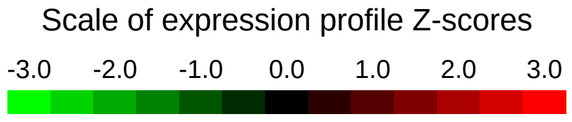

GEO Link:	http://www.ncbi.nlm.nih.gov/geo/query/acc.cgi?acc=GSE16355
Status:	Public on Sep 30 2009
Title:	Lymphatic endothelial cells (LEC) transfected with the KSHV microRNA cluster
Organism:	Homo sapiens
Experiment type:	Expression profiling by array
Platform:	GPL570
Pubmed ID:	20080955
Summary & Design:	**Summary:** Kaposi sarcoma is the most common cancer in AIDS patients and is typified by red skin lesions. The disease is caused by the KSHV virus (HHV8) and is recognisable by its distinctive red skin lesions. The lesions are KSHV-infected spindle cells, most commonly the lymphatic endothelial and blood vessel endothelial cells (LEC and BEC), plus surrounding stroma. The KSHV virus expresses multiple microRNA in a single cluster. Here we test the effects of this KSHV microRNA cluster in LEC cells using Affymetrix hgu133plus2 chips. **Overall design:** There are n=3 of: 1. LEC control with empty vector pSIN-MCS (LEC), 2. LEC transfected with the same vector containing the KSHV microRNA cluster.

Background corr dist: KL-Divergence = 0.0418, L1-Distance = 0.0160, L2-Distance = 0.0002, Normal std = 0.6022

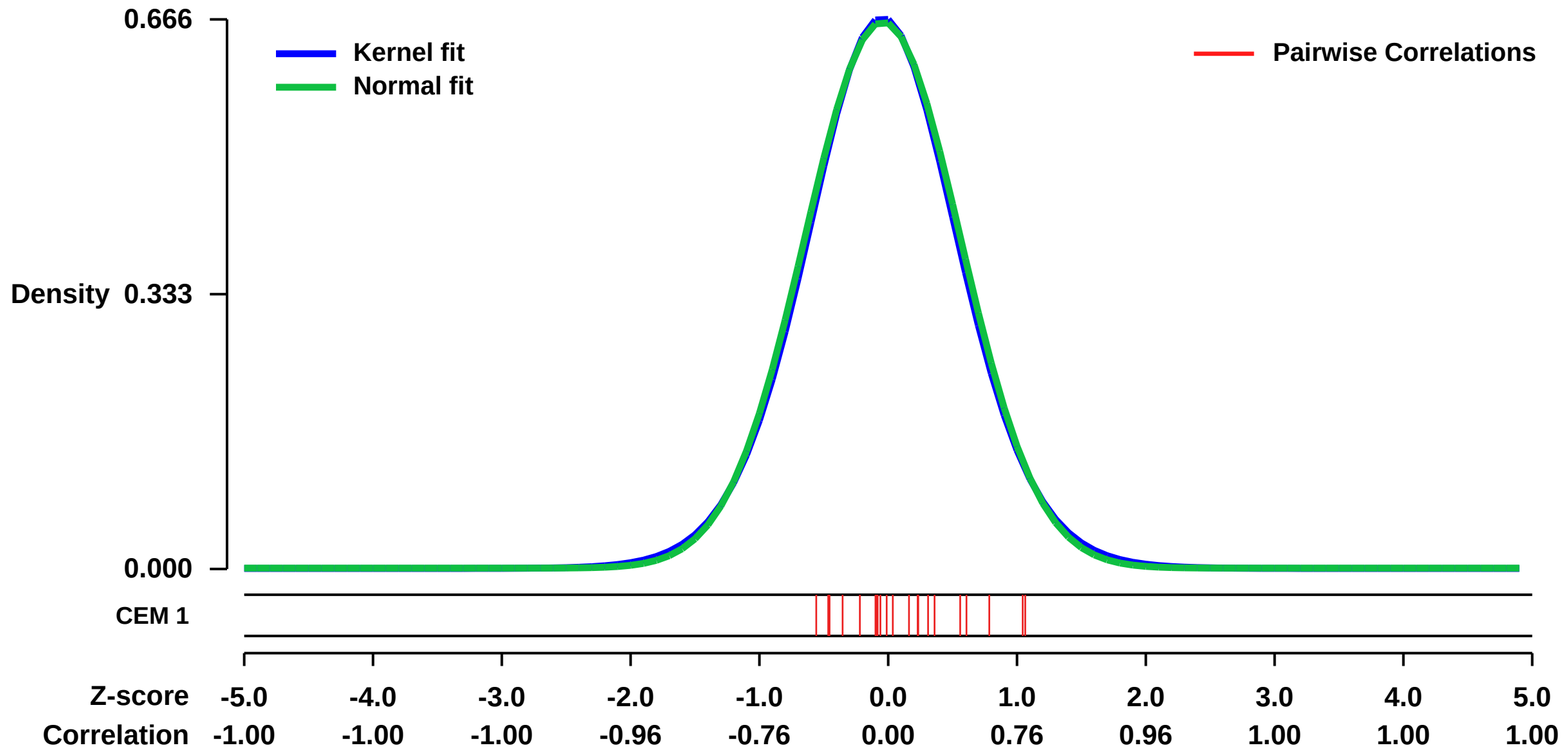

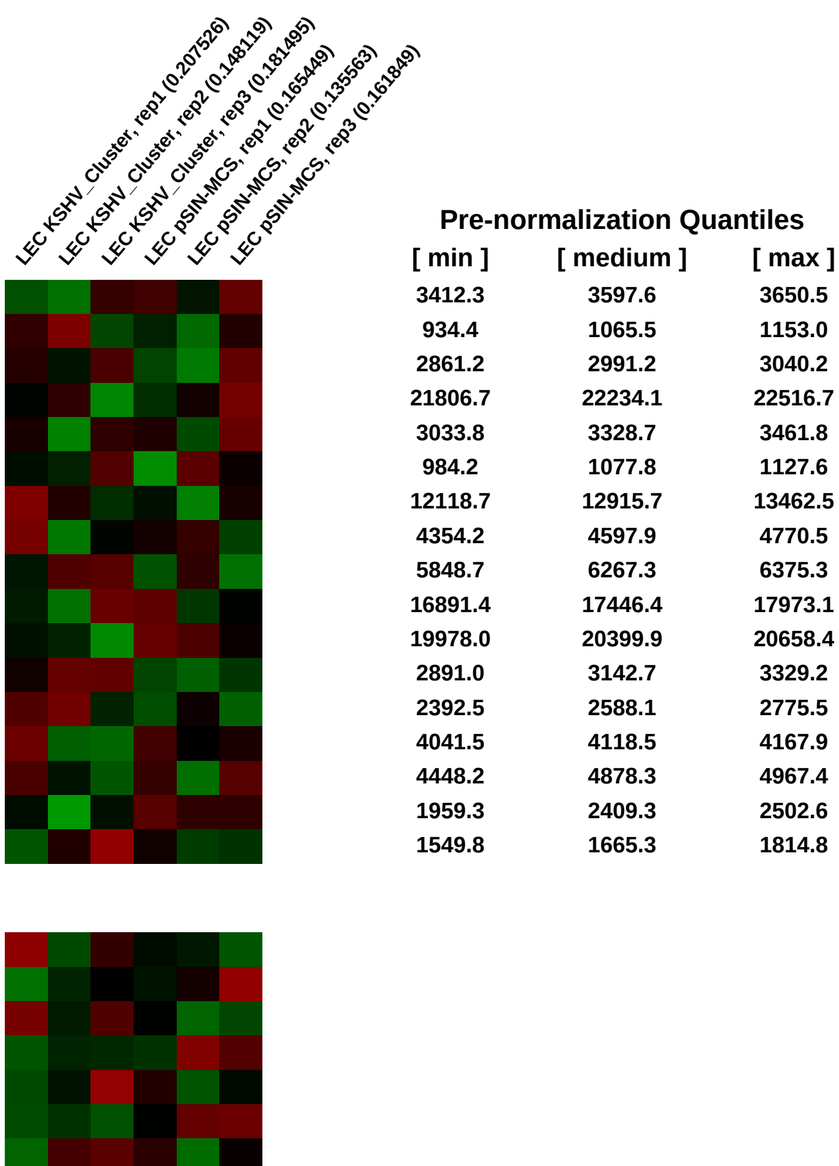

GEO Series "GSE12485" Expression Profiles

Num of samples in this series: 10

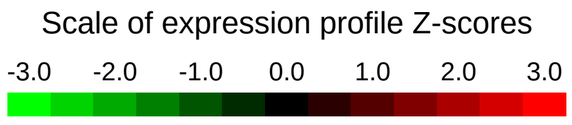

GEO Link:	http://www.ncbi.nlm.nih.gov/geo/query/acc.cgi?acc=GSE12485
Status:	Public on Jun 22 2010
Title:	Changes in cardiac transcription profiles following off-pump coronary revascularization surgery
Organism:	Homo sapiens
Experiment type:	Expression profiling by array
Platform:	GPL570
Pubmed ID:	20332183
Summary & Design:	**Summary:** To investigate changes in cardiac transcription profiles caused by off-pump cardiac surgery, we collected myocardial samples, prior and after grafting, from patients undergoing off-pump coronary revascularization surgery. The transcriptional profile of the mRNA in these samples was measured with gene array technology. Changes in transcriptional profiles can be correlated with the stress response of heart to off-pump surgery. **Keywords:** human, cardiac, OPCAB coronary surgery, gene expression. **Overall design:** Myocardial samples were collected, prior and after grafting, from patients undergoing off-pump coronary artery bypass grafting.

Background corr dist: KL-Divergence = 0.0799, L1-Distance = 0.0285, L2-Distance = 0.0014, Normal std = 0.4728

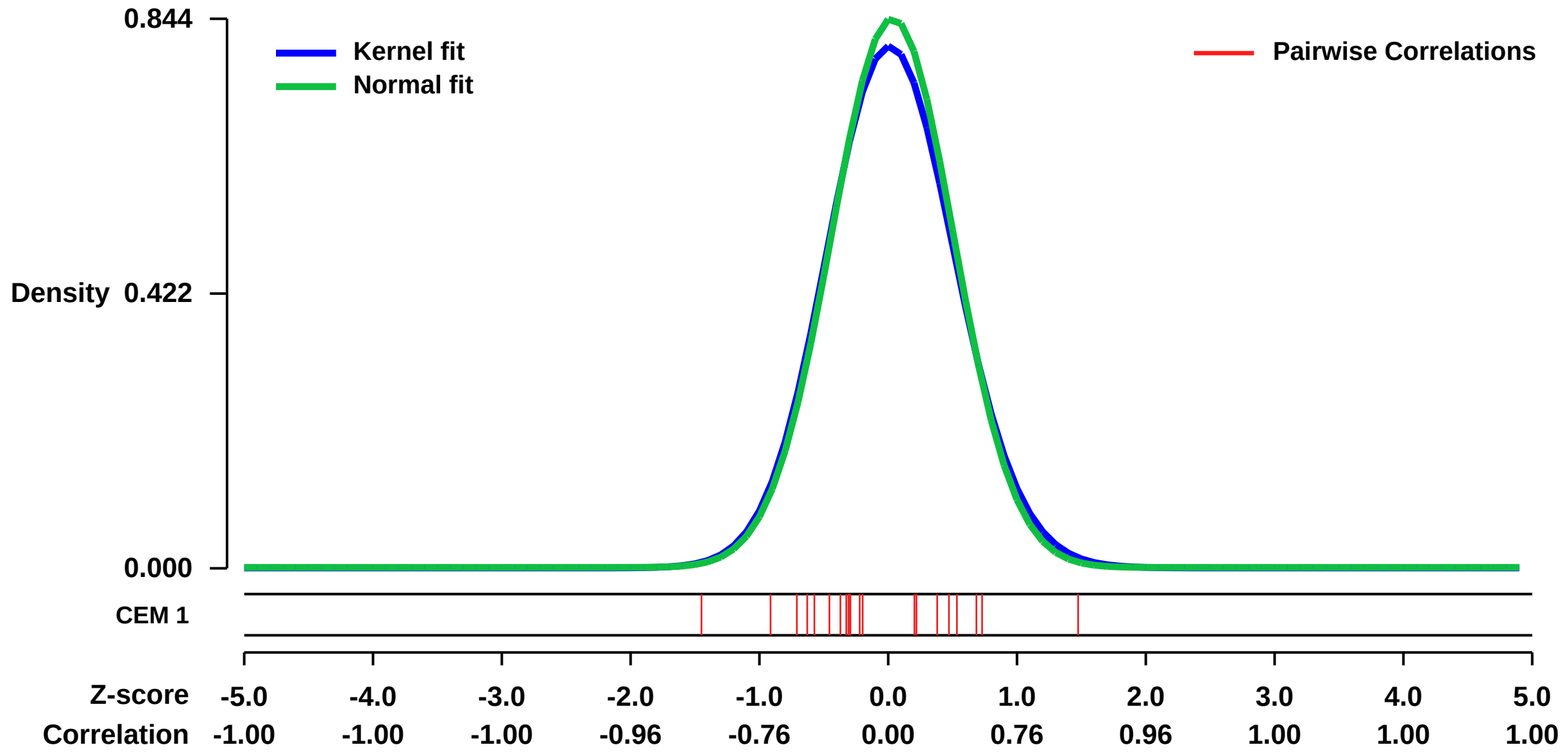

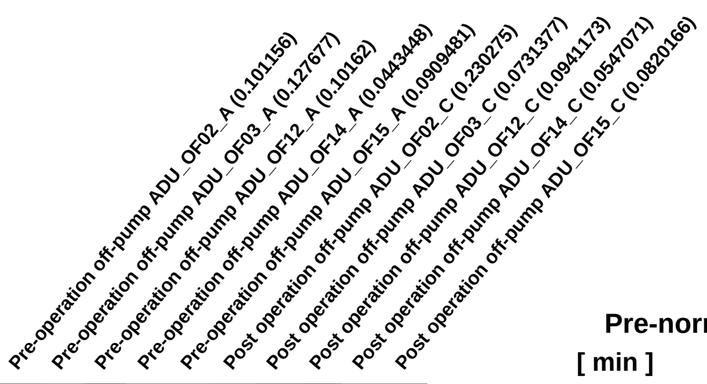

CEM 1
P (S | Z, I) = 0.00
Mean Corr = -0.08906

CEM 1 + Top 10 Genes

Null module

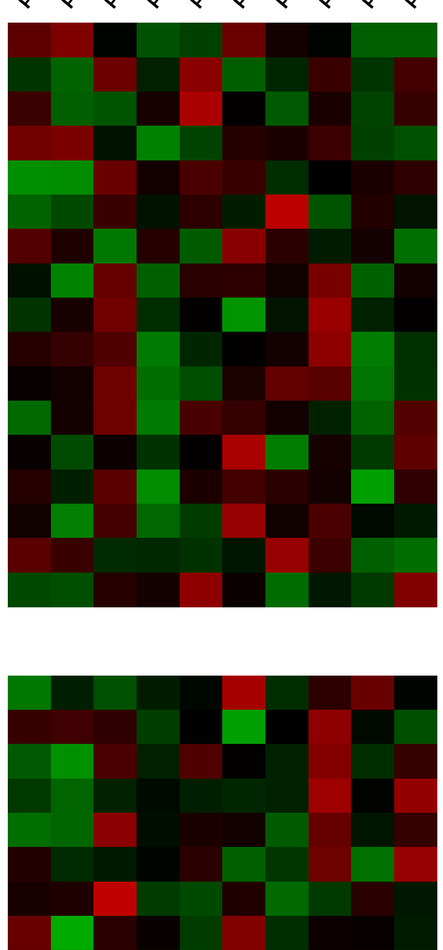

	Pre-normalization Quantiles [min]	[medium]	[max]
MANF	1446.1	1838.1	2403.9
SDF2L1	484.9	561.8	760.7
CRELD2	1175.1	1326.6	1514.2
HSPA5	8377.2	11726.0	13730.3
HYOU1	978.8	1961.0	2410.1
PDIA4	218.5	265.8	386.7
PDIA6	6168.6	7831.5	8996.2
DNAJB11	984.4	1161.5	1280.1
HSP90B1	596.4	1213.6	1834.7
PDIA3	2790.0	4273.9	5541.9
PPIB	1433.1	3042.7	4138.4
C19orf10	857.1	1116.0	1280.7
SLC35B1	2547.6	2952.1	3462.7
SEC61A1	1002.8	1229.6	1290.2
RPN1	734.4	1210.3	1660.7
DNAJC3	1421.3	1805.5	2558.1
CDK2AP2	592.9	1021.9	1507.3
ARID5B			
XBP1			
HNRNPAB			
SGK1			
HSPB1			
DDIT4			
ARL4D			
SAP30			
KIAA0408			
GPR17			
HSPH1			
DNASE1L2			
SLC5A3			
GNAS			
GPR3			
TNFRSF25			
TM6SF2			
MKKS			
PLEKHF1			
ZMYM1			
DOK3			
FGF20			
SLC39A2			
KCNIP2			
ERRFI1			
DEDD2			
CCDC117			
USP31			
AHSA2			
CYS1			
CNIH2			
BANP			
CHORDC1			
P4HA1			

GEO Series "GSE21270" Expression Profiles

Num of samples in this series: 18

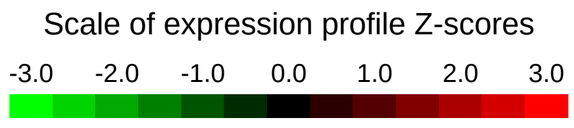

GEO Link: http://www.ncbi.nlm.nih.gov/geo/query/acc.cgi?acc=GSE21270

Status: Public on Jul 01 2013

Title: Genome-wide screening of temporal responsive genes induced by a low concentration of the carcinogen N-methyl-N'-nitro-N-nitrosoguanidine in a normal human cell line

Organism: Homo sapiens

Experiment type: Expression profiling by array

Platform: GPL570

Pubmed ID:

Summary & Design:

Summary:
The alkylating agent N-methyl-N'-nitro-N-nitrosoguanidine (MNNG) is a direct mutagen and carcinogen, causing DNA damage and other comprehensive alterations that lead to chromosomal aberrations, mutations, tumor initiation, and cell death. Our previous study revealed that MNNG at different concentrations could induce extensive changes in gene expression at an early stage of exposure. To further understand the dynamic cellular responses and hazardous effects caused by this environmental carcinogen, we used a whole-genome time-course screening methods to find out the gene expression changes induced by a low concentration of MNNG in human normal amnion epithelial FL cells. The cells were exposed to 1.0 ´µM MNNG, and differential gene expression profiles at 3, 12, and 24 h after MNNG treatment were obtained by use of Affymetrix HG-U133 Plus 2.0 oligonucleotide microarray technology, followed by quantitative real-time RT-PCR validation. The results showed that the low-dose MNNG exposure triggered extensive but moderate changes in gene expression at these three experiment time points after exposure. The responsive genes encode important proteins, including cell cycle regulators, transcription factors and signal transducers that determine cell cycle progression, cell fate and other activities associate with pro-oncogenic potentials. The differential gene expression profiles at the three time points varied greatly, and generally reflected a cellular responsive process from initiation to progression and to recovery after MNNG exposure. These results will aid our understanding of the complicated mechanisms of MNNG-induced cellular responses.

Keywords: N-methyl-N'-nitro-N-nitrosoguanidine; Cellular response; Temporal gene expression change; Oligonucleotide microarray; Quantitative real-time RT-PCR

Overall design:
Human amnion epithelial FL cells were exposed to vehicle control (dimethyl sulfoxide) and a low concentration (1.0 ´µM) MNNG for 2 h, respectively. The differential gene expression profiles at 3, 12 and 24 h post MNNG treatment were obtained using Affymetrix HG-U133 Plus 2.0 oligonucleotide microarrays. The transcriptomic changes at different time points post MNNG treatment would provide insight into the dynamic processes of cellular response to this genotoxic agent.

Background corr dist: KL-Divergence = 0.0810, L1-Distance = 0.0653, L2-Distance = 0.0097, Normal std = 0.4841

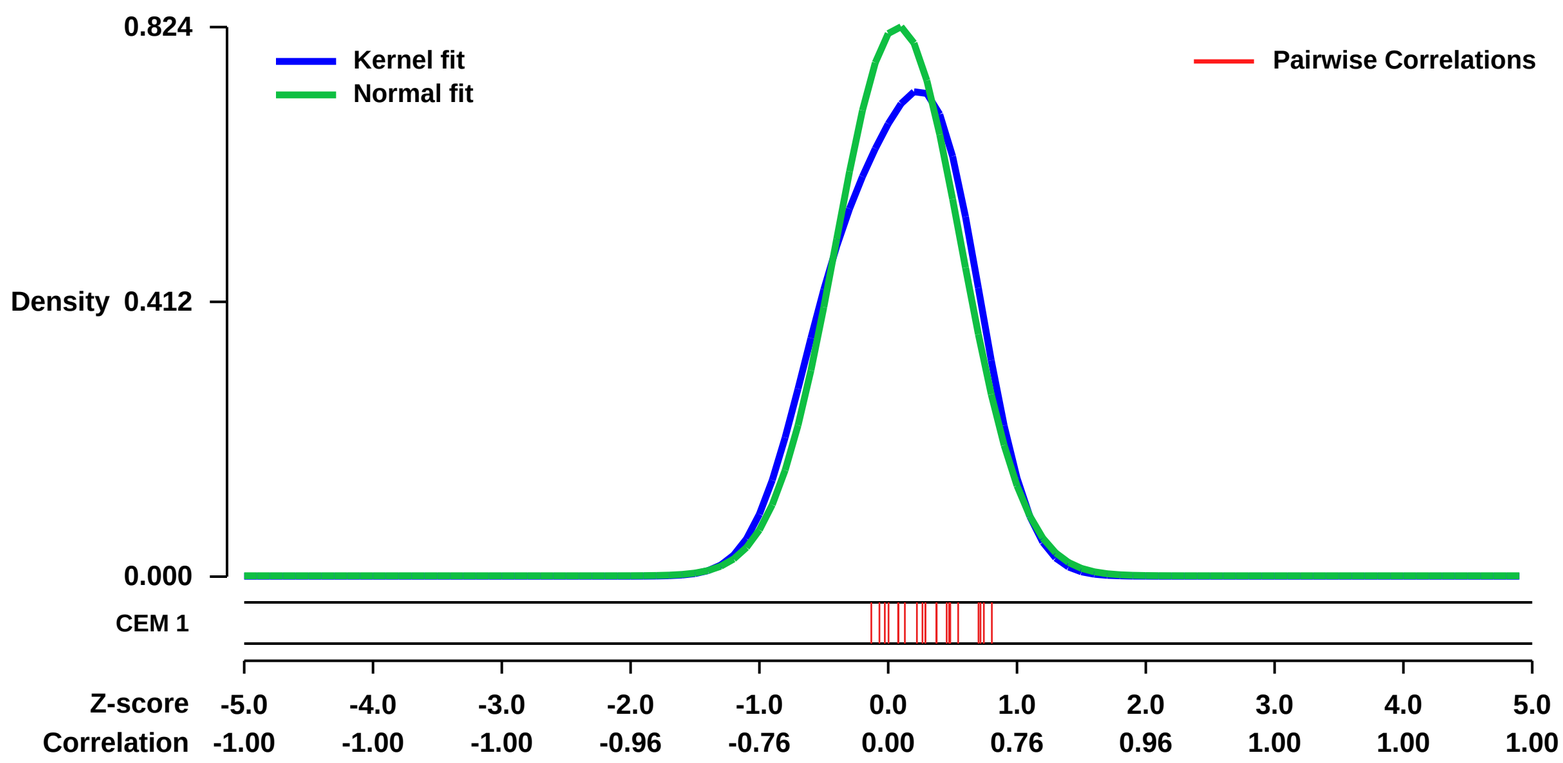

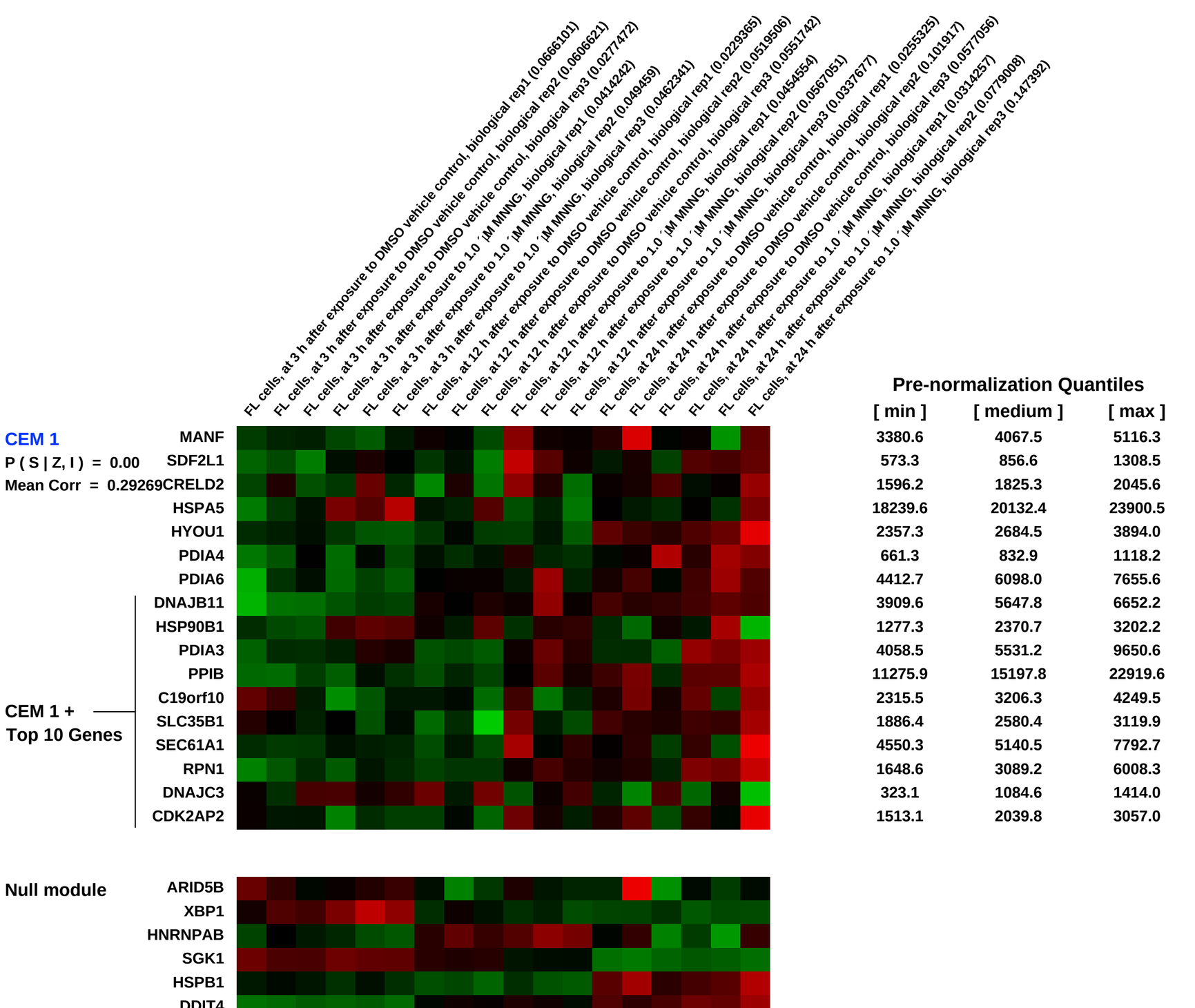

GEO Series "GSE55624" Expression Profiles

Num of samples in this series: 18

Scale of expression profile Z-scores

-3.0 -2.0 -1.0 0.0 1.0 2.0 3.0

GEO Link:	http://www.ncbi.nlm.nih.gov/geo/query/acc.cgi?acc=GSE55624
Status:	Public on Mar 06 2014
Title:	Inhibiting tankyrases sensitizes KRAS mutant cancer cells to MEK inhibitors by FGFR2 feedback signaling
Organism:	Homo sapiens
Experiment type:	Expression profiling by array
Platform:	GPL570
Pubmed ID:	24747911
Summary & Design:	**Summary:** Tankyrases (TNKS) play roles in Wnt signaling, telomere homeostasis and mitosis, offering attractive targets for anti-cancer treatment. Using unbiased combination screening in a large panel of cancer cell lines, we have identified a strong synergy between TNKS and MEK inhibitors in KRAS mutant cancer cells. Our study uncovers a novel function of TNKS in the relief of a feedback loop induced by MEK inhibition on FGFR2 signaling pathway. Moreover, dual inhibition of TNKS and MEK leads to more robust apoptosis and anti-tumor activity both in vitro and in vivo than effects observed by previously reported MEK inhibitor combinations. Altogether, our results show how a novel combination of TNKS and MEK inhibitors can be highly effective in targeting KRAS mutant cancers by suppressing a newly discovered resistance mechanism. This experiment is designed to detect genes differentially expressed in the combination treatment compared to others **Overall design:** SW480 cells were seeded in 10cm dishes and treated for 4h and 16h with DMSO, TNKS inhibitor (TNKSi : NVP-TNKS656), MEK inhibitor (MEKi : AZD6244) or the combination of both at 1uM final

Background corr dist: KL-Divergence = 0.1740, L1-Distance = 0.0301, L2-Distance = 0.0017, Normal std = 0.3550

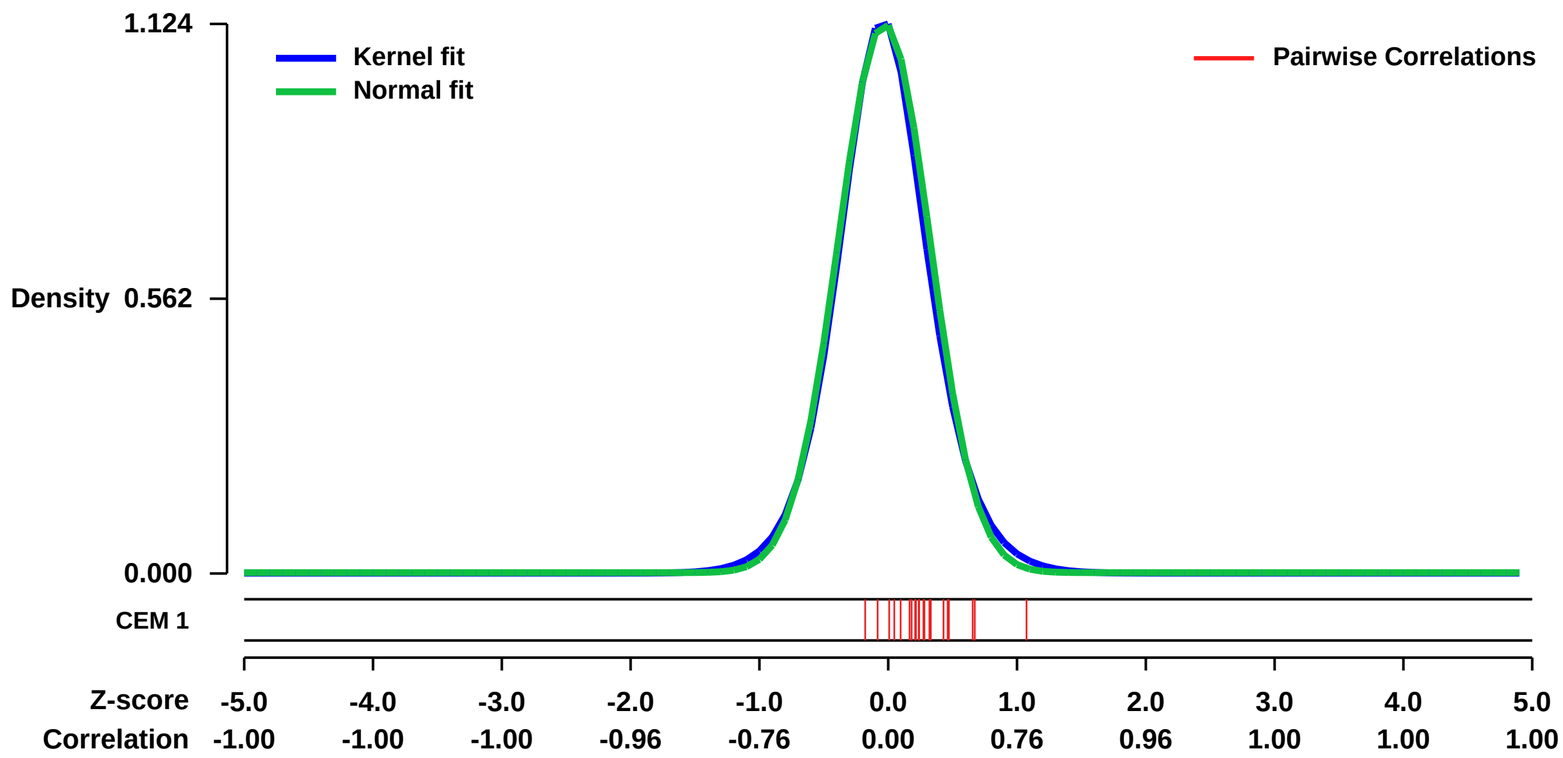

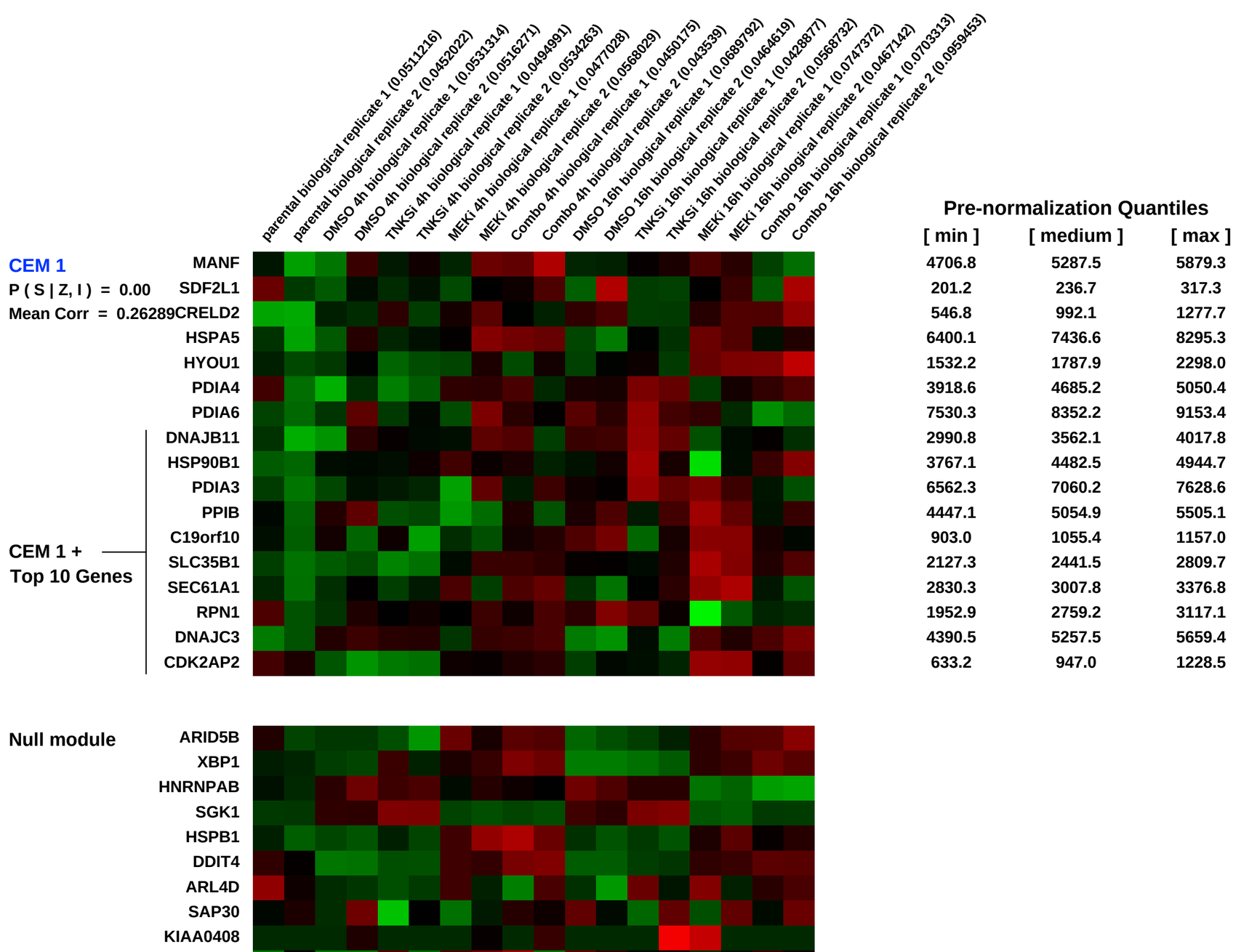

Pre-normalization Quantiles

	[min]	[medium]	[max]
MANF	4706.8	5287.5	5879.3
SDF2L1	201.2	236.7	317.3
CRELD2	546.8	992.1	1277.7
HSPA5	6400.1	7436.6	8295.3
HYOU1	1532.2	1787.9	2298.0
PDIA4	3918.6	4685.2	5050.4
PDIA6	7530.3	8352.2	9153.4
DNAJB11	2990.8	3562.1	4017.8
HSP90B1	3767.1	4482.5	4944.7
PDIA3	6562.3	7060.2	7628.6
PPIB	4447.1	5054.9	5505.1
C19orf10	903.0	1055.4	1157.0
SLC35B1	2127.3	2441.5	2809.7
SEC61A1	2830.3	3007.8	3376.8
RPN1	1952.9	2759.2	3117.1
DNAJC3	4390.5	5257.5	5659.4
CDK2AP2	633.2	947.0	1228.5

GEO Series "GSE11324" Expression Profiles

Num of samples in this series: 12

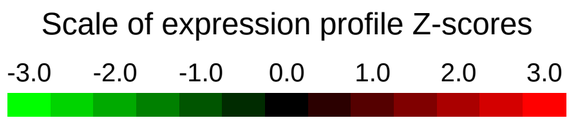

GEO Link:	http://www.ncbi.nlm.nih.gov/geo/query/acc.cgi?acc=GSE11324
Status:	Public on May 02 2008
Title:	Genome-wide analysis of estrogen receptor binding sites
Organism:	Homo sapiens
Experiment type:	Expression profiling by array
Platform:	GPL570
Pubmed ID:	17013392
Summary & Design:	**Summary:** The estrogen receptor is the master transcriptional regulator of breast cancer phenotype and the archetype of a molecular therapeutic target. We mapped all estrogen receptor and RNA polymerase II binding sites on a genome-wide scale, identifying the authentic cis binding sites and target genes, in breast cancer cells. Combining this unique resource with gene expression data demonstrates distinct temporal mechanisms of estrogen-mediated gene regulation,particularly in the case of estrogen-suppressed genes. Furthermore, this resource has allowed the identification of cis-regulatory sites in previously unexplored regions of the genome and the cooperating transcription factors underlying estrogen signaling in breast cancer. **Keywords:** estrogen effect, time course **Overall design:** This Series currently contains the gene expression data accompaning Carroll JS et al. Nature Genetics 38,1289-1297(2006). MCF7 cells were stimulated with 100 nM estrogen for 0, 3, 6, or 12h. All experiments were performed in triplicate.

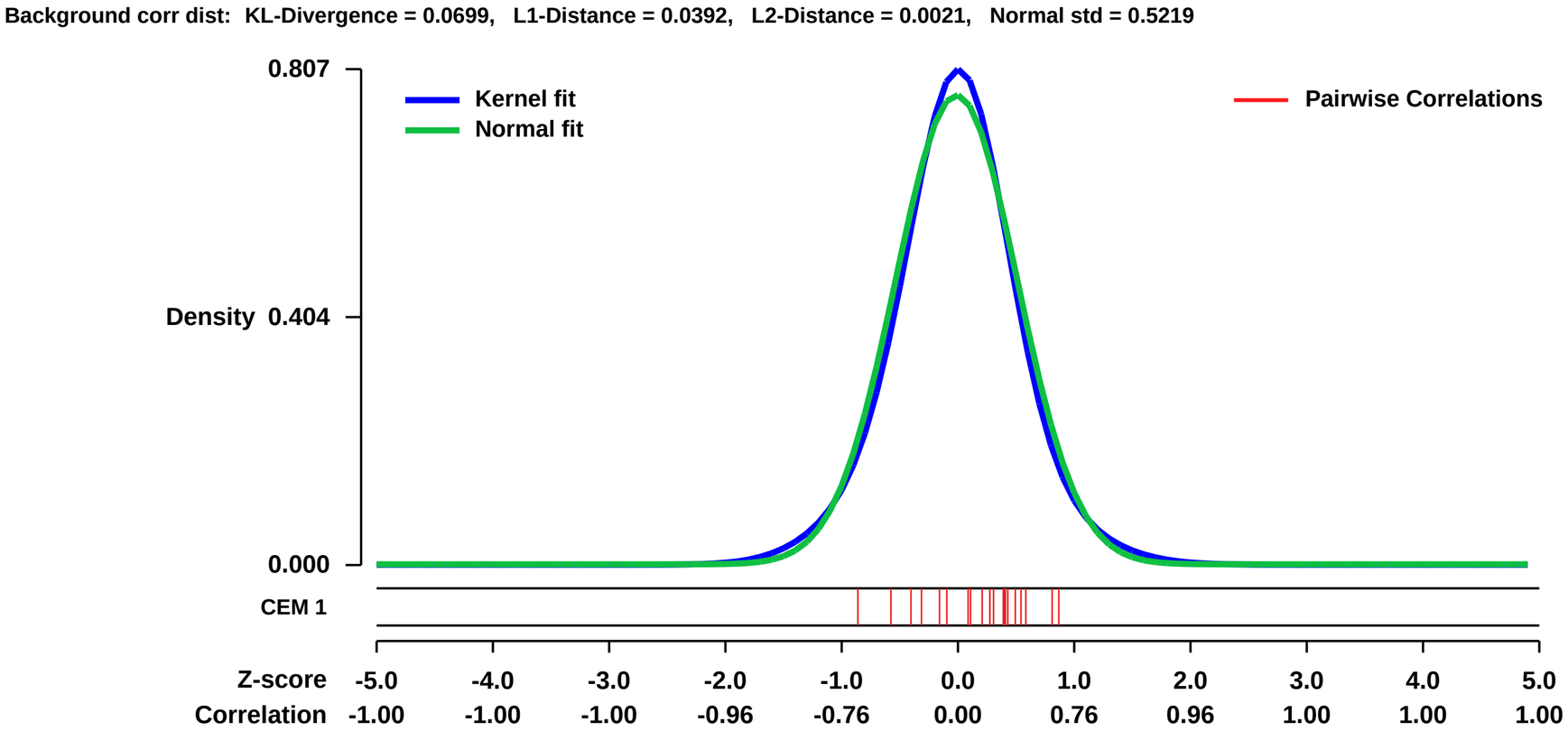

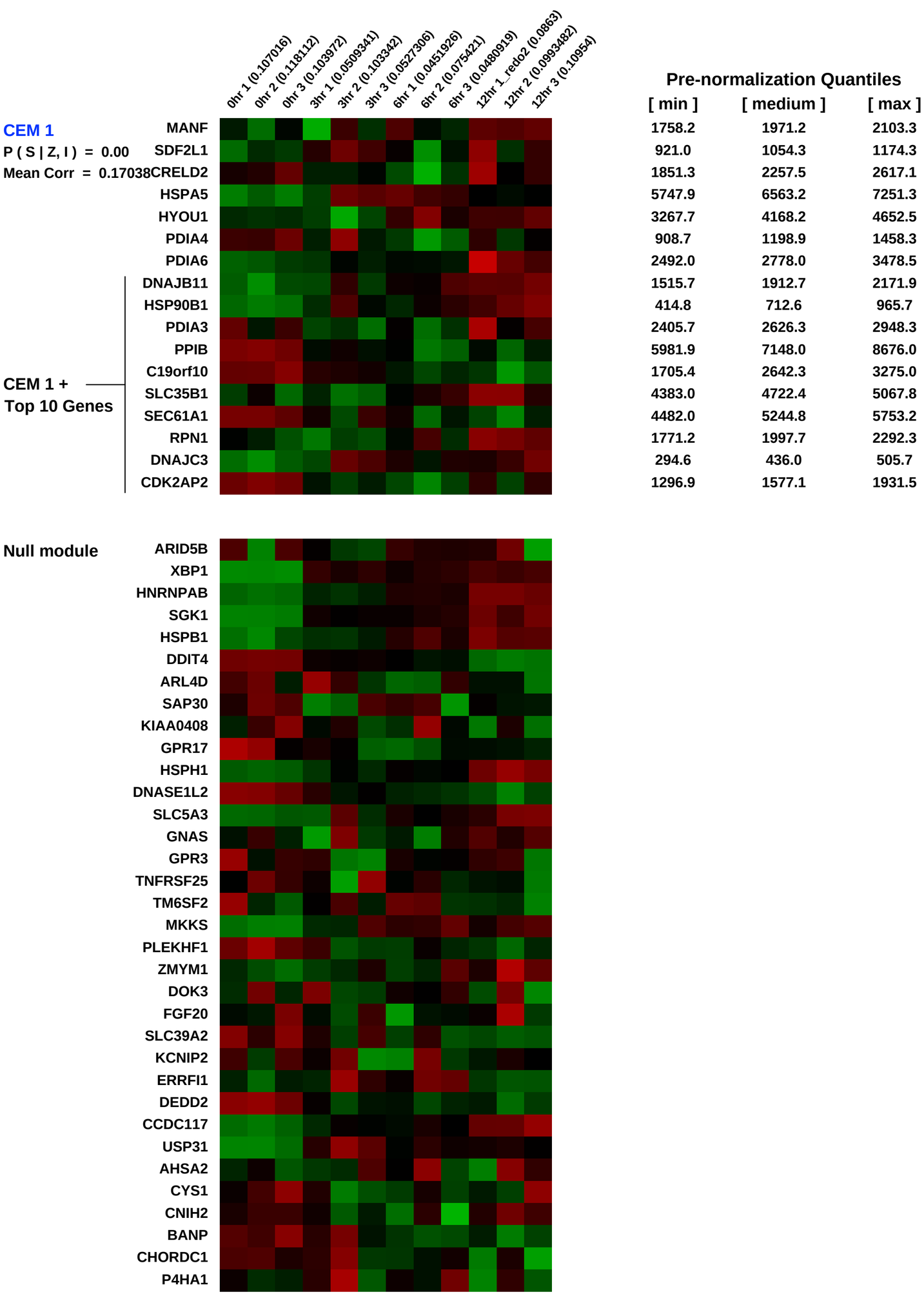

GEO Series "GSE13806" Expression Profiles

Num of samples in this series: 17

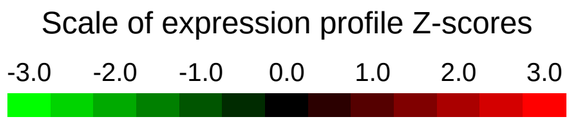

GEO Link:	http://www.ncbi.nlm.nih.gov/geo/query/acc.cgi?acc=GSE13806
Status:	Public on May 01 2009
Title:	Effect of ectopic expression of sFRP1 on MDA-MB-231 human breast cancer cells in vitro and in vivo as xenograft
Organism:	Homo sapiens
Experiment type:	Expression profiling by array
Platform:	GPL570
Pubmed ID:	
Summary & Design:	**Summary:** RNA was isolated from ectopically sFRP1-expressing MDA-MB-231 cells and control MDA-MB-231 cells and as well from tumor lysates arising from these cells as nude mouse xenograft. Gene expression profiles for these samples were investigated using Affymetrix arrays. **Overall design:** MDA-MB-231 human breast cancer cells were stably transfected with human sFRP1 encoding vector or empty vector as control. After the selection with antibiotics, three clones of MDA-MB-231/sFRP1 and three clones of MDA-MB-231/control were selected. These six clones were cultured individually in DMEM 10% FCS with 1mg/ml G-418. When cells reached 70-80% confluence, RNA was isolated from the cells. In parallel, the three clones of MDA-MB-231/sFRP1 and the three clones of MDA-MB-231/control were pooled respectively. One million of cells from each pool were suspended in 100ul PBS and injected to fat pads of female balb/c nude mice (6 mice were injected with MDA-MB-231/sFRP1 and 5 mice were injected with MDA-MB-231/control) to do a xenograft experiment. A few - several weeks after, mice were sacrificed when tumor reached a certain size, tumors were taken and RNA was isolated using trizol reagent.

Background corr dist: KL-Divergence = 0.0927, L1-Distance = 0.0427, L2-Distance = 0.0035, Normal std = 0.4689

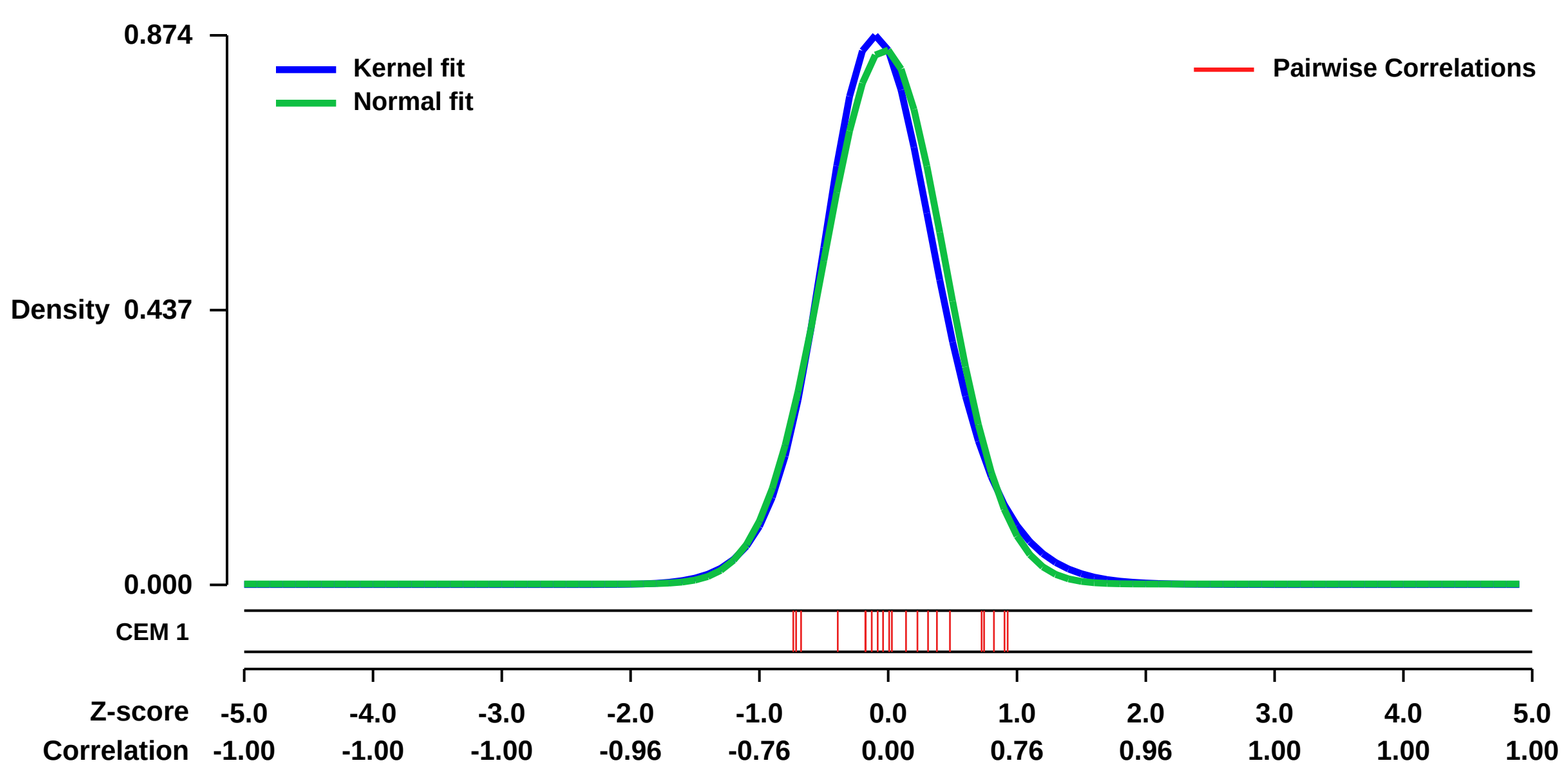

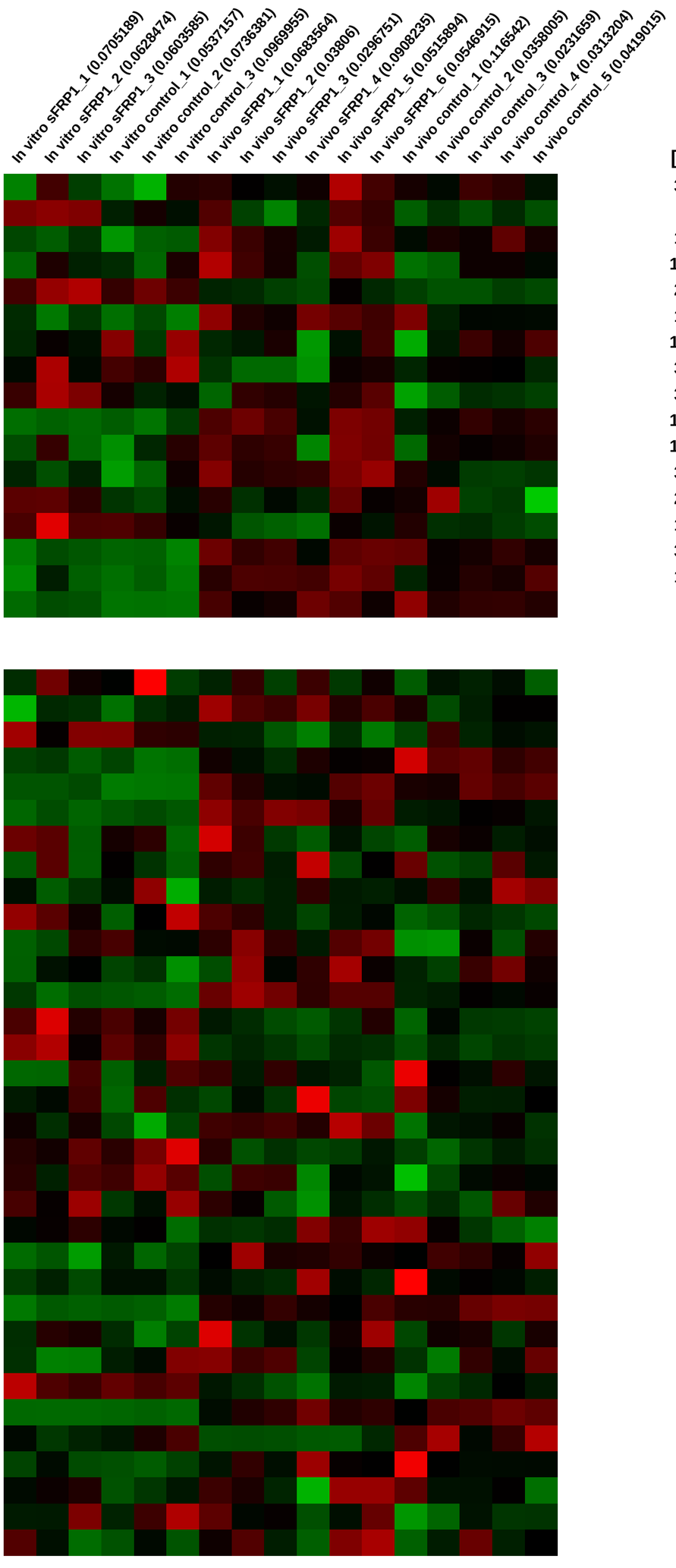

	Pre-normalization Quantiles		
	[min]	[medium]	[max]
MANF	3486.9	5805.2	7745.0
SDF2L1	463.2	844.6	1490.9
CRELD2	1716.9	2707.8	3597.2
HSPA5	14937.6	18845.3	23952.6
HYOU1	2525.7	3073.5	5806.7
PDIA4	1094.7	1761.1	2595.8
PDIA6	10659.5	12634.4	14755.4
DNAJB11	3375.4	4712.3	6302.6
HSP90B1	3636.1	6842.7	10873.4
PDIA3	13101.0	19360.2	24888.2
PPIB	18709.8	24466.7	28281.8
C19orf10	3559.5	4941.5	6474.9
SLC35B1	2224.8	2985.4	3647.7
SEC61A1	1707.7	2467.6	4494.1
RPN1	3543.8	5725.0	6984.5
DNAJC3	1944.2	3582.7	4561.4
CDK2AP2	884.0	2560.6	4079.5

GEO Series "GSE16837" Expression Profiles

Num of samples in this series: 113

Details of this dataset are not shown due to large number of samples and the page size limit.

Find details in http://www.ncbi.nlm.nih.gov/geo/query/acc.cgi?acc=GSE16837

Background corr dist: KL-Divergence = 0.1987, L1-Distance = 0.0557, L2-Distance = 0.0074, Normal std = 0.3314

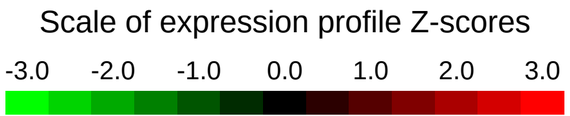

GEO Series "GSE6400" Expression Profiles

Num of samples in this series: 12

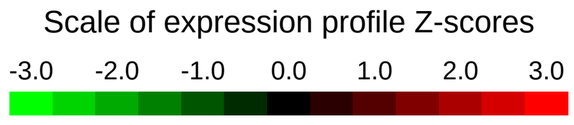

GEO Link:	http://www.ncbi.nlm.nih.gov/geo/query/acc.cgi?acc=GSE6400
Status:	Public on Dec 01 2006
Title:	Cultured A549 lung cancer cells treated with actinomycin D and sapphyrin PCI-2050
Organism:	Homo sapiens
Experiment type:	Expression profiling by array
Platform:	GPL570
Pubmed ID:	17233922
Summary & Design:	**Summary:** The goal of this project was to characterize changes in gene expression in response to the anti-cancer agent sapphyrin PCI-2050. Cultured A549 human lung cancer cells were treated with sapphyrin PCI-2050 or actinomycin D, a known transcripitonal inhibitor. The gene expression profiles of drug-treated and control A549 cultures were determined using Human Genome U133 Plus 2.0 Arrays (Affymetrix, Santa Clara, CA). Further details are provided in our published manuscript: <http://www.molecular-cancer.com/content/6/1/9>. **Keywords:** responses to treatments with anti-cancer agents **Overall design:** A549 human lung cancer cells (1 x 10^5 cells per T-25 flask in 7 mL complete RPMI 1640 medium) were seeded eight days prior to treatment of non-cycling plateau phase cultures with drug. At four hours prior to RNA isolation, sapphyrin PCI-2050 (1.25 or 2.5 ¿…M final concentration), actinomycin D (5 ¿…g/mL final concentration), or control (5% mannitol) solution was added to the cultures. Each experiment was performed in triplicate. After incubation, all cultures were washed twice with HBSS supplemented with 0.5% BSA and total RNA was isolated and subjected to analysis on Human Genome U133 Plus 2.0 Arrays (Affymetrix, Santa Clara, CA).

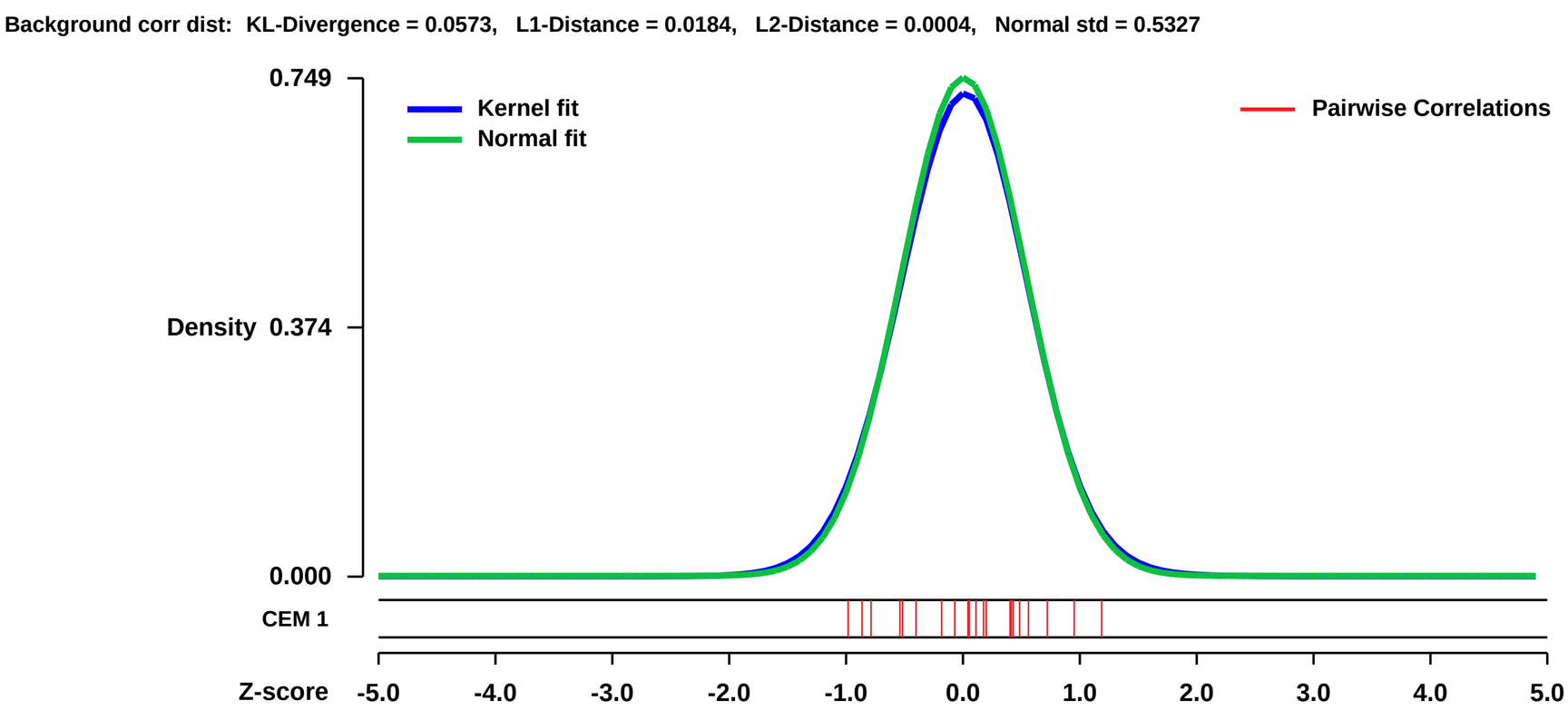

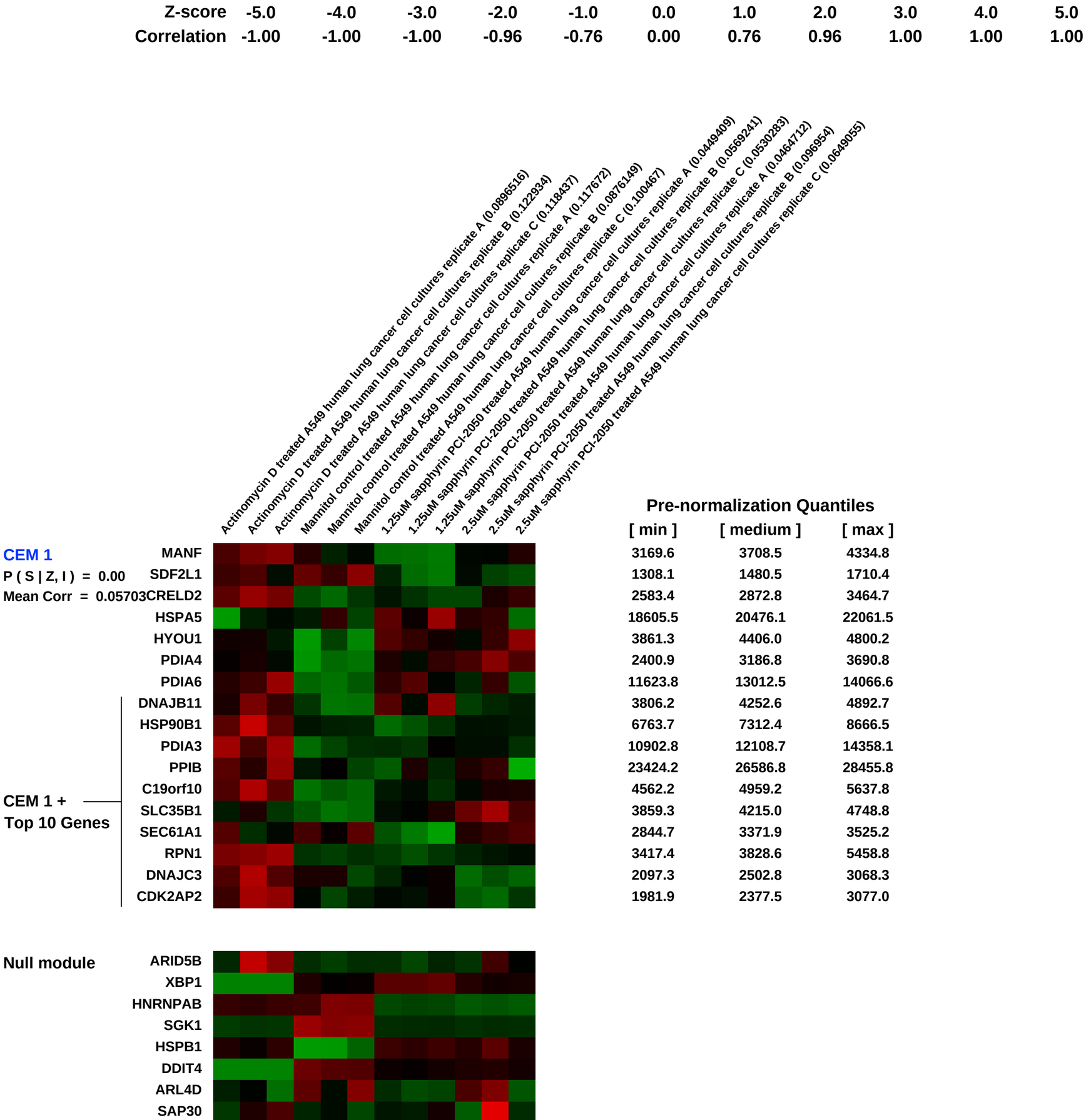

GEO Series "GSE55810" Expression Profiles

Num of samples in this series: 10

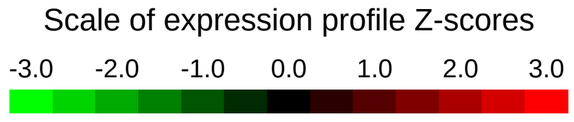

GEO Link:	http://www.ncbi.nlm.nih.gov/geo/query/acc.cgi?acc=GSE55810
Status:	Public on Mar 12 2014
Title:	Effect of co-culture with macrophages on two colon cancer cell lines.
Organism:	Homo sapiens
Experiment type:	Expression profiling by array
Platform:	GPL570
Pubmed ID:	
Summary & Design:	**Summary:** These data suggest that co-culture with macrophages increases expression of NDRG-1 in epithelial cell lines. The finding is confirmed in 1 mouse epithelial cell line, and in tissue derived from mice genetically and dietetically altered to increase macrophage infiltration of the small and large intestinal epithelium. NDRG1 is identified as a potential mediator of macrophage effects on tumorigenesis in the large and small intestine. Array data is part of a larger study involving the effects of Vitamin D, in concert with macrophages, on intestinal homeostasis and tumorigenesis, entitled Cell autonomous and non-autonomous interactions of a western-style diet and the vitamin D receptor in intestinal homeostasis and tumorigenesis **Overall design:** Cells from human colon cancer cell lines were cultured either alone, with Vitamin D3, with THP1 macrophages, or with THP1 macrophages and Vitamin D3, in a system which allowed no physical contact but exchange of soluble factors between the cell types.

Background corr dist: KL-Divergence = 0.0427, L1-Distance = 0.0589, L2-Distance = 0.0048, Normal std = 0.6724

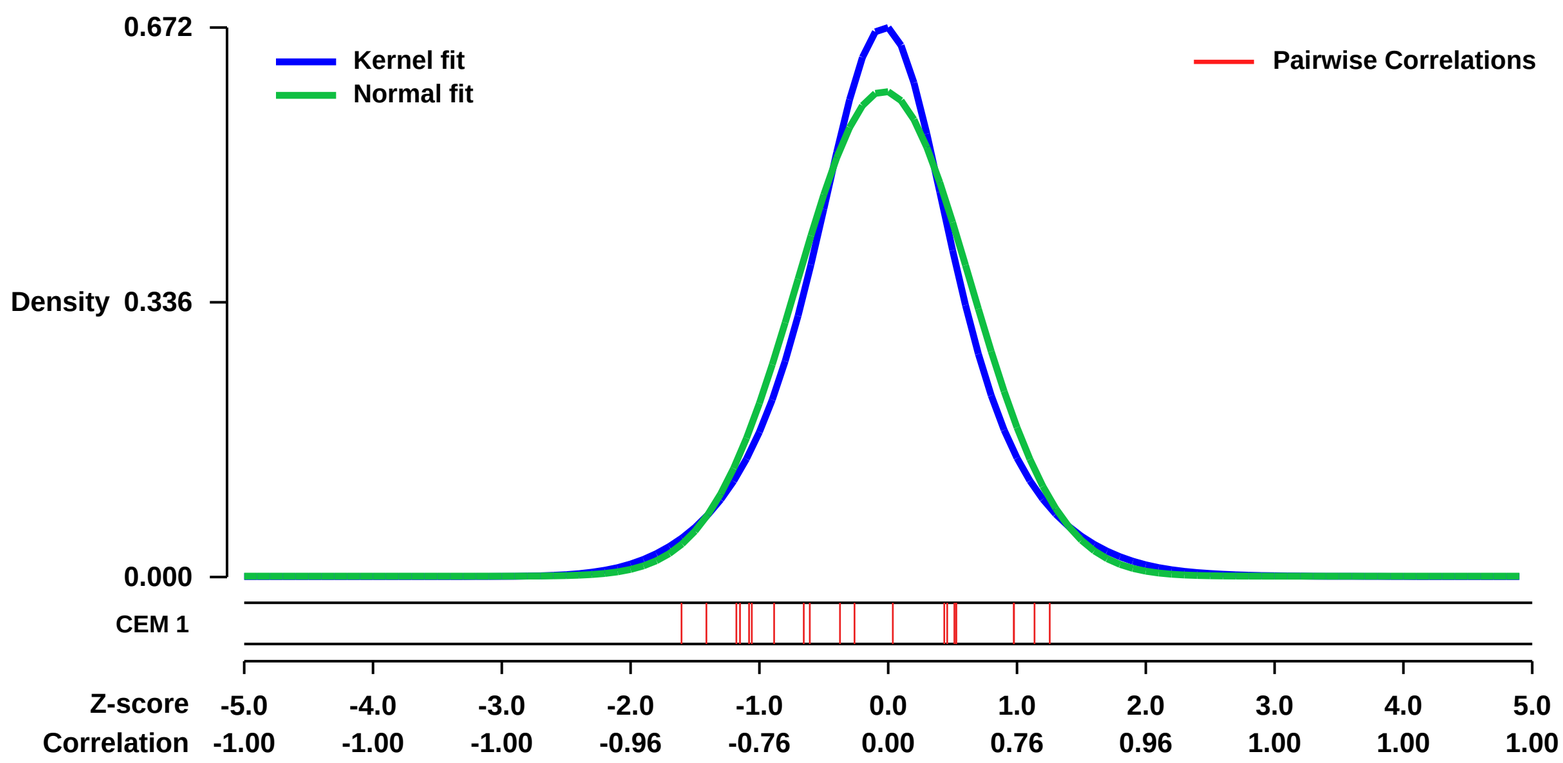

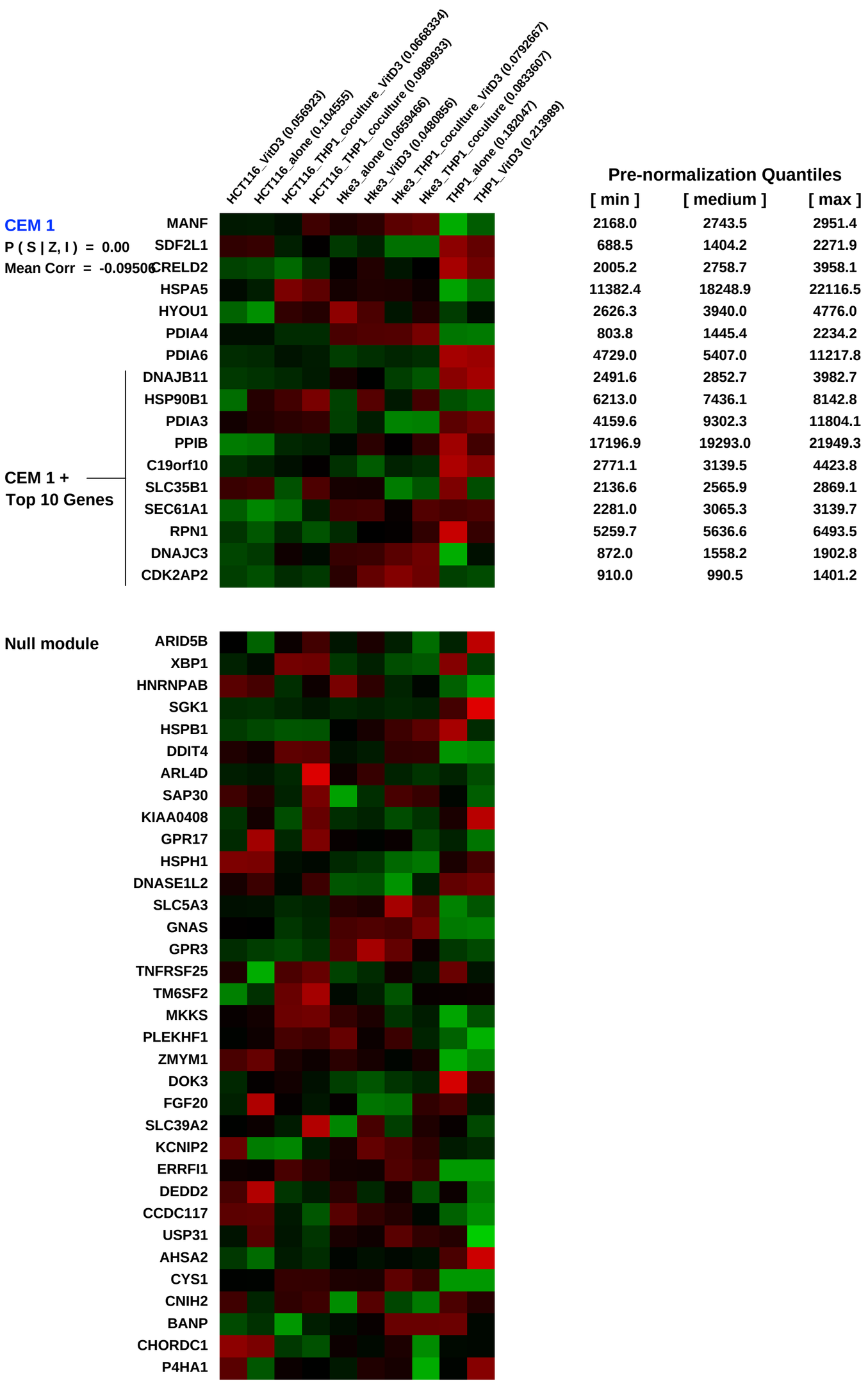

Pre-normalization Quantiles

	[min]	[medium]	[max]
MANF	2168.0	2743.5	2951.4
SDF2L1	688.5	1404.2	2271.9
CRELD2	2005.2	2758.7	3958.1
HSPA5	11382.4	18248.9	22116.5
HYOU1	2626.3	3940.0	4776.0
PDIA4	803.8	1445.4	2234.2
PDIA6	4729.0	5407.0	11217.8
DNAJB11	2491.6	2852.7	3982.7
HSP90B1	6213.0	7436.1	8142.8
PDIA3	4159.6	9302.3	11804.1
PPIB	17196.9	19293.0	21949.3
C19orf10	2771.1	3139.5	4423.8
SLC35B1	2136.6	2565.9	2869.1
SEC61A1	2281.0	3065.3	3139.7
RPN1	5259.7	5636.6	6493.5
DNAJC3	872.0	1558.2	1902.8
CDK2AP2	910.0	990.5	1401.2

GEO Series "GSE44867" Expression Profiles

Num of samples in this series: 16

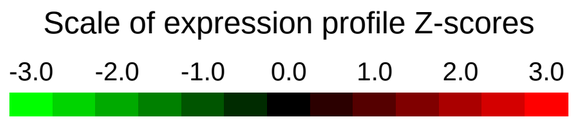

GEO Link:	http://www.ncbi.nlm.nih.gov/geo/query/acc.cgi?acc=GSE44867
Status:	Public on Mar 06 2013
Title:	Identification of targets regulated by HSF1 in response to HSP90 inhibitors
Organism:	Homo sapiens
Experiment type:	Expression profiling by array
Platform:	GPL570
Pubmed ID:	
Summary & Design:	**Summary:** A375 cells with inducible knockdown HSF1 with and without HSP90 inhibitor treatment **Overall design:** A375 cells were seeded in 6-well plates for 3d with 100ng/ml doxycycline prior to treatment with 0.1% DMSO or 100nM HSP990 for 3h

Background corr dist: KL-Divergence = 0.1562, L1-Distance = 0.0314, L2-Distance = 0.0019, Normal std = 0.3671

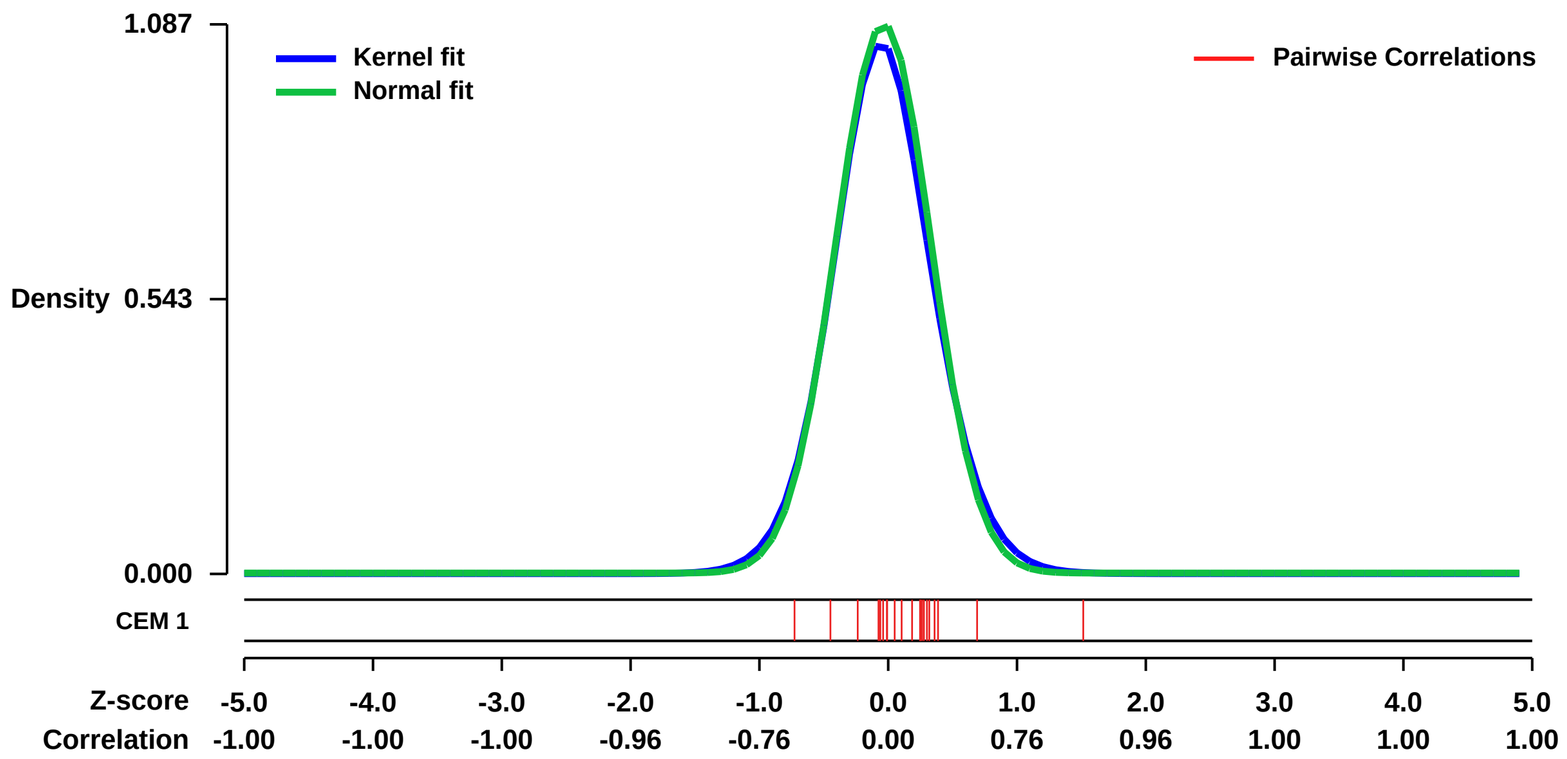

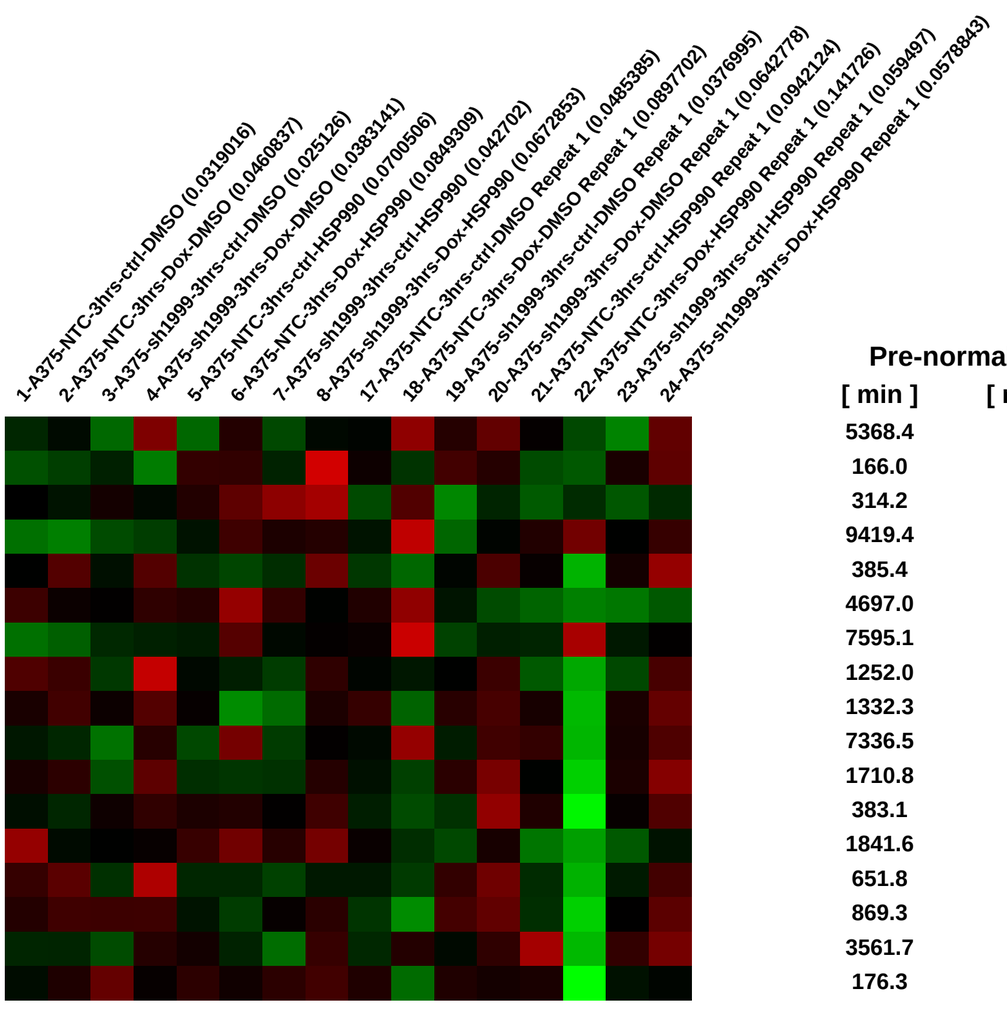

Pre-normalization Quantiles

	[min]	[medium]	[max]
MANF	5368.4	6414.3	7626.0
SDF2L1	166.0	230.3	323.3
CRELD2	314.2	563.4	902.8
HSPA5	9419.4	12051.5	16049.6
HYOU1	385.4	1142.2	1775.7
PDIA4	4697.0	6307.0	7899.5
PDIA6	7595.1	8760.5	11784.0
DNAJB11	1252.0	2329.7	3658.1
HSP90B1	1332.3	5544.8	7036.4
PDIA3	7336.5	9156.4	10596.8
PPIB	1710.8	3751.0	4708.0
C19orf10	383.1	752.8	939.5
SLC35B1	1841.6	2388.1	2858.1
SEC61A1	651.8	2027.4	3795.7
RPN1	869.3	1777.1	2009.1
DNAJC3	3561.7	4162.4	4590.3
CDK2AP2	176.3	536.7	627.7

GEO Series "GSE30775" Expression Profiles

Num of samples in this series: 6

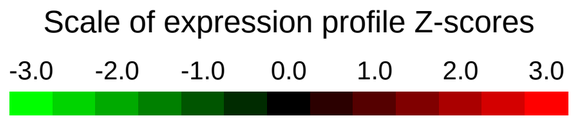

GEO Link:	http://www.ncbi.nlm.nih.gov/geo/query/acc.cgi?acc=GSE30775
Status:	Public on Jul 20 2011
Title:	Gene expression change after LSD1 siRNA treatment in ER-negative breast cancer cells MDA-MB-231
Organism:	Homo sapiens
Experiment type:	Expression profiling by array
Platform:	GPL570
Pubmed ID:	22542627
Summary & Design:	**Summary:** Knock-down of LSD1 using siRNA approach induced regulation of several proliferation-associated genes in ER-negative breast cancer cells MDA-MB-231. **Overall design:** To identify changes on gene expression caused by treatment with siRNA directed against LSD1 (si) or control siRNA (control) in MDA-MB-231 cells, total RNA was purified from the cells after treatment for 6 days (2 rounds of transfection). Three biological replicates were used.

Background corr dist: KL-Divergence = 0.0328, L1-Distance = 0.0402, L2-Distance = 0.0018, Normal std = 0.7030

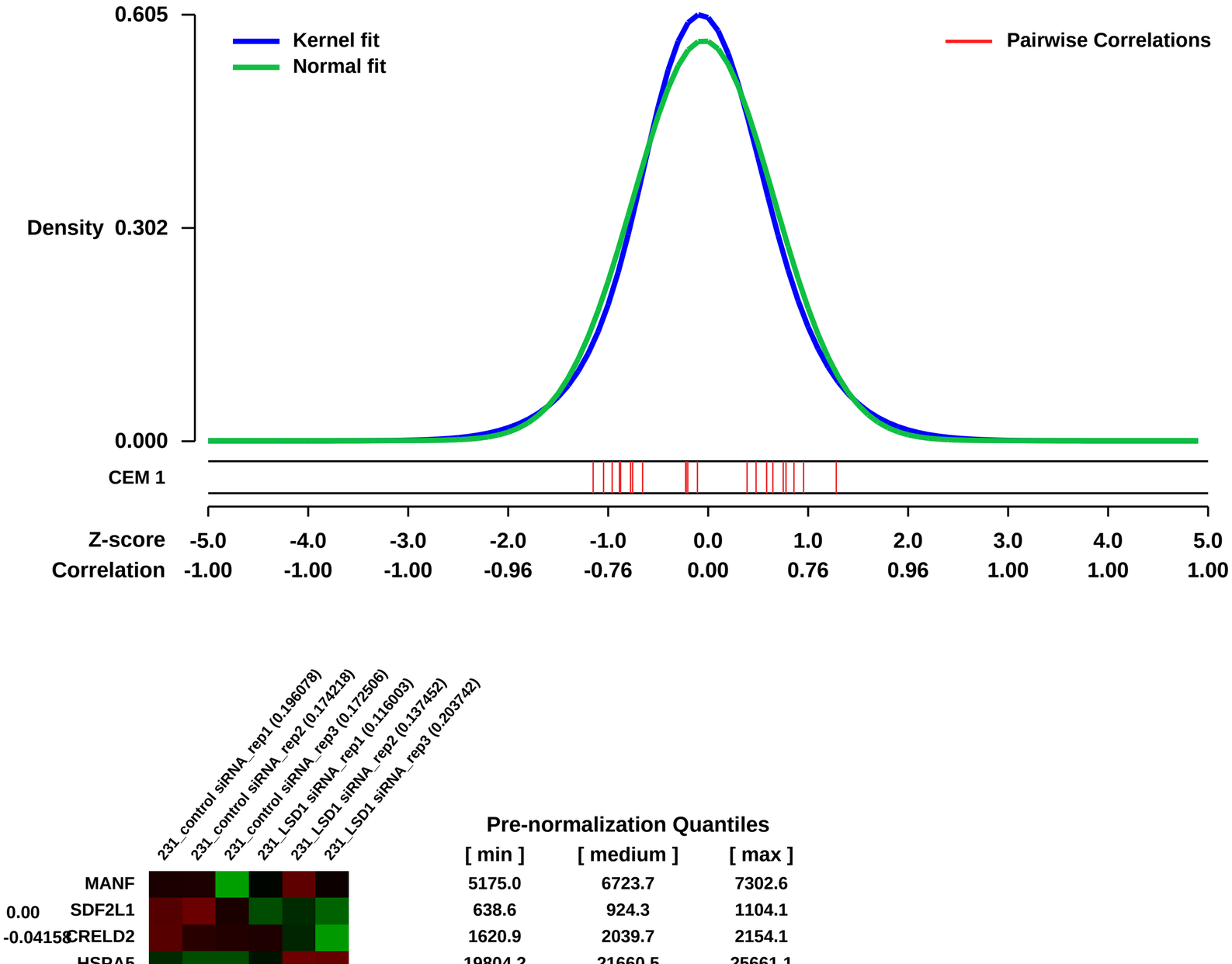

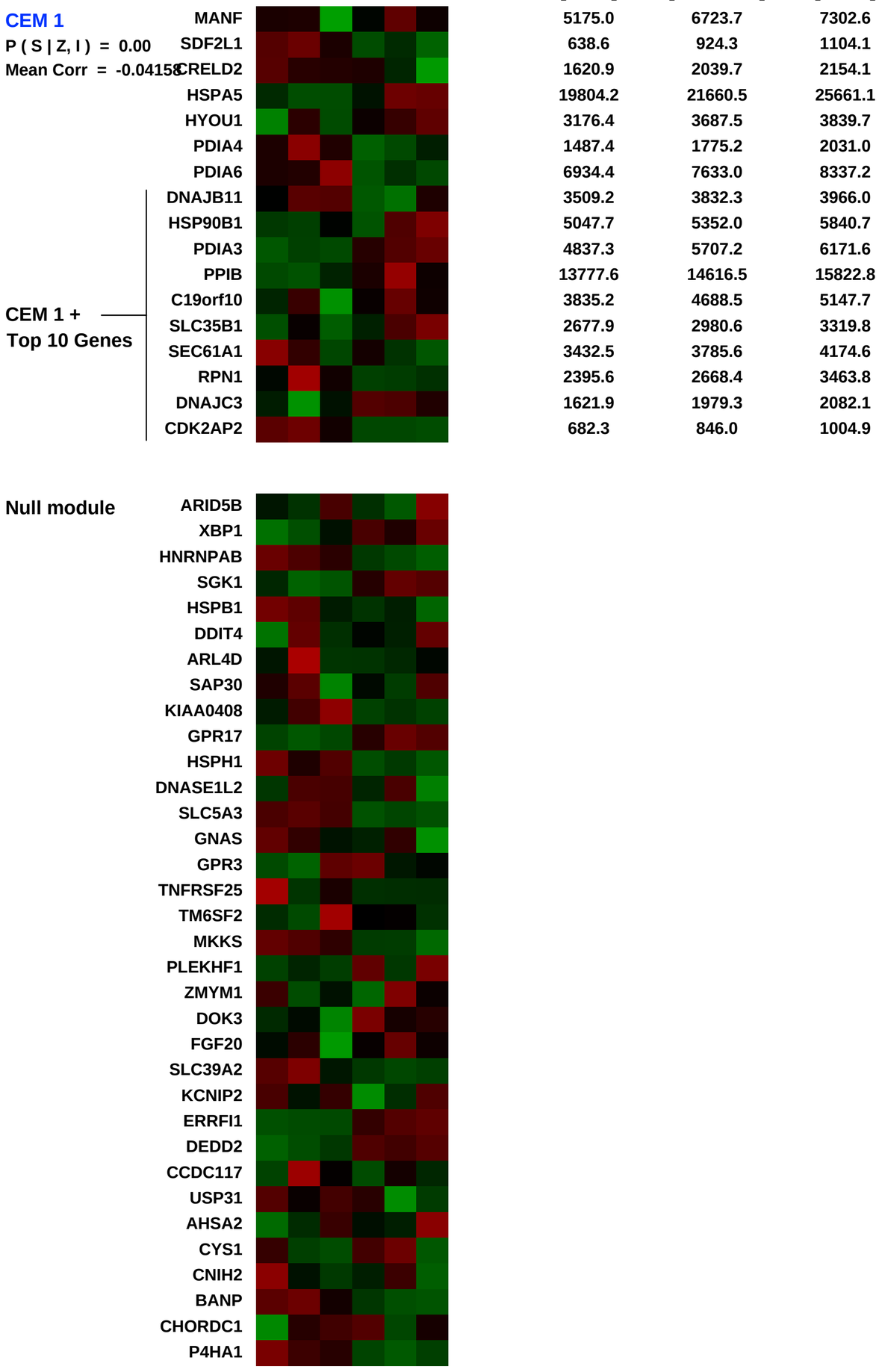

GEO Series "GSE27670" Expression Profiles

Num of samples in this series: 6

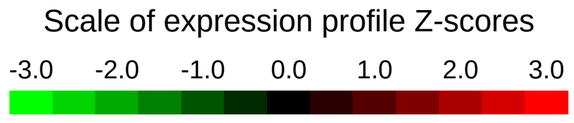

GEO Link:	http://www.ncbi.nlm.nih.gov/geo/query/acc.cgi?acc=GSE27670
Status:	Public on Jul 27 2011
Title:	Down-regulation of BLIMP1-alpha by the EBV oncogene, LMP1, disrupts the plasma cell differentiation program and prevents viral replication in B cells
Organism:	Homo sapiens
Experiment type:	Expression profiling by array
Platform:	GPL570
Pubmed ID:	21411757
Summary & Design:	**Summary:** In this study, we have investigated the effect of BLIMP1$_{c}$– on gene expression, cell differentiation and pathogenesis in normal human GC B cells using a non-viral vector based system **Overall design:** Gene expression was compared among BLIMP1$_{c}$–, LMP1-transfected and control vector-transfected GC B cells from two patients. RNA from the FACS-sorted transfected GC B cells was amplified. Fragmented cRNA was hybridized to HG-U133 Plus 2.0 microarrays. Differentially expressed genes were identified using the GCOS pair-wise analysis.

Background corr dist: KL-Divergence = 0.0433, L1-Distance = 0.0442, L2-Distance = 0.0029, Normal std = 0.6328

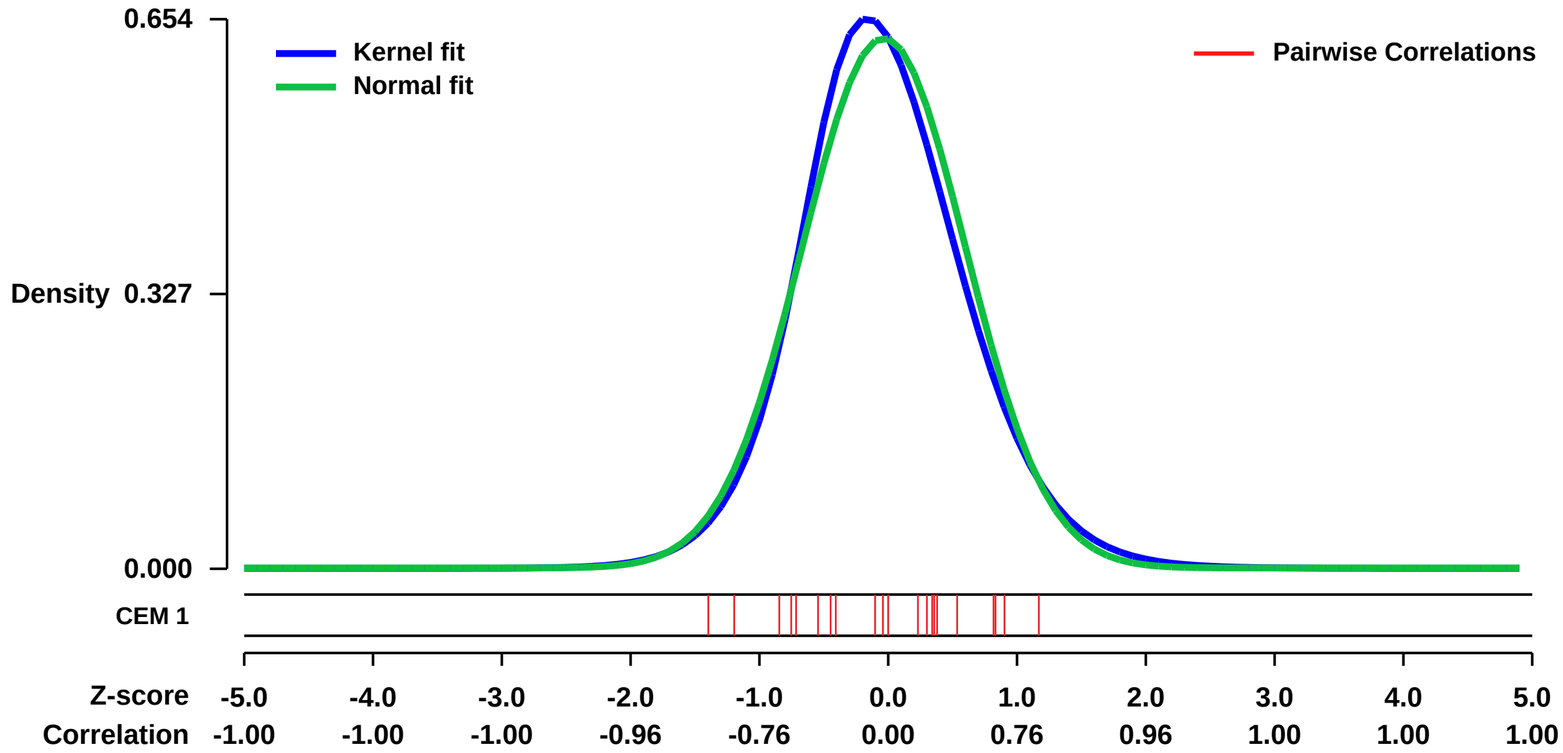

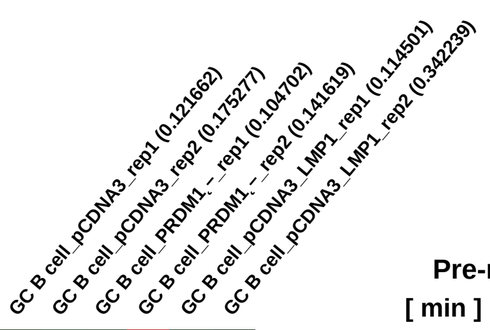

Pre-normalization Quantiles

[min] [medium] [max]

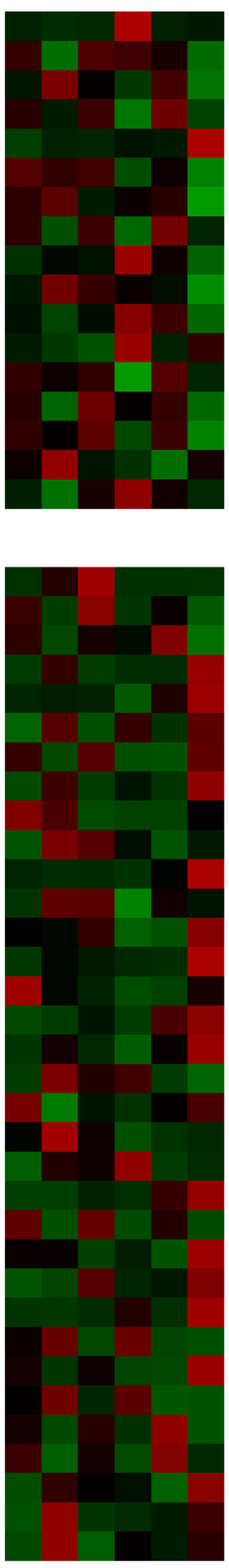

MANF	4042.8	4600.1	15293.3
SDF2L1	1923.2	4816.8	5273.8
CRELD2	5362.7	10189.1	14933.5
HSPA5	4206.5	13133.1	17295.2
HYOU1	191.6	353.9	1181.3
PDIA4	235.7	813.6	921.8
PDIA6	11637.2	16545.5	17838.0
DNAJB11	2185.8	5131.4	6608.2
HSP90B1	725.4	1356.6	2539.2
PDIA3	1529.3	2673.9	3414.6
PPIB	2790.8	3972.9	5937.5
C19orf10	2986.3	3377.1	4670.0
SLC35B1	1584.6	2234.7	2350.7
SEC61A1	377.9	772.2	957.1
RPN1	196.3	1162.5	1404.1
DNAJC3	441.7	844.1	1272.1
CDK2AP2	157.2	567.2	953.9
ARID5B			
XBP1			
HNRNPAB			
SGK1			
HSPB1			
DDIT4			
ARL4D			
SAP30			
KIAA0408			
GPR17			
HSPH1			
DNASE1L2			
SLC5A3			
GNAS			
GPR3			
TNFRSF25			
TM6SF2			
MKKS			
PLEKHF1			
ZMYM1			
DOK3			
FGF20			
SLC39A2			
KCNIP2			
ERRFI1			
DEDD2			
CCDC117			
USP31			
AHSA2			
CYS1			
CNIH2			
BANP			
CHORDC1			
P4HA1			

GEO Series "GSE41137" Expression Profiles

Num of samples in this series: 140

Details of this dataset are not shown due to large number of samples and the page size limit.

Find details in http://www.ncbi.nlm.nih.gov/geo/query/acc.cgi?acc=GSE41137

Background corr dist: KL-Divergence = 0.2600, L1-Distance = 0.0707, L2-Distance = 0.0149, Normal std = 0.2971

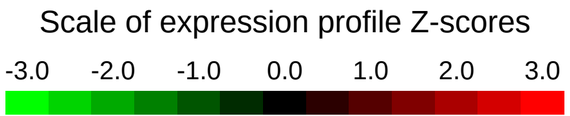

GEO Series "GSE37934" Expression Profiles

Num of samples in this series: 6

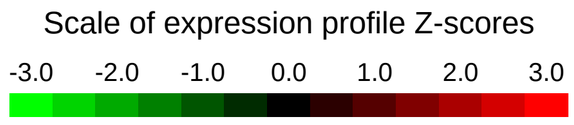

GEO Link:	http://www.ncbi.nlm.nih.gov/geo/query/acc.cgi?acc=GSE37934
Status:	Public on May 12 2012
Title:	Differential gene expression profiles between SKOV3.ip1-S116A cells (Ser116 of PEA-15 substituted with alanine) and SKOV3.ip1-S116D cells (Ser116 of PEA-15 substituted
Organism:	Homo sapiens
Experiment type:	Expression profiling by array
Platform:	GPL570
Pubmed ID:	23543364
Summary & Design:	**Summary:** To dissect the molecular mechanisms of PEA-15-mediated paclitaxel sensitization in ovarian cancer cells, we performed cDNA microarray analysis using SKOV3.ip1-S116A cells (Ser116 of PEA-15 substituted with alanine) and SKOV3.ip1-S116D cells (Ser116 of PEA-15 substituted with aspartic acid). cDNA microarray data analysis showed that SCLIP (SCG10-like protein), also known as STMN3, was highly expressed in SKOV3.ip1-S116D cells and was involved in pPEA-15-mediated paclitaxel sensitization in ovarian cancer cells. **Overall design:** SKOV3.ip1-S116A cells (Ser116 of PEA-15 substituted with alanine) and SKOV3.ip1-S116D cells (Ser116 of PEA-15 substituted with aspartic acid) were used. Total RNA was extracted and purified using RNeasy mini kit (Qiagen, Inc.) according to the manufacturerâ s instructions. The integrity of the obtained RNA was assessed using an Agilent 2100 BioAnalyzer (Agilent Technologies). The Affymetrix HGU133 plus platform was used for hybridization, staining, and imaging of the arrays by following the manufacturerâ s instructions. Gene expression analysis was performed in triplicate.

Background corr dist: KL-Divergence = 0.0302, L1-Distance = 0.0177, L2-Distance = 0.0003, Normal std = 0.6687

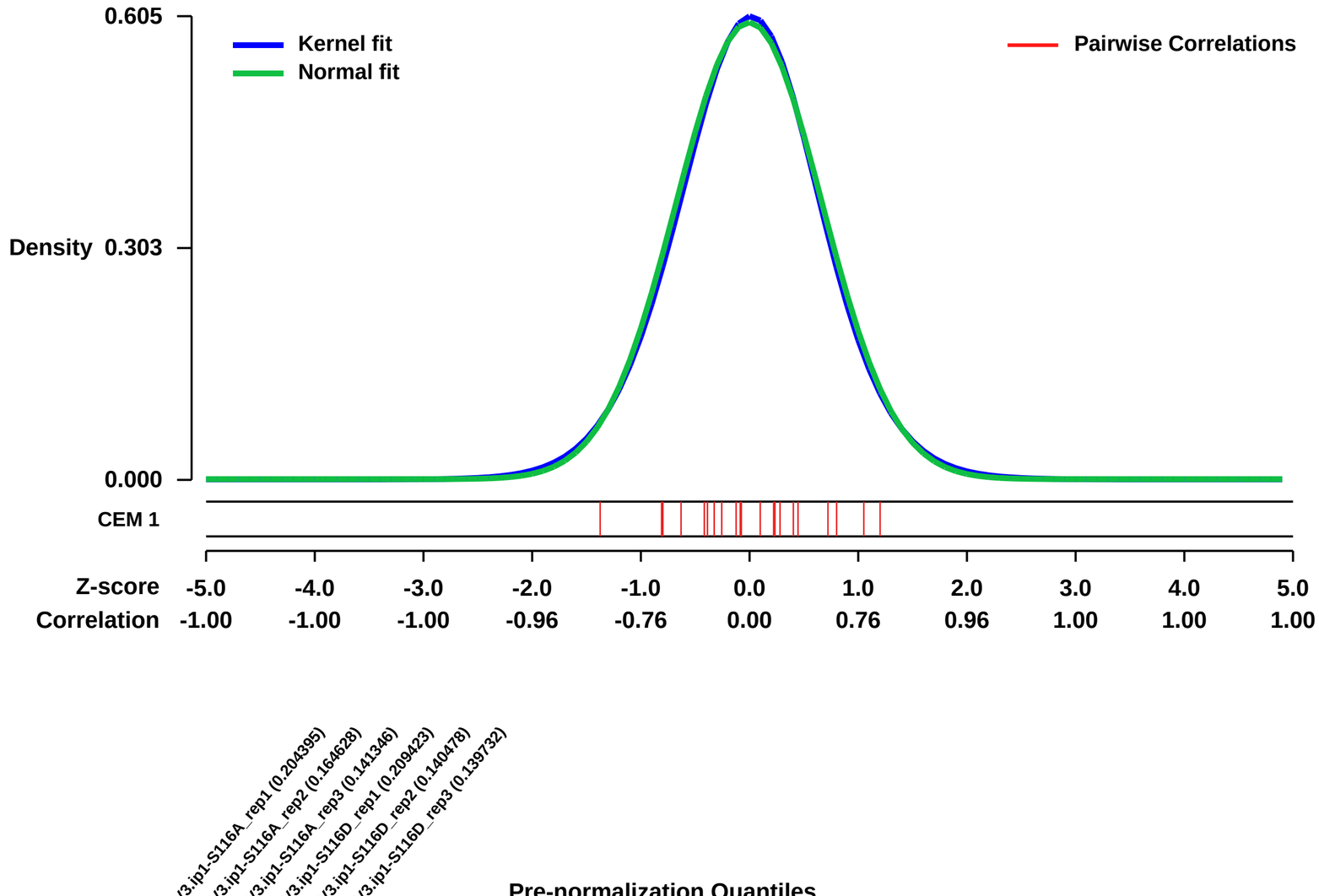

Pre-normalization Quantiles

	[min]	[medium]	[max]
CEM 1			
P (S | Z, I) = 0.00			
Mean Corr = 0.00653			
MANF	2565.5	2971.7	3385.3
SDF2L1	650.6	913.8	1089.5
CRELD2	1681.9	1984.1	2202.2
HSPA5	10416.5	11575.6	12891.0
HYOU1	2705.5	3204.7	3380.9
PDIA4	1127.5	1281.0	1320.7
PDIA6	9670.0	9980.4	10408.0
CEM 1 + Top 10 Genes			
DNAJB11	2396.3	2540.8	2777.8
HSP90B1	2822.0	3250.6	3399.5
PDIA3	5238.4	5578.6	6051.8
PPIB	6048.3	6409.0	6850.0
C19orf10	2846.2	3570.8	3724.2
SLC35B1	2965.7	3565.7	3739.3
SEC61A1	2451.2	3197.7	3664.2
RPN1	2516.2	2959.7	3148.0
DNAJC3	1466.9	1900.6	2135.2
CDK2AP2	347.1	375.7	420.6
Null module			
ARID5B			
XBP1			
HNRNPAB			
SGK1			
HSPB1			
DDIT4			
ARL4D			
SAP30			
KIAA0408			
GPR17			
HSPH1			
DNASE1L2			
SLC5A3			
GNAS			
GPR3			
TNFRSF25			
TM6SF2			
MKKS			
PLEKHF1			
ZMYM1			
DOK3			
FGF20			
SLC39A2			
KCNIP2			
ERRFI1			
DEDD2			
CCDC117			
USP31			
AHSA2			
CYS1			
CNIH2			
BANP			
CHORDC1			
P4HA1			

GEO Series "GSE10147" Expression Profiles

Num of samples in this series: 6

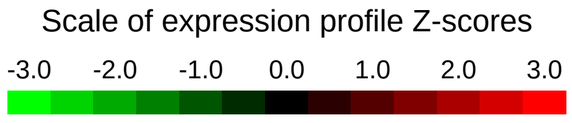

GEO Link:	http://www.ncbi.nlm.nih.gov/geo/query/acc.cgi?acc=GSE10147
Status:	Public on Feb 14 2008
Title:	Expression data from human plasmacytoid dendritic cells treated with p17 or CpG
Organism:	Homo sapiens
Experiment type:	Expression profiling by array
Platform:	GPL570
Pubmed ID:	18310327
Summary & Design:	**Summary:** We used microarrays to detail the global program of gene expression underlying the effect of p17 on human plasmacytoid dendritic cells and was compared to CpG profile. **Keywords: gene expression study** **Overall design:** Human plasmacytoid dendritic cells were purified from two donors and cultured in the presence of p17 or CpG for 18 h.

Background corr dist: KL-Divergence = 0.0440, L1-Distance = 0.0181, L2-Distance = 0.0003, Normal std = 0.5954

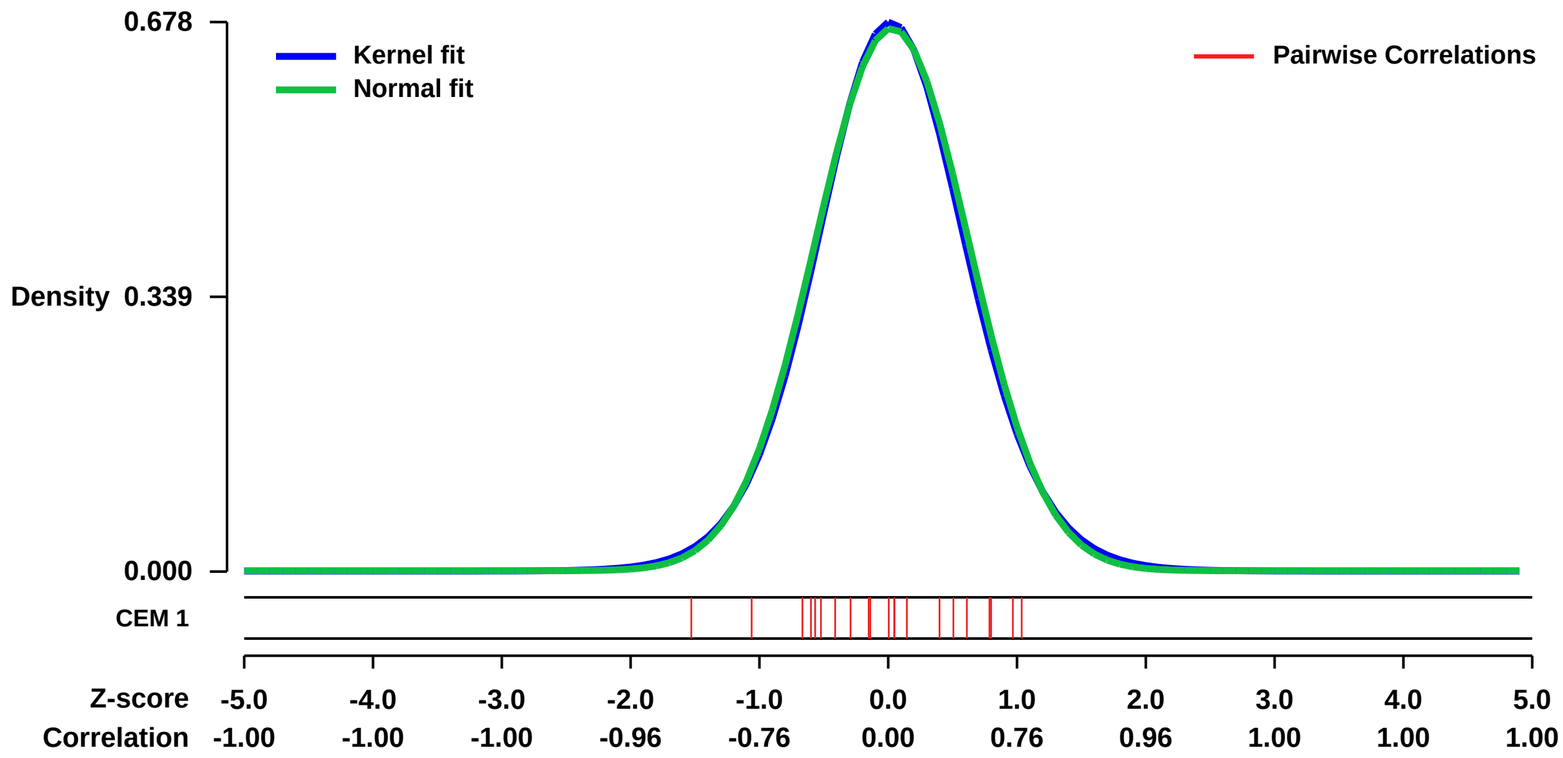

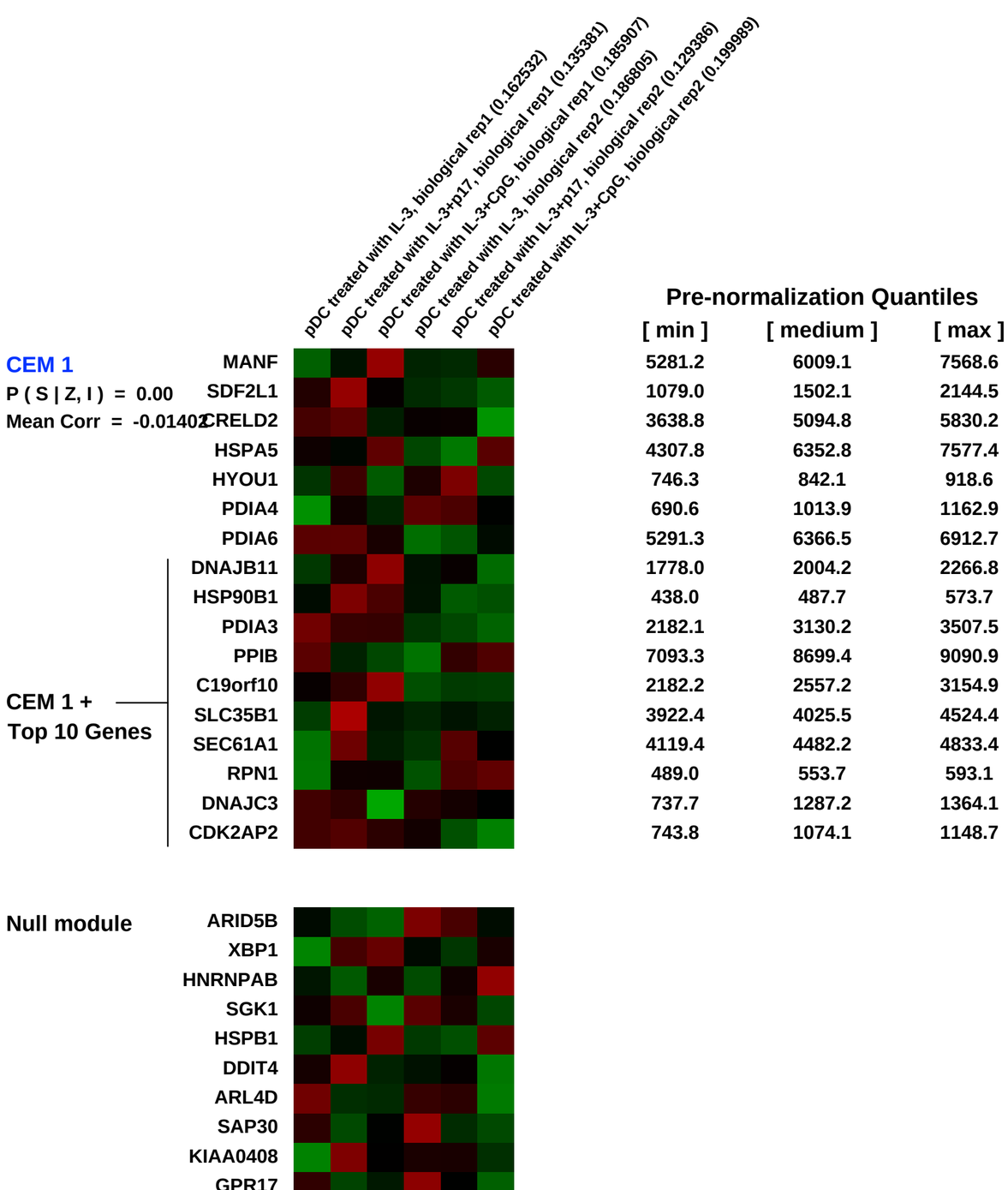

GEO Series "GSE42045" Expression Profiles

Num of samples in this series: 50

Scale of expression profile Z-scores

-3.0 -2.0 -1.0 0.0 1.0 2.0 3.0

GEO Link:	http://www.ncbi.nlm.nih.gov/geo/query/acc.cgi?acc=GSE42045
Status:	Public on Oct 04 2013
Title:	TWEAK-treated time course in MDA-MB-436 cells
Organism:	Homo sapiens
Experiment type:	Expression profiling by array
Platform:	GPL570
Pubmed ID:	23974006
Summary & Design:	**Summary:** Tumor necrosis factor-related weak inducer of apoptosis, TWEAK, is a TNF superfamily member that mediates signaling through its receptor fibroblast growth factor inducible-14, Fn14. In tumor cell lines, TWEAK induces proliferation, survival and NF-kappaB signaling and gene expression that promote tumor growth and suppress antitumor immune responses. Anti-TWEAK antibody, RG7212, inhibits tumor growth in vivo with decreases in pathway activation markers and modulation of tumor, blood and spleen immune cell composition. Candidate response prediction markers, including Fn14, have been identified in mouse models. Phase I pharmacodynamic data from patients are consistent with preclinical results. TWEAK:Fn14 signaling is upregulated in human cancer and pathway activation induces tumor proliferation and survival signaling. Blockade with anti-TWEAK mAb, RG7212, inhibits tumor growth in multiple models in mice. TWEAK induces changes that suppress anti-tumor immune responses and RG7212 blocks these effects resulting in changes in tumor immune cell composition and decreases in cytokines that promote immunosuppression. Antitumor efficacy in mice was observed in a range of Fn14 expressing models with pathway activation and expressing either wild-type or mutant p53, BRAF or KRAS suggesting both a patient selection strategy and potential broad clinical applicability. Preclinical mechanism of action hypotheses are supported by Phase I clinical data, with decreases in proliferation markers and increased tumor T cell infiltration. **Overall design:** MDA-MB-436 cells untreated or treated with 1090-TW (TWEAK) for 15 minutes, 1 hour, 4 hours, 8 hours, or 24 hours. Five replicates for each condition were performed.

Background corr dist: KL-Divergence = 0.3353, L1-Distance = 0.0593, L2-Distance = 0.0091, Normal std = 0.2682

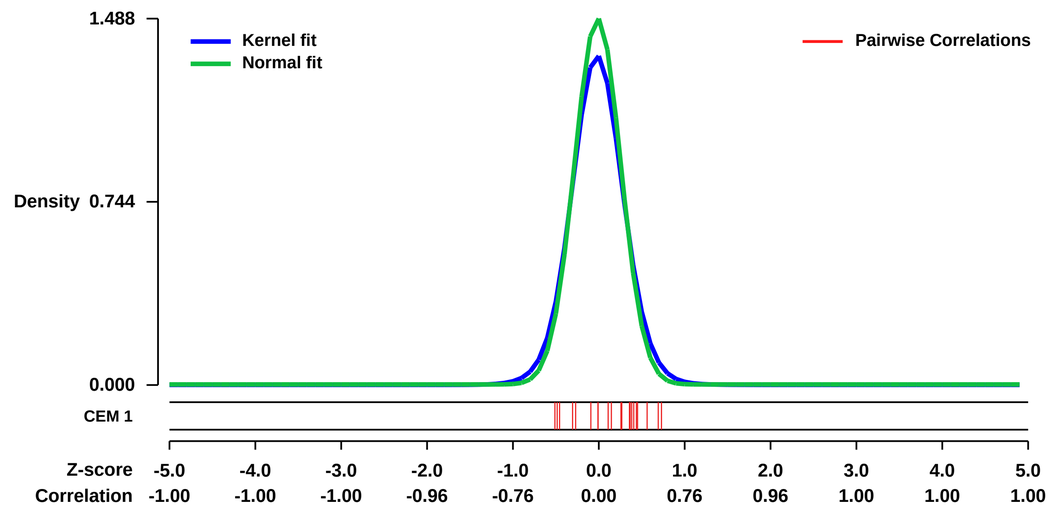

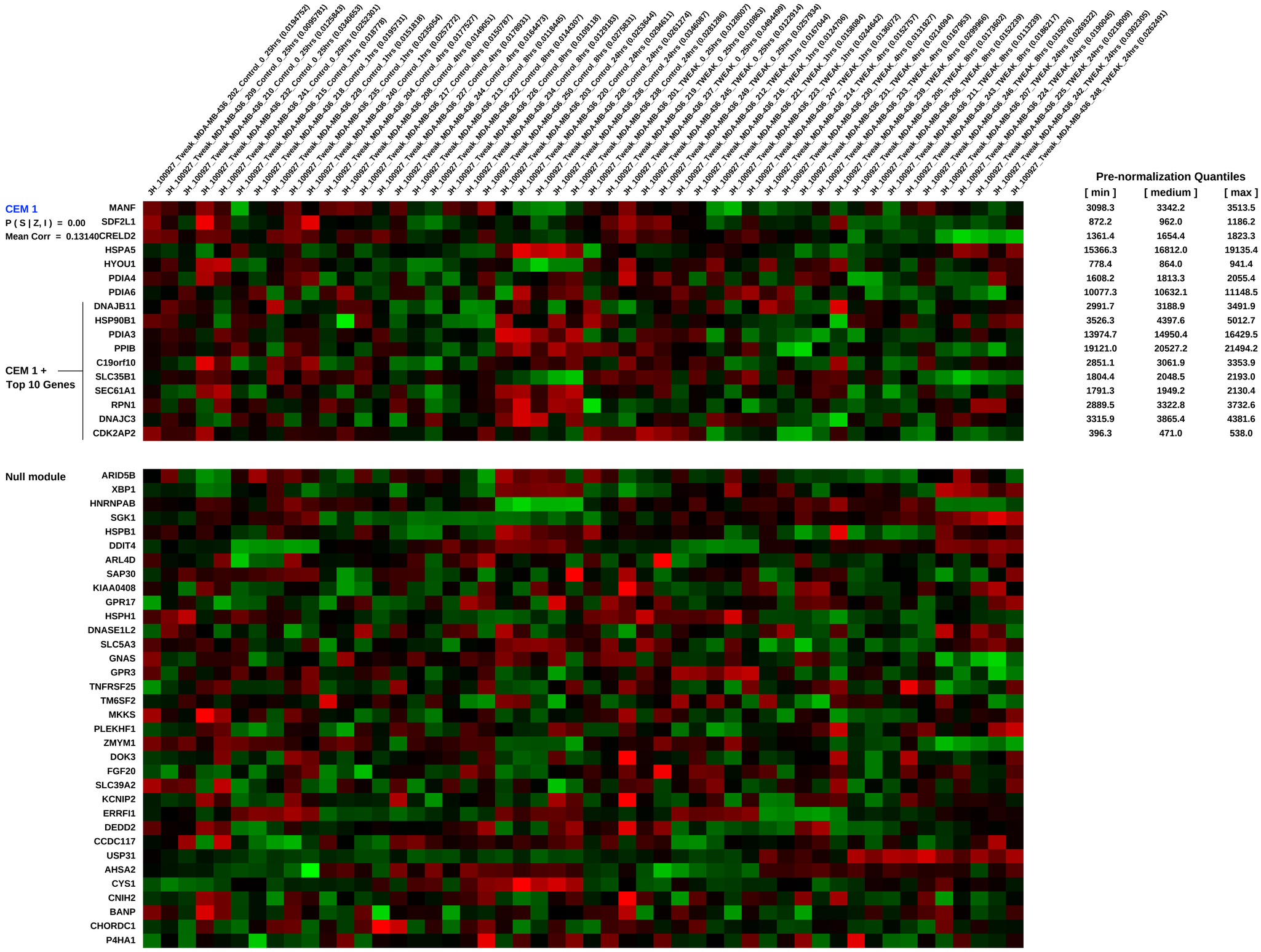

Pre-normalization Quantiles

[min]	[medium]	[max]
3098.3	3342.2	3513.5
872.2	962.0	1186.2
1361.4	1654.4	1823.3
15366.3	16812.0	19135.4
778.4	864.0	941.4
1608.2	1813.3	2055.4
10077.3	10632.1	11148.5
2991.7	3188.9	3491.9
3526.3	4397.6	5012.7
13974.7	14950.4	16429.5
19121.0	20527.2	21494.2
2851.1	3061.9	3353.9
1804.4	2048.5	2193.0
1791.3	1949.2	2130.4
2889.5	3322.8	3732.6
3315.9	3865.4	4381.6
396.3	471.0	538.0

GEO Series "GSE24244" Expression Profiles

Num of samples in this series: 8

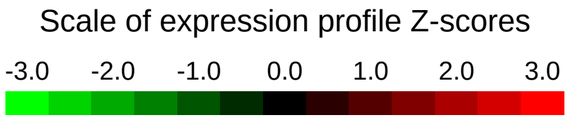

GEO Link:	http://www.ncbi.nlm.nih.gov/geo/query/acc.cgi?acc=GSE24244
Status:	Public on Nov 21 2010
Title:	Gene expression profiling of four subpopulations in GBM
Organism:	Homo sapiens
Experiment type:	Expression profiling by array
Platform:	GPL570
Pubmed ID:	21102433
Summary & Design:	**Summary:** GBM is a heterogenous brain tumor with hyperproliferation of endothelial cells. In order to understand the cellular mechanism of vasculogenesis in GBM, four fractions of cells are seperated. Microarray assays was performed to examine the potential lineage relationship and the signal pathways involved in determining the cell identity and function. **Overall design:** Four subpopulation of cells were seperated from two independent GBM dissociates by FCAS assay based on the expression of membrane marker CD133 and CD144. Total RNA was extracted from freshly sorted cells without any culture.

Background corr dist: KL-Divergence = 0.0522, L1-Distance = 0.0338, L2-Distance = 0.0018, Normal std = 0.5746

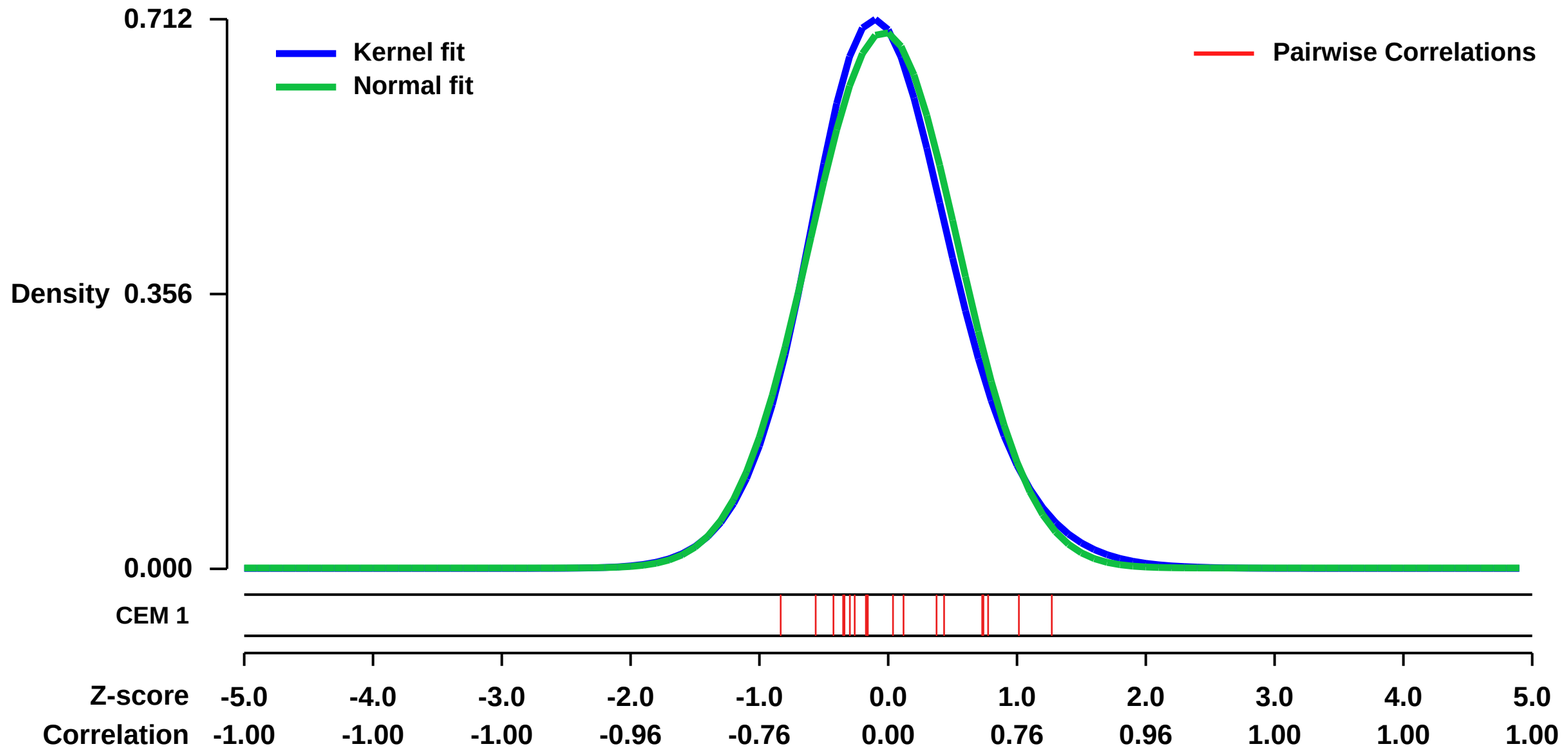

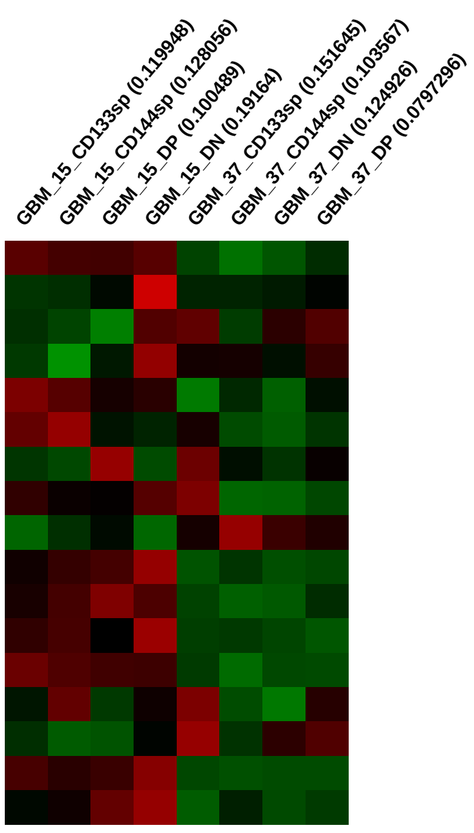

GEO Series "GSE7508" Expression Profiles

Num of samples in this series: 6

Scale of expression profile Z-scores

-3.0 -2.0 -1.0 0.0 1.0 2.0 3.0

GEO Link:	http://www.ncbi.nlm.nih.gov/geo/query/acc.cgi?acc=GSE7508
Status:	Public on Apr 13 2007
Title:	Identification of LEDGF-responsive genes in Jurkat cells
Organism:	Homo sapiens
Experiment type:	Expression profiling by array
Platform:	GPL570
Pubmed ID:	17545577
Summary & Design:	**Summary:** The LEDGF transcript from the PSIP1 gene was knocked down in Jurkat cells using RNAi technology. The resulting Jurkat-derived cell line (Jurkat-siJK2) was compared to a control cell line (wild type Jurkat) using microarray analysis. Genes identified as being modulated by LEDGF were preferential targets of HIV integration. **Keywords: effects of gene knockdown** **Overall design:** 2 cell lines were used, Jurkat-siJK2 (experimental) and wild-type Jurkat (control). 3 independent cultures of each cell line were used for independent RNA extractions, labeling reactions and array hybridizations.

Background corr dist: KL-Divergence = 0.0448, L1-Distance = 0.0264, L2-Distance = 0.0008, Normal std = 0.6016

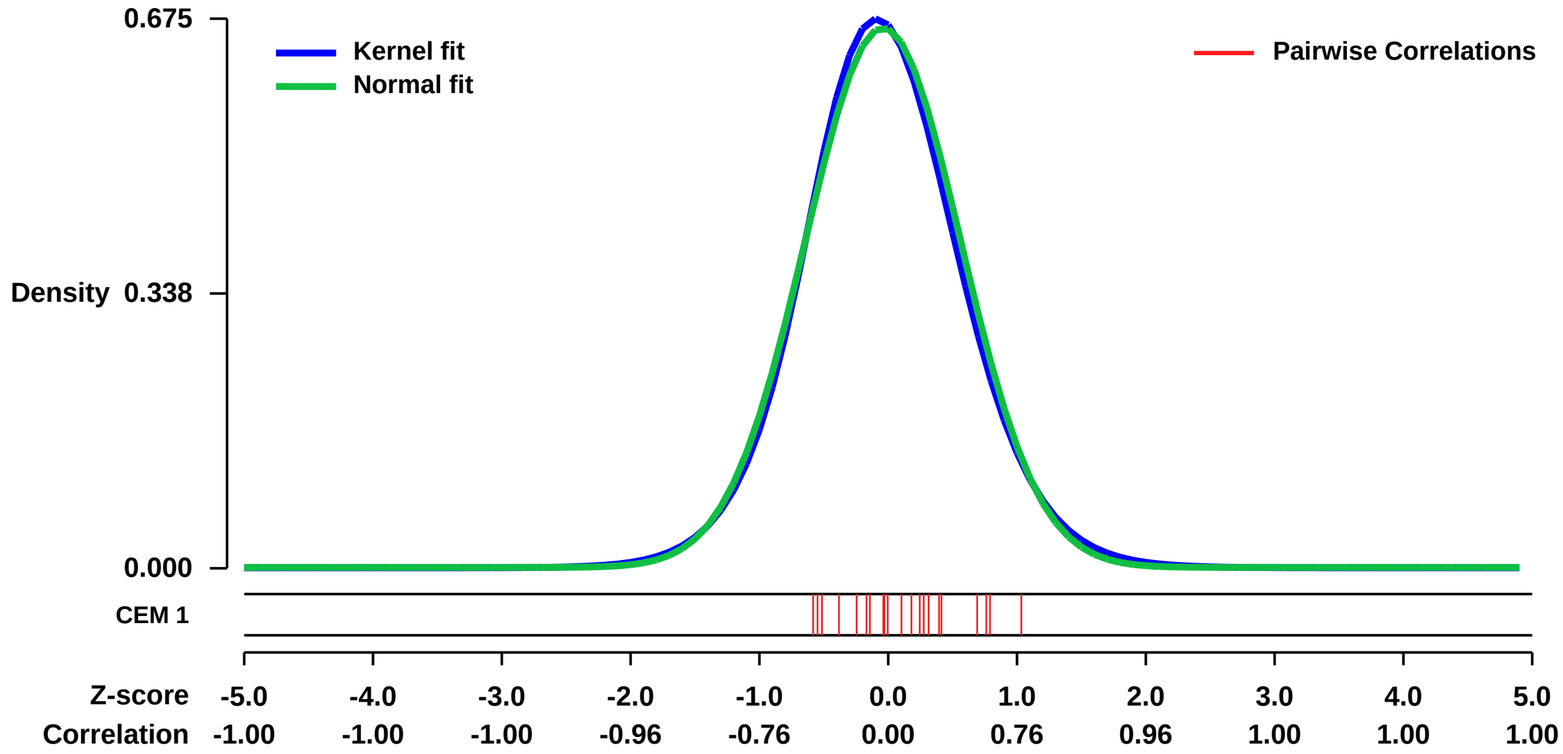

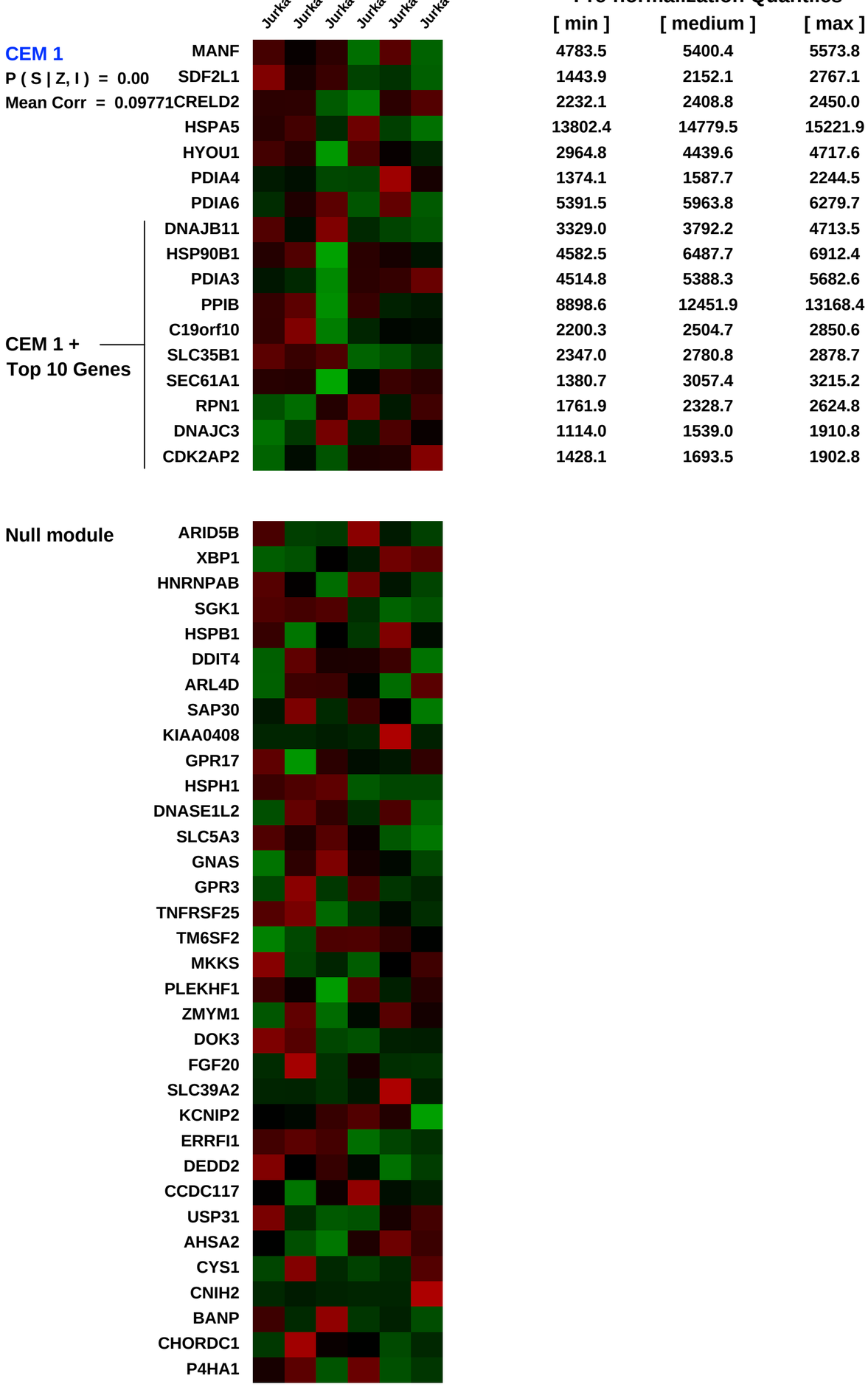

GEO Series "GSE17508" Expression Profiles

Num of samples in this series: 6

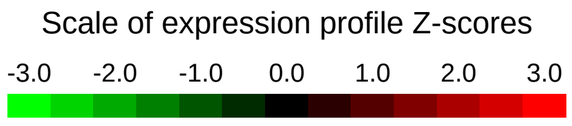

GEO Link:	http://www.ncbi.nlm.nih.gov/geo/query/acc.cgi?acc=GSE17508
Status:	Public on Dec 01 2012
Title:	Identification of human miR-22-responsive transcripts in MCF7 cells
Organism:	Homo sapiens
Experiment type:	Expression profiling by array
Platform:	GPL570
Pubmed ID:	
Summary & Design:	**Summary:** To examine the expression patterns of human miR-22-responsive transcripts in estrogen receptor alpha positive cell line MCF7, we transfected miR-22 duplex or negative control RNA duplex into MCF7 cells. Gene expression patterns were then evaluated using Affymetrix Human Genome U133 Plus 2.0 Array microarrays. **Keywords: comparision of expression patterns in MCF7 cells with or without human miR-22 overexpression.** **Overall design:** Total RNA was collected from two groups MCF7-NC (MCF7 cells transfected with negative control RNA duplex) and MCF7-miR (MCF7 cells transfected with miR-22 duplex) and hybridized to Affymetrix microarrays. Each group has three repeat samples.

Background corr dist: KL-Divergence = 0.0484, L1-Distance = 0.0220, L2-Distance = 0.0005, Normal std = 0.5819

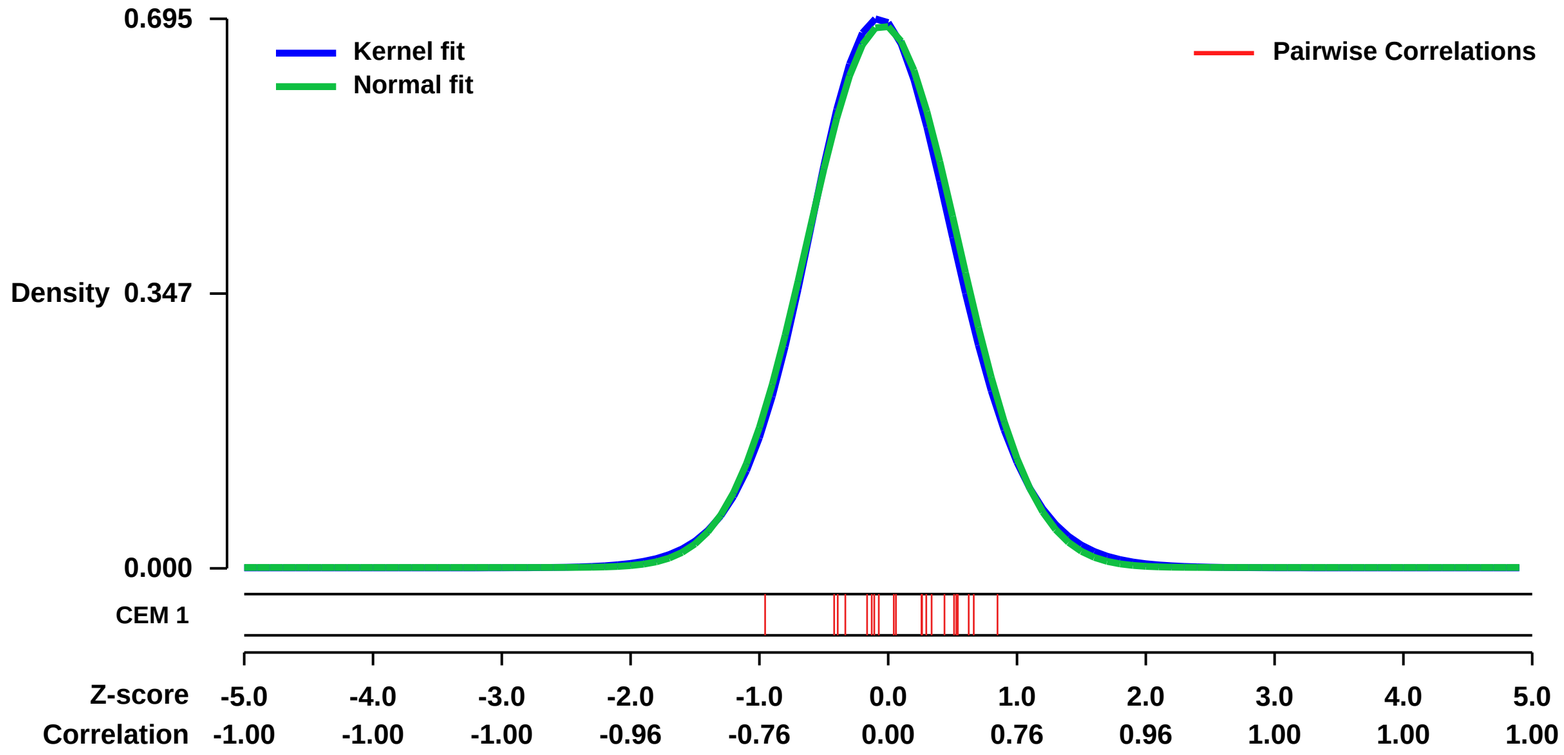

CEM 1
P (S | Z, I) = 0.00
Mean Corr = 0.12418

CEM 1 + Top 10 Genes

Null module

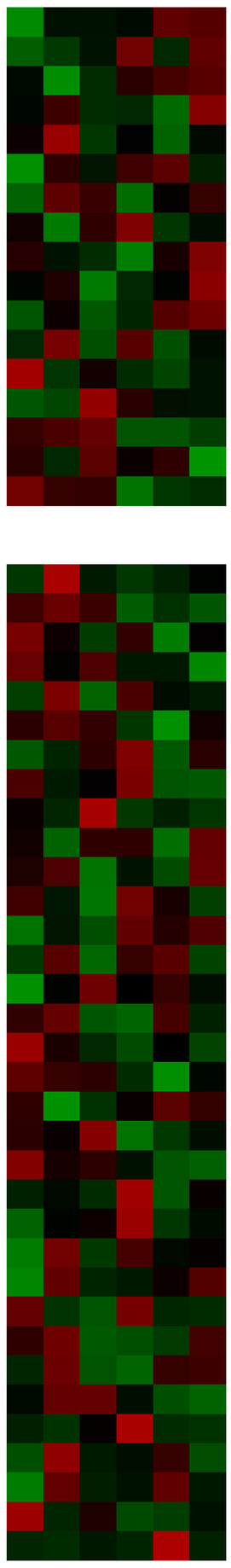

MANF	2973.8	3390.2	3730.5
SDF2L1	2343.9	2508.7	2802.1
CRELD2	3237.5	3919.8	4098.7
HSPA5	10895.7	11801.0	13085.9
HYOU1	1338.0	1600.6	2010.9
PDIA4	931.0	1161.4	1215.4
PDIA6	6247.6	6846.9	7000.5
DNAJB11	3794.6	4409.1	4904.2
HSP90B1	1107.8	1871.5	2378.9
PDIA3	9247.9	9701.5	10251.4
PPIB	15948.8	16397.8	16837.6
C19orf10	2704.3	2920.0	3327.7
SLC35B1	4306.5	4502.6	5212.6
SEC61A1	1042.0	1188.2	1524.8
RPN1	4541.2	5259.5	5517.2
DNAJC3	1361.6	1624.7	1689.7
CDK2AP2	919.6	1143.1	1228.6
ARID5B			
XBP1			
HNRNPAB			
SGK1			
HSPB1			
DDIT4			
ARL4D			
SAP30			
KIAA0408			
GPR17			
HSPH1			
DNASE1L2			
SLC5A3			
GNAS			
GPR3			
TNFRSF25			
TM6SF2			
MKKS			
PLEKHF1			
ZMYM1			
DOK3			
FGF20			
SLC39A2			
KCNIP2			
ERRFI1			
DEDD2			
CCDC117			
USP31			
AHSA2			
CYS1			
CNIH2			
BANP			
CHORDC1			
P4HA1			

GEO Series "GSE35659" Expression Profiles

Num of samples in this series: 24

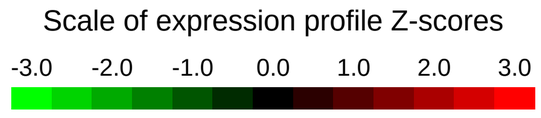

GEO Link:	http://www.ncbi.nlm.nih.gov/geo/query/acc.cgi?acc=GSE35659
Status:	Public on Feb 10 2012
Title:	A transcriptional map of the impact of endurance exercise training on skeletal muscle phenotype (resting muscle after endurance training)
Organism:	Homo sapiens
Experiment type:	Expression profiling by array
Platform:	GPL570
Pubmed ID:	20930125
Summary & Design:	**Summary:** The molecular pathways which are activated and contribute to physiological remodeling of skeletal muscle in response to endurance exercise have not been fully characterized. We previously reported that ~800 gene transcripts are regulated following 6 weeks of supervised endurance training in young sedentary males, referred to as the training responsive transcriptome (TRT). Here we utilized this database together with data on biological variation in muscle adaptation to aerobic endurance training in both humans and a novel out-bred rodent model to study the potential regulatory molecules that coordinate this complex network of genes. We identified three DNA sequences representing RUNX1, SOX9, and PAX3 transcription factor binding sites as over-represented in the TRT. In turn, miRNA profiling indicated that several miRNAs targeting RUNX1, SOX9 and PAX3 were down-regulated by endurance training. The TRT was then examined by contrasting subjects who demonstrated the least vs. the greatest improvement in aerobic capacity (low vs. high responders), and at least 100 of the 800 TRT genes were differentially regulated, thus suggesting regulation of these genes may be important for improving aerobic capacity. In high responders, pro-angiogenic and tissue developmental networks emerged as key candidates for coordinating tissue aerobic adaptation. Beyond RNA level validation there were several DNA variants that associated with VO(2)max trainability in the HERITAGE Family Study but these did not pass conservative Bonferroni adjustment. In addition, in a rat model selected across 10 generations for high aerobic training responsiveness, we found that both the TRT and a homologous subset of the human high responder genes were regulated to a greater degree in high responder rodent skeletal muscle. This analysis provides a comprehensive map of the transcriptomic features important for aerobic exercise-induced improvements in maximal oxygen consumption. **Overall design:** This data is from skeletal muscle post 6 weeks of endurance exercise training.

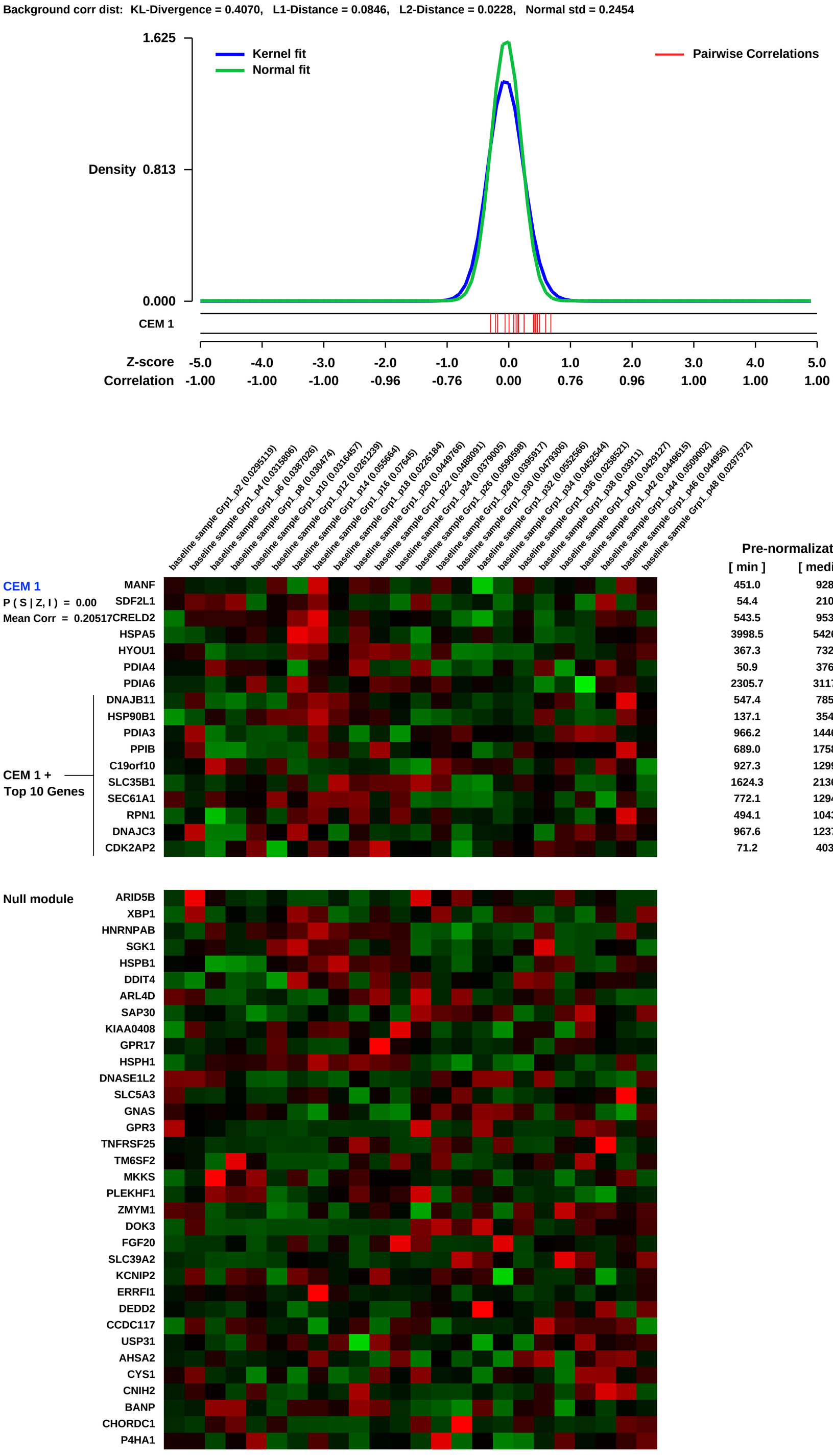

Pre-normalization Quantiles

[min]	[medium]	[max]
451.0	928.1	1464.2
54.4	210.8	395.1
543.5	953.1	1454.1
3998.5	5426.6	8407.8
367.3	732.5	1106.6
50.9	376.1	645.4
2305.7	3117.9	3764.4
547.4	785.8	1297.7
137.1	354.1	687.8
966.2	1446.5	2105.4
689.0	1758.0	3300.2
927.3	1299.3	1904.0
1624.3	2136.5	2808.8
772.1	1294.0	1702.2
494.1	1043.4	1751.4
967.6	1237.3	1641.5
71.2	403.1	750.2

GEO Series "GSE48101" Expression Profiles

Num of samples in this series: 9

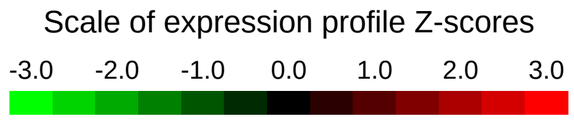

GEO Link:	http://www.ncbi.nlm.nih.gov/geo/query/acc.cgi?acc=GSE48101
Status:	Public on Mar 21 2014
Title:	A conditionally immortalized human pancreatic beta cell line
Organism:	Homo sapiens
Experiment type:	Third-party reanalysis
Platform:	GPL570
Pubmed ID:	24667639
Summary & Design:	**Summary:** Access to an unlimited number of human pancreatic beta cells represents a major challenge in the field of diabetes to better dissect human beta cell functions and to make significant progress in drug discovery and cell replacement therapies. We previously reported the generation of the EndoC-bH1 human beta cell line that was generated by targeted oncogenesis in human fetal pancreases followed by in vivo cell differentiation in mice. Such cell line displayed many functional properties of adult beta cells. Here we devised a novel strategy to generate conditionally immortalized human beta cell lines based on CRE-mediated excision of immortalizing transgenes. The resulting EndoC-bH2 cell line can be massively amplified in vitro. Transgenes are next efficiently excised upon CRE expression leading to cell proliferation arrest and strong enhancement of beta cell specific features such as insulin expression, content and secretion. Excised EndoC-bH2 cells are close to authentic human beta cells and represent a unique tool to further study beta cell function and to understand why adult human beta cells are refractory to proliferation and how to achieve drug-dependent mobilization towards beta cell expansion. **Overall design:** Expression profile of human beta cell lineEndoC-bH2 before and after excision of an immortalization cassette (SV40 LT and hTERT) is compared to human exocrine pancreas cell line SKPC and adult human islets from cadaveric donors. Three replicates were used for each sample group. The three adult human islets samples were taken from GEO series GSE40709 (GSM999550, GSM999551 and GSM999552) and normalized with H357 and SKPC cell line samples using RMA.

Background corr dist: KL-Divergence = 0.0138, L1-Distance = 0.0369, L2-Distance = 0.0013, Normal std = 0.8893

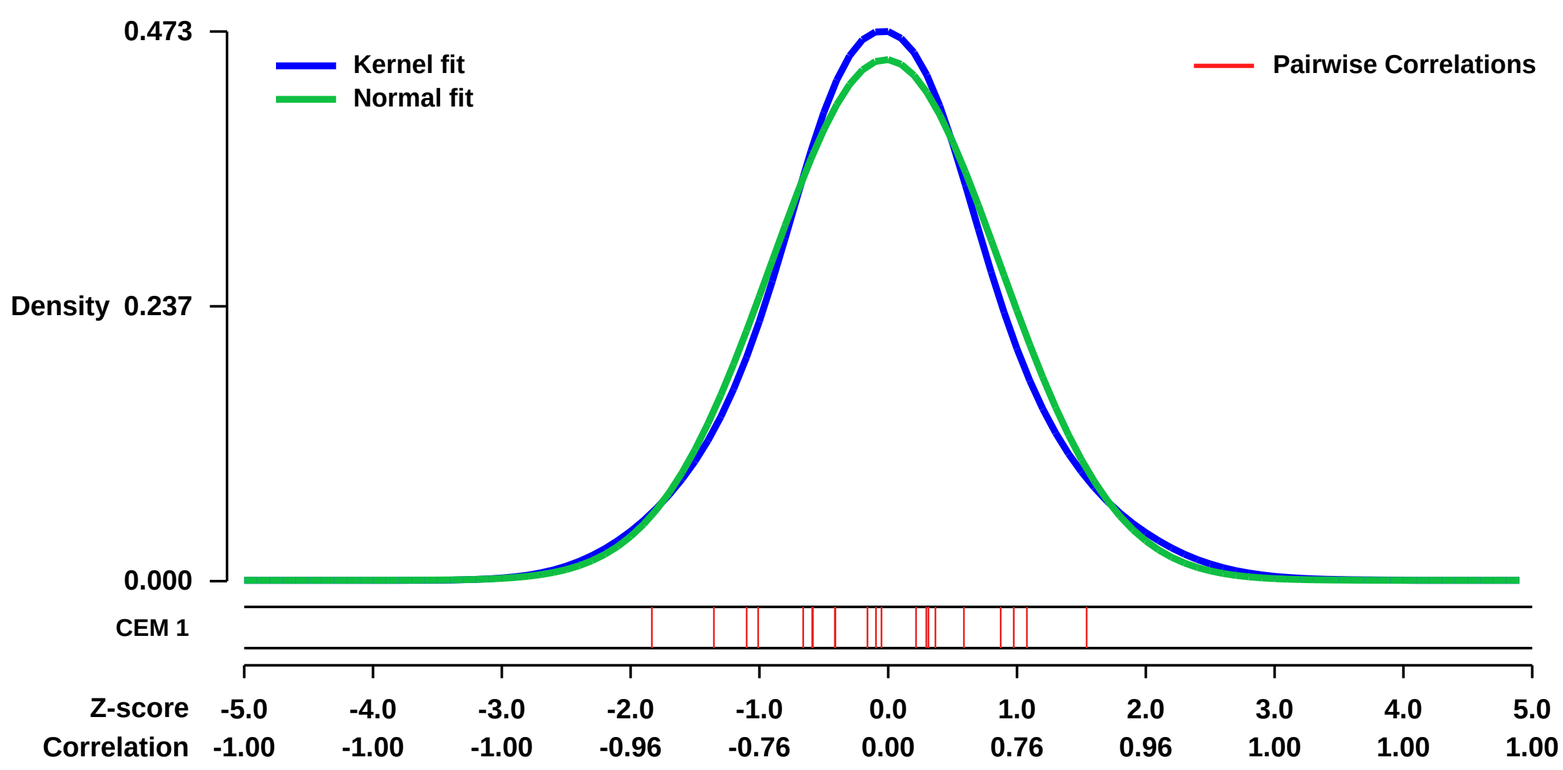

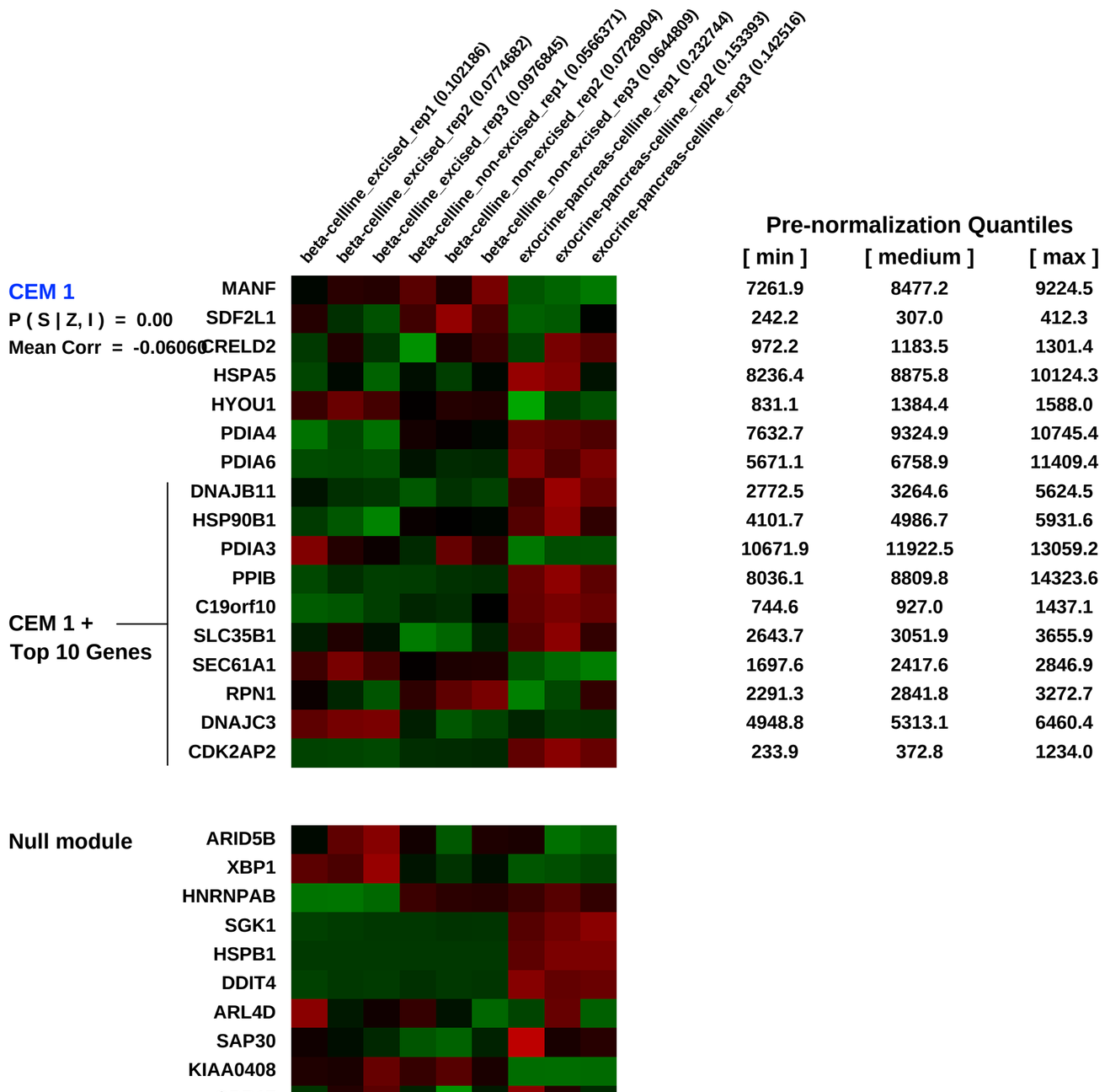

Pre-normalization Quantiles

	[min]	[medium]	[max]
MANF	7261.9	8477.2	9224.5
SDF2L1	242.2	307.0	412.3
CRELD2	972.2	1183.5	1301.4
HSPA5	8236.4	8875.8	10124.3
HYOU1	831.1	1384.4	1588.0
PDIA4	7632.7	9324.9	10745.4
PDIA6	5671.1	6758.9	11409.4
DNAJB11	2772.5	3264.6	5624.5
HSP90B1	4101.7	4986.7	5931.6
PDIA3	10671.9	11922.5	13059.2
PPIB	8036.1	8809.8	14323.6
C19orf10	744.6	927.0	1437.1
SLC35B1	2643.7	3051.9	3655.9
SEC61A1	1697.6	2417.6	2846.9
RPN1	2291.3	2841.8	3272.7
DNAJC3	4948.8	5313.1	6460.4
CDK2AP2	233.9	372.8	1234.0

GEO Series "GSE46925" Expression Profiles

Num of samples in this series: 6

Scale of expression profile Z-scores

-3.0 -2.0 -1.0 0.0 1.0 2.0 3.0

GEO Link:	http://www.ncbi.nlm.nih.gov/geo/query/acc.cgi?acc=GSE46925
Status:	Public on Aug 01 2013
Title:	Aerobic training modulation of the host systemic milieu directly alters breast cancer cell phenotype in vitro.
Organism:	Homo sapiens
Experiment type:	Expression profiling by array
Platform:	GPL570
Pubmed ID:	
Summary & Design:	**Summary:** Aberrant production and/or function of multiple host systemic factors (e.g., metabolic and immune-inflammatory mediators) act in concert to promote a â tumorigenicâ host milieu that directly promotes an aggressive malignant phenotype as well as drug resistance. Hence, strategies with the capacity to simultaneously act across multiple host systemic pathways may be required to optimize therapeutic outcomes in solid tumors. We hypothesized that chronic aerobic training, a pleiotropic whole-body intervention, modulates multiple systemic host pathways that, in turn, effectively alters cancer cell phenotype in vitro. Plasma samples from patients with solid tumors exposed to chronic aerobic training or sedentary control were comprehensively characterized for changes in immune, inflammatory, and metabolic pathways. Compared with sedentary control, aerobic training caused significant reductions in interleukin (IL)-4, macrophage inflammatory protein-1 beta (MIP1-¿†), vascular endothelial growth factor (VEGF), tumor necrosis factor-alpha (TNF-¿–), and hepatocyte growth factor (HGF). There were no significant changes in leukocyte phenotype or any plasma metabolite signatures. Exposure of estrogen receptor (ER) distinct human breast cancer cell lines (MCF-7 and MDA-MB-231) to post-intervention serum from breast cancer patients exposed to aerobic training caused marked increases in proliferation, migration, and apoptosis, compared to control patient serum. Only the combination of cytokines significantly reduced in plasma following aerobic training recapitulated the phenotype observed with patient serum in MCF-7 cells whereas only the single addition of MIP-1¿† or HGF significantly increased apoptosis in MDA-MB-231 cells. Co-culturing of MDA-MB-231 cells with patient exercise serum and a HGF neutralizing antibody increased proliferation and completely abrogated exercise serum-induced apoptosis. Finally, whole-genome microarray of MDA-MB-231 cells exposed to exercise or control patient serum revealed differential modulation of 310 genes including PTEN, CDK3, and IGFBP1. Our findings indicate the widespread potential of chronic aerobic training to modulate host immune-inflammatory systemic factors in patients with solid tumors. Modulation of such pathways directly alters breast cancer phenotypes providing novel insight into the molecular pathways by which exercise may inhibit malignant progression. **Overall design:** MDA-MB-231 cells were plated at 250,000 cells/well in triplicate with 10% FBS in 6-well plates and left overnight to adhere. Media was suctioned off and replaced with serum free media. Patient serum was then added to the wells at a 10% final concentration and RNA was harvested using Qiagen RNeasy kit after 4 days.

Background corr dist: KL-Divergence = 0.0409, L1-Distance = 0.0142, L2-Distance = 0.0002, Normal std = 0.6049

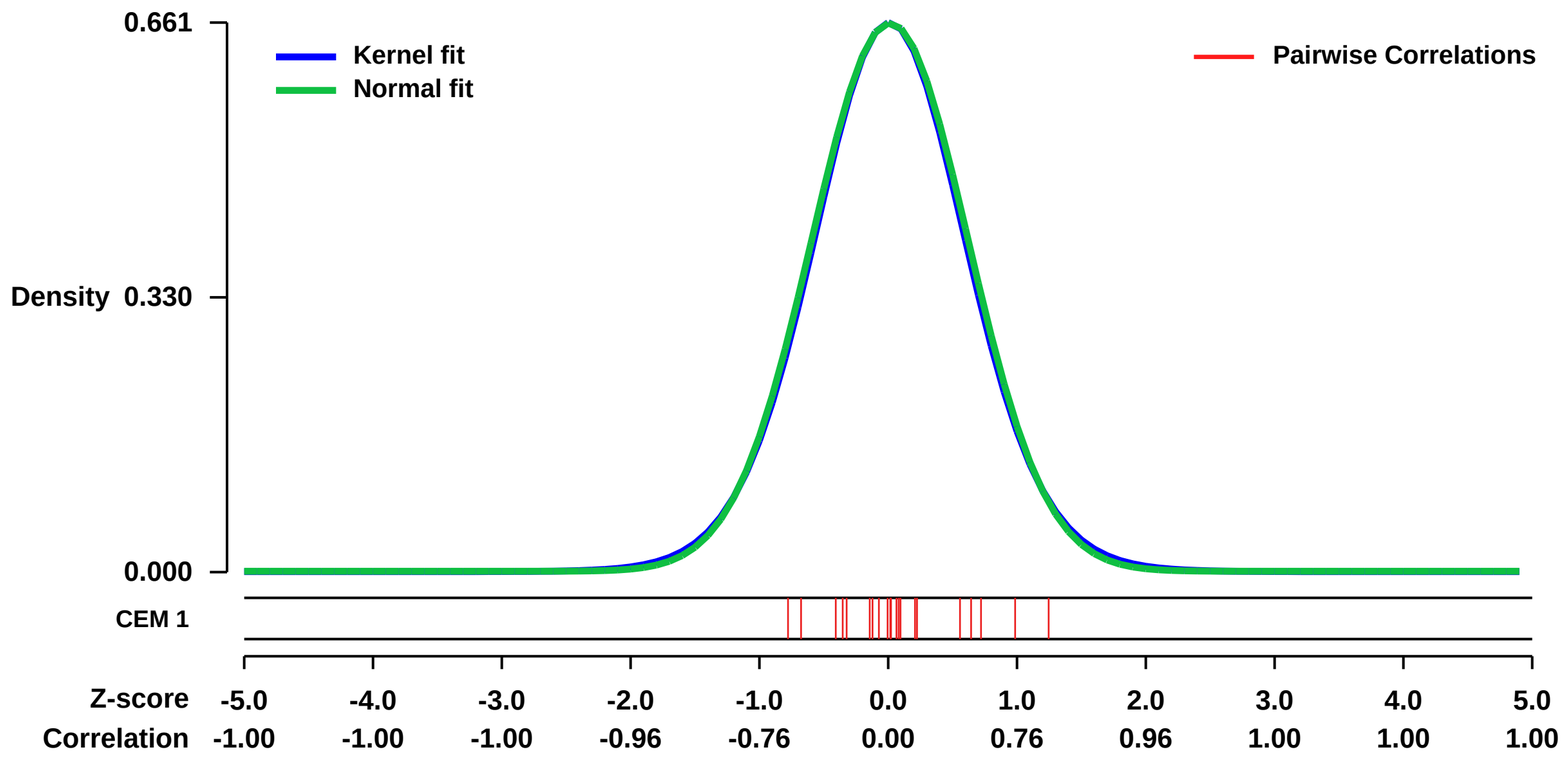

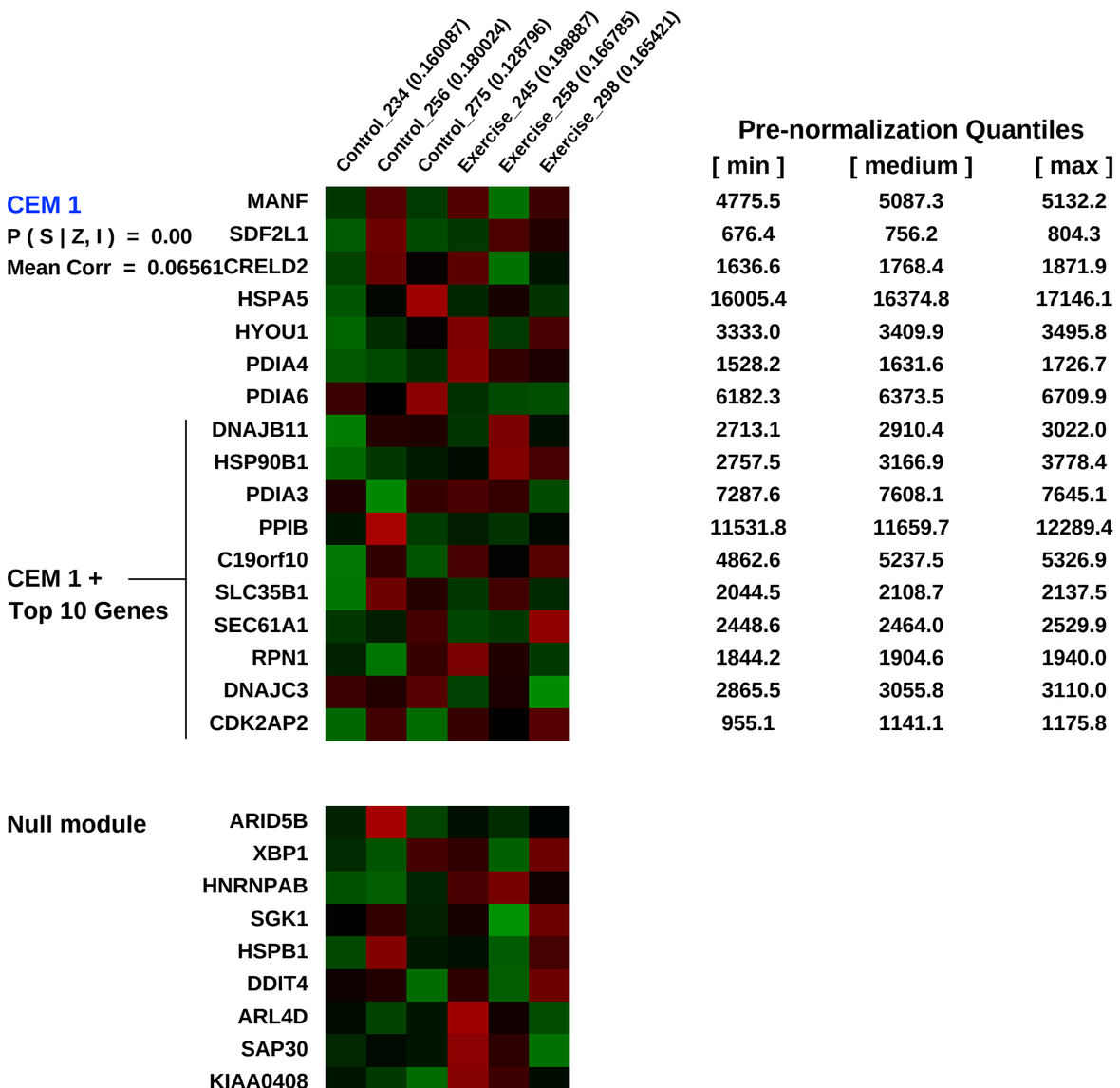

Pre-normalization Quantiles

	[min]	[medium]	[max]
MANF	4775.5	5087.3	5132.2
SDF2L1	676.4	756.2	804.3
CRELD2	1636.6	1768.4	1871.9
HSPA5	16005.4	16374.8	17146.1
HYOU1	3333.0	3409.9	3495.8
PDIA4	1528.2	1631.6	1726.7
PDIA6	6182.3	6373.5	6709.9
DNAJB11	2713.1	2910.4	3022.0
HSP90B1	2757.5	3166.9	3778.4
PDIA3	7287.6	7608.1	7645.1
PPIB	11531.8	11659.7	12289.4
C19orf10	4862.6	5237.5	5326.9
SLC35B1	2044.5	2108.7	2137.5
SEC61A1	2448.6	2464.0	2529.9
RPN1	1844.2	1904.6	1940.0
DNAJC3	2865.5	3055.8	3110.0
CDK2AP2	955.1	1141.1	1175.8

GEO Series "GSE46801" Expression Profiles

Num of samples in this series: 9

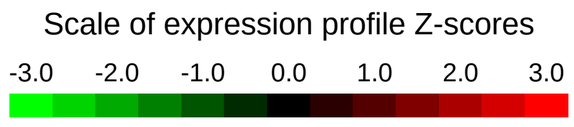

GEO Link:	http://www.ncbi.nlm.nih.gov/geo/query/acc.cgi?acc=GSE46801
Status:	Public on Aug 01 2013
Title:	Expression data from Control, Uninfected and BRAF infected cells
Organism:	Homo sapiens
Experiment type:	Expression profiling by array
Platform:	GPL570
Pubmed ID:	24043806
Summary & Design:	**Summary:** Melanocytes within benign human nevi are the paradigm for tumor suppressive senescent cells in a pre-malignant neoplasm. These cells typically contain mutations in either the BRAF or N-RAS oncogene and express markers of senescence, including p16. However, a nevus can contain 10s to 100s of thousands of clonal melanocytes and approximately 20-30% of melanoma are thought to arise in association with a pre-existing nevus. Neither observation is indicative of fail-safe senescence-associated proliferation arrest and tumor suppression. We set out to better understand the status of nevus melanocytes. Proliferation-promoting Wnt target genes, such as cyclin D1 and c-myc, were repressed in oncogene-induced senescent melanocytes in vitro, and repression of Wnt signaling in these cells induced a senescent-like state. In contrast, cyclin D1 and c-myc were expressed in many melanocytes of human benign nevi. Specifically, activated Wnt signalling in nevi correlated inversely with nevus maturation, an established dermatopathological correlate of clinical benignancy. Single cell analyses of lone epidermal melanocytes and nevus melanocytes showed that expression of proliferation-promoting Wnt targets correlates with prior proliferative expansion of p16-expressing nevus melanocytes. In a mouse model, activation of Wnt signaling delayed, but did not bypass, senescence of oncogene-expressing melanocytes, leading to massive accumulation of proliferation-arrested, p16-positive non-malignant melanocytes. We conclude that clonal hyperproliferation of oncogene-expressing melanocytes to form a nevus is facilitated by transient delay of senescence due to activated Wnt signaling. The observation that activation of Wnt signaling correlates inversely with nevus maturation, an indicator of clinical benignancy, supports the notion that persistent destabilization of senescence by Wnt signaling contributes to the malignant potential of nevi. We used microarrays to detail the global programme of gene expression after lentiviral infection of BRAF in 3 replicates. **Overall design:** Primary human melanocytes were infected/uninfected with lentivirus containing either an Empty Vector or activated BRAFV600E mutant in three biological replicates

Background corr dist: KL-Divergence = 0.0475, L1-Distance = 0.0450, L2-Distance = 0.0027, Normal std = 0.6185

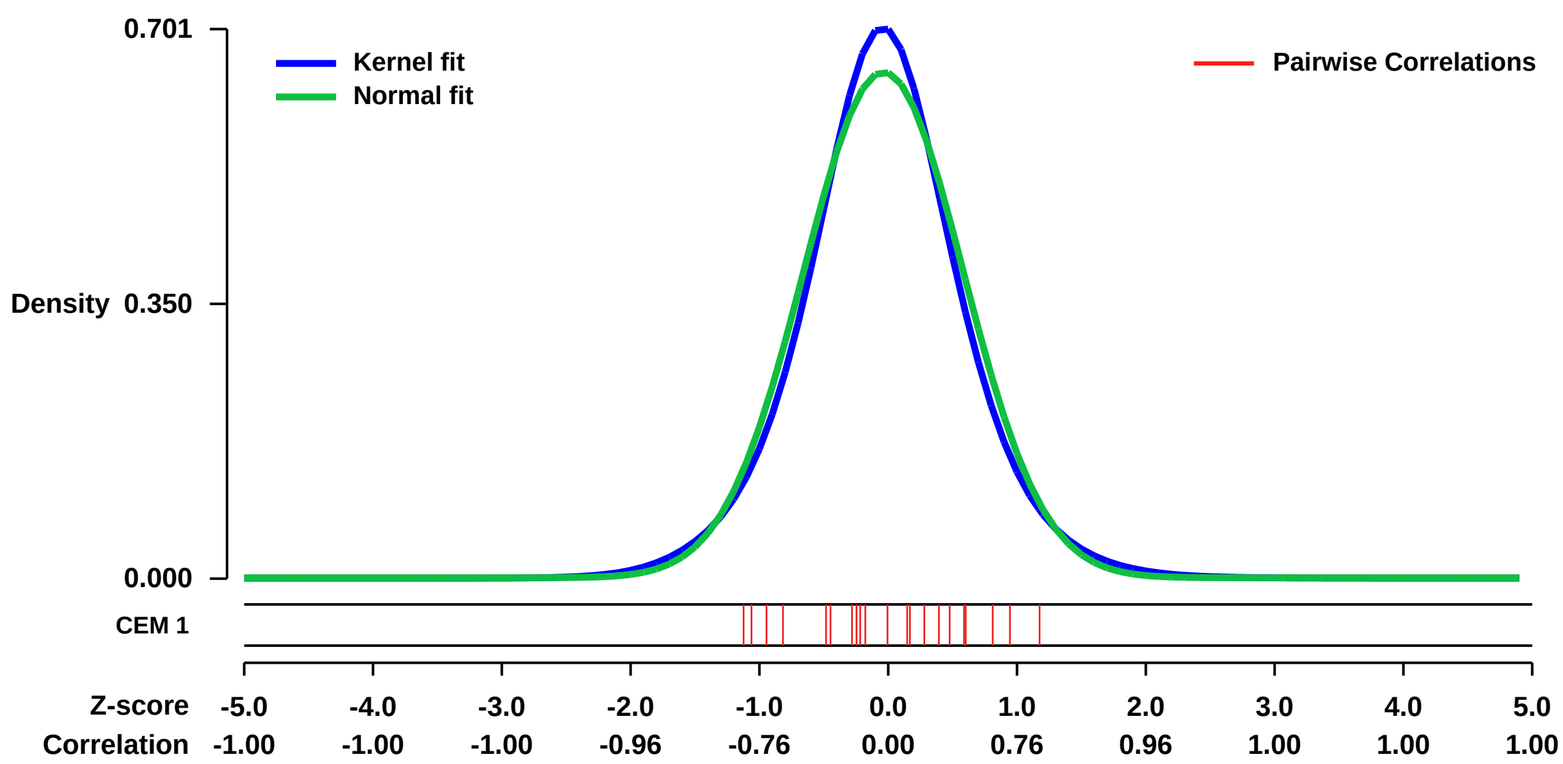

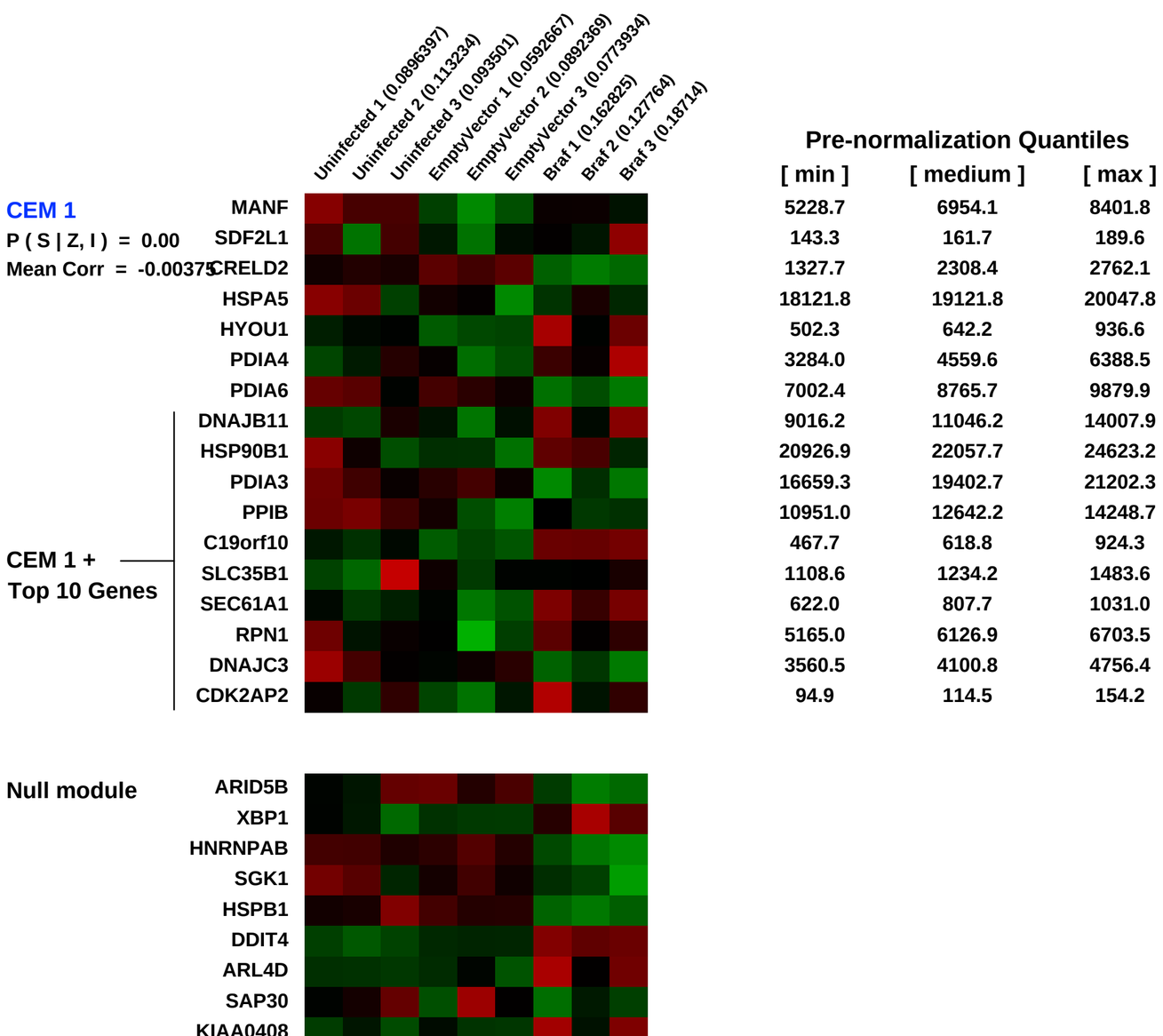

Pre-normalization Quantiles

	[min]	[medium]	[max]
MANF	5228.7	6954.1	8401.8
SDF2L1	143.3	161.7	189.6
CRELD2	1327.7	2308.4	2762.1
HSPA5	18121.8	19121.8	20047.8
HYOU1	502.3	642.2	936.6
PDIA4	3284.0	4559.6	6388.5
PDIA6	7002.4	8765.7	9879.9
DNAJB11	9016.2	11046.2	14007.9
HSP90B1	20926.9	22057.7	24623.2
PDIA3	16659.3	19402.7	21202.3
PPIB	10951.0	12642.2	14248.7
C19orf10	467.7	618.8	924.3
SLC35B1	1108.6	1234.2	1483.6
SEC61A1	622.0	807.7	1031.0
RPN1	5165.0	6126.9	6703.5
DNAJC3	3560.5	4100.8	4756.4
CDK2AP2	94.9	114.5	154.2

GEO Series "GSE42407" Expression Profiles

Num of samples in this series: 6

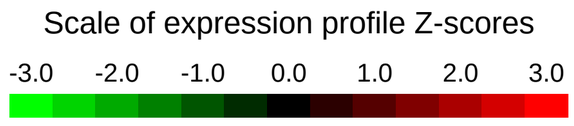

GEO Link:	http://www.ncbi.nlm.nih.gov/geo/query/acc.cgi?acc=GSE42407
Status:	Public on Dec 11 2012
Title:	Expression data from CL1-0 and CL1-5 lung cancer cell line.
Organism:	Homo sapiens
Experiment type:	Expression profiling by array
Platform:	GPL570
Pubmed ID:	23267084
Summary & Design:	**Summary:** A lung cancer cell model of invasive transformation was developed to select progressively invasive cell populations from a parental cell line of human lung adenocarcinoma, CL1. Five progressive sub-clones namely, CL1-1, CL1-2, CL1-3 CL1-4, and CL1-5 were selected using transwell and displayed increasing invasion potential (Chu et al, 1997). Here, we used microarrays to analyze and compare gene expression profiles between CL1-0 and CL1-5 for the identification of invasion/metastasis associated gene signatures. **Overall design:** CL1-0 and CL1-5 lung cancer cell lines were used for RNA extraction and hybridization on Affymetrix microarrays. A total of 6 chips were used for microarray analysis including three biological repeats from CL1-0 and three biological repeats from CL1-5.

Background corr dist: KL-Divergence = 0.0199, L1-Distance = 0.0477, L2-Distance = 0.0025, Normal std = 0.8472

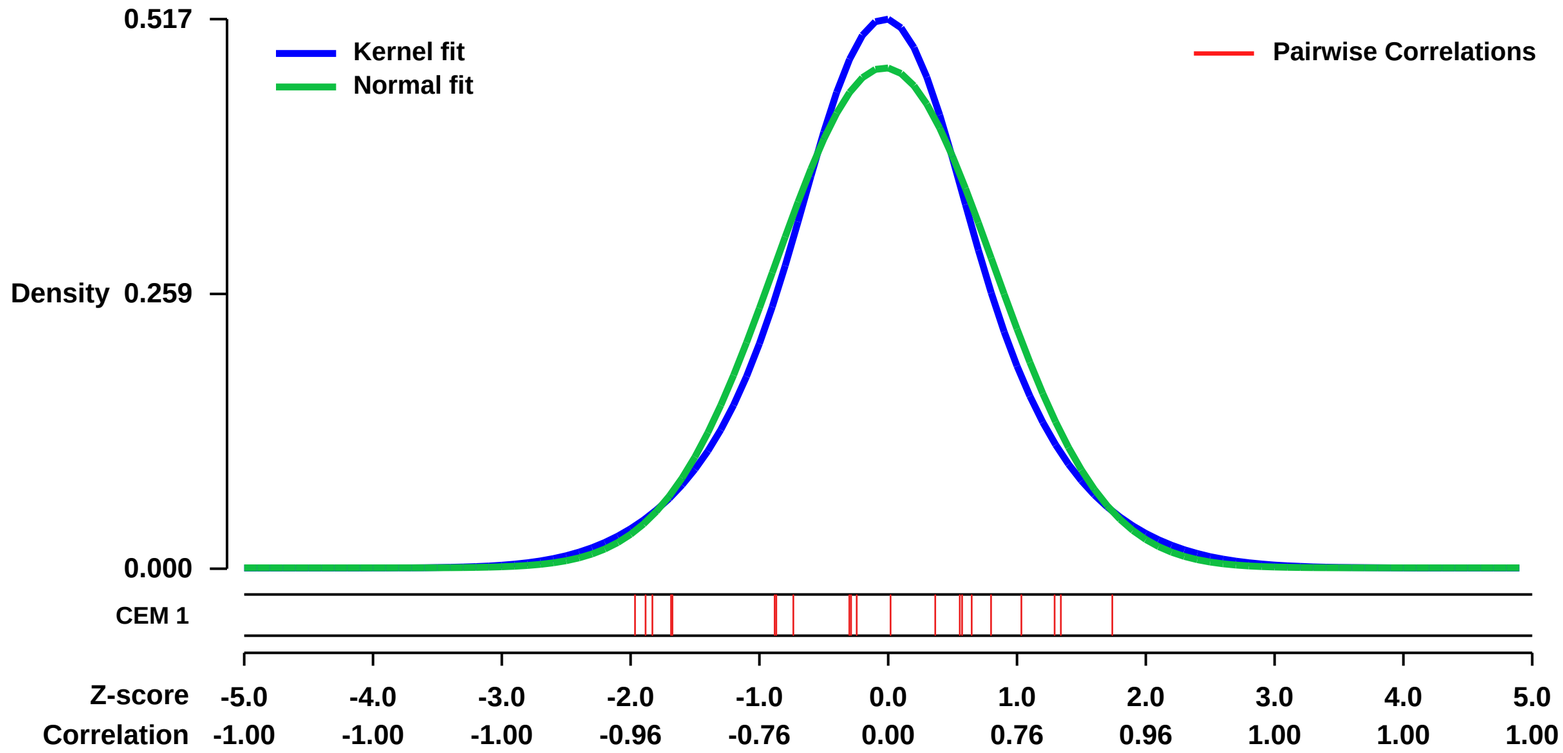

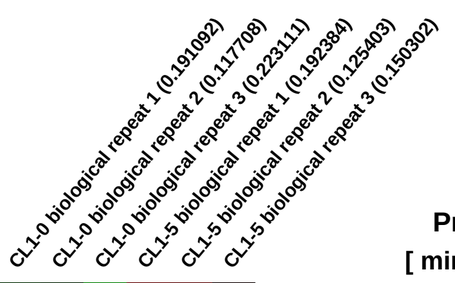

Pre-normalization Quantiles

CEM 1
P (S | Z, I) = 0.00
Mean Corr = -0.07186

CEM 1 + Top 10 Genes

Null module

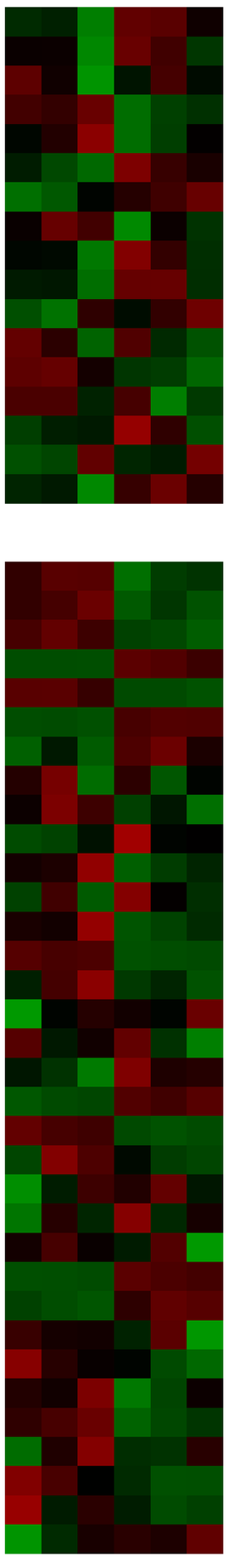

	[min]	[medium]	[max]
MANF	2807.3	3881.9	4509.3
SDF2L1	752.3	1122.9	1359.6
CRELD2	3498.2	4082.2	4357.3
HSPA5	23252.8	31310.3	33976.0
HYOU1	4074.7	4971.7	6069.8
PDIA4	758.6	939.9	1079.5
PDIA6	7216.0	8777.4	9475.4
DNAJB11	3253.0	3685.3	3950.5
HSP90B1	3007.0	4307.3	5848.6
PDIA3	5947.0	9146.9	13696.1
PPIB	13796.7	16144.9	17074.8
C19orf10	3247.7	3887.1	4142.2
SLC35B1	3607.0	4245.1	4664.4
SEC61A1	2710.8	3213.9	3224.2
RPN1	4515.6	4594.4	4847.1
DNAJC3	975.9	1059.9	1283.8
CDK2AP2	1039.6	1334.2	1451.5
ARID5B			
XBP1			
HNRNPAB			
SGK1			
HSPB1			
DDIT4			
ARL4D			
SAP30			
KIAA0408			
GPR17			
HSPH1			
DNASE1L2			
SLC5A3			
GNAS			
GPR3			
TNFRSF25			
TM6SF2			
MKKS			
PLEKHF1			
ZMYM1			
DOK3			
FGF20			
SLC39A2			
KCNIP2			
ERRFI1			
DEDD2			
CCDC117			
USP31			
AHSA2			
CYS1			
CNIH2			
BANP			
CHORDC1			
P4HA1			

GEO Series "GSE19533" Expression Profiles

Num of samples in this series: 10

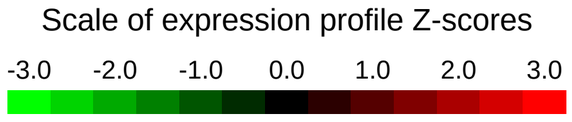

GEO Link:	http://www.ncbi.nlm.nih.gov/geo/query/acc.cgi?acc=GSE19533
Status:	Public on Jan 04 2012
Title:	Gene expression changes in the human diaphragm following cardiothoracic surgery
Organism:	Homo sapiens
Experiment type:	Expression profiling by array
Platform:	GPL570
Pubmed ID:	21463877
Summary & Design:	**Summary:** It is unknown how soon the diaphragm begins to start the process of atrophy following the start of MV. We hypothesized that genes responsible for maintaining diaphragmatic contractile function, stress response, energy transduction would be altered over the course of a 5 hour cardiothoracic surgery. **Overall design:** Two diaphragm biopsies were obtained from 5 male patients (~67 +/- 11 years) undergoing cardiothoracic surgery. The first biopsy was obtained as soon as the diaphragm was exposed; the second biopsy was obtained as late in the surgery as possible (4.9 +/- 1.8 hours). We profiled mRNA from the 5 pairs of muscle biopsies with a microarray (Affymetrix Human Genome U133 Plus 2.0).

Background corr dist: KL-Divergence = 0.0581, L1-Distance = 0.0256, L2-Distance = 0.0010, Normal std = 0.5302

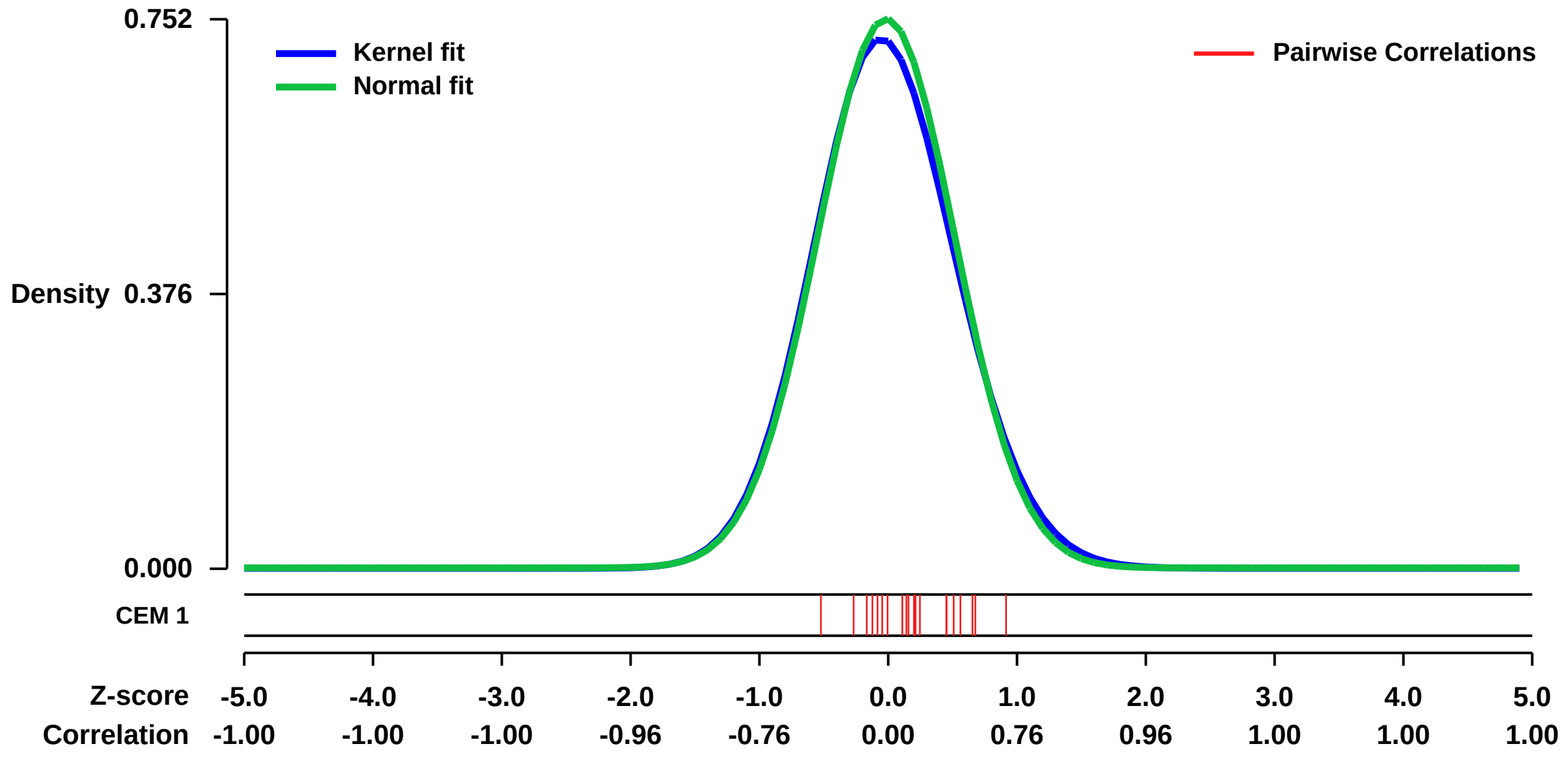

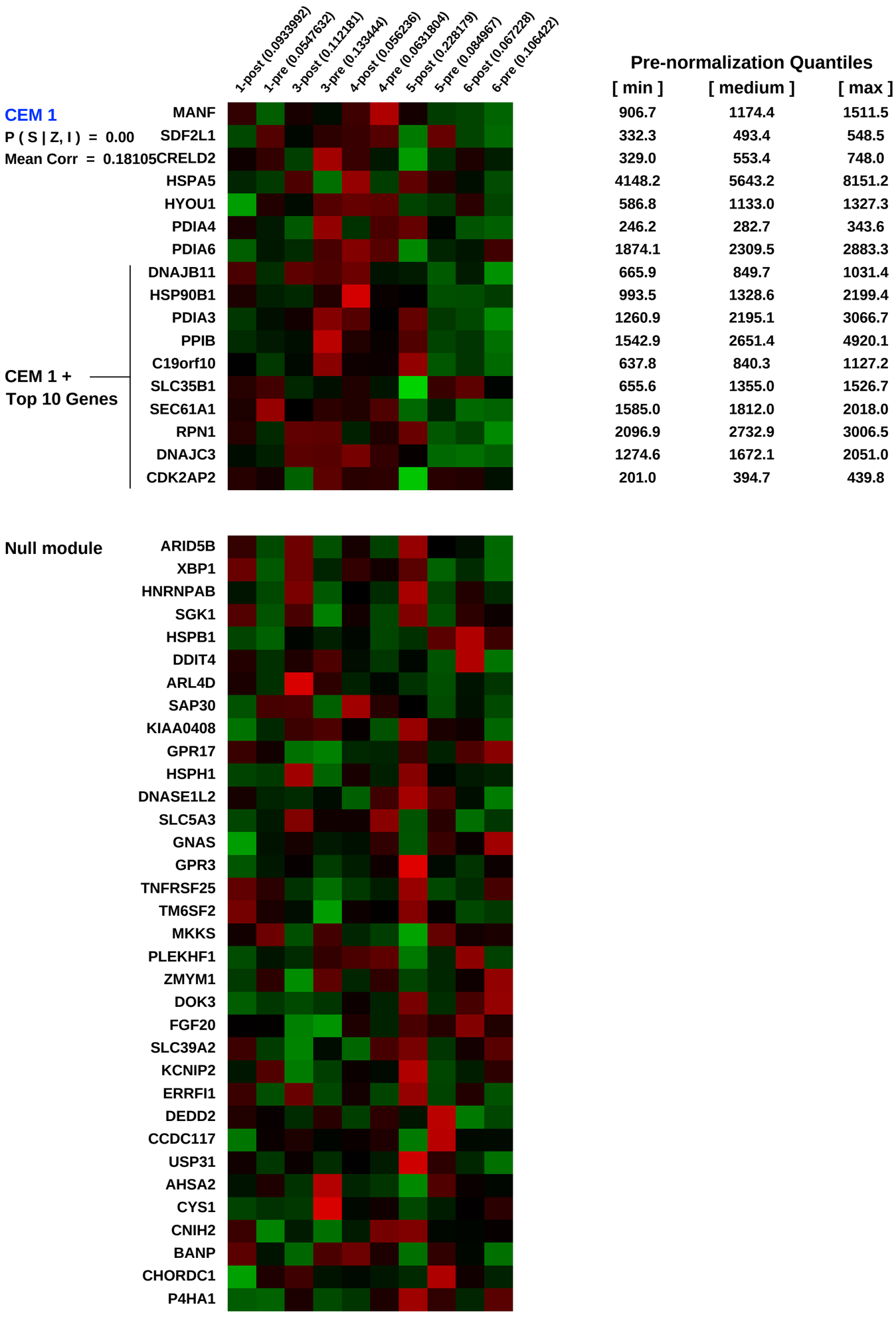

GEO Series "GSE40301" Expression Profiles

Num of samples in this series: 12

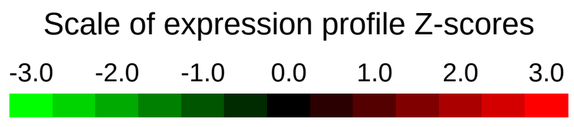

GEO Link:	http://www.ncbi.nlm.nih.gov/geo/query/acc.cgi?acc=GSE40301
Status:	Public on Aug 23 2012
Title:	GPI-anchored Timp1 protein
Organism:	Homo sapiens
Experiment type:	Expression profiling by array
Platform:	GPL570
Pubmed ID:	
Summary & Design:	**Summary:** Tissue inhibitor of metalloproteinase 1 (TIMP-1) controls matrix metalloproteinase (MMP) activity through 1:1 stochiometric binding. Human TIMP-1 fused to a glycosylphosphatidylinositol (GPI) anchor (TIMP-1-GPI) shifts the activity of TIMP-1 from the extracellular matrix to the cell surface. TIMP-1-GPI treated renal cell carcinoma cells (RCC) show increased apoptosis and reduced proliferation. Transcriptomic profiling and regulatory pathway mapping were used to identify potential mechanisms driving these effects. Significant changes in inhibitor of DNA binding (IDs), TGF-¸†1/SMAD and BMP pathways resulted from TIMP-1-GPI treatment. These events were linked to reduced TGF-¸†1 signaling mediated by inhibition of proteolytic processing of latent TGF-¸†1 by TIMP-1-GPI. Activity of TIMP-1 from the extracellular matrix to the cell surface. TIMP-1-GPI treated renal cell carcinoma cells (RCC) show increased apoptosis and reduced proliferation. Transcriptomic profiling and regulatory pathway mapping were used to identify potential mechanisms driving these effects. Significant changes in inhibitor of DNA binding (IDs), TGF-¸†1/SMAD and BMP pathways resulted from TIMP-1-GPI treatment. These events were linked to reduced TGF-¸†1 signaling mediated by inhibition of proteolytic processing of latent TGF-¸†1 by TIMP-1-GPI. **Overall design:** Renal cell carcinoma cells were transfected with empty vector, rhTimp1 and 2 concentrations of Timp1-GPI fusion protein

Background corr dist: KL-Divergence = 0.0740, L1-Distance = 0.0258, L2-Distance = 0.0011, Normal std = 0.4863

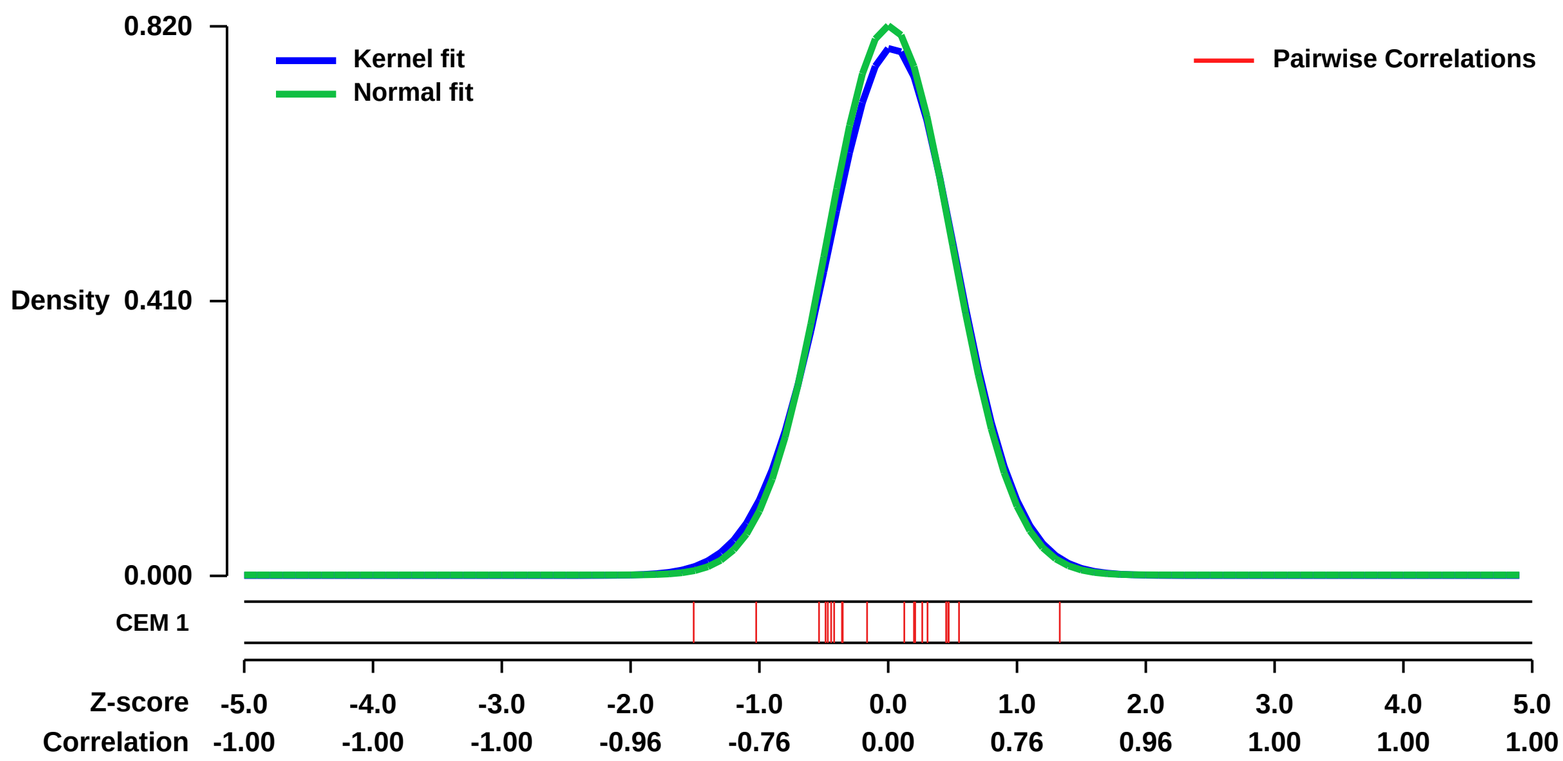

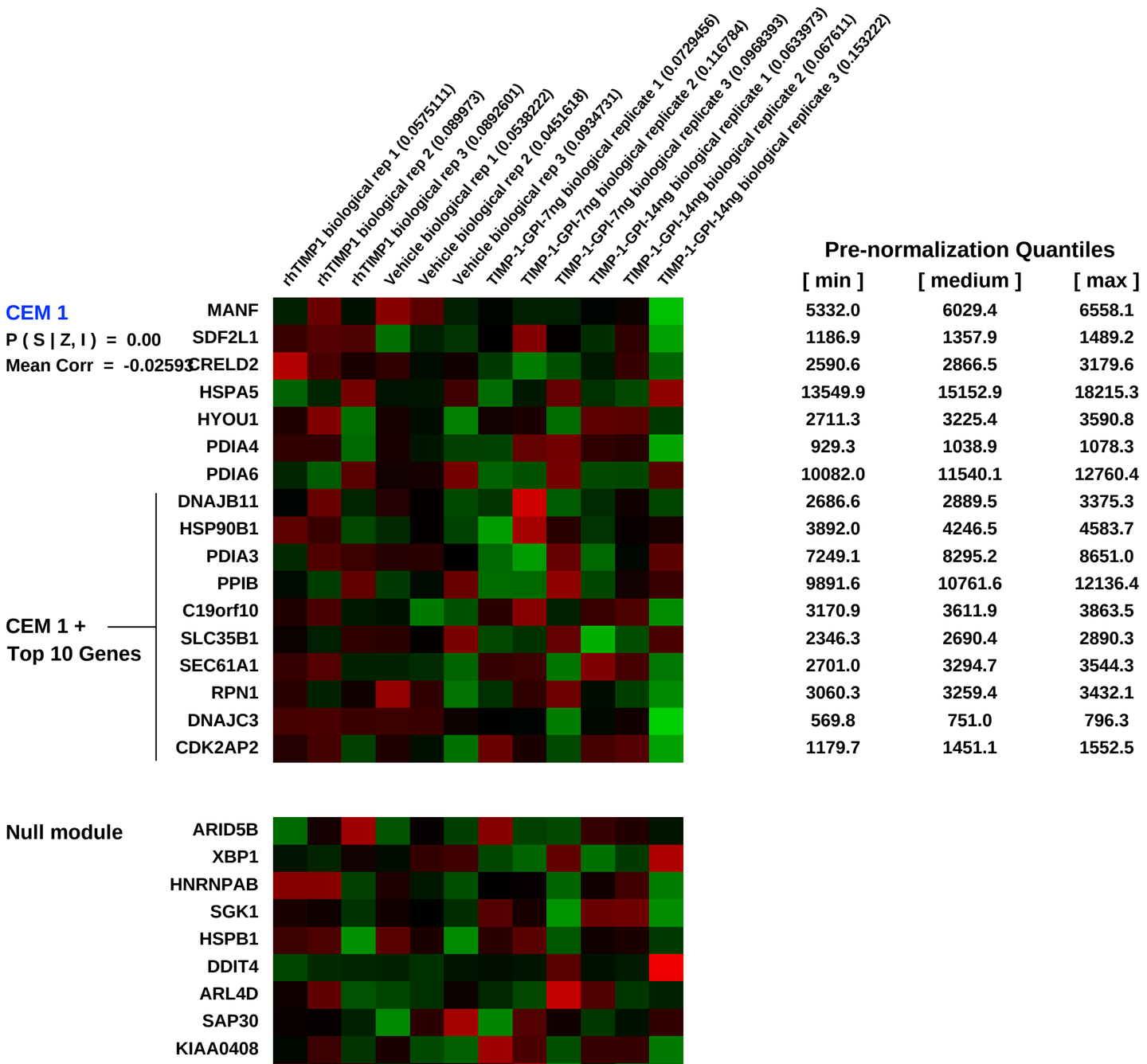

Pre-normalization Quantiles

	[min]	[medium]	[max]
MANF	5332.0	6029.4	6558.1
SDF2L1	1186.9	1357.9	1489.2
CRELD2	2590.6	2866.5	3179.6
HSPA5	13549.9	15152.9	18215.3
HYOU1	2711.3	3225.4	3590.8
PDIA4	929.3	1038.9	1078.3
PDIA6	10082.0	11540.1	12760.4
DNAJB11	2686.6	2889.5	3375.3
HSP90B1	3892.0	4246.5	4583.7
PDIA3	7249.1	8295.2	8651.0
PPIB	9891.6	10761.6	12136.4
C19orf10	3170.9	3611.9	3863.5
SLC35B1	2346.3	2690.4	2890.3
SEC61A1	2701.0	3294.7	3544.3
RPN1	3060.3	3259.4	3432.1
DNAJC3	569.8	751.0	796.3
CDK2AP2	1179.7	1451.1	1552.5

GEO Series "GSE34828" Expression Profiles

Num of samples in this series: 6

Scale of expression profile Z-scores

-3.0 -2.0 -1.0 0.0 1.0 2.0 3.0

GEO Link:	http://www.ncbi.nlm.nih.gov/geo/query/acc.cgi?acc=GSE34828
Status:	Public on Dec 03 2013
Title:	Expression data from fibroblast growth factor receptor 4 (FGFR4) knock down ovarian cancer cell lines
Organism:	Homo sapiens
Experiment type:	Expression profiling by array
Platform:	GPL570
Pubmed ID:	23344261
Summary & Design:	**Summary:** Advanced ovarian cancer is the most lethal gynecologic malignancy in the United States. Currently patients are treated by surgical cytoreductive surgery with the aim of reducing tumor burden to microscopic disease followed by adjuvant combined treatment with a platinum and taxane containing chemotherapy, which affords 80% of patients an initial complete response. However, Abdominal and pelvic recurrence rates are high and response to further chemotherapy is limited. Attempts at introducing biologic therapeutic agents to improve outcome in this disease are ongoing, while prognostic or predictive biomarkers that can stratify patients for treatment are still lacking. Using a 60-mer 22K oligonucleotide-based array comparative genome hybridization (CGH) platform combined with DNA isolated from microdissected tumor tissue samples, Birrer et. al. reported that the amplification of 5q31-35.3 in ovarian cancer cells is a negative prognostic indicator for patients with advanced stage high-grade serous ovarian cancer (HGSC). Further studies showed that fibroblast growth factor 1 (FGF1) located in the amplicon, may be one of the driving genes for ovarian cancer progression (Birrer et. al., 2007). Besides FGF1, located on the same amplicon is one of its receptors fibroblast growth factor receptor 4 (FGFR4), suggesting that it may also be amplified and may be another driving gene involved in ovarian cancer pathogenesis.In this study, we used microarrays to explore and compare gene expression profiles between FGFR4 knock down ovarian cancer cell lines and their corresponding parental cell lines. **Overall design:** Two high grade serous ovarian cancer cell lines: SKOV3 and OVCA432 were selected for this study. For each of the cell lines, two different siRNA sequences which both target human FGFR4 were used. While a non-target scramble siRNA sequence was used as control. Ovarian cancer cells were transfected with siRNA using lipofectamine (Invitrogen). RNA extraction was performed 72 hours post-transfection, followed by hybridization on Affymetrix microarrays.

Background corr dist: KL-Divergence = 0.0336, L1-Distance = 0.0242, L2-Distance = 0.0007, Normal std = 0.6546

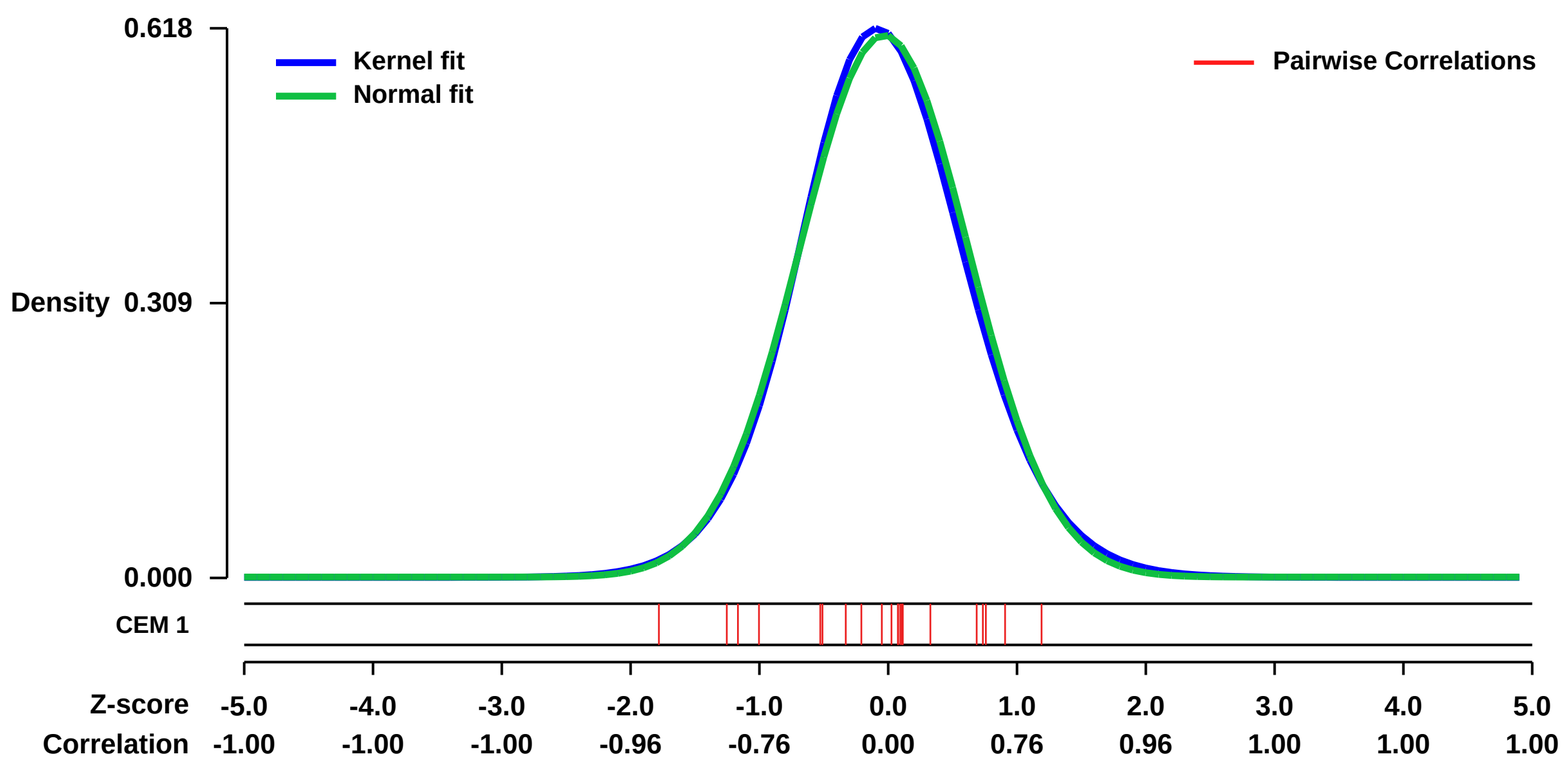

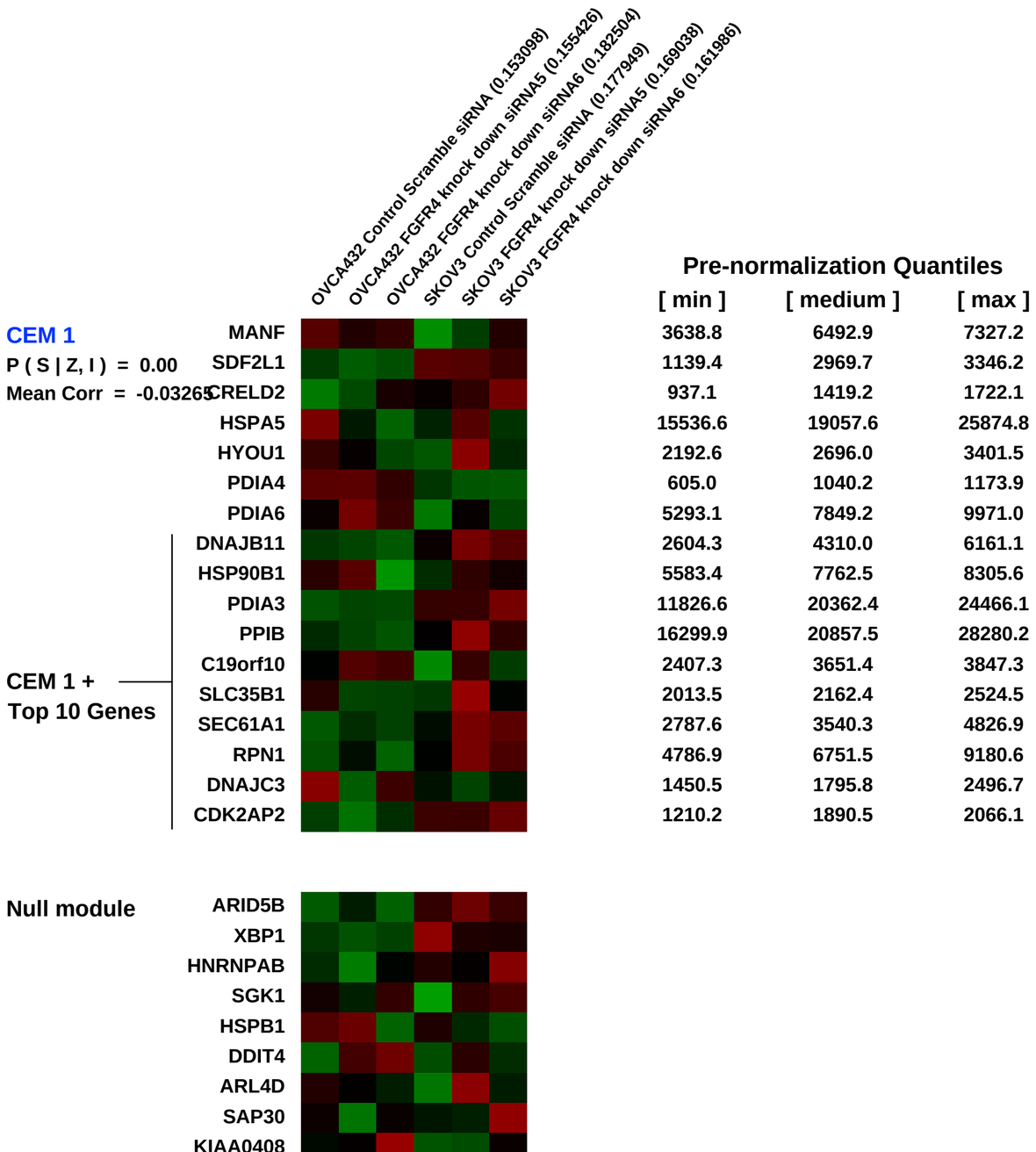

	Pre-normalization Quantiles		
	[min]	[medium]	[max]
MANF	3638.8	6492.9	7327.2
SDF2L1	1139.4	2969.7	3346.2
CRELD2	937.1	1419.2	1722.1
HSPA5	15536.6	19057.6	25874.8
HYOU1	2192.6	2696.0	3401.5
PDIA4	605.0	1040.2	1173.9
PDIA6	5293.1	7849.2	9971.0
DNAJB11	2604.3	4310.0	6161.1
HSP90B1	5583.4	7762.5	8305.6
PDIA3	11826.6	20362.4	24466.1
PPIB	16299.9	20857.5	28280.2
C19orf10	2407.3	3651.4	3847.3
SLC35B1	2013.5	2162.4	2524.5
SEC61A1	2787.6	3540.3	4826.9
RPN1	4786.9	6751.5	9180.6
DNAJC3	1450.5	1795.8	2496.7
CDK2AP2	1210.2	1890.5	2066.1
ARID5B			
XBP1			
HNRNPAB			
SGK1			
HSPB1			
DDIT4			
ARL4D			
SAP30			
KIAA0408			
GPR17			
HSPH1			
DNASE1L2			
SLC5A3			
GNAS			
GPR3			
TNFRSF25			
TM6SF2			
MKKS			
PLEKHF1			
ZMYM1			
DOK3			
FGF20			
SLC39A2			
KCNIP2			
ERRFI1			
DEDD2			
CCDC117			
USP31			
AHSA2			
CYS1			
CNIH2			
BANP			
CHORDC1			
P4HA1			

GEO Series "GSE28274" Expression Profiles

Num of samples in this series: 6

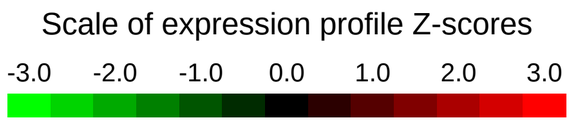

GEO Link:	http://www.ncbi.nlm.nih.gov/geo/query/acc.cgi?acc=GSE28274
Status:	Public on Apr 04 2011
Title:	Real-time Monitoring of Cisplatin Toxicity on Cancer Cells
Organism:	Homo sapiens
Experiment type:	Expression profiling by array
Platform:	GPL570
Pubmed ID:	21603599
Summary & Design:	**Summary:** Treatment of MCF7 breast cancer cells by cisplatin leads to a very specific metabolic response and an onset of cell death about 10-11 h after beginning of treatment. For more detailed understanding of the molecular processes underlying the specific metabolic response, mRNA was isolated from MCF7 cells when the specific changes, (i) induction of glycolysis and (ii) onset of cell death, were detected during online measurement in the cell biosensor system. **Overall design:** MCF7 breast cancer cells were treated with cisplatin in the BIONAS 2500 cell biosensor chip system, and samples were collected from the biosensor chip module at time points when glycolysis was induced (change of ph; 8-9h) and at the beginning of cell death (change of impedance; 10-11h).

Background corr dist: KL-Divergence = 0.0327, L1-Distance = 0.0211, L2-Distance = 0.0005, Normal std = 0.6534

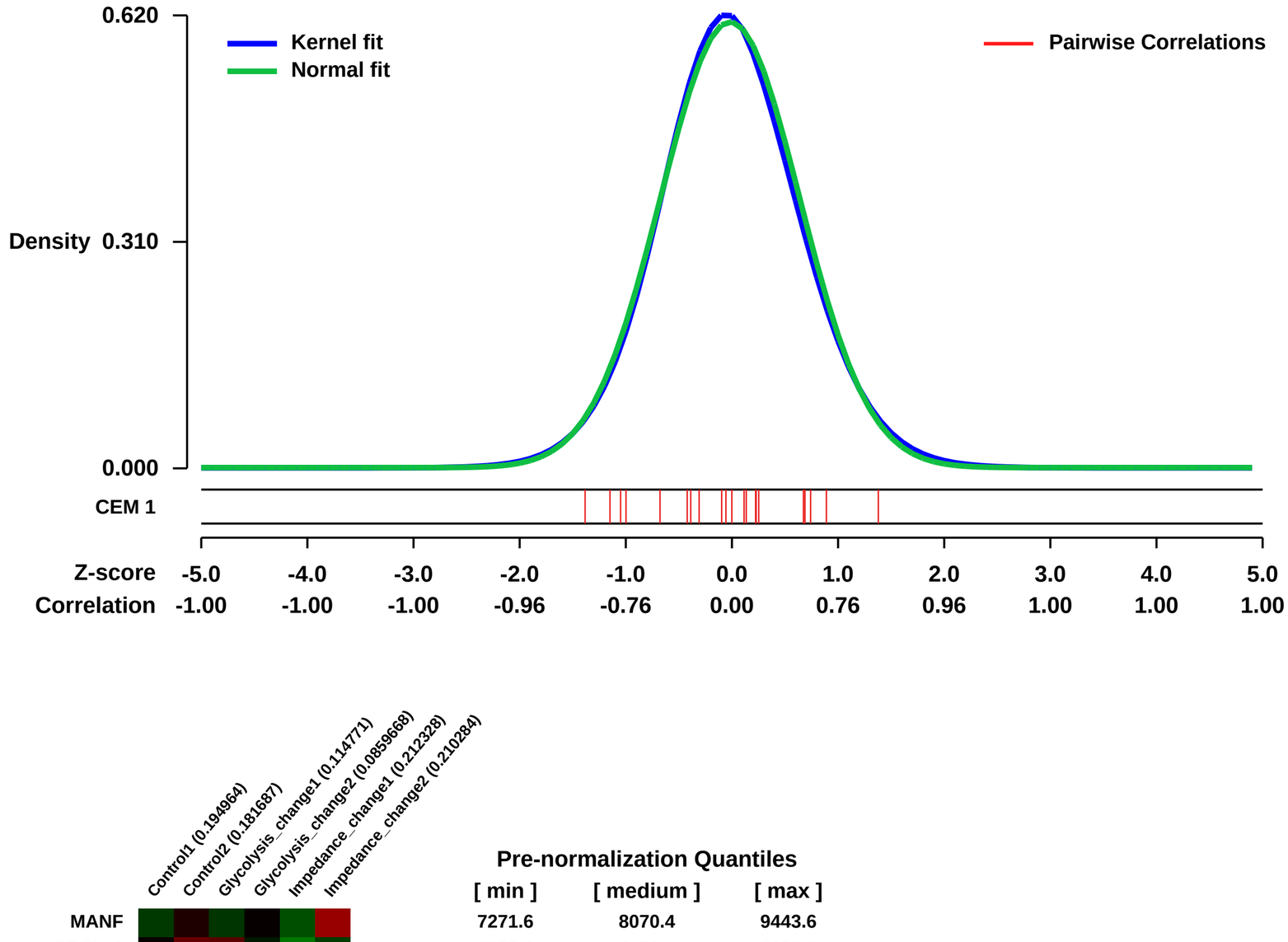

CEM 1
P (S | Z, I) = 0.00
Mean Corr = -0.03367

CEM 1 + Top 10 Genes

Null module

MANF	7271.6	8070.4	9443.6
SDF2L1	3975.4	4651.6	5152.9
CRELD2	6243.8	6659.6	7139.7
HSPA5	16569.8	24959.4	26320.0
HYOU1	8288.4	10851.0	12175.5
PDIA4	2541.1	2942.1	3404.8
PDIA6	10301.9	11184.8	12123.6
DNAJB11	4027.0	6477.7	7571.3
HSP90B1	347.9	6170.8	6700.7
PDIA3	4853.1	9299.2	9912.0
PPIB	10549.5	13707.0	14802.1
C19orf10	3053.9	3809.5	4336.2
SLC35B1	5568.2	6105.4	6424.4
SEC61A1	4546.1	4941.7	5771.0
RPN1	6472.6	7519.4	8347.0
DNAJC3	1545.8	2466.8	3862.2
CDK2AP2	3588.8	4593.0	5332.2
ARID5B			
XBP1			
HNRNPAB			
SGK1			
HSPB1			
DDIT4			
ARL4D			
SAP30			
KIAA0408			
GPR17			
HSPH1			
DNASE1L2			
SLC5A3			
GNAS			
GPR3			
TNFRSF25			
TM6SF2			
MKKS			
PLEKHF1			
ZMYM1			
DOK3			
FGF20			
SLC39A2			
KCNIP2			
ERRFI1			
DEDD2			
CCDC117			
USP31			
AHSA2			
CYS1			
CNIH2			
BANP			
CHORDC1			
P4HA1			

GEO Series "GSE11919" Expression Profiles

Num of samples in this series: 9

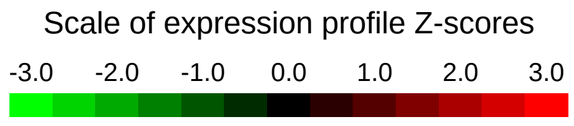

GEO Link:	http://www.ncbi.nlm.nih.gov/geo/query/acc.cgi?acc=GSE11919
Status:	Public on Feb 10 2009
Title:	Vitamin C-induced gene expression profiling in GM5659 human skin fibroblasts
Organism:	Homo sapiens
Experiment type:	Expression profiling by array
Platform:	GPL570
Pubmed ID:	18973801
Summary & Design:	**Summary:** The skin is a protective barrier against external insults and any lesion must be rapidly and efficiently repaired. Dermal fibroblasts are the major source of extracellular connective tissue matrix and play an important role in wound healing. Vitamin C is an important water-soluble free radical scavenger and an essential cofactor for collagen synthesis by dermal fibroblasts and, consequently, may contribute to the maintenance of healthy skin. Using microarray analysis, we investigated the effects of long-term exposure to a stable vitamin C derivative, ascorbic acid 2-phosphate (AA2P), in contact-inhibited populations of primary human dermal fibroblasts. Compared with ""scorbutic"" cells, cells exposed to AA2P increased the expression of genes associated with DNA replication and repair and with the G(2)/M phase of the cell cycle. Consistent with the gene expression changes, AA2P increased the mitogenic stimulation of quiescent fibroblasts by serum factors and cell motility in the context of wound healing. Furthermore, AA2P-treated fibroblasts showed faster repair of oxidatively damaged DNA bases. We propose that vitamin C may protect the skin by promoting fibroblast proliferation, migration, and replication-associated base excision repair of potentially mutagenic DNA lesions, and we discuss the putative involvement of hypoxia-inducible transcription factor-1 and collagen receptor-related signaling pathways. **Overall design:** Gene expression changes in response to vitamin C were analysed by Microarray technology in GM5659 human skin fibroblasts. Cells were treated with 100 ´µM of AA or AA2P (or growth medium alone) added fresh every day for a period of 5 days before the vitamin C-induced gene expression changes were investigated. Control, AA- and AA2P-treated samples were collected from three independent experiments each.

Background corr dist: KL-Divergence = 0.0749, L1-Distance = 0.0192, L2-Distance = 0.0004, Normal std = 0.4944

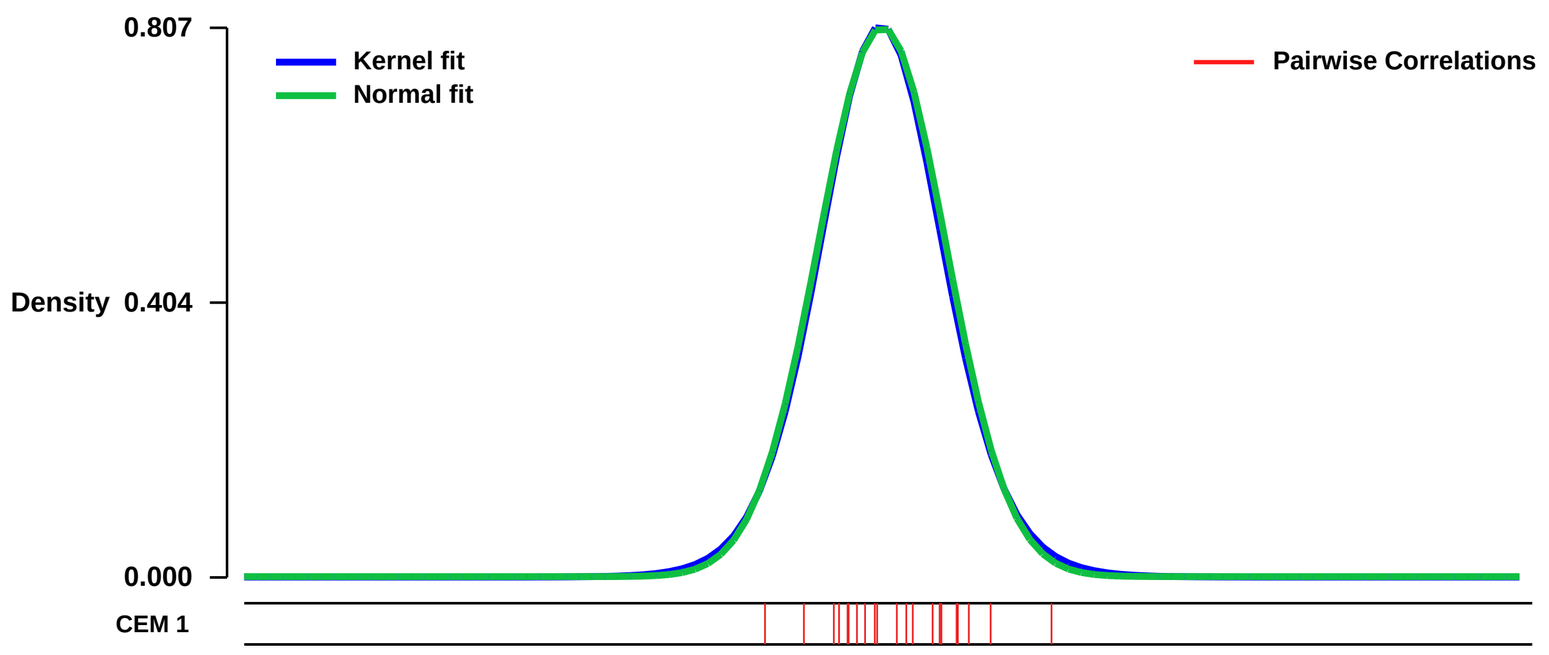

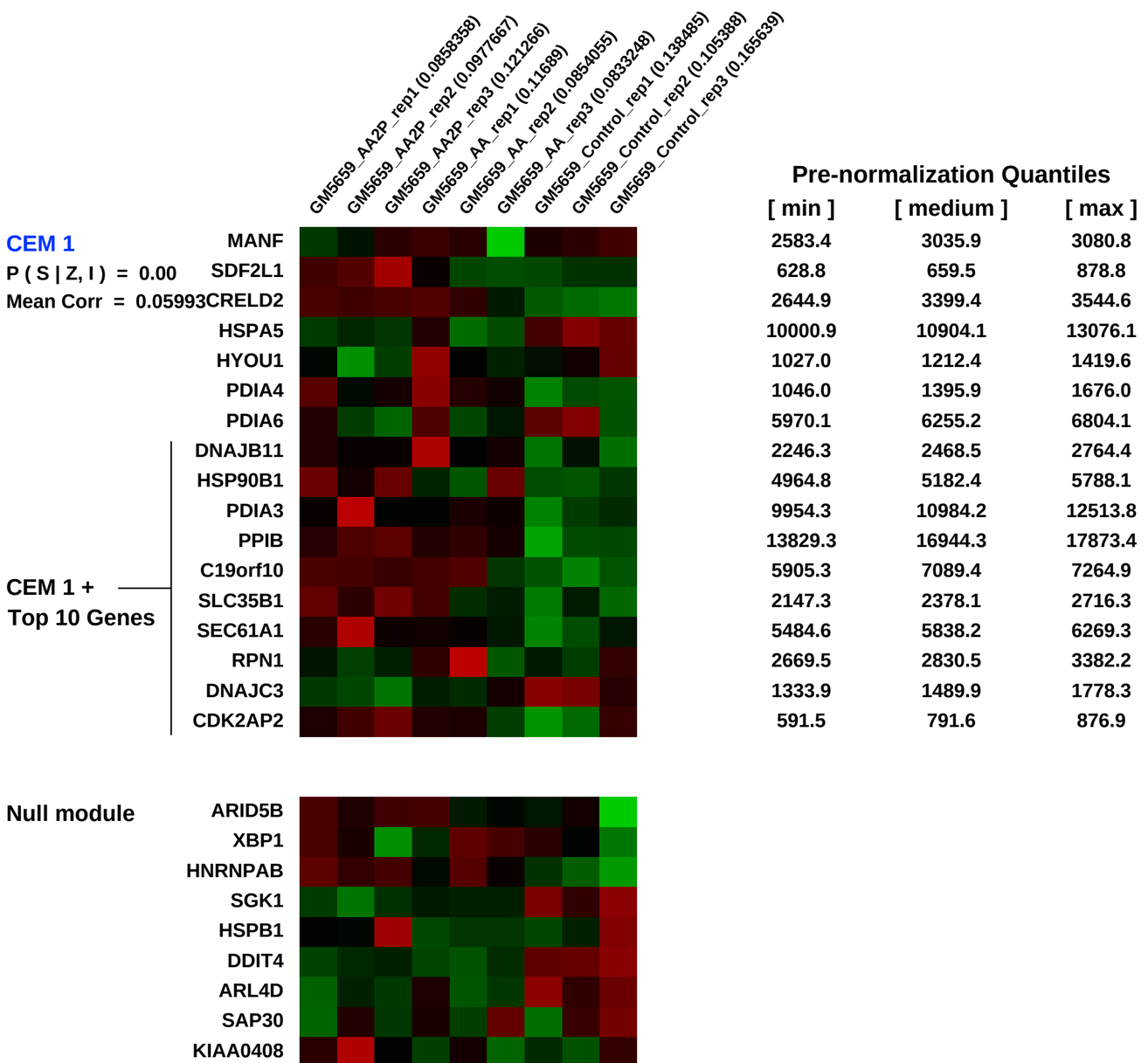

Pre-normalization Quantiles

	[min]	[medium]	[max]
MANF	2583.4	3035.9	3080.8
SDF2L1	628.8	659.5	878.8
CRELD2	2644.9	3399.4	3544.6
HSPA5	10000.9	10904.1	13076.1
HYOU1	1027.0	1212.4	1419.6
PDIA4	1046.0	1395.9	1676.0
PDIA6	5970.1	6255.2	6804.1
DNAJB11	2246.3	2468.5	2764.4
HSP90B1	4964.8	5182.4	5788.1
PDIA3	9954.3	10984.2	12513.8
PPIB	13829.3	16944.3	17873.4
C19orf10	5905.3	7089.4	7264.9
SLC35B1	2147.3	2378.1	2716.3
SEC61A1	5484.6	5838.2	6269.3
RPN1	2669.5	2830.5	3382.2
DNAJC3	1333.9	1489.9	1778.3
CDK2AP2	591.5	791.6	876.9

GEO Series "GSE56037" Expression Profiles

Num of samples in this series: 6

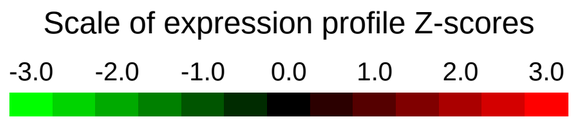

GEO Link:	http://www.ncbi.nlm.nih.gov/geo/query/acc.cgi?acc=GSE56037
Status:	Public on Aug 01 2014
Title:	Effect of increased FOXA1 on gene expression in bladder cancer cells
Organism:	Homo sapiens
Experiment type:	Expression profiling by array
Platform:	GPL570
Pubmed ID:	
Summary & Design:	**Summary:** Urothelial cell carcinoma of the bladder (UCC) is a common disease characterized by FGFR3 mutation. Whilst upregulation of this oncogene occurs most frequently in low-grade non-invasive tumors, recent data reveal increased FGFR3 expression characterizes a common sub-type of invasive UCC sharing genetic similarities with lobular breast cancer. These similarities include upregulation of the FOXA1 transcription factor and reduced expression of microRNAs-99a/100. We have previously identified direct regulation of FGFR3 by these two microRNAs and now search for further targets. Using a microarray meta-database we find potential FOXA1 regulation by microRNAs-99a/100. We confirm direct targeting of the FOXA1 3â UTR by microRNAs-99a/100 and also potential indirect regulation through microRNA-485-5p/SOX5/JUN-D/FOXL1 and microRNA-486/FOXO1a. In 292 benign and malignant urothelial samples, we find an inverse correlation between the expression of FOXA1 and microRNAs-99a/100 (r=-0.33 to -0.43, p<0.05). As for FGFR3 in UCC, tumors with high FOXA1 expression have lower rates of progression than those with low expression (Log rank p=0.009). Using global gene expression and CpG methylation profiling we find genotypic consequences of FOXA1 upregulation in UCC. These are associated with regional hypomethylation and near FOXA1 binding sites, and mirror patterns previously reported in FGFR3 mutant UCC. These include gene silencing through aberrant hypermethylation (e.g. IGFBP3) and affect genes that characterize lobular breast cancer (e.g. ERBB2, XBP1). In conclusion, we have identified microRNAs-99a/100 mediate a direct relationship between FGFR3 and FOXA1, and potentially facilitate cross talk between these pathways in UCC. **Overall design:** Gene expression profiling of EJ Bladder cancer cells transfected with FOXA1 construct or with empty pUC19 vector.

Background corr dist: KL-Divergence = 0.0445, L1-Distance = 0.0222, L2-Distance = 0.0006, Normal std = 0.5948

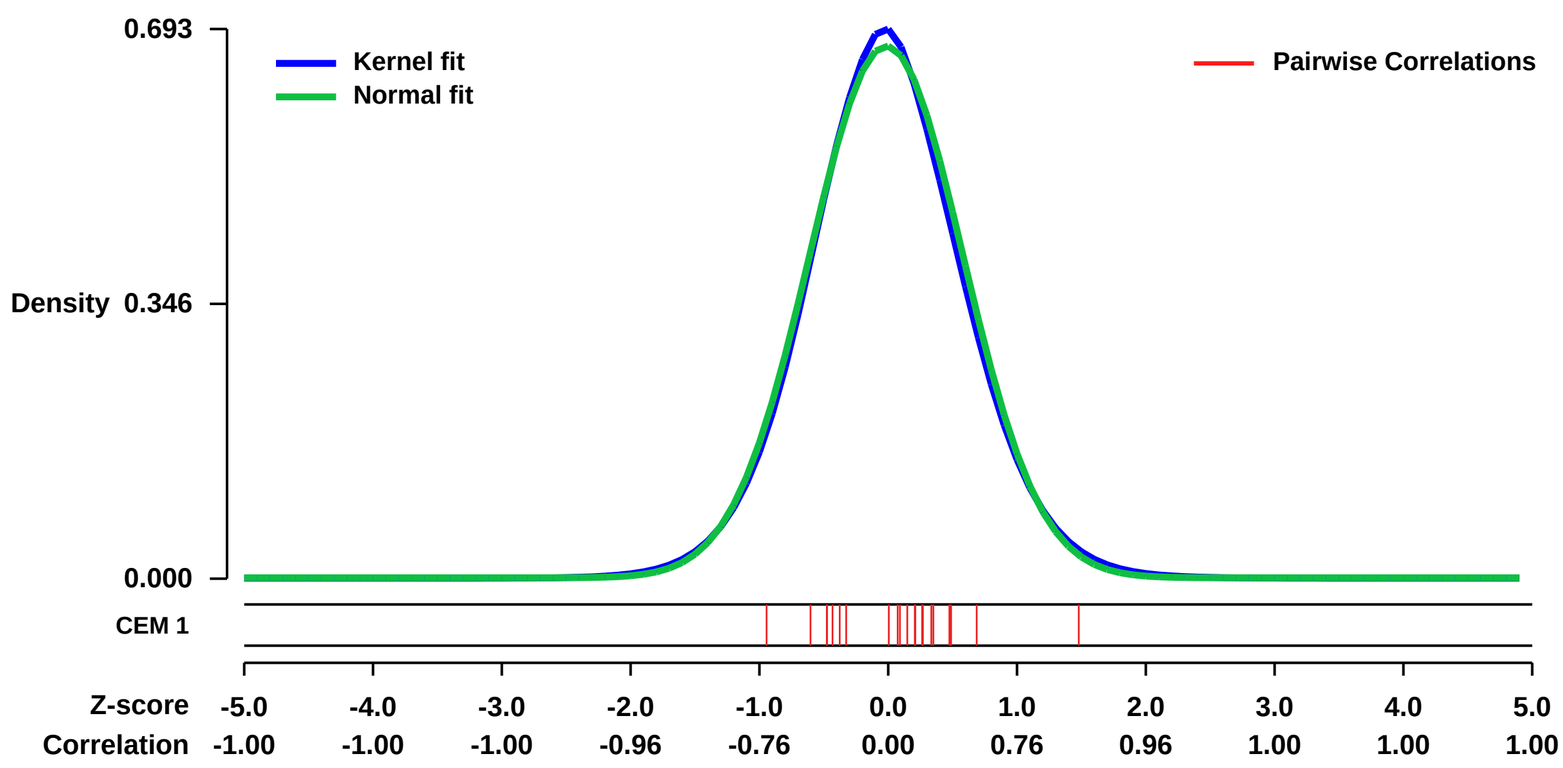

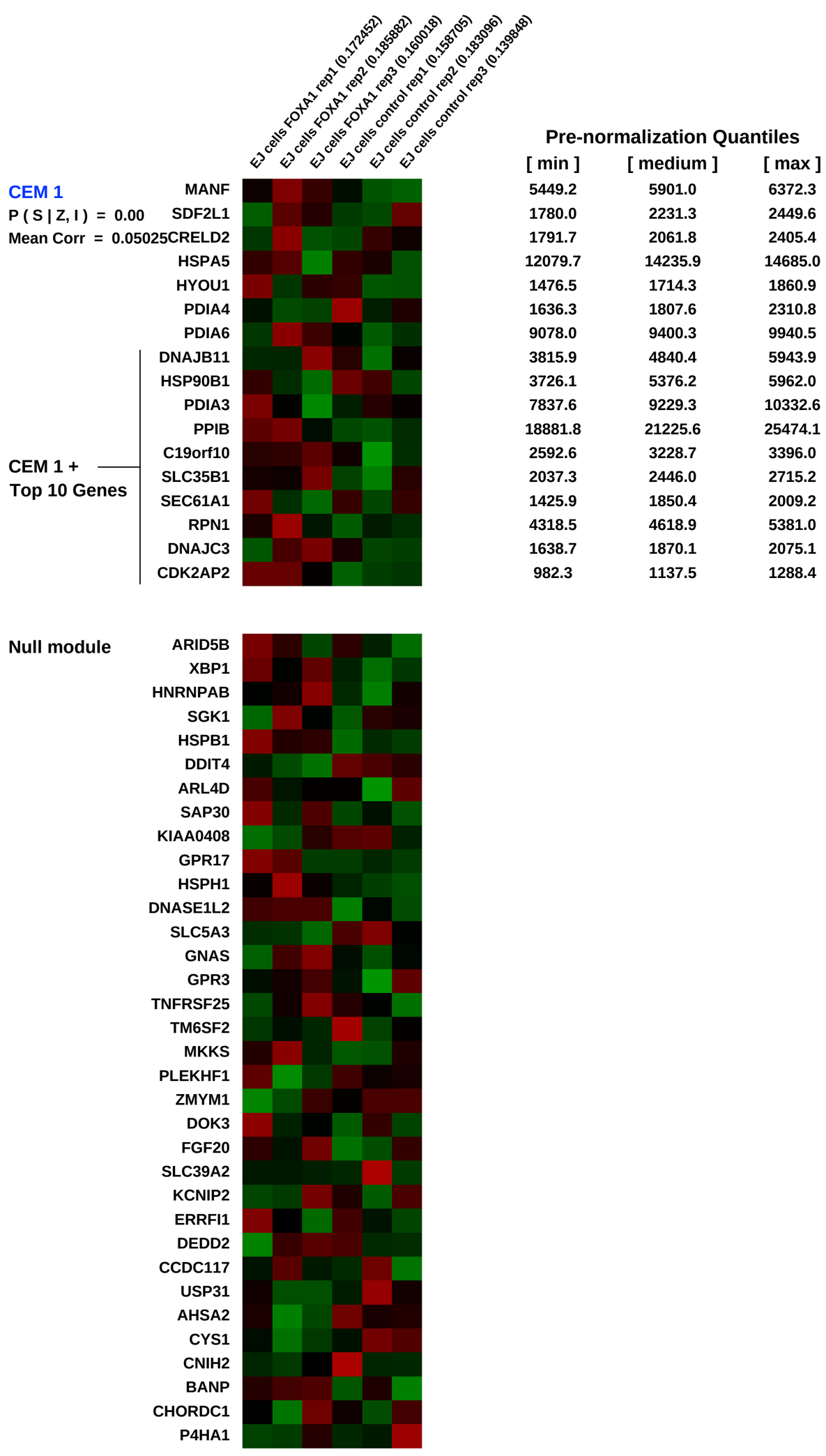

	Pre-normalization Quantiles		
	[min]	[medium]	[max]
MANF	5449.2	5901.0	6372.3
SDF2L1	1780.0	2231.3	2449.6
CRELD2	1791.7	2061.8	2405.4
HSPA5	12079.7	14235.9	14685.0
HYOU1	1476.5	1714.3	1860.9
PDIA4	1636.3	1807.6	2310.8
PDIA6	9078.0	9400.3	9940.5
DNAJB11	3815.9	4840.4	5943.9
HSP90B1	3726.1	5376.2	5962.0
PDIA3	7837.6	9229.3	10332.6
PPIB	18881.8	21225.6	25474.1
C19orf10	2592.6	3228.7	3396.0
SLC35B1	2037.3	2446.0	2715.2
SEC61A1	1425.9	1850.4	2009.2
RPN1	4318.5	4618.9	5381.0
DNAJC3	1638.7	1870.1	2075.1
CDK2AP2	982.3	1137.5	1288.4
ARID5B			
XBP1			
HNRNPAB			
SGK1			
HSPB1			
DDIT4			
ARL4D			
SAP30			
KIAA0408			
GPR17			
HSPH1			
DNASE1L2			
SLC5A3			
GNAS			
GPR3			
TNFRSF25			
TM6SF2			
MKKS			
PLEKHF1			
ZMYM1			
DOK3			
FGF20			
SLC39A2			
KCNIP2			
ERRFI1			
DEDD2			
CCDC117			
USP31			
AHSA2			
CYS1			
CNIH2			
BANP			
CHORDC1			
P4HA1			

GEO Series "GSE28019" Expression Profiles

Num of samples in this series: 24

Scale of expression profile Z-scores

-3.0 -2.0 -1.0 0.0 1.0 2.0 3.0

GEO Link:	**http://www.ncbi.nlm.nih.gov/geo/query/acc.cgi?acc=GSE28019**
Status:	**Public on Mar 16 2013**
Title:	**Neuroblastoma cell line profiling**
Organism:	**Homo sapiens**
Experiment type:	**Expression profiling by array**
Platform:	**GPL570**
Pubmed ID:	
Summary & Design:	**Summary:** **24 standard human Neuroblastoma Cell lines were profiled without applying any transfections in order to measure the expression profiles.** **Keywords: cell line, neuroblastoma, mRNA profiling** **Overall design:** **24 human Neuroblastoma cell line samples were analyzed**

Background corr dist: **KL-Divergence = 0.3915, L1-Distance = 0.0785, L2-Distance = 0.0192, Normal std = 0.2514**

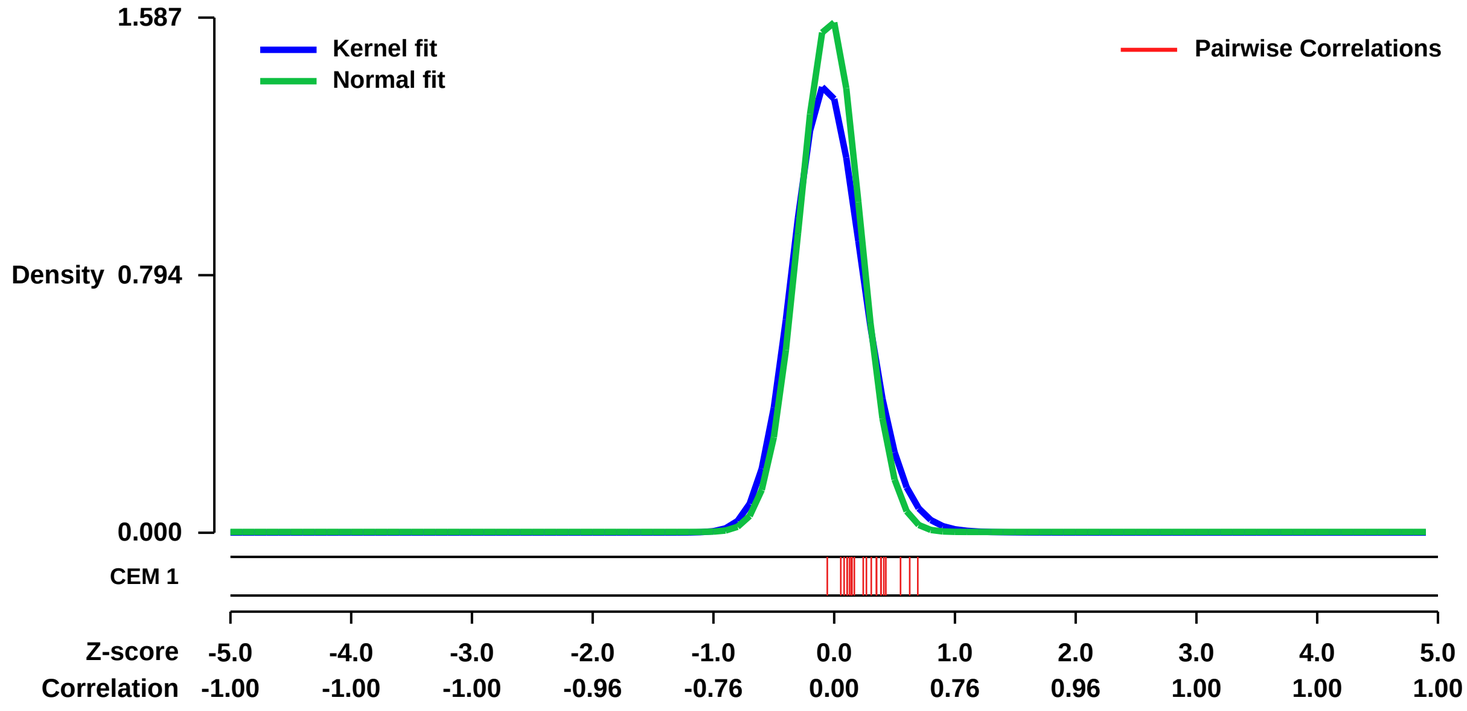

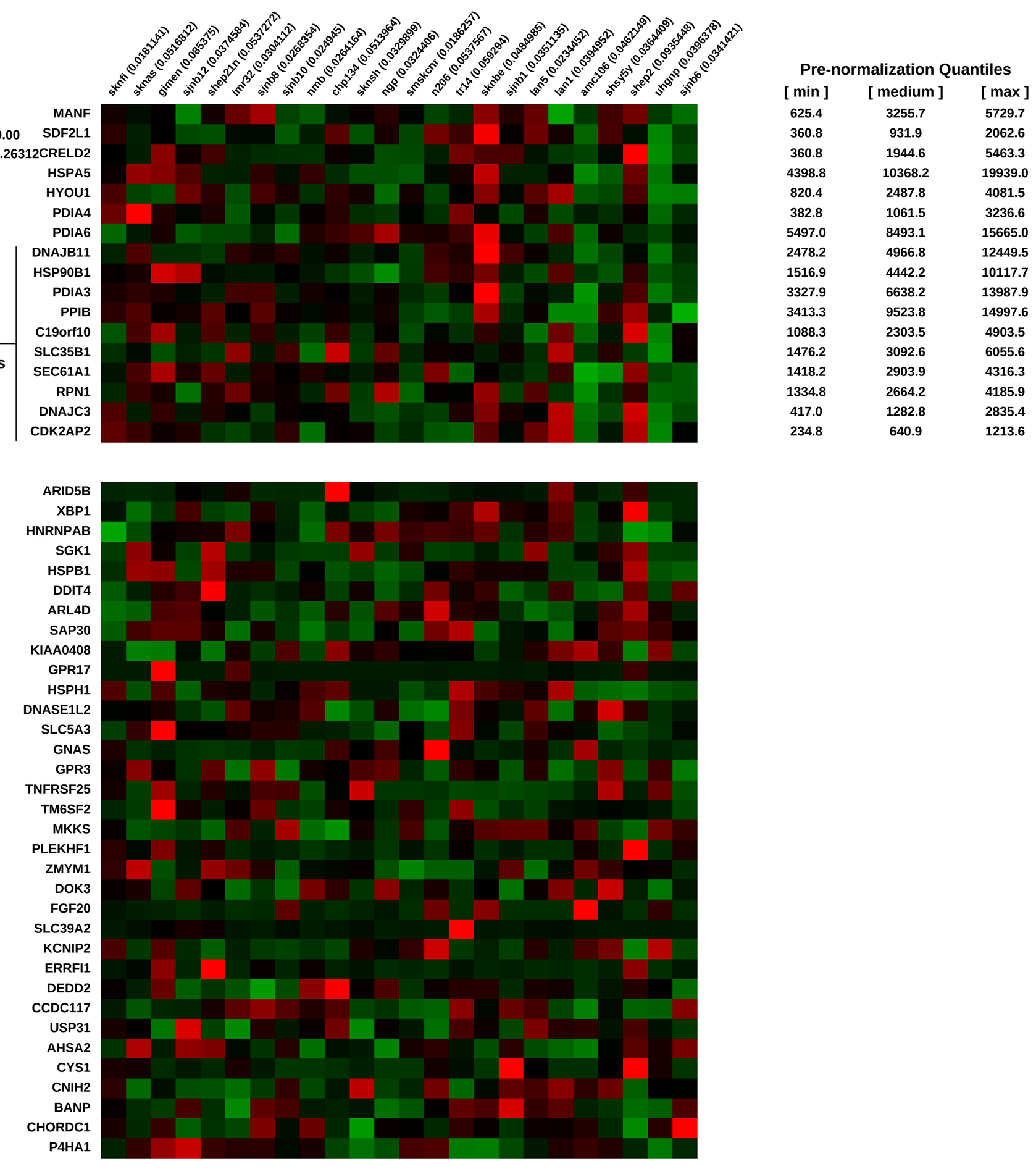

	Pre-normalization Quantiles		
	[min]	[medium]	[max]
MANF	625.4	3255.7	5729.7
SDF2L1	360.8	931.9	2062.6
CRELD2	360.8	1944.6	5463.3
HSPA5	4398.8	10368.2	19939.0
HYOU1	820.4	2487.8	4081.5
PDIA4	382.8	1061.5	3236.6
PDIA6	5497.0	8493.1	15665.0
DNAJB11	2478.2	4966.8	12449.5
HSP90B1	1516.9	4442.2	10117.7
PDIA3	3327.9	6638.2	13987.9
PPIB	3413.3	9523.8	14997.6
C19orf10	1088.3	2303.5	4903.5
SLC35B1	1476.2	3092.6	6055.6
SEC61A1	1418.2	2903.9	4316.3
RPN1	1334.8	2664.2	4185.9
DNAJC3	417.0	1282.8	2835.4
CDK2AP2	234.8	640.9	1213.6

GEO Series "GSE53091" Expression Profiles

Num of samples in this series: 125

Details of this dataset are not shown due to large number of samples and the page size limit.

Find details in http://www.ncbi.nlm.nih.gov/geo/query/acc.cgi?acc=GSE53091

Background corr dist: KL-Divergence = 0.0488, L1-Distance = 0.0775, L2-Distance = 0.0100, Normal std = 0.6307

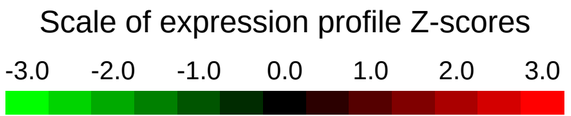

GEO Series "GSE45276" Expression Profiles

Num of samples in this series: 12

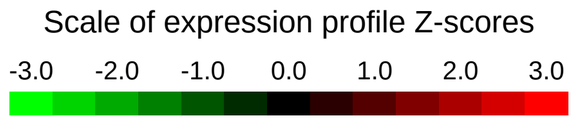

GEO Link:	http://www.ncbi.nlm.nih.gov/geo/query/acc.cgi?acc=GSE45276
Status:	Public on Mar 19 2013
Title:	Expression data from Control, AKT and RAS transduced cells
Organism:	Homo sapiens
Experiment type:	Expression profiling by array
Platform:	GPL570
Pubmed ID:	21474066
Summary & Design:	**Summary:** Mutations in both RAS and the PTEN/PIK3CA/AKT signaling module are found in the same human tumors. PIK3CA and AKT are downstream effectors of RAS, and the selective advantage conferred by mutation of two genes in the same pathway is unclear. Based on a comparative molecular analysis, we show that activated PIK3CA/AKT is a weaker inducer of senescence than is activated RAS. More-over, concurrent activation of RAS and PIK3CA/AKT impairs RAS-induced senescence. We used microarrays to detail the global programme of gene expression after transduction of AKT and RAS **Overall design:** IMR90 cells were transfected with Control, AKT and RAS retrovirus containing medium in 4 replicates. Fibroblasts were drug selected and kept in drug for duration of experiments.

Background corr dist: KL-Divergence = 0.0670, L1-Distance = 0.0467, L2-Distance = 0.0031, Normal std = 0.5419

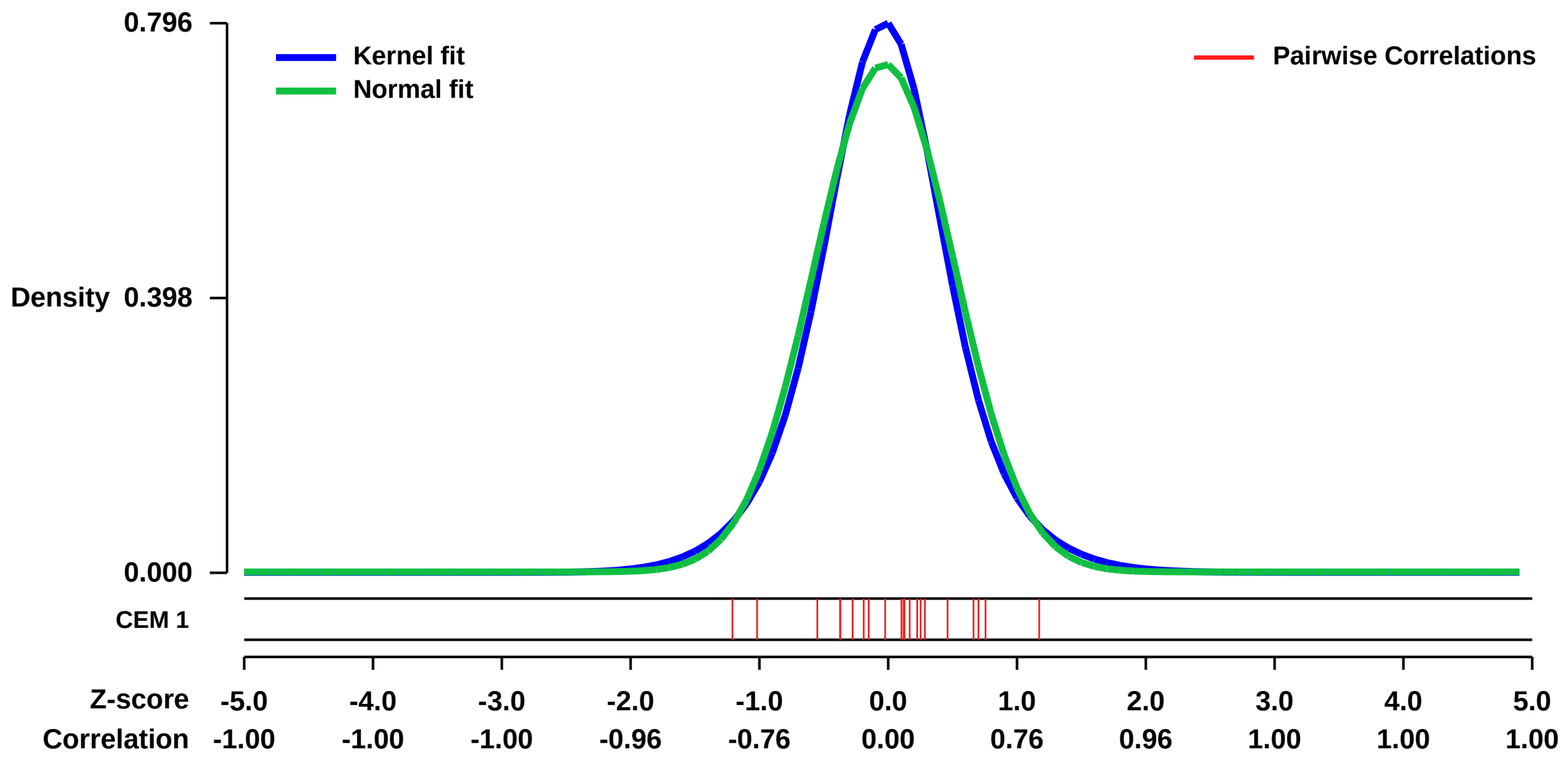

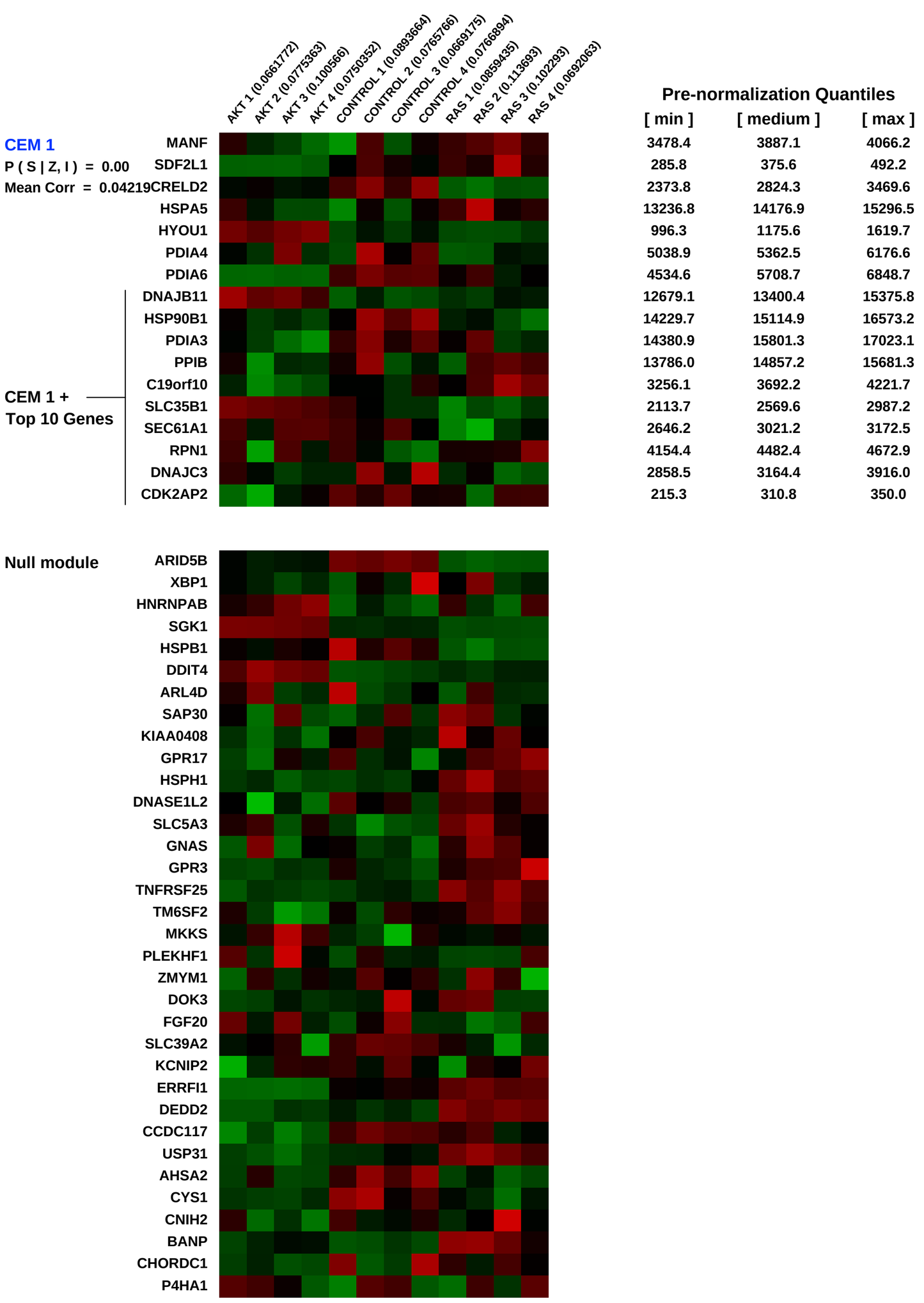

GEO Series "GSE24224" Expression Profiles

Num of samples in this series: 6

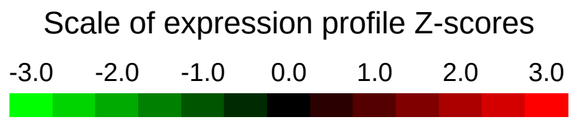

GEO Link:	http://www.ncbi.nlm.nih.gov/geo/query/acc.cgi?acc=GSE24224
Status:	Public on Sep 21 2010
Title:	Analysis of genome-wide methylation and gene expression induced by decitabine treatment in HL60 leukemia cell line
Organism:	Homo sapiens
Experiment type:	Methylation profiling by genome tiling array
Platform:	GPL570
Pubmed ID:	21077739
Summary & Design:	**Summary:** Epigenetic changes play a role in the pathogenesis of myeloid malignancies and hypomethylating agents have shown efficacy in these diseases. We studied the apoptotic effect, the genome-wide methylation and gene expression profiles in HL60 cells following decitabine treatment, using micro-array technologies. Decitabine treatment resulted in a decrease in global DNA methylation, corresponding to 4876 probeset IDs with significantly reduced methylation levels, while expression of 2583 IDs was induced. The integrated analysis identified 160 genes demethylated and upregulated by decitabine, mainly including development and differentiation pathways genes. Genes target of polycomb group protein regulation were overrepresented in this group. Apoptosis was induced by decitabine and apoptosis-specific PCR arrays more precisely indicated decitabine-induced upregulation of 13 apoptosis-related genes, in particular Dap-kinase 1 and Bcl2L10. Correspondingly, in primary patient samples, BCL2L10 was hypermethylated in 45% of AML, 43% of therapy-related myeloid neoplasms, 12% of MDS and in none of the controls. **Overall design:** In this work, we were interested in the identification of key pathways involved in the global methylation and gene expression changes induced by decitabine in a myeloid cell line model. The human acute myeloid leukemia cell line HL60 was treated with 1 ´µM decitabine or the same volume of vehicle (mock sample) for 3 days. At the end of treatment DNA and total RNA were extracted for methylation and gene expression studies, to identify genes hypermethylated in HL60 cells and that could be targets of hypomethylating treatment. Methylation profiling was performed by the Methylated DNA Immunoprecipitation (MeDIP) using an anti-5-Methylcytidine Antibody (GeneTex Inc). Methylation-enriched DNA and total DNA were labeled and hybridized on the Affymetrix GeneChip Human Promoter 1.0R Tiling Arrays (Affymetrix, USA). Gene expression profiling (GEP) was performed using the Affymetrix U133 Plus 2.0 expression array. All hybridization reactions were performed using GeneChip Fluidics Station 450, and GeneChips were scanned using the Affymetrix GeneChip Scanner 3000 (Affymetrix, USA). The MeDIP.CEL files for biological triplicates of HL60 mock and decitabine-treated were log2 transformed, normalized and imported into the Partek Genomic Suite software (PGS). The differences between treated and control samples were performed using a t-Test (p-value 0.05). Significantly enriched regions were obtained by the MAT algorithm (Model-based Analysis of Tiling arrays). The expression array .CEL files for HL60 mock and decitabine-treated cells were imported in PGS using the Gene Expression Workflow tool, after GC-RMA normalization and log2 transformation. Significantly over and under-expressed genes were detected using the 1-way ANOVA tool at p<0.01 and +/- 2 fold enrichment. The integration between significantly demethylated and induced genes upon decitabine treatment was performed using the VENN diagram tool in PGS.

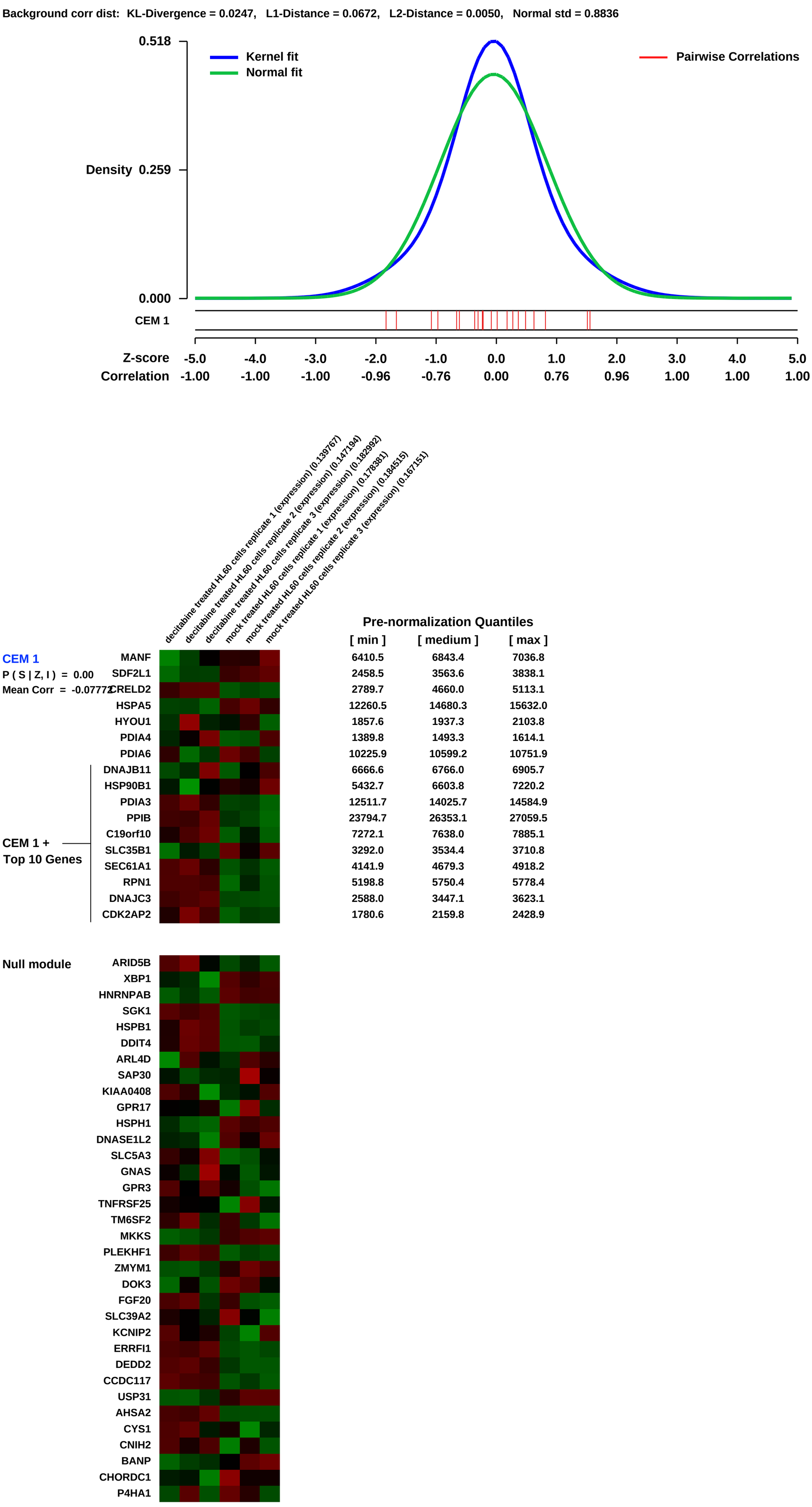

GEO Series "GSE45029" Expression Profiles

Num of samples in this series: 6

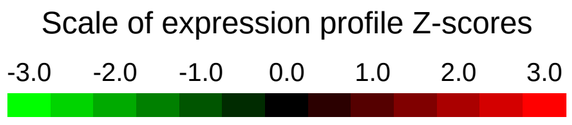

GEO Link:	http://www.ncbi.nlm.nih.gov/geo/query/acc.cgi?acc=GSE45029
Status:	Public on Apr 22 2013
Title:	Doxycycline alters metabolism and proliferation of human cell lines
Organism:	Homo sapiens
Experiment type:	Expression profiling by array
Platform:	GPL570
Pubmed ID:	23741339
Summary & Design:	**Summary:** The tetracycline antibiotics are widely used in biomedical research as mediators of inducible gene expression systems. Despite many known effects of tetracyclines on mammalian cells -- including inhibition of the mitochondrial ribosome -- there have been few reports on potential off-target effects at concentrations commonly used in inducible systems. Here, we report that in human cell lines, commonly used concentrations of doxycycline change gene expression patterns and concomitantly shift metabolism towards a more glycolytic phenotype, evidenced by increased lactate secretion and reduced oxygen consumption. We also show that these concentrations are sufficient to slow proliferation and alter cell cycle progression in vitro. These findings suggest that researchers using doxycycline in inducible expression systems should design appropriate controls to account for potential confounding effects of the drug on cellular metabolism. **Overall design:** Total RNA was extracted from MCF12A cells treated with either vehicle control or Dox at 1 ug/mL. The experiment was performed in biological triplicate. Microarray results were processed using the RMA method.

Background corr dist: KL-Divergence = 0.0444, L1-Distance = 0.0214, L2-Distance = 0.0005, Normal std = 0.5968

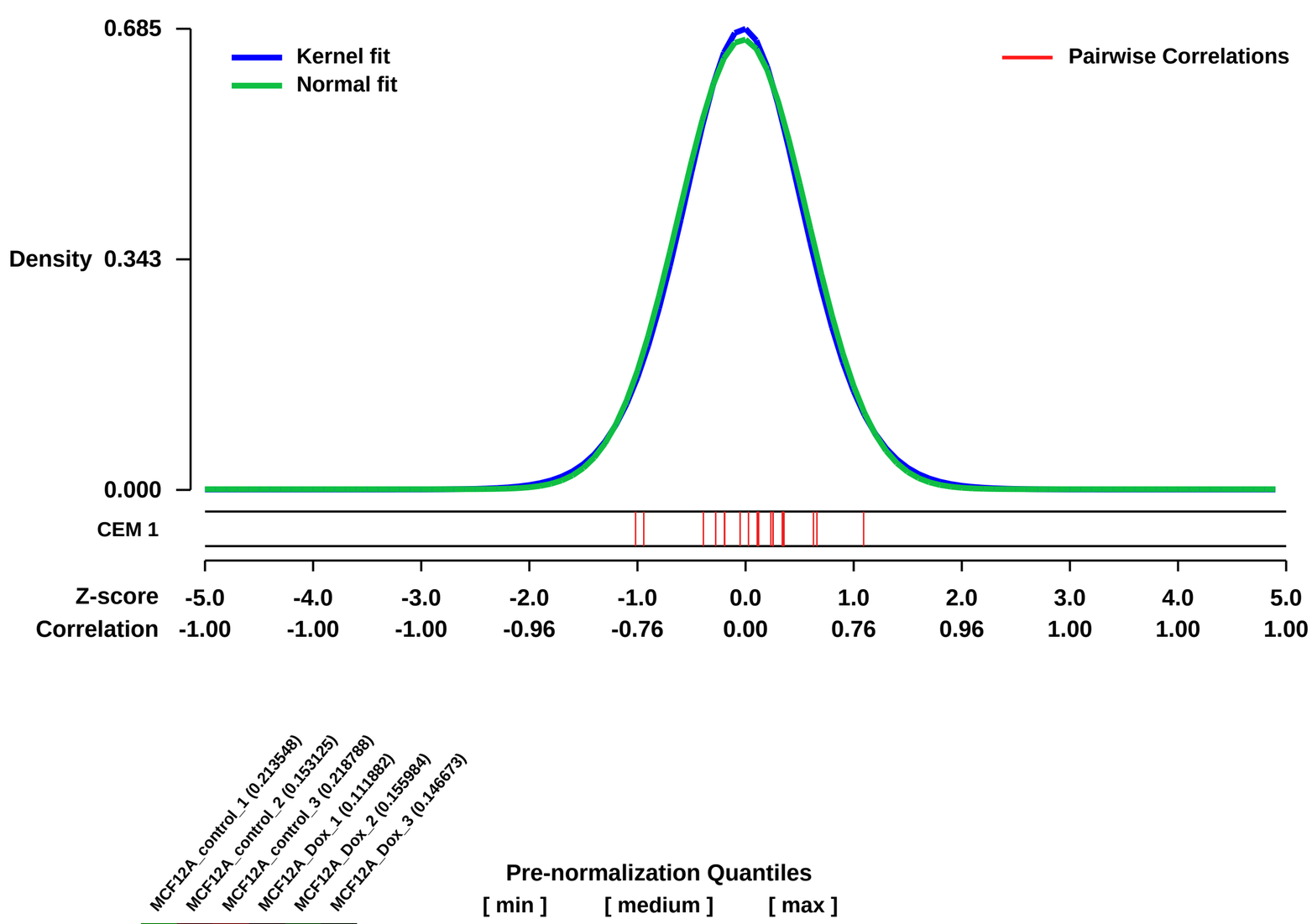

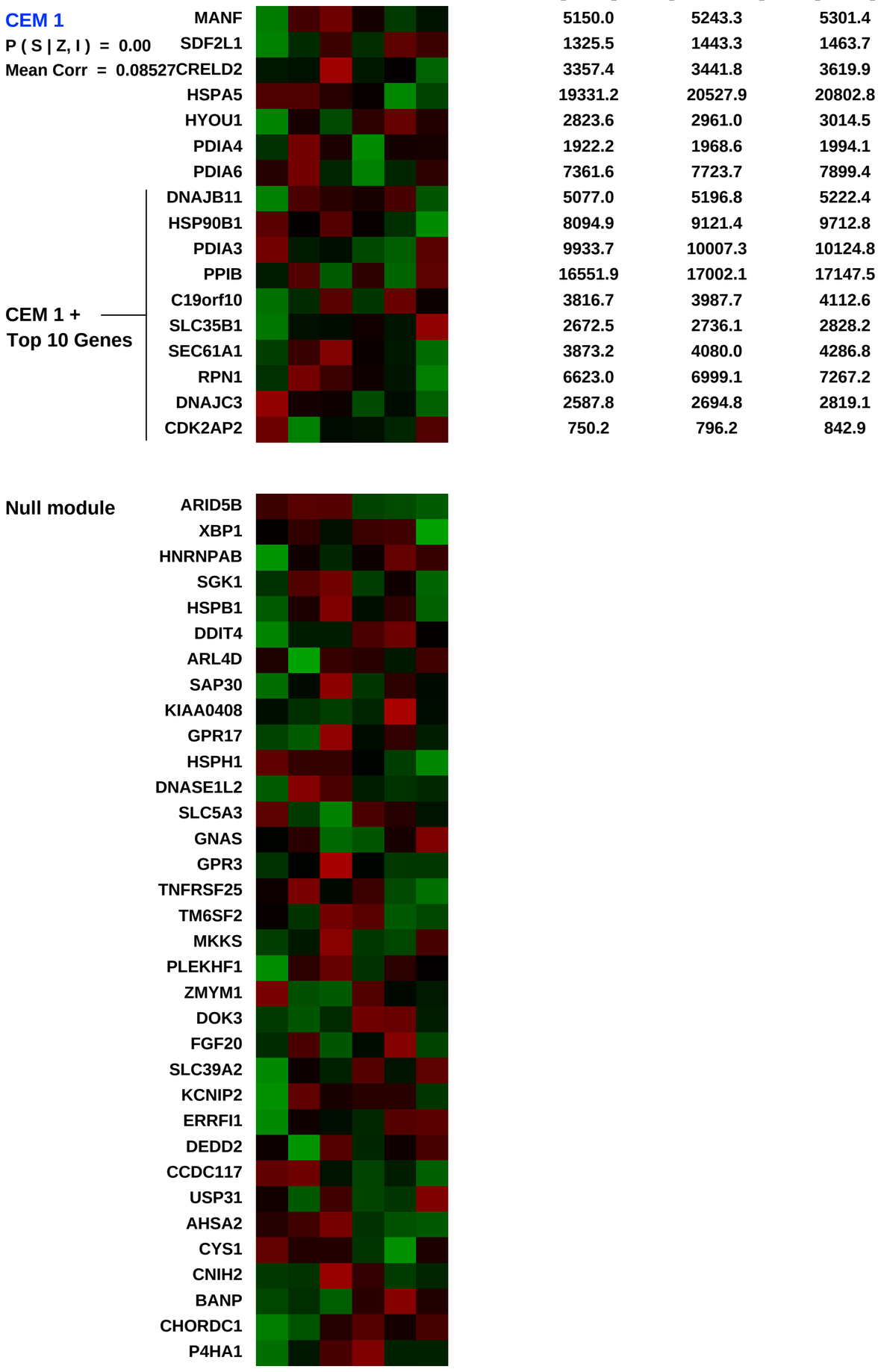

Pre-normalization Quantiles

	[min]	[medium]	[max]
MANF	5150.0	5243.3	5301.4
SDF2L1	1325.5	1443.3	1463.7
CRELD2	3357.4	3441.8	3619.9
HSPA5	19331.2	20527.9	20802.8
HYOU1	2823.6	2961.0	3014.5
PDIA4	1922.2	1968.6	1994.1
PDIA6	7361.6	7723.7	7899.4
DNAJB11	5077.0	5196.8	5222.4
HSP90B1	8094.9	9121.4	9712.8
PDIA3	9933.7	10007.3	10124.8
PPIB	16551.9	17002.1	17147.5
C19orf10	3816.7	3987.7	4112.6
SLC35B1	2672.5	2736.1	2828.2
SEC61A1	3873.2	4080.0	4286.8
RPN1	6623.0	6999.1	7267.2
DNAJC3	2587.8	2694.8	2819.1
CDK2AP2	750.2	796.2	842.9

GEO Series "GSE29783" Expression Profiles

Num of samples in this series: 10

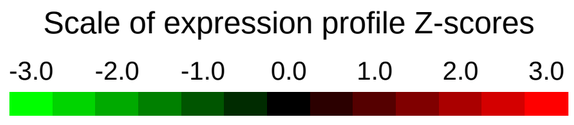

GEO Link:	http://www.ncbi.nlm.nih.gov/geo/query/acc.cgi?acc=GSE29783
Status:	Public on Jun 29 2012
Title:	Expression data from hESCs expressing RB7LP or T121
Organism:	Homo sapiens
Experiment type:	Expression profiling by array
Platform:	GPL570
Pubmed ID:	
Summary & Design:	**Summary:** We used microarray analysis to study the expression differences between controls and hESCs expressing RB7LP for 3 days, and controls and hESCs expressing T121 for 3 days. RB7LP is the large pocket fragment of the retinoblastoma protein (RB) fused to GFP, in which seven phosphorylation sites for Cdk have been mutated (Angus, SP et al. Mol Cell Biol 23, 8172 (Nov, 2003). T121 is a truncated form of the SV40 Large T (LT) viral oncoprotein that inactivates the function of the three members of the retinoblastoma (RB) protein family (RB, p107, p130). **Overall design:** We plated hESCs that had been infected with inducible lentiviruses to express either RB7LP or T121. The day after plating, one well from each virus was treated with doxycyline to induce expression of either RB7LP or T121 and after 3 days were harvested for microrarray analysis.

Background corr dist: KL-Divergence = 0.0376, L1-Distance = 0.0582, L2-Distance = 0.0058, Normal std = 0.6451

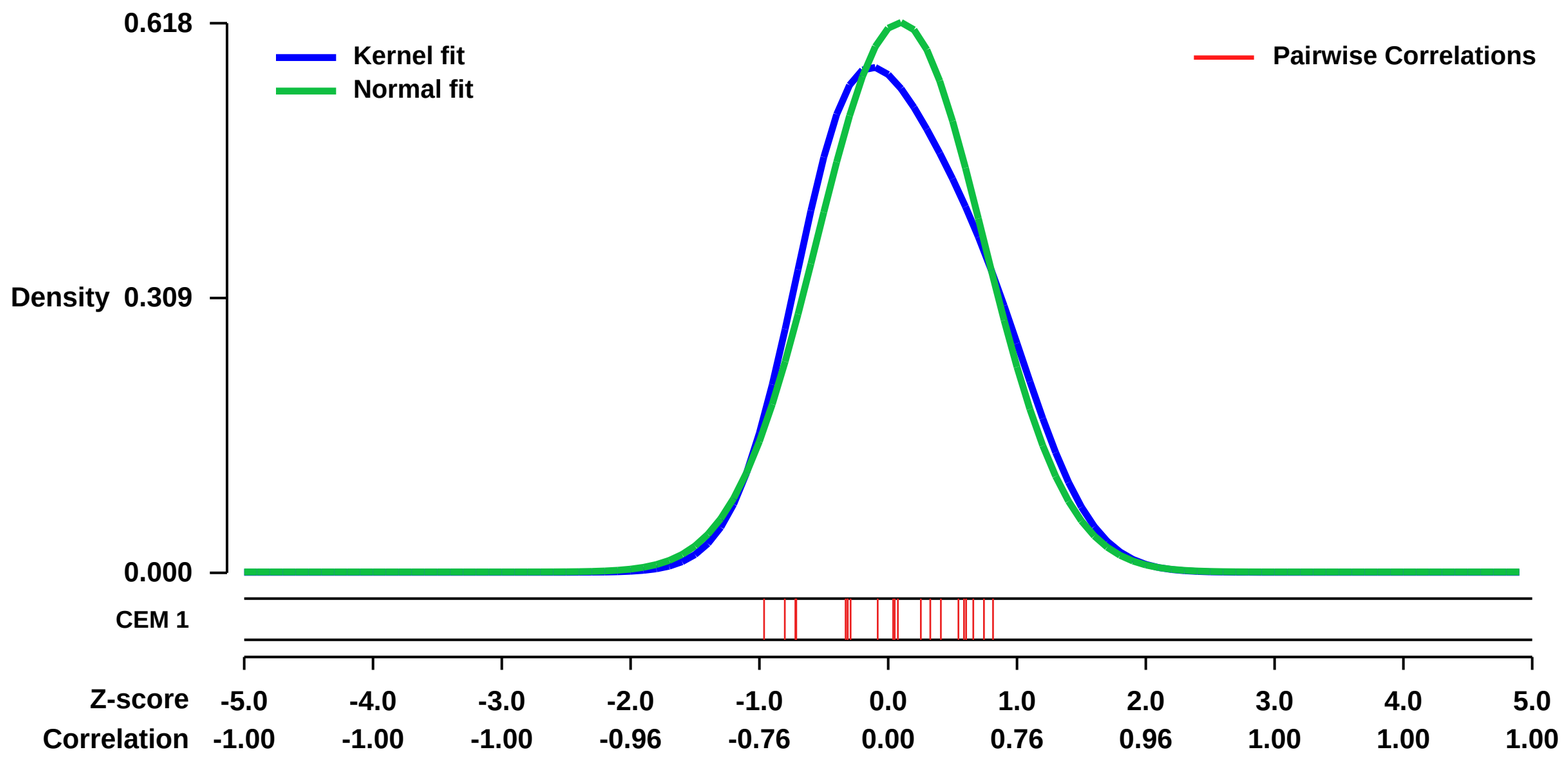

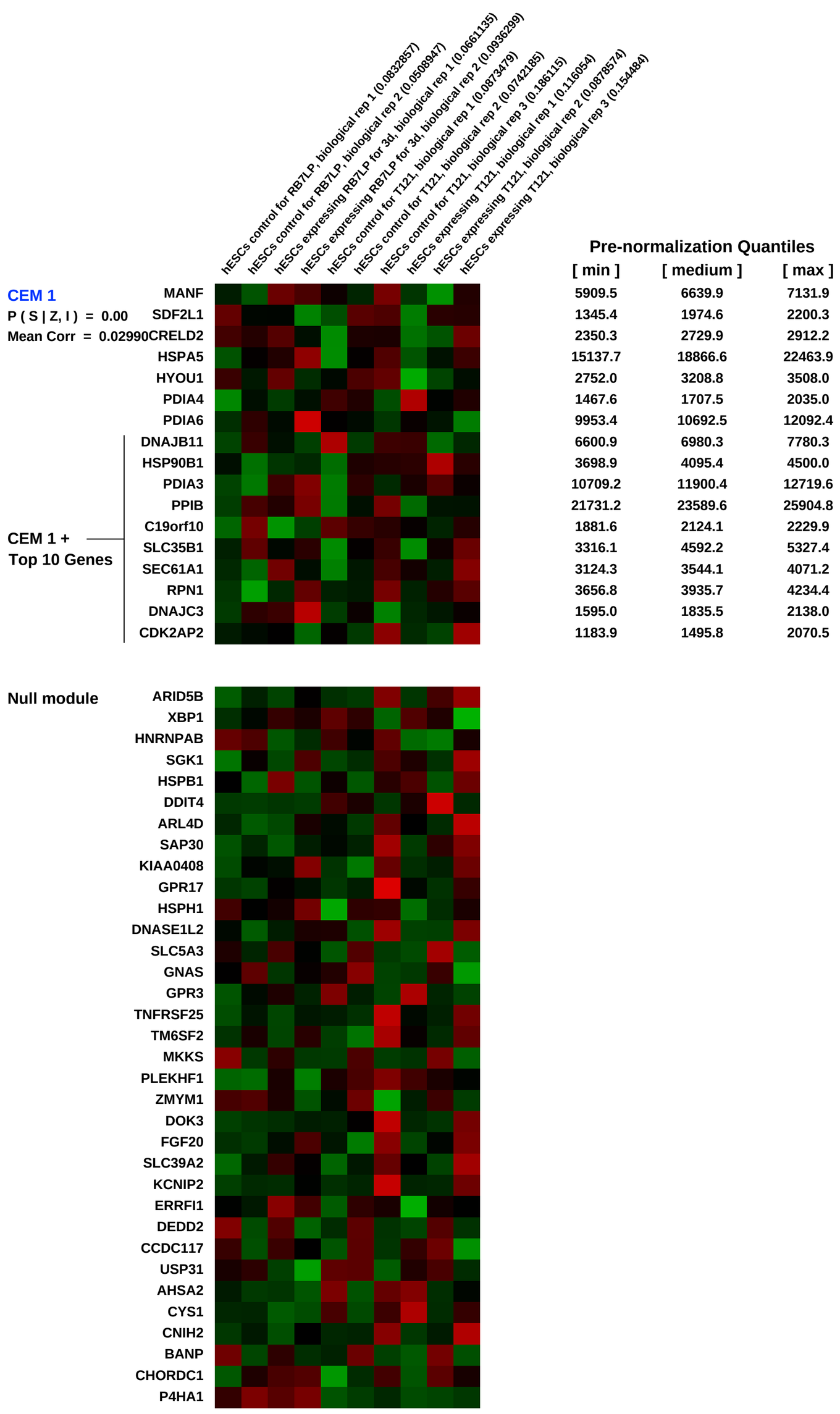

GEO Series "GSE16870" Expression Profiles

Num of samples in this series: 36

Scale of expression profile Z-scores

-3.0 -2.0 -1.0 0.0 1.0 2.0 3.0

GEO Link:	http://www.ncbi.nlm.nih.gov/geo/query/acc.cgi?acc=GSE16870
Status:	Public on Jul 22 2010
Title:	HeLa cells treated with V-ATPase inhibitors or with desoxyferramine compared to HeLa in DMSO or medium with low LDL
Organism:	Homo sapiens
Experiment type:	Expression profiling by array
Platform:	GPL570
Pubmed ID:	20661293
Summary & Design:	**Summary:** Expression data from HeLa cells treated with V-ATPase inhibitors or with desoxyferramine compared to HeLa treated with DMSO or medium with low LDL To determine which genes respond first to low concentrations of V-ATPase inhibition, we treated HeLa cells with two different V-ATPase inhibitors, bafilomycin and phenylsalicylihalamide (LX1077) at concentrations that slow cell growth by only 20%. To identify genes responding to expected effects of inhibiting the V-ATPase, expression data from inhibiting the V-ATPase was compared to that of chelating iron or incubating cells in medium with low LDL. **Overall design:** HeLa cells were also treated with the iron chelator, desoxiferamine for 6 or 12 hours or with medium with low LDL for 12 hours to identify genes that respond to low iron or low cholesterol. Each timepoint and each treatment has two independent replicates. Experimental samples were compared to control samples grown on the same day.

Background corr dist: KL-Divergence = 0.4787, L1-Distance = 0.0884, L2-Distance = 0.0255, Normal std = 0.2291

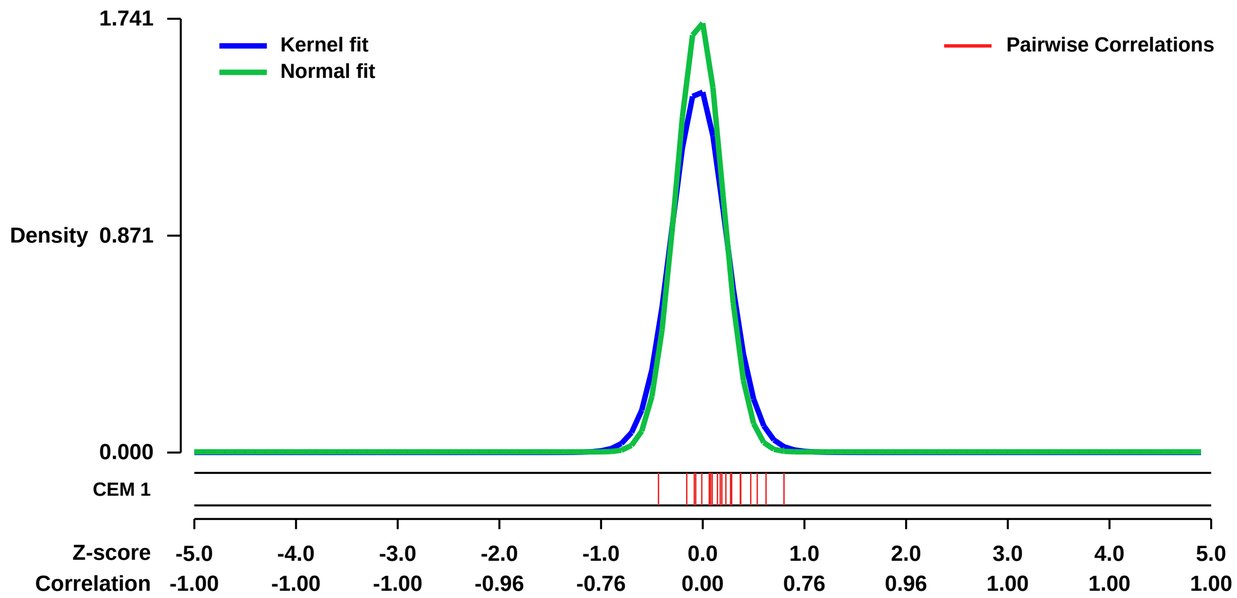

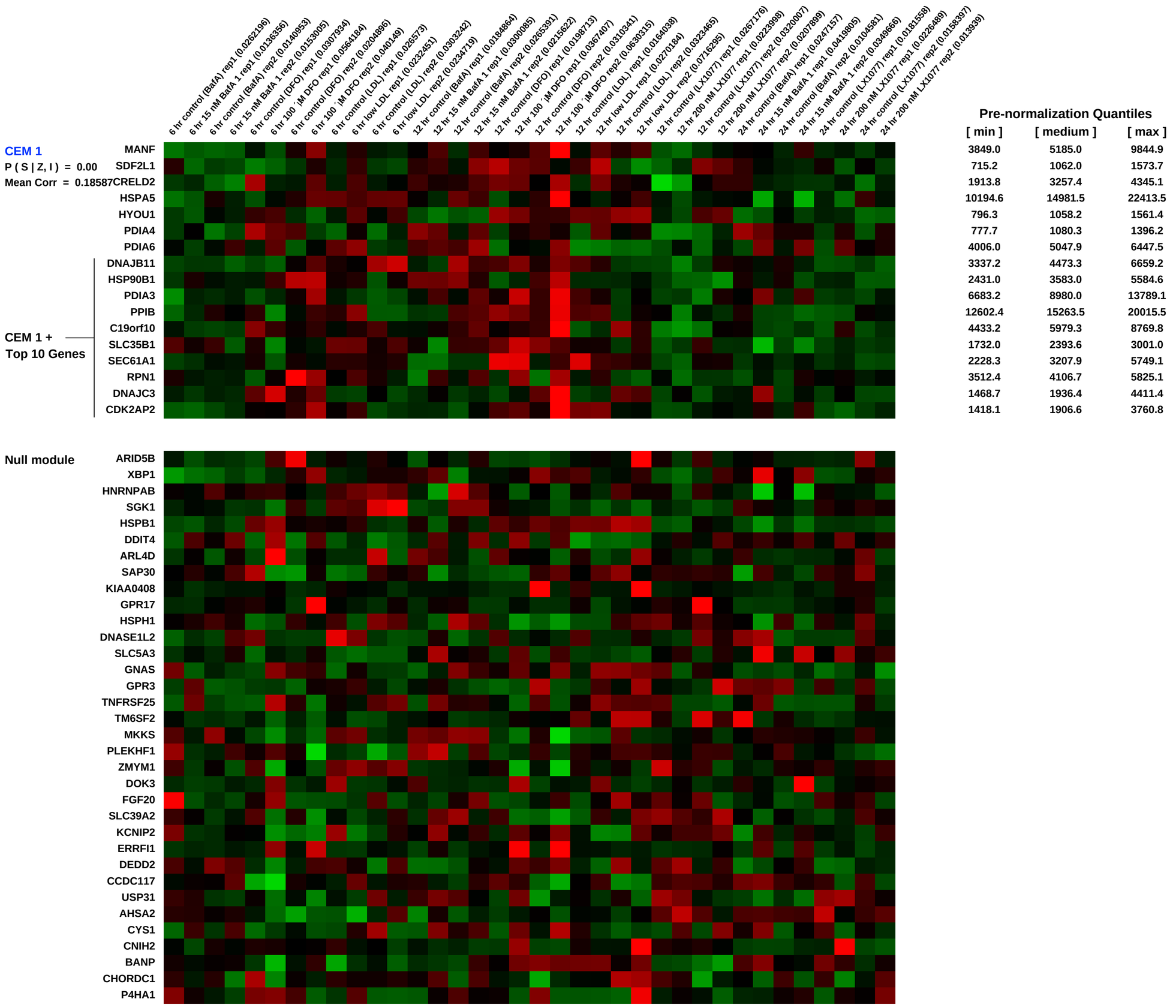

Pre-normalization Quantiles

	[min]	[medium]	[max]
MANF	3849.0	5185.0	9844.9
SDF2L1	715.2	1062.0	1573.7
CRELD2	1913.8	3257.4	4345.1
HSPA5	10194.6	14981.5	22413.5
HYOU1	796.3	1058.2	1561.4
PDIA4	777.7	1080.3	1396.2
PDIA6	4006.0	5047.9	6447.5
DNAJB11	3337.2	4473.3	6659.2
HSP90B1	2431.0	3583.0	5584.6
PDIA3	6683.2	8980.0	13789.1
PPIB	12602.4	15263.5	20015.5
C19orf10	4433.2	5979.3	8769.8
SLC35B1	1732.0	2393.6	3001.0
SEC61A1	2228.3	3207.9	5749.1
RPN1	3512.4	4106.7	5825.1
DNAJC3	1468.7	1936.4	4411.4
CDK2AP2	1418.1	1906.6	3760.8

GEO Series "GSE8596" Expression Profiles

Num of samples in this series: 12

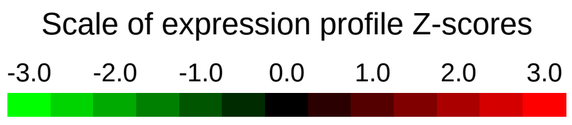

GEO Link:	http://www.ncbi.nlm.nih.gov/geo/query/acc.cgi?acc=GSE8596
Status:	Public on Jul 27 2007
Title:	Expression profiles of pediatric solid tumor cell lines
Organism:	Homo sapiens
Experiment type:	Expression profiling by array
Platform:	GPL570
Pubmed ID:	18212050
Summary & Design:	**Summary:** For identification of candidate genes that is specifically expressed in Ewing family tumor (EFT) cells, we performed DNA microarray-based global expression profiling using Affymetrix Human Genome U133 Plus 2.0 Array and analyxed expression profiles from EFT cell lines (7 lines), neuroblastoma (NB) cell lines (3 lines), a Rhabdomyosarcoma (RMS) cell line, and a human immortalized mesenchymal progenitor cells UET-13 cells. **Keywords: Ewing family tumor** **Overall design:** Expression profiles of pediatric solid tumor cell lines were analyzed and compared using Affymetrix HG-U133 Plus 2.0 (GPL570).

Background corr dist: KL-Divergence = 0.1713, L1-Distance = 0.0526, L2-Distance = 0.0071, Normal std = 0.3654

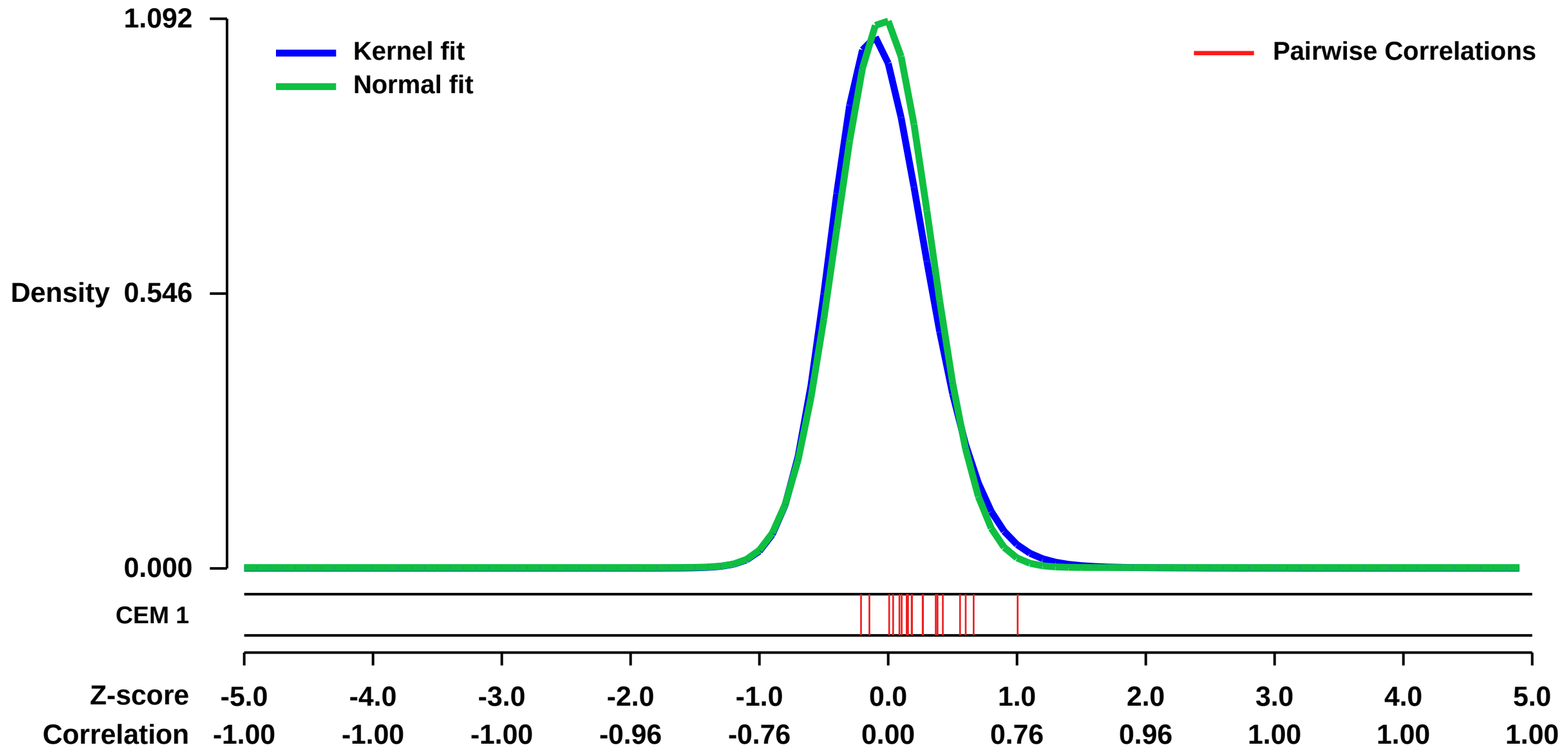

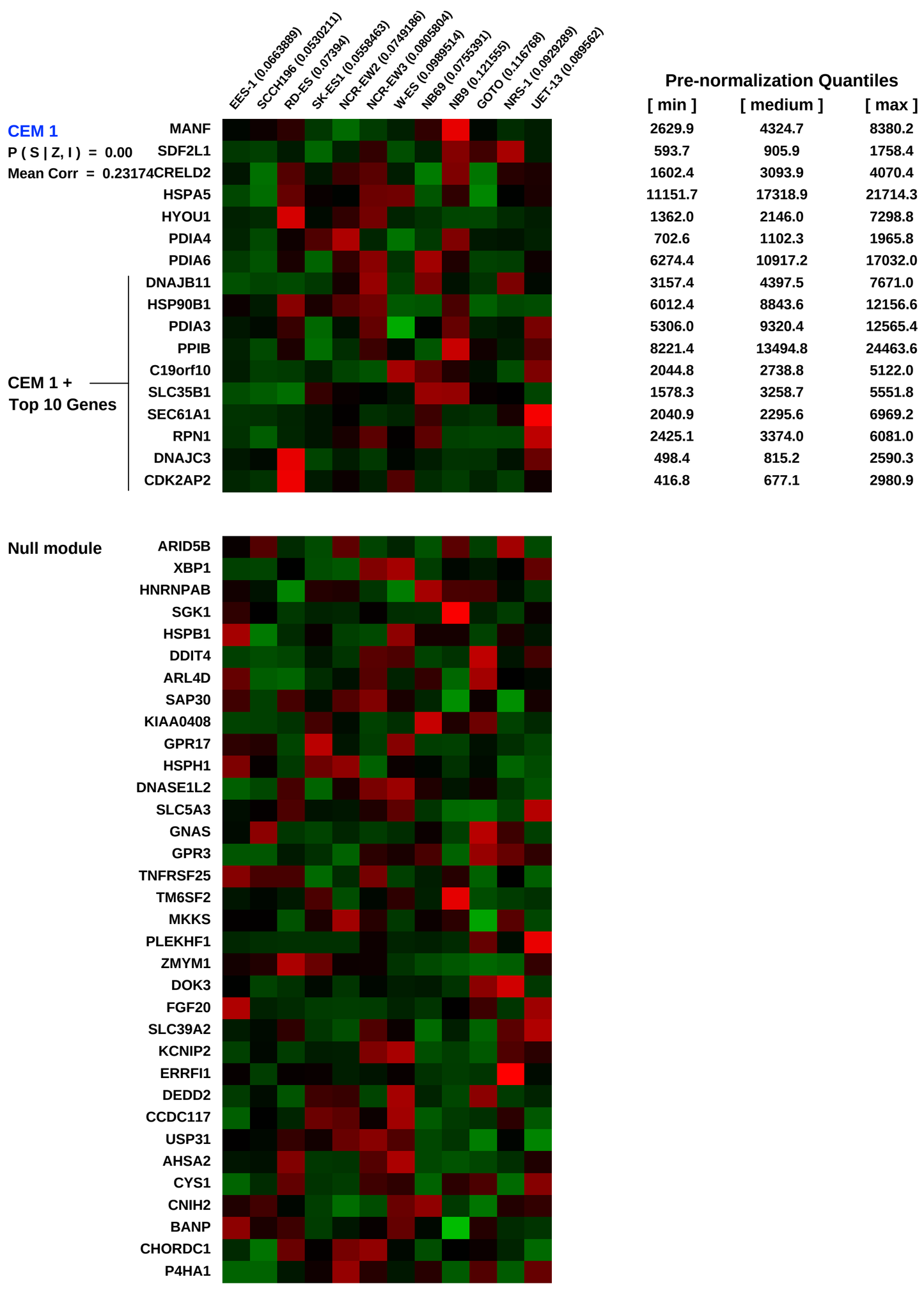

GEO Series "GSE32108" Expression Profiles

Num of samples in this series: 15

Scale of expression profile Z-scores

-3.0 -2.0 -1.0 0.0 1.0 2.0 3.0

GEO Link:	http://www.ncbi.nlm.nih.gov/geo/query/acc.cgi?acc=GSE32108
Status:	Public on Sep 15 2011
Title:	Knockdown effect of CDK8 or CDK19 in HeLa S3 cell
Organism:	Homo sapiens
Experiment type:	Expression profiling by array
Platform:	GPL570
Pubmed ID:	22117896
Summary & Design:	**Summary:** Mediator complex has been known as pivotal regulator of RNA polymerase II. Mediator complex has two CDK subunits in vertebrates, named CDK8 and CDK19. To elucidate functional difference between CDK8 and CDK19 in human cell, we employ siRNA mediate knockdown assay using HeLa S3 cell line. According to this assay these CDKs possess highly redundancy in HeLa S3 cell transcription regulation mechanism but in several genes, each CDK shows gene specific regulatory function. **Overall design:** HeLa S3 cells were seeded on 6-well plate at 4 x 104 cells per well in 2ml antibiotic free DMEM medium before 24hr transfection. We transfect siRNA using Lipofectamine 2000 (invitrogen) according to its manual and siRNA final concentration in the medium was 20nM. After culturing for 48hr, transfection medium was changed to fresh antibiotic containing medium. Then the cells were incubated for additional 12hr and then RNA was prepared using RNeazy column (QIAGEN). Five ¸…g of prepared RNA was subjected to the gene expression analysis using Human Genome U133 Plus 2.0 (Affymetrix) followed by characterizations with GeneSpring software (Agilent) and Pathway Analysis software (Ingenuity). In this analysis we employ two individual siRNA against each CDK and three replicates in each condition.
Background corr dist:	KL-Divergence = 0.0801, L1-Distance = 0.0416, L2-Distance = 0.0037, Normal std = 0.4736

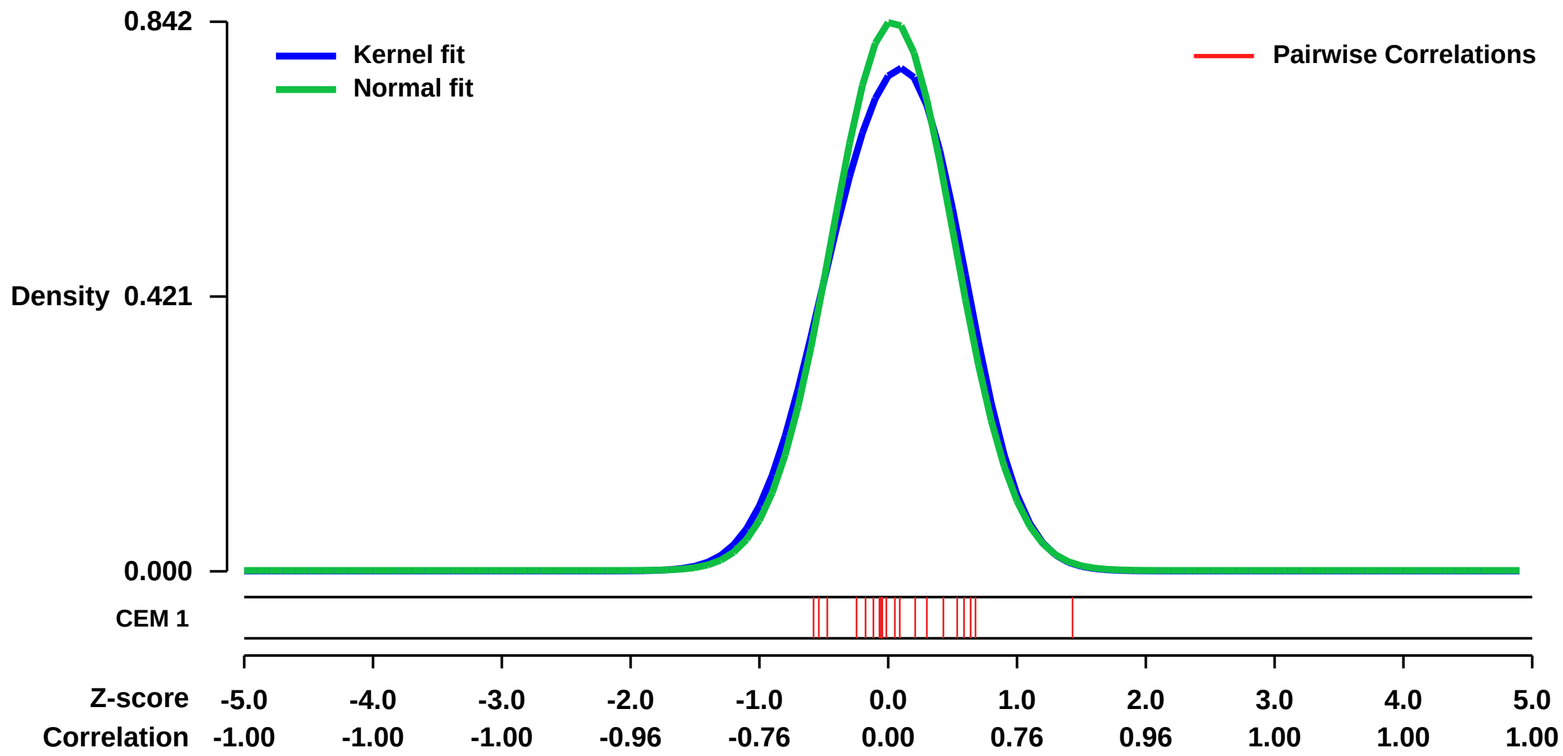

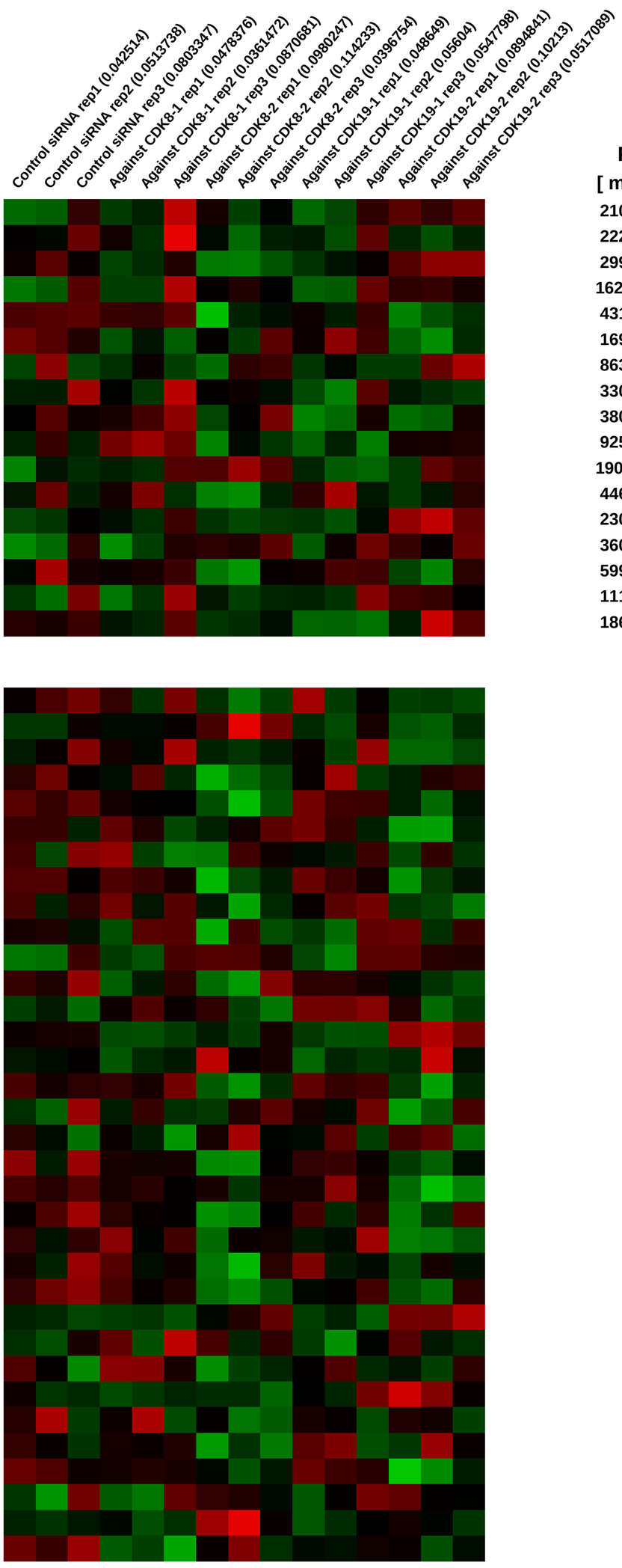

Pre-normalization Quantiles

	[min]	[medium]	[max]
Control siRNA rep1 (0.042514)	2108.3	3051.7	4813.1
Control siRNA rep2 (0.0513738)	2226.1	2758.4	4488.9
Control siRNA rep3 (0.0803347)	2991.8	3780.4	4596.5
Against CDK8-1 rep1 (0.0478376)	16290.7	22011.6	30193.2
Against CDK8-1 rep2 (0.0361472)	4316.5	5706.4	6236.5
Against CDK8-1 rep3 (0.0870681)	1694.6	2074.0	2426.9
Against CDK8-2 rep1 (0.0980247)	8633.5	9154.7	10963.2
Against CDK8-2 rep2 (0.114233)	3308.9	4889.9	8070.7
Against CDK8-2 rep3 (0.0396754)	3800.8	4639.7	5361.1
Against CDK19-1 rep1 (0.048649)	9255.6	10160.1	11380.5
Against CDK19-1 rep2 (0.05604)	19035.2	20234.9	22407.7
Against CDK19-1 rep3 (0.0547798)	4464.9	5280.9	6533.7
Against CDK19-2 rep1 (0.0894841)	2306.5	2473.0	3541.8
Against CDK19-2 rep2 (0.10213)	3606.2	4748.4	5277.0
Against CDK19-2 rep3 (0.0517089)	5997.5	7018.9	7975.6
	1113.6	1361.0	1919.7
	1867.1	2114.6	2683.5

GEO Series "GSE9974" Expression Profiles

Num of samples in this series: 6

Scale of expression profile Z-scores

-3.0 -2.0 -1.0 0.0 1.0 2.0 3.0

GEO Link: http://www.ncbi.nlm.nih.gov/geo/query/acc.cgi?acc=GSE9974

Status: Public on Mar 20 2008

Title: The effect of the HDAC inhibitor OSU-HDAC42 on gene expression in esophageal tissues and adenocarcinoma cells I

Organism: Homo sapiens

Experiment type: Expression profiling by array

Platform: GPL570

Pubmed ID:

Summary & Design:

Summary:
Title: In vitro and in vivo effects of the orally bioavailable phenylbutyrate-derived histone deacetylase inhibitor OSU-HDAC42 on gene expression in esophageal tissues and in esophageal adenocarcinoma cells

Histone deacetylases (HDACs) modulate nucleosomal packaging of DNA, thereby influencing gene transcription and multiple cancer-associated processes.

Thus, we conducted microarray analysis at multiple time-points to assess the ability of OSU-HDAC42, the S enantiomer of the previously published compound HDAC-42, to modulate key acid-induced changes as well as to impact other genes altered as the normal esophageal epithelium progresses along the metaplasia-dysplasia-esophageal adenocarcinoma continuum.

Keywords: acid-pulsed cells pretreated with OSU-HDAC42 or vehicle

Overall design:
SEG-1 cells were pretreated for 24 hours with vehicle or OSU-HDAC42, pulsed with acidified media (pH 3.5; 20 mins at 37C), replenished with media or OSU-HDAC42, and harvested 3, 6 and 24 hours later. Global gene expression analysis was conducted using the human genome chip U133 2.0 Plus.

Background corr dist: KL-Divergence = 0.0359, L1-Distance = 0.0235, L2-Distance = 0.0007, Normal std = 0.6370

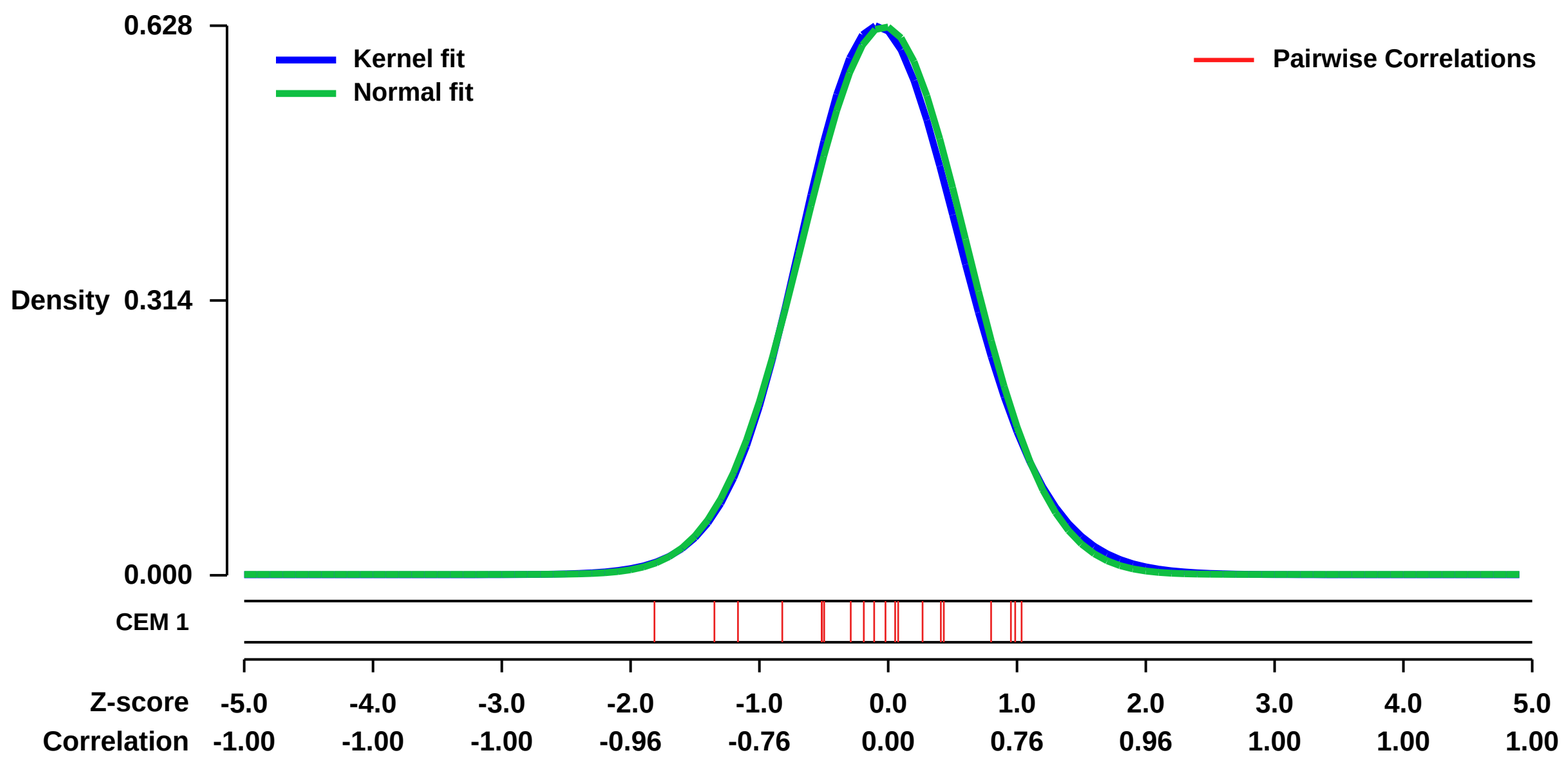

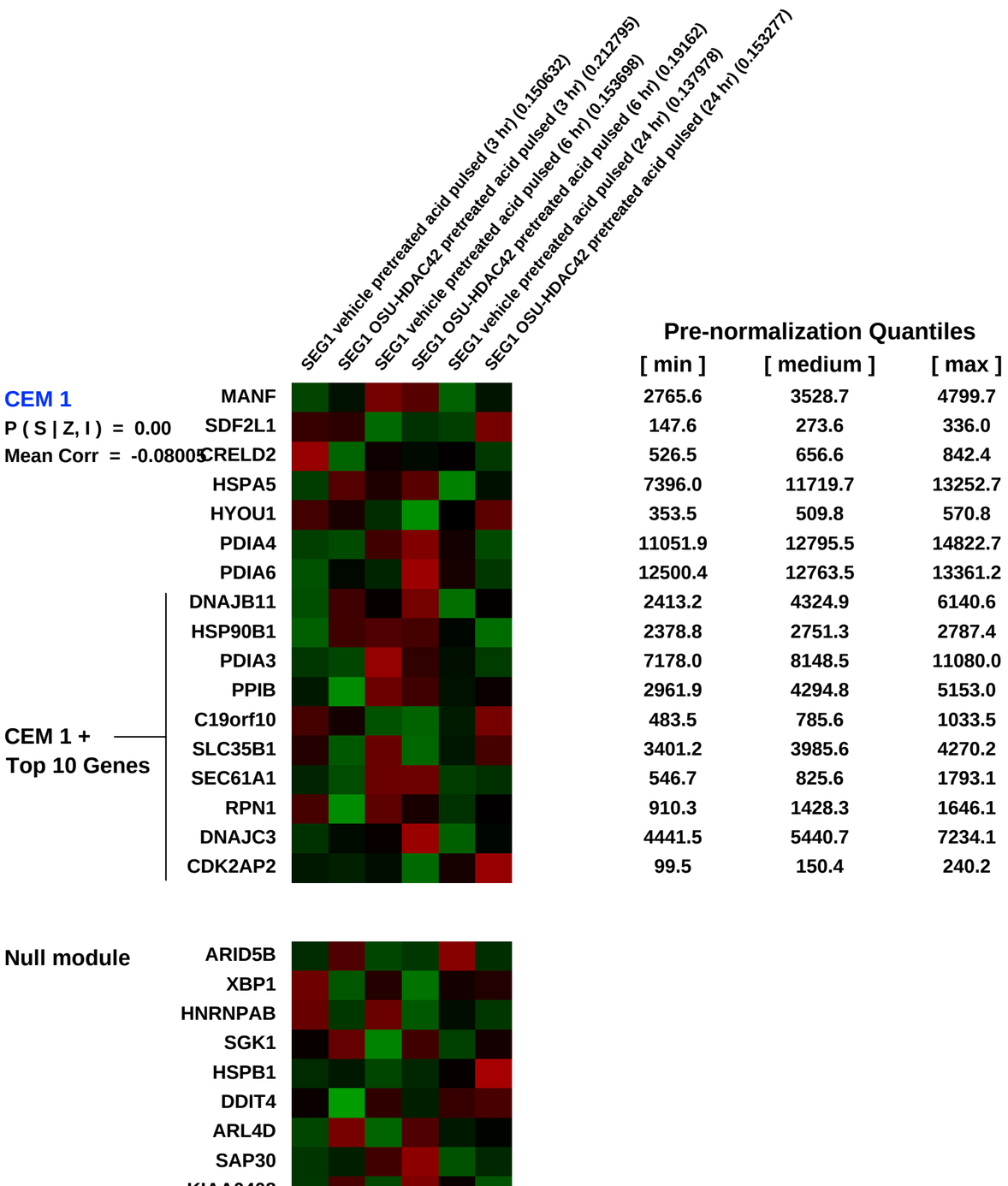

Pre-normalization Quantiles

	[min]	[medium]	[max]
MANF	2765.6	3528.7	4799.7
SDF2L1	147.6	273.6	336.0
CRELD2	526.5	656.6	842.4
HSPA5	7396.0	11719.7	13252.7
HYOU1	353.5	509.8	570.8
PDIA4	11051.9	12795.5	14822.7
PDIA6	12500.4	12763.5	13361.2
DNAJB11	2413.2	4324.9	6140.6
HSP90B1	2378.8	2751.3	2787.4
PDIA3	7178.0	8148.5	11080.0
PPIB	2961.9	4294.8	5153.0
C19orf10	483.5	785.6	1033.5
SLC35B1	3401.2	3985.6	4270.2
SEC61A1	546.7	825.6	1793.1
RPN1	910.3	1428.3	1646.1
DNAJC3	4441.5	5440.7	7234.1
CDK2AP2	99.5	150.4	240.2

GEO Series "GSE29327" Expression Profiles

Num of samples in this series: 6

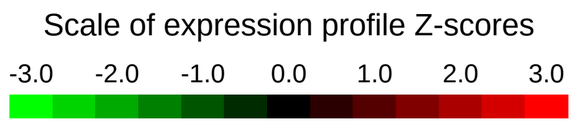

GEO Link:	http://www.ncbi.nlm.nih.gov/geo/query/acc.cgi?acc=GSE29327
Status:	Public on Jun 14 2011
Title:	Gene expression profiling of MCF10A (miR-221/222 vs control)
Organism:	Homo sapiens
Experiment type:	Expression profiling by array
Platform:	GPL570
Pubmed ID:	21673316
Summary & Design:	**Summary:** Analysis of gene expression of MCF10A to identify the targets of miR-221 and miR-222 **Keywords: MCF10, miR-221, miR-222** **Overall design:** RNA profiles of human MCF10A cell line

Background corr dist: KL-Divergence = 0.0118, L1-Distance = 0.0335, L2-Distance = 0.0016, Normal std = 0.8889

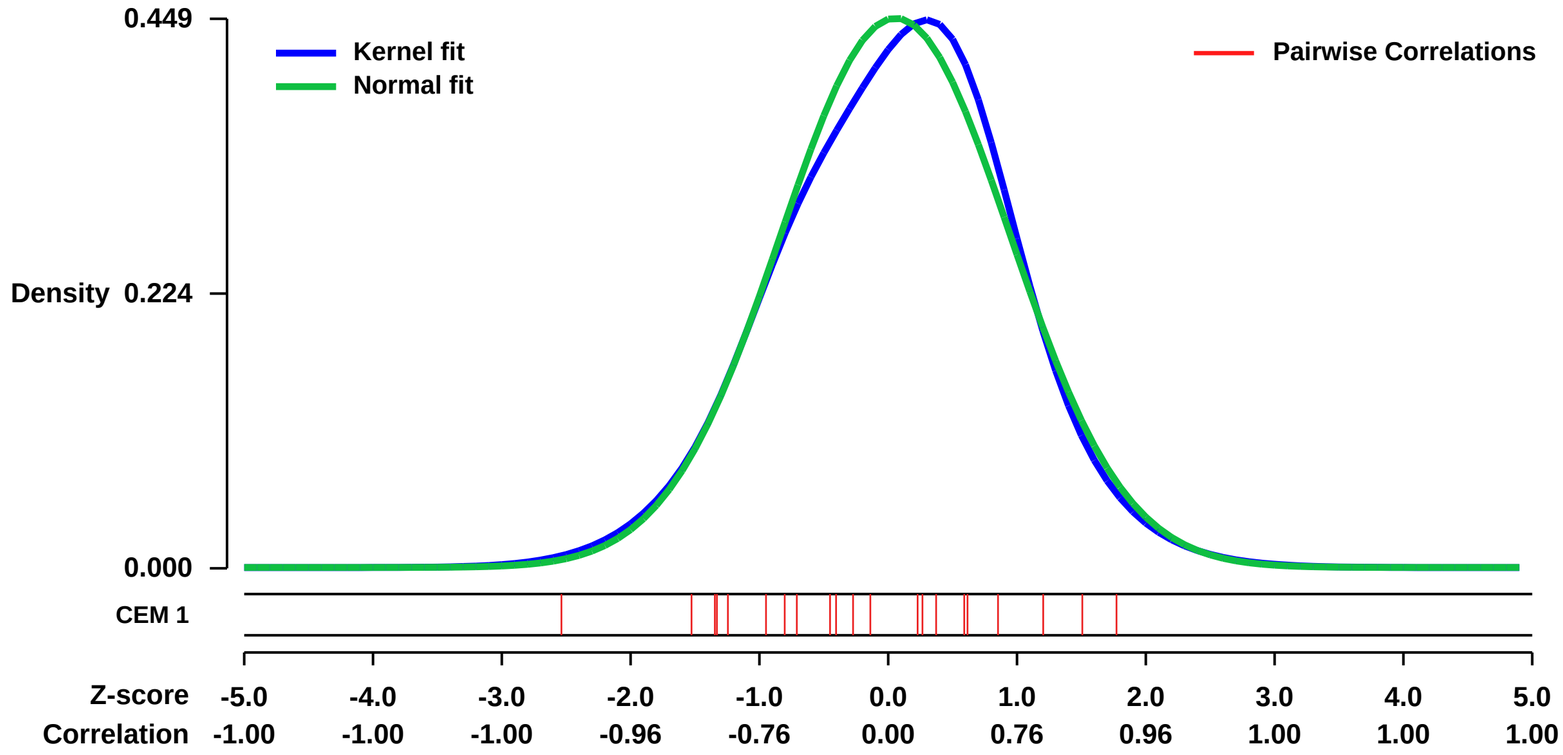

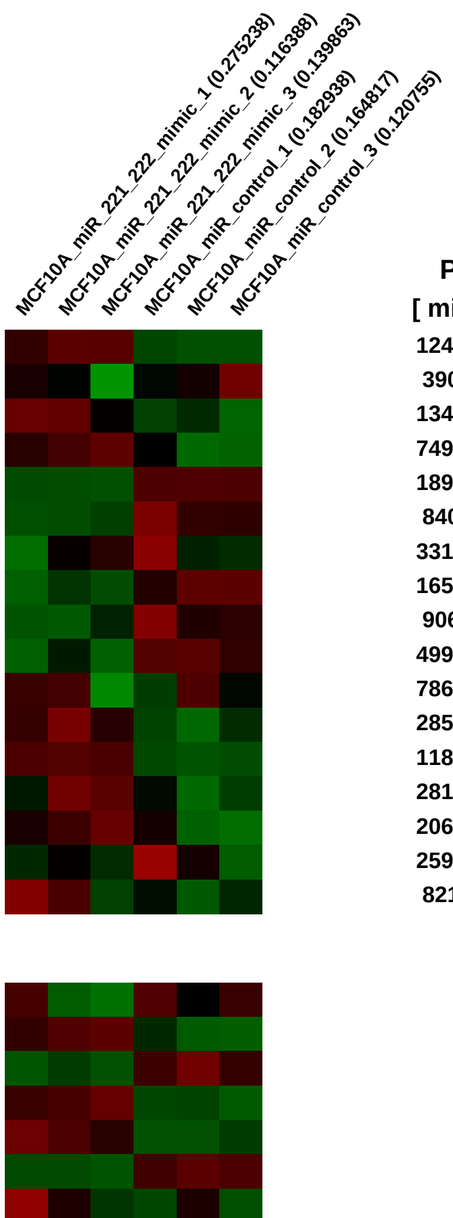

Pre-normalization Quantiles

		[min]	[medium]	[max]
CEM 1	MANF	1240.0	1727.4	1874.5
P (S | Z, I) = 0.00	SDF2L1	390.9	426.7	446.7
Mean Corr = -0.11512	CRELD2	1342.3	1568.7	1793.8
	HSPA5	7495.2	8272.7	8581.6
	HYOU1	1897.3	3841.2	3877.1
	PDIA4	840.7	1028.1	1142.6
	PDIA6	3312.6	3490.3	3688.5
CEM 1 + Top 10 Genes	DNAJB11	1652.8	1753.2	1799.5
	HSP90B1	906.9	1088.8	1235.7
	PDIA3	4999.1	5984.0	6264.0
	PPIB	7868.4	8401.1	8458.8
	C19orf10	2853.2	3202.0	3406.0
	SLC35B1	1188.8	2064.4	2113.8
	SEC61A1	2814.5	2976.5	3187.7
	RPN1	2069.7	2243.9	2345.2
	DNAJC3	2595.6	2710.4	2886.0
	CDK2AP2	821.0	850.2	906.2
Null module	ARID5B			
	XBP1			
	HNRNPAB			
	SGK1			
	HSPB1			
	DDIT4			
	ARL4D			
	SAP30			
	KIAA0408			
	GPR17			
	HSPH1			
	DNASE1L2			
	SLC5A3			
	GNAS			
	GPR3			
	TNFRSF25			
	TM6SF2			
	MKKS			
	PLEKHF1			
	ZMYM1			
	DOK3			
	FGF20			
	SLC39A2			
	KCNIP2			
	ERRFI1			
	DEDD2			
	CCDC117			
	USP31			
	AHSA2			
	CYS1			
	CNIH2			
	BANP			
	CHORDC1			
	P4HA1			

GEO Series "GSE39889" Expression Profiles

Num of samples in this series: 16

Scale of expression profile Z-scores

-3.0 -2.0 -1.0 0.0 1.0 2.0 3.0

GEO Link:	http://www.ncbi.nlm.nih.gov/geo/query/acc.cgi?acc=GSE39889
Status:	Public on Jan 10 2013
Title:	Neutrophil gene expression in response to Mycobacterium abscessus
Organism:	Homo sapiens
Experiment type:	Expression profiling by array
Platform:	GPL570
Pubmed ID:	23451220
Summary & Design:	**Summary:** The response of human neutrophils to the emerging pathogen Mycobacterium abscessus has not been described. However, M. abscessus infections are frequently associated with neutrophil-rich abscesses. To better understand the reponse of neutrophils to M. abscessus we performed gene expression analysis using Affymetrix HG-U133A Plus 2.0 microarrays. Human neutrophils from healthy donors were stimulated with isogenic rough and smooth morphotypes of M. abscessus. Staphylococcus aureus was used as a control. Gene expression was compared to neutrophils left unstimulated. Neutrophils from four individual donors were isolated on separate days and stimulated with freshly prepared bacteria. Neutrophils (stimulated and control) were left for 2 hours before total RNA was isolated, and biotinylated cRNA was prepared by standard methods. Analysis indicates that M. abscessus morphotypes induce a limited number of genes, when compared to S. aureus, which are enriched in genes for cytokines and chemokines, including neutrophil-specific chemokines. These data suggest that neutrophils have a limited response to M. abscessus, which may contribute to neutrophil-rich abscess formation.!Series_overall_design = Human neutrophils from healthy donors were exposed to rough Mab (ATCC 19977T), smooth Mab (ATCC 19977T) and S. aureus (CF clinical strain) for two hours; control cells were exposed to saline. **Overall design:** Human neutrophils from healthy donors were exposed to rough Mab (ATCC 19977T), smooth Mab (ATCC 19977T) and S. aureus (CF clinical strain) for two hours; control cells were exposed to saline.

Background corr dist: KL-Divergence = 0.2005, L1-Distance = 0.0492, L2-Distance = 0.0060, Normal std = 0.3359

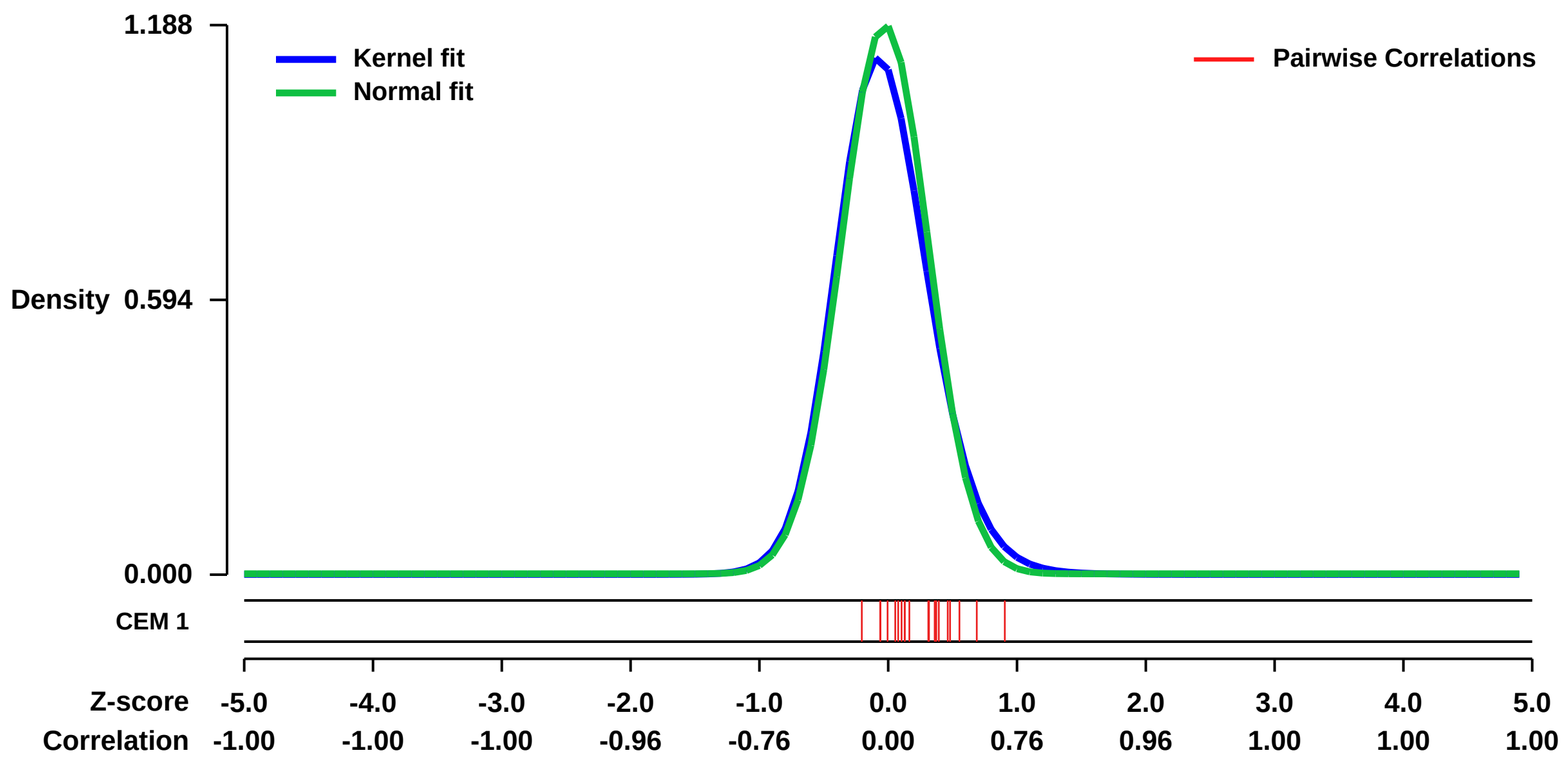

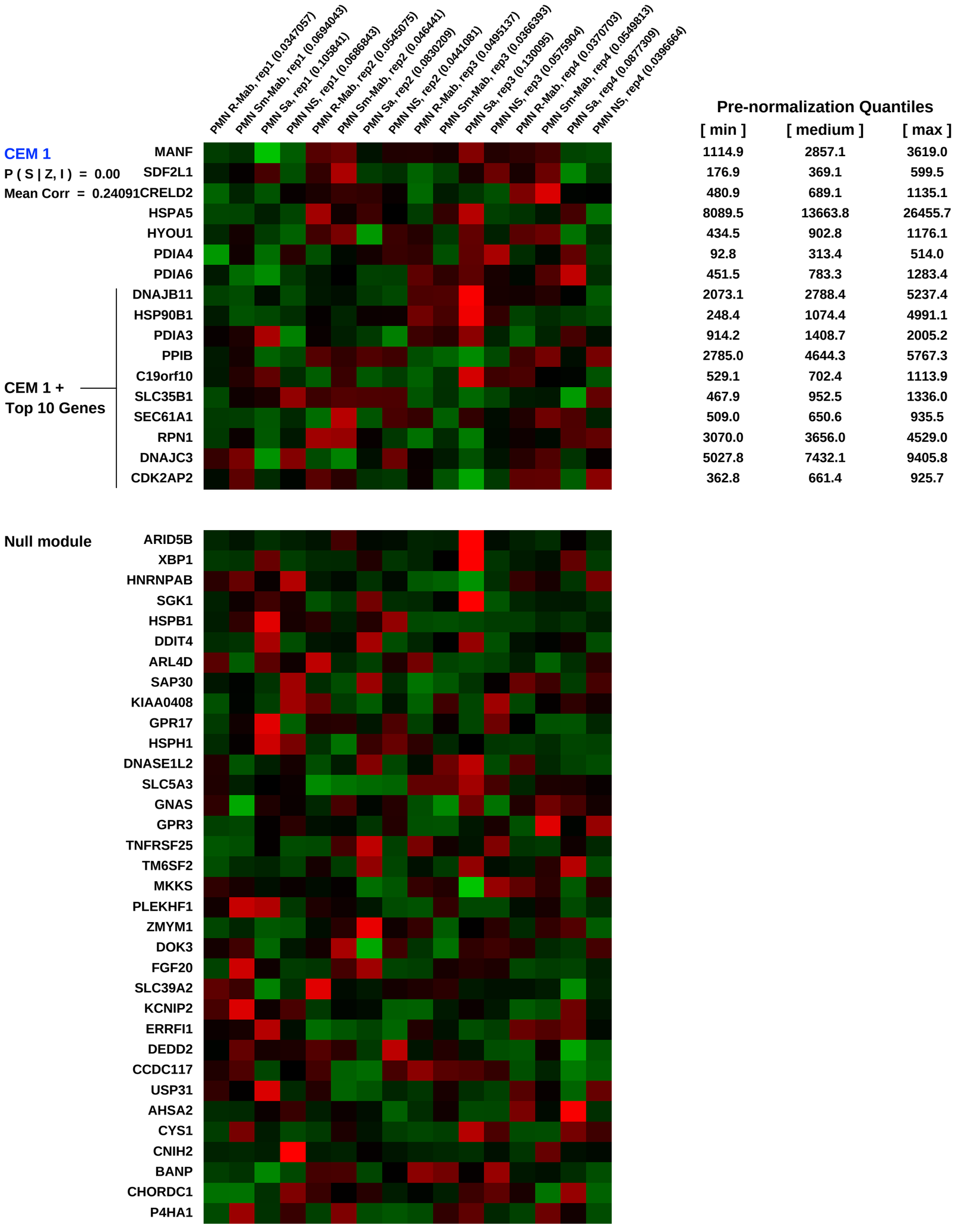

Pre-normalization Quantiles

	[min]	[medium]	[max]
MANF	1114.9	2857.1	3619.0
SDF2L1	176.9	369.1	599.5
CRELD2	480.9	689.1	1135.1
HSPA5	8089.5	13663.8	26455.7
HYOU1	434.5	902.8	1176.1
PDIA4	92.8	313.4	514.0
PDIA6	451.5	783.3	1283.4
DNAJB11	2073.1	2788.4	5237.4
HSP90B1	248.4	1074.4	4991.1
PDIA3	914.2	1408.7	2005.2
PPIB	2785.0	4644.3	5767.3
C19orf10	529.1	702.4	1113.9
SLC35B1	467.9	952.5	1336.0
SEC61A1	509.0	650.6	935.5
RPN1	3070.0	3656.0	4529.0
DNAJC3	5027.8	7432.1	9405.8
CDK2AP2	362.8	661.4	925.7

GEO Series "GSE33943" Expression Profiles

Num of samples in this series: 58

Scale of expression profile Z-scores

-3.0 -2.0 -1.0 0.0 1.0 2.0 3.0

GEO Link: http://www.ncbi.nlm.nih.gov/geo/query/acc.cgi?acc=GSE33943
Status: Public on Oct 04 2013
Title: Gene expression profiles of pediatric IBD remission patients
Organism: Homo sapiens
Experiment type: Expression profiling by array
Platform: GPL570
Pubmed ID: 24260248

Summary & Design:

Summary:
Clinical remission is apparent when laboratory markers of inflammation are normal and clinical symptoms are absent. However, sub-clinical inflammation can still be present. A detailed analysis of the immune status during this inactive state of disease may provide a useful tool to subcategorize patients with subclinical immune activation

We performed (un)supervised clustering analysis of IBD-associated genes and applied Ingenuity´fi pathway software to identify specific molecular profiles between patients.

Overall design:
We analyzed RNA gene expression profiles of peripheral blood leucocytes (PBL) from pediatric IBD patients in clinical remission and age-matched controls.

Background corr dist: KL-Divergence = 0.1113, L1-Distance = 0.0906, L2-Distance = 0.0211, Normal std = 0.4424

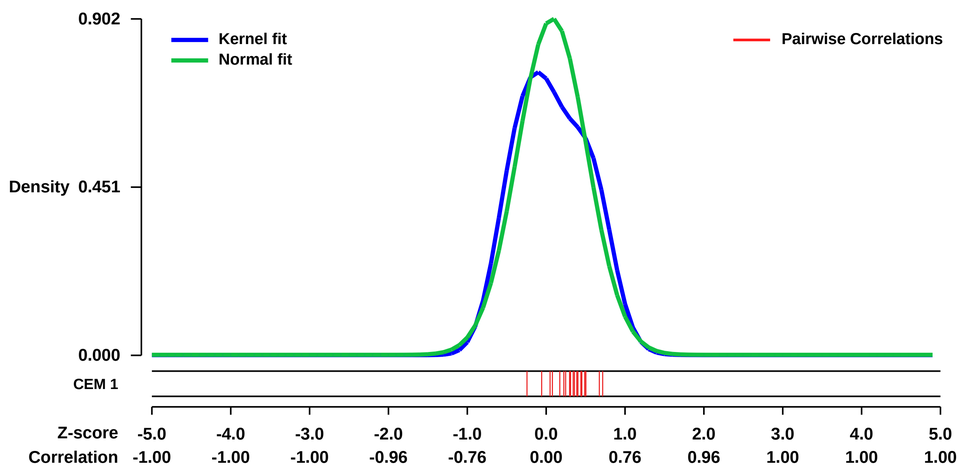

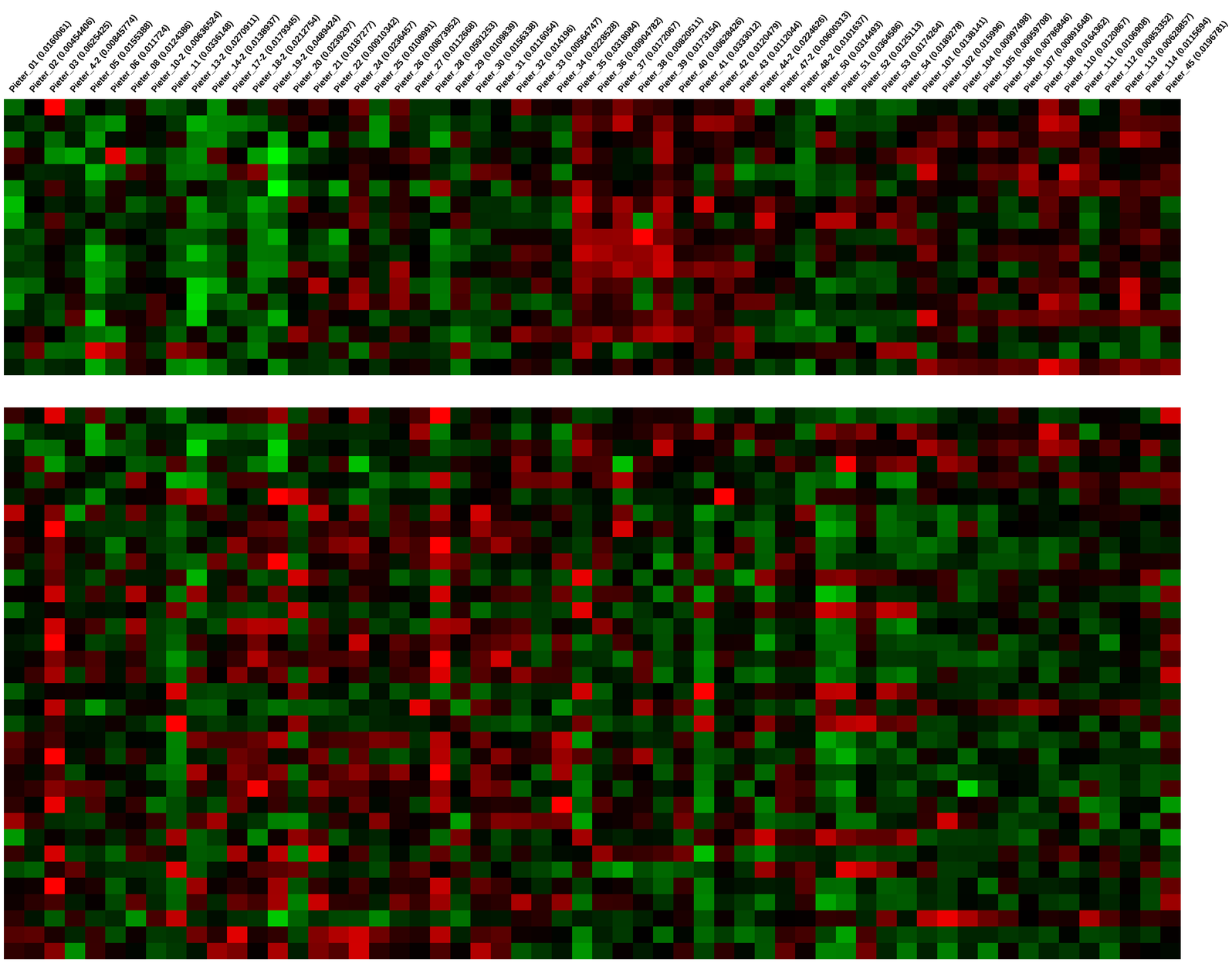

Pre-normalization Quantiles		
[min]	[medium]	[max]
1980.2	2756.2	4368.1
699.8	1023.5	1393.9
1059.5	1478.5	1906.7
1656.8	3311.1	4772.1
1049.1	1684.1	2393.6
512.4	985.7	1258.9
1161.7	2410.9	3785.5
830.3	1176.5	1712.9
731.6	1233.8	2125.2
2953.3	5508.8	8631.8
7829.2	11445.7	16444.8
1124.4	1660.5	2206.5
735.1	1052.0	1372.2
1414.6	2083.4	2797.0
2008.5	2816.7	3873.7
1101.9	1870.6	3369.0
937.3	1536.8	2349.3

GEO Series "GSE7678" Expression Profiles

Num of samples in this series: 8

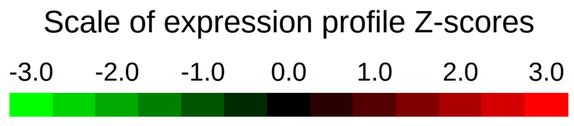

GEO Link:	http://www.ncbi.nlm.nih.gov/geo/query/acc.cgi?acc=GSE7678
Status:	Public on Aug 20 2007
Title:	miRNA34 expression in SW480 cells
Organism:	Homo sapiens
Experiment type:	Expression profiling by array
Platform:	GPL570
Pubmed ID:	17656095
Summary & Design:	**Summary:** SW480 were stably transfected with an episomal plasmid expressing GFP and miRNA34 from a bidirectional doxycyclin regulatable promoter (Bornkamm et al Nucleic Acids Res. 2005 Sep 7;33(16)). Polyclonal cell lines were obtained by selection with Hygromycin at 350ug/ml for 10 days. The cell llnes identified as GFP only express GFP, whereas the cell lines identified as miRNA34a express both GFP and miRNA34 under doxycyclin control. For the present experiment, cells were treated with 1ug/ml Docycyclin for 72h. Cells were harvested and total RNA was isolated using Trizol (Invitrogen). After RNA cleanup (RNeasy, Qiagen) Affymetrix 133 Plus 2.0 micorarrays were hybridized using standard techniques. **Keywords:** Cell line transfection **Overall design:** The log-transformed probe-set values and the results of the statistical analysis for each probe-set, and the associated README file, are included as Supplementary files.

Background corr dist: KL-Divergence = 0.0420, L1-Distance = 0.0168, L2-Distance = 0.0003, Normal std = 0.5989

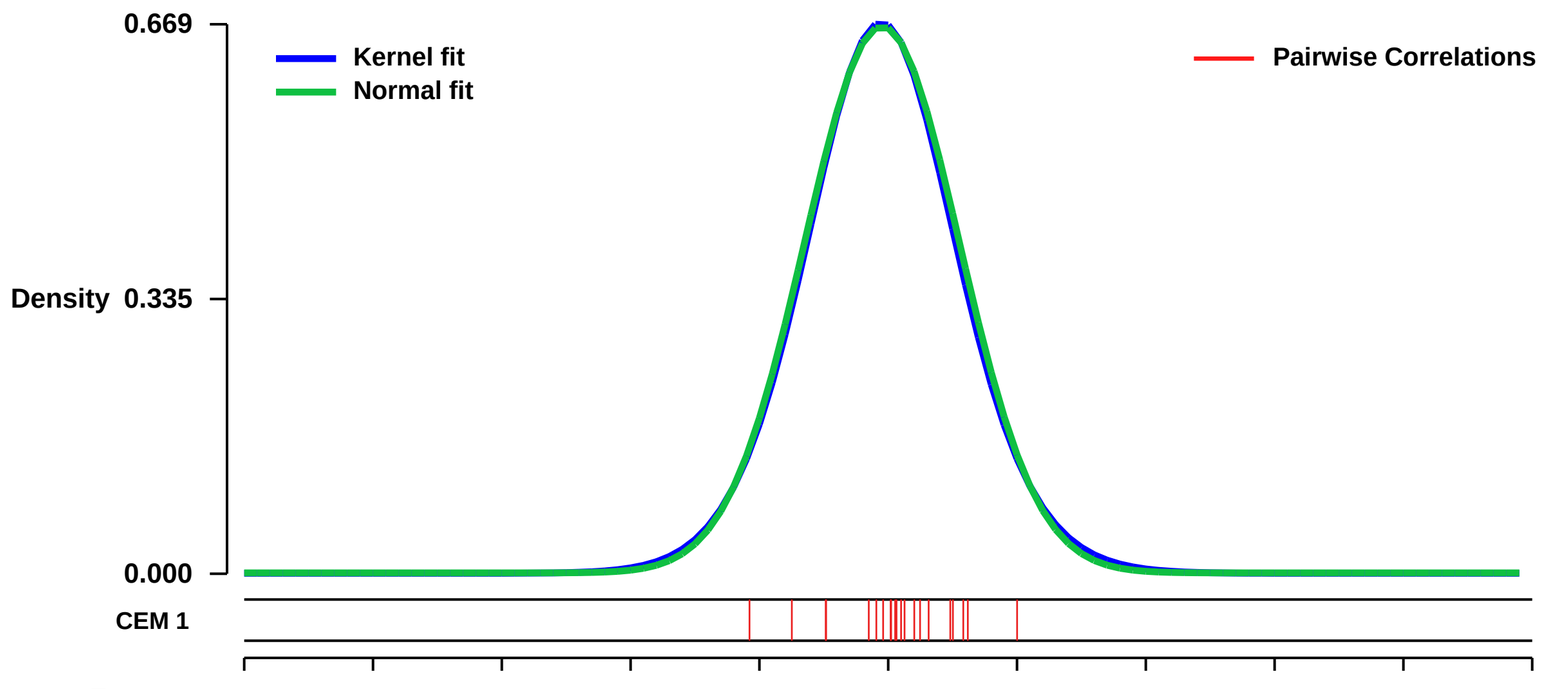

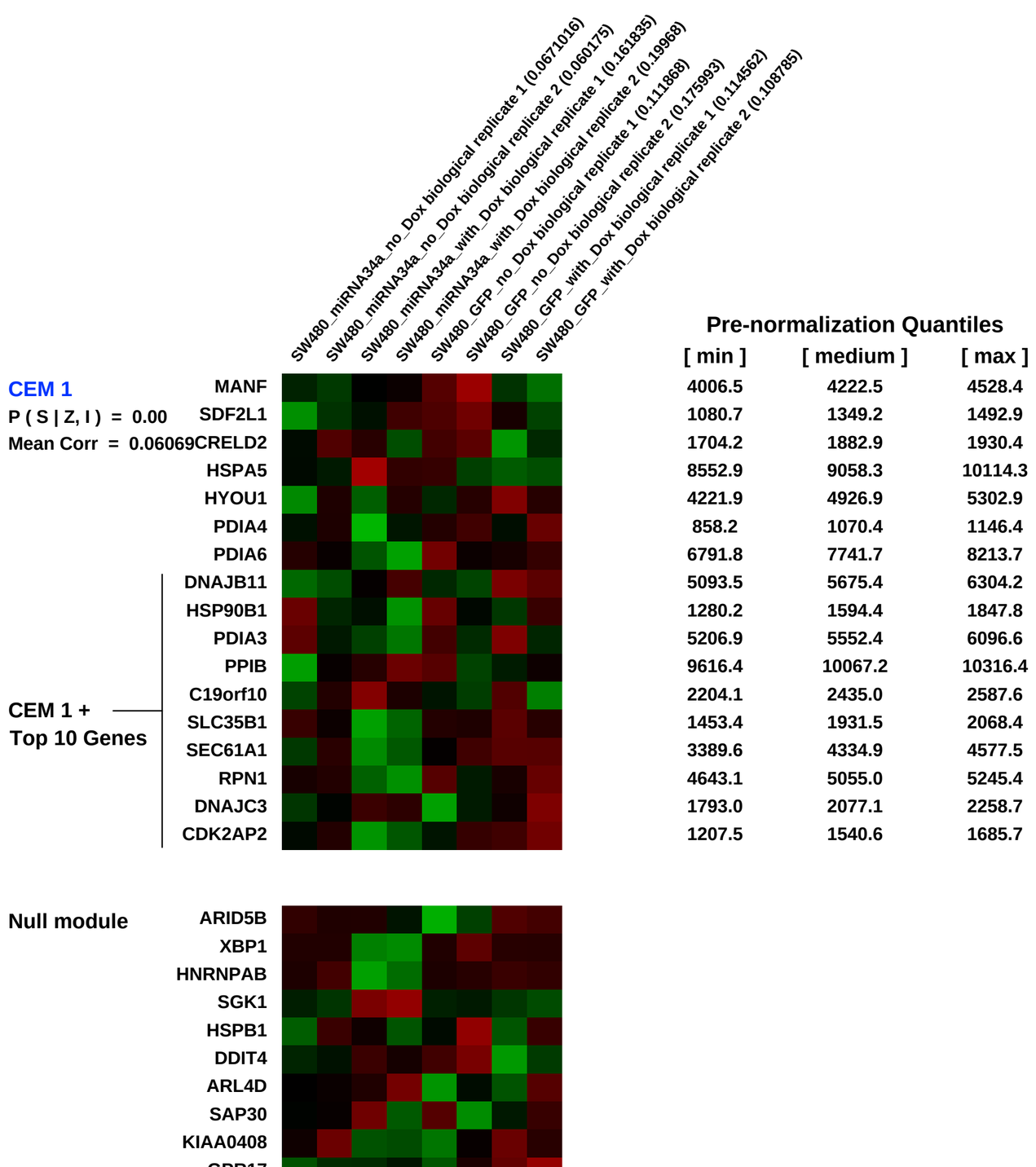

Pre-normalization Quantiles

	[min]	[medium]	[max]
MANF	4006.5	4222.5	4528.4
SDF2L1	1080.7	1349.2	1492.9
CRELD2	1704.2	1882.9	1930.4
HSPA5	8552.9	9058.3	10114.3
HYOU1	4221.9	4926.9	5302.9
PDIA4	858.2	1070.4	1146.4
PDIA6	6791.8	7741.7	8213.7
DNAJB11	5093.5	5675.4	6304.2
HSP90B1	1280.2	1594.4	1847.8
PDIA3	5206.9	5552.4	6096.6
PPIB	9616.4	10067.2	10316.4
C19orf10	2204.1	2435.0	2587.6
SLC35B1	1453.4	1931.5	2068.4
SEC61A1	3389.6	4334.9	4577.5
RPN1	4643.1	5055.0	5245.4
DNAJC3	1793.0	2077.1	2258.7
CDK2AP2	1207.5	1540.6	1685.7

GEO Series "GSE28715" Expression Profiles

Num of samples in this series: 12

Scale of expression profile Z-scores

-3.0 -2.0 -1.0 0.0 1.0 2.0 3.0

GEO Link:	http://www.ncbi.nlm.nih.gov/geo/query/acc.cgi?acc=GSE28715
Status:	Public on Sep 01 2011
Title:	Identification of Med26 target genes in Human HEK 293T cells
Organism:	Homo sapiens
Experiment type:	Expression profiling by array
Platform:	GPL570
Pubmed ID:	21729782
Summary & Design:	**Summary:** Med26 is a subunit of the Human Mediator complex. The Mediator complex is an evolutionarily conserved coregulatory complex that interacts with RNA polymerase II to regulate gene expression. In metazoa, Mediator is composed of some 30 distinct subunits. Mediator exists in multiple, functionally distinct forms that share a common core of subunits and can be distinguished by the presence or absence of a kinase module composed of Med12, Med13, Cdk8, and Cyclin C. In higher eukaryotes, a subset of Mediator complexes is associated with an additional subunit, Med26. This Med26-containing Mediator copurifies from cells with little or no kinase module, but near-stoichiometric Pol II. Evidence suggests that Med26-containing Mediator plays a key role in transcriptional activation however, the mechanism(s) by which Med26 contributes to this process are not known. To identify Med26 target genes, we used Affymetrix U133A plus 2.0 expression arrays to analyze mRNA expression in 293T cells from which Med26 had been depleted by transient transfection by each of three different siRNAs. **Overall design:** Three different independent Med26 siRNA knockdowns were compared to a non-targeting control in triplicate, for a total of 12 samples.

Background corr dist: KL-Divergence = 0.1217, L1-Distance = 0.0275, L2-Distance = 0.0011, Normal std = 0.4059

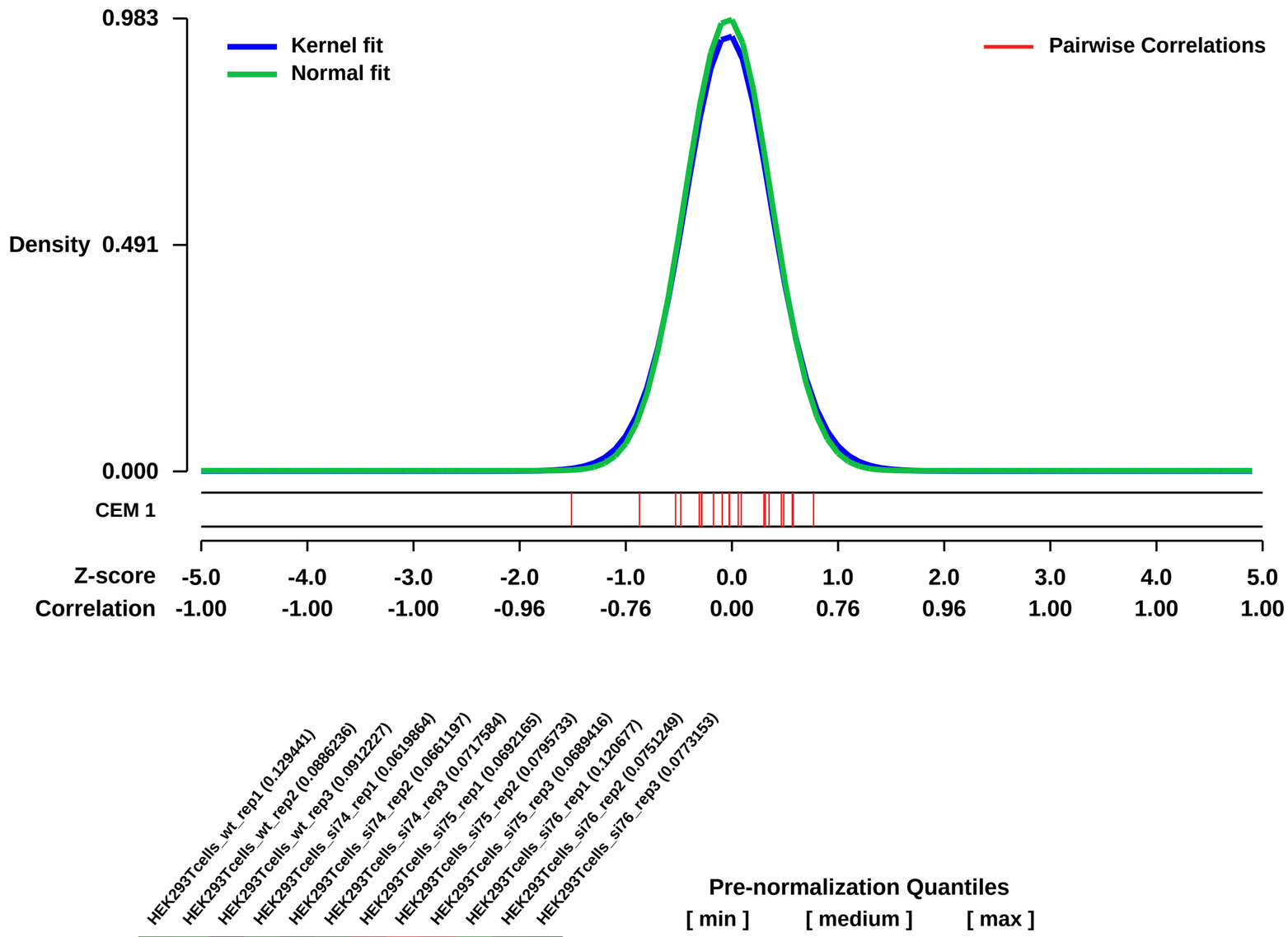

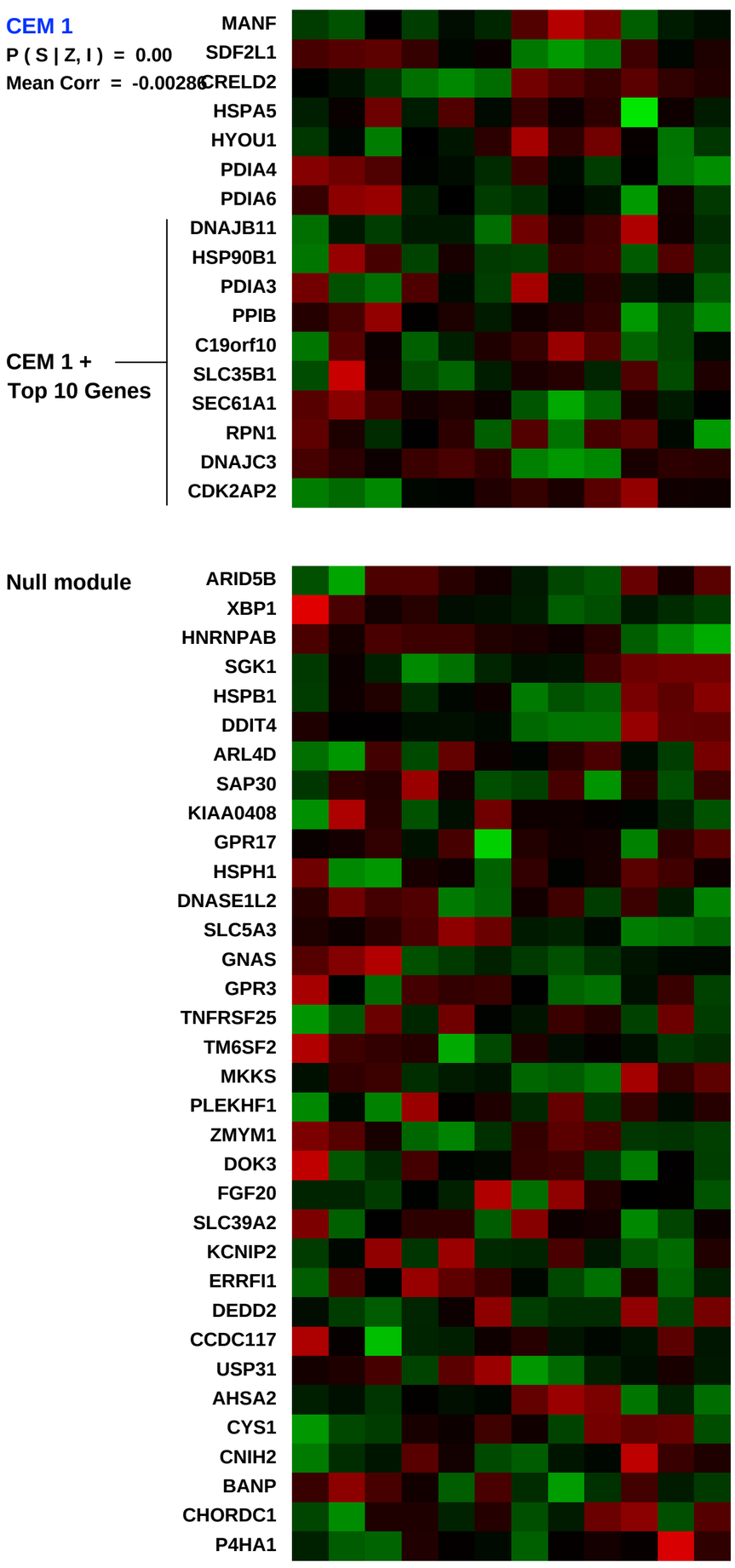

Pre-normalization Quantiles

	[min]	[medium]	[max]
MANF	6240.5	6678.2	7750.1
SDF2L1	1810.9	2471.2	2702.8
CRELD2	3464.5	4352.5	4769.7
HSPA5	10385.9	12556.1	13412.9
HYOU1	3756.5	4170.1	4699.3
PDIA4	1116.4	1325.9	1532.0
PDIA6	6028.9	7078.9	8162.5
DNAJB11	3022.7	3213.8	3642.3
HSP90B1	1250.7	1631.7	1975.4
PDIA3	8117.3	8901.3	10279.2
PPIB	11690.7	13842.6	15240.4
C19orf10	3281.4	3764.8	4277.0
SLC35B1	3065.8	3324.0	3726.4
SEC61A1	2752.1	3440.4	3867.5
RPN1	4407.5	4684.1	4783.0
DNAJC3	1161.2	2207.1	2360.7
CDK2AP2	948.1	1097.3	1225.3

GEO Series "GSE26051" Expression Profiles

Num of samples in this series: 46

Scale of expression profile Z-scores

-3.0 -2.0 -1.0 0.0 1.0 2.0 3.0

GEO Link:	http://www.ncbi.nlm.nih.gov/geo/query/acc.cgi?acc=GSE26051
Status:	Public on Jun 07 2011
Title:	Analysis of Human Tendinopathy Gene Expression
Organism:	Homo sapiens
Experiment type:	Expression profiling by array
Platform:	GPL570
Pubmed ID:	21539748
Summary & Design:	**Summary:** Chronic tendon injuries, also known as tendinopathy, are common among professional and recreational athletes. These injuries result in a significant amount of morbidity and health care expenditure and yet little is known about the molecular mechanism leading to tendinopathy. We have used histological evaluation and molecular profiling to determine the gene expression changes in 23 human patients undergoing surgical procedures for the treatment of chronic tendinopathy. Diseased tendons have altered extracellular matrix, fiber disorientation, increased cellular content and vasculature and the absence of inflammatory cells. Global gene expression profiling identified 1783 transcripts with significant different expression patterns in the diseased tendons. Global pathway analysis further suggests altered expression of extracellular matrix proteins and the lack of an appreciable inflammatory response. We have identified pathways and genes regulated in tendinopathy samples that will help contribute to the understanding of the disease towards the development of novel therapeutics. **Overall design:** A prospective study was initiated to collect tissue from patients undergoing surgery as standard of care for tendinopathy. Biopsies (~3mm^3) of diseased tendons as well as a section of grossly normal appearing tendon were collected from 23 patients. Written informed consent was obtained from all patients prior to any study related procedure.

Background corr dist: KL-Divergence = 0.4366, L1-Distance = 0.0829, L2-Distance = 0.0228, Normal std = 0.2415

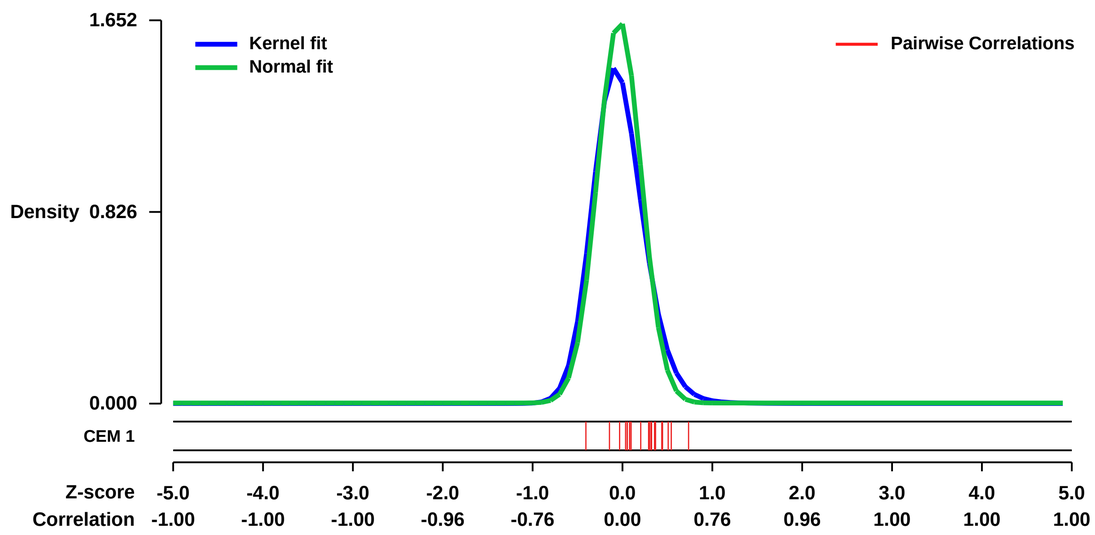

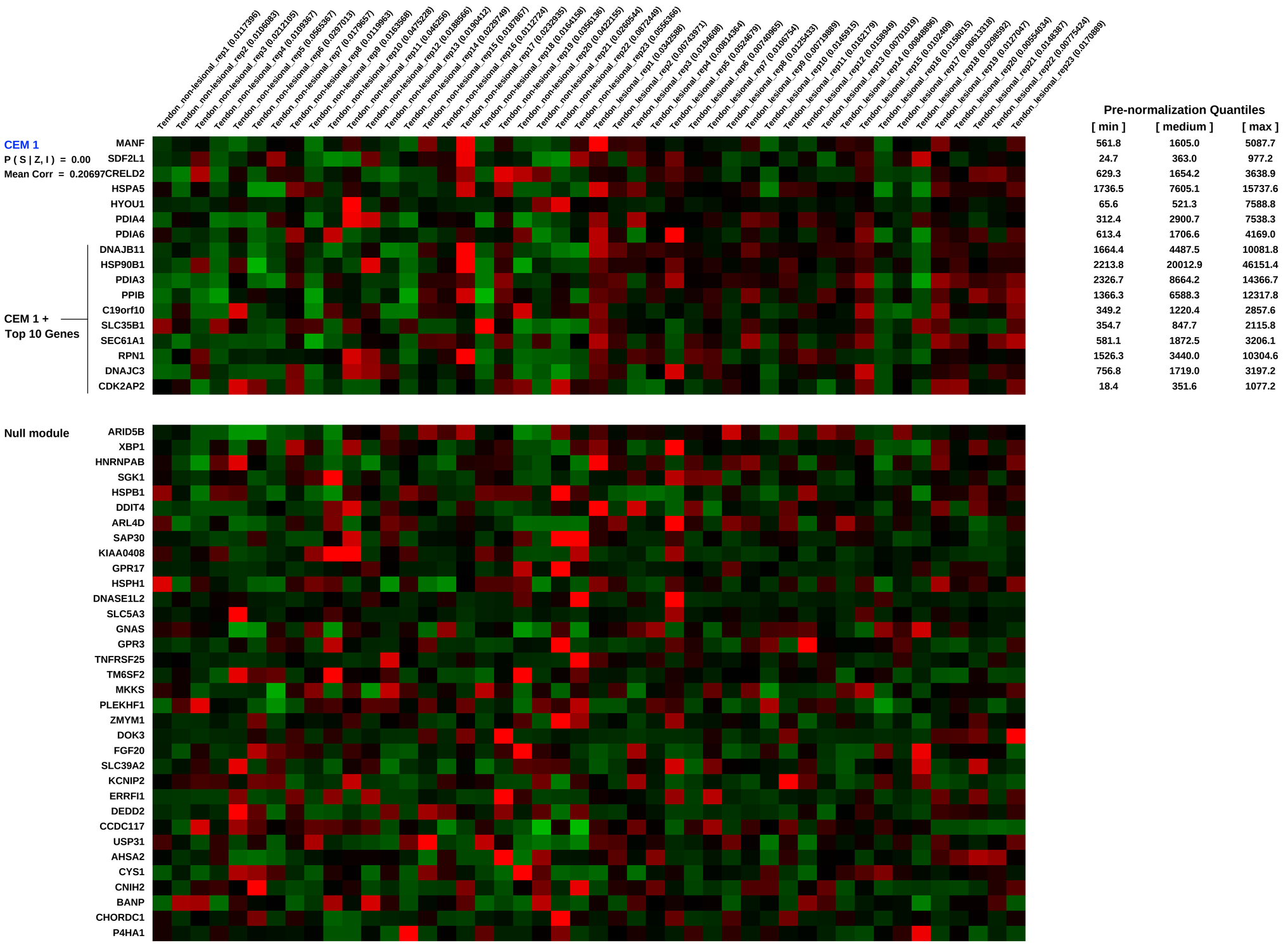

Pre-normalization Quantiles		
[min]	[medium]	[max]
561.8	1605.0	5087.7
24.7	363.0	977.2
629.3	1654.2	3638.9
1736.5	7605.1	15737.6
65.6	521.3	7588.8
312.4	2900.7	7538.3
613.4	1706.6	4169.0
1664.4	4487.5	10081.8
2213.8	20012.9	46151.4
2326.7	8664.2	14366.7
1366.3	6588.3	12317.8
349.2	1220.4	2857.6
354.7	847.7	2115.8
581.1	1872.5	3206.1
1526.3	3440.0	10304.6
756.8	1719.0	3197.2
18.4	351.6	1077.2

GEO Series "GSE24468" Expression Profiles

Num of samples in this series: 20

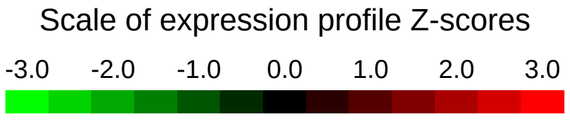

GEO Link:	http://www.ncbi.nlm.nih.gov/geo/query/acc.cgi?acc=GSE24468
Status:	Public on Oct 01 2010
Title:	Elucidation of the Mechanisms by which the Progesterone Receptor Inhibits Inflammatory Responses in Cellular Models of Breast Cancer
Organism:	Homo sapiens
Experiment type:	Expression profiling by array
Platform:	GPL570
Pubmed ID:	20980435
Summary & Design:	**Summary:** Both pro- and anti-mitogenic activities have been ascribed to progesterone receptor (PR) agonists and antagonists in breast cancer cells, however, the transcriptional responses that underlie these paradoxical functions are not apparent. Using non-transformed, normal human mammary epithelial cells (hMECs) engineered to express PR, and standard microarray technology, we defined 2,370 genes that were significantly regulated by the PR agonist R5020. Gene Ontology (GO) analysis revealed that GO-terms involved in inflammation and NF-¸”B signaling were among the most significantly regulated. Interestingly, on those NF-¸”B responsive genes that were inhibited by agonist-activated PR, antagonists either (a) mimicked the actions of agonists or (b) reversed the inhibitory actions of agonists. This difference in pharmacological response could be attributed to the fact that although agonist and antagonist-activated PR is recruited to the promoters of NF-¸”B responsive promoters, the physical presence of PR tethered to the promoter of some genes is sufficient for transcriptional inhibition whereas on others an agonist-activated PR conformation is required for inhibition of NF-¸”B signaling. Importantly, the actions of PR on the latter class of genes were reversed by an AF-2 inhibiting, LXXLL-containing peptide. Consideration of the relative activities of these distinct anti-inflammatory pathways in breast cancer may be instructive with respect to the likely therapeutic activity of PR agonists or antagonists in the treatment of breast cancer. **Overall design:** Human mammary epithelial cells treated with R5020 or vehicle.

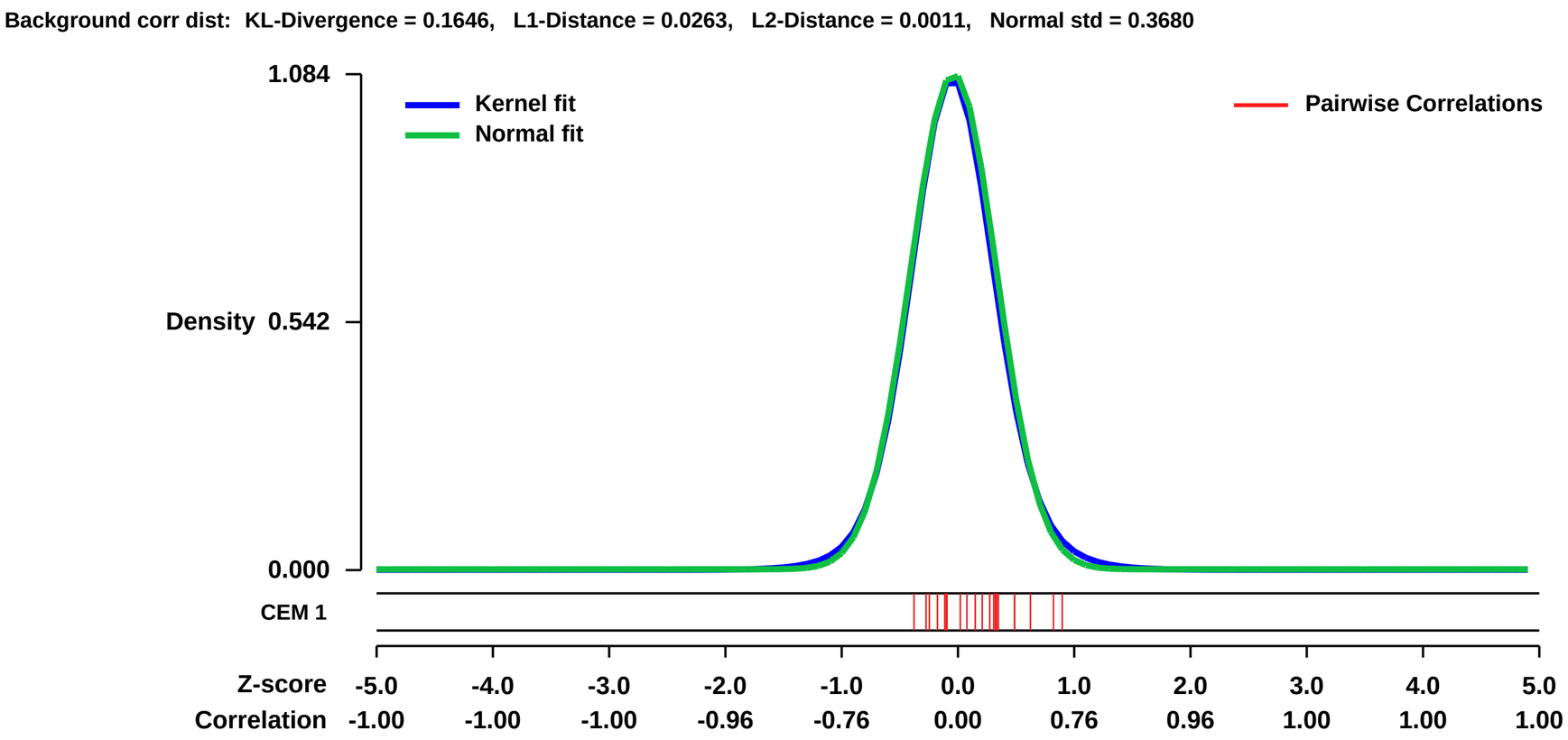

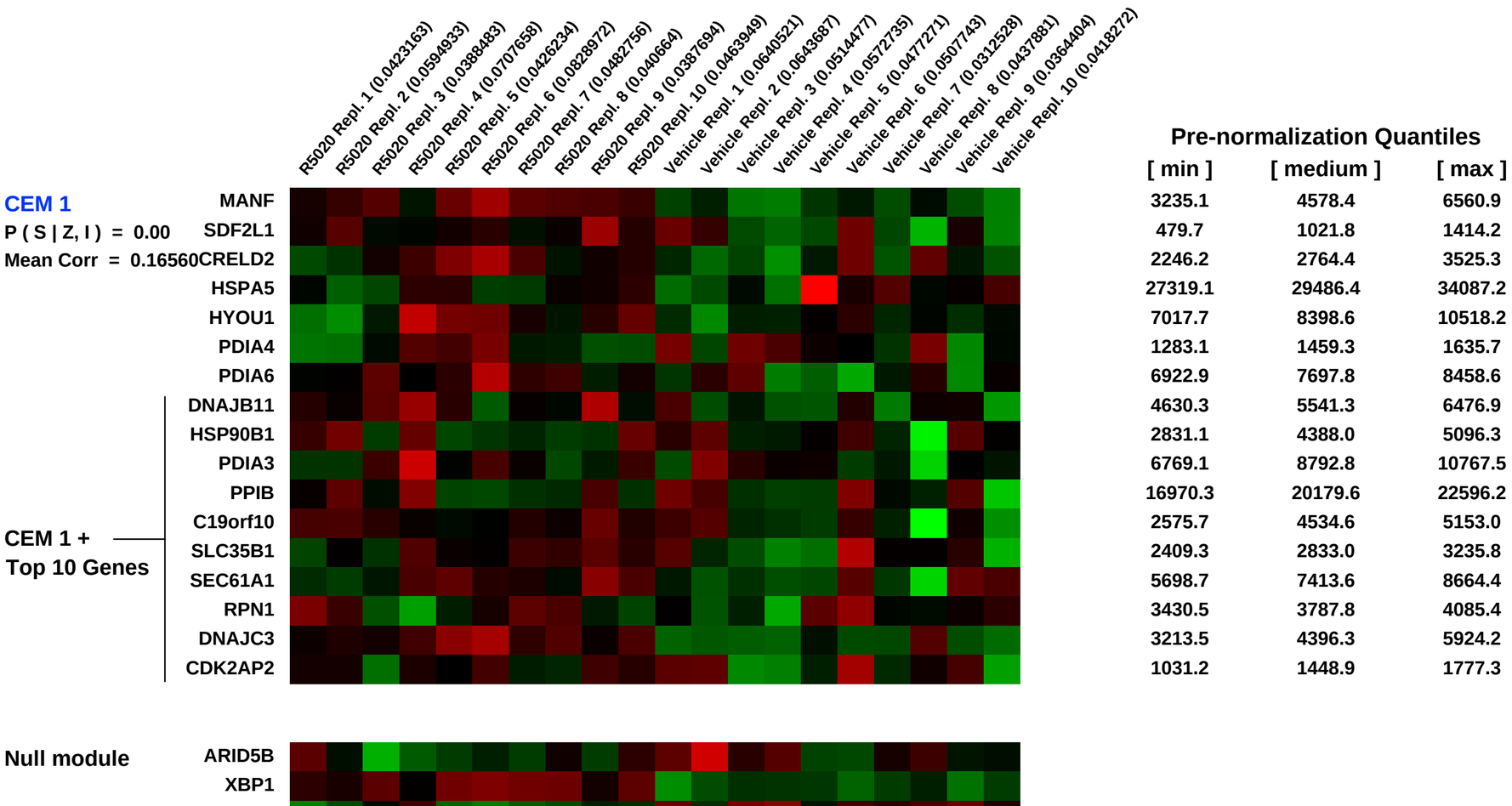

Pre-normalization Quantiles

[min]	[medium]	[max]
3235.1	4578.4	6560.9
479.7	1021.8	1414.2
2246.2	2764.4	3525.3
27319.1	29486.4	34087.2
7017.7	8398.6	10518.2
1283.1	1459.3	1635.7
6922.9	7697.8	8458.6
4630.3	5541.3	6476.9
2831.1	4388.0	5096.3
6769.1	8792.8	10767.5
16970.3	20179.6	22596.2
2575.7	4534.6	5153.0
2409.3	2833.0	3235.8
5698.7	7413.6	8664.4
3430.5	3787.8	4085.4
3213.5	4396.3	5924.2
1031.2	1448.9	1777.3

GEO Series "GSE16836" Expression Profiles

Num of samples in this series: 8

Scale of expression profile Z-scores

-3.0 -2.0 -1.0 0.0 1.0 2.0 3.0

GEO Link: http://www.ncbi.nlm.nih.gov/geo/query/acc.cgi?acc=GSE16836
Status: Public on Aug 31 2009
Title: Transcriptional profiling of CD16+ and CD16- peripheral blood monocytes from healthy individuals
Organism: Homo sapiens
Experiment type: Expression profiling by array
Platform: GPL570
Pubmed ID: 19712453

Summary & Design:

Summary:
Human peripheral blood monocytes (Mo) consist of subsets distinguished by expression of CD16 (FCGRIII) and chemokine receptors. Classical CD16- Mo express CCR2 and migrate in response to CCL2, while a minor CD16+ Mo subset expresses CX3CR1 and migrates into tissues expressing CX3CL1. CD16+ Mo produce pro-inflammatory cytokines and are expanded in certain inflammatory conditions including HIV infection.

To gain insight into the developmental relationship and functions of CD16+ and CD16- Mo, we examined transcriptional profiles of these Mo subsets in peripheral blood from healthy individuals. Of 16,328 expressed genes, 2,759 genes were differentially expressed and 228 and 250 were >2-fold upregulated and downregulated, respectively, in CD16+ compared to CD16- Mo. CD16+ Mo were distinguished by upregulation of dendritic cell (DC) (SIGLEC10, CD43, RARA) and macrophage (MF) (CSF1R/CD115, MafB, CD97, C3aR) markers together with transcripts relevant for DC-T cell interaction (CXCL16, ICAM-2, LFA-1), cell activation (LTB, TNFRSF8, LST1, IFITM1-3, HMOX1, SOD-1, WARS, MGLL), and negative regulation of the cell cycle (CDKN1C, MTSS1), whereas CD16- Mo were distinguished by upregulation of myeloid (CD14, MNDA, TREM1, CD1d, C1qR/CD93) and granulocyte markers (FPR1, GCSFR/CD114, S100A8-9/12). Differential gene expression in CD16+ and CD16- Mo was confirmed by quantitative real time RT-PCR (i.e., CD16, C3AR1, C1QR1, ICAM-2, CSF1R, CSF3R, CDKN1C, TNFRSF1, and LTB) and flow cytometry (i.e., CSF1R, CSF3R, C1QR1, C3AR1, CD1d, CD43, CXCL16, and CX3CR1). Furthermore, increased expression of RARA and KLF2 transcripts in CD16+ Mo coincided with absence of cutaneous lymphocyte associated antigen (CLA) expression, indicating potential imprinting for non-skin homing.

These results suggest that CD16+ and CD16- Mo originate from a common myeloid precursor, with CD16+ Mo having a more MF- and DC-like transcription program suggesting a more advanced stage of differentiation. Distinct transcriptional programs, together with their recruitment into tissues via different mechanisms, also suggest that CD16+ and CD16- Mo give rise to functionally distinct DC and MF in vivo.

Overall design:
Total Mo were isolated by negative selection using magnetic immunobeads (Monocyte Isolation Kit II, Miltenyi). CD16+ and CD16- Mo fractions were further isolated using CD16 magnetic immunobeads (Miltenyi). Total RNA from Mo pellets was isolated by Trizol extraction and purified using RNeasy columns (Qiagen). The quality of RNA was assessed by visualization of intact bands corresponding to 18S and 28S rRNA on formaldehyde agarose gels. Total RNA (10 ´µg) from matched CD16+ and CD16- Mo samples isolated from 4 different healthy donors was quality tested using an Agilent 2100 Bioanalyzer chip, reverse transcribed, and hybridized on the GeneChip Human Genome U133 Plus 2.0 Array (Affymetrix), which includes 54,000 probe sets on a single array (i.e., 47,000 transcripts and variants, including 38,500 well-characterized human genes). Primary data analysis performed using GeneSpring software (Biopolymer core facility, Harvard Medical School) generated Excel spreadsheets with relative gene expression values for the 4 matched CD16+ and CD16- Mo subsets.

Background corr dist: KL-Divergence = 0.0657, L1-Distance = 0.0328, L2-Distance = 0.0019, Normal std = 0.5243

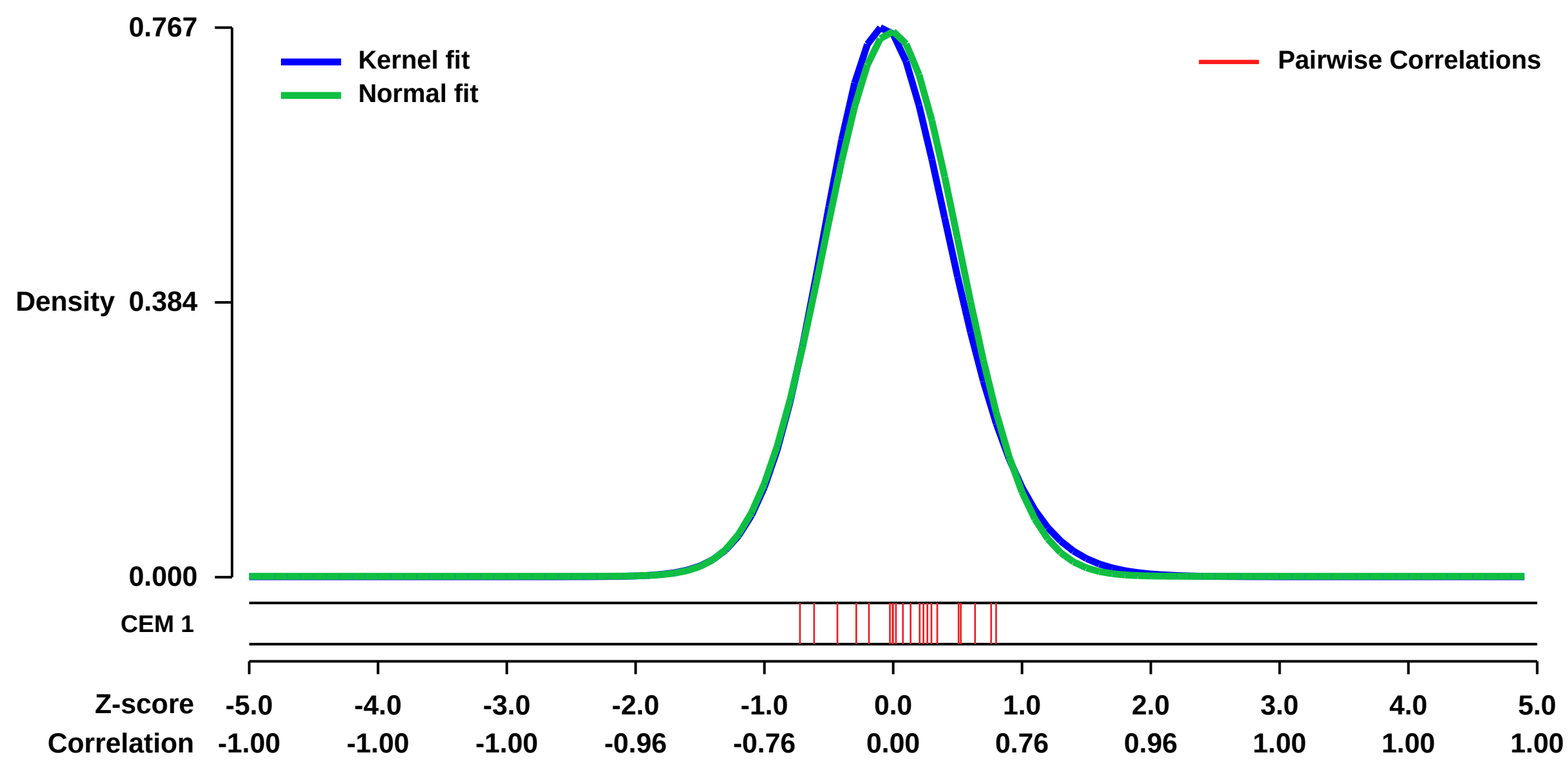

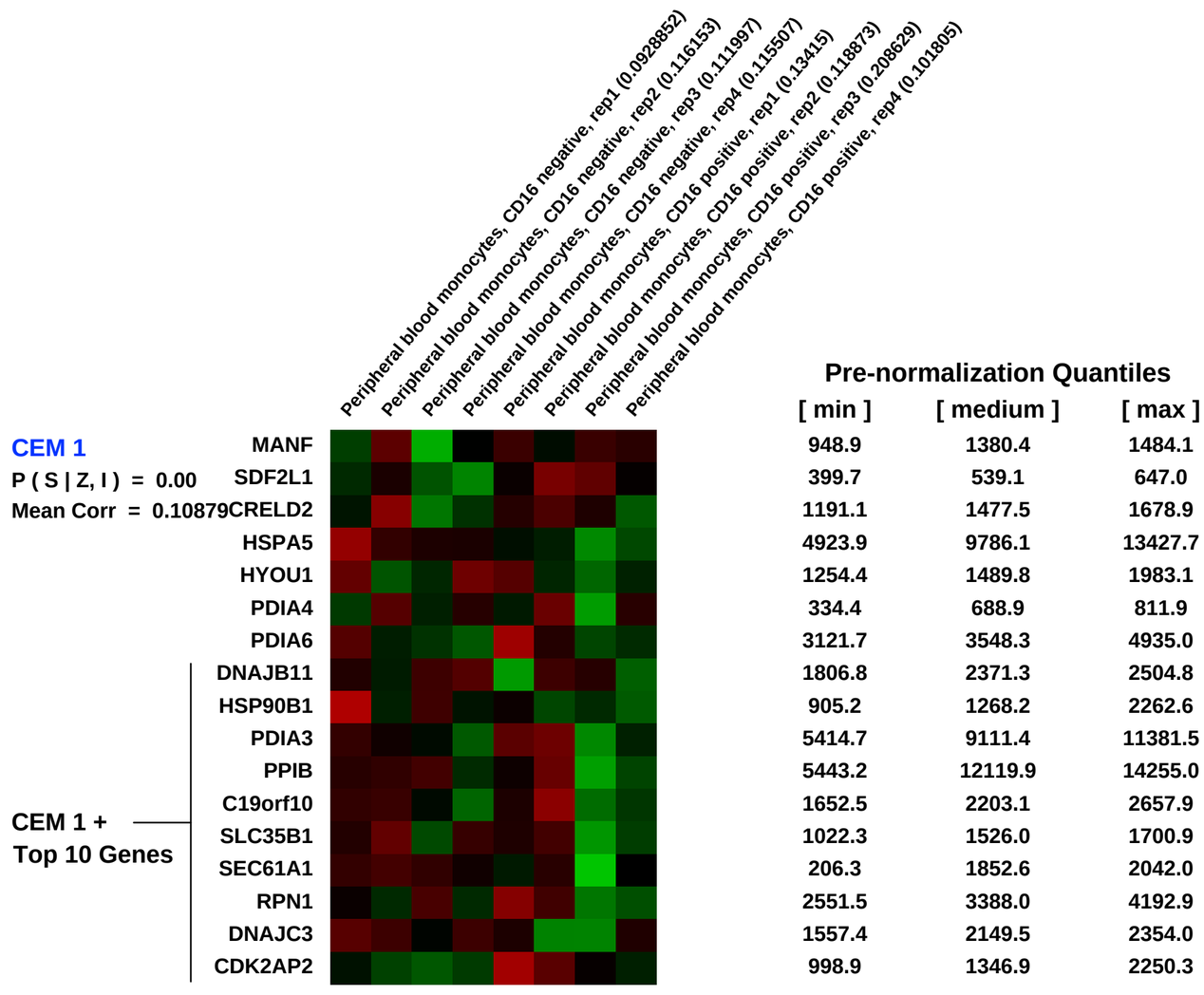

CEM 1
P (S | Z, I) = 0.00
Mean Corr = 0.10879

CEM 1 + Top 10 Genes

	Pre-normalization Quantiles [min]	[medium]	[max]
MANF	948.9	1380.4	1484.1
SDF2L1	399.7	539.1	647.0
CRELD2	1191.1	1477.5	1678.9
HSPA5	4923.9	9786.1	13427.7
HYOU1	1254.4	1489.8	1983.1
PDIA4	334.4	688.9	811.9
PDIA6	3121.7	3548.3	4935.0
DNAJB11	1806.8	2371.3	2504.8
HSP90B1	905.2	1268.2	2262.6
PDIA3	5414.7	9111.4	11381.5
PPIB	5443.2	12119.9	14255.0
C19orf10	1652.5	2203.1	2657.9
SLC35B1	1022.3	1526.0	1700.9
SEC61A1	206.3	1852.6	2042.0
RPN1	2551.5	3388.0	4192.9
DNAJC3	1557.4	2149.5	2354.0
CDK2AP2	998.9	1346.9	2250.3

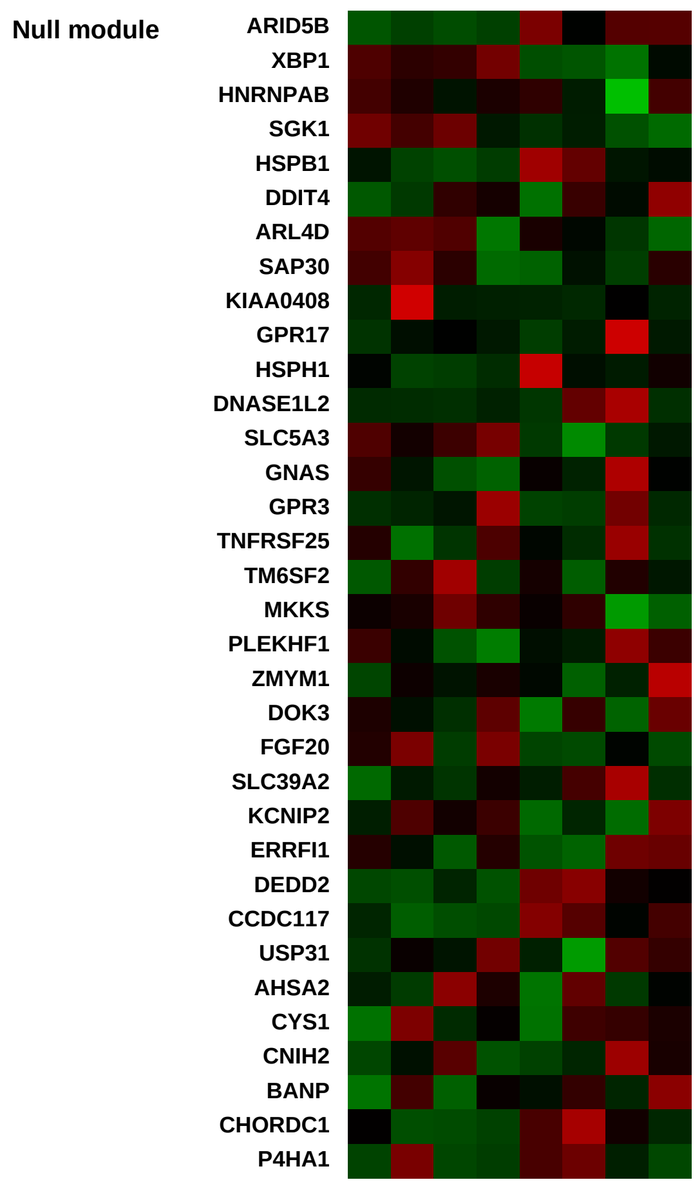

Null module

ARID5B
XBP1
HNRNPAB
SGK1
HSPB1
DDIT4
ARL4D
SAP30
KIAA0408
GPR17
HSPH1
DNASE1L2
SLC5A3
GNAS
GPR3
TNFRSF25
TM6SF2
MKKS
PLEKHF1
ZMYM1
DOK3
FGF20
SLC39A2
KCNIP2
ERRFI1
DEDD2
CCDC117
USP31
AHSA2
CYS1
CNIH2
BANP
CHORDC1
P4HA1

GEO Series "GSE48541" Expression Profiles

Num of samples in this series: 9

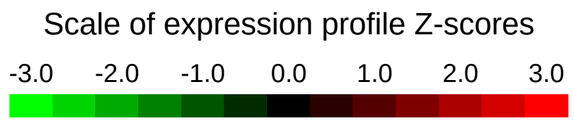

GEO Link:	http://www.ncbi.nlm.nih.gov/geo/query/acc.cgi?acc=GSE48541
Status:	Public on Sep 12 2013
Title:	Prostaglandin dose response on hematopoietic stem cells (25 & 37 deg C)
Organism:	Homo sapiens
Experiment type:	Expression profiling by array
Platform:	GPL570
Pubmed ID:	23996087
Summary & Design:	**Summary:** Umbilical cord blood (UCB) is a valuable source of hematopoietic stem cells (HSCs) for use in allogeneic transplantation. Key advantages of UCB are rapid availability and less stringent requirements for HLA matching. However, UCB contains an inherently limited HSC count, which is associated with delayed time to engraftment, high graft failure rates and early mortality. 16,16 dimethyl prostaglandin E2 (dmPGE2) was previously identified to be a critical regulator of HSC homeostasis and we hypothesized that a brief ex vivo modulation could improve patient outcomes by increasing the ""effective dose"" of HSCs. Molecular profiling with Affymetrix GeneChips were used to evaluate if increasing the concentration of prostaglandin at 25 and 37 deg C could increase biological responses. **Overall design:** Isolated human CD34+ cells from umbilical cord blood were incubated ex vivo in Stem Span (SS) media evaluating five concentrations of 16,16-dmPGE2 (0.1uM, 1uM, 10uM, 50uM, and 100uM) or Vehicle (DMSO) for 2 hours at 25 or 37 deg C. Total RNA was isolated post incubation and analyzed on Affymetrix microarrays for pathway activation.

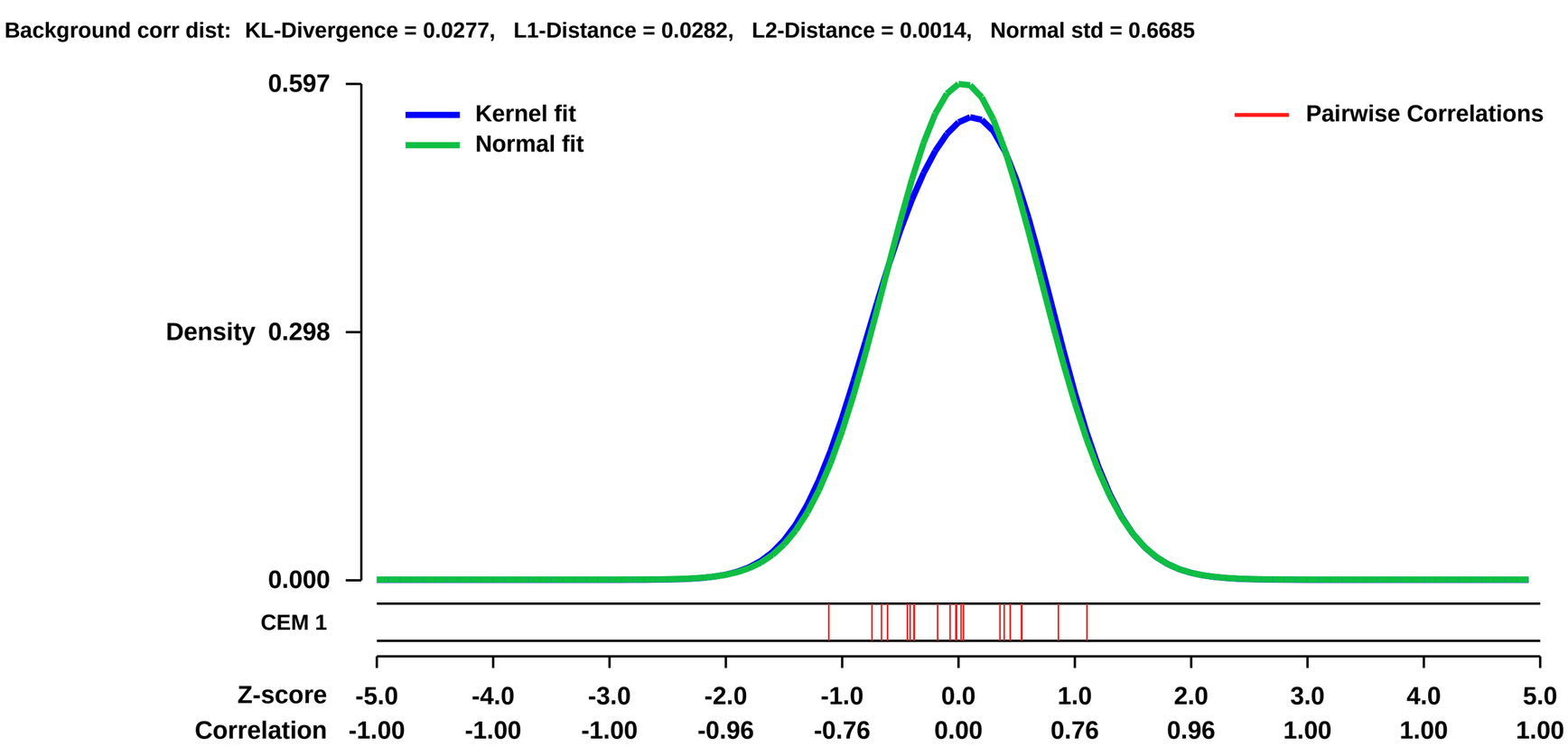

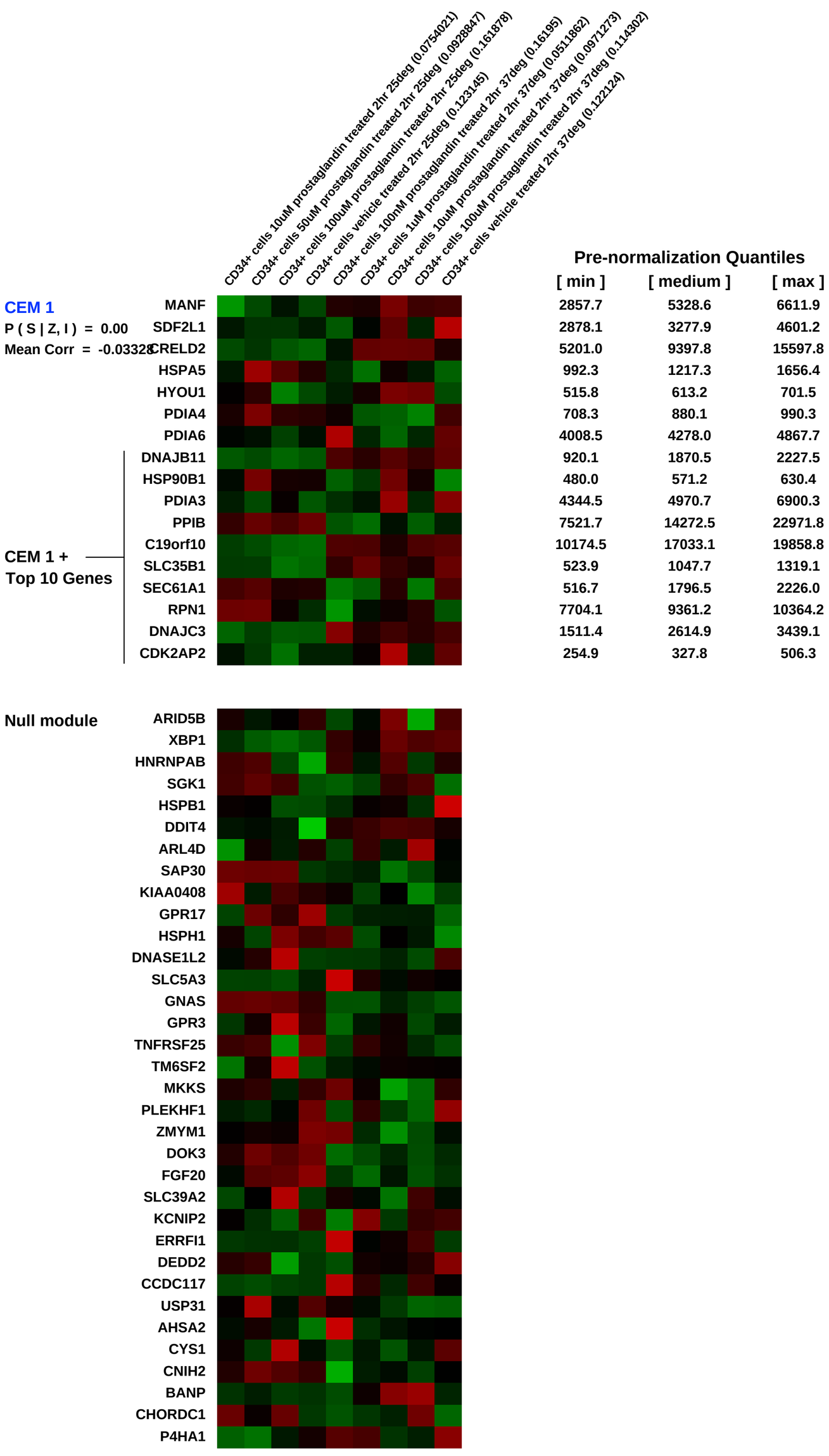

GEO Series "GSE12261" Expression Profiles

Num of samples in this series: 12

Scale of expression profile Z-scores

-3.0 -2.0 -1.0 0.0 1.0 2.0 3.0

GEO Link:	http://www.ncbi.nlm.nih.gov/geo/query/acc.cgi?acc=GSE12261
Status:	Public on Dec 31 2008
Title:	Global effects of 2-methoxyestradiol on smooth muscle cell hyperproliferation and vascular remodeling in atherosclerosis
Organism:	Homo sapiens
Experiment type:	Expression profiling by array
Platform:	GPL570
Pubmed ID:	
Summary & Design:	**Summary:** We used microarrays to detail transcriptional changes in cultured human smooth muscle cells in response to acute and chronic 2-methoxyestradiol treatment 2-ME, an endogenous metabolite. of estradiol, not only exerts cytotoxic effects on cancer cells but it also protects against multiple proliferative disorders, including atherosclerosis and injury-induced intimal thickening Keywords: treatment vs. control **Overall design:** Human aortic smooth muscle cells cultures with/without 2-methoxyestradiol (acute/chronic treatment)

Background corr dist: KL-Divergence = 0.1334, L1-Distance = 0.0305, L2-Distance = 0.0015, Normal std = 0.3914

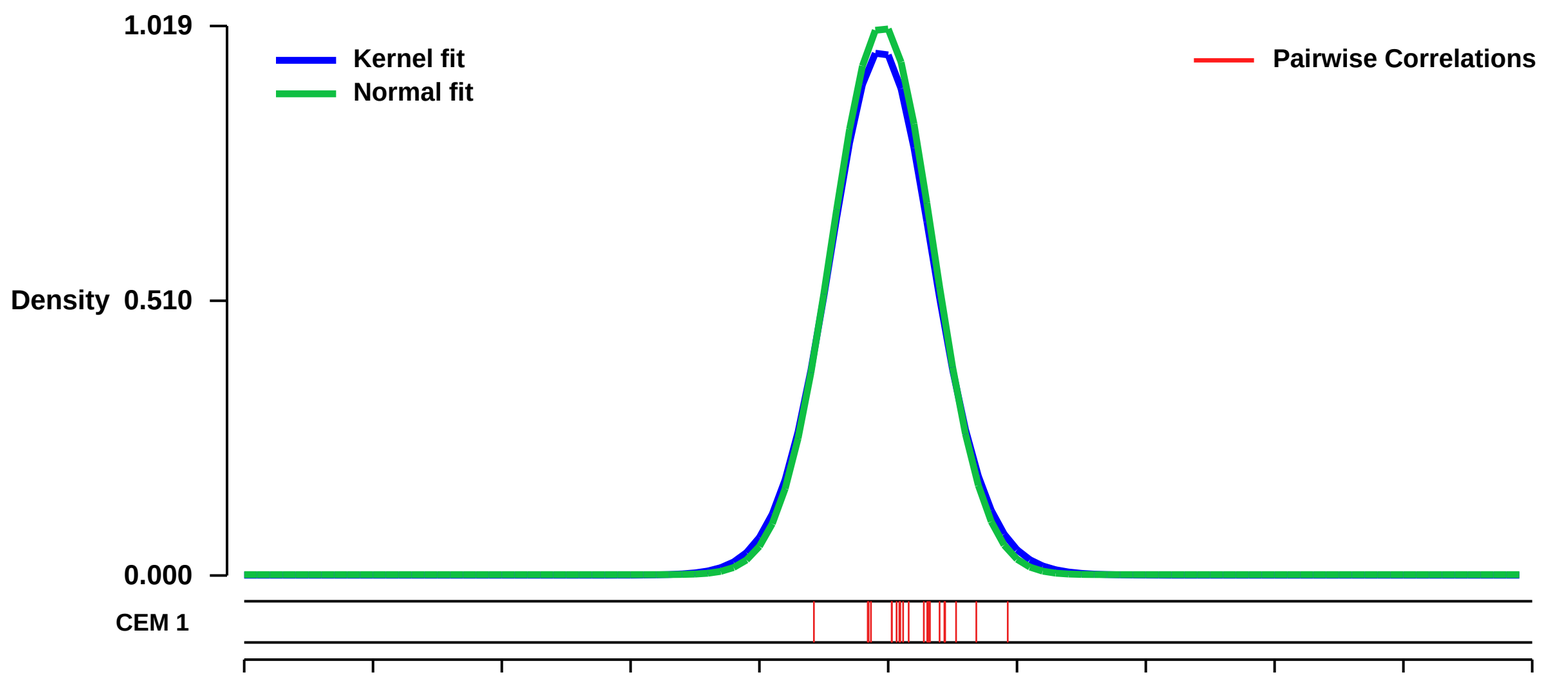

Z-score	-5.0	-4.0	-3.0	-2.0	-1.0	0.0	1.0	2.0	3.0	4.0	5.0
Correlation	-1.00	-1.00	-1.00	-0.96	-0.76	0.00	0.76	0.96	1.00	1.00	1.00

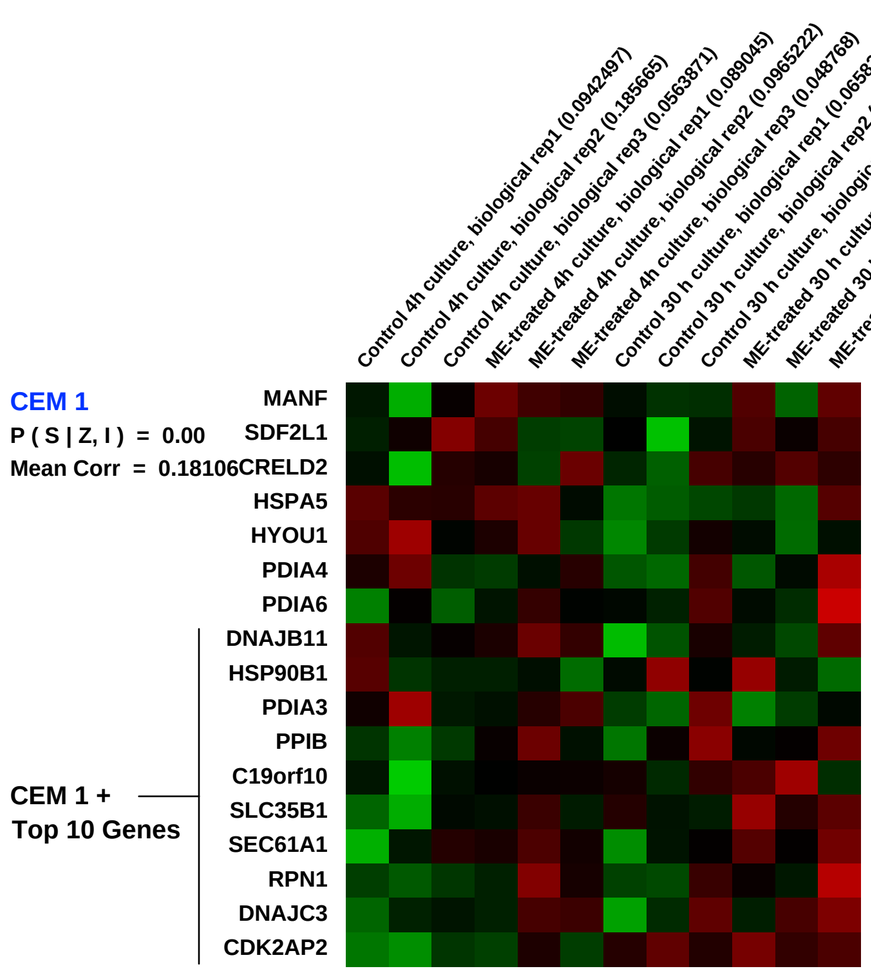

Pre-normalization Quantiles

	[min]	[medium]	[max]
MANF	5401.4	6235.8	6700.5
SDF2L1	974.3	1211.3	1354.0
CRELD2	4847.7	5465.5	5654.9
HSPA5	20792.5	24993.5	26660.7
HYOU1	4907.7	5521.7	6277.7
PDIA4	1160.3	1276.3	1495.7
PDIA6	13642.1	14873.2	17006.0
DNAJB11	3933.2	4405.2	4588.5
HSP90B1	9712.1	10180.4	11001.9
PDIA3	9280.5	11654.4	14955.1
PPIB	29415.7	30223.5	31043.1
C19orf10	4972.6	6079.4	6854.8
SLC35B1	2252.5	2494.0	2731.2
SEC61A1	7229.6	7886.8	8211.3
RPN1	5557.2	5734.1	6286.8
DNAJC3	4250.7	4553.7	4866.1
CDK2AP2	1062.3	1300.7	1414.9

GEO Series "GSE52724" Expression Profiles

Num of samples in this series: 286

Details of this dataset are not shown due to large number of samples and the page size limit.

Find details in http://www.ncbi.nlm.nih.gov/geo/query/acc.cgi?acc=GSE52724

Background corr dist: KL-Divergence = 0.2979, L1-Distance = 0.0833, L2-Distance = 0.0212, Normal std = 0.2806

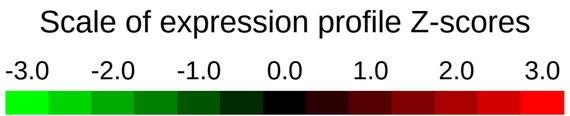

GEO Series "GSE18206" Expression Profiles

Num of samples in this series: 48

Scale of expression profile Z-scores

-3.0 -2.0 -1.0 0.0 1.0 2.0 3.0

GEO Link:	http://www.ncbi.nlm.nih.gov/geo/query/acc.cgi?acc=GSE18206
Status:	Public on Aug 20 2010
Title:	Analysis of human in vivo irritated epidermis: differential profiles induced by sodium lauryl sulphate and nonanoic acid
Organism:	Homo sapiens
Experiment type:	Expression profiling by array
Platform:	GPL570
Pubmed ID:	20428187
Summary & Design:	**Summary:** Irritant contact dermatitis (ICD) pathogenesis is not completely understood and the genes participating in the epidermal response towards chemical irritants are only partly known. It is commonly accepted that different irritants have different mechanisms of action in the development of ICD. To define the differential molecular events induced in the epidermis by different irritants, we collected sequential biopsies (´‰, 4 and 24 hours after a single exposure and at day 11 after repeated exposure) from human volunteers exposed to sodium lauryl sulphate (SLS) or nonanoic acid (NON). Gene expression analysis using high-density oligonucleotide microarrays revealed essentially different pathway responses ´‰ h after exposure: NON transiently induced the IL-6 pathway as well as a number of mitogen activated signalling cascades including ERK and growth factor receptor signalling, whereas SLS transiently downregulated cellular energy metabolism pathways. Differential expression of the cyclooxygenase-2 and matrix metalloproteinase 3 transcripts was confirmed immunohistochemically. After cumulative exposure, 883 genes were differentially expressed while 26 suggested common biomarkers were identified . In conclusion, we bring new insights into two hitherto less well elucidated phases of skin irritancy: the very initial as well as the late phase after single and cumulative exposure, respectively. **Overall design:** 36 healthy volunteers were exposed to the skin irritants SLS (n=18) or NON (n=18). Samples from 18 volunteers (9 SLS and 9 NON-exposed) were selected for the microarray experiment. Samples were obtained according to elapsed time following a single cutaneous exposure: 0.5 h, 4h and 24h. Moreover, samples were obtained at day 11 coresponding to a cumulatively (10 min for 5+4 days) irritated skin site. A balanced incomplete block design was used to obtain samples from the 4 time points; however, 0h samples (controls) were obtained for all subjects. Samples from the time point 0.5 h were of special interest and therefore doubled. Thus, 24 chips were hybridized for each irritant giving a total of 48 chips in the experiment. The relative contribution of chips per timepoint for each irritant: 0h (n=9), 0.5h (n=6), 4h (n=3), 24h (n=3), day 11 (n=3).

Background corr dist: KL-Divergence = 0.2048, L1-Distance = 0.0460, L2-Distance = 0.0046, Normal std = 0.3297

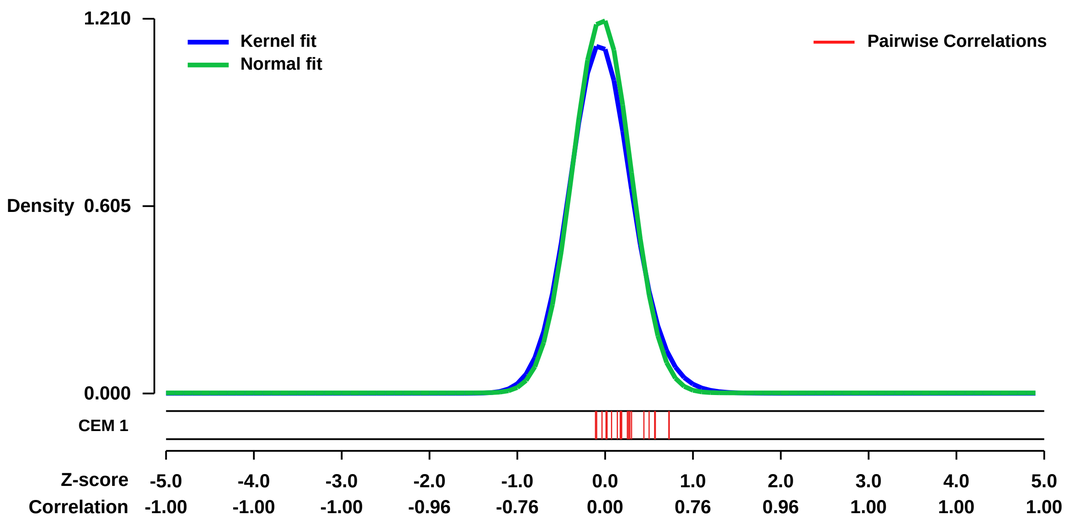

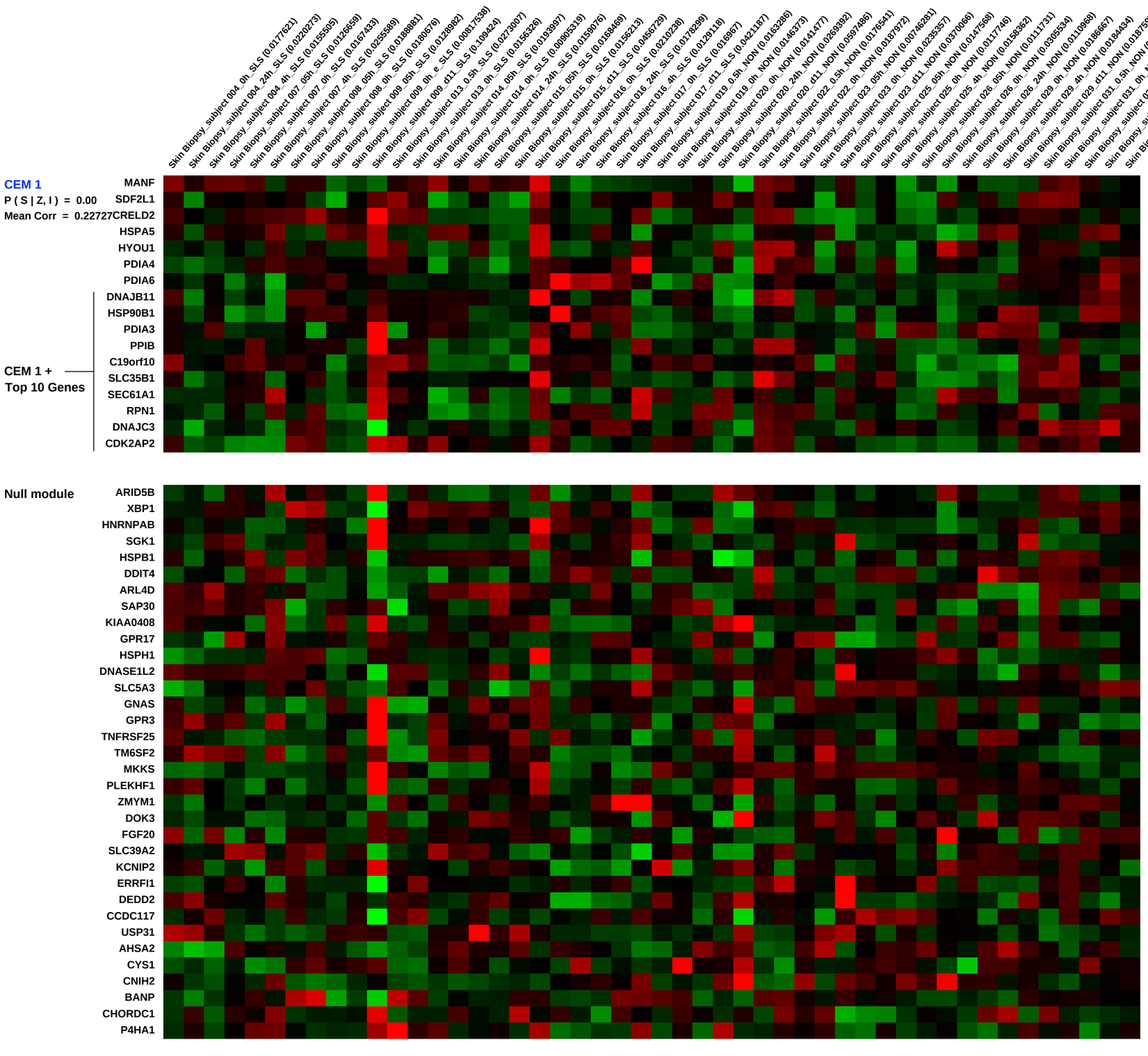

Pre-normalization Quantiles

[min]	[medium]	[max]
1394.5	1885.0	2408.0
350.1	475.2	566.4
1000.8	1306.7	1809.4
2193.6	3159.5	4224.8
1023.5	1370.8	1906.2
382.6	504.7	703.8
1282.2	1892.3	2834.0
971.9	1278.6	1684.1
129.0	307.7	607.5
1866.0	2656.1	4188.4
2676.7	3274.4	5118.6
978.2	1273.5	1484.5
843.4	1003.4	1273.2
982.6	1322.5	1717.5
2077.2	2516.3	3168.3
1022.6	1529.0	1924.0
368.8	480.9	668.4

GEO Series "GSE13818" Expression Profiles

Num of samples in this series: 26

Scale of expression profile Z-scores

-3.0 -2.0 -1.0 0.0 1.0 2.0 3.0

GEO Link: http://www.ncbi.nlm.nih.gov/geo/query/acc.cgi?acc=GSE13818
Status: Public on Jan 01 2009
Title: Small molecule inhibitors of HIF-2a translation link its 5â -UTR Iron-Responsive Element (IRE) to oxygen sensing
Organism: Homo sapiens
Experiment type: Expression profiling by array
Platform: GPL570
Pubmed ID: 20354189

Summary & Design:

Summary:
Cells transiently adapt to hypoxia by globally decreasing protein translation. However, specific proteins needed to respond to hypoxia evade this translational repression. The mechanisms of this phenomenon remain unclear. We screened for and identified small molecules that selectively decrease HIF-2a translation in an mTOR independent manner, by enhancing the binding of Iron Regulatory Protein 1 (IRP1) to a recently reported Iron-Responsive Element (IRE) within the 5â -untranslated region (UTR) of the HIF-2a message. Knocking down the expression of IRP1 by shRNA abolished the effect of the compounds. Hypoxia de-represses HIF-2a translation by disrupting the IRP1-HIF-2a IRE interaction. Thus, this chemical genetic analysis describes a molecular mechanism by which translation of the HIF-2a message is maintained during conditions of cellular hypoxia through inhibition of IRP-1 dependent repression. It also provides the chemical tools for studying this phenomenon.

Overall design:
3 replicate samples of 786-O human Clear Cell Renal Carcinoma cells untreated, mock treated with DMSO or treated with either of 4 HIF-2a inhibitor compounds identified by chemical genetic screening.

Background corr dist: KL-Divergence = 0.3941, L1-Distance = 0.0773, L2-Distance = 0.0183, Normal std = 0.2492

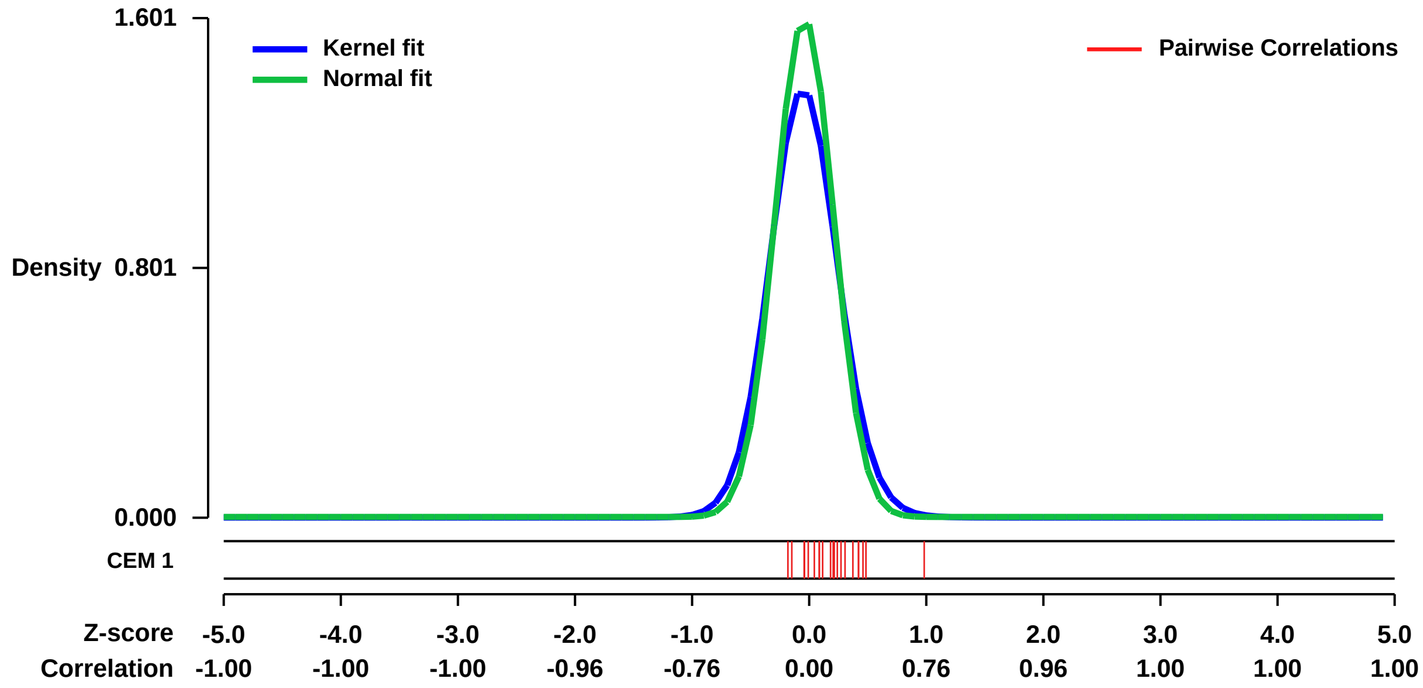

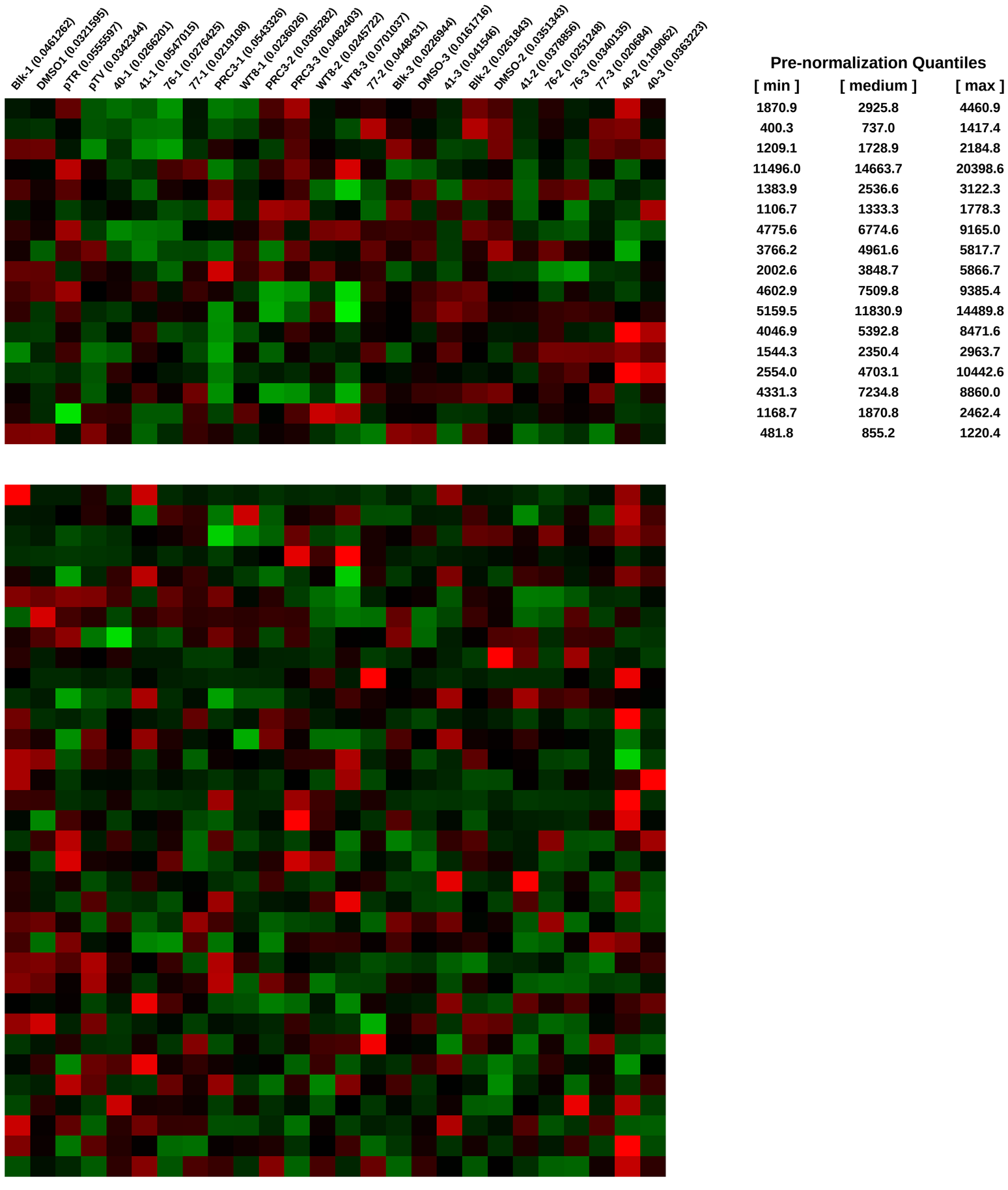

Pre-normalization Quantiles	[min]	[medium]	[max]
1870.9	2925.8	4460.9
400.3	737.0	1417.4
1209.1	1728.9	2184.8
11496.0	14663.7	20398.6
1383.9	2536.6	3122.3
1106.7	1333.3	1778.3
4775.6	6774.6	9165.0
3766.2	4961.6	5817.7
2002.6	3848.7	5866.7
4602.9	7509.8	9385.4
5159.5	11830.9	14489.8
4046.9	5392.8	8471.6
1544.3	2350.4	2963.7
2554.0	4703.1	10442.6
4331.3	7234.8	8860.0
1168.7	1870.8	2462.4
481.8	855.2	1220.4

GEO Series "GSE46714" Expression Profiles

Num of samples in this series: 6

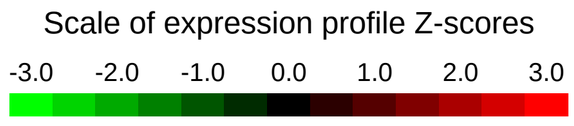

GEO Link:	http://www.ncbi.nlm.nih.gov/geo/query/acc.cgi?acc=GSE46714
Status:	Public on Sep 12 2013
Title:	Prostaglandin duration required to elicit maximum response on hematopoietic stem cells
Organism:	Homo sapiens
Experiment type:	Expression profiling by array
Platform:	GPL570
Pubmed ID:	23996087
Summary & Design:	**Summary:** Umbilical cord blood (UCB) is a valuable source of hematopoietic stem cells (HSCs) for use in allogeneic transplantation. Key advantages of UCB are rapid availability and less stringent requirements for HLA matching. However, UCB contains an inherently limited HSC count, which is associated with delayed time to engraftment, high graft failure rates and early mortality. 16,16 dimethyl prostaglandin E2 (dmPGE2) was previously identified to be a critical regulator of HSC homeostasis and we hypothesized that a brief ex vivo modulation could improve patient outcomes by increasing the â effective doseâ of HSCs. Molecular profiling with Affymetrix GeneChips were used to evaluate if prostgandin is required for the entire 2 hour incubation to elicit the maximum pathway activated gene expression response. **Overall design:** Isolated human CD34+ from umbilical cord blood were incubated ex vivo in Stem Span (SS) media with 10uM 16,16-dimethyl prostaglandin E2 for varying amounts of time within a two hour incubation window to evaluate if the entire 120 minutes is required to elicit the maximum pathway activated gene expression response or if shorter incubation times were sufficent. Total RNA was isolated post incubation and analyzed on Affymetrix microarrays for pathway activation.

Background corr dist: KL-Divergence = 0.0167, L1-Distance = 0.0339, L2-Distance = 0.0018, Normal std = 0.7829

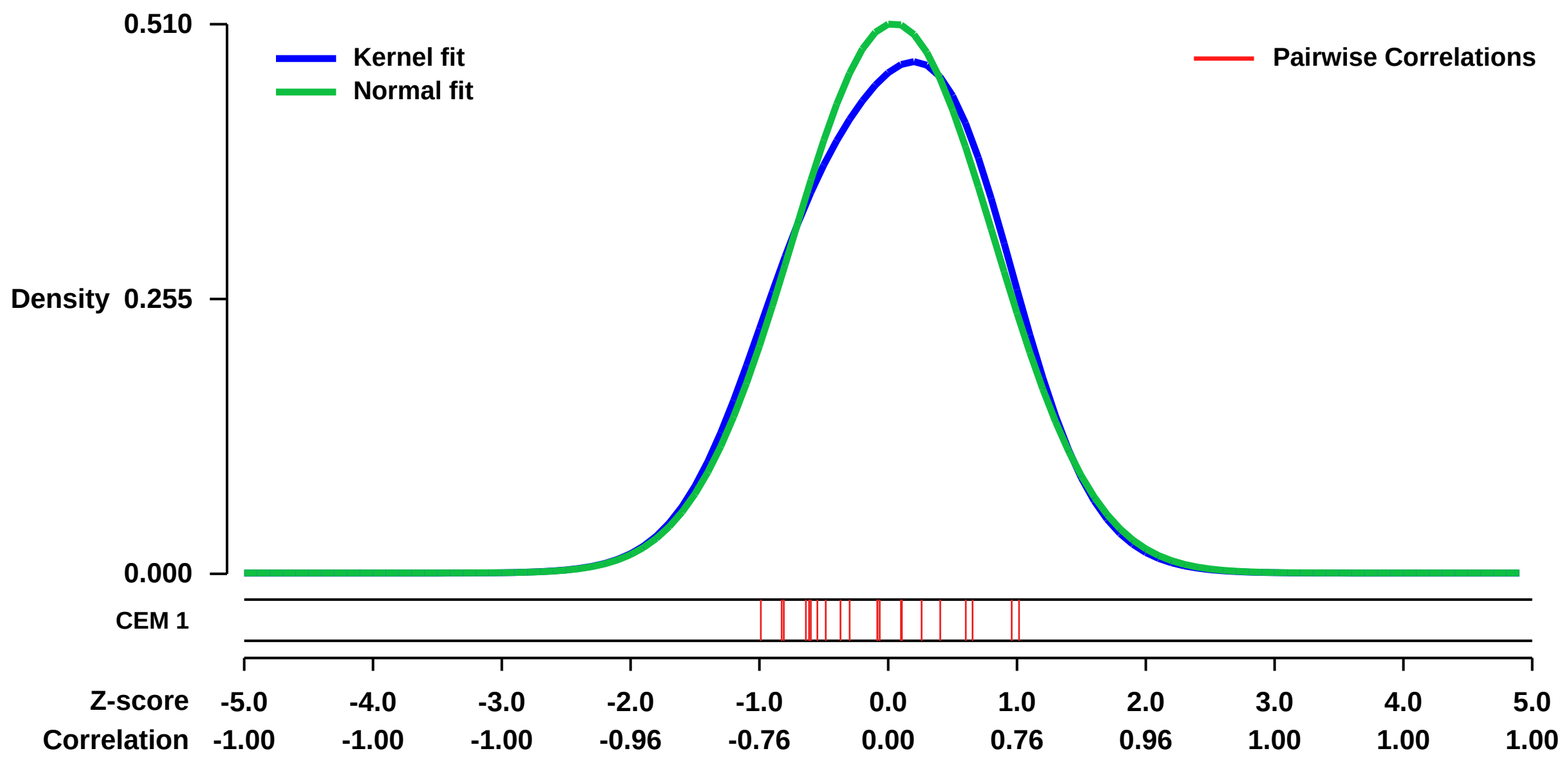

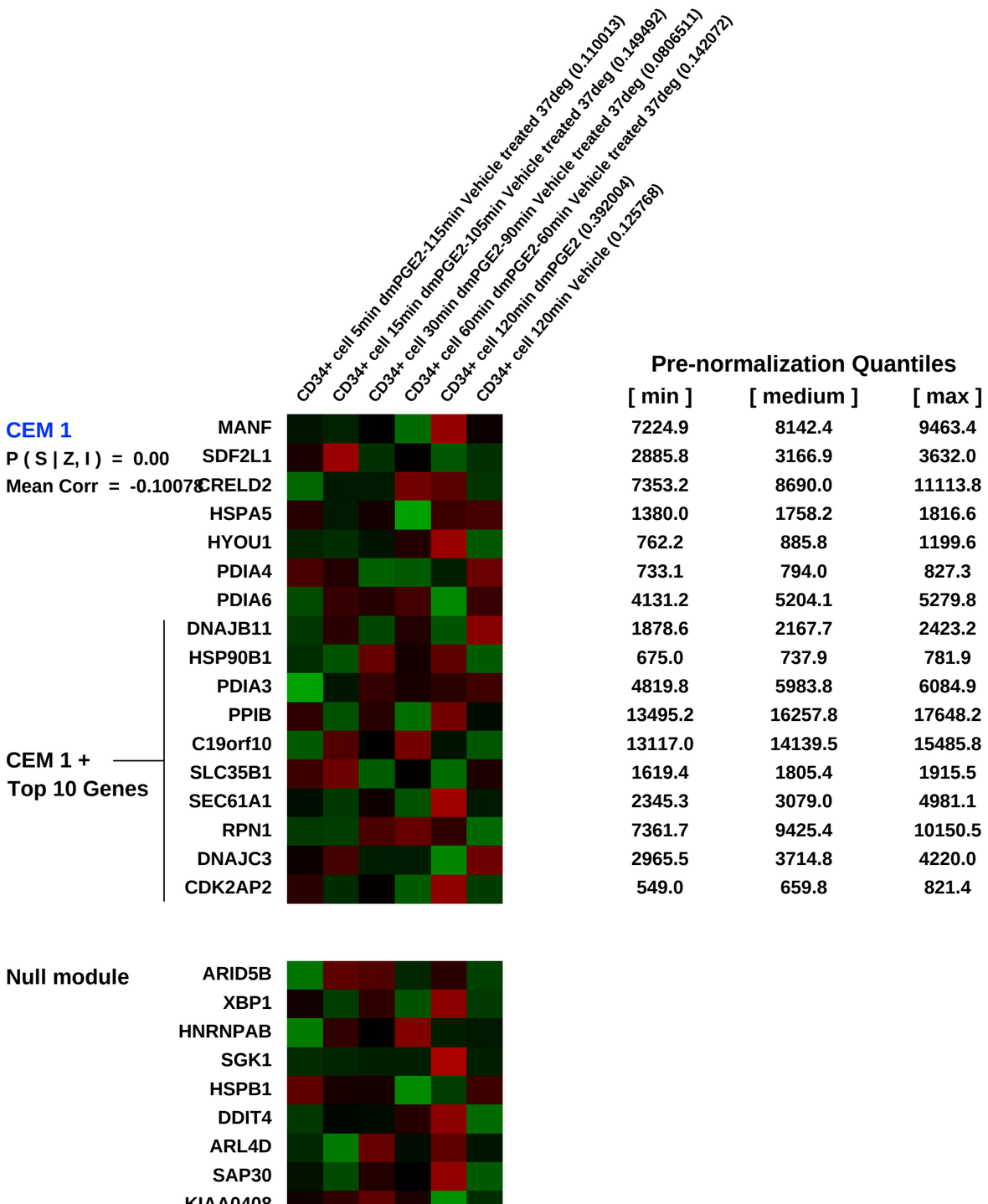

GEO Series "GSE41827" Expression Profiles

Num of samples in this series: 6

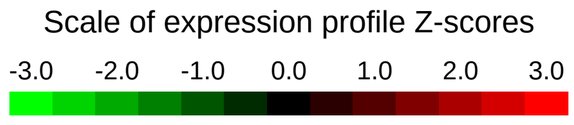

GEO Link:	http://www.ncbi.nlm.nih.gov/geo/query/acc.cgi?acc=GSE41827
Status:	Public on Oct 31 2012
Title:	Expression data from HeLa cells treated with Casiopeina Cas-II-gly
Organism:	Homo sapiens
Experiment type:	Expression profiling by array
Platform:	GPL570
Pubmed ID:	23382936
Summary & Design:	**Summary:** Copper-based chemotherapeutic compounds Casiopeinas, have been presented as able to promote selective programmed cell death in cancer cells, thus being proper candidates for targeted cancer therapy. DNA fragmentation and apoptosis -in a process mediated by reactive oxygen species- for a number of tumor cells, have been argued to be the main mechanisms. However, a detailed functional mechanism (a model) is still to be defined and interrogated for a wide variety of cellular conditions; before establishing settings and parameters needed for their wide clinical application. Microarrays were used to determine the expression profile from HeLa cells in order to propose a model for the role played by intrinsic apoptosis triggered by the oxidative stress caused by Cas-II-gly. **Overall design:** The cervix-uterine cell line HeLa´ ´ was´ maintained at 37C in 5% CO2´ under sterile conditions in Dulbecco's modified Eagle medium (DMEM, Sigma), supplemented with 10% fetal bovine serum (Sigma). Cells were treated with Cas II-gly in 96-well microplates by 6 h.´ ´ HeLa cells whole genome gene expression experiments (triplicates for cases/controls) were performed in total mRNA extracted under the GPL570 protocol.

Background corr dist: KL-Divergence = 0.0187, L1-Distance = 0.0399, L2-Distance = 0.0015, Normal std = 0.8563

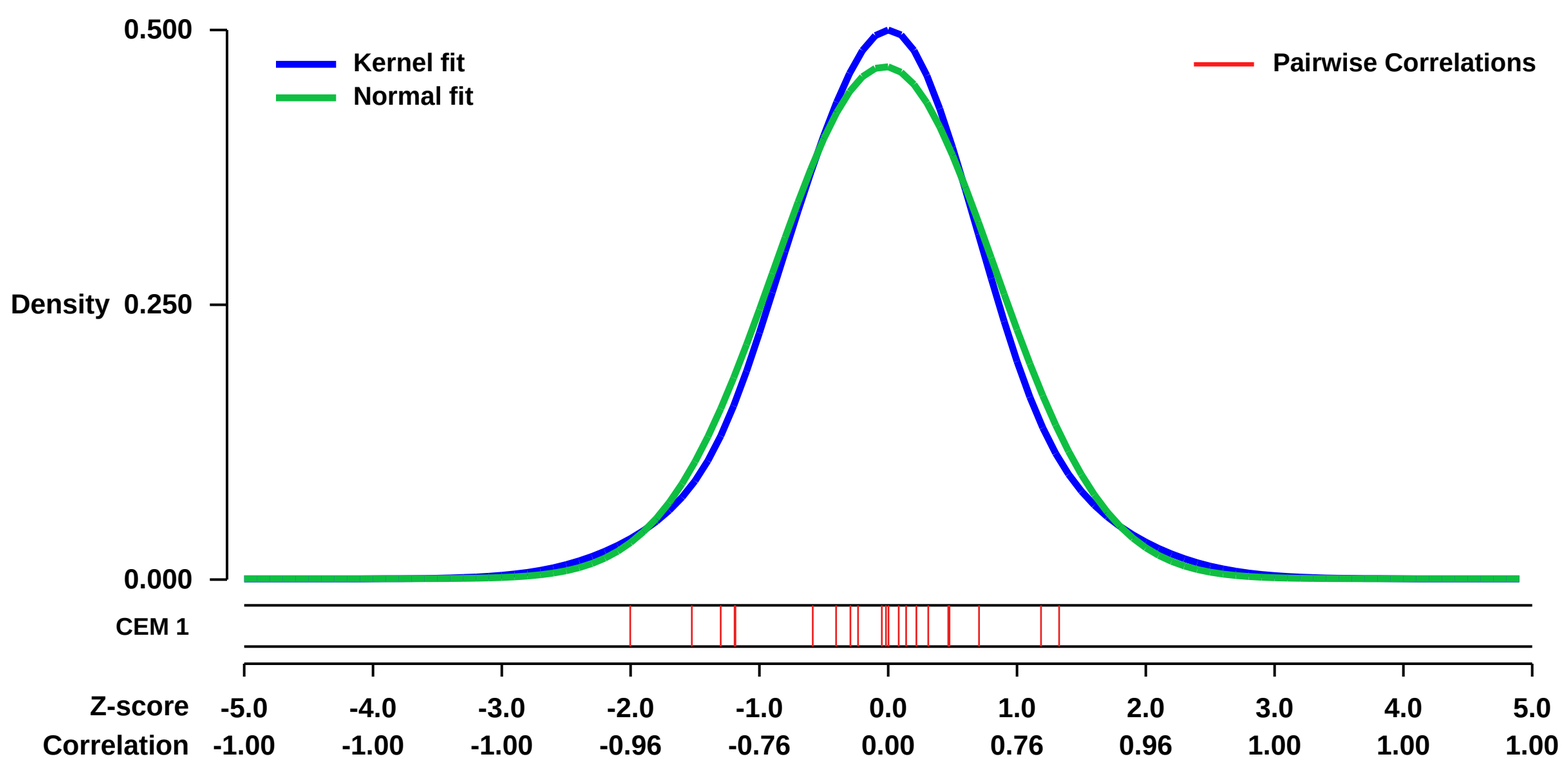

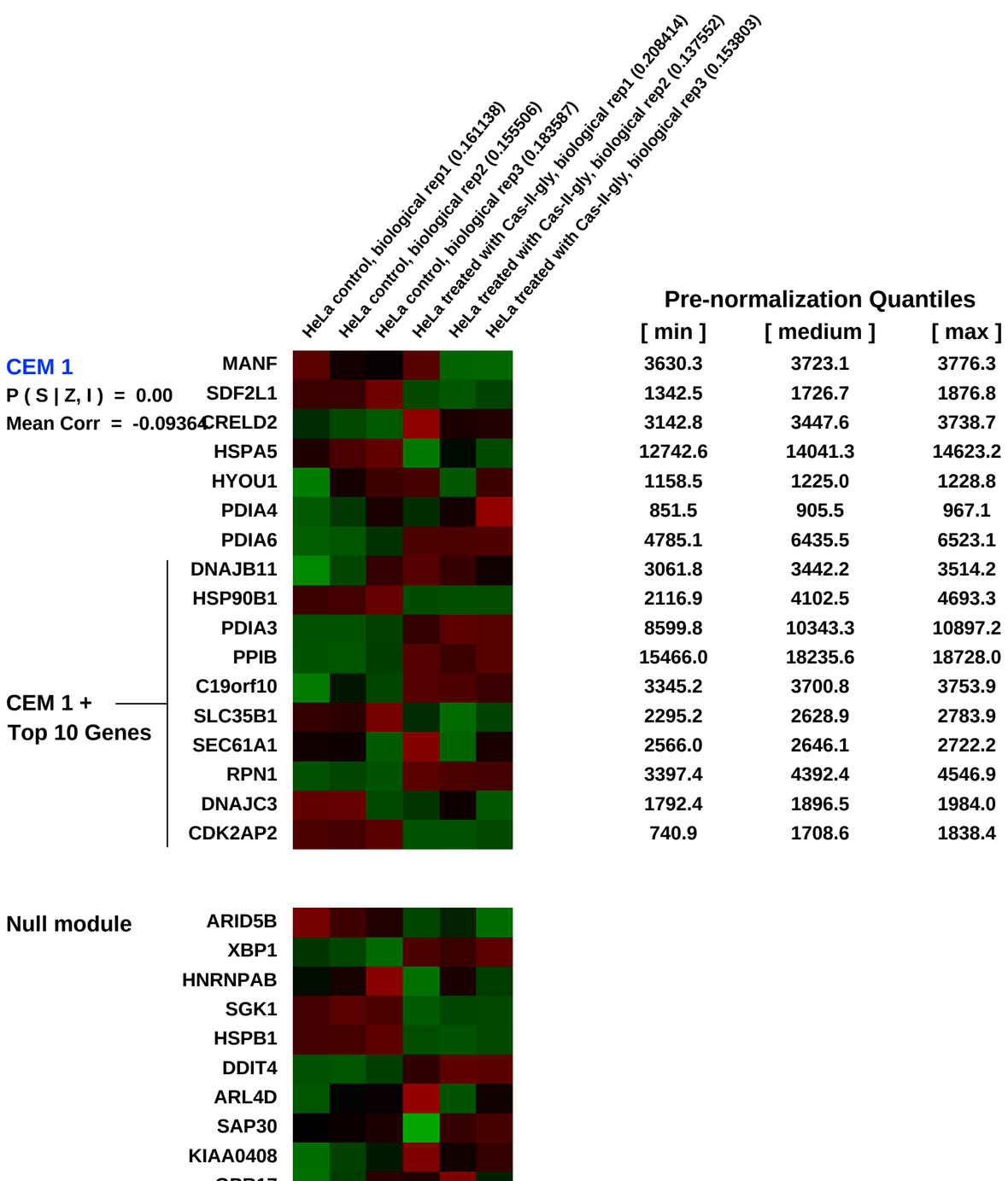

	Pre-normalization Quantiles		
	[min]	[medium]	[max]
MANF	3630.3	3723.1	3776.3
SDF2L1	1342.5	1726.7	1876.8
CRELD2	3142.8	3447.6	3738.7
HSPA5	12742.6	14041.3	14623.2
HYOU1	1158.5	1225.0	1228.8
PDIA4	851.5	905.5	967.1
PDIA6	4785.1	6435.5	6523.1
DNAJB11	3061.8	3442.2	3514.2
HSP90B1	2116.9	4102.5	4693.3
PDIA3	8599.8	10343.3	10897.2
PPIB	15466.0	18235.6	18728.0
C19orf10	3345.2	3700.8	3753.9
SLC35B1	2295.2	2628.9	2783.9
SEC61A1	2566.0	2646.1	2722.2
RPN1	3397.4	4392.4	4546.9
DNAJC3	1792.4	1896.5	1984.0
CDK2AP2	740.9	1708.6	1838.4
ARID5B			
XBP1			
HNRNPAB			
SGK1			
HSPB1			
DDIT4			
ARL4D			
SAP30			
KIAA0408			
GPR17			
HSPH1			
DNASE1L2			
SLC5A3			
GNAS			
GPR3			
TNFRSF25			
TM6SF2			
MKKS			
PLEKHF1			
ZMYM1			
DOK3			
FGF20			
SLC39A2			
KCNIP2			
ERRFI1			
DEDD2			
CCDC117			
USP31			
AHSA2			
CYS1			
CNIH2			
BANP			
CHORDC1			
P4HA1			

GEO Series "GSE59666" Expression Profiles

Num of samples in this series: 26

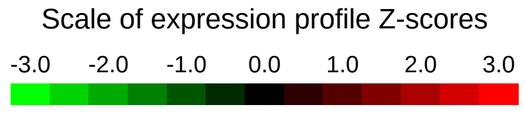

GEO Link:	http://www.ncbi.nlm.nih.gov/geo/query/acc.cgi?acc=GSE59666
Status:	Public on Jul 23 2014
Title:	Temporal Endogenous Gene Expression Profiles in Response to Lipid-Mediated Transfection
Organism:	Homo sapiens
Experiment type:	Expression profiling by array
Platform:	GPL570
Pubmed ID:	
Summary & Design:	**Summary:** The current understanding of the molecular factors underlying LF2000-mediated transfection is largely unknown. Cationic LF2000 gene delivery system was used to transfer GFP transgene to HEK293T cells. FACS separation of transfected (GFP positive), untransfected (GFP negative), and untreated cells enabled gene expression profiles to be obtained using Affymetrix´fi HG-U133A 2.0 microarrays for each cell population. Gene profiles were differentially compared for each population combination. **Overall design:** Control (untreated), transfected (GFP positive), and untransfected (GFP negative) RNA samples were purified from HEK293T cells after FACS isolation. Treated experiments were repeated on triplicate days to run 3 microarrays for each cell population. Controls were run on duplicate to give 2 microarrays for each population.

Background corr dist: KL-Divergence = 0.0603, L1-Distance = 0.0634, L2-Distance = 0.0063, Normal std = 0.5749

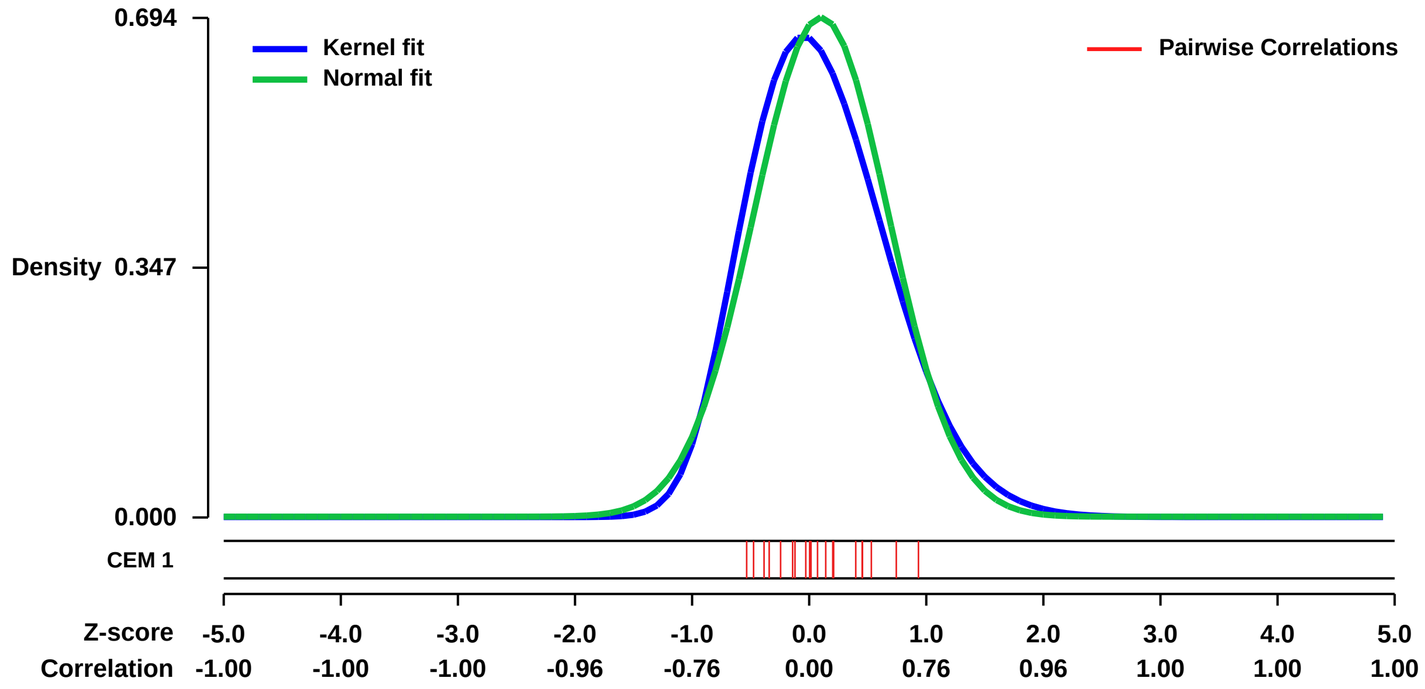

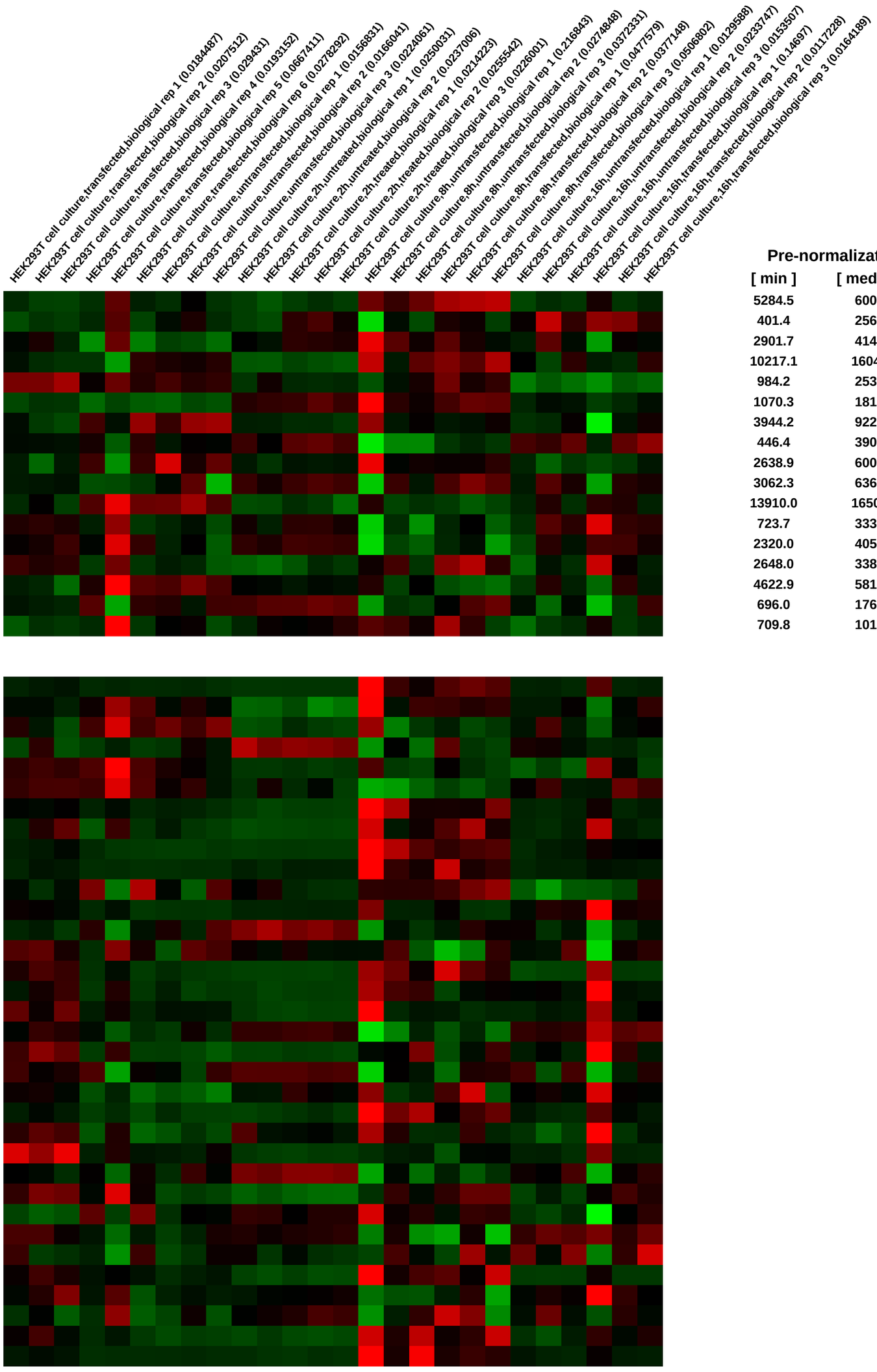

GEO Series "GSE32523" Expression Profiles

Num of samples in this series: 8

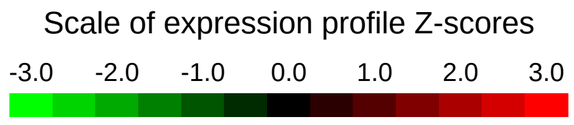

GEO Link:	http://www.ncbi.nlm.nih.gov/geo/query/acc.cgi?acc=GSE32523
Status:	Public on Dec 13 2012
Title:	shRNA knockdown of ZMIZ1 in human T-cell Acute Lymphoblastic Leukemia cell line CEM
Organism:	Homo sapiens
Experiment type:	Expression profiling by array
Platform:	GPL570
Pubmed ID:	23161489
Summary & Design:	**Summary:** Human T-cell Acute lymphoblastic Leukemia cell line CEM was transfected with either shRNA against ZMIZ1 or scrambled shRNA. Four (non-paired) biological replicates of each condition had mRNA assays performed using Affymetrix HG_U133_plus_2 arrays, with 54675 probe-sets. A supplementary Excel workbook holding the same processed data as the series matrix file is provided, with some probe set annotation, and a simple statistical comparison. The raw (.CEL) files are also provided. **Keywords: Expression profiling by array** **Overall design:** Human T-cell Acute lymphoblastic Leukemia cell line CEM was transfected with either shRNA against ZMIZ1 or scrambled shRNA. Four (non-paired) biological replicates of each condition had mRNA assays performed using Affymetrix HG_U133_plus_2 arrays, with 54675 probe-sets.

Background corr dist: KL-Divergence = 0.0536, L1-Distance = 0.0220, L2-Distance = 0.0006, Normal std = 0.5571

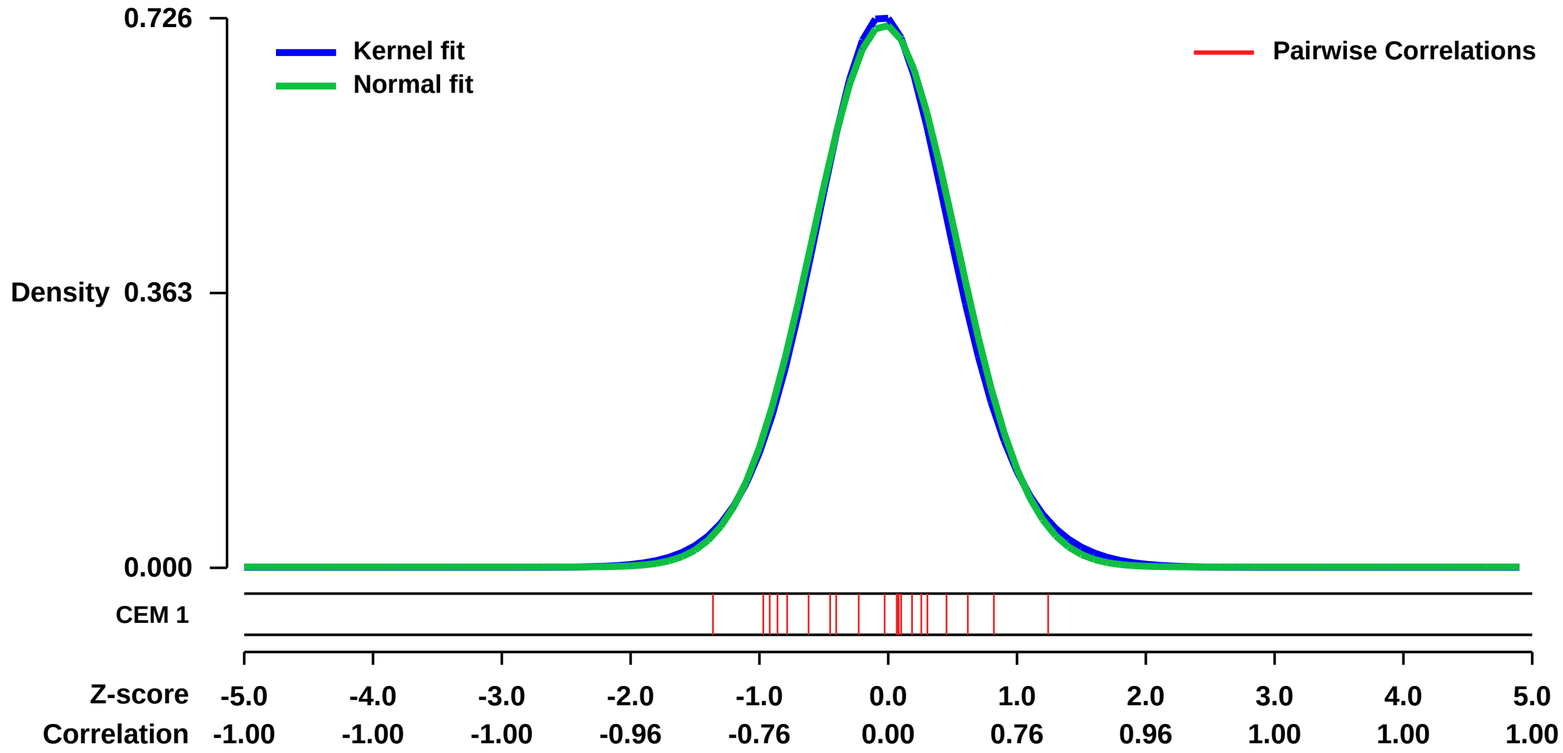

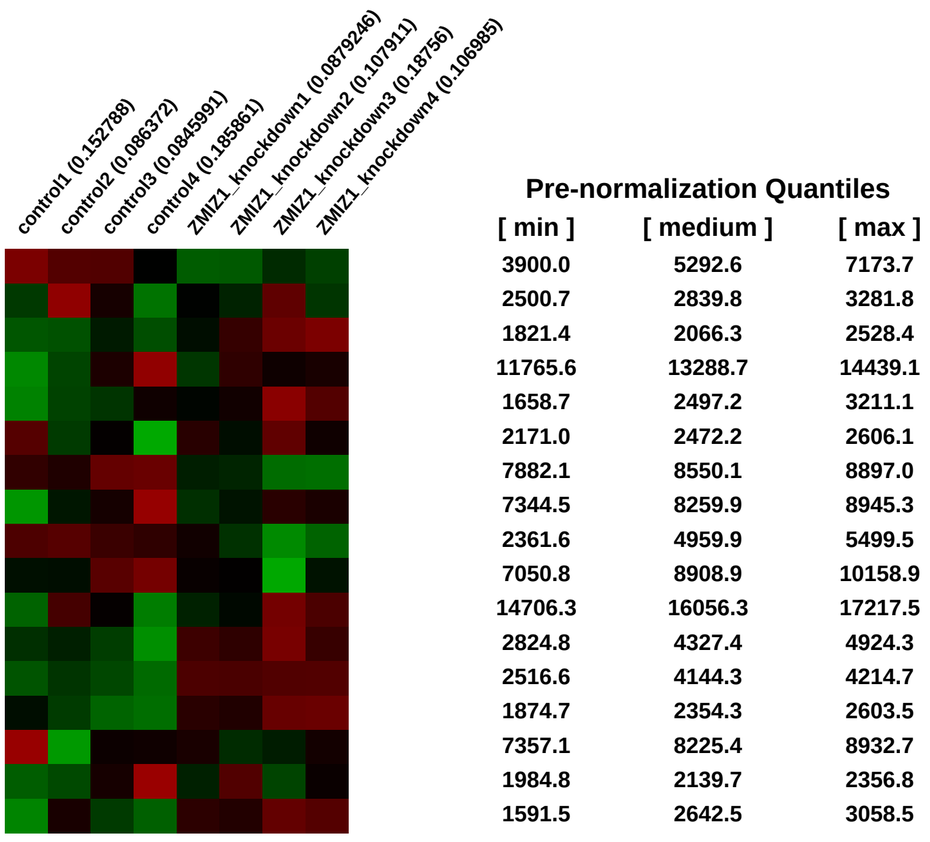

GEO Series "GSE14671" Expression Profiles

Num of samples in this series: 59

Scale of expression profile Z-scores

-3.0 -2.0 -1.0 0.0 1.0 2.0 3.0

GEO Link: http://www.ncbi.nlm.nih.gov/geo/query/acc.cgi?acc=GSE14671
Status: Public on Jan 01 2010
Title: EXPRESSION SIGNATURE TO PREDICT MAJOR CYTOGENETIC RESPONSE IN CHRONIC PHASE CML PATIENTS TREATED WITH IMATINIB
Organism: Homo sapiens
Experiment type: Expression profiling by array
Platform: GPL570
Pubmed ID: 19837975

Summary & Design:

Summary:
Newly diagnosed chronic phase chronic myeloid leukemia (CML) patients with a major cytogenetic response (MCyR) after 12 months of imatinib therapy have an excellent long-term outcome, while patients without MCyR have a high progression risk. Since patients with primary cytogenetic resistance may benefit from more intensive therapy up-front, we sought to identify biomarkers to predict MCyR.

Keywords: Two group comparison to identify trasncriptomic signature that predicts response to therapy

Overall design:
CD34+ cells were isolated from cryopreserved mononuclear cells of chronic phase CML patients with a complete cytogenetic response (CCyR) or >65% Ph-positive metaphases after 12 months of imatinib therapy (training set N=36). Gene expression profiles generated on amplified RNA using Affymetrix HG-U133 Plus 2.0 arrays were compared between responders and non-responders, using the criteria ANOVA p<0.1 and fold difference >|1.5|. A minimal response classifier derived from the comparison was used to predict response in a prospectively collected validation set using same criteria for responders/nonresponders (N=23).

Background corr dist: KL-Divergence = 0.2172, L1-Distance = 0.0614, L2-Distance = 0.0100, Normal std = 0.3215

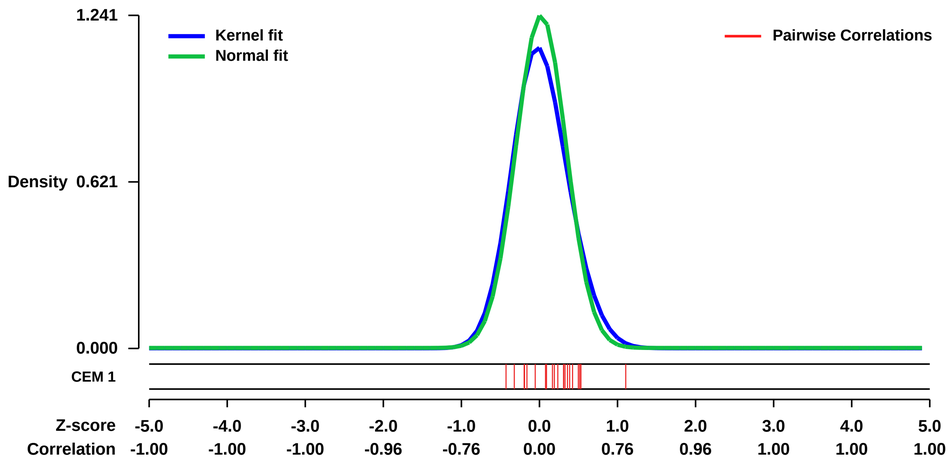

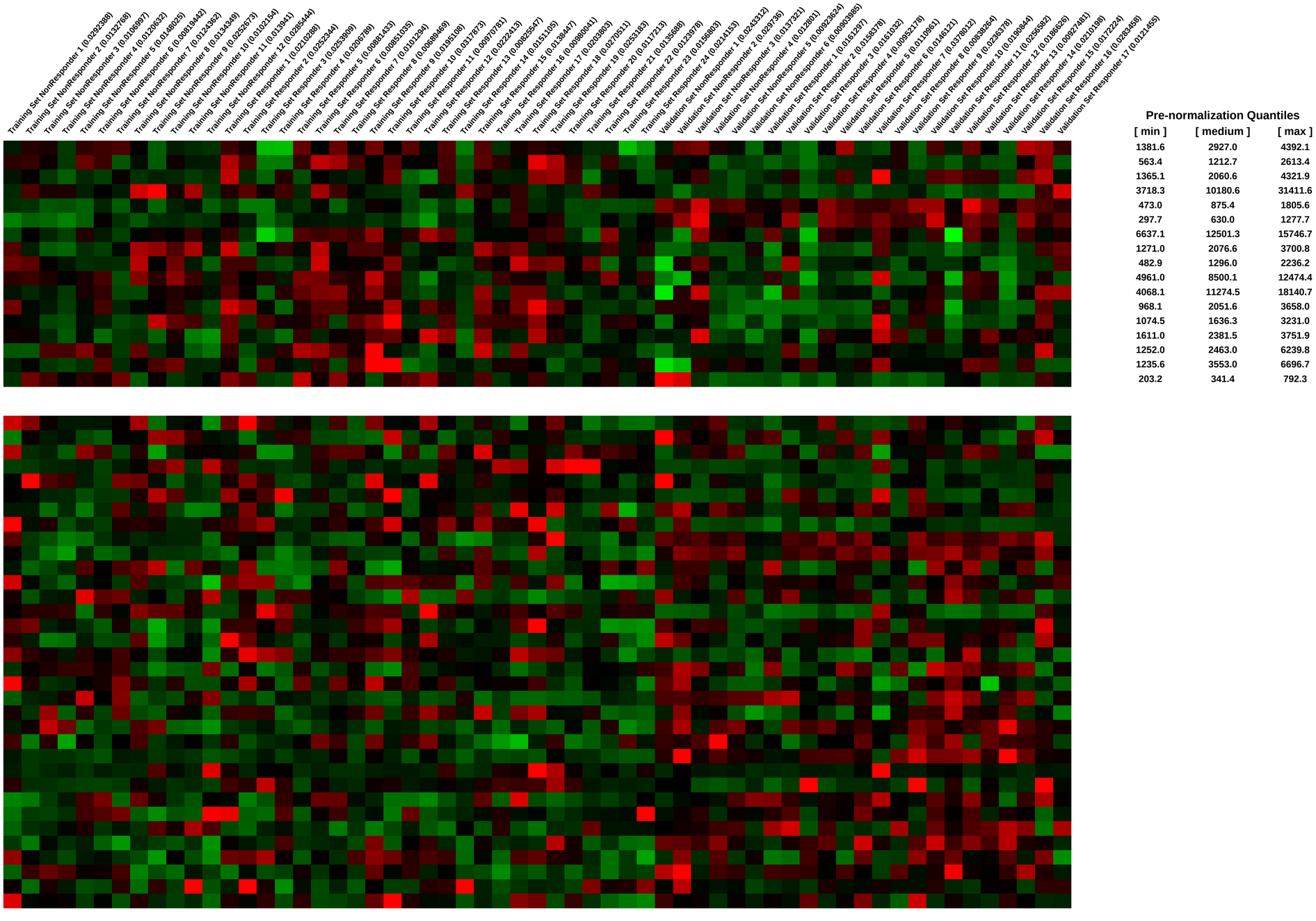

Pre-normalization Quantiles		
[min]	[medium]	[max]
1381.6	2927.0	4392.1
563.4	1212.7	2613.4
1365.1	2060.6	4321.9
3718.3	10180.6	31411.6
473.0	875.4	1805.6
297.7	630.0	1277.7
6637.1	12501.3	15746.7
1271.0	2076.6	3700.8
482.9	1296.0	2236.2
4961.0	8500.1	12474.4
4068.1	11274.5	18140.7
968.1	2051.6	3658.0
1074.5	1636.3	3231.0
1611.0	2381.5	3751.9
1252.0	2463.0	6239.8
1235.6	3553.0	6696.7
203.2	341.4	792.3

GEO Series "GSE20193" Expression Profiles

Num of samples in this series: 9

Scale of expression profile Z-scores

-3.0 -2.0 -1.0 0.0 1.0 2.0 3.0

GEO Link:	http://www.ncbi.nlm.nih.gov/geo/query/acc.cgi?acc=GSE20193
Status:	Public on Mar 15 2010
Title:	Altered levels of MOF and decreased levels of H4K16ac correlate with a defective DNA damage response (DDR).
Organism:	Homo sapiens
Experiment type:	Expression profiling by array
Platform:	GPL570
Pubmed ID:	20479123
Summary & Design:	**Summary:** **Full title: Altered levels of MOF (member of MYST family histone acetyl transferase) and decreased levels of H4K16ac correlate with a defective DNA damage response (DDR).** **The human MOF gene encodes a protein that specifically acetylates histone H4 at lysine 16 (H4K16ac). Here we show that altered levels of H4K16ac correlate with a defective DNA damage response (DDR) to ionizing radiation (IR). The defect however is not due to altered expression of proteins involved in DDR. Specific inhibition of H4K16ac deacetylation in MOF-depleted cells rescued IR-induced abrogation of DDR. MOF was found associated with DNA-dependent protein kinase catalytic subunit (DNAPKcs), a protein involved in non-homologous end joining (NHEJ) repair, whose ATMdependent IR-induced phosphorylation was abrogated in MOF-depleted cells. Our data indicate that MOF depletion greatly decreased the repair of DNA double-strand breaks (DSBs) by NHEJ and homologous recombination (HR). In addition, the MOF protein activity associates with chromatin upon DNA damage and colocalizes with the synaptonemal complex in male meiocytes. We propose that MOF, through H4K16ac, plays a critical role in the cellular DNA damage response.** **Keywords: Cell type comparison** **Overall design:** **HEK293 cells were transfected with plasmids encoding hMOF for over-expression of the histone acetyl transferase that leads to elevated levels of acetylation of Lysine 16 of histone H4. siRNA mediated knock-down of hMOF was performed to deplete the H4K16ac levels. Total RNA samples for expression profiling was obtained from wild type (293 cells without any treatment), hMOF over-expressed and hMOF knock-down 293 cell lines. Each sample was analyzed in triplicates using EGPF dsRNA treated samples as control.**

Background corr dist: KL-Divergence = 0.0858, L1-Distance = 0.0209, L2-Distance = 0.0006, Normal std = 0.4656

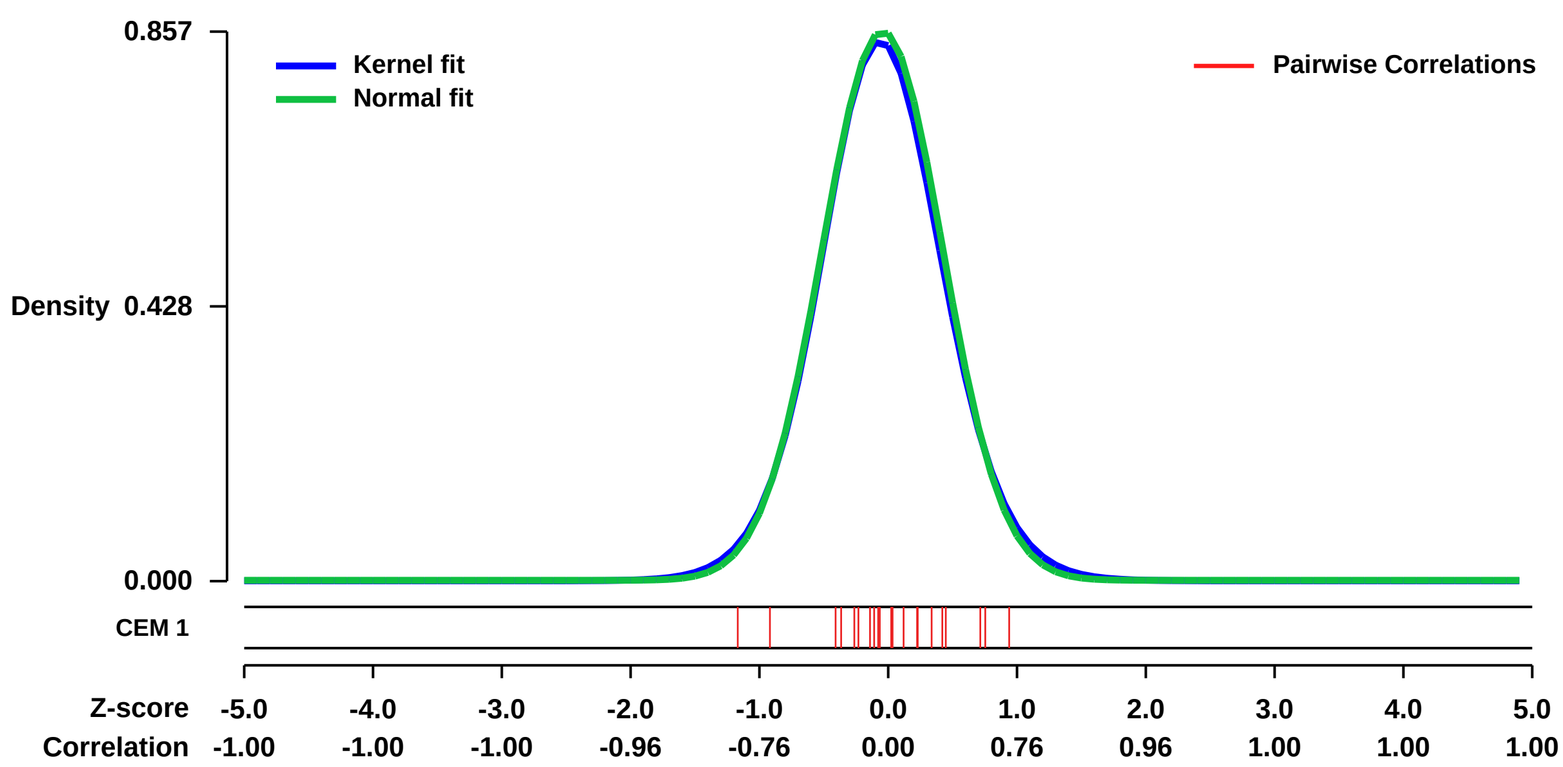

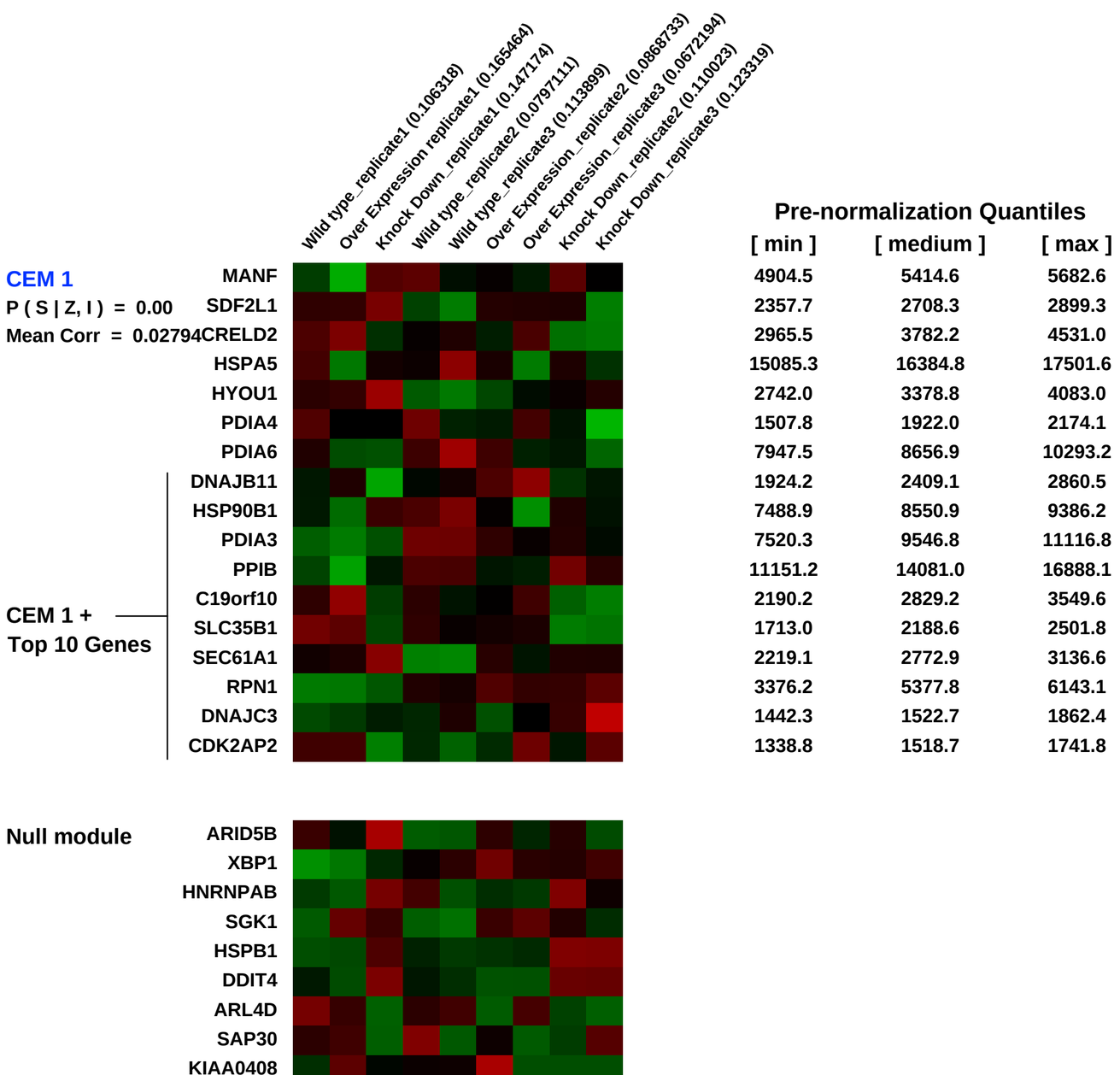

Pre-normalization Quantiles

	[min]	[medium]	[max]
MANF	4904.5	5414.6	5682.6
SDF2L1	2357.7	2708.3	2899.3
CRELD2	2965.5	3782.2	4531.0
HSPA5	15085.3	16384.8	17501.6
HYOU1	2742.0	3378.8	4083.0
PDIA4	1507.8	1922.0	2174.1
PDIA6	7947.5	8656.9	10293.2
DNAJB11	1924.2	2409.1	2860.5
HSP90B1	7488.9	8550.9	9386.2
PDIA3	7520.3	9546.8	11116.8
PPIB	11151.2	14081.0	16888.1
C19orf10	2190.2	2829.2	3549.6
SLC35B1	1713.0	2188.6	2501.8
SEC61A1	2219.1	2772.9	3136.6
RPN1	3376.2	5377.8	6143.1
DNAJC3	1442.3	1522.7	1862.4
CDK2AP2	1338.8	1518.7	1741.8

GEO Series "GSE33109" Expression Profiles

Num of samples in this series: 39

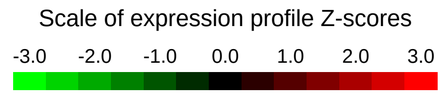

GEO Link:	http://www.ncbi.nlm.nih.gov/geo/query/acc.cgi?acc=GSE33109
Status:	Public on Oct 21 2011
Title:	Gene expression changes in human neural cells exposed to VX (O-ethyl S-[2-(diisopropylamino)ethyl] methylphosphonothiolate)
Organism:	Homo sapiens
Experiment type:	Expression profiling by array
Platform:	GPL570
Pubmed ID:	23440544
Summary & Design:	**Summary:** Organophosphorus compounds may induce neurotoxicity through mechanisms other than the cholinergic pathway, which need to be unraveled by a comprehensive and systematic approach such as genome-wide gene expression analysis. We used microarrays to study gene expression changes in human neural cells after exposure to VX, and identified pathways underlying these changes. **Overall design:** Human neural cells were exposed to sublethal concentrations (0, 0.1, 10 ¸…M) of VX. RNA were extracted at different timepoints (0, 6, 24, 72 h) after VX exposure and hybridized to Affymetrix microarrays. Four biological repeats were used for each condition.

Background corr dist: KL-Divergence = 0.2977, L1-Distance = 0.0471, L2-Distance = 0.0048, Normal std = 0.2835

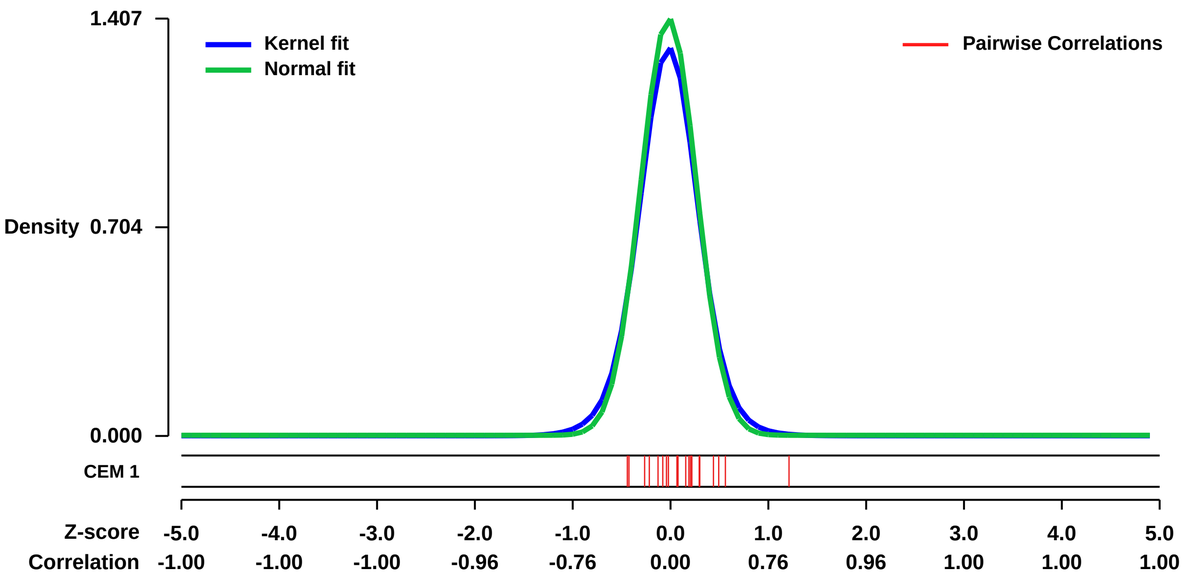

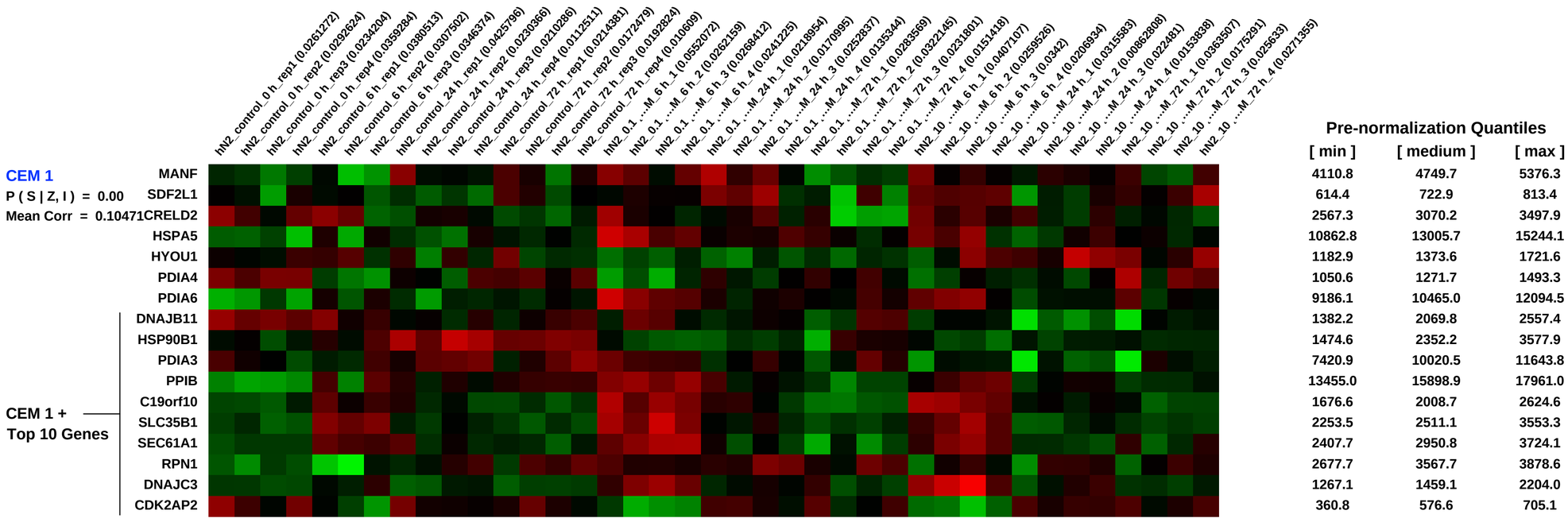

Pre-normalization Quantiles

[min]	[medium]	[max]
4110.8	4749.7	5376.3
614.4	722.9	813.4
2567.3	3070.2	3497.9
10862.8	13005.7	15244.1
1182.9	1373.6	1721.6
1050.6	1271.7	1493.3
9186.1	10465.0	12094.5
1382.2	2069.8	2557.4
1474.6	2352.2	3577.9
7420.9	10020.5	11643.8
13455.0	15898.9	17961.0
1676.6	2008.7	2624.6
2253.5	2511.1	3553.3
2407.7	2950.8	3724.1
2677.7	3567.7	3878.6
1267.1	1459.1	2204.0
360.8	576.6	705.1

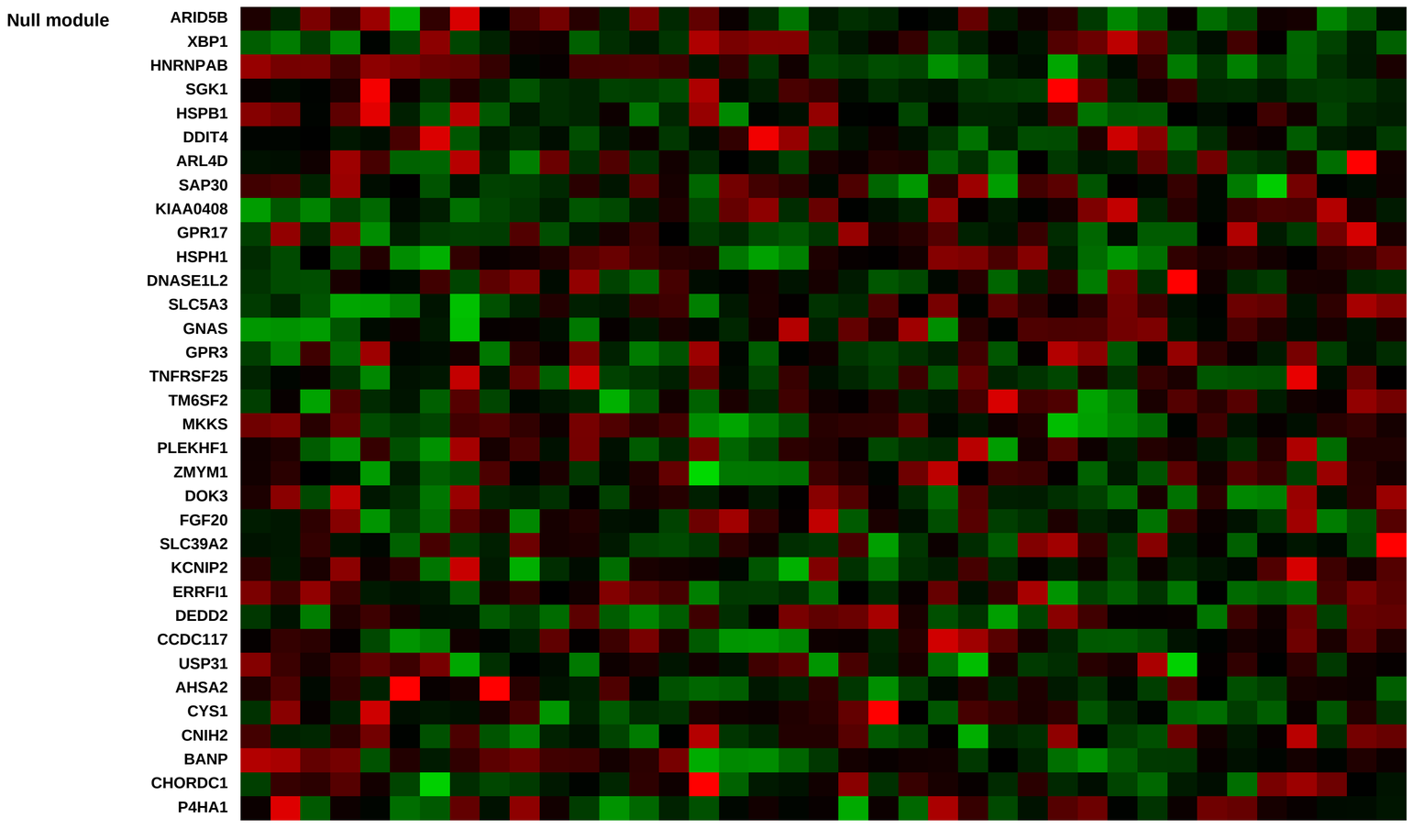

GEO Series "GSE56582" Expression Profiles

Num of samples in this series: 9

Scale of expression profile Z-scores

-3.0 -2.0 -1.0 0.0 1.0 2.0 3.0

GEO Link: http://www.ncbi.nlm.nih.gov/geo/query/acc.cgi?acc=GSE56582
Status: Public on Apr 08 2014
Title: Expression data from PC3 cocultured with Osteoblasts
Organism: Homo sapiens
Experiment type: Expression profiling by array
Platform: GPL570
Pubmed ID:

Summary & Design:

Summary:
Inhibitors of Wnt signaling have been previously shown to be involved in prostate cancer (PC) metastasis; however the role of Sclerostin (Sost) has not yet been explored. Here we show that elevated Wnt signaling derived from Sost deficient osteoblasts (OBSOSTKO) promotes PC invasion while rhSOST has an inhibitory effect. In contrast, rhDKK1 promotes PC elongation and filopodia formation, morphological changes characteristic of an invasive phenotype. Furthermore, rhDKK1 was found to activate canonical Wnt signaling in PC3 cells as quantified by TOPFLASH reporter and b-catenin activity, suggesting that SOST and DKK1 have opposing roles on Wnt signaling in this context. Gene expression analysis of PC3 cells co-cultured with OBs exhibiting varying amounts of Wnt signaling identified CRIM1 as one of the transcripts up-regulated under highly invasive conditions. Following further analysis we found that CRIM1 increases PC3 invasion, complexes with b-catenin, and promotes cell-adhesion, suggesting that elevated Wnt signaling secreted from the bone may promote PC tropism by promoting CRIM1 expression and facilitating cancer cell invasion and adhesion to bone. We concluded that SOST and DKK1 have opposing effects on PC3 cell invasion and that bone-derived Wnt signaling positively contributes to the invasive phenotypes of metastatic cancer cells by activating CRIM1 expression and facilitating PC-OB physical interaction. As such, we investigated the effects of high concentrations of SOST in vivo. We found that PC3-cells overexpressing SOST injected via tail vein did not readily metastasize in NSG xenografts, suggesting that targeting the molecular bone environment may influence bone metastatic outcome in clinical settings.

Overall design:
PC3 cells were cultured for 48 hours in specified conditions prior to RNA extraction and hybridization on Affymetrix Human Genome U133 Plus 2.0 Array. All experiments were performed in at least duplicates. Total RNA was collected from PC3 cells cultured in normal growth media, cocultured with WT mouse osteoblasts supplemented with recombinant human DKK1, cells cocultured with WT mouse osteoblasts supplemented with recombinant human SOST, or cocultured with SostKO mouse osteoblasts.

Background corr dist: KL-Divergence = 0.0703, L1-Distance = 0.0208, L2-Distance = 0.0005, Normal std = 0.4967

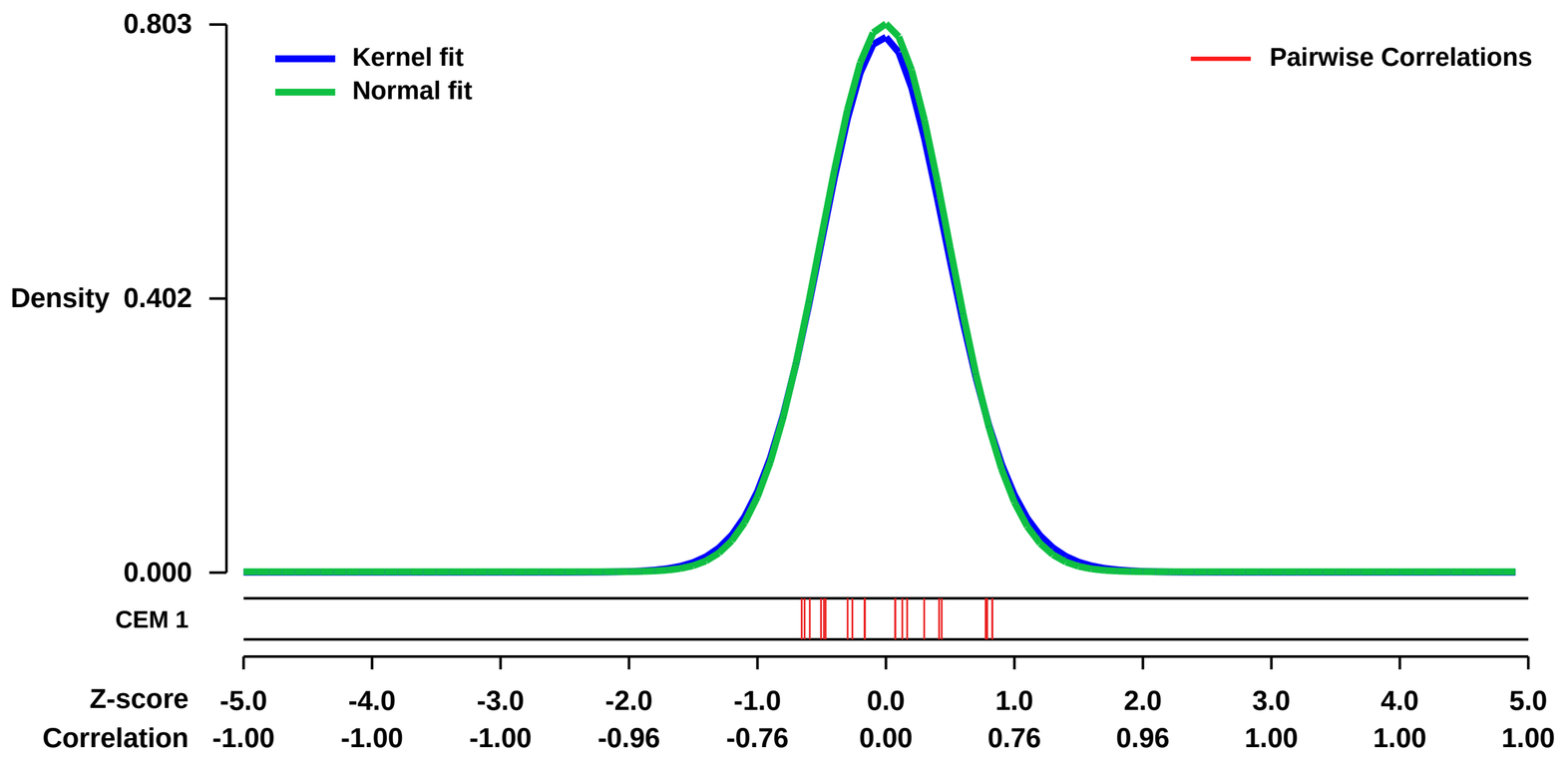

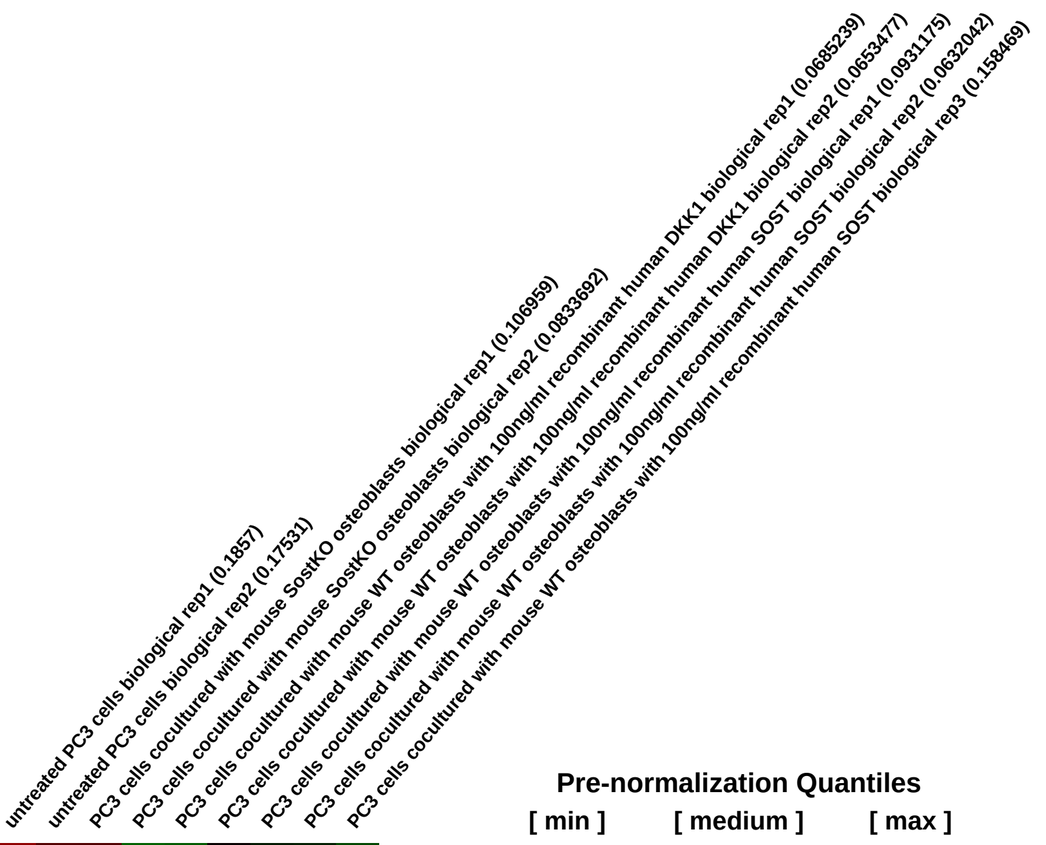

CEM 1
P (S | Z, I) = 0.00
Mean Corr = 0.01415

CEM 1 + Top 10 Genes

	Pre-normalization Quantiles		
	[min]	[medium]	[max]
MANF	6364.2	6786.2	7779.8
SDF2L1	1859.8	2010.8	2635.6
CRELD2	3160.0	3352.9	3556.8
HSPA5	14382.8	14782.8	15535.5
HYOU1	2846.3	3294.4	4976.5
PDIA4	2407.1	2830.5	3174.8
PDIA6	10779.2	11253.3	11811.0
DNAJB11	5753.7	6054.7	7018.5
HSP90B1	4200.7	6182.5	8190.6
PDIA3	12474.8	14282.9	15410.4
PPIB	14102.0	15006.1	16012.0
C19orf10	6759.1	7149.0	8135.2
SLC35B1	4789.0	4986.0	5651.7
SEC61A1	3336.8	3546.9	4026.7
RPN1	4947.9	5251.1	5922.8
DNAJC3	1817.2	1917.3	2007.8
CDK2AP2	1314.7	1665.0	1830.1

Null module

ARID5B
XBP1
HNRNPAB
SGK1
HSPB1
DDIT4
ARL4D
SAP30
KIAA0408
GPR17
HSPH1
DNASE1L2
SLC5A3
GNAS
GPR3
TNFRSF25
TM6SF2
MKKS
PLEKHF1
ZMYM1
DOK3
FGF20
SLC39A2
KCNIP2
ERRFI1
DEDD2
CCDC117
USP31
AHSA2
CYS1
CNIH2
BANP
CHORDC1
P4HA1

GEO Series "GSE31315" Expression Profiles

Num of samples in this series: 12

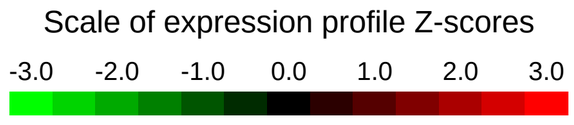

GEO Link:	http://www.ncbi.nlm.nih.gov/geo/query/acc.cgi?acc=GSE31315
Status:	Public on Aug 08 2012
Title:	Expression data from SP and non-SP sorted anti-EpCAM treated A549 cells
Organism:	Homo sapiens
Experiment type:	Expression profiling by array
Platform:	GPL570
Pubmed ID:	
Summary & Design:	**Summary:** Targeted therapies against cancer stem cells which are enriched in side populations (SP) involves interruption of Wnt-signalling. Furthermore, EpCAM is a SP marker and modulator of Wnt-signalling. Therefore, the effects of an anti-EpCAM treatment on SP-cells and WNT/¸†-catenin signalling was studied. SP of the human lung adenocarcinoma cell line A549 was obtained by fluorescence activated cell sorting and whole genome scans helped to define their molecular phenotype after anti-EpCAM antibody treatment. **Overall design:** Anti-EpCAM treated and untreated A549 cells were subjected to Hoechst 33342 dye exclusion assay and sorted to SP and non-SP fractions by FACS. Three biological replicates.

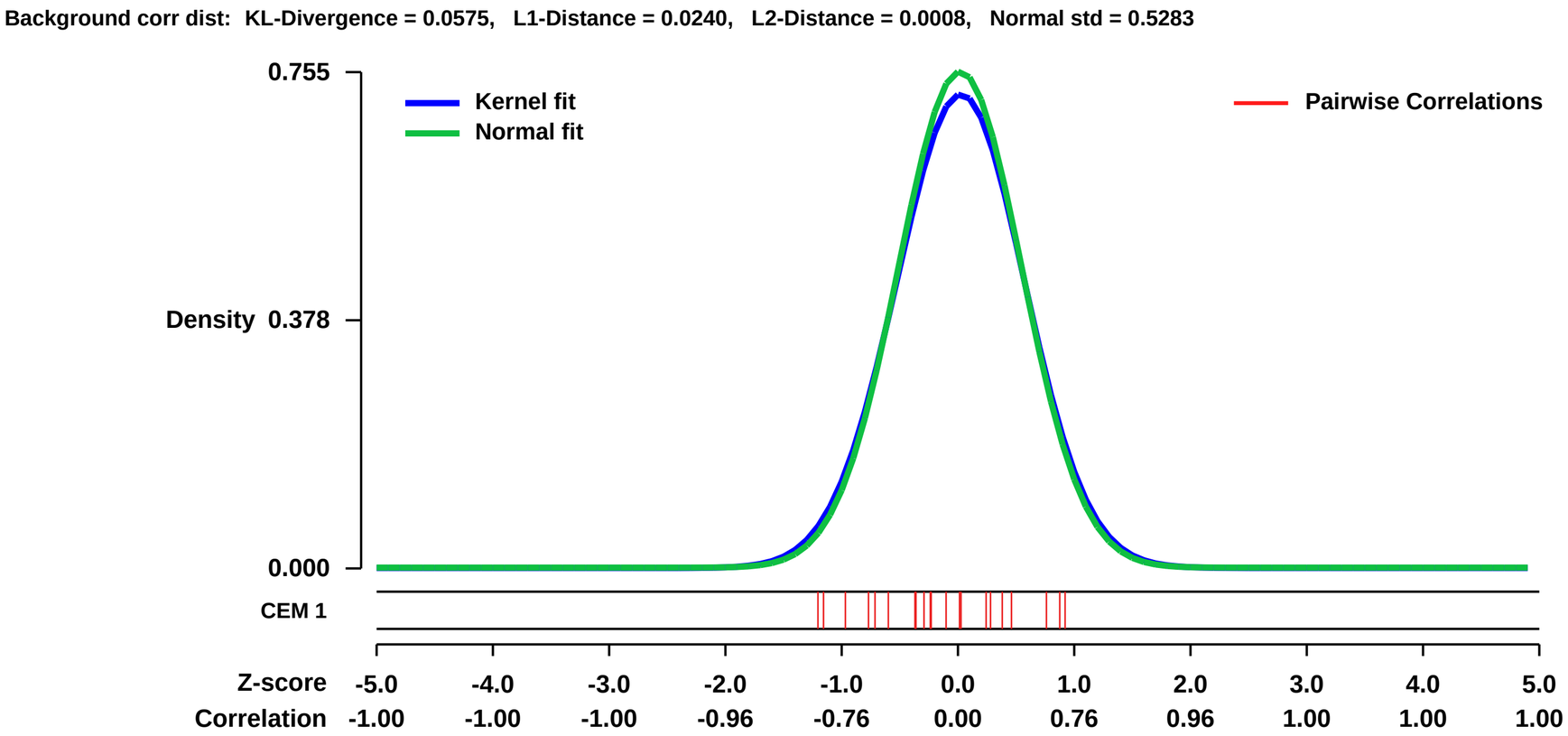

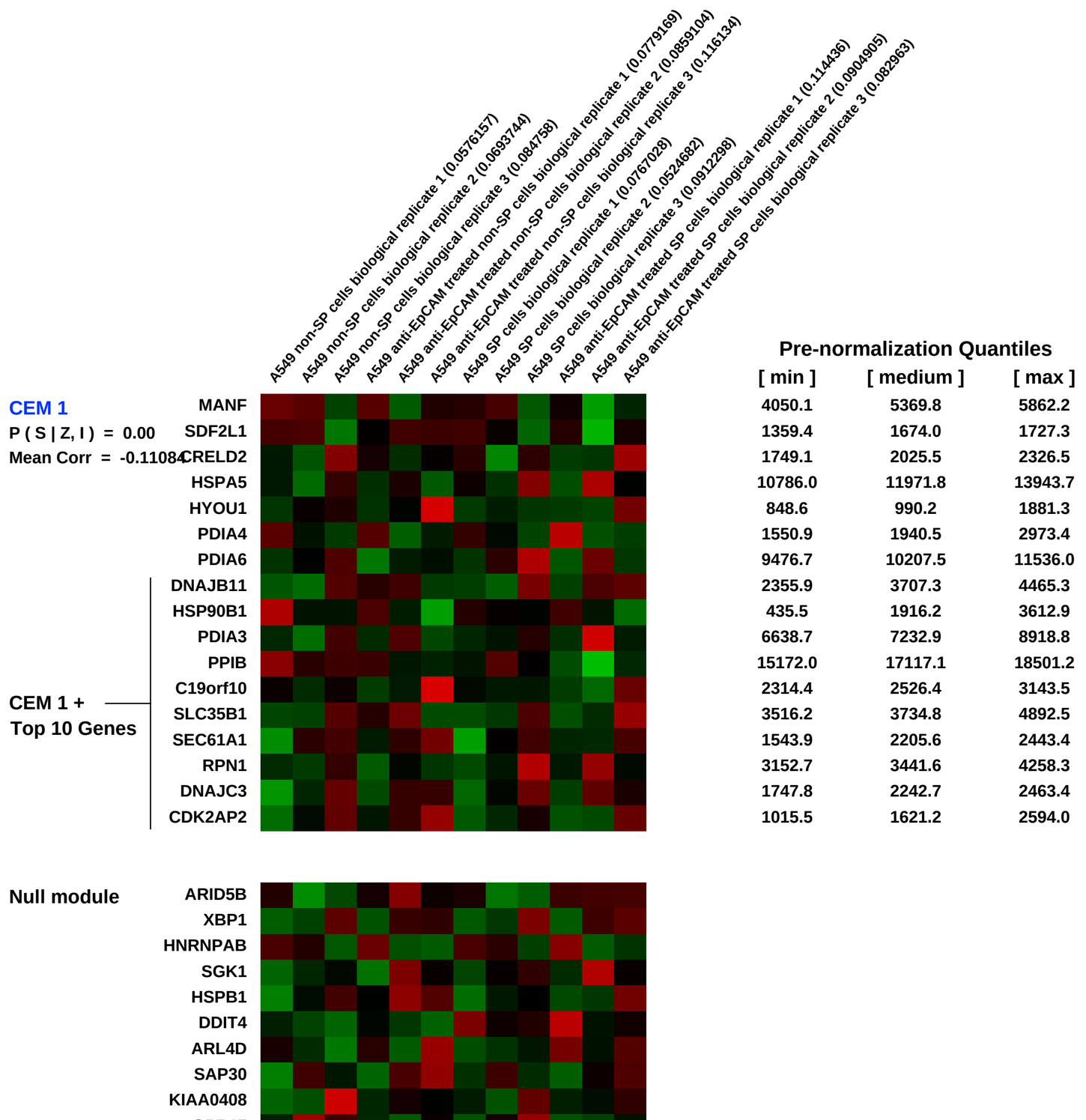

GEO Series "GSE50547" Expression Profiles

Num of samples in this series: 6

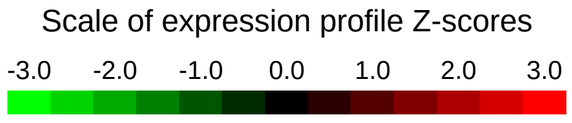

GEO Link:	http://www.ncbi.nlm.nih.gov/geo/query/acc.cgi?acc=GSE50547
Status:	Public on Sep 24 2013
Title:	Global mRNA gene expression analysis profiling control HEK293 cell and cells expressing HSP70K71E
Organism:	Homo sapiens
Experiment type:	Expression profiling by array
Platform:	GPL570
Pubmed ID:	
Summary & Design:	**Summary:** This is global mRNA gene expression data for HEK293 and cells expressing HSP70K71E ; most genes were down-regulated for HSP70K71E compared to the control **Keywords: Global mRNA expression** **Overall design:** We overexpressed pCI1-EGFP (control) and Hsp70K71E-EGFP to HEK293 and collected total RNA from each condition to analyze global mRNA expression
Background corr dist:	**KL-Divergence = 0.0477, L1-Distance = 0.0203, L2-Distance = 0.0005, Normal std = 0.5826**

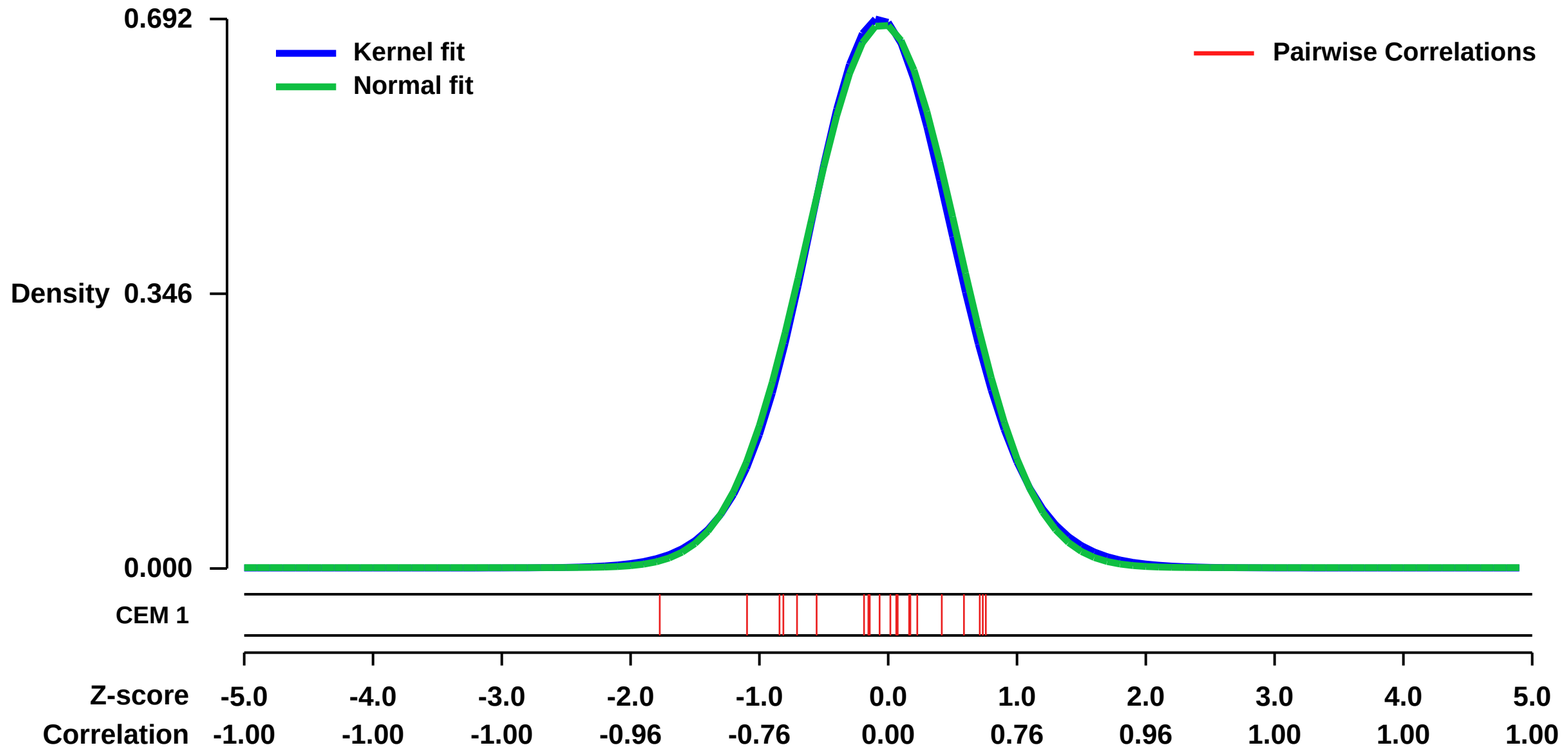

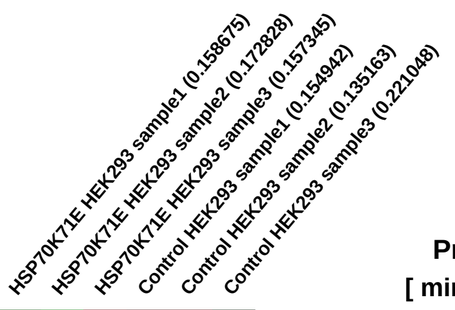

Pre-normalization Quantiles

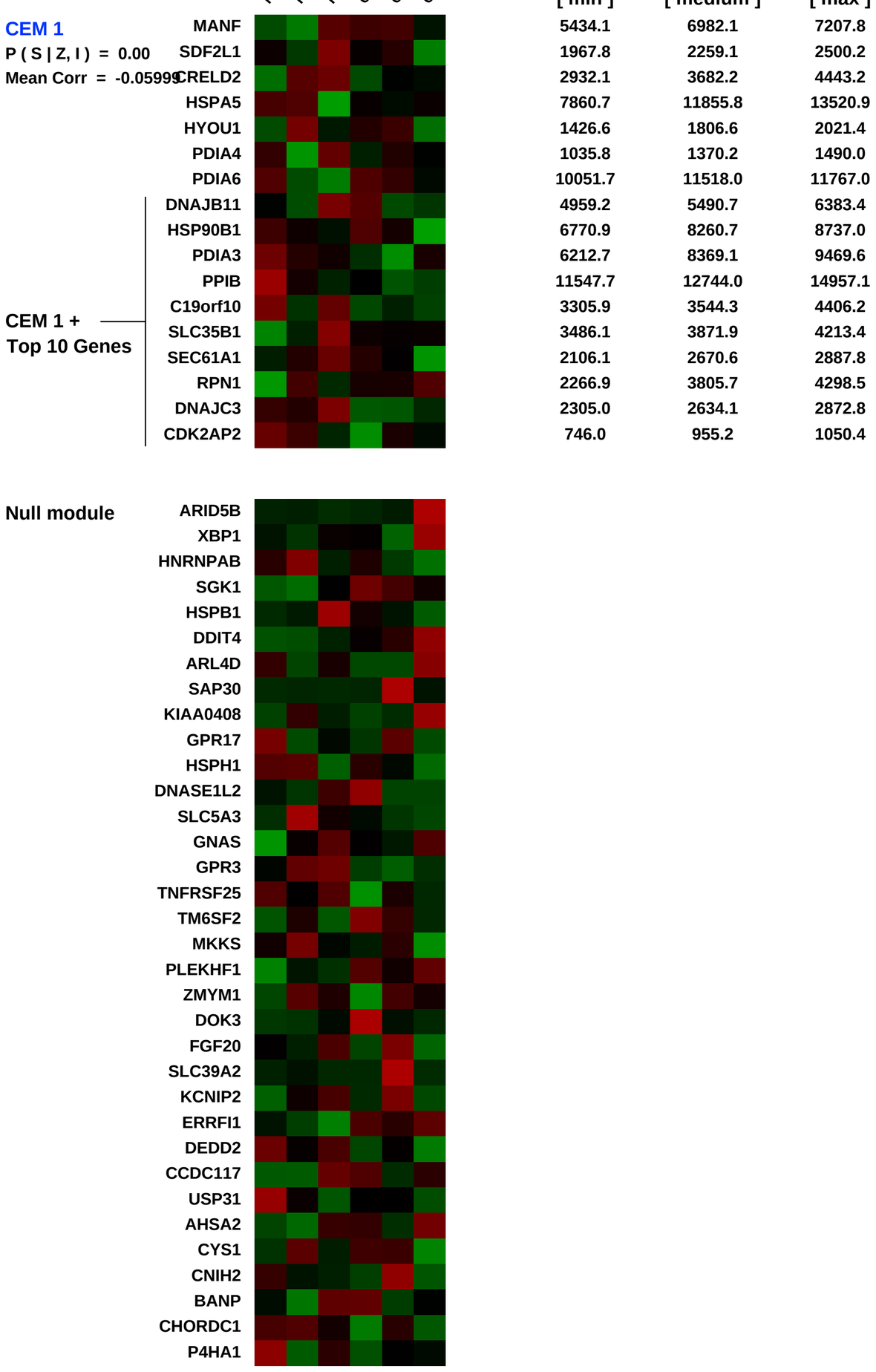

GEO Series "GSE14970" Expression Profiles

Num of samples in this series: 12

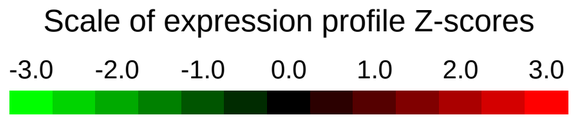

GEO Link:	http://www.ncbi.nlm.nih.gov/geo/query/acc.cgi?acc=GSE14970
Status:	Public on Feb 23 2010
Title:	Transcription profile in patients with acyanotic or cyanotic Tetralogy of Fallot
Organism:	Homo sapiens
Experiment type:	Expression profiling by array
Platform:	GPL570
Pubmed ID:	20416888
Summary & Design:	**Summary:** To determine cardiac transcription profiles, we collected myocardial samples immediately after institution of cardiopulmonary bypass from acyanotic or cyanotic Tetralogy of Fallot patients undergoing corrective surgery. The transcriptional profile of the mRNA in these samples was measured with gene array technology. **Overall design:** Myocardial samples were collected, immediately after institution of cardiopulmonary bypass from acyanotic or cyanotic Tetralogy of Fallot patients undergoing corrective surgery.

Background corr dist: KL-Divergence = 0.0960, L1-Distance = 0.0317, L2-Distance = 0.0018, Normal std = 0.4405

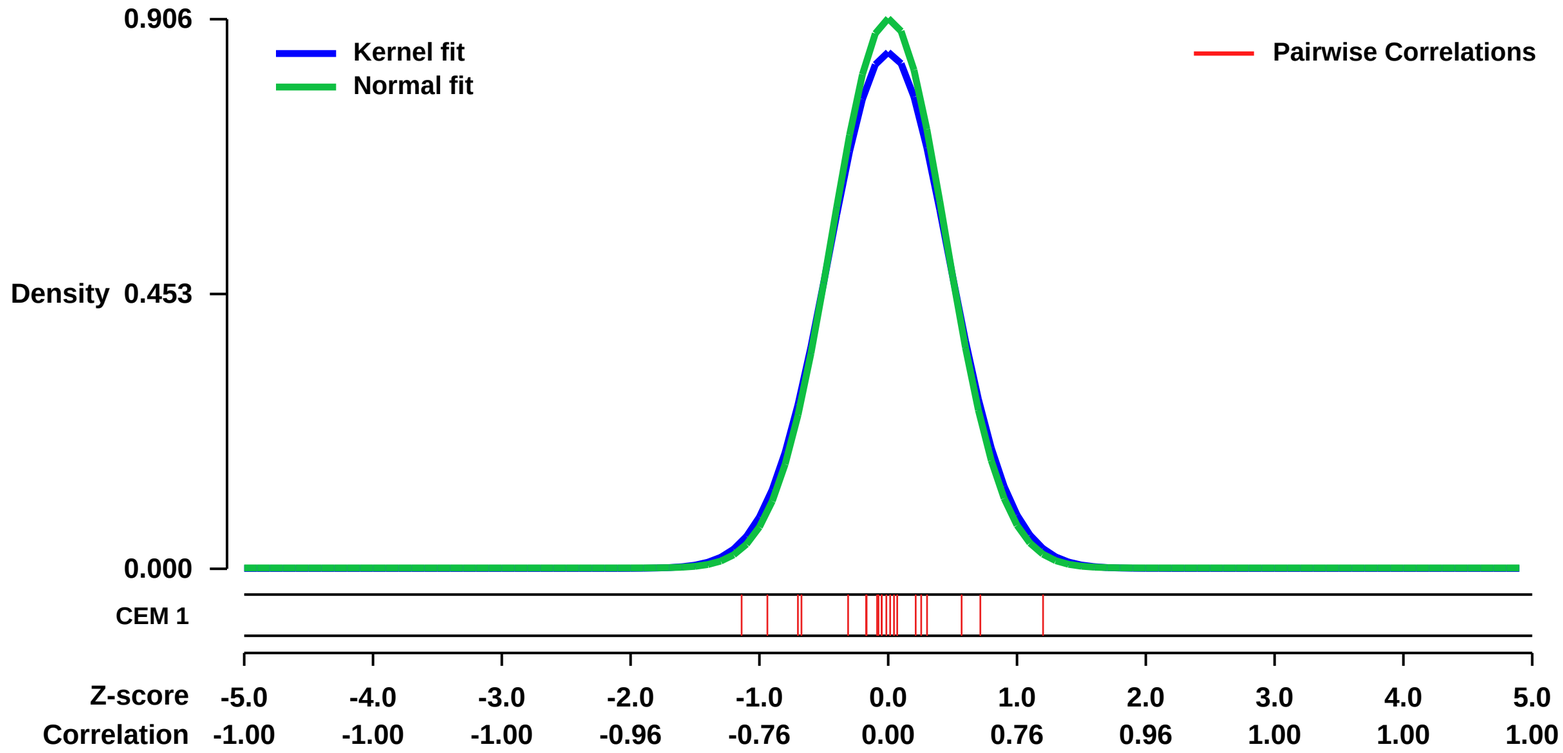

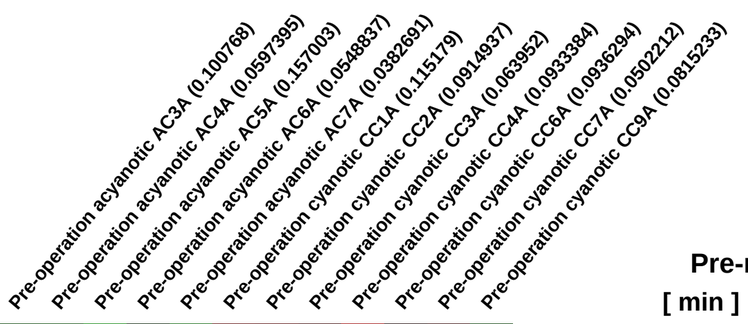

Pre-normalization Quantiles

		[min]	[medium]	[max]
CEM 1	MANF	1750.1	2256.3	2708.4
P (S | Z, I) = 0.00	SDF2L1	589.5	807.3	1319.2
Mean Corr = -0.03846	CRELD2	1139.8	1377.7	1648.4
	HSPA5	10454.3	13303.3	15436.0
	HYOU1	1070.5	1603.2	2051.9
	PDIA4	268.6	339.7	401.5
	PDIA6	6884.7	9101.7	10851.2
CEM 1 + Top 10 Genes	DNAJB11	1007.2	1659.7	2347.4
	HSP90B1	1060.6	1613.5	2079.1
	PDIA3	3306.2	4409.7	5117.4
	PPIB	3446.9	4221.3	6088.5
	C19orf10	926.1	1238.6	1307.1
	SLC35B1	2303.3	2532.9	3230.4
	SEC61A1	745.1	1523.8	1797.7
	RPN1	1026.8	1243.5	1651.3
	DNAJC3	1288.0	1924.7	2592.1
	CDK2AP2	739.2	1268.4	1987.6
Null module	ARID5B			
	XBP1			
	HNRNPAB			
	SGK1			
	HSPB1			
	DDIT4			
	ARL4D			
	SAP30			
	KIAA0408			
	GPR17			
	HSPH1			
	DNASE1L2			
	SLC5A3			
	GNAS			
	GPR3			
	TNFRSF25			
	TM6SF2			
	MKKS			
	PLEKHF1			
	ZMYM1			
	DOK3			
	FGF20			
	SLC39A2			
	KCNIP2			
	ERRFI1			
	DEDD2			
	CCDC117			
	USP31			
	AHSA2			
	CYS1			
	CNIH2			
	BANP			
	CHORDC1			
	P4HA1			

GEO Series "GSE9361" Expression Profiles

Num of samples in this series: 9

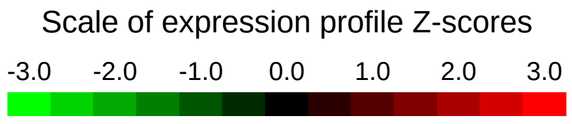

GEO Link:	http://www.ncbi.nlm.nih.gov/geo/query/acc.cgi?acc=GSE9361
Status:	Public on Feb 25 2008
Title:	Functional interaction between a PIP2 novel polyA polymerase and type 1 PIPKIalpha
Organism:	Homo sapiens
Experiment type:	Expression profiling by array
Platform:	GPL570
Pubmed ID:	18288197
Summary & Design:	**Summary:** A loss of StarPap would be predicted to result in a decrease in cellular levels of mRNAs which it polyadenylates. Moreover, if PIPKIalpha has a function relationship with StarPap, knockdown of PIPKIalpha should cause a decrease in a pool of target mRNAs which require both StarPap and PIPKIalpha for their maturation. To test this, we independently knocked down StarPap and PIPKIalpha, and performed microarray analysis of total polyadenylated mRNAs from each group. **Keywords:** Gene expression after siRNA knockdown **Overall design:** HEK293 cells were transfected with siRNA specific for StarPap or PIPKIalpha or control siRNA. N=3

Background corr dist: KL-Divergence = 0.0474, L1-Distance = 0.0258, L2-Distance = 0.0007, Normal std = 0.5859

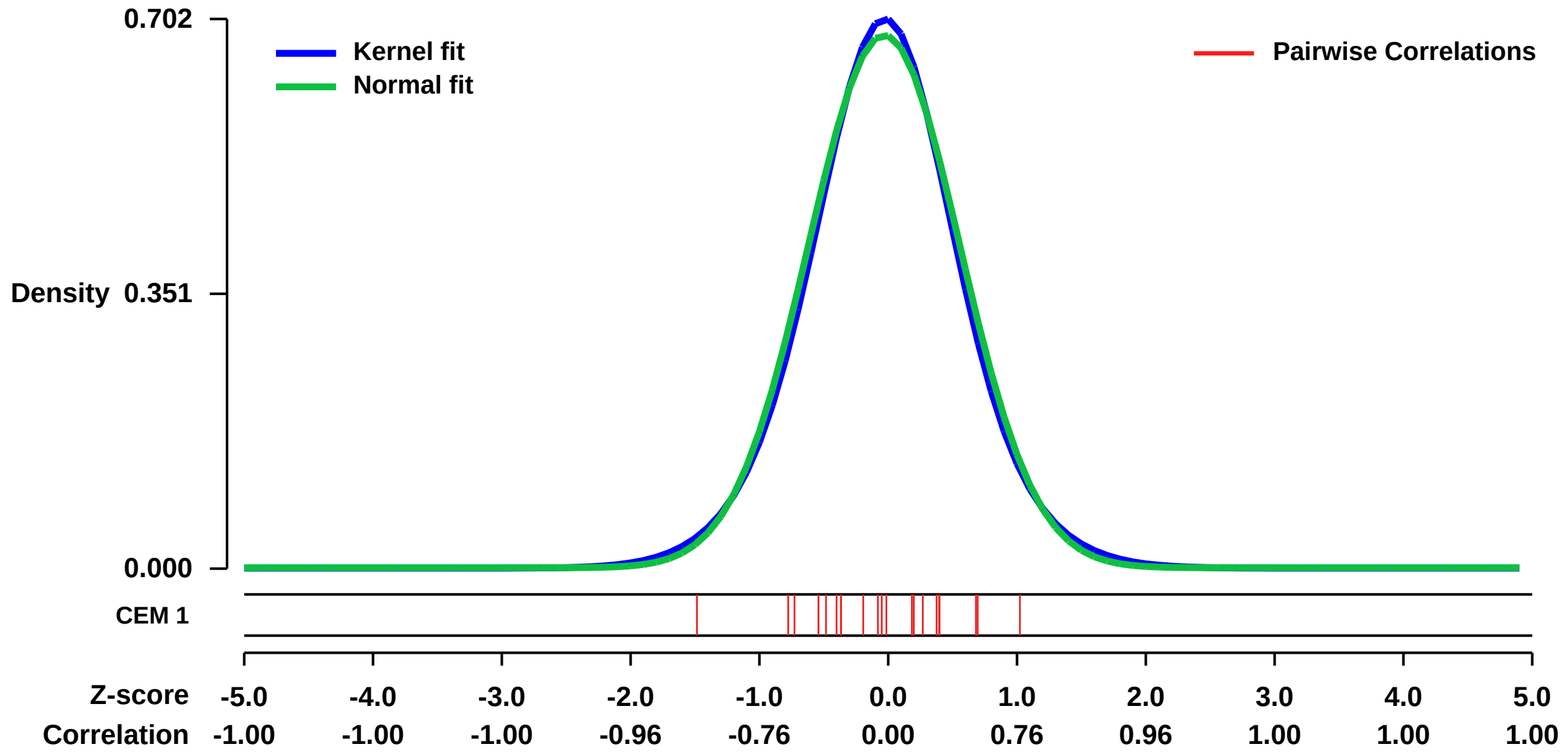

		Pre-normalization Quantiles [min]	[medium]	[max]
CEM 1	MANF	1998.2	2713.4	2951.5
P (S | Z, I) = 0.00	SDF2L1	1392.4	1735.4	2246.2
Mean Corr = -0.03899	CRELD2	3087.1	5177.0	6149.5
	HSPA5	9914.0	10926.0	12077.5
	HYOU1	3185.9	3723.0	4161.6
	PDIA4	746.7	1366.2	1537.4
	PDIA6	4714.6	5030.5	6195.7
CEM 1 + Top 10 Genes	DNAJB11	4679.2	5298.4	6432.9
	HSP90B1	5470.0	5690.2	6642.3
	PDIA3	7836.0	8746.4	9748.7
	PPIB	7699.1	11782.9	15836.8
	C19orf10	2397.8	3101.9	3813.8
	SLC35B1	2044.4	2610.2	3769.1
	SEC61A1	1886.3	2043.8	2326.7
	RPN1	3918.1	4203.2	5220.8
	DNAJC3	466.7	998.1	1155.5
	CDK2AP2	630.6	923.0	1133.0
Null module	ARID5B			
	XBP1			
	HNRNPAB			
	SGK1			
	HSPB1			
	DDIT4			
	ARL4D			
	SAP30			
	KIAA0408			
	GPR17			
	HSPH1			
	DNASE1L2			
	SLC5A3			
	GNAS			
	GPR3			
	TNFRSF25			
	TM6SF2			
	MKKS			
	PLEKHF1			
	ZMYM1			
	DOK3			
	FGF20			
	SLC39A2			
	KCNIP2			
	ERRFI1			
	DEDD2			
	CCDC117			
	USP31			
	AHSA2			
	CYS1			
	CNIH2			
	BANP			
	CHORDC1			
	P4HA1			

GEO Series "GSE30985" Expression Profiles

Num of samples in this series: 24

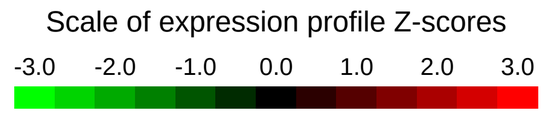

GEO Link:	**http://www.ncbi.nlm.nih.gov/geo/query/acc.cgi?acc=GSE30985**
Status:	**Public on Dec 01 2011**
Title:	**Expression profiling of DNMT1 inhibitors in HCT116 cells**
Organism:	**Homo sapiens**
Experiment type:	**Expression profiling by array**
Platform:	**GPL570**
Pubmed ID:	
Summary & Design:	**Summary:** **Epigenetic changes accompany tumorigenesis and are required for tumor maintenance. Modulation of DNA methylation state, histone acetylation, and histone methylation, as well as reversal of disease-associated epigenetic state aberrations, can be disruptive to malignant disease progression. We produced lipophilic prodrugs of decitabine, which is a DNA methyltransferase inhibitor and is efficacious in treatment of myelodysplastic syndromes when dosed subcutaneously. Comparison of parent and prodrug activities in vitro and in vivo revealed comparable effects and unveiled several novel features of nucleoside analog molecular activity in vitro.** **Overall design:** **HCT116 were treated for 72 hour with Decitabine, Azacytidine and various prodrugs in duplicates at different dose concentrations. Cells were also treated with DMSO as control (quadrpulets), RNA was extracted and samples were hybridized to Affymetrix Hu133plus 2.0 arrays.**

Background corr dist: **KL-Divergence = 0.1018, L1-Distance = 0.0366, L2-Distance = 0.0027, Normal std = 0.4345**

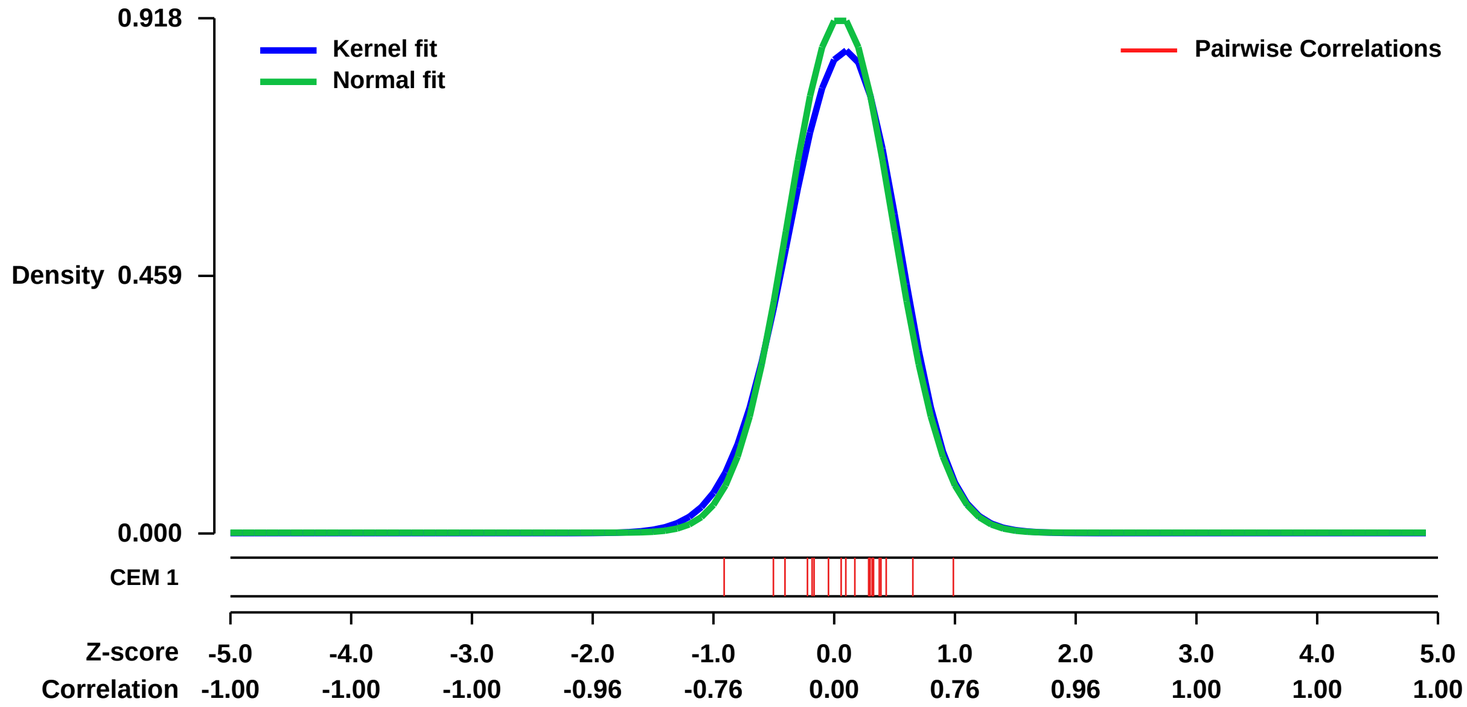

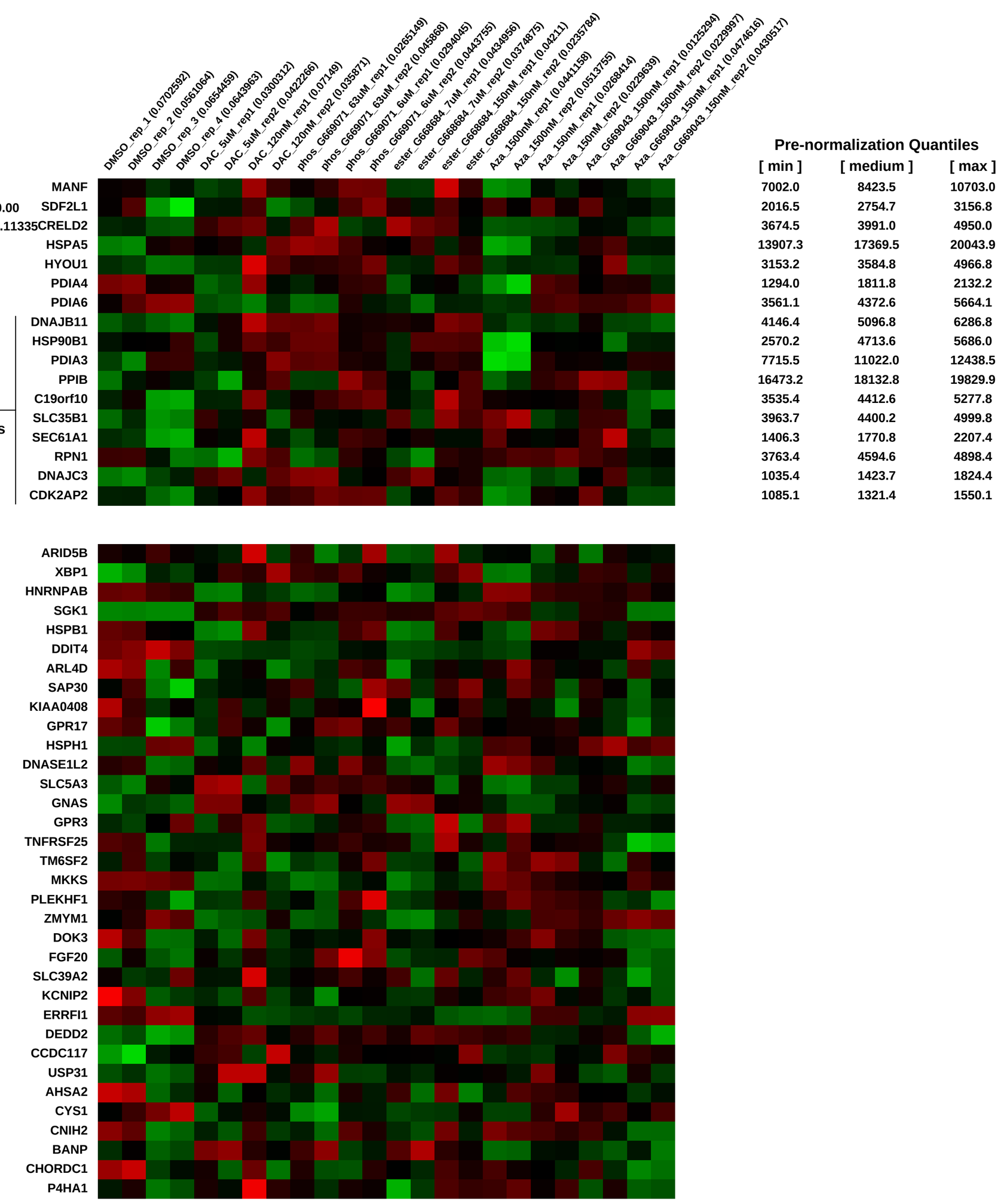

GEO Series "GSE3485" Expression Profiles

Num of samples in this series: 8

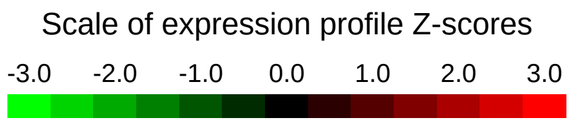

GEO Link:	http://www.ncbi.nlm.nih.gov/geo/query/acc.cgi?acc=GSE3485
Status:	Public on Nov 07 2005
Title:	Identification of LEDGF-regulated genes.
Organism:	Homo sapiens
Experiment type:	Expression profiling by array
Platform:	GPL570
Pubmed ID:	16311605
Summary & Design:	**Summary:** The LEDGF transcript from the PSIP1 gene was knocked down using RNAi technology. The resulting 293T derived cell line (293TsiLL) was compared to a control cell line (293TsiScram) using microarray analysis. Genes identified as being modulated by LEDGF were preferential targets of HIV integration. **Keywords: gene knockdown effects** **Overall design:** 2 cell lines were used, 293TsiLL (experimental) and 293TsiScram (control). 4 independent cultures of each cell line were used for independent RNA extractions, labeling reactions and array hybridizations.

Background corr dist: KL-Divergence = 0.0630, L1-Distance = 0.0183, L2-Distance = 0.0004, Normal std = 0.5173

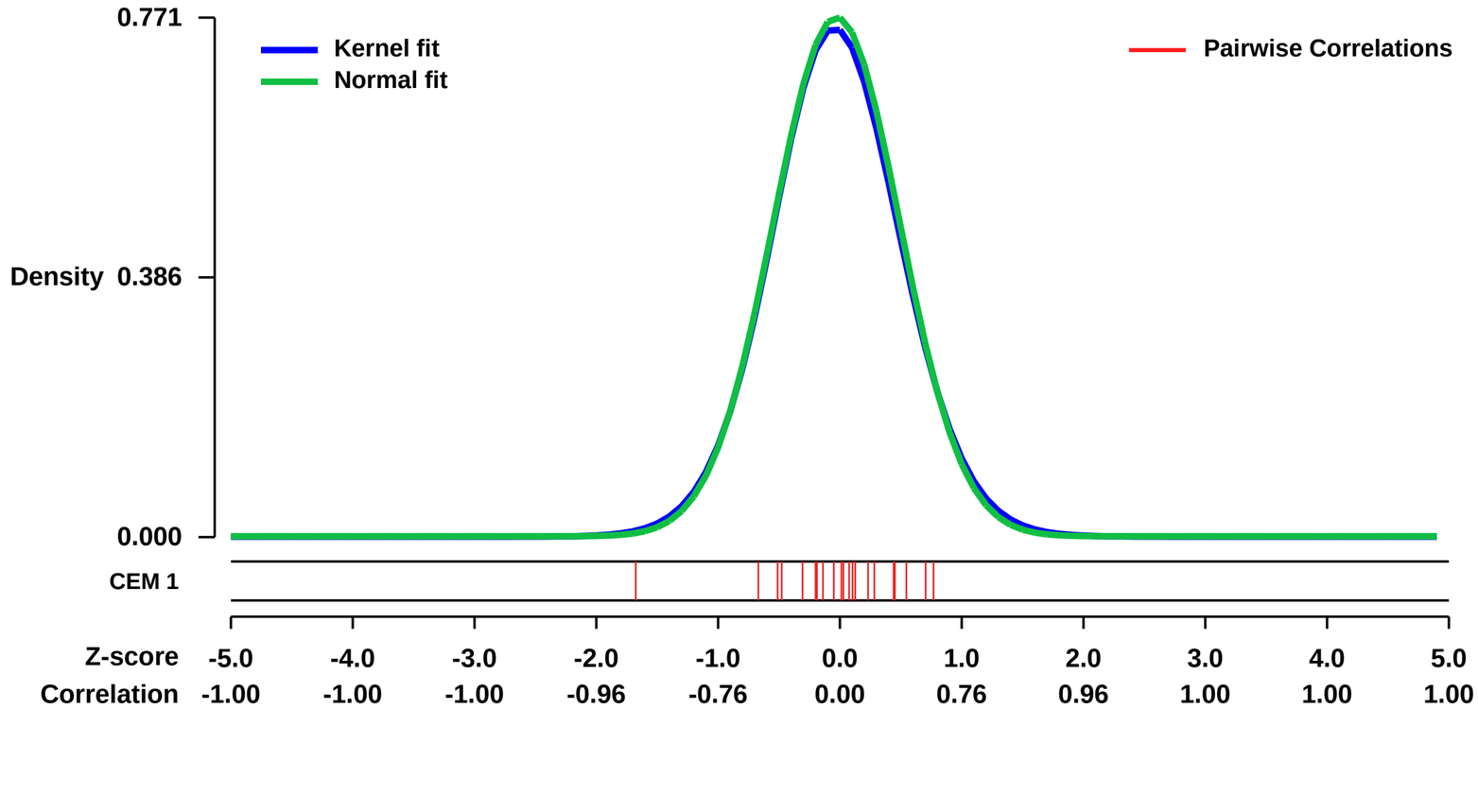

CEM 1
P (S | Z, I) = 0.00
Mean Corr = 0.00636

CEM 1 + Top 10 Genes

MANF	3338.1	3893.2	4226.6
SDF2L1	991.6	1677.3	2172.7
CRELD2	2955.0	3637.1	3836.3
HSPA5	10698.4	12106.6	13301.4
HYOU1	2889.5	3803.8	4502.8
PDIA4	1429.4	1486.9	1599.3
PDIA6	6354.0	7257.4	8217.1
DNAJB11	2105.8	3198.8	3943.2
HSP90B1	2823.5	3931.4	4249.3
PDIA3	4907.5	6083.3	6700.0
PPIB	6141.2	8704.8	9911.1
C19orf10	2267.6	3130.2	3709.9
SLC35B1	2872.9	3136.1	3383.7
SEC61A1	2614.3	3853.8	4682.8
RPN1	2884.5	4041.6	4203.3
DNAJC3	924.1	1076.8	1274.1
CDK2AP2	429.7	511.9	614.8

Null module

ARID5B
XBP1
HNRNPAB
SGK1
HSPB1
DDIT4
ARL4D
SAP30
KIAA0408
GPR17
HSPH1
DNASE1L2
SLC5A3
GNAS
GPR3
TNFRSF25
TM6SF2
MKKS
PLEKHF1
ZMYM1
DOK3
FGF20
SLC39A2
KCNIP2
ERRFI1
DEDD2
CCDC117
USP31
AHSA2
CYS1
CNIH2
BANP
CHORDC1
P4HA1

GEO Series "GSE29384" Expression Profiles

Num of samples in this series: 6

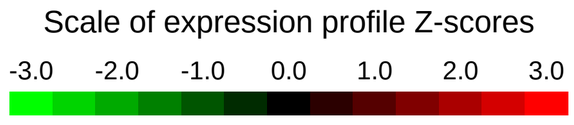

GEO Link:	http://www.ncbi.nlm.nih.gov/geo/query/acc.cgi?acc=GSE29384
Status:	Public on Apr 04 2012
Title:	Tetracycline-Inducible Cyr61 effect on LN229 glioma cells
Organism:	Homo sapiens
Experiment type:	Expression profiling by array
Platform:	GPL570
Pubmed ID:	22282654
Summary & Design:	**Summary:** Glioblastoma multiforme is the most common and aggressive form of brain cancer. The use of oncolytic HSV-1 (oHSV) to selectively target brain cancer cells leading to their lytic destruction has shown to be very promising in a preclinical setting, but is lacking efficacy in clinical trials. Cyr61, a secreted extracellular matrix protein which functions to promote angiogenesis, migration, proliferation and tumorigenesis, was found to be upregulated rapidly following oHSV infection. Here we show, using microarray analysis, that Cyr61 expression leads to the induction of several genes with type 1 interferon function. We show that Cyr61 mediated type 1 IFN induction is through its interaction with integrin alpha6beta1 on the cell surface and results in oHSV inhibition, reducing the efficacy of this therapy. We used microarray to detail the global program of gene expression underlying Cyr61 mediated oncolytic HSV-1 inhibition and identified distinct classes of up-regulated genes during this process. **Overall design:** Tetracycline-Inducible glioma cells expressing Cyr61 protein in the presence of doxycycline were treated with or without doxycycline for 24 hours. RNA was extracted and hybridized on Affymetrix microarray. Two groups: ´– dox to induce cyr61, performed in triplicate.

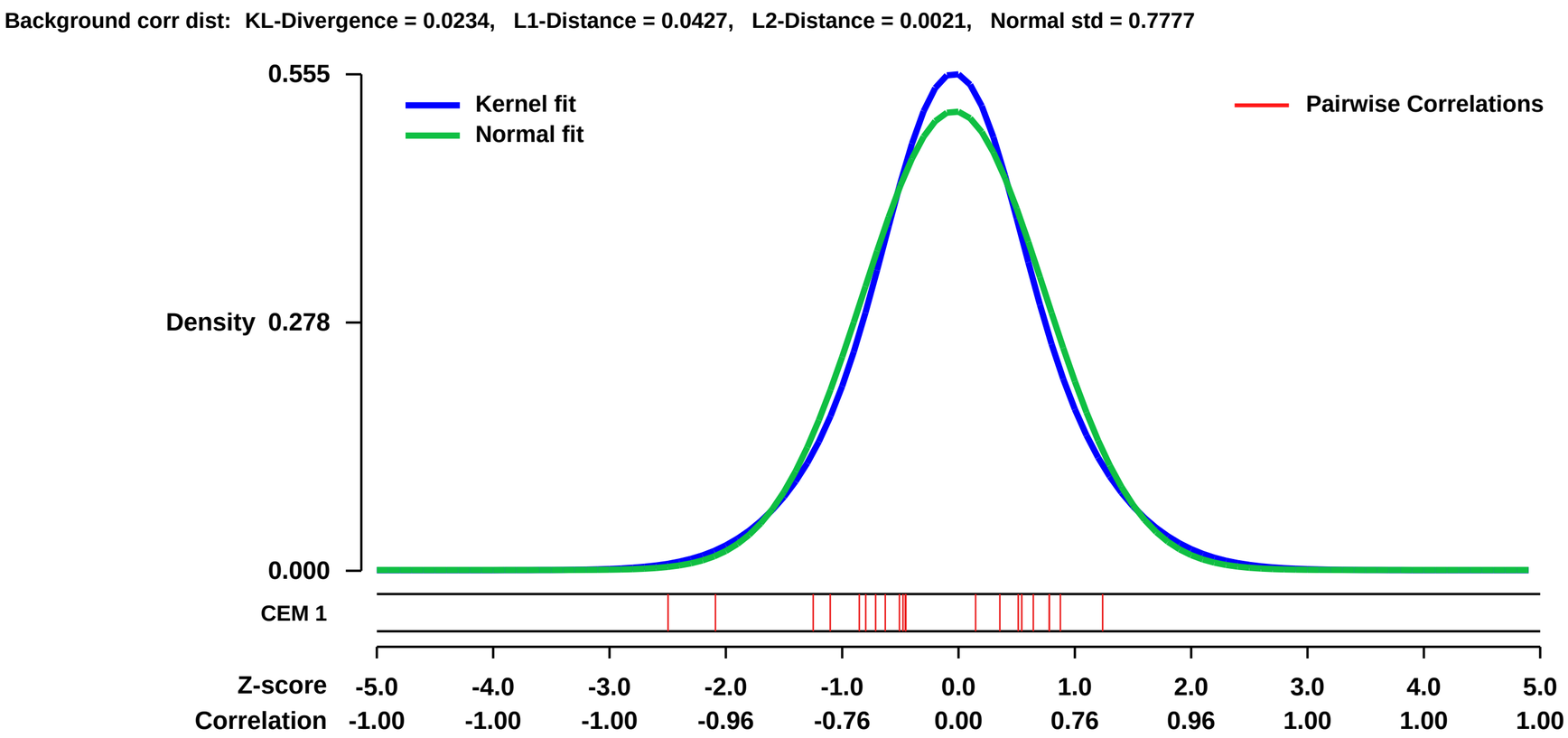

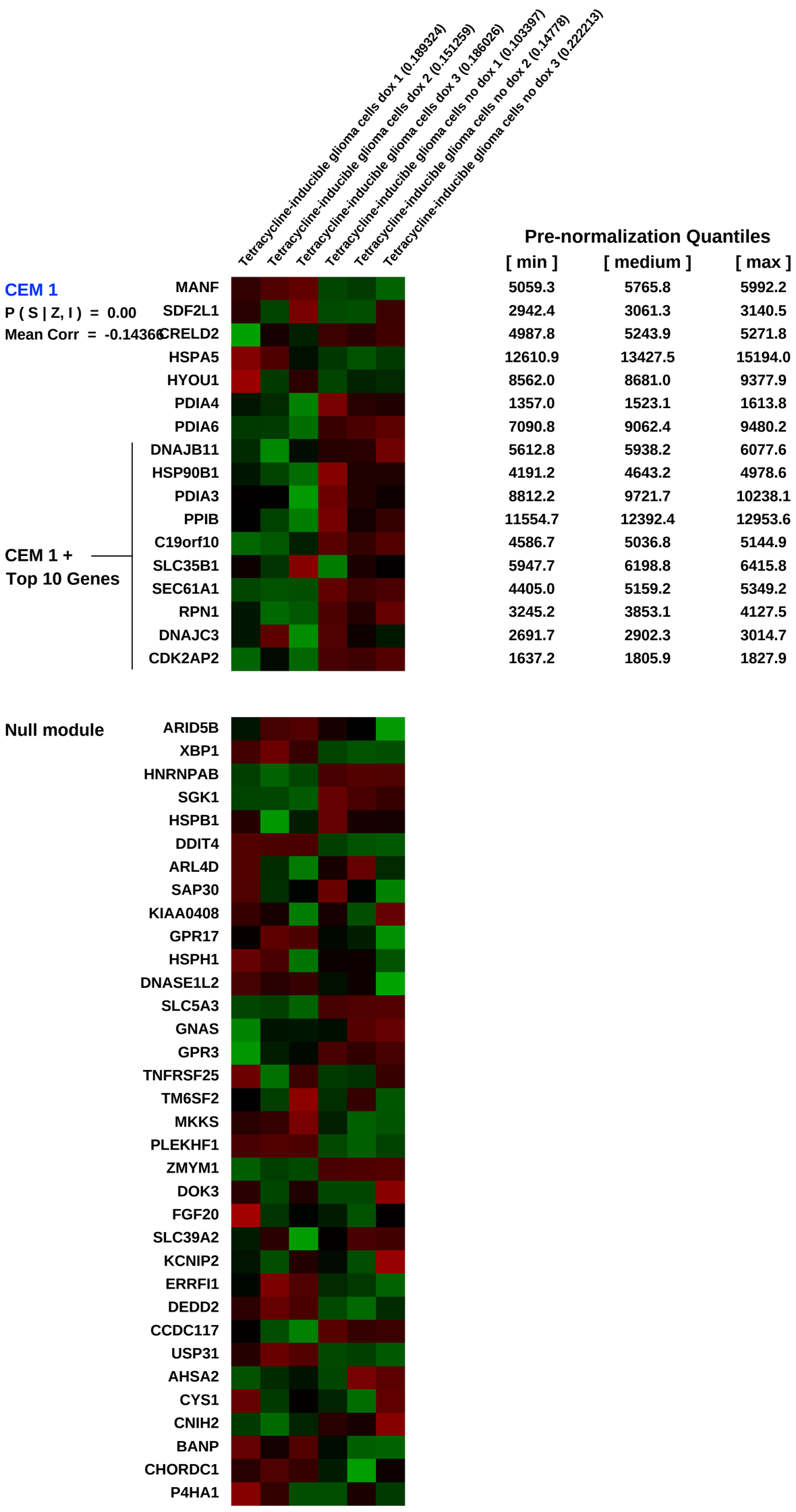

GEO Series "GSE34455" Expression Profiles

Num of samples in this series: 9

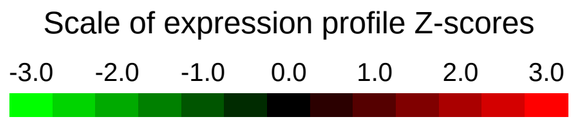

GEO Link:	http://www.ncbi.nlm.nih.gov/geo/query/acc.cgi?acc=GSE34455
Status:	Public on Jun 01 2012
Title:	Expression data from transfection of U87 glioma cells with miR-376a* for 24 hours
Organism:	Homo sapiens
Experiment type:	Expression profiling by array
Platform:	GPL570
Pubmed ID:	23093778
Summary & Design:	**Summary:** Enforced expression of miRNAs in cells leads to down-regulation of several mRNAs, which harbour binding sites in their 3'UTRs for the overexpressed miRNA and represent potential target genes of the miRNA We transfected unedited miR-376a* (376a*A) and edited miR-376a* (376a*G) into U87 cells to identify transcripts down-regulated by each in comparison to control miRNA transfection. The aim was to identify target genes directly subject to regulation by miR-376a*A and by miR-376a*G **Overall design:** U87 cells (100,000) were transfected with 50 nM of miR-376a*A, miR-376a*G or miR-control. Following incubation for 24 hours, total RNA was isolated from transfected cells. For each (miR-376a*A or miR-376a*G), genes differentially expressed upon miRNA transfection were determined based on comparison with miR-control-transfected samples. Biological triplicates were used for each sample type.

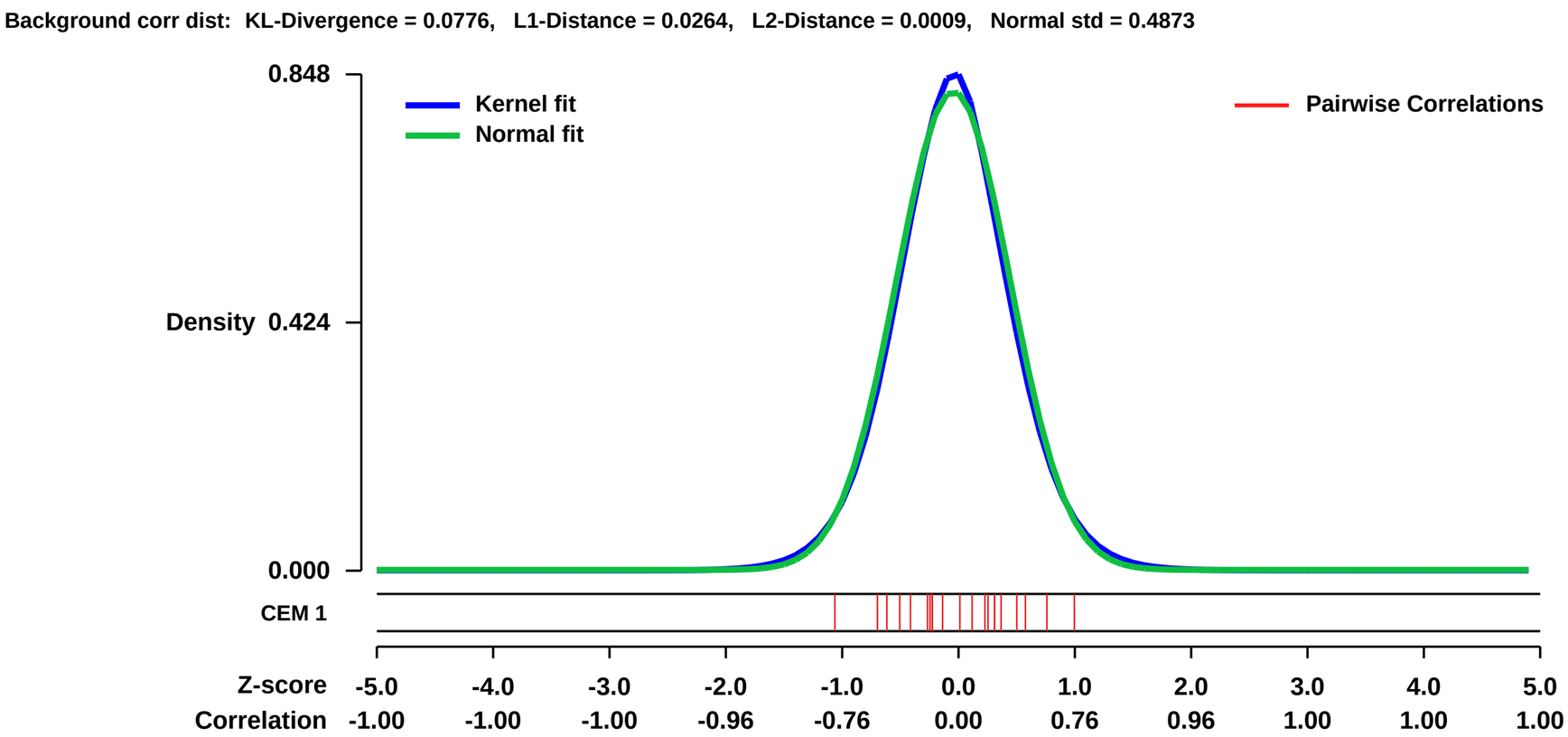

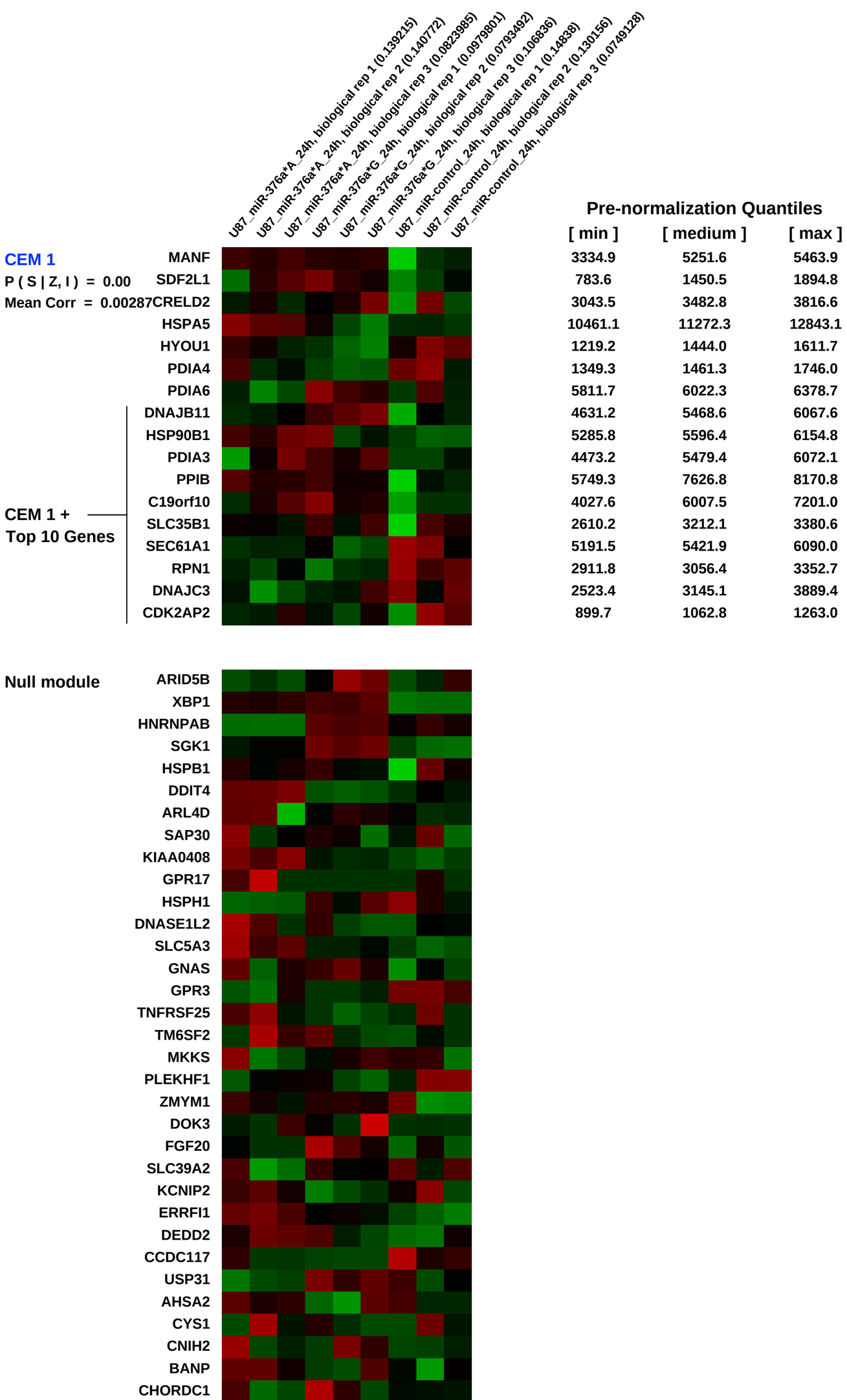

GEO Series "GSE59665" Expression Profiles

Num of samples in this series: 23

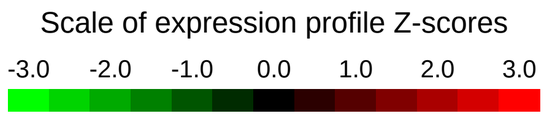

GEO Link:	http://www.ncbi.nlm.nih.gov/geo/query/acc.cgi?acc=GSE59665
Status:	Public on Jul 23 2014
Title:	Temporal Endogenous Gene Expression Profiles in Response to Polymer-Mediated Transfection and Profile Comparison to Lipid-Mediated Transfection
Organism:	Homo sapiens
Experiment type:	Expression profiling by array
Platform:	GPL570
Pubmed ID:	
Summary & Design:	**Summary:** The current understanding of the molecular factors underlying polyethylenimine(PEI)-mediated transfection is largely unknown. Cationic PEI was used to transfer GFP transgene to HEK293T cells. FACS separation of transfected (GFP positive), untransfected (GFP negative), and untreated cells enabled gene expression profiles to be obtained using Affymetrix´fi HG-U133A 2.0 microarrays for each cell population. Gene profiles were differentially compared for each population combination. **Overall design:** Control (untreated), transfected (GFP positive), and untransfected (GFP negative) RNA samples were purified from HEK293T cells after FACS isolation. Treated experiments were repeated on triplicate days to run 3 microarrays for each cell population. Controls were run on duplicate to give 2 microarrays for each population.

Background corr dist: KL-Divergence = 0.1038, L1-Distance = 0.0403, L2-Distance = 0.0033, Normal std = 0.4294

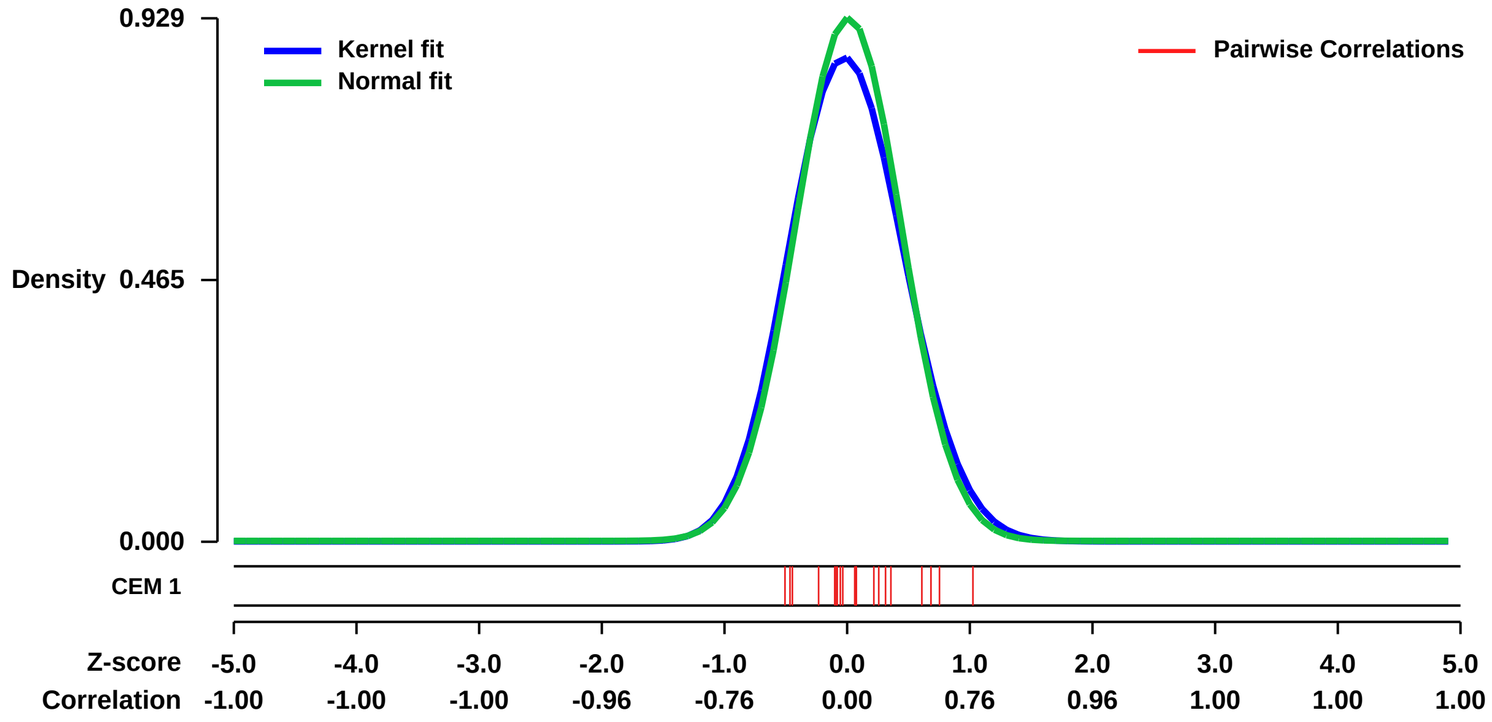

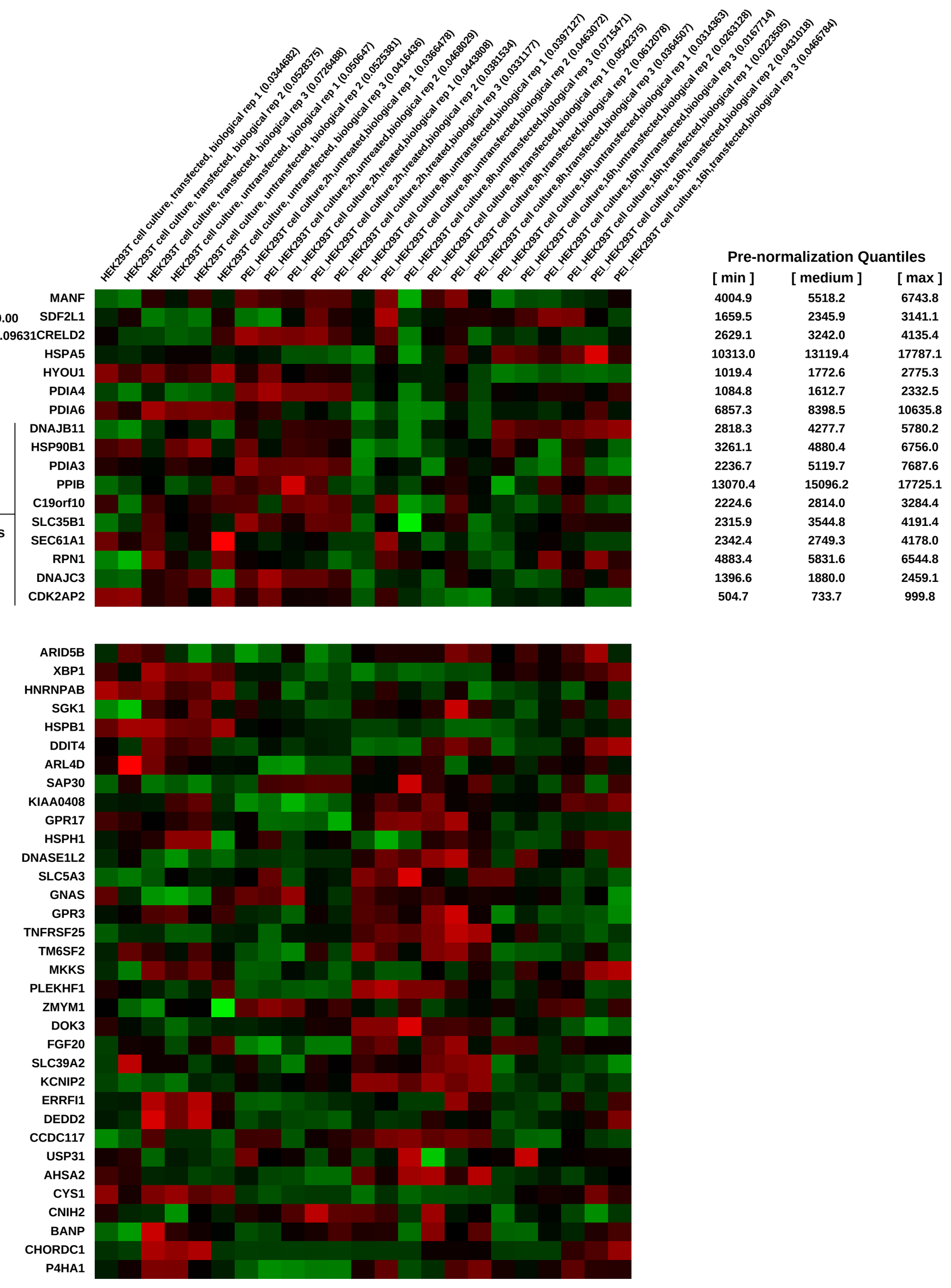

GEO Series "GSE25458" Expression Profiles

Num of samples in this series: 12

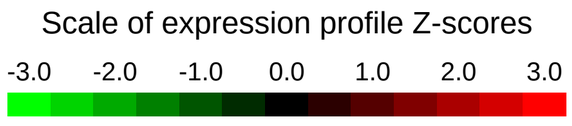

GEO Link:	http://www.ncbi.nlm.nih.gov/geo/query/acc.cgi?acc=GSE25458
Status:	Public on Nov 18 2010
Title:	Gene expression in endometrial cancer cells treated with metastin-10 (kp10)
Organism:	Homo sapiens
Experiment type:	Expression profiling by array
Platform:	GPL570
Pubmed ID:	21282360
Summary & Design:	**Summary:** Invasion into deep myometrium and/or lymphovascular space is a well-known risk factor for endometrial cancer metastasis, resulting in poor prognosis. It is therefore clinically important to identify novel molecules that suppress tumor invasion. Reduced expression of the metastasis suppressor, KISS1 (kisspeptin), and its endogenous receptor, GPR54, has been reported in several cancers, but the significance of the KISS1/GPR54 axis in endometrial cancer metastasis has not been clarified. Metastin-10 is the minimal bioactive sequence of genetic products of KISS1. Clinicopathological analysis of 92 endometrial cancers revealed overall survival is improved in cancers with high expression of GPR54. Through RNAi and mousemodel analyses, metastin-10 was predicted to suppress invasion and metastasis of GPR54-expressing endometrial cancers. These data suggest that metastin-10 may induce genetic changes in the metastatic character of endometrial cancers. **Overall design:** Gene expression microarray data (Affymetrix U133 Plus 2.0) for Ishikawa cells treated with or without 10¸…M metastin-10 and/or GPR54 siRNA were generated in triplicate and RMA-normalized.

Background corr dist: KL-Divergence = 0.1034, L1-Distance = 0.0304, L2-Distance = 0.0016, Normal std = 0.4296

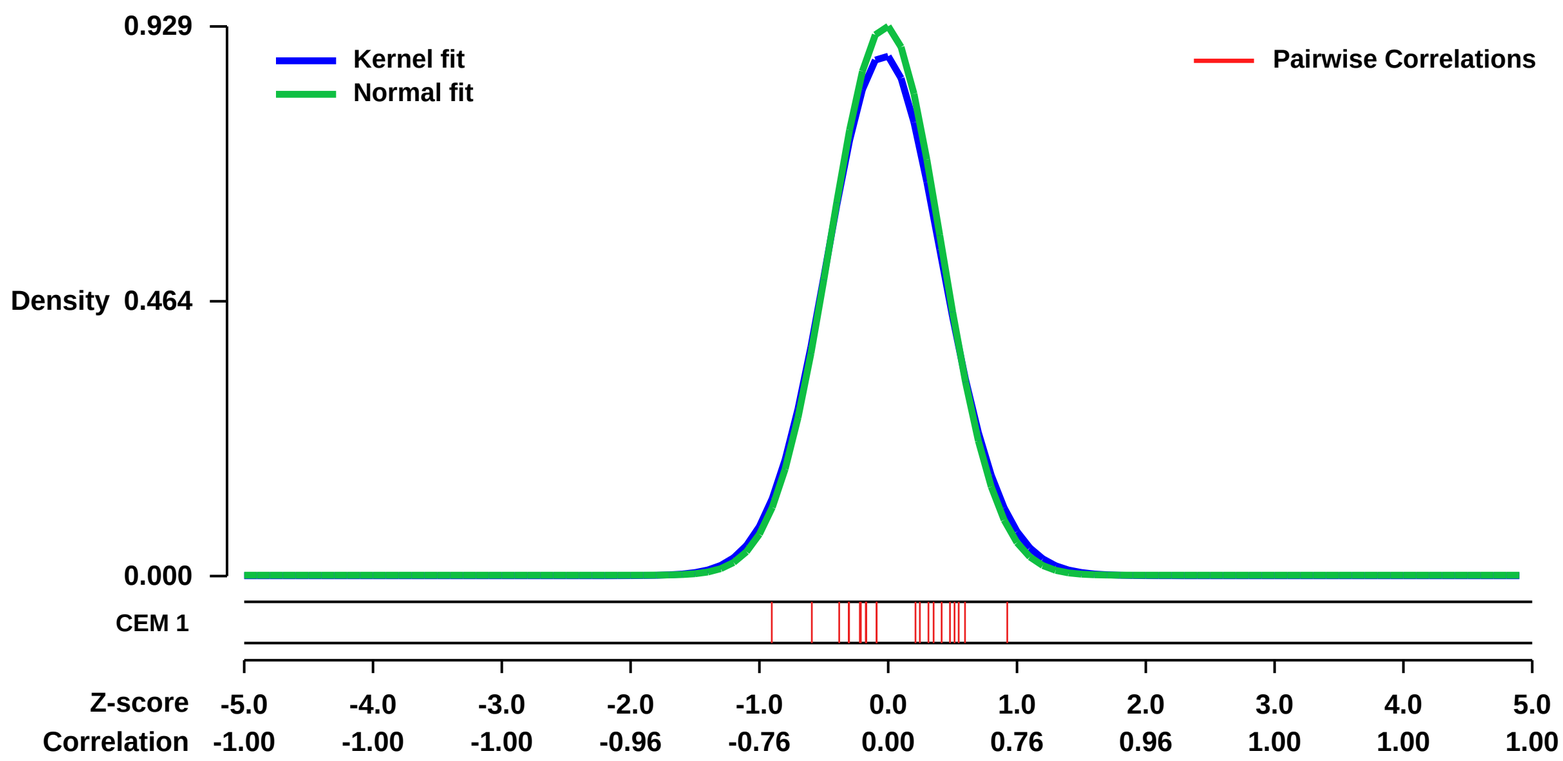

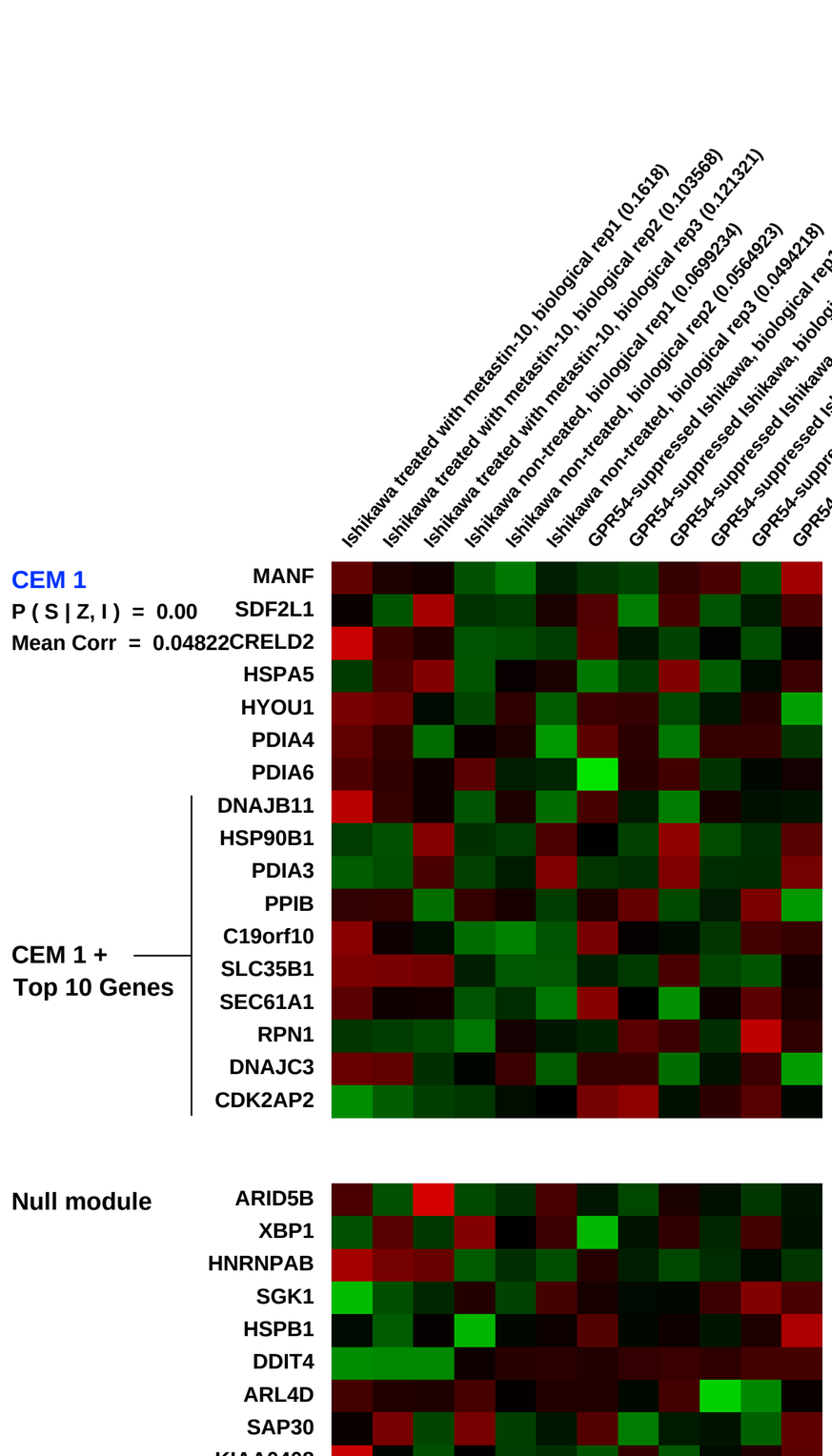

Pre-normalization Quantiles

	[min]	[medium]	[max]
MANF	3871.8	4187.4	4519.7
SDF2L1	1501.0	1752.7	2039.6
CRELD2	3869.5	4087.5	4641.3
HSPA5	18344.6	20048.2	21697.4
HYOU1	3273.5	4112.4	4455.1
PDIA4	1607.8	2012.8	2124.6
PDIA6	12316.5	13613.9	13987.6
DNAJB11	4960.3	5469.4	6073.9
HSP90B1	4965.3	5358.5	7354.6
PDIA3	8712.8	10158.4	15085.7
PPIB	19542.9	21503.2	22487.4
C19orf10	2253.6	2454.5	2650.2
SLC35B1	3940.6	4069.3	4407.9
SEC61A1	2706.0	2945.4	3123.3
RPN1	6170.6	6445.3	7063.2
DNAJC3	1481.8	2067.3	2208.4
CDK2AP2	1332.9	1496.4	1674.8

GEO Series "GSE15162" Expression Profiles

Num of samples in this series: 8

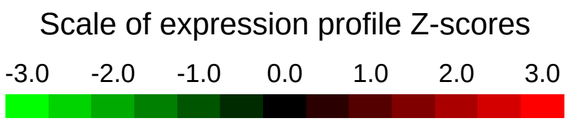

GEO Link:	http://www.ncbi.nlm.nih.gov/geo/query/acc.cgi?acc=GSE15162
Status:	Public on Mar 11 2009
Title:	Quercetin effect on gene expression in HepG2 hepatocellular cancer cells
Organism:	Homo sapiens
Experiment type:	Expression profiling by array
Platform:	GPL570
Pubmed ID:	21782406
Summary & Design:	**Summary:** Quercetin is a flavonol modifying numerous cell processes with potent antiproliferative effects on cancer cell-lines. The aim of this study was to explore by gene-array analysis the effect of quercetin on cancer-related gene expression in HepG2 cells, followed by verification with RT-PCR and analysis of the expected phenotypic changes (migration, cell cycle, cell proliferation). Quercetin induces significant changes on cell-adhesion related genes, leading to reduced migratory capacity and disorganization of the actin cytoskeleton. Several genes related to DNA functions, cellular metabolism and signal-transducer activities were also modified, while an early effect on Gâ protein related cascades possibly via protease-activated receptor 2 and phospholipase C-¿‡1 was identified. Cyclin-D associated events in G1 and ubiquitin-dependent degradation of cyclin-D1 were also affected, resulting in cell-cycle arrest without activation of apoptosis pathways. In conclusion quercetin (3¿…M) exerts its cellular effects by modifying numerous genes related to mechanisms involved in cancer initiation and promotion. **Overall design:** HepG2 cells were serum starved for 24 hours and were then treated with serum free medium with or without quercetin (3¿…M). Total RNA was collected at 2, 4, 12 and 24 hours and was used for gene-array experiments.

Background corr dist: KL-Divergence = 0.0302, L1-Distance = 0.0401, L2-Distance = 0.0028, Normal std = 0.6627

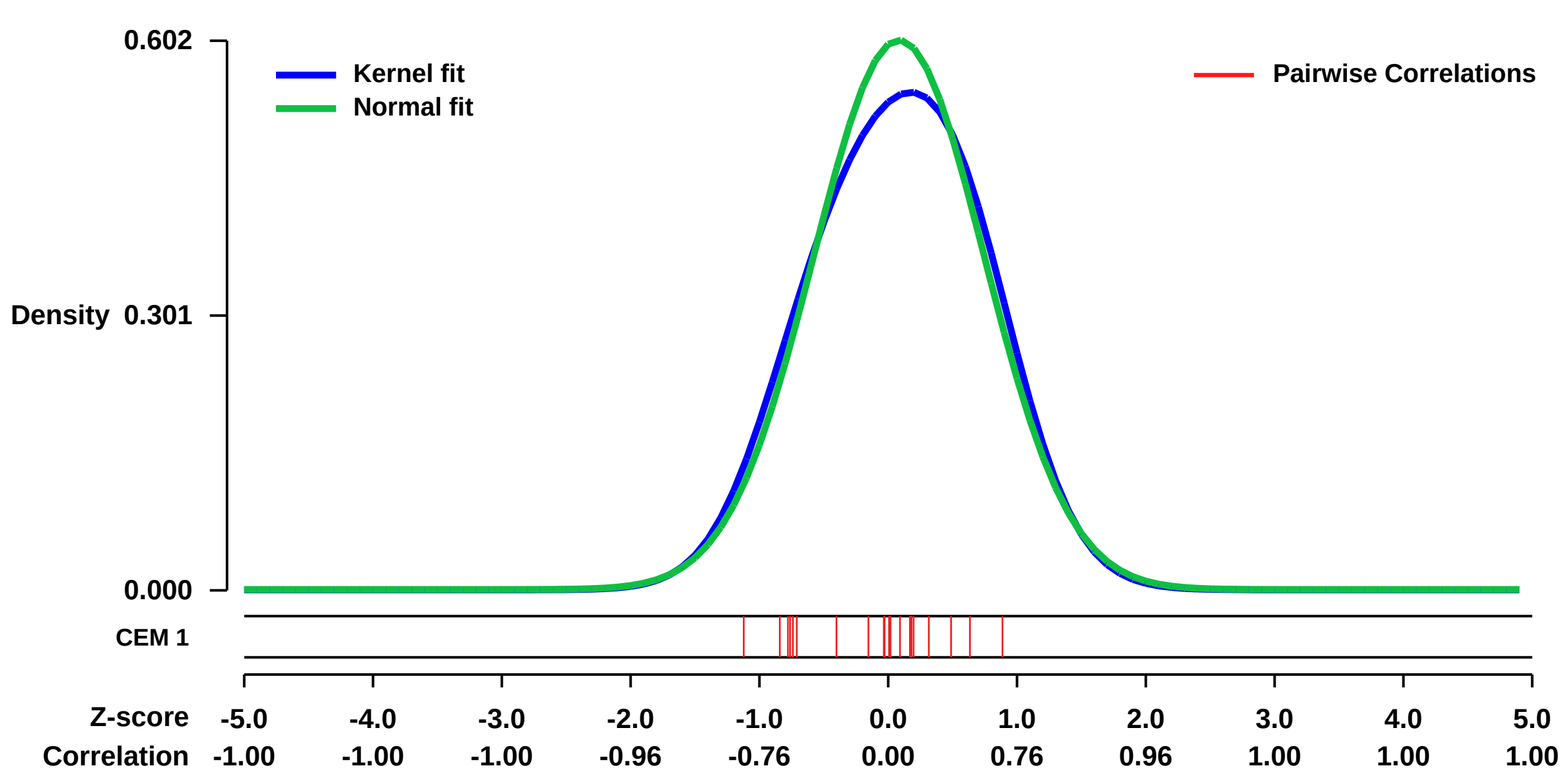

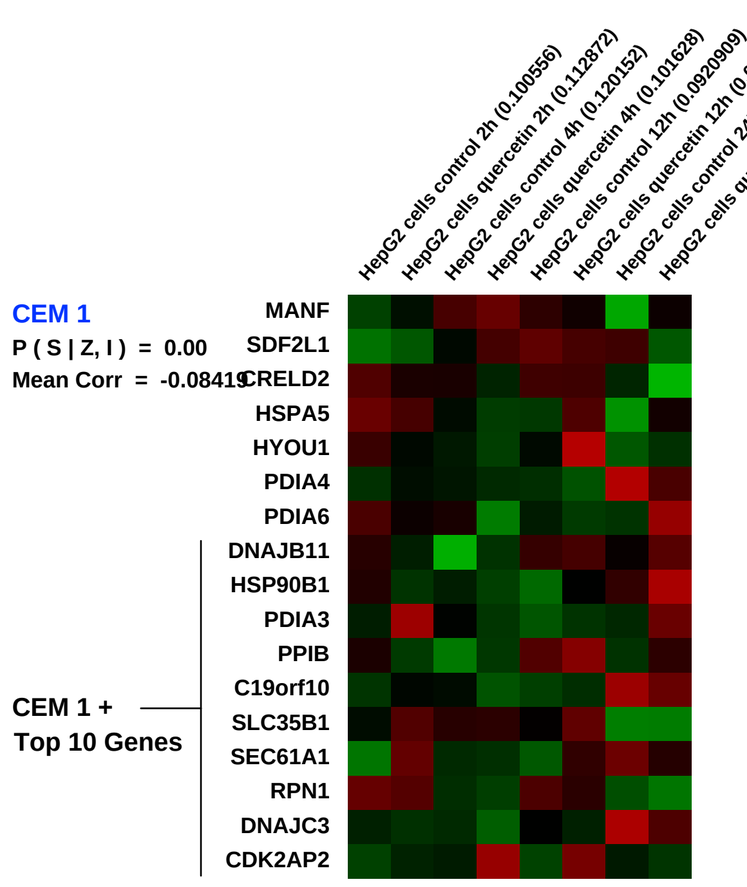

Pre-normalization Quantiles

	[min]	[medium]	[max]
MANF	2877.0	3525.4	3835.8
SDF2L1	1262.4	1479.5	1520.2
CRELD2	1233.2	1697.1	1818.1
HSPA5	14800.5	17187.2	18456.3
HYOU1	3985.8	4515.5	5805.8
PDIA4	1454.5	1675.8	2399.7
PDIA6	7656.7	8816.3	10000.2
DNAJB11	2346.8	3530.7	3786.0
HSP90B1	2434.1	2984.3	3887.5
PDIA3	8586.5	9018.2	10476.4
PPIB	12742.6	15876.7	18133.7
C19orf10	2851.9	3260.5	4197.0
SLC35B1	1960.7	2600.0	2822.6
SEC61A1	3370.0	3804.1	4005.5
RPN1	4164.3	5331.4	5759.9
DNAJC3	1713.6	1956.6	2762.3
CDK2AP2	1344.4	1400.3	1657.9

GEO Series "GSE19670" Expression Profiles

Num of samples in this series: 10

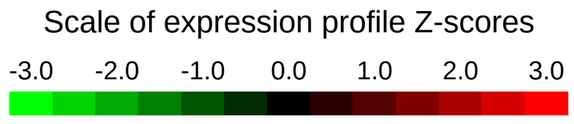

GEO Link:	http://www.ncbi.nlm.nih.gov/geo/query/acc.cgi?acc=GSE19670
Status:	Public on Dec 29 2009
Title:	Expression array analysis of the effects of vitamin D3 and mutp53
Organism:	Homo sapiens
Experiment type:	Expression profiling by array
Platform:	GPL570
Pubmed ID:	20227041
Summary & Design:	**Summary:** We wanted to examine the effect of vitamin D3 and endogenous mutant p53 expressed in SKBR3 cells on gene expression paterns. Expression microarray analysis was performed on SKBR3 cells without or with endogenous mutp53 knockdown, with or without 1a25-vitamin D3 treatment. **Overall design:** SKBR3 cells expressing p53R175H, transfected either with siRNA for p53 (p53i) or with control LacZ siRNA, 48h after transfection, three samples of each transfection were treated with 1a25(OH)2D3 (D3;100nM) for different time points; 8 houres, 20 hours and 50 hours. Cells were subjected to RNA extraction and hybridization on Affymetrix microarrays.

Background corr dist: KL-Divergence = 0.1230, L1-Distance = 0.0311, L2-Distance = 0.0018, Normal std = 0.4033

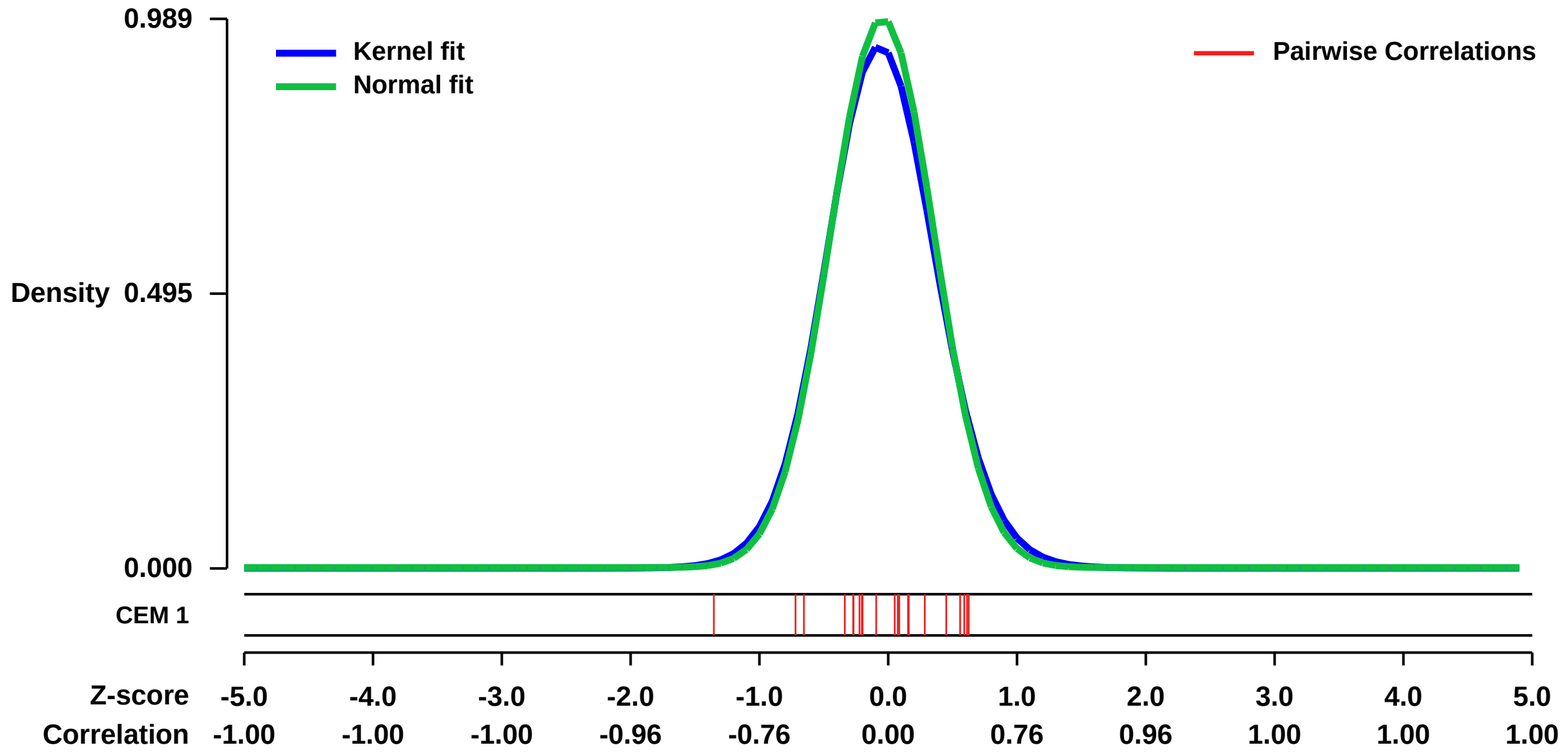

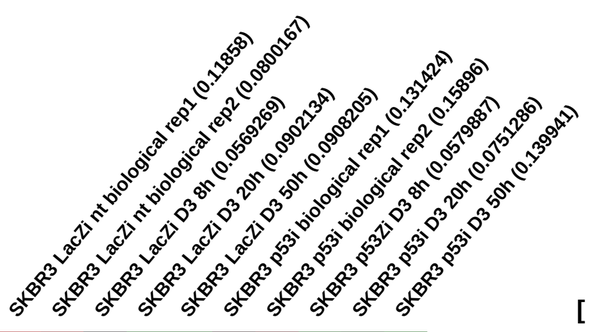

Pre-normalization Quantiles

[min] [medium] [max]

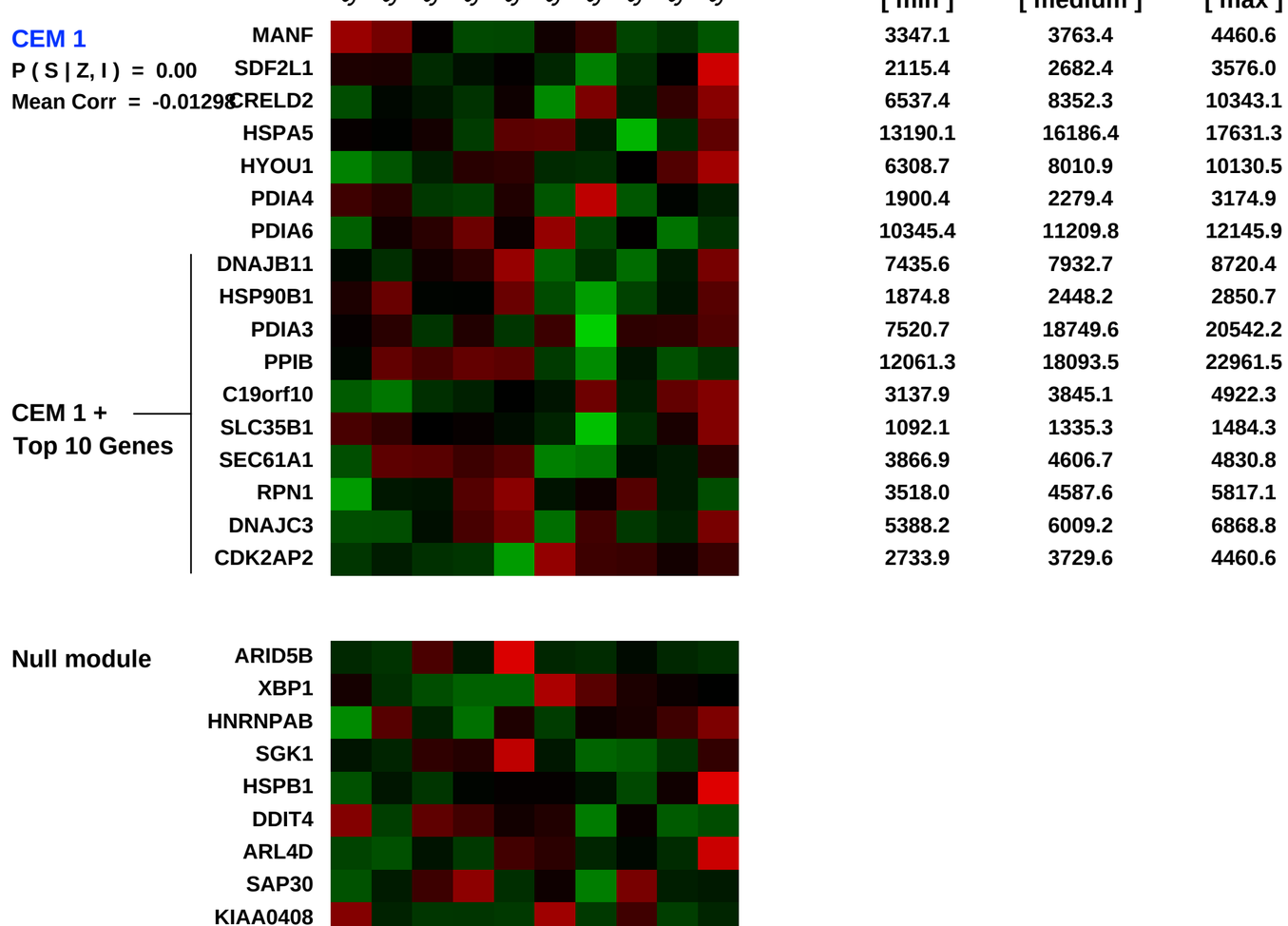

GEO Series "GSE9647" Expression Profiles

Num of samples in this series: 12

Scale of expression profile Z-scores

-3.0 -2.0 -1.0 0.0 1.0 2.0 3.0

GEO Link:	http://www.ncbi.nlm.nih.gov/geo/query/acc.cgi?acc=GSE9647
Status:	Public on Nov 21 2007
Title:	Comparative transcriptomic profiling of unstimulated and inflamed HUVEC exposed to apple procyanidin oligomers
Organism:	Homo sapiens
Experiment type:	Expression profiling by array
Platform:	GPL570
Pubmed ID:	18979505
Summary & Design:	**Summary:** We used microarrays to investigate changes in gene expression of human vascular endothelial cells (HUVEC) exposed to an apple extract enriched in procyanidins of low-medium molecular weight (dp3.9) to determine possible protective effects induced by these plant derived compounds on the endothelial cells. **Keywords: Comparative gene expression, Control vs Treated cells (response to exposure with xenobiotics plant polyphenols)** **Overall design:** We used unstimulated and TNF-¿–-inflamed confluent monolayers of HUVEC exposed to low doses of oligomeric procyanidins extracted from apple, to determine whether these apple polyphenols exerted any protective effects on human endothelial cells.

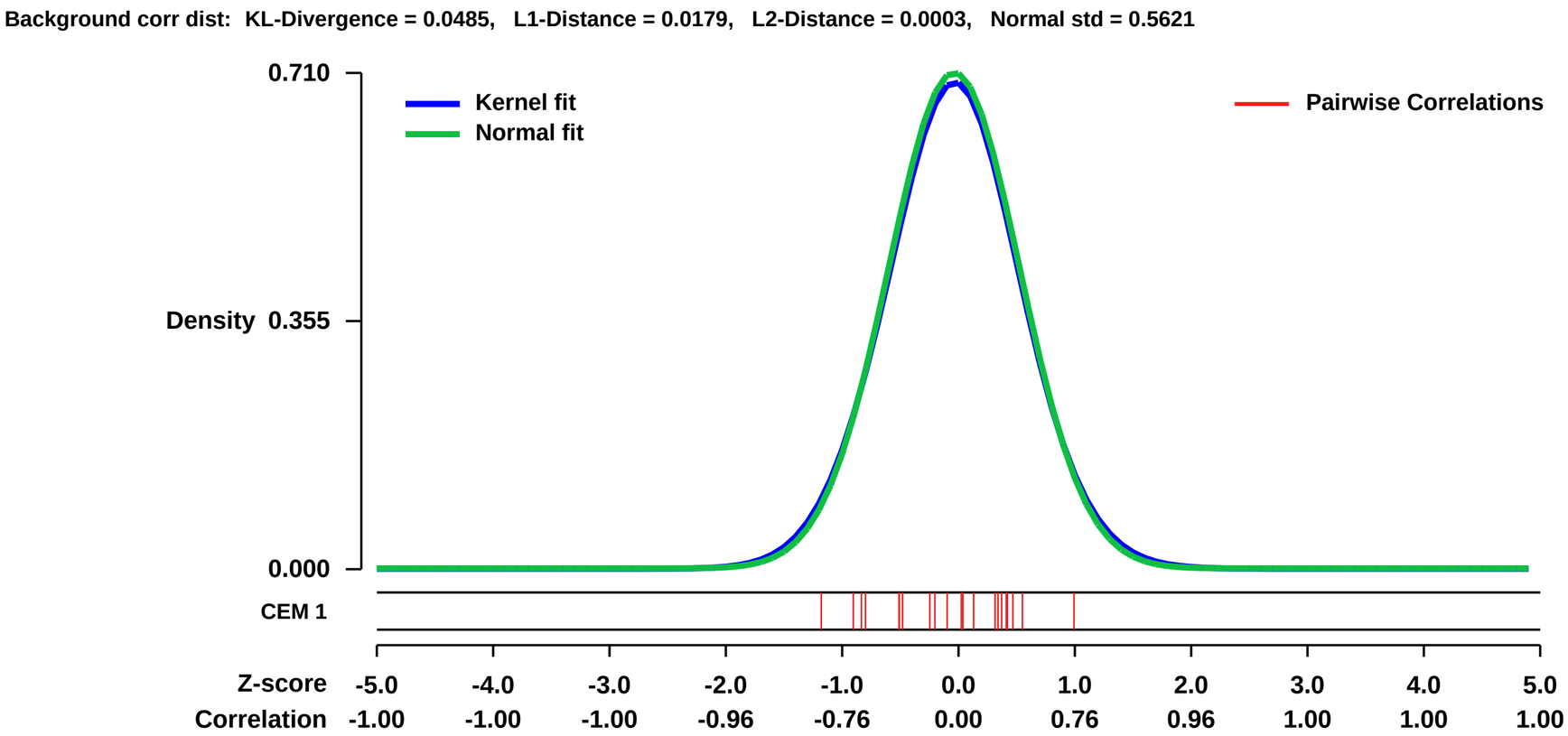

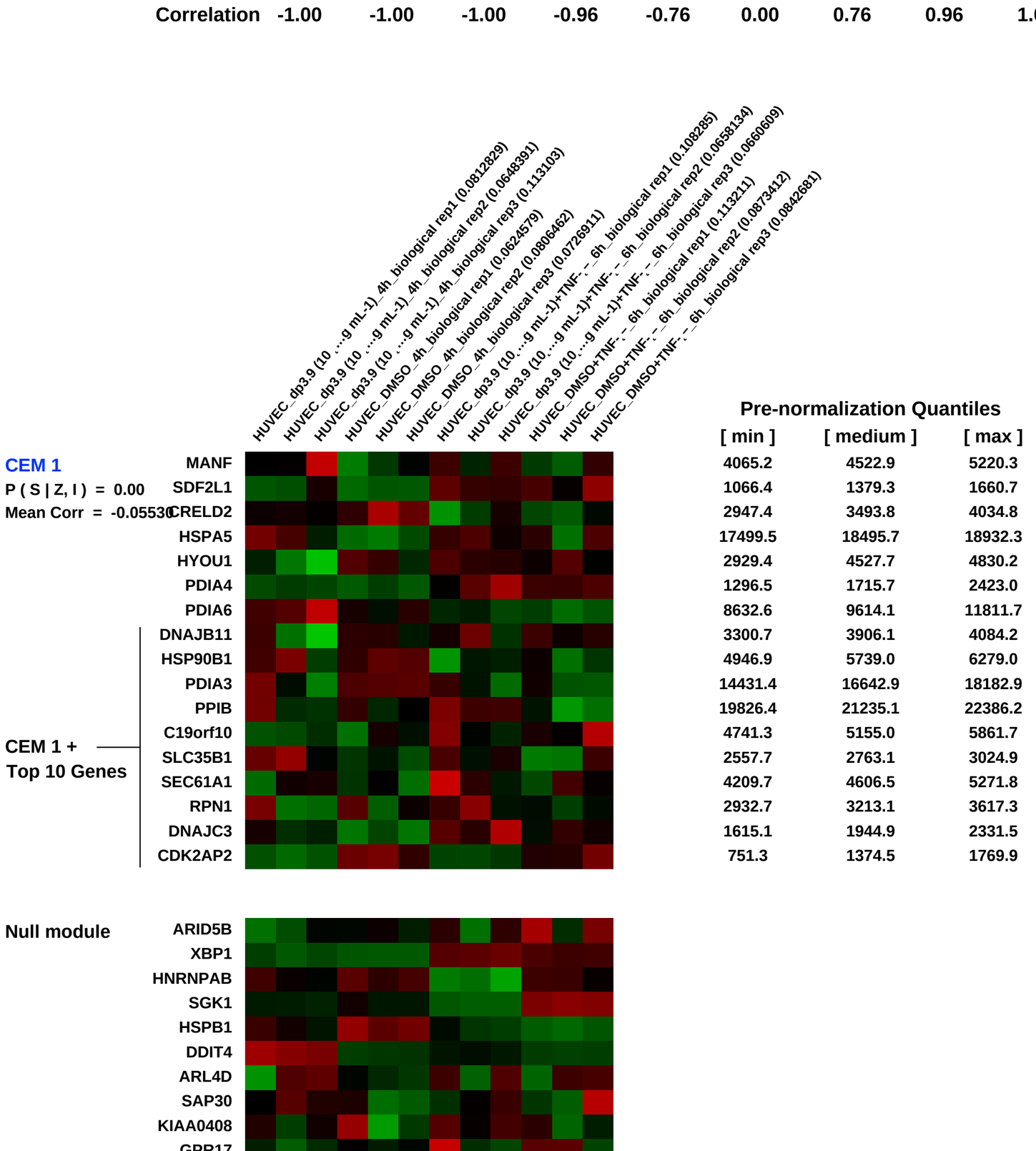

GEO Series "GSE12155" Expression Profiles

Num of samples in this series: 24

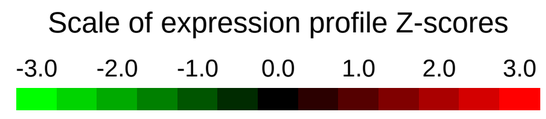

GEO Link:	http://www.ncbi.nlm.nih.gov/geo/query/acc.cgi?acc=GSE12155
Status:	Public on Dec 19 2008
Title:	Characterization of a Colony Assay Used to Investigate Endothelial Progenitor Cells
Organism:	Homo sapiens
Experiment type:	Expression profiling by array
Platform:	GPL570
Pubmed ID:	19092138
Summary & Design:	**Summary:** Subjects underwent endothelial testing and blood sampling at baseline and after 3 months of exercise training. Microarray and flow cytometry-based characterization of cells from an endothelial progeniator colony assay was consistent with T lymphocytes, but not endothelial cells. **Keywords: expression analysis** **Overall design:** blood samples from 12 healthy subjects at baseline (A) and after 3 months (B) of exercise.

Background corr dist: KL-Divergence = 0.2510, L1-Distance = 0.0572, L2-Distance = 0.0085, Normal std = 0.3019

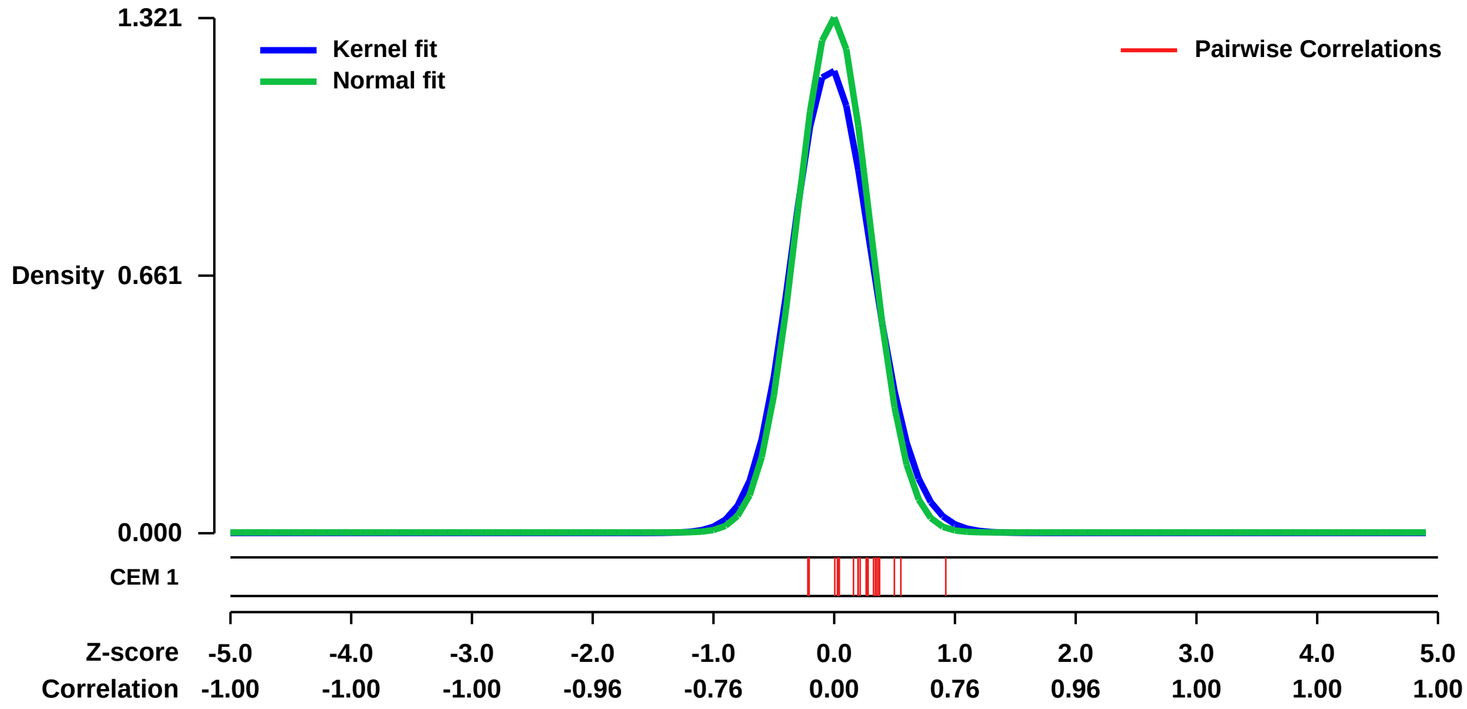

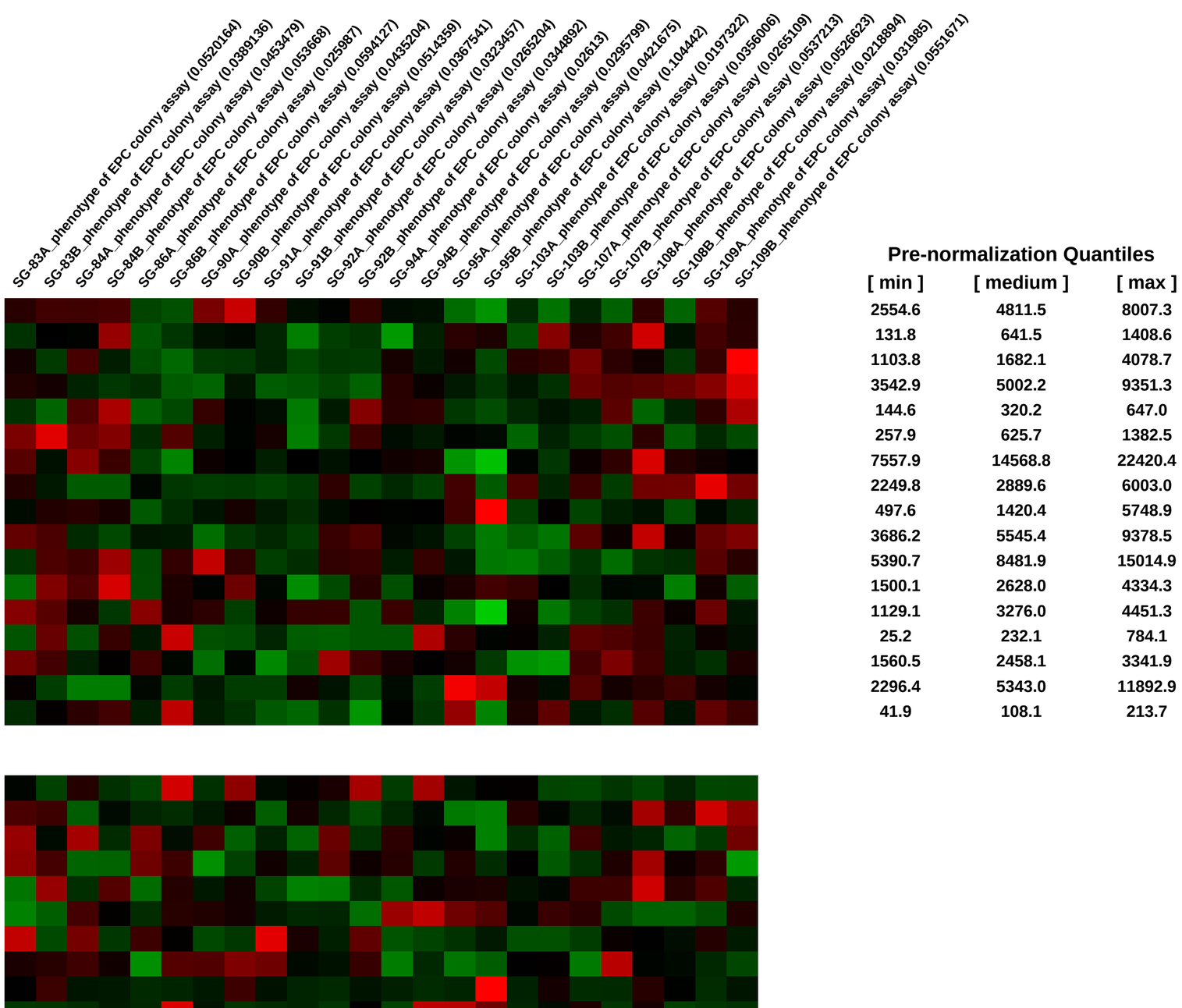

Pre-normalization Quantiles		
[min]	[medium]	[max]
2554.6	4811.5	8007.3
131.8	641.5	1408.6
1103.8	1682.1	4078.7
3542.9	5002.2	9351.3
144.6	320.2	647.0
257.9	625.7	1382.5
7557.9	14568.8	22420.4
2249.8	2889.6	6003.0
497.6	1420.4	5748.9
3686.2	5545.4	9378.5
5390.7	8481.9	15014.9
1500.1	2628.0	4334.3
1129.1	3276.0	4451.3
25.2	232.1	784.1
1560.5	2458.1	3341.9
2296.4	5343.0	11892.9
41.9	108.1	213.7

GEO Series "GSE27526" Expression Profiles

Num of samples in this series: 6

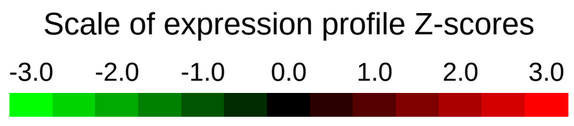

GEO Link:	http://www.ncbi.nlm.nih.gov/geo/query/acc.cgi?acc=GSE27526
Status:	Public on Jul 01 2011
Title:	ChIP-seq defined genome-wide map of TGFbeta/SMAD4 targets: implications with clinical outcome of ovarian cancer patients
Organism:	Homo sapiens
Experiment type:	Expression profiling by array
Platform:	GPL570
Pubmed ID:	21799915
Summary & Design:	**Summary:** Deregulation of the transforming growth factor-¸† (TGF¸†) signaling pathway in epithelial ovarian cancer has been reported, but the precise mechanism underlying disrupted TGF¸† signaling in the disease remains unclear. We performed chromatin immunoprecipitation followed by sequencing (ChIP-seq) to investigate genome-wide screening of TGF¸†-induced SMAD4 binding in epithelial ovarian cancer. Following TGF¸† stimulation of the A2780 epithelial ovarian cancer cell line, we identified 2,362 SMAD4 binding loci and 318 differentially expressed SMAD4 target genes. Comprehensive examination of SMAD4-bound loci, revealed four distinct binding patterns: 1) Basal; 2) Shift; 3) Stimulated Only; 4) Unstimulated Only. SMAD4-bound loci were primarily classified as either Stimulated only (74%) or Shift (25%), indicating that TGF¸†-stimulation alters SMAD4 binding patterns in epithelial ovarian cancer cells compared to normal epithelial cells. Furthermore, based on gene regulatory network analysis, we determined that the TGF¸†-induced SMAD4-dependent regulatory network was strikingly different in ovarian cancer compared to normal cells. Importantly, the TGF¸†/SMAD4 target genes identified in the A2780 epithelial ovarian cancer cell line were predictive of patient survival, based on in silico mining of publically available patient data bases. In conclusion, our data highlight the utility of next generation sequencing technology to identify genome-wide SMAD4 target genes in epithelial ovarian cancer. The results link aberrant TGF¸†/SMAD signaling to ovarian tumorigenesis. Furthermore, the identified SMAD4 binding loci, combined with gene expression profiling and in silico data mining of patient cohorts, may provide a powerful approach to determine potential gene signatures with biological and future translational research in ovarian and other cancers. **Overall design:** Gene expression: 3 technical replicates each of SMAD4 stimulated and SMAD4 unstimulated cells

Background corr dist: KL-Divergence = 0.0410, L1-Distance = 0.0225, L2-Distance = 0.0006, Normal std = 0.6146

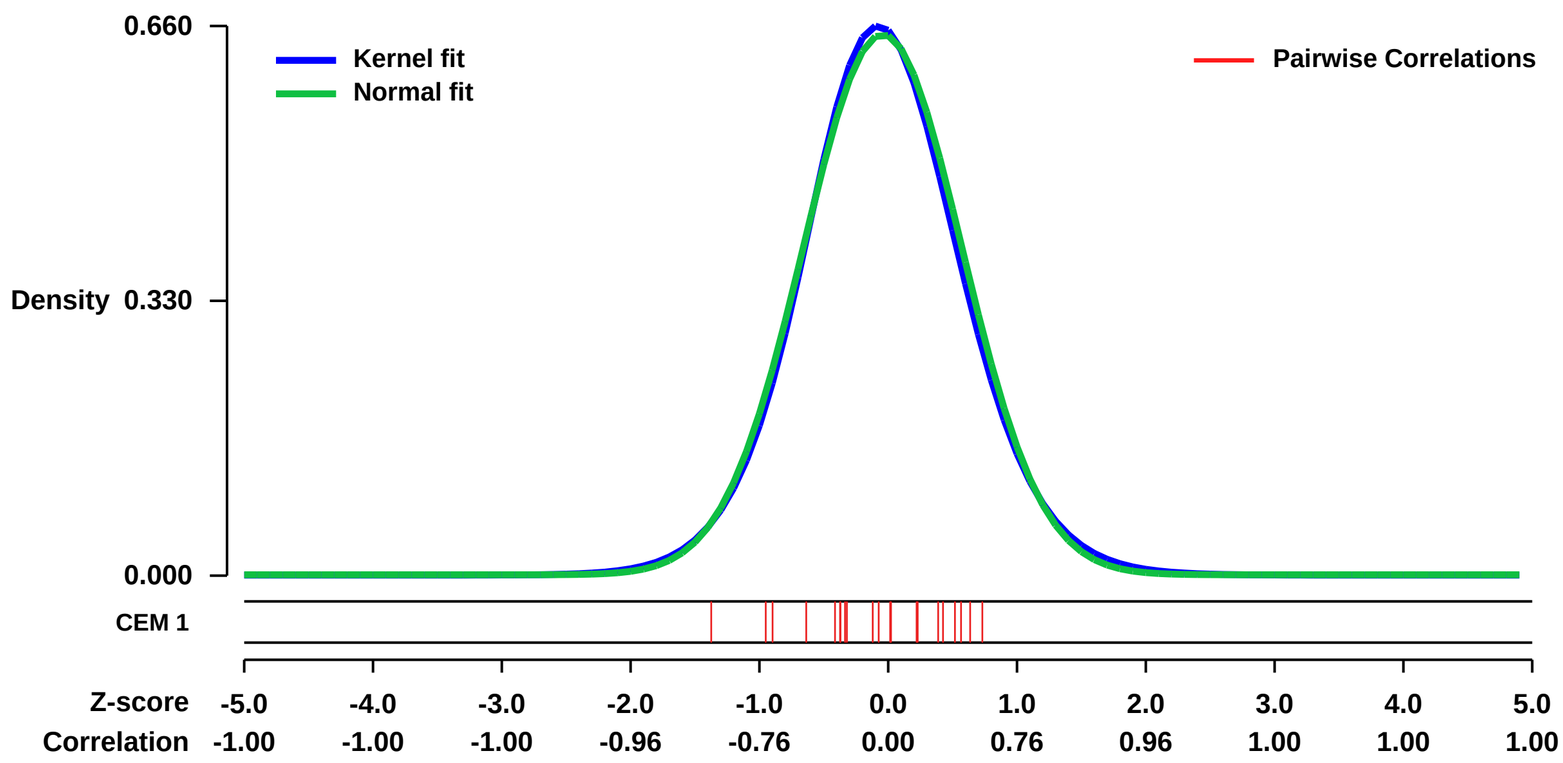

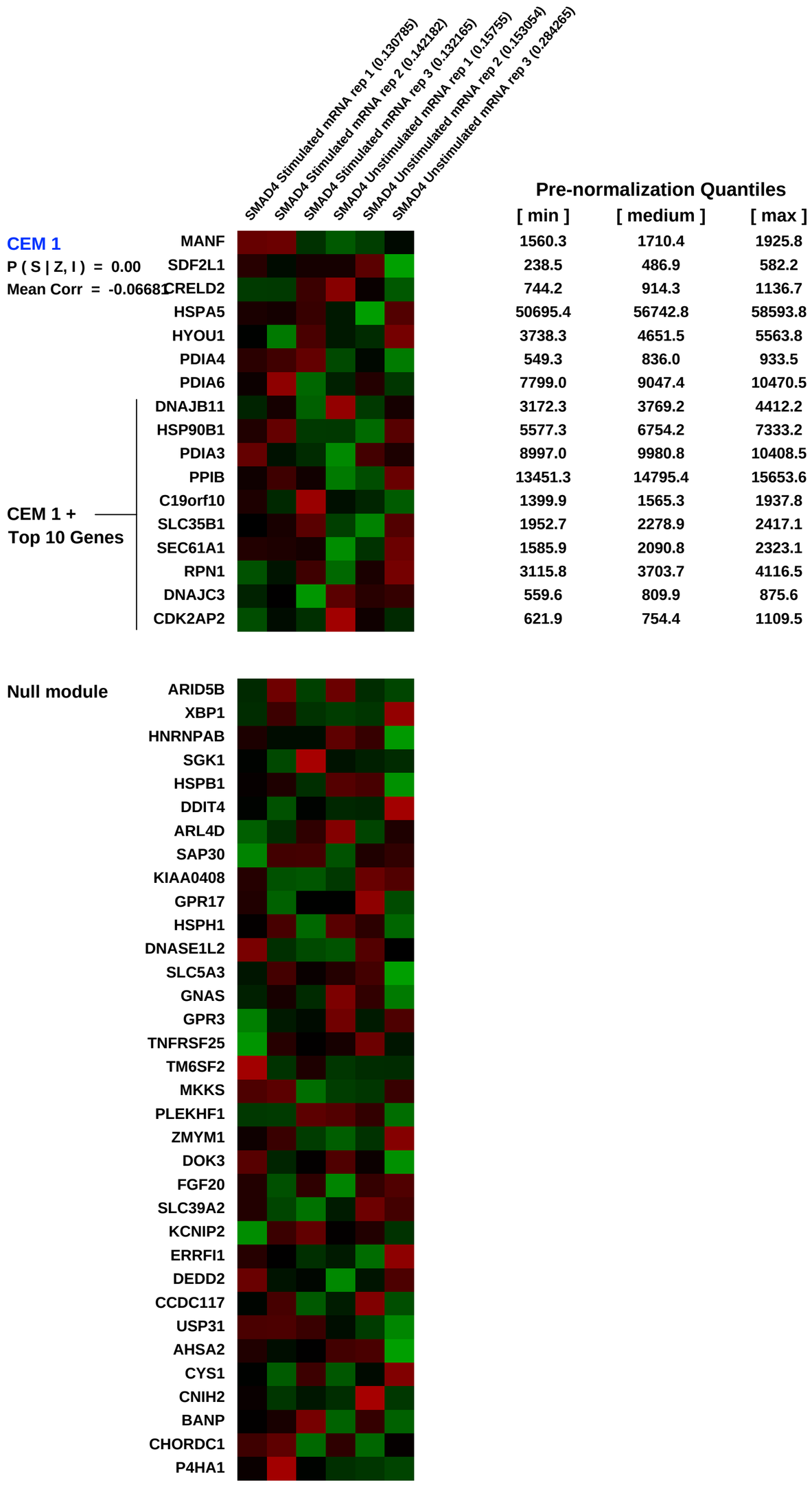

GEO Series "GSE40960" Expression Profiles

Num of samples in this series: 6

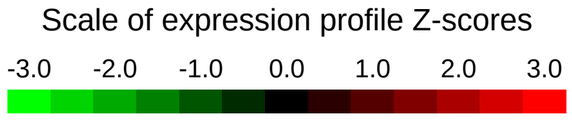

GEO Link:	http://www.ncbi.nlm.nih.gov/geo/query/acc.cgi?acc=GSE40960
Status:	Public on Sep 19 2012
Title:	Expression data from BMP9-treated human dermal microvascular endothelial cells (HMVEC-D)
Organism:	Homo sapiens
Experiment type:	Expression profiling by array
Platform:	GPL570
Pubmed ID:	23018639
Summary & Design:	**Summary:** BMP9 signaling has been implicated in hereditary hemorrhagic telangiectasia and vascular remodeling, acting via the HHT target genes, endoglin and ALK1. This study sought to identify endothelial BMP9-regulated proteins that could affect the HHT phenotype. Gene ontology analysis of cDNA microarray data obtained following BMP9 treatment of primary human endothelial cells indicated regulation of chemokine, adhesion, and inflammation pathways. **Overall design:** The sample set is comprised of three biological replicate control human dermal microvascular endothelial cells, and three treated (5 ng/ml human recombinant BMP9) biological replicate human dermal microvascular endothelial cells

Background corr dist: KL-Divergence = 0.0501, L1-Distance = 0.0260, L2-Distance = 0.0008, Normal std = 0.5775

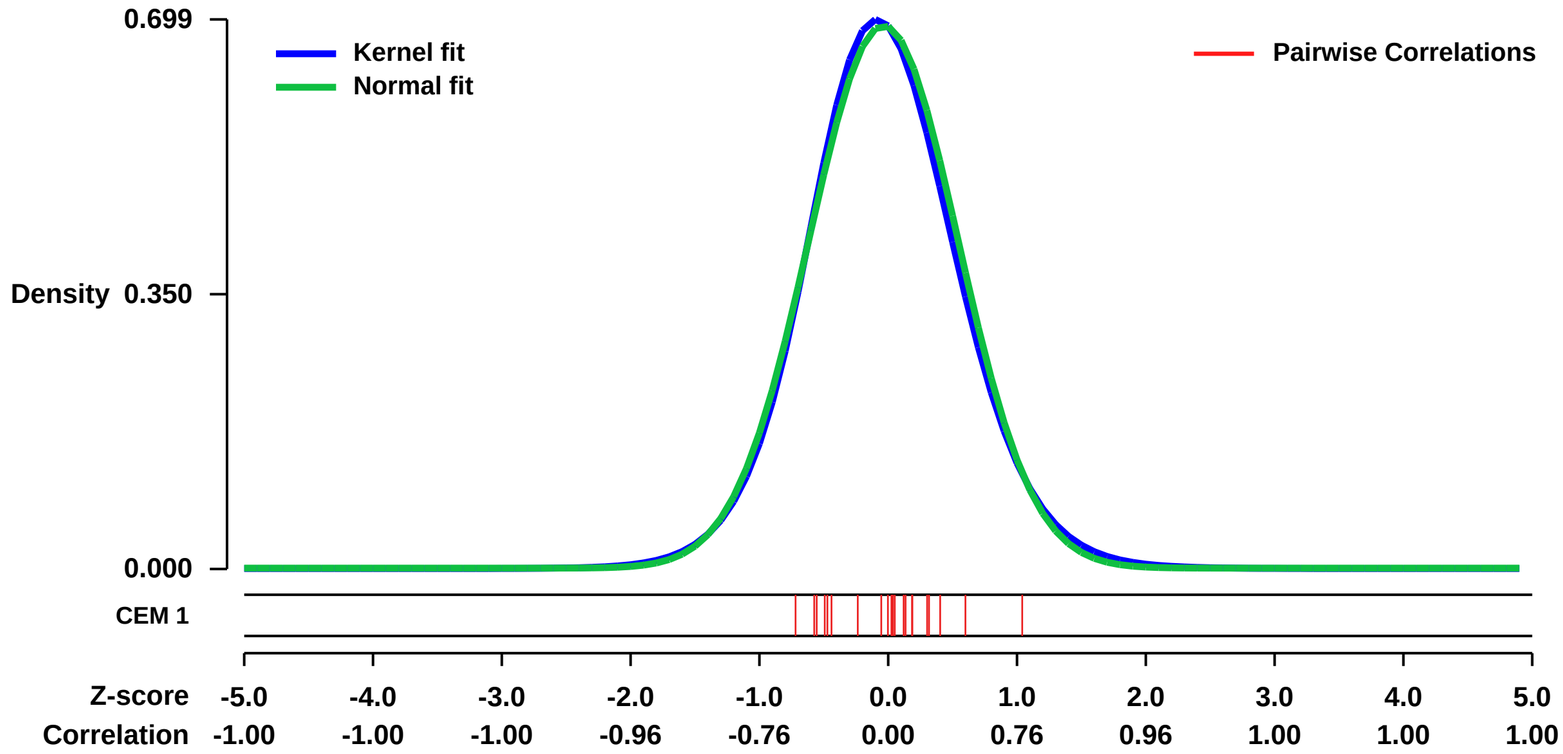

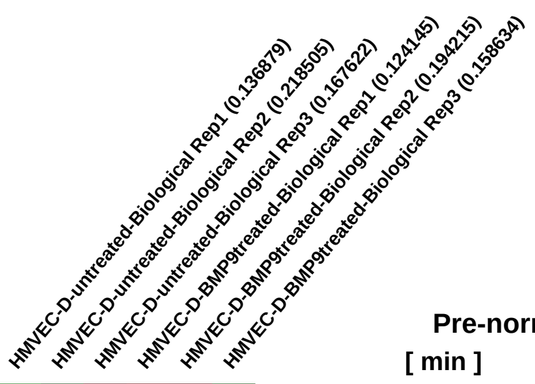

Pre-normalization Quantiles

[min] [medium] [max]

CEM 1
P (S | Z, I) = 0.00
Mean Corr = -0.00978

CEM 1 + Top 10 Genes

Null module

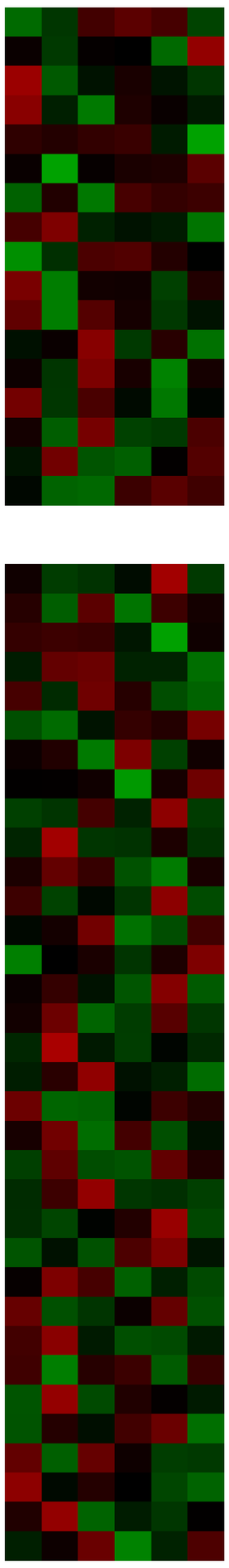

MANF	10419.8	12112.8	12357.9
SDF2L1	308.7	399.0	515.5
CRELD2	1266.4	1409.4	1758.1
HSPA5	8696.2	10993.8	13270.6
HYOU1	223.6	1333.1	1385.6
PDIA4	1359.1	1873.9	2047.9
PDIA6	26235.1	30081.6	30514.5
DNAJB11	1334.6	1464.6	1655.9
HSP90B1	2620.9	3184.0	3326.4
PDIA3	4264.0	5650.7	6646.7
PPIB	6016.3	8545.7	9829.5
C19orf10	2626.8	3221.4	3829.2
SLC35B1	561.3	857.8	1059.1
SEC61A1	1098.5	2016.1	2979.3
RPN1	1432.0	1675.6	1886.3
DNAJC3	5280.2	5947.8	6689.5
CDK2AP2	9.2	263.1	311.0
ARID5B			
XBP1			
HNRNPAB			
SGK1			
HSPB1			
DDIT4			
ARL4D			
SAP30			
KIAA0408			
GPR17			
HSPH1			
DNASE1L2			
SLC5A3			
GNAS			
GPR3			
TNFRSF25			
TM6SF2			
MKKS			
PLEKHF1			
ZMYM1			
DOK3			
FGF20			
SLC39A2			
KCNIP2			
ERRFI1			
DEDD2			
CCDC117			
USP31			
AHSA2			
CYS1			
CNIH2			
BANP			
CHORDC1			
P4HA1			

GEO Series "GSE36609" Expression Profiles

Num of samples in this series: 9

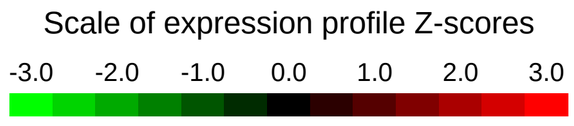

GEO Link:	http://www.ncbi.nlm.nih.gov/geo/query/acc.cgi?acc=GSE36609
Status:	Public on Mar 20 2012
Title:	Gene expression profile of human embryonic stem cells growth in low concentrations of nitric oxide
Organism:	Homo sapiens
Experiment type:	Expression profiling by array
Platform:	GPL570
Pubmed ID:	
Summary & Design:	**Summary:** Identification of genes regulated in human embryonic stem cells by the effect of low concentrations of nitric oxide. The transcriptome of cells treated with NO were compared with that of cells cultured in abscense of LIF, and undifferentiated ES cells cultured in presence of LIF. The H181 hES cell line was used for the experiments. These data complement a previous study realized in mES cells under the same NO conditions . The aim of the work is to know how NO modify transcriptome of ES cells and how participate in the modulation of self renewal and differentiation. **Overall design:** Passages between 72 and 74 of the H181 cell line were cultured on Matrigel-coated tissue culture plates in presence of 8ng/ml of bFGF for maintain them undifferentiated (control). For treatments, cells were cultured in the absence of bFGF to induce differentiation and treat cells with 2uM of DETA/NO. Cells were grown for 6 days mantaining the conditions of the treatment each 19 hours. Dietilentriamine-NO (DETA-NO) (Sigma) was used as donor of nitric oxide. Expression data of cells treated with NO in absence of bFGF were compared with cells cultured in absence of this, in order to observe how the treatment affects the transcriptome, and if there is some similarity with undifferentiated condition in presence of bFGF.

Background corr dist: KL-Divergence = 0.0928, L1-Distance = 0.0239, L2-Distance = 0.0009, Normal std = 0.4496

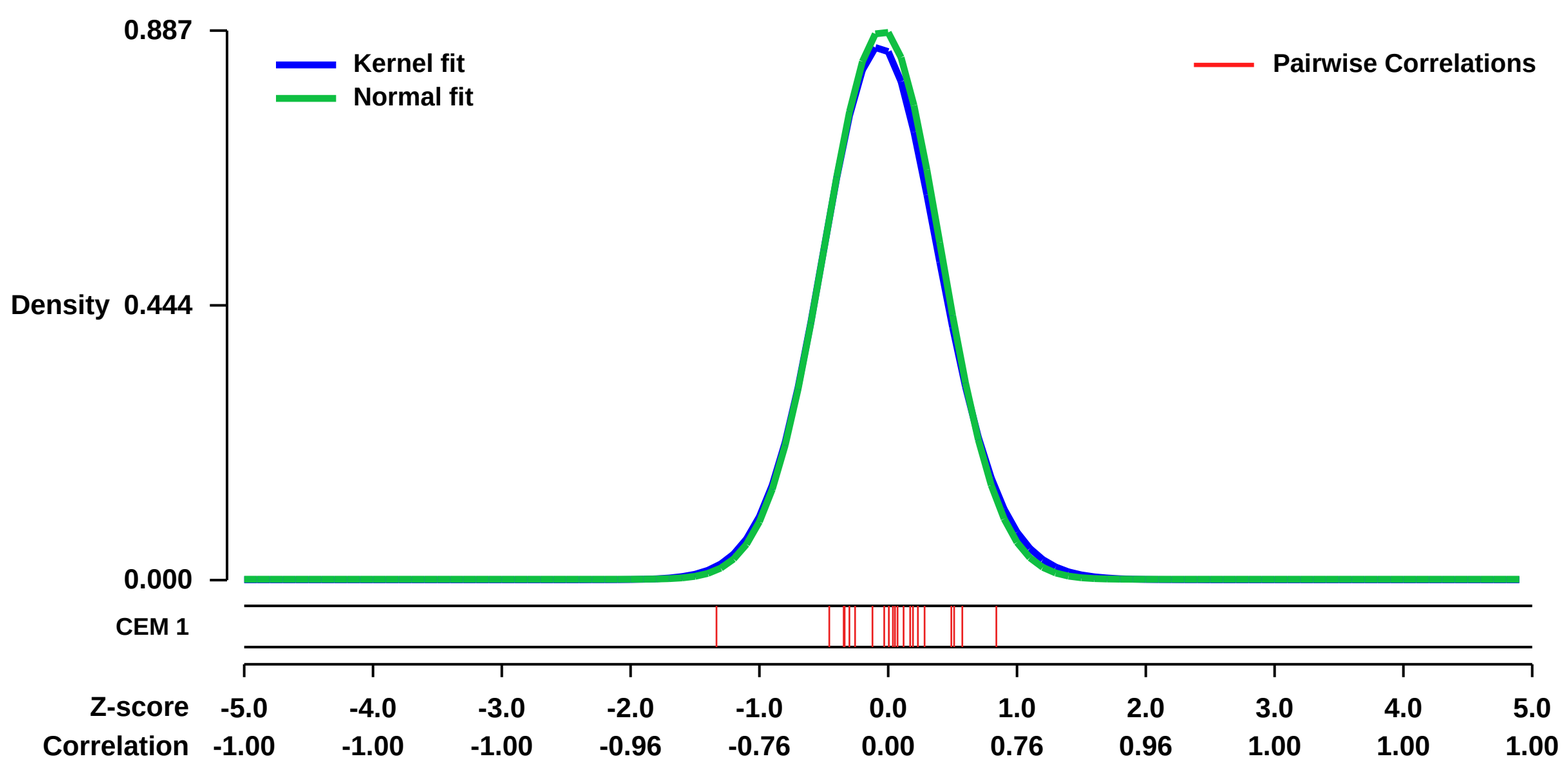

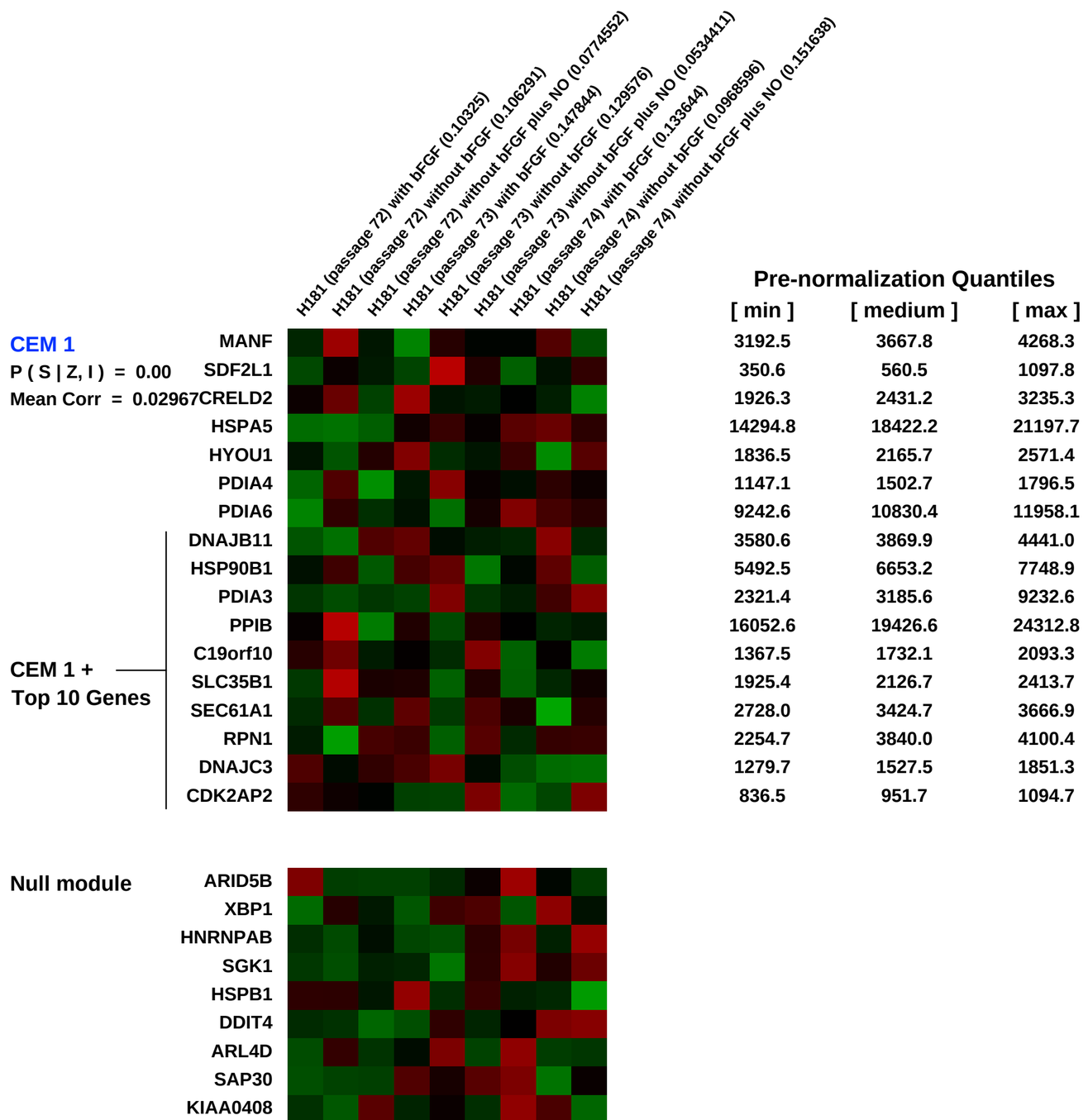

Pre-normalization Quantiles

	[min]	[medium]	[max]
MANF	3192.5	3667.8	4268.3
SDF2L1	350.6	560.5	1097.8
CRELD2	1926.3	2431.2	3235.3
HSPA5	14294.8	18422.2	21197.7
HYOU1	1836.5	2165.7	2571.4
PDIA4	1147.1	1502.7	1796.5
PDIA6	9242.6	10830.4	11958.1
DNAJB11	3580.6	3869.9	4441.0
HSP90B1	5492.5	6653.2	7748.9
PDIA3	2321.4	3185.6	9232.6
PPIB	16052.6	19426.6	24312.8
C19orf10	1367.5	1732.1	2093.3
SLC35B1	1925.4	2126.7	2413.7
SEC61A1	2728.0	3424.7	3666.9
RPN1	2254.7	3840.0	4100.4
DNAJC3	1279.7	1527.5	1851.3
CDK2AP2	836.5	951.7	1094.7

GEO Series "GSE10979" Expression Profiles

Num of samples in this series: 18

Scale of expression profile Z-scores

-3.0 -2.0 -1.0 0.0 1.0 2.0 3.0

GEO Link:	http://www.ncbi.nlm.nih.gov/geo/query/acc.cgi?acc=GSE10979
Status:	Public on Jan 01 2009
Title:	A study of temporal transcriptional changes induced by a low concentration BPDE in cultured human cells
Organism:	Homo sapiens
Experiment type:	Expression profiling by array
Platform:	GPL570
Pubmed ID:	20018196
Summary & Design:	**Summary:** The environmental carcinogen, (´–)-anti-benzo[a]pyrene-7,8-diol-9,10-epoxide (BPDE), causes bulky-adduct DNA damages, triggers certain signaling pathways, and elicits gene expression changes. Here, we focused on the temporal gene expression changes induced by a low concentration (0.05 ´µM) BPDE in human amnion epithelial FL cells. Differential gene expression profiles at 1, 10 and 22 h post BPDE treatment were obtained using Affymetrix HG-U133 Plus 2.0 oligonucleotide microarrays. A cohort of gene expression changes related to cell cycle progression, cell growth or apoptosis, stress response, and post-transcriptional regulation was validated with quantitative real-time RT-PCR. The alteration of several cell cycle-related genes was correlated and possibly contributed to the cell cycle arrest phenotype. Paradoxical transcriptional regulations regarding cell growth or apoptosis emerged in response to BPDE treatment, which indicated that cell fate was determined by integrated signals. The temporal transcriptional changes would be of help to clarify the molecular mechanism of cellular response to BPDE. **Keywords:** time course **Overall design:** Human amnion epithelial FL cells were exposed to vehicle control (dimethyl sulfoxide) and a low concentration (0.05 ´µM) (´–)-anti-benzo[a]pyrene-7,8-diol-9,10-epoxide, respectively. The differential gene expression profiles at 1, 10 and 22 h post BPDE treatment were obtained using Affymetrix HG-U133 Plus 2.0 oligonucleotide microarrays. The transcriptomic changes at different time points post BPDE treatment would provide insight into the dynamic processes of cellular response to this genotoxic agent.

Background corr dist: KL-Divergence = 0.2294, L1-Distance = 0.0516, L2-Distance = 0.0067, Normal std = 0.3136

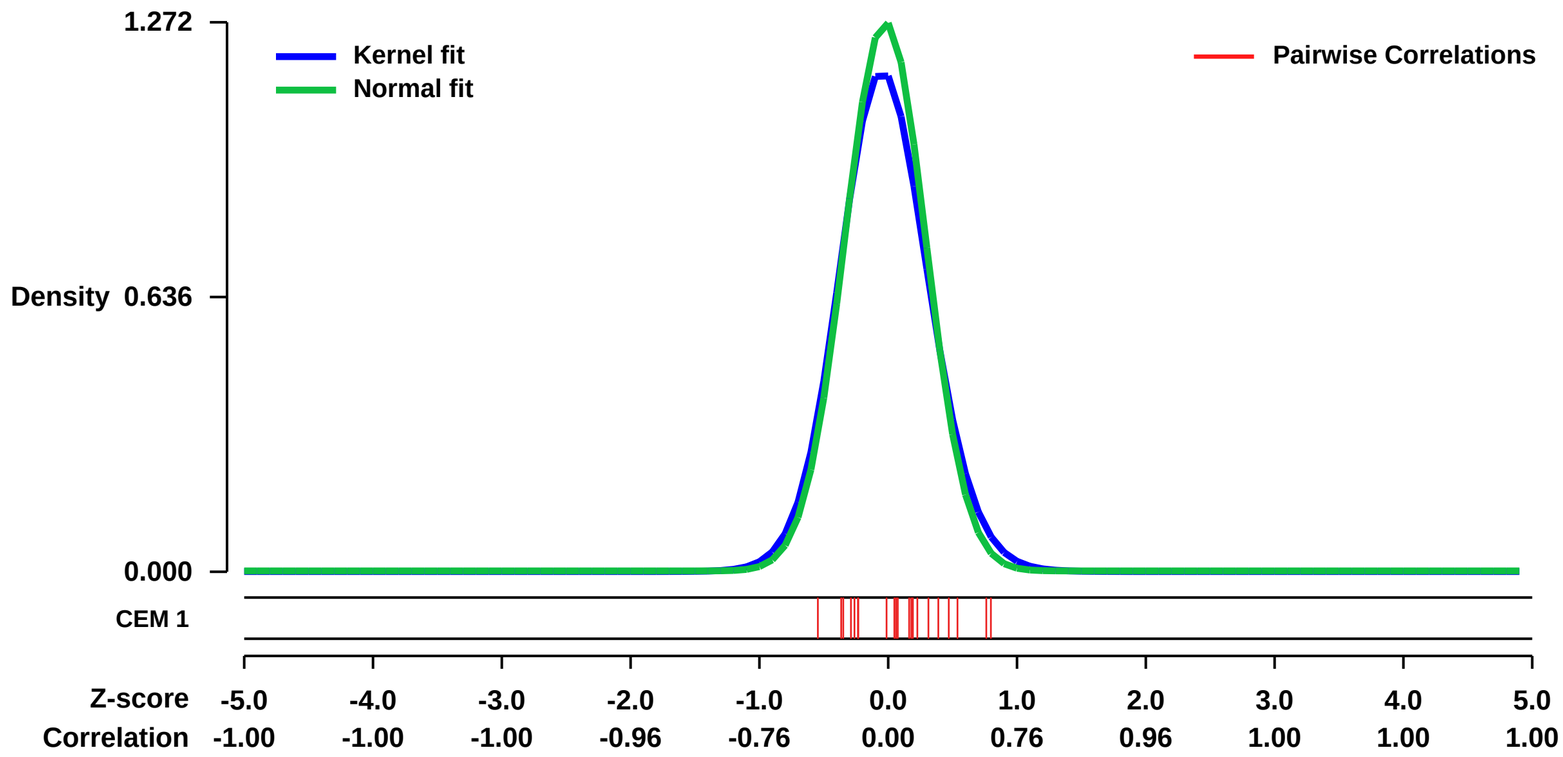

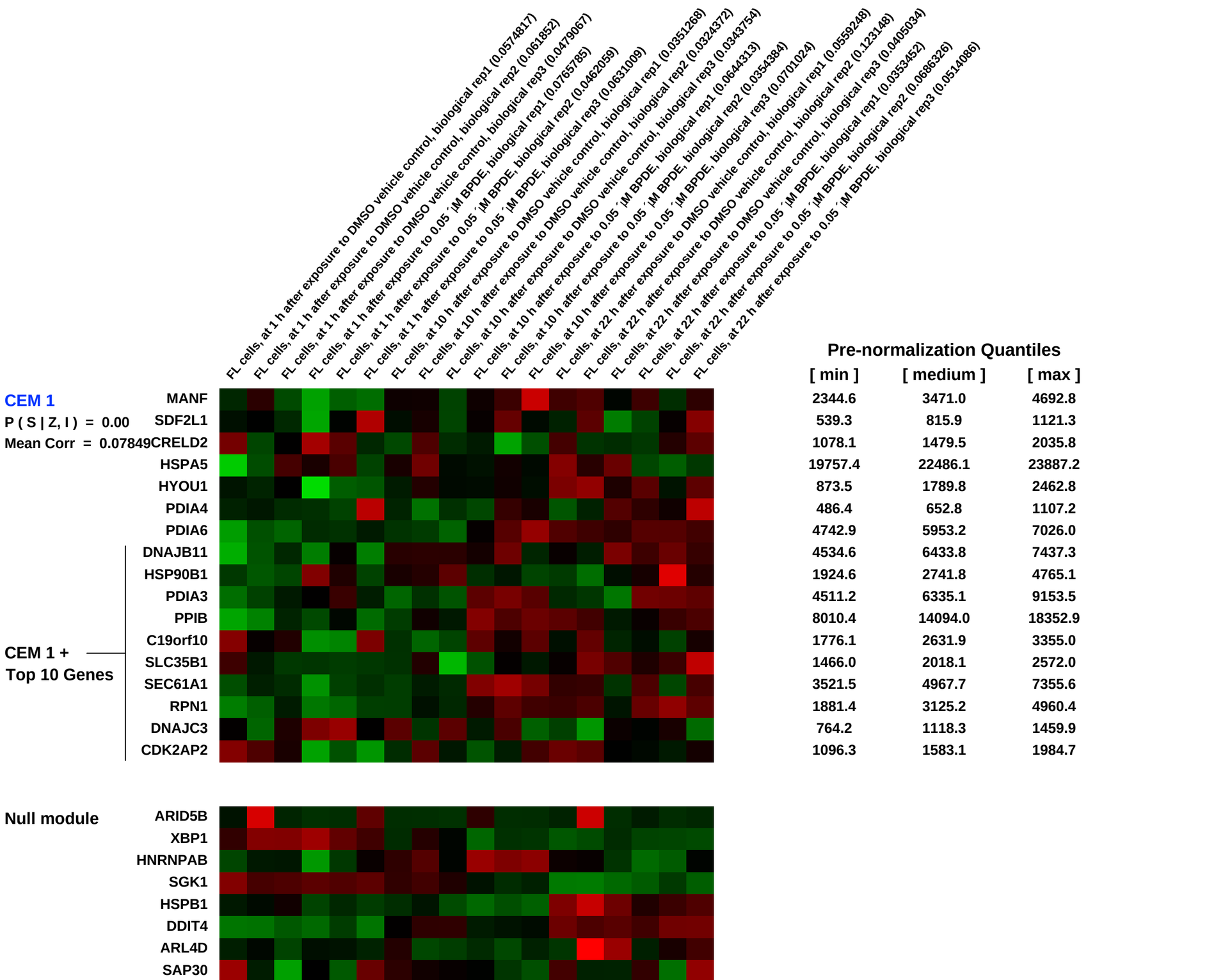

GEO Series "GSE3202" Expression Profiles

Num of samples in this series: 23

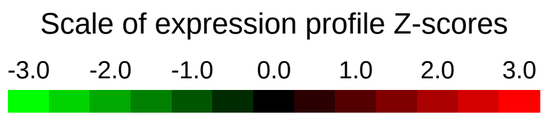

GEO Link:	http://www.ncbi.nlm.nih.gov/geo/query/acc.cgi?acc=GSE3202
Status:	Public on Sep 10 2005
Title:	MK886 treatment of H720 non-small cell lung cancer cell line
Organism:	Homo sapiens
Experiment type:	Expression profiling by array
Platform:	GPL570
Pubmed ID:	16551867
Summary & Design:	**Summary:** **In this experiments different treatments were applied to lung cancer cell lines** **1)H720 cell line suspension was treated by 1 micromole of 5-lipoxygenase activating protein inhibitor MK886 serum-free in TIS medium for 24 h.** **2) A549 cell line was treated as H720 by MK886** **3) A549 was treated by 100 nM of silencing cocktail (siRNA) prepared against the 4-th exon of the gene and generated by RNASEIII digestion of double stranded RNA. The cocktail was prepared by Ambion technology, see the manufacturer's protocol. The observed silencing was >90%** **4) Based on Oligoengine vectors, silencing constructs were created against HRPA2B1 transcript(HNRPA2B1 is a subunit of spliceosome). Stable transfectants were raised harboring the construct.** **Keywords: drug treatment** **Overall design:** **4) FLAP silencing: 1 control, 2 treatments**

Background corr dist: KL-Divergence = 0.1427, L1-Distance = 0.0271, L2-Distance = 0.0011, Normal std = 0.3878

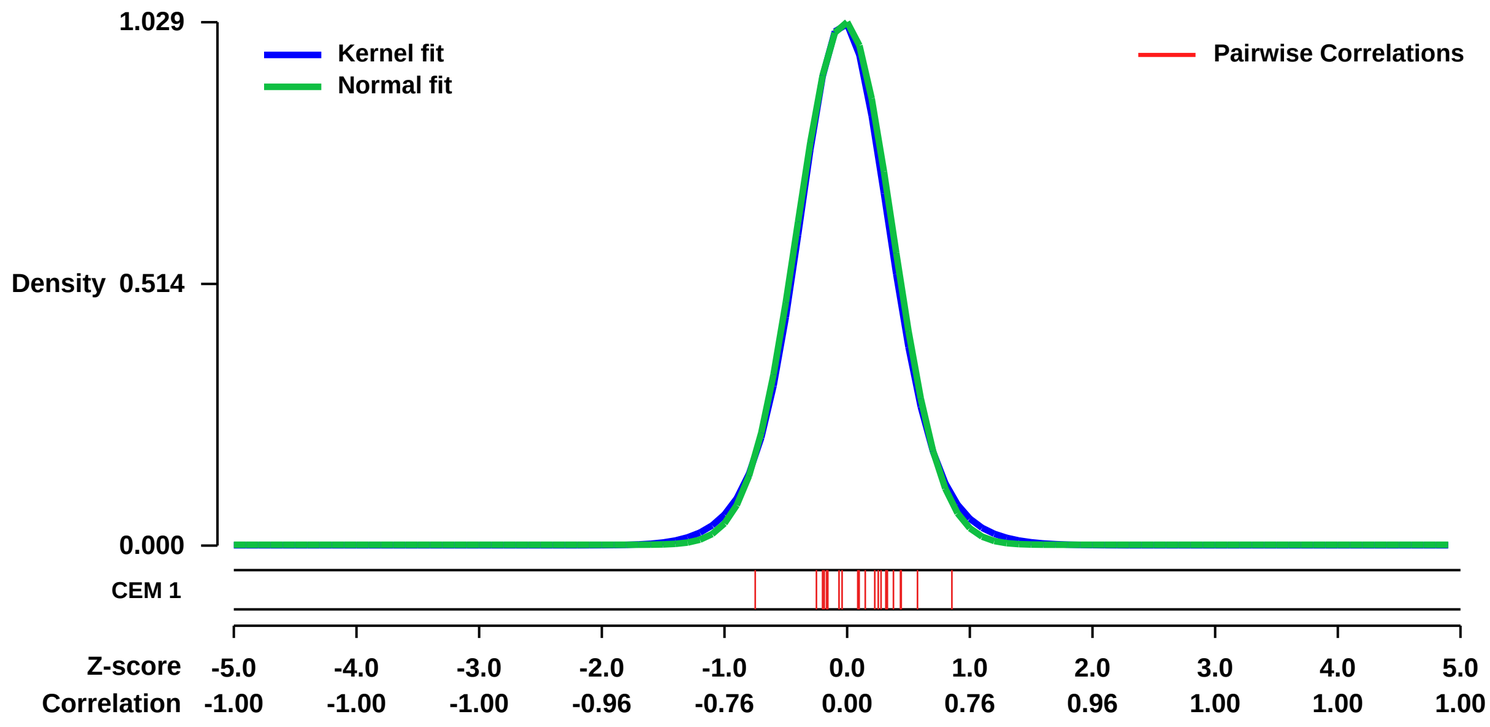

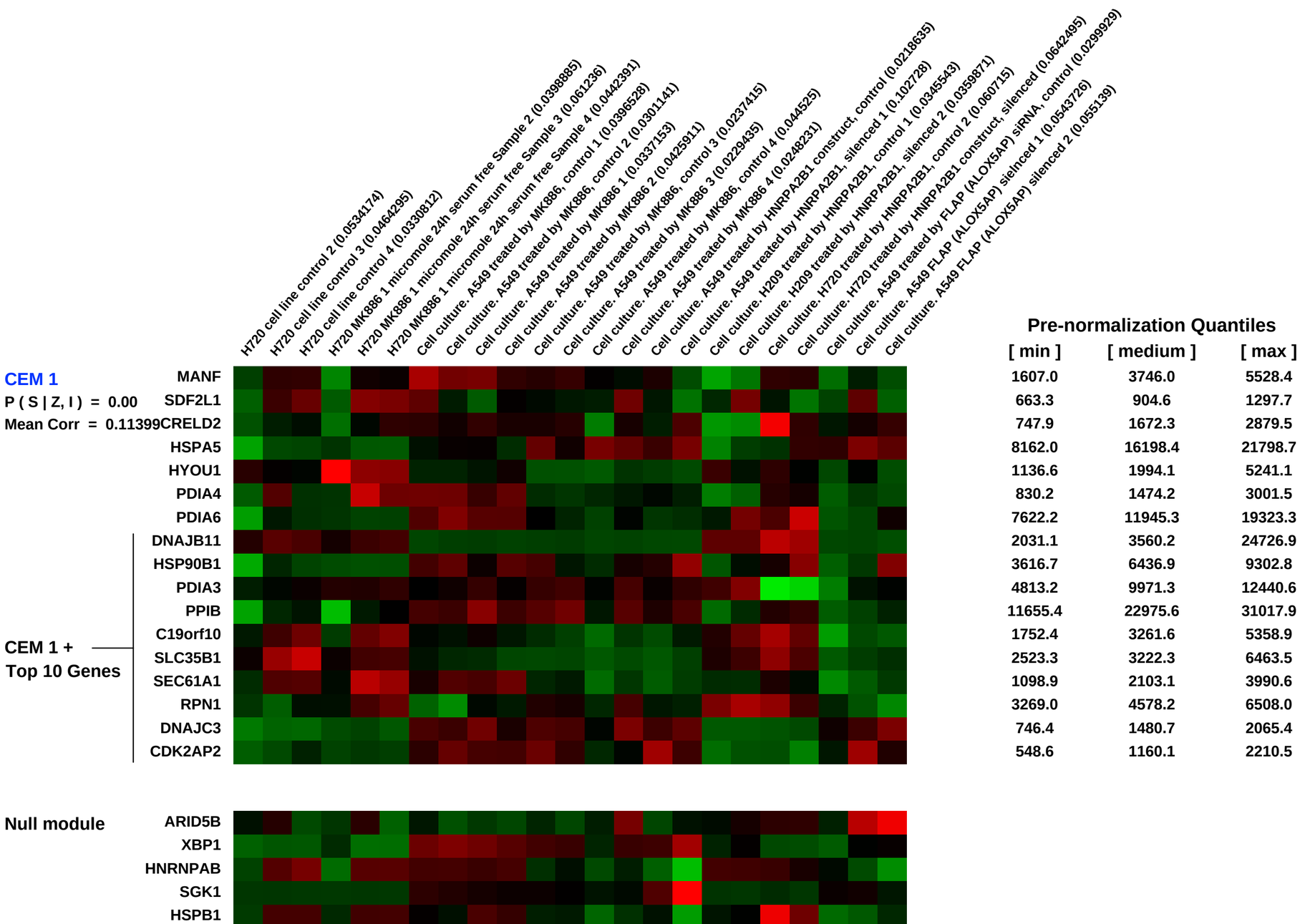

GEO Series "GSE17861" Expression Profiles

Num of samples in this series: 16

Scale of expression profile Z-scores

-3.0 -2.0 -1.0 0.0 1.0 2.0 3.0

GEO Link:	http://www.ncbi.nlm.nih.gov/geo/query/acc.cgi?acc=GSE17861
Status:	Public on Aug 28 2009
Title:	Analyses of heterogeneous renal allograft biopsies reveal conserved rejection signatures and molecular pathways I, partB
Organism:	Homo sapiens
Experiment type:	Expression profiling by array
Platform:	GPL570
Pubmed ID:	19017305
Summary & Design:	**Summary:** Specific early diagnosis of renal allograft rejection is gaining importance in the current trend to minimize and individualize immunosuppression. Gene expression analyses could contribute significantly by defining â molecular Banffâ signatures. Several previous studies have applied transcriptomics to distinguish different classes of kidney biopsies. However, the heterogeneity of microarray platforms, clinical samples and data analysis methods complicates the identification of robust signatures for the different types and grades of rejection. To address these issues, a comparative meta-analysis was performed across five different microarray datasets of heterogeneous sample collections from two published clinical datasets and three own datasets including biopsies for clinical indications, protocol biopsies, as well as comparative samples from non-human primates (NHP). This work identified conserved gene expression signatures that can differentiate groups with different histopathological findings in both human and NHP, regardless of the technical platform used. The marker panels comprise genes that clearly support the biological changes known to be involved in allograft rejection. A characteristic dynamic expression change of genes associated with immune and kidney functions was observed across samples with different grades of CAN. In addition, differences between human and NHP rejection were essentially limited to genes reflecting interstitial fibrosis progression. This data set comprises all renal allograft biopsies for clinical indications from patients at Hˆ·pital Tenon, Paris (February 2003 until September 2004) and few respective patients from Hˆ·pital Bicˆ“tre, Paris, Hˆ·pital Pellegrin, Bordeaux, and Hˆ·pital Dupuytren, Limoges, plus control normal kidney samples from Hˆ·pital Tenon, Paris, France (first batch). We used microarrays to identify different gene expression signatures of renal allograft biopsies that can classify them according to different types of allograft rejection or CAN. **Keywords:** disease state analysis **Keywords:** Expression profiling by array **Overall design:** 16 renal allograft core biopsies for clinical indications with different histopathological diagnoses according to BANFF'97 criteria (additional samples associated with GSE9489)

Background corr dist: KL-Divergence = 0.1811, L1-Distance = 0.0471, L2-Distance = 0.0051, Normal std = 0.3474

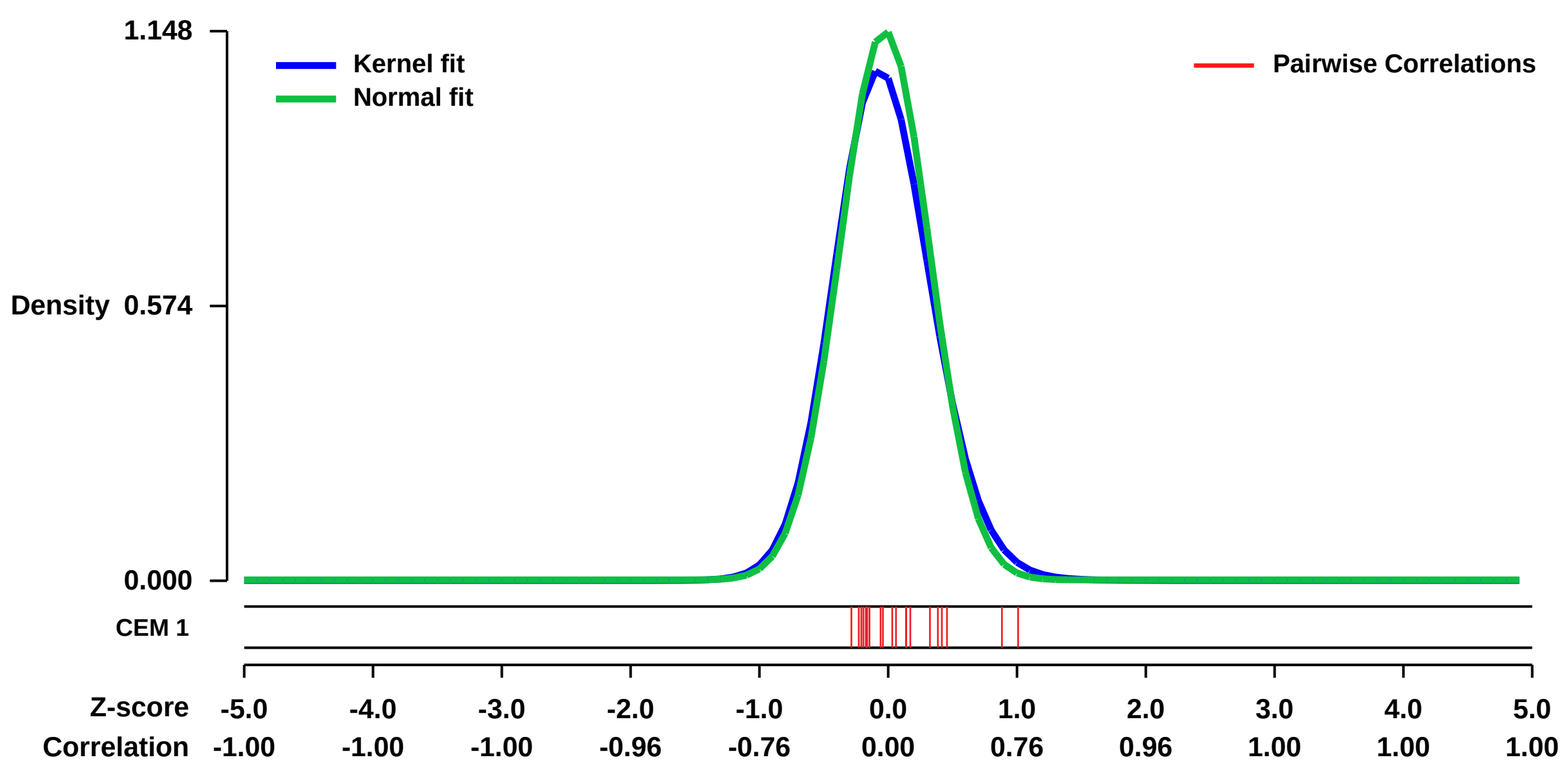

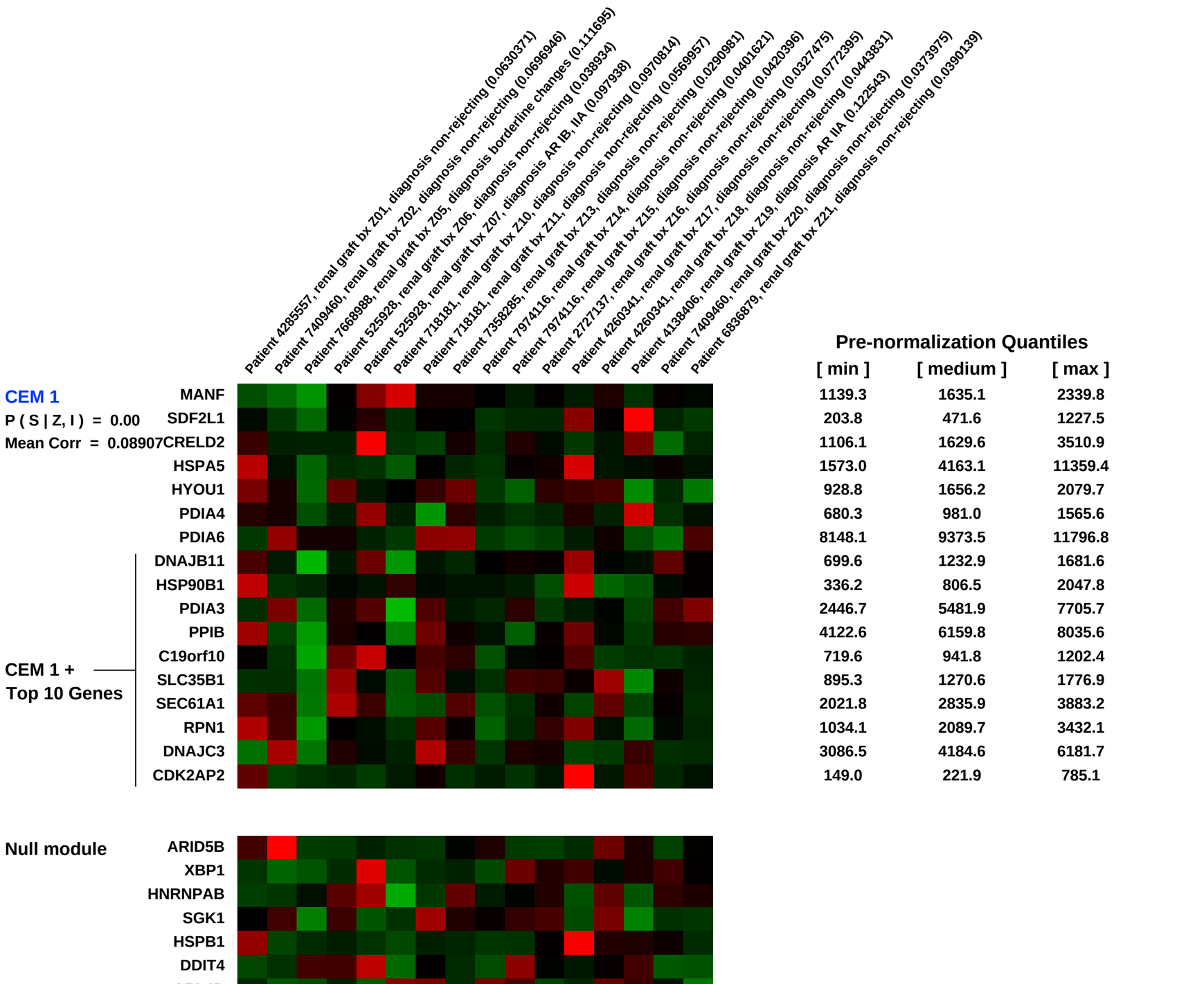

GEO Series "GSE5679" Expression Profiles

Num of samples in this series: 11

Scale of expression profile Z-scores

-3.0 -2.0 -1.0 0.0 1.0 2.0 3.0

GEO Link:	http://www.ncbi.nlm.nih.gov/geo/query/acc.cgi?acc=GSE5679
Status:	Public on Sep 19 2006
Title:	Comparative gene expression profile of PPARg and RARa ligand treated human dendritic cells
Organism:	Homo sapiens
Experiment type:	Expression profiling by array
Platform:	GPL570
Pubmed ID:	16982809
Summary & Design:	**Summary:** Our data indicated that activation of the PPARg nuclear receptor induces a retinoid response in human dendritic cells. In order to assess the contribution of retinoid signaling to the PPARg response we decided to use a combination of pharmacological activators and inhibitors of these pathways. Cells were treated with the synthetic PPARg ligand rosiglitazone (RSG), or with RSG along with the RARa antagonist (AGN193109) to block RARa mediated gene expression, or the RARa specific agonists (AM580) alone. This design allows one to determine if retinoid signaling is a downstream event of PPARg activation and what portion of PPARg regulated genes are regulated via induced retinoid signaling. **Keywords:** ligand response **Overall design:** Monocytes were cultured for 5 days with 500 U/ml IL-4 and 800 U/ml GM-CSF, cytokine treatment was repeated at day 3. Ligands were added at the beginning of differentiation but AGN193109 (AGN) treatment was repeated at day 3. Cells were obtained from three healthy individuals (three biological replicates) and cells were treated with vehicle (DC), 2.5 uM rosiglitazone (DC RSG), 100 nM AM580 (DC AM). RSG treatment was also combined with 1 uM AGN193109 (DC RSG AGN) in this case two biological replicates was used (RNA was obtained from 2. and 3. individuals).

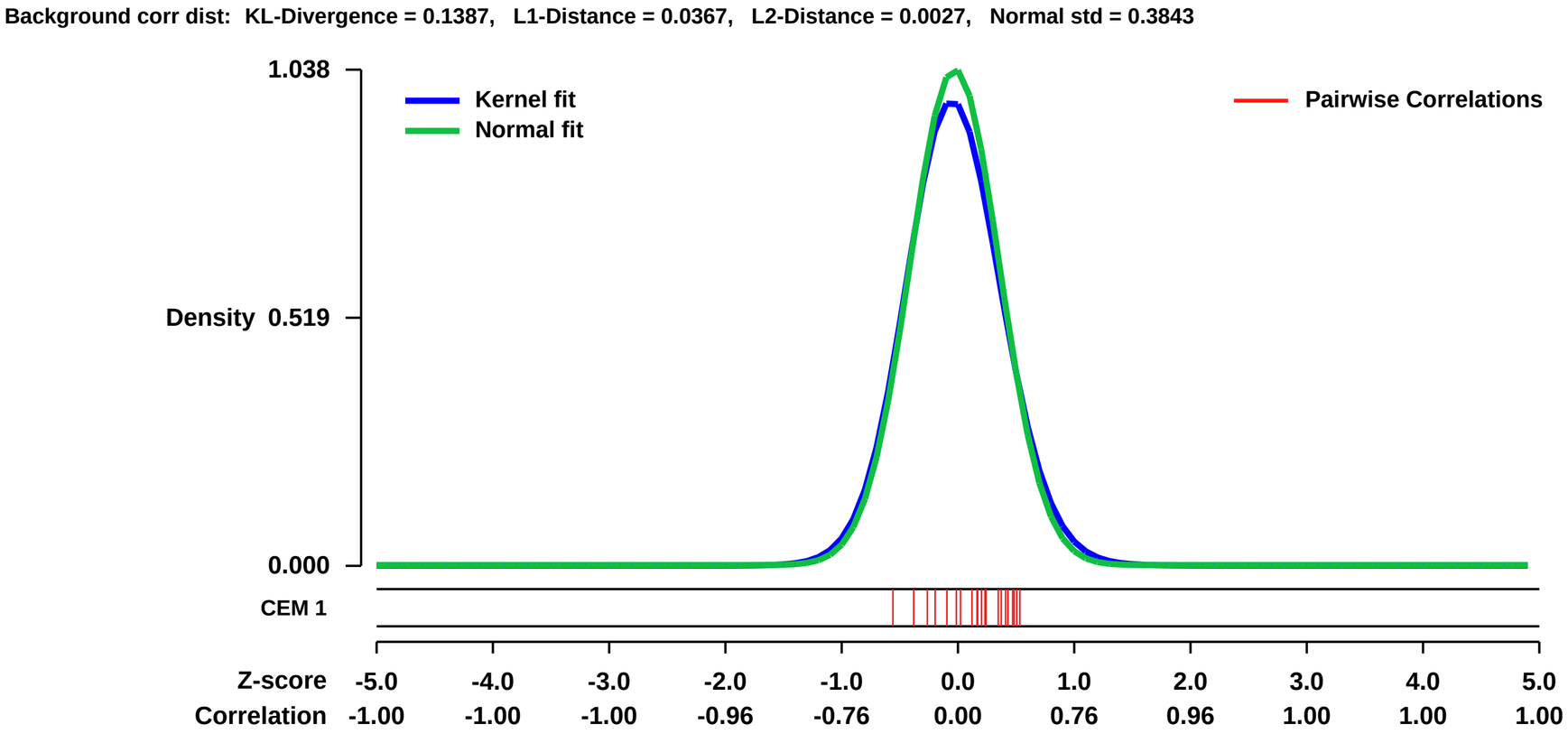

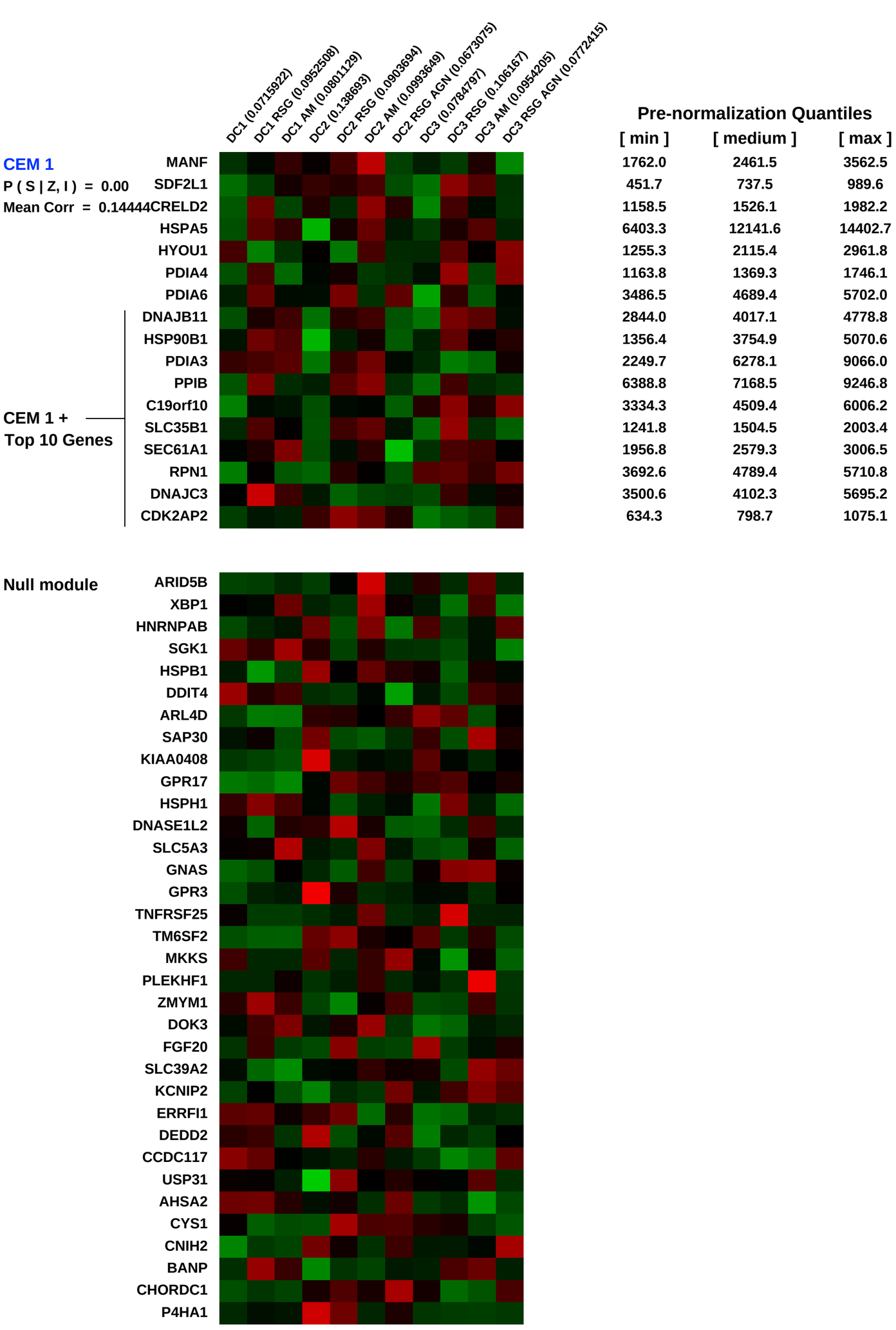

GEO Series "GSE15918" Expression Profiles

Num of samples in this series: 9

Scale of expression profile Z-scores

-3.0 -2.0 -1.0 0.0 1.0 2.0 3.0

GEO Link: http://www.ncbi.nlm.nih.gov/geo/query/acc.cgi?acc=GSE15918
Status: Public on May 02 2009
Title: Torcetrapib induces aldosterone and cortisol production in an intracellular calcium-dependent mechanism
Organism: Homo sapiens
Experiment type: Expression profiling by array
Platform: GPL570
Pubmed ID: 19164467

Summary & Design:

Summary:
ILLUMINATE (Investigation of Lipid Level Management to Understand its Impact in Atherosclerotic Events), the phase 3 morbidity and mortality trial of torcetrapib, a cholesteryl ester transfer protein (CETP) inhibitor, identified previously undescribed changes in plasma levels of potassium, sodium, bicarbonate, and aldosterone. A key question after this trial is whether the failure of torcetrapib was a result of CETP inhibition or of some other pharmacology of the molecule. The direct effects of torcetrapib and related molecules on adrenal steroid production were assessed in cell culture using the H295R as well as the newly developed HAC15 human adrenal carcinoma cell lines. Torcetrapib induced the synthesis of both aldosterone and cortisol in these two in vitro cell systems. Analysis of steroidogenic gene expression indicated that torcetrapib significantly induced the expression of CYP11B2 and CYP11B1, two enzymes in the last step of aldosterone and cortisol biosynthesis pathway, respectively. Transcription profiling indicated that torcetrapib and angiotensin II share overlapping pathways in regulating adrenal steroid biosynthesis. Hormone-induced steroid production is mainly mediated by two messengers, calcium and cAMP. An increase of intracellular calcium was observed after torcetrapib treatment, whereas cAMP was unchanged. Consistent with intracellular calcium being the key mediator of torcetrapibâ s effect in adrenal cells, calcium channel blockers completely blocked torcetrapib-induced corticoid release and calcium increase. A series of compounds structurally related to torcetrapib as well as structurally distinct compounds were profiled. The results indicate that the pressor and adrenal effects observed with torcetrapib and related molecules are independent of CETP inhibition.

Overall design:
Experimental Background: Aldosterone production by H295R adrenocortical carcinoma cells in response to the treatments described [dimethyl sulfoxide (vehicle), angiotensin II (a CETP inhibitor), or test compound CP-529414 (a CETP inhibitor)] will be analyzed.

Background corr dist: KL-Divergence = 0.0717, L1-Distance = 0.0209, L2-Distance = 0.0006, Normal std = 0.4931

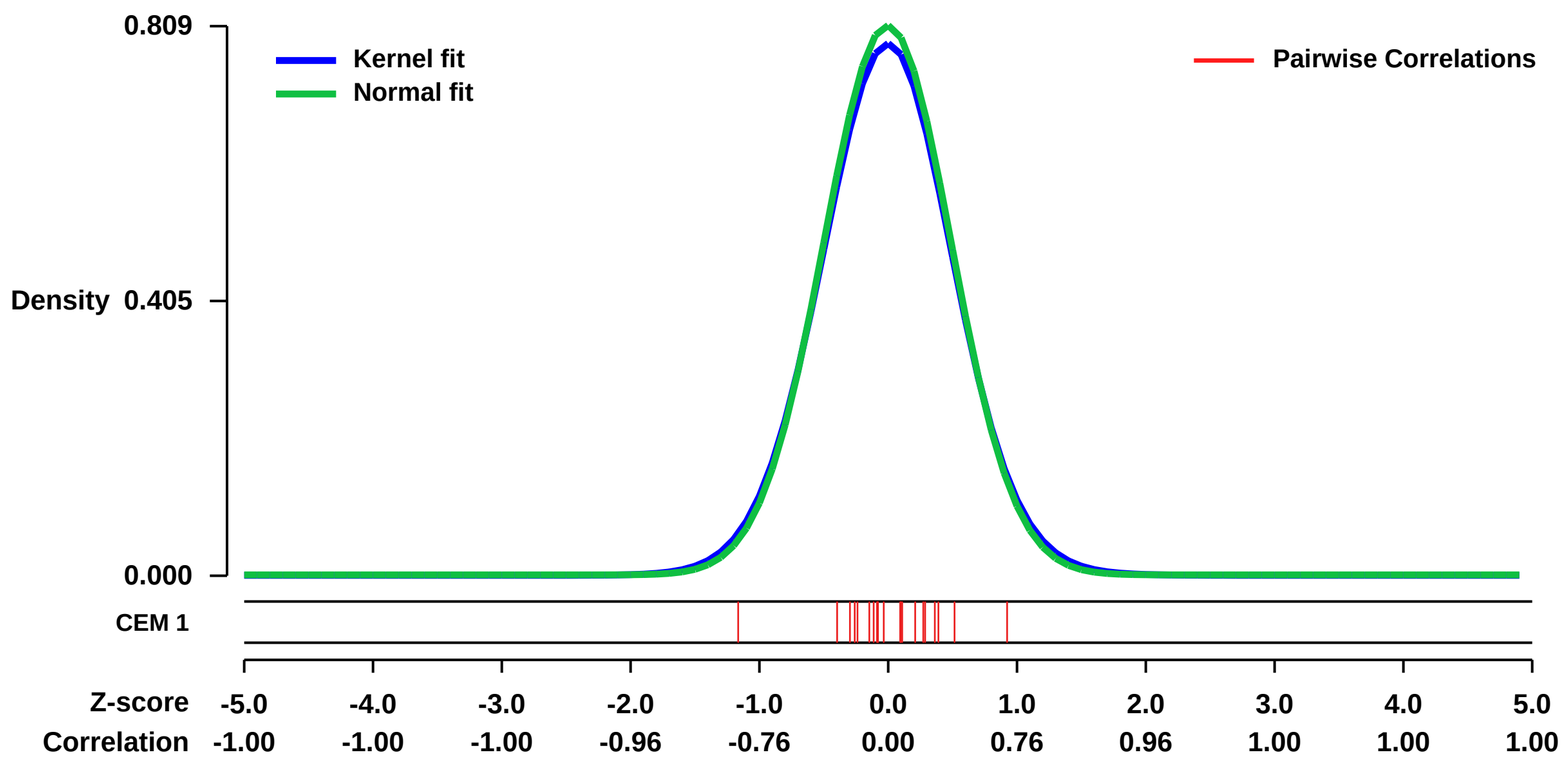

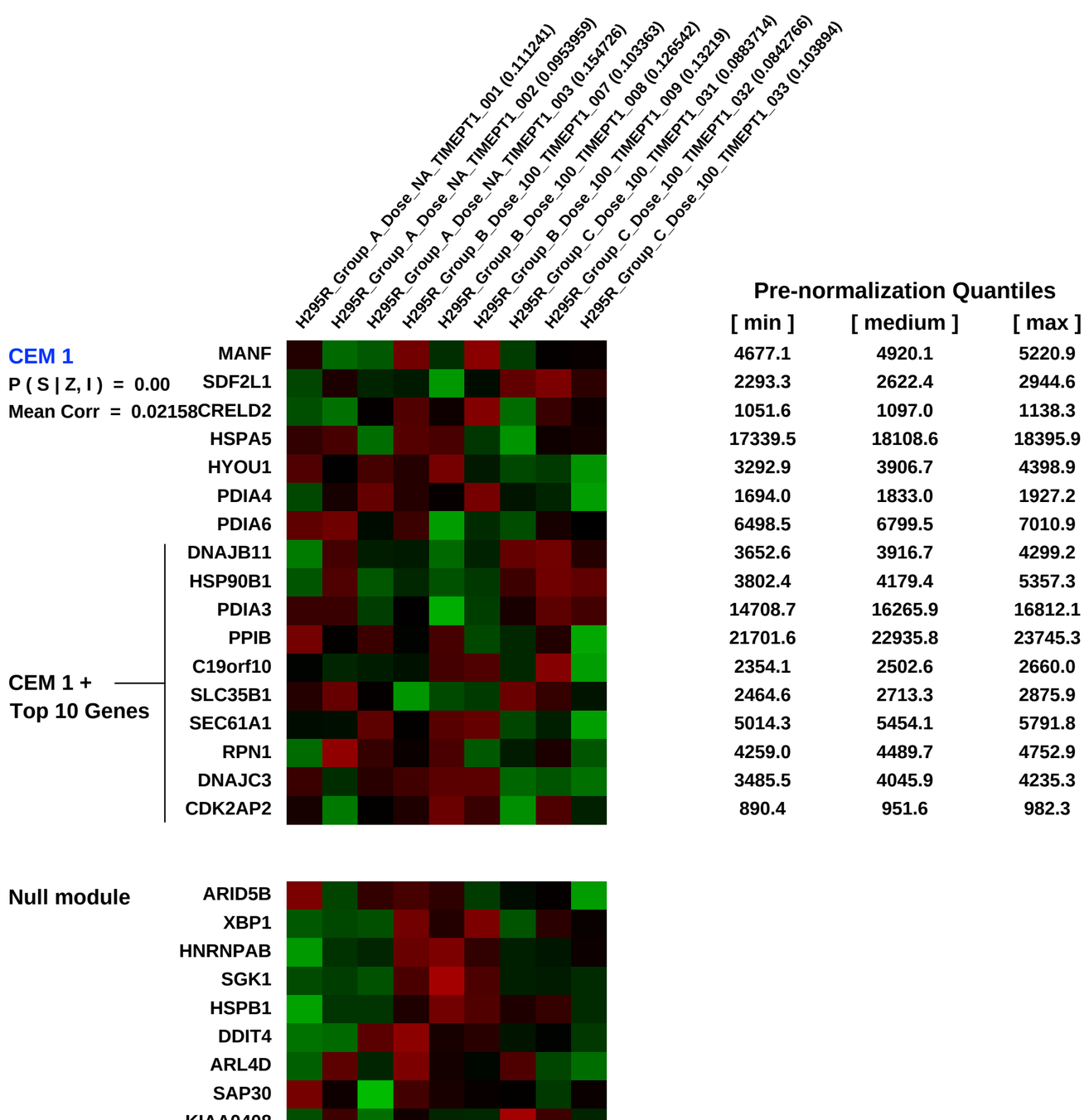

		Pre-normalization Quantiles		
		[min]	[medium]	[max]
CEM 1	MANF	4677.1	4920.1	5220.9
	SDF2L1	2293.3	2622.4	2944.6
	CRELD2	1051.6	1097.0	1138.3
	HSPA5	17339.5	18108.6	18395.9
	HYOU1	3292.9	3906.7	4398.9
	PDIA4	1694.0	1833.0	1927.2
	PDIA6	6498.5	6799.5	7010.9
CEM 1 + Top 10 Genes	DNAJB11	3652.6	3916.7	4299.2
	HSP90B1	3802.4	4179.4	5357.3
	PDIA3	14708.7	16265.9	16812.1
	PPIB	21701.6	22935.8	23745.3
	C19orf10	2354.1	2502.6	2660.0
	SLC35B1	2464.6	2713.3	2875.9
	SEC61A1	5014.3	5454.1	5791.8
	RPN1	4259.0	4489.7	4752.9
	DNAJC3	3485.5	4045.9	4235.3
	CDK2AP2	890.4	951.6	982.3
Null module	ARID5B			
	XBP1			
	HNRNPAB			
	SGK1			
	HSPB1			
	DDIT4			
	ARL4D			
	SAP30			
	KIAA0408			
	GPR17			
	HSPH1			
	DNASE1L2			
	SLC5A3			
	GNAS			
	GPR3			
	TNFRSF25			
	TM6SF2			
	MKKS			
	PLEKHF1			
	ZMYM1			
	DOK3			
	FGF20			
	SLC39A2			
	KCNIP2			
	ERRFI1			
	DEDD2			
	CCDC117			
	USP31			
	AHSA2			
	CYS1			
	CNIH2			
	BANP			
	CHORDC1			
	P4HA1			

GEO Series "GSE26511" Expression Profiles

Num of samples in this series: 39

Scale of expression profile Z-scores

-3.0 -2.0 -1.0 0.0 1.0 2.0 3.0

GEO Link:	http://www.ncbi.nlm.nih.gov/geo/query/acc.cgi?acc=GSE26511
Status:	Public on Feb 15 2011
Title:	Involvement of the TGF-ع† and ع†-catenin pathways in pelvic lymph node metastasis in early stage cervical cancer
Organism:	Homo sapiens
Experiment type:	Expression profiling by array
Platform:	GPL570
Pubmed ID:	21385933
Summary & Design:	**Summary:** **Purpose: Presence of pelvic lymph node metastases is the main prognostic factor in early stage cervical cancer patients, primarily treated with surgery. Aim of this study was to identify cellular tumor pathways associated with pelvic lymph node metastasis in early stage cervical cancer.** **Experimental Design: Gene expression profiles (Affymetrix U133 plus 2.0) of 20 patients with negative (N0) and 19 with positive lymph nodes (N+), were compared with gene sets that represent all 285 presently available pathway signatures. Validation immunostaining of tumors of 274 consecutive early stage cervical cancer patients was performed for representatives of the identified pathways.** **Results: Analysis of 285 pathways resulted in identification of five pathways (TGF-ع†, NFAT, ALK, BAD, and PAR1) that were dysregulated in the N0, and two pathways (ع†-catenin and Glycosphingolipid Biosynthesis Neo Lactoseries) in the N+ group. Class comparison analysis revealed that five of 149 genes that were most significantly differentially expressed between N0 and N+ tumors (P<0.001) were involved in ع†-catenin signaling (TCF4, CTNNAL1, CTNND1/p120, DKK3 and WNT5a). Immunohistochemical validation of two well-known cellular tumor pathways (TGF-ع† and ع†-catenin) confirmed that the TGF-ع† pathway (positivity of Smad4) was related to N0 (OR:0.20, 95%CI:0.06-0.66) and the ع†-catenin pathway (p120 positivity) to N+ (OR:1.79, 95%CI:1.05-3.05).** **Conclusions: Our study provides new, validated insights in the molecular mechanism of lymph node metastasis in cervical cancer. Pathway analysis of the microarray expression profile suggested that the TGF-ع† and p120-associated non-canonical ع†-catenin pathways are important in pelvic lymph node metastasis in early stage cervical cancer.** **Overall design:** **For the microarray experiment, we selected fresh frozen primary cervical cancer tissue, containing at least 80% tumor cells, of patients with histologically confirmed N0 (n=20) and of patients with N+ (n=19). The N0 and N+ groups were matched for age, FIGO stage and histology (all squamous cell carcinoma).**

Background corr dist: KL-Divergence = 0.2375, L1-Distance = 0.0867, L2-Distance = 0.0216, Normal std = 0.3254

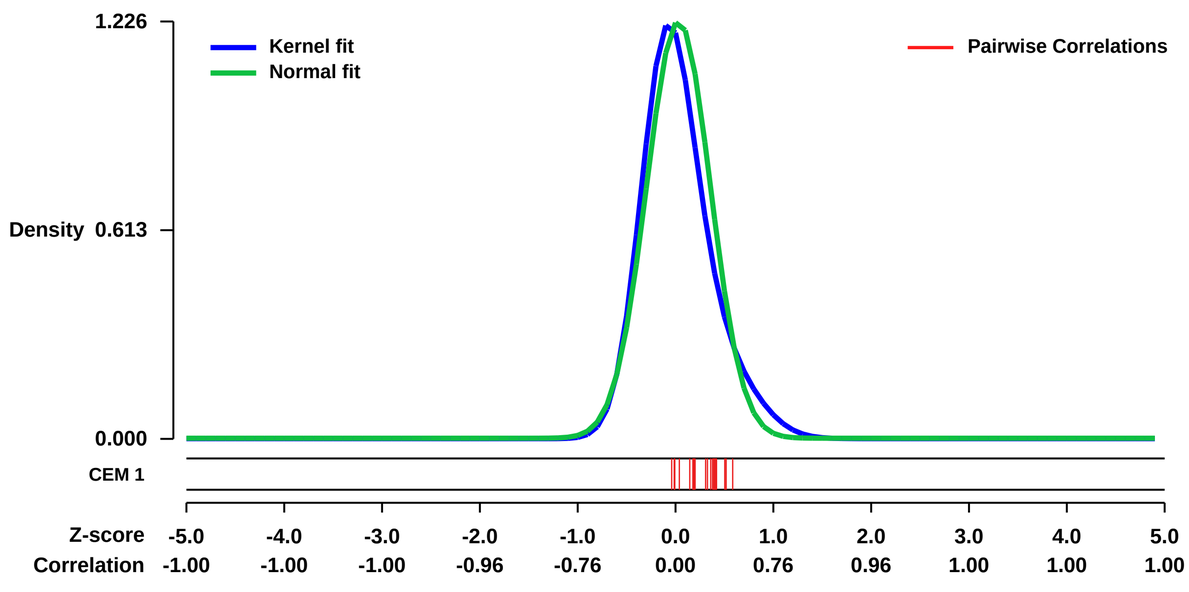

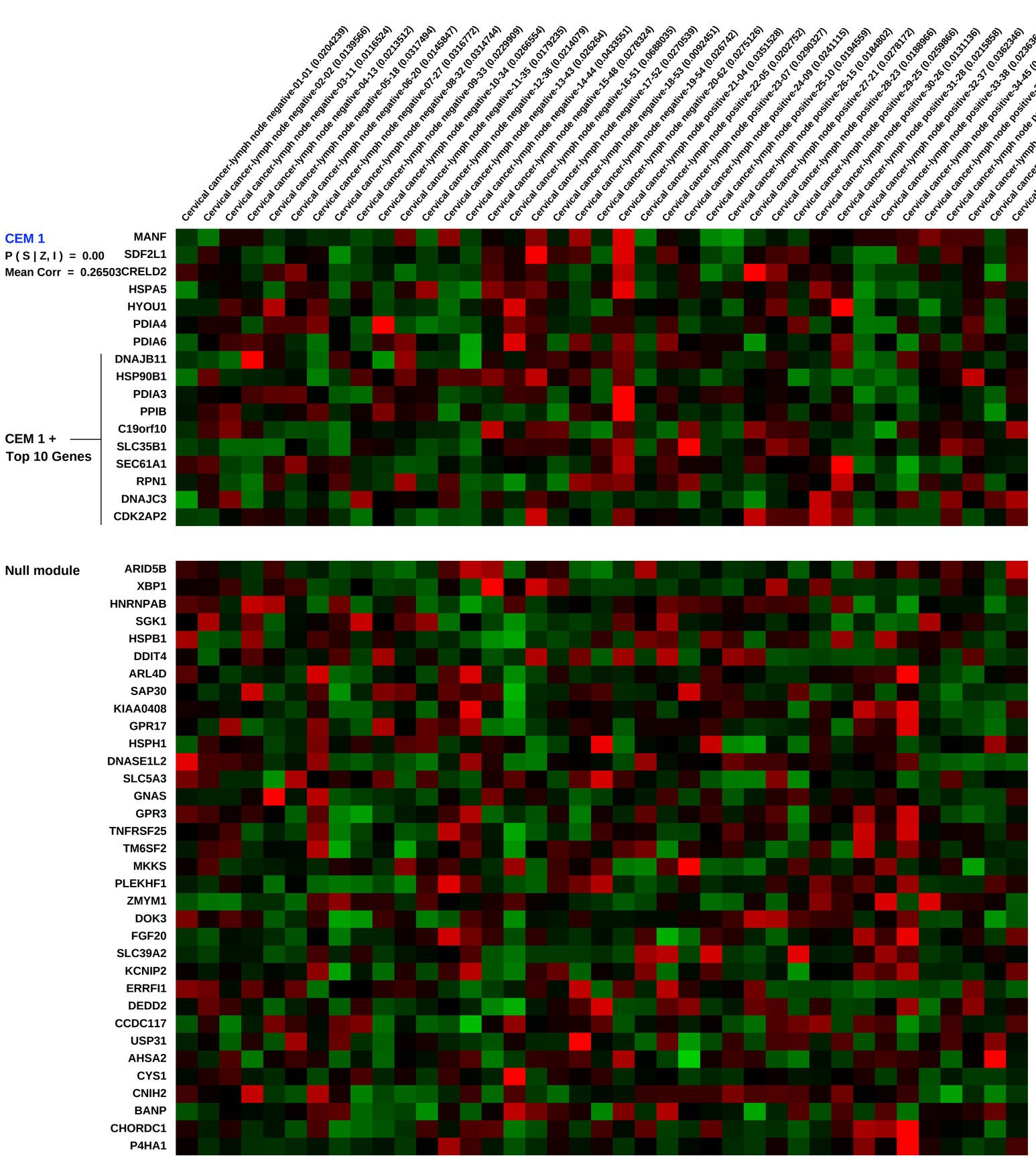

Pre-normalization Quantiles

[min]	[medium]	[max]
1349.0	2114.4	3457.5
615.7	1344.4	2711.5
1265.9	2034.0	3594.0
5900.3	8461.3	13115.0
1273.6	2228.9	4389.9
619.2	973.3	1925.1
2807.5	5255.8	8745.8
1867.7	4208.5	8172.0
1480.2	2145.0	3117.7
2667.2	5965.9	15522.0
3775.3	7185.2	17011.5
1362.7	1894.0	2745.4
1449.2	1910.9	3309.2
1137.3	2492.7	5523.5
2302.3	3970.6	6990.9
1090.0	1814.5	2932.8
659.8	1070.8	1984.1

GEO Series "GSE24235" Expression Profiles

Num of samples in this series: 28

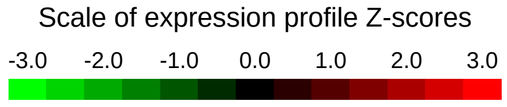

GEO Link:	http://www.ncbi.nlm.nih.gov/geo/query/acc.cgi?acc=GSE24235
Status:	Public on Dec 06 2010
Title:	Skeletal muscle gene expression in response to resistance exercise: sex specific regulation
Organism:	Homo sapiens
Experiment type:	Expression profiling by array
Platform:	GPL570
Pubmed ID:	21106073
Summary & Design:	**Summary:** The molecular mechanisms underlying the sex differences in human muscle morphology and function remain to be elucidated. The purpose of the study was to detect the sex differences in the skeletal muscle transcriptome in both the resting state and following anabolic stimuli, resistance exericse. **Overall design:** We used microarrays to profile the transcriptome of the biceps brachii of young men and women who underwent an acute unilateral RE session following 12 weeks of progressive training. Bilateral muscle biopsies were obtained either at an early (4h post-exercise) or late recovery (24h post-exercise) time point. Muscle transcription profiles were compared in the resting state between men (n=6) and women (n=8), and in response to acute RE in trained exercised vs. untrained non-exercised control muscle for each sex and time point separately (4h post-exercise, n=3 males, n=4 females; 24h post-exercise, n=3 males, n=4 females). A logistic regression-based method (LRpath), following Bayesian moderated t-statistic (IMBT), was used to test gene functional groups and biological pathways enriched with differentially expressed genes.

Background corr dist: KL-Divergence = 0.2506, L1-Distance = 0.0668, L2-Distance = 0.0121, Normal std = 0.3012

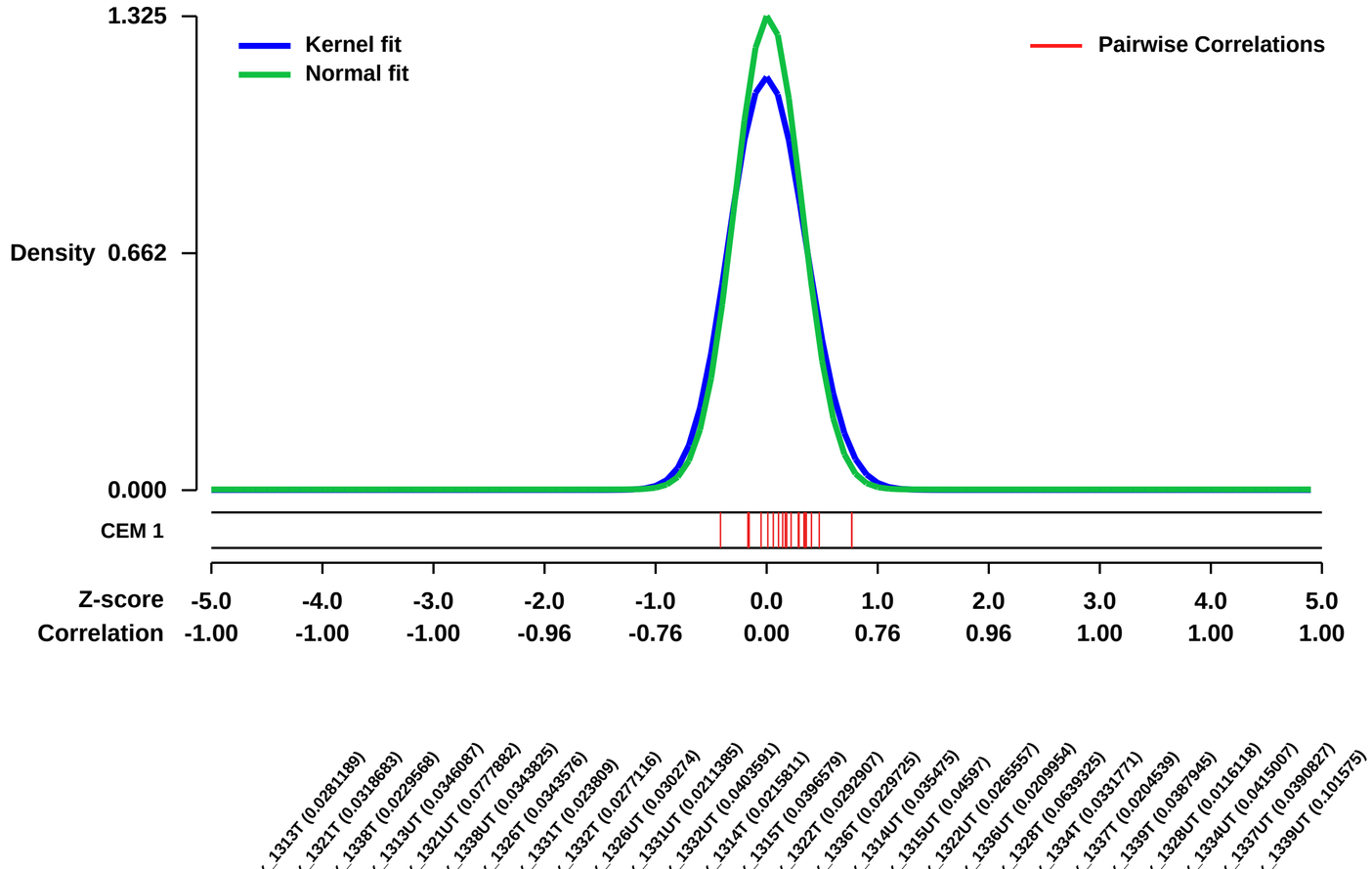

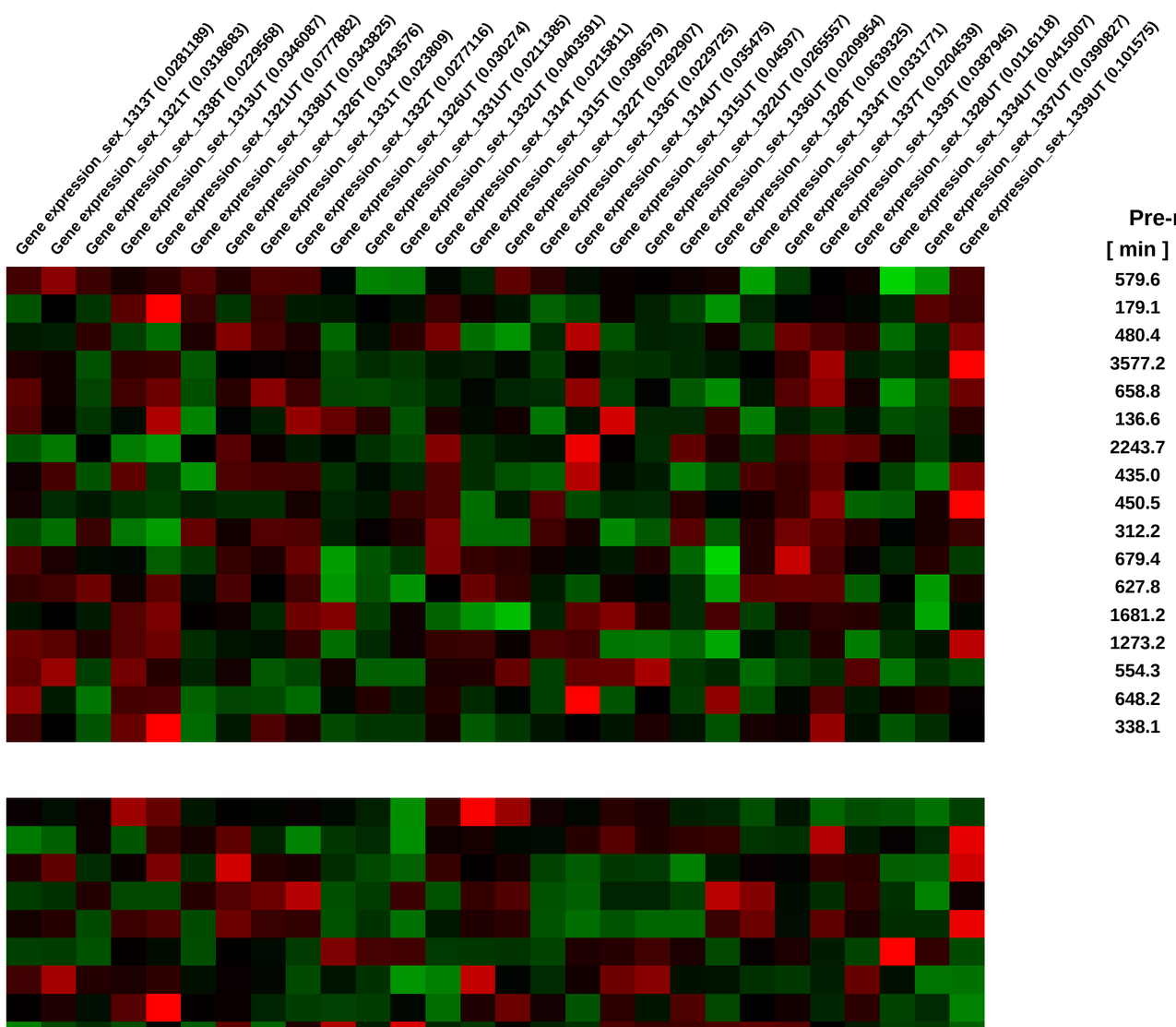

Pre-normalization Quantiles

[min]	[medium]	[max]
579.6	1102.1	1385.5
179.1	274.9	505.3
480.4	581.1	727.9
3577.2	4461.7	9421.0
658.8	957.8	1276.2
136.6	175.4	247.1
2243.7	2878.4	3927.4
435.0	626.7	903.0
450.5	553.8	953.1
312.2	880.0	1191.3
679.4	1908.7	2893.2
627.8	858.3	985.2
1681.2	2174.2	2503.1
1273.2	2008.1	2742.1
554.3	791.2	1371.1
648.2	892.1	1478.8
338.1	504.4	1107.6

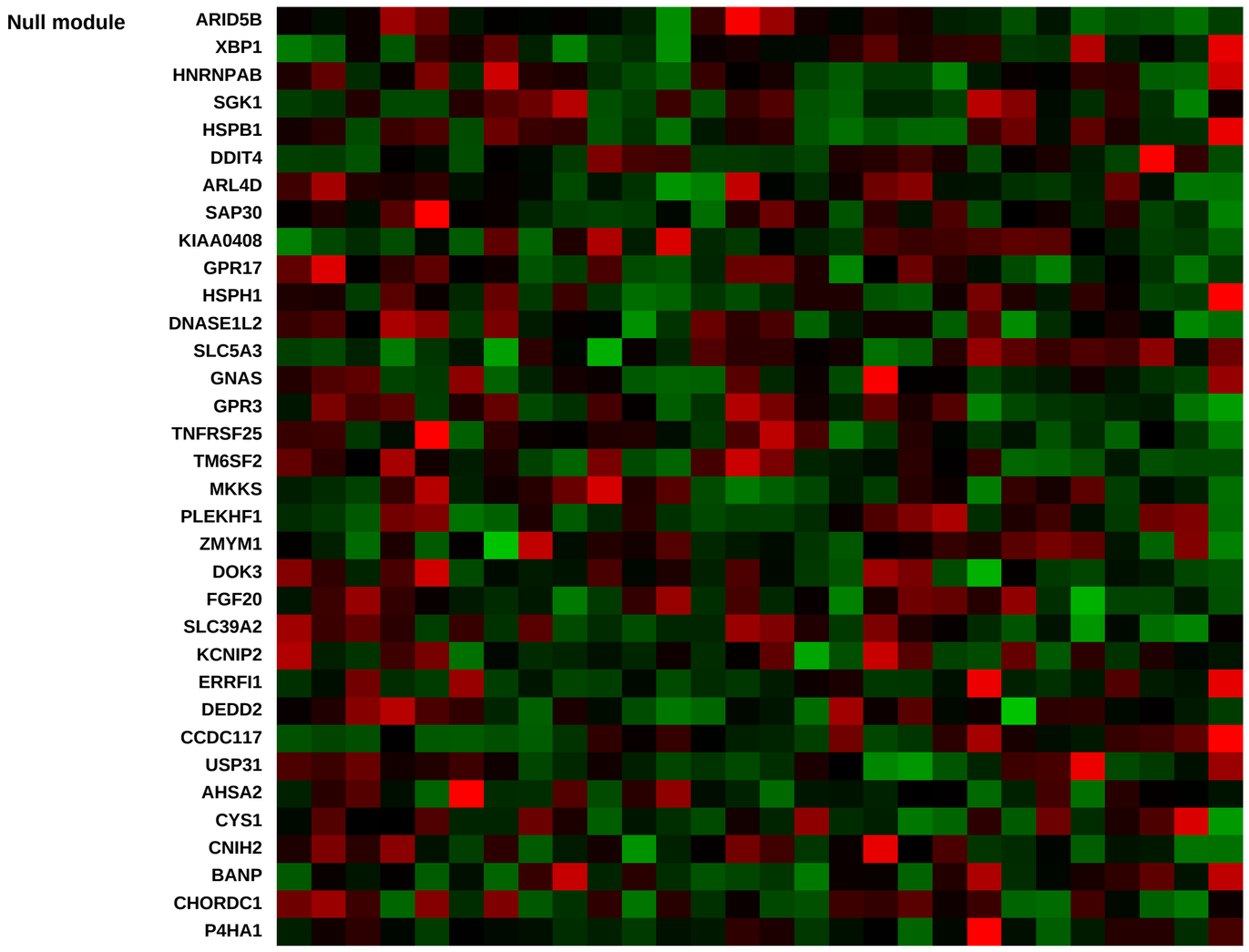

GEO Series "GSE31469" Expression Profiles

Num of samples in this series: 12

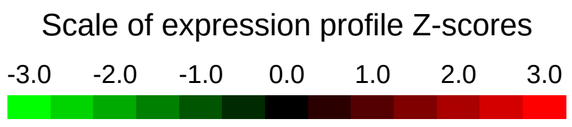

GEO Link:	http://www.ncbi.nlm.nih.gov/geo/query/acc.cgi?acc=GSE31469
Status:	Public on Jan 03 2013
Title:	Host cell gene expression in Influenza A/WSN/33 (H1N1) infected A549 cells at 2, 4 and 6 hours post infection
Organism:	Homo sapiens
Experiment type:	Expression profiling by array
Platform:	GPL570
Pubmed ID:	22470468
Summary & Design:	**Summary:** We used the microarray data to analyze host cells response on A549 cells infected with A/WSN/33 (H1N1) **Overall design:** The A/WSN/33 (H1N1) infected A549 cells were harvested at 2, 4 and 6 hpi and RNA extraction was performed using standard protocol as described by Affymetrix. The aim of this experiment is to analyze host response to Influenza A/WSN/33 (H1N1) infection.

Background corr dist: KL-Divergence = 0.1705, L1-Distance = 0.0423, L2-Distance = 0.0039, Normal std = 0.3536

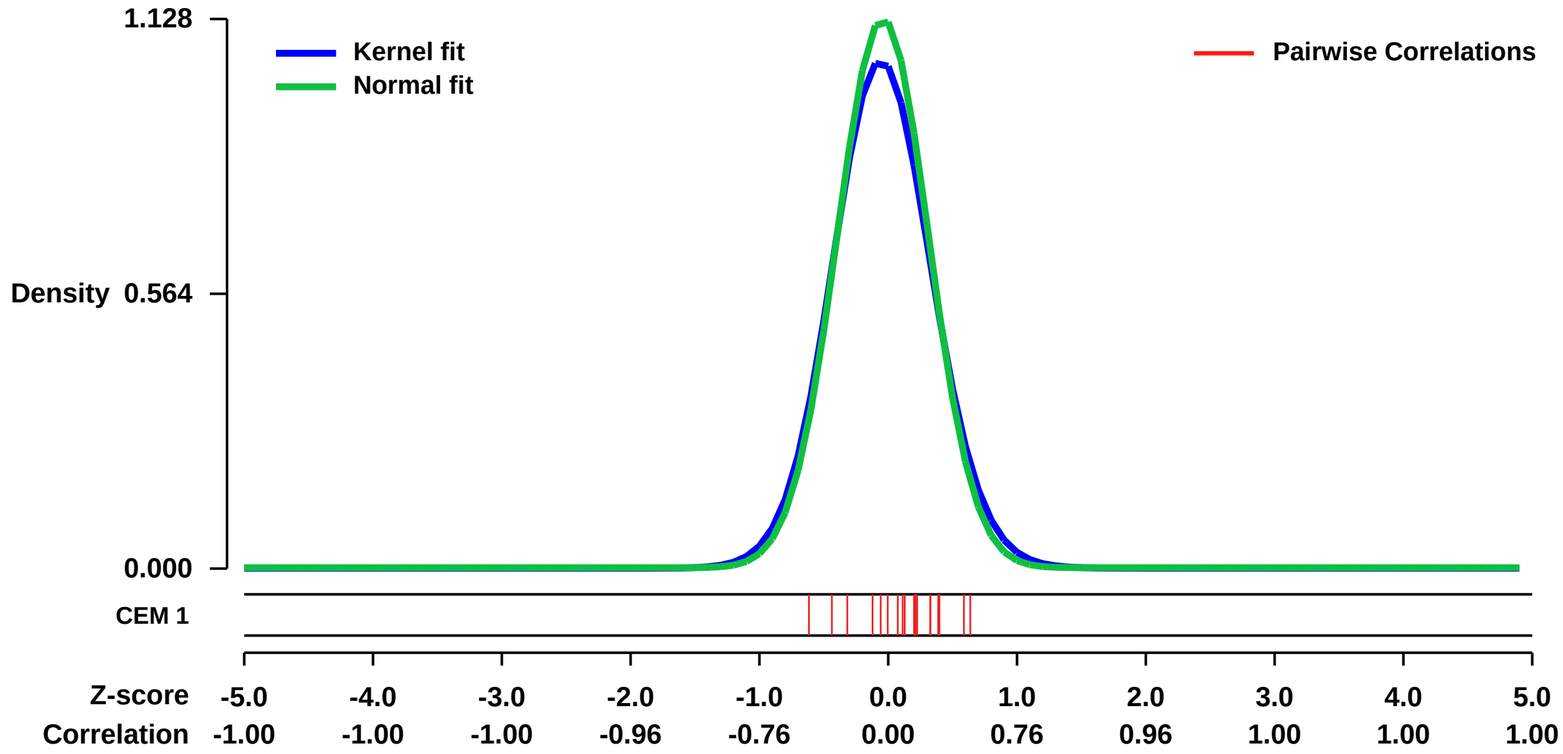

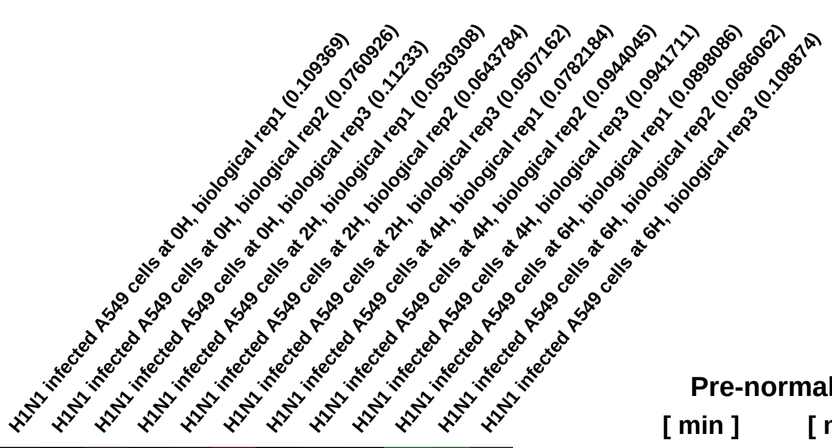

Pre-normalization Quantiles

[min] [medium] [max]

CEM 1
P (S | Z, I) = 0.00
Mean Corr = 0.13079

CEM 1 + Top 10 Genes

Null module

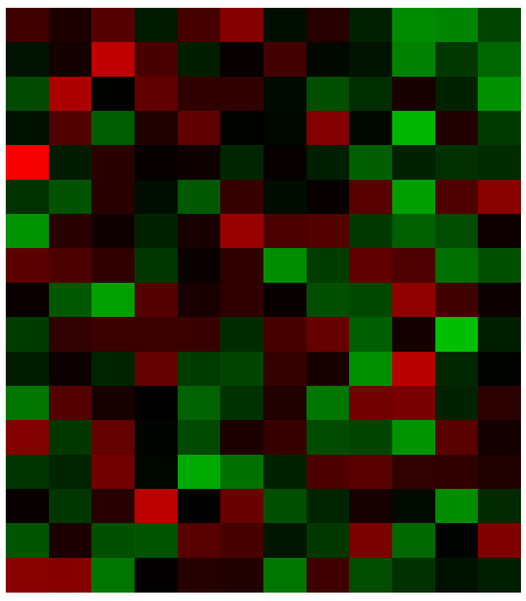

MANF	2897.1	3443.5	3778.9
SDF2L1	726.7	904.5	1195.7
CRELD2	1257.1	1600.4	2019.1
HSPA5	14188.3	16529.1	18238.8
HYOU1	1154.7	1348.4	2129.2
PDIA4	1722.1	2132.0	2450.7
PDIA6	10340.7	11188.8	11901.6
DNAJB11	2309.8	2993.3	3177.9
HSP90B1	7559.2	8334.8	8916.7
PDIA3	5599.4	7269.8	7631.2
PPIB	17721.3	19526.2	21895.1
C19orf10	2578.8	3047.1	3379.9
SLC35B1	2981.8	3129.2	3227.3
SEC61A1	2410.6	2835.2	3010.3
RPN1	2488.4	2911.9	3487.3
DNAJC3	787.4	943.5	1142.1
CDK2AP2	1690.6	1965.2	2276.4
ARID5B			
XBP1			
HNRNPAB			
SGK1			
HSPB1			
DDIT4			
ARL4D			
SAP30			
KIAA0408			
GPR17			
HSPH1			
DNASE1L2			
SLC5A3			
GNAS			
GPR3			
TNFRSF25			
TM6SF2			
MKKS			
PLEKHF1			
ZMYM1			
DOK3			
FGF20			
SLC39A2			
KCNIP2			
ERRFI1			
DEDD2			
CCDC117			
USP31			
AHSA2			
CYS1			
CNIH2			
BANP			
CHORDC1			
P4HA1			

GEO Series "GSE45434" Expression Profiles

Num of samples in this series: 16

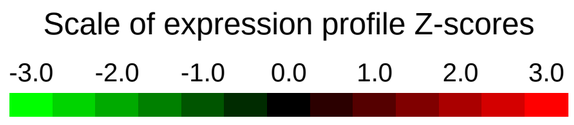

GEO Link:	http://www.ncbi.nlm.nih.gov/geo/query/acc.cgi?acc=GSE45434
Status:	Public on Jul 31 2014
Title:	Gene expression profiles of human hepatocellular carcinoma (training set 2)
Organism:	Homo sapiens
Experiment type:	Third-party reanalysis
Platform:	GPL570
Pubmed ID:	
Summary & Design:	**Summary:** Hepatocellular carcinoma (HCC) in young subjects is rare but more devastating. We hypothesize that genes and etiological pathways are unique to young HCC (yHCC; â40 years old at diagnosis) patients. We therefore compared the gene expression profiles between yHCCs and HCCs from elderly patients. **Overall design:** 16 young HCC were collected from patients aged less than 40. 16 elder HCC profiles were downloaded from the Expression Project for Oncology (expO) of the International Genomics Consortium, with accession number GSE2109 in GEO database.

Background corr dist: KL-Divergence = 0.1636, L1-Distance = 0.0917, L2-Distance = 0.0207, Normal std = 0.3910

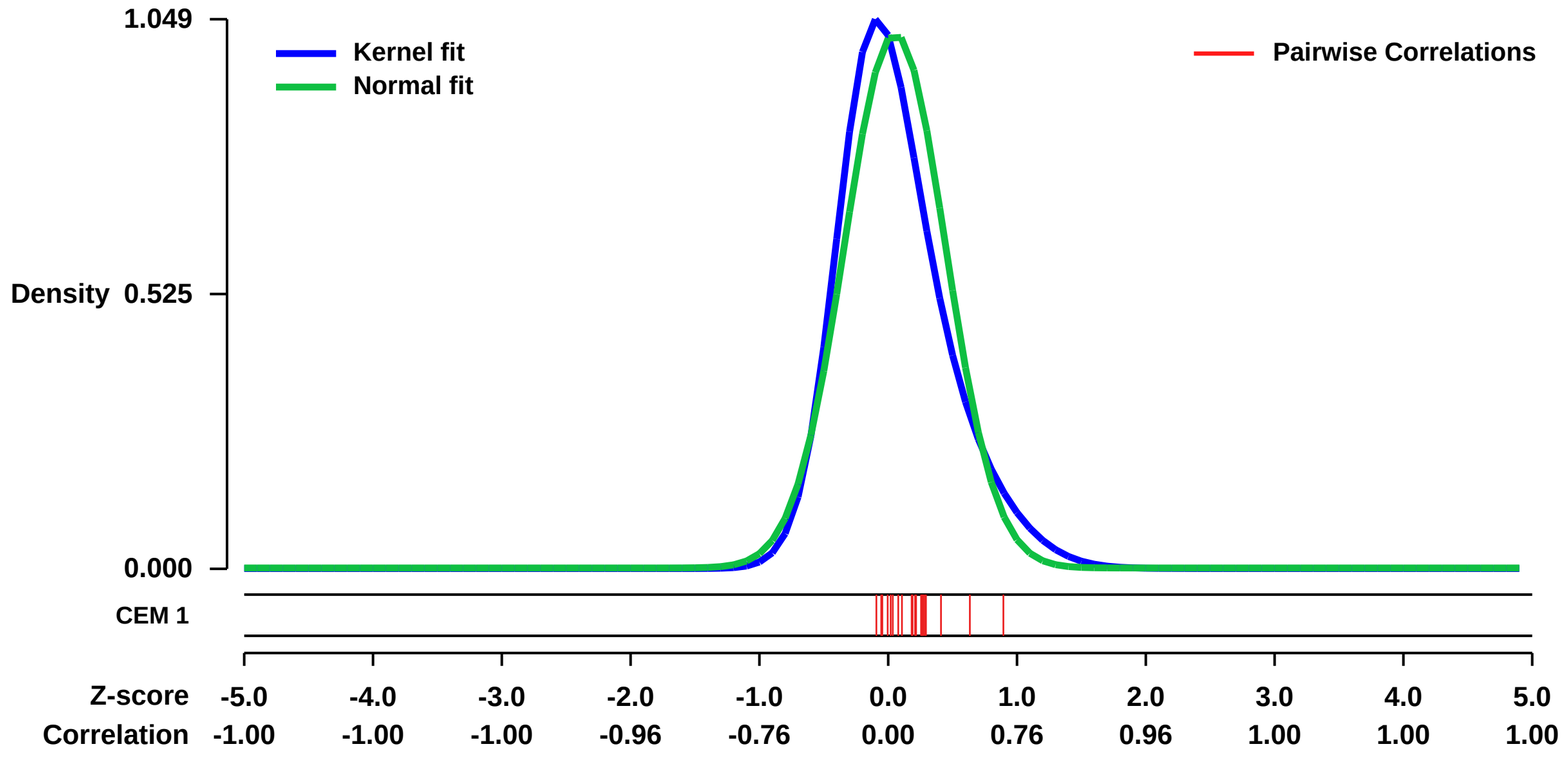

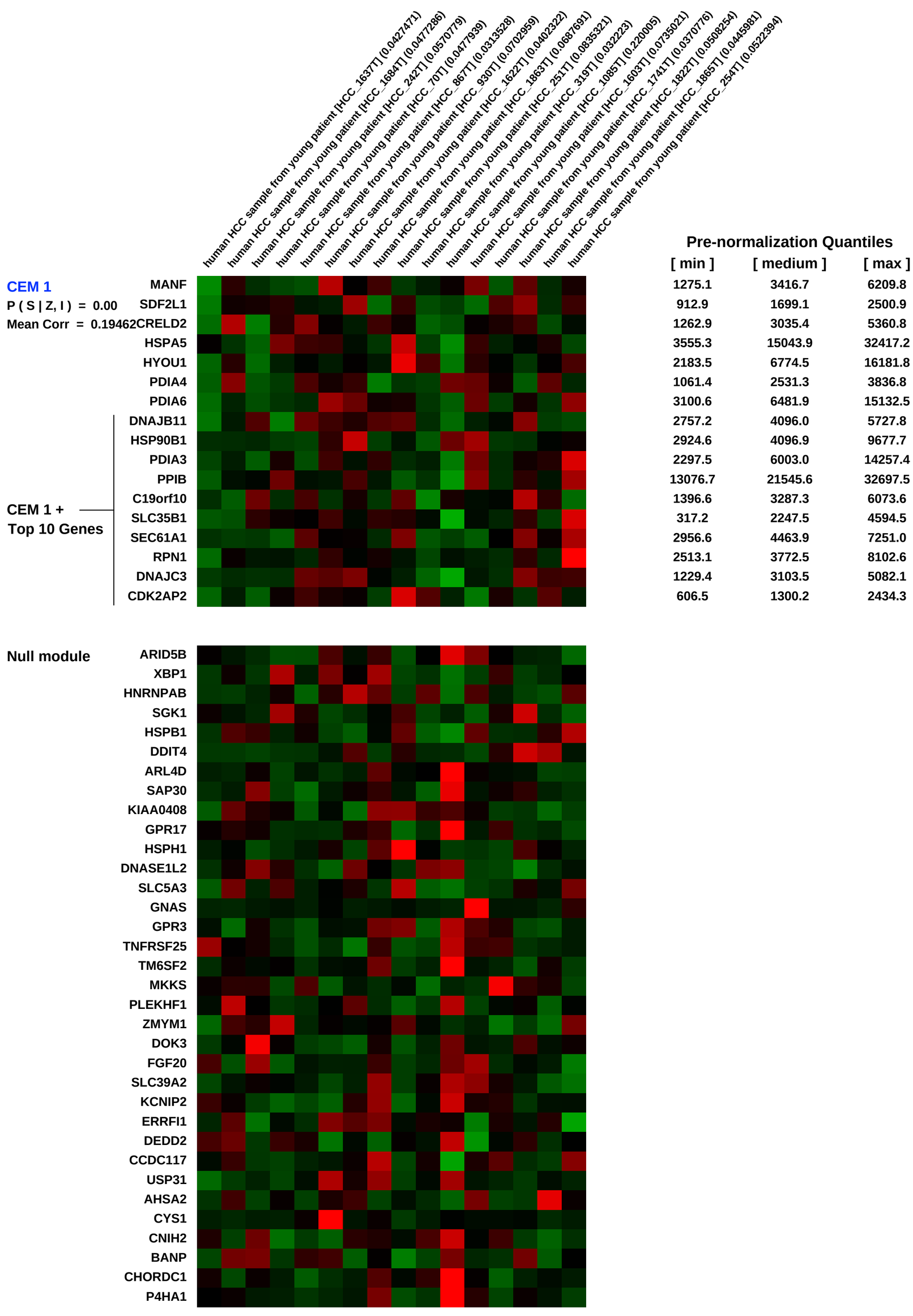

GEO Series "GSE11622" Expression Profiles

Num of samples in this series: 38

Scale of expression profile Z-scores

-3.0 -2.0 -1.0 0.0 1.0 2.0 3.0

GEO Link: http://www.ncbi.nlm.nih.gov/geo/query/acc.cgi?acc=GSE11622
Status: Public on May 20 2009
Title: Molecular Analysis of the Vaginal Response to Estrogens in the Ovariectomized Rat and Postmenopausal Woman
Organism: Homo sapiens
Experiment type: Expression profiling by array
Platform: GPL570
Pubmed ID: 18578861

Summary & Design:

Summary:
Background. Vaginal atrophy (VA) is the thinning of the vaginal epithelial lining, typically the result of lowered estrogen levels during menopause. Some of the consequences of VA include increased susceptibility to bacterial infection, pain during sexual intercourse, and vaginal burning or itching. Although estrogen treatment is highly effective, alternative therapies are also desired for women who are not candidates for hormone replacement therapy (HRT). The ovariectomized (OVX) rat is widely accepted as an appropriate animal model for many estrogen-dependent responses in humans; however, since reproductive biology can vary significantly between mammalian systems, this study examined how well the OVX rat recapitulates human biology at the transcriptional level. This report describes an analysis of expression profiling data, comparing the responses of rat and human vaginae to estrogen treatment. Results. The level of differential expression between pre- vs. post- estrogen treatment was calculated for each of the human and OVX rat datasets. Probe sets corresponding to orthologous rat and human genes were mapped to each other using NCBI Homologene. A positive correlation was observed between the rat and human responses to estrogen. Genes belonging to several biological pathways and GO categories were similarly differentially expressed in rat and human. A large number of the coordinately regulated biological processes are already known to be involved in human VA, such as inflammation, epithelial development, and EGF pathway activation. Conclusions. At the transcriptional level, there is evidence of significant overlap of the effects of estrogen treatment between the OVX rat and human VA samples.

Keywords: Disease State Analysis: Animal Model Validation

Overall design:
We analyzed vaginal biopsies from 19 woman pre and post 3 month estradiol treatment and compared to OVX rats treated with E2 for 6 hr, 3 days or 5 days (N=5)

Background corr dist: KL-Divergence = 0.3617, L1-Distance = 0.0643, L2-Distance = 0.0113, Normal std = 0.2601

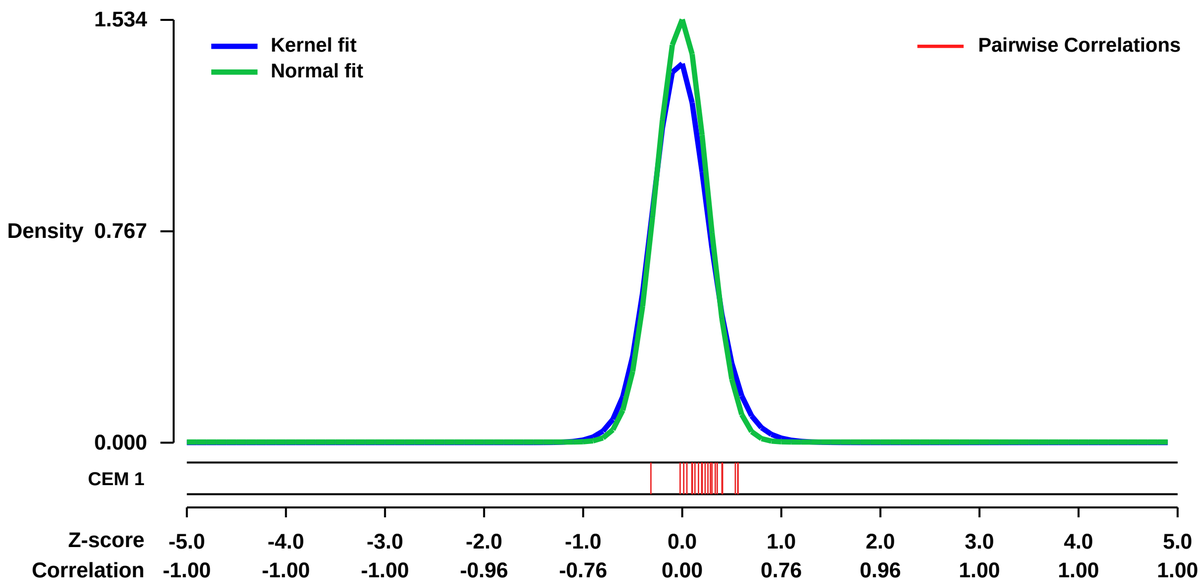

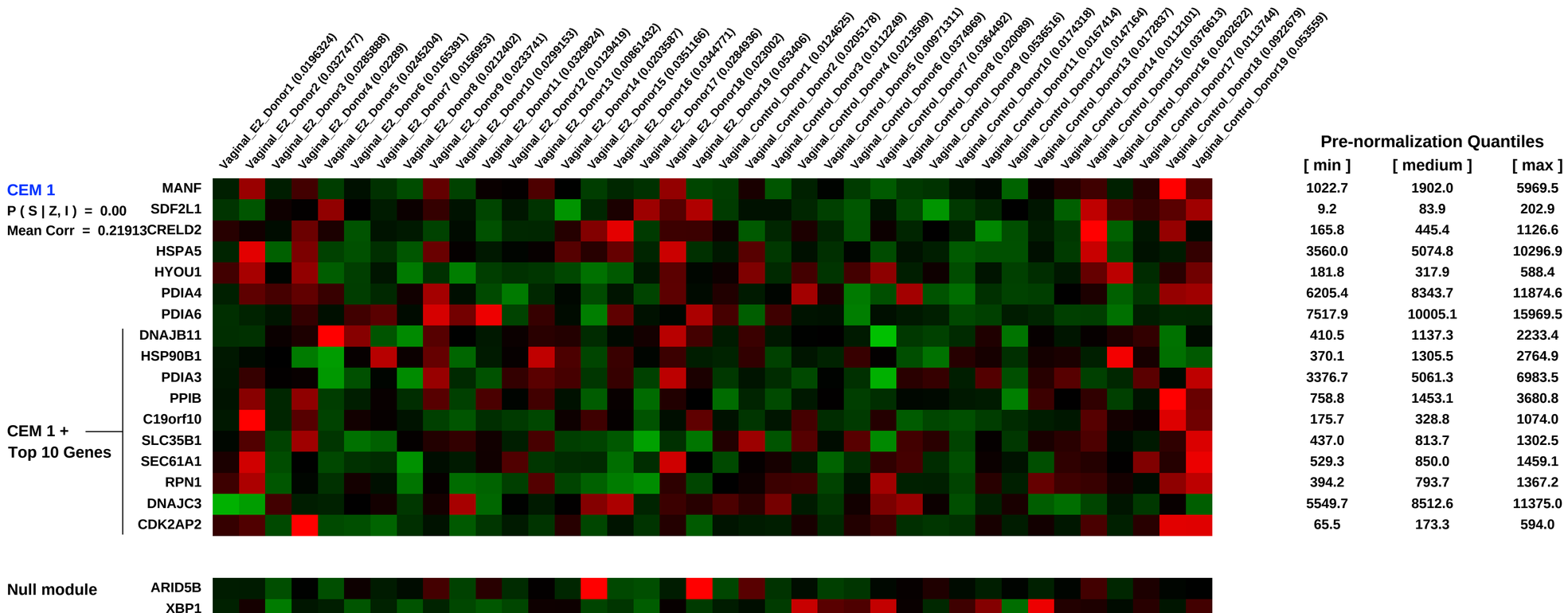

Pre-normalization Quantiles

	[min]	[medium]	[max]
MANF	1022.7	1902.0	5969.5
SDF2L1	9.2	83.9	202.9
CRELD2	165.8	445.4	1126.6
HSPA5	3560.0	5074.8	10296.9
HYOU1	181.8	317.9	588.4
PDIA4	6205.4	8343.7	11874.6
PDIA6	7517.9	10005.1	15969.5
DNAJB11	410.5	1137.3	2233.4
HSP90B1	370.1	1305.5	2764.9
PDIA3	3376.7	5061.3	6983.5
PPIB	758.8	1453.1	3680.8
C19orf10	175.7	328.8	1074.0
SLC35B1	437.0	813.7	1302.5
SEC61A1	529.3	850.0	1459.1
RPN1	394.2	793.7	1367.2
DNAJC3	5549.7	8512.6	11375.0
CDK2AP2	65.5	173.3	594.0

GEO Series "GSE12734" Expression Profiles

Num of samples in this series: 14

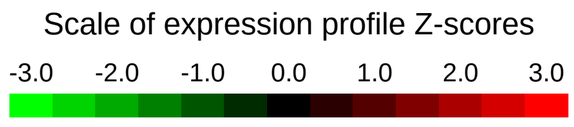

GEO Link:	http://www.ncbi.nlm.nih.gov/geo/query/acc.cgi?acc=GSE12734
Status:	Public on Apr 18 2009
Title:	Comparison of Chronic Lymphocytic Leukemia patients expressing high or low levels of ZAP70 mRNA
Organism:	Homo sapiens
Experiment type:	Expression profiling by array
Platform:	GPL570
Pubmed ID:	19377082
Summary & Design:	**Summary:** **Comparison of Chronic Lymphocytic Leukemia patients expressing high or low levels of ZAP70 mRNA: prognostic factors and interaction with the microenvironment.** **Zeta-associated protein 70 (ZAP70) is a widely recognized prognostic factor in chronic lymphocytic leukemia (CLL), but mechanisms by which its higher expression leads to a poor outcome remain to be fully explained.** **In an attempt to unveil unfavorable cellular properties linked to high ZAP70 expression, we used gene expression profiling to identify genes associated with disparities in B-cells from CLL patients expressing high versus low ZAP70 mRNA, measured by quantitative real-time PCR.** **Keywords: comparison of poor and good prognosis CLL patient transcriptome regarding ZAP70 expression** **Overall design:** **Two groups of seven CLL patients were compared, selected on the basis of either high or low ZAP70 mRNA expression. Total RNA from CD19+ purified cells was exctracted and hybidyzed on Affymetrix GeneChip´fi Human Genome U133 Plus 2.0 Array. Amplification, hybridization and scanning were done according to standard Affymetrix protocols (www.affymetrix.com). CEL files were ,normalized with RMA method.**

Background corr dist: KL-Divergence = 0.1320, L1-Distance = 0.0470, L2-Distance = 0.0050, Normal std = 0.3948

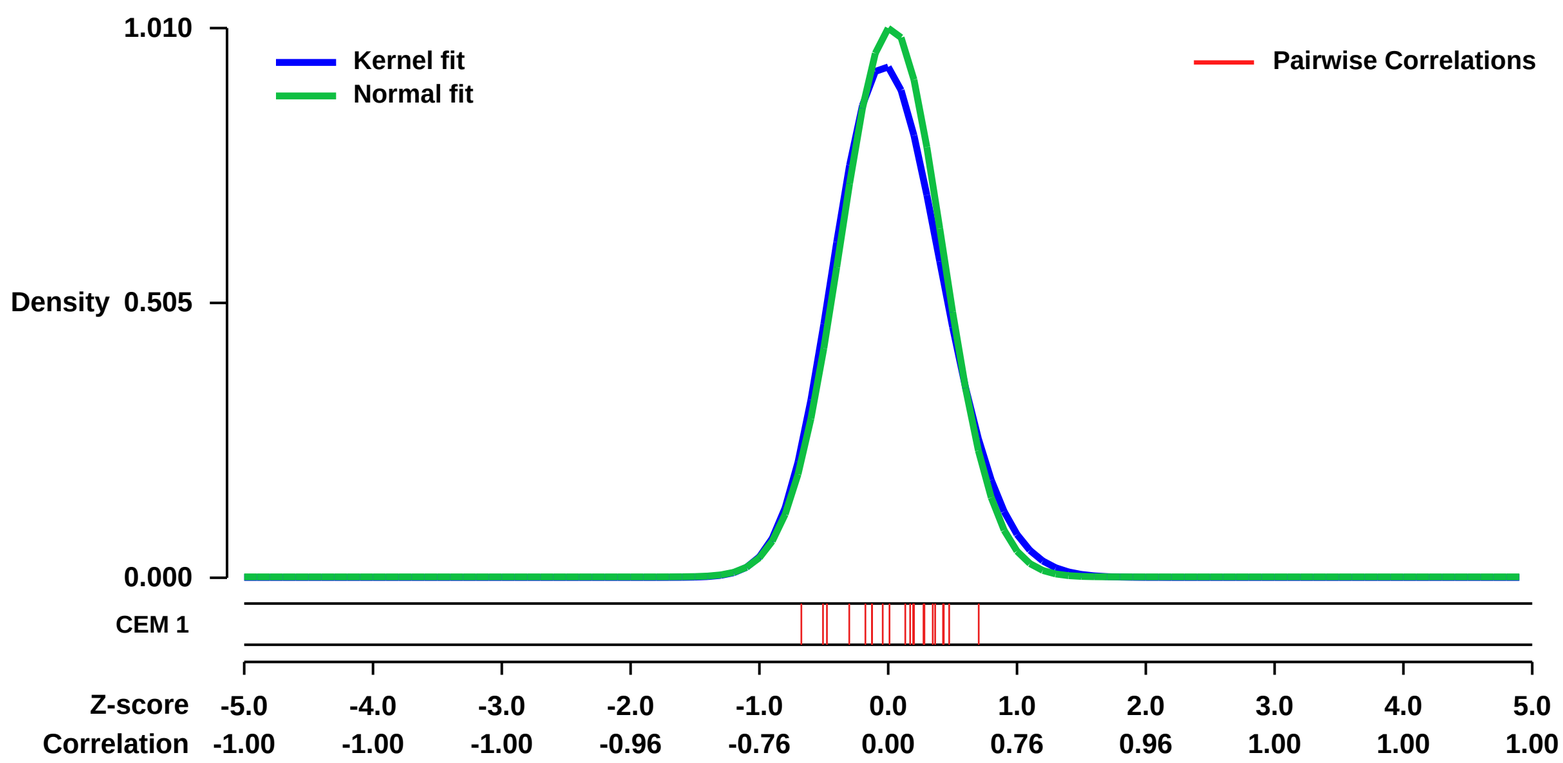

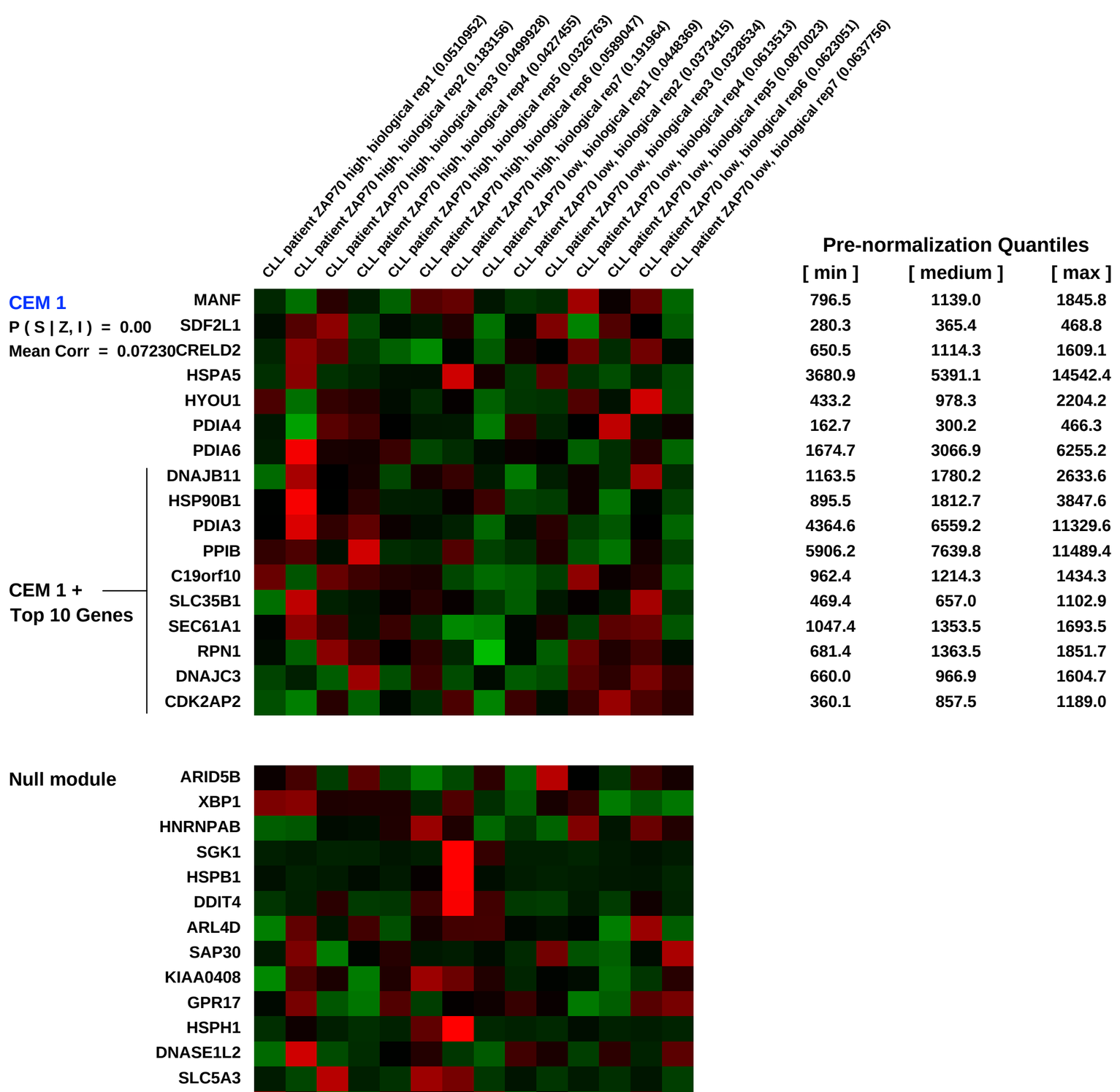

Pre-normalization Quantiles

	[min]	[medium]	[max]
MANF	796.5	1139.0	1845.8
SDF2L1	280.3	365.4	468.8
CRELD2	650.5	1114.3	1609.1
HSPA5	3680.9	5391.1	14542.4
HYOU1	433.2	978.3	2204.2
PDIA4	162.7	300.2	466.3
PDIA6	1674.7	3066.9	6255.2
DNAJB11	1163.5	1780.2	2633.6
HSP90B1	895.5	1812.7	3847.6
PDIA3	4364.6	6559.2	11329.6
PPIB	5906.2	7639.8	11489.4
C19orf10	962.4	1214.3	1434.3
SLC35B1	469.4	657.0	1102.9
SEC61A1	1047.4	1353.5	1693.5
RPN1	681.4	1363.5	1851.7
DNAJC3	660.0	966.9	1604.7
CDK2AP2	360.1	857.5	1189.0

GEO Series "GSE28998" Expression Profiles

Num of samples in this series: 14

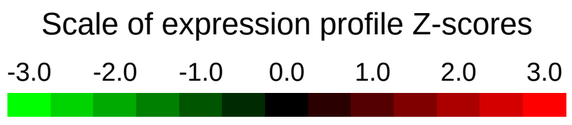

GEO Link:	http://www.ncbi.nlm.nih.gov/geo/query/acc.cgi?acc=GSE28998
Status:	Public on Dec 15 2011
Title:	Human skeletal muscle transcriptional response to exercise
Organism:	Homo sapiens
Experiment type:	Expression profiling by array
Platform:	GPL570
Pubmed ID:	22052873
Summary & Design:	**Summary:** The aim of this investigation was to evaluate the effect of training on the global transcriptional response of skeletal muscle to an acute bout of resistance exercise. **Overall design:** Seven young healthy men and women underwent a 12-week supervised progressive unilateral arm resistance exercise (RE) training program. One week after the last session of training, subjects performed an acute bout of bilateral arm RE in which the trained and the untrained arm exercised at the same relative intensity. A muscle biopsy was obtained 4h post exercise from the biceps brachii of the trained and untrained arm. Trained and untrained muscle samples were analyzed for mRNA levels of over 20,000 annotated genes using Affymetrix U133 Plus 2.0 microarrays.

Background corr dist: KL-Divergence = 0.1173, L1-Distance = 0.0375, L2-Distance = 0.0028, Normal std = 0.4087

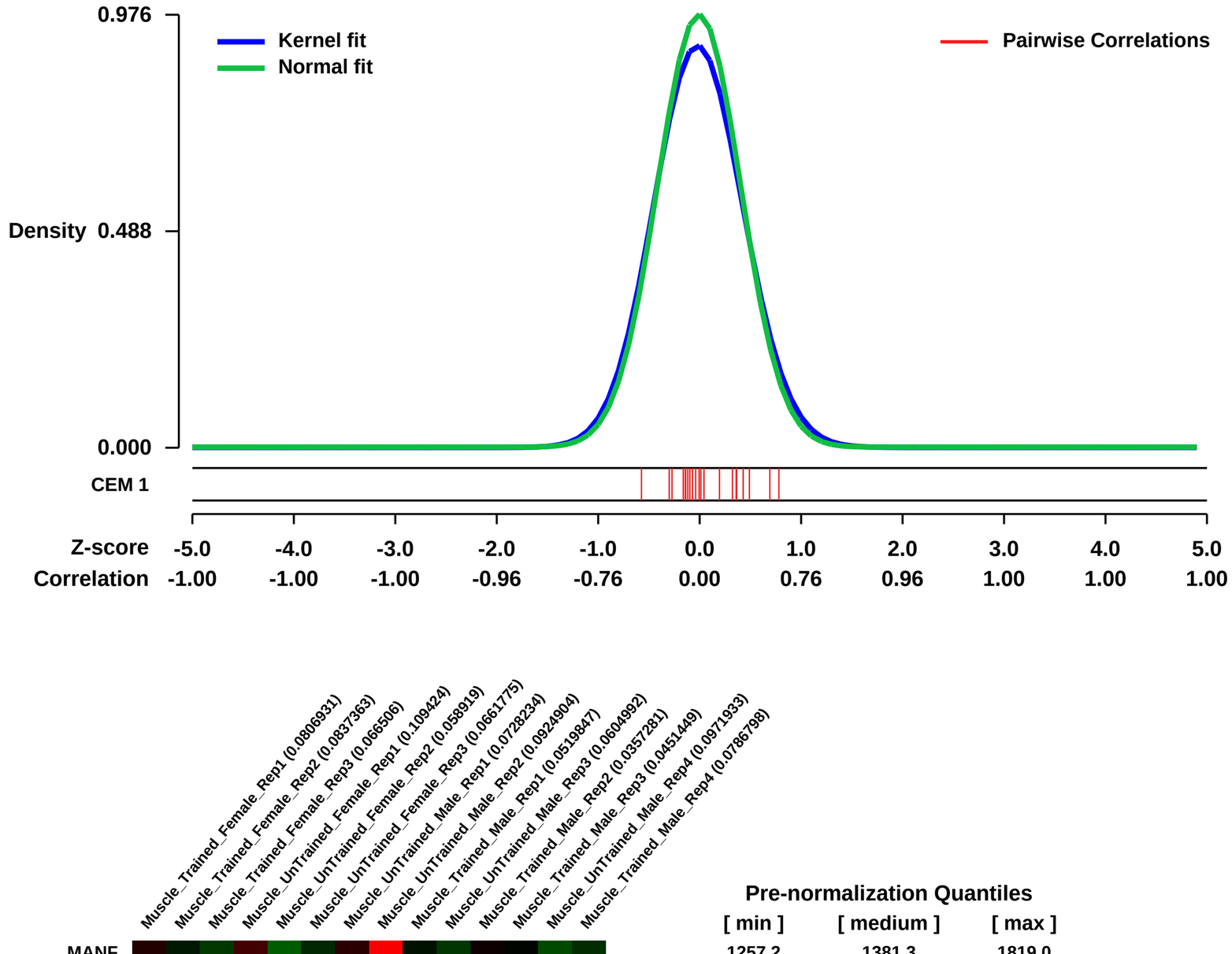

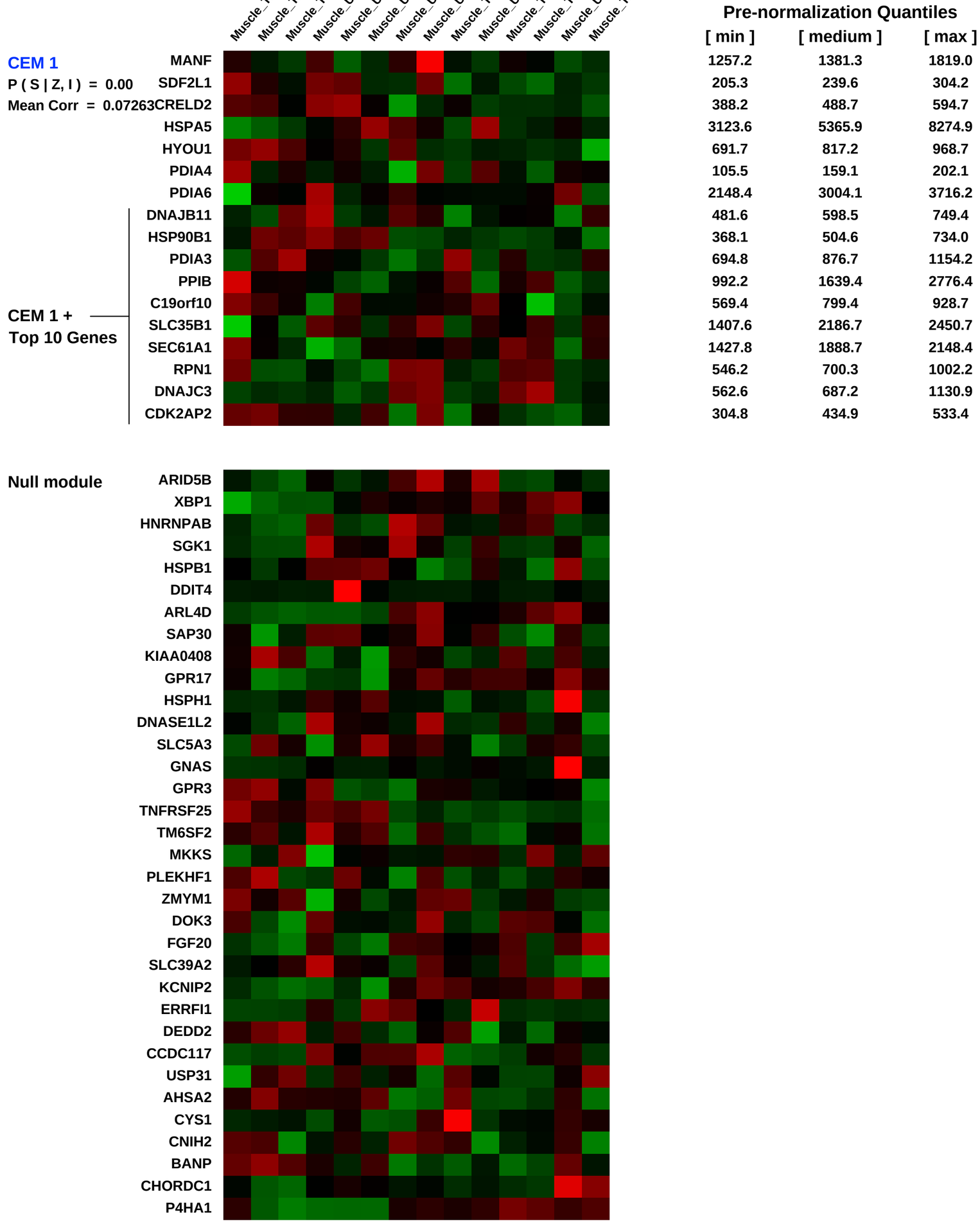

Pre-normalization Quantiles

[min]	[medium]	[max]
1257.2	1381.3	1819.0
205.3	239.6	304.2
388.2	488.7	594.7
3123.6	5365.9	8274.9
691.7	817.2	968.7
105.5	159.1	202.1
2148.4	3004.1	3716.2
481.6	598.5	749.4
368.1	504.6	734.0
694.8	876.7	1154.2
992.2	1639.4	2776.4
569.4	799.4	928.7
1407.6	2186.7	2450.7
1427.8	1888.7	2148.4
546.2	700.3	1002.2
562.6	687.2	1130.9
304.8	434.9	533.4

GEO Series "GSE32547" Expression Profiles

Num of samples in this series: 18

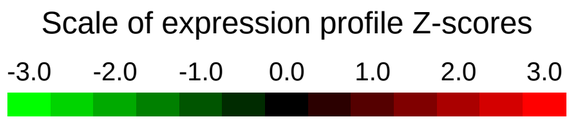

GEO Link:	http://www.ncbi.nlm.nih.gov/geo/query/acc.cgi?acc=GSE32547
Status:	Public on Jan 01 2013
Title:	Expression data of HUVEC cells after statin treatment
Organism:	Homo sapiens
Experiment type:	Expression profiling by array
Platform:	GPL570
Pubmed ID:	
Summary & Design:	**Summary:** 3-hydroxy-3-methylglutaryl coenzyme A reductase inhibitors, statins, are known to exert endothelial athero-protective effects through the induction of specific transcriptional factors and their downstream target genes besides lowering LDL-cholesterol. However its critical mechanism has not still been elucidated. Here we report the comprehensive change of transcripts induced by pitavastatin. We used repeated microarray analysis of HUVECs treated with pitavastatin for 4-hours, we identified a group of consistently up - or down - regulated genes. **Overall design:** HUVECs were used within the first 6 passages. For studies, HUVECs were cultivated in medium EGM2MV containing pitavastatin at a concentration of 1 ¸…M, and same concentration of DMSO was used as a control sample.

Background corr dist: KL-Divergence = 0.2214, L1-Distance = 0.0446, L2-Distance = 0.0045, Normal std = 0.3191

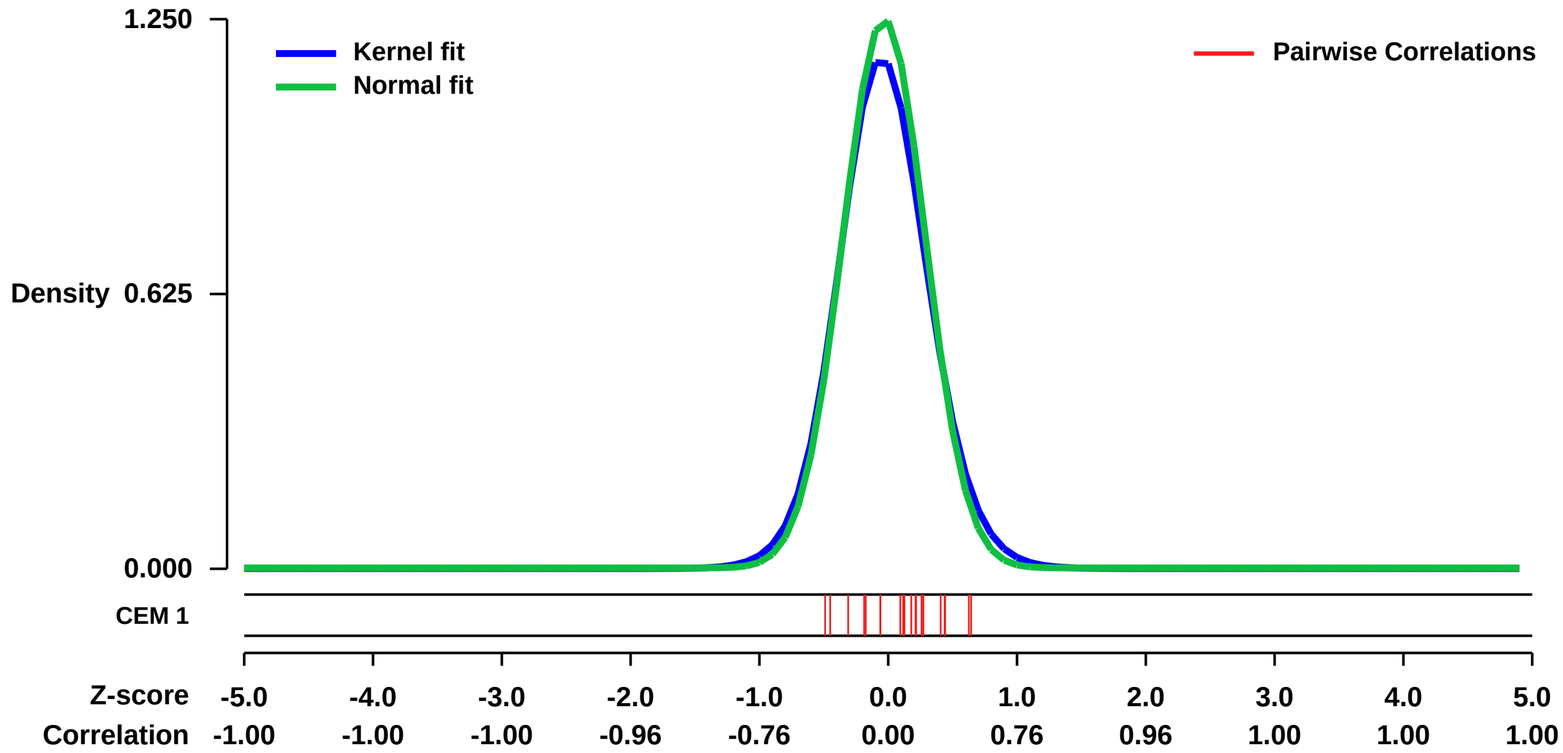

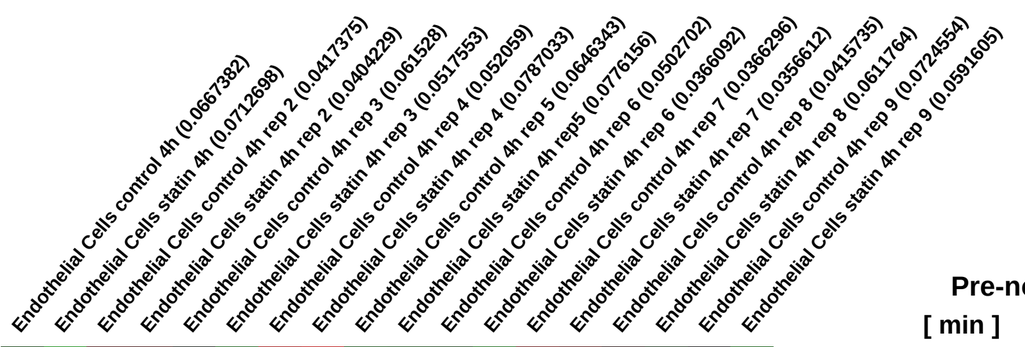

Pre-normalization Quantiles

	[min]	[medium]	[max]
CEM 1			
P (S | Z, I) = 0.00			
Mean Corr = 0.11412			
MANF	2759.8	3704.8	5136.6
SDF2L1	651.6	890.1	1280.4
CRELD2	2732.8	3375.7	4695.3
HSPA5	15745.9	21480.3	25284.8
HYOU1	1837.8	3445.8	5374.5
PDIA4	662.4	1372.0	2273.6
PDIA6	7245.6	10345.8	11693.1
CEM 1 + Top 10 Genes			
DNAJB11	2496.8	3746.3	5116.0
HSP90B1	4046.7	9120.2	15677.7
PDIA3	7488.3	14189.2	17023.0
PPIB	7603.8	15529.8	19535.4
C19orf10	3844.6	4589.4	6646.5
SLC35B1	2018.7	2525.2	3340.5
SEC61A1	3789.1	5038.4	5982.4
RPN1	2071.6	3342.5	4132.2
DNAJC3	1520.2	2284.0	2880.9
CDK2AP2	644.3	1285.7	2121.8
Null module			
ARID5B			
XBP1			
HNRNPAB			
SGK1			
HSPB1			
DDIT4			
ARL4D			
SAP30			
KIAA0408			
GPR17			
HSPH1			
DNASE1L2			
SLC5A3			
GNAS			
GPR3			
TNFRSF25			
TM6SF2			
MKKS			
PLEKHF1			
ZMYM1			
DOK3			
FGF20			
SLC39A2			
KCNIP2			
ERRFI1			
DEDD2			
CCDC117			
USP31			
AHSA2			
CYS1			
CNIH2			
BANP			
CHORDC1			
P4HA1			

GEO Series "GSE18043" Expression Profiles

Num of samples in this series: 12

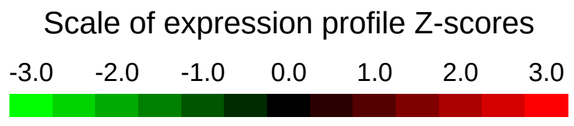

GEO Link:	http://www.ncbi.nlm.nih.gov/geo/query/acc.cgi?acc=GSE18043
Status:	Public on Sep 10 2009
Title:	Priming integrin alpha5 promotes human mesenchymal stromal cell osteoblast differentiation and osteogenesis
Organism:	Homo sapiens
Experiment type:	Expression profiling by array
Platform:	GPL570
Pubmed ID:	19843692

Summary & Design:

Summary:
Human adult mesenchymal stromal cells (hMSC) have the potential to differentiate into chondrogenic, adipogenic or osteogenic lineages, providing a potential source for tissue regeneration. An important issue for efficient bone regeneration is to identify factors that can be targeted to promote the osteogenic potential of hMSCs. Using transcriptomic analysis, we found that integrin alpha5 (ITGA5) expression is upregulated during dexamethasone-induced hMSCs osteoblast differentiation. Gain-of-function studies showed that ITGA5 promotes the expression of osteoblast phenotypic markers as well as in vitro osteogenesis in hMSCs. Downregulation of endogenous ITGA5 using shRNA blunted osteoblast marker expression and osteogenic differentiation. Pharmacological and molecular analyses showed that the enhanced hMSCs osteoblast differentiation induced by ITGA5 was mediated by activation of FAK/ERK1/2-MAPKs and PI3K signaling pathways. Remarkably, activation of ITGA5 using a specific antibody that primes the integrin or a peptide that specifically activates ITGA5 was sufficient to enhance ERK1/2-MAPKs and PI3K signaling and to promote osteoblast differentiation and osteogenic capacity of hMSCs. We also demonstrate that hMSCs engineered to over-express ITGA5 exhibited a marked increase in their osteogenic potential in vivo. These findings not only reveal that ITGA5 is required for osteoblast differentiation of adult human MSCs but also provide a novel targeted strategy using ITGA5 agonists to promote the osteogenic capacity of hMSCs, which may be used for tissue regeneration in bone disorders where the recruitment or capacity of MSCs is compromised.

Keywords: Time course of osteogenic differentiation processes

Overall design:
Gene expression profiles were generated from bone marrow MSC before and 1, 3 and 7 days after stimulation with 10E-7M dexamethasone to study the early molecular processes of osteogenic differentiation. 3 replicates per timepoint.

Background corr dist: KL-Divergence = 0.1086, L1-Distance = 0.0323, L2-Distance = 0.0020, Normal std = 0.4255

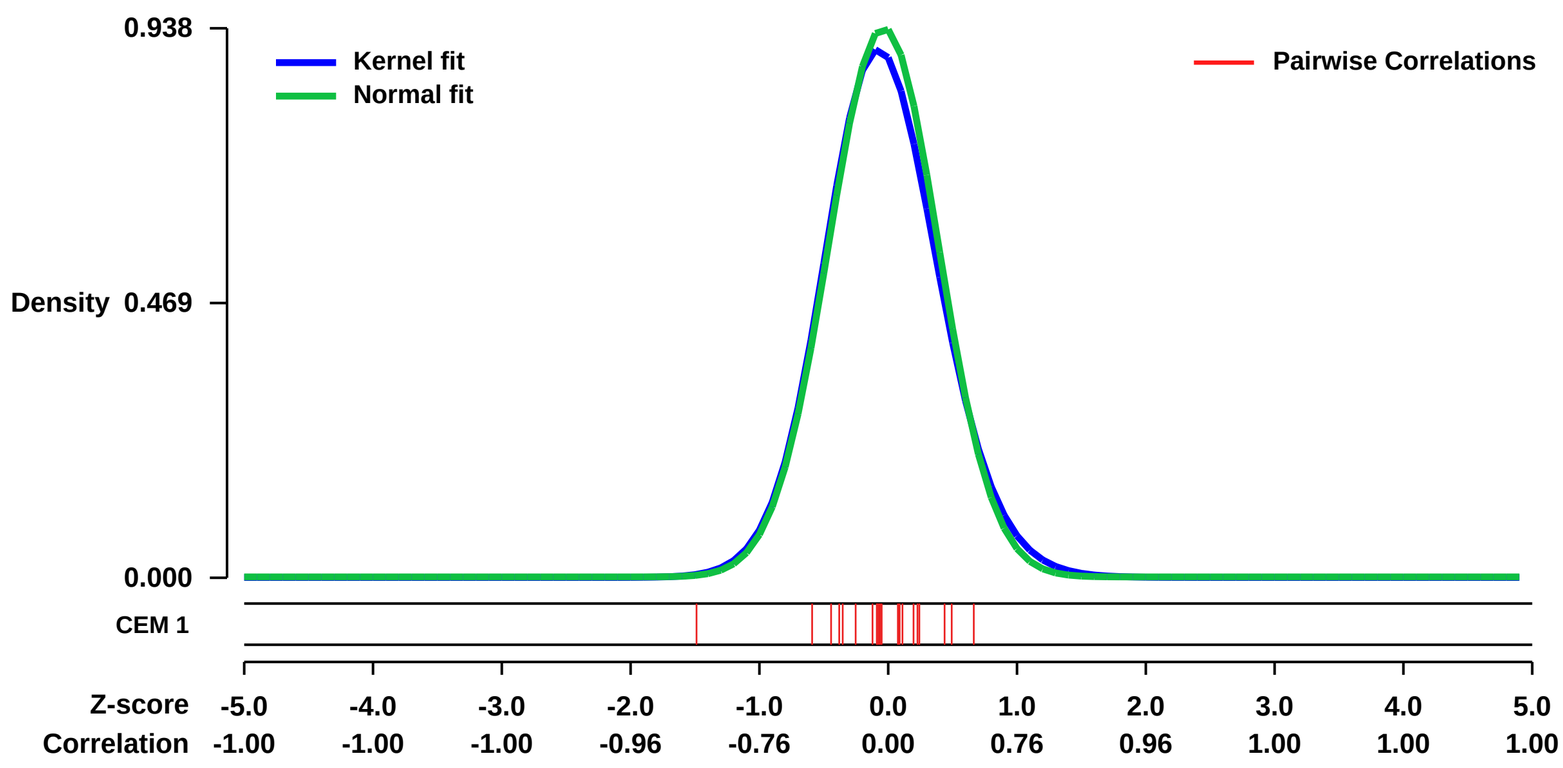

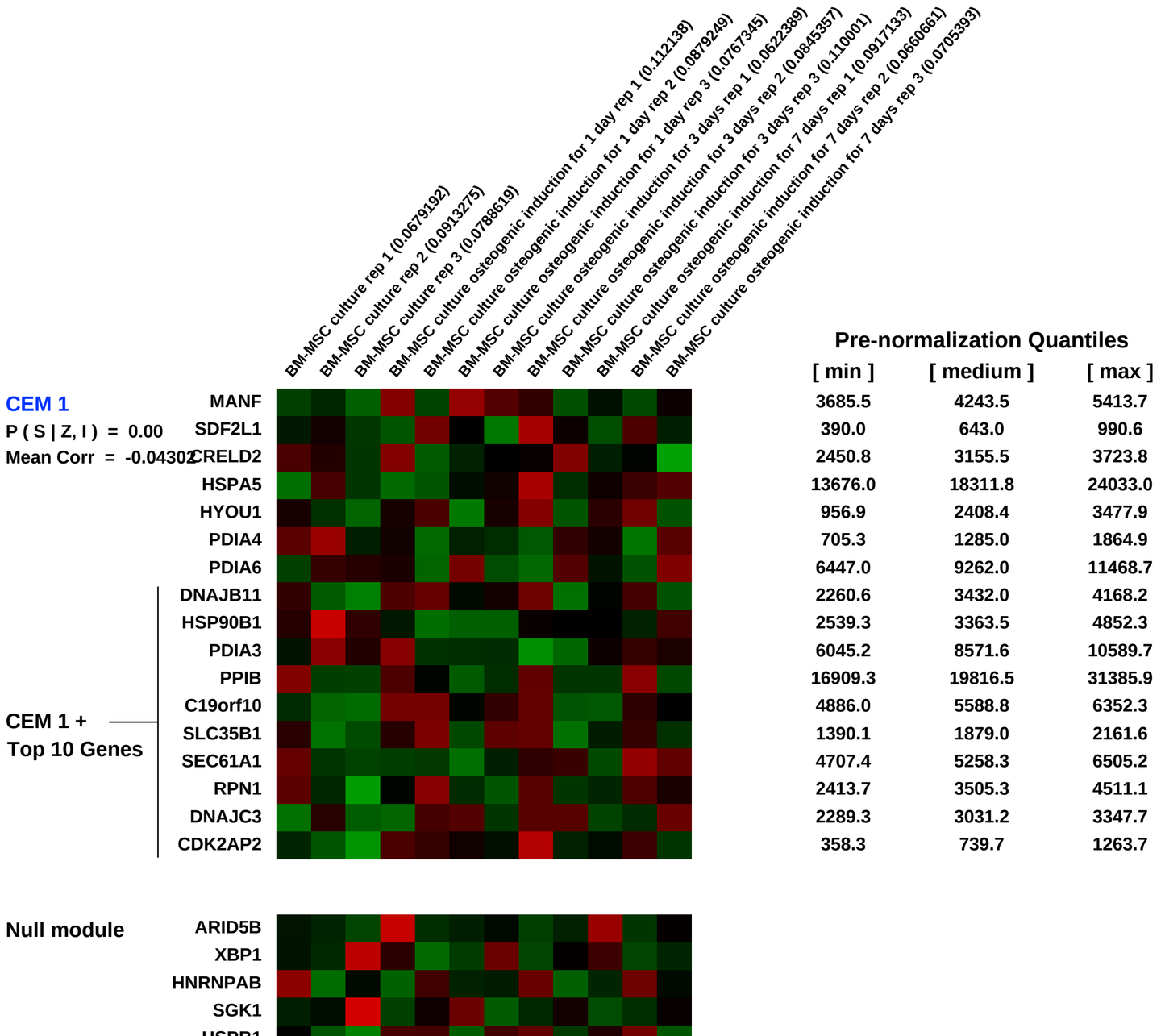

GEO Series "GSE13136" Expression Profiles

Num of samples in this series: 30

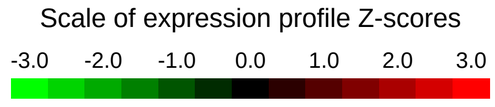

GEO Link:	http://www.ncbi.nlm.nih.gov/geo/query/acc.cgi?acc=GSE13136
Status:	Public on Oct 09 2008
Title:	Identification of candidate neuroblastoma genes by combining genomic and expression microarrays: expression data
Organism:	Homo sapiens
Experiment type:	Expression profiling by array
Platform:	GPL570
Pubmed ID:	17533364
Summary & Design:	**Summary:** Gene expression analysis was performed on 30 Neuroblastomas to identify genes whose transcription is significantly altered by recurrent chromosomal alterations. Genomic copy number losses and gains had been delineated in the tumours using FISH and SNP arrays. We have identified genes significantly altered by 7 recurrent alterations: 1p, 3p, 4p, 10q and 11q loss, 2p and 17q gain, and genes co-amplified and over-expressed as a result of MYCN amplification. Identifying genes whose expression is consistently altered by chromosomal gains or losses is an important step in defining genes of biological relevance in a wide variety of tumour types. However, additional criteria are needed to discriminate further among the large number of candidate genes identified. This is particularly true for neuroblastoma, where multiple genomic copy number changes of proven prognostic value exist. We have used Affymetrix microarrays and a combination of fluorescent in-situ hybridisation and single nucleotide polymorphism (SNP) microarrays to establish expression profiles and delineate copy number alterations in 30 primary neuroblastomas. **Keywords: Disease State Analysis** **Overall design:** 30 neuroblastomas were obtained from patients of all stages (10 patients - stage 1, 2, 3 or 4s disease, 20 patients - stage 4 disease). RNA samples were extracted and analysed using Affymetrix Human Genome U133 Plus 2.0 Arrays. Patient were treated according to the United Kingdom Childrenâ s Cancer Study Group [UKCCSG], European Neuroblastoma Study Group and Localised Neuroblastoma European Study Group protocols.

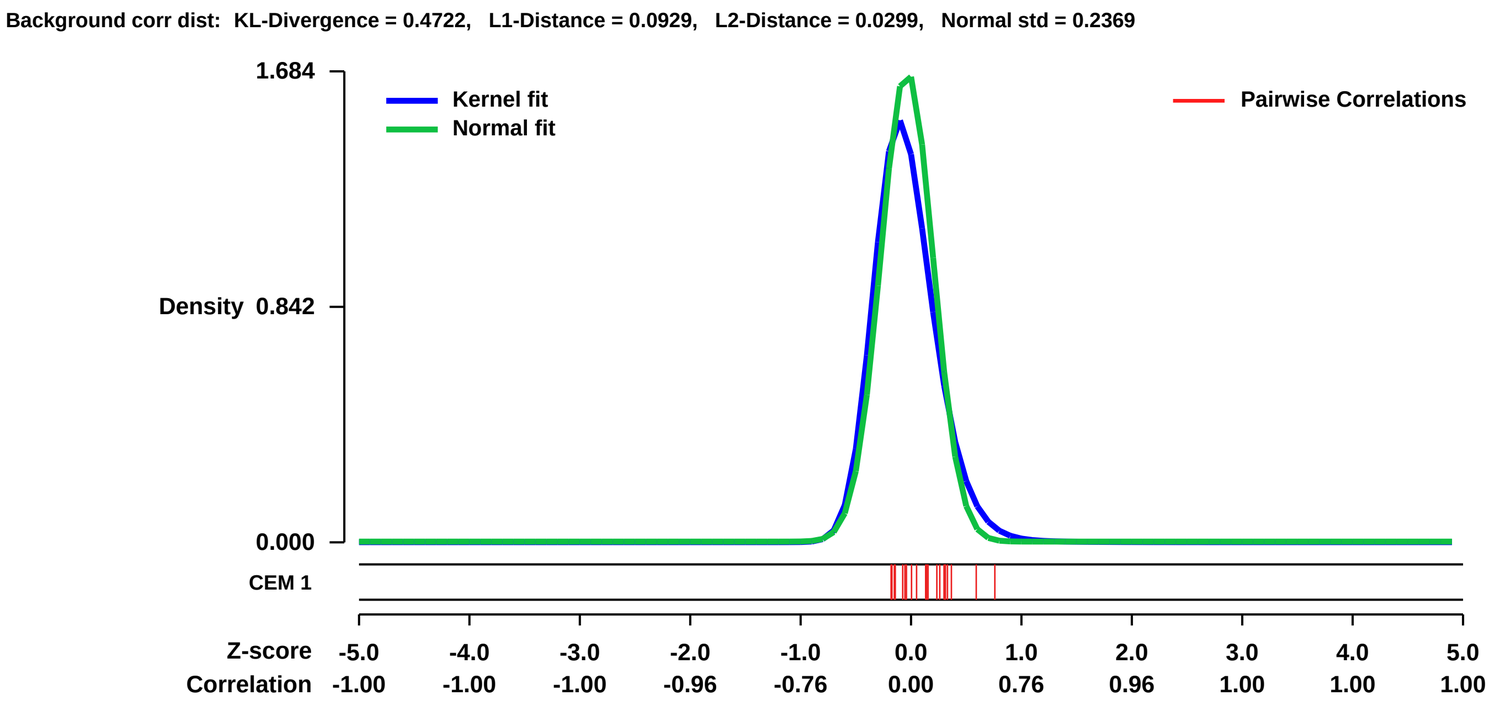

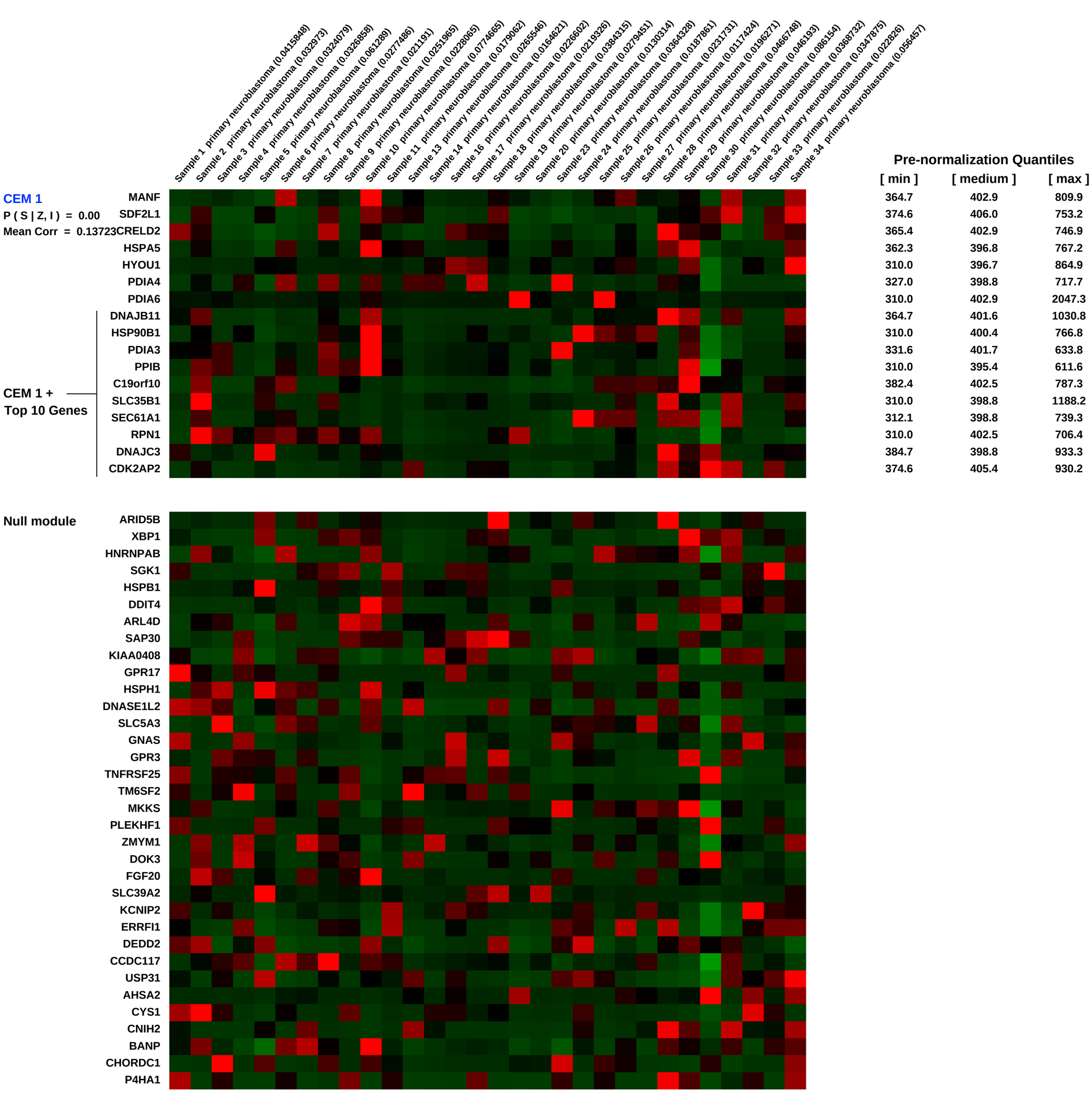

GEO Series "GSE29652" Expression Profiles

Num of samples in this series: 18

Scale of expression profile Z-scores

-3.0 -2.0 -1.0 0.0 1.0 2.0 3.0

GEO Link:	http://www.ncbi.nlm.nih.gov/geo/query/acc.cgi?acc=GSE29652
Status:	Public on Jun 01 2011
Title:	Microarray analysis of the astrocyte transcriptome in the ageing brain: relationship to Alzheimer’s pathology and ApoE genotype
Organism:	Homo sapiens
Experiment type:	Expression profiling by array
Platform:	GPL570
Pubmed ID:	21705112
Summary & Design:	**Summary:** Astrocyte dysfunction impacts their normal function, including neuronal support, thereby contributing to neurodegenerative pathologies including Alzheimer’s disease (AD). Therefore to understand the role of astrocytes in the pathogenesis of age-related disorders we analysed the gene expression profile of astrocytes with respect to Alzheimer-type pathology. The aim of the present study was to combine immuno-LCM and microarray analysis to characterise the astrocyte transcriptome at different Braak stages, and with respect to ApoE genotype, in post-mortem human temporal cortex sampled dervied from the Medical Research Council Cognitive Function and Ageing Study (MRC-CFAS). **Overall design:** keywords: human GFAP-positive astrocytes

Background corr dist: KL-Divergence = 0.1660, L1-Distance = 0.0512, L2-Distance = 0.0062, Normal std = 0.3600

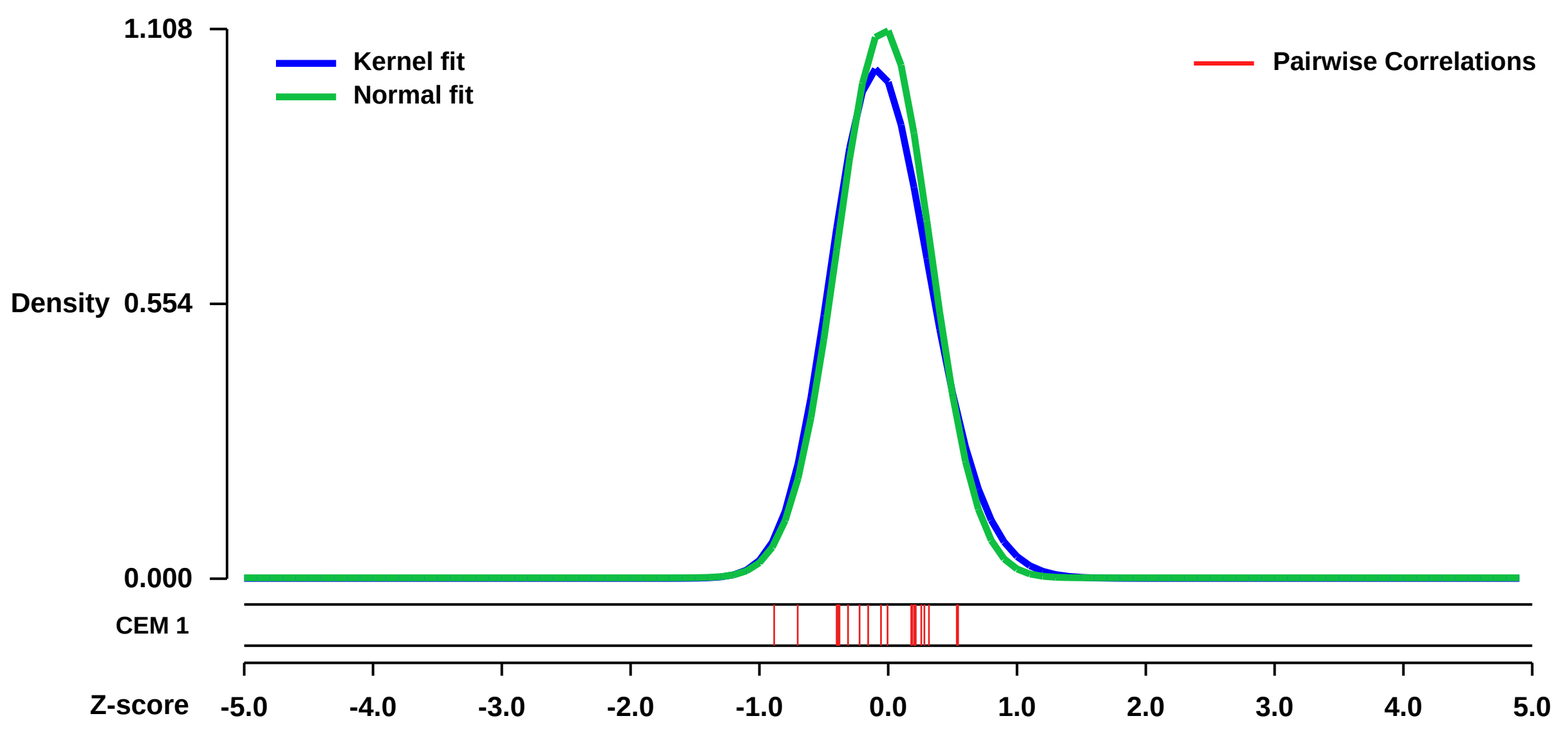

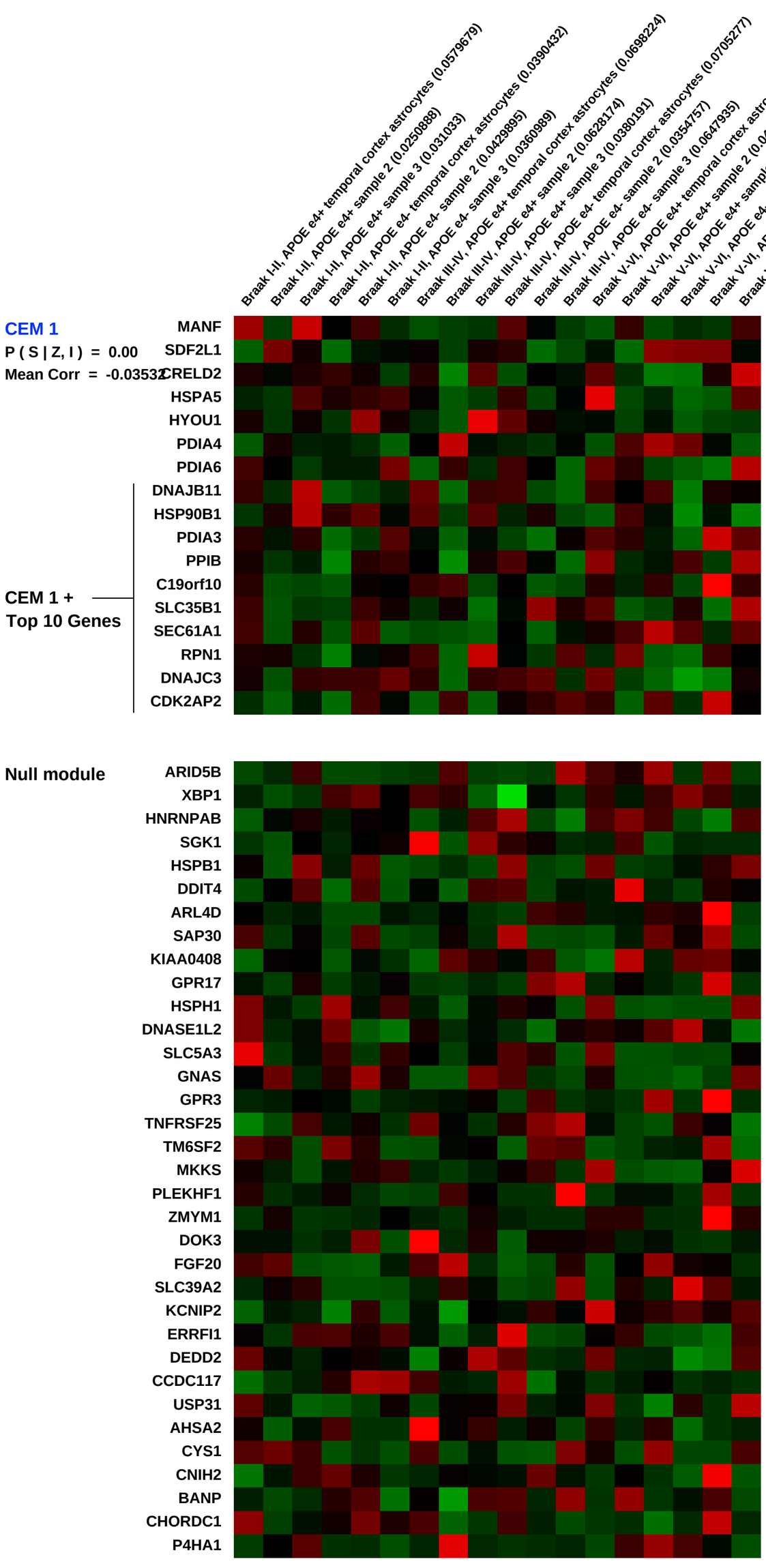

Pre-normalization Quantiles

	[min]	[medium]	[max]
MANF	15.1	164.1	1090.8
SDF2L1	31.2	228.4	519.7
CRELD2	29.6	1137.7	2504.8
HSPA5	42.7	884.9	2844.8
HYOU1	369.8	1042.7	3161.6
PDIA4	277.2	659.6	1662.9
PDIA6	49.7	1421.3	3556.5
DNAJB11	36.6	497.1	1086.8
HSP90B1	162.1	947.7	2065.8
PDIA3	65.5	586.5	1683.1
PPIB	16.0	825.4	1801.7
C19orf10	68.0	355.5	1157.4
SLC35B1	127.5	603.1	1206.7
SEC61A1	36.3	427.4	1181.0
RPN1	62.8	705.0	1712.3
DNAJC3	190.7	1233.3	1561.4
CDK2AP2	17.6	242.2	621.1

GEO Series "GSE22435" Expression Profiles

Num of samples in this series: 17

Scale of expression profile Z-scores

-3.0 -2.0 -1.0 0.0 1.0 2.0 3.0

GEO Link:	http://www.ncbi.nlm.nih.gov/geo/query/acc.cgi?acc=GSE22435
Status:	Public on Aug 03 2011
Title:	Expression of Splicing Factor Genes is Reduced in Human Obesity and Contributes to Enhanced Lipogenesis
Organism:	Homo sapiens
Experiment type:	Expression profiling by array
Platform:	GPL570
Pubmed ID:	21803291
Summary & Design:	**Summary:** Alternative mRNA splicing provides transcript diversity and has been proposed to contribute to several human diseases. Here, we demonstrate that expression of genes regulating RNA processing is decreased in both liver and skeletal muscle of obese humans. To determine the metabolic impact of reduced splicing factor expression, we further evaluated the splicing factor, SFRS10, identified as down-regulated in obese human liver and skeletal muscle and in high fat fed rodents. siRNA-mediated reductions in SFRS10 expression induced lipogenesis and lipid accumulation in cultured hepatocytes. Moreover, SFRS10 heterozygous mice have both increased hepatic lipogenic gene expression and hypertriglyceridemia. We also demonstrate that LPIN1, a key regulator of lipid metabolism, is a splicing target of SFRS10, with reduced SFRS10 levels favoring the lipogenic ¸† isoform of LPIN1. Importantly, LPIN1¸†-specific siRNA abolished the lipogenic effects of decreased SFRS10 expression. Together, our results indicate reduced expression of SFRS10 alters LPIN1 splicing and induces lipogenesis, demonstrating that reduced splicing factor expression observed in human tissues may contribute to metabolic phenotypes associated with human obesity. **Overall design:** Skeletal muscle samples were obtained from 10 lean control subjects and 7 obese subjects with either IGT or DM2 undergoing elective cholecystectomy. Data for liver samples presented in the same manuscript are available at GEO GSE15653. In this analysis RNA was isolated for cRNA preparation and hybridized to Affymetrix Human Genome U133 Plus 2.0 microarrays.

Background corr dist: KL-Divergence = 0.2142, L1-Distance = 0.0516, L2-Distance = 0.0065, Normal std = 0.3226

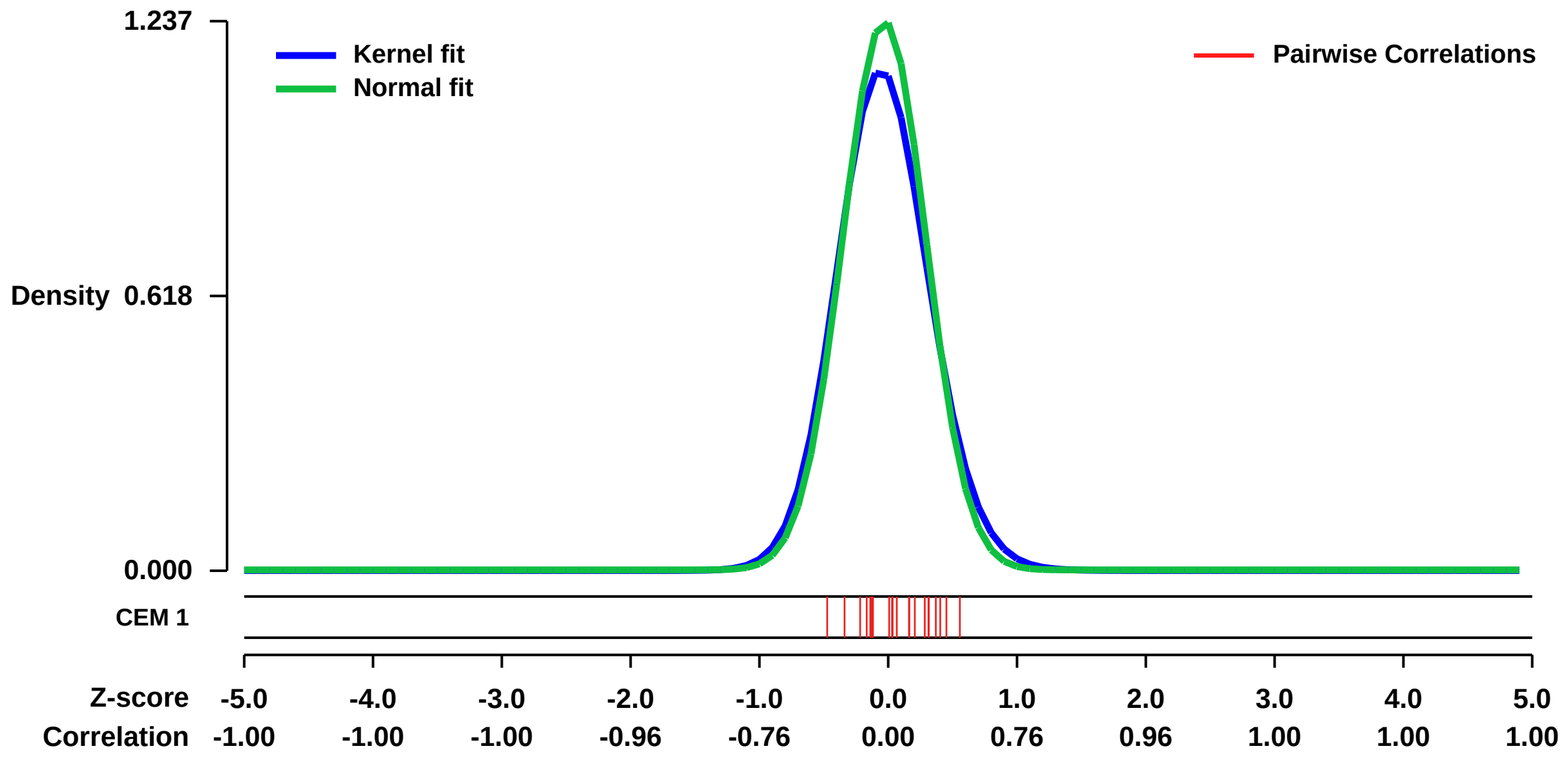

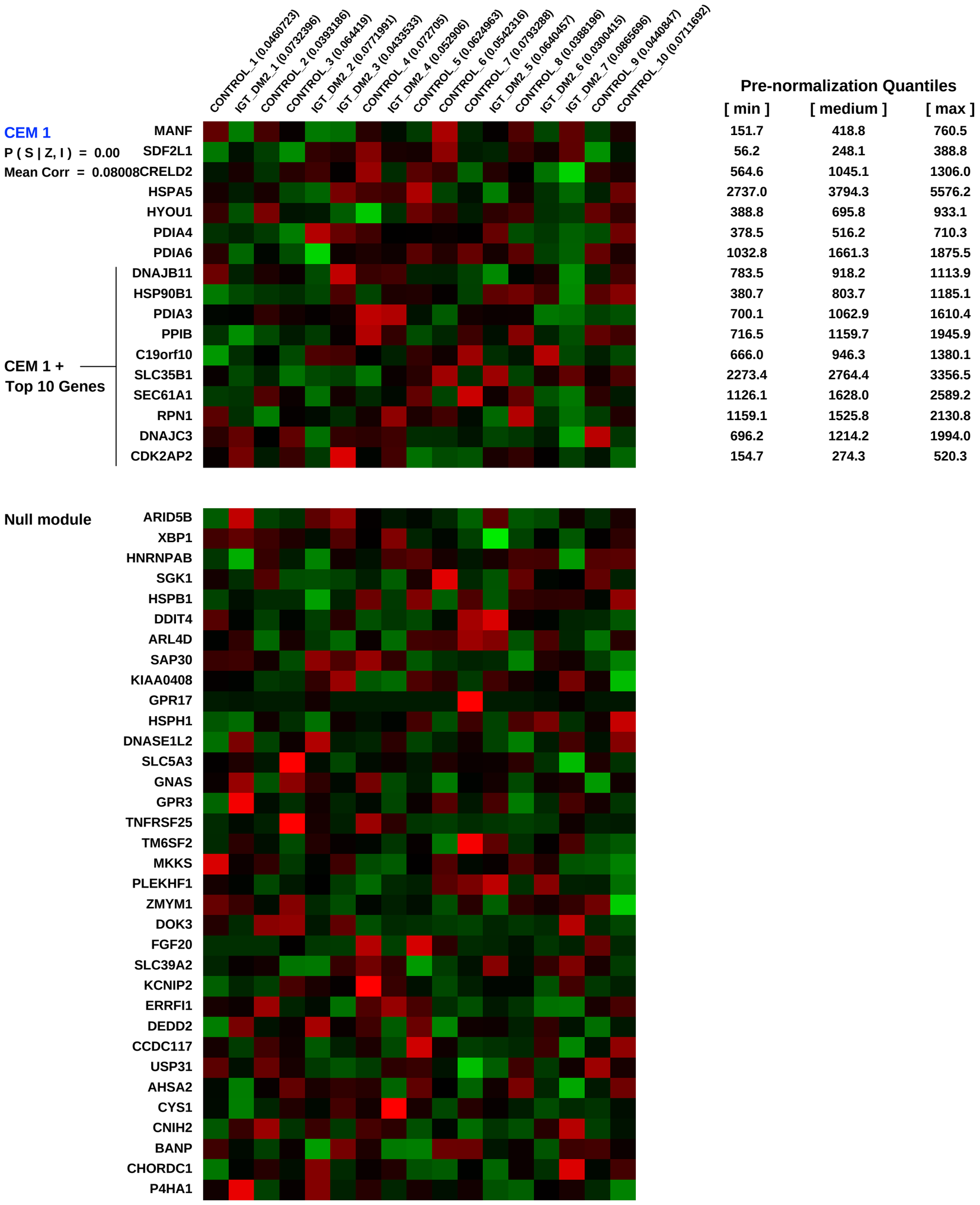

Pre-normalization Quantiles

[min]	[medium]	[max]
151.7	418.8	760.5
56.2	248.1	388.8
564.6	1045.1	1306.0
2737.0	3794.3	5576.2
388.8	695.8	933.1
378.5	516.2	710.3
1032.8	1661.3	1875.5
783.5	918.2	1113.9
380.7	803.7	1185.1
700.1	1062.9	1610.4
716.5	1159.7	1945.9
666.0	946.3	1380.1
2273.4	2764.4	3356.5
1126.1	1628.0	2589.2
1159.1	1525.8	2130.8
696.2	1214.2	1994.0
154.7	274.3	520.3

GEO Series "GSE12710" Expression Profiles

Num of samples in this series: 20

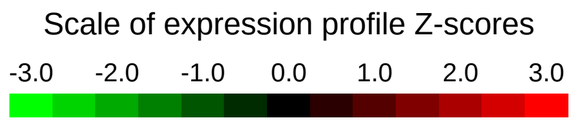

GEO Link:	http://www.ncbi.nlm.nih.gov/geo/query/acc.cgi?acc=GSE12710
Status:	Public on Oct 30 2008
Title:	Differential gene expression profiles are dependent upon method of peripheral blood RNA isolation (direct, heparin)
Organism:	Homo sapiens
Experiment type:	Expression profiling by array
Platform:	GPL570
Pubmed ID:	18847473
Summary & Design:	**Summary:** RNA isolation and purification steps greatly influence the results of gene expression profiling. There are two commercially available products for whole blood RNA collection, PAXgene and Tempus blood collection tubes, and each comes with their own RNA purification method. We examined the impact of RNA isolation methods on gene expression profiles. We demonstrated that peripheral blood RNA isoaltion can critically impact differential expression results, particularly in the clinical setting where fold-change differences are typically small and there is inherent variability within biological corhorts Keywords: micorarray quality assurance **Overall design:** Comparison of 5 healthy control samples drawn directly in PAXgene or Tempus tubes vs. the same 5 healthy control samples drawn in Li Heparin tubes with no PHA stimulation.

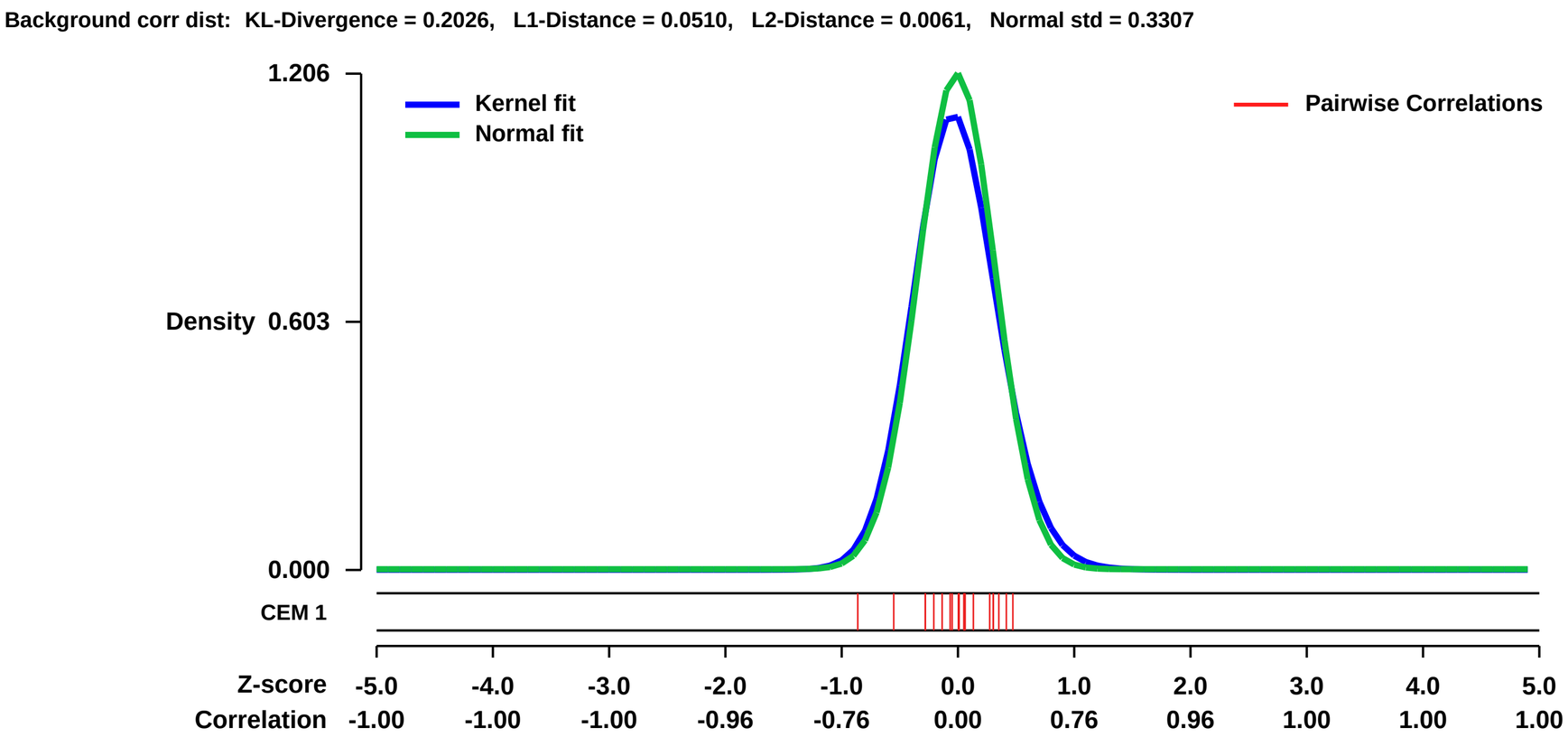

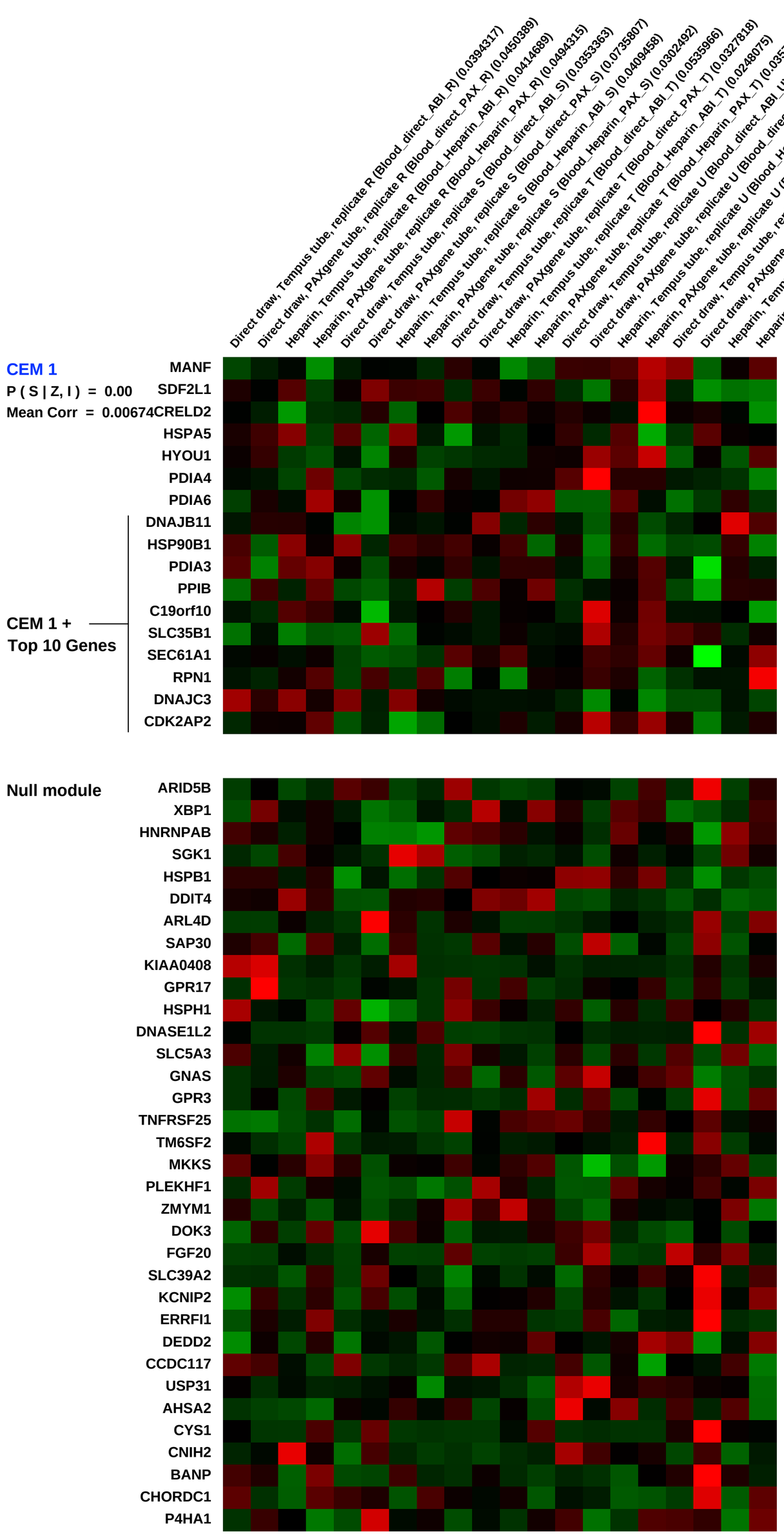

Pre-normalization Quantiles

	[min]	[medium]	[max]
MANF	1289.1	1944.1	2833.7
SDF2L1	177.1	469.0	759.4
CRELD2	436.5	730.2	1174.5
HSPA5	3434.2	5043.3	6310.2
HYOU1	703.1	1272.5	2050.9
PDIA4	583.4	947.7	1918.3
PDIA6	1948.7	2642.9	3423.1
DNAJB11	1321.6	1803.5	2565.9
HSP90B1	261.2	915.0	1368.6
PDIA3	3114.4	6316.3	7752.9
PPIB	8122.4	12608.8	17092.2
C19orf10	368.9	1000.9	1752.7
SLC35B1	625.1	816.3	1123.0
SEC61A1	567.0	1625.4	2165.4
RPN1	2124.2	2812.8	4121.3
DNAJC3	1907.3	3583.9	5925.1
CDK2AP2	470.4	1269.2	2059.3

GEO Series "GSE21497" Expression Profiles

Num of samples in this series: 20

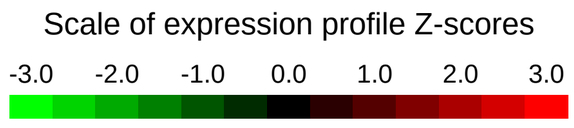

GEO Link:	http://www.ncbi.nlm.nih.gov/geo/query/acc.cgi?acc=GSE21497
Status:	Public on Oct 23 2010
Title:	Common Gene Transcriptional Patterns Following Immobilization, Spinal Cord Injury, and Unloading in Human Skeletal Muscle
Organism:	Homo sapiens
Experiment type:	Expression profiling by array
Platform:	GPL570
Pubmed ID:	20798274
Summary & Design:	**Summary:** Following spinal cord injury, skeletal muscle loss is rapid. This severe atrophy is attributed to declines in protein synthesis and increases in protein breakdown. However, the signaling mechanisms controlling these changes are not well understood. Nine male patients and one female patient with spinal cord injury (SCI) (Mean ´– SEM = 43.9 ´– 6.7 yrs) were recruited for this study. Six patients were quadriplegics and four patients were paraplegics. Inclusion criteria were as follows: patients above the age of 18 yrs, absence of severe brain injury (Glasgow Coma Scale > 13), absence of muscle-crush injury or compartment syndrome, absence of all of the following conditions: hypoxic injury, systemic sepsis, systemic inflammatory or autoimmune disease, and malignancy. Muscle biopsies were obtained from the vastus lateralis muscles of the SCI patients two days and five days post-SCI. Biopsies collected two days post-SCI were included in the current analysis. Expression changes were measured by microarray and gene clustering; identification of enriched functions and canonical pathways were performed using the Database for Annotation, Visualization and Integrated Discovery (DAVID) and Ingenuity Pathway Analysis (IPA). Functional analysis found that 48h following SCI expression, gene expression changes were related to decreases in metabolic functions such as the tricarboxylic acid cycle and oxidative phosphorylation as well as increases in functions associated with protein degradation such as proteasome activity and ubiquitination. Furthermore, increases in expression of metallothioneins were found to be the most over-represented functional group in the DAVID analysis. Results from this study showed that functional categories of gene expression changes in human skeletal muscle are consistent with previous findings in animals. **Overall design:** Muscle biopsies were obtained from the vastus lateralis muscles of the SCI patients two days and five days post-SCI. (N = 10). A 5mm Berstrom biopsy needle was used. Biopsy samples were immediately snap-frozen in liquid nitrogen upon excision. All samples were stored at -80´°C until analysis.

Background corr dist: KL-Divergence = 0.3256, L1-Distance = 0.0686, L2-Distance = 0.0138, Normal std = 0.2705

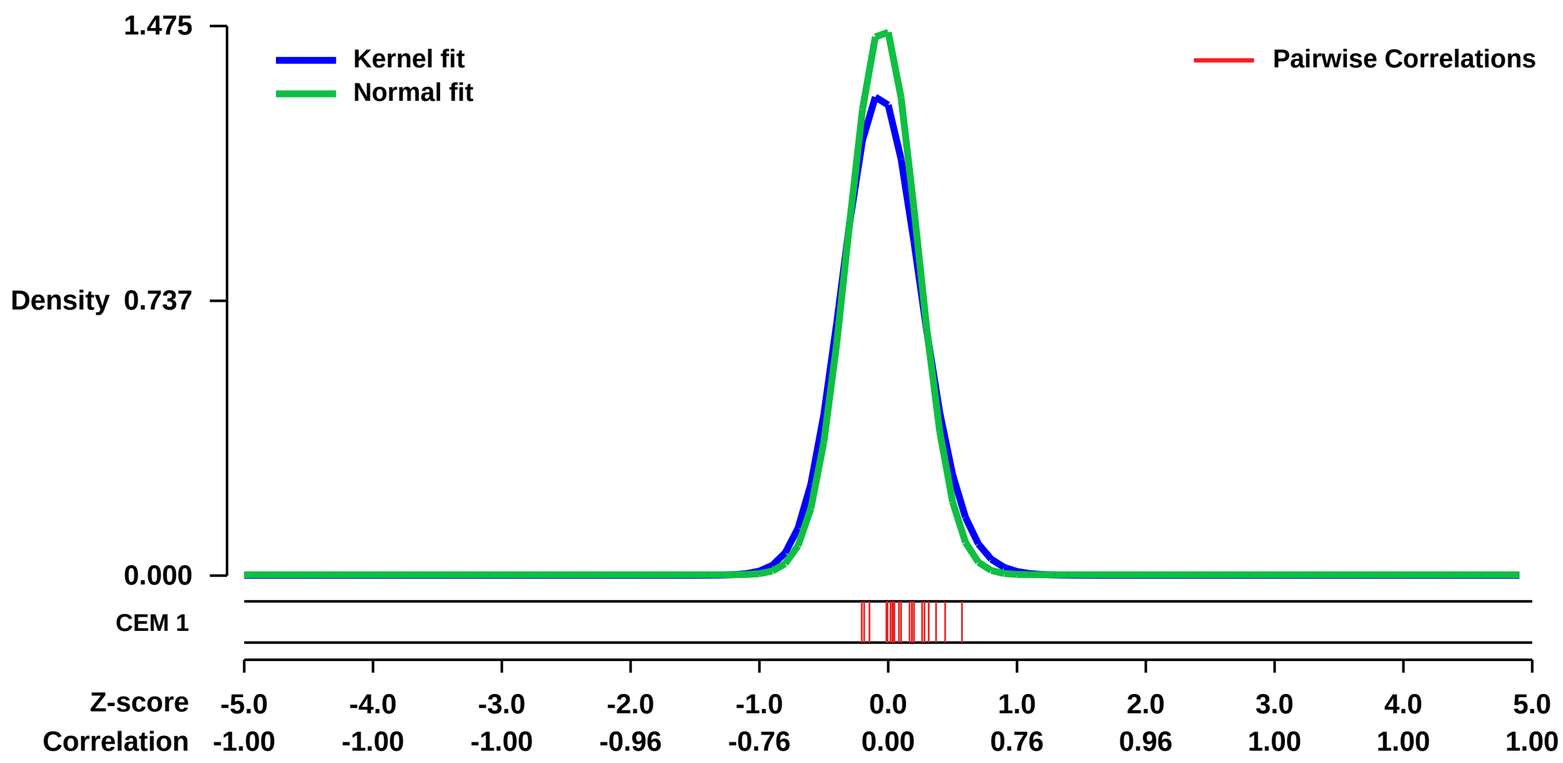

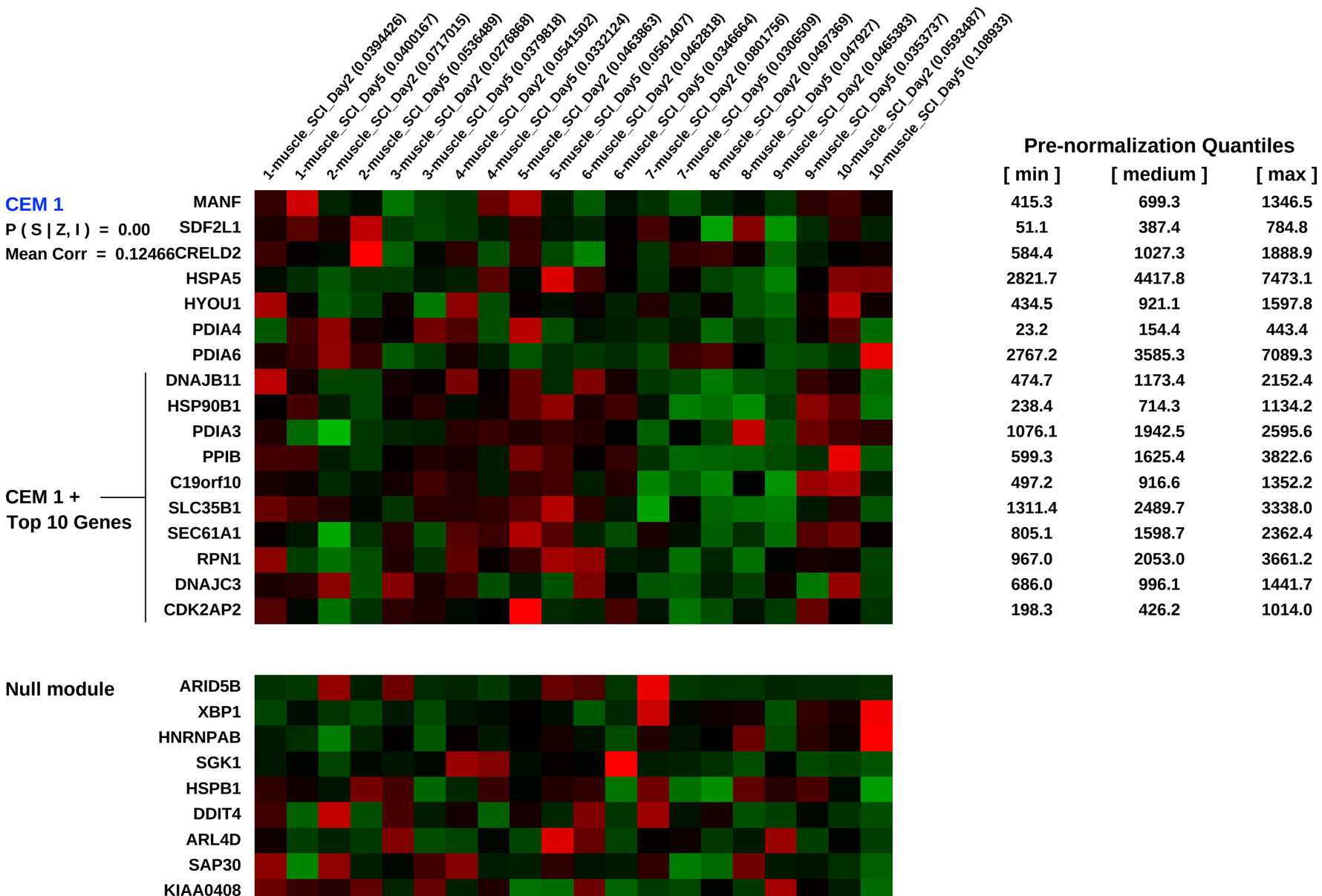

Pre-normalization Quantiles

	[min]	[medium]	[max]
MANF	415.3	699.3	1346.5
SDF2L1	51.1	387.4	784.8
CRELD2	584.4	1027.3	1888.9
HSPA5	2821.7	4417.8	7473.1
HYOU1	434.5	921.1	1597.8
PDIA4	23.2	154.4	443.4
PDIA6	2767.2	3585.3	7089.3
DNAJB11	474.7	1173.4	2152.4
HSP90B1	238.4	714.3	1134.2
PDIA3	1076.1	1942.5	2595.6
PPIB	599.3	1625.4	3822.6
C19orf10	497.2	916.6	1352.2
SLC35B1	1311.4	2489.7	3338.0
SEC61A1	805.1	1598.7	2362.4
RPN1	967.0	2053.0	3661.2
DNAJC3	686.0	996.1	1441.7
CDK2AP2	198.3	426.2	1014.0

GEO Series "GSE31471" Expression Profiles

Num of samples in this series: 18

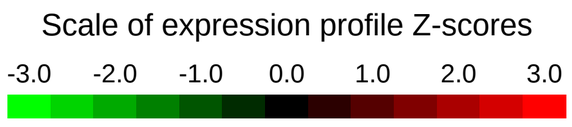

GEO Link:	http://www.ncbi.nlm.nih.gov/geo/query/acc.cgi?acc=GSE31471
Status:	Public on Jan 03 2013
Title:	Host cell gene expression in Influenza A/Duck/Malaysia/01 (H9N2) infected A549 cells at 2, 4, 6, 8 and 10 hours post infection
Organism:	Homo sapiens
Experiment type:	Expression profiling by array
Platform:	GPL570
Pubmed ID:	22470468
Summary & Design:	**Summary:** We used the microarray data to analyze host cells response on A549 cells infected with A/Duck/Malaysia/01 (H9N2) **Overall design:** The A/Duck/Malaysia/01 (H9N2) infected A549 cells were harvested at 2, 4, 6, 8 and 10 hpi and RNA extraction was performed using standard protocol as described by Affymetrix. The aim of this experiment is to analyze host response to Influenza A/Duck/Malaysia/01 (H9N2) infection.

Background corr dist: KL-Divergence = 0.0135, L1-Distance = 0.0438, L2-Distance = 0.0025, Normal std = 0.9059

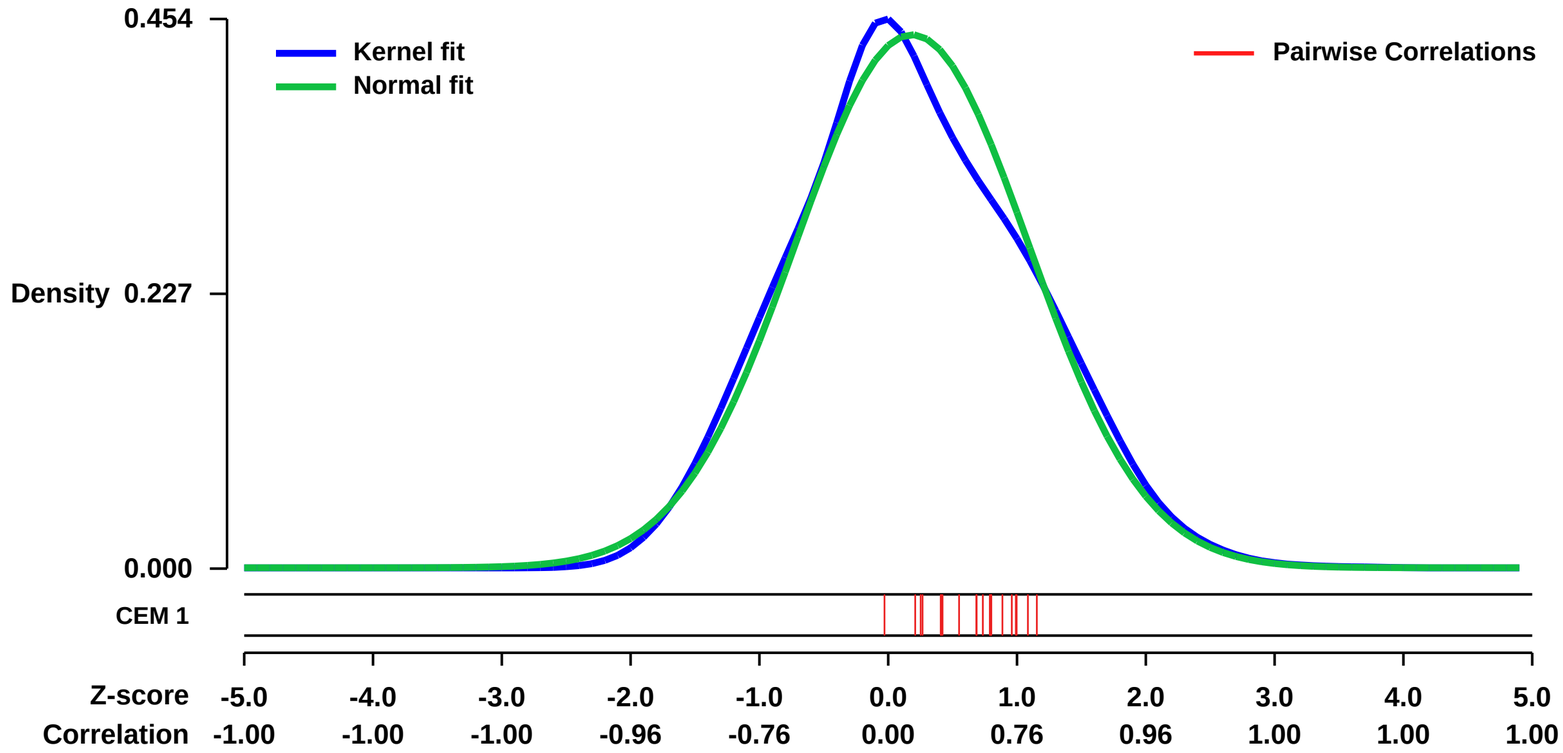

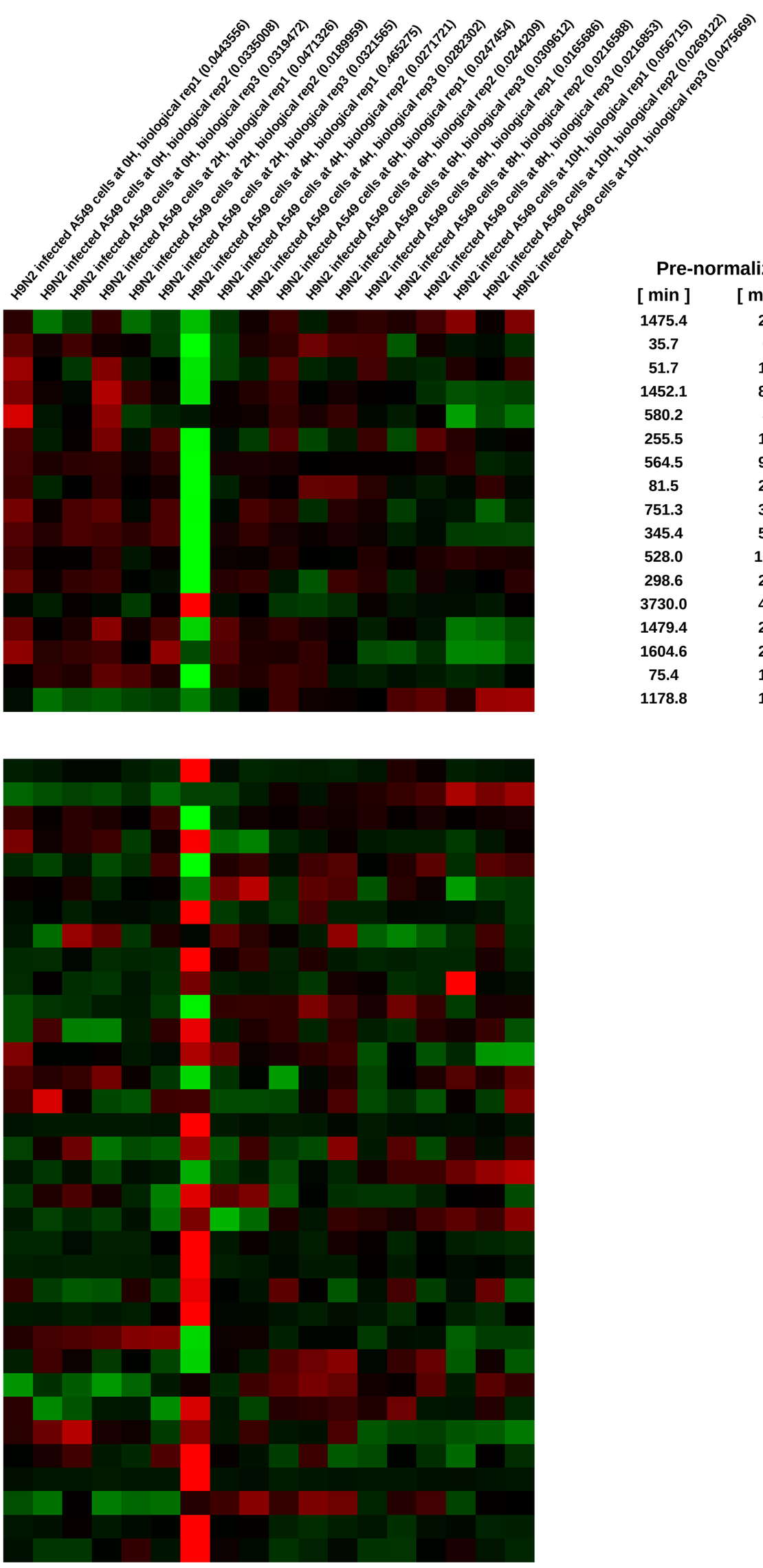

GEO Series "GSE21832" Expression Profiles

Num of samples in this series: 9

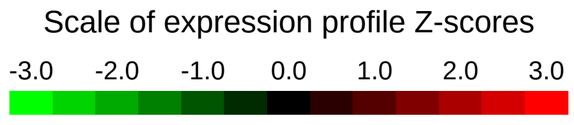

GEO Link:	http://www.ncbi.nlm.nih.gov/geo/query/acc.cgi?acc=GSE21832
Status:	Public on Dec 31 2010
Title:	Identification of the receptor tyrosine kinase AXL in triple negative breast cancer as a novel target for the human miR-34a microRNA (gene expression)
Organism:	Homo sapiens
Experiment type:	Expression profiling by array
Platform:	GPL570
Pubmed ID:	21814748

Summary & Design:

Summary:
Triple negative breast cancer (TNBC) is histologically characterized by the absence of the hormone receptors estrogen and progesterone, in addition to having a negative immunostain for HER-2. The aggressiveness of this disease and lack of targeted therapeutic options for treatment is of high clinical importance. MicroRNAs are short 21- to 23 nucleotide endogenous non-coding RNAs that regulate gene expression by binding to mRNA transcripts, resulting in either decreased protein translation or mRNA degradation. Dysregulated expression of miRNAs is now a hallmark of many human cancers. In order to identify a miRNA/mRNA interaction that is biologically relevant to the triple negative breast cancer genotype/phenotype, we initially conducted a miRNA profiling experiment to detect differentially expressed miRNAs in cell line models representing the triple negative (MDA-MB-231), ER+ (MCF7), and HER-2 overexpressed (SK-BR-3) histotypes. We identified human miR-34a expression as being >3-fold down (from its median expression value across all cell lines) in MDA-MB-231 cells, and identified AXL as a putative mRNA target using multiple miRNA/target prediction algorithms. The miR-34a/AXL interaction was functionally characterized through ectopic overexpression experiments with a miR-34a mimic. In reporter assays, miR-34a binds to the putative target site within the AXL 3â UTR to affect luciferase expression. We also observed degradation of AXL mRNA and decreased AXL protein levels, as well as cell signaling effects on AKT phosphorylation and phenotypic effects on cell migration. Finally, we present an inverse correlative trend in miR-34a and AXL expression for both cell line and patient tumor samples.
Comparison of the changes in gene expression as a result of transfections with miR-34a mimic molecules (representing two different vendors; Qiagen and Dharmacon) in MDA-MB-231 cells.

Overall design:
MDA-MB-231 cells were transfected in 6-well dishes (600,000 cells) with either AllStar negative control, Qmimic, or Dmimic at 10 nM final concentration using Lipofectamineâ¢ 2000 (Invitrogen; Carlsbad, CA). All transfections were performed in triplicate. Forty-eight hours post-transfection, total RNA was isolated from each sample using Qiagenâ s miRNeasy extraction kit (Qiagen; Germantown, MD). Total RNA samples were sent to the Laboratory of Molecular Technology (National Cancer Institute at Frederick; Frederick, MD), for processing on Affymetrix GeneChip Human Genome U133 Plus 2.0 microarrays (Affymetrix; Santa Clara, CA). Expression values were normalized using Robust Multichip Averaging (RMA). Only gene probes (AllStar vs. Mimic) that passed a log2 1.5-fold change, p < 0.05 threshold using an Empirical Bayes moderated t statistics with a Benjamini-Hochberg correction for the false discovery rate were reported. All analyses were performed with Bioconductor packages AFFYGUI and LIMMA on a R environment.

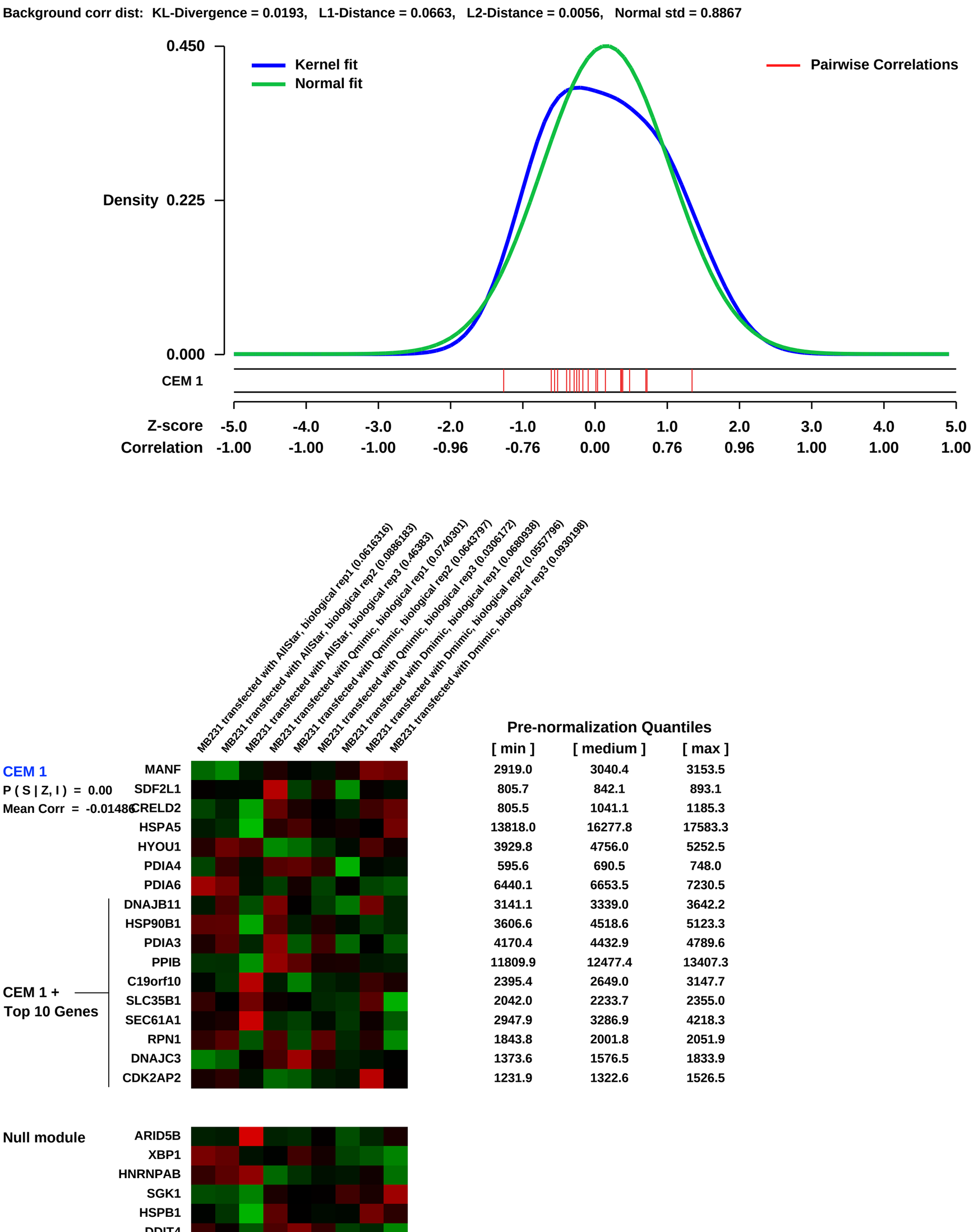

GEO Series "GSE6022" Expression Profiles

Num of samples in this series: 6

Scale of expression profile Z-scores

-3.0 -2.0 -1.0 0.0 1.0 2.0 3.0

GEO Link: http://www.ncbi.nlm.nih.gov/geo/query/acc.cgi?acc=GSE6022
Status: Public on Oct 14 2006
Title: Immunoprecipitation of U2AF65 associated mRNAs
Organism: Homo sapiens
Experiment type: Expression profiling by array
Platform: GPL570
Pubmed ID: 17137510

Summary & Design:

Summary:
U2AF65 is an essential splicing factor involved in the 3'splice site recognition dureing the first steps of spliceosome assembly. In addition, this protein has nucleocytoplasmic shuttling activity and the Drosophila homologue has been implicated in mRNA export.

We have used microarray hybridization coupled to RNA immunoprecipitation from HeLa cell cytoplasmic extracts using anti-U2AF65 antibodies to identify mRNA molecules associated with the U2AF65 splicing factor

Sample preparation methods (Gama-Carvalho et al, 2006, submitted)

Suspension HeLa cells were grown in DMEM, 10% FCS, Pen/Strep and split 1:2 the day before harvesting. Post-nuclear cytoplasmic extracts were obtained as described (Herbert and Hecht 1999), using 5x107 cells/ml of lysis buffer. mRNAs were isolated by immunoprecipitation from 200ul of precleared HeLa cell extract, using the anti-U2AF65 MC3 mAb (Gama-Carvalho, Krauss et al. 1997) or the Bb7 anti-PTB mAb (ATCC) for 2h at 4´"C. Immune complexes were precipitated with a slurry with 50% of protein A/protein G agarose beads (Amersham), blocked with 100ug/ul of tRNA and RNAse free BSA (Ambion), by rotating for 1h at 4´"C and washed with lysis buffer. Complexes bound to the beads were eluted with TES buffer (10mM Tris, 0.5M EDTA, 0.5% SDS, pH 8.0) by heating at 65´"C for 10 minutes and Trizol extracted. Polyadenilated RNA in the cell extract (input) and in the immunoprecipitation sample was reverse transcribed, end-tagged and PCR amplified using the Super SMART PCR cDNA synthesis kit from Clontech, following manufacturer instructions. 1ug of input or precipitated RNA was used per RT-PCR reaction to produce samples for microarray hybridization. For each set of samples (input and immunoprecipitated) a 100ul test PCR reaction was performed according to manufacturer instructions and analyzed by agarose gel electrophoresis to select ideal conditions for amplification in the linear range. PCR reactions were pooled to obtain enough material for microarray hybridization. 15ug of PCR amplified cDNA from input and immunoprecipitated samples were fragmented, end labeled with biotin and hybridized to Affymetrix GeneChip Human Genome U133 Plus 2.0 Arrays as described (Brodsky, Meyer et al. 2005), following standard Affymetrix hybridization protocols.

Brodsky, A. S., C. A. Meyer, et al. (2005). ""Genomic mapping of RNA polymerase II reveals sites of co-transcriptional regulation in human cells."" Genome Biol 6(8): R64.

Gama-Carvalho, M., R. D. Krauss, et al. (1997). ""Targeting of U2AF65 to sites of active splicing in the nucleus."" J Cell Biol 137(5): 975-87.

Herbert, T. P. and N. B. Hecht (1999). ""The mouse Y-box protein, MSY2, is associated with a kinase on non-polysomal mouse testicular mRNAs."" Nucleic Acids Res 27(7): 1747-53.

Keywords: RNA immunoprecipitation

Overall design:
RNA immunoprecipitation was performed from HeLa cell extracts with anti-U2AF65 antibodies. For each immunoprecipitation experiment, two Affimetrix microarrays were hybridized with equal amount of total extract cDNA or cDNA from the immunoprecipitated sample. This series contains microarray data from three independant RNA immunoprecipitation experiments

Background corr dist: KL-Divergence = 0.0325, L1-Distance = 0.0173, L2-Distance = 0.0003, Normal std = 0.6552

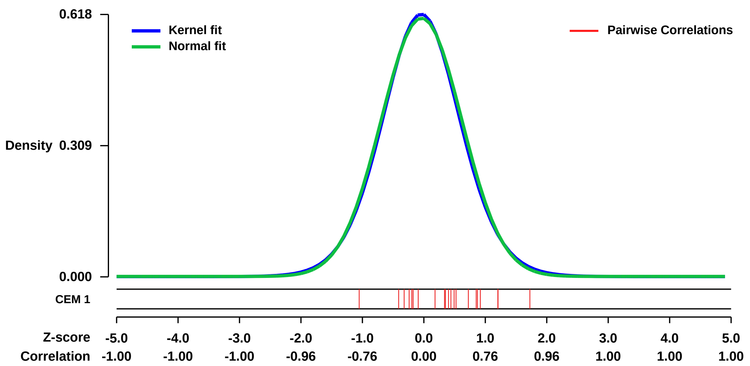

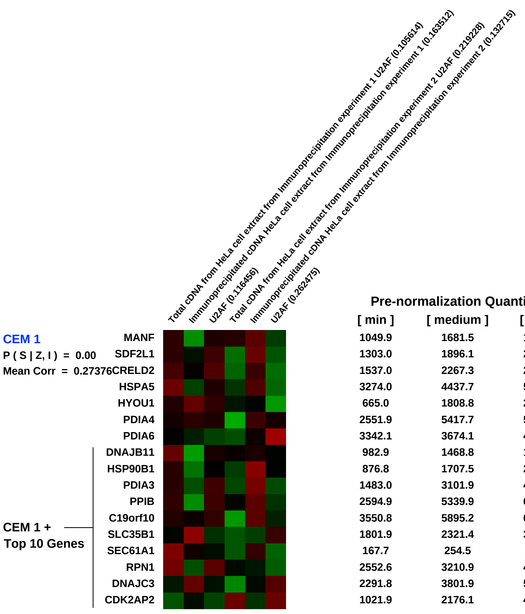

Pre-normalization Quantiles

	[min]	[medium]	[max]
MANF	1049.9	1681.5	1876.2
SDF2L1	1303.0	1896.1	2133.7
CRELD2	1537.0	2267.3	2361.9
HSPA5	3274.0	4437.7	5097.3
HYOU1	665.0	1808.8	2216.0
PDIA4	2551.9	5417.7	5834.2
PDIA6	3342.1	3674.1	4332.8
DNAJB11	982.9	1468.8	1670.6
HSP90B1	876.8	1707.5	2697.0
PDIA3	1483.0	3101.9	4140.9
PPIB	2594.9	5339.9	6015.6
C19orf10	3550.8	5895.2	6606.4
SLC35B1	1801.9	2321.4	3266.7
SEC61A1	167.7	254.5	336.5
RPN1	2552.6	3210.9	4203.6
DNAJC3	2291.8	3801.9	5096.6
CDK2AP2	1021.9	2176.1	4168.4